EUROPEAN CONGRESS OF RADIOLOGY

ECR 2020

Book of abstracts

CONTENTS

Springer

myESR.org

EUROPEAN SOCIETY OF RADIOLOGY

Disclaimer

The ECR 2020 Book of Abstracts is published by the European Society of Radiology (ESR) and summarises the presentations that were accepted to be held at the European Congress of Radiology 2020 (programme status as per January 31, 2020). Due to the outbreak of the coronavirus pandemic, the meeting originally planned for March 2020 could not be held.

Abstracts were submitted by the authors warranting that good scientific practice, copyrights and data privacy regulations have been observed and relevant conflicts of interest declared.

Abstracts reflect the authors' opinions and knowledge. The ESR does not give any warranty about the accuracy or completeness of medical procedures, diagnostic procedures or treatments contained in the material included in this publication. The views and opinions presented in ECR abstracts and presentations, including scientific, educational and professional matters, do not necessarily reflect the views and opinions of the ESR.

In no event will the ESR be liable for any direct or indirect, special, incidental, consequential, punitive or exemplary damages arising from the use of these abstracts.

The Book of Abstracts and all of its component elements are for general educational purposes for health care professionals only and must not take the place of professional medical advice. Those seeking medical advice should always consult their physician or other medical professional.

In preparing this publication, every effort has been made to provide the most current, accurate, and clearly expressed information possible. Nevertheless, inadvertent errors in information can occur. The ESR is not responsible for typographical errors, accuracy, completeness or timeliness of the information contained in this publication.

The ECR 2020 Book of Abstracts is a supplement to Insights into Imaging (1869-4101) and published under the Creative Commons Attribution License 4.0 (CC BY 4.0).

Insights Imaging (2020) 11 (Suppl 1): 34
https://doi.org/10.1186/s13244-020-00851-0
Published Online: 5 May 2020

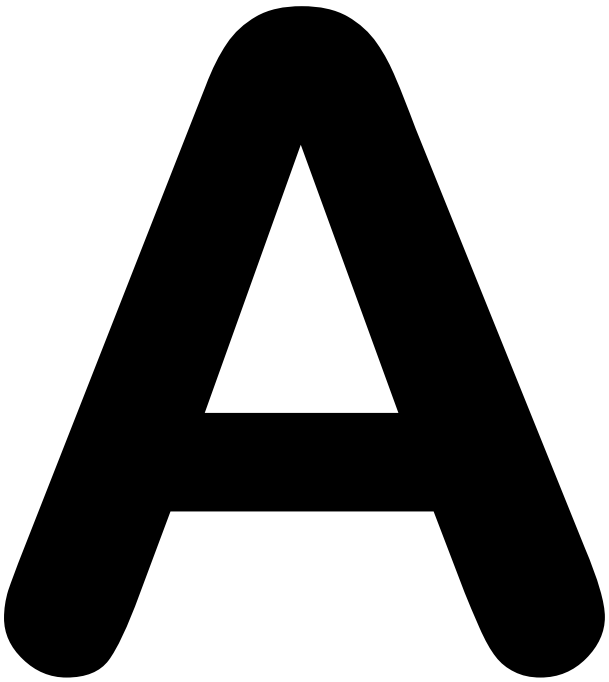

Postgraduate Educational Programme

Children in Focus (IF)
Coffee & Talk (open forum) Sessions (C)
EFOMP Workshop (EF)
ESR at Work Sessions
ESR/EFRS/ISRRT meets Sessions (Meets)
European Excellence in Education (E³)
EuroSafe Imaging Sessions
Joint Sessions
Multidisciplinary Sessions (MS)
New Horizons Sessions (NH)
Plenary Lectures (PL)
Professional Challenges Sessions (PC)
Pros & Cons Session (PS)
Refresher Courses (RC)
Special Focus Sessions (SF)
State of the Art Symposia (SA)
Transatlantic Course of ESR and RSNA (TC)

Wednesday, March 11

08:30 - 10:00 **Room X**

Joint Session of the ESR and ESTRO

ESR/ESTRO

Radiology and radiotherapy in liver tumours

ESR/ESTRO-1/ESR/ESTRO-2 08:30
Chairpersons' introduction
R. G. H. Beets-Tan*; Amsterdam/NL (r.beetstan@nki.nl)*
B. J. Slotman*; Amsterdam/NL (bj.slotman@amsterdamumc.nl)*
Session objectives:
1. To learn about the entire spectrum of radiation treatment of liver tumours.
2. To know its indications.
3. To understand the value of imaging as a guidance for these procedures.
4. To learn about the performance in evaluating response.
Author Disclosures:
R. G. H. Beets-Tan: nothing to disclose; B. J. Slotman: Speaker at ViewRay Inc, Research/Grant Support at ViewRay, Research/Grant Support at Varian medical systems

ESR/ESTRO-3 08:35
Stereotactic body radiation therapy (SBRT) in liver tumours
M. Hawkins*; London/UK (maria.hawkins@oncology.ox.ac.uk)*
Learning objectives:
1. To learn about indications for using SBRT in liver tumours.
2. To understand outcomes after SBRT in liver tumours.
3. To appreciate potential toxicities of SBRT in this setting.
4. To become familiar with future directions in SBRT for liver malignancies.
Author Disclosures:
M. Hawkins: nothing to disclose

ESR/ESTRO-4 08:50
MRI-guided RT in liver tumours
L. Boldrini*; Rome/IT (lucaboldrini@hotmail.it)*
Learning objectives:
1. To become familiar with the MRI guided RT workflow.
2. To describe the applications of MRI guided RT in liver tumours.
3. To provide an overview of the existing MRI guided RT evidence and further developments.
Author Disclosures:
L. Boldrini: Advisory Board at IBA, Research/Grant Support at ViewRay, Consultant at KBMS, KBO Lab

ESR/ESTRO-5 09:05
Selective internal radiation therapy (SIRT) for liver tumours
J. I. Bilbao Jaureguizar*; Pamplona/ES (jibilbao@unav.es)*
Learning objectives:
1. To describe the most common indications of radioembolisation (selective internal radiation therapy).
2. To be familiar with the main anatomical and haemodynamical aspects that will lead to a successful technique.
3. To know how complications can be avoided.
Author Disclosures:
J. I. Bilbao Jaureguizar: Speaker at Sirtex Medical

ESR/ESTRO-6 09:20
Post-selective intra-arterial radiation therapy (SIRT) response evaluation: what a radiologist should know
N. Lev Cohain*; Jerusalem/IL (NAAMAL@HADASSAH.ORG.IL)*
Learning objectives:
1. To describe what is the ideal timeframe for a follow-up protocol.
2. To present tumour response assessment after SIRT.
3. To provide an overview of benign post-SIRT imaging findings.
4. To present possible complications.
Author Disclosures:
N. Lev Cohain: nothing to disclose

09:35
Panel discussion: Radiologists and radiotherapists: how can they help each other to achieve the best care for the patient with liver tumours

08:30 - 10:00 **Room N**

Neuro

RC 111

Craniocervical junction

RC 111-1 08:30
Chairperson's introduction
J. van Goethem*; Antwerp (Edegem)/BE (johan.vangoethem@uantwerpen.be)*
Session objectives:
1. To become familiar with the anatomy and congenital anomalies of the craniocervical junction.
2. To recognise fractures and ligamentous injury of the craniocervical junction.
3. To be aware of craniocervical abnormalities in systemic diseases.
Author Disclosures:
J. van Goethem: nothing to disclose

RC 111-2 08:35
A. Congenital abnormalities
A. Rossi*; Genoa/IT (andrearossi@gaslini.org)*
Learning objectives:
1. To become familiar with the congenital bone anomalies and variants of the craniocervical junction.
2. To learn about associated cerebellar and spinal cord abnormalities.
3. To illustrate craniocervical anomalies in syndromes.
Author Disclosures:
A. Rossi: Consultant at Bracco Group, Speaker at Bracco Group, Speaker at Telemedicine Clinic

RC 111-3 08:58
B. Trauma
A. Adams*; London/UK (ashokadams@hotmail.com)*
Learning objectives:
1. To be able to categorise the spectrum of fractures.
2. To develop an understanding of the biomechanics and management options.
3. To appreciate the imaging findings in ligamentous craniocervical injuries.
Author Disclosures:
A. Adams: nothing to disclose

RC 111-4 09:21
C. Systemic diseases and tumours
K.-O. Loevblad*; Geneva/CH (Karl-Olof.Lovblad@hcuge.ch)*
Learning objectives:
1. To recognise craniocervical injuries in rheumatoid arthritis.
2. To differentiate systemic diseases from other pathology involving the craniocervical junction.
3. To become familiar with retro-odontoid pseudotumours without rheumatoid arthritis.
Author Disclosures:
K.-O. Loevblad: nothing to disclose

09:44
Panel discussion: Imaging strategies for assessing the craniocervical junction

09:00 - 10:00 **Coffee & Talk 2**

Coffee & Talk (open forum) Session

Organised by EuroSafe Imaging

C 9

Radiation protection: more opportunities than risks

C 9-1/C 9-2 09:00
Chairpersons' introduction
G. Frija*; Paris/FR (guy.frija@aphp.fr)*
I. Kralik*; Zagreb/HR (ikralik@kbd.hr)*

Wednesday

Session objectives:
1. To highlight the benefit of imaging procedures.
2. To promote clinical guidelines.
3. To promote equipment and software for significant dose reduction.
Author Disclosures:
G. Frija: nothing to disclose, I. Kralik: nothing to disclose

C 9-3 09:05
What is the ideal referral that we wish to receive?
A. Brady*; Cork/IE (adrianbrady@me.com)*
Learning objectives:
1. To outline the importance of providing appropriate clinical information when requesting imaging studies.
2. To emphasise the two-way conversation between referrers and radiologists inherent in good radiology practice.
3. To reinforce the centrality of radiologist input in choosing the most effective use of imaging to answer clinical problems.
Author Disclosures:
A. Brady: nothing to disclose

C 9-4 09:15
Very low dose: a paradigm shift in radiation protection?
R. W. Loose*; Nuremberg/DE (r.loose@mail.de)*
Learning objectives:
1. To highlight the ALARA principle and requirements for diagnostic image quality.
2. To promote and demonstrate the chances of new dose reduction techniques.
3. To outline diagnostic limitations in cases of too-low dose protocols.
Author Disclosures:
R. W. Loose: nothing to disclose

C 9-5 09:25
Defensive medicine: how to avoid inappropriate "rule-out" referrals
F. Kainberger*; Vienna/AT (franz.kainberger@meduniwien.ac.at)*
Learning objectives:
1. To assess the relevance of overutilisation, overdiagnosis, and overtreatment.
2. To use a simple grading for expressing the pre-test probability in referrals for imaging.
3. To assess the usefulness of strategies for reducing the rate of "rule-out" referrals.
Author Disclosures:
F. Kainberger: nothing to disclose

09:35
Open forum discussion

08:30 - 10:00 **Room E**

E³ - Advanced Course: Interactive Teaching Session for Young (and not so Young) Radiologists

E³ 121a
Musculoskeletal tumours

E³ 121a-1 08:30
A. Soft tissue tumours
F. M. H. M. Vanhoenacker*; Antwerp/BE (filip.vanhoenacker@telenet.be)*
Learning objectives:
1. To describe the imaging findings of soft tissue tumours.
2. To list the differential diagnosis of soft tissue tumours and tumour-like conditions.
Author Disclosures:
F. M. H. M. Vanhoenacker: nothing to disclose

E³ 121a-2 09:15
B. Bone tumours
F. B. B. Ergen*; Ankara/TR (bergen@delta-eur.com)*
Learning objectives:
1. To describe imaging findings of musculoskeletal tumours and tumour-like conditions.
2. To recognise imaging pitfalls of musculoskeletal tumours and tumour-like conditions.
Author Disclosures:
F. B. B. Ergen: nothing to disclose

08:30 - 10:00 **Room F1**

E³ - Advanced Course: Interactive Teaching Session for Young (and not so Young) Radiologists

E³ 121b
Emergency and chest radiology

E³ 121b-1 08:30
A. Dyspnoea in oncologic patients: how to approach it
C. M. M. Schaefer-Prokop*; Amersfoort/NL (cornelia.schaeferprokop@gmail.com)*
Learning objectives:
1. To learn about the role of imaging in these patients.
2. To understand the importance of clinical data for narrowing the differential diagnosis.
Author Disclosures:
C. M. M. Schaefer-Prokop: nothing to disclose

E³ 121b-2 09:15
B. Blunt thoracic trauma: from the plain film to CT
A. Oikonomou*; Toronto, ON/CA (anastasia.oikonomou@sunnybrook.ca)*
Learning objectives:
1. To learn about the spectrum of radiological findings in blunt thoracic trauma.
2. To emphasise the importance of CT reformations for the detection of severe complex traumatic injuries.
Author Disclosures:
A. Oikonomou: nothing to disclose

08:30 - 10:00 **Room F2**

GI Tract

RC 101
Colon cancer: a multidisciplinary approach

Moderator:
L. C. O. K. Blomqvist; Stockholm/SE

RC 101-1 08:30
A. What are the expectations from the surgeon?
D. Ignjatovic*; Oslo/NO (dejan.ignjatovic@medisin.uio.no)*
Learning objectives:
1. To learn about the clinical background and surgical techniques for colon cancer.
2. To learn the surgical nomenclature used for the different variants of surgical procedures, in particular that related to the vasculature.
3. To understand how different imaging features on CT related to anatomical vascular variants can affect the surgical procedure.
Author Disclosures:
D. Ignjatovic: nothing to disclose

RC 101-2 09:00
B. My CT protocol for staging colon cancer
A. Drolsum*; Oslo/NO (adrolsum@gmail.com)*
Learning objectives:
1. To demonstrate the CT acquisition protocol relevant for staging of colon cancer that also allows demonstration of bowel vasculature.
2. To learn about the vascular anatomy of the colon and nodal pathways as visualised on CT.
3. To understand how software post-processing can facilitate assessment and demonstration of vascular anatomy.

Author Disclosures:
A. Drolsum: nothing to disclose

RC 101-3 09:30
C. Integrated staging and vascular assessment
A. Negaard*; Lørenskog/NO (anne.negard@ahus.no)*
Learning objectives:
1. To present clinical cases that demonstrates the use of CT to illustrate local and distant staging in a structured report.
2. To demonstrate how the vascular assessment is performed in the same examination.
3. To present typical cases that demonstrate the importance of assessment, both in relation to the extent of disease as well as the vascular anatomy.
Author Disclosures:
A. Negaard: nothing to disclose

08:30 - 10:00 **da Vinci (Room D1)**

Cardiac

RC 103

Imaging the complexity of pulmonary hypertension (PH) "syndrome"

Moderator:
M. Francone; Rome/IT

RC 103-1 08:30
A. Uncoupling right ventricular physiology with cardiovascular magnetic resonance (CMR): from early adaptation to heart failure
F. Pontana*; Lille/FR (fpontana@gmail.com)*
Learning objectives:
1. To review peculiarities of right heart physiology and ventricular interdependence in pulmonary hypertension.
2. To outline early and late morpho-functional changes associate with right ventricular pressure overload.
3. To understand the primary role of CMR in the evaluation of different forms of pulmonary hypertension.
Author Disclosures:
F. Pontana: Speaker at Siemens Healthcare, Speaker at GE Heathcare, Speaker at Bracco, Speaker at Bayer

RC 103-2 09:00
B. Assessment of PH by CT
E. Mershina*; Moscow/RU (elena_mershina@mail.ru)*
Learning objectives:
1. To review the spectrum of currently available techniques, from pulmonary angiography to CT perfusion, with spectral imaging.
2. To list typical and subtle CT imaging parenchymal and vascular features in primary and secondary forms of disease.
3. To review the current role of CT in clinical guidelines for the diagnosis and treatment of pulmonary hypertension.
Author Disclosures:
E. Mershina: nothing to disclose

RC 103-3 09:30
C. Cardiac imaging to monitor therapeutic response and predict outcome
J. Vogel-Claussen*; Hanover/DE (vogel-claussen.jens@mh-hannover.de)*
Learning objectives:
1. To discuss the advances in treatment and importance of imaging to guide therapy.
2. To understand the predictive role of CT and MRI.
3. To analyse the importance and respective roles of CT and MRI to monitor response to therapy.
Author Disclosures:
J. Vogel-Claussen: Consultant at BMBF, Novartis, Boehringer Ingelheim, GSK, Siemens Healthineers, Grant Recipient at BMBF, Novartis, Boehringer Ingelheim, GSK, Siemens Healthineers

08:30 - 10:00 **Darwin (Room D2)**

Radiographers

RC 114

The role of radiographers in ensuring quality in practice

RC 114-1/RC 114-2 08:30
Chairpersons' introduction
J. Ferda*; Plzen/CZ (ferda@fnplzen.cz)*
D. Pekarovic*; Ljubljana/SI (dean.pekarovic@kclj.si)*
Session objectives:
1. To understand the importance of quality in daily practice.
2. To appreciate the role of radiographers in promoting and delivering quality improvements.
3. To promote discussion on practical approaches to developing a quality culture in medical imaging.
Author Disclosures:
J. Ferda: nothing to disclose, D. Pekarovic: nothing to disclose

RC 114-3 08:36
A. The radiographers' role in justification
P. Bezzina*; Malta/MT (paul.bezzina@um.edu.mt)*
Learning objectives:
1. To review the relevant EU legislation.
2. To understand the impact of legislation on the practice of radiographers.
3. To consider the potential for continuous professional development to support justification across modalities.
Author Disclosures:
P. Bezzina: nothing to disclose

RC 114-4 08:59
B. Quality assurance to guarantee safe and secure procedures
M.-L. Ryan*; Dublin/IE (marielouise.ryan@ucd.ie)*
Learning objectives:
1. To review the concept of quality assurance and its impact on enhancing service delivery.
2. To recognise the need for quality assurance to be part of a radiographer's routine practice.
3. To discuss actual examples highlighting the impact of quality assurance on practices.
Author Disclosures:
M.-L. Ryan: nothing to disclose

RC 114-5 09:22
C. Multimodality intervention: the importance of a quality culture
M. Halbwachs*; Strasbourg/FR (madeline.halbwachs@chru-strasbourg.fr)*
Learning objectives:
1. To understand the complexity of imaging quality assurance in multimodality interventional suites.
2. To be aware of how to manage quality assurance in this complex environment.
3. To consider potential continuous professional development needs in multimodality interventional imaging.
Author Disclosures:
M. Halbwachs: nothing to disclose

09:45
Panel discussion: Monitoring and ensuring quality: the professional role of radiographers

08:30 - 10:00 **Descartes (Room D3)**

Special Focus Session

SF 1a

Evaluating oncologic treatment response in clinical practice and trials

SF 1a-1 08:30
Chairperson's introduction
M. Dewey*; Berlin/DE*
Session objectives:
1. To explain the role of imaging in response evaluation in clinical trials and routine.
2. To explain the role of integrating quantitative imaging into clinical practice.
3. To describe the role of quantification of metastases in clinical practice.
Author Disclosures:
M. Dewey: Patent Holder at Patent on fractal analysis of perfusion imaging (jointly with Florian Michallek, PCT/EP2016/071551), Board Member at M.D. is European Society of Radiology (ESR) Research Chair (2019–2022) and the opinions expressed in this presentation are the author's own and do not represent the view of ESR., Grant Recipient at EU (603266-2) DFG (DE 1361/14-1, DE 1361/18-1, BIOQIC GRK 2260/1, Radiomics DE 1361/19-1 and 20-1 in SPP 2177/1), Berlin University Alliance (GC_SC_PC 27), Berlin Institute of Health (Digital Health Accelerator)., Speaker at Canon, Guerbet. , Author at Editor: Cardiac CT (Springer Nature)., Other at Organisation of Hands-on cardiac CT courses (www.ct-kurs.de) , Other at Institutional research agreements: Siemens, General Electric, Philips, Canon.

SF 1a-2 08:40
Insights from trials about endpoints for response evaluation in clinical practice
L. Fournier*; Paris/FR*
Learning objectives:
1. To list the features of trials using imaging for response evaluation.
2. To explain the limitations of applying this knowledge in clinical practice.
3. To describe how to best use imaging for response evaluation.
Author Disclosures:
L. Fournier: Grant Recipient at Invectys, Speaker at General Electric, Speaker at Novartis, Speaker at Janssen, Speaker at Sanofi, Speaker at Bayer, Speaker at Pfizer, Research/Grant Support at Philips, Research/Grant Support at Ariana Pharma, Research/Grant Support at Evolucare

SF 1a-3 09:00
Integrating quantitative imaging into clinical practice
N. deSouza*; Surrey/UK*
Learning objectives:
1. To describe approaches to integrating quantitative imaging into clinical practice.
2. To explain the limitations of quantitative imaging in clinical practice.
3. To describe how to use quantitative imaging for clinical care.
Author Disclosures:
N. deSouza: nothing to disclose

SF 1a-4 09:20
Quantification of bone metastases becomes possible in clinical practice
F. Lecouvet*; Brussels/BE (frederic.lecouvet@uclouvain.be)*
Learning objectives:
1. To explain the possibilities of bone metastasis quantification.
2. To list the limitations of bone metastasis quantification.
3. To describe how to best use bone metastasis quantification in patient care.
Author Disclosures:
F. Lecouvet: nothing to disclose

09:40
Panel discussion: How to best evaluate oncologic response in clinical practice?

08:30 - 10:00 **Room K**

E³ - European Diploma Prep Session

E³ 123

Paediatric

E³ 123-1 08:30
Chairperson's introduction
J.-F. Chateil*; Bordeaux/FR (jean-francois.chateil@chu-bordeaux.fr)*
Session objectives:
1. To understand the imaging features of the most common congenital and neoplastic disorders of the brain in children and adolescents.
2. To describe the imaging presentations of the most common disorders of the lung and mediastinum in the paediatric age group.
3. To become familiar with the imaging features of important congenital, acute, and neoplastic diseases of the abdomen in children and adolescents.
Author Disclosures:
J.-F. Chateil: nothing to disclose

E³ 123-2 08:36
A. Paediatric neuro imaging
M. Argyropoulou*; Ioannina/GR (margyrop@cc.uoi.gr)*
Learning objectives:
1. To describe the normal development of the brain.
2. To explain the most common congenital disorders of the brain.
3. To understand the most common brain tumours in children and adolescents.
Author Disclosures:
M. Argyropoulou: nothing to disclose

E³ 123-3 09:04
B. Paediatric chest imaging
C. Owens*; London/UK (owens.catherine.5@gmail.com)*
Learning objectives:
1. To describe the normal development of the lung and mediastinum.
2. To explain imaging features of congenital disorders of the lung and mediastinum.
3. To understand the imaging manifestations of respiratory distress and bronchopulmonary dysplasia in infants.
4. To describe the most common tumours of the chest in children.
Author Disclosures:
C. Owens: Consultant at Sidra Medicine , Speaker at Sidra

E³ 123-4 09:32
C. Paediatric abdominal imaging
T. A. Watson*; London/UK*
Learning objectives:
1. To understand the imaging features of congenital disorders of the abdomen.
2. To describe the diagnostic evaluation and imaging presentation of the most common emergencies in children according to age.
3. To understand the imaging presentation of the most common oncologic disorders of the abdomen in children.
Author Disclosures:
T. A. Watson: nothing to disclose

08:30 - 10:00 **Room M 4**

E³ - Rising Stars Programme: Basic Session

BS 1

Radiologic anatomy: abdomen

Moderator:
S. Gourtsoyianni; Athens/GR

BS 1-1 08:30
Small bowel
S. A. Taylor*; London/UK (csytaylor@yahoo.co.uk)*

Learning objectives:
1. To appreciate the embryological development of the small bowel.
2. To learn about the anatomy of the small bowel relevant to radiological imaging.
3. To understand the pitfalls of the normal small bowel appearance during imaging interpretation.
Author Disclosures:
S. A. Taylor: Consultant at Robarts plc

BS 1-2 09:00
Anorectal
A. Palkó; *Szeged/HU (palkoand@gmail.com)*
Learning objectives:
1. To review the normal anatomy of the anorectum.
2. To learn how well depicted the different anatomical landmarks of the anorectum are with different available imaging methods.
3. To discuss the clinical scenarios for which it is necessary to be aware of the anatomy of the anorectum.
Author Disclosures:
A. Palkó: nothing to disclose

BS 1-3 09:30
Peritoneum and mesentery
P. K. Prassopoulos; *Thessaloniki/GR (pprasopo@auth.gr)*
Learning objectives:
1. To review the radiologic anatomy of peritoneal ligaments, mesenteries, and omenta on cross-sectional imaging.
2. To describe the most clinically important peritoneal compartments and fluid collections.
3. To discuss the key role of anatomy in the dissemination of malignancies or the restriction of inflammatory processes in the abdomen.
Author Disclosures:
P. K. Prassopoulos: nothing to disclose

08:30 - 10:00 **Room M 5**

E³ - Advanced Course: Artificial Intelligence

E³ 120

Artificial intelligence in radiology: the basics you need to know

E³ 120-1 08:30
Chairperson's introduction: Artificial intelligence, machine learning and deep learning: what is the difference?
G. Langs; *Vienna/AT*
Session objectives:
1. To become familiar with the different definitions of artificial intelligence domains.
2. To understand that most of the current hype in radiology is about deep learning.
3. To learn about the history of deep learning and why it is so popular now.
Author Disclosures:
G. Langs: disclosure/affirmation information not submitted

E³ 120-2 08:36
A. Conventional machine learning vs deep learning
M. de Bruijne; *RotterdamNL (marleen.debruijne@erasmusmc.nl)*
Learning objectives:
1. To understand the difference between machine learning and deep learning.
2. To learn about the various conventional machine learning techniques.
3. To learn about pros and cons of conventional machine learning vs deep learning.
Author Disclosures:
M. de Bruijne: Research/Grant Support at COSMONiO, Research/Grant Support at Quantib, Patent Holder at US8811724, EP2240904A1,EP2240904B1,US8126240B2,US8811724B2,US7844090B2,US7463758B2,, Research/Grant Support at Vertex

E³ 120-3 09:04
B. Training data for deep learning: what is needed?
B. Glocker; *London/UK (b.glocker@imperial.ac.uk)*
Learning objectives:
1. To understand how deep learning algorithms are trained.
2. To learn about methods to perform deep learning in case of limited training data.
3. To understand the limits of deep learning approaches.
Author Disclosures:
B. Glocker: Advisory Board at Definiens AG, Employee at HeartFlow Ltd., Employee at Microsoft Research Ltd., Advisory Board at Kheiron Medical Technologies, Research/Grant Support at HeartFlow Ltd., Grant Recipient at European Research Council, Grant Recipient at National Institute of Health Research, Grant Recipient at Engineering and Physical Sciences Research Council

E³ 120-4 09:32
C. Clinical applications of artificial intelligence (AI) in medical imaging
N. Papanikolaou; *Lisbon/PT (nickolas.papanikolaou@research.fchampalimaud.org)*
Learning objectives:
1. To learn about the current state of the art of AI applications in medical imaging.
2. To focus on the current challenges related to AI development and deployment in clinical conditions.
3. To understand how AI will transform medical imaging in the long term.
Author Disclosures:
N. Papanikolaou: Shareholder at MRIcons LTD, Advisory Board at Advantis Medical Imaging

08:30 - 10:00 **Tech Gate Auditorium**

Special Focus Session

SF 1b

CEUS in children

SF 1b-1 08:30
Chairperson's introduction
M. Wozniak; *Lublin/PL (mwozniak@hoga.pl)*
Session objectives:
1. To learn about the current role of intravenous applications of CEUS (contrast-enhanced ultrasound) in the paediatric population.
2. To understand the technique and current place of contrast-enhanced voiding urosonography (ce-VUS) in children in diagnostic algorithms.
3. To become familiar with the usefulness of CEUS in paediatric trauma.
Author Disclosures:
M. Wozniak: nothing to disclose

SF 1b-2 08:40
Liver and extrahepatic intravenous applications
D. Ključevšek; *Ljubljana/SI (damjana.kljucevsek@siol.net)*
Learning objectives:
1. To learn about the most common indications for intravenous CEUS in children.
2. To become familiar with the technique and the most common findings.
3. To discuss the limitations of the imaging method.
Author Disclosures:
D. Ključevšek: nothing to disclose

SF 1b-3 09:00
Vesicoureteral (VU) reflux
G. Roic; *Zagreb/HR (goran.roic@kdb.hr)*
Learning objectives:
1. To learn about the indications for CEUS in vesicoureteral reflux in children.
2. To become familiar with the technique and the most common findings.
3. To discuss the limitations of the imaging method in reflux evaluation.
Author Disclosures:
G. Roic: nothing to disclose

SF 1b-4 09:20
Traumas
H.-J. Mentzel; *Jena/DE (hans-joachim.mentzel@med.uni-jena.de)*

Learning objectives:
1. To learn about when CEUS may be useful in trauma evaluation in children.
2. To become familiar with the technique and the most common findings.
3. To discuss the limitations of the imaging methods in a trauma setting.
Author Disclosures:
H.-J. Mentzel: Speaker at Bracco, Speaker at Samsung, Investigator at Bayer, Grant Recipient at Sunlight

09:40
Panel discussion: Is off-label use of CEUS in children a cause for concern?

10:30 - 12:00 **Room N**

Special Focus Session

SF 2a
Prostate embolisation

SF 2a-1 10:30
Chairperson's introduction: New developments in managing benign prostatic disease
H. Hoppe*; Berne/CH (hanno.hoppe@web.de)*
Session objectives:
1. To learn about the results of the underlying cause of prostatic obstruction.
2. To become familiar with the results of current surgical treatments.
3. To learn about the results of current medical therapies.
Author Disclosures:
H. Hoppe: Research/Grant Support at Cook Medical, Research/Grant Support at Boston Scientific

SF 2a-2 10:40
Patient selection and assessment
T. Bilhim*; Lisbon/PT (tiagobilhim@hotmail.com)*
Learning objectives:
1. To learn about the assessment methods and grading systems for prostate outflow obstruction.
2. To learn about consent and who are the optimal patients for treatments.
3. To understand which patients should not be primarily treated with prostate embolisation.
Author Disclosures:
T. Bilhim: Consultant at Merit Medical, Consultant at Terumo, Speaker at Cook, Speaker at Philips, Shareholder at EmbolX

SF 2a-3 10:57
Anatomy, imaging and planning
C. R. Tapping*; Oxford/UK (charles.tapping@ouh.nhs.uk)*
Learning objectives:
1. To become familiar with the normal anatomy and blood supply of the prostate gland.
2. To learn about the pre-procedural imaging methodologies.
3. To understand pre-procedural planning, including blood and drug management.
Author Disclosures:
C. R. Tapping: Speaker at Merit Medical, Speaker at Boston Scientific

SF 2a-4 11:14
Embolisation technique
K. Wilhelm*; Bonn/DE (Kai.wilhelm@johanniter-kliniken.de)*
Learning objectives:
1. To become familiar with the standard equipment required for prostate embolisation.
2. To learn about the techniques for selective cannulation of the prostate arteries.
3. To understand the role of dyna CT, and tricks and tips for embolisation.
Author Disclosures:
K. Wilhelm: nothing to disclose

SF 2a-5 11:31
Outcome and results from trials
F. Wolf*; Vienna/AT (florian.wolf@meduniwien.ac.at)*
Learning objectives:
1. To understand the technical success.
2. To become familiar with short and long term clinical success, and how it compares with medical and surgical techniques.
3. To be aware of the complications.
Author Disclosures:
F. Wolf: nothing to disclose

11:48
Panel discussion: New developments in managing benign prostatic disease

10:30 - 12:00 **Room O**

Abdominal Viscera

RC 201
Benign and malignant lesions in "forgotten organs"

Moderator:
I. Petkovska; New York, NY/US

RC 201-1 10:30
A. Imaging of the spleen
C. S. Reiner*; Zurich/CH*
Learning objectives:
1. To be aware of the most common benign and malignant lesions in the spleen and their differential diagnoses.
2. To know about imaging strategies and protocols with ultrasound, CT, and MRI of the spleen.
3. To know about the management of splenic lesions.
Author Disclosures:
C. S. Reiner: nothing to disclose

RC 201-2 11:00
B. Imaging of mesentery and omentum
M. J. Lahaye*; Amsterdam/NL (MJ.Lahaye@gmail.com)*
Learning objectives:
1. To understand the anatomical landmarks of the mesentery and omentum.
2. To be aware of the most common pathological findings of the mesentery and omentum.
3. To learn to avoid diagnostic mistakes when findings of the mesentery and omentum are seen.
Author Disclosures:
M. J. Lahaye: nothing to disclose

RC 201-3 11:30
C. Imaging of the gallbladder
B. J. Op de Beeck*; Edegem/BE (bart.op.de.beeck@uza.be)*
Learning objectives:
1. To become familiar with most common benign and malignant changes of the gallbladder.
2. To be aware of the strengths and shortcomings of different imaging techniques including ultrasound, CT, and MRI.
3. To understand diagnostic pitfalls of gallbladder imaging.
Author Disclosures:
B. J. Op de Beeck: nothing to disclose

11:00 - 12:00 **Coffee & Talk 2**

Coffee & Talk (open forum) Session
Organised by EuroSafe Imaging

C 10
Quality and safety in paediatric imaging

C 10-1/C 10-2 11:00
Chairpersons' introduction
C. Granata*; Genoa/IT*
D. P. Frush*; Durham, NC/US (dfrush@stanford.edu)*

Session objectives:
1. To understand how to implement best practice in radiation protection of newborns in neonatal intensive care units.
2. To gain an overview on the most important aspects of optimisation of paediatric protocols in CT.
3. To learn how exposure indicators can be used for optimisation in paediatric digital radiography.
Author Disclosures:
C. Granata: Speaker at Guerbet Italia, D. P. Frush: nothing to disclose

C 10-3 11:05
Radiation protection in the neonatal intensive care unit
S. Salerno*; Palermo/IT*
Learning objectives:
1. To learn the requisites of quality for radiologic studies commonly performed in NICU.
2. To gain an overview on related diagnostic reference levels (DRLs) and technique optimisation.
3. To gain an overview on shielding.
Author Disclosures:
S. Salerno: disclosure/affirmation information not submitted

C 10-4 11:15
Optimising protocol parameters in paediatric conventional radiology and CT
E. Sorantin*; Graz/AT (erich.sorantin@medunigraz.at)*
Learning objectives:
1. To appreciate the importance of dose optimisation in children.
2. To learn how to optimise CT protocols in children to avoid the most common pitfalls.
Author Disclosures:
E. Sorantin: nothing to disclose

C 10-5 11:25
Understanding dose indices and exposure indicators in digital radiography
R. Seuri*; HUS, Helsinki/FI (raija.seuri@hus.fi)*
Learning objectives:
1. To understand what exposure indicators are and what they are not.
2. To learn how exposure indicators play a role in ensuring correct use of the equipment and optimising radiation dose in paediatric digital radiology.
Author Disclosures:
R. Seuri: nothing to disclose

11:35
Open forum discussion

10:30 - 12:00 **Room E**

E³ - Rising Stars Programme: Basic Session

BS 2
Radiologic anatomy: chest

Moderator:
F. Rengier; Heidelberg/DE

BS 2-1 10:30
Mediastinal
M. Occhipinti*; Florence/IT (mariaelena.occhipinti@gmail.com)*
Learning objectives:
1. To review the mediastinal anatomy according to old and new classifications.
2. To define "normal" and "abnormal" mediastinal anatomy.
3. To use radiologic anatomy to characterise mediastinal lesions and to stage tumours.
Author Disclosures:
M. Occhipinti: Research/Grant Support at Fondazione Menarini

BS 2-2 11:00
Lungs
C. M. M. Schaefer-Prokop*; Amersfoort/NL (cornelia.schaeferprokop@gmail.com)*
Learning objectives:
1. To know how to interpret mediastinal lines and contours in chest radiography.
2. To become familiar with "signs" in chest radiography helpful for diagnosis.
3. To know the normal appearance of lung parenchyma on CT and to use the anatomy of the secondary lobule for analysis of chest diseases.
Author Disclosures:
C. M. M. Schaefer-Prokop: nothing to disclose

BS 2-3 11:30
Vasculature
I. Žuža*; Kostrena/HR*
Learning objectives:
1. To identify thoracic vascular structures on chest x-rays.
2. To interpret chest vasculature, including aorta and coronary arteries, major aortic branches, and pulmonary arteries and veins by using multidetector CT (MDCT).
3. To review and illustrate the most common variants and anomalies.
4. To discuss the challenges and limitations in interpretation based on particular CT scanning protocols.
Author Disclosures:
I. Žuža: nothing to disclose

10:30 - 12:00 **Room F2**

Musculoskeletal

RC 210
Musculoskeletal tumours

Moderator:
F. B. B. Ergen; Ankara/TR

RC 210-1 10:30
A. Bone tumours and tumour-like conditions
P. G. O'donnell*; St Albans/UK (paulodonnell@nhs.net)*
Learning objectives:
1. To explain the imaging findings of bone tumours.
2. To describe how to differentiate benign from malignant bone lesions.
Author Disclosures:
P. G. O'donnell: nothing to disclose

RC 210-2 11:00
B. Soft tissue tumours
A. Bazzocchi*; Bologna/IT (abazzo@inwind.it)*
Learning objectives:
1. To explain the imaging findings of soft tissue tumours.
2. To describe differential diagnostic considerations in imaging soft tissue tumours.
Author Disclosures:
A. Bazzocchi: nothing to disclose

RC 210-3 11:30
C. Tumours of the spinal column
F. M. H. M. Vanhoenacker*; Antwerp/BE (filip.vanhoenacker@telenet.be)*
Learning objectives:
1. To explain the imaging findings of spinal tumours.
2. To describe differential diagnostic considerations in imaging spinal tumours.
Author Disclosures:
F. M. H. M. Vanhoenacker: nothing to disclose

10:30 - 12:00 **da Vinci (Room D1)**

Special Focus Session

SF 2b

My three most dreaded head and neck requests

SF 2b-1 10:30
Chairperson's introduction
P. Golofit*; Szczecin/PL (piotrgolofit@gmail.com)*
Session objectives:
1. To address the dilemmas of common requests in head and neck radiology.
2. To discuss imaging approaches in tinnitus, lymphadenopathies, and hoarseness.
3. To debate negative imaging findings in symptomatic patients.
Author Disclosures:
P. Golofit: nothing to disclose

SF 2b-2 10:36
Tinnitus
B. Verbist*; Leiden/NL (b.m.verbist@lumc.nl)*
Learning objectives:
1. To review imaging modalities used for the workup of tinnitus.
2. To give an overview of underlying lesions in pulsatile tinnitus.
3. To compare imaging for pulsatile and non-pulsatile tinnitus.
Author Disclosures:
B. Verbist: Grant Recipient at HPTC-Varian consortium, Research/Grant Support at Advanced Bionics, Research/Grant Support at Cochlear

SF 2b-3 10:57
Enlarged lymph nodes
R. Maroldi*; Brescia/IT (roberto.maroldi@unibs.it)*
Learning objectives:
1. To discuss the imaging approach for suspected enlarged lymph nodes.
2. To review the differential diagnoses in lymphadenopathies.
3. To advise when fine needle aspiration cytology or biopsy is needed.
Author Disclosures:
R. Maroldi: nothing to disclose

SF 2b-4 11:18
Hoarseness
E. Vassallo*; Msida/MT (edithvassallo@gmail.com)*
Learning objectives:
1. To explain the value of CT and MRI in the evaluation of hoarseness.
2. To show lesions causing hoarseness.
3. To reflect on the incidence of underlying lesions in hoarseness.
Author Disclosures:
E. Vassallo: nothing to disclose

11:39
Panel discussion: How to deal with symptomatic patients without definite imaging findings?

10:30 - 12:00 **Darwin (Room D2)**

Paediatric

RC 212

Fluoroscopy: a mainstay state of the art in paediatric radiology

RC 212-1 10:30
Chairperson's introduction
N. Mitreska*; Skopje, MK/MK*
Session objectives:
1. To learn about the most common indications for fluoroscopy in neonates, infants and children.
2. To optimise protocols with a special concern for dose management.
3. To be aware of limits and pitfalls.
Author Disclosures:
N. Mitreska: disclosure/affirmation information not submitted

RC 212-2 10:35
A. Use of fluoroscopy in neonates with suspected gastrointestinal pathology
I. Aagenæs*; Oslo/NO (iaagenes@gmail.com)*
Learning objectives:
1. To learn about the most common indications for fluoroscopy in non-urogenital queries in neonates.
2. To become familiar with the technique, findings, and pitfalls for the most common fluoroscopy non-urogenital queries in the neonate.
3. To discuss the best fluoroscopic approach in suspected bowel obstruction in a neonate.
Author Disclosures:
I. Aagenæs: nothing to disclose

RC 212-3 11:00
B. Gastrointestinal and other applications in the older child
J. Barber*; London/UK*
Learning objectives:
1. To learn about the most common indications for fluoroscopy in non-urogenital queries in infant and older children.
2. To become familiar with the technique of the most common fluoroscopy queries in this patient group.
3. To discuss the most common findings and pitfalls.
Author Disclosures:
J. Barber: nothing to disclose

RC 212-4 11:25
C. Urogenital applications
G. Perucca*; Turin, TO/IT (giuliaperucca@yahoo.it)*
Learning objectives:
1. To learn about the indications for fluoroscopy in urogenital queries in children.
2. To become familiar with the technique in fluoroscopic urogenital queries.
3. To discuss the most common findings and pitfalls.
Author Disclosures:
G. Perucca: nothing to disclose

11:50
Panel discussion: When can ultrasound imaging replace fluoroscopy?

10:30 - 12:00 **Descartes (Room D3)**

ESR Ultrasound Subcommittee Session

US 2

Ultrasound (US) incidental findings

Moderators:
C. M. Nyhsen; Haguenau/FR
P. Ricci; Rome/IT

US 2-1 10:30
Thyroid and lymph node
D.-A. A. Clevert*; Munich/DE (Dirk.Clevert@med.uni-muenchen.de)*
Learning objectives:
1. To learn how to manage incidental findings.
2. To appreciate the accuracy of multiparametric ultrasound imaging for immediate diagnosis of incidentaloma.
3. To understand the differential diagnosis and correct or best multimodalities management of incidental findings.
Author Disclosures:
D.-A. A. Clevert: Speaker at Siemens, Bracco, Samsung, Philips, Advisory Board at Philips, Samsung

US 2-2 10:50
Liver and pancreas
M. D'onofrio*; Verona/IT (mirko.donofrio@univr.it)*
Learning objectives:
1. To learn how to manage incidental findings.
2. To appreciate the accuracy of multiparametric ultrasound imaging for immediate diagnosis of incidentaloma.
3. To understand the differential diagnosis and correct or best multimodalities management of incidental findings.

Author Disclosures:
M. D'onofrio: Speaker at Siemens, Speaker at Hitachi, Speaker at Bracco, Advisory Board at Siemens, Research/Grant Support at Hitachi

US 2-3 11:10
Spleen and kidney
M. Bertolotto*; Trieste/IT (bertolot@units.it)*
Learning objectives:
1. To learn how to manage incidental findings.
2. To appreciate the accuracy of multiparametric ultrasound imaging for immediate diagnosis of incidentaloma.
3. To understand the differential diagnosis and correct or best multimodalities management of incidental findings.
Author Disclosures:
M. Bertolotto: nothing to disclose

US 2-4 11:30
Testis and ovary
P. S. Sidhu*; London/UK (paulsidhu@nhs.net)*
Learning objectives:
1. To learn how to manage incidental findings.
2. To appreciate the accuracy of multiparametric ultrasound imaging for immediate diagnosis of incidentaloma.
3. To understand the differential diagnosis and correct or best multimodalities management of incidental findings.
Author Disclosures:
P. S. Sidhu: Advisory Board at Samsung, Consultant at Itreas, Speaker at Bracco, Speaker at Siemens, Speaker at Philips, Speaker at GE Healthcare

11:50
Panel discussion: Diagnostics and treatment

10:30 - 12:00 **Room K**

Neuro

RC 211
Sellar and suprasellar lesions

RC 211-1 10:30
Chairperson's introduction
M. Z. Karlovic Vidakovic*; Mostar/BA (karlovicmarijana@yahoo.com)*
Session objectives:
1. To present an imaging strategy for imaging pituitary adenoma.
2. To learn about anatomical variations and congenital sellar pathology.
3. To become familiar with craniopharyngioma and Rathke cleft cyst.
Author Disclosures:
M. Z. Karlovic Vidakovic: nothing to disclose

RC 211-2 10:35
A. Anatomy, variants and function of the pituitary gland
S. Looby*; Dublin/IE (seamuslooby@beaumont.ie)*
Learning objectives:
1. To review the anatomy of the sellar and parasellar region.
2. To recognise sellar variants.
3. To be able to appropriately image the patient with diabetes insipidus.
Author Disclosures:
S. Looby: nothing to disclose

RC 211-3 10:58
B. Imaging of sellar and suprasellar lesions
Z. Rumboldt*; Rijeka/HR (puz3@yahoo.com)*
Learning objectives:
1. To recognise pituitary and sellar neoplasms other than adenoma.
2. To describe perisellar and suprasellar pathology.
3. To provide an overview of sellar and suprasellar childhood lesions.
Author Disclosures:
Z. Rumboldt: Speaker at Bracco (last time in 2016), Research/Grant Support at Bayer (in 2013)

RC 211-4 11:21
C. Post-treatment findings and follow-up
F. Bonneville*; Toulouse/FR (bonneville.f@chu-toulouse.fr)*
Learning objectives:
1. To become familiar with the different types of pituitary adenoma.
2. To define the most effective imaging strategy for pituitary adenoma.
3. To learn about the role of MRI after surgical and/or medical treatment.
Author Disclosures:
F. Bonneville: nothing to disclose

11:44
Panel discussion: Imaging sellar and suprasellar lesions

10:30 - 12:00 **Room M 1**

Radiographers

RC 214
The role of medical imaging in radiotherapy

RC 214-1/RC 214-2 10:30
Chairpersons' introduction
C. A. Beardmore*; London/UK (charlotteb@sor.org)*
K. Galumyan*; Yerevan/AM*
Session objectives:
1. To understand CT and MRI specifications for treatment and planning.
2. To be aware of imaging positioning verification options.
3. To highlight the radiographers' role in radiotherapy planning and dosimetry.
Author Disclosures:
C. A. Beardmore: nothing to disclose, K. Galumyan: disclosure/affirmation information not submitted

RC 214-3 10:36
A. CT and MRI in treatment and planning
J. G. Couto*; Msida/MT (jose.g.couto@um.edu.mt)*
Learning objectives:
1. To highlight the imaging specifications for planning.
2. To understand the role of CT in current radiotherapy practice.
3. To be familiar with the role of MRI in current radiotherapy practice.
Author Disclosures:
J. G. Couto: nothing to disclose

RC 214-4 10:59
B. Role of imaging in positioning verification
A. Raith*; Vienna/AT (alexander.raith@gmx.at)*
Learning objectives:
1. To discuss the use of different imaging modalities for position verification.
2. To be familiar with modification techniques to address deviations in treatment planning.
3. To identify practical tips for MRI Linac use.
Author Disclosures:
A. Raith: Speaker at FH Campus Wien

RC 214-5 11:22
C. The radiographers' role in radiation planning and dosimetry
N. Rodrigues*; Melres/PT*
Learning objectives:
1. To identify advantages and disadvantages of different methods for radiation planning and dosimetry.
2. To be familiar with strategies to decrease organ risk.
3. To understand the importance of adaptive radiotherapy.
Author Disclosures:
N. Rodrigues: disclosure/affirmation information not submitted

11:45
Panel discussion: The future role of radiographers in radiotherapy treatment and planning: opportunities for the advancement of roles

10:30 - 12:00 **Room M 2**

E³ - Advanced Course: Hot Topics in Emergency Radiology

E³ 218

Pregnancy and postpartum abdominal acute conditions

E³ 218-1 10:30
Chairperson's introduction
M. de la Hoz Polo*; London/UK (mdelahozpolo@gmail.com)*
Session objectives:
1. To review imaging of common acute abdominal and pelvic conditions (medical and surgical) presenting during pregnancy.
2. To review imaging of common postpartum period conditions.
3. To describe the interventional radiology procedures used to treat ante- and postpartum complications of pregnancy.
Author Disclosures:
M. de la Hoz Polo: nothing to disclose

E³ 218-2 10:36
A. The acute abdomen in pregnancy
M. Javitt*; Haifa/IL (m_javitt@rambam.health.gov.il)*
Learning objectives:
1. To briefly describe the role of CT, MRI, and US in the detection of acute abdominal conditions during pregnancy, and radiation dose effect on the foetus (radiation dose, use of contrast agents, suggested protocol, and teratogenicity).
2. To review the imaging findings of abdominal non-pregnancy related complications such as appendicitis, urolithiasis, hepatobilliary conditions (fatty liver of pregnancy, cholestasis in pregnancy, HELLP syndrome), intestinal obstruction, and vascular related complications (ovarian vein thrombosis, splenic artery aneurysm rupture).
3. To review the imaging findings of abdominal pregnancy related complications such as ectopic pregnancy, molar pregnancy, placental abruption, adnexal torsion, and pelvic inflammatory disease.
Author Disclosures:
M. Javitt: nothing to disclose

E³ 218-3 11:04
B. Acute postpartum conditions
A. D. Karaosmanoğlu*; Ankara/TR (alidevrim76@yahoo.com)*
Learning objectives:
1. To become familiar with the normal postpartum appearances on US, CT, and MRI, both immediately and up to 6 weeks postpartum.
2. To review imaging of common postpartum period conditions such as causes of postpartum haemorrhage, retaining products of conception, puerperal septic thrombophlebitis, and other infective/inflammatory puerperal conditions.
3. To discuss protocols for breastfeeding and expressing of breast milk in relation to CT and MRI imaging.
Author Disclosures:
A. D. Karaosmanoğlu: nothing to disclose

E³ 218-4 11:32
C. Interventional radiology in postpartum haemorrhage
R. Patel*; Oxford/UK*
Learning objectives:
1. To briefly review the vascular imaging features that are relevant for planning or verifying transcatheter embolisation of obstetric and gynaecologic conditions.
2. To describe the interventional radiology procedures that are used to treat various complications of pregnancy such ectopic gestational sac, aspiration of symptomatic ovarian cyst, and obstructive uropathy.
3. To describe the interventional radiology procedures that are used to treat various complications of the postpartum period, such as uterine artery embolisation (UAE) for cases of post-partum haemorrhage, drainage of postcesarean abscess collection, and treatment of vesicouterine fistula.
Author Disclosures:
R. Patel: nothing to disclose

10:30 - 12:00 **Room M 3**

Vascular

RC 215

Venous thrombotic disease

RC 215-1 10:30
Chairperson's introduction
M. Krokidis*; Athens/GR (mkrokidis@hotmail.com)*
Session objectives:
1. To understand the importance of the appropriate diagnosis and treatment of acute and chronic venous disease.
2. To become familiar with the optimal diagnostic tools.
3. To learn when and how interventional radiology techniques can help in venous thromboembolic disease.
Author Disclosures:
M. Krokidis: Consultant at Terumo

RC 215-2 10:35
A. Acute deep vein thrombosis: diagnosis, interventional radiology (IR) treatment and outcomes
G. Maleux*; Leuven/BE*
Learning objectives:
1. To learn about the clinical symptoms and diagnosis of deep vein thrombosis (DVT).
2. To become familiar with the different conservative and IR treatment options.
3. To discuss the short-, mid-, and long-term outcomes.
Author Disclosures:
G. Maleux: disclosure/affirmation information not submitted

RC 215-3 10:58
B. Diagnosis and treatment of central venous occlusions
S. D. Qanadli*; Lausanne/CH (Salah.Qanadli@chuv.ch)*
Learning objectives:
1. To learn about clinical symptoms and the appropriate diagnostic tools.
2. To become familiar with which patients IR treatment is indicated.
3. To understand how to treat a central venous occlusion using IR methods.
Author Disclosures:
S. D. Qanadli: nothing to disclose

RC 215-4 11:21
C. Chronic deep vein thrombosis: diagnosis, IR treatment and outcomes
R. Leffroy*; Dijon/FR*
Learning objectives:
1. To learn about the clinical symptoms and diagnosis of chronic DVT.
2. To become familiar with preinterventional imaging and appropriate treatment planning.
3. To discuss different IR techniques and outcomes.
Author Disclosures:
R. Leffroy: disclosure/affirmation information not submitted

11:44
Panel discussion: Should emergency treatment for deep vein thrombosis become part of IR service?

10:30 - 12:00 **Room M 4**

E³ - Advanced Course: Interactive Teaching Session for Young (and not so Young) Radiologists

E³ 221

Paediatric brain imaging

E³ 221-1 10:30
A. Head and neck emergencies in children
A. Rossi*; Genoa/IT (andrearossi@gaslini.org)*
Learning objectives:
1. To become familiar with the different entities.
2. To identify the key imaging findings.

Author Disclosures:
A. Rossi: Advisory Board at Bracco Group, Speaker at Bracco group, Speaker at Telemedicine Clinic

E³ 221-2 11:15
B. Acute neurological child beyond trauma
B. Nedregaard*; Oslo/NO (bnedr@frisurf.no)*
Learning objectives:
1. To become familiar with the most common cause of acute neurological emergencies.
2. To learn the imaging criteria for differentiation.
Author Disclosures:
B. Nedregaard: nothing to disclose

10:30 - 12:00 **Room M 5**

E³ - Advanced Course: Artificial Intelligence

E³ 220

Artificial intelligence for image reconstruction: towards deep imaging?

E³ 220-1 10:30
Chairperson's introduction
D. Le Bihan*; Gif Sur Yvette/FR (denis.lebihan@gmail.com)*
Session objectives:
1. To understand what is hype and what can be expected in deep learning based reconstruction.
2. To understand the impact of artificial intelligence vs other developments in image reconstruction.
3. To learn about the expected developments coming in the next 5 years.
Author Disclosures:
D. Le Bihan: nothing to disclose

E³ 220-2 10:36
A. Deep learning for MRI reconstruction
K. Hammernik*; London/UK (k.hammernik@imperial.ac.uk)*
Learning objectives:
1. To show how with deep learning we can learn the entire MRI reconstruction procedure.
2. To understand the advantages and disadvantages of using deep learning in MRI reconstruction.
3. To show the application of deep learning in the reconstruction of MRI musculoskeletal images.
Author Disclosures:
K. Hammernik: nothing to disclose

E³ 220-3 11:04
B. Deep learning in cardiovascular MRI
D. Rueckert*; London/UK (D.Rueckert@imperial.ac.uk)*
Learning objectives:
1. To understand how MRI acquisition time can be reduced with deep learning.
2. To understand potential artefacts related to deep learning based image reconstruction.
3. To show applications of deep learning in the reconstruction of cardiovascular MRI data.
Author Disclosures:
D. Rueckert: Consultant at IXICO, Consultant at Circle Cardiovascular Imaging, Consultant at Heartflow

E³ 220-4 11:32
C. Deep learning in CT imaging
M. M. Prokop*; Nijmegen/NL (mathias.prokop@radboudumc.nl)*
Learning objectives:
1. To learn how deep learning can be used to improve CT image quality.
2. To understand how deep learning can be used to speed up CT image acquisition.
3. To learn about clinical applications of deep learning based CT reconstruction.
Author Disclosures:
M. M. Prokop: Research/Grant Support at Canon Medical Systems, Research/Grant Support at Siemens Healthineers, Speaker at Bracco, Speaker at Bayer, Speaker at Siemens Healthineers, Speaker at Canon Medical Systems

10:30 - 12:00 **Tech Gate Auditorium**

E³ - ECR Master Class (Molecular Imaging)

E³ 226

Quantitative imaging in oncology

E³ 226-1 10:30
Chairperson's introduction
J. O'Connor*; Manchester/UK (James.O'Connor@manchester.ac.uk)*
Session objectives:
1. To understand the impact of tumour heterogeneity on diagnosis and treatment.
2. To learn the basics of quantifying heterogeneity in tumours.
3. To review the future impact of imaging heterogeneity in tumours.
Author Disclosures:
J. O'connor: Grant Recipient at Cancer Research UK, Owner at Mediknow Ltd

E³ 226-2 10:35
A. Intra- and intertumoural heterogeneity and the impact for cancer diagnostics
M. Eisenblaetter*; Freiburg/DE (michel.eisenblaetter@uniklinik-freiburg.de)*
Learning objectives:
1. To learn about tumour heterogeneity.
2. To review current strategies to explore biological heterogeneity.
3. To understand how this heterogeneity impacts diagnosis and treatment.
Author Disclosures:
M. Eisenblaetter: Speaker at Bracco Imaging Spa, Research/Grant Support at Pfizer Specialty Care

E³ 226-3 11:00
B. Quantitative image biomarkers for targeted tumour therapies
R. Garcia Figueiras*; Santiago de Compostela/ES (roberto.garcia.figueiras@sergas.es)*
Learning objectives:
1. To learn how heterogeneity can be quantified from images.
2. To understand the main classes of heterogeneity on imaging.
3. To review limits and pitfalls of features extraction.
Author Disclosures:
R. Garcia Figueiras: nothing to disclose

E³ 226-4 11:25
C. From quantitative imaging to radiomics and deep learning
H. K. Hahn*; Bremen/DE*
Learning objectives:
1. To learn how to optimise the acquisition of images for quantitative imaging.
2. To understand image processing which may impact quantification.
3. To become familiar with the concepts behind quantification, including machine learning approaches.
Author Disclosures:
H. K. Hahn: disclosure/affirmation information not submitted

11:50
Panel discussion: What can we quantify and why is it essential?

12:45 - 13:45 **Coffee & Talk 1**

Coffee & Talk (open forum) Session

Organised by ESOR

C 1

The scholar and fellow's experience

C 1-1 12:45
Chairperson's introduction
N. I. Traikova*; Plovdiv/BG (nikoletatraikova@gmail.com)*
Author Disclosures:
N. I. Traikova: nothing to disclose

C 1-2 12:50
Visiting scholar in Europe
F. Pesapane*; Milan/IT (filippopesapane@gmail.com)*
Learning objectives:
1. To understand that the mobility of radiology trainees is an indispensable prerequisite to facing new challenges, promoting collaboration among centres/systems that cannot remain isolated, positively impacting the quality of research, and applying artificial intelligence to medical imaging.
2. To become familiar with the need to promote scientific international multicentre collaboration to identify a best practice, to standardise it, and to share it.
3. To learn about ESR's role supporting international training opportunities for young radiologists, enhancing scientific mobility, and promoting cooperation between centres of different countries.
4. To become familiar with the cultural-knowledge and the networks developed during mobility that can be used by the trainees to advance in their career.
Author Disclosures:
F. Pesapane: nothing to disclose

C 1-3 12:50
Visiting scholar in USA
J. Kirchner*; Düsseldorf/DE (Julian.Kirchner@med.uni-duesseldorf.de)*
Learning objectives:
1. To learn about application process for visiting scholar in USA.
2. To understand the usefulness of getting in touch with the American medical system.
3. To appreciate to work with people from all over the world.
Author Disclosures:
J. Kirchner: nothing to disclose

C 1-4 13:04
Exchange Fellow in Europe
N. Bogveradze*; Tbilisi/GE (bogveradze.nino@gmail.com)*
Learning objectives:
1. To learn how to apply for an exchange fellowship program in Europe.
2. To understand the role of the exchange fellowship program for the participant.
3. To become familiar with all aspects of the exchange fellowship program.
4. To appreciate the chance to work in a world-leading team.
Author Disclosures:
N. Bogveradze: nothing to disclose

C 1-5 13:11
Bracco Clinical Fellow
C. Standaert*; Veurne/BE*
Learning objectives:
1. To learn how to apply for a BRACCO clinical fellowship.
2. To become familiar with the practical aspects of preparing a clinical fellowship in the UK such as language requirements, GMC application and housing.
3. To understand the advantages of clinical fellowships in centres of excellence that give the framework to become an expert radiologist in the field and stimulate research.
4. To learn about personal development and growth by conducting a fellowship abroad.
Author Disclosures:
C. Standaert: nothing to disclose

13:18
Open forum discussion

12:45 - 13:45 **Room F1**

E³ - The Beauty of Basic Knowledge: Breast

E³ 24A

Basics of mammography

Moderators:
E. M. Fallenberg; Munich/DE
K. Kinkel; Chêne-Bougeries/CH

E³ 24A-1 12:45
Cookbook for image analysis and interpretation
A. Tardivon*; Paris/FR (anne.tardivon@curie.fr)*
Learning objectives:
1. To assess mammographic image quality and mammographic breast density.
2. To recognise and name main imaging findings using the breast imaging reporting and data system (BIRADS) lexicon.
Author Disclosures:
A. Tardivon: Research/Grant Support at PHRCH -K- 2018

E³ 24A-2 13:15
Differences in mammography techniques and image analysis
S. Zackrisson*; Malmö/SE (sophia.zackrisson@med.lu.se)*
Learning objectives:
1. To learn about the technique and purpose of tomosynthesis compared to digital mammography.
2. To understand differences in reading a screening and diagnostic mammography.
3. To become familiar with work-up possibilities after a positive screening mammography, taking into account psychological consideration.
Author Disclosures:
S. Zackrisson: Speaker at Siemens Healthcare AG, Consultant at Collective Minds Radiology, Founder at Z Imagination AB

12:45 - 13:45 **Coffee & Talk 3**

Coffee & Talk (open forum) Session

C 19

Structured reporting: how to provide the key information - application to thoracic imaging

C 19-1 12:45
Chairperson's introduction
H.-U. Kauczor*; Heidelberg/DE*
Session objectives:
1. To explain the advantages of structured reports.
2. To illustrate their use in dedicated clinical indications.
3. To understand their role for practice and research.
Author Disclosures:
H.-U. Kauczor: Research/Grant Support at Siemens, Philips, Bayer, Speaker at Siemens, Philips, Astra Zeneca, Merck Sharp Dohme, Boehringer Ingelheim

C 19-2 12:50
Pulmonary embolism
B. Ghaye*; Brussels/BE (benoit.ghaye@uclouvain.be)*
Learning objectives:
1. To learn how to comment on the quality of computed tomography angiography (CTA).
2. To be able to indicate the level of arterial obstruction.
3. To learn how to report signs of pulmonary embolism severity.
Author Disclosures:
B. Ghaye: nothing to disclose

C 19-3 12:58
Pulmonary nodules in lung cancer screening
M. Silva*; Parma/IT (mariosilvamed@gmail.com)*

Learning objectives:
1. To learn about which nodule characteristics to report.
2. To be informed of which extranodular findings to report.
3. To understand the importance of mentioning guidelines for management.
Author Disclosures:
M. Silva: nothing to disclose

C 19-4 13:06
Diffuse parenchymal lung disease
H. Prosch; *Vienna/AT (helmut.prosch@meduniwien.ac.at)*
Learning objectives:
1. To become familiar with the pivotal patterns.
2. To learn how to assess change in surveillance or therapy response.
3. To consolidate knowledge about quantitative imaging biomarkers.
Author Disclosures:
H. Prosch: nothing to disclose

13:14
Open forum discussion

12:45 - 13:45 **Room G**

E³ - The Beauty of Basic Knowledge: Pancreas

E³ 25A
Acute pancreatitis

Moderator:
R. Manfredi; Rome/IT

E³ 25A-1 12:45
Atlanta classification of acute pancreatitis
T. L. Bollen; *Nieuwegein/NL (tlbollen@hotmail.com)*
Learning objectives:
1. To understand grading of acute pancreatitis: Atlanta classification.
2. To learn about the clinical impact of Atlanta classification.
3. To understand the follow up of acute pancreatitis.
Author Disclosures:
T. L. Bollen: nothing to disclose

E³ 25A-2 13:15
Role of imaging
C. Triantopoulou; *Athens/GR (ctriantopoulou@gmail.com)*
Learning objectives:
1. To learn about the diagnosis of acute pancreatitis.
2. To understand how to apply Atlanta classification to imaging.
3. To learn about new trends in the diagnosis of acute pancreatitis.
Author Disclosures:
C. Triantopoulou: nothing to disclose

12:45 - 13:15 **Room M 5**

EDiR Session

EDiR 1
An instrument to develop excellence in your career: practical session (part 1)

Moderator:
L. Oleaga Zufiria; Barcelona/ES

EDiR 1-1 12:45
EDiR teaser
L. Oleaga Zufiria; *Barcelona/ES (lauraoleaga@gmail.com)*
Learning objectives:
1. To present the EDiR examination.
2. To show the structure of the EDiR exam.
3. To review some practical cases: multiple response questions, short cases, and CORE cases.
Author Disclosures:
L. Oleaga Zufiria: Consultant at TMC Academy

EDiR 1-2 13:05
Tips from an EDiR holder
A. Pons Escoda; *Barcelona/ES (aponse@hotmail.com)*
Learning objectives:
1. To review ten essential tips to succeed in the EDiR.
2. To highlight the importance of the EDiR.
3. To explain the advantages of having the EDiR.
Author Disclosures:
A. Pons Escoda: nothing to disclose

14:00 - 15:30 **Room N**

EuroSafe Imaging Session

EU 3
Cumulative dose: too often and too much

EU 3-1/EU 3-2 14:00
Chairpersons' introduction
K. Applegate; *Zionsville, IN/US (keapple5123@gmail.com)*
G. Frija; *Paris/FR (guy.frija@aphp.fr)*
Session objectives:
1. To understand the clinical context of cumulative dose.
2. To report on some data from Europe.
3. To propose technical and clinical solutions to avoid a too high cumulative dose.
Author Disclosures:
K. Applegate: nothing to disclose, G. Frija: nothing to disclose

EU 3-3 14:10
Cumulative doses: an awareness problem
J. Vassileva; *Vienna/AT (J.N.Vassileva@gmail.com)*
Learning objectives:
1. To present a summary of the recent data on patient cumulative exposure from recurrent imaging procedures, and the actions proposed during the IAEA meeting on this topic.
2. To ensure medical benefits always exceed risks for patients who need frequent radiological imaging for diagnosing and monitoring their diseases.
Author Disclosures:
J. Vassileva: nothing to disclose

EU 3-4 14:30
Defining scenarios with a risk for cumulative dose
F. Kainberger; *Vienna/AT (franz.kainberger@meduniwien.ac.at)*
Learning objectives:
1. To identify scenarios where patients have an increased probability of reaching or exceeding the cumulative dose limits.
2. To develop methods of early detection of scenarios with a potential higher dose risk, and how alert systems can be implemented.
3. To learn how to document and communicate in situations with a higher risk of cumulative dose with a view on the patient's outcome.
Author Disclosures:
F. Kainberger: nothing to disclose

EU 3-5 14:50
EuroSafe Imaging: opportunities to reduce cumulative doses in children
R. Seuri; *HUS, Helsinki/FI (raija.seuri@hus.fi)*
Learning objectives:
1. To illustrate that there are groups of patients at risk of receiving high cumulative doses during childhood.
2. To understand the role of justification in avoiding unnecessary high cumulative doses.
3. To understand the role of dose tracking in optimisation.
Author Disclosures:
R. Seuri: nothing to disclose

15:10
Panel discussion: Next steps for reducing cumulative doses

14:00 - 15:30 **Room O**

Chest

RC 304

Thoracic emergencies: part 1

Moderator:
B. Ghaye; Brussels/BE

RC 304-1 14:00
A. Chest trauma
M. Brink; *Nijmegen/NL (Mobrink@hotmail.com)*
Learning objectives:
1. To describe the CT features of pulmonary contusion.
2. To learn about signs of diaphragmatic rupture.
3. To know when to suspect and how to confirm aortic injury.
Author Disclosures:
M. Brink: Grant Recipient at Canon Medical Systems, Speaker at Canon Medical Systems

RC 304-2 14:22
B. Lung ultrasound: only for the intensive care doctors?
D. Lichtenstein; *Paris/FR (D.Licht@free.fr)*
Learning objectives:
1. To become familiar with the normal and abnormal findings.
2. To be aware of the limits of lung ultrasound.
3. To learn how to incorporate lung ultrasound in the diagnostic workup of intensive care patients.
Author Disclosures:
D. Lichtenstein: nothing to disclose

RC 304-4 14:45
C. Infectious emergencies
I. J. Hartmann; *Zwijndrecht/NL (i.j.c.hartmann@gmail.com)*
Learning objectives:
1. To learn about signs of invasive fungal infections.
2. To review the signs of pneumocystis infection.
3. To learn about acute viral infections of the chest.
Author Disclosures:
I. J. Hartmann: nothing to disclose

RC 304-3 15:07
D. Diagnosing pulmonary embolism (PE)
G. Aviram; *Tel-Aviv/IL (aviramgalit@hotmail.com)*
Learning objectives:
1. To learn about optimising CT angiography indications.
2. To be aware of the causes of imaging inconclusiveness.
3. To learn how to identify signs of acute right ventricular dysfunction.
Author Disclosures:
G. Aviram: Research/Grant Support at Philips Healthcare

14:00 - 15:30 **Room E**

E³ - Rising Stars Programme: Basic Session

BS 3

Musculoskeletal: essentials of trauma imaging

Moderator:
A. S. Vieira; Porto/PT

BS 3-1 14:00
Fractures and dislocations in the extremities
R. Sutter; *Zurich/CH*
Learning objectives:
1. To describe imaging features of fractures and dislocations.
2. To list imaging findings that help in identifying subtle fractures.
3. To explain imaging features of fracture healing and non-healing.
Author Disclosures:
R. Sutter: nothing to disclose

BS 3-2 14:30
Acetabular fractures demystified
Ü. Aydingöz; *Ankara/TR (ustunaydingoz@yahoo.com)*
Learning objectives:
1. To describe the rationale behind the classification of acetabular fractures.
2. To explain imaging findings of acetabular fractures important for the orthopaedist.
Author Disclosures:
Ü. Aydingöz: nothing to disclose

BS 3-3 15:00
Cervical spine trauma
P. J. MacMahon; *Dublin/IE (pmacmahon@mater.ie)*
Learning objectives:
1. To describe the mechanisms of cervical spine injury.
2. To explain imaging findings of cervical spine injury.
Author Disclosures:
P. J. Macmahon: nothing to disclose

14:00 - 15:30 **Room F1**

Oncologic Imaging

RC 316

Peritoneal carcinomatosis: the role of imaging in detection and treatment planning?

Moderator:
M. J. Lahaye; Amsterdam/NL

RC 316-1 14:00
A. Detection and characterisation: tips and tricks
L. Fournier; *Paris/FR*
Learning objectives:
1. To become familiar with imaging strategies for assessment of peritoneal carcinomatosis.
2. To discuss multimodal concepts for detection and characterisation.
3. To learn about the limitations of non-invasive imaging approaches.
Author Disclosures:
L. Fournier: Grant Recipient at Invectys, Speaker at General Electric, Speaker at Sanofi, Speaker at Bayer, Speaker at Pfizer, Speaker at Novartis, Speaker at Janssen, Research/Grant Support at Philips, Research/Grant Support at Ariana Pharma, Research/Grant Support at Evolucare

RC 316-2 14:30
B. Surgical view: citoreductive surgery
A.-S. Bats; *Paris/FR (anne-sophie.bats@aphp.fr)*
Learning objectives:
1. To understand the surgeon's view on imaging strategies.
2. To learn about surgical strategies for treatment of peritoneal carcinomatosis.
3. To discuss the role of the radiologist in preoperative management.
Author Disclosures:
A.-S. Bats: nothing to disclose

RC 316-3 15:00
C. Imaging in treatment planning and follow-up
G. Zamboni; *Verona/IT (gzamboni@hotmail.com)*
Learning objectives:
1. To become familiar with the role of imaging for systemic and local treatment planning.
2. To discuss the value of imaging modalities.
3. To understand the limitations and pitfalls of imaging.
Author Disclosures:
G. Zamboni: nothing to disclose

14:00 - 15:30 **Room F2**

Breast

RC 302

New developments in mammographic breast imaging

RC 302-1 14:00
Chairperson's introduction
M. Sklair-Levy*; Ramat Gan/IL (miri.sklairlevy@sheba.health.gov.il)*
Session objectives:
1. To recognise the advantages and disadvantages of digital breast tomosynthesis and contrast enhanced mammography techniques.
2. To learn about the challenges between different 3D mammography systems.
3. To understand the future potential of new breast imaging techniques in lesion assessment.
Author Disclosures:
M. Sklair-Levy: nothing to disclose

RC 302-2 14:05
A. Tomo, 2D-Synthetic and artefacts: is it the same in all machines?
I. Sechopoulos*; Nijmegen/NL (ioannis.sechopoulos@radboudumc.nl)*
Learning objectives:
1. To know the different scan and reconstruction protocols.
2. To learn the impact on resolution and lesion delineation.
3. To get an idea of adequate quality control in tomosynthesis.
Author Disclosures:
I. Sechopoulos: Research/Grant Support at Siemens Healthcare, Research/Grant Support at Canon Medical Systems, Speaker at Siemens Healthcare, Speaker at Hologic Inc.

RC 302-3 14:28
B. Contrast mammography alone or combined with tomosynthesis: which is the way to go?
P. Clauser*; Vienna/AT (clauser.p@hotmail.it)*
Learning objectives:
1. To learn the basics of contrast enhanced mammography.
2. To understand the role of these new techniques in different clinical settings.
3. To learn about the new potential of combining mammography with molecular imaging, optical imaging, and texture analysis.
Author Disclosures:
P. Clauser: Speaker at Siemens

RC 302-4 14:51
C. Phase-contrast mammography and future techniques
M. Stampanoni*; Zurich/CH (marco.stampanoni@psi.ch)*
Learning objectives:
1. To understand the technique of phase-contrast breast imaging.
2. To learn about the potential in lesion differentiation.
3. To get an idea of further implementation and developments.
Author Disclosures:
M. Stampanoni: Board Member at GratXray AG, Shareholder at GratXray AG

15:14
Panel discussion: Mammography, digital breast tomosynthesis, and contrast-enhanced mammography: where will we stand in 10 years?

14:00 - 15:00 **Coffee & Talk 3**

Coffee & Talk (open forum) Session

Organised by WHO

C 34

Oncologic imaging and the World Health Organisation (WHO)

C 34-1 14:00
Chairperson's introduction
E. Denton*; Norwich/UK (erika.denton@nnuh.nhs.uk)*
Session objectives:
1. To understand how the International Agency for Research on Cancer IARC at The World Health Organisation currently collaborates with radiology experts.
2. To understand the outputs and publications from IARC and how imaging involvement is proposed and how radiology will be reflected in future governance and publications.
3. To understand current oncologic imaging standards for reporting.
Author Disclosures:
E. Denton: nothing to disclose

C 34-2 14:05
The work of the World Health Organisation in oncologic imaging
I. A. Cree*; Lyons/FR (creei@iarc.fr)*
Learning objectives:
1. To understand work of the World Health Organisation Classification of Tumours Editorial Board.
2. To understand the publications produced by the WHO for oncological reporting and where imaging will be represented.
Author Disclosures:
I. A. Cree: nothing to disclose

C 34-3 14:15
How do radiologists currently standardise oncologic reporting?
A. Rockall*; London/UK (a.rockall@imperial.ac.uk)*
Learning objectives:
1. To understand the standards radiologists currently use to report oncologic imaging.
2. To understand how international standards might impact oncologic imaging.
Author Disclosures:
A. Rockall: Speaker at Guerbet

14:25
Open forum discussion

14:00 - 15:30 **da Vinci (Room D1)**

Genitourinary

RC 307

The retroperitoneal "non-renal" mass

RC 307-1 14:00
Chairperson's introduction
M. Bertolotto*; Trieste/IT (bertolot@units.it)*
Session objectives:
1. To understand the imaging features of primary retroperitoneal tumours.
2. To know the imaging role in patients with "functioning" adrenal lesions.
3. To be able to recognise non-neoplastic retroperitoneal diseases and to guide patient management.
Author Disclosures:
M. Bertolotto: nothing to disclose

RC 307-2 14:05
A. Imaging primary retroperitoneal tumours
G. Heinz*; St. Pölten/AT (gertraud.heinz@stpoelten.lknoe.at)*
Learning objectives:
1. To know the imaging findings that allow recognising a mass as retroperitoneal.
2. To understand how to differentiate among different retroperitoneal tumours.
3. To be able to provide guidance to the surgical approach of these lesions.
Author Disclosures:
G. Heinz: nothing to disclose

RC 307-3 14:28
B. The "functioning" adrenal mass
A. Cieszanowski*; Warsaw/PL (andrzej.cieszanowski@wum.edu.pl)*
Learning objectives:
1. To understand the role of radiology in patients with "functioning" adrenal tumours.
2. To know how to look for small/difficult to see "functioning" lesions.
3. To know how to provide guidance to the surgeon who is planning a minimally invasive surgical approach.

Author Disclosures:
A. Cieszanowski: Speaker at Philips, Speaker at Siemens, Speaker at Bayer, Speaker at GE

RC 307-4 14:51
C. "Non-neoplastic" retroperitoneal diseases
M. Scaglione*; Middlesborough/UK (mscaglione@tiscali.it)*
Learning objectives:
1. To know the imaging features of retroperitoneal abscesses and haematomas.
2. To understand the role of imaging in patients with retroperitoneal fibrosis.
3. To understand how radiology can help planning management of these lesions.
Author Disclosures:
M. Scaglione: nothing to disclose

15:14
Panel discussion: Highlights in non-renal retroperitoneal masses

14:00 - 15:30 **Darwin (Room D2)**

EFRS Workshop

EFRS WS 3
Growing radiography research

Moderators:
A. England; Manchester/UK
J. McNulty; Dublin/IE

EFRS WS 3-1 14:00
Building research collaboration: my top tips
C. Buissink*; Groningen/NL (c.buissink@pl.hanze.nl)*
Learning objectives:
1. To explore key considerations to establishing good research collaborations.
2. To appreciate how to avoid unsuccessful collaborations.
Author Disclosures:
C. Buissink: nothing to disclose

EFRS WS 3-2 14:15
The EFRS Research Hub
L. A. Rainford*; Dublin/IE (louise.rainford@ucd.ie)*
Learning objectives:
1. To understand the purpose of the EFRS Research Hub.
2. To review aspects of the EFRS Research Hub launched at ECR 2019.
3. To consider future opportunities and the value of the EFRS Research Hub.
Author Disclosures:
L. A. Rainford: nothing to disclose

EFRS WS 3-3 14:30
Grant writing: my top tips
K. Knapp*; Exeter/UK (K.M.Knapp@exeter.ac.uk)*
Learning objectives:
1. To explore key considerations for writing a successful grant application.
2. To consider intellectual property issues when writing a grant.
3. To understand the common pitfalls in grant writing.
Author Disclosures:
K. Knapp: Author at Carver's Medical Imaging, Research/Grant Support at Wellcome / Stryker

EFRS WS 3-4 14:45
Considering doctoral studies: my top tips
J. McNulty*; Dublin/IE (jonathan.mcnulty@ucd.ie)*
Learning objectives:
1. To learn about the current status of doctoral opportunities across Europe.
2. To explore key considerations to make before commencing doctoral studies.
Author Disclosures:
J. McNulty: nothing to disclose

EFRS WS 3-5 15:00
Making the most of the EFRS Radiographer Research Network
A. England*; Manchester/UK (A.England@salford.ac.uk)*
Learning objectives:
1. To learn about the EFRS Radiographer Research Network.
2. To consider how the EFRS Radiographer Research Network could support research-related activities.
Author Disclosures:
A. England: nothing to disclose

15:15
Panel discussion: Is radiographer research essential for all radiographers?

14:00 - 15:30 **Room G**

GI Tract

RC 301
Imaging the acute abdomen: new insights

Moderator:
D. E. Malone; Dublin/IE

RC 301-1 14:00
A. Acute mesenteric ischaemia
M. Ronot*; Clichy/FR (maxime.ronot@aphp.fr)*
Learning objectives:
1. To learn about the different types of acute mesenteric ischaemia and the clinical conditions in which they occur.
2. To understand how the imaging features are related to the underlying pathophysiology.
3. To appreciate the role of endovascular interventional procedures in the management of acute mesenteric ischaemia.
Author Disclosures:
M. Ronot: nothing to disclose

RC 301-2 14:30
B. Low-dose abdominal CT for evaluating suspected appendicitis
K. H. Lee*; Seongnam/KR (kholeemail@gmail.com)*
Learning objectives:
1. To emphasise the need for reducing radiation exposure in adolescents and young adults with suspected appendicitis.
2. To critically review published evidence indicating that low-dose CT is comparable with normal-dose CT for diagnostic performance and clinical outcome.
3. To review low-dose CT imaging techniques and other practical issues for the successful implementation of low-dose CT in practice.
Author Disclosures:
K. H. Lee: Grant Recipient at Korea Health Technology R&D Project through the Korea Health Industry Development Institute of the Ministry of Health & Welfare, , Grant Recipient at Seoul National University Bundang Hospital, Grant Recipient at Dasol Life Science, Grant Recipient at Bracco Imaging Korea, Grant Recipient at GE Healthcare Medical Diagnostics, Korea, Grant Recipient at Mid-Career Researcher Program of National Research Foundation of Korea

RC 301-3 15:00
C. Acute colonic diverticulitis
S. Schmidt*; Lausanne/CH (sabine.schmidt@chuv.ch)*
Learning objectives:
1. To review the typical and atypical imaging features of acute colonic diverticulitis and their influence on patient management.
2. To become familiar with the complications and the most important differential diagnoses of acute colonic diverticulitis.
3. To understand the importance of image-guided interventions for the management of complicated acute colonic diverticulitis.
Author Disclosures:
S. Schmidt: nothing to disclose

14:00 - 15:30 **Room K**

E³ - European Diploma Prep Session

E³ 323

Interventional

E³ 323-1 14:00
Chairperson's introduction
J. I. Bilbao; *Pamplona/ES (jibilbao@unav.es)*
Session objectives:
1. To understand the principles and techniques of angiography and image-guided interventions.
2. To become familiar with the most common percutaneous and intra-arterial interventions in oncology.
3. To describe the most common vascular interventions.
Author Disclosures:
J. I. Bilbao Jaureguizar: Speaker at Sirtex Medical

E³ 323-2 14:06
A. Basic principles of angiography and image-guided interventions
L. Cambj-Sapunar; *Split/HR*
Learning objectives:
1. To describe the normal anatomy and normal variants of the arterial and venous vascular system.
2. To understand the importance of pre-procedure planning and selection of image guidance techniques.
3. To explain basic percutaneous image-guided techniques, including arterial access as well as biopsy and drainage.
Author Disclosures:
L. Cambj-Sapunar: nothing to disclose

E³ 323-3 14:34
B. Image-guided interventions in oncology
T. Bilhim; *Lisbon/PT (tiagobilhim@hotmail.com)*
Learning objectives:
1. To describe the basic technical methodological principles and indications of imaging-guided interventions in oncological disorders, including thermal ablation techniques.
2. To understand the principles and indications for vascular interventions in cancer, e.g., transarterial treatment of liver tumours.
3. To become familiar with post-treatment follow-up, highlighting normal and abnormal pathological imaging findings.
Author Disclosures:
T. Bilhim: Consultant at Merit Medical, Consultant at Terumo, Speaker at Cook, Speaker at Philips, Shareholder at EmbolX

E³ 323-4 15:02
C. Vascular interventions
D. Kuhelj; *Ljubljana/SI (dimitrij.kuhelj@guest.arnes.si)*
Learning objectives:
1. To become familiar with the pretreatment imaging flow-chart in atherosclerotic diseases.
2. To describe indications and techniques for arterial angioplasty and stenting.
3. To explain techniques of arterial embolisation and coiling, as well as thromboaspiration.
Author Disclosures:
D. Kuhelj: Speaker at ABBOTT

14:00 - 15:30 **Room M 2**

E³ - Advanced Course: Hot Topics in Emergency Radiology

E³ 318

Assessing neurological complications and brain death in ICU patients

E³ 318-1 14:00
Chairperson's introduction
M. C. Çalli; *Izmir/TR (cem.calli@gmail.com)*
Session objectives:
1. To become familiar with common and less frequent neurological complications in ICU patients.
2. To be able to proactively help the ICU team to best diagnose and manage these complications.
3. To become familiar with the protocols in imaging of brain death and potential organ donation.
Author Disclosures:
M. C. Çalli: nothing to disclose

E³ 318-2 14:05
A. CT and MRI in neurologically impaired ICU patients
F. J. A. Meijer; *Nijmegen/NL (Anton.Meijer@radboudumc.nl)*
Learning objectives:
1. To understand the main neurological complication in intensive care patients.
2. To understand the value of MRI in coma patients with unclear brain pathology.
3. To understand how different imaging sequences of CT and MRI can help to identify and classify neurological complications.
Author Disclosures:
F. J. A. Meijer: Speaker at Canon Medical Systems at ECR 2020

E³ 318-3 14:30
B. Brain death evaluation
O. Bronov; *Moscow/RU (doctorbronov@gmail.com)*
Learning objectives:
1. To become familiar with the most typical constellations.
2. To learn about appropriate imaging protocols.
3. To understand the context of transplantation units and imaging of potential organ donors.
Author Disclosures:
O. Bronov: nothing to disclose

E³ 318-4 14:55
C. Imaging of potential organ donors
S. Roosendaal; *Amsterdam/NL (stefanmed@fastmail.nl)*
Learning objectives:
1. To learn about correct indication.
2. To learn about appropriate imaging protocols.
3. To be able proceed appropriately in the case of inconclusive findings.
Author Disclosures:
S. Roosendaal: nothing to disclose

15:20
Panel discussion: Combined imaging of brain death and organ donation: is this feasible?

14:00 - 15:30 **Room M 3**

Head and Neck

RC 308

Head and neck imaging: when does it become abnormal?

Moderator:
N. Thieme; Berlin/DE

RC 308-1 14:00
A. Normative measures in the temporal bone
F. Veillon; *Strasbourg/FR (francis.veillon@chru-strasbourg.fr)*
Learning objectives:
1. To learn about the normal appearance of the temporal bone.
2. To understand how to assess when the anatomy is abnormal.
3. To show clinical cases where structures are too large or too small.
Author Disclosures:
F. Veillon: nothing to disclose

RC 308-2 14:22
B. Normative measures in the orbit
R. Kohler; *Sion/CH*

Learning objectives:
1. To understand differences in the size and shape of the eye.
2. To learn about the normal appearance and anatomic variations of the optic nerve.
3. To use clinical cases to discuss normative measures of the soft tissue structures in the orbit.
Author Disclosures:
R. Kohler: Grant Recipient at not yet known

RC 308-3 14:45
C. Anatomical variations of importance in dental implant planning
S. Cappabianca*; Naples/IT (salvatore.cappabianca@unicampania.it)*
Learning objectives:
1. To discuss the role of cone beam CT in dental imaging.
2. To review anatomical variations of the mandibular canal and interforaminal region.
3. To show examples of implant injuries.
Author Disclosures:
S. Cappabianca: nothing to disclose

RC 308-4 15:07
D. Growing up or growing wrong
B. Verbist*; Leiden/NL (b.m.verbist@lumc.nl)*
Learning objectives:
1. To learn about the normal development of the head and neck area.
2. To understand how to assess clinically-relevant developmental defects.
3. To highlight important variants using clinical cases.
Author Disclosures:
B. Verbist: Grant Recipient at HPTC-Varian consortium, Research/Grant Support at Advanced Bionics, Research/Grant Support at Cochlear

14:00 - 15:30 **Room M 4**

E³ - Advanced Course: Interactive Teaching Session for Young (and not so Young) Radiologists

E³ 321

Paediatric radiology for the general radiologist

E³ 321-1 14:00
A. Pitfalls in paediatric chest and abdomen
B. Coley*; Columbus, OH/US (brian.coley@cchmc.org)*
Learning objectives:
1. To review the basic principles of the paediatric chest radiographs through common mistakes.
2. To emphasise pitfalls when imaging the paediatric abdomen.
3. To learn to avoid the most common pitfalls.
Author Disclosures:
B. Coley: Author at Elsevier, Board Member at Neoview

E³ 321-2 14:45
B. Paediatric musculoskeletal imaging: normal variants or real injuries?
F. M. Saez Garmendia*; Bilbao/ES (fersaez@yahoo.com)*
Learning objectives:
1. To become familiar with the normal variants.
2. To identify the key imaging findings to differentiate between normal variants and disease.
3. To learn how to integrate age, location, and clinical history with the radiological features before establishing a diagnosis.
Author Disclosures:
F. M. Saez Garmendia: nothing to disclose

14:00 - 15:30 **Room M 5**

E³ - Advanced Course: Artificial Intelligence

E³ 320

Artificial intelligence and translations to clinical practice

E³ 320-1 14:00
Chairperson's introduction
W. J. Niessen*; Rotterdam/NL (w.niessen@erasmusmc.nl)*
Session objectives:
1. To become familiar with international initiatives to bring machine learning and radiology communities together.
2. To discuss how societies such as ESR, RSNA, and ACR should work together with the machine learning community to bring artificial intelligence into clinical practice.
3. To understand the complementary nature of data science and medical imaging.
Author Disclosures:
W. J. Niessen: Shareholder at Quantib BV, Founder at Quantib BV, Consultant at Quantib BV

E³ 320-2 14:06
A. Artificial intelligence (AI) use cases
K. Dreyer*; Boston, MA/US*
Learning objectives:
1. To introduce the audience to the AI use cases as developed by the American College of Radiology.
2. To learn about an ecosystem for developing AI algorithms that can be translated to clinical practice.
3. To discuss hurdles and proposed solutions in getting AI techniques regulatory approved.
Author Disclosures:
K. Dreyer: nothing to disclose

E³ 320-3 14:34
B. Challenges to objectively compare performance of AI applications
L. Maier-Hein*; Heidelberg/DE (l.maier-hein@dkfz-heidelberg.de)*
Learning objectives:
1. To learn the outcomes of a review of more than 150 challenges in medical imaging.
2. To learn about the metrics allowing the objective evaluation of AI algorithm performance.
3. To understand how new developments in AI challenges help to objectively evaluate the performance of algorithms.
Author Disclosures:
L. Maier-Hein: nothing to disclose

E³ 320-4 15:02
C. How far are we in getting AI into clinical practice?
L. Marti-Bonmati*; Valencia/ES (Luis.Marti@uv.es)*
Learning objectives:
1. To critically review the current level of AI adoption in clinical practice.
2. To understand the need of data scientists working in radiology departments.
3. To discuss what next steps need to be taken in order to increase take-up in clinical practice.
Author Disclosures:
L. Marti-Bonmati: nothing to disclose

16:00 - 17:30 **Room X**

Imaging Informatics

RC 405

Effect of the EU General Data Protection Regulations (GDPR): moving patients' data across hospitals, regions, countries

Moderator:
O. Ratib; Geneva/CH

RC 405-1 16:00
A. The GDPR: an overview
C. D. Becker; *Geneva/CH*
Learning objectives:
1. To learn about the content of the GDPR.
2. To understand the effects of GDPR for scientific use of imaging data.
3. To become familiar with the terminology as used in GDPR.
Author Disclosures:
C. D. Becker: nothing to disclose

RC 405-2 16:25
B. Transferring patients' data across hospitals, regions, countries: pros and cons
E. Kotter; *Freiburg/DE (elmar.kotter@uniklinik-freiburg.de)*
Learning objectives:
1. To understand how imaging data can be shared.
2. To learn about the influence of GDPR on data sharing.
3. To appreciate the challenges when sharing imaging data.
Author Disclosures:
E. Kotter: nothing to disclose

RC 405-3 16:50
C. Anonymous or pseudo-anonymous 2D-3D data: is privacy really warranted?
T. de Bondt; *Antwerp/BE (timo.debondt@gmail.com)*
Learning objectives:
1. To learn about the methods to de-identify (imaging) data.
2. To understand the pitfalls of de-identification methods.
3. To understand how to approach de-identification for research.
Author Disclosures:
T. de Bondt: nothing to disclose

RC 405-4 17:10
D. Management of data for clinical trials
D. Regge; *Candiolo-Torino/IT*
Learning objectives:
1. To learn about data management for clinical trials.
2. To understand imaging biobank concepts.
3. To appreciate the requirements for building proper imaging biobanks.
Author Disclosures:
D. Regge: Speaker at GE Medical Systems

16:00 - 17:00 **Coffee & Talk 1**

Coffee & Talk (open forum) Session

Organised by ESOR

C 2

Quality and standards

Moderator:
H.-U. Kauczor; Heidelberg/DE

C 2-1 16:00
What a fellow should learn about "Quality and Standards"
A. Brady; *Cork/IE (adrianbrady@me.com)*
Learning objectives:
1. To understand the need for common standards in the delivery of radiology services.
2. To learn about the ways the quality of radiological service delivery can be measured and enhanced.
3. To appreciate the benefits of patient satisfaction and safety when maintaining quality standards in radiology.
Author Disclosures:
A. Brady: nothing to disclose

C 2-2 16:10
What a fellow wants to learn about "Quality and Standards"
M. Marolt Music; *Ljubljana/SI (mmusic@onko-i.si)*
Learning objectives:
1. To understand the importance of quality control in a radiology department.
2. To become familiar with radiology standards in a fellow's daily practice.
3. To consider the role of radiology fellows in improving quality in radiology.
Author Disclosures:
M. Marolt Music: nothing to disclose

C 2-3 16:20
Role of radiographers in "Quality and Standards"
H. H. Hjemly; *Sorumsand/NO (hakon@radiograf.no)*
Learning objectives:
1. To learn about radiographers' scope of practise related to quality assurance and quality control in medical imaging.
2. To understand the essential role radiographers have in the radiological team to assure the delivery of safe, cost-effective, and high-quality diagnostic imaging.
3. To become familiar with recommended learning objectives related to quality and standards for radiography students.
Author Disclosures:
H. H. Hjemly: nothing to disclose

C 2-4 16:30
Role of structured reporting to foster "Quality and Standards"
W. Sommer; *Munich/DE*
Learning objectives:
1. To learn about different forms of structured reporting.
2. To understand the implication of structured reporting on report quality and completeness.
Author Disclosures:
W. Sommer: Founder at Smart Reporting GmbH, CEO at Smart Reporting GmbH

16:40
Open forum discussion

16:00 - 17:30 **Room N**

EuroSafe Imaging Session

EU 4a

Why do we need to know radiation doses in imaging procedures?

Moderator:
G. N. Paulo; Coimbra/PT

EU 4a-1 16:00
Chairperson's introduction
E. Vaño; *Madrid/ES (eliseov@med.ucm.es)*
Session objectives:
1. To highlight the importance of the dosimetric aspects for the optimisation of imaging procedures as required by the European directive.
2. To recognise the differences between the dosimetric quantities used for diagnostic reference levels and those used for the epidemiological studies and population dose evaluation.
3. To identify the benefits and limitations of the automatic patient dose registries in imaging procedures.
Author Disclosures:
E. Vaño: nothing to disclose

EU 4a-2 16:10
Relevance of patient dose evaluation in the MEDIRAD project
J. Damilakis*; Iraklion/GR (John.Damilakis@med.uoc.gr)*
Learning objectives:
1. To learn about the objectives of the MEDIRAD project and the expected impact on radiology practice.
2. To appreciate the potential of the automatic patient dose registries to improve epidemiological research.
3. To understand the role of the different dosimetric tools developed and used by MEDIRAD to improve the accuracy of patient dose evaluations.
Author Disclosures:
J. Damilakis: Research/Grant Support at European Commission H2020

EU 4a-3 16:25
Diagnostic reference levels in paediatrics
C. Granata*; Genoa/IT*
Learning objectives:
1. To learn the importance of patient dose reduction in paediatric imaging and the relevance of the European guidelines on diagnostic reference levels.
2. To appreciate the difficulties in collecting and analysing patient dose values in paediatric imaging, but the need to audit these doses.
3. To understand the importance of guidelines to improve the radiation protection in paediatric imaging and the evaluation of population dose in paediatrics.
Author Disclosures:
C. Granata: Speaker at Guerbet Italia

EU 4a-4 16:40
Diagnostic reference levels (DRLs) and image quality: the need to use clinical indication
E. P. Efstathopoulos*; Alimos/GR (stathise@med.uoa.gr)*
Learning objectives:
1. To learn what diagnostic reference levels are and what they are not, and the limitations of DRLs.
2. To appreciate the trade-off between radiation dose and image quality.
3. To understand the need for the establishment of clinical indication-based DRLs.
Author Disclosures:
E. P. Efstathopoulos: nothing to disclose

EU 4a-5 16:55
Optimisation and radiation dose in medical imaging
R. M. Sanchez*; Madrid/ES (robertomariano.sanchez@salud.madrid.org)*
Learning objectives:
1. To learn that the new European directive requires estimating, registering, and analysing patient dose values for medical imaging.
2. To appreciate the role of automatic patient dose registries in optimisation, and the impact of new technology in reducing patient doses in medical imaging.
3. To understand the differences between the different dosimetric quantities to optimise the imaging procedures and to estimate population doses.
Author Disclosures:
R. M. Sanchez: nothing to disclose

17:10
Panel discussion: What basic dosimetric information in medical imaging has to be known by the referrers, by the radiologists, and by the patients?

16:00 - 17:30 **Room O**

Chest

RC 404
Thoracic emergencies: part 2

Moderator:
G. Mostbeck; Vienna/AT

RC 404-1 16:00
A. Emergencies in thoracic oncology
C. Beigelman-Aubry*; Lausanne/CH*
Learning objectives:
1. To learn about various causes of dyspnea in thoracic oncology.
2. To learn about cardiac complications of thoracic malignancies.
3. To learn how to suggest an appropriate differential diagnosis.
Author Disclosures:
C. Beigelman-Aubry: Speaker at Gilead, Speaker at Boehringer, Speaker at Astra Zeneca

RC 404-2 16:22
B. Haemoptysis
A. Khalil*; Paris/FR (antoine.khalil@aphp.fr)*
Learning objectives:
1. To understand the role of multidetector CT angiography.
2. To learn about the planning of endovascular interventions.
Author Disclosures:
A. Khalil: nothing to disclose

RC 404-3 16:45
C. Non-ischaemic cardiac emergencies
C. Loewe*; Vienna/AT (christian.loewe@meduniwien.ac.at)*
Learning objectives:
1. To learn how to evaluate acute pericarditis.
2. To learn how to explore patients with suspected myocarditis.
3. To learn about takotsubo features on MRIs.
Author Disclosures:
C. Loewe: Speaker at Siemens Healthineers; , Speaker at BRACCO, Speaker at GE Healthcare

RC 404-4 17:07
D. Postoperative and iatrogenic complications
J. D. Dodd*; Dublin/IE (jonniedodd@gmail.com)*
Learning objectives:
1. To learn about signs of bronchopleural fistula and lobar torsion.
2. To review the signs of chemotherapy-induced pulmonary toxicity.
3. To learn about thoracic complications of interventional radiology.
Author Disclosures:
J. D. Dodd: Speaker at Boehringer Ingelheim, Research/Grant Support at St. Vincent's Foundation, Research/Grant Support at FP7 Program of the European Commission

16:00 - 17:30 **Coffee & Talk 2**

EuroSafe Imaging Session

EU 4b
Building capacity and quality/safety awareness in Africa

Moderators:
M. Abdel-Wahab; Vienna/AT
S. Abdulrazak; Vienna/AT
G. Frija; Paris/FR

C11-1/C 11-2/C 11-3 16:00
Introduction
B. Brkljačić*; Zagreb/HR*
G. Frija*; Paris/FR (guy.frija@aphp.fr)*
S. Abdulrazak*; Vienna/AT*
Author Disclosures:
B. Brkljačić: disclosure/affirmation information not submitted, G. Frija: nothing to disclose, S. Abdulrazak: disclosure/affirmation information not submitted

C 11-4 16:20
Strengthening radiology in Africa: the IAEA multifactorial approach
D. Paez*; Vienna/AT (d.paez@iaea.org)*
Learning objectives:
1. To provide an overview of IAEA's capacity building activities in Africa.
2. To learn how African countries can concretely benefit from IAEA support.
3. To explore synergies between IAEA, ESR, and Africa.
Author Disclosures:
D. Paez: nothing to disclose

C 11-5 16:30
IAEA policy in Africa
P. Johnston*; Vienna/AT*
Learning objectives:
1. To provide an overview of IAEA's efforts to promote radiation protection in patients in Africa.
2. To understand the challenges and opportunities to improve patient safety in Africa through the demonstration of successful examples.
3. To provide a roadmap for improving radiation protection of patient activities in Africa.
Author Disclosures:
P. Johnston: disclosure/affirmation information not submitted

C 11-6 16:40
African Society of Radiology (ASR) expectations
T. El-Diasty*; Mansoura/EG (teldiasty@hotmail.com)*
Learning objectives:
1. To understand the role of the African Society of Radiology in promoting quality and safety in radiology practice in Africa.
2. To understand the needs of different African countries.
3. To discuss methods of promoting the exchange of knowledge between African countries via ESR and IAEA.
Author Disclosures:
T. El-Diasty: nothing to disclose

C 11-7 16:50
EuroSafe Imaging Star concept in Africa
B. Mansouri*; Algiers/DZ (boudjema.mansouri@gmail.com)*
Learning objectives:
1. To integrate the AFROSAFE Rad Stars initiative into the AFROSAFE Rad radiation safety campaign (action plan 2019-2021).
2. To define new criteria and rates adapted for the specificities of African countries, the practice of medical imaging, and the implementation of radiation protection.
3. To learn about the impact of EuroSafe Imaging on the launch of AFROSAFE Rad Stars.
Author Disclosures:
B. Mansouri: nothing to disclose

C 11-8/**C 11-9** 17:00
Introducing ESR iGuide Clinical Decision Support in Africa
D. Husseiny Salama; *Cairo/EG*,
M. Kawooya; *Kampala/UG*
Author Disclosures:
D. Husseiny Salama: disclosure/affirmation information not submitted,
M. Kawooya: disclosure/affirmation information not submitted

C 11-10 17:15
EuroSafe Imaging: ISR vision for imaging in Africa
G. Frija; *Paris/FR*
Author Disclosures:
G. Frija: disclosure/affirmation information not submitted

17:25
Discussion

16:00 - 17:30 **Room E**

Pros & Cons Session

PS 427
Breast cancer: to screen or not to screen?

PS 427-1 16:00
Chairperson's introduction
F. J. Gilbert*; Cambridge/UK (fjg28@cam.ac.uk)*
Session objectives:
1. To understand how the effectiveness of breast screening is assessed.
2. To learn about the key controversies for and against screening.
3. To decide whether or not the benefits outweigh the harms of breast screening.
Author Disclosures:
F. J. Gilbert: Consultant at Alphabet Inc., Equipment Support Recipient at GE Healthcare, Grant Recipient at Hologic, Research/Grant Support at GE Healthcare, Research/Grant Support at Bayer

PS 427-2 16:05
A. The evidence for breast screening
M. Broeders*; Nijmegen/NL (mireille.broeders@radboudumc.nl)*
Learning objectives:
1. To understand the evidence from population trials.
2. To learn about the effectiveness and potential benefits of breast screening.
3. To become familiar with the rational for screening and types of cancers detected.
Author Disclosures:
M. Broeders: Employee at Dutch Expert Centre for Screening, Nijmegen, the Netherlands, Speaker at Hologic, Siemens

PS 427-3 16:30
B. The evidence against breast screening
P. Autier*; Dardilly/FR (philippe.autier@i-pri.org)*
Learning objectives:
1. To understand overdiagnosis and overtreatment in relation to screening.
2. To learn about the potential harms of screening.
3. To become familiar with the costs associated with screening.
Author Disclosures:
P. Autier: nothing to disclose

16:55
Discussion

16:00 - 17:30 **Room F1**

E³ - Advanced Course: Interactive Teaching Session for Young (and not so Young) Radiologists

E³ 421
Imaging of the liver

E³ 421-1 16:00
A. CT and MRI liver imaging reporting and data system (LIRADS): how to use it and what to expect
A. Darnell*; Barcelona/ES (andarnel@clinic.cat)*
Learning objectives:
1. To become familiar with LIRADS categories, definitions, and algorithms.
2. To discuss the confusing features of LIRADS with examples.
3. To understand what the probability of hepatocellular carcinoma is for each LIRADS category.
Author Disclosures:
A. Darnell: Speaker at Bayer

E³ 421-2 16:45
B. Focal lesions in non-cirrhotic liver: how to diagnose, differentiate and manage
G. Brancatelli*; Palermo/IT (gbranca@yahoo.com)*
Learning objectives:
1. To learn how to differentiate focal liver lesions in non-cirrhotic patients with CT and MRI.
2. To know how to manage non-cirrhotic patients with focal liver lesions.
Author Disclosures:
G. Brancatelli: Consultant at Bayer, Speaker at Bayer, Other at General Electric, Other at Bracco

16:00 - 17:30 **Room F2**

Musculoskeletal

RC 410
Imaging of chronic forefoot pain

Moderator:
M. S. Posadzy; Poznan/PL

RC 410-1 16:00
A. Articular disorders
M. Shahabpour*; Brussels/BE (maryam.shahabpour@uzbrussel.be)*

Learning objectives:
1. To explain the disease spectrum and pathophysiology of articular sources of chronic forefoot pain.
2. To describe the imaging findings of articular disorders that present with chronic forefoot pain.
Author Disclosures:
M. Shahabpour: nothing to disclose

RC 410-2 16:30
B. Extra-articular source of pain
G. Bierry*; Strasbourg/FR (guillaume.bierry@chru-strasbourg.fr)*
Learning objectives:
1. To explain the disease spectrum and pathophysiology of extra-articular sources of chronic forefoot pain.
2. To describe the imaging findings of extra-articular conditions that are present in chronic forefoot pain.
Author Disclosures:
G. Bierry: Advisory Board at General Electric

RC 410-3 17:00
C. Imaging-guided percutaneous treatment of forefoot pain
R. L. Cazzato*; Strasbourg/FR (gigicazzato@hotmail.it)*
Learning objectives:
1. To explain the rationale behind the imaging-guided percutaneous treatment of forefoot pain.
2. To describe the imaging-guided percutaneous procedures for the treatment of forefoot pain.
Author Disclosures:
R. L. Cazzato: nothing to disclose

16:00 - 17:00 **Coffee & Talk 3**

Coffee & Talk (open forum) Session

C 20

Imaging biobanks: from concept to implementation

C 20-1 16:00
Chairperson's introduction: What is an imaging biobank?
E. Neri*; Pisa/IT (emanueleneri1@gmail.com)*
Session objectives:
1. To define an imaging biobank.
2. To describe ESR activities in imaging biobanks.
3. To provide a brief overview of imaging biobank trials in Europe.
Author Disclosures:
E. Neri: Advisory Board at QUIBIM, Speaker at GE/Healthcare

C 20-2 16:06
HORIZON 2020 PRIMAGE biobank
L. Marti-Bonmati*; Valencia/ES (Luis.Marti@uv.es)*
Learning objectives:
1. To describe the scope of the PRIMAGE project.
2. To report the ongoing activities.
3. To foresee the expected impact.
Author Disclosures:
L. Marti-Bonmati: Research/Grant Support at H2020

C 20-3 16:14
Dutch biobank
A. van der Lugt*; Rotterdam/NL (a.vanderlugt@erasmusmc.nl)*
Learning objectives:
1. To describe the population imaging trial in Rotterdam.
2. To discuss the expected impact of the trial.
3. To discuss the pros and cons of population imaging (incidental findings, costs, etc.).
Author Disclosures:
A. van der Lugt: Grant Recipient at Stryker, Grant Recipient at Medtronic, Grant Recipient at Penumbra, Grant Recipient at Ceronovus, Grant Recipient at Siemens, Grant Recipient at GE Healthcare, Grant Recipient at Philips Healthcare

C 20-4 16:22
Artificial intelligence (AI) for analysis in large-scale population studies: UK biobank
D. Rueckert*; London/UK (D.Rueckert@imperial.ac.uk)*
Learning objectives:
1. To report the rationale of the UK biobank.
2. To describe the imaging workflow used.
3. To discuss the application of AI tools.
Author Disclosures:
D. Rueckert: Consultant at IXICO, Consultant at Circle Cardiovascular Imaging, Consultant at Heartflow

16:30
Open forum discussion

16:00 - 17:30 **da Vinci (Room D1)**

Physics in Medical Imaging

RC 413

Blue skies and current trends in digital radiography (DR), computed tomography (CT) and interventional radiology (IR)

RC 413-1 16:00
Chairperson's introduction: Overview of multi-front development in x-ray
J. Sjöberg*; Stockholm/SE (johan.a.sjoberg@sll.se)*
Session objectives:
1. To learn about existing technologies.
2. To learn about state of the art in x-ray imaging modalities.
3. To predict future developments.
Author Disclosures:
J. Sjöberg: nothing to disclose

RC 413-2 16:05
A. Updates and future perspectives to DR technology
J. I. Peltonen*; Helsinki/FI (juha.peltonen@hus.fi)*
Learning objectives:
1. To learn about existing DR technologies.
2. To learn about state of the art in DR imaging.
3. To predict future developments in DR imaging.
Author Disclosures:
J. I. Peltonen: nothing to disclose

RC 413-3 16:28
B. Updates and future perspectives to CT technology
M. Kachelrieß*; Heidelberg/DE (marc.kachelriess@dkfz.de)*
Learning objectives:
1. To learn about existing CT technologies.
2. To learn about state of the art in CT imaging.
3. To predict future developments in CT imaging.
Author Disclosures:
M. Kachelrieß: nothing to disclose

RC 413-4 16:51
C. Updates and future perspectives to IR and angiography technology
N. Marshall*; Leuven/BE (nicholas.marshall@uzleuven.be)*
Learning objectives:
1. To learn about existing IR technologies.
2. To learn about state of the art in IR.
3. To predict future developments in IR.
Author Disclosures:
N. Marshall: nothing to disclose

16:14
Panel discussion: What can we expect from new detectors, equipment designs and post-processing/reconstruction?

16:00 - 17:30 **Darwin (Room D2)**

EFRS Workshop

EFRS WS 4

Public and patient involvement (PPI)

Moderators:
C. A. Beardmore; London/UK
E. Briers; Brussels/BE

EFRS WS 4-1 16:00
The patient's perspective: considering our voice
E. Briers*; Brussels/BE (erikbriers@telenet.be)*
Learning objectives:
1. To learn how to improve engagement with the public and patients in relation to delivering quality medical imaging, interventional radiology, and radiotherapy services.
2. To discuss what matters to patients within medical imaging, interventional radiology, and radiotherapy services.
3. To learn how to capture effective patient feedback for continuous service improvement.
Author Disclosures:
E. Briers: nothing to disclose

EFRS WS 4-2 16:18
Patient, public and practitioner partnerships at a national level: a UK case study
R. Harris*; London/UK (rachelh@sor.org)*
Learning objectives:
1. To learn about the development of a guiding principles strategy for partnership working.
2. To describe the key priorities within the strategy.
3. To consider the steps in supporting implementation of the principles at a national level.
Author Disclosures:
R. Harris: nothing to disclose

EFRS WS 4-3 16:33
Public and patient involvement in education and training
H. Precht*; Middelfart/DK (hepr@ucl.dk)*
Learning objectives:
1. To learn about the importance of patient engagement in education and training.
2. To consider how the public and patients can contribute to radiographers' education.
3. To understand how patient feedback helps support professional and service development.
Author Disclosures:
H. Precht: nothing to disclose

EFRS WS 4-4 16:48
Public and patient involvement in research
A. Negrouk*; Brussles/BE*
Learning objectives:
1. To understand how the public and patients can help research trial and protocol development.
2. To learn how patients and researchers can work together in managing research projects.
3. To understand how patients can help disseminate research results at the end of a study.
Author Disclosures:
A. Negrouk: nothing to disclose

EFRS WS 4-5 17:03
The role of the EFRS in supporting public and patient engagement
J. McNulty*; Dublin/IE (jonathan.mcnulty@ucd.ie)*
Learning objectives:
1. To consider the opportunities for patient, public, and practitioner engagement at the European level.
2. To showcase ongoing activity that will help support improved patient and public partnerships.
3. To learn about future EFRS plans for partnership working.
Author Disclosures:
J. McNulty: nothing to disclose

17:18
Panel discussion: Public and patient involvement: are we doing enough?

16:00 - 17:30 **Descartes (Room D3)**

Radiographers

RC 414

Practical magnetic resonance imaging tips for radiographers

RC 414-1/RC 414-2 16:00
Chairpersons' introduction
A. I. Holodny*; New York, NY/US*
V. G. Syrgiamiotis*; Goudi/GR (syrgiamiotisvasilis@gmail.com)*
Session objectives:
1. To understand practical tips to optimise MRI examinations at 3 Tesla.
2. To be aware of practical tips applicable to paediatric examinations.
3. To discuss the latest issues in MRI safety and how these can be better managed.
Author Disclosures:
A. I. Holodny: disclosure/affirmation information not submitted, V. G. Syrgiamiotis: nothing to disclose

RC 414-3 16:06
A. Practical tips to optimise your examinations at 3 Tesla
J. Podobnik*; Ljubljana/SI (janez.podobnik@kclj.si)*
Learning objectives:
1. To review MRI at 3 Tesla, the benefits it provides, and the associated challenges.
2. To recognise artefacts related to 3 Tesla MRI and to be aware of how these can be reduced.
3. To be familiar with tips for examination optimisation at 3 Tesla.
Author Disclosures:
J. Podobnik: nothing to disclose

RC 414-4 16:29
B. Practical tips in paediatric MRI
U. Weinberger*; Vienna/AT (ulrike.weinberger@fh-campuswien.ac.at)*
Learning objectives:
1. To be aware of special patient care considerations for paediatric patients in MRI.
2. To be familiar with MRI examinations which are routinely, and often exclusively, performed on paediatric patients.
3. To understand methods for paediatric image optimisation in routine practice.
Author Disclosures:
U. Weinberger: Speaker at FH Campus Wien

RC 414-5 16:52
C. What is new in MRI safety?
V. M. F. Silva*; Porto/PT (vitorsoft@gmail.com)*
Learning objectives:
1. To be familiar with key MRI safety issues.
2. To understand how recent and future developments are introducing new safety issues.
3. To be aware of how new safety issues should be managed, and to understand the importance of continuous professional development in MRI safety.
Author Disclosures:
V. M. F. Silva: nothing to disclose

17:15
Panel discussion: How can we ensure MRI radiographers keep up to date with evolving safety requirements?

16:00 - 17:30 **Room G**

Genitourinary

RC 407

Acute and chronic pelvic pain

RC 407-1 16:00
Chairperson's introduction
O. Nikolic*; Novi Sad/RS (nikolic.olivera@gmail.com)*
Session objectives:
1. To learn about the cause of acute and chronic pelvic pain.
2. To understand what the radiologist needs to know about imaging findings in pelvic pain.
Author Disclosures:
O. Nikolic: nothing to disclose

RC 407-2 16:05
A. Acute pelvic pain
M. Basta Nikolic*; Novi Sad/RS (drmarijanabastanikolic@gmail.com)*
Learning objectives:
1. To discuss gynaecological disorders causing acute pelvic pain and differential diagnosis.
2. To present a radiological approach in management of acute pelvic pain.
Author Disclosures:
M. Basta Nikolic: nothing to disclose

RC 407-3 16:24
B. Chronic non-endometriotic pelvic pain
M. M. Otero-Garcia*; Vigo/ES (Maria.Milagros.Otero.Garcia@sergas.es)*
Learning objectives:
1. To know the different causes of chronic pelvic pain.
2. To understand what the radiologist can offer to the clinical referee in patients with chronic pelvic pain.
Author Disclosures:
M. M. Otero-Garcia: nothing to disclose

RC 407-4 16:43
C. Endometriosis
R. A. Kubik-Huch*; Baden/CH (rahel.kubik@ksb.ch)*
Learning objectives:
1. To learn about the clinical features of endometriosis with an emphasis on chronic pelvic pain.
2. To become familiar with the increasing role of MRI for the workup and management of endometriosis.
3. To learn how to optimise MRI of the female pelvis in patients with suspected endometriosis.
4. To illustrate the MRI features of ovarian and peritoneal endometriosis.
Author Disclosures:
R. A. Kubik-Huch: nothing to disclose

RC 407-5 17:02
D. Embolisation of pelvic congestion syndrome
R. Uberoi*; Oxford/UK (raman.uberoi@ouh.nhs.uk)*
Learning objectives:
1. To understand the pathophysiology underlying pelvic congestion syndrome.
2. To learn about the common presentations.
3. To learn about the treatment options, particularly venous embolisations.
Author Disclosures:
R. Uberoi: Grant Recipient at Gore, Advisory Board at Minova, Grant Recipient at Vascutek, Investigator at Vascutek

17:21
Panel discussion: What radiologists have to know in female pelvic pain imaging

16:00 - 17:30 **Room K**

Paediatric

RC 412

Intensive care paediatric radiology: the very sick neonate

RC 412-1 16:00
Chairperson's introduction
S. Stafrace*; Doha/QA (samstafrace01@gmail.com)*
Session objectives:
1. To learn about the most common neurological emergencies in intensive care neonates.
2. To understand the wide variety of thoracic devices that may be used in these patients.
3. To discuss the role of US in abdominal emergencies in the critically ill child.
Author Disclosures:
S. Stafrace: nothing to disclose

RC 412-2 16:05
A. Neuroimaging in the neonatal intensive care unit
M. Argyropoulou*; Ioannina/GR (margyrop@cc.uoi.gr)*
Learning objectives:
1. To learn the most common neurological emergencies in the intensive care patient.
2. To understand the preferential use of US and MRI as imaging techniques.
3. To discuss the key findings that may be useful for differential diagnosis.
Author Disclosures:
M. Argyropoulou: nothing to disclose

RC 412-3 16:30
B. Chest imaging in the ICU: tubes and catheters
M. L. L. Lobo*; Lisbon/PT (mluisalobo@gmail.com)*
Learning objectives:
1. To learn the crucial role of simple views in critically ill children.
2. To understand the variety of devices used in the intensive care unit.
3. To discuss how to avoid the most common pitfalls.
Author Disclosures:
M. L. L. Lobo: nothing to disclose

RC 412-4 16:55
C. Emergencies in the critically ill neonate: abdominal US applications and beyond
M. Riccabona*; Graz/AT*
Learning objectives:
1. To learn about typical body (abdomen, chest and other) emergencies that can be addressed by US in the neonatal intensive care unit (NICU).
2. To understand some typical findings that may help in disease characterisation.
3. To appreciate the considerable impact on prognosis and survival of the critically ill neonate.
Author Disclosures:
M. Riccabona: nothing to disclose

17:20
Panel discussion: Is there a role for FAST scan in the paediatric ICU?

16:00 - 17:30 **Room M 1**

Molecular Imaging

RC 406

Merging the best: hybrid imaging

Moderator:
G. Antoch; Düsseldorf/DE

RC 406-1 16:00
A. Hybrid imaging with SPECT/CT
A. Scarsbrook*; York/UK (a.scarsbrook@nhs.net)*

Wednesday

Learning objectives:
1. To learn the basic principles of hybrid SPECT/CT imaging.
2. To understand what complementary information can be provided by SPECT/CT.
3. To learn the clinical applications of SPECT/CT.
Author Disclosures:
A. Scarsbrook: nothing to disclose

RC 406-2 16:30
B. Hybrid imaging with PET/MRI
F. Kiessling; *Aachen/DE (fkiessling@ukaachen.de)*
Learning objectives:
1. To learn the basic principles of hybrid PET/MRI.
2. To understand what new information can be provided by PET/MRI.
3. To learn about emerging clinical applications of PET/MRI.
Author Disclosures:
F. Kiessling: Speaker at RWTH Aachen University

RC 406-3 17:00
C. Hyperpolarised MRI
F. A. Gallagher; *Cambridge/UK (fag1000@cam.ac.uk)*
Learning objectives:
1. To learn the basic principles of hyperpolarisation.
2. To understand what new information can be provided by hyperpolarised MRI.
3. To learn about oncological and non-oncological applications of hyperpolarised MRI.
Author Disclosures:
F. A. Gallagher: Grant Recipient at GSK, Research/Grant Support at GE Healthcare

16:00 - 17:30 **Room M 2**

E³ - Advanced Course: Hot Topics in Emergency Radiology

E³ 418

Non-neurological complications in intensive care patients

E³ 418-1 16:00
Chairperson's introduction
M.-A. Weber; *Rostock/DE (marc-andre.weber@med.uni-rostock.de)*
Session objectives:
1. To become familiar with common and less frequent complications in ICU patients.
2. To be able to proactively help the ICU team to best diagnose and manage these complications.
3. To become familiar with common diagnostic questions, treatments, and interventions arising in ICU.
Author Disclosures:
M.-A. Weber: nothing to disclose

E³ 418-2 16:06
A. The white chest and severe dyspnoea
M. Herman; *Olomouc/CZ (miroslav.herman@fnol.cz)*
Learning objectives:
1. To understand the physiopathology of the severe respiratory complications in emergency and ICU scenarios.
2. To know when a computed tomography can be decisive.
3. To learn the differential diagnosis patterns for the imaging findings in chest x-ray and CT.
Author Disclosures:
M. Herman: nothing to disclose

E³ 418-3 16:34
B. Acute abdominal complications
M. Scaglione; *Middlesborough/UK (mscaglione@tiscali.it)*
Learning objectives:
1. To become familiar with the most common requests: infection, bleeding, ischaemia, leakage, and obstruction.
2. To learn about the different imaging protocols (when to use intravenous and enteral contrast agent).
3. To learn the main imaging findings.
Author Disclosures:
M. Scaglione: nothing to disclose

E³ 418-4 17:02
C. Image-guided interventions in ICU patients
L. Appelbaum; *Jerusalem/IL (liata@hadassah.org.il)*
Learning objectives:
1. To learn about the role of emergency CT/US-guided intervention.
2. To learn about the optimal utilisation of materials, equipment, and imaging including low-dose CT.
3. To learn the management of patients after failed interventional treatments.
Author Disclosures:
L. Appelbaum: nothing to disclose

16:00 - 17:30 **Room M 3**

Head and Neck

RC 408

Imaging of eye and orbital pathologies

Moderator:
M. Lemmerling; Beervelde/BE

RC 408-1 16:00
A. Traumatic lesions of the eye and orbit
A. Ailianou; *Neuchâtel/CH (a_ailianou@yahoo.com)*
Learning objectives:
1. To become familiar with imaging features of orbital fractures.
2. To learn about traumatic lesions of the eye and orbital soft tissues.
3. To review acute and chronic complications after orbital trauma.
Author Disclosures:
A. Ailianou: nothing to disclose

RC 408-2 16:30
B. Infection and inflammation in the eye and orbit
K. Erb-Eigner; *Berlin/DE (Katharina.Erb@charite.de)*
Learning objectives:
1. To become familiar with infections and inflammation in different orbital structures.
2. To discuss imaging features of infection and inflammation in the eye and orbit.
3. To learn how to reach the final diagnosis.
Author Disclosures:
K. Erb-Eigner: nothing to disclose

RC 408-3 17:00
C. Benign and malignant masses of the eye and orbit
P. de Graaf; *Amsterdam/NL (p.degraaf@amsterdamumc.nl)*
Learning objectives:
1. To discuss advanced imaging techniques in tumoural orbit lesions.
2. To review intraocular tumours.
3. To become familiar with intraorbital masses.
Author Disclosures:
P. de Graaf: nothing to disclose

16:00 - 17:30 **Room M 5**

E³ - Advanced Course: Artificial Intelligence

E³ 420

Radiomics: principles and applications

E³ 420-1 16:00
Chairperson's introduction
S. Klein*; Rotterdam/NL (s.klein@erasmusmc.nl)*
Session objectives:
1. To become familiar with the basic principles of radiomics.
2. To understand that radiomics is a specific branch of machine learning.
3. To learn about the difference between radiomics and deep learning.
Author Disclosures:
S. Klein: nothing to disclose

E³ 420-2 16:06
A. Radiomics: images are data!
G. Cicchetti*; Rome/IT (cicchetti.giuseppe88@gmail.com)*
Learning objectives:
1. To understand the design of a pipeline to develop a radiomics signature.
2. To learn about the current state of the art in radiomics.
3. To learn about the impact of radiomics for precision medicine.
Author Disclosures:
G. Cicchetti: nothing to disclose

E³ 420-3 16:34
B. Radiomics applications
T. Penzkofer*; Berlin/DE*
Learning objectives:
1. To learn about the state of the art of radiomics in prostate cancer.
2. To learn about the state of the art of radiomics in gliomas.
3. To learn about other promising application areas of radiomics.
Author Disclosures:
T. Penzkofer: Research/Grant Support at research agreements (no personal payments, outside of submitted work) with AGO, Aprea AB, ARCAGY-GINECO, Astellas Pharma Global Inc (APGD), Astra Zeneca, Clovis Oncology, Inc., Dohme Corp, Holaira, Incyte Corporation, Karyopharm, Lion Biotechnologies, In

E³ 420-4 17:02
C. Multicentre studies for more robust radiomics signatures
M. P. A. Starmans*; Rotterdam/NL (m.starmans@erasmusmc.nl)*
Learning objectives:
1. To introduce a framework for rapid development of radiomics signatures.
2. To explain how the parameters of a radiomics pipeline can be automatically optimised.
3. To show the performance of the framework for a number of applications.
Author Disclosures:
M. P. A. Starmans: nothing to disclose

16:00 - 17:30 **Tech Gate Auditorium**

Special Focus Session

SF 4

Interventional radiology in oncology

SF 4-1 16:00
Chairperson's introduction
N.N.
Session objectives:
1. To become familiar with current percutaneous ablation and embolisation techniques.
2. To learn about the clinical indications of percutaneous ablation and embolisation.
3. To understand the advantages and limitations of each ablation and embolisation technique.
Author Disclosures: -

SF 4-2 16:05
Ablation techniques in the lung
C. A. Ridge*; Dublin/IE (caroleridge@hotmail.com)*
Learning objectives:
1. To become familiar with current percutaneous ablation techniques in the lung.
2. To learn about the clinical indications of percutaneous ablation in lung lesions.
3. To understand the advantages and limitations of each ablation technique.
Author Disclosures:
C. A. Ridge: Research/Grant Support at Siemens

SF 4-3 16:30
Ablation and embolisation techniques in the liver
P. L. L. Pereira*; Heilbronn/DE (philippe.pereira@slk-kliniken.de)*
Learning objectives:
1. To become familiar with current percutaneous ablation and embolisation techniques in the liver.
2. To learn about the clinical indications of percutaneous ablation and embolisation in liver tumours.
3. To understand the advantages and limitations of each ablation and embolisation technique.
Author Disclosures:
P. L. L. Pereira: Advisory Board at Bayer, Roche, BMS, Terumo, Siemens, Medtronic, Consultant at Medtronic, Terumo, Grant Recipient at Siemens Healthineers, BTG, Terumo, Research/Grant Support at Siemens Healthineers, BTG, Terumo, Speaker at Sirtex, Guerbet, Terumo, Angiodynamics, Pharmacept, Medtronic

SF 4-4 16:55
Ablation techniques in the bone
A. Gangi*; Strasbourg/FR (Afshin.Gangi@chru-strasbourg.fr)*
Learning objectives:
1. To become familiar with current percutaneous ablation techniques in the bone.
2. To learn about the clinical indications of percutaneous ablation in bone lesions.
3. To understand the advantages and limitations of each ablation technique.
Author Disclosures:
A. Gangi: Other at Proctoring BTG

17:20
Panel discussion: The role of interventional radiologist in the treatment of lung, liver and bone lesions

Thursday, March 12

08:30 - 10:00 **Room B**

E³ - Rising Stars Programme: Basic Session

BS 5a

Abdominal viscera: abdominal emergencies

Moderator:
A. Palkó; Szeged/HU

BS 5a-1 08:30
Perforation of the GI tract
V. Maniatis; *Aabenraa/DK (vmaniatis67@gmail.com)*
Learning objectives:
1. To review the aetiologies of perforation.
2. To present current imaging techniques for evaluation of perforation.
3. To describe the typical features of perforation.
Author Disclosures:
V. Maniatis: nothing to disclose

BS 5a-2 09:00
Bowel obstruction
A. Filippone; *Pescara/IT (filipponea378@gmail.com)*
Learning objectives:
1. To review the most common causes of bowel obstruction.
2. To present current imaging techniques for evaluation of bowel obstruction.
3. To become familiar with the typical findings of bowel obstruction.
Author Disclosures:
A. Filippone: Employee at Bracco Imaging S.p.A.

BS 5a-3 09:30
Vascular emergencies
V. E. Sinitsyn; *Moscow/RU (vsini@mail.ru)*
Learning objectives:
1. To review the most common causes.
2. To present current imaging techniques.
3. To be familiar with the role of interventional radiology.
Author Disclosures:
V. E. Sinitsyn: nothing to disclose

08:30 - 10:00 **Room C**

Chest

RC 504

Lung nodule management in 2020

RC 504-1 08:30
Chairperson's introduction
R.-I. Milos; *Vienna/AT (ruxandra-iulia.milos@meduniwien.ac.at)*
Session objectives:
1. To avoid common errors in nodule categorisation or measurement.
2. To summarise the recent knowledge about nodule management.
3. To understand the place of risk prediction models.
Author Disclosures:
R.-I. Milos: nothing to disclose

RC 504-2 08:35
A. Radiological assessment
T. Frauenfelder; *Zurich/CH (thomas.frauenfelder@usz.ch)*
Learning objectives:
1. To learn how to recognise false nodules.
2. To learn how to classify lung nodules as solid, part solid, or non-solid.
3. To be aware of the typical and atypical characteristics of perifissural opacities.
Author Disclosures:
T. Frauenfelder: nothing to disclose

RC 504-3 08:58
B. Computer-aided diagnosis (CAD) and artificial intelligence (AI) perspective
A. R. Larici; *Rome/IT (annarita.larici@unicatt.it)*
Learning objectives:
1. To review the capabilities and limitations of CAD for the detection of lung nodules.
2. To learn about the performance of AI in the detection and characterisation of lung nodules.
3. To understand the basic concepts of machine learning as applied to imaging.
4. To summarise currently available machine learning techniques in radiology.
Author Disclosures:
A. R. Larici: Advisory Board at Boehringer-Ingelheim, Speaker at Boehringer-Ingelheim, MSD, Roche, GE, Astra Zeneca

RC 504-4 09:21
C. Management guidelines
A. Bankier; *Boston, MA/US (alexander.bankier@umassmemorial.org)*
Learning objectives:
1. To review the incidentally-found nodule management guidelines.
2. To become familiar with the LungRADS classification of screen-detected nodules.
3. To learn about Brock and Herder and other prediction models for evaluating the malignancy risk.
Author Disclosures:
A. Bankier: Consultant at Daiichi Pharmaceutical, Consultant at Spiration (Olympus)

09:44
Panel discussion: What do radiologists need to better manage pulmonary nodules?

08:30 - 10:00 **Room X**

Professional Challenges Session

PC 5

Audit and value in clinical radiology: enhancing quality

PC 5-1 08:30
Chairperson's introduction
A. Brady; *Cork/IE (adrianbrady@me.com)*
Session objectives:
1. To provide an ESR perspective on clinical audit.
2. To discuss the benefits of multidisciplinary working.
3. To consider existing programmes for national audit.
Author Disclosures:
A. Brady: nothing to disclose

PC 5-2 08:35
Developing and implementing a national audit programme
J. Suutari; *Helsinki/FI*
Learning objectives:
1. To consider potential obstacles to national audit programme development.
2. To discuss the establishment of a national audit model.
3. To emphasise the benefits associated with a large scale, national audit.
Author Disclosures:
J. Suutari: nothing to disclose

PC 5-3 08:55
Audit and quality improvement: the UK perspective
D. Howlett; *Eastbourne/UK (david.howlett@nhs.net)*
Learning objectives:
1. To review the existing UK radiology audit/quality improvement (QI) programme.
2. To demonstrate the UK experience in clinical audit.
3. To consider the challenges and benefits of multiagency collaboration in radiology audit.
Author Disclosures:
D. Howlett: nothing to disclose

PC 5-4 09:15
Clinical audit: the radiographer's perspective
G. N. Paulo; *Coimbra/PT (graciano@estescoimbra.pt)*
Learning objectives:
1. To discuss multidisciplinary working in the context of clinical audit.
2. To consider mechanisms of facilitating multidisciplinary involvement.
3. To evaluate multidisciplinary audit in practice.
Author Disclosures:
G. N. Paulo: nothing to disclose

PC 5-5 09:35
Adding value in radiology
J. P. Borgstede; *Colorado Springs, CO/US (borgrad@msn.com)*
Learning objectives:
1. To discuss "value" in radiology.
2. To consider the importance of adding value in radiological practice.
3. To evaluate wider concepts of value and their relationship to QI.
Author Disclosures:
J. P. Borgstede: nothing to disclose

09:55
Panel discussion: Auditing: cumbersome formality or beneficial value-adding activity?

09:00 - 10:00 **Coffee & Talk 1**

Coffee & Talk (open forum) Session
Organised by ESOR

C 3
Imaging research: making the most of our opportunities

C 3-1 09:00
Chairperson's introduction
V. Goh; *London/UK (vicky.goh@kcl.ac.uk)*
Session objectives:
1. To understand that research is central to evidence-based medicine.
2. To appreciate the different types of research in radiology and how radiologists have approached this in their practice.
3. To learn how to maximise opportunities and understand how artificial intelligence is shaping future research.
Author Disclosures:
V. Goh: Research/Grant Support at Siemens, Speaker at Siemens

C 3-2 09:05
Why is imaging research important?
G. Cook; *London/UK (gary.cook@kcl.ac.uk)*
Learning objectives:
1. To understand that research is central to evidence-based medicine.
2. To appreciate the basic principles of imaging research.
3. To learn the different types of research in radiology.
Author Disclosures:
G. Cook: Consultant at NanoMab Technology, Research/Grant Support at NanoMab Technology, Research/Grant Support at Theragnostics Ltd, Research/Grant Support at Serac Healthcare Ltd

C 3-3 09:15
Why should you undertake a PhD?
D. Caruso; *Rome, LT/IT (dcaruso85@gmail.com)*
Learning objectives:
1. To understand the reason behind the decline of interest in an academic career.
2. To learn about the qualities of a successful PhD.
3. To appreciate the skills that a PhD program will provide you.
Author Disclosures:
D. Caruso: nothing to disclose

C 3-4 09:25
Being an academic radiologist: what does this really mean in practice?
S. Gourtsoyianni; *Athens/GR (sgty76@gmail.com)*
Author Disclosures:
S. Gourtsoyianni: nothing to disclose

C 3-5 09:35
Research in the artificial intelligence era: how can we compete?
K. G. Foley; *Llantrisant/UK*
Learning objectives:
1. To learn about the central role that radiologists have in artificial intelligence research.
2. To understand the importance of collaboration in imaging research.
Author Disclosures:
K. G. Foley: Grant Recipient at Welsh Government & Intel

C 3-6 09:45
Making the most of interdisciplinary research: artificial intelligence and beyond
V. Goh; *London/UK (vicky.goh@kcl.ac.uk)*
Learning objectives:
1. To appreciate how interdisciplinary research is important to advancing knowledge.
2. To be aware of the opportunities available to radiologists.
3. To understand how this could work in the artificial intelligence era and beyond.
Author Disclosures:
V. Goh: Research/Grant Support at Siemens, Speaker at Siemens

09:55
Open forum discussion

08:30 - 10:00 **Room N**

E³ - ECR Master Class (Paediatric)

E³ 526a
Whole-body MRI in children

E³ 526a-1 08:30
Chairperson's introduction
G. Roic; *Zagreb/HR (goran.roic@kdb.hr)*
Session objectives:
1. To discuss the technical challenges in whole-body MRI (WBMRI) in children.
2. To get an overview of the applications of WBMRI in children in oncological and inflammatory conditions.
3. To discuss the future of WBMRI and whole-body hybrid imaging in children.
Author Disclosures:
G. Roic: nothing to disclose

E³ 526a-2 08:35
A. Technical considerations: the basics
L. Tanturri de Horatio; *Rome/IT (laura.tanturri@opbg.net)*
Learning objectives:
1. To learn about the software and hardware for WBMRI.
2. To understand the choice of protocol in WBMRI in children.
3. To discuss technical challenges in paediatric WBMRI.
Author Disclosures:
L. Tanturri de Horatio: nothing to disclose

E³ 526a-3 08:53
B. Whole-body MRI in oncological conditions
A. S. Littooij; *Utrecht/NL (alittooij@hotmail.com)*
Learning objectives:
1. To learn about WBMRI in staging and response evaluation in children with cancer.
2. To understand typical findings.
3. To discuss how WBMRI may replace other imaging modalities.
Author Disclosures:
A. S. Littooij: nothing to disclose

E³ 526a-4 09:11
C. Whole-body MRI in musculoskeletal inflammation
E. V. Brandis; *Oslo/NO (elisabeth@vonbrandis.net)*
Learning objectives:
1. To learn about the indications for WBMRI in children with musculoskeletal inflammation.
2. To understand typical findings and differential diagnosis including normal variants that may mimic disease.
3. To discuss current clinical practice for WBMRI in non-bacterial osteomyelitis.

Author Disclosures:
E. V. Brandis: nothing to disclose

E³ 526a-5 09:29
D. The future role of MR-PET
S. Gatidis*; Tübingen/DE (sergios.gatidis@med.uni-tuebingen.de)*
Learning objectives:
1. To learn about the current clinical and scientific state of the art.
2. To learn about the limitations and pitfalls of MR-PET.
3. To discuss future developments.
Author Disclosures:
S. Gatidis: nothing to disclose

09:47
Panel discussion: Whole-body MRI in children: what to expect in the future?

08:30 - 10:00 **Room O**

Joint Session of the ESR and EFLM

ESR/EFLM
Integrated diagnostics: are we ready for it?

ESR/EFLM-1 08:30
Chairpersons' introduction (part 1)
A.-M. Simundic*; Zagreb/HR (am.simundic@gmail.com)*
Session objectives:
1. To present EFLM and its aims.
2. To appreciate the major challenges in laboratory medicine.
3. To explain the rationale behind featured topics.
Author Disclosures:
A.-M. Simundic: nothing to disclose

ESR/EFLM-2 08:35
Chairpersons' introduction (part 2)
B. Brkljačić*; Zagreb/HR (boris@brkljacic.com)*
Session objectives:
1. To identify the potential benefits of a partnership between EFLM and ESR.
2. To understand the major overlaps of laboratory medicine and radiology where integrated diagnostics could aid in patient management.
3. To identify major challenges in radiology as a diagnostic discipline.
Author Disclosures:
B. Brkljačić: nothing to disclose

ESR/EFLM-3/ESR/EFLM-4 08:40
Can we improve patient outcome by integrating radiology and laboratory medicine?
M. Neumaier*; Mannheim/DE (michael.neumaier@medma.uni-heidelberg.de)*
S. O. Schönberg*; Mannheim/DE*
Learning objectives:
1. To become familiar with the term "integrated diagnostics".
2. To learn why the current diagnostic approach needs improvement.
3. To understand how integrated diagnostics can improve patient outcome.
Author Disclosures:
M. Neumaier: nothing to disclose, S. O. Schönberg: nothing to disclose

ESR/EFLM-5 09:00
How to improve cancer detection through integrated diagnostics?
V. Haselmann*; Mannheim/DE*
Learning objectives:
1. To learn the biomarkers available for improved cancer diagnostics in the medical laboratory.
2. To appreciate the impact of detection of nucleic acids in body fluids for clinical decision-making and therapy stratification.
3. To understand the synergistic effects of integrated diagnostics for improved follow-up of systemic disease and the potentials for early detection of cancer in primary diagnosis.
Author Disclosures:
V. Haselmann: nothing to disclose

ESR/EFLM-6 09:15
Diagnosing heart failure: is there a better way?
P. Collinson*; London/UK (paul.collinson@stgeorges.nhs.uk)*
Learning objectives:
1. To understand the current limitations of biomarkers used to diagnose heart failure.
2. To appreciate the impact of heart failure biomarker measurement for clinical decision-making and therapy stratification.
3. To identify opportunities for combining radiological and laboratory investigations for more efficient management of patients with heart failure.
Author Disclosures:
P. Collinson: nothing to disclose

ESR/EFLM-7 09:30
Integrating blood biomarkers and radiology to achieve optimal detection and management of pulmonary embolism
G. Lippi*; Verona/IT (giuseppe.lippi@univr.it)*
Learning objectives:
1. To learn the diagnostic performance, clinical significance, and biological and analytical drawbacks of laboratory tests currently used for diagnosing and managing pulmonary embolism.
2. To appreciate the role of thrombus-targeted fibrinolysis as a promising theranostic approach in diagnosing and managing pulmonary embolism.
3. To understand the potentialities of combining radiological and laboratory investigations for more efficient management of patients with pulmonary embolism.
Author Disclosures:
G. Lippi: nothing to disclose

09:45
Panel discussion: Integrating the diagnostic strategies in radiology and laboratory medicine: a "nice to have" or a necessity?

08:30 - 10:00 **Studio 2020**

Genitourinary

RC 507
Imaging in pregnancy

RC 507-1 08:30
Chairperson's introduction
G. Masselli*; Rome/IT (gabriele.masselli@uniroma1.it)*
Session objectives:
1. To understand how to safely perform imaging procedures in pregnant women.
2. To become familiar with the most relevant pathological conditions in pregnancy.
3. To learn about the indications of imaging procedures in pregnancy.
Author Disclosures:
G. Masselli: nothing to disclose

RC 507-2 08:35
A. Safety issues in pregnancy: what radiologists need to know
C. Bourgioti*; Athens/GR (charisbourgioti@yahoo.com)*
Learning objectives:
1. To learn about safe radiology practices and procedures in pregnant women.
2. To understand how to minimise the radiation burden in pregnant women.
3. To learn how and when to use contrast media in pregnancy.
Author Disclosures:
C. Bourgioti: nothing to disclose

RC 507-3 08:58
B. Imaging acute abdomen in pregnancy
M. Weston*; Leeds/UK (michael.weston2@nhs.net)*
Learning objectives:
1. To become familiar with the different causes of acute abdominal pain in pregnancy.
2. To learn about the imaging features of the different causes of acute abdominal pain in pregnancy.
3. To learn how to use different imaging modalities in the setting of acute abdominal pain in pregnancy.
Author Disclosures:
M. Weston: nothing to disclose

RC 507-4 09:21
C. Imaging the placenta
H. C. Addley; *Cambridge/UK (helenclareaddley@hotmail.co.uk)*
Learning objectives:
1. To understand the appearance of the placenta with different imaging modalities.
2. To become familiar with the imaging appearance of the most common pathological conditions of the placenta.
3. To discuss the added value of cross-sectional imaging in the evaluation of placental abnormalities.
Author Disclosures:
H. C. Addley: nothing to disclose

09:44
Panel discussion: How should we image the pregnant woman, and when?

08:30 - 09:30 **Coffee & Talk 2**

Coffee & Talk (open forum) Session

Jointly organised by WHO and EuroSafe Imaging

C 12

Using CT in asymptomatic people: are we doing more harm than good?

C 12-1 08:30
Chairperson's introduction
M. D. R. D. R. Perez; *Geneva/CH (perezm@who.int)*
Session objectives:
1. To review the status and trends in the use of CT in asymptomatic people for individual health assessment (IHA).
2. To discuss the potential benefits and harms of CT-IHA practice in different scenarios, and the associated challenges in terms of quality and safety of health care.
3. To propose a framework for enhancing justification, regulatory compliance, and clinical governance of CT-IHA practices.
Author Disclosures:
M. D. R. D. R. Perez: nothing to disclose

C 12-2 08:40
Setting the scene
G. Frija; *Paris/FR (guy.frija@aphp.fr)*
Learning objectives:
1. To define individual health assessment.
2. To see where imaging and, especially, CT are implied.
3. To see how to improve current existing guidelines.
Author Disclosures:
G. Frija: nothing to disclose

C 12-3 08:50
Individual health assessment (IHA) in the regulations
N.N.
Learning objectives:
1. To describe the specific requirements for exposure of asymptomatic individuals in the Euratom Basic Safety Standards Directive.
2. To describe the specific requirements for exposure of asymptomatic individuals in the International Basic Safety Standards.
3. To discuss the implications and challenges of these standards regarding justification, optimisation, and referral guidelines.
Author Disclosures: -

C 12-4 09:00
Korean experience
M.-J. Kim; *Anyang-si/KR*
Learning objectives:
1. To outline cultural and societal approaches in Korea to IHA as part of health care provision.
2. To describe briefly the findings relating to thyroid screening conducted outside a national screening programme.
3. To discuss the potential evaluation of IHA provided by NECA or similar organisations, including the value added and the challenges faced.
Author Disclosures:
M.-J. Kim: disclosure/affirmation information not submitted

C 12-5 09:10
Open forum discussion
J. Griebel; *Neuherberg/DE (jgriebel@bfs.de)*
Author Disclosures:
J. Griebel: nothing to disclose

08:30 - 10:00 **Room E**

Musculoskeletal

RC 510

MRI of the knee

Moderator:
E. Oei; Rotterdam/NL

RC 510-1 08:30
A. Anterior knee pain
M. Tzalonikou; *Athens/GR*
Learning objectives:
1. To describe the normal anatomy and MRI appearances of the anterior knee structures (including the extensor mechanism, fat pads and synovial plicae).
2. To explain the imaging appearances of pathological conditions that present with anterior knee pain.
Author Disclosures:
M. Tzalonikou: nothing to disclose

RC 510-2 09:00
B. Meniscal abnormalities: obvious and subtle
P. Omoumi; *Lausanne/CH (Patrick.Omoumi@chuv.ch)*
Learning objectives:
1. To describe the anatomy of the menisci and the classification of meniscal tears.
2. To explain unusual imaging appearances of meniscal tears and potential pitfalls.
Author Disclosures:
P. Omoumi: nothing to disclose

RC 510-3 09:30
C. Cruciate and collateral ligaments
A. P. Parkar; *Bergen/NO (apparkar@gmail.com)*
Learning objectives:
1. To describe the normal anatomy and MRI appearances of the cruciate and collateral ligaments.
2. To explain the imaging appearances of pathological conditions involving the cruciate and collateral ligaments.
3. To specify the indirect signs that occur with ligament injury.
Author Disclosures:
A. P. Parkar: nothing to disclose

08:30 - 10:00 **Room F1**

E³ - Advanced Course: Interactive Teaching Session for Young (and not so Young) Radiologists

E³ 521

Small bowel imaging

E³ 521-1 08:30
A. CT and MR enterography: my technical tips for preparation and scanning
A. J. J. Madureira; *Porto/PT*
Learning objectives:
1. To understand the importance of proper preparation for enterography.
2. To be familiar with technical details that ensures high imaging quality.
Author Disclosures:
A. J. J. Madureira: nothing to disclose

E³ 521-2 09:15
B. Detection of small bowel involvement in patients with peritoneal carcinomatosis before hyperthermic intraperitoneal chemotherapy (HIPEC)?
M. R. Torkzad; *Stockholm/SE (michael.torkzad@gmail.com)*
Learning objectives:
1. To understand how to optimise imaging techniques to detect peritoneal involvement of the small bowel.
2. To be familiar the various imaging characteristics of peritoneal involvement of the small bowel.
Author Disclosures:
M. R. Torkzad: nothing to disclose

08:30 - 10:00 **Room F2**

Special Focus Session

SF 5
MRI of rectal carcinoma

SF 5-1 08:30
Chairperson's introduction
I. Blazic; *Belgrade/RS (ivanablazic@yahoo.com)*
Session objectives:
1. To understand the role of magnetic resonance imaging in rectal cancer patient management.
2. To learn how MRI findings influence the initial therapeutic approach in rectal cancer patients.
3. To discuss the report on post neoadjuvant treatment MRI findings and its impact on further therapeutic approach in patients with rectal cancer.
Author Disclosures:
I. Blazic: nothing to disclose

SF 5-2 08:36
Keynote lecture: The disappearing rectal cancer: the radio-surgical challenge of our time
R. J. Heald; *Southampton/UK (bill.heald@me.com)*
Learning objectives:
1. Up to a third of rectal cancers undergoing chemoradiotherapy may achieve complete regression so that post-treatment MRI may save them from surgery.
2. The radiologist must increasingly understand the regression process and timing of the replacement of cancer by scar tissue.
3. Tumour regression grading (TRG) and its relationship to endoscopic and histological criteria must be understood. A new sign, the split scar (SSS), may be a predictor of the permanence of the regression.
Author Disclosures:
R. J. Heald: nothing to disclose

SF 5-3 08:56
Rectal cancer revisited: Dutch perspective
R. G. H. Beets-Tan; *Amsterdam/NL (r.beetstan@nki.nl)*
Learning objectives:
1. To explain rectal cancer patient management in the Netherlands and the role of the radiologist in the multidisciplinary team.
2. To understand the importance of rectal cancer MRI and how MRI findings influence clinical decisions.
3. To discuss current pitfalls and challenges in rectal cancer imaging and ways to overcome them.
Author Disclosures:
R. G. H. Beets-Tan: nothing to disclose

SF 5-4 09:14
Rectal cancer revisited: UK perspective
G. Brown; *London/UK (gina.brown@rmh.nhs.uk)*
Learning objectives:
1. To explain rectal cancer patient management in the UK and the role of the radiologist in the multidisciplinary team.
2. To understand the importance of rectal cancer MRI and how MRI findings influence clinical decisions.
3. To discuss current pitfalls and challenges in rectal cancer imaging and ways to overcome them.
Author Disclosures:
G. Brown: nothing to disclose

SF 5-5 09:32
Rectal cancer: old challenges, new tools
L. C. O. K. Blomqvist; *Stockholm/SE (lennart.k.blomqvist@gmail.com)*
Learning objectives:
1. To offer an overview of advanced imaging techniques and new modalities applied in rectal cancer imaging.
2. To explain the advantages and drawbacks of different modalities.
3. To discuss future perspectives in imaging of rectal cancer.
Author Disclosures:
L. C. O. K. Blomqvist: Founder at Collective Minds Radiology

09:50
Panel discussion: Role of the radiologist in diagnosis and management of rectal cancer

08:30 - 09:15 **Coffee & Talk 3**

Coffee & Talk (open forum) Session

C 21
Statistics resources for radiology research

C 21-1 08:30
Chairperson's introduction
Ü. Aydingöz; *Ankara/TR (ustunaydingoz@yahoo.com)*
Session objectives:
1. To list books, journal articles, and internet sources for learning and applying statistics.
2. To describe how books, journal articles, and online sources can be used for statistical analysis in radiology research.
3. To explain the current controversy regarding the use of the p-value in statistics.
Author Disclosures:
Ü. Aydingöz: nothing to disclose

C 21-2 08:35
Books and journal articles for learning and applying statistics in radiology research
G. Di Leo; *San Donato Milanese/IT (gianni.dileo77@gmail.com)*
Learning objectives:
1. To list books and journal articles for learning and applying statistics.
2. To describe how books and online articles can be used for statistical analysis in radiology research.
Author Disclosures:
G. Di Leo: Author at Springer Verlag

C 21-3 08:45
Internet sources for learning and applying statistics in radiology research
V. Wieske; *Berlin/DE*
Learning objectives:
1. To list internet sources for learning and applying statistics.
2. To describe how internet sources can be used for statistical analysis in radiology research.
Author Disclosures:
V. Wieske: Research/Grant Support at Grant support from the FP7 Program of the European Commission for the randomized multicenter DISCHARGE trial (603266-2, HEALTH-2012.2.4.-2)

C 21-4 08:55
The p-value controversy in statistics: what the radiologist needs to know
T. Akıncı D'Antonoli; *Basel/CH (drtugba@hotmail.com)*
Learning objectives:
1. To explain the uses and misuses of the p-value in statistical analyses.
2. To describe the ways to overcome the misuse of the p-value in statistical analyses.
Author Disclosures:
T. Akıncı D'Antonoli: nothing to disclose

09:05
Open forum discussion

08:30 - 10:00 **da Vinci (Room D1)**

E³ - ECR Master Class (Cardiac)

E³ 526b

Cardiac imaging in arrhythmia and sudden cardiac death

E³ 526b-1 08:30
Chairperson's introduction
P. Donato*; Coimbra/PT (donato.pj@gmail.com)*
Session objectives:
1. To learn about existing imaging biomarkers to prevent sudden cardiac death.
2. To understand how to face the challenge of arrhythmia in cardiac imaging.
3. To become familiar with the prerequisites for MRI in patients with active implants.
Author Disclosures:
P. Donato: nothing to disclose

E³ 526b-2 08:35
A. The role of cardiovascular magnetic resonance (CMR) in sudden cardiac death
D. Piotrowska-Kownacka*; Warsaw/PL*
Learning objectives:
1. To become familiar with the pathophysiology of sudden cardiac death.
2. To introduce CMR biomarkers to prevent sudden cardiac death.
3. To learn how to perform and how to interpret CMR to prevent sudden cardiac death.
Author Disclosures:
D. Piotrowska-Kownacka: nothing to disclose

E³ 526b-3 09:00
B. Preventing sudden cardiac death with CT: pure theory or new diagnostic paradigm?
K. Gruszczyńska*; Katowice/PL (kgruszczynska@poczta.onet.pl)*
Learning objectives:
1. To learn what to look for in CT to prevent sudden cardiac death.
2. To get an overview about existing evidence of cardiac CT in this indication.
3. To discuss the possible future role of cardiac CT in preventing sudden cardiac death.
Author Disclosures:
K. Gruszczyńska: nothing to disclose

E³ 526b-4 09:25
C. Imaging to drive electrophysiology procedures
G. Pontone*; Milan/IT (gianluca.pontone@ccfm.it)*
Learning objectives:
1. To learn about the importance of early identification of potentially lethal arrhythmias.
2. To become familiar with tips and tricks for successful CMR in patients with arrhythmia.
3. To understand the role of imaging for planning of electrophysiological procedures.
Author Disclosures:
G. Pontone: nothing to disclose

09:50
Panel discussion: Should we screen, who should we screen and how should we screen in order to prevent sudden cardiac death?

08:30 - 10:00 **Darwin (Room D2)**

ISRRT meets Japan

Meets 5

Radiography profession performance and future challenges in Japan

Presiding:
H. H. Hjemly; Sorumsand/NO
D. E. Newman; Fargo, ND/US

Meets 5-1/Meets 5-2 08:30
Chairpersons' introduction
H. H. Hjemly*; Sorumsand/NO (hakon@radiograf.no)*
D. E. Newman*; Fargo, ND/US (donnaenewman@gmail.com)*
Session objectives:
1. To recognise the demographics and patient accessibility to health care services in the country.
2. To understand the infrastructure of imaging health services and their contribution to the primary and hospital health services to sustain the population and individual health.
3. To inform on the role of the professional society in influencing the future educational programme of radiographers in the country.
4. To inform on how the professional society supports and promotes the radiographers' role in the community and the health care system.
5. To receive information on radiography career structure and opportunities for professional development of radiographers in Japan.
6. To appreciate the radiographers' post-graduation professional requirements and relevant opportunities, and to keep up to date with evidence-based practice in imaging services.
7. To inform on what society believes about artificial intelligence, and what preparatory action have been undertaken (if any) to get radiographers ready to embrace the changes.
Author Disclosures:
H. H. Hjemly: nothing to disclose, D. E. Newman: nothing to disclose

Meets 5-3 08:35
Education system and career structure of radiological technologists in Japan
N. Kodama*; Niigata/JP (n_kodama@jart.or.jp)*
Learning objectives:
1. To explain the education and license system of radiological technologists in Japan.
2. To understand current problems of radiological technologist education, especially clinical training.
3. To explain the career structure of radiological technologists in Japan.
4. To understand the expansion of the work of radiological technologist in the future.
5. To inform on task shifting (delegation of medical practice) to radiological technologist in Japan.
6. To inform on the relationship between radiological technologists and artificial intelligence (AI).
Author Disclosures:
N. Kodama: Board Member at The Japan Association of Radiological Technologists

Meets 5-4 08:53
Latest optimal CT imaging technology and radiation dose reduction
T. Masuda*; Hiroshima/JP (takanorimasuda@yahoo.co.jp)*
Learning objectives:
1. To explain the outlines of a brief history of CT equipment.
2. To understand the current problems of radiation dose in Japan compared to other countries by using diagnostic reference levels (DRLs).
3. To understand the latest CT imaging technology and radiation dose reduction methods for maintaining image quality and diagnostic accuracy.
4. To inform about artificial intelligence for machine and deep learning.
5. To learn about how to use machine and deep learning in the clinical CT examination.
Author Disclosures:
T. Masuda: nothing to disclose

Meets 5-5 09:11
The role of radiological technologists in emergency medicine: a contribution of ultrasound
A. Kasuya*; Kariya/JP (akihirokasuya1224@gmail.com)*

Learning objectives:
1. To learn about the current status of emergency imaging in Japan.
2. To appreciate the usefulness of ultrasound by radiological technologists in emergency imaging.
3. To share the ultrasound educational program by sonographers.
Author Disclosures:
A. Kasuya: nothing to disclose

Meets 5-6 09:29
Radiation therapy in Japan: current status and recent topics of radiation therapy in Japan
H. Monzen*; OsakaSayama/JP (hmon@med.kindai.ac.jp)*
Learning objectives:
1. To recognise the scale of the cancer burden in Japan, and a brief history of radiotherapy.
2. To understand current problems and recent research topics for radiological technologists.
3. To inform on accreditation guidelines for radiotherapy technologists.
4. To receive information on radiotherapy technologists' carrier structure and opportunities for professional development for radiotherapy technologists.
5. To appreciate the role of radiotherapy technologists and their professional requirements: knowledge of the special techniques and safety protocols for precision radiation therapy, including intensity-modulated radiation therapy, stereotactic radiation therapy, and image-guided radiation therapy.
6. To inform on research topics: new materials and methods for radiotherapy as part of an academic-industrial alliance.
7. To learn about how to use machine learning and knowledge-based radiation treatment plans in volumetric modulated arc therapy.
Author Disclosures:
H. Monzen: Speaker at Kindai University

09:47
Panel discussion: How will you describe the future opportunities and challenges for radiographers in Japan? Do you think the emerging technology will change the profession, and in what way?

08:30 - 10:00 **Descartes (Room D3)**

Paediatric

RC 512

Optimising the management of children with cancer: how to improve?

RC 512-1 08:30
Chairperson's introduction
K. Rosendahl*; Bergen/NO (karen.rosendahl@unn.no)*
Session objectives:
1. To discuss the role of SPECT/CT and PET/MRI in diagnosis and follow-up of children with cancer.
2. To get an overview of indications for nuclear medicine in paediatric oncology.
3. To understand the clinical significance of hybrid imaging in children.
Author Disclosures:
K. Rosendahl: nothing to disclose

RC 512-2 08:36
A. The role of SPECT and SPECT/CT
B. Johnsen*; Bergen/NO (boel.johnsen@helse-bergen.no)*
Learning objectives:
1. To learn the differences of SPECT-CT and PET-CT in paediatric oncology.
2. To understand the molecular basis of the different radiotracers available.
3. To gain insight into future directions.
Author Disclosures:
B. Johnsen: nothing to disclose

RC 512-3 08:59
B. Can PET/MRI replace PET/CT?
H. R. Nadel*; Vancouver, BC/CA (hnadel@stanford.edu)*
Learning objectives:
1. To become familiar with the differences between PET/MR and PET/CT in children.
2. To learn about optimising protocols for paediatric PET/MR.
3. To be able to identify specific indications for PET/MR in children with cancer.
Author Disclosures:
H. R. Nadel: Consultant at Beacon BIoscience, Inc D/B/A ICON Medical Imaging

RC 512-4 09:22
C. Radiation doses and patient exposure issues
H. Kertész*; Vienna/AT (hunor.kertesz@meduniwien.ac.at)*
Learning objectives:
1. To understand the source of the total effective dose for hybrid imaging techniques.
2. To appreciate recent advances of PET imaging technologies/methodologies that could lower the effective patient dose.
3. To understand the novel image reconstruction algorithms for PET image reconstruction that could lead to the same image quality with less injected activity.
4. To review clinically viable approaches to dose reduction in oncology PET/CT examinations.
Author Disclosures:
H. Kertész: nothing to disclose

09:45
Panel discussion: The future direction of nuclear medicine imaging in paediatric oncology

08:30 - 10:00 **Room G**

Physics in Medical Imaging

RC 513

Demystifying MRI: things you always wanted to know

Moderator:
P. Gilligan; Dublin/IE

RC 513-1 08:30
A. Basic MRI: the building blocks of pulse sequences
A. G. Webb*; Leiden/NL (a.webb@lumc.nl)*
Learning objectives:
1. To learn about how NMR signals are produced.
2. To understand the basic concepts of relaxation.
3. To learn about the operation of inversion recovery and spin echo pulse sequences.
Author Disclosures:
A. G. Webb: nothing to disclose

RC 513-2 09:00
B. MRI basic concepts: how to turn signals into images
D. J. Lurie*; Aberdeen/UK (d.lurie@abdn.ac.uk)*
Learning objectives:
1. To learn how magnetic field gradients encode spatial information.
2. To understand the main ways in which field gradients are used.
3. To appreciate the basic concepts of data collection and image reconstruction in MRI.
Author Disclosures:
D. J. Lurie: Research/Grant Support at GE Healthcare

RC 513-3 09:30
C. Practical MRI: a toolkit of standard MR pulse sequences
I. Seimenis*; Athens/GR (iseimen@med.uoa.gr)*
Learning objectives:
1. To learn about common types of MR pulse sequence.
2. To understand the difference between gradient echo and spin echo.
3. To appreciate the factors influencing choice of pulse sequence.
Author Disclosures:
I. Seimenis: nothing to disclose

08:30 - 10:00 **Room K**

E³ - European Diploma Prep Session

E³ 523

Head and neck

E³ 523-1 08:30
Chairperson's introduction
M. G. Mack*; Munich/DE (m.mack@radiologie-muenchen.de)*
Session objectives:
1. To become familiar with the anatomy and imaging presentation of the most common disorders of the temporal bone and skull base.
2. To understand the imaging presentation of common inflammatory and neoplastic disorders of the nose, paranasal sinuses, and nasopharynx.
3. To describe the typical imaging features of the most common neoplastic disorders of the oral cavity, oropharynx, hypopharynx, and larynx.
Author Disclosures:
M. G. Mack: nothing to disclose

E³ 523-2 08:36
A. Temporal bone and skull base
A. Trojanowska*; Lublin/PL*
Learning objectives:
1. To differentiate the anatomy, normal variants, and congenital disorders of the temporal bone.
2. To understand the causes and imaging features of hearing and vestibular disorders.
3. To describe the imaging presentation of the most common tumours of the skull base.
Author Disclosures:
A. Trojanowska: disclosure/affirmation information not submitted

E³ 523-3 09:04
B. Nose, paranasal sinuses and nasopharynx
F. A. Pameijer*; Utrecht/NL (f.a.pameijer@umcutrecht.nl)*
Learning objectives:
1. To describe the anatomy and normal variants of the nose, paranasal sinuses, and nasopharynx.
2. To differentiate the imaging features of acute and chronic inflammatory changes of the nose and paranasal sinuses.
3. To understand the imaging features of benign and malignant tumours of the nose, paranasal sinuses, and nasopharynx.
Author Disclosures:
F. A. Pameijer: nothing to disclose

E³ 523-4 09:32
C. Oral cavity, oropharynx, hypopharynx and larynx
M. Becker*; Geneva/CH*
Learning objectives:
1. To describe the normal imaging anatomy of the oral cavity, oropharynx, hypopharynx, and larynx.
2. To understand the imaging features of tumours of the oral cavity and oropharynx.
3. To understand the imaging features of tumours of the hypopharynx and larynx.
Author Disclosures:
M. Becker: nothing to disclose

08:30 - 10:00 **Room M 1**

Joint Session of the ESR and UEMS

ESR/UEMS

Visibility of imaging professionals in the EU

ESR/UEMS-1/ESR/UEMS-2 08:30
Chairpersons' introduction
M. Adriaensen*; Heerlen/NL (miraude@gmail.com)*
L. Bonomo*; Rome/IT (lorenzo.bonomo.md@gmail.com)*
Session objectives:
1. To describe the role of the UEMS and ESR within the EU.
2. To understand the differences between the ESR and the UEMS.
3. To understand the importance of cooperation between ESR and UEMS.
Author Disclosures:
M. Adriaensen: nothing to disclose, L. Bonomo: nothing to disclose

Putting your interests first: two approaches, one goal

ESR/UEMS-3 08:36
The ESR approach
L. E. Derchi*; Genoa/IT (derchi@unige.it)*
Learning objectives:
1. To understand the structure of the ESR.
2. To understand the differences between the ESR and the UEMS.
3. To understand the importance of UEMS/ESR political involvement in the EU affairs.
Author Disclosures:
L. E. Derchi: nothing to disclose

ESR/UEMS-4 08:41
The UEMS approach
B. Maillet*; Brussels/BE (bernie.mail@skynet.be)*
Learning objectives:
1. To understand the structure of the UEMS.
2. To understand the differences between the ESR and the UEMS.
3. To understand the importance of UEMS/ESR political involvement in the EU affairs.
Author Disclosures:
B. Maillet: nothing to disclose

What does the EU mean for me? A radiologist's guide

ESR/UEMS-5 08:46
To be or not to be at the table: why advocacy matters for radiologists?
K. Riklund*; Umeå/SE (katrine.riklund@umu.se)*
Learning objectives:
1. To understand the concept of advocacy.
2. To understand the importance of advocacy at the EU level.
3. To understand the influence of EU directives on national legislation and daily practice.
Author Disclosures:
K. Riklund: Board Member at CMRAD AB, Board Member at Dicom Port AB

ESR/UEMS-6/ESR/UEMS-7 08:54
Creating a European radiology workforce: the value of qualifications across borders
C. Catalano*; Rome/IT (carlo.catalano@uniroma1.it)*
V. Papalois*; London/UK*
Learning objectives:
1. To understand the value of qualifications across borders and mobility of health care workers.
2. To understand the three levels of the European Legislation process.
3. To understand the influence of EU directives on national legislation and daily practice.
Author Disclosures:
C. Catalano: nothing to disclose, V. Papalois: disclosure/affirmation information not submitted

ESR/UEMS-8 09:10
Setting European standards for radiology: making your qualifications count at home and abroad
L. Oleaga Zufiria*; Barcelona/ES (lauraoleaga@gmail.com)*
Learning objectives:
1. To get an overview of the existing European Training Curriculum in radiology.
2. To know about the value of the European Diploma in Radiology (EDiR).
3. To learn about the European Training Assessment Programme (ETAP) 2.0.
Author Disclosures:
L. Oleaga Zufiria: Consultant at TMC Academy

ESR/UEMS-9 09:18
Setting European standards for interventional neuroradiology: the UEMS ETR in INR
M. Sąsiadek*; Wroclaw/PL (marek.sasiadek@umed.wroc.pl)*

Learning objectives:
1. To learn about a harmonised, comprehensive, structured, and balanced set of standards for interventional neuroradiology.
2. To understand the importance of a European training programme in interventional neuroradiology.
3. To defend the professional interests of interventional neuroradiologists in Europe.
Author Disclosures:
M. Sąsiadek: nothing to disclose

ESR/UEMS-10 09:26
Setting European standards for ultrasound: which way to go?
P. Ricci*; Rome/IT (paolo.ricci@uniroma1.it)*
Learning objectives:
1. To understand the importance of a set of recommendations and guidelines for the training of non-radiologists in ultrasound.
2. To learn about the importance of improving the medical services of ultrasound, avoiding malpractice, and protecting patient safety.
3. To learn about the involvement of ESR and UEMS in the field of ultrasound.
Author Disclosures:
P. Ricci: Board Member at UEMS

Staying ahead of the curve with CME/CPD

ESR/UEMS-11 09:34
The importance of CME/CPD across Europe: the role of EACCME
V. Papalois*; London/UK*
Learning objectives:
1. To understand the difference between Continuing Medical Education (CME) and Continuing Professional Development (CPD).
2. To learn about the European Accreditation Council for Continuing Medical Education (EACCME).
3. To learn about the Accreditation Council in Imaging (ACI).
Author Disclosures:
V. Papalois: disclosure/affirmation information not submitted

ESR/UEMS-12 09:42
Which kind of European CME/CPD do the radiologists want to gain?
M. A. Lucic*; Sremska Kamenica/RS (milos.a.lucic@gmail.com)*
Learning objectives:
1. To know about the existence of European CME credits (ECMEC).
2. To learn about the importance of credits in different European countries.
3. To predict future trends in CME/CPD within the field of radiology.
Author Disclosures:
M. A. Lucic: Research/Grant Support at Secretariat for Science and Technology Development of the Autonomous Province of Vojvodina; Grant Nr. 142-451-2151/2019

09:50
Panel discussion: The state of radiology in the EU

08:30 - 10:00 **Room M 2**

E³ - Advanced Course: Hot Topics in Emergency Radiology

E³ 518

The role of radiology in the management of mass casualty incidents

E³ 518-1 08:30
Chairperson's introduction
A. Blanco Barrio*; Murcia/ES (anablancowhite@gmail.com)*
Session objectives:
1. To understand the mass casualty patient pathway from scene to hospital.
2. To understand how a lack of advanced planning can make radiology a roadblock to forward patient flow and can increase mortality and morbidity.
3. To learn which imaging protocols to use to make rapid, brief, accurate diagnoses in multiple casualties.
4. To learn about communication, including communication failure, during a mass casualty incident.
Author Disclosures:
A. Blanco Barrio: nothing to disclose

E³ 518-2 08:36
A. Before the disaster: preparations and standards
F. Mück*; Munich/DE (fabian.mueck@donau-isar-klinikum.de)*
Learning objectives:
1. To understand how to establish the capabilities and limitations of the emergency radiology department.
2. To learn how to decide what protocols to use in case of a mass casualty incident.
3. To learn the importance of the disaster management plan and team practice.
Author Disclosures:
F. Mück: nothing to disclose

E³ 518-3 09:04
B. CT findings of mass casualty incidents, terror attacks and assaults
E. A. Dick*; London/UK (elizabethdick2010@gmail.com)*
Learning objectives:
1. To learn about the typical injuries of knife or gunshot wounds.
2. To understand the physics of bomb blasts and the corresponding injuries.
3. To appreciate the role of radiology in disaster settings and to discuss scenarios of biological, chemical, or radiation attacks.
Author Disclosures:
E. A. Dick: Board Member at European Society of Emergency Radiology, Speaker at Guerbert

E³ 518-4 09:32
C. The role of interventional radiology in mass casualty incidents
A. Bloom*; Jerusalem/IL (allan@hadassah.org.il)*
Learning objectives:
1. To present the unique features of interventional radiology in mass casualty incident settings.
2. To provide examples of interventional radiology use in mass casualty incidents.
3. To present new tools used for the treatment of patients.
Author Disclosures:
A. Bloom: nothing to disclose

08:30 - 10:00 **Room M 3**

E³ - Rising Stars Programme: Basic Session

BS 5b

Career opportunities for radiographers

Moderator:
J. McNulty; Dublin/IE

BS 5b-1 08:30
The specialised paediatric radiographer
J. Gardling*; Lund/SE (jenny.gardling@med.lu.se)*
Learning objectives:
1. To become familiar with the key differences in paediatric patient care.
2. To appreciate the additional knowledge, skills, and attributes of a paediatric radiographer.
3. To understand the need for education, training, and continuous professional development for specialised paediatric radiographers.
Author Disclosures:
J. Gardling: nothing to disclose

BS 5b-2 08:55
Radiographers in ultrasound
G. Harrison*; London/UK (gillhaha@gmail.com)*
Learning objectives:
1. To understand the ultrasound education and training requirements.
2. To become familiar with the potential scope of practice for, and impact of, sonographers.
3. To identify the sonographers' role within medical imaging and the wider multidisciplinary team.
Author Disclosures:
G. Harrison: Employee at Society and College of Radiographers. Employee at City, University of London

BS 5b-3 09:20
The radiation protection officer
E. Gruppetta*; Msida/MT (egrupetta@yahoo.co.uk)*
Learning objectives:
1. To understand the education and training needs of the radiation protection officer (RPO).
2. To become familiar with the important roles and responsibilities of the RPO across different modalities.
3. To highlight the responsibilities of an RPO within a wider medical imaging team.
Author Disclosures:
E. Gruppetta: nothing to disclose

09:45
Panel discussion: Things to consider when starting your career

08:30 - 10:00 **Room M 4**

Neuro

RC 511

Brain tumours: new things you should know

RC 511-1 08:30
Chairperson's introduction
D. Zlatareva*; Sofia/BG (dorazlat@yahoo.com)*
Session objectives:
1. To become familiar with the new World Health Organisation (WHO) classification for brain neoplasms.
2. To appreciate the role of the radiologist in the diagnostic workup of glioma.
3. To understand perfusion imaging and its role in diagnosis and follow-up of glioma.
Author Disclosures:
D. Zlatareva: nothing to disclose

RC 511-2 08:35
A. Low grade glioma
M. Smits*; Rotterdam/NL (marion.smits@erasmusmc.nl)*
Learning objectives:
1. To become familiar with the changes in the new WHO classification for low grade glioma.
2. To understand the role of functional imaging and perfusion imaging in the diagnostic workup of low grade glioma.
3. To present the differential diagnosis and pitfalls in imaging low grade glioma.
Author Disclosures:
M. Smits: Speaker at GE Healthcare (honorarium paid to institution), Consultant at reviewer for Parexel Ltd (honorarium paid to institution)

RC 511-3 08:58
B. High grade glioma
T. A. Yousry*; London/UK (t.yousry@ucl.ac.uk)*
Learning objectives:
1. To become familiar with the changes in the new WHO classification for high grade glioma.
2. To describe the different findings in true progression and pseudoprogression.
3. To learn about the role of radiomics in imaging high grade glioma.
Author Disclosures:
T. A. Yousry: Speaker at Hikma, Research/Grant Support at Wellcome, MRC, Stroke Association, British Hear Foundation, NIHR BRC, Other at Paraxel International, Biogen, Speaker at ParadigmMS

RC 511-4 09:21
C. Posterior fossa tumours
S. L. Kumar*; Singapore/SG*
Learning objectives:
1. To become familiar with the changes in the new WHO classification for posterior fossa neoplasms.
2. To learn about the role of diffusion and perfusion imaging in posterior fossa tumours.
3. To list the various posterior fossa neoplasms in adults and children.
Author Disclosures:
S. L. Kumar: nothing to disclose

09:44
Panel discussion: Radiomics in brain tumour imaging

08:30 - 10:00 **Room M 5**

E³ - Advanced Course: Artificial Intelligence

E³ 520

Artificial intelligence and clinical decision support

E³ 520-1 08:30
Chairperson's introduction
A. Alberich-Bayarri*; Valencia/ES (angel@quibim.com)*
Session objectives:
1. To become familiar with the different parts of the workflow where artificial intelligence may play a role.
2. To understand the challenges of using artificial intelligence for decision support.
3. To learn about the process required to get artificial intelligence empowered diagnoses to the clinic.
Author Disclosures:
A. Alberich-Bayarri: CEO at QUIBIM SL, Board Member at QUIBIM SL, Founder at QUIBIM SL

E³ 520-2 08:36
A. Clinical decision support workflow improved by artificial intelligence (AI)
E. R. Ranschaert*; Turnhout/BE (erik.ranschaert@gmail.com)*
Learning objectives:
1. To learn how decision support workflow can be supported and improved by AI.
2. To understand the different workflow parts in which AI can play a role.
3. To discuss how to evaluate the clinical value of AI in decision support.
Author Disclosures:
E. R. Ranschaert: Consultant at Barco NV, Consultant at Robovision BVBA, Shareholder at Osimis SA, Shareholder at Diagnose.me BV

E³ 520-3 09:04
B. Data mining and machine learning for integrated clinical decision support
G. Boland*; Wellesley, MA/US (gboland@partners.org)*
Learning objectives:
1. To understand how data mining can help in clinical decision support.
2. To learn about the needs and limitations of standardisation for AI assisted clinical decision support.
3. To learn about the state of the art in AI assisted clinical decision support.
Author Disclosures:
G. Boland: Consultant at Siemens Healthineers

E³ 520-4 09:32
C. AI to predict treatment response
N. deSouza*; Surrey/UK*
Learning objectives:
1. To understand the role of AI in moving towards precision medicine.
2. To understand the current potential of AI for monitoring response.
3. To understand how to manage AI in a clinical workflow as a decision support tool.
Author Disclosures:
N. deSouza: nothing to disclose

09:30 - 10:15 **Coffee & Talk 3**

Coffee & Talk (open forum) Session

C 22

How to organise research in radiology

C 22-1 09:30
Chairperson's introduction
F. A. Gallagher*; Cambridge/UK (fag1000@cam.ac.uk)*
Session objectives:
1. To understand the challenges of being a successful researcher in radiology.
2. To become familiar with the skills required for imaging research.
3. To learn how to develop a research group.
Author Disclosures:
F. A. Gallagher: Grant Recipient at GSK, Research/Grant Support at GE Healthcare

C 22-2 09:35
A research group as a small business: managing and running research
G. P. Krestin*; Rotterdam/NL*
Learning objectives:
1. To understand how to manage a research group.
2. To understand how to acquire funding for research.
3. To learn how to write a successful grant.
Author Disclosures:
G. P. Krestin: Consultant at Bracco Imaging, Board Member at Quantib BV, Research/Grant Support at GEHC, Research/Grant Support at Bayer AG, Research/Grant Support at Siemens Healthineers

C 22-3 09:43
Starting an academic career: balancing clinical work and research
R. A. Woitek*; Cambridge/UK (ramona.woitek@meduniwien.ac.at)*
Learning objectives:
1. To learn the challenges of being a clinician and a researcher.
2. To become familiar with the leadership skills required to be an excellent researcher.
3. To understand how to develop a career in academic radiology.
Author Disclosures:
R. A. Woitek: nothing to disclose

09:51
Open forum discussion: the challenges of clinical research and how to succeed

10:30 - 11:00 **Forum (Room A)**

Plenary Lecture

PL 1

Imaging at a different scale: the wide lives of our cells

Presiding:
B. Brkljačić; Zagreb/HR

PL 1-1 10:30
Imaging at a different scale: the wild lives of our cells
R. Weissleder*; Boston, MA/US (rweissleder@mgh.harvard.edu)*
Author Disclosures:
R. Weissleder: Advisory Board at Accure Health, Consultant at Alivio Therapeutics, Advisory Board at Bioanalytix, Advisory Board at Elsevier Inc., Advisory Board at Lumicell, Advisory Board at Moderna Therapeutics, Consultant at Moderna Therapeutics, Advisory Board at Seer Bioscience, Advisory Board at Tarveda Therapeutics, Consultant at Tarveda Therapeutics

12:45 - 13:45 **Room B**

E^3 - The Beauty of Basic Knowledge: Breast

E^3 24B

Basis of breast ultrasound and multimodality readings

Moderators:
P. Kapetas; Vienna/AT
K. Kinkel; Chêne-Bougeries/CH

E^3 24B-1 12:45
Practical ultrasound of the breast: how I do it
A. Athanasiou*;Athens/GR (aathanasiou@mitera.gr)*
Learning objectives:
1. To learn about patient positioning and image quality control.
2. To understand the value of colour Doppler ultrasound and elastography.
3. To learn about applying ultrasound breast imaging reporting and data systems (BIRADS).
Author Disclosures:
A. Athanasiou: nothing to disclose

E^3 24B-2 13:15
Integrating ultrasound findings into the final mammography report
J. Lee*; New York, NY/US (jiyon_L@hotmail.com)*
Learning objectives:
1. To understand how to assess concordance between mammography and ultrasound results.
2. To learn to give a final recommendation (no further action required, short-term follow-up, biopsy, other imaging modality, etc.).
Author Disclosures:
J. Lee: nothing to disclose

12:45 - 13:45 **Room C**

E^3 - The Beauty of Basic Knowledge: Pancreas

E^3 25B

Chronic pancreatitis

Moderator:
C. Matos; Lisbon/PT

E^3 25B-1 12:45
How to diagnose and classify
G. Zamboni*; Verona/IT (gzamboni@hotmail.com)*
Learning objectives:
1. To learn about the diagnosis of chronic pancreatitis.
2. To understand the classification of chronic pancreatitis.
3. To appreciate the role of imaging in the follow-up of chronic pancreatitis.
Author Disclosures:
G. Zamboni: nothing to disclose

E^3 25B-2 13:15
Functional evaluation of chronic pancreatitis
M. A. Bali*; Brussels/BE (mbali@ulb.ac.be)*
Learning objectives:
1. To appreciate functional evaluation of chronic pancreatitis.
2. To learn about the role of imaging in recurrent pancreatitis.
Author Disclosures:
M. A. Bali: nothing to disclose

12:45 - 13:45 **Coffee & Talk 1**

Coffee & Talk (open forum) Session

Organised by ESOR

C 4

ESOR and its role in online education

C 4-1 12:45
Chairperson's introduction
C. Loewe*; Vienna/AT (christian.loewe@meduniwien.ac.at)*
Author Disclosures:
C. Loewe: Speaker at Siemens Healthineers, Speaker at BRACCO, Speaker at GE Healthcare

C 4-2 12:50
ESR Education on demand: how does it work, what is there for you
S. Barter*; Bedford/UK*
Learning objectives:
1. To learn about the relaunched ESR Education on Demand Platform.
2. To appreciate what's new in 2020.
3. To understand the functionality and feedback for the user.
4. To become familiar with the personalised learning progress feature.
Author Disclosures:
S. Barter: nothing to disclose

C 4-3 13:05
ESOR in ESR Connect: where is the future?
V. Vilgrain*; Clichy/FR (valerie.vilgrain@aphp.fr)*
Learning objectives:
1. To learn about ESR Connect.
2. To understand online education ESOR in ESR Connect.
3. To appreciate the future developments of online education ESOR.
Author Disclosures:
V. Vilgrain: Speaker at Hopsital Beaujon

13:20
Open forum discussion

12:45 - 13:45 **Coffee & Talk 2**

Coffee & Talk (open forum) Session

Organised by EuroSafe Imaging

C 13

ESR iGuide: more appropriate imaging through clinical decision support

C 13-1 12:45
Chairperson's introduction: Update on Croatia adoption
B. Brkljačić; *Zagreb/HR (boris@brkljacic.com)*
Session objectives:
1. To understand the impact of clinical decision support on appropriate imaging utilisation.
2. To learn about the implementation of evidence-based guidelines in clinical practice.
3. To learn from user and healthcare provider experiences in Europe and the Middle East.
Author Disclosures:
B. Brkljačić: nothing to disclose

C 13-2 12:53
Medical imaging decision and support study (MIDAS)
T. J. Kroencke*; Augsburg/DE*
Learning objectives:
1. To learn about the history of initiatives to guide tailored and appropriate imaging, and reduce waste and harm to patients.
2. To understand why radiologists need to spearhead development of clinical decision support in imaging as a component of value-based radiology.
3. To appreciate decision support as a possible method to promote the appropriate, meaningful, value-based, and personalised use of medical imaging.
4. To become familiar with the MIDAS study: a multi-centre study that evaluates the impact of iGuide on overuse and inappropriate use of imaging tests.
Author Disclosures:
T. J. Kroencke: Grant Recipient at Research Grant, Innovationsfunds Germany

C 13-3 13:01
ESR iGuide implementation in Saudi Arabia
F. Garni*; Riyadh/SA*
Learning objectives:
1. To understand the problem with ordering radiology exams in Saudi government hospitals i.e. MNG-HA.
2. To explain the operational, clinical, and technical challenges in implementing CDSS for diagnostic services such as radiology.
3. To discuss why MNG-HA did a proof of concept (PoC).
4. To detail the impact of PoC on operational and clinical factors, and costs.
5. To explain the full implantation approach and the lesson learned.
Author Disclosures:
F. Garni: disclosure/affirmation information not submitted

C 13-4 13:09
ESR guideline localisation and version upgrade experience
H. Stahlbrandt*; Eksjo/SE (henriettae@stahlbrandt.com)*
Learning objectives:
1. To learn about iGuide and its versions as a tool for more appropriate imaging and what goes on in the background.
2. To understand why and how to upgrade iGuide.
3. To appreciate the value of iGuide and its localisation tools.
4. To become familiar with the value of iGuide and its localisation tools.
Author Disclosures:
H. Stahlbrandt: nothing to disclose

13:17
Open forum discussion

12:45 - 13:45 **Coffee & Talk 3**

Coffee & Talk (open forum) Session

Organised by ESR Publications

C 23

How to get my manuscript accepted: tips and tricks from the editors

C 23-1 12:45
Chairperson's introduction
M. Smits*; Rotterdam/NL (marion.smits@erasmusmc.nl)*
Session objectives:
1. To interact with the editors-in-chief of the ESR journals.
2. To discuss all elements of scientific peer review.
3. To understand what to consider when submitting a manuscript.
4. To learn how to respond to referees' comments.
Author Disclosures:
M. Smits: Consultant at reviewer for Parexel Ltd (honorarium paid to institution), Speaker at GE Healthcare (honorarium paid to institution)

C 23-2 12:50
How to "polish" a submission
Y. Menu*; Paris/FR (yves.menu@aphp.fr)*

Learning objectives:
1. To learn the importance of the cover letter.
2. To understand how the title and key points are instrumental in drawing the reader's attention.
3. To become familiar with the optimal construction of the introduction and the discussion.
4. To be able to differentiate what should be in the "Material and Method" or in the "Results" sections.
5. To learn how a bibliography should be built and checked.
Author Disclosures:
Y. Menu: nothing to disclose

C 23-3 12:55
How to reply to reviewers' criticism
F. Sardanelli*; Milan/IT*
Learning objectives:
1. What to do when the reviewer is right.
2. What to do when the reviewer is wrong.
3. What to do when two reviewers disagree.
4. Making the revised manuscript easier to read.
Author Disclosures:
F. Sardanelli: Advisory Board at Bracco, Research/Grant Support at Bayer, Bracco, General Electric, Speaker at Bayer, Bracco, General Electric

C 23-4 13:00
How to manage critical reviews
L. Marti-Bonmati*; Valencia/ES (Luis.Marti@uv.es)*
Learning objectives:
1. To understand how critical reviews should be conducted.
2. To learn how critical reviews are reviewed.
3. To be able to manage levels of evidence and recommendations.
Author Disclosures:
L. Marti-Bonmati: nothing to disclose

13:05
Open forum discussion

12:45 - 13:15 **Room M 5**

EDiR Session

EDiR 2

An instrument to develop excellence in your career: practical session (part 2)

Moderator:
L. Oleaga Zufiria; Barcelona/ES

EDiR 2-2 12:45
EDiR teaser
L. Oleaga Zufiria*; Barcelona/ES (lauraoleaga@gmail.com)*
Learning objectives:
1. To present the EDiR examination.
2. To show the structure of the EDiR exam.
3. To review some practical cases: multiple response questions, short cases, and CORE cases.
Author Disclosures:
L. Oleaga Zufiria: Consultant at TMC Academy

EDiR 2-3 13:05
Tips from an EDiR holder
C. J. Tolman*; Rotterdam/NL (christinetolman@hotmail.nl)*
Learning objectives:
1. To review ten essential tips to succeed in the EDiR.
2. To highlight the importance of the EDiR.
3. To explain the advantages of having the EDiR.
Author Disclosures:
C. J. Tolman: nothing to disclose

14:00 - 15:30 **Room B**

Neuro

RC 711

Inflammatory and infectious central nervous system (CNS) pathology

RC 711-1 14:00
Chairperson's introduction
A. M. Koc*; Izmir/TR (alimuratkoc@gmail.com)*
Session objectives:
1. To understand the role of imaging in the diagnosis and monitoring of inflammatory and infectious diseases of the central nervous system.
2. To learn basic principles in the use of imaging in neuroinfection and neuroinflammation.
3. To appreciate the added value of imaging in addition to clinical findings and laboratory tests, including cerebrospinal fluid analysis.
Author Disclosures:
A. M. Koc: nothing to disclose

RC 711-2 14:05
A. Autoimmune encephalitis
P. Demaerel*; Leuven/BE*
Learning objectives:
1. To describe the imaging pattern of autoimmune encephalitis.
2. To learn about imaging patterns in autoimmune pathology.
3. To appreciate the role of imaging in a multidisciplinary and multimodal approach.
Author Disclosures:
P. Demaerel: nothing to disclose

RC 711-3 14:28
B. Infectious encephalitis
A. Zimny*; Wroclaw/PL (abernac@wp.pl)*
Learning objectives:
1. To learn about the correct choice of imaging modalities and image acquisition parameters for the detection and monitoring of infectious diseases of the central nervous system.
2. To understand the benefits and challenges of image pattern recognition for diagnostic purposes.
3. To appreciate the heterogeneity of the disease spectrum, and challenges to interpreting imaging findings in the context of clinical presentation and possible comorbidities.
Author Disclosures:
A. Zimny: nothing to disclose

RC 711-4 14:51
C. Inflammatory and infectious myelitis
M. M. Thurnher*; Vienna/AT (majda.thurnher@meduniwien.ac.at)*
Learning objectives:
1. To learn about the spectrum of infectious diseases of the spinal cord and their most characteristic imaging features.
2. To understand the difficulties in image acquisition and image interpretation.
3. To appreciate the clinical relevance of early diagnosis and therapeutic intervention.
Author Disclosures:
M. M. Thurnher: Speaker at Biogen, Speaker at Guerbet, Speaker at Bracco

15:14
Panel discussion: Ask the expert: is imaging the key diagnostic modality for an early and specific diagnosis of infectious diseases leading to a better functional outcome?

14:00 - 15:30 **Room C**

Special Focus Session

SF 7a

Addressing challenges in imaging of larger patients

SF 7a-1/SF 7a-2 14:00
Chairpersons' introduction
V. Løgager; *Herlev/DK (Vibeke.Loegager@regionh.dk)*
J. McNulty; *Dublin/IE (jonathan.mcnulty@ucd.ie)*
Session objectives:
1. To consider the impact of an increasingly overweight population and increased obesity on medical imaging examinations and service provision.
2. To evaluate how we can optimise imaging in this population across different modalities.
Author Disclosures:
V. Løgager: nothing to disclose, J. McNulty: nothing to disclose

SF 7a-3 14:06
Key considerations in general radiography examinations of larger patients
K. Knapp; *Exeter/UK (K.M.Knapp@exeter.ac.uk)*
Learning objectives:
1. To discuss the impact of patient size on image quality and dose.
2. To review the limitations and opportunities presented by state-of-the-art equipment.
3. To explore key optimisation steps for the examination of larger patients, children and adults, in general radiography.
Author Disclosures:
K. Knapp: Author at Carver's Medical Imaging, Grant Recipient at Wellcome, Stryker

SF 7a-4 14:24
Modification of ultrasound technique and protocols for larger patients
B. Kraus; *Vienna/AT*
Learning objectives:
1. To discuss the impact of patient size on ultrasound technique and image quality.
2. To consider current ultrasound technology, systems, and probes.
3. To explore key optimisation steps, techniques and protocols, for the examination of larger patients.
Author Disclosures:
B. Kraus: nothing to disclose

SF 7a-5 14:42
Diagnostic image quality considerations for larger patients in computed tomography
S. J. Foley; *Dublin/IE (shane.foley@ucd.ie)*
Learning objectives:
1. To discuss the impact of patient size on image quality and dose for paediatric and adult examinations.
2. To review the limitations and opportunities presented by state-of-the-art equipment.
3. To explore key optimisation steps, techniques and protocols, for the examination of larger patients.
Author Disclosures:
S. J. Foley: nothing to disclose

SF 7a-6 15:00
Optimal imaging of larger patients in magnetic resonance imaging
E. Thiry; *Strasbourg/FR (thiry_elise@outlook.fr)*
Learning objectives:
1. To discuss the impact of patient size on image quality in MRI.
2. To consider current scanner, coil, and sequence design in terms of larger patients.
3. To explore key optimisation steps, techniques and protocols, for the examination of larger patients.
Author Disclosures:
E. Thiry: nothing to disclose

15:18
Panel discussion: How such patient diversity can impact on daily practice and how we can improve our services?

14:00 - 15:30 **Room N**

Physics in Medical Imaging

RC 713

Current and future trends in personalised clinical dosimetry

RC 713-1 14:00
Chairperson's introduction
E. T. Samara; *Sion/CH (elina.samara@hopitalvs.ch)*
Session objectives:
1. To understand the needs for personalised dosimetry.
2. To learn about existing and new methodologies used for patient dosimetry.
3. To understand the challenges for the implementation of patient-specific dosimetry.
Author Disclosures:
E. T. Samara: nothing to disclose

RC 713-2 14:05
A. Breast imaging dosimetry
I. Sechopoulos; *Nijmegen/NL (ioannis.sechopoulos@radboudumc.nl)*
Learning objectives:
1. To understand the current method to estimate organ dose in mammography and its limitations.
2. To understand breast dosimetry in emerging modalities.
3. To learn about upcoming approaches in breast dosimetry.
Author Disclosures:
I. Sechopoulos: Research/Grant Support at Siemens Healthcare, Research/Grant Support at Canon Medical Systems, Speaker at Siemens Healthcare, Speaker at Hologic Inc.

RC 713-3 14:25
B. Patient dosimetry in CT
S. Edyvean; *Didcot/UK (Sue.Edyvean@phe.gov.uk)*
Learning objectives:
1. To review the basic dose quantities in CT.
2. To understand the limitation of the basic dose quantities in describing patient doses in CT.
3. To learn about potential physical, computational, and monitoring methods in personalised CT dosimetry.
Author Disclosures:
S. Edyvean: nothing to disclose

RC 713-4 14:45
C. Patient dosimetry in cone beam computed tomograph (CBCT)
R. Pauwels; *Aarhus/DK (pauwelsruben@hotmail.com)*
Learning objectives:
1. To review the basic dose quantities that has been applied in CBCT scanners.
2. To understand how the current dose quantities relate to actual patient dose in different CBCT applications.
3. To learn about the possible future methods in personalised CBCT dosimetry and dose monitoring.
Author Disclosures:
R. Pauwels: Consultant at International Atomic Energy Agency

RC 713-5 15:00
D. Patient dose in fluoroscopy and interventional radiology
A. Trianni; *Udine/IT (annalisa.trianni@asuiud.sanita.fvg.it)*
Learning objectives:
1. To review the fundamental patient dosimetry quantities.
2. To learn about calculation of patient dose for interventional procedures.
3. To learn about real-time patient dose monitoring strategies.
Author Disclosures:
A. Trianni: nothing to disclose

15:20
Panel discussion: The future of patient-specific dosimetry

14:00 - 15:30 **Room O**

Children in Focus

IF 7

The patient journey: from foetus to adulthood

IF 7-1 14:00
Chairperson's introduction
C. Owens; *London/UK (owens.catherine.5@gmail.com)*
Session objectives:
1. To set the scene for the Children in Focus sessions.
2. To emphasize the importance of investment in the future of our world.
3. To introduce the programme.
Author Disclosures:
C. Owens: nothing to disclose

IF 7-2 14:05
In memoriam Prof. Helen M.L. Carty
A. T. Carty; *Liverpool/UK*
Author Disclosures:
A. T. Carty: nothing to disclose

IF 7-3 14:07
From Women in Focus to Children in Focus
H. Hricak; *New York/US*
Author Disclosures:
H. Hricak: Speaker at Memorial Sloan Kettering Cancer Center, Board Member at IBA

IF 7-4 14:12
Inspiration behind Children in Focus
B. Brkljačić; *Zagreb/HR (boris@brkljacic.com)*
Author Disclosures:
B. Brkljačić: nothing to disclose

IF 7-5 14:17
The foetus: from imagination to imaging
L. E. Derchi; *Genoa/IT (derchi@unige.it)*
Learning objectives:
1. To learn the status of the unborn child in history.
2. To appreciate the historical understanding of life in utero.
3. To present images from carvings, paintings and illustrations along human history.
Author Disclosures:
L. E. Derchi: nothing to disclose

IF 7-6 14:35
The impact of advanced medical intervention on childhood malignancy: where we are now and why we need to be here
P. Veys; *London/UK (paul.veys@gosh.nhs.uk)*
Learning objectives:
1. To learn how we have moved on over the decades to more sophisticated, less toxic therapies for cancer treatment in childhood.
2. To appreciate the importance and human impacts of these advances.
3. To understand the vital differences we are making with more bespoke treatments and the impact on the individual.
Author Disclosures:
P. Veys: Grant Recipient at Servier, Grant Recipient at Medical Research Council, Grant Recipient at Wellcome, Advisory Board at Novartis

IF 7-7/**IF 7-8** 14:53
My personal journey through childhood cancer in pictures: a ten year marathon
O. Parry; *London/UK,*
P. Parry; *London/UK*
Learning objectives:
1. To learn how it feels to be a child with cancer.
2. To appreciate the personal journey taken over time and the consequences to the individual.
3. To understand the impact of historical therapy on future adult life.
Author Disclosures:
O. Parry: disclosure/affirmation information not submitted, P. Parry: disclosure/affirmation information not submitted

15:11
Panel discussion: Where are we now and what has really changed?

14:00 - 15:30 **Room E**

E³ - Advanced Course: Interactive Teaching Session for Young (and not so Young) Radiologists

E³ 721a

Errare humanum est

E³ 721a-1 14:00
A. Errors in chest radiograph
D. Tack; *Braine-L'Alleud/BE (denis.tack@skynet.be)*
Learning objectives:
1. To learn to recognise ambiguous signs in plain films.
2. To learn to avoid the most common pitfalls in reading plain chest films.
Author Disclosures:
D. Tack: nothing to disclose

E³ 721a-2 14:45
B. Errors in CT of the chest
J. Vilar; *Valencia/ES (vilarsamper@gmail.com)*
Learning objectives:
1. To learn to interpret ambiguous chest CT signs.
2. To learn to avoid the most common pitfalls in reading chest CT images.
Author Disclosures:
J. Vilar: nothing to disclose

14:00 - 15:30 **Room F1**

E³ - ECR Master Class (Neuro)

E³ 726

How to implement MRI neuro advanced techniques at home

Moderator:
I. Tsougos; Larissa/GR

E³ 726-1 14:00
A. Practical approach to cerebral perfusion techniques
H. R. R. Jäger; *London/UK*
Learning objectives:
1. To understand the essentials in MRI perfusion techniques.
2. To describe how to interpret the data in brain perfusion MRI.
3. To know the limitations of perfusion MRI studies.
Author Disclosures:
H. R. R. Jäger: disclosure/affirmation information not submitted

E³ 726-2 14:30
B. How to read spectroscopy
C. Hoffmann; *Tel Hashomer/IL (chen.hoffmann@sheba.health.gov.il)*
Learning objectives:
1. To describe the role of 1H spectroscopy in daily practice.
2. To become familiar with 1H spectroscopic imaging and post processing techniques.
3. To be aware of other MRI spectroscopy techniques e.g. 31P.
Author Disclosures:
C. Hoffmann: nothing to disclose

E³ 726-3 15:00
C. How to read diffusion tensor imaging (DTI)
R. Gasparotti*; Brescia/IT (roberto.gasparotti@unibs.it)*
Learning objectives:
1. To learn the principals of DTI in neuroradiology.
2. To appreciate the practical value of DTI in different neurological disorders.
3. To be familiar with pitfalls of diffusion-weighted imaging (DWI) and DTI – common language with neurosurgeons.
Author Disclosures:
R. Gasparotti: nothing to disclose

14:00 - 15:00 **Coffee & Talk 3**

Coffee & Talk (open forum) Session

Organised by ESR Publications

C 24

How to get my manuscript accepted: getting help from reporting guidelines

C 24-1 14:00
Chairperson's introduction
Y. Menu*; Paris/FR (yves.menu@aphp.fr)*
Session objectives:
1. To learn about the concept of different reporting guidelines and how they are adapted to specific types of research.
2. To understand why these guidelines are most useful when considered early in the study/manuscript preparation, avoiding major errors in the construction of the manuscript.
3. To be aware that these guidelines are useful for reviewers and editors.
Author Disclosures:
Y. Menu: nothing to disclose

C 24-2 14:03
Why are STARD and STROBE useful and how do they help authors and editors?
F. Sardanelli*; Milan/IT*
Learning objectives:
1. To learn about the definition of these guidelines.
2. To understand the major benefit of including these guidelines early in the study.
3. To be aware of other guidelines that may be useful for specific purposes, like CONSORT or ARRIVE.
Author Disclosures:
F. Sardanelli: Advisory Board at Bracco, Research/Grant Support at Bayer, Bracco, General Electric, Speaker at Bayer, Bracco, General Electric

C 24-3 14:08
What is PRISMA, and what is the recipe for a relevant meta-analysis?
M. Dewey*; Berlin/DE*
Learning objectives:
1. To understand the relationship between systematic review and meta-analysis.
2. To become familiar with the PRISMA checklist and flow diagram, and to understand how they can provide useful guidance for authors towards a successful meta-analysis.
3. To assess PRISMA as a tool for critical appraisal of published systematic reviews.
Author Disclosures:
M. Dewey: Grant Recipient at EU (603266-2) DFG (DE 1361/14-1, DE 1361/18-1, BIOQIC GRK 2260/1, Radiomics DE 1361/19-1 and 20-1 in SPP 2177/1), Berlin University Alliance (GC_SC_PC 27), Berlin Institute of Health (Digital Health Accelerator)., Patent Holder at Patent on fractal analysis of perfusion imaging (jointly with Florian Michallek, PCT/EP2016/071551), Speaker at Canon, Guerbet. , Author at Editor: Cardiac CT (Springer Nature)., Other at Organisation of Hands-on cardiac CT courses (www.ct-kurs.de) , Other at Institutional research agreements: Siemens, General Electric, Philips, Canon.

C 24-4 14:13
Can we elaborate guidelines or a checklist for radiomics studies?
D. Pinto Dos Santos*; Cologne/DE (daniel.pinto-dos-santos@uk-koeln.de)*
Learning objectives:
1. To learn about the most common weaknesses in published/submitted manuscripts dealing with artificial intelligence/radiomics.
2. To understand how reporting guidelines can help authors avoid these errors by providing a checklist.
3. To be aware of ongoing efforts in adapting reporting guidelines to the field of artificial intelligence.
Author Disclosures:
D. Pinto Dos Santos: Advisory Board at Cook Medical, Advisory Board at mediaire GmbH

14:18
Open forum discussion

14:00 - 15:30 **da Vinci (Room D1)**

Special Focus Session

SF 7b

How radiologists can help the infertile couple

SF 7b-1 14:00
Chairperson's introduction
M. Studniarek*; Gdansk/PL (mstud@gumed.edu.pl)*
Session objective:
1. To learn about infertility: definition, epidemiology, infertility types and mechanisms, patients' expectations.
Author Disclosures:
M. Studniarek: nothing to disclose

SF 7b-2 14:04
Andrology expert's view on the role of radiology in infertility
D. Jezek*; Zagreb/HR (davor.jezek@mef.hr)*
Learning objectives:
1. To learn about male infertility problems and causes.
2. To understand when infertility is reversible and the role of accurate diagnosis, adequate medication when needed, and surgical and interventional radiology procedures in solving infertility problems from a clinical point of view.
3. To become familiar with the role of the andrologist, and the information needed by clinicians in decision making.
Author Disclosures:
D. Jezek: nothing to disclose

SF 7b-3 14:19
Imaging the infertile men: when and how?
M. Bertolotto*; Trieste/IT (bertolot@units.it)*
Learning objectives:
1. To learn about the radiological evaluation of infertile men. When, why, and what should be examined.
2. To understand the clinician's expectations and when radiologists can help.
3. To become familiar with the radiological procedures helpful in the diagnosis, and differentiation of infertility causes: radiological signs of varicocele, obstructive and non-obstructive azoospermia, where and how to find cryptorchid testis.
Author Disclosures:
M. Bertolotto: nothing to disclose

SF 7b-4 14:39
Imaging the infertile women: when and how?
R. Forstner*; Salzburg/AT (r.forstner@salk.at)*
Learning objectives:
1. To learn the various causes of female infertility.
2. To understand the appropriate use of MRI in assessing infertility.
3. To illustrate uterine and extrauterine conditions impairing fertility.
Author Disclosures:
R. Forstner: nothing to disclose

SF 7b-5 14:59
Interventional radiology in male and female infertility
R. Uberoi*; Oxford/UK (raman.uberoi@ouh.nhs.uk)*

Learning objectives:
1. To learn about the contemporary methods of infertility treatment including in vitro fertilisation.
2. To understand the main differences between radiological methods and other methods applied in infertility. How interventional radiologists can help in female or male infertility.
3. To become familiar with the methodology of interventional radiology procedures applied in the diagnosing and treatment of male and female infertility.
Author Disclosures:
R. Uberoi: Grant Recipient at Gore, Grant Recipient at Terumo

14:19
Panel discussion: What is the role of the radiologist in the workup of infertility?

14:00 - 15:30 **Darwin (Room D2)**

Special Focus Session

SF 7c
BasiCardiac for non-cardiac radiologists

SF 7c-1 14:00
Chairperson's introduction
L. Natale*; Rome/IT (luigi.natale@unicatt.it)*
Session objectives:
1. To familiarise general radiologists with cardiac findings in ungated chest CT.
2. To discuss the major indication for gated cardiac CT.
3. To explain MR imaging of myocardial infarction.
4. To review the MR role in acute chest pain with normal coronary arteries.
Author Disclosures:
L. Natale: nothing to disclose

SF 7c-2 14:05
Cardiac findings in ungated chest CT
K. Nikolaou*; Tübingen/DE (Konstantin.Nikolaou@med.uni-tuebingen.de)*
Learning objectives:
1. To refresh knowledge surrounding cardiac anatomy and normal variants.
2. To review common pathological cardiac findings.
3. To become familiar with possible relationships between lung and cardiac findings.
Author Disclosures:
K. Nikolaou: Research/Grant Support at Siemens Healthcare, Bracco, GE, Bayer

SF 7c-3 14:25
Coronary artery disease: how, why, and when a cardiac CT?
R. Vliegenthart*; Groningen/NL (r.vliegenthart@umcg.nl)*
Learning objectives:
1. To discuss the technical aspects of gated cardiac CT.
2. To be familiar with the appropriateness criteria for CT use in cardiac diseases.
3. To understand the most frequent indication to cardiac CT.
Author Disclosures:
R. Vliegenthart: Research/Grant Support at Institutional research grant, Siemens Healthineers

SF 7c-4 14:45
CMR: characterising myocardial damage
M. Francone*; Rome/IT (marco.francone@uniroma1.it)*
Learning objectives:
1. To become familiar with basic MR sequences to detect myocardial damage.
2. To learn about the differential diagnosis of ischemic and non ischemic cardiomyopathies.
3. To recognise the prognostic implications of MRI data.
Author Disclosures:
M. Francone: nothing to disclose

SF 7c-5 15:00
Acute chest pain with normal coronaries: a clear indication for CMR
M. Gutberlet*; Leipzig/DE (matthias.gutberlet@helios-gesundheit.de)*
Learning objectives:
1. To review differential diagnosis of acute chest pain.
2. To understand the role of CMR in characterisation of acute presentation and normal invasive coronary angiography.
3. To become familiar with prognostic implications of MRI data in acute settings.
Author Disclosures:
M. Gutberlet: Speaker at Bayer, Philips, Siemens, Bracco and Circle

15:15
Panel discussion: The heart is not a black hole in the chest

14:00 - 15:30 **Descartes (Room D3)**

Genitourinary

RC 707
Prostate cancer management: pushing the diagnostic frontier

RC 707-1 14:00
Chairperson's introduction
O. Ratib*; Geneva/CH (osman.Ratib@hcuge.ch)*
Session objectives:
1. To learn about the state of the art of prostate cancer imaging.
2. To understand how to skip the hurdles of implementing this into European and national prostate cancer guidelines.
3. To learn the next steps in the evolution of imaging of prostate cancer.
Author Disclosures:
O. Ratib: nothing to disclose

RC 707-2 14:05
A. The role of MRI
V. Panebianco*; Rome/IT (valeria.panebianco@uniroma1.it)*
Learning objectives:
1. To illustrate the evolution of MRI in terms of technical and standardisational improvement.
2. To understand the clinical impact of MRI in the era of the prostate imaging reporting and data system (PI-RADS).
3. To become familiar with the MRI strategies for risk-adapted prostate cancer diagnosis.
Author Disclosures:
V. Panebianco: nothing to disclose

RC 707-3 14:25
B. The role of molecular imaging: PSMA-PET/CT and PET/MR
H.-P. Schlemmer*; Heidelberg/DE*
Learning objectives:
1. To become familiar with the key clinical issues and imaging strategies for risk-adapted prostate cancer diagnosis.
2. To understand the significance and complementary roles of whole-body MRI and PSMA-PET/CT for tumour detection, (re)staging, as well as therapy planning and monitoring.
3. To learn the clinical indications for risk-adapted whole-body PSMA-PET/CT and PET/MRI according to current guidelines.
Author Disclosures:
H.-P. Schlemmer: Advisory Board at Siemens Healthineers, Advisory Board at Bayer, Grant Recipient at Siemens Healthineers, Grant Recipient at Bayer, Speaker at Siemens Healthineers, Speaker at Bayer

RC 707-4 14:45
C. Theranostic approaches to prostate cancer management
H. Ilhan*; Munich/DE (harun.ilhan@med.lmu.de)*
Learning objectives:
1. To review and evaluate current approaches for hybrid imaging in prostate cancer.
2. To analyse the impact of imaging on several therapeutic approaches for prostate cancer.
3. To look ahead for future approaches for prostate cancer theranostics.
Author Disclosures:
H. Ilhan: Advisory Board at Bayer, Research/Grant Support at Novartis, Speaker at Bayer, Speaker at Sirtex Medical

15:05
Panel discussion: Investigating patients with suspected and proven prostate cancer in 2025

14:00 - 15:30 **Room G**

Multidisciplinary Session

MS 7a

Multidisciplinary team for breast cancer

MS 7a-1 14:00
Chairperson's introduction
G. Ivanac*; Zagreb/HR (gordana.augustan@gmail.com)*
Session objectives:
1. To highlight the importance of multidisciplinary breast teams in the diagnosis and treatment of breast cancer.
2. To introduce the EU guidelines for breast centres.
3. To introduce the 'key disciplines' for a multidisciplinary breast centre.
Author Disclosures:
G. Ivanac: nothing to disclose

MS 7a-2 14:03
Radiologist's perspective
E. Divjak*; Zagreb/HR*
Learning objectives:
1. To learn about the role of different imaging modalities in detecting and characterising breast lesions precisely.
2. To understand the importance of needle biopsy and of pathologic "b-classification" in the management of women with breast cancer.
3. To understand the role of a multidisciplinary approach based on case presentation.
Author Disclosures:
E. Divjak: nothing to disclose

MS 7a-3 14:21
Pathologist's perspective
C. Tomasovic-Loncaric*; Zagreb/HR (ctomasov@kbd.hr)*
Learning objectives:
1. To learn about the advantages and deficiencies of pathological examination in the non-invasive diagnosis of breast lesions.
2. To understand the impact of the recommended standard surgical and radiological procedures on the accuracy of pathological diagnosis.
3. To understand the impact of good communication with radiologists and clinicians on the accuracy of pathological diagnosis.
Author Disclosures:
C. Tomasovic-Loncaric: nothing to disclose

MS 7a-4 14:39
Surgeon's perspective
R. Zic*; Zagreb/HR*
Learning objectives:
1. To learn about different surgical options in the treatment of breast cancer patients.
2. To understand the rationale behind current perioperative and adjuvant treatment approaches.
3. To understand the principles of individualised treatment according to the biology of breast cancer.
Author Disclosures:
R. Zic: disclosure/affirmation information not submitted

MS 7a-5 14:57
Oncologist's perspective
N. Dedic-Plavetic*; Zagreb/HR (ndedic@kbc-zagreb.hr)*
Learning objectives:
1. To learn about the current medical treatment options and modalities.
2. To understand the indications for the neoadjuvant treatment approach and the appropriate modalities.
3. To understand the interactions of known predictive factors, current neoadjuvant/adjuvant treatment options, and prognosis within an interdisciplinary treatment concept.
Author Disclosures:
N. Dedic-Plavetic: Advisory Board at Roche, Advisory Board at Mylan, Investigator at Roche, Speaker at Roche, Advisory Board at Novartis, Speaker at Pfizer, Speaker at Novartis, Investigator at Roche, Advisory Board at Pfizer

MS 7a-6 15:15
Multidisciplinary case presentation and discussion
G. Ivanac*; Zagreb/HR (gordana.augustan@gmail.com)*
Author Disclosures:
G. Ivanac: nothing to disclose

14:00 - 15:30 **Room K**

Multidisciplinary Session

MS 7b

Liver transplantation in patients with hepatocellular carcinoma: a multidisciplinary approach

MS 7b-1 14:00
Chairperson's introduction
I. G. Lupescu*; Bucharest/RO (ilupescu@gmail.com)*
Session objectives:
1. To highlight the crucial role of the multidisciplinary team (MDT) in prompt early diagnosis, staging of hepatocellular carcinoma (HCC), and formulating an individualised treatment plan.
2. To present the key role of the radiologist in the MDT in pre-transplant and post-transplant liver evaluation of patients with HCC.
3. To discuss the gastroenterologist's and the surgeon's point of view for liver transplantation in patients with "early-stage" HCC.
Author Disclosures:
I. G. Lupescu: nothing to disclose

MS 7b-2 14:06
Surveillance of hepatocelular carcinoma in patients with cirrhosis and indications for liver transplantation: the gastroenterologist's perspective
L. Gheorghe*; Bucharet/RO (drlgheorghe@gmail.com)*
Learning objectives:
1. To redefine the appropriate candidates and the current methodology for HCC surveillance in cirrhosis.
2. To update the recommendations for liver transplantation in patients with HCC.
3. To discuss the management of patients with liver cirrhosis and hepatocellular carcinoma while on the transplant wait list.
Author Disclosures:
L. Gheorghe: Speaker at Fundeni Clinical Institute, Gastroenterology and Hepatology Center; Carol Davila University of Medicine and Pharmacy

MS 7b-3 14:28
Imaging and interventional radiology in preoperative liver transplantation: from diagnosis to bridging
R. L. Dumitru*; Bucharest/RO (radu.dumitru@gmail.com)*
Learning objectives:
1. To raise awareness of the radiological findings and their role in patient preparation.
2. To identify the normal and variant hepatic arterial, hepatic venous, portal venous, and bile duct anatomy.
3. To become familiar with interventional radiology (IR) procedures for patients on the waiting list for liver transplantation (ablation, TACE).
Author Disclosures:
R. L. Dumitru: nothing to disclose

MS 7b-4 14:43
The point of view of the surgeon: what the surgeon needs to know?
I. Popescu*; Bucharest/RO*
Learning objectives:
1. To describe the different types of liver transplantation.
2. To emphasise the importance of knowing, prior to the liver transplantation, the anatomical vascular and biliary tree variants.
3. To discuss current surgical techniques and their importance in pre-transplantation evaluation.

Author Disclosures:
I. Popescu: disclosure/affirmation information not submitted

MS 7b-5 15:05
Post-transplant complications: from diagnosis to treatment
C. M. Grasu*; Bucharest/RO (mugur.grasu@gmail.com)*
Learning objectives:
1. To identify the normal post-transplantation imaging findings.
2. To discuss post-transplantation complications and their imaging characteristics.
3. To present interventional radiology techniques in liver translate complications.
Author Disclosures:
C. M. Grasu: Consultant at Boston Scientific, Consultant at Terumo Europe NV, Speaker at Bayer

MS 7b-6 15:20
Multidisciplinary case presentation and discussion
I. G. Lupescu*; Bucharest/RO (ilupescu@gmail.com)*
Author Disclosures:
I. G. Lupescu: nothing to disclose

14:00 - 15:30 **Room M 2**

E³ - Advanced Course: Interactive Teaching Session for Young (and not so Young) Radiologists

E³ 721b
Head and neck imaging

E³ 721b-1 14:00
A. Cystic neck lesions
A. Borges*; Lisbon/PT (borgalexandra@gmail.com)*
Learning objectives:
1. To become familiar with the differential diagnosis.
2. To know the usefulness of the biochemistry of fine needle aspiration in the differential diagnosis.
Author Disclosures:
A. Borges: nothing to disclose

E³ 721b-2 14:45
B. Non-traumatic head and neck emergencies
A. Rovira Cañellas*; Barcelona/ES (alex.rovira@idi.gencat.cat)*
Learning objectives:
1. To become familiar with the most common cause of emergencies.
2. To learn the imaging criteria for differentiation.
Author Disclosures:
A. Rovira Cañellas: nothing to disclose

14:00 - 15:30 **Room M 3**

ESOR Session

ESOR
Education in research

Moderators:
M. Fuchsjäger; Graz/AT
V. Vilgrain; Clichy/FR

ESOR-1 14:00
Introduction
M. Fuchsjäger*; Graz/AT (michael.fuchsjaeger@medunigraz.at)*
Author Disclosures:
M. Fuchsjäger: nothing to disclose

ESOR-2 14:05
ESOR in action 2020
V. Vilgrain*; Clichy/FR (valerie.vilgrain@aphp.fr)*
Learning objectives:
1. To become familiar with ESOR.
2. To learn about ESOR activities in 2020.
3. To understand the new topics of the ESOR Educational Programme.
Author Disclosures:
V. Vilgrain: Speaker at Hospital Beaujon

ESOR-3 14:10
Getting involved in clinical trials: it is never too early
V. Goh*; London/UK (vicky.goh@kcl.ac.uk)*
Learning objectives:
1. To understand the rationale for clinical trials.
2. To learn about the different types of clinical trials.
3. To appreciate the role of radiologists in clinical trials.
Author Disclosures:
V. Goh: Research/Grant Support at Siemens, Speaker at Siemens

ESOR-4 14:30
The importance of networking in research
C. Catalano*; Rome/IT (carlo.catalano@uniroma1.it)*
Author Disclosures:
C. Catalano: nothing to disclose

ESOR-5 14:50
My experience: Bracco research fellowship
Ž. Snoj*; Ljubljana/SI (ziga.snoj@gmail.com)*
Learning objectives:
1. To appreciate the opportunity of a research fellowship.
2. To become familiar with research fellowship goals.
3. To gain insight into the fellowship course based on the scholar's experience.
Author Disclosures:
Ž. Snoj: nothing to disclose

15:00
Awards

14:00 - 15:30 **Room M 4**

State of the Art Symposium

SA 7
Musculoskeletal ultrasound of the extremities

SA 7-1 14:00
Chairperson's introduction
G. M. Allen*; Oxford/UK (gina_m_allen@btinternet.com)*
Session objectives:
1. To describe the anatomical considerations for ultrasonography of the extremities.
2. To define the pathologic conditions whereby diagnostic ultrasonography of the extremities is utilised.
3. To explain the ultrasonography findings of the pathologic conditions of the extremities.
Author Disclosures:
G. M. Allen: nothing to disclose

SA 7-2 14:06
Tendons, ligaments and retinaculae of the wrist and hand
M. Faruch-Bilfeld*; Toulouse/FR (mariefaruch@hotmail.com)*
Learning objectives:
1. To describe the anatomical considerations for ultrasonography of the wrist and hand.
2. To define the pathologic conditions whereby diagnostic ultrasonography of the tendons, ligaments and retinaculae of the wrist and hand is utilised.
3. To explain the ultrasonography findings of the pathologic conditions of the tendons, ligaments and retinaculae of the wrist and hand.
Author Disclosures:
M. Faruch-Bilfeld: nothing to disclose

SA 7-3 14:24
Tendons, ligaments and retinaculae of the ankle and foot
G. M. Allen; *Oxford/UK (gina_m_allen@btinternet.com)*
Learning objectives:
1. To describe the anatomical considerations for ultrasonography of the ankle and foot.
2. To define the pathologic conditions whereby diagnostic ultrasonography of the tendons, ligaments and retinaculae of the ankle and foot is utilised.
3. To explain the ultrasonography findings of the pathologic conditions of the tendons, ligaments and retinaculae of the ankle and foot.
Author Disclosures:
G. M. Allen: nothing to disclose

SA 7-4 14:42
Soft tissue masses
E. Drakonaki; *Iraklion/GR (drakonaki@yahoo.gr)*
Learning objectives:
1. To describe the anatomical considerations for ultrasonography of the soft tissues in the extremities.
2. To define the soft tissue masses whereby diagnostic ultrasonography is utilised in the extremities.
Author Disclosures:
E. Drakonaki: nothing to disclose

SA 7-5 15:00
Peripheral nerve disorders
C. Martinoli; *Genoa/IT (carlo.martinoli@unige.it)*
Learning objectives:
1. To describe the anatomical considerations for ultrasonography of the nerves in the extremities.
2. To define the pathologic conditions whereby diagnostic ultrasonography of the nerves in the extremities is utilised.
3. To explain the ultrasonography findings of the pathologic conditions of the nerves in the extremities.
Author Disclosures:
C. Martinoli: nothing to disclose

15:18
Panel discussion: How can we, as radiologists, best serve the interest of the patient in musculoskeletal ultrasound of the extremities while protecting our turf?

14:00 - 15:30 **Room M 5**

E³ - Advanced Course: Artificial Intelligence

E³ 720

Challenges and solutions for introducing artificial intelligence (AI) in daily clinical workflow

E³ 720-1 14:00
Chairperson's introduction
E. Kotter; *Freiburg/DE (elmar.kotter@uniklinik-freiburg.de)*
Session objectives:
1. To become familiar with the current state of AI implementation in radiology departments.
2. To understand how you can start implementing AI based solutions.
3. To learn about challenges and pitfalls in implementing AI in your department.
Author Disclosures:
E. Kotter: nothing to disclose

E³ 720-2 14:06
A. Implementation of AI algorithms in picture archiving and communication systems (PACS)
W. B. Veldhuis; *Utrecht/NL (w.veldhuis@umcutrecht.nl)*
Learning objectives:
1. To learn about how you can start experimenting with AI in daily clinical routine.
2. To learn about developments to integrate multiple AI tools within one framework.
3. To learn about processes to evaluate AI algorithms for clinical use cases.
Author Disclosures:
W. B. Veldhuis: Founder at QuantibU BV

E³ 720-3 14:27
B. How to best complement human intelligence with AI
C. J. Herold; *Vienna/AT (Christian.Herold@meduniwien.ac.at)*
Learning objectives:
1. To understand current and emerging concept for AI and machine learning in imaging.
2. To explore whether it is possible to success fully integrate AI into clinical practice today.
3. To learn how the radiologists can be assisted by AI.
Author Disclosures:
C. J. Herold: CEO at Medical University of Vienna

E³ 720-4 14:48
C. AI, ethics and radiology
A. Brady; *Cork/IE (adrianbrady@me.com)*
Learning objectives:
1. To understand ethical aspects related to data use in AI.
2. To learn about possible bias in AI algorithms.
3. To learn how to prepare radiology policies for AI.
Author Disclosures:
A. Brady: nothing to disclose

E³ 720-5 15:09
D. AI in radiology: culture change
H. Fleishon; *Atlanta, GA/US (hfleishon@outlook.com)*
Learning objectives:
1. To review possible changes in radiology practices and departments due to implementation of AI workflows.
2. To present possible impact of AI on radiology macroeconomics.
3. To discuss educational innovations to introduce AI into radiology resident training.
Author Disclosures:
H. Fleishon: nothing to disclose

14:00 - 15:30 **Tech Gate Auditorium**

Imaging Informatics

RC 705

Everything you need to know about 3D post-processing

RC 705-1 14:00
Chairperson's introduction
E. Sorantin; *Graz/AT*
Session objectives:
1. To learn about the state-of-the-art information regarding 3D post-processing.
2. To understand how 3D post-processing can be used optimally in daily clinical practice.
3. To appreciate how automated 3D post-processing and quantification will lead to increased use of 3D visualisations for diagnostics and therapy planning over 2D viewing.
Author Disclosures:
E. Sorantin: nothing to disclose

RC 705-2 14:05
A. 3D post-processing in 2020
A. Alberich-Bayarri; *Valencia/ES (angel@quibim.com)*
Learning objectives:
1. To learn about recent advances in 3D post-processing techniques.
2. To understand how these techniques can now be used in clinical practice.
3. To learn new tips and tricks to use in your daily practice.
Author Disclosures:
A. Alberich-Bayarri: CEO at QUIBIM SL, Board Member at QUIBIM SL, Founder at QUIBIM SL

RC 705-3 14:28
B. Making better use of your 3D package: tips and tricks
P. M. van Ooijen*; Groningen/NL (p.m.a.van.ooijen@umcg.nl)*
Learning objectives:
1. To learn about the functionality of state-of-the-art 3D packages.
2. To understand the pitfalls in use of 3D post-processing.
3. To appreciate the need for training in 3D post-processing techniques.
Author Disclosures:
P. M. van Ooijen: nothing to disclose

RC 705-4 14:51
C. Interpretation of 3D processing results: from image to volume reading
T. Frauenfelder*; Zurich/CH (thomas.frauenfelder@usz.ch)*
Learning objectives:
1. To learn about different developments in creating 3D anatomical and functional models for diagnostic and therapy planning purposes.
2. To understand the pros and cons of such technologies.
3. To appreciate that automated 3D image analysis will lead to new ways in which diagnosis and therapy planning will be performed.
Author Disclosures:
T. Frauenfelder: nothing to disclose

16:14
Panel discussion: Will we still look at 2D images in 10 years' time?

16:00 - 17:30 **Room B**

E³ - Rising Stars Programme: Basic Session

BS 8
Genitourinary

Moderator:
L. E. Derchi; Genoa/IT

BS 8-1 16:00
Adrenal pathologies
M. Stajgis*; Poznan/PL (stajgis@gmail.com)*
Learning objectives:
1. To review the most common pathologies.
2. To present current imaging techniques for evaluation of adrenal pathologies.
3. To demonstrate the most important findings of the common adrenal pathologies.
Author Disclosures:
M. Stajgis: nothing to disclose

BS 8-2 16:30
Prostate cancer
B. Hamm*; Berlin/DE*
Learning objectives:
1. To review the most common pathologies.
2. To present current imaging techniques for evaluation of the prostate.
3. To demonstrate the most important findings of prostate pathologies.
Author Disclosures:
B. Hamm: disclosure/affirmation information not submitted

BS 8-3 17:00
Foetal MRI
D. Prayer*; Vienna/AT (daniela.prayer@meduniwien.ac.at)*
Learning objectives:
1. To learn about the indications of foetal MRI.
2. To describe the foetal MRI technique.
3. To illustrate the imaging features in most common foetal pathologies.
Author Disclosures:
D. Prayer: nothing to disclose

16:00 - 17:30 **Room on demand Room C or Room M 3**

Musculoskeletal

RC 810
Inflammatory and infectious diseases of the spine: how to differentiate from degeneration

Moderator:
I. Engele; Riga/LV

RC 810-1 16:00
A. Spondyloarthritis: a diagnostic chameleon
V. Zubler*; Zurich/CH*
Learning objectives:
1. To explain the disease spectrum and pathophysiology of spondyloarthritides.
2. To describe the imaging findings of spondyloarthritides.
Author Disclosures:
V. Zubler: nothing to disclose

RC 810-2 16:30
B. Crystals: may also affect the spine
M. Reijnierse*; Leiden/NL (m.reijnierse@lumc.nl)*
Learning objectives:
1. To explain the disease spectrum and pathophysiology of crystal deposition diseases that affect the spine.
2. To describe the imaging findings of crystal deposition diseases that affects the spine.
Author Disclosures:
M. Reijnierse: nothing to disclose

RC 810-3 17:00
C. Infection: imaging, indication and techniques for biopsy
J.-L. Drape*; Paris/FR (jean-luc.drape@cch.aphp.fr)*
Learning objectives:
1. To describe the imaging findings of spinal infection.
2. To explain the biopsy indication and techniques in spinal infection.
Author Disclosures:
J.-L. Drape: Speaker at HOPITAL COCHIN

16:00 - 17:00 **Coffee & Talk 1**

Coffee & Talk (open forum) Session
Organised by the European Board of Radiology (EBR)

C 35
ETAP 2.0: a certification of excellence for radiology training departments

C 35-1 16:00
Chairperson's introduction
D. Negru*; Iasi/RO (draneg@gmail.com)*
Session objectives:
1. To learn about ETAP 2.0.
2. To understand the importance of the assessment of training programmes.
3. To learn about facts and figures of ETAP.
Author Disclosures:
D. Negru: nothing to disclose

C 35-2 16:10
Steps for the certification
A. Montvila*; Kaunas/LT (montvila.antanas@gmail.com)*
Learning objectives:
1. To show the phases of the ETAP 2.0 certification process.
2. To learn how to prepare for the audit process.
3. To learn how the outcome of the certification is determined.
Author Disclosures:
A. Montvila: Board Member at European Junior Doctors Association

C 35-3 16:30
Benefits of getting ETAP 2.0 certified
J. Kraft*; Leeds/UK (Jeannette.Kraft@nhs.net)*
Learning objectives:
1. To know the different reasons for obtaining the certification.
2. To check the quality of the training programme.
3. To learn how to improve the training programme.
Author Disclosures:
J. Kraft: nothing to disclose

16:50
Open forum discussion

16:00 - 17:30 **Room N**

EuroSafe Imaging Session

EU 8
European study on clinical diagnostic reference levels (DRLs) (EUCLID) project: final results

Moderators:
J. Damilakis; Iraklion/GR
G. Frija; Paris/FR

EU 8-1 16:00
An overview of the EUCLID project
J. Damilakis*; Iraklion/GR (John.Damilakis@med.uoc.gr)*
Learning objectives:
1. To understand why clinical DRLs are needed in adult imaging.
2. To learn about the EUCLID methodology of establishing DRLs.
3. To give an overview of the EUCLID results.
Author Disclosures:
J. Damilakis: Research/Grant Support at European Commission

EU 8-2 16:15
EUCLID clinical DRLs values in CT and European comparisons
V. Tsapaki*; Nea Ionia/GR (virginia@otenet.gr)*
Learning objectives:
1. To present EUCLID CT data analysis in the attempt to define EUCLID CT DRLs.
2. To compare with existing clinical CT DRLs.
3. To present the challenges and limitations, as well as methods, to improving surveys for DRLs determination.
Author Disclosures:
V. Tsapaki: nothing to disclose

EU 8-3 16:30
EUCLID clinical DRLs values in interventional radiology and European comparisons
W. Jaschke*; Innsbruck/AT (werner.jaschke@i-med.ac.at)*
Learning objectives:
1. To learn the differences between clinical DRL and DRL.
2. To report the EUCLID clinical DRL values in interventional radiology.
3. To provide information on DRL values for procedures in Europe.
Author Disclosures:
W. Jaschke: nothing to disclose

EU 8-4 16:45
Implementation of clinical DRLs in practice: ask one centre
S. T. Schindera*; Riehen/CH (sebastian.schindera@ksa.ch)*
Learning objectives:
1. To discuss the main challenges in the implementation of clinical DRLs.
2. To present the major benefits when applying clinical DRLs.
3. To discuss future application of clinical DRLs in CT.
Author Disclosures:
S. T. Schindera: nothing to disclose

EU 8-5 16:55
The European Commission's perspective
G. Simeonov*; Luxembourg/LU (georgi.simeonov@ec.europa.eu)*
Learning objectives:
1. To understand the role of DRLs in the European system for radiation protection in medicine.
2. To understand the European Commission's reasoning behind supporting the EUCLID project.
3. To obtain insights into the position of the European Commission with respect to EUCLID project results.
4. To discuss needs for further European work on DRLs, including the wider context of quality and safety in radiology.
Author Disclosures:
G. Simeonov: nothing to disclose

17:10
Panel discussion: How can clinical DRLs be introduced into daily clinical routine?

16:00 - 17:30 **Room O**

Children in Focus

IF 8
Medicolegal dilemmas in paediatric medicine

IF 8-1 16:00
Chairperson's introduction
A. C. Offiah*; Sheffield/UK (amaka.offiah@nhs.net)*
Author Disclosures:
A. C. Offiah: Advisory Board at Alexion, Advisory Board at BioMarin, Speaker at InfoMed, Grant Recipient at Alexion, Other at Expert witness for cases of suspected child abuse

IF 8-2 16:06
Child abuse, creation of a non-disease? The Swedish report versus IPR/ESPR white paper: is anything really ever black and white?
A. Choudhary*; Little Rock, AR/US (achoudhary@uams.edu)*
Learning objectives:
1. To learn how effective the radiologist is at diagnosing abusive head trauma.
2. To appreciate the difficulties of creating high-level scientific evidence for radiological signs of child abuse.
3. To discuss the dilemmas when selecting studies for meta-analysis of medical signs of child abuse.
Author Disclosures:
A. Choudhary: Shareholder at GE, Speaker at Honorarium for lectures at meetings, Other at Expert witness for medicolegal cases

IF 8-3 16:22
Medical evidence from a legal perspective
W. Duijst*; Maastricht/NL (ackenniscentrum.nl@gmail.com)*
Learning objectives:
1. To understand the true impact of legal evidence and the role of medical expert witnesses.
2. To appreciate the differences between legal and medical evidence.
3. To discuss legal dilemmas when medical scientific evidence is sparse. How does the court evaluate the reliability and credibility of the expert witnesses?
Author Disclosures:
W. Duijst: nothing to disclose

IF 8-4 16:38
The EU perspective: is child abuse a homogenous 'disease' across Europe? Cultural aspects
M. Raissaki*; Iraklion/GR (mraissaki@yahoo.gr)*
Learning objectives:
1. To present examples of cultural differences in what is perceived as 'abuse'.
2. To understand the difficulties in appreciation of demographics of child abuse across Europe.
3. To discuss how potential cultural differences can create medical and legal dilemmas in defining child abuse.
4. To discuss the importance of prevention.
Author Disclosures:
M. Raissaki: nothing to disclose

IF 8-5 16:54
Child sexual abuse in India among children from marginalised backgrounds
R. M. George; *Vienna/AT (reena.mary.george@univie.ac.at)*
Learning objectives:
1. To learn about health services available to survivors of child sexual abuse and awareness programmes currently available to deal with this issue.
2. To appreciate the paradox in law relating to child sexual abuse in India.
3. To discuss positive and negative examples of services provided to children after reporting their abuse, and examples of the impact of child sexual abuse in some cases.
Author Disclosures:
R. M. George: nothing to disclose

17:10
Panel discussion: How can we secure credible evidence regarding child abuse in order to protect both children and their carers?

16:00 - 17:30 **Studio 2020**

Special Focus Session

SF 8a

How to diagnose and manage abdominal, retroperitoneal and pelvic incidentalomas

SF 8a-1 16:00
Chairperson's introduction
A. Rockall; *London/UK (a.rockall@imperial.ac.uk)*
Session objectives:
1. To illustrate the frequency of incidentalomas on imaging studies.
2. To discuss the pros and cons of incidental detection of abnormalities during imaging studies.
3. To highlight the economic aspects of management of incidentally diagnosed lesions.
Author Disclosures:
A. Rockall: Speaker at Guerbet

SF 8a-2 16:05
Liver, pancreatic and splenic incidentalomas
A. Cieszanowski; *Warsaw/PL (andrzej.cieszanowski@wum.edu.pl)*
Learning objectives:
1. To explain the frequency of incidental findings in the liver, pancreas, and spleen according to age and applied imaging modality.
2. To highlight the role of current imaging techniques in the differentiation of abdominal incidentalomas.
3. To describe the present guidelines and recommendations for the follow-up of incidental findings in the abdomen.
Author Disclosures:
A. Cieszanowski: Speaker at Siemens, Speaker at GE, Speaker at Philips, Speaker at Bayer, Speaker at Bracco

SF 8a-3 16:30
Adrenal and renal incidentalomas
M. Hellström; *Gothenburg/SE (mikael.hellstrom@xray.gu.se)*
Learning objectives:
1. To discuss the frequency and significance of cystic and solid renal incidentalomas.
2. To highlight the prevalence of incidental adrenal findings.
3. To describe the role of different diagnostic methods in the characterisation of renal and adrenal incidentalomas, including renal biopsy.
4. To underline the recommendations for the workup of adrenal lesions as well as for cystic and solid renal incidentalomas.
Author Disclosures:
M. Hellström: nothing to disclose

SF 8a-4 16:55
Pelvic incidentalomas
D. Akata; *Ankara/TR (akataden@gmail.com)*
Learning objectives:
1. To outline the prevalence of pelvic incidentalomas in male and female populations in different age groups.
2. To highlight the role of US, CT, and MRI in differentiation of pelvic incidentalomas.
3. To explain how to follow-up and manage incidentally detected pelvic masses.
Author Disclosures:
D. Akata: nothing to disclose

17:20
Panel discussion: The management of incidentalomas: when to dismiss, follow-up or treat them?

16:00 - 17:00 **Coffee & Talk 2**

Coffee & Talk (open forum) Session

Organised by the ESR Subcommittee on Audit and Standards

C 14

Clinical audit and the European-Basic Safety Standards (EU-BSS): where are we now?

C 14-1 16:00
Chairperson's introduction
D. Howlett; *Eastbourne/UK (david.howlett@nhs.net)*
Session objectives:
1. To reinforce the importance of a clinical audit for radiology departments.
2. To update on Esperanto: distribution and feedback.
3. To consider the future direction for the European clinical audit.
Author Disclosures:
D. Howlett: nothing to disclose

C 14-2 16:05
Clinical audit: EU-BSS uptake, the ESR perspective
A. Brady; *Cork/IE (adrianbrady@me.com)*
Learning objectives:
1. To review the requirements of the EU-BSS.
2. To present updated survey findings of EU-BSS uptake amongst European radiology departments.
3. To consider the challenges around EU-BSS uptake and transposition.
Author Disclosures:
A. Brady: nothing to disclose

C 14-3 16:20
Clinical audit: EU-BSS uptake, the regulator perspective
A. Karoussou-Schreiner; *Louxembourg/LU*
Learning objectives:
1. To update on EU-BSS transposition across Europe.
2. To update on the Heads of the European Radiological Protection Competent Authorities (HERCA) position.
3. To discuss the process and requirements of inspection.
Author Disclosures:
A. Karoussou-Schreiner: disclosure/affirmation information not submitted

C 14-4 16:30
Case example: clinical audit template
T. Ø. Holter; *Oslo/NO (uxtaho@ous-hf.no)*
Learning objectives:
1. To review a clinical audit performed at a local level.
2. To appreciate the challenges and hurdles encountered.
3. To discuss the benefits of a clinical audit at the departmental level.
Author Disclosures:
T. Ø. Holter: nothing to disclose

16:45
Open forum discussion: To discuss the potential for future pan European projects

16:00 - 17:30 **Room F1**

ESR meets Israel

Meets 8a

Radiology in Israel: technology and professionalism

Presiding:
B. Brkljačić; Zagreb/HR
J. Sosna; Jerusalem/IL

Meets 8a-1 16:00
Welcome from the ESR President
B. Brkljačić*; Zagreb/HR (boris@brkljacic.com)*
Author Disclosures:
B. Brkljačić: nothing to disclose

Meets 8a-2 16:02
Introduction
J. Sosna*; Jerusalem/IL (jacobs@hadassah.org.il)*
Learning objectives:
1. To present the fundamentals of radiology in Israel.
2. To present and discuss the role of artificial intelligence (AI) and technology in radiology in Israel.
3. To discuss the humanistic aspects of radiology.
Author Disclosures:
J. Sosna: Consultant at Xact, Grant Recipient at Philips

Meets 8a-3 16:12
Will artificial intelligence (AI) replace the radiologist?
E. Konen*; Ramat Gan/IL (eli.konen@sheba.health.gov.il)*
Learning objectives:
1. To describe AI principles.
2. To present current AI applications.
3. To discuss the role of the future radiologist (AI, human, both).
Author Disclosures:
E. Konen: Consultant at AIDOC, Shareholder at Voxallence

16:32
Interlude 1: Israel: a rich history and bright future

Meets 8a-5 16:37
Doctor-patient communication in radiology
D. Shaham*; Jerusalem/IL (dshaham@hadassah.org.il)*
Learning objectives:
1. To present the human aspects of radiology work.
2. To describe the interpersonal interactions of the radiologist.
3. To present cultural differences in the perception of radiologists.
Author Disclosures:
D. Shaham: nothing to disclose

16:57
Interlude 2: Musical piece

Meets 8a-7 17:02
Imaging technology development: the Israeli experience
J. Sosna*; Jerusalem/IL (jacobs@hadassah.org.il)*
Learning objectives:
1. To present Israel as a start-up nation.
2. To describe technological developments that originated from Israel.
3. To present imaging technology innovations in development and in clinical practice.
Author Disclosures:
J. Sosna: Consultant at Xact, Grant Recipient at Philips

17:22
Panel discussion: The future of radiology: technology- or human-centred?

16:00 - 17:30 **Room F2**

Head and Neck

RC 808

Differential diagnoses you don't want to miss

Moderator:
E. B. Arkink; Reykjavík/IS

RC 808-1 16:00
A. Differential diagnoses of bone lesions in the head and neck: excluding dental cysts
V. Lenoir*; Geneva/CH*
Learning objectives:
1. To understand how to classify bone lesions in the head and neck.
2. To recognise which bone lesions you should be concerned about.
3. To become familiar with the most appropriate imaging modalities and protocols to use.
Author Disclosures:
V. Lenoir: nothing to disclose

RC 808-2 16:30
B. Differential diagnoses of cystic lesions in the head and neck: including dental cysts
S. Robinson*; Vienna/AT (s.robinson@dzu.at)*
Learning objectives:
1. To become familiar with the common cystic lesions in the neck.
2. To understand the pitfalls when assessing cystic lesions.
3. To learn about the most appropriate imaging techniques to use.
Author Disclosures:
S. Robinson: nothing to disclose

RC 808-3 17:00
C. Differential diagnoses of soft tissue masses of the face and neck in adults
D. Farina*; Brescia/IT (davide.farina@unibs.it)*
Learning objectives:
1. To become familiar with the anatomy.
2. To learn which imaging technique to use.
3. To understand the typical imaging appearance of soft tissue masses.
Author Disclosures:
D. Farina: Speaker at BAYER 2019, Other at BRACCO 2019

16:00 - 17:00 **Coffee & Talk 3**

Coffee & Talk (open forum) Session

C 25

Publishing in the radiography journal

C 25-1 16:00
Chairperson's introduction
J. M. Nightingale*; Sheffield/UK (J.Nightingale@shu.ac.uk)*
Session objectives:
1. To discuss all elements of scientific peer review.
2. To understand what to consider when submitting a manuscript.
3. To learn how to respond to referees' comments.
4. To interact with the radiography journal editorial team
Author Disclosures:
J. M. Nightingale: nothing to disclose

C 25-2 16:02
A tool to help establish the evidence base for the profession
H. Precht*; Middelfart/DK (hepr@ucl.dk)*
Learning objectives:
1. To consider why publishing is important for the development of the radiographer profession.
2. To explore the importance of publishing for individual researchers and practitioners.
3. To explore the importance of publishing for clinical and academic departments

Author Disclosures:
H. Precht: Board Member at University College Lillebelt

C 25-3 16:07
Review articles: how to get your work published
F. Zarb*; Msida/MT (francis.zarb@um.edu.mt)*
Learning objectives:
1. To explore what constitutes a strong review article and appropriate review methodologies.
2. To consider the use of reporting guidelines such as PRISMA and STARD
Author Disclosures:
F. Zarb: nothing to disclose

C 25-4 16:12
The reviewer's perspective and how to respond
A. England*; Manchester/UK (A.England@salford.ac.uk)*
Learning objectives:
1. To identify the purpose of peer review and to explain the steps within the peer review process.
2. To understand the qualities of a good review.
3. To learn how best to respond to reviewers' comments
Author Disclosures:
A. England: nothing to disclose

C 25-5 16:17
Editor-in-chief's top ten tips for publishing success
J. M. Nightingale*; Sheffield/UK (J.Nightingale@shu.ac.uk)*
Learning objectives:
1. To discuss reasons why a manuscript may be rejected.
2. To emphasise how common manuscript errors can be avoided.
3. To highlight the author's responsibilities in promoting their article.
Author Disclosures:
J. M. Nightingale: nothing to disclose

16:25
Open forum discussion

16:00 - 17:30 **da Vinci (Room D1)**

Special Focus Session

SF 8b
Quantitative MRI: from MR-physics to tissue microstructure

SF 8b-1 16:00
Chairperson's introduction
L. Mascaro*; Brescia/IT (lmascaro@libero.it)*
Session objectives:
1. To understand the principles and methods of quantitative MRI modalities that are used to measure tissue microstructure.
2. To highlight the pros and cons of quantitative imaging as compared to weighted imaging.
3. To show the potentials and limitations of the mapping technique for providing sub-voxel metrics for tissue characterisation.
4. To give updates on the role of quantitative MRI in research and routine clinical applications.
Author Disclosures:
L. Mascaro: nothing to disclose

SF 8b-2 16:05
T1, T2, and PD: direct mapping or not?
M. J. B. Warntjes*; Linköping/SE (marcel.warntjes@cmiv.liu.se)*
Learning objectives:
1. To present current methods for T1, T2, and PD mapping.
2. To understand how mathematical multicompartment analysis of relaxation times can describe complex biophysical models of tissue microstructure.
3. To underline how relaxation and PD mapping give novel information related to tissue microstructure at the subvoxel level.
Author Disclosures:
M. J. B. Warntjes: Consultant at SyntheticMR, Linköping, Sweden, Shareholder at SyntheticMR, Linköping, Sweden

SF 8b-3 16:28
Bringing quantitative magnetic susceptibility mapping into the clinic
C. Langkammer*; Graz/AT*
Learning objectives:
1. To present current methods for quantitative susceptibility mapping (QSM).
2. To understand which biophysical tissue properties can affects magnetic susceptibility, and to identify which tissues benefit from a QSM analysis.
3. To highlight the potentials of QSM to assess tissue function and disease, and to describe the actual limits of the technique as a standard tool for clinical diagnostic imaging.
Author Disclosures:
C. Langkammer: nothing to disclose

SF 8b-4 16:51
Promises and pitfalls of magnetisation transfer and diffusion
M. Cercignani*; Brighton/UK (m.cercignani@bsms.ac.uk)*
Learning objectives:
1. To present basic and advanced methods for magnetisation transfer (MT) and diffusion quantification.
2. To define the tissue microstructure and structural connectivity features that affect diffusion, and to give updates on novel quantitative diffusion metrics, their potential, and limits for clinical applications.
3. To understand MT modelling and feature extraction, and to describe the state of the art of MT quantification in clinical and pre-clinical studies.
Author Disclosures:
M. Cercignani: nothing to disclose

16:19
Panel discussion: From direct mapping to extrapolating MR-properties

16:00 - 17:30 **Darwin (Room D2)**

ISRRT meets Canada

Meets 8b
Radiography profession performance and future challenges in Canada

Presiding:
E. Agadakos; Athens/GR
D. Katsifarakis; Athens/GR

Meets 8b-1/Meets 8b-2 16:00
Chairpersons' introduction
E. Agadakos*; Athens/GR (eagadakos@gmail.com)*
D. Katsifarakis*; Athens/GR (dikatsifarakis@gmail.com)*
Session objectives:
1. To recognise the demographics and patient accessibility to health care services in the country.
2. To understand the infrastructure of the imaging health services and their contribution to the primary and hospital health services to sustain the population and individual health.
3. To inform on the role of the professional society in influencing the future educational programme of radiographers in the country.
4. To become aware of the strategies employed by the professional society to support and promote the radiographers' role in the community and the health care system.
5. To gain information on radiography career structure and opportunities for professional development of radiographers in Canada.
6. To appreciate the radiographers' post-graduation professional requirements and relevant opportunities, and to keep up to date with evidence-based practice in imaging services.
7. To communicate the society's position on artificial intelligence and preliminary actions undertaken to prepare radiographers in embracing the changes.
Author Disclosures:
E. Agadakos: Board Member at ISRRT , D. Katsifarakis: nothing to disclose

Meets 8b-3 16:05
The regulatory situation in Canada for radiographers and radiological technologists
A. Cromp*; St-Léonard, QC/CA (acromp@ac-consultant.ca)*

Learning objectives:
1. To learn how the profession of radiographers is regulated in Canada.
2. To understand how the regulation differs from one province to another, and the challenges of mobility for radiographers.
3. To become familiar with the continuing professional development obligations imposed by regulators.
4. To understand the difference between regulators, the National Alliance of Regulators, and the Canadian Association of Medical Radiation Technologists (CAMRT).
Author Disclosures:
A. Cromp: nothing to disclose

Meets 8b-4 16:23
The current and evolving state of medical radiation technology (MRT) education in Canada
C. Bru*; Ottawa, ON/CA (cbru@camrt.ca)*
Learning objectives:
1. To examine the different models of entry-level MRT education in Canada.
2. To identify trends impacting entry-level MRT education.
3. To discuss Canada's transition to a role-based competency framework.
4. To describe the advanced practice landscape in Canada.
Author Disclosures:
C. Bru: nothing to disclose

Meets 8b-5 16:41
Artificial intelligence (AI) and the medical radiation profession: how our advocacy must inform future practice
A. Murphy*; Vancouver/CA (aandrewfmurphy@gmail.com)*
Learning objectives:
1. To learn about the overall applications of AI in medical imaging.
2. To understand the methods in which these applications are being researched, tested, and sold to health care professionals, and the steps radiology groups are taking to educate their members.
3. To appreciate the value that both radiographers and radiographer societies around the world can provide by ensuring safe, accountable rollouts of AI tools.
4. To become familiar with AI as a clinical tool rather than an overcomplicated, inaccessible entity.
Author Disclosures:
A. Murphy: nothing to disclose

Meets 8b-6 16:59
Quality, safety and peer review: a Canadian experience
S. DeColle*; Edmonton, AB/CA (Steve.DeColle@albertahealthservices.ca)*
Learning objectives:
1. To learn about technologist peer learning.
2. To appreciate the value of peer learning to the patient experience.
3. To understand the implications peer learning has on quality and safety.
Author Disclosures:
S. Decolle: nothing to disclose

17:17
Panel discussion

16:00 - 17:30 **Descartes (Room D3)**

Professional Challenges Session

PC 8

Patient engagement, visible radiology and eHealth

PC 8-1/PC 8-2 16:00
Chairpersons' introduction
N. Bedlington*; Vienna/AT*
E. Kotter*; Freiburg/DE (elmar.kotter@uniklinik-freiburg.de)*
Session objectives:
1. To learn about the challenges of eHealth today and tomorrow.
2. To appreciate the communication and cooperation of patients using eHealth.
3. To understand the relevance of visible and communicating radiologists.
Author Disclosures:
N. Bedlington: disclosure/affirmation information not submitted, E. Kotter: nothing to disclose

PC 8-3 16:06
Clinical services, communication with patients: which kind of report/language is expected
J. M. L. Bosmans*; Ghent/BE (janbosmans@telenet.be)*
Learning objectives:
1. To learn about the pros and cons of radiologists' communication of imaging results to patients.
2. To appreciate the opportunities for direct communication with patients.
3. To understand the potential of structured reporting providing patient-tailored reports.
Author Disclosures:
J. M. L. Bosmans: nothing to disclose

PC 8-4 16:22
Patient engagement in research: donation of data, risk-sharing in oncology, incentives for screening
E. Briers*; Brussels/BE (erikbriers@telenet.be)*
Learning objectives:
1. To learn about the need for clinical data for research and artificial intelligence developments.
2. To appreciate that patients with serious, life-threatening diseases perform a benefit/risk assessment in making decisions.
3. To understand the value of imaging in screening, and ways to improve acceptance.
Author Disclosures:
E. Briers: nothing to disclose

PC 8-5 16:38
Patient access to reports and images: solutions and experiences
W. Gibbs*; Scottsdale/US (wendeNgibbs@gmail.com)*
Learning objectives:
1. To appreciate the risks of misinterpretation of radiology reports by clinicians.
2. To recognise the importance of clear radiology reporting for patients.
3. To understand the necessity of standardised language and structured reporting.
Author Disclosures:
W. Gibbs: nothing to disclose

PC 8-6 16:54
Education and training
L. Oleaga Zufiria*; Barcelona/ES (lauraoleaga@gmail.com)*
Learning objectives:
1. To learn about the need for education in non-imaging competences.
2. To appreciate inter-professional training in communication techniques.
3. To understand patients' expectations.
Author Disclosures:
L. Oleaga Zufiria: Consultant at TMC Academy

17:10
Panel discussion: Should radiology be more active in direct communication with patients?

16:00 - 17:30 **Room G**

Special Focus Session

SF 8c

Fibrotic lung diseases: what radiologists should know or learn

SF 8c-1 16:00
Chairperson's introduction
S. R. Desai*; London/UK*
Session objectives:
1. To review the common and distinctive imaging features of lung fibrosis.
2. To clarify the differences between idiopathic and secondary manifestations of lung fibrosis.
3. To learn about novel diagnostic and quantification imaging methods.
Author Disclosures:
S. R. Desai: disclosure/affirmation information not submitted

SF 8c-2 16:05
Fleischner updated criteria for the diagnosis of idiopathic pulmonary fibrosis (IPF)
N. Sverzellati; *Parma/IT (nicola.sverzellati@unipr.it)*
Learning objectives:
1. To become familiar with the patterns of definite or probable usual interstitial pneumonia (UIP).
2. To understand the implications of the new criteria for patient care.
3. To learn about the remaining indications of lung biopsy for confirmation of diagnosis.
Author Disclosures:
N. Sverzellati: nothing to disclose

SF 8c-3 16:30
Drug and radiation-induced lung fibrosis
C. M. M. Schaefer-Prokop; *Amersfoort/NL (cornelia.schaeferprokop@gmail.com)*
Learning objectives:
1. To learn about current medications potentially causing lung fibrosis.
2. To review the imaging patterns of drug-induced fibrosis.
3. To learn about the longitudinal evolution of post-radiation fibrosis.
Author Disclosures:
C. M. M. Schaefer-Prokop: nothing to disclose

SF 8c-4 16:55
Connective tissue disease-related lung fibrosis
G. Chassagnon; *Paris/FR*
Learning objectives:
1. To review the CT features of non-specific interstitial pneumonia (NSIP).
2. To learn about new detection and follow-up techniques based on elastic registration.
3. To learn about deep learning-based quantification of connective tissue disease-related lung fibrosis.
Author Disclosures:
G. Chassagnon: disclosure/affirmation information not submitted

17:20
Panel discussion: The pivotal role of radiologists for lung fibrosis management

16:00 - 17:30 **Room K**

Emergency Imaging

RC 817
Why do I miss fractures in emergency?

RC 817-1 16:00
Chairperson's introduction
S. Wirth; *Munich/DE (wirth.online@googlemail.com)*
Session objectives:
1. To learn the typical constellations and findings of missed fractures.
2. To understand the potential complications resulting from missing fractures.
3. To appreciate direct and indirect fracture signs with different imaging modalities.
Author Disclosures:
S. Wirth: nothing to disclose

RC 817-2 16:05
A. Missed fractures in children
K. Johnson; *Birmingham/UK (karl.johnson2@nhs.net)*
Learning objectives:
1. To become familiar with commonly missed fractures in children.
2. To understand the choice of the most suited imaging modality.
3. To learn about atypical imaging findings in different clinical scenarios.
Author Disclosures:
K. Johnson: nothing to disclose

RC 817-3 16:30
B. Missed fractures in adults
S. Döring; *Brussels/BE (seema.doering@gmx.net)*
Learning objectives:
1. To become familiar with the most commonly missed fractures in adult patients.
2. To understand which additional information will influence the choice of imaging modality.
3. To learn about atypical imaging findings in adult patients after trauma.
Author Disclosures:
S. Döring: nothing to disclose

RC 817-4 16:55
C. Missed musculoskeletal injuries in whole-body trauma
A. Platon; *Geneva/CH (Alexandra.Platon@hcuge.ch)*
Learning objectives:
1. To become familiar with the most commonly missed musculoskeletal injuries in patients after polytrauma.
2. To understand the clinical impact of missed subtle injuries on clinical outcome of trauma victims.
3. To be familiar with less typical imaging findings in musculoskeletal injuries.
Author Disclosures:
A. Platon: nothing to disclose

17:20
Panel discussion: How to reduce the rate of missed fractures most effectively and efficiently

16:00 - 17:30 **Room M 1**

Hybrid Imaging

RC 806
Advancing clinical hybrid imaging

RC 806-1 16:00
Chairperson's introduction
T. H. Helbich; *Vienna/AT (Thomas.Helbich@meduniwien.ac.at)*
Session objectives:
1. To understand the basic concepts of hybrid imaging.
2. To appreciate the clinical role of hybrid imaging.
3. To learn how hybrid imaging can be used more effectively in routine practice.
Author Disclosures:
T. H. Helbich: nothing to disclose

RC 806-2 16:06
A. Cost-effectiveness of hybrid imaging
B. M. Fischer; *London/UK (Malene.fischer@kcl.ac.uk)*
Learning objectives:
1. To discuss why clinicians often consider hybrid imaging as the expensive choice, and whether the notion of PET/CT as an expensive technology is fair.
2. To obtain knowledge of basic concepts of health economy.
3. To present and discuss examples of cost-effectiveness studies on the use of PET/CT in oncology.
4. To evaluate how hybrid imaging may be incorporated as a cost-effective tool into routine clinical practice.
Author Disclosures:
B. M. Fischer: Speaker at Takeda, Research/Grant Support at Siemens Heathineers

RC 806-3 16:29
B. PET/MRI in clinical routine
V. Goh; *London/UK (vicky.goh@kcl.ac.uk)*
Learning objectives:
1. To learn about the basic concepts underlying PET/MRI.
2. To understand the potential clinical advantages of combining PET and MRI.
3. To discuss how PET/MRI may find a role as a routine clinical test in the future.
Author Disclosures:
V. Goh: Research/Grant Support at Siemens, Speaker at Siemens

RC 806-4 16:52
C. How PET/MRI enables accurate fusion of radiation treatment?
U. van der Heide; *Amsterdam/NL (u.vd.heide@nki.nl)*

Learning objectives:
1. To learn about the role of MRI and PET/MRI in radiation oncology.
2. To understand how MRI and/or PET/MRI can be used to monitor radiotherapy response.
3. To appreciate the role of hybrid imaging in targeting and modulating radiation therapy.
Author Disclosures:
U. van der Heide: Grant Recipient at Philips Healthcare, Grant Recipient at Elekta AB

17:15
Panel discussion: Clinical hybrid imaging in the real world

16:00 - 17:30 **Room M 2**

E³ - Advanced Course: Hot Topics in Emergency Radiology

E³ 818

Occlusive vascular diseases: no time to lose!

E³ 818-1 16:00
Chairperson's introduction
R. Basilico; *Chieti/IT*
Session objectives:
1. To understand common pathways for acute infarction throughout the body.
2. To identify early signs of ischaemia.
3. To appreciate how early diagnosis can affect outcome favourably.
Author Disclosures:
R. Basilico: nothing to disclose

E³ 818-2 16:06
A. Acute stroke: CT and MRI findings
K. Katulska; *Poznań/PL (katarzyna_katulska@op.pl)*
Learning objectives:
1. To understand the role of CT and MRI in acute stroke.
2. To recognise the imaging findings on CT and MRI in acute stroke.
3. To become familiar with the findings that influence patient management.
Author Disclosures:
K. Katulska: nothing to disclose

E³ 818-3 16:27
B. Acute chest pain
H. Alkadhi; *Zurich/CH*
Learning objectives:
1. To learn about the imaging assessment of acute chest pain.
2. To become familiar with cardiac CT findings in the emergency setting.
3. To understand the importance to establish gated CT protocols covering more than the heart alone.
Author Disclosures:
H. Alkadhi: nothing to disclose

E³ 818-4 16:48
C. Acute mesenteric ischaemia
M. Zins; *Paris/FR (mzins@hpsj.fr)*
Learning objectives:
1. To learn about the imaging protocols for the detection of mesenteric ischaemia.
2. To become familiar with the detection of the crucial findings of mesenteric ischaemia.
3. To become familiar with the role of diagnostic and interventional radiologists in the assessment of mesenteric ischaemia.
Author Disclosures:
M. Zins: nothing to disclose

E³ 818-5 17:09
D. Interventional radiology in acute mesenteric ischaemia
A. Krajina; *Hradec Králové/CZ (antonin.krajina@fnhk.cz)*
Learning objectives:
1. To learn about the indications and contraindications for endovascular treatment.
2. To learn about the available techniques for urgent revascularisation.
3. To learn about the outcomes following endovascular revascularisation, including the complications.
Author Disclosures:
A. Krajina: nothing to disclose

16:00 - 17:30 **Room on demand**
Room C or Room M 3

Oncologic Imaging

RC 816

Role of imaging in cancer of unknown primary (CUP)

Moderator:
N. I. Traikova; Plovdiv/BG

RC 816-1 16:00
A. CT: the useful report
S. Gourtsoyianni; *Athens/GR (sgty76@gmail.com)*
Learning objectives:
1. To become familiar with the potential of CT and its limitations.
2. To discuss the value of morphological imaging for assessment of unknown primaries.
3. To learn about the pitfalls of CT.
Author Disclosures:
S. Gourtsoyianni: nothing to disclose

RC 816-2 16:22
B. MRI with diffusion weighted imaging (DWI) and dynamic contrast-enhancement (DCE)
A. R. R. Padhani; *London/UK (anwar.padhani@stricklandscanner.org.uk)*
Learning objectives:
1. To understand the benefit of MRI in contrast to other modalities.
2. To learn about functional MRI techniques.
3. To discuss the limitations of DWI and DCE for CUP diagnostics.
Author Disclosures:
A. R. R. Padhani: nothing to disclose

RC 816-3 16:45
C. Nuclear medicine: (PET/CT, PET/MRI, novel tracers)
T. Bäuerle; *Erlangen/DE (tobias.baeuerle@uk-erlangen.de)*
Learning objectives:
1. To learn about the benefits and limitations of hybrid imaging for assessment of CUP.
2. To understand novel concepts in tracer development.
3. To discuss the future role of nuclear medicine and radiology for CUP.
Author Disclosures:
T. Bäuerle: nothing to disclose

RC 816-4 17:07
D. Unknown primary: emerging challenges for imaging and the importance of integrated diagnostics
H. Hricak; *New York/US*
Learning objectives:
1. To gain familiarity with the tests and procedures used to evaluate CUP.
2. To understand the pitfalls and benefits of different imaging modalities.
3. To grasp essentials in integrating imaging, molecular genetics, tumour markers, and therapy.
Author Disclosures:
H. Hricak: Speaker at Memorial Sloan Kettering Cancer Center, Board Member at IBA

16:00 - 17:30 **Room M 4**

E³ - Advanced Course: Interactive Teaching Session for Young (and not so Young) Radiologists

E³ 821

Imaging of the brain

E³ 821-1 16:00
A. Stroke mimics
M. M. Thurnher; *Vienna/AT (majda.thurnher@meduniwien.ac.at)*
Learning objectives:
1. To become familiar with the different entities that can mimic a stroke.
2. To know the usefulness of perfusion studies in the differential diagnosis.
Author Disclosures:
M. M. Thurnher: Speaker at Biogen, Speaker at Guerbet, Speaker at Bracco

E³ 821-2 16:45
B. Acquired toxic-metabolic encephalopathies
M. Spero; *Zagreb/HR (martina.spero@gmail.com)*
Learning objectives:
1. To review the most common causes.
2. To learn the MRI and CT appearances of these lesions.
Author Disclosures:
M. Spero: nothing to disclose

16:00 - 17:30 **Room M 5**

E³ - Advanced Course: Artificial Intelligence

E³ 820

Making visible the invisible: pushing the boundaries in multimodality radiomic quantification

Moderator:
N. deSouza; Surrey/UK

E³ 820-1 16:00
Chairperson's introduction
L. Fournier; *Paris/FR*
Session objectives:
1. To introduce the subject of radiomic analyses across imaging modalities.
2. To highlight the potentials and limitations to be discussed by speakers.
3. To introduce the speakers.
Author Disclosures:
L. Fournier: Grant Recipient at Invectys, Speaker at General Electric, Speaker at Bayer, Speaker at Pfizer, Speaker at Novartis, Speaker at Janssen, Speaker at Sanofi, Research/Grant Support at Philips, Research/Grant Support at Ariana Pharma, Research/Grant Support at Evolucare

E³ 820-2 16:05
A. Unravelling the mysteries of the black box: does radiomics enhance or complement biomarker data?
A. Jimenez-Pastor; *Valencia/ES (anajimenez@quibim.com)*
Learning objectives:
1. To learn what radiomic analyses add to current biomarker evaluation.
2. To appreciate the limitations and pitfalls of such analyses.
3. To understand the most robust statistical methods for carrying out the analyses.
Author Disclosures:
A. Jimenez-Pastor: nothing to disclose

E³ 820-3 16:28
B. Working across modalities: how do we progress from redundant to relevant data?
H. C. Woodruff; *Maastricht/NL (h.woodruff@maastrichtuniversity.nl)*
Learning objectives:
1. To learn how radiomic outputs differ across modalities.
2. To appreciate the variability of the method and how to ensure data is robust.
3. To understand the relevance of the findings.
Author Disclosures:
H. C. Woodruff: Shareholder at OncoRadiomics

E³ 820-4 16:51
C. Using radiomics in the clinic: a decision support tool?
M. E. Mayerhöfer; *Vienna/AT (marius.mayerhoefer@meduniwien.ac.at)*
Learning objectives:
1. To learn the clinical scenarios where radiomic analyses may be helpful.
2. To appreciate the place of these analyses in the context of other quantifiable biomarkers.
3. To understand the implications of using these analyses in the clinic.
Author Disclosures:
M. E. Mayerhöfer: Speaker at Siemens, Research/Grant Support at Siemens, Speaker at Bristol-Myers Squibb

17:14
Panel discussion: How do we make sure radiomic analyses are ready for prime time use?

16:00 - 17:30 **Tech Gate Auditorium**

E³ - ECR Master Class (Vascular)

E³ 826

Cone-beam, 4D and more: new diagnostic tools for vascular diseases

Moderator:
T. Jakobs; Munich/DE

E³ 826-1 16:00
A. The role of intraprocedural perfusion assessment in peripheral arterial disease
J. A. Reekers; *Amsterdam/NL*
Learning objectives:
1. To understand the technique of intraprocedural perfusion assessment.
2. To learn how to target peripheral revascularisation therapy based on perfusion assessment.
3. To discuss the value of using intraprocedural perfusion assessment on the outcome of endovascular therapy for peripheral artery disease.
Author Disclosures:
J. A. Reekers: disclosure/affirmation information not submitted

E³ 826-2 16:30
B. CT 4D imaging after thoracic endovascular aortic repair (TEVAR)
R. Schernthaner; *Vienna/AT (ruediger.schernthaner@meduniwien.ac.at)*
Learning objectives:
1. To understand the challenges of imaging follow-up after TEVAR.
2. To become familiar with the technique of 4D CT.
3. To learn how to establish treatment recommendations based on 4D CT results after TEVAR.
Author Disclosures:
R. Schernthaner: Research/Grant Support at Siemens Healthineers

E³ 826-3 17:00
C. How cone-beam CT can change your practice in interventional radiology
R. Uberoi; *Oxford/UK (raman.uberoi@ouh.nhs.uk)*
Learning objectives:
1. To understand the technique of cone-beam CT.
2. To learn about the role and applications of the cone-beam in the angio suite.
3. To discuss the influence on daily clinical practice in interventional radiology.
Author Disclosures:
R. Uberoi: Grant Recipient at Gore, Grant Recipient at Terumo

Friday, March 13

08:30 - 10:00 **Room B**

E³ - Rising Stars Programme: Basic Session

BS 9a

Radiologic anatomy: head and neck

Moderator:
M. Becker; Geneva/CH

BS 9a-1 08:30
Neck spaces
N. I. Traikova; *Plovdiv/BG (nikoletatraikova@gmail.com)*
Learning objectives:
1. To learn the anatomy of the neck spaces.
2. To discuss current imaging techniques for their evaluation.
3. To describe the imaging appearance of most common pathological findings.
Author Disclosures:
N. I. Traikova: nothing to disclose

BS 9a-2 09:00
Temporal bone
J. W. Casselman; *Bruges/BE*
Learning objectives:
1. To know which technique is best suited to visualise specific anatomical structures of the temporal bone.
2. To recognise the clinically most important anatomical structures of the middle and inner ear.
3. To learn how the anatomical structures of the temporal bone appear in the transverse, coronal, and double oblique plane.
Author Disclosures:
J. W. Casselman: Speaker at Cefla S.A. (Newtom), Speaker at Philips Healthcare

BS 9a-3 09:30
Larynx
R. Maroldi; *Brescia/IT (roberto.maroldi@unibs.it)*
Learning objectives:
1. To understand the anatomy and signals of the cartilage framework of the larynx.
2. To learn the surgical subdivision of the paraglottic space of the larynx into its key compartments.
3. To learn the anatomy and signals of the muscles within the larynx.
Author Disclosures:
R. Maroldi: nothing to disclose

08:30 - 10:00 **Room X**

Special Focus Session

SF 9a

Hybrid imaging: beyond FDG PET/CT

SF 9a-1 08:30
Chairperson's introduction
T. Beyer; *Vienna/AT*
Session objectives:
1. To provide an overview of non-FDG PET/CT imaging.
2. To learn about the range of PET tracers that are in widespread use.
3. To consider the potential clinical advantages of these tracers.
Author Disclosures:
T. Beyer: Founder at cmi-experts GmbH, Founder at Dedicaid GmbH, Research/Grant Support at Siemens Healthineers

SF 9a-2 08:36
Prostate specific membrane antigen (PSMA) hybrid imaging in guiding prostate cancer therapy
C. C. Cyran; *Munich/DE (clemens.cyran@med.uni-muenchen.de)*
Learning objectives:
1. To understand the biology of PSMA.
2. To consider different approaches to imaging PSMA and its use in therapy.
3. To learn about current clinical applications for guiding prostate therapy.
Author Disclosures:
C. C. Cyran: Speaker at Goetz Partners Ltd, Consultant at Sandoz

SF 9a-3 08:54
Somatostatin receptor imaging and therapy
L. Aloj; *Cambridge/UK*
Learning objectives:
1. To understand the biology underlying somatostatin-based agents.
2. To consider different approaches to imaging and therapy through the use of the somatostatin receptor.
3. To learn about the current clinical applications guiding neuroendocrine tumour therapy.
Author Disclosures:
L. Aloj: nothing to disclose

SF 9a-4 09:12
Hybrid PET and SPECT for cardiovascular imaging
A. Flotats; *Barcelona/ES*
Learning objectives:
1. To learn the clinical need for hybrid imaging in cardiovascular diseases.
2. To consider the role for both PET and SPECT imaging.
3. To learn the range of cardiovascular tracers that are used clinically and their role.
Author Disclosures:
A. Flotats: nothing to disclose

SF 9a-5 09:30
Imaging to guide immuno-oncology
U. Mahmood; *Oak Brook/US (umahmood@mgh.harvard.edu)*
Learning objectives:
1. To understand the challenges of imaging response to immunomodulatory therapy.
2. To understand current standard of care imaging for immuno-oncology.
3. To understand some of the novel PET imaging approaches in clinical trials and development.
Author Disclosures:
U. Mahmood: Founder at CytoSite Biopharma, Shareholder at CytoSite Bippharma, Research/Grant Support at CytoSite Bippharma

09:48
Panel discussion: New trends in hybrid imaging

09:00 - 10:00 **Coffee & Talk 1**

Coffee & Talk (open forum) Session

Organised by ESOR

C 5

What would the next generation of radiologists look like?

Moderator:
C. Catalano; Rome/IT

C 5-1 09:00
A clinical radiologist
R. Mansour; *Oxford/UK*
Learning objective:
1. To learn about the challenges and opportunities for the next generation clinical radiologists.
Author Disclosures:
R. Mansour: nothing to disclose

C 5-2 09:08
An interventional radiologist
A. Napoli; *Rome/IT (alessandro.napoli@uniroma1.it)*

Learning objectives:
1. To learn new trends in interventional radiology.
2. To understand the evolving role of interventional radiology.
3. To appreciate new technology advances within the interventional radiology domain.
4. To become familiar with future assets of interventional radiology culture for residents and professionals.
Author Disclosures:
A. Napoli: nothing to disclose

C 5-3 09:16
An "artificial intelligent" radiologist
L. Marti-Bonmati; *Valencia/ES (Luis.Marti@uv.es)*
Learning objectives:
1. To learn about the use of artificial intelligence and deep learning (AI/DL) tools during each step of the radiology value chain.
2. To understand how AI/DL solutions can improve radiological reporting.
3. To appreciate the AI/DL approaches towards automatic segmentation and properties extraction in medical imaging.
4. To become familiar with the main limitations of AI/DL tools in the radiological environment.
Author Disclosures:
L. Marti-Bonmati: Advisory Board at QUIBIM SME

C 5-4 09:24
A researcher
O. Clement; *Paris/FR (olivier.clement@aphp.fr)*
Learning objectives:
1. To learn about the opportunities to do research in radiology.
2. To understand the funding programmes and the role of EIBIR.
3. To become familiar with the different aspect of an academic career.
Author Disclosures:
O. Clement: Speaker at Bracco, Speaker at Bayer, Speaker at Guerbet

09:32
Open forum discussion

08:30 - 10:00 **Room O**

Paediatric

RC 912
Foetal imaging and postnatal correlation

RC 912-1 08:30
Chairperson's introduction
D. Prayer; *Vienna/AT (daniela.prayer@meduniwien.ac.at)*
Author Disclosures:
D. Prayer: nothing to disclose

RC 912-2 08:35
A. Foetal MRI advanced techniques
G. Kasprian; *Vienna/AT (gregor.kasprian@meduniwien.ac.at)*
Learning objectives:
1. To learn about the principles of advanced techniques in foetal MRI.
2. To understand the potential for their use.
3. To discuss the limitations and disadvantages of these techniques.
Author Disclosures:
G. Kasprian: nothing to disclose

RC 912-3 08:53
B. Corpus callosum anomalies: pre- and postnatal correlation
E. Vazquez Mendez; *Barcelona/ES (evazquez@vhebron.net)*
Learning objectives:
1. To evaluate the diagnostic accuracy of foetal MRI for diagnosis.
2. To compare pre- and postnatal MRI data.
3. To ascertain the outcome in cases of isolated complete or partial agenesis.
Author Disclosures:
E. Vazquez Mendez: nothing to disclose

RC 912-4 09:11
C. Foetal MRI of acquired brain pathology
L. Guibaud; *Bron/FR*
Learning objectives:
1. To learn about the various types of acquired brain pathology in the foetus.
2. To understand the limitations in the comprehension of the underlying cause.
3. To discuss the best estimates of the prevalence of acquired brain pathology.
Author Disclosures:
L. Guibaud: disclosure/affirmation information not submitted

RC 912-5 09:29
D. Pre- and postnatal congenital cystic renal diseases
F. E. Avni; *Lille/FR (favni@skynet.be)*
Learning objectives:
1. To learn about differential diagnosis of hyperechoic kidneys in foetuses and children.
2. To become familiar with the latest classification of inherited renal cystic diseases.
3. To discuss the limitations of the imaging methods for diagnosis.
Author Disclosures:
F. E. Avni: nothing to disclose

09:47
Panel discussion: How to overcome the challenges in foetal MRI in routine practice and research

08:30 - 10:00 **Studio 2020**

Special Focus Session

SF 9b
Imaging of migrant and refugee children

SF 9b-1 08:30
Chairperson's introduction
M. Soudack; *Ramat Gan/IL (michalle.soudack@health.sheba.gov.il)*
Session objectives:
1. To learn about challenges in providing healthcare to migrant and refugee children in Europe.
2. To be aware of emerging diseases in migrant and refugee children.
3. To discuss the scientific and medicolegal dilemmas when using radiological methods for age determination in unaccompanied refugee minors.
Author Disclosures:
M. Soudack: nothing to disclose

SF 9b-2 08:35
Challenge of promoting health of refugee and migrant children in Europe
A. Hjern; *Stockholm/SE (anders.hjern@su.se)*
Learning objectives:
1. The epidemiology of infectious and chronic diseases in this population compared to domestic children: the clinician's perspective.
2. To learn about the challenges of promoting health of refugee and migrant children in Europe.
3. To discuss how to improve the management of migrant and refugee children and carers, with a special focus on imaging and intervention.
Author Disclosures:
A. Hjern: nothing to disclose

SF 9b-3 08:59
Imaging of emerging diseases in refugee and migrant children
B. Oğuz; *Ankara/TR (oguzberna@yahoo.com)*
Learning objectives:
1. The epidemiology of infectious and chronic diseases in this population compared to domestic children: the radiologist's perspective.
2. To learn about the spectrum of findings on imaging in migrant and refugee children.
3. To discuss new diagnostic and practical challenges for radiologists.
Author Disclosures:
B. Oğuz: nothing to disclose

SF 9b-4 09:23
Age determination for legal purpose
L.-S. O. Müller; *Oslo/NO (lilmul@ous-hf.no)*

Learning objectives:
1. To learn about the principles and limitations of radiological age determination.
2. To define the role of the paediatric radiologist in age determination for legal purposes.
3. To discuss ethical considerations in medical age determination.
Author Disclosures:
L.-S. O. Müller: nothing to disclose

09:47
Panel discussion: The role of the radiologist in the management of refugee and migrant children

08:30 - 09:30 **Coffee & Talk 2**

Coffee & Talk (open forum) Session
Organised by EuroSafe Imaging

C 15
ESR and EuroSafe Imaging initiatives: improving justification

C 15-1 08:30
Chairperson's introduction
G. Frija*; Paris/FR (guy.frija@aphp.fr)*
Session objectives:
1. To describe the importance of justification as a principle of radiation protection and medicine.
2. To describe four key implications for the justification process resulting from European legislation.
3. To provide a brief historical perspective of deficiencies in justification.
Author Disclosures:
G. Frija: nothing to disclose

C 15-2 08:35
Audit and Standards Subcommittee's published surveys
D. Howlett*; Eastbourne/UK (david.howlett@nhs.net)*
Learning objectives:
1. To consider the requirements of the European basic safety standards directive (EU-BSS) with an emphasis on clinical audit.
2. To present the results of EU-BSS uptake surveys amongst European radiology departments.
3. To discuss the implications of survey findings and mechanisms to enhance departmental clinical audit processes.
Author Disclosures:
D. Howlett: nothing to disclose

C 15-3 08:45
Overview of justification processes following previous HERCA initiatives and potential new ones
A. Karoussou-Schreiner*; Louxembourg/LU*
Learning objectives:
1. To outline the actions conducted by regulatory authorities in Europe within HERCA on justification.
2. To discuss the findings following the inspection action conducted on justification in radiology in 2016.
3. To present the campaign "Getting the right image for my patient" that promotes the appropriate use of medical imaging.
Author Disclosures:
A. Karoussou-Schreiner: disclosure/affirmation information not submitted

C 15-4 08:55
Giving a practical, on the ground view of how justification is handled on a day-to-day basis
A. Palkó*; Szeged/HU (palkoand@gmail.com)*
Learning objectives:
1. To demonstrate how dose monitoring is built into the daily workflow of a tertiary diagnostic radiology centre.
2. To understand the effect of required justification, in cases of dose exceeding DRL, on the attitude and practice of physicians and technicians.
Author Disclosures:
A. Palkó: nothing to disclose

C 15-5 09:05
Activities undertaken during 2019/20 to assess and improve matters
G. Frija*; Paris/FR (guy.frija@aphp.fr)*
Learning objectives:
1. To discuss the roles of professionals in the justification process.
2. To outline the key aspects of a draft EuroSafe discussion paper on improving justification.
3. To describe initial feedback on the paper from EuroSafe Imaging Star centres.
Author Disclosures:
G. Frija: nothing to disclose

09:15
Open forum discussion

08:30 - 10:00 **Room E**

Special Focus Session

SF 9c
My top three tips for breast imaging

SF 9c-1 08:30
Chairperson's introduction
M. Fuchsjäger*; Graz/AT (michael.fuchsjaeger@medunigraz.at)*
Session objectives:
1. To appreciate the fundamental tips and tricks of the most renowned European breast radiologists for clinical practice.
2. To acknowledge the single most important aspects for successfully performing breast examinations.
3. To learn how to avoid common pitfalls in breast radiology.
Author Disclosures:
M. Fuchsjäger: nothing to disclose

SF 9c-2 08:35
Screening with tomosynthesis
S. Zackrisson*; Malmö/SE (sophia.zackrisson@med.lu.se)*
Learning objectives:
1. To understand why tomosynthesis is better than mammography for breast cancer screening.
2. To appreciate the current scientific evidence of tomosynthesis in screening.
3. To acknowledge what further steps are needed before implementation in screening.
Author Disclosures:
S. Zackrisson: Speaker at Siemens Healthcare AG, Consultant at Collective Minds Radiology, Founder at Z Imagination AB

SF 9c-3 08:41
Automated breast ultrasound
A. Vourtsis*; Athens/GR (athinavourtsi@yahoo.gr)*
Learning objectives:
1. To recognise artefacts specific to automated breast ultrasound (ABUS).
2. To appreciate the value of multiplanar reconstruction and the coronal spiculation pattern.
3. To gain insight into possible indications for ABUS.
Author Disclosures:
A. Vourtsis: Consultant at General Electric Company Educator, ABUS, Advisory Board at Noncorporate Member of Medical Advisory Board of Volpara Solutions

SF 9c-4 08:47
Complex cystic and solid lesions
P. Kapetas*; Vienna/AT (panagiotis.kapetas@meduniwien.ac.at)*
Learning objectives:
1. To understand the difference between complex cystic and solid lesions from other cystic lesions of the breast.
2. To become familiar with complementary sonographic techniques for the accurate characterisation of cystic breast lesions.
3. To be able to properly manage complex cystic and solid lesions of the breast.
Author Disclosures:
P. Kapetas: nothing to disclose

Questions and discussion

SF 9c-6 08:59
Imaging the axilla
A. O. Oktay Alfatli*; Izmir/TR (aysenur.oktay@ege.edu.tr)*
Learning objectives:
1. To understand the clinical role of axillary staging.
2. To learn the imaging features of abnormal lymph nodes and the criteria for biopsy.
3. To understand the importance of discriminating minimal vs advanced nodal disease.
Author Disclosures:
A. O. Oktay Alfatli: nothing to disclose

SF 9c-7 09:05
Contrast-enhanced spectral mammography
C. S. Balleyguier*; Villejuif/FR*
Learning objectives:
1. To understand the technical principles of contrast-enhanced spectral mammography.
2. To understand the added value of information provided by contrast-enhanced spectral mammography.
3. To become familiar with the information provided by contrast-enhanced spectral mammography and breast MRI regarding lesion morphology and enhancement.
Author Disclosures:
C. S. Balleyguier: disclosure/affirmation information not submitted

SF 9c-8 09:11
Stereotactic-guided biopsy
D. Djilas*; Sremska Kamenica/RS*
Learning objectives:
1. To understand the indications for stereotactic-guided breast biopsy.
2. To learn about the technical aspects of stereotactic biopsy.
3. To understand the importance of marker clip placement post-biopsy.
Author Disclosures:
D. Djilas: disclosure/affirmation information not submitted

Questions and discussion

SF 9c-10 09:23
US-guided biopsy
G. Ivanac*; Zagreb/HR (gordana.augustan@gmail.com)*
Learning objectives:
1. To understand current indications, contraindications, and possible complications of US-guided biopsy.
2. To be familiar with different available biopsy systems and to know which one to choose according to the clinical setting.
3. To learn the most important technical tips for performing a US-guided biopsy successfully.
Author Disclosures:
G. Ivanac: nothing to disclose

SF 9c-11 09:29
MRI-guided biopsy
R. M. Mann*; Nijmegen/NL (r.mann@rad.umcn.nl)*
Learning objectives:
1. To understand the importance of pre-biopsy preparation including patient information.
2. To be familiar with how to relate lesion and needle positions.
3. To appreciate tricks for targeting lesions in complicated locations (superficial, deep, retroareolar).
Author Disclosures:
R. M. Mann: Grant Recipient at Siemens Healthineers, Bayer Healthcare, Screenpoint medical, Seno medical, Medtronic, Bard/BD, Advisory Board at Transonic Imaging

SF 9c-12 09:35
Treatment response and therapy monitoring
E. M. Fallenberg*; Munich/DE*
Learning objectives:
1. To learn what is important in the reporting of the treatment response.
2. To understand the accuracy of mammography, ultrasound, and magnetic resonance in the monitoring of therapy.
Author Disclosures:
E. M. Fallenberg: Advisory Board at Transsonic, Speaker at Guerbet, Speaker at Bayer, Speaker at GE, Board Member at EUSOBI, Board Member at DRG AG Mamma

SF 9c-13 09:41
Post-therapy evaluation
J. Camps Herrero*; Valencia/ES (juliacamps@gmail.com)*
Learning objectives:
1. To understand and learn the different phases of fat necrosis and its imaging correlates in all modalities.
2. To know what to report in patients with breast implants and oncoplastic reconstructions.
3. To learn the different appearances of breast cancer recurrence.
Author Disclosures:
J. Camps Herrero: nothing to disclose

09:47
Questions and discussion

08:30 - 10:00 **Room F1**

ESR meets Croatia, Slovakia and Slovenia

Meets 9

Interventional neuroradiology, cardiac MRI and EVAR: our experience

Presiding:
B. Brkljačić; Zagreb/HR
D. Miletic; Rijeka/HR
V. Lehotska*;* Bratislava/SK
M. Marolt Music; Ljubljana/SI

Meets 9-1 08:30
Welcome from the ESR President
B. Brkljačić*; Zagreb/HR (boris@brkljacic.com)*
Author Disclosures:
B. Brkljačić: nothing to disclose

Meets 9-2/Meets 9-3/Meets 9-4 08:32
Introduction
D. Miletic*; Rijeka/HR (damir.miletic@medri.hr)*
V. Lehotska*; Bratislava/SK (viera.lehotska@ousa.sk)*
M. Marolt Music*; Ljubljana/SI (mmusic@onko-i.si)*
Session objectives:
1. To learn about the interventional neuroradiology (INR) techniques and indications for aneurysm and stroke treatment, and to acknowledge the impact of mechanical thrombectomy.
2. To demonstrate various applications of cardiac MRI including alternative methods in cardiac imaging.
3. To learn about indications, technical aspects and clinical outcomes of endovascular aortic repair.
Author Disclosures:
D. Miletic: nothing to disclose, V. Lehotska: nothing to disclose,
M. Marolt Music: nothing to disclose

Meets 9-5 08:37
Interventional neuroradiology: from coil to clot
D. Ozretic*; Zagreb/HR (david.ozretic@ck.t-com.hr)*
Learning objectives:
1. To present developments of INR in Croatia and its current place in clinical practice.
2. To learn about the INR techniques and indications for aneurysm and stroke treatment.
3. To acknowledge the impact of mechanical thrombectomy on the patients, and on the referring and performing physicians.
Author Disclosures:
D. Ozretic: nothing to disclose

08:57
Interlude: Promotional video about Croatia

Meets 9-7 09:02
Cardiac MRI and beyond
Z. Berecova*; Bratislava/SK (hapka78@hotmail.com)*
Learning objectives:
1. To illustrate organisation and implementation of cardiac imaging, particularly cardiac MRI, in Slovakia.
2. To demonstrate various applications of cardiac MRI.
3. To learn more about the value of alternative methods in cardiac imaging.
Author Disclosures:
Z. Berecova: nothing to disclose

09:22
Interlude: Promotional video about Slovakia

Meets 9-9 09:27
EVAR: two decades of experience in Slovenia
V. Salapura*; Ljubljana/SI (salapura@siol.net)*
Learning objectives:
1. To present developments of endovascular aortic interventions (EVAR) in Slovenia.
2. To learn about indications, technical aspects and clinical outcomes of endovascular aortic repair.
3. To emphasise the importance of continuous progress of minimally invasive endovascular aortic interventions.
Author Disclosures:
V. Salapura: nothing to disclose

09:47
Interlude: Promotional video about Slovenia

09:52
Panel discussion: What is the impact of cardiac MRI, neurovascular and aortic interventions on turf battles in Croatia, Slovakia and Slovenia?

08:30 - 10:00 **Room F2**

Neuro

RC 911
Neuromuscular imaging

RC 911-1 08:30
Chairperson's introduction
L. Ten Dam*; Amsterdam/NL (l.tendam@amc.uva.nl)*
Session objectives:
1. To provide an imaging strategy for neuromuscular diseases.
2. To become familiar with congenital and acquired neuromuscular diseases.
3. To demonstrate the role of imaging in muscular atrophy.
Author Disclosures:
L. Ten Dam: nothing to disclose

RC 911-2 08:35
A. How to image patients with neuromuscular disease
M.-A. Weber*; Rostock/DE (marc-andre.weber@med.uni-rostock.de)*
Learning objectives:
1. To be aware of the recent developments in muscle imaging.
2. To understand the role of imaging in muscle atrophy.
3. To become familiar with the expectations from the neurologist.
Author Disclosures:
M.-A. Weber: nothing to disclose

RC 911-3 08:58
B. How to report congenital myopathies
A. Pichiecchio*; Pavia/IT (anna.pichiecchio@mondino.it)*
Learning objectives:
1. To appreciate muscle MRI findings in neuromuscular disorders.
2. To learn about structured reporting in neuromuscular diseases.
3. To understand the role of various imaging modalities in the workup of congenital myopathies.
Author Disclosures:
A. Pichiecchio: Advisory Board at G-enzyme, Consultant at Prex srl

RC 911-4 09:21
C. How to recognise adult neuromuscular disease?
S. Shah*; London/UK*
Learning objectives:
1. To apply the optimal imaging protocol.
2. To appreciate the role of quantitative imaging in genetic and acquired myopathies.
3. To illustrate the role of brain imaging in neuromuscular disorders.
Author Disclosures:
S. Shah: disclosure/affirmation information not submitted

09:44
Panel discussion: Recent developments in muscle imaging

09:00 - 10:00 **Coffee & Talk 3**

Coffee & Talk (open forum) Session

C 26
Embolisation techniques: tips and tricks

C 26-1 09:00
Chairperson's introduction
T. J. Kroencke*; Augsburg/DE*
Session objectives:
1. To become familiar with the varied indications for embolisation.
2. To understand the basic embolisations techniques.
3. To be familiar with the different types of embolic agents.
Author Disclosures:
T. J. Kroencke: nothing to disclose

C 26-2 09:04
Embolisation in trauma
S. Anthony*; Oxford/UK*
Learning objectives:
1. To understand the indications for embolisation in trauma.
2. To understand the selection of embolisation materials for small and large vessels.
3. To appreciate the outcomes of embolisation in trauma.
Author Disclosures:
S. Anthony: disclosure/affirmation information not submitted

C 26-3 09:10
Embolisation for endoleaks post endovascular aneurysm repair (EVAR)
F. Fanelli*; Florence/IT (fabrizio.fanelli@unifi.it)*
Learning objectives:
1. To appreciate the types of endoleaks post EVAR.
2. To become familiar with the techniques for embolisation for endoleaks.
3. To appreciate the outcomes following embolisation.
Author Disclosures:
F. Fanelli: Advisory Board at Philips, Advisory Board at Medtronic, Consultant at Philips, Consultant at Medtronic, Speaker at Cook, Speaker at Medtronic, Speaker at Philips, Speaker at Volcano Philips, Speaker at WL Gore & Associates, Research/Grant Support at Surmodics, Advisory Board at Bayer, Speaker at Penumbra

C 26-4 09:16
Gonadal vein embolisation
A. Basile*; Catania/IT (antodoc@yahoo.com)*
Learning objectives:
1. To understand the indications for gonadal vein embolisation.
2. To appreciate the techniques for embolisation.
3. To become familiar with the outcomes of gonadal vein embolisation.
Author Disclosures:
A. Basile: disclosure/affirmation information not submitted

C 26-5 09:22
Oncology embolisation of liver tumours
P. Reimer*; Karlsruhe/DE*
Learning objectives:
1. To appreciate the indications for embolisation in liver tumours.
2. To understand the principles and techniques of embolisation in liver tumours.
3. To become familiar with the outcomes of embolisation for common lesions in liver tumours.
Author Disclosures:
P. Reimer: nothing to disclose

09:28
Open forum discussion

08:30 - 10:00 **da Vinci (Room D1)**

Physics in Medical Imaging

RC 913

Radiation dose monitoring systems (RDMS): from commissioning to effective use

RC 913-1 08:30
Chairperson's introduction: RDMS: big data and tons of information
V. Tsapaki*; Nea Ionia/GR (virginia@otenet.gr)*
Session objectives:
1. To learn about the basic elements to consider when purchasing and commissioning an RDMS.
2. To be able to increase the effectiveness of using your RDMS.
3. To understand how to manage the situation of patients with recurrent exams.
Author Disclosures:
V. Tsapaki: nothing to disclose

RC 913-2 08:35
A. Supply and commissioning of an RDMS to meet all your needs
N. Fitousi*; Leuven/BE (niki.fitousi@qaelum.com)*
Learning objectives:
1. To understand how to select the right system for each hospital.
2. To learn how data should be validated after being collected.
3. To understand how derived quantities are calculated.
Author Disclosures:
N. Fitousi: Employee at Qaelum NV

RC 913-3 08:58
B. How to manage the data and extract the relevant information
O. Rampado*; Turin/IT (orampado@cittadellasalute.to.it)*
Learning objectives:
1. To learn about methods of data extraction.
2. To be able to query the database with different filters.
3. To understand how to use this data to guide optimisation actions.
Author Disclosures:
O. Rampado: nothing to disclose

RC 913-4 09:21
C. Monitoring and analysis of patients with high cumulative risks
J. Vassileva*; Vienna/AT*
Learning objectives:
1. To learn the strategies to define attention levels and possible intervention thresholds.
2. To understand how to correlate cumulative dose indices with cumulative risks.
3. To evaluate which procedures and clinical pathways involve high cumulative risks.
Author Disclosures:
J. Vassileva: nothing to disclose

09:44
Panel discussion: Are RDMS useful to share data between the main players in the optimisation process?

08:30 - 10:00 **Darwin (Room D2)**

Special Focus Session

SF 9d

Cardiac imaging to drive clinical decision making

SF 9d-1 08:30
Chairperson's introduction
L. Natale*; Rome/IT (luigi.natale@unicatt.it)*
Session objectives:
1. To become familiar with the inevitable role of advanced cardiac imaging for clinical decision making in ischaemic and structural heart disease.
2. To learn about the importance of outcome prediction for appropriate treatment decision making.
3. To understand the essential role of cardiac radiology in the management of cardiac patients.
Author Disclosures:
L. Natale: nothing to disclose

SF 9d-2 08:35
Cardiac imaging as decision maker in coronary artery disease
M. Hrabak Paar*; Zagreb/HR (majahrabak@gmail.com)*
Learning objectives:
1. To understand the importance of myocardial assessment for treatment decision making in coronary artery disease.
2. To become familiar with imaging techniques to assess ischaemic myocardial disease.
3. To learn about imaging derived biomarkers to predict the outcome of coronary revascularisation and to assess prognosis of patients with coronary artery disease.
Author Disclosures:
M. Hrabak Paar: nothing to disclose

SF 9d-3 08:59
Cardiac imaging as inevitable prerequisite to indicate minimal-invasive valvular repair
G. Feuchtner*; Innsbruck/AT (Gudrun.Feuchtner@i-med.ac.at)*
Learning objectives:
1. To become familiar with minimal-invasive treatment options for valvular heart disease.
2. To learn about the information required to indicate and plan minimal-invasive valvular repair.
3. To understand the importance of cardiac imaging to identify the best time and the best technique for valvular repair.
Author Disclosures:
G. Feuchtner: nothing to disclose

SF 9d-4 09:23
Cardiac MRI to explore the grey zones of the athletes' hearts
A. Kallifatidis*; Thessaloniki/GR (alexandros.kallifatidis@yahoo.gr)*
Learning objectives:
1. To understand the important difference between well-trained and hypertrophic myocardium.
2. To learn about the imaging techniques to differentiate between athlete's heart and hypertrophic cardiomyopathy.
3. To become familiar with imaging derived biomarkers to predict prognosis and to indicate treatment of patients with myocardial hypertrophy
Author Disclosures:
A. Kallifatidis: nothing to disclose

09:47
Panel discussion: Not without radiology! Could there be any treatment of ischemic or structural heart disease without advanced cardiac imaging anymore? And what does this mean for radiology service?

08:30 - 10:00 **Descartes (Room D3)**

Professional Challenges Session

PC 9

Postgraduate and speciality training for radiographers

PC 9-1/PC 9-2 08:30
Chairpersons' introduction
D. Akata; *Ankara/TR (akataden@gmail.com)*
B. Kraus; *Vienna/AT*
Session objectives:
1. To consider the importance of further education and training beyond Bachelor level (EQF Level 6).
2. To discuss the importance of tailoring education and training for specialist areas.
Author Disclosures:
D. Akata: nothing to disclose, B. Kraus: nothing to disclose

PC 9-3 08:35
Postgraduate radiographer training across Europe
L. A. Rainford; *Dublin/IE (louise.rainford@ucd.ie)*
Learning objectives:
1. To discuss the current landscape of postgraduate training opportunities for radiographers across Europe.
2. To review the range of approaches to the purpose, design, and delivery of programmes.
3. To explore future opportunities to progress postgraduate radiography education.
Author Disclosures:
L. A. Rainford: nothing to disclose

PC 9-4 08:53
Ultrasound training requirements
R. A. M. Santos; *Coimbra/PT (rutemartinssantos@gmail.com)*
Learning objectives:
1. To describe the range of approaches to postgraduate ultrasound education for radiographers.
2. To explore the key considerations for postgraduate ultrasound education.
3. To discuss the potential impact of high-quality ultrasound training programmes on service delivery.
Author Disclosures:
R. A. M. Santos: nothing to disclose

PC 9-5 09:11
In-house cardiovascular interventional training
H. Faltot; *Colmar/FR (herve.faltot@cardio-paramed.com)*
Learning objectives:
1. To discuss the specific requirements and considerations for radiographers training in vascular interventional radiology and interventional cardiology.
2. To review the structure and impact of an in-house training programme.
3. To consider future opportunities to link with a formal postgraduate training programme.
Author Disclosures:
H. Faltot: nothing to disclose

PC 9-6 09:29
Paediatric radiography training in specialised and non-specialised centres
J. L. Portelli; *Msida/MT (jonathan.portelli@um.edu.mt)*
Learning objectives:
1. To review potential deficits in the education and training of radiographers in paediatrics.
2. To discuss the need for paediatric radiography to be considered as a specialty in radiography.
3. To consider potential solutions to improve the knowledge, skills, and competence of radiographers in paediatric imaging.
Author Disclosures:
J. L. Portelli: nothing to disclose

09:47
Panel discussion: Overcoming the challenges in postgraduate radiography education

08:30 - 10:00 **Room G**

Abdominal Viscera

RC 901

CT protocol selection for imaging of abdominal viscera

Moderator:
D. J. M. Tolan; Leeds/UK

RC 901-1 08:30
A. CT protocol of the liver
F. Caseiro Alves; *Coimbra/PT (caseiroalves@gmail.com)*
Learning objectives:
1. To learn about the indication of different CT protocols of the liver.
2. To understand the value of correct contrast media timing.
3. To recognise how to avoid the most common mistakes in a clinical setting.
Author Disclosures:
F. Caseiro Alves: nothing to disclose

RC 901-2 09:00
B. CT protocol of the pancreas
W. Schima; *Vienna/AT (wolfgang.schima@khgh.at)*
Learning objectives:
1. To be able to understand differences between standard and dedicated pancreas CT protocols.
2. To discuss the value of intravenous and oral contrast media for pancreas imaging.
3. To be aware of potential pitfalls in diagnosing pancreatic tumours or inflammatory lesions.
Author Disclosures:
W. Schima: nothing to disclose

RC 901-3 09:30
C. CT protocol in trauma patients
A. G. Schreyer; *Brandenburg a.d.H./DE (andreas.schreyer@mac.com)*
Learning objectives:
1. To understand the particularities of CT protocols in trauma patients.
2. To be aware of the most common differential diagnoses in a trauma setting.
3. To learn to avoid mistakes and to deal with pitfalls in trauma patients.
Author Disclosures:
A. G. Schreyer: nothing to disclose

08:30 - 10:00 **Room K**

Joint Session of the ESR and EFOMP

ESR/EFOMP

Photon counting detectors: system design and clinical applications of an emerging technology

Moderators:
V. Gershan; Skopje/MK
T. Sella; Jerusalem/IL

ESR/EFOMP-1 08:30
Photon counting CT: detector, prototypes and scan modes
M. Kachelrieß; *Heidelberg/DE (marc.kachelriess@dkfz.de)*
Learning objectives:
1. To learn which kind of detectors are currently available for performing photon counting.
2. To become familiar with the existing prototypes of photon counting CT and with their scan modes.
3. To understand the advantages of photon counting CT.

Author Disclosures:
M. Kachelrieß: nothing to disclose

ESR/EFOMP-2 08:50
Pre-clinical and clinical applications of spectral photon-counting CT (SPCCT)
P. C. Douek*; Lyons/FR (philippe.douek@chu-lyon.fr)*
Learning objectives:
1. To learn the potentials of pre-clinical and clinical application of SPCC.
2. To appreciate the potential value of SPCCT in terms of spatial resolution, low-dose, and ultra-low-dose imaging.
3. To understand the potential of K-edge icontrast agent imaging.
Author Disclosures:
P. C. Douek: Grant Recipient at H2020

ESR/EFOMP-3 09:10
Physics evaluation and initial clinical results with the first full-field photon counting CT system based on silicon
M. Danielsson*; Stockholm/SE (md@mi.physics.kth.se)*
Learning objectives:
1. To learn about the recent advancements of photon-counting technology using silicon sensors.
2. To understand the differences between conventional sensors and alternative materials.
3. To appreciate the possibility offered by photon counting technology to perform quantitative material decomposition.
Author Disclosures:
M. Danielsson: Shareholder at Prismatic Sensors AB

ESR/EFOMP-4 09:30
Digital mammography screening with photon counting technique: high diagnostic performance at low mean glandular dose
M. F. J. Ryan*; Cork/IE (maxf.ryan@gmail.com)*
Learning objectives:
1. To learn of the recent advancements of photon counting technology in digital mammography screening.
2. To appreciate the possibility offered by photon counting technology to perform digital mammography screening.
3. To understand the differences of conventional tomosynthesis using energy-integrating flat-panel detectors
Author Disclosures:
M. F. J. Ryan: nothing to disclose

09:50
Panel discussion: Which clinical applications are foreseeable for the photon counting technology?

08:30 - 10:00 **Room M 1**

E³ - Rising Stars Programme: Basic Session

BS 9b
Bone health and osteoporosis imaging

Moderator:
J.-P. Dillenseger; Strasbourg/FR

BS 9b-1 08:30
Osteoporosis: epidemiology, risk factors, and screening
K. Knapp*; Exeter/UK (K.M.Knapp@exeter.ac.uk)*
Learning objectives:
1. To become familiar with epidemiological considerations and risk factors.
2. To be aware of screening and imaging in osteoporosis patient follow-up.
Author Disclosures:
K. Knapp: Author at Carver's Medical Imaging, Research/Grant Support at Wellcome, Stryker

BS 9b-2 08:55
Dual-energy x-ray absorptiometry and other modalities
R. M. Lopes*; Vila Nova de Gaia/PT (rogeriolopes87@gmail.com)*
Learning objectives:
1. To become familiar with the evolution of dual-energy x-ray absorptiometry (DXA) systems.
2. To understand the important role of the radiographer in DXA examinations: optimisation, reproducibility, and quality assurance.
3. To become aware of the importance of understanding the scan generated report information.
Author Disclosures:
R. M. Lopes: nothing to disclose

BS 9b-3 09:20
Opportunities for radiographers in bone health
E. McDermott*; Dublin/IE (eilish.mcdermott@ucd.ie)*
Learning objectives:
1. To explore potential opportunities for radiographers to increase their contribution in this field.
2. To be aware of the limitations with current osteoporosis imaging structures and roles.
3. To discuss the importance of education, training, and continuous professional development for radiographers specialising in this field.
Author Disclosures:
E. McDermott: nothing to disclose

09:45
Panel discussion: How can we further develop the radiographers' role in osteoporosis imaging?

08:30 - 10:00 **Room M 2**

E³ - Advanced Course: How to Improve Your Expertise in Cardiothoracic Imaging

E³ 919
Low-dose thoracic CT: only screening for lung cancer?

E³ 919-1 08:30
Chairperson's introduction
N. Howarth*; Chêne-Bougeries/CH (nigel.howarth@grangettes.ch)*
Session objectives:
1. To learn how to optimise CT protocols in the context of screening.
2. To be aware of the false positive risk.
3. To learn about the key features to report during screening.
Author Disclosures:
N. Howarth: nothing to disclose

E³ 919-2 08:36
A. Overview of lung cancer screening activities in European countries
S. Diederich*; Düsseldorf/DE (Stefan.Diederich@vkkd-kliniken.de)*
Learning objectives:
1. To be aware of the latest results of lung cancer screening trials.
2. To learn about the best technical standards for lung cancer screening.
3. To learn about the performance of artificial intelligence algorithms for lung cancer prediction.
Author Disclosures:
S. Diederich: nothing to disclose

E³ 919-3 09:04
B. Lung nodule management
A. R. Larici*; Rome/IT (annarita.larici@unicatt.it)*
Learning objectives:
1. To be aware of the common causes of solitary pulmonary nodules.
2. To learn about key radiological features suggesting a benign cause.
3. To learn about the methods allowing identifying malignant nodules.
Author Disclosures:
A. R. Larici: Advisory Board at Boehringer-Ingelheim, Speaker at Boehringer-Ingelheim, MSD, Roche, GE

E³ 919-4 09:32
C. Coronary artery disease assessment as part of a lung cancer screening programme: how to do it?
R. Vliegenthart*; Groningen/NL (r.vliegenthart@umcg.nl)*

Learning objectives:
1. To become familiar with the importance and predictive power of coronary calcium assessment.
2. To discuss the possibilities of combining coronary calcium assessment and lung cancer screening.
3. To learn about the practical implementation of coronary calcium assessment in the routine chest.
Author Disclosures:
R. Vliegenthart: nothing to disclose

08:30 - 10:00 **Room M 4**

Musculoskeletal

RC 910

The old spine: challenges of imaging and treatment

Moderator:
M. Adriaensen; Heerlen/NL

RC 910-1 08:30
A. Degeneration of the old spine: relevance of findings and differential diagnosis
V. Cassar-Pullicino*; Oswestry/UK (Victor.Pullicino@nhs.net)*
Learning objectives:
1. To explain the pathophysiology of degenerative changes in the spine.
2. To describe the imaging findings of degenerative diseases of the spine.
Author Disclosures:
V. Cassar-Pullicino: nothing to disclose

RC 910-2 09:00
B. Fractures: bone fragility in the elderly, assessing osteoporosis and bone quality, and differential diagnosis
G. Guglielmi*; Andria/IT*
Learning objectives:
1. To explain the pathophysiology of osteoporosis in the spine.
2. To describe the imaging findings of spinal osteoporosis and its consequences.
Author Disclosures:
G. Guglielmi: Speaker at University of Foggia

RC 910-3 09:30
C. Interventional radiology: is there still a place for vertebroplasty and kypho-/stentoplasty
C. A. Binkert*; Winterthur/CH (christoph.binkert@ksw.ch)*
Learning objectives:
1. To explain the procedures of vertebroplasty and kyphoplasty.
2. To discuss the current role of vertebroplasty and kyphoplasty in spinal fractures.
Author Disclosures:
C. A. Binkert: Advisory Board at CTI vascular, Merit Medical, Research/Grant Support at Abbott, Philips

08:30 - 10:00 **Room M 5**

E³ - Advanced Course: Hot Topics in GU Cancer

E³ 922

Whole-body imaging in metastatic urinary tract and prostate cancer

E³ 922-1 08:30
Chairperson's introduction
A. R. R. Padhani*; London/UK (anwar.padhani@stricklandscanner.org.uk)*
Author Disclosures:
A. R. R. Padhani: Research/Grant Support at Siemens Healthineers, Advisory Board at Siemens Healthineers, Other at Siemens Healthineers, Janssen, Sanofi, Mint

E³ 922-2 08:45
A. Whole-body MRI: technique and reporting system Met Rads P
F. Lecouvet*; Brussels/BE (frederic.lecouvet@uclouvain.be)*
Learning objectives:
1. To review patient selection for whole-body MRI in prostate cancer.
2. To learn state-of-the-art technical tips.
3. To learn a systematic reporting system.
Author Disclosures:
F. Lecouvet: nothing to disclose

E³ 922-3 09:10
B. Whole-body MRI and response assessment
N. Tunariu*; Sutton, London/UK (nina.tunariu@icr.ac.uk)*
Learning objectives:
1. To recognise active disease.
2. To learn pitfalls of interpretation.
3. To recognise the appearance of treatment response.
Author Disclosures:
N. Tunariu: Speaker at Janssen, Advisory Board at Janssen, Advisory Board at Bayer

E³ 922-4 09:35
C. PET and PET/MRI in prostate cancer
I. A. Burger*; Zurich/CH*
Learning objectives:
1. To learn about the role of PET in prostate cancer.
2. To understand the advantages and limitations of PET and PET/MRI.
3. To become familiar with potential pitfalls through case review.
Author Disclosures:
I. A. Burger: nothing to disclose

08:30 - 10:00 **Tech Gate Auditorium**

State of the Art Symposium

SA 9

Immunotherapy: what the radiologist needs to know

SA 9-1 08:30
Chairperson's introduction
J. Sosna*; Jerusalem/IL (jacobs@hadassah.org.il)*
Session objectives:
1. To describe the basics of immunotherapy in oncology.
2. To demonstrate the scope of clinical uses and the clinical impact.
3. To familiarise radiologists with the evaluation criteria.
Author Disclosures:
J. Sosna: Consultant at Xact, Grant Recipient at Philips

SA 9-2 08:35
Immunotherapy: the basics for radiologists
T. Ng*; London/UK (tony.ng@kcl.ac.uk)*
Learning objectives:
1. To describe the basic changes in the immune system in oncology patients.
2. To describe the means by which immunotherapy can be used.
3. To present different immune modulation therapies in various neoplastic diseases.
Author Disclosures:
T. Ng: Grant Recipient at Daiichi Sankyo Inc.

SA 9-3 09:00
Assessment of tumour response
C. Suzuki*; Stockholm/SE (chikako.suzuki@ki.se)*
Learning objectives:
1. To describe the current practice of oncology evaluation in cross sectional imaging.
2. To present the difficulties of the common techniques.
3. To provide an overview of novel assessment techniques and their applicability.
Author Disclosures:
C. Suzuki: nothing to disclose

SA 9-4 09:25
The immune response in interventional oncology: challenges and opportunities
N. Goldberg; *Jerusalem/IL (sgoldber@bidmc.harvard.edu)*
Learning objectives:
1. To describe the current practice of interventional oncology (IO).
2. To present applications in which the immune system can be modulated by IO.
3. To discuss challenges and opportunities of immune system modulation in IO.
Author Disclosures:
N. Goldberg: Advisory Board at Xact Robotics, Consultant at Angiodynamics, Consultant at Cosman Company

09:50
Panel discussion: Role of radiologists in immunotherapy

10:30 - 11:00 **Forum (Room A)**

Plenary Lecture

PL 2

Presiding:
B. Brkljačić; Zagreb/HR

PL 2-1 10:30
Digitalisation: the journey to a more human healthcare
B. Montag; *Erlangen/DE*
Author Disclosures:
B. Montag: disclosure/affirmation information not submitted

12:45 - 13:45 **Room B**

E³ - The Beauty of Basic Knowledge: Breast

E³ 24C

Basics of breast MRI

Moderators:
J. Camps Herrero; Valencia/ES
K. Kinkel; Chêne-Bougeries/CH

E³ 24C-1 12:45
When is breast MRI indicated and what protocol to use?
R. M. Mann; *Nijmegen/NL (r.mann@rad.umcn.nl)*
Learning objectives:
1. To know the guidelines for accepted indications of breast MRI.
2. To learn the basic protocol for screening and diagnostic breast MRI.
Author Disclosures:
R. M. Mann: Grant Recipient at Siemens Healthineers, Bayer Healthcare, Screenpoint medical, Seno medical, Medtronic, BD/BARD, Advisory Board at Transonic imaging

E³ 24C-2 13:15
How to read breast MRI
F. Pediconi; *Rome/IT (federica.pediconi@uniroma1.it)*
Learning objectives:
1. To understand morphological and kinetic findings.
2. To know the value of diffusion-weighted imaging.
3. To learn about reporting by using the breast imaging reporting and data system (BIRADS).
Author Disclosures:
F. Pediconi: Speaker at Bayer, Speaker at Bracco imaging

12:45 - 13:45 **Room C**

E³ - The Beauty of Basic Knowledge: Pancreas

E³ 25C

Cystic neoplasms

Moderator:
T. Lauenstein; Düsseldorf/DE

E³ 25C-1 12:45
Intraductal papillary neoplasms
S. Skehan; *Dublin/IE*
Learning objectives:
1. To learn about the classification of cystic pancreatic neoplasms.
2. To appreciate the classification of intraductal papillary mucinous neoplasms (IPMNs).
3. To understand the diagnostic imaging findings of IPMNs.
Author Disclosures:
S. Skehan: nothing to disclose

E³ 25C-2 13:15
Other cystic pancreatic neoplasms
R. M. Pozzi-Mucelli; *Stockholm/SE (raffaella.pozzi-mucelli@sll.se)*
Learning objectives:
1. To understand diagnostic imaging findings of other cystic neoplasms.
2. To appreciate differential diagnosis of pancreatic cystic lesions.
3. To understand the follow-up of cystic pancreatic neoplasms.
Author Disclosures:
R. M. Pozzi-Mucelli: nothing to disclose

12:45 - 13:45 **Coffee & Talk 2**

Coffee & Talk (open forum) Session

Organised by EuroSafe Imaging

C 16

Dose management (DM): requirements, promises and reality

C 16-1 12:45
Chairperson's introduction
R. W. Loose; *Nuremberg, DE/DE (r.loose@mail.de)*
Session objectives:
1. To stress the impact of DM on quality assurance and optimisation.
2. To demonstrate how DM can help to implement the requirements of the European basic safety standards directive (EU-BSS).
3. To discuss different complexity levels of DM.
Author Disclosures:
R. W. Loose: nothing to disclose

C 16-2 12:50
DICOM image and radiation dose structured report (RDSR) dose parameters: what do we have, what do we need?
E. Vaño; *Madrid/ES (eliseov@med.ucm.es)*
Learning objectives:
1. To appreciate the relevance of the dosimetric information available during and at the end of interventional procedures to help in optimisation.
2. To learn that additional details on technical parameters are available in the DICOM RDSR, helping to audit individual procedures.
3. To understand how the information contained in the RDSR for radiation events may be helpful in optimising some individual procedures.
Author Disclosures:
E. Vaño: nothing to disclose

C 16-3 13:00
Workflow of dose management in the context of PACS, RIS, HIS, IHE
P. Mildenberger; *Mainz/DE (mildenbe@uni-mainz.de)*

Learning objectives:
1. To demonstrate the available tools for DM in hospital information systems/radiology information systems/picture archiving and communication systems (HIS-RIS-PACS).
2. To explain the health care enterprise (IHE) concept for DM.
3. To discuss the potential of new developments for DM.
Author Disclosures:
P. Mildenberger: nothing to disclose

C 16-4 13:10
Requirements on dose management system in terms of dose storage, processing, reporting, tracking, quality assurance and the directive EU-BSS 2013/59
S. T. Schindera*; Riehen/CH (sebastian.schindera@ksa.ch)*
Learning objectives:
1. To demonstrate examples of how to use dose management software for quality improvement.
2. To demonstrate the pitfalls of using dose management software.
3. To discuss future applications for dose management systems.
Author Disclosures:
S. T. Schindera: nothing to disclose

C 16-5 13:20
Experiences in practice between vendor promises and clinical reality
V. Tsapaki*; Nea Ionia/GR (virginia@otenet.gr)*
Learning objectives:
1. To demonstrate the real practice of DM procurement to installation.
2. To show the possible challenges during the procedure of DM purchase and installation.
3. To discuss necessary implementation steps.
Author Disclosures:
V. Tsapaki: nothing to disclose

13:30
Open forum discussion

12:45 - 13:45 **Coffee & Talk 3**

Coffee & Talk (open forum) Session
Organised by EIBIR

C 27
Artificial intelligence (AI) and the future of imaging: European funding prospects

C 27-1 12:45
Chairperson's introduction
G. P. Krestin*; Rotterdam/NL*
Session objectives:
1. To learn about the mission of the European Institute for Biomedical Imaging Research (EIBIR).
2. To become familiar with the European research landscape and EIBIR support.
3. To learn about the need for AI in imaging research.
Author Disclosures:
G. P. Krestin: Consultant at Bracco Imaging, Board Member at Quantib BV, Research/Grant Support at GEHC, Research/Grant Support at Bayer AG, Research/Grant Support at Siemens Healthineers

C 27-2 12:55
The importance of artificial intelligence in imaging research
W. J. Niessen*; Rotterdam/NL (w.niessen@erasmusmc.nl)*
Learning objectives:
1. To learn about AI and its role in imaging research.
2. To appreciate the importance of AI in imaging research.
3. To learn about EIBIR initiatives on AI.
Author Disclosures:
W. J. Niessen: Founder at Quantib BV, Shareholder at Quantib BV, Consultant at Quantib BV

C 27-3 13:05
Deep learning in imaging and cancer care
G. Langs*; Vienna/AT*
Learning objectives:
1. To learn about applications of deep learning.
2. To understand how deep learning is used in imaging and cancer care.
Author Disclosures:
G. Langs: Founder at contextflow GmbH, Grant Recipient at Novartis, Grant Recipient at Siemens Healthineers, Grant Recipient at NVIDIA

C 27-4 13:15
Applying artificial intelligence for biomarker discovery
A. Alberich-Bayarri*; Valencia/ES (angel@quibim.com)*
Learning objectives:
1. To learn about applications of AI.
2. To understand how AI can be used for biomarker discovery.
Author Disclosures:
A. Alberich-Bayarri: CEO at QUIBIM SL, Founder at QUIBIM SL, Board Member at QUIBIM SL

C 27-5 13:25
European funding and support services for AI and imaging research
P. Zolda*; Vienna/AT*
Learning objectives:
1. To learn about the types of funding available for AI and biomedical imaging research.
2. To learn about the support EIBIR offers imaging researchers.
3. To appreciate EIBIR's effectiveness in helping researchers secure funding.
Author Disclosures:
P. Zolda: nothing to disclose

13:35
Open forum discussion

12:45 - 13:45 **Room M 5**

EDiR Session

EDiR 3
The Essential Guide by Springer and other new tools to prepare the examination

Moderator:
L. Oleaga Zufiria; Barcelona/ES

EDiR 3-1 12:45
The Essential Guide publication by Springer
L. Oleaga Zufiria*; Barcelona/ES (lauraoleaga@gmail.com)*
Learning objectives:
1. To present the new e-book for EDiR preparation.
2. To present a guide on how to use the book.
3. To present the setup of the chapters of the book.
Author Disclosures:
L. Oleaga Zufiria: Consultant at TMC Academy

EDiR 3-2 12:57
EDiR App: self-assessment
W. van Lankeren*; Rotterdam/NL (w.vanlankeren@erasmusmc.nl)*
Learning objectives:
1. To present the self-assessment cases available in the app.
2. To show the utility of self-assessment for EDiR preparation.
3. To demonstrate the importance of using new learning approaches.
Author Disclosures:
W. van Lankeren: nothing to disclose

EDiR 3-3 13:09
EDiR App: structured reporting
F. M. Saez Garmendia*; Bilbao/ES (fersaez@yahoo.com)*
Learning objectives:
1. To become familiar with the new CORE cases with structured reports available in the EDiR app.
2. To help candidates facing the CORE exam to use structured reports.
3. To show the advantages of using structured reports when preparing for the CORE examination.
Author Disclosures:
F. M. Saez Garmendia: nothing to disclose

EDiR 3-4 13:21
EDiR blog
W. van Lankeren; *Rotterdam/NL*
Learning objectives:
1. To present the recent blogs incorporated in the app.
2. To show the process of blog preparation.
3. To show examples of flash and long cases.
Author Disclosures:
W. van Lankeren: nothing to disclose

13:33
Discussion

14:00 - 15:30 **Room N**

Breast

RC 1102

State of the art and recent developments in breast ultrasound

Moderator:
A. Athanasiou; Athens/GR

RC 1102-1 14:00
A. Breast ultrasound: tell me the value of coloured images
C. S. Balleyguier; *Villejuif/FR*
Learning objectives:
1. To learn the correct setting and interpretation of Doppler and elastography.
2. To realise the added value in lesion assessment.
3. To know the roll in follow-up and therapy monitoring.
Author Disclosures:
C. S. Balleyguier: disclosure/affirmation information not submitted

RC 1102-2 14:30
B. Automated breast ultrasound (ABUS): the right add-on in screening dense breast
A. Vourtsis; *Athens/GR (athinavourtsi@yahoo.gr)*
Learning objectives:
1. To learn how to perform, assess image quality, interpret, and recognise artefacts.
2. To review the current literature of ABUS in women with dense breasts.
3. To understand the value of 3D multiplanar images and ABUS workflow implementation compared to handheld US (HHUS).
Author Disclosures:
A. Vourtsis: Advisory Board at Noncorporate Member of Medical Advisory Board of Volpara Solutions, Consultant at Consultant, General Electric Company Educator, ABUS

RC 1102-3 15:00
C. Can artificial intelligence (AI) be helpful in the US-screening setting?
P. Kapetas; *Vienna/AT (panagiotis.kapetas@meduniwien.ac.at)*
Learning objectives:
1. To understand the current status of the use of AI in breasts US.
2. To realise the limitations in the implementation of US in screening and of AI in US examinations.
3. To explore potential future applications.
Author Disclosures:
P. Kapetas: nothing to disclose

14:00 - 15:30 **Room O**

Children in Focus

IF 11

Against all odds: bringing health care to children in low-resource areas

IF 11-1 14:00
Chairperson's introduction
K. Rosendahl; *Bergen/NO (karen.rosendahl@unn.no)*
Author Disclosures:
K. Rosendahl: nothing to disclose

IF 11-2 14:06
Child health in the Sustainable Development Goals (SDG) era
A. Banerjee; *Geneva/CH (banerjeea@who.int)*
Learning objectives:
1. To recognise the changes in mortality and morbidity patterns.
2. To understand the new directions in child health.
3. To discuss the life course approach to child health.
Author Disclosures:
A. Banerjee: Employee at World Health Organization, Speaker at World Health Organization

IF 11-3 14:26
The challenges of health care delivery to refugee and migrant children
G. Bernini; *Milan/IT (gaela.bernini@bracco.com)*
Learning objectives:
1. To learn the current status of health care delivery in this vulnerable population.
2. To appreciate the acute impact on the child.
3. To understand the late effects to these children and impact on their future lives.
Author Disclosures:
G. Bernini: Employee at Bracco Foundation

IF 11-4 14:46
ESPR Outreach task force: what is our best way to help?
J. Kasznia-Brown; *Bristol/UK (joanna.brown@tst.nhs.uk)*
Learning objectives:
1. To learn about the aims of the ESPR outreach task force.
2. To illustrate with details of ongoing projects.
3. To discuss the best way for paediatric radiologists to influence health care for children in low-resource areas.
Author Disclosures:
J. Kasznia-Brown: nothing to disclose

15:06
Panel discussion: How can we efficiently reach out to children in low resource areas to develop self-sustainable aid-programs?

14:00 - 15:30 **Studio 2020**

Joint Session of the EFRS and ISRRT

EFRS/ISRRT

Artificial intelligence and the radiographer profession

EFRS/ISRRT-1/EFRS/ISRRT-2 14:00
Chairpersons' introduction
J. McNulty; *Dublin/IE (jonathan.mcnulty@ucd.ie)*
D. E. Newman; *Fargo, ND/US (donnaenewman@gmail.com)*
Session objectives:
1. To discuss artificial intelligence in the context of the radiographer profession.
2. To explore the key considerations for the profession related to artificial intelligence.
Author Disclosures:
J. McNulty: nothing to disclose, D. E. Newman: nothing to disclose

EFRS/ISRRT-3 14:06
Exploring the current landscape and evidence-base relating to artificial intelligence (AI) and the radiographer profession
N. H. Woznitza; *London/UK (nicholas.woznitza@nhs.net)*
Learning objectives:
1. To summarise the existing evidence of the impact of AI on radiographers.
2. To recognise the risks and benefits when introducing AI into clinical practice.
3. To explore the opportunities that AI could present in radiographer role development.
Author Disclosures:
N. H. Woznitza: Consultant at InHealth

EFRS/ISRRT-4 14:24
Ethical considerations in AI
A. Brady; *Cork/IE (adrianbrady@me.com)*
Learning objectives:
1. To learn the ethical controversies that AI is introducing in medical imaging.
2. To provide an overview of the professional and legal implications.
3. To explore/elaborate on the need for a code of conduct.
Author Disclosures:
A. Brady: nothing to disclose

EFRS/ISRRT-5 14:42
Considering AI in our education and training programmes
M. Hardy; *Bradford/UK (M.L.Hardy1@bradford.ac.uk)*
Learning objectives:
1. To consider what our students need to know about AI.
2. To discuss opportunities to use AI to supplement radiographer education.
3. To identify future concepts that radiographers will require to work with integrated AI.
Author Disclosures:
M. Hardy: nothing to disclose

EFRS/ISRRT-6 15:00
Horizon scanning: the future of AI and the radiographer profession
M. Jackowski; *Angier, NC/US (mjackowski@asrt.org)*
Learning objectives:
1. To discuss how radiographers can contribute to the development of AI in medical imaging.
2. To summaries barriers to the implementation of AI in clinical practice.
3. To illustrate the potential contribution of AI to patient safety.
Author Disclosures:
M. Jackowski: Board Member at American Society of Radiologic Technologists, Employee at Siemens Healthineers

15:18
Panel discussion: What steps can be taken to better prepare radiographers for AI?

14:00 - 15:30 **Darwin (Room D2)**

Emergency Imaging

RC 1117
Complications of endovascular interventions

Moderator:
M. C. Firetto; Milan/IT

RC 1117-1 14:00
A. Complications in thoracic and abdominal endovascular aneurysm procedures
R. A. Morgan; *London/UK (robert.morgan@stgeorges.nhs.uk)*
Learning objectives:
1. To become familiar with the most common endovascular thoracic and abdominal procedures.
2. To understand the mechanism of the possible risks during endovascular procedures.
3. To recognise these acute complications in different imaging modalities.
Author Disclosures:
R. A. Morgan: Speaker at Cook, Speaker at Bard

RC 1117-2 14:30
B. Imaging and management of complication of peripheral arterial revascularisation
M. J. Lee; *Dublin/IE (mlee@rcsi.ie)*
Learning objectives:
1. To become familiar with the possible complication of endovascular treatments.
2. To recognise findings of complications in different imaging modalities.
3. To learn about the management of common complications.
Author Disclosures:
M. J. Lee: nothing to disclose

RC 1117-3 15:00
C. Imaging appearance of typical complications after liver embolisation: what is normal and what needs to be reported
T. J. Kroencke; *Augsburg/DE*
Learning objectives:
1. To become familiar with the possible endovascular typical complications and normal findings.
2. To become familiar with the interventional radiologist's needs imaging to plan treatment after complications.
3. To recognise when to call surgical colleagues.
Author Disclosures:
T. J. Kroencke: nothing to disclose

14:00 - 15:30 **Descartes (Room D3)**

EFOMP Workshop

EF 11
CT protocol management and optimisation: management (part A)

Moderator:
M. Brambilla; Novara/IT

EF 12-1 14:00
Chairperson's introduction
K. N. Bolstad; *Bergen/NO*
Session objectives:
1. To become familiar with the concept of CT protocol management systems (CT-PMS).
2. To discuss the opportunities provided by the standardisation of CT protocols in the optimisation process.
3. To understand how dose tracking systems can be used in quality assurance of CT-PMS.
Author Disclosures:
K. N. Bolstad: nothing to disclose

EF 11-2 14:05
Developing a CT protocol management system (CT-PMS)
J. Sjöberg; *Stockholm/SE (johan.a.sjoberg@sll.se)*
Learning objectives:
1. To learn how to set up a review committee and the role of each member (radiologist, medical physicist, radiographer).
2. To understand why implementing a CT-PMS is a prerequisite for optimisation.
3. To become familiar with existing CT-PMS systems.
Author Disclosures:
J. Sjöberg: nothing to disclose

EF 11-3 14:35
A general framework for monitoring CT acquisition workflow
T. Szczykutowicz; *Madison, WI, WI/US (tszczykutowicz@uwhealth.org)*
Learning objectives:
1. To learn how to maintain consistency in CT acquisition protocols throughout a large radiology department.
2. To understand how technologist quality can be monitored using informatics tools.
3. To discuss the current state of informatics solutions to facilitate protocols management in radiology.
Author Disclosures:
T. Szczykutowicz: Advisory Board at imalogix LLC, Consultant at GE Healthcare, Consultant at Takeda Pharmecuitcals , Owner at protocolshare.org LLC, Grant Recipient at GE Healthcare

EF 11-4 15:05
Dose tracking systems as a tool for CT-PMS
F. Zanca; *Leuven/BE (federica.zanca@palindromo.consulting)*
Learning objectives:
1. To understand how dose management systems can be used in quality assurance of CT-PMS.
2. To become familiar with applications of this method through worked examples.
3. To discuss the application in multicentre studies.
Author Disclosures:
F. Zanca: Owner at Palindromo Consulting

14:00 - 15:30 **Room G**

E³ - ECR Master Class (Head and Neck)

E³ 1126

Improving staging and treatment outcomes in head and neck cancer

E³ 1126-1 14:00
Chairperson's introduction
M. Horta; *Lisbon/PT (mariana_horta@hotmail.com)*
Session objectives:
1. To learn about new developments in MRI for early tumour detection.
2. To understand the changing role of imaging with human papillomavirus (HPV) related disease.
3. To learn how to improve detection of recurrence and prediction of outcome.
Author Disclosures:
M. Horta: nothing to disclose

E³ 1126-2 14:05
A. Nasopharynx: early tumour detection and imaging markers for treatment response
A. D. King; *Hong Kong/CN*
Learning objectives:
1. To learn how best to detect early nasopharyngeal carcinoma (NPC).
2. To understand how to assess tumour response.
3. To highlight how imaging response may alter the treatment pathway.
Author Disclosures:
A. D. King: nothing to disclose

E³ 1126-3 14:28
B. Early glottic carcinoma: new insights relevant for tumour staging and patient management
D. Farina; *Brescia/IT (davide.farina@unibs.it)*
Learning objectives:
1. To become acquainted with treatment options for early glottic cancer.
2. To understand the best imaging techniques for assessing early glottic cancer.
3. To learn which imaging features affect patient management.
Author Disclosures:
D. Farina: Speaker at BAYER 2019, Other at BRACCO 2019

E³ 1126-4 14:51
C. Oropharynx: risk stratification related to HPV association
A. Trojanowska; *Lublin/PL*
Learning objectives:
1. To understand the role of HPV in treatment and outcome of oropharyngeal cancer.
2. To learn about the impact of HPV on tumour staging.
3. To reflect on imaging features differentiating HPV+ from HPV-.
Author Disclosures:
A. Trojanowska: disclosure/affirmation information not submitted

15:14
Panel discussion: Will new developments in imaging alter staging and treatment in head and neck oncology?

14:00 - 15:30 **Room M 2**

E³ - Advanced Course: Hot Topics in Emergency Radiology

E³ 1118

Dual-energy and subtraction CT in emergency radiology

E³ 1118-1 14:00
Chairperson's introduction
S. Wirth; *Munich/DE (wirth.online@googlemail.com)*
Session objectives:
1. To become familiar with dual-energy CT techniques and reconstruction possibilities.
2. To understand the clinical applications and added value of dual-energy CT in emergency pathologies.
3. To learn about the anatomical and functional information of different organ systems provided by dual-energy CT.
4. To become familiar with the impact of dual-energy CT on radiation dose and required iodine volume.
5. To become familiar with the possible future applications of dual-energy CT in combination with deep learning techniques.
Author Disclosures:
S. Wirth: nothing to disclose

E³ 1118-2 14:06
A. Blood and bleeding
M. Brink; *Nijmegen/NL (Mobrink@hotmail.com)*
Learning objectives:
1. To understand the advantages of dual-energy CT in neuro, aortic, and PE diagnoses.
2. To understand how virtual non-contrast images might replace the precontrast phase.
3. To highlight the superiority of dual-energy CT in the demonstration of enhancement.
Author Disclosures:
M. Brink: Grant Recipient at Canon Medical Systems, Speaker at Canon Medical Systems

E³ 1118-3 14:34
B. The usual suspects: urogenital and musculoskeletal
R. Guggenberger; *Zurich/CH (roman.guggenberger@usz.ch)*
Learning objectives:
1. To learn about the differentiation of stones.
2. To understand the advantages of duel-energy CT in recognising subtle/occult fractures.
3. To highlight the role of dual-energy CT in reducing metal-related artefacts in musculoskeletal imaging.
Author Disclosures:
R. Guggenberger: nothing to disclose

E³ 1118-4 15:02
C. Dual-energy CT in acute emergency conditions in the abdomen and pelvis
J. Sosna; *Jerusalem/IL (jacobs@hadassah.org.il)*
Learning objectives:
1. To describe dual-energy CT techniques.
2. To provide an overview of dual-energy tools used in the evaluation of ED patients.
3. To present the role of dual-energy CT in emergency situations.
Author Disclosures:
J. Sosna: nothing to disclose

16:00 - 17:30 **Room C**

Breast

RC 1202

Evidence-based breast MRI: when, how and why

RC 1202-1 16:00
Chairperson's introduction
F. Sardanelli; *Milan/IT*
Session objectives:
1. To understand the contribution of MRI to preoperative staging and the context within which it should be recommended.
2. To understand the importance of the multiparametric protocol and robust image quality.
3. To recognise the steps required to move to abbreviated MRI for high-risk screening.
Author Disclosures:
F. Sardanelli: Advisory Board at Bracco, Speaker at Bayer, Bracco, General Electric, Research/Grant Support at Bayer, Bracco, General Electric

RC 1202-2 16:05
A. Preoperative staging with MRI: fresh data on an old mantra
R. M. Trimboli*; San Donato Milanese/IT (trimboli.rm@gmail.com)*
Learning objectives:
1. To learn about the evidence for and against the use of MRI in preoperative staging.
2. To understand the background, design, and early results of the MIPA trial and recent literature.
3. To be able to explain the role of preoperative MRI during multidisciplinary tumour board meetings.
Author Disclosures:
R. M. Trimboli: nothing to disclose

RC 1202-3 16:30
B. Abbreviated protocols: are we ready?
C. K. Kuhl*; Aachen/DE (ckuhl@ukaachen.de)*
Learning objectives:
1. To learn about the evidence for abbreviated MRI and the comparison with standard protocols.
2. To understand the different protocols for abbreviated MRI and the merits of each sequence used.
3. To appreciate the advantages and limitations for abbreviated MRI.
Author Disclosures:
C. K. Kuhl: nothing to disclose

RC 1202-4 16:55
C. How can we make use of MRI biomarkers in clinical practice?
L. Martincich*; Candiolo/IT*
Learning objectives:
1. To learn about the different biomarkers that are available and the evidence for using them in patients with breast cancer.
2. To understand in which clinical settings biomarkers might be of value now and in the future.
3. To recognise the limits for a widespread application.
Author Disclosures:
L. Martincich: disclosure/affirmation information not submitted

17:20
Panel discussion: Why is the adoption of MRI in clinical practice still so difficult?

16:00 - 17:00 **Coffee & Talk 1**

Coffee & Talk (open forum) Session
Organised by ESOR

C 6
The European Diploma in Radiology (EDiR) as an instrument to develop a professional career

C 6-1 16:00
Chairperson's introduction
L. Oleaga Zufiria*; Barcelona/ES (lauraoleaga@gmail.com)*
Session objectives:
1. To present EDiR: the essential guide.
2. To describe the new EDiR innovative tools to prepare the exam.
3. To describe the advantages of being an EDiR holder.
4. To present quiz examination cases (MRQs, short cases, CORE cases).
Author Disclosures:
L. Oleaga Zufiria: Consultant at TMC Academy

C 6-2 16:05
How to succeed in the EDiR examination: presentation of "EDiR: the essential guide" and new innovative tools to prepare for the EDiR examination
L. Oleaga Zufiria*; Barcelona/ES (lauraoleaga@gmail.com)*
Learning objectives:
1. To present the script for reading the e-book.
2. To present the setup of the chapters following the scheme of the three sections in which EDiR is organised.
3. To demonstrate the links to ESR online educational content.
4. To show the self-assessment cases available in the app.
5. To show the new CORE cases with structured report.
6. To present the recent blogs incorporated in the app.
Author Disclosures:
L. Oleaga Zufiria: Consultant at TMC Academy

C 6-3 16:20
Why EDiR certification matters
A. Soler Perromat*; Barcelona/ES (alexandresolerp@gmail.com)*
Learning objectives:
1. To describe the experience of taking the exam.
2. To explain the reasons why it is worth taking the exam.
3. To understand the benefits of having the European Diploma in Radiology.
Author Disclosures:
A. Soler Perromat: nothing to disclose

C 6-4 16:30
Interactive quiz
W. van Lankeren*; Rotterdam/NL (w.vanlankeren@erasmusmc.nl)*
Learning objectives:
1. To familiarise the EDiR candidate with the way of testing.
2. To more effectively prepare for the EDiR exam after interactive participation in the quiz.
3. To practice the skills of how to tackle and address the questions in the exam.
Author Disclosures:
W. van Lankeren: nothing to disclose

16:50
Open forum discussion

16:00 - 17:30 **Room N**

EuroSafe Imaging Session

EU 12
Dose reduction in quantitative single- and multi-energy computed tomography

EU 12-1/EU 12-2 16:00
Chairpersons' introduction
S. T. Schindera*; Riehen/CH (sebastian.schindera@ksa.ch)*
W. Stiller*; Heidelberg/DE*
Session objectives:
1. To raise awareness of available technology and methods for quantitative computed tomography imaging.
2. To become familiar with clinical applications of single- and multi-energy CT for the acquisition of quantitative imaging biomarkers.
3. To learn about the potential for dose reduction in the field of quantitative CT and its effects on analyses results.
Author Disclosures:
S. T. Schindera: nothing to disclose, W. Stiller: Advisory Board at Philips Medical Systems Nederland B.V., Veenpluis 4-6, 5684 Best, The Netherlands

EU 12-3 16:05
Dual- and multi-energy CT: physical background and concepts
P. B. Noel*; Philadelphia, PA/US (peter.noel@uphs.upenn.edu)*
Learning objectives:
1. To introduce the basic concept of spectral imaging.
2. To illustrate the technical implementations of dual- and multi-energy CT.
3. To demonstrate dose reduction potentials in spectral CT.
Author Disclosures:
P. B. Noel: Advisory Board at Philips Healthcare, Research/Grant Support at Philips Healthcare, Speaker at Philips Healthcare, Consultant at Stryker , Shareholder at MITOS GmbH

EU 12-4 16:20
Spectral photon-counting CT: technical concepts for quantitative multi-energy imaging and dose reduction
L. Boussel*; Lyons/FR*
Learning objectives:
1. To become familiar with photon-counting CT technology and its differences to conventional CT detectors.
2. To understand the technical concepts of photon counting for quantitative multi-energy imaging.
3. To learn about the potential of photon-counting technology for enabling future dose reduction in CT.
Author Disclosures:
L. Boussel: nothing to disclose

EU 12-5 16:35
Single dual-energy iodine maps with organ-specific acquisition timing as a quantitative imaging biomarker replacing abdominal CT perfusion
S. Skornitzke*; Heidelberg/DE (Stephan.Skornitzke@med.uni-heidelberg.de)*
Learning objectives:
1. To learn about the potential of dual-energy CT for iodine quantification in the abdomen as a quantitative imaging biomarker
2. To understand the link between conventional dynamic CT perfusion and quantitative dual-energy iodine maps.
3. To raise awareness of dual-energy iodine maps with organ-specific acquisition times as a dose-reduced alternative to abdominal CT perfusion.
Author Disclosures:
S. Skornitzke: Shareholder at Investment funds containing shares of healthcare companies

EU 12-6 16:50
Effects of dose reduction on quantitative analyses of chest CT
J. M. Goo*; Seoul/KR (jmgoo@plaza.snu.ac.kr)*
Learning objectives:
1. To understand the dose reduction approaches in chest CT.
2. To review the quantitative analyses used in chest CT.
3. To learn about the impact of dose reduction approaches on quantitative analyses.
Author Disclosures:
J. M. Goo: Research/Grant Support at Infinitt Healthcare

EU 12-7 17:05
Perfusion CT as quantitative imaging biomarker in acute ischaemic stroke and brain trauma: what about the dose?
I. Shelef*; Beer-Sheva/IL (shelef@bgu.ac.il)*
Learning objectives:
1. To become familiar with perfusion CT as a quantitative imaging biomarker in acute ischemic stroke and brain trauma.
2. To learn about the potential for, and limitations of, dose reduction in neurologic perfusion CT imaging.
3. To understand the use and limitations of perfusion CT for the assessment of acute ischemic stroke and brain trauma.
Author Disclosures:
I. Shelef: nothing to disclose

17:20
Panel discussion: Which role does quantitative single- and multi-energy computed tomography play in daily practice, and is it compatible with dose reduction?

16:00 - 17:30 **Room O**

Children in Focus

IF 12

The child as an individual: whose life is it anyway?

IF 12-1 16:00
Chairperson's introduction
B. Said*; London/UK (Bella.Said@gosh.nhs.uk)*
Author Disclosures:
B. Said: nothing to disclose

IF 12-2 16:05
Use of restraints in children: what is acceptable, when and why?
J. Dahlberg*; Oslo/NO (jorged@medisin.uio.no)*
Learning objectives:
1. To learn about the legal aspects/laws/UN/European children's convention.
2. To describe ethical and judicial dilemmas regarding restraint.
3. To discuss who defines what is to the "benefit to the child".
Author Disclosures:
J. Dahlberg: nothing to disclose

IF 12-3 16:25
Parental and cultural autonomy: can carers make any decisions on behalf of their child?
E. Verhagen*; Gronigen/NL (a.a.e.verhagen@umcg.nl)*
Learning objectives:
1. To discuss who owns the child's data and the ethical dilemmas of sharing children's medical stories in magazines, TV programmes, social media etc.
2. To learn about the value of childrens' data for medical research.
3. To what extent can parents decide what is best for their child? Using examples including vaccination, alternative therapies, and circumcision/genital mutilation etc.
Author Disclosures:
E. Verhagen: nothing to disclose

IF 12-4 16:45
Paediatric radiology: is there really any point?
Ø. E. E. Olsen*; London/UK (oystein.e.olsen@googlemail.com)*
Learning objectives:
1. To appreciate the evidence available for how a child-friendly/age-adjusted environment increases the diagnostic quality of radiological examinations.
2. To learn the importance of not treating children as small adults (results from adult research not applicable for children, normal variants, different diseases, age-adjusted care).
3. To discuss variations in the practice and availability of specialised paediatric radiology practice across Europe.
Author Disclosures:
Ø. E. E. Olsen: nothing to disclose

17:05
Panel discussion: Who defines what is best for the child?

IF 12-6/IF 12-7 17:25
Closing remarks
L.-S. O. Müller*; Oslo/NO (lilmul@ous-hf.no)*
C. Owens*; London/UK (owens.catherine.5@gmail.com)*
Author Disclosures:
L.-S. O. Müller: nothing to disclose, C. Owens: nothing to disclose

16:00 - 17:30 **Studio 2020**

E³ - ECR Master Class (Oncologic Imaging)

E³ 1226

Whole-body MRI (and PET/MRI)

Moderator:
D. Prezzi; London/UK

E³ 1226-1 16:00
A. Metastatic bone prostate cancer
F. Lecouvet*; Brussels/BE (frederic.lecouvet@uclouvain.be)*
Learning objectives:
1. To define imaging strategies in newly diagnosed, recurrent, and advanced disease.
2. To become able to use MET-RADS-P guidelines for whole-body MRI acquisition, reading, and response assessment.
3. To illustrate recent therapeutic advances: i.e. oligometastatic disease and precision medicine approaches.
Author Disclosures:
F. Lecouvet: nothing to disclose

E³ 1226-2 16:30
B. Multiple myeloma
L. A. Moulopoulos*; Athens/GR (lmoulop@med.uoa.gr)*

Learning objectives:
1. To become aware of the value of whole-body MRI in myeloma.
2. To understand current imaging protocols.
3. To learn about its roles: detect, monitor, and provide prognostic information.
Author Disclosures:
L. A. Moulopoulos: nothing to disclose

E³ 1226-3 17:00
C. Lymphoma
M. E. Mayerhöfer*; Vienna/AT (marius.mayerhoefer@meduniwien.ac.at)*
Learning objectives:
1. To introduce the role of whole-body MRI and PET/MRI for imaging lymphoma subtypes.
2. To know its value for detection, assessment of response, and prognosis.
3. To understand the current advantages and limitations of whole-body MRI and PET/MRI.
Author Disclosures:
M. E. Mayerhöfer: Speaker at Siemens, Research/Grant Support at Siemens, Speaker at Bristol-Myers Squibb

16:00 - 17:30 **Room E**

E³ - Advanced Course: Interactive Teaching Session for Young (and not so Young) Radiologists

E³ 1221a

Genitourinary radiology for the general radiologist

E³ 1221a-1 16:00
A. Cystic pelvic masses: differential diagnosis and management
O. Nikolic*; Novi Sad/RS (nikolic.olivera@gmail.com)*
Learning objectives:
1. To learn the imaging characteristics of the different entities.
2. To become familiar with the practical workflow in everyday clinical practice
Author Disclosures:
O. Nikolic: nothing to disclose

E³ 1221a-2 16:45
B. Gynaecological emergencies
M. Weston*; Leeds/UK (michael.weston2@nhs.net)*
Learning objectives:
1. To become familiar with the differential diagnosis.
2. To identify the key imaging findings.
Author Disclosures:
M. Weston: nothing to disclose

16:00 - 17:30 **Room F1**

E³ - Advanced Course: Interactive Teaching Session for Young (and not so Young) Radiologists

E³ 1221b

Gastrointestinal radiology

E³ 1221b-1 16:00
A. Inflammatory bowel disease
J. Rimola*; Barcelona/ES (jrimola@clinic.cat)*
Learning objectives:
1. To review the spectrum of imaging findings in inflammatory bowel disease, mainly in Crohn's disease.
2. To learn about the management options.
Author Disclosures:
J. Rimola: Advisory Board at Takeda, Advisory Board at Gilead, Advisory Board at Robarts Clinical Reserach, Research/Grant Support at Abbvie, Research/Grant Support at Genentech

E³ 1221b-2 16:45
B. Rectal cancer staging: key findings
I. Blazic*; Belgrade/RS (ivanablazic@yahoo.com)*
Learning objectives:
1. To understand the imaging technique.
2. To identify the key imaging findings.
Author Disclosures:
I. Blazic: nothing to disclose

16:00 - 17:30 **Room F2**

E³ - Rising Stars Programme: Basic Session

BS 12

Vascular: US and vascular disease

Moderator:
J. Bremerich; Basel/CH

BS 12-1 16:00
Abdominal aorta
D.-A. A. Clevert*; Munich/DE (Dirk.Clevert@med.uni-muenchen.de)*
Learning objectives:
1. To learn how to perform the examination and its role in diagnostic assessment.
2. To learn about US findings in abdominal aortic aneurysm (AAA) treatment planning and post-treatment evaluation.
3. To appreciate the role of contrast enhanced ultrasound (CEUS) and technological innovations in routine practice.
Author Disclosures:
D.-A. A. Clevert: Speaker at Bracco, Samsung, Philips, Siemens, Advisory Board at Philips, Samsung

BS 12-2 16:30
Upper and lower limb: arterial
E. Divjak*; Zagreb/HR*
Learning objectives:
1. To understand how to perform the examination and its role in diagnostic assessment.
2. To understand US findings for diagnostic and follow-up.
3. To underline tips and tricks to start your activity.
Author Disclosures:
E. Divjak: nothing to disclose

BS 12-3 17:00
Lower limb: venous
S. M. Dudea*; Cluj/RO (sdudea1@gmail.com)*
Learning objectives:
1. To understand how to perform the examination and its role in diagnostic assessment.
2. To understand US findings for diagnostic and follow-up.
3. To underline tips and tricks to start your activity.
Author Disclosures:
S. M. Dudea: nothing to disclose

16:00 - 17:00 **Coffee & Talk 3**

Coffee & Talk (open forum) Session

Organised by the ESR Subcommittee on Value-Based Radiology

C 28

Value in radiology: in the eye of the beholder

C 28-1 16:00
Chairperson's introduction
M. Fuchsjäger*; Graz/AT (michael.fuchsjaeger@medunigraz.at)*

Session objectives:
1. To understand the concept of value in radiology.
2. To learn about the challenges of developing a concept of value-based radiology.
3. To learn about experiences with value-based approaches in practice.
Author Disclosures:
M. Fuchsjäger: nothing to disclose

C 28-2 16:10
Artificial intelligence and value-based health care
P. Algra*; Heiloo/NL*
Learning objectives:
1. To learn about the Value-based Healthcare Centre's implementation of value-based health care (VBHC).
2. To understand the practical challenges of organising health care delivery based on value.
3. To understand the administrative, managerial, and financial processes of VBHC in practice.
Author Disclosures:
P. Algra: disclosure/affirmation information not submitted

C 28-3 16:15
What do patients value?
C. Justich*; Vienna/AT (cjustich@me.com)*
Learning objectives:
1. To learn about how to mutually interact with one another in a way that is optimised for both sides.
2. To understand what matters most to patients.
3. To appreciate the need to get prepared for further steps.
Author Disclosures:
C. Justich: Speaker at ESR PAG

C 28-4 16:20
Results of the ESR patient survey on value-based radiology (VBR)
M. Fuchsjäger*; Graz/AT (michael.fuchsjaeger@medunigraz.at)*
Learning objectives:
1. To learn about the results of the ESR value-based radiology patient survey.
2. To appreciate how value is perceived by radiology patients.
3. To understand which factors determine quality and value for patients in radiology.
Author Disclosures:
M. Fuchsjäger: nothing to disclose

C 28-5 16:25
Value-based pay models for radiology
V. M. Rao*; Philadelphia/US*
Learning objectives:
1. To learn about the status quo of value-based pay and reimbursement models.
2. To understand the challenges in monetising "value".
3. To learn about the differences between value-based and volume-based pay models.
Author Disclosures:
V. M. Rao: disclosure/affirmation information not submitted

C 28-6 16:30
Value of radiology: the Canadian perspective
E. Lee*; Vancouver/CA (ejlee888@gmail.com)*
Learning objectives:
1. To become familiar with the challenges facing health care delivery in Canada.
2. To understand the value of radiology from a quantitative perspective within the Canadian health care system.
3. To become familiar with the key stakeholders and target audiences that can influence radiology practice and improved patient care.
Author Disclosures:
E. Lee: nothing to disclose

C 28-7 16:35
VBR concepts around the globe: similarities and contrasts
J. A. Brink*; Boston, MA/US*
Learning objectives:
1. To understand the different approaches to VBR internationally.
2. To learn about the differences in practical implementations of VBR concepts.
3. To understand the importance of professional societies in promoting best (value-based) practices.
Author Disclosures:
J. A. Brink: Board Member at Accumen, Inc.

C 28-8 16:40
Joint paper on value-based radiology
A. Brady*; Cork/IE (adrianbrady@me.com)*
Learning objectives:
1. To explain the origin and purpose of the multi-society paper on value-based radiology.
2. To highlight the commonalities and differences between countries relating to value in medicine.
3. To understand how the value contributed to health care by radiology can be objectified and quantified.
Author Disclosures:
A. Brady: nothing to disclose

16:45
Open forum discussion: International perspectives on value in radiology

16:00 - 17:30 **da Vinci (Room D1)**

Chest

RC 1204

Pulmonary neuroendocrine proliferations and neoplasms

Moderator:
M. Silva; Parma/IT

RC 1204-1 16:00
A. Diffuse idiopathic pulmonary neuroendocrine cell hyperplasia (DIPNECH)
G. Chassagnon*; Paris/FR (gchassagnon@gmail.com)*
Learning objectives:
1. To learn about the diagnostic criteria of this syndrome.
2. To understand the correspondence between imaging and pathology.
3. To know when to suggest this diagnosis on CT.
Author Disclosures:
G. Chassagnon: nothing to disclose

RC 1204-2 16:30
B. Carcinoid tumours
H. Prosch*; Vienna/AT (helmut.prosch@meduniwien.ac.at)*
Learning objectives:
1. To learn about the radiological features of central and peripheral carcinoids.
2. To know when to suspect a carcinoid tumour in a case of bronchial obstruction.
3. To learn about the role of FDG and DOTATOC PET/CT in the evaluation of carcinoid tumours.
Author Disclosures:
H. Prosch: nothing to disclose

RC 1204-3 17:00
C. Small cell lung cancer (SCLC)
M. Das*; Duisburg/DE (Marco.Das@helios-gesundheit.de)*
Learning objectives:
1. To learn about the common radiological manifestations of small cell lung cancer.
2. To learn how to distinguish between limited or extensive forms.
3. To learn how the TNM staging system should be integrated into the classification of SCLC.
Author Disclosures:
M. Das: nothing to disclose

16:00 - 17:30 **Darwin (Room D2)**

EFRS meets Slovenia

Meets 12

A guided tour of Slovenia through the modalities

Presiding:
J. McNulty; Dublin/IE
U. Gačnik; Ljubljana/SI

Meets 12-1 16:00
Session introduction
J. McNulty; *Dublin/IE (jonathan.mcnulty@ucd.ie)*
Author Disclosures:
J. McNulty: nothing to disclose

Meets 12-2 16:05
Introduction: Radiographers in Slovenia
U. Gačnik; *Ljubljana/SI (uros.gacnik@gmail.com)*
Session objectives:
1. To introduce the radiography profession in Slovenia and the priorities of the National Society.
2. To introduce Slovenia as a country, Slovenian life, and culture.
Author Disclosures:
U. Gačnik: Speaker at SLOVENIAN SOCIETY OF RADIOGRAPHERS

Meets 12-3 16:10
The radiographers' role in hybrid imaging
S. Rep; *Ljubljana, SLO/SI*
Learning objectives:
1. To understand the advantages and disadvantages of hybrid imaging.
2. To understand the importance of protocol optimisation and the important role of the radiographer.
3. To become familiar with the impact of quality control processes on image and data quality.
Author Disclosures:
S. Rep: nothing to disclose

Meets 12-4 16:26
The effective use of negative contrast agents in magnetic resonance cholangiopancreatography (MRCP)
A. Breznik; *Celje/SI (abreznik@gmail.com)*
Learning objectives:
1. To become familiar with different types of negative contrast agents in MRCP imaging.
2. To acknowledge the impact of using different negative contrast agents.
3. To learn about the possibilities of protocol optimisation in MRCP imaging.
Author Disclosures:
A. Breznik: nothing to disclose

16:42
Interlude: I feel Slovenia

Meets 12-6 16:47
Protocol designing and optimisation in cardiac CT
J. Mišič; *Ljubljana/SI (jure.misic@gmail.com)*
Learning objectives:
1. To become familiar with different cardiac CT scan modes.
2. To learn about the possibilities of protocol optimisation.
3. To understand the challenges in cardiac CT examination.
Author Disclosures:
J. Mišič: Employee at University medical centre Ljubljana

Meets 12-7 17:03
Quality assurance in mammography: evaluation of radiographs
E. Alukić; *Ljubljana/SI*
Learning objectives:
1. To present evaluation criteria for mammographic images from the Slovenian screening programme.
2. To review the most common positioning errors from across the Slovenian screening programme.
3. To address the challenges of the manual assessment of mammograms.
Author Disclosures:
E. Alukić: Speaker at UL, Faculty of Health Sciences

17:19
Panel discussion

16:00 - 17:30 **Descartes (Room D3)**

EFOMP Workshop

EF 12

CT protocol management and optimisation: optimisation (part B)

Moderator:
A. Trianni; Udine/IT

EF 12-2 16:00
Chairperson's introduction
M. Kortesniemi; *Hus/FI (mika.kortesniemi@hus.fi)*
Session objectives:
1. To understand why standardisation of acquisition and reconstruction protocols is needed in quantitative radiology.
2. To provide an overview of CT acquisition and reconstruction protocols based on clinical indications (low-dose and high-dose protocols as examples).
3. To understand the need for benchmarking optimised protocols in everyday clinical practice.
Author Disclosures:
M. Kortesniemi: nothing to disclose

EF 12-2 16:05
Optimised acquisition and reconstruction protocols: chest CT
E. Castellano; *London/UK (elly.castellano@rmh.nhs.uk)*
Learning objectives:
1. To give an overview of optimised protocols.
2. To understand issues related to the technical implementation of these protocols.
3. To discuss specific issues related to different scanners.
Author Disclosures:
E. Castellano: nothing to disclose

EF 12-3 16:30
Optimised acquisition and reconstruction protocols: cardiac CT
M. Kalra; *Boston, MA/US (MKALRA@mgh.harvard.edu)*
Learning objectives:
1. To give an overview of optimised protocols.
2. To understand issues related to the technical implementation of these protocols.
3. To discuss specific issues related to different scanners.
Author Disclosures:
M. Kalra: Research/Grant Support at Siemens Healthineers, Research/Grant Support at Riverain Inc.

EF 12-4 17:00
Optimised acquisition and reconstruction protocols: abdomen and CT angiography
N. Buls; *Brussels/BE (nico.buls@uzbrussel.be)*
Learning objectives:
1. To give an overview of optimised protocols.
2. To understand issues related to the technical implementation of these protocols.
3. To understand issues related to the role of iodine volume, concentration, and flow rate.
Author Disclosures:
N. Buls: Grant Recipient at GE Healthcare, Advisory Board at GE Healthcare

16:00 - 17:30 **Room G**

Multidisciplinary Session

MS 12a

Revisiting screening for developmental dysplasia of the hip (DDH)

MS 12a-1 16:00
Chairperson's introduction
K. Rosendahl*; Bergen/NO (karen.rosendahl@unn.no)*
Session objectives:
1. To explain the rationale behind US screening for developmental dysplasia of the hip.
2. To explain how a nation-wide screening programme could be established for developmental dysplasia of the hip.
3. To describe the current challenges and opportunities in the screening for developmental dysplasia of the hip.
Author Disclosures:
K. Rosendahl: nothing to disclose

MS 12a-2 16:15
The need for a standardised approach to US screening for DDH
K. G. Chlapoutakis*; Iraklion/GR (kgchlapoutakis@outlook.com)*
Learning objectives:
1. To explain the rationale behind US screening for developmental dysplasia of the hip.
2. To describe the method for US screening for developmental dysplasia of the hip.
Author Disclosures:
K. G. Chlapoutakis: nothing to disclose

MS 12a-3 16:35
A paediatrician's perspective on screening DDH: Swiss-Mongolian Paediatric Project
T. Baumann*; Solothurn/CH (tombaum@gawnet.ch)*
Learning objectives:
1. To explain how a nation-wide screening programme could be established for developmental dysplasia of the hip.
2. To describe the challenges and opportunities posed by a nation-wide screening for developmental dysplasia of the hip.
Author Disclosures:
T. Baumann: Investigator at Swiss international pediatric project

MS 12a-4 16:55
A paediatric orthopaedist's perspective: who, when and how to screen for DDH
C. Maizen*; London/UK (maizen.claudia@gmail.com)*
Learning objectives:
1. To explain the paediatric orthopaedic perspective on who, when and how to screen for developmental dysplasia of the hip.
2. To describe the challenges and opportunities in the screening for developmental dysplasia of the hip.
Author Disclosures:
C. Maizen: nothing to disclose

17:15
Panel discussion: How can we improve early detection of developmental dysplasia of the hip?

16:00 - 17:30 **Room K**

Multidisciplinary Session

MS 12b

Multidisciplinary team for epilepsy

MS 12b-1 16:00
Chairperson's introduction
P. Demaerel*; Leuven/BE*
Session objectives:
1. To understand the clinical aspects and treatment dilemmas of epileptic disease.
2. To review the role of imaging in the diagnosis and treatment planning of epilepsy.
3. To learn about image-guided resective epilepsy surgery and the postoperative outcome.
Author Disclosures:
P. Demaerel: nothing to disclose

MS 12b-2 16:05
Clinical presentation and treatment options in epileptic disease
A. Schulze-Bonhage*; Freiburg/DE (andreas.schulze-bonhage@uniklinik-freiburg.de)*
Learning objectives:
1. To review the clinical presentation of epilepsy.
2. To describe localising information in seizure semiology and EEG.
3. To discuss medical and surgical treatment options.
Author Disclosures:
A. Schulze-Bonhage: Grant Recipient at BIAL, Investigator at UCB, Precisis, Speaker at BIAL, EISAI, UCB, Advisory Board at GW, Lundbek, Synergia

MS 12b-3 16:20
Radiological workup in epilepsy: (functional) MRI
H. Urbach*; Freiburg/DE (horst.urbach@uniklinik-freiburg.de)*
Learning objectives:
1. To describe options for the detection of epileptogenic foci.
2. To explore the value of functional imaging techniques in epilepsy.
3. To show how to perform a pre-surgical imaging workup.
Author Disclosures:
H. Urbach: Shareholder at Veobrain GmbH

MS 12b-4 16:35
Stereotactic techniques
V. Coenen*; Freiburg/DE (Volker.coenen@uniklinik-freiburg.de)*
Learning objectives:
1. To describe general options of stereotactic techniques in epilepsy.
2. To discuss stereotactic lesioning techniques in different indications.
3. To show state-of-the-art SEEG technique.
Author Disclosures:
V. Coenen: Advisory Board at CorTec, Advisory Board at Cortics, Other at Medtronic, Other at Boston Scientific

MS 12b-5 16:50
Image-guided epilepsy surgery
J. Beck*; Freiburg/DE*
Learning objectives:
1. To describe non-invasive and invasive pre-surgical diagnostic modalities.
2. To review surgical treatment options and the postoperative outcome.
3. To discuss how to deal with MRI-negative epilepsy.
Author Disclosures:
J. Beck: disclosure/affirmation information not submitted

17:05
Multidisciplinary case presentation and discussion

16:00 - 17:30 **Room M 1**

ESHI^{MT} Session

ESHI(MT)

The importance of identifying technical errors in hybrid imaging: pitfalls and artefacts in PET/CT and PET/MRI

Moderators:
M. D'Anastasi; Msida/MT
J. Rübenthaler; Munich/DE

ESHI(MT)-1 16:00
Artefacts on PET/CT and PET/MRI
I. Rausch*; Vienna/AT*
Learning objectives:
1. To understand image distortions, artefacts, and bias from methodological pitfalls in PET/CT and PET/MR imaging.
2. To learn about possible solutions to frequent image distortions.
3. To understand the methodological limitations of PET/CT and PET/MRI.
Author Disclosures:
I. Rausch: nothing to disclose

ESHI(MT)-2 16:23
Pitfalls in FDG-PET/CT
J. L. Vercher Conejero*; Barcelona/ES (jlvercher@hotmail.com)*
Learning objectives:
1. To become familiar with the different types of pitfalls in FDG-PET/CT imaging and how to minimise them.
2. To understand the strengths and limitations of FDG-PET/CT as a hybrid imaging modality.
3. To learn about the correct patient preparation, relevant patient history, and data and study acquisition.
Author Disclosures:
J. L. Vercher Conejero: Advisory Board at AAA

ESHI(MT)-3 16:46
Beyond FDG: pitfalls and artefacts
C. C. Cyran*; Munich/DE (clemens.cyran@med.uni-muenchen.de)*
Learning objectives:
1. To learn about the most frequent pitfalls and artefacts of PET tracers beyond FDG.
2. To appreciate the most important risks of misinterpretation with PET tracers beyond FDG.
3. To understand the physiological background of pitfalls and artefacts when imaging with PET tracers beyond FDG.
Author Disclosures:
C. C. Cyran: Consultant at Sandoz, Speaker at Goetz Partners Ltd

17:09
Panel discussion: Clinical relevance of misinterpreting pitfalls and artefacts in hybrid imaging. How can we augment diagnostic confidence in hybrid imaging?

16:00 - 17:30 **Room M 2**

E^3 - Advanced Course: How to Improve Your Expertise in Cardiothoracic Imaging

E^3 1219

Infections of the chest

E^3 1219-1 16:00
Chairperson's introduction
R. Cesar*; Golnik/SI (rok.cesar@klinika-golnik.si)*
Session objectives:
1. To review the role of imaging in infectious lung diseases.
2. To learn about cardiac complications of infections.
Author Disclosures:
R. Cesar: nothing to disclose

E^3 1219-2 16:06
A. Pulmonary infections
J. Neuwirth*; Prague 10/CZ (neuwirthj@gmail.com)*
Learning objectives:
1. To review the role and limitations of chest-x ray for diagnosing community-acquired pneumonia.
2. To learn about pulmonary infections in immunocompromised hosts.
3. To become familiar with CT signs suggesting fungal infection.
Author Disclosures:
J. Neuwirth: Speaker at IPVZ, Chair of radiology, Prague

E^3 1219-3 16:34
B. Tuberculosis (TB)
I. E. Tyurin*; Moscow/RU (igortyurin@gmail.com)*
Learning objectives:
1. To evaluate the imaging patterns of thoracic tuberculosis.
2. To review the different imaging features of the disease in immune compromised patients.
3. To discuss the current role of imaging in nontuberculous mycobacterial disease.
Author Disclosures:
I. E. Tyurin: nothing to disclose

E^3 1219-4 17:02
C. Infectious endocarditis
H. Alkadhi*; Zurich/CH*
Learning objectives:
1. To review the valvular consequences of untreated infections.
2. To become familiar with the CT signs of endocarditis in native valves.
3. To learn about the typical appearance of infectious complications after valvular surgery.
Author Disclosures:
H. Alkadhi: nothing to disclose

16:00 - 17:30 **Room M 3**

RTF - Radiology Trainees Forum

TF

Highlighted Lectures

Moderators:
M. Marolt Music; Ljubljana/SI
N. I. Traikova; Plovdiv/BG

TF-1 16:00
Imaging of knee in sports injuries
Ž. Snoj*; Ljubljana/SI (ziga.snoj@gmail.com)*
Learning objectives:
1. To understand the most common sports-related injury patterns in the knee.
2. To learn what to include in the MRI report.
3. To be familiar with diagnostic features after post-treatment procedures in the knee.
Author Disclosures:
Ž. Snoj: nothing to disclose

TF-2 16:30
Benign lesions in head and neck: what is really benign?
R. Maroldi*; Brescia/IT*
Learning objectives:
1. To be familiar with the most common benign findings in head and neck imaging.
2. To understand what benign lesions could cause potential complications and where is the need to be extremely cautious.
3. To know what to include in the MRI report.
Author Disclosures:
R. Maroldi: nothing to disclose

TF-3 17:00
Bone lesions: an integrated approach
V. Cassar-Pullicino*; Oswestry/UK (Victor.Pullicino@nhs.net)*

Learning objectives:
1. To describe typical features of normal bone marrow.
2. To understand normal bone marrow transformation over maturation.
3. To get familiar with MRI pattern of malignant bone marrow lesions.
4. To get familiar with MRI pattern of benign bone marrow lesions.
5. To get familiar with bone marrow MRI pattern as a consequence of iatrogenic (radiotherapy etc.) or metabolic (bone marrow transformation etc.).
Author Disclosures:
V. Cassar-Pullicino: nothing to disclose

16:00 - 17:30 **Room M 4**

Transatlantic Course of ESR and RSNA (Radiological Society of North America): Stroke Imaging and Endovascular Treatment: Now and the Future

TC 1228

Current status of stroke workup and treatment

Moderators:
R. Uberoi; Oxford/UK
A. Vagal; Cincinnati, OH/US

TC 1228-1 16:00
A. Current status of endovascular management of acute ischaemic stroke: evidence and guidelines
R. Uberoi*; Oxford/UK (raman.uberoi@ouh.nhs.uk)*
Learning objectives:
1. To learn about current evidence of endovascular treatment in acute ischaemic stroke.
2. To become familiar with evidence-based guidelines (AHA/ASA and ESO/ESMINT) in stroke treatment.
Author Disclosures:
R. Uberoi: Grant Recipient at Gore, Grant Recipient at Terumo

TC 1228-2 16:25
B. CT-based evaluation of acute stroke: advantages and challenges
A. Vagal*; Cincinnati, OH/US (vagala@ucmail.uc.edu)*
Learning objectives:
1. To learn about the advantages and challenges of CT-based stroke imaging workup.
2. To become familiar with the pitfalls of CT perfusion imaging.
Author Disclosures:
A. Vagal: Research/Grant Support at NIH/NINDS, Cerovenus

TC 1228-3 16:50
C. MRI-based evaluation of acute stroke: advantages and challenges
M. Wintermark*; Stanford, CA/US*
Learning objectives:
1. To learn about the advantages of MRI-based stroke imaging workup.
2. To become familiar with the challenges of MRI-based stroke imaging workup.
Author Disclosures:
M. Wintermark: Advisory Board at Icometrix, Advisory Board at MoreHealth, Advisory Board at Magnetic Insight, Advisory Board at Nines, Advisory Board at Subtle

17:15
Panel discussion: Strategy for acute stroke imaging and intervention

16:00 - 17:30 **Room M 5**

E^3 - Advanced Course: Hot Topics in GU Cancer

E^3 1222

Whole-body imaging in gynaecological malignancy

E^3 1222-1 16:00
Chairperson's introduction
P. Rousset*; Pierre-Bénite/FR (roussetpascal@gmail.com)*
Author Disclosures:
P. Rousset: nothing to disclose

E^3 1222-2 16:15
A. Whole-body MRI for staging and treatment planning in ovarian cancer
V. Vandecaveye*; Leuven/BE (vincent.vandecaveye@uz.kuleuven.ac.be)*
Learning objectives:
1. To learn the MRI technique for imaging the peritoneum in advanced ovarian cancer.
2. To learn the appearances of whole-body MRI in metastatic ovarian cancer.
3. To be aware of the pitfalls to interpretation.
Author Disclosures:
V. Vandecaveye: nothing to disclose

E^3 1222-3 16:40
B. PET/CT and PET/MRI in cervix and endometrial cancer: current status
L. Umutlu*; Essen/DE (Lale.Umutlu@uk-essen.de)*
Learning objectives:
1. To learn the indications for use of hybrid imaging in cervix and endometrial cancer.
2. To know the strengths and weaknesses of the technique.
3. To be familiar with the role of hybrid imaging in patient prognosis.
Author Disclosures:
L. Umutlu: Speaker at Siemens Healthineers, Speaker at Bayer Healthcare, Grant Recipient at Siemens Healthineers

E^3 1222-4 17:05
C. Advanced imaging techniques in metastatic gynaecological cancer
E. Sala*; Cambridge/UK (es220@medschl.cam.ac.uk)*
Learning objectives:
1. To learn about the concept and technique of texture analysis.
2. To be familiar with the key associations between biology and texture features.
3. To be familiar with the potential added value of texture analysis in image interpretation.
Author Disclosures:
E. Sala: nothing to disclose

16:00 - 17:30 **Tech Gate Auditorium**

Special Focus Session

SF 12

Update in head and neck cancer imaging

SF 12-1 16:00
Chairperson's introduction
M. Ravanelli*; Brescia/IT*
Session objectives:
1. To learn about the role of functional imaging in the diagnosis, treatment planning, and evaluation of head and neck cancer.
2. To become acquainted with the technique, current status, and future directions of quantitative imaging analysis in head and neck oncology.
Author Disclosures:
M. Ravanelli: disclosure/affirmation information not submitted

SF 12-2 16:05
Functional imaging for characterisation of primary tumours
M. de Win*; Amsterdam/NL (m.m.dewin@amsterdamumc.nl)*
Learning objectives:
1. To review functional imaging techniques applied in head and neck oncology.
2. To gain an understanding of the underlying biologic phenomena represented by the different techniques.
3. To appreciate their usefulness for histopathologic differentiation of a primary head and neck tumour.
Author Disclosures:
M. de Win: nothing to disclose

SF 12-3 16:30
Functional imaging for treatment prediction and treatment monitoring
M. Becker*; Geneva/CH*
Learning objectives:
1. To understand the role of functional imaging in treatment planning of head and neck cancers.
2. To become familiar with the role of functional imaging in the evaluation of therapeutic response.
3. To recognise the challenges of the execution and interpretation of hybrid imaging, and to learn about solutions.
Author Disclosures:
M. Becker: Grant Recipient at Swiss National Science Foundation

SF 12-4 16:55
Texture analysis and radiogenomics in head and neck carcinoma
A. D. King*; Hong Kong/CN*
Learning objectives:
1. To learn about the rationale and technique of texture analysis and radiogenomics.
2. To acquire knowledge of the current results of these techniques in head and neck oncology.
3. To get an insight into the challenges of these techniques and future directions.
Author Disclosures:
A. D. King: nothing to disclose

17:20
Panel discussion: New tools in head and neck oncology: fancy follies or must haves?

Saturday, March 14

08:30 - 10:00 **Room C**

Abdominal Viscera

RC 1301

Common benign and malignant liver lesions: unusual radiological appearance

Moderator:
S. M. Ertürk; Istanbul/TR

RC 1301-1 08:30
A. Features of benign liver lesions
M. M. França*; Maia/PT (mariamanuela.franca@gmail.com)*
Learning objectives:
1. To know the most common benign liver lesions.
2. To learn about unusual appearances of benign liver tumours.
3. To develop an algorithm in order to find the correct differential diagnosis.
Author Disclosures:
M. M. França: nothing to disclose

RC 1301-2 09:00
B. Features of primary malignant liver lesions
V. Vilgrain*; Clichy/FR (valerie.vilgrain@aphp.fr)*
Learning objectives:
1. To understand the typical features and prevalence of hepatocellular carcinomas (HCCs) and cholangiocellular carcinomas (CCCs).
2. To learn about the reasons why HCCs and CCCs do not always show typical imaging features.
3. To establish a strategy as to how to differentiate atypical HCCs and CCCs from other liver tumours.
Author Disclosures:
V. Vilgrain: Speaker at Hospital Beaujon

RC 1301-3 09:30
C. Features of liver metastases
Y. Menu*; Paris/FR (yves.menu@aphp.fr)*
Learning objectives:
1. To learn about the primary tumours often leading to liver metastases.
2. To understand why liver metastases can have different imaging characteristics.
3. To know the imaging features of liver metastases after systemic chemotherapy or loco-regional therapy.
Author Disclosures:
Y. Menu: nothing to disclose

08:30 - 10:00 **Room X**

Joint Session of the ESR and ESMRMB

ESR/ESMRMB

Ultrahigh-field (UHF) MRI goes clinical and beyond

Moderators:
R. Kreis; Bern/CH
A. Rockall; London/UK

ESR/ESMRMB-1 08:30
Challenges and solutions
A. G. Webb*; Leiden/NL (a.webb@lumc.nl)*
Learning objectives:
1. To learn about the challenges due to theoretical differences between MRI at very high and low field.
2. To understand the physical basis for improved imaging at very high fields.
3. To appreciate the technical solutions and the promise of ultrahigh-field MRI.
Author Disclosures:
A. G. Webb: nothing to disclose

ESR/ESMRMB-2 08:55
The clinical use today
T. Sinnecker*; Basel/CH (tim.sinnecker@miac.ch)*
Learning objectives:
1. To learn about currently available imaging methods available at UHF.
2. To appreciate the clinical benefits of UHF MRI in neurologic and non-neurologic diseases.
3. To recognise the potential of UHF MRI in MS.
Author Disclosures:
T. Sinnecker: Employee at Medical Image Analysis Center (MIAC), Other at Travel support from Roche and Actelion outside of this work

ESR/ESMRMB-3 09:20
New horizons
J. Wijnen*; Utrecht/NL (jwijnen@umcutrecht.nl)*
Learning objectives:
1. To learn about non-standard contrasts becoming available thanks to UHF.
2. To appreciate the clinical potential of proton and heteronuclear spectroscopy at UHF.
3. To catch a glimpse of heteronuclear MRI at 7T and beyond.
Author Disclosures:
J. Wijnen: nothing to disclose

09:45
Panel discussion: Does UHF MRI add more than cost?

09:00 - 10:00 **Coffee & Talk 1**

Coffee & Talk (open forum) Session

Organised by ESOR

C 7

Why are research fellowships important for young radiologists?

C 7-1 09:00
Chairperson's introduction
L. Marti-Bonmati*; Valencia/ES (Luis.Marti@uv.es)*
Session objectives:
1. To interact with young and senior radiologists to foster research.
2. To discuss all elements of researchers' involvement.
3. To understand enhanced critical-thinking and problem-solving skills.
4. To provide data for discussions in competencies and in healthcare innovation.
Author Disclosures:
L. Marti-Bonmati: nothing to disclose

C 7-2 09:10
My experience as a young research fellowship recipient
J. Amorim*; Porto/PT (joaopinheiroamorim@gmail.com)*
Learning objectives:
1. To comment on the lessons learned and opportunities for young researchers.
2. To understand how research and clinical practice can be related.
3. To become familiar with main radiological research methodologies.
4. To learn how a research relationship can be built and followed-up.
Author Disclosures:
J. Amorim: Grant Recipient at Bracco Fellowship from the European School of Radiology (ESOR)

C 7-3 09:20
Multidisciplinary collaboration to improve research in radiology
A. Alberich-Bayarri*; Valencia/ES (angel@quibim.com)*
Learning objectives:
1. To comment on the relevance of multidisciplinary collaboration in all steps of research.
2. To become familiar with the creation of, and problems related to, collaborative research.
3. To learn how knowledge, innovation, improvements, and visibility are distributed in healthcare.
Author Disclosures:
A. Alberich-Bayarri: CEO at QUIBIM SL, Board Member at QUIBIM SL, Founder at QUIBIM SL

C 7-4 09:30
How to mentor research fellowship programmes
R. Manfredi*; Rome/IT*
Learning objectives:
1. To understand how to develop or set up a research institutional programme.
2. To learn how to attract the best residents, fellows, and staff radiologists.
3. To be able to manage levels of involvement, tasks, and times (chronograms).
Author Disclosures:
R. Manfredi: Speaker at Bracco

09:40
Open forum discussion

08:30 - 10:00 **Room N**

EuroSafe Imaging Session

EU 13
Paediatric CT doses and risks (MEDIRAD)

Moderator:
I. Thierry-Chef; Barcelona/ES

EU 13-1 08:30
Chairperson's introduction
J. Damilakis*; Iraklion/GR (John.Damilakis@med.uoc.gr)*
Author Disclosures:
J. Damilakis: Research/Grant Support at European Commission H2020

EU 13-2 08:35
The use of CT in paediatrics: examination frequencies and common practices
M. Kaijser*; Danderyd/SE*
Learning objectives:
1. To provide information on the role of CT in the paediatric population.
2. To describe historical and current trends of CT usage in the paediatric population.
3. To discuss what can be expected of paediatric imaging in the future.
Author Disclosures:
M. Kaijser: disclosure/affirmation information not submitted

EU 13-3 08:50
CT dosimetry in children: patient-specific dosimetry and dose reduction tools
J. Damilakis*; Iraklion/GR (John.Damilakis@med.uoc.gr)*
Learning objectives:
1. To learn the strengths and limitations of patient-specific CT dosimetry.
2. To become familiar with dose reduction tools in paediatric CT.
3. To be updated about radiation doses in paediatric CT.
Author Disclosures:
J. Damilakis: Research/Grant Support at European Commission H2020

EU 13-4 09:05
Radiation exposure from CT in childhood and subsequent risk of haematological malignancies, brain and other cancers
I. Thierry-Chef*; Barcelona/ES*
Learning objectives:
1. To present the results of the EPI-CT European study concerning haematological malignancies.
2. To present the results of the EPI-CT European study concerning brain cancers and other solid tumours.
3. To discuss extension of follow-up and the need for a more detailed nested case-control study.
4. To share the lessons learned for optimisation of paediatric imaging protocols.
Author Disclosures:
I. Thierry-Chef: Employee at ISGlobal

EU 13-5 09:20
Risk communication and risk optimisation
C. Granata*; Genoa/IT*
Learning objectives:
1. To learn how to establish an effective dialogue in a clinical setting with parents and carers.
2. To understand how the principles of justification and optimisation, and their implementation, are the basis of risk optimisation in radiologic imaging.
Author Disclosures:
C. Granata: Speaker at Guerbet

09:35
Panel discussion: Radiation safety in paediatric CT: what are the challenges?

08:30 - 10:00 **Room O**

E³ - ECR Master Class (Breast)

E³ 1326a
Artificial intelligence (AI) in breast imaging: potential perspectives and (unjustified) fears

Moderator:
T. H. Helbich; Vienna/AT

E³ 1326a-1 08:30
A. What a breast radiologist should know about artificial intelligence
E. Giannotti*; Nottingham/UK (ytteb84@hotmail.com)*
Learning objectives:
1. To define all terms used in artificial intelligence topics.
2. To know the main domains of applications in breast imaging.
3. To understand the principles of deep learning algorithm.
Author Disclosures:
E. Giannotti: nothing to disclose

E³ 1326a-2 09:00
B. Deep learning algorithm applications in breast imaging
I. Thomassin-Naggara*; Paris/FR (isabellethomassin@gmail.com)*
Learning objectives:
1. To understand when we need to train, validate, and apply an AI in clinical routine.
2. To appreciate the real value for diagnosis of the different existing algorithms.
3. To learn how we could use it for personalised screening.
Author Disclosures:
I. Thomassin-Naggara: Advisory Board at siemens, Research/Grant Support at GE, Research/Grant Support at Canon, Speaker at GE, Speaker at Canon, Speaker at Guerbet, Speaker at Hologic

E³ 1326a-3 09:30
C. Radiomics and breast imaging
K. Pinker-Domenig*; New York, NY/US (pinkerdk@mskcc.org)*
Learning objectives:
1. To learn how a radiomic model may be built.
2. To know the main applications of radiomics in breast imaging.
3. To understand potential clinical implications of this domain.
Author Disclosures:
K. Pinker-Domenig: Research/Grant Support at Katja Pinker is funded in part through the NIH/NCI Cancer Center Support Grant P30 CA008748., Speaker at Katja Pinker received payment for activities not related to the present article including lectures, service on speakers bureaus and for travel/accommodations/meeting expenses from the European Society of Breast Imaging (MRI educational course, annual scie, Research/Grant Support at Digital Hybrid Breast PET/MRI for Enhanced Diagnosis of Breast Cancer (HYPMED) H2020 - Research and Innovation Framework Programme PHC-11-2015 # 667211-2, Research/Grant Support at A Body Scan for Cancer Detection using Quantum Technology (CANCERSCAN) H2020-FETOPEN-2018-2019-2020-01 # 828978, Research/Grant Support at ultiparametric 18F-Fluoroestradiol PET/MRI coupled with Radiomics Analysis and Machine Learning for Prediction and Assessment of Response to Neoadjuvant Endocrine Therapy in Patients with Hormone Receptor+/HER2− Invasive Breast Cancer 02.09.2019 / 31.08.2

08:30 - 10:00 **Studio 2020**

Special Focus Session

SF 13

The abused child: the key role of imaging

SF 13-1 08:30
Chairperson's introduction
S. M. Aukland; *Bergen/NO (stein.magnus.aukland@helse-bergen.no)*
Session objectives:
1. To learn about existing imaging guidelines in suspected physical child abuse.
2. To learn about the typical radiological findings in physical child abuse and how to differentiate inflicted from accidental injury.
3. To discuss the radiological evidence and the medico-legal role of the radiologist in physical child abuse.
Author Disclosures:
S. M. Aukland: nothing to disclose

SF 13-2 08:34
Skeletal injury: should we use radiography or CT?
R. R. van Rijn; *Amsterdam/NL (r.r.vanrijn@amsterdamumc.nl)*
Learning objectives:
1. To learn about usual aspects of skeletal injury in non-accidental trauma.
2. To learn about appropriate workup and existing guidelines.
3. To discuss respective indications for radiography and CT.
Author Disclosures:
R. R. van Rijn: nothing to disclose

SF 13-3 08:52
Head injury CT and/or MRI?
A. Choudhary; *Little Rock, AR, AR/US (achoudhary@uams.edu)*
Learning objectives:
1. To learn about usual aspects of abusive head injury.
2. To learn about appropriate workup and existing guidelines.
3. To discuss respective indications for CT and MRI.
Author Disclosures:
A. Choudhary: Shareholder at GE, Speaker at Honorarium for lectures for child abuse courses, Other at expert witness for child abuse cases

SF 13-4 09:10
Inflicted abdominal injury
M. Raissaki; *Iraklion/GR (mraissaki@yahoo.gr)*
Learning objectives:
1. To learn about typical imaging findings in abdominal trauma.
2. To learn about appropriate radiology workup in suspected inflicted abdominal injuries.
3. To discuss indications for imaging.
Author Disclosures:
M. Raissaki: nothing to disclose

SF 13-5 09:28
Testimony in court
A. C. Offiah; *Sheffield/UK (amaka.offiah@nhs.net)*
Learning objectives:
1. To learn about the paediatric radiologist as a medico-legal expert.
2. To describe the role of the paediatric radiologist as part of the multidisciplinary team in suspected child abuse.
3. To learn about the role and the challenges for the paediatric radiologist during testimony in court.
Author Disclosures:
A. C. Offiah: Advisory Board at Alexion, Board Member at BioMarin, Grant Recipient at Alexion, Speaker at InfoMed, Other at Expert witness in cases of suspected child abuse

09:46
Panel discussion: Imaging in non-accidental injury: the role of the paediatric radiologist

08:30 - 09:30 **Coffee & Talk 2**

Coffee & Talk (open forum) Session

Organised by EuroSafe Imaging

C 17

International Society of Radiology (ISR) call for action on quality and safety

Moderators:
D. P. Frush; Durham/US
G. Frija; Paris/FR

C 17-1 08:30
Introduction to the concept of the International Atomic Energy Agency (IAEA) Bonn Call for Action
O. Holmberg; *Vienna/AT (O.Holmberg@iaea.org)*
Learning objectives:
1. To learn what the Bonn Call for Action is, and how it helps strengthen radiation protection in medicine.
2. To understand the involvement of international organisations, radiation protection campaigns, and other interested parties in the implementation of the Bonn Call for Action.
3. To gain knowledge on different radiation protection initiatives and activities that link to the Bonn Call for Action.
Author Disclosures:
O. Holmberg: nothing to disclose

C 17-2 08:40
The World Health Organisation (WHO) vision
M. D. R. D. R. Perez; *Geneva/CH (perezm@who.int)*
Learning objectives:
1. To present the WHO views and actions to promote quality and safety in health care.
2. To identify the challenges and opportunities for enhancing radiation safety culture in health care.
3. To discuss strategies for integrating radiation safety into the concept of patient safety and quality of care, enhancing stakeholders' engagement, and strengthening global cooperation.
Author Disclosures:
M. D. R. D. R. Perez: nothing to disclose

C 17-3 08:50
The Middle East vision
S. Hagi; *Jeddah/SA (sarahhagi@gmail.com)*
Learning objectives:
1. To present the current status of quality and safety issues in the Middle East region.
2. To address expectations and challenges for ArabSafe.
3. To identify opportunities of increased cross-fertilization between ArabSafe and ISRQSA.
Author Disclosures:
S. Hagi: nothing to disclose

C 17-4 09:00
The African vision
T. El-Diasty; *Mansoura/EG (teldiasty@hotmail.com)*
Learning objectives:
1. To highlight the interest of the ISR and EuroSafe Imaging in promoting quality and safety issues in Africa.
2. To address challenges regarding quality/safety awareness in Africa.
3. To present the situation in Africa and the expectations of the African Society of Radiology (ASR) and AFROSAFE.
Author Disclosures:
T. El-Diasty: nothing to disclose

C 17-5 09:10
The Chinese vision
Z. Y. Jin; *Beijing/CN*

Learning objectives:
1. To highlight the current status of quality and safety in the Chinese radiology field.
2. To address challenges to quality and safety control of clinical radiology practice in China.
3. To present EuroSafe's potential in promoting quality and safety issues in China.
Author Disclosures:
Z. Y. Jin: disclosure/affirmation information not submitted

09:20
Open forum discussion

08:30 - 10:00 **Room E**

E³ - Advanced Course: Interactive Teaching Session for Young (and not so Young) Radiologists

E³ 1321

Musculoskeletal radiology: arthropathies

E³ 1321-1 08:30
A. Extremities
Ü. Aydingöz; *Ankara/TR (ustunaydingoz@yahoo.com)*
Learning objectives:
1. To explain the key points in the differential diagnosis of common arthropathies in the extremities.
2. To describe the imaging findings of common arthropathies in the extremities as they relate to pathophysiology.
Author Disclosures:
Ü. Aydingöz: nothing to disclose

E³ 1321-2 09:15
B. The axial skeleton
A. H. Karantanas; *Iraklion/GR (akarantanas@gmail.com)*
Learning objectives:
1. To explain the key points in the differential diagnosis of arthropathies in the axial skeleton.
2. To describe the imaging findings of arthropathies in the axial skeleton as they relate to pathophysiology.
Author Disclosures:
A. H. Karantanas: nothing to disclose

08:30 - 10:00 **Room F1**

E³ - ECR Master Class (Chest)

E³ 1326b

Autoimmune thoracic diseases

Moderator:
P. A. Grenier; Paris/FR

E³ 1326b-1 08:30
A. Relapsing polychondritis
A.-L. Brun; *Suresnes/FR (annelaure.brun@gmail.com)*
Learning objectives:
1. To learn about the pathophysiology and clinical manifestations of this disease.
2. To learn when to suggest this diagnosis on CT.
3. To review the other causes of tracheobronchial wall thickening.
Author Disclosures:
A.-L. Brun: nothing to disclose

E³ 1326b-2 09:00
B. Alveolar proteinosis
A. Oikonomou; *Toronto, ON/CA (anastasia.oikonomou@sunnybrook.ca)*
Learning objectives:
1. To learn about the CT manifestations of alveolar proteinosis.
2. To review the other causes of crazy paving on CT.
3. To be aware of infectious complications, especially superinfection by Nocardia.
Author Disclosures:
A. Oikonomou: nothing to disclose

E³ 1326b-3 09:30
C. Goodpasture syndrome and differentials
A. Devaraj; *London/UK*
Learning objectives:
1. To learn about the pathophysiology and the clinical manifestations of this disease.
2. To learn about CT signs of intra-alveolar haemorrhage.
3. To review the other causes of intra-alveolar haemorrhage.
Author Disclosures:
A. Devaraj: Advisory Board at Boehringer Ingelheim

09:00 - 10:00 **Coffee & Talk 3**

Coffee & Talk (open forum) Session -

Organised by the ESR Subcommittee on Undergraduate Education

C 29

Developing the next generation radiologist by targeting undergraduates

C 29-1 09:00
Welcome and introduction: It's never too early to develop the next generation radiologist
V. Goh; *London/UK (vicky.goh@kcl.ac.uk)*
Session objectives:
1. To understand why it is important to target medical students.
2. To highlight the current undergraduate engagement programmes.
3. To identify further strategies for ESR to improve undergraduate engagement.
Author Disclosures:
V. Goh: Research/Grant Support at Siemens, Speaker at Siemens

C 29-2 09:05
Why I chose radiology as a future career
A. Sharkey; *London/UK (AmyRose.Sharkey@gstt.nhs.uk)*
Learning objectives:
1. To appreciate the factors influencing career decision-making at the undergraduate level.
2. To highlight the challenges in making radiology an attractive career.
3. To learn of successful practices in promoting radiology to undergraduates.
Author Disclosures:
A. Sharkey: nothing to disclose

C 29-3 09:13
Engaging undergraduates: lessons learnt from a young teacher's perspective
A. Svare; *Riga/LV (atis.svare@gmail.com)*
Learning objectives:
1. To understand the challenges of engaging undergraduates from a teacher's perspective.
2. To highlight current best practice in teaching radiology.
3. To learn potential ways to improve radiology engagement in undergraduate education.
Author Disclosures:
A. Svare: nothing to disclose

C 29-4 09:21
Interactivity: using software teaching platforms to inspire undergraduates
T. Vincent; *Brighton/UK (T.R.Vincent@bsms.ac.uk)*

Learning objectives:
1. To understand the key educational design principles that help make digital learning resources effective for learners.
2. To explore how digital learning resources can help attract undergraduates to radiology.
3. To discuss how ESR could improve undergraduate engagement with teaching and learning platforms.
Author Disclosures:
T. Vincent: nothing to disclose

C 29-5 09:29
How could the ESR develop the next generation radiologists? Delivering the undergraduate curriculum
C. Catalano; *Rome/IT (carlo.catalano@uniroma1.it)*
Learning objectives:
1. To highlight how the ESR undergraduate curriculum was conceived and developed.
2. To highlight how ESR is delivering the curriculum.
3. To highlight how ESR is developing undergraduate engagement.
Author Disclosures:
C. Catalano: nothing to disclose

C 29-6 09:37
Open forum discussion: The next generation radiologist: next steps in producing a white paper
V. Goh; *London/UK,* A. Sharkey; *London/UK,* A. Svare; *Riga/LV,* T. Vincent; *Brighton/UK,* C. Catalano; *Rome/IT,* L. Oleaga Zufiria; *Barcelona/ES (lauraoleaga@gmail.com)*
Author Disclosure:
L. Oleaga Zufiria: Consultant at TMC Academy

08:30 - 10:00 **da Vinci (Room D1)**

Emergency Imaging

RC 1317
Imaging of 'foreign bodies'

RC 1317-1 08:30
Chairperson's introduction
J. B. Dormagen; *Oslo/NO (jobador@gmail.com)*
Session objectives:
1. To become familiar with commonly used surgical and orthopaedic devices and materials.
2. To learn their proper positioning, and the early signs of postoperative complications.
3. To understand the imaging pathway in management of ingested foreign bodies.
Author Disclosures:
J. B. Dormagen: nothing to disclose

RC 1317-2 08:35
A. Surgical and orthopaedic devices: are they really properly positioned?
E. A. Dick; *London/UK (elizabethdick2010@gmail.com)*
Learning objectives:
1. To become familiar with different types of commonly used surgical, neurosurgical, and orthopaedic devices in clinical practice.
2. To understand how to evaluate their proper positioning.
3. To be familiar with imaging signs of incorrect implementation of neurosurgical and orthopaedic devices.
Author Disclosures:
E. A. Dick: Board Member at ESER

RC 1317-3 09:00
B. Did I swallow that? US and CT of sharp foreign bodies penetrating stomach and bowel
J. B. C. M. Puylaert; *The Hague/NL (dr.jbcmpuylaert@wxs.nl)*
Learning objectives:
1. To be familiar with characteristics of commonly ingested foreign bodies.
2. To understand which imaging modalities are best suited for detection of foreign bodies in different clinical scenarios.
3. To recognise the first signs of early complications resulting from ingested foreign bodies.
Author Disclosures:
J. B. C. M. Puylaert: nothing to disclose

RC 1317-4 09:25
C. The role of interventional radiology in the management of foreign bodies and following complications
H. Leonhardt; *Gothenburg/SE (henrik.leonhardt@vgregion.se)*
Learning objectives:
1. To recognise the role of interventional radiology in the treatment of complications resulting from the presence of foreign bodies.
2. To learn when to call the interventional radiologist.
3. To learn about techniques of the removal of foreign bodies with an endovascular approach.
Author Disclosures:
H. Leonhardt: nothing to disclose

09:50
Panel discussion: Common language with clinicians: how to report 'foreign bodies' presence and indicate the optimal management

08:30 - 10:00 **Darwin (Room D2)**

EFRS meets the Netherlands

Meets 13
Safety in the Netherlands

Presiding:
J. McNulty; Dublin/IE
S. Geers van Gemeren; Utrecht/NL

Meets 13-1 08:30
Session introduction
J. McNulty; *Dublin/IE (jonathan.mcnulty@ucd.ie)*
Author Disclosures:
J. McNulty: nothing to disclose

Meets 13-2 08:35
Introduction: Radiographers in the Netherlands
S. Geers van Gemeren; *Utrecht/NL (s.geers@nvmbr.nl)*
Session objectives:
1. To introduce the radiography profession in the Netherlands and the priorities of the National Society.
2. To introduce the Dutch country and culture.
3. To introduce the important role of radiographers in safety.
Author Disclosures:
S. Geers van Gemeren: nothing to disclose

Meets 13-3 08:40
Hybrid imaging: the merge between radiology and nuclear medicine
P. Liedorp; *Raamsdonkveer/NL (peter@pi-medical.nl)*
Learning objectives:
1. To understand the advantages and disadvantages of merging radiology and nuclear medicine departments.
2. To understand the history of hybrid imaging.
3. To become familiar with the safety issues in hybrid imaging and the change in education of radiographers.
Author Disclosures:
P. Liedorp: nothing to disclose

Meets 13-4 08:56
Gonad shielding guidelines for radiographers
A. Vegter; *Stadskanaal/NL (a.vegter@treant.nl)*
Learning objectives:
1. To learn about the Dutch gonad shielding guidelines for radiographers.
2. To acknowledge the impact of using guidelines and standards for the profession.
3. To learn about the import role of clinical reasoning for radiation protection.
Author Disclosures:
A. Vegter: nothing to disclose

09:12
Interlude: Feel the Netherlands

Meets 13-6 09:17
REVIVE: Radiology during pregnancy: translating risk factor publications and international guidelines into practice when communicating with pregnant patients
C. Vroonland*; Haarlem/NL (colinda.vroonland@inholland.nl)*
Learning objectives:
1. To become familiar with the multidisciplinary project REVIVE.
2. To learn about the Dutch guidelines.
3. To understand the challenges in implementing guidelines and standards.
Author Disclosures:
C. Vroonland: Research/Grant Support at SIA

Meets 13-7 09:33
Electromagnetic field risk assessment and evaluation in MRI
J. Meedendorp*; Utrecht/NL*
Learning objectives:
1. To learn about the EU directive 2013/15 on electromagnetic fields.
2. To learn about the Dutch guidelines on electromagnetic field risk assessment and evaluation.
3. To learn about the challenges and import role for radiographers.
Author Disclosures:
J. Meedendorp: disclosure/affirmation information not submitted

09:49
Panel discussion

08:30 - 10:00 **Descartes (Room D3)**

Professional Challenges Session

PC 13
Equipment purchasing decisions: a team approach

PC 13-1 08:30
Chairperson's introduction
A. Trianni*; Udine/IT (annalisa.trianni@asuiud.sanita.fvg.it)*
Session objectives:
1. To become familiar with the general procurement process.
2. To address the general challenges of the process regarding multiple modalities.
3. To introduce the different roles of the team professionals.
Author Disclosures:
A. Trianni: nothing to disclose

PC 13-2 08:35
Preliminary evaluation of the need and utilisation
E. Kotter*; Freiburg/DE (elmar.kotter@uniklinik-freiburg.de)*
Learning objectives:
1. To learn about utilisation/need aspects and related values for further planning of specifications.
2. To discuss the differences between smaller and larger organisations' needs for evaluation.
3. To present the preliminary evaluation process with an example case(s).
Author Disclosures:
E. Kotter: nothing to disclose

PC 13-3 08:49
Technical specification as the prerequisite for clinical use
A. T. Rogers*; Nottingham/UK (andy.rogers@nuh.nhs.uk)*
Learning objectives:
1. To become familiar with the different types of technical specification to satisfy the utilisation criteria.
2. To address the pitfalls of specifications related to neutrality, independence, and relativity aspects.
3. To learn to grade tenders against specifications with an example case(s).
Author Disclosures:
A. T. Rogers: Speaker at Nottingham University Hospitals

PC 13-4 09:03
Site planning and project management
M. N. N. Özmen*; Ankara/TR (mozmen@hacettepe.edu.tr)*
Learning objectives:
1. To address issues related to site construction requirements.
2. To discuss potential collaboration in purchasing between engineering, physics, and imaging experts.
3. To highlight approaches for success in imaging equipment installation.
Author Disclosures:
M. N. N. Özmen: nothing to disclose

PC 13-5 09:17
Legal and financial aspects of procurement
A. Giovagnoni*; Ancona/IT (a.giovagnoni@univpm.it)*
Learning objectives:
1. To describe tender requirements in different countries.
2. To discuss financial options in equipment purchasing.
3. To describe ways for planning departmental equipment upgrades and maintenance.
Author Disclosures:
A. Giovagnoni: nothing to disclose

PC 13-6 09:31
Economic issues
E. Schouman-Claeys*; Paris/FR*
Learning objectives:
1. To discuss negotiation strategies.
2. To discuss short and long term financial plans for imaging equipment purchasing.
3. To describe the means for planning return on investment for expensive imaging scanners.
Author Disclosures:
E. Schouman-Claeys: disclosure/affirmation information not submitted

09:45
Panel discussion: How to choose the right machine?

08:30 - 10:00 **Room G**

New Horizons Session

NH 13
Alzheimer's disease and neurodegeneration: visualising the invisible

NH 13-1 08:30
Chairperson's introduction
S. Haller*; Geneva/CH (sven.haller@me.com)*
Session objectives:
1. To appreciate that dementia is more than Alzheimer's.
2. To understand that neurodegenerative diseases are overlapping and may co-exist.
3. To acknowledge the need for early and specific detection of cognitive decline for future, hopefully successful, clinical trials.
Author Disclosures:
S. Haller: Consultant at Spineart, Advisory Board at EPAD, Board Member at Neuroradiology, Speaker at GE

NH 13-2 08:35
Visualising the human glymphatic system
G. A. Ringstad*; Oslo/NO (geirringstad@yahoo.no)*
Learning objectives:
1. To become familiar with the glymphatic system.
2. To appreciate the role of the glymphatic system in the clearance of amyloid-β and tau.
3. To highlight experiences with MRI of the glymphatic system in normal pressure hydrocephalus dementia.
4. To understand how reduced glymphatic and lymphatic clearance function may be associated with neurodegenerative disease.
Author Disclosures:
G. A. Ringstad: Shareholder at Brainwidesolutions AS, Speaker at Bayer AG

NH 13-3 08:53
PET as part of the biomarker toolbox for early clinical diagnosis of Alzheimer's disease
J. Arbizu; *Pamplona/ES (jarbizu@unav.es)*
Learning objectives:
1. To learn about the different radiotracers available to evaluate the specific processes involved in the neurodegenerative conditions found in dementia.
2. To understand the benefit of PET molecular imaging in the diagnostic workup of Alzheimer's disease.
3. To appreciate the role of different PET and SPECT techniques in the differential diagnosis of neurodegenerative disorders.
4. To become familiar with the methodology to perform and read PET molecular imaging in dementia.
Author Disclosures:
J. Arbizu: Research/Grant Support at Lilli-Avid, Research/Grant Support at General Electric, Research/Grant Support at Piramal , Advisory Board at Advanced Accelerator Applications, Advisory Board at Bayer, Advisory Board at Araclon-Biotech, Speaker at Advanced Accelerator Applications, Speaker at Isoder, Advisory Board at Biogen, Speaker at Eisai, Speaker at Genzyme

NH 13-4 09:11
Imaging beyond beta-amyloid and tau: insights from high-field MRI
L. van der Weerd; *Leiden/NL*
Learning objectives:
1. To appreciate the technical advantages and disadvantages in the use of ultra-high field MRI.
2. To learn about the mechanisms of MRI contrasts at ultra-high field.
3. To learn about underlying pathophysiological sources of MRI contrast and the disease specificity of different MRI biomarkers.
4. To list promising applications of ultra-high field MRI in Alzheimer's disease and other neurodegenerative diseases.
Author Disclosures:
L. van der Weerd: nothing to disclose

NH 13-5 09:29
Integrating population imaging with clinical imaging for the memory clinic: the Oxford Brain Health Centre
C. Mackay; *Oxford/UK (clare.mackay@psych.ox.ac.uk)*
Learning objectives:
1. To overview current practice for memory clinic imaging in the UK and beyond and appreciate the limitations for research.
2. To describe the recent major initiatives in population imaging and understand some of the technical and logistical challenges these studies face.
3. To describe the opportunities and challenges associated with integrating high quality individual imaging with large population datasets such as the UK Biobank for the clinic.
Author Disclosures:
C. Mackay: nothing to disclose

09:47
Panel discussion: Over 100 years of hype and hope in dementia and Alzheimer's research: what lessons have we learned, and what are the future directions?

08:30 - 10:00 **Room K**

E³ - European Diploma Prep Session

E³ 1323
Urogenital

E³ 1323-1 08:30
Chairperson's introduction
V. Løgager; *Herlev/DK (Vibeke.Loegager@regionh.dk)*
Session objectives:
1. To become familiar with the imaging presentation of common neoplastic and infectious disorders of the kidneys.
2. To describe the typical imaging features of obstructive uropathy and neoplastic disorders of the ureter and bladder.
3. To understand the imaging presentation of benign and malignant disorders of the prostate.
Author Disclosures:
V. Løgager: nothing to disclose

E³ 1323-2 08:36
A. Renal and adrenal imaging
N. Grenier; *Bordeaux/FR (nicolas.grenier@chu-bordeaux.fr)*
Learning objectives:
1. To describe the normal imaging anatomy and variants of the kidney and the adrenal glands.
2. To understand the imaging features of benign and malignant tumours of the kidneys.
3. To describe imaging features of benign and malignant tumours of the adrenal glands.
4. To explain the imaging features of infectious disorders of the kidneys.
Author Disclosures:
N. Grenier: Advisory Board at Supersonic Imagine

E³ 1323-3 09:04
B. Imaging of the ureter and bladder
M. Seçil; *Izmir/TR (mustafa.secil@deu.edu.tr)*
Learning objectives:
1. To explain the imaging anatomy and variants of the ureter and bladder.
2. To understand the diagnostic evaluation and imaging features of obstructive uropathy.
3. To describe the imaging features of benign and malignant tumours of the ureter and bladder.
Author Disclosures:
M. Seçil: nothing to disclose

E³ 1323-4 09:32
C. Prostate imaging
H. C. Thoeny; *Fribourg/CH (Harriet.thoeny@h-fr.ch)*
Learning objectives:
1. To explain the prostate imaging reporting and data system (PIRADS) in prostate imaging.
2. To describe the imaging features of benign prostatic hypertrophy.
3. To understand the imaging features of prostate cancer.
4. To describe the imaging features of inflammatory changes of the prostate.
Author Disclosures:
H. C. Thoeny: Advisory Board at Guerbet

08:30 - 10:00 **Room M 2**

E³ - Advanced Course: How to Improve Your Expertise in Cardiothoracic Imaging

E³ 1319
Cardiovascular imaging in pregnancy

E³ 1319-1 08:30
Chairperson's introduction
J.-N. Dacher; *Rouen/FR (jean-nicolas.dacher@chu-rouen.fr)*
Session objectives:
1. To learn about risk factors, incidence, and outcomes of acute cardiovascular events during pregnancy.
2. To learn how to adapt CT acquisition protocol during pregnancy.
3. To become familiar with alternative imaging techniques.
Author Disclosures:
J.-N. Dacher: nothing to disclose

E³ 1319-2 08:36
A. Pulmonary embolism: optimising patient's selection and radiation protection
C. Loewe; *Vienna/AT (christian.loewe@meduniwien.ac.at)*
Learning objectives:
1. To learn how to adapt CT acquisition protocol during pregnancy.
2. To become familiar with alternative imaging techniques.
3. To become familiar with alternative diagnoses.
Author Disclosures:
C. Loewe: Speaker at Siemens Healthineers , Speaker at BRACCO, Speaker at GE Healthcare

E³ 1319-3 09:04
B. Acute aortic disease in pregnancy
R. P. J. Budde; *Rotterdam/NL (r.budde@erasmusmc.nl)*

Learning objectives:
1. To learn about risk factors and prevalence of acute aortic syndromes during pregnancy.
2. To learn how to adapt CT acquisition protocol during pregnancy.
3. To become familiar with alternative imaging techniques.
Author Disclosures:
R. P. J. Budde: nothing to disclose

E³ 1319-4 09:32
C. Imaging peripartum cardiomyopathy and other cardiac complications
A. Jacquier*; Marseille/FR (alexis.jacquier@ap-hm.fr)*
Learning objectives:
1. To learn about prevalence and clinical presentation of cardiomyopathy during pregnancy.
2. To learn an appropriate diagnostic algorithm.
3. To become familiar with prognosis and outcome.
Author Disclosures:
A. Jacquier: nothing to disclose

08:30 - 10:00 **Room M 3**

Cardiac

RC 1303

New techniques in cardiac CT: game changers or money makers?

RC 1303-1 08:30
Chairperson's introduction: Will the new techniques overcome the clinical underuse of cardiac CT?
K. Nikolaou*; Tübingen/DE (Konstantin.Nikolaou@med.uni-tuebingen.de)*
Session objectives:
1. To understand the importance of combining morphological and functional information in ischemic heart disease.
2. To understand the reasons for persisting underuse.
3. To get an overview about new techniques able to change this underuse.
Author Disclosures:
K. Nikolaou: Research/Grant Support at Siemens, GE, Bracco, Bayer

RC 1303-2 08:35
A. Morphology matters: cardiac CT can improve the outcome
G. Muscogiuri*; Milan/IT (g.muscogiuri@gmail.com)*
Learning objectives:
1. To underline the high predictive value of cardiac CT.
2. To emphasise the impact of cardiac CT on the outcome.
3. To discuss the role of cardiac CT in the clinical management of coronary artery disease patients.
Author Disclosures:
G. Muscogiuri: nothing to disclose

RC 1303-3 09:00
B. CT perfusion: integration of function will change the game
R. Vliegenthart*; Groningen/NL (r.vliegenthart@umcg.nl)*
Learning objectives:
1. To learn about the technical challenges of performing CT perfusion.
2. To understand the opportunities of combining functional and morphological information by adding perfusion to cardiac CT.
3. To become familiar with the interpretation of CT perfusion results.
Author Disclosures:
R. Vliegenthart: nothing to disclose

RC 1303-4 09:25
C. CT-derived fractional flow reserve (FFR) is the future!
U. J. Schoepf*; Charleston, SC/US (schoepf@musc.edu)*
Learning objectives:
1. To understand the principle of CT derived fractional flow reserve (CT FFR).
2. To learn about the possible added value of CT derived FFR to cardiac CT.
3. To discuss the influence of availability of CT derived FFR in the clinical management of CAD patients.
Author Disclosures:
U. J. Schoepf: Research/Grant Support at Astellas; Bayer; Bracco; Elucid Bioimaging; GE; Heartflow; Siemens

09:50
Panel discussion: Artificial intelligence to overcome clinical underuse of these techniques

08:30 - 10:00 **Room M 4**

Transatlantic Course of ESR and RSNA (Radiological Society of North America): Stroke Imaging and Endovascular Treatment: Now and the Future

TC 1328

Practical stroke imaging and mimics

Moderators:
J.-P. Pruvo; Lille/FR
A. Vagal; Cincinnati, OH/US

TC 1328-1 08:30
A. Stroke mimics and "chameleons": how to recognise them
D. Leys*; Lille/FR (didier.leys@univ-lille.fr)*
Learning objectives:
1. To learn about the definitions of stroke mimics and chameleons.
2. To understand the clinical challenges of stroke mimics.
3. To become familiar with the imaging signs and differential diagnosis of stroke mimics.
Author Disclosures:
D. Leys: Advisory Board at Pfizer 2017, 2018, Advisory Board at Bayer 2017, Investigator at Boehringer Ingelheim, Research/Grant Support at University of Heidelberg

TC 1328-2 09:00
B. Practical review of stroke imaging and triage: within six hours and beyond including wake-up strokes
L. Hacein-Bey*; Carmichael, CA/US (lhaceinbey@yahoo.com)*
Learning objectives:
1. To learn about optimal patient triage in acute ischaemic stroke in early and delayed time windows.
2. To understand stroke imaging in wake-up strokes and unknown onset time.
3. To appreciate the importance of efficient workup and time metrics.
Author Disclosures:
L. Hacein-Bey: nothing to disclose

TC 1328-3/TC 1328-4 09:30
C. Interactive case discussion
L. Hacein-Bey*; Carmichael, CA/US (lhaceinbey@yahoo.com)*
D. Leys*; Lille/FR (didier.leys@univ-lille.fr)*
Learning objectives:
1. To learn how imaging can help in decision making in acute stroke.
2. To consolidate the knowledge gained from the session with interactive cases.
Author Disclosures:
L. Hacein-Bey: nothing to disclose, D. Leys: Advisory Board at Pfizer 2017, 2018, Advisory Board at Bayer 2017, Investigator at Boehringer Ingelheim, Grant Recipient at University of Heidelberg

08:30 - 10:00 **Room M 5**

E³ - Advanced Course: Hot Topics in GU Cancer

E³ 1322

Tumour relapse in gynaecological cancer

E³ 1322-1 08:30
Chairperson's introduction
S. Nougaret*; Montpellier/FR*
Author Disclosures:
S. Nougaret: nothing to disclose

E³ 1322-2 08:45
A. Differentiating relapse from post-treatment appearances
R. Forstner*; Salzburg/AT (r.forstner@salk.at)*
Learning objectives:
1. To learn post radiotherapy appearances in cervix cancer.
2. To recognise the appearances of disease relapse.
3. To be familiar with the complications of treatment seen on imaging.
Author Disclosures:
R. Forstner: nothing to disclose

E³ 1322-3 09:10
B. Planning exenterative surgery
H. A. H. Vargas*; New York, NY/US*
Learning objectives:
1. To learn the important criteria for patient selection.
2. To learn the critical anatomy for surgical planning.
3. To be familiar with the post-surgical appearances and follow-up plan.
Author Disclosures:
H. A. H. Vargas: nothing to disclose

E³ 1322-4 09:35
C. Salvage treatment with image directed therapy: high-intensity focused US (HIFU) and stereotactic radiotherapy
N. deSouza*; Surrey/UK*
Learning objectives:
1. To be familiar with the imaging considerations for stereotactic radiotherapy in relapsed disease.
2. To be familiar with the concepts of imaging in directing a radiotherapy treatment plan.
3. To be familiar with the use of HIFU for treatment of pelvic relapse.
Author Disclosures:
N. deSouza: nothing to disclose

08:30 - 10:00 **Tech Gate Auditorium**

Joint Session of the ESR and EFSUMB

ESR/EFSUMB
Bosniak cyst classification

ESR/EFSUMB-1/ESR/EFSUMB-2 08:30
Chairpersons' introduction
D.-A. A. Clevert*; Munich/DE (Dirk.Clevert@med.uni-muenchen.de)*
P. S. Sidhu*; London/UK (paulsidhu@nhs.net)*
Session objectives:
1. To review the classification of complex renal cysts and the relationship to malignancy.
2. To appreciate the need for a contrast-enhanced ultrasound (CEUS) classification of these complex cysts.
3. To review and understand the nature of the enhancement of complex cysts with CEUS.
Author Disclosures:
D.-A. A. Clevert: Speaker at Bracco, Speaker at Siemens, Speaker at Samsung, Speaker at Philips, Advisory Board at Philips, Advisory Board at Samsung; P. S. Sidhu: Advisory Board at Samsung Inc, Seoul Korea, Consultant at Itreas Inc, Amsterdam, Speaker at Bracco, SpA Milan, Speaker at Philips, Netherlands, Speaker at Siemens Healthineers, Speaker at GE healthcare

ESR/EFSUMB-3 08:35
Contrast-enhanced ultrasound (CEUS) in the classification of Bosniak cysts: is it better?
V. Cantisani*; Rome/IT (vito.cantisani@uniroma1.it)*
Learning objectives:
1. To provide CEUS features for characterising cystic lesions.
2. To discuss literature evidence on the reliability of CEUS.
3. To compare CEUS properties with CT and MRI for better kidney cystic characterisation.
Author Disclosures:
V. Cantisani: Speaker at Samsung, Speaker at Bracco, Speaker at Canon

ESR/EFSUMB-4 08:53
Role of CT and MRI
T. Fischer*; Berlin/DE (thom.fischer@charite.de)*
Learning objectives:
1. To review the pros and cons of each approach, including safety of CT.
2. To become familiar with the Bosniak cyst classification for MRI and CT.
3. To discuss the evidence for the use of these methods in routine clinical practice.
Author Disclosures:
T. Fischer: Advisory Board at Canon, Siemens, Bracco, Speaker at Canon, Siemens, Bracco

ESR/EFSUMB-5 09:11
Key recommendations of the EFSUMB clinical position paper on US-based Bosniak cyst classification
M. Bertolotto*; Trieste/IT (bertolot@units.it)*
Learning objectives:
1. To review the differences between CEUS and contrast-CT/MRI in cystic renal lesion characterisation.
2. To describe the key features of CEUS that enables estimation of the risk of malignancy and assigns a Bosniak score.
3. To illustrate the EFSUMB key recommendations for renal cyst classification at CEUS.
Author Disclosures:
M. Bertolotto: nothing to disclose

ESR/EFSUMB-6/ESR/EFSUMB-7 09:29
Interactive cases presentation with renal cysts
J. Webb*; Liverpool/UK (JOLANTA.WEBB@liverpoolft.nhs.uk)*
M. Ragel*; Liverpool/UK (mragel@blueyonder.co.uk)*
Learning objectives:
1. To understand which features of a renal cyst to assess during CEUS in order to assign a Bosniak classification, especially to distinguish between benign and malignant lesion.
2. To know the pitfalls of CEUS renal cyst characterisation and how to counteract them.
3. To understand the place of CEUS in renal cyst characterisation and the follow-up.
Author Disclosures:
J. Webb: nothing to disclose, M. Ragel: nothing to disclose

09:47
Panel discussion: How would you classify this complex renal cyst?

10:30 - 11:00 **Forum (Room A)**

Plenary Lecture

PL 3
Building the human brain: molecular logic of neural circuit formation

Presiding:
B. Brkljačić; Zagreb/HR

PL 3-1 10:30
Building the human brain: molecular logic of neural circuit formation
N. Šestan*; New Haven, CT/US*
Author Disclosures:
N. Šestan: disclosure/affirmation information not submitted

12:45 - 13:45 **Room B**

E³ - The Beauty of Basic Knowledge: Breast

E³ 24D
Basics of interventional breast imaging

Moderators:
F. J. Gilbert; Cambridge/UK
K. Kinkel; Chêne-Bougeries/CH

E³ 24D-1 12:45
Ultrasound-guided interventional imaging: when and how?
M. Mahoney; *Cincinnati, OH/US (mary.mahoney@uc.edu)*
Learning objectives:
1. To learn about cyst aspiration and biopsy techniques.
2. To understand contraindication and complications.
3. To understand the correlation between imaging and pathology.
Author Disclosures:
M. Mahoney: Board Member at RSNA, Board Member at ACR, Author at Elsevier

E³ 24D-2 13:05
When and how to biopsy under mammographic guidance?
D. Djilas; *Sremska Kamenica/RS*
Learning objectives:
1. To learn about the techniques and limitations.
2. To become familiar with the quality control of stereotactic or tomosynthesis guided breast biopsy.
Author Disclosures:
D. Djilas: disclosure/affirmation information not submitted

E³ 24D-3 13:25
When and how to biopsy under MRI guidance?
P. A. T. Baltzer; *Vienna/AT (patbaltzer@gmail.com)*
Learning objectives:
1. To learn about the techniques and limitations.
2. To become familiar with the quality control of MRI guided breast biopsy.
Author Disclosures:
P. A. T. Baltzer: nothing to disclose

12:45 - 13:45 **Room C**

E³ - The Beauty of Basic Knowledge: Pancreas

E³ 25D
Solid pancreatic neoplasms

Moderator:
B. I. Choi; Seoul/KR

E³ 25D-1 12:45
Diagnosis
M. Zins; *Paris/FR (mzins@hpsj.fr)*
Learning objectives:
1. To learn about diagnostic imaging findings of solid pancreatic neoplasms.
2. To understand treatment planning.
3. To appreciate differential diagnosis of solid pancreatic neoplasms.
Author Disclosures:
M. Zins: nothing to disclose

E³ 25D-2 13:15
Staging
N. Kartalis; *Stockholm/SE (nikolaos.kartalis@me.com)*
Learning objectives:
1. To learn how to stage pancreatic adenocarcinoma.
2. To understand resectability criteria.
3. To appreciate the role of imaging in treatment planning.
Author Disclosures:
N. Kartalis: nothing to disclose

12:45 - 13:45 **Coffee & Talk 3**

Coffee & Talk (open forum) Session
Organised by the ESR Patient Advisory Group (ESR-PAG)

C 30
Innovative tools to improve the communication between radiologists and patients

C 30-1 12:45
Chairperson's introduction
N. Bedlington; *Vienna/AT*
Session objectives:
1. To understand why patient-centred communication is key for achieving better outcomes in the radiology department.
2. To identify room for improvement in patient communication based on experience reports by patient representatives.
3. To learn how radiologists can implement efficient communication strategies to better divide time between patient consultations and clinical practice.
Author Disclosures:
N. Bedlington: disclosure/affirmation information not submitted

C 30-2 12:50
Sharing best practices in engaging with radiologists
C. Cruwys; *Haute Vienne/FR (CCruwys@dense-info.org)*
Learning objectives:
1. To appreciate practical tools that help to streamline the flow of information between patients and radiologists.
2. To learn about programs that help patients to better engage with professionals in the radiology department.
3. To understand how patients can participate in decision-making regarding the care pathway.
Author Disclosures:
C. Cruwys: nothing to disclose

C 30-3 12:58
The radiologist's perspective: effectively dividing time for communication with patients
D.-G. Carrie; *Balma/FR (dominiquecarrie@wanadoo.fr)*
Learning objectives:
1. To learn how to better organise direct contact with the patient in the radiology department.
2. To demonstrate how language can be adapted to meet expectations for understandable and clear communication.
3. To understand what practical tools are available in the radiology department to communicate more effectively with patients.
Author Disclosures:
D.-G. Carrie: nothing to disclose

C 30-4 13:06
Patient experiences on optimising communication in the radiology department
B. Bauer; *Abensberg/DE*
Learning objectives:
1. To demonstrate how digital tools can contribute to improving the communication between patients and radiologists.
2. To learn about practical solutions in hospital departments in order to explain clinical results.
3. To outline how patients can more adequately educate themselves to better understand radiology procedures.
Author Disclosures:
B. Bauer: nothing to disclose

C 30-5 13:14
Achieving better patient outcomes through effective communication and empowerment
C. Justich; *Vienna/AT (cjustich@me.com)*

Learning objectives:
1. To outline which initiatives could be introduced in the hospital department to involve patients in seeking effective communication tools.
2. To learn practical solutions in hospital departments to meet patients' demands for involvement in decision-making regarding the care pathway.
3. To understand why patient empowerment and engagement will result in more effective communication in the hospital department.
Author Disclosures:
C. Justich: Speaker at ESR PAG

13:22
Open forum discussion: How to implement a system of effective patient-professional communication

14:00 - 15:30 **Room B**

Head and Neck

RC 1508
Skull base

RC 1508-1 14:00
Chairperson's introduction
B. Schuknecht*; Zurich/CH (bschuknecht@mri-roentgen.ch)*
Session objectives:
1. To become familiar with normal skull base anatomy and variants.
2. To understand how to review skull base pathology.
3. To know how to differentiate infection/inflammation from a tumour.
Author Disclosures:
B. Schuknecht: nothing to disclose

RC 1508-2 14:05
A. Skull base anatomy
E. Loney*; Halifax/UK (elizabeth.loney@cht.nhs.uk)*
Learning objectives:
1. To understand how to classify skull base anatomy.
2. To become acquainted with clinically relevant anatomical variants.
3. To review the important anatomical subsites.
Author Disclosures:
E. Loney: nothing to disclose

RC 1508-3 14:28
B. Infectious and inflammatory diseases of the skull base
J. Goh*; Singapore/SG (Julian_Goh@ttsh.com.sg)*
Learning objectives:
1. To understand how to recognise infectious and inflammatory skull base pathology.
2. To become familiar with the imaging modalities used to diagnose and assess treatment response.
3. To recognise the important review areas and complications.
Author Disclosures:
J. Goh: nothing to disclose

RC 1508-4 14:51
C. Benign and malignant tumours of the skull base
A. Borges*; Lisbon/PT (borgalexandra@gmail.com)*
Learning objectives:
1. To learn how to make an accurate differential diagnosis.
2. To become familiar with important review areas and the staging of malignant tumours.
3. To recognise tumour mimics.
Author Disclosures:
A. Borges: nothing to disclose

15:14
Panel discussion: What are the challenges in assessing the skull base?

14:00 - 15:30 **Room C**

Musculoskeletal

RC 1510
Imaging of forgotten small joints

Moderator:
P. N. M. Tyrrell; Oswestry/UK

RC 1510-1 14:00
A. Sterno-clavicular joints: from trauma to inflammation
A.-G. Jurik*; Aarhus/DK (jurik@dadlnet.dk)*
Learning objectives:
1. To explain the pathological conditions that involve the sterno-clavicular joints.
2. To describe the imaging findings of abnormalities that involve the sterno-clavicular joints.
Author Disclosures:
A.-G. Jurik: nothing to disclose

RC 1510-2 14:30
B. Symphysis pubis and its surroundings
A. Kassarjian*; Pozuelo de Alarcón/ES (akassarjian@gmail.com)*
Learning objectives:
1. To explain the pathological conditions that involve the symphysis pubis and its surroundings.
2. To describe the imaging findings of abnormalities that involve the symphysis pubis and its surroundings.
Author Disclosures:
A. Kassarjian: nothing to disclose

RC 1510-3 15:00
C. Proximal tibio-fibular joint: a cause for lateral knee pain
A. Cotten*; Lille/FR (anne.cotten@chru-lille.fr)*
Learning objectives:
1. To explain the pathological conditions that involve the proximal tibio-fibular joint.
2. To describe the imaging findings of abnormalities that involve the proximal tibio-fibular joint.
Author Disclosures:
A. Cotten: Author at CHU de Lille

14:00 - 15:30 **Room X**

ESR Patient Advisory Group (ESR-PAG)

PA
Artificial intelligence (AI) in radiology: meeting expectations and benefiting outcomes

PA-1/**PA-2** 14:00
Chairpersons' introduction
B. Bauer*; Abensberg/DE*
N. I. Traikova*; Plovdiv/BG (nikoletatraikova@gmail.com)*
Session objectives:
1. To understand how patients can benefit from the application of AI in radiology.
2. To learn which management changes the introduction of AI in radiology triggers for professionals in clinical practice.
3. To learn how the use of AI in radiology raises ethical questions that need to be answered in view of a patient-centred approach.
Author Disclosures:
B. Bauer: nothing to disclose, N. I. Traikova: nothing to disclose

PA-3 14:05
The untapped potential of AI in radiology
J. A. Brink*; Boston, MA/US*

Learning objectives:
1. To learn how AI is currently used in radiology to generate more effective outcomes.
2. To understand how AI will transform clinical practice for radiologists in the next few decades.
3. To identify best practices for bridging the gap between radiologist and patient due to technological developments.
Author Disclosures:
J. A. Brink: Board Member at Accumen, Inc.

PA-4 14:20
Managing expectations for a patient-centred application of AI in radiology
E. Briers; *Brussels/BE (erikbriers@telenet.be)*
Learning objectives:
1. To understand what benefits patients expect from introducing AI in radiology.
2. To demonstrate how patients can contribute to better outcomes through shared-decision making and active involvement in utilising AI.
3. To learn how patients can be encouraged to co-develop AI in radiology that is patient-centred and adapted to patient expectations.
Author Disclosures:
E. Briers: nothing to disclose

PA-5 14:35
A patient perspective on data privacy in AI
C. Isaacs; *Woking/UK (chrisisaacs83@googlemail.com)*
Learning objectives:
1. To learn which measures need to be introduced from a patient's point of view to uphold the highest data privacy standards.
2. To provide examples of how patient involvement in data collection and analysis contributes to an accelerated diagnosis and treatment.
3. To understand how patient education and communication in the field of AI is crucial in order to maintain the patient's trust in clinical practice and research.
Author Disclosures:
C. Isaacs: nothing to disclose

PA-6 14:50
Putting ethics fist: key questions concerning AI in radiology
A. Brady; *Cork/IE (adrianbrady@me.com)*
Learning objectives:
1. To understand which ethical implications accompany the introduction of AI in radiology.
2. To learn about practical solutions to uphold the highest ethical standards in radiology.
3. To share best practices of collaboration between patients and radiologists in developing guidelines and ethical standards.
Author Disclosures:
A. Brady: nothing to disclose

PA-7 15:05
Data sets for training and validation of AI-tools
L. Marti-Bonmati; *Valencia/ES (Luis.Marti@uv.es)*
Learning objectives:
1. To learn about the relevance of training for AI development.
2. To appreciate the opportunities of collaborative developments of data sets for training.
3. To understand the need for validation of AI tools.
Author Disclosures:
L. Marti-Bonmati: nothing to disclose

15:20
Panel discussion: How to embed AI in radiology to the benefit of a patient-centred approach

14:00 - 15:00 **Coffee & Talk 1**

Coffee & Talk (open forum) Session
Organised by ESOR

C 8
ESOR one-year fellowship

C 8-1 14:00
Chairperson's introduction
R. G. H. Beets-Tan; *Amsterdam/NL (r.beetstan@nki.nl)*
Session objectives:
1. To understand the goal of a one year ESOR research fellowship and to learn about the expectations.
2. To know how this fellowship could help you boost your career.
Author Disclosures:
R. G. H. Beets-Tan: nothing to disclose

C 8-2/**C 8-3** 14:05
Why should you apply for a one-year fellowship?
T. D. L. Nguyen-Kim; *Zurich/CH (thidanlinh.nguyen@usz.ch)*
E. K. Hong; *Seoul/KR (amyh0803@gmail.com)*
Learning objectives:
1. To learn from their experiences during their visit to the centre.
2. To know how it improved their scientific skills.
3. To learn how their fellowship had an impact on their academic career.
Author Disclosures:
T. D. L. Nguyen-Kim: nothing to disclose, E. K. Hong: nothing to disclose

14:35
Open forum discussion

14:00 - 15:30 **Room N**

Breast

RC 1502
Interventional breast imaging: the increasing role of the radiologist

Moderator:
C. Kurtz; Lucerne/CH

RC 1502-1 14:00
A. Fine needle aspiration cytology (FNAC), core needle or vacuum assisted biopsy (VAB): what, when and how?
A. Evans; *Dundee/UK (a.z.evans@dundee.ac.uk)*
Learning objectives:
1. To get to know the different needle systems.
2. To become familiar with potential pitfalls.
3. To be able to choose the right needle for the right indication.
Author Disclosures:
A. Evans: nothing to disclose

RC 1502-2 14:30
B. Breast lesion localisation: going beyond wires
M. Marolt Music; *Ljubljana/SI (mmusic@onko-i.si)*
Learning objectives:
1. To appreciate the importance of image-guided preoperative wire localisation for non-palpable lesions.
2. To get to know alternative localisation techniques.
3. To become familiar with the limitations of different techniques.
Author Disclosures:
M. Marolt Music: nothing to disclose

RC 1502-3 15:00
C. Percutaneous ablation of breast cancer: a step forward
G. Mauri; *Milan/IT (vanni.mauri@gmail.com)*

Learning objectives:
1. To become familiar with the different techniques for tumour ablation.
2. To acknowledge the value of each technique for the treatment of breast lesions.
3. To identify factors that affect success.
Author Disclosures:
G. Mauri: Consultant at Elesta SrL

14:00 - 15:30 **Room O**

ESTI Session: Lung Cancer Screening Certification Programme

ESTI

Lung nodule management: case-based session

Moderator:
M. Silva; Parma/IT

ESTI-1 14:00
Solid nodule morphological evaluation: how to recognise obviously benign/malignant nodules, intrapulmonary lymph nodes, and pitfalls
A. Devaraj; *London/UK*
Learning objectives:
1. To learn how to recognise obviously benign/malignant nodules.
2. To become familiar with intrapulmonary lymph nodes characteristics.
3. To be aware of the common pitfalls.
Author Disclosures:
A. Devaraj: nothing to disclose

ESTI-2 14:30
Solid nodule measurement, follow-up and criteria of positive screens
H. Prosch; *Vienna/AT (helmut.prosch@meduniwien.ac.at)*
Learning objectives:
1. To understand the limitations of diameter measurement.
2. To appreciate the role of computed assisted diagnosis (CAD) tools for volume measurement and doubling time estimation.
3. To learn about the criteria of positive screens.
Author Disclosures:
H. Prosch: Research/Grant Support at Siemens

ESTI-3 15:00
Subsolid nodules evaluation, follow-up and criteria of positive screens
M.-P. Revel; *Paris/FR (marie-pierre.revel@aphp.fr)*
Learning objectives:
1. To learn how to categorise nodules as solid, part-solid, or non solid.
2. To learn how to define subsolid nodule evolutivity during follow-up.
3. To learn about the criteria of positive screens.
Author Disclosures:
M.-P. Revel: Other at GUERBET

14:00 - 15:00 **Coffee & Talk 2**

Coffee & Talk (open forum) Session

Organised by EuroSafe Imaging

C 18

EuroSafe meets ArabSafe

C 18-1/**C 18-2** 14:00
Chairpersons' introduction
G. Frija; *Paris/FR (guy.frija@aphp.fr)*
B. Mansouri; *Algiers/DZ (boudjema.mansouri@gmail.com)*
Session objectives:
1. To highlight the EuroSafe Imaging strategy.
2. To discuss optimisation and justification.
3. To share common experiences.
Author Disclosures:
G. Frija: nothing to disclose, B. Mansouri: nothing to disclose

C 18-3 14:10
EuroSafe Imaging campaign: is the EuroSafe Imaging Call for Action relevant for ArabSafe?
G. Frija; *Paris/FR (guy.frija@aphp.fr)*
Learning objectives:
1. To highlight the EuroSafe Imaging Call for Action.
2. To detail how optimisation is handled.
3. To provide an update on the EuroSafe Imaging Stars concept.
Author Disclosures:
G. Frija: nothing to disclose

C 18-4 14:20
ArabSafe campaign: which are the most important challenges in implementing radiation protection?
B. Mansouri; *Algiers/DZ (boudjema.mansouri@gmail.com)*
Learning objectives:
1. To update and highlight the implementation of the ArabSafe campaign, including the results and constraints.
2. To highlight the implementation of the Bonn Call for Action into Arabic countries though the ArabSafe campaign, taking into consideration the peculiarities or similarities at a regional level (north Africa or the Middle East).
3. To expand on issues relating to radiation safety and, in particular, how to tackle the challenges of encouraging adherence to standards, policies strategies, and activities.
Author Disclosures:
B. Mansouri: nothing to disclose

C 18-5 14:30
Use case in Saudi Arabia. Presentation of the first Saudi National DRLs for CT in adults and children: implementation plan and the effect of the implementation of dose monitoring in mammography screening practice in Saudi Arabia
S. Hagi; *Jeddah/SA (sarahhagi@gmail.com)*
Learning objectives:
1. To present the results of the Saudi Food & Drug Authority (SFDA) National DRLs for CT practice.
2. To highlight the modification to paediatric practices.
3. To present the features of mammography practice in Saudi Arabia and its limitations.
4. To introduce the Saudi FDA national project for establishing mammography DRLs.
5. To discuss the effect of using dose monitoring software on mean glandular dose in a teaching hospital.
Author Disclosures:
S. Hagi: nothing to disclose

C 18-6 14:40
Use case in Egypt
D. Husseiny Salama; *Cairo/EG (drdinahusseiny@yahoo.com)*
Learning objectives:
1. To present Egypt's key use cases in radiation safety technology.
2. To highlight the interaction between the available tools and the needs of the end users.
3. To introduce the radiation safety model in Egypt and how the technology functions through it.
Author Disclosures:
D. Husseiny Salama: nothing to disclose

14:50
Open forum discussion

14:00 - 15:30 **Room E**

Special Focus Session

SF 15

My top three tips for imaging musculoskeletal injury

SF 15-1 14:00
Chairperson's introduction
Ü. Aydingöz; *Ankara/TR (ustunaydingoz@yahoo.com)*

Session objectives:
1. To describe clinically useful imaging tips to diagnose and manage musculoskeletal injuries.
2. To explain the relevance and diagnostic accuracy of the presented imaging findings.
3. To list pitfalls and the differential diagnosis of imaging findings.
Author Disclosures:
Ü. Aydingöz: nothing to disclose

SF 15-2 14:05
Wrist
J.-L. Drape*; Paris/FR (jean-luc.drape@cch.aphp.fr)*
Learning objectives:
1. To describe clinically useful imaging tips to diagnose and manage wrist injuries.
2. To explain the relevance and diagnostic accuracy of the presented imaging findings.
3. To list the pitfalls and the differential diagnosis of imaging findings.
Author Disclosures:
J.-L. Drape: nothing to disclose

SF 15-3 14:20
Shoulder
K. Wörtler*; Munich/DE (klaus.woertler@tum.de)*
Learning objectives:
1. To describe clinically useful imaging tips to diagnose and manage shoulder injuries.
2. To explain the relevance and diagnostic accuracy of the presented imaging findings.
3. To list the pitfalls and the differential diagnosis of imaging findings.
Author Disclosures:
K. Wörtler: nothing to disclose

SF 15-4 14:35
Hip
V. V. Mascarenhas*; Lisbon/PT (vmascarenhas@me.com)*
Learning objectives:
1. To describe clinically useful imaging tips to diagnose and manage hip injuries.
2. To explain the relevance and diagnostic accuracy of the presented imaging findings.
3. To list the pitfalls and the differential diagnosis of imaging findings.
Author Disclosures:
V. V. Mascarenhas: nothing to disclose

SF 15-5 14:50
Knee
C. W. A. Pfirrmann*; Forch/CH*
Learning objectives:
1. To describe clinically useful imaging tips to diagnose and manage knee injuries.
2. To explain the relevance and diagnostic accuracy of the presented imaging findings.
3. To list the pitfalls and the differential diagnosis of imaging findings.
Author Disclosures:
C. W. A. Pfirrmann: nothing to disclose

SF 15-6 15:05
Ankle
B. Forster*; Vancouver/CA (bruce.forster@vch.ca)*
Learning objectives:
1. To describe clinically useful imaging tips to diagnose and manage ankle and foot injuries.
2. To explain the relevance and diagnostic accuracy of the presented imaging findings.
3. To list the pitfalls and the differential diagnosis of imaging findings.
Author Disclosures:
B. Forster: Shareholder at Canada Diagnostic Centres, Grant Recipient at SECTRA AB; Remuneration of travel expenses for educational conference

15:20
Panel discussion: My single best tip in improving diagnostic accuracy in musculoskeletal injury

14:00 - 15:30 **Room F1**

ESR meets Canada

Meets 15
Tales from the Canadian Frontier

Presiding:
B. Brkljačić; Zagreb/HR
M. Barry; Ottawa, ON/CA

Meets 15-1 14:00
Welcome from the ESR President
B. Brkljačić*; Zagreb/HR (boris@brkljacic.com)*
Author Disclosures:
B. Brkljačić: nothing to disclose

Meets 15-2 14:02
Introduction: Fun facts about Canada
M. Barry*; Ottawa, ON/CA (mbarry@car.ca)*
Session objectives:
1. To learn about cultural anecdotes associated with Canada.
2. To appreciate the vastness in diversity and landscape of the country.
3. To become familiar with the economic disposition of the national healthcare system in Canada.
Author Disclosures:
M. Barry: nothing to disclose

Meets 15-3 14:04
Overview of radiology in Canada
M. Barry*; Ottawa, ON/CA (mbarry@car.ca)*
Learning objectives:
1. To have a better understanding of the Canadian healthcare landscape and radiology practice in a single-payer system.
2. To learn about advocacy strategies that have been successful in raising awareness for radiology and garnering support from key decision makers.
3. To appreciate the challenges that exist in medical imaging in Canada and explore solutions/best practices for navigating through these difficulties.
Author Disclosures:
M. Barry: nothing to disclose

Meets 15-4 14:19
Artificial intelligence: a global phenomenon changing the way radiologists practice
J. J. R. Chong*; Montreal, QC/CA (jaronchong@gmail.com)*
Learning objectives:
1. To become familiar with the status of artificial intelligence in Canada.
2. To learn about how deep learning and algorithms can impact the way data is interpreted in relation to medical imaging.
3. To understand how artificial intelligence will change the way radiologists practice within Canada.
Author Disclosures:
J. J. R. Chong: nothing to disclose

Meets 15-5 14:34
Hot topic - Physician burnout: a Canadian perspective
M. N. Patlas*; Hamilton, ON/CA (patlas69@yahoo.com)*
Learning objectives:
1. To understand burnout in the Canadian context and the contributing factors to stress.
2. To learn strategies in mitigating burnout in a clinical environment.
Author Disclosures:
M. N. Patlas: Author at Springer

Meets 15-6 14:49
Canadian interlude with embassy

Meets 15-7 14:54
Transcontinental thematic analysis of gender role in medical schools leadership: a message to academic radiology and hospital administration
W. Abdellatif*; Vancouver, BC/CA*
Author Disclosures:
disclosure/affirmation information not submitted

Meets 15-8 14:59
Can CTA differentiate free-floating thrombus in the internal carotid artery from atherosclerotic plaque in patients evaluated for stroke or transient ischemic attack? A Canadian multi-centre study
P. Puac Polanco; *Ottawa, ON/CA*
Author Disclosures:
disclosure/affirmation information not submitted

Meets 15-9 15:04
Traumatic bowel injuries increased detectability with dual-energy CT virtual monoenergetic with color-coded iodine overlay imaging
F. Macri; *Vancouver, BC/CA*
Author Disclosures:
disclosure/affirmation information not submitted

Meets 15-10 15:09
The history of Medicare in Canada
E. Lee*; Vancouver/CA (ejlee888@gmail.com)*
Learning objectives:
1. To describe the Canadian medical system.
2. To recognise the journey and evolution to a publicly funded health system.
3. To identify the advantages and challenges within the Canadian medical system.
Author Disclosures:
E. Lee: nothing to disclose

15:24
Questions

14:00 - 15:30 **Room F2**

E³ - Rising Stars Programme: Basic Session

BS 15a
Hybrid imaging

Moderator:
U. Mahmood; Oak Brook/US

BS 15a-1 14:00
Clinical applications of hybrid imaging
K. Riklund*; Umeå/SE (katrine.riklund@umu.se)*
Learning objectives:
1. To understand the indications and limitations of hybrid imaging in common diseases.
2. To discuss the added value of hybrid imaging.
Author Disclosures:
K. Riklund: Board Member at CMRAD AB, Board Member at Dicom Port AB

BS 15a-2 14:30
Hybrid imaging: thorax
D. Neriman*; London, LONDON/UK (deena.neriman@nhs.net)*
Learning objectives:
1. To learn about the indications for thoracic pathologies.
2. To discuss limitations and pitfalls in thoracic pathologies.
3. To demonstrate the most important findings.
Author Disclosures:
D. Neriman: nothing to disclose

BS 15a-3 15:00
Hybrid imaging: abdomen and pelvis
S. Gatidis*; Tübingen/DE (sergios.gatidis@med.uni-tuebingen.de)*
Learning objectives:
1. To learn about the indications for abdominal and pelvic pathologies.
2. To discuss limitations and pitfalls in abdominal and pelvic pathologies.
3. To demonstrate the most important findings.
Author Disclosures:
S. Gatidis: nothing to disclose

14:30 - 15:30 **Coffee & Talk 3**

Coffee & Talk (open forum) Session

C 31
Addressing shortages in the medical imaging workforce

Moderators:
B. Verbist; Leiden/NL
D. Katsifarakis; Athens/GR

C 31-1 14:30
Overview from the WHO on the health care worker shortages and contributing factors
M. D. R. D. R. Perez*; Geneva/CH (perezm@who.int)*
Learning objectives:
1. To summarise the existing shortages, the WHO's High-Level Commission on Health Employment and Economic Growth, and the ILO-WHO-OECD Working for Health Five Year Action Plan.
2. To discuss the adopted World Health Assembly resolution on the Global Strategy on Human Resources for Health: Workforce 2030.
3. To explain the Call for Action Campaign that has been established to address the global health care worker shortfall.
Author Disclosures:
M. D. R. D. R. Perez: nothing to disclose

C 31-2 14:35
The view of the International Society of Radiology
L. Donoso*; Barcelona/ES (ldonoso@clinic.cat)*
Learning objectives:
1. To provide an overview of global radiologist shortfalls.
2. To discuss the ISR's contributions and strategies to counter the global radiologist workforce shortage.
Author Disclosures:
L. Donoso: Advisory Board at Context Flow, Advisory Board at Methinks, Advisory Board at iVascular, Author at Affidea, Shareholder at Vivo Diagnostico

C 31-3 14:40
The view of the European Society of Radiology
L. E. Derchi*; Genoa/IT (derchi@unige.it)*
Learning objectives:
1. To provide an overview of current, and future, radiologist shortfalls in Europe.
2. To discuss opportunities and efforts to counter the radiologist workforce shortages in Europe.
Author Disclosures:
L. E. Derchi: nothing to disclose

C 31-4 14:45
The view of the International Society of Radiographers and Radiologic Technologists
D. E. Newman*; Fargo, ND/US (donnaenewman@gmail.com)*
Learning objectives:
1. To provide an overview of global radiographer/radiologic technologist shortages.
2. To discuss ISRRT's collaborative efforts and strategies, submitted to WHO, to counter these shortages.
3. To discuss the ISRRT partnership with the EFRS to disseminate strategies within Europe to help counter these shortages.
Author Disclosures:
D. E. Newman: nothing to disclose

C 31-5 14:50
The views of the European Federation of Radiographer Societies
J. McNulty*; Dublin/IE (jonathan.mcnulty@ucd.ie)*
Learning objectives:
1. To provide an overview of the current status of the radiographer workforce across Europe.
2. To discuss opportunities and efforts to counter shortages across Europe through collaborative efforts.
Author Disclosures:
J. McNulty: nothing to disclose

14:55
Open forum discussion

14:00 - 15:30 **da Vinci (Room D1)**

Physics in Medical Imaging

RC 1513
Striking the balance: image quality assessment in radiological optimisation

RC 1513-1 14:00
Chairperson's introduction: The big picture: can we be objective about image quality?
M. Kortesniemi*; Hus/FI (mika.kortesniemi@hus.fi)*
Session objectives:
1. To appreciate the reasons why image quality is important in radiological optimisation.
2. To understand the main methods of image quality assessment and optimisation.
3. To learn how image quality assessment is applied in clinical practice.
Author Disclosures:
M. Kortesniemi: nothing to disclose

RC 1513-2 14:05
A. From signal to image: the basics of image quality assessment
A. Mackenzie*; Guildford/UK (alistairmackenzie@nhs.net)*
Learning objectives:
1. To learn the basics of signal formation and image quality assessment.
2. To understand how they are applied in radiological imaging.
3. To identify limitations.
Author Disclosures:
A. Mackenzie: nothing to disclose

RC 1513-3 14:28
B. Between a ROC(k) and a hard place: methods of determining clinical image quality
O. J. O Connor*; Cork/IE (oj.oconnor@ucc.ie)*
Learning objectives:
1. To learn about traditional and practical methods of determining image quality.
2. To understand how the methods are applied to projection radiography, interventional radiology, and CT.
3. To identify limitations of current techniques.
Author Disclosures:
O. J. O Connor: nothing to disclose

RC 1513-4 14:51
C. Bridging the gap between physical and clinical image quality
C. Hoeschen*; Magdeburg/DE*
Learning objectives:
1. To learn about physics-based methods of determining image quality.
2. To understand how they are applied to projection radiography, interventional radiology, and CT.
3. To identify how to bridge the gap between the physics methods and the clinical image quality assessment.
Author Disclosures:
C. Hoeschen: disclosure/affirmation information not submitted

14:14
Panel discussion: Can we balance image quality and dose needs in an objective manner?

14:00 - 15:30 **Darwin (Room D2)**

E³ - ECR Master Class (Abdominal Viscera)

E³ 1526
Update of diffusion-weighted MRI

Moderator:
S. R. Rafaelsen; Vejle/DK

E³ 1526-1 14:00
A. Technical advances of diffusion-weighted imaging (DWI)
N. Papanikolaou*; Lisbon/PT*
(nickolas.papanikolaou@research.fchampalimaud.org)
Learning objectives:
1. To learn about the strengths and shortcomings of different DWI techniques.
2. To understand how to integrate and optimise DWI in MRI protocols.
3. To be able to avoid pitfalls in DWI.
Author Disclosures:
N. Papanikolaou: Advisory Board at Advantis Medical Imaging, Shareholder at MRIcons LTD

E³ 1526-2 14:30
B. DWI of abdominal organs
D. Caruso*; Rome, LT/IT (dcaruso85@gmail.com)*
Learning objectives:
1. To learn how to integrate DWI in your abdominal MRI protocol.
2. To understand the clinical value of DWI for the depiction of abdominal pathologies.
3. To be able to deal with technical difficulties of DWI in the upper abdomen and subphrenic space.
Author Disclosures:
D. Caruso: nothing to disclose

E³ 1526-3 15:00
C. DWI of pelvic organs
E. Sala*; Cambridge/UK (es220@medschl.cam.ac.uk)*
Learning objectives:
1. To understand the correct implementation of DWI for pelvic imaging.
2. To learn how to avoid imaging artefacts in pelvic DWI.
3. To become familiar with typical findings and pitfalls of pelvic DWI.
Author Disclosures:
E. Sala: nothing to disclose

14:00 - 15:30 **Descartes (Room D3)**

Vascular

RC 1515
No time to lose: aortic disease, revisited

Moderator:
T. Jargiello; Lublin/PL

RC 1515-1 14:00
A. Diagnosis and treatment of abdominal aortic aneurysms
F. Wolf*; Vienna/AT (florian.wolf@meduniwien.ac.at)*
Learning objectives:
1. To learn about the definition and classification of abdominal aortic aneurysms.
2. To understand the relevant information and measurements to plan an endovascular aortic repair.
3. To become familiar with the different possibilities of endovascular treatment including anchors, snorkels, branches, and chimneys.
Author Disclosures:
F. Wolf: nothing to disclose

RC 1515-2 14:30
B. Acute diagnosis and imaging in aortic dissection
R. Iezzi*; Rome/IT (roberto.iezzi@policlinicogemelli.it)*

Learning objectives:
1. To learn about definition and classification of aortic dissections and subtypes.
2. To understand the importance of accurate diagnosis for appropriate treatment planning.
3. To appreciate the need for acute diagnosis and treatment indication.
Author Disclosures:
R. Iezzi: Advisory Board at Terumo, Guerbet, Speaker at Terumo, Pharmacept, Bracco

RC 1515-3 15:00
C. Endovascular treatment in aortic dissection
P. J. Schaefer*; Kiel/DE (jp.schaefer@rad.uni-kiel.de)*
Learning objectives:
1. To learn about endovascular treatment possibilities for aortic dissections.
2. To understand the role of radiology in modern treatment of aortic dissections.
3. To appreciate the need to combine radiological information with the clinical situation.
Author Disclosures:
P. J. Schaefer: nothing to disclose

14:00 - 15:30 **Room G**

Neuro

RC 1511
Update on cerebrospinal fluid (CSF) diseases

Moderator:
Z. Merhemic; Sarajevo/BA

RC 1511-1 14:00
A. Imaging strategies for hydrocephalus
J. Bladowska*; Wroclaw/PL (asia.bladowska@gmail.com)*
Learning objectives:
1. To describe the different types of hydrocephalus and how to distinguish them in imaging.
2. To understand the pathophysiology of CSF circulation.
3. To apply MRI techniques for diagnosing abnormalities of the CSF flow.
Author Disclosures:
J. Bladowska: nothing to disclose

RC 1511-2 14:22
B. Diagnosis and treatment of intracranial hypotension
E. Papadaki*; Iraklion/GR (fpapada@otenet.gr)*
Learning objectives:
1. To understand the underlying pathophysiology of spontaneous intracranial hypotension (SIH).
2. To understand imaging strategies for this condition.
3. To clarify myths and misperceptions of intracranial hypotension.
Author Disclosures:
E. Papadaki: nothing to disclose

RC 1511-3 14:45
C. Reversible cerebral vasoconstriction syndrome (RCVS), posterior reversible encephalopathy syndrome (PRES), and others
J. Linn*; Munich/DE (Jennifer.Linn@uniklinikum-dresden.de)*
Learning objectives:
1. To understand the current controversial mechanism of posterior reversible encephalopathy syndrome (PRES).
2. To understand therapeutic and prognostic implications of PRES and reversible cerebral vasoconstriction syndrome (RCVS) diagnosis.
3. To appreciate imaging features of PRES, RCVS, and their differentials.
Author Disclosures:
J. Linn: Speaker at Bayer Healthcare, Advisory Board at mediaire GmbH

RC 1511-4 15:07
D. Hypertension-associated brain changes
A. Krainik*; Grenoble/FR (akrainik.esr@gmail.com)*
Learning objectives:
1. To understand the causes of intracranial hypertension.
2. To understand the threats of intracranial hypertension on the central nervous system and arterial integrity.
3. To recognise intracranial hypertension and its complications on CT and MRI.
Author Disclosures:
A. Krainik: nothing to disclose

14:00 - 15:30 **Room K**

E³ - European Diploma Prep Session

E³ 1523
Cardiac and vascular

E³ 1523-1 14:00
Chairperson's introduction
K.-F. Kreitner*; Mainz/DE (karl-friedrich.kreitner@unimedizin-mainz.de)*
Session objectives:
1. To understand the basic principles and techniques of cardiovascular imaging, including CT and MRI of the heart and great vessels.
2. To become familiar with the imaging presentations of disorders of the endocardium, the pericardium, and the cardiac valves.
3. To understand the MRI presentation of disorders of the myocardium.
Author Disclosures:
K.-F. Kreitner: nothing to disclose

E³ 1523-2 14:06
A. Cardiovascular imaging: the basics
R. Marano*; Rome/IT (riccardo.marano@unicatt.it)*
Learning objectives:
1. To understand the anatomy, normal variants, and abnormalities of the heart and great vessels.
2. To describe the technical aspects and methodology of cardiac and vascular CT.
3. To describe the technical aspects and methodology of cardiac and vascular MRI.
Author Disclosures:
R. Marano: nothing to disclose

E³ 1523-3 14:34
B. Cardiovascular imaging: valves, endocardium and aorta
C. Loewe*; Vienna/AT (christian.loewe@meduniwien.ac.at)*
Learning objectives:
1. To recognise the imaging presentation of the different forms of valvular disease.
2. To understand the causes and imaging presentations of endocarditis.
3. To describe the diagnostic evaluation and imaging presentation of common diseases of the great vessels, including aortic dissection and aneurysms.
Author Disclosures:
C. Loewe: Speaker at Siemens Healthineers, Speaker at BRACCO, Speaker at GE Healthcare

E³ 1523-4 15:02
C. Cardiovascular imaging: myocardium and pericardium
J. Bogaert*; Leuven/BE (Jan.Bogaert@uzleuven.be)*
Learning objectives:
1. To describe the diagnostic evaluation and imaging presentation of ischaemic heart disease.
2. To understand the diagnostic evaluation and imaging presentation of myocarditis.
3. To become familiar with the causes and imaging presentations of pericardial effusion.
Author Disclosures:
J. Bogaert: nothing to disclose

14:00 - 15:30 **Room M 1**

E³ - Rising Stars Programme: Basic Session

BS 15b

Radiographer research: tips to get you started

Moderator:
G. Unterhumer; Vienna/AT

BS 15b-1 14:00
Undertaking a systematic review
L. J. O. C. Lanca*; Singapore/SG (Luis.Lanca@singaporetech.edu.sg)*
Learning objectives:
1. To become familiar with the aims of systematic reviews.
2. To understand the systematic reviews process and explore methodologies.
3. To be aware of the importance of identifying the appropriate keywords, databases, and search strategies to promote a robust systematic review.
Author Disclosures:
L. J. O. C. Lanca: nothing to disclose

BS 15b-2 14:25
Planning and undertaking interviews
M. D. Davis*; Dublin/IE (michaela.davis@ucd.ie)*
Learning objectives:
1. To become familiar with interview-focused methodologies.
2. To understand the importance of a well-designed and thorough interview process.
3. To learn how to present interview findings.
Author Disclosures:
M. D. Davis: nothing to disclose

BS 15b-3 14:50
Conducting survey-based research
A. M. Bolejko*; Malmö/SE (anetta.bolejko@med.lu.se)*
Learning objectives:
1. To be aware of appropriate methodologies for performing surveys and questionnaires (paper-based and online).
2. To become familiar with survey validation methods.
3. Tips to promote effective survey dissemination and higher response rates.
Author Disclosures:
A. M. Bolejko: Speaker at Lund university, Author at Lund university

15:15
Panel discussion: Research mentorship: getting help from the experts

14:00 - 15:30 **Room M 2**

E³ - Advanced Course: How to Improve Your Expertise in Cardiothoracic Imaging

E³ 1519

Mediastinal and cardiac tumours in adults

E³ 1519-1 14:00
Chairperson's introduction
E. Coche*; Brussels/BE (emmanuel.coche@uclouvain.be)*
Session objectives:
1. To review the main causes of mediastinal and cardiac tumours.
2. To become familiar with the new classification of mediastinal compartments.
3. To appreciate the need for defining a standardised management.
Author Disclosures:
E. Coche: Speaker at Cliniques Universitaires St-Luc

E³ 1519-2 14:06
A. Prevascular compartment of the mediastinum
J. Vilar*; Valencia/ES (vilarsamper@gmail.com)*
Learning objectives:
1. To become familiar with the main causes of prevascular tumours.
2. To review the CT features of thymic malignancies.
3. To learn when to suspect lymphoma and when to suggest percutaneous biopsy.
Author Disclosures:
J. Vilar: nothing to disclose

E³ 1519-3 14:34
B. Paravertebral space
M. Occhipinti*; Florence/IT (mariaelena.occhipinti@gmail.com)*
Learning objectives:
1. To become familiar with the posterior mediastinal pathology.
2. To review the typical and atypical features of neurogenic tumours.
3. To learn about less frequent causes of paravertebral space masses.
Author Disclosures:
M. Occhipinti: Research/Grant Support at Fondazione Menarini

E³ 1519-4 15:02
C. Cardiac masses: a survival guide
V. E. Sinitsyn*; Moscow/RU (vsini@mail.ru)*
Learning objectives:
1. To learn how to differentiate thrombi from tumours of the cardiac cavities.
2. To review the main differential diagnosis of cardiac tumours.
3. To learn about the role of US, CT, and MRI for diagnosis and characterisation.
Author Disclosures:
V. E. Sinitsyn: nothing to disclose

14:00 - 15:30 **Room M 4**

Transatlantic Course of ESR and RSNA (Radiological Society of North America): Stroke Imaging and Endovascular Treatment: Now and the Future

TC 1528

Endovascular treatment

Moderators:
J.-P. Pruvo; Lille/FR
R. Uberoi; Oxford/UK

TC 1528-1 14:00
A. Endovascular treatment of acute ischaemic stroke: practical pearls
A. Berlis*; Augsburg/DE*
Learning objectives:
1. To learn about endovascular treatment in ischaemic stroke.
2. To understand the different approaches of endovascular treatment.
3. To appreciate the importance of efficient workup and time metrics in angiosuite.
Author Disclosures:
A. Berlis: disclosure/affirmation information not submitted

TC 1528-2 14:30
B. Where to perform and how to organise thrombectomy
J. Heit*; Stanford/US (jheit@stanford.edu)*
Learning objectives:
1. To learn about the number of persons and regulatory recommendations.
2. To understand the optimal organisation in angiosuite and workflow.
3. To appreciate the implications and management for continuity of care.
Author Disclosures:
J. Heit: Consultant at Medtronic, Consultant at MicroVention, Advisory Board at iSchemaView

TC 1528-3/TC 1528-4/TC 1528-5 15:00
C. Interactive discussion with illustrative cases of endovascular thrombectomy
A. Berlis*; Augsburg/DE*
J. Heit*; Stanford/US (jheit@stanford.edu)*
G. Boulouis*; Paris/FR (gregoireboulouis@gmail.com)*

Learning objectives:
1. To learn about tricks and tips of endovascular treatment using illustrative cases.
2. To appreciate the optimal time metrics in angiosuite.
3. To become familiar with the different approaches (stent retriever, ADAPT) and challenging cases (tandem occlusions, distal occlusions).
Author Disclosures:
A. Berlis: disclosure/affirmation information not submitted;
J. Heit: Consultant at Medtronic, Consultant at MicroVention, Advisory Board at iSchemaView
G. Boulouis: nothing to disclose

14:00 - 15:30 **Room M 5**

E³ - Advanced Course: Hot Topics in GU Cancer

E³ 1522

Tumour relapse in urological cancer

E³ 1522-1 14:00
Chairperson's introduction
V. Løgager*; Herlev/DK (Vibeke.Loegager@regionh.dk)*
Author Disclosures:
V. Løgager: nothing to disclose

E³ 1522-2 14:15
A. Prostate cancer relapse
V. Panebianco*; Rome/IT (valeria.panebianco@uniroma1.it)*
Learning objectives:
1. To learn the follow-up strategy post radical prostatectomy.
2. To recognise relapse and know the patterns of spread.
3. To learn about the use of imaging in planning salvage therapy.
Author Disclosures:
V. Panebianco: nothing to disclose

E³ 1522-3 14:40
B. Non-prostate urological cancer relapse
H. A. H. Vargas*; New York, NY/US*
Learning objectives:
1. To recognise the expected post treatment appearances.
2. To know follow-up strategies for detection of relapse.
3. To learn to recognise pitfalls by case review.
Author Disclosures:
H. A. H. Vargas: nothing to disclose

E³ 1522-4 15:05
C. Theranostics in urological cancer
M. Hartenbach*; Vienna/AT (markus.hartenbach@me.com)*
Learning objectives:
1. To learn about theranostic options in urological cancers.
2. To understand the advantages and limitations of theranostic approaches.
3. To become familiar with the new indications and outcomes of theranostic approaches.
Author Disclosures:
M. Hartenbach: CEO at MINUTEmedical Inc.

14:00 - 15:30 **Tech Gate Auditorium**

ESR Ultrasound Subcommittee Session

US 15

Common applications of dermatologic ultrasound

Moderators:
O. Catalano; Naples/IT
D. E. Gaitini; Haifa/IL

US 15-1 14:00
Chairperson's introduction
X. Wortsman*; Santiago/CL (xworts@yahoo.com)*
Session objectives:
1. To review the normal anatomy of the skin, nails, and hair, and to review the guidelines and technical considerations for performing dermatologic ultrasound examinations.
2. To provide an overview of the frequent applications of ultrasound in benign dermatologic conditions.
3. To learn the ultrasonographic features of the most common types of skin cancer.
Author Disclosures:
X. Wortsman: nothing to disclose

US 15-2 14:05
Dermatologic ultrasound: essential anatomy, guidelines, and technical considerations
D. E. Gaitini*; Haifa/IL (d_gaitini@rambam.health.gov.il)*
Learning objectives:
1. To learn the requisites for practising dermatologic ultrasound examinations.
2. To become familiar with the normal ultrasound anatomy of skin, nail, and hair.
3. To review and understand the current guidelines for dermatologic ultrasound examinations.
Author Disclosures:
D. E. Gaitini: nothing to disclose

US 15-3 14:25
Top ten applications of ultrasound in benign dermatologic conditions
X. Wortsman*; Santiago/CL (xworts@yahoo.com)*
Learning objectives:
1. To learn the most common benign dermatologic conditions that can benefit from an ultrasound examination.
2. To appreciate the clinical and ultrasonographic correlations of these dermatologic entities.
3. To understand the ultrasound appearance of these conditions.
Author Disclosures:
X. Wortsman: nothing to disclose

US 15-4 14:45
Ultrasonographic signs and locoregional staging of skin cancer
O. Catalano*; Naples/IT*
Learning objectives:
1. To learn the most common types of skin cancer.
2. To appreciate the ultrasonographic appearance of the most common types of skin cancer.
3. To understand and review the protocol for an ultrasonographic locoregional staging of skin cancer.
Author Disclosures:
O. Catalano: nothing to disclose

15:05
Panel discussion: Questions and answers

16:00 - 17:30 **Room B**

Emergency Imaging

RC 1617

Blunt polytrauma: CT protocols, CT interpretation and interventional radiology options

RC 1617-1 16:00
Chairperson's introduction
K. H. Nieboer*; Brussels/BE (k.hans.nieboer@gmail.com)*
Session objectives:
1. To understand the different CT and contrast protocols that can be performed in blunt polytrauma patients and when to apply them.
2. To be able to quickly identify and classify solid organ injuries.
3. To recognise injuries that can be treated with interventional radiology.
Author Disclosures:
K. H. Nieboer: Speaker at GE Healthcare

RC 1617-2 16:05
A. CT protocols in blunt polytrauma
E. Kashef*; London/UK (elikadoc@icloud.com)*
Learning objectives:
1. To understand the advantages and disadvantages of different CT protocols adopted in blunt polytrauma patients.
2. To learn the goal of use of single and dual phase contrast injection protocols in trauma.
3. To be able to incorporate the most suitable CT protocol in defined clinical scenarios.
Author Disclosures:
E. Kashef: Speaker at Guerbet , Consultant at Rocket medical

RC 1617-3 16:30
B. Solid organs injuries: a tailored approach
M. N. Patlas*; Hamilton, ON/CA (patlas69@yahoo.com)*
Learning objectives:
1. To learn about the main traumatic injuries that can be detected in solid organs.
2. To understand which crucial findings will change patient management.
3. To understand what surgical and intensive care teams need to know about detected injuries.
Author Disclosures:
M. N. Patlas: Other at Springer

RC 1617-4 16:55
C. Interventional radiology in trauma: diagnosis and management
T. Jargiello*; Lublin/PL (tojarg@interia.pl)*
Learning objectives:
1. To learn which vascular injuries in solid organs can be treated with interventional radiology.
2. To become familiar with the imaging findings of great vessel injuries.
3. To understand how vascular injuries can be treated.
Author Disclosures:
T. Jargiello: nothing to disclose

17:20
Panel discussion: What is the best CT protocol in the evaluation of blunt trauma patients?

16:00 - 17:30 **Room N**

EuroSafe Imaging Session

EU 16
Technology developments which impact dose delivery

EU 16-1/**EU 16-2** 16:00
Chairpersons' introduction: Setting the scene of modern technology for exposure efficient medical imaging
C. Hoeschen*; Magdeburg/DE*
G. Frija*; Paris/FR (guy.frija@aphp.fr)*
Session objectives:
1. To introduce why optimisation of dose is important in certain imaging tasks.
2. To highlight the importance of efficient technology use.
3. To introduce speakers and their topics in terms of potential of imaging technology.
Author Disclosures:
C. Hoeschen: disclosure/affirmation information not submitted;
G. Frija: nothing to disclose

EU 16-3 16:05
Overarching technological developments for producing x-rays in medical imaging for reducing dose
C. Hoeschen*; Magdeburg/DE*
Learning objectives:
1. To learn about the possibilities for dose efficient imaging using scanning imaging geometries and/or monoenergetic x-rays.
2. To understand new concepts for source developments that could be used in medical surroundings to offer advantages in reducing dose.
3. To discuss the chances and limits of such approaches, especially with respect to three-dimensional and interventional imaging.
Author Disclosures:
C. Hoeschen: disclosure/affirmation information not submitted

EU 16-4 16:23
Applying algorithmic approaches for efficient imaging technologies
M. Rafecas*; Lübeck/DE (rafecas@imt.uni-luebeck.de)*
Learning objectives:
1. To learn about the different reconstruction and noise reduction methods.
2. To understand potentials and limitations of such technologies.
3. To see examples from various imaging modalities.
Author Disclosures:
M. Rafecas: nothing to disclose

EU 16-5 16:41
Optimising radiation efficiency in interventional imaging
M. Pech*; Magdeburg/DE*
Learning objectives:
1. To learn about the possibilities to improve image quality and dose management in CT fluoroscopy.
2. To understand the concept of iterative 3D image reconstruction.
3. To learn how to estimate the radiation dose to the hand during interventions correctly.
Author Disclosures:
M. Pech: Speaker at Universitätsklinikum Magdeburg A.ö.R.

EU 16-6 16:59
New concepts for dose determination for staff and patients, and ist importance for optimisation
L. Struelens*; Mol/BE (lstruele@sckcen.be)*
Learning objectives:
1. To learn about the possibilities of changing the way personal dosimetry of staff is performed by using computational methods.
2. To learn about new developments to improve the monitoring of patient doses by using computational methods.
Author Disclosures:
L. Struelens: nothing to disclose

17:17
Panel discussion: Future chances for radiation protection by efficient use of technological developments

16:00 - 17:30 **Room O**

New Horizons Session

NH 16
Lung cancer screening implementation in Europe: is it inevitable?

NH 16-1 16:00
Chairperson's introduction
M. M. Prokop*; Nijmegen/NL (mathias.prokop@radboudumc.nl)*
Session objectives:
1. To summarise the current status of CT lung cancer screening from a national and international perspective.
2. To analyse common hurdles to recruitment, retention, and access.
3. To determine future directions into which CT lung cancer screening should evolve.
Author Disclosures:
M. M. Prokop: Research/Grant Support at Canon Medical Systems, Research/Grant Support at Siemens Healthineers, Speaker at Siemens Healthineers, Speaker at Bracco, Speaker at Bayer, Speaker at Canon Medical Systems

NH 16-2 16:05
NELSON trial latest results
H. J. de Koning*; Rotterdam/NL (h.dekoning@erasmusmc.nl)*
Learning objectives:
1. To review the NELSON trial design and settings.
2. To learn about the final mortality reduction results.
3. To learn about causes of death unrelated to lung cancer.
Author Disclosures:
H. J. de Koning: Research/Grant Support at HORIZON2020 4-in-the-lung run, Speaker at Univ Zurich/Astra Zeneca, Research/Grant Support at NIH/NCI CISNET

NH 16-3 16:23
Lung cancer screening in Europe
M. Silva; *Parma/IT (mariosilvamed@gmail.com)*
Learning objectives:
1. To review the European guidelines for screening.
2. To learn about the Lung Cancer Screening (LCS) certification project.
3. To describe the currently active nationwide screening programmes.
Author Disclosures:
M. Silva: nothing to disclose

NH 16-4 16:41
Challenges to implementing lung cancer screening: US experience
A. Bankier; *Boston, MA/US (alexander.bankier@umassmemorial.org)*
Learning objectives:
1. To learn about ways to promote lung cancer screening.
2. To review the strategies for a high adherence and retention rate.
3. To learn how to optimise lung cancer screening implementation in clinical practice.
Author Disclosures:
A. Bankier: Consultant at Daiichi Pharmaceutical, Consultant at Spiration (Olympus)

NH 16-5 16:59
Lung cancer screening: will humans still be needed?
B. van Ginneken; *Nijmegen/NL (bramvanginneken@gmail.com)*
Learning objectives:
1. To learn about computer-aided detection (CAD) tools for lung nodule detection and characterisation.
2. To review automated screening opportunities beyond lung nodule detection.
3. To learn about the current and projected future artificial intelligence performance in lung cancer detection.
Author Disclosures:
B. van Ginneken: Founder at Thirona, Grant Recipient at MeVis Medical Solutions, Shareholder at Thirona, Grant Recipient at Delft Imaging Systems, Grant Recipient at Thirona

NH 16-6 17:17
Panel discussion: Lung cancer screening, from trial to practice
M. M. Prokop; *Nijmegen/NL,* H. J. de Koning; *Rotterdam/NL,* M. Silva; *Parma/IT,* A. Bankier; *Boston, MA/US,* B. van Ginneken; *Nijmegen/NL,* S. Vallone; *Turin/IT*

16:00 - 17:30 **Studio 2020**

E³ - ECR Master Class (Musculoskeletal)

E³ 1626a
State-of-the-art imaging of postoperative joints

Moderator:
F. Kainberger; Vienna/AT

E³ 1626a-1 16:00
A. Postoperative shoulder
C. W. A. Pfirrmann; *Forch/CH*
Learning objectives:
1. To explain the most frequently used surgical techniques for glenohumeral instability, subacromial decompression, rotator cuff repair and arthroplasty, and their imaging appearance.
2. To describe potential postoperative complications and their imaging apprearance.
Author Disclosures:
C. W. A. Pfirrmann: nothing to disclose

E³ 1626a-2 16:30
B. Postoperative knee
E. Oei; *Rotterdam/NL (e.oei@erasmusmc.nl)*
Learning objectives:
1. To explain the most frequently used surgical techniques for meniscal repair, ligament reconstruction and cartilage repair, and their imaging appearance.
2. To describe potential postoperative complications and their imaging appearance.
Author Disclosures:
E. Oei: Research/Grant Support at GE Healthcare

E³ 1626a-3 17:00
C. Postoperative hip
P. D. Afonso; *Lisbon/PT (p.diana.a@gmail.com)*
Learning objectives:
1. To explain the most frequently used surgical techniques for femoroacetabular impingement and degenerative hip joint disease, and their imaging appearance.
2. To describe potential postoperative complications and their imaging appearance.
Author Disclosures:
P. D. Afonso: nothing to disclose

16:00 - 17:30 **Room on demand Room E or Room F2**

Abdominal Viscera

RC 1601
Imaging of pancreatitis

Moderator:
K. I. Ringe; Hannover/DE

RC 1601-1 16:00
A. Focal pancreatitis vs adenocarcinoma
T. L. Bollen; *Nieuwegein/NL (tlbollen@hotmail.com)*
Learning objectives:
1. To learn about the prevalence and clinical markers of focal pancreatitis and adenocarcinoma.
2. To understand the difficulties in differentiating these entities and to develop imaging-based problem solving tools.
3. To become familiar with follow-up strategies in non-conclusive cases or when the biopsy is negative.
Author Disclosures:
T. L. Bollen: nothing to disclose

RC 1601-2 16:22
B. IgG4 autoimmune pancreatitis
A. Arora; *Liverpool/UK*
Learning objectives:
1. To know the imaging characteristics of autoimmune pancreatitis compared to other forms of pancreatitis.
2. To learn about the value of different imaging tool including US, CT, and MRI for the diagnosis of autoimmune pancreatitis.
3. To be aware of imaging markers indicating therapeutic success in patients with autoimmune pancreatitis.
Author Disclosures:
A. Arora: disclosure/affirmation information not submitted

RC 1601-3 16:45
C. Imaging of chronic pancreatitis
N. Kartalis; *Stockholm/SE (nikolaos.kartalis@me.com)*
Learning objectives:
1. To understand the strengths and weaknesses of different imaging tools for the diagnosis of chronic pancreatitis.
2. To be aware of typical and atypical imaging findings in patients with chronic pancreatitis.
3. To learn about the pitfalls and how to avoid diagnostic mistakes in patients with chronic pancreatitis.
Author Disclosures:
N. Kartalis: nothing to disclose

RC 1601-4 17:07
D. Interventions in acute pancreatitis
M. Maher; *Dublin/IE (m.maher@ucc.ie)*
Learning objectives:
1. To recognise the techniques of interventions in acute pancreatitis.
2. To understand the indications of transgastral vs percutaneous drainage.
3. To learn how to avoid complications following pancreatic interventions.
Author Disclosures:
M. Maher: nothing to disclose

16:00 - 17:30 **Room F1**

State of the Art Symposium

SA 16

Hepatocellular carcinoma (HCC): the role of radiology

SA 16-1 16:00
Chairperson's introduction
F. Caseiro Alves*; Coimbra/PT (caseiroalves@gmail.com)*
Session objectives:
1. To discuss the role of radiologists in the management of patients with HCC.
2. To learn the imaging findings of HCC and the differentials.
3. To become familiar with treatment options.
Author Disclosures:
F. Caseiro Alves: nothing to disclose

SA 16-2 16:05
A clinician's perspective on the role of radiology in HCC: any room for improvement?
M.-A. Woerns*; Mainz/DE (marcus-alexander.woerns@unimedizin-mainz.de)*
Learning objectives:
1. To review how the clinician benefits from imaging in the management of patients with HCC.
2. To become familiar with the clinician's questions and the answers radiology may provide.
3. To learn from a clinician's perspective how radiologists can improve in their role in the management of patients with HCC.
Author Disclosures:
M.-A. Woerns: Advisory Board at Abbvie, Bayer, Bristol-Myers Squibb, Eisai, Ipsen, Roche Pharma, Speaker at Abbvie, Bayer, Bristol-Myers Squibb, Celgene, Gilead Science, Incyte, Ipsen, Janssen-Cilag, MSD Sharp & Dohme, Research/Grant Support at Abbvie, Ipsen

SA 16-3 16:20
Guidelines and beyond: the non-invasive diagnosis of HCC
C. B. Sirlin*; San Diego/US (csirlin@ucsd.edu)*
Learning objectives:
1. To understand similarities and differences in the current guidelines for the diagnosis of HCC worldwide.
2. To understand the algorithmic approach to imaging diagnosis: liver imaging reporting and data system (LI-RADS).
3. To review the pros and cons of the different systems.
Author Disclosures:
C. B. Sirlin: Consultant at Consultancy as representative of UC Regents: GE Healthcare, Bayer, AMRA, Fulcrum Therapeutics, IBM/Watson Health, Advisory Board at Advisory Board as representative of UC Regents: AMRA, Guerbet, Bristol Myers Squibb, Grant Recipient at Gilead, GE Healthcare, Siemens, GE MRI, Bayer, GE Digital, GE US, ACR Innovation, Philips, Celgene, Speaker at Speaking services, money deposited to UC Regents: GE Healthcare, Bayer , Other at Development of educational presentations or articles, money paid to UC Regents: Medscape, Resoundant, Research/Grant Support at Lab Service Agreements: Enanta, ICON Medical Imaging, Gilead, Shire, Virtualscopics, Intercept, Synageva, Takeda, Genzyme, Janssen, NuSirt, Celgene-Parexel, Organovo, Consultant at Independent Consulting: Epigenomics, Blade Therapeutics , Author at Royalty from educational article, paid to UC Regents: Wolters Kluwer Health (UpToDate Publishing): , Other at Development of educational presentations or articles, money paid to Claude Sirlin: Medscape, Board Member at SAR Board of Directors, no fees received, travel expenses reimbursed

SA 16-4 16:40
How to approach a small lesion in cirrhosis
G. Brancatelli*; Palermo/IT (gbranca@yahoo.com)*
Learning objectives:
1. To review typical and atypical forms of small HCC in the cirrhotic liver.
2. To describe the most common lesions and pseudolesions occurring in the cirrhotic liver beyond HCC.
3. To understand strategies to improve diagnosis of small lesions in the cirrhotic liver.
Author Disclosures:
G. Brancatelli: Consultant at Bayer, Speaker at Bayer, Other at General Electric, Other at Bracco

SA 16-5 17:00
How imaging can help choose treatment of HCC and the role of interventional radiology
V. Vilgrain*; Clichy/FR (valerie.vilgrain@aphp.fr)*
Learning objectives:
1. To learn the key factors for the treatment of HCC patients.
2. To understand the role of imaging in choosing treatment.
3. To become familiar with the role of interventional radiology in HCC.
Author Disclosures:
V. Vilgrain: Speaker at Hospital Beaujon

17:20
Panel discussion: How can we improve the diagnosis of HCC?

16:00 - 17:30 **Room on demand**
Room E or Room F2

Musculoskeletal

RC 1610

Musculoskeletal infection

Moderator:
M. Rupreht; Maribor/SI

RC 1610-1 16:00
A. Imaging osteomyelitis: an update
J. Fritz*; Baltimore, MD/US (janfritz777@gmail.com)*
Learning objectives:
1. To describe the role of imaging in diagnosing osteomyelitis.
2. To explain the role of intravenous contrast medium material in diagnosing osteomyelitis.
3. To list the differential diagnostic considerations in imaging osteomyelitis.
Author Disclosures:
J. Fritz: Research/Grant Support at Siemens Healthcare, Advisory Board at Siemens Healthcare, Advisory Board at GE Healthcare, Patent Holder at Siemens Healthcare, Patent Holder at Johns Hopkins University

RC 1610-2 16:30
B. Soft tissue infections
S. Martin*; Palma de Mallorca/ES (silvia.m.martin@gmail.com)*
Learning objectives:
1. To describe the role of imaging in soft tissue infections.
2. To explain the role of intravenous contrast medium material in diagnosing soft tissue infections.
3. To list the differential diagnostic considerations in imaging soft tissue infections.
Author Disclosures:
S. Martin Martin: nothing to disclose

RC 1610-3 17:00
C. Septic arthritis
R. K. Lalam*; Oswestry/UK (radhesh.lalam@nhs.net)*
Learning objectives:
1. To describe the role of imaging in septic arthritis.
2. To explain the role of intravenous contrast medium material in diagnosing septic arthritis.
3. To list the differential diagnostic considerations in imaging septic arthritis.
Author Disclosures:
R. K. Lalam: nothing to disclose

16:00 - 17:00 **Coffee & Talk 3**

Coffee & Talk (open forum) Session

C 32

How to advance the academic ladder

C 32-1 16:00
Chairperson's introduction
J. Sosna*; Jerusalem/IL (jacobs@hadassah.org.il)*
Session objectives:
1. To describe promotion tracks in academic radiology.
2. To present quality metrics in judging publications.
3. To highlight the importance of grants in the production of valuable research.
Author Disclosures:
J. Sosna: Consultant at Xact, Grant Recipient at Philips

C 32-2 16:05
Judging publications for academic promotions
L. Marti-Bonmati*; Valencia/ES (Luis.Marti@uv.es)*
Learning objectives:
1. To present how publications are judged in academic committees.
2. To describe bibliometric measures.
3. To emphasise the value of publications in academic radiology.
Author Disclosures:
L. Marti-Bonmati: nothing to disclose

C 32-3 16:15
Grants: importance for science and academia
G. P. Krestin*; Rotterdam/NL*
Learning objectives:
1. To describe the value of raising grants for performing research.
2. To present possible sources of funding and means for acquiring them.
3. To present how grant-raising is judged in universities.
Author Disclosures:
G. P. Krestin: Consultant at Bracco Imaging, Board Member at Quantib BV, Research/Grant Support at GEHC, Research/Grant Support at Bayer AG, Research/Grant Support at Siemens Healthineers

16:25
Open forum discussion

16:00 - 17:30 **da Vinci (Room D1)**

Vascular

RC 1615

Visceral arteries

RC 1615-1 16:00
Chairperson's introduction
J. A. Reekers*; Amsterdam/NL*
Session objectives:
1. To learn about incidence and aetiology of visceral arteries diseases.
2. To become familiar with clinical symptoms and evaluation in visceral arteries diseases.
3. To indicate the role of radiology in diagnosis and treatment of the visceral arteries.
Author Disclosures:
J. A. Reekers: disclosure/affirmation information not submitted

RC 1615-2 16:05
A. Diagnosis of abdominal vascular compression syndromes
B. E. Çil*; Istanbul/TR (bcil@kuh.ku.edu.tr)*
Learning objectives:
1. To become familiar with abdominal arterial and venous compression syndromes.
2. To learn about functional imaging techniques in assessment of vascular compression syndromes.
3. To become familiar with the typical imaging findings in abdominal compression syndromes and their clinical relevance.
Author Disclosures:
B. E. Çil: nothing to disclose

RC 1615-3 16:28
B. Acute and chronic mesenteric ischaemia
M. Zins*; Paris/FR (mzins@hpsj.fr)*
Learning objectives:
1. To become familiar with occlusive and non-occlusive mesenteric ischaemia.
2. To understand the differences between acute and chronic ischaemia.
3. To learn about the importance of fast and correct diagnosis in acute mesenteric ischaemia.
Author Disclosures:
M. Zins: nothing to disclose

RC 1615-4 16:51
C. Endovascular treatment of mesenteric ischaemia
R. A. Morgan*; London/UK (robert.morgan@stgeorges.nhs.uk)*
Learning objectives:
1. To review indications for endovascular treatment of mesenteric ischaemia.
2. To become familiar with the technical possibilities of endovascular repair of visceral arteries.
3. To learn about risks and complications of endovascular treatment of mesenteric ischaemia.
Author Disclosures:
R. A. Morgan: Speaker at Cook, Speaker at Bard

17:14
Panel discussion: Radiologists as the best case managers in acute and chronic mesenteric ischaemia

16:00 - 17:30 **Darwin (Room D2)**

Breast

RC 1602

Update on lesions with uncertain malignant potential (B3)

Moderator:
C. Van Ongeval; Leuven/BE

RC 1602-1 16:00
A. Wrap-up of the newest literature on the most important B3 lesions
Z. Varga*; Zurich/CH*
Learning objectives:
1. To know about the biological behaviour of the most important B3 lesions.
2. To understand the difference between B3a and B3b lesions.
3. To recognise the most worrisome entities.
Author Disclosures:
Z. Varga: nothing to disclose

RC 1602-2 16:30
B. Imaging lesions of uncertain potential
A. Linda*; Udine/IT (annalinda33@gmail.com)*
Learning objectives:
1. To become familiar with the most common imaging findings in B3 lesions.
2. To identify the most appropriate imaging modality.
3. To identify the factors that limit patient compliance to the management recommendations after a pathologic result of a high-risk breast lesion.
Author Disclosures:
A. Linda: nothing to disclose

RC 1602-3 17:00
C. How to handle them: update on B3 guidelines
N. Sharma*; Leeds/UK (Nisha.sharma2@nhs.net)*
Learning objectives:
1. To learn about the most recent international recommendations on the management of B3 lesions.
2. To differentiate between the results of a core needle and a vacuum assisted biopsy (VAB).
3. To be able to identify cases when VAB excision may pose a valid alternative to a surgical one.
Author Disclosures:
N. Sharma: nothing to disclose

16:00 - 17:30 **Descartes (Room D3)**

Radiographers

RC 1614

Practical computed tomography tips for radiographers

RC 1614-1/RC 1614-2 16:00
Chairpersons' introduction
H. Husejnagic*; Tuzla/BA*
J. Santos*; Coimbra/PT (joanasantos@estescoimbra.pt)*
Session objectives:
1. To understand the impact of CT scanner development on the radiographers' role.
2. To be aware of practical optimisation tips for routine CT examinations based on clinical indications in adults and children.
Author Disclosures:
H. Husejnagic: disclosure/affirmation information not submitted;
J. Santos: Speaker at ESTESC-IPC

RC 1614-3 16:06
A. The practical implications of CT scanner development: where we have come from and where we are now
D. Hribar*; Ljubljana/SI (dejan.hribar@kclj.si)*
Learning objectives:
1. To appreciate the developments in CT technology over time.
2. To understand the implications of technological advancements upon current clinical practice.
3. To be aware of key aspects of technology developments with which radiographers should be fully familiar.
Author Disclosures:
D. Hribar: Other at Siemens Healthineers

RC 1614-4 16:29
B. Practical tips for radiographers in CT scanning of the thorax and abdomen
S. D. Mørup*; Kolding/DK (sdmo@ucl.dk)*
Learning objectives:
1. To review CT examinations of the thorax and abdomen, and subsequent dose implications.
2. To be aware of recent research relevant to the optimisation of CT examination of the thorax and abdomen.
3. To understand key principles of optimisation for specific clinical indications when performing a CT examination of the thorax and abdomen.
Author Disclosures:
S. D. Mørup: nothing to disclose

RC 1614-5 16:52
C. Practical tips for radiographers when scanning paediatric imaging
B. Møller Christensen*; Jönköping/SE (berit.moller-christensen@ju.se)*
Learning objectives:
1. To review examinations that are routinely performed on paediatric patients.
2. To understand key evidence-based principles of optimisation and how these can be applied in routine practice.
3. To be aware of how European and international guidelines and legislation in different geographical jurisdictions should empower active optimisation in paediatric CT.
Author Disclosures:
B. Møller Christensen: nothing to disclose

17:15
Panel discussion: How can we ensure CT radiographers keep up to date with changes in CT technology?

16:00 - 17:30 **Room G**

Paediatric

RC 1612

Imaging in abdominal emergencies: an (evidence-based) update

Moderator:
C. de Lange; Oslo/NO

RC 1612-1 16:00
A. The acute abdomen in neonates
A. Coma*; Barcelona/ES (coma.ana@gmail.com)*
Learning objectives:
1. To learn about typical neonatal abdominal emergencies.
2. To understand the choice of modalities in acute abdomen emergencies in neonates.
3. To appreciate typical findings and 'red flag' features.
Author Disclosures:
A. Coma: nothing to disclose

RC 1612-2 16:30
B. The acute abdomen in young children
A. D. Calder*; London/UK (Alistair.Calder@gosh.nhs.uk)*
Learning objectives:
1. To learn about the causes of acute abdominal pain in children.
2. To understand the choice of imaging techniques and their limitations.
3. To appreciate typical radiological features of abdominal emergencies.
Author Disclosures:
A. D. Calder: nothing to disclose

RC 1612-3 17:00
C. Polytrauma: differences between adult and paediatric protocols
C. J. L. Eriksen*; Oslo/NO (cornelialind@gmail.com)*
Learning objectives:
1. To learn how paediatric trauma differs from adult trauma.
2. To understand how examination techniques and protocols must be tailored accordingly.
3. To appreciate the importance of multidisciplinary team collaboration in planning and conducting radiological investigations in a trauma setting.
Author Disclosures:
C. J. L. Eriksen: nothing to disclose

16:00 - 17:30 **Room K**

Cardiac

RC 1603

Dead or alive: imaging of myocardial viability

RC 1603-1 16:00
Chairperson's introduction
C. Peebles*; Southampton/UK (Charles.Peebles@uhs.nhs.uk)*
Session objectives:
1. To understand the concept of myocardial viability.
2. To understand the current state of the art to image myocardial viability.
3. To outline the role of echocardiography, single-photon emission computed tomography (SPECT), CT, and MRI.
Author Disclosures:
C. Peebles: nothing to disclose

RC 1603-2 16:05
A. MRI: why and when
T. Leiner*; Utrecht/NL (t.leiner@umcutrecht.nl)*
Learning objectives:
1. To learn about how MRI should be performed to assess viability.
2. To understand the strengths and weaknesses of MRI compared to other techniques.
3. To learn how to report MRI for viability assessment.

Author Disclosures:
T. Leiner: Research/Grant Support at Bayer Healthcare, Research/Grant Support at Philips Healthcare, Board Member at International Society for Magnetic Resonance in Medicine (ISMRM)

RC 1603-3 16:28
B. Hybrid imaging
F. Caobelli*; Basel/CH (federico.caobelli@usb.ch)*
Learning objectives:
1. To learn about how hybrid imaging should be performed to assess viability.
2. To understand the strengths and weaknesses of hybrid imaging compared to other techniques.
3. To understand how hybrid imaging could be developed in clinical practice.
Author Disclosures:
F. Caobelli: nothing to disclose

RC 1603-4 16:51
C. CT: how and why
F. Bamberg*; Freiburg/DE (fabian.bamberg@uni-tuebingen.de)*
Learning objectives:
1. To learn about the potential of CT to assess viability.
2. To understand the strengths and weaknesses of CT imaging compared to other techniques.
3. To understand how to report CT for viability assessment.
Author Disclosures:
F. Bamberg: Research/Grant Support at Siemens Healthineers, Research/Grant Support at Bayer Healthcare, Speaker at Siemens Healthineers, Speaker at Siemens Healthineers, Speaker at Bracco

17:14
Panel discussion: What imaging test for which patient?

16:00 - 17:30 **Room M 1**

E³ - ECR Master Class (Genitourinary)

E³ 1626b

Prostate MRI: the accreditation issue

E³ 1626b-1 16:00
Chairperson's introduction
J. Richenberg*; Brighton/UK (jonathan.richenberg@nhs.net)*
Session objectives:
1. To understand the emerging role of the multidisciplinary approach for prostate cancer.
2. To discuss the role of the radiologist in the multidisciplinary approach to prostate cancer.
3. To discuss the accreditation and certification issues for prostate imaging.
Author Disclosures:
J. Richenberg: nothing to disclose

E³ 1626b-2 16:05
A. Prostate MRI: minimum and optimal requirements
J. O. Barentsz*; Nijmegen/NL (Jelle.Barentsz@radboudumc.nl)*
Learning objectives:
1. To understand the minimum requirements for multiparametric MRI of prostate cancer.
2. To understand how to optimise MRI technique at 3T and 1.5T.
3. To review sequence parameters and scan optimisation for prostate imaging.
Author Disclosures:
J. O. Barentsz: Advisory Board at SPL Medical, Advisory Board at Soteria

E³ 1626b-3 16:28
B. Towards a European accreditation of prostate imaging centres
V. Løgager*; Herlev/DK (Vibeke.Loegager@regionh.dk)*
Learning objectives:
1. To learn about the role of the radiologist in the multidisciplinary approach for prostate cancer.
2. To discuss the requirements for a specialist prostate centre, with emphasis to the imaging issue.
3. To understand quality indicators for prostate MRI.
Author Disclosures:
V. Løgager: nothing to disclose

E³ 1626b-4 16:51
C. Towards a certified radiologist
H. C. Thoeny*; Fribourg/CH (Harriet.thoeny@h-fr.ch)*
Learning objectives:
1. To understand the need for a certified radiologist in a prostate unit.
2. To illustrate the level III European Training Curriculum for prostate imaging.
3. To discuss how to certify radiologists for prostate imaging.
Author Disclosures:
H. C. Thoeny: Advisory Board at Guerbet

17:14
Panel discussion: Prostate units: the radiologist must be in the core team

16:00 - 17:30 **Room M 2**

E³ - Advanced Course: How to Improve Your Expertise in Cardiothoracic Imaging

E³ 1619

Pulmonary embolism/pulmonary hypertension

E³ 1619-1 16:00
Chairperson's introduction
G. Aviram*; Tel-Aviv/IL (aviramgalit@hotmail.com)*
Session objectives:
1. To review the current controversies regarding pulmonary embolism diagnosis.
2. To review the role of CT in pulmonary hypertension.
3. To appreciate the need for defining a standardised management.
Author Disclosures:
G. Aviram: Research/Grant Support at Philips Healthcare

E³ 1619-2 16:06
A. Diagnosis of acute pulmonary embolism (PE)
M.-P. Revel*; Paris/FR (marie-pierre.revel@aphp.fr)*
Learning objectives:
1. To review the role of clinical probability scores and D-dimer assessment.
2. To learn about tips and tricks to optimise arterial opacification on CT.
3. To learn about key features to report in acute PE.
Author Disclosures:
M.-P. Revel: Other at GUERBET

E³ 1619-3 16:34
B. Pulmonary hypertension
A. P. Parkar*; Bergen/NO (apparkar@gmail.com)*
Learning objectives:
1. To become familiar with the causes of pulmonary hypertension.
2. To learn about the radiological presentation of pulmonary artery hypertension.
3. To understand how imaging helps patient management.
Author Disclosures:
A. P. Parkar: nothing to disclose

E³ 1619-4 17:02
C. The heart in pulmonary hypertension
K.-F. Kreitner*; Mainz/DE (karl-friedrich.kreitner@unimedizin-mainz.de)*
Learning objectives:
1. To learn about cardiac causes of pulmonary hypertension.
2. To become familiar with cardiac assessment in pulmonary hypertension.
3. To recognise the prognostic importance of right ventricle dysfunction in pulmonary hypertension.
Author Disclosures:
K.-F. Kreitner: nothing to disclose

16:00 - 17:30 **Room M 3**

E³ - Rising Stars Programme: Basic Session

BS 16

The importance of good patient positioning in imaging

Moderator:
A. Ohmstede; Oldenburg/DE

BS 16-1 16:00
Positioning tips and tricks for musculoskeletal radiography
J. Jensen*; Odense/DK*
Learning objectives:
1. To understand how correct positioning is assessed.
2. To understand the impact of incorrect patient positioning on radiation dose and image quality.
3. To highlight appropriate actions to correct poor positioning.
Author Disclosures:
J. Jensen: nothing to disclose

BS 16-2 16:25
Positioning tips and tricks for CT
R. Booij*; Rotterdam/NL (r.booij@erasmusmc.nl)*
Learning objectives:
1. To become familiar with the impact on image quality and radiation exposure due to the isocenter in CT.
2. To be aware of tools to adapt protocols according to clinical indications.
3. To understand the impact of patient positioning in image post-processing.
Author Disclosures:
R. Booij: Research/Grant Support at Siemens Healthineers

BS 16-3 16:50
Positioning tips and tricks for MRI
C. Malamateniou*; London/UK (christina.malamateniou@city.ac.uk)*
Learning objectives:
1. To understand the importance of appropriate coil positioning as part of sequence optimisation.
2. To understand the importance of careful patient positioning in terms of image quality, diagnostic accuracy, and reproducibility.
3. To be aware of further positioning considerations for claustrophobic, paediatric, and other patient groups.
Author Disclosures:
C. Malamateniou: nothing to disclose

17:15
Panel discussion: The importance of patient positioning: do we have to go back to basics?

16:00 - 17:30 **Room M 4**

Transatlantic Course of ESR and RSNA (Radiological Society of North America): Stroke Imaging and Endovascular Treatment: Now and the Future

TC 1628

The future strategy for stroke thrombectomy

Moderators:
J.-P. Pruvo; Lille/FR
R. Uberoi; Oxford/UK
A. Vagal; Cincinnati, OH/US

TC 1628-1 16:00
A. Addressing workforce needs: who and how to train specialists
H. van Overhagen*; Den Haag, ZH/NL (hansvo@xs4all.nl)*
Learning objectives:
1. To learn about the number and type of specialists trained.
2. To understand the global organisation of stroke interventionists and neurologists.
3. To appreciate the future potential number of cases.
Author Disclosures:
H. van Overhagen: nothing to disclose

TC 1628-2 16:30
B. The future for stroke thrombectomy: what is next?
M. V. Jayaraman*; Providence, RI/US (MJayaraman@Lifespan.org)*
Learning objectives:
1. To learn about the subgroups that were not studied in the recent stroke trials.
2. To understand about use of artificial intelligence in stroke.
3. To become familiar with use of artificial intelligence in stroke.
Author Disclosures:
M. V. Jayaraman: nothing to disclose

TC 1628-3 17:00
C. New innovations in stroke thrombectomy techniques and technology
K. A. Hausegger*; Klagenfurt/AT (klaus.hausegger@kabeg.at)*
Learning objectives:
1. To understand the limitations of current devices and techniques.
2. To appreciate the evolution in stroke thrombectomy technology.
3. To understand how the different devices and techniques may improve outcomes.
Author Disclosures:
K. A. Hausegger: nothing to disclose

16:00 - 17:30 **Room M 5**

E³ - Advanced Course: Hot Topics in GU Cancer

E³ 1622

Early detection of ovarian cancer

E³ 1622-1 16:00
Chairperson's introduction
R. Forstner*; Salzburg/AT (r.forstner@salk.at)*
Author Disclosures:
R. Forstner: nothing to disclose

E³ 1622-2/ **E³ 1622-3** 16:15
A. Current guidance on screening and familial ovarian cancer
A. George*; London/UK (angela.george@rmh.nhs.uk)*
A. Rockall*; London/UK (a.rockall@imperial.ac.uk)*
Learning objectives:
1. To be aware of the implications of the results of recent screening trials.
2. To be aware of breast cancer (BRCA) gene testing and treatment implications.
3. To know the guidance on screening high risk groups.
Author Disclosures:
A. George: Advisory Board at Astra Zeneca, Tesaro/GSK, Roche, Speaker at Astra Zeneca, Tesaro/GSK, Roche, Clovis;
A. Rockall: Speaker at Guerbet

E³ 1622-4 16:40
B. Ultrasound in ovarian tumours: the role of pattern recognition, IOTA, and O-RADS
J. Yazbek*; London/UK (joseph.yazbek@nhs.net)*
Learning objectives:
1. To explore various methods used in the ultrasound assessment of adnexal masses.
2. To understand a new lexicon for ovarian/adnexal mass evaluation on ultrasound.
3. To explore the clinical application of the lexicon and the development of a risk stratification and management system.
Author Disclosures:
J. Yazbek: nothing to disclose

E³ 1622-5 17:05
C. O-RADS: MRI
I. Thomassin-Naggara*; Paris/FR (isabellethomassin@gmail.com)*
Learning objectives:
1. To understand a new lexicon for ovarian/adnexal mass evaluation on MRI.
2. To understand the use of the lexicon in the development of a risk stratification and management system.
3. To apply O-RADS-MRI to case management.
Author Disclosures:
I. Thomassin-Naggara: Speaker at General Electric, Advisory Board at Siemens, Speaker at Canon, Research/Grant Support at General Electric, Research/Grant Support at Canon, Speaker at Guerbet, Speaker at Hologic

16:00 - 17:30 **Tech Gate Auditorium**

ESR Ultrasound Subcommittee Session

US 16

Ultrasound-guided interventional procedures: new techniques and applications

Moderator:
D.-A. A. Clevert; Munich/DE

US 16-1 16:00
Liver
E. Leen*; London/UK*
Learning objectives:
1. To learn about the new results and applications of ultrasound in guided interventional procedures: liver malignancy biopsy, primary liver malignancy ablation, secondary liver malignancy ablation.
2. To understand consolidated and new indications of ultrasound-guided interventional procedures: PEI, RFA, MWA, IRE.
3. To appreciate the accuracy of ultrasound-guided interventional procedures from consolidated to new applications: analysis of data from personal experiences and literature series comparison and discussion.
4. To become familiar with the new techniques of ultrasound guidance and the new diagnostic and therapeutic indications for ultrasound-guided interventional procedures: CEUS imaging, fusion imaging, elastosonographic imaging for liver malignancy biopsy and treatment, MWA, IRE, combination treatment.
Author Disclosures:
E. Leen: disclosure/affirmation information not submitted

US 16-2 16:15
Pancreas
M. D'onofrio*; Verona/IT (mirko.donofrio@univr.it)*
Learning objectives:
1. To learn about new results and applications of ultrasound-guided interventional procedures: pancreatic
malignancy FNA and biopsy, primary pancreatic malignancy ablation.
2. To understand consolidated and new indications of ultrasound-guided interventional procedures: FNA and biopsy, RFA.
3. To appreciate the accuracy of ultrasound-guided interventional procedures from consolidated to new applications: analysis of data from personal experiences and literature series comparison and discussion.
4. To become familiar with the new techniques of ultrasound guidance and with the new diagnostic and therapeutic indications for ultrasound-guided interventional procedures: CEUS imaging, fusion imaging, elastosonographic imaging for pancreatic malignancy biopsy and treatment, RFA, MWA, IRE, combination treatment.
Author Disclosures:
M. D'onofrio: Speaker at Siemens, Speaker at Hitachi, Speaker at Bracco, Advisory Board at Siemens, Research/Grant Support at Hitachi

US 16-3 16:30
Kidney
J.-M. Correas*; Paris/FR*
Learning objectives:
1. To learn about new results and applications of ultrasound-guided interventional procedures: renal malignancy FNA and biopsy, primary renal malignancy ablation.
2. To understand consolidated and new indications of ultrasound-guided interventional procedures: FNA and biopsy, RFA.
3. To appreciate the accuracy of ultrasound-guided interventional procedures from consolidated to new applications: analysis of data from personal experiences and literature series comparison and discussion.
4. To become familiar with the new techniques of ultrasound guidance and with the new diagnostic and therapeutic indications for ultrasound-guided interventional procedures: CEUS imaging, fusion imaging, elastosonographic imaging for renal malignancy biopsy and treatment, RFA, cryoablation, MWA, combination treatment.
Author Disclosures:
J.-M. Correas: disclosure/affirmation information not submitted

US 16-4 16:45
Thyroid
G. Mauri*; Milan/IT (vanni.mauri@gmail.com)*
Learning objectives:
1. To learn about new results and applications of ultrasound-guided interventional procedures: thyroid malignancy FNA, thyroid nodule ablation.
2. To understand consolidated and new indications of ultrasound-guided interventional procedures: FNA, RFA.
3. To appreciate the accuracy of ultrasound-guided interventional procedures from consolidated to new applications: analysis of data from personal experiences and literature series comparison and discussion.
4. To become familiar with the new techniques of ultrasound guidance and with the new diagnostic and therapeutic indications for ultrasound-guided interventional procedures: CEUS imaging, fusion imaging, elastosonographic imaging for thyroid malignancy FNA.
Author Disclosures:
G. Mauri: Consultant at Elesta SrL

US 16-5 17:00
Vascular
D.-A. A. Clevert*; Munich/DE (Dirk.Clevert@med.uni-muenchen.de)*
Learning objectives:
1. To learn about new results and application of ultrasound-guided vascular interventional procedures.
2. To understand consolidated and new indications to ultrasound-guided vascular interventional procedures.
3. To become familiar with the new techniques of ultrasound guidance and with the new diagnostic and therapeutic indications for ultrasound vascular interventional procedures: CEUS imaging and fusion imaging.
Author Disclosures:
D.-A. A. Clevert: Speaker at Bracco, Siemens, Philips, Samsung, Advisory Board at Philips, Samsung

17:15
Panel discussion: How to be prepared for ultrasound-guided interventions?

Sunday, March 15

08:30 - 09:30 **Room B**

E³ - The Beauty of Basic Knowledge: Breast

E³ 24E

How to deal with common clinical breast symptoms

Moderators:
G. Forrai; Budapest/HU
K. Kinkel; Chêne-Bougeries/CH

E³ 24E-1 08:30
The acute painful breast
M. Lesaru*; Bucharest/RO (m.lesaru@gmail.com)*
Learning objectives:
1. To learn about the choice of imaging modality.
2. To understand management options and treatment of common breast lesions causing pain, including mastitis.
Author Disclosures:
M. Lesaru: nothing to disclose

E³ 24E-2 09:00
How to manage nipple discharge
I. Thomassin-Naggara*; Paris/FR (isabellethomassin@gmail.com)*
Learning objectives:
1. To identify causes of nipple discharge unrelated to the breast or physiology.
2. To learn about the choice and sequence of imaging modalities to identify breast lesions causing nipple discharge.
3. To understand the spectrum of common benign and malignant breast lesions in relationship to nipple discharge.
Author Disclosures:
I. Thomassin-Naggara: Advisory Board at Siemens, Speaker at GE, Speaker at Canon, Research/Grant Support at GE, Research/Grant Support at Canon, Speaker at Guerbet, Speaker at Hologic

08:30 - 09:30 **Room C**

E³ - The Beauty of Basic Knowledge: Pancreas

E³ 25E

Pancreatic adenocarcinoma mimickers

Moderator:
R. Negrelli; Verona/IT

E³ 25E-1 08:30
Autoimmune pancreatitis
R. Manfredi*; Rome/IT (riccardo.manfredi@unicatt.it)*
Learning objectives:
1. To learn about autoimmune pancreatitis.
2. To understand imaging findings of pancreatic adenocarcinoma mimickers.
3. To appreciate differential diagnosis criteria for pancreatic adenocarcinoma.
Author Disclosures:
R. Manfredi: Speaker at Bracco

E³ 25E-2 09:00
Paraduodenal pancreatitis
G. Morana*; Treviso/IT (giovanni.morana@aulss2.veneto.it)*
Learning objectives:
1. To learn about autoimmune paraduodenal pancreatitis.
2. To understand imaging findings of paraduodenal pancreatitis.
3. To appreciate differential diagnosis criteria for paraduodenal pancreatitis.
Author Disclosures:
G. Morana: Speaker at BRACCO

08:30 - 10:00 **Room N**

Physics in Medical Imaging

RC 1713

Dose management in paediatric radiology

RC 1713-1 08:30
Chairperson's introduction
C. Saidlear*; Dublin/IE (colm.saidlear@cuh.ie)*
Session objectives:
1. To become familiar with modern dose management methods in paediatric radiology.
2. To understand the important aspects of paediatric dose management.
3. To appreciate the current trends and limitations.
Author Disclosures:
C. Saidlear: nothing to disclose

RC 1713-2 08:35
A. The special case of the paediatric patient: risks and justification
C. Owens*; London/UK (owens.catherine.5@gmail.com)*
Learning objectives:
1. To learn about risks and justification techniques in paediatric radiology.
2. To understand how these methods are applied in a clinical setting.
3. To appreciate the benefits of new information and the current limitations.
Author Disclosures:
C. Owens: Consultant at Sidra Medicine

RC 1713-3 08:58
B. Optimisation and technology in neonate and paediatric CT scanning
P. Nowik*; Stockholm/SE (patrik.nowik@ki.se)*
Learning objectives:
1. To review the dose assessment and dose management methods in paediatric CT imaging.
2. To understand the technical possibilities for CT optimisation between different vendors.
3. To learn how to implement optimisation in protocol management and at the multiprofessional team level.
Author Disclosures:
P. Nowik: Consultant at Siemens Healthcare Sweden

RC 1713-4 09:21
C. Optimisation and technology in neonate and paediatric projection radiography (PR) and interventional radiology (IR)
H. Delis*; Patras/GR (hdelis@gmail.com)*
Learning objectives:
1. To understand the dose management and technical optimisation methods in paediatric PR.
2. To understand the dose management and technical optimisation methods in paediatric IR.
3. To learn how to implement optimisation in protocol management and at the multiprofessional team level.
Author Disclosures:
H. Delis: nothing to disclose

09:44
Panel discussion: Paediatric dose management: are we doing enough for the next generation?

08:30 - 10:00 **Studio 2020**

Special Focus Session

SF 17a

Colorectal liver metastasis: treatment planning and management

SF 17a-1 08:30
Chairperson's introduction
O. Akhan*; Ankara/TR (akhano@tr.net)*
Session objectives:
1. To mention the clinical importance of colorectal cancer (CRC) liver metastasis.
2. To describe the best diagnostic methods for both the diagnosis and treatment decision.
3. To make an overview on the treatment options.
4. To discuss the importance of combined therapies.
Author Disclosures:
O. Akhan: nothing to disclose

SF 17a-2 08:34
Surgeon's perspective: what is needed?
J. Conneely*; Dublin/IE*
Learning objectives:
1. To underline what a surgeon would like to know from diagnostic radiologists.
2. To teach which surgical treatment options we have.
3. To discuss the role of surgery for treatment through comparing or combining with the other options.
Author Disclosures:
J. Conneely: disclosure/affirmation information not submitted

SF 17a-3 08:52
Radiologist's perspective: what should be shown?
D. Miletic*; Rijeka/HR (damir.miletic@medri.hr)*
Learning objectives:
1. To describe the best techniques and their indications for diagnosis.
2. To teach important radiological features for diagnosis and treatment decision.
3. To teach how the patients are evaluated after treatment.
Author Disclosures:
D. Miletic: nothing to disclose

SF 17a-4 09:10
Interventional radiology in oncology perspective: which therapies are recommended?
R. Iezzi*; Rome/IT (roberto.iezzi@policlinicogemelli.it)*
Learning objectives:
1. To mention the interventional radiological treatment options and the role of local ablation alternatives.
2. To teach the role of transarterial treatment alternatives and their results.
3. To discuss the importance of combined therapies.
Author Disclosures:
R. Iezzi: Advisory Board at Terumo, Guerbet, Speaker at Terumo, Pharmacept, Bracco

SF 17a-5 09:28
Immunotherapy and the role of the radiologist
J. Podgorska*; Warsaw/PL (jpodgo@gmail.com)*
Learning objectives:
1. To understand the mechanisms of actions of immunotherapy.
2. To recognise different patterns of response to immunotherapy.
3. To be aware of adverse reactions related to novel drugs.
Author Disclosures:
J. Podgorska: Investigator at TG THERAPEUTICS, ICON CLINICAL RESEARCH LIMITED, MSD POLSKA SP. Z O.O., IQVIA RDS EASTERN HOLDINGS GMBH, Speaker at GE MEDICAL SYSTEMS POLSKA, Siemens Healthcare Sp. z o.o.

09:46
Panel discussion: The role of diagnostic and interventional radiology in diagnosis and management of colorectal liver metastasis

08:30 - 10:00 **Room F1**

E^3 - Advanced Course: Interactive Teaching Session for Young (and not so Young) Radiologists

E^3 1721

Neuroradiology: paediatric and adult

E^3 1721-1 08:30
A. Imaging in epilepsy: how to scan and find the suspect
M. Okujava*; Tbilisi/GE (okujava@gmx.net)*
Learning objectives:
1. To describe best imaging protocols when considering the patient's age.
2. To review common epileptogenic lesions and their imaging features.
3. To define contributions from advanced imaging.
Author Disclosures:
M. Okujava: nothing to disclose

E^3 1721-2 09:15
B. Imaging in movement disorders: keeping up with the neurologist
H. K. Karli Oğuz*; Ankara/TR (kaderkarlioguz@gmail.com)*
Learning objectives:
1. To review common movement disorders and basic mechanisms.
2. To define the role of radiologic examinations and review ideal imaging protocols.
3. To review diagnostic radiologic patterns in classified movement disorders
Author Disclosures:
H. K. Karli Oğuz: nothing to disclose

08:30 - 10:00 **Room F2**

Musculoskeletal

RC 1710

Muscle oedema, injury and atrophy

Moderator:
M. F. Reiser; Munich/DE

RC 1710-1 08:30
A. Non-infectious causes of muscle inflammation and muscle injury due to nerve entrapment
N. Mamisch-Saupe*; Zurich/CH (nsaupe@hotmail.com)*
Learning objectives:
1. To explain the non-infectious causes of muscle inflammation and muscle injury due to nerve entrapment.
2. To describe the imaging findings of non-infectious causes of muscle inflammation and muscle injury due to nerve entrapment.
Author Disclosures:
N. Mamisch-Saupe: Speaker at Hirslanden Clinic Zurich

RC 1710-2 09:00
B. Traumatic and overuse injuries of the muscles
F. Kainberger*; Vienna/AT (franz.kainberger@meduniwien.ac.at)*
Learning objectives:
1. To explain the pathophysiology of overuse injuries of the muscles.
2. To describe the imaging findings of overuse injuries of the muscles.
Author Disclosures:
F. Kainberger: nothing to disclose

RC 1710-3 09:30
C. Sarcopenia: more than just atrophy
V. Vasilevska Nikodinovska*; Skopje/MK (v_vasilevska@yahoo.com)*
Learning objectives:
1. To describe the emerging concept of sarcopenia.
2. To explain how imaging modalities are used in the diagnosis and management of sarcopenia.
Author Disclosures:
V. Vasilevska Nikodinovska: nothing to disclose

08:30 - 10:00 **da Vinci (Room D1)**

Professional Challenges Session

PC 17

Challenges facing the radiology workforce

PC 17-1 08:30
Chairperson's introduction
S. Morozov*; Moscow/RU (morozov@npcmr.ru)*
Session objectives:
1. To learn about the challenges of radiology today.
2. To appreciate the value of subspecialisation and its risks to radiology as a general discipline.
3. To understand the need for interdisciplinary and inter-professional cooperation.
Author Disclosures:
S. Morozov: Speaker at Siemens, CEO at Moscow CDT, Advisory Board at Agfa

PC 17-2 08:36
Strategies to overcome radiologists shortage including "turf battles - a friend or a foe?", teleradiology, artificial technology, delegation to radiographers
N. Dugar*; Doncaster/UK (Neelam.Dugar@gmail.com)*
Learning objectives:
1. To learn about the different situations across Europe.
2. To appreciate the potential of supportive solutions.
3. To understand the opportunities and threads of delegation.
Author Disclosures:
N. Dugar: nothing to disclose

PC 17-3 08:54
Education and training challenges
C. Catalano*; Rome/IT (carlo.catalano@uniroma1.it)*
Learning objectives:
1. To learn about the differences in concepts for education and training across Europe.
2. To appreciate the potential of efficient education and training in radiology.
3. To understand the need for appropriate support to implement education and training structures.
Author Disclosures:
C. Catalano: nothing to disclose

PC 17-4 09:12
Challenges and opportunities with subspecialisation in radiology
C. D. Becker*; Geneva/CH*
Learning objectives:
1. To learn about the spectrum of highly subspecialised radiology.
2. To appreciate the potential of subspecialisation.
3. To understand the risks for radiology from turf battles (or not providing specialised services).
Author Disclosures:
C. D. Becker: nothing to disclose

PC 17-5 09:30
Radiologists' workload and risks for burnout
B. Forster*; Vancouver/CA (bruce.forster@vch.ca)*
Learning objectives:
1. To learn about typical administrative tasks and physician/manager balance.
2. To understand the value of analytics and efficiency optimisation.
3. To appreciate the support by business and management experts in radiology departments.
Author Disclosures:
B. Forster: Shareholder at Canada Diagnostic Centres, Grant Recipient at SECTRA AB; Remuneration of travel expenses as educational speaker

09:48
Panel discussion: Is radiology at risk due to shortages, subspecialisation and other challenges?

08:30 - 10:00 **Darwin (Room D2)**

Radiographers

RC 1714

Leadership and management in radiography

RC 1714-1/RC 1714-2 08:30
Chairpersons' introduction
F. Birsasteanu*; Timisoara/RO*
T. Starc*; Brezovica/SI*

Session objectives:
1. To appreciate the key principles for all current and future radiographer leaders.
2. To discuss the impact of quality leadership within profession and within departments.
Author Disclosures:
F. Birsasteanu: disclosure/affirmation information not submitted;
T. Starc: nothing to disclose

RC 1714-3 08:36
A. Effective communication: a key leadership and management tool
J. M. Nightingale*; Sheffield/UK (J.Nightingale@shu.ac.uk)*
Learning objectives:
1. To be aware of the theories underpinning effective communication.
2. To understand the meaning and impact of effective communication within radiography practice.
3. To explore which steps can be taken to improve communication techniques.
Author Disclosures:
J. M. Nightingale: nothing to disclose

RC 1714-4 08:59
B. Leading change: key considerations and tools to motivate radiography teams in quality management
Z. Läänelaid*; Tartu/EE*
Learning objectives:
1. To understand the key principles of change management.
2. To be familiar with motivators relevant to radiography teams.
3. To become aware of practical tips to support radiographers responsible for change within their professional roles.
Author Disclosures:
Z. Läänelaid: disclosure/affirmation information not submitted

RC 1714-5 09:22
C. Inclusive leadership: equality, diversity and inclusion
L. A. Rainford*; Dublin/IE (louise.rainford@ucd.ie)*
Learning objectives:
1. To understand the breadth of which radiographers should reflect on inclusivity in the profession.
2. To be familiar with the changing landscape of inclusivity in academic and clinical environments.
3. To be familiar with specific initiatives, guidelines, and directives driving improvements in inclusivity through inclusive leadership.
Author Disclosures:
L. A. Rainford: nothing to disclose

09:45
Panel discussion: Developing future radiographer leaders: what support do current clinical and academic leaders need?

08:30 - 10:00 **Descartes (Room D3)**

Oncologic Imaging

RC 1716

Tumour response assessment in abdominal imaging

Moderator:
O. V. Kucheruk; Moscow/RU

RC 1716-1 08:30
A. Size-based assessment: metrics and pitfalls
M. D'Anastasi*; Msida/MT (melvin.a.danastasi@gov.mt)*
Learning objectives:
1. To learn about the current size-based assessment concepts.
2. To understand classification strategies, including response evaluation criteria in solid tumours (RECIST).
3. To discuss potential pitfalls of treatment response assessment based on tumour size.
Author Disclosures:
M. D'Anastasi: Advisory Board at Keosys Medical Imaging

RC 1716-2 08:52
B. Diffusion weighted imaging (DWI) and dynamic contrast-enhancement (DCE): opportunities
D.-M. Koh*; London/UK*
Learning objectives:
1. To become familiar with the rationale of DWI and DCE images for tumour response assessment.
2. To learn about the application of functional imaging strategies in abdominal imaging.
3. To consider an integration of DWI and DCE in classification systems.
Author Disclosures:
D.-M. Koh: nothing to disclose

RC 1716-3 09:15
C. Nuclear medicine and molecular approaches
C. C. Cyran*; Munich/DE (clemens.cyran@med.uni-muenchen.de)*
Learning objectives:
1. To appreciate basic concepts of nuclear medicine for response monitoring.
2. To learn about different radiotracers for abdominal tumours.
3. To discuss quantitative assessment strategies from nuclear medicine.
Author Disclosures:
C. C. Cyran: Consultant at Sandoz, Speaker at Goetz Partners Ltd

RC 1716-4 09:37
D. Immunotherapy and imaging
D. Regge*; Candiolo-Torino/IT (daniele.regge@ircc.it)*
Learning objectives:
1. To learn about current aspects of immunotherapy in tumour response assessment.
2. To discuss strategies for quantitative tumour monitoring in abdominal imaging.
3. To become familiar with the pitfalls in imaging the response to immunotherapy.
Author Disclosures:
D. Regge: Speaker at GE Medical Systems

08:30 - 10:00 **Room G**

New Horizons Session

NH 17

MRI of the future

NH 17-1 08:30
Chairperson's introduction
F. A. Gallagher*; Cambridge/UK (fag1000@cam.ac.uk)*
Session objectives:
1. To provide an overview of recent advances in MRI.
2. To discuss potential clinical applications.
3. To explain the challenges in translating these new approaches into patient care.
Author Disclosures:
F. A. Gallagher: Grant Recipient at GSK, Grant Recipient at GE Healthcare

NH 17-2 08:35
Is there a future for gadolinium-based contrast agents?
O. Clement*; Paris/FR (olivier.clement@aphp.fr)*
Learning objectives:
1. To discuss the risks of gadolinium-based contrast agents.
2. To learn about the role of targeted gadolinium agents.
3. To learn about new MRI contrast agents.
Author Disclosures:
O. Clement: Speaker at Bracco, Speaker at Bayer, Grant Recipient at Guerbet

NH 17-3 08:50
High field MRI: is higher better and is there a limit?
S. Trattnig*; Vienna/AT (siegfried.trattnig@meduniwien.ac.at)*
Learning objectives:
1. To discuss the advantages of high field MRI.
2. To learn about the challenges of using high field imaging.
3. To consider potential clinical roles for high field MRI.
Author Disclosures:
S. Trattnig: nothing to disclose

NH 17-4 09:05
Novel MRI contrast methods: CEST, hyperpolarisation
S. Aime*; Turin/IT (silvio.aime@unito.it)*
Learning objectives:
1. To present novel methods to generate MRI contrast.
2. To understand the underlying biology.
3. To consider potential clinical applications in the future.
Author Disclosures:
S. Aime: nothing to disclose

NH 17-5 09:20
Quantitative MRI: fingerprinting and beyond
V. Gulani*; n/a*
Learning objectives:
1. To understand the principles underlying magnetic resonance fingerprinting (MRF).
2. To learn how the method can be applied clinically.
3. To discuss potential roles of MRF in healthcare.
Author Disclosures:
V. Gulani: disclosure/affirmation information not submitted

NH 17-6 09:35
Matrix in vision: non-invasive imaging of the extracellular matrix
B. Hamm*; Berlin/DE*
Learning objectives:
1. To learn about the extracellular matrix as an imaging target.
2. To understand the role of molecular imaging.
3. To understand the role of magnetic resonance elastography.
Author Disclosures:
B. Hamm: disclosure/affirmation information not submitted

09:50
Panel discussion: What are the promising emerging areas in MRI?

08:30 - 10:00 **Room K**

E³ - European Diploma Prep Session

E³ 1723

Gynaecology and obstetrics

E³ 1723-1 08:30
Chairperson's introduction
M. Bekiesinska-Figatowska*; Warsaw/PL (m.figatowska@mp.pl)*
Session objectives:
1. To understand the imaging presentation of the most common benign and malignant disorders of the uterus.
2. To become familiar with inflammatory and neoplastic disorders of the adnexa.
3. To understand the imaging features of acute gynaecological disorders and of acute diseases in pregnancy.
Author Disclosures:
M. Bekiesinska-Figatowska: nothing to disclose

E³ 1723-2 08:36
A. Imaging of the uterus
R. A. Kubik-Huch*; Baden/CH (rahel.kubik@ksb.ch)*
Learning objectives:
1. To comprehend the imaging anatomy of the uterus and its changes throughout life and during pregnancy.
2. To understand typical imaging features and the local imaging-based staging of cervical cancer.
3. To become familiar with the typical imaging features of benign disorders of the uterus, especially uterine leiomyomas, adenomyosis, and endometriosis.
Author Disclosures:
R. A. Kubik-Huch: nothing to disclose

E³ 1723-3 09:04
B. Disorders of the adnexa
R. Forstner*; Salzburg/AT (r.forstner@salk.at)*
Learning objectives:
1. To describe the imaging features of benign tumours of the ovaries.
2. To understand the diagnostic evaluation and imaging features of malignant tumours of the ovaries.
3. To identify imaging features in regard to the stage and extent of adnexal tumours.
4. To become familiar with the imaging features useful for differentiating adnexal masses.
Author Disclosures:
R. Forstner: nothing to disclose

E³ 1723-4 09:32
C. Acute gynaecological and obstetric disorders
G. Masselli*; Rome/IT (gabriele.masselli@uniroma1.it)*
Learning objectives:
1. To become familiar with the typical and atypical imaging features of acute disorders of the uterus.
2. To understand the common emergencies associated with acute gynaecological disorders, including ectopic pregnancy, placenta previa, and emergencies related to abortion.
Author Disclosures:
G. Masselli: nothing to disclose

08:30 - 10:00 **Room M 2**

E³ - ECR Master Class (Emergency Imaging)

E³ 1726

Post-treatment emergencies in oncologic patients

E³ 1726-1 08:30
Chairperson's introduction: The role of imaging in the early detection of complications in oncologically treated patients
N.N.

Session objectives:
1. To learn about different approaches in modern tumour therapy.
2. To understand the radiological appearance of complications following treatment in oncologic patients.
3. To appreciate the role of different imaging modalities in further management of patients.
Author Disclosures: -

E³ 1726-2 08:35
A. Chest
S. Bommart*; Montpellier/FR (s-bommart@chu-montpellier.fr)*
Learning objectives:
1. To become familiar with the modern approach to malignant chest tumour therapy.
2. To learn how to differentiate clinically important complications.
3. To understand how to look for early signs of severe and urgent conditions.
Author Disclosures:
S. Bommart: nothing to disclose

E³ 1726-3 09:00
B. Abdomen
R. Basilico*; Chieti/IT (raffaellabasilico@gmail.com)*
Learning objectives:
1. To learn about different therapies used in abdominal tumours.
2. To become familiar with possible complications.
3. To understand the effectiveness of imaging modalities in the evaluation of emergent complications.
Author Disclosures:
R. Basilico: nothing to disclose

E³ 1726-4 09:25
C. How can interventional radiologists help in the management of oncological treatment complications?
K. K. Pyra*; Lublin/PL (k.pyra@poczta.fm)*
Learning objectives:
1. To be aware of the importance of early detection of treatment associated complications in oncological therapy.
2. To learn which tumour therapy complications can be treated with interventional radiology.
3. To be familiar with interventional techniques used in the treatment of complications of different tumour therapies.
Author Disclosures:
K. K. Pyra: Speaker at Medical University of Lublin

09:50
Panel discussion: What is the impact of complication findings on the continued management of oncologic patients?

08:30 - 10:00 **Room M 3**

E³ - Rising Stars Programme: Basic Session

BS 17

Communication as a safety tool

Moderator:
A. Santos; Coimbra/PT

BS 17-1 08:30
The relevance of patient communication
U. L. Jakobsen*; Odense M/DK (ulja1@ucl.dk)*
Learning objectives:
1. To understand the need for effective communication to guarantee the appropriate examination of the correct patient.
2. To become familiar with various communication techniques to increase patient cooperation.
3. To be aware of the potential of communication to enhance the quality of patient services.
Author Disclosures:
U. L. Jakobsen: nothing to disclose

BS 17-2 08:55
Communication of radiation risk
J. L. Portelli*; Msida/MT (jonathan.portelli@um.edu.mt)*
Learning objectives:
1. To become familiar with practical tips to support effective patient risk communication.
2. To be aware of the risk communication challenges for vulnerable patients.
3. To understand the obligations of communicating risk under EU legislation.
Author Disclosures:
J. L. Portelli: nothing to disclose

BS 17-3 09:20
Radiographers as communication role models
D. Toonen-Bok*; Groningen/NL*
Learning objectives:
1. To become familiar with models of communication.
2. To be aware of radiographers' appropriate attitudes and posture as a means of communication.
3. To be aware of how to develop and promote an optimal communication training setting for students.
Author Disclosures:
D. Toonen-Bok: Speaker at Hanzehogeschool

09:45
Panel discussion: Communication as a tool to improve the patient experience: how can we build an effective communication culture?

08:30 - 10:00 **Room M 4**

Special Focus Session

SF 17b
When stroke happens in children

SF 17b-1 08:30
Chairperson's introduction
M. Argyropoulou*; Ioannina/GR (margyrop@cc.uoi.gr)*
Session objectives:
1. To learn about the aetiology and imaging features of stroke in children.
2. To learn about the imaging protocols for stroke in children.
3. To discuss the optimal diagnostic and treatment pathway when stroke happens in children.
Author Disclosures:
M. Argyropoulou: nothing to disclose

SF 17b-2 08:35
Stroke in neonates
M. H. Lequin*; Rotterdam/NL (m.h.lequin@umcutrecht.nl)*
Learning objectives:
1. To learn about the indications for neonatal stroke imaging.
2. To discuss the role of ultrasonography and MRI in neonatal stroke imaging.
3. To understand the different imaging patterns in neonatal stroke and their prognostic implications.
Author Disclosures:
M. H. Lequin: Speaker at UMCU

SF 17b-3 09:00
Stroke in older children
T. von Kalle*; Stuttgart/DE (t.vonkalle@klinikum-stuttgart.de)*
Learning objectives:
1. To learn about the imaging protocols used in older children presenting with stroke.
2. To discuss the aetiologies of stroke in older children.
3. To understand the stroke imaging patterns and their prognostic implications in older children.
Author Disclosures:
T. von Kalle: nothing to disclose

SF 17b-4 09:25
Interventional radiology in paediatric stroke
O. Naggara*; Paris/FR*
Learning objectives:
1. To discuss the indications for interventions in paediatric stroke.
2. To learn about the techniques used in interventional radiology for paediatric stroke.
3. To understand the limitations and risks of interventions in children with stroke.
Author Disclosures:
O. Naggara: disclosure/affirmation information not submitted

09:50
Panel discussion: How to organise stroke care related to age?

08:30 - 10:00 **Room M 5**

E³ - Advanced Course: Hot Topics in GU Cancer

E³ 1722
Early detection of prostate cancer

E³ 1722-1 08:30
Chairperson's introduction
A. Stanzione*; Naples/IT (arnaldostanzione@yahoo.it)*
Author Disclosures:
A. Stanzione: nothing to disclose

E³ 1722-2/E³ 1722-3 08:45
A. Screening for prostate cancer: where are we now?
S. A. Sohaib*; Sutton/UK*
A. George*; London/UK (angela.george@rmh.nhs.uk)*
Learning objectives:
1. To be aware of important prostate cancer genetics and familial cancer.
2. To learn about the difference in low risk vs high risk genetic groups.
3. To be aware of the use of imaging and other biomarkers.
Author Disclosures:
S. A. Sohaib: nothing to disclose;
A. George: Advisory Board at Astra Zeneca, Tesaro/GSK, Roche, Speaker at Astra Zeneca, Tesaro/GSK, Roche, Clovis

E³ 1722-4 09:10
B. Pre-biopsy detection and new techniques for detection in prostate cancer
S. Punwani*; London/UK*
Learning objectives:
1. To understand the role of multi-parametric magnetic resonance imaging (mpMRI) in tumour detection.
2. To be aware of texture features of prostate cancer.
3. To learn how texture analysis differentiates benign from malignant prostate lesions.
Author Disclosures:
S. Punwani: disclosure/affirmation information not submitted

E³ 1722-5 09:35
C. Active surveillance: best practice
J. J. Futterer*; Nijmegen/NL (jurgenfutterer@gmail.com)*
Learning objectives:
1. To be familiar with case selection for active surveillance.
2. To know the frequency of imaging.
3. To understand when treatment will be commenced.
Author Disclosures:
J. J. Futterer: nothing to disclose

08:30 - 10:00 **Tech Gate Auditorium**

Cardiac

RC 1703

Cardiac imaging in structural heart disease

RC 1703-1 08:30
Chairperson's introduction
L. Natale*; Rome/IT (luigi.natale@unicatt.it)*
Session objectives:
1. To become familiar with the concept of "structural" heart disease in modern cardiovascular medicine.
2. To get an overview about the minimally invasive treatment possibilities in structural heart diseases.
3. To learn about the requirements and possibilities of modern cardiac imaging in structural heart diseases.
Author Disclosures:
L. Natale: nothing to disclose

RC 1703-2 08:35
A. CT-guided planning of minimally invasive procedures
R. Salgado*; Antwerp/BE (r.salgado@outlook.com)*
Learning objectives:
1. To learn about the requirements prior to minimally invasive valvular repair and other diseases.
2. To outline the most appropriate imaging protocols.
3. To gain insights into future developments in devices and minimally invasive treatments.
Author Disclosures:
R. Salgado: nothing to disclose

RC 1703-3 08:58
B. Defining the optimal time to treat valvular heart disease: role of MRI
A. Redheuil*; Paris/FR*
Learning objectives:
1. To outline the clinical problem and approach treatment decision-making in valvular heart disease.
2. To become familiar with the MRI derived imaging biomarkers in valvular heart disease.
3. To discuss the possible future role of MRI in outcome prediction in valvular heart disease.
Author Disclosures:
A. Redheuil: disclosure/affirmation information not submitted

RC 1703-4 09:21
C. Follow-up after minimally invasive valvular repair
H. Alkadhi*; Zurich/CH*
Learning objectives:
1. To become familiar with the appropriate imaging technique after minimally invasive valvular repair.
2. To learn about the different devices currently used in treatment of structural heart disease.
3. To become familiar with the normal outcomes and most common procedural complications.
Author Disclosures:
H. Alkadhi: nothing to disclose

09:44
Panel discussion: How to face the challenges of the increasing demand for imaging evaluation in structural heart disease

10:30 - 12:00 **Room B**

E³ - Rising Stars Programme: Basic Session

BS 18

Cardiothoracic emergencies

Moderator:
A. Santa; Sibiu/RO

BS 18-1 10:30
Acute aortic syndrome
T. Jargiello*; Lublin/PL (tojarg@interia.pl)*
Learning objectives:
1. To become familiar with the most common aetiologies of acute aortic diseases.
2. To present current imaging techniques for evaluation of acute aortic diseases.
3. To demonstrate the most important imaging findings.
Author Disclosures:
T. Jargiello: nothing to disclose

BS 18-2 11:00
Pulmonary embolism
I. Vlahos*; London/UK*
Learning objectives:
1. To review the most common pathologies leading to pulmonary embolism.
2. To present current imaging techniques for evaluation of pulmonary embolism.
3. To become familiar with the typical findings in acute and chronic pulmonary embolism.
Author Disclosures:
I. Vlahos: Consultant at Previously: GE Healthcare (not current), Consultant at Previously: Siemens Healthcare (not current)

BS 18-3 11:30
Acute coronary syndrome
R. M. M. Hinzpeter*; Zurich/CH (Ricarda.Hinzpeter@usz.ch)*
Learning objectives:
1. To become familiar with segmental coronary anatomy.
2. To present different techniques for assessment of acute coronary syndrome.
3. To become familiar with the typical findings of acute coronary syndrome.
Author Disclosures:
R. M. M. Hinzpeter: nothing to disclose

10:30 - 12:00 **Room N**

EuroSafe Imaging Session

EU 18

Artificial intelligence for dose optimisation

Moderator:
M. Kortesniemi; Hus/FI

EU 18-1 10:30
Chairperson's introduction
M. Fachet*; Magdeburg/DE (melanie.fachet@ovgu.de)*
Session objectives:
1. To understand how artificial intelligence (AI) can help in radiation dose optimisation in medical imaging.
2. To learn about practical use cases of AI applications for radiation dose optimisation in medical imaging.
3. To appreciate potential challenges associated with the implementation of AI applications for radiation dose optimisation in medical imaging.
Author Disclosures:
M. Fachet: nothing to disclose

EU 18-2 10:35
Technology using AI for radiation protection
M. Kortesniemi*; Hus/FI (mika.kortesniemi@hus.fi)*

Learning objectives:
1. To understand the revised process of radiation protection and optimisation.
2. To understand the need for more comprehensive imaging quality data extending to the clinical level.
3. To learn how radiomics and AI may help in more clinically adjusted and quantitative optimisation.
Author Disclosures:
M. Kortesniemi: nothing to disclose

EU 18-3 10:55
What is the limit of dose reduction by artificial intelligence methods: 2D and 3D?
C. Hoeschen*; Magdeburg/DE*
Learning objectives:
1. To name a number of very drastic claims of dose reduction using AI in x-ray based imaging.
2. To show that AI methods will, for diagnostic purposes, be limited based on physical information theory aspects, and why some approaches seem to be able to go beyond due to methodological errors.
3. To learn exemplary methods on how to detect methodological errors and construct test cases for ensuring to avoid such errors in your own research.
Author Disclosures:
C. Hoeschen: disclosure/affirmation information not submitted

EU 18-4 11:15
Chances and limitations of AI for nuclear medical imaging
C. Hoeschen*; Magdeburg/DE*
Learning objectives:
1. To understand the nuclear imaging processes and to identify in which steps AI can be of help.
2. To focus on some selected applications, e.g. towards reduction of the administered dose or costs of scanners.
3. To analyse possible drawbacks and bottlenecks.
Author Disclosures:
C. Hoeschen: disclosure/affirmation information not submitted

11:35
Panel discussion: Towards AI for dose optimisation in medical imaging: where are we using it in clinical practice?

10:30 - 12:00 **Room O**

Abdominal Viscera

RC 1801
Imaging of the biliary system

Moderator:
P. K. Prassopoulos; Thessaloniki/GR

RC 1801-1 10:30
A. Magnetic resonance cholangiopancreatography (MRCP): state of the art
C. Matos*; Lisbon/PT*
Learning objectives:
1. To know the different techniques of MRCP including their advantages and disadvantages.
2. To discuss differences of MRCP at 1.5T and 3.0T.
3. To understand how to deal with pitfalls in MRCP.
Author Disclosures:
C. Matos: nothing to disclose

RC 1801-2 11:00
B. Primary sclerosing cholangitis (PSC)
G. Morana*; Treviso/IT (giovanni.morana@aulss2.veneto.it)*
Learning objectives:
1. To be aware of the pathophysiological background of PSC.
2. To learn about typical and atypical imaging features of PSC.
3. To understand follow-up imaging strategies in patients with PSC.
Author Disclosures:
G. Morana: Speaker at BRACCO

RC 1801-3 11:30
C. Biliary drainage and stenting
T. K. Helmberger*; Munich/DE (Thomas.Helmberger@muenchen-klinik.de)*
Learning objectives:
1. To understand the access routes for biliary drainage and stenting.
2. To be aware of pitfalls and complications during and after biliary interventions.
3. To know the strengths and shortcomings of different imaging techniques for therapeutic control and follow-up examinations.
Author Disclosures:
T. K. Helmberger: nothing to disclose

10:30 - 12:00 **Studio 2020**

Neuro

RC 1811
State-of-the-art paediatric neuroradiology

RC 1811-1 10:30
Chairperson's introduction
M. C. Çalli*; Izmir/TR (cem.calli@gmail.com)*
Session objectives:
1. To list the spectrum of applications and indications for imaging in paediatric neuroradiology.
2. To apply the appropriate image acquisition protocols for diseases in the field.
3. To appreciate the clinical relevance of imaging for the diagnostic process of neurological disorders in infants and children.
Author Disclosures:
M. C. Çalli: nothing to disclose

RC 1811-2 10:35
A. Imaging myelin maturation disorders
F. Triulzi*; Milano (MI)/IT (fabio.triulzi@unimi.it)*
Learning objectives:
1. To describe normal and pathological patterns of myelination.
2. To understand the role of imaging with respect to narrowing the differential diagnosis and supporting the clinical diagnosis.
3. To appreciate the importance of pattern recognition for the diagnosis of myelination disorders in children.
Author Disclosures:
F. Triulzi: nothing to disclose

RC 1811-3 10:58
B. Imaging of developmental disorders
B. B. Ertl-Wagner*; Toronto, ON/CA (BirgitBetina.Ertl-Wagner@sickkids.ca)*
Learning objectives:
1. To describe the spectrum of developmental disorders of the brain.
2. To understand the key imaging features that lead to the correct diagnosis.
3. To appreciate the importance of making a correct imaging diagnosis.
Author Disclosures:
B. B. Ertl-Wagner: Spouse/Partner at employee of Siemens Healthineers

RC 1811-4 11:21
C. Imaging in paediatric neuro-oncology
G. Morana*; Genoa/IT (giomorana@yahoo.it)*
Learning objectives:
1. To learn about the spectrum of neuro-oncological diseases in children.
2. To understand the role of imaging beyond the diagnostic process.
3. To appreciate the increasing clinical relevance of advanced imaging techniques in paediatric neuro-oncology.
Author Disclosures:
G. Morana: nothing to disclose

11:44
Panel discussion: Ask the expert: what is relevant for my own daily clinical practice?

10:15 - 12:15 **Room E**

E³ - Rising Stars Programme: Case-Based Diagnosis Training

CB
Case-Based Diagnosis Training

Moderators:
S. Robinson; Vienna/AT
K. M. Friedrich; Vienna/AT

CB-1 10:15
Liver
F. Caseiro Alves; *Coimbra/PT (caseiroalves@gmail.com)*
Author Disclosures:
F. Caseiro Alves: nothing to disclose

CB-2 10:24
Neuro
D. Prayer; *Vienna/AT (daniela.prayer@meduniwien.ac.at)*
Author Disclosures:
D. Prayer: nothing to disclose

CB-3 10:33
Musculoskeletal
F. Kainberger; *Vienna/AT (franz.kainberger@meduniwien.ac.at)*
Author Disclosures:
F. Kainberger: nothing to disclose

CB-4 10:42
Maxillofacial
S. Robinson; *Vienna/AT (s.robinson@dzu.at)*
Author Disclosures:
S. Robinson: nothing to disclose

CB-5 10:51
Genitourinary
M. Toepker; *Vienna/AT (mt@dz10.at)*
Author Disclosures:
M. Toepker: nothing to disclose

CB-6 11:00
Interlude: Air in the wrong place
B. Özgen Mocan; *Chicago, IL/US (burcem@gmail.com)*
Author Disclosures:
B. Özgen Mocan: nothing to disclose

CB-7 11:30
Head and neck
C. Czerny; *Vienna/AT (christian.czerny@meduniwien.ac.at)*
Author Disclosures:
C. Czerny: nothing to disclose

CB-8 11:39
Chest
H. Prosch; *Vienna/AT (helmut.prosch@meduniwien.ac.at)*
Author Disclosures:
H. Prosch: nothing to disclose

CB-9 11:48
Spine
K. M. Friedrich; *Vienna/AT*
Author Disclosures:
K. M. Friedrich: nothing to disclose

CB-10 11:57
Gastrointestinal
W. Schima; *Vienna/AT (wolfgang.schima@khgh.at)*
Author Disclosures:
W. Schima: nothing to disclose

CB-11 12:06
Breast
M. Fuchsjäger; *Graz/AT (michael.fuchsjaeger@medunigraz.at)*
Author Disclosures:
M. Fuchsjäger: nothing to disclose

10:30 - 12:00 **Room F1**

E³ - Advanced Course: Interactive Teaching Session for Young (and not so Young) Radiologists

E³ 1821a
Cardiac imaging: an update

E³ 1821a-1 10:30
A. Coronary artery disease - reporting and data system (CAD-RADS): a new tool for reporting coronary CT angiograms (CTAs)
B. Szilveszter; *Budapest/HU (szilveszter.balint@gmail.com)*
Learning objectives:
1. To be familiar with standardised reporting of coronary CTA findings.
2. To know the impact of CAD-RADS in management and treatment.
Author Disclosures:
B. Szilveszter: nothing to disclose

E³ 1821a-2 11:15
B. Athlete's heart
J. Bogaert; *Leuven/BE (Jan.Bogaert@uzleuven.be)*
Learning objectives:
1. To learn about the different entities that cause left ventricular thickening.
2. To understand the role of the different techniques in the study of this patients.
Author Disclosures:
J. Bogaert: nothing to disclose

10:30 - 11:30 **Coffee & Talk 3**

Coffee & Talk (open forum) Session
Organised by the ESR Subcommittee on PIER

C 33
Guidance for IT in radiology: how radiologist can benefit from DIAM (Digital Imaging Adoption Model)

C 33-1 10:30
Chairperson's introduction
L. Donoso; *Barcelona/ES (ldonoso@clinic.cat)*
Session objectives:
1. To explain the relevance of IT in radiology.
2. To provide an overview of criteria for benchmarking.
3. To discuss the role of audit tools like DIAM.
Author Disclosures:
L. Donoso: Advisory Board at Context Flow, Advisory Board at Methinks, Advisory Board at Affidea, Shareholder at Vivo Diagnostico

C 33-2 10:35
Overview and update on DIAM radiology
P. Mildenberger; *Mainz/DE (mildenbe@uni-mainz.de)*
Learning objectives:
1. To explain the methodology of DIAM radiology.
2. To provide examples of departments' experiences with DIAM radiology.
3. To discuss further opportunities for DIAM radiology.
Author Disclosures:
P. Mildenberger: nothing to disclose

C 33-3 10:45
Overview and international experiences with DIAM enterprise imaging (EI)
J. Studzinski; *Leipzig/DE (jstudzinski@himssanalytics.eu)*
Learning objectives:
1. To explain the methodology of DIAM EI.
2. To provide examples of departments' experiences with DIAM EI.
3. To discuss further opportunities for DIAM EI.
Author Disclosures:
J. Studzinski: nothing to disclose

C 33-4 10:55
The value of DIAM Gap analyses
P. Hoogland; *Utrecht/NL (phoogland@phit.nl)*
Learning objectives:
1. To explain the value of DIAM in consulting radiology departments and national screening programmes.
2. To showcase the benefit of DIAM as a strategic tool for IT development.
3. To discuss the value of DIAM Gap analyses.
Author Disclosures:
P. Hoogland: nothing to disclose

11:05
Open forum discussion: DIAM radiology or DIAM enterprise imaging, which one to go for?

10:30 - 12:00 **da Vinci (Room D1)**

Paediatric

RC 1812

Imaging of frequent queries in children: an evidence-based approach

RC 1812-1 10:30
Chairperson's introduction
S. Franchi-Abella; *Le Kremlin-Bicêtre/FR (stephanie.franchi@aphp.fr)*
Session objectives:
1. To learn about four common queries for radiological investigations in children.
2. To understand the evidence-based indication for imaging and the choice of imaging modalities in these queries.
3. To discuss the importance of good collaboration with the referring clinician when selecting children for imaging and potential further workup in these queries.
Author Disclosures:
S. Franchi-Abella: nothing to disclose

RC 1812-2 10:35
A. Abdominal pain: constipation and beyond
I. Robinson; *Dublin/IE (ihwrobinson@hotmail.com)*
Learning objectives:
1. To learn about the most common causes of chronic abdominal pain in children.
2. To understand indications for imaging and choice of imaging modalities in paediatric abdominal pain.
3. To appreciate typical findings and 'red flag' features.
Author Disclosures:
I. Robinson: nothing to disclose

RC 1812-3 10:53
B. Respiratory tract infections
P. Ciet; *Rotterdam/NL (p.ciet@erasmusmc.nl)*
Learning objectives:
1. To learn about the role of imaging in childhood respiratory tract infections.
2. To understand the indications and limitations for radiography, CT, and ultrasound.
3. To discuss typical radiological findings and their clinical implications in a child with a respiratory tract infection.
Author Disclosures:
P. Ciet: Grant Recipient at Italian Cystic Fibrosis Foundation, Patent Holder at Erasmus MC - MRI diaphragm, Consultant at Vertex Pharmaceutical

RC 1812-4 11:11
C. Large and small heads: when and how to image
U. Y. Ayaz; *Mersin/TR (umityasarayaz@yahoo.com)*
Learning objectives:
1. To learn the indications for imaging in deviating head circumference.
2. To understand examination techniques and imaging algorithms.
3. To appreciate the most common pathologies and their clinical implications.
Author Disclosures:
U. Y. Ayaz: nothing to disclose

RC 1812-5 11:29
D. The limping child
I. Barber Martinez; *Esplugues de Llobregat (Barcelona)/ES (ibarber@sjdhospitalbarcelona.org)*
Learning objectives:
1. To learn about the most important differential diagnosis in a limping child.
2. To understand indications for imaging and choice of imaging modalities in a child with a limp.
3. To appreciate the most important findings and 'red flag' features.
Author Disclosures:
I. Barber Martinez: nothing to disclose

11:47
Panel discussion: The requisites for usual paediatric indications

10:30 - 12:00 **Darwin (Room D2)**

Oncologic Imaging

RC 1816

Functional and molecular imaging techniques in oncology: how to use them in routine practice

RC 1816-1 10:30
Chairperson's introduction: What are the problems of morphologic evaluation
L. Marti-Bonmati; *Valencia/ES (Luis.Marti@uv.es)*
Session objectives:
1. To address the limitations of morphological imaging modalities.
2. To introduce the basic concepts of functional imaging in oncology.
3. To learn the current status of these techniques in routine clinical practice.
Author Disclosures:
L. Marti-Bonmati: nothing to disclose

RC 1816-2 10:35
A. CT perfusion techniques
H. Schoellnast; *Graz/AT*
Learning objectives:
1. To learn about current approaches to CT perfusion.
2. To understand the basic principles behind each technique.
3. To discuss radiation exposure from CT perfusion techniques.
4. To appreciate the clinical usefulness of these techniques in routine clinical practice.
Author Disclosures:
H. Schoellnast: nothing to disclose

RC 1816-3 10:58
B. Functional MRI techniques
V. Goh; *London/UK (vicky.goh@kcl.ac.uk)*
Learning objectives:
1. To learn about different functional MRI techniques, such as diffusion and perfusion.
2. To understand the basic principles behind each technique.
3. To appreciate the clinical usefulness of these techniques in routine clinical practice.
Author Disclosures:
V. Goh: Research/Grant Support at Siemens, Speaker at Siemens

RC 1816-4 11:21
C. Assessment by molecular imaging
J. Grimm; *New York/US (grimmj@mskcc.org)*

Learning objectives:
1. To learn about the basic concepts in molecular imaging.
2. To understand how molecular imaging might be integrated into patient care.
3. To discuss clinical examples of where molecular imaging is already established in clinical practice.
Author Disclosures:
J. Grimm: nothing to disclose

11:44
Panel discussion: Where are we using functional evaluations in clinical practice?

10:30 - 12:00 **Descartes (Room D3)**

Musculoskeletal

RC 1810

Elbow imaging: from detailed anatomy to pathology

Moderator:
A. B. Rosskopf; Zurich/CH

RC 1810-1 10:30
A. The medial and lateral epicondyle
M. C. de Jonge*; Amsterdam/NL (milkodejonge@gmail.com)*
Learning objectives:
1. To explain the anatomical considerations and pathophysiology of abnormalities that involve the medial and lateral epicondyles of the humerus.
2. To describe the imaging findings of abnormalities that involve the medial and lateral epicondyles of the humerus.
Author Disclosures:
M. C. de Jonge: nothing to disclose

RC 1810-2 11:00
B. Biceps and triceps
A. Tagliafico*; Genoa/IT (albertotagliafico@gmail.com)*
Learning objectives:
1. To explain the anatomical considerations and pathophysiology of abnormalities that involve the biceps and triceps brachii.
2. To describe the imaging findings of abnormalities that involves the biceps and triceps brachii.
Author Disclosures:
A. Tagliafico: nothing to disclose

RC 1810-3 11:30
C. Plicae and articular cartilage
A. Alcala-Galiano Rubio*; Madrid/ES (andrearoob@hotmail.com)*
Learning objectives:
1. To explain the anatomical considerations and pathophysiology of abnormalities that involve the elbow plicae and articular cartilage.
2. To describe the imaging findings of abnormalities that involve the elbow plicae and articular cartilage.
Author Disclosures:
A. Alcala-Galiano Rubio: nothing to disclose

10:30 - 12:00 **Room K**

Genitourinary

RC 1807

Contrast media: acute kidney injury and acute adverse reactions

RC 1807-1 10:30
Chairperson's introduction
M.-F. Bellin*; Le Kremlin-Bicêtre/FR*
Session objectives:
1. To learn about emergent issues regarding the safe use of contrast media.
2. To understand the mechanisms underlying acute reactions and renal function deterioration after contrast media injection.
3. To provide evidence-based recommendations for safe use of contrast media and for the management of acute reactions.
Author Disclosures:
M.-F. Bellin: Board Member at IRSN Institut de Radioprotection et Sureté Nucléaire

RC 1807-2 10:35
A. Post-contrast acute kidney injury (PC-AKI)
A. J. van der Molen*; Leiden/NL*
Learning objectives:
1. To understand the definition of PC-AKI.
2. To learn about the possible causes for PC-AKI.
3. To review current evidence regarding PC-AKI.
Author Disclosures:
A. J. van der Molen: Speaker at Bayer Healthcare, Other at Thieme Verlag

RC 1807-3 11:00
B. Iodine-based contrast media in myeloma patients
G. Heinz*; St. Pölten/AT (gertraud.heinz@stpoelten.lknoe.at)*
Learning objectives:
1. To learn about the relationships between iodine-based contrast media and myeloma.
2. To understand the mechanisms of AKI in myeloma patients.
3. To review current evidence regarding the risk of PC-AKI in myeloma patients.
Author Disclosures:
G. Heinz: nothing to disclose

RC 1807-4 11:15
C. Ongoing evidence for acute adverse reactions
O. Clement*; Paris/FR (olivier.clement@aphp.fr)*
Learning objectives:
1. To learn about the acute adverse reactions from contrast media.
2. To understand the current evidence regarding risk factors.
3. To illustrate the first-line treatment of acute adverse reactions.
Author Disclosures:
O. Clement: Speaker at Bracco, Speaker at Bayer, Speaker at Guerbet

11:40
Panel discussion: Towards a safer use of contrast media

10:30 - 12:00 **Room M 1**

Joint Session of the ESR and EORTC

ESR/EORTC

Advanced imaging for stratifying treatment in oligometastatic prostate cancer

Moderator:
N. deSouza; Surrey/UK

ESR/EORTC-1 10:30
Chairperson's introduction
F. Lecouvet*; Brussels/BE (frederic.lecouvet@uclouvain.be)*
Session objectives:
1. To highlight the role of imaging for detecting oligometastatic prostate cancer.
2. To introduce image-based treatment stratification.
3. To introduce the speakers.
Author Disclosures:
F. Lecouvet: nothing to disclose

ESR/EORTC-2 10:36
Prostate cancer: managing the oligometastatic patient
M. Spahn*; Zurich/CH*

Learning objectives:
1. To learn about the classification of oligometastatic prostate cancer.
2. To appreciate the local and systemic management options for patients with oligometastatic prostate cancer.
3. To understand the impact on the outcome by stratifying patients for treatment.
Author Disclosures:
M. Spahn: nothing to disclose

ESR/EORTC-3 10:59
Whole-body MRI: is it ready for prime time to detect oligometastatic prostate cancer?
F. D. de Keyzer*; Leuven/BE (frederik.de.keyzer@hotmail.be)*
Learning objectives:
1. To learn about whole-body MRI: how to optimise the technique.
2. To appreciate the technical challenges and limitations of the technique in prostate cancer patients.
3. To understand how the output may be quantified and assessed.
Author Disclosures:
F. D. de Keyzer: nothing to disclose

ESR/EORTC-4 11:22
Molecular imaging for directing and delivering therapy in oligometastatic prostate cancer
D. E. Oprea-Lager*; Amsterdam/NL (d_e_oprea@yahoo.com)*
Learning objectives:
1. To learn about targeted imaging and radionuclide therapy in oligometastatic prostate cancer.
2. To appreciate how molecular imaging may be used to stratify therapy.
3. To understand how to devise trials that establish an evidence-based use of modern imaging techniques.
Author Disclosures:
D. E. Oprea-Lager: nothing to disclose

11:45
Panel discussion: How, whom and when to image oligometastatic prostate cancer?

10:30 - 12:00 **Room M 2**

Vascular

RC 1815
Carotid disease 2.0

Moderator:
V. Bérczi; Budapest/HU

RC 1815-1 10:30
A. Carotid plaque imaging: tool or fool?
L. Saba*; Cagliari/IT (lucasabamd@gmail.com)*
Learning objectives:
1. To learn about radiological methods to analyse carotid plaque morphology.
2. To critically review the influence of plaque morphology on actual treatment guidelines.
3. To discuss the possible future role of carotid plaque imaging for treatment decision making.
Author Disclosures:
L. Saba: nothing to disclose

RC 1815-2 11:00
B. Carotid involvement in inflammatory arterial disease
A. J. J. Madureira*; Porto/PT*
Learning objectives:
1. To provide an overview about inflammatory arterial disease.
2. To become familiar with the involvement of supraaortic arteries in inflammatory arterial disease.
3. To learn about radiological diagnosis of supraaortic involvement in inflammatory arterial disease.
Author Disclosures:
A. J. J. Madureira: nothing to disclose

RC 1815-3 11:30
C. Carotid stent: medical history or part of the future?
K. A. Hausegger*; Klagenfurt/AT (klaus.hausegger@kabeg.at)*
Learning objectives:
1. To learn about the technique of carotid stent implantation.
2. To review current indications for carotid stent implantation.
3. To discuss the future role of carotid stent implantation.
Author Disclosures:
K. A. Hausegger: nothing to disclose

10:30 - 12:00 **Room M 3**

Emergency Imaging

RC 1817
Acute conditions in the elderly

RC 1817-1 10:30
Chairperson's introduction
M. Stajgis*; Poznan/PL (stajgis@gmail.com)*
Session objectives:
1. To learn the typical constellations and findings of elderly patients.
2. To understand the potential complications connected with ageing.
3. To appreciate direct and indirect radiological findings.
Author Disclosures:
M. Stajgis: nothing to disclose

RC 1817-2 10:35
A. Confusion in the elderly: what can we expect in imaging of acute conditions?
M. Wykretowicz*; Poznan/PL*
Learning objectives:
1. To become familiar with acute pathology causing confusion in the elderly.
2. To recognise specific pathologies on acute imaging.
3. To understand which complications we can expect in the confused elderly.
Author Disclosures:
M. Wykretowicz: nothing to disclose

RC 1817-3 11:00
B. Grandparent has a high fever and thoracic/abdominal pain
I. Millet*; Montpellier/FR*
Learning objectives:
1. To become familiar with acute pathology causing high fever in the elderly.
2. To recognise which specific pathologies should be ruled out on acute chest and abdomen imaging.
3. To understand the complications we have to look for in the elderly with a high fever.
Author Disclosures:
I. Millet: nothing to disclose

RC 1817-4 11:25
C. Postoperative complications in the elderly
F. Iacobellis*; Naples/IT (iacobellisf@gmail.com)*
Learning objectives:
1. To learn about the most common complications in the acute postoperative elderly.
2. To become familiar with the imaging signs of these acute postoperative complications.
3. To recognise the indications for imaging guided treatment of these postoperative complications.
Author Disclosures:
F. Iacobellis: nothing to disclose

11:50
Panel discussion: Imaging of the elderly patient: A forgotten task?

10:30 - 12:00 **Room M 4**

Chest

RC 1804

Back to basics: how to interpret a chest radiograph?

RC 1804-1 10:30
Chairperson's introduction
R. Cesar*; Golnik/SI (rok.cesar@klinika-golnik.si)*
Session objectives:
1. To increase the radiologists' confidence in chest radiography reading.
2. To recognise and interpret the typical abnormalities.
3. To understand the limitations of chest radiography.
Author Disclosures:
R. Cesar: nothing to disclose

RC 1804-2 10:35
A. A chest radiography reading guide
N. H. Strickland*; London/UK*
Learning objectives:
1. To learn about chest radiography quality criteria.
2. To learn about the normal features.
3. To learn which difficult areas to concentrate on.
Author Disclosures:
N. H. Strickland: nothing to disclose

RC 1804-3 10:52
B. Alveolar, interstitial and nodular syndromes
F. Molinari*; Tourcoing/FR (francescomolinari.dr@gmail.com)*
Learning objectives:
1. To learn about alveolar opacities characteristics.
2. To learn how to recognise the presence of interstitial changes.
3. To understand the chest radiography limitations for lung nodule detection.
Author Disclosures:
F. Molinari: nothing to disclose

RC 1804-4 11:09
C. Lobar atelectasis
D. Tack*; Braine-L'Alleud/BE (denis.tack@skynet.be)*
Learning objectives:
1. To review the signs of lobar atelectasis in frontal chest radiography.
2. To learn about the complementary role of the lateral view.
3. To explain the differences with other causes of lung opacity.
Author Disclosures:
D. Tack: nothing to disclose

RC 1804-5 11:26
D. Pleural syndrome
A. P. Parkar*; Bergen/NO (apparkar@gmail.com)*
Learning objectives:
1. To learn how to identify partial pneumothorax.
2. To be able to identify signs of compressive pleural effusion.
3. To be aware of the limitations of bedside chest x-ray for pneumothorax detection.
Author Disclosures:
A. P. Parkar: nothing to disclose

RC 1804-6 11:43
E. Mediastinal syndrome
M. Occhipinti*; Florence/IT (mariaelena.occhipinti@gmail.com)*
Learning objectives:
1. To review the normal mediastinal lines.
2. To learn about the normal and abnormal mediastinal contour.
3. To know how to use the silhouette sign to localise mediastinal opacities.
Author Disclosures:
M. Occhipinti: Research/Grant Support at Fondazione Menarini

10:30 - 12:00 **Room M 5**

E³ - Advanced Course: Interactive Teaching Session for Young (and not so Young) Radiologists

E³ 1821b

Breast imaging

E³ 1821b-1 10:30
A. Imaging of ductal abnormalities
D. Djilas*; Sremska Kamenica/RS*
Learning objectives:
1. To understand the most common ductal lesions.
2. To learn how to recognise ductal pathology using different imaging modalities.
3. To discuss the importance of finding different types of ductal carcinoma in situ (DCIS).
Author Disclosures:
D. Djilas: disclosure/affirmation information not submitted

E³ 1821b-2 11:15
B. Diffusion-weighted imaging (DWI) of the breast
N. Radovic*; Zagreb/HR*
Learning objectives:
1. To gain familiarity with the principles of DWI in breast imaging.
2. To learn how to acquire qualitative and quantitative information for lesion assessment on DWI.
3. To understand the limitations and pitfalls of DWI in clinical practice.
Author Disclosures:
N. Radovic: nothing to disclose

B

Scientific Programme

Clinical Trials in Radiology (CTiR)
My Thesis in 3 Minutes (MyT3)
Research Presentation Sessions (RPS)
Student Sessions (S)

Wednesday, March 11

08:30 - 10:00 **Room O**

Oncologic Imaging

RPS 116

Oncologic imaging in genitourinary: kidney and prostate, advanced topics

Moderators:
G. Frauenfelder; Rome/IT
H.-P. Schlemmer; Heidelberg/DE

RPS 116-K 08:30
Keynote lecture
H. Hricak; *New York, NY/US*

Author Disclosures:
H. Hricak: nothing to disclose

RPS 116-1 08:40
Upgrading to significant disease with monitoring prostate MRI scans and repeat biopsy in men on active surveillance for low-risk prostate cancer: are confirmatory biopsies still necessary?
D. F. Osses, F.-J. Drost, J. F. M. Verbeek, M. J. Roobol, I. G. Schoots; *Rotterdam/NL (i.schoots@erasmusmc.nl)*

Purpose: To investigate whether serial prostate magnetic resonance imaging (MRI) may guide the utility of repeat targeted (TBx) and systematic biopsy (SBx) in monitoring men with low-risk prostate cancer (PCa) at one year in active surveillance (AS).
Methods and materials: We included 111 consecutive men with low-risk (ISUP grade 1) PCa who received protocolled repeat MRIs with or without TBx and repeat SBx at one-year AS. TBx was performed in PI-RADS score ≥3 lesions. Upgrading defined as ISUP grade ≥2 PCa (I), grade ≥2 PCa with cribriform growth/intraductal carcinoma (II), and grade ≥3 PCa (III) was investigated.
Results: Upgrading (I) was 32% (35/111). Upgrading in MRI-positive and MRI-negative men was 48% (30/63) and 10% (5/48) (p<0.001), respectively. In MRI-positive men, upgrading was 23% (7/30) by TBx only and 33% (10/30) by SBx only. Progressive change (PRECISE score 4-5) on positive MRI was observed in 27% (17/63). Upgrading (I) occurred in 41% (7/17) of these men, which was 50% (23/46) in men without progressive change (PRECISE score 1-3) on positive MRI (p=0.534). Upgrading (II) was 15% (17/111). Upgrading in MRI-positive and MRI-negative men was 22% (14/63) and 6% (3/48) (p=0.021), respectively. Upgrading (III) was 5% (5/111). Upgrading in MRI-positive and MRI-negative men was 6% (4/63) and 2% (1/48) (p=0.283), respectively.
Conclusion: In serial MRI-negative men, the added value of repeat SBx at one-year surveillance is limited and should be balanced individually against the harms. In serial MRI-positive men, the added value of repeat SBx is substantial. SBx should be performed together with TBx in all MRI-positive men at one-year surveillance. Biopsy should not be omitted in men without progressive disease on positive MRI.
Limitations: n/a
Ethics committee approval: n/a
Funding: No funding was received for this work.
Author Disclosures:
D. F. Osses: nothing to disclose
F.-J. Drost: nothing to disclose
J. F. M. Verbeek: nothing to disclose
M. J. Roobol: nothing to disclose
I. G. Schoots: nothing to disclose

RPS 116-2 08:46
ECE score: a new MRI scale to evaluate and stratify the risk of extracapsular extension in patients with prostate cancer
S. Varello, M. Gatti, F. Gentile, I. Ruggirello, L. Allois, A. Carisio, C. Dianzani, P. Fonio, R. Faletti; *Turin/IT (sara.varello@gmail.com)*

Purpose: To analyse the performance of different prostate imaging features associated with prostate cancer (PCa) extracapsular extension (ECE) in order to develop an ECE-score.
Methods and materials: A retrospective study on 114 patients who underwent multiparameter prostate MRI (mp-MRI) at 1.5Tesla using a 32 phased-array coil before radical prostatectomy was conducted. mp-MRIs were analysed for the length of contact between PCa and the prostatic capsule, capsule irregularity, bulge, loss of capsule, neurovascular bundle thickening, measurable extra-capsular disease, and DWI signal increase in extra-capsular location, and ADC value and PSA density were calculated. The data was analysed with a parametric test and 5 diagnostic parameters. A threshold of 90% in specificity and positive predictive value was used to distinguish between major and minor criteria. The ECE-score was tested with the ROC curve procedure.
Results: ECE was found at histopathological review in 41 patients (ECE+). Capsule irregularity, bulge, loss of capsule, neurovascular bundle thickening, DWI signal increase in extra-capsular location, and measurable extra-capsular disease had a highly significant difference between ECE+ and others (p<0.0001). Capsule irregularity, bulge, and loss of capsule were included in the minor criteria and neurovascular bundle thickening and DWI signal increase in the extra-capsular location were included in the major criteria. The ECE-score was equal to 1 for the presence of 0 criteria, 2 for 1 minor, 3 for 2 minor, 4 for 3 minor or 1 major, and 5 for 2 major criteria or the presence of measurable extra-capsular disease. The ROC curve procedure established the good ability of the ECE-score to discriminate ECE+ with an AUC of 0.93 (0.87-0.98).
Conclusion: The ECE-score proposed can improve the detection of ECE and allow for more accurate staging, providing important additional information for optimal patient-tailored treatment planning.
Limitations: A monocentric and retrospective study. The absence of interobserver variability.
Ethics committee approval: n/a
Funding: No funding was received for this work.
Author Disclosures:
S. Varello: nothing to disclose
R. Faletti: nothing to disclose
M. Gatti: nothing to disclose
F. Gentile: nothing to disclose
P. Fonio: nothing to disclose
I. Ruggirello: nothing to disclose
L. Allois: nothing to disclose
A. Carisio: nothing to disclose
C. Dianzani: nothing to disclose

RPS 116-3 08:52
Influence of the minimum b-value on prostate cancer assessment using conventional DWI and DKI models
N. Adubeiro[1], L. Nogueira[1], R. G. Nunes[2], H. A. Ferreira[2], E. F. C. Ribeiro[1], J. M. La Fuente[1]; *[1]Porto/PT, [2]Lisbon/PT (nca.estsp@gmail.com)*

Purpose: To investigate the influence of the minimum b-value in diffusion parameters estimated for prostate tissues using mono-exponential and kurtosis models.
Methods and materials: 58 patients were prospectively enrolled to perform magnetic resonance imaging of the prostate at 3.0T. A diffusion-weighted sequence using 11 b-values ranging from 0-2,000 s/mm^2 was used.
Mono-exponential and kurtosis models were fitted to the diffusion signal. 6 different b-value combinations were used to estimate the apparent diffusion coefficient (ADC) while varying the minimum b-value (0, 50, 100, 150, 200, and 500 s/mm^2) and b-values up to 1,100 s/mm^2. Diffusion kurtosis imaging (DKI) metrics were computed using b-values ranging from 0-2,000 s/mm^2 and considering the same minimum b-values.
The Mann-Whitney test was used to assess differences in diffusion metrics between prostate cancer (PCa) and normal tissue. Differences in b-value combinations were assessed with the Friedman test. Receiver operating characteristics curves were performed for each metric.
Results: ADC and the mean diffusivity (MD) were significantly lower and the mean kurtosis (MK) was significantly higher (p<0.001) in PCa compared to normal tissue for all b-values combinations.
MK did not change with the minimum b-value for normal tissue or PCa (p>0.05), but ADC and MD differed significantly.
The MK metric achieved the highest AUC (96.0%) and accuracy (93.8%) using all b-values (0-2,000 s/mm^2) but the diagnostic performance was not statistically improved when compared to ADC or MD.
Conclusion: MK values were not influenced by the chosen low b-value, indicating that microperfusion effects do not influence MK, contrarily to ADC and MD.
The diagnostic performances of ADC, MD, and MK were similar.
Limitations: Prostate lesions were confirmed by transrectal ultrasound-guided biopsy.
Ethics committee approval: Approved by the hospital ethics committee [number 251/12 (190-DEFI/195-CES)] and all patients gave written informed consent.
Funding: No funding was received for this work.
Author Disclosures:
N. Adubeiro: nothing to disclose
L. Nogueira: nothing to disclose
R. G. Nunes: nothing to disclose
H. A. Ferreira: nothing to disclose
J. M. La Fuente: nothing to disclose
E. F. C. Ribeiro: nothing to disclose

RPS 116-4 08:58

Characterising the appearance of clinically significant prostate cancer on pre-surgical MRI in a radiopathomic study

M. Rusu, C. Kunder, R. Fan, R. West, P. Ghanouni, J. Brooks, G. Sonn; *Stanford/US (mirabela.rusu@stanford.edu)*

Purpose: Magnetic resonance imaging (MRI) has great potential to improve prostate cancer diagnosis. Yet, the subtle differences between low-grade cancers, high-grade cancers, and benign conditions render the interpretation of prostate MRI challenging. We propose to characterise the radiologic appearance of clinically significant (Gleason group >2) prostate cancers on a multi-parametric MRI. We are focusing on patients that underwent radical prostatectomy and had pre-surgical MRIs.
Methods and materials: We aligned the radiology and histopathology images using our RAPSODI platform that registers corresponding histopathology and MRI slices, assuming slice-to-slice correspondences. The labels obtained were used in a radiomic study that relies on the established QIFP platform (http://qifp.stanford.edu) in which 900 textural and morphologic features were computed for each lesion. Our study included 20 patients for which Gleason grades were outlined on 1-2 histopathology slices.
Results: Preliminary results showed statistically significant differences between Gleason groups ≤2 and Gleason groups >2 on the radiomic features of T2-weighted MRI and the apparent diffusion coefficient. The combination of multiple image-derived features resulted in better separation between the two groups.
Conclusion: Differences between clinically significant and insignificant prostate cancers were revealed on pre-surgical multi-parametric MRI via radiomic analysis using labels derived from an alignment of histopathology and MRI images. Future work will focus on using the identified differences to predict high-grade disease on MRI.
Limitations: Our preliminary study included 20 subjects and was focused on assessing MRI differences on account of low-grade and high-grade disease in a radiomic study without the use of an external validation set.
Ethics committee approval: The study was approved by the Institutional Review Board (IRB) of Stanford University. Informed consent was waived for this retrospective study.
Funding: Department of Radiology, Stanford University, NIH-U01CA196387-01.
Author Disclosures:
R. Fan: nothing to disclose
M. Rusu: nothing to disclose
G. Sonn: nothing to disclose
P. Ghanouni: nothing to disclose
J. Brooks: nothing to disclose
R. West: nothing to disclose
C. Kunder: nothing to disclose

RPS 116-5 09:04

Multiparamateric MRI characteristics of cribriform growth in prostate cancer in comparison to other Gleason sub-patterns

G. Ghobadi[1], P. J. van Houdt[1], E. Bekers[1], I. G. Schoots[2], H. G. van der Poel[1], F. J. Pos[1], L. Bentzen[3], K. Haustermans[4], U. van der Heide[1]; *[1]Amsterdam/NL, [2]Rotterdam/NL, [3]Aarhus/DK, [4]Leuven/BE (g.ghobadi@nki.nl)*

Purpose: Distinguishing Gleason 4 from Gleason 3 pattern in prostate cancer diagnosis is challenging, owing to overlapping mpMRI characteristics of some Gleason sub-patterns. Cribriform growth is a known prognostic Gleason 4 sub-pattern. The purpose of this study was to identify mpMRI characteristics of cribriform growth and to separate them from non-cribriform Gleason pattern 4 and Gleason pattern 3.
Methods and materials: In a prospective 3-centre study, mpMRI parameters (T2 map, ADC map derived from DWI, and K^{trans} and k_{ep} maps from DCE-MRI) were acquired in 30 patients prior to prostatectomy. Gleason sub-patterns, [Gleason pattern 3 intermediate/dense (based on the density of neoplastic glands) and Gleason pattern 4 with/without cribriform growth] were manually segmented on digital H&E slices. Patient-customised molds enabled the registration of histopathology and MRI. We compared the median mpMRI values for Gleason sub-patterns with a non-parametric Kruskal-Wallis test.
Results: Gleason pattern 4 was determined in 18 patients and cribriform growth was found in 6. Of all cancer volume, 27% was Gleason 4 and 37% of this was cribriform growth. T2 and ADC of cribriform areas were not different from non-cribriform and dense Gleason 3 areas. Only intermediate Gleason 3 areas had higher T2 and ADC values than the other sub-patterns ($p<0.001$). DCE parameters, K^{trans}, and k_{ep} were significantly lower in cribriform versus non-cribriform areas ($p<0.001$). k_{ep} was also lower in areas with cribriform compared to Gleason 3 intermediate ($p<0.001$) and Gleason 3 dense areas ($p<0.001$).
Conclusion: Our results indicate that mp-MRI may help in distinguishing cribriform growth from other sub-patterns based on DCE k_{ep}.
Limitations: The size of the dataset.
Ethics committee approval: Institutional review boards approval and written informed consent obtained.
Funding: This study was part of the DR THERAPAT project (FP7-ICT-2011-9, Project No. 600852).
Author Disclosures:
G. Ghobadi: Speaker at the Netherlands Cancer Institute
P. J. van Houdt: nothing to disclose
E. Bekers: nothing to disclose
I. G. Schoots: nothing to disclose
H. G. van der Poel: nothing to disclose
F. J. Pos: nothing to disclose
L. Bentzen: nothing to disclose
K. Haustermans: Grant Recipient at University Hospitals Leuven
U. van der Heide: Grant Recipient at the Netherlands Cancer Institute

RPS 116-6 09:10

Automated artificial intelligence-based measurements of biomarkers in ^{18}F-choline PET/CT are associated with disease-specific survival of high-risk prostate cancer patients

E. Polymeri[1], H. Kjölhede[1], O. Enqvist[1], J. Ulén[2], M. H. Poulsen[3], J. A. Simonsen[3], Å. Johnsson[1], P. F. Høilund-Carlsen[3], L. Edenbrandt[1]; *[1]Gothenburg/SE, [2]Malmö/SE, [3]Odense/DK (eirinipol@hotmail.com)*

Purpose: Artificial intelligence (AI) offers new possibilities for obtaining objective quantitative measurements of biomarkers from positron-emission tomography/computed tomography (PET/CT). The aim of this study was to evaluate the prognostic significance of automated quantification of tumour infiltration in the prostate gland in ^{18}F-Choline PET/CT of high-risk prostate cancer patients in respect to age, PSA, and a Gleason score.
Methods and materials: Training of the AI-algorithm was performed on PET/CT scans of 143 patients. Validation of the algorithm was carried out in ^{18}F-choline PET/CT scans of 272 high-risk prostate cancer patients. Automated measurements of the radiotracer uptake in voxels in the region automatically segmented as prostate by the AI-algorithm were performed. Voxels with a standardised uptake value (SUV) above 2.65g/ml were considered abnormal. The following calculations were obtained: lesion VOLUME (volume of abnormal voxels, ml), total lesion uptake (TLU, defined as the product of SUVmean x lesion VOLUME), and lesion FRACTION (the quotient of VOLUME and total prostate volume). Associations between automated measurements, age, prostate-specific antigen (PSA) level (logarithmic), Gleason score, and prostate cancer-specific survival were studied using a univariate Cox-regression model.
Results: 20 patients died of prostate cancer during follow-up. The PET/CT measurements were significantly associated with prostate cancer-specific survival [VOLUME (HR 1.03, p <0.001); TLU (HR 1.9, p<0.001); lesion FRACTION (HR 1.05, p <0.001)], while age, PSA, and Gleason score were not.
Conclusion: ^{18}F-choline uptake, determined by automatically-derived measurements, was significantly associated with disease-specific survival in this patient cohort.
Limitations: The small number of events during the follow-up period in this patient group prevented us from performing multivariate analyses.
Ethics committee approval: Research ethical review board in Denmark and Sweden.
Funding: Gothenburg University (Medical Faculty ALF Grants), Sweden, and EXINI Diagnostics AB, Lund, Sweden.
Author Disclosures:
E. Polymeri: nothing to disclose
H. Kjölhede: nothing to disclose
O. Enqvist: nothing to disclose
J. Ulén: nothing to disclose
Å. Johnsson: nothing to disclose
L. Edenbrandt: Employee at EXINI Diagnostics AB, Lund, Sweden, Research/Grant Support at EXINI Diagnostics AB, Lund, Sweden
J. A. Simonsen: nothing to disclose
M. H. Poulsen: nothing to disclose
P. F. Høilund-Carlsen: nothing to disclose

RPS 116-7 09:16

Diffusion-weighted imaging in prostate cancer: a descriptor of tumour habitat differentiates high-risk and low-risk lesions

A. Bevilacqua[1], M. Mottola[1], F. Ferroni[2], D. Barone[2], G. Gavelli[2]; [1]*Bologna/IT,* [2]*Meldola/IT (margherita.mottola@unibo.it)*

Purpose: To discriminate between patients with high-risk (HR) and low-risk (LR) prostate cancer (PCa) in order to support radiologists in deciding on the most proper therapy strategy.
Methods and materials: 42 patients with a clinical suspicion of PCa were consecutively selected from the database of our institution. All patients underwent 3T-mpMRI and TRUS biopsy and, based on their Gleason scores (GS), were assigned to the HR (GS≥3+4) or LR class, the latter including, besides patients with GS=3+3, patients with a negative biopsy, whether they have positive or negative mpMRI. 84 radiomic features were extracted on DWI sequences and related ROC curves computed. The feature showing the lowest p-value in discriminating HR from LR was selected.
Results: The mean of the local coefficient of variation (CV_L-m), representing local DWI variance, performed the best ($p \sim 10^{-6}$) and discriminated HR from LR with AUC=0.91 (95% CI, 0.75-0.97), specificity=85%, sensitivity=87% (4 FP and 2 FN), and all FPs were GS=3+3. These results yielded the probability of FDR=24% of the overtreatment for LR patients and the probability of FOR=8% that a HR patient is not treated.
Conclusion: One of our radiomic features derived from DWI sequences was enough to differentiate HR from LR PCa. Since the level of restriction to the motion of water molecules in the extracellular compartment affects tumour behaviour, radiomic features extracted from DWI sequences result in the best candidate to quantify relevant properties of tumour habitats needed to characterise the different tumour heterogeneities.
Limitations: Patients were not enough to reliably include clinical parameters in the PCa risk assessment. Although they could be crucial to help to improve the radiomic model, a higher number of parameters require a number of patients growing exponentially to have a representative sample size.
Ethics committee approval: IRB approval. Written, informed consent was waived.
Funding: No funding was received for this work.
Author Disclosures:
M. Mottola: nothing to disclose
A. Bevilacqua: nothing to disclose
G. Gavelli: nothing to disclose
D. Barone: nothing to disclose
F. Ferroni: nothing to disclose

RPS 116-8 09:22

Can PSMA PET CT rule out all relapses of prostate cancer?

M. Garcia Fontes, L. Valuntas, M. Rodríguez Parodi, G. Dos Santos, V. Gigirey, O. Alonso*; Montevideo/UY*

Purpose: To determine if a negative PSMA PET CT can ever rule out tumour recurrences in prostate cancer.
Methods and materials: In a period of 6 months, 246 PET CT PSMAs with biochemical relapse were performed. Those with negative or indeterminate findings were selected to be studied with a multiparametric prostate MRI. 12 patients, 58-75 years old, with a PSA between 0.9 and 22 ng/ml were included. Prostate multiparametric resonance was performed with a Discovery 750W General Electric 3 Tesla. The study protocol included axial T2 panoramic, axial and coronal T2 high resolution of the prostate, diffusion (DWI), and ADC focus and perfusion sequences.
PET CT acquisition was performed 60 minutes after intravenous administration of 2 MBq/Kg of 68Ga-PSMA with 64-slice equipment (General Electric Discovery 690 VCT) from the skull to mid-thigh. The images were corrected for "flight time" (TOF correction).
Results: Of the 12 included patients, 10 presented with local tumour recurrences at the level of the prostate, periprostatic region, or bladder wall. These lesions were not seen with PET PSMA due to the concentration of the radiopharmaceutical in the bladder.
All lesions presented a pathological signal in T2, restriction in DWI, and early enhancement in the perfusion sequence. This last sequence is essential for the detection of tumour recurrences due to the neoangiogenesis of tumoural tissue.
Conclusion: We can conclude that in cases of a negative PSMA PET CT, a multiparametric prostate MRI must be suggested. This study may show relapses in regions not seen with PET PSMA and may change patient management. The main sequence that represents the key of diagnosis is perfussion.
Limitations: Few patients.
Ethics committee approval: Written informed consent obtained.
Funding: No funding was received for this work.
Author Disclosures:
M. Garcia Fontes: nothing to disclose
L. Valuntas: nothing to disclose
M. Rodríguez Parodi: nothing to disclose
G. Dos Santos: nothing to disclose
V. Gigirey: nothing to disclose
O. Alonso: nothing to disclose

RPS 116-9 09:28

VERDICT MRI fractional intracellular volume assessment could help avoid unnecessary biopsies in men assessed for prostate cancer with multi-parametric MRI

S. Singh, H. Rogers, E. W. Johnston, B. Kanber, C. M. Moore, D. Atkinson, E. Panagiotaki, S. Punwani*; London/UK*

Purpose: To determine whether the quantitative fractional intracellular volume (FIC) from VERDICT MRI (vascular, extracellular, and restricted diffusion for cytometry in tumours) and/or ADC (apparent diffusion coefficient) can prospectively identify men undergoing prostate mpMRI with significant cancer.
Methods and materials: We previously demonstrated FIC has a higher ROC-AUC (0.93) than ADC (0.85) for differentiating clinically-significant from benign/non-significant prostate cancer. In this study, we derived and prospectively applied FIC and ADC thresholds based on Youden's index (from previous ROC-analysis using men with Likert≥3): FIC:0.41, ADC:1.12×10^{-3} to a cohort of 30 men with Likert≥3 mpMRI lesions who underwent targeted biopsy. The mean lesion FIC, ADC, sensitivity, and specificity of the derived thresholds were calculated.
Results: Biopsies revealed 16 clinically-significant (3+4=2, ≥4+3=4) cancers and 14 benign/non-significant cancers (benign=12, 3+3=2). Clinically-significant lesions had higher FIC (mean: 0.43±0.22) compared to benign/non-significant lesions (mean: 0.26±0.15) p=0.035. ADC was not significantly different between the two groups (significant: $1.06 \pm 0.16 \times 10^{-3}$ vs benign/non-significant: $0.93 \pm 0.33 \times 10^{-3}$, p=0.12).
The FIC threshold correctly classified 86% of men (n=12) with a benign/non-significant biopsy as negative for significant-cancer compared with 36% of men (n=5) for the ADC threshold. 62% of men with significant cancer (n=10) were classified as positive for significant cancer by the FIC threshold, compared with 81% of men (n=13) using the ADC threshold.
Combining Likert≥4 and FIC threshold, 12/14 men with benign/non-significant pathology could have avoided biopsy. However, 1/16 men with significant cancer would not have been biopsied. Combining Likert≥4 and ADC threshold, 4/14 men with benign/non-significant pathology could have avoided a biopsy and all men with significant cancer would have undergone a biopsy.
Conclusion: A combined Likert score and FIC thresholds could help avoid unnecessary biopsies in men being investigated for prostate cancer.
Limitations: n/a
Ethics committee approval: London–Surrey Borders REC approval, written informed consent obtained.
Funding: Prostate Cancer UK (PG14-018-TR2).
Author Disclosures:
S. Singh: nothing to disclose
E. W. Johnston: nothing to disclose
S. Punwani: nothing to disclose
H. Rogers: nothing to disclose
B. Kanber: nothing to disclose
C. M. Moore: nothing to disclose
D. Atkinson: nothing to disclose
E. Panagiotaki: nothing to disclose

RPS 116-10 09:34

Renal oncocytoma versus chromophobe renal cell carcinoma: radiomics uncovering the secrets in MRI images

N. Gündüz, M. B. Eser, A. Yıldırım, A. Kabaalioğlu*; Istanbul/TR (bilgineser@hotmail.com)*

Purpose: A preoperative distinction between renal oncocytoma (RON) and chromophobe renal cell carcinoma (cRCC) remains challenging based on the visual interpretation of multiparametric magnetic resonance imaging (mp-MRI) including apparent diffusion coefficient (ADC) or dynamic sequences. We aimed to evaluate the ability of radiomics, a recently emerged tool for mathematical tissue characterisation based on tumour heterogeneity, in differentiating both tumours.
Methods and materials: This single-centre retrospective study included 14 patients with histopathologically proven RON (n=6) and cRCC (n=8). All cases were imaged before surgery by mp-MRI. Axial MRI-ADC mapping images were used for the manual segmentation of the masses by two radiologists using open-source PyRadiomics software. The radiomics features were extracted from 3 categories: shape and size, histogram-based first-order texture, and high-order texture. Interobserver reliability was assessed using the intraclass correlation coefficient (ICC). Features with excellent (ICC>0.90) agreement were compared

between RON and cRCC groups. The features with a p<0.05 were analysed by the receiver operating curve for the precision of RON.
Results: 16 radiomics features (2 shape and size, 5 first-order, and 8 high-order texture) provided an ICC>0.90 and p<0.05. Histogram-based first-order features using 3-dimensional whole tumour ADC showed the highest diagnostic performance for predicting RON (median ADC cut-off ≥1.84x10^{-3} mm/s, sensitivity=100%, and specificity 100%, p=0.002). Among high order texture features, 5 grey-level run-length matrixes and 3 grey-level size zone matrixes related features predicted RON with considerably high performance (area under the curve >0.90, sensitivity and specificity >0.80, p<0.05).
Conclusion: Radiomics analysis of MRI-ADC mapping can successfully distinguish between RON and cRCC with a quite high diagnostic precision performance.
Limitations: The small sample size and retrospective design.
Ethics committee approval: Institutional ethics committee approval number: 2019/0283.
Funding: No funding was received for this work.
Author Disclosures:
M. B. Eser: nothing to disclose
N. Gündüz: nothing to disclose
A. Yıldırım: nothing to disclose
A. Kabaalioğlu: nothing to disclose

RPS 116-11 09:40

The development of postoperative image-guided tissue sampling using 3D-printed tumour moulds enabling multi-omics data integration

S. Ursprung, M. Crispin-Ortuzar, M. Gehrung, A. Priest, F. A. Gallagher, A. Warren, G. Stewart, E. Sala, F. Markowetz*; Cambridge/UK (su263@cam.ac.uk)*

Purpose: Renal cancer is phenotypically and genetically highly heterogeneous. Genetic intratumoral heterogeneity plays a determining role in tumour aggressiveness, metastasis, and treatment resistance. Precise spatial registration of imaging and molecular data is required for multi-omics data integration to leverage the full potential of personalised cancer care. We describe the development of an automated pipeline for producing 3D-printed tumour moulds for image-guided tissue sampling.
Methods and materials: Following preoperative multiparametric, morphologic, and physiological MRI and image registration, the renal tumour, normal kidney, and anatomical structures that needed preserving during tissue sampling were manually segmented. 3D-printed tumour moulds were generated and cutting-guides with 1 cm spacing were introduced. The direction of the cutting-guides can be selected according to pathologists' preferences. The design of the mould was improved in an iterative process involving pathologists, urologists, radiologists, and imaging scientists to ensure accuracy, universal applicability, and minimal disturbance to workflows. The accuracy of the spatial registration was determined by the Dice similarity coefficient between predicted and observed tissue cross-sections.
Results: 6 patients (age 62.7±8.3 years) were included in the iterative mould design process. High morphological correspondence of anatomy between tissue and predicted cross-sections from imaging were seen, as well as a good agreement of predicted and observed tumour cross-sections. In the latest iteration of the mould, Dice similarity coefficients of 0.92 and 0.76 were observed for the tumour and normal kidney, respectively, thanks to the introduction of orientation landmarks.
Conclusion: A highly automated pipeline for the acquisition of tissue samples registered to imaging data was developed in an iterative process. The involvement of urologists and pathologists ensured maximum clinical acceptability of the mould and resulted in a pathway for multi-regional, multi-omics data integration.
Limitations: Recruitement for this study is ongoing.
Ethics committee approval: UK-REC-Numbers: 5/EE/0378, 03/018.
Funding: Cancer Research UK.
Author Disclosures:
S. Ursprung: nothing to disclose
M. Crispin-Ortuzar: nothing to disclose
M. Gehrung: nothing to disclose
A. Priest: nothing to disclose
F. A. Gallagher: nothing to disclose
G. Stewart: Board Member at Pfizer, Board Member at AstraZeneca, Grant Recipient at Intuitive Surgical, Consultant at Merck, Consultant at Pfizer, Consultant at EUSA Pharma, Consultant at Cambridge Medical Robotics, Speaker at Pfizer
E. Sala: Speaker at Siemens
F. Markowetz: nothing to disclose
A. Warren: nothing to disclose

RPS 116-12 09:46

Radiomic analysis in renal cell carcinoma: the impact of computed tomography vascular phase on parameter quantification

A. Azam[1], A. Jahangeer[1], C. Kelly-Morland[1], M. M. Siddique[1], G. Cook[1], F. Collinson[2], J. Swaine[2], J. Brown[2], V. Goh[1]*; [1]London/UK, [2]Leeds/UK (aishah2018@hotmail.co.uk)*

Purpose: Radiomic analysis and quantification of tumour heterogeneity may capture additional treatment effects beyond current standards and predict clinical outcomes, however, how CT acquisition affects quantifiable parameters should be considered. This prospective study aims to explore the impact of an arterial or portal venous phase acquisition on radiomic features in patients with metastatic renal cell carcinoma.
Methods and materials: 33 adults (31 male; mean age 65.5±9.1) with 61 lesions underwent contrast-enhanced CT. Volumetric regions-of-interest were delineated around the primary±metastatic lesion(s) in both arterial and portal phases. Radiomic features were extracted using validated in-house software. A total of 183 first, second, and high-order statistical parameters were compared using a Wilcoxon signed-rank test, with a Bonferroni correction for multiple comparisons, p<0.005.
Results: Pixel intensity parameters differed between phases e.g. the mean intensity (58.6 vs 68.6, p=0.0015), variance (4,778.9 vs 5,251.3, p=0.0019) (portovenous and arterial, respectively). There was no significant difference in shape, histogram, fractal, second-order grey-level co-occurrence matrix or high-order grey-level run length, grey-level dependence matrix, grey-level run-length size zone matrix, and neighbourhood grey-tone difference matrix parameters.
Conclusion: As expected, histogram parameters differed between phases. However, the stability of radiomics parameters between phases indicates their robustness to acquisition timing and is promising for their use as biomarkers of the treatment response.
Limitations: The small sample size and heterogeneity in CT acquisition parameters.
Ethics committee approval: Ethical approval and informed consent - NRES Committee North West Liverpool Central, 06/06/2011, REC ref: 11/NW/0246.
Funding: The National Institute for Health Research Health Technology Assessment Programme (project number 09/91/21).
Author Disclosures:
A. Azam: nothing to disclose
A. Jahangeer: nothing to disclose
C. Kelly-Morland: nothing to disclose
M. M. Siddique: nothing to disclose
G. Cook: nothing to disclose
F. Collinson: nothing to disclose
J. Swaine: nothing to disclose
J. Brown: nothing to disclose
V. Goh: nothing to disclose

RPS 116-13 09:52

Patterns of response and comparison of RECIST1.1, irRECIST, and iRECIST criteria in a population of patients treated by nivolumab for a metastatic clear renal cell carcinoma

P. Iorio[1], C. S. Balleyguier[2], N. Lassau[2], M. Tazdait[2], A. Benchimol[2], J. Arfi[2], E. Zareski[3], D. L. Albiges[2], C. Caramella[2]*; [1]Paris/FR, [2]Villejuif/FR, [3]Neuilly/Seine/FR*

Purpose: Immune checkpoint inhibitors (ICIs) now have a place in the treatment of metastatic renal cell carcinomas (mRCC). Atypical responses have been described under ICI in several types of cancer such as pseudoprogression that are not captured by the conventional RECIST 1.1 criteria. Therefore, new criteria have been proposed, irRC, irRECIST, and iRECIST, but little is known about their usefulness in mRCC evaluation.
Methods and materials: This monocentric study included patients treated in a clinical trial with nivolumab for mRCC. We retrospectively analysed the response patterns, their frequency, the discrepancies between the RECIST 1.1, irRECIST, and iRECIST criteria, and overall survival by response type.
Results: Of the 56 patients included, 81% presented a conventional response (objective response or stability 18% and progression 63%) and 19% an atypical response (pseudoprogression 5% and dissociated response 14%). The irRECIST and iRECIST criteria captured the phenomenon of pseudoprogression in all patients, but 3 had no therapeutic impact. Patients with a dissociated response had the lowest overall survival with a significant difference compared to the progression subgroup.
Conclusion: Atypical patterns of response occur in 19% of the patients treated by nivolumab for mRCC. Further studies are needed to confirm our findings of dissociated response patients who seem to have a worse prognosis than classical progressive patients.

Limitations: A monocentric study involving a small number of patients, which does not allow the results to be generalised and significant prognostic factors to be identified. The patients were included in a therapeutic protocol and this could have constituted a selection bias.
Ethics committee approval: n/a
Funding: No funding was received for this work.
Author Disclosures:
P. Iorio: nothing to disclose
D. L. Albiges: nothing to disclose
C. Caramella: nothing to disclose
N. Lassau: nothing to disclose
M. Tazdait: nothing to disclose
C. S. Balleyguier: nothing to disclose
J. Arfi: nothing to disclose
A. Benchimol: nothing to disclose
E. Zareski: nothing to disclose

08:30 - 10:00 **Room Y**

Head and Neck

RPS 108

Advanced imaging in head and neck tumours

Moderators:
C. Czerny; Vienna/AT
T. D'Angelo; Messina/IT

RPS 108-K 08:30
Keynote lecture
S. Bisdas*; London/UK (sotirios.bisdas@nhs.net)*

Author Disclosures:
S. Bisdas: nothing to disclose

RPS 108-1 08:40
The value of venous phase dual-layer spectral CT in the visualisation of laryngeal carcinoma: a preliminary study
G. Hong, Z. Yang, M. Zou*; Guangzhou/CN (trueangel_xun@163.com)*

Purpose: To explore the value of venous phase dual-layer spectral CT (DLSCT) in detecting and staging laryngeal carcinoma.
Methods and materials: 21 patients with a proven diagnosis of laryngeal carcinoma were examined with a DLSCT scanner and retrospectively analysed. Images were acquired in the venous phase. MonoE40 images were reconstructed on a workstation and compared to poly-energetic reconstruction images. Data from the ROIs of the lesion, the adjacent sternocleidomastoid muscle, adipose tissue, the common carotid artery, and the jugular vein were recorded, including iodine content (mg/mL), Z_{eff} values, virtual non-contrast attenuation (HU), and attenuation values at 40, 70, and 100 keV (HU). The steepness of the Hounsfield unit (HU)-increase at the tumour margin was analysed. Means were compared using a Student's t-test. ANOVA was used for multiple comparisons.
Results: MonoE40 images were superior to poly-energetic reconstructions in tumour detection and margin delineation. MonoE40 showed significantly higher attenuation differences between tumour and healthy tissue compared to poly-energetic reconstructions ($p<0.01$). The HU-increase at the boundary of the tumour was significantly steeper in MonoE40 images compared to poly-energetic reconstructions ($p<0.01$). Iodine uptake and Z_{eff} values in the tumour was significantly higher compared to healthy tissue ($p<0.01$). MonoE40 compared to conventional poly-energetic images improved the visualisation of the vessel from the venous phase ($p<0.01$).
Conclusion: Virtual mono-energetic reconstructions of venous phase DLSCT enables improved visualisation of laryngeal carcinoma, quantification of tumour iodine uptake, and Z_{eff} values. Improved contrast of MonoE40 compared to conventional poly-energetic reconstructions enables higher diagnostic confidence concerning tumour margin detection and vessel evaluation.
Limitations: Limitations of the number of cases.
Ethics committee approval: This study was approved by the medical ethics committee of the hospital.
Funding: No funding was received for this work.
Author Disclosures:
G. Hong: nothing to disclose
Z. Yang: nothing to disclose
M. Zou: nothing to disclose

RPS 108-2 08:46
Primary tumour and lymph node radiomics assessment in PET-CT in non-metastatic nasopharyngeal carcinoma patients
C. Xie[1], Y. Chen[2], V. Vardhanabhuti[1]; [1]*Hong Kong/HK,* [2]*Beijing/CN*

Purpose: To evaluate the prognostic value of radiomic features extracted from pre-treatment PET-CT images of the primary tumours (PT) and lymph nodes (LNs) in locally advanced nasopharyngeal carcinoma (NPC) patients.
Methods and materials: A total of 145 consecutive patients (median age 48 years, 75.2% male) with newly diagnosed NPC were included. Radiomics analysis was performed on 118 PT and 66 LN images. Conventional PET parameters (SUV_{max}, SUV_{mean}, and TLG), shape-based features, and 6 robust texture features were extracted. This data was used to analyse the correlation with 3-year overall survival (OS) and progression-free survival (PRFS) based on a Kaplan-Meier log-rank test.
Results: One PET radiomics feature (LN sphericity) was significantly predictive of OS ($p=0.024$) and PRFS ($p=0.002$). Independent CT predictive radiomic features were PT GLRM LRE ($p=0.011$), LN sphericity ($p=0.011$), and compactness ($p=0.042$) for OS, and PT GLRM LRE ($p = 0.039$) and LN sphericity ($p = 0.008$) for PRFS.
Conclusion: CT shape-based features and texture features extracted from primary tumours and LNs provide significant predictive value for survival in patients with NPC. LN PET radiomics information was significantly predictive for survival and performed better than primary features. The unity of LN radiomics can be further validated by prospective randomised trials, considering their potential in predicting clinical outcomes of tumour patients.
Limitations: A retrospective study and small sample size.
Ethics committee approval: This study has been approved by IRB.
Funding: No funding was received for this work.
Author Disclosures:
V. Vardhanabhuti: nothing to disclose
Y. Chen: nothing to disclose
C. Xie: nothing to disclose

RPS 108-3 08:52
Machine learning re-sampling techniques in imbalanced datasets improve prognostication performance in a multicentre cohort of head and neck cancer patients using a PET-based radiomics model
C. Xie, J. Ho, H. Pang, R. Du, K. Chiu, E. Lee, V. Vardhanabhuti*; Hong Kong/CN*

Purpose: Achieving good performance on real biomedical data that frequently contains imbalance characteristics remains a challenging task. This study aimed to investigate the impact of re-sampling techniques in imbalanced datasets for PET radiomics-based prognostication in head and neck (HNC) cancer patients.
Methods and materials: PET-based radiomics analysis was performed in 166 patients (median age 49.3 years, 77.1% male) diagnosed with nasopharyngeal carcinoma (NPC) in our centre and 182 HNC patients from the TCIA database. Conventional PET and 15 robust texture features were extracted for the correlation analysis of overall survival (OS) and disease progression-free survival (DFS). We investigated cross-combination of 10 re-sampling methods and 4 classifiers for radiomics-based survival prediction.
Results: Re-sampling techniques including oversampling and hybrid sampling achieved significant improvement on the area under the receiver operating characteristic curve (AUC) and prediction of the minority class in terms of precisions, recalls, and F-measures in both cohorts, as compared to no oversampling (Wilcoxon signed rank-sum test, $p < 0.05$). We observed that the combination method ADASYN oversampling+XGboost classifier (AUC of 0.70, accuracy of 0.74, sensitivity of 0.75, and specificity of 0.70) presented the highest performance for DFS prediction. ADASYN+SVM performed best (AUC of 0.80, accuracy of 0.76, sensitivity of 0.74, and specificity of 0.86) for OS prediction in our NPC cohort.
Conclusion: We identified optimal machine learning methods for the prediction of prognostication in NPC, which enhanced the applications of radiomics in precision oncology and clinical practice. Of note, re-sampling techniques showed a significant positive impact on prediction performance in imbalanced datasets.
Limitations: Our study is limited by retrospective datasets in terms of relatively small numbers of instances.
Ethics committee approval: n/a
Funding: No funding was received for this work.
Author Disclosures:
C. Xie: nothing to disclose
V. Vardhanabhuti: nothing to disclose
K. Chiu: nothing to disclose
H. Pang: nothing to disclose
J. Ho: nothing to disclose
E. Lee: nothing to disclose
R. Du: nothing to disclose

RPS 108-4 08:58

Correlation between histogram-based DCE-MRI parameters and ^{18}F-FDG PET values in oropharyngeal squamous cell carcinoma: evaluation in primary tumours and metastatic nodes

A. Vidiri, E. Gangemi, E. Ruberto, R. Pasqualoni, R. Sciuto, A. Farneti, M. Benevolo, R. Pellini, S. Marzi; *Rome/IT (emma_gan86@yahoo.it)*

Purpose: To investigate the correlation between histogram-based dynamic contrast-enhanced MRI (DCE-MRI) parameters and ^{18}F-FDG-PET values in oropharyngeal squamous cell carcinoma (OPSCC), both in primary tumours (PT) and in metastatic nodes (LNs).
Methods and materials: 52 patients with a new diagnosis of OPSCC were enrolled in the present study. Imaging including DCE-MRI and ^{18}F-FDG PET/CT scans was acquired from all patients. Both PT and the largest LN, if present, were volumetrically contoured.
Quantitative parameters, including the transfer constant K^{trans} and Kep, and the volume of extravascular extracellular space v_e, were calculated from DCE-MRI. The percentiles, P10, P25, P50, P75, P90, and skewness, and kurtosis and entropy were obtained from the histogram-based analysis of each perfusion parameter. Standardised uptake values, SUV_{max}, SUV_{peak}, SUV_{mean}, metabolic tumour volume (MTV), and total lesion glycolysis (TLG) were calculated applying an SUV threshold of 40%.
The correlations between all variables were investigated with the Spearman-rank correlation test. To exclude false-positive results under multiple testing, the Benjamini and Hockberg method was applied.
Results: No significant correlation was found in PT, while significant associations emerged between K^{trans} and ^{18}F-FDG PET parameters in LNs.
Conclusion: Evident relationships emerged between DCE-MRI and ^{18}F-FDG PET parameters in OPSCC LNs, while no association was found in PTs. The complex relationships between perfusion and metabolic biomarkers should be interpreted separately for primary tumours and lymph nodes. A multiparametric approach to analyse PTs and LSs before treatment is advisable in HNSCC.
Limitations: The retrospective nature of this study may have introduced bias and confounding factors.
Ethics committee approval: The study was authorised by the hospital ethics committee
Funding: This study was conducted retrospectively on a patient population included in a larger prospective study funded by the Italian Association for Cancer Research.
Author Disclosures:
E. Gangemi: nothing to disclose
A. Vidiri: nothing to disclose
E. Ruberto: nothing to disclose
R. Pasqualoni: nothing to disclose
R. Sciuto: nothing to disclose
A. Farneti: nothing to disclose
M. Benevolo: nothing to disclose
R. Pellini: nothing to disclose
S. Marzi: nothing to disclose

RPS 108-5 09:04

A comparison among gamma distribution, intravoxel incoherent motion, and mono-exponential models of orofacial tumours: a preliminary study

W. Panyarak, T. Chikui, K. Tokumori, Y. Yamashita, K. Yoshiura; *Fukuoka/JP (wpanyarak@gmail.com)*

Purpose: We compared the parameters of gamma distribution (GD), intravoxel incoherent motion (IVIM), and mono-exponential (ME) models based on the goodness-of-fit, correlations, and effectiveness in the differential diagnosis among various orofacial lesions.
Methods and materials: 57 patients underwent 3-Tesla MRI examinations including TSE-DWI with 6 b-values (0-1000 s/mm^2). The shape parameter k, scale parameter θ, and fractions of diffusion (f_1, f_2, and f_3, which represent the cell component, parenchyma, and perfusion component, respectively) were obtained by GD model. D, D*, and f were obtained by IVIM model. ADC was obtained by ME model. Akaike information criterion was used to evaluate the goodness-of-fit. Correlations of the three methods were then assessed. All parameters were compared among inflammatory lesions (n=5) and benign (n=14) and malignant tumours (n=38).
Results: There was no significant difference between the GD and IVIM models, but both models showed a better goodness-of-fit than the ME model (p<0.0001). The f_1 showed strong negative correlations with D (ρ=–0.906) while the f_3 showed moderately positive correlations with f (ρ=0.583). The malignant tumours showed significantly lower k, D, and ADC values (p<0.0001), which reflected their higher cellularity (higher f_1 values) of benign tumours. No significant differences were found in any parameters between inflammatory lesions and either type of tumour.
Conclusion: The GD and IVIM models displayed comparable correlations and a better goodness-of-fit than the ME model. The GD model clearly showed that malignant tumours had higher cellularity than did benign tumours, which was attributed to their lower D and ADC values.
Limitations: There was a limited number of benign tumours included.
Ethics committee approval: This study was approved by the institutional ethics committee.
Funding: This research is supported by a JSPS KAKENHI (C) 18K09770.
Author Disclosures:
W. Panyarak: nothing to disclose
Y. Yamashita: nothing to disclose
K. Tokumori: nothing to disclose
T. Chikui: nothing to disclose
K. Yoshiura: nothing to disclose

RPS 108-6 09:10

Magnetic resonance imaging (MRI) driven cytology: from a comparison of diagnostic accuracy to a proposal for a new diagnostic algorithm in the preoperative work-up of parotid lesions

G. Guazzarotti, E. Venturini, R. Mellone, A. de Gaspari, D. Di Santo, F. de Cobelli; *Milan/IT*

Purpose: To determine the diagnostic accuracy (AC) of multiparametric MRI (mp-MRI), fine-needle aspiration cytology (FNAC) and their combined use in differential diagnosis of parotid tumours.
Methods and materials: 89 consecutive patients with clinical evaluation and mp-MRI (T2-T1-DWI[b:0-1000]-DCE) for parotid lesion were prospectively enrolled; 80/89 patients underwent FNAC. ADC was measured by ROI avoiding necrosis and, by ROC analysis, 2 ADC thresholds were identified. Time-intensity curves (TIC) were classified as A (time to peak[TTP]≥120s), B (TTP<120s+washout ratio[WR]≥30%), C (TTP<120s+WR<30%), and D (flat). The first 30 patients were retrospectively analysed. Using morphological features, ADC value, TIC, and T2 signal an mp-MRI diagnostic algorithm validated on the remaining patients was constructed. Sensitivity (SE), specificity (SP), positive and negative predictive values (VPP and VPN), and AC were evaluated using histology as a gold standard. AC of FNAC and algorithm was calculated before and after modification of diagnosis referring to anamnestic data and FNAC results.
Results: We evaluated 68 benign (37 pleomorphic adenomas [PA], 23 Warthin tumours, 2 cysts [Cy], and 6 other benign lesions) and 21 malignant lesions (16 carcinomas, 5 lymphomas [L]). 2 ADC thresholds were identified to distinguish PA/Cy (ADC>1.3) and L (ADC<0.6) from other lesions. Adenopathies (p=.003), infiltration of adjacent structures (p<.001), hypointense/heterogeneous T2 signal (p=.002), and type C TIC (p<.001) were significantly related to malignancy and used in the definition of diagnostic algorithm. Applied to the validation group, it showed SE=69.23%, SP=95.24%, PPV=81.81%, NPV=90.90%, and AC=89.09%. Adding anamnestic data, it showed SE=78.57%, SP=95.24%, PPV=84.61%, NPV=93.02, and AC=89.47%.
FNAC demonstrated SE=77.78%, SP=100%, PPV=100%, NPV=96%, and AC=96.49%, with non-diagnostic/indeterminate results in 28.75% of cases.
When FNAC was used to characterise indeterminate lesions after mp-MRI, we obtained SE=80%, SP=95.34%, PPV=85.71%, NPV=93.18%, and AC=91.38%.
Conclusion: Preoperative mp-MRI, associated with FNAC in doubt lesions, reaches a high diagnostic accuracy and should be proposed as a preoperative diagnostic work-up of parotid lesions.
Limitations: A relatively small sample size.
Ethics committee approval: Approved by the Institutional Review Board; each patient signed a specific written informed consent.
Funding: No funding was received for this work.
Author Disclosures:
G. Guazzarotti: nothing to disclose
E. Venturini: nothing to disclose
R. Mellone: nothing to disclose
A. de Gaspari: nothing to disclose
D. Di Santo: nothing to disclose
F. de Cobelli: nothing to disclose

RPS 108-7 09:16

Prognostic role of diffusion-weighted and dynamic contrast-enhanced MRI in loco-regionally advanced head and neck cancer treated with concomitant chemoradiotherapy

M. Garbajs[1], S. Bisdas[2], P. Strojan[1], K. Surlan Popovic[1]; [1]*Ljubljana/SI,* [2]*London/UK (manca.garbajs@gmail.com)*

Purpose: In this prospective study, the value of pre-treatment dynamic contrast-enhanced (DCE) and diffusion-weighted (DW) MRI-derived parameters, as well as their changes early during treatment, was evaluated for predicting disease-free survival (DFS) and overall survival (OS) in patients with loco-regionally

advanced head and neck squamous cell carcinoma (HNSCC) treated with concomitant chemo-radiotherapy (cCRT) with cisplatin.
Methods and materials: MRI examinations were performed in 20 consecutive patients with loco-regionally advanced HNSCC at baseline and after 10 Grays (Gy) of cCRT. Tumour apparent diffusion coefficient (ADC) and DCE parameters (volume transfer constant [K_{trans}], extracellular extravascular volume fraction [v_e], and plasma volume fraction [V_p]) were measured. Relative changes in parameters from baseline to 10 Gy were calculated. Univariate and multivariate Cox regression analysis were conducted. Receiver operating characteristic (ROC) curve analysis was employed to identify parameters with the best diagnostic performance.
Results: None of the parameters was identified to predict for DFS. On univariate analysis of OS, lower pre-treatment ADC (p=0.012), higher pre-treatment K_{trans} (p=0.026), and higher reduction in K_{trans} (p=0.014) from baseline to 10 Gy were identified as significant predictors. Multivariate analysis identified only higher pre-treatment K_{trans} (p=0.026; 95% confidence interval (CI): 0.000–0.132) as an independent predictor of OS. At ROC curve analysis, pre-treatment K_{trans} yielded an excellent diagnostic accuracy (area under curve [AUC]=0.95, sensitivity 93.3%, and specificity 80%).
Conclusion: In our group of HNSCC patients treated with cisplatin-based cCRT, pre-treatment K_{trans} was found to be a good predictor of OS.
Limitations: A small sample size and high number of parameters to analyse.
Ethics committee approval: At Ministry of Health, Republic of Slovenia No.22k/03/13.
Funding: No funding was received for this work.
Author Disclosures:
M. Garbajs: nothing to disclose
S. Bisdas: nothing to disclose
P. Strojan: nothing to disclose
K. Surlan Popovic: nothing to disclose

RPS 108-8 09:22

Correlation between oropharyngeal squamous cell carcinoma and human papilloma virus: MRI volumetric texture analysis

L. Bertana[1], A. Florio[1], N. Landini[1], A. Menegaldo[1], D. Caruso[2], P. Boscolo Rizzo[3], A. C. Frigo[3], A. Laghi[2], G. Morana[1]; [1]*Treviso/IT,* [2]*Rome/IT,* [3]*Padua/IT (lucabertana82@gmail.com)*

Purpose: To predict the presence of human papilloma virus (HPV) in oropharyngeal squamous cell carcinomas (OPSCC) with volumetric MRI texture analysis.
Methods and materials: We retrospectively analysed 47 patients with T1-T4 OPSCC histologically confirmed after a biopsy. HPV was determined as both positive of HPV DeoxyriboNucleic Acid and p16 immunochemistry. All patients underwent MR examinations with the following sequences: pre- and post-contrast T1-w, T2-w, and DWI at 5b-values (0, 50, 100, 500, 750, and 1,000 s/mm²). ADC maps were computed. Texture analysis was performed on a hand-drawn region of interest (ROI) of the entire primary tumour volume on T2-w, DWI at b1000, ADC, and post-contrastography T1-w sequences. Mean value (MV), standard deviation (SD), mean positive pixel (MPP), entropy, skewness, and kurtosis were extracted and compared between HPV+ and HPV- patients with a Student's T-test. Parameters were clustered in three groups (HPV+ smokers, HPV- smokers, and non-smokers). The analysis of variance was computed. False discovery rate was checked with Benjamini-Hochberg correction. Multivariable logistic regression was adopted for an HPV presence predictive model
Results: 18 (38%) patients were HPV+ and 29 (62%) patients were HPV-. HPV+ patients had a significantly lower ADC MV and ADC MPP with respect to HPV- patients (p<0.001). No statistically differences were detected between smokers and non-smokers (p>0.05). The predictive model based on mean ADC resulted in a sensitivity of 89% and specificity of 90% for both parameters
Conclusion: Primary tumour ADC MV and ADC MPP were significantly lower in HPV+ patients than for HPV- patients. Further studies will be necessary to validate these results.
Limitations: Limitation in the number of patients.
Ethics committee approval: Approval from ethic committee for this retrospective study.
Funding: No funding was received for this work.
Author Disclosures:
A. Florio: nothing to disclose
A. C. Frigo: nothing to disclose
L. Bertana: nothing to disclose
N. Landini: nothing to disclose
A. Laghi: nothing to disclose
A. Menegaldo: nothing to disclose
G. Morana: nothing to disclose
P. Boscolo Rizzo: nothing to disclose
D. Caruso: nothing to disclose

RPS 108-9 09:28

Histogram analysis parameters derived from DCE-MRI in head and neck squamous cell cancer: associations with microvessel density

H.-J. Meyer[1], G. Hamerla[1], A. K. Höhn[1], L. Leifels[1], A. Surov[2]; [1]*Leipzig/DE,* [2]*Ulm/DE (hans-jonas.meyer@medizin.uni-leipzig.de)*

Purpose: DCE-MRI is a functional imaging modality which is widely acknowledged to be linked to microvessel density in tissues. Therefore, it might be able to predict vessels in tumours. The present study sought to elucidate possible associations between microvessel density and histogram parameters in head and neck squamous cell carcinomas (HNSCC).
Methods and materials: 30 participants with a histologically proven HNSCC were included in the study. DCE-MRI was performed with a 3T MRI and histogram analysis was calculated with a whole lesion measurement. In every case, microvessel density was estimated with CD105 stained specimens.
Results: The median derived from Ktrans correlated with vessel area (ρ=0.39, P=0.034). No other Ktrans or Ve parameters reached statistical significance. Several Kep derived parameters correlated with vessel area as well as with vessel count. MinKep had the highest correlation coefficient with the vessel area (ρ=0.45, P=0.01). ModeKep had the highest coefficient with vessel count (ρ=0.41, P=0.03).
Conclusion: Histogram parameters derived from Kep might be used as surrogate imaging biomarkers for microvessel density parameters in HNSCC. MinKep showed the highest correlation with the vessel area and ModeKep with vessel count.
Limitations: Firstly, the patient sample is rather small, but larger than in two comparable preliminary studies published previously. Secondly, the histopathology analysis was performed on a bioptic specimen, which might not be fully representative of the whole tumour, whereas the MRI analysis was performed as a whole lesion measurement. This might result in some incongruities.
Ethics committee approval: n/a
Funding: No funding was received for this work.
Author Disclosures:
H.-J. Meyer: nothing to disclose
G. Hamerla: nothing to disclose
A. K. Höhn: nothing to disclose
L. Leifels: nothing to disclose
A. Surov: nothing to disclose

RPS 108-10 09:34

Parallel imaging with and without compressed sensing: utility for head and neck MR imaging in patients with different diseases

H. Ikeda[1], Y. Ohno[1], K. Murayama[1], K. Yamamoto[2], A. Iwase[1], T. Fukuba[1], D. Tabata[1], M. Ikedo[2], H. Toyama[1]; [1]*Toyoake/JP,* [2]*Otawara/JP (ikeda-gif@umin.net)*

Purpose: To determine the utility of compressed sensing (CS) for head and neck MR imaging obtained with parallel imaging (PI) in patients with different diseases.
Methods and materials: 30 consecutive patients with various head and neck diseases underwent T2-weighted imaging by a 3T MR system (Vantage Galan 3T, Canon Medical Systems, Otawara, Japan) by PI with and without CS. On the quantitative assessment of the image quality, signal-to-noise ratio (SNR), percentage of the coefficient of variation (%CV), and contrast-to-noise ratio (CNR) in each patient were determined by ROI measurement. For qualitative assessment, two board-certified radiologists visually evaluated overall image quality, artefacts, and diagnostic performance by a 5-point scoring system. To compare quantitatively assessed image qualities, all indexes were compared between PI with and without CS by t-test. Interobserver agreements on each method were assessed by kappa statistics. To compare qualitative scores, a Wilcoxon's singed-rank test was performed. Finally, mean examination time was compared between PI with and without CS.
Results: SNR, %CV, and CNR of PI with CS were significantly better than those of PI without CS (p<0.0001). Interobserver agreements were assessed as significant and substantial (overall image quality: 0.67<κ<0.71, artefact: 0.65<κ<0.81, diagnostic performance: 0.62<κ<0.73). All qualitative image qualities had no significant differences (p>0.05). Examination time of PI with CS (83s ± 11s) was significantly shorter than without CS (173s ± 54s, p<0.0001).
Conclusion: Compressed sensing combined with parallel imaging is more useful than parallel imaging for head and neck MR examination in patients with different diseases.
Limitations: A limited study population.
Ethics committee approval: This study was a retrospective study and written informed consent was waived. This study was approved by the institutional review board of Fujita Health University Hospital.
Funding: This study was technically supported by Canon Medical Systems Corporation.

Author Disclosures:
H. Ikeda: nothing to disclose
Y. Ohno: Research/Grant Support at Canon Medical Systems Corporation
K. Murayama: Research/Grant Support at Canon Medical Systems Corporation
K. Yamamoto: Employee at Canon Medical Systems Corporation
A. Iwase: nothing to disclose
T. Fukuba: nothing to disclose
D. Tabata: nothing to disclose
M. Ikedo: Employee at Canon Medical Systems Corporation
H. Toyama: Research/Grant Support at Canon Medical Systems Corporation

RPS 108-11 09:40
Comparison between simultaneous multi-slice and integrated slice-by-slice shimming readout-segmented echo-planar imaging in head and neck tumours
T. Su, Y. Chen, Z. Xu, Z. Zhang, Z. Jin*; Beijing/CN (angelasu.love@163.com)*

Purpose: To compare the simultaneous multi-slice (SMS) and integrated slice-by-slice shimming (iShim) readout-segmented echo-planar imaging (rs-EPI, RESOLVE) for diffusion-weighted imaging (DWI) in head and neck tumours.
Methods and materials: 20 patients with histologically proven head and neck malignant tumours were included in this prospective study. The MR exam included the prototype sequences SMS-RESOLVE and iShim-RESOLVE, acquired at b-values of 0 and 800 s/mm2. Image quality was evaluated quantitatively (distortion rate, signal-to-noise ratio SNR, and ADC values), and compared. The acquisition time was 2:47 for SMS-RESOLVE and 3:09 for iShim-RESOLVE.
Results: 20 primary tumours and 7 metastatic lymph nodes were analysed. The lesion distortion rate of iShim-RESOLVE was significantly lower than that of SMS-RESOLVE. And the SNR of iShim-RESOLVE images were significantly higher than that of SMS-RESOLVE. The primary signal intensities of lesions obtaine by iShim-RESOLVE were significantly higher than that of SMS-RESOLVE images. In addition, there was no significant difference in the ADC values of primary lesions and lymph nodes between iShim-RESOLVE and SMS-RESOLVE sequences.
Conclusion: IShim-RESOLVE can improve image quality in head and neck DWI practice with substantially decreased lesion distortion and increased SNR, and it showed comparable ADC values of tumours and total acquisition time compared to an SMS-RESOLVE sequence.
Limitations: The study population was rather small. The clinical practice values of these protocols should be researched further.
Ethics committee approval: This prospective study was approved by the local ethics committee and written informed consent was obtained from all subjects.
Funding: No funding was received for this work.
Author Disclosures:
T. Su: nothing to disclose
Y. Chen: nothing to disclose
Z. Xu: nothing to disclose
Z. Zhang: nothing to disclose
Z. Jin: nothing to disclose

RPS 108-12 09:46
Low-tube voltage 80-kVp neck CT with an adaptive statistical iterative reconstruction (ASIR)-V algorithm: preliminary results in the evaluation of the loco-regional extension of head and neck cancer
C. Giannitto[1], G. Vatteroni[1], O. G. Santonocito[2], G. Ferrillo[1], R. Ramberti[3], G. Mercante[1], B. Fiamengo[1], G. Spriano[1], L. Balzarini[1];
[1]*Milan/IT,* [2]*Mascalucia/IT,* [3]*Rozzano/IT*
(caterina.giannitto@gmail.com)

Purpose: To evaluate the diagnostic accuracy of low-tube voltage 80-kV (peak) neck CT acquisition in the loco-regional extension of head and neck cancer, analysing the impact of ASIR-V algorithm on signal, noise, and image quality.
Methods and materials: Two radiologists (with 5 and 10 years experience in head and neck cancer) separately analysed standard 120-kVp neck CTs and anonymised 80-kVp neck CTs of 20 patients with head and neck cancer who underwent CT (Revolution CT; GE Healthcare, Milwaukee, WI). 10 patients (6 oral cancers, 4 laryngeal cancers) who underwent surgery were unrolled. Images were reconstructed using an adaptive statistical iterative reconstruction (ASIR)-V algorithm on image quality. Image noise, the signal-to-noise ratio (SNR), and the contrast-to-noise ratio (CNR) were calculated for the lesions and were compared between the different post-processing ASIR-V % used. Reviewers were blinded to histology results. Sensitivity (SE), specificity (SP), positive predictive value (PPV), and negative predictive value (NPV) were calculated for standard 120-kVp CT and 80-kVp CT evaluations.
Results: Low-tube voltage 80-kVp neck CT acquisition (SE 94%, SP 92.2%, VVP 95.1%, and NPV 90.3 %) is more accurate than 120-kVp CT (SE 85.7%, SP 77.8%, VVP 85.7 %, and NPV 77.8%) in the definition of the loco-regional extension in head and neck cancer. Compared to ASIR-V 0%, image reconstructed with ASIR-V demonstrated a significant reduction of image noise in 80-kVp CT images ($P < 0.05$).
Conclusion: Low-tube voltage 80-kVp neck CT acquisition and reconstruction with ASIR-V could provide a better definition of the loco-regional extension in head and neck cancer.
Limitations: The small cohort and the monocentric experience. Results must be validated in a large cohort.
Ethics committee approval: The study was approved by an ethics committee.
Funding: No funding was received for this work.
Author Disclosures:
L. Balzarini: nothing to disclose
C. Giannitto: nothing to disclose
G. Vatteroni: nothing to disclose
O. G. Santonocito: nothing to disclose
G. Ferrillo: nothing to disclose
B. Fiamengo: nothing to disclose
G. Mercante: nothing to disclose
G. Spriano: nothing to disclose
R. Ramberti: nothing to disclose

RPS 108-13 09:52
MRI accuracy in the detection of optic nerve invasion in retinoblastomas: a radio-pathologic correlation
R. Costa, J. Albuquerque, V. R. F. Simonini, H. S. D. Souza, M. Decnop, C. Mattosinho*; Rio de Janeiro/BR (rangeldesousa1@gmail.com)*

Purpose: To determine the sensitivity, specificity, and accuracy of MRIs in detecting optic nerve invasion in patients with retinoblastoma.
Methods and materials: A retrospective study with inclusion criteria of patients with a diagnosis of retinoblastoma who attended a reference centre in oncology from 2009-2019 and who had MRIs of orbits and a subsequent enucleation procedure. The criteria for invasion by imaging was a thickening and enhancement of the nerves as well as morphological changes. The results obtained were compared with the histopathological reports, confirming or discarding the optic nerve invasion and determining the sensitivity, specificity, and accuracy.
Results: 50 patients were included, with a predominance of females with a mean age of 4 years and a mean lesion diameter of 1.5 cm. In the analysed group, MRI showed a sensitivity of 21%, specificity of 74%, and negative predictive value of 61%. The estimated accuracy was 54%.
Conclusion: In the studied group, MRI showed low accuracy for the detection of optic nerve invasion, considering that in most retinoblastomas the invasion is microscopic. The false-positive cases are mostly due to the related inflammatory process, which mimics the radiological findings of invasion.
Limitations: A small number of patients (50) and unicentric study.
Ethics committee approval: n/a
Funding: No funding was received for this work.
Author Disclosures:
R. Costa: nothing to disclose
J. Albuquerque: nothing to disclose
V. R. F. Simonini: nothing to disclose
H. S. D. Souza: nothing to disclose
M. Decnop: nothing to disclose
C. Mattosinho: nothing to disclose

08:30 - 10:00 **Coffee & Talk 3**

Physics in Medical Imaging

RPS 113

Advances in CT

Moderators:
N. Saltybaeva; Zug/CH
O. Rampado; Turin/IT

RPS 113-1 08:30

Physical evaluation of a novel ultra-high-resolution CT scanner

L. J. Oostveen[1], K. Boedeker[2], M. Brink[1], M. M. Prokop[1], F. de Lange[1], I. Sechopoulos[1]; [1]*Nijmegen/NL,* [2]*Otawara/JP (luuk.oostveen@radboudumc.nl)*

Purpose: To evaluate the technical performance of an ultra-high-resolution CT (UHRCT) system.
Methods and materials: Standard procedures and phantoms were used to measure the modulation transfer function (MTF), slice sensitivity profile, uniformity, CT number accuracy, noise power spectrum (NPS), and low-contrast detectability of a UHRCT (Aquilion Precision, Canon Medical Systems) and compare them to a multidetector-row CT (MDCT, Aquilion ONE Genesis). The super-high-resolution (SHR) mode of the UHRCT uses detector elements (dels) with an effective size of 0.25x0.25 mm^2 at the isocentre. The high-resolution (HR) mode bins two dels in the longitudinal direction. The normal-resolution (NR) mode bins 2x2 del, resulting in a del size equivalent to that of the MDCT system.
Results: The UHRCT limiting-resolution MTF (10% MTF: 4.1 lp/mm) is twice as high as that in the NR mode and of the MDCT (10% MTF: 1.7 and 1.9 lp/mm, respectively). The slice sensitivity profile in the SHR mode (FWHM: 0.45 mm) is 40% narrower than that of the MDCT (0.77 mm). Uniformity and CT numbers are within the expected range for all UHRCT modes. Noise in the SHR and HR modes has a higher magnitude and higher frequency components than MDCT. Low-contrast detectability is lower for all UHRCT modes compared to MDCT, but a dose increase of about 14% for NR, and about 23% for HR and SHR, results in matching low contrast performance.
Conclusion: HR and SHR modes of UHRCT result in twice the limiting spatial resolution of MDCT, requiring only a 23% increase in dose to achieve the same low-contrast detectability.
Limitations: The use of linear metrics with non-linear reconstruction algorithms must be performed with care and only for the evaluation of the relative differences between techniques, as done here.
Ethics committee approval: n/a
Funding: Funding received from Canon.
Author Disclosures:
L. J. Oostveen: Research/Grant Support at Canon Medical Systems Corporation
K. Boedeker: Employee at Canon Medical Systems Corporation
M. Brink: nothing to disclose
M. M. Prokop: Research/Grant Support at Canon Medical Systems Corporation, Speaker at Canon Medical Systems Corporation, Research/Grant Support at Siemens Healthineers, Speaker at Siemens Healthineers, Speaker at Bracco, Speaker at Bayer
F. de Lange: nothing to disclose
I. Sechopoulos: Research/Grant Support at Canon Medical Systems Corporation, Research/Grant Support at Siemens Healthineers, Speaker at Siemens Healthineers, Speaker at Hologic

RPS 113-2 08:36

Context-sensitive ultrahigh-resolution bone imaging in whole-body photon-counting CT

L. Klein, E. Wehrse, C. Amato, C. H. Ziener, M. Uhrig, S. Heinze, H.-P. Schlemmer, M. Kachelrieß, S. Sawall; *Heidelberg/DE (laura.klein@dkfz.de)*

Purpose: To improve the diagnostic workflow of bone imaging by providing organ-specific, context-sensitive images in whole-body photon-counting (PC) CT showing osseous structures at ultrahigh resolution (UHR) and soft tissue at standard resolution with reduced noise within a single image.
Methods and materials: Acquisitions of the lumbar spine and pelvis were acquired in 5 patients and 10 forensic specimens using the UHR mode (pixel size 0.25 mm at the isocenter) of a PC CT prototype (SOMATOM CounT, Siemens Healthineers). Acquisitions are performed using 120 kV/300 mAs over a longitudinal scan range of 10 cm ($CTDI_{vol\ 32cm}$=24 mGy, D_{eff}=2.8 mSv). Images are reconstructed using sharp kernels (e.g. U70f) for bones and smoother kernels (e.g. D40f) for diagnostic tasks in soft tissue. Reconstruction of UHR data with low spatial resolution results in reduced noise compared to acquisitions with standard pixels sizes at the same dose [MedPhys 32(5):1321ff, 2005]. Bones, contrast agent, and soft tissue regions are automatically identified by decomposing the intrinsically acquired spectral data of the system. A context-sensitive image [Med. Phys. 45(10): 4541ff, 2018] is computed pixelwise using the sharp reconstruction for osseous structures and smooth reconstruction for soft tissue.
Results: The resulting context-sensitive images simultaneously provide mutually exclusive image properties: low noise and moderate spatial resolution (7.4 lp/cm for D40f) in soft tissue and the highest spatial resolution in osseous structures (16.0 lp/cm for U70f).
Conclusion: Context-sensitive images including UHR data improve clinical workflow by presenting mutually exclusive image properties within a single image and hence increased information content. This also may increase the rate of incidental findings.
Limitations: The proposed method has only been applied to a limited number of patients and forensic specimens.
Ethics committee approval: n/a
Funding: No funding was received for this work.
Author Disclosures:
S. Sawall: nothing to disclose
M. Kachelrieß: nothing to disclose
L. Klein: nothing to disclose
E. Wehrse: nothing to disclose
C. Amato: nothing to disclose
C. H. Ziener: nothing to disclose
M. Uhrig: nothing to disclose
S. Heinze: nothing to disclose
H.-P. Schlemmer: nothing to disclose

RPS 113-3 08:42

Kernel considerations for high-resolution photon-counting CT: dose reduction versus spatial resolution

L. Klein, J. Hardt, A. Byl, E. Wehrse, S. Heinze, M. Uhrig, H.-P. Schlemmer, M. Kachelrieß, S. Sawall; *Heidelberg/DE (laura.klein@dkfz.de)*

Purpose: To evaluate the dependency of noise reduction of high-resolution whole-body photon-counting (PC) CT compared to conventional energy-integrating (EI) CT as a function of reconstruction kernel.
Methods and materials: A semi-anthropomorphic liver phantom and forensic human specimens were measured using a prototype CT equipped with an EI and a PC detector (SOMATOM CounT, Siemens Healthineers). Images were acquired using the ultrahigh-resolution mode of the PC detector (PC-UHR, pixel size 0.25 mm at the isocenter) and the EI detector (0.6 mm at the isocenter). Reconstructions were performed using all available reconstruction kernels and resulted in different noise and spatial resolution levels. Theory predicts that PC-UHR images reconstructed to a lower spatial resolution result in reduced noise compared to EI at the same resolution and dose [MedPhys 32(5):1321ff, 2005]. Dose-normalised noise is evaluated and compared between both detector types for different kernels. Phantom results are verified in post mortem lung scans that typically require reconstructions using smooth and sharp kernels.
Results: Low-resolution images (below $MTF_{10\%}$=6.5 lp/cm, B40f kernel) show no significant difference in image noise between both detector types. PC-UHR reconstructed with a higher target MTF ($MTF_{10\%}$=9.3 lp/cm, B80f) achieves a noise reduction of up to 30% at the same dose and resolution as the EI detector. A noise evaluation in bronchioli typically performed at low spatial resolution does not benefit from acquisitions with small detector pixels while the visualisation of fine lung structures using sharp resolution kernels improves significantly using PC-UHR.
Conclusion: Clinical applications requiring medium or high resolution will be improved by the usage of PC-UHR and the consequent noise reduction equivalent to a radiation dose reduction.
Limitations: The effect has only been evaluated in phantoms and forensic specimens.
Ethics committee approval: n/a
Funding: No funding was received for this work.
Author Disclosures:
S. Heinze: nothing to disclose
L. Klein: nothing to disclose
J. Hardt: nothing to disclose
A. Byl: nothing to disclose
E. Wehrse: nothing to disclose
H.-P. Schlemmer: nothing to disclose
M. Uhrig: nothing to disclose
M. Kachelrieß: nothing to disclose
S. Sawall: nothing to disclose

RPS 113-4 08:48

Dedicated metal artefact reduction for photon-counting CT

A. Byl, L. Klein, J. Hardt, E. Wehrse, H.-P. Schlemmer, S. Heinze, M. Uhrig, S. Sawall, M. Kachelrieß; *Heidelberg/DE (achim.byl@dkfz-heidelberg.de)*

Purpose: To reduce metal artefacts in photon-counting (PC) CT.
Methods and materials: CT systems with PC detectors usually provide multiple energy bins and acquire spectral information by default. In the presence of metal artefacts, the bin images require metal artefact reduction. We linearly combined (LC) the bin images in two ways: a) to produce an image with reduced artefacts and b) to minimise noise. A corrected LC (CLC) image was obtained by applying frequency split (FS) normalised metal artefact reduction (NMAR), the gold standard MAR algorithm, to the LC with minimum noise, inserting the high-frequency components of the LC with reduced artefacts. Then, each bin was corrected with FSNMAR using the CLC as a prior and corresponding FS image. Images of forensic specimens containing metal implants were acquired at the SOMATOM CounT PC prototype CT system (Siemens Healthineers, Germany) at 140 kV with a tube current of 300 mAs and thresholds of 25, 45, 70, and 90 keV, resulting in 4 bin images. To quantify the artefact content standard deviations in 3 ROIs (metal artefact, soft tissue without artefacts, and bone), our new PC-FSNMAR were compared to conventional FSNMAR applied to each bin separately (binwise FSNMAR).
Results: Compared to binwise FSNMAR, PC-FSNMAR shows several advantages: a reduced noise and artefact level of up to 70% close to the metal, fewer metal artefacts even in the low-energy bins due to the usage of an optimal prior image, and preserved spectral information in all bins.
Conclusion: PC-FSNMAR significantly improves image quality compared to conventional binwise FSNMAR, in particular in regions close to the metal and for low-energy bins, which suffer most from metal artefacts.
Limitations: n/a
Ethics committee approval: n/a
Funding: No funding was received for this work.
Author Disclosures:
A. Byl: nothing to disclose
L. Klein: nothing to disclose
H.-P. Schlemmer: nothing to disclose
S. Sawall: nothing to disclose
M. Kachelrieß: nothing to disclose
J. Hardt: nothing to disclose
E. Wehrse: nothing to disclose
S. Heinze: nothing to disclose
M. Uhrig: nothing to disclose

RPS 113-5 08:54

Development of an articulated anthropomorphic 3D-printed arm phantom for image quality and dosimetry optimisation of CT protocols

O. V. Ivashchenko[1], H. Ruitenbeek[2], M. Boonekamp[1], M. Fusaglia[3], I. Hernandez-Giron[1]; *[1]Leiden/NL, [2]Enschede/NL, [3]Amsterdam/NL (o.ivashchenko@lumc.nl)*

Purpose: To guarantee optimal diagnostic image quality to dose trade-off in CT, acquisition and reconstruction parameters are optimised for standardised patient positions. For indications related to anatomical regions from the lower abdomen up to the head, arms should be placed outside the field-of-view. However, for a large group of patients, including trauma or restricted shoulder mobility cases, one or both arms can be fully immobilised. Then, arm-positioning-specific instructions do not apply, affecting dose and image quality. This could be overcome using trauma-specific CT protocols adapted for non-trivial arm positions. CT-manufacturers allow for complex dose modulation with non-trivial arm-positioning, but implementation and optimisation in clinical practice is rare. One of the reasons is the scarcity of commercially available anthropomorphic phantoms for CT-dosimetry with articulated arms. Our goal was to develop affordable and reproducible production methods of totally articulated arm extensions of the RANDO-phantom, widely used for CT QC in radiology and radiotherapy.
Methods and materials: 3D-modelling, 3D-printing, and moulding techniques were used to manufacture the phantom, using anthropomorphic bones and soft-tissue-like materials. After testing various 3D-printing, silicone, gels, and polyurethane materials, a nylon-aluminium mix aluminide and a custom polyurethane-rubber mix were selected, corresponding to average HUs of human hard bone and fat-muscle mix, respectively. Image quality, attenuation, and dose modulation properties of the phantom, attached to RANDO-phantom, were evaluated for trauma-CT protocols.
Results: Attenuation of the phantom [bone: (562±336) HU, soft tissue: (56±24) HU] closely mimicked values of the human arm [compact-bone: (800±400) HU, fat-to-muscle: (-80:100) HU] and is stable within the 80-140kV range. CTDIvol dose of the thorax trauma-CT varied by 12% (0.3 mGy) for various arm positions (arms-up, down, and mixed).
Conclusion: A reproducible method for the production of totally-articulated arm phantom for CT-imaging was developed to optimise new CT protocols with complex arm positions.
Limitations: The simplified soft tissue anatomy.
Ethics committee approval: n/a
Funding: No funding was received for this work.
Author Disclosures:
O. V. Ivashchenko: nothing to disclose
H. Ruitenbeek: nothing to disclose
M. Boonekamp: nothing to disclose
M. Fusaglia: nothing to disclose
I. Hernandez-Giron: nothing to disclose

RPS 113-6 09:00

The characterisation of the stellar detector and admire iterative reconstruction using a channelised hotelling observer and noise power spectrum metric

C. Ghetti[1], O. Ortenzia[1], A. D'alessio[2], L. Noferini[3]; *[1]Parma/IT, [2]Novara/IT, [3]Arezzo/IT (CGhetti@ao.pr.it)*

Purpose: To investigate the performances of two CT systems produced by the same manufacturer (Siemens Somatom Flash/Edge) with different detector technologies and different generations of iterative reconstruction (IR) algorithms (Safire and Admire).
Methods and materials: A homemade phantom was scanned on Flash CT equipped with ultrafast ceramic (UFC) detector and Edge CT with a stellar detector. Images were reconstructed with filtered back-projection (FBP) and IR algorithms. Image quality was evaluated in terms of low-contrast detectability using a channelised hotelling observer (CHO). The performance on signal detection predicted by the CHO was compared to the outcomes of three expert readers for tuning the model-observer (MO). The noise reduction, image texture, and the effects of IR algorithms were evaluated in terms of the noise power spectrum (NPS).
Results: The analysis with MO showed the best performance of Edge respect to Flash system for both FBP and IR algorithms. The better stellar detector efficiency improved the signal detection of the Edge versus the Flash system of about 20%. The IR algorithms further improved the detectability of the signal on both systems. The evaluated noise reduction due to the stellar detector was 57%. Admire IR preserved a more traditional CT image texture appearance due to lower NPS peak shift.
Conclusion: The stellar detector implemented on Edge CT showed an overall greater improvement in low-contrast detectability performance compared to the CT scanner equipped with a conventional detector. Large differences in NPS were observed between Safire and Admire.
Limitations: A very simple detection task, i.e. detecting a known symmetric object placed on a uniform background which is very far from the clinical condition.
Ethics committee approval: n/a
Funding: No funding was received for this work.
Author Disclosures:
C. Ghetti: nothing to disclose
O. Ortenzia: nothing to disclose
A. D'alessio: nothing to disclose
L. Noferini: nothing to disclose

RPS 113-7 09:06

Threshold-dependent dual-energy performance and spectral separation in a clinical whole-body photon-counting CT

S. Sawall, L. Klein, C. Amato, E. Wehrse, J. Maier, H.-P. Schlemmer, C. H. Ziener, S. Heinze, M. Kachelrieß; *Heidelberg/DE (stefan.sawall@dkfz.de)*

Purpose: To evaluate the dual-energy (DE) performance and spectral separation in a clinical, photon counting CT (PCCT) and compare it to dual-source CT (DSCT) DE imaging.
Methods and materials: Semi-anthropomorphic phantoms (abdomen/thorax) extendable with fat rings (S/M/L) equipped with iodine vials (5-30 mg/mL) were measured in a clinical PCCT prototype (SOMATOM CounT, Siemens). The system is comprised of a PC detector with two energy bins, [20 keV, T] and [T, eU] with T=threshold and U=tube voltage. PCCT measurements were performed at all tube voltages (80-140 kV) and threshold settings (50-90 keV). Further measurements were performed using energy integrating DSCT (SOMATOM Flash, Siemens) using 100 kV/Sn 140 kV. Spectral separation was quantified as the relative contrast media ratio (RelCM) between the energy bins and low/high images. Image noise and the dose-normalised contrast-to-noise ratio (CNRD) were evaluated in the resulting virtual non-contrast and iodine images.

Results: RelCM of the PC detector varied between 1.2 and 2.7 and increased with higher thresholds and higher tube voltage, and slightly decreased with larger phantoms. RelCM of the DSCT was found as 2.20 on average over all phantoms. The maximum CNRD in the iodine images was found for T=67/68/70/71 keV for 80/100/120/140 kV. This corresponds to CNRD values of 1.07/1.21/1.32/1.40 $mGy^{-1/2}$ for the small phantom, while the EI DSCT achieves 1.67 $mGy^{-1/2}$ in this case.
Conclusion: Intrinsically acquired PC data are able to provide VNC and iodine images similar to conventional DSCT and allow for a retrospective spectral analysis. Quantitatively, the CNRD is 16% lower with PC than with dual-source dual-energy CT.
Limitations: The presented experiments are limited to phantoms. A forensic study is pending.
Ethics committee approval: n/a
Funding: No funding was received for this work.
Author Disclosures:
H.-P. Schlemmer: nothing to disclose
S. Sawall: nothing to disclose
L. Klein: nothing to disclose
C. Amato: nothing to disclose
E. Wehrse: nothing to disclose
J. Maier: nothing to disclose
C. H. Ziener: nothing to disclose
S. Heinze: nothing to disclose
M. Kachelrieß: nothing to disclose

RPS 113-8 09:12
Does patient off-centring impact the accuracy of dual-energy CT-based iodine quantification in liver tumours?
C. S. Schmidt, B. Baessler, D. N. Nakhostin, H. Alkadhi, A. Euler*; Zurich/CH*

Purpose: To assess the impact of patient off-centring to the absolute error of dual-energy CT-based iodine quantification (DECT-IQ) in liver tumours.
Methods and materials: A liver phantom with 3 cylindrical liver lesions (diameter 15 mm; iodine concentration of 0, 3, and 5 mgI/mL) was imaged repeatedly at 7 vertical table positions ranging from -6 to + 4 cm from the centred 0-position. Scans were performed in dual-energy mode on a dual-source (DS) DECT at 100/Sn150 kV (Somatom Force, Siemens Healthineers) and a single-source (SS) split-filter DECT at AuSn120 kV (Somatom Edge Plus, Siemens Healthineers). The radiation dose was kept constant at 8 mGy. 10 repeated measurements of each lesion's iodine concentration were averaged to obtain the concentration at each off-centre position. The absolute error of iodine quantification was calculated by comparing the measured to the known iodine concentrations. Absolute errors were compared using robust repeated-measures ANOVAs with robust posthoc comparisons.
Results: Absolute errors varied considerably between the 7 different off-centre positions (DS: range 0-1 mgI/mL, mean error 0.31±0.23 mgI/mL; SS: range 0-2.8 mgI/mL, mean error 1.08±0.66 mgI/mL). Group-wise comparisons yielded statistically different error values for multiple lesions and off-centre positions. However, no consistent trend could be observed for absolute error rates depending on off-centre position. Overall, larger error ranges and variations were observed for SS compared to DS.
Conclusion: Patient off-centring has a considerable, yet non-systematic, impact on iodine quantification in DECT and should be considered as an important confounding factor. However, this impact was smaller for DS DECT than for SS DECT.
Limitations: A phantom study.
Ethics committee approval: n/a
Funding: No funding was received for this work.
Author Disclosures:
C. S. Schmidt: nothing to disclose
B. Baessler: nothing to disclose
D. N. Nakhostin: nothing to disclose
H. Alkadhi: nothing to disclose
A. Euler: nothing to disclose

RPS 113-9 09:18
A 3D generalisation of a detectability index in computed tomography: a feasible approach?
R. Villa, N. Paruccini, M. Signoriello, E. de Ponti*; Monza/IT*
(raffaele.vill@gmail.com)

Purpose: Computed tomography (CT) devices acquire and reconstruct volumetric data. In this condition, the 2D analysis of the target transfer function (TTF) and noise power spectrum (NPS) may cause an overestimation of the detectability index, in particular, when iterative reconstruction (IR) algorithms are used. 3D detectability index generalisations have been used to evaluate low-contrast CT performance.
Methods and materials: A cylindrical water-filled phantom was equipped with a central cylindrical PMMA insert and then scanned changing CTDIvol, reconstruction algorithm, filter, and slice thickness; 2D TTF was evaluated.
3D TTF was investigated using a central PMMA spherical insert in the same cylindrical water phantom.
2D and 3D NPS were calculated in a homogeneous phantom. Furthermore, FFT and NPS results were combined in non-pre-whitening (NPW) model to obtain the 3D detectability index.
Results: 3D TTFs show a spherical symmetry for low CTDI level. NPS analysis shows that the variation between 2D and 3D NPS is around 10% in terms of variance for FBP and iterative noise-based reconstruction; the difference increases significantly for model-based iterative reconstruction (from 20% to 180%). The 2D NPS and 3D NPS ratio are flat for FBP, while it depends on spatial frequency for model-based IR; it is higher for lower frequencies. A comparison between 3D and 2D detectability indexes shows a reduction of 15 and 35% for FBP and IR, respectively.
Conclusion: The 3D generalisation of the detectability index shows a lower performance for a model-based IR algorithm when compared with the one obtained with standard 2D metrics.
Limitations: A comparison with a human observer has to be performed in order to check absolute performances.
Ethics committee approval: n/a
Funding: No funding was received for this work.
Author Disclosures:
N. Paruccini: nothing to disclose
R. Villa: nothing to disclose
M. Signoriello: nothing to disclose
E. de Ponti: nothing to disclose

RPS 113-10 09:24
CT imaging texture analysis: evaluation of variability sources in the different steps of radiomic workflow
F. Calderoni[1], C. de Mattia[1], F. Rizzetto[2], P. E. Colombo[1], A. Vanzulli[3], A. Torresin[1]; *[1]Milan/IT, [2]Rho/IT, [3]Segrate/IT (francesca.calderoni@unimi.it)*

Purpose: To analyse the main sources of textural radiomic features (RFs) variability in the different steps of radiomic workflow to quantify the effect on trial results and to evaluate possible recommendations for its reduction.
Methods and materials: Radiomic workflow consists of several steps (imaging acquisition and reconstruction, segmentation, and features extraction) and for each of them, potential sources of variability were analysed.
The analyses were performed on Catphan® acquisitions or patients' images for parameters not significant on the phantom. A wide set of scanner manufacturers and models were considered, involving different centres.
The software used for segmentation and features extraction were IntelliSpace Portal 8, 3DSlicer, and IBEX.
Results: In the imaging acquisition step, repeatability, inter-scanner reproducibility, and tube voltage caused high RFs variability, with a mean relative standard deviation of 30% (range 0%-800%), while the workload was demonstrated to not affect RFs values strongly.
Regarding imaging reconstruction, the most crucial parameters were the algorithm and kernel, with RFs mean variations of 50% and 20%, respectively (maximum 600% and 400%).
The inter-reader variation in contouring was the overall largest source of variability, with a mean value of 60% (maximum 1000%).
In the RFs extraction step, the inter-slice resampling seemed not to be a useful solution and the choice of the feature category parameters was the most critical point to standardising in the radiomic workflow.
Conclusion: A phantom study is preparatory to determine an optimal workflow that maximises RFs predictivity on patients. Once the main variability sources are identified, these can be limited or removed through a reasoned and shared standardisation. Nevertheless, a compromise between RFs stability and predictivity must be evaluated and tailored on each specific trial.
Limitations: The conclusions derive from choices made for the analysis.
Ethics committee approval: n/a
Funding: No funding was received for this work.
Author Disclosures:
C. de Mattia: nothing to disclose
F. Calderoni: nothing to disclose
P. E. Colombo: nothing to disclose
A. Vanzulli: nothing to disclose
A. Torresin: nothing to disclose
F. Rizzetto: nothing to disclose

RPS 113-11 09:30

Stable and harmonisable radiomics features: a guide to robust radiomics analysis

A. Ibrahim[1], H. C. Woodruff[1], S. Primakov[1], R. Granzier[1], R. Leijenaar[1], J. E. Wildberger[1], F. Mottaghy[2], P. Lambin[1]; [1]Maastricht/NL, [2]Aachen/DE (a.ibrahim@maastrichtuniversity.nl)

Purpose: Radiomics features have been reported to be sensitive to differences in image acquisition and reconstruction, which affects the generalisability of radiomics signatures. We aim to identify radiomics features that are insensitive to these differences and to investigate the potential of ComBat harmonisation in radiomics analysis.
Methods and materials: Publicly available credence cartridge radiomics (CCR) phantom data (13 CT scans of a 10-layer phantom) was used. Features were extracted using 2 toolboxes (RadiomiX and Pyradiomics). An overall concordance correlation coefficient (OCCC) with a cut-off of 0.9 was used to identify stable and "ComBatable" features. ComBat was applied using the scanner directly as the source of feature variation and also in a step-wise manner to remove intra-scanner and inter-scanner batch effects.
Results: 6% and 10% of RadiomiX and Pyradiomics features, respectively, were insensitive to differences in imaging vendors and/or reconstruction settings. After direct ComBat application, 21% and 14% of RadiomiX and Pyradiomics features, respectively, were found to be 'ComBatable'. Following step-wise ComBat application, 40% and 29% RadiomiX and Pyradiomics features, respectively, were "ComBatable".
Conclusion: We identified a subset of radiomics features that can be directly compared when the images being analysed were acquired using different vendors. ComBat harmonisation can significantly increase the number of radiomics features that can be used for analysis across varied cohorts. We propose a new methodology for performing radiomics analysis to produce more generalisable radiomics signatures.
Limitations: Taking reconstruction settings per scan as a source of a batch effect. The lack of scans generated by other commonly used scanners in the clinics. The lack of scans with the same settings acquired using different scanners.
Ethics committee approval: n/a
Funding: No funding was received for this work.
Author Disclosures:
A. Ibrahim: nothing to disclose
H. C. Woodruff: Shareholder at Oncoradiomics
P. Lambin: Advisory Board at Oncoradiomics, Shareholder at Oncoradiomics, Patent Holder at Oncoradiomics, Research/Grant Support at Oncoradiomics, Research/Grant Support at Varian medical, Research/Grant Support at ptTheragnostic, Research/Grant Support at Health Innovation Ventures , Research/Grant Support at DualTpharma, Advisory Board at Convert pharmaceuticals, Advisory Board at BHV, Advisory Board at Merck, Shareholder at Convert pharmaceuticals, Patent Holder at Oncoradiomics, Patent Holder at ptTheragnostic/DNAmito
J. E. Wildberger: Grant Recipient at Agfa, Grant Recipient at Bard, Grant Recipient at Bayer, Grant Recipient at GE, Grant Recipient at Optimed, Grant Recipient at Philips, Grant Recipient at Siemens
F. Mottaghy: nothing to disclose
R. Leijenaar: Shareholder at Oncoradiomics
R. Granzier: nothing to disclose
S. Primakov: nothing to disclose

RPS 113-12 09:36

CT imaging texture analysis: evaluation of the effect of reconstruction algorithms and kernels by different vendors

F. Calderoni[1], C. de Mattia[1], P. E. Colombo[1], A. Vanzulli[2], G. Feliciani[3], A. Sarnelli[4], A. Torresin[1]; [1]Milan/IT, [2]Segrate/IT, [3]Meldola/IT, [4]Forli/IT (francesca.calderoni@unimi.it)

Purpose: Iterative reconstruction (IR) techniques allow for radiation dose savings through noise reduction in CT image processing. This effect on imaging texture and on radiomic features (RFs) was analysed.
Methods and materials: The analyses were performed on Catphan® acquisitions on 3 scanners of different vendors (Siemens Healthineers, Philips Healthcare, and GE Healthcare) reconstructed with several combinations of an algorithm (filtered back projection (FBP) or IR), IR blending, and kernel.
RFs were extracted from the same cylindric region using IBEX.
The following variability sources were considered as relative discrepancy (RD) or relative standard deviation (RSD) of RFs values: FBP and IR algorithms with a fixed kernel, different blending, and different kernels with the same algorithm.
Results: The RD between FBP and IR was feature, vendor, and kernel dependent. The Siemens scanner showed the highest variability (up to 2,469%), while the Philips scanner the lowest (up to 73%).
The effect of blending values was strongly vendor dependent with RSDs higher than the variability due to FBP-IR reconstruction.
Considering similar kernels as in clinical situations, the greatest effect can be seen in the Philips scanner (up to 70%).
The RFs trend as a function of the different kernels suggests differences among kernels of the 3 vendors but also highlights the physical meaning that lies under some RFs definitions.
Conclusion: The imaging reconstruction step introduces a not negligible variability in the radiomic workflow.
A second reconstruction, other than the diagnostic one, could be proposed to reduce the variability affecting patient studies, fixing the most similar algorithm and kernel among the different vendors. Nevertheless, a residual difference which affects inter-scanner reproducibility is inevitable and must be taken into account.
Limitations: The use of a uniform target within the phantom.
Ethics committee approval: n/a
Funding: No funding was received for this work.
Author Disclosures:
F. Calderoni: nothing to disclose
G. Feliciani: nothing to disclose
C. de Mattia: nothing to disclose
P. E. Colombo: nothing to disclose
A. Vanzulli: nothing to disclose
A. Sarnelli: nothing to disclose
A. Torresin: nothing to disclose

RPS 113-13 09:42

The evaluation of CT image quality with patient-mimicking phantoms: the development of phantoms with anatomic detail and low-contrast lesions for detectability experiments

G. Ardila Pardo, J. Conzelmann, U. Genske, B. Hamm, M. Scheel, P. Jahnke; Berlin/DE (paul.jahnke@charite.de)

Purpose: Detectability experiments aim to assess the diagnostic performance of CT images and are of particular relevance for studying iterative reconstruction. The purpose was to develop anatomically realistic phantoms with low-contrast lesions for detectability experiments.
Methods and materials: Low-contrast lesions were digitally inserted into a neck CT image of a patient. The original and the manipulated CT images were used to create 5 phantoms: 1 phantom without any lesion and 4 phantoms with lesions of 10, 20, 30, and 40 HU contrast. Radiopaque 3D printing was used with potassium iodide doped ink (600 mg/mL). The phantoms were scanned with different CT settings. The lesion contrast was analysed with HU measurements. A 2-alternative forced-choice experiment was performed with 7 radiologists to study the impact of lesion contrast on detection accuracy (DA) and reader confidence (1=lowest, 5=highest).
Results: The developed phantoms reproduced the patient size, shape, and anatomy. The measured mean±SD contrast values of the low contrast lesions were 9.7±1.2 HU (10 HU contrast lesion), 18.2±2 HU (20 HU contrast), 30.2±2.7 HU (30 HU contrast), and 37.7±3.1 HU (40 HU contrast). Mean±SD detection accuracy and confidence values were not significantly different for 10 and 20 HU lesion contrast (82.1±6.3% vs 83.9±9.4%, p=0.863 and 1.7±0.4 vs 1.8±0.5, p=0.159). They increased to 95±5.7% and 2.6±0.7 for 30 HU lesion contrast and 99.5±0.9% and 3.8±0.7 for 40 HU lesion contrast (p<0.005).
Conclusion: A flexible method was developed to produce anatomically realistic phantoms for detectability experiments. The method creates the groundwork for the assessment of CT image quality in a clinical context.
Limitations: n/a
Ethics committee approval: IRB approval was obtained.
Funding: BMWi.
Author Disclosures:
P. Jahnke: Patent Holder at PhantomX GmbH, Shareholder at PhantomX GmbH, Research/Grant Support at BMWi
G. Ardila Pardo: nothing to disclose
J. Conzelmann: nothing to disclose
U. Genske: nothing to disclose
B. Hamm: nothing to disclose
M. Scheel: Patent Holder at PhantomX GmbH, Shareholder at PhantomX GmbH

RPS 113-14 09:48
Systematic CT protocol optimisation: how to improve patient safety with available CT techniques
P. Jahnke, J. Conzelmann, U. Genske, M. Nunninger, B. Hamm, M. Scheel, T. Diekhoff; *Berlin/DE (paul.jahnke@charite.de)*

Purpose: CT acquisition protocols frequently use available CT techniques inefficiently, but cannot be systematically optimised in clinical trials. The purpose was to develop a method to test and improve CT protocol settings for safer patient diagnostics with lower dose exposure.
Methods and materials: 7 patient-mimicking phantoms were used to simulate neck CT imaging of patients. 6 phantoms contained low-contrast lesions in different localisations in the parapharyngeal space and 1 phantom did not contain any lesion. The phantoms were scanned twice and different settings for tube voltage (ATPS, 120 kVp), tube current (ATCM SD 14, 10, and 7.5, and 150, 200, and 250 mA), pitch (0.6, 0.8, and 1.4), and image reconstruction (FBP, AIDR-3D) were systematically combined. Lesion detectability was assessed in a reader experiment with 14 radiologists. ROC statistics were performed and the area under the curve (AUC) was determined. The results were compared with a reference protocol (120 kVp, ATCM SD 7.5, pitch 0.8, AIDR-3D).
Results: All acquisitions using ATPS were performed with 100 kVp tube voltage. A tube voltage reduction from 120 to 100 kVp increased AUC values (p=0.002) and reduced the dose (p=0.005). In combination with 100 kVp tube voltage and AIDR-3D (but not with 120 kVp and FBP), an ATCM noise level increase reduced the dose (p<0.005) without decreasing AUC values (p>0.7). A protocol modification to ATPS, ATCM SD 10, pitch 0.8, and AIDR-3D reduced the dose by 71% and non-significantly increased mean±SD AUC values from 0.84±0.09 to 0.88±0.07 (p=0.215).
Conclusion: Patient-mimicking phantoms were used to systematically evaluate CT protocol settings. A 71% dose reduction was possible through the improved use of available CT techniques.
Limitations: n/a
Ethics committee approval: IRB approval was obtained.
Funding: BMWi.
Author Disclosures:
P. Jahnke: Patent Holder at PhantomX GmbH, Shareholder at PhantomX GmbH, Research/Grant Support at BMWi
J. Conzelmann: nothing to disclose
U. Genske: nothing to disclose
M. Nunninger: nothing to disclose
B. Hamm: nothing to disclose
M. Scheel: Patent Holder at PhantomX GmbH, Shareholder at PhantomX GmbH
T. Diekhoff: nothing to disclose

RPS 113-15 09:54
The interplay between radiation dose, convolution kernel, and advanced CT reconstructions
A. Hasegawa[1], T. Pan[2]; *[1]Chapel Hill/US, [2]Houston, TX/US (akira.hasegawa@algomedica.com)*

Purpose: To evaluate how noise reduction and image texture are affected by radiation exposure and convolution kernel in ADMIRE of Siemens and PixelShine of AlgoMedica based on deep learning.
Methods and materials: The homogeneous module of an ACR CT phantom was scanned at radiation exposures between 1.9 and 3.1 mGy (CTDI-16) and reconstructed with Hr40, Hr44, and Hr49 on Force using FBP and ADMIRE. The FBP images were processed by PixelShine.The noise power spectrum (NPS) of each reconstruction was computed. The centroid frequency ratio (CFR) of the NPS centroid frequencies and noise magnitude ratio (NMR) of the areas under the NPS curves of noise reduction and FBP were compared. A smaller CFR means more image blurring and a smaller NMR means more noise reduction. An ideal reconstruction should maintain CFR of close to 1 and NMR of close to 0.
Results: In all radiation exposures, ADMIRE reduced more noise with Hr49 (NMR=0.47) than Hr44 (0.67) or Hr40 (0.78) at the same image blurring (CFR≈0.8). Noise reduction by ADMIRE was not dependent on radiation exposure. The application of PixelShine reduced noise at the same image blurring for all kernels Hr49 (0.92 to 0.45), Hr44 (0.85 to 0.48), and Hr40 (0.87 to 0.56), and was less dependent on the selection of kernel compared to ADMIRE.
Conclusion: Both CFR and NMR were affected by the convolution kernel but not by radiation exposure in both methods. PixelShine (based on deep learning) had less centroid frequency shift for all kernels and was less dependent on kernel selection compared to ADMIRE.
Limitations: We didn't try all available convolution kernels. To change the dose levels, we only changed the tube current.
Ethics committee approval: n/a
Funding: No funding was received for this work.
Author Disclosures:
A. Hasegawa: Employee at AlgoMedica, Inc.
T. Pan: Consultant at Bracco Diagnostic, Inc.

08:30 - 10:00 **Room G**

Breast

RPS 102

Mammography and breast ultrasound: technical advances

Moderators:
C. S. Balleyguier; Villejuif/FR
N. Healy; Cambridge/UK

RPS 102-1 08:30
Detection of micro-calcifications of breast lesion on ultrasound elastography
S. Sampangi[1], Y. Kumarswamy[1], S. Swamy[1], M. Ashok Kumar[2], A. A. R. Kesari[1], I. Desai[1], N. K. Jain[1], N. Reddy[1]; *[1]Bangalore/IN, [2]Bikaner/IN (dr_sudhakar79@yahoo.com)*

Purpose: To identify and characterise breast lesions with micro-calcifications using ultrasound elastography.
Methods and materials: All patients with breast lesions and micro-calcifications on digital mammogram were subjected for ultrasound and elastography for further characterisation of the lesion. Siemens ACUSON S2000 machine with 14L5 and 9L4 probes were used for the ultrasound scan. Greyscale images of the lesions were described as per ACR BIRADS category. Elastography with VTI images were obtained in and around the lesion. VTI showed the lesion as soft or hard compared to adjacent parenchyma. Elastography/B Mode Ratio was calculated. E/B Ratio of 1 or <1 was considered as benign and > 1 was considered as malignant. Micro-calcifications with hypoechoic lesions were visualised, however in absence of hypoechoic mass, micro-calfications werenot seen in greyscale. VTI images showed micro-calcifications as bright dot like appearence in a hard tumour background along with E/B Ration > 1.
Results: Out of 105 breast lesions with micro-calcifications on a mammogram, the ultrasound scan could identify micro-calcifications in only 20 lesions. However, elastography identified 102 cases. On elastography, the micro-calcifications showed as bright spots in a dark or hard tumour background. Another 3 lesion showed it as a harder area. This gives confidence for radiologists to identify lesions even in the absence of a hypoechoic mass in the breast. Cases of DCIS without mass lesion are generally difficult to identify on the greyscale, but VTI will detect it as a hard area with bright specks of calcifications, like a starry sky appearance. These are also seen along the duct wall and cyst wall in fibro-cystic disease.
Conclusion: Elastography will detect micro-calcifications even in the absence of mass lesions on greyscale.
Limitations: Necrotic changes in breast lesion will be mask micro-calcification on elastography.
Ethics committee approval: n/a
Funding: No funding was received for this work.
Author Disclosures:
S. Sampangi: nothing to disclose
S. Swamy: nothing to disclose
Y. Kumarswamy: nothing to disclose
M. Ashok Kumar: nothing to disclose
A. A. R. Kesari: nothing to disclose
I. Desai: nothing to disclose
N. K. Jain: nothing to disclose
N. Reddy: nothing to disclose

RPS 102-2 08:36
Acoustic radiation force impulse elastography as an alternative to diffusion-weighted imaging for the characterisation of breast lesions
P. Kapetas[1], P. Clauser[1], S. Viganò[2], T. H. Helbich[1], P. A. T. Baltzer[1]; *[1]Vienna/AT, [2]Cernusco Sul Naviglio/IT (panagiotis.kapetas@meduniwien.ac.at)*

Purpose: Diffusion-weighted imaging (DWI) and acoustic radiation force impulse (ARFI) elastography are techniques investigating microstructural tissue properties. We hypothesised that the information provided by ultrasound-acquired ARFI and magnetic resonance imaging (MRI)-acquired DWI for breast lesion characterisation is largely redundant, and that ARFI could be applied similarly as DWI, skipping the additional MRI scan.

Methods and materials: 60 patients (18-84 years, mean 51.9), each with one breast lesion, underwent both breast ultrasound including ARFI and MRI including DWI. For each lesion, maximum shear wave velocity (SWV) and mean apparent diffusion coefficient (ADC) were recorded. Histology was the reference standard. Diagnostic performance was assessed with receiver operating characteristics (ROC) curve analysis. Independent predictors of malignancy were evaluated using multivariate logistic regression. Correlation between SWV and ADC was assessed by the Pearson correlation coefficient (r).
Results: Both ARFI and DWI showed high diagnostic performance in differentiating benign (n=15) from malignant (n=45) breast lesions as measured by the area under the ROC curve (0.817 and 0.863 respectively, p=0.535). The corresponding sensitivity and specificity for each modality was 88.9%, 73.3%, 80%, and 86.7%. Correlation analysis demonstrated a significant (p<0.001) moderate (r=-0.492) negative correlation between SWV and ADC. Multivariate logistic regression showed that the combination of ARFI and DWI did not improve the results of the single modalities.
Conclusion: There is significant correlation between ultrasound-acquired SWV and MRI-acquired ADC values of breast lesions. Since both modalities have a similar accuracy for the differentiation of benign from malignant lesions, application of ARFI elastography may obviate the need for an additional MRI examination including DWI for breast lesion characterisation.
Limitations: Limited patient number.
Ethics committee approval: IRB-approved, retrospective study. The need for an informed consent was waived.
Funding: No funding was received for this work.
Author Disclosures:
P. Kapetas: nothing to disclose
P. Clauser: nothing to disclose
S. Viganò: nothing to disclose
T. H. Helbich: nothing to disclose
P. A. T. Baltzer: nothing to disclose

RPS 102-3 08:42

Shear wave elastography stiffness as an independent predictor of axillary lymph node metastases in patients with invasive breast cancer

S. B. Grover[1], A. K. Nag[1], S. Patra[1], H. Grover[2], A. Katyan[1], S. K. Jain[1], A. K. Mandal[1]; [1]*New Delhi/IN,* [3]*New York/US (shabnamgrover@yahoo.com)*

Purpose: To evaluate shear wave elastography tumour stiffness as an independent predictor of axillary lymph node metastases in patients with invasive breast cancer.
Methods and materials: In this institutional review board-approved prospective cross-sectional study, 81 consenting female patients with newly diagnosed, biopsy-proven, single lesion, invasive breast cancer >15 mm diameter were recruited. Patients were examined on Siemens Acuson S-3000 using a 4-9 MHz linear probe. Having assessed SWE quality, the built-in colour overlay was placed, including tumour and surrounding tissue. SWE stiffness was obtained by placing ROI in the region of maximum stiffness on the colour map. At least three E-max values (kPa) were obtained for each tumour. Following surgical resection, tumour type, grade, and axillary lymph node involvement were evaluated at histopathology. Diagnostic performance of mean SWE stiffness for prediction of axillary LN metastases was evaluated using Chi-square test and ROC curve.
Results: Out of 81 interrogated tumours, 40 were axillary node-positive and 41 were negative. SWE stiffness values were higher in lymph node-positive cases (p<0.001). Using E-max cut-off value of >215 kPa for positive axillary LN metastases, sensitivity of 92.3%, false-positive rate of 7.7%, with calculated specificity 92.8%, PPV 92.3%, and NPV 92.8% were obtained.
Conclusion: SWE evaluated tumour stiffness is a reliable independent predictor of axillary lymph node metastasis in invasive breast cancer. Further validation of this technique can lead to its routine application for superior risk stratification and individualised management decisions regarding neoadjuvant chemotherapy and axillary lymph node dissection.
Limitations: Studies with larger cohorts are required for further revalidation of results.
Ethics committee approval: Informed consent obtained from all patients.
Funding: No funding was received for this work.
Author Disclosures:
S. B. Grover: Author at Vardhman Mahavir Medical College and Safdarjung Hospital
A. K. Nag: Author at Vardhman Mahavir Medical College and Safdarjung Hospital
H. Grover: Author at Mount Sinai West, New York, USA
A. Katyan: Author at Vardhman Mahavir Medical College and Safdarjung Hospital
S. K. Jain: Author at Vardhman Mahavir Medical College and Safdarjung Hospital
A. K. Mandal: Author at B R Ambedkar Medical College, Rohini, New Delhi,India
S. Patra: Author at Vardhman Mahavir Medical College and Safdarjung Hospital

RPS 102-4 08:48

Combination use of quantitative parameters for shear wave elastography and superb microvascular imaging to evaluate breast masses

E. J. Lee, Y.-W. Chang; *Seoul/KR (demian3923@naver.com)*

Purpose: To evaluate the diagnostic value of adding quantitative parameters of SWE and SMI to breast US in differentiating benign and malignant breast masses.
Methods and materials: 200 pathologically proven breast lesions in 193 patients were retrospectively reviewed using breast US with greyscale, SWE, and SMI. The AUC in the combination of BI-RADS, Emax, Eratio, and SMI_{VI} were compared using calculated cut-off values for two sets of cases. Set 1 included only downgrade C4a. Set 2 included upgrade of C3 and downgrade of C4a. The diagnostic performance was compared between greyscale US and US with the additional combination of quantitative parameters.
Results: There were 115 (57.5 %) benign lesions and 85 (42.5%) malignant lesions. Emax with a cut-off value of 84.45 kPa had the highest AUC value compared to Eratio of 3.35% or SMI_{VI} of 3.57%. In set 1, the combination of BI-RADS with Emax or SMI_{VI} had a significantly higher AUC value compared to BI-RADS alone (p<0.05). BI-RADS with the addition of Emax, Eratio, and SMI_{VI} had the best diagnostic performance compared to BI-RADS alone, with an accuracy of 84.0%. The specificity increased significantly from 46.1% (53 of 115) to 79.1% (91 of 115), and the sensitivity was slightly reduced but not statistically significant.
Conclusion: Combining all quantitative values of SWE and SMI with BI-RADS improved the diagnostic performance in differentiating between benign and malignant breast lesions.
Limitations: This study was a retrospective design and inter- or intraobserver variability was not evaluated. We only investigated the quantitative values of SWE and SMI.
Ethics committee approval: This retrospective study was approved by the institutional review board for ethical issues in clinical research.
Funding: This work received Soonchunhyang University research funding.
Author Disclosures:
E. J. Lee: nothing to disclose
Y.-W. Chang: nothing to disclose

RPS 102-5 08:54

What is the most predictive parameter in shear wave elastography to differentiate breast cancer and to predict tumour characteristics and immunohistochemical subtypes?

H. Kim, J. Lee, B. J. Kang, S. H. Kim; *Seoul/KR (kimhj2577@gmail.com)*

Purpose: To identify the most predictive parameter using shear wave elastography (SWE) to differentiate breast cancer and to predict tumour characteristics and immunohistochemical subtypes.
Methods and materials: From November 2018 to February 2019, conventional breast ultrasound (US) and SWE were consecutively performed in women with BI-RADS category of 3 or above breast lesions. A total of 211 breast lesions from 190 patients were enrolled for the study and BI-RADS categories and qualitative and quantitative SWE parameters for each lesion were prospectively obtained. Pathologic results including immunopathologic factors were evaluated. The diagnostic performance of each parameter and its correlation with immunohistochemical subtypes of breast cancer were analysed.
Results: Among the 211 breast lesions, there were 82 malignant and 129 benign lesions, and 69 invasive ductal cancer (IDC) and 142 noninvasive ductal cancer (non-IDC) lesions. Of all the SWE parameters, Emax showed the highest accuracy in differentiating malignancy from benign (AUC=0.891) and IDC from non-IDC (AUC=0.884). Also, Emax was less affected by the lesion depth and size. Poorly differentiated and PR-negative tumours showed higher Emax (p<0.05). Ki-67 positive breast cancer showed more heterogeneous shear wave (high SDmean) and colour distribution (p<0.05). KI-67 and CK5/6 positive breast cancers showed higher Emax/Efat ratio (p<0.05).
Conclusion: Emax is a relatively accurate and stable parameter to differentiate malignancy from benign and IDC from non-IDC. In addition, the Emax/Efat ratio and heterogeneous SWE colour distribution could be a predictive factor in differentiating Ki-67 positive breast cancer.
Limitations: Our research has been conducted using a relatively small sample size and limited within a single centre.
Ethics committee approval: n/a
Funding: No funding was received for this work.
Author Disclosures:
H. Kim: nothing to disclose
J. Lee: nothing to disclose
B. J. Kang: nothing to disclose
S. H. Kim: nothing to disclose

RPS 102-6 09:00
DIMASOS: a German multi-centre trial for density-indicated mammography sonography screening
S. H. Heywang-Köbrunner[1], A. Hacker[1], M. Hertlein[1], C. Mieskes[1], E. Mieskes[1], S. Elsner[2], A. Katalinic[2]; [1]Munich/DE, [2]Lübeck/DE
(sylvia.heywang@referenzzentrum-muenchen.de)

Purpose: Population-based centralised screening programs to date rely on mammography-screening only. However, even with latest digital technology, sensitivity drops strongly in the upper 5-15% density range. Feasibility and outcome of quality-assured density-adapted mammographic-sonographic screening is tested.
Methods and materials: Density is prospectively calculated on approximately 240,000 mammograms to select 30,000 patients with a density exceeding the upper 15% density range. These women are offered participation. Mammographic 1st, 2nd, and consensus readings are followed by independent combined mammographic-sonographic 1st, 2nds and consensus readings.
Results: For women with breast density > upper 15% range, incremental cancer detection, incremental false-positive rate, biopsy rate, and costs will be recorded. Acceptance by patients, feasibility for screeners, and quality assurance will be tested. Incremental detection of at least 60 cancers is expected.
Conclusion: A significant impact on screening effect is expected for women with very high breast densities.
Limitations: Due to wide availability of ultrasound, the ethical requirement of patient information in a randomised controlled trial design is impossible. Two different control groups are possible: either a historical group or a prospective parallel control group (completely anonymised) from women in the same SUs (selected by mammography unit or date).
Effect on interval cancer rate and stage distribution in the follow-up round will be evaluated after completion of the follow-up phase.
Ethics committee approval: Expected 11/2019.
Funding: The study is payed through the National German Innovation Fund.
Author Disclosures:
S. H. Heywang-Köbrunner: Author at Reference Center Mammography Munich
A. Hacker: Employee at Reference Center Mammography Munich
C. Mieskes: Employee at Reference Center Mammography Munich
M. Hertlein: Other at IT-Consultant
A. Katalinic: Author at Institut für Sozialmedizin Universität Lübeck
E. Mieskes: Employee at Reference Center Mammography Munich
S. Elsner: Employee at Institut für Sozialmedizin Universität Lübeck

RPS 102-7 09:06
Sonoelastography in the evaluation of fibrocystic breast disease
N. Jain, R. Rastogi*; Moradabad/IN (neha11aug@gmail.com)*

Purpose: Fibrocystic breast disease or fibroadenosis is a benign disease of the breast characterised clinically by mastalgia, firm palpable regions in the breast, and a suspicious palpable lump. Mastalgia is characteristically premenstrual and is partially or completely relieved with menstrual flow associated with decreased firmness. High-resolution ultrasonography (HRUS) is being utilised for differentiating benign from malignant breast diseases. Recently, sonoelastography, especially acoustic radiation forced impulse (ARFI) imaging, is being evaluated in breast imaging.
Methods and materials: This pilot study aimed to evaluate sonoelastography in fibrocystic breast disease and ARFI in differentiating normal from fibrocystic breast parenchyma.
30 breasts, 15 each with normal and clinically-suspected fibrocystic disease, were evaluated by sonoelastography using a high-resolution, linear-array transducer. Data from virtual touch tissue quantification (VTTQ) was collected from fibroglandular parenchyma in the axillary tail and superolateral quadrant of the breast in both normal and clinical disease groups, as fibrocystic breast disease is more common in the superolateral quadrant. The data obtained from the control group was then compared with that from clinically suspected cases of fibrocystic breast disease. The patients with a diagnosis of fibrocystic breast disease on sonoelastography were followed-up clinically or with tissue diagnosis.
Results: Sonoelastography picked up 10 out of 12 clinically/tissue-proven cases with elasticity values lower than that of the normal breast (usually less than 2m/sec)
Conclusion: Sonoelastography (both VTI and VTTQ) shows highly accurate results allowing for the confident diagnosis of fibrocystic disease, thus obviating the need for tissue diagnosis. Given the high prevalence of benign fibrocystic disease of the breast and high accuracy of sonoelastography, imaging can be used with high confidence in not only reaching the diagnosis but also in monitoring the treatment of disease, thus optimising the cost and duration of treatment.
Limitations: n/a
Ethics committee approval: n/a
Funding: No funding was received for this work.
Author Disclosures:
N. Jain: nothing to disclose
R. Rastogi: nothing to disclose

RPS 102-8 09:12
Does image fusion technique improve the sonographic and histopathologic detection rate of conventional B-mode occult MRI-detected breast lesions?
S. Nakano[1], K. Fujii[2], Y. Mouri[2], J. Kousaka[2], T. Ando[2], M. Goto[2], K. Suzuki[2]; [1]Aichi/JP, [2]Nagakute/JP (snakano1@aichi-med-u.ac.jp)

Purpose: MRI-guided breast biopsy aids in the histopathologic diagnosis of conventional B-mode (cB-mode) occult MRI-detected lesions. Recently, real-time virtual sonography (RVS), a coordinated US and MRI with electromagnetic tracking system, was developed. By using its imaging fusion technique, we can sonographically biopsy for cB-mode occult MRI-detected lesions without special technique. Our aim was to retrospectively evaluate the utility of second-look US using RVS for detection of cB-mode occult MRI-detected lesions.
Methods and materials: Between 2016 and 2018, 27 consecutive patients who underwent second-look US to identify cB-mode occult MRI-detected lesions were enrolled in this study. Second-look US using RVS was performed after an additional supine MRI.
Results: Of the 28 lesions in the 27 patients, all were re-identified in supine MRI and 24 (86%) were detected by second-look US using RVS. MRI morphology types of the 24 lesions were as follows: mass, 10; non-mass enhancement, 14; and focus, 4. US-guided biopsy under RVS or excisional biopsy demonstrated that of the 24 lesions, 8 (33%) were malignant and the remaining 16 (66%) were benign. Of the 8 malignant, 4 were DCIS, 3 were IDC, and one was ILC. All the subtype of invasive carcinomas were ER/PgR positive, HER2 negative, and Ki-67 negative. All 4 remaining US-occult lesions could be followed up under RVS after the enhancing area was marked on the breast surface using RVS.
Conclusion: The findings of our study suggest that second-look US using RVS with additional supine MRI could improve the sonographic and histopathologic detection rate of cB-mode occult MRI-detected lesions.
Limitations: Small number. Retrospective study. Single institute study.
Ethics committee approval: This pilot study was approved by the Institutional Review Board at our hospital. The written informed consent for this evaluation was obtained.
Funding: No funding was received for this work.
Author Disclosures:
S. Nakano: nothing to disclose
K. Fujii: nothing to disclose
Y. Mouri: nothing to disclose
J. Kousaka: nothing to disclose
T. Ando: nothing to disclose
M. Goto: nothing to disclose
K. Suzuki: nothing to disclose

RPS 102-9 09:18
Real-time MRI-US imaging fusion technique for breast lesion characterisation
A. Abate[1], R. Giovanazzi[2], C. Di Bella[2], S. de Beni[3], S. D'onofrio[3], M. Cereseto[3], G. Querques[2], V. Besostri[4], R. Corso[2]; [1]Lesmo/IT, [2]Monza/IT, [3]Esaote/IT, [4]Pavia/IT (abate.anna75@gmail.com)

Purpose: Evaluation of novel MRI-US fusion imaging technique based on model-adaptive artificial intelligence (AI) algorithms and focused on improving diagnostic confidence and multimodal-localisation of breast lesions.
Methods and materials: In 6 months, 80 female patients (mean age: 56 ys) underwent breast ultrasound (US), using MyLab9eXP (Esaote, Italy) with fusion-imaging technology (VirtualNavigator and BreastNav), linear probe, and dedicated tracking sensor.
On 22 out of 80 patients, with evident mammographic suspicion and negative US examination, diagnostic completion with MRI was performed in prone and supine position, after locating 9 skin-landmarks (SL) on the patients' breast, to evaluate morphological modifications in prone-supine change.
Results: In 22 MRI examinations, 27 lesions were identified by a target placed on MRI supine image. VirtualNavigator in all cases visualised the target on US through fusion-imaging with supine-MRI. Nevertheless, radiological daily workflow contemplates breast MRI with the prone patient. To manage the relevant deformations due to prone-supine change, a new fusion-imaging AI-modelling algorithm was developed (BreastNav). To assess algorithm accuracy in the two different positions, 5 out of the 22 acquired MRI, with different age and breast morphology, were selected. For each, one SL was identified on prone-MRI. BreastNav automatically determined the new SL position on supine-MRI and the accuracy (in terms of Euclidean error and RMSE) in the 3 dimensions was measured. This assessment enabled the AI-algorithm to be validated, as it responded correctly to the different SL positions with an average error of 1.14 cm.

Conclusion: The AI-modelling algorithm of BreastNav manages important deformations induced by a patient's different positions between US and MRI, in order to optimise lesion identification, visible mainly on MRI, directly on US and to guide subsequent biopsy procedures.
Limitations: n/a
Ethics committee approval: n/a
Funding: No funding was received for this work.
Author Disclosures:
A. Abate: Speaker at ASST Monza, Author at ASST Monza
R. Giovanazzi: Author at ASST Monza
C. Di Bella: Author at ASST Monza
S. de Beni: Author at ESAOTE
S. D'onofrio: Author at ESAOTE
M. Cereseto: Author at ESAOTE
G. Querques: Author at ASST Monza
V. Besostri: Author at ASST Monza
R. Corso: Author at ASST Monza

RPS 102-10 09:24

Digital breast tomosynthesis versus MRI in the detection and loco-regional presurgical staging of breast cancer: correlation with breast density and background parenchymal enhancement

S. Messina, A. Orlando, S. Busalacchi, L. Spatafora, G. Milia, F. Midiri, R. Ienzi, M. Midiri, T. V. Bartolotta*; Palermo/IT (silviamessina9106@gmail.com)*

Purpose: To assess the role of digital breast tomosynthesis (DBT) and MRI in detection and loco-regional presurgical staging (LoPreSS) of breast cancer (BC).
Methods and materials: 78 women (age: 32-76), undergone both DBT and breast MRI for biopsied suspicious breast lesions or for equivocal findings at conventional imaging, were divided into two groups on the basis of mammographic density (MD), in non-dense (A-B) and dense (C-D) breasts, and two groups according to the background parenchymal enhancement (BP), 1-2 and 3-4. Sensitivity, specificity, negative and positive predictive values (NPV and PPV), and accuracy in LoPreSS in unifocal, multifocal, multicentric and bilateral BC, were calculated.
Results: 28/78 lesions were benign and 48/78 malignant (17/48 unifocal, 9/48 multifocal, 20/48 multicentric, 2/48 bilateral). MRI showed higher sensitivity (100% vs 87,5%, p=0.0013), specificity (76,7% vs 46,7%, p=0.0001), PPV (87,3% vs 72,4%, p=0.0208), and NPV (100% vs 70%, p<0.0001) than DBT. MRI showed a significantly higher accuracy in LoPreSS than DBT for multicentric (100% vs 45%, p=0.0001), multifocal (100% vs 55%, p=0.0274), and bilateral (100% vs 50%, p=0.3173), but not for unifocal (82,3% vs 64.7%, p=0.2520) BC. 20/48 BC patients showed non-dense and 28/48 dense breasts. DBT showed higher accuracy in LoPreSS in the non-dense group (17/20- 85% -vs 9/28- 32.1%-p=0.0081). With MRI, no differences in LoPreSS between non-dense and dense breast were noted (95% vs 92,8 %, p=0), as well as between BPE 1-2 group and 3-4 group (93,5% and 94,1%, p=0.93) respectively. Among non-dense breasts, MRI and DBT showed no significant differences in preoperative staging accuracy (95% vs 85%; p=0.30).
Conclusion: In BC, LoPreSS breast MRI showed higher accuracy in dense breasts than DBT. No significant differences in non-dense breasts were noted.
Limitations: Single-centre study.
Ethics committee approval: n/a
Funding: No funding was received for this work.
Author Disclosures:
T. V. Bartolotta: nothing to disclose
S. Messina: nothing to disclose
M. Midiri: nothing to disclose
A. Orlando: nothing to disclose
S. Busalacchi: nothing to disclose
L. Spatafora: nothing to disclose
G. Milia: nothing to disclose
F. Midiri: nothing to disclose
R. Ienzi: nothing to disclose

RPS 102-11 09:30

Reduction of pressure sensor artifacts in the simultaneous acquisition of wide-angle breast tomosynthesis and mechanical imaging

P. Bakic[1], M. Dustler[2], A. D. A. Maidment[1], S. Zackrisson[2], A. Tingberg[2]; [1]Philadelphia/US, [2]Malmö/SE (predrag.bakic@pennmedicine.upenn.edu)

Purpose: Mechanical imaging (MI) maps tissue stiffness, which increases in breast tumours. The simultaneous acquisition of digital breast tomosynthesis (DBT) and MI combines the information about the anatomical structure and tissue stiffness of breast findings. This combination has the potential to reduce the number of false-positives and help avoid biopsies by resolving ambiguous DBT findings based upon their MI data. In simultaneous imaging, the MI pressure sensor is present during the DBT acquisition, producing visible artefacts. These artefacts may be reduced by preprocessing DBT projections, modifying the reconstruction algorithm, or designing radiolucent sensors. In this paper, we characterised artefacts seen in wide-angle DBT images with and without preprocessing.
Methods and materials: We have used a clinically available wide-angle DBT system to image a structured physical breast phantom on top of a commercial MI sensor. DBT images were acquired using the standard clinical protocol and automatic exposure control. We preprocessed DBT projections by flat fielding, using sensor images with and without the phantom. Images obtained with and without flat fielding were assessed visually by experienced medical physicists.
Results: Simultaneous DBTMI acquisition shows sensor artefacts in reconstructed images within ~1/3 of the phantom thickness above the detector. These artefacts are less prominent as compared to our previous study of simultaneous DBTMI using a narrow-angle DBT system. Flat-fielded images show substantially reduced appearance of artefacts, with slightly increased noise.
Conclusion: The simultaneous DBTMI imaging removes the requirement for two separate acquisitions. However, it produces noticeable artefacts due to the presence of the MI sensor. These artefacts overlap breast anatomical structures and may compromise diagnosis. Flat fielding of DBT projections substantially eliminates artefacts. Quantitative validation and method optimisation is ongoing.
Limitations: n/a
Ethics committee approval: n/a
Funding: Supported by the H2020 Marie Skłodowska-Curie Fellowship #846540.
Author Disclosures:
A. D. A. Maidment: nothing to disclose
S. Zackrisson: Speaker at Siemens, Research/Grant Support at Siemens
P. Bakic: nothing to disclose
M. Dustler: nothing to disclose
A. Tingberg: Research/Grant Support at Siemens

RPS 102-12 09:36

Impact of digital breast tomosynthesis (DBT) on dose when assessing breast masses

N. Anandan[1], M. A. McMahon[1], B. J. G. Dall[1], I. Haigh[1], Y. Chen[2], N. Sharma[1]; [1]Leeds/UK, [2]Nottingham/UK (nevine.anandan@nhs.net)

Purpose: The impact of DBT on dose when assessing masses.
Methods and materials: All women recalled between 13/11/15 and 29/07/16 following an abnormal screening mammogram had triple assessment and biopsy if required.
A DBT study was read within 6 weeks of assessment clinic. The number of additional mammographic views, doses (mGy), and DBT examination was recorded.
Statistics: Doses analysed in a mixed design, 2x2 ANOVA, looking at dose with and without DBT (within cases).
Results: 1,470 women attended screening assessment and 835 women consented. 810 had complete data on dose and screening outcome.
353 cases recalled for a mass (351 women) and 316 biopsies performed (314 women). 74 cancers identified.
Tomosynthesis/ultrasoud recommended 97 biopsies and 73/74 cancers would have been identified with one case of DCIS missed.
Significant effect of use of DBT, $F(1,339) = 4.80$, $p = .029$, $\omega = .11$ (within cases): mean dose without DBT was higher than with DBT.
When a biopsy was undertaken that tomosynthesis/ultrasound indicated should not have taken place, mean dose was higher without DBT.
When a biopsy was taken that tomosynthesis/ultrasound agreed should have taken place, there was no significant difference in dose without/with DBT.
Reduction in the number of films used, associated with the use of DBT, was analysed in a one way, between cases ANOVA looking at whether cases were biopsied or not. The overall reduction in the number of films used, associated with the use of DBT, was 3.61 (SD = 2.12).
Conclusion: DBT in assessment has the potential to reduce the dose and number of additional mammographic images in diagnostic workup of masses.
Limitations: This was a single-centre study.
Ethics committee approval: IRB approved the prospective study.
Funding: No funding received for this work.
Author Disclosures:
N. Anandan: nothing to disclose
M. A. McMahon: nothing to disclose
B. J. G. Dall: nothing to disclose
I. Haigh: nothing to disclose
Y. Chen: nothing to disclose
N. Sharma: nothing to disclose

RPS 102-13 09:42

Impact of a pressure-based flexible paddle in digital breast tomosynthesis on the participant and technologist

K. J. Schilling[1], M. van Lier[2], S. Muller[3]; [1]Boca Raton/US, [2]Amsterdam/NL, [3]Buc/FR (monique.van.lier@sigmascreening.com)

Purpose: Mammographic breast compression using compression paddles equipped with a pressure indicator (pressure-based compression) has not yet been reported for flexible paddles in digital breast tomosynthesis (DBT). We aimed to evaluate the effect of a new DBT pressure-based flexible paddle (DBT-PBFP) on the technologist and patient experience. The impact on radiation dose and compression parameters variability was also addressed.
Methods and materials: Women with a DBT appointment, agreeing with study participation, received PBFP-guided breast compression on a GE-Senographe-Pristina. Mean compression pressure (force over contact area) was visualised during compression to the technologist and participant using 8 LED's (2kPa per LED), aiming for an 8-14kPa target range. Compression parameters were retrospectively obtained from the study examinations and priors. The participant and technologist experiences were assessed using a questionnaire.
Results: From 94 participants, four-views conventional prior and study DBT examinations (total: 376 paired-views) and completed questionnaires were available. Technologists indicated that DBT-PBFP use eased explaining breast-compression (100%) and improved their workflow (97%). From all women, 89% would recommend DBT-PBFP-compression to friends. The compression force (mean±standard deviation) did not differ in CC-views (prior:82.3±20.6N, PBFP:86.4±34.2N, p=0.11), but increased in MLO-views (prior:85.2±21.9N, PBFP:103.1±31.5N, p<0.0001). Compression pressure variability decreased with 50% (p<0.0001) for CC-views and 34% (p<0.0001) for MLO-views, along with a decreased breast thickness (CC-view:8%, p<0.0001, MLO-view:10%, p<0.0001). Sub-group analysis (100 paired-views) showed overall average glandular dose reduction (prior:1.65±0.38mGy, PBFP:1.59±0.37mGy), with MLO-views as main contributor.
Conclusion: Using the new DBT-PBFP improved the participant and technologist experience and workflow while significantly reducing compression pressure variability, breast thickness, and average glandular dose.
Limitations: In some patients, a different DBT-system and/or technologist performed the study compared to prior examination, which may impact on the patient-comfort and radiation-dose comparability.
Ethics committee approval: Institutional review-board approved. Written informed-consent.
Funding: No funding was received for this work.
Author Disclosures:
M. van Lier: Employee at Sigmascreening, Shareholder at Sigmascreening
K. J. Schilling: Consultant at GE Healthcare, Investigator at GE Healthcare
S. Muller: Employee at GE Healthcare

RPS 102-14 09:48

What is the impact of intraoperative specimen tomosynthesis in determination of surgical margin of breast conserving surgery?

I. Başara Akin, G. Tokatli Camkerten, E. Akyol, A. Balci, M. Guray Durak, S. O. Aksoy, P. Balci; Izmir/TR (slbasara@yahoo.com)

Purpose: Breast conserving surgery (BCS) has become a routine procedure in early-stage breast cancer. Because of the risk of local recurrence, the most important aim of BCS is the removal of a malignant mass with no tumour margin. However, it has been shown that surgical margin negativity rates are still low. The sensitivity of specimen mammography (SMG) in terms of surgical margin negativity is low. Specimen tomosynthesis (STS) has increased the diagnostic efficacy lesion detection. The aim of this study was to determine the efficacy of STS added to SMG in the intraoperative process to evaluate the surgical margin in excised tissue.
Methods and materials: SMG and STS findings of BIRADS 4-5 specimens were evaluated retrospectively by two different observers. The observers were unaware of the histopathological outcome during the evaluation process. The SMG and the STS findings were compared in terms of BIRADS classification and histopathology. Inter- and intraobserver correlation analyses were performed. Chi-square test and compatibility Kappa (K) analysis were performed.
Results: 89 patients were included in this study. SMG-STS findings for observer 1 was K 0,80 (excellent) and for observer 2 was K 0,77 (good). Interobserver Ks were 0.48 and 0.43 (moderate), respectively. Sensitivities in SMG were 45% and 23%, the specificities were 90% and 74%, PPVs were 88% and 70%, NPVs were 50% and 42%, respectively. The sensitivities in the STS were 53% and 43%, specificities were 90% and 78%, PPVs were 87% and 48%, and NPVs were 61% and 49%, respectively.
Conclusion: In BCS, using STS in the intraoperative process provides the optimal evaluation of the surgical margin, a shortening of the duration of surgery, and a decrease in re-excision rates.
Limitations: Limited patients number.
Ethics committee approval: n/a
Funding: No funding was received for this work.
Author Disclosures:
G. Tokatli Camkerten: Author at Dokuz Eylül University School of Medicine, Department of Radiology
I. Başara Akin: Author at Dokuz Eylül University School of Medicine, Department of Radiology
E. Akyol: Author at Dokuz Eylül University School of Medicine, Department of Radiology
A. Balci: Author at Dokuz Eylül University School of Medicine, Department of Radiology
M. Guray Durak: Author at Dokuz Eylül University School of Medicine, Department of Pathology
S. O. Aksoy: Author at Dokuz Eylül University School of Medicine, Department of General Surgery
P. Balci: Author at Dokuz Eylül University School of Medicine, Department of Radiology

RPS 102-15 09:54

Association between patient and physical acquisition parameters and mammography positioning errors

M. Abdolell[1], N. Paquet[1], J. I. Payne[1], K. Tsuruda[2], O. Tong[1], P. Barnes[1], P. Brown[1], J. Caines[1], S. E. Iles[1]; [1]Halifax, NS/CA, [2]Oslo/NO (Sian.Iles@nshealth.ca)

Purpose: To identify which mammographic image positioning errors are associated with patient and physical acquisition parameters in the general screening population.
Methods and materials: Image quality assessments were performed on mammograms of 9259 subjects included in a population-based case-control study. The following mammography positioning errors were assessed (densitas qualityaiTM) on MLO and CC images from each subject's most recent screening exam: exaggeration, skin folds, portion cut-off, patient-related artefacts, posterior tissues missing, improper pectoralis muscle positioning, inadequate IMF, sagging, and proper height on image receptor. Logistic regression was used to model the presence of positioning errors as a function of patient/physical acquisition parameters including age, breast volume, and compression pressure partitioned into deciles. The Mantel-Haenszel test for linear trend was used to assess a dose-response relationship between the risk of errors and patient/physical acquisition parameters.
Results: When examining individual patient/physical acquisition parameters, patient age was found to be linearly associated with 10 of the 13 errors ($p < 0.05$), and breast volume and compression pressure were each found to be associated with 12 of the 13 errors ($p < 0.05$).
Conclusion: This study shows that patient and physical acquisition parameters, such as age, breast volume, and compression pressure, are related to elevated or diminished risk of mammography image positioning errors during a screening exam.
Limitations: This study requires external validation.
Ethics committee approval: REB Approval was received and a waiver of consent was granted.
Funding: There was no funding received for this specific study, but the images used in this study were obtained from a previously funded study.
Author Disclosures:
M. Abdolell: CEO at Densitas Inc.
P. Brown: nothing to disclose
J. I. Payne: Other at Densitas Inc.
K. Tsuruda: nothing to disclose
P. Barnes: nothing to disclose
N. Paquet: Employee at Densitas Inc.
S. E. Iles: nothing to disclose
O. Tong: nothing to disclose
J. Caines: Advisory Board at Densitas Inc.

08:30 - 10:00 **Room M 1**

Musculoskeletal

RPS 110

Cartilage, bone marrow oedema, tissue and body imaging

Moderators:
N.N.
E. Vassalou; Iraklion/GR

RPS 110-1 08:30

Sub-regional morphological assessment of normal and degenerative articular cartilage

R. Khandelwal[1], A. Kharat[1], K. Saoji[1], A. Jaju[1], D. Kumar[2]; [1]*Pune/IN,* [2]*Bangalore/IN (rachit.khandelwal@gmail.com)*

Purpose: To assess morphological changes in the sub-regions of knee articular cartilage in the presence of pathologic/degenerative or traumatic disease through automated and quantitative computation method.
Methods and materials: This prospective observational study was designed to assess 35 normal and 20 patients (chondromallacia patellae=8, osteoarthritis=7, and traumatic injuries with degraded cartilage=5). MR scanning was performed on 3T MAGNETOM Vida (Siemens Healthineers, Germany) using an 18-channel knee coil. Regional and sub-regional analysis of the cartilage in terms of morphological changes such as thickness and volume were performed using an MR chondral health (Version 2.1) work-in-progress (WIP) package provided by Siemens Healthineers.
Results: Cartilage was segmented in various zones and regions, which were colour demarcated, and quantitative measurements in terms of thickness and volume were performed. Mean thicknesses of the femur, patella, and tibia of normal subjects were1.63±0.22 mm, 2.11±0.38mm, and 1.51±0.20 mm, respectively, while mean volumes were 10.17±2.39, 3.11±0.79, and 3.74±0.85, respectively. Thicknesses in OA (femur=1.59 mm, tibia=1.45 mm), traumatic (femur-=1.59 mm, tibia=1.50 mm) and chondromallacia patellae (femur=1.57 mm, tibia=1.48 mm) patients were found to be slightly decreased compared to normal, while it was increased for the patella region (OA=2.15 mm, traumatic=1.97 mm, and chondrmallacia patellae=2.15 mm). A similar pattern was observed for volume, in OA (femur=9.52 ml, tibia=3.37 ml), traumatic (femur=9.04 ml, tibia=3.13 ml), and chondromallacia patellae (femur=9.24 mm, tibia=3.32 ml) patients were found to be slightly decreased compared to normal, while it was increased for the patella region (OA=3.18 ml, traumatic=2.7 ml, and chondromallacia patellae=3.20 ml). This evidenced the degenerative changes in the morphology of cartilage.
Conclusion: Automated cartilage segmentation and quantitative measurements in terms of thickness and volume have significantly reduced time and improved diagnostic accuracies quantitatively.
Limitations: A small sample size.
Ethics committee approval: Ethics committee approval obtained.
Funding: WIP loaned by Siemens under Master Research Agreement.
Author Disclosures:
R. Khandelwal: Speaker at Dr D Y Patil Hospital
A. Kharat: Consultant at Dr D Y Patil Hospital
K. Saoji: Consultant at Dr D Y Patil Hospital
A. Jaju: Consultant at Dr D Y Patil Hospital
D. Kumar: Employee at Siemens

RPS 110-2 08:36

The evaluation of cartilage degeneration using quantitative ultrashort echo time magnetisation transfer (UTE-MT): a feasibility study

J. Yang[1], H. Shao[1], Y. Ma[2], L. Wan[2], J. Du[2], G. Tang[1]; [1]*Shanghai/CN,* [2]*San Diego/US (yangjiaweitj@126.com)*

Purpose: To investigate the feasibility of using a quantitative ultrashort echo time magnetisation transfer (UTE-MT) technique to evaluate cartilage degeneration.
Methods and materials: 20 human anterolateral condyle specimens were obtained from total knee arthroplasty and then underwent MR scans on a clinical 3.0T scanner. 72 regions of interest (ROI) were manually drawn on specimens for UTE-MT measurement and the corresponding cartilage-bone regions were further divided into normal, mild, moderate, and severe degeneration groups based on histological measures of degeneration (Mankin scores) as a reference standard. 20 healthy volunteers and 15 osteoarthritis patients (the anterolateral condyle was involved) underwent MRI scans with UTE-MT and clinical sequences. The cartilage regions were grouped according to MRI Recht grades and UTE-MTR were obtained by drawing the ROI in the corresponding regions. The differences in quantitative results among different grades were compared.
Results: Ex vivo results showed that the UTE magnetisation transfer ratio (UTE-MTR) in the normal group was significantly different from the mild group (P=0.021), moderate group (P<0.001), and severe group (P<0.001). UTE-MTR strongly correlated with histological grades of cartilage degeneration (Mankin scores) (P=-0.678, P<0.001). In vivo results showed that UTE-MTR in the normal group was significantly different from the moderate group (P=0.02).
Conclusion: UTE-MT may provide a promising imaging biomarker with potential application in the diagnosis and monitoring of cartilage degeneration.
Limitations: MTR values are susceptible to many factors, including deviation fre-quencies, radio-frequency angles, and field intensities. We have not been confirmed using the corresponding histological measures of a degeneration in vivo study.
Ethics committee approval: The study was approved by the ethics committee at our research hospital (shsy-iec-ky-3964).
Funding: National Natural Science Foundation of China (81871325,81801656).
Author Disclosures:
J. Yang: nothing to disclose
H. Shao: nothing to disclose
Y. Ma: nothing to disclose
L. Wan: nothing to disclose
J. Du: nothing to disclose
G. Tang: nothing to disclose

RPS 110-3 08:42

Quantitative cartilage mapping using synthetic MR sequences: a comparative study of magnetic resonance image compilation (MAGiC) cartilage mapping and multi-echo T2 cartilage mapping

S. Rajan, V. K. Venugopal, M. Murugavel, V. Mahajan, H. Mahajan; *New Delhi/IN (drsriramrajan@gmail.com)*

Purpose: To compare a cartilage map created using synthetic MRI images using magnetic resonance image compilation (MAGiC) versus a conventional T2 multi-echo cartilage map. A comparison of normal and abnormal values.
Methods and materials: 30 subjects were scanned on a 3.0T scanner, first with multi-echo T2 cartilage map and then with a MAGiC sequence. 20 slices were obtained with the multi-echo and similar synthetic multi-echo images, with the MAGIC technique in a sagittal plane and reconstructed to yield cartilage maps. The T2 relaxation values were calculated by carefully placed ROIs on the weight-bearing segments of the medial (MFC) and lateral femoral cartilage segments (LFC) on both the multi-echo T2 maps and synthetic MR T2 maps. Pearson's correlation coefficient was calculated between these two sets of values.
Results: There was a moderate positive correlation between the T2 relaxation values generated on multi-echo T2W sequences and the synthetic MR generated T2 maps on both the medial and lateral femoral cartilage segments. Pearson's correlation coefficient (R) was 0.5365 and 0.5174 for MFC and LFC, respectively (p<0.05). The exact cartilage thickness was better seen on the synthetic MR images.
Conclusion: We conclude that a cartilage map could be created from virtual multiple echoes synthesised using a single MAGIC acquisition, resulting in both anatomical and cartilage map images.
Limitations: The small sample size.
Ethics committee approval: Approval was obtained from the institutional ethics committee.
Funding: No funding was received for this work.
Author Disclosures:
S. Rajan: nothing to disclose
V. K. Venugopal: Consultant at CARING, Other at Research collaboration, General Electric Company Research collaboration, Koninklijke Philips NV Research collaboration, Qure.ai Research collaboration, Predible Health

M. Murugavel: nothing to disclose
V. Mahajan: nothing to disclose
H. Mahajan: nothing to disclose

RPS 110-4 08:48

Regional bone mineral density assessed by statistical parametric mapping in patients with and without reoperation following instrumented lumbar spinal fusion: a case-control study

M. T. Löffler, A. Valentinitsch, C. Zimmer, Y.-M. Ryang, J. S. Kirschke; *Munich/DE (m_loeffler@web.de)*

Purpose: To opportunistically assess regional bone mineral density (BMD) at the lumbar spine using statistical parametric mapping (SPM) of existing CTs in patients with and without reoperation following instrumented lumbar spinal fusion (LSF).

Methods and materials: 17 patients (69.2±9.4 years) who had reoperation after y median 593 days (range 49–2,259) following LSF were matched to 17 patients (70.3±8.4 years) who did not have reoperation (matched by sex, age±5 years, and fused levels). In the hospital's records, patients without reoperation did not present with a sensory-motor deficit or severe pain at the last visit after a median follow-up of 135 days (range 5–1,129). Opportunistic screening of regional BMD was performed using SPM of ≥1 lumbar vertebra in preoperative or immediate postoperative CT. Vertebral bodies were segmented by our in-house algorithm. SPM involves normalisation to a common template and calculation of voxel-wise statistics in relation to a group of 18 young healthy individuals yielding T_{spm}-scores.
Results: Patients with and without reoperation presented normal BMD without significant difference (135.3±50.9 vs 132.1±51.6 mg/cm³). Compared to young healthy individuals, patients with and without reoperation showed equally reduced T_{spm}-scores (inferior vertebral region: -2.52±1.48 vs -2.53±1.40).
Conclusion: Opportunistic osteoporosis screening by SPM at the lumbar spine can be performed in presurgical CT even on a single vertebra, thus informing the surgeon about reduced BMD. In these matched groups undergoing LSF, regional BMD was not associated with the risk of reoperation as it was not in the osteoporotic range.
Limitations: Due to the retrospective design of this case-control study, loss of follow-up is a potential confounding factor.
Ethics committee approval: This retrospective study was approved by the IRB.
Funding: European Research Council (No 637164, iBack, ERC-2014-STG).
Author Disclosures:
M. T. Löffler: nothing to disclose
A. Valentinitsch: nothing to disclose
Y.-M. Ryang: nothing to disclose
J. S. Kirschke: Grant Recipient at ERC
C. Zimmer: nothing to disclose

RPS 110-5 08:54

The diagnostic accuracy of colour-coded virtual noncalcium dual-energy CT for the depiction of traumatic bone marrow oedema in sacral insufficiency fractures in comparison to MRI

C. Booz, I. Yel, L. Lenga, S. S. Martin, K. Eichler, R. Hammerstingl, T. J. Vogl[1], M. H. Albrecht; *Frankfurt am Main/DE*
(boozchristian@gmail.com)

Purpose: To evaluate the diagnostic accuracy of dual-energy CT virtual non-calcium (VNCa) reconstructions for the depiction of traumatic bone marrow oedema in sacral insufficiency fractures using MRI as a standard of reference.
Methods and materials: Data from 52 consecutive patients who had undergone third-generation dual-source dual-energy CT and 3T MRI within 7 days from January 2017-December 2018 due to low back pain were retrospectively analysed. 5 radiologists, blinded to clinical and MRI information, independently assessed a conventional grey-scale dual-energy CT series for fractures according to the Denis classification. After 8 weeks, readers re-evaluated all cases using colour-coded VNCa reconstructions for sacral bone marrow oedema. Quantitative analysis of CT numbers on VNCa reconstructions was performed by a sixth radiologist. Two additional experienced radiologists, blinded to clinical and CT information, defined the reference standard in consensus MRI reading sessions. Sensitivity, specificity, and the area under the curve (AUC) were primary indices for diagnostic accuracy.
Results: MRI revealed a total of 39 zones with focal traumatic bone marrow oedema in 27 patients. Fracture lines were detected in 12 patients on conventional grey-scale CT. In the qualitative analysis, VNCa showed high overall sensitivity (96%) and specificity (93%) for the depiction of bone marrow oedema. CT numbers obtained from VNCa were significantly different in zones with or without oedema (P<0.001). The overall AUC was 0.965. A cut-off value of -32 Hounsfield units provided a sensitivity of 92% and a specificity of 88% for differentiating bone marrow oedema.
Conclusion: Dual-energy CT VNCa reconstructions yield excellent diagnostic accuracy for colour-coded depictions of traumatic bone marrow oedema in sacral insufficiency fractures compared to MRI.
Limitations: The retrospective single-centre study design.
Ethics committee approval: This study was approved by the local IRB.
Funding: No funding was received for this work.
Author Disclosures:
C. Booz: Speaker at Siemens Healthinners
I. Yel: nothing to disclose
L. Lenga: nothing to disclose
S. S. Martin: nothing to disclose
K. Eichler: nothing to disclose
R. Hammerstingl: nothing to disclose
T. J. Vogl: nothing to disclose
M. H. Albrecht: Speaker at Siemens Healthineers, Speaker at Bracco

RPS 110-6 09:00

The effectiveness of methotrexate in the management of localised scleroderma (morphea) according to an ultrasound activity score

C. Vera-Kellet, R. Meza-Romero, C. Moll-Manzur, C. Ramírez-Cornejo, X. Wortsman; *Santiago/CL (xworts@yahoo.com)*

Purpose: Methotrexate (MTX) is a first-line treatment for morphea (cutaneous scleroderma). To date, no studies have evaluated the effectiveness of MTX in morphea considering colour Doppler ultrasonography. We aimed to assess the effectiveness of using MTX in patients with morphea according to ultrasound activity.
Methods and materials: A retrospective cohort study with 22 morphea patients treated with MTX was evaluated clinically and ultrasonographically (July 2014-July 2019). Clinical data, dose, and duration of treatment were correlated with an ultrasound activity score (UAS). The UAS was based on the presence of increased hypodermal hyperechogenicity and dermal-hypodermal hypervascularity, type of vessels, number, and the type of involved corporal segments in consecutive ultrasound examinations per patient. Statistics included Wilcoxon and Fisher exact tests, the odds ratio (OR), and the risk ratio (RR) with their 95% confidence intervals. Significance was set at 0.05.
Results: Between the first and second ultrasound, there was a significant decrease of one point of the UAS (p<0.05) and 7.9 times more chance of lowering the UAS in the group exposed to >15 mg/week of MTX versus the group exposed to ≤15 mg/week of MTX. However, between the first and last ultrasound, there was an increase in a point of the UAS (p<0.05), and only 3.6 times more chance of lowering the activity score in the group exposed to concentrations >15 mg/week of MTX. A non-significant decrease of the activity was detected in the group exposed to ≤15 mg/week of MTX.
Conclusion: A decrease of activity is seen in patients treated with MTX doses ≥15 mg/week, but there is a long-term loss of the effect of MTX.
Limitations: The small size of the sample.
Ethics committee approval: Approved by the ethics committee.
Funding: No funding was received for this work.
Author Disclosures:
X. Wortsman: nothing to disclose
R. Meza-Romero: nothing to disclose
C. Moll-Manzur: nothing to disclose
C. Ramírez-Cornejo: nothing to disclose
C. Vera-Kellet: nothing to disclose

RPS 110-7 09:06

Bone marrow oedema in the non-traumatic hip: high accuracy of dual-energy CT with water-hydroxyapatite decomposition imaging

W. Son[1], C. Park[1], H. S. Jeong[1], Y. S. Song[2], I. S. Lee[2]; *[1]Yangsan/KR, [2]Busan/KR (andywson@gmail.com)*

Purpose: To evaluate the diagnostic performance of dual-energy CT with water-hydroxyapatite (HAP) imaging for bone marrow oedema in patients with non-traumatic hip pain.
Methods and materials: 40 patients (mean age, 58 years; 16 male and 24 female) who underwent rapid kVp-switching dual-energy CT and MRI within 1 month from April 2018-February 2019 with hip pain but no trauma were enrolled. Two radiologists retrospectively evaluated 80 hip joints for the presence, extent (femoral head involved, head and neck, and head to intertrochanter), and severity (mild oedema, moderate, and severe) of bone marrow oedema on dual-energy water-HAP images. Water mass density (mg/cm³) on water-HAP images was determined with a region-of-interest-based quantitative analysis. MRI served as the standard of reference.
Results: Sensitivity, specificity, and accuracy of readers 1 and 2 for the identification of bone marrow oedema in water-HAP images were 85% and 85%, 93% and 73%, and 89% and 79%, respectively. The area under the receiver operating characteristic curve was 0.96 for reader 1 and 0.91 for reader 2 for the differentiation of the presence of oedema from no oedema. The optimal water mass density to classify the presence of oedema for reader 1 was 951 mg/cm³ with 93% sensitivity and 93% specificity, and for reader 2 was 957 mg/cm³ with 80% sensitivity and 80% specificity.
Conclusion: Dual-energy water-HAP images showed good diagnostic performance for bone marrow oedema in patients with non-traumatic hip pain.
Limitations: Only two readers were involved in this study. Subcortical zones could not be evaluated to reduce artefacts. We evaluated only water-HAP images without conventional CT images to minimise bias.
Ethics committee approval: This retrospective study was approved by IRB.
Funding: No funding was received for this work.
Author Disclosures:
W. Son: nothing to disclose
C. Park: nothing to disclose
H. S. Jeong: nothing to disclose
Y. S. Song: nothing to disclose
I. S. Lee: nothing to disclose

RPS 110-8 09:12

Early functional and morphological changes of calf muscles in delayed onset muscle soreness (DOMS) assessed with 7T MRI

R. Heiß, R. Janka, M. S. May, W. Wuest, T. Hotfiel, M. Uder, A. Nagel, F. W. Roemer*; Erlangen/DE (Rafael.Heiss@uk-erlangen.de)*

Purpose: To assess morphological and functional alterations of the skeletal muscle after induction of delayed onset muscle soreness (DOMS) using 7 Tesla (T) magnetic resonance imaging (MRI).
Methods and materials: DOMS was induced in 16 participants who performed a standardised eccentric exercise protocol of the calf muscles. 7T MRI including 2D T1w- (0.18x0.18x1 mm^3), 2D T2w-sequences (0.2x0.2x2 mm^3), T2-mapping (0.5x0.5x5 mm^3), and 3D quantitative susceptibility mapping (QSM, 0.7x0.7x0.7 mm^3) was acquired at baseline (prior the exercise), directly (t1), and 60 hours (t2) after the exercise. T2 signal intensity (SI), T2 values [ms], T1 SI, and computed quantitative susceptibility maps [ppb] were assessed in the medial (MG) and lateral gastrocnemius muscle (LG), in the soleus muscle (SM), and in the tibialis anterior muscle (AM).
Results: Directly after exercise (t1), T2 SI (p=0.03) and T2-values (p=0.03) had increased significantly in the LG, whereas no change was observed for MG, SM, or AM. At t2, T2 SI and T2-values of LG (p=0.001, p=0.02) and MG (p=0.04, p=0.03) had increased significantly compared to baseline. T1 SI and susceptibility did not change in any muscle at any time point. No structural muscle injuries could be visually detected, regardless of the degree of intramuscular oedema. Clinical parameters confirmed the induction of DOMS in every participant.
Conclusion: MRI at 7T allows the visualisation of DOMS immediately after the inducing exercise, whereas expected changes in susceptibility e.g. reflecting micro-haemorrhage could not be detected with quantitative susceptibility mapping.
Limitations: The limited number of patients.
Ethics committee approval: Institutional review board approval was obtained from Friedrich-Alexander-University Erlangen-Nuremberg, Germany.
Funding: Funded by the German Society of Musculoskeletal Radiology (DGMSR).
Author Disclosures:
R. Heiß: nothing to disclose
R. Janka: nothing to disclose
M. S. May: nothing to disclose
W. Wuest: nothing to disclose
M. Uder: nothing to disclose
A. Nagel: nothing to disclose
F. W. Roemer: nothing to disclose
T. Hotfiel: nothing to disclose

RPS 110-9 09:18

Clinical usefulness of cross-sectional imaging modalities in grading the severity of sarcopenia in liver cirrhosis patients and its impact on morbidity and mortality

H. A. Kamal, N. E. M. A. El Liethy*; Cairo/EG (hebakamala@gmail.com)*

Purpose: To assess the severity of sarcopenia in liver cirrhosis patients by quantifying muscle mass through CT at L3 level, measuring appendicular muscle thickness by musclo-skeletal ultrasound, then correlating their results with handgrip strength as representative of functional status.
Methods and materials: This study included 100 cirrhotic patients/30 controls who had a CT to calculate the psoas muscle cross-sectional area, volume, and muscle index, musculoskeletal ultrasound to calculate the anterior mid-arm/mid-thigh muscle thickness and quadriceps muscle index, and lastly handgrip strength calculated by dynamometry.
Results: This study included 130 subjects, 71 men and 49 females. Cirrhotic patients were graded into three groups according to a Child scoring system. The mean CT psoas volume, psoas surface area, and psoas muscle index for Child (A+B) were 25.44±6.96, 7.97±2.23, and 4.58±1.21, while for Child C were 15.85±6.02, 5.02±1.80, and 2.96±1.00. The musculoskeletal ultrasound mean mid-arm, mid-thigh, and quadriceps thickness index were 2.00±0.29, 2.93±0.33, and 1.69±0.17 for Child (A+B), while were 1.53±0.25, 2.30±0.45, and 1.36±0.26 for Child C. The quadriceps thickness index cut-off was 1.6750 $cm/m^2$and psoas muscle index cut off was 4.5 cm^2/m^2.
Conclusion: Psoas muscle index as well as appendicular muscle thickness measurements were well correlated with handgrip strength and proved to be independent prognostic factors for grading sarcopenia in cirrhotic patients.
Limitations: There are no normal values for muscle thickness among Egyptians. We didn't follow up patients after discharge for quality of life, readmissions, and post-hospital mortality.
Ethics committee approval: The study had been approved by the research ethics committee of the Faculty of Medicine at Cairo University in Egypt on201572016 in compliance with the Helsinki declaration (DoH-oct20081).
Written and informed consent was obtained.
Funding: No funding was received for this work.
Author Disclosures:
H. A. Kamal: nothing to disclose
N. E. M. A. El Liethy: nothing to disclose

RPS 110-10 09:24

Low skeletal muscle mass is a predictor of hospitalisation length in patients with a sternal fracture and concomitant injuries

H. G. Yavaş, A. Akçay, F. Ufuk*; Denizli/TR (huseyingokhanyavas@gmail.com)*

Purpose: Total muscle area (TMA) and psoas muscle area (PMA) at the L3 vertebrae level have been shown as strong indicators of skeletal muscle mass (SMM). Our aim was to investigate the prognostic significance of SMM in patients with sternal fractures and concomitant injuries due to blunt trauma on full-body computed tomography (CT).
Methods and materials: CT reports of patients who had full-body CT due to blunt chest trauma were analysed retrospectively from 01/01/2009-06/01/2019. Patients with sternal fracture were re-evaluated. TMA and PMA were measured separately at the L3 vertebrae level.
Results: A total of 55 patients with sternal fracture were evaluated. Isolated sternal fractures were detected in 20% (n=11) of the patients. The most common mechanism of injury was motor vehicle collisions (n=45) and the predominant fracture location was in the manubrium sterni (n=36). The most common injuries accompanying sternum fracture were rib fracture (n=30) and lung contusion (n=24). There was a statistically significant relationship between PMA (p=0.0001, r=-0.587, and r=-0.471, respectively) and TMA (p=0.0001, r=-0.376, and r=-0.263, respectively) values, and hospitalisation length and length of stay in an intensive care unit. There was a positive correlation between the sternal displacement grade (mild, moderate, and severe) and the death of the patient within one-month and the presence and thickness of a retrosternal haematoma. The presence of a retrosternal haematoma, vertebra corpus fracture, pneumothorax, haemothorax, splenic injury, and the inferior part of the sternum body fracture were significantly correlated with hospitalisation length.
Conclusion: Low TMA and PMA are strong predictors of hospitalisation length in patients with sternal fractures and concomitant injuries.
Limitations: The descriptive data was retrospectively collected. The number of patients was relatively low.
Ethics committee approval: Ethics committee approval obtained.
Funding: No funding was received for this work.
Author Disclosures:
A. Akçay: nothing to disclose
F. Ufuk: nothing to disclose
H. G. Yavaş: nothing to disclose

RPS 110-11 09:30

The assessment of intramuscular tissue perfusion in PRICE therapy using contrast-enhanced ultrasound (CEUS)

R. Heiß[1], M. Hoppe[2], C. Lutter[3], R. Forst[1], M. S. May[1], W. Wuest[1], P. D. M. Engelhardt[2], C. Grim[2], T. Hotfiel[1]; *[1]Erlangen/DE, [2]Osnabrück/DE, [3]Rostock/DE (Rafael.Heiss@uk-erlangen.de)*

Purpose: To investigate intramuscular tissue perfusion (ITP) in athletes before, during, and after PRICE-therapy in sport-specific conditions and to prove the hypothesis of reactive hyperemia after PRICE-therapy.
Methods and materials: 20 healthy athletes (11 female, 9 males: age 25±3; 21-30 years (mean±SD; range), BMI 23±3 kg/m^2) were randomised into a PRICE or control group. Quantifiable contrast-enhanced ultrasound (CEUS) was assessed to analyse microvascular blood flow of the anterior thigh (rectus femoris muscle, RF; vastus intermedius muscle, VI). Baseline perfusion measurements (T_0) were compared to exercise (cycling, T_1), intervention (PRICE or control (rest), (T_2)), and to 60 min follow-up (T_3). PRICE included rest, cryotherapy (3° celsius), compression (35 mmHg), and elevation.
Results: After cycling, an upregulation of ITP was observed in the VI and RF for both groups. The PRICE measurements revealed a decrease of ITP, corresponding to a 47% and 53% decrease in the VI (WiAUC, PE; p=0.01, n.s.) and a 50% and 72% decrease in the RF (p=0.037; p=0.002). In contrast, an increase of ITP was observed for the control group at T_1 and T_2. At T_3, the superficial RF (PRICE) revealed a significant persistent decrease of 15% and 50% (n.s.; p=0.003), whereas the RF (control) and VI (both groups) showed no significant changes to baseline conditions.
Conclusion: Our study highlights the fundamental impact of PRICE on ITP. PRICE applied after exercise leads to a downregulation of microvascular blood flow in superficial as well as deep muscle layers. The termination of PRICE is not associated with a reactive hyperemia.
Limitations: The imited number of participants. No cross-over design.
Ethics committee approval: IRB approval was obtained from Friedrich-Alexander-University Erlangen-Nuremberg, Germany. All participants signed an institutionally approved informed-consent document.
Funding: No funding was received for this work.

Author Disclosures:
R. Heiß: nothing to disclose
M. Hoppe: nothing to disclose
C. Lutter: nothing to disclose
R. Forst: nothing to disclose
M. S. May: nothing to disclose
W. Wuest: nothing to disclose
C. Grim: nothing to disclose
P. D. M. Engelhardt: nothing to disclose
T. Hotfiel: nothing to disclose

RPS 110-12 09:36
Evaluation of aortic inflammation on ^{18}F-FDG PET/CT in rheumatoid arthritis patients treated with biologic therapies
T. T. Dam, K. Okamura, T. Nakajima, Y. Yonemoto, T. Suto, H. Sakane, H. Chikuda, Y. Tsushima*; Maebashi/JP*
(trangbeo.fsh@gmail.com)

Purpose: Biologic therapies have been shown to reduce cardiovascular risk in rheumatoid arthritis (RA) patients. We evaluated the inflammatory activity of the ascending aorta in RA patients who received biologic treatment and to assess the RA-related factors that influence the aortic status.
Methods and materials: ^{18}F-fluorodeoxyglucose (FDG) positron emission tomography/computed tomography scans were performed for 64 patients with RA, before and after 6 months of biologic therapies, and the clinical characteristics were evaluated. The aortic wall inflammation was assessed by the FDG uptake in the ascending aorta, calculated as the standardised uptake value (SUV) and the target-to-background ratio (TBR). Clinical evaluations included the disease activity scores 28-joint erythrocyte sedimentation rate (DAS28-ESR) and several serum markers (ESR, C-reactive protein [CRP], anti-cyclic citrullinated peptide antibody [ACPA], and rheumatoid factor (RF).
Results: At 6 months, the decrease in TBR value was observed in 44% of patients. The FDG parameters, the DAS28-ESR, ESR, CRP, ACPA, and RF in the decreased-TBR group changed significantly after the treatment. The FDG parameters at baseline in the decreased-TBR group were significantly higher than those in the increased-TBR group. In a logistic regression analysis, the SUV at baseline was the most important contributor to the decrease in the aortic TBR after biologic treatment.
Conclusion: The cardioprotective effects of biologics might not apply to all RA patients. The SUV at baseline of the ascending aorta was identified as the significant factor predicting the improvement of the aortic wall inflammatory state after biologic therapies.
Limitations: The choice of biologic agents for RA patients might lead to bias since each drug has its own mechanism on RA pathogenesis.
Ethics committee approval: The study protocol was approved by the IRB of Gunma University Hospital.
Funding: No funding was received for this work.
Author Disclosures:
T. T. Dam: nothing to disclose
K. Okamura: nothing to disclose
T. Nakajima: nothing to disclose
Y. Tsushima: nothing to disclose
Y. Yonemoto: nothing to disclose
T. Suto: nothing to disclose
H. Chikuda: nothing to disclose
H. Sakane: nothing to disclose

RPS 110-13 09:42
Osteophytes, osteochondrosis, and a sclerotic aorta: to use or not to use lumbar spine dual-energy x-ray absorptiometry (DXA)?
M. Radeva[1], A. Malich[1], N. Valous[2], A. Pfeil[3], I. Papageorgiou[1]*;*
[1]Nordhausen/DE, [2]Heidelberg/DE, [3]Jena/DE
(ismini.e.papageorgiou@gmail.com)

Purpose: Dual-energy x-ray absorptiometry (DXA) quantifies the bone mass density (BMD) and reports it as the number of standard deviations from the sex-and-race-norm (T-score). Osteophytes, osteochondrosis, arthrosis, and atherosclerosis are known to contaminate the BMD, hence affecting the diagnostic accuracy. Although the confounding effect of large scale degeneration is undoubted, the influence of low-grade degenerative changes is a grey-zone in DXA interpretation.
The aim is to quantify the influence of low- and intermediate-grade degenerative changes in the lumbar spine DXA.
Methods and materials: A retrospective diagnostic accuracy study for N=446 female patients 65±14 years was conducted. The degree of spinal degeneration was described with a custom-developed point-system assessing arthrosis, end-plate osteophytes, and atherosclerotic plaques in a semiquantitative scale 0-4. The inclusion criteria were female, adult, and DXA from the hip and lumbar spine within 3 months. The index test was a DXA T-score. The ground truth was a hip total T-score <-2.5. Statistical analysis in MatLab 2017b.
Results: For spinal degeneration grade of 0/1/2/3/4, N=98/121/96/71/60 (total 446). Pearson's analysis returned a positive correlation between the spinal T-score and degeneration rate (P 0.0004).
The ROC analysis showed that, in the absence of degeneration (grade 0), DXA of the spine was a very sensitive surrogate marker for osteoporosis (AUC 0.97), sensitivity/specificity (Se/Spe) 100/81%. This declined upon low- or intermediate-grade degenerative changes, grade-1 AUC 0.83 (Se/Spe 91/67%), Fisher p<0.0001; grade-2 AUC 0.66 (Se/Spe 54/72%), Fisher p=0.03.
Conclusion: Even low- or intermediate grade degenerative changes in the lumbar spine significantly influence the sensitivity of DXA and should be considered as a significant confounding factor in the diagnosis of osteoporosis.
Limitations: The retrospective design not adjusted for other confounding factors.
Ethics committee approval: The study was approved by the local ethics committee.
Funding: No funding was received for this work.
Author Disclosures:
I. Papageorgiou: nothing to disclose
M. Radeva: nothing to disclose
N. Valous: nothing to disclose
A. Pfeil: nothing to disclose
A. Malich: nothing to disclose

RPS 110-14 09:48
MRI lumbosacral spine: is the workload really justified? An audit of indications and referral patterns at a tertiary care hospital
A. Faryad, A. Mansoor, M. Masood*; Lahore/PK*
(mahjabeentafazzul@gmail.com)

Purpose: To evaluate the clinical indications of MRI for the lumbosacral spine; referral sources and appropriateness of requests with respect to the appropriateness criteria of the American College of Radiology for MRI in low back pain patients.
Methods and materials: This study was conducted in the MRI centre of the radiology department, Mayo Hospital Lahore, which is a tertiary care hospital. From July 1, 2019-August 31, 2019, about 1,285 MRIs were done, of which 303 (23%) were MRI lumbosacral spine for low back pain. We included 200 patients between ages 18-80 years who were referred from different sources with a complaint of low back pain within a period of 2 months in our study. These were then assessed for indications and appropriateness criteria.
Results: Out of 200 patients who underwent MRI lumbosacral spine for LBP within a period of 2 months, 32.5% requests were “usually appropriate”, 24.5% “may be appropriate”, and 43% were “usually not appropriate” according to the appropriateness criteria of the American College of Radiology.
Conclusion: Judicious use of MRIs in patients with low back pain is necessary to avoid wastage of resources and a burden on healthcare facilities.
Limitations: No local guidelines available regarding appropriateness.
Ethics committee approval: Ethics committee approval was sought.
Funding: No funding was received for this work.
Author Disclosures:
A. Mansoor: nothing to disclose
A. Faryad: Author at Mayo Hospital Lahore, Speaker at Mayo Hospital Lahore
M. Masood: nothing to disclose

RPS 110-15 09:54
Synthetic imaging MAGIC (magnetic resonance image compilation) applications beyond the brain
R. Vadapalli[1], A. S. Vadapalli[2]*; [1]Hyderabad/IN, [2]London/UK*
(rammohanvsv@gmail.com)

Purpose: To elucidate the emerging clinical applications of MAGIC (magnetic resonance image compilation) beyond the brain.
Methods and materials: 79 subjects aged from 28-64 years with a M:F ratio of 3:2 who were referred for MR examinations for neck mass (n=3), pelvis (n=16), knee pain (n=19), hip pain (n=9), shoulder injury (n=11), ankle and foot pain (n=16), and wrist and hand (n=5) were included in the study.
MR imaging protocols were supplemented with the MAGIC sequence with 6 image contrasts. T1, T2, PD, STIR, DIR, and PSIR with quantitative T1 and T2 R1.R2 maps in 4 minutes.
The images were randomised and independently assessed for diagnostic quality, morphologic legibility, and diagnostic radiologic findings. The MAGIC T2 quantitative maps of the knee and hip with ROIs on cartilage were compared with cartigram maps.
Results: The overall diagnostic quality of synthetic MR images was non-inferior to conventional MR imaging on a 5-level Likert scale (P<0.001).

The legibility of synthetic and conventional morphology agreed in >95%.
Morphological findings like joint effusion, erosions, chondromalacia, ligament, tendon injuries, meniscal and labral tears, and sacroiliitis showed acceptable concordance.
STIR and DIR views of MAGIC contributed the maximum for detections of sacroiliitis, tenosynovitis, and chondromalacia, and so as quantitative T2 maps of MAGIC. Interobserver variability was in acceptable limits (Cohen's kappa 0.9).
Conclusion: Synthetic MR imaging quality was similar to that of conventional joint and MSK imaging with the facility of additional contrast views: STIR, PSIR and DIR quantitative T1, T2, R1, and R2 maps thus increasing the sensitivity and specificity.
Limitations: The small sample size.
Ethics committee approval: Waiver from ERB as it is a supplementary sequence to conventional imaging.
Funding: No funding was received for this work.
Author Disclosures:
R. Vadapalli: Consultant at GE Healthcare, Speaker at Philips health care
A. S. Vadapalli: nothing to disclose

08:30 - 10:00 **Room M 2**

Artificial Intelligence and Machine Learning

RPS 105

Artificial intelligence and machine learning of the lungs

Moderators:
O. Weinheimer; Heidelberg/DE
N.N.

RPS 105-K 08:30
Keynote lecture
N.N.

RPS 105-1 08:40
Deep learning to increase lung cancer detection in chest x-rays: a retrospective cohort analysis of national lung screening trial participants
H. Yoo[1], K. H. Kim[1], S. Park[1], M. Kalra[2]; [1]Seoul/KR, [2]Boston, MA/US
(hyunsuky@lunit.io)

Purpose: To verify whether lung cancer detection can be improved if radiologists use an artificial intelligence (AI) algorithm in a chest x-ray (CXR) screen setting.
Methods and materials: The testing was based on the data from the ACRIN of the National Lung Screening Trial (NLST) (n=5491), a multicentre cohort of current and formerly heavy smokers. We estimated the performance of radiologists in detecting lung cancer diagnosed at baseline (T0) or first (T1) study year if the AI algorithm was used during initial radiologic evaluation and compared it with raw radiologist performance. The algorithm used in this study was a deep learning-based model (Lunit INSIGHT CXR1) trained from an external dataset, which produced an abnormality score that ranged from 0-100%, reflecting the probability that the lesion was malignant. A threshold abnormality score of 30% was adopted as the cut-off for classification. TNM stage, size, location, and overlapping anatomical areas in CXR of the lesion detected by radiologists and the algorithm were compared.
Results: Radiologists with the AI algorithm showed a significantly higher detection rate (73.5%(64.0%-83.0%)[61/83] vs. 53.0%(42.3%-63.7%)[44/83]; P<0.001) than without the algorithm. The lesions missed by radiologists but found by the algorithm mostly had no annotated abnormalities (6/17) or abnormalities that did not warrant further workup (8/17). There was no significant difference in TNM stage, size, location, and overlapping anatomical areas between lung cancer found with and without the algorithm.
Conclusion: The detection rate of the radiologists with AI significantly improved compared to raw radiologists. Using AI during lung cancer screening may lead to earlier diagnosis, due to the detection of nodules not suspected by radiologists.
Limitations: Because of retrospective design of our study, AI analysis was performed after radiologist reading.
Ethics committee approval: n/a
Funding: No funding was received for this work.
Author Disclosures:
H. Yoo: Author at Lunit, Investigator at Lunit, Employee at Lunit
K. H. Kim: Employee at Lunit, Investigator at Lunit, Author at Lunit
S. Park: Author at Lunit, Investigator at Lunit, Employee at Lunit
M. Kalra: Grant Recipient at NIH (R57), Siemens Healthineers, Riverain Inc.

RPS 105-2 08:46
AI-based non-small cell lung cancer detection and segmentation on CT images with RECIST functionality
S. Primakov[1], A. Ibrahim[1], S. Sanduleanu[1], G. Wu[1], H. Gietma[1], L. Hendriks[1], O. Morin[2], H. C. Woodruff[1], P. Lambin[1]; [1]Maastricht/NL, [2]San Francisco/US
(s.primakov@maastrichtuniversity.nl)

Purpose: Localising and delineating lung tumours is essential for radiotherapy planning and various quantitative imaging workflows. However, manual contouring is highly laborious and time-consuming, as well as being prone to variability and poor reproducibility. To address these issues we created a fully automated pipeline for detecting and segmenting lung tumours on CT images.
Methods and materials: Multicentric CT images from 1,043 NSCLC patients with expert delineations of the gross tumour volume were used to train, test, and validate our detection and segmentation method. A three-step approach was developed, consisting of data pre-processing, lung isolation, and tumour segmentation. A pre-processing algorithm was developed with regard to hardware and acquisition parameters. A 2D U-net type convolutional neural network with test-time augmentation and volumetric post-processing was trained on 936 CT scans. We evaluated model performance on the remaining 107 scans by using a Dice similarity coefficient (DSC), Jaccard index (J), and 95th Hausdorff distance (H95th). In addition, we implemented the RECIST and volumetric-RECIST (VRECIST) functionality.
Results: On the external validation dataset, we achieved a median slice-wise detection accuracy of 0.99 (IQR=0.01), a specificity of 0.99, and a sensitivity of 0.90. Generated segmentations achieved an average DSC of 0.81, median of 0.88 (IQR = 0.12), average J of 0.71, median of 0.78 (IQR = 0.19), and H95th of 6 mm.
Conclusion: The proposed pipeline can potentially provide a low-cost, observer-independent, and reproducible method for the detection and segmentation of lung cancers on CT images. Moreover, it can be used for automated tumour response evaluation using RECIST or VRECIST.
Limitations: The ground truth depended on the quality of doctor's contours.
Ethics committee approval: n/a
Funding: European Program H2020 (PREDICT-ITN-766276); KWF Kankerbestrijding 12085/2018-2.
Author Disclosures:
S. Primakov: nothing to disclose
A. Ibrahim: nothing to disclose
H. C. Woodruff: Shareholder at Oncoradiomics
P. Lambin: Shareholder at Oncoradiomics, Shareholder at Convert pharmaceuticals, Patent Holder at Oncoradiomics, Patent Holder at ptTheragnostic/DNAmito, Research/Grant Support at Varian medical, Research/Grant Support at Oncoradiomics, Research/Grant Support at ptTheragnostic, Research/Grant Support at Health Innovation Ventures, Research/Grant Support at DualTpharma
G. Wu: nothing to disclose
L. Hendriks: nothing to disclose
O. Morin: nothing to disclose
S. Sanduleanu: nothing to disclose
H. Gietma: nothing to disclose

RPS 105-3 08:52
Automated detection of primary lung cancer of all stages and associated metastases on FDG-PET/CT using three retina U-Net algorithms
T. J. Weikert[1], P. Jäger[2], J. Bremerich[1], G. Sommer[1], B. Stieltjes[1], S. Yang[1], K. H. Maier-Hein[2], A. W. Sauter[1]; [1]Basel/CH, [2]Heidelberg/DE
(thomas.weikert@usb.ch)

Purpose: To develop and evaluate Retina U-net algorithms with a different fore- and background balance for the detection of primary lung tumours of all stages and associated lymphatic and non-lymphatic metastases on FDG-PET-CTs.
Methods and materials: We selected 364 patients with histologically confirmed lung cancer that underwent FDG-PET/CT between 01/2010-06/2016. The dataset comprised tumours of all stages according to the 8th edition of TNM classification in lung cancer. To establish a standard of reference, all lung tumours (T), lymphatic metastases (N), and distant metastases (M) were manually segmented as 3D-volumes using the transverse, fused whole-body PET/CT series. The dataset was split in a training (n=216), validation (n=74), and testing dataset (n=74). We trained and validated three Retina-U-net-based algorithms on (A) solely T-lesions, (B) T&N-lesions, and (C) T,N&M-lesions. We evaluated the performance of the algorithms for detection of all lesions at

multiple classifier-thresholds, calculating sensitivity, specificity, false-positive findings-per-case (FPC), area-under-the-ROC, and free-response-ROC-curves.
Results: We found very good detection rates of more than 90% for T3 and T4 lesions at low FPCs of 1.1 for the algorithm (C) trained on T,N&M-lesions. Performance of the algorithms (A) and (B) were worse. The detection rate of M-lesions in approach (C) was 72.3 %.
Conclusion: The algorithms presented in this study can serve as a foundation for automated detection of TNM-lesions in PET/CTs. This can reduce the rate of missed lesions. Training on all T,N&M-lesions yielded better results than training on solely T- or T&N-lesions.
Limitations: There was no distinction of T-/N- and M-lesions by the algorithm. 3D image segmentation for the establishment of ground truth was complete by only two readers.
Ethics committee approval: Written informed consent was waived by the Swiss regional ethics committee (project number: 2016-01649).
Funding: No funding was received for this work.
Author Disclosures:
T. J. Weikert: nothing to disclose
P. Jäger: nothing to disclose
J. Bremerich: nothing to disclose
G. Sommer: nothing to disclose
B. Stieltjes: nothing to disclose
S. Yang: nothing to disclose
K. H. Maier-Hein: nothing to disclose
A. W. Sauter: nothing to disclose

RPS 105-4 08:58
Evolving UNet architecture for lung cancer segmentation
S. Thulasi Seetha[1], K. Driessens[2], H. C. Woodruff[2], U. Pastorino[1], E. Bertocchi[1], P. Lambin[2]; [1]Milan/IT, [2]Maastricht/NL
(s.thulasiseetha@maastrichtuniversity.nl)

Purpose: Automatic image segmentation through deep learning currently requires a laborious trial-and-error search for a bespoke network architecture. Our aim was to automate this search using an evolutionary algorithm we named gNEAT (gradient-based NEAT) and test it for lung cancer segmentation.
Methods and materials: gNEAT searched for a fitting neural network starting from a fixed, UNet-based, outer-skeleton and evolves the convolutional blocks within it. The computational complexity of training each candidate network through gradient descent was offset by using a proxy dataset (a resizing of the original images) during the search. By grouping similar networks as species, diversity was kept intact. gNEAT's incremental growth feature allowed a compact architectural search and removed the need for a customised initialisation. We also evaluated the influence of the model augmentation trick on the hand-designed and the model generated by gNEAT.
We tested the approach on the open-source lung-1 CT imaging data containing manually delineated tumours.
Results: The final model evolved by gNEAT yielded higher Dice scores than a through trial-and-error designed model (based on domain knowledge). Moreover, the augmented models have a better Dice score on both validation and test set.
Conclusion: gNEAT may replace the laborious but necessary task of hand-designing task-specific deep network architectures. The outcome also suggests that the performance of a model can be boosted by augmenting its depth.
Limitations: gNEAT is computationally complex and the generational approach taken can be difficult to parallelise efficiently.
Ethics committee approval: n/a
Funding: Funding from European Program H2020 (PREDICT - ITN - n° 766276).
Author Disclosures:
S. Thulasi Seetha: nothing to disclose
H. C. Woodruff: Shareholder at Oncoradiomics
U. Pastorino: nothing to disclose
P. Lambin: Research/Grant Support at Varian Medical, Research/Grant Support at Oncoradiomics, Research/Grant Support at ptTheragnostic, Research/Grant Support at Health Innovation Ventures, Research/Grant Support at DualTpharma, Other at Oncoradiomics, Other at BHV, Other at Merck, Other at Convert Pharmaceuticals, Shareholder at Oncoradiomics SA, Shareholder at Convert Pharmaceuticals SA, Patent Holder at Oncoradiomics, Patent Holder at ptTheragnostic/DNAmito
K. Driessens: nothing to disclose
E. Bertocchi: nothing to disclose

RPS 105-5 09:04
The effectiveness of deep learning combined with multiple tumour-related antigen autoantibodies to diagnose lung cancers at T0-TⅡ stages
Q. Meng[1], J. Ding[2], X. J. Chen[1]; [1]Zhengzhou/CN, [2]Beijing/CN
(mengke436@163.com)

Purpose: To estimate the value of combining deep learning (DL) with seven tumour-related antigen autoantibodies (7-TAAbs) to diagnose lung cancers (LC) at T0-TII stages.
Methods and materials: 136 patients who underwent LDCT and serum 7-TAAbs pre-operative tests were reviewed and analysed by deep learning (DL). The inclusion criteria for the study are as follows: 1) chest CT revealed one or more indeterminate pulmonary nodules, 2) no history of tuberculosis, 3) no history of lung cancer, and 4) no currently known extrathoracic malignancies. The sensitivity, specificity, accuracy, and receiver operating characteristics curve of diagnosing LC among DL, 7-TAAbs, and DL and/or 7-TAAbs were analysed.
Results: The positive expression rate of 7-TAAbs in LC patients was 45.4% (54/119), which had no relation to the gender or age of patients and size or type of nodule, TNM stage, and CT signs (all $P > 0.05$), but was related only to the type of pathology. The predictive ability of 7-TAAbs in LC diagnosis was better than that of DL or DL and 7-TAAbs, which had the best specificity, YI, +LR, PPV, and SUV. The performance of DL or 7-TAAbs for LC screening had a higher sensitivity, accuracy, YI, and lower FNR than those of DL and 7-TAAbs.
Conclusion: The 7-TAAbs was the best method for diagnosing LC and showed good performance for screening when assisted by DL, which could benefit scaled LDCT screening of LC.
Limitations: The limitations for this retrospective single-centre study was selection bias according to small number of patients and lack of tumour control group
Ethics committee approval: This single-centre study protocol was approved by the Affiliated Tumor Hospital of Zhengzhou University Medical Ethics Committee according to the established legal regulations.
Funding: No funding was received for this work.
Author Disclosures:
Q. Meng: nothing to disclose
J. Ding: nothing to disclose
X. J. Chen: nothing to disclose

RPS 105-6 09:10
Lung screening assistance: how to cut down the false-positive rate and detect lung cancer earlier (a retrospective study)
S. Lopez[1], P. Fillard[2], Y. Diascorn[1], B. Padovani[1]; [1]Nice/FR, [2]Palaiseau/FR
(stephanie.lopez@univ-cotedazur.fr)

Purpose: Is it possible to significantly reduce false-positive candidates while detecting all true-positive cases, considering prior chest CT-scans? What about detecting lung cancer earlier?
Methods and materials: In our retrospective study based on the NLST dataset, we included 1,102 patients with 3 annual chest CT-scans (T_0, T1, and T_2): 104 being diagnosed with cancer at T_2 and 998 with no cancer evidence 3 years after the last CT-scan. We developed an AI algorithm based on neural networks using these 3 CT-scans to predict the cancer status.
Results: We developed an AI algorithm that detected all cancers at T_2 (100% sensitivity).
Considering the CT-scan at T_2 only, algorithm specificity is 64% compared to 22% for radiologists (+42%). When considering the prior (T_0 and T_1), AI specificity was 82% versus 58% for radiologists (+24%). Based on the data, this implies that the AI would reduce the number of unnecessary exams by half. The same AI algorithm executed on scans at T_1 was able to classify correctly 76% of the cancer-positive patients at T_2, while radiologists screened positively 70% of them (+6%). AI specificity was measured at 80% versus 25% for radiologists (+55%) at T_1.
Conclusion: Our preliminary results show that radiologists could be provided with reliable guidance based on AI to detect cancer earlier (76% and 64%, respectively, 1 and 2 years before).
The data indicates many patients with negative biopsies that then developed cancer 1 or 2 years later. The reasons remain unclear and further research should focus on automated nodule detection and guided biopsies.
Limitations: The NLST dataset is large but geographically limited to a North American screening population.
Ethics committee approval: n/a
Funding: This work was supported by UCAJEDI (French National Research Agency grant) ANR-15-IDEX-01.
Author Disclosures:
S. Lopez: nothing to disclose
P. Fillard: nothing to disclose
Y. Diascorn: nothing to disclose
B. Padovani: nothing to disclose

RPS 105-7 09:16

Impact of computed tomography reconstruction kernel selection on the performance of deep learning based lung nodule detection

S. K. Verma[1], S. Vaidya[2], K. Vaidhya[2], D. S. Mahra[2], K. C. Kaluva[2], A. Chunduru[2], S. Dhawan[3]; [1]Delhi/IN, [2]Bengaluru/IN, [3]New Delhi/IN (dr.sdhawan@gmail.com)

Purpose: To evaluate the relationship between computed tomography reconstruction kernels and the sensitivity of deep learning algorithms for lung nodule detection. We attempted to understand consistencies and discrepancies for the same.

Methods and materials: A 20-layer deep residual convolutional neural network based on 3D Feature pyramid networks was trained and validated on 888 CTs from the LIDC-IDRI dataset for lung nodule detection. The LIDC-IDRI dataset had a good mixture of CTs with different reconstruction kernels: soft-tissue (58%), lung (27%), and sharp (13%).

100 pairs of CTs with soft-tissue and lung kernels were randomly sampled from the NLST dataset. Ground truth for the same studies was annotated by a pair of junior and senior radiologists, with the AI's prediction used as priors.

A post-study analysis was done to measure the relationship between sensitivity and the reconstruction kernels (soft-tissue and lung) used in the CTs from NLST at different false-positive rates.

Results: The AI showed a sensitivity of 88% at 1 FP/scan for detection of >= 4 mm nodules on 177 LIDC-IDRI CTs when compared against the consensus of 3 out of 4 radiologists, and a sensitivity of 75% at 1.5 FPs/scan for 100 lung kernel CTs and 75% at 1.6 FPs/scan for 100 soft-tissue kernel CTs from NLST with AI + radiologists as ground truth.

The difference in performance by the AI in soft-tissue kernel CTs and lung kernel CTs was not found to be statistically significant as the one-way ANOVA revealed p=0.9938 and p=0.90, respectively, for sensitivity and false-positives per scan.

Conclusion: Deep learning algorithms are proving to be robust in the detection of lung nodules between CTs reconstructed from different kernels.

Limitations: The analysis of differences.

Ethics committee approval: Ethics committee approval obtained.

Funding: No funding was received for this work.

Author Disclosures:
S. Vaidya: Founder at Predible Health
S. K. Verma: nothing to disclose
S. Dhawan: nothing to disclose
K. Vaidhya: Employee at Predible Health
D. S. Mahra: Employee at Predible Health
A. Chunduru: Founder at Predible Health
K. C. Kaluva: Employee at Predible Health

RPS 105-8 09:22

The influence of kernel reconstruction and nodule size in computer-aided detection (CAD) of lung nodules

A. Paternain Nuin, I. Soriano Aguadero, P. Malmierca Ordoqui, A. C. Igual Rouilleault, L. García Del Barrio, J. Larrache, J. C. Pueyo Villoslada, G. Bastarrika Alemañ; Pamplona/ES (alberpanu@gmail.com)

Purpose: To determine the impact of two different reconstruction filters in the performance of a commercially available computer-aided detection (CAD) software for lung nodule detection.

Methods and materials: 78 patients who underwent a low-dose chest CT scan for lung cancer screening were prospectively recruited. Each scan was read by a radiologist and by a CAD software (syngo.CT Lung CAD, Siemens Healthineers) using filter reconstructions for soft tissues (kernel A) and for lung parenchyma (kernel B). Nodules less than 3 mm in size were excluded from the analysis. The detection rate (DR) of both reconstructions was analysed according to the nodule size, considering a diameter of 6 mm as clinically relevant. The consensus between the radiologist and CAD software was set as the reference standard. Features like nodule composition, location, and relation to anatomical structures were also evaluated. Data analysis was performed with a Chi-square test and Student t-tests. A p-value <0.05 was considered statistically significant.

Results: 301 lung nodules were detected. Overall, kernel A had significantly higher DR (65.1%) than kernel B (56.8%) (p<0.01), even considering the pulmonary nodules larger than 6 mm (DR of 85.7% vs 77.1%, respectively, p<0.01). There were no significant differences in the average number of false-positive results per scan (1.33 for kernel A vs. 1.00 for kernel B, p=0.21).

Conclusion: In the evaluated CAD system, the use of a soft tissue reconstruction filter allowed for higher detection rates than the lung parenchyma filter with a similar number of false-positive results, even for clinically relevant nodules.

Limitations: A small sample size.

Ethics committee approval: Ethics committee approval obtained.

Funding: No funding was received for this work.

Author Disclosures:
A. Paternain Nuin: nothing to disclose
I. Soriano Aguadero: nothing to disclose
P. Malmierca Ordoqui: nothing to disclose
G. Bastarrika Alemañ: nothing to disclose
A. C. Igual Rouilleault: nothing to disclose
L. García Del Barrio: nothing to disclose
J. Larrache: nothing to disclose
J. C. Pueyo Villoslada: nothing to disclose

RPS 105-9 09:28

A comparison of lung nodule detection sensitivity of deep learning algorithms in comparison with 3 radiologists of varying experience levels

K. C. Kaluva[1], S. Vaidya[1], V. K. Venugopal[2], S. Rajan[2], P. S. Shad[3], V. Mahajan[2], H. Mahajan[2], A. Raj[1], S. Upadhyay[1]; [1]Bengaluru/IN, [2]New Delhi/IN, [3]Delhi/IN (vasanthdrv@gmail.com)

Purpose: To compare the performance of deep learning algorithms for lung nodule detection against 3 independent radiologists of different experience levels (28 yrs, 20 yrs, and 14 yrs) on a retrospective chest CT dataset of 240 patients

Methods and materials: In a retrospective clinical validation study, three independent radiologists were required to annotate 240 chest CTs for all visible nodules between 5-30 mm in size. The annotations were compared with outputs of a deep learning algorithm (Predible Health) for nodule detection

All nodules were sub-classified as having consensus among 1, 2, or 3 radiologists. The deep learning algorithm was individually tested on nodule datasets with varying consensus levels. When testing on the 2/3 and 3/3 consensus dataset, we marked the 1/3 consensus nodules as irrelevant findings and did not penalise the algorithm for its detection.

Results: After considering for overlaps, there were a total of 146 nodules marked by the radiologists. The algorithm had a sensitivity of 96% (47/49) on nodules with 3/3 consensus and sensitivity of 91.1% (72/79) on nodules with 2/3 consensus, both at 1 false-positives per scan. The algorithm had an overall FROC score of 0.91 on nodules with 3/3 consensus and 0.86 on nodules with 2/3 consensus. Combining the algorithms' findings with each radiologist' and comparing with the consensus of the other two as ground truth, we observe an increased sensitivity ranging from 5 to 20%.

Conclusion: This study demonstrates that lung nodule detection algorithms can improve the sensitivity of radiologists by as much as 20%, helping them report quicker.

Limitations: A possible improvement in study design if nodules without consensus can be adjudicated by an experienced thoracic radiologist.

Ethics committee approval: Required Ethics Committee approvals were obtained for the study.

Funding: Funded by Predible Health.

Author Disclosures:
S. Vaidya: Founder at Predible Health
K. C. Kaluva: Employee at Predible Health
H. Mahajan: Founder at Mahajan Imaging, Research/Grant Support at General Electric Company, Research/Grant Support at Koninklijke Philips NV, Research/Grant Support at Qure.ai, Research/Grant Support at Predible Health
V. Mahajan: Research/Grant Support at General Electric Company, Research/Grant Support at Koninklijke Philips NV, Research/Grant Support at Qure.ai, Research/Grant Support at Predible Health
V. K. Venugopal: Consultant at Mahajan Imaging, Research/Grant Support at General Electric Company, Research/Grant Support at Koninklijke Philips NV, Research/Grant Support at Qure.ai, Research/Grant Support at Predible Health
S. Rajan: nothing to disclose
P. S. Shad: nothing to disclose
A. Raj: Employee at Predible Health
S. Upadhyay: Employee at Predible Health

RPS 105-10 09:34

Classification of lung opacities in supine chest radiographs: artificial intelligence approach (external algorithm evaluation) versus a radiological assessment

J. Rueckel[1], W. G. Kunz[1], B. Hoppe[1], M. Notohamiprodjo[2], F. Meinel[3], C. C. Cyran[1], M. Ingrisch[1], J. Ricke[1], B. O. T. Sabel[1]; [1]Munich/DE, [2]Tübingen/DE, [3]Rostock/DE (johannes.rueckel@googlemail.com)

Purpose: We evaluated an AI algorithm aiming to automatically classify basal lung opacities in SCXRs according to underlying pneumonia or pleural effusions. Algorithm accuracy was compared with radiologist's (board-certified) diagnostic performance.

Methods and materials: The algorithm was trained on publicly available datasets. A retrospectively identified evaluation dataset was analysed (166 patients with SCXR and CT scan both within 90 minutes without any intervention

in between). Radiologists evaluated SCXRs according to following reading-scores: 0="no pneumonia/effusion", 1="possible pneumonia/effusion" and 2="highly suspected pneumonia/effusion".
Algorithm performance was quantified by receiver-operating curves (ROCs), hereby statistically compared with radiologist's operating points characterised by sensitivity/specificity and corresponding 95%CIs.
Results: Radiologists achieved a maximum diagnostic accuracy for pneumonia detection up to 0.87 (95%CI 0.78-0.93) when considering only the SCXR-reading-score 2 as positive for pneumonia. Radiological assessment achieved non-significant numerically higher results compared with algorithm ROCs (AUROC 0.737/0.796/0.834 with reference standard CT/SCXR-reading-score 0 and 1 as negative for pneumonia/SCXR-reading-score 1 and 2 as positive for pneumonia).
Regarding pleural effusion detection, there was no significant difference between the radiologist's diagnostic accuracy (sensitivity/specificity/PPV/NPV/accuracy 0.67/0.69/0.71/0.68) and the AI algorithm (AUROC 0.740/0.847/0.883 with reference standard CT/SCXR-reading-score 0 and 1 as negative for pleural effusions/SCXR-reading-score 1 and 2 as positive for pleural effusions).
Conclusion: Considering the minor level of performance differences between the AI algorithm and radiological assessment, we regard AI to be a promising clinical decision support tool in clinical routine.
Limitations: Limitations mainly refer to the labelling of the underlying public datasets used for algorithm training, but also to the limited number of radiological readers not allowing for inter-reader variability analysis.
Ethics committee approval: Approval was obtained for this study.
Funding: Funding by/in cooperation with Siemens Healthineers
Author Disclosures:
J. Rueckel: nothing to disclose
W. G. Kunz: nothing to disclose
B. Hoppe: nothing to disclose
M. Notohamiprodjo: nothing to disclose
F. Meinel: nothing to disclose
C. C. Cyran: nothing to disclose
M. Ingrisch: nothing to disclose
J. Ricke: nothing to disclose
B. O. T. Sabel: nothing to disclose

RPS 105-11 09:40

Takeaways from the validation of an AI-based malignancy likelihood estimation for lung cancer screening when used on routine CT studies in a tertiary care hospital

V. Chaudhry[1], V. Saxena[1], S. Vaidya[2], D. S. Mahra[2], K. Vaidhya[2], A. Chunduru[2], B. Aggarwal[3]; [1]*Delhi/IN*, [2]*Bengaluru/IN*, [3]*New Delhi/IN* *(vivek_saxena67@hotmail.com)*

Purpose: To assess the performance of a deep learning-based malignancy likelihood estimation system trained on screening data from the National Lung Cancer Screening Trial (NLST) on a retrospective dataset of biopsy-proven studies from a large tertiary hospital in North India. The retrospective clinical validation dataset consisted of cases with primary cancers (64%), metastatic cancers (13%), and benign conditions (23%).
Methods and materials: The deep learning algorithm was trained on 1,245 scans from the NLST trial with pathologically proven ground truths to determine the malignancy status of a lung nodule. Retrospective data of 123 patients over 20 months who underwent CT-guided lung biopsy were chosen as suitable for the validation study. All patient studies were evaluated on follow-up scans to ensure conformance with biopsy results.
Results: The AI model showed a sensitivity of 75% (95% CI: 64%-83%) on 95 malignant nodules with a PPV of 86% (95% CI: 79%-90%). It is notable that 6 studies that appeared negative on histological findings were correctly predicted by the AI model as malignant, as confirmed by follow-up scans and re-biopsy. The AI model had a specificity of 58% (95% CI: 37%-76%) on 28 benign nodules with an NPV of 40% (95% CI: 29%-51%).
Conclusion: The algorithm can be positioned as an adjunct tool to the histology report that sometimes suffers an error rate due to erroneous sampling. Cancer screening settings only account for a limited context in training data due to specific inclusion criteria and hence further enhancement using a larger and more diverse training dataset is required before it can be used in routine practice.
Limitations: A studying mechanism of failure by the AI algorithm.
Ethics committee approval: Ethics committee approved.
Funding: Funded by Predible Health.
Author Disclosures:
S. Vaidya: Founder at Predible Health
V. Chaudhry: nothing to disclose
V. Saxena: nothing to disclose
B. Aggarwal: nothing to disclose
D. S. Mahra: Employee at Predible Health
K. Vaidhya: Employee at Predible Health
A. Chunduru: Founder at Predible Health

RPS 105-12 09:46

Deep learning-based automatic biomarkers extraction from chest CT in diffuse interstitial lung diseases: a correlation study with pulmonary function tests

M. Colevray, P.-J. Lartaud, O. Nempont, T. K. Y. Broussaud, V. Cottin, L. Boussel*; Lyons/FR (marion.colevray@yahoo.fr)*

Purpose: Lung volume monitoring is essential to assess the evolution of pulmonary fibrosis in diffuse interstitial lung diseases (DILD), however, current automatic software often fails to accurately segment lungs.
We aimed to develop a deep learning-based automatic segmentation tool to quantify lungs parameters on unenhanced chest CT and validate the results in comparison with pulmonary function test (PFT) parameters.
Methods and materials: A 3D-U-net convolutional neural network was trained on 90 randomly selected unenhanced chest CT scans of patients presenting with DILD and validated on 50 others (sex ratio M/F=34/16, mean age=60±15.2 years). The mean Dice coefficient and root mean squared error (RMSE) were calculated on the validation dataset. The network was then applied on 1,171 CT exams (from 424 adult DILD patients, sex-ratio M/F=256/168, mean age=64.6±13.29 years) and the following parameters were calculated: total lung volume (CT_{vol}), mean (CT_{dens}), kurtosis (CT_{kurt}), and skewness (CT_{skew}) of lung density. Pearson correlation coefficients (r) and regression analysis were performed to assess the relationship between CT and PFT parameters (forced vital capacity (FVC), total lung capacity (TLC), and carbon monoxide diffusing capacity (DLCO)).
Results: On the validation dataset, the mean Dice was 0.97±0.01 (range 0.91-0.99) with an RMSE of 0.007 l.
The mean CT_{vol} was 3.33±1.23 l with an overestimation of FCV (2.51±0.91 l) and an underestimation of TLC (4.18±1.34 l). Very good correlations were found between CT_{vol} and FVC and TLC (r=0.87 and 0.85, respectively, p<0.0001). DLCO was poorly correlated with CT parameters with r-values of -0.31, 0.48, and 0.51 (p<0.0001) for CT_{dens}, CT_{kurt}, and CT_{skew}, respectively.
Conclusion: Our deep learning-based automated segmentation method allows for the accurate quantification of lung volume on chest CT with a good correlation with FVC and TLC.
Limitations: n/a
Ethics committee approval: n/a
Funding: No funding was received for this work.
Author Disclosures:
M. Colevray: nothing to disclose
P.-J. Lartaud: nothing to disclose
O. Nempont: nothing to disclose
T. K. Y. Broussaud: nothing to disclose
V. Cottin: nothing to disclose
L. Boussel: nothing to disclose

RPS 105-13 09:52

Automatic pleural effusion detection on chest x-ray as a triage tool

J. J. Visser[1], M. Rossius[1], Y. Blinder[2], M. Cohen-Sfady[2], C. Brestel[2], E. Ziv[2], A. Akselrod-Ballin[2], E. Elnekave[3], E. Goz[4], E. Zvi[4], R. Wities[4]; [1]*Rotterdam/NL*, [2]*Kibbutz Shefayim/IL*, [3]*Petach Tikva/IL*, [4]*Shefayim/IL* *(m.rossius@erasmusmc.nl)*

Purpose: A shortage of radiologists, combined with the progression of radiological training toward cross-sectional exams, has combined to create a growing gap in the time to CXR reporting. An automatic chest x-ray (CXR) triage tool could mitigate the clinical consequences of interpretation delays. One common corollary sign of acute disease is the presence of pleural effusion. Our purpose was to validate an AI based CXR-pleural effusion detection algorithm.
Methods and materials: 488 consecutive CXRs were included in the analysis. Each study was scored algorithmically for the detection of pleural effusion. A gold standard was established independently by an expert radiologist with 10 years of clinical experience.
Results: 105/488 cases showed pleural effusion. The algorithm achieved 92.4% sensitivity and 90.1% specificity. In this series, the corresponding positive predictive value was 71.9% and the negative predictive value was 97.7%.
Of note, 64/105 of the positive cases were accompanied by other findings of acute disease such as consolidation. 13/38 of the false-positive results were, in fact, positive for acute consolidations. All 8 false-negative cases involved small pleural effusions.
Conclusion: We observed an excellent capability for automatic detection of pleural effusion, which in this random sample was highly correlated with other findings of acute cardiopulmonary disease. Further investigation and development is warranted to accomplish more comprehensive triage capability for chest x-rays.
Limitations: The retrospective nature of the study. A gold standard based on single chest x-ray interpretation.
Ethics committee approval: Institutional Review Board approval was obtained.
Funding: No funding was received for this work.

Author Disclosures:
J. J. Visser: nothing to disclose
E. Elnekave: Employee at Zebra Medical Vision
Y. Blinder: Employee at Zebra Medical Vision
M. Cohen-Sfady: Employee at Zebra Medical Vision
C. Brestel: Employee at Zebra Medical Vision
E. Ziv: Employee at Zebra Medical Vision
A. Akselrod-Ballin: Employee at Zebra Medical Vision
M. Rossius: nothing to disclose
E. Goz: Employee at Zebra Medical Vision
E. Zvi: Employee at Zebra Medical Vision
R. Wities: Employee at Zebra Medical Vision

08:30 - 10:00 **Room M 3**

Interventional Radiology

RPS 109

Liver malignancies: HCC and metastases

Moderators:
E. Pinto; Liverpool/UK
N.N.

RPS 109-1 08:30
Palliative ablation by CT brachytherapy in hepatic metastatic NET
F. Feldhaus[1], H. Jann[1], M. Jonczyk[1], G. Wieners[1], U. Fehrenbach[1], M. Pavel[1], B. Gebauer[1], B. Wiedenmann[1], T. Denecke[2]; [1]*Berlin/DE,* [2]*Leipzig/DE (felix.feldhaus@charite.de)*

Purpose: Hepatic metastases of gastroenteropancreatic neuroendocrine tumours (GEP-NETs) may induce prognosis-relevant complications in an otherwise stable systemic disease after resection of the primary. The present study should determine the period by which the CT-guided high-dose-rate brachytherapy (CT-HDRBT) of rapidly growing liver metastases can delay the onset of palliative systemic therapy with an otherwise stable disease course.
Methods and materials: In this retrospective, monocentric observational study, a total of n=23 patients (n=37 CT-HDRBT sessions) from one nationwide ENETS centre were included. In addition to parameters described in previous studies (local tumour control (LTC), progression-free survival (PFS), and overall survival (OS)), this study intended to determine the delay of a therapy escalation by individual, highly selective CT-HDBRT in oligotopic hepatic progression (due to ENETS-tumour board vote).
Results: For n=23 patients (n=37 CT-HDRBT sessions) with GEP-NET hepatic metastases, the median follow up was 31 months, range 6-87, and OS was 82% after 84 months. The median LTC was 16 months (quartiles, 7.5-34), the median PFS (RECIST oriented) was 10.5 months (quartiles 2.0-24.25), and the median OS was 27.5 months (quartiles, 10.0-38.25). No further escalation of therapy (watch and wait- and/or SSA-therapy) after solitary HDRBT was necessary in 11/23 cases (48%). In the case of systemic therapy, a delay of a mean 16 (±16) months and a median of 12 months (range, 0-60 months) compared to an immediate escalation of therapy was achieved.
Conclusion: In patients with disseminated GEP-NET and oligotopic hepatic progression within essentially stable disease, CT-guided interstitial HDRBT can delay the onset of systemic therapy escalation. As shown in a pilot study, CT-HDRBT is a reliable and effective treatment option for local ablation of GEP-NET hepatic metastases.
Limitations: A retospective and observational study design with pre-selected patients.
Ethics committee approval: n/a
Funding: No funding was received for this work.
Author Disclosures:
F. Feldhaus: nothing to disclose
H. Jann: nothing to disclose
M. Jonczyk: nothing to disclose
G. Wieners: nothing to disclose
M. Pavel: nothing to disclose
B. Gebauer: nothing to disclose
B. Wiedenmann: nothing to disclose
T. Denecke: nothing to disclose
U. Fehrenbach: nothing to disclose

RPS 109-2 08:36
Ultrasound fusion imaging in the percutaneous ablation of focal liver malignancies
A. Drudi, A. Lucarelli, A. Beleù, A. Giaretta, G. Rizzo, S. Conci, M. D'onofrio; *Verona/IT (drudi.ale@gmail.com)*

Purpose: To evaluate the efficacy, advantages, and limitations of the ultrasound fusion imaging (US-FI) technique in percutaneous ablation of focal hepatic malignant tumours and to assess the change in the timing of the procedures performed under US-FI guidance.
Methods and materials: 16 consecutive patients with 33 focal hepatic malignant tumours (27 hepatocellular carcinomas, 6 metastases) were prospectively enrolled between January and May 2019 and treated with percutaneous radiofrequency ablation or ethanol injection under US-FI guidance. Procedures were performed by two expert radiologists who answered several scored questions (from 1 to 10) of a survey about US-FI technique at the end of every procedure. The times of the procedure with and without US-FI were monitored and compared. The mean qualitative and quantitative parameters of the tumour were evaluated by CT/MRI before and after the procedures.
Results: US-FI was judged more useful, the less conspicuous the lesion was in B-mode ($p<0.001$), increasing operator confidence in 88.2% of cases. US-FI changed the perception of lesion size in 70.5% of cases, correcting the choice of needle path in 76.5% of the procedures. The synchronization process is more precise when the lesion diameter is larger ($p=0.047$). The mean time of the procedures was 17min and 50s and the total duration of the procedure did not influence the radiologists' judgment about the utility of US-FI ($p>0.05$). The complete ablation of lesions was achieved in 67% of tumours. No post-procedural complication was observed.
Conclusion: US-FI significantly increases the confidence of operators, enhancing the conspicuity of the target lesion and permitting to plan the needle path more precisely. The technique does not significantly prolong the total time of the procedure.
Limitations: Interoperator variability.
Ethics committee approval: n/a
Funding: No funding was received for this work.
Author Disclosures:
A. Drudi: nothing to disclose
A. Lucarelli: nothing to disclose
A. Beleù: nothing to disclose
A. Giaretta: nothing to disclose
G. Rizzo: nothing to disclose
S. Conci: nothing to disclose
M. D'onofrio: nothing to disclose

RPS 109-3 08:42
Transcatheter arterial chemoembolisation of liver metastases by degradable starch microspheres (DSM-TACE) loaded with different chemotherapeutic drugs: a retrospective single-center analysis
R. Marcello, G. Marcello, G. Assegnati, D. Konda, E. Pofi; *Rome/IT, (robermarcello@gmail.com)*

Purpose: To evaluate the effectiveness and safety of DSM-TACE using irinotecan, oxaliplatin, and adriblastine loaded with absorbable microspheres (50 micron in size) for the treatment of colorectal, gastro-oesophagal breast cancer, NET and GIST liver metastases in a salvage setting of patients refractory to or not able to tolerate chemotherapy.
Methods and materials: A total of 39 DSM-TACE were performed in 29 patients (mean 2.4/patient, range 1-3). The interval between treatments ranged from 4 to 6 weeks (mean 5.0 weeks, median 4 weeks). TACE was done with lobar delivery (22 via the right hepatic artery, 17 via the left hepatic artery). Microcatheters 2.7 Fr in diameter were used for all treatments (Progreat Terumo, JAP). C-arm CT was performed during arterial test injections (flow 2 cc/sec, volume 24 cc, delay 4s, scan 8s,) before TACE in 31 procedures to confirm the appropriate catheter position.
Results: All patients had upper abdominal pain and nausea lasting for 1-3 days after TACE. The pain was graded severe in 32%, moderate in 40%, and mild in 28% of procedures. Nausea was graded ECOG 3 in 12%, ECOG 2 in 43%, and ECOG 1 in 45%.
At 3 months, the complete absence of tumour enhancement during CT was seen in 9 patients and necrosis comprising about 50% of tumour volume in 16 patients.
Conclusion: TACE using DSM-TACE is safe and effective in patients with liver metastases who had been treated with systemic chemotherapy before. The median time to progression was 5 months, however, all patients showed intrahepatic tumour progression during follow-up (median follow-up 9 months).
Limitations: No potential bias.
Ethics committee approval: n/a
Funding: No funding was received for this work.

Author Disclosures:
R. Marcello: nothing to disclose
G. Marcello: nothing to disclose
G. Assegnati: nothing to disclose
D. Konda: nothing to disclose
E. Pofi: nothing to disclose

RPS 109-4 08:48

Real-time CT thermometry during hepatic radiofrequency ablation: an investigation of the correlation between CT number shift, tissue temperature, and feasibility in a clinical setting

P. L. Cheah, C. H. Yeong, N. Sulaiman, Y. H. Wong, D. L. Lee, D. Tan, K.-S. Lim, B. J. Abdullah*; Kuala Lumpur/MY (pengloon78@hotmail.com)*

Purpose: Post-radiofrequency ablation (RFA) evaluation of liver tumours are currently based on visual inspection of computed tomography (CT) images. This study aimed to investigate the correlation between CT number shift and temperature change in order to create CT thermal maps for objective assessment of ablation margins.
Methods and materials: RFA was conducted on ex-vivo bovine livers (n=40) with constant temperature monitoring via embedded fibre-optic sensors at various locations within the ablation volume. CT scans were performed at 3-minute intervals throughout the ablation and cooling process. CT numbers were obtained from points that corresponded to the locations of the temperature sensors. The correlation between CT number shift and temperature change was analysed using SPSS and MATLAB software. CT thermal maps for the real-time monitoring of tissue temperature were then developed and tested on patients undergoing hepatic RFA.
Results: A negative linear correlation was found between CT number shift (y) and temperature change (x): y =-4.99-1.16x (r=0.84). CT number decreased as tissue temperature increased during ablation and vice versa during the cooling period at a rate of 1.16 HU/°C. In clinical settings, the CT thermal maps were feasible in the intra-ablation scans but demonstrated poor results in delayed post-ablation scans.
Conclusion: There was a strong correlation between CT number shift and tissue temperature during RFA. Using the equation developed from this study and the aid of thermal map algorithms, it is possible to estimate tissue temperature based on CT number shift during real-time CT-guided RFA. This approach would improve the objective evaluation of ablation margins.
Limitations: The small number of human subjects with RFA images suitable for thermal map testing.
Ethics committee approval: University of Malaya Medical Centre MREC ID No:20161025-4414.
Funding: University of Malaya Postgraduate Research Fund (PO057-2015B).
Author Disclosures:
P. L. Cheah: nothing to disclose
C. H. Yeong: nothing to disclose
N. Sulaiman: nothing to disclose
Y. H. Wong: nothing to disclose
D. L. Lee: nothing to disclose
D. Tan: nothing to disclose
K.-S. Lim: nothing to disclose
B. J. Abdullah: nothing to disclose

RPS 109-5 08:54

The role of intra-arterial ^{177}Lu-DOTATATE therapy in the treatment of hepatic metastasis from neuroendocrine tumours

M. Rajasekaran, I. Subbanna, V. Bhargavi, J. Moideen*; Bangalore/IN, (muthusubramanian1989@gmail.com)*

Purpose: The propensity of currently practised intravenous 177Lu therapy to produce side-effects warrants any novel techniques to reduce the side-effects without compromising the dose delivered to the target areas. GEP-NETs have the tendency to metastasize to the liver, but seldomly to other organs. We have postulated the selective intra-arterial administration of 177Lu-DOTATATE to hepatic arteries will reduce unwanted side-effects and increasing the dose delivered to target areas due to the first-pass extraction of the radiopeptides by the tumour.
Methods and materials: A prospective evaluation of 36 patients who underwent intra-arterial Lu-177 DOTATATE therapy for hepatic neuroendocrine metastasis in our institution from June 2014-September 2018 was done. CAPTEM-PRRT regimen based on Columbia University protocol was adopted in our study. RECIST and PERCIST crieterias were used for reponse evaluation based on pre-procedure and follow-up ^{68}Ga-DOTANOC PET-CT.
Results: We found that 88% (CR+PR) of patients had a significant radiological tumour response and 12% showed a stabilisation of the disease. No patients were found to have progressive disease. We observed the highest proportion of radiological responders in our study when compared to previous intra-arterial studies.
Conclusion: We conclude that intra-arterial ^{177}Lu DOTATATE therapy is a promising effective treatment option for hepatic metastasis from neuroendocrine tumours. Given the limited success in the management of metastatic NETs with surgery, long-acting octreotide therapy, and chemotherapy, and the tendency of intravenous PRRT to produce side-effects, intra-arterial ^{177}Lu DOTATATE therapy stands alone as a novel technique with fewer side-effects and commendable outcomes.
Limitations: A single-centre study. Resources for evaluation of serum chromogranin A levels are limited and expensive in Indian.
Ethics committee approval: Ethics committee approval obtained.
Funding: No funding received for this work.
Author Disclosures:
M. Rajasekaran: nothing to disclose
I. Subbanna: nothing to disclose
V. Bhargavi: nothing to disclose
J. Moideen: nothing to disclose

RPS 109-6 09:00

Introduction and early experience with percutaneous microwave ablation in Croatia: our first 150 cases

L. Novosel*; Zagreb/HR (novosel_luka@hotmail.com)*

Purpose: To show the road we took to introduce percutaneous ablative therapy for tumours in Croatia, which was practically non-existing until 2017, to now having a growing demand by oncologists and surgeons after treating our first 150 patients.
Methods and materials: This is a retrospective analysis of 150 patients treated with percutaneous CT-guided microwave ablation from January 2017-October 2019. We treated 78 kidney tumours, 42 liver tumours (including 34 CRC metastasis and 8 HCC), 9 bone tumours, and 22 lung tumours (including 14 metastases and 8 lung cancers).
We used HS Amica, Emprint, and Eco ablation devices, with internally cooled ablation probes, usually 14 or 16G, with high energy output.
Results: Best results were achieved with kidney cancer ablation, with only 3 cases of residual tumour after the initial treatment, which were additionally treated with second MWA. Our secondary efficacy is 100% until now. There was only one case of severe bleeding after ablation which was treated with embolisation in the angio suite.
We had the highest rate of recurrence with CRC liver metastases, where 18 patients showed residual tumour tissue. In 12 cases, there were adittional new metastases found in the follow-up period. There were 2 cases of significant complications with biliary tree injury and colon injury that were treated surgicaly.
Conclusion: Percutaneous CT-guided microwave ablation has a growing role in the therapy of liver, kidney, lung, and bone tumours in Croatia, and with our good results in the first 150 patients since 2017, there is a higher awareness about the role of interventional radiology in cancer treatment.
Limitations: A retrospective observational study.
Ethics committee approval: n/a
Funding: No funding was received for this work.
Author Disclosures:
L. Novosel: nothing to disclose

RPS 109-7 09:06

Contrast-enhanced ultrasound-guided feeding artery ablation as an add-on to percutaneous radiofrequency ablation for hepatocellular carcinoma: technical feasibility and therapeutic outcomes

X. Li, M. Xu, X. Xie*; [1]Guangzhou/CN (johnsylee@foxmail.com)*

Purpose: To evaluate the technical feasibility and therapeutic outcomes of contrast-enhanced ultrasound-guided feeding artery ablation (FAA) as an add on to percutaneous radiofrequency ablation (RFA) for hepatocellular carcinoma (HCC), and to compare with conventional RFA (con-RFA).
Methods and materials: For this retrospective study, June 2014-August 2016, 49 patients were assigned to a FAA-RFA or con-RFA group according to the technical feasibility evaluated by 2D- and real-time 3D-contrast-enhanced ultrasound (CEUS). Technical success of FAA and subsequent tumour perfusion change was evaluated. Ablation sizes and therapeutic outcomes were compared between the two groups.
Results: FAA was considered feasible in 25 (51.0%) of 49 HCCs. The most common reason for FAA infeasibility was that the presumed FAA point was less than 1 cm to the bifurcation of non-feeding branches. The technical success rate of FAA was 100%. 13/25 (52.0%) target tumours were evaluated as complete perfusion response, while 12/25 (48.0%) were partial perfusion response. The ablation volume was 41.9±17.5cm^3 (14.9-78.2) in the FAA-RFA group, which was larger than that of 26.2±8.2cm^3 (12.4-45.5) in the con-RFA group ($p < 0.001$). The cumulative rates of LTP at 1-, 2-, and 3-year were respectively 0.0%,

4.2%, and 4.2% for the FAA-RFA group versus 8.3%, 18.7%, and 25.0% for the con-RFA group (p=0.073). Con-RFA and target tumour size were independent risk factors of LTP. The major complications rate did not differ between the two groups.
Conclusion: As an add on to conventional percutaneous RFA, FAA tailored to feeding artery characteristics provides larger ablation size and good local control for HCC.
Limitations: The retrospective nature and relatively small sample size.
Ethics committee approval: This technique was approved by the institutional review board of the hospital. Informed consent was waived.
Funding: National Natural Science Foundation of China (No.81371555).
Author Disclosures:
X. Li: Speaker at The First Affiliated Hospital, Sun Yat-sen University
M. Xu: Author at The First Affiliated Hospital, Sun Yat-sen University
X. Xie: Author at The First Affiliated Hospital, Sun Yat-sen University

RPS 109-8 09:12

The role of intravoxel incoherent motion (IVIM) MRI imaging in the response evaluation of hepatocellular carcinoma after transarterial chemoembolisation (TACE)

M. R. Bursupalle, V. Jineesh, A. Ayyappan, A. Alex*; Trivandrum/IN (maheshreddy.bursupalle@gmail.com)*

Purpose: To evaluate the role of IVIM imaging in the response evaluation of HCC after TACE.
Methods and materials: 15 patients underwent TACE with 40-60 mg epirubicin from April 2018-Oct 2019. MRI-DWI with IVIM and T1 dynamic CEMR imaging was done in 3T GE machine before TACE procedure and at 6 weeks and 12 weeks after TACE. Response evaluation was analysed by comparing IVIM parameters (like D*,f, and ADC) before and after TACE procedure and also with dynamic CEMR imaging.
Results: IVIM parameters after TACE showed a decrease in values when compared to pre-TACE values. Decreased IVIM values correlated well with nonenhancing and minimal enhancing regions. Before TACE, mean D*, f, and ADC values were 25x10-4 +/- 5x10-4 mm2/s, 12+/- 6%, and 750x10-6 +/- 150x10-6 mm2/s, respectively. After TACE, mean D*, f, and ADC values were 15x10-4 +/- 5x10-4 mm2/s, 5 +/- 2% and 1500x10-6 +/- 150x10-6 mm2/s, respectively
Conclusion: IVIM is useful to evaluate tumour response and may obviate the need for contrast usage in some situations.
Limitations: Small sample size and lack of pathological validation of the MRI results.
Ethics committee approval: Approved by Ethics committee of SCTIMST, Trivandrum, Kerala, India.
Funding: Funding received from the STIMST institute.
Author Disclosures:
M. R. Bursupalle: nothing to disclose
V. Jineesh: nothing to disclose
A. Ayyappan: nothing to disclose
A. Alex: nothing to disclose

RPS 109-9 09:18

Yttrium-90 transarterial radioembolisation in advanced-stage HCC: the impact of portal vein thrombosis on survival

L. D'acierno, F. Somma, V. Stoia, R. D'angelo, F. Fiore*; Naples/IT (ludovicad.a@gmail.com)*

Purpose: To assess and compare the effectiveness and safety of HCC patients with PVT and without PVT, after Y-90 Transarterial radioembolisation (TARE).
Methods and materials: From November 2005-November 2012, Y-90 resin-based TARE was performed in an IRB-approved prospective protocol, on 89 patients with unresectable HCC. 33/89 patients had PVT, the remaining 56 were resistant-to-cTACE or underwent TARE as a downstaging therapy. All patients were studied with multi-detector computed tomography (MDCT), angiography, 99mTc-MAA-scintigraphy, and a liver biopsy. The gastroduodenal artery was embolised in most cases. Proton-pump inhibitors were administered to prevent gastritis and ulcers. A $\chi 2$ test with Yates correction and log-rank test were used to compare the two proportions and Kaplan-Meier survival curves, respectively.
Results: The average activity administered was 1.7 ± 0.4 GBq. After the treatment, CTCAE grade 2 adverse events occurred in 46% (41/89) patients. In particular, fever and abdominal pain were found in 25 and 16 patients, respectively. No major side-effect was observed. According to the mRECIST criteria, partial response or complete response was found in 70% of patient three months after the treatment and in 90.5% nine months after the treatment. No significant difference was found in the survival of patients with PVT compared to those without PVT (p=0.672). Complete regression of PVT was observed in almost half of the patients (13/27, 48.1%).
Conclusion: Portal vein invasion does not affect survival in advanced-stage HCC-patients undergoing TARE using Y-90 resin-based microspheres. The Y90 procedure is associated with a regression of portal vein tumour thrombus.
Limitations: A single-centre, retrospective study.
Ethics committee approval: n/a
Funding: No funding was received for this work.
Author Disclosures:
L. D'acierno: nothing to disclose
V. Stoia: nothing to disclose
F. Somma: nothing to disclose
F. Fiore: nothing to disclose
R. D'angelo: nothing to disclose

RPS 109-10 09:24

Balloon-occluded microwave ablation plus balloon-occluded TACE in patients with a single large HCC: preliminary results

A. Tanzilli, R. Iezzi, A. Posa, F. Carchesio, A. Gasbarrini, R. Manfredi*; Rome/IT (alessandrotanzilli93@gmail.com)*

Purpose: To evaluate the feasibility, safety, and efficacy of combined single-step therapy in patients with an unresectable single large (>3 cm) hepatocellular carcinoma (HCC) with balloon-occluded microwave ablation (BO-MWA) plus transcatheter arterial balloon-occluded chemoembolisation (BO-TACE).
Methods and materials: 10 consecutive child-A patients (mean age: 69.7±9y, range: 62-78y) with an unresectable single large HCC (>3 cm) (mean size: 5.6±0.43 cm-range: 4.2-8 cm) were enrolled in our pilot study. The schedule consisted of percutaneous microwave ablation of the lesion during occlusion of the hepatic artery supplying the tumour (BO-MWA), followed by TACE under the occlusion of feeding arteries by a micro-balloon catheter (BO-TACE). Adverse events and intra and periprocedural complications were clinically assessed. Early local efficacy was evaluated on 1-month follow-up multiphasic computed tomography (CT) on the basis of m-RECIST criteria.
Results: Technical success was obtained in all procedures. No major complications occurred. A mean necrotic area of 6.2±1.03 cm was obtained, with a complete response of 80% obtained at 1-month follow-up, with 2 partial responses (less than 30% of residual tumour). All lesions smaller than 5 cm in size were completely necrotic.
Conclusion: Our preliminary experience seems to demonstrate that BO-MWA plus BO-TACE could be a safe and effective combined therapy for unresectable large HCC lesions, allowing a high rate of local response also in lesion exceeding 5 cm in size.
Limitations: A small number of cases.
Ethics committee approval: Written informed consent was obtained.
Funding: No funding was received for this work.
Author Disclosures:
A. Tanzilli: nothing to disclose
R. Iezzi: nothing to disclose
A. Posa: nothing to disclose
F. Carchesio: nothing to disclose
A. Gasbarrini: nothing to disclose
R. Manfredi: nothing to disclose

RPS 109-11 09:30

The treatment of hepatocellular carcinoma (HCC) using thermal ablation: microwave ablation (MWA) versus laser-induced thermotherapy (LITT) regarding local tumour control, side-effects, and survival rates

T. J. Vogl, H. Adwan, N.-E. A. Nour-Eldin, T. Gruber-Rouh*; Frankfurt am Main/DE (t.vogl@em.uni-frankfurt.de)*

Purpose: To compare microwave ablation (MWA) with laser-induced thermotherapy (LITT) in the treatment of hepatocellular carcinoma (HCC) regarding local tumour control, survival rate, and complications.
Methods and materials: Of 277 patients, 231 patients (177 males, 54 females; mean:65.8 years) were treated with MWA and 46 patients (36 males, 10 females; mean:67.1 years) with LITT. All ablations were evaluated for the location of the lesion, diameter, volume, post-ablation volume, device, power, duration of therapy, and local tumour control.
Results: The mean tumour diameter and volume were 21.13 mm and 4.8 cm^3 in the MWA group and 24.33 mm and 5.4 cm^3 in the LITT group. The mean post-ablation volume was 30 cm^3 in the MWA group and 47.6 cm^3 in the LITT group. The local recurrence rate was 4.3% (10/231) in the MWA group and 2.2% (1/46) in the LITT group. The complete remission rate was 23.8% (55/231) in the MWA group and 34.8% (16/46) in the LITT group. The rate of newly developed HCC lesions was 71.9% (166/231) in the MWA group and 63% (29/46) in the LITT group. The complication rate was 4.32% in the MWA group versus 13% (6/46)

in LITT. Survival time was 922 days in the MWA group versus 1,293 days in the LITT group, with a significant difference in the survival time (p=0.002).
Conclusion: MWA and LITT are both effective for the local treatment of HCC. LITT patients had an overall longer survival time than MWA patients with a higher rate of complications.
Limitations: A retrospective study design.
Ethics committee approval: Approved by the Institutional Review Board.
Funding: No funding was received for this work.
Author Disclosures:
T. J. Vogl: nothing to disclose
H. Adwan: nothing to disclose
N.-E. A. Nour-Eldin: nothing to disclose
T. Gruber-Rouh: nothing to disclose

RPS 109-12 09:54
Radiofrequency ablation versus repeat resection for recurrent hepatocellular carcinoma (≤5 cm) after initial curative resection
X. Zhao; *Jinan/CN (zhaoxinya2000@126.com)*

Purpose: To compare the efficacy and safety of radiofrequency ablation (RFA) and repeat resection as the first-line treatment in recurrent HCC.
Methods and materials: This retrospective study analysed 290 patients who underwent RFA (n=199) or repeat resection (n=91) between January 2006 and December 2016 for locally recurrent HCC (≤5 cm) following primary resection. We compared overall survival (OS), progression-free survival (PFS), and complications between the two treatment groups for the total cohort and the propensity score matched (PSM) cohort.
Results: The 1, 3, and 5-year OS (90.7%, 69.04%, 55.6% versus 87.7%, 62.9%, 38.1%, p=0.11) and PFS (56.5%, 27.9%, 14.6% versus 50.2%, 21.9%, 19.2%, p=0.80) were similar in the RFA group and the repeat resection group. However, RFA was superior to repeat resection in the complication rate and hospital stay (p≤0.001). We observed similar findings in the PSM cohort of 50 pairs of patients and when OS and PFS were measured from the time of the primary resection. The OS of the RFA group was significantly better than the repeat resection group among those with 2 or 3 recurrent tumour nodules in both the total cohort (p=0.009) and the PSM cohort (p=0.038).
Conclusion: RFA has the same efficacy as repeat resection in recurrent HCC patients, but with fewer complications. RFA is more efficient and safer than repeat resection in patients with 2 or 3 recurrent tumour nodules.
Limitations: Our study is limited by the noninterventional nonrandomised study design, but we used the propensity score matching method.
Ethics committee approval: The study was approved by Shandong Provincial Hospital review board with a waiver of patient informed consent.
Funding: This work was supported by Shandong Provincial Medical Health Technology Development Projects (No. 2017WS472).
Author Disclosures:
X. Zhao: nothing to disclose

RPS 109-13 09:36
Percutaneous thermal ablation of colorectal liver metastases: CT radiomic features of the surrounding liver parenchyma as predictors of local tumour progression
F. Fumarola[1], M. Calandri[1], V. Giannini[2], D. Regge[3], P. Fonio[1], A. Veltri[4], C. Gazzera[1]; *[1]Turin/IT, [2]Candiolo/IT, [3]Candiolo-Torino/IT, [4]Orbassano/IT*

Purpose: To investigate the correlation between radiomic features of the surrounding liver parenchyma and local tumour progression (LTP) after ablative treatments of colorectal liver metastases (CLM). No pertinent data concerning the role of radiomics in this setting are present in the literature.
Methods and materials: 39 CT-based radiomic features were extracted from 37 CLM in 35 consecutive patients who underwent image-guided thermal ablation. Patients with preprocedural CT acquired earlier than 30 days before the procedure were excluded. Ablation margins, size of the lesion, chemotherapy regimens, and technology (radiofrequency or microwave) were also evaluated.
CT images of CLM were manually segmented on portal phase acquisitions (ITKsnap software, version 3.6.0). Subsequently, a volume including 1 cm in width of surrounding liver parenchyma was automatically generated. Radiomic features were extrapolated using in-house software developed in C++ with ITK libraries. Statistical analysis was performed using a Mann-Whitney U test and Pearson test. ROC curves and AUC were also evaluated.
Results: 1st percentile (p=0.023; AUC=0.738) and 10st percentile (p=0.043; AUC=0.713) had a direct correlation with LTP in all pre-treatment lesions. In the 24 lesions with ablation margins ≥5 mm (LTP in 7/24 cases, 29.2%), 7 features (1st percentile, contrast, entropy, diffEntropy, infCorr1, dissimilarity, and SRE) and 6 features (including correlation, energy, homogeneity, infCorr2, diffVariance, and maxGLCM), respectively showed a direct and an indirect correlation with LTP (p<0.005).
Conclusion: CT radiomic features of the surrounding liver parenchyma of CLM with LTP significantly differ from ablated CLM without LTP, especially in the case of adequate safety margins (≥5 mm). These preliminary findings suggest a role for radiomic features as predicting factors of the outcome of CLM ablation.
Limitations: The limited number of patients.
Ethics committee approval: n/a
Funding: No funding was received for this work.
Author Disclosures:
F. Fumarola: nothing to disclose
D. Regge: nothing to disclose
V. Giannini: nothing to disclose
P. Fonio: nothing to disclose
A. Veltri: nothing to disclose
C. Gazzera: nothing to disclose
M. Calandri: nothing to disclose

RPS 109-14 09:42
Advanced cholangiocarcinoma with data from a tertiary referral centre: best supportive care versus TACE versus systemic chemotherapy
T. J. Vogl, C. Koch, W. Bechstein, A. Schnitzbauer, N. Filmann, T. Gruber-Rouh, S. Zeuzem, O. Waidmann, J. Trojan; *Frankfurt am Main/DE (t.vogl@em.uni-frankfurt.de)*

Purpose: To evaluate the role of best supportive care (BSC) versus systemic chemotherapy versus regional chemoembolisation (TACE) in patients with unresectable cholangiocarcinoma (CCC). The treatment performed was documented and the survival of the patients with unresectable CCC treated at a tertiary referral centre was analysed.
Methods and materials: In 220 consecutive patients with CCC, systemic chemotherapy, using cisplatin and gemcitabine, and TACE using mitomycin, cisplatin, and lipiodol, was performed. Survival curves were calculated according to the Kaplan-Meier method and the log-rank test was applied for survival analysis.
Results: Any palliative treatment was beneficial for patients with unresectable CCC when compared to BSC alone; the median OS with BSC was 10 weeks (BSC vs. TACE p=0.017, HR=0.36; BSC vs. TACE/chemotherapy p<0.001, HR=0.24; BSC vs. chemotherapy p<0.001, HR=0.31). A combination of TACE and chemotherapy prolonged overall survival as compared to TACE alone (105 weeks vs. 43 weeks, p=0.045).
Conclusion: The majority of patients with biliary tract cancer are diagnosed with intrahepatic CCC and have a poor prognosis with advanced stage CCC. Multimodal treatment in palliative patients significantly prolongs survival.
Limitations: A retrospective study design.
Ethics committee approval: Approval by the Institutional Review Board.
Funding: No funding was received for this work.
Author Disclosures:
T. J. Vogl: nothing to disclose
C. Koch: nothing to disclose
W. Bechstein: nothing to disclose
A. Schnitzbauer: nothing to disclose
N. Filmann: nothing to disclose
T. Gruber-Rouh: nothing to disclose
S. Zeuzem: nothing to disclose
O. Waidmann: nothing to disclose
J. Trojan: nothing to disclose

RPS 109-15 09:48
Percutaneous thermal ablation of neuroendocrine liver metastases
F. Darvizeh[1], F. Ullo[1], M. Calandri[1], B. C. Odisio[2], S. Yevich[2], A. Veltri[1], P. Fonio[1], C. Gazzera[1]; *[1]Turin/IT, [2]Houston/US (fdarvizeh@gmail.com)*

Purpose: To evaluate the local tumour progression (LTP) and overall survival (OS) in patients with neuroendocrine liver metastases (NLMs) who have undergone percutaneous thermal ablation.
Methods and materials: The retrospective two-centre study was conducted on 36 patients (67 lesions) with NLM who were treated with percutaneous thermal ablation and subsequent intra-arterial therapy, if necessary. Uni/multivariate analyses were performed using logistic regression and Cox-regression models.
Results: The midgut was the most frequent primary tumour site (34.3%) followed by the pancreas (21%).
100% of the secondary hepatic lesions were ablated completely at the first cross-sectional imaging control and only 6% showed LTP (4/67).
The median OS was calculated as 11.26 years and the midgut (site of origin) was shown as the main independent predictor of OS (HR: 7.39, p=0.001). Furthermore, patients with non-functional NETs had a reduced OS compared to functional NET (HR: 0.027, p=0.027). No immediate post-procedural complications were found.

Conclusion: Percutaneous thermal ablation procedures appear feasible and safe in the treatment of well-differentiated NLMs and allow an effective local tumour control with a low LTP rate. However, furthur study is required to show if radiologic procedures themself might really improve the relatively high OS.
Limitations: A relatively small series.
Ethics committee approval: Ethics committee approval obtained.
Funding: No funding was received for this work.
Author Disclosures:
F. Darvizeh: nothing to disclose
F. Ullo: nothing to disclose
M. Calandri: nothing to disclose
B. C. Odisio: nothing to disclose
S. Yevich: nothing to disclose
P. Fonio: nothing to disclose
C. Gazzera: nothing to disclose
A. Veltri: nothing to disclose

10:30 - 12:00 **Room X**

Radiographers

RPS 214

Image quality considerations and challenges: radiography and mammography

Moderators:
U. Bick; Berlin/DE
K. Borg Grima; Naxxar/MT

RPS 214-1 10:30
The effect of humour as a cognitive technique for decreasing anxiety during mammography
A. M. A. Oliveira[1], A. F. Abrantes[2], L. P. V. Ribeiro[3], R. P. P. Almeida[2], A. D. M. Ribeiro[1], S. Rodrigues[2], K. B. Azevedo[2]; [1]*Portimão/PT,* [2]*Faro/PT,* [3]*Parchal/PT (alexandra.m.oliveira@hotmail.com)*

Purpose: Mammography is the most effective method available for the early detection of breast cancer but many women report experiencing some anxiety, pain, and discomfort when they undergo these procedures. In recent years, substantial research claims that humour and laughter possess unique characteristics for coping with pain and stress. The aim of this study was to determine the effect of humour on levels of anxiety during mammography.
Methods and materials: A total sample of 120 outpatients from public and private facilities was divided into a control group (n=60) and an experimental group (n=60). Sociodemographic interview and state-trait anxiety inventory were applied to both after consent of participation in the study. The experimental group watched funny videos before mammography while the control group did not watch any videos.
Results: Cronbach's alpha coefficient was excellent (0.909). No significant correlations between the control group and the experimental group (r=0.831, P=0.831) were observed. However, in the private facility, there was a slight decrease in anxiety levels in the experimental group (66% of the patients who watched the videos had a low state of anxiety compared to 60% in the control group), but the levels were the same in the public facility for both groups (90% of women reported a low to moderate state of anxiety).
Conclusion: Results from this study have provided important information regarding anxiety levels during mammography but can't confirm that humour techniques can decrease anxiety. Additional research on the effects of humour and other techniques (such as music) is recommended to explore new skills that can help to decrease patient's anxiety, pain, and discomfort.
Limitations: The sample size.
Ethics committee approval: The ethics committee approved the study and written informed consent was obtained.
Funding: No funding was received for this work.
Author Disclosures:
A. M. A. Oliveira: nothing to disclose
A. F. Abrantes: nothing to disclose
L. P. V. Ribeiro: nothing to disclose
R. P. P. Almeida: nothing to disclose
A. D. M. Ribeiro: nothing to disclose
S. Rodrigues: nothing to disclose
K. B. Azevedo: nothing to disclose

RPS 214-2 10:36
Improving the performance of mammographers in a breast cancer screening program: the ASL Latina experience
S. Pacifici[1], G. P. Fanelli[2], N. Ravazzolo[1], A. Tomei[1], P. Bellardini[3]; [1]*Rome/IT,* [2]*Borgo Carso Latina/IT,* [3]*Latina/IT (s_pacifici@virgilio.it)*

Purpose: The success of a screening program is guaranteed, among other things, by the synergy between the radiologist and the mammographer. The mammographer is the main actor, as both the quality of the services and the adherence to the program is subordinate to its technical-professional and relational skills. Thus, a mammography screening program needs mammographers trained, responsible, and aware; all qualities that can be developed and consolidated solely through a theoretical-practical training program tailored to the specific needs of each service. With this background, a training project was launched at the ASL of Latina.
Methods and materials: The quality assessment and training activities were entrusted to an external senior mammographer consultant with specific skills and qualifications in breast imaging. The choice of an external professional ensured the establishment of a fiduciary and peer relationship with the recipients of the project. The project included theoretical and practical meetings.
A PGMI system was used to evaluate the images.
Results: The scores of 136 images randomly selected before the project started were as follows: P 9.5%, G 7.5%, M 50%, and I 33%.
23 mammograms contained at least one inadequate image (67.50% of the total) and 8 inadequate to recall (6% of the total). At one month from the end of both training and corrective steps, the images classified as M presented a strong percentage reduction (30% vs 50%) for the benefit of the images classified as P and G (now, respectively 51.25% and 30%), with a total reset of I images.
Conclusion: The excellent results of the project confirmed that the verification and monitoring of a mammographer's performance is a powerful tool for improving the technical-diagnostic quality of mammography screening programs.
Limitations: n/a
Ethics committee approval: n/a
Funding: No funding was received for this work.
Author Disclosures:
S. Pacifici: nothing to disclose
G. P. Fanelli: nothing to disclose
N. Ravazzolo: nothing to disclose
P. Bellardini: nothing to disclose
A. Tomei: nothing to disclose

RPS 214-3 10:42
Supplementary imaging procedures for women with dense breasts undergoing breast cancer screening: a systematic review
D. Mizzi[1], P. H. Hogg[2], A. England[3], J. F. Kelly[4], F. Zarb[1], N. Mercieca[5]; [1]*Msida/MT,* [2]*Salford/UK,* [3]*Manchester/UK,* [4]*Chester/UK,* [5]*Gozo/MT (deborah.mizzi@um.edu.mt)*

Purpose: To evaluate published evidence and calculate the diagnostic test performance of supplementary imaging procedures for breast cancer screening in women with dense breasts.
Methods and materials: Data sources for identifying journal publications included MEDLINE (ProQuest), CINAHL, Health and Medicine Databases (ProQuest), Web of Science, and the Cochrane library. Reference lists of the studies and relevant systematic reviews that were retrieved were reviewed to identify relevant articles that were not identified in the literature searches. Two reviewers independently reviewed the titles, abstracts, and full-text articles to determine if studies met the inclusion and exclusion criteria. All studies were required to report diagnostic test performance characteristics using a supplementary screening with any imaging modality after a negative digital screening mammogram in asymptomatic women with dense breasts (BI-RADS C/D) as the sole risk factor. Discordance throughout the process was resolved by a third reviewer. Study quality was assessed using QUADAS-2 tool.
Results: 28 journal publications satisfied the inclusion criteria. 16 of these reported on hand-held ultrasound, 2 reported on automated whole breast ultrasound, 5 reported on MRI, 2 reported on digital breast-tomosynthesis, and 2 reported on molecular breast imaging. Only 1 study reported on contrast-enhanced digital mammography. Overall, the evidence indicates that supplementary screening among women with dense breasts and recent negative mammography can consistently identify additional cancers, most of which are invasive, but also leads to unnecessary recalls and biopsies.
Conclusion: Supplementary imaging procedures consistently detected additional breast cancers not identified by digital mammography in asymptomatic women with dense breasts. The inclusion of supplementary imaging into routine screening of dense breasts is recommended but will need to consider the availability and local yield.
Limitations: n/a
Ethics committee approval: n/a
Funding: No funding was received for this work.

Author Disclosures:
D. Mizzi: nothing to disclose
J. F. Kelly: nothing to disclose
P. H. Hogg: nothing to disclose
A. England: nothing to disclose
F. Zarb: nothing to disclose
N. Mercieca: nothing to disclose

RPS 214-4 10:48
The impact of self-compression on breast dose and thickness in mammography
P. Bravhar[1], N. Mekis[2], E. Alukić[2]; [1]*Breazovica/SI,* [2]*Ljubljana/SI*

Purpose: To determine whether the use of self-compression in mammography increases compression force, which will lead to a decreased thickness of breast and lower mean glandular dose (MGD).
Methods and materials: Measurements were performed on 132 patients that were referred to mammography. Patients were randomly divided into two equal groups. In one group, women compressed the right breast themselves and the radiographer compressed the left, and in the other group, they switched roles. MGD, compression force, and thickness of the breast were obtained for each patient. The image quality was not assessed in this part of the study. Data comparison was done with a related-samples Wilcoxon signed rank test.
Results: When the compression was done by the trained radiographer, the average compression force was 89.9 N, average breast thickness was 52.3 mm, and MGD was 1.48 mGy when compared to the self-compression, where the average compression force was 107.9 N, thickness 48.9 mm, and MGD 1.36 mGy, respectively. We have proven a significant increase in average compression force for 20% ($p<0.001$), and a decrease in breast thickness by 7% ($p<0.001$) and MGD by 8% ($p=0.002$).
Conclusion: The results showed that the use of self-compression in mammography in CC projection leads to a decrease of MGD and thickness, which is the result of greater compression force. All the stated facts could lead to better image quality, which will be assessed in the second part of the study.
Limitations: Due to the limitations of the mammography unit, self-compression could only be performed on craniocaudal (CC) projection.
Ethics committee approval: Approved by the national medical ethics committee. Patient consent was obtained.
Funding: No funding was received for this work.
Author Disclosures:
E. Alukić: Speaker at University of Ljubljana, Faculty of Health Sciences
N. Mekis: nothing to disclose
P. Bravhar: nothing to disclose

RPS 214-5 10:54
The eye-tracking system as an assessment tool for mammography positioning
H. Yamashina[1], A. Yagahara[1], T. Suzuki[2], K. Ogasawara[1]; [1]*Sapporo/JP,* [2]*Iwamizawa/JP (y-hiroko@med.hokudai.ac.jp)*

Purpose: In Japan, an objective structured clinical examination (OSCE) is an emerging trend. One of the most difficult positioning techniques to be acquired is breast positioning in mammography. In this study, we evaluated the effectiveness of the eye-tracking system as an assessment tool.
Methods and materials: Two skilled mammographers (A and B) and two third-year university students (C and D) were recruited for a preliminary study. Three areas of interest (AOIs) were selected to detect visual attention: a) the juxtathoracic region (pectoral muscle), b) entire glandular tissue, and c) abdominal tissue (infra-mammary fold). Saccade-fixation eye movements were detected using gaze plots and heat maps. Dwell time was also assessed within selected AOIs.
Results: Heat maps during the moving of the compression device into the position illustrated the differences of visual attention among participants. Expert A was gazing at the pectoral muscle and glandular tissue but had no gaze at the infra-mammary fold. Expert B was found to have strong visual attention on the pectoral muscle. Student C did not show any gaze within the selected AOIs. Student D was gazing at the pectoral muscle and infra-mammary fold. In addition, gaze at the display of the compression force was observed among students. Dwell time within AOIs also showed the differences in visual attention among participants.
Conclusion: An eye-tracking system can be used as an assessment tool for mammography positioning. Using both a heat map and dwell time within AOIs should be applied for a more accurate assessment.
Limitations: We need to further examine the association between the obtained clinical images with visual attention to investigate the effectiveness of the eye-tracking system.
Ethics committee approval: Informed consent was obtained from all participants.
Funding: No funding was received for this work.
Author Disclosures:
H. Yamashina: nothing to disclose
T. Suzuki: nothing to disclose
K. Ogasawara: nothing to disclose
A. Yagahara: nothing to disclose

RPS 214-6 11:00
The influence of digital breast tomosynthesis on PGMI classification of 2D screening-detected cancers and baseline 2D screening examinations of interval cancer (IC) in the Oslo tomosynthesis screening trial
R. Gullien[1], A. E. Haakull[1], A. S. Bakken[2], J.-G. Andersen[1]; [1]*Oslo/NO,* [2]*Royken/NO (uxraul@ous-hf.no)*

Purpose: To examine whether tomosynthesis has an impact on the classification of mammograms classified as moderately-good (M) when DBT was used in addition to 2D.
Methods and materials: 130 of 230 SDC from OTST with at least one normal score at independent double reading and 51 IC were included. Two incomplete exams were excluded. 179 cases with CC and MLO (2D and 2D+DBT) of each breast, n=716 mammograms, were included. Two radiographers independently assessed mammograms using criteria from a quality-assurance manual (QAM) from BreastScreen Norway. 2D and DBT were classified separately: P=perfect, G=good, M=moderately-good, and I=inadequate. P+G were pooled. Images classified as M were selected for analysis and divided into sub-groups: a=pectoral muscle not to nipple level, b=nipple not in profile, c=inframammary angle not clearly demonstrated, d=skin folds/overlying tissue, and e=asymmetry.
Results: PGMI results for 2D were P+G=498/716 (70%), M=24% 173/716 (24%), and I=6% 45/716 (6%). Images classified as M included 39/173 (23%) in CC projection and 134/173 (77%) in MLO projection. All 39 CC images (22 RCC and 17 LCC) retained the classification. 93/134 (69%) of MLO images were upgraded from M to G when 2D+DBT images were used for comparison. The remaining 41/134 (31%) M MLO images retained classification. No CC or MLO were downgraded. The main reasons for re-classifying MLO images to M were sub-group d 44/134 (33%), followed by sub-group c 44/134 (33%), sub-group a 26/134 (19%), sub-group b 20/134 (15%) and no images in sub-group e. In sub-group d, 39/44 89% were upgraded. In sub-group a, 2/26 (8%) were upgraded. In sub-group b and c, all retained the classification.
Conclusion: Most moderately-good images were in MLO-projection. Adding DBT to 2D for PGMI classification resulted in upgrading moderately-good MLO images to good when reasons were skin folds/overlying tissue.
Limitations: n/a
Ethics committee approval: n/a
Funding: No funding was received for this work.
Author Disclosures:
R. Gullien: nothing to disclose
A. E. Haakull: nothing to disclose
A. S. Bakken: nothing to disclose
J.-G. Andersen: nothing to disclose

RPS 214-7 11:06
Retrospective PGMI classifys and examines compression force (CF) of screening-detected cancers and mammograms prior to diagnosis interval cancer from the Oslo tomosynthesis screening trial
R. Gullien[1], A. E. Haakull[1], A. S. Bakken[2], J.-G. Andersen[1]; [1]*Oslo/NO,* [2]*Royken/NO (uxraul@ous-hf.no)*

Purpose: To examine if CF on mammograms of screening-detected cancers (SDC) and screening mammograms prior to an interval cancer (IC) diagnose classified as inadequate had any impact on the PGMI classification.
Methods and materials: 130 of 230 SDC from OTST with at least one normal score at independent double reading and 51 IC were included. Two incomplete exams were excluded. 179 cases with CC and MLO (2D and 2D+DBT) of each breast, n=716, mammograms were included. Two radiographers independently assessed the mammograms using criteria from a quality-assurance manual (QAM) from BreastScreen Norway, 2003 edition. 2D and DBT were classified separately: P=perfect, G=good, M=moderately-good, and I=inadequate. P+G were pooled. The QAM recommend CF between 10N and 18N, usually between 12N and 15N. Images with CF outside the recommendation (10-18N) and images classified as inadequate were selected for analysis.
Results: The mean CF for all images was 12, 4N, the median of all CC images=12N, and the median of all MLO images=13N, and were within the recommendations. 64 images had a lower (42 CC projection, 22 MLO projection) and 2 CC images had a higher CF than recommended. Overall, the lowest CF was 6, 0N (LMLO=inadequate) and the highest was 18, 3N (LCC=perfect). 45 images were classified as inadequate, (26 RCC, 17 LCC, 1 RMLO, and 1 LMLO). 19 of the 26 RCC images were within recommendations, 7 were lower, and none were higher than recommended. Of the 17 LCC images, 16 images were within the recommendations and 1 was lower. 1 inadequate MLO image was lower than

recommended. The main reason for classifying images as inadequate was that part of the breast tissue was missing.
Conclusion: It seems that there were no correlations between the compression-force and mammograms classified as inadequate. Inadequate mammograms and reasons for low compression force should be further investigated.
Limitations: Only internal radiographers classified the mammograms. No control group with CF, only recommendations in the QAM for comparison.
Ethics committee approval: Clinical Trials NCT 01248546, Regional Ethic Committees 2010/144.
Funding: No funding was received for this work.
Author Disclosures:
R. Gullien: nothing to disclose
A. E. Haakull: nothing to disclose
A. S. Bakken: nothing to disclose
J.-G. Andersen: nothing to disclose

RPS 214-8 11:12

Identification of image quality criteria for the assessment of mammography images with breast implants using the Delphi method by radiographers and radiologists

C. S. D. Reis, I. Gremion, N. Richli*; Lausanne/CH*

Purpose: To identify the most relevant image quality (IQ) criteria that should be used to assess breast implants mammograms (BIM) according to radiographers' and radiologists' working in breast cancer screening programs perspectives.
Methods and materials: A two-round Delphi method using a questionnaire was applied, asking the experts to rank each image criteria encountered in the literature according to 4 possible answers: 1=need to have/2=nice to have/3=not relevant/4=does not know. Criteria for craniocaudal, mediolateral-oblique, and lateral, performed with and without Ecklund manoeuvre, were included. This process was repeated modifying criteria in the second round by removing the less relevant criteria highlighted during the first round and including participants' suggestions.
Results: Visualisation of anatomical details (extension of the pectoral muscle, nipple in profile) was considered the most relevant criteria by radiographers during the first round, while general criteria were prioritised by radiologists in both rounds, namely the sharpness of glandular tissue, absence of artefacts, and the spread of breast tissue. The analysis of implant flow, the BI anterior edge, and its maximum retropulsion when the Eklund manoeuvre was performed were the specific criteria for BIM considered as the most relevant to be assessed. The visualisation of retroglandular adipose tissue and axillary tail were considered as "nice to have".
Conclusion: The importance of each criterion used to assess BIM was not the same for radiographers and radiologists, which suggests the two groups of experts are looking for different aspects of the image. Further education and training are necessary to align the strategy to assess IQ of BIM and reduce subjectivity.
Limitations: This study did not include all BCS centres available in the country, not being possible to generalise these results.
Ethics committee approval: n/a
Funding: Funding provided by HES-SO.
Author Disclosures:
C. S. D. Reis: nothing to disclose
N. Richli: nothing to disclose
I. Gremion: nothing to disclose

RPS 214-9 11:18

Does radiographer assessment of image quality align with that required for diagnosis?

R. G. L. Decoster, R. Toomey, M.-L. Ryan*; Dublin/IE*

Purpose: Previous research indicates that radiologists and radiographers agree on the visibility of anatomical structures in radiographs but not on the clinical usability. The impact of the differences in the acceptance of a radiograph on the radiologist's confidence to diagnose is unknown.
Methods and materials: 24 radiographers and 6 radiologists scored 40 PA chest radiographs (24 without and 16 with pathology) for clinical usability (RadLex) in the detection of lung lesions. Additionally, radiologists classified the radiographs as normal or abnormal and scored their confidence on a 5-point scale. AUC_{ROC}were calculated for each RadLex category to evaluate the alignment between the radiographer's assessment and the radiologist's performance.
Results: Based on the AUC_{ROC}, the classification of the radiographs by radiographers in terms of clinical usability was no predictor for the clinical performance of the radiologist. A significant different ($p<0.01$) classification was noticed between radiographers and radiologists. 25.3% of the cases, rejected by the radiographers (rejected 56%), sufficiently supported the detection of pathology for the radiologist (rejected 30.7%).
Conclusion: Almost half of the radiographs rejected by radiographers were potentially diagnostic, with useful doses likely being discarded. The discrepancy between professions in the evaluation of clinical usability alludes to a different approach in image evaluation. Future research is needed to align both professions, with agreement and collaboration being untapped niches for potential dose optimisation strategies.
Limitations: The number of cases was relatively low to facilitate observers with limited availability and so the prevalence did not reflect the clinical practice.
Ethics committee approval: n/a
Funding: No funding was received for this work.
Author Disclosures:
R. G. L. Decoster: nothing to disclose
M.-L. Ryan: nothing to disclose
R. Toomey: nothing to disclose

RPS 214-10 11:24

Are image quality judgements by radiographers guided by a global signal or "gist"?

R. Toomey, J. Ryan, R. G. L. Decoster, J. G. Stowe, M. O'connor, K. G. Cronin, L. A. Rainford*; Dublin/IE*

Purpose: Radiographers differ from radiologists in their assessment of image quality, which may have connotations for patient diagnosis and radiation dose. Understanding the perceptual basis for these judgements is warranted.
Expert radiologists are thought to be guided in pathology detection by an initial global impression, detecting abnormalities at a rate higher than chance in under 250 ms. This study aims to determine whether radiographers employ a similar process, detecting a global signal for "inadequate" image quality.
Methods and materials: 27 qualified radiographers attending the EFRS Research Hub 2019 viewed 24 chest radiographs of varying quality under two conditions and rated the image quality of each on a scale of 1 (very inadequate) to 5 (excellent); ratings of 1 or 2 indicated a repeat image was necessary.
In the first condition ("flash"), a sequence of fixation cross (750 ms), radiograph (200 ms), mask (50 ms), and a blank screen with rating scale (unlimited) were presented for each radiograph. In the second condition ("free"), images were presented in a different order with unlimited time, representing standard viewing conditions.
Results: 35.69% of the images had identical ratings in each condition. 69.61% were given the same decision to accept/reject in both conditions. Where the decision changed, 74.6% were initially accepted. Flash and free ratings were correlated ($r=0.507$, $p<0.01$); mean flash ratings were higher than free ($p<0.01$).
Conclusion: Radiographers may use a global impression in determining image quality, though further research is required.
Limitations: Selection bias is possible as all participants were ECR attendees. The limited number and range of images limits the findings.
Ethics committee approval: The work was submitted to the home institution human research ethics committee and declared exempt from a full review.
Funding: The study was conducted at the EFRS Research Hub and used monitors donated by Barco.
Author Disclosures:
R. Toomey: nothing to disclose
R. G. L. Decoster: nothing to disclose
L. A. Rainford: nothing to disclose
J. Ryan: CEO at Ziltron Ltd.
J. G. Stowe: nothing to disclose
M. O'connor: nothing to disclose
K. G. Cronin: nothing to disclose

RPS 214-11 11:30

Radiographers' visual acuity performance can impact image quality evaluation

C. S. D. Reis[1], F. A. P. S. Soares[2], G. M. Bartoli[1], K. Dastan[3], Z. Dhlamini[4], A. Hussain[5], D. Kroode[6], M. F. M. McEntee[7], J. D. Thompson[3], N. Mekis[8]; *[1]Lausanne/CH, [2]Florianopolis/BR, [3]Salford/UK, [4]Bloemfontein/ZA, [5]Derby/UK, [6]Groningen/NL, [7]Cork/IE, [8]Ljubljana/SI*

Purpose: To determine the impact of reduced visual acuity on object counting and image evaluation of anatomical details in appendicular radiographs.
Methods and materials: Phantom images were produced for the purpose of counting objects and image appraisal of anatomical structures was performed on anonymised radiographies. A 4-point Likert-scale was applied to characterise the level of anatomical definition (1-not defined; 4-clearly defined). The tasks were performed under 3 conditions: wearing 2, 1, and 0 pairs of simulation glasses, which provided different magnitudes of reduced visual acuity. Inferential statistics were carried out using SPSS and areas under the visual grading characteristic curve (AUC_{VGC}) were used as figure-of-merit. The tasks were completed by radiography students participating in a research summer school.
Results: Observers were not able to count low-contrast objects with 2 pairs of glasses (13). The evaluation of anatomical details was performed by 7 radiography students wearing 0 and 2 pairs of glasses, but total interpretation

time was longer when visual acuity was reduced (15.4 versus 8.9min). VGC analysis showed that observers can lose the ability to detect anatomical and contrast differences when they have a simulated visual acuity reduction, with low-contrast detection presenting more of a challenge (soft tissues). No simulation glasses compared with 1 pair gives binomial AUC_{VGC} of 0.302 (0.280, 0.333), that decreases to 0.197 (0.175, 0.223) when using 2 pairs.
Conclusion: Reduced visual acuity has a negative impact on the evaluation of test-objects and clinical images. Further work is required to test the reduced visual acuity impact on the technical evaluation of different imaging, pathologies, and levels of experience.
Limitations: There was no optometrist available to measure the differences on observers' visual acuity.
Ethics committee approval: HSR1819-115.
Funding: No funding was received for this work.
Author Disclosures:
C. S. D. Reis: nothing to disclose
F. A. P. S. Soares: nothing to disclose
G. M. Bartoli: nothing to disclose
K. Dastan: nothing to disclose
Z. Dhlamini: nothing to disclose
A. Hussain: nothing to disclose
D. Kroode: nothing to disclose
M. F. M. McEntee: nothing to disclose
J. D. Thompson: nothing to disclose
N. Mekis: nothing to disclose

RPS 214-12 11:36
Quality assessment of paediatric chest radiographs: differences between radiologists and radiographers
C. I. D. C. T. Martins[1], F. M. Nogueira[1], J. Santos[2];
[1]Lisbon/PT, [2]Coimbra/PT
(claudia.teles.martins@gmail.com)

Purpose: To characterise differences in the evaluation of the quality of paediatric chest radiographs between radiographers and radiologists.
Methods and materials: 24 paediatric chest radiographs, performed before and after the implementation of a dose optimisation program, were analysed by 5 observers: 2 radiologists and 3 radiographers. This evaluation was performed blindly, independently, and without a time limit. The evaluation included an analysis of anatomical criteria (1 to 5-point Likert scale) and visual perception of physical image characteristics (1 to 3-point Likert scale) such as noise, resolution, and contrast (11 criteria). Visual grading analysis and visual grading characteristics analysis were performed.
Results: The analysis of the scores was performed by criterion and by phase in the different weight ranges, and 1,320 scores were obtained. No statistically significant differences were found for scores between both phases (p=0.131). Regarding the differences between professional classes, radiographers gave lower scores than radiologists in almost all criteria and all weight levels, regardless of the phase. The average scores assigned by radiographers ranged from 1.3-4.9, with the most frequent average score being 4.7 (8.0%). The average scores given by the radiologists ranged from 2.0-5.0, with the most frequent mean score being 5.0 (43.2%). In the two analysed phases (before and after optimisation), in all weight ranges and criteria, statistically significant differences ($p<0.05$) were found between the evaluations performed by radiographers and radiologists.
Conclusion: The evaluation of the quality of chest radiographs was influenced by the evaluator's academic background, which may have implications for adherence to x-ray exposure optimisation programs.
Limitations: The number of images and observers were limited.
Ethics committee approval: Approved by the ethical board of the hosting hospital.
Funding: No funding was received for this work.
Author Disclosures:
C. I. D. C. T. Martins: nothing to disclose
F. M. Nogueira: nothing to disclose
J. Santos: nothing to disclose

RPS 214-13 11:42
A comparison of the success rate and radiation burden between radiography students when imaging the thoracic and lumbar spine
R. Viltužnik, N. Mekis; *Ljubljana/SI*

Purpose: To investigate if there are differences in the radiation burden (DAP, effective dose) and success rate among radiography students in Slovenia.
Methods and materials: 124 students participated in the study: 1st (n=39), 2nd (n=30), and 3rd (n=30) year students of the 1st cycle degree and students from both 2nd cycle degree years that were put in one group (n=25) due to the poor representation of each study year. The students were unaware of what kind of study they participated in. They were asked to perform thoracic and lumbar spine imaging in both standard projections on an anthropomorphic phantom. DAP measurements and field size were obtained and the effective dose and dose to organs were calculated. All images were evaluated according to the criteria in professional literature. Only the optimal images were further included in the analysis.
Results: There were no significant differences between the number of rejected and optimal images in thoracic spine radiography in both projections. In the AP view of the thoracic spine, the 1st year students had the best results in DAP and effective dose. In the lateral view, the 2nd year students used the smallest field size. Significant differences were found between the number of optimal and rejected images in lumbar spine radiography, where the 1st year students had the far higher number of rejected images. No significant differences in image field size, DAP, and effective dose between all four groups in lumbar spine radiography were found.
Conclusion: We cannot point out the best group of students based on imaging field size, DAP, and effective dose. However, the best results in the number of optimal images were achieved by the 2nd cycle degree students.
Limitations: All students should have participated.
Ethics committee approval: n/a
Funding: No funding was received for this work.
Author Disclosures:
R. Viltužnik: Speaker at Faculty of health sciences
N. Mekis: nothing to disclose

RPS 214-14 11:48
An investigation of how exposure faults can be accounted for in the reject analysis of digital radiographs
C. Mc Keown, K. Matthews; *Dublin/IE (ciaramck97@gmail.com)*

Purpose: Reject analyses (RA) in digital radiography report low reject rates for inadequate exposure because digital systems can produce diagnostic images over a broad range of exposure levels. A review of current literature indicates a lack of investigation into whether reduced rates of exposure error are actual or whether they are masked by post-processing techniques that optimally render images for display such that less-than-optimal exposure goes unnoticed. The current study aimed to investigate how exposure faults can be accounted for in the RA of digital radiographs.
Methods and materials: A system to store digital reject images was set up. Rejects and their associated anonymised data were collected over an audit period of one month. To facilitate the analysis of exposure through the calculation of the deviation index (DI), examination specific target exposure values were derived in compliance with IEC advice. An objective quality analysis of the images was conducted at a RIS-PACS workstation at the researchers' university.
Results: A comparison of the frequency of exposure error reported in the RA (5.7%) and DI analysis (20%) revealed that RA of itself is not effective in identifying exposure error in digital radiographs. Image quality evaluation using Spearman's non-parametric test of correlation confirmed that no significant correlation existed between SNR or CNR and DI values.
Conclusion: RA without further consideration of exposure is not effective in identifying exposure error in digital radiographs. The addition of exposure analysis using DIs provides information that can be used to inform optimisation strategies for digital radiographs. Thresholds for SNR and CNR in terms of diagnostic efficacy should be investigated to determine whether target exposures could be reduced without an image detriment.
Limitations: The study is specific to a site using Siemens technology. The method, however, is robust/reproducible and could be adapted/replicated in other sites.
Ethics committee approval: Ethical approval from UCD SM UREC was granted (November 2018).
Funding: No funding was received for this work.
Author Disclosures:
C. Mc Keown: nothing to disclose
K. Matthews: nothing to disclose

RPS 214-15 11:54
A reject analysis targeted to identify the techniques of undergraduate radiographers that may benefit from further development
C. Lynch, K. Matthews; *Dublin/IE (chloe.lynch@ucdconnect.ie)*

Purpose: As well as contributing to quality assurance, reject analysis can provide staff and students with targeted feedback so they can learn from mistakes and improve practice. However, in the study centres, there were no mechanisms in place to retrieve rejected images specifically for student feedback. The aims of this study were to develop a mechanism to retrieve images performed by student radiographers for reject analysis across multiple sites and analyse the findings of reject analysis on these images to establish any themes that might contribute to focused teaching.
Methods and materials: An archive folder in the RIS-PACS was established to receive images identified as rejected and performed by students. From a list of 8 categories, reasons for rejection were recorded by the researcher. For quality

assurance, a small sample was also assessed blindly by an expert radiographer with Cramer's V revealing a significant, strong association (V=1.0, p=0.00) between the two sets of data and thus establishing the credibility of the researcher reject analysis.
Results: 164 rejected images across 42 different projections were harvested. The lower limb was the most repeated body region. Positioning, centring, and artefact were the most frequent reasons for rejection. Lateral knees, lateral wrists, and PA chests were the most frequently rejected projections. These findings strongly aligned with findings reported in published papers.
Conclusion: Detailed reject analysis provides information that can enhance optimisation. Consideration of reasons for rejection can provoke staff consideration of technique and highlight areas where the teaching of students could be focussed. These could lead to a reduction in repeats and reduced patient doses.
Limitations: The overall reject rate could not be calculated.
Ethics committee approval: An ethical exemption was granted by the undergraduate research and ethics committee.
Funding: No funding was received for this work.
Author Disclosures:
C. Lynch: nothing to disclose
K. Matthews: nothing to disclose

10:30 - 12:00 **Room F1**

Neuro

RPS 211
Spine and nerves

Moderators:
H. Ozdemir; Adana/TR
S. Gerevini; Bergamo/IT

RPS 211-1 10:30
A new insight of brain reorganisation in the sensorimotor cortex after spinal cord injury
Q. Chen, N. Chen, Z. Wang*; Beijing/CN (chenqian8319@163.com)*

Purpose: To investigate possible brain reorganisation after spinal cord injury (SCI) using multimodal fMRI and to further study their association with clinical variables.
Methods and materials: 21 traumatic SCI patients and 21 healthy controls (HCs) were recruited. The 3D whole-brain structural and resting-state functional images were acquired from all participants using a 3.0 Tesla MRI system. VBM and TBSS analysis were conducted to investigate the differences in brain structure between SCI patients and HCs, separately. Seed-based FC analysis was performed to explore the whole-brain functional changes using the results of brain structure as seeds. The association between brain changes and clinical variables was performed.
Results: SCI patients showed GMV decrease in the dorsal anterior cingulate cortex (dACC), bilateral anterior insular cortex (aIC), bilateral orbital frontal cortex (OFC), and right superior temporal gyrus (STG). No significant difference in WM was found. When the seeds were located in the left aIC and right STG, SCI patients showed decreased FC in the bilateral primary sensorimotor cortex and left inferior parietal lobule (IPL), separately. Additionally, the FC value in the right primary sensorimotor cortex was positively correlated with the total motor score, while the FC value in the left IPL was positively correlated with the left/right/total motor score in SCI patients.
Conclusion: These findings indicate that SCI can cause brain reorganisation in some higher cognitive areas, which are not related to sensorimotor function directly. More importantly, reorganisation of these regions may be vital factors in sensorimotor dysfunction through the decreased FC with sensorimotor areas after SCI.
Limitations: We did not conduct a longitudinal study.
Ethics committee approval: The study protocol was approved by the ethics committee of our hospital.
Funding: National Natural Science Foundation of China (No.81871339).
Author Disclosures:
Q. Chen: nothing to disclose
N. Chen: nothing to disclose
Z. Wang: nothing to disclose

RPS 211-2 10:36
Paediatric retroclival epidural haematoma in the acute trauma setting: a sign of tectorial membrane stripping injury
P. Fiester, D. Rao, S. Andreou, E. Soule, J. Patel*; Jacksonville, FL/US, (peterfiester@gmail.com)*

Purpose: A traumatic retroclival epidural haematoma (REH) is a rare sign of significant cervical flexion-extension injury in the paediatric population. The purpose of our study was to identify paediatric patients with an REH and a record the haematoma size and extent and examine the major craniocervical ligaments for injury.
Methods and materials: Paediatric patients who suffered a REH were identified retrospectively using the keywords 'clivus', 'epidural haematoma', and 'retroclival' included in head CT reports from 2012-2018 using Nuance mPower software. The cervical and brain MRI exams for these patients were reviewed for craniocervical ligament injury by two CAQ certified neuroradiologists. Detailed descriptions of patient injuries were recorded along with demographic information, clinical history, patient management, and outcome.
Results: Ten paediatric patients were identified with an acute, post-traumatic REH with an average anteroposterior size of 4.4 mm and craniocaudal size of 4.3 cm. All patients demonstrated either a stripping (90%) or partial stripping (10%) injury of the tectorial membrane. The disruption of the additional major craniocervical ligaments (alar ligament, transverse ligament, longitudinal ligaments, and ligamentum flavum) was relatively rare. The most common associated ligamentous injuries involved the anterior atlantooccipital membrane, apical ligament, and interspinous ligaments. The majority of patients were managed conservatively with excellent clinical outcomes.
Conclusion: A post-traumatic REH in the paediatric population is associated with a stripping of the tectorial membrane from the posterior clivus. We propose that the identification of an REH on initial head CT should trigger a cervical MRI to evaluate the integrity of the tectorial membrane and other craniocervical ligaments.
Limitations: The mall sample size for this rare injury.
Ethics committee approval: A waiver of informed consent was granted by the University of Florida Health Jacksonville IRB-03 chairman.
Funding: No funding was recieved for this work.
Author Disclosures:
E. Soule: nothing to disclose
P. Fiester: nothing to disclose
D. Rao: nothing to disclose
S. Andreou: nothing to disclose
J. Patel: nothing to disclose

RPS 211-3 10:42
Impact of incomplete investigation of suspected cauda equina syndrome before referral to specialist spinal units
R. Duarte Armindo[1], D. Fountain[2], S. Davies[1], D. Ballard[1]*; [1]London/UK, [2]Cambridge/UK (ruimigueldarmindo@gmail.com)*

Purpose: International guidelines state that patients with suspected cauda equina syndrome (CES) should undergo urgent lumbar MRI, ideally before referral to specialist spinal surgery units. This work, part of the evaluation of national treatment and investigation of cauda equina (ENTICE) study, aims to characterise the implications on patient care and for the receiving units of referrals with an incomplete investigation in this setting.
Methods and materials: A retrospective, multicentre observational study of the investigation and management of patients with suspected CES was conducted across the UK, including all patients referred to a spinal unit from 1st October 2016-31st March 2017.
Results: From a total of 4,441 referrals to 28 UK spinal units, more than half were made without any previous imaging and less than a fifth resulted in surgical decompression. In patients with incomplete initial studies, there was a statistically significant increase in time from presentation to MRI (median 13.9 vs 3.1 hours, p<0.001), but no significant increase in time from presentation to decompression. Approximately 85% of patients transferred for MRI were discharged without surgical intervention. Strict adherence to existing guidelines over this period would have resulted in a reduction of referrals and transfers by over 70%.
Conclusion: For the majority of cases, an adequate investigation was not completed prior to a referral to specialist centres. Previous studies suggest that the costs associated with an incomplete investigation before referral clearly outweigh those of providing access to MRI scanning 24/7 in smaller hospitals. More studies, from countries with different levels of MRI availability and/or other systems of patient referral, are needed to understand the clinical magnitude of this problem and to establish transversally applicable guidelines.
Limitations: A retrospective study with little information on long-term clinical outcomes.
Ethics committee approval: n/a
Funding: No funding was received for this work.

Author Disclosures:
R. Duarte Armindo: nothing to disclose
D. Fountain: nothing to disclose
S. Davies: nothing to disclose
D. Ballard: nothing to disclose

RPS 211-4 10:48
T2-mapping of the distal sciatic nerve in healthy subjects and patients suffering from lumbar disc herniation with nerve compression
N. Sollmann, D. Weidlich, E. Klupp, B. Cervantes, C. Ganter, C. Zimmer, T. Baum, J. S. Kirschke, D. C. Karampinos*; Munich/DE (nico.sollmann@tum.de)*

Purpose: To provide reference T2 values for magnetic resonance neurography (MRN) of the distal sciatic nerve and compare these to T2 changes in patients with nerve compression.
Methods and materials: 22 subjects (28.3±3.5 years) and 5 patients with unilateral sciatica due to degenerative disc disease with disc herniation underwent MRN using a T2-prepared turbo spin-echo (TSE) sequence of the distal sciatic nerve bilaterally. 5 and 2 healthy subjects further underwent a commonly used multi-echo spin-echo (MESE) sequence and magnetic resonance spectroscopy (MRS) as the gold-standard method, respectively. Measurements of T2 values were performed by two readers.
Results: T2 values based on the T2-prepared TSE sequence were 44.4±3.0 ms (left) and 44.5±2.7 ms (right; p>0.05) in the healthy subjects and showed good inter-reader reliability. In patients, distal sciatic nerves showed T2 values of 61.5±6.2 ms (side of nerve affection) vs 43.3±2.4 ms (unaffected side). T2 values of MRS were in good agreement with measurements from the T2-prepared TSE sequence. However, they were not in agreement with those of the MESE sequence, which showed clearly higher values (62.8±3.2 ms [left] and 62.7±2.8 ms [right]).
Conclusion: A T2-prepared TSE sequence enables the determination of accurate T2 values of the distal sciatic nerve, whereas a commonly used MESE sequence tends to overestimate nerve T2. Our approach may enable to quantitatively assess direct nerve affection in patients with nerve compression.
Limitations: The small size of the patient cohort, but it is only intended to form a first case series for comparison to reference values.
Ethics committee approval: This prospective study was approved by the IRB.
Funding: ERC and Philips Healthcare.
Author Disclosures:
N. Sollmann: nothing to disclose
D. Weidlich: nothing to disclose
E. Klupp: nothing to disclose
B. Cervantes: nothing to disclose
C. Ganter: nothing to disclose
C. Zimmer: nothing to disclose
T. Baum: nothing to disclose
J. S. Kirschke: Research/Grant Support at Philips Healthcare, Research/Grant Support at ERC
D. C. Karampinos: Research/Grant Support at Philips Healthcare

RPS 211-5 10:54
Advanced trends in magnetic resonance imaging in the assessment of lumbar intervertebral degenerative disc disease
R. S. Abou Khadrah*; Tanta/EG (rotinia2009@gmail.com)*

Purpose: To evaluate the sensitivity of T2-mapping and the apparent diffusion coefficient in the determination of an early stage of intervertebral disc degeneration.
Methods and materials: 60 patients (mean age of 47.50±7.88) and 20 volunteers presenting with low-back pain underwent T2-mapping and DWI. All the lumber discs were evaluated morphologically and given a grade according to Pfirrmann's grading (I to IV). Every disc was divided into three parts: central, peripheral, and all-disc. The values of both T2 and ADC were calculated and analysis. The different correlation between the result and age were done using a ROC curve for both T2-mapping and ADC value, aiming to determine the cut-off values.
Results: There was a negative correlation between T2 values and semi-quantitative grading (Pfirrmann grading) of disc degeneration and T2 values were significantly different when comparing grade I to V. A T2 value of nucleus pulposus was more sensitive than annulus fibrosus and the entire disc. ADC values were found to decrease with the increased degree of disc degeneration. There was a weakly significant negative correlation between age and T2-mapping values, ADC values of nucleus pulposus, and the entire disc.
Conclusion: T2-mapping was significantly different when comparing grade I to V while ADC value had a significant weak negative correlation with age. T2-mapping and, to a smaller extent, ADC can be used for quantitative analysis of early disc degeneration for early diagnosis and better management.
Limitations: The absence of histological correlation with the results, absence of direct relation between the morphological changes of disks and T2-mapping and DWI, and the subjective grading of disks by Pfirrmann grading.
Ethics committee approval: The study was approved by the ethical committee of Tanta University Hospital.
Funding: No funding was received for this work.
Author Disclosures:
R. S. Abou Khadrah: Author at Tanta university Hospital, Speaker at Tanta university Hospital

RPS 211-6 11:00
T2-mapping of the intervertebral disc: pre-treatment assessment, evaluation of changes, and the prognostic value in patients undergoing O2-O3 chemodiscolysis
F. Bruno, E. Tommasino, M. Varrassi, E. Di Cesare, A. Barile, C. Masciocchi, A. Splendiani*; L'Aquila/IT*

Purpose: To assess the MRI modifications of the intervertebral disc (IVD) treated by chemodiscolysis using T2-mapping sequences and possible associations with clinical and instrumental outcomes.
Methods and materials: 37 sciatica patients (20 males, 17 females; mean age 46.15 years) were enrolled for percutaneous CT-guided O2-O3 chemodiscolysis treatment. As a control group, we enrolled 28 patients treated by CT-guided periradicular injections. All patients were submitted to clinical (using visual analogue scale and Oswestry disability index) and imaging studies to evaluate the intervertebral disc area (IDA) and T2-mapping values of the IVD before, at 1-month, and 6-months follow-up.
Results: The mean pre-treatment T2 relaxation time values were 38.80±4.51ms, 44.05±0.91ms, and 45.45±14.11ms for anterior annulus fibrosus (aAF), nucleus pulposus (NP), and posterior annulus fibrosus (pAF), respectively, with a significant increase at the level of the NP (p<0.05) at the 1-month follow-up. The 6-months follow-up showed a reduction with normalisation of intradiscal T2-mapping values. The mean ODI and VAS scores showed significant improvement at the post-treatment follow-up (p<0.05). Correlation analysis of T2 relaxation time values showed a significant correlation of NP values with both the reduction of IDA (0.81, p<0.001) and the improvement of clinical scores (0.86, p<0.001). In the control group, despite the clinical improvement, we did not find significant IVA reduction nor significant T2 values changes after treatment.
Conclusion: T2-mapping may be a useful indicator to predict disc shrinkage and the clinical response to CT-guided O2-O3 injection.
Limitations: The relatively small patient sample.
Ethics committee approval: All procedures were in accordance with the ethical standards of the institutional and/or national research committee and with the Helsinki declaration.
Funding: No funding was received for this work.
Author Disclosures:
F. Bruno: nothing to disclose
E. Tommasino: nothing to disclose
M. Varrassi: nothing to disclose
E. Di Cesare: nothing to disclose
A. Barile: nothing to disclose
A. Splendiani: nothing to disclose
C. Masciocchi: nothing to disclose

RPS 211-7 11:06
Virtual non-calcium dual-energy CT: diagnostic accuracy for the colour-coded depiction of cervical disk herniation and spinal nerve root impingement in comparison with standard grey-scale CT
C. Booz, I. Yel, L. Lenga, S. S. Martin, K. Eichler, J. L. Wichmann, R. Hammerstingl, T. J. Vogl, M. H. Albrecht*; Frankfurt am Main/DE (MoritzAlbrecht@gmx.net)*

Purpose: To investigate the diagnostic accuracy of colour-coded dual-energy CT virtual non-calcium (VNCa) reconstructions for the depiction of cervical disk herniation and spinal nerve root impingement compared to conventional grey-scale CT.
Methods and materials: Data from 57 patients (337 intervertebral disks, 30 women and 27 men) who had undergone third-generation dual-source dual-energy CT and 3.0T MRI of the cervical spine within two weeks from January 2017-December 2018 were retrospectively analysed. 5 blinded radiologists independently analysed conventional grey-scale dual-energy CT series for the presence and degree of cervical disk herniation and spinal nerve root impingement. After 8 weeks, readers reassessed examinations by using colour-coded VNCa reconstructions. Two additional experienced blinded radiologists defined the reference standard in consensus MRI reading sessions. Sensitivity and specificity were primary indices of diagnostic accuracy.

Results: A total of 103 cervical disk herniations were visualised by MRI. Colour-coded VNCa reconstructions yielded significantly higher overall sensitivity (487/515 [95%] vs 392/515 [76%]) and specificity (1107/1170 [95%] vs 906/1170 [77%]) for depicting cervical disk herniation compared to standard CT (all comparisons, P<0.001). Regarding spinal nerve root impingement, VNCa reconstructions revealed higher diagnostic accuracy compared to standard CT (sensitivity, 195/230 [85%] vs 115/230 [50%]; specificity, 1430/1455 [98%] vs 1325/1455 [91%]; all comparisons, P<0.001). VNCa reconstructions provided improved diagnostic confidence (mean scores 4.85 vs 2.94) and image quality (mean scores 4.50 vs 3.15) compared with standard CT images (all comparisons, P<0.001).
Conclusion: Colour-coded VNCa reconstructions substantially improve diagnostic accuracy and confidence for the depiction of cervical disk herniation and spinal nerve root impingement compared to conventional grey-scale CT.
Limitations: The retrospective single-centre study design.
Ethics committee approval: This study was approved by the local IRB.
Funding: No funding was received for this work.
Author Disclosures:
I. Yel: nothing to disclose
C. Booz: Speaker at Siemens Healthineers
L. Lenga: nothing to disclose
S. S. Martin: nothing to disclose
K. Eichler: nothing to disclose
J. L. Wichmann: Employee at Siemens Healthineers, Speaker at Siemens Healthineers, Speaker at GE Healthcare
R. Hammerstingl: nothing to disclose
T. J. Vogl: nothing to disclose
M. H. Albrecht: Speaker at Siemens Healthineers, Speaker at Bracco

RPS 211-8 11:12

Sciatic nerve characteristics in follow-up patients with deep gluteal syndrome (DGS) who underwent surgery

S. B. Stajic[1], A. Vojvodic[2], M. Misic[2], M. Gasic[3], G. Lukic[2], D. Domokos Simic[2]; [1]*Pancevo/RS,* [2]*Belgrade/RS,* [3]*Kosovska Mitrovica/KV*
(stajicsava34@gmail.com)

Purpose: The hypothesis is the relevance of sciatic nerve stiffness in follow-up patients with deep gluteal syndrome (DGS) who underwent surgery. Neurological examinations, pelvic MRI, and electromyography (EMG) were performed. Our focus was to follow-up sciatic nerve characteristics in patients after surgery compared with data one year later.
Methods and materials: The sciatic nerve was scanned by strain elastography using ARFI (colour elastogram and stiffness ratio-SR), during knee movements in patients with DGS without surgery (89) and in patients (24) before and after surgery (follow-up 3 months) and one year later in 21 patients.
Results: The evidently based recovery of sciatic nerve diameter (4.9 to 8 mm, in extension, and 3.9 to 4.6 mm, in flexion) and stiffness (7.3 to 1.3SR in extension, 3.9 to 4.6SR in flexion) shortly after surgery (p<0.01) was partially annulled (6.8 mm, 3.2SR, in extension, 4.4 mm, 6.7SR, in flexion) one year later (p<0.05). Sciatic nerve recovery after surgery was marked (r=0.881) relative to one year later (r=0.579). The correlation between MRI and EMG findings and ARFI nerve stiffness values in patients scheduled for surgery was high (r=0.963) and in those one year later (r=0.749). The overall specificity of the method was 83.8%, sensitivity was 78.4%, and accuracy of 83.9%. Compression processes and the accrual of nerve fibrous strips were evident (MRI) in some patients one year later.
Conclusion: Elastography was a useful tool in decision-making for surgery and in the follow-up.
Limitations: The study has to be developed with more observed cases, but limitations depend on surgical procedures and MRI findings.
Ethics committee approval: n/a
Funding: No funding was received for this work.
Author Disclosures:
S. B. Stajic: Author at Clinical Hospital Center Dr Dragisa Misovic Dedinje, Belgrade, Serbia
A. Vojvodic: Investigator at Clnical Hospital Center Zemun, Belgrade, Serbia
M. Misic: Investigator at Academy of Profession Studies, High Health School, Belgrade, Serbia
M. Gasic: Investigator at Institute of Anatomy, University of Kosovska Mitrovica, Kosovo
G. Lukic: Investigator at Clinical Hospital Center Dr Dragisa Misovic Dedinje, Belgrade, Serbia
D. Domokos Simic: Investigator at Clinical Hospital Center Dr Dragisa Misovic Dedinje, Belgrade, Serbia

RPS 211-9 11:18

Whether brain reorganisation occurs in patients with medullary cone injury: a pilot fMRI study

Q. Chen, N. Chen, Z. Wang*; Beijing/CN (chenqian8319@163.com)*

Purpose: To explore possible brain changes after MCI and to further study their associations with clinical variables.
Methods and materials: 10 MCI patients and 10 healthy controls (HCs) were recruited. The 3D high-resolution structural images and resting-state functional magnetic resonance imaging of all subjects were obtained using a 3.0 Tesla MRI system. VBM and TBSS analysis were conducted to investigate the differences in brain structure between MCI patients and HCs. ALFF and fALFF were used to characterise changes in regional neural activity. Seed-based functional connectivity (FC) analysis was performed to study the whole-brain changes using the results of structural and ALFF/fALFF as seed regions. Associations between brain changes and clinical variables were also analysed.
Results: MCI patients showed decreased ALFF in the right frontal lobe (FL). Additionally, when choosing the right FL as seed, MCI patients showed increased FC in the left orbital frontal cortex (OFC) and right cerebellum posterior lobe (CPL), separately. No significant difference was found in brain structure. The increased FC in the right CPL was negatively correlated with the VAS score.
Conclusion: MCI can cause alterations in brain function and have not yet reached the brain structure. All the changes were within the cognitive-related areas or between these areas and the sensorimotor region, which are closely associated with patients' neuropathic pain. These findings suggest that the real cause of neuropathic pain in MCI patients may be the functional change of cognitive-related brain areas or the change of the connectivity between cognitive-related brain areas and sensorimotor areas.
Limitations: We didn't conduct it as a longitudinal study.
Ethics committee approval: The study protocol was approved by the ethics committee of our hospital.
Funding: National Natural Science Foundation of China (No.81871339).
Author Disclosures:
N. Chen: nothing to disclose
Q. Chen: nothing to disclose
Z. Wang: nothing to disclose

RPS 211-10 11:24

Association of statin dose and nerve damage in type 2 diabetes

J. M. E. Jende, D. S. Kopf, D. Z. Kender, D. J. Gröner, S. Heiland, P. D. P. Nawroth, M. Bendszus, F. Kurz*; Heidelberg/DE*
(johann.jende@gmx.de)

Purpose: Lowering serum cholesterol is an established treatment in type 2 diabetes (T2D). A recent study found that nerve lesions in T2D increase with low serum cholesterol levels, indicating that lowering serum cholesterol levels may contribute to diabetic neuropathy (DN) in T2D. The objective of this study was to investigate whether there is a correlation between statin doses and peripheral nerve lesions in T2D patients.
Methods and materials: 100 participants (52 under statin treatment, 48 without statin treatment) underwent magnetic resonance neurography (MRN) of the right leg at 3 Tesla and clinical, serological, and electrophysiological assessment. Three-dimensional reconstruction of the sciatic nerve was performed to quantify the nerve's diameter and lipid equivalent lesion load (LEL) with a subsequent correlation-analysis of all acquired clinical and serological data.
Results: LEL correlated negatively with nerve conduction velocities and amplitudes of the tibial (r=-0.33; p=0.014 and r=-0.31; p=0.020, respectively) and peroneal nerve (r=-0.51; p<0.001 and r=-0.28; p=0.034, respectively). The statin dose, calculated as the equivalent of simvastatin, correlated positively with the nerve's LEL (r=0.39; p=0.005) and the nerve's mean cross-sectional area (r=0.40;p=0.005). All correlations remained significant after multivariate analysis for patients' sex, age, disease duration, body-mass-index, HbA1c levels, triglycecides, and glomerular filtration rate.
Conclusion: Our findings indicate that the intake of statins in T2D DN is associated with a higher amount of nerve lesions and nerve swelling. These findings are relevant with regards to emerging therapies that promote an aggressive lowering of serum cholesterol in T2D. Further longitudinal studies on the impact of lipid lowering therapies on the course of DN are required.
Limitations: Only cross-sectional data was acquired.
Ethics committee approval: Local ethics number S-383/2016, clinicaltrials.gov identifier (NCT03022721).
Funding: German Research Council (Deutsche Forschungsgesellschaft, DFG).
Author Disclosures:
J. M. E. Jende: nothing to disclose
D. S. Kopf: nothing to disclose
D. Z. Kender: nothing to disclose
P. D. P. Nawroth: nothing to disclose
S. Heiland: nothing to disclose
M. Bendszus: nothing to disclose
D. J. Gröner: nothing to disclose
F. Kurz: nothing to disclose

RPS 211-11 11:30

Troponin T and peripheral nerve damage in type 2 diabetes

J. M. E. Jende, D. S. Kopf, D. Z. Kender, D. J. Gröner, P. D. P. Nawroth, M. Bendszus, F. Kurz*; Heidelberg/DE (johann.jende@gmx.de)*

Purpose: Clinical studies have suggested that changes in peripheral nerve microcirculation may contribute to nerve damage in diabetic neuropathy (DN). It has recently been shown that both high-sensitivity troponin assays (hsTNT) and N-terminal brain natriuretic peptide (pro-BNP) provide predictive values for both cardiac and peripheral microangiopathy in type 2 diabetes (T2D). The aim of this study was to investigate the association of sciatic nerve integrity in 3 Tesla magnetic resonance neurography (MRN) with hsTNT and pro-BNP serum levels in T2D patients.
Methods and materials: 51 patients with T2D (23 without DN, 28 with DN) and 10 control subjects without diabetes underwent diffusion-weighted MRN at 3 Tesla. The sciatic nerve's fractional anisotropy (FA), a marker for structural nerve integrity, was calculated in an automated approach. Results were correlated with clinical, electrophysiological, and serological data.
Results: In T2D patients, hsTNT showed a negative correlation with the sciatic nerve's FA (r=-0.52; p<0.001) with a closer correlation in DN patients (r=-0.66; p<0.001). HsTNT further correlated positively with the neuropathy disability score (NDS; r=0.39, p=0.005). Negative correlations were found with sural nerve conduction velocities (NCVs; r=-0.65; p<0.001), tibial and peroneal NCVs (r=-0.44; p=0.002 and r=-0.42; p=0.003, respectively), and tibial and peroneal amplitudes (r=-0.53; p<0.001 and r=-0.29; p=0.044, respectively). No such correlations were found for pro-BNP.
Conclusion: This study is the first to show that hsTNT is a potential indicator for structural nerve damage in T2D. Our results support the hypothesis that peripheral microangiopathy is a key contributor to diabetic neuropathy in T2D.
Limitations: The number of participants precludes multivariate analysis for all parameters acquired.
Ethics committee approval: Local ethics number S-383/2016, clinicaltrials.gov identifier (NCT03022721).
Funding: The German research council (Deutsche Forschungsgesellschaft, SFB1158).
Author Disclosures:
J. M. E. Jende: nothing to disclose
D. Z. Kender: nothing to disclose
D. J. Gröner: nothing to disclose
D. S. Kopf: nothing to disclose
M. Bendszus: nothing to disclose
P. D. P. Nawroth: nothing to disclose
F. Kurz: nothing to disclose

RPS 211-12 11:36

The role of pre-operative MR and polysomnography in children with achondroplasia

N. Jenko, D. Connolly, A. Raghavan, H. Elphick, J. Fernandes, S. Ushewokunze, P. Arundel, A. C. Offiah*; Sheffield/UK (n@jenko.eu)*

Purpose: All children with achondroplasia have craniocervical junction (CCJ) stenosis, which may lead to cardio-respiratory arrest. There is an on-going debate as to whether routine MRI screening is indicated in infants. Our aim was to assess MR findings in a cohort of children with achondroplasia.
Methods and materials: The severity of stenosis was assessed independently by 2 observers in the following way: 1=narrowing of CCJ, 2=complete effacement of CSF, 3=distortion and compression of the spinal cord, and 4=T2 changes in the cord. MR findings, MR assessment of CSF flow, polysomnography results, and history of surgical decompression were recorded. Interobserver reliability was assessed using Cohen's kappa.
Results: A total of 85 children under the care of our institution were identified. 52 patients underwent MRI. 7 were excluded due to insufficient pre-decompression imaging.
Lumbar stenosis was demonstrated in 13 of the 36 patients for whom whole-spine imaging was available. The median age for children with distal stenosis was 12 years, compared to 1 year for children without. Interobserver reliability of the scoring was 0.60 (moderate), which improved to 0.81 (strong) when grades 1 and 2 were merged.
Conclusion: The distortion of the spinal cord at the CCJ (grades 3 and 4) correlates well with abnormal polysomnography. The presence of CSF flow does not exclude stenosis. In older children, we advocate acquiring whole-spine imaging due to the high prevalence of distal stenosis. To improve observer reliability, a 3 rather than 4-point MRI scoring system should be considered, merging the current grades 1 and 2.
Limitations: This work is a single-centre retrospective analysis. The grading system has not been validated.
Ethics committee approval: n/a
Funding: No funding was received for this work.
Author Disclosures:
A. Raghavan: nothing to disclose
N. Jenko: nothing to disclose
A. C. Offiah: nothing to disclose
P. Arundel: nothing to disclose
D. Connolly: nothing to disclose
J. Fernandes: nothing to disclose
H. Elphick: nothing to disclose
S. Ushewokunze: nothing to disclose

RPS 211-13 11:42

The role of diffusion tensor imaging in Hirayama disease

A. Ignatius, B. P. S., D. R. S.*; Chennai/IN (dr.amalanignatius@gmail.com)*

Purpose: Hirayama's disease (HD) is a benign, self-limited, motor neuron disease that results in sporadic juvenile muscular atrophy of the distal upper extremities. The aim is to analyse diffusion tensor imaging (DTI) parameters of HD which helps in earlier diagnosis and predicts the microarchitectural damage of the spinal cord and to assess the DTI parameters in both neutral and flexion positions of patients with HD and compare that with normal sex and age-matched controls. The diagnosis will be confirmed based on clinical, electromyographic, MRI findings, and follow-up.
Methods and materials: This is a prospective study conducted in Barnard Institute of Radiology, MMC, and RGGGH. Consecutive subjects undergoing routine clinical spinal magnetic resonance for Hirayama Disease were invited to participate in this study. RESOLVE (readout segmentation of long variable echo trains) DTI was performed using a 1.5T scanner (Avato, Siemens) and FA, ADC (MD), E1 (AD), E2, E3, and RD values were analysed.
Results: 9 patients with HD had decreased FA and increased ADC values in the neutral position compared to age and sex-matched controls, among whom 8 patients had further decreased FA and increased ADC in the flexion position. 1 patient with HD had FA and ADC values similar to the controls.
Conclusion: DTI parameters confirm the damage of the cervical cord during flexion and non-invasively reveal the neural status of HD patients. FA and ADC is a useful micro-biomarker in diagnosing Hirayama disease.
Limitations: Further studies with larger cohorts are needed to infer a definite conclusion. Observer bias while marking the region of interest.
Ethics committee approval: The study in approved by Institutional Ethical Committee of Madras Medical College.
Funding: No funding was received for this work.
Author Disclosures:
A. Ignatius: nothing to disclose
B. P. S.: nothing to disclose
D. R. S.: nothing to disclose

RPS 211-14 11:48

Morphometric analysis of the atlas in Down syndrome patients

F. Albadr, A. Al-Habib, A. Abujamea, A. Alatar, A. Alahmari, E. Alshail*; Riyadh/SA (abdul.alatar@gmail.com)*

Purpose: Atlantoaxial instability (AAI) is considered the most prevalent cervical abnormality in patients with Down syndrome (DS). No previous study has described the anatomy of the atlas lateral mass (ALM) in DS comparative to non-DS patients. This study aimed to provide a quantitative analysis of ALM morphology in DS patients to identify differences that might be relevant for safe instrumentation.
Methods and materials: A retrospective study. DS cases were identified. A control group included age-and sex-matched patients without DS who had a cervical CT scan were included. CT image reconstructions of these scans were made using Siemens syngo via Workstation to adjust any rotated images of C1. A neuroradiologist performed the measurements of anatomic details of ALM. The included radiologic measurements were the anterior height (AH), posterior height (PH), posterior height inferior to arch (PHIA), anteroposterior diameter (APD), and mid-width (MW), which were measured bilaterally. The posterior-to-anterior height ratio (PH/AH*100) was calculated. The measurements of patients with/without DS were compared.
Results: A total of 1,265 patients with DS were identified. 40 met our criteria, 18 of them were excluded due to poor CT quality. A total of 22 patients with and 22 without DS were included in the analysis. The median age for DS and non-DS was 15 years and 14.5 years, respectively. Three measurements were significantly smaller in patients with DS; anterior-height (p=0.001), posterior-height (p<0.001), and the posterior-anterior height ratio (p=0.001).
Conclusion: Patients with DS had a trapezoid-like geometry of their ALM with smaller heights of the posterior wall compared to the anterior wall. The distance available for screw insertion (below the posterior arch of ALM) is significantly smaller in DS patients. These variations should be considered during surgical planning for the safe placement of instrumentation.

Limitations: The retrospective nature of the study.
Ethics committee approval: Ethics committee approval obtained.
Funding: No funding was received for this work.
Author Disclosures:
F. Albadr: nothing to disclose
A. Alatar: nothing to disclose
A. Al-Habib: nothing to disclose
A. Alahmari: nothing to disclose
A. Abujamea: nothing to disclose
E. Alshail: nothing to disclose

RPS 211-15 11:54
MR cisternography with 3DCISS as a screening test for the detection of active CSF leaks: a comparison with standard CT and MR cisternography
P. Reddy[1], S. Ismail[2], B. B. Das[3], B. Nagabhushana Reddy[1], S. Viswamitra[1]; *[1]Bangalore/IN, [2]Puttaparthi, [3]Bangalore, Karnataka/IN (86prashanth.reddy@gmail.com)*

Purpose: To assess the diagnostic performance of the 3DCISS MRI sequence in the detection of CSF rhinorrhea in patients with active leaks.
Methods and materials: A retrospective review of our database was performed and imaging studies meeting the inclusion criteria were used for the study. The inclusion criteria were patients with active CSF leak due to any aetiology and patients with both 3DCISS MRI and conventional CT or MR cisternography. The exclusion criteria were recurrent CSF leaks following endoscopic surgery and studies with suboptimal image quality. The sample size was 21 patients.
All CT images were acquired using a 128 slice CT scanner. MR imaging was performed on 1.5T a scanner (Siemens Aera). CT/MR cisternography was performed as per standard protocol.
Images were analysed for the presence, site, and the number of skull-base defects by 2 blinded reviewers with 5 years and 6 years of experience in neuroradiology.
Results: 25 cases were included in the study. 11 patients had spontaneous leaks and 14 had non-spontaneous leaks.
3DCISS MRI had a sensitivity, specificity, positive predictive value, and negative predictive value of 100%, 71.4%, 90%, and 100%, respectively, with p=0.00085 for the detection of a CSF leak irrespective of aetiology.
For spontaneous CSF leaks, the sensitivity, specificity, positive predictive value, and negative predictive value were 100%, 62.5%, 85.7%, and 100%, respectively, with p=0.09.
Conclusion: 3D CISS MR cisternography has very high sensitivity and negative predictive value for the detection of CSF leaks, irrespective of aetiology, and may be used as an initial screening test.
Limitations: The small sample size and retrospective design.
Ethics committee approval: The need for informed consent was waived due to the retrospective nature of the study.
Funding: No funding was received for this work.
Author Disclosures:
P. Reddy: nothing to disclose
S. Ismail: nothing to disclose
B. B. Das: nothing to disclose
B. Nagabhushana Reddy: nothing to disclose
S. Viswamitra: nothing to disclose

10:30 - 12:00 **Room Y**

My Thesis in 3 Minutes

MyT3 2
Breast

Moderators:
I. Gheonea; Craiova/RO
S. Zackrisson; Malmö/SE

MyT3 2-1 10:30
Axillary lymph node status in BIRADS 4-5 female patients: a management cornerstone. Can ultrasound elastography help?
S. T. Hamed, O. M. M. N. Nada, O. Zakaria, D. Elmesidy, M. A. G. A. M. Eissa; *Cairo/EG (dr.chipsy@gmail.com)*

Purpose: Assess accuracy and additive value of breast elastography in evaluation of axillary lymph node status in patients with BIRADS 4 and 5 breast lesions, diagnosed on sono-mammography.
Methods and materials: 60 female patients with BIRADS 4 or 5 lesions were included. Conventional ultrasonography "US", strain "SE" and shear wave "SWE" elastography examinations for their lymph nodes done and their imaging findings evaluated individually and correlated with pathology. US: lymph nodes were evaluated regarding shape (ovoid or non-ovoid), cortical thickening > 3mm "according to its calculated cutoff value" (present or not, and if present "diffuse or focal or irregular mass"), Hilum (central, effaced, eccentric or not-preserved), Vascularity (hilar or non-hilar). Elastography: lymph nodes were evaluated regarding the percentage of the stiff cortex on colour-coded images with a modulated scoring system. Also cutoff values for strain ratio "SR" (in SE) and maximum elasticity "Emax", elasticity ratio "Eratio" (in SWE) calculated.
Results: In US, Cortical thickness was the most sensitive criteria (100% sensitivity). And the vascular pattern was the second sensitive. Eratio showed the highest diagnostic indices compared to rest of SWE criteria with sensitivity, specificity, accuracy (76.9%,100%,85% respectively). SR showed higher specificity & accuracy than qualitative SE (76.2% vs 57.14% and 83.33% vs 80% respectively), with relatively lower sensitivity (87.2 % vs 92.31% respectively). US showed highest sensitivity & accuracy (100%, 88.33% respectively) among the rest of used modalities. with relatively lower specificity (66.67%).
Conclusion: Addition of strain or shear wave elastogrphy offer no significant benefit over conventional ultrasound alone in evaluation of axillary lymph nodes in breast cancer patients.
Limitations: Tissue compression extent influences elasticity image.
Ethics committee approval: All participated patients provided informed written consents following our institutional ethical committee approval.
Funding: No funding was received for this work.
Author Disclosures:
M. A. G. A. M. Eissa: nothing to disclose
S. T. Hamed: nothing to disclose
O. M. M. N. Nada: nothing to disclose
D. Elmesidy: nothing to disclose
O. Zakaria: nothing to disclose

MyT3 2-2 10:34
Mammographic density and risk factors collected by direct interview in breast interval and screen-detected cancers
L. La Corte[1], L. Baglietto[1], D. Caramella[1], C. Iacconi[2]; *[1]Pisa/IT, [2]Carrara/IT (lacorte.luisa@gmail.com)*

Purpose: To evaluate risk factors in a cohort of women in a mammographic screening programme.
Methods and materials: In a retrospective cohort of 140.504 women, 45 to 70 years old between 2007 and 2017, a total of 94 interval cancers (IC), 501 screen-detected cancers (SDC) and 282 healthy women (CONTROLS) were recruited. For each IC, a blind experienced radiologist compared the last negative mammogram and the diagnostic one to classify cancers (true interval, minimal sign, occult, false negative). On every mammogram the ACR BI-RADS density score was reported; each woman received a phone interview to collect data on risk factors.
Results: Mammographic density in IC and SDC was distributed as follows: A 13% vs 29%, B 24% vs 49%, C 59% vs 17%, D 5% in both types. Proportion of tumour subtypes is similar in both cancer types with a prevalence of LUM B HER2- (41-48%). Tumour dimensions: prevalent size IC > 1 cm (66%) vs SDC <1cm (55%). The evaluation of BMI in IC and SDC and its comparison with controls results in a p value < 0.002. Death rate is 1,4% for SDC vs. 7,4 for IC. Other risk factors were not significantly different.
Conclusion: In our analysis, we found a higher mammographic density in IC than in SDC, confirming dense breast as one of the most important factors linked to intervals. The higher tumour dimensions in IC may depends on faster spreading and higher aggressiveness of the cancer and could explain the higher death rate. The result of the chi square test underlines the importance of BMI as an independent risk factor and the necessity to control body weight for breast cancer prevention.
Limitations: Retrospective analysis.
Ethics committee approval: The study was approved by the ethics committee.
Funding: No funding was received.
Author Disclosures:
L. La Corte: nothing to disclose
C. Iacconi: nothing to disclose
L. Baglietto: nothing to disclose
D. Caramella: nothing to disclose

MyT3 2-3 10:38
MRI and PET/CT in parallel for the detection of axillary lymph node metastases in breast cancer patients: a meta-analysis
X. Zhang, H. Luo, J. Zhang, Y. Liu; *Chengdu/CN*

Purpose: To evaluate the diagnostic accuracy of MRI and PET/CT in direct comparative studies as noninvasive modalities in detecting axillary lymph node metastases in breast cancer patients.
Methods and materials: A systematic literature search in the PubMed, EMBASE, Web of Science, Cochrane, and Chinese Biomedical Literature Databases to identify relevant original studies. Study quality was assessed using the Quality Assessment of Diagnostic Accuracy Studies (version 2). Study data

were independently extracted to calculate sensitivity and specificity, as well as areas under summary receiver operating characteristic curves (AUCs).
Results: The sample comprised 9 studies including patients with breast cancer, and in which MRI and PET/CT were both performed to assess axillary lymph node status. Pooled sensitivity were 0.56 (95% confidence interval [CI] 0.51–0.61) on both MRI and PET/CT; pooled specificity were 0.87 (95% confidence interval [CI] 0.85–0.90) and 0.93 (95% CI 0.91–0.95) on MRI and PET/CT respectively. The diagnostic odds ratio was 7.62 (95% CI 5.52–10.52) on MRI and 14.45 (95% CI 9.95–20.99) on PET/CT respectively. The AUC and Q* index were 0.8333 and 0.7656 on MRI; the AUC and Q* index were 0.8772 and 0.8076 on PET/CT.
Conclusion: For detecting lymph node metastases noninvasively, MRI and PET/CT both had low sensitivity; MRI had moderately high specificity, while PET/CT had high specificity. Large-scale, quality-controlled, prospective studies are needed to verify the diagnostic accuracy of these modalities.
Limitations: First, a small number of studies was included. Second, most included studies were retrospective, which may have caused patient selection bias. Third, most studies used only morphologic features (without functional features) on MRI as criteria for detecting axillary lymph node metastases, which may have contributed to the low sensitivity and specificity of MRI.
Ethics committee approval: n/a
Funding: No funding was received for this work.
Author Disclosures:
Y. Liu: nothing to disclose
X. Zhang: nothing to disclose
H. Luo: nothing to disclose
J. Zhang: nothing to disclose

MyT3 2-4 10:42
A preliminary study of the combination of ultrafast and abbreviated dynamic contrast-enhanced breast MRI
S. Jeong, S. M. Ha, H. S. Ahn, S. Woo, H.-C. Shin*; Seoul/KR (fofrl@naver.com)*

Purpose: We combined the abbreviated and ultrafast MRI technique with the standard MRI protocol and compared lesion characterisation quantitatively and qualitatively to the standard MRI protocol.
Methods and materials: Fifty-six patients with breast cancer who underwent MRI from June 2017 to May 2018 and fulfilled our inclusion criteria were included. Three radiologists measured the lesion sizes, described the MRI findings using BI-RADS lexicon and demarcated the regions of interest to extract the volumetric quantitative and semi-quantitative parameters. We used Pearson's correlation analysis comparing the quantitative and semi-quantitative parameters. To evaluate the inter-observer variability, we calculated the intra-correlation coefficient. We also analysed the correlation in BI-RADS lexicon.
Results: There were 45 (80.4%) luminal and 11 (19.6%) non-luminal breast cancers, and the most common tumour subtype was invasive carcinoma (n=48, 85.7%), followed by ductal carcinoma in situ (n=8, 14.3%). Regarding correlation between the quantitative and semi-quantitative parameters, K^{trans} significantly correlated with the wash-in factor (r, 0.862; $p < 0.001$) and AUC value (r, 0.951; $p < 0.001$). The lesion size measured by standard and combined abbreviated-ultrafast phases and that from the surgical pathological specimens showed moderate agreement (ICC range, 0.516−0.578). The ICCs among the three readers were excellent for lesion size measurement, BI-RADS lexicon regarding lesion type, mass shape, margin, internal enhancement, non-mass enhancement distribution, and internal enhancement by the standard and combined abbreviated-ultrafast protocols.
Conclusion: The use of the modified and combined abbreviated-ultrafast MRI protocol provides a reliable measurement of the quantitative parameters and may aid in the screening of breast cancer.
Limitations: This study was a retrospective one and conducted in a single centre. Further, this study involved a small number of cases with only breast cancer.
Ethics committee approval: n/a
Funding: No funding was received for this work.
Author Disclosures:
S. Jeong: Speaker at Chung-Ang University Hospital, Author at Chung-Ang University Hospital
S. M. Ha: Author at Seoul National University Hospital
H. S. Ahn: Author at Chung-Ang University Hospital
S. Woo: nothing to disclose
H.-C. Shin: nothing to disclose

MyT3 2-5 10:46
Missed breast lesions in mammography: what factors are we overlooking?
M. Malik*; Islamabad/PK (xz.mariam@gmail.com)*

Purpose: To determine frequency of false negative mammograms and various factors leading to missed breast lesions in mammography.
Methods and materials: This study was conducted at the radiology department of Combined Military Hospital Rawalpindi. 150 patients were included between 15th December 2014 till 10th January 2017. Patients in whom no con-commitment ultrasound or only unilateral mammography was done were excluded. Cases assigned BIRAD 4 and 5 in whom no other multicentric, multifocal or contralateral breast carcinoma was detected were excluded. Two standard views of mammography namely craniocaudal and mediolateral oblique positions of both breasts were obtained. Cause of missed breast carcinoma on the initial mammogram was analysed and classified into the four factors of patient, tumour, technical and provider. Frequency of false-negative mammograms was recorded.
Results: In our study, the percentage of the false-negative mammogram was 29.59%. Lesion factors were seen in 59 (39.67%) patients and included subtle carcinomas, signs of malignancy, small groups of amorphous or punctuate microcalcifications, focal asymmetric densities, dilated ducts, relatively well-circumscribed masses, masked carcinomas, multifocal carcinomas, multicentric and synchronous carcinomas and diffuse oedema pattern. Patient factors were seen in 40 (26.67%) patients and included dense breasts. Provider factors of mis-interpretation and bad interpretation were seen in 29 (19.33%) patients and technical factors of bad exposure and malpositioned breasts in 22 (26.67%) patients.
Conclusion: Lesion factors were the most common cause of false-negative mammograms followed by patient factors, technical factors and provider factors respectively. Recognition of these would decrease the frequency of false-negative mammogram and in turn breast cancer morbidity and mortality.
Limitations: There are no potential limitations of our study.
Ethics committee approval: Study was approved by Institutional Review Board of Combined Military Hospital Rawalpindi.
Funding: No funding was received.
Author Disclosures:
M. Malik: nothing to disclose

MyT3 2-6 10:50
Breast lesions of uncertain malignant potential (B3): can different vacuum-assisted biopsy needles (11G vs 8G) affect the outcome?
A. Franconeri[1], C. Bellini[2], G. Bicchierai[2], D. de Benedetto[2], F. Di Naro[2], J. Nori[2], V. Miele[2]*; [1]Pavia/IT, [2]Florence/IT (afrancon88@gmail.com)*

Purpose: To evaluate if the use of 11G or 8G needle in vacuum-assisted biopsy (VAB) can predict different outcomes of breast lesions of uncertain malignant potential (B3).
Methods and materials: We retrospectively screened 1025 women with a histological diagnosis of B3 from 2000 to 2018. All patients underwent needle core biopsy (NCB) or vacuum-assisted biopsy (VAB) at our centre. We selected patients with VAB and histological surgical specimen after open excision (OE) or vacuum-assisted excision (VAE) or proof of stability on follow-up, with a final population of 378 women. Biopsy guidance systems were stereotactic/tomosynthesis (STX/TOMO) and ultrasound (US). We evaluated positive predictive values (PPV) of the malignant outcome of the two biopsy needles in each B3 histological subtype. Chi-square test and Fisher exact test were used to compare groups.
Results: Out of 378 VABs, 377 were STX/TOMO-guided and 1 US-guided. 86 (22.8%) were performed with 11G and 292 (77.2%) with 8G. Overall VAB PPV of malignant outcome was 16.1% (9.3% carcinoma in situ, 6.9% invasive). 11G and 8G PPV was 20.9% vs 14.7%, respectively (p-value=0.2271). No statistically significant differences in upgrade rates were found between 11G and 8G in not pure ADH (p=0.1043), pure ADH (p=0.0685), FEA (p=1), not pure LN (p=0.8595), pure LN (p=0.7973).
Conclusion: Our results showed that 11G or 8G needle in VAB does not affect B3 outcome in any subtype. In the special case of ADH, we think that the limited group sample may have affected the statistical significance between the two groups.
Limitations: The retrospective nature of the study and different numeric sample between 11G and 8G.
Ethics committee approval: n/a
Funding: No funding was received for this work.
Author Disclosures:
A. Franconeri: nothing to disclose
C. Bellini: nothing to disclose
G. Bicchierai: nothing to disclose
D. de Benedetto: nothing to disclose
F. Di Naro: nothing to disclose
J. Nori: nothing to disclose
V. Miele: nothing to disclose

MyT3 2-7 10:54

Breast arterial calcification on mammography does not predict coronary artery disease on invasive coronary angiography

A. Fathala; *Riyadh/SA (ahm35799@hotmail.com)*

Purpose: The main purpose of this retrospective associated was to investigate the association between visually detected BAC on screening mammography and coronary artery disease based on conventional invasive coronary angiography (CAG).
Methods and materials: The sample was formed of 190 female patients, with a mean age of 60.5 ± 7 years old ranging from 51 to 87 years. All our patients had undergone a mammography screening and cardiac catheterisations with mean interval 3.6 ± 2.8 months ranging from 1 to 12 months. Digital mammography: grades of calcification: (1) scattered calcifications, (2) few punctate vascular calcifications, (3) coarse or tram track calcifications affecting < 3 vessels, (4) coarse or tram track calcifications affecting ≥3 vessels. Conventional invasive coronary angiography (CAG). Two main groups based on the presence or absence of luminal stenosis were formed: patients without (CHD−) and patients with (CHD+) CHD.
Results: The sample was formed of 190 female patients, with a mean age of 60.5 ± 7 years old ranging from 51 to 87 years. Out of 190, BAC was found in 113 (60%). There was strong association between BAC and CAD risk factors (hypertension (P-value 0.01), diabetes (P-value <0.03), and chronic kidney disease (P-value <0.001). There was no association between BAC and dyslipidemia and smoking. The strongest predictors of CAD on CAG were bAC and hyperlipidemia.
Conclusion: BAC on mammography does not predict angiographically proven CAD. There is a strong association between BAC and age and many other conventional CAD risk factors.
Limitations: This study is a retrospective, single-centre study.
Ethics committee approval: The study was approved by the hospital research ethics committee.
Funding: No funding was received.
Author Disclosures:
A. Fathala: nothing to disclose

MyT3 2-8 10:58

Diagnostic performance of unenhanced T2-weighted and IVIM DW MRI for axillary lymph nodal staging in breast cancer

Y. Liu, H. Luo, C. Wang, M. Wang, J. Ren; *Chengdu/CN*

Purpose: To investigate the performance of IVIM parameters compared with unenhanced T2-weighted traditional features in diagnosing axillary lymph nodes (LN) metastases in newly diagnosed breast cancer patients.
Methods and materials: 88 patients with histopathologically proven breast cancer were prospectively enrolled, who underwent 3.0 T T2-weighted imaging (T2WI) and IVIM DWI. Two radiologists independently identified metastatic LN by traditional features (including long axis [L] , short axis [S], L/S ratio [<1.6], fatty hilum, margin, signal intensity). Then on IVIM DW imaging, IVIM parameters (including ADC value, D, D* and f) were obtained. The Mann-Whitney U test was used to compare the performance of the aforementioned criteria to determine benignity or malignancy of axillary LN.
Results: 38 patients were found with metastatic LN, while 50 patients with non-metastatic LN. All above IVIM parameters, L, S, L/S ratio, fatty hilum and margin showed no significant differences between the two groups. Metastatic LNs were with abnormal signal intensity compared with non-metastatic LNs (P =0.007); sensitivity and specificity of which for differentiation were 73% and 60% respectively. If combing all the features on T2WI, the sensitivity and specificity for diagnosing metastatic LN were 69% and 66% respectively.
Conclusion: IVIM DWI was not useful to distinguish metastatic from non-metastatic LNs in axilla. The features on unenhanced T2WI also had low sensitivity and specificity.
Limitations: First, the patient number was small. Second, most axillary LNs with a short diameter smaller than 5 mm, which would prone to be influenced by artefact or partial volume effect from adjacent tissue. Third, we used only unenhanced features (not including features on dynamic contrast-enhanced MRI) as criteria for detecting LN metastases.
Ethics committee approval: This prospective study was approved by the institutional review board of our hospital.
Funding: No funding was received for this study.
Author Disclosures:
M. Wang: nothing to disclose
Y. Liu: nothing to disclose
H. Luo: nothing to disclose
C. Wang: nothing to disclose
J. Ren: nothing to disclose

MyT3 2-9 11:02

Role of ultrasound vs contrast-enhanced mammography in the characterisation of lesions in dense breasts

R. R. M. Abdel Gawad; *Cairo/EG (reemramadan1@hotmail.com)*

Purpose: Breast density affects mammographic sensitivity by a masking phenomenon; as the dense tissue may obscure an underlying malignancy. Breast density has been reported to be a strong independent risk factor for breast cancer. Purpose of this work is to study the impact of breast ultrasound vs contrast-enhanced spectral mammography in the detection and diagnosis of lesions in the mammography dense breasts.
Methods and materials: This study was done on 50 cases with mammography dense breast classified as (C) or (D). All patients underwent digital mammography, breast ultrasound and contrast-enhanced spectral mammography.
Results: By comparing both modalities, they both revealed the same specificity 65%, with higher sensitivity in CESM 97% compared to 88% in ultrasound and thus total accuracy was higher in CESM 85% compared to 79% in ultrasound.
Conclusion: CESM revealed superior diagnostic accuracy and higher sensitivity than ultrasound and hence, permitted better detection of malignant lesions. CESM can be performed in routine practice changing the diagnostic, and further, the treatment strategy. Bilateral CESM is feasible, easily accomplished and well-tolerated. CESM is cost-effective, easily feasible and radiation dose is a minor drawback as it is only slightly higher than for conventional mammography. Future studies should investigate the performance of CESM in larger population groups to evaluate the diagnostic accuracy of this promising imaging method particularly in women at high risk and women with dense breasts.
Limitations: Our study is limited by small sample size and the fact that was performed in a single institution. Multi-centre with multi-reader studies are needed. Also the increased number of malignant lesions 33/53 lesions (62.3 %), this could be attributed to the work nature of the institute and the targeted study population.
Ethics committee approval: n/a
Funding: No funding was received for this work.
Author Disclosures:
R. R. M. Abdel Gawad: Speaker at National cancer institute

MyT3 2-10 11:06

Outcome of B3 breast lesions with 14G needle core biopsy (NCB): 18-years monocentric experience

C. Bellini[1], A. Franconeri[2], G. Bicchierai[1], D. de Benedetto[1], F. Di Naro[1], J. Nori[1], V. Miele[1]; *[1]Florence/IT, [2]Pavia/IT (1chiarabellini@gmail.com)*

Purpose: To evaluate the outcome of histological subtypes of breast lesions of uncertain malignant potential (B3), using 14G needle core biopsy.
Methods and materials: We retrospectively screened 1025 women with a histological diagnosis of B3 from 2000 to 2018. All patients underwent needle core biopsy (NCB) or vacuum-assisted biopsy (VAB) at our centre. We selected patients with 14G NCB and histological surgical specimen after open excision (OE) or vacuum-assisted excision (VAE) or proof of stability on follow-up, with a final population of 400 women. Biopsy guidance systems were ultrasound (US) and clinical (freehand). We evaluated positive predictive values (PPV) of malignant outcome in each B3 histological subtype. Chi-square and t student tests were used to assess statistically significant differences between groups.
Results: Out of 400 NCBs, 394 (98.5%) were US-guided and 6 (1.5%) freehand. Overall NCB PPV of malignant outcome was 27.3% (13% carcinoma in situ, 14.3% invasive). Out of 44 carcinomas in situ, 14 (32%) were G1, 25 (57%) G2 and 5 (11%) G3, while out of 45 invasive, 21 (47%) were G1, 20 (44%) G2 and 4 (9%) G3. Mean size of carcinomas in situ and invasive was 18.43±10.32 mm (range: 4.00-80.00) vs 41.88±65.63 mm (range: 4.00-200.00), respectively (p= 0.0215). The histological subtypes with the highest association with malignancy were pure atypical ductal hyperplasia-ADH (68.3%), not pure ADH (64.3%), flat epithelial atipia-FEA (26.9%), pure lobular neoplasia-LN (20%) and not pure LN (21.7%). No statistically significant difference was found between pure ADH and not pure ADH (p=0.725) and between pure LN and not pure LN (p =1).
Conclusion: Our results using 14G NCB showed the highest malignancy outcome rates for ADH (64.3%), FEA (26.9%) and LN (21.7%).
Limitations: This study is a retrospective study.
Ethics committee approval: n/a
Funding: No funding received for this work.
Author Disclosures:
A. Franconeri: nothing to disclose
C. Bellini: nothing to disclose
G. Bicchierai: nothing to disclose
D. de Benedetto: nothing to disclose
F. Di Naro: nothing to disclose
J. Nori: nothing to disclose
V. Miele: nothing to disclose

MyT3 2-11 11:10

Whole-lesion texture analysis of apparent diffusion coefficients for monitoring early response in patients with breast cancer undergoing concurrent chemotherapy

W. Wang, J. Cheng*; Zhengzhou/CN*

Purpose: To explore the role of whole-tumour texture analysis of apparent diffusion coefficient (ADC) related parameters in the early assessment of treatment response during the concurrent chemotherapy (CCT) course of breast cancer.
Methods and materials: We retrospectively evaluated findings in 42 patients with breast cancer who underwent diffusion-weighted imaging (b=0,800 s/mm^2) at 3T with the acquisition of corresponding ADC maps before CCT, at the end of 2nd and 4th week during chemotherapy. Whole lesion ADC texture analysis generated several texture analysis-related parameters including skewness, kurtosis, mean, variance and per cent. The ADC texture analysiss of 42 patients were generated to visually observe dynamic changes in the texture analysis parameters following CCT.
Results: All parameters except mean and variance showed significant changes during CCT (all $P < 0.05$). Skewness and kurtosis both showed high early decline rate (25%, 32 %) at the end of 2nd week of CCT. The percent of ADC texture analysis also changed obviously following CCT.
Conclusion: Whole lesion texture analysis of ADC held the potential in monitoring early tumour response in patients with breast cancer undergoing CCT.
Limitations: It is a small-scale retrospective research in which the number of patients per tumour is unbalanced. The correlation between ADC texture analysis parameters and histopathological characteristics needs further study.
Ethics committee approval: No ethics committee approval was obtained.
Funding: National Key R&D Program of China (2016YFC0106900). The investigation of equipment evaluation and clinical applications in magnetic resonance imaging.
Author Disclosures:
W. Wang: Author at First Affiliated Hospital of Zhengzhou University
J. Cheng: Author at First Affiliated Hospital of Zhengzhou University

MyT3 2-12 11:14

Digital breast tomosynthesis-guided vacuum-assisted breast biopsy (DBT-VABB): comparing two different ways of local anaesthesia administration

M. A. Orsi, F. Leone, M. Cellina, G. Oliva*; Milan/IT (m.orsi83@gmail.com)*

Purpose: To understand if the adjunction of a small amount of lidoicaine, directly administered via the biopsy needle, could reduce the pain in DBT-VABB.
Methods and materials: Between November 2017 and September 2019, consecutive patients subjected to DBT-VABB performed in a single institution, were randomly selected to receive or local needle lidocaine injection before biopsy (lido 1) or local needle lidocaine injection plus direct lidocaine administration via the biopsy needle (4 cc) (lido 2). Right after the biopsy a pain scale chart from 1 to 10 was collected.
Results: Out of 124 consecutive patients treated, 61 were "lido 1" and 63 "lido 2". The "lido 2" group experienced less pain than the "lido 1" group: the mean pain scale value for "lido 1" group was 5.3 and for "lido 2" group was 3.7.
Conclusion: Adding local anaesthesia administration via the biopsy needle could reduce the pain in DBT-VABB. This is a preliminary prospective experience; more cases are needed to confirm these preliminary data.
Limitations: This study has following limitations: a single centre study, operators not blinded to the patient's assigned group, more lidocaine administration in the "lido 2" group.
Ethics committee approval: Written informed consent was obtained.
Funding: No funding was received for this work.
Author Disclosures:
M. A. Orsi: nothing to disclose
F. Leone: nothing to disclose
M. Cellina: nothing to disclose
G. Oliva: nothing to disclose

MyT3 2-13 11:18

Breast's density and CAD: could a suspicous lesion change the assessment of computer-aided detection? A retrospective study

F. Leone, M. A. Orsi, M. Cellina, G. Oliva*; Milan/IT (federica-leone@live.it)*

Purpose: To compare mammograms density rated by radiologists and computer-aided detection (CAD) in order to investigate how a suspicious lesion could change the assessment.
Methods and materials: We reviewed a retrospective cohort of 6453 patients with mammograms acquired in a single hospital between January and September 2019. We included the mammograms with breast suspicious lesion (BIRADS 4 and 5) histopathology proven, with a focus on microcalcification, and images in full compliance with standard quality. We evaluated radiologist's breast density and CAD's breast density.
Results: We obtained a final cohort of 68 images (CC and MLO) and a total of 40 cases of breast lesions (with benign and malignant histopathology). We found not statistically significant differences between the two assessments.
Conclusion: CAD is not susceptible of error in breast density evaluation even for mammograms within a suspicious lesion which gives to CAD a main role in the breast cancer risk assessment.
Limitations: We evaluated a small cohort of mammograms since CAD is available in our center starting in January in just one mammography. The cohort was from screening programme where patients are asymptomatic so we collected suspicious lesions chatateriser by a diameter in a range of 0.4-1.8 mm. It is a retrospective study.
Ethics committee approval: n/a
Funding: No funding was received for this work.
Author Disclosures:
F. Leone: nothing to disclose
M. Cellina: nothing to disclose
M. A. Orsi: nothing to disclose
G. Oliva: nothing to disclose

MyT3 2-14 11:22

Value of machine learning with MRI radiomics for early prediction of pathological complete response to neoadjuvant chemotherapy in HER2-positive invasive breast cancer

L. Qin, G. Yajia*; Shanghai/CN (liqincelery@163.com)*

Purpose: To assess the value of machine learning with radiomics based on DCE-MRI for early prediction of pCR to NAT in HER2 positive invasive breast cancer.
Methods and materials: 127 patients with HER2 positive invasive breast cancer confirmed by pathology were enrolled in this retrospective study. All patients underwent DCE-MRI before NAT, and performed surgery after completion of NAT. 1316 radiomic features for every patient were extracted. To avoid overfitting, a forward stepwise regression was used to select potential features. The number of selected features was determined by Akaike information criterion. 23 classifiers based on the 1st postcontrast and multi-phases DCE-MRI were constructed respectively. The performence of the classifiers were assessed by accuracy, sensitivity, specificity, and AUC.
Results: For pCR classification, 6 features from the 1st post-contrast phase and 6 from multiphases DCE-MRI scan were selected. The linear SVM based on multiphase DCE-MRI scans outperformed the logistic regression model using the single 1st post-contrast DCE-MRI sequence with an AUC of 0.84 vs 0.69. In mass and non-mass enhancement groups, the accuracy of linear SVM achieved 76% and 84%.
Conclusion: Machine learning based on pretreatment multi phases DCE-MRI may offer more information for early prediction of pCR to NAC in patients with locally HER2 positive invasive breast cancer.
Limitations: The work presented in our study had several limitations. First, this was a retrospective study and all patients were recruited from a single centre. Second, we compared the performance of machion learning models based on radiomic of pretreatment the 1st postcontrast sequence and multiphases DCE-MRI imaging. However, the study lacked an independent validation cohort, external validation of our results pending adequate patient follow-up will be entailed in the future work.
Ethics committee approval: n/a
Funding: No funding was received for this work.
Author Disclosures:
G. Yajia: nothing to disclose
L. Qin: nothing to disclose

MyT3 2-15 11:26

Ultrasonographical evaluation of BI-RADS® 4 breast injuries and their histological correlation

L. L. Ospino Ortiz[1], A. P. Ortiz Gomez[2], K. Catein[2]*; [1]Rio de Janeiro/BR, [2]Petropolis/BR (loreospino_1991@hotmail.com)*

Purpose: Does the histopathological diagnosis of ultrasound-guided core biopsy breast agree with the morphological characteristics of the lesions in patients previously classified as BIRADS 4?
Methods and materials: Patients with category 4 BI-RADS ultrasound reports performed outside the study period and those whose BI-RADS classification did not have any of the 4A, 4B and 4C subdivisions were excluded; patients with incomplete medical records and lack of access to the histopathological report of the core biopsy. From the reports selected according to the inclusion and exclusion criteria: identification, age, breast distinction, diagnostic hypothesis and ultrasound-based BI-RADS classification, in addition to the final diagnosis after histopathological results.

Results: The mean age of the patients was 52.58 years (±17.05), with prevalence for the involvement of left breast lesions (n=104, 52%) and for the BI-RADS® 4C classification (n=87, 43.5%), and most had a positive final diagnosis for breast cancer (58.3%). This level of agreement was statistically (p=0.00) higher in patients diagnosed with cancer (72.1%).
Conclusion: The use of the BI-RADS® system showed a high predictive value for cases classified in category 4, with an accuracy level of 80%, except for patients with inconclusive final diagnosis and those without initial diagnosis in the medical records. It was concluded that the BI-RADS® category 4 ultrasound classification system associated with the histopathological result of core biopsies is an effective method to predict and aid the management of breast cancer, and further studies are needed to confirm the findings.
Limitations: The percentage of population treated in preventive medicine that uses the radiology service and the possible underreporting bias that may exist due to using the clinical file as a source of information.
Ethics committee approval: n/a
Funding: No funding was received.
Author Disclosures:
L. L. Ospino Ortiz: nothing to disclose
A. P. Ortiz Gomez: nothing to disclose
K. Catein: nothing to disclose

MyT3 2-16 11:30

In-vivo measurements of ADC of invasive ductal breast cancer: a multicentric study to assess the quality of DWI protocols in breast MRI at 1.5T

S. Atzori[1], L. Baglietto[1], M. Fornili[1], D. della Latta[2], D. Caramella[1], C. Iacconi[3]; *[1]Pisa/IT, [2]Massa/IT, [3]Carrara/IT (s.atzori1@libero.it)*

Purpose: Evaluating the diagnostic performances of diffusion-weighted Imaging (DWI) sequences of three magnetic resonance (MR) scanners in women undergoing breast MR for breast cancer.
Methods and materials: 90 women aged 28-78, 30 for each centre, underwent multiparametric contrast-enhanced breast MR with DWI for invasive ductal carcinoma with mass-like features. Every centre has a 1.5T MR scanner with similar DWI protocols. For every tumour, a circular ROI encompassing the lesion was drawn in the ADC sequence. Centimetric ROIs were drawn in the contralateral healthy breast in the retro areolar and upper outer quadrant (UOQ) as normal glandular controls. ROI in the normal tissue was not registered in case of bilateral tumours (n=3), and in in one case of extremely fatty breasts, obtaining 86 normal controls (29 in centre 1, 29 in centre 2 and 28 in centre 3). Fibroglandular tissue (FGT) was annotated as well. Data were compared for age, FGT (1-4 BIRADS classes), tumour size (1-2cm, 2-4cm, >4cm) and ADC values. Fisher exact test for size and FGT and Kruskal-Wallis test for continuous variables were used.
Results: Age, size and FGT don't vary significantly between the three centres (p=0.15, 0.82 and 0.96, respectively). Tumoural ADC values vary significantly (p=0.001), with an inter-centre mean variation of 17%. Retroareolar and UOQ ADC values don't vary significantly (p=0.76 and 0.43, respectively), as well as their mean (p=0.87).
Conclusion: With similar DWI protocols, ADC values in breast tumours vary significantly between the three centres. Multicentric trials should consider this difference in the quantitative evaluation of lesions.
Limitations: Scarce cohort numerosity and inhomogeneity of breast tumours (even of similar histology) may influence the significativity of some results.
Ethics committee approval: n/a
Funding: No funding was received for this work.
Author Disclosures:
S. Atzori: nothing to disclose
L. Baglietto: nothing to disclose
M. Fornili: nothing to disclose
D. della Latta: nothing to disclose
D. Caramella: nothing to disclose
C. Iacconi: nothing to disclose

MyT3 2-17 11:34

The use of digital breast tomosynthesis in the surveillance of breast cancer patients following breast conservative surgery

S. Ahmed, R. Hassan*; Assiut/EG (shimaaabdalla@aun.edu.eg)*

Purpose: To evaluate the added value of DBT in the surveillance of patients following breast conservative surgery (BCS) and evaluate its role in the management of the architectural distortion (AD).
Methods and materials: 410 asymptomatic breast cancer patients underwent both DM and DBT for routine surveillance following BCS. Three radiologists reviewed all examinations. The area under the ROC curve (AUC) was calculated for BI-RADS assessment by DM and DM + DBT. Multivariate logistic regression analysis was performed to identify the imaging features that can predict outcome in AD.
Results: DM + DBT detected 212 mammographic abnormalities in 170 (41.55) patients, the final diagnosis was benign in 109 (64.1%) patients and second breast cancer was diagnosed in 61(35.9%) patients. Masses had the highest PPV for malignancy (43.8%), while asymmetry had the lowest (16.7%). AUC for BI-RADS assessment increased significantly (P=0.01) from 0.696 for DM to 0.843 for DM+ DBT. In the setting of AD, multivariate analysis demonstrated that scar area AD and non-scar area AD with negative sonographic correlation are significantly associated with benign outcome. Only DBT detected AD, and positive sonographic correlation in non-scar area AD was not significantly associated with malignancy.
Conclusion: DBT is strongly recommended to be a standard combination in the surveillance of patients following BCS. In the setting of AD, DBT can accurately exclude postoperative bed recurrence, non-scar area AD with negative sonographic correlation was significantly associated with the benign outcome; however, a biopsy cannot be omitted because 50% of the surgically excised, only DBT-detected AD were malignant.
Limitations: The present study was not a part of an integrated population-based surveillance programme for patients with CBS.
Ethics committee approval: IRB approval was obtained.
Funding: No funding was received.
Author Disclosures:
R. Hassan: nothing to disclose
S. Ahmed: nothing to disclose

MyT3 2-18 11:38

Prognostic value of MRI complete radiological response in breast cancer patients after neadjuvant chemotherapy

M. Costilla Frías, J. H. Del Riego Ferrari, L. Tortajada Gimenez, A. Martín Oloriz, C. Aynes, M. T. Villajos, F. Escribano Alcantara, C. Codina*; Sabadell/ES (mcostilla@tauli.cat)*

Purpose: Neoadjuvant chemotherapy (NAC) has an essential role in the treatment of patients with breast cancer. A subgroup of these patients achieves a pathologic complete response (pCR) after NAC, defined as the absence of invasive cancer in breast surgery. pCR is related to higher long-term survival, especially in aggressive phenotypes. MRI is able to predict non-invasively and accurately the presence of pCR by rCR, defined as the absence of enhancement at tumour bed after NAC. The main purpose of our study is to assess rCR as a surrogate outcome of survival in breast cancer patients treated with NAC.
Methods and materials: We retrospectively reviewed contrast-enhanced and diffusion-weighted MRI studies of breast cancer patients treated with NAC at the diagnosis, during (early response) and after NAC (late response) and determined if they presented a complete, partial or not radiological response. We reviewed survival outcomes (overall survival and disease-free survival) and assessed its realationship to rCR.
Results: Preliminary data: We included >200 patients. The hypothesis is that the presence of rCR was related to a higher short and long-term survival, with differences according to the tumour fenotype. The combined use of CE and DW-MRI rCR had good correlation when predicting pCR.
Conclusion: rCR seems to be a prognostic survival outcome in breast cancer patients treated with NAC. The combined use of CE and DW-MRI is accurate in predicting pCR.
Limitations: The main limitation is the change of diagnostic methods and criteria in evaluating radiological response. To try to compensate it, a review of all MRI studies was done by two radiologists with exclusive dedication to breast radiology (JdR and LT).
Ethics committee approval: n/a
Funding: No funding was received for this work.
Author Disclosures:
M. Costilla Frías: nothing to disclose
J. H. Del Riego Ferrari: nothing to disclose
L. Tortajada Gimenez: nothing to disclose
A. Martín Oloriz: nothing to disclose
C. Aynes: nothing to disclose
M. T. Villajos: nothing to disclose
F. Escribano Alcantara: nothing to disclose
C. Codina: nothing to disclose

MyT3 2-19 11:42

Radiomic features of tumour and fibro-grandular tissue for predicting sentinel lymph node metastasis of breast cancer

X. Chen*; Chengdu/CN (1121790150@qq.com)*

Purpose: This study aimed to predict sentinel lymph node metastasis (SLNM) of breast cancer via radiomic features of tumour and fibro-glandular tissue based on the contrast-enhanced magnetic resonance imaging (DCE-MRI).
Methods and materials: Preoperative magnetic resonance imaging data from 36 women with histopathologically confirmed breast cancer, consisting of 16 SLNM positive and 20 SLNM negative proven by surgery, were retrospectively studied.198 radiomic features of the whole tumours and 198 radiomic features

of ipsilateral fibro-grandular tissue were extracted, based on pharmacokinetic modelling dynamic contrast-enhanced magnetic resonance imaging (PK-DCE-MRI). The least absolute shrinkage and selection operator (LASSO) regression was used to select useful radiomic features. Logistic regression was used to build predictive models for SLNM in breast cancer.
Results: All the radiomic features of the whole tumour and ipsilateral fibro-grandular tissue were reduced to 33 SLN status-related features by LASSO. The predictive model based on radiomic features of tumour's radiomic features and ipsilateral fibro-grandular tissue was developed. Their prediction ability was moderate, with an area under the curve (AUC) of 0.682.
Conclusion: Radiomic analysis of radiomic features of tumour and fibro-grandular tissue based on the DCE-MRI has the potential to more accurately predicting SLNM in breast cancer patients.
Limitations: Case source is not multi-centre.
Ethics committee approval: n/a
Funding: No funding was received for this work.
Author Disclosures:
X. Chen: nothing to disclose

MyT3 2-20 11:46
Comparison of prone digital breast tomosynthesis–guided vacuum-assisted biopsy (DBT-guided VAB) and prone atereotactic-guided vacuum-assisted biopsy (S-guided VAB)
G. Boffelli[1], C. Ferranti[2], C. Depretto[2], C. G. Monaco[2], A. Liguori[2], A. Borelli[2], G. Scaperrotta[2]; *[1]Bergamo/IT, [2]Milan/IT (giuliaboffelli@hotmail.it)*

Purpose: To compare the performance of prone DBT–guided VAB with prone S-guided VAB, focusing on time of procedure, number of expositions, average glandular dose and complications.
Methods and materials: The institutional review board approved this retrospective study and informed consent was waived. From July 2015 to January 2017, 306 patients with 306 suspicious mammographic findings (BI-RADS ≥4) underwent to a mammography-guided biopsy, prone S-guided or prone DBT-guided VAB. T student Test, Chi-squared and multivariate regression statistics were used.
Results: During the study period, 155 prone S-guided VAB in 155 patients (mean age, 56 years; age range, 39–84 years) and 151 DBT guided VAB in 151 patients (mean age, 57 years; age range, 33–84 years) were performed. Mean procedure time was briefer with DBT-guided VAB versus S-guided VAB (14,5 vs 17,4 minutes, respectively; P <0,001), and fewer expositions were acquired with DBT-guided VAB versus S-guided VAB (8 vs 11, respectively; P <0,001); therefore the average glandular dose (AGD) was significantly lower in DBT-guided VAB versus S-guided VAB (11,8 mGy vs 18 mGy respectively; P <0,001). There were no differences in the distribution of histologic results (P = 0,74) and in breast density (P = 0,09) between the two groups. No major complications were observed in either group.
Conclusion: Performance of prone DBT-guided VAB was superior to prone S-guided VAB, because it allows a faster procedure, with a fewer radiological expositions and lower radiation dose.
Limitations: We included in our study all the procedures that were actually performed in our institution, so technical success was not considered.
Ethics committee approval: The institutional review board approved this retrospective study and informed consent was waived.
Funding: No funding was received for this work.
Author Disclosures:
G. Boffelli: nothing to disclose
C. Ferranti: nothing to disclose
C. Depretto: nothing to disclose
C. G. Monaco: nothing to disclose
A. Liguori: nothing to disclose
A. Borelli: nothing to disclose
G. Scaperrotta: nothing to disclose

10:30 - 12:00 **Coffee & Talk 3**

Cardiac

RPS 203

Myocardial perfusion imaging and infarct characterisation: diagnosis and prognosis

Moderators:
T. Emrich; Mainz/DE
R. Vliegenthart; Groningen/NL

RPS 203-1 10:30
Improved sensitivity in diagnosing myocardial infarction using frequency selective nonlinear blending in computed tomography
E. Stock, R. Schwarz, J. Herrmann, C. Artzner, K. Nikolaou, M. Bongers; *Tübingen/DE (eva.stock@med.uni-tuebingen.de)*

Purpose: To evaluate the effect of frequency selective nonlinear blending (NLB) on the detectability of clinically suspected myocardial infarction in computed tomography (CT) images.
Methods and materials: A retrospective patient search in our institution's PACS yielded 32 patients with myocardial infarction who underwent both contrast-enhanced CT (CECT) and invasive coronary angiography (ICA) between 2015 and 2019. ICA was used as a standard of reference. NLB was applied to CECT images, which were obtained in the portal-venous phase. Two readers independently determined optimal NLB settings and independently rated image quality (equidistant Likert). Objective image quality was determined using a ROI-based calculation of contrast-to-noise ratios (CNR). The acquired data was statistically compared between CECT and NLB using non-parametric tests. Interobserver agreement was calculated using kappa statistics.
Results: On average, a centre of 110 HU, a delta of 20 HU, and a slope of 5 resulted in the best overall delineation of hypodense areas of myocardial infarction. Averaged CNR of myocardial infarctions could be significantly increased using NLB (CECT:5, 73 [2,88;12,83]; NLB:11, 28 [6,56;23,19]; p<0,0001). Interobserver agreement showed substantial agreement (kappa: 0,70). Subjective image quality was significantly higher for NLB CT images in comparison with CECT images (CECT:2 [2;2],NLB:4 [3;4],p<0,0001).
Conclusion: This pilot study demonstrated that frequency selective nonlinear blending of CECT images allows a significant improvement of the delineation of myocardial infarction. Further clinical studies are warranted in order to validate these initial results.
Limitations: A small study population.
Ethics committee approval: This study was approved by our local ethics committee.
Funding: No funding was received for this work.
Author Disclosures:
E. Stock: nothing to disclose
R. Schwarz: nothing to disclose
J. Herrmann: nothing to disclose
C. Artzner: nothing to disclose
M. Bongers: nothing to disclose
K. Nikolaou: Speaker at Siemens, Bayer, Bracco, Advisory Board at Siemens, Bayer, Bracco

RPS 203-2 10:36
Myocardial perfusion status in patients with coronary chronic total occlusion: evaluated by 16-cm wide detector CT
K. Liu, Z. Li; *Chengdu/CN (634270986@qq.com)*

Purpose: To evaluate the myocardial perfusion status of patients with coronary chronic total occlusion (CTO) by 16-cm wide detector CT and explore the differences of perfusion parameters between myocardial segments dominated by CTO and non-CTO vessels.
Methods and materials: 34 patients with CTO confirmed by coronary angiography (CAG) were enrolled and their data about dynamic myocardial computed tomography perfusion (CTP) imaging on a 16-cm wide detector CT was analysed retrospectively. Based on a standardised 17-segment model of AHA, perfusion parameters of myocardial segments were measured using a "CT dynamic myocardial perfusion" module on Ziostation2 software, including myocardial blood volume (MBV) and myocardial blood flow (MBF). CT attenuation values of each myocardial segment were alsoi measured. The occlusive vessel was determined by CAG results and the differences of parameters between myocardial segments dominated by CTO and non-CTO vessels were analysed.

Results: There was a significant difference in CT attenuation values between myocardial segments dominated by CTO and non-CTO vessels [(94.9±25.4) Hu vs. (114.0±24.6) Hu, P=0.003). Compared with myocardial segments dominated by non-CTO vessels, MBV and MBF of myocardial segments dominated by CTO vessels significantly decreased [MBV: (17.09±7.9) ml/100ml vs. (23.6±8.5) ml/100ml, P=0.002; MBF: (226.5±85.2) ml/(100ml·s) vs. (334.7±163.3) ml/(100ml·s), P=0.001].
Conclusion: Myocardial perfusion status was different in myocardial segments dominated by CTO and non-CTO vessels. MBV and MBF may have the potential to differentiate normal myocardium from ischemic myocardium in CTO patients.
Limitations: A small sample size and a lack of studies about the diagnostic performance of MBV and MBF.
Ethics committee approval: This study was approved by the Institutional Medical Ethics Committee of our institute. Written informed consent was obtained.
Funding: This work was supported by the "1.3.5" project for disciplines of excellence, West China Hospital, Sichuan University, China [ZYGD18019].
Author Disclosures:
K. Liu: nothing to disclose
Z. Li: nothing to disclose

RPS 203-3 10:42

Extracellular volume fraction and infarct size determined by LGE CMR predict left ventricular remodeling within the first 6 months following an acute myocardial infarction

E. Tahir, M. Sinn, J. Stáreková, M. Avanesov, U. Radunski, K. Müllerleile, C. Stehning, G. Adam, G. Lund*; Hamburg/DE (e.tahir@uke.de)*

Purpose: Tissue characterisation could provide incremental information to predict left ventricular (LV) remodeling after myocardial infarction (MI). We investigated the clinical utility of an approach using novel mapping techniques compared to standard CMR to predict LV remodeling.
Methods and materials: 74 patients with reperfused MI were enrolled. CMRs were obtained at 8±5 days after MI. Cine sequences were used to determine LV remodelling at baseline and 6 months after infarction. T2 relaxation times were quantified using a free-breathing, navigator-gated multi-echo sequence. T1 relaxation times were measured using the modified look-locker inversion recovery sequence. Parametric maps were generated with OsiriX. LGE was used to identify the infarcted areas.
Results: A total of 11 patients (15%) developed LV remodelling. ECV and infarct size had the best predictive performance to identify patients at risk of LV remodelling after AMI with AUCs of 0.843 and 0.806, respectively. Infarct size was significantly better than native T1 with an AUC of 0.549 (P<0.05). T2 and oedema size also showed good AUCs of 0.768 and 0.743, respectively. The optimal cut-off of ≥57% for ECV provided a sensitivity and specificity of 86% and 85%, respectively. The optimal cut-off of ≥17.2 %LV for infarct size provided a sensitivity and specificity of 82% and 76%, respectively. The optimal cut-offs for the other CMR parameters were oedema size ≥27 %LV, ≥1236ms for native T1 and ≥88ms for T2.
Conclusion: ECV and infarct size are the best predictors for LV remodelling within a follow-up period of 6 months and show a better discriminatory performance than non-contrast standard and parametric mapping techniques.
Limitations: The main limitation of this study is the small number of patients.
Ethics committee approval: This study was approved by the Ärztekammer Hamburg.
Funding: No funding was received for this work.
Author Disclosures:
E. Tahir: nothing to disclose
M. Sinn: nothing to disclose
J. Stáreková: nothing to disclose
M. Avanesov: nothing to disclose
U. Radunski: nothing to disclose
C. Stehning: Employee at Philips Research
G. Adam: nothing to disclose
G. Lund: nothing to disclose
K. Müllerleile: nothing to disclose

RPS 203-4 10:48

The prognostic value of the myocardial salvage index measured by magnetic resonance imaging after ST-segment elevation myocardial infarction: a systematic review and meta-regression analysis

B. Kendziora, M. Dewey*; Berlin/DE (benjamin.kendziora@charite.de)*

Purpose: To summarise published data on the prognostic value of the proportion of salvaged myocardium inside previously ischaemic myocardium (myocardial salvage index) measured by T2-weighted and T1-weighted late gadolinium enhancement magnetic resonance imaging (MRI) after ST-segment elevation myocardial infarction (STEMI).
Methods and materials: We systematically searched for studies stating both the myocardial salvage index measured by T2-weighted and T1-weighted late gadolinium enhancement MRI after STEMI and the incidence of major cardiac events (MACE) during follow-up, defined as cardiac death, nonfatal myocardial infarction, or admission for heart failure. Random and mixed effects models were used for data analysis.
Results: The search revealed 10 studies with 2,697 patients. The pooled myocardial salvage index, calculated as the proportion of nonnecrotic myocardium inside edematous myocardium measured by T2-weighted and T1-weighted late gadolinium enhancement MRI after STEMI, was 43.0% (95% confidence interval [CI]: 37.4, 48.6). The pooled length of follow-up was 12.3 months (95 % CI: 7.0, 17.6). The pooled incidence of MACE during follow-up was 10.6 % (95% CI: 5.7, 15.5). With every 1% increase in the myocardial salvage index, there was an absolute decrease of 1.7% in the incidence of MACE during follow-up (95 % CI: 1.6, 1.9). Heterogeneity between studies was considerable ($\tau = 21.3$).
Conclusion: An analysis of the published data suggests that the myocardial salvage index measured by T2-weighted and T1-weighted late gadolinium enhancement MRI after STEMI provides prognostic information on the risk of MACE. However, there is considerable heterogeneity between studies.
Limitations: In consequence of the heterogeneity between studies, exact thresholds of the myocardial salvage index for low or high risk of MACE cannot be provided.
Ethics committee approval: n/a
Funding: We acknowledge support from the German Research Foundation and the Open Access Publication Fund of Charité - Universitätsmedizin Berlin.
Author Disclosures:
B. Kendziora: nothing to disclose
M. Dewey: Grant Recipient at German Foundation of Heart Research, Grant Recipient at GE Healthcare, Grant Recipient at Bracco, Grant Recipient at Guerbet, Grant Recipient at Toshiba, Grant Recipient at Siemens Medical Solutions, Grant Recipient at Philips Medical Systems, Grant Recipient at German Research Foundation, Grant Recipient at European Union, Other at Cardiac MR Academy Berlin, Other at Bayer-Schering, Other at Toshiba Medical Systems, Author at Springer

RPS 203-6 10:54

Normal range of quantified myocardial perfusion with whole heart coverage CT scanner in subjects with normal coronary artery

Y. Gao, N. Zhao, W. Ma, W. Geng, B. Lyu*; Beijing/CN (gaoyang226@126.com)*

Purpose: To determine the range and regional heterogeneity of myocardial perfusion in subjects with normal coronary artery on dynamic perfusion computed tomography.
Methods and materials: Participants without a history of hypertension, hyperlipidemia, diabetes, smoking, and chest pain were prospectively enrolled. Coronary computed tomography angiography was performed to verify the normal coronary artery without any plaque or stenosis. Myocardial perfusion was assessed at rest and during triphosadenine-induced hyperemia using a Revolution CT (GE Healthcare, Milwaukee, Wisconsin). Myocardial blood flow (MBF) and myocardial blood volume (MBV) were quantified based on a 17-segment American Heart Association model.
Results: 34 (age 33–65 years; 15 men) participants were enrolled. The mean global MBF_{rest} and MBF_{stress}, MBV_{rest} and MBV_{stress} were 116.2±39.2 ml/100g/min and 210.7±56.3 ml/100g/min, 17.6±4.8 ml/100g and 25.7±5.6 ml/100g, respectively. Mean MBF_{rest} (123.9±39.4 ml/100g/min) and MBF_{stress} (216.9±56.5 ml/100g/min) of the anterior region were higher than in other regions. The mean MBF_{rest} (103.2±34.2 ml/100g/min) and MBF_{stress} (205.8±50 ml/100g/min) of the inferoseptum regions were lower than in other regions. The mean variation of MBF_{rest} was significantly higher than MBF_{stress} (21.1±6.4% vs. 17.7±4.3%, P=0.016) and MBV as well (15.9±6.1% vs. 11.8±5.5%, p<0.001). MBF_{stress} and MBV_{stress} of female were significantly higher than male subjects (226.4±56.9 ml/100g/min vs. 190.8±48.9 ml/100g/min, p<0.001 and 26.8±5.9 ml/100g vs. 24.3±4.8 ml/100g, p<0.001, respectively).
Conclusion: This study reveals normal myocardial perfusion parameter and regional heterogeneity on dynamic CT perfusion. Myocardial flow reserve were significantly higher in female than male participants.
Limitations: The results were from a single institution and the number of subjects was small. We did not compare CT MBF values to a reference standard from PET or cardiac MR.
Ethics committee approval: The institutional ethics committee of Fuwai Hospital approved this study.
Funding: The study received a grant from the National Key Research and Development Program of China (2016YFC1300402).
Author Disclosures:
B. Lyu: nothing to disclose
Y. Gao: nothing to disclose
N. Zhao: nothing to disclose
W. Ma: nothing to disclose
W. Geng: nothing to disclose

RPS 203-7 11:00

A comparison of iodine distribution characteristics in rest and stress first-pass perfusion of healthy myocardium as obtained by a dual-layer CT scanner

S. Boccalini[1], S. A. Si-Mohamed[2], L. Hanquier[1], L. Boussel[2], D. Revel[1], P. C. Douek[1]; [1]Lyons/FR, [2]Bron/FR (sara.boccalini@yahoo.com)

Purpose: To compare iodine distribution in healthy myocardium at first-pass perfusion imaging between stress and rest acquisitions using dual-layer CT (DLCT).
Methods and materials: Between May 2019 and September 2019, patients undergoing coronary-CT for typical thoracic pain without troponin elevation and patients with borderline stenosis at coronary CT underwent an additional CT acquisition after pharmacological stress. Both exams were performed on a DLCT. The injection protocols were 50mL of contrast material at 5mL/sec at rest 35mL in patients <80kg and 0.5mL/kg in patients >80 kg (maximum 45mL) at 2.5mL/sec under stress. Patients with coronary stenosis >50% and/or with positive invasive FFR were excluded. Regions-of-interest were manually drawn on the 16 AHA myocardial segments. Iodine concentration was measured on iodine-maps in mg/mL.
Results: 224 segments (112 rest/112 stress of the same patients) were analysed. No significant difference in iodine concentration was found between rest (median=1.48mg/mL; IQR=0.44) and stress (median=1.44mg/mL; IQR=0.53) (p=0.4). At rest, a significant difference between coronary territories was demonstrated (p=0.02; highest values in the territory of the circumflex (median=1.66mg/mL; IQR=0.49). After stress iodine concentration was homogeneous in different coronary territories (p=0.2). The difference of iodine values between rest and stress was not significantly different in the 16 segments (p=0.94) nor in coronary territories (p=0.37).
Conclusion: In healthy myocardium, significant differences between coronary territories were shown at rest but not after stress, probably because of different injection protocols. Therefore, an injection protocol with a low dose and slow flow is preferable to evaluate myocardial perfusion after pharmacological stress. The difference between rest and stress iodine values of healthy myocardium was homogeneous, without focal reduction of iodine content.
Limitations: Few patients.
Ethics committee approval: n/a
Funding: No funding was received for this work.
Author Disclosures:
S. Boccalini: nothing to disclose
S. A. Si-Mohamed: nothing to disclose
L. Hanquier: nothing to disclose
L. Boussel: nothing to disclose
D. Revel: nothing to disclose
P. C. Douek: nothing to disclose

RPS 203-8 11:06

Histological validation of cardiac magnetic resonance T1 mapping for evaluating the myocardial alterations on day 1, day 7, and 3 months in a swine model with myocardial infarction

L. Zhang, Y.-K. Guo, C. Fu, H.-Y. Xu, M.-X. Yang, R. Xu, L. Chen; *Chengdu/CN (zhanglu_scu2018@163.com)*

Purpose: To explore how native T1 and extracellular volume (ECV) measured on CMR changed with time in infarcted myocardium after myocardial infarction (MI) and the correlation between ECV and native T1 against histopathological findings.
Methods and materials: A total of 22 pigs were subjected to occlude anterior descending artery and underwent serial CMR examinations in acute (within 24h, n = 22), subacute (7 days, n = 13), and chronic (3 months, n = 6). The CMR protocol included cine, modified look-lock inversion (MOLLI) recovery and late gadolinium enhancement (LGE). Hematoxylin-eosin and Masson trichrome staining were conducted following scanning. The CMR and histopathological examinations were performed on the same day.
Results: Infarcted native T1 changed with peaking at 7 days ($p < 0.05$), while a progressive increase was observed in ECV during 3 months ($p < 0.05$). The histology-evaluated ECV demonstrated a good correlation in the comparison with native T1 (acute, $r = 0.89$, $p < 0.001$; subacute, $r = 0.94$, $p < 0.001$; chronic, $r = 0.83$, $p < 0.001$) and a similar correlation was found compared with CMR-measured ECV (acute, $r = 0.89$, $p < 0.001$; subacute, $r=0.96$, $p < 0.001$; chronic, $r = 0.82$, $p < 0.001$).
Conclusion: Both native T1 and ECV in infarcted myocardium demonstrated a dynamical change in time and had a good correlation with histology. This may be explained by the severe interstitial oedema and the progressive collagenous deposition, indicating the implication for the timing of CMR imaging early after MI for individual therapy and prognosis.
Limitations: The experimental setup did not allow for baseline examination.
Ethics committee approval: The experimental study was approved by the institutional ethics review board.
Funding: No funding was received for this work.
Author Disclosures:
L. Zhang: Author at West China Second University Hospital, Sichuan University, Speaker at West China Second University Hospital, Sichuan University
Y.-K. Guo: nothing to disclose
C. Fu: nothing to disclose
H.-Y. Xu: nothing to disclose
M.-X. Yang: nothing to disclose
R. Xu: nothing to disclose
L. Chen: nothing to disclose

RPS 203-9 11:12

Fractal analysis of perfusion using 4D dynamic CT to differentiate microvascular and macrovascular ischemia

F. Michallek[1], S. Nakamura[2], H. Ota[3], H. Sakuma[2], M. Dewey[1], K. Kitagawa[2]; [1]Berlin/DE, [2]Tsu/JP, [3]Sendai/JP (florian.michallek@charite.de)

Purpose: To understand the chaos of myocardial perfusion under physiological and ischaemic conditions, and to non-invasively differentiate microvascular and macrovascular causes of ischaemia.
Methods and materials: Four-dimensional dynamic first-pass perfusion CT (4D-CTP) data from the AMPLIFiED multicentre study was assessed using 4D fractal analysis. The chaos of perfusion was quantified by fractal dimension (FD). As combined reference, invasive coronary angiography and CTP defined coronary macrovascular artery disease (CAD, ≥80% diameter stenosis or positive FFR with abnormal subendocardial perfusion on CTP), coronary microvascular disease (CMD, <30% diameter stenosis and negative FFR with abnormal subendocardial perfusion on CTP), and normal controls. Analysis was conducted per-segment according to the AHA-17-segments model. Differences in median FD (with interquartile range, IQR) after elimination of intrapatient-clustering were tested using Kruskal-Wallis and Mann-Whitney-U-test (post hoc). Analysis software was developed by the first-author (FM). The STARD-guidelines have been adhered to.
Results: A cohort of n=30 patients was analysed (CMD: n=10 [123 segments]; CAD: n=10 [93 segments]; normal: n=10 [170 segments]). In normal perfusion, physiological chaos was high ($FD_{normal} = 4.49$, $IQR_{normal} = 0.07$). In ischaemia, perfusion was markedly more homogeneous compared to normal perfusion with significantly ($p<0.001$) less chaos in macrovascular ($FD_{CAD}=4.26$, $IQR_{CAD}=0.03$) than microvascular ischaemia ($FD_{CMD} = 4.37$, $IQR_{CMD} = 0.01$) with a coefficient of determination $r^2 = 0.82$.
Conclusion: Perfusion features inherent physiological chaos, which is reduced in ischaemia. Reduction of perfusion chaos depends on the underlying pathophysiology with perfusion being more homogeneous in macrovascular (CAD) than microvascular (CMD) ischaemia.
Limitations: It remains to be determined if fractal analysis can predict clinical outcomes.
Ethics committee approval: n/a
Funding: No funding was received for this work.
Author Disclosures:
H. Sakuma: nothing to disclose
F. Michallek: Grant Recipient at F.M. has received grant support from the German Research Foundation (DFG, project number: 392304398) and the Digital Health Accelerator of the Berlin Institute of Health., Patent Holder at F.M. has filed a patent application on fractal analysis of perfusion imaging (together with Marc Dewey, PCT/EP2016/071551).
S. Nakamura: nothing to disclose
H. Ota: nothing to disclose
M. Dewey: Grant Recipient at M.D. has received grant support from the Heisenberg Program of the German Research Foundation (DFG) for a professorship (DE 1361/14-1), the Digital Health Accelerator of the Berlin Institute of Health, and the DFG graduate program on quantitative biomedic, Other at M.D. was elected European Society of Radiology (ESR) Research Chair (2019–2022) and the opinions expressed in this article are the author's own and do not represent the view of ESR. M.D. is also the editor of Coronary CT Angiography and Cardiac CT, both p, Patent Holder at M.D. has filed a patent application on fractal analysis of perfusion imaging (together with Florian Michallek, PCT/EP2016/071551)., Speaker at M.D. has received lecture fees from Toshiba Medical Systems, Guerbet, Cardiac MR Academy Berlin, and Bayer (Schering-Berlex).
K. Kitagawa: nothing to disclose

RPS 203-10 11:18

Diagnosing and predicting performance of myocardial injury in acute STEMI based on texture analysis of non-contrast-enhanced T1-mapping

Q. Ma[1], Y. Hou[1], X. Lu[1], J. Wang[2], X. Wang[1]; [1]Shenyang/CN, [2]Beijing/CN (444656285@qq.com)

Purpose: To evaluate the feasibility of texture analysis on non-contrast-enhanced T1 maps of cardiac MRI for the diagnosis of myocardial injury in acute myocardial infarction.
Methods and materials: 68 ST-segment–elevation myocardial infarction patients (mean age 55.7 ± 10.5 years, 57 males and 11 females) underwent acute 3T CMR after a percutaneous coronary intervention (PCI), 40 of whom also underwent a 6-month follow-up CMR. Texture analysis was applied to the T1 maps using a software package that was freely available (MaZda, version 4.6). Stepwise dimension reduction and selection of texture features were performed to evaluate the myocardial injury severity using late gadolinium enhancement (LGE) as the standard reference.
Results: A total of 1,088 segments of the acute CMR images were analysed, where 103 (9.5%) segments showed MVO and 557 (51.2%) segments showed myocardial infarction. A total of 244 (38.1%) segments showed irreversible myocardial infarction. A radiomics signature based on T1 maps resulted in a good diagnostic performance of MVO in the training set (AUC: 0.85, 95% CI, 0.80 – 0.89) and the validation set (AUC: 0.85, 95% CI, 0.78 – 0.93), and a fair diagnostic performance of myocardial infarction in the training set (AUC: 0.78, 95% CI, 0.75 – 0.82) and the validation set (AUC: 0.79, 95% CI, 0.74 – 0.84). The radiomics signature also predicted the irreversible myocardial at 6 months with a good performance in the training set (AUC: 0.78, 95% CI, 0.74 – 0.83) and the validation set (AUC: 0.80, 95% CI, 0.74 – 0.86).
Conclusion: Non-contrast-enhanced T1-mapping allows the assessment of the severity of the acute myocardial injury, especially MVO. It also predicted irreversible myocardial damage at 6 months.
Limitations: n/a
Ethics committee approval: n/a
Funding: No funding was received for this work.
Author Disclosures:
Q. Ma: nothing to disclose
Y. Hou: nothing to disclose
X. Lu: nothing to disclose
J. Wang: nothing to disclose
X. Wang: nothing to disclose

RPS 203-11 11:24

Sequential strategy including FFR_{CT} plus stress-CTP impacts on the management of patients with stable chest pain: the stress-CTP RIPCORD study

A. Baggiano[1], M. Guglielmo[1], G. Muscogiuri[1], L. Fusini[1], A. Del Torto[1], A. I. Guaricci[2], A. L. Bartorelli[1], M. Pepi[1], G. Pontone[1]; [1]Milan/IT, [2]Bari/IT (andrea.baggiano@ccfm.it)

Purpose: Stress computed tomography perfusion (Stress-CTP) and CT-derived fractional flow reserve (FFR_{CT}) are functional techniques that can be added to coronary CT angiography (cCTA) to improve management of patients with suspected coronary artery disease (CAD).
We sought to determine impact of FFR_{CT} and Stress-CTP added to cCTA on management of patients with suspected CAD.
Methods and materials: Patients scheduled for invasive coronary angiography (ICA) were evaluated with cCTA, FFR_{CT}, and stress-CTP. A management plan defined as optimal medical therapy (OMT) or revascularisation was recorded for the following strategies: cCTA alone, cCTA+FFR_{CT}, cCTA+stress-CTP, and cCTA+FFR_{CT}+stress-CTP. These strategies were then compared with the clinical decision based on ICA plus invasive FFR. Endpoints for each strategy were overall evaluability, effective radiation dose (ED), rate of reclassification, agreement with therapeutic decision making, and the rate of agreement in terms of vessels to be revascularised.
Results: 291 consecutive patients were enrolled. cCTA alone, cCTA+FFR_{CT}, cCTA+stress-CTP, and cCTA+FFR_{CT}+stress-CTP showed similar evaluability (91%, 89%, 90%, and 87%, respectively) and a similar rate of reclassification of cCTA findings when FFR_{CT} and stress-CTP were added (28% and 34%, respectively). cCTA, cCTA+FFR_{CT}, cCTA+stress-CTP, and cCTA+FFR_{CT}+stress-CTP showed a rate of agreement versus the final therapeutic decision and a rate of agreement in terms of vessels to be revascularised of 63%, 71%, 89%, and 84% (cCTA+stress-CTP and cCTA+FFR_{CT}+stress-CTP vs cCTA and cCTA+FFR_{CT}:p<0.01), and 57%, 64%, 74%, and 71% (cCTA+stress-CTP and cCTA+FFR_{CT}+stress-CTP vs cCTA and cCTA+FFR_{CT}:p<0.01), respectively, with an ED of 2.9±1.3mSv, 2.9±1.3mSv, 5.9±2.7mSv, and 3.1±2.1mSv (cCTA+FFR_{CT}+stress-CTP vs cCTA+stress-CTP:p<0.001).
Conclusion: The addition of functional assessment with FFR_{CT} and stress-CTP provides incremental therapeutic decision-making value compared to cCTA alone. Sequential strategy with cCTA+FFR_{CT}+stress-CTP is associated with the best compromise in terms of clinical impact and radiation exposure.
Limitations: A single-centre study.
Ethics committee approval: Ethical committee registration number:R250/15-CCM262.
Funding: Grant from General Electric.
Author Disclosures:
A. Baggiano: nothing to disclose
A. L. Bartorelli: nothing to disclose
M. Guglielmo: nothing to disclose
G. Muscogiuri: nothing to disclose
L. Fusini: nothing to disclose
A. Del Torto: nothing to disclose
A. I. Guaricci: nothing to disclose
M. Pepi: nothing to disclose
G. Pontone: nothing to disclose

RPS 203-12 11:30

Invisible to the eye: radiomics revealing alterations in apparently healthy myocardial tissue of patients with ischemic disease

A. Cavaliere[1], L. Baffoni[2], R. Motta[1], B. Giorgi[1], E. Quaia[1], M. de Lazzari[1], M. Perazzolo Marra[1], C. Giraudo[1]; [1]Padua/IT, [2]Montebelluna/IT (annachiara88cavaliere@gmail.com)

Purpose: To characterise by radiomic analyses the healthy myocardial tissue (i.e. without any visual alteration at MR imaging) of patients with ischaemic and non-ischaemic myocardial disease.
Methods and materials: Patients with ischaemic and non-ischaemic disease who underwent a contrast-enhanced cardiac MR from January 2018 to September 2019 were included in this retrospective study. One radiologist expert in cardiovascular imaging, blind to the clinical information, applied a 5 mm standardised region of interest (i.e. using the phase-sensitive inversion recovery images) on the healthy myocardial tissue of each patient and on the myocardium of 10 controls (patients without myocardial infarction) using a 3D Slicer. 56 radiomic features belonging to three categories were extracted: first-order statistics (FOS), grey-level co-occurrence matrix (GLCM), and grey-level run-length matrix (GLRLM). One-way repeated-measures analysis of variance (ANOVA) with Greenhouse-Geisser correction and Bonferroni post hoc tests were used to evaluate the differences among all datasets (p<0.05).
Results: 10 patients with ischaemic injury (1 female; mean age 60.6 ±10.8 yrs), 11 with non-ischaemic infarction (3 females, mean age 51.8 ±21.4), and 10 controls (3 females, mean age 35.1 ±15.1) were examined. For 25/56 investigated features, the myocardium of the ischaemic patients differed from that of the non-ischaemic patients and controls (4 FOS, 13 GLCM, and 8 GLRLM features; p<0.05 each). No statistically significant differences emerged between the non-ischaemic patients and the controls for any of the examined variables (p>0.05, each).
Conclusion: Radiomic analyses suggest that ischaemic injuries also affect myocardial tissue visually healthy on MR imaging.
Limitations: Further studies including a larger population and a longitudinal approach are necessary to fully address this evidence and its clinical implications.
Ethics committee approval: Ethics committee approval obtained.
Funding: No funding was received for this work.
Author Disclosures:
L. Baffoni: nothing to disclose
A. Cavaliere: nothing to disclose
R. Motta: nothing to disclose
B. Giorgi: nothing to disclose
E. Quaia: nothing to disclose
M. de Lazzari: nothing to disclose
M. Perazzolo Marra: nothing to disclose
C. Giraudo: nothing to disclose

RPS 203-13 11:36

DWI sequence in cardiac imaging: a valid contrast-free substitute for late gadolinium enhancement (LGE) and T2-STIR in patients with acute myocardial infarction

C. Marzi[1], C. Martini[2], N. Gaibazzi[2], A. Palumbo[2], G. W. Antonucci[3]; [1]Reggio Emilia/IT, [2]Parma/IT, [3]Barletta/IT (martinic@ao.pr.it)

Purpose: To prove that the use of DWI sequences in C-MRI could be even better than T2-STIR in identifying an oedema zone after myocardial infarction and to demonstrate the potential for DW-CMR as a contrast-free alternative to LGE.
Methods and materials: Study eligibility criteria: studies about the comparison between DWI and T2-STIR in patients with acute myocardial infarction and studies about the possible substitution of late gadolinium enhancement (LGE)

with cardiac DWI. The information and the articles were mostly queried via PubMed and ResearchGate. Starting with 87 articles, a total of 28 relevant studies pertaining to cardiac DWI met the eligibility criteria. The MR equipment, the cardiac DWI type, the b factor values used for each sequence, the scan-time duration, the slice thickness, and/or the number of slices were extracted from the selected trials.
Results: DWI vs T2-STIR: the sensitivity was higher on DWI images (83% vs 61%) and the specificity was 90% for both sequences. The area of oedema was higher in DWI images.
DWI vs LGE: the area of infarct-related high intensity on DW-MRI showed significant linear correlation with LGE area in 20 patients with AMI.
Conclusion: DWI has been more sensitive than T2-STIR in all the studies performed. While it has been equally effective in DWI vs LGE, the advantage of using DWI would be in its ability to detect the ischaemic area even in the absence of the contrast agent. The possibility of eliminating contrast media from this exam would lead to a reduction in the cost of the whole examination for the hospital and there would be a total elimination of renal stress for the patient, which would be especially useful for patients suffering from kidney failure.
Limitations: The operator skills.
Ethics committee approval: n/a
Funding: No funding was received for this work.
Author Disclosures:
N. Gaibazzi: nothing to disclose
C. Marzi: nothing to disclose
C. Martini: nothing to disclose
A. Palumbo: nothing to disclose
G. W. Antonucci: nothing to disclose

RPS 203-14 11:42
A comparison of qualitative tagging and late gadolinium enhancement with PET- CT in the evaluation of myocardial viability
M. Y. A. Moideenbawa Abdulmajed[1], U. Debi[1], V. Bhatia[2], A. Sood[1], R. M. Kumar, M. S. Sandhu; *Chandigarh/IN*
(aser2125@gmail.com)

Purpose: To compare the efficacy of tagging and late gadolinium enhancement in assessing myocardial viability, keeping PET CT as a gold standard.
Methods and materials: We conducted a prospective analytical study comprised of 28 adult patients with perfusion/metabolism matched or mismatched defects in PET CT. These patients were taken for cardiac MR evaluation, mainly assessing tagging and late gadolinium enhancement for motion and scar respectively. Tagging was assessed using wall grid motion and grid crunching. Scoring was from 1 to 5 in increasing order of wall motion abnormality. Late gadolinium enhancement was graded from 0 to 4, ranging from no enhancement to complete transmural enhancement.
Results: Out of 448 myocardial segments, 6% (n=27) of the segments were considered non-viable with the matched defect, 56.5% (n=253) were normal, and 37.5% (n=168) were hibernating according to PET CT. 51.1 % (n= 86) of the hibernating segments were akinetic and 48% (n=82) were hypokinetic with the sensitivity of 66.03% (P < 0.001). However, 88.8% (n=24) of the non-viable segments showed severe akinesia with specificity and PPV of tagging of 88.89% and 98.93%, respectively (P<0.001). There was a good concordance between regional wall motion abnormalities detected using tagging and the percentage of transmural enhancement detected using LGE. LGE showed good sensitivity, 91.7%, as compared to PET CT in identifying hibernating myocardium. However, specificity was low at 44.4%.
Conclusion: Tagging has a good correlation with the late gadolinium enhancement, and as a standalone, MRI parameter shows increased specificity and positive predictive value in identifying non-viable myocardium compared with PET/CT.
Limitations: A small sample size. Stress examination was not done.
Ethics committee approval: Approved by an institutional ethics committee.
Funding: No funding was received for this work.
Author Disclosures:
M. Y. A. Moideenbawa Abdulmajed: nothing to disclose
U. Debi: nothing to disclose
V. Bhatia: nothing to disclose
A. Sood: nothing to disclose
M. S. Sandhu: nothing to disclose
R. M. Kumar: nothing to disclose

RPS 203-15 11:48
Myocardial perfusion recovery after steroid therapy predicts cardiac events in cardiac sarcoidosis
K. Koyanagawa[1], M. Naya[2], T. Aikawa[2], O. Manabe[2], S. Furuya[2], M. Kuzume[2], S. Tsuneta[1], N. Oyama-Manabe[2], T. Anzai[2];
[1]Sapporo, Hokkaido/JP, [2]Sapporo/JP
(k.koyanagawa0607@med.hokudai.ac.jp)

Purpose: Whether immunosuppression therapy improves myocardial perfusion in patients with cardiac sarcoidosis (CS) and the association between myocardial perfusion recovery and prognosis are unknown. This study aimed to clarify myocardial perfusion recovery after steroid therapy and its prognostic value for major adverse cardiac events (MACE) in CS patients.
Methods and materials: 38 consecutive patients with steroid-naive CS (median age, 63 IQR 51–68 years; 10 men) underwent electrocardiography (ECG)-gated ^{99m}Tc-MIBI SPECT pre- and post-steroid therapy. Patients were classified based on summed rest score (SRS) of pre-steroid therapy and ΔSRS values ($SRS_{post} - SRS_{pre}$) as follows: improvement ($SRS_{pre} > 0$ and ΔSRS < 0), non-improvement ($SRS_{pre} > 0$ and ΔSRS ≥ 0), preservation ($SRS_{pre} = 0$ and ΔSRS = 0), and progression ($SRS_{pre} = 0$ and ΔSRS > 0) groups. In addition, we defined the improvement and preservation groups as the recovery group, whereas the non-improvement and progression groups were the non-recovery group.
Results: From the results of SPECT, 23, 10, 3, and 2 patients were classified into the improvement, non-improvement, preserved, and progression group, respectively. Therefore, 26 patients were assigned to the recovery group and 12 patients to the non-recovery group. MACE occurred in 8 patients after 2.88 years of follow-up. The Kaplan-Meier curves revealed a significantly higher rate of MACE in the non-recovery group (17.4%/y vs. 2.9%/y, P = 0.007).
Conclusion: Myocardial perfusion was recovered by steroid therapy in 23 (61%) and preserved in 3 (8%) CS patients. Myocardial perfusion recovery after steroid therapy was significantly associated with a low incidence of MACE.
Limitations: A single-centre study with a small number of patients and events.
Ethics committee approval: Approved by the Ethics Committee of Hokkaido University Hospital.
Funding: No funding was received for this work.
Author Disclosures:
K. Koyanagawa: nothing to disclose
M. Naya: nothing to disclose
T. Aikawa: nothing to disclose
O. Manabe: nothing to disclose
S. Furuya: nothing to disclose
M. Kuzume: nothing to disclose
S. Tsuneta: nothing to disclose
N. Oyama-Manabe: nothing to disclose
T. Anzai: nothing to disclose

10:30 - 12:00 **Room G**

Paediatric

RPS 212

New insights in paediatric body imaging

Moderators:
G. Perucca; Turin/IT
S. Stafrace; Doha/QA

RPS 212-1 10:30
Intravoxel incoherent motion imaging for the study of placental microstructure in intrauterine growth restriction: a prenatal in vivo MR study
A. Antonelli[1], S. Capuani[1], G. Ercolani[1], S. Bernardo[1], B. Kuehn[2], R. Grimm[2], A. de Rinaldis[2], L. Manganaro[1], C. Catalano[1]; *[1]Rome/IT, [2]Erlangen/DE*
(amanda.antonelli@uniroma1.it)

Purpose: To investigate the role of intravoxel incoherent motion (IVIM) MRI for the study of placental microvascular and microstructural impairment in intrauterine growth restriction (IUGR) compared to normal placentae.
Methods and materials: 63 singleton pregnancies (49 normal and 14 IUGR subjects) were enrolled. Advanced diffusion-weighted EPI with 10 b-values (0, 10, 30, 50, 75, 100, 150, 400, 700, and 1,000s/mm2) was performed at 1.5T. MR body diffusion toolbox prototype software was used to obtain perfusion fraction (f), pseudo-diffusion coefficient (D*), and diffusion coefficient (D) maps. For each subject, ROIs were manually placed in whole foetal and whole maternal placenta and in three parenchymal areas (umbilical (U), central (C), and peripheral (P)) in both the foetal and maternal side. Differences between f, D, and D* mean values and their correlation with gestational age (GA) were investigated in both the normal and IUGR group.
Results: f was significantly lower ($p=10^{-9}$) in IUGR compared to the normal group in whole maternal and whole foetal ROIs, in U-, C-, and P- maternal and foetal ROIs, whereas D was higher in IUGR compared to normal pregnancies (p=0.01) in whole, U-, C-, and P- foetal ROIs. D* was significantly lower in IUGR than in the healthy group in the whole maternal side (p=0.02) and in the foetal P-ROI. D showed a significant negative correlation with GA in the whole placenta (p<0.0001) and in U-, C-, and P- maternal and foetal ROIs.

Conclusion: According to our results, the IVIM model is able to quantify in vivo microvascular and microstructural impairment of placental parenchyma in IUGR compared to normal pregnancies, detecting dysfunctional perfusion and diffusion qualities in vivo. Placental IVIM-MRI is a useful tool in the microstructural analysis of placental insufficiency affecting IUGR pregnancies.
Limitations: The heterogeneity of the IUGR group.
Ethics committee approval: The study was approved by the local ethics committee.
Funding: No funding was received for this work.
Author Disclosures:
A. Antonelli: nothing to disclose
L. Manganaro: nothing to disclose
G. Ercolani: nothing to disclose
S. Capuani: nothing to disclose
C. Catalano: nothing to disclose
S. Bernardo: nothing to disclose
B. Kuehn: Employee at Siemens Healthineers
R. Grimm: Employee at Siemens Healthineers
A. de Rinaldis: Employee at Siemens Healthineers

RPS 212-2 10:36

Is there a worldwide standard normal foetal lung volume by MRI measurement?

S. Sefidbakht[1], A. Dehdashtian[1], S. Bagheri[1], F. Bagheri[1], N. Rahimirad[1], P. Keshavarz[1], B. Bijan[2]; [1]*Shiraz/IR,* [2]*Sacramento, CA/US*
(SepidehSefidbakht@yahoo.com)

Purpose: To evaluate the application of prenatal magnetic resonance imaging in order to predict pulmonary hypoplasia, the foetal lung volume (FLV) was measured with the aim to establish reference data in normal foetuses.
Methods and materials: 342 foetuses with abnormal ultrasound findings underwent fast spin-echo T2-weighted MR imaging. Data of 241 foetuses at 18-36 weeks gestation without thoracic malformations were obtained for an FLV normative curve. This resulted in a formula calculating the expected foetal lung volume dependent on the gestational age.
Results: Normal FLV increased with the gestational age as the spread of values. The expected foetal lung volume was derived from the following formula: foetal lung volume (mL)=0.002×(GA^2.913), in which GA is the gestational weeks. FLV in our population had a more consistent correlation with Japanese foetuses than European or American foetuses.
Conclusion: In foetuses with normal lungs, FLV distribution against the gestational age is simply measured prenatally with MR imaging. A single universal formula might not be suitable for foetuses worldwide. In our region, acquired data was more consistent with Asian normal values.
Limitations: Sampling was not performed among a strictly healthy population and it may involve foetuses with structural abnormalities outside the chest cavity referred for prenatal MR imaging. Lung volume measurements may alter with the cardiac cycle or foetal breathing. In this study, such an effect tried to be degraded via the acquisition time and by multiple measurements, and by obtaining a mean foetal lung volume. Two plane measurement and 3D volumetry were not accessible for comparison.
Ethics committee approval: The study protocol was approved by the local institutional review board and informed consent was waived by the institutional ethics committee.
Funding: No funding was received for this work.
Author Disclosures:
S. Bagheri: nothing to disclose
S. Sefidbakht: nothing to disclose
A. Dehdashtian: nothing to disclose
F. Bagheri: nothing to disclose
N. Rahimirad: nothing to disclose
P. Keshavarz: nothing to disclose
B. Bijan: nothing to disclose

RPS 212-3 10:42

CMR imaging derived systemic to pulmonary collateral flow exceeding 20% of stroke volume considerably reduces antegrade pulmonary flow in univentricular heart patients

A. Yanovskiy, L. Martelius, J. Salminen, T. Ojala; *Helsinki/FI*
(yanovskiy.anna@gmail.com)

Purpose: Systemic to pulmonary collateral flow (SPCF) is a significant haemodynamic burden in univentricular heart (UVH) patients after a bidirectional Glenn operation and diminishes to some extent after a total cavopulmonary connection (TCPC). By cardiac magnetic resonance imaging (CMR), pulmonary flow (Qp) and pulmonary-to-systemic-blood-flow ratio (Qp/Qs) can be estimated from pulmonary arteries and pulmonary veins. Our objective was to define if these methods differ in operated UVH patients and if this difference correlates to the amount of SPCF.
Methods and materials: A retrospective single-centre study included 82 consecutive CMR examinations of patients with UVH (pre-TCPC stage n=17 (21%), post-TCPC n=65 (79%)) was conducted. For each patient, phase-contrast velocity mapping derived Qp was calculated twice; as the sum of the pulmonary arteries flows (QpPA) and pulmonary vein flows (QpPV). Qp/Qs ratios were calculated based on both QpPA and QpPV. The relationship between delta Qp/Qs (calculated as $[(Qp_{PV}/Qs)-(Qp_{PA}/Qs)]$) and the SPCF was computed using the Pearson correlation coefficient. Minimal clinically important difference (MCID) in Qp/Qs ratios was estimated as ≥0.5, ROC curve, and cut-off analyses were performed.
Results: In the pre-TCPC group, SPCF was significantly higher compared to the post-TCPC group (26%(10%-60%) and 14%(3%-37%), respectively, p<0.001). In both groups, QpPA/Qs was smaller or rarely equal to QpPV/Qs (p<0.001). Delta Qp/Qs and SPCF showed a strong positive correlation (r=0.85, p<0.001). ROC analysis suggests the cut-off for MCID ≥0.5 at about 20% of SPCF with a sensitivity of 80%, specificity of 84%, and excellent accuracy (AUC=0.92±0.04).
Conclusion: SPCF violates Qp and Qp/Qs ratio measurements based only on PA, resulting in their underestimation. At any stage of UVH palliation, SPCF exceeding 20% of stroke volume decreases the antegrade pulmonary artery flow remarkably.
Limitations: n/a
Ethics committee approval: n/a
Funding: No funding was received for this work.
Author Disclosures:
L. Martelius: nothing to disclose
A. Yanovskiy: nothing to disclose
J. Salminen: nothing to disclose
T. Ojala: nothing to disclose

RPS 212-4 10:48

Left atrial dysfunction in children and adolescents with severe obesity: a cardiac magnetic resonance imaging myocardial strain study

E. Xu[1], N. Kachenoura[1], V. della Valle[1], B. Dubern[1], A. Karsenty[1], R. Layese[2], J. Lamy[1], A. Redheuil[1], E. Blondiaux[1]; [1]*Paris/FR,* [2]*Créteil/FR*
(ericxu.pro@gmail.com)

Purpose: Paediatric severe obesity has tripled in the last decades along with associated complications. Less is known regarding left atrial (LA) dysfunction and its association with left and right ventricular (LV, RV) remodelling. Our aim was to assess the effects of severe childhood obesity using strain analysis by cardiac magnetic resonance (CMR).
Methods and materials: Children prospectively recruited were categorised into two groups according to their body mass index (BMI). Strain measurements were derived from standard cine images using a dedicated CMR imaging feature-tracking (FT) software.
Results: 36 children were recruited. Reduced values were found in children with obesity for LA reservoir function (23.9% vs 32%, p=0.008), contractile function (4.6% vs 10.9%, p=0.004), and LA ejection fraction (EF). An increasing BMI was significantly associated with decreasing absolute values in LA strain in reservoir and contraction phases and in LAEF. Absolute RV radial motion fraction was reduced by 42% and circumferential strain by 31% in children with obesity. Obese children showed a reduced LV radial strain.
Conclusion: CMR FT identifies LA dysfunction in severely obese children with impaired reservoir and atrial contraction phases, suggesting an early loss in the compensatory ability of atrial contraction in case of severe obesity. CMR FT strain measurements could help to detect early signs of cardiac dysfunction related to obesity in childhood and adolescence.
Limitations: The limited sample size of our study population. We also lacked the availability of several clinical data e.g. the percentage of body fat that could have been valuable clinical parameter to correlate with our CMR findings.
Ethics committee approval: Ethical approval was obtained and patients and parents gave informed consent.
Funding: This work was supported by the French Society of Radiology.
Author Disclosures:
E. Xu: nothing to disclose
E. Blondiaux: nothing to disclose
N. Kachenoura: nothing to disclose
V. della Valle: nothing to disclose
J. Lamy: nothing to disclose
A. Redheuil: nothing to disclose
B. Dubern: nothing to disclose
A. Karsenty: nothing to disclose
R. Layese: nothing to disclose

RPS 212-5 10:54
Chest x-ray or lung ultrasound in neonatal lung disease?
S. Deftereos, S. Foutzitzi; *Alexandroupolis/GR*
(foutzita@gmail.com)

Purpose: Early and reliable diagnosis is important for neonatal patients with respiratory diseases (RD) which are common in the neonatal intensive care unit (NICU). Lung ultrasound (LUS) on the contrary of chest x-ray (CXR) and computed tomography present increased use in everyday practice due to their safety and mobility (bedside method) as well as their ability to produce real-time continuous images.
Methods and materials: 99 neonates from NICU with a gestational age ranging from 25 weeks-40 weeks and respiratory distress were included in this study. All babies after clinical estimation (Apgar score, vital signs, and laboratory tests etc.) underwent CXR followed by LUS. The findings were compared between them.
Results: Clinically 77 (78.8%) neonates suffered from respiratory distress syndrome (RDS), 3 (3%) revealed pneumothorax, and 14 (14.1%) full-term neonates presented with transient tachypnea of the newborn. 2 (2%) neonates with pleural fluids, 1 (1%) with meconium aspiration syndrome, 1 (1%) with a hernia, and 2 (2%) with right upper lobe collapse were diagnosed. The basis of our diagnosis was clinical decision. According to this, the severity of illness was estimated by chest x-ray as well as by LUS. CXR had the most sensitivity and specificity in pneumothorax and hernia (100%) while LUS had 66% and 100%, respectively. In RDS, CXR achieved 73.9% sensitivity and 82% specificity, and in LUS, had 99% sensitivity but only 64.1% specificity.
Conclusion: CXR remains the method of choice in RD diagnosis. LUS is a useful tool in NICU. It is reliable, easy-to-use, convenient, non-invasive, and free of a radiation method with the potential to become a tool for bedside dynamic respiratory monitoring.
Limitations: n/a
Ethics committee approval: n/a
Funding: No funding was received for this work.
Author Disclosures:
S. Foutzitzi: nothing to disclose
S. Deftereos: nothing to disclose

RPS 212-6 11:00
Chronic aspiration in children: a retrospective study of CT findings and videofluoroscopy correlations
R. Meshaka, S. Zimmels, A. Kelly, T. R. Semple; *London/UK*
(riwa.meshaka@nhs.net)

Purpose: Chronic aspiration is a common childhood cause of recurrent lower respiratory tract infection. Diagnosis is made clinically and supported by videofluoroscopy (VF), but chronic aspiration is often suggested when right upper and bilateral lower lobe disease is seen on chest radiography or CT, despite limited evidence to support this. The objective of this study was to investigate CT findings in VF-proven aspiration.
Methods and materials: Children under 5 years with VF and CT data were identified from a speech and language therapy referrals database. Aspiration was assessed as present/absent on VF. 9 CT features of aspiration (atelectasis, bronchial wall thickening, mosaic attenuation, mucus plugging, bronchiectasis, ground glass, consolidation, volume loss, and interstitial lung disease) were assessed as present/absent and scored for severity/extent on a 3-point scale.
Results: 61 patients were identified (44 aspiration, 17 no aspiration, mean age 1.5 vs 2.1 years respectively, p=0.22). There were more CT features in the aspiration group (mean 6 vs 4.8) with greater extent/severity scores (7.3 vs 5.0), but neither reached significance (p=0.24 and 0.46). The presence of atelectasis (in any lobe) suggested aspiration (p=0.04), with aspiration extent nearing significance (p=0.07). No other feature reached statistical significance. Most features demonstrated a right upper, right lower, and left lower lobe predominance in both cohorts.
Conclusion: Our small cohort supports the use of atelectasis on CT as a prompt for the investigation of aspiration. The RUL, RLL, and LLL predominant distribution alone is not diagnostic and VF continues as the gold standard investigation for aspiration.
Limitations: Our small cohort is based at a tertiary heart and lung centre; patients often have other comorbidities.
Ethics committee approval: Currently under submission.
Funding: No funding was received for this work.
Author Disclosures:
R. Meshaka: nothing to disclose
S. Zimmels: nothing to disclose
A. Kelly: nothing to disclose
T. R. Semple: nothing to disclose

RPS 212-7 11:06
The upper airway after open airway surgery for laryngotracheal stenosis: a magnetic resonance study
B. Elders, B. Pullens, H. A. W. M. Tiddens, P. A. Wielopolski, P. Ciet; *Rotterdam/NL (b.elders@erasmusmc.nl)*

Purpose: Laryngotracheal stenosis (LTS) is often successfully corrected with open airway surgery. However, the majority of patients remain with respiratory and vocal sequelae. A better understanding of these sequelae is needed to improve clinical care and surgical interventions. The aim of this study was to image the upper airway of paediatric patients with a history of open airway surgery for LTS using magnetic resonance imaging (MRI).
Methods and materials: 48 patients (age 14.4 (range 7.5-30.7) years) and 11 healthy volunteers (age 15.9 (range 8.2-28.8) years) were included, spirometry and static and dynamic upper airway MRI (30 minutes, 3T GE scanner, 6CH carotid coil, spatial resolution 0.5x0.5 (in-plane) x2 mm, temporal resolution: 240 ms) were conducted. MRI analysis included the assessment of post-operative anatomy and measurements of airway areas and diameters during static and dynamic (inspiration and phonation) acquisitions.
Results: Good image quality was achieved for static and dynamic images (61.4% and 70.2%) without artefacts (70.2%). Excellent MRI visualisation showed vocal cord thickening in 80.9% of patients and a significant decrease in lumen area at the vocal cord level (22.0 (IQR 17.7-30.3) mm^2 vs 35.1 (IQR 21.2-54.7) mm^2, p=0.03) but not the cricoid (62.0 ± 27.3 mm^2 vs 66.2 ± 34.8 mm^2, p=0.68) compared to healthy volunteers. Furthermore, 53.2% of patients had an a-frame deformation of the trachea at the site of the previous tracheal cannula, showing even further lumen collapse during inspiration. 37 (78.7%) patients showed signs of possible fibrosis/chronic oedema, mostly located at the arytenoids or vocal cords.
Conclusion: Static and dynamic MRI is suitable for the extensive evaluation of the upper airway in post LTS children.
Limitations: n/a
Ethics committee approval: Local medical ethics committee approval (MEC-2018-013) and written informed consent obtained.
Funding: Funding provided by the 'Vrienden van het Sophia Foundation'.
Author Disclosures:
B. Elders: nothing to disclose
B. Pullens: nothing to disclose
H. A. W. M. Tiddens: nothing to disclose
P. A. Wielopolski: nothing to disclose
P. Ciet: nothing to disclose

RPS 212-8 11:12
3Tesla lung MRI in children with pneumonia
S. Yücel[1], T. Aycicek[2], M. Ceyhan Bilgici[2], O. S. Dincer[1], L. Tomak[2], S. G. Sensoy[2]; *[1]Mus/TR, [2]Samsun/TR (serapyucl@gmail.com)*

Purpose: As an alternative to chest x-ray and CT, which exposes patients to ionising radiation, this paper aims to investigate the utility of fast 3T sequences for the detection of pulmonary abnormalities in children with pneumonia.
Methods and materials: 47 children with clinically suspected pneumonia were prospectively included in this study. All children underwent thoracic MRI (3T) and PA chest x-ray. 15 patients had contrast-enhanced thorax CT or HRCT. MRI protocol included axial and coronal T2-weighted spectral presaturation with inversion recovery (SPIR) MultiVane XD, axial echo-planar imaging (EPI), and diffusion-weighted imaging (DWI) with respiratory gating. Kappa statistics, Cochran Q and McNemar tests were used to investigate the results.
Results: There was a statistically substantial agreement between chest radiographs and MRIs in detecting consolidation/infiltration (k=0.64), peribronchial thickening (0.78), and bronchiectasis (k=1), a moderate agreement for detecting cavities (k=0.54) and pleural effusion n (k=0.44), and a fair agreement for detecting empyema (k=0.32) and bilateral involvement of the lungs (k=0.23). MRI was superior to chest x-ray in detecting bilateral involvement (p=0.000), lymph nodes (p=0.000), pleural effusion (p=0.000), and empyema (p=0.003). MRI detected all consolidation or infiltration detected on CT imaging. The kappa test showed a moderate agreement between MRI and CT in detecting pleural effusion (k=0.48) and ground-glass opacity (k=0.44), and a substantial agreement for all other pathologies (k=0.61-0.99). No statistically significant difference was observed between MRI and MDCT for detecting pneumonia associated pathologies by the McNemar test.
Conclusion: Thoracic 3T MRI is an accurate and effective technique to evaluate children with pneumonia. MRI detected more pathologies than chest x-ray and had similar results compared with thorax CT.
Limitations: The timeline between imaging modalities was 0-3 days. Patients older than 6 years old were included to avoid giving sedation to patients.
Ethics committee approval: The study was approved by the Ondokuz Mayis University Ethical Committee on 30th of March, 2017.
Funding: Ondokuz Mayis University BAP-project office.

Author Disclosures:
S. Yücel: Author at Mus State Hospital
O. S. Dincer: Investigator at Mus State Hospital
M. Ceyhan Bilgici: Investigator at Ondokuz Mayis Faculty of Medicine
T. Aycicek: Investigator at Ondokuz Mayis Faculty of Medicine
L. Tomak: Investigator at Ondokuz Mayis Faculty of Medicine
S. G. Sensoy: Investigator at Ondokuz Mayis Faculty of Medicine

RPS 212-9 11:18
Acoustic radiation force impulse imaging for predicting liver cirrhosis in infants with biliary atresia
Y. Chen, S. Gu, Y. Zhu*; Shanghai/CN (joychen1266@126.com)*

Purpose: To evaluate acoustic radiation force impulse (ARFI) in assessing liver cirrhosis preoperatively in infants with biliary atresia (BA).
Methods and materials: A total of 138 infants with BA scheduled for Kasai surgery were enrolled in this retrospective cohort study. All infants underwent ARFI imaging to evaluate liver stiffness by measuring shear-wave speeds (SWSs) followed by a liver biopsy within 3 days after imaging. The liver fibrosis stages of specimens were classified using the Batts-Ludwig scoring system. The Spearman correlation coefficient value between the SWSs and fibrosis stage was calculated. Receiver operating characteristic (ROC) curves were used for evaluating the diagnostic performance of ARFI imaging in diagnosing liver cirrhosis (fibrosis stage F4).
Results: The median age of infants at the day of imaging was 56d. The biopsy histopathology confirmed 27 infants with fibrosis stage F1, 42 infants with fibrosis stage F2, 55 infants with fibrosis stage F3, and 14 infants with fibrosis stage F4. The median SWS of infants with F1, F2, F3, and F4 was 1.43m/s, 1.61m/s, 1.95m/s, and 2.39m/s, respectively (P<0.001). A significant correlation was found between SWS values and the fibrosis stage with a Spearman correlation coefficient of 0.744 (P<0.001). The AUC of SWS values for diagnosing cirrhosis was 0.948 (95% CI: 0.896, 0.978). The best cut-off value for predicting cirrhosis was 2.06m/s, with the sensitivity of 92.9% and specificity of 91.1%.
Conclusion: The SWS value measured by ARFI imaging showed excellent correlation with the liver fibrosis stage and might be an ideal non-invasive approach in predicting liver cirrhosis in infants with BA preoperatively.
Limitations: The retrospective study design.
Ethics committee approval: Appoved by insitute ethics committee (XHEC-D-2015-160).
Funding: No funding was received for this work.
Author Disclosures:
S. Gu: nothing to disclose
Y. Chen: nothing to disclose
Y. Zhu: nothing to disclose

RPS 212-10 11:24
ARFI elastography of the liver and spleen in patients with Gaucher disease type 1: correlations with clinical data and markers of disease severity
A. Lollert, C. Hoffmann, M. Lache, J. König, M. Brixius-Huth, J. Hennermann, C. Düber, G. Staatz*; Mainz/DE (andre.lollert@unimedizin-mainz.de)*

Purpose: To evaluate the feasibility of acoustic force impulse (ARFI) elastography of the liver and spleen in patients with Gaucher disease type 1 (GD1) and to assess correlations between organ stiffness and clinico-radiologic data, such as the Gaucher disease type 1 severity scoring system (GD-DS3).
Methods and materials: We retrospectively evaluated the results of ARFI elastography as measures of liver and spleen stiffness in 57 patients with GD1. The feasibility of the method was assessed. Correlations between elastography data and clinical data related to the metabolic syndrome, laboratory tests, and GD1-related clinico-radiologic data (bone marrow burden score, GD-DS3) were assessed.
Results: ARFI elastography provided reliable results (i.e. standard deviation <30% of the mean value between the measurements) in 50/57 patients. Significant liver fibrosis was present in 35/50 patients (70%). Liver stiffness correlated significantly with the GD-DS3 score (P=0.029). Spleen stiffness correlated significantly with age (P=0.021), body mass index (P=0.002), several laboratory parameters, and near-significantly with the GD-DS3 score (P=0.059).
Conclusion: ARFI elastography is a useful tool for a more profound assessment of disease severity in patients with GD1, which adds relevant information to the standard clinical scores. Thus, elastography might allow for extended therapy monitoring, especially in patients with significant liver fibrosis. Spleen elastography showed promising results and its role should be further investigated.
Limitations: The retrospective study design and heterogeneity of the study cohort. Therapy-related factors were not analysed.
Ethics committee approval: The study was approved by the local independent ethics committee.
Funding: Sanofi-Genzyme.

Author Disclosures:
A. Lollert: Research/Grant Support at Sanofi-Genzyme
C. Hoffmann: nothing to disclose
M. Lache: nothing to disclose
J. König: nothing to disclose
M. Brixius-Huth: nothing to disclose
J. Hennermann: Research/Grant Support at Sanofi-Genzyme
C. Düber: Research/Grant Support at Sanofi-Genzyme
G. Staatz: Research/Grant Support at Sanofi-Genzyme

RPS 212-11 11:30
Diffusion-weighted imaging for the differentiation of biliary atresia and grading of hepatic fibrosis in infants
J. Kim, H. J. Shin, H. Yoon, S. J. Han, H. Koh, M.-J. Kim, M.-J. Lee*; Seoul/KR*

Purpose: To determine whether the values of the hepatic apparent diffusion coefficient (ADC) can differentiate biliary atresia (BA) from non-BA or be correlated with the grade of hepatic fibrosis in infants with cholestasis.
Methods and materials: This retrospective cohort study included infants who received liver MRI examinations to evaluate cholestasis from July 2009-October 2017. Liver ADC, ADC ratio of liver/spleen, aspartate aminotransferase to platelet ratio index (APRI), and spleen size were compared between the BA and non-BA groups. The diagnostic performances of all parameters for significant fibrosis (F3-4) were obtained by receiver-operating characteristics (ROC) curve analysis.
Results: A total of 227 infants (M:F=98:129; mean age=57±36.3), including 125 BA patients, were analysed. Liver ADC values were lower (p=0.012) and spleen size was larger (p<0.001) in the BA group compared to the non-BA group. There were 34 patients with F0, 15 with F1, 71 with F2, 36 with F3, and 12 with F4. There were significant correlations between fibrosis grades and all 4 parameters of APRI (τ=0.289), spleen size (τ=0.297), liver ADC (τ=-0.206), and ADC ratio (τ=-0.249) (all, p<0.001). The cut-off values for significant fibrosis (F3-4) were 0.712 for APRI (area under the ROC curve [AUC], 0.712), 5.9 cm for spleen size (AUC, 0.701), 1.044×10^{-3} mm/sec for liver ADC (AUC, 0.666), and 1.22 for ADC ratio (AUC, 0.647).
Conclusion: Liver ADC values could be helpful in differentiating BA from non-BA and predicting significant hepatic fibrosis in infants with cholestasis.
Limitations: A retrospective study. The lack of evaluation for additional effects on conventional US or MR-based diagnoses.
Ethics committee approval: n/a
Funding: No funding was received for this work.
Author Disclosures:
J. Kim: nothing to disclose
H. J. Shin: nothing to disclose
H. Yoon: nothing to disclose
S. J. Han: nothing to disclose
H. Koh: nothing to disclose
M.-J. Kim: nothing to disclose
M.-J. Lee: nothing to disclose

RPS 212-12 11:36
Postoperative hepatic artery ultrasound evaluation of liver transplants in children: the results from a tertiary-care paediatric hospital
A. Antón Jiménez, A. Coma, J. Piqueras Pardellans, L. Riera Soler, L. Riaza Martin, E. Vazquez Mendez*; Barcelona/ES (alba.antonj@gmail.com)*

Purpose: To establish the normal reference values of a hepatic artery US Doppler postoperative evaluation after liver transplant in the paediatric population and to associate acute vascular complications with these US Doppler parameters.
Methods and materials: A retrospective study of US Doppler parameters of liver transplants in children from 2016-2019 in a tertiary-care paediatrics hospital was performed.
Patient age, liver underlying disease, the introduction of enteral feeding, and surgical technique were recorded.
Peak systolic velocity (psV) and resistive index (RI) at US Doppler studies were analysed every 24 hours during the first 5 days after liver transplantation.
Results: 40 children (19 girls and 21 boys; mean age 5.4 years) enrolled during 2016-2019. One patient required retransplantation.
Of the 41 liver transplantations performed, 21 were living donor and deceased split-liver grafts.
6 acute arterial complications occurred, 4 anastomotic stenosis, and 2 arterial thromboses.
There was a significant association between psV and RI and with arterial complications. Range interval psV was inferior in partial-liver compared to total-liver transplants and in paediatric transplants compared to adults. A value of psV ≤30 cm/s after transplantation correlated with a risk of acute vascular complication and it was frequently observed after the 3rd day. A reduction of RI usually happened 1-2 days after the psV decrease.

Conclusion: Normal reference psV range is inferior in paediatric liver transplant compared to that described in adults.
psV and RI correlate with arterial complications in the postoperative period. psV ≤30 cm/s value can predict potential acute arterial complications before RI.
CT should be performed to confirm US findings when psV ≤30 cm/s.
Limitations: A retrospective study.
Ethics committee approval: n/a
Funding: No funding was received for this work.
Author Disclosures:
A. Antón Jiménez: nothing to disclose
J. Piqueras Pardellans: nothing to disclose
L. Riera Soler: nothing to disclose
L. Riaza Martin: nothing to disclose
E. Vazquez Mendez: nothing to disclose
A. Coma: nothing to disclose

RPS 212-13 11:42
Dynamic MR lymphangiography to find the location of chylus leakage in children
W. M. Klein, B. Verhoeven, F. Udink Ten Cate, L. J. Schultze Kool; *Nijmegen/NL (willemijn.klein@radboudumc.nl)*

Purpose: Chylus leakage can occur in cases with congenital lymphatic malformations or flow abnormalities. The loss of proteins and fat leads to severe morbidity, social impairment, and mortality. Standard treatment is a low-fat diet, drainage, and ultimately radiological or surgical intervention.
Dynamic MRI lymphangiography (DMRL) is a minimal-invasive imaging method to detect the location of leakage and therefore guide intervention. We present this innovative technique in paediatric cases.
Methods and materials: Paediatric patients with severe congenital chylus leakage and failing conservative treatment were included. Lower inguinal lymph nodes were punctured using ultrasound guidance with the placement of 25G spinal needles. The MRI scan consisted of T1- and T2-weighted imaging of the thorax and abdomen, followed by intranodal injection of gadolinium and dynamic lymphangiography demonstrating the lymph flow and any leakage.
Results: 6 children were included who underwent DMRL. 2 boys with scrotal chylus leakages appeared to have retroperitoneal retrograde flow; both improved with interventional embolisation. One boy with severe chylothorax showed mediastinal leakage, which was successfully embolised. A syndromal boy showed an abnormal thoracic duct for which we have no treatment options. Two Noonan-like neonates with severe chylothorax showed extensive leakages. They had embolising interventions, however, leakages could not be stopped and both eventually died.
Conclusion: DMRL is a minimally invasive method to demonstrate flow and leakage of lymph or chylus and can serve as well as a guiding map for intervention.
More knowledge of congenital lymph malformations and flow abnormalities is needed to help more patients who have no current treatment options.
Limitations: This is a pilot study with a small number of patients.
Ethics committee approval: n/a
Funding: No funding was received for this work.
Author Disclosures:
W. M. Klein: nothing to disclose
B. Verhoeven: nothing to disclose
F. Udink Ten Cate: nothing to disclose
L. J. Schultze Kool: nothing to disclose

RPS 212-14 11:48
A comparison of image quality between single- and split-filter dual-energy paediatric abdominal CTs for radiation dose optimisation: a phantom study
K. Zhang[1], Y. Dou[2], W. Shen[1]; *[1]Tianjin/CN, [2]Beijing/CN (13516258019@163.com)*

Purpose: To compare the image quality of abdominal split-filter dual-energy CT (SF-DECT) to single-energy CT (SECT) and optimise the radiation dose using the paediatric phantom.
Methods and materials: The abdomen regions of an anthropomorphic phantom representing a 5-year-old patient were scanned using SECT and SF-DECT retrospectively in different radiation dose groups. SF-DECT scans were reconstructed into composed images. Objective image quality, including CT values, image noise and contrast-to-noise (CNR) of liver and kidney, was measured and compared between SF-DECT and SECT in every radiation dose group. The results between SF-DECT and SECT were compared using the Mann–Whitney U test. After performing a Kruskal–Wallis test, objective image quality parameters were analysed among the different dose groups.
Results: Image noise of SF-DECT was significantly lower than SECT in 3 mGy and 4 mGy ($p < 0.001$), and there was no difference in the 1 mGy and 2 mGy group (p=0.925 and 0.547, respectively). CNR of the liver and kidney of SF-DECT was significantly higher than SECT in all dose groups, except CNR of kidney in the 1 mGy group (p=0.862) and CNR of the liver in the 1 mGy and 2mGy group. The image noise decreased with the increase of dose in SF-DECT with the CNR increasing ($p < 0.001$). Furthermore, there were no differences between 3 mGy and 4 mGy groups for both the image noise and CNR.
Conclusion: The use of split-filter dual-energy in paediatric abdominal CT could provide comparable, even superior image quality at different levels of radiation dose compared to standard SECT.
Limitations: This is a phantom study that does not fully represent the condition of real children. We do not implement the subjective score of image quality.
Ethics committee approval: n/a
Funding: No funding was received for this work.
Author Disclosures:
K. Zhang: Author at Department of Radiology, Tianjin First Center Hospital
W. Shen: Author at Department of Radiology, Tianjin First Center Hospital
Y. Dou: Author at Siemens Healthcare Ltd,HC NEA DI CT SMK

RPS 212-15 11:54
A comparison of image quality and radiation dose between split-filter dual-energy images and single-energy images in paediatric abdominal CTs
Y. Gao, Y. Chen, Y. Dai; *Guangzhou/CN (gyinger423@163.com)*

Purpose: Few studies have reported the use of split-filter dual-energy CT (SF-DECT) in paediatric patients. This study aims to compare image quality and radiation dose of paediatric abdominal SF-DECT to single-energy CT (SECT) with automatic voltage selection (ATVS).
Methods and materials: 30 paediatric patients prospectively underwent abdominal SF-DECT (70Kev and 150Kev, Force, Siemens). Another 30 paediatric patients who received abdominal SECT with ATVS (80kv for baby<1y and 100kv for others, Aquilion One, Toshiba) were also reviewed. Objective and subjective image quality were compared. CNR and FOM were separately calculated for the liver (CNR_{liv}) and the portal vein (CNR_{pv}). Size-specific dose estimate (SSDE) was used to compare the radiation dose. A Mann-Whitney U test was used to compare the ranked data. T-tests were used to compare the numeric data.
Results: The radiation dose was 57% lower for SF-DECT compared to SECT (22.7±3.7 vs 9.6±2.4, p<0.01). Though CNR_{liv} and CNR_{pv} and noise were slightly higher in DECT images (15.6±3.6 vs 11.5±1.5, 2.2±0.9 vs 1.6±0.6, and 12.3±1.9 vs 15.3±1.6, p<0.05), FOM_{liv} and FOM_{pv} were equal between the two groups (12.9±8.8 vs 14.6±4.2 and 0.25±0.20 vs 0.31±0.28, p>0.05). Subjective artefacts, noise, sharpness, and diagnostic confidence were equal between the two groups (p>0.05).
Conclusion: The use of split-filter dual-source dual-energy CT images can significantly reduce the radiation dose compare to SECT with ATVS, which still provides comparable objective and subjective image quality.
Limitations: Further multicentre studies with larger sample sizes are needed.
Ethics committee approval: This study was approved by the IRB of the First Affiliated Hospital, Sun Yat-sen University.
Funding: No funding was reveived for this work.
Author Disclosures:
Y. Gao: nothing to disclose
Y. Chen: nothing to disclose
Y. Dai: nothing to disclose

14:00 - 15:30 **Room X**

Neuro

RPS 311

Gadolinium retention and neurovascular imaging

Moderators:
N.N.
Z. T. Kincses; Szeged/HU

RPS 311-K 14:00
Keynote lecture
D. Stojanov; *Nis/RS (drstojanov@gmail.com)*

Author Disclosures:
D. Stojanov: nothing to disclose

RPS 311-1 14:10

Gadolinium retention in the human body: the awareness of radiologists and impacts on daily radiology practice

M. E. Adin; *Istanbul/TR (emin.adin@gmail.com)*

Purpose: To assess the awareness and impact of awareness of the emerging gadolinium retention data on the preferences of radiologists in daily radiology practice and to demonstrate gadolinium-enhanced MRI exercise diversities across radiologists with respect to background factors like the type of affiliations, experience in radiology, attendance to scientific events, and scope of daily radiology practice.
Methods and materials: A 21 question survey was addressed to radiologists who were at least one year from completing residency and/or fellowship training. A closed survey link was emailed to the members of the Turkish Society of Radiology and was active for four weeks (October-November 2018). The results were presented as descriptive data and grouped findings were statistically analysed.
Results: 1,133 eligible members received the emails and 335 radiologists completed the survey. 89% of respondents were aware of emerging gadolinium retention data. 45% of respondents decreased the amount of gadolinium administration and/or the frequency of gadolinium-enhanced scans since the emergence of gadolinium retention data. 88% of radiologists, who were aware of the molecular classification, used a macrocyclic agent. 39% (n=130) switched to a macrocyclic agent from linear agents within the last three years. Radiologists' attitude toward gadolinium retention was significantly associated with their background factors. The observance of HDN due to gadolinium retention was uncommon in daily practice (64% never observed).
Conclusion: Gadolinium retention data affected radiologists' approach to contrast-enhanced MRI scans, mostly in the form of switching to a macrocyclic gadolinium agent and increasing the indicative threshold for gadolinium administration. The translation of recent gadolinium retention data to clinical practice varied among radiologists with respect to background factors like experience in radiology and subspeciality training.
Limitations: The study was conducted in a single European country and may not necessarily be applicable worldwide.
Ethics committee approval: n/a
Funding: No funding was received for this work.
Author Disclosures:
M. E. Adin: nothing to disclose

RPS 311-2 14:16

MRI evidence of progressive gadolinium deposition in bone during monthly triple-dose gadolinium CE-MRIs and its relationship to hypophosphataemia

J. J. Debevits[1], D. Bageac[1], P. Dicamillo[2], R. Munbodh[1], R. Wu[1], S. Dhin-Jalbut[3], L. J. Wolansky[1], D. Karimeddini[1]; [1]*Farmington, CT/US,* [2]*Cleveland/US,* [3]*New Brunswick/US (debevits@uchc.edu)*

Purpose: To investigate for MRI evidence of calvarial gadolinium (Gd) deposition during monthly high-dose contrast administration over two years and at 10 years, and to interrogate whether osseous Gd deposition correlates with hypophosphataemia.
Methods and materials: The study cohort consisted of a retrospective analysis of 67 patients with MS or CIS who had participated in the BECOME trial and who received monthly off-label triple-dose gadopentetate dimeglumine (0.3mmol/kg) enhanced MRIs for up to 26 months. Pre-MRI blood samples were collected. An ROI mask was created in the diploic space (DS) using manual segmentation and co-registered to track signal intensity (SI) changes on fat-suppressed non-Gd T1-weighted. S/N ratios (SI Bone/SI Air) established an average SI change over time. To evaluate the association between SI changes and hypophosphataemia, we performed linear mixed regression modelling with a random intercept to test the linear trend in the SI change between the groups with and without hypophosphataemia.
Results: The monthly rate of T1-SI change in the diploic space during the first 14 months of triple-dose Gd administration was S/N=0.039 (S.E. 0.008; p<0.0001). ~10 years after the study termination, diploic S/N decreased to pre-study levels (N=28). Patients who developed hypophosphataemia (<2.5 mg/dl) at least once experienced a significantly slower increase of T1-hyperintensity compared to patients without hypophosphataemia (mean monthly S/N difference=0.034; p=0.037). Those who experienced >=1 episode of moderate hypophosphataemia (<2.0 mg/dl) did not experience any significant change in monthly diploic S/N.
Conclusion: Monthly administration of triple-dose Gd is associated with progressive T1 hyperintensity in the cranial diploic space, suggesting Gd deposition in bone. This change was lower in patients who developed hypophosphataemia and washed out after 10 years.
Limitations: The volume averaging, segmentation technique, and updates in MRI technique.
Ethics committee approval: n/a
Funding: Guerbet.
Author Disclosures:
J. J. Debevits: nothing to disclose
L. J. Wolansky: Research/Grant Support at Guerbet
D. Bageac: nothing to disclose
R. Munbodh: nothing to disclose
R. Wu: nothing to disclose
P. Dicamillo: nothing to disclose
S. Dhin-Jalbut: nothing to disclose
D. Karimeddini: nothing to disclose

RPS 311-3 14:22

Gadolinium-based contrast agent in the aqueous chamber of infantile healthy eyes promptly after intravenous injection

K. Deike-Hofmann[1], P. von Lampe[2], H.-P. Schlemmer[1], N. Bechrakis[2], C. Kleinschnitz[2], M. Forsting[2], A. Radbruch[2]; [1]*Heidelberg/DE,* [2]*Essen/DE (k.deike@dkfz-heidelberg.de)*

Purpose: To investigate whether a gadolinium-based contrast agent (GBCA) can be detected on T1-weighted MRIs in the anterior chamber of infantile eyes promptly post-injection (p.i.).
Methods and materials: Orbital MRIs of 200 healthy eyes of children suffering from retinoblastoma were assessed. The MRIs were performed with orbital coils with the children under general anaesthesia. Differences of signal intensity ratios (ΔSIRs) of the AC to the lense were determined between pre- and post-contrast-enhanced T1-weighting (Dotarem®, 0.1 ml/kg, mean p.i. time=12min).
Results: A highly significant signal intensity increase was found in the AC of healthy eyes 12min p.i. (median ΔSIR=+0.08, p<0.0001). In addition, gadolinium-enhancement showed a strong negative correlation with children's age in multivariate analysis with adjustment for p.i. time (p<0.0001).
Conclusion: GBCA leakage into the AC of healthy infantile eyes was found promptly after injection. The negative correlation between the patient's age and GBCA-enhancement might be explained by a maturation process of the blood-aqueous barrier or Schlemm's canal. Future studies should assess the duration and potential diagnostic applications as well as possible safety concerns of gadolinium presence in the AC.
Limitations: T1-weighting is semi-quantitative in nature, that's why the calculated ΔSIRs do not allow conclusions to be drawn regarding true GBCA concentrations. Furthermore, serial p.i. scans would have been desirable as the concentration peak of the GBCA in the AC might have exceeded the p.i. time. However, ΔSIRs of the longest p.i. times did not clearly surpass the other ΔSIRs, which suggests that AC enhancement might have already reached saturation.
Ethics committee approval: This retrospective study was approved by the ethics committee of the University of Essen.
Funding: No funding was received for this work.
Author Disclosures:
K. Deike-Hofmann: nothing to disclose
P. von Lampe: nothing to disclose
H.-P. Schlemmer: nothing to disclose
N. Bechrakis: nothing to disclose
C. Kleinschnitz: nothing to disclose
M. Forsting: nothing to disclose
A. Radbruch: nothing to disclose

RPS 311-4 14:28

High signal intensity in the globus pallidus (GP) and dentate nucleus (DN) on unenhanced T1-weighted magnetic resonance images: an assessment of two macrocyclic gadolinium-based agents

S. Rozenblatt[1], J. Luckman[2]; [1]*Tel Aviv/IL,* [2]*Ramat Hasharon/IL (rozshira@gmail.com)*

Purpose: To compare changes in the signal intensity (SI) measured at the dentate nucleus (DN) and globus pallidus (GP) on unenhanced T1-weighted magnetic resonance (MR) images in patients who received gadobutrol (gadavist) to those who received gadoterate meglumine (dotarem).
Methods and materials: 47 patients with CNS tumours who had undergone at least 4 MRI exams were divided into two groups. Group 1=25 patients who underwent gadoterate meglumine-enhanced MR imaging. Group 2=22 patients who underwent gadobutrol-enhanced MR imaging. Region of interest measurements were applied to unenhanced T1-weighted images by two radiologists. GP to the thalamus (TH), DN to middle cerebellar peduncle (MCP) SI ratio, and relative change (Rchange) between the initial and final examinations were calculated for each patient. The differences in the mean Rchange were analysed using a non-parametric regression test. The relationship between Rchange and the number of enhanced MR imaging examinations was evaluated using a Pearson correlation coefficient.
Results: Gadobutrol-enhanced MR imaging showed a significant increase in Rchange for DN-MCP (P<0.004). Contrarily, gadoterate meglumine-enhanced MR imaging showed no significant increase in Rchange for DN-MCP. There was a significant linear association between the number of MRI examinations and an

increase in Rchange for DN-MCP (r=0.56, P=0.001) and for GP-TH (r=0.53, P=0.007) in patients who received gadobutrol.
Conclusion: A statistically significant dose-dependent T1-weighted signal increment observed in DN and GP is associated with multiple gadobutrol administrations but not with gadoterate meglumine administrations.
Limitations: A retrospective design consisting of patients with CNS tumours and damaged blood brain barrier, lacking a control group of patients who never received GBCAs.
Ethics committee approval: The institutional review board approved this study.
Funding: No funding was received for this work.
Author Disclosures:
S. Rozenblatt: nothing to disclose
J. Luckman: nothing to disclose

RPS 311-5 14:34
The absence of T1 hyperintensity in the brain of high-risk iron-loaded thalassemia patients after multiple administrations of high-dose gadobutrol
A. Meloni[1], D. Montanaro[1], M. C. Resta[2], P. Keilberg[1], L. Pistoia[1], T. Casini[3], S. de Cori[1], V. Positano[1], A. Pepe[1]; [1]Pisa/IT, [2]Bari/IT, [3]Florence/IT
(alessia.pepe@ftgm.it)

Purpose: We evaluated signal changes in the dentate nucleus, globus pallidus, pons, and thalamus (normalised to the deep cerebellum white matter) in T1-weighted magnetic resonance (MR) images after serial injections of gadobutrol in patients with thalassemia without neurological lesions.
Methods and materials: Three study groups were scanned at both 1.5T and 3T: 15 thalassemia patients who were transfused and chelated with ≥4 gadobutrol administrations at a high dose (0.2 mmol/Kg per scan) for cardiovascular MR, 8 thalassemia patients, and 13 healthy subjects who never received gadolinium-based contrast agents (GBCA). The iron overload was assessed by the T2* technique.
Results: Demographics were comparable among the groups. Signal intensity (SI) ratios and T2* values at 1.5T in all regions were comparable among the three groups. No correlation was detected between SI ratios and T2* values. In patients with more than 4 GBCA administrations, the SI ratios were not associated with the total cumulative gadolinium dose and the total number of contrast-enhanced examinations. The SI ratios at 1.5T were significantly higher than those obtained at 3T. Moreover, no correlation was found between SI ratios at 1.5T and 3T.
Conclusion: Our study describes the lack of increased SI in T1-weighted MR images after repeated administrations of gadobutrol for cardiovascular MR studies in a high-risk population (high dose per scan, iron overload that can facilitate the transmetallation of gadolinium). A potential role of chelation therapy cannot be excluded. Moreover, SI ratios in the sampled anatomical areas differ between 1.5T and 3T machine, which is to be taken into account in trials or group analysis studies.
Limitations: The limited sample size.
Ethics committee approval: Ethics committee approval obtained.
Funding: E-MIOT project: “no-profit support” from industrial sponsorships (Chiesi Farmaceutici, ApoPharma, Bayer).
Author Disclosures:
A. Pepe: nothing to disclose
A. Meloni: nothing to disclose
D. Montanaro: nothing to disclose
M. C. Resta: nothing to disclose
P. Keilberg: nothing to disclose
L. Pistoia: nothing to disclose
T. Casini: nothing to disclose
S. de Cori: nothing to disclose
V. Positano: nothing to disclose

RPS 311-6 14:40
No changes in T1 relaxometry after a mean of eleven administrations of gadobutrol
K. Deike-Hofmann[1], J. Reuter[1], R. Haase[1], T. Kuder[1], D. Paech[1], M. Forsting[2], H.-P. Schlemmer[1], C. P. Heußel[1], A. Radbruch[1]; [1]Heidelberg/DE, [2]Essen/DE
(k.deike@dkfz-heidelberg.de)

Purpose: Quantitative T1 relaxometry is the benchmark in imaging potential gadolinium deposition and is known to be superior to semi-quantitative signal-intensity-ratio analyses. However, T1 relaxometry studies are rare, commonly limited to a few target structures, and reported results are inconsistent.
We systematically investigated quantitative T1 relaxation times (qT1) of a variety of brain nuclei after serial application of gadobutrol.
Methods and materials: Retrospectively, qT1 measurements were performed in a patient cohort with a mean number of 11 gadobutrol applications (n=46) compared to a control group with no prior GBCA administration (n=48). 13 target structures were evaluated including the dentate nucleus, globus pallidus (GP), thalamus, hippocampus, putamen, caudate, amygdala, and frontal white matter. Subsequently, a multivariate regression analysis was performed.
Results: No assessed site revealed a significant correlation between qT1 and the number of gadobutrol administrations in multivariate regression analyses. A significant negative correlation between qT1 and age was found for the GP and thalamus ($p<0.05$ each).
Conclusion: No T1 relaxation time shortening was found in any assessed brain structure after the serial injection of 11 doses gadobutrol.
Limitations: Unknown injections of GBCAs cannot definitely be excluded. However, a potentially higher GBCA exposition would have increased the probability of qT1 changes even more. Moreover, cerebral involvement was more frequent in the GBCA group. Therefore, this potential confounder was included in the multivariate analysis even though this would have theoretically just meant an even higher vulnerability for cerebral GBCA leakage and deposition.
Ethics committee approval: Written informed consent was waived due to the retrospective character of this institutional review board approved study.
Funding: This study was financially supported by Bayer AG (Berlin, Germany). The authors had sole control of the data and the information submitted for publication.
Author Disclosures:
R. Haase: nothing to disclose
K. Deike-Hofmann: Research/Grant Support at Bayer AG
J. Reuter: nothing to disclose
T. Kuder: nothing to disclose
D. Paech: nothing to disclose
M. Forsting: nothing to disclose
H.-P. Schlemmer: nothing to disclose
C. P. Heußel: nothing to disclose
A. Radbruch: Research/Grant Support at Bayer AG

RPS 311-7 14:46
A comparison of the effects of gadolinium-based contrast agents on neuronal cells
M. A. Erdogan, M. Apaydin, G. Armagan, D. Taskiran; *Izmir/TR*
(meldapaydin@gmail.com)

Purpose: Gadolinium-based contrast agents (GBCAs) are widely used in magnetic resonance imaging (MRI). Recently, an increased signal intensity has been reported in specific brain areas such as the dentate nucleus, globus pallidus, and cerebellum after repeated administrations of GBCAs. The aim of the study was to investigate the toxic effects of GBCAs on neuronal cells by using SH-SY5Y neuroblastoma cells.
Methods and materials: For toxicity assays, SH-SY5Y cells were seeded in 96-well dishes (5,000 cells/well) and incubated with different doses (0-1,000 µM) of several macrocyclic (gadoteric acid and gadobutrol) and linear GBCAs (gadoversetamide, gadopentetic acid, gadodiamide, and gadoxetic acid) for 72 hours. Cell viability and mitochondrial activity were evaluated by using MTS assay, colony-forming assay, and Hoechst staining. Alpoptotic markers, Bax and Bcl-2, were assessed by Western blotting. The results were expressed as mean ± SEM. A $p<0.05$ was accepted as statistically significant.
Results: Both macrocyclic and linear GBCAs significantly and dose-dependently reduced cell viability in neuronal cells compared to untreated cells. Cell viability was measured between 89.49±4.09 % and 60.99±0.77% in GBCAs-treated groups. In addition, neurotoxicity was more prominent in linear GBCAs-treated cultures ($p<0.0005$). Bax protein levels were increased in GBCA-treated cells, especially those treated with linear agents, whereas Bcl-2 expression was decreased concomitantly.
Conclusion: The results of the study indicate that exposure to specific GBCAs, even at low micro-molar concentrations, may have detrimental effects on neuronal survival. Further investigations are required to clarify the molecular mechanism underlying GBCAs-induced cell death.
Limitations: The in vitro study should be supported an in vivo study.
Ethics committee approval: n/a
Funding: No funding was received for this work.
Author Disclosures:
M. Apaydin: nothing to disclose
M. A. Erdogan: nothing to disclose
G. Armagan: nothing to disclose
D. Taskiran: nothing to disclose

RPS 311-8 14:52
Dynamic susceptibility MR perfusion imaging of the brain: not just a question of contrast molarity
V. Panara, P. Chiacchiaretta, M. Parenti, M. Caulo; *Chieti/IT*
(valepana@libero.it)

Purpose: Dynamic-susceptibility-contrast (DSC) perfusion (PWI) MR is based on the quantification of the signal loss on T2*-weighted images during the first pass of a contrast bolus through the brain immediately after injection of a

gadolinium (Gd)-based contrast agent. Gd-based contrast agents with higher molarity are generally considered more suitable for DSC imaging, although a greater loss of signal intensity can be achieved using a faster bolus of a less viscous contrast agent that might compensate for lower molarity. The aim of this cross-sectional study was to retrospectively analyse and compare DSC PWI studies performed with gadobutrol (1M) and gadoteridol (0.5M) on the healthy hemisphere of patients with brain tumours.
Methods and materials: DSC-PWI MRs of 36 patients (9 pts gadobutrol flow 4 ml/s, 15 pts gadoteridol 4 ml/s, and 12 pts gadoteridol 6 ml/s) with brain tumours involving only one hemisphere were retrospectively evaluated. A quantitative assessment was performed. A neuroradiologist manually positioned 4 ROIs (2 in proximity to MCA and 2 in proximity of the occipital cortex) in the healthy hemispheres. A simplified formulation of the gamma-variate (GV) model function was applied to estimate the mean of maximum (peak), AUC, and FHWM of the perfusion parameter derived from DR2* signal. Each derived CBV parametric map was qualitatively reviewed by two neuroradiologists by assigning a 4-point imaging quality score.
Results: No quantitative nor qualitative differences between the two contrast agents were observed in terms of peak, AUC, FHWM, and quality score. The agreement between readers was excellent (k=0.81).
Conclusion: In this DSC MRI study, no significant differences were found between gadobutrol and gadoteridol in terms of quantitative and qualitative perfusional parameters.
Limitations: A single-center cross-sectional study with a small group of patients.
Ethics committee approval: n/a
Funding: No funding was received for this work.
Author Disclosures:
V. Panara: nothing to disclose
M. Caulo: nothing to disclose
P. Chiacchiaretta: nothing to disclose
M. Parenti: nothing to disclose

RPS 311-9 14:58

Impact of the novel contrast agent gadopiclenol on decision making in patients with brain metastases

F. A. Giordano[1], J. Fleckenstein[1], M. Eckl[1], L. Hoppen[1], F. Wenz[1], M. Essig[2], M. Bendszus[3]; [1]*Mannheim/DE,* [2]*Winnipeg, MB/CA,* [3]*Heidelberg/DE (Frank.Giordano@umm.de)*

Purpose: Brain metastases (BM) are either treated with stereotactic radiosurgery (SRS) or whole-brain radiotherapy (WBRT), whereas the number of lesions detected is crucial for choosing adequate modality. Here we evaluate the impact on decision making and treatment planning of BM using the novel contrast agent, gadopiclenol.
Methods and materials: This is a post-hoc analysis of data from a phase IIb study, where patients underwent two separate MRI scans with gadopiclenol and gadobenate dimeglumine, both at 0.1 mmol/kg. Patients with ≥1BM detected in any scan were subjected to an investigator-blinded analysis. Radiation treatment plans (SRS or WBRT) were calculated for both MRIs, with the gross tumour volume (GTV) indicating the contrast-enhancing aspects of the tumour and the V_{12Gy} indicating the volume receiving ≥12Gy.
Results: A total of 13 patients (31% females) were eligible for this analysis. In 2 patients, gadopiclenol-based MRI scanning detected additional BMs that were undetected with gadobenate-based scans. In one patient, a single metastasis was seen only with gadopiclenol, changing the decision from no treatment to SRS. In the second patient, gadopiclenol detected 5 additional metastases, changing the decision from SRS to WBRT. In addition, the mean GTV was higher in therapy plans calculated on gadopiclenol-based scans than on gadobenate-based scans (4.74 vs 4.32 cm^3), indicating a different appearance of BM sizes. Logically, the mean V_{12Gy} was also higher with gadopiclenol than with gadobenate-based scans (14 vs 11 cm^3).
Conclusion: Gadopiclenol improved the detection of BM in 2 of 13 patients, which led to a change in treatment decisions (from no therapy to SRS and from SRS to WBRT) and to treatment plans with larger GTVs.
Limitations: The small patient numbers.
Ethics committee approval: Ethics committee approval obtained.
Funding: The study was sponsored by Guerbet.
Author Disclosures:
F. A. Giordano: Investigator at Guerbet
J. Fleckenstein: nothing to disclose
M. Eckl: nothing to disclose
L. Hoppen: nothing to disclose
F. Wenz: nothing to disclose
M. Essig: nothing to disclose
M. Bendszus: Investigator at Guerbet, Consultant at Guerbet

RPS 311-10 15:04

The value of 4D-MR angiography at 3T compared to DSA for the follow-up of treated dural arteriovenous fistulas

B. Dissaux[1], F. Eugene[2], J. Ognard[1], J.-C. Gentric[1], J.-C. Ferre[2]; [1]*Brest/FR,* [2]*Rennes/FR (brieg.dissaux@gmail.com)*

Purpose: The value of 4D-MRA for the follow-up of treated dural arteriovenous fistulas (DAVF) has rarely been evaluated.
We hypothesized that this technique could be valuable for the follow-up and post-therapeutic assessment of DAVF. The purpose of this study was to evaluate the performance of 4D-MRA at 3T for the follow-up of patients with treated DAVF.
Methods and materials: Patients treated for a DAVF in two centres from 2008-2019 were included if they met the following criteria: DAVF treated by embolisation or surgery and imaging during the follow-up with both 4D-MRA at 3T and DSA performed within 6 months. One reader analysed DSA and two readers analysed 4D-MRA.
For both modalities, 4D-MRA and DSA, readers first evaluated in a binary fashion whether a residual/recurrent DAVF was present or not. Then, when present, each residual/recurrent DAVF was classified according to the criteria of Cognard et al. The intertechnic agreement was assessed for detection of residual/recurrent DAVF and bleeding risk grading using Cohen's kappa.
Results: We recorded 59 couples of examinations for 52 patients with a median age of 64 years (range 24-86 years). Sensibility, specificity, predictive positive value, and predictive negative values of 4D-MRA for the detection of a residual/recurrent DAVF were 58.3% (95% CI: 41.8% to 74.8%) and 91.4% (95% CI: 83.9% to 98.8%), respectively. Predictive positive value and predictive negative values of 4D-MRA for the detection of a residual/recurrent DAVF were 82% (95% CI: 71.6% to 93%) and 76% (95% CI: 63.7% to 88.6%). The intertechnic agreement was moderate with k=0.5 (95% CI: 0.3 to 0.7).
Conclusion: 4D-MRA at 3T could be interesting for the follow-up of treated DAVF.
Limitations: A retrospective study.
Ethics committee approval: n/a
Funding: No funding was received for this work.
Author Disclosures:
B. Dissaux: nothing to disclose
F. Eugene: nothing to disclose
J. Ognard: nothing to disclose
J.-C. Gentric: nothing to disclose
J.-C. Ferre: nothing to disclose

RPS 311-11 15:10

The application of neurovascular 4Dflow MRI in the assessment of haemodynamics on patients with Moyamoya disease

J.-G. Zhang, Z. Li*; Chengdu/CN (zjgscuhx@126.com)*

Purpose: To analyse and compare the change of haemodynamics between pre and postoperation on patients of Moyamoya disease (MMD) using neurovascular 4Dflow MRI (phase-contrast MRA).
Methods and materials: In this study, 28 MMD patients who underwent an operation of encephaloduroarteriosynangiosis (EDAS) were enrolled. We analysed the haemodynamics of these patients by 4Dflow MRI scanning and compared the parameters between pre and postoperation including wall shear stress (WSS), flow rate, and relative pressure.
Results: The WSS and relative pressure of postoperation measured at the distal part of the internal carotid artery (ICA), the initial part of the anterior cerebral artery (ACA), and the middle cerebral artery (MCA) were significantly lower than those of preoperation (all $P < 0.05$). The flow rate significantly increased (all $P < 0.05$) after the operation.
Conclusion: The operation of EDAS can effectively improve the blood flow of MMD patients and decrease the pressure on the cerebral vascular wall. As a non-invasive, multi-parameter, and quantitative imaging technique, 4Dflow MRI has the potential to improve the diagnosis and assessment of cerebrovascular diseases.
Limitations: The sample size was small.
Ethics committee approval: This study was approved by the Ethics Committee of West China Hospital and written informed consent was obtained.
Funding: 1.3.5 project for disciplines of excellence, West China Hospital, Sichuan University (Program Number: ZYGD18019).
Author Disclosures:
J.-G. Zhang: nothing to disclose
Z. Li: nothing to disclose

RPS 311-12 15:16

Deep learning-based automated detection of cerebral aneurysms: a comparison of reading performance between radiologists and neurosurgeons

S. Koshino, A. Choppin, M. Suzuki, T. Takamura, Y. Adachi, O. Abe, S. Aoki; *Tokyo/JP (saori.koshino@gmail.com)*

Purpose: To demonstrate the effects of deep learning-based computer-aided detection (CAD) on the reader's performance for the detection of cerebral aneurysms in MR angiography (MRA).
Methods and materials: 200 brain MRA datasets (93 men and 107 women; mean age, 64.7 years±15.3 [standard deviation]; mean aneurysm size, 3.3 mm±1.74), 50 with unruptured cerebral aneurysms and 150 without, were acquired on scanners from 3 different vendors at 1.5 or 3T and were retrospectively evaluated. 20 physicians (10 radiologists including 5 certificated radiologists and 5 non-certificated radiologists, and 10 neurosurgeons including 4 certificated neurosurgeons and 6 non-certificated neurosurgeons) were asked to detect cerebral aneurysms on MRA scans and associated projection images without and with CAD using ResNet–18, a convolutional neural network. The observers' performance was evaluated using a jackknife free-response receiver operating characteristics (JAFROC) analysis.
Results: The figure-of-merit (FOM) values computed using the JAFROC program significantly improved from 0.717 without CAD to 0.751 with CAD for all readers (P<0.001). The average sensitivity increased from 68.2% to 77.2% for all readers, whereas the average specificity decreased from 79.4% to 72.1%. On subgroup analyses, the FOM values increased from 0.647 to 0.697 for non-certificated radiologists, from 0.799 to 0.822 for certificated radiologists, from 0.645 to 0.681 for non-certificated neurosurgeons, and from 0.810 to 0.836 for certificated neurosurgeons. There was no statistical significance in the reading performances between radiologists and neurosurgeons both without CAD (P=0.826) and with CAD (P=0.753). However, the performances between non-certificated neurosurgeons and certificated neurosurgeons with CAD showed a significant difference (P=0.0479).
Conclusion: The diagnostic accuracy of cerebral aneurysms improved for radiologists and neurosurgeons with CAD.
Limitations: n/a
Ethics committee approval: This study was approved by the institutional review board.
Funding: This work was funded by LPixel Inc.
Author Disclosures:
S. Koshino: nothing to disclose
A. Choppin: nothing to disclose
M. Suzuki: nothing to disclose
T. Takamura: nothing to disclose
Y. Adachi: nothing to disclose
O. Abe: nothing to disclose
S. Aoki: nothing to disclose

14:00 - 15:30 **Coffee & Talk 1**

Genitourinary

RPS 307

Deep learning and radiomics in prostate imaging

Moderators:
T. Durmus; Berlin/DE
P. A. B. Puech; Lille/FR

RPS 307-1 14:00

Value of histogram analysis from a stretched exponential model on diffusion-weighted imaging in evaluating clinically significant prostate cancer

K. E. Kim, C. K. Kim; *Seoul/KR (ganne1113@gmail.com)*

Purpose: To evaluate the usefulness of histogram analysis of a stretched exponential model (SEM) on diffusion-weighted imaging (DWI) in evaluating clinically significant prostate cancer (CSC).
Methods and materials: 85 patients were enrolled who had prostate cancer and underwent 3-T multiparametric MRI, followed by radical prostatectomy. Histogram parameters of the tumour from the SEM (distributed diffusion coefficient [DDC] and alpha) and the monoexponential model (MEM; apparent diffusion coefficient [ADC]) were evaluated. The associations between parameters and a Gleason score (GS) or prostate imaging reporting and data system (PI-RADS) v2 were evaluated. The area under the receiver operating characteristics curve (AUC) was calculated to evaluate the diagnostic performance of parameters in predicting CSC.
Results: The values of histogram parameters of DDC and ADC were significantly lower in patients with CSC than in patients without CSC (P<0.05), except for skewness and kurtosis. The value of the 25th percentile of alpha was significantly lower in patients with CSC than in patients without CSC (P=0.014). Histogram parameters of ADC and DDC had significant weak to moderate negative associations with the Gleason score (GS) or PI-RADS v2 (P<0.001), except for skewness and kurtosis. For predicting CSC, the AUCs of mean ADC (0.856), 50th percentile DDC (0.852), and 25th percentile alpha (0.707) yielded the highest values compared to other histogram parameters from each group.
Conclusion: Histogram analysis of the SEM on DWI may be a useful quantitative tool for evaluating CSC. However, the SEM did not outperform the MEM.
Limitations: A retrospective study at a single institution, inevitable errors for quantitative measurements, and no application of multiexponential diffusion attenuation.
Ethics committee approval: Our institutional review board approved this retrospective study and the requirement for informed consent was waived.
Funding: No funding was received for this work.
Author Disclosures:
K. E. Kim: nothing to disclose
C. K. Kim: nothing to disclose

RPS 307-2 14:06

Individualised prostate cancer risk assessment using MRI-based deep learning compared to multivariate risk modelling including PI-RADSv2: a decision curve analysis

D. Deniffel[1], N. Abraham[1], K. Namdar[1], S. Motamed[1], I. Gujrathi[2], E. Salinas-Miranda[1], F. Khalvati[1], M. A. Haider[1]; [1]*Toronto/CA,* [2]*Boston/US (ddeniffel@lunenfeld.ca)*

Purpose: To compare the clinical utility of a convolutional neural network (CNN)-based model applied to multiparametric MRI (mpMRI) with a risk model (RM) combining PI-RADSv2 and clinical parameters, for risk assessment of clinically significant prostate cancer (csPCa; ISUP≥grade 2).
Methods and materials: We retrospectively analysed 499 patients who underwent mpMRI and MRI-targeted biopsy. A 3D-CNN classifier was trained on diffusion-weighted MRIs and ADC maps of 400 patients (training cohort). CNN output probabilities were recalibrated to provide interpretable risk estimates for csPCa. A subset of the training cohort (n=290) was used to build an RM incorporating PI-RADSv2 scores and clinical parameters (prostate volume, PSA density, and age). Model discrimination in the validation cohort (n=99) was compared using the area under the ROC curve (AUC). Clinical usefulness of both models and PI-RADSv2 (cut-off≥4) was assessed using decision curves illustrating the clinical net benefit, which balances the benefits of detecting csPCa against the harms of unnecessary biopsies.
Results: The CNN's discrimination (AUC=0.83) was not superior to the RM (AUC=0.83) (p=0.95); however, across the entire range of clinically relevant risk thresholds (5-20%), the CNN had a higher net benefit than PI-RADSv2 and the RM. The CNN showed a clear net benefit at a risk threshold ≥5% for biopsy referral, resulting in a biopsy reduction of 21% (21/99) without missing csPCa (0/37). Applying a risk threshold ≥10% for the CNN and RM resulted in a 25% (25/99) and 7% (7/99) biopsy reduction, missing 3% (1/37) and 0% (0/37) of csPCas, respectively.
Conclusion: Our CNN model with calibrated risk estimates could reduce biopsies by 21% without missing any csPCa and is potentially superior to a multivariate RM combining PI-RADSv2 and clinical parameters.
Limitations: A single-centre, retrospective study.
Ethics committee approval: IRB-approved study.
Funding: OICR; DFG-fellowship[DE 3207/1-1].
Author Disclosures:
D. Deniffel: nothing to disclose
N. Abraham: nothing to disclose
K. Namdar: nothing to disclose
S. Motamed: nothing to disclose
I. Gujrathi: nothing to disclose
E. Salinas-Miranda: nothing to disclose
F. Khalvati: nothing to disclose
M. A. Haider: nothing to disclose

RPS 307-3 14:12

Independent validation of deep learning-based automated patient assessment on prostate MRI: the influence of image co-registration

P. Schelb[1], X. Wang[1], S. Kohl[1], M. Görtz[1], M. Wiesenfarth[1], M. Hohenfellner[1], H.-P. Schlemmer[1], K. H. Maier-Hein[1], D. Bonekamp[2]; [1]*Heidelberg/DE,* [2]*Hirschberg/DE*

Purpose: To apply a previously developed convolutional neural network (CNN) ensemble to a new set of prostate MRI examinations from consecutive patients for further validation and to examine the influence of different image co-registration approaches on CNN predictions.
Methods and materials: 3 Tesla MRI from 147 consecutive patients with 251 MR lesions (70 sPC positive) were included. DICOM images of T2-weighted, DWI b=1500 s/mm2, and corresponding ADC maps were analysed by a fully automatic analysis pipeline consisting of DWI/ADC to T2W image co-registration utilising three approaches (rigid, affine, and b-spline) prior to evaluation by the CNN ensemble. Maximum CNN tumour map probability above 0.33 (calibrated previously to correspond to PI-RADS>=4 assessment) indicated positive, otherwise regarded as negative. Both individual and combined maximum probability of the three co-registrations was evaluated.
Results: Sensitivity/specificity/accuracy was 65%/84%/75% for rigid, 71%/73%/72% for b-spline, 73%/72%/71% for affine, and 77%/70%/71% for combined compared to 89%/60%/73% for PI-RADS>=4. Accuracy (p=0.87), sensitivity (p=0.08), and specificity (p=0.36) of CNN predictions on combined co-registration were not significantly different from PI-RADS>=4 assessment.
Conclusion: The best CNN sensitivity was achieved by combined registration, highlighting the importance of registration on the performance for detection of small lesions. While achieving a lower sensitivity than PI-RADS at higher specificity, the CNN approach showed promising performance. Importantly, lowering the probability threshold of the CNN ensemble could increase the sensitivity more to match the specificity of PI-RADS. However, more data is required to justify adjusting the threshold.
Limitations: This is a single institution, single scanner CNN model, which requires multi-institutional, multi-scanner validation in the future, however, benefits from standardised conditions in the current setting.
Ethics committee approval: Approved by an ethics committee. Written informed consent waived (S-156/2018).
Funding: No funding was received for this work.
Author Disclosures:
D. Bonekamp: Speaker at Profound Medical Inc.
P. Schelb: nothing to disclose
X. Wang: nothing to disclose
S. Kohl: Employee at Google Inc.
M. Görtz: nothing to disclose
M. Wiesenfarth: nothing to disclose
M. Hohenfellner: nothing to disclose
H.-P. Schlemmer: Consultant at Siemens, Curagita, Profound, Bayer, Board Member at Curagita, Grant Recipient at BMBF, Deutsche Krebshilfe, Dietmar-Hopp-Stiftung, Roland-Ernst-Stiftung
K. H. Maier-Hein: nothing to disclose

RPS 307-4 14:18

PI-RADS 3 lesions: role of prostate MRI texture analysis in the identification of prostate cancer

R. Cannella, D. Giambelluca, F. Vernuccio, A. Comelli, A. Pavone, L. Salvaggio, M. Midiri, R. Lagalla, G. Salvaggio*; Palermo/IT (rob.cannella89@gmail.com)*

Purpose: To determine the diagnostic performance of the texture analysis of prostate MRI for the diagnosis of prostate cancer among PI-RADS 3 lesions.
Methods and materials: 43 patients with at least one PI-RADS 3 lesion on prostate MRI performed between June 2016 and January 2019 were retrospectively included. The reference standard was a pathological analysis of radical prostatectomy specimens or MRI-targeted biopsies. Texture analysis extraction of target lesions and non-lesional prostate glands was performed on axial T2-weighted images and ADC maps using a radiomic software. Lesions were categorised as prostate cancer (Gleason score≥6) and no prostate cancer. Statistical analysis was performed using the generalised linear model (GLM) regression and the discriminant analysis (DA). AUROC with 95% C.I. were calculated to assess the diagnostic performance of standalone features and predictive models for the diagnosis of prostate cancer.
Results: The analysis of 46 PI-RADS 3 lesions (i.e. 27 [58.7%] no prostate cancers; 19 [41.3%] prostate cancers) revealed 9 and 6 independent texture parameters significantly correlated with the final histopathological results on T2-weighted and ADC maps images (r_{pb} of 0.274-0.387 and 0.293-0.371), respectively. The resulting GLM and DA predictive models for the diagnosis of prostate cancer yielded an AUROC of 0.775 and 0.779 on T2-weighted images or 0.815 and 0.821 on ADC maps images.
Conclusion: Texture analysis of PI-RADS 3 lesions on T2-weighted and ADC maps images helps to identify prostate cancer. The good diagnostic performance of the combination of multiple radiomic features for the diagnosis of prostate cancer may help in predicting lesions where aggressive management may be warranted.
Limitations: Retrospective analysis, only pathologically proven lesions, and small sample size.
Ethics committee approval: IRB-approved study, informed consent was waived.
Funding: No funding was received for this work.
Author Disclosures:
R. Cannella: nothing to disclose
D. Giambelluca: nothing to disclose
F. Vernuccio: nothing to disclose
A. Comelli: nothing to disclose
A. Pavone: nothing to disclose
L. Salvaggio: nothing to disclose
R. Lagalla: nothing to disclose
M. Midiri: nothing to disclose
G. Salvaggio: nothing to disclose

RPS 307-5 14:24

Added value of quantitative DCE imaging on mpMRI prediction of stage ≥pT3 prostate cancer

A. Cretese, F. Bonato, L. Cereser, G. Como, C. Zuiani, R. Girometti*; Udine/IT (rgirometti@sirm.org)*

Purpose: To investigate whether quantitative dynamic contrast-enhanced imaging (DCE) can improve the diagnosis of pathological stage ≥T3 (≥pT3) when staging prostate cancer (PCa) with multiparametric magnetic resonance imaging (mpMRI).
Methods and materials: Over a three year period, we retrospectively included 63 patients with biopsy-proven PCa who underwent preoperative mpMRI on 3.0T equipment, using a prostate imaging reporting and data system version 2 (PI-RADSv2)-compliant protocol. The study included two readers in consensus (3 and 10 years of experience), blinded to final pathology, manually drawn volumetric regions of interest over PI-RADS ≥2 observations, calculating the volume transfer constant (K^{trans}) and rate constant (K_{ep}) with the Tofts extended model. Readers assessed extraprostatic disease by using a morphological 1-5 PI-RADSv2-derived score. We calculated the sensitivity and specificity for stage ≥pT3 of mpMRI alone, mpMRI+K^{trans}, mpMRI+ K_{ep}, and mpMRI+ K^{trans}+ K_{ep}. Thresholds for K^{trans}/K_{ep} and areas under the curve (AUC) were derived from a receiver operating characteristic analysis.
Results: The final pathology found 70 cancers, showing stage ≥pT3 in 30.0% of cases. mpMRI alone showed 61.9% (95%CI 38.4-81.9) sensitivity, 89.8% (95%CI 77.8-96.6) specificity, and AUC of 0.76 (95%C.I. 0.64-0.85). Cut-off values for K^{trans} and K_{ep} were 0.28 and 1.39, respectively. Sensitivity, specificity, and AUC were 95.2% (95%CI 76.2-99.9), 55.1% (95%CI 40.2-69.3), and 0.75 (95%C.I. 0.634- 0.847) for mpMRI+k^{trans}, 95.2% (95%CI 76.2-99.9), 63.3% (95%CI 48.3-76.6), and 0.79 (95%CI 0.68 to 0.88) for mpMRI+k_{ep}, and 90.5% (95%CI 69.6-98.8), 75.5% (95%CI 61.1-86.7), and 0.83 (95%CI 0.72-0.91) for mpMRI+k^{trans}+k_{ep}.
Conclusion: Adding K^{trans} and K_{ep} to mpMRI significantly increased the sensitivity for stage ≥pT3. DCE-derived parameters might be useful in the routine staging setting.
Limitations: A monocentric retrospective study and lack of absolute threshold for quantitative DCE values.
Ethics committee approval: IRB approval and informed consent waived.
Funding: No funding was received for this work.
Author Disclosures:
R. Girometti: nothing to disclose
A. Cretese: nothing to disclose
F. Bonato: nothing to disclose
L. Cereser: nothing to disclose
G. Como: nothing to disclose
C. Zuiani: nothing to disclose

RPS 307-6 14:30

Comparison of first-order radiomic parameters to the mean ADC for the prediction of clinically significant cancer from prostate MRI

X. Wang[1], V. Schütz[1], M. Görtz[1], D. Tichy[1], P. D. A. Stenzinger[1], M. Hohenfellner[1], H.-P. Schlemmer[1], D. Bonekamp[2]; *[1]Heidelberg/DE, [2]Hirschberg/DE*

Purpose: To explore first-order ADC radiomics metrics other than the ADC mean value (known to be one of the strongest monoparameteris in quantitative assessment) regarding their ability to further increase the predictive value of prostate MRI for detecting clinically significant prostate cancer (csPC).
Methods and materials: Consecutive patients with a clinical suspicion for csPC examined on a single 3 Tesla MR scanner who underwent MR-guided targeted and systematic biopsy in 2017 and had visible MR lesions were included. A board-certified radiologist re-reviewed MRIs blinded to clinical information and segmented lesions on MRI images. The mean ADC (mADC) and 18 other first-order ADC radiomic parameters were calculated. Logistic regression with variable selection was used to determine the optimal parameters for csPC prediction. Receiver operating characteristics (ROC) and a likelihood-ratio test (LRT) were used for comparison of performance.

Results: 253 patients harboured 392 MR lesions (302 in the peripheral zone), of which 129 lesions were csPC positive. The univariate model ROC area under the curve (AUC) was 0.66 for mADC and 0.68 for entropy. Variable selection retained only mADC and entropy in the final model, while none of the other radiomic parameters contributed further. The combined model had ROC AUC of 0.73 (p<0.001 LRT compared to the univariate mADC model).
Conclusion: Entropy provides important additional information to mADC, thereby improving quantitative assessment of prostate MRI.
Limitations: All patients were examined on a single scanner system, limiting the generalisability of our results, however, providing a highly standardised mADC measurement which entropy was able to provide added value to.
Ethics committee approval: Approved by an ethics committee with written informed consent waived (S-156/2018).
Funding: No funding was received for this work.
Author Disclosures:
D. Bonekamp: Speaker at Profound Medical Inc.
P. D. A. Stenzinger: Consultant at Astra Zeneca,BMS, Novartis, Roche, Illumina, Thermo Fisher, Board Member at Astra Zeneca, BMS, Novartis, Thermo Fisher
X. Wang: nothing to disclose
V. Schütz: nothing to disclose
M. Görtz: nothing to disclose
D. Tichy: nothing to disclose
M. Hohenfellner: nothing to disclose
H.-P. Schlemmer: Consultant at Siemens, Curagita, Profound, Bayer, Board Member at Curagita, Grant Recipient at BMBF, Deutsche Krebshilfe, Dietmar-Hopp-Stiftung, Roland-Ernst-Stiftung

RPS 307-7 14:36

Added-value of dynamic contrast-enhanced (DCE) MRI in a lesion-based quantitative analysis of multiparametric prostate MRI in consecutive at-risk patients

A. A. Tavakoli[1], P. Badura[1], T. Tubtawee[2], V. Schütz[1], D. Tichy[1], A. Stenzinger[1], M. Hohenfellner[1], H.-P. Schlemmer[1], D. Bonekamp[3]; [1]Heidelberg/DE, [2]Songkhla/TH, [3]Hirschberg/DE*

Purpose: To examine the added-value of DCE in multi-parametric prostate MRI with a region-of-interest based quantitative evaluation.
Methods and materials: Clinical lesions reported in 3 Tesla MR exams from 315 consecutive patients with suspicion for prostate cancer were retrospectively segmented on ADC maps and a visually identified early DCE time-point. DCE was normalised to minimally enhancing parenchyma (DCEnorm). Multiple heuristic and pharmacokinetic parameters were determined, including the difference in bolus arrival time between the femoral artery and lesion (BATlesdiff) and normalised lesion AUC (AUCnorm). A basic logistic regression model included mean ADC and DCEnorm while a second model was extended by heuristic and pharmacokinetic parameters. The binary outcome was a Gleason grade group (GGG) >=2 from a targeted biopsy core for lesion-based analysis and maximum targeted GGG for patient-based analysis.
Results: Of 308 patients with successful exams, 274 had 454 MR lesions that served as biopsy targets. 211 patients had a total of 275 MR lesions in the PZ. In the PZ, the model was simplified to ADCmean, DCEnorm (both p<0.001), BATlesdiff (p=0.04), and AUCnorm (p=0.15) by variable selection. This model performed significantly better (patient-based: AUROC 0.84 vs 0.80, p=0.04; lesion-based: AUROC 0.80 vs 0.76, p=0.03) than the ADC-only model. In the TZ, the model was reduced to the ADC-only model and no added benefit of any DCE-parameter was found.
Conclusion: In a comprehensive quantitative ROI-based analysis, DCE demonstrates the ability to improve MRI assessment in the peripheral zone but not the transition zone.
Limitations: Our results provide data on a typical PI-RADS compliant DCE protocol, however, cannot provide information on how to best trade off spatial for temporal resolution.
Ethics committee approval: Approved by an ethics committee with written informed consent waived (S-156/2018).
Funding: No funding was received for this work.
Author Disclosures:
D. Bonekamp: Speaker at Profound Medical Inc.
A. A. Tavakoli: nothing to disclose
T. Tubtawee: nothing to disclose
V. Schütz: nothing to disclose
D. Tichy: nothing to disclose
A. Stenzinger: Consultant at Astra Zeneca,BMS, Novartis, Roche, Illumina, Thermo Fisher, Board Member at Astra Zeneca, BMS, Novartis, Thermo Fisher, Speaker at Astra Zeneca,BMS, Novartis, Roche, Illumina, Thermo Fisher
M. Hohenfellner: nothing to disclose
H.-P. Schlemmer: Consultant at Siemens, Curagita, Profound, Bayer, Board Member at Curagita;, Grant Recipient at BMBF, Deutsche Krebshilfe, Dietmar-Hopp-Stiftung, Roland-Ernst-Stiftung
P. Badura: nothing to disclose

RPS 307-8 14:42

Texture analysis on multiparametric prostate magnetic resonance imaging (mpMRI) for evaluation of prostate cancer (PCa) aggressiveness

I. Ruggirello[1], M. Gatti[1], A. Motta[1], V. Giannini[2], M. Petracchini[1], S. Cirillo[1], D. Regge[2], P. Fonio[1], R. Faletti[1]; [1]Turin/IT, [2]Candiolo/IT (ireneruggirello@gmail.com)*

Purpose: To develop and validate a classifier system for the prediction of prostate cancer (PCa) aggressiveness using MRI texture analysis.
Methods and materials: 106 patients with histologically confirmed PCa were included in this retrospective study for model development and internal validation. Another 51 patients were included for independent external validation. A total of 64 first-order parameters and second-order texture parameters derived from the grey-level co-occurrence matrix were extracted from manually segmented tumours on T2w MRI and ADC maps. Data was analysed with a parametric test and Lasso logistic regression was used for feature selection and developing radiomics signatures to discriminate tumours with 4+3 vs > 3+4 GS high- and low-grade disease respectively (HG and LG). The predictive performance of the signature was evaluated via a receiver operating curve (ROC).
Results: A total of 25 radiomics features significantly different between the two groups (highest correlation for ADC entropy: r=0.33, p<0.001) in the training group. We developed two radiomics signature based on 6 (l=min) and 1 (l=1.SE) features, respectively. The signatures resulted in AUC of 0.74 (0.65-0.84), p<0.001 and AUC of 0.73 (0.63-0.82), p<0.001, in the training group, and 0.64 (0.48-0.80), p<0.001 and AUC of 0.65 (0.49-0.80), p<0.001, in the validation set.
Conclusion: MRI texture features could serve as potential diagnostic markers in assessing PCa biological aggressiveness.
Limitations: A retrospective analysis, the absence of evaluation of contrast-enhanced sequences and maps, and relatively poor AUC values.
Ethics committee approval: n/a
Funding: No funding was received for this work.
Author Disclosures:
I. Ruggirello: nothing to disclose
M. Gatti: nothing to disclose
R. Faletti: nothing to disclose
V. Giannini: nothing to disclose
D. Regge: nothing to disclose
A. Motta: nothing to disclose
M. Petracchini: nothing to disclose
S. Cirillo: nothing to disclose
P. Fonio: nothing to disclose

RPS 307-9 14:48

Radiomics in DW-MRI detects non-clinically significant prostate cancer and reduces overtreatment

A. Bevilacqua[1], M. Mottola[1], F. Ferroni[2], G. Gavelli[2], D. Barone[2]; [1]Bologna/IT, [2]Meldola/IT (margherita.mottola@unibo.it)*

Purpose: To assess to what extent radiomic features computed on high b-value DWI sequences (b=2000s/mm^2) could reliably detect non-clinically significant (NCS) prostate cancer and reduce overtreatment.
Methods and materials: This study retrospectively enrolled 25 patients of our institution, randomly extracted from PACS with a clinical suspicion of PCa who underwent prostate 3T-mpMRI. 10 patients reported NCS-PCa after TRUS biopsy, with a Gleason Score (GS)≤3+3, 15 were CS-PCa. PCa regions of interest (ROIs) were outlined in all slices by two experienced radiologists in consensus and reported on the DWI sequences, when needed, where 84 radiomic features with the corresponding ROC curves were computed. In order to prevent overfitting, a one-only feature was selected yielding the highest AUC and p-value<0.001 at the one-tail Wilcoxon rank-sum test.
Results: The dispersion of local skewness (LS) of DWI values is higher for CS-PCa (p-value~10^{-4}) and AUC=0.92 (95%CI, 0.70-0.99). Sensitivity and specificity for NCS were 90% and 87%, respectively (1 FN and 2 FP), with a false omission rate (FOR) equal to 7%, this representing a very low risk of overtreatment. Moreover, the two FPs have GS=3+4, the CS-PCa group closest to NCS one.
Conclusion: Radiomic features extracted from high b-values DWI sequences allows highlighting non-visible image properties related to the complexity of the tumour habitat. The higher variability of LS hints at increasing heterogeneity of tumour micro-environment for CS-PCa. In addition, this excellent performance stresses the promising role of DWI-based radiomics in discriminating CS-PCa from NCS-PCa.
Limitations: No clinical parameters were considered for differentiation. However, at most, they could improve these results. In addition, the number of patients is limited, but uneven in their characteristics, since not derived from any dedicated study.
Ethics committee approval: IRB approval, written informed consent was waived.
Funding: No funding was received for this work.

Author Disclosures:
M. Mottola: nothing to disclose
A. Bevilacqua: nothing to disclose
G. Gavelli: nothing to disclose
D. Barone: nothing to disclose
F. Ferroni: nothing to disclose

RPS 307-10 14:54

The role of dynamic contrast-enhanced sequences on the learning curve in prostate MRI interpretation: a comparison with biparametric examinations in readers with different experiences

L. Panebianco, M. Martino, A. Izzo, G. Bianchi, F. Formiconi, C. Gianneramo, A. Pace, R. Manetta, C. Masciocchi; *L'Aquila/IT (aivlim@hotmail.it)*

Purpose: To assess the value of dynamic contrast-enhancement (DCE) use in detecting prostatic index lesions when evaluating the performance of two radiologists with different experience with biparametric (bpMRI) and multiparametric (mpMRI) examinations.
Methods and materials: A retrospective study of 150 patients was performed including 3 Tesla prostate mpMRI.
Two radiologists, with advanced and limited experience, respectively, blinded to clinical and histological data, classified each index lesion using PI-RADS v2. Images were revisited with a reading, including diffusion-weighted imaging (DWI), apparent diffusion coefficient (ADC) maps, T2-weighted (T2W) imaging, and, after 3 months, DCE.
Results were matched with Gleason patterns. The performance was quantified by sensitivity (SNS), specificity (SPC), and area under the curve (AUC) of the ROC (receiver operating characteristics).
Results: Concordance was good for the expert reader: weighted Cohen's k ≈ 0.809 (95% CI 0.707-0.912), unlike the performance of the inexperienced reader, which resulted in a Cohen's k 0.396 (95% CI 0.241-0.551). The expert reader performed as well in bpMRI as in mpMRI (SNS=0.73–0.70, AUC=0.744–0.819; p=0.087). The inexperienced reader performed well in mpMRI, but significantly worse in bpMR: SNS=27.94 versus 64.71 and AUC=0.634 versus 0.807 (p=0.0024).
Conclusion: Results based on the expert reader showed no substantial differences between the performance with bpMRI and mpMRI. The experience gained in mpMRI could advantage the reader in the transition to bpMRI.
Quite differently, the outcome for the inexperienced reader in mpMRI was similar to the expert reader, but in the absence of DCE, the performance dropped significantly.
Limitations: The involvement of one radiologist for each category (experienced and non-experienced) could be limiting in the evaluation of results.
Ethics committee approval: n/a
Funding: No funding was received for this work.
Author Disclosures:
L. Panebianco: nothing to disclose
M. Martino: nothing to disclose
A. Izzo: nothing to disclose
F. Formiconi: nothing to disclose
R. Manetta: nothing to disclose
C. Masciocchi: nothing to disclose
C. Gianneramo: nothing to disclose
A. Pace: nothing to disclose
G. Bianchi: nothing to disclose

RPS 307-11 15:00

A multicentre-multivendor study to evaluate the generalisability of a radiomics model for classifying prostate cancer

J. M. Castillo[1], M. P. A. Starmans[2], M. Arif[1], W. J. Niessen[2], S. Klein[2], I. G. Schoots[2], J. Veenland[2]; [1]*Rotterdam, Zuid-Holland/NL,* [2]*Rotterdam/NL (j.castillotovar@erasmusmc.nl)*

Purpose: Radiomics applied to magnetic resonance imaging (MRI) has shown promising results in classifying prostate cancer (PCa). However, the effects of these models on unseen data from different centres have rarely been addressed. Our goal is to evaluate the generalisability of radiomic models in the context of PCa classification and to compare the performance between our models and radiologists using prostate imaging reporting and data system (PIRADS) v2.
Methods and materials: The data comprised multiparametric MRI, histology of radical prostatectomy, and pathology reports of 107 patients from three centres. By correlating the MRI with histology, 204 lesions were identified. From each lesion, radiomics features were extracted. Radiomics models for discriminating between high-grade and low-grade lesions were automatically developed using machine learning, either single-centre through cross-validation, or multicenter. For comparison with the multicentre setting, a subset of the dataset was classified by two expert radiologists using PIRADS.
Results: The single-centre models obtained a mean AUC of 0.75 for the internal cross-validation; when testing on unseen data, the mean AUC decreased to 0.54. In the multicentre setting, the radiologists obtained a mean AUC of 0.47, while the radiomics model obtained a mean AUC of 0.75.
Conclusion: Radiomic models may obtain a decent performance when tested in a single-centre setting. However, there can be a considerable drop in classification performance when testing these models on data from different centres. On a multicenter dataset, our radiomics model outperformed PIRADS and may represent a more accurate alternative for malignancy prediction.
Limitations: Despite developing a multicenter-multivendor study, our cohort size is limited.
Ethics committee approval: The Medical ethics review committee of Erasmus MC (NL32105.078.10). The national Dutch trials register (ID: NL2368).
Funding: Partly financed by the Netherlands Organization for Scientific Research.
Author Disclosures:
M. Arif: nothing to disclose
J. M. Castillo: nothing to disclose
M. P. A. Starmans: nothing to disclose
W. J. Niessen: nothing to disclose
S. Klein: nothing to disclose
I. G. Schoots: nothing to disclose
J. Veenland: nothing to disclose

RPS 307-12 15:06

Multi-parametric magnetic resonance imaging of prostate cancer: correlation between Ktrans, a Gleason score, and a PI-RADS score

E. Lucertini[1], D. Caruso[1], M. Zerunian[1], D. de Santis[1], T. Biondi[2], N. Panvini[3], A. Laghi[1]; [1]*Rome/IT,* [2]*Belvedere Marittimo/IT,* [3]*Latina/IT (elena.lucertini@gmail.com)*

Purpose: To measure K^{trans} and correlate it with a Gleason score (GS) and a PI-RADS score in patients with prostate cancer.
Methods and materials: This retrospective study included patients with pathologically proven prostate cancer who had undergone clinically indicated 1.5 Tesla multi-parametric magnetic resonance imaging (MRI) examination. T2 weighted (T2w) images, diffusion-weighted images (DWI), and dynamic contrast-enhanced (DCE) sequences were obtained. A PI-RADS score was calculated for all tumour lesions. From a DCE-MRI dataset, K^{trans} was computed and compared between patients with clinically insignificant (GS≤6) and clinically significant (GS≥7) prostate cancer. The Spearman rank-order correlation coefficient (ρ) was used to assess the correlation strength between K^{trans} and GS and between K^{trans} and a PI-RADS score.
Results: 21 patients (age: 67±12 years; BMI: 26.63±4.04 Kg/m^2) with a PSA of 7.91±3.01 were included in the study. 7 patients (33.3%) had clinically insignificant prostate cancer while 14 patients (66.7%) were diagnosed with clinically significant prostate cancer. The mean K^{trans} value was 0.42±0.20 min^{-1} (range: 0.15–0.75). K^{trans} was significantly higher (0.52±0.14 min^{-1}) in clinically significant prostate cancer compared to clinical insignificant prostate cancer (0.23±0.15 min^{-1}; P=0.016). K^{trans} showed moderate significant correlation with GS (ρ=0.575, P=0.006), while it showed no significant correlation with PI-RADS (ρ=0.386, P=0.069).
Conclusion: K^{trans} may discriminate between clinically insignificant and significant prostate cancer and show a moderate correlation with GS. This MP-MRI may serve as an imaging biomarker in prostate cancer.
Limitations: Limitations of this study are the small sample size and the inclusion of only patients with proven prostate cancer, despite its design requiring a selected patient population to assess the correlation between K^{trans} and GS.
Ethics committee approval: Written informed consent obtained.
Funding: No funding was received for this work.
Author Disclosures:
E. Lucertini: nothing to disclose
D. Caruso: nothing to disclose
M. Zerunian: nothing to disclose
D. de Santis: nothing to disclose
T. Biondi: nothing to disclose
N. Panvini: nothing to disclose
A. Laghi: nothing to disclose

RPS 307-13 15:12

A comparison between biparametric and multiparametric prostatic MRI: added value of DCE in PCa detection using new PI-RADS v 2.1 classification

A. Grecchi, M. C. Ambrosetti, A. Mazzaro, G. Zamboni, G. Mansueto; *Verona/IT (annamaria.grecchi88@gmail.com)*

Purpose: The indiscriminate use of contrast-enhanced MRI for the detection of PCa has been questioned in the new PIRADS v2.1. Our purpose is to compare

multiparametric MRI (mpMRI) and biparametric MRI (bpMRI) for prostatic cancer (PCa) detection using PIRADSv 2.1.
Methods and materials: The mpMRI exams performed between June and October 2019 were considered and lesions with a PIRADS from 3 to 5 in the reports were independently reviewed by two radiologists having 3 (reader A) and 10 (reader B) years experience. Evaluation of T2, DWI, ADC (bpMRI), and DCE (mpMRI) was performed, indicating a partial score for each parameter of bpMRI and a final PIRADS score for every lesion, both with and without DCE. Inter-rater agreement (Cohen's Kappa) was calculated regarding PIRADS for bpMRI and mpMRI. Data analysis was performed for cases upgraded to PIRADS 4-5 after DCE.
Results: 47 prostate MRIs were considered for 61 total lesions (47 PZ, 14 TZ). Inter-rater agreement was Kappa=0.9 and 0.8 (very good) for assigned PIRADS, respectively, for bpMRI and mpMRI. Inter-rater agreement was only moderate (Kappa=0.5) for T2 score: 11/13 lesions were in PZ and therefore this had little impact.
23 PZ lesions with PIRADS 3 were upgraded to PIRADS 4 or 5 after DCE (the same lesions for both readers). Out of 23 upgraded lesions, 13 for reader A and 6 for reader B did not show any worrisome feature in DWI or ADC map, while in the other cases, either DWI or ADC was considered as “markedly abnormal”.
Conclusion: DCE appears to have a useful role in staging lesions with PIRADSv2.1 only for PZ lesions with a PIRADS 3 score, independent of the DWI features.
Limitations: A small series.
Ethics committee approval: Written informed consent obtained.
Funding: No funding was received for this work.
Author Disclosures:
A. Grecchi: nothing to disclose
M. C. Ambrosetti: nothing to disclose
A. Mazzaro: nothing to disclose
G. Zamboni: nothing to disclose
G. Mansueto: nothing to disclose

RPS 307-14 15:18
A stepwise logistic regression model based on MRI radiomic features to predict histopathological aggressiveness of prostate cancer (PCa)
G. Stranieri[1], D. Basile[2], M. Calandri[3], V. Giannini[4], S. Mazzetti[4], A. de Pascale[5], F. Russo[3], A. Veltri[5], D. Regge[4]; [1]Catanzaro/IT, [2]Rivoli/IT, [3]Turin/IT, [4]Candiolo/IT, [5]Orbassano/IT
(giuseppestranieri92@gmail.com)

Purpose: To develop and externally validate a stepwise logistic regression model based on MRI radiomic features to predict different Gleason scores (GS) of prostate cancer (PCa).
Methods and materials: A dataset was composed of 97 patients (105 PCas), enrolled in two institutions with different MRI scanners and protocols, who underwent robot-assisted radical-prostatectomy for PCa after mpMRI. Lesions were classified as low aggressive (LA) if their pathological Gleason score was ≤3+4 and high aggressive (HA) if it was ≥4+3. A previously developed computer-aided diagnosis (CAD) system able to detect PCas was applied to the dataset and the output of CAD was used as a PCa segmentation mask. From the segmented masks of ADC maps and T2w images, 59 first- and second-order radiomics features were extracted (i.e. skewness, kurtosis, and texture parameters from GLCM and GLRLM matrices). Patients from institution-A were used as training and testing dataset, while patients from institution-B as a validation set. A stepwise logistic regression model was created using 70% of lesions as a training set and 30% as a testing set, all randomly selected. Since the composition of a training and testing set might affect the performance of the model, this selection was repeated 5 times and the model reaching the highest accuracy in the testing set was chosen and applied to the validation set.
Results: Accuracy of the training set was 96.6% (54/56), with a sensitivity in detecting HA PCas of 95.6% (22/23) and a specificity of 96.9% (32/33). The accuracy of the testing set was 83.3% (20/24), with a sensitivity of 60% (6/10) and a specificity of 100% (14/14). the accuracy of the validation set was 68% (17/25), with a sensitivity of 40% (4/10) and a specificity of 86.7% (13/15).
Conclusion: MRI radiomic features are promising markers in discriminating PCa aggressiveness on the histopathological level.
Limitations: Further confirmations are required by larger series.
Ethics committee approval: Approved by an ethical committee.
Funding: No funding was received for this work.
Author Disclosures:
G. Stranieri: nothing to disclose
D. Basile: nothing to disclose
D. Regge: nothing to disclose
A. Veltri: nothing to disclose
V. Giannini: nothing to disclose
F. Russo: nothing to disclose
S. Mazzetti: nothing to disclose
A. de Pascale: nothing to disclose
M. Calandri: nothing to disclose

RPS 307-15 15:24
Assessment of prostate cancer aggressiveness using deep learning and radiomic data: a pilot study
L. Mercatelli[1], E. Bertelli[1], M. A. Pascali[2], S. Colantonio[2], D. Germanese[2], A. Barucci[1], C. Caudai[2], S. Agostini[1], V. Miele[1]; [1]Florence/IT, [2]Pisa/IT
(mercatelli.laura@gmail.com)

Purpose: To investigate the potential role of radiomic and deep learning features extracted from multiparametric MRI (mp-MRI) in predicting prostate cancer (PCa) aggressiveness, correlated with a Gleason score (GS). The aim of this study is to define a predictive model to distinguish low--grade (GS <=3+4) from intermediate/high-grade (GS >=4+3) PCa.
Methods and materials: Our population was composed of 50 peripheral zone PCa patients (PIRADS score 3--5) who underwent a 1.5 T mp-MRI and freehand transperineal MRI/US fusion-guided targeted biopsy (62 lesions: 41 with GS<=3+4 and 21 with GS>=4+3). The lesions were segmented on T2w images and ADC maps. Two analyses were then carried out. (i) Radiomic features were computed, identifying the most discriminative set (signature). A support vector machine was trained on 52 cases (35 GS<=3+4 and 17 GS>=4+3) and tested on the remaining 10 (6 GS<=3+4 and 4 GS>=4+3). (ii) Three deep learning architectures were trained on the same dataset, augmented with rigid and non-rigid deformations, in order to limit overfitting.
Results: The radiomic approach, using 6 features, allowed the correct classification of all cases (accuracy 100%, sensitivity 100%, and specificity 100%). The best performing DL model (based on VGG16) achieved accuracy 87.3%, sensitivity 97.2%, and specificity 74% on T2w images.
Conclusion: Radiomic features can be useful in the assessment of lesion aggressiveness. The DL features need more investigations on a larger population and a more balanced distribution.
Limitations: Our main limitation is the small number of patients.
Ethics committee approval: The study was approved by our Institutional Review Board.
Funding: No funding was received for this work.
Author Disclosures:
L. Mercatelli: nothing to disclose
E. Bertelli: nothing to disclose
S. Agostini: nothing to disclose
V. Miele: nothing to disclose
A. Barucci: nothing to disclose
M. A. Pascali: nothing to disclose
S. Colantonio: nothing to disclose
D. Germanese: nothing to disclose
C. Caudai: nothing to disclose

14:00 - 15:30 **Coffee & Talk 2**

Cardiac

RPS 303

Advanced CT and MR techniques

Moderators:
G. De Rubeis; Rome/IT
K. Gruszczyńska; Katowice/PL

RPS 303-1 14:00
Comparison of free breathing 3D mDIXON with 3D inversion recovery and 3D spectral presaturation with inversion recovery sequences for the assessment of late gadolinium enhancement
R. A. K. Dessouky[1], V. Destasio[2], S. Boccalini[3], S. A. Si-Mohamed[3], T. K. Y. Broussaud[4], P. C. Douek[4], M. Sigovan[5]; [1]Zagazig/EG, [2]Rome/IT, [3]Bron/FR, [4]Lyons/FR, [5]Villeurbanne/FR (rihamdessouky@gmail.com)

Purpose: Three dimensional (3D) late gadolinium enhancement (LGE) MRI sequences are increasingly used in clinical practice. Knowledge of strengths/limitations of each sequence can guide sequence choice. We aimed to evaluate technical and diagnostic performance of three dimensional (3D) mDIXON versus 3D inversion recovery (3D VIAB) and 3D spectral presaturation with inversion recovery (3D SPIR) LGE sequences.
Methods and materials: A total of 78 patients (50 males and 28 females, age 49±18 years) with 1.5T CMR including 3 different 3D LGE sequences (3D mDIXON, 3D VIAB, and 3D SPIR) were evaluated for technical and diagnostic performance by two readers. Qualitative scores and quantitative signal to noise (SNR) and contrast to noise (CNR) measurements were compared among sequences. Qualitative comparisons were made using Friedman and Wilcoxon signed rank tests. Quantitative comparisons were made using one way ANOVA. Reader agreements were tested using Kohen’s Kappa. Any p-value <0.05 was significant.

Results: Technically, 19 out of 78 (24 %) patients were excluded due to poor (grade 4) image quality and reader agreements were excellent (= 0.91-0.96, p<0.001) for all sequences. Diagnostically, 3D mDIXON showed higher confidence in the diagnosis of pericardial enhancement (p-values =0.007, 0.034 and 0.025 for three sequences, 3D VIAB, and 3D SPIR comparisons). 3D mDIXON outperformed 3D SPIR in both visualisation of LGE (p=0.02) and quality of fat suppression (p=0.001).
Conclusion: 3D mDIXON is a diagnostic problem-solving tool, especially when making a diagnosis of epicardial enhancement and/or fat suppression is needed. Choice of 3D LGE sequence should be based on a patient's breath-hold ability, diagnostic needs, and institutional availability considering the strengths and limitations of each sequence.
Limitations: A possible differences in timing between gadolinium injection and image acquisition.
Ethics committee approval: n/a
Funding: No funding was received for this work.
Author Disclosures:
R. A. K. Dessouky: nothing to disclose
V. Destasio: nothing to disclose
S. Boccalini: nothing to disclose
T. K. Y. Broussaud: nothing to disclose
P. C. Douek: nothing to disclose
M. Sigovan: nothing to disclose
S. A. Si-Mohamed: nothing to disclose

RPS 303-2 14:06
Late gadolinium enhancement at right ventricular insertion points in subjects with structurally normal hearts is prognostically irrelevant
C. Grigoratos[1], A. Pantano[2], L. Ait-Ali[1], A. Barison[1], G. Todiere[1], G. Festa[3], G. Sinagra[2], G. D. Aquaro[1]; [1]Pisa/IT, [2]Trieste/IT, [3]Massa/IT
(cgrigoratos@ftgm.it)

Purpose: Late gadolinium enhancement (LGE) is the current non-invasive gold standard for fibrosis assessment. The diagnostic and prognostic significance of different LGE patterns have already been described, but the clinical importance of isolated right ventricular insertion points (RVIP) LGE is yet to be defined.
Methods and materials: We retrospectively analysed 420 patients (270 males, mean age 38±17 years) with structurally normal hearts except for the presence of RVIP-LGE (44 patients), other-LGE (midwall or subepicardial; 36 patients), or no-LGE (340 patients). All patients underwent cardiac magnetic resonance with LGE sequences. Clinical follow-up was performed for a median of 2,177 days. The primary composite endpoint included cardiac death, resuscitated cardiac arrest, and appropriate implantable cardiac defibrillator shock.
Results: The prevalence of cardiac events was significantly lower in RVIP-LGE than those with other-LGE (p=0.006). The Kaplan Meier curve analysis demonstrated no significant differences between patients with RVIP-LGE and no-LGE for the primary endpoint. On contrast, patients with other-LGE had a worse prognosis than those with RVIP-LGE or no-LGE (p<0.0001). Among patients with other-LGE, the midwall pattern of LGE distribution was associated with a worse prognosis than a subepicardial one (p =0.0044).
Conclusion: RVIP-LGE in subjects without additional evidence of cardiac damage does not convey a worse prognosis when compared with subjects without LGE and it is therefore not to be considered a marker of disease. Its diagnostic and prognostic significance is to be considered irrelevant.
Limitations: A small number of cardiac events occurred as expected given the low cardiac risk population considered. To overcome this limit, a bigger follow-up period was obtained. Parametric imaging such as T1 and T2 mapping was not routinely performed. The main reason was that this technique was not commercially available when the majority of patients were scanned.
Ethics committee approval: n/a
Funding: No funding was received for this work.
Author Disclosures:
C. Grigoratos: nothing to disclose
A. Pantano: nothing to disclose
L. Ait-Ali: nothing to disclose
A. Barison: nothing to disclose
G. Todiere: nothing to disclose
G. Festa: nothing to disclose
G. Sinagra: nothing to disclose
G. D. Aquaro: nothing to disclose

RPS 303-3 14:12
Correcting versus resolving respiratory motion in free-breathing whole-heart MRA: a comparison in patients with thoracic aortic disease
T. Leonard[1], R. Stroud[1], D. Piccini[2], U. J. Schoepf[1], J. Heerfordt[2], J. Yerly[2], L. Di Sopra[2], P. Suranyi[1], A. Varga-Szemes[1]; [1]Charleston, SC/US, [2]Lausanne/CH *(leonarty@musc.edu)*

Purpose: Whole-heart magnetic resonance angiography (MRA) requires sophisticated methods accounting for respiratory motion. Our purpose was to evaluate the image quality of compressed sensing-based respiratory motion-resolved three-dimensional (3D) whole-heart MRA compared with self-navigated motion-corrected whole-heart MRA in patients with known thoracic aorta dilation.
Methods and materials: 25 patients were prospectively enrolled in this ethically approved study. Whole-heart 1.5T MRA was acquired using a prototype 3D radial steady-state free-precession free-breathing sequence. The same data was reconstructed with a one-dimensional motion-correction algorithm (1D-MCA) and an extradimensional golden-angle radial sparse parallel reconstruction (XD-GRASP). Subjective image quality was scored and objective image quality was quantified (signal intensity ratio, SIR, and vessel sharpness). Wilcoxon, McNemar, and paired t-tests were used.
Results: Subjective image quality was significantly higher using XD-GRASP compared to 1D-MCA (median 4.5, interquartile range 4.5–5.0 versus 4.0 [2.25–4.75]; p < 0.001), as well as signal homogeneity (3.0 [3.0–3.0] versus 2.0 [2.0–3.0]; p = 0.003), and image sharpness (3.0 [2.0–3.0] vs 2.0 [1.25–3.0]; p < 0.001). SIR with the 1D-MCA and XD-GRASP was 6.1±3.9 versus 7.4±2.5, respectively (p < 0.001), while signal homogeneity was 274.2±265.0 versus 199.8±67.2 (p = 0.129). XD-GRASP provided a higher vessel sharpness (45.3±10.7 versus 40.6±101, p = 0.025).
Conclusion: XD-GRASP-based motion-resolved reconstruction of free-breathing 3D whole-heart MRA datasets provides improved image contrast, sharpness, and signal homogeneity, and seems to be a promising technique that overcomes some of the limitations of motion correction or respiratory navigator gating.
Limitations: A limited sample size and computational power heavy post-processing.
Ethics committee approval: IRB approved and written informed consent was obtained.
Funding: Siemens.
Author Disclosures:
T. Leonard: nothing to disclose
R. Stroud: nothing to disclose
U. J. Schoepf: Grant Recipient at Astellas, Bayer, Siemens, HeartFlow, Bracco, Guerbet, Elucid BioImagining , Consultant at Siemens, Guerbet, HeartFlow, Elucid BioImaging
D. Piccini: Employee at Siemens
J. Heerfordt: Other at Siemens
J. Yerly: nothing to disclose
L. Di Sopra: nothing to disclose
P. Suranyi: nothing to disclose
A. Varga-Szemes: Grant Recipient at Siemens, Consultant at Elucid BioImaging

RPS 303-4 14:18
Delayed enhancement of papillary muscles on cardiac MRI in patients with mitral regurgitation
S. J. Lim, H. J. J. Koo, J.-W. Kang, D. H. Yang; *Seoul/KR*
(vitamindasa@hanmail.net)

Purpose: Left ventricular (LV) fibrosis in patients with mitral regurgitation (MR) has been reported due to mitral valve prolapse (MVP) and MVP has been associated with sudden cardiac death. We evaluated the presence and characteristics of late gadolinium enhancement (LGE) at mitral apparatus on cardiac magnetic resonance imaging (MRI) in MR patients with and without MVP.
Methods and materials: Between January 2000 and December 2017, 88 patients (mean age, 58.3±12.0; male, 42%) with MR underwent cardiac MRI. LGE on cardiac MRI, clinical characteristics including echocardiographic findings, and a history of arrhythmia were reviewed. After patients were classified into an MVP or non-MVP group, clinical and imaging parameters were compared. Factors associated with LGE were evaluated using logistic regression analysis.
Results: In 88 MR patients (43 MVP, 45 non-MVP), LV myocardial enhancement was more common in the MVP group (28% vs. 11%, p <0.046). Papillary muscle enhancement was found in 8 (9.1%) patients (1 pure MVP, 3 MVP with TR, 2 functional MR with TR, and 2 rheumatic MR). In 31 pure MVP patients, 9 showed LGE (8 LV myocardium and 1 papillary muscle). One of them had bilateral diffuse papillary muscle enhancement and an event of sudden cardiac arrest due to ventricular fibrillation. Systolic blood pressure (BP) (odds ratio [OR], 1.08; 95% confidence interval [CI], 1.02 – 1.14; p=0.01) and ventricular arrhythmia (OR, 22.58; 95% CI, 2.32 – 219.60; p=0.01) were associated with LGE at papillary muscles.
Conclusion: LGE at papillary muscles was not uncommon (9.1%) in MR. High systolic BP and ventricular arrhythmia were associated with LGE at papillary muscles. Papillary muscle enhancement on cardiac MRI should not be overlooked.
Limitations: Not all patients were evaluated by Holter monitoring. Quantification of LGE was unavailable.
Ethics committee approval: n/a
Funding: No funding was received for this work.

Author Disclosures:
S. J. Lim: nothing to disclose
H. J. J. Koo: nothing to disclose
J.-W. Kang: nothing to disclose
D. H. Yang: nothing to disclose

RPS 303-5 14:24

Compressed sensing 4D flow assessment of aortic and pulmonary artery flow volumes

U. Reiter[1], C. Reiter[1], N. Jin[2], F. Testud[3], V. Nizhnikava[1], D. Giese[3], A. Triebl[1], M. Fuchsjäger[1], G. Reiter[1]; [1]Graz/AT, [2]Chicago/US, [3]Malmö/SE
(ursula.reiter@medunigraz.at)

Purpose: Although cardiac magnetic resonance four-dimensional (4D) flow imaging is considered an adequate technique for the assessment and "conservation of mass" comparisons of flow volumes, its widespread use is limited by long scan times. The purpose of the study was to investigate if the acceleration of whole-heart 4D flow imaging by compressed sensing (CS) can be employed to derive aortic and pulmonary flow volumes.
Methods and materials: 11 prospectively recruited cardiac patients without known or suspected shunts and with a regular heart rhythm underwent 3T (Magnetom Skyra, Siemens Healthcare, Erlangen, Germany) retrospectively ECG- and navigator-gated whole-heart 4D flow imaging with (acceleration-factor=7.6) and without CS (parallel acquisition acceleration-factor=3) employing a prototype sequence. Spatial resolution and the number of reconstructed frames were matched in the respective 4D flow protocols. For both data sets, aortic (Qa) and pulmonary (Qp) net flow volumes were evaluated using prototype software (4DFlow, Siemens Healthcare, Erlangen, Germany). The relationships between results derived with and without compressed sensing were analysed by correlation analysis; means and variances were compared employing t- and Levene test.
Results: Scan times were significantly shorter when employing CS (369±92 s vs. 618±119 s, p<0.01). Flow volumes from CS measurements (Qa=81±20 ml; Qp=82±18 ml) had no significant bias compared to measurements without CS (Qa=83±21 ml, p=0.42; Qp=82±19 ml, p=0.80) and demonstrated strong correlations (r=0.97 and 0.95, for Qa and Qp, respectively). Pulmonary-to-systemic blood flow ratios (Qp/Qa=1.02±0.11 and Qp/Qa=1.01±0.09, with and without CS, respectively) did not differ significantly, neither in means (p=0.80) nor in variances (p=0.67).
Conclusion: Compressed sensing allows for substantial acceleration of 4D flow acquisition without significant impact on the precision of derived aortic and pulmonary flow volumes.
Limitations: A small patient number.
Ethics committee approval: Medical University Graz (24-126ex11/12).
Funding: OeNB Anniversary Fund (17934).
Author Disclosures:
U. Reiter: nothing to disclose
C. Reiter: nothing to disclose
N. Jin: Employee at Siemens Medical Solutions USA
F. Testud: Employee at Siemens Healthcare AB
V. Nizhnikava: Grant Recipient at ESOR Fellowship
D. Giese: Employee at Siemens Healthcare GmbH
A. Triebl: nothing to disclose
M. Fuchsjäger: nothing to disclose
G. Reiter: Employee at Siemens Healthcare Diagnostics GmbH

RPS 303-6 14:30

Compressed sensing 4DFlow MRI for the assessment of the left ventricular stroke volume

B. Longere[1], G. Braye[1], V. Silvestri[1], N. Jin[2], S. Toupin[3], A. Simeone[1], J. Pagniez[1], F. Pontana[1]; [1]Lille/FR, [2]Chicago/US, [3]Paris/FR
(fpontana@gmail.com)

Purpose: 4DFlow MRI provides haemodynamic assessment but is time-consuming. The aim of our study was to evaluate the accuracy of a prototype 4DFlow sequence featuring acceleration technique based on compressed sensing for the assessment of the left ventricular (LV) stroke volume.
Methods and materials: 22 adult patients referred for cardiac MRI underwent a comprehensive protocol on a 1.5T scanner (MAGNETOM Aera, Siemens Healthcare) including at least (a) standard segmented steady-state-free precession cine sequences with one short-axis stack, one vertical, and one horizontal 2-chamber slice for measuring LV stroke volume (cineSV), (b) a single-breath-hold 2D phase-contrast sequence (2D-PC) at the level of the sino-tubular junction for direct quantification of the aortic forward volume (2DSV), and (c) a prototype free-breathing compressed sensing 4DFlow (CS4DF) sequence covering the entire thoracic aorta. Multiplanar reconstructions were used to place the region of interest at the same anatomical level as the 2D-PC sequence.
Results: CS4DF sequence mean scan time was 4.2 ±0.8 min. A mean cineSV of 96.3 ±28.4 mL was provided by LV contouring, a mean 2DSV was 92.0 ±26.7 mL and a mean 4DSV was 89.9 ±25.4 mL (p=0.944). Linear regression demonstrated strong correlation of 4DSV with 2DSV (R^2=0.89). There was a very good inter-rater and intra-rater agreement with an ICC of 0.96 and 0.97, respectively.
Conclusion: CS4DF is a robust and fast option to quantify aortic forward volume, with excellent intra- and inter-observer agreement. This sequence is promising to reach widespread clinical practice of 4DFlow imaging since the thoracic aorta could be scanned in less than 5 minutes.
Limitations: No major limitation except sample size.
Ethics committee approval: Each patient gave written informed consent.
Funding: No funding was received for this work.
Author Disclosures:
F. Pontana: Speaker at Siemens Healthcare, Speaker at GE Healthcare, Speaker at Bracco, Speaker at Bayer
B. Longere: nothing to disclose
G. Braye: nothing to disclose
V. Silvestri: nothing to disclose
S. Toupin: Employee at Siemens Healthcare
N. Jin: Employee at Siemens Healthcare
J. Pagniez: nothing to disclose
A. Simeone: nothing to disclose

RPS 303-7 14:36

Value of T2 mapping in patients with chronic thromboembolic pulmonary hypertension (CTEPH) before and after balloon pulmonary angioplasty (BPA)

A. Hasse[1], V. Bethke[1], A. Brose[1], A. Breithecker[1], C. B. Wiedenroth[2], K. Tello[1], W. Seeger[1], G. Krombach[1], F. Roller[1]; [1]Giessen/DE, [2]Bad Nauheim/DE
(alexander.hasse@mail.de)

Purpose: Native T1 mapping as a marker of myocardial fibrosis showed promising correlations to right heart function and pulmonary haemodynamics in pulmonary hypertension. However, myocardial texture changes, like oedema, occur long before fibrosis arises. Therefore, the aim of this study was to assess the value of T2 mapping in patients with inoperable CTEPH before and after BPA.
Methods and materials: MRI at 1.5 Tesla including T2 mapping and right heart catheterisation were performed before and 6 months after BPA in 30 consecutive patients (mean age 63.4 ± 10.6 years; 17 female). T2 values were measured in the right ventricular insertion points (upper and lower RVIP) and in the interventricular septum at the basal short-axis section. The results were correlated to right ventricular function (RVEF) and pulmonary haemodynamics (mPAP and PVR).
Results: RVEF, mPAP, and PVR significantly improved after BPA (all p<0.0001). T2 values were elevated and decreased significantly after BPA (upper RVIP 61.6ms ± 6.1 to 57.0ms ± 4.5 and lower RVIP 64.4ms ± 5.6 to 58.9ms ± 4.5, p<0.0001, septum 60.2ms ± 4.0 to 58.9ms ± 3.9, p<0.02). The T2 values of the lower RVIP revealed the best correlations to RVEF, mPAP, and PVR before (r=-0.33, r=0.45 and r = 0.45 both p=0.013) and after BPA (r=-0.16, r=0.35 and r=0.14).
Conclusion: In our cohort of CTEPH patients, septal and RVIP myocardial T2 times were elevated before BPA and decreased significantly after BPA. It is therefore highly suspected that myocardial oedema is present in mechanically demanded myocardium in pulmonary hypertension and that BPA leads to a significant oedema reduction. Therefore, we conclude that T2 mapping might enable new insights regarding therapy-response, monitoring, and prognosis.
Limitations: A small study cohort.
Ethics committee approval: n/a
Funding: No funding was received for this work.
Author Disclosures:
A. Hasse: nothing to disclose
F. Roller: nothing to disclose
V. Bethke: nothing to disclose
A. Brose: nothing to disclose
A. Breithecker: nothing to disclose
C. B. Wiedenroth: nothing to disclose
K. Tello: nothing to disclose
W. Seeger: nothing to disclose
G. Krombach: nothing to disclose

RPS 303-8 14:42

The impact of a new deep learning denoising algorithm on LGE images

G. Muscogiuri[1], S. Dell'aversana[2], F. Ricci[3], M. Gatti[4], A. I. Guaricci[5], M. Guglielmo[1], A. Baggiano[1], M. Pepi[1], G. Pontone[1]; [1]Milan/IT, [2]Naples/IT, [3]Rome/IT, [4]Turin/IT, [5]Bari (BA)/IT (g.muscogiuri@gmail.com)

Purpose: To assess the reliability of 2D segmented late gadolinium enhancement (2D-S_{LGE}) reconstructed with a DL denoising approach of 50% and 75% of strength.

Methods and materials: 20 patients who underwent cardiac MR were enrolled in September 2019. 2D-S_{LGE} were retrospectively reconstructed in magnitude and phase-sensitive sequences using the DL denoising approach with respectively 50% and 75%. Overall subjective image quality in both magnitude and phase-sensitive sequences with standard and DL denoising reconstructions was evaluated using a 3-point Likert scale image. Objective image quality was evaluated calculating the signal to noise ratio (SNR) and contrast to noise ratio (CNR) using different images DL denoising reconstruction. A cut off value of $p<0.05$ was considered statistically significant.
Results: The overall analysis of subjective image quality was statistically significant (p:0.004), better only in magnitude images reconstructed with 75% of DL denoising compared to standard magnitude images. The CNR between scar and myocardium in phase-sensitive was not significantly different between the standard and DL denoising approach. Conversely in magnitude, the CNR improve significantly in the 50% DL denoising (p:0.01) and 75% DL denoising (p:0.02) approaches. A statistically significant improvement of SNR compared to standard magnitude reconstruction was observed for 50% DL denoising in terms of scar (p:0.02). While myocardial magnitude SNR resulted in significant improvement if compared to reconstruction in 50% DL denoising (p:0.01) and 75% DL denoising (p:0.01).
Conclusion: The best DL denoising approach seems to be shown in magnitude reconstruction with 75% DL denoising.
Limitations: Diagnostic accuracy should be performed.
Ethics committee approval: Still in process.
Funding: No funding was received for this work.
Author Disclosures:
G. Muscogiuri: nothing to disclose
S. Dell'aversana: nothing to disclose
F. Ricci: nothing to disclose
M. Gatti: nothing to disclose
A. I. Guaricci: nothing to disclose
M. Guglielmo: nothing to disclose
A. Baggiano: nothing to disclose
M. Pepi: nothing to disclose
G. Pontone: nothing to disclose

RPS 303-9 14:48

4D-flow assessment of early-diastolic mitral annular peak tissue velocity: a comparison with echocardiography

C. Reiter, G. Reiter, C. Kräuter, E. Kolesnik, A. Schmidt, D. Scherr, A. Triebl, M. Fuchsjäger, U. Reiter*; Graz/AT (Clemens.Reiter@medunigraz.at)*

Purpose: Early-diastolic mitral annular peak tissue velocities represent important parameters in the evaluation of left ventricular diastolic function. Their measurement is well-established in echocardiography but not in cardiac magnetic resonance (CMR) imaging. The purpose of the present study was to investigate the feasibility of derivation of early-diastolic mitral annular peak tissue velocities from CMR four-dimensional (4D) flow imaging and to compare the results with echocardiography.
Methods and materials: 74 subjects (male/female, 33/41; age 60±10 years) were prospectively recruited to undergo echocardiography and CMR whole heart 4D-flow imaging at 3 Tesla. Echocardiographic medial (e' medial) and lateral (e' lateral) early-diastolic mitral annular peak tissue velocities were acquired following current guidelines. Corresponding 4D-flow-based early-diastolic mitral annular peak tissue velocities were determined as early-diastolic peak mean through-plane tissue velocities in the inferoseptal (4DFe' medial) and the anterolateral (4DFe' lateral) segments of multiplanar reformatted short-axis planes just below the mitral valve using a prototype software (4DFlow, Siemens Healthcare, Erlangen, Germany). A comparison of CMR and echocardiography data was performed by means of correlation and a Bland-Altman analysis.
Results: Tissue velocities from 4D-flow measurements (4DFe' medial=7.4±2.3cm/s; 4DFe' lateral=9.3±2.5cm/s) had no significant bias compared to echocardiographically obtained tissue velocities (e' medial=7.6±2.4cm/s, p=0.43; e' lateral=9.3±2.9cm/s, p=0.95) while showing strong correlations (r=0.77 and 0.84, for medial and lateral assessment, respectively). The clinically frequently used average of medial and lateral velocities showed even stronger correlation (r=0.90) without bias (4DFe' average=8.4±2.2cm/s vs. e' average = 8.5±2.4cm/s, p=0.52).
Conclusion: Early-diastolic mitral annular peak tissue velocities from echocardiography and CMR 4D-flow correlate strongly and demonstrate no bias, suggesting 4D-flow as a potential technique for its assessment interchangeable with echocardiography.
Limitations: A single observer and single-centre study.
Ethics committee approval:
NCT01728597, NCT03253835.
Funding: OeNB-Anniversary-Fund Nr.17934.
Author Disclosures:
C. Reiter: nothing to disclose
G. Reiter: Employee at Siemens Healthcare Diagnostics GmbH
U. Reiter: nothing to disclose
C. Kräuter: nothing to disclose
E. Kolesnik: nothing to disclose
A. Schmidt: nothing to disclose
D. Scherr: nothing to disclose
A. Triebl: nothing to disclose
M. Fuchsjäger: nothing to disclose

RPS 303-10 14:54

Prognostic validity of coronary flow reserve (CFR) derived from mapping-stress MRI in the risk stratification of chronic coronary syndrome patients

P. Palumbo, E. Cannizzaro, C. de Cataldo, S. Torlone, M. C. de Donato, A. Corridore, M. Latessa, E. Di Cesare, C. Masciocchi*; L'Aquila/IT (palumbopierpaolo89@gmail.com)*

Purpose: The need for a prognostic assessment of CAD patients is continuously increasing. Some studies have tried to validate the accuracy of novel T1 mapping application during adenosine stress in detecting coronary flow alteration. The purpose of our study was to evaluate its prognostic validity during an intermediate-to-long term follow-up.
Methods and materials: 34 patient (68,42±8,9 y; 30 males; 4 females) submitted on a 3.0T stress CMR with a CT evidence of CAD were included. Ischaemic or infarctuated CAD patients were distinguished from non-obstructive CAD patients (negative first-pass perfusion or LGE). A major adverse cardiac event and secondary cardiac outcomes were reported. The mean follow-up was 30.26±5.28 months.
Results: All measurements were firstly repeated with two different vendors and inter-vendor agreement were calculated. Secondly, cardiac outcomes were compared with T1 values. A high incidence of cardiac outcomes was recorded in the ischaemic/infarctuated CCS patients, with no significant increase in T1 values during adenosine infusion (p-value=0,158). Among non-obstructive patients, the 56.25% referred mainly secondary cardiac outcomes. Interestingly, a lack of T1 mapping stress reactivity was found. A significant difference was found between different T1 responders and non-responders group in a Kaplan-Meier survival analysis (p-value=0,001).
Conclusion: Our study confirms the prevalent role of stress CMR as a predictive prognostic factor in the outcome of a heart patient. T1 mapping sequences result in more sensitive and specific identification of microvascular abnormalities, increasing the clinical utility of stress CMR in identifying high-risk patients.
Limitations: A lack of catheter-based FFR and myocardial blood flow estimation do not allow a definitive comparison with the current gold standard to confirm our findings. Moreover, the small sample size was considered with potential selection bias.
Ethics committee approval: Our study was conducted in accordance with the declaration of Helsinki.
Funding: No funding was received for this work.
Author Disclosures:
P. Palumbo: nothing to disclose
E. Cannizzaro: nothing to disclose
C. de Cataldo: nothing to disclose
S. Torlone: nothing to disclose
M. C. de Donato: nothing to disclose
M. Latessa: nothing to disclose
A. Corridore: nothing to disclose
E. Di Cesare: nothing to disclose
C. Masciocchi: nothing to disclose

RPS 303-11 15:00

Two-shot compressed sensing techniques accelerate cardiac cine sequence acquisition and quantitative evaluation of diagnostic efficacy

J. Wang[1], L. Lin[1], J. An[1], M. Schmidt[2], C. Forman[2], Y. Wang[1]*; [1]Beijing/CN, [2]Erlangen/DE (wangjian_511@sina.com)*

Purpose: In this prospective study, we tried to introduce a 2-shot compressed sensing (CS) cine technique in cardiac magnetic resonance (CMR) to obtain fast high-quality cine images and accurately access cardiac function close to standard cine sequence than the single-shot (ss) CS cine technique.
Methods and materials: Enrolled patients underwent CMR on a 3T scanner from July to December, 2018. Cine image was performed with 3 different methods: a standard segment cine sequence, a real-time single-shot CS (ss CS) cine sequence, and a prototype 2-shot CS cine sequence. Quantitative analysis of image quality used a 0-4 score system and cardiac function analysis was performed on all 3 types of cine images.

Results: 35 patients completed all 3 types of cine sequences. The average scan time was (100.3±20.6)s for standard cine, (20.1±4.1)s for ss CS cine, and (30.1±6.2)s for 2-shot CS cine. The median total image quality score was 4 for standard and 2-shot CS cine and 3 for ss CS cine. There was a significant difference in total quality between standard cine and ss CS cine, but not with 2-shot CS cine. The differences between the standard cine and the ss CS cine were not statistically significant except for LV mass and LVESV, and there were no statistical differences between the standard cine and the 2-shot cine. There was a good correlation between standard cine and ss CS cine, and standard cine and 2-shot CS cine (P<0.01).
Conclusion: The 2-shot cine sequence can acquire images that are closer to the quality of the standard cine sequence and can be used to accurately evaluate the cardiac function.
Limitations: A small study cohort.
Ethics committee approval: n/a
Funding: No funding was received for this work.
Author Disclosures:
J. Wang: nothing to disclose
L. Lin: nothing to disclose
J. An: nothing to disclose
Y. Wang: nothing to disclose
M. Schmidt: nothing to disclose
C. Forman: nothing to disclose

RPS 303-12 15:06
A prospective randomised non-inferiority study of low iodine dual-energy coronary CT-angiography
D. C. Rotzinger[1], S. A. Si-Mohamed[2], L. Boussel[2], R. A. Meuli[1], P. C. Douek[3]; [1]Lausanne/CH, [2]Bron/FR, [3]Lyons/FR (david.rotzinger@chuv.ch)

Purpose: To demonstrate the non-inferiority of low iodine dose dual-layer spectral detector coronary CTA (CCTA) compared to standard injection conventional CCTA for the evaluation of coronary artery disease and to compare the contrast-to-noise ratio between monochromatic and conventional CCTA reconstructions.
Methods and materials: 108 patients were randomised to undergo either a standard iodine injection protocol A (flow rate, 5 mL/s) or a reduced flow rate protocol B (flow rate, 2.5 mL/s) CCTA on a dual-layer spectral detector CT system. Conventional images only were reconstructed for protocol A. For protocol B, 55 keV monochromatic images were reconstructed. Contrast-to-noise ratio (CNR) between lumen and fat was measured in 5 coronary segments (LM, distal LAD, distal LCx, proximal RCA, and distal RCA). Two independent radiologists rated 17 coronary segments per patient regarding image quality on a 4-point Likert scale (4=best score). An examination was considered diagnostic if no segment was scored 1.
Results: The injected contrast agent volume was 72.2±9.8 mL and 42.5±10.5 mL for protocol A and B, respectively (p<0.001). CNR was 23.3±14.2 and 28.9±18.2 in protocol A and B, respectively (p=0.015). The rate of diagnostic CCTA was 89.3% (n=50/56) and 96.2% (n=50/52) in protocols A and B, respectively. Non-inferiority of protocol B compared to A was inferred (95% CI of the difference= -0.1651 to 0.0277), with a pre-specified non-inferiority margin of 10%.
Conclusion: Spectral CCTA with 55 keV monochromatic reconstructions allows for a 40% reduction in iodine dose compared to conventional CT angiography of the coronary arteries. Additionally, monochromatic reconstructions can improve the CNR between the coronary lumen and surrounding fat.
Limitations: Only one monochromatic energy level (55 keV) was evaluated.
Ethics committee approval: Ethics committee approval and written informed consent were received.
Funding: Funding was received from Bracco.
Author Disclosures:
D. C. Rotzinger: nothing to disclose
S. A. Si-Mohamed: nothing to disclose
L. Boussel: nothing to disclose
R. A. Meuli: nothing to disclose
P. C. Douek: nothing to disclose

RPS 303-13 15:12
Improvement of image quality in high-resolution coronary computed tomography angiography when using a new deep learning image reconstruction algorithm
L. Macron, J. Feignoux, C. Le Goff, J.-L. Sablayrolles; Saint-Denis/FR, (laurentmacron@gmail.com)

Purpose: High resolution (HiRes) acquisition mode is highly valuable for assessing challenging lesions on coronary computed tomography angiography (CCTA), especially for severely calcified plaques and stents. However, HiRes acquisition mode introduces higher noise due to lower tube current availability, limiting its use for large patients. The aim of this study was to assess the impact of a new deep learning-based image reconstruction (DLIR) algorithm (TrueFidelity, GE Healthcare) on imageqQuality (IQ) for HiRes CCTA.
Methods and materials: HiRes CCTA exams from 29 patients were reconstructed with adaptive statistical iterative reconstruction V 50% (ASIRV50) and DLIR. IQ of both data sets was assessed quantitatively by measuring signal-to-noise and contrast-to-noise ratios (SNR and CNR) of the left ventricle and ascending aorta, and subjectively by two radiologists on a 5-points Likert scale. One-way ANOVA and Kruskall-Wallis test were used to compare quantitative metrics and subjective IQ respectively; p value <0.05 was considered significant.
Results: The mean age was 67+/-8 years, 55% were men, median Body Mass Index was 23 kg/m^2 (from 18 to 28), and mean DLP was 149+/-40mGy/cm. The mean SNR and CNR were significantly higher with DLIR images compared to ASIRV50 (left ventricle: SNR = 17.7vs9.3, CNR = 21.6vs13.6; ascending aorta: SNR = 18.4vs10.9, CNR = 19.8vs9.3, respectively; p <0.0001 each) and subjective IQ was significantly improved with DLIR (4.6+/-0.5) compared to ASIRV50 (3.8+/-0.4; p<0.0001).
Conclusion: By further reducing image noise magnitude without altering texture compared to ASIRV50, DLIR could expand the use of HiRes acquisition mode for CCTA in clinical routine and improve coronary stenosis depiction and quantification.
Limitations: Only 29 patients were included.
Ethics committee approval: n/a
Funding: No funding was received for this work.
Author Disclosures:
L. Macron: nothing to disclose
J.-L. Sablayrolles: nothing to disclose
J. Feignoux: nothing to disclose
C. Le Goff: Consultant at GE Healthcare

RPS 303-14 15:18
A new dual-energy algorithm for better displaying vessel wall borders of the coronary artery on coronary CT angiography
F. Zhang[1], W. Deng[2], K. Chen[2], H. Tan[3]; [1]Sanya, Hainan/CN, [2]Shanghai/CN, [3]Beijing/CN (fanzradiology@126.com)

Purpose: To evaluate the potential ability of better displaying the distal coronary artery by using a new algorithm which depicts only water attenuation contribution of each voxel on CTA.
Methods and materials: Coronary CTAs were acquired using a dual-layer detector CT (Spectral IQON®, Philips Healthcare, the Netherlands) on 23 patients with a normal body mass index (BMI, 20-25 kg/m^2). Conventional images (group A), the new algorithm images (group B), and Z effective images (group C) of each patient were divided into three groups. The mean image noise and CNR of different groups were measured on CT images compared using the one-way ANOVA test. In addition, image quality and vessel wall contour evaluation were performed by two radiologists, who were blinded to the reconstruction algorithm, using a five-point confidence scale (1 [poor] to 5 [excellent]). The results of the three groups were compared with the Mann-Whitney U-test.
Results: There was a significant difference in mean image noise, CNR, image quality, and the contour of the vessel wall in the three groups (p<0.00). By using the new algorithm, the CNR and image quality of images were better than conventional images and Z effective images. The vessel wall contour can be clearly displayed in group B, but not in group A and C.
Conclusion: A new dual-energy algorithm could significantly improve displaying distal coronary artery on CCTA.
Limitations: A lack of in vitro experiments to determine the accuracy of the new algorithm.
Ethics committee approval: n/a
Funding: Social development special project of hainan key research and development plan.
Author Disclosures:
F. Zhang: nothing to disclose
W. Deng: nothing to disclose
K. Chen: nothing to disclose
H. Tan: nothing to disclose

RPS 303-15 15:24
CT-FFR profiles in patients without coronary artery disease
T. Leonard[1], C. N. de Cecco[1], U. J. Schoepf[1], S. S. Martin[2], A. M. Fischer[1], R. R. Bayer[1], R. H. Savage[1], A. Varga-Szemes[1], M. van Assen[3]; [1]Charleston, SC/US, [2]Frankfurt am Main/DE, [3]Groningen/NL (leonarty@musc.edu)

Purpose: To evaluate the effect of measurement location and lumen area changes on CT-FFR values in patients without coronary artery disease (CAD).
Methods and materials: Patients who underwent calcium scoring (CACS) and CCTA with CT-FFR were retrospectively included. Exclusion occurred if their CACS was >0, troponin levels were elevated, or any cardiac-abnormality was found on CCTA studies. On-site CT-FFR based on an artificial intelligence,

deep-learning algorithm was computed for each coronary artery at proximal, mid, and distal segments. At each location, the lumen area and Hounsfield Unit (HU) value were measured. CT-FFR was considered positive with values <0.75. The relationship between lumen areas, HU-values, and CT-FFR was evaluated for each coronary artery and each location. Ratios between mid and distal values compared to proximal-values for lumen and HU parameters were calculated.
Results: 106 patients were included. In 39 (37%) patients, the LAD had CT-FFR values <0.75, with a decrease in CT-FFR from 0.97 (SD:0.04) proximally to 0.62 (SD:0.10) distally in the abnormal patients. The Cx showed a limited number of patients with CT-FFR values <0.75 (n=16, 15%), with a decrease in CT-FFR values from 0.96 (SD:0.04) proximally to 0.65 (SD:0.09) distally in those patients. The RCA had 36 (34%) patients with CT-FFR <0.75, with distal CT-FFR values of 0.61 (SD:0.12) and proximal CT-FFR values of 0.98 (SD:0.02). 12 abnormal CT-FFR values were measured mid-segment, while all others were measured at distal-segments. The lumen area was not significantly different between the abnormal and normal CT-FFR groups, while both HU and HU-ratios were significantly lower in the abnormal CT-FFR group for all three major coronary arteries.
Conclusion: CT-FFR values in patients without CAD can become abnormal at a distal location without indicating flow-limiting stenosis, which depends strongly on HU-values.
Limitations: A retrospective single-centre study with limited subject-availability.
Ethics committee approval: Institutional-Review-Board approval.
Funding: Siemens Healthineers.
Author Disclosures:
T. Leonard: nothing to disclose
C. N. de Cecco: Grant Recipient at Bayer, Siemens
U. J. Schoepf: Grant Recipient at Siemens, GE, Astllas, Bayer, Elucid Bioimaging, GE, Guerbet, HeartFlow Inc, , Consultant at Siemens, Elucid Bioimaging
S. S. Martin: nothing to disclose
R. R. Bayer: Grant Recipient at HeartFlow, Bayer
R. H. Savage: nothing to disclose
A. M. Fischer: nothing to disclose
A. Varga-Szemes: Grant Recipient at Siemens , Consultant at Elucid Bioimaging
M. van Assen: nothing to disclose

14:00 - 15:30 **Room Y**

CTiR 3
Clinical Trials in Radiology 1

Moderators:
M. Dewey; Berlin/DE
U. Mahmood; Oak Brook/US

CTiR 3-1 14:00
Stopping anticoagulation for isolated or incidental sub-segmental pulmonary embolism (STOAPE) trial
G. Robinson[1], D. Lasserson[2], S. Jowett[2], A. Turner[2], S. Greenfield[2], C. Cummins[2], M. Newnham[2], J. C. L. Rodrigues[1]; [1]Bath/UK, [2]Birmingham/UK (grobinson1@nhs.net)

Purpose: The UK National Institute for Health Research (NIHR) posed: Should patients with incidental or isolated subsegmental pulmonary emboli identified on imaging be treated with anticoagulants?
Methods and materials: A randomised prospective open blinded endpoint trial. 1466 patients enrolled across 50 sites with an entry criteria of an isolated/incidental SSPE on CTPA. Patients will be randomly allocated to anticoagulation or no anticoagulation for 3 months. Imaging will be reviewed by an 'expert panel'. Primary outcome: VTE recurrence and major bleeding and CRNMB at 3 months. Secondary outcomes: hospitalisations for VTE or bleeding events, VTE recurrence, cost-effectiveness, EQ-5D-5L, unscheduled healthcare visits, PE/VTE deaths.
Results: Patients will be recruited from 1st June 2020. Study Objectives: (1) Determine whether not anticoagulating for isolated SSPE reduces harm compared with three months of full anticoagulation. (2) Determine the rate of complications of anticoagulation therapy in patients with SSPE. (3) Determine whether not treating SSPE is acceptable to patients and clinicians. (4) Determine the reclassification rate of SSPE diagnoses made by acute reporting radiologists when reviewed by thoracic radiologists. (5) Assess cost-effectiveness of the no-treatment approach in patients with SSPE, taking a health service perspective. (6) Set up an acute PE research network to support follow-on research studies.
Conclusion: This will be the first randomised controlled trial of anticoagulation in subsegmental pulmonary embolism to establish the risks and benefits of treatment. This presentation shows the study design, discusses the role of radiology, and the imaging data/outcomes that can be captured.
Limitations: Radiological limitiation: misdiagnosis of sub-segmental pulmonary embolism as the main entry criteria; however, this reflects 'real-world practice' and has been considered by the authors and NIHR.
Ethics committee approval: UK National Institute for Health Research (NIHR).
Funding: UK National Institute for Health Research (NIHR).
Author Disclosures:
G. Robinson: nothing to disclose
D. Lasserson: nothing to disclose
S. Jowett: nothing to disclose
A. Turner: nothing to disclose
S. Greenfield: nothing to disclose
C. Cummins: nothing to disclose
M. Newnham: nothing to disclose
J. C. L. Rodrigues: nothing to disclose

CTiR 3-2 14:10
Discussant
E. Castañer González; *Sabadell/ES (ecastaner@tauli.cat)*

Author Disclosures:
E. Castañer González: Speaker at UDIAT-CD Institut Universitari del Parc Tauli

CTiR 3-3 14:15
Can additional cancers detected by digital breast tomosynthesis in screening be detected on the corresponding mammography examination using artificial intelligence?
V. Dahlblom, A. Tingberg, K. Lang, I. Andersson, S. Zackrisson, M. Dustler; *Malmö/SE (victor.dahlblom@med.lu.se)*

Purpose: To investigate whether additional digital breast tomosynthesis (DBT) screen-detected cancers could be detected on the corresponding digital mammography (DM) examination by a deep-learning based AI system, using paired data from a prospective tomosynthesis screening trial.
Methods and materials: We used a subgroup of 14768 women from the Malmö Breast Tomosynthesis Screening Trial. All participants were examined with both DM and DBT with independent readings. Of 136 screen-detected cancers, 41 cancers were detected only on DBT. We analysed DM with a mammography AI software (ScreenPoint Transpara™). The software identifies and scores suspicious areas in the images with a score between 1 and 100 (highest risk), and also provides a composite cancer risk score between 1 and 10 (highest risk) for the whole examination. A cancer was defined as detected by the software if the examination got the highest risk score and the cancer lesion was correctly localised and scored over 60. Descriptive statistics were used.
Results: 1797 examinations (12%) got the highest examination risk score. The AI software detected 15 of the 41 DBT-only detected cancers (37 %) on DM. A majority were invasive cancers, with 8 invasive ductal carcinomas, 4 invasive lobular carcinomas, and 1 invasive tubular carcinoma. Three cancers had histological grade 3, and 2 had lymph node metastases.
Conclusion: A substantial number of the additional DBT screen-detected cancers were also detected on DM with AI. The possibilities of using mammography plus AI in screening should be further investigated, taking effects on e.g. false positive recalls into account.
Limitations: Single-centre study with a single vendor.
Ethics committee approval: Approved, informed consent used.
Funding: AIDA Fellowship, Vinnova (V. Dahlblom) and Governmental Funding for Clinical Research, Region Skåne. ScreenPoint Medical provided the software, but did not participate in the study.
Author Disclosures:
V. Dahlblom: nothing to disclose
M. Dustler: Patent Holder at US 9 833 203, Equipment Support Recipient at Screenpoint Medical
S. Zackrisson: Other at Speaker fees from Siemens, Other at Travel support from Siemens, Patent Holder at US 9 833 203
A. Tingberg: nothing to disclose
I. Andersson: nothing to disclose
K. Lang: Other at Speaker fees from Siemens Healthineers

CTiR 3-4 14:25
Discussant
E. Szabó; *Szeged/HU*

Author Disclosures:
E. Szabó: nothing to disclose

CTiR 3-5 14:30
Digital Breast Tomosynthesis (CBT) as a primary screening test in a population-based screening program: results from the "Trento DBT pilot study" including interval carcinoma anlysis
D. Bernardi[1], M. A. Gentilini[2], M. Pellegrini[2], C. Fantò[2], M. Valentini[2], V. Sabatino[2], M. de Nisi[2], N. Houssami[3]; [1]Milan/IT, [2]Trent/IT, [3]Sydney/AU (Daniela.Bernardi@humanitas.it)

Purpose: To report the results of a prospective trial on the use of DBT in place of digital mammography (DM) in women who attended screening invitation.
Methods and materials: From mid October 2014 to December 2016, a prospective cohort of 46,343 women presenting for screening had a DBT mammography; synthetic 2D images were reconstructed and read in combination with DBT. Main screening-parameters, including interval cancer rate (IRC) at 2-year follow up and DBT sensitivity, were assessed and compared with those of a historical cohort of 37,436 women previously screened with DM. Rate ratio (RR) and 95% CI statistics were used.
Results: Cancer detection rate (CDR) was 8.67% for DBT versus 5.48 for MX (RR 1.58, 95% CI 1.34-1.87). DBT-screened had lower recall rate (RR) compared to DM-screened cohort (2.55% and 3.21% respectively; RR 0.79, 95% CI 0.73-0.86) and increased PPV (34.07% for DBT and 17.07 for MX; RR 1.99, 95% CI 1.68-2.37). DBT implementation was associated with a significantly higher CDR for stage I-II invasive cancers across all tumour size and grade categories. Most of the cancers detected by DBT were node-negative. Interval cancer rate (IRC) for DBT-screened were comparable to MX-screened cohort (1.10 and 1.36 per 1000 screens respectively; RR 0.81, 95% CI 0.55-1.19). Screening sensitivity was higher for DBT than MX although not significantly (88.74 % vs 80.08%; RR 1.11, 95% CI 0.94-1.31).
Conclusion: Population-based implementation of DBT screening was associated with increased CDR and reducing RR, but no significant change for interval cancer rate.
Limitations: The pilot is a non-randomised clinical trial.
Ethics committee approval: Approval by local health authorities.
Funding: No funding was received for this work.
Author Disclosures:
D. Bernardi: nothing to disclose
M. A. Gentilini: nothing to disclose
M. Pellegrini: nothing to disclose
C. Fantò: nothing to disclose
M. Valentini: nothing to disclose
V. Sabatino: nothing to disclose
N. Houssami: nothing to disclose
M. de Nisi: nothing to disclose

CTiR 3-6 14:40
Discussant
P. A. T. Baltzer; *Vienna/AT (patbaltzer@gmail.com)*

Author Disclosures:
P. A. T. Baltzer: nothing to disclose

CTiR 3-7 14:45
MRI screening in women with extremely dense breasts: patient and MRI characteristics to distinguish between false-positives and true-positives
B. M. Den Dekker, M. F. Bakker, S. V. de Lange, R. M. Pijnappel, W. B. Veldhuis, C. van Gils; *Utrecht/NL (bm.den.dekker@hotmail.com)*

Purpose: To identify patient and MRI characteristics that are useful to distinguish true-positive screening MRI examinations from false-positives in women with extremely dense breasts.
Methods and materials: Patient and MRI characteristics of 454 Dutch breast cancer screening participants (50-75 years) with Volpara density category 4 on mammography and a positive first-round MRI screening result (BI-RADS 3/4/5) after a normal screening mammography, were collected prospectively (DENSE trial). Positive predictive values for malignancy in relation to patient and MRI characteristics were assessed. Multivariable logistic regression analysis with stepwise backward selection using AIC was used to find the optimal model to distinguish true-positives from false-positives.
Results: Of 454 women with a positive MRI screening examination, 79 were diagnosed with breast cancer, the remaining 375 MRI examinations were considered false-positive. In univariate analysis age (p-value<0.03), BMI (p-value 0.01), first degree relatives with breast cancer (p-value 0.002), MRI BI-RADS (p-value<0.001), lesion type (p-value 0.02) and lesion kinetics (p-value 0.02) were associated with breast cancer diagnosis. The optimal multivariable prediction model included MRI BI-RADS, age, previous breast biopsy, first degree relatives with breast cancer, and menopausal status (AUROC 0.829, 95%CI 0.779-0.880).
Conclusion: In addition to BI-RADS classification of screening MRI, the patient characteristics of age, previous breast biopsy, first degree relatives with breast cancer, and menopausal status might be useful to distinguish true-positive MRI examinations from false-positives in women with extremely dense breasts.
Limitations: The model has not yet been validated in an independent dataset.
Ethics committee approval: Ethical approval for the DENSE trial was obtained from the Dutch Minister of Health, Welfare and Sport (2011/19). Written informed consent from study participants was obtained.
Funding: Supported by UMC Utrecht, ZonMw, Dutch Cancer Society, Dutch Pink Ribbon/A Sister's Hope, Bayer AG Pharmaceuticals, stichting Kankerpreventie Midden-West, Volpara Health Technologies.
Author Disclosures:
S. V. de Lange: Research/Grant Support at Bayer AG Pharmaceuticals, Research/Grant Support at Volpara Health Technologies
B. M. Den Dekker: nothing to disclose
M. F. Bakker: Research/Grant Support at Bayer AG Pharmaceuticals, Research/Grant Support at Volpara Health Technologies
W. B. Veldhuis: nothing to disclose
R. M. Pijnappel: nothing to disclose
C. van Gils: Research/Grant Support at Bayer AG Pharmaceuticals, Research/Grant Support at Volpara Health Technologies

CTiR 3-8 14:55
Discussant
U. Bick; *Berlin/DE (Ulrich.Bick@charite.de)*

Author Disclosures:
U. Bick: Patent Holder at Hologic, Inc.

CTiR 3-9 15:00
Dose reference levels during fluoroscopically-guided procedures performed using mobile X-ray systems in operating rooms
L. Hadid-Beurrier[1], M. Demonchy[2], J. Le Roy[3], B. Royer[4], D. Dabli[5]; [1]Paris/FR, [2]Frejus/FR, [3]Montpellier/FR, [4]Maxéville/FR, [5]Angers/FR (lama.hadid@aphp.fr)

Purpose: The French Society of Medical Physics (SFPM) initiated a task group to establish dose reference levels (DRL) for the most common procedures performed in operating rooms using mobile X-ray systems.
Methods and materials: This multicenter prospective study involved 57 french medical institutions of different categories. Anonymised data was collected for 10 to 30 consecutive interventions from a list of 62 procedures types, belonging to 7 surgery specialties (neurosurgery, orthopaedics, digestive, urology, cardiology, vascular, and multi-specialty). Dose-Area-Product (DAP) and fluoroscopy time Reference Levels (RL) were established based on the 3rd quartile of distributions. Correction coefficients from quality assurance reports were applied to DAP displayed values to improve their accuracy. The impact of the procedure complexity was also investigated.
Results: DRLs were established for 31 procedures performed with mobile C-arms. Important variations were observed between the different surgery specialties. Lowest doses were reported for orthopaedic procedures (DAP=0.07 $Gy.cm^2$ for hallux valgus, elbow, and hands), while highest doses were found in vascular procedures (DAP=85 $Gy.cm^2$ for abdominal aortic aneurysm repair). In urology, DRLs ranged between 2 $Gy.cm^2$ for ureteroscopy and 10 $Gy.cm^2$ for lithotripsy. In cardiology, DRLs were higher for 3-leads pacemakers than for 1 or 2-leads pacemakers. Moreover, results show values below those obtained from fixed interventional radiology facilities. Indeed, when compared to the french RL using fixed modalities, DAP is 6 times lower for lower-extremity arteriography and 3 times lower for biliary drainage.
Conclusion: DRLs were established to help medical physicists and surgeons to evaluate their practice and optimise patient radiation safety.
Limitations: Patients' body mass index was not considered.
Ethics committee approval: This study was approved by the National Commission for Data Protection and Liberties and registered in Clinicaltrials.gov.
Funding: No funding has been obtained.
Author Disclosures:
L. Hadid-Beurrier: nothing to disclose
J. Le Roy: nothing to disclose
M. Demonchy: nothing to disclose
B. Royer: nothing to disclose
D. Dabli: nothing to disclose

CTiR 3-10 15:10
Discussant
A. Trianni; *Udine/IT (annalisa.trianni@asuiud.sanita.fvg.it)*

Author Disclosures:
A. Trianni: nothing to disclose

CTiR 3-11 15:15
CT screening for early lung cancer, cardiovascular disease, and COPD in China: rationale and design of the NELCIN-B3 study
Y. Du[1], M. Vonder[1], Q. Li[2], G. Sidorenkov[1], Z. Ye[3], X. Xie[2], W. Wang[2], M. Oudkerk[1], S. Liu[2]; [1]Groningen/NL, [2]Shanghai/CN, [3]Tianjin/CN (marleenvonder@gmail.com)

Purpose: To determine and optimise the diagnostic performance of the Netherlands-China Big-3 screening (NELCIN-B3) protocol for early detection of lung cancer, cardiovascular disease (CVD), and COPD by low-dose CT in a Chinese population.
Methods and materials: Diagnostic randomised controlled and prospective cohort studies are conducted in three hospitals in China. 14,000 participants between 40-74 y will be randomly allocated to intervention and control groups. Risk-factor questionnaires, lung function, and blood samples will be collected. Intervention group participants will undergo low-dose chest CT and management according to NELCIN-B3 protocol. Quantitative assessment of Big-3 imaging biomarkers will be performed: lung nodule volume, volume doubling time, coronary calcium score, and emphysema score. Control group participants will undergo default chest CT and be managed according to hospital protocol based on lung nodule diameter and visual assessment of COPD and coronary calcium. Four years after the initial assessment, the referral rate, incidence of the Big-3, and related mortality will be evaluated.
Results: The effectiveness of quantitative assessment of CT imaging biomarkers for the Big-3 in the intervention group will be evaluated and compared to the control group with regards to referral rate, clinical diagnosis of the Big-3, and related mortality.
Conclusion: We expect that the quantitative assessment of the CT imaging biomarkers will reduce the number of unnecessary referrals for early detected lung nodules and improve the early detection of CVD and COPD in a Chinese population.
Limitations: Management of non-solid nodules in the intervention group will be based on the diameter due to lack of validated volume-based protocol.
Ethics committee approval: Approval was issued by the Biomedical Research Ethics Committee of Shanghai Changzheng Hospital and written informed consent collected.
Funding: This study is funded by the Chinese Ministery of Sciences and Technology (MOST) and the Royal Dutch Academy of Sciences (KNAW).
Author Disclosures:
M. Vonder: nothing to disclose
G. Sidorenkov: nothing to disclose
Y. Du: nothing to disclose
Z. Ye: nothing to disclose
X. Xie: nothing to disclose
M. Oudkerk: Other at Institute for Diagnostic Accuracy
S. Liu: nothing to disclose
Q. Li: nothing to disclose
W. Wang: nothing to disclose

CTiR 3-12 15:25
Discussant
M. Benegas Urteaga; Barcelona/ES (benegasmariana@gmail.com)

Author Disclosures:
M. Benegas Urteaga: nothing to disclose

14:00 - 15:30 **Descartes (Room D3)**

Paediatric

RPS 312

New insights in paediatric head and neck imaging

Moderators:
I. L. Štěpán-Buksakowska; Prague/CZ
E. Vazquez Mendez; Barcelona/ES

RPS 312-1 14:00
Neurodevelopmental outcomes of posterior fossa anomalies diagnosed by foetal MRI
S. Sefidbakht[1], A. Teimouri[1], P. Katibeh[1], N. Rahimirad[1], N. Asadi[1], P. Keshavarz[1], P. Iranpour[1], F. Zarei[1], B. Bijan[2]; [1]Shiraz/IR, [2]Sacramento, CA/US (Arashteimourirad@gmail.com)

Purpose: To retrospectively evaluate neurodevelopmental outcomes (NDO) of prenatally diagnosed isolated posterior fossa abnormalities characterised on foetal MRI.
Methods and materials: Out of 821 foetal MRIs performed on pregnant women referred to a tertiary referral centre from May 2015-July 2018, 66 were done for the further evaluation of isolated posterior fossa abnormalities suspected in ultrasound. Post-delivery follow-up was done by a trained examiner using national registry data and parental phone calls. The abnormal outcome was defined as an ASQ score below the cut-off for age and related skill. Pregnancy termination due to a foetal anomaly or foetal death (TOPFA/FD) was recorded.
Results: The maternal age was 29.3±5.7. Gestational ages at the time of the MRI were 24.7±5.9. Out of 66 cases, 19 cases were diagnosed as normal, 3 were lost to follow-up (LTFU), 1 foetal death, 13 normal, and 2 abnormal NDO (minor communication, fine motor, and problem-solving issues). Out of 36 foetuses referred for possible vermian hypoplasia, 15 foetuses were diagnosed with inferior vermian hypoplasia (4 TOPFA/FD, 6 LTFU, 3 normal, and 2 abnormal NDO), 14 were diagnosed as possible BPC before 19 wks GA (2 LTFU, 2 TOPFA/FD, 8 normal, and 2 abnormal NDO (mean ASQ 217, minor communication issues)), and 5 were diagnosed as mega cisterna magna (1 LTFU and 4 normal NDO). The worse outcome was with cerebellar hypoplasia (5 TOPFA/FD and 1 LTFU) and dandy-walker malformation (6 TOPFA/FD and one abnormal NDO).
Conclusion: MRI is fairly accurate in ruling out clinically significant posterior fossa abnormality even before 19 weeks GA. Prenatally diagnosed cerebellar hypoplasia and DWM are uniformly associated with a poor prognosis. Most cases of BPC have a normal and most cases of IVH have an abnormal NDO.
Limitations: n/a
Ethics committee approval: n/a
Funding: No funding was received for this work.
Author Disclosures:
A. Teimouri: nothing to disclose
S. Sefidbakht: nothing to disclose
P. Katibeh: nothing to disclose
N. Rahimirad: nothing to disclose
N. Asadi: nothing to disclose
P. Keshavarz: nothing to disclose
P. Iranpour: nothing to disclose
F. Zarei: nothing to disclose
B. Bijan: nothing to disclose

RPS 312-2 14:06
Foetal optic structures: a postmortem MRI study
F. Prayer, C. Seitz, M. Weber, D. Prayer, P. Brugger, G. M. Gruber; Vienna/AT

Purpose: To establish normal values of foetal optic structures as a reference for future in vivo imaging studies.
Methods and materials: Postmortem foetal MRI data of 33 foetuses with normal development of optical structures and 25 foetuses with pathologies (GW 16-42) were analysed. The pathology group included complex malformations (15), intrauterine growth restriction (2), premature rupture of membranes (4), twin-associated problems (3), and stillbirth (1). MRI was performed on a 3 Tesla scanner utilising an 8-channel knee coil. Retrobulbar and intracranial optic nerve diameters, optic nerve length, the angle between optic nerves, and minimum transverse diameter of the optic chiasm were obtained. Correlations with gestational age were performed. Measurements were performed using free Image J software on T2-weighted images (TR 300ms, TE 140 ms, and isovoxel 0.4mm ciss 3d sequence).
Results: The optic nerve length increased from 10.5-29.41 mm within 26 GW. The retrobulbar optic nerve diameter increased from 0.83 (right)/0.860 (left) mm to 2.13 (right)/ 2.10 (left) mm. The transverse diameter of the optic chiasm increased from 4.1-6.7 mm within 24 weeks. The angle between the optic nerves decreased by 36.5 degrees within 26 weeks. Optic structure measurements correlated significantly with gestational age. Foetuses in the pathology group had at least one aberration from the normal values.
Conclusion: Postmortem foetal MRI-based optic structure measurements correlated with gestational age and showed a change in orientation of the optic chiasm from a U shape at early gestation towards a V shape at later gestation. Based on the presented normal values, developmental defects can be detected sensitively.
Limitations: More studies are needed to investigate translation to in vivo foetal MRI.
Ethics committee approval: This study was approved by the institutional review board.
Funding: No funding was received for this work.

Author Disclosures:
F. Prayer: nothing to disclose
C. Seitz: nothing to disclose
G. M. Gruber: nothing to disclose
M. Weber: nothing to disclose
P. Brugger: nothing to disclose
D. Prayer: nothing to disclose

RPS 312-3 14:12

Paediatric orbital masses: the value of adding diffusion-weighted imaging to conventional MRI in lesion categorisation

A. Youssef, I. Zaky, A. Mohammed Aly, D. Elgalaly, M. Afifi, H. Taha, H. Elzomor, A. Alieldin; *Cairo/EG (aydayoussefegypt@gmail.com)*

Purpose: To assess the diagnostic contribution of diffusion-weighted (MRI) using apparent diffusion coefficient (ADC) values for the characterisation of orbital masses and differentiation of benign and malignant lesions.
Methods and materials: 130 patients with recently diagnosed orbital masses who underwent preoperative conventional MRI and DWI were included. The average ADC obtained from each tumour was compared with the histopathological diagnosis determined from the subsequent surgical sample.
Results: 70 girls and 60 boys (age range: 1 month-18 years) with orbital masses were included. The globe was the seat of lesions in 33% of cases, optic nerve in 20.7%, and 7 cases had lesions in the lacrimal gland. 45 cases were diagnosed as benign masses and 85 as malignant lesions.
There was a statistically significant difference between the mean ADC value of the benign lesions (1.39±0.52 $x10^{-3}$ mm^2/s) and those of the malignant lesions (0.69±0.22 $x10^{-3}mm^2/s$).
The optimal ADC cut-off value that was deter-mined for the discrimination between these lesions was 1.075 $x10^{-3}mm^2/s$, with a sensitivity of 97.14% and specificity of 75%.
Using conventional MRI alone in predicting benign and malignant lesions has the sensitivity of 76% and specificity of 91%, with 94% positive predictive value and 67% negative predicative value.
Combining DWI and conventional MRI has increased accuracy, as the sensitivity 95% and specificity 86%, with 93% positive predictive value and 90% negative predictive value.
Conclusion: ADC values provide an accurate, sensitive, fast, and non-invasive means of characterising paediatric orbital tumours. A priori tumour characterisation is useful in timing and treatment planning for orbital tumours.
Limitations: Variable pathological subtypes in all orbital compartments were included.
Ethics committee approval: n/a
Funding: No funding was received for this work.
Author Disclosures:
A. Youssef: nothing to disclose
I. Zaky: nothing to disclose
A. Mohammed Aly: nothing to disclose
D. Elgalaly: nothing to disclose
M. Afifi: nothing to disclose
H. Taha: nothing to disclose
H. Elzomor: nothing to disclose
A. Alieldin: nothing to disclose

RPS 312-4 14:18

Neurosensory hearing loss in children with Zika virus microcephaly and brain MRI evaluation

N. Anaissi Rocha Pessoa[1], M. de Carvalho Leal[1], S. Caldas Da Silva Neto[1], L. Ferreira Muniz[1], P. M Parizel[2], M. D. F. Vasco Aragao[1]; [1]*Recife/BR,* [2]*Perth/AU (fatima.vascoaragao@gmail.com)*

Purpose: To describe the findings of brain MRI in children affected by congenital Zika virus syndrome (CZS) and sensorineural hearing loss (SHL).
Methods and materials: A retrospective cross-sectional study with two groups was conducted. Group A consisted of 6 children with microcephaly and SHL and group B consisted of 27 children with microcephaly without SHL. All children had a diagnosis of CZS confirmed in a previous study, had a hearing evaluation through BERA, and had brain and/or inner ear MRI. The images were qualitatively evaluated by a radiologist and two otolaryngologists.
Results: In a partial result, we observed a frequency of brainstem hypoplasia in all patients in group A, being 17% moderate, 33% severe, and 50% very serious. In group B, it was 18.5% mild, 25.9% moderate, 44.4% severe, and 11.1% very serious. Regarding hypoplasia of regions of the lower frontal parenchyma, in group A there were 3 (50%) severe cases and 3 (50%) very serious cases. In group B, this division was 3.7% normal, 25.9% mild/moderate, 51.8% severe, and 18.5% very serious. In the evaluation of the temporal parenchyma, in group A we found 7% of severe cases and 83% of very serious cases. In group B, the numbers found were equal to the frontal parenchyma evaluation.
Conclusion: We can observe that the group of patients with hearing loss presents more severity in the classification of their brain alterations, which may reflect in the hearing ability.
Limitations: The small sample of children with CZS with sensorineural hearing loss.
Ethics committee approval: Ethics committee approval obtained.
Funding: No funding was received for this work.
Author Disclosures:
M. D. F. Vasco Aragao: nothing to disclose
N. Anaissi Rocha Pessoa: nothing to disclose
M. de Carvalho Leal: nothing to disclose
S. Caldas Da Silva Neto: nothing to disclose
L. Ferreira Muniz: nothing to disclose
P. M Parizel: nothing to disclose

RPS 312-5 14:24

Chronic rhinosinusitis in patients with primary ciliary dyskinesia: comparison with findings in cystic fibrosis

F. Wuennemann[1], O. Sommerburg[1], M. Stahl[1], H.-U. Kauczor[1], I. Baumann[1], M. A. Mall[2], M. Eichinger[1], M. O. Wielpütz[1]; [1]*Heidelberg/DE,* [2]*Berlin/DE*

Purpose: Primary ciliary dyskinesia (PCD) and cystic fibrosis (CF) are characterised by impaired mucociliary clearance. Though pulmonary involvement has been the focus of research in the past, upper airway manifestations with chronic rhinosinusitis (CRS) has been rarely studied. CRS results in an increased disease burden and might be a reservoir for recurrent pulmonary pathogens. Our aim was to evaluate the extent of CRS in patients with PCD and CF using MRI.
Methods and materials: MRI of the paranasal sinuses was performed in 12 PCD patients with 25 MR-examinations (mean age 10.21y, range 0.21-18.22y) and compared to 21 age-matched CF patients with 49 MR examinations (mean 10.78y, range 0.13-18.71y). Abnormalities of the paranasal sinuses (mucosal swelling, mucopyoceles, effusion, polyps, and displacement of the medial maxillary sinus wall) were assessed using a newly developed CRS MRI scoring system.
Results: The overall sum score was significantly lower in PCD compared to CF ($p=0.0011$). With respect to the individual sinuses, scores of the maxillary sinus, the frontal sinus, the sphenoid sinus, and ethmoid cells were significantly lower in PCD. The involvement of the mastoid cells was significantly higher in PCD ($p<0.001$). The prevalence of mucopyoceles per individual sinus was significantly higher in CF ($p<0.001$ per sinus).
Conclusion: MRI is sensitive in detecting CRS across the whole paediatric age range. The novel score is applicable to patients with PCD and revealed a lower extent of CRS in patients with PCD compared to CF, despite similar pathophysiology.
Limitations: Differences in structural abnormalities of CRS in PCD and CF were not yet correlated to clinical outcome parameters.
Ethics committee approval: Approved by the institutional ethics committee. Written consent was obtained from parents or legal guardians.
Funding: Supported by the German BMBF, the Mukoviszidose e.V., and the Einstein Foundation.
Author Disclosures:
F. Wuennemann: nothing to disclose
O. Sommerburg: nothing to disclose
M. Stahl: Grant Recipient at Vertex
I. Baumann: nothing to disclose
M. A. Mall: Advisory Board at Bayer, Vertex, Boehringer Ingelheim, Polyphor, Arrowhead, ProQr, Spyryx, Santera, Enterprise Therapeutics, Research/Grant Support at German Ministry of Education, Einstein Foundation, Mukoviszidose e.V., Speaker at Bayer, Vertex, Boehringer Ingelheim, Polyphor, Arrowhead, ProQR, Spyryx, Santera, Galapagos, Sterna, Enterprise Therapeutics, Celtaxys
H.-U. Kauczor: Advisory Board at Boehringer Ingelheim, Research/Grant Support at Siemens, Philips, Speaker at Siemens, Philips, Boehringer Ingelheim, Astra Zeneca, MSD Sharp & Dome
M. O. Wielpütz: Grant Recipient at Vertex, Boehringer Ingelheim, Advisory Board at Vertex, Boehringer Ingelheim
M. Eichinger: nothing to disclose

RPS 312-6 14:30

The paediatric voice after airway reconstruction on MRI

B. Elders, M. Hakkesteegt, B. Pullens, H. A. W. M. Tiddens, P. A. Wielopolski, P. Ciet; *Rotterdam/NL (b.elders@erasmusmc.nl)*

Purpose: Although the focus in patients after laryngotracheal stenosis (LTS) is mainly on airway function, dysphonia is a common sequela that strongly influences the quality of life of patients. Dysphonia is caused by pre-existing stenosis and anatomical distortion due to airway reconstruction. Magnetic resonance imaging (MRI) is ideal to assess the vocal cords in static and dynamic conditions. The aim of this study was to image the vocal cords in children post

airway reconstruction for LTS on static and dynamic MRI and to compare these findings to voice outcome.
Methods and materials: Patients filled out a voice-related questionnaire ((paediatric) voice handicap index (p)VHI), the quality of the voice was tested with the dysphonia severity index (DSI), and static and dynamic upper airway MRI during free-breathing, inspiration and phonation (3T GE scanner, 6CH carotid coil, spatial resolution 0.5x0.5 (in plane) x2 mm, temporal resolution: 240 ms) was performed. Post-surgical anatomy, areas, diameters, and movement of the vocal cords were analysed.
Results: 48 patients (age 14.4 (11.7-19.4) years) and 11 healthy volunteers (age 15.9 (8.4-20) years) were included. Patients showed a high score on the (p)VHI (26.2±18.6%) and a decrease in DSI score (-2.6±2.4 vs 0.68±2.9, p<0.001) compared to healthy volunteers, representing dysphonia. MRI showed vocal cord (80.9%) and arytenoid thickening (59.6%). Furthermore, impaired adduction during phonation (61.7%) was seen, highly correlated to both (p)VHI and DSI score (odds 1.05 (1.01-1.09), p=0.02 and 0.65 (0.48-0.88), p=0.006).
Conclusion: Static and dynamic MRI is an excellent, non-invasive method to visualise the causes of dysphonia in combination with anatomy in paediatric patients with a history of LTS.
Limitations: n/a
Ethics committee approval: Approval by the local medical ethics committee (MEC-2018-013) and written informed consent was obtained.
Funding: Funded by the Vrienden van het Sophia Foundation.
Author Disclosures:
B. Elders: nothing to disclose
M. Hakkesteegt: nothing to disclose
B. Pullens: nothing to disclose
H. A. W. M. Tiddens: nothing to disclose
P. A. Wielopolski: nothing to disclose
P. Ciet: nothing to disclose

RPS 312-7 14:36

A preliminary study assessing a novel neonatal brain MRI in the neonatal ICU

N. Berkovitz[1], E. Ben-David[2], A. Pais[3], D. Rosenbaum[4], Y. Kassierer[2], A. Bin Nun[2]; [1]*Yad-Binyamin/IL,* [2]*Jerusalem/IL,* [3]*Shoham/IL,* [4]*New York/US (nadavber@gmail.com)*

Purpose: To compare images from an experimental 1T permanent MRI scanner in the NICU to clinical 1.5T images.
Methods and materials: This was a prospective, non-randomised, feasibility study. Stable premature infants born prior to 28th week, or born between the 28th-32nd week of pregnancy with IVH, US abnormalities, severe morbidity, or abnormal neurological exam, underwent scanning at near term equivalent age with both conventional 1.5T and dedicated neonatal 1T MRI. MRI scans included T1, T2, and diffusion-weighted imaging performed on a conventional 1.5T (Aera, Siemens) and on a novel 1T MRI (Embrace, Aspect) located in the NICU. No more than 72 hours elapsed between the two studies. 3 radiologists blindly reviewed the images for the following: 10 predetermined anatomical structures, bilateral measurement of ADC values in the supraventricular white matter and vitreous humour, and notation of pathological findings. Findings and comparisons were subject to statistical analysis.
Results: 55 neonates were included in the study. 17 were scanned only on the 1T NICU scanner due to lack of parental consent for a second scan. Identification of the anatomical structures was similar for all 10 locations (P=0.64). Normalised ADC values of the white matter were similar (P=0.31, 0.44 for left and right, respectively). Bland Altman analysis demonstrated excellent agreement. 131 pathological findings were noted involving the parenchyma and ventricles on both scanners. Conspicuity of haemorrhage was slightly better on the 1.5T scanner (P<0.01).
Conclusion: The 1T neonatal scanner performs as well as a clinical scanner and is a potential clinical tool for use in the NICU.
Limitations: At the time of the study, SWI imaging was not available on the 1T scanner.
Ethics committee approval: Approved by IRB. Parental consent required.
Funding: Aspect Imaging.
Author Disclosures:
N. Berkovitz: nothing to disclose
E. Ben-David: nothing to disclose
A. Bin Nun: nothing to disclose
Y. Kassierer: nothing to disclose
A. Pais: Employee at Aspect Imaging
D. Rosenbaum: nothing to disclose

RPS 312-8 14:42

Cerebral white matter alterations in very preterm infants: the contribution of 2D shear-wave elastography

M. Francavilla[1], P. Picq[2], P. Boizeau[2], M. Tanter[2], O. Baud[3], S. Guilmin Crepon[2], V. Biran[2], M. Alison[4]; [1]*Bari/IT,* [2]*Paris/FR,* [3]*Geneva/CH,* [4]*Saint Mande/FR (marianto_fra@hotmail.it)*

Purpose: To describe the brain elasticity of very preterm infants during development compared to term-born controls and to determine the diagnostic role of cerebral quantitative shear-wave elastography (SWE) in preterm children compared to standard cranial ultrasound (US) examination.
Methods and materials: 34 very preterm from 24 to 27+6 gestational weeks (GW) and 47 preterms (28 to 31+6 GW) underwent sequential brain US with elasticity measurement from birth to term.
18 term-born controls had the same protocol at birth.
On conventional US, frontal and parietal white matter (WM) was classified as normal or abnormal according to its echogenicity compared to plexus. Quantitative measurements of brain stiffness were performed with SWE in bilateral frontal and parietal WM and thalami.
Descriptive statistical analysis and multivariate analysis (ANOVA) for comparison between groups were performed.
Results: A progressive increase of brain stiffness was demonstrated with increased gestational age in all brain areas.
Brain stiffness was higher in parietal than in frontal WM at any gestational age.
WM elasticity values measured at term remained significantly lower in both subgroups of preterms compared to controls (p=0.04 and p=0.003 in frontal WM; p=0.003 and p=0.09 in parietal WM).
Brain WM elasticity was similar between preterm infants with or without abnormal WM on standard US examination.
Conclusion: Brain stiffness values change according to the gestational age with an anteroposterior gradient that might reflect normal brain maturation.
WM stiffness of very preterm infants remains lower than control newborns even at term.
Brain stiffness values do not seem to reflect the WM alterations found on conventional US but should be compared to MRI as the gold standard method.
Limitations: The lack of interobserver correlation and the decreasing number of preterms throughout the study.
Ethics committee approval: Ethics committee approval obtained.
Funding: No funding was received for this work.
Author Disclosures:
M. Francavilla: nothing to disclose
M. Alison: nothing to disclose
V. Biran: nothing to disclose
P. Picq: nothing to disclose
P. Boizeau: nothing to disclose
S. Guilmin Crepon: nothing to disclose
O. Baud: nothing to disclose
M. Tanter: nothing to disclose

RPS 312-9 14:48

The neurodevelopmental effect of intracranial haemorrhage observed in hypoxic-ischaemic brain injury in hypothermia-treated asphyxiated neonates: an MRI study

A. Lakatos[1], M. Kolossvary[2], M. Szabó[2], Á. Jermendy[2], H. Barta[2], G. Gyebnár[2], G. Rudas[2], L. R. Kozák[2]; [1]*Miskolc/HU,* [2]*Budapest/HU (drea820317@gmail.com)*

Purpose: The importance of intracranial haemorrhage (ICH) being present concomitantly to hypoxic-ischaemic encephalopathy (HIE) in hypothermia-treated asphyxiated neonates had not been investigated despite the known influence of hypothermia on haemostasis. We aimed to determine whether the presence of ICH on MRI alongside the signs of HIE have an impact on prognosis.
Methods and materials: A retrospective study of 108 asphyxiated term infants treated with whole-body hypothermia having a brain MRI within one week of life was conducted. The presence or absence of HIE signs on MRI and on MR spectroscopy (MRS) and/or of the 5 major types of ICH were recorded. The neurodevelopmental outcome was measured with the BSID-II test. Death or abnormal neurodevelopment (BSID-II score<85) was considered a poor outcome in a Chi-square test. Multivariate logistic regression analysis was performed on the survivors.
Results: MRI and MRS signs of HIE were present in 72% and ICH in 36% of neonates. The Chi-square test showed a relationship between the neurodevelopmental outcome and initial MRI. Unadjusted logistic regression showed that neonates presenting imaging signs of HIE have 6.23 times higher odds for delayed mental development (OR=6.2292; CI95%=[1.2642; 30.6934], p = 0.0246) than infants without imaging alterations, with no ICH effect on the outcome. Adjustment for clinical and imaging parameters did not change the pattern of results.
Conclusion: HIE related MRI abnormalities proved to be important prognostic factors of poor outcome in cooled asphyxiated infants, suggesting that early MRI with MRS is beneficial for prognostication. Interestingly, ICHs present in 36% of

patients had no significant effect on the outcome, despite the known haemostasis altering effects of hypothermia.
Limitations: The retrospective nature of the study.
Ethics committee approval: Institutional and Medical Research Council Ethics Committee of Hungary approved this study. Written informed consent was obtained.
Funding: AJ[PPD460004]; LRK[Bolyai Research Fellowship]; GyGy[EFOP-3.6.3-VEKOP-16-2017-00009].
Author Disclosures:
A. Lakatos: nothing to disclose
M. Kolossvary: nothing to disclose
M. Szabó: nothing to disclose
Á. Jermendy: nothing to disclose
H. Barta: nothing to disclose
G. Gyebnár: nothing to disclose
G. Rudas: nothing to disclose
L. R. Kozák: nothing to disclose

RPS 312-10 14:54

Quantitative paediatric MRI going clinical: comprehensive brain assessment from a single sequence based on quantitative brain maturation atlases

B. Morel[1], G. F. Piredda[2], T. Hilbert[2], C. Tauber[1], J. P. Cottier[1], B. Maréchal[2], T. Kober[2]; [1]*Tours/FR,* [2]*Lausanne/CH (doc.baptiste@gmail.com)*

Purpose: A quantitative anatomical 3D sequence was optimised for paediatric application and used to build quantitative brain maturation atlases, mapping both the volumetric and T1-relaxometry changes. This allows for a comprehensive assessment of anatomy, morphometry, and a marker for brain microstructure (T1 relaxometry).
Methods and materials: We performed a two-year single-centre prospective study recruiting infants aged 1-16 years from a university hospital to be scanned at 1.5T (MAGNETOM Aera, Siemens Healthcare, Erlangen, Germany) using a 20-channel head coil without sedation. A single prototype MP2RAGE scan (TI1/TI2=600/2,000 ms, TR=5,000 ms, voxel size=1.33x1.33x1.25 mm^3 isotropic, TA=6:42 min) was performed. The supposed medical condition was an isolated headache with spontaneously favourable evolution. Brain maturation was modelled based on resulting T1 maps and volumetry (using the MorphoBox prototype adapted for paediatrics).
Results: 63 normal brain MRIs (33 female) were obtained. Automated segmentation and T1-mapping was successful in all scans. The evolution of volumes and T1 values were modelled over age to obtain reference ranges (without gender difference). The absolute volume of white matter increased continuously during childhood, with stable cortical grey matter volumes. Reference regional T1 values decreased rapidly during the first two years of age (supposedly showing myelinisation) and then more smoothly.
Conclusion: In addition to anatomical T1 images, the 3D MP2RAGE sequence allows for automated morphometric and relaxometry assessment. Based on this data, we created reference brain maturation atlases covering the entire childhood which have the potential to quantitatively support clinical decision making in paediatrics.
Limitations: A single-centre study with a limited sample of patients.
Ethics committee approval: Approved by the local ethics committee for human research (RNI-2017-093).
Funding: GF Piredda, T Hilbert, B Maréchal, and T Kober are Siemens Healthineers employees.
Author Disclosures:
B. Morel: nothing to disclose
G. F. Piredda: nothing to disclose
T. Hilbert: Employee at Siemens Healthineers
J. P. Cottier: nothing to disclose
B. Maréchal: Employee at Siemens Healthineers
C. Tauber: nothing to disclose
T. Kober: Employee at Siemens Healthineers

RPS 312-11 15:00

Frequency-dependent changes of interhemispheric functional connectivity and aberrant cerebral synchronisation in idiopathic generalised epilepsy

X. Ma, L. Jiang, S. Li, T. Zhang*; Zunyi/CN (mxj2439630056@163.com)*

Purpose: To characterise the functional connectivities (FC) frequency-dependency between hemispheres and the alteration within the cerebral in patients with idiopathic generalised epilepsy (IGE).
Methods and materials: Resting-state functional imaging was performed in 21 patients with IGE and 22 healthy controls. The FC for different frequency bands between the bilateral hemispheres and within the cerebral were calculated and within-group differences were analysed. Altered interhemispheric FC regions shown in patients were selected as seed regions for cerebral FC analysis. Two-way ANOVA and threshold-free cluster enhancement were performed.
Results: Compared with the controls, patients with IGE showed decreased interhemispheric FC between the bilateral orbitofrontal cortex in the full frequency band (0.01-0.1 Hz) the putamen and the superior temporal gyrus in the slow-4 band (0.027-0.073 Hz), and the orbitofrontal cortex and lingual gyrus in the slow-5 band (0.01-0.027 Hz). Moreover, the cortical-subcortical FC was decreased, the connection within the default mode network (DMN) was segregated into the front and back parts, and the DMN and auditory perceptual processing network was enhanced.
Conclusion: Our findings suggested that the FC in patients with IGE is frequency-dependent and the interaction alteration of cortical-subcortical and the coupling change of brain functional networks may play a crucial role in the pathophysiology of IGE.
Limitations: We acquired the r-fMRI data without recording the patient's simultaneous EEG data. Some patients in this study are taking antiepileptic drugs, which may have effects on cognitive ability and inhibiting the functional synchronisation of brain networks. The sample size of our study is relatively small.
Ethics committee approval: The retrospective study was approved by the local medical ethics committee and written informed consent was obtained.
Funding: Zunyi Science and Technology Cooperation Program (Number: (2017) 46).
Author Disclosures:
X. Ma: nothing to disclose
L. Jiang: nothing to disclose
S. Li: nothing to disclose
T. Zhang: nothing to disclose

RPS 312-12 15:06

Fibre tractography and diffusion tensor imaging in children with corpus callosum anomalies: a clinico-radiologic correlation

N. F. El Ameen, M. Ibraheim, S. Mounir*; ElMinia/EG (nadia.elameen@yahoo.com)*

Purpose: To evaluate the role of fibre tractography (FT) and diffusion tensor imaging (DTI) of the brain in paediatric patients with corpus callosum anomalies and correlate the findings with the clinical presentation.
Methods and materials: A prospective study included 115 children with CT findings suggested corpus callosum anomalies. Their ages ranged from 4 months-8 years old. All patients were referred from a paediatric neurology unit to the radiology department from April 2018-December 2018. All patients underwent MRI tractography and diffusion tensor imaging.
Results: Our study included 42 males and 73 females. They were reviewed for the presence and type of corpus callosum anomalies according to the Hanna classification. The most common type was hypoplasia without dysplasia 37/115 (32 %). An isolated anomaly was seen in 90/115 (78.3%). Using DTI and fibre tractography, corpus callosum fibre defects were classified into fronto-rostral, caudal, and whole body. A significant statistical correlation was found between ADHD as well as autism and loss of fronto-rostral fibres. Epilepsy and developmental delay were correlated to a whole-body defect and caudal fibre tract defects.
Conclusion: Fibre tractography and diffusion tensor imaging are promising techniques in the assessment of patients with corpus callosum anomalies. They provide accurate localisation of the affected segment of callosal fibres and help to predict the clinical prognosis of patients that could not be explained by the morphological changes seen in conventional MRI alone.
Limitations: The small number of patients and the need for anesthesia in most of the patient cohort.
Ethics committee approval: The study was done after the approval of ethical committee of our institution and after written informed consent of patients' parent before the examination and before anesthesia.
Funding: No funding was received for this work.
Author Disclosures:
N. F. El Ameen: nothing to disclose
M. Ibraheim: nothing to disclose
S. Mounir: nothing to disclose

RPS 312-13 15:12

Posterior reversible encephalopathy syndrome in children: the association of blood pressure with imaging severity

K. Khandwala[1], K. Hilal[1], N. Sajjad[1], A. Malik[2]; [1]*Karachi/PK,* [2]*Atlanta/US (kumail.khandwala@gmail.com)*

Purpose: To evaluate the association and correlation between blood pressure (BP) and posterior reversible encephalopathy syndrome (PRES) imaging severity in the paediatric population in whom radiological features and pathophysiology remains obscure.

Methods and materials: A retrospective evaluation of paediatric patients diagnosed with PRES over the last 10 years at Aga Khan University was performed. Radiological findings were reviewed by two paediatric radiologists along with the clinical profile and outcome. Imaging severity was categorised into mild, moderate, and severe. The distribution of lesions, enhancement, diffusion restriction, and haemorrhage were assessed. Various conditions that may resemble PRES were excluded.
Results: Out of 43 children, 20 were males and 23 were females with a mean age of 10.7 years. The most common primary disease was malignancy (28%) out of which lymphoma predominated. The mean systolic BP was 131.5 (70-205) mmHg and diastolic was 82.9 (35-170) mmHg. 14 children had hypertension higher than autoregulatory limits. Imaging showed a parieto-occipital lobe involvement pattern in 42% of cases, holohemisphereic pattern in 30.2%, cerebellar involvement in 23.3%, and superior frontal sulcus pattern in 2.3%. 4.7% had a haemorrhage, 25.6% had contrast enhancement, and 27.9% had a positive diffusion restriction (cytotoxic oedema). No statistically significant association of imaging severity with BP (P=0.70), imaging severity with haemorrhage (P=0.30), and diffusion restriction (P=0.64) with imaging severity and with each other (P=1) was seen.
Conclusion: We did not find any statistically significant association of blood pressure with imaging severity, haemorrhage, and diffusion restriction (cytotoxic oedema). Further prospective studies are needed to determine the pathophysiological mechanisms and their correlation with imaging findings in PRES in children.
Limitations: The retrospective study design and single-centre study.
Ethics committee approval: Ethics committee approval obtained.
Funding: No funding was received for this work.
Author Disclosures:
K. Khandwala: nothing to disclose
K. Hilal: nothing to disclose
N. Sajjad: nothing to disclose
A. Malik: nothing to disclose

RPS 312-14 15:18
Cerebral perfusion in children sedated with propofol: an arterial spin labelling (ASL) study
V. Maruotti, E. Piccirilli, P. Chiacchiaretta, A. Ferretti, V. Panara, M. Caulo; *Chieti/IT (valeriomaruotti@gmail.com)*

Purpose: Paediatric MRI is highly dependent on anaesthesia, but sedative-hypnotic drugs can modify the cerebral metabolic rate and cerebral perfusion. Arterial spin labelling (ASL) MRI allows the investigation of brain perfusion without administrating contrast material.
We sought to evaluate the effects of propofol on the dynamic of cerebral perfusion in early childhood.
Methods and materials: 21 young children (2-5 years old) had an MRI performed using a 3T scanner. None of the children were premature, nor had a stroke, brain tumour, metabolic diseases, seizure, or brain malformations. Patients were sedated immediately before the MRI with an intravenous bolus of propofol. ASL was performed after the reference scout in 7 children (t1a), 3 minutes later in 7 children (t1b), and 6 minutes later in 7 children (t1c). All children underwent ASL at the end of sedation (t2 a, b, c). Individual brain perfusion maps were extracted to evaluate the average whole-brain perfusion (WBP). Mean values of CBF for each group were determined and the differences between groups using a t-test.
Results: The mean CBF (mL/100 g/min) were (t1) 34.7 ±6.4 and (t2) 32.6 ±6.7 (p= 0.0004). The subgroup values were (t1a) 34.6 ± 5, (t2a) 31.2 ± 5.1, (t1b) 31.3 ± 6, (t2b) 29.4 ± 5.1, (t1c) 38.2 ± 6.8, and (t2c) 37.3 ± 7.7. The difference between t1a and t2a (p= 0.004) was more significant than between t1b and t2b (P=0.028). The difference between t1c and t2c (P=0.363) was not statistically significant.
Conclusion: During sedation with propofol, cerebral perfusion decreases from oversedation.
Limitations: The small size.
Ethics committee approval: The institutional review board approved this prospective study.
Funding: No funding was received for this work.
Author Disclosures:
V. Maruotti: nothing to disclose
E. Piccirilli: nothing to disclose
P. Chiacchiaretta: nothing to disclose
A. Ferretti: nothing to disclose
V. Panara: nothing to disclose
M. Caulo: nothing to disclose

14:00 - 15:30 **Room M 1**

Abdominal Viscera

RPS 301a

Pancreas and biliary disease

Moderators:
M. C. Ambrosetti; Verona/IT
S. K. Puri; New Delhi/IN

RPS 301a-1 14:00
Magnetic resonance (MR) in the identification of mural nodules of intraductal papillary mucinous neoplasms (IPMN) of the pancreas
G. Giannotti, A. Drudi, A. Lucarelli, A. Beleù, G. Rizzo, C. Longo, N. Cardobi, R. de Robertis Lombardi, M. D'onofrio; *Verona/IT (gabriele200590@gmail.com)*

Purpose: To evaluate the diagnostic accuracy of dynamic magnetic resonance (MR) with diffusion weighted imaging (DWI) in the identification of mural nodules of intraductal papillary mucinous neoplasms (IPMN) of the pancreas.
Methods and materials: 91 preoperative MRI scans with histopathological diagnosis of IPMN were reviewed by two radiologists. They evaluated the presence, number, and size of mural nodule, the SI of the nodule on T1-WI after i.v. contrast medium administration and on DWI, and the size of the cystic lesion and dilation of the main pancreatic duct. Two pathologists reviewed each case, evaluating the presence, number, and size of papillary structures, and the degree of epithelial dysplasia. Qualitative and quantitative analysis were performed. Interobserver agreement was calculated.
Results: Statistically significant differences were found for the following correlations: presence of nodules >5mm on MRI and confirmed by pathological review, size and number of mural nodule on pathological review and degree of dysplasia, size and number of mural nodule evaluated on MRI and tumoral dysplasia, presence of nodule >5mm with post-contrast enhancement and hyperintensity on DWI and degree of dysplasia, dilation of MPD and tumoral dysplasia. Interobserver agreement was moderate for the presence of mural nodule (K=0.56), the presence of high signal intensity on DWI (K=0.60), and enhancement of mural nodule (K= 0.58). Histogram analysis of ADC map showed a correlation between entropy of the entire cystic lesion and the degree of dysplasia.
Conclusion: Dynamic MRI with DW imaging has a good accuracy in the detection of IPMN mural nodule >5mm. DWI and T1-WI after contrast medium administration can be useful in the evaluation of malignancy of IPMN. Entropy could be used as a predictive parameter of malignancy of IPMN.
Limitations: None
Ethics committee approval: n/a
Funding:
No funding was received for this work.
Author Disclosures:
G. Giannotti: nothing to disclose
A. Drudi: nothing to disclose
A. Lucarelli: nothing to disclose
A. Beleù: nothing to disclose
G. Rizzo: nothing to disclose
C. Longo: nothing to disclose
N. Cardobi: nothing to disclose
R. de Robertis Lombardi: nothing to disclose
M. D'onofrio: nothing to disclose

RPS 301a-2 14:06
Branch-duct intraductal papillary mucinous neoplasms of the pancreas: a 10 year follow-up of the safety of a surveillance MRI protocol
P. Boraschi, G. Tarantini, F. M. Donati, R. Cervelli, P. Scalise, D. Caramella; *Pisa/IT (p.boraschi@gmail.com)*

Purpose: To assess the safety of a surveillance MRI protocol through a 10 year follow-up of patients with branch-duct intraductal papillary mucinous neoplasms (BD-IPMNs) of the pancreas.
Methods and materials: All patients with “presumed” MR diagnosis of BD-IPMNs observed from 2008 to 2009 were retrospectively recruited from our radiological database. Only patients without worrisome features (WF) and/or high-risk stigmata (HRS) at diagnosis were enrolled. MRI protocol included axial T1w/T2w sequences, MRCP, and diffusion-weighted MRI with multiple b values. Contrast-enhanced T1-weighted sequences were obtained only at the baseline and if there was a suspicion of degeneration during the follow-up. The policy for follow-up consisted of abdominal MRI/MRCP every 6 months in the first 2 years from diagnosis and then each year in absence of clinical/radiological signs of progression. Cyst growth rate analysis and development of WF, HRS, and

pancreatic cancer (PC) during follow-up were evaluated. Patients with missing data and/or without 10 years follow-up were excluded from analysis.
Results: 69 patients fulfilling all the inclusion criteria represented our study group. During surveillance, five out of 69 patients (7%) underwent surgery (PC, n=2; IPMN with low grade dysplasia, n=3). WF and HRS developed in 10/69 (14,5%) and 3/69 (4%) cases, respectively. The cysts were dimensionally unchanged or slightly reduced in size in 18/69 (26%) and 3/69 (4,3%) patients, respectively. In the remaining 48/69 (69,5%) cases, cyst enlargement was appreciable with a median annual growth rate of 0,97±0,87 mm/yr (range: 0,13-5,0 mm).
Conclusion: In our series, pancreatic BD-IPMNs slowly grow over the time. Worrisome features, high-risk stigmata, and pancreatic cancer developed in a low percentage of patients, supporting the safety of our surveillance MRI protocol.
Limitations: Retrospective study.
Ethics committee approval: n/a
Funding:
No funding was received for this work.
Author Disclosures:
P. Boraschi: nothing to disclose
G. Tarantini: nothing to disclose
F. M. Donati: nothing to disclose
R. Cervelli: nothing to disclose
P. Scalise: nothing to disclose
D. Caramella: nothing to disclose

RPS 301a-3 14:12
Magnetic resonance morphologic features predict progression of incidental pancreatic cystic lesions during follow-up
S. Zhu, S.-X. Rao*; [1]Shanghai/CN (616209440@qq.com)*

Purpose: To evaluate which magnetic resonance (MR) morphologic features could predict the progression of pancreatic cystic lesions (PCLs) that were suitable for follow-up.
Methods and materials: A total of 2,176 MR images of PCLs were retrospectively reviewed between January 2009 and December 2016. The study population was composed of 223 patients. Clinical data and MR morphologic features of PCLs were recorded. We divided the individuals into two subgroups according to the final MR features. Univariable and multivariable regression analyses were performed to identify independent risk factors for progression of PCLs.
Results: 37.7% (84/223) PCLs progressed during follow-up, compared to 62.3% (139/223) PCLs that were stable. Age (odds ratio (OR) = 1.042; p = 0.017), number of lesions (OR = 0.491; p = 0.048), communication to pancreatic duct (PD) (OR = 2.425; p = 0.007), and the septa (OR = 6.105; p < 0.001) were significant independent factors for progression of PCLs. Among 84 lesions of progression, 27.4% (23/84) lesions increased to ≥ 30 mm or showed worrisome imaging features at the end of follow-up, which needs clinical interventions. The initial size and communication to PD were independent factors for progression of PCLs which needs clinical interventions (p < 0.001 and 0.011, respectively).
Conclusion: Age, number of the lesions, communication to PD, and the septa were independent risk factors for the progression of PCLs, and the initial size and communication to PD could potentially predict PCLs needing clinical interventions.
Limitations: We selected patients by reviewing the diagnostic reports. We did not collect the laboratory results. There is a difference in magnetic field strength.
Ethics committee approval: The Ethics Committee at Zhongshan Hospital of Fudan approved this retrospective research and waived the informed patient consent.
Funding: No funding was received for this work.
Author Disclosures:
S. Zhu: nothing to disclose
S.-X. Rao: nothing to disclose

RPS 301a-4 14:18
The value of diffusion-weighted imaging in the grading of pancreatic neuroendocrine neoplasms
W. Mingliang, Z. Mengsu*; Shanghai/CN (wang.mingliang@zs-hospital.sh.cn)*

Purpose: To evaluate the value of diffusion-weighted imaging (DWI) for the grading of pancreatic neuroendocrine neoplasms (pNEN).
Methods and materials: MR images and pathological data of 72 patients with pathologically confirmed pNEN were analysed retrospectively. PNEN was classified into pNETG1, pNETG2, pNETG3, and pNECG3 according to WHO's 2017 latest classification. ADC values of tumour and pancreas were measured.
Results: All 72 cases of pNEN were single lesion and the pathological grade was 18 cases of pNETG1, 36 cases of pNETG2, 13 cases of pNETG3, and 5 cases of pNECG3. ADC value of pNEN was negatively correlated with ki-67 (r=-0.845, P < 0.001). There were statistically significant differences in ADC values between pNETG1 and pNETG2, pNETG1 and pNETG3, pNETG1 and pNECG3, pNETG2 and pNETG3, and pNETG2 and pNECG3 groups (P < 0.001). There was no statistically significant difference in ADC values between pNETG3 and pNECG3 groups (P=0.233). The ADC value =1.596x10^{-3}mm^2/s was used as the cutoff value to distinguish the sensitivity and specificity of 97.22% and 83.33% of grade G1 and G2 pNEN, and the area under ROC curve was 0.941 (Z=13.340, P < 0.001). The ADC value =1.103x10^{-3}mm^2/s was used as the cutoff value to distinguish the sensitivity of 83.33% and specificity of 100% of G2 and G3 panNEN, and the area under ROC curve was 0.968 (Z=18.830, P < 0.001).
Conclusion: ADC values of tumours are helpful for the grading of pancreatic neuroendocrine neoplasms.
Limitations: The number of cases included in G3 (both pNETG3 and pNECG3) was small.
Ethics committee approval: The retrospective study was approved by the institutional review board of our hospital.
Funding: No funding was received for this work.
Author Disclosures:
W. Mingliang: nothing to disclose
Z. Mengsu: nothing to disclose

RPS 301a-5 14:24
The relationship between the portal radiomics score and G1/2 non-functional pancreatic neuroendocrine tumours
Y. Bian, H. Zhang, X. Fang, L. Wang, J. Lu, G. Jin*; Shanghai/CN (bianyun2012@foxmail.com)*

Purpose: To explore the exact relationship between the portal radiomics score (rad-score) and the grading in non-functional pancreatic neuroendocrine tumours (NF-pNETs), and evaluate the diagnostic performance of the rad-score.
Methods and materials: In this retrospective study, 102 patients with surgically resected, pathologically confirmed NF-pNETs underwent MSCT from January 2014 to December 2017. Radiomic features were extracted from portal venous CT scans. The least absolute shrinkage and selection operator method was used to select the features. Multivariate logistic regression models were utilised to analyse the association between the portal rad-score and grades of NF-pNETs. The portal rad-score performance was determined by its discrimination and clinical usefulness.
Results: The portal rad-score, which consisted of 4 selected features, was significantly associated with grades of NF-pNETs. High-risk patients had a 1.56-fold increased risk of G2 compared with low-risk patients. The portal rad-score was in its high accuracy (AUC=0.86 in all size, AUC=0.81 in size 2 cm). The best cut point based on maximising the sum of sensitivity and specificity was -0.134. The decision curves showed that if the threshold probability is above 0.02, using the rad-score in the current study to G1/2 NF-pNETs adds more benefit than the treat-all-patients scheme or the treat-none scheme.
Conclusion: The portal rad-score is a potentially valuable noninvasive tool for accurate preoperative prediction of grades for NF-pNETs.
Limitations: Firstly, this study was retrospective in nature. Secondly, we did not validate the rad-score with an external data cohort - this could form the topic of a future study.
Ethics committee approval: This retrospective single-center cross-sectional study was reviewed and approved by the Biomedical Research Ethics Committee of Changhai hospital.
Funding: National Science Foundation for Scientists of China (81871352, 81701689), Top Project of the Military Medical Science and Technology Youth Training Program (17QNP017).
Author Disclosures:
Y. Bian: nothing to disclose
H. Zhang: nothing to disclose
X. Fang: nothing to disclose
L. Wang: nothing to disclose
J. Lu: nothing to disclose
G. Jin: nothing to disclose

RPS 301a-6 14:30
Diffusion-weighted imaging of autoimmune pancreatitis: how good is it as an imaging biomarker for disease activity?
L. Zhu[1], P. Asbach[2], T. Denecke[3], B. Hamm[2], Z. Jin*[1]; [1]Beijing/CN, [2]Berlin/DE, [3]Leipzig/DE*

Purpose: To evaluate diffusion-weighted imaging (DWI) features of autoimmune pancreatitis (AIP) at baseline, under treatment, and at relapse, and to compare with a disease-free pancreas.
Methods and materials: 62 patients with AIP (48 with initial attack and 14 with relapsed disease) underwent MRI with DWI (b =0 and 800sec/mm^2) at 3T. All patients received corticosteroid therapy (CST) with MR follow-up. 17 relapses were found during follow-up, whereas the remaining remained clinically stable. 40 gender-and age-matched patients without pancreatic disease served as control.

Results: The ADC value of AIP at baseline was significantly decreased compared to a disease-free pancreas (985.5±116.5 mm^2/s vs 1256.7±102.4 mm^2/s, p<0.001). During CST, the ADC value increased within 6 months, and further increased after 1 year (1174.8±122.1 mm^2/s and 1230.1±157.5 mm^2/s, respectively). At relapse, there was an relative decrease of ADC value (1104.8±200.5 mm^2/s), however, the value was significantly higher compared to the initial attack (p<0.001). Receiver-operating curve analysis yielded an area under the curve (AUC) of 0.876 for differentiating baseline AIP from a normal pancreas, an AUC of 0.701 for clinically active AIP (baseline + relapse) vs a normal pancreas, and an AUC of 0.544 for relapsed AIP vs a normal pancreas.
Conclusion: DWI might be useful in monitoring the dynamic change of AIP under CST. However, relapsed disease show less diffusion restriction than the initial attack and the absolute ADC value doesn't determine the disease activity of AIP.
Limitations: This was a retrospective study from a single institution and further multicenter validation studies are needed.
Ethics committee approval: The institutional review board approved this study and all patients gave written informed consent that their clinical and imaging data could be used for scientific purposes.
Funding: This study was founded by the national natural science foundation of China (81901716).
Author Disclosures:
L. Zhu: nothing to disclose
P. Asbach: nothing to disclose
T. Denecke: nothing to disclose
B. Hamm: nothing to disclose
Z. Jin: nothing to disclose

RPS 301a-7 14:36
Differentiation of pancreatic adenocarcinoma from surrounding pancreatic tissue using the shortened MR protocol: histogram analysis of T2W signal intensity and ADC
D. T. Šarac, A. Djuric-Stefanovic*; Belgrade/RS (dimitrije.sarac89@gmail.com)*

Purpose: To evaluate whether pancreatic adenocarcinoma (PAC) could be accurately differentiated from the surrounding pancreatic tissue (PT) using the shortened MR scanning protocol by quantitative analysis of ADC and T2W signal intensity including the histogram-derived analysis.
Methods and materials: We retrospectively analysed 31 cases of PAC who underwent shortened 1.5T-MRI scanning protocol, which consisted of T2W FSSE and diffusion-weighted imaging (DWI) sequence with the apparent diffusion coefficient (ADC) by using two b values (0 and 800 mm^2/s). Tumour and surrounding pancreatic tissue were segmented on three consecutive the-largest-tumour-area sections in T2W series and the corresponding ADC map. Histogram analysis of T2W signal of PAC and PT was performed using MAZDA software. Mean values of ADC and T2W signal intensity and histogram-derived quantitative parameters (variance, skewness, kurtosis, minimum and maximum normalised values) of PAC and PT were compared using the paired-samples-t or Wilcoxon test depending on normality of parameter distribution, which was explored using the Shapiro-Wilk test.
Results: Mean ADC of PAC (1.537±0.221x10^{-3} mm^2/s) did not significantly differ from PT (1.555±0.196x10^{-3} mm^2/s) (p=0.644). Mean value of T2W signal intensity of PAC (median, 639.46) was non-significantly higher (p=0.410) than PT (589.76). Of histogram-derived parameters, variance of T2W signal intensity was significantly lower (p=0.030), kurtosis of histogram was higher (p=0.050), and minimum normalised signal intensity was significantly higher (p<0.001) in PAC than in PT.
Conclusion: Histogram-derived quantitative analysis of T2W signal intensity improves accuracy in differentiation of PAC from surrounding pancreatic tissue on shortened MRI scanning protocol.
Limitations: There were no obvious limitations.
Ethics committee approval: n/a
Funding: No funding was received for this work.
Author Disclosures:
D. T. Šarac: nothing to disclose
A. Djuric-Stefanovic: nothing to disclose

RPS 301a-8 14:42
Imaging-related delays in the diagnosis of pancreatic ductal adenocarcinoma: a multi-centered population-based observational study
J. Kang, S. Clarke, M. Abdolell, R. Ramjeesingh, J. I. Payne, A. Costa*; Halifax/CA (jessie-dain@Dal.Ca)*

Purpose: To determine the diagnostic interval of patients with pancreatic ductal adenocarcinoma (PDAC) in our region's population and which factors, including imaging-related delays, may impact survival.
Methods and materials: This study evaluated 257 patients (129 men, 128 women; mean 71.8 years) diagnosed with PDAC from 2014-2015. Patient data was retrieved from the Cancer Registry database, including demographics, stage, and dates of initial presentation/diagnosis and death.
The imaging archive was searched for US, CT, and MRI examinations performed during the diagnostic interval; these were independently rated by two radiologists according to the American College of Radiology RADPEER system. Univariate Kaplan-Meier analysis was performed for age (<65, 65-79, 80), sex, tumour location, stage, surgery, and RADPEER score. Multivariate Cox proportion hazards model was performed to assess for association between these covariates and survival.
Results: RADPEER 1-2 and 3 scores were assigned to 219 and 38 patients, respectively. The overall diagnostic interval was 77 days; this was much longer in the RADPEER 3 group (190 vs. 58 days, p=0.018). However, K-M analysis showed worse survival in the RADPEER 1-2 group (p=0.007).
Survival was also worse with distal PDAC (p=0.016), stage (p<0.0001), and no surgery (p<0.001). Survival was similar amongst the sexes (p=0.083). The Cox proportional hazards model showed better survival in women (p=0.008) and surgical patients (p<0.001), and worse survival in patients aged >80 years (p=0.016) and with stage IV disease (p=0.006).
Conclusion: Imaging-related delays are associated with much longer diagnostic intervals. However, this did not impact survival in our population.
Limitations: Retrospective study, registry data, other factors associated with survival: patient's comorbidities.
Ethics committee approval: Research ethics board approval and PHIA adherence.
Funding: No funding was received for this work.
Author Disclosures:
J. Kang: nothing to disclose
A. Costa: nothing to disclose
S. Clarke: Research/Grant Support at GE Healthcare
M. Abdolell: CEO at Densitas Inc.
J. I. Payne: nothing to disclose
R. Ramjeesingh: nothing to disclose

RPS 301a-9 14:48
The prevalence and stability predictors of pancreatic lesions screened by non-contrast whole-body MRI
C. Xue[1], G. Lo[2], O. L. Wong[3], J. Yuan[3]; *[1]Hong Kong/HK, [2]Happy Valley/CN, [3]Hong Kong/HK (cindy.xue21@gmail.com)*

Purpose: To evaluate prevalence and stability predictors of pancreatic lesions (PLs) using non-contrast whole-body MRI (WBMRI) screening.
Methods and materials: 3236 consecutive healthy subjects (1765 male, 1471 female, mean: 55±13 years, range: 20-92 years) receiving non-contrast WBMRI using 1.5T or 3T MRI scanners covering brain, neck, thorax, abdomen, pelvis, and spine from 2008-2018 were retrospectively analysed. Abdomen protocol included T2w-TSE, T1w-FS, and DWI. Images were evaluated by radiologists (10+ years of experience). Subjects with PLs were identified and necessary follow-ups (interval: 1-9 years) were conducted to confirm the PLs' nature. Prevalence was counted as the proportion of PL reported to the total of WBMRI cases. PLs were divided into 2 groups (I: need treatment/close-monitor, II: simple/benign cysts). Pearson-correlation was conducted to evaluate the relationship between prevalence of PL and age. Chi-square and t-test were used to evaluate PL stability regarding sex and PL size.
Results: In this study, 74 (2.3%) subjects (40 males, 34 females) with PL were observed using WBMRI. Group I included 2 pancreatic carcinoma, 9 intraductal papillary mucinous neoplasms (IPMN), 1 serous cystadenoma, and 4 pancreatic cysts with changes in size/number/density. Group II consisted of 58 stable pancreatic cysts. PLs' size ranged from 0.1-4 cm (mean:0.6±0.6mm). Group I had significantly larger PLs (size:1±0.95mm) compared to group II (size:0.52±0.5mm)(p<0.05), with no significant difference in gender (p=0.066) or age (p=0.42) between groups.
Prevalence of PL was age-dependent (Pearson-coef.=0.35;p<0.005), with no pancreatic lesion found in subjects under 30 years old, and gender-independent (p=0.8;2.3%(male),2.3%(female)).
Conclusion: Prevalance of PL screened by WBMRI is 2.3%, and is age-dependent but gender-independent. PL size might be a potential predictor of whether further treatment/close-monitoring is needed.
Limitations: This is a retrospective study, hence, an inadvertent bias could not be excluded.
Ethics committee approval: Ethical approval has been obtained.
Funding: No funding was received for this work.
Author Disclosures:
C. Xue: nothing to disclose
G. Lo: nothing to disclose
O. L. Wong: nothing to disclose
J. Yuan: nothing to disclose

RPS 301a-10 14:54

Quantitative magnetic resonance imaging of the pancreas in patients with type-2 diabetes mellitus

T. H. Waddell, D. Halliday, A. Dennis, H. R. Wilman, R. Nicholls, M. Kelly, R. Banerjee*; Oxford/UK (tom.waddell@perspectum.com)*

Purpose: Traditional techniques for characterising pancreatic tissue such as endoscopy and computed tomography are invasive, limited by interobserver variability and lack sensitivity. Magnetic resonance imaging (MRI) successfully predicts liver outcomes, correlates with histology, and does not use ionizing radiation. MRI is emerging as a promising technique for monitoring the pancreas in patients with T2DM. Here we explore the utility of multiparametric MRI of the pancreas within a cohort of T2DM participants compared to healthy participants.
Methods and materials: 459 participants underwent a pancreatic MRI scan as part of the UK Biobank imaging study. 3 regions of interest (10mm) were placed on proton density fat fraction (PDFF) and T1 (a fibroinflammation biomarker) maps in the head, body, and tail of the pancreas. PDFF and T1 values were successfully acquired from 90.8% and 90.4% of scans, respectively. Participants were excluded if pancreatic T2* measured < 23.1 ms (high iron). Data from 126 participants (20 T2DM/106 healthy) were included for analysis.
Results: Two-sample Kolmogorov-Smirnov tests revealed T2DM participants had significantly greater PDFF than healthy participants (6.79% vs 3.09%, p < 0.0001), and there was a trend towards increased T1 in T2DM patients (639ms vs 603ms, p = 0.2). PDFF was not uniformly distributed within the pancreas with a trend towards increased fat in the body compared to the head and tail of the pancreas (T2DM: head 4.94%, body 7.06%, tail 4.57%; healthy: head 2.69%, body 3.28%, tail 3.07%). Data is presented as median.
Conclusion: Multi-parametric MRI had a high success rate for quantitative characterisation of pancreatic tissue, even in this high-throughput epidemiological study. Pancreatic PDFF, but not T1, was significantly higher in patients with T2DM vs heathy participants.
Limitations: Single analyst.
Ethics committee approval: n/a
Funding: No funding was received for this work.
Author Disclosures:
T. H. Waddell: Employee at Perspectum Diagnostics , Shareholder at Perspectum Diagnostics
D. Halliday: Other at Perspectum Diagnostics
A. Dennis: Employee at Perspectum Diagnostics , Shareholder at Perspectum Diagnostics
H. R. Wilman: Other at Perspectum Diagnostics
R. Nicholls: Employee at Perspectum Diagnostics , Shareholder at Perspectum Diagnostics
M. Kelly: Employee at Perspectum Diagnostics , Shareholder at Perspectum Diagnostics
R. Banerjee: CEO at Perspectum Diagnostics , Board Member at Perspectum Diagnostics , Shareholder at Perspectum Diagnostics , Founder at Perspectum Diagnostics

RPS 301a-11 15:00

The relationship between pancreas divisum subtypes, bile duct variation, and portal vein variation

M. K. Şimşek, C. Altay, H. A. Özgül, I. Başara Akin, M. Seçil*; Izmir/TR (mkursatsimsek9@gmail.com)*

Purpose: To evaluate the incidence of the biliary duct (BD) and portal vein (PV) variations by magnetic resonance cholangiopancreatography (MRCP), contrast-enhanced computed tomography (CECT), and MR imaging (MRI) in patients with pancreatic divisum (PD) and control group patients.
Methods and materials: A retrospective study was performed from January 2010 to October 2018 in a single high-volume centre. Patients who had hepatobiliary surgery, malignancy, or pancreatitis were excluded. 199 patients with PD (age: 57.6±15,2 years, F=114, M=85), and 55 patients without any pancreatic variation (age: 61,1±14,3 years, F=28, M=27) who underwent MRCP, CECT, and/or MRI were enrolled. Two experienced radiologists assessed all the images for the variation of the BD and PV. The Chi-Square test was used with IBM SPSS 24.0 package program (SPSS Inc, Chicago, IL, USA).
Results: Of all 199 patients with PD, 57 patients (28,6%) were classified as PD type I, 48 (24,1%) were type II, and 94 (47,3%) were type III. BD and PV variations were found in 61.4% and 51.1% of the patients with PD, respectively. 11 patients without PD (20%) have BD variations, and 9 (16,3%) have PV variations. There were statistically significant differences between the control group and patients with PD, and PD subtypes and PV and BD variations ratio (P<0.05).
Conclusion: PD is the most common pancreatic variation. To have knowledge about pancreas divisum, bile duct and portal vein variations is essential in hepatobiliary surgery planning.
Limitations: The number of the patients was limited.
Ethics committee approval: Ethical committee approval was obtained.
Funding: No funding was received for this work.
Author Disclosures:
M. K. Şimşek: nothing to disclose
C. Altay: nothing to disclose
M. Seçil: nothing to disclose
I. Başara Akin: nothing to disclose
H. A. Özgül: nothing to disclose

RPS 301a-12 15:06

Camera-based respiratory triggering improves image quality of 3D magnetic resonance cholangiopancreatography

F. N. Harder, F. Lohöfer, G. Kaissis, C. Zöllner, O. Kamal, A. Hock, E. J. Rummeny, D. C. Karampinos, R. Braren*; Munich/DE (Felix.Harder@tum.de)*

Purpose: To evaluate the performance of a novel camera-based breathing navigation system in respiratory-triggered (CRT) 3D-magnetic resonance cholangiopancreatography (MRCP) at 3T MRI.
Methods and materials: Two compressed sensing (CS) accelerated 3D-MRCP data sets were acquired subsequently within one imaging session with traditional respiratory belt- (BRT) or camera- (CRT) based triggering in 28 patients. The CS factor was 15. Overall image quality, blurring, motion artifacts, and discernibility of the pancreaticobiliary tree (PBT) were scored on a 4-point scale retrospectively by two radiologists. The contrast ratio between the common bile duct and its adjacent tissue was measured by region-of-interest (ROI) analysis. Signal intensity increase at the boundaries of the ducts was quantified byline profilesto objectify blurring and motion artifacts. Furthermore, extracted respiratory signal curves were analysed for signal quality and trigger timing.
Results: Total scan time was 72s for both acquisitions. CRT yielded significantly better ratings in image quality, background suppression, blurring, and discernibility of PBT structures compared to BRT. Contrast ratios were significantly higher in CRT (0.94 ± 0.03) than in BRT (0.93±0.03) exams; paired t test P=0.0017. Line profileslopes through the common bile duct revealed significantly higher values in CRT (42.23 ± 8.74 % of maximum intensity/mm) compared to BRT (36.06 ± 8.96 % of maximum intensity/mm; paired t testP<0.0001). Camera-derived respiratory signal curves showed a higher SNR, lower standard deviation of the signal amplitude, and less incorrect triggering than the respiratory belt-derived respiratory signal curves.
Conclusion: Camera-based respiratory triggering significantly improves image quality of 3D-MRCP compared to conventional respiratory belt triggering.
Limitations: n/a
Ethics committee approval: n/a
Funding: No funding was received for this work.
Author Disclosures:
D. C. Karampinos: nothing to disclose
E. J. Rummeny: nothing to disclose
F. N. Harder: nothing to disclose
G. Kaissis: nothing to disclose
F. Lohöfer: nothing to disclose
C. Zöllner: nothing to disclose
O. Kamal: nothing to disclose
R. Braren: nothing to disclose
A. Hock: Employee at Philips

RPS 301a-13 15:12

Clinical feasibility of compress SENSE 3D MR cholangiopancreatography (CS-MRCP) with real-time tracking (vital eye) in pancreaticobiliary disorders: a preliminary study

M. He, J. Xu, X. Wang, J. Wang, H. Xue, Z. Jin*; Beijing/CN (377174431@qq.com)*

Purpose: To prospectively evaluate the clinical feasibility of a CS-MRCP using real-time tracking (vital eye) (CS-VE-MRCP) and to compare its performance with original navigator-triggered (NT) CS-MRCP and NT-MRCP.
Methods and materials: A total of 27 patients (11 males, 16 females, age range:15-60 years, mean age: 45.67±16.72 years) with suspected pancreaticobiliary pathologies were prospectively enrolled and completed the three MRCP protocols randomly. The acquisition time was recorded. The entire pancreaticobiliary system was divided into 12 segments and evaluated on a 5-point scale by 2 radiologists independently. The Friedman test with a post hoc test was performed to compare image acquisition time, the presence of artifacts, background suppression, overall image quality, and duct visualisation among the three protocols. The diagnosis performance of the three protocols was evaluated by AUC value and compared by McNemar's test. Interobserver agreement was evaluated by linearly weighted kappa coefficients.
Results: Compared to NT-MRCP, the acquisition time of CS-NT-MRCP and CS-VE-MRCP was significantly decreased (both P < 0.001). There is no significant difference in imaging quality (P> 0.05) between the NT-MRCP and CS-VE-MRCP protocols. NT-MRCP depicted pancreatic duct and intrahepatic duct better than CS-NT-MRCP (all P < 0.05) and was comparable with CS-VE-MRCP

(all P> 0.05). For detecting pancreatobiliary pathologies, both CS-VEMRCP and NT-MRCP had significantly better performance compared to CS-NT-MRCP (AUC was 0.955 (95%CI:0.918,1) for NT-MRCP, 0.677 (95%CI:0.573,0.781) for CS-NT-MRCP, and 0.903 (95%CI:0.839, 0.968) for CS-VE-MRCP, both P < 0.05). All evaluation reached good to excellent agreement (0.619-0.897).
Conclusion: Vital eye can feasibly improve imaging quality and diagnostic performance of CS-MRCP protocols.
Limitations: Small sample size and lack of histopathological results.
Ethics committee approval: Institutional review board approval and written informed consent was obtained.
Funding: No funding was received for this work.
Author Disclosures:
M. He: nothing to disclose
Z. Jin: nothing to disclose
H. Xue: nothing to disclose
J. Xu: nothing to disclose
X. Wang: Consultant at Philip healthcare
J. Wang: Consultant at Philip healthcare

RPS 301a-14 15:18
Gadoxetic acid-enhanced MRI in primary sclerosing cholangitis: added value in liver function evaluation and monitoring of disease progression
A. Elkilany[1], T. Müller[1], A. Fischer[1], T. Denecke[2], D. Geisel[1]; [1]*Berlin/DE,* [2]*Leipzig/DE*

Purpose: To evaluate the added value of gadoxetic acid-enhanced magnetic resonance imaging (MRI) in the monitoring of disease progression and liver function in patients with primary sclerosing cholangitis (PSC).
Methods and materials: We retrospectively identified 120 patients (87 male, 33 female; mean age 42.58±12.3 years) with confirmed diagnosis of PSC who underwent 259 gadoxetic acid-enhanced MRI examinations between January 2008 and May 2019. Relative enhancement (RE) in hepatobiliary phase (HBP) was calculated in each Couinaud liver segment and in the whole liver and correlated with liver function tests (LFTs) and different prognostic clinical scoring systems, including model for end-stage liver disease (MELD) score, Mayo risk score, and Amsterdam-Oxford-PSC score. Furthermore, RE was correlated with qualitative MRI parameters including lobar atrophy, T2 hyperintensity, significant bile duct stenosis, and bile duct irregularities (pruning and beading).
Results: There was a significant negative correlation between RE in HBP and Mayo risk score (r = -0.716), MELD score (r = -0.554), Amsterdam-Oxford-PSC score (r = -0.465), LFTs including bilirubin (r=-0.521), aspartate aminotransferase (r=-0.449), alkaline phosphatase (r=-0.428), INR (r = -0.552), Alanine aminotransferase (r=-0.286) and Gamma-glutamyl transferase (r=-0.202) and a significant positive correlation with albumin (r=0.552). Furthermore, correlation between RE in HBP and qualitative MRI findings revealed a significant negative correlation with biliary duct dilatation (r=-0.286), significant bile duct stenosis (r=-0.204), lobar atrophy (r=-0.122), T2 hyperintensity (r=-0.096), and bile duct caliber irregularity (r=-0.112).
Conclusion: Gadoxetic acid-enhanced MRI can be used as a surrogate parameter for the evaluation of liver function and monitoring of disease progression in patients with PSC.
Limitations: No correlation with ERCP or clinical outcome.
Ethics committee approval: The study was approved by the institutional review board.
Funding: No funding was received for this work.
Author Disclosures:
A. Elkilany: nothing to disclose
T. Müller: nothing to disclose
A. Fischer: nothing to disclose
T. Denecke: nothing to disclose
D. Geisel: nothing to disclose

RPS 301a-15 15:24
Hepatobiliary phase gadoxetic acid excretion in gadoxetic acid-enhanced MRI as a prognostic factor in patients with primary sclerosing cholangitis
A. Elkilany[1], T. Müller[1], A. Fischer[1], T. Denecke[2], D. Geisel[1]; [1]*Berlin/DE,* [2]*Leipzig/DE*

Purpose: To evaluate the utilisation of gadoxetic acid excretion in the hepatobiliary phase of gadoxetic acid-enhanced magnetic resonance imaging (MRI) as a prognostic parameter for disease progression and liver function in patients with primary sclerosing cholangitis (PSC).
Methods and materials: We retrospectively identified 120 patients (87 male, 33 female; mean age 42.58±12.3 years) with confirmed diagnosis of PSC who underwent 259 gadoxetic acid-enhanced MRI examinations between January 2008 and May 2019. Patients were divided into excreting (181 patients) and non-excreting (78 patients) groups depending on the presence or absence of gadoxetic acid excretion in the common bile duct (CBD) in hepatobiliary phase (HBP) respectively. Both groups were compared regarding relative liver enhancement (RE) in HBP, liver function tests (LFTs), and different prognostic clinical scoring systems including model for end-stage liver disease (MELD) score, Mayo risk score, and Amsterdam-Oxford-PSC score.
Results: Relative liver enhancement (RE) in HBP was significantly higher (P < 0.005) in the excreting group while clinical scoring systems (Mayo risk score, MELD score, and Amsterdam-Oxford-PSC score) were significantly higher (P < 0.005) in the non-excreting group. LFTs comparison between both groups demonstrated a significantly higher levels of bilirubin (P < 0.005), aspartate aminotransferase (P = 0.001), alkaline phosphatase (P < 0.005), and INR (P = 0.001) in the non-excreting group and a significantly higher level of serum albumin (P < 0.005) in the excreting group.
Conclusion: Gadoxetic acid excretion in the hepatobiliary phase of gadoxetic acid-enhanced MRI can be used as a prognostic parameter for monitoring of disease progression and evaluation of liver function in patients with PSC.
Limitations: No comparison regarding clinical outcomes or ERCP findings.
Ethics committee approval: The study was approved by the institutional review board.
Funding: No funding was received for this work.
Author Disclosures:
A. Elkilany: nothing to disclose
T. Müller: nothing to disclose
A. Fischer: nothing to disclose
T. Denecke: nothing to disclose
D. Geisel: nothing to disclose

14:00 - 15:30 **Tech Gate Auditorium**

Abdominal Viscera

RPS 301b

The role of imaging in hepatocellular carcinoma (HCC) management

Moderators:
M. C. Burgmans; Leiden/NL
R. Sartoris; Clichy/FR

RPS 301b-K 14:00
Keynote lecture
A. Ba-Ssalamah; *Vienna/AT*

Author Disclosures:
A. Ba-Ssalamah: nothing to disclose

RPS 301b-2 14:10
Short MRI surveillance protocol for the detection of hepatocellular carcinoma: the SMS protocol
F. Willemssen, Q. G. de Lussanet de la Sablonière, R. S. Dwarkasing; *Rotterdam/NL (f.willemssen@erasmusmc.nl)*

Purpose: The purpose of this study was to explore if a short MRI surveillance protocol, the SMS protocol, can be used as surveillance examination for detection of hepatocellular carcinoma.
Methods and materials: Between 2010 and 2018, all patients who underwent yearly CE-MRI because of US screening failure as surveillance for HCC, with at least 2 examinations, were included. Second last negative MRI examination or MRI examination with HCC detected on full CE-MRI protocol, were selected. Axial T2 weighted images, axial DWI (b=600), and axial T1-in and opposed phase images were sent to a separated server. Three independent reviewers with 18, 13 and 5 years' experience in abdominal imaging evaluated these series. The presence of HCC was scored using a three-point scale as definitely HCC, uncertain, and no HCC. Reference standard was the full CE-MRI according to the international guidelines of the AASLD and EASL.
Results: 215 patients were included in our cohort follow-up study. 39 patients developed HCC (18,1%), of which 37 were detected (94,9%) by the SMS protocol. 2 HCCs were missed (0,9%). 31 patients (14,4%) had suspect lesions, which proved to be false positive. Interobserver agreement was high, the area under the curve was 0.909.
Conclusion: Surveillance of HCC using the SMS protocol has an excellent accuracy with high interobserver agreement. The SMS protocol might be a promising technique to replace US as screening tool for surveillance of HCC.
Limitations: Retrospective analysis. No direct comparison with US.
Ethics committee approval: Our local medical ethical committee granted permission for the study and informed consent was waived.
Funding: No funding was received for this work.

Author Disclosures:
F. Willemssen: nothing to disclose
Q. G. de Lussanet de la Sablonière: nothing to disclose
R. S. Dwarkasing: nothing to disclose

RPS 301b-3 14:16

Diagnostic performance of an abbreviated non-contrast MRI for hepatocellular carcinoma surveillance

J. S. Kim, J. K. Lee, S. Y. Baek, S. Jang*; Seoul/KR (truth0508@nate.com)*

Purpose: To evaluate per-patient diagnostic performance of a minimised non-contrast MRI protocol for hepatocellular carcinoma (HCC) surveillance in cirrhotic liver, as well as factors affecting diagnostic sensitivity.
Methods and materials: A total of 226 patients who underwent MRI for HCC surveillance over an eight year period were included in this retrospective study. Set1 consisted of diffusion-weighted imaging and respiratory-triggered, fast-spin echo T2-weighted imaging with fat suppression. Set2 included T1-weighted in/opposed-phase images added to images from Set1. Image sets were scored as positive or negative for HCC according to predetermined criteria by two readers independently. The diagnostic performance of the two sets in conjunction with α-fetoprotein (AFP) was assessed and compared using the McNemar test.
Results: The sensitivity, specificity, and accuracy of Set1 of reader1/reader2 were 84.4%/87.3%, 86.8%/86.8%, and 85.0%/87.2%, respectively. Those for Set2 were 87.3%/89.6%, 81.1%/79.2%, and 85.8/87.2%, respectively. The sensitivities of the sets were not significantly different (p=0.063). Sensitivities of both sets in conjunction with AFP were higher than those of MRI alone without statistical significance (87.3%/89.6% and, p=0.063/>0.99; 89.6%/89.6%, p=0.125/>0.99). In very early stage HCC, the sensitivities of Set1 and Set2 were 73.1%/76.9% and 76.9%/82.7%, respectively.
Conclusion: An abbreviated non-contrast MRI protocol consisting of Fat-sat T2WI and DWI is highly sensitive and may be a viable method for HCC surveillance of the cirrhotic liver. The inclusion of T1-weighted in/opposed-phase and AFP may increase this sensitivity.
Limitations: This was a retrospective study.
Ethics committee approval: Our institutional review board approved this retrospective study; informed consent was waived.
Funding: No funding was received for this work.
Author Disclosures:
J. S. Kim: nothing to disclose
J. K. Lee: nothing to disclose
S. Y. Baek: nothing to disclose
S. Jang: nothing to disclose

RPS 301b-4 14:22

Abbreviated magnetic resonance imaging (AMRI) for HCC detection: a five-year single-center experience

A. Pecorelli[1], P. M. Dautt Medina[1], N. Layyous[1], J. Y. An[1], A. Mamidipalli[1], R. L. Brunsing[2], M. T. Booker[1], C. B. Sirlin[1], K. J. Fowler[1]*; [1]San Diego, CA/US, [2]Stanford/US (pecorelli.anna@gmail.com)*

Purpose: Our center initiated in June 2014 hepatobiliary-phase AMRI for clinical HCC surveillance in patients with cirrhosis or chronic hepatitis B in whom ultrasound surveillance was compromised by obesity or other factors. The exam acquires 3 sequences (T1w fat-suppressed, T2w single shot fast spin echo, diffusion weighted) about 20 minutes after gadoxetate disodium (0.025 mmol/kg) administration with a total scanner time ≤ 15 minutes. The aim of the study is to describe the 5-year, single-center clinical experience of AMRI for HCC surveillance.
Methods and materials: Reports for AMRIs performed through May 2019 were retrospectively reviewed. Results were scored as negative (no or only definitely benign observations), subthreshold (observations < 10 mm), or positive (observations ≥ 10 mm). Each patient was categorised surveillance-negative, surveillance-subthreshold, or surveillance-positive according to their highest AMRI score. Outcomes were evaluated using all available clinical, imaging, and pathological data.
Results: 1160 AMRIs were performed in 561 patients between June 2014-May 2019. 185 (33%) patients were lost to follow-up. Of the remaining 376 patients, 295 (79%) were surveillance-negative, 23 (6%) surveillance-subthreshold, and 58 (15%) surveillance-positive. Based on the composite reference standard, 292/295 (99%) surveillance-negative and 20/23 (87%) surveillance-subthreshold patients were HCC-negative (true negatives); 29/58 (50%) of surveillance-positive patients were HCC-positive (true positives). Sensitivity, specificity, and accuracy of surveillance AMRI were 86%, 91%, and 90% respectively.
Conclusion: Hepatobiliary-phase AMRI surveillance is feasible clinically in patients in whom ultrasound surveillance is compromised. Our preliminary single-center experience suggests it provides higher sensitivity (86% vs 78%) and specificity (98% vs 89%) with lower loss to follow-up (33% vs 38%) than historically reported ultrasound surveillance.
Limitations: Retrospective study.
Ethics committee approval: IRB approval has been granted.
Funding: No funding was received for this work.
Author Disclosures:
A. Pecorelli: nothing to disclose
P. M. Dautt Medina: nothing to disclose
N. Layyous: nothing to disclose
J. Y. An: nothing to disclose
A. Mamidipalli: nothing to disclose
M. T. Booker: nothing to disclose
R. L. Brunsing: nothing to disclose
C. B. Sirlin: Consultant at Blade, Boehringer, Epigenomics, Research/Grant Support at Bayer, Celgene, GE, Gilead, Philips, Siemens
K. J. Fowler: Consultant at 12sigma, Epigenomics, Medscape, Research/Grant Support at GE, Bayer

RPS 301b-5 14:28

Radiomics model to predict hepatocellular carcinoma on liver MRI of high-risk patients in surveillance: a proof-of-concept study

M. P. A. Starmans, C. J. Els, F. Fiduzi, W. J. Niessen, S. Klein, R. S. Dwarkasing*; Rotterdam/NL (m.starmans@erasmusmc.nl)*

Purpose: Hepatocellular carcinoma (HCC) is the most common primary liver cancer. Many guidelines recommend surveillance with ultrasound twice per year for patients at risk (e.g. with hepatitis or cirrhosis). However, ultrasound has limited sensitivity for detecting early HCC. We present radiomics based on MRI of the liver parenchyma as an alternative.
Methods and materials: In our center, high risk patients deemed unsuitable for ultrasound surveillance for HCC had undergone yearly liver MRI. As a proof-of-concept, we aimed to distinguish two extrema: livers in which no HCC developed (i.e. HCC-naive livers) and livers with HCC at first detection. To this end, T2W and diffusion-weighted MRI (B-values: 0/50 and 600+) were collected from 154 patients (74 HCC, 80 HCC-naive). A clinician delineated the liver parenchyma, excluding HCC if present. Within the liver, 410 radiomics features, excluding shape and volume measures, were extracted per sequence. Three decision models, using 1) T2W; 2) DWI; and 3) T2W+DWI, were created through an automated search amongst a variety of machine learning algorithms to find the combination that maximises performance. Evaluation was implemented through a 100x random-split cross-validation, with 80% of the data used for training and model optimisation, and 20% for testing.
Results: The T2W+DWI radiomics model had a mean area under the curve (AUC) of 0.77. The models using only the T2W or DWI faired similar (AUC of 0.74 and 0.74, respectively).
Conclusion: Our radiomics approach showed that livers in which a HCC has developed differ in appearance from HCC-naive livers. Our next step includes the extension to longitudinal analysis of the liver to predict HCC development at an earlier stage.
Limitations: First step towards ultimate aim: prediction in longitudinal setting.
Ethics committee approval: Erasmus MC IRB (MEC-2018-1621)
Funding: NWO #14929-14930
Author Disclosures:
M. P. A. Starmans: nothing to disclose
C. J. Els: nothing to disclose
F. Fiduzi: nothing to disclose
W. J. Niessen: Founder at Quantib, Advisory Board at Quantib, Shareholder at Quantib
S. Klein: nothing to disclose
R. S. Dwarkasing: nothing to disclose

RPS 301b-6 14:34

Combining CT-liver perfusion and MRI with hepatobiliary contrast agent to increase diagnostic accuracy in patients with suspected hepatocellular carcinoma

G. Kalarakis[1], E. Chryssou[2], K. Perisinakis[2], D. Samonakis[2], M. Koulentaki[2], I. Karageorgiou[2], E. Akoumianakis[2], A. A. Hatzidakis[3]*; [1]Stockholm/SE, [2]Heraklion/GR, [3]Thessaloniki/GR (kagiorgos@gmail.com)*

Purpose: We sought to compare the diagnostic accuracy of CT-liver perfusion (CTLP) plus MR imaging versus MR imaging alone for detection and characterisation of suspected HCC lesions.

Methods and materials: 33 patients (31 male, 25 cirrhotic) under HCC surveillance underwent Gadoxetic-Acid-Enhanced (GaE) MRI and CTLP in a 6-week interval. In total, 88 pairs of CTLP and GaE-MRI examinations were studied (17 pre-treatment, 67 post-TACE, 4 post-ablation). GaE-MRI was performed on a 1.5T-system (Siemens Vision-Hybrid). Lesions were characterised on MRI using established criteria. CTLP studies were performed on a 128-CT-system (GE Revolution HD) with 140mm z-axis coverage. Lesions with mean value greater than 1.4 HU/sec and 35 ml/100g/min on Mean-Slope-of-Increase and Hepatic-Arterial-Blood-Flow parametric maps respectively were considered as HCC on CTLP. Diagnoses based on GaE-MRI alone and GaE-MRI plus CTLP, were compared with DSA-angiography and 6-month follow-up as gold standard.
Results: Of the total identified 282 lesions (median diameter 15mm, range 5-110mm), 111 were considered as viable HCCs. GaE-MRI identified 98 true-positive, 157 true-negative lesions, and misdiagnosed 14 false-positive and 13 false-negative lesions, providing 88.3% sensitivity (95%CI; 80.8%-93.6%) and 91.8% specificity (95%CI; 86.6%-95.4%). The combination of GaE-MRI and CTLP identified 102 true-positive, 166 true-negative, 5 false-positive, and 9 false-negative lesions, increasing sensitivity and specificity to 91.9% (95%CI 85.1%-96.2%) and 97% (95%CI 93.3%-99%), respectively.
Conclusion: The combination of MRI and CTLP may increase accuracy of hepatic nodule characterisation, enabling more efficient patient selection for early and individualised loco-regional treatment.
Limitations: Use of single manufacturer's software platform and absence of histological verification can be considered the main limitations of this study.
Ethics committee approval: Institutional Ethics Committee approved the study. All patients provided informed consent.
Funding: No funding was received for this work.
Author Disclosures:
G. Kalarakis: nothing to disclose
A. A. Hatzidakis: nothing to disclose
E. Chryssou: nothing to disclose
I. Karageorgiou: nothing to disclose
E. Akoumianakis: nothing to disclose
K. Perisinakis: nothing to disclose
D. Samonakis: nothing to disclose
M. Koulentaki: nothing to disclose

RPS 301b-7 14:40

Atypical enhancement pattern of hepatocellular carcinoma on multiphasic CT due to presence of portal vein thrombosis: a potential pitfall in imaging-based diagnosis

M. Rauf, C. Bai, S. Gul, B. Yawar Faiz*; Islamabad/PK (mari23392@gmail.com)*

Purpose: The American Association for Study of Liver Diseases diagnostic criteria allows non-invasive diagnosis of hepatocellular cancer (HCC) by imaging on basis of arterial phase enhancement followed by washout in portal venous phase. Portal vein thrombosis (PVT) is a common finding in the setting of cirrhosis where venous flow within the liver is altered. Also in our experience, presence of PVT leads to high incidence of atypical arterial enhancement, which may be secondary to compensatory increased arterial supply to the background liver. Our aim is to determine incidence of atypical enhancement pattern in HCCs with PVT as it remains a potential cause for delayed imaging diagnosis.
Methods and materials: 300 patients with HCC and portal vein thrombosis who underwent pretreatment multiphasic CT imaging were drawn retrospectively from our database. Arterial, portal venous, and delayed phase images were assessed qualitatively for lesion hypervascularity and washout by two independent consultant radiologists. Arterioportal shunting was also documented if present. Results were compiled using spss v21, results and p value determined.
Results: 201 lesions (66.8%) lacked typical arterial phase enhancement, however lesion washout was present, while 99 lesions (32.9%) showed typical arterial enhancement with washout (P< 0.001). Tumour thrombus was seen in 263 lesions (87.4%) while bland thrombus documented in 37 lesions (12.3%). Lesions with tumour thrombus showed high incidence of atypical lesion enhancement as compared to bland thrombus 76.4% (P< 0.001).
Arterioportal shunting was seen in 188 lesions (62.5%) (P< 0.001).
Conclusion: A large proportion of HCC with PVT lack characteristic arterial phase enhancement. This should be given a consideration when making imaging diagnosis of HCC.
Limitations: Relatively small sample size.
Ethics committee approval: Approved by institutional review board.
Funding: No funding was recieved for this work.
Author Disclosures:
M. Rauf: nothing to disclose
C. Bai: nothing to disclose
S. Gul: Consultant at shifa international hospital islamabad
B. Yawar Faiz: Consultant at shifa international hospital islamabad

RPS 301b-8 14:46

Radiomic analysis of contrast-enhanced CT predicts microvascular invasion and outcome in hepatocellular carcinoma

X. Xu, Y.-D. Zhang*; Nanjing/CN (xufast@hotmail.com)*

Purpose: To estimate whether radiomics can provide complementary value for predicting MVI risk in HCC patients.
Methods and materials: 495 patients with histologically confirmed HCC were retrospectively reviewed. All the patients have intact preoperative clinicoradiological records. 93 radiomic features were extracted from each patient and radiomics signatures were built by using the RFE-SVM method. Odds-ratio (OR) regression model was performed to determine risk factors of MVI and construct the predictive nomogram. A decision curve analysis was applied to test the incremental value of radiomics score (RS) to LI-score for predicting MVI.
Results: 9 radiomics features were selected to build a radiomics signature that was significantly associated with MVI ($p < 0.001$). An MVI risk estimation nomogram, which incorporated higher aspartate aminotransferase (AST), higher α-fetoprotein (AFP), non-smooth tumour margin, extrahepatic growth pattern, ill-defined pseudo-capsule, peritumoral arterial enhancement, positive radio-genomic venous invasion (RVI) score, and higher RS, was established with an area under curve (AUC) of 0.894 (95%CI, 0.864-0.920). Adding RS to LI-score scheme did not achieve significant improvement in predictive performance and did not add additional net benefits in a decision curve analysis.
Conclusion: Radiomics is still a complemental tool that offers limited additional benefit to the conventional radiologic method for predicting MVI risk of HCC.
Limitations: We restricted our study to the analysis of portal-phase CT images and cannot rule out the possibility that arterial phase CT are interrogating different tumour characteristics. The data was retrospectively evaluated. This study is a single-centre experience.
Ethics committee approval: Ethics committee approval was granted by local institutional ethics review board with a waiver of written informed consent.
Funding: No funding was received for this work.
Author Disclosures:
X. Xu: nothing to disclose
Y.-D. Zhang: nothing to disclose

RPS 301b-9 14:52

Radiological appearance of HCC recurrence after orthotopic liver transplantation (OLT) in adult patients: practical approach for an effective imaging follow-up

A. Pecorelli, M. Pace, P. A. Bonaffini, F. Sala, M. Lucà, S. Fagiuoli, S. Sironi*; Bergamo/IT (pecorelli.anna@gmail.com)*

Purpose: To describe the imaging pattern of hepatocellular carcinoma (HCC) recurrence after OLT in adult patients. To find recurrence predictors to improve follow-up strategies.
Methods and materials: We retrospectively reviewed 154 patients transplanted for HCC inside Milan criteria (MC) at a single transplant centre between 2001-2013. All the patients underwent a multiphasic liver CECT on a 256-row scanner for follow-up. Recurrence diagnosis was based on histology when available or imaging according to international guidelines. The following data was collected: sex, age, liver disease aetiology, radiological appearance at OLT, alfaphetoprotein (AFP) levels before and after OLT, histology, microvascular invasion, tumour grade, site, number, radiological appearance, and treatment of HCC recurrence.
Results: 31 (20.1%) patients developed HCC recurrence (median time 27 months; range 3-144). The most common site was liver allograft (61.3%) followed by lungs (35.6%), lymph nodes (12.9%), skin (9.7%), bones (9.7%), and brain (3.2%). In 10 (32.3%) cases, HCC recurred as diffuse metastatic disease (two/more sites) and in 21 cases (67.7%) as a single site (1-, 3- and 5-years disease-free survival (DFS) rates of 63.6%, 18.2%, 9.1% vs 90.0%, 50.0%, 35.0%; p=0.049). Twelve cases had typical CT pattern (hyper-vascularisation and wash-out), 7 atypical (2 hypervascular without washout, 5 hypodense in all phases). No correlation of imaging patterns was found with clinical characteristics of recurrence. DFS independent prognostic factors at the multivariate analysis were sex and AFP levels at OLT and at HCC recurrence.
Conclusion: Metastatic disease recurrence in OLT-HCC adult patient is not uncommon, with a trend toward a poor survival rates. No specific imaging predictors for recurrence are available. Six months CECT follow-up for the first year and once a year for the following 3 years might help to improve management strategies.
Limitations: Retrospective study.
Ethics committee approval: IRB approval was granted.
Funding: No funding was received for this work.

Author Disclosures:
A. Pecorelli: nothing to disclose
F. Sala: nothing to disclose
M. Pace: nothing to disclose
M. Lucà: nothing to disclose
P. A. Bonaffini: nothing to disclose
S. Sironi: nothing to disclose
S. Fagiuoli: nothing to disclose

RPS 301b-10 14:58
Risk of liver cirrhosis and hepatocellular carcinoma after Fontan operation: a need for surveillance
D. H. Lee*; Seoul/KR (dhlee.rad@gmail.com)*

Purpose: The aims of this study were to investigate the cumulative incidence of cirrhosis and HCC and to identify specific features distinguishing HCC from benign arterial phase hyper-enhancing (APHE) nodules that developed after the Fontan operation.
Methods and materials: We retrospectively enrolled 313 post-Fontan patients who had been followed for more than 5 years and had undergone ultrasound or computed tomography (CT) of the liver between January 2000 and August 2018. Cirrhosis was diagnosed clinically.
Results: During the 5,882.7 person-years follow-up, the estimated cumulative incidence rates of cirrhosis at 5-, 10-, 20-, and 30-years after the Fontan operation were 1.3%, 9.2%, 56.6%, and 97.9%, respectively. On multiphasic CT, 18 patients had APHE nodules ≥1 cm showing washout in the portal venous phase (PVP)/delayed phase, which met current non-invasive HCC diagnosis criteria. Among them only 7 patients (38.9%, 7/18) were diagnosed with HCC. Thus, the annual incidence of HCC was 0.12% during 5,875.9 person-years of follow-up after the Fontan operation. After cirrhosis developed, the annual incidence of HCC was greater: 1.04% (7 HCCs per 672.7 person-years). The appearance of washout in the PVP (P=0.006), the long time elapsed since the initial Fontan operation (P=0.04), the large diameter of nodule (P=0.03), and elevated AFP level (P<0.001) were significantly more common in patients with HCC than those with a benign APHE nodule.
Conclusion: In post-Fontan patients, cirrhosis is a frequent late complication, especially after 10 years, and HCC is not a rare complication after cirrhosis development. Diagnosis of HCC should not be based solely on the current imaging criteria.
Limitations: Retrospective design with potential selection bias.
Ethics committee approval: This study was approved by the Institutional Review Board of Seoul National University Hospital (IRB No. 1812-158-998).
Funding: No funding was received for this work.
Author Disclosures:
D. H. Lee: nothing to disclose

RPS 301b-11 15:04
Hepatocellular carcinoma: MRI texture analysis as a predictive biomarker of survival after Yttrium-90 radioembolisation
S. Liu, M. King, C. Zhan, A. Tong, B. Dane, C. Huang, K. Shanbhogue*; New York, NY/US (Shu.Liu@nyumc.org)*

Purpose: To assess the utility of pretreatment MRI texture analysis (TA) in predicting tumour free survival (TFS) and overall survival (OS) in patients with hepatocellular carcinoma (HCC) treated with Yttrium-90 radioembolisation (Y-90).
Methods and materials: This retrospective study included 52 treatment naïve patients with 70 HCC lesions treated with Y-90. TA was performed on MRI obtained within one month prior to Y-90 on T2-weighted, diffusion, and hepatic arterial (HAP) and portal venous phase (PVP) post-contrast images. The texture features, mean, kurtosis, skewness, and entropy were correlated with qEASL score on 2 post-Y-90 MRIs. Receiver operator characteristic (ROC) curves were calculated for predicting treatment response. The association of texture features with TFS and OS after adjusting for significant clinical factors was assessed with Cox proportional hazard regression.
Results: The median TFS and OS were 386 and 450 days, respectively. 26 patients demonstrated residual disease or progression and 5 patients died with median survival of 476 days. Entropy was lower in patients with complete response than with stable or progressive disease on HAP and PVP of both follow-up MRI (p=0.007-0.043). Average entropy on PVP was a predictor for residual disease or progression (p=0.05, AUC 0.66, at cutoff 2.7, specificity=92%, sensitivity=54%). Maximum skewness on diffusion was the most accurate predictor for complete response on first follow-up MRI (AUC 0.73, p=0.01). After adjusting for significant clinical predictors, minimal kurtosis on HAP was found to be a predictor of OS (p=0.028, HR=0.025).
Conclusion: Pretreatment texture features can be valuable predictive biomarkers for treatment response and overall survival.
Limitations: This study is limited by the retrospective nature, performance of TA by a single operator, and inherent sensitivity of TA to imaging artifact.
Ethics committee approval: IRB approved.
Funding: No funding was received for this work.
Author Disclosures:
S. Liu: nothing to disclose
K. Shanbhogue: nothing to disclose
C. Huang: nothing to disclose
M. King: nothing to disclose
C. Zhan: nothing to disclose
A. Tong: nothing to disclose
B. Dane: nothing to disclose

RPS 301b-12 15:10
Predicting the therapeutic response of hepatocellular carcinoma to transcatheter arterial chemoembolisation based on CT texture analysis: evaluation of a multiparametric prediction model
J. Vosshenrich, C. J. Zech, T. Boldanova, M. Heim, D. Boll*; Basel/CH (jan.vosshenrich@usb.ch)*

Purpose: To investigate the value of texture analysis of pretherapeutic dynamic CT for prediction of therapeutic response of hepatocellular carcinoma (HCC) to transcatheter arterial chemoembolisation (TACE) according to mRECIST.
Methods and materials: Pre- and post-therapeutic 4-phase CT scans of 92 biopsy proven HCCs in 37 patients treated with TACE were retrospectively analysed. Patients with and without liver cirrhosis were included. Pretherapeutic CT was performed directly prior to TACE, initial post-therapeutic imaging four weeks after TACE, and subsequently at 3-month intervals. Each HCC was manually segmented according to mRECIST criteria. Measurements and quantitative texture parameters were extracted and included area, long axis, mean of positive pixels (MPP), and uniformity of positive pixel distribution (UPP). Lesions were grouped into virgin lesions (primary TACE) and lesions undergoing re-TACE. Prediction models were calculated and visualised as decision trees.
Results: Texture parameters from pretherapeutic CT imaging are good discriminators when aiming to predict complete response (CR) or progressive disease (PD) in virgin lesions as well as lesions undergoing repeated TACE.
ROC curve analysis showed excellent results for the prediction of CR in virgin lesions with an AUC of 0.964 (positive predictive value: 96.9%, negative predictive value: 82.5%, accuracy: 88.9%).
Performance of our model to predict PD in virgin lesions was just slightly inferior with an AUC of 0.883 (accuracy: 80.1%) as well as for CR in re-TACE lesions (AUC: 0.833, accuracy: 75%) and PD in re-TACE lesions (AUC: 0.859, accuracy: 80%).
Conclusion: A multiparametric model based on texture analysis of pretherapeutic CT-imaging may predict response of HCCs to subsequent TACE treatment. This could serve as a valuable tool for radiologists and clinicians when triaging patients to TACE.
Limitations: n/a
Ethics committee approval: Approved by institutional ethics committee.
Funding: No funding was received for this work.
Author Disclosures:
J. Vosshenrich: nothing to disclose
C. J. Zech: nothing to disclose
T. Boldanova: nothing to disclose
M. Heim: nothing to disclose
D. Boll: nothing to disclose

RPS 301b-13 15:16
Impact of skeletal muscle mass loss and sarcopenia on cumulative survival and procedure success in hepatocellular carcinoma (HCC) patients who have undergone transarterial chemoembolisation (TACE)
L. Allois, A. Depaoli, E. Mosso, S. Gaia, A. Ferraris, P. Carucci, C. Guarnaccia, E. Rolle, P. Fonio*; Turin/IT*

Purpose: This study aimed to evaluate the impact of sarcopenia and skeletal muscle mass loss in the first year after TACE on complete response (CR) and overall survival (OS) in cirrhotic patients with HCC.
Methods and materials: In a retrospective trial conforming to the Helsinki Declaration, we selected 44 cirrhotic patients treated with TACE between 2014 to 2018 as first therapy for early or intermediate HCC. We divided patients in two groups on the basis of complete or no complete response to treatment (CR/NCR, mRECIST Criteria). We calculated L3-Skeletal Muscle Index (L3SMI) on two CT examinations (before treatment (pre-L3SMI) and after 12 months) and its variation in this period (ΔL3SMI). We also compared OS in patient with ΔL3SMI<0 and ΔL3SMI≥0 and the CR rate between sarcopenic (L3SMI<39 cm^2/m^2 for female, <50 cm^2/m^2 for male) and no sarcopenic patients.

Results: The two groups were homogeneous in terms of sex, age, BMI, smoke and alcohol habits, Child-Pugh Score, and radiologic appearance lesion (nodular, non-nodular, infiltrative). Univariate analysis demonstrated no significant differences in pre-L3SMI in the two groups (52.8 cm^2/m^2 vs 52.2 cm^2/m^2; p=0,82) and in ΔL3SMI (-3,57% NCR vs -1,33% CR; p=0,62). Patients with ΔL3SMI<0 and ≥0 had a comparable OS (OS 3-year 13% vs 90%; p=0,17). No differences were highlighted between sarcopenic patients (n=13) and no sarcopenic patients in terms of CR rate (30% vs 58%; p=0,18).
Conclusion: We observed a lower reduction of muscle mass in patients with CR, a better survival of patients with increased or stable muscle mass, and a higher response rate in no-sarcopenic patients, but without reaching statistical significance. For these reasons, we need further studies.
Limitations: The cohort was small.
Ethics committee approval: n/a
Funding: No funding was received for this work.
Author Disclosures:
L. Allois: nothing to disclose
A. Ferraris: nothing to disclose
A. Depaoli: nothing to disclose
C. Guarnaccia: nothing to disclose
E. Mosso: nothing to disclose
S. Gaia: nothing to disclose
P. Carucci: nothing to disclose
E. Rolle: nothing to disclose
P. Fonio: nothing to disclose

16:00 - 17:30 **Room Y**

My Thesis in 3 Minutes

MyT3 4
Vascular

Moderators:
T. Bilhim; Lisbon/PT
P. Chabrot; Clermont-Ferrand/FR

MyT3 4-1 16:00
Clinical applications of partial splenic artery embolisation
A. M. Teama; *Kafrelsheikh/EG (amr.teama@hotmail.com)*

Purpose: Partial splenic embolisation is a safe and effective method in the management of certain clinical conditions related to splenic pathologies.
Methods and materials: During the period from April 2016 to November 2016, the present study included 20 patients 11 males, 9 females, with different splenic pathologies candidate to splenic artery embolisation. Their ages ranged between 37- 72 years with a mean age of 55 years old. Patient inclusion criteria include adult males and females, patients candidate to the procedures, patients haemodynamically stable for procedure and patients with signs and symptoms of thrombocytopenia. Patients with hypersensitivity of contrast materials and haemodynamically unstable for procedure and pregnant females were excluded from the study.
Results: The technical success reflects in the success of all procedures in all cases. The technical complications occurred are puncture site haematoma, 4 cases developed haematoma at the puncture site and were resolved conservative. There is high significant increase in platelet count one month after PSE in all patients presented by hypersplenism. Before PSE platelet count means was 59.6±29.83 K/UL and increased to mean of 72.3±38.9 K/UL after one month of the procedure.
Conclusion: PSE is effective in improving thrombocytopenia due to hypersplenism with a statistically significant mean improvement of platelet counts. PSE is an alternative endovascular procedure for patients with portal hypertension complications. Splenic embolisation proved to be a lifesaving treatment in autoimmune haemolytic anaemia resistant to immunosuppressive and biological therapies, not eligible for surgical intervention because of critical condition.
Limitations: Patients presented with hypersensitivity of contrast materials, who were haemodynamically unstable for procedure and renal impairment.
Ethics committee approval: A written informed consent was done for all patients.
Funding: No funding was rcieved for this work.
Author Disclosures:
A. M. Teama: nothing to disclose

MyT3 4-2 16:04
Endovascular management of cerebral arteriovenous malformations
M. T. N. Mekhail[1], A. Bessar[1], T. Elserafy[1], M. Teaema[1], F. Youssef[2]; *[1]Zagazig/EG, [2]Cairo/EG*

Purpose: Endovascular management is effective and safe in management of cerebral AVMs to improve the outcome of patients with cerebral AVMs.
Methods and materials: 25 patients with cerebral AVMs are subjected to CT, MRI, MRA, CT angiography and four-vessel angiography for detection of angioarchitexture of cerebral AVMs locations and grading.
Results: 25 patients with cerebral AVMs, one patient (4%) with a family history of cerebral AVMs. 10 patients (40%) were presented with intracranial haemorrhage, 7 patients (28%) with epilepsy, 6 patients (24%) with headache and 2 patients with weakness due to AVM itself (8%). The cerebral AVMs were present in the eloquent area in 11 patients (44%) and 14 patients (56%) in non-eloquent area. The Spetzler grading was grade II) in 3 patients (12%), grade III in 15 patients (60%), grade IV in 5 patients (20%) and G V in 2 patients (8%). 10 patients (40%) showed complete occlusion of the nidus and 15 patients (60%) had a partial reduction of the nidus and were candidates for radiosurgery (48%) and surgery (12%). The periprocedural problems were vaospasm in 2 patients (8%), one patient (4%) with microcatheter stuck in the 2 cm Onyx plug and broke during the removal attempt, temporary deficit in 2 patients (8%) due to Onyx reflux and extravasation of Onyx so we recommend uses of pressure cooker technique. Regarding outcome of epilepsy after 6 months we found that 5 of the 7 patients (71.4%) were well controlled while in other 2 patients (28.6%), the fits became infrequent.
Conclusion: Endovascular management of cerebral AVMs is a valid, effective and safe approach for AVM treatment with high rates of total and near-total occlusion with acceptable complications.
Limitations: There are no limitations to this study.
Ethics committee approval: n/a
Funding: No funding was received for this work.
Author Disclosures:
M. T. N. Mekhail: nothing to disclose
A. Bessar: nothing to disclose
T. Elserafy: nothing to disclose
M. Teaema: nothing to disclose
F. Youssef: nothing to disclose

MyT3 4-3 16:08
Evaluating the vessel wall permeability of abdominal aortic aneurysm using 3D dynamic contrast-enhanced MRI
B. Tian, X. Tian, Z. Shi, J. Lu; *Shanghai/CN (bing.tian@hotmail.com)*

Purpose: This study aims to 1) investigate the feasibility of 3D dynamic contrast-enhanced (DCE) MRI to evaluate the vessel wall permeability of abdominal aortic aneurysm(AAA), and 2) assess the relationship between Ktrans and AAA diameter/intraluminal thrombus (ILT).
Methods and materials: 13 patients with AAAs were scanned on a 3T Siemens Skyra scanner. MRI was acquired using 1) a 3D T1-weighted black blood FSE sequence and 2) a 3D DCE sequence using fast gradient-echo. AAA diameter and ILT thickness were measured. Based on the volume distribution of ILT on the black blood MRI, patients were divided into two types: Type 1: Fresh ILT was present; Type 2: Without fresh ILT. 3D DCE MRI images were analysed. ROIs were carefully drawn on aneurysm wall and ILT (if available) and Ktrans was obtained for both aneurysm wall and ILT. Spearman's r was used to evaluate the correlation of DCE Ktrans with AAA diameter and ILT thickness. Mann-Whitney test was used to compare DCE Ktrans between the aneurysm wall and ILT. DCE Ktrans differences were also investigated as a function of ILT types.
Results: 11/13 patients were found to have ILT and 3/13 patients' AAA diameter was ≥5.5cm. There was a positive correlation between Ktrans and AAA diameter (r=-0.57; P=0.01). A relatively weak, non-significant negative correlation was found between Ktrans and ILT thickness (r=-0.32; P=0.34). DCE Ktrans of aneurysm wall was significantly higher than that of ILT(P=0.01). There was no significant difference in DCE Ktrans between different types of ILT.
Conclusion: 3D DCE MRI can be used to evaluate the vessel wall permeability of AAA with high temporal and spatial resolution.
Limitations: Small patients number, and further larger scale study is needed.
Ethics committee approval: n/a
Funding: No funding was received for this work.
Author Disclosures:
B. Tian: nothing to disclose
X. Tian: nothing to disclose
Z. Shi: nothing to disclose
J. Lu: nothing to disclose

MyT3 4-4 16:12

Evaluation of different keV-settings in dual-energy CT angiography of the siphon of internal carotid artery using noise-optimised virtual monoenergetic imaging

J. Fu, Y. Zeng, J. Zhang; *Shanghai/CN (kdidjs_fu@163.com)*

Purpose: The aim of this study was to perform an objective image analysis of traditional and noise-optimised virtual monoenergetic imaging (VMI & VMI+) algorithms in third generation dual-source dual-energy computed tomography angiography (DE-CTA), for showing the siphon of internal carotid artery more clearly.
Methods and materials: Twenty-eight patients who underwent DE-CTA of brain were evaluated in this retrospective study. On the VMI and VMI+, images were reconstructed from 40-keV to 190-keV. Then, attenuation and noise were measured in the siphon of bilateral internal carotid artery, and muscle and fat in the back of the neck. The signal-to-noise ratio (SNR) and contrast-to-noise ratio (CNR) were calculated.
Results: Attenuation values were highest both on 40-keV VMI and VMI+ (745.55±184.87 vs 721.38±174.89, p=0.409). Although noise values were also greatest at 40-keV in the two reconstructions (117.40±39.97 vs 75.18±28.66, p<0.001), the values on 40-keV VMI+ were significantly lower compared to the VMI. SNR was the highest in 75-keV VMI and 84-keV VMI+, and there was no significant difference between the two datasets (11.39±2.72 vs 11.62±3.27, p=0.572). CNR was the greatest in 64-keV VMI and 40-keV VMI+ respectively (15.87±6.02 vs 29.95±10.94, p＜0.001), and it was were higher in 40-keV VMI+.
Conclusion: The 40-keV VMI+ reconstruction was recommended for showing the siphon of internal carotid artery more clearly in third generation dual-source DE-CTA of brain.
Limitations: This study only involved objective evaluation and did not mention subjective evaluation.
Ethics committee approval: This retrospective study was approved by the institutional review board of our hospital.
Funding: This study was supported by the National Key Research and Development Program of China.
Author Disclosures:
Y. Zeng: Author at Huashan Hospital, Fudan University
J. Zhang: Author at Huashan Hospital, Fudan University
J. Fu: Author at Huashan Hospital, Fudan University, Speaker at Huashan Hospital, Fudan University

MyT3 4-5 16:16

The use of near-infrared spectroscopy (NIRS) to measure vascular haemodynamics within bone tissue in vivo

R. Meertens, K. Knapp, F. Casanova, W. D. Strain; *Exeter/UK (r.m.meertens@exeter.ac.uk)*

Purpose: Measuring vascular haemodynamics within bone tissue is difficult with existing imaging modalities due to bone's high density and mineral content. Near-infrared spectroscopy (NIRS) has the potential to safely measure markers of blood oxygenation and vascular responsiveness. The aim of this PhD project was to explore if NIRS could be an accurate, reliable and precise diagnostic tool for measuring markers of bone haemodynamics in vivo.
Methods and materials: A systematic review was undertaken, establishing existing evidence around the use of NIRS for measuring in vivo haemodynamics in bone tissue. Arterial occlusion protocols were developed to measure haemodynamics at the tibia using NIRS. Thirty-six participants were recruited to assess if NIRS could obtain reproducible measurements which correlate with other markers of bone health, including dynamic contrast-enhanced magnetic resonance imaging (DCE-MRI), bone mineral densitometry, trabecular bone scoring, and blood markers of bone metabolism.
Results: Markers of NIRS at the tibia were identified with within-subject coefficients of variation ranging from 3.0% to 27.7%. These markers demonstrated statistically significant associations with bone density and relatable DCE-MRI haemodynamic markers at the tibia.
Conclusion: NIRS can produce reproducible markers of oxygen extraction and microvascular reactivity at the tibia. NIRS markers show promising associations with other markers of bone health which may facilitate future research into the vascular role of common bone pathologies such as osteoporosis.
Limitations: This PhD project explored a relatively small participant sample at one testing site. However, the study has demonstrated promise worthy of further investigations in wider populations using different commercially available NIRS systems.
Ethics committee approval: Reseach involving human participants was undertaken with ethical approval from the NHS Health Research Authority (16/SW/0254).
Funding: Funding for this PhD projet was gratefully received via the College of Radiographers Doctoral Fellowship Grant.

Author Disclosures:
R. Meertens: nothing to disclose
K. Knapp: nothing to disclose
F. Casanova: nothing to disclose
W. D. Strain: nothing to disclose

MyT3 4-6 16:20

How we see congenital portosystemic shunts through CT-angiography

M. Akyüz[1], I. Akdulum[1], M. Öztürk[2], Ö. L. Boyunağa[1], A. Sigirci[3]; *[1]Ankara/TR, [2]Aksaray/TR, [3]Malatya/TR (melih.akyuz.md@gmail.com)*

Purpose: Portosystemic shunts(PSS) are rarely-observed anomalies. Depending on the shunt localisation, there are two types extrahepatic and intrahepatic. There are few studies related to paediatric age group in the literature. The aim of the study is to evaluate the computerised tomography angiography (CTA) findings according to PSS types.
Methods and materials: The study included US and CTA exams of 8 patients (7 m-16 yr). US and CTA findings were recorded and classified by Blanc et al anatomical classification.
Results: 2 patients were female and the remaining 6 were male. 5 out of 8 patients had extrahepatic PSS - 3 children had type 1 and the remaining 2 had type 2 - 3 patients had type 3 intrahepatic PSS. One patient was tested with a pulmonary artery-vein shunt suspicion. Additionally, in that case, the pathologic signal was visualised in globus pallidus suggesting hepatic encephalopathy. Abdomen CT - Angiography imaging showed large shunt between the portal vein and the vena cava inferior (VCI). Another patient was tested due to primary pulmonary hypertension. In partially included abdominal sections, coincidentally detected a shunt between the portal vein and the VCI. No follow-up examination was performed in five patients. Two extrahepatic PSS patients were treated with coil occlusion by interventional radiologists. During the angiographic examination of one patient portal vein could not be visualised therefore could not be treated.
Conclusion: Small shunts may not be visualised via US. To demonstrate PSS, CTA might be necessary. In addition, CTA findings in the PSS could be a guide for tailoring clinical management and planning treatment by interventional radiologist or surgeons prior to the procedure.
Limitations: The study was limited by a few patient number and no follow-up with five patients.
Ethics committee approval: n/a
Funding: No funding was received for this work.
Author Disclosures:
M. Akyüz: nothing to disclose
I. Akdulum: nothing to disclose
M. Öztürk: nothing to disclose
Ö. L. Boyunağa: nothing to disclose
A. Sigirci: nothing to disclose

MyT3 4-7 16:24

Resting-state functional connectivity in patients with asymptomatic stenoses of the internal carotid arteries

A. Lepekhina; *St. Petersburg/RU (anna20.04.1994@yandex.ru)*

Purpose: To determine changes in the functional connectivity of the brain in patients with asymptomatic atherosclerotic stenoses of internal carotid arteries (ICA) arteries by performing resting-state functional magnetic resonance imaging (fMRI).
Methods and materials: Resting-state fMRI was performed to 23 patients with asymptomatic atherosclerotic stenosis of one or several ICA to 60-75% (14 women, 9 men, 55 to 81 y.o., mean age 69 ± 5.4 y.o.) and healthy controls (13 women, 10 men) on 3.0T MR-scanner. All patients from the study group suffered from arterial hypertension. Carotids stenting was performed to 4 patients. We used CONN v.18 software package for statistical processing and result evaluation (rfMRI).
Results: Intergroup statistical analysis (ROI-ROI, Seed-to-Voxel) showed differences in functional connectivity in 19 patients (p <0.001). Right hemisphere: a significant increase in negative functional connections (FC) of the medial prefrontal cortex (MPFC) with the insula and the marginal gyrus was determined; decrease of positive FC of MPFC with the anterior and posterior part of the parahippocampal, middle and inferior temporal gyri. Left hemisphere: decrease of the positive functional connectivity of MPFC with the middle temporal gyrus and hippocampus (3.54 ≥ T ≥ 3.09). In 4 patients who underwent ICA stenting, there were no changes in the functional connections, compared to the control group.

Conclusion: Our findings confirm that brain connectome (and DMN in particular) alterations are most likely caused by contributions made by presence of asymptomatic atherosclerotic stenoses of the ICA.
Limitations: Our study had limitation as the sample size was relatively small. Limitations include evaluating only diseases mediated through BP and aCAS.
Ethics committee approval: n/a
Funding: No funding was received for this work.
Author Disclosures:
A. Lepekhina: Author at Almazov National Medical Research Centre

MyT3 4-8 16:28

Angiographic analysis on posterior fossa haemorrhages and vascular malformations using computed tomographic angiography and digital subtraction angiography

V. Selvamurugan, V. Singh, R. V. Phadke, Z. Neyaz*; Lucknow/IN (vigneshmdrd@gmail.com)*

Purpose: The purpose of this study is to analyse the various causes of posterior fossa haemorrhages and to compare the diagnostic accuracy of computed tomography angiography (CTA) with digital subtraction angiography (DSA) in detecting various posterior fossa vascular pathologies.
Methods and materials: From January 2017 – October 2018, 80 patients (49 males, 31 females) were included who had symptoms of non-traumatic posterior fossa haemorrhage or vascular pathologies. The mean age of the patients was 43.59 ± 1.58 years. Among 80 patients, 31 patients underwent both CTA and DSA with a mean interval of 6.2 ± 1.1 days.
Results: Out of 80 patients, 47 (58.8%) had aneurysms, 29 (36.3%) had arteriovenous malformations (AVMs), one patient had developmental venous anomaly (DVA) and one patient had brainstem cavernoma. No cause could be detected in two patients. There was a statistically significant difference in the age groups of patients with aneurysms (46.96 ± 1.88 years) and AVMs (36.24 ± 2.56 years) ($p<0.05$). The correct diagnosis was made with CTA in 24 out of 25 aneurysms and 2 of the 4 AVMs. The cause of haemorrhage was found to be aneurysms in two missed cases of AVMs. The sensitivity and specificity of CTA in detecting aneurysms was 95.7 and 100% respectively, and in diagnosing AVM was 66.7 and 100% respectively. The overall sensitivity, specificity and diagnostic accuracy of CTA as compared to DSA were 96.6, 100 and 97% respectively.
Conclusion: CTA is a simple, fast and non-invasive imaging modality that can be used to detect and characterise the vascular pathologies in posterior fossa.
Limitations: The main limitations in our study was the unavoidable selection bias and smaller sample size.
Ethics committee approval: n/a
Funding: n/a
Author Disclosures:
V. Selvamurugan: nothing to disclose
V. Singh: nothing to disclose
Z. Neyaz: nothing to disclose
R. V. Phadke: nothing to disclose

MyT3 4-9 16:32

A multidisciplinary approach to the diagnosis and treatment of kaposiform hemangioendothelioma in newborn children

S. Riebienkov, I. Benzar*; Kiev/UA (rebenkov@gmail.com)*

Purpose: The aim of the study is the determination of the clinical course, the choice of the diagnostic and treatment methods and evaluating the effectiveness of treatment in newborn children with Kaposiform hemangioendothelioma (KHE) and Kasabach-Merritt phenomenon.
Methods and materials: The study enrolled 6 newborn patients with Kaposiform hemangioendothelioma (KHE) and Kasabach-Merritt phenomenon within a period from 2013 - 2018. US, MRI (CT) performed for a primary diagnosis, and MRI follow-up investigations to evaluate treatment effectiveness.
Results: An infiltrative hypervascular lesion with the involvement of muscles, fat spaces and reticular lymphedema was observed. Possible involvement of bones, skin. Thrombocytopenia 8-20 x 10 9 /l was diagnosed in all patients. Corticosteroids treatment lead to platelet count normalization in 7-15 days, but minimal decreasing of tumour size. A sustained clinical and laboratory remission was achieved in 2 patients after propranolol monotherapy in daily dose 2,5 mg/kg. In other 3 patients vincristine was prescribed in a dosage of 1,5 mg/m 2 once a week with following positive clinical outcome. Vincristine treatment duration was 6 - 12 months. An outcome was considered to be good in 5 patients and as satisfactory in 1. No excellent outcome was observed as in all patients MRI showed a residual tumor mass in 6 months after treatment termination.
Conclusion: The diagnosis of kaposhiform hemangioendothelioma can be made without invasive procedures, based on data from radiological studies and laboratory parameters (Kasabach-Merritt phenomenon). Short courses of corticosteroids are effective for thrombocytopenia relief in KHE patients. The sustained remission was achieved with treatment by propranolol (n=2), vincristine (n=1), and propranolol+vincristine combination (n=3). The course of chemotherapy can be cancelled after stabilization of the size of the residual tumour.
Limitations: n/a
Ethics committee approval: n/a
Funding: No funding was received for this work.
Author Disclosures:
S. Riebienkov: nothing to disclose
I. Benzar: nothing to disclose

MyT3 4-10 16:36

Diagnostic yield of CT angiography in penetrating lower extremity trauma

A. P. Le Roux, A.-M. Du Plessis, R. D. Pitcher*; Cape Town/ZA (alwynleroux@gmail.com)*

Purpose: Injury is a major public health challenge, placing a significant demand on hospital resources, particularly in resource-limited settings. With the rise of interpersonal and gang violence, there has been an increase in penetrating injuries to the lower extremities, and the use of CT angiography (CTA) for suspected arterial injuries. Over-utilization of expensive imaging - with a relatively low yield - significantly increases healthcare costs. The implementation of value-based care is paramount in a resource-limited setting. The aim is to determine the value of CTA in penetrating lower extremity injuries in a resource-limited setting.
Methods and materials: This retrospective descriptive study from 1 July 2013 – 31 June 2018 included all Tygerberg Hospital patients undergoing penetrating trauma-related emergency lower extremity CTA for suspected arterial injury. The yield of clinically significant injuries and the positive predictive value of specific clinical signs were calculated.
Results: 982 patients (median age 27 years, 91% male) were included. 90% (885/982) had gunshots, 9% (89/982) stabs and 0.5% (5/982) other injuries. 33% (23/68) of patients with hard signs of vascular injury and 7.9% (73/914) with soft signs/no indication for imaging had clinically significant injuries. Significant ($p<0.05$) correlations were a rapidly expanding haematoma (PPV 40%), an absent pulse (PPV 39%), and a diminished pulse (PPV 18%). There was a year-on-year rise in the number of studies, but no significant difference in injury yield.
Conclusion: The current utilisation of CTA has a low yield in detecting clinically significant vascular injuries in penetrating lower extremity trauma. There is a poor correlation between the clinical indication provided and imaging findings.
Limitations: Retrospective study design.
Ethics committee approval: Stellenbosch University ethics approval (S18/10/219).
Funding: No funding was received for this work.
Author Disclosures:
A. P. Le Roux: nothing to disclose
A.-M. Du Plessis: nothing to disclose
R. D. Pitcher: nothing to disclose

MyT3 4-11 16:40

Optimisation of window settings on traditional and noise-optimised virtual monoenergetic imaging for displaying intracranial arterial aneurysm in dual-energy CT angiography

Y. Zeng, X. Cao, H. Li, J. Fu, J. Zhang*; Shanghai/CN (18211220088@fudan.edu.cn)*

Purpose: To determine the optimal window settings for displaying intracranial aneurysm more clearly on virtual monoenergetic imaging (VMI) reconstructions of third generation dual-source, dual-energy CT angiography (DE-CTA).
Methods and materials: A total of 28 intracranial aneurysms were retrospectively evaluated in 26 patients who underwent cerebral angiography in third-generation dual-source dual-energy CT (DECT). Images were reconstructed with traditional VMI and noise-optimised VMI reconstructions at 1-keV intervals from 40-keV to 190-keV. Attenuation and noise were measured in the intracranial aneurysm, brain tissue around the aneurysm, fat in the posterior neck, and internal carotid arteries. A contrast-to-noise (CNR) was calculated. At the energy level where the dataset had highest CNR respectively on the traditional and noise-optimised VMI reconstructions, the subjectively best window setting (width and level, B-W/L) was independently determined by two observers and subsequently related with internal carotid arteries attenuation to calculate separate optimised values (O-W/L) using linear regression.
Results: The CNR was highest at 64-keV (M64) and 40-keV (M40+) respectively on the traditional and noise-optimised VMI reconstructions (21.29±8.51 vs 34.34±11.41, $p<0.001$). The B-W/L for M64 and M40+ was 690/190 and 1570/450, respectively. Results from regression analysis inferred an O-W/L of 650/180 for M64 and 1480/420 for M40+.
Conclusion: In order to display aneurysms more clearly on third-generation dual-source DE-CTA, we recommended 64-keV and 40-keV as the energy level on traditional and noise-optimised VMI reconstructions, respectively. And the W/L settings of 650/180 for M64 and 1480/420 for M40+ were suggested.

Limitations: There was no comparison between traditional and noise-optimised VMI in intracranial aneurysm visualisation.
Ethics committee approval: This study was approved by ethics committee of our hospital.
Funding: This study was supported by the National Key Research and Development Program of China.
Author Disclosures:
Y. Zeng: Author at Huashan Hospital, Fudan University, Speaker at Huashan Hospital, Fudan University
X. Cao: Author at Huashan Hospital, Fudan University
H. Li: Author at Huashan Hospital, Fudan University
J. Fu: Author at Huashan Hospital, Fudan University
J. Zhang: Author at Huashan Hospital, Fudan University

MyT3 4-12 16:44
Comparison of moving bed contrast-enhanced MR angiography vs digital subtraction angiography in peripheral arterial disease
E. Ozgul*; Afyonkarahisar/TR (dresrayam@gmail.com)*

Purpose: Peripheral arterial disease is partial or total occlusion of one or more peripheral arteries due to atherosclerosis. The aim of this study is to evaluate the accuracy of contrast-enhanced moving bed MRA for significant stenosis and occlusions vs DSA serving as the gold standard.
Methods and materials: We have evaluated retrospectively 1118 arterial segments of 43 patients with a known or suspicious PAD who underwent DSA after MRA within 30 days. DSA was accepted as the gold standard and the sensitivity, specificity and accuracy of MRA were determined. MRA and DSA images were examined by two different radiologists as a double-blind study. McNemar test was used to evaluate the significant difference in diagnostic aspect between DSA and MRA. Specificity, sensitivity, positive and negative estimated values, diagnostic accuracy rate were calculated. Kappa coefficient (κ) was calculated to determine the significance of diagnostic compliance between DSA and MRA. Results for $p<0.05$ were accepted statistically significant.
Results: The overall sensitivity and specificity values of contrast-enhanced moving bed MRA for significant (>70%) stenosis were 91% and 97.3%; for total occlusion, sensitivity and specificity values were 90% and 99.3% respectively. For both of them, the accuracy was 96%. No significant difference is found between contrast-enhanced moving bed MRA and DSA for the diagnosis of peripheral arterial disease ($p>0.05$).
Conclusion: Contrast-enhanced moving bed MRA is a reliable, fast, noninvasive imaging modality in the diagnosis of patients, in planning of interventional procedures and follow-up of the patients with peripheral arterial disease.
Limitations: 14 segments in 5 patients were excluded because of metallic artefact due to iliac stents. Lower sensitivity ratios were calculated from iliac arteries. It was due to a decrease in the number of iliac segments.
Ethics committee approval: n/a
Funding: No funding was received for this work.
Author Disclosures:
E. Ozgul: nothing to disclose

MyT3 4-13 16:48
Quality control studies of dynamic contrast-enhanced 3-dimensional magnetic resonance angiography for spinal vascular
J. Cao, L.-L. Cui*; Shenyang/CN (cmucao@163.com)*

Purpose: A spinal vascular malformation is rare in clinics, with a high disabling rate. Dynamic contrast-enhanced 3-dimensional magnetic resonance angiography（DCE-3D-MRA) for spinal vascular play an important role in the diagnosis and treatment of spinal vascular malformations and postoperative follow-up. In this study, we investigated the protocol for scanning spinal vascular to improve the success rate of DCE-3D-MRA for spinal vascular.
Methods and materials: We developed a protocol for assessment of anterior spinal artery based on anatomic, morphologic of anterior spinal artery in 24 research participants using DCE-3D-MRA in the area between T8 and L5. Real-time sequence was used to monitor the time of administration. The contrast agent was injected through antecubital veins with high pressure syringe at a rate of 3ml/s in 16 research participants and 2ml/s in 17 research participants.
Results: Although the average enhanced scan time we detected was 16s, individualised scanning was essential. Then we can get a better image quality by the dosing speed of 3ml/s.
Conclusion: The quality of images of DCE-3D-MRA for spinal vascular can be improved by using optimal scanning protocol.
Limitations: The study is limited by the small sample.
Ethics committee approval: n/a
Funding: No funding was received for this work.
Author Disclosures:
J. Cao: Author at The First Hospital of China Medical University
L.-L. Cui: Author at The First Hospital of China Medical University

MyT3 4-14 16:52
Contrast-enhanced perfusion patterns and serum lipid signatures specific of vulnerable plaque in predicting stroke: a cohort study of carotid stenosis in Chinese patients
H. Yunqian, W. Zhu, M. Chen*; Shanghai/CN (18721619656@163.com)*

Purpose: To investigate the correlation between contrast-enhanced ultrasound (CEUS) perfusion patterns and serum lipid signatures specific of carotid artery vulnerable plaque with the degree of carotid stenosis, which provide the basis for early diagnosis of cerebral ischaemic stroke.
Methods and materials: From March 2018 to June 2018, 202 patients with carotid plaque who underwent CEUS were enrolled in this study. The patients who did not undergo CTA or DSA examination within 1 week after CEUS examination were excluded. 80 patients were analysed. All subjects underwent a contrast-enhanced ultrasound, CTA or DSA, and serum lipid testing. In face-to-face interviews with participants, trained investigators used questionnaires to get information about their routine cardiovascular and cerebrovascular risk factors, demographic characteristics, smoking history, lifestyle, atrial fibrillation history and other disease histories.
Results: Serum-free fatty acid was significantly associated with CVA events ($P<0.05$). Serum-free fatty acid was significantly associated with the different contrast agent enhancement level and difference contrast-enhanced perfusion patterns ($P<0.05$).
Conclusion: The enhancement levels and the CEUS perfusion patterns with microbubbles are infused from the surface to the interior of the plaque was increased with the degree of carotid stenosis, the CEUS perfusion pattern of moderate or higher carotid stenosis plaques is mainly infused from the surface to the interior of the plaque, serum-free fatty acid was increased with the enhancement levels of the plaques. These may evidence that the plaque begins to become vulnerable.
Limitations: This is an observational study. We did not analyse the morphology and properties of plaques in this study.
Ethics committee approval: n/a
Funding: No funding was received for this work.
Author Disclosures:
H. Yunqian: Author at Tong Ren Hospital, Shanghai Jiao Tong University School of Medicine, Speaker at Tong Ren Hospital, Shanghai Jiao Tong University School of Medicine
W. Zhu: Employee at Tong Ren Hospital, Shanghai Jiao Tong University School of Medicine
M. Chen: Other at Tong Ren Hospital, Shanghai Jiao Tong University School of Medicine

MyT3 4-15 16:56
Non-contrast MR venography in the diagnosis of post-thrombotic iliac vein obstruction and extravascular compression
V. Shebryakov, O. Karpov, Y. Stoyko, O. Bronov, M. Yashkin, D. Lutarevich*; Moscow/RU (VSHEBRYAKOV@MAIL.RU)*

Purpose: Evaluate value of non-contrast MRI in the diagnosis of post-thrombotic iliac vein obstruction and extravascular compression.
Methods and materials: The study included 228 patients with CVD (clinical class C3-C6 according to the CEAP classification), including 110 males and 118 females. The average age of the patients was 43.6±11.6 years. All patients underwent ultrasound angioscanning veins of the lower extremities and MRI of the iliac veins and inferior vena cava. Studies were performed on MRI using a special protocol non-contrast sequences: 1. BH TRUFI/FIESTA 3D using Valsalva manoeuvre; 2. INHANCE 3D using the free-breathing technique, with subsequent 3D reconstruction.
Results: 107 patients have been diagnosed with stenosis of the left common iliac vein due to compression of the right common iliac artery (May-Thurner syndrome). 65 patients underwent stenting of left common iliac vein with the May-Turner syndrome. Two patients underwent stenting of the left external and common iliac veins with post-thrombotic obstruction. 50 post-thrombotic deep vein changes have been revealed.
Conclusion: MR-venography is the most optimal method in the diagnosis of the causes of extra and intravenous pathology of the IVC and its basin. There is no radiation exposure, no use of contrast agent and short time relation. 3D-reconstruction of the IVC and iliac veins can be used for planning corrective treatment and reconstructive operations. MR-venography is equal to contrast angiographic methods in detecting extravasal compression and is recommended in the initial evaluation of suspected May-Thurner syndrome and post-thrombotic iliac vein obstructions.

Limitations: n/a
Ethics committee approval: n/a
Funding: No funding was received for this work.
Author Disclosures:
V. Shebryakov: nothing to disclose
O. Karpov: nothing to disclose
Y. Stoyko: nothing to disclose
O. Bronov: nothing to disclose
M. Yashkin: nothing to disclose
D. Lutarevich: nothing to disclose

MyT3 4-16 17:00

Carotid stenosis evaluation by 128-slice CT: comparison of NASCET, ECST and CC grading methods, and comparison with colour-Doppler ultrasonography

F. M. H. Rijnberg, A. Lammertink*; Groningen/NL (frankrijnberg@hotmail.nl)*

Purpose: Purpose is to evaluate the intra- and interobserver variability of the North American Symptomatic Carotid Endarterectomy Trial (NASCET), European Carotid Surgery Trial (ECST), and Common Carotid (CC) methods, which are used to measure the degree of carotid stenosis, using 128-slice CT and to compare the measurements made by these three methods, and to compare those methods with the gold standard, ultrasound.
Methods and materials: Of the initial 25 included patients, five patients were excluded during the study because the percentage of stenosis of these five patients could not be determined using the NASCET, ECST and/or CC method. CT-Angiography (CTA) examination was performed by a 128-slice scanner (Siemens SOMATOM Definition AS 128). Retrospective data from the CT scan and the ultrasound examination were used. In addition, prospective data has been collected. Two neuroradiologists measured the degree of carotid stenosis by using the NASCET-, ECST-, and CC-method. Intra-observeragreement and inter-observeragreement were determined by intraclass correlation coefficient (ICC).
Results: The similarity between neuroradiologists and ultrasound examination was highest in the ECST and CC method (85%). The similarity between neuroradiologists themselves was highest with the use of the ECST and CC method (95%). The inter-observer agreement is highest with the ECST method (0.672), followed by the NASCET method (0.667) and the CC method (0.532). The intra-observer agreement within the NASCET method is “moderate" while within the ECST and CC methods it was "fair".
Conclusion: The ECST method is the most reliable way to determine the extent of carotid stenosis based on the high similarity with the golden method, the high similarity between neuroradiologists and the high inter-observer agreement compared to the NASCET and CC method.
Limitations: n/a
Ethics committee approval: n/a
Funding: No funding was received for this work.
Author Disclosures:
F. M. H. Rijnberg: nothing to disclose
A. Lammertink: nothing to disclose

MyT3 4-17 17:04

Prediction of early haematoma expansion in cerebral haemorrhage based on non-contrast CT

L. Song[1], T. Guo[1], J. Wang[2], H. Ren[1]*; [1]Xiangyang/CN, [2]Xiang/CN (song580lei@163.com)*

Purpose: Patients with intracerebral haemorrhage (ICH) were divided into haematoma expansion group and non-haematoma expansion group. The clinical features of the two groups of patients and the imaging features of non-contrast CT were analysed to explore the relationship between the two groups and the early haematoma expansion.
Methods and materials: Consecutive adult patients with spontaneous ICH who had undergone baseline CT within 6 hours after ICH symptom onset were screened for inclusion. A follow-up CT scan was performed within 24 hours after the initial CT scan. Baseline clinical data, including age, sex, diabetes mellitus, coronary heart disease, past stroke history, onset to CT scan time, and CT features (haematoma volume, haematoma morphology, haematoma site, delayed intraventricular haemorrhage and island sign), were prospectively collected and recorded in our ICH research database. We also prospectively recorded admission blood pressure, admission Glasgow Coma Scale (GCS) score.
Results: 140 patients with haematoma expansion group (37.8%) and 230 patients with non-haematoma expansion group (62.2%) were enrolled. Multivariate logistic regression analysis showed irregular haematoma shape (OR=2.289, 95% CI=1.131-4.631, P=0.021), island sign (OR=2.327, 95% CI=1.139-4.751, P=0.020) and delayed intraventricular haemorrhage (OR=4.979, 95% CI=1.423-17.429, P=0.012) are the independent predictor of early haematoma expansion. The predicted sensitivity and specificity were 71.45% and 54.78%, 51.4% and 81.7%, 23.07% and 71.3%, respectively.
Conclusion: Irregular haematoma shape, island sign and delayed intraventricular haemorrhage expansion based on non-contrast CT are the independent predictors of early haematoma expansion. Irregular haematoma shape has the higher sensitivity and island sign has the highest specificity.
Limitations: This study is based on a single centre retrospective study.
Ethics committee approval: n/a
Funding: n/a
Author Disclosures:
H. Ren: Author at Xiangyang Central Hospital, Affiliated Hospital of Hubei University of Arts and Science
L. Song: Author at Xiangyang Central Hospital, Affiliated Hospital of Hubei University of Arts and Science
T. Guo: Author at Xiangyang No.1 People’s Hospital, Hubei University of Medicine
J. Wang: Author at Xiangyang Central Hospital, Affiliated Hospital of Hubei University of Arts and Science

MyT3 4-18 17:08

Application of FLAIR vascular hyperintensity-DWI mismatch in ischaemic stroke, depending on semi-quantitative DWI-Alberta stroke programme early CT score

L. Song[1], J. Wang[2]*; [1]Xiangyang/CN, [2]Xiang/CN (song580lei@163.com)*

Purpose: Our aim is to determine whether there is a relationship between (DWI)-Alberta Stroke Programme Early CT Score (ASPECTS) and fluid-attenuated inversion recovery (FLAIR) vascular hyperintensity (FVH)-DWI mismatch and to better quantify FVH-DWI mismatch to assess the prognosis of cerebral infarction.
Methods and materials: A retrospective analysis of 109 patients with MCA stenosis or occlusion with cerebral infarction was performed by dividing this cohort into FVH-DWI match group and FVH-DWI mismatch group based on FVH and DWI results. The clinical and imaging data of these two groups of patients were reviewed and analysed to identify associations between FVH-DWI mismatch and prognosis of patients for the preservation of neurological function. Correlation between DWI-ASPECTS and FVH-DWI mismatch was also performed.
Results: FVH-DWI mismatch was present in 66/109 (60.55%) patients, and FVH-DWI match was present in 43/109 (39.45%). Patients with FVH-DWI mismatch had higher DWI-ASPECTS (7.0 vs 4.0, P < 0.001) and lower mRS at 3 months (3.0 vs 4.0, P <0.001) than patients without FVH-DWI mismatch. Multiple regression analysis suggested that DWI-ASPECTS (OR = 4.7, 95% CI = 2.5–9.2, P < 0.001) remained significantly associated with FVH-DWI mismatch. Two threshold points for DWI-ASPECTS of 3 and 8 can be used to distinguish whether there is a mismatch in FVH-DWI by smooth curve fitting.
Conclusion: The DWI-ASPECTS score was an independent predictor of FVH-DWI mismatch. At DWI-ASPECTS ≤ 3, the FVH-DWI mismatch offers no prognostic value; whereas, at DWI ASPECTS ≥ 8, the FVH-DWI mismatch had the highest prognostic value. DWI-ASPECTS can roughly determine whether there is a FVH-DWI mismatch in order to select optimal clinical treatment and accurately assess prognosis.
Limitations: This study is based on a single centre retrospective study.
Ethics committee approval: n/a
Funding: n/a
Author Disclosures:
L. Song: Author at Department of Radiology, Xiangyang Central Hospital, Affiliated Hospital of Hubei University of Arts and Science, Investigator at Department of Radiology, Affiliated Hospital of Guizhou Medical University, Guiyang, China
J. Wang: Author at Department of Radiology, Xiangyang Central Hospital, Affiliated Hospital of Hubei University of Arts and Science

MyT3 4-19 17:12

Factors resulting in the increase of the total dose received by the patient during endovascular procedures performed within the region of the central nervous system

S. Modlińska[1], M. M. Cebula[1], J. Komenda[2], J. Baron[1]*; [1]Katowice/PL, [2]Czeladź/PL*

Purpose: The aim of the study was to analyse factors influencing the total radiation dose during diagnostic and therapeutic procedures in the field of neuroradiology, obtained by a patient with suspicion of intracranial pathology.
Methods and materials: The retrospective analysis involved 419 procedures. The following group can be divided into 321 panangiography and 98 embolisations preceded by panangiography procedures. For each of the procedures the total dose absorbed by the patient was calculated on the basis of the "cumulative air kerma" parameter. In the analysed group aneurysms were found in 318 patients, arteriovenous malformations in 46 patients, and in 54 cases no pathology was revealed. The collected data was subjected to statistical

analysis. The relationship between the total dose received by the patient during procedures and the location of the pathology, the type of surgery, the type of embolisation material used, the presence of subarachnoid haemorrhage (SAH) and the type of embolisation were analysed.
Results: There was a statistically significant correlation between the total radiation dose absorbed by the patient and the type of procedure (p <0.000), the amount of embolisation material used (p <0.05) and the presence of SAH (p <0.000). There was no significant effect of the type of pathology and pathology location on the total dose received by the patient during the procedure.
Conclusion: The total dose received by the patient during neuroradiology procedures depends on the type of intervention, the type of material used during embolisation and the presence of SAH.
Limitations: n/a
Ethics committee approval: n/a
Funding: No funding was received for this work.
Author Disclosures:
S. Modlińska: Author at Medical University of Silesia, Speaker at Medical University of Silesia
M. M. Cebula: Author at Medical University of Silesia
J. Komenda: Author at Medical University of Silesia
J. Baron: Author at Medical University of Silesia

MyT3 4-20 17:16
Non-contrast magnetic resonance angiography in renal artery assessment
S. Sethu Madhavan[1], V. Bhat[2], K. Ga[2]; [1]*Kannur/IN,* [2]*Bengaluru/IN*
(sreesm7@gmail.com)

Purpose: To evaluate renal artery anatomy in cases of suspected renovascular hypertension using INHANCE non-contrast MR angiography and determine its significance in diagnosing renal artery stenosis.
Methods and materials: Non-contrast MR angiography using INHANCE was performed on a 1.5T MRI system for assessing renal arteries in 114 patients referred with clinically suspected renovascular hypertension for a period of three years (June 2014 to May 2017). Out of this, 10 patients further underwent Contrast enhanced-MR Angiography, 7 underwent CT-angiography and one patient underwent both contrast-enhanced MR angiography and CT angiography.
Results: We evaluated the findings on non-contrast INHANCE MR angiography in suspected cases of renal artery hypertension in 114 subjects. Its validity was calculated in comparison with contrast-enhanced MR angiography and/or CT Angiography in 18 patients. In our study, renal artery stenosis was found in 21.2% arteries out of the 214 arteries examined. Also, there was noted a significant association between renal artery stenosis identified on non-contrast INHANCE MR angiography and that on contrast-enhanced MR angiography and CT angiography (p<0.001).
Conclusion: Non-contrast INHANCE MR angiography can be used as a significant and valuable screening investigation for renal artery assessment especially in patients with impaired renal functions where contrast-based investigations carry a high risk.
Limitations: No comparisons are available with the gold standard, digital subtraction angiography. INHANCE NC-MRA sequence was done in the axial plane and other planes could not be evaluated. Our study population may not be a true representation of all clinically suspicious cases of renovascular hypertension hence derived values may not be truly representative.
Ethics committee approval: Ethics committee approval was received.
Funding: No funding was received for this work.
Author Disclosures:
S. Sethu Madhavan: nothing to disclose
K. Ga: nothing to disclose
V. Bhat: nothing to disclose

16:00 - 17:30 **Room M 4**

Neuro

RPS 411

Paediatric neuroimaging and neuroanatomy

Moderators:
N. Plakhotina; St. Petersburg/RU
N.N.

RPS 411-1 16:00
Long term neurodevelopmental outcomes of children with foetal isolated vermian anomaly
L. Ben-Sira, R. Shperling, L.-T. Pratt, *Tel-Aviv/IL*
(bensiraliat@gmail.com)

Purpose: To evaluate the neurodevelopmental performance of children with abnormal isolated vermian during foetal life.
Methods and materials: A historical cohort study (2000-2017) of women referred due to suspected central nervous system abnormalities. Of 447 fetuses suspected with anomalies of the PF, 79 were considered as an isolated vermian abnormality; of these, 15 cases were lost to follow-up and 26 underwent termination of pregnancy (TOP). The remaining 38 composed the study and control groups; 3 foetuses were excluded since they were diagnosed postpartum with genetic syndromes. 9 had an isolated vermian anomaly (IVA) (study group). 26 of these foetuses were diagnosed as having Blakes' pouch cyst (BPC) or arachnoid cyst. The structures of the PF were assessed quantitatively by measuring vermian length, width, pons diameter, transverse cerebellar diameter (TCD), and additional biometry. The neurodevelopmental performance was assessed using the Vineland adaptive behaviour scale II (VABS-II) questionnaire (parental interview).
Results: Children with IVA showed significantly lower scores on the VABS-II and in its subdomains. This group presented with developmental difficulties and attention deficits when compared to foetuses with BPC.
Conclusion: IVA, when diagnosed prenatally, is a significant risk factor for later neurodevelopmental performance in contrast with other posterior fossa cysts (PFC).
This study highlights the importance of a correct classification and prenatal diagnosis of “true IVA”, which enables accurate neurodevelopmental prognostication.
Limitations: The study had a wide-ranging age groups; the median age in the control group was 3.85 years-old and in the study group II 9.3 years-old. The developmental milestones are very different.
The small sample size limits our ability to conclude unequivocally whether IVA is associated with genetic syndromes.
Ethics committee approval: The study was approved by the Helsinki committee at our medical centre. Approval number: 0419-17-TLV.
Funding: No funding was received for this work.
Author Disclosures:
L. Ben-Sira: nothing to disclose
R. Shperling: nothing to disclose
L.-T. Pratt: nothing to disclose

RPS 411-2 16:06
Imaging the foetal brainstem: an in vivo MRI study
G. O. Dovjak, P. Brugger, G. M. Gruber, D. Prayer, G. Kasprian; *Vienna/AT*
(gregor.dovjak@meduniwien.ac.at)

Purpose: The brainstem is involved in different types of hindbrain anomalies, which are nowadays increasingly detected by prenatal sonography. However, little is known about the proportions of different foetal brainstem segments and their evolution throughout pregnancy. This study aimed to assess the midsagittal two-dimensional area of brainstem substructures with foetal MRI.
Methods and materials: Prenatal cases with normal brain development were retrospectively assessed. The midbrain, pons, and medulla oblongata were segmented using a T2-weighted median sagittal slice and ITK snap. The ratios of the brainstem substructures were calculated and correlated to gestational age.
Results: 148 brain-normal foetal MRI with a mean age of 25.26±4.12 gestational weeks (GW) showed a sufficient image quality to be assessed. The ratio midbrain:pons significantly decreased (p<0.01) from 0.6 to 0.5 between 18 and 40 GW, whereas the ratio pons:medulla oblongata increased significantly (p<0.01) from 1.5 to 1.8. The ratio midbrain:medulla oblongata remained 0.9 throughout gestation (p=0.91).

Conclusion: Two-dimensional segmentation of brainstem substructures revealed that there was an increase in the size of pons compared to midbrain and medulla oblongata during the 2nd and 3rd trimester. Brainstem proportions at the early second trimester (midbrain:pons:medulla=3:4:3) differ from those postnatally (1:2:1), which has to be acknowledged when assessing the brainstem in foetal hindbrain malformations.
Limitations: An inherently limiting factor of foetal imaging is the small size of the posterior fossa. The size and limited resolution make segmentation prone to partial volume effects. Although movement artefacts can be a limiting factor, we were able to bypass them by repeating the desired image plane.
Ethics committee approval: Ethics committee approval and written informed consent were obtained.
Funding: No funding was received for this work.
Author Disclosures:
G. O. Dovjak: nothing to disclose
P. Brugger: nothing to disclose
G. M. Gruber: nothing to disclose
D. Prayer: nothing to disclose
G. Kasprian: nothing to disclose

RPS 411-3 16:12

An apparent diffusion coefficient of different areas of the brain in growth-restricted foetuses

B. Moradi[1], Z. Alibeigi Nezhad[2], N. Seyed Saadat[1], M. A. Kazemi[1], M. Shirazi[1], A. Borhani[1]; [1]*Tehran/IR,* [2]*Alibeigi Nezhad/IR (Aliborhani@gmail.com)*

Purpose: To compare the apparent diffusion coefficient (ADC) values of different areas of the brain in foetuses with intrauterine growth restriction (IUGR) and control cases.
Methods and materials: A total of 38 foetuses with IUGR and 18 control foetuses with similar gestational age were compared using a 3T magnetic resonance scanner. IUGR cases included 23 foetuses with clinical severity signs (group A) and 15 foetuses without these signs (group B). ADC values were measured in different brain regions and compared among the groups. Foetuses with brain structural abnormalities were excluded.
Results: Foetal brain signal and anatomy were normal in all foetuses. Head circumference <5% was more common in IUGR compared to IUGR B (56.5% vs 13.3%, p<0.0001). In comparison to the normal group, the ADC values in IUGR foetuses were significantly lower in the cerebellar hemisphere (CH) (1.239 vs 1.280.5 x10-3 mm2/sec, p=0.045), thalami (1.205 vs 1.285 x10-3 mm2/sec, p=0.031), and caudate nucleus (CN) (1.319 vs 1.394 x10-3 mm2/sec, p=0.04). However, ADC values were not significantly different between IUGR subtypes. Pons had the lowest ADC values among all brain regions.
Conclusion: In a comparison with a control group, ADC values of some brain areas (thalami, CN, and CH) were found to be significantly lower in IUGR foetuses, though there were not any significant differences in IUGR subtypes.
Limitations: The specificity and sensitivity might be overestimated because the ADC value cut-off was calculated from our own cases.
Ethics committee approval: Institutional review board approval and parents' informed consent were obtained.
Funding: No funding was received for this work.
Author Disclosures:
A. Borhani: nothing to disclose
B. Moradi: nothing to disclose
Z. Alibeigi Nezhad: nothing to disclose
N. Seyed Saadat: nothing to disclose
M. A. Kazemi: nothing to disclose
M. Shirazi: nothing to disclose

RPS 411-4 16:18

Widespread cortical dyslamination in epilepsy patients with periventricular heterotopia and focal cortical dysplasia

E. Lotan[1], O. Tomer[2], I. Tavor[2], I. Blatt[1], H. Goldberg-Stern[3], C. Hoffmann[1], G. Tsarfaty[1], D. Tanne[2], Y. Assaf[2]; [1]*Tel Hashomer/IL,* [2]*Tel Aviv/IL,* [3]*Petah Tikva/IL*

Purpose: Emerging research confirms our understanding of epilepsy as a network disorder that involves more widespread cortical compromise than previously assumed. However, little is known about the developed laminar-specific cortical disruption. We aimed to investigate the cortical laminar architecture of the neocortex beyond the measurement of cortical thickness using clinically feasible structural MRI.
Methods and materials: Epilepsy patients with focal cortical dysplasia (FCD; n=9), periventricular nodular heterotopia (PVH; n=9), and age-matched healthy controls (HC; n=9) underwent T1 relaxation 3T-MRI, of which component probability T1-maps were utilised to extract a sub-voxel composition of 6 T1 cortical layers. 78 cortical areas of the automated anatomical labelling (AAL) atlas were divided into 1,000 equal-volume sub-areas and logistic regressions were performed to compare FCD/PNH patients to HC, with the T1-layers composing each sub-area as regressors. The significance maps were projected on MNI brain templates.
Results: Widespread cortical dyslamination was observed in the patient groups compared to the HC. Out of 1,000 sub-areas, 291 bilateral hemispheric cortical sub-areas were found to predict FCD and 256 to predict PNH. For each of these sub-areas, we were able to identify the T1-layer, which contributed the most to the prediction.
Conclusion: Our results reveal similar widespread cortical dyslamination in epilepsy patients with FCD and PNH, which supports the concept of epilepsy as a network disease, although intrinsic abnormalities of neuronal development may be a contributory factor. As the ability to assess structural and functional connections in the human brain increases through both diffusion tensor imaging and functional MRI, using qualitative and quantitative information of cortical laminar patterns in epilepsy patients as a sensitive imaging biomarker could potentially elucidate pathophysiologic mechanisms and facilitate patient management towards developing individually tailored treatment.
Limitations: n/a
Ethics committee approval: Ethics committee approval obtained.
Funding: No funding was received for this work.
Author Disclosures:
E. Lotan: nothing to disclose
O. Tomer: nothing to disclose
I. Blatt: nothing to disclose
I. Tavor: nothing to disclose
C. Hoffmann: nothing to disclose
G. Tsarfaty: nothing to disclose
D. Tanne: nothing to disclose
H. Goldberg-Stern: nothing to disclose
Y. Assaf: nothing to disclose

RPS 411-5 16:24

Isolated and subtle abnormality of the corpus callosum: correlation with postnatal clinical outcome

L. Ben-Sira[1], N. Feldman[1], L.-T. Pratt[1], K. Kradjen[1], G. Malinger[2]; [1]*Tel-Aviv/IL,* [2]*Holon/IL (bensiraliat@gmail.com)*

Purpose: To examine the correlation between isolated and subtle abnormality of the CC with postnatal clinical outcomes.
Methods and materials: This retrospective study included all women referred for foetal neurosonogram and foetal MRI in Tel Aviv Sourasky medical centre from 2006-2017 due to suspected CC abnormality. Classification of the cases to anomaly subtypes was made by two independent observers according to CC integrity, width, length, shape, and additional brain findings. 44 isolated cases excluding complete CC agenesis and 44 control cases paired by age and gender to the study group who performed foetal MRI and were normal were included in the study. The clinical outcome was assessed by the adaptive behaviour assessment scale (ABAS-II) and by medical review questionnaires.
Results: The study group scored lower in all of the ABAS-II sub-domains and a significant difference between the study and control groups was found in the conceptual, practical, and general domains (p=0.005, 0.009, and 0.006). Special education placement was reported only in the study group (in 3 children) and the children in this group received neurodevelopmental interventions more often than the control group. In addition, individual comparisons were made for each CC anomaly subtype which included short, thick, thin, and dysmorphic CC. A similar trend of impaired functional abilities was evident in both short and thick CC subgroups.
Conclusion: This study sheds light on the unresolved question regarding the clinical outcome of isolated subtle anomalies in the CC during pregnancy. Subtle CC anomaly, especially short and thick, manifest mild functional difficulties. No major handicaps were found in our study group.
Limitations: Larger studies on this subject matter are still required.
Ethics committee approval: Ethics committee approval obtained.
Funding: No funding was received for this work.
Author Disclosures:
L. Ben-Sira: nothing to disclose
N. Feldman: nothing to disclose
L.-T. Pratt: nothing to disclose
K. Kradjen: nothing to disclose
G. Malinger: nothing to disclose

RPS 411-6 16:30

Differentiation of genetic subtypes of medulloblastomas using qualitative and quantitative (ADC) MRI features

J. Reis, H. Zimmermann, V. Ruf, N. Thon, T. Liebig, R. Forbrig; *Munich/DE*

Purpose: According to the updated WHO 2016 classification of CNS tumours, diagnosis of a medulloblastoma now demands genetic subgroup information (in addition to histopathology), defining the tumour biology, therapy and prognosis more precisely. The aim of this study was to assess potential correlations of

qualitative and quantitative MRI features for differentiation of genetic subtypes of medulloblastomas.
Methods and materials: A retrospective single-centre analysis of all patients with medulloblastomas from 2015-2019 with available genetic subgroup information (WNT, SHH, and non-WNT/non-SHH) was conducted. Regarding qualitative MRI analysis, tumour location as well as presence/absence of contrast-enhancement, oedema, cysts, and signs of metastatic disease were evaluated. Quantitative MRI analysis consisted of manual region-of-interest (ROI) based on ADC_{mean} calculation within the solid tumour. Statistical analysis included a comparison of ADC_{mean} between the genetic subgroups and a correlation with histopathological and imaging features.
Results: 30 patients (8 female, mean age=12 years) were included. 3/30 tumours were WNT-activated (10%), 11/30 (37%) SHH-activated, and 16/30 (53%) were classified as non-WNT/non-SHH. The tumour was located centrally in 19/30 (63%) and laterally in 7/30 (23%) patients. Distinct contrast enhancement was present in 3/30 (10%), oedema in 6/30 (20%; exclusively SHH subtypes), cysts in 25/30 (83%), and signs of metastatic disease in 13/30 (43%) patients. ADC_{mean} [$10^{-6}mm^2/s$] was 484 for WNT, 566 for SHH, and 624 for non-WNT/non-SHH subtypes ($p>0.05$). We found a significant negative correlation between ADC_{mean} and the proliferation parameter ki67 ($r=-0.469$, $p=0.009$, $n=30$).
Conclusion: In our study, peritumoral oedema was only present in SHH subtypes. Quantitative DWI analysis alone was not sufficient for the differentiation of genetic subtypes. However, a comparably lower ADC value was associated with a higher proliferation rate.
Limitations: n/a
Ethics committee approval: n/a
Funding: No funding was received for this work.
Author Disclosures:
J. Reis: nothing to disclose
H. Zimmermann: nothing to disclose
R. Forbrig: nothing to disclose
N. Thon: nothing to disclose
T. Liebig: nothing to disclose
V. Ruf: nothing to disclose

RPS 411-7 16:36

Imaging in neonatal encephalitis due to Chikungunya vertical transmission

N. Sachdev, S. Sana, A. Prasad, Y. Singh*; New Delhi/IN (namritasach@rediffmail.com)*

Purpose: Imaging modalities like neurosonogram and CT have a limited role in evaluation. MRI with diffusion-weighted imaging shows features of viral encephalitis involving frontoparietal subcortical and deep white matter and corpus callosum.
Methods and materials: 10 neonates of Chikungunya encephalitis born of mothers with Chikungunya in the last 2 weeks prior to delivery underwent MRI evaluation included T1, T2, FLAIR diffusion-weighted, gradient echo, and post-contrast images. A neurosonogram was done in one child and a CT scan in another. Follow-up MRI was done at 1 month or 3 months, depending on the clinical evaluation of the neurodevelopmental delay.
Results: 2/10 neonates showed normal MRIs. All the cases showed bilateral involvement affecting frontal, parietal, and occipital lobes. The infratentorial compartment with the cerebellum and brain stem were not involved. T2 and FLAIR hyperintensities diffuse as well as discrete in appearance were seen in the subcortical and deep white matter periventricular location with sparing of the U fibres. Follow-up MRIs showed a significant reversal in diffusion restriction in the 1-month scan. Cystic encephalomalacia with ventricular dilatation was seen with a reduction in white matter volume in the 3-month follow-up scan in 2 cases.
Conclusion: Encephalitis is the most common neurological presentation in the Chikungunya infected neonates after mother-to-child transmission. Neuro imaging is essential with MRI, with diffusion-weighted imaging being the primary imaging modality. DWI images may show changes prior to signal intensity changes on T2 images. DWI can also demonstrate progress as well as as prognosticate. Long-term MRI imaging is important in neonates who have neurodevelopmental delays.
Limitations: n/a
Ethics committee approval: n/a
Funding: No funding was received for this work.
Author Disclosures:
N. Sachdev: nothing to disclose
S. Sana: nothing to disclose
A. Prasad: nothing to disclose
Y. Singh: nothing to disclose

RPS 411-8 16:42

Orbito-facial dysmorphology in patients with different degrees of trigonocephaly severity: quantitative morpho-volumetric analysis in infants with non-syndromic metopic craniosynostosis

A. Marrazzo[1], R. Calandrelli[2], M. Panfili[2], F. Pilato[2], L. Massimi[2], C. Colosimo[2]; *[1]Taranto/IT, [2]Rome/IT (arm.marrazzo@gmail.com)*

Purpose: Craniofacial dysmorphology varies significantly along a wide spectrum of severity in metopic cranial synostosis (MCS). This study aimed to quantify craniofacial changes to investigate their relationships with the severity of trigonocephaly.
Methods and materials: Among 59 infants with MCS, we identified 3 groups according to the severity of trigonocephaly combining the metopic ridge and interfrontal angles (mild, moderate, and severe). We performed a quantitative analysis using high-resolution CT images evaluating: 1) cranial fossae dimensions; 2) vault indices and ratios: interparietal/intercoronal (IPD/ICD ratio), interparietal/intertemporal (IPD/ITD), cephalic index, vertico-longitudinal index; 3) orbito-facial distances (midfacial depth, maxillary height, upper facial index, orbital distances, globe protrusions), maxilla and orbital volumes; 4) supratentorial (ICV) and infratentorial (PCFV) cranial volume, supratentorial (WBV) and infratentorial (PCFBV) brain volume.
Results: In all groups, middle skull base lengths and upper midface indexes (n-pr/af-af) were increased.
In moderate and severe groups, anterior hemifossae lengths were reduced, IPD/ICD and vertico-longitudinal index were changed, interzygomatic buttre distance, midfacial depth (af-ans), anterior, and mild and lateral interorbital distances were reduced and globe protrusions were increased.
The comparison between moderate and severe groups showed a worsening of globe protrusions and IPD/ICD in the severe group and only in the severe group were ICV and WBV resulted reduced.
Conclusion: This morpho-volumetric study provides new insights in understanding the craniofacial changes occurring in infants at different severities of trigonocephaly. The increase of globe protrusions and the reduction of sovratentorial volumes found in the severe group reflect the severity of trigonocephaly; these patients might require early surgical cranial expansion.
Limitations: A retrospective study
Ethics committee approval: n/a
Funding: No funding was received for this work.
Author Disclosures:
A. Marrazzo: nothing to disclose
R. Calandrelli: nothing to disclose
M. Panfili: nothing to disclose
F. Pilato: nothing to disclose
L. Massimi: nothing to disclose
C. Colosimo: nothing to disclose

RPS 411-9 16:48

Dural venous sinuses and subarachnoid spaces in foetuses with MMC correlate with sac morphology: implications for the pathophysiology of abnormal brain development

I. Shelef[1], N. Boniel[2], L. L Tene[1], R. Goldstein[3], N. Gupta[3], O. Glenn[3]; *[1]Beer Sheva/IL, [2]Winnipeg, MB/CA, [3]San Francisco, CA/US (shelef@bgu.ac.il)*

Purpose: We hypothesise a significant size difference exists in the subarachnoid spaces (SAS) and dural venous sinuses (DVS) of myelomeningocele (MMC) infants in utero and that these differences vary depending on the morphology of the MMC sac.
Methods and materials: 76 foetuses with MMC underwent MRI prior to foetal surgery (mean gestational age 23.55+/-2.85 weeks) and repeat MRI postnatally (mean age at MRI 24.07+/-85.37 weeks). Head MRIs of 74 gestational-age matched normal foetuses were used for comparison. The MMC prenatal group was subdivided based on the presence or absence of a spinal sac. SAS depth and DVS diameters were compared between all groups.
Results: All parameters were significantly different between prenatal MMC group and normal foetus group ($p<0.001$). All SAS measurements were significantly smaller in the prenatal MMC group compared to the normal foetus group ($p<0.001$). SAS in the subgroup of MMC with an absent or flaccid sac was significantly less than those with an apparently tense sac. All DVS were found to be significantly narrower in the prenatal MMC group compared to the normal foetus group ($p<0.001$). The superior sagittal sinus was narrower in the subgroup of MMC with an absent sac versus those with an apparently tense sac.
Conclusion: This is the first report of mismatch between DVS and SAS diameters in foetuses with MMC and normal foetuses. Preliminary results suggest a contradiction in DVS size; when no sac (or a flaccid sac) is present, the veins are significantly narrowed and vice versa. We postulate that in the presence of a sac, there is less leakage of cerebrospinal fluid and the vein morphology is closer to normal.
Limitations: The potential sources of bias and small study group.
Ethics committee approval: n/a
Funding: No funding was received for this work.

Author Disclosures:
I. Shelef: nothing to disclose
N. Boniel: nothing to disclose
L. L Tene: nothing to disclose
R. Goldstein: nothing to disclose
N. Gupta: nothing to disclose
O. Glenn: nothing to disclose

RPS 411-10 16:54
MRI anatomical variants of the head of the hippocampus
E. Piccirilli, L. Gentile, V. Panara, V. Maruotti, P. A. Mattei, M. Caulo*; Chieti/IT (ele.piccirilli@gmail.com)*

Purpose: The head of the hippocampus (H) is classically described as having 2 -4 digitations both in ex-vivo specimens and in-vivo coronal MRI. Our aim was to develop a new MR-based classification of the anatomical variants of H in a large sample population of healthy subjects
Methods and materials: Brain MRIs of 247 young healthy subjects (138 M, age 18-39) were analysed. The H was identified on coronal reformatted 3D T1-w MRI. The H of a subset of 100 subjects were analysed and classified according to number of sulci and number and size of digitations. This classification was used to assess the frequencies of anatomical variants in a larger subset of 247 subjects for hemisphere and sex. Statistically significant differences were assessed by Chi-Square or marginal homogeneity tests (level of significance ρ<0.05)
Results: 8 variants of the H were described. Class 0 (11.3%) describes a total lack of sulci and is subdivided in 0A (one digitation, 10.1%) and 0B (no digitations or "null variant", 1.1%). Class 1 (25.6%, one single sulcus) is subdivided into 4 types according to location and width of the sulcus [1A (8.8%), 1B (12.8%), 1C (1.3%), and 1D (2.7%)]. Class 2 ("classical variant", 2 symmetrical sulci and 3 digitations equal in size) is the most frequent overall (63.0%). A statistically significant difference between the H classification of the two hemispheres was observed only in women (ρ=0.035) and overall (ρ=0.047). Variants prevalence did not differ between genders.
Conclusion: We described a new morphologic classification of the H which should allow minimisation of the risk of misinterpreting anatomical variants as pathologic conditions.
Limitations: Only T1w coronal images were assessed, not T2w.
Ethics committee approval: n/a
Funding: No funding was received for this work.
Author Disclosures:
E. Piccirilli: nothing to disclose
V. Panara: nothing to disclose
P. A. Mattei: nothing to disclose
M. Caulo: nothing to disclose
V. Maruotti: nothing to disclose
L. Gentile: nothing to disclose

RPS 411-11 17:00
Age-related differences in subfields and subregions of the hippocampus in normal volunteers
N. Ananyeva, E. Andreev, R. Ezhova, T. Salomatina, L. Akhmerova*; St. Petersburg/RU (ananieva_n@mail.ru)*

Purpose: To define the changes in subfields and subregions of the hippocampus in normal ageing.
Methods and materials: We examined 83 normal volunteers without neurological or psychiatric disorders divided into groups: 15-19, 20-24, 25-29, 30-39, 40-49, 50-59, 60-69 years old, and older than 70.
MR VBM was performed using 3D MPRAGE on MRI 1.5T XGV (Canon, Japan) with Freesurfer 6.0.
Results: A comparative analysis using the Mann-Whitney criteria defined the increase of the whole hippocampal volume until the age of 29. Then until 39, there was no difference. After that first slow (until 69) and after 70, a quick decrease of 17% of a significance level, p≤0.05.
The most significant difference occurred in the CA3 Broadmann area increasing until 24 years old, 12% of a significance level, p≤0.05. Until 49, there was no difference. There was a decrease of 7% until 70 years, and after 70 years, a decrease of 19% of a significance level, p≤0,01. The same results we found in the CA1 Brodmann area: increasing until age 29 years then a slow decreasing. After 70 years, a decrease of 18% of a significance level, p≤0,05, was seen. A significant difference was found in the hippocampal sulcus of 20% of a significance level, p≤0.05.
In old age, a significance level, p≤0.05, was found in the decrease in the volume of the hippocampal tail of 23%, molecular layer of hippocampus (14%), and of the dentate gyrus (19%), fimbria (37%), and subiculum (16%).
Conclusion: In our research, we found significant dynamics of differences in the whole volume of the hippocampus. The most significant changes were found in the CA1 and CA3 Broadmann areas, hippocampal sulcus, fimbria, hippocampal tail, subiculum, molecular layer of hippocampus, and dentate gyrus.
Limitations: n/a
Ethics committee approval: Ethics committee approval obtained.
Funding: No funding was received for this work.
Author Disclosures:
N. Ananyeva: Author at Bekhterev NMIC NP
E. Andreev: Author at Bekhterev NMIC NP
R. Ezhova: Author at Bekhterev NMIC NP
T. Salomatina: Author at Bekhterev NMIC NP
L. Akhmerova: Author at Bekhterev NMIC NP

RPS 411-12 17:06
The measurement of hippocampal dimensions versus hippocampal volumetry via the automated segmentation on MRI for the validation of hippocampal sclerosis
X. C. Liew[1], K. Rahmat[2], N. Ramli[2], F. B. Fadzli[2], K. S. Lim[2]; [1]*Lembah Pantai/MY,* [2]*Kuala Lumpur/MY (katt_xr2000@yahoo.com)*

Purpose: To develop a simple quantitative technique for hippocampal atrophy which is comparable to hippocampal volumetry on MRI and to specifically delineate and obtain the cut-off value for normal and abnormal hippocampal volume, height, and width.
Methods and materials: A cross-sectional MRI study of 43 temporal lobe epilepsy and 49 control subjects was conducted. MRI brain assessment by two readers was based on standard visual diagnostic criteria by identifying hippocampal atrophy and hyperintensity on axial T2 FSE/coronal FLAIR CUBE sequences. The mean manual measurement of the hippocampal head height and width were performed using MANGO (multi-image analysis GUI) software by two readers. The hippocampal volume was measured by Free Surfer automated segmentation.
Results: A moderate positive correlation between the hippocampal volume and height/width bilaterally (p <0.001) was seen. Wilcoxon rank tests demonstrated a significant difference between bilateral hippocampal volume and width. A Mann-Whitney test showed that hippocampal volume, height, and width in the control group were significantly higher than the patient group (p<0.001).
The optimal cut-point value by (ROC) curve and Youden index for the left hippocampal volume was 3257 mm³ (sensitivity: 91.3%, specificity:88.4%, PPV:72.4%, and NPV:96.8%), left hippocampal height was 7 mm (sensitivity: 84.6%, specificity: 89.4%, PPV:75.9%, and NPV:93.7%), and left hippocampal width was 15 mm (sensitivity: 61.3%, specificity: 83.6%, PPV: 65.5%, and NPV: 81.0%). The optimal cut-point value for the right hippocampal volume was 3761 mm³ (sensitivity: 87.5%, specificity: 97.1%, PPV: 91.3%, and NPV: 95.7%), right hippocampal height was 7 mm (sensitivity: 88.2%, specificity: 89.3%, PPV: 65.2%, and NPV: 97.1%), and right hippocampal width was 17 mm (sensitivity: 61.5%, specificity: 89.4%, PPV: 69.6%, and NPV: 85.5%).
Conclusion: Manual measurement of hippocampal dimension is simple and reliable with a strong positive correlation between the hippocampal volume, height, and width in combination with semiology and MRI visual assessment.
Limitations: n/a
Ethics committee approval: Approval by the institutional ethics board.
Funding: University Malaya research grant.
Author Disclosures:
K. Rahmat: nothing to disclose
N. Ramli: nothing to disclose
X. C. Liew: nothing to disclose
F. B. Fadzli: nothing to disclose
K. S. Lim: nothing to disclose

RPS 411-13 17:12
Brain size matters: a comparative study between Indian and caucasian brains and intracranial volumes
J. Desai[1], A. Joshi[1], R. Kulkarni[1], L. Poonamallee[2], A. Sakegaonkar[1]; [1]*Pune/IN,* [2]*New York/US (juhi.desai@in-medprognostics.com)*

Purpose: Quantitative MRI has been proven to aid in identifying subtle volumetric changes in the brain. Studies have stated regional and global differences in shape, size, and volume between the caucasian and eastern populations. Chinese, Korean, and Japanese populations have also shown significant differences in brain shape and size between the western and eastern population. Our objective was to study the differences between the Indian and caucasian populations.

Methods and materials: 100 healthy control T1 3d MRIs of brains were collected from Indian and caucasian (XNAT database) populations, cross-matched between the ages of 20-85 years. A semi-automated clustering segmentation technique of ITK-SNAP was used to segment brain volumes. MRIs with motion artefacts were rejected to reduce error.
Results: Data had a normal distribution between ages, with a skewness coefficient of 0.05. The age and gender-matched comparison of Indian (group 1) and caucasian (group 2) brains and intracranial volumes (ICV) showed significant differences. The average volumes for Indians were 1,122.48 ml (whole-brain) and 1,339.75 ml (ICV) as compared to 1,222.68 ml (whole-brain) and 1,482.87 ml (ICV) in caucasians. One way anova for brain and ICV were found significant at $p<0.5$.
Conclusion: To our knowledge, this is the first large-scale study examining the differences in the volumes of brains and intracranial volumes between Indians and caucasians. The statistical analysis confirms the vast differences in the volumes of the brain in the two population. For the use of the quantitative analysis based on MRI to be clinically relevant, new references need to be build based on the type of population.
Limitations: The relationship between brain volumes and ICV described here are based on cross-sectional data and await refinement in future analyses.
Ethics committee approval: n/a
Funding: No funding was received for this work.
Author Disclosures:
J. Desai: Author at PROGNOSTICS IN-MED PVT LTD
A. Joshi: Author at Deenanath Mangeshkar hospital
L. Poonamallee: Founder at PROGNOSTICS IN-MED PVT LTD
R. Kulkarni: nothing to disclose
A. Sakegaonkar: Employee at PROGNOSTICS IN-MED PVT LTD

RPS 411-14 17:18

Applying clinical 7 Tesla MRI scanners for postmortem examinations in forensic medicine

D. Gascho, E. Deininger-Czermak, N. Zoelch, M. Thali*; Zurich/CH (dominic.gascho@irm.uzh.ch)*

Purpose: The role of postmortem magnetic resonance imaging (MRI) is becoming more important in forensic medicine. The purpose of this study was to assess the potential advantages in using 7 Tesla MRI versus 3 Tesla MRI in forensic medicine for the assessment of cerebral haemorrhages.
Methods and materials: Decedents with cerebral haemorrhages (n=10) after blunt trauma or in accordance with a natural cause of death underwent head examinations using a 3 Tesla MRI unit and using a 7 Tesla MRI unit. The case selection was based on the detection of a cerebral haemorrhage on a previously performed computed tomography scan. The MRI protocol included 3D T2, T1, and susceptibility-weighted sequences. Additionally, high-resolution 3D in-phase gradient-echo sequences were performed for the visualisation of the bones. The images were visually compared by two radiologists.
Results: 7 Tesla MRI was superior to 3 Tesla MRI with regard to the detailed visualisation of anatomical structures due to the high contrast and high spatial resolution of the 7 Tesla MRI. Additionally, microhaemorrhages could be visualised on 7 Tesla MRI due to an increased susceptibility compared to 3 Tesla MRI. Overall, 7 Tesla MRI allowed for a more precise assessment of cerebral bleeding. A drawback of 7 Tesla MRI was the increased B1 inhomogeneities compared to 3 Tesla MRI, which caused signal differences across the brain. Small osseous fractures could be visualised on both MRI units, albeit 7 Tesla MRI presented a higher spatial resolution.
Conclusion: 7 Tesla MRI enables a more precise examination of cerebral haemorrhages, which may provide new opportunities for their radiological assessment in forensic as well as in clinical radiology.
Limitations: A small number of cases.
Ethics committee approval: n/a
Funding: No funding was received for this work.
Author Disclosures:
D. Gascho: nothing to disclose
E. Deininger-Czermak: nothing to disclose
N. Zoelch: nothing to disclose
M. Thali: nothing to disclose

RPS 411-15 17:24

TI optimisation for postmortem FLAIR MRI: a pilot study

C. Bruguier, J.-F. Knebel, V. Magnin, P. Genet, V. Dunet*; Lausanne/CH (christine.bruguier@chuv.ch)*

Purpose: During the radiological evaluation of the FLAIR sequence for postmortem cases, a wide variety of image contrast is observed, different from that encountered in living patients. We aimed at evaluating the impact of two variables (temperature and delay from death) suspected of having an influence on the optimal inversion time (TI) value, which allows obtaining the living patient-like image contrast.
Methods and materials: In 24 postmortem cases, brain MRIs were performed and 3D FLAIR sequences with TI varying from 1,660 ms-900 ms, every 110 ms, were acquired. Two radiologists independently evaluated the images and were asked to choose which TI corresponded to the image of a standard patient-like FLAIR contrast. Rectal temperature and delay between the death of the cases and MRI were recorded. Pearson's correlation tests between the mean TI value, temperature, and delay were performed, as well as an evaluation of interobserver reliability with the prevalence-adjusted and bias-adjusted Kappa (PABAK).
Results: The temperature ranged from 5.7°-29.7°, while the death-MRI delay ranged from 12.3h to 74.4h. The optimal TI value ranged from 1,330 ms-1,100 ms, with moderate interobserver reliability (PABAK=0.56, 95%CI [0.28-0.84]). The optimal TI value was significantly correlated with the temperature (Pearson R=0.70; p=0.0014) and the delay from death (Pearson R=-0.67; p=0.00027). Rectal temperature was inversely correlated with the delay from death (Pearson R=-0.79; p<0.00001).
Conclusion: Postmortem brain FLAIR imaging contrast is significantly related to body temperature and delay from death. The TI value should be adapted to obtain living patient-like image contrast. A larger study cohort is needed to confirm these preliminary results and to evaluate whether the TI value could be used as an additional tool for dating the postmortem interval.
Limitations: The size sample.
Ethics committee approval: n/a
Funding: No funding was received for this work.
Author Disclosures:
C. Bruguier: Author at University Hospital of Lausanne, Speaker at University Hospital of Lausanne
J.-F. Knebel: nothing to disclose
V. Magnin: nothing to disclose
P. Genet: nothing to disclose
V. Dunet: nothing to disclose

Thursday, March 12

08:30 - 10:00 **Room Y**

My Thesis in 3 Minutes

MyT3 5

Musculoskeletal

Moderators:
N.N.

MyT3 5-1 08:30

Diffusion-weighted magnetic resonance imaging of the normal bone marrow in children and the effects of local and systemic cancer therapies

E. Pace, E. Clarke, A. Mackinnon, H. Mandeville, S. Vaidya, N. Desouza;
London/UK (ERIKA.PACE@RMH.NHS.UK)

Purpose:
To establish apparent diffusion coefficient (ADC) values for normal paediatric clival marrow and variation with age, gender, and puberty. To compare post-photon and proton-therapy clival ADC changes. To examine chemotherapy effects on ADC in the spine. To develop a longitudinal study to assess post-transplant bone marrow changes.
Methods and materials: Inclusion criteria: 5-17 years old, iso-DW-MRI ISO, non-oncological population (aim 1). Exclusion criteria: drugs (aim 1), dental brace, DW-MRI artefacts. Image acquisition/analysis: 1.5 T scanner. DWI with b = 0 and 1000 s/mm2. A 4-6 mm region-of-interest drawn within the clivus (Adept®, The Institute of Cancer Research) and at L3-S1. ADC calculated on a voxel-by-voxel basis through a monoexponential fit of the data yielded mean, median, 10th, 25th, 75th, and 90th centile ADC values.
Results: With chemotherapy, a reduction in vertebral ADC at 3 months was stabilised or decreased by 6 months. Although no oedematous response developed, fat replacement of haematopoetic tissue still resulted.
Conclusion: As paediatric prospective studies to investigate normal bone marrow are ethically difficult, the work in this thesis was largely retrospective. A first innovative attempt to establish the influence of age, gender and puberty on ADC values of clival marrow in cancer-free children alongside an assessment of oncological local and systemic treatment-related effects have been made.
Limitations: Unnumerous cohorts. Non-standardised acquisition timing of the follow-up scans; different tumour types, photon/proton dose, and chemotherapy. PUMA (Paediatric osseoUs Marrow Assessment) trial recruitment still in progress.
Ethics committee approval: Service Evaluations (562 and 756) approved by The Marsden. Approval from the Joint Research Committee to import MR scans performed at St George's Hospital. PUMA trial approved by the Health Research Authority.
Funding: Cancer Research United Kingdom grant (2013-2018).
Author Disclosures:
E. Pace: Author at The Royal Marsden
A. Mackinnon: nothing to disclose
H. Mandeville: nothing to disclose
S. Vaidya: nothing to disclose
N. Desouza: nothing to disclose
E. Clarke: nothing to disclose

MyT3 5-2 08:34

Application of "Trigger Drop" in patients enrolled for percutaneous treatment of symptomatic discal hernia: preliminary results

A. Paladini[1], I. Percivale[1], A. Carriero[1], M. Spinetta[1], G. Guzzardi[1], Z. Falaschi[1], M. Cernigliaro[1], S. Bor[2], D. Zagaria[1]; [1]*Novara/IT,* [2]*Santhià/IT*
(andreapaladini1988@gmail.com)

Purpose: Trigger drop® is a muscle mediator that reduces the pain due to articular and muscular etiology. The device acts on crossed muscular chains and on neuro-lymphatic points with antalgic effect. We performed "dropping technique" applying inherit devices with different shapes in different positions on the body surface.
Methods and materials: From January to June 2019, 19 symptomatic patients have been enrolled. All patients were candidates to either cervical (5 patients) or lumbar (14 patients) disc treatment. Primary and secondary endpoints have been evaluated: efficacy of Trigger-Drop® has been evaluated in stopping analgesic drugs assumption and reducing back-pain through the visual analogic scale (VAS) evaluated before and soon after the device positioning. We performed a clinical follow-up three weeks after Trigger-drop positioning.
Results: In 89,5% (17 Patients) the device had immediate pain relief with a VAS reduction >4 compared to the initial value. 87.5% of patients stopped painkillers therapy after the application of Trigger-Drop®. Only one minor side effect was reported (localised cutaneous erythema), which disappeared by itself.
Conclusion: In our experience the positioning of Trigger-drop®, in patients waiting for percutaneous disc treatment, has been effective and safe in relieving back pain for a short period (three weeks), improving the overall quality of life of patients. Trigger-Drop® therapy allowed the pharmacologic therapy suspension for pain management.
Limitations: Not a large cohort of patients included.
Ethics committee approval: n/a
Funding: No funding was received for this work.
Author Disclosures:
A. Paladini: nothing to disclose
I. Percivale: nothing to disclose
A. Carriero: nothing to disclose
M. Spinetta: nothing to disclose
G. Guzzardi: nothing to disclose
M. Cernigliaro: nothing to disclose
S. Bor: nothing to disclose
D. Zagaria: nothing to disclose
Z. Falaschi: nothing to disclose

MyT3 5-3 08:38

Staging of osteochondral lesions of the talus: comparison of cone-beam CT arthrography with MR imaging

J. Desimpel[1], F. M. H. M. Vanhoenacker[2]; [1]*Antwerp/BE,* [2]*Duffel/BE*
(julie_desimpel@hotmail.com)

Purpose: An osteochondral lesion (OCL) is defined as damage involving both articular cartilage and subchondral bone. OCL of the talus is frequently detected by routine MRI by identification of bone marrow oedema as an indirect marker of overlying cartilage lesion. The articular cartilage of the talus and the distal tibia is thin compared to the knee joint hampering precise staging of osteochondral lesions of the talus on MRI. CBCT-arthrography has a better spatial resolution than MRI and visualises the articular cartilage more in detail. The purpose of this study was to compare the value of CBCT-arthrography as staging method of talar OCL.
Methods and materials: 35 patients with a talar OCL underwent both MR imaging (1.5T) and CBCT-arthrography within a time frame of maximum 1 month to avoid significant lesion progression between both examinations. The following parameters were scored individually by two radiologists: depth of the cartilage lesion, degree of detachment (no, partial or complete), size and the presence of subchondral bone changes.
Results: CBCT-arthrography led to an upstaging of the OCL in 28 cases. 13 patients subsequently underwent surgery of which 6 patients had an upstaging of the degree of detachment on CBCT-arthrography (upstaging to partial detachment in 2 cases and to complete detachment in 4 cases). Surgery was recommended in 3 cases of which 2 patients had an upstaging of the degree of detachment on CBCT-arthrography (1 patient with partial and 2 patients with complete detachment).
Conclusion: CBCT-arthrography is a very promising technique for staging of cartilage lesions of the ankle. Improved staging is very useful in those clinical scenarios where arthroscopic treatment of the lesion is considered.
Limitations: This stud is limited by the number of patients.
Ethics committee approval: Ethics committee approval.
Funding: No funding was received for this work.
Author Disclosures:
J. Desimpel: nothing to disclose
F. M. H. M. Vanhoenacker: nothing to disclose

MyT3 5-4 08:42

Diagnostic accuracy of dual-energy CT in assessment of traumatic bone marrow oedema of lower limb and its correlation with MRI

H. Yadav[1], S. Khanduri[2], P. Yadav[2]; [1]*New Delhi/IN,* [2]*Lucknow/IN*
(harshyadav.kgmc@gmail.com)

Purpose: To assess the diagnostic accuracy of dual-energy CT in detecting bone marrow oedema in patients of trauma of lower limb and correlate it with MRI.
Methods and materials: The study included 40 patients aged between 15–70 years of either sex. All the patients of lower extremity trauma after clinical evaluation underwent DECT and MRI evaluation. All the images were postprocessed on a work station and were further evaluated by a radiologist.
Results: Mean attenuation at fractured site observed by dual-energy CT was found to be significantly higher as compared to that at the adjacent site (170.75±33.99 vs 19.73±22.50 HU). Sensitivity, the specificity of dual-energy CT as compared to MRI in detecting bone marrow oedema were 94.1%, 91.3% respectively. Out of 40 cases enrolled in the study, agreement of MRI and dual-energy CT was observed in 37 (92.5%).

Conclusion: Dual-energy CT can be an effective alternative to MRI in detection of bone marrow oedema in patients of lower limb trauma. Dual-energy CT can also be used in patients in whom MRI is contraindicated.
Limitations: Not applicable.
Ethics committee approval: Not applicable.
Funding: No funding was received for this work.
Author Disclosures:
H. Yadav: Author at Lady Hardinge Medical College
S. Khanduri: nothing to disclose
P. Yadav: nothing to disclose

MyT3 5-5 08:46
The role of bone marrow lesions in acute joint injury
L. Selvarajah[1], A. Curtis[2], O. Kennedy[2]; [1]*Limerick/IE,* [2]*Dublin/IE (logesselva@gmail.com)*

Purpose: Post-traumatic osteoarthritis (PTOA) mainly affects a younger population cohort and poses significant costs to healthcare systems. Recent developments have identified that joint injury is initiated in the sub-chondral region of the joint despite the initial intra-articular cartilage injury. Of particular interest is bone marrow oedema or lesions (BMLs) that appear in the sub-chondral region almost immediately after initial joint injury.
Methods and materials: A review is undertaken on what is known about these phenomena (microcracks and BMLs) in the literature and discuss potential mechanisms by which they may be linked. Papers published in the last 10 years relating to bone remodeling in joint injury, subchondral microdamage, BMLs, bone-cartilage crosstalk and novel imaging models demonstrating acute knee injury were reviewed.
Results: The recent findings in this field have shown that microcracks in bone initiate targeted remodelling via RANKL expression in osteocytes. Other work has shown that subchondral microcracks co-localise with BMLs as viewed by MRI. Finally, BMLs are associated with and predict subsequent pain and structural joint degeneration.
Conclusion: This paper demonstrates that subchondral microcracks likely occur during acute joint injury, and are closely linked to BML that are seen by clinical MRI and thus are potentially involved in the subsequent joint degeneration that occurs after injury. BMLs could serve as a potential site of radiological monitoring and therapeutic intervention to better tailor patient management.
Limitations:
The precise way in which subchondral activities are linked with those in the articular compartment is not yet known but defining these events using additional imaging sequences (DWI-ADC/T1rho) will be an important next step in this field.
Ethics committee approval:
This article does not contain any studies with human or animal subjects performed by any of the authors.
Funding: No funding was received for this work.
Author Disclosures:
L. Selvarajah: nothing to disclose
O. Kennedy: nothing to disclose
A. Curtis: nothing to disclose

MyT3 5-6 08:50
T2-mapping evaluation of long-term cartilage alteration of humeral head for arthroscopic Bankart repair with or without remplissmage
Y. Xie, S. Chen*; Shanghai/CN (xieyuxue1994@gmail.com)*

Purpose: To quantitatively evaluate the cartilage alteration of humeral head after Bankart repair with or without remplissmage using T2-mapping.
Methods and materials: Fifty-six patients, including 28 with isolated Bankart repair surgery (group A) and 28 with combined remplissmage (group B), and 20 healthy subjects (control group) were recruited. All participants underwent T2-mapping scan and were evaluated with American Shoulder and Elbow Surgeon scores（ASES）and range of motion (ROM) at a minimal of 2 years' follow-up (average, 8.9 years). The total humeral head cartilage was segmented into six compartments (I-VI) along the coronal oblique plane.
Results: Of the 56 patients, 3 (5.4%) had recurrent dislocation during daily activities. There was no significant difference in preoperative and postoperative ASES between group A and group B (P=0.82). The mean external rotator loss was 6.3 degrees for group A and 9.8 degrees for group B (P=0.12). The T2 values in the middle-to-inferior subregions were significantly higher than those in the superior subregions (P<0.05). The total and all the compartments of T2 values in the patient groups were higher than those in the control group (P<0.05). For the two patient groups, there was no significant difference of T2 values between all regions (P>0.05). Moreover, the T2 values in both patient groups were negatively correlated with ASES scores, especially for the middle-to-inferior compartments (r= –0.52 to -0.6, P < 0.05).
Conclusion: Shoulder instability after repair showed increasing cartilage T2 values in humeral head, mainly involving middle-to-inferior compartments, which could be the main cartilage compartment that may affect the patient's clinical symptoms.
Limitations: The cohort of patient was small.
Ethics committee approval: This study was approved by the Health Sciences Institutional Review Board of our hospital (2015M-010).
Funding: Grant support was received from the National Natural Science Foundation, China (No. 81671652).
Author Disclosures:
Y. Xie: Author at huashan hospital, Speaker at huashan hospital
S. Chen: Research/Grant Support at huashan hospital

MyT3 5-7 08:54
MRI evaluation to predict tendon size for knee ligament reconstruction
G. Di Nino, E. Grassedonio, P. Toia, L. La Grutta, M. Nobile, T. Smeraldi, F. Midiri, M. Galia, M. Midiri*; Palermo/IT*

Purpose: The aim of this study is to evaluate a possible correlation between anthropometric parameters and sizes of knee tendons used for ACL reconstruction. We hypothesised that specific clinical and radiological knee measurements could be better tendon sizes predictors than anthropometric parameters.
Methods and materials: 110 patients were enrolled and 80 patients met the inclusion criteria of the study. All patients underwent an MRI of the knee with a 1.5 T MRI. For each patient, anthropometric data such as gender, height, weight, body mass index (BMI) and knee circumference were recorded. MRI knee measurements were performed on each study: patellar tendon (PT) thickness and length, quadriceps tendon (QT) thickness, semitendinosus tendon (ST), gracilis tendon (GR) diameter, the largest patella and intercondylar width.
Results: The ST, QT and PT thickness were higher in males than in females and no significant GT and knee circumference differences were. Significant, but weak correlations were found between patient anthropometric data and hamstrings diameter, PT length, and QT and PT thickness. Intercondylar and patellar width present a moderate correlation between PT thickness, PT length and ST diameter.
Conclusion: The intercondylar and patellar width presented a moderate correlation with PT thickness, PT length and ST diameter. Further, weak correlations were found between patient anthropometric data (gender, weight, height, BMI) and GR and ST diameter, PT length, and QT and PT thickness. This results may help surgeons during preoperative planning, specifically regarding graft choice and size.
Limitations: The study is preformed as a single centre study.
Ethics committee approval: n/a
Funding: No funding was received for this work.
Author Disclosures:
E. Grassedonio: Author at A.O.U.P Paolo Giaccone
G. Di Nino: Author at A.O.U.P Paolo Giaccone, Speaker at A.O.U.P Paolo Giaccone
P. Toia: Author at A.O.U.P Paolo Giaccone
L. La Grutta: Author at A.O.U.P Paolo Giaccone
M. Nobile: Author at A.O.U.P Paolo Giaccone
T. Smeraldi: Author at A.O.U.P Paolo Giaccone
F. Midiri: Author at A.O.U.P Paolo Giaccone
M. Galia: Author at A.O.U.P Paolo Giaccone
M. Midiri: Author at A.O.U.P Paolo Giaccone

MyT3 5-8 08:58
Hand extensor compartments: how to study them and is it always their fault?
C. A. B. Oliveira[1], F. M. F. Gomes[2], F. Vieira[1], V. Mendes[1]; [1]*Braga/PT,* [2]*Vila Nova de Sande/RO (carlosaboliveira2014@gmail.com)*

Purpose: To evaluate 100 patients with pain referred to the dorsal compartment, by grading the lesions in a three-way system (mild, moderate and high) and to examine the correlation between the physical exam and the ultrasound findings.
Methods and materials: Hand ultrasound was done to 100 patients with evaluation of the dorsal and volar hand. A review of the literature was made.
Results: In 72% of cases, pathology was found in the dorsal hand: 48% tendinitis of the I compartment, 22% tendinitis of the III compartment and the rest of the patients with multicompartment extensor pathology. 28% of cases with tenosynovitis of the flexor compartment lesion - 75% of cases; median nerve compression - 15% of cases and other pathology. Physical exam was according in 80 % of cases and pain referred to the lateral compartment was found in 68 %.

Conclusion: Hand pathology is complex and demands a correct grading and evaluation by the radiologist.
Limitations: This study is limited by its sample and a one radiologist reader.
Ethics committee approval: N/A
Funding: No funding was received.
Author Disclosures:
C. A. B. Oliveira: nothing to disclose
F. M. F. Gomes: nothing to disclose
F. Vieira: nothing to disclose
V. Mendes: nothing to disclose

MyT3 5-9 09:02
Diffusion tensor imaging of annulus fibrosus in subjects with discogenic low back pain
S. Tian, H. Yuan*; Beijing/CN (ts@bjmu.edu.cn)*

Purpose: Observe the morphology and integrity of annulus fibrosus by diffusion tensor imaging (DTI), and quantitatively analyse the annulus fibrosus by measuring the apparent diffusion coefficient (ADC) and fractional anisotropy (FA) in subjects with discogenic low-back pain (DLBP).
Methods and materials: Subjects with DLBP confirmed by discography were selected as the DLBP group and healthy volunteers as the healthy control (HC) group. The ADC, FA and λ1, λ2, λ3 values were measured by axial DTI of L3-S1 levels. The differences of ADC, FA and λ1, λ2, λ3 values between two groups were compared. The data conforming to normal distribution were tested by t-test, while the data not conforming to normal distribution were tested by nonparametric test.
Results: 30 subjects in the DLBP group and 24 subjects in the HC group were included in the study. The ADC value of ROI in the DLBP group was significantly lower than that in the HC group (6.10 ± 3.17 vs 9.84 ± 4.01, P = 0.0002), and the FA value was significantly higher than that in the HC group (0.341 ± 0.201 vs 0.231 ± 0.150, P = 0.007). Compared with the HC group, the DLBP group showed significantly lower λ1 (4.44 ± 0.36 vs 4.75 ± 0.35), λ2 (4.19 ± 0.34 vs 4.50 ± 0.36), and λ3 values (3.97 ± 0.34 vs 4.27 ± 0.38; all P < 0.05).
Conclusion: Diffusion tensor imaging has guiding significance in the clinical diagnosis of DLBP and preoperative localisation of the responsible segment.
Limitations: Retrospective design and the small sample sizes.
Ethics committee approval: Peking University Third Hospital Medical Science Research Ethics Committee approved this study (16-45-QX-TTK).
Funding: No funding was received for this work.
Author Disclosures:
S. Tian: nothing to disclose
H. Yuan: nothing to disclose

MyT3 5-10 09:06
Accuracy of volumetric trabecular bone mineral density assessment using dual-source dual-energy CT: a prospective phantom study and comparison with quantitative CT
C. Booz[1], I. Yel[1], N. Grosse Hokamp[2], J. Borggrefe[2], L. Lenga[1], S. S. Martin[1], J. L. Wichmann[1], T. J. Vogl[1], M. H. Albrecht[1]; [1]*Frankfurt am Main/DE,* [2]*Cologne/DE (boozchristian@gmail.com)*

Purpose: To assess the accuracy of phantomless volumetric bone mineral density (BMD) assessment of trabecular bone using dual-source dual-energy computed tomography (DECT) in comparison to quantitative CT (QCT).
Methods and materials: Data from a validated anthromorphic spine phantom consisting of three lumbar vertebra equivalents containing 50, 100 and 200 mg/cm³ calcium hydroxyapatite (HA) concentrations which had been scanned using third-generation dual-source DECT, QCT and dual x-ray absorptiometry (DXA) was analyzed. For volumetric BMD assessment based on DECT, dedicated postprocessing software using material decomposition was applied, which enables phantomless BMD assessment of the trabecular bone through semi-manual definition of the volume of interest (VOI). Scans of all modalities were repeated three times and measurements per vertebrae were also repeated three times, and averaged values were recorded. The accuracy of DECT and QCT for BMD assessment was compared; additionally, calculated BMD values were correlated with DXA, the standard of reference for BMD assessment according to the WHO.
Results: Significantly higher correlations between actual and measured HA concentrations were found for DECT (r=0.98) compared to QCT (r=0.93, P<.001). Mean error for all measurements was -2.8 ± 3.3 mg/cm³ (DECT) and –8.3 ± 9.5 mg/cm³ (QCT) (P<.001). There was significantly higher correlation between BMD values of DECT and DXA (r=0.99) compared to BMD values of QCT and DXA (r=0.96, P<.001).
Conclusion: Phantomless volumetric BMD assessment of trabecular bone using dedicated DECT material decomposition achieves substantially improved accuracy and significantly higher correlation with DXA in comparison to QCT.
Limitations: Small number of BMD measurements in this phantom study.
Ethics committee approval: This study was approved by the local IRB. Written informed consent was waived.
Funding: No funding was received for this work.
Author Disclosures:
C. Booz: Speaker at Siemens Healthineers
I. Yel: nothing to disclose
N. Grosse Hokamp: Speaker at Philips
J. Borggrefe: Speaker at Philips
L. Lenga: nothing to disclose
S. S. Martin: nothing to disclose
J. L. Wichmann: Employee at Siemens Healthineers, Speaker at Siemens Healthineers, Speaker at GE Healthcare
M. H. Albrecht: Speaker at Siemens Healthineers, Speaker at Bracco
T. J. Vogl: nothing to disclose

MyT3 5-11 09:10
Complex radiological diagnosis of osteonecrosis in desomorphine dependence patients on the pre-operative stage of treatment
A. Babkova, N. S. Serova, S. P. Pasha, S. K. Ternovoy*; Moscow/RU (an4i1@ya.ru)*

Purpose: To determine the diagnostic efficiency of methods of complex radiological diagnosis (ortopantomography, conventional radiography, MSCT, CBCT) in the evaluation of osteonecrosis in patients on the preoperative stage.
Methods and materials: In the period from 2014 to 2018, a total of 108 drug addicts with a history of abuse desomorphine were evaluated at the clinics of the Sechenov University. The age of patients varied from 18 to 48 years. The median age was 28 years. Among the patients, the number of women was 11 (10,1%), men – 97 (89,9%). The duration of administration of desomorphine in this group of patients ranged from 2 months to 10 years. Orthopantomography, radiography of the skull, MSCT and CBCT were performed on 108 patients (100%) in the preoperative stage. Also 25 patients (21%) underwent radionuclide diagnostics: planar bone scan, SPECT.
Results: The application of complex highly informative radiological methods (MSCT, CBCT, radionuclide diagnostics) in desomorphine dependence patients at the preoperative stage of treatment enables full investigation of character and the prevalence of the pathological process, to plan further tactics of surgical treatment.
Conclusion: The diagnostic efficiency parameters at the preoperative stage for MSCT were: the sensitivity – 98,1%, the specificity – 99,6%, the accuracy – 98,8%, for CBCT were: the sensitivity – 97,3%, the specificity – 99,1%, the accuracy – 98,4%, for orthopantomography: the sensitivity – 78,6%, the specificity – 76,3%, the accuracy – 77,4%, for skull xray: the sensitivity – 61,1%, the specificity – 59,2%, the accuracy – 60,2%.
Limitations: No limitations.
Ethics committee approval: n/a
Funding: No funding was received for this work.
Author Disclosures:
A. Babkova: nothing to disclose
N. S. Serova: nothing to disclose
S. P. Pasha: nothing to disclose
S. K. Ternovoy: nothing to disclose

MyT3 5-12 09:14
Long-term comparison between blind and ultrasound-guided injection in Morton neuroma
F. Ruiz Santiago, N. Prados Olleta, P. Tomás Muñoz, A. J. Láinez Ramos-Bossini*; Granada/ES (ferusan12@gmail.com)*

Purpose: This study aims to compare the effectiveness of blind vs ultrasound-guided injections in Morton neuroma until one year of follow-up.
Methods and materials: This is an evaluator blinded randomised trial. 31 patients with Morton neuroma were injected based on anatomic landmarks and 33 patients under ultrasound guidance. Patients were clinically assessed by the VAS score (0-10), and by the Manchester Foot Pain and Disability Index (MFPDI) –17 items; total score: 17 (best state) - 51 (worst state). Injections containing 1 ml of 2% mepivacaine and 40 mg triamcinolone were administered in the web space. Follow-up was performed at 15 days, 1 month, 45 days, 2 months, 3 months, 6 months and 1 year.
Results: Improvement in the VAS score was superior in the ultrasound group at all points of follow-up (p<0.05) except at 1 year when differences did not reach statistical significance (VAS: 4.6 ± 0.6 vs 5.9 ± 0.6, p=0.16). The improvement according to the MFDI was superior in the ultrasound group from 45 days to one-year follow-up (31.4± 1.7 vs 36.8± 1.9, p<0.05).

Conclusion: Ultrasound-guided injections in Morton neuroma led to greater long-term clinical improvement than blind injections. Although differences in pain tend to disappear at one-year follow-up, the disability index remains statistically improved in the ultrasound-guided group in comparison with the blind group.
Limitations: MN was not confirmed by histological examination in all our patients, but the overall accuracy of clinical and imaging diagnosis altogether has been reported to be very high, over 95%. Another limitation of the study is the sample size, which may have prevented differences from reaching stronger statistical significance.
Ethics committee approval: The study was approved by the local ethics committee (code: 0565-N-16).
Funding: No funding was received for this work.
Author Disclosures:
F. Ruiz Santiago: nothing to disclose
N. Prados Olleta: nothing to disclose
P. Tomás Muñoz: nothing to disclose
A. J. Láinez Ramos-Bossini: nothing to disclose

MyT3 5-13 09:18
Shoulder stability: where does it fail?
C. A. B. Oliveira, F. D. S. Costeira, V. Mendes, F. Vieira*; Braga/PT (carlosaboliveira2014@gmail.com)*

Purpose: To evaluate the stability of the upper limb when pathology is present. Shoulder findings when there's elbow pathology and vice-versa. Grading of interstitial oedema in muscle for compensations/stability.
Methods and materials: 80 patients with elbow or shoulder pathology confirmed with ultrasound. When elbow pathology was found the integrity of the biceps anchor, conjoined tendon and pectoral major were evaluated with a 3 stage system (mild, moderate and high-grade oedema). When shoulder pathology was found, common insertion of the biceps, distal coracobrachial insertion and triceps distal insertion were evaluated with a 3 grade system (mild, moderate and high-grade oedema).
Results: Shoulder pathology was documented in 40 cases: Common insertion of the biceps- stage II oedema in 85% of cases, distal coracobrachial insertion- stage II oedema in 70% of cases, and triceps distal insertion- stage II oedema in 50% of cases. Elbow pathology was documented in 40 cases: biceps anchor- stage II oedema in 90% of cases, conjoined tendon- stage II oedema in 81% of cases, and pectoral major - stage II oedema in 72 % of cases. Complete tear of the tendon was found in 6 cases involving the biceps anchor and common insertion. Shoulder assimetry was found in 75% of cases. In 54% of cases cervical and dorsal spine x-ray was done with scoliosis found in only 10 %.
Conclusion: Upper limb stability is a hard problem with compensations consituting a common difficulty.
Limitations: This study is limited by its sample and one radiologist bias.
Ethics committee approval: N/A
Funding: No funding was received for this work.
Author Disclosures:
C. A. B. Oliveira: nothing to disclose
V. Mendes: nothing to disclose
F. D. S. Costeira: nothing to disclose
F. Vieira: nothing to disclose

MyT3 5-14 09:22
Pitfalls in imaging of TFCC
O. Balazs*; Timisoara/RO (oanabalazs@yahoo.com)*

Purpose: The triangular fibrocartilage complex plays an important role in wrist biomechanics and is prone to traumatic and degenerative injury, making it a common source of ulnar-sided wrist pain. Diagnosis of injuries to the ligamentous structures of the wrist can be a challenge, particularly when there is involvement of the small, complex structures of the proximal wrist. A detailed understanding of the triangular fibrocartilage complex anatomy and injury patterns is critical in generating an accurate report to help guide treatment.
Methods and materials: A retrospective review of MR wrists done in our institution over a two-year period was performed and illustrative cases were selected. A review of the normal anatomy of TFCC, imaging technique, normal MR appearance, Palmer classification, variant anatomy that mimic TFCC disease and spectrum of imaging findings in TFCC injury are discussed in the study.
Results: Advances in magnetic resonance imaging have facilitated a better visualisation of the triangular fibrocartilage complex structures. However, there are a number of pitfalls that may cause difficulty in diagnosis of injuries to the triangular fibrocartilage complex, lunotriquetral ligament, and scapholunate ligament. The accuracy of diagnosis of injuries to the TFCC and wrist ligaments may decrease due to use of inappropriate MR imaging sequences or MR imaging artifacts, whereas variant anatomy of the proximal wrist structures may mimic disease of the TFCC and wrist ligaments.
Conclusion: Knowledge of the detailed anatomy of the wrist, as well as variant patterns of structure morphology and signal intensity, can help differentiate actual disease from normal or variant appearances at the assessment with MR imaging.
Limitations: None.
Ethics committee approval: N/A
Funding: No funding was received for this work.
Author Disclosures:
O. Balazs: nothing to disclose

MyT3 5-15 09:26
Sarcopenia in total hip replacement and its effects on complications
M. Ay, H. Çetin, N. Çay*; Ankara/TR (mesutay0929@yandex.com)*

Purpose: The aim of this study was to evaluate the psoas muscle and paravertebral muscle in terms of sarcopenia in patients with total hip replacement and to investigate the effect of sarcopenia on prosthetic complications.
Methods and materials: The area of the bilateral paravertebral and psoas muscles and the density of the software-selected area were independently calculated by the prosthesis of the patients. In addition, normal or possible complications of the final prosthesis were noted in each patient. While evaluating the images, paravertebral and psoas muscle boundaries were drawn at level of the L3 or L4 vertebrae in accordance with the previously accepted studies and maximum area measurement was performed.
Results: Although there was no significant difference in bilateral paravertebral muscle areas, there was a decrease in muscle density when hip prosthesis patients were compared with normal group regardless of side. There was a statistically significant decrease in left psoas muscle area and density in patients with left hip replacement compared to normal group. There was a statistically significant decrease in the right psoas muscle area and density in patients with right hip replacement compared to the normal group. Although there was no significant difference in the right psoas muscle area, there was a decrease in the psoas muscle density complications in patients with the right hip prosthesis. Although there was no significant difference in the right psoas muscle area in patients with left hip prosthesis compared to patients with prosthesis complications and healthy prosthesis, there was a decrease in the psoas muscle density complications.
Conclusion: We concluded that the prevalence of sarcopenia is higher in patients with prosthesis compared to the normal population and that sarcopania may be one of the reasons that increase at the prosthesis complications.
Limitations: No limitations.
Ethics committee approval: N/A
Funding: N/A
Author Disclosures:
M. Ay: Author at Ankara Bilkent City Hospital
N. Çay: Author at Ankara Bilkent City Hospital
H. Çetin: nothing to disclose

MyT3 5-16 09:30
MRI findings and their correlations in patients with symptomatic subtle cavovarus hindfoot deformity
I. Menkova*; St. Petersburg/RU (irina.s.menkova@gmail.com)*

Purpose: To find significant associations of ligamentous, tendon, osseous abnormalities in patients with symptomatic subtle cavovarus hindfoot deformity.
Methods and materials: Ankle MRI of 35 patients (18 male; mean age 52±5,6) with clinical and radiographic evidence of subtle cavovarus hindfoot deformity was assessed by 2 musculoskeletal radiologists. Pearson's, Spearman's Rank correlation coefficients were used for analysing.
Results: All patients with cavovarus hindfoot deformity underwent weight-bearing radiographic measurement of Cobey angle, a measurement of the modified Cobey angle on MRI. All patients were divided into the groups according to Cobey angle range. Group I: 19 patients with Cobey angle of 1-4°, group II: 10 patients - 5-9°, group III - 6 patients – >9°. Signs of peroneal tendinopathy were found in all patients. The severity of the peroneal tendons tears (according to Sobel classification) correlated with the hindfoot varus severity. III-IV grade of the peroneal tendons tears was observed more often in patients of II-III groups (p=0.0065). Hypertrophy and degenerative changes of the peroneal tubercle were revealed in 18 patients (fig.1). Oedematous changes of the peroneal tubercle were found mostly in the patients with the highest rates of calcaneus deviation (group III) (p=0.0016). In all the patients with symptomatic idiopathic cavovarus hindfoot, chronic lateral ligaments tears were found. Other pathologic conditions of ankle structures in these patients had no significant associations between them and hindfoot varus severity (p>0.05).

Conclusion: Painful peroneal tubercle hypertrophy associated with peroneal tendinopathy is evident in patients with more pronounced cavovarus hindfoot deformity. The grade of peroneal tendons tears also increases with an increasing of hindfoot varus severity. Such pathologic conditions exacerbate chronic pain and the degree of ankle lateral instability and often require surgical correction.
Limitations: n/a
Ethics committee approval: n/a
Funding: No funding was received.
Author Disclosures:
I. Menkova: nothing to disclose

MyT3 5-17 09:34
The role of diffusion-weighted MRI in the assessment of treatment response to chemotherapy in osteosarcoma
R. Kaddah[1], T. Raafat[1], L. M. E.-M. S. A. Bokhary[2]; [1]Cairo/EG, [2]Giza/EG *(dr-lobna2011@hotmail.com)*

Purpose: To investigate whether DWI is useful for monitoring the therapeutic response after chemotherapy in osteosarcoma by comparing the ADC values pre and post-treatment. And to determine if osteosarcomas change their water diffusion during preoperative chemotherapy in relation to the amount of tumour necrosis.
Methods and materials: Inclusion criteria: osteosarcoma patients coming to the National Cancer Institue (NCI). Exclusion criteria: patients who have implanted electric and electronic devices and those who are intolerant to contrast administration. MRI techniques: conventional MRI, DWI and postgadolinium DTPA MR imaging initially and 3-6 months after chemotherapy administration. DWI analysis: qualitative analysis was done by studying the signal intensity of different lesions on both the DWIs (at the highest b value i.e. at 800sec/mm2) and the ADC map. Quantitative analysis: ADC calculation by using the electronic cursor on the ADC map in 3 different ROI of the lesion which was placed on the solid and preferably enhancing parts of the lesion excluding necrotic, fibrotic and haemorrhagic areas as well as adjacent fat, normal tissue and bone.
Results: The study showed 17 patients with regressive response, 7 with a progressive response and only one case remained stationary. Follow-up MR after treatment showed increased intra-tumoural breaking down in (52%) of patients.
Conclusion: DWI and ADC value in following-up the treatment of osteosarcoma revealed to increase the mean ADC value in regressive cases and vice versa in progressive cases. Following-up by MRI revealed increased in tumour breaking down in post-therapeutic conventional MRI.
Limitations: None.
Ethics committee approval: Informed written consent was obtained from the patients after explanation of the procedure.
Funding: No funding was received for this work.
Author Disclosures:
L. M. E.-M. S. A. Bokhary: nothing to disclose
R. Kaddah: nothing to disclose
T. Raafat: nothing to disclose

MyT3 5-18 09:38
Immediate morphological spine modification after positioning of removable interspinous spacer for unifocal lumbar canal stenosis
L. J. Pavan[1], F. Torre[1], J. Yazbek[2], A. Prestat[1], S. Guinebert[3], D. S. Palominos Pose[4], N. Stacoffe[5], N. Amoretti[1]; [1]Nice/FR, [2]Bordeaux/FR, [3]Paris/FR, [4]Santiago/CL, [5]Lyons/FR

Purpose: To evaluate the immediate morphological modifications on pre and post-procedural CT scan after percutaneous positioning of a removable interspinous spacer (ISS) for unifocal lumbar canal stenosis under fluoroscopic and CT guidance.
Methods and materials: Patients treated in our centre between 12/2018 and 09/2019 with a percutaneous removable interspinous spacer (LobsterProject®, Techlamed®) for symptomatic unifocal lumbar stenosis were retrospectively selected. After general or epidural anaesthesia, under fluoroscopic and CT guidance, the ISS was percutaneously placed by two interventional radiologists in the central part of the interspinous ligament with lateral access. For each patient interspinous space, intradiscal space, intra-articular space and foraminal area (based on bone cortical on sagittal imaging) were measured on pre- and post-procedural low dose CT by two operators (OP1-OP2).
Results: Nine patients were selected with a mean age of 80,1[68-92] years. Interspinous space significantly increased (-OP1:3.3 vs 8.8mm, p<0.01 -OP2:3.4 vs 9.7mm, p<0.01) as well as foraminal area (-OP1:132 vs 155mm2, p<0.01 -OP2:132 vs 163mm2, p<0.01), according to both operators. Intradiscal space (-OP1:6.2 vs 6.8mm, p=0.069 -OP2:6.3vs6.9mm, p=0.021) and intra-articular space (OP1:2.1 vs 2.9mm, p=0.076 -OP2:2.1 vs 3.3mm, p=0.011) increased too (statistically significant according to one operator). Mean operative time was 44 minutes. Technical positioning was satisfying in 8/9 cases.
Conclusion: Interspinous spacer has immediate significant effects on lumbar morphology, significantly increasing interspinous space, foraminal area, intradiscal space and intra-articular space. The reduced invasiveness of the procedure and the possibility of percutaneous removal allows to avoid a major surgery, even if the ISS is not tolerated.
Limitations: Limits of the study are the analysis on low-dose CT and lack of a long term clinical follow-up.
Ethics committee approval: n/a
Funding: No funding was received for this work.
Author Disclosures:
L. J. Pavan: nothing to disclose
F. Torre: nothing to disclose
A. Prestat: nothing to disclose
N. Amoretti: nothing to disclose
J. Yazbek: nothing to disclose
S. Guinebert: nothing to disclose
D. S. Palominos Pose: nothing to disclose
N. Stacoffe: nothing to disclose

MyT3 5-19 09:42
Use of DISCOGEL® to treat cervical and lumbar discal bulging: results and consideration in our monocentric experience
A. Paladini[1], G. Guzzardi[1], M. Spinetta[1], A. Galbiati[1], M. Cernigliaro[1], D. Negroni[1], I. Percivale[1], Z. Falaschi[1], G. F. Buoni[2]; [1]Novara/IT, [2]Turin/IT *(20027467@studenti.uniupo.it)*

Purpose: Intervertebral disc bulging is a radiologic sign due to the weakness of annulus fibrosus that causes compression on the inter-vertebral foramina with a symptoms characterized by back pain with or without limbs irradiation and functional limitation
Methods and materials: We retrospectively evaluated our monocentric experience in 78 Patients affected by cervical and lumbar disc bulging treated with DISCOGEL®. Inclusion criteria were: at least 6 weeks failure of medical therapy and disc degeneration classified as Pfirmann grade 1-3. Patients selection was based on the evaluation of a spine MRI and clinical symptoms
Results: We performed all the procedures in angiographic suite, with prone (lumbar treatment) or supine (cervical) position and in all of cases we injected 0,8 ml DISCOGEL® for every disc treated. No major adverse events have been reported. According to MacNab scale, in our experience, clinical success was achieved in the 75,7 % of cases (59/78 Patients). In the 24,3% of cases (19/78 Patients) the treatment was not efficient
Conclusion: Our study demonstrates that DISCOGEL® is safe and efficient in the treatment of cervical and lumbar disc bulging, with a good clinical success and a low adverse events rate.
Limitations: no randomization of our cohort of patients
Ethics committee approval: n/a
Funding: No funding was received for this work
Author Disclosures:
D. Negroni: nothing to disclose
A. Paladini: nothing to disclose
G. Guzzardi: nothing to disclose
M. Spinetta: nothing to disclose
A. Galbiati: nothing to disclose
M. Cernigliaro: nothing to disclose
I. Percivale: nothing to disclose
Z. Falaschi: nothing to disclose
G. F. Buoni: nothing to disclose

08:30 - 10:00 **Tech Gate Auditorium**

Breast

RPS 502

Breast cancer screening scenarios with and without tomosynthesis

Moderators:
S. B. Grover; New Delhi/IN
M. A. Marino; Messina/IT

RPS 502-K 08:30
Keynote lecture
N.N.

RPS 502-1 08:40

Discordant and false-negative screen-detected cancers at independent double reading: a comparison of digital mammography and digital breast tomosynthesis in a population-based screening program

P. Skaane, S. Y. Yanakiev, T. Lie, E. E. Eben, R. Gullien, S. B. Brandal; *Oslo/NO (PERSKA@ous-hf.no)*

Purpose: To review screening-detected cancers (SDC) missed by one or both readers at independent double reading comparing digital mammography (DM) and digital breast tomosynthesis (DM+DBT) in population-based screening.
Methods and materials: A prospective study comparing DM and 2D+DBT included 24,301 women aged 50-69. A paired design with independent double reading for 2D and for 2D+DBT. Four readers interpreted each examination using a breast-based 5-point rating scale. SDC with at least one false-negative score were retrospectively reviewed by four radiologists using the same 5-point scale, giving an individual score for each breast, for CC- and MLO-view, and for DM and DBT. A consensus meeting categorised the findings as normal, nonspecific, or significant minimal signs, and false-negative ("miss"). Mammographic findings were grouped as circumscribed mass, spiculated mass, architectural distortion, asymmetry, and calcifications.
Results: 230 SDC (4 bilateral) were found, 175 at DM and 227 at DM+DBT. Prospective interpretation had a positive score in all arms for 100 SDC, but a normal score in at least one arm for 130 SDC. Normal score, discordant positive, and concordant positive for the 130 SDC (134 breasts) were for 2D 57, 53, 24, and for 2D+DBT 3, 75, and 56, respectively. Mammographic features in these 130 SDC revealed 89 spiculated masses, 23 calcifications, and 11 distortions. SDC presenting as spiculated mass and visible in retrospect had improved conspicuity on CC-views as compared with MLO-views at DBT.
Conclusion: Spiculated mass was the most common feature of missed SDC with a high interobserver variability in DBT-screening, probably caused by perception errors. Missed SDC presenting as calcifications might more often represent classification errors.
Limitations: The screening examinations including DM and DBT were interpreted sequentially in one reading session, the 2D images first and then immediately after the 3D (DBT) images.
Ethics committee approval: Oslo Tomosynthesis Screening Trial (OTST): Clinical Trials.gov nr.: NCT 01248546. Regional Ethics Committee reference number: 2010/144
Funding: No funding was received for this work.
Author Disclosures:
S. B. Brandal: nothing to disclose
P. Skaane: Speaker at Hologic, GE Healthcare
S. Y. Yanakiev: nothing to disclose
T. Lie: nothing to disclose
E. E. Eben: nothing to disclose
R. Gullien: nothing to disclose

RPS 502-2 08:46

Delayed breast cancer diagnosis after repeated recall at biennial screening mammography: an observational follow-up study from the Netherlands

J. L. R. Lameijer[1], A. C. Voogd[2], R. M. Pijnappel[3], W. Setz[1], M. Broeders[4], V. C. G. Tjan-Heijnen[2], L. Duijm[4]; *[1]Eindhoven/NL, [2]Maastricht/NL, [3]Utrecht/NL, [4]Nijmegen/NL (joostlameijer@gmail.com)*

Purpose: To investigate delayed breast cancer diagnosis after repeated recall for the same screening mammographic abnormality.
Methods and materials: This was a retroprospective observational study performed in a cohort of women enrolled in a mammography screening programme in the Netherlands. All women aged 50-75 who underwent biennial screening mammography in the south of the Netherlands between January 1, 2007, and December 31, 2016, were included. Follow-up of recalled women was at least 2 years.
Results: A delayed diagnosis of breast cancer was seen in 2.8% of all recalled women with breast cancer. Most delays were caused by incorrect BI-RADS classifications after recall (74.2%). Tumour characteristics of breast cancers with a diagnostic delay were comparable to those of cancers without delay, except for proportions of DCIS and tumour histology. The delayed confirmation of breast cancer significantly increased the mean tumour size (P<0.001). The proportion of women who experienced a diagnostic delay in the confirmation of their breast cancer significantly varied among hospitals (P=0.027).
Conclusion: We found that the proportion of women with a long delay of their breast cancer confirmation following recall did not decrease during 20 years of screening. These delays worsen the tumour size and may negatively influence prognosis of survival. We suggest that quality assurance not only covers the screening programmes, but also the hospitals handling recall.
Limitations: Screening mammography programmes are constantly subject to changes. These parameters influence accuracy and may limit extrapolation of our findings to other programmes.
Ethics committee approval: Ethical approval was not required for this observational follow-up study. The screening programme requires women to 'opt-out' of mammography screening. Three recalled women refused and were excluded.
Funding: No funding was received for this work.
Author Disclosures:
J. L. R. Lameijer: nothing to disclose
A. C. Voogd: nothing to disclose
R. M. Pijnappel: nothing to disclose
W. Setz: nothing to disclose
M. Broeders: nothing to disclose
V. C. G. Tjan-Heijnen: nothing to disclose
L. Duijm: nothing to disclose

RPS 502-3 08:52

Predicting the long-term impact of breast tomosynthesis on the cancer detection rate in a screening programme

F. Caumo[1], G. Gennaro[1], A. Pittaro[1], G. Romanucci[2], C. Fedato[3], S. A. Montemezzi[2]; *[1]Padua/IT, [2]Verona/IT, [3]Treviso/IT (francesca.caumo@iov.veneto.it)*

Purpose: To evaluate the long-term impact on cancer detection rate (CDR) of breast tomosynthesis (DBT) used as screening test.
Methods and materials: From April 2015 to March 2017, 34,688 women were enrolled in a screening programme where digital mammography (FFDM) was replaced by DBT combined with synthetic mammography (SM). The rescreening round was split in two: about half the population was rescreened by DBT+SM and the second half by FFDM. CDR was calculated for the first screening round dividing between prevalent and incident cancers and compared with CDRs obtained by FFDM before using DBT. $CDR_{prevalent}$ found in the second round by DBT+SM and by FFDM respectively were compared with values found in the first round and with those associated with former FFDM screening. CDR differences were tested by the Chi-square test.
Results: In the first DBT round, cancer detection of prevalent and incident cancers was respectively 11.8/1000 and 8.6/1000. Both values were significantly higher than CDRs found in the former FFDM screening ($CDR_{prevalent}$ = 8.4/1000; $CDR_{incident}$ = 5.7/1000; p<0.0001). At the rescreening with DBT+SM, $CDR_{incident}$ decreased at 8.1/1000 but the difference with the first round was not significant; a significant decrease was found at the rescreening by FFDM, with a $CDR_{incident}$=3.5. The difference between incident CDRs by FFDM before and after the introduction of DBT was also significant (5.7/1000 vs. 3.5/1000, p<0.0001).
Conclusion: Rescreening with DBT detected more cancers than FFDM, anticipating cancers which might have been detected in the following rounds. The decrease in CDR of rescreening by FFDM after DBT compared to FFDM CDR before DBT shows that DBT also found cancers which might have shown up within two years.
Limitations: Case-control study.
Ethics committee approval: Approved by the IRB. Patient informed consents collected.
Funding: No funding was received for this work.
Author Disclosures:
F. Caumo: nothing to disclose
G. Gennaro: nothing to disclose
A. Pittaro: nothing to disclose
G. Romanucci: nothing to disclose
C. Fedato: nothing to disclose
S. A. Montemezzi: nothing to disclose

RPS 502-4 08:58

The early effects of a mammography screening program on advanced breast cancer incidence in the Friuli Venezia Giulia Italian region

F. Giudici[1], M. Tonutti[1], M. Bortul[1], F. Zanconati[1], A. Zucchetto[2], A. Franzo[3], M. Gobbato[3], M. A. Cova[1], L. Bucchi[4]; *[1]Trieste/IT, [2]Cro-Aviano/IT, [3]Udine/IT, [4]Forli'-Meldola/IT (giudici.ctf@gmail.com)*

Purpose: Breast cancer (BC) screening aims to reduce BC mortality. Effects on mortality require more time to become evident making an evaluation of its effectiveness difficult. This study assessed incidence rates of advanced breast cancer (ABC) and a surrogate measure of mortality reduction based on the attendance to Friuli-Venezia Giulia (FVG) region mammography screening programme (MSP). It has been the first to evaluate, on a regional basis, the effectiveness of MPS implemented in Italy in 2000.
Methods and materials: Administrative databases were record-linked with the FVG cancer registry. The cohort included women aged 50-69 years invited to the first screening round. Attenders were women who responded to at least one of the first two screening rounds (2006-2007 and 2008-2009) and non-attenders who responded to neither of them. ABC was defined as tumour ≥ 2 cm (T2+), lymph-node-positive (N+), or TNM Stage greater than II (stage II+). Age-standardised incidence rate ratios (IRR) of attenders versus non-attenders, with

95% confidence intervals (95%CI), were calculated. IRRs were adjusted for age and socio-economic status by fitting a Poisson regression.
Results: The cohort included 104,488 attenders and 49,839 non-attenders (154,327 women). During the follow-up period (median 7.02 years), 3,866 invasive BC were diagnosed (2,717 and 1,149 among attender and non-attenders respectively). Attenders had lower rates of T2+ BC (IRR=0.64; 95% CI: 0.56-0.72), N+ BC (IRR=0.87; 95% CI: 0.78-0.98), and Stage II+ BC (IRR=0.78; 95% CI: 0.70-0.87). The self-selection bias was limited.
Conclusion: The attendance to the FVG MPS was associated to a significant decrease in the risk of advanced BC that was independent of self-selection biases. This early effect is suggestive of a future impact of the screening programme on BC mortality.
Limitations: Short follow-up.
Ethics committee approval: n/a
Funding: No funding was received for this work.
Author Disclosures:
F. Giudici: nothing to disclose
M. Tonutti: nothing to disclose
M. Bortul: nothing to disclose
F. Zanconati: nothing to disclose
L. Bucchi: nothing to disclose
A. Zucchetto: nothing to disclose
M. Gobbato: nothing to disclose
A. Franzo: nothing to disclose
M. A. Cova: nothing to disclose

RPS 502-5 09:04

Unenhanced MRI combined with digital breast tomosynthesis: diagnostic accuracy for breast cancer detection of a double-reading strategy

V. Marconi, R. Girometti, A. Linda, L. Di Mico, F. Bondini, C. Zuiani*; Udine/IT (rgirometti@sirm.org)*

Purpose: To evaluate the accuracy for breast cancer (BC) detection of a double-reading approach involving combined unenhanced breast magnetic resonance imaging and digital breast tomosynthesis (UMRI-DBT).
Methods and materials: We retrospectively included 93 patients (mean age 57.5±10.4 years) who underwent both 1.5T magnetic resonance imaging and DBT from January 2016 to December 2017. Three readers (R1, R2, and R3), ranging from 3 to 10 years experience, blinded to clinical information and histology, independently evaluated a combination of UMRI (transverse T1-weighted imaging and diffusion-weighted imaging [DWI]) and DBT, using a Likert-score and the BI-RADS scale to provide final a categorisation of observations. Using postoperative pathology and a ≥2-years follow-up as the standard of reference, we calculated per-lesion sensitivity and positive predictive value (PPV) for BC of individual readings (R1, R2, and R3), as well as combined pairwise readings (R1+R2, R1+R3, R2+R3), assuming as positive a finding with a score ≥4 for at least one reader. The McNemar test was used for comparisons.
Results: A total of 105 findings were operated or referred to follow-up, including 65/105 (61.9%) cancers and 40/105 (38.1%) benign findings. On a single-reader basis, sensitivity and PPV ranged 73.8-80% and 83.9-87.9%, respectively. Double-reading significantly increased the sensitivity in the case of R1+R2 (83.1%) versus R2 (73.8%) (p=0.0001), and R1+R3 (86.2%) versus R3 (78.5%) (p=0.0005). After double-reading, there was a slight decrease in PPV (ranging 81.8-87.7%).
Conclusion: Combined UMRI and DBT showed acceptable accuracy for detecting BC. A double-reading strategy has the potential to increase the sensitivity, at the cost of a slight decrease in PPV.
Limitations: Monocentric retrospective study on relatively small population.
Ethics committee approval: Approved by our IRB. Informed consent acquisition was waived due to the retrospective design.
Funding: No funding was received for this work.
Author Disclosures:
R. Girometti: nothing to disclose
V. Marconi: nothing to disclose
A. Linda: nothing to disclose
L. Di Mico: nothing to disclose
F. Bondini: nothing to disclose
C. Zuiani: nothing to disclose

RPS 502-6 09:10

Delayed breast cancer diagnoses in women recalled at screening mammography: trends in the proportions and lengths of delay over two decades of screening

L. Duijm[1], J. L. R. Lameijer[2], M. Broeders[1], R. M. Pijnappel[3], L. J. A. Strobbe[1], V. C. G. Tjan-Heijnen[4], A. C. Voogd[4]; [1]*Nijmegen/NL,* [2]*Eindhoven/NL,* [3]*Utrecht/NL,* [4]*Maastricht/NL (lemduijm@hotmail.com)*

Purpose: To determine trends in the frequency and length of delay in breast cancer diagnosis in women recalled at screening mammography.
Methods and materials: We included a consecutive series of 817,656 screens of women who received biennial screening mammography between January 1, 1997, and December 31, 2016. During at least 2.5 year follow-up, radiological reports and biopsy reports were collected of all recalled women. The 20 year inclusion period was divided into 4 cohorts of 5 years each (1997-2001, 2002-2006, 2007-2011, 2012-2016). For each cohort, we determined the number and tumour characteristics of screen detected cancers and assessed the proportion of recalled women who experienced a diagnostic delay of at least four months in breast cancer confirmation.
Results: The proportion of recalled women who experienced a diagnostic delay of at least four months decreased from 7.5% in 1997-2001 (47/623) to 3.0% in 2012-2016 (67/2223, P<0.001). Among all delays, the proportion of women with a delay of at least two years increased from 27.7% (13/47) in 1997-2001 to 74.6% (50/67) in 2012-2016 (P<0.001), that is of all recalled women 2.1% (13/623) and 2.5% (50/2223), respectively. Most of these were only detected and re-recalled at the following screening round. Cancers with a diagnostic delay >2 years were more frequently invasive (P=0.009) and showed a less favourable B&R grading (P<0.001) than cancers with a diagnostic delay of 4-24 months.
Conclusion: The proportion of recalled women with a diagnostic delay in confirmation of breast cancer has more than halved during two decades of screening mammography. Unfortunately, long delays now constitute the majority of women who face a delay, which may worsen breast cancer survival.
Limitations: n/a
Ethics committee approval: n/a
Funding: No funding was received for this work.
Author Disclosures:
L. Duijm: nothing to disclose
J. L. R. Lameijer: nothing to disclose
M. Broeders: nothing to disclose
R. M. Pijnappel: nothing to disclose
L. J. A. Strobbe: nothing to disclose
V. C. G. Tjan-Heijnen: nothing to disclose
A. C. Voogd: nothing to disclose

RPS 502-7 09:16

Classification of interval cancers on digital breast tomosynthesis compared to digital mammography in the Malmö breast tomosynthesis screening trial

K. Johnson[1], K. Lang[2], I. Andersson[2], D. M. Ikeda[3], S. Zackrisson[2]; [1]*Lund/SE,* [2]*Malmö/SE,* [3]*Stanford/US (kristin.johnson@med.lu.se)*

Purpose: To evaluate cancer visibility with digital breast tomosynthesis (DBT) in screening, we classified interval cancers (ICs) on DBT versus digital mammography (DM) in the Malmö breast tomosynthesis screening trial (MBTST).
Methods and materials: The MBTST is a prospective, paired, population-based one-arm screening trial comparing one-view DBT with two-view DM. 14,848 women were enrolled from January 2010 to February 2015. ICs were identified in the Swedish Cancer Registry. The DM and DBT images were reviewed retrospectively, side-by-side, in consensus by two experienced breast radiologists who classified the types of ICs as true negative, minimal sign, or false negative. The distribution of IC types for the two modalities was assessed. Breast density was classified into fatty or dense.
Results: There were 22 ICs following the MBTST. The distribution of IC types on prior DBT was 46% (10/22) true negatives, 18% (4/22) minimal signs, and 36% (8/22) false negatives. As judged on prior DM, the same ICs were 46% (10/22) true negatives, 9% (2/22) minimal signs, and 46% (10/22) false negatives. 13 (59%) women had dense breasts.
Conclusion: The majority of the ICs were true negative on both DBT and DM. A slight shift was noted from false negative ICs on prior DM to ICs with a minimal sign on prior DBT, which suggests a challenge of increased retrospective cancer visibility when introducing a more sensitive screening method. The numbers are, however, small and the result needs to be confirmed in larger samples.
Limitations: Single-centre trial. Few interval cancers
Ethics committee approval: Lund University Ethics Committee approval. Written informed consent.
Funding: Governmental funding for clinical research.
Author Disclosures:
K. Johnson: nothing to disclose
K. Lang: Other at Speaker fees Siemens, Other at Travel support Siemens
I. Andersson: nothing to disclose
D. M. Ikeda: Board Member at Grail Inc, Consultant at Hologic Inc
S. Zackrisson: Other at Speaker fees Siemens, Patent Holder at US 9 833 203, Other at Travel support Siemens

RPS 502-8 09:22

First Australian pilot trial of digital breast tomosynthesis (3D-mammography) population-based screening in BreastScreen Victoria

D. J. Lockie[1], N. Houssami[2], M. E. Clemson[3]; [1]Southbank/AU, [2]Sydney/AU, [3]Ringwood East, Vl/AU (lockie.darren@gmail.com)

Purpose: To assess cancer detection rates, recall rates, and reading time, as well as the feasibility of population-based tomosynthesis screening, in BreastScreen Victoria, Australia.
Methods and materials: Women ≥40 years presenting for routine screening (August 2017–November 2018) to Maroondah BreastScreen were prospectively recruited and received tomosynthesis (with synthesised 2D-images) or standard 2D mammography for routine screening.
Reading outcome (clear or recall), final screening outcome for 3D and 2D cohorts, and screen reading times were obtained from the client information system (CIS).
Results: Amongst 5,018 tomosynthesis screens, 49 cancers (40 invasive, 9 in situ) were detected representing a CDR of 9.77/1,000 (95%CI 7.23–12.89/1,000). Amongst 5,166 2D-mammography screens, 34 cancers were detected (30 invasive, 4 in situ), a CDR of 6.58/1,000 (4.56–9.18/1,000). The difference in CDR was 3.18/1,000 (-0.32–6.84); the difference in CDR between screening modalities was shown for repeat screening rounds (3.47/1,000; -0.26–7.52) and was evident in women ≥ 60 years (6.96/1,000; 1.05–13.91) in stratified analyses.
Tomosynthesis screening had higher recall (4.18%; 3.65–4.78%) than mammography (3.00%; 2.55–3.50%); the difference in recall was 1.18% (0.46–1.92%).
Screen-reading time for tomosynthesis was approximately 3 times that of mammography.
Approximately 5% of women opted out of tomosynthesis screening.
Conclusion: Tomosynthesis screening seems feasible (given adequate infrastructure and service preparation). Tomosynthesis increased breast cancer detection, recall to assessment, and screen-reading time compared to mammography.
Our findings can underpin large-scale evaluation of tomosynthesis in Australia's BreastScreen program that examines longer-term end-points.
Limitations: Study design was intentionally not a RCT.
Ethics committee approval: Trial Registration: ACTRN-12617000947303.
Funding: This study was funded by a National Breast Cancer Foundation (NBCF) Australia pilot study grant.
Author Disclosures:
D. J. Lockie: Grant Recipient at Australian NBCF
N. Houssami: Grant Recipient at Australian NBCF
M. E. Clemson: Grant Recipient at Australian NBCF

RPS 502-9 09:28

Breast cancer detection rate of screening digital breast tomosynthesis versus 2D mammography: a meta-analysis

A. Wadera[1], M. Alabousi[2], D. N. Zha[2], J.-P. Salameh[3], L. Samoilov[4], A. Dehmoobad Sharifabadi[3], A. Pozdynakov[2], B. Sadeghirad[2], A. Alabousi[2]; [1]Valhalla, NY/US, [2]Hamilton, ON/CA, [3]Ottawa/CA, [4]London/CA (akshay_wadera@student.nymc.edu)

Purpose: To perform a systematic review and meta-analysis comparing the breast cancer detection rate (CDR) and positive predictive value (PPV) of digital breast tomosynthesis (DBT), combined DBT, and 2-D mammography (2-D MMG), and 2-D MMG alone in screening populations.
Methods and materials: MEDLINE and Embase were searched to identify studies reporting patients undergoing 2-D MMG alone and DBT with or without 2-D MMG for breast cancer screening. CDR and PPV were pooled using a random-effects model meta-analysis of proportions. Heterogeneity was assessed based on visual inspection of individual forest plots.
Results: A total of 24 studies were included, reporting on 215,225 patients for DBT (1,313 with breast cancer), 385,200 for combined DBT and 2-D MMG (2,683 with breast cancer), and 764,166 for 2-D MMG alone (3,443 with breast cancer). The CDR of DBT (6.0 per 1,000, 95% confidence interval [CI] 4.7-7.4) demonstrated no statistically significant difference compared to combined DBT and 2-D MMG (7.5 per 1,000, CI 6.5-8.6), or 2-D MMG alone (4.6 per 1,000, CI3.6-5.7). Combined DBT and 2-D MMG showed a statistically significant higher CDR compared to 2-D MMG alone. No difference was identified in the PPV between DBT (15%, CI 9-23), combined DBT and 2-D MMG (15%, CI 10-20), and 2-D MMG alone (9%, CI 6-12).
Conclusion: Combined DBT and 2-D MMG detect more cases of breast cancer than 2-D MMG alone. DBT was no different than 2-D MMG alone, which may be related to the study heterogeneity. The study's results support the implementation of combined DBT and 2-D MMG in screening practice.
Limitations: This study was limited by mild to moderate study heterogeneity.
Ethics committee approval: n/a
Funding: No funding was received for this work.
Author Disclosures:
A. Wadera: nothing to disclose
M. Alabousi: nothing to disclose
D. N. Zha: nothing to disclose
J.-P. Salameh: nothing to disclose
L. Samoilov: nothing to disclose
A. Pozdynakov: nothing to disclose
A. Dehmoobad Sharifabadi: nothing to disclose
B. Sadeghirad: nothing to disclose
A. Alabousi: nothing to disclose

RPS 502-10 09:34

A survey of technical repeats and recalls in the UK Breast Screening Service

M. L. Hill[1], M. Halling-Brown[2], P. Whelehan[3], R. Highnam[4]; [1]Issy-Les-Moulineaux/FR, [2]Guildford/UK, [3]Dundee/UK, [4]Wellington/NZ (melissa.hill@volparasolutions.com)

Purpose: This study surveyed reasons for repeat examinations (TR) due to clinical image quality (IQ) deficiencies within the United Kingdom National Health Service Breast Screening Programme (NHSBSP). Understanding TR is a first step towards improving IQ, the patient experience, and reducing inefficiencies.
Methods and materials: TR exams include technical repeats (TP), where additional views are acquired during screening, and technical recalls (TC), where women are invited to a second appointment to repeat views. Study cases coded with a repeat reason were obtained from the OPTIMAM image database among women with normal four-view screening exams acquired between 2011 and 2018. Distributions of repeats according to reason and breast laterality were analysed with repeat codes grouped into inadequate positioning (IP), image blurring (IB), and other factors (OF) categories.
Results: In total, 3,821 cases were included, with 3,846 TR split between 3,228 TP and 618 TC. Of the TR, 2,053 and 1,438 were unilateral for right or left breast repeated views, respectively. The remaining 355 TR were for the same repeat reason bilaterally. Comparing repeat classifications by proportions of TP, TC, and total TR, IP accounted for 90%, 31%, and 80%, respectively, IB represented 8%, 66%, and 17%, respectively, and OF was consistently around 3%.
Conclusion: The majority of TR were related to IP, but among TC, IB was the predominant repeat reason. A focused effort to reduce both IP and IB at the time of the screening exam has the potential to improve IQ and substantially reduce the number of TC in the NHSBSP.
Limitations: Potential for population and practice bias due to case collection from two screening centres, predominantly using Hologic equipment.
Ethics committee approval: Source database REC approval: 19/SC/0284.
Funding: Volpara Solutions Ltd. and CRUK support for OPTIMAM image database.
Author Disclosures:
M. L. Hill: Consultant at Volpara Solutions Ltd.
M. Halling-Brown: Grant Recipient at CRUK
P. Whelehan: nothing to disclose
R. Highnam: CEO at Volpara Solutions Ltd.

RPS 502-11 09:40

A multicentre, retrospective analysis of interval cancers to determine clinicopathological factors that correlate with increased growth rates

N. Sharma[1], S. Duffy[2], M. G. Wallis[3], L. S. Wilkinson[4], K. Satchithananda[2], R. Rahim[2], A. Turnbull[5], E. G. E. Macinnes[6], J. Simpson[1]; [1]Leeds/UK, [2]London/UK, [3]Cambridge/UK, [4]Oxford/UK, [5]Derby/UK, [6]York/UK (Nisha.sharma2@nhs.net)

Purpose: This multicentre, retrospective review of intervals cancers aimed to identify clinicopathological factors that correlate with increased tumour volume doubling times. The potential impact of delayed diagnosis was also explored.
Methods and materials: Data from interval cancer diagnoses with retrospective screening mammographic changes classified as either uncertain or suspicious were collated from five English breast screening units. Tumour volume doubling time was calculated based on the time from screening to diagnosis and the observed size difference. Demographic data and pathology and radiological details were noted, including mammographic density, grade, and nodal and hormone receptor status.
Results: Data was available for 306 patients with interval cancers. 81% were diagnosed at least 12 months after screening with 19% presenting within the first year. Average time to diagnosis was 644 days (SD 276 days). Average tumour volume doubling time, based on the difference in radiological sizes and assuming volume and size proportionality, was 167 days (95% CI 151-186). Age (p=0.01), grade (p<0.001), and ER status (p<0.001) correlated with TVDTs, with women under 60, grade 3 cancers, and ER negative cancers having significantly shorter doubling times. HER2 positive tumours had shorter doubling times than

the negative, but this difference was not statistically significant. There was no correlation between breast density and tumour growth rate.
Conclusion: Cancers diagnosed in women under the age of 60, Grade 3 and hormone receptor negative cancers were found to have shorter tumour volume doubling times. BIRADS breast density did not correlate with tumour growth rates. Delay in diagnosis in this group of screening patients is likely to result in a modest increase in breast cancer mortality.
Limitations: Small numbers.
Ethics committee approval: n/a
Funding: No funding was received for this work.
Author Disclosures:
N. Sharma: nothing to disclose
J. Simpson: nothing to disclose
M. G. Wallis: nothing to disclose
L. S. Wilkinson: nothing to disclose
K. Satchithananda: nothing to disclose
R. Rahim: nothing to disclose
A. Turnbull: nothing to disclose
S. Duffy: nothing to disclose
E. G. E. Macinnes: nothing to disclose

RPS 502-12 09:46
An analysis of screen-detected invasive cancers by grade in the English breast cancer screening programme: are we failing to detect enough small grade 3 cancers?
R. G. Blanks[1], M. G. Wallis[2], R. Alison[1], R. Given-Wilson[3]; [1]*Oxford/UK,* [2]*Cambridge/UK,* [3]*London/UK (matthewwallis492@btinternet.com)*

Purpose: Detection of small high grade invasive cancers contributes disproportionately to mortality reduction from mammographic screening. We have studied the relative sensitivity of detection of invasive cancers by grade in the English breast screening programme (NHSBSP).
Methods and materials: This study examined data from national returns from the NHSBSP for 7 years, 2009/2010 to 2015/2016. Information on size and grade of invasive cancers was collected for first/prevalent (age 45-52) and routine repeat/incident (age 53-70) screens.
Results: Data was analysed from 11.3 million screens when 67,681 invasive cancers were diagnosed. 29% of prevalent cancers were grade 1, 52% grade 2, and 18% grade 3. At all screens, the rate of detection of small (<15mm) grade 3 cancers and large (15mm) grade 1 cancers was disproportionately low. We estimate a relative sensitivity of mammography for grade 3 detection of 52% and grade 2 detection of 62% relative to the sensitivity for grade 1 cancers.
Conclusion: Published data shows the majority of the mortality reduction from screening is attributable to the detection of grade 3 invasive cancers, and these are over-represented in interval cancers. In our study, the sensitivity of the NHSBSP for small high grade cancers appears similar to that reported from the Swedish Two Counties study. It has not been improved by the introduction of digital mammography. Technological advances should focus on improving high-grade cancer detection.
Limitations: Retrospective data from a 3-year programme but prevalent/first screen is independent of screening interval.
Ethics committee approval: The study has no patient contact, intervention, or use of identifiable patient data, and is therefore exempted from ethical review in the UK.
Funding: Roger Blanks and Rupert Alison received funding from Public Health England to perform this work.
Author Disclosures:
M. G. Wallis: nothing to disclose
R. G. Blanks: nothing to disclose
R. Given-Wilson: nothing to disclose
R. Alison: nothing to disclose

RPS 502-13 09:52
Trends in recall and outcome of screen-detected microcalcifications during two decades of screening mammography in the Netherlands
L. Duijm[1], J. Luiten[2], E. Luiten[3], M. Broeders[1], K. Roes[1], V. C. G. Tjan-Heijnen[4], A. Voogd[4]; [1]*Nijmegen/NL,* [2]*Tilburg/NL,* [3]*Breda/NL,* [4]*Maastricht/NL (lemduijm@hotmail.com)*

Purpose: To determine trends in recall and outcome of screen-detected microcalcifications during 20 years of screening mammography.
Methods and materials: We included a consecutive series of 817,656 screens obtained in a Dutch breast cancer screening region between January 1997 and January 2017. In 2009/2010 (transition period) screen-film mammography (SFM) was gradually replaced by full-field digital mammography (FFDM). We focused on the recall of suspicious microcalcifications and obtained all radiology reports and pathology outcomes of recalled women, with a 2-year follow-up. Screening outcomes during the period of SFM (1997-2010) and FFDM (2009-2016) were compared.
Results: A total of 18,565 women were recalled, of whom 3,556 had suspicious microcalcifications. The recall rate for microcalcifications per 1,000 screens increased from 1.0 in 1997-1998 to 7.2 during the transition (p<0.001) and afterwards gradually decreased to 5.2 at the latest digital screening period (p<0.001). The recalls yielding DCIS increased from 0.3 per 1,000 screens to 1.1 per 1,000 screens, respectively. More than half of the DCIS lesions were high grade (393/747, 52.6%). The distribution in DCIS grading was stable during the 20-year screening period (p= 0.362).
Conclusion: The recall rate for suspicious microcalcifications at mammographic screening significantly increased over the past two decades, while the DCIS detection rate increased less rapidly, resulting in a lower positive predictive value of recall. Since it is not yet clear to which degree histological features of DCIS can be estimated by the patterns of microcalcifications alone, a stereotactic core-needle biopsy is currently still mandatory in the workup of these lesions.
Limitations: n/a
Ethics committee approval: Ethical approval was not required for the current study.
Funding: No funding was received for this work.
Author Disclosures:
L. Duijm: nothing to disclose
J. Luiten: nothing to disclose
E. Luiten: nothing to disclose
V. C. G. Tjan-Heijnen: nothing to disclose
A. Voogd: nothing to disclose
M. Broeders: nothing to disclose
K. Roes: nothing to disclose

11:15 - 12:30 **Room B**

Musculoskeletal

RPS 610

Ultrasound, interventions and new techniques

Moderators:
G. M. Allen; Oxford/UK
N.N.

RPS 610-K 11:15
Keynote Lecture
B. Bignotti; *Genoa/IT*

Author Disclosures:
B. Bignotti: nothing to disclose

RPS 610-1 11:25
Accuracy of ultrasound in the characterisation of superficial soft tissue tumours: a prospective study
S. W. Y. Yip[1], J. F. F. Griffith[1], E. H. Hung[2], W. H. A. Ng[2], C. S. Tong[3], K. L. L. Lee[3]; [1]*Shatin/HK,* [2]*Hong Kong/CN,* [3]*Hong Kong/HK (stefaniewyip@gmail.com)*

Purpose: To prospectively evaluate the accuracy of ultrasound in characterising superficial soft tissue tumours.
Methods and materials: 830 superficial soft tissue tumours were prospectively evaluated with ultrasound by 5 experienced musculoskeletal radiologists. The radiologist at the time of examination provided 1-3 specific differential diagnoses and the perceived level of confidence with regard to each diagnosis. The clinical diagnosis was recorded. Ultrasound and clinical diagnoses were compared with the histological diagnosis to determine the accuracy. Tumour malignancy was determined by histology or clinical follow-up.
Results: 234 (28.2%) of 830 tumours had a subsequent histological correlation. Compared with histology, the accuracy of clinical and ultrasound examination for determining the specific tumour type was 32.9% and 82.1%, respectively, considering all differential diagnoses provided. Radiologists were “fully confident” about the ultrasound diagnoses in 136 (58.1%) of 234 superficial soft tissue tumours and, in this setting, the diagnostic accuracy of ultrasound was 95.6%. When the radiologist was “not fully confident”, accuracy was 45.9% for the first ultrasound differential diagnosis and 63.2% for all differential diagnoses. Sensitivity, specificity, positive predictive value, and negative predictive value of ultrasound for identifying malignant soft tissue tumours was 91.7%, 94.1%, 45.8%, and 99.5%, respectively.
Conclusion: Based on the ultrasound appearances alone, the radiologist can be ‘fully confident’ with providing a specific diagnosis in over half of the cases and, in this setting, diagnostic accuracy is very high. Ultrasound is also highly accurate at discriminating benign from malignant superficial soft tissue tumours.

Limitations: Only one-quarter of tumours examined had a final histological diagnosis as it is common for soft tissue tumours with a clear diagnosis to forgo excision.
Moreover, a referral bias may have existed with more clinically atypical tumours referred for an ultrasound examination.
Ethics committee approval: This study was approved by the institutional review board.
Funding: No funding was received for this work.
Author Disclosures:
S. W. Y. Yip: nothing to disclose
J. F. F. Griffith: nothing to disclose
E. H. Hung: nothing to disclose
W. H. A. Ng: nothing to disclose
C. S. Tong: nothing to disclose
K. L. L. Lee: nothing to disclose

RPS 610-2 11:31

Quantitative evaluation of muscle stiffness with shear-wave elastography in children with cerebral palsy after a botulinum toxin A injection

N. Dağ, M. N. Cerit, B. N. Muşmal, M. Zinnuroğlu, S. Ozhan Oktar*; Ankara/TR (drndag@icloud.com)*

Purpose: To evaluate the changes in medial gastrocnemius muscle (GCM) stiffness after a botulinum toxin A (BTA) injection in children with cerebral palsy (CP) by using shear-wave elastography (SWE) and to investigate the usability of this technique in the evaluation of treatment efficacy and correlation with clinical measurements. SWE is used to assess whether treatment for GCM spasticity causes an alteration in the stiffness of the anterior tibial (TA) muscle, which is its antagonist.
Methods and materials: 43 spastic lower extremities of 24 children with CP were evaluated. BTA injection treatment was applied to the medial GCM. Muscle stiffness was measured with the SWE technique before the procedure and one month after the procedure. The patients were evaluated with the modified Ashworth scale (MAS) and modified Tardieu scale (MTS) in the physiotherapy department at about the same time.
Results: Mean SWE values of GCM muscle were measured as 45.9±6.5 kPa before BTA and 25.0±5.7 kPa after BTA, and the difference between them was statistically significant ($p<0.01$). A statistically significant difference was found between MAS and MTS results. There was a statistically significant high correlation between SWE values and MAS scores (rho: 0.77; $p<0.01$). A statistically significant correlation was found between SWE values and MTS parameters. Mean SWE values of TA muscle were measured as 36.9±7.9 kPa before BTA and 28.4±5.2 kPa after BTA, and the difference between them was statistically significant ($p<0.01$).
Conclusion: Quantitative measurement of muscle stiffness with SWE might provide important information for evaluating spasticity and treatment efficacy in children with CP.
Limitations: A small number of patients.
Ethics committee approval: The study was approved by the institutional ethics committee.
Funding: No funding was received for this work.
Author Disclosures:
N. Dağ: nothing to disclose
M. N. Cerit: nothing to disclose
B. N. Muşmal: nothing to disclose
M. Zinnuroğlu: nothing to disclose
S. Ozhan Oktar: nothing to disclose

RPS 610-3 11:37

The role of ultrasound and Doppler in callus formation in diaphyseal fractures of long bones treated by internal fixation

C. Mehta, U. Gohil, K. K. Kartik*; Vadodara/IN (drchetan_mehta@yahoo.com)*

Purpose: To evaluate callus formation and the role of Doppler in diaphyseal fractures of long bones treated by internal fixation.
Methods and materials: 100 patients with a diaphyseal fracture of long bones treated with internal fixation underwent ultrasonography of the fractured site at 6 weeks, 12 weeks, 18 weeks, and 24 weeks. The presence of callus and its echogenicity were evaluated. Doppler was applied to evaluate the vascularity within callus and spectral trace for the resistance index. Radiographs were obtained in AP and lateral views.
Results: Out of the 100 patients evaluated, 87% progressed to union and 13% progressed to non-union of the fracture.
At 6 weeks, hypoechoic callus was seen in 83 patients progressing to union and 9 patients progressing to non-union. Callus formation on ultrasound at 6 weeks yielded a sensitivity and specificity of 95.4% and 69.2%, respectively. Callus on x-ray at 6 weeks yielded a sensitivity and specificity of 80.6% and 92.3%, respectively.
At 12 weeks, 100% of fractures demonstrated a hypoechoic callus with the presence of vascularity on the application of Doppler in 82% of uniting fractures and 84% of non-uniting fractures. The resistance index ranged from 0.56-0.89 in uniting fractures and 0.73-1.57 in non-uniting fractures, with cut-off below <0.88 yielding a sensitivity of 98% and specificity of 90%for uniting fractures.
At 18 weeks, 85% of patients progressing to union had a hyperechoic callus and 100% had a hyperechoic callus at 24 weeks.
Conclusion: Ultrasound proved to be more sensitive for detecting the presence of early callus than radiographs. Colour Doppler and spectral trace add additional functional data on bone callus and neovascularisation with low resistive index in callus of uniting fractures.
Limitations: Orthopaedic implants can limit the evaluation.
Ethics committee approval: Ethics committee approval obtained.
Funding: No funding was received for this work.
Author Disclosures:
C. Mehta: nothing to disclose
U. Gohil: nothing to disclose
K. K. Kartik: nothing to disclose

RPS 610-4 11:43

Detection of intra-articular urate deposition in gout: an ultrasound and dual-energy CT study

J. Legrand[1], F. Becce[2], C. Marzin[1], L. Norberciak[1], J.-F. Budzik[1], T. Pascart[1]; *[1]Lille/FR, [2]Lausanne/CH*

Purpose: To determine if dual-energy computerised tomography (DECT) was able to detect intra-articular monosodium urate (MSU) deposits, identified with ultrasonography (US), in patients with gout.
Methods and materials: Knees of patients with a diagnosis of gout via US and DECT scans were prospectively assigned to DC+ or DC- groups depending on the presence or absence of the US double-contour sign (DC).
Standardised regions of interest were drawn in the patellofemoral joint space, the menisci, and the femorotibial cartilage. 5 DECT parameters were obtained: CT numbers in Hounsfield Unit (HU) at 80 and 140 kV, effective atomic number (Z_{eff}), electron density (ρ_e), and the dual-energy index (DEI). Zones were compared between the two groups using linear mixed models.
In a preliminary study, we used a phantom constituted of 3 rods of MSU (0, 200, and 600mg/ml) which were scanned to determine the in vitro DECT parameters of different concentrations of MSU.
Results: 115 patients were included. The mean gout duration was 9.0±9.8 years, mean serum urate level was 7.3±2.3 mg/dL, and mean DECT volume of urate deposition was 1.2cm^3±3.8. 225 knees were analysed. 36 knees were assigned to the DC+ group.
No significant differences were found between DC+ and DC- knees for Zeff, ρe, and DEI in menisci ($p=0.94$, 0.72, and 0.97, respectively), femorotibial cartilage ($p=0.94$, 0.89, and 0.97, respectively), or patellofemoral joint space ($p= 0.48$, 0.89, and 0.54, respectively).
Phantoms exhibited increasing values in ρ_e ($p=0.03$) with growing MSU concentrations.
Conclusion: This study shows that, in vivo, DECT is not able to identify intra-articular MSU deposition in patients with gout, although it has the ability to detect in vitro growing concentrations of MSU.
Limitations: n/a
Ethics committee approval: n/a
Funding: No funding was received for this work.
Author Disclosures:
J. Legrand: nothing to disclose
F. Becce: nothing to disclose
L. Norberciak: nothing to disclose
J.-F. Budzik: nothing to disclose
T. Pascart: nothing to disclose
C. Marzin: nothing to disclose

RPS 610-6 11:49

Quantitative evaluation of image quality of reduced-dose cone-beam CT images using an adaptive image noise optimiser

R. H. H. Wellenberg, G. J. Streekstra, M. Maas*; Amsterdam/NL (r.h.wellenberg@amc.uva.nl)*

Purpose: To quantitatively assess the image quality of reduced-dose CBCT images, reconstructed with different levels of adaptive image noise optimiser (AINO).
Methods and materials: A fresh frozen cadaver lower leg was scanned on a Planmed verity cone-beam CT-scanner using ultra-low-dose parameters of 0.4 mm resolution, 300 projections, 15 ms pulse length, and a sharp reconstruction kernel. The kV was varied between 96–80 and mA was reduced from 6.3 to 4, 2, and 1 mA. Acquisitions were reconstructed without AINO and with AINO (levels light/medium/strong), which resulted in a total of 80 reconstructions. CT-numbers, standard deviations as a noise estimate, and contrast-to-noise-ratios (CNR) were quantitatively assessed in regions-of-interest placed in the bone and

soft tissue. Quantitative results of standard protocol images using 96kV and 6.3mA, without AINO, served as a reference.
Results: $CTDI_{vol}$ reduced 92%, from 2.74 mGy in 96kV/6.3mA acquisitions to 0.21 mGy in 80kV/1mA acquisitions. Standard deviations and CNR decreased while CT-numbers remained constant in reduced-dose results. AINO reduced standard deviations of noise, and increased CNR, while CT numbers remained constant. Increasing levels of AINO results in higher CNR (p<0.001). Based on the quantitative analysis on CNR, AINO potentially enables a radiation dose reduction of 15-85%, depending on the level of AINO, kV, and mA. Photon-starvation artefacts appear at low kV and mA.
Conclusion: Based on the quantitative analysis on CNR, AINO potentially enables a radiation dose reduction of 15-85%, depending on the level of AINO, kV, and mA. However, AINO is incapable of eliminating photon-starvation artefacts and images appear smoother due to noise reduction.
Limitations: The sample size and quantitative assessment of image quality only.
Ethics committee approval: n/a
Funding: No funding was received for this work.
Author Disclosures:
R. H. H. Wellenberg: nothing to disclose
G. J. Streekstra: nothing to disclose
M. Maas: nothing to disclose

RPS 610-7 11:55
Prognostic prediction in initially diagnosed multiple myeloma patients using IVIM-DWI and multi-echo Dixon MR imaging
A. Jo, J.-Y. Jung, S. E. Lee, S.-Y. Lee, S.-E. Lee*; Seoul/KR (JARSW2011@gmail.com)*

Purpose: To evaluate the feasibility of the multi-parametric MRI including intravoxel incoherent motion-diffusion-weighted imaging (IVIM-DWI) and multi-echo Dixon on a prediction of the prognosis in initially diagnosed multiple myeloma (MM)
Methods and materials: This retrospective study included 78 patients who were initially diagnosed with MM. All patients received MRIs of lumbar and/or thoracic spines, including IVIM-DWI and multi-echo Dixon prior to initiation of the therapy. The freehand region of interest was drawn within the marrow space of the vertebral body: pure diffusion coefficient (Dslow), pseudo-diffusion coefficient (Dfast), and perfusion fraction (Pf) maps from IVIM-DWI, and proton-density fat-fraction (PDFF) maps from multi-echo Dixon MR imaging. All patients were classified into 3 groups according to the international staging system (ISS) and compared using ANOVA with a Scheffe test. A logistic regression model was built to predict the prognosis between the two groups (early stage-ISS I vs advanced stage-ISS II and III).
Results: 38 patients were ISS-1, 22 ISS-II, 18 ISS-III. The higher grade of ISS demonstrated significantly lower PDFF and higher Dslow (Dslow: 355.6±19 vs 408.1±19 vs 579.8±17 $\mu m^2/s$, P<0.001/PDFF: 46% vs 30% vs 15%, p<0.001). In the prediction model using logistic regression by stepwise selection, PDFF was the single most significant factor to differentiate early and advanced stages of MM with an accuracy of 76% and AUC of 0.83.
Conclusion: Dslow from IVIM-DWI and PDFF from multi-echo Dixon were significantly associated with prognosis in initially diagnosed MM.
Multi-parametric bone marrow imaging with IVIM-DWI and multi-echo Dixon could be used to predict the prognosis in initially diagnosed MM.
Limitations: A retrospective study with a limited number of patients. Our MR imaging examinations were limited to the lumbosacral and thoracic spine.
Ethics committee approval: n/a
Funding: No funding was received for this work.
Author Disclosures:
A. Jo: nothing to disclose
J.-Y. Jung: nothing to disclose
S. E. Lee: nothing to disclose
S.-Y. Lee: nothing to disclose
S.-E. Lee: nothing to disclose

RPS 610-8 12:01
Change of apparent diffusion coefficient during CT-guided periradicular infiltration as an indicator of therapy success
S. Talarczyk[1], D. F. P. Uhlenbrock[1], P. Haage[2], C. A. Stückle[3]; *[1]Dortmund/DE, [2]Wuppertal/DE, [3]Witten/DE*

Purpose: To analyse changes in the apparent diffusion coefficient in patients with specific low back pain following CT-guided interventional therapy.
Methods and materials: From 11/2017-2/2018, 14 MRI examinations in 7 patients suffering from low back pain were compared before and after CT-guided periradicular infiltration therapy in respect to the ADC value of the affected and treated nerve root. Two radiologists independently measured the ADC value of the affected nerve twice and the mean value was calculated. Before and, in average, 11 days after CT-guided treatment where a glucocorticoid, a local anaesthetic, and a contrast agent were injected close to the affected nerve root, the same nerve root was measured. The affected nerve root was compared by the same procedure to a non-affected nerve root. We asked the patients before each intervention to point out their actual pain on an analogue pain score ranging from 0-10. We calculated the correlation between the change in ADC value and the development of the pain score as a one-sided Pearson correlation.
Results: There is a strong negative correlation of -0.698 (p=0.017) between the change of ADC value and the improvement of the pain score under therapy. For the reference nerve, no significant change of ADC over time was shown.
Conclusion: Effective periradicular CT-guided infiltration leads to a significant ADC increase of the affected nerve.
Limitations: The small number of patients.
Ethics committee approval: The presented study was approved by the local ethic committee.
Funding: No funding was received for this work.
Author Disclosures:
S. Talarczyk: nothing to disclose
P. Haage: nothing to disclose
D. F. P. Uhlenbrock: nothing to disclose
C. A. Stückle: nothing to disclose

RPS 610-9 12:07
Chondroblastoma treatment by radiofrequency thermal ablation
F. Ruiz Santiago, L. Guzman Alvarez, A. Martinez Martinez, A. J. Láinez Ramos-Bossini*; Granada/ES (ferusan12@gmail.com)*

Purpose: To present our experience in the treatment of chondroblastoma by radiofrequency thermal ablation.
Methods and materials: In the last 15 years, we treated 9 patients (8 males) with chondroblastoma using RTA under CT-guidance. Tumours were located in the humeral head (3), the femoral head (2), and the distal femoral epiphysis (4). Age ranged from 11-20 years (median: 15 years). Tumour size ranged from 12-34 mm (median: 22 mm).
According to tumour size and location, the electrode's active tip ranged from 1-3 cm. Dry ablation or perfused monopolar electrodes were used to treat smaller (6) and larger (3) lesions, respectively. Cementation was added in 3 cases.
Imaging follow-up was performed by MRI (7), CT (1), and radiography (9). Follow-up ranged from 6 months to 15 years.
Results: Total pain control was achieved in all cases. A follow-up MRI demonstrated resolution of oedema, as well as a necrotic area extending beyond the outer edge of the lesion. Radiography showed stability of the lesions, with increased sclerosis and no cortex collapse.
In one case, a 4 cm shortening of the humerus was observed at the end of skeletal development (7 years after treatment). In another case, early hip osteoarthritis was developed (15 years after treatment).
Conclusion: Successful treatment of chondroblastoma can be achieved by RTA. MRI hallmarks associated with clinical success were resolution of bone marrow oedema and an area of necrosis extending beyond the tumour edge. Radiography remains a useful exam to demonstrate cortex integrity.
Limitations: A retrospective review of the cases, although data and images were acquired prospectively, according to hospital clinical protocols.
Ethics committee approval: This work was approved by the local ethics committee (0847-N-19).
Funding: No funding was received for this work.
Author Disclosures:
F. Ruiz Santiago: nothing to disclose
L. Guzman Alvarez: nothing to disclose
A. Martinez Martinez: nothing to disclose
A. J. Láinez Ramos-Bossini: nothing to disclose

RPS 610-10 12:13
Clinical utility of dual-energy CT used as an add-on to 18F FDG PET/CT in the preoperative staging of resectable NSCLC with suspected single osteolytic metastases
H. Wu, S. Dong*; Guangzhou/CN (15876530875@163.com)*

Purpose: To determine the clinical value of ^{18}F-FDG-PET/CT and dual-energy virtual noncalcium CT for detecting and identifying single osteolytic metastases (SOM) in participants with non-small cell lung cancer (NSCLC).
Methods and materials: 42 participants (mean age, 63.5 years ± 10.1; range, 41–81 years) with suspected SOM diagnosed by whole-body ^{18}F-FDG-PET/CT underwent non-enhanced dual-energy CT. All images were visually and quantitatively evaluated by two nuclear medicine physicians (R1 and R2) and two radiologists (R3 and R4), independently. The results of visual and quantitative analysis of ^{18}F-FDG-PET/CT and dual-energy CT were compared with pathological results.
Results: In the visual analysis, the specificity and positive predictive value of dual-energy CT for reader 1 and reader 2 were larger than the corresponding figures of ^{18}F-FDG-PET/CT for reader 3 and reader 4 (94.1% each vs 82.4%/76.5%; 95.2%/95.0% vs 88.9%/86.2%). The sensitivity and negative

predictive value of dual-energy CT was relatively lower than the number of ^{18}F-FDG-PET/CT for readers (80.0%/76.0% vs 96.0%/100.0%; 76.2%/72.7% vs 93.3%/100.0%, respectively). ROI-based analysis of SUV_{max} on PET/CT images and CT numbers on VNCa images showed a significant difference between metastases and non-metastases (P<0.001 each).
Conclusion: Pre-surgical evaluation by the combination of whole-body ^{18}F-FDG-PET/CT and dual-energy CT could improve the classification of SOM and may further guide surgical decision-making in participants with NSCLC.
Limitations: Results should be interpreted with caution because of the relatively small numbers of selected participants included in this exploratory analysis.
Ethics committee approval: Ethics committee approval obtained.
Funding: Natural Science Foundation of Guangdong Province (nos. 2017A020215192) and Guangzhou Science and Technology Project (CN) (nos. 201804010049).
Author Disclosures:
H. Wu: nothing to disclose
S. Dong: nothing to disclose

RPS 610-11 12:19
Dynamics of muscle injuries and recovery in diffusion-tensor imaging
I. Yel, K. Eichler, C. Booz, T. Gruber-Rouh, T. J. Vogl, B. Kaltenbach;
Frankfurt am Main/DE (Dr.IbrahimYel@gmail.com)

Purpose: MR imaging of muscle injuries in clinical routine is limited to assessing muscle morphology and integrity. Essential information about the healing process and return-to-play decisions are mainly determined clinically by sports medicine specialists. The aim was to establish measurable parameters on diffusion-tensor imaging to assess stages of muscle recovery.
Methods and materials: 25 male soccer players with a non-contact hamstring injury were included. 3 consecutive MR-examinations on a 3-Tesla-MRI were performed at initial injury (within 72 hours), and three and six weeks after injury. Freehand ROI-measurements were placed in the injured muscle to assess ADC-, fractional anisotropy (FA), and the sum of eigenvalues (TRACE). For comparison, the same ROI-measurements were also performed on the contralateral healthy muscle.
Results: Overall mean DTI-values for the injured muscle were as followed (initial examination, first follow-up, and second follow-up): ADC ($10^{-3}mm^2/s$): 1.9±0.2, 1.8±0.1, and 1.7±0,1; FA: 263±66, 305 ±73, and 259±53; TRACE: 40.7±10.2, 37.0±8.9, and 36.9±9.2. Throughout the healing course initial ADC- and TRACE-values of the injuries were significantly higher compared to the second follow-up (P≤0.016), whereas FA-values in the first follow-up increased significantly compared to baseline und final examinations (P≤0.036). When comparing the injured muscle with the contralateral healthy muscle, significant differences could be found for the initial FA-values (261.7±62.7 vs 301.7±101.1, P= 0.006) and all three TRACE-values (39.9±10.2 vs 29.3±8.5, 37.0±8.9 vs 31.3±8.8, and 36.9±9.2 vs 30.7±8.6; P≤0.023).
Conclusion: Measurements of ADC, FA, and TRACE could facilitate more a reliable clinical application of MRI imaging, especially to provide further information and more confident clinical application regarding the stage of recovery and healing process.
Limitations: A mono-centre study with high interindividual differences in injury pattern of the hamstrings.
Ethics committee approval: Approval by local IRB.
Funding: No funding was received for this work.
Author Disclosures:
I. Yel: nothing to disclose
C. Booz: Speaker at Siemens Healthineers
T. J. Vogl: nothing to disclose
K. Eichler: nothing to disclose
B. Kaltenbach: nothing to disclose
T. Gruber-Rouh: nothing to disclose

RPS 610-12 12:25
The effect of radiofrequency pulse transmission polarisation on metal-related artefacts in 3T magnetic resonance imaging: circular versus elliptical polarisation
I. Khodarahmi[1], G. Chang[1], J. Fritz[2]; [1]*New York, NY/US,* [2]*Baltimore, MD/US (iman.khodarahmi@nyumc.org)*

Purpose: To investigate the effect of circular and elliptical polarisation of the radiofrequency (RF) pulse on metal-related artefacts in total hip arthroplasty implants during a metal artefact reduction sequence MRI at 3T.
Methods and materials: A cobalt-chromium total hip arthroplasty system with a polyethylene liner immersed in a standard ASTM gel phantom underwent an MRI with high-bandwidth turbo spin-echo (HBW-TSE), slice encoding for metal artefact correction (SEMAC), and compressed sensing (CS) SEMAC in axial, coronal, and sagittal planes using proton density weighting. Each scan was acquired twice with circular (CP) and elliptical (EP) RF polarisation, while keeping other sequence parameters identical. After anonymisation/randomisation, artefacts were volumetrically quantified for CP and EP images using manual segmentation. Additionally, observers compared the two modes for overall image quality through a side-by-side display of each image pair and selection of the preferred polarisation mode.
Results: On quantitative analysis, artefact degraded regions were significantly smaller on EP images compared to the CP images of the same location/pulse sequence (paired t-test: p<0.02 for all pulse sequences). The overall artefact volume (including the implant itself) calculated using axial HBW-TSE images was 19% lower for EP (510 cm^3) compared to CP (608 cm^3). Readers chose the image quality of EP in 56% (95% CI: 51%-61%) and CP in 7% (95% CI: 4%-9%) of the cases with significantly superior image quality of EP (signed test: p<0.001 for all sequences).
Conclusion: 3T MRI with elliptical RF pulse polarisation results in stronger metal artefact reduction and overall superior image quality than circular polarisation. Switching to elliptical polarisation for 3T imaging of metal-containing body parts may eventually hold promise for in vivo clinical imaging.
Limitations: The in-vitro nature of the study.
Ethics committee approval: n/a
Funding: RSNA fellow research grant.
Author Disclosures:
I. Khodarahmi: nothing to disclose
J. Fritz: Research/Grant Support at Siemens AG, Research/Grant Support at Johnson & Johnson, Research/Grant Support at Zimmer Biomet Holdings, Inc, Research/Grant Support at Microsoft Corporation, Research/Grant Support at BTG International Ltd , Advisory Board at Siemens AG, Advisory Board at General Electric Company, Advisory Board at BTG International Ltd, Speaker at Siemens AG Patent agreement, Siemens AG
G. Chang: nothing to disclose

11:15 - 12:30 **Room C**

GI Tract
RPS 601a
Advances in rectal cancer imaging

Moderators:
B. J. Op De Beeck; Edegem/BE
N.N.

RPS 601a-1 11:15
The predictive value of pre- and post-neoadjuvant chemoradiotherapy MRI characteristics for patient outcomes in locally advanced rectal cancer
Y. Meng[1], C. Wang[2], P. Dou[1], H. Zhang[3], K. Xu[1], C. Zhou[3]; [1]*Xuzhou/CN,* [2]*Jiangsu/CN,* [3]*Beijing/CN (mengyankai@126.com)*

Purpose: To investigate the predictive value of pre- and post-neoadjuvant chemoradiotherapy (nCRT) magnetic resonance imaging (MRI) characteristics for the long-term survival outcomes in patients with locally advanced rectal cancer (LARC).
Methods and materials: We retrospectively evaluated pre- and post-nCRT MR characteristics of LARC patients. The 3 year DFS was estimated using the Kaplan-Meier product-limit method. Associations between MRI variabilities and survival outcomes were assessed using Cox proportional hazards model.
Results: In total, 171 LARC patients (112 men and 59 women) with a median age of 55 years (range, 27-82 years) treated with nCRT were evaluated. MRI assessment of extramural venous invasion (mrEMVI) positivity was a significant independent adverse factor of long-term survival (HR=2.589, 95% CI=1.398-4.794, P=0.002) on multivariate analysis. Patients with positive mrEMVI had significantly lower 3-year DFS than those with negative mrEMVI (52.6 months vs 65.1 months; P=0.003). Moreover, the tumour regression grade on MRI (mrTRG) also significantly correlated with survival outcomes in patients with LARC. Patients with partial response on post-nCRT MRI (mrPR) showed worse DFS than those with complete response (mrCR) (HR=4.914, 95% CI=1.176-20.533, P=0.029).
Conclusion: mrEMVI positivity was an independent adverse prognostic indicator for 3-year DFS. Further, mrTRG may also be a predictive factor for the prognosis of LARC patients.
Limitations: A single-centre retrospective analysis.
Ethics committee approval: This retrospective study was approved by our Institutional Review Board and the need for informed consent was waived owing to the retrospective nature of the study.
Funding: This study was funded by the National Natural Science Foundation of China (81771904), Beijing Science and Technology Program (Z161100000516101), and Beijing Hope Run Special Fund of Cancer Foundation of China (LC2016A05).

Author Disclosures:
Y. Meng: nothing to disclose
H. Zhang: nothing to disclose
K. Xu: nothing to disclose
C. Zhou: nothing to disclose
C. Wang: nothing to disclose
P. Dou: nothing to disclose

RPS 601a-2 11:21
What's in a name? "Polypoid" as a descriptor in pelvic MRI synoptic reporting for rectal cancer
J. S. Golia Pernicka[1], D. Bates[2], J. Fuqua[2], A. Knezevic[2], J. Yoon[3], L. Nardo[4], I. Petkovska[2], V. Paroder[2], M. J. Gollub[2]; [1]*Bridgeport, CT/US,* [2]*New York, NY/US,* [3]*Montreal, QC/CA,* [4]*Sacramento, CA/US* *(gollubm@mskcc.org)*

Purpose: To compare MR imaging morphology of rectal cancer with clinicopathologic features.
Methods and materials: 50 rectal MRI reports with the synoptic term "polypoid" tumour were reviewed retrospectively and 90 reports containing "circumferential" and "partially circumferential" tumours were randomly selected to serve as controls. Preoperative tumour (T) and lymph node (N) stages of the polypoid tumours were determined by two readers and compared to reported T-stages for the controls. To assess the difference in degrees of attachment to wall circumference (WC) (≤¼ or >¼) and the presence of a pedicle, 25 randomly selected polypoid tumours and 25 randomly selected controls were reviewed by two additional readers. Inter-reader agreement was assessed using the kappa statistics for binary measures, weighted kappa for ordinal measures, and nonparametric interclass correlation coefficient (ICC) for continuous measures. Features were compared between cases and controls using Fisher's exact test for categorical variables and Wilcoxon rank-sum test for continuous variables.
Results: Polypoid shape, pedicle presence, and degree of attachment showed moderate agreement (k=0.41-0.76). N size showed good agreement (ICC=0.83-0.91). Distinguishing characteristics of polypoid tumours were an attachment to < ¼ WC (p<0.001, 0.002) and presence of a pedicle (p<0.001, both) in significantly more cases compared to controls. Lower T and N stages, smaller largest node, and fewer number of nodes > 3mm were significantly associated with polypoid morphology compared to controls (p<0.001 to 0.008).
Conclusion: Primary "polypoid" tumours at rectal MRI represent a distinct phenotype with lower pathologic T and N stages. If the above definition of "polypoid" is validated, this synoptic term may be more than descriptive and could potentially inform patient prognostication.
Limitations: Retrosepctive study.
Ethics committee approval: IRB waiver of patient consent.
Funding: NCI P30 CA008748 Cancer Center Support Grant.
Author Disclosures:
M. J. Gollub: nothing to disclose
J. S. Golia Pernicka: nothing to disclose
D. Bates: nothing to disclose
J. Fuqua: nothing to disclose
A. Knezevic: nothing to disclose
J. Yoon: nothing to disclose
L. Nardo: nothing to disclose
I. Petkovska: nothing to disclose
V. Paroder: nothing to disclose

RPS 601a-3 11:27
Clinical T4a rectal cancer at MRI: do these patients develop peritoneal carcinomatosis?
C. Simmers[1], M. Capanu[1], D. Bates[1], J. Fuqua[1], J. S. Golia[2], S. Javed-Tayyab[1], V. Paroder[1], I. Petkovska[1], M. J. Gollub[1]; [1]*New York, NY/US,* [2]*Bridgeport, CT/US* *(gollubm@mskcc.org)*

Purpose: To evaluate development of peritoneal carcinomatosis or other adverse short- or long-term outcomes in patients with MRI-based T4a rectal cancer.
Methods and materials: In the 5 year period from 2013-2018, the clinico-pathologic records of all patients with pretreatment rectal MRI with reported clinical (c) T3c, T3d, T4a, and T4b primary rectal adenocarcinoma were retrospectively reviewed by one radiology fellow. All MRI reported features such as nodal stage and tumour height were collected. Pathologic T and N stages were summarised among patients undergoing curative resection. Recurrence-free survival (RFS) and overall survival (OS) were estimated using the Kaplan-Meier method. Differences in survival were compared using the log-rank test. Descriptive statistics were used to describe distant metastases.
Results: 256 patients were included with 28 clinical T4a, 135 T3cd, and 93 T4b patients reported at MRI. Median follow-up among survivors was 27 months (range 0.36-70 months). All patients underwent neoadjuvant treatment and, at surgical pathology, only 3 cases were pT4a. 9 patients developed peritoneal carcinomatosis (9/256 3.5%) who had been clinical T3cd (n=5/135, 3%), T4a (n=2/28, 7%), and T4b (n=2/93, 2%). 5 of the 9 patients underwent surgery and all had pT3 disease. RFS (p=0.065) and OS (p=0.1694) did not differ between cT3cd and cT4a nor between cT4a and cT4b. RFS was worse in cT4b compared with cT3cd (p=0.03).
Conclusion: Peritoneal carcinomatosis occurs rarely in rectal cancer, even in cases diagnosed as cT4a on baseline MRI. Overall and recurrence-free survival in patients with MRI-based T4a was not worse than those with T3cd disease.
Limitations: Retrospective study.
Ethics committee approval: IRB waived the need for consent.
Funding: This research was funded in part through the NIH/NCI Cancer Center Support Grant P30 CA008748.
Author Disclosures:
M. J. Gollub: nothing to disclose
C. Simmers: nothing to disclose
M. Capanu: nothing to disclose
D. Bates: nothing to disclose
J. Fuqua: nothing to disclose
J. S. Golia: nothing to disclose
S. Javed-Tayyab: nothing to disclose
V. Paroder: nothing to disclose
I. Petkovska: nothing to disclose

RPS 601a-4 11:33
MRI texture analysis for the early prediction of therapeutic response to neoadjuvant chemoradiotherapy and tumour recurrence of locally advanced rectal cancer
H. Park, K. A. Kim, S. S. Hwang, S. Y. Park, H. A. Kim; *Suwon-si/KR*

Purpose: To evaluate the efficiency of texture analysis (TA) based on baseline rectal MRI for the early prediction of therapeutic response to neoadjuvant chemoradiotherapy (nCRT) and tumour recurrence in patients with locally advanced rectal cancer (LARC).
Methods and materials: Consecutive patients with LARC who underwent rectal MRI between January 2014 and December 2015, and surgical resection after completing nCRT, were retrospectively enrolled and divided into responder and nonresponder groups according to tumour regression grade (TRG). Tumour recurrence was evaluated. TA parameters were extracted from the tumour volume of interest (VOI) from the baseline rectal T2W MRI using LifeX Software. Receiver operating characteristic (ROC) curve analysis was performed to evaluate the optimal TA parameter cut-off values to stratify the patients. Univariate and multivariate analyses were performed to assess the efficacy of each texture parameter in predicting tumour response and disease-free survival with logistic and Cox regression tests.
Results: In total, 78 consecutive patients were enrolled. In the logistic regression, good treatment response was associated with low Conv_Min (OR=0.300, p=0.013) and high Conv_Std (OR=3.174, p=0.016), Shape_Sphericity (OR=3.170, p=0.015), and Shape_Compacity (OR=2.779, p=0.032). In the Cox regression, a greater risk of tumour recurrence was related to higher grey-level run-length matrix_long-run low grey-level emphasis (GLRLM_LRLGE) (HR=2.268, p=0.046).
Conclusion: Texture analysis based on baseline rectal T2W MRI could be valuable for predicting the treatment response to nCRT for rectal cancer and tumour recurrence
Limitations: While many factors were used in our study, the small number of subjects is the limitation.
Ethics committee approval: This study was approved by the institutional review board of our institution.
Funding: No funding was received for this work.
Author Disclosures:
H. Park: nothing to disclose
K. A. Kim: nothing to disclose
S. S. Hwang: nothing to disclose
S. Y. Park: nothing to disclose
H. A. Kim: nothing to disclose

RPS 601a-5 11:39
Value of high-resolution MRI in detecting lymph node calcifications in patients with rectal cancer
Y. Chen[1], Z. Wen[1], Y. Liu[1], X. Yang[1], Y. Ma[1], B. Lu[1], X. Xiao[2], S. Yu[1]; [1]*Guangzhou/CN,* [2]*Shenzhen/CN (chenyan_me@163.com)*

Purpose: To analyse imaging findings for nodal metastasis calcifications on MSCT and high-resolution MRI, and determine the value of high-resolution MRI in detecting nodal calcifications in rectal cancer patients.
Methods and materials: In a respective study, 229 consecutive rectal cancer patients who underwent total mesorectal excision following pelvic MSCT and rectal high-resolution MRI were included. MSCT was reviewed for the presence of nodal calcifications by two radiologists. To analyse nodal calcifications, high-

resolution two-dimensional turbo spin-echo T2-weighted imaging (2D-TSE-T2WI) and fat-suppressed gadolinium-enhanced isotropic high-resolution three-dimensional gradient-echo T1-weighted imaging (3D-GRE-T1WI) were independently reviewed by two radiologists at one-month and two-month intervals, respectively. The sensitivities, specificities, and accuracies of the two high-resolution MRI for detecting nodal calcifications were calculated using MSCT results as a reference.
Results: Regional calcified metastatic nodes were found in 28 patients. Node-to-node evaluation showed 55 of 56 calcified nodes to be metastatic. Fifty-one calcified metastatic nodes displayed scattered fine punctate calcifications to different degrees on MSCT. By the two high-resolution techniques, the calcifications demonstrated patchy, marked reductions in signal intensity in corresponding areas, but were larger than those on MSCT. The sensitivity and accuracy of the high-resolution 3D-GRE-T1WI were significantly higher than those of high-resolution 2D-TSE-T2WI (76.8% vs. 58.9%, P = 0.013; 98.3% vs. 97.9%, P = 0.007, respectively).
Conclusion: Metastatic nodal calcifications are characteristic of imaging findings in rectal cancer. Calcifications are indicated by extremely low signal intensity or extremely low enhancement within nodes on high-resolution 2D-TSE-T2WI and the high-resolution 3D-GRE-T1WI, which will aid in the accurate diagnosis of metastatic nodes.
Limitations: Did not apply diffusion-weighted imaging to evaluate nodal calcifications.
Ethics committee approval: Approved by an institutional review board. Written informed consent was obtained.
Funding: Science and Technology Planning Project of Guangdong Province (2014A020212126).
Author Disclosures:
Y. Chen: nothing to disclose
Z. Wen: nothing to disclose
Y. Liu: nothing to disclose
X. Yang: nothing to disclose
B. Lu: nothing to disclose
X. Xiao: nothing to disclose
S. Yu: nothing to disclose
Y. Ma: nothing to disclose

RPS 601a-6 11:45

Humans cannot distinguish mucinous rectal cancer from acellular mucin post-treatment: can computers? A multi-institutional pilot study of MRI radiomics

M. J. Gollub[1], M. Fox[2], N. Horvat[3], I. Petkovska[1], S. P. Sheedy[4], E. Korngold[5], C. Moreno[6], S. Nougaret[7], P. Gibbs[1]; *[1]New York, NY/US, [2]Hull/UK, [3]Sao Paulo/BR, [4]Rochester, MN/US, [5]Portland/US, [6]Atlanta/US, [7]St Clement de Riviere/FR (gollubm@mskcc.org)*

Purpose: To determine the accuracy of MRI radiomics to distinguish between post-treatment residual cellular and acellular mucinous rectal neoplasms.
Methods and materials: At 5 institutions from the Rectal and Anal Disease Focused Panel of the Society of Abdominal Radiology, a retrospective study of all patients with rectal adenocarcinoma containing mucin on post-neoadjuvant CRT MRI and prior to surgery between 2003 and 2017 (n= 362) was performed. Patients with <75% mucin on MRI were excluded (n=308). Manual volumetric segmentation of mucinous masses was performed on Terra Recon software (Aquarius iNtuition Viewer v 4.4.13.P4) by one experienced radiologist. Radiomics and machine learning models were performed using CERR within MatLab (2017b) to generate 22 first order and 80 second order parameters. Statistical analysis was performed with SPSS (v.25) using ROC curves to determine significant individual parameters (AUC > 0.70).
Results: 54 patients, 30 males, mean age 58yr (39-75yr), and 24 females, mean age 58yr (32-87yr), had stage 0-2 and 3 disease (n= 41, 13, respectively). 54 patients underwent neoadjuvant CRT. Histopathology showed 10 acellular, mucinous, non-neoplastic masses and 44 mucinous adenocarcinomas. In univariate testing, 4/102 parameters were of significance, with the best performing radiomic model for neoplasm classification showing an AUC of 0.63 using a cubic support vector machine with 10-fold cross-validation.
Conclusion: An MRI radiomic model performed modestly in distinguishing post-treatment acellular, non-neoplastic masses from residual mucinous rectal adenocarcinoma with an AUC 0.63. While not ready for clinical dissemination, such modeling may be a step forward for informing treatment decisions in these aggressive tumours.
Limitations: Retrospective, a small number of cases.
Ethics committee approval: Waiver of consent from IRB.
Funding: No funding was received for this work.
Author Disclosures:
M. J. Gollub: nothing to disclose
M. Fox: nothing to disclose
N. Horvat: nothing to disclose
I. Petkovska: nothing to disclose
S. P. Sheedy: nothing to disclose
E. Korngold: nothing to disclose
C. Moreno: nothing to disclose
S. Nougaret: nothing to disclose
P. Gibbs: nothing to disclose

RPS 601a-7 11:51

T and N staging of rectal cancer: comparison between the 2012 and 2016 structured MRI report templates proposed by the European Society of Gastrointestinal and Abdominal Radiology (ESGAR)

F. M. Donati, R. Cervelli, P. Boraschi, N. Furbetta, G. Tarantini, L. Morelli, D. Caramella*; Pisa/IT (p.boraschi@gmail.com)*

Purpose: To compare the 2012 and 2016 structured MRI report templates proposed by the European Society of Gastrointestinal and Abdominal Radiology (ESGAR) for the TN staging of rectal cancer.
Methods and materials: 47 consecutive patients affected by biopsy-proven rectal cancer were included in this retrospective study. 19 out of 47 had undergone neoadjuvant chemoradiation therapy (nCRT) before surgery. All patients performed MR examination within 20 days before surgery. A comparison between the radiological TN staging obtained according to both 2012 and 2016 ESGAR guidelines and the pathological TN staging was performed.
Results: The radiological T stage did not differ between 2012 and 2016 ESGAR guidelines. It was classified as T1, T2, T3, T4 in 1, 5, 20, and 2 patients directly resected, and as T0, T2, T3, T4 in 4, 7, 6, and 2 patients who underwent nCRT, respectively. A statistical correlation was found between the radiological and pathological T stage ($p<0.0001$;ρ of Spearman=0.62). As to the radiological N stage, according to 2012 and 2016 guidelines, in 24 and 32 patients no metastatic lymph-nodes were found. The N1 stage was classified in 22 and 14 patients respectively, whereas the N2 stage in only one patient, according to both guidelines. The pathological N stage was N0, N1, N2 in 27, 16, and 4 patients. A statistical correlation was found between the radiological-pathological N stage comparison by applying both the 2012 ($p=0.009$) and the 2016 guidelines ($p<0.0001$). However, the updated 2016 version showed a stronger correlation (ρ of Spearman=0.60).
Conclusion: Both the 2012 and the 2016 ESGAR structured MRI report templates were reliable tools to assess the radiological T and N stage of rectal cancer. The 2016 templates were more accurate in estimating lymph-nodes involvement.
Limitations: Retrospective study.
Ethics committee approval: n/a
Funding: No funding was received for this work.
Author Disclosures:
P. Boraschi: nothing to disclose
F. M. Donati: nothing to disclose
R. Cervelli: nothing to disclose
N. Furbetta: nothing to disclose
L. Morelli: nothing to disclose
D. Caramella: nothing to disclose
G. Tarantini: nothing to disclose

RPS 601a-8 11:57

The role of high-resolution apparent diffusion coefficient histogram analysis in evaluating tumour response of locally advanced rectal cancer after neoadjuvant chemoradiotherapy

L. Yang, C. Xia, D. Liu, B. Wu*; Chengdu/CN (lqyang95@163.com)*

Purpose: To evaluate the role of high-resolution ADC map based on read-out segmented echo-plannar imaging (rs-EPI) in assessing tumour response before and after neoadjuvant chemoradiotherapy (CRT) by using histogram analysis in locally advanced rectal cancer (LARC).
Methods and materials: 63 LARC who received neoadjuvant CRT and surgery were enrolled retrospectively. They all underwent pre- and post-CRT MR examinations, including DWI using rs-EPI. According to pathological results, patients were grouped as pathological complete responder (pCR, n=16) and non-pCR (n=47). Visual assessment of residual tumour and whole-tumour histogram analysis of pre- and post-CRT ADC map was performed by two radiologists, and tumour volume on the ADC map was also recorded.
Results: Overall interobserver agreement was good for histogram analysis (ICC=0.543-0.999). Tumour volume reduction rate on the ADC map showed no significant difference between two groups (P=0.468). Post-CRT mean, quantile values, and their percentage changes were higher in the pCR group (all P<0.001). Post-CRT mean value had a good diagnostic power in selecting pCR (AUCs=0.855), with a cut-off value of $1.345´10^{-3}mm^2/s$, yielding a sensitivity of 83%, specificity of 81.3%. Post-CRT quantile 95% value had the highest AUCs (AUCs=0.868) among quantile values and higher specificity (87.5% vs. 81.3%) than mean value with comparable overall diagnostic performance (P=0.563). The visual assessment showed a sensitivity of 85.1%, specificity of 68.8% in selecting pCR.

Conclusion: Quantitative ADC value of rs-EPI DWI could reliably evaluate tumour response in patients with LARC. Post-CRT 95% quantile ADC value could help mean value to more accurately identify pCR.
Limitations: This is a retrospective study with a relative small number of patients.
Ethics committee approval: This retrospective study was approved by our Institutional Review Board and the requirement for informed consent was waived.
Funding: No funding was received for this work.
Author Disclosures:
L. Yang: nothing to disclose
C. Xia: nothing to disclose
B. Wu: nothing to disclose
D. Liu: nothing to disclose

RPS 601a-9 12:03

Performance and inter-reader reproducibility of MRI using a simplified response template to help (pre-) select rectal cancer patients for surgery versus organ preservation after chemoradiotherapy

H. E. Haak[1], M. Maas[1], T. N. Boellaard[1], A. Delli Pizzi[2], C. Mihl[3], D. van der Zee[4], G. L. Beets[1], R. G. H. Beets-Tan[1], D. M. J. Lambregts[1]; [1]Amsterdam/NL, [2]Chieti/IT, [3]Maastricht/NL, [4]Uden/NL (doenja.lambregts@gmail.com)

Purpose: To assess the inter-reader reproducibility and performance of MRI using a simplified response template (designed for this study) to differentiate between patients likely requiring surgery and potential organ-preservation (watch-and-wait) candidates who would benefit from more detailed response assessment with endoscopy.
Methods and materials: 7 independent readers (varying from resident level to MRI-expert) retrospectively evaluated the restaging MRIs (T2W+DWI) of 62 rectal cancer patients after chemoradiotherapy using a simplified response template, taking into account the morphology on T2W-MRI (degree of fibrosis) and signal pattern on DWI (no/focal/scattered high signal). They categorised patients as poor response (tumour certain/surgery definitely required), intermediate response (tumour likely/surgery probably required), and good response (potential complete response, endoscopy required to determine eligibility for watch-and-wait). The reference standard was histopathology (and/or long-term follow-up). Inter-reader reproducibility was tested using Kendall's coefficient of concordance.
Results: 48 patients had a residual tumour and 14 were confirmed complete responders. Overall interobserver reproducibility was good (W0.65). The median % of patients categorised as good/intermediate/poor responders was 29%/50%/21%. The vast majority of MR-categorised poor and intermediate responders had confirmed residual tumour (median 100%, range 95-100% for the 7 different readers; and median 88%, range 76-100%, respectively). The majority (median 71%, range 57-93% for the 7 different readers) of the in total 14 confirmed complete responders were correctly classified in the "good response" group. The remaining ones were almost exclusively classified as intermediate responders (except for 1 complete responder who was misclassified as a poor responder by 1/7 readers).
Conclusion: MRI using a simplified structured response template can aid radiologists with varying levels of expertise in pre-selecting which patients will require surgery versus potential watch-and-wait candidates who will benefit from further endoscopic response assessment.
Limitations: This study is based on a small cohort with retrospectively included patients.
Ethics committee approval: n/a
Funding: No funding was received for this work.
Author Disclosures:
M. Maas: nothing to disclose
H. E. Haak: nothing to disclose
T. N. Boellaard: nothing to disclose
A. Delli Pizzi: nothing to disclose
C. Mihl: nothing to disclose
D. van der Zee: nothing to disclose
G. L. Beets: nothing to disclose
R. G. H. Beets-Tan: nothing to disclose
D. M. J. Lambregts: nothing to disclose

RPS 601a-11 12:09

Patho-radiomic signatures predict pathological complete response to neoadjuvant chemoradiotherapy in rectal cancer

W. Lijuan[1], H. Zhang[2], Z. Sun[2], W. Peng[2], L. Wan[2]; [1]Beijing, Chaoyang/CN, [2]Beijing/CN (18345195352@163.com)

Purpose: To investigate the diagnostic performance of the patho-radiomic signatures from pathology and radiology features for predicting pathological complete response (pCR) after neoadjuvant chemoradiotherapy (nCRT) in patients with rectal cancer (RC).
Methods and materials: A total of 156 patients with RC were enrolled in this retrospectively study between March 2015 and March 2018. All patients underwent MR examination before and after nCRT, and all pathological sections were harvested from proctoscopic biopsy before nCRT. 512 pathomic features were extracted from each patient pathological section and 190 radiomic features were obtained from T2-weighted MR imaging (MRI). The least absolute shrinkage and selection operator (LASSO) method was used for pathology and radiology features selection and building signatures. The patho-radiomic signatures, other conventional MRI parameters, and clinical factors were integrated into a multivariable logistic regression analysis to determine if the signatures were independent prognostic factors for pCR.
Results: Overall, 25 patients (16.0%) achieved pCR. The pathomics and radiomics signature, which both comprised 3 selected features, was significantly associated with pCR after nCRT. On multivariate analysis, the patho-radiomic signatures were independent prognostic factors. The area under the receiver operating curve (AUC-ROC) of the multivariable regression model for pCR prediction was 0.845 (95% CI, 0.762 to 0.928).
Conclusion: In RC patients who underwent nCRT, the patho-radiomic signatures created by combining pathology and radiology features exhibited favourable for pCR prediction and can increase the confidence of the organ-preserving strategy.
Limitations: The first limitation was the relatively small size. The second is a retrospective design. Next, we need more samples to verify the diagnostic performance of the patho-radiomic signatures.
Ethics committee approval: This study was approved by our institutional ethics committee.
Funding: The special scientific research projects of the Beijing science and technology project [Grant Number Z16110000051610].
Author Disclosures:
W. Lijuan: nothing to disclose
H. Zhang: nothing to disclose
Z. Sun: nothing to disclose
W. Peng: nothing to disclose
L. Wan: nothing to disclose

RPS 601a-12 12:15

Rectal cancer: a methodological approach for matching PET/MRI to histopathology

M. K. Rutegård[1], M. Båtsman[1], J. Axelsson[1], F. Brännström[2], L. C. O. K. Blomqvist[3], I. Ljuslinder[1], R. Palmqvist[1], M. Rutegård[1], K. Riklund[1]; [1]Umeå/SE, [2]Södertälje/SE, [3]Stockholm/SE (miriam.rutegard@diagrad.umu.se)

Purpose: The role of hybrid imaging with magnetic resonance imaging (MRI) and ^{18}F-fluoro-2-deoxy-D-glucose positron-emission tomography (FDG-PET) in the preoperative staging and restaging in rectal cancer is not clear. To enable evaluation of locoregional disease in the on-going RECTOPET (REctal Cancer Trial on PET/MRI/CT) study, a methodology to match mesorectal imaging findings to histopathology is presented, along with initial observations.
Methods and materials: 24 patients with rectal adenocarcinoma underwent FDG-PET/MRI. In 9 patients, of whom 5 received neoadjuvant treatment, an MRI of the surgical specimen was performed. The pathological cut-out was done according to clinical routine with the addition of photodocumentation of each slice of the specimen, noting the location, size, and type of pathology of each mesorectal finding. This allowed matching individual nodal structures from preoperative MRI examinations, via the specimen MRI, to histopathological findings.
Results: Preoperative MRI identified 197 mesorectal nodal structures, of which 92 (47%) could be anatomically matched to histopathology. Of the matched nodal structures identified in both MRI and histopathology, 25% were found to be malignant. These malignant structures consisted of lymph nodes (43%), tumour deposits (48%), and extramural venous invasion (9%).
Conclusion: We have been able to anatomically match individual nodal structures at preoperative MRI with dedicated histopathology, thus devising a method to study the characteristics of benign and malignant mesorectal structures on a finding-by-finding basis. Initial observations suggest that small malignant nodal structures assessed as lymph nodes at MRI in the majority of cases comprise other forms of mesorectal tumour spread.

Limitations:
This is a single-centre study with a small sample size.
Ethics committee approval:
This study was approved by the Regional Ethical Review Board in Umeå and participation required written informed consent.
Funding:
This work was supported by Umeå University and Umeå University Hospital.
Author Disclosures:
R. Palmqvist: nothing to disclose
M. K. Rutegård: nothing to disclose
K. Riklund: nothing to disclose
L. C. O. K. Blomqvist: nothing to disclose
M. Båtsman: nothing to disclose
J. Axelsson: nothing to disclose
F. Brännström: nothing to disclose
I. Ljuslinder: nothing to disclose
M. Rutegård: nothing to disclose

11:15 - 12:30 **Room X**

Vascular

RPS 615

CT in vascular imaging

Moderators:
V. Rafailidis; London/UK
N.N.

RPS 615-K 11:15
Keynote lecture
M. Radzina*; Riga/LV (mradzina@gmail.com)*

Author Disclosures:
M. Radzina: nothing to disclose

RPS 615-1 11:25
Impact on clinical practice of updated guidelines on iodinated contrast material: CINART
E. C. Nijssen[1], P. J. Nelemans[1], R. Rennenberg[1], A. J. van der Molen[2], V. van Ommen[1], J. E. Wildberger[1]*; [1]Maastricht/NL, [2]Leiden/NL (j.wildberger@mumc.nl)*

Purpose: Guidelines on the safe use of iodinated contrast material recommend intravenous prophylactic hydration to prevent post-contrast adverse (renal) effects. The AMACING trial showed that standard prophylaxis was not (cost-) effective in the bulk of patients targeted by the guidelines and the latter have been updated accordingly. The current study aims to evaluate the consequences for the clinical practice in terms of reductions in complications, hospitalisations, and costs.
Methods and materials: The Contrast-Induced Nephropathy After Reduction of the Threshold for prophylaxis (CINART) project is a retrospective observational study. All elective procedures with intravascular iodinated contrast administration at Maastricht University Medical Centre (UMC+) in patients aged >18 years, formerly eligible for prophylaxis (eGFR30-44ml/min/1.73m^2 or eGFR45-59ml/min/1.73m^2 in combination with diabetes or >1 predefined risk factor) and currently eligible for prophylaxis (eGFR<30ml/min/1.73m^2), were included. Data was used to calculate the relative reductions in complications, hospitalisations, and costs associated with standard prophylactic intravenous hydration. CINART is registered with Clinicaltrials.gov: NCT03227835.
Results: From July 1, 2017-July 1, 2018, 1,992 elective procedures with intravascular iodinated contrast in patients formerly and currently eligible for prophylaxis were identified: 1,808 in patients formerly eligible for prophylaxis and 184 in patients currently eligible for prophylaxis. At Maastricht UMC+, guideline updates led to large relative reductions in the number of complications from prophylaxis, e.g. symptomatic heart failure (-89%), extra hospitalisations (-93%), and costs (-91%).
Conclusion: Guideline updates have had a demonstrable impact on daily clinical practice, benefiting patients, hospitals, and health care budgets. The local impact on costs, hospitalisations, and complications can be calculated using the interactive calculator.
Limitations: A single-centre study at Maastricht UMC+. Parameters may vary at other centres.
Ethics committee approval: The Medical Research Ethics Committee Maastricht UMC+ waived the requirement for informed consent.
Funding: Stichting de Weijerhorst.

Author Disclosures:
E. C. Nijssen: nothing to disclose
J. E. Wildberger: nothing to disclose
P. J. Nelemans: nothing to disclose
R. Rennenberg: nothing to disclose
A. J. van der Molen: nothing to disclose
V. van Ommen: nothing to disclose

RPS 615-2 11:31
Time-resolved dual-source CT angiography: an evaluation of type II endoleaks after endovascular aneurysm repair
N. Schicchi, M. Fogante, P. Esposto Pirani, G. Agliata, A. Giovagnoni*; Ancona/IT*

Purpose: To evaluate the sensibility in type II endoleak detection and compare the performance in arterial supply vessel identification between standard and time-resolved protocols after endovascular aneurysm repair (EVAR).
Methods and materials: In this prospective study, 83 consecutive patients referred for CT after EVAR were enrolled. All patients had at least one non-treated type II endoleak detected with a previous CT using a standard protocol (SP), consisting of unenhanced, arterial and venous acquisitions, serving as the reference standard. All exams were performed with DSCT (SOMATOM Force, Germany). A time-resolved protocol consisted of 8 unidirectional scan phases followed by dual-energy acquisition was used. The sensibility in endoleak detection was evaluated. The performance in arterial supply vessel identification and radiation dose were compared between 2 protocols.
Results: Using SP, 102 type II endoleaks and 69 arterial supply vessels were identified; 42 were lumbar arteries (LAs), 11 were inferior mesenteric arteries (IMA), and 16 were both. Using a time-resolved protocol, 85 type II endoleaks and arterial supply vessels were identified in all patients; 51 were LAs, 14 were IMA, and 20 were both. The sensibility in endoleak detection was 100%. The performance in arterial supply vessels identification with the time-resolved protocol was significantly higher (p<000.1). The radiation dose was 6.93±1.86 mSv with SP and 7.12± .95 mSv with the time-resolved protocol (p<0.304).
Conclusion: The time-resolved protocol compared to SP demonstrated very high sensibility in type II endoleak detection and better performance in arterial supply vessels identification with no significant difference in radiation dose.
Limitations: No external reference standard.
Ethics committee approval: Our ethics committee approved this study. Written informed consent was obtained.
Funding: No funding was received for this work.
Author Disclosures:
M. Fogante: nothing to disclose
N. Schicchi: nothing to disclose
P. Esposto Pirani: nothing to disclose
G. Agliata: nothing to disclose
A. Giovagnoni: nothing to disclose

RPS 615-3 11:37
The clinical application of adaptive statistical iterative reconstruction V combined with a low tube current technique in head dual-energy spectral imaging CTA
T. Song, Z. Li*; Chengdu/CN*

Purpose: To explore the feasibility and clinical value of dual-energy spectral imaging combined with low tube current and ASiR-V for dose reduction on head CTA.
Methods and materials: Phantom study: An anthropomorphic PBU-60 angiographic head phantom was examined on a revolution CT using spectral imaging mode at different tube currents (280, 320, 365, 405, and 445 mA) and images were reconstructed with the filtered back-projection (FBP) 20%, 40%, 60%, and 80% ASiR-V algorithm.
Clinical study: 40 patients who underwent head dual-energy spectral imaging CTA were prospectively enrolled and randomly divided into two groups. Group A (low tube current) was the experimental group and the parameters were set according to the results of the phantom study. Group B was the control group with 445 mA tube current and the FBP algorithm.
Results: Phantom study: The image noise decreased as the tube current increased and the SNR and CNR were on the rise. With the same tube current, the image noise decreased and SNR and CNR increased as the proportion of ASiR-V increased. The noise reduction rate reached 46.73±4.27% at ASiR-V 80%. The CTDI increased as the tube current rose and there was a significant positive correlation between them.
Clinical study: The radiation dose of group A was 39% lower than group B and no significant difference was noted on the subjective scores.

Conclusion: Low tube current (280 mA) combined with ASiR-V 80% can effectively reduce the radiation dose and obtain satisfactory images for diagnosis on head CTA spectral imaging.
Limitations: This study was a single-centre study.
Ethics committee approval: This study was approved by the biomedical ethics committee of our hospital.
Funding: 1.3.5 project for disciplines of excellence, West China Hospital, Sichuan University (ZYGD18019).
Author Disclosures:
T. Song: nothing to disclose
Z. Li: nothing to disclose

RPS 615-4 11:43

Split-phase aortic CTA for TAVI planning using a dual-layer spectral CT with reconstruction of low-keV virtual monoenergetic images

D. Mangold, J. Riffel, H.-U. Kauczor, T. F. Weber*; Heidelberg/DE (dav.mangold@gmail.com)*

Purpose: CT protocols for TAVI planning have to be adapted when using a dual-layer spectral CT scanner (DLCT) with 4 cm detector width instead of a conventional single-layer CT with 8 cm detector width (SLCT). The purpose of this study was to compare the objective image quality of aortic CT angiograms (CTA) performed for TAVI planning using a split-phase technique with the reconstruction of 40keV virtual monoenergetic images (VMI40) obtained with DLCT versus a single-phase technique with the reconstruction of standard polychromatic images obtained with SLCT.
Methods and materials: 115 CTA from each scanner were retrospectively analysed. For SLCT, spiral CTA with retrospective ECG-gating was performed for heart and vessel assessment at once. For DLCT, spiral CTA without ECG-synchronisation was performed immediately after a retrospectively ECG-gated spiral acquisition covering the heart. For the image quality assessment, SNR and CNR were calculated on the basis of abdominal aortic and lumbar muscle ROI analyses. Sufficient aortic enhancement was considered at attenuation >250HU.
Results: Contrast material volume was comparable for DLCT and SLCT (82±6ml vs 81±4ml, p=0.191). Aortic enhancement of VMI40 DLCT-CTA was significantly higher than of SLCT-CTA (610±273HU vs 413±127 HU, p<0.001). No significant differences were found for SNR (21±11 vs 21±8, p=0.420) and CNR (24±15 vs 24±10, p=0.524). Sufficient aortic enhancement was achieved in 97% for DLCT-CTA and in 93% for SLCT-CTA. Total dose length products of TAVI planning examinations were 2003±417mGy*cm for DLCT and 2401±754mGy*cm for SLCT (p<0.001).
Conclusion: Using a split-phase acquisition technique with the reconstruction of VMI40, CTA for TAVI planning can be obtained with similar objective image quality with DLCT compared to an ECG-gated CT acquisition of the whole aorta performed with conventional SLCT.
Limitations: n/a
Ethics committee approval: This study was approved by our local ethical committee.
Funding: No funding was received for this work.
Author Disclosures:
D. Mangold: nothing to disclose
T. F. Weber: nothing to disclose
H.-U. Kauczor: nothing to disclose
J. Riffel: nothing to disclose

RPS 615-5 11:49

Artificial intelligence and the thoracic aorta: do we still have to measure manually?

M. Pradella[1], T. J. Weikert[1], J. Cyriac[1], R. Kärgel[2], J. Bremerich[1], G. Sommer[1], A. W. Sauter[1], B. Stieltjes[1], P. Brantner[1]*; [1]Basel/CH, [2]Nuremberg/DE (maurice.pradella@usb.ch)*

Purpose: Thoracic aorta dilatation is a major risk factor for dissection or rupture. Diameter measurements on cross-sectional imaging are time-consuming and show inter-reader variability.
We evaluated an artificial intelligence (AI)-Rad companion (AI-RC, Siemens Healthineers) which automatically performs guideline-based measurements of the thoracic aorta and compares them to radiologists' measurements.
Methods and materials: We identified ECG-gated scans of patients (pts) which were suspected or already diagnosed with dilatation. AHA guideline-based diameter measurements were included in the report. In parallel, those cases were processed with AIRC according to current AHA guidelines. Measurements of the aortic sinus (AS) and ascending aorta (AA) were compared. Cases with a difference of 5 mm or less between AIRC and manual measurements were considered plausible. If the difference was >5 mm, further evaluation was performed.
Results: 367 scans of 346 patients (mean age 64.5 yrs, 261 male (75.4%)) were included in this study.
The mean difference between reported and AIRC measurements were 0.26 mm for AS (95% CI: -0.71-0.40 mm) and 0.03 mm for AA (95% CI: -0.34-0.34 mm), respectively. Correlations coefficients (Pearson) were high for AS (0.702) and very high for AA (0.912).
Of 367 pts measurements, 270 (74%) were within 5 mm. 97 cases showed a difference >5 mm between measurements. 70 of those 97 cases (72%) showed a misidentification of AS, 4 (4%) a sole misidentification of AA, and 19 (20%) were correctly measured by AIRC. In total, 289/367 cases (79%) were correctly measured by AIRC.
Conclusion: AIRC shows the potential to assist radiologists since it automatically performs measurements of the thoracic aorta. It reliably measures AA but struggles in identifying the AS in some cases.
Limitations: A single-centre study and retrospective analysis.
Ethics committee approval: Approved by the regional ethics committee. Informed consent was waived.
Funding: No funding was received for this work.
Author Disclosures:
M. Pradella: nothing to disclose
P. Brantner: nothing to disclose
T. J. Weikert: nothing to disclose
R. Kärgel: Consultant at Siemens Healthineers
J. Bremerich: nothing to disclose
G. Sommer: nothing to disclose
A. W. Sauter: nothing to disclose
B. Stieltjes: nothing to disclose
J. Cyriac: nothing to disclose

RPS 615-6 11:55

Identification of fast-growing abdominal aortic aneurysms (AAAs) via radiomics analysis of contrast-enhanced computed tomography (CE-CT) imaging

F. Xiong, Y. Wang, J. Leach, E. Kao, D. Mitsouras, D. Saloner*; San Francisco/US (xiongfei0129@gmail.com)*

Purpose: To investigate the feasibility of radiomics analysis of AAA CE-CT images to predict fast growth 0.3 cm/year.
Methods and materials: This retrospective cross-sectional study included 84 AAAs (44 fast-growing, 40 stable) with an index CE-CT for morphologic assessment. Growth was calculated from subsequent clinically-indicated imaging (mean follow-up 3.3±2.6 years). A semi-automated algorithm isolated the AAA outer wall and 1,130 quantitative shape, and 1st-order and texture features were extracted for each segmentation using an open-source package. Recursive feature elimination (RFE) was used to select the maximally-independent features robustly associated with growth. A random forest (RF) classifier then classified AAAs as fast-growing or stable on the basis of the selected features. The performance of the classifier and a model using conventional risk factors (maximum diameter, age, BMI, diabetes, hypertension, and smoking) were evaluated via 5-fold cross-validation. These two were compared by the area under the receiver operating characteristic (ROC) curve (AUC) using DeLong's test. Finally, using multivariate logistic regression, the RFE-selected radiomics features and clinical factors were examined for independent association with the growth outcome.
Results: The mean AUC of the radiomics classification model was 0.80±0.09 and was statistically significantly different (P=0.017) from the conventional risk factor model (mean AUC=0.59±0.12). In multivariate regression, 10 radiomics features independently predicted fast growth. The overall model achieved an odds ratio of 63.20 (95% CI: 8.15-490.06, p<0.001).
Conclusion: Radiomics features of AAAs in CT images appear to have value in detecting fast growth and may assist in rupture risk stratification.
Limitations: The small sample size and lacked an independent stability test for the selected radiomics features.
Ethics committee approval: IRB approved.
Funding: No funding was received for this work.
Author Disclosures:
F. Xiong: nothing to disclose
Y. Wang: nothing to disclose
E. Kao: nothing to disclose
J. Leach: nothing to disclose
D. Mitsouras: nothing to disclose
D. Saloner: nothing to disclose

RPS 615-7 12:01

Twin-beam dual-energy CT for the diagnosis of pulmonary embolisms: first clinical results

B. M. W. Petritsch, A. Weng, P. Pannenbecker, S. Veldhoen, T. A. Bley, A. Kosmala*; Würzburg/DE (petritsch_b@ukw.de)*

Purpose: To compare image quality and radiation dose of a new technical dual-energy (DE) approach using a split-filter design versus standard CTA at a single-source CT scanner in patients with suspected pulmonary embolism.
Methods and materials: Computed tomography pulmonary angiography (CTPA) was performed with 2 protocols at the same 128-row CT system (SOMATOM Edge, Siemens Healthineers). Group 1 (n=22) received standard single-energy CTPA and group 2 (n=17) received a split-filter dual-energy CTPA (Twin-Beam $_{50}$Sn & $_{120}$Au). The CT attenuation in the pulmonary artery and signal-to-noise ratio (SNR) and contrast-to-noise ratio (CNR) were compared. The subjective image quality of standard CTPA and iodine maps was assessed (5-point Likert-scale). The DLP was reported and the effective radiation dose was estimated.
Results: Pulmonary artery attenuation was higher in the standard CTPA (447±146 HU) compared to the DE group (329±127 HU) ($p<0.05$). In contrast, SNR (17.0±4.6 vs 23.6±6.0) and CNR (14.8±4.6 vs 19.3±6.3) were both higher in the DE group ($p<0.05$). The subjective image quality of CTPA was rated excellent (=1) in group 1 and good (=2) in group 2. In the DE cohort, 4 iodine maps were of non-diagnostic quality (=5), possibly due to breathing artefacts. The mean DLP (138.6±61.4 mGy*cm/182.1±85.2 mGy*cm) and effective radiation dose (2.49±1.10 mSv/3.28±1.53 mSv) were similar in both groups (p=n.s).
Conclusion: Twin-beam DE CT offers the possibility to gain dual-energy information from a single-source single-layer CT system. The new technique provides higher SNR and CNR with an effective radiation dose similar to standard CT.
Limitations: A comparison of twin-beam DE with more established dual-source DE CTPA is pending and should be performed in further studies.
Ethics committee approval: This prospective study was approved by the institutional review board.
Funding: No funding was received for this work.
Author Disclosures:
B. M. W. Petritsch: nothing to disclose
A. Weng: nothing to disclose
P. Pannenbecker: nothing to disclose
S. Veldhoen: nothing to disclose
T. A. Bley: nothing to disclose
A. Kosmala: nothing to disclose

RPS 615-8 12:07

Low-contrast media dose protocol in renal CT angiography for non-obese patients: the usefulness of low virtual mono-energetic images derived from a dual-layer spectral detector CT

Y. Yang, F. Yan, R. Chang, X. Chen, Q. Han, H. Dong*; Shanghai/CN (yyz01a15@rjh.com.cn)*

Purpose: To evaluate the image quality and artery conspicuity of renal CTA with low virtual mono-energetic images (VMI) derived from a dual-layer spectral detector CT (DLCT) using low contrast media (CM) dose protocol.
Methods and materials: 60 non-obese (BMI≤28 kg/m^2) patients referred for renal CTA were prospectively enrolled in this study using a low CM protocol of 110 mgI/kg. Both conventional 120kVp polyenergetic images (PI) and VMIs (40-70keV) were reconstructed. CT attenuation and SD of the abdominal artery (AA), left renal arteries (LR), and right renal arteries (RR) were measured. The contrast-to-noise ratio (CNR) was calculated. The subjective image quality (IQ) was assessed using a 5-point scale and compared between VMIs and PI.
Results: The CT value of VMIs increased (AA: 187.42±38.92HU-518.80±127.50HU; LR: 174.68±36.18HU-455.25±121.47HU; RR: 179.20±39.03HU-470.98±129.88HU) as energy level decreased (70keV-40keV). VMIs from 40-60keV had a higher attenuation value than PI ($p<0.05$). The noise of VMIs subtle increased (AA: 15.39±1.92HU-18.02±2.91HU; LR: 13.77±2.52HU-17.58±2.96HU; RR: 13.60±2.67HU-17.81±3.06HU) as energy levels decreased. VMIs from 50-70keV had lower image noise than PI (all $p<0.05$). The CNR steeply increased as energy levels decreased and had significant higher CNR than PI.
Conclusion: The low CM protocol proposed was clinically feasible using low energy VMIs (40-50 keV) derived from DLCT, which could provide superior image quality in comparison to the conventional 120 kVp PI for renal CTA in terms of both objective and subjective evaluation.
Limitations: No control group of PI with routine CM protocol was introduced.
Ethics committee approval: Written informed consent was obtained.
Funding: No funding was received for this work.
Author Disclosures:
Y. Yang: nothing to disclose
F. Yan: nothing to disclose
R. Chang: nothing to disclose
X. Chen: Employee at Clinical Science, Philips Healthcare, Shanghai
Q. Han: Employee at Clinical Science, Philips Healthcare, Shanghai
H. Dong: nothing to disclose

RPS 615-9 12:13

A preoperative MDCT angiography study of hepatic arterial and portal venous anatomy in liver donors

P. Saraswat, S. Vohra*; New Delhi/IN*

Purpose: To study the various anatomical variations in the branching patterns and origins of the arterial supply to the liver and portal vein and discuss their surgical implications in living donor liver transplant (LDLT).
Methods and materials: The study included an MDCT angiography evaluation of 450 liver donors. The hepatic artery and portal vein branching patterns were described according to Michel's and Nakamura et al classification and miscellaneous findings were discussed separately.
Results: Standard arterial anatomy was seen in 66% of cases. The most common arterial variant was type V followed by type III and II. The remaining Michel's variants including type IV, VI, VIII, and IX were seen in 8% cases. The origin of the segment 4 artery was seen most commonly from LHA. In the remaining cases, it was seen originating from RHA, CHA, HAP, and both LHA and RHA.
Miscellaneous arterial anatomy was seen in 4% cases, including segmental arterial supply to the right lobe from LHA, GDA, CHA, and CA , early branching of the hepatic artery from CHA, aberrant origin of RHA from CA, GDA, and the aorta, and the origin of CA from SMA and the aorta.
Type A portal vein anatomy was seen in 83% cases followed by type C and B. Type D anatomy was seen in 1 case. Type E portal vein anatomy was seen in 2 cases. In 5 cases, branches to segment 7 and 8 were seen arising from LPV. In one case, the accessory segment 8 branch was arising from the MPV bifurcation.
Conclusion: Variant hepatic vascular anatomy is seen in a significant number of donors and its evaluation allows the selection of suitable donors and operative procedures, and hence decreases intra-operative time and complications.
Limitations: A single-centre study.
Ethics committee approval: n/a
Funding: No funding was received for this work.
Author Disclosures:
P. Saraswat: nothing to disclose
S. Vohra: nothing to disclose

RPS 615-10 12:19

The diagnostic utility of hybrid: three-phase scintigraphy and CT angiography imaging in patients with acute lower limb ischaemia

O. V. Leshchinskaya, N. E. Kudryashova, I. P. Mikhailov, E. V. Migunova, O. G. Sinyakova, O. A. Lbova, E. A. Nikolaeva*; Moscow/RU (Leschinskaya78@mail.ru)*

Purpose: CT angiography (CTA) provides information on the patency of peripheral arteries and 3-phase scintigraphy can assess perfusion and viability of affected tissues. Our aim was to evaluate the utility of hybrid imaging comprising CTA and three-phase scintigraphy using osteotropic or perfusion radiotracers.
Methods and materials: From September 2018-August 2019, we examined 79 patients (mean age 68.3±9.7) with acute lower limb ischaemia. The hybrid studies comprised CT angiography (CTA) and three-phase scintigraphy performed on Discovery 670NM/16-rowCT, GE, USA. Scintigraphy was performed in group 1 in 63/79 patients using ^{99m}Tc-pyrophosphate (500MBq, 2.85mSv) and in group 2 - in 16/79 using ^{99m}Tc-MIBI (500MBq, 4.5mSv).
Results: We evaluated two groups of patients based on the severity of ischaemia: grade 1-2A-51 (45/6), grade 2B-18 (13/5), and grade 3-10 (5/5); groups 1 and 2, respectively. 51/79 patients with grades 1-2A had either normal or slightly decreased tissue blood flow. 28/79 patients with grades 2B-3 had a significant decrease in tissue blood flow. In group 1, the washout index in tissue and bone phases ("muscle/muscle") was decreasing and the "muscle/bone ratio" index in bone phase was increasing, with a clear difference between grades 1-2A, 2B, and 3. 4/5 patients from group 1 (grade 3) had areas of necrotic changes. In group 2, the washout index was significantly different between 1-2A-2B and 3 ($p\leq0.05$). ^{99m}Tc-pyrophosphate studies were more informative for acute ischaemia grades with less radiation 2.85mSv vs 4.5mSv.
Conclusion: CTA and scintigraphy are complementary and their fusion provides a reliable diagnosis of patency and grades of ischaemia. Moreover, hybrid imaging using osteotropic radiotracer defines the areas of aseptic necrosis, which is essential in planning endovascular or surgical intervention. ^{99m}Tc-pyrophosphate studies were more informative than ^{99m}Tc-MIBI with less patient exposure.
Limitations: The retrospective design.
Ethics committee approval: n/a
Funding: No funding was received for this work.

Author Disclosures:
O. V. Leshchinskaya: nothing to disclose
N. E. Kudryashova: nothing to disclose
I. P. Mikhailov: nothing to disclose
E. V. Migunova: nothing to disclose
O. G. Sinyakova: nothing to disclose
O. A. Lbova: nothing to disclose
E. A. Nikolaeva: nothing to disclose

RPS 615-11 12:25
Application of dual-layer spectral detector CT angiography in improving the imaging quality of lower extremity arteries
N. Wang, Z. Liu, X. Lu, Y. Hou*; Shenyang/CN*
(wangning19900508@126.com)

Purpose: To evaluate the application value of dual-layer spectral detector CT (DLCT) in CT angiography (CTA) of the lower extremities.
Methods and materials: 48 patients (12 males; mean age, 62.37±16.83 years) with suspected lower extremity arterial disease underwent CTA by DLCT in this prospective study. Virtual monoenergetic images (VMIs) were reconstructed at 60-80 keV, with a 5-keV increment. Attenuation, noise, the corresponding contrast noise ratios (CNR), and signal noise ratio (SNR) were assessed in the iliac artery, femoral artery, popliteal artery, and anterior tibial artery. Comparisons between VMIs and conventional images (CIs) were performed by one-way ANOVA test. The image quality was graded on a 5-point scale, 5 being the best.
Results: In CI and VMI studies, 60 keV VMI showed the highest subjective score (217 points). CNR and SNR at 60 keV and 65 keV were statistically significantly higher than other VMIs and CIs ($p < 0.01$). The image noise at 60 keV and 65 keV was significantly lower than CIs ($p<0.05$). The attenuation of each target vessel at 60 keV was significantly higher than at 65 keV and other level VMIs ($p<0.05$). The overall image quality was best at 60 keV.
Conclusion: A VMI level at 60 keV for lower extremity CTA can notably improve the overall image quality and may be used in clinical routine imaging protocols.
Limitations: The examinations used only 120 kVp and comparable imaging protocols. We only included a limited number of patients. Large-scale studies should consider a variety of different protocols.
Ethics committee approval: n/a
Funding: No funding was received for this work.
Author Disclosures:
N. Wang: nothing to disclose
X. Lu: nothing to disclose
Z. Liu: nothing to disclose
Y. Hou: nothing to disclose

11:15 - 12:30 **Coffee & Talk 1**

Oncologic Imaging

RPS 616a

Musculoskeletal tumours and body composition quantitation

Moderators:
A. Isaac; London/UK
L. Kintzelé; Heidelberg/DE

RPS 616a-1 11:15
Distinguishing well-differentiated liposarcomas from lipomas on MR images using a radiomics approach
M. P. A. Starmans, M. Vos, M. J. M. Timbergen, S. R. van der Voort, D. J. Grünhagen, S. Sleijfer, C. Verhoef, J. J. Visser, S. Klein*; Rotterdam/NL*
(m.starmans@erasmusmc.nl)

Purpose: Well-differentiated liposarcomas (WDLPS) are difficult to distinguish from lipomas. This distinction is currently made through an invasive biopsy to test for MDM2-amplification. We present a non-invasive alternative using radiomics based on MRI. This work has been accepted for publication by the British Journal of Surgery.
Methods and materials: Our dataset consisted of 116 patients (58 MDM2-negative lipomas, 58 MDM2-positive WDLPS) with at least a pre-treatment T1-weighted MRI scan who were referred to the Erasmus MC between 2009-2018. When available, T2-weighted scans were included. A clinician manually segmented the tumours, from which 113 radiomics features were extracted. Decision models were created through an automated search amongst a variety of machine learning algorithms to find the combination that maximizes performance. The evaluation was implemented through 100x random-split cross-validation, using 80% for training and model optimisation and 20% for testing. For comparison, the tumours were manually scored by 3 radiologists. Agreement was determined through Cohen's kappa.
Results: The T1w-based radiomics model had a mean area under the curve (AUC) of 0.83, a sensitivity of 0.68, and specificity of 0.84. Adding T2w MRI improved the performance to an AUC of 0.89, a sensitivity of 0.74, and a specificity of 0.88. The 3 radiologists had an AUC of 0.74/0.72/0.61, a sensitivity of 0.74/0.91/0.64, and a specificity of 0.55/0.36/0.59. The mean Cohen's kappa between the radiologists was 0.23, indicating poor interobserver agreement.
Conclusion: Our radiomics model was able to distinguish WDLPS from lipomas, with a performance superior to 3 experienced radiologists. Hence, radiomics may serve as an objective, non-invasive aid in diagnostic work-up to differentiate between lipomas and WDLPS.
Limitations: A potential volume bias, which has been assessed in additional subanalyses.
Ethics committee approval: Erasmus MC IRB (MEC-2016-339).
Funding: NWO #14929-14930, Stichting Coolsingel #567.
Author Disclosures:
M. P. A. Starmans: nothing to disclose
M. Vos: nothing to disclose
M. J. M. Timbergen: nothing to disclose
S. R. van der Voort: nothing to disclose
D. J. Grünhagen: nothing to disclose
S. Sleijfer: nothing to disclose
C. Verhoef: nothing to disclose
J. J. Visser: nothing to disclose
S. Klein: nothing to disclose

RPS 616a-2 11:21
Progressive desmoid tumours: a comparison of radiomics and conventional response criteria for predicting progression during systemic therapy
A. Crombe[1], M. Kind[1], A. Bouhamama[2], A. Italiano[1]*; [1]Bordeaux/FR, [2]Lyons/FR*
(crombeamandine2@gmail.com)

Purpose: The response of desmoid tumours (DTs) to chemotherapy is evaluated with RECIST in daily practice and clinical trials. MRI demonstrates an early change in heterogeneity in responding tumours due to a decrease in cellular area and increase in fibro-necrotic content before a dimensional response. Heterogeneity can be quantified with radiomics. Our aim was to develop radiomics-based response criteria and to compare their performances with the usual criteria.
Methods and materials: 42 patients (median age: 38.2) were included, presenting with progressive DT, MRI at baseline (MRI-0), and early evaluation (3 months later, MRI-1). After signal intensity normalisation, voxel size standardisation, discretisation, and segmentation of DT volume on fat-suppressed contrast-enhanced T1-weighted-imaging, 90 baseline and delta 3D-radiomics features (RFs) were extracted. Using cross-validation and least absolute shrinkage and selection operator penalised Cox regression, a radiomics score was generated. The performances of models based on the radiomics score, modified-RECIST, EASL, Cheson, Choi and revised-Choi criteria from MRI-0 to MRI-1 to predict the progression-free survival (PFS, per RECIST) were assessed with a concordance-index. The results were adjusted for performance-status, tumour volume, prior chemotherapy, current chemotherapy, and beta-catenin mutation.
Results: There were 10 progressions. The radiomics score included 4 variables. A high score indicated a poor prognosis. The radiomics score correlated with PFS (adjusted hazard ratio=12.02, p=0.002) but none of the usual response criteria. The prognostic model based on the radiomics score had the highest concordance-index (0.85, 95% confidence interval=(0.72-0.99)).
Conclusion: Quantifying early changes in heterogeneity through a dedicated radiomics score can improve the response evaluation for DT patients undergoing chemotherapy.
Limitations: A relatively small population study, a small number of events (: progression), and a lack of standardisation of the MRI protocol.
Ethics committee approval: IRB-approved. Written informed consent obtained.
Funding: No funding was received for this work.
Author Disclosures:
A. Crombe: nothing to disclose
M. Kind: nothing to disclose
A. Bouhamama: nothing to disclose
A. Italiano: nothing to disclose

RPS 616a-3 11:27

MRI contrast-enhanced T1 signal intensity: a potential imaging biomarker for prediction efficacy in desmoid-type fibromatosis treated with imatinib

H. C. Zhu, X. T. Li, Y. S. Sun*; Beijing/CN (zulo1481@126.com)*

Purpose: Recent studies showed that MRI signal intensity was a prognostic marker for progression-free survival (PFS) and an association has been demonstrated between desmoid tumour growth and T2 signal intensity. In this study, we present the predictive value of the hyperintensity percentage of tumours on pre-therapy MRI for PFS in patients with desmoid-type fibromatosis (DF) treated with imatinib.
Methods and materials: We enrolled 38 DF patients treated with imatinib. The evaluation of areas of signal hyperintensity on pre-therapy MRI images was performed on T2 and T1 contrast enhancement (CE) sequences. Two radiologists defined the whole tumour areas and areas of signal hyperintensity by manually drawing on each slice of stacked MR images on axial T2 and axial T1 CE sequences. Associations of clinical or radiographic characteristics with PFS (by RECIST1.1) were evaluated by Cox regression and Kaplan-Meier statistics.
Results: Hyperintense T1 CE proportion (hazard ratio [HR], 3.37; 95% confidence interval [CI], 1.23-9.25) was identified as independent predictors for PFS ($p<0.05$). Kaplan-Meier analysis showed that the hyperintense T1 CE proportion (less than 75%) was associated with improved PFS ($p<0.05$). No progression disease was exhibited in patients with a hyperintense T1 CE proportion less than 75%, while 78.4% progression disease was exhibited in patients with a hyperintense T1 CE proportion more than 75%.
Conclusion: Our study showed that hyperintense T1 CE proportion is a prognostic predictor in DF patients treated with imatinib. Those tumours with a hyperintense T1 CE proportion less than 75% have less likelihood of progressing during treatment with imatinib. Hence, MR imaging is a valuable imaging biomarker for predicting the prognosis of DF treated with imatinib, thereby contributing to personalised medicine.
Limitations: A retrospective study and a relatively small patient population.
Ethics committee approval: n/a
Funding: No funding was received for this work.
Author Disclosures:
H. C. Zhu: Author at Beijing Cancer Hospital, Speaker at Beijing Cancer Hospital
X. T. Li: Author at Beijing Cancer Hospital
Y. S. Sun: Author at Beijing Cancer Hospital

RPS 616a-4 11:33

Distinguishing desmoid-type fibromatosis from soft tissue sarcoma on MRI using a radiomics approach

M. P. A. Starmans, M. J. M. Timbergen, G. A. Padmos, D. J. Grünhagen, G. J. van Leenders, D. Hanff, S. Sleijfer, J. J. Visser, S. Klein*; Rotterdam/NL (m.starmans@erasmusmc.nl)*

Purpose: Diagnosing desmoid-type fibromatosis (DTF) is challenging due to its rarity, requiring an invasive biopsy with β-catening staining and CTNNB1 mutational analysis. We evaluated radiomics based on MRI as an alternative for distinguishing DTF from soft tissue sarcoma (STS) and determining the DTF CTNNB1 mutation (S45F, T41A or wild-type).
Methods and materials: T1-weighted MRIs were gathered from 203 patients, including 72 DTFs and 131 STS (64 fibromyxosarcomas, 36 myxoid liposarcomas, and 31 leiomyosarcomas), all pathologically proven. A clinician segmented the tumours, from which 424 radiomics features were extracted. Sex, age, and tumour location were collected. A decision model was created through an automated search amongst a variety of machine learning algorithms to find the combination that maximizes performance. The evaluation was implemented through 100x random-split cross-validation, with 80% of the data used for training and model optimisation and 20% for testing. For comparison, a location-matched subset of tumours was manually scored by two radiologists.
Results: The mean area under the curve (AUC) of the DTF versus STS radiomics imaging model was 0.79 on the full database and 0.88 on the location-matched database. The two radiologists had an AUC of 0.80 and 0.88, respectively, on the location-matched database. Age and gender performed well on their own (AUC of 0.93) and combined with imaging (AUC of 0.98). The CTNNB1 radiomics model showed a mean AUC of 0.61, 0.56, and 0.74 for S45F, T41A, and wild-type, respectively.
Conclusion: Our radiomics model is capable of distinguishing DTF from STS with a performance similar to that of two experienced radiologists. However, the model was not able to predict the CTNNB1 mutation status.
Limitations: A potential age/gender bias.
Ethics committee approval: Erasmus MC IRB (MEC-2016-339).
Funding: NWO #14929-14930, Stichting Coolsingel #567.
Author Disclosures:
M. P. A. Starmans: nothing to disclose
M. J. M. Timbergen: nothing to disclose
G. A. Padmos: nothing to disclose
D. J. Grünhagen: nothing to disclose
G. J. van Leenders: nothing to disclose
D. Hanff: nothing to disclose
S. Sleijfer: nothing to disclose
J. J. Visser: nothing to disclose
S. Klein: nothing to disclose

RPS 616a-5 11:39

Desmoid-type fibromatosis: a pilot study of tumour response assessment by using MRI signal combined size criteria

H. C. Zhu, X. T. Li, Y. S. Sun*; Beijing/CN (zulo1481@126.com)*

Purpose: Desmoid-type fibromatosis (DF) is a locally aggressive tumour. RECIST 1.1 is generally used for assessing the response of DF, but the role of MRI signal isn't defined. We aimed to establish a specified MRI signal criterion for assessing the response of DF and to test the performance of signal criterion combined with RECIST 1.1.
Methods and materials: This retrospective study included 129 DF patients who received systematic therapy or were closely followed up without surgery. All patients underwent pre-treatment and six-month-interval follow-up MRIs for more than 3 years (a total of 6 follow-ups). The correlation between signal grade and size was tested, and the signal grade and size among 3 response groups (partial response (PR), stable disease (SD), and progression disease (PD)) was compared. A specified signal and size criterion was established, which was used to assess the tumour response at each follow-up and compared with the reference. The RECIST1.1 criterion at the end of 3rd year was the reference.
Results: Changes in T2 grade and size among the 3 response categories were significantly different (all $p<0.01$). The signal and size criterion accurately predicted 95% of PR patients at the 2nd follow-up and 81.2% of PD patients at the 3rd follow-up, while only 13.1% of PR and 56.3% of PD were predicted by RECIST1.1. However, the accuracy of the signal and size criterion for predicting SD was lower than RECIST1.1.
Conclusion: This study verified that MRI signal is useful for assessing the tumour response of DF and could be added to establish a specified signal and size criterion. A signal and size criterion can identify PR and PD patients earlier than RECIST1.1.
Limitations: n/a
Ethics committee approval: n/a
Funding: No funding was received for this work.
Author Disclosures:
H. C. Zhu: Author at Beijing Cancer Hospital, Speaker at Beijing Cancer Hospital
X. T. Li: Author at Beijing Cancer Hospital
Y. S. Sun: Author at Beijing Cancer Hospital

RPS 616a-6 11:45

High-grade soft-tissue sarcomas: can optimising DCE-MRI post-processing improve prognostic radiomics models?

A. Crombe[1], D. Fadli[1], X. Buy[1], A. Italiano[1], O. Saut[2], M. Kind[1]*; [1]Bordeaux/FR, [2]Talence/FR (crombeamandine2@gmail.com)*

Purpose: Heterogeneity on DCE-MRIs of sarcomas may be prognostic. The aim was to investigate the best method to extract prognostic data from baseline DCE-MRIs.
Methods and materials: 50 uniformly-treated adults with non-metastatic high-grade sarcomas and pre-treatment DCE-MRIs at 1.5T were included in this retrospective single-centre study. 92 radiomics features (RFs) were extracted at each DCE-MRI phase (11 from t=0s to 88s). Relative changes in RFs (rRFs) since the acquisition baseline were calculated (11x92 rRFs). Curves of rRF as a function of time post-injection were integrated (92 integrated-rRFs [irRFs]). K^{trans} and the area under the time-intensity curve at 88s parametric maps were computed and 2x92 parametric-RFs (pRFs) were extracted. 5 DCE-MRI-based radiomics models were built on an RFs subset (32s, 64s, 88s), all rRFs, all irRFs, and all pRFs. Two additional models were elaborated as a reference on conventional radiological features and T2-WI RFs. A common machine-learning approach was applied to the radiomics models. Features with $p<0.05$ at univariate analysis were entered in a LASSO-penalised Cox regression including bootstrapped 10-fold cross-validation. Resulting radiomics scores (RScores) were dichotomised as per their median and entered into multivariate Cox models for predicting metastatic relapse-free survival. Models were compared with a concordance-index.
Results: Only dichotomised RScores from models based on the rRFs subset, all rRFS, and irRFS correlated with prognostic ($p=0.0107$-0.0377). The models including all rRFs and irRFs had the highest c-index (0.83) followed by the radiological model. The radiological and full rRFs models were significantly better than the T2-based radiomics model ($p=0.02$).

Conclusion: The initial DCE-MRI of STS contains prognostic information. It seems more relevant to make predictions on rRFs instead of pRFs.
Limitations: A retrospective study, heavy post-processing to homogenise DCE-MRI temporal parameters, with no validation cohort.
Ethics committee approval: IRB approved.
Funding: No funding was received for this work.
Author Disclosures:
A. Crombe: nothing to disclose
D. Fadli: nothing to disclose
X. Buy: nothing to disclose
A. Italiano: nothing to disclose
O. Saut: nothing to disclose
M. Kind: nothing to disclose

RPS 616a-7 11:51

The utility of 18F-FDG PET and DWI data for the assessment of therapy response of soft tissues sarcomas under neoadjuvant ILP

J. Grueneisen[1], M. Chodyla[1], B. M. Schaarschmidt[2], A. Demircioglu[1], O. Martin[2], K. Herrmann[1], M. Forsting[1], L. Podleska[1], L. Umutlu[1]; [1]*Essen/DE,* [2]*Düsseldorf/DE (johannes.grueneisen@uk-essen.de)*

Purpose: To evaluate the clinical applicability of quantitative 18F-FDG PET and DWI datasets for the prediction of therapy response of soft tissue sarcomas (STS) under neoadjuvant isolated limb perfusion (ILP).
Methods and materials: 37 patients with a confirmation of an STS of the extremities underwent an 18F-FDG PET/MR examination before and after neoadjuvant ILP with melphalan and TNF-α. Data analysis comprised measurements of the tumour size, metabolic activity (SUVs), and diffusion-restriction (ADC-values) in pre- and post-therapeutic examinations and percentage changes during treatment were calculated. A Mann-Whitney-U test and ROC analysis were used to compare the results of the different quantitative imaging parameters. Histopathological results after subsequent tumour resection served as a reference standard and patients were categorised as responders or non-responders based on the regression grading scale by Salzer-Kuntschik.
Results: Histopathological analysis categorised 22 (59%) patients as therapy responders (grade I-III) and 15 (41%) patients as non-responders (grade IV-VI). Tumours in the responder group showed a reduction in size (-9.7%) and metabolic activity (SUVpeak: -51.9%; SUVmean: -37.2%), and an increase of the ADC values (ADCmin: +23.1%; ADCmean: +31.8%) under treatment. Percentage changes in the non-responder group amounted to: tumour size -6.2%, SUVpeak: -17.3%, SUVmean: -15.1%, ADCmin: +16.1%, and ADCmean: +14.6%. The differences of the SUVs and ADCmean values between responders and non-responders were significantly different (<0.01). The corresponding AUCs were 0.63 (tumour size), 0.87 (SUVpeak), 0.78 (SUVmean), 0.54 (ADCmin), and 0.84 (ADCmean), respectively.
Conclusion: Our study demonstrates good performance of 18F-FDG PET/MR-derived quantitative imaging parameters for response prediction of STS under ILP. Integrated PET/MRI could serve as a valuable tool for monitoring neoadjuvant treatment strategies of STS.
Limitations: The limited patient cohort.
Ethics committee approval: The study was approved by the local ethics committee.
Funding: No funding was received for this work.
Author Disclosures:
J. Grueneisen: nothing to disclose
M. Chodyla: nothing to disclose
B. M. Schaarschmidt: nothing to disclose
K. Herrmann: nothing to disclose
M. Forsting: nothing to disclose
A. Demircioglu: nothing to disclose
L. Podleska: nothing to disclose
L. Umutlu: nothing to disclose
O. Martin: nothing to disclose

RPS 616a-8 11:57

Low skeletal muscle mass and postoperative morbidity in surgical oncology: a systematic review and meta-analysis

L. Weerink[1], A. van der Hoorn[2], B. van Leeuwen[2], G. de Bock[2]; [1]*Almelo/NL,* [2]*Groningen/NL (lweerink@gmail.com)*

Purpose: To meta-analyse the relationship between preoperative sarcopenia and the development of severe postoperative complications in patients undergoing oncological surgery.
Methods and materials: PubMed and Embase databases were systematically searched from inception until May 2018. Studies reporting on the incidence of severe postoperative complications and radiologically determined preoperative sarcopenia were included. Data was extracted independently by two reviewers. Random effect meta-analyses were applied to estimate the pooled odds ratio (OR) with 95% confidence intervals (95CI) for severe postoperative complications, defined as Clavien-Dindo grade ≥3, including 30-day mortality. Heterogeneity was evaluated with I^2-testing. Analyses were performed overall and stratified by the measurement method, tumour location, and publication date.
Results: A total of 1,924 citations were identified and 53 studies (14,295 patients) included. When measuring the total skeletal muscle area, 43% of the patients were sarcopenic versus 33% when measuring the psoas area. Severe postoperative complications were present in 20% of patients where 30-day mortality was 3%. Preoperative sarcopenia was associated with an increased risk of severe postoperative complications (OR_{pooled}: 1.44, 95CI: 1.24-16.8, P<0.001, I^2=55%) and 30-day mortality (OR_{pooled}: 2.15, 95CI: 1.46-3.17, P<0.001, I^2=14%). A low psoas mass was a stronger predictor for severe postoperative complications compared to a low total skeletal muscle mass (OR_{pooled}: 2.06, 95CI: 1.37-3.09, OR_{pooled}: 1.32, 95CI: 1.14-1.53, respectively) and 30-day mortality (OR_{pooled}: 6.17 (95CI: 2.71-14.08, OR_{pooled}: 1.80 (95CI: 1.24-2.62), respectively). The effect was independent of tumour location and publication date.
Conclusion: The presence of low psoas mass prior to surgery as an indicator for sarcopenia is a common phenomenon and is a strong predictor for the development of postoperative complications and 30-days mortality. The presence of low total skeletal muscle mass, which is even more frequent, is a less informative predictor.
Limitations: n/a
Ethics committee approval: n/a
Funding: No funding was received for this work.
Author Disclosures:
L. Weerink: nothing to disclose
A. van der Hoorn: nothing to disclose
B. van Leeuwen: nothing to disclose
G. de Bock: nothing to disclose

RPS 616a-9 12:03

Do CT-based body composition parameters at baseline or their early changes correlate with progression in metastatic solid tumour patients treated with immunotherapy?

A. Crombe, M. Kind, M. Toulmonde, A. Italiano, S. Cousin*; Bordeaux/FR (crombeamandine2@gmail.com)*

Purpose: To investigate associations between CT-scan-based body composition (BC) parameters (and their early changes) with progression-free survival (PFS) in metastatic cancer patients treated with immunotherapy.
Methods and materials: Patients were consecutively included as they were treated with immunotherapy at our institution for a metastatic tumour with an available baseline CT-scan (CT0, ≤28 days before beginning immunotherapy) and early evaluation CT-scan (CT1, 2 months later ± 28 days). At each evaluation, the areas corresponding to psoas alone, skeletal muscle, subcutaneous, visceral, and total adipose tissues at the L3 vertebral level were extracted and weighted by height^2, providing wSMAI, SMI, SATI, VATI, and TATI, respectively, and their changes (Δt-) from the 1st day of treatment to CT1. After assessing the optimal cut-point for each BC-parameter (which maximised the bootstrapped concordance-index and balance between the subgroups of patients), correlations with PFS were evaluated using multivariate Cox models.
Results: Between December 2013-December 2016, 117 patients were included (55 female, median age: 63 years). After cut-point optimisation and adjustment with clinical covariables, 7 BC-parameters correlated with PFS: baseline BMI, SMI, VATI, Δt-wSMAI, Δt-SMI, Δt-SATI, and Δt-VATI (p-values range: <0.001-0.03). At multivariate analysis, 4 remained independently associated with lower PFS, namely: SMI <35.2cm^2/m^2 (HR=3.5, p=0.006), VATI ≥11cm^2/m^2 (HR=2.1, p=0.02), Δt-wSMAI <-0.7 cm^2/m^2/day (HR=6, p<0.001), and Δt-SATI <-0.02 cm^2/m^2/day (HR=1.9, p=0.026). Adding these BC-parameters significantly improved the prediction of PFS compared with a model that only included baseline clinical features and BMI (concordance-index=0.76 vs 0.68, p=0.007).
Conclusion: CT-based BC-parameters and their early changes could help in anticipating the outcome in metastatic cancer patients. Further prospective evaluations are required to validate these findings and to determine whether nutritional interventions are indicated.
Limitations: The retrospective, single-centre design, manual segmentation, and lack of standardisation in CT acquisition protocols.
Ethics committee approval: IRB approved.
Funding: No funding was received for this work.
Author Disclosures:
A. Crombe: nothing to disclose
M. Kind: nothing to disclose
M. Toulmonde: nothing to disclose
A. Italiano: nothing to disclose
S. Cousin: nothing to disclose

RPS 616a-10 12:09

Evaluating body composition by combining quantitative spectral detector computed tomography and deep learning-based image segmentation

N. Grosse Hokamp[1], D. Zopfs[1], K. Bousabarah[1], S. Lennartz[1], M. Merkt[2], D. Maintz[3], S. Haneder[1]; [1]Cologne/DE, [2]Coblenz/DE, [3]Münster/DE
(nils.grosse-hokamp@uk-koeln.de)

Purpose: To develop and evaluate an automated machine learning algorithm to segment abdominal muscle mass and visceral and subcutaneous fat mass using conventional images (CI) and iodine maps (IM) from spectral-detector computed tomography (SDCT).
Methods and materials: A deep convolutional neural network (DCNN) was trained/validated with 74/14 chest-abdomen-pelvis studies to identify the abdominal region. Afterwards, a DCNN U-Net was trained to perform segmentation of subcutaneous fat based on 1,153/203 segmented slices (training/validation). The aforementioned DCNNs were used to classify images to the abdominal region and subtract subcutaneous fat. Thresholding based on attenuation and iodine uptake was used to segment muscle mass. Test re-test matrices and Bland-Altman plots were obtained by comparing the fat-muscle ratio in 14 patients undergoing repetitive examination within a time interval of <21 days for clinical indications.
Results: The classifier DCNN assigned images to the abdominal region with an accuracy of 98.7%. Regarding the segmentation of subcutaneous fat, the mean Dice similarity coefficient per case compared to the segmented ground truth on the validation data was 0.95. Test re-test matrices for the prediction of subcutaneous fat, visceral fat, and muscle mass were well indicated by a mean difference of 9%.
Conclusion: The proposed quantitative image analysis algorithm for predicting subcutaneous and visceral fat as well as muscle mass utilises machine learning in combination with advanced reconstructions from dual-energy CT. It allows for a reproducible estimation of body composition and potentially facilitates the opportunistic and automated evaluation of body composition, allowing for risk stratification, for example, in the setting of sarcopenia.
Limitations: The small sample size.
Ethics committee approval: Obtained, informed consent was waived.
Funding: Else Kröner-Fresenius-Stiftung and Koeln-Fortune-Program/University of Cologne.
Author Disclosures:
N. Grosse Hokamp: Speaker at Philips, Research/Grant Support at Philips
D. Zopfs: nothing to disclose
K. Bousabarah: nothing to disclose
D. Maintz: Speaker at Philips
S. Haneder: nothing to disclose
M. Merkt: nothing to disclose
S. Lennartz: Research/Grant Support at Philips

RPS 616a-11 12:15

The evaluation of various diffusion models for the differentiation of peripheral nerve sheath tumours with neurofibromatosis type 1

M. Kaul, L. Well, V.-F. Mautner, G. Adam, J. Salamon; Hamburg/DE
(mkaul@uke.uni-hamburg.de)

Purpose: Diffusion-weighted imaging is a tool for the sensitive and specific identification of malignancy in NF1. We studied various diffusion models for the ability to map parameters of significance and to test their numerical stability.
Methods and materials: Diffusion measurements were performed at 3T with b-values of 0, 10, 20, 30, 50, 70, 100, 300, 400, 600, and 800s/mm². We analysed 44 benign and 15 malign PNST tumours in 29 patients. Regions-of-interest were set manually and evaluated by fitting model functions: ADC, IVIM, kurtosis, stretched-kurtosis, gamma, and truncated-gamma. T-tests were applied to investigate significant differences in benign and malign PNST for the model parameters. The information criteria AIC, BIC, and R^2 values were compared. Numerical stability was evaluated by the number of analysable pixels normed by the tumour size.
Results: Conventional ADC-DWI fitting b-values (0 and >100s/mm²) is the most robust technique in comparison to the more complex models which provide additional parameters on the costs of larger variances and less numerical stability, as the smallest AIC and BIC value indicates. Generally, benign tumours result in better fit results as R^2 are higher and the normed area values are larger. In contrast, AIC and BIC do not differ much. The gamma-function, and especially the stretched-kurtosis model, perform on a similar level concerning robustness as the ADC model but offer additional information.
Conclusion: Various models are able to differentiate between malignant and benign PNST. ADC-mapping is a solid way. Nevertheless, using a gamma-function or the stretched-kurtosis model offers additional parameters which might also be of interest as it also offers differences detection.
Limitations: Malign PNST were larger, which probably has an effect.
Ethics committee approval: Approval by the local ethics board was given.
Funding: No funding was received for this work.
Author Disclosures:
M. Kaul: nothing to disclose
L. Well: nothing to disclose
V.-F. Mautner: nothing to disclose
G. Adam: nothing to disclose
J. Salamon: nothing to disclose

RPS 616a-12 12:21

Genotype-phenotype correlation in neurofibromatosis type 1: whole NF1 gene deletion (type 1) leads to high tumour-burden and increased tumour-growth in affected patients

L. Well, K. Döbel, S. Farschtschi, V.-F. Mautner, G. Adam, J. Salamon; Hamburg/DE

Purpose: Neurofibromatosis type-1 (NF1) is a dominantly inherited tumour-predisposition syndrome and patients develop large plexiform (PNF) or cutaneous (NF) neurofibromas. High tumour-burden and tumour-growth are indicators for malignant transformation. Studies indicate that large deletions of the NF1 gene and its flanking regions (type-1-deletion) lead to more severe manifestations of NF1 compared to NF1 caused by smaller intragenic changes. Therefore, the purpose of our study was to evaluate the tumour-burden and tumour-growth of patients with type-1-deletions and to compare these with NF1 patients without large deletions of the NF1 gene (non-type-1-deletion patients).
Methods and materials: We retrospectively evaluated whole-body MRI examinations (1.5T; T1wTSE coronal, T2wTIRM coronal, T2wHASTE TIRM axial, and T2wTSE sagittal) of verified type-1-deletion patients and an age- and sex-matched collective of non-type-1-deletion NF1-patients (both n=38; 20 male vs 18 female; mean age deletion 26.2 years vs non-deletion 25.4 years). Patients were further divided into age-dependent subgroups (0-10; 11-18; 19-49; ≥ 50 years of age). All patients had received follow-up MRIs (mean observed time-period: deletion 6.3 vs non-deletion 5.5 years). Whole-body tumour-volume was semi-automatically assessed (MedX) and tumour-growth over time was calculated.
Results: NF1 patients with type-1-deletions showed a significantly higher tumour-burden on initial examination (mean volume 884.8 ml) compared to non-type-1-deletion patients (mean volume 357.1ml; p=0.0087) and an increased tumour-growth over time (mean growth/year deletion 61.4 ml vs non-deletion 9.2 ml; p<0.0001). Tumour-burden and tumour-growth were significantly higher for type 1 deletion patients in all age subgroups (all p<0.05).
Conclusion: NF1 caused by type 1 deletions leads to a high tumour-burden and an increased tumour-growth in affected patients.
Limitations: The relatively small number of patients studied.
Ethics committee approval: The study was approved by the local ethics review board.
Funding: No funding was received for this work.
Author Disclosures:
L. Well: nothing to disclose
K. Döbel: nothing to disclose
S. Farschtschi: nothing to disclose
V.-F. Mautner: nothing to disclose
G. Adam: nothing to disclose
J. Salamon: nothing to disclose

11:15 - 12:30 **Room N**

Artificial Intelligence and Machine Learning

RPS 605a

Artificial intelligence and MRI radiomics

Moderators:
M. Novikov; Kiev/UA
O. Pianykh; Newton Highlands/US

RPS 605a-1 11:15

Radiomics versus visual assessment of T2-weighted MR images: which is better to define T-stage in rectal cancer?

J. M. Moreira[1], I. Santiago[1], J. Santinha[1], V. Maniatis[2], M. Lisitskaya[3], N. Figueiredo[1], C. Matos[1], N. Papanikolaou[1]; [1]Lisbon/PT, [2]Aabenraa/DK, [3]Moscow/RU

Purpose: To evaluate radiomics performance in comparison to radiological visual assessment for the discrimination between ≤T2 and ≥T3 rectal cancer tumours on T2-weighted (T2w) MR images.
Methods and materials: This multi-institutional study included two datasets of consecutive patients with rectal cancer who underwent total mesorectal excision as primary curative treatment, without neoadjuvant therapy (n=23-institution A;

n=20-institution B). Two patient groups were formed based on pathological stage, <=T2 (n=22) and >=T3 (n=21). Patients underwent staging MRI before surgery comprising high-resolution T2w imaging. T2w images were blindly reviewed by 2 radiologists and primary tumours were classified as <=T2 or >=T3. A volume of interest around the whole primary tumour was drawn by the 2 radiologists and the corresponding datasets were analysed using PyRadiomics. Feature stability was tested using a correlation coefficient cutoff of 0.75. Feature reduction was performed, excluding highly correlated features. A general linear model (w/LASSO) was then run to select the best performance feature. Repeated cross-validation was performed. Interobserver agreement was estimated for T2w visual assessment by the 2 radiologists. A DeLong test was employed to assess if the differences between auROC were statistically significant.
Results: 'Spherical disproportion' was the best discriminator with an accuracy upon cross-validation of 72.3% +- 12.6%. The accuracy of the T2w visual analysis was 63% and 77% for the two reader with an intraclass correlation coefficient of 0.71 [95CI:0.46-0.84]. Comparison between radiomics analysis and visual analysis revealed no statistically significant differences (p=0.95 and p=0.14).
Conclusion: The performance of radiomics analysis based on T2w is similar to that of visual assessment by radiologists.
Limitations: An additional study to include radiomic features of the surroundings of the tumour might lead to better staging discrimination.
Ethics committee approval: Ethics committee approval obtained.
Funding: No funding was received for this work.
Author Disclosures:
I. Santiago: nothing to disclose
V. Maniatis: nothing to disclose
J. Santinha: nothing to disclose
J. M. Moreira: nothing to disclose
M. Lisitskaya: nothing to disclose
C. Matos: nothing to disclose
N. Papanikolaou: nothing to disclose
N. Figueiredo: nothing to disclose

RPS 605a-2 11:21

Radiomics to detect SDHx mutation in paragangliomas and pheochromocytomas on MRI

A. Tran, L. Duron, C. Lussey Lepoutre, L. Fournier*; Paris/FR*
(tranalexia@yahoo.com)

Purpose: To identify potential imaging biomarkers of SDHx mutation in paragangliomas and pheochromocytomas on MRI using radiomics.
Methods and materials: Mice with a subcutaneous tumour carrying a homozygous knockout of the SDHB gene ($SDHB^{-/-}$) or the wild type (WT) counterpart ($SDHB^{lox/lox}$) were studied on MRI, respectively 22 $SDHB^{-/-}$ and 16 WT tumours. Analysis of the True Fisp-weighted images using a radiomics workflow allowed for the extraction of 105 features. Feature reduction based on reproducibility and statistical analysis evaluated the performance of each feature to detect the SDHB mutation. The candidate features were then tested in patients with paragangliomas or pheochromocytomas: 9 with SDHx mutations, 10 with no mutation, and 13 with a mutation other than SDHx.
Results: In the 38 mice studied by MRI, 17 features were significantly different between the $SDHB^{-/-}$ tumours and WT tumours, using a Benjamini and Hochberg correction with a False Discovery Rate of 0.1. When the 17 features were tested in the 32 patients, only 2 remained significantly associated to the presence of the SDHx mutation in humans: 1) the glcm_JointEnergy (0.009 vs 0.004; p=0.03 between SDHx mutations and no mutation and p=0.003 between SDHx mutations and any mutation other than SDHx or no mutation) and 2) the glcm_JointEntropy (7.9 vs 8.6 ; p=0.01 between SDHx mutations and any mutation other than SDHx or no mutation).
Conclusion: Using radiomics and a data-driven and big-data method on MR images, a texture feature reflecting tumour heterogeneity was shown to be predictive of SDHx-mutation status both in a mouse model and in patients.
Limitations: Few SDHB patients. The Fiesta sequence is not systematic in the MRI protocol of paragangliomas and pheochromocytomas. A monocentric study.
Ethics committee approval: Ethical and regulatory authorisations were obtained for both the pre-clinical and clinical studies.
Funding: No funding was received for this work.
Author Disclosures:
A. Tran: nothing to disclose
L. Duron: nothing to disclose
C. Lussey Lepoutre: nothing to disclose
L. Fournier: nothing to disclose

RPS 605a-3 11:27

Radiomics analysis of gradient-echo MRI for lymph node classification in rectal cancer

J. M. Moreira, I. Santiago, J. Santinha, M. J. M. Barata, N. Shemesh, C. Matos, N. Papanikolaou*; Lisbon/PT*

Purpose: To characterise mesorectal lymph nodes (LNs) extracted from rectal cancer patients employing radiomics analysis on gradient-echo MRI images.
Methods and materials: 29 benign and 35 malignant LNs retrieved from 11N+ rectal cancer patient specimens were examined in a 16.4T scanner. A T2* multi-gradient-echo sequence was acquired (50 TEs starting at 1.6ms and 1.4ms interval). Datasets were denoised while a radiologist segmented the central slice of each node and the third echo was considered for radiomics analysis. 757 radiomics features were extracted from the original, Laplacian of Gaussian, and wavelet images. Feature extraction was performed using pyradiomics. Stratified partition was used to divide data into training (80%-52 LNs) and test sets (20%-12 LNs). Feature reduction was performed by removing near-zero and zero variance, as well as highly correlated features. Univariate analysis was performed while the Bonferroni test was employed for multiple comparisons correction. Significant features were used to create a logistic regression model, which was optimised using 100-times repeated 5-fold cross-validation. The fine-tuned model was applied to the test set and the area under the receiver operating characteristic curve (auROC) was calculated.
Results: The 5 features selected from the training set had auROCs between 0.79 and 0.82. After repeated cross-validation, the logistic regression model applied on the training set provided a mean auROC of 0.81, with a standard deviation of 0.12. The optimised logistic regression model applied to the test set provided an auROC of 0.89.
Conclusion: Radiomics analysis based on gradient-echo MRI has excellent performance for the distinction between benign and malignant mesorectal LNs extracted from rectal cancer patients.
Limitations: The low number of patients might be a limitation of this work.
Ethics committee approval: Ethics committee approval obtained.
Funding: No funding was received for this work.
Author Disclosures:
J. M. Moreira: nothing to disclose
I. Santiago: nothing to disclose
J. Santinha: nothing to disclose
M. J. M. Barata: nothing to disclose
C. Matos: nothing to disclose
N. Shemesh: nothing to disclose
N. Papanikolaou: nothing to disclose

RPS 605a-4 11:33

Development and external validation of automatic diagnostic aid for multiple sclerosis using a radiomics analysis of white matter on clinical and quantitative MRI

E. Lavrova[1], H. C. Woodruff[1], C. Phillips[2], E. Salmon[2], E. Lommers[2], P. Lambin[1], P. Maquet[2]*; [1]Maastricht/NL, [2]Liege/BE*
(elizaveta.lavrova@uliege.be)

Purpose: To achieve high diagnostic precision in multiple sclerosis (MS) and to enable fast clinical decision support, it is necessary to monitor brain injury appearing in white matter (WM) with a reliable and robust method. We investigated the ability of a radiomics models to differentiate between MS patients and healthy subjects (HS) based on clinical T1w and quantitative MRI (qMRI) of WM.
Methods and materials: A dataset containing T1w and qMRI (R1, R2*, MT, PD maps) of 36 MS patients and 37 HS was used for training. Two external datasets containing T1w images of 359 HS and 15 MS patients were combined for validation. From each MRI scan, 107 radiomics features were extracted and feature selection with bootstrap sampling was performed on the training set. Various binary classification models informed by T1w and both single and mixed qMRI features were trained. Models were assessed using accuracy and “area under the receiver operator characteristic curve” (AUC) metrics. Classifiers based on T1w were tested on the external datasets using resampling, while qMRI models were tested on the training set using a standard cross-validation.
Results: The 5 most informative and reproducible features were selected for T1w and for quantitative MRI data. On the training (and external) datasets, the best performance was achieved by a support vector classifier using mixed qMRI features.
Conclusion: Brain WM radiomics features extracted from MRI can be used for automatic status estimation in multiple sclerosis. The best classification performance is achieved with mixed qMRI models. Models are based on simple features, which makes them easily interpretable.
Limitations: For external validation, available qMRI data is needed.
Ethics committee approval: The study was approved by the local ethic committee (approval B707201213806). Written informed consent was obtained from all participants.
Funding: Maastricht-Liege Imaging Valley, FRS-FNRS Belgium.

Author Disclosures:
E. Lavrova: nothing to disclose
H. C. Woodruff: Shareholder at Oncoradiomics
C. Phillips: nothing to disclose
P. Lambin: Research/Grant Support at Varian medical, Research/Grant Support at Oncoradiomics, Research/Grant Support at ptTheragnostic, Research/Grant Support at Health Innovation Ventures , Research/Grant Support at DualTpharma, Consultant at Oncoradiomics, Consultant at BHV, Consultant at Merck, Consultant at Convert pharmaceuticals, Shareholder at Oncoradiomics, Shareholder at Convert pharmaceuticals, Patent Holder at Oncoradiomics, Patent Holder at ptTheragnostic/DNAmito, Other at ptTheragnostic/DNAmito, Other at Oncoradiomics, Other at Health Innovation Ventures
E. Salmon: nothing to disclose
E. Lommers: nothing to disclose
P. Maquet: nothing to disclose

RPS 605a-5 11:39

Exploring breast cancer response prediction to neoadjuvant systemic therapy using MRI-based radiomics: a systematic review

R. Granzier, T. Nijnatten, H. C. Woodruff, M. Smidt, M. B. I. Lobbes*; Maastricht/NL (r.granzier@maastrichtuniversity.nl)*

Purpose: MRI-based tumour response prediction to neoadjuvant systemic therapy (NST) in breast cancer patients is increasingly being studied using radiomics with outcomes that appear to be promising. The aim of this study was to systematically review the current literature and reflect on its quality.
Methods and materials: A systematic literature search was performed using PubMed and EMBASE databases until May 8th, 2019. Abstracts were read and screened by two reviewers independently. The quality of the radiomics workflow of all eligible studies was assessed using the radiomics quality score (RQS). An overview of the methodologies used in all steps of the radiomics workflow and current results are presented.
Results: 16 studies were selected for inclusion with cohort sizes ranging from 35 to 414 patients. The RQS scores varied from 0% to 41.2%. Methodologies used in the radiomics workflow varied greatly, especially for region of interest (ROI) segmentation, features selection, and model development with heterogeneous outcomes as a result. 7 studies applied univariate analysis and 9 studies applied multivariate analysis. The majority of the studies performed their analysis on the pretreatment dynamic contrast-enhanced T1 weighted (DCE T1W) sequence. Entropy was the best performing individual feature, with AUC values ranging from 0.83 to 0.85. The best performing multivariate prediction model, based on logistic regression analysis, scored an AUC of 0.94 in the validation cohort.
Conclusion: This systematic review revealed large methodological heterogeneity for each step of the MRI-based radiomics workflow, consequently, the (overall promising) results are difficult to compare. Consensus for standardisation of MRI-based radiomics workflow for tumour response prediction to NST in breast cancer patients is needed to further improve research in this field.
Limitations: Publication bias and data heterogeneity.
Ethics committee approval: n/a
Funding: No funding was received for this work.
Author Disclosures:
R. Granzier: nothing to disclose
T. Nijnatten: nothing to disclose
H. C. Woodruff: Shareholder at Oncoradiomics
M. Smidt: Research/Grant Support at Servier
M. B. I. Lobbes: nothing to disclose

RPS 605a-6 11:45

MRI-based radiomics in breast cancer: feature robustness and its interoperability with respect to interobserver segmentation variability

R. Granzier, N. Verbakel, A. Ibrahim, J. van Timmeren, T. Nijnatten, R. Leijenaar, M. B. I. Lobbes, M. Smidt, H. C. Woodruff*; Maastricht/NL (r.granzier@maastrichtuniversity.nl)*

Purpose: In order to extract clinically useful information from medical images, it is of utmost importance that extracted features are reproducible and standardised. This study investigates the robustness of radiomics features, extracted using two commonly used radiomics software, with respect to interobserver manual segmentation variability on dynamic contrast-enhanced breast MRI. In addition, the differences in feature robustness and interobserver segmentation variability between easy-to-segment tumours and more challenging ones, as perceived by the expert, were investigated.
Methods and materials: 129 histologically confirmed breast tumours were segmented manually in three dimensions on the first post-contrast T1-weighted MR exam by four observers: a breast radiologist, a radiologist in training, a PhD candidate with a medical degree, and a medical student. Features were extracted using the RadiomiX and the open-source Pyradiomics softwares. Features with an intraclass correlation coefficient (ICC>0.9) were considered robust. Interobserver variability was evaluated using the volumetric Dice similarity coefficient (DSC).
Results: The mean DSC for all tumours was 0.81 (range 0.19-0.96). The mean DSC was higher for the easy tumours compared to the challenging tumours (0.83 vs 0.75, respectively, p<0.001). In total, 41.6% (552/1328) and 32.8% (273/833) of all RadiomiX and Pyradiomics features were identified as robust, respectively. Of the 94 easy tumours, 57.5% RadiomiX and 35.7% Pyradiomics features were robust. Of the 35 challenging tumours, only 17.2% RadiomiX and 28.6% Pyradiomics features were robust.
Conclusion: This study shows conclusively the intuitive notion that more complex, challenging tumours lead to less robust features, and that robust features are not simply interchangeable between radiomics software with respect to interobserver segmentation variability. Ultimately, a list of robust radiomics features which is independent of interobserver segmentation variability in breast MRI was identified for two commonly used software.
Limitations: n/a
Ethics committee approval: n/a
Funding: No funding was received for this work.
Author Disclosures:
R. Granzier: nothing to disclose
N. Verbakel: nothing to disclose
A. Ibrahim: nothing to disclose
J. van Timmeren: nothing to disclose
R. Leijenaar: Shareholder at Oncoradiomics
T. Nijnatten: nothing to disclose
M. B. I. Lobbes: nothing to disclose
M. Smidt: Research/Grant Support at Servier
H. C. Woodruff: Shareholder at Oncoradiomics

RPS 605a-7 11:51

Reproducibility of radiomics in pelvic MRI: the effect of variations between readers, segmentation methodology, and software

N. Schurink, J. J. M. van Griethuysen, L. A. Min, R. G. H. Beets-Tan, S. R. van Kranen, D. M. J. Lambregts*; Amsterdam/NL*

Purpose: Although several studies have investigated the reproducibility of radiomics data derived from CT and PET/CT, data on the reproducibility of MR-based radiomics are scarce. This study aims to assess the reproducibility of radiomic features derived from pelvic MRI data and study the effects of variations between readers, segmentation methodology, and feature extraction software packages.
Methods and materials: 25 pelvic MRIs (T2W-MRI of anal cancer) were retrospectively analysed and segmented by two readers to include the: [1] whole-tumour volume and [2] largest single axial tumour-slice. Pixel intensities were normalised to mean=300/SD=100 and images were resampled isotropically (2x2x2mm^3). Radiomic features were extracted using 2 open-source packages (PyRadiomics-v2.2.0, CaPTk-v1.7.3), using comparable settings without image filtration. Segmented pixel intensities were quantised using a fixed bin width of 5. Only features defined in both packages were extracted (first-order, shape, GLCM, GLRLM, GLSZM, and NGTDM features, 51 total). For each feature, the intraclass correlation coefficient (ICC) was calculated between the [1] two readers, [2] two segmentation methods (whole-volume vs. single-slice), and [3] two software packages. When comparing segmentation methods, shape features were excluded from the analysis.
Results: Inter-reader reproducibility was moderate (20/51 features;0.5<ICC<=0.75) to good (15/51 features;0.75<ICC<=0.9). Between segmentation methods, the majority of features (in particular GLRLM, GLSZM, and NGTDM) showed poor reproducibility (31/45 features; ICC<0.5), though most first-order features showed good (7/15 features; 0.75<ICC<=0.9) to excellent (2/15 features; ICC>0.9) reproducibility. Between software packages, the majority of first-order, shape, GLCM, and GLRLM features showed excellent reproducibility (23/30 features; ICC>0.9). The remaining higher-order features (GLSZM and NGTDM) were all poorly reproducible (21/21 features; ICC<0.5).
Conclusion: Variations in software and segmentation methodology negatively affected measurement reproducibility in MRI-based radiomics, in particular for higher-order features. Inter-reader reproducibility was moderate-good.
Limitations: n/a
Ethics committee approval: n/a
Funding: No funding was received for this work.
Author Disclosures:
N. Schurink: nothing to disclose
J. J. M. van Griethuysen: nothing to disclose
L. A. Min: nothing to disclose
R. G. H. Beets-Tan: nothing to disclose
S. R. van Kranen: nothing to disclose
D. M. J. Lambregts: nothing to disclose

RPS 605a-8 11:57

Staging of endometrial cancer using MRI: prediction of deep myometrial infiltration using radiomics-powered machine learning

R. Del Grosso, A. Stanzione, R. Cuocolo, V. Romeo, A. Nardiello, A. Travaglino, P. P. Mainenti, L. Insabato, M. P. S. Maurea; *Naples/IT (renatadelgrosso91@gmail.com)*

Purpose: Deep myometrial invasion (≥ 50% wall thickness, DMI) is the most important morphological prognostic factor for endometrial cancer (EC). While DMI can be assessed on MRI, it often proves challenging, reader-experience dependent, and with interobserver variability. Radiomics allow quantification of tumour heterogeneity and has been successfully paired to machine learning (ML). We aimed to detect DMI in EC patients using radiomics-powered ML.
Methods and materials: One operator manually segmented lesion volumes of interest (VOIs) to extract radiomic features from T2-weighted images. Two additional readers performed lesion segmentation on 30 random patients to test feature stability. Patients were randomly split into model development and validation sets. Multistep feature reduction was performed on the first set. Only stable features (interobserver correlation coefficient ≥ 0.75) were employed. A variance threshold ≤ 0.01 was applied. Highly intercorrelated features (≥ 0.80) were also discarded. Finally, a random forest wrapper was used to select the most significant features. These were employed to train and test via 10-fold cross-validation an ensemble algorithm, a bagged J48 decision tree, whose performance was also assessed on the validation set.
Results: Retrospectively, 54 patients were identified (DMI histopathologically was proven in 17). 1,132 features were extracted and 144 were stable. Then, 21 were discarded due to low variance. After the removal of the highly intercorrelated ones, the set was reduced to 19 features. The random forest wrapper finally identified the 3 most useful ones. In the cross-validation testing, an 86% accuracy was obtained with an AUC of 0.92. In the validation set, these were respectively 91% and 0.94.
Conclusion: Radiomics-powered ML appears as a promising tool to accurately detect DMI in EC patients on MRI.
Limitations: No external validation and a small population.
Ethics committee approval: IRB approved and consent waived.
Funding: No funding was received for this work.
Author Disclosures:
R. Del Grosso: nothing to disclose
A. Nardiello: nothing to disclose
R. Cuocolo: nothing to disclose
A. Stanzione: nothing to disclose
P. P. Mainenti: nothing to disclose
M. P. S. Maurea: nothing to disclose
L. Insabato: nothing to disclose
A. Travaglino: nothing to disclose
V. Romeo: nothing to disclose

RPS 605a-9 12:03

A radiomics-based model to identify the aetiology of liver cirrhosis using gadoxetic acid–enhanced MRI

A. Elkilany[1], T. Müller[1], M. Demir[1], M. Schmelzle[1], T. Denecke[2], D. Geisel[1]; *[1]Berlin/DE, [2]Leipzig/DE*

Purpose: To develop and validate a radiomics-based model as a noninvasive method for the accurate detection of the cause of liver cirrhosis using gadoxetic acid-enhanced magnetic resonance imaging (MRI).
Methods and materials: In this retrospective study, 104 patients (68 male, 36 female; mean age, 61.38 ± 12.8 years; age range, 22–84 years) with a known aetiology of liver cirrhosis who underwent gadoxetic acid-enhanced MRI between January 2014 and August 2019 were included. The patients were classified into 4 groups according to the aetiology of liver cirrhosis: 30 patients had alcoholic cirrhosis, 40 patients had hepatitis-induced cirrhosis, 18 patients had cirrhosis due to primary sclerosing cholangitis (PSC), and 15 patients had cirrhosis following non-alcoholic steatohepatitis (NASH). Radiomics features were extracted from the hepatobiliary phase of gadoxetic acid-enhanced MRI on 2D and 3D region of interest samples using LIFEx, version 5.10. Then, radiomic signatures were classified using a fine Gaussian support vector machine (SVM) as a classification method using a one-vs-one multiclass Gaussian kernel in MathWorks MATLAB R2019b.
Results: The radiomics model demonstrated a 99.5% accuracy in identifying the aetiology of the liver cirrhosis, preliminary without validation of the classification.
Conclusion: Radiomics analysis of gadoxetic acid-enhanced MRI is a promising approach to identify the aetiology of liver cirrhosis.
Limitations: No limitations.
Ethics committee approval: The study was approved by the institutional review board.
Funding: No funding was received for this work.
Author Disclosures:
A. Elkilany: nothing to disclose
T. Müller: nothing to disclose
M. Schmelzle: nothing to disclose
T. Denecke: nothing to disclose
D. Geisel: nothing to disclose
M. Demir: nothing to disclose

RPS 605a-10 12:09

Pituitary adenoma surgical consistency prediction on T2-weighted MRI: a radiomics machine learning analysis

M. B. Cipullo[1], R. Cuocolo[1], L. Ugga[2], D. Solari[1], A. D' Amico[3], L. M. Cavallo[1], P. Cappabianca[1], A. Brunetti[1]; *[1]Naples/IT, [2]Scafati/IT, [3]Salerno/IT*

Purpose: Pituitary macroadenomas are the most common tumours of the pituitary gland. As far as they are usually soft masses, some of them may present with a harder consistency, making it difficult to remove them by using their standard surgical technique, transsphenoidal adenomectomy. The objective of the following study was to determine the accuracy of machine learning texture analysis in assessing the consistency of pituitary macroadenomas in patients subdued to endoscopic endonasal surgery.
Methods and materials: A total of 89 patients (68 soft, 11 rubbery, and 10 fibrous adenomas) who underwent an endoscopic endonasal procedure for pituitary adenoma removal were retrospectively included. Two readers independently segmented the lesions on T2-weighted MR images for the extraction and stability testing of radiomic features. Oversampling of the minority classes was used to balance the data. A 75/25% training-testing split was used for model validation. During feature selection on the training data, unstable, low-variance, and highly-intercorrelated parameters were removed. Subsequently, the most informative features were identified with a random forest-based wrapper and a random forest was employed for consistency prediction in the validation set.
Results: Of the 1,118 features extracted, 599 were stable with an ICC >= 0.90. Only one of these showed a variance <= 0.01, while 526 were highly intercorrelated (>= 0.80). Among the remaining 72 features, the wrapper selected 10 as most useful. The finalised random forest model achieved an overall accuracy of 84.31% with an AUC of 0.97.
Conclusion: Radiomics and machine learning showed high accuracy in the prediction of pituitary adenoma consistency on pre-operative T2-weighted MR images, promising to be a useful tool in the surgical approach choice.
Limitations: A single institution study.
Ethics committee approval: IRB approved. Written informed consent was waived.
Funding: No funding was received for this work.
Author Disclosures:
M. B. Cipullo: nothing to disclose
R. Cuocolo: nothing to disclose
L. Ugga: nothing to disclose
D. Solari: nothing to disclose
A. Brunetti: nothing to disclose
A. D' Amico: nothing to disclose
P. Cappabianca: nothing to disclose
L. M. Cavallo: nothing to disclose

RPS 605a-11 12:15

Using magnetic resonance-based machine learning radiomics to predict diagnosis and prognosis in gliosarcoma

X. Yi[1], B. Chen[2], J. Li[1]; *[1]Changsha/CN, [2]Los Angeles/US (yixiaoping@csu.edu.cn)*

Purpose: To develop and evaluate a MRI derived machine learning radiomics method to preoperatively differentiate gliosarcoma (GSM) from glioblastoma (GBM) and predict survival.
Methods and materials: A single-centre retrospective review was conducted on 39 GSM patients and 316 GBM patients [training cohort: GSM n=27, GBM n=221; validation cohort: GSM n=12, GBM n=95]. Machine learning radiomics models were built by combining the least absolute shrinkage and selection operator (LASSO), random forest (RF), and support vector machine (SVM) methods.
Results: The final SVM model provided an AUC of 0.9420 (95% CI: 0.8922–0.9918) with an accuracy of 0.9280 (95% CI: 0.8119-0.9760) in the training cohort and an AUC of 0.9447 (95% CI: 0.9025–0.9870) with an accuracy of 0.8972 (95% CI: 0.8318-0.9533) in the validation cohort. A radiomics score (Rad-score) was calculated which was computed based on Cox regression coefficients of the multivariate Cox regression. All GSM patients were separated into two groups, the low and high risk groups, which are the patients with Risk-score ≤median and Risk-score > median, respectively. The result of a lokrank test indicated that the median survival of the two groups was statistically significant (P = 0.00007).

Conclusion: This study presents a pre-enhanced MRI image-based machine learning radiomics method that could potentially facilitate the preoperative identification of GSM tumour from GBM and predict the prognosis for GSM.
Limitations: Our study was a retrospective study conducted in a single institution. Therefore, there might be case selection bias and a shortage of accurate radiology-pathology correlation study to reveal the underlying pathology.
Ethics committee approval: Our Institutional Review Board approved this retrospective study (No. 201709995) and waived informed consents as this study was retrospective.
Funding: This study is partially supported by China Postdoctoral Science Foundation funded project (2018M632997).
Author Disclosures:
X. Yi: nothing to disclose
B. Chen: nothing to disclose
J. Li: nothing to disclose

RPS 605a-12 12:21
MRI-based radiomics to predict treatment outcome in oropharyngeal cancer patients
P. Bos[1], M. W. M. van Den Brekel[1], Z. A. R. Gouw[1], A. Al-Mamgani[1], M. Taghavi[1], C. Parmar[2], H. J. W. L. Aerts[2], R. G. H. Beets-Tan[1], B. Jasperse[1]; [1]*Amsterdam/NL,* [2]*Boston, MA/US (pa.bos@nki.nl)*

Purpose: Prognostic markers calculated from diagnostic imaging, also called radiomics, have shown promising results in predicting treatment outcomes of different cancer types. This study assessed MR-based radiomics to predict locoregional failure (LRF) after chemoradiation treatment in oropharyngeal squamous cell carcinoma (OPSCC) patients. The added value of radiomic features to traditional clinical outcome predictors was evaluated.
Methods and materials: 177 patients were included in the study, 76 (43%) HPV positive tumours and 77 (44%) negative HPV tumours. Pretreatment MRI, clinical variables, and outcome data were retrospectively collected from OPSCC patients. In addition, 824 radiomic features were extracted within the manually delineated primary tumour region. Three machine learning models based on either clinical variables (clinical model), radiomic features (radiomic model), and both combined (combined model) were created. The latter two were constructed using wrapper feature selection in combination with random forest, while the clinical model was based on a support vector machine. Prediction quality was assessed using area under the curve (AUC). Different models were compared using the McNeil test. All analyses were performed for the total population and stratified for the tumour human papillomavirus (HPV) status.
Results: Within the total patient cohort, the radiomic model showed the best predictive performance with an AUC of 0.65 compared to the clinical model (AUC: 0.41, p=0.04) and combined model (AUC: 0.63, p=0.07). The same trend was seen in HPV subgroups, however, without reaching statistical significance.
Conclusion: MR-based radiomics is able to predict LRF after chemoradiation in OPSCC patients and performed better compared to clinical variables.
Limitations: All patients were selected from a single-centre while applying radiomics in multicentre cohorts is preferred. Another limitation is the single reader design of the delineations.
Ethics committee approval: IRBd18047.
Funding: Verwelius Foundation.
Author Disclosures:
M. Taghavi: nothing to disclose
P. Bos: nothing to disclose
M. W. M. van Den Brekel: nothing to disclose
B. Jasperse: nothing to disclose
H. J. W. L. Aerts: nothing to disclose
Z. A. R. Gouw: nothing to disclose
R. G. H. Beets-Tan: nothing to disclose
C. Parmar: nothing to disclose
A. Al-Mamgani: nothing to disclose

11:15 - 12:30 **Room O**

Breast

RPS 602a

Contrast-enhanced breast MRI and beyond

Moderators:
N.N.
O. Puchkova; Moscow/RU

RPS 602a-K 11:15
Keynote lecture
J. Camps Herrero*; Valencia/ES*
Author Disclosures:
J. Camps Herrero: nothing to disclose

RPS 602a-1 11:25
The additional utility of ultrafast MRI on conventional DCE-MRI in evaluating preoperative MRI of breast cancer patients
A. Y. Park, S. J. Lee, K. H. Ko, H. K. Jung, J. E. Koh*; Seongnam-si/KR*

Purpose: To investigate whether the additional use of ultrafast MRI can improve the diagnostic performance of conventional dynamic contrast-enhanced MRI (DCE-MRI) in evaluating MRI-detected lesions in breast cancer patients.
Methods and materials: This retrospective study enrolled 103 consecutive breast cancer patients with 204 breast lesions (62 benign and 142 malignant) who underwent preoperative DCE-MRI with ultrafast imaging (9 image sets with 6.5-second temporal resolution). Two reviewers assessed the BI-RADS categories of breast lesions using conventional DCE-MRI and assessed the following parameters on the ultrafast MRI: initial enhancement phase, maximum relative enhancement, slope, and maximum slope ($slope_{max}$) on the kinetic curve. Interobserver agreement was analysed between the two reviewers. The ultrafast MRI parameters were compared between benign and malignant tumours, and cut-off values were determined. For 97 additional MRI-detected lesions, the BI-RADS category was re-assessed using the cut-off values and the diagnostic performance was compared between the conventional DCE-MRI and the combined conventional and ultrafast DCE-MRI.
Results: All ultrafast MRI parameters differed significantly between malignant and benign tumours (all, p<0.001). Initial enhancement phase by reviewer and $slope_{max}$ were the top two parameters showing significant differences between benign and malignant tumours with high reliability. With the use of cut-off values for initial enhancement phase (≤phase 2) and $slope_{max}$ (>9.8%/sec), the specificity of conventional DCE-MRI was significantly increased (29.4% vs 64.7%, p<0.001) without loss of sensitivity (100% vs 88.2%, p=0.157) in evaluating masses.
Conclusion: The additional use of ultrafast MRI can improve the specificity of conventional DCE-MRI when evaluating MRI-detected masses in breast cancer patients.
Limitations: A large proportion of malignant lesions might have influenced the study results. The kinetic curve analysis for conventional and ultrafast DCE-MRI was performed by manually selecting the most enhanced voxel.
Ethics committee approval: n/a
Funding: No funding was received for this work.
Author Disclosures:
A. Y. Park: nothing to disclose
S. J. Lee: nothing to disclose
K. H. Ko: nothing to disclose
H. K. Jung: nothing to disclose
J. E. Koh: nothing to disclose

RPS 602a-2 11:31
The usefulness of postoperative surveillance MR for women after breast-conservation therapy: focusing on MR features of early and late recurrent breast cancer
H. Kim[1], J. Lee[1], H. Kim[2], B. J. Kang[1], S. H. Kim[1]; [1]*Seoul/KR,* [2]*Cheonbo-ro/KR (amgaemi@gmail.com)*

Purpose: To investigate the diagnostic performance of mammography, ultrasonography, and breast magnetic resonance imaging (MRI) for early and late recurrences in patients who underwent breast-conservation therapy (BCT) for breast cancer.
Methods and materials: This retrospective study was conducted between January 2014 and August 2018. 1,312 women with 2,026 surveillance breast MR examinations after BCT were studied. We assessed the cancer detection rate of each postoperative imaging modalities and feature of recurrent lesion in postoperative MRI.
Results: Of 2,026 cases of surveillance postoperative MRI, 103 cases were confirmed as recurrent breast cancer through biopsy. 31 cases occurred within 12 months after BCT, which was defined as an early recurrence. The other 72 cases were found to recur after 13 months after BCT and were defined as late recurrence. There were no statistically significant differences between 2 groups for patients' demographics with p > 0.05, except for the presence of symptoms. In both early and late recurrence groups, MRI showed a significantly higher cancer detection rate than other modalities (p < 0.01), and there were cases which could be diagnosed by postoperative MRI only. Recurrent lesions showed fast enhancement in the early phase regardless of their delayed phase pattern in the early recurrence group. In the late recurrence group, recurrences also showed significantly fast enhancement in the early phase, but they showed a washout pattern in the delayed phase.

Conclusion: In breast cancer patients with BCT, breast MRI showed a significantly higher cancer detection rate than others. The fast enhancing lesion in the early phase of postoperative MRI should be conscious and need further workup, such as biopsy, due to the high possibility of recurrence.
Limitations: n/a
Ethics committee approval: Approved by our institutional review board.
Funding: No funding was received for this work.
Author Disclosures:
H. Kim: nothing to disclose
J. Lee: nothing to disclose
H. Kim: nothing to disclose
B. J. Kang: nothing to disclose
S. H. Kim: nothing to disclose

RPS 602a-3 11:37

A systematic review on variability in studies of breast diffusion-weighted imaging for treatment monitoring

K. van der Hoogt, R.-J. Schipper, G. Winter-Warnars, L. C. Ter Beek, C. Loo, R. M. Mann, R. G. H. Beets-Tan*; Amsterdam/NL*

Purpose: Breast diffusion-weighted imaging (DWI) appears to have strong potential for prediction of therapy outcome in patients treated with neoadjuvant systemic therapy (NST). While summary statistics show decent results in recent meta-analyses, absolute data are variable between studies. This systematic review aims to identify methodological differences between studies and their effect on reported results in order to improve the value of DWI as a biomarker for the monitoring of NST.
Methods and materials: Pubmed was searched for papers reporting on DWI for response prediction/monitoring/evaluation of NST in breast cancer, published before February 2019. The selection was first performed on title/abstract by two independent researchers and, subsequently, full texts were screened for eligibility. Quality of selected studies was assessed using QUADAS2. Population and cancer characteristics (e.g. age, tumour types, type of NST), MRI parameters (e.g. field strength, b-values, voxel size), and post-processing approaches (e.g. ADC mapping, region of interest (ROI) selection) were extracted.
Results: The search yielded 31 papers. After assessment, 15 papers were included in this analysis. Risk of bias of included studies was low. Studies varied with regard to breast cancer types, NST types and pCR-definition (in-/exclusion of residual DCIS). Technical variation was observed in MRI-settings including b-values, ROI-selection, and timing of the MRI scans. These differences all contribute to the observed overlapping ranges of ADC values for pCR and non-pCR.
Conclusion: This systematic review reveals strong heterogeneity in DWI-studies on prediction of NST response. Consequently, DWI metrics for response monitoring should be interpreted with caution. Standardisation of the technique is important.
Limitations: The risk of bias of included studies was low.
Ethics committee approval: n/a
Funding: No funding was received for this work.
Author Disclosures:
K. van der Hoogt: nothing to disclose
R.-J. Schipper: nothing to disclose
G. Winter-Warnars: nothing to disclose
L. C. Ter Beek: nothing to disclose
C. Loo: nothing to disclose
R. M. Mann: nothing to disclose
R. G. H. Beets-Tan: nothing to disclose

RPS 602a-4 11:43

A novel model for the evaluation of breast DWI: is it possible to predict BI-RADS categories?

Y. Selek[1], I. Durur Subaşi[2], A. T. Arikok[1], B. Hekimoğlu[1]; [1]*Ankara/TR,* [2]*Istanbul/TR (irmakdurur@yahoo.com)*

Purpose: To determine BI-RADS categories of patients based on diffusion-weighted imaging (DWI) by a novel evaluation model and compare DWI-derived categories to the previous multiparametric magnetic resonance imaging (MP-MRI) interpretations of the same group and the histopathology data.
Methods and materials: The anonymised DWIs of consecutive 400 patients were evaluated retrospectively according to a classification system based on lesion morphology and pattern of diffusion changes. To investigate the performance of DWI, the highest BI-RADS category for each patient was determined and the results were compared with BI-RADS categories found in MP-MRI reports, and, in possible cases, were also compared to pathology results. nADC values were measured and the diagnostic performance of nADC in benign and malignant discrimination and the threshold values were analysed.
Results: Evaluation system based on DWI findings provided 64% sensitivity, 98% specificity, 90% positive predictive value (PPV), 89% negative predictive value (NPV), and 89.5% accuracy when the MP-MRI was accepted as the reference standard. 87% sensitivity, 68% specificity, 70% PPV, 86% NPV, and 77% accuracy were determined according to pathology results. A threshold value of 0.784 for nADC provided 68% sensitivity, 73% specificity, 72% PPV, 69% NPV, and 71% accuracy for benign-malignant discrimination. nADC values were significantly lower in malignant lesions.
Conclusion: In this study, DWI-derived new conceptualise provided acceptable accuracy rates. Although DWI is a functional examination, its morphological data may also aid in the characterisation of suspicion of lesions.
Limitations: The evaluation was made by two radiologists in consensus, intraobserver and interobserver comparisons could not be made. For technical reasons, some patients were excluded. No reflection of the general population due to MRI indications. Retrospective design.
Ethics committee approval: DYBEAH 29.04.2019-62/18.
Funding: No funding was received for this work.
Author Disclosures:
I. Durur Subaşi: nothing to disclose
Y. Selek: nothing to disclose
B. Hekimoğlu: nothing to disclose
A. T. Arikok: nothing to disclose

RPS 602a-5 11:49

Diffusion-weighted imaging for breast lesion detection and characterisation: additional value of synthetic higher b-values

I. Daimiel Naranjo, R. Lo Gullo, C. Rossi Saccarelli, A. Bitencourt, S. Thakur, E. A. Morris, K. Pinker-Domenig;
New York, NY/US

Purpose: To assess the performance of diffusion-weighted imaging (DWI) for breast cancer detection and characterisation by combining acquired b-values (800 s/mm2) and different synthetic b-values (1000, 1200, 1500, and 1800 s/mm2).
Methods and materials: In this IRB-approved retrospective study, 80 women with 103 benign and malignant breast lesions underwent multiparametric breast MRI at 3T with dynamic contrast-enhanced images (DCE-MRI) and DWI were included. Three readers (r1, r2, r3) independently evaluated CE-MRI and DWI combined with ADC maps for lesion visibility, malignancy likelihood, and preferred b-value. Histopathology was the standard of reference for all the lesions.
Results: Synthetic intermediate b-values (1200–1500 s/mm2) provided the best lesion conspicuity and image quality across all readers. Only 9 (8.7%) enhancing lesions (5 benign, 4 malignant) were missed by all readers, comprising diffuse tumours and masses <1cm. Overall lesion detectability for DWI ranged between 79.6%-83.4% and was 100% for DCE-MRI.
Sensitivity and specificity for lesion characterisation with DWI was r1 61.7% and 94.1%, r2 61.7% and 82.4%, and r3 65% and 82.4%, respectively. Sensitivity and specificity for DCE-MRI was r1 88.3% and 76.5%, 95% and 50%, and r3 86.7% and 70.6%. DWI was significantly less sensitive across all readers ($p<0.001$) but significantly more specific for two readers ($p=0.007$) than DCE-MRI.
Conclusion: Synthetic intermediate b-values (1200–1500 s/mm2) provided the best lesion conspicuity and image quality. DWI with synthetic high b-values increases specificity as a valuable adjunct to DCE-MRI.
Limitations: No normal cases were included in this study and therefore specificity values were unable to be obtained for lesion detectability.
Ethics committee approval: IRB-approved.
Funding: Spanish Foundation Alfonso Martin Escudero, the NIH/NCI Cancer Center Support Grant (P30 CA008748) and the Breast Cancer Research Foundation.
Author Disclosures:
I. Daimiel Naranjo: nothing to disclose
S. Thakur: nothing to disclose
R. Lo Gullo: nothing to disclose
C. Rossi Saccarelli: nothing to disclose
A. Bitencourt: nothing to disclose
E. A. Morris: nothing to disclose
K. Pinker-Domenig: nothing to disclose

RPS 602a-6 11:55

Value of multiparametric MRI with dynamic contrast-enhanced and diffusion-weighted imaging in non-mass enhancing breast tumours

M. A. Marino[1], D. B. Avendano[2], D. Leithner[3], P. Clauser[4], S. Thakur[5], P. A. T. Baltzer[4], M. S. Jochelson[5], E. A. Morris[5], K. Pinker-Domenig[5];
[1]*Messina/IT,* [2]*Monterrey, Nuevo Leon/MX,* [3]*Frankfurt am Main/DE,* [4]*Vienna/AT,* [5]*New York, NY/US (mariaadele.marino@gmail.com)*

Purpose: To evaluate the diagnostic performance of multiparametric magnetic resonance imaging (mpMRI) with dynamic contrast-enhanced (DCE) and diffusion-weighted imaging (DWI) in non-mass enhancing (NME) breast tumours.
Methods and materials: A prospectively populated database was searched for patients who underwent MRI of the breast with T2wi, DWI, and DCE MRI for a BIRADS 45 imaging abnormality, and demonstrated a suspicious NME tumour on DCE-MRI NME according to the 5th edition of the BI-RADS lexicon. Two readers independently assessed DWI and DCE, as well as the two combined as mpMRI. Appropriate statistical tests were used to compare diagnostic values with respect to sensitivity, specificity, diagnostic accuracy, and AUC.
Results: 66 patients with 66 NME breast lesions were included: 37/66 (56%) malignant and 29/66 (44%) non-malignant. DCE-MRI had a sensitivity and specificity of 94.9%, 67% (r1) and 100%, 77.8% (r2). DWI 84.1%,55.6% (r1) and 76.9%,81.5% (r2), respectively. Diagnostic accuracy was 78.8% (r1), 72.7% (r2) for DWI, and 83.3% (r1), 90.1% (r2) for DCE-MRI, respectively. When both parameters were used together as mpMRI, sensitivity was 87.2% (r1), 90% (r2), and specificity 85.2% (r1 and r2), resulting in the best diagnostic accuracy of 90.6% (r1) and 86.2% (r2). MpMRI allowed a reduction of false positives of 33.3% (6 vs 4) (r1) and 55.5% (9 vs 4) (r2). There was substantial inter-reader agreement for both DCE-MRI and MpMRI readings (k=0.610 vs k=0.719), while scarce for DWI (k=0.380)
Conclusion: Multiparametric MRI using DWI and DCE-MRI increases diagnostic accuracy for breast cancer detection for lesions presenting as NME on DCE MRI.
Limitations: Retrospective study.
Ethics committee approval: Institutional review board-approved study
Funding: Breast Cancer Research Foundation.
Author Disclosures:
M. A. Marino: nothing to disclose
D. B. Avendano: nothing to disclose
D. Leithner: nothing to disclose
P. Clauser: Speaker at Siemens
S. Thakur: nothing to disclose
E. A. Morris: Board Member at Medscape
P. A. T. Baltzer: nothing to disclose
M. S. Jochelson: Speaker at GE
K. Pinker-Domenig: Grant Recipient at Katja Pinker received payment for activities not related to the present article including lectures, service on speakers bureaus and for travel/accommodations/meeting expenses from the European Society of Breast Imaging (MRI educational course, annual scie

RPS 602a-7 12:01

A multiparametric approach of diagnosing breast lesions using diffusion-weighted imaging and ultrafast dynamic contrast-enhanced MRI

A. Ohashi[1], M. Kataoka[1], M. Iima[1], M. Honda[1], Y. Urushibata[2], M. Nickel[3], E. Weiland[3], M. Toi[1], K. Togashi[1]; [1]Kyoto/JP, [2]Tokyo/JP, [3]Erlangen/DE (amaoh135@gmail.com)

Purpose: We aimed to evaluate the diagnostic performance of multiparametric approach for breast lesions using maximum slope (MS) from ultrafast dynamic contrast-enhanced (UF-DCE) sequence, apparent diffusion coefficient (ADC), lesion size, and patient's age.
Methods and materials: Two different groups with different UF-DCE sequences were analysed. Group 1: 204 lesions (152 malignant, 52 benign) with k-space-weighted image contrast (KWIC) sequence, and group 2: 114 lesions (78 malignant, 36 benign) with improved 3D-gradient-echo volumetric interpolated breath-hold examination (VIBE) sequence with compressed sensing (both were prototype sequences). Each UF-DCE sequence acquired the image up to 1 min after gadolinium injection. DWI sequences were the same between two groups with b value of 0 and 1,000 s/mm^2. MS and ADC values were measured by two radiologists and their inter-reader agreements were evaluated using intra-class correlation coefficients (ICC). MS derived from UF-DCE sequences, ADC value from DWI, lesion size, and patients' age were used for a multiparametric model using ROC analysis. Univariate and multivariate logistic regression analysis were performed.
Results: Inter-rater agreements were excellent (≥0.95). Univariate logistic regression analysis showed that all parameters differed significantly between malignant and benign lesion (p<0.05). AUC of MS and ADC were 0.74/ 0.92 in group 1 and 0.77/ 0.86 in group 2. The combination of all parameters using multiparametric model yielded an AUC of 0.95 for group 1 and 0.91 for group 2, respectively.
Conclusion: A multiparametric approach based on UF-DCE MRI, DWI, lesion size, and patient's age provides excellent diagnostic performance.
Limitations: Retrospective design.
Ethics committee approval: This study protocol was approved by our institutional review board. The written informed consent was waived because of the retrospective design.
Funding: JP15K09922, MEXT 25120002, 25120008.
Author Disclosures:
A. Ohashi: nothing to disclose
M. Kataoka: nothing to disclose
M. Iima: nothing to disclose
M. Honda: nothing to disclose
Y. Urushibata: Employee at Siemens Healthcare K.K.
M. Nickel: Employee at Siemens Healthcare GmbH
E. Weiland: Employee at Siemens Healthcare GmbH
M. Toi: nothing to disclose
K. Togashi: nothing to disclose

RPS 602a-8 12:07

Comparing zoom diffusion-weighted imaging with standard diffusion-weighted imaging in MRI of the breasts

S. Panwar, H. Mahajan, R. Bhattacharjee; New Delhi/IN (panshikha@rediffmail.com)

Purpose: Diffusion-weighted imaging (DWI) forms an integral part of breast MRI to detect cancer and assess disease response following neoadjuvant chemotherapy. Apparent diffusion coefficient (ADC) allows quantification of diffusion signal and facilitates differentiating benign from malignant lesions. Zoom DWI combines 2D spatially-selective RF excitation pulses for single-shot echo-planar-imaging with reduced field-of-view in the phase-encoding direction. It leads to a decreased number of k-space acquisition lines, significantly shortening EPI echo train and susceptibility artefacts, hence reducing image distortion and blurr. This study evaluates the feasibility of zoom DWI versus standard DWI in terms of ADC quantification.
Methods and materials: 25 patients with 30 lesions, 18 malignant, including 3 post NACT followup, and 12 benign (histopathologically proven) were scanned on 3T MRI, Ingenia, Philips, using a dedicated multichannel phased-array breast coil. The comparative protocol comprised of zoom DWI and routine DWI sequence (b0 & b1000). Both sets of images were used to generate ADC maps using in-house diffusion tool. ROI were drawn at corresponding points to obtain ADC1 (zoom DWI) and ADC2 (routine DWI) by the same radiologist with 14 years experience in reading breast MRI. The mean and standard deviation of ADC values were noted.
Results: ADC1 values were lower than ADC2 in malignant lesions and were higher in most benign and post NACT lesions. Reference cut-off used for malignant lesions was < 1.2x10-2 mm2/s and for benign > 1.2. The explanation could be better image quality with less or no image distortion, blurring, and aliasing in zoom DWI, hence improved ADC map generation and accurate quantification.
Conclusion: Zoom DWI enables accurate breast lesion characterisation, especially for those with borderline ADC values, into benign and malignant on 3T imaging due to better image quality.
Limitations: n/a
Ethics committee approval: n/a
Funding: No funding was received for this work.
Author Disclosures:
S. Panwar: nothing to disclose
H. Mahajan: nothing to disclose
R. Bhattacharjee: nothing to disclose

RPS 602a-9 12:13

Diffusion with very high b-value in breast MRI: the end of the contrast injection?

H. Hamri[1], Z. Jolibois[2], M. Scholer[3], E. Weiland[2], C. de Bazelaire[2]; [1]Rabat/MA, [2]Paris/FR, [3]Vincennes/FR (hamri.hajar@yahoo.fr)

Purpose: To evaluate the diagnostic yield of diffusion-weighted imaging (DWI) with very high b-value combined with T2 weighted sequence in breast MRI.
Methods and materials: 130 patients were included consecutively in this retrospective study approved by our IRB.
All patients underwent breast MRI (MAGNETOM Aera, Siemens 1.5T, 18-channel breast antenna) with a 2D-SS-EPI-SPAIR diffusion sequence (TR/TE: 5200/67ms, b 2500s/mm²) in addition to the standard protocol with 2D-T1-FSE, 3D-T2-SPAIR, and 3D-T1-VIBE-SPAIR -DCE.
Two independent readings were performed by 2 radiologists in consensus: 1) combined analysis of the DWI and T2W sequences, and 2) analysis of the standard protocol according to BIRADS lexicon. All findings with hypersignal DWI and low T2 signal were considered as suspicious. All suspicious lesions were biopsied. BIRADS 1-3 lesions had at least 2 years follow-up or histological proof. Diagnostic yields were compared using ROC curves.
Results: A total of 180 lesions were analysed of which 27% were malignant. Low sensitivity but higher specificity were found with the combined analysis of DWI and T2W sequences compared with T1W, T2W, and DCE sequences (92%, 92% vs 96%, 82%, respectively). However, the comparison of ROC curves showed no significant difference (AUC= 0.92 vs 0.89, respectively, p= 0,364).

Conclusion: Combined analysis of DWI with a b-value of 2500s/mm² and T2W sequences could be a reliable alternative to gadolinium injection, particularly for the screening of women with a high risk of breast cancer.
Limitations: No ADC calculated with a single b-value of 2500s/mm².
Ethics committee approval: Study approved by our institutional review board.
Funding: No funding was received for this work.
Author Disclosures:
H. Hamri: nothing to disclose
Z. Jolibois: nothing to disclose
M. Scholer: nothing to disclose
E. Weiland: nothing to disclose
C. de Bazelaire: nothing to disclose

RPS 602a-10 12:19
Feasibility of diffusion-weighted imaging (DWI) for lesion localisation during MRI-guided breast biopsy avoiding contrast-agent administration: a single-centre experience
S. Storer, R. Menghini, L. Camera, S. A. Montemezzi*; Verona/IT (storersilvia@gmail.com)*

Purpose: MRI-guided breast vacuum biopsy is used to analyse suspicious lesions if no correlation is found on US or mammography. DWI employs the differential diffusion rate of water molecules in normal and pathologic tissue, while contrast-enhanced (CE) sequences reflect tissue vascularity. Our purpose was to evaluate the feasibility of DWI for targeting lesions in MRI-guided breast biopsy without applying a contrast agent.
Methods and materials: Out of 59 MRI-guided breast biopsies performed in our institution between January 2019 and September 2019, 29 patients acquired both DWI (b value 1300 s/mm^2) and dynamic contrast-enhanced (CE) sequences during the biopsy to target the lesion in a 3T Machine. The puncture was carried out using a coaxial 9G system and DWI was repeated to evaluate the correct position of the needle. Finally, a site marker was placed.
Results: Out of 29 lesions, 21 presented DWI restriction (9 resulted B5-, 6 B2-, 6 B3-lesions). 19 lesions presented "mass-like" enhancement (size 5 mm-30 mm) and 14 of them (73,7%) demonstrated diffusion restriction, 10 lesions presented "non-mass" enhancement (5 mm-35 mm) and 7 of them showed DWI restriction (70%). DWI acquisition time was shorter than CE-sequences (4.26 min vs 5.35 min).
Correct positioning of coaxial system was confirmed on DWI as a signal loss (2 cases were limited by artefacts due to anaesthetic injection). The site marker was identified using T1-weighted images (acquisition time 1.52 min).
Conclusion: DWI can been used as an alternative to dynamic sequences for targeting lesions with a minimum size of 5 mm, mainly with "mass-like" enhancement. The most important advantages of this approach are targeting bilateral lesions, reducing use of contrast agent, with a shorter acquisition time.
Limitations: n/a
Ethics committee approval: n/a
Funding: No funding was received for this work.
Author Disclosures:
S. Storer: nothing to disclose
R. Menghini: nothing to disclose
L. Camera: nothing to disclose
S. A. Montemezzi: nothing to disclose

RPS 602a-11 12:25
Breast DTI: mean diffusivity and fractional anisotropy of IDC and DCIS
M. Nadrljanski, Z. Milosevic*; Belgrade/RS (dr.m.nadrljanski@gmail.com)*

Purpose: To assess breast DTI (mean diffusivity (MD) and fractional anisotropy (FA)) in patients with invasive ductal carcinoma (IDC) and ductal carcinoma in situ (DCIS) in comparison with DWI (apparent diffusion coefficient (ADC)).
Methods and materials: A retrospective analysis of breast MRI (N=30) included consecutive patients with unilateral lesion: IDC (n1=15) and DCIS (n2=15). All patients were examined with a 1.5T MRI system with DTI and DCE sequences. FA, MD, and ADC were computed for all lesions, and FA and MD were computed for parenchyma. Mann Whitney U test and Spearman correlations were performed.
Results: MD is significantly different between IDC and DCIS: 0.991+/-0.006 vs. 1.331+/-0.053, p<0.0001. FA is not considered significantly different between IDC and DCIS: 0.300+/-0.021 vs. 0.318+/-0.027, p=0.085. MD and FA are considered significantly different between DCIS and parenchyma (1.331+/-0.053 vs. 1.627+/-0.026, p<0.0001; 0.318+/-0.027 vs. 0.351+/-0.021, p=0.002, respectively). Correlation between DTI parameters in DCIS (MD and FA) and ADC was considered significant (r=0.581, p=0.023; r=0.710, p=0.003, respectively).
Conclusion: MD in DCIS is significantly lower in comparison with values for IDC and is significantly higher than parenchymal MD. FA is significantly different in DCIS compared to parenchyma. In correlation with ADC, DTI parameters may contribute to a better characterisation of non-mass enhancement.
Limitations: A retrospective, single-centre study on a small sample of patients may lead to lower generalisability. Manually drawn ROI definition may be the source of bias. Technical limitations include EPI-based artefacts and the 1.5T field strength in DTI.
Ethics committee approval: Referent board approval obtained for retrospective analysis.
Funding: No funding was received for this work.
Author Disclosures:
M. Nadrljanski: nothing to disclose
Z. Milosevic: nothing to disclose

11:15 - 12:30 **Studio 2020**

Cardiac

RPS 603a

Cardiomyopathies: functional assessment and deep phenotyping

Moderators:
N. Galea; Rome/IT
A. Jacquier; Marseille/FR

RPS 603a-K 11:15
Keynote lecture
M. Pirnat*; Maribor/SI (majapirnat@gmail.com)*

Author Disclosures:
M. Pirnat: nothing to disclose

RPS 603a-1 11:25
Similar but not identical: radiomic analyses of areas with late gadolinium enhancement in patients with ischaemic and non-ischaemic disease
L. Baffoni1, A. Cavaliere[2], R. Motta[2], B. Giorgi[2], R. Stramare[2], M. de Lazzari[2], M. Perazzolo Marra[2], E. Quaia[2], C. Giraudo[2]*; [1]Montebelluna/IT, [2]Padua/IT (baffoniluca@gmail.com)*

Purpose: To characterise by radiomic analyses the injured myocardial tissue, shown via late gadolinium enhancement MR imaging, of patients with ischaemic (ISd) and non-ischaemic (nISd) myocardial disease.
Methods and materials: Patients with ISd and nISd who underwent a contrast-enhanced cardiac MR from January 2018 to May 2019 were included in this retrospective study. One radiologist expert in cardiovascular imaging, blind to the clinical information, applied a 3 mm standardised region of interest (i.e. using the phase-sensitive inversion recovery images) on the scar of the myocardial tissue of each patient, using a 3D slicer. 56 radiomic features belonging to three categories were extracted: first-order statistics (FOS), grey-level co-occurrence matrix (GLCM), and grey-level run length matrix (GLRLM). The student's t-test was used to compare the two groups of patients for each radiomic feature (p<0.05). The accuracy of the variables showing a statistically significant difference was assessed by receiver operating characteristic curves.
Results: 10 patients with ISd (1 female; mean age±SD 60.6±10.8 yrs) and 11 nISd (3 females, mean age±SD 51.8±21.4 yrs) were examined. For 41 out of the 56 investigated features, a significant difference between the two groups occurred (8 FOS, 17 GLCM, and 16 GLRLM; p<0.05 each). The area under the curve was excellent only for Imc1 (AUC=.982) and good only for minimum and the tenth percentile (respectively AUC=.773 and AUC=.782). All other features showed a low accuracy.
Conclusion: 3 features can be considered as good radiomic markers of ischaemic injury. Radiomic analyses support that ischaemic injuries differ from non-ischaemic lesions, despite both appearing visually very similar on late gadolinium enhanced MR sequence.
Limitations: Future studies on a larger population are necessary to confirm this finding and its clinical implications.
Ethics committee approval: Ethics committee approval obtained.
Funding: No funding was received for this work.
Author Disclosures:
L. Baffoni: nothing to disclose
A. Cavaliere: nothing to disclose
R. Motta: nothing to disclose
B. Giorgi: nothing to disclose
R. Stramare: nothing to disclose
M. de Lazzari: nothing to disclose
M. Perazzolo Marra: nothing to disclose
E. Quaia: nothing to disclose
C. Giraudo: nothing to disclose

RPS 603a-2 11:31
Global longitudinal diastolic strain rate as an early marker for predicting adverse outcomes in hypertrophic cardiomyopathy by cardiac magnetic resonance feature tracking
X. Chunchao, Z. Li; *Chengdu/CN*
(xiachunchao@126.com)

Purpose: Diastolic dysfunction acts as one of the predominant mechanisms responsible for main adverse cardiovascular events (MACE) in hypertrophic cardiomyopathy (HCM). The aim of this study is to explore the potential value of global diastolic strain-rate (PDSR) derived from cardiac magnetic resonance feature tracking (CMR-FT) in predicting adverse outcomes in HCM population.
Methods and materials: 98 HCM patients [including 44 patients with left ventricular outflow tract obstruction (LVOTO) and 54 patients without] were enrolled and followed for a mean (+SD) of 4.50 ± 1.89 years. LV global myocardial mechanics were assessed for each one by CMR-FT at study entry.
Results: Compared with the nonobstructive subgroup, the obstructive subgroup demonstrated a deteriorated magnitude of LV global radial, circumferential, and longitudinal peak diastolic strain rate (PDSR) at study entry (all $P < 0.05$). During a long-term follow-up, a total of 24 patients suffered from MACE. Furthermore, when applying the specified cut-off value of 0.33 1/s for longitudinal PDSR, the Kaplan-Meier curve demonstrated that patients with lower longitudinal PDSR experienced significantly lower freedom from MACE when compared with their counterparts among nonobstructive, obstructive, and overall cohorts, respectively (all log-rank $P < 0.05$). Multivariable analysis demonstrated that longitudinal PDSR remained the independent predictor of outcome despite adjusting for other confounding factors (hazard ratio: 3.17, 95% confidence interval: 1.20-8.37; $P < 0.05$).
Conclusion: CMR-FT derived longitudinal PDSR probably serves as an early marker for predicting adverse outcomes in an HCM population, which is beneficial for risk stratification. Further confirmatory studies are needed.
Limitations: A limited study population and retrospective nature of the study.
Ethics committee approval: The institutional ethics committee of our hospital approved this retrospective study.
Funding: 1.3.5 project for disciplines of excellence, West China Hospital, Sichuan University.
Author Disclosures:
X. Chunchao: nothing to disclose
Z. Li: nothing to disclose

RPS 603a-3 11:37
Rare disease: cardiac risk assessment with MRI in patients with myotonic dystrophy type 1
M. Alì, C. B. Monti, R. Cardani, L. Melazzini, F. Secchi, G. Meola, F. Sardanelli; *Milan/IT (marco.ali90@gmail.com)*

Purpose: To evaluate myocardial extracellular volume and strain in myotonic dystrophy type I patient (DM1) and appraise whether they could be viable imaging-biomarkers of subclinical cardiac pathology.
Methods and materials: We retrospectively analysed 9 DM1 without apparent cardiac disease who had undergone a cardiac magnetic resonance (CMR) examination. They were age- and sex-matched with healthy controls. Cardiac strain (CS) and extracellular volume (ECV) were calculated from CMR images. Mann-Whitney U test was used to compare independent distributions, Spearman's ρ for correlations, and t-test was used to compare the ECV obtained in DM1 with that in healthy subjects. Data was reported as median and interquartile range.
Results: The main findings were the follows:
- Global CS (-19.1%;-20.5%,-16.5%) in DM1 was lower ($p=0.011$) than that in controls (-21.7%;-22.7%,-21.3%).
- Global ECV in DM1 (32.3%;29.3%,36.8%) was significantly ($p=0.008$) lower than that reported in literature (Di Leo et al. Eur Radiol. 2019) in healthy subjects (25.6%;19.9%,31.9%).
- Global CS showed a strong, positive correlation with septal CS ($\rho=0.767$, $p=0.016$) and with both global ($\rho=0.733$ $p=0.025$) and septal ECV ($\rho=0.767$, $p=0.016$). A very strong positive correlation was observed between global ECV and septal ECV ($\rho=0.983$, $p<0.001$).
Conclusion: In DM1, the increase in ECV and decrease in CS may be taken into consideration as a trigger for follow-up and implementation of preventive measures. Physicians dealing with DM1 may potentially take into consideration CMR as an early screening tool to identify initial cardiac involvement.
Limitations: A small sample size due to the prevalence of DM1 in the population.
Ethics committee approval: Ethics committee approved.
Funding: No funding was received for this work.
Author Disclosures:
M. Alì: nothing to disclose
F. Sardanelli: Grant Recipient at Bayer, Grant Recipient at Bracco, Grant Recipient at General Electric, Speaker at Bayer, Speaker at Bracco, Speaker at General Electric, Advisory Board at Bracco
F. Secchi: nothing to disclose
C. B. Monti: nothing to disclose
G. Meola: nothing to disclose
R. Cardani: nothing to disclose
L. Melazzini: nothing to disclose

RPS 603a-4 11:43
Right ventricular involvement in Fabry's disease
T. Emrich[1], S. Benz[1], I. A. Abidoye[2], C. Düber[1], L. Arash-Kaps[1], J. B. Hennermann[1], C. Kampmann[1], K.-F. Kreitner[1]; *[1]Mainz/DE, [2]Ado-Ekiti/NG (tilman.emrich@gmail.com)*

Purpose: Involvement of the right ventricle is associated with a poor prognosis in several cardiomyopathies because of the increased risk for arrhythmias and subsequent sudden cardiac arrest. In Fabry's disease (FD), the myocardium is affected by the accumulation of sphingolipids. Current diagnostic tests for cardiac involvement in FD focus on the left ventricle. The purpose of this retrospective study was to evaluate right ventricular involvement in FD by CMR.
Methods and materials: We compared 61 FD patients and 56 healthy volunteers using CMR at 3T. T1 mapping, mass, and global strains were acquired for both ventricles using dedicated software. For group analysis, FD patients were divided by the severity of cardiac involvement into three stages.
Results: RV mass rose with increasing accumulation of sphingolipids. All feature tracking strain parameters of the right ventricle showed significant differences in comparison with healthy volunteers ($p<0.0001$). The most altered parameter was global right ventricular longitudinal strain with a mean of -25.3% (± 8.4) for healthy volunteers and -17.1% (±5.8) in FD. Split by the different stages of cardiac involvement, the decrease of strain parameters rose with a higher stage of the disease. Notably, even in stage I, there was already an elevation of RV mass and reduction of LV global longitudinal strain.
Conclusion: CMR parameters of the right ventricle show significant differences in all disease stages compared to healthy volunteers. RV changes (mass and strain) seem to occur earlier compared to an elevation of left ventricular mass. Therefore, analysis of the RV should be routinely included in the detailed assessment of patients with Fabry's disease.
Limitations: A single-centre study.
Ethics committee approval: The study was approved by the local ethics committee (837.196.13/837.477.14).
Funding: No funding was received for this work.
Author Disclosures:
L. Arash-Kaps: nothing to disclose
J. B. Hennermann: nothing to disclose
T. Emrich: nothing to disclose
S. Benz: nothing to disclose
I. A. Abidoye: nothing to disclose
C. Düber: nothing to disclose
C. Kampmann: nothing to disclose
K.-F. Kreitner: nothing to disclose

RPS 603a-5 11:49
Texture analysis of cine CMR sequences in patients with dilated cardiomyopathy: may the radiomic signature predict the prognosis?
N. Di Meo, L. Zanolini, G. M. Agazzi, L. Lupi, M. Ravanelli, D. Farina; *Brescia/IT (nunzia.dimeo@hotmail.it)*

Purpose: To explore the potential of texture analysis (TA) of cardiac MR (CMR) sequences in predicting major adverse cardiovascular events (MACE) in a population of patients affected by dilated cardiomyopathy (DCM).
Methods and materials: A retrospective study on 170 CMR scans performed on patients with DCM. CMR was acquired on a 1.5T scanner using a standardised protocol composed of morphologic, cine, and late gadolinium enhancement (LGE) sequences. The cine CMR short-axis stack (10-12 sections per patient) was post-processed with a freeware software (3D slicer, www.slicer.org). Circumferential ROIs were traced semi-automatically by a single operator on the entire left ventricular (LV) myocardium. TA was then performed using the pyRadiomics library which extracted 107 TA features for each ROI. Patients were followed up for 5 years during which MACE was recorded. Statistical analysis of TA features was performed applying the least absolute shrinkage and selection operator (LASSO) method in order to discard non-significant features. A radiomic score was calculated from statistically significant features.
Results: 59.5% of participants had a MACE during the follow-up. A radiomic signature including 5 TA features (Elongation, RobustMeanAbsoluteDeviation, Minimum, X10Percentile, GrayLevelVariance) allowed for diving of the population into two subgroups: patients with a low score had better prognosis (MACE free-survival: 80% at 4 years) than patients with high score (MACE free-survival: 50% at 4 years). Survival curves showed significant divergence between the two subgroups after the 2nd year of follow-up (HR 0,31; P<0,001).

Conclusion: TA of standard cine-CMR sequences on the whole LV allows to create a radiomic score which may predict the midterm prognosis of patients with DCM.
Limitations: A single-centre, retrospective study with a small sample.
Ethics committee approval: All patients gave written consent to CMR.
Funding: No funding was received for this work.
Author Disclosures:
N. Di Meo: nothing to disclose
L. Zanolini: nothing to disclose
G. M. Agazzi: nothing to disclose
L. Lupi: nothing to disclose
M. Ravanelli: nothing to disclose
D. Farina: nothing to disclose

RPS 603a-6 11:55

Manually measured global longitudinal strain in cardiac MRI scans: the evaluation of myocardial longitudinal kinesia in patients affected by hypertrophic cardiomyopathy

E. Muscogiuri, D. Caruso, T. Polidori, M. Pignatelli, G. Fraietta, M. Di Girolamo, A. Laghi*; Rome/IT (e.muscogiuri@gmail.com)*

Purpose: To evaluate manually measured global longitudinal strain (GLS) in MRI scans as a technique to detect myocardial kinesia impairment in patients affected by hypertrophic cardiomyopathy.
Methods and materials: We retrospectively evaluated 36 patients who underwent cardiac magnetic resonance imaging (MRI) between 2011 and 2019. The study population has been divided into two groups: the first group (control group) was composed of 16 patients who resulted negative for any detectable pathology and the second group was composed of 20 patients affected by hypertrophic cardiomyopathy (HCM) with preserved ejection fraction. Two radiologists independently measured global longitudinal strain (GLS) by tracing endocardial border lengths in routinely acquired cine images on vertical (VLA) and horizontal long axis (HLA). We calculated the mean values of GLS for each group and Student's test was used to compare the means as proof that they were significantly different. Possible correlations between GLS and functional parameters were also analysed (e.g. ejection fraction, volumes, and presence of fibrosis).
Results: The mean GLS values we obtained concerning the first (6 M, mean ejection fraction 63%) and the second group (13 M, mean ejection fraction 72%) were 22,9 ± 2,3 % and 16 ± 2,1%, respectively. The GLS values regarding the second group were significantly lower than the first group (p<0.01). GLS did not correlate with other parameters, such as the presence of fibrosis replacement or left ventricle volumes.
Conclusion: We demonstrated that manually measured GLS is a useful tool to detect longitudinal kinesia impairment in patients affected by hypertrophic cardiomyopathy. Thus, the parameter we measured allows to rapidly estimate myocardial longitudinal kinesia without using any dedicated software.
Limitations: A small study population and heterogeneous types of HCM.
Ethics committee approval: n/a
Funding: No funding was received for this work.
Author Disclosures:
E. Muscogiuri: nothing to disclose
D. Caruso: nothing to disclose
T. Polidori: nothing to disclose
M. Pignatelli: nothing to disclose
G. Fraietta: nothing to disclose
M. Di Girolamo: nothing to disclose
A. Laghi: nothing to disclose

RPS 603a-7 12:01

Left ventricular feature tracking strain analysis for the detection of early cardiac involvement in Anderson Fabry disease

M. Richter, V. Bethke, A. Hasse, A. Brose, S. Harth, C. Tanislav, G. Krombach, F. Roller*; Giessen/DE (richter.martinjo@gmail.com)*

Purpose: Anderson Fabry disease (AFD) is an X-linked multi-organ disorder of lysosomal metabolism with cardiac disease being the leading cause of death. Cardiac MRI, especially native T1 mapping, showed great potential for the detection of early cardiac involvement. As a further increment, feature tracking strain analysis (FT-SA) showed promising results in other cardiac diseases. Therefore the goal of the current study is to evaluate the potential of FT-SA in AFD.
Methods and materials: 16 consecutive AFD patients (9 female) with a mean age of 49.9 years ± 16.8 standard deviation (SD) and 16 control patients (9 female; 47.5 years ± 13.2 SD) were investigated at 1.5 Tesla. Global native T1 values were evaluated and left ventricular global longitudinal feature tracking strain analysis was performed (LV-GL). Results were correlated against serum Lyso-Gb3-Levels.
Results: Native T1 values were significantly lower in all AFD patients 913.3ms ± 40.0 SD compared to control patients 959.0ms ± 23.6 SD (p<0.0004), whereas ventricular functions and strain parameters did not differ significantly between both groups. Moreover, native T1 values were significantly lower in Lyso-Gb3 positive AFD patients with 870.9ms ± 41.5 SD (p <0.0001). Lyso-Gb3 (mean level 19.3ng/ml ± 30.0 SD) showed a moderate negative correlation to native T1 (r=-0.38) and a moderate positive correlation to LV-GL strain (r=0.39). Furthermore, native T1 showed a good significant negative correlation to LV-GL strain (r = -0.69, p=0.047).
Conclusion: Although ventricular function and strain values do not differ significantly between AFD patients and controls, the moderate and good correlations of LV-GL strain to Lyso-Gb3 and native T1 values suggest that wall motion anomalies might occur early in cardiac AFD involvement. Large scale trials are needed to verify our findings.
Limitations: A small study cohort.
Ethics committee approval: n/a
Funding: No funding was received for this work.
Author Disclosures:
M. Richter: nothing to disclose
V. Bethke: nothing to disclose
A. Hasse: nothing to disclose
A. Brose: nothing to disclose
S. Harth: nothing to disclose
C. Tanislav: nothing to disclose
G. Krombach: nothing to disclose
F. Roller: nothing to disclose

RPS 603a-8 12:07

Texture analysis and machine learning of T1 maps and ECV compared with strain parameters: differentiation among hypertrophic cardiomyopathy, hypertensive heart disease, and normal control

R.-Y. Shi, L. Wu, J.-R. Xu*; Shanghai/CN (ryshicn@hotmail.com)*

Purpose: To assess the diagnostic potential of texture analysis (TA) applied in T1 maps and extracellular volume (ECV) obtained from cardiac magnetic resonance (CMR) for the diagnosis of hypertrophic cardiomyopathy (HCM) and hypertensive heart disease (HHD) from normal controls (NC) and compared with strain parameters.
Methods and materials: The study included 35 HCM patients, 20 HHD patients, and 21 normal NCs. Regions of interest (ROI) for TA were drawn on T1 maps and ECV by open-source software. Stepwise dimension reduction and feature selection were performed by reproducibility, machine learning, and collinearity and multivariable regression analysis for selecting features enable differential HCM and HHD. Strain parameters were calculated by cine sequences.
Results: 3 independent features allowed differentiation between abnormal (HCM and HHD) and NC in T1 map and 2 features in ECV analysis. Of the best-calculated model, the areas under the receiver operating curve (ROC) were as follows: 0.977 for T1 map and 0.909 for ECV. To distinguish HCM from HHD, 2 independent features were screen out for both T1 and ECV maps. The areas under the ROC were as follows: 0.906 for T1 map and 0.906 for ECV. Strain parameters of 3 direction could differentiate abnormal from NC, but only longitudinal strain indicated a significant difference between HCM and HHD with the area 0.703 under the ROC curve.
Conclusion: Texture analysis of T1 maps and ECV show a high accuracy for diagnosis of hypertrophy myocardium from NC and also differentiate HCM from HHD. The result of strain parameters was not ideal.
Limitations: For the software property, the 2D texture features may produce selection bias.
Ethics committee approval: The institutional review board approved this retrospective study. Informed consent was obtained from all subjects.
Funding: No funding was received for this work.
Author Disclosures:
R.-Y. Shi: nothing to disclose
L. Wu: nothing to disclose
J.-R. Xu: nothing to disclose

RPS 603a-9 12:13

Quantification of right ventricular strain and strain rate using cardiac magnetic resonance feature tracking in hypertrophic cardiomyopathy subjects with preserved ejection fraction

L. Yang, K. Wang*; Harbin/CN (970082484@qq.com)*

Purpose: To evaluate the feasibility and reproducibility of using CMR-FT for analysis of bi-ventricular strain and strain rate in HCM patients as well as to explore the correlation between RV and LV deformation.
Methods and materials: A total of 60 HCM patients and 48 controls were studied. Global and segmental peak values of bi-ventricular longitudinal, circumferential, radial strain, and systolic SR were analysed. Pearson analysis

was performed to investigate the correlation between RV and LV deformation. Intraobserver and interobserver reproducibility were also assessed.
Results: Left ventricular mass in the HCM group was significantly higher than in the control group. Left ventricular end-systolic volume, left ventricular end-diastolic volume, right ventricular end-systolic volume, and right ventricular end-diastolic volume in the HCM group were significantly lower than the correlated parameters in the control group (P<0.001), whereas there was no statistical difference in ejection fraction (p >0.05). Global longitudinal strain (GLS), global longitudinal strain rate (GLSR), global circumferential strain (GCS), global circumferential strain rate (GCSR), global radial strain (GRS), and global radial strain rate (GRSR) of the LV and RV were all significantly lower compared with the control group. Segmental strain and SR were also true (p <0.001). Bi-ventricular strain and SR measurements were highly reproducible at both intra and interobserver levels. Pearson analysis showed RV GCS, GLS, and GRS positively correlated with LV GCS, GLS, and GRS (r=0.713, p<0.001; r=0.728, p<0.001; r=0.730, p<0.001).
Conclusion: CMR-FT is a promising approach to the analyse impairment of global and segmental myocardium deformation in HCM patients non-invasively and quantitatively.
Limitations: n/a
Ethics committee approval: The protocol was approved by institutional review boards of the 2nd, the 3rd, and the 4th Affiliated Hospital of Harbin Medical University.
Funding: This paper was supported by the National Natural Science Foundation of China General Projects (81571740) (KW).
Author Disclosures:
L. Yang: Author at The third affiliated hospital of Harbin Medical University
K. Wang: Founder at The third affiliated hospital of Harbin Medical University

RPS 603a-10 12:19
Using myocardial extracellular volume fraction to differentiate healthy from cardiomyopathic myocardium using dual-source dual-energy CT
A. F. Abadia[1], V. Vingiani[2], M. van Assen[3], S. S. Martin[1], A. Varga-Szemes[1], U. J. Schoepf[1]; [1]*Charleston, SC/US,* [2]*Rome/IT,* [3]*Groningen/NL*
(vincenzovingiani@gmail.com)

Purpose: To evaluate the feasibility of dual-energy CT (DECT)-based iodine quantification to estimate myocardial extracellular volume fraction (ECV) in patients with and without cardiomyopathy (CM), and assess its ability to distinguish healthy myocardial tissue from cardiomyopathic, with the goal of defining a threshold ECV value for disease detection.
Methods and materials: 10 healthy subjects and 60 patients with CM (mean age 66.4±9.4; 59 males; 40 ischemic and 20 non-ischemic CM) underwent late-iodine-enhanced DECT-imaging. Myocardial iodine maps were obtained using 3-material decomposition. ECV was estimated from haematocrit levels and the iodine maps, using the AHA 16-segment model of the left ventricle. ROC curve analysis was performed with corresponding AUC, along with Youden's index assessment, to establish a threshold for CM detection.
Results: The median ECV for ischaemic CM, non-ischaemic CM, and healthy myocardium were 36.9% (32.4-41.1), 38.3% (33.7-43.0), and 25.4% (22.9-27.3), respectively. Healthy myocardium showed significantly lower median ECV values compared to ischaemic and non-ischaemic CM (p<0.001). From Youden's index analysis, an ECV>29.48% would indicate the presence of CM (sensitivity=90.3; specificity=90.3). The AUC for the ROC curve was 0.950 (p<0.001).
Conclusion: Our study findings resulted in a promising threshold ECV value that could facilitate the differentiation between healthy and diseased myocardium, and highlights the potential of this DECT methodology to detect cardiomyopathic tissue. The threshold found is not intended to be used as an absolute diagnostic test, but rather as a tool that could provide additional value for the characterisation of myocardial tissue.
Limitations: A retrospective single-centre study with limited availability of healthy-subjects' contrast-enhanced DECT delayed scans.
Ethics committee approval: Approved by the Institutional Review Board and written informed consent was obtained from all subjects.
Funding: No funding was received for this work.
Author Disclosures:
A. F. Abadia: nothing to disclose
V. Vingiani: nothing to disclose
M. van Assen: nothing to disclose
S. S. Martin: nothing to disclose
A. Varga-Szemes: Research/Grant Support at Siemens, Consultant at Elucid Bioimaging
U. J. Schoepf: Research/Grant Support at Astellas, Bayer, Elucid Bioimaging, GE, Guerbet, HeartFlow Inc., and Siemens, Consultant at Astellas, Bayer, Elucid Bioimaging, GE, Guerbet, HeartFlow Inc., and Siemens

RPS 603a-11 12:25
Differences in myocardial segmental strain between obstructive and non-obstructive hypertrophic cardiomyopathy assessed by feature tracking cardiovascular magnetic resonance
V. Palmisano, S. Cossa, M. Porcu, R. Cau, L. Saba*; Cagliari/IT*
(vitanio88@gmail.com)

Purpose: To evaluate whether there are any significant differences in myocardial strain parameters between obstructive hypertrophic cardiomyopathy (HOCM) and non-obstructive hypertrophic cardiomyopathy (HCM) as assessed by cardiovascular magnetic resonance feature tracking (CMR-FT).
Methods and materials: Cardiovascular magnetic resonance (CMR) was performed in 32 patients. 17 patients (mean age, 51 ± 17, 65% man) had an echocardiography diagnosis of HCM (aortic transvalvular pressure gradient (ATPG) < 30 mmHg) and 15 patients (mean age, 62 ± 15, 53% man) had a diagnosis of HOCM (ATPG > 30 mmHg). Left ventricle (LV) late gadolinium enhancement (LGE) was quantified. CMR-FT was used to estimate LV global and segmental strain parameters in both groups.
Results: All of the patients had normal LV volumes and ejection fraction (EF). Global radial, circumferential, and longitudinal strain and strain rate were lower than normal value reference, but there were no significant differences in both groups. Segmental strain analysis showed significantly higher values of almost all 3 components of strain, strain rate, displacement, and velocity in HOCM than HCM, in mid anteroseptal, mid anterior, and all apical myocardial segments (p <0,05). These values were independent by almost all segmental thickness and LGE.
Conclusion: Obstructive hypertrophic cardiomyopathy patients have higher left ventricle segmental strain parameters than non-obstructive patients in apex and mid anterior wall. This may represent a greater work load for the LV and explain the major risk in HOCM patients of development myocardial dysfunction.
Limitations: The small sample size of the study may introduce not optimal quantification in regional strain. We did not have a control group. We did not evaluate the inter and intravariability of the feature tracking cardiovascular magnetic resonance analysis.
Ethics committee approval: Patients provided written informed consent.
Funding: No funding was received for this work.
Author Disclosures:
V. Palmisano: nothing to disclose
S. Cossa: nothing to disclose
M. Porcu: nothing to disclose
R. Cau: nothing to disclose
L. Saba: nothing to disclose

11:15 - 12:30 **Coffee & Talk 2**

Oncologic Imaging

RPS 616b

Metastatic malignancies: advanced diagnosis and radiomics data

Moderators:
R. Perez Lopez; Barcelona/ES
N.N.

RPS 616b-1 11:15
Preoperative prediction of peritoneal metastasis in colorectal cancer using a clinical-radiomics model
M. Li, T. T. Tong*; Shanghai/CN (17211230001@fudan.edu.cn)*

Purpose: To establish and validate a combined clinical-radiomics model for preoperative prediction of synchronous peritoneal metastasis (PM) in patients with colorectal cancer (CRC).
Methods and materials: We enrolled 779 patients (585 in the training set and 194 in the validation set) with clinicopathologically confirmed CRC. Significant clinical risk factors were used to build the clinical model. The least absolute shrinkage and selection operator (LASSO) algorithm was adopted to construct a radiomics signature, which included imaging features of the primary lesion and the largest peripheral lymph node, and stepwise logistic regression was applied to select the significant variables to develop the clinical-radiomics model. We used the Akaike information criterion (AIC) and receiver operating characteristic analysis to compare the goodness of fit and the prediction performance of the three models, respectively. An independent validation cohort, containing 139 consecutive patients from February-September 2018 was used to evaluate the performance of the optimal model.

Results: Among the three models, the clinical-radiomics model (AIC=1,043.2) was identified as the optimal model with the minimum AIC value (the clinical-only model: AIC=1,277.7; radiomics-only model: AIC=1,280.5). The clinical-radiomics model also showed good discrimination in both the training cohort (AUC=0.855) and the validation cohort (AUC=0.793).
Conclusion: The present study proposes a clinical-radiomics model created with a CT-based radiomics signature and key clinical features that can potentially be applied in the individual preoperative prediction of PM for CRC patients.
Limitations: The potential sources of bias and limitations of the design.
Ethics committee approval: Our institutional review board (Fudan University Shanghai Cancer Center Medical Ethics Committee) approved this study and waived the need for informed consent from the patients.
Funding: No funding was received for this work.
Author Disclosures:
M. Li: nothing to disclose
T. T. Tong: nothing to disclose

RPS 616b-2 11:21

A comparison of whole-body MRI and 68Ga-DOTATATE PET/CT findings in patients with suspected peritoneal metastases from neuroendocrine tumours

M. P. Engbersen, M. Versleijen, D. M. J. Lambregts, R. G. H. Beets-Tan, M. Tesselaar, M. J. Lahaye*; Amsterdam/NL*

Purpose: To compare whole-body MRI and 68Ga-DOTATATE PET/CT in detecting metastatic lesions from neuroendocrine tumours suspected of peritoneal metastases.
Methods and materials: In this retrospective study, patients that have undergone a whole-body MRI and a 68Ga-DOTATATE PET/CT with suspicion of peritoneal metastases from neuroendocrine origin between 2016-2019 were included. The MRI consisted of diffusion-weighted, T2-weighted, and post-contrast T1-weighted imaging of the thorax, abdomen, and pelvis. The 68Ga-DOTATATE PET/CT acquisitions were made 45 minutes after the intravenous injection of the tracer. To identify all potentially malignant lesions, the MRI images and the PET/CT images were respectively evaluated by an abdominal radiologist and a nuclear medicine physician. The findings were compared for discrepancies.
Results: 16 patients were included and 89 suspicious lesions were identified by either MRI or PET/CT. The median time between imaging modalities was 40 days (range: 1-100 days). On average, MRI and PET/CT identified 31 and 17 peritoneal lesions, 36 and 17 liver lesions, and 6 and 12 suspicious lymph-nodes, respectively. In one patient, diffuse sub-centimetre liver lesions were found that were not visible on PET/CT. The agreement of MRI over all PET/CT positive lesions was 81.2%. The overall agreement between MRI and PET/CT findings was 50.6%. Of all 18 suspected lesions found on MRI under 5 mm, only 3 were detected on PET/CT.
Conclusion: 68Ga-DOTATATE PET/CT is currently the standard staging tool for metastatic neuroendocrine tumours, however, whole-body MRI can detect more small lesions. More research is needed to determine whether detecting more peritoneal and liver metastases with MRI will have clinical implications.
Limitations: The retrospective nature and standard of reference.
Ethics committee approval: n/a
Funding: No funding was received for this work.
Author Disclosures:
M. P. Engbersen: nothing to disclose
M. Versleijen: nothing to disclose
D. M. J. Lambregts: nothing to disclose
R. G. H. Beets-Tan: nothing to disclose
M. Tesselaar: nothing to disclose
M. J. Lahaye: nothing to disclose

RPS 616b-3 11:27

A comparison of diffusion-weighted MRI (DWI) and 68Ga-DOTATATE PET/CT to assess tumour response of liver metastases of primary neuroendocrine tumours (NET) following Yttrium-90 radioembolisation

M. Ingenerf, N. Fink, J. Sauerbeck, H. Ilhan, J. Ricke, C. Schmid-Tannwald*; Munich/DE*

Purpose: To compare ADC values of DWI and SUV of 68Ga-DOTATATE PET/CT in assessing treatment response in patients with hepatic metastases of primary NET undergoing selective internal radiotherapy.
Methods and materials: 30 patients with 80 target liver lesions of primary NET who underwent abdominal MRI with DWI and 68Ga-DOTATATE PET/CT before and after SIRT were included. Tumour size, mean ADC values of the lesions and normal liver parenchyma, intralesional SUVmax and SUV mean, tumour to spleen ratio (T/S ratio), and tumour to liver ratio (T/L ratio) were measured. Tumour response to radioembolisation was classified with respect to response evaluation criteria in solid tumours v1.1 (RECIST) on a follow-up examination.
Results: 67/80 metastases were categorised as stable disease (SD) and 13/80 metastases as partial remission (PR). Intralesional ADCmin and ADCmean increased significantly ($p<0.006$) after SIRT in the group of PR and SD, with a significantly higher increase of ADCmin values in the PR group (54.1±14.6% vs 24±4.9%, $p=0.02$). Currently used SUV measurements showed a significant decrease in the PR group (SUVmax, SUVmean, T/S ratio, and T/L ratio), while in the SD group, only SUVmax, SUVmean, and T/S ratio (max/max) decreased significantly. Using ROC curves, SUVmean was found as the best metric (AUC 0.75), however, similar results were obtained for ADCmin (AUC 0.7).
Conclusion: DW-MRI may be used as an alternative to 68Ga-DOTATATE PET/CT for quantitative response assessment in patients with hepatic metastases of NET following SIRT and may represent a valuable functional marker to guide the further management of these patients.
Limitations: A retrospective study.
Ethics committee approval: Approval was obtained from the LMU ethics commission. Written informed consent was waived due to fully (irreversible) anonymised data.
Funding: No funding was received for this work.
Author Disclosures:
M. Ingenerf: nothing to disclose
C. Schmid-Tannwald: nothing to disclose
H. Ilhan: nothing to disclose
N. Fink: nothing to disclose
J. Ricke: nothing to disclose
J. Sauerbeck: nothing to disclose

RPS 616b-4 11:33

Predicting the response of individual liver metastases with radiomics in HER2 amplified patients undergoing dual-targeted therapy

G. Cappello, V. Giannini, A. Defeudis, S. Mazzetti, L. Vassallo, D. Regge*; Candiolo/IT (giovanni.cappello@ircc.it)*

Purpose: To validate a machine learning algorithm to predict the response of individual liver metastases (LM) in heavily pretreated HER2 amplified metastatic colorectal cancer (mCRC) patients undergoing dual-target therapy within a phase II clinical study.
Methods and materials: 38 patients with amplified HER2 mCRC enrolled in the multicentre HERACLES trial (NCT03225937) were randomly divided into a training set (28 patients) and a validation set (10 patients). All received anti-HER2 treatment (trastuzumab plus lapatinib) and underwent CT examination every 8 weeks until disease progression. The largest diameter of each LM was measured before and after 3 months of treatment to classify metastases in responders (R+) and non-responders (R-). All LM with a diameter >10 mm were manually contoured on the baseline and 24 texture features were extracted. After selecting the most discriminative features using a genetic algorithm, a Gaussian Naïve Bayes classifier was trained on the training set and applied to the validation dataset.
Results: The dataset was composed of 141 metastases: 108 (75R+, 33R-) in the training set and 33 (21R+, 12R-) in the validation set. The classifier reached a sensitivity, specificity, PPV, and NPV of 89%, 85%, 93%, and 78% for the training set and 90%, 42%, 73%, and 71% for the validation set, respectively. Difference variance and homogeneity were the two most important radiomics features in our model.
Conclusion: Our study demonstrated the feasibility of developing a radiomics model able to predict the likelihood of response of individual LM in patients with HER+ mCRC undergoing dual-target therapy.
Limitations: The low number of lesions in the validation dataset, low specificity, especially in the validation dataset, and the manual segmentation with consequent interobserver variability.
Ethics committee approval: Ethics committee approval obtained.
Funding: AIRC 5x1000 2018-ID.21091, AIRCx1000-ID 9970, and contribution from F Hoffmann-La Roche.
Author Disclosures:
G. Cappello: nothing to disclose
V. Giannini: nothing to disclose
A. Defeudis: nothing to disclose
S. Mazzetti: nothing to disclose
L. Vassallo: nothing to disclose
D. Regge: nothing to disclose

RPS 616b-5 11:39

The value of apparent diffusion coefficients (ADC) to assess the response of hepatic metastases of primary neuroendocrine tumours (NET) undergoing selective internal radiotherapy with 90Yttrium-microspheres

M. Ingenerf, N. Fink, J. Sauerbeck, H. Ilhan, J. Ricke, C. Schmid-Tannwald*; Munich/DE*

Purpose: To evaluate the role of diffusion-weighted imaging (DWI) with ADC measurements in the assessment of tumour response in patients with liver metastases of primary NET undergoing Yttrium-90 radioembolisation.
Methods and materials: 43 patients with hepatic metastases of primary NET who underwent abdominal MRI with DWI 39±28 days before and 74±46 days after SIRT were included. Tumour size, intralesional minimal, and maximal and mean ADC (ADCmin, ADCmax, and ADCmean, respectively) were measured for a maximal 3 target lesions per patient on pre- and post-interventional DWI by two readers independently. The tumour response to radioembolisation was classified corresponding to response evaluation criteria in solid tumours v1.1 (RECIST) on a follow-up examination.
Results: A total of 120 metastases with a mean pre-interventional diameter of 3.04 cm±1.59was analysed. 27/120 target lesions were categorised as partial remission (PR), 87/120 lesions as stable disease (SD), and 6 lesions as progressive disease (PD). After radioembolisation, ADC values (ADC min, max, and mean) increased significantly ($p<0.005$) in the group of PR and SD, whereas there was no significant change of ADC values in the group of PD. Between the group of PR and PD, a significant difference in the percentage change of ADCmean (61% vs 11%, respectively, $p<0.05$) was found before and after SIRT.
Conclusion: ADC values, especially ADCmean changes on DWI, appear to represent a valuable quantitative marker to assess the response of hepatic metastases of primary NET beyond morphologic changes and may help in assessing further therapeutic strategies of patients who undergo SIRT.
Limitations: A retrospective study.
Ethics committee approval: Approval was obtained by the LMU ethics commission. Written informed consent was waived due to fully (irreversible) anonymised data.
Funding: No funding was received for this work.
Author Disclosures:
M. Ingenerf: nothing to disclose
N. Fink: nothing to disclose
H. Ilhan: nothing to disclose
J. Ricke: nothing to disclose
C. Schmid-Tannwald: nothing to disclose
J. Sauerbeck: nothing to disclose

RPS 616b-6 11:45

The impact of inter-reader contouring variability on textural radiomics of CRC liver metastases

F. Rizzetto[1], C. de Mattia[2], F. Calderoni[2], L. Vassallo[3], V. Giannini[4], A. Defeudis[4], D. Regge[4], A. Torresin[2], A. Vanzulli[5]; *[1]Rho/IT, [2]Milan/IT, [3]Monasterolo di Savigliano/IT, [4]Candiolo/IT, [5]Segrate/IT (Francesco.rizzetto@studenti.unimi.it)*

Purpose: Radiomics is actually at the forefront of precision medicine, but to fully develop it requires multicentre collaboration. In this context, the impact of inter-reader contouring variability on radiomics features (RFs) must be evaluated.
Methods and materials: The liver metastases (n=70) from colorectal cancers were segmented on CT scans by two readers. RFs from grey-level co-occurrence and run-length matrices were extracted from the whole-lesion volume (3D ROIs) and from the largest cross-section (2D ROIs) for each metastasis. Inter-reader contouring variability was evaluated with the Dice coefficient (DC) and Hausdorff distance (HD), while its impact on RFs was assessed using the mean relative discrepancy and intraclass correlation coefficient (ICC). For the main lesion of each patient, one reader also delineated circular ROIs in the same slice of the 2D ROIs.
Results: According to the similarity indices, the best inter-reader contouring agreement was observed for 2D ROIs (mean DC: 0.83±0.09; mean HD: 0.25±0.18). Comparing RFs values, the mean relative discrepancy was lower from 2D than 3D ROIs for 24/32 (75%) RFs, ranging from 0.04%-1,567% and from 0.02%-752%, respectively. Correspondingly, an ICC >0.9 was observed for more RFs from 2D ROIs (53%) than from 3D ones (34%). The variability between 2D and circular ROIs was equal or lower than inter-reader variability for 94% of RFs.
Conclusion: As automatic segmentation tools are currently lacking, a careful selection of the contouring methods is required to minimise differences in the results of texture analysis. 2D contouring seems to reduce this variability but it could be less informative than a whole-lesion analysis.
Limitations: The choice of different preprocessing parameters could impact on the results.
Ethics committee approval: All patients signed informed consent.
Funding: Supported by a grant from AIRC 5 x mille.
Author Disclosures:
F. Rizzetto: nothing to disclose
F. Calderoni: nothing to disclose
C. de Mattia: nothing to disclose
A. Torresin: nothing to disclose
V. Giannini: nothing to disclose
A. Defeudis: nothing to disclose
L. Vassallo: nothing to disclose
D. Regge: nothing to disclose
A. Vanzulli: nothing to disclose

RPS 616b-7 11:51

Baseline clinical and imaging predictors of treatment response and overall survival of patients with metastatic melanoma undergoing immunotherapy

A. E. E. Othman, A. Schraag, S. Afat, T. Eigentler, B. Klumpp; *Tübingen/DE*

Purpose: To identify predictive clinical and CT imaging biomarkers and assess their predictive capacity regarding overall survival (OS) and treatment response in patients with metastatic melanoma undergoing immunotherapy.
Methods and materials: 103 patients with immunotherapy for metastatic melanoma were randomly divided into a training (n=69) and validation cohort (n=34). Baseline tumour markers (LDH, S100B), baseline CT imaging biomarkers (tumour burden and Choi density), and CT texture parameters (entropy, kurtosis, skewness, uniformity, MPP, and UPP) of the largest target lesion were extracted. To identify treatment response predictors, binary logistic regression analysis was performed in the training cohort and tested in the validation cohort. For OS, Cox regression and Kaplan Maier analyses were performed in the training cohort. Bivariate and multivariate models were established. The goodness of fit was assessed with Harrell's C-index. Potential predictors were tested in the validation cohort also using Cox-regression and Kaplan-Meier analyses.
Results: Baseline S100B (hazard ratio (HR)=2.543, p=0.018), tumour burden (HR=1.657, p=0.002), and kurtosis (HR=2.484, $p<0.001$) were independent predictors of OS and were confirmed in the validation cohort ($p<0.048$). Tumour burden and kurtosis showed incremental predictive capacity, allowing a good predictive model when combined with baseline S100B levels (C-index=0.720). Only S100B was predictive of treatment response (OR=0.630, p=0.022). Imaging biomarkers did not predict treatment response.
Conclusion: We identified easily obtainable baseline clinical (S100B) and CT predictors (tumour burden and kurtosis) of OS in patients with metastatic melanoma undergoing immunotherapy. However, imaging predictors did not predict treatment response.
Limitations: A retrospective, single-centre predictive study.
Ethics committee approval: The institutional ethics committee of the university hospital approved this retrospective study and waived informed patient consent.
Funding: No funding was received for this work.
Author Disclosures:
A. E. E. Othman: nothing to disclose
A. Schraag: nothing to disclose
S. Afat: nothing to disclose
T. Eigentler: nothing to disclose
B. Klumpp: nothing to disclose

RPS 616b-8 11:57

Changes in tumour heterogeneity with tyrosine kinase inhibitor therapy in metastatic renal cell carcinoma: preliminary results from the STAR trial

A. Azam[1], A. Jahangeer[1], L. Gervais-Andre[1], C. Kelly-Morland[1], M. M. Siddique[1], G. Cook[1], F. Collinson[2], V. Goh[1], J. Brown[2]; *[1]London/UK, [2]Leeds/UK (aishah2018@hotmail.co.uk)*

Purpose: Quantification of tumour heterogeneity potentially captures anti-vascular treatment effects beyond mean attenuation and size change during anti-angiogenic drug therapy. We aimed to assess global and locoregional heterogeneity changes during tyrosine kinase inhibitor therapy in metastatic renal cell carcinoma patients within the multicentre STAR trial.
Methods and materials: 59 prospective adults (54 male; mean age 67.5±7.0) with 108 lesions underwent arterial-phase contrast-enhanced CT prior to (T0) and 3 months after treatment (T1). Volumetric regions-of-interest were delineated for the same lesions (5 maximum) at each time point. 183 radiomic features (including surface, shape, fractal, histogram, and second and high-order features) were derived using validated in-house software. Highly correlated features ($r>0.80$) were excluded prior to further analysis. Changes on treatment were compared using the Wilcoxon signed-rank test (correcting for multiple comparisons, $p<0.0025$).

Results: Accompanying a tumour volume decrease on treatment (100.22 cm^3 vs 74.77 cm^3, p<0.001), global tumour attenuation also decreased (41.6 vs 38.2, p<0.001) while negative skewness improved (-1.4 vs -0.94, p<0.001) in keeping with lower vascularisation. Additionally, locoregional GLCM contrast (37.89 vs 48.77, p<0.001), GLSZM intensity variability (0.003 vs 0.004, p<0.001), and GLTDM texture strength (2.52 vs 3.78, p<0.001) increased. GLRL long-run high-grey-level emphasis (1,857 vs 1,611, p<0.001) decreased, indicating greater local texture variation and higher texture visibility and granularity.
Conclusion: Following tyrosine kinase inhibitor therapy, a global reduction in tumour attenuation and negative skewness during the arterial phase is accompanied by increasing locoregional variability capturing the spatial heterogeneity of therapy anti-vascular effects.
Limitations: The small sample and heterogeneity in CT parameters.
Ethics committee approval: Ethical board approval and informed consent - NRES Committee REC ref: 11/NW/0246.
Funding: The National Institute for Health Research Health Technology Assessment Programme (project number 09/91/21).
Author Disclosures:
C. Kelly-Morland: nothing to disclose
A. Azam: nothing to disclose
A. Jahangeer: nothing to disclose
L. Gervais-Andre: nothing to disclose
M. M. Siddique: nothing to disclose
G. Cook: nothing to disclose
F. Collinson: nothing to disclose
V. Goh: nothing to disclose
J. Brown: nothing to disclose

RPS 616b-9 12:03
Patterns of progression under immunotherapy in metastatic kidney cancer
S. Mezghani[1], B. Rance[2], A. Simonaggio[2], J. Deidier[2], A. Bellucci[3], M. Florin[2], S. Oudard[2], Y. Vano[2], L. Fournier[2]; *[1]Boulogne-Billancourt/FR, [2]Paris/FR, [3]Issy Les Moulineaux/FR (sarah.mezghani@gmail.com)*

Purpose: To determine patterns of progression or pseudoprogression in patients with mRCC treated by immunotherapy.
Methods and materials: A retrospective monocentric ethics committee-approved study included patients with mRCC treated by immunotherapy between January 2013-January 2019 for which all the imaging history was available on our PACS. Tumour response was evaluated using RECIST 1.1 and iRECIST criteria. The numbers of responders and pseudoprogression were collected. Patterns of unconfirmed progression (iUPD) and confirmed progression (iCPD) were analysed.
Results: 96 patients met the inclusion criteria. The median follow-up was 13 months. Only 4/96 pseudoprogressions were observed during follow-up. Including pseudoprogressions, 34/96 (35%) patients were responders. 55/96 (57%) patients progressed according to RECIST, with a median PFS of 2.6 months. Progression was confirmed according to iRECIST in 18/22 (82%) cases during the next follow-up, 4/22 (18%) cases after 2 follow-ups. In 3/33 (9%) cases, patients remained iUPD and continued immunotherapy with a clinical benefit despite RECIST progression. 7/96 (7%) patients were lost to follow-up. There was no preferential organ in which response, pseudoprogression, unconfirmed, or confirmed progression occurred.
Conclusion: Pseudoprogressions seem rare in mRCC under immunotherapy. However, some patients do not confirm progression immediately, or at all, and may benefit from continuing therapy beyond RECIST progression.
Limitations: A retrospective monocentric study.
Ethics committee approval: Ethics committee approval was obtained.
Funding: No funding was received for this work.
Author Disclosures:
S. Mezghani: nothing to disclose
B. Rance: nothing to disclose
A. Simonaggio: nothing to disclose
J. Deidier: nothing to disclose
A. Bellucci: nothing to disclose
M. Florin: nothing to disclose
S. Oudard: nothing to disclose
Y. Vano: nothing to disclose
L. Fournier: nothing to disclose

RPS 616b-10 12:09
Diagnostic performance of trimodality imaging follow-up in bladder cancer patients treated with preservation therapy
S. Ahmed; *Assiut/EG (shimaaabdalla@aun.edu.eg)*

Purpose: To evaluate the diagnostic accuracy of abdominopelvic ultrasound (US), virtual cystoscopy (VC), and MRI diffusion (MRI DWI) compared to conventional cystoscopy (CC) in the diagnosis of bladder lesions after transurethral resection (TURT).
Methods and materials: 45 patients with a history of high-grade T1 or T2-T4a bladder cancer who underwent TURT and received chemoradiation schedule were included. They were followed-up on the basis of serial cystoscopies. Before each cystoscopy, the patients underwent bladder ultrasound, CT-based virtual cystoscopy, and diffusion-weighted MRI. The results of these 3 non-invasive modalities were compared with those of cystoscopy and with histological findings obtained by (repeat) transurethral resection. Sensitivity, specificity, positive and negative predictive values, and accuracy were calculated and compared to CC and histopathology as a gold standard.
Results: After a median 24 month follow-up, US, CT VC, and MRI DWI detected 23, 28, and 29 lesions respectively of the 30 lesions detected at CC. There was pathology-confirmed local recurrence in 18 lesions (40%) and benign changes in 12 lesions (27%), while the remaining 15 patients were negative. 18 lesions (60 %) were larger than 1 cm and 23 lesions showed polypoidal morphology (77 %). The accuracy of US, CT VC, and MRI DWI in the diagnosis of bladder lesions were 73%, 93%, and 93%, respectively (P>0.10).
Conclusion: Imaging surveillance in bladder cancer preservation should include MRI DWI as part of the surveillance programme to reduce the frequency of cystoscopy. MRI and CT VC were of comparable accuracy and US had the lowest sensitivity, however, it is still can be used as the first step of surveillance.
Limitations: The lack of standardisation of the time interval among the studied imaging modalities.
Ethics committee approval: The study protocol was approved by the local institutional review board (IRB: IORG0006563).
Funding: No funding was received for this work.
Author Disclosures:
S. Ahmed: nothing to disclose

RPS 616b-11 12:15
Whole-body MRI: a 'one-stop-shop' for staging high-risk prostate cancer?
N. Ali[1], P. Charters[1], N. Burns-Cox[2], P. Burn[2]; *[1]Bristol/UK, [2]Taunton/UK (noorali@doctors.org.uk)*

Purpose: To determine if whole-body MRI (WBMRI) has a role as a single imaging test for patients with newly diagnosed prostate cancer with a high risk of metastatic disease.
Methods and materials: Patients newly presenting with serum prostatic specific antigen (PSA) of ≥50 ng/mL who had undergone WBMRI as part of clinical staging were assessed retrospectively. For each scan, the nodal and metastatic status were recorded. In addition, tumour conspicuities (lesion ADC to background gland ADC) within the prostate were recorded and compared with tumour conspicuities on contemporaneous dedicated prostate MRIs (in patients in whom both tests were performed).
Results: 50 patients were assessed, with a serum PSA range of 50-4,751 ng/mL (median 150 ng/mL). 68% (35/50) of patients had metastases on WBMRI (15/50 bone only, 3/50 lymph node only, and 16/50 both bone and lymph node metastases). Of patients with serum PSA ≥100 ng/mL, 87% (26/30) had metastases. The primary prostate tumour was positively identified in all cases. 20/50 patients had both prostate MRI and WBMRI; for these, reciprocal of the ratio of the mean prostate tumour ADC to the mean background gland ADC for prostate MRI was 2.0 (range 1.2-3.1) compared to 1.7 for WBMRI (range 1.2-2.3).
Conclusion: In patients with PSA ≥50, WBMRI identified metastases in a high proportion of patients. Lesion conspicuity within the prostate gland was found to be relatively similar to that on dedicated prostate MRI. WBMRI may, therefore, have a 'one-stop-shop' role in selected high-risk patients for both directing the targeted biopsy of the prostate tumour and for the staging of metastatic disease.
Limitations: A restrospective study with small numbers.
Ethics committee approval: n/a
Funding: No funding was received for this work.
Author Disclosures:
N. Ali: nothing to disclose
P. Burn: nothing to disclose
P. Charters: nothing to disclose
N. Burns-Cox: nothing to disclose

RPS 616b-12 12:21
The role of PET-CT with 18F-FDG in the initial assessment of patients with carcinoma of an unknown primary origin (CUP)
S. Yaremenko, N. Rucheva, V. E. Sinitsyn; *Moscow/RU (yaremenkosa@yandex.ru)*

Purpose: To assess the effectiveness of PET-CT with 18-fluorodeoxyglucose (FDG) in patients with carcinoma of an unknown primary origin (CUP).
Methods and materials: 187 patients diagnosed with CUP were included in the single-centre retrospective study from September 2018-March 2019: m/f ratio was 123/64 (65.8%/34.2%) and the mean age of patients was 61.9±7.5 years. All patients had a biopsy of at least one metastatic lesion and the malignant

nature of the neoplasm was histologically verified. The standard oncological evaluation (including body CT) done before the PET/CT failed to detect the primary tumour.
Results: Among 187 patients included in the study, the biopsy-proven histological diagnoses were squamous cell cancer (n=87, 46.5%), melanoma (n=15, 8%), undifferentiated carcinoma (n=45, 24.1%), adenocarcinoma (n=23, 12.3%), and undifferentiated malignant neoplasm (n=17, 9.1%). After PET-CT, the primary tumour was detected in 93 (49.7%) patients. New metastatic lesions were revealed in 93 (49.7%) patients. Re-classification of the TNM stage after PET/CT was recorded in 131 (70.1%) cases. TNM stage reclassification was significantly more often observed in patients with an identified primary tumour (100%) compared to the group with an unknown location of the primary tumour (40.4%, p<0.01).
Conclusion: PET-CT with 18F-FDG allows the performance of significantly more accurate diagnostic workup and tumour staging in the majority of patients with CUP. PET-CT with 18F-FDG is an essential part of the diagnostic protocol in patients with CUP.
Limitations: A single-centre study.
Ethics committee approval: The study was approved by the local ethics committee.
Funding: No funding was received for this work.
Author Disclosures:
S. Yaremenko: Author at Lomonosov State University Faculty of Medicine
N. Rucheva: Author at Lomonosov State University Faculty of Medicine
V. E. Sinitsyn: Author at Lomonosov State University Faculty of Medicine

11:15 - 12:30 **Room E**

Breast

RPS 602b

High-risk situations in breast cancer

Moderators:
M. A. Lúðvíksson; Reykjavik/IS
S. Sauer; Würzburg/DE

RPS 602b-1 11:15

Identification of women at high risk of breast cancer and in need of supplementary screening

M. Eriksson[1], K. Czene[1], S. Zackrisson[2], P. Hall[1]; [1]Stockholm/SE, [2]Malmö/SE (mikael.eriksson@ki.se)

Purpose: Mammography screening reduces breast cancer mortality but a large proportion of breast cancers are missed and detected at later stages, or develop in between screening intervals. We developed the KARMA model, taking the risk of breast cancer into consideration. This model identifies women who are likely to be diagnosed with breast cancer before or at the next screen.
Methods and materials: The study was based on the KARMA cohort, a prospective screening cohort including 70,877 participants. We identified 974 incident cancers and sampled 9,376 healthy individuals from the cohort. Risk scores were developed using mammographic features (density, masses, microcalcifications) and their asymmetry, age, menopausal status, family history of breast cancer, body-mass index, hormone replacement therapy, tobacco and alcohol, and a polygenic risk score including 313 SNPs. The KARMA score was developed from the risk scores using age stratified logistic regression.
Results: The full model reached an area under the curve of 0.77 (95% CI 0.76, 0.79) with good model fit (Hosmer-Lemeshow = 0.2). There was an 8-fold difference in risk between the 8% of women at high risk and at general risk. Women identified as high risk were more likely to be diagnosed with more aggressive cancers. The image-based model was validated in two independent cohorts.
Conclusion: By combining mammographic features, lifestyle factors, family history, and a polygenic risk score, we generated a model that identifies women with a high likelihood of being diagnosed with breast cancer within two years and in need of supplementary screening.
Limitations: Limited to model 1 validation.
Ethics committee approval: Karolinska Institutet dnr 2010/958-31/1, 2016/2600-31. Lund dnr 2009/770.
Funding: Märit and Hans Rausing's Initiative Against Breast Cancer. The Kamprad Foundation.
Author Disclosures:
M. Eriksson: nothing to disclose
K. Czene: nothing to disclose
P. Hall: nothing to disclose
S. Zackrisson: nothing to disclose

RPS 602b-2 11:21

Comparing contrast-enhanced spectral mammography with breast MRI in high and intermediate risk women: preliminary results

V. Pasqualino, G. Gennaro, A. Pittaro, E. Baldan, E. Bezzon, I. Polico, F. Caumo; *Padua/IT (vincenzopasqualino@gmail.com)*

Purpose: To compare contrast-enhanced spectral mammography (CESM) with breast MRI and in a women population at high and intermediate risk of developing breast cancer.
Methods and materials: 59 women at high and intermediate risk for breast cancer, aged above 35 years, without known allergies to iodine and gadolinium contrast-agents, were prospectively recruited. CESM and MRI were performed with a minimum 72-hour interval to avoid nephrotoxicity. CESM images were evaluated independently by two breast radiologists, while MRI studies were interpreted by two different independent breast radiologists. Background parenchymal enhancement (BPE) and breast density (BD) were scored in 4 classes, while possible lesions were classified according to BIRADS scale. Sensitivity, specificity, positive-predictive-value (PPV), and negative-predictive-value (NPV) were compared by modality, and inter- and intra-modality agreement evaluated.
Results: Sensitivity was 100% for both modalities, while specificity was 81.1% with CESM and 71.6% with MRI. PPV was 76.6% with CESM and 66.4% with MRI, while NPV was 100% for both modalities. Neither specificity nor NPV differences were significant. The agreement for BPE and BD was from good to excellent for both modalities. The agreement between CESM and MRI for BPE was fair (k=0.34), probably due to the different phase of the ovarian cycle at the time of the two examinations.
Conclusion: CESM showed the same sensitivity as MRI, with some benefits in terms of specificity, even if not significant.
Limitations: Small sample size (preliminary results). BPE inter-modality disagreement likely influenced by the possible different phase of the ovarian cycle at the time of examinations.
Ethics committee approval: Study approved by the IRB. Patient informed consent collected.
Funding: Research project.
Author Disclosures:
V. Pasqualino: nothing to disclose
G. Gennaro: nothing to disclose
A. Pittaro: nothing to disclose
E. Baldan: nothing to disclose
E. Bezzon: nothing to disclose
I. Polico: nothing to disclose
F. Caumo: nothing to disclose

RPS 602b-3 11:27

Radiation dose with contrast-enhanced spectral mammography as a screening test for high and intermediate risk population

G. Gennaro, V. Pasqualino, E. Baldan, E. Bezzon, A. Pittaro, F. Caumo; *Padua/IT (gisella.gennaro@iov.veneto.it)*

Purpose: To estimate the amount of radiation dose associated with contrast-enhanced spectral mammography (CESM).
Methods and materials: CESM is a dual-energy technique consisting in the sequential acquisition of two images, one at low-energy, equivalent to a standard mammogram, and the second at higher energy, both after the injection of iodine contrast agent. The two paired images are recombined to provide a "subtraction" image where possible lesions are contrast-enhanced. CESM was used within a clinical study comparing the clinical performance of CESM and breast MRI for the screening of women at high and intermediate risk of breast cancer. Patients enrolled in the study underwent both bilateral CESM in two views and breast MRI. Dosimetric data from the first 60 CESM examinations (486 images) was extracted from the DICOM header of all low- and high-energy image pairs acquired for each patient. Mean glandular dose (MGD) per-view was compared between low- and high-energy images and the increase in MGD compared to standard mammography was calculated.
Results: The mean compressed breast thickness was 50.8±15.8 mm. The average total MGD per view was 2.22±0.44 mGy; 70% due to the low-energy image, 1.53±0.42 mGy, obtained with the same exposure parameters as for a standard mammogram, while the remaining 30% of the dose, 0.70±0.07 mGy, was due to the high-energy image. Compared to standard mammography, the mean dose increase associated with CESM was 48%. For any breast thickness per-view, CESM dose was either within or below MGD limiting values established for both standard mammography and tomosynthesis.
Conclusion: The modest increase in radiation dose by CESM should not be an obstacle for its use as a screening test for women at high and intermediate risk of breast cancer.
Limitations: Relatively small sample size.
Ethics committee approval: Study approved by the Institutional Ethics Committee.
Funding: Regional Healthcare System.

Author Disclosures:
G. Gennaro: nothing to disclose
V. Pasqualino: nothing to disclose
E. Baldan: nothing to disclose
E. Bezzon: nothing to disclose
A. Pittaro: nothing to disclose
F. Caumo: nothing to disclose

RPS 602b-4 11:33
Effect of BPE on cancer detection in MRI-guided biopsies for high-risk lesions distinguished only on MRI
K. Sirkovich[1], T. Arazi-Kleinman[2], G. Bar On[3]; [1]Holon/IL, [2]Zeriffin/IL, [3]Natanya/IL (kserkovich@hotmail.com)

Purpose: To evaluate the effect of background parenchymal enhancement (BPE) on cancer detection in patients undergoing magnetic resonance imaging (MRI)-guided biopsy for lesions that were perceived on MRI but were not appreciated on other modalities, such as mammography (MG) or ultrasound (US).
Methods and materials: An analysis of 145 MRI-guided biopsies for high-risk lesions on MRI that were not visible on MG or US was conducted. The procedures were performed in Wolfson Medical Center by two experienced breast radiology specialists from January 2017 to December 2018 and recorded retrospectively. BPE was evaluated on the latest MRI examination for each patient. Pathology was compared between women, low BPE (mild or minimal) to high BPE (moderate to marked), by using Fisher's exact test.
Results: Of 145 MRI guided biopsies, 126 were classified with low BPE and 19 were classified with high BPE (87% vs. 13%, P>0.999). In the low BPE group, 74 biopsies confirmed a malignant process, while 52 were benign (59% vs. 41%, P>0.999). In the high BPE group, 11 biopsies confirmed a malignant process, while 8 were benign (58% vs. 42%, P>0.999).
Conclusion: Different BPE levels had no significant impact on rates of breast cancer in MRI-guided biopsy for high-risk lesions detected only on MRI.
Limitations: Larger samples are needed.
Ethics committee approval: n/a
Funding: No funding was received for this work.
Author Disclosures:
K. Sirkovich: nothing to disclose
T. Arazi-Kleinman: nothing to disclose
G. Bar On: nothing to disclose

RPS 602b-5 11:39
Six-month interval screening with mammography and ultrasound in BRCA mutation carriers who undergo annual MRI: does it improve cancer detection?
B. Musaiev, K. A. Musaieva, D. L. Kaduri, E. Carmon, T. Sella; Jerusalem/IL (tamarse@hadassah.org.il)

Purpose: Alternating breast cancer screening for patients with the highest risk suggests performing annual MRI and annual mammography (MG) and/or ultrasound (US) at 6-month intervals. The purpose of this study was to evaluate the supplemental benefit of 6-month interval MG/US in patients who undergo this alternating screening.
Methods and materials: We retrospectively reviewed MG, US, and MRI screening images and clinical charts of 177 women with known BRCA mutations. The study group included 83 women (age 26-70, mean 42) who underwent between 2-12 annual rounds of alternating screening for a total of 380 rounds (mean 8.5).
The control group was compromised of 94 women (age 25-67, mean 44) with between 5-14 annual rounds of MR only screening for a total of 646 rounds (mean 7.5).
Results: Overall, 14 cancers were detected among the 177 women (7.9%), 6/83 women in the study group (7.2%) and 8/94 women in the control group (8.5%).
Two malignancies were clinically missed on MRI and diagnosed on 6-month interval MG/US, however, on retrospective blinded review by an expert radiologist, both were detected on 6-month prior MRI, hence, all malignancies were initially present on MRI.
Amongst the study group, 39 findings were referred for biopsy with 6 cancers diagnosed (15%), 4 based on MR findings, 1 on US, and 1 on MG. 33 benign biopsies (85%) were performed, 20 detected on MR, 12 on US, and 1 on MG.
A total of 29 biopsies were performed in the MR only control group with 8 yielding malignancy (27.5%) and 21 benign (72.5%).
Conclusion: Six-month interval MG/US screening in BRCA woman undergoing annual MR screening did not add to cancer detection, while increasing the rate of FP benign biopsies.
Limitations: A retrospective study.
Ethics committee approval: Informed consent was waived.
Funding: No funding was received for this work.
Author Disclosures:
T. Sella: nothing to disclose
B. Musaiev: nothing to disclose
K. A. Musaieva: nothing to disclose
E. Carmon: nothing to disclose
D. L. Kaduri: nothing to disclose

RPS 602b-6 11:45
Surveillance scheme after risk-reducing mastectomy in BRCA1 BRCA2 mutation carriers: to screen or not to screen?
N. Kanana[1], M. Sklair-Levy[1], E. Friedman[2], E. Klang[1], Y. Yagil[3], A. Shalmon[1], M. Gotlieb[1], D. Madorsky Feldman[1], M. A.Ban David[1]; [1]Ramat Gan/IL, [2]Tel Aviv/IL, [3]Herzliya/IL (Nayruz.Knaana@sheba.health.gov.il)

Purpose: To assess the rate of breast cancer diagnosis in BRCA mutation carriers after bilateral mastectomy and the need for ongoing MRI surveillance.
Methods and materials: This retrospective study focused on Jewish female carriers of pathogenic BRCA1 or BRCA2 mutation who underwent bilateral mastectomy at BC diagnosis. All participants underwent breast imaging (MRI alternating with US at 6-12 month intervals) after mastectomy. Data on subsequent BC diagnosis and timing and the diagnostic breast imaging modality were collected, and BC recurrence rates were calculated.
Results: Overall, 189 female mutation carriers (133 BRCA1, 45 BRCA2, 5 both BRCA genes, 6 unknown) with BC underwent mastectomy between April 1, 2009, and August 31, 2018. During a mean follow-up of 6.1±4.2 years, 13 (6.9%) were diagnosed with BC: 12 ipsilateral BC (range from surgery 0.4-28.8 years) and 1 contralateral BC (15.9 years from risk-reducing surgery RRS). Notably, clinical suspicion of BC diagnosis was prompted by palpation (6, 46%), imaging surveillance (5, 38%; 4 MRI, 1 US), tumour markers (1, 8%), and, in one case, unknown.
Conclusion: BRCA1/2 mutation carriers who undergo RRS (risk-reducing surgery) after BC diagnosis should be considered for ongoing breast imaging surveillance.
Limitations: A retrospective study conducted in one institute in carriers of a limited spectrum of BRCA1/2 mutations with different surgical approaches performed by several surgical teams. Although follow-up encompassed a fair amount of women of different ages, the total number of women with post risk-reducing surgery cancer diagnosis was relatively limited.
Ethics committee approval: The Institutional Review Board approved the study. The need for a specific informed consent was waived by the Sheba Ethics committee.
Funding: No funding was received for this work.
Author Disclosures:
M. A.Ban David: nothing to disclose
M. Gotlieb: nothing to disclose
N. Kanana: nothing to disclose
M. Sklair-Levy: nothing to disclose
E. Klang: nothing to disclose
E. Friedman: nothing to disclose
Y. Yagil: nothing to disclose
A. Shalmon: nothing to disclose
D. Madorsky Feldman: nothing to disclose

RPS 602b-7 11:51
Ductal carcinoma in situ as seen on MRI in BRCA mutation carriers
R. Faermann, M. Brodsky, J. Weidenfeld, O. Halshtok, A. Shalmon, M. Gotlieb, Y. Yagil, M. Sklair-Levy; Ramat Gan/IL (rfaermann@gmail.com)

Purpose: Recent studies have shown that BRCA mutation carriers are prone to earlier onset of DCIS and invasive breast cancer with a higher prevalence of DCIS in BRCA carriers than non-carriers. Most of BRCA-associated tumours have DCIS present, favouring the existence of a premalignant pathway. However, DCIS in those studies was diagnosed with mammography (calcifications).
MRI screening has become an important tool for screening and early detection in BRCA carriers. MRI can detect DCIS even if non-calcified on mammography. The aim of our study was to analyse BRCA patients with DCIS on MRI biopsy and the MRI presentation.
Methods and materials: A retrospective study of BRCA patients with pure DCIS diagnosed with MRI biopsy between 2015 until 2019 at the Sheba Medical Center. All MRI and mammography studies were analysed by a fellowship-trained radiologist.
Results: 950 BRCA carriers underwent surveillance MRI. 22 had a diagnosis of DCIS on MRI biopsy. 14 patients (64%) were BRCA1 carriers, while 8 patients (36%) were BRCA2 carriers. The median age of BRCA1 patients was 40 years old, which was lower than of BRCA2 patients (66 years old) (p<.05). The most common MRI presentation was non-mass enhancement. BRCA 1 patients were more commonly hormone receptors negative (9 patients, 64%) and had high-grade DCIS (100%), while BRCA2 patients were more commonly hormone

receptors positive (5 patients, 63%) and had more commonly intermediate grade DCIS (5 patients, 63%).
Conclusion: MRI detected non-calcified DCIS is more common in BRCA1 gene-mutation carriers and presents earlier than in BRCA2 patients, usually as a high-grade disease. This finding is opposite to calcified DCIS detected on mammography, which is more common in BRCA2 carriers.
Limitations: Single-centre only, retrospective study.
Ethics committee approval: n/a
Funding: No funding was received for this work.
Author Disclosures:
R. Faermann: nothing to disclose
M. Sklair-Levy: nothing to disclose
A. Shalmon: nothing to disclose
O. Halshtok: nothing to disclose
M. Brodsky: nothing to disclose
M. Gotlieb: nothing to disclose
Y. Yagil: nothing to disclose
J. Weidenfeld: nothing to disclose

RPS 602b-8 11:57
Association of the differences in average glandular dose with breast cancer risk
L. Ma, X. Lin, G. Qin, Y. Cai, W. Chen*; Guangzhou/CN*
(male2@mail2.sysu.edu.cn)

Purpose: To compare the differences in average glandular dose (AGD) between both breasts of healthy subjects and those of breast cancer patients, and to investigate if the AGD difference is associated with breast cancer risk and improves breast cancer classification.
Methods and materials: The craniocaudal-view and mediolateral-view full-field digital mammography (FFDM) images from 1,005 healthy subjects whose both breasts were BI-RADS categorised as I or II and 475 biopsy-confirmed unilateral breast cancer patients whose breast at the contralateral side was category I or II were collected. Both two populations were randomised into training and test sets. Multivariate logistic regression analysis was used to build the breast cancer risk assessment model and the area under the receiver operating characteristic curve (A_z) was used to evaluate the model. An independent 24 breast cancer patients who originally were BI-RADS categorised I or II for both breasts, but were diagnosed with unilateral biopsy-confirmed breast cancer later, were included to validate the model.
Results: The AGD differences in both FFDM images between tumour-bearing and healthy breasts of patients were significantly higher than those in healthy subjects ($P<0.001$). The model with AGD differences had a higher A_z value than the model without AGD differences. While there were no AGD differences between originally healthy breasts of breast cancer patients, significant AGD differences between now tumour-bearing breasts and the then previously healthy breasts were found in both FFDM images.
Conclusion: The AGD differences between both breasts could be included in the breast cancer risk assessment model to evaluate breast cancer risk.
Limitations: The follow-up sample size was small.
Ethics committee approval: This study was approved by institutional review board. The necessity to obtain written informed consent was waived.
Funding: Medical Scientific Research Foundation of Guangdong Province, China (B2018017).
Author Disclosures:
L. Ma: nothing to disclose
G. Qin: nothing to disclose
X. Lin: nothing to disclose
Y. Cai: nothing to disclose
W. Chen: nothing to disclose

RPS 602b-9 12:03
Breast density from low-dose risk assessment mammograms
G. Ionescu[1], S. Squires[1], E. F. Harkness[1], A. Mackenzie[2], D. G. Evans[1], A. J. J. Maxwell[1], S. Howell[1], S. M. Astley[1]; *[1]Manchester/UK, [2]Guildford/UK*
(sue.astley@manchester.ac.uk)

Purpose: To quantify breast density from low-dose mammograms and hence facilitate screening stratification for young women.
Methods and materials: We analysed routine screening mammograms from women in the Predicting Risk of Cancer at Screening study (PROCAS) and from a study of Automated Low Dose Risk Assessment Mammography (ALDRAM) in which both standard and low-dose mammograms (one-tenth the original dose) were acquired. We simulated low dose mammograms in a PROCAS case-control set of 335 prior mammograms of women with interval and subsequent screen-detected cancers, each matched with three controls on age, BMI group, menopausal status, and parity. We developed an automated breast density method using a convolutional neural network trained on the average visual assessment of two readers who recorded percent mammographic density on visual analogue scales (VAS). With this, we predicted density in the 1,340 simulated low-dose PROCAS images and in the low-dose and standard mammograms from 148 women aged 31-45 in ALDRAM. For the case-control set, we computed odds ratios (OR) of developing breast cancer between the highest and lowest quintiles of predicted density. We also calculated the per-breast Pearson correlation between predicted density on standard and low dose mammograms in ALDRAM.
Results: The OR between the highest and lowest quintiles of mammographic density in the simulated low-dose case-control set was 3.57 (95% CI 2.25-5.68). In the ALDRAM cohort, the correlation between density in standard mammograms and their low-dose equivalents was 0.987.
Conclusion: Automated assessment of breast density in mammograms taken with one-tenth of the usual dose is feasible and has the potential to be used for stratification of young women in personalised breast screening programmes.
Limitations: Only GE mammograms were used.
Ethics committee approval: NHS-REC ref:19/NW/0037.
Funding: MRC-CiC award.
Author Disclosures:
S. M. Astley: nothing to disclose
G. Ionescu: nothing to disclose
S. Squires: nothing to disclose
E. F. Harkness: nothing to disclose
D. G. Evans: nothing to disclose
S. Howell: Speaker at G.E.
A. Mackenzie: nothing to disclose
A. J. J. Maxwell: nothing to disclose

RPS 602b-10 12:09
Measurement of breast density in each breast: is it also suggestive of breast cancer risk?
J. L. Browne, L. Casas, G. Santandreu, A. Rincon, I. Rodriguez, M. A. Pascual*; Barcelona/ES*
(juabro@dexeus.com)

Purpose: Previous studies of breast density (BDen) suggest a 4 to 6-fold increase in breast cancer risk (BCR) for high density relative to non-dense breasts. However, many incidental factors have to be accounted for in these studies: family and personal history, BMI, obstetric history, hormonal treatment, and age.
Our objective was to compare glandular volume (GVol), breast volume (BVol), and breast density (BDen) in each breast of women with unilateral breast cancer (UBC) versus no cancer contralateral breast (NCCB), and determine if BDen is an independent BCR.
Methods and materials: We reported the results of GVol, BVol, and BDen measured during clinical practice in 216 women with unilateral invasive cancers from 4/2014 to 12/2015.
All women had mammography performed with photon counting equipment. The detector separates photons in low and high energy photons, allowing spectral determination of GVol, BVol, and calculates BDen.
Cancers were detected using mammography, ultrasound, or MRI.
Results: Of the 216 cases, 104 were right NCCB/left UCB and 112 were left NCCB/UCB. Mean BDen was 30.1% in UBC vs 28.8% for NCCB and mean GVol was 160.3cc vs 147,4cc, respectively (both $P<0.0001$). BVol differences were not significant ($P= 0.199$). In 117 cases, BDen was higher in UCB than NCCB, in 59 cases lower, and in 40 cases the same. In 131 cases, GVol was higher in UCB, while lower in 85.
Conclusion: Our results indicate that even with identical hormonal status, immunologic system, genetic background, BMI, and habits, higher BDen and higher GVol are significantly associated with a higher BCR. Our study shows that even clinically non-appraisable BDen and GVol differences are independently associated with a higher BCR.
Limitations: n/a
Ethics committee approval: n/a
Funding: No funding was received for this work.
Author Disclosures:
J. L. Browne: nothing to disclose
L. Casas: nothing to disclose
G. Santandreu: nothing to disclose
A. Rincon: nothing to disclose
I. Rodriguez: nothing to disclose
M. A. Pascual: nothing to disclose

RPS 602b-11 12:15
Characterisation of sub-centimetre enhancing breast masses on MRI with radiomics in BRCA mutation carriers
R. Lo Gullo, I. Daimiel Naranjo, C. Rossi, A. Bitencourt, P. Gibbs, M. Fox, E. A. Morris, K. Pinker-Domenig*; New York, NY/US*
(logullor@mskcc.org)

Purpose: To verify whether radiomics features extracted from MRI of BRCA-positive patients with breast masses smaller than 1 cm can differentiate benign from malignant lesions using model-free parameter maps.
Methods and materials: In this retrospective study, 96 BRCA mutation carriers (mean age at the time of biopsy = 45.5±13.5 years) as assessed with genetic testing and who had an MRI from November 2013–February 2019 that led to a biopsy (BI-RADS 4) or imaging follow up (BI-RADS 3) were included. Two radiologists assessed all lesions independently and in consensus according to the breast imaging and reporting and data system (BI-RADS) lexicon. Radiomics features, based on first-order statistics, the grey level co-occurrence matrix (GLCM), run length matrix (RLM), size zone matrix (SZM), neighbourhood grey level dependence matrix, and neighbourhood grey tone difference matrix, were calculated
Results: Consensus BI-RADS classification assessment achieved a diagnostic accuracy of 53.4%, a sensitivity of 73.1%, a specificity of 42.1%, a positive predictive value (PPV) of 40.5%, and a negative predictive value (NPV) of 76.2%. The model combining 5 parameters (age, lesion location, GLCM-based correlation from the pre-contrast phase, first-order coefficient of variation from the 1st post-contrast phase, and SZM-based grey level variance from the 1st post-contrast phase) achieved a diagnostic accuracy of 81.5%, a sensitivity of 63.2% (24/38), a specificity of 91.4% (64/70), PPV of 80.0% (24/30), and NPV of 82.1% (64/78).
Conclusion: Radiomics improves diagnostic accuracy compared to qualitative morphological assessment with BI-RADS classification alone in BRCA mutation carriers.
Limitations: Using only single-centre data. Relatively small sample size. We included small breast masses which constitute few pixels in the final ROI.
Ethics committee approval: IRB approved.
Funding: This work was partially supported by the NIH/NCI Cancer Center Support Grant (P30 CA008748) and the Breast Cancer Research Foundation.
Author Disclosures:
R. Lo Gullo: nothing to disclose
I. Daimiel Naranjo: nothing to disclose
C. Rossi: nothing to disclose
A. Bitencourt: nothing to disclose
P. Gibbs: nothing to disclose
M. Fox: nothing to disclose
K. Pinker-Domenig: nothing to disclose
E. A. Morris: nothing to disclose

RPS 602b-12 12:21
Correlation of 18F-FDG PET/MRI imaging information with relevant immunohistochemical markers in breast cancer patients: could PET/MRI identify high-risk patients?
O. Martin[1], J. Kirchner[1], N.-M. Bruckmann[1], B. M. Schaarschmidt[1], J. Grueneisen[2], L. Umutlu[2], G. Antoch[1], L. M. Sawicki[1]; [1]Düsseldorf/DE, [2]Essen/DE (o.f.martin@web.de)

Purpose: To correlate prognostically relevant immunohistochemical parameters of breast cancer with simultaneously acquired standardised uptake values (SUV) and apparent diffusion coefficient (ADC) derived from hybrid PET/MRI.
Methods and materials: 56 female patients with therapy-naive, histologically-proven breast cancer (mean age 54.1±12.0 years) underwent dedicated prone 18F-FDG breast PET/MRI and supine whole-body 18F-FDG PET/MRI. Diffusion-weighted imaging (DWI, b values: 0, 500, 1000 s/mm²) was performed simultaneously with PET acquisition. A region of interest (ROI) encompassing the entire primary tumour was drawn into each patient's breast and prone PET/MR images to determine the glucose metabolism represented by maximum and mean SUV and into ADC maps to assess tumour cellularity represented by mean and minimum ADC values. Histopathological tumour grading, as well as additional prognostically relevant immunohistochemical markers, i.e. Ki-67, progesterone, estrogen receptor, and human epidermal growth factor receptor 2 (HER2/neu), were determined.
Results: We found a significant inverse correlation between both SUV- and ADC-values derived from breast PET/MRI (r=-0.49 for SUVmean vs. ADCmean and r=-0.43 for SUVmax vs. ADCmin, both p<0.001). Tumour grading, as well as Ki67, showed a significant positive correlation with SUVmean from both whole-body PET/MRI (r=0.42 and r=0.37, p<0.001) and breast PET/MRI (r=0.37 and r=0.32, p<0.01). For immunohistochemical markers, HER2/neu significantly correlates inverse with ADC-values from breast PET/MRI (r=-0.35, p<0.01).
Conclusion: The present data show a correlation between increased glucose-metabolism, cellularity, degree of differentiation, as well as Ki67 and HER2/neu expression of breast cancer primaries. 18F-FDG-PET and DWI from hybrid PET/MRI may offer complementary information for the evaluation of breast cancer aggressiveness in initial staging and treatment response.
Limitations: A small population and potential measurement error in ADC-values due to centrally necrotising tumours.
Ethics committee approval: Review board approval. Written informed consent was obtained
Funding: No funding was received for this work.

Author Disclosures:
O. Martin: nothing to disclose
J. Kirchner: nothing to disclose
N.-M. Bruckmann: nothing to disclose
L. M. Sawicki: nothing to disclose
B. M. Schaarschmidt: nothing to disclose
J. Grueneisen: nothing to disclose
G. Antoch: nothing to disclose
L. Umutlu: nothing to disclose

11:15 - 12:30 **Room F1**

Abdominal Viscera
RPS 601b
Elastography

Moderators:
I. Abelskaia; Minsk/BY
C. Pozzessere; Florence/IT

RPS 601b-K 11:15
Keynote lecture
R. Maxime; Clichy/FR (maxime.ronot@aphp.fr)

Author Disclosures:
R. Maxime: nothing to disclose

RPS 601b-1 11:25
Two-dimensional shear wave elastography for significant liver fibrosis in patients with chronic hepatitis B: a systematic review and meta-analysis
H. Wei, H. Jiang, B. Song; Chengdu/CN (weih_cat@163.com)

Purpose: To assess the diagnostic performance of two-dimensional shear wave elastography (2D SWE) for detecting significant liver fibrosis in patients with chronic hepatitis B (CHB).
Methods and materials: A systematic literature search of the PubMed, EMBASE, Cochrane Library databases, and Web of Science was conducted. Bivariate modelling and hierarchical summary receiver-operating-characteristic modelling were constructed to summarise the diagnostic performance of 2D SWE. Subgroup analyses were performed to explore the source of heterogeneity.
Results: 11 eligible studies with 2592 patients were included. 2D SWE showed a summary sensitivity of 88% (95% CI: 83–91), specificity of 83% (95% CI: 78–88), and summary AUC of 0.92 (95% CI: 0.89-0.94) for detecting significant liver fibrosis in CHB patients. Subgroup analysis revealed that sensitivity was significantly higher for prospective studies than retrospective studies (89% vs 82%, p <0.01) and for studies excluding patients receiving antiviral therapies than studies without excluding patients with antiviral treatment (89% vs 82%, p <0.01). Specificity was significantly higher for studies with larger populations (≥110) than those with smaller sample size (<110) (85% vs 75%, p <0.05). In particular, the cutoff values in studies exclusively including antiviral treatment-naïve CHB patients were generally lower than studies without excluding patients receiving antiviral treatment, with an average of 6.91 kPa and 8.87 kPa, respectively (p <0.01).
Conclusion: 2D SWE is an excellent modality for the prediction of significant liver fibrosis in CHB populations. Further work is required to establish the cutoff values that account for antiviral treatment as a potential confounding factor.
Limitations: A small number of studies were included in our research.
Ethics committee approval: n/a
Funding: This work was supported by the National Natural Science Foundation of China (No. 81771797).
Author Disclosures:
H. Wei: nothing to disclose
H. Jiang: nothing to disclose
B. Song: nothing to disclose

RPS 601b-2 11:31
Etiology of the liver stiffness assessed with ultrasound elastography: a cross sectional twin study
D. L. Tarnoki[1], M. O. Erdei[2], M. Piroska[1], A. Hernyes[1], H. Szabó[1], M. Fekete[3], A. Tarnoki[1]; [1]Budapest/HU, [2]Linz/AT, [3]Kaposvar/HU (tarnoki4@gmail.com)

Purpose: Non-alcoholic fatty liver disease (NAFLD) is an epidemic and a common radiological finding. However, the background of liver stiffness assessed with the ultrasound based noninvasive shear wave elasticity imaging (SWEI) method is still sparse. Our aim was to determinate whether the SWEI

based liver stiffness has a heritable component or if it is determinated by the environment.
Methods and materials: 160 Hungarian twins (97 monozygotic, MZ, 62 dizygotic, DZ; mean age 50.6±14.7 years) recruited from the Hungarian Twin Registry underwent a cross sectional ultrasonographic SWEI between 2016 and 2018. Patients with cirrhosis or a history of oncologic disease were excluded. Heritability was calculated using univariate ACE model.
Results: Men had higher Young-modulus values than the women (8.47±3.52 vs. 6.83±3.09, p=0.01). Young-modulus values were higher in patients with ultrasound based steatosis (6.36±2.55 vs. 8.42±3.57, p=0.001) which was confirmed by increasing mild and moderate steatosis compared to healthy patients without NAFLD. In MZ twins, there was a lower intrapair correlation for the Young-modulus (r=0.32, 95% CI, 0.011 to 0.569) than in DZ twins (r=0.507, 95% CI, 0.172 to 0.734), which demonstrated no additive genetic component, a high unique environmental (E=0.609, 95% CI, 0.427 to 0.831), and moderately common environmental effect (C=0.391, 95% CI, 0.169 to 0.573), respectively.
Conclusion: SWEI assessed liver stiffness is elevated in men and in patients with NAFLD and demonstrates no heritability. Our results might stimulate further studies to understand the environmental factors determining the liver stiffness.
Limitations: Relatively low number of DZ twins compared to MZ twins might slightly bias the heritability results.
Ethics committee approval: The local ethical committee approved the study (approval number: 189-1/2014). All participants gave informed consent.
Funding: No funding was received for this work.
Author Disclosures:
D. L. Tarnoki: nothing to disclose
A. Hernyes: nothing to disclose
M. O. Erdei: nothing to disclose
M. Piroska: nothing to disclose
H. Szabó: nothing to disclose
M. Fekete: nothing to disclose
A. Tarnoki: nothing to disclose

RPS 601b-3 11:37

Comparison of sound touch elastography (STE), shear wave elastography (SWE), and vibration controlled transient elastography (VCTE) using liver biopsy as reference for chronic liver disease assessment

I. Gatos[1], P. Drazinos[2], S. Yarmenitis[3], I. Theotokas[1], E. Panteleakou[1], A. Soultatos[1], P. S. Zoumpoulis[1]; *[1]Athens/GR, [2]Kifissia/GR, [3]Marousi/GR (p.drazinos@echomed.gr)*

Purpose: Chronic liver disease (CLD) is currently one of the major causes of death and the major cause of hepatocellular carcinoma development. Accurate diagnosis regarding CLD progress is very important. Although liver biopsy (LB) is considered 'gold standard' for diagnosis, several non-invasive methods exist in order to avoid LB complications. Sound touch elastography (STE) that is available in the Resona 7 ultrasound (US) device and is similar to shear wave elastography (SWE) seems promising but needs to be validated. Our aim is to evaluate and compare a new commercial variant of US elastography, STE, against already established methods such as SWE and vibration controlled transient elastography (VCTE), using LB as a 'gold standard'.
Methods and materials: 139 subjects, 28 normal (F0) and 111 with CLD (F1-F4), were included in the study. A B-Mode and elastographic examination was performed on each patient with Resona 7, Aixplorer (SWE), and Fibroscan (VCTE) US devices. The STE, SWE, and VCTE measurements were performed on the right lobe (RL) of each patient and were compared to LB results according to the Metavir Classification System (F0-F4). Receiver operating characteristic (ROC) analysis was performed for all methods to obtain best cut-off stiffness values.
Results: ROC analysis showed AUC (STE/SWE/VCTE) 0.9541/0.9581/0.9632 for F=F4, 0.9591/0.9623/0.9631 for F≥F3, 0.9346/0.9481/0.9415 for F≥F2, and 0.9224/0.9397/0.9348 for F≥F1. Best cut-off stiffness values calculated (STE/SWE/VCTE) in kPa: F=F4: 11.05/10.5/10.6, F≥F3: 9.05/8.7/8.8, F≥F2: 8.0/8.3/7.6, F≥F1: 7.15/7.05/6.2, respectively.
Conclusion: In conclusion, STE performs similarly to VCTE and SWE in terms of accuracy and could be used as alternative to the other methods.
Limitations: n/a
Ethics committee approval: All subjects participating in this study signed an informed consent.
Funding: No funding was received for this work.
Author Disclosures:
P. Drazinos: nothing to disclose
P. S. Zoumpoulis: Equipment Support Recipient at Mindray
S. Yarmenitis: nothing to disclose
I. Theotokas: nothing to disclose
I. Gatos: nothing to disclose
E. Panteleakou: nothing to disclose
A. Soultatos: nothing to disclose

RPS 601b-4 11:43

Preoperative evaluation of the liver using 2D-shear wave elastography with propagation map for prediction of post-hepatectomy liver failure: comparison with transient elastography

D. H. Lee, J. Y. Lee, J. Bae*; Seoul/KR (dhlee.rad@gmail.com)*

Purpose: To evaluate whether 2D-shear wave elastography (SWE) could predict post-hepatectomy liver failure (PHLF) in patients who underwent resection for liver tumours in comparison with transient elastography (TE).
Methods and materials: Between July 2018 and March 2019, we prospectively enrolled 49 patients who underwent surgical resection for liver tumours. After liver resection, development of PHLF was assessed using criteria proposed by an international study group of liver surgery. Association between liver stiffness values obtained by TE/SWE and development of PHLF was assessed using ROC analysis.
Results: After liver resection, 15 patients (15/49, 30.1%) experienced PHLF. Mean liver stiffness value obtained from TE in 15 patients with PHLF was higher than in 34 patients without PHLF, but there was no statistically significant difference (9.3 kPa vs. 10.5 kPa, P=0.086). The area under the curve (AUC) of TE for prediction of PHLF was 0.655 (P=0.082, 95% confidence interval [CI]; 0.505-0.785). Regarding liver stiffness value obtained 2D-SWE, 15 patients with PHLF had significantly higher liver stiffness value compared to 34 patients without PHLF (8.1 kPa vs. 10.6 kPa, P=0.011). The AUC of 2D-SWE for prediction of PHLF was 0.729 (P=0.006, 95% CI; 0.584-0.846), which was not significantly different from TE (P=0.275). The estimated sensitivity and specificity of 2D-SWE for detecting PHLF was 80.0% and 73.5% when the cut-off value was set at 7.8 kPa.
Conclusion: 2D-SWE with propagation map could have a potential to predict PHLF in patients who underwent resection for liver tumour.
Limitations: Small number of partcipants.
Ethics committee approval: Our institutional review board approved this prospective study.
Funding: Canon medical system supported this study. Whole data was collected and analysed by the authors.
Author Disclosures:
D. H. Lee: nothing to disclose
J. Y. Lee: nothing to disclose
J. Bae: nothing to disclose

RPS 601b-5 11:49

Comparison between transient elastography and liver surface nodularity for detecting clinically significant portal hypertension

R. Sartoris[1], A. Souhami Amanou[1], A. Calandra[2], P.-E. Rautou[1], F. Cauchy[1], V. Vilgrain[1], R. Maxime[1]; *[1]Clichy/FR, [2]Palermo/IT*

Purpose: To compare the performance of liver surface nodularity (LSN) and transient elastography (TE,Fibroscan®) for the detection of clinically significant portal hypertension (CSPH), and to propose a combined algorithm to improve diagnostic performance.
Methods and materials: This study included patients with compensated cirrhosis who underwent CT, TE, and hepatic venous pressure gradient (HVPG) measurement within 30 days between 2015-2018. Accuracy of TE and LSN for predicting CSPH was evaluated with AUROC. Student t-test and Pearson correlation coefficient were used. Rule-in and rule-out values were evaluated.
Results: 140 patients underwent both tests: 109 men (78%,mean age 63±9 yrs), including 39 (28%) with CSPH. LSN was valid in 130 patients (93%) and correlated with HVPG (r=0.68;P<.001). Patients with CSPH had a higher LSN than those without (mean 3.14±0.15 vs. 2.50±0.03,P<.001; AUROC=0.87±0.03). TE was valid in 132 patients (94%) and correlated with HVPG (r=0.75,P<.001; AUROC=0.87±0.03). In patients with both valid LSN and TE values (n=122), no significant difference in terms of diagnostic performance was found (DeLong, P=.54). In this group, using cutoff values of 2.57 (LSN) and 21.5kPa (TE) correctly classified 75% and 80% patients, respectively (p=0.36). Patients with 0 (n=45), 1 (n=51), and both tests (n=26) above cutoff values had 0%-24%-92% CSPH.
Conclusion: LSN score showed similar diagnostic performance and feasibility as transient elastography for detecting CSPH. Combination of both tests improved correct patient classification.
Limitations: This study only included patients with cirrhosis during pre-surgery evaluation for hepatocellular carcinoma.
The study did not analyse the predictive role of LSN score for portal hypertension–related complications such as bleeding esophageal varices or death.
Ethics committee approval: n/a
Funding: No funding was received for this work.

Author Disclosures:
R. Sartoris: nothing to disclose
A. Souhami Amanou: nothing to disclose
A. Calandra: nothing to disclose
P.-E. Rautou: nothing to disclose
F. Cauchy: nothing to disclose
V. Vilgrain: nothing to disclose
R. Maxime: nothing to disclose

RPS 601b-6 11:55

Liver stiffness and fatty liver quantification in high risk patients

I. Sporea, R. Mare, S. Nistorescu, A. Vitel, R. Sirli, A. S. Popescu, A. Sima, R. Timar, M. Tomescu; *Timisoara/RO (isporea@umft.ro)*

Purpose: To assess the severity of liver fibrosis and steatosis in both type 2 diabetes patients (T2DM) and those with metabolic syndrome (MS) using non-invasive methods: transient elastography (TE) and controlled attenuation parameter (CAP).
Methods and materials: The study included 704 T2DM and 150 MS patients who were prospectively evaluated in the same session by means of TE and CAP (FibroScan EchoSens) to assess liver fibrosis and steatosis. Reliable liver stiffness measurements (LSM) were defined as the median value of 10 LSM with an IQR/median <30%. A cut-off value of 10.1 kPa was used to define severe fibrosis (F≥3). For differentiation between stages of steatosis we used the following cut-off values proposed by the manufacturer: S1 (mild) 230-275, S2(moderate) 275-300 db/m, S3(severe) > 300 db/m.
Results: Of 854 patients screened, we excluded those with associated viral hepatitis, those with an AUDIT-C score ≥8, and those with unreliable LSM. The final analysis included 546 T2DM and 133 MS patients. BMI ≥ 30 kg/m^2 was found in 59.9% T2DM and in 72.2% (96/133) of MS patients (p<0.001). There were no significant differences between grades of steatosis by means of CAP in patients with T2DM (S1-15.6%, S2-15.6 % and S3-59.3%) and those with MS (S1-22.5%, S2-10.5% and S3-54.1%). Severe fibrosis was detected by means of TE in 19% (104/546) of subjects with T2DM and in 18% (24/133) with MS.
Conclusion: In our group, 79.5% obtained reliable LSM by means of TE and CAP. Presence of steatosis was found in 88.7% of patients by means of CAP and 18.8% of them had severe fibrosis suggesting the need for further assessment.
Limitations: Some patients with metabolic syndrome had diabetes.
Ethics committee approval: Written consent.
Funding: No funding was received for this work.
Author Disclosures:
I. Sporea: Consultant at Emergency County Hospital Timisoara, Advisory Board at GE, Philips
R. Mare: nothing to disclose
S. Nistorescu: nothing to disclose
A. Vitel: nothing to disclose
R. Sirli: nothing to disclose
A. S. Popescu: nothing to disclose
A. Sima: nothing to disclose
R. Timar: nothing to disclose
M. Tomescu: nothing to disclose

RPS 601b-7 12:01

Spleen stiffness for predicting the presence of high risk varices: comparison between two different elastography techniques

F. Renata, I. Sporea, B. Felix, R. Lupusoru, M. Danila, P. Alina, S. Roxana; *Timisoara/RO (renata.fofiu@yahoo.com)*

Purpose: To establish the usefulness of spleen stiffness (SS) values measured using two elastography techniques, point shear wave elastography (pSWE) and 2D-shear wave elastography (2D-SWE), as non-invasive markers for predicting the presence of high risk varices (HRV) in patients with compensated liver cirrhosis and to compare their performances.
Methods and materials: A prospective study was performed, including 107 subjects with compensated liver cirrhosis who underwent both upper endoscopy and SS measurements (SSM) by means of two elastographic techniques: pSWE - using virtual touch quantification (VTQ) technology (Acuson S2000-Siemens); and 2D-SWE (LOGIQ E9-General Electric), in the same admission. Reliable SSM were defined for both techniques as the median value of 10 measurements acquired in a homogenous area with IQR/M<0.30. HRV were defined as grade II, III esophageal and gastric varices. Compensated liver cirrhosis was diagnosed based on clinical, biological, and elastographic criteria (liver transient elastography>12.5 kPa).
Results: We obtained reliable SSM in 96.2% (103/107) by means of 2D-SWE.GE and in 94.4 (101/107) subjects by means of pSWE-VTQ. 98 subjects were included in the final analysis, 40.8% (40/98) had HRV. The mean SS values were significantly higher for patients with HRV as compared to those with first grade or no varices for both techniques (16.74±3.42 kPa vs. 12.71±2.2 kPa,p<0.0001 for 2D-SWE.GE; 3.52±0.49 m/s vs. 2.7±0.3 m/s,p<0.0001 for pSWE-VTQ). The best SS cut-off value by 2D-SWE.GE for predicting the presence of HRV was 13.2 kPa (AUROC–0.84; sensitivity-87.5%; specificity-69%; PPV-66%; NPV-88.9%), while for pSWE-VTQ was 2.91 m/s (AUROC–0.9; sensitivity-85%; specificity-75.8%; PPV-70.8%; NPV-88%). Based on AUROC comparison, there was no significant difference between the performance of the two techniques for predicting the presence of HRV (p=0.2191).
Conclusion: SS has a good accuracy for predicting HRV with both elastography techniques, 2D-SWE.GE and pSWE-VTQ.
Limitations: n/a
Ethics committee approval: n/a
Funding: No funding was received for this work.
Author Disclosures:
P. Alina: nothing to disclose
F. Renata: nothing to disclose
I. Sporea: nothing to disclose
B. Felix: nothing to disclose
R. Lupusoru: nothing to disclose
M. Danila: nothing to disclose
S. Roxana: nothing to disclose

RPS 601b-8 12:07

Measurement of the relationship between the histologic stage of liver fibrosis and the spatial variability of liver shear stiffness (kPa) using 2D magnetic elastography (MRE)

N. Layyous[1], C. B. Sirlin[2], K. J. Fowler[2], E. Z. Sy[2], T. Wolfson[2], A. Pecorelli[3], T. I Delgado[2], A. S. Boehringer[2], R. Loomba[2]; *[1]Rancho Santa Margarita, CA/US, [2]San Diego/US, [3]Milan/IT (nadera.layyous@ucdconnect.ie)*

Purpose: To investigate the relationship between the histologic stage of liver fibrosis and the spatial variability of liver shear stiffness (kPa) as measured by 2D magnetic elastography (MRE) in adults with known/suspected non-alcoholic fatty liver disease (NAFLD). Secondarily, to explore possible confounders (age, sex, and body mass index (BMI)).
Methods and materials: We retrospectively identified 156 adult patients with known or suspected NAFLD who underwent research 2D MRE exams (4 slices per patient) at 3T between 2014 and 2015 and for whom the following was available: age, sex, BMI, and liver biopsies performed within 180 days before or after MRE. Analysts placed regions of interest (ROI) on each of the four slices in areas of liver parenchyma with planar wave propagation. Number of pixels, mean stiffness, and standard deviation (SD) of stiffness was computed across the four ROIs. Stiffness SD was used as a metric of spatial variability. An expert pathologist scored liver fibrosis stage for each patient using the NASH CRN system. Stiffness SD was correlated with fibrosis stage (Spearman correlation). A multivariable linear regression was used to model stiffness SD as a function of fibrosis stage and possible confounders (stiffness mean, age, sex, and BMI).
Results: Stiffness SD positively correlated fibrosis stage. In multivariable analysis, the strongest predictor of stiffness SD was stiffness mean. Sex and fibrosis stage had trend-wise significant association with stiffness SD, while BMI and age did not.
Conclusion: Spatial variability of liver stiffness increases with fibrosis stage. Further research is needed to determine whether spatial variability of stiffness reflects the spatial variability in fibrosis or other factors.
Limitations: Stiffness measured by MRE comes from only within the ROI.
Ethics committee approval: All patients gave informed consent.
Funding: NIH grant and in part from GE.
Author Disclosures:
N. Layyous: nothing to disclose
T. I Delgado: nothing to disclose
A. Pecorelli: nothing to disclose
T. Wolfson: nothing to disclose
C. B. Sirlin: Consultant at Blade, Boehringer, Epigenomics, Grant Recipient at Bayer, GE, Gilead, Philips, Siemens, Other at Representative for institutional consultation for BMS, Exact Sciences, IBM-Watson, Other at Active lab service agreements with Enanta, Gilead, ICON, Intercept, Nusirt, Shire, Synageva, Takeda, Other at Completed lab service agreements with Alexion, AstraZeneca, Bristol-Myers Squibb, Celgene, Galmed, Genzyme, Isis, Janssen, Pfizer, Roche, Sanofi, Virtualscopics
K. J. Fowler: Consultant at 12 sigma, Medscape, Research/Grant Support at Bayer, GE
E. Z. Sy: nothing to disclose
A. S. Boehringer: nothing to disclose
R. Loomba: Grant Recipient at NIH, Grant Recipient at GE

RPS 601b-9 12:13

Interobserver variability in the evaluation of magnetic resonance elastography in patients with fibrotic liver disease

M. W. Raudner[1], D. Bencikova[1], S. Pötter-Lang[1], N. Bastati[1], K. Grąt[2], G. Reiter[3], S. Kannengiesser[4], S. Trattnig[1], M. Krssak[1], A. Ba-Ssalamah[1]; [1]Vienna/AT, [2]Warsaw/PL, [3]Graz/AT, [4]Erlangen/DE (marcus.raudner@meduniwien.ac.at)

Purpose: To assess the feasibility of a manual segmentation approach in magnetic resonance elastography (MRE) using a spin echo echo-planar imaging (EPI) prototype sequence in patients with various hepatic diseases.
Methods and materials: In total, 111 (46 female, mean age 61.0±13.6 years) individuals were examined at 3T (Magnetom PRISMAfit, Siemens Healthineers, Erlangen, Germany) using a prototype spin echo EPI sequence. The derived MRE images were independently evaluated by two readers, both qualitatively and quantitatively (in kPa) with strict adherence to the QIBA Consensus Profile for MRE of the Liver of the RSNA.
Results: The wave propagation was graded as disorganised in 11 and 9 cases, suboptimal in 34 and 28 cases, and optimal in 66 and 74 cases, by both readers respectively.
Mean stiffness was 3.2±1.8 kPa for reader 1 and 3.4±1.8 kPa for reader 2. The agreement of both readers was excellent with an ICC of 0.969 (95%CI 0.950-0.980) with only a minimal bias of -0.14 kPa (95%CI -0,228023 to -0,0532536). There was no correlation between disagreement and increasing kPa (r_{sp}=0.019, p=0.856). Also, the mean difference between both readers did not differ between groups with better or worse wave propagation (p=0.549 and p=0.584).
Conclusion: Based upon the presented data, assessing the agreement of manual stiffness assessment in MRE at 3T using a spin echo EPI prototype sequence, the interobserver agreement was excellent. However, evaluating the cause-specific sources for suboptimal wave propagation is warranted.
Limitations: There is no gold standard for in vivo MRE using a spin echo EPI sequence at 3T. This study was conducted retrospectively with various hepatic diseases.
Ethics committee approval: Approved by the ERB of the Medical University of Vienna. Written and informed consent received from all participants.
Funding: No funding was received for this work.
Author Disclosures:
S. Pötter-Lang: nothing to disclose
M. W. Raudner: nothing to disclose
D. Bencikova: nothing to disclose
N. Bastati: nothing to disclose
K. Grąt: nothing to disclose
G. Reiter: Employee at Siemens Healthineers
S. Kannengiesser: Employee at Siemens Healthineers
M. Krssak: nothing to disclose
A. Ba-Ssalamah: nothing to disclose
S. Trattnig: nothing to disclose

RPS 601b-10 12:19

Single- and multi-frequency MR elastography with gradient-recalled echo and spin-echo echo-planar acquisitions: comparison of robustness and intersegmental liver stiffness variation

V. C. Obmann[1], R. Kreis[1], I. Sack[2], A. Berzigotti[1], M. M. Obmann[3], J. T. Heverhagen[1], A. Christe[1], A. T. Huber[1]; [1]Berne/CH, [2]Berlin/DE, [3]Basel/CH (verena.obmann@insel.ch)

Purpose: To assess the agreement between single-frequency (sf) gradient recalled echo (GRE), sf spin echo echoplanar (SE-EP) and multifrequency (mf) SE-EP magnetic resonance elastography (MRE) sequences of the liver for the assessment of liver fibrosis.
Methods and materials: In this prospective proof-of-concept study, 22 patients (11 male, mean age 57 year, range 30-80 years) with histologically proven different degree of liver fibrosis (F0-F4) underwent MRE at 3T with three different MRE methods at 4 slices through the liver: i) sf 2D GRE MRE (sf-greMRE), ii) sf 2D SE-EP MRE (sf-se-epiMRE) and iii) multifrequency SE-EP MRE (mfMRE). Sequence robustness was assessed as number of segments per sequence in which image quality was good enough to measure liver stiffness. Intrasequence consistency was assessed by the coefficient of variance (CV) over regional stiffness estimates. For statistical analysis, ANOVA with post-hoc group comparison was performed.
Results: Evaluable segments for sf-greMRE, sf-se-epiMRE, and mfMRE were 3.0±1.5, 6.9±1.6, and 5.9±2.5; p<0.001. In pairwise comparison, sf-greMRE showed significantly fewer evaluable segments than sf-se-epiMRE and mfMRE (both p<0.001), while there was no significant difference between sf-se-epiMRE and mfMRE (p=0.147). The CV between segments for sf-greMRE, sf-se-epiMRE, and mfMRE was 15.0±9.5, 16.1±9.4, and 12.0±4.3; p=0.234. There was a trend towards lower CV in mfMRE.
Conclusion: Our data suggest that sf-se-epiMRE and mfMRE may be more robust alternatives to sf-greMRE, although a bigger sample size is needed for diagnostic accuracy to assess grading of liver fibrosis with these sequences.
Limitations: We acknowledge small study population as the main limitation of our study.
Ethics committee approval: This study was approved by the cantonal ethics committee Bern. Written informed consent was given.
Funding: This project was funded by the Swiss National Science Foundation (SNF) grant # 320030_188591.
Author Disclosures:
V. C. Obmann: nothing to disclose
R. Kreis: nothing to disclose
I. Sack: nothing to disclose
A. Berzigotti: nothing to disclose
M. M. Obmann: nothing to disclose
J. T. Heverhagen: nothing to disclose
A. Christe: nothing to disclose
A. T. Huber: nothing to disclose

RPS 601b-11 12:25

Can T1-mapping serve as an alternative to MR-elastography in the staging of liver fibrosis?

S. Freiin von Ulmenstein[1], S. Bogdanovic[2], H. Honcharova-Biletska[1], S. Blümel[1], A. Deibel[1], C. Jüngst[1], A. Weber[1], C. Gubler[1], C. S. Reiner[1]; [1]Zurich/CH, [2]Gossau/CH (sophie.vonulmenstein@usz.ch)

Purpose: To compare the diagnostic performance of T1-mapping and MR-elastography (MRE) for staging of hepatic fibrosis with histopathology as standard of reference.
Methods and materials: 48 patients who underwent liver biopsy for suspected fibrosis or were diagnosed with alcohol-toxic cirrhosis prospectively underwent look-locker inversion recovery T1-mapping and MRE. T1 relaxation time and liver stiffness (LS) were measured in the right and left liver lobe by two readers. Hepatic fibrosis was histopathologically staged according to a standardised fibrosis score (F0-F4). For statistical analysis independent t-test, Mann-Whitney-U-Test and ROC analysis were performed. ROC analysis was performed to determine accuracy of T1-mapping and MRE for fibrosis staging.
Results: Histopathological analysis diagnosed 3 patients with F0 (6%), 14 with F1 (29%), 13 with F2 (27%), 7 with F3 (15%), and 11 with F4 (23%, including previously diagnosed cirrhotic patients). T1-mapping and MRE both showed significantly higher values for patients with significant fibrosis (F0-1 vs. F2-4; T1-mapping p=0.001, MRE p<0.0001) as well as for patients with severe fibrosis or cirrhosis (F0-2 vs. F3-4; T1-mapping p=0.010, MRE p<0.0001). The diagnostic performance of T1-mapping and MRE was similarly high for significant fibrosis (F2-4) (AUC 0.798 vs. 0.868, p=0.39), but was significantly higher for MRE for severe fibrosis (F3/4) (AUC 0.952 vs. 0.745, p=0.02).
Conclusion: T1-mapping may be used as an alternative to MRE for diagnosing fibrosis in patients with different liver diseases, especially for the detection of clinically significant fibrosis.
Limitations: T1-maps were not fat-corrected, which might have influenced the results and should be a target of further studies.
Ethics committee approval: The local ethics committee approved this prospective study and all patients gave written informed consent.
Funding: No funding was received for this work.
Author Disclosures:
S. Freiin von Ulmenstein: nothing to disclose
S. Bogdanovic: nothing to disclose
H. Honcharova-Biletska: nothing to disclose
S. Blümel: nothing to disclose
A. Deibel: nothing to disclose
C. Jüngst: nothing to disclose
A. Weber: nothing to disclose
C. Gubler: nothing to disclose
C. S. Reiner: nothing to disclose

11:15 - 12:30 **Room F2**

Neuro

RPS 611a

Neurodegenerative diseases

Moderators:
J. Boban; Sremska Kamenica, Novi Sad/RS
B. M. Góraj; Nijmegen/NL

RPS 611a-1 11:15

Classifying white matter hyperintensities according to intensity and spatial localisation reveals a specific association with cognition

L. Melazzini[1], V. Bordin[1], S. Suri[2], E. Zsoldos[2], K. Ebmeier[2], M. Jenkinson[2], C. Mackay[2], F. Sardanelli[1], L. Griffanti[2]; [1]Milan/IT, [2]Oxford/UK
(lucamelazzini@yahoo.it)

Purpose: White matter hyperintensities (WMH) on T2-weighted images are imaging biomarkers of brain small vessel disease. When classified according to location (periventricular/deep), they have shown different associations with cognition. WMH can also appear hypointense on T1-weighted (T1w) images as a possible sign of irreversible tissue damage.
We hypothesise that sub-classifying WMH combining intensity information and spatial localisation may provide better insight into the association with cognition, not detectable for the total WMH burden.
Methods and materials: We analysed data from 680 subjects of the Whitehall II imaging sub-study. A supervised machine learning method (BIANCA) was used to segment WMH. An automatic method based on cluster localisation and image intensity were then applied to classify WMH into 4 categories according to adjacency to the ventricles (periventricular/deep) and appearance on T1w images (either T1w-hypointense or not). Derived volumes were entered into a general linear model as predictors of the participants' cognitive scores on neuropsychological tests.
Results: Periventricular T1w-hypointense WMH were significantly related to worse performance in trail-making test A (p=0.006), trail-making test B (p=0.028), digit-symbol coding (p=0.018), and digit-span (p=0.032) tests. When including only the total WMH burden in the model, the only significant associations between WMH and cognition were with trail-making test A (p=0.040) and the digit-symbol coding task (p=0.022).
Conclusion: Sub-classifying WMH according to both location and appearance on T1w images provided added value compared to total WMH burden alone. These are promising findings for WMH interpretation in the clinical practice and for the development of methods for analysing imaging biomarkers related to cognition.
Limitations: This study is cross-sectional in its design.
Ethics committee approval: n/a
Funding: MRC (G1001354), MRC-DPUK, and Parkinson's UK.
Author Disclosures:
L. Melazzini: nothing to disclose
L. Griffanti: nothing to disclose
F. Sardanelli: Grant Recipient at Bayer, Grant Recipient at General Electric, Grant Recipient at Bracco, Speaker at Bayer, Speaker at General Electric, Speaker at Bracco, Advisory Board at Bracco
C. Mackay: nothing to disclose
M. Jenkinson: nothing to disclose
K. Ebmeier: nothing to disclose
V. Bordin: nothing to disclose
S. Suri: nothing to disclose
E. Zsoldos: nothing to disclose

RPS 611a-2 11:21

Brain structural covariance in subtypes of mild cognitive impairment at risk of disease progression

H. Yao[1], L. Zhao[2], Y. Luo[2], L. Shi[2], D. Lew[2], V. Mok[3], B. Zhou[1], X. Zhang[1], N. An[1]; [1]Beijing/CN, [2]Shenzhen/CN, [3]Hong Kong/HK

Purpose: To investigate the structural covariance in mild cognitive impairment (MCI) subtypes and a newly defined MCI subgroup with more severe Alzheimer's disease (AD)-like brain atrophy pattern.
Methods and materials: We included 72 subjects with AD, 96 with MCI, and 108 normal controls (NC). The MCI subjects were further grouped into amnestic MCI (aMCI, n=72) and non-amnestic MCI (naMCI, n=24). T1-weighted MRI scans were collected for all the participants and were processed with AccuBrain for brain volume quantification of basal ganglia structures. An AD resemblance atrophy index (AD-RAI) was generated by AccuBrain to evaluate the severity of AD-like brain atrophy patterns. Based on this index, the MCI group was subdivided into MCI-L (AD-RAI<0.5, with a lower risk of progression to AD, n=70) and MCI-H (AD-RAI>0.5, with a higher risk of progression to AD, n=26). We compared the volumetric measures of the different groups, with multiple comparison corrections where appropriate. Structural covariance, which was calculated by correlations of brain volumes between regions, was compared between MCI subgroups and NC or AD.
Results: MCI-L and naMCI presented similar brain volumes of basal ganglia structures with the NC group, while MCI-H and aMCI presented similar brain volumes with the AD group. Subjects with aMCI had more extensive volumetric connections than naMCI and the MCI-H group triggered even more extensive brain volumetric connections than AD.
Conclusion: AD-RAI that measures the AD-like brain atrophy degree identified a subgroup of MCI with more extensive network-level brain structural changes than AD and other subtypes of MCI. Future study should aim to validate the structural covariance of this MCI subgroup in possible progression to AD in a longitudinal dataset.
Limitations: The generalisability of the findings warrants further validation due to the small sample size.
Ethics committee approval: n/a
Funding: No funding was received for this work.
Author Disclosures:
L. Zhao: Employee at BrainNow Research Institute
H. Yao: nothing to disclose
Y. Luo: Employee at BrainNow Research Institute
L. Shi: Founder at BrainNow Research Institute
D. Lew: Employee at BrainNow Research Institute
V. Mok: Consultant at BrainNow Research Institute
B. Zhou: nothing to disclose
X. Zhang: nothing to disclose
N. An: nothing to disclose

RPS 611a-3 11:27

Study on feasible elemental statistics of MR-phase information for AD diagnosis

S. Shinohara[1], T. Yoneda[1], Y. Tatewaki[2], B. Thyreau[2], T. Nagasaka[2], T. Mutoh[3], H. Arai[3], Y. Taki[3]; [1]Kuhonji Chuo-Ward, Kumamoto/JP, [2]Sendai/JP
(sabo30115@gmail.com)

Purpose: MR-phase can detect iron in the amyloid plaque (AP) as a pathological feature of Alzheimer's disease (AD). This study aimed to suggest a reliable evaluating method of AP via statistics of MR-phase information.
Methods and materials: 20 MRIs of AD, MCI due to AD, and normal cognition patients visiting Tohoku University Hospital (April-July 2017, m/w=9/11, 78.6±8.0y, MMSE=22.6±4.1) were used. The scan was done by SWIp (echo space=4, 1st TE/DTE=7.3/8 ms) and MPRAGE on 3T-MRI. We automatically classified brain areas using AAL atlas equipped in SPM12 on native space of phase image using MATLAB. We derived elemental statistics (mean value, SD, skewness, and kurtosis) of extracted phase histograms derived from each cortex area and evaluated them by changing TE.
Results: All statistics linearly changed proportionally to TE. The proportional coefficient of skewness to TE showed a high correlation to MMSE (r^2>0.4; SFG, >0.6; PrCn, p<0.01) that the rest of parameters didn't show (r^2<0.1; p>0.05). The histogram analysis showed that skewness changing was coming from the lower lobe distortion of phase histogram, which might be corresponding to AP iron loading in the cortex. Although some of the data couldn't fit the Gaussian model as reported previously to derive AP, we could derive statistics in all cases.
Conclusion: We could derive elemental statistics of MR-phase histogram in all data. The proportional coefficient of skewness to TE might be a candidate of novel quantity to bring to the clinical site for AD diagnosis using MRI.
Limitations: Truncation artefact around the brain boundary and phase distortion near the vessel may affect phase distribution.
Ethics committee approval: This study was approved by IRB (approved #2017-1-1097).
Funding: No funding was received for this work.
Author Disclosures:
Y. Tatewaki: nothing to disclose
B. Thyreau: nothing to disclose
T. Yoneda: nothing to disclose
S. Shinohara: nothing to disclose
T. Nagasaka: nothing to disclose
T. Mutoh: nothing to disclose
H. Arai: nothing to disclose
Y. Taki: nothing to disclose

RPS 611a-4 11:33

Prediction of Alzheimer's disease by using a novel 3D deep learning model

J. Ma, Q. Chu, B. Pan, J. Gu, S. Wang; *Shenzhen/CN (wangsilun@gmail.com)*

Purpose: It has been shown that deep learning methods provide high diagnostic accuracy for Alzheimer's disease diagnosis. We aim to investigate the novel deep learning model named 3D Deepbrain for AD diagnosis and applied it to real-world data.
Methods and materials: 391 AD patients and 492 age- and sex-matched controls (mean age 73.8±15.1 vs 74.9±15.5, p>0.05) from the ADNI database were recruited for Deepbrain model training. The model was tested by 71 AD patients and 77 matched controls (mean age 64.5±10.3 vs 64.4±0.2, p>0.05). All 3D MRI images were preprocessed by using the SPM12 software package to generate the grey and white matter. Diagnostic accuracy were compared by the Deepbrain model and VGG16 model. The Deepbrain model introduces the squeeze and excitation blocks as the deeper feature extractors which can enhance the capability of channel-wise feature extraction.
Results: For the testing dataset of ADNI, the Deepbrain model has a better diagnostic accuracy of 89.26%, sensitivity of 87.67%, precision 86.48%, specificity of 90.38%, and NPV of 91.26% than the VGG16 (accuracy 87.00%, sensitivity 82.43%, precision 85.91%, specificity 90.29%, and NPV 87.73%). For the real-world data, the Deepbrain model achieved an accuracy of 81.08%, sensitivity of 61.97%, precision 97.77%, specificity of 98.70%, and NPV of 73.78%, which was also better than VGG16 (accuracy 75.51%, sensitivity 42.29%, precision 99.99%, specificity 99.99%, and NPV 67.85%).
Conclusion: A novel 3D Deepbrain model was developed which can achieve promising AD diagnostic accuracy when compared to a conventional model in both public and real-world datasets. The Deepbrain model has the potential to be used in clinical tasks.
Limitations: More real-world data needs to be tested.
Ethics committee approval: n/a
Funding: No funding was received for this work.
Author Disclosures:
S. Wang: nothing to disclose
J. Gu: nothing to disclose
B. Pan: nothing to disclose
J. Ma: nothing to disclose
Q. Chu: nothing to disclose

RPS 611a-5 11:39

Abnormal cerebral microstructures revealed by diffusion kurtosis imaging in amyotrophic lateral sclerosis

H.-J. Huang, H.-J. Chen, T.-X. Zou; *Fuzhou/CN (chj0075@126.com)*

Purpose: To investigate cerebral microstructural changes in amyotrophic lateral sclerosis (ALS) using diffusion kurtosis imaging (DKI) for the first time.
Methods and materials: 18 ALS patients and 20 controls were included and underwent DKI scanning. A revised-ALS functional rating scale (ALSFRS-R) was administered to assess disease severity. Disease duration and progression rate were also recorded. Voxel-based analysis was applied to examine the alteration of DKI metrics (i.e. mean(MK)/axial(AK)/radial(RK) kurtosis) and conventional diffusion metrics (i.e. fractional anisotropy and mean/axial/radial diffusivity).
Results: ALS patients showed MK reductions in grey-matter areas, including the bilateral precentral gyrus, bilateral paracentral lobule, and left anterior cingulate gyrus. They also showed decreased MK values in white matter (WM) in the bilateral precentral gyrus, bilateral corona radiata, bilateral middle corpus callosum, left occipital lobe, and right superior parietal lobule. The spatial distribution of regions with reduced RK was similar to those with decreased MK. No between-group AK difference was found. The correlation analysis revealed significant associations between DKI metrics and clinical assessments such as the ALSFRS-R score and disease duration. Additionally, several WM regions showed between-group differences in conventional diffusion metrics, but the spatial extent was smaller than that with reduced DKI metrics.
Conclusion: The reduction in DKI metrics indicates decreased microstructural complexity in ALS, involving both motor-related areas and extra-motor regions. DKI measurements can serve as potential biomarkers for assessing disease severity and provide supplementary information to the conventional diffusion in relecting ALS-related WM abnormalities.
Limitations: The sample size is relatively small.
Ethics committee approval: Approval for this evaluation was obtained from the Research Ethics Committee of Fujian Medical University Union Hospital, China. All of the subjects provided written informed consent.
Funding: National Natural Science Foundation of China (No. 81501450).
Author Disclosures:
H.-J. Chen: nothing to disclose
T.-X. Zou: nothing to disclose
H.-J. Huang: nothing to disclose

RPS 611a-6 11:45

Diffusion basis spectrum imaging quantifies microstructural changes of the substantia nigra in early-stage Parkinson's disease

Z. Hu[1], P. Sun[2], X. Ceng[1], A. George[2], R. Yang[1], S. Song[2]; *[1]Guangzhou/CN, [2]Saint Louis/US (jassica1227@126.com)*

Purpose: To examine the microstructural changes in the substantia nigra (SN) of patients with early-stage Parkinson's disease (PD) using diffusion basis spectrum imaging (DBSI).
Methods and materials: 37 age- and sex-matched early-stage PD patients and 22 healthy controls (HCs) were enrolled. All participants underwent clinical assessments and diffusion-weighted MRI scans. SN regions were manually drawn then analysed by diffusion tensor imaging (DTI) and DBSI to assess the microstructural integrity of SN, using both DTI- and DBSI-derived diffusion metrics to reflect tissue loss (DBSI-fiber-fraction and DTI-fraction-anisotropy(FA)), dendritic injury (DBSI-fiber-axial-diffusivity (AD) and DTI-AD/mean-diffusivity(MD)), inflammation (DBSI-restricted-fraction), and oedema (DBSI non-restricted-fraction).
Results: Only DTI-FA among DTI metrics was significantly decreased in PD (PD: 0.32±0.03 vs HCs: 0.33±0.02, p=0.015), suggesting potential but not specific tissue damage in SN. Interestingly, DBSI-restricted-fraction was significantly increased (PD: 0.13±0.05 vs HCs: 0.11±0.04, p=0.031), potentially reflecting increased inflammatory cell infiltration in PD. More importantly, the significantly increased DBSI non-restricted-fraction (PD: 0.15±0.05 vs HCs: 0.12±0.05, p=0.02) and decreased DBSI-fiber-fraction (PD: 0.72±0.07 vs HCs: 0.77±0.07, p=0.003) in PD, potentially indicating the presence of oedema and/or coexisting tissue loss, further reflecting the dopaminergic neuronal loss and/or dendritic loss in SN. Other DBSI metrics were insignificantly altered. Furthermore, DBSI-restricted-fraction was negatively correlated with the Hamilton anxiety rating scale (HAMA) (r=-0.501, p=0.005), but no correlation was found between DTI-FA and clinical scales.
Conclusion: DBSI detected and quantified the extent of SN dendritic and/or neuronal loss with coexisting oedema and increased inflammatory cellularity, consistent with the hallmark SN pathologies in PD. DBSI results potentially indicate the specific pathological changes in SN with early-stage PD. A finding remains to be further investigated through more extensive longitudinal DBSI analysis of PD patients.
Limitations: There is no intergroup comparison within different stages of PD.
Ethics committee approval: Ethics committee approval and written informed consent were obtained.
Funding: No funding was received for this work.
Author Disclosures:
Z. Hu: nothing to disclose
P. Sun: nothing to disclose
X. Ceng: nothing to disclose
A. George: nothing to disclose
R. Yang: nothing to disclose
S. Song: nothing to disclose

RPS 611a-7 11:51

Comparing "swallow tail sign" and striatal uptake in early-stage Parkinson's disease: a potential surrogate of 18F-DTBZ PET

N. W. Wang, X. Liu, Y. Li; *Shanghai/CN (wangna100medical@126.com)*

Purpose: To compare the changes of "swallow tail sign" (STS) and striatal uptake on PET to construct an evaluating scale based on bilateral STS in each patient and to estimate its diagnostic performance in early-stage Parkinson's disease (PD).
Methods and materials: 39 patients with early-stage PD and 28 healthy controls (HC) underwent quantitative susceptibility mapping scanning on 3T MRI, of whom 35 patients were assessed on [^{18}F]9-fluoropropyl-(+)-dihydrotetra-benazine (^{18}F-DTBZ) PET. The alterations of STS and striatal uptake in each hemisphere were visually rated as 0-2 points, respectively, with the concordance rate being calculated. In the participant level, an evaluating scale was acquired by adding the bilateral STS points and its diagnostic power was being estimated.
Results: The concordance rate of rating points on STS and ipsilateral striatal binding was 94.3% in the right side and 91.4% in the left. Of 70 nuclei, 28 STS showed a total loss, all of the ipsilateral striatum exhibited decreased uptake, and 39 STS displayed partial loss, 36 ipsilateral striatum presented decreased uptake. Bilateral total loss was in 7 patients, unilateral total loss with contralateral partial loss in 14 patients, bilateral partial loss in 14 patients, and unilateral partial loss with contralateral normal in 1 patient. Using the bilateral partial loss of STS as the threshold, the sensitivity and specificity achieved 94.59% and 92.49% for discriminating PD from HC. The specificity was 100% when the total loss of STS was found in the unilateral hemisphere.
Conclusion: The alterations of STS correspond well with striatal uptake in early-stage PD. The evaluating scale of STS change has a satisfactory diagnostic performance in discriminating the disease. Given that unilateral total loss of STS is detected, the PET examination would not be necessarily applied.

Limitations: n/a
Ethics committee approval: Ethics committee approval obtained.
Funding: National Natural Science Foundation of China (no. 61672236).
Author Disclosures:
N. W. Wang: nothing to disclose
X. Liu: nothing to disclose
Y. Li: nothing to disclose

RPS 611a-8 11:57

Intra-network functional connectivity changes of the frontoparietal network in Parkinson's disease

N. A. Teichert[1], C. Rubbert[1], C. Mathys[2], S. B. Eickhoff[3], M. Südmeyer[1], C. J. Hartmann[1], B. Turowski[1], A. Schnitzler[1], J. Caspers[1]; [1]*Düsseldorf/DE,* [2]*Oldenburg/DE,* [3]*Jülich/DE*
(nikolas.teichert@med.uni-duesseldorf.de)

Purpose: The frontoparietal network (FPN) is involved in cognitive action control mediating between the dorsal attention (DAN) and default mode (DMN) networks. While neuroimaging studies have shown network alterations of DMN and DAN in Parkinson's disease (PD), the role of FPN in PD is unclear. Hence, we investigated functional connectivity changes of the FPN in PD.
Methods and materials: Resting-state functional magnetic resonance imaging (3T, EPI, TR=2.2s TE=30ms, 3.1mm³, 11min) was assessed in 38 PD patients and 43 healthy controls (HC, matched for age, gender, and movement). Patients were scanned under dopaminergic medication (ON) and after >12h withdrawal (OFF). The preprocessed fMRI time-series were split into 20 intrinsic brain networks using independent component analysis and left and right FPN were identified. For both FPN, voxel-wise group differences in functional connectivity (PD vs HC, for both medical conditions) were determined using a dual regression approach and permutation testing (n=5000; TFCE; p<0.05, FWE-corrected).
Results: Compared to HC, there was increased connectivity with right FPN in ipsilateral sensorimotor, inferior parietal, parietal opercular, and extrastriate visual areas in PD OFF. For left FPN, PD OFF showed increased connectivity with ipsilateral postcentral, inferior parietal, intraparietal sulcus, extrastriate visual, and frontopolar regions. In PD ON, there was decreased connectivity with contralateral primary sensorimotor areas for both FPN. For left FPN and PD ON, there was increased connectivity with ipsilateral postcentral, inferior parietal, inferior frontal, parietal opercular, thalamic, frontopolar, and ventral visual areas.
Conclusion: Both FPN show increased connectivity in PD. After dopaminergic treatment, there seems to be a connectivity shift from right to left FPN with a decoupling of right FPN from its contralateral counterpart and an increase of ipsilateral connectivity in left FPN.
Limitations: n/a
Ethics committee approval: Approved by the local ethics committee.
Funding: No funding was received for this work.
Author Disclosures:
N. A. Teichert: nothing to disclose
J. Caspers: nothing to disclose
A. Schnitzler: nothing to disclose
S. B. Eickhoff: nothing to disclose
C. Mathys: nothing to disclose
C. Rubbert: nothing to disclose
M. Südmeyer: nothing to disclose
C. J. Hartmann: nothing to disclose
B. Turowski: nothing to disclose

RPS 611a-9 12:03

Histogram analysis of DTI metrics of grey and white matter in the cognitive decline of Parkinson's disease

C. V. Gkizas[1], L. G. Astrakas[1], M. Chondrogiorgi[1], S. Konitsiotis[1], J.-P. Pruvo[2], M. Argyropoulou[1]; [1]*Ioannina/GR,* [2]*Lille/FR (chgkizas@gmail.com)*

Purpose: To investigate the role of histogram analysis of diffusion tensor imaging (DTI) metrics in detecting microstructural changes of grey (GM) and white matter (WM) associated with cognitive decline in Parkinson's disease (PD).
Methods and materials: 21 PD-patients with dementia (PDD), 21 with mild cognitive impairment (PD-MCI), and 20 without dementia (PD-CTRL) were enrolled in the study. The Parkinson's disease-cognitive rating scale (PDCRS) was used for neuropsychological assessment. Histogram scalars for fractional anisotropy (FA), mean diffusivity (MD), axial diffusivity (AD), and radial diffusivity (RD) were assessed. Differences between groups were evaluated using a Mann Whitney U-test. P<0.05 was considered statistically significant.
Results: In GM compared to PD-CTRLs, the MD showed higher mean, median, mode, and percentile prc75 in PDDs, the FA showed higher mean, median, maxima, and prc25 in PDD and MCI, the AD and RD showed increased maxima, median, and prc75 in PDD, and the AD showed increased median, prc25, and prc75 in PD-MCI. In WM compared to PD-CTRLs, the MD, RD, and AD showed decreased mean, median, mode, and prc25 in PD-MCI, and the FA showed increased mean and prc25. The RD showed higher mean and maxima in PDD than in the PD-MCI group.
Conclusion: GM abnormalities underlying cognitive decline in PD follow a continuum starting with increased AD and ending with additional RD and MD increases. A loss of WM diffusion restriction is present from the early stages of cognitive decline. Neuronal and axonal losses at early stages and additional demyelination might be the histological substrate explaining these microstructural changes.
Limitations: The use of 1.5T MRI.
Ethics committee approval: All patients signed a detailed consent. The study was approved by our hospital's ethics committee.
Funding: No funding was received for this work.
Author Disclosures:
M. Chondrogiorgi: nothing to disclose
L. G. Astrakas: nothing to disclose
C. V. Gkizas: nothing to disclose
S. Konitsiotis: nothing to disclose
J.-P. Pruvo: nothing to disclose
M. Argyropoulou: nothing to disclose

RPS 611a-10 12:09

Measuring the midsagittal midbrain area in T1-weighted 3D MRI to differentiate between TDP-43-proteinopathies (ALS) and tauopathies (PSP)

D. Cantré, C. Koch, M. Dyrba, J. Prudlo*; Rostock/DE*
(daniel.cantre@med.uni-rostock.de)

Purpose: Amyotrophic lateral sclerosis (ALS, TDP-43-proteinopathy) and progressive supranuclear palsy (PSP, tauopathy) are histopathologically different neurodegenerative diseases. In cases with overlapping clinical features (i.e. frontotemporal dementia and predominant upper motoneuron symptoms), the prediction of the underlying histopathology can be impossible by clinical criteria alone but is important for adequate therapy. To our knowledge, data regarding midbrain morphology in ALS-patients is not available. The aim of this study was to investigate whether the neuroimaging markers midsagittal midbrain area (MBA) and midbrain-to-pons-ratio (MB/P-ratio) can differentiate between both histopathological entities.
Methods and materials: We assessed T1-weighted 3D MPRAGE sequences in patients with ALS (n=71), PSP (n=36), and in healthy controls (HC, n=72). Two blinded investigators performed manual planimetric measurements to obtain MBA and MB/P-ratios for all individuals. For statistical analysis, inter-rater-reliability, regression analysis, and receiver-operating-characteristics (ROC) were calculated.
Results: Pearson correlation coefficients were r=0.98 for the MBA and r=0.96 for MB/P-ratio. Both MBA and MB/P-ratio were significantly higher in individuals with ALS compared to PSP-patients (p<0.001 for both parameters) and showed no difference compared to healthy controls (p>0.5 for both parameters). Areas under the ROC-curves were 0.935 for MBA and 0.899 for MB/P-ratio (ALS vs PSP).
Conclusion: Our data shows that no measurable midbrain atrophy occurs in ALS-patients. Results for PSP-patients with significantly reduced MBA are in line with the findings of previous studies. Therefore, measuring the MBA is a suitable surrogate marker to differentiate TDP-43-proteinopathies (ALS) from tauopathies (PSP). As a single measurement, the MBA can be easily determined in clinical routine MRI-assessment. MB/P-ratio may be used alternatively but requires two measurements and, therefore, is more time-consuming.
Limitations: A potential selection bias may exist because of the matching algorithm.
Ethics committee approval: n/a
Funding: No funding was received for this work.
Author Disclosures:
D. Cantré: nothing to disclose
C. Koch: nothing to disclose
M. Dyrba: nothing to disclose
J. Prudlo: nothing to disclose

RPS 611a-11 12:15

Multimodal imaging to quantify serial changes of the putaminal region during a precursor state and the early stage of Parkinson's disease

H. Takahashi[1], Y. Watanabe[2], H. Tanaka[3], H. Kato[3], H. Adachi[3], M. Mihara[1], H. Mochizuki[3], N. Tomiyama[3]; [1]*Osaka/JP,* [2]*Otsu/JP,* [3]*Suita/JP*
(hiroto.takahashi07@gmail.com)

Purpose: Rapid eye movement sleep behaviour disorder (RBD) is known as a precursor to Parkinson's disease (PD) and identifying a predictor is important to assess PD development from RBD. We aimed to assess the serial putamen changes in a precursor state and determine a predictive image marker for PD development from RBD.

Methods and materials: 8 patients with RBD (RBD group) and 16 patients (PD group) with early PD (Hoehn and Yahr scale: 1-2) underwent dopamine transporter (DAT) imaging and diffusion tensor magnetic resonance imaging (DTI).
The DAT-specific binding ratio (SBR) and the putamen DTI value [mean diffusivity (MD) and fractional anisotropy (FA) values] were calculated.
For each value, the time course in the RBD group and the significance of intergroup differences using a Mann-Whitney's U test were assessed.
Logit (p) was used to estimate the probability of early PD from RBD in relation to the SBR and the DTI value, and the performance of each value to discriminate early PD from RBD was assessed using receiver operating characteristic (ROC) analysis.
Results: During the time course of RBD, there were no significant changes in any value. Both the SBR and the FA value were significantly less in the PD group than in the RBD group.
RBD and PD groups can be separated clearly with the SBR and the FA value. The respective areas under the ROC curve (AUCs) for SBR/FA value were 0.95/0.80 and the AUC for logit (p) was 1.00.
Conclusion: The use of both DAT-SBR and DTI-FA can provide a high performance to discriminate early PD from RBD.
Limitations: The RBD group underwent a short time follow-up.
Ethics committee approval: Our institutional review board approved this study.
Funding: Two of co-authors were supported by the Japan Agency for Medical Research and development.
Author Disclosures:
H. Takahashi: nothing to disclose
Y. Watanabe: nothing to disclose
H. Tanaka: nothing to disclose
H. Kato: nothing to disclose
H. Adachi: nothing to disclose
M. Mihara: Research/Grant Support at Japan Agency for Medical Research and development
H. Mochizuki: Research/Grant Support at Japan Agency for Medical Research and development
N. Tomiyama: nothing to disclose

RPS 611a-12 12:21
Neurite orientation dispersion and density imaging in the substantia nigra and striatum in early-stage idiopathic Parkinson disease
X. Zeng, Y. Xu, C. Ye, H. Yuan*; Beijing/CN (xiangzhuzeng@126.com)*

Purpose: Neurite orientation dispersion and density imaging (NODDI) was used to quantify microstructural changes in substantia nigra (SN) and striatum in early stage of Parkinson disease (PD).
Methods and materials: 19 PD and 20 healthy control cases were investigated. All PD patients were at stage ≤2.5 on the Hoehn and Yahr (H-Y) Scale.
The NODDI sequence consists of one shell with 30 gradient directions and b=711 s/mm^2, and the other with 60 directions and b=2855 s/mm^2. T2 FLAIR images were also acquired.
All DWI data was fitted to the NODDI model using the AMICO algorithm where intracellular volume fraction (Vic), orientation dispersion index (OD), and isotropic volume fraction (Viso) maps were generated. An experienced neuroradiologist drew both sides of the head of the caudate nucleus (CN), putamen (Pu), globus pallidus (GP), substantia nigra pars compacta (SNpc), substantia nigra pars reticulate (SNpr), and thalamus on T2 FLAIR images. T2 FLAIR images were registered to the b_0 images using FSL. Then we extracted the values of each parameter of NODDI and calculated the average values of the nuclei.
Results: Compared with HC, the OD of PD group was significantly different in bilateral GP and right thalamus ($p_{right\ GP}$=0.02, t=-2.39; $p_{left\ GP}$=0.01, t=-2.65; $p_{right\ Thalamus}$=0.005, t=-3.30). There was no significant difference in Vic and Viso between the two groups among the nuclei.
Compared with PD patients whose H-Y Scale was equal or greater than 2, those less than 2 have a significant difference of OD in the right CN (p=0.048, t=-2.13).
Conclusion: As a potential biomarker, OD of NODDI is effective to measure regional neurite changes in early PD patients.
Limitations: The sample size is relatively small.
Ethics committee approval: Ethics committee approval and informed consent was obtained.
Funding: No funding was received for this work.
Author Disclosures:
X. Zeng: nothing to disclose
Y. Xu: nothing to disclose
H. Yuan: nothing to disclose
C. Ye: nothing to disclose

11:15 - 12:30 **Room Y**

Head and Neck

RPS 608

Thyroid gland

Moderators:
E. Gotsiridze; Tbilisi/GE
N.N.

RPS 608-K 11:15
Keynote lecture
A. S. McQueen*; Newcastle Upon Tyne/UK (andrewmcqueen7@hotmail.com)*

Author Disclosures:
A. S. McQueen: nothing to disclose

RPS 608-1 11:25
The value of superb microvascular imaging for evaluating indeterminate lymph nodes in patients with papillary thyroid carcinoma
S. Y. Lee, J. Y. Lee, R. G. Yoon*; Seoul/KR (20170141@eulji.ac.kr)*

Purpose: Ultrasound (US) is regarded as a primary imaging modality for the diagnosis of lateral cervical lymph node (LN) metastasis from papillary thyroid cancer (PTC). However, US has limitations for evaluating metastatic LNs in the indeterminate LN category. Recently, a detailed analysis of vascular structures on US became feasible with the application of superb microvascular imaging (SMI). We aimed to assess the value of SMI for detecting metastasis in indeterminate LNs in PTC.
Methods and materials: This retrospective study included 80 lateral cervical lymph nodes with indeterminate grey-scale US features (41 metastatic and 39 benign) from 80 patients with PTC (70 initially diagnosed and 10 recurrences). Patients underwent power Doppler US and SMI before US-guided biopsy. Two readers independently analysed the distribution of feeding vessels and the number and appearance of internal vessels, and compared them between metastatic and benign LNs. Inter-reader agreement was assessed. The diagnostic performance of SMI for distinguishing between benign and malignant LNs was calculated and compared.
Results: Interobserver agreement was strong for SMI. There was no significant difference in vascular patterns between benign and metastatic LNs on PDUS (distribution of feeding vessels, P=0.59; the number of internal vessels, P=0.52; internal vessel appearance, P=0.59). SMI depicted significant difference in vascular patterns between metastatic and benign LNs (distribution of feeding vessels, number of internal vessels, internal vessel appearance, P<0.001). SMI showed a diagnostic sensitivity, specificity, and accuracy of 82.9%, 79.5%, and 81.3%, respectively.
Conclusion: SMI can improve the identification of lateral lymph node metastasis in patients with indeterminate LNs.
Limitations: It was a retrospective observational study, which might have a possibility for selection bias.
Ethics committee approval: This study was approved by the IRB and requirement for written informed consent was waived.
Funding: No funding was received for this work.
Author Disclosures:
S. Y. Lee: nothing to disclose
J. Y. Lee: nothing to disclose
R. G. Yoon: nothing to disclose

RPS 608-2 11:31
Diagnostic performance of US-guided core-needle biopsy versus fine-needle aspiration for diagnosing thyroid neoplasm as a first-line biopsy method: a propensity score matching study
J. Y. Lee[1], S. L. Jung[1], H. K. Lim[1], J. H. Shin[1], S. Y. Han[1], J. E. Lee[2]*; [1]Seoul/KR, [2]Bucheon/KR (peachwh@naver.com)*

Purpose: The efficacy and safety of CNB for initially detected thyroid nodules remain unclear. The purpose of this study was to evaluate the diagnostic performance of CNB as a first-line diagnostic method for diagnosing thyroid neoplasms and compare against those of FNA via a propensity score analysis.
Methods and materials: This study included 2,898 thyroid nodules from 2,662 patients from three institutions. Adjustments for differences in baseline characteristics were done by using a propensity score analysis. The rates of non-diagnostic and inconclusive results, diagnostic accuracy for diagnosing malignancy, neoplastic follicular patterns lesions (NFPLs), and thyroid neoplasms were compared. Subgroup analyses were performed according to the K-TIRADS categories.

Results: After 1:1 matching, 753 nodules with CNB and 753 nodules with FNA were enrolled. The non-diagnostic and inconclusive results were significantly lower in the CNB group than the FNA group (all, P<0.001). For diagnosing malignancy, the diagnostic performance of CNB did not significantly differ from FNA. For diagnosing NFPLs, CNB showed significantly higher sensitivity (P<0.001) and AUC (P<0.001) than FNA. On subgroup analysis according to K-TIRADS category, CNB showed significantly higher sensitivity in the low suspicion category (P<0.001) for diagnosing malignancy. For diagnosing NFPLs, CNB showed significantly higher sensitivity and AUCs than FNA in all K-TIRADS categories (all, P<0.001). Regarding thyroid neoplasms, CNB showed significantly higher sensitivity than FNA in low and intermediate suspicion categories (all, P<0.001). The complication rate was similar between groups in matched cohorts.
Conclusion: CNB might be useful and safe for initially detected thyroid nodules, especially in the low and intermediate suspicion category.
Limitations: It was a retrospective observation study.
Ethics committee approval: This study was approved by the IRB and requirement for written informed consent was waived.
Funding: No funding was received for this work.
Author Disclosures:
J. Y. Lee: nothing to disclose
S. L. Jung: nothing to disclose
H. K. Lim: nothing to disclose
J. H. Shin: nothing to disclose
S. Y. Han: nothing to disclose
J. E. Lee: nothing to disclose

RPS 608-3 11:37

The role of repeated fine-needle aspiration for Bethesda I thyroid nodules: a 12-year single-centre experience

M. Daud, H. Maze, B. Mali, K. Atlan, P. Lebensart, K. Azam, Y. Azrak, N. Goldberg, L. Appelbaum*; Jerusalem/IL (marron.daud01@ateneopv.it)*

Purpose: Fine-needle aspiration of the thyroid is the gold-standard method for the assessment of thyroid nodules, with results expressed by the Bethesda system. Bethesda I, "non-diagnostic", is noted in up to 15% of the cases, which by definition presents a diagnostic dilemma. The aim of this study is to determine whether repeated FNA for patients receiving an initial Bethesda I provides substantial additional diagnostic information.
Methods and materials: A retrospective review of Bethesda I cases which underwent repeated FNA of the same nodule between 2006-2018 in our institution was performed. Demographic data, sonographic features, TIRADS classification, results of the repeated FNA, and surgical pathology reports were collected and analysed.
Results: Of 1,200 patients, 144 (12%) were classified as Bethesda I (117 females, 27 males) with a median age of 52 years (16-85). Among them, only 36 (25%) remained in the same category after the second aspiration. 85 (59%) were reclassified as B2, 4 (2%) as B3, 5 (3.4%) as B4, 7 (4.8%) as B5, and 8 (5.5%) as B6. Retrospective analysis determined that 90% of these 36 cases were mainly cystic or spongiform benign-appearing nodules with a pre-biopsy indication such as symptomatic or growing nodules. Upon subsequent 3rd FNA, 18 (50%) of these patients remained in the same category (BI) and 2 (5.5%) had B2. The remainder 16 (44.5%) received only follow-up.
Conclusion: Repeat aspiration of non-diagnostic thyroid nodules has a positive impact, with diagnostic resolution in over 70% of the cases. However, for nodules with classic benign cystic or spongiform features, follow-up only should be considered.
Limitations: n/a
Ethics committee approval: n/a
Funding: No funding was received for this work.
Author Disclosures:
M. Daud: nothing to disclose
Y. Azrak: nothing to disclose
H. Maze: nothing to disclose
K. Atlan: nothing to disclose
P. Lebensart: nothing to disclose
K. Azam: nothing to disclose
N. Goldberg: nothing to disclose
L. Appelbaum: nothing to disclose
B. Mali: nothing to disclose

RPS 608-4 11:43

Radiological-pathological correlation of thyroid nodule ultrasound and cytology using the TIRADS and Bethesda classifications

S. Aslan*; Giresun/TR (serdaraslan28@hotmail.com)*

Purpose: To compare the thyroid imaging reporting and data system (TIRADS) of classifying thyroid nodules with the findings on fine-needle aspiration cytology (FNAC) reported using the Bethesda system.
Methods and materials: A prospective analysis of 250 patients was performed comparing thyroid nodule ultrasound findings based on the TIRADS classification to the FNAC report based on the Bethesda classification. TIRADS 1 and biopsy-proven malignancy were excluded. Benign-appearing nodules were reported as TIRADS 2 and 3. Indeterminate or suspected follicular lesions were reported as TIRADS 4 and malignant-appearing nodules were reported as TIRADS 5. All the nodules were performed to FNAC and TIRADS findings were compared to Bethesda classification.
Results: Of the 250 patients, 137 were TIRADS 2, 48 were TIRADS 3, 26 were TIRADS 4, and 39 were TIRADS 5. The probability of a malignant FNAC (Bethesda V-VI) in TIRADS 2, 3, 4, and 5 classes were 0%, 6.9%, 18.9%, and 92.3%, respectively. The benign FNAC (Bethesda II) in TIRADS 2 was 100%, while for TIRADS 3, 4, and 5 were 74.5%, 25.8%, and 7.6%, respectively. Of the 39 patients that were TIRADS 5, 36 patients had a biopsy-proven cancer (92.3% concordance), but 3 were benign (false-positive sonographic impression). Overall concordance rate with FNAC was 94% and the sensitivity, specificity, and negative predictive value were 89%, 90.5%, and 96%, respectively.
Conclusion: Our study shows a fairly good correlation of thyroid ultrasound reporting using the TIRADS classification with the Bethesda classification of FNAC.
Limitations: Being a single-centre study can be seen as a limitation.
Ethics committee approval: This prospective study was approved by our institutional ethics committee. Informed consent was obtained from all individual participants included in the study.
Funding: No funding was received for this work.
Author Disclosures:
S. Aslan: nothing to disclose

RPS 608-5 11:49

Correlation of ACR 2017 thyroid imaging reporting and data system (ACR TI-RADS) scoring on ultrasound and Bethesda cytopathology for thyroid nodule risk stratification

A. A. Singhal, D. Sarin, H. Sarin, A. Mithal, S. S. Baijal*; Gurgaon/IN (dr.alkaasinghal@gmail.com)*

Purpose: To assess the efficiency of the ACR TI-RADS 2017 in selecting the thyroid nodules on ultrasound for FNAC and its correlation with Bethesda cytopathology classification.
Methods and materials: A prospective study was conducted of 1,000 thyroid nodules evaluated on ultrasound in the radiology department from 2015-2019 at our tertiary hospital. Selection criteria included all discrete thyroid nodules where ACR TI-RADS was applied and the patients had an ultrasound-guided fine-needle aspiration cytology (FNAC) done at our institute as per TI-RADS criteria. TIRADS 1 nodules were excluded from the study. Cytopathology Bethesda classification findings were compared with TI-RADS score on ultrasound.
Results: Of the 1,000 nodules, 398 nodules were TIRADS 2 (39.8%), 256 nodules were TIRADS 3 (25.6%), 152 nodules were TIRADS 4 (15.2%), and 194 nodules were TIRADS 5 (19.4%). Of the 400 TIRADS 2 nodules, 98 % were benign (Bethesda II). The remaining 2 % were Bethesda III. TIRADS 3 were benign in 72% and malignant in 28% cases. TIRADS 4 nodules were benign in 24% and malignant in 76% cases. TIRADS 5 nodules were malignant in 98% cases (2% false-positive). Overall concordance of ACR TI-RADS and FNAC Bethesda classification was 92% for benign nodules and 95% for malignant nodules. The sensitivity, specificity, and negative predictive value were 90%, 93%, and 96%, respectively.
Conclusion: Ultrasound ACR TI-RADS 2017 scoring is an efficient system for selecting thyroid nodules on ultrasound for FNAC and has a fairly good correlation with Bethesda cytopathology classification.
Limitations: Ultrasound being an operator dependent modality, the skill and experience of the operator with thyroid imaging may impact the results.
Ethics committee approval: Ethics committee approval from MIER (Medanta Institute of Education and Scientific Research) was obtained.
Funding: No funding was received for this work.
Author Disclosures:
A. A. Singhal: Author at Medanta Medicity Hospital Gurgaon Delhi NCR India, Consultant at Medanta Division of radiology and Nuclear Medicine, Employee at Medanta Medicity Hospital Gurgaon Delhi NCR India, Investigator at Medanta Medicity Hospital Gurgaon Delhi NCR India, Speaker at Medanta Medicity Hospital Gurgaon Delhi NCR India
D. Sarin: Author at Medanta Medicity Hospital Gurgaon Delhi NCR India
S. S. Baijal: Author at Medanta Medicity Hospital Gurgaon Delhi NCR India
A. Mithal: Author at Medanta Medicity Hospital Gurgaon Delhi NCR India
H. Sarin: Author at Medanta Medicity Hospital Gurgaon Delhi NCR India

RPS 608-6 11:55

Comparative evaluation of conventional ultrasound-based thyroid imaging reporting and data system (TIRADS) and contrast-enhanced ultrasound qualitative parameters in the differentiation of thyroid nodules

L. Garg, S. B. Grover, S. Patra, Chintamani, G. Khanna*; New Delhi/IN (lovishgarg05@gmail.com)*

Purpose: To compare the diagnostic accuracy of conventional ultrasound-based thyroid imaging reporting and data system (TIRADS) and contrast-enhanced ultrasound (CEUS) qualitative parameters in the differentiation of benign and malignant thyroid nodules using histopathology as a gold standard.
Methods and materials: This prospective IRB approved study comprised 60 patients with thyroid nodules at primary presentation. In patients with multiple nodules, the single most suspicious nodule was interrogated. All patients were examined with conventional ultrasound and classification of nodules was performed following ACR TIRADS, followed by CEUS using 2.4 ml of intravenous second-generation contrast agent. Nodules were categorised as benign or malignant based upon both TIRADS and CEUS. The CEUS qualitative parameters evaluated were enhancement degree, homogeneity, margins, order, and wash-out pattern. The diagnosis obtained by each technique were compared with histopathology as a gold standard. Statistical analysis was done to calculate sensitivity, specificity, NPV, and PPV.
Results: In the series of nodules evaluated, 28 were benign and 32 were malignant on histopathology. TIRADS classified 29 nodules as benign and 31 as malignant. Whereas on CEUS, 27 were classified as benign and 33 as malignant. For TIRADS, sensitivity was 75%, specificity was 75%, PPV was 77.4%, and NPV was 72.4%. For CEUS, sensitivity was 84.4%, specificity was 78.6%, PPV was 81.8%, and NPV was 81.5%.
Conclusion: CEUS qualitative parameters were found to have superior diagnostic accuracy to conventional ultrasound-based TIRADS in the differential diagnosis of thyroid nodules. Therefore, CEUS is a valuable supplementary technique in the definitive diagnosis of thyroid nodules and should be exploited further.
Limitations: A single-centre study.
Ethics committee approval: Informed consent from all patients. Animal board approval n/a.
Funding: No funding was received for this work.
Author Disclosures:
.. Chintamani: nothing to disclose
L. Garg: Author at VMMC and Safdarjung Hospital, New Delhi
S. B. Grover: Author at VMMC and Safdarjung Hospital, New Delhi
S. Patra: nothing to disclose
G. Khanna: nothing to disclose

RPS 608-7 12:01

Thyroid multimodal-imaging comprehensive risk stratification scoring (TMC-RSS) system: a quantitative scoring system for characterising thyroid nodules

A. Mahajan, N. Sable, R. Vaish, S. V. Kane, D. Chaukar, A. Dcruz*; Mumbai/IN (drabhishek.mahajan@yahoo.in)*

Purpose: To create an algorithm (TMC-RSS-system) using ultrasound features in combination with Doppler and elastography (ES-Asteria) and to test its diagnostic performance.
Methods and materials: A prospective study over 2 years, with all studies performed on the same equipment and US, Doppler, and elastography performed by same observer. The gold standard was the pathology. 650 nodules (560 patients) with a final analysis of 616 nodules. 47.2% benign and 52.8% malignant. TMC-RSS system scoring showed malignant characteristics plus (+)3 points for ES-score 3/4 and malignant nodes, (+)1 point for taller than wider, microcalcification, hypoechogenicity, solid composition, ill-defined margins, and central+/-peripheral vascularity, and (+)0.5 point for an irregular halo, size >1 cm. For benign characteristics, minus (-)3 points for purely cystic, ES-score-1, (-)1 point for a spongiform, comet-tail artefact, complete halo, and (-)0.5 point for peripheral vascularity. Final TMC-RSS-score was calculated by addition and subtraction of positive and negative points.
Results: The mean age was 52.1 yrs. The mean size was 2.6+/-1.9 cm. Diagnostic performance of combined US, ES, TIRADS, and CD (sensitivity: 96%, specificity: 95%, PPV: 95%, NPV: 96%, and kappa: 0.911) was statistically ($p<0.001$) higher than either combination of US, TIRADS, ES, and CD. On univariate analysis, all US features and on multivariate analysis all except taller than wider was statistically significant for predicting malignancy ($p>0.05$). TMC-RSS score had a 90% sensitivity, 89% specificity, and 91% accuracy for characterising the nodules. On the ROC curve, the cut-off for best performance of TMC-RSS score was 5.75. The cumulative risk of malignancy based on TMC-RSS score was 2.4% for <3.0 score, 18% for score 3-6, and >80% for score >6.1.
Conclusion: TMC-RSS is easy-to-use, robust, reproducible, and provides a higher degree of confidence to an average non-expert radiologist.
Limitations: Match-pair analysis with other scoring systems.
Ethics committee approval: Ethics committee approval obtained.
Funding: No funding was received for this work.
Author Disclosures:
A. Mahajan: nothing to disclose
N. Sable: nothing to disclose
R. Vaish: nothing to disclose
S. V. Kane: nothing to disclose
D. Chaukar: nothing to disclose
A. Dcruz: nothing to disclose

RPS 608-8 12:07

The determination of diagnostic accuracy of ACR (TI-RADS) in thyroid nodules on ultrasonography

G. Jameel*; Islamabad/PK (ghazal.jameel@yahoo.com)*

Purpose: TIRADS (thyroid imaging reporting and data system) is a risk stratification system for classifying thyroid lesions and was recognised by the American College of Radiology (ACR) in 2017. TIRADS classification is now being used in the daily routine categorisation of sonographically visualised thyroid nodules. The aim of the study was to categorise all solid nodules of thyroids identified sonographically according to the TIRADS score and correlating the TIRADS score with BETHESDA histopathological category of the same nodule after FNAC. This correlation, if validated, could help to avoid many unnecessary aspirations and thyroid-related surgical procedures in cases where both sonographic and histopathological grades are low and to warrant early intervention in case of high-scores with increasing risk of malignancy.
Methods and materials: Ultrasound of the thyroid was carried out on GE logic with a linear transducer of 7.5–12 MHz frequency. 210 patients referred for sonography of thyroid nodules were included in the study from 1st January 2018-31st July 2019. Fine-needle aspiration was carried out under ultrasound guidance and cytology was done on all nodules categorised according to TIRADS. TIRADS and Bethesda scores were correlated.
Results: A total of 210 patients with 233 nodules of a mean size of 2.5 ± 1.5 cm were included. The risk of malignancy of the TIRADS categories were as follows: TIRADS 2 0%, TIRADS 3 2.2%, TIRADS 4A 5.9%, TIRADS 4B 57.9%, and TIRADS 5 100%.
Conclusion: TIRADS is a useful diagnostic classification in predicting malignancy and with FNAC using BETHESDA classification, unnecessary surgical procedures can be avoided.
Limitations: n/a
Ethics committee approval: n/a
Funding: No funding was received for this work.
Author Disclosures:
G. Jameel: Consultant at PAEC General Hospital Pakistan

RPS 608-9 12:13

Malignancy in the contralateral lobe and the role of surveillance US after hemithyroidectomy for thyroid cancer

O. O'brien, S. Wright, O. Hilmi, C. McArthur*; Glasgow/UK (owen.o'brien@nhs.net)*

Purpose: There is a limited consensus on the duration of surveillance neck ultrasound (US) in hemithyroidectomy-only differentiated thyroid cancer (DTC) patients. Our aim was to determine follow-up US findings, when available, and identify rates of contralateral malignancy in patients with DTC at hemithyroidectomy.
Methods and materials: A retrospective observational study of all patients who underwent hemithyroidectomy between 01/12/13–31/01/15 in the Greater Glasgow and Clyde (GG&C) healthboard.
Results: 49 patients had DTC identified following hemithyroidectomy (46) or isthmusectomy (3). Based on largest/worst prognostic cancer if multifocal, subtypes were papillary (36), follicular (8), and Hurthle cell (5) with a mean diameter of 23 mm (range 0.3-75 mm). 20 were papillary microcarcinomas (PMC) and 16 of these were incidental. 13 patients had multifocal lobar disease. 36/49 proceeded to initial completion thyroidectomy. 30 completions would have been recommended/reasonable with the current guidelines. Further malignancy was found in 16/36 (44%), all PMC.
The remaining 13 patients had US follow-up over 0.5-5.5 years. In one, a contralateral U3/Thy3f nodule on 1st surveillance US 2 years postoperatively had PMC at completion. A further case had a contralateral U2 nodule upgraded to U3/Thy3a at 3rd annual US/FNA, which was benign on completion. Otherwise, there was normal appearances or sonographically benign nodules with no lymphadenopathy demonstrated.

Conclusion: In patients with hemithyroidectomy DTC not meeting criteria for initial completion, US/FNA follow-up prompted later completion in 2/13, with one case of completion malignancy, PMC. Otherwise, US findings were limited.
Overall completion malignancy rate was 45%, all PMC.
PMC is often undetectable at US and the role of repeated post-hemithyroidectomy US surveillance is of doubtful benefit in this group.
Limitations: A small sample size. Future collaborating studies with other Scottish/UK healthboards would be beneficial.
Ethics committee approval: n/a
Funding: No funding was received for this work.
Author Disclosures:
O. O'brien: nothing to disclose
C. McArthur: nothing to disclose
S. Wright: nothing to disclose
O. Hilmi: nothing to disclose

RPS 608-11 12:19
The size did matter: radiofrequency ablation for benign thyroid nodules
N. Kan, W.-C. Lin*; Kaohsiung/TW (naning@hotmail.com.tw)*

Purpose: To compare the effectiveness of radiofrequency ablation (RFA) for thyroid nodules among groups with different volume of nodules.
Methods and materials: This retrospective study evaluated 186 patients with benign thyroid nodules (BTNs) who underwent ultrasound-guided RFA treatment. The BTNs were categorised into group 1 (≤10 ml), group 2 (10-30 ml), and group 3 (> 30 ml), according to the initial volume of BTNs before ablation. The RFA procedures were performed using the moving shot technique. The volume reduction ratio (VRR) of each nodule, cosmetic score, symptomatic score, and complications were analysed at 1, 3, and 6 months after RFA among the three groups.
Results: At 1-month follow-up, group 3 showed significantly greater VRR compared to the other two groups (group 1, 31.88 ± 37.91%; group 2, 38.9 ± 19.18%; group 3, 48.7 ± 20.43%, $p < 0.05$). At 6-month follow-up, there was no significant difference of VRR among the three groups (group 1, 74.6 ± 20.92%; group 2, 68.1 ± 17.07%; group 3, 75.0 ± 11.88%). The major complication was temporary vocal palsy. One skin burn, one haematoma, and nodular rupture occurred during or after the procedure. The complication rate of group 3 was higher compared to the other two groups, but there was no statistical significance.
Conclusion: RFA was effective in patients with larger thyroid nodules (>30 ml) and its therapeutic efficacy and safety were similar to those in patients with smaller thyroid nodules.
Limitations: A retrospective single-centre study and a relatively short-term follow-up period (6 months).
Ethics committee approval: This study was approved by the institutional review board and informed consent for each procedure was obtained.
Funding: No funding was received for this work.
Author Disclosures:
N. Kan: Speaker at Kaohsiung Chang Gung Memorial Hospital, Author at Kaohsiung Chang Gung Memorial Hospital
W.-C. Lin: Author at Kaohsiung Chang Gung Memorial Hospital

11:15 - 12:30 **Coffee & Talk 3**

Physics in Medical Imaging

RPS 613

Artificial intelligence (AI) revising the physics in medical imaging

Moderators:
L. Fournier Pompidou; Paris/FR
K. N. Bolstad; Bergen/NO

RPS 613-1 11:15
A task-based MTF comparison between a new deep learning-based CT reconstruction and current iterative methods
T. Szczykutowicz[1], B. Nett[2], J. Tang[2], J. Hsieh[3]; *[1]Madison, WI/US, [2]Waukesha, WI/US, [3]Brookfield, WI/US (tszczykutowicz@uwhealth.org)*

Purpose: With filtered back-projected image reconstruction, spatial resolution performance is not dependent on image contrast or noise/dose. Existing iterative methods have been shown to produce a spatial resolution that is dependent on image contrast or noise/dose. Here, we characterise the contrast and dose dependence of TrueFidelity (GE Healthcare), a CE marked new deep learning image reconstruction (DLIR) approach.
Methods and materials: We imaged acrylic, bone, polyethylene, and air phantom inserts. We imaged at dose levels of 16, 8, and 4 mGy. Images were reconstructed using 6 methods: filtered back projection (FBP), 2 levels of a statistical iterative reconstruction (ASiR-V), and 3 levels of the vendor's new deep learning (DLIR) approach. The ASiR-V level was chosen based on a vendor recommendation (AR50, 50%). The tasked-based modulation transfer function (MTF task) methodology was used to obtain contrast dependent spatial resolution for each insert.
Results: The 50% and 10% MTF task values for all DLIR strengths were all comparable to FBP and all ASiR-V levels. The 10% MTF task at 8 mGy for FBP was 0.69/0.65/0.65/0.66 for poly/air/acrylic/bone, respectively. The 10% MTF task at 8 mGy for 50% ASiR-V was 0.7/0.65/0.68/0.66 for poly/air/acrylic/bone, respectively. The 10% MTF task at 8 mGy for medium-strength DLIR was 0.71/0.69/0.69/0.69 for poly/air/acrylic/bone, respectively. All reconstruction methods showed an expected decreased performance when the focal spot switched from medium to large between the 8/4 and 16 mGy levels, respectively.
Conclusion: Unlike other advanced iterative CT algorithms, this deep learning method did not exhibit contrast or noise/dose dependencies with respect to spatial resolution.
Limitations: Other abstracts address noise texture differences.
Ethics committee approval: n/a
Funding: GE Healthcare.
Author Disclosures:
T. Szczykutowicz: Consultant at GE Healthcare, Advisory Board at iMALOGIX LLC, Consultant at Takeda, Founder at protocolshare.org LLC
B. Nett: Employee at GE Healthcare
J. Tang: Employee at GE Healthcare
J. Hsieh: Founder at GE Healthcare

RPS 613-2 11:21
How does a deep learning image reconstruction algorithm affect image quality in CT abdominal imaging?
X. Liu[1], J. Rong[1], C. T. Jensen[1], A. G. Chandler[2]; *[1]Houston, TX/US, [2]Waukesha, WI/US (xliu@mdanderson.org)*

Purpose: To access noise characteristics of a new deep learning image reconstruction (DLIR) and compare its performance with adaptive statistical iterative reconstruction (ASiR-V) and filtered back-projection (FBP).
Methods and materials: The uniform section of an ACR CT phantom was surrounded by an oval-shaped fat-equivalent ring to mimic the patient size/shape and scanned on a GE Revolution CT scanner using a clinical abdominal CT protocol at 4 dose levels to simulate ultra-low, low, routine, and high-quality dose CT abdominal imaging with reported $CTDI_{vol}$ of 2, 6, 20, and 50mGy, respectively. Images reconstructed with ASiR-V and DLIR at various noise reduction strengths were compared with baseline FBP. Additionally, modulation transfer functions (MTF) were measured to assess the spatial resolution properties of different reconstructions.
Results: Both DLIR and ASiR-V reduced noise when compared with baseline FBP, while DLIR also maintained the shape of NPS distribution across the spatial frequency to be similar to FBP. In contrast, high strength ASiR-V (60% and 90%) reduced noise significantly at the higher spatial frequency but the peak frequency of NPS shifted toward the lower frequency end as ASiR-V strength increased, demonstrating a different image texture to that of FBP. Similar behaviours of NPS have been observed at all radiation levels. Both ASiR-V and DLIR improved the spatial resolution compared with FBP. DLIR resulted in the best MTF performance regardless of the strength applied.
Conclusion: DLIR has the potential to achieve an optimised image quality with reduced noise and hence the option for patient dose reduction; at the same time, the image texture was maintained similarly to that of FBP.
Limitations: This study was conducted using a phantom. The outcome of clinical patient imaging needs to be investigated and is under evaluation.
Ethics committee approval: n/a
Funding: No funding was received for this work.
Author Disclosures:
X. Liu: nothing to disclose
J. Rong: nothing to disclose
C. T. Jensen: nothing to disclose
A. G. Chandler: Employee at GE Healthcare

RPS 613-3 11:27
The performance assessment of a novel deep learning CT reconstruction algorithm: a phantom study
C. Franck[1], P. D. Deak[2], G. Zhang[3], F. Zanca[4]; *[1]Edegem/BE, [2]Berlin/DE, [3]Leuven/BE, [4]Heverlee/BE*

Purpose: For the past few years, "low dose" was the benchmark for image quality in CT and the introduction of iterative reconstruction (IR) allowed dose reductions by about 50% compared to filtered back projection (FBP) at the expense of image texture. In this study, we aimed to assess whether a novel

deep learning (DL) reconstruction can preserve the FPB-like image texture at dose levels attained by IR.
Methods and materials: Noise (SD), NPS, and MTF were measured on Catphan phantom derived images. The acquisition occurred on a 512-slice GE Revolution at 100kVp, 350 ms, 0.98 pitch, 40 mm collimation, and 1.25 mm thickness. Two different dose levels (3.0 and 7.6mGy $CTDI_{vol}$) were used, relevant for clinical practice and reconstructed with FBP, ASIR-V (50% and 100% blending), and DL.
Results: Compared to FBP, both ASIR-V and DL reduced image noise. At 3.0mGy, SD decreased by 37%, 69%, and 35% and NPS area by 53%, 83%, and 54% using 50% ASIR-V, 100% ASIR-V, and DL, respectively. While the NPS apex of 50% and 100% ASIR-V (f_{peak}=0.23, 0.13 mm^{-1}; f_{avg}=0.28, 0.18 mm^{-1}) shifted towards lower frequencies with respect to FBP (f_{peak}=0.28 mm^{-1}; f_{avg}=0.33 mm^{-1}), no difference was observed with DL (f_{peak}=0.28 mm^{-1}; f_{avg}=0.31 mm^{-1}).
Noise and NPS of 3.0mGy DL (SD=13.5; f_{peak}=0.28 mm^{-1}; f_{avg}=0.31 mm^{-1}) and 7.6mGy FBP (SD=13.9; f_{peak}=0.30 mm^{-1}; f_{avg}=0.3 $3mm^{-1}$) were similar, suggesting a 60% dose reduction is possible with DL, while preserving the image texture.
No spatial frequency differences were observed between FBP, ASIR-V, and DL ($MTF_{50\%}$=0.36 mm^{-1}).
Conclusion: The DL-based reconstruction reduces noise with respect to FBP without modifying the image texture. Moreover, it has the potential to reduce the dose with respect to FBP, in a similar way as IR.
Limitations: No clinical images were used to evaluate the radiologists' perception of image quality and texture.
Ethics committee approval: n/a
Funding: No funding was received for this work.
Author Disclosures:
C. Franck: nothing to disclose
F. Zanca: nothing to disclose
P. D. Deak: Employee at GE Healthcare
G. Zhang: nothing to disclose

RPS 613-4 11:33
Equal CNR at thinner slice thicknesses enabled the use of a CE-marked deep learning reconstruction method for CT
T. Szczykutowicz[1], B. Nett[2], J. Tang[2], J. Hsieh[3]; *[1]Madison, WI/US, [2]Waukesha, WI/US, [3]Brookfield, WI/US (tszczykutowicz@uwhealth.org)*

Purpose: New CT image reconstruction frameworks can alter the fundamental tradeoffs between spatial resolution, noise, and dose. Here, we investigate the performance of a new deep learning-based CT image reconstruction algorithm (TrueFidelity, GE Healthcare).
Methods and materials: We imaged a phantom with low and high contrast inserts at a slice thickness ranging from 0.625 mm-5 mm. We imaged at dose levels of 16, 8, and 4 mGy. All measurements were repeated 5 times. Images were reconstructed using filtered back projection (FBP), 2 levels of an advanced statistical iterative reconstruction (ASiR-V), and 3 levels of a deep learning image reconstruction (DLIR) approach. The ASiR-V levels were chosen based on institutional (20%) and vendor (50%) recommended levels. CNR, uniformity, and CT number were assessed for each slice thickness, reconstruction type, and dose level.
Results: All slice thicknesses, reconstruction types, and dose levels exhibited acceptable results for uniformity and CT number for all algorithms. The performance of CNR was highest for DLIR, followed closely by 50% ASiR-V, and was lowest for FBP. At 5 mm slice thickness and 16 mGy, DLIR low/medium/high CNR was 1.18/1.33/1.53 compared to 1.03 for FBP and 1.17/1.47 for 20%/50% ASiR-V. DLIR allowed for equal CNR as FBP at smaller slice thicknesses. For example, at 16 mGy, DLIR had the same CNR at 1.25 mm thickness as FBP had at 5 mm thickness.
Conclusion: The new TrueFidelity DLIR method outperforms existing ASiR-V and FBP. Our results have motivated several sections in our institution to utilise thin 1.25 mm images for tasks for which they used to use a thicker 5 mm slice.
Limitations: Additional abstracts address spatial resolution and noise texture.
Ethics committee approval: n/a
Funding: GE Healthcare.
Author Disclosures:
T. Szczykutowicz: Consultant at GE Healthcare, Advisory Board at iMALOGIX LLC, Consultant at Takeda , Founder at protocolshare.org LLC
B. Nett: Employee at GE Healthcare
J. Tang: Employee at GE Healthcare
J. Hsieh: Employee at GE Healthcare

RPS 613-5 11:39
The potential of deep learning image reconstruction for CT for reducing radiation exposure: a phantom study
N. Nagasawa, K. Kitagawa, N. Kubooka, Y. Ichikawa, A. Yamazaki, H. Maki, H. Sakuma*; Tsu/JP*
(nagasawa@clin.medic.mie-u.ac.jp)

Purpose: Deep learning image reconstruction (DLIR) is a new reconstruction method which can provide efficient noise reduction. The purpose of this phantom study was to investigate the relationship between radiation dose and physical metrics of the latest DLIR algorithm.
Methods and materials: Acquisitions on a physical evaluation phantom (Catphan 700, The Phantom Laboratory, Salem, NY, USA) equipped with low-(⊿60H.U.) and high(⊿240H.U.)-contrast model objects were performed at 120kV and 10 dose levels (CTDIvol: 1-10mGy in 1mGy steps) with a multidetector CT scanner (Revolution CT, GE Healthcare, Milwaukee, WI, USA). Raw data was reconstructed with a 1.25 mm slice thickness using standard kernel for FBP, hybrid iterative reconstruction (HIR), and 3 strength levels of DLIR (low, med, high, TrueFidelity, GE Healthcare, Milwaukee, WI, USA). The noise power spectrum (NPS), modulation transfer function (MTF), and detectability index (SNR^2) were computed.
Results: The 50% MTF and 10% MTF of DLIR were comparable to those of FBP for low-contrast objects and were higher for high-contrast objects at all dose levels. The NPS peak frequency of DLIR was similar to FBF and was higher than HIR, indicating less noise texture change from FBP compared to HIR. The highest SNR^2 was obtained with DLIR-high for both low- and high-contrast models. FBP-equivalent image quality can be achieved with -40% radiation dose for HIR, -50% for DLIR-low, -60% for DLIR-med, and -70% for DLIR-high for the high-contrast model. These values were -29%, -46%, -55%, and -64%, respectively, for the low-contrast model.
Conclusion: DLIR can substantially reduce noise without sacrificing spatial resolution or changing noise texture, which might provide a dose reduction of up to -70%.
Limitations: A phantom study
Ethics committee approval: n/a
Funding: No funding was received for this work.
Author Disclosures:
N. Nagasawa: nothing to disclose
K. Kitagawa: nothing to disclose
A. Yamazaki: nothing to disclose
Y. Ichikawa: nothing to disclose
H. Maki: nothing to disclose
H. Sakuma: nothing to disclose
N. Kubooka: nothing to disclose

RPS 613-6 11:45
Deep learning reconstruction and hybrid-iterative reconstruction for ultrahigh-resolution CT: the impact of radiation dose on spatial resolution and noise texture
L. J. Oostveen, M. M. Prokop, F. de Lange, I. Sechopoulos*; Nijmegen/NL*
(luuk.oostveen@radboudumc.nl)

Purpose: To determine how radiation dose affects spatial resolution and noise in ultra-high-resolution CT (UHRCT) using deep learning reconstruction (DLR) and hybrid-iterative reconstruction (Hybrid-IR) algorithms.
Methods and materials: We acquired images of a Catphan 500 phantom and a 320 mm water phantom using a UHRCT system with 0.25 mm effective detector size (Aquilion Precision, Canon Medical Systems) in high-resolution mode at $CTDI_{vol}$ values of 4.3, 9.1, and 22.3 mGy. The images were reconstructed with DLR (AiCE body standard) and Hybrid-IR (AiDR3D-enhanced, FC08). Modulation transfer functions (MTFs) at the isocentre were determined using the edge of the teflon rod of the catphan images. Image noise (standard deviation, SD) and noise power spectra (NPSs) were determined from the water phantom images, with the frequency where the NPS peaks used to quantify noise texture.
Results: All results are provided in increasing dose order. The MTF of DLR is higher than that of Hybrid-IR at all dose-levels. The 50% of the MTFs is crossed at 9, 10, 10 lp/cm for DLR; Hybrid-IR: 6, 7, 7 lp/cm. SD values for DLR are 13.6, 18.7, and 17.1, while for Hybrid-IR these values are 21.9, 27.0, and 27.5. For both techniques, the NPS peak shifts with dose. Peak frequencies for DLR are 0.4, 0.7, and 0.9 lp/cm, while for Hybrid-IR these values are 0.7, 1.1, and 1.3 lp/cm.
Conclusion: DLR creates higher-resolution images with lower noise compared to Hybrid-IR at all dose levels. As opposed to with filtered back projection, spatial resolution and noise coarseness are a function of the dose with these reconstruction algorithms.

Limitations: The use of linear metrics with non-linear reconstruction algorithms must be performed with care and only for the evaluation of relative differences between techniques, as done here.
Ethics committee approval: n/a
Funding: Funding received from Canon.
Author Disclosures:
L. J. Oostveen: Research/Grant Support at Canon Medical Systems Corporation
M. M. Prokop: Research/Grant Support at Canon Medical Systems Corporation, Speaker at Canon Medical Systems Corporation, Research/Grant Support at Siemens Healthineers, Research/Grant Support at Siemens Healthineers, Speaker at Bracco, Speaker at Bayer
F. de Lange: nothing to disclose
I. Sechopoulos: Research/Grant Support at Canon Medical Systems Corporation, Speaker at Siemens Healthineers, Speaker at Hologic

RPS 613-7 11:51

Impact of a deep learning-based reconstruction algorithm on pulmonary nodule detection in chest CT

C. Franck[1], M. J. Spinhoven[1], A. Snoeckx[1], H. El Addouli[1], S. Nicolay[1], A. van Hoyweghen[1], P. D. Deak[2], F. Zanca[3]; [1]*Edegem/BE,* [2]*Berlin/DE,* [3]*Heverlee/BE*

Purpose: Detection of pulmonary nodules is a challenging task in low-dose CT. Dose reduction using iterative reconstruction (IR) results in image texture changes, impacting pathological structures. A novel deep learning (DL) reconstruction technique can suppress noise without impacting image texture, using dose levels comparable to IR. Our aim was to assess whether DL is non-inferior to IR for the clinical task of nodule detection.
Methods and materials: Up to 6 (range 3-6, mean 4.2) artificial lung nodules (diameter: 3, 5, and 8mm; density: -800, -630, and +100HU) were inserted at different locations in the Lungman anthropomorphic phantom (Kyoto Kagaku). 6 configurations were imaged (10 abnormal and 6 normal). Each configuration was scanned at 7.6mGy (clinical protocol) and 3 different levels of dose reduction: 60% (3mGy), 80% (1.6mGy), and 95% (0.38mGy). Images were reconstructed using 2 different algorithms (50% ASIR-V and DL with low, medium, and high strength). The 256 CT-scans (160 abnormal, 96 normal) were evaluated by 4 chest radiologists. Nodules were located and scored on a 5-point scale, blinded for dose and reconstruction algorithm. Data was analysed by the jackknife free-response receiver operating characteristic method.
Results: We found no statistically significant difference in nodule detection among the image reconstruction algorithms (p=0.987, the average across readers AUC: 0.555, 0.561, 0.557, and 0.558 for 50% ASIR-V, DL-L, DL-M, and DL-H, respectively) for all dose reduction levels together. When stratifying per dose, no statistical difference (p=0.97) was found for the lowest dose (0.38mGy).
Conclusion: Our study suggests that this DL algorithm is non-inferior to IR for the clinical task of nodule detection, even at very low dose levels.
Limitations: Research assessing the change in image texture has been conducted in a separate study to uncover the full potential of DL.
Ethics committee approval: n/a
Funding: No funding was received for this work.
Author Disclosures:
C. Franck: nothing to disclose
F. Zanca: nothing to disclose
M. J. Spinhoven: nothing to disclose
H. El Addouli: nothing to disclose
A. van Hoyweghen: nothing to disclose
A. Snoeckx: nothing to disclose
S. Nicolay: nothing to disclose
P. D. Deak: Employee at GE Healthcare

RPS 613-8 11:57

A comparison of advanced AI-based CT reconstructions by noise magnitude and centroid frequency ratios

T. Pan[1], A. Hasegawa[2]; [1]*Houston, TX/US,* [2]*Chapel Hill/US (akira.hasegawa@algomedica.com)*

Purpose: To compare noise reduction and texture change of CT images reconstructed by True Fidelity (TF), ASiR-V of GE, and PixelShine of AlgoMedica. Both TF and PixelShine are deep-learning algorithms.
Methods and materials: The homogeneous module of an ACR CT phantom was scanned at radiation levels ranging from 1.4-4.8mGy (CTDI-16) and reconstructed using FBP, ASiR-V, and TF. All FBP reconstructions were further processed by PixelShine. Noise power spectrum (NPS) was computed. The centroid frequency ratio (CFR) of NPS centroid frequencies and the noise magnitude ratio (NMR) of areas under NPS between noise reduction and FBP were compared. An ideal reconstruction should maintain CFR close to 1 (less image blurring) and NMR close to 0 (more noise reduction).
Results: All reconstructions reduced more noise at a higher dose than a lower dose. However, there was a larger change of NMR for TF than for ASiR-V or PixelShine at the same CFR, suggesting the performance of TF was highly dependent on the amount of image noise. At 1.4mGy and the same CFR (same image blurring), PixelShine>ASiR-V>TF, where '>' means more noise reduction (lower NMR). At 3.4mGy, PixelShine>ASiR-V=TF. At 4.8mGy, PixelShine>TF>ASiR-V. TF and ASiR-V switched places from 1.4mGy to 4.8mGy.
Conclusion: The performance of TF was highly dependent on image noise. TF reduced more noise than ASiR-V at 4.8mGy. Conversely, ASiR-V reduced more noise at 1.4mGy than TF. PixelShine reduced more noise at the same CFR than TF and ASiR-V at all dose levels.
Limitations: The limited range of doses and that we only used tube current to change the dose.
Ethics committee approval: n/a
Funding: No funding was received for this work.
Author Disclosures:
A. Hasegawa: Employee at AlgoMedica, Inc.
T. Pan: Consultant at Bracco Diagnostic, Inc.

RPS 613-9 12:03

Deep learning applied to low kV imaging in CT

T. Szczykutowicz[1], B. Nett[2], J. Tang[2], J. Hsieh[3]; [1]*Madison, WI/US,* [2]*Waukesha, WI/US,* [3]*Brookfield, WI/US (tszczykutowicz@uwhealth.org)*

Purpose: This work characterises the use of low kV imaging on Revolution Apex (GE Healthcare) with a new x-ray tube and TrueFidelity, a CE marked deep learning-based image reconstruction (DLIR) technique.
Methods and materials: We imaged a CT phantom (30 by 40 cm solid water with 2, 5, and 15 mg/cc of iodine, fat, brain, and blood inserts) at 70, 80, 100, 120, and 140 kVp. We imaged at dose levels of 18, 8, and 4 mGy. Images were reconstructed using 3 methods: filtered back projection (FBP), a statistical iterative reconstruction (ASiR-V), and the vendor's new deep learning image reconstruction approach. The ASiR-V levels were chosen based on institutional (20%) and vendor (50%) recommended levels. DLIR was set at medium strength. The relative dose reduction factor (RDF) methodology was applied to quantify the potential of changing kVp and or applying the ASiR-V/DLIR methods to reduce the dose.
Results: As expected, for materials that increase the CT number while decreasing kVp, the RDF predicted a dose reduction for all recon types. For materials like the brain where FBP exhibited a dose penalty with decreasing kVp, DLIR enabled lowering of the kVp without any dose penalty (RDF for brain tissue FBP at 70 kVp was 1.10 while DLIR had a brain RDF at 70 kVp of 0.26). For 5 mg/cc strength iodine at 16 mGy and 70 kVp, FBP/ASiR-V 20%/ASiR-V 50%/DLIR had RDF values of 0.49/0.36/0.20/0.10, respectively.
Conclusion: New deep learning reconstruction (TrueFidelity, GE Healthcare) allowed for a better simultaneous realisation of iodine and non-iodine imaging tasks on the same exam.
Limitations: Noise texture and spatial resolution are evaluated in other abstracts.
Ethics committee approval: n/a
Funding: GE Healthcare.
Author Disclosures:
T. Szczykutowicz: Consultant at GE Healthcare, Board Member at iMALOGIX LLC, Consultant at Takeda, Founder at protocolshare.org LLC
B. Nett: Employee at GE Healthcare
J. Tang: Employee at GE Healthcare
J. Hsieh: Employee at GE Healthcare

RPS 613-11 12:09

Image quality capabilities and dose reduction opportunities of a deep learning image reconstruction algorithm: a phantom study

J. Greffier[1], H. Pasquier[2], A. Hamard[1], J. P. Beregi[1], J. Frandon[1]; [1]*Nîmes/FR,* [2]*Buc/FR (joel.greffier@chu-nimes.fr)*

Purpose: To assess the impact on image quality and dose reduction opportunities of a deep learning image reconstruction (DLIR) algorithm compared to a model-based iterative reconstruction (MBIR) algorithm.
Methods and materials: Acquisitions were performed on an image quality phantom at 7 dose levels (CTDIvol: 15/10/7.5/5/2.5/1/0.5mGy). Raw data was reconstructed using the filtered back-projection (FBP), 2 levels of MBIR, and 3 levels of DLIR algorithms. The mean attenuation, noise, contrast-to-noise ratio (CNR), noise-power-spectrum (NPS), and task-based transfer function (TTF) were computed. The detectability index (d') was computed to model the detection of a large mass in the liver, a small calcification, and small lesion with low-contrast.
Results: CNR values obtained with all DLIR levels were lower than AV100 and higher than AV50 (except with DLIR-L). NPS peaks were higher with AV50 than with all DLIR levels and only higher with AV100 than with DLIR-L. The average NPS spatial frequencies were higher with DLIR than with MBIR. For all DLIR

levels, $TTF_{50\%}$ obtained with DLIR were higher than MBIR. d' values increased with the level of DLIR and the percentage of MBIR. d' were higher with DLIR than with AV50, but lower with DLIR-L and DLIR-M than with AV100. d' values were higher with DLIR-H than with AV100 for the small lesion with low-contrast (10%±4%) and in the same range for other simulated lesions.
Conclusion: DLIR algorithms reduced noise and improved spatial resolution and detectability without changing the noise texture. Images obtained with DLIR seem to be more adapted to a dose optimisation process than those with MBIR.
Limitations: Raw-data was reconstructed using the single-kernel "standard" and conducted on a phantom that does not take into account the difference in morphology between patients.
Ethics committee approval: n/a
Funding: No funding was received for this work.
Author Disclosures:
J. Greffier: nothing to disclose
H. Pasquier: Employee at GE Healthcare
J. P. Beregi: nothing to disclose
J. Frandon: nothing to disclose
A. Hamard: nothing to disclose

RPS 613-12 12:15
Towards 4D interventional guidance: reconstructing interventional tools from four x-ray projections using a deep neural network
E. Eulig[1], J. Maier[1], N. R. Bennett[2], M. Knaup[1], D. K. Hörndler[3], A. Wang[2], M. Kachelrieß[1]; [1]*Heidelberg/DE,* [2]*Palo Alto/US,* [3]*Nuremberg/DE (elias.eulig@dkfz-heidelberg.de)*

Purpose: To reconstruct interventional tools from only 4 x-ray CBCT projections for tomographic interventional guidance.
Methods and materials: Single or biplane x-ray fluoroscopy is the standard imaging technique for interventional guidance. Due to its projective nature, it only provides a limited ability to resolve three-dimensional structures. While tomographic (3D+time) interventional guidance could overcome this drawback, it is currently infeasible due to the exceedingly high dose to both the patient and the surgeon. Prior work demonstrated that interventional tools can be reconstructed from 10 to 20 cone-beam CT (CBCT) projections by using prior knowledge of an appropriately sampled patient scan together with principles from a compressed sensing theory. To achieve a further dose reduction, which is necessary to make tomographic interventional guidance clinically feasible, we trained a deep neural network to segment interventional tools (stents and guidewires) from CT reconstructions of only 4 x-ray projections. We assumed to have a perfect prior scan, therefore subtracted the prior scan from any interventional scan results in a sparse volume consisting of only interventional tools and noise. The network was trained on simulated CBCT data of several different stent models and guidewires and tested on both simulated data and measured data of a Siemens Zeego robot-driven C-arm system.
Results: For both the simulated and the measured data, we observed very good agreement with the ground truth, indicating that the network is able to generalise from simulated to measured data while having been trained exclusively on the former.
Conclusion: Deep learning-based reconstruction of interventional tools has the ability to overcome the dose issue of tomographic interventional guidance.
Limitations: Currently, the method assumes to have a perfect patient prior. We want to address this limitation in the future.
Ethics committee approval: n/a
Funding: No funding was received for this work.
Author Disclosures:
E. Eulig: nothing to disclose
M. Kachelrieß: nothing to disclose
N. R. Bennett: nothing to disclose
J. Maier: nothing to disclose
M. Knaup: nothing to disclose
D. K. Hörndler: CEO at Ziehm Imaging GmbH
A. Wang: nothing to disclose

11:15 - 12:30 **da Vinci (Room D1)**

Genitourinary

RPS 607

New ultrasound modalities in the genitourinary system

Moderators:
E. Bertelli; Florence/IT
G. Roic; Zagreb/HR

RPS 607-K 11:15
Keynote lecture
V. E. Gazhonova; *Moscow/RU (vx969@yandex.ru)*

Author Disclosures:
V. E. Gazhonova: nothing to disclose

RPS 607-1 11:25
Contrast-enhanced ultrasound (CEUS) following renal cryoablation: potential and limits
I. Campo, C. Sachs, R. Ciabattoni, M. A. Cova; *Triest/IT (irenecampo11@gmail.com)*

Purpose: To investigate how long after cryoablation successfully ablated tumours became completely avascular at CEUS.
Methods and materials: Between January 2012 and January 2018, 79 patients (55 men, 24 women, median and average age: 73 yo; range 46-89 yo) with 82 renal tumours treated with percutaneous cryoablation underwent CEUS before the procedure and at postoperative day one. If the lesion was avascular at the CEUS performed at postoperative day one, no further imaging was obtained before the reference contrast-CT/MR scheduled six months after the procedure. If the lesion still displayed enhancement at postoperative day one, CEUS was repeated up to the disappearance of the intralesional vascularity after one week, two weeks, one month, and three months, if necessary.
Results: The reference contrast-CT/MR obtained six months after the ablation procedure showed 80 successfully ablated tumours and two cases of tumour persistence. 46/80 (57%) successfully ablated tumours were avascular on postoperative day one, 67/80 (84%) within one week, 72/80 (90%) within two weeks. All successfully ablated tumours were avascular after one month. The two lesions with tumour persistence displayed intralesional vascularity after three months.
Conclusion: After successful cryoablation, intralesional enhancement disappears within two weeks in the majority of cases but can persist for up to one month.
Limitations: A retrospective study.
Ethics committee approval: n/a
Funding: No funding was received for this work.
Author Disclosures:
I. Campo: nothing to disclose
C. Sachs: nothing to disclose
R. Ciabattoni: nothing to disclose
M. A. Cova: nothing to disclose

RPS 607-2 11:31
Accuracy of contrast-enhanced ultrasound qualitative parameters for the characterisation of complex cystic and solid renal masses: a comparative study
S. B. Grover[1], M. Altamash[1], S. Patra[1], H. Grover[2], A. Katyan[1], A. Kumar[1], A. K. Mandal[1]; [1]*New Delhi/IN,* [2]*New York/US (shabnamgrover@yahoo.com)*

Purpose: To compare the diagnostic accuracy of contrast-enhanced ultrasound (CEUS) qualitative parameters for the characterisation of complex cystic and solid renal masses, using histopathology as a gold standard.
Methods and materials: This Institutional Review Board approved prospective study comprised 102 consenting patients, including 50 complex cystic and 52 solid renal masses. Conventional ultrasound (US) was performed, followed by CEUS with 1.2 ml intravenous injection of second-generation ultrasound contrast agent. For complex cystic renal masses, contrast-enhancement within septae/mural nodule/s was observed and classified using a Bosniak system. For solid renal masses, wash-in pattern, degree of peak enhancement, homogeneity at peak enhancement, wash-out pattern, and peripheral rim enhancement were recorded, using adjacent normal parenchyma as control. Parametric diagnostic

tests were applied to evaluate the diagnostic accuracy of CEUS qualitative parameters for both complex cystic and solid renal masses.
Results: Of 102 patients, 38 (37.3%) were benign and 64 (62.7%) malignant on histopathology. Sensitivity, specificity, positive predictive value (PPV), negative predictive value (NPV), and accuracy of CEUS qualitative parameters for complex cystic masses were 77.78%, 100%, 100%, 88.89%, and 92%, respectively. For solid masses, sensitivity was 65.22%, specificity was 100%, PPV was 100%, NPV was 55.56%, and accuracy was 69.99%.
Conclusion: CEUS quantitative parameters show comparable diagnostic accuracy for the characterisation of both complex cystic and solid renal masses as benign or malignant. The technique holds promise not only for reducing exposure to radiation but for great clinical utility in patients with impaired renal function, in whom iodinated/gadolinium-based contrast agents are contraindicated.
Limitations: A single-centre study and limited cohort of patients.
Ethics committee approval: Informed consent from all patients. Animal board approval N/A.
Funding: No funding was received for this work.
Author Disclosures:
S. B. Grover: Author at VMMC and Safdarjung Hospital, New Delhi, India
M. Altamash: Author at VMMC and Safdarjung Hospital, New Delhi, India
S. Patra: Author at VMMC and Safdarjung Hospital, New Delhi, India
H. Grover: Author at Mt. Sinai West, New York, USA
A. Kumar: Author at VMMC and Safdarjung Hospital, New Delhi, India
A. K. Mandal: Author at VMMC and Safdarjung Hospital, New Delhi, India
A. Katyan: nothing to disclose

RPS 607-3 11:37

A comparison between the diagnostic accuracy of CEUS qualitative parameters and conventional ultrasound-based IOTA simple rules (SR) for the sonographic characterisation of complex adnexal masses

S. Patra[1], S. B. Grover[1], H. Grover[3], P. Mittal[1], G. Khanna[1]; [1]*New Delhi/IN,* [2]*New York, NY/US (patrasayantan92@gmail.com)*

Purpose: The purpose of this study was to compare diagnostic accuracy between contrast-enhanced ultrasound (CEUS) qualitative parameters and conventional ultrasound (US) based IOTA simple rules (SR) in patients with sonographically complex adnexal masses, using histopathology as a gold standard.
Methods and materials: This Institutional Review Board approved prospective study consisted of 70 consenting patients with 70 complex adnexal masses. Conventional US examination was followed by CEUS using intravenous administration of 4.8 ml of second-generation ultrasound contrast agent. Tumours larger than 10 cm were examined by a transabdominal route and the rest transvaginally. Tumours were categorised into “benign”, “malignant”, or “inconclusive” based on IOTA SR. CEUS qualitative parameters evaluated were enhancement order, extent, and pattern relative to the myometrium, with at least two features required for categorisation. Histopathology diagnosis was obtained for all tumours. The diagnostic accuracy of qualitative parameters and IOTA SR was obtained.
Results: Of 70 patients, 34 (48.6%) were benign and 36 (51.4%) were malignant. Sensitivity, specificity, positive predictive value (PPV), and negative predictive value (NPV) for IOTA SR were 87.5%, 79.2%, 89.5%, and 76%, while for CEUS qualitative parameters these were 93.6%, 86.4%, 96.1%, and 79.2%.The type of enhancement showed highest sensitivity (94.9%), specificity (90.5%), PPV (97.4%), and NPV (82.6%). Accuracy for CEUS qualitative parameters was 92%, while for conventional US based IOTA SR was 84.7%, p <0.05.
Conclusion: CEUS qualitative parameters were found to have better diagnostic accuracy than conventional US-based IOTA SR for the characterisation of sonographically complex adnexal masses. The technique holds potential not only for reducing invasive biopsies/diagnostic laparotomy but also is of immense clinical utility in patients with impaired renal function.
Limitations: A single-centre study with a imited number of patients.
Ethics committee approval: Ethics committee approval obtained.
Funding: No funding was received for this work.
Author Disclosures:
S. Patra: Author at VMMC and Safdarjung Hospital, New Delhi
S. B. Grover: Author at VMMC and Safdarjung Hospital, New Delhi
H. Grover: Author at Mt. Sinai West, New York, USA
P. Mittal: Author at VMMC and Safdarjung Hospital, New Delhi
G. Khanna: Author at VMMC and Safdarjung Hospital, New Delhi

RPS 607-4 11:43

Evaluation of diagnostic accuracy of contrast-enhanced ultrasound (CEUS) quantitative parameters for the characterisation of solid renal masses

S. B. Grover[1], M. Altamash[1], S. Patra[1], H. Grover[2], A. Katyan[1], A. Kumar[1], A. K. Mandal[1]; [1]*New Delhi/IN,* [2]*New York/US (shabnamgrover@yahoo.com)*

Purpose: To evaluate the diagnostic accuracy of contrast-enhanced ultrasound (CEUS) quantitative parameters for the characterisation of solid renal masses, using histopathology as a gold standard.
Methods and materials: In this Institutional Review Board approved prospective study, 52 consenting patients with solitary solid renal masses were recruited. Conventional ultrasound (US) was performed, followed by CEUS with 1.2 ml bolus intravenous injection of second-generation ultrasound contrast agent. For every tumour, a time-intensity curve was constructed and peak enhancement (PE), time to peak (TTP), area under the time-intensity curve (AUTIC), and mean transit time (MTT) were documented. Multiple linear regression and ROC curves were used to evaluate cut-off values and the diagnostic accuracy of CEUS quantitative parameters.
Results: Of 52 patients evaluated, 6 (11.5%) were benign and 46 (88.5%) malignant on histopathology. TTP and MTT showed reliable accuracy for the characterisation of solid renal masses. For TTP, considering cut-off of 18s, sensitivity, specificity, PPV, and NPV were 97.73%, 75%, 95.56%, and 85.71%, respectively (AUC 0.94). For MTT, considering cut-off of 28s, the same were 95.65%, 83.33%, 97.78%, and 71.43%, respectively (AUC 0.93). Neither AUTIC (cut-off >3100, AUC 0.68) nor PE (cut-off >17, AUC 0.65) were independently capable for the characterisation of solid renal masses. Using all four criteria, sensitivity, specificity, PPV, and NPV were 95.4%, 47.1%, 90.2%, and 66.7%, respectively (p<0.05).
Conclusion: CEUS quantitative parameters have a significant role in the characterisation of solid renal masses. The technique holds potential not only for reducing exposure to iodinated contrast and radiation dosage but is of great clinical utility in patients with impaired renal function, in whom iodinated/gadolinium-based contrast agents are contraindicated.
Limitations: A single-centre study.
Ethics committee approval: Informed consent from all patients. Animal board approval N/A.
Funding: No funding was received for this work.
Author Disclosures:
S. B. Grover: Author at VMMC and Safdarjung Hospital, New Delhi, India
M. Altamash: Author at VMMC and Safdarjung Hospital, New Delhi, India
S. Patra: Author at VMMC and Safdarjung Hospital, New Delhi, India
H. Grover: Author at Mt. Sinai West, New York, USA
A. Kumar: Author at VMMC and Safdarjung Hospital, New Delhi, India
A. K. Mandal: Author at VMMC and Safdarjung Hospital, New Delhi, India
A. Katyan: nothing to disclose

RPS 607-5 11:49

Shall we use contrast-enhanced ultrasound (CEUS) for the characterisation of nonpalpable testicular lesions? An analysis from a cost-effectiveness perspective

J. Rübenthaler[1], S. H. Kim[2], W. G. Kunz[1], W. Sommer[1], D.-A. A. Clevert[1], M. F. Froelich[3]; [1]*Munich/DE,* [2]*Frankfurt am Main/DE,* [3]*Mannheim/DE*

Purpose: Accurate characterisation of testicular lesions is crucial to allow for the correct treatment of malignant tumours and to avoid unnecessary procedures in benign ones. In recent years, contrast-enhanced ultrasound (CEUS) proved to be superior in specifying the dignity of small, nonpalpable testicular lesions (<1.5 cm) compared to B-mode and colour-Doppler ultrasound, which were previously regarded as the primary imaging method. The aim of this study was to analyse the cost-effectiveness of CEUS as compared to unenhanced ultrasound for the characterisation of nonpalpable testicular lesions.
Methods and materials: A decision model based on Markov simulations estimated lifetime costs and quality-adjusted life-years (QALYs) associated with unenhanced ultrasound and CEUS. Model input parameters were obtained from recent literature. A deterministic sensitivity analysis of diagnostic parameters and costs was performed. Probabilistic sensitivity analysis using Monte-Carlo modelling was also applied. The willingness-to-pay (WTP) was set to $100,000/QALY.
Results: In the base-case scenario, unenhanced ultrasound resulted in total costs of $5,113.14 and an expected effectiveness of 8.29 QALYs, whereas CEUS resulted in total costs of $4,397.77 with 8.35 QALYs. Therefore, the strategy unenhanced ultrasound was dominated by CEUS in the base-case scenario. Sensitivity analysis showed CEUS to be the cost-effective alternative along with a broad range of costs.
Conclusion: Contrast-enhanced ultrasound is a cost-effective imaging method for the characterisation of nonpalpable testicular lesions.
Limitations: There is only little published and available data for sensitivities and specificities of colour-Doppler and CEUS for the evaluation of small non-palpable testicular lesions, and the current model is based on a single study with 115 patients instead of a meta-analysis which would be the more preferred option.
Ethics committee approval: n/a
Funding: No funding was received for this work.

Author Disclosures:
J. Rübenthaler: nothing to disclose
M. F. Froelich: Employee at Smart Reporting
S. H. Kim: Employee at Smart Reporting
W. G. Kunz: nothing to disclose
W. Sommer: Founder at Smart Reporting
D.-A. A. Clevert: nothing to disclose

RPS 607-6 11:55
Strain elastography: is it valuable in the assessment of cervical incompetence during pregnancy?
E. Elkayal; *ElFayoum/EG (engy.elkayal@gmail.com)*

Purpose: Can strain elastography assess the elasticity characteristics of the cervix between 12-14 weeks of pregnancy?
Methods and materials: We conducted a descriptive cross-sectional study in the ultrasound unit of the radiology department, Fayoum University Hospital, between January 2018 and January 2019. This study included 40 women presenting for the routine first trimester. The following data was recorded: elastographic colour assessment of the cervical canal and ultrasound cervical length, maternal age, obstetrical history, and the gestational age at birth. Elastographic assessment of the cervical canal was performed using a colour map: red (soft), yellow (medium-soft), green (medium-hard), and purple (hard). If two colours were visible in the region of the cervical canal, the softer option was noted.
Results: It was found that the red colour group (soft cervix in elastography reading) had a 62.5% sensitivity and 70.9% specificity, with a total diagnostic accuracy of 70% in predicting preterm delivery. When adding the "yellow colour", the sensitivity was raised to 87.5%, the specificity to 72.5%, and the total accuracy increased to 74.3% of cases of preterm delivery. The number of preterm deliveries (<37 weeks of pregnancy) was significantly higher in the red and yellow groups than in the green and purple groups.
Conclusion: Elastography has been increasingly used in the assessment of the cervical canal at 12-14 weeks of pregnancy and can identify patients with a high-risk of preterm delivery in women with cervical incompetence.
Limitations: There is no distinction between a reference tissue and the target tissue in the cervix. There are multiple pressure sources such as a patient's respiration, arterial pulsations, foetal movements, and the shaking hands of the operator.
Ethics committee approval: Ethics committee of Fayoum University.
Funding: No funding was received for this work.
Author Disclosures:
E. Elkayal: nothing to disclose

RPS 607-7 12:01
Shear-wave elastography of the prostate for the detection of Ca prostate in cases of elevated PSA and BPH
S. S. Sachar[1], S. Sachar[2]; *[1]New Delhi/IN, [2]Muzaffarnagar/IN (drsacharsaurabh@gmail.com)*

Purpose: To conduct a prospective study to evaluate transrectal shear-wave elastography (SWE) in the detection of prostate cancer (PC) in patients with elevated PSA and enlarged prostate, and to correlate with TRUS-guided biopsy and CE-MRI (3 Tesla) findings and detect the sensitivity, specificity, PPV, and NPV for SWE.
Methods and materials: A total of 26 male patients with a minimum cut-off age of 60 years, minimum grade II prostatomegaly/prostatic hyperplasia on grey-scale imaging and PSA levels of at least 10.0 ng/mL were evaluated, and their transrectal SWE findings were correlated with CE-MRI and TRUS biopsy findings.
Results: Cross imaging and biopsy data analysed per core for SWE findings showed that for patients with PSA <20 µg/L, the sensitivity and specificity of SWI for prostate cancer detection were 90% and 88%, while in patients with PSA >20 µg/L, the sensitivity and specificity were 93% and 93%, respectively. Prostate cancer had significantly higher stiffness values compared to benign tissues, with a trend toward stiffness differences in different Gleason grades.
Conclusion: Shear-wave elastography has a high sensitivity, specificity, PPV, and NPV for the detection of PC. With a high PPV, patients with elevated PSA levels, prostatomegaly on routine grey-scale imaging or abnormal results in digital rectal examination and negative SWE may not require a biopsy. This could significantly reduce the need for uncomfortable interventions like TRUS-guided biopsy's negative biopsy rate in prostate cancer detection.
Limitations: Uncooperative patients due to very old age, a user bias, and unavailability of a full spectrum of diagnostic capabilities including PSA and CE-MRI (3T).
Ethics committee approval: Written and informed consent was obtained.
Funding: No funding was recieved for this work.
Author Disclosures:
S. S. Sachar: nothing to disclose
S. Sachar: nothing to disclose

RPS 607-8 12:07
Does shear-wave elastography correlate with biopsies in acute renal graft dysfunction patients? Preliminary results
C. G. García Roch[1], G. F. Maria Esther[1], A. Roca Muñoz[1], F. X. Aragon Tejada[1], S. Aso Manso[1], P. A. A. Barón Rodiz[2], F. García García[2]; *[1]Toledo/ES, [2]Madrid/ES (carmen.roch@gmail.com)*

Purpose: Can shear-wave elastography provide early and confident diagnosis of parenchymal injury in acute kidney graft dysfunction patients compared to biopsies?
Methods and materials: A single-centre, prospective, longitudinal, and analytical study that included all kidney transplanted patients referred for biopsy at our institution due to acute graft failure (post-implantation dysfunction or >20% baseline Cr increase) between January 2018-March 2019.
Within 24 hours after laboratory tests and after a baseline ultrasound examination to rule out non-parenchymal complications, six quantitative shear-wave elastography (SWE) valid measurements (kPa) at graft's cortical interpolar region were acquired by the same senior ultrasound specialist radiologist.
From each graft, kPa range, mean, median, standard deviation, and interquartile range were collected. Shortly after, same-point biopsies were performed and informed by two pathologists according to the 2013 Banff classification.
Exclusion criteria were age <18 years, non-informed consent, adjacent collections, hydronephrosis, vascular stenosis/thrombosis, drug toxicity, recurrent graft disease, and pyelonephritis.
Results: 6 patients were finally enrolled (4 women, 2 men). Allograft age ranged between 5-3,320 days. Creatinine values ranged between 1.8-5.0mg/dL and SWE measurements ranged between 12.7-25.6kPa.
Biopsies resulted in Banff II category in 2 patients, Banff III category in 1 case, and Banff IV category in 3 cases.
After statistical analysis, we found a positive correlation of creatinine levels with SWE values.
Surprisingly, sex seemed to be positively related to SWE values, whereas we found no statistical significance of SWE with the type of Banff classification.
Conclusion: Forthcoming investigations with a larger sample size are needed to validate our findings and define if SWE could be proposed as a future alternative to biopsy in graft dysfunction.
Limitations: A single-centre study with a small sample size.
Ethics committee approval: n/a
Funding: No funding was received for this work.
Author Disclosures:
C. G. García Roch: nothing to disclose
G. F. Maria Esther: nothing to disclose
A. Roca Muñoz: nothing to disclose
F. X. Aragon Tejada: nothing to disclose
S. Aso Manso: nothing to disclose
P. A. A. Barón Rodiz: nothing to disclose
F. García García: nothing to disclose

RPS 607-9 12:13
Comparing computed tomography (CT) and contrast-enhanced ultrasound (CEUS) in the management of complex renal cysts: a single-centre experience
E. Gioulis[1], L. Angelini[2], N. Civitareale[2], A. Zago[2], M. Coss[2], G. Piccoli[2], R. Napoli[2], S. Valerio[2], M. Salemi[2]; *[1]Vittorio Veneto/IT, [2]Conegliano/IT (egioulis@sirm.org)*

Purpose: To gauge the correspondence between CT Bosniak classification, CEUS modified Bosniak classification, and clinical/histological outcomes.
Methods and materials: From March 2017-September 2018, 60 patients underwent CT and CEUS. 65 complex renal cysts were evaluated first by CT and then by CEUS. Benign lesions were defined as those with a Bosniak classification of 2-2F and malignant lesions as those with a Bosniak classification of 3-4, or those with histological diagnosis or those that showed progression during follow-up. Cohen K test, CEUS, CT sensitivity and specificity, and ROC curves were performed.
Results: Bosniak score from CT to CEUS: 17 downgraded ● 11 concluded the follow-up (CEUS Bosniak I) ● 1 operated: pseudocyst (CT Bosniak 4 → CEUS Bosniak 3) ● 5 continue to be monitored 31 maintained ● 4 surgeries: 3 RCC (1 Bosniak 2F, 1 Bosniak 3, 1 Bosniak 4), 1 oncocytoma (Bosniak 4) ● 1 biopsy: HG B-Cell Lymphoma (Bosniak 4) ● 24 continue to be monitored ● 2 were lost to follow-up
17 upgraded ● 6 surgeries: 4 RCC (1 CT Bosniak 2F, 3 CT Bosniak 3 → 4 CEUS Bosniak 4), 1 MCRNLMP (CT Bosniak 2F → CEUS Bosniak 3) 1 simple cyst (CT Bosniak 2F → CEUS Bosniak 3) ● 9 continue to be monitored ● 2 were lost to follow-up
Cohen Kappa test = 0.658 "good"
Conclusion: CEUS can help to better define a Bosniak score, being an alternative to CT when iodinated contrast is contraindicated. CEUS can be

performed bedside. CEUS can reduce ionising radiation exposure and CT scanner workload.
Limitations: CEUS limitations consist in the patients constitutions, location of the renal cyst, and bowel gas.
Ethics committee approval: Written informed consent obtained. Specific literature reviewed.
Funding: No funding was received for this work.
Author Disclosures:
E. Gioulis: nothing to disclose
L. Angelini: nothing to disclose
N. Civitareale: nothing to disclose
M. Coss: nothing to disclose
R. Napoli: nothing to disclose
A. Zago: nothing to disclose
G. Piccoli: nothing to disclose
S. Valerio: nothing to disclose
M. Salemi: nothing to disclose

RPS 607-10 12:19
Association between 2D transperineal ultrasound and physical examination in evaluation of pelvic floor muscle functions
A. Aryan, M. Arab Ahmadi*; Tehran/IR (arvinaryan@yahoo.com)*

Purpose: Transperineal ultrasound has been introduced for the assessment of pelvic floor muscles functional status, however, the accuracy of these modalities as compared to physical examination remains uncertain. Moreover, the assessment of levator ani function status via physical examination is subjective and requires high gynaecological experience. The study aimed to compare the correlation between 2D transperineal ultrasonography and physical examination (intravaginal palpation) for the evaluation of pelvic levator ani function.
Methods and materials: This cross-sectional study was performed on 40 women aged 29 to 75 years who were candidates for structural evaluation due to the suspicion of pelvic floor muscles dysfunction. The status was assessed by both physical examination (graded based on the Oxford Grading System) and transperineal 2D ultrasound.
Results: Strong correlations were revealed between the Oxford physical examination score and both US parameters as levator ani assessment in the midsagittal plan, the difference between AP dimension of hiatus at rest and at squeezing ($r=0.671$, $p<0.001$), and also the cranial shift of muscle ($r=0.498$, $p<0.001$). The decrease in hiatus dimension and cranial shift assessed by ultrasound was found by an increase in the Oxford physical examination score.
Conclusion: Because of the high correlation between physical and ultrasound examination in assessing pelvic floor muscle performance, ultrasound, as an available low-cost method, can be used safely instead of a physical evaluation for this purpose. The assessment of levator ani function by mid sagital 2D transperineal ultrasound should be using the two indices including cranial shift and the decrease in hiatus dimension during squeezing.
Limitations: A small sample size.
Ethics committee approval: The study was approved by the ethical committees at the University of Medical Sciences.
Funding: No funding was received for this work.
Author Disclosures:
A. Aryan: nothing to disclose
M. Arab Ahmadi: nothing to disclose

RPS 607-11 12:25
How to increase eligibility in MRgFUS (magnetic resonance-guided focused ultrasound surgery) to treat difficult cases of uterine fibroids (UFs): tips and tricks
L. P. Vazzana, S. Iafrate, I. Capretti, F. Arrigoni, M. Di Luzio, S. Mascaretti, G. Mascaretti, C. Masciocchi*; L'Aquila/IT (luciavazzana@gmail.com)*

Purpose: To investigate additional tips and tricks to increase the eligibility of MRgFUS in patients showing some limitation.
Methods and materials: From September 2015 to June 2017, we evaluated 19 women with UFs showing an inadequate acoustic window to MRgFUS. Additional to the common techniques used to obtain an adequate acoustic window, such as filling the bladder with saline and filling the rectum with ultrasound gel, we tried to evaluate some strategies to increase the eligibility to the procedure. We used an inversion table with the patients in an antigravity position in order to move up the bowel loops. Furthermore, a low-fibre diet for a week before the MRgFUS was advised to reduce intestinal bloating, distension, and intestinal peristalsis. The volume of treated fibroid and non-perfused volume (NPV) were calculated with specific software.
Results: Out of 19 patients, 12 showed an adequate acoustic window and underwent MRgFUS after using inversion table (21%), filling the bladder and rectum (48%), and a low-fibre diet (31%). The UFs presented a mean extension of the NPV of about 50-65%, with good effectiveness of the treatment. 7 patients, despite these strategies, continued to display an inadequate acoustic window and were not treated.
Conclusion: Some practical tips and tricks to get an adequate acoustic window for the ultrasound beam may increase the eligibility of patients to MRgFUS, thus allowing the procedure. Furthermore, in these patients, MRgFUS shows good safety profile and an improvement of clinical outcomes.
Limitations: A small number of patients.
Ethics committee approval: n/a
Funding: No funding was received for this work.
Author Disclosures:
M. Di Luzio: nothing to disclose
L. P. Vazzana: nothing to disclose
S. Iafrate: nothing to disclose
I. Capretti: nothing to disclose
F. Arrigoni: nothing to disclose
S. Mascaretti: nothing to disclose
G. Mascaretti: nothing to disclose
C. Masciocchi: nothing to disclose

11:15 - 12:30 **Darwin (Room D2)**

Chest

RPS 604a

Evaluation of interstitial lung disease: recent advances and new techniques

Moderators:
E. Baratella; Trieste/IT
E. J. Stern; Seattle, WA/US

RPS 604a-K 11:15
Keynote Lecture
M. Benegas Urteaga*; Barcelona/ES (benegasmariana@gmail.com)*

Author Disclosures:
M. Benegas Urteaga: nothing to disclose

RPS 604a-1 11:25
The effect of deep learning reconstruction on cyst scores in patients with cystic lung diseases
C. Steveson[1], J. Schuzer[2], S. Rollison[2], T. Machado[2], A. Jones[2], P. Julien-Williams[2], J. Moss[2], M. Chen[2]; *[1]Adelaide/AU, [2]Bethesda/US (chloe.steveson@medical.canon)*

Purpose: To investigate the effect of a deep learning image reconstruction algorithm on cyst scores (percentage of lung volume occupied by cysts) in chest CT scans.
Methods and materials: 105 consecutive patients with cystic lung diseases underwent chest CT at standard radiation doses on a 320 detector row CT scanner with the following scan parameters: Helical scan, 0.5mm x 80 detector rows, 120 or 100kV, automatic exposure control, 0.275s rotation speed, and standard pitch. Each scan was reconstructed using a soft tissue kernel with hybrid iterative reconstruction (AIDR3D) and deep learning reconstruction (AiCE) techniques. Cyst scores were quantified by semi-automated software. The signal to noise ratio was calculated for each reconstruction. The data was analysed by linear correlation, paired t-test, and Bland-Altman.
Results: Patients averaged 49.1 years (range 27-76yrs), 91% were female. The mean radiation dose was 4.50 mSv ±2.24 mSv. The mean cyst score was 8.9±10.8 (range 0-43.8) for clinical AIDR 3D reconstruction and 9.2±11.2 (range 0-45.1) for deep learning reconstruction AiCE, representing an insignificant difference of 0.28%. Linear correlation coefficient was excellent at 0.99 ($p<0.0001$). Signal-to-noise for AiCE images was higher than AIDR3D images (8.76 vs. 7.38, respectively, $p<0.001$).
Conclusion: Deep learning image reconstruction has an excellent correlation with conventional AIDR 3D reconstruction for chest CT at standard radiation doses.
Limitations: A single-centre study.
Ethics committee approval: Institutional ethics approval obtained (National Institutes of Health, USA).
Funding: No funding was received for this work.

Author Disclosures:
C. Steveson: Employee at Canon Medical Systems
J. Schuzer: Employee at Canon Medical Research
S. Rollison: nothing to disclose
M. Chen: nothing to disclose
J. Moss: nothing to disclose
T. Machado: nothing to disclose
A. Jones: nothing to disclose
P. Julien-Williams: nothing to disclose

RPS 604a-2 11:31

From infancy to adulthood: developmental changes in pulmonary quantified computed tomography parameters

J. F. M. Gawlitza[1], F. Trinkmann[2], F. Trudzinski[1], H. Wilkens[1], A. Bücker[1], J. Stroeder[1], P. Fries[1]; [1]*Homburg/DE,* [2]*Mannheim/DE (joshua.gawlitza@uks.eu)*

Purpose: Quantified computed tomography (qCT) is known for correlations with airflow obstruction and fibrotic changes of the lung. However, as qCT studies often focus on diseased and elderly subjects, current literature lacks physiological qCT values during body development. We evaluated the chest CT examinations of a healthy cohort, reaching from infancy to adulthood, in order to determine physiological qCT values and changes during body development
Methods and materials: Dose-optimised chest CT examinations performed over the last 3 years using a dual-source CT scanner were retrospectively analysed. Exclusion criteria were age >30 years and any known or newly diagnosed lung pathology (n = 151). Lung volume, mean lung density, full-width-at-half-maximum, and low attenuated volume (LAV) were semi-automated quantified. qCT values between different age groups as well as unenhanced (Group 1) and contrast-enhanced (Group 2) protocols were compared. Models for the projection of age-dependent changes in qCT values were fitted.
Results: Significant differences in qCT parameters were found between the age subgroups ($p < 0.05$). All parameters except LAV merge into a plateau level above this age as shown by fitted polynomial models (r^2 between 0.85 and 0.67). In group 2, this plateau phase is shifted back around 5 years. Except for the volume, significant differences in all qCT values were found between group 1 and 2 ($p < 0.01$).
Conclusion: qCT parameters underlie a specific age-dependant dynamic from infancy to adulthood. Except for LAV, qCT parameters reach a plateau phase around adolescence. Contrast-enhanced protocols seem to shift this plateau backwards.
Limitations: Group findings are projected on individuals. Nonetheless, a yearly CT for lung evaluation in healthy patients would be unacceptable. No spirometric triggering. The sample size.
Ethics committee approval: Institutional Review Board Waiver.
Funding: No funding was received for this work.
Author Disclosures:
F. Trinkmann: nothing to disclose
J. F. M. Gawlitza: nothing to disclose
F. Trudzinski: nothing to disclose
H. Wilkens: nothing to disclose
A. Bücker: nothing to disclose
J. Stroeder: nothing to disclose
P. Fries: nothing to disclose

RPS 604a-3 11:37

Interstitial lung abnormality in abdominal and thoracoabdominal computed tomography scans performed for routine clinico-surgical indications

G. Milanese, M. Silva, V. R. Papapietro, E. Bacchini, G. Capretti, F. Specchia, S. E. Gazzani, E. Iezzi, N. Sverzellati*; Parma/IT*

Purpose: To define the prevalence of interstitial lung abnormality (ILA) in patients undergoing routine abdominal and/or thoracic-abdominal computed tomography (CT) without clinical indication for pulmonary disease (PD). To evaluate the percentage of radiological under-reporting of CT features of ILA.
Methods and materials: This retrospective study included patients undergoing an abdominal or thoracoabdominal CT scan for clinico-surgical indications other than PD.
The detection of CT features of ILA was visually performed by a group of investigators. Subsequently, selected subjects were evaluated by an expert thoracic radiologist for classification into $ILA_{fibrotic}$/$ILA_{non-fibrotic}$/$ILA_{equivocal}$ /ILA_{absent}. Patients with $ILA_{fibrotic}$ were classified according to the 2017 Fleischner Society criteria for IPF, including a description of individual abnormalities. The pattern of $ILA_{non-fibrotic}$ was also evaluated.
Results: ILAs were assessed in 26,295 consecutive subjects of whom 663 (2.5%) subjects had ILA on at least one CT as follows: 255 (1%) had $ILA_{fibrotic}$ (0.22% typical UIP, 0.24% probable UIP, 0.33% indeterminate for UIP, and 0.17% most consistent with a non-IPF diagnosis), 161 (0.6%) had $ILA_{non-fibrotic}$, and 247 (0.9%) had $ILA_{equivocal}$.
A total of 374 out of 663 ILA (56.4%) were unreported in the original radiology reports of baseline abdominal/thoraco-abdominal CT scans.
Conclusion: In this large study cohort of unselected subjects undergoing abdominal/thoracoabdominal CT for clinical indications other than PD, the frequency of ILA, particularly that of $ILA_{fibrotic}$, was not negligible, with substantial under-reporting.
Limitations: A monocentric setting.
Ethics committee approval: 210/2017/OSS/AOUPR.
Funding: Roche.
Author Disclosures:
G. Milanese: nothing to disclose
M. Silva: nothing to disclose
V. R. Papapietro: nothing to disclose
E. Bacchini: nothing to disclose
G. Capretti: nothing to disclose
F. Specchia: nothing to disclose
S. E. Gazzani: nothing to disclose
E. Iezzi: nothing to disclose
N. Sverzellati: nothing to disclose

RPS 604a-4 11:43

Cross-border knowledge sharing in the diagnostic workup of a rare disease: experiences with a Trans-European teleradiology project on idiopathic pulmonary fibrosis

T. J. Weikert, G. Sommer, M. Tamm, P. Haegler, J. Cyriac, A. W. Sauter, K. Hostettler, J. Bremerich*; Basel/CH (thomas.weikert@usb.ch)*

Purpose: To share experience from a large, ongoing expert reading teleradiology program in Europe and Asia aiming at supporting referring centres to interpret high-resolution computed tomography (HRCT) with respect to the presence of usual interstitial pneumonia (UIP)-pattern in patients with suspected idiopathic pulmonary fibrosis (IPF).
Methods and materials: We analysed data from 01/2014 to 05/2019, including HRCTs from 239 medical centres in 12 European and Asian countries that were transmitted to our picture archiving and communication system (PACS) via a secured internet connection. Structured reports were generated in consensus by a radiologist with over 20 years experience in thoracic imaging and a pulmonologist with specific expertise in interstitial lung disease according to current guidelines on IPF. Reports were sent to referring physicians. We evaluated patient characteristics, technical issues, report turnaround times, and frequency of diagnoses. We also conducted a survey to collect feedback from referring physicians.
Results: HRCT image data from 703 patients was transmitted (53.5% male). The mean age was 63.7 years (SD:17). In 35.1% of all cases, the diagnosis was “UIP”/”Typical UIP”. The mean report turnaround time was 1.7 days (SD:2.9). Data transmission errors occurred in 7.1%. The overall satisfaction rate among referring physicians was high (8.4 out of 10; SD:3.2).
Conclusion: This Eurasian teleradiology program demonstrates the feasibility of cross-border teleradiology for the provision of state-of-the-art structured reporting to centres with limited expertise in chest radiology.
Limitations: A low response rate of the survey. No cost-effectiveness analysis was conducted.
Ethics committee approval: Informed conset was waived by the local ethics committee (Project ID: Req-2019-00403).
Funding: No funding was received for this work. The teleradiology program is financially supported by Boehringer Ingelheim.
Author Disclosures:
T. J. Weikert: nothing to disclose
G. Sommer: nothing to disclose
M. Tamm: nothing to disclose
P. Haegler: Employee at Boehringer Ingelheim
J. Cyriac: nothing to disclose
A. W. Sauter: nothing to disclose
K. Hostettler: nothing to disclose
J. Bremerich: nothing to disclose

RPS 604a-5 11:49

Characteristics of lung disease patterns on CT scans in patients with idiopathic inflammatory myopathies: association with myositis specific auto-antibodies

A. Laporte, K. Mariampillai, Y. Allenbach, O. Benveniste, P. Grenier, S. Boussouar*; Paris/FR (mandine_31@hotmail.fr)*

Purpose: To identify different lung patterns associated with idiopathic inflammatory myopathies (IIM) and to evaluate the potential relationship between the CT findings of interstitial lung disease (ILD) and myositis specific antibodies (MSA).

Methods and materials: All consecutive IIM patients referred to the internal medicine department between 2004 and 2019 were included and chest CT scans were retrospectively assessed by two radiologists. The CT findings were used for multivariate analysis to identify subgroups of patients.
Results: CT scans of 257 patients with IIM including inclusion body myositis (IBM) (n=68), dermatomyositis (DM) (n=67), immune-mediated necrotising myopathy (IMNM) (n= 63), and antisynthetase syndrome (ASS) (n=59) were analysed. MSA were present in 173 patients (67.3%). 94 patients (36%) had ILD. The cluster analysis identified three subgroups of patients. The first cluster (n= 21) was characterised by consolidation (95%). DM with anti-MDA5 was significantly more present in this cluster. All the patients of the second cluster (n=34) presented cysts (including honeycombing). The patients in the last cluster (n=39) had significantly more intralobular-reticulations, an absence of cysts, and 17% of consolidation. Patients with ASS were significantly more present in cluster 2 and 3.
Conclusion: Despite the heterogeneity of ILD observed in IMM, ILD could be split among 3 clusters according to CT-scan criteria and theses clusters were associated to MSA. The identification by radiologists of those clusters could facilitate diagnostic screening, following, and prognostic value.
Limitations: It was a monocentric, retrospective study and we didn't take into account the evolution of lung pattern through different CT scans for each patient.
Ethics committee approval: Written informed consent was provided by all patients for use of the database.
Funding: No funding was received for this work.
Author Disclosures:
A. Laporte: nothing to disclose
P. Grenier: nothing to disclose
S. Boussouar: nothing to disclose
O. Benveniste: nothing to disclose
Y. Allenbach: nothing to disclose
K. Mariampillai: nothing to disclose

RPS 604a-6 11:55

Evaluation of the relationship between pulmonary manifestations and laboratory findings in rheumatoid arthritis patients

H. Çelik, N. S. Gezer, G. O. Simsek, A. Ozgen Alpaydın, S. Tarhan, E. Yilmaz, P. Balci*; Izmir/TR (dr.celik90@gmail.com)*

Purpose: The relationship between radiological and laboratory findings in rheumatoid arthritis (RA) patients is not fully documented in the literature. We aimed to show the correlation between chest computed tomography (CT) findings and laboratory tests used in the diagnosis and follow-up of patients with RA.
Methods and materials: Chest CT scans of 263 patients with RA were evaluated for a rheumatoid nodule, serositis, bronchiectasis, constrictive bronchiolitis, follicular bronchiolitis, and interstitial fibrosis pattern (Figure 1-3). Anti-nuclear antibody (ANA), rheumatoid factor (RF), C-reactive protein (CRP), and erythrocyte sedimentation rate (ESR) values synchronous with CT scans were recorded. The relationship between the radiological findings and laboratory data was analysed.
Results: 70% of patients were female. CT scans revealed rheumatoid nodules in 25% and cavitation in at least one rheumatoid nodule in 21% of patients with rheumatoid nodules. Nonspecific interstitial pneumonia (NSIP) was the most common fibrosis pattern (% 65). Serositis, bronchiectasis, and constrictive bronchiolitis were defined in 18%, 36%, and 22% of the patients, respectively. A statistically significant relationship was found between constrictive bronchiolitis and ESR (p: 0.001), between serositis, ESR, and CRP (p=0.003 ve p<0001 respectively), and between bronchiectasis and CRP (p=0.005) (Table 1). There was no statistically significant relationship between ANA values and any radiological findings.
Conclusion: This study suggests that some specific laboratory tests used in the diagnosis and follow-up of RA may predict lung involvement patterns that may develop due to rheumatoid arthritis such as constructive bronchiolitis, serositis, and bronchiectasis.
Limitations: There were differences in some of the chest CT protocols such as the use of high-resolution CT or contrast media. Also, some laboratory tests were not performed in all patients.
Ethics committee approval: Ethics committee approval is available.
Funding: No funding was received for this work.
Author Disclosures:
H. Çelik: nothing to disclose
N. S. Gezer: nothing to disclose
G. O. Simsek: nothing to disclose
A. Ozgen Alpaydın: nothing to disclose
S. Tarhan: nothing to disclose
E. Yilmaz: nothing to disclose
P. Balci: nothing to disclose

RPS 604a-7 12:01

Comparison of the relevancies of different reconstruction kernels and slices thickness for disease progression in idiopathic pulmonary fibrosis

J. Pan[1], J. Hofmanninger[1], S. Röhrich[1], F. Prayer[1], N. Sverzellati[2], H. Prosch[1], G. Langs[1]*; [1]Vienna/AT, [2]Parma/IT (jeanny.pan@meduniwien.ac.at)*

Purpose: To compare image markers and the importance of the different reconstruction kernels and slice thickness in chest CT scans in idiopathic pulmonary fibrosis (IPF) using unsupervised machine learning (ML).
Methods and materials: CT scans from 106 IPF patients were reconstructed with 5 different reconstruction kernels and 3 different slice thicknesses. Firstly, supervoxels were computed using autonomously segmented lung regions. The texture grey-level co-occurrence matrix was computed for assigning 1 to 20 cluster labels to each supervoxel. Cluster label volume maps were generated for each scan. The differences between the label maps of two subsequent scans were computed for different combinations of slice thickness and reconstruction kernels. The volume differences between subsequent scans with different kernel combinations were tested. The computed globally labelled volume fractions were utilised as input to train a random forest classifier. The trained classifier identified progression markers by predicting the sequence of longitudinal examinations for randomly chosen patients.
Results: The classifier's performance was evaluated with 10 different runs. 10% of the patients were used as test data. The mean accuracies after 10 runs were 76% for subsequent scans with the same kernel, 79% for scans with all 5 kernels combined, 88% for scans with Boneplus and Bone kernels, 85% for scans with Boneplus, and 60% for scans with Bone kernel alone. 2 clusters are identified as stable texture clusters for the assessment of IPF progression with different combinations of kernels and slice thickness.
Conclusion: The proposed ML methods were able to identify the relevance of different combinations of kernels. For applying a machine learning approach, homogeneous slice thickness is more relevant than reconstruction kernels. 2 stable texture patterns are shown as markers for the assessment of IPF.
Limitations: n/a
Ethics committee approval: n/a
Funding: No funding was received for this work.
Author Disclosures:
J. Pan: Research/Grant Support at Boehringer Ingelheim
N. Sverzellati: nothing to disclose
J. Hofmanninger: nothing to disclose
G. Langs: Research/Grant Support at Siemens, Research/Grant Support at Novartis
S. Röhrich: nothing to disclose
F. Prayer: nothing to disclose
H. Prosch: Research/Grant Support at Boehringer Ingelheim

RPS 604a-8 12:07

The evaluation of lung CT densitometry in interstitial lung diseases

Y. Şengül, D. Kocakaya, C. Ilgin, E. Eryuksel, N. Inanc, N. C. Cimsit*; Istanbul/TR (yldzsngl34@gmail.com)*

Purpose: To evaluate the relationship between changes in the density in lung parenchyma with pulmonary function test (PFT) and visual CT features, regardless of the pattern differences in ILD, and also to investigate the threshold values of densitometric parameters in predicting the severity of pulmonary fibrosis.
Methods and materials: 69 patients with idiopathic pulmonary fibrosis (IPF), systemic sclerosis (SSc), and rheumatoid arthritis (RA) were evaluated who had no more than a 1-month interval between thorax CT and PFT measurements. CT scans were scored visually then processed to obtain mean lung density (MLD), the percentage of high attenuation area (HAA%), and the HU value in 85th percentile. The relationships between the densitometry with PFT and semiquantitative scoring were evaluated.
Results: All densitometry values in patients with ILD were significantly higher than the control group. MLD threshold value was -760 (sensitivity 50%, specificity 81%), the HAA% 7.3 (sensitivity 65%, specificity 81%), 85th perc -660 (sensitivity 62%, specificity 81%) based on DLCO% predicted value of 70 in determining the severity of pulmonary fibrosis.
Densitometric parameters showed a statistically significant correlation with physiologic quantities and fibrosis score (r: -0.40 to -0.50) and (r:0.52 to 0.66), respectively.
The fibrosis score and densitometry parameters were high in patients with a pulmonary artery diameter greater than 29 mm.
Conclusion: Quantitative densitometric CT parameters correlate with pulmonary function test results and visual scoring. This objective method may be useful for determining the extent and severity of fibrosis in ILD.
Limitations: A retrospective study and the low number of samples.
Ethics committee approval: The local Medical Ethical Committee permission (09.2018.782) was obtained.
Funding: No funding was received for this work.

Author Disclosures:
Y. Şengül: Author at Marmara University Pendik Research and Educational Hospital
E. Eryuksel: Author at Marmara University Pendik Research and Educational Hospital
D. Kocakaya: Author at Marmara University Pendik Research and Educational Hospital
N. Inanc: Author at Marmara University Pendik Research and Educational Hospital
C. Ilgin: Author at Marmara University Pendik Research and Educational Hospital
N. C. Cimsit: Author at Marmara University Pendik Research and Educational Hospital

RPS 604a-9 12:13
The impact of hybrid iterative reconstruction on quantitative analysis with pulmonary CT
Z. Liu*; Beijing/CN (liuzhuormyy@sina.cn)*

Purpose: To investigate the impact of hybrid iterative reconstruction blending levels on quantitative analysis and objective image quality of pulmonary CT.
Methods and materials: Pulmonary CT images were acquired from 52 subjects and reconstructed using different hybrid iterative reconstruction blending levels including FBP, ASIR-V30%, ASIR-V50%, ASIR-V70%, and ASIR-V100%. Quantitative analyses were compared including emphysema index(EI), total lung volume, luminal area, wall area, wall thickness, diameter of airway, and nodule volume. CT value and standard deviation (SD) were also measured and compared.
Results: EIs were found statistically different [FBP (3.34 %), ASIR-V30% (2.13 %), ASIR-V50% (1.46 %), ASIR-V70% (0.98 %), and ASIR-V100% (0.57 %)(P<0.001)]. SDs decreased dramatically with the increase of ASIR-V percentage [air in trachea: FBP (29.8HU), ASIR-V30% (25.5HU), ASIR-V50% (22.6HU), ASIR-V70% (19.6HU), ASIR-V100% (15.2HU), descending aorta: FBP (35.2HU), ASIR-V30% (27.6HU), ASIR-V50% (22.7HU), ASIR-V70% (18.0HU), ASIR-V100% (12.1HU) (P<0.001)]. There was no statistically significant difference of CT values, airway dimensions, nodule volumes, and lung volumes among different blending levels (P>0.05).
Conclusion: With the increase of blending level of ASIR-V, EI and SD decreased significantly, while volumetric quantification of lung nodule and airway dimensions were not affected.
Limitations: The results of this single-centre study were limited to only one scanner and one iterative reconstruction algorithm. The sample size of patients in our study was small, which may affect the statistical results.
Ethics committee approval: n/a
Funding: No funding was received for this work.
Author Disclosures:
Z. Liu: nothing to disclose

RPS 604a-10 12:19
A comparison between the ATS/ERS/JRS/ALAT criteria of 2011 and 2018 for usual interstitial pneumonia on HRCT: a cross-sectional study
L. L. Wuyts, M. Camerlinck, D. de Surgeloose, L. Vermeiren, D. Ceulemans, J. Clukers, H. Slabbynck*; Antwerp/BE*

Purpose: To determine whether the revised 2018 ATS/ERS/JRS/ALAT radiological criteria for usual interstitial pneumonia (UIP) provide better diagnostic agreement compared to those published in 2011.
Methods and materials: The cohort for this cross-sectional study (single-centre, nonacademic) was recruited from a multidisciplinary ILD team discussion (MDD) from July 2010 to December 2018, with clinical suspicion of idiopathic pulmonary fibrosis (n= 325). Exclusion criteria were technical HRCT issues, images not acquired within reference centre, the presence of lung neoplasm, the patient suffering from known connective tissue disease, drug exposure to pulmonary toxins, or a lack of a working diagnosis after MDD (Figure 1). Four readers with varying degrees of experience in the interpretation of HRCT independently assessed 192 HRCT scans for the presence of fibrotic lung disease characteristics. A diagnostic category was assigned to each HRCT according to both the previous (2011) and current (2018) radiological criteria based on the ATS/ERS/JRS/ALAT statements on IPF (Figures 2 and 3). An inter-rater variability analysis (Gwet's second-order agreement coefficient) was performed.
Results: The resulting estimate of Gwet's AC_1 coefficient for the use of the ATS/ERS/JRS/ALAT radiological criteria for 2011 and 2018 is 0.62 (± 0.06) and 0.65 (± 0.06), respectively (Table 1). The inter-rater variability improved for every pair of readers, except for one. Considering the varying degree of experience of these 4 radiologists, we report only minor differences in the agreement level.
Conclusion: No statistically significantly higher degree of diagnostic agreement is observed when applying the revised ATS/ERS/JRS/ALAT radiological criteria for UIP of 2018 compared to those of 2011. The estimated inter-rater variability for assigning the diagnostic categories is moderate for both classification systems, although it improves consistently, independent from the degree of experience in HRCT interpretation.
Limitations: n/a
Ethics committee approval: Ethics committee approval was obtained.
Funding: No funding was received for this work.
Author Disclosures:
L. L. Wuyts: nothing to disclose
M. Camerlinck: nothing to disclose
D. de Surgeloose: nothing to disclose
L. Vermeiren: nothing to disclose
D. Ceulemans: nothing to disclose
J. Clukers: nothing to disclose
H. Slabbynck: nothing to disclose

RPS 604a-11 12:25
Can we improve the prediction of survival in fibrotic interstitial lung diseases? Texture-based quantitative CT model outperforms expert diagnosis
E. J. M. Barbosa Jr., W. Gefter, D. Kontos, B. Haghighi*; Philadelphia, PA/US*

Purpose: Usual interstitial pneumonia (UIP) is generally associated with a worse prognosis than other types of non-UIP fibrotic interstitial lung diseases (ILD). We hypothesised that a texture-based model utilising high-resolution quantitative HRCT (qCT) imaging features can better predict survival in ILD patients when compared to the clinical standard of UIP versus non-UIP expert diagnostic labels.
Methods and materials: 40 ILD patients (20 UIP, 20 non-UIP ILD) were classified by expert consensus of 2 radiologists and followed for 7 years. Clinical variables (CVs) such as age, gender, smoking status, and co-morbidities, as well as the outcomes such as time to death or lung transplantation, were recorded. A survival analysis (Kaplan-Meier with Cox regression) was performed, comparing expert diagnostic labels (UIP vs non-UIP) versus a texture-based model utilising 26 higher-order 3D imaging metrics derived from quantitative HRCT, with varying region of interest (ROI) sizes, controlling for age and co-morbidities.
Results: Survival curves of UIP vs non-UIP ILD patients (using expert diagnostic labels) were not statistically different (p=0.59). In contrast, our texture-based qCT model with CVs achieved statistically significant partition of the cohort (p=0.029, c-statistic = 0.73) into distinct survival sub-groups.
Conclusion: Our texture-based qCT model substantially outperformed expert diagnostic labels (UIP vs non-UIP expert) to predict survival in ILD patients. These models, by capturing latent HRCT derived lung parenchymal texture biomarkers that are not explicitly accounted for in clinical standard diagnostic labels, may provide more accurate prognostication, ultimately contributing to more effective patient management, treatment planning, and possibly improving long-term outcomes.
Limitations: The retrospective nature and sample size of the study.
Ethics committee approval: Approved by the local IRB (#821679) with HIPAA waiver of informed consent.
Funding: This research was supported by a Radiological Society of North America (RSNA) Research Seed Grant to the lead author (EB).
Author Disclosures:
E. J. M. Barbosa Jr.: nothing to disclose
W. Gefter: nothing to disclose
D. Kontos: nothing to disclose
B. Haghighi: nothing to disclose

11:15 - 12:30 **Descartes (Room D3)**

Interventional Radiology

RPS 609a

Lung and mediastinal interventions

Moderators:
M. Krokidis; Cambridge/UK
L. Musayeva; Baku/AZ

RPS 609a-1 11:15
Bronchial artery diameter as a predictor of haemoptysis: a single-centre experience
B. S. R. Reddy[1], P. Chatterjee[2], K. Sunder[3], R. Kumar[3], V. Mazumdar[3]; *[1]Chennai, Tamil Nadu/IN, [2]Guwahati, ASSAM/IN, [3]Chennai/IN (sudeepreddy2009@gmail.com)*

Purpose: To evaluate the bronchial artery diameter in multidetector CT angiography (MDCTA) as a predictor of haemoptysis and to compare this with digital subtraction angiography (DSA) prior to bronchial artery embolisation.
Methods and materials: MDCTA was performed in 40 patients (35 men, 5 women; age range=19-82 years; mean=52.6 years) with haemoptysis who were referred for bronchial artery embolisation. Bronchial arteries with a diameter of more than 2 mm were considered abnormal and hypertrophied. Transverse, multiplanar reconstruction, and 3-dimensional reconstruction (maximum intensity projection and volume-rendered) images were analysed to identify the abnormal hypertrophied bronchial arteries causing haemoptysis. Their origin and course were noted. DSA was performed with the knowledge of findings from MDCTA. Selective arteriograms of abnormal bronchial arteries were performed. Embolisation was done for all patients using polyvinyl alcohol particles (300-500 µm), gel foam, or coils.
Results: DSA was performed for all cases and the results were compared with MDCTA. MDCTA shows a 96.2% sensitivity and 100% specificity in identifying abnormal hypertrophied bronchial arteries with a diameter of more than 2 mm.
Conclusion: There is a strong positive correlation of bronchial artery diameter of more than 2 mm in MDCTA for predicting haemoptysis.
Limitations: A small sample size. A multicenteric study may be required for further evalution.
Ethics committee approval: n/a
Funding: No funding was received for this work.
Author Disclosures:
B. S. R. Reddy: Other at apollo main hospital
P. Chatterjee: Consultant at apollo main hospital
K. Sunder: Consultant at apollo main hospital
R. Kumar: Consultant at apollo main hospital
V. Mazumdar: Consultant at apollo main hospital

RPS 609a-2 11:21

Transpulmonary chemoembolisation (TPCE) and transarterial chemoperfusion (TACP) in patients with primary and secondary lung neoplasms: evaluation of apparent diffusion coefficient (ADC) values
T. J. Vogl, T. Hoppe, N. N. N. Naguib, N.-E. A. Nour-Eldin, T. Gruber-Rouh, L. Basten*; Frankfurt am Main/DE*
(t.vogl@em.uni-frankfurt.de)

Purpose: To evaluate the predictive value of the apparent diffusion coefficient (ADC) for the treatment response in unresectable primary and secondary lung neoplasms using transpulmonary chemoembolisation (TPCE) and transarterial chemoperfusion (TACP).
Methods and materials: 42 primary (n=13) and secondary (n=29) unresectable lung lesions of 31 patients undergoing TPCE and TACP were included. Lesion diameter, volume, and ADC values were measured on an MRI series including a diffusion-weighted imaging (DWI) sequence at the beginning and end of each treatment cycle. Treatment response was evaluated on a per-lesion basis. Partial response (PR) was defined as a size decrease of ≥30%, progressive disease (PD) as an increase of≥20%, and stable disease (SD) was the remaining lesions. A statistical analysis of ADC values was performed using t-tests, an analysis of variance, and receiver-operating characteristic curves.
Results: 9 lesions recorded PR: the mean pre-treatment ADC was $1.164x10^{-3}$ mm²/s and the mean ADC increase was 32.9%. 19 lesions recorded SD: the mean pre-treatment ADC was $1.449x10^{-3}$ mm²/s and the mean ADC increase was 6.9%. 14 lesions recorded PD: the mean pre-treatment ADC was $1.418x10^{-3}$ mm²/s and the increase in the mean ADC was 5.0%. The difference in ADC changes between response groups was significant (p≤0.02). Pre-treatment ADC recorded an area under the curve (AUC) of 0.774 for response prediction. A threshold ADC increase of 20.7% showed 88% sensitivity and 78% specificity for response prediction (AUC 0.838).
Conclusion: The study showed significant differences in mean ADC changes comparing PR to SD (p=0.02) and PR to PD (p<0.01) groups with a correlation between lesion volume reduction and an early increase in ADC in patients undergoing TPCE and TACP.
Limitations: A retrospective study design with a small number of patients.
Ethics committee approval: Approval by the Institutional Review Board.
Funding: No funding was received for this work.
Author Disclosures:
T. J. Vogl: nothing to disclose
T. Hoppe: nothing to disclose
N. N. N. Naguib: nothing to disclose
N.-E. A. Nour-Eldin: nothing to disclose
T. Gruber-Rouh: nothing to disclose
L. Basten: nothing to disclose

RPS 609a-3 11:27

Lung cancer CT-guided FNAC with rapid on-site evaluation (ROSE)
F. Fiore, L. D'acierno, V. Stoia, N. Martucci, R. D'angelo, F. Somma*; Naples/IT*
(ludovicad.a@gmail.com)

Purpose: To evaluate the efficacy and accuracy of CT-guided fine-needle aspiration citology (FNAC) in lung cancer typing.
Methods and materials: From January 2013-December 2017, 640 FNAC specimens were collected from 640 patients and examined with rapid on-site evaluation (ROSE), and subsequently underwent immunological tests (TTF-1, p40, CK 5/6, CK 7, and Napsin). Afterwards, cytological findings were compared with final histologic diagnoses. Overall adequacy and accuracy rates were determined by comparison with the final diagnosis.
Results: Of the 640 cases, concordance between "adequate" interpretation by ROSE and unequivocal malignant or benign diagnoses on final interpretation was 100%. In 80% of the specimens, it was possible to perform immunohistological analysis. The complication rate was 7%; no bleeding occurred but we did observe pneumothorax, which was distinguished in "early", when it was diagnosed during or at the end of the procedure and treated percutaneously, or "delayed", when it occurred in the first 24 hours and was surgically treated.
Conclusion: Lung cancer typing according to cytological criteria is feasible, accurate, and comparable with results of a histological analysis on small specimens. In addition, the possibility of immunological testing combined with the minimally invasive specimen harvesting can come up to the oncologists' increasing demands of a specific target for the new therapeutic frontiers (chemoimmunotherapy, radiotherapy, or surgery).
Limitations: A retrospective study and a single-centre experience.
Ethics committee approval: n/a
Funding: No funding was received for this work.
Author Disclosures:
L. D'acierno: nothing to disclose
V. Stoia: nothing to disclose
F. Fiore: nothing to disclose
F. Somma: nothing to disclose
R. D'angelo: nothing to disclose
N. Martucci: nothing to disclose

RPS 609a-4 11:33

Correlation between the length of embolisation material pulmonary arteriovenous malformation and the distal pulmonary hypoperfusion evaluated by spectral imaging in patients with HHT
J. Bizouerne, L. Cassagnes*; Clermont-Ferrand/FR*
(julie.bizouerne@gmail.com)

Purpose: Pulmonary arteriovenous malformation (PAVM) embolisation creates a ventilation-perfusion mismatch (V/Q defect). The pulmonary hypoperfused volume generated can be viewed on an iodine map with a dual-energy computed tomography as a defect, like acute pulmonary embolism. Our objective was to evaluate a correlation between the distance embolisation material PAVM, and the pulmonary hypoperfused volume, using spectral imaging in patients with hereditary haemorrhagic telangiectasia (HHT).
Methods and materials: 5 patients with HHT who had at least one embolised PAVM at our university hospital between March 2018 and May 2019 were included prospectively. A chest dual-energy computed tomography was performed. The distal pulmonary hypoperfused volume was quantified with manual segmentation using an iodine map. This distal pulmonary hypoperfused volume and the distance embolisation material PAVM were compared.
Results: 9 PAVM were studied. We found a high correlation between the distance embolisation material PAVM and the distal pulmonary hypoperfused volume (0.77, p=0.02), and between the diameter of the embolised artery and the distal pulmonary hypoperfused volume (0.88, p=0.004). The correlation between the distance embolisation material PAVM and the distal pulmonary hypoperfused volume still remained after exclusion of the effect of the diameter of the embolised artery (0.35, p=0.03).
Conclusion: Our study found a correlation between the distance embolisation material PAVM and the distal pulmonary hypoperfused volume, independent of the diameter of the embolised artery. It suggests an importance to realise the most distal embolisation possible.
Limitations: A monocentric study.
Ethics committee approval: The study was approved by CERIM (IRB: CRM-1904-005).
Funding: No funding was received for this work.
Author Disclosures:
J. Bizouerne: Author at CHU CLERMONT FERRAND
L. Cassagnes: Author at CHU CLERMONT FERRAND

RPS 609a-5 11:39

Endovascular treatment of haemoptysis: a study of failures and relapses
W. Mohammad[1], E. Mahdjoub[1], L. Saker[1], T. Israel[2], M.-P. Debray[1], A. Khalil[1]; *[1]Paris/FR, [2]Tros-Rivières, Guadeloupe/FR (antoine.khalil@aphp.fr)*

Purpose: To identify the causes of failure and/or relapse of the endovascular treatment of haemoptysis.
Methods and materials: We conducted a retrospective study from a prospective database of all patients who underwent endovascular treatment for haemoptysis from September 2015-March 2019. We collected clinical data such as age, gender, volume, the tolerability of haemoptysis, and the cause of haemoptysis. We reviewed CT-angiography and digital angiography. We defined failure (failure of catheterism or persistence of haemoptysis), short-term relapse (<1 month), and long-term relapse (>1 month).
Results: 148 patients (114 men and 34 women, median age: 57 y) were included in the study. Cancer (51 cases), tuberculosis (22 cases), bronchiectasis (20 cases), aspergillosis (15 cases), and cryptogenic haemoptysis (14 cases) accounted for more than 80% of causes. Failures and relapses were observed in 38 patients (26%). Failure, short-term relapse, and long-term relapse were respectively observed in 6 (4%), 23 (16%), and 9 (6%) patients. Among the 29 patients who experienced a failure of treatment or a short-term relapse, the two most common causes of failure and relapse were an incomplete embolisation (17 patients/29; 59%) and an error concerning the involved circulation (4 patients/29; 14 %). A re-embolisation enabled the control of haemoptysis in 22 of 29 patients (76%), for a total of 141/148 patients in the whole study (95%).
Conclusion: Incomplete embolisation and an error concerning involved circulation are the most frequent causes (21 patients/29) of failure/relapse in patients who experienced a failure of treatment and short-term relapse. Re-embolisation enables the control of haemoptysis in 22 of these 29 patients (76%).
Limitations: A retrospective monocentric analysis of a patient series with haemoptysis.
Ethics committee approval: n/a
Funding: No funding was received for this work.
Author Disclosures:
A. Khalil: nothing to disclose
W. Mohammad: nothing to disclose
M.-P. Debray: nothing to disclose
E. Mahdjoub: nothing to disclose
L. Saker: nothing to disclose
T. Israel: nothing to disclose

RPS 609a-6 11:45

Multiparametric evaluation of CT-guided local thermal ablation of inoperable lung tumours

E. H. A. Emara[1], E. Elhawash[2], T. J. Vogl[3], N. N. N. Naguib[3], N.-E. A. Nour-Eldin[3], H. Mansour[4], S. Saber[4], S. E. Hegab[2], M. Abouelezz[4]; *[1]Kafr ElSheikh/EG, [2]Alexandria/EG, [3]Frankfurt am Main/DE, [4]Zagazig/EG (emademara85@yahoo.com)*

Purpose: To determine the value of conventional MRI with contrast, apparent diffusion coefficient (ADC) value calculation, and CT with contrast in the assessment of early- and long-term treatment response after ablation of inoperable lung tumours with microwave ablation (MWA) and radiofrequency (RFA).
Methods and materials: 58 patients with 86 lung lesions were treated with MWA and RFA according to the guidelines and evaluated by MRI with contrast including T1.T2 WI, T1 post-contrast, and diffusion-weighted imaging (DWI) using b-values (50, 400, and 800 mm2/s) and ADC value measurement before and 24 hours after ablation. Follow-up by chest CT and/or MRI after 24 hours, three, six, nine months, one year, and every 6 months onwards to determine response to ablation was conducted. ADC value changes after ablation were compared to NRT response.
Results: 56 lesions (65.1%) showed complete response and 30 lesions (34.9%) showed a local progression (residual activity). There was a statistical significant difference in T2 WI signal intensity after ablation in both groups (P=0.047) but no significant difference in T1 WI at all over the follow-up period (P=0.914). There was a statistical significant difference in contrast enhancement between local progression lesions and responsive lesions during the follow-up period (P=0.001).
The ADC value measured 24 hours after ablation in the responding groups (1.71 ± 0.3× 10^{-3} mm^2/s) was statistically significantly higher than in the non-responding groups (1.42 ± 0.3×$10^3$$mm^2$/s) (P=0.001).
A cut-off ADC value (1.42) has been suggested as a reference point to predict the response (66.69% sensitivity, 84.23% specificity, 66.8% PPV, and 84.3% NPV).
Conclusion: MRI with contrast is effective in the evaluation of local tumour control after thermal ablation of inoperable lung tumours. ADC value measurement may allow early prediction of the treatment efficacy before morphological changes in conventional imaging can be detected.
Limitations: Respiratory motion artefacts and difficulty in small lesion detection.
Ethics committee approval: n/a
Funding: No funding was received for this work.
Author Disclosures:
T. J. Vogl: nothing to disclose
E. H. A. Emara: nothing to disclose
E. Elhawash: nothing to disclose
N. N. N. Naguib: nothing to disclose
N.-E. A. Nour-Eldin: nothing to disclose
H. Mansour: nothing to disclose
S. Saber: nothing to disclose
S. E. Hegab: nothing to disclose
M. Abouelezz: nothing to disclose

RPS 609a-7 11:51

CT fluoroscopy-guided single-needle core biopsy of anterior mediastinal masses: retrospective analysis of accuracy and complications

G. Vatteroni[1], E. Lanza[2], D. Poretti[1], V. Pedicini[1], R. Lutman[2], C. Sicuso[2], L. Trieste[3], F. D'antuono[4]; *[1]Milan/IT, [2]Rozzano/IT, [3]Pisa/IT, [4]Rocchetta S. Antonio/IT (giulia.vatteroni@gmail.com)*

Purpose: To retrospectively evaluate the safety, diagnostic yield, and risk factors of the diagnostic failure of CT fluoroscopy-guided core-needle biopsy (CNB) of anterior mediastinal masses performed with a large calibre single-needle technique.
Methods and materials: We retrospectively evaluated 85 patients who underwent CT fluoroscopy-guided CNB of anterior mediastinal masses between June2017-June2019. All procedures were performed using an automated cutting needle (14 to 18G, 10 cm length), collecting at least one specimen considered adequate. The biopsy results were compared with the final diagnosis in order to evaluate the diagnostic accuracy. The procedures were divided into diagnostic success and diagnostic failure groups. Variables related to patients (age, sex, and presence of PET-CT or CE-CT/MRI prior to biopsy), lesions (size, presence of calcification, and fluid and/or fat), and procedures (patient position, approach type, size of needle, number of samples, operator's experience, procedure time, and complications) were assessed to determine the risk factors for diagnostic failure.
Results: Procedures were performed on 48 women and 37 men (mean age 47.7±19years). In 35 (41%) and 57 (67%) patients, PET-CT and/or CE-CT/MRI were available before performing the biopsy. The mean lesion size was 68±32.9 mm (range 9-159); 10 and 22 lesions demonstrated respectively calcification and fluid on CT images. On 85 procedures, 78 (92%) were diagnostic successes and 7 (8%) were diagnostic failures. The diagnosed masses included 42 lymphomas, 17 thymomas, 7 thymic carcinomas, 3 liposarcomas, and 10 others. The variables between the two groups were compared using Fisher's exact test. No significant risk factor for diagnostic failure was identified.
Conclusion: CT fluoroscopy-guided biopsy of anterior mediastinal masses performed with a large calibre (≤18G) single-needle technique is a safe and highly accurate procedure with a low complications rate (4%).
Limitations: A retrospective study.
Ethics committee approval: n/a
Funding: No funding was received for this work.
Author Disclosures:
G. Vatteroni: nothing to disclose
E. Lanza: nothing to disclose
D. Poretti: nothing to disclose
R. Lutman: nothing to disclose
F. D'antuono: nothing to disclose
C. Sicuso: nothing to disclose
V. Pedicini: nothing to disclose
L. Trieste: nothing to disclose

RPS 609a-9 12:03

The effect of an autologous blood clot seal to prevent and minimise the risk of pneumothorax in CT-guided lung and mediastinal biopsy: an initial experience

B. K. Choudhury; *Guwahati/IN (choudhury60@gmail.com)*

Purpose: To determine whether an autologous blood clot seal (ABCS) after lung and mediastinal biopsy can prevent and minimise the risk of pneumothorax.
Methods and materials: A prospective study enrolling 20 patients was conducted from August 2018-July 2019. Patients undergoing CT-guided biopsy of lung and mediastinal masses were candidates. A biopsy path of at least 2 cm aerated lung was selected so that an effective blood clot seal might be applied and any blebs, fissures, and blood vessels in the pathway were avoided. The biopsy was performed with CT guidance using a 20-gauge coaxial system. The patient's clotted blood, which ranged from 1 ml to 5 ml, was injected into the needle track while the guiding needle was withdrawn, filling the entire needle track to the visceral pleura. Immediately after withdrawing the needle, the puncture site was put in a dependent position.

Results: ABCS after a biopsy was performed in 20 deep-seated and risky lung and mediastinal masses ranging from 10 mm-25 mm in the age group of 35-68 years. Only one patient developed a very small pneumothorax, which was revealed only in post-procedure CT and was not seen in a chest skiagram taken one hour after the procedure.
Conclusion: The use of autologous blood clot seal after biopsy of deep lung and mediastinal lesions significantly prevents and minimizes the risk of pneumothorax. It appears to be more beneficial when a 20 gauge coaxial needle and immediate dependant positioning of the puncture site is used.
Limitations: An ongoing study with a limited number of patients within a one year period. Long-term study with more number of patients is needed.
Ethics committee approval: n/a
Funding: No funding was received for this work.
Author Disclosures:
B. K. Choudhury: nothing to disclose

RPS 609a-10 12:09

Retrievable covered metallic segmented Y airway stents modified with 3D printing for gastro-respiratory fistulas involving carina and bronchi distal to carina: a preliminary retrospective study

Q. Shan, W. Huang, Z. Wang*; Shanghai/CN (1010818490@qq.com)*

Purpose: To evaluate the efficacy and safety of retrievable covered metallic segmented Y airway stents modified with 3D printing for gastro-respiratory fistulas involving carina and bronchi distal to carina.
Methods and materials: We designed a new covered metallic segmented Y airway stent for fistulas involving carina and bronchi distal to carina. All stents were individually customised with the aid of 3D printing. 6 patients with gastro-respiratory fistulas after an oesophagectomy of oesophagal cancer underwent stent implantation. Stents were retrieved when the fistula was cured or stent-related complications occurred.
Results: 7 Y stents were successfully implanted and removed in 6 patients (100%). All stents expanded well and the fistulas were sealed completely. Excessive granulation tissue proliferation was found in 1 patient (16.7%), which was treated by cryotherapy under bronchoscope. The stent was removed and second stenting was performed afterwards. The median KPS of patients after stenting significantly improved compared with that prior to stent implantation. Sputum retention was the most common complication after stenting (83.33%). The indwelling time of the stent was 61.00±9.43 (50-70) days. After stent removal, the bronchoscopy showed a cure of the fistula in all patients and no stents showed fracture after the removal.
Conclusion: Retrievable covered metallic segmented Y airway stents modified with 3D printing appears to be effective and safe in the treatment of gastro-respiratory fistulas involving carina and bronchi distal to carina.
Limitations: The small sample size and retrospective nature. In addition, the assessment of long-term outcome and complication after stent removal is needed. Larger prospective controlled studies are warranted.
Ethics committee approval: This retrospective study was approved by the institutional review board and written informed consent was obtained.
Funding: No funding was received for this work.
Author Disclosures:
Q. Shan: nothing to disclose
W. Huang: nothing to disclose
Z. Wang: nothing to disclose

RPS 609a-11 12:15

The role of multi-detector computed tomography angiography for preprocedural planning and radiation dose reduction in bronchial artery embolisation

B. S. R. Reddy[1], P. Chatterjee[2], K. Sunder[3], R. Kumar[3], V. Mazumdar[3];
[1]Chennai, Tamil Nadu/IN, [2]Guwahati, Assam/IN, [3]Chennai/IN
(sudeepreddy2009@gmail.com)

Purpose: To evaluate prospectively bronchial and non-bronchial systemic arteries with MDCT angiography (MDCTA) prior to bronchial artery embolisation (BAE) in patients with haemoptysis and the amount of radiation dose reduction when BAE is performed with the knowledge of MDCTA.
Methods and materials: MDCTA was performed in 40 patients with haemoptysis who were referred for BAE. Transverse, multiplanar reconstruction, and 3-dimensional reconstruction images were analysed to identify the abnormal hypertrophied arteries causing haemoptysis. Their origin and course were noted. Digital subtraction angiography (DSA) was performed with the knowledge of findings of MDCTA. Selective arteriograms of abnormal arteries were performed. DSA findings were compared with MDCTA. Embolisation was done in all the patients using polyvinyl alcohol particles (300-500 µm), gel foam, or coils. The total cumulative dose for a single BAE intervention ranges from 0.2–2.7 Gy as a standard range and we compared this with our radiation dose parameters. Radiation dose parameters were recorded for all cases.
Results: MDCTA shows a 96.2% sensitivity and 100% specificity in identifying abnormal bronchial arteries, and a 64.7% sensitivity and 100% specificity in identifying abnormal non-bronchial systemic arteries. There was 40.2% reduction in cumulative DAP, 30.7% reduction in cumulative air kerma, and 77.1% reduction in contrast dose when BAE was performed with the knowledge of MDCTA.
Conclusion: MDCTA allows for the rapid and detailed identification of abnormal arteries using a variety of reformatted images. This information may be helpful for the interventional radiologist in order to avoid thoracic aortography and ro attempt direct catheterisation of the arteries to be occluded, resulting in reducing the examination time in the angiography suite and minimising contrast load and radiation dose.
Limitations: A small sample size. A multicentric study may be required for further evaluation.
Ethics committee approval: n/a
Funding: No funding was received for this work.
Author Disclosures:
B. S. R. Reddy: Other at apollo main hospital
P. Chatterjee: Consultant at apollo main hospital
K. Sunder: Consultant at apollo main hospital
R. Kumar: Consultant at apollo main hospital
V. Mazumdar: Consultant at apollo main hospital

RPS 609a-12 12:21

Transvenous pulmonary chemoembolisation (TPCE) and intra-arterial chemoperfusion (IACP) in primary lung malignancies: a palliative treatment approach

T. J. Vogl[1], A. I. Mekkawy[2], M. El-Sharkaway[2], D. B. Thabet[2], N. N. N. Naguib[1], N.-E. A. Nour-Eldin[1], T. Gruber-Rouh[1], R. Hammerstingl[1], A. Hasan[2];
[1]Frankfurt am Main/DE, [2]Assiut/EG
(t.vogl@em.uni-frankfurt.de)

Purpose: To evaluate tumour response, local tumour control, and patient survival after the palliative treatment of primary lung cancer using transpulmonary chemoembolisation (TPCE) and intra-arterial chemoperfusion (IACP).
Methods and materials: 118 patients with unresectable primary lung cancer not responding to systemic chemotherapy underwent either repetitive TPCE (n=56) or IACP (n=62) from 01/2006-04/2017 (mean number of sessions/patient: 5.3±2.2, median number of nodules: 3, bilateral lung involvement 45.8%). The chemotherapeutic agents used were mitomycin C and gemcitabine (n=14), without cisplatin (n=98), or other combinations (n=6).
Regional delivery of the chemotherapeutic agents was performed either through selective catheterisation of the tumour-supplying pulmonary arteries with subsequent embolisation or through non-selective IACP. Tumour response was assessed according to the rRECIST criteria.
Results: Partial response was achieved in 15.3%, stable disease in 60.2%, and progressive disease in 24.6%. The estimated mean survival time (MST) and time-to-progression were 15.8±1.7 and 9.2 ±1.3 months in the TPCE group and 20±3.8 and 11.1±1.7 months in the IACP group, respectively. These differences were statistically insignificant.
Patients with advanced disease who underwent subsequent ablative therapy had a significantly longer mean survival time of 24.6±4 months versus the non-ablation group (MST=15.3±2.8; p=0-001).
Conclusion: TPCE and IACP have the potential to improve local tumour control and prolong survival in a selected group of patients who have limited treatment options.
Limitations: Patients were assigned to each treatment case-by-case. It might be better to do perfusion in less vascular tumours and embolisation in highly vascular ones.
The effects of critical prognostic factors were difficult to evaluate due to insufficient information in the database.
Ethics committee approval: Institutional Review Board approval was obtained. Written informed consent was not required due to the retrospective design.
Funding: No funding was received for this work.
Author Disclosures:
T. J. Vogl: nothing to disclose
A. I. Mekkawy: nothing to disclose
M. El-Sharkaway: nothing to disclose
D. B. Thabet: nothing to disclose
N. N. N. Naguib: nothing to disclose
N.-E. A. Nour-Eldin: nothing to disclose
T. Gruber-Rouh: nothing to disclose
R. Hammerstingl: nothing to disclose
A. Hasan: nothing to disclose

11:15 - 12:30 **Room G**

Artificial Intelligence and Machine Learning

RPS 605b

Artificial intelligence and machine learning in breast cancer

Moderators:
P. Clauser; Vienna/AT
M. A. Guevara Lopez; Guimaraes/PT

RPS 605b-K 11:15
Keynote lecture
S. Vinnicombe; *Cheltenham/UK (sarah.vinnicombe@nhs.net)*

Author Disclosures:
S. Vinnicombe: nothing to disclose

RPS 605b-1 11:25
Accelerating breast cancer screening using an abbreviated MRI protocol and artificial intelligence
X. Jing, M. Wielema, L. Cornelissen, S. Zheng, J. Guo, P. Sijens, M. Oudkerk, M. Dorrius, P. M. van Ooijen*; Groningen/NL (x.jing@umcg.nl)*

Purpose: Breast MRI is not considered a cost-effective tool for breast cancer screening. Abbreviated protocols combined with artificial intelligence (AI) could achieve high efficiency, rapid throughput, and lower costs. The aim of this study was to investigate the feasibility of automatically pinpointing abnormality using a convolutional neural network (CNN) in breast MRI screening with different shortened protocols.
Methods and materials: 96 breast MRI exams (61 normal, 35 abnormal) were collected and labelled by radiologists. For each exam, maximum intensity projection (MIP) images were generated from both Twist (time-resolved angiography with interleaved stochastic trajectories) and dynamic contrast-enhanced T1-weighted sequences (T1) at different time points after contrast agent administration. Three MIP images from 1) Twist, 2) Twist + T1, and 3) T1 were stacked together to generate a composite image, where the different combinations represent different MRI protocols. The composite images, assigned the same label as their original exams, were then used for the training of CNN (ResNet18). During testing, the result of an exam was determined by the majority of the predictions on all composite images generated from the exam under test. The performance of the proposed method was evaluated using 4-fold cross-validation, where each fold contains 15 normal and 8 abnormal exams.
Results: Twist alone achieved a sensitivity of 97%, specificity of 98%, positive predictive value (PPV) of 97%, and negative predictive value (NPV) of 98%. Twist+T1 achieved the same sensitivity and NPV, but lower specificity (93%) and PPV (89%). T1 alone gained the lowest performance on any metrics.
Conclusion: Use of an abbreviated protocol without T1 sequence, in combination with AI, could accelerate the breast MRI screening without affecting performance, leading to reduced costs.
Limitations: n/a
Ethics committee approval: n/a
Funding: No funding was received for this work.
Author Disclosures:
X. Jing: nothing to disclose
M. Wielema: nothing to disclose
L. Cornelissen: nothing to disclose
S. Zheng: nothing to disclose
J. Guo: nothing to disclose
P. Sijens: nothing to disclose
M. Oudkerk: nothing to disclose
M. Dorrius: nothing to disclose
P. M. van Ooijen: nothing to disclose

RPS 605b-2 11:31
Mammographic breast density classification and risk assessment using deep learning
M. Jie[1], M. Xu[1], X. Lin[1], S. Wu[1], Y. Zhang[2], Z. Cao[2], L. Huang[1], M. Wu[1], Y. Wang[1]*; [1]Shenzhen/CN, [2]Palo Alto/US (majie688@hotmail.com)*

Purpose: High consistency and accuracy of breast density assessment are necessary and routinely visually assessed by radiologists. Furthermore, breast density is a vital risk factor for breast cancer diagnosis. However, qualitative assessment of mammographic breast density is subjective and differs largely between radiologists.
Methods and materials: We designed two models of two-category, including scatted density and heterogeneously density, and four-category, including almost entirely fatty, scattered areas of fibroglandular tissue, heterogeneously dense, and extremely dense. The novelty of the presented method employed pyramidal residual units instead of down-sampling to a concatenate feature map by increasing it gradually. Data augmentation implemented by this investigation involved several real-time transforms source images during the training progress. Additionally, image preprocessing, extracting the region of interest of breast, and normalising images by using adjudgment of window-width and window-centre were adopted to keep the training-set from different vendors consistent and uniform. In this retrospective study, the developed method was trained and validated by utilising 40,364 and 9,000 mammograms from in-house hospital, respectively.
Results: The presented CNN-based breast density classification models were tested directly by using 1,821 images. The two-classification accuracy was 94.56% and the area under ROC curve (AUC) 96.8%, respectively. The other four-classification accuracy was 81.88% and AUC 94.40%, respectively.
Conclusion: Our experimental results demonstrated high classification accuracies between two hard to distinguish breast density categories. It is helpful for addressing inconsistency in density assessment of mammograms. Importantly, we anticipate that the proposed method will improve assessment of breast density and promote risk judgment of breast cancer. It assists radiologists to provide better notification to patients in breast cancer screening.
Limitations: The bias caused by race difference was not well considered.
Ethics committee approval: n/a
Funding: No founding was received for this work.
Author Disclosures:
M. Jie: Employee at Shenzhen People's Hospital
S. Wu: Employee at PingAn Technology
M. Xu: Employee at Shenzhen People's Hospital
X. Lin: Employee at Shenzhen People's Hospital
Y. Zhang: Employee at PingAn Tech, US Research Lab
Z. Cao: Employee at PingAn Tech, US Research Lab
L. Huang: Employee at PingAn Technology
M. Wu: Employee at Shenzhen People's Hospital
Y. Wang: Employee at Shenzhen People's Hospital

RPS 605b-3 11:37
Performance of radiologists versus a machine learning classifier for optoacoustic imaging of the breast
G. Menezes, S. Dykes, B. A. Clingman, A. T. Stavros*; San Antonio, TX/US (giselalgm@gmail.com)*

Purpose: Our imaging device fuses laser optical imaging with grey-scale ultrasound (OA/US) to differentiate between benign and malignant masses of the breast. The study compared the performance of radiologists to a machine learning (ML) classifier.
Methods and materials: We used a subset of 1,585 masses from the PIONEER trial (USA, December 2012-September 2015) to train the ML classifier. The training set consisted of image feature scores that were assigned by 7 independent breast radiologists (5 ultrasound and 5 OA/US features), in addition to mass size, mass depth, patient age, and the mammogram BI-RADS category. We then tested the classifier using all 213 masses from the MAESTRO OA/US trial (Netherlands, March 2015-February 2016). Sensitivity, specificity, and AUC were calculated for both the radiologists and classifier predictions.
Results: The classifier's sensitivity was 97.0% versus 95.5% obtained by the radiologists. The classifier also outperformed the radiologists in specificity (55.5% vs 41.1%). AUC was 86.9% for the classifier and 83.1% for the radiologists. Partial AUC (over the sensitivity range 95.0% to 100%) was 73.9% (classifier) versus 61.0% (radiologists). Because the classifier and the radiologists use the same feature scores, the only difference between the classifier and the radiologist results is how those feature scores are combined into a final likelihood of malignancy score.
Conclusion: The ML classifier exceeds the performance of radiologists on new/external data. This indicates that the classifier might help radiologists improve their final OA/US assessment. The correct assignment of OA/US features is essential for an optimal classifier performance.
Limitations: The main limitations of our study were sample size and inclusion criteria of the Maestro trial. Only 213 BI-RADS 4A and 4B masses were included.
Ethics committee approval: n/a
Funding: This study was funded by Seno Medical Instruments, Inc.
Author Disclosures:
G. Menezes: Employee at Seno Medical Instruments, Inc.
S. Dykes: Employee at Seno Medical Instruments, Inc.
B. A. Clingman: Employee at Seno Medical Instruments, Inc.
A. T. Stavros: Employee at Seno Medical Instruments, Inc.

RPS 605b-4 11:43

Detecting and delineating suspicious masses in contrast-enhanced mammography (CEM) using a deep learning workflow

M. Beuque, Y. van Wijk, H. C. Woodruff, Y. Widaatalla, M. B. I. Lobbes, P. Lambin*; Maastricht/NL (m.beuque@maastrichtuniversity.nl)*

Purpose: CEM has superior diagnostic accuracy compared to conventional mammography. Applying machine learning techniques would potentially increase the accuracy of CEM even more, but is hampered by the labour-intensive process of contouring lesions. Automated detection and ranking of lesions seen on CEM would shorten this process and facilitate automated classification as part of a machine learning workflow.
Methods and materials: Our dataset (n=828) included both craniocaudal (CC) and mediolateral oblique (MLO) views consisting of low-energy and recombined images. All images contained manual delineations of lesions made by expert radiologists. Pre-processing consisted of: (1) cropping the image around the breast, (2) merging of 2x low-energy and 1x recombined image as layers into an RGB image, and (3) rebinning from 16 to 8 bits using adaptive histogram equalisation. A retinaNet model was trained with ResNet50 as a backbone. We considered a mass to be 'detected' when the intersection over union (IoU) of the detected mass area and expert delineation was greater than 0.1.
Results: When looking at both views separately, our model correctly detected 87% of the masses in the test set with an average IoU of 0.7 for detected masses. On the training set, it detected 84% of masses with an average IoU of 0.7. When combining different views, 90 (97)% of the (cancerous) masses were detected on a patient level in the training set (88 (91)% in the test set).
Conclusion: Our automated detection and localisation tool was able to detect the vast majority of masses seen on CEM. The machine learning workflow can be accelerated significantly using this tool as this is normally a time consuming and labour intensive process.
Limitations: This workflow is not applicable for micro-calcification.
Ethics committee approval: n/a
Funding: European Program H2020 (PREDICT-ITN-766276) ; KWF Kankerbestrijding 12085/2018-2.
Author Disclosures:
M. Beuque: nothing to disclose
Y. van Wijk: Employee at ptTheragnostic/DNAmito
H. C. Woodruff: Shareholder at Oncoradiomics
M. B. I. Lobbes: nothing to disclose
P. Lambin: Research/Grant Support at Varian medical, Research/Grant Support at Oncoradiomics, Research/Grant Support at ptTheragnostic, Research/Grant Support at Health Innovation Ventures , Research/Grant Support at DualTpharma, Other at Oncoradiomics, Other at BHV, Other at Merck , Other at Convert pharmaceuticals, Shareholder at Oncoradiomics SA , Shareholder at Convert pharmaceuticals SA , Patent Holder at Oncoradiomics , Patent Holder at ptTheragnostic/DNAmito
Y. Widaatalla: nothing to disclose

RPS 605b-5 11:49

Can artificial intelligence reduce the interval cancer rate in mammography screening?

K. Lang[1], S. Hofvind[2], A. Rodriguez Ruiz[3], I. Andersson[1]; *[1]Malmö/SE, [2]Oslo/NO, [3]Nijmegen/NL (kristina.lang@med.lu.se)*

Purpose: To analyse the detection performance of interval cancers (ICs) on prior standard digital screening mammograms using an artificial intelligence (AI) system.
Methods and materials: 430 IC screening exams acquired with different mammography devices at four screening sites in Southern Sweden (2013–2017) were analysed with a deep learning-based AI system. The system assigns risk scores from 1 to 10 with an increasing risk of malignancy. Recall recommendations were also provided by the AI tool at approximately 4% and 1% recall rates (risk score ≥ 9.67, and ≥ 9.92, respectively). For the cases with recommended recall, two experienced breast radiologists classified the IC type in consensus (true-negative, minimal sign, or false-negative) and whether the AI system correctly localised the lesion.
Results: A large number of the ICs had an AI risk score of 10 (33%, 143/430), while 40% were assigned scores 1 to 7 (part of the 70% of the screening population with a lower likelihood of cancer by the AI). At a 4% recall rate, 17% of the ICs (73/430) were included, 74% of which were visible in retrospect (28 minimal sign, 26 false-negative), and all but 7 were correctly localised. At a 1% recall rate, 6% of the ICs (24/430) were included, 79% of which were visible in retrospect (12 minimal sign, 7 false-negative), and all were correctly localised.
Conclusion: The AI system was able to detect a substantial number of interval cancers on the prior screening exam. Applying an AI-derived recall rate recommendation for the most suspicious cases to, for example, a 3rd reader or a consensus discussion, might provide means to help the radiologist reduce the interval cancer rate.
Limitations: A single AI vendor. A retrospective review of IC cases
Ethics committee approval: Ethics committee approval and informed consent obtained.
Funding: No funding was received for this work.
Author Disclosures:
K. Lang: Speaker at Siemens Healthineers
S. Hofvind: nothing to disclose
I. Andersson: nothing to disclose
A. Rodriguez Ruiz: Employee at ScreenPoint Medical

RPS 605b-6 11:55

Breast cancer detection by mammographic view with artificial intelligence in digital breast tomosynthesis

E. F. Conant[1], A. Y. Toledano[2], S. Periaswamy[3], S. Fotin[3], H. Haldankar[3], J. Go[3], J. Boatsman[4], J. Hoffmeister[3]; *[1]Philadelphia, PA/US, [2]Washington/US, [3]Nashua, NH/US, [4]San Antonio/US (emily.conant@pennmedicine.upenn.edu)*

Purpose: To evaluate the performance of artificial intelligence (AI) with digital breast tomosynthesis (DBT) by craniocaudal (CC) versus mediolateral oblique (MLO) mammographic views.
Methods and materials: A diagnostic accuracy study of an AI system was conducted with 260 retrospectively collected DBT exams, 65 biopsy-proven cancer, and 195 non-cancer, from sequential blocks of cases from seven U.S. sites, randomly selected to match a screening population. The maximum AI scores overall and across breasts within mammographic view (CC versus MLO) were compared to a previously validated threshold for cancer detection. 95% confidence intervals (CI) for the difference in correlated proportions for sensitivity and specificity were calculated using a McNemar test.
Results: The estimated sensitivity (95% CI) for CC and MLO were 0.74 (0.62, 0.83) and 0.77 (0.65, 0.85), respectively; a difference of -0.03 (-0.30, 0.24). The estimated specificity with CC images was 0.64 (0.57, 0.70), which is significantly higher than that of MLO images at 0.54 (0.47, 0.61), giving a difference of 0.10 (0.01, 0.19). Among the 65 cancer cases, 9 were detected by CC alone, 11 by MLO alone, and 39 by both. Among the 195 non-cancer cases, 45 were correctly ruled out by CC, 26 by MLO, and 79 by both. Overall, the AI system detected 91% (59/65) of cancers and ruled out 41% (79/195) non-cancer cases.
Conclusion: While the AI system was not trained to maximise performance within mammographic view, these results suggest that unbalanced conspicuity across mammographic views may have implications for AI performance with single-view exams.
Limitations: The performance of AI may not be indicative of radiologists in clinical practice.
Ethics committee approval: IRB approval and waiver of informed consent was obtained for HIPAA-compliant retrospective case collection.
Funding: iCAD (Nashua, NH) funded this work.
Author Disclosures:
E. F. Conant: Advisory Board at iCAD, Inc., Grant Recipient at iCAD, Inc., Advisory Board at Hologic, Inc., Grant Recipient at Hologic, Inc.
A. Y. Toledano: Consultant at iCAD, Inc.
S. Periaswamy: Employee at iCAD, Inc.
S. Fotin: Employee at iCAD, Inc., Shareholder at iCAD, Inc.
H. Haldankar: Employee at iCAD, Inc.
J. Go: Employee at iCAD, Inc., Shareholder at iCAD, Inc.
J. Boatsman: Employee at Intrinsic Imaging, Shareholder at Intrinsic Imaging
J. Hoffmeister: Employee at iCAD, Inc.

RPS 605b-7 12:01

Deep learning model used in mammographic breast density assessment

J. Tao, F. Yang, J. Liu*; Wuhan/CN (2014xh0917@hust.edu.cn)*

Purpose: To investigate if the clinical value of a deep learning (DL) model can be used to help radiologists improving the diagnostic efficiency of mammography.
Methods and materials: In this prospective study, 50 cases were randomly selected each week, 2,548 mammograms of 637 women, from November 2018 to February 2019. All evaluations were performed by four radiologists. The ResNet-18 model was used to evaluate breast density. 200 digital mammograms of 50 women were collected 4 weeks later. The density of each mammogram was evaluated by machine and four radiologists provide breast density classification based on the DL model results independently. The final gold standard was determined by majority decision and joint discussion.
Results: The consistency of the four images' overall assessment evaluated by the four radiologists in each patient (K=0.75) was higher than the assessment of unilateral breast images (0.718) and single image (0.696). The accuracy of the four images' overall assessment, unilateral breast images assessment, and single image assessment in patients were 0.856, 0.834, and 0.825. The consensual assessment of single image evaluated between DL model and four

radiologists（K=0.675）was higher than the overall assessment given by a single radiologist (0.675) and the assessment of unilateral breast images (0.599). The consistency of 200 breast densities in March evaluated by four radiologists who refer to AI results increased to 0.825.
Conclusion: Adding four experienced radiologists evaluating all cases independently is where we differ from previous studies. The evaluations of a DL model and four radiologists agree well with each other, the consistency of evaluations by four radiologists assisting with DL model increase.
Limitations: The limitation of our experiment is that we have fewer cases. We will add more cases and multiple centres in the future.
Ethics committee approval: n/a
Funding: No funding was received for this work.
Author Disclosures:
J. Tao: Author at Tongji medical college union hospital of huazhong university of science and technology
F. Yang: Author at Tongji medical college union hospital of huazhong university of science and technology
J. Liu: Board Member at Tongji medical college union hospital of huazhong university of science and technology

RPS 605b-8 12:07

Comparing the mammography screening performance of three external AI CAD algorithms and radiologists within a true population-based screening cohort

M. Salim, E. Wåhlin, K. Dembrower, M. Eklund, K. Smith, F. Strand*; Stockholm/SE (mattiesalim@gmail.com)*

Purpose: To examine if there was any difference in cancer detection between various state-of-the-art AI CAD algorithms applied as independent readers of screening mammography and if they reached radiologist-level performance.
Methods and materials: This case-control study, nested within a population-based screening cohort during 2008 to 2015, consisted of the latest screening examination for 740 women diagnosed with breast cancer (positive) and a random sample of 8,066 healthy controls (negative). Positive ground truth was determined by pathology-verified diagnosis at screening or within 12 months thereafter. Negative ground truth was determined by 2-year cancer-free follow-up. There were 25 original first-reader radiologists, one for each examination. Three AI CAD algorithms, sourced from different vendors, yielded a continuous prediction score for the suspicion of cancer of each examination. For a binary decision, the cut-point was defined by the mean specificity of the original first-reader radiologists (96.56%). The processing of one of the three AI algorithms has not yet been completed and those results cannot currently be reported.
Results: The average age was 58.2 and 55.1 years for positive and negative cases, respectively. AUC was 0.96 (95%CI: 0.95 to 0.97) and 0.91 (95%CI: 0.90 to 0.92) for AI algorithm 1 and 2, respectively (p<0.001). At radiologists' specificity, the sensitivity was 82%, 66%, and 76% for AI algorithm 1, AI algorithm 2, and the original first-reader radiologists, respectively (p<0.001 for each pair-wise comparison).
Conclusion: One AI algorithm outperformed the other AI algorithm and the original first-reader radiologists. The time has come for prospective screening trials using carefully chosen AI CAD algorithms under controlled circumstances.
Limitations: n/a
Ethics committee approval: Our ethical review board approved the research in this study and waived the need for individual informed consent.
Funding: Stockholm County Council Dnr 20170802.
Author Disclosures:
M. Salim: nothing to disclose
E. Wåhlin: nothing to disclose
K. Dembrower: nothing to disclose
M. Eklund: nothing to disclose
K. Smith: nothing to disclose
F. Strand: nothing to disclose

RPS 605b-9 12:13

Evaluating the feasibility of fully automated mammography image positioning assessments

M. Abdolell[1], N. Paquet[1], R. Duggan[1], N. Sharma[2], S. Hofvind[3], S. E. Iles[1]; *[1]Halifax/CA, [2]Leeds/UK, [3]Oslo/NO (Nisha.sharma2@nhs.net)*

Purpose: To evaluate the level of agreement between an automated mammography image positioning assessment tool and a panel of experts to determine if such a tool may be practically integrated in routine breast screen activities.
Methods and materials: 672 FFDM studies rejected due to positioning errors were independently reviewed by 5 Radiographers and 2 Radiologists. Reviewers evaluated studies for positioning errors including (1) portion cut off, (2) inadequate inframammary fold (IMF), (3) pectoralis muscle position, and (4) pectoralis muscle thickness. Inter-rater agreement was evaluated between the consensus of the 7 reviewers and the automated tool using weighted Fleiss' Kappa.
Results: Inter-rater agreement between the algorithm and the panel of experts ranged from good to excellent (kappa = 0.546-0.84).
Conclusion: An automated mammography image positioning error algorithm demonstrates good to excellent agreement with a consensus of experts and may be effective for continual quality assurance efforts in routine breast screening activities.
Limitations: A limitation in this analysis is that the expert reviewers were not given a training session or training dataset prior to performing their assessments for this study.
Ethics committee approval: n/a
Funding: There was no funding recieved for this study. Densitas Inc. provided in-kind support, such as the use of their Image Review Tool.
Author Disclosures:
M. Abdolell: CEO at Densitas Inc.
N. Paquet: Employee at Densitas Inc.
R. Duggan: Employee at Densitas Inc.
S. E. Iles: nothing to disclose
N. Sharma: Advisory Board at Densitas Inc.
S. Hofvind: nothing to disclose

RPS 605b-10 12:19

Differential diagnosis of benign and malignant breast lesions using ultrasound-derived texture analysis features and a machine learning approach

V. Romeo[1], R. Cuocolo[1], R. Apolito[2], A. Ventimiglia[3], A. Vitale[1], R. Buonocore[4], M. R. Argenzio[2], M. P. S. Maurea[1], M. Imbriaco[1]; *[1]Naples/IT, [2]Salerno/IT, [3]Castellamare di Stabia/IT, [4]Pontecagnano Faiano/IT (valeria.romeo@unina.it)*

Purpose: To assess the applicability of a machine learning (ML) approach using texture analysis (TA) features extracted from ultrasound (US) images acquired in two different institutions to differentiate benign from malignant breast lesions.
Methods and materials: Ultrasound examinations of 117 patients with 135 breast lesions (benign n=91, malignant n=44) from institution 1 and 55 patients with 57 breast lesions (benign=19, malignant n=38) from institution 2 were retrospectively selected. Fine needle aspiration and/or tru-cut biopsy or follow-up were used as a standard of reference. The breast lesions of institution 1 were used as a training set, while the breast lesions of institution 2 were used as a validation set. After grey-scale image normalisation and data discretisation using a bin width=3, breast lesions were manually segmented on 2D US images delineating regions of interest (ROIs). ROIs and images were imported in a dedicated software to extract first, second, and higher-order TA features. Features were then normalised according to the training set population. ML analysis was then conducted to obtain the highest accuracy, expressed as the percentage of correctly classified instances.
Results: A total of 697 features were extracted. Among these, 579 highly correlated (r>0.8) and 37 showing a variance <0.01 were excluded from the final dataset, with 81 features left. A data mining software was then run using the subset evaluator that identified 5 final features. Employing such features with a random forest algorithm, 1,000 iterations, and a 10-fold cross validation, an accuracy of 80.7% was obtained on both training and validation sets.
Conclusion: A ML approach using US-derived features may represents a promising tool to discriminate benign from malignant breast lesions.
Limitations: A retrospective study.
Ethics committee approval: IRB approved.
Funding: No funding was received for this work.
Author Disclosures:
V. Romeo: nothing to disclose
R. Cuocolo: nothing to disclose
R. Apolito: nothing to disclose
A. Ventimiglia: nothing to disclose
A. Vitale: nothing to disclose
R. Buonocore: nothing to disclose
M. R. Argenzio: nothing to disclose
M. P. S. Maurea: nothing to disclose
M. Imbriaco: nothing to disclose

RPS 605b-11 12:25

Machine learning ensembled a with deep learning model to classify density and detect lesions in mammography studies

M. Shoura[1], S. Halabi[2], W. Taha[3], O. Mahanna[3], J. Tonthat[3], E. Abdelfatah[3], I. Hasan[4], Y. Shalaby[5]; *[1]Newton, MA/US, [2]San Francisco/US, [3]Boston/US, [4]Kuwait/KW, [5]Cairo/EG (mohamed.shoura@paxerahealth.com)*

Purpose: We have developed an ensemble model of multiple machine learning and deep learning algorithms to detect lesions, detect density levels, and show the overall probability of malignancy in mammography studies.

Methods and materials: We used a pre-trained model that used a DenseNet-121 architecture to train a model against a labelled dataset that consists of 200K+ high-resolution mammography exams to detect lesions and show in an ROI or heatmap. We also used 500K+ labelled exams with structured reports to be used for building a density classification model. We balanced a dataset of 90K studies and used a GoogleNet architecture to train a model that classifies images into two levels (Low and High dense) with an AUC of 89%. Another patch classifier pre-trained model for detecting the probability in malignancy was run against a balanced dataset of 2.5K studies (10K images). This generated a structured dataset that represents predicted lesions locations and classifications per breast (MLO/CC). The dataset was enriched with some more tags like malignant probability, benign probability, number of malignant/benign lesions, age, density (High/Low), and exposure time. ML Models used: ridge classifier, decision tree, random forest, ExtraTree, voting classifier, and AdaBoost. The voting classifier model provided the best results with an AUC of 88%.
Results: The ensemble model was tested with experienced radiologists on a subset of 100 studies as phase one and it managed to classify malignancy and density with an accuracy rate of 87%.
Conclusion: The ensemble model improves the accuracy of the models by 6%. A built-in chatbot embedded in the PACS viewer helped radiologists to verify the results in a much easier way.
Limitations: The model will be tested with more datasets to increase the accuracy of the detection.
Ethics committee approval: n/a
Funding: PaxeraHealth.
Author Disclosures:
M. Shoura: CEO at PaxeraHealth Corp
S. Halabi: Advisory Board at PaxeraHealth Corp
W. Taha: Consultant at PaxeraHealth Corp
O. Mahanna: Employee at PaxeraHealth Corp
J. Tonthat: Employee at PaxeraHealth Corp
E. Abdelfatah: Employee at PaxeraHealth Corp
I. Hasan: Consultant at PaxeraHealth Corp

11:15 - 12:30 **Room K**

Radiographers

RPS 614

Computed tomography: examination improvement

Moderators:
S. J. Foley; Dublin/IE
T. A. Yalynska; Kiev/UA

RPS 614-K 11:15
Keynote lecture
F. Zarb; *Msida/MT (francis.zarb@um.edu.mt)*

Author Disclosures:
F. Zarb: nothing to disclose

RPS 614-1 11:25
Lead shielding significantly reduces the dose to the breasts during head CT: a phantom study
N. Zalokar[1], N. Mekis[2]; *[1]Slovenska Bistrica/SI, [2]Ljubljana/SI*

Purpose: Since the breasts are considered one of the most radiosensitive organs in the human body, the aim of this study was to investigate whether the dose to the breasts during head CT is reduced with the use of lead shielding.
Methods and materials: The research was carried out on an anthropomorphic phantom of body and head PBU 60 in two major hospitals (hospital A and B) in Slovenia using axial and helical protocols. The breast implant size of 340 ml was attached to the phantom and served to simulate the breast. The dose to the breasts was measured 20 times during each protocol. Half of the measurements conducted during each protocol were performed with the use of lead shielding of 0.5 mm equivalent lead density. Measurements were carried out on the General Electric Healthcare Revolution EVO and the Toshiba Aquilion 64 slice CT unit; 40 measurements' data was collected. The absorbed dose was measured with the EDD30 dosimeter, which was positioned to the centre of the breast implant.
Results: A significant decrease of the absorbed dose to the breasts in both hospitals was shown. The use of lead shielding reduced the absorbed dose to the breast by 95% ($p<0.001$) in hospital A and 86% ($p<0.001$) in hospital B during the axial head CT examination. A significant dose reduction was also shown during the helical head CT examination; 96% ($p<0.001$) dose reduction in hospital A and 82% ($p<0.001$) in hospital B.
Conclusion: The use of lead shielding to the breasts is highly recommended during a head CT examination, regardless of the used protocol, due to the significant dose reduction.
Limitations: The study was only conducted on a phantom.
Ethics committee approval: n/a
Funding: No funding was received for this work.
Author Disclosures:
N. Zalokar: Speaker at Faculty of Health Sciences, University of Ljubljana
N. Mekis: nothing to disclose

RPS 614-2 11:31
A comparison between two trauma CT protocols: can a multiphase contrast injection, single-pass acquisition be a viable technique in major trauma?
D. J. Biddle, S. Freeman, S. Upponi; *Cambridge/UK (david.biddle@nhs.net)*

Purpose: A comparison between two trauma CT protocols. Can a multiphase contrast injection, single-pass acquisition be a viable technique in major trauma?
Methods and materials: A retrospective analysis of 100 consecutive major trauma patients referred for CT from January-February 2019 was conducted. 50 patients were imaged with the established two-pass protocol (arterial thoracoabdominal and portal venous abdominopelvic phases) and 50 patients underwent the single-pass, multiphase injection protocol (mixed arterial and venous phase of chest, abdomen, and pelvis). Patients were imaged on a Siemens Definition AS+ 128 slice scanner. Both trauma protocols were bolus-triggered using a region-of-interest (ROI) placed over the descending thoracic aorta. Hounsfield unit measurements were obtained from the main pulmonary artery, thoracic aorta, and portal vein. Two consultant radiologists assessed the overall quality of the studies, rating the studies as diagnostic or non-diagnostic. Splenic enhancement was specifically assessed as a marker of solid organ enhancement. Radiation dose and injury severity score (ISS) data were evaluated for each cohort.
Results: The single-pass cohort had significant dose reduction compared to the two-pass method (DLP 903.84 vs 1856.42 mGycm: $p=0.0001$). Pulmonary artery enhancement was comparable ($p=0.3247$), whilst the aortic ($p=0.0026$) and portal vein ($p=0.0118$) attenuation was significantly higher in the single-pass cohort. Both cohorts had excellent diagnostic quality: 100%. There was no significance between splenic attenuation ($p=0.6845$) in both techniques. There was no significance relating to ISS ($p=0.1668$).
Conclusion: The single-pass, multiphase technique significantly reduces the radiation dose in trauma patients whilst maintaining excellent diagnostic accuracy.
Limitations: The study cohort was limited to 50 patient from each technique. A larger inclusion would provide more diversity of trauma referrals to evaluate the technique
Ethics committee approval: n/a
Funding: No funding was received for this work.
Author Disclosures:
D. J. Biddle: nothing to disclose
S. Freeman: nothing to disclose
S. Upponi: nothing to disclose

RPS 614-3 11:37
The factors associated with radiation dose variation in cardiac CT angiography
M. F. M. McEntee[1], A. B. Alhailiy[2], E. U. Ekpo[2], P. Kench[2], E. Ryan[3], P. C. Brennan[2]; *[1]Cork/IE, [2]Sydney/AU, [3]Brisbane/AU (mark.mcentee@ucc.ie)*

Purpose: To examine the factors associated with dose variation during cardiac CT angiography (CCTA).
Methods and materials: A questionnaire was distributed to CT centres across Australia and Saudi Arabia. All participating centres collected data for adults who underwent a CCTA procedure. The questionnaire gathered information about the examination protocol, scanning parameters, patient parameters, volume CT dose index ($CTDI_{vol}$), and dose length product (DLP). A stepwise regression analysis was performed to assess the contribution of tube voltage (kV), padding time, cross-sectional area (CSA) of the chest, and weight to DLP.
Results: A total of 17 CT centres provided data for 423 CCTA examinations. The median $CTDI_{vol}$ and DLP were 18 mGy and 256 mGy.cm, respectively. There was a statistically significant difference in DLP between retrospective and prospective ECG gated modes ($p=0.001$). The median DLP from CCTA using a padding technique was 61% higher than CCTA without padding ($p=0.001$). The stepwise regression showed that kV is the most significant predictor of DLP followed by the padding technique then CSA. Correlation analysis showed a strong positive correlation between weight and CSA ($r=0.78$), and there was a moderate positive correlation between weight and DLP ($r=0.42$), as well as CSA and DLP ($r=0.48$).

Conclusion: Findings show radiation dose variations for CCTA. The factors associated with dose variation found in this study are scanning mode, kV, padding time technique, and CSA of the chest.
Limitations: Only Australia was included.
Ethics committee approval: Approved the human research ethics committee of the University of Sydney.
Funding: No funding was received for this work.
Author Disclosures:
M. F. M. McEntee: Employee at University College Cork
P. C. Brennan: CEO at DirectED, Employee at University of Sydney
A. B. Alhailiy: nothing to disclose
E. U. Ekpo: nothing to disclose
P. Kench: nothing to disclose
E. Ryan: nothing to disclose

RPS 614-4 11:43

The accuracy of Hounsfield values with "artificial 120 kVp" reconstruction kernel on different tissues and kVp at multislice CT: a phantom study

M. Kusk, M. Vestergaard*; Esbjerg/DK (martin.weber.kusk@rsyd.dk)*

Purpose: Advances have made scanning at kVps other than 120 feasible; optionally with spectral filtering for dose reduction. This has prompted “artificial 120 kVp” kernels scoring to correct Hounsfield values acquired at other kVps, primarily for coronary calcium scoring. Our purpose is to assess the accuracy of this kernel compared to “true” 120 kVp scans over a wider range of kVps and tissue equivalents.
Methods and materials: Images were acquired on Siemens Somatom FORCE scanner. A Gammex-RMI 461 phantom with 5 different density inserts was scanned 5 times in 10 kV steps from 70-150 plus at 100 and 150 kV with a spectral filter. CTDI was kept constant. 3 mm slices were reconstructed at standard and “artificial 120 kVp” kernel. Measurements of Hounsfield value and standard deviation were performed. ANOVA was used to test for differences from 120 kV scans.
Results: For soft-tissue and fat equivalent tissues, "artificial 120 kVp" kernel did not significantly alter Hounsfield values for images acquired without spectral filtration, regardless of kVp. The difference from "true" 120 kVp varied by up to 30%. At 100 kVp with tin filter, Hounsfield values matched within 1%. 150 kVp images with tin filter differed by 35%. Bone/calcium equivalent tissue Hounsfield values matched "true" 120 kVp images to within 4%.
Conclusion: Hounsfield values of soft tissue and adipose tissue are not recovered by the "artificial 120 kVp" kernel and observers should be aware of these limitations when viewing images reconstructed with this kernel. Hounsfield values are accurate for calcifications.
Limitations: As a phantom study, results should be verified on real patients before results can be generalised.
Ethics committee approval: n/a
Funding: No funding was received for this work.
Author Disclosures:
M. Kusk: nothing to disclose
M. Vestergaard: nothing to disclose

RPS 614-5 11:49

40keV virtual mono-energetic image quality and optimisation of window settings in pancreas dynamic contrast enhancement

J. Xu, Y. Yang, R. Chang, Q. Han, X. Chen, H. Dong*; Shanghai/CN (919669640@qq.com)*

Purpose: To explore virtual monoenergetic (MonoE) image quality and determine the optimal window settings for Mone-E40 keV images in pancreatic multiphase enhanced scans based on spectral detector CT (SDCT).
Methods and materials: In this retrospective study, 30 patients suspected for pancreatic neuroendocrine tumour (PNET) underwent a pancreatic multiphase-enhanced CT scan on an SDCT. The polyenergetic (PolyE) and MonoE-40keV images of arterial phase portal venous phase were reconstructed respectively. CT values, noise values, background noise, signal-to-noise ratio (SNR_{pnet}), and contrast-noise ratio (CNR_{pent}) in the lesion area were recorded to reflects the image quality between all groups. The best individual window settings for $MonoE_{AP}$-40keV and $MonoE_{PVP}$-40keV were also recorded to assess the display of the pancreas and its lesion area. Through regression analysis, the optimal window settings were obtained from the resulting equations. Subjective image quality scores and lesion diameter were measured to determine the effects of different W/L settings.
Results: The CT value, SNR, and CNR of MonoE-40keV were significantly higher than those of PolyE images, both in the arterial phase and the portal venous phase. For MonoE-40keV images, the optimal window settings were 880/230 and 840/260. All adjusted W/L settings were significantly different and produced a higher subjective score than the standard window settings (350/60). There was no difference between the manual adjustment and the math calculated W/L settings ($p > 0.05$) and no significant differences in lesion diameter were found between all of the window settings ($p > 0.05$).
Conclusion: In pancreatic multiphase SDCT enhanced scan, the quality of virtual monoenergetic 40keV images is better than polyenergetic images. For MonoE-40keV, the appropriate window setting is required to achieve the best pancreatic lesion visualisation.
Limitations: The number of patients was relatively small.
Ethics committee approval: Written informed consent was obtained.
Funding: No funding was received for this work.
Author Disclosures:
J. Xu: nothing to disclose
Y. Yang: nothing to disclose
Q. Han: Employee at Philips Clinical Medical Research Division, Shanghai
X. Chen: Employee at Philips Clinical Medical Research Division, Shanghai
H. Dong: nothing to disclose
R. Chang: nothing to disclose

RPS 614-6 11:55

Establishing DRLs for the most common CT procedures based on patients' body mass indexes

N. Zalokar[1], M. Kukuljan[2], M. Karić[2], A. Diklić[2], N. Mekis[3]; *[1]Slovenska Bistrica/SI, [2]Rijeka/HR, [3]Ljubljana/SI*

Purpose: To establish DRLs based on patients' body mass indexes and compare them with DRLs established based on patients' weight.
Methods and materials: Data for 1,633 patients that were imaged on a single CT unit in a time span of 6 months were collated. Only adult patients were included in the study. Filtration of the data was made based on patients' weights which was selected according to the ICRP 135 publication; patients with 70±10 kg were included in the study. Another filtration of the data was made in the second part of the study based on the patients’ average BMIs; patients with BMI 27 ± 5 were included in the study. Examinations performed less than 20 times were excluded. The DRLs were established at the 75th percentile for the total DLP.
Results: The data of 621 patients was analysed after the filtration based on patients’ weights. After the filtration based on the average BMI, 1,152 patients remained for the analysis. DRLs were established for 7 examinations (abdomen, abdomen-pelvis, CT angiography, extremity, head, pulmonary angiography, and the thorax). Established DRLs based on patients’ BMIs were increased by 11%, 22%, 10%, 46%, 6%, 22%, and 11% for the abdomen, abdomen-pelvis, CT angiography, extremity, head, pulmonary angiography, and the thorax, respectively, compared to the DRLs based on patients’ weights. It has to be stated that the average patient weight from our collected data was 80.3 kg and the median was 80 kg.
Conclusion: Based on our results and the fact that the population is becoming heavier, we would recommend that DRLs should be established based on patients’ BMIs to get more accurate results.
Limitations: No CTDIvol data.
Ethics committee approval: n/a
Funding: No funding was received for this work.
Author Disclosures:
M. Kukuljan: nothing to disclose
A. Diklić: nothing to disclose
N. Zalokar: Speaker at Faculty for Health Sciences, University of Ljubljana
M. Karić: nothing to disclose
N. Mekis: nothing to disclose

RPS 614-7 12:01

The influence of a scan projection radiograph sequence and decentring on a total dose at thoracoabdominal CT: a phantom study

M. Kusk, M. B. Vestergaard*; Esbjerg/DK (martin.weber.kusk@rsyd.dk)*

Purpose: To examine the influence on the sequence of lateral and frontal scan projection radiographs (SPR), with and without patient de-centring, on dose-length-product using CAREDose4D tube current modulation at thoracoabdominal CT.
Methods and materials: Two scanners were examined: A) Definition FLASH and B) Definition AS (Siemens Healthcare AG). A full-body anthropomorphic phantom was marked for placement reproducibility and placed in the standard position. 5 identical thoracoabdominal scans were performed for each of the SPR combinations as follows: A-P, P-A, lateral, A-P plus lateral, lateral plus A-P, PA-plus lateral, and lateral plus P-A. All series were repeated three times: with an iso-centred phantom and 5 cm decentring anterior and posterior, respectively. DLP was noted for each scan. mAs vs Z-position was plotted.
Results: For both scanners, A-P or P-A SPRs alone resulted in higher doses than lateral alone. Scans with P-A or A-P SPR followed by lateral SPR resulted in 30% lower DLP than with A-P or P-A performed first. With decentring, the variation in the dose was less than 5% when lateral SPR performed alone or after A-P or P-A SPR. When P-A or A-P performed alone or after lateral SPR,

decentring resulted in differences of up to 50%. Relative variations were largest in denser regions, but lower in the thorax.
Conclusion: Incorrect sequencing of SPRs can seriously alter the patient radiation dose when using CAREDose4D, especially when the patient is not centred. Radiographers must be aware of this when designing protocols or prescribing additional SPRs.
Limitations: As this was only a phantom study and dose variations were not uniform across anatomy, the effective total dose variations are not necessarily linearly correlated with DLP. Other software versions may exhibit other behavior.
Ethics committee approval: n/a
Funding: No funding was received for this work.
Author Disclosures:
M. Kusk: nothing to disclose
M. B. Vestergaard: nothing to disclose

RPS 614-8 12:07
Dose outliers in computed tomography
L. Kuopusjärvi, M. Hanni, A. Kotiaho*; Oulu/FI (lassi.kuopusjarvi@gmail.com)*

Purpose: Abnormal doses in CT examinations have been studied in the past, although often with complex methods. We developed a practical method to detect abnormal radiation doses in CT examinations via Radimetrics.
Methods and materials: 4 CT protocols were chosen for evaluation from 1/10/2017-22/08/2019: routine head (n=23985), abdomen in venous phase (n=4445), pulmonary embolism (n=2404), and thorax/abdomen/pelvis suspected malignancy scan (n=3668). Examinations were investigated with the following parameters: $CTDI_{VOL}$/SSDE vs WED, acquisition count vs scan length, and maximum DLP recorded per protocol. Dose outliers were visually inspected based on the graphs containing these parameters.
Results: Some dose outliers were excluded based on patient-based reasons such as hands inside the scan FOV, wrongly registered protocol name, or unusual imaging instructions given by the radiologist. We observed the following outliers per protocol: routine head (n=5), abdomen in venous phase (n=13), pulmonary embolism (n=26), and thorax/abdomen/pelvis scan (n=8). Out of 52 outliers, 33 included double scanning. Too long scan length or scanning outside of survey radiograph was present in 27 incidents. 8 incidents included contrast media extravasation and in 7 of those, a second scan was required. 17 examinations had to be repeated because of a failed timing of a contrast media bolus. Most commonly, this was because the patient held their hands down. This caused image quality degradations in the monitoring phase of i.v. contrast injection, yielding a scan start delay.
Conclusion: This project led to clarifications in CT-examination instructions, detailed presentations on the causes of dose outliers, and changes in CT imaging protocols. For example, the lateral survey radiographs were optimised in pulmonary embolism to make the pulmonary area more visible.
Limitations: This method is applicable to other CT protocols as well.
Ethics committee approval: The institutional review board approved the study (204/2019).
Funding: No funding was received for this work.
Author Disclosures:
L. Kuopusjärvi: nothing to disclose
M. Hanni: nothing to disclose
A. Kotiaho: Speaker at Tromp Medical

RPS 614-9 12:13
Acceptable quality dose (AQD) for common CT examinations: a UAE multicentre study
W. Elshami[1], M. M. Abuzaid[1], D. Z. Joseph[2], I. H. M. Elhag[3], M. A. Musallam[1]; *[1]Sharjah/AE, [2]Kano/NG, [3]Abu Dhabi/AE (welshami@sharjah.ac.ae)*

Purpose: Acceptable quality dose (AQD) is a bottom-top optimisation approach based on image quality, radiation dose, and a patient's weight. The standard dose value is used as an optimisation tool for producing a quality image in the diagnostic examination. The primary purpose of this study is to determine the AQD resulting from various protocols for adult patients undergoing CT examinations in 4 hospitals in the UAE.
Methods and materials: The data used in this study was collected from 4 CT scanners for adult patients undergoing brain, chest, abdomen, and chest-abdomen CT. 320 patients were included in the study. Patient information and exposure parameters were extracted. All images were assessed for image quality according to scoring criteria 1, 2, 3, and 4 corresponding to bad, not acceptable, acceptable, and higher than necessary quality, respectively. Only images with acceptable quality (score of 3) were selected and grouped into 8 weight groups. The median values for CTDIvol and DLP were determined as the AQD.
Results: The results were depicted in table form.
Conclusion: AQD is a bottom-top optimisation approach based on image quality, radiation dose, and a patient's weight. The integration of image quality scoring with dose might result in the detection of situations with higher-than-necessary image quality. Thus, awareness and orientation of radiologists in image quality are essential to optimise image quality and patient dose.
Limitations: The study focused on the common examinations only, thus, other examinations such as angiography and the spine were not included in the study.
Ethics committee approval: Approval Reference No: MOHP/REC-18/2018.
Funding: No funding was received for this work.
Author Disclosures:
W. Elshami: nothing to disclose
M. M. Abuzaid: nothing to disclose
D. Z. Joseph: nothing to disclose
I. H. M. Elhag: nothing to disclose
M. A. Musallam: nothing to disclose

RPS 614-10 12:19
Optimisation of post-processing parameters for abdominal forensic CT scans
J. B. Nielsen[1], P. A. Nielsen[2], D. M. Bech[3], P. L. Hansen[4], S. Deppe Mørup[5], P. M. Leth[6], H. Precht[7]; *[1]Odense V/DK, [2]Odense C/DK, [3]Odense SØ/DK, [4]Odense/DK, [5]Kolding/DK, [6]Esbjerg/DK, [7]Middelfart/DK (juliebn@live.dk)*

Purpose: Forensic institutes have widely embraced the use of postmortem CT (PMCT) as a supplement or replacement of autopsy in postmortem examinations. However, imaging of the deceased provides an array of challenges not observed in the living: rigor mortis, damage by fire, severe decomposition, or dismemberment not only complicates the proper identification of anatomy but also affects the positioning and centring of the diseased. Consequently, there is a need for reconstruction methods aimed specifically for postmortem conditions to compensate for the variable states of the bodies. In this study, alternative reconstruction methods were tested.
Methods and materials: 4 reconstruction protocols, 3 newly constructed and 1 standard, were compared using a visual grading analysis with 4 observers. The study population was 20 retrospective PMCT scans with different degrees of decomposition. Interobserver agreement was assessed using Fleiss Kappa, with a 95% confidence interval.
Results: The stage of decomposition highly influenced the evaluation from the observer of the usefulness of the reconstruction. Excluding the severely decomposed bodies, 93.4-100% of the 20 PMCTs evaluated were found to be useful for diagnosis using the 4 reconstructions. One newly constructed protocol scored higher in VGAS compared to the standard protocol, with respect to usefulness and beam hardening, indicating a better diagnostic value.
Conclusion: There is a need for improved reconstruction parameters in PMCT, focusing on an increase of details otherwise lost to decay. Moreover, protocols must be targeted to the condition of the body, as highly decomposed, incinerated, and waterlogged bodies all differ structurally from the recently deceased as well as pose-practical problems in relation to positioning.
Limitations: Observers had limited experience in forensic imaging. A limited study population. The question for noise assessment was worded ambiguously.
Ethics committee approval: n/a
Funding: No funding was received for this work.
Author Disclosures:
J. B. Nielsen: nothing to disclose
P. A. Nielsen: nothing to disclose
D. M. Bech: nothing to disclose
P. L. Hansen: nothing to disclose
S. Deppe Mørup: nothing to disclose
H. Precht: nothing to disclose
P. M. Leth: nothing to disclose

RPS 614-11 12:25
A model-based iterative reconstruction with a lung image filter versus filtered back projection and adaptive statistical reconstruction in chest CT: a comparative assessment of image quality
M. Tsuda[1], K. Ichikawa[2], S. Yata[1], A. Murakami[1], H. Yunaga[1]; *[1]Yonago-Shi Tottori-Ken/JP, [2]Kanazawa/JP*

Purpose: To assess the image quality of chest CT using a model-based iterative reconstruction (MBIR) with a lung-image filter.
Methods and materials: The image quality was assessed subjectively and objectively. In the subjective assessment of overall image quality, 25 clinical lung images were assessed by 3 radiologists and scored using a 5-point scale. The images were reconstructed using filtered back projection (FBP), adaptive statistical iterative reconstruction (ASiR-V), and MBIR with a lung-image filter. ASiR-V blending level was 50%. Modulation transfer function (MTF) and noise power spectrum (NPS) were measured in the objective image quality assessment. The MTF measurement phantom has 20, 100, 200, and 500 Hounsfield unit (HU) blocks. The blocks were set into a water phantom and 4 contrast MTFs were obtained using the phantom. NPS measurements were obtained using a water phantom. All measurements in the objective assessment

were made using the "CT measure" application (Japanese Society of Technology).
Results: The images obtained by MBIR with lung-image filter received the highest scores in the subjective assessment and showed improved spatial resolution under high-contrast conditions. NPS showed mostly good noise reduction at the MBIR with a lung-image filter.
Conclusion: Using MBIR with a lung-image filter significantly improved the image quality in chest CT.
Limitations: Objective assessments were not made using task-based methods.
Ethics committee approval: This study has been approved by Certified Review Board, Tottori University Hospital.
Funding: No funding was received for this work.
Author Disclosures:
M. Tsuda: nothing to disclose
K. Ichikawa: nothing to disclose
S. Yata: nothing to disclose
A. Murakami: nothing to disclose
H. Yunaga: nothing to disclose

11:15 - 12:30 **Room M 1**

Cardiac

RPS 603b

Connecting the heart with the lungs and the rest of the body

Moderators:
I. Carbone; Rome/IT
V. Wieske; Berlin/DE

RPS 603b-K 11:15
Keynote lecture
M. Nedevska; *Sofia/BG (nedevska_maria@yahoo.com)*

Author Disclosures:
M. Nedevska: nothing to disclose

RPS 603b-1 11:25
Ventricular mass index for non-invasive treatment control of balloon pulmonary angioplasty in chronic thromboembolic pulmonary hypertension
A. Brose[1], M. Richter[1], V. Bethke[1], A. Hasse[1], M. Richter[1], K. Tello[1], C. B. Wiedenroth[2], G. Krombach[1], F. Roller[1]; *[1]Giessen/DE, [2]Bad Nauheim/DE (alexander.brose@radiol.med.uni-giessen.de)*

Purpose: Within the last decade, balloon pulmonary angioplasty (BPA) has grown as a valuable therapy option for inoperable CTEPH, accompanied by invasive right heart catheterisation as the gold standard in therapy monitoring. The purpose of this study was to investigate the ventricular mass index as a non-invasive parameter to monitor BPA treatment success.
Methods and materials: 26 patients with CTEPH who underwent BPA received cardiac MRI and right heart catheterisation (RHC) prior to and 6 months after treatment. Ventricular mass index (VMI) was evaluated by two experienced radiologists and the mean pulmonary arterial pressure (mPAP) was derived from RHC. Paired testing of the pre- and post-interventional values was performed with a Wilcoxon signed-rank test. The Spearman-Rho correlation coefficient was used to correlate invasive and non-invasive parameters. Univariate linear regression analysis was performed to show the impact of mPAP on VMI.
Results: VMI and mPAP both showed a mean decrease by 20% 6 months after BPA (VMI -19.0% vs mPAP -23.4%). The VMI ratio (postBPA/preBPA) correlated significantly with the mPAP ratio (r=0,403*) and the ratio of brain natriuretic peptide (r=0,577**), whereas the ratio of right or left ventricular mass showed only mediocre correspondence. In addition, the total decrease in VMI also correlated significantly with the total change in mPAP (r=0,457*) and NT-proBNP (r=0,452*). Univariate linear regression analysis between VMI and mPAP showed significant interrelation (R=0,401; p=0,042 and R=0,474; p=0,014).
Conclusion: Cardiac MRI allows for non-invasive assessment of therapy outcomes in BPA treated CTEPH. Thereby, VMI is a better parameter than right or left ventricular mass only.
Limitations: The study comprises only a small number of patients.
Ethics committee approval: Institutional Review Board approval was obtained.
Funding: No funding was received for this work.

Author Disclosures:
A. Brose: nothing to disclose
M. Richter: nothing to disclose
V. Bethke: nothing to disclose
A. Hasse: nothing to disclose
M. Richter: nothing to disclose
K. Tello: nothing to disclose
C. B. Wiedenroth: nothing to disclose
G. Krombach: nothing to disclose
F. Roller: nothing to disclose

RPS 603b-2 11:31
Association of left and right ventricular strains with presence of pulmonary hypertension: a cine realtime feature-tracking study
V. Nizhnikava, G. Reiter, U. Reiter, C. Kräuter, C. Reiter, G. Kovacs, H. Olschewski, M. Fuchsjäger; *Graz/AT (volha.nizhnikava@gmail.com)*

Purpose: Pulmonary hypertension (PH) is associated with left (LV) and right ventricular (RV) myocardial alterations, which should be reflected in alterations of LV and RV strain parameters. The aim of the current study was to analyse if global myocardial strain parameters derived from cine realtime feature-tracking predict the presence of PH.
Methods and materials: 65 patients with known or suspected PH underwent right heart catheterisation and free-breathing cardiac MR cine realtime imaging at 3T (Skyra, Siemens Healthcare) within 1±3 days (mPAP=43.47±11.07mmHg in PH; mPAP=18.97±3.7mmHg in non-PH, n=34 and 31, respectively). LV and RV global radial (GRS), circumferential (GCS), and longitudinal (GLS) strains and strain rates (GRS_{rate}, GCS_{rate}, and GLS_{rate}, respectively) were evaluated by cvi42 (Circle Cardiovascular Imaging, Canada) using a two-dimensional approach. Group differences of resulting strain parameters and their association with PH were analysed employing t-test, correlation, and receiver operating characteristic curve analysis.
Results: Apart from RV diastolic GRS_{rate} and GCS_{rate}, all RV strains and strain rates, as well as LV diastolic GRS_{rate} and GCS_{rate}, differed significantly between PH and non-PH subjects and correlated significantly with mPAP.
The strongest correlation with mPAP (r=0.59) was found for RV-GLS (-21±4% vs. -15±4%, p<0.0001, in PH and non-PH, respectively). RV-GLS also demonstrated the highest area under the curve (AUC) for the prediction of PH (AUC=0.86, 95% confidence interval: 0.75-0.94). A cut-off RV-GLS>-17.6% resulted in a sensitivity of 79% (95% confidence interval: 62-91%) and a specificity of 86% (95% confidence interval: 67-96%) for the diagnosis of PH.
Conclusion: Despite the significant association of global LV and RV strains and strain rates derived from cine realtime feature-tracking with PH, the prediction of PH from global myocardial strain parameters is limited.
Limitations: A single-centre study.
Ethics committee approval: NCT01725763.
Funding: OeNB-Anniversary-FundNr.17934.
Author Disclosures:
V. Nizhnikava: Grant Recipient at ESOR fellowship
G. Reiter: Employee at Siemens Healthcare Diagnostics GmbH
G. Kovacs: nothing to disclose
U. Reiter: nothing to disclose
C. Reiter: nothing to disclose
C. Kräuter: Grant Recipient at OeNB Anniversary Fund
H. Olschewski: nothing to disclose
M. Fuchsjäger: nothing to disclose

RPS 603b-3 11:37
Atrial measurements: can they predict adverse events in patients with acute pulmonary embolism (PE)?
R. R. Kirkbride[1], A. C. Monteiro[1], D. C. Dabreo[2], B. H. Heidinger[3], D. M. Tridente[1], C. Wiest[1], G. Aviram[4], B. J. Carroll[1], D. Litmanovich[1]; *[1]Boston, MA/US, [2]Kingston, ON/CA, [3]Vienna/AT, [4]Tel-Aviv/IL (rachaelkirkbride1@gmail.com)*

Purpose: To determine the association between atrial size and adverse events (AE) in patients with acute PE.
Methods and materials: Left (LA) and right atrial (RA) volume (Image 1), area (largest axial), and diameter (perpendicular to interatrial septum), along with ventricular diameters and pulmonary artery (PA) diameter, were retrospectively measured in 493 patients with acute PE. Interventricular septal bowing and reflux of contrast into the inferior vena cava was also assessed. Tricuspid annular plane systolic excursion (TAPSE) was measured as a representative echocardiography parameter and ECG evidence of right-heart strain documented. AE was defined as 30-day PE-related mortality or the need for advanced therapy i.e. thrombolysis, thrombectomy, or vasopressors. Mann-Whitney and Chi-squared tests were used to compare those with and without

AE. The area under the curve values and multivariate logistic regression were used for prediction analysis.
Results: There was 62/493 patients with AE. There was no significant sex (p=0.6) or age (p=0.2) difference between the groups. Decreased LA volume, area, and diameter, along with increased RA/LA volume, area, and diameter ratios, septal bowing, and contrast reflux were associated with AE. PA diameter was not associated.
LA volume was the best atrial predictor of AE (AUC=0.67) and was an equivocal predictor compared to the combination of RV/LV diameter ratio, TAPSE, and ECG (AUC=0.71)(P=0.07).
Conclusion: Decreased LA measurements along with septal bowing and contrast reflux are associated with acute PE-related adverse events. LA volume is of similar predictive value compared to a combination of ventricular diameter ratio, TAPSE, and ECG.
Limitations: A retrospective study with selection bias as only patients with acute PE and echo were included. Non-gated images were degraded by motion.
Ethics committee approval: IRB waived informed consent(#2015P000425).
Funding: No funding was received for this work.
Author Disclosures:
A. C. Monteiro: nothing to disclose
R. R. Kirkbride: nothing to disclose
D. M. Tridente: nothing to disclose
D. C. Dabreo: nothing to disclose
G. Aviram: nothing to disclose
B. H. Heidinger: nothing to disclose
C. Wiest: nothing to disclose
B. J. Carroll: nothing to disclose
D. Litmanovich: nothing to disclose

RPS 603b-4 11:43
Unmasking the occult heart involvement in systemic sclerosis of recent onset: the role of strain imaging by using cardiac magnetic resonance
P. Palumbo, E. Cannizzaro, C. de Cataldo, F. Cobianchi Bellisari, P. Ruscitti, R. Giacomelli, P. Cipriani, E. Di Cesare, C. Masciocchi*; L'Aquila/IT (palumbopierpaolo89@gmail.com)*

Purpose: To assess the occult cardiac involvement in asymptomatic SSc participants of recent onset by strain imaging derived from cardiac magnetic resonance (CMR) for very early identification of myocardial involvement associated with a poor prognosis
Methods and materials: 16 consecutive SSc participants of recent onset were included. We considered SSc of recent onset, all those participants fulfilling the ACR/EULAR 2013 classification criteria, in less than 1 year from the onset of Raynaud's phenomenon. All the participants underwent pharmacological stress, rest perfusion, and late enhancement (LE) CMR. Strain evaluations of the left ventricle were performed on cine-images and the values were compared with 15 healthy controls (HCs). All 2-d radial, circumferential, and longitudinal strain values were analysed
Results: No SSc participant showed internal organs or skin involvement, "traditional" cardiovascular risk factors, episodes of chest pain, and all were naïve to any medication. Perfusions defects were detected in 5 SSc participants and LE in 1 participant. By analysing strain values, we observed a significant reduction of radial (SSc: 29.47% ±4.41 vs HCs: 40.43% ± 13.24, p= 0.006) and longitudinal (SSc: -15.36% ± 1.72 vs HCs: -17.94% ±1.84, p= 0.002) values in SSc. Conversely, the comparison of circumferential values did not result in statistical difference (SSc: -19.17% ± 2.52 vs HCs: -20.30% ± 3.32, p= 0.348).
Conclusion: The decreased radial and longitudinal strain values could unmask an early sub-endocardial involvement in asymptomatic SSc participants, which is independent from traditional cardiovascular risk factors and seems to be a specific hallmark of recent onset of the disease.
Limitations: A small sample size.
Ethics committee approval: The study was conducted in accordance with Helsinki declaration.
Funding: No funding was received for this work.
Author Disclosures:
P. Palumbo: nothing to disclose
E. Cannizzaro: nothing to disclose
C. de Cataldo: nothing to disclose
F. Cobianchi Bellisari: nothing to disclose
E. Di Cesare: nothing to disclose
C. Masciocchi: nothing to disclose
P. Ruscitti: nothing to disclose
R. Giacomelli: nothing to disclose
P. Cipriani: nothing to disclose

RPS 603b-6 11:49
Myocardial deformation in patients having Takayasu's arteritis with pulmonary artery involvement using cardiac magnetic resonance feature tracking
X. Guo, M. Liu, Z. Ma, T. Jiang, J. Gong*; Beijing/CN (xjguo1001@126.com)*

Purpose: To explore the feasibility of a CMR-derived feature tracking algorithm for assessing left ventricular myocardial deformation in patients having Takayasu's arteritis with pulmonary artery involvement (PTA), and to determine if these parameters are correlated to clinical assessments.
Methods and materials: Patients with PTA (n = 25) and healthy controls (n=17) were enrolled and underwent CMR examination. Feature tracking of CMR cine imaging was used to obtain left ventricular global, segmental longitudinal, circumferential, radial strain, and their respective strain rates. Clinical assessments were performed concurrently. ROC curve was performed to detect patients with PTA.
Results: PTA patients had significantly reduced global peak longitudinal strain (GLS) (-12.7± 3.9%,-14.9± 2.5%), a peak longitudinal diastolic strain rate (GLDSR) (0.65± 0.57%,0.94± 0.28%), and a peak radial diastolic strain rate (GRDSR) (-2.08±1.22,-2.85±0.87%). The basal peak circumferential strain (CS), peak radial diastolic strain rate (RDSR), mid-ventricular CS, peak circumferential diastolic strain rate, LDSR, and RDSR were also decreasing (P<0.05). GLS was correlated to ESRs (r=-0.48, P=0.02). GLS had the highest sensitivity (84%), specificity (53%), and accuracy (75%) for the identification of PTA patients.
Conclusion: The abnormal LV myocardial deformation of PTA patients with preserved LVEF can be detected early using feature tracking CMR. GLS is associated with ESR and had a high sensitivity for PTA patients.
Limitations: The patients included in our study were limited to PTA. Most patients in our study were enrolled later into the disease course. This likely influences the strength of associations between clinical and imaging assessments. There was an insufficient sample size and this may affect the strength of our results.
Ethics committee approval: The study protocol was approved by the Beijing Chao-Yang Hospital Ethics Committee (2017-K-127).
Funding: This study was supported by the National Natural Science Foundation of China (81871328).
Author Disclosures:
X. Guo: nothing to disclose
M. Liu: nothing to disclose
Z. Ma: nothing to disclose
T. Jiang: nothing to disclose
J. Gong: nothing to disclose

RPS 603b-7 11:55
Left ventricular function assessment in significant hypertension with primary aldosteronism: evaluation by cardiac magnetic resonance feature tracking
R. Shi, Z.-G. Yang, X.-M. Li, T. Pang*; Chengdu/CN*

Purpose: To evaluate left ventricular (LV) global myocardial strain in newly diagnosed primary aldosteronism (PA) patients compared with healthy controls.
Methods and materials: Form May 2018 to April 2019, 33 significant hypertension patients with newly diagnosed PA and 20 healthy controls were enrolled retrospectively. Cardiac magnetic resonance (CMR) was used to determine LV feature-tracking parameters. Global peak strain (PS), peak systolic strain rate (PSSR), and peak diastolic strain rate (PSDR) were measured and compared among patients and controls. Clinical variables, medication, and other cardiovascular risk factors were obtained through patient questionnaires or medical records.
Results: PA patients had a higher LV mass than normal controls (71.74 ± 16.87 vs. 94.44 ± 24, p=0.002). A decrease in global circumferential PSSR, longitudinal, and radial PSDR were found in PA patients compared to healthy individuals (all p<0.05). Systolic blood pressure and serum aldosterone concentration (SAC) was closely related to LV mass index and LV deformation (all p < 0.05).
Conclusion: Our findings may indicate that in PA patients, CMR-feature tracking could quantify LV deformation effectively. Further, systolic blood pressure and SAC may induce LV hypertrophy and functional impairment.
Limitations: Our study is single-centred and retrospective, based on a small sample size, which may cause bias. Patients with subclinical coronary heart disease and kidney disease may affect the outcome.
Ethics committee approval: This study was approved by the Institutional Review Board of West China Hospital, Sichuan University (Chengdu, Sichuan, China) with a waiver of informed consent due to the retrospective nature of this investigation.
Funding: No funding was received for this work.
Author Disclosures:
R. Shi: nothing to disclose
Z.-G. Yang: nothing to disclose
X.-M. Li: nothing to disclose
T. Pang: nothing to disclose

RPS 603b-8 12:01

People living with HIV have diverse and independent forms of cardiac involvement: insights from cardiac magnetic resonance imaging

C. Arendt, D. Leithner, T. Wolf, A. Haberl, C. Stephan, T. J. Vogl, E. Nagel, P. de Leuw, V. Puntmann*; Frankfurt am Main/DE (crt.arendt@gmail.com)*

Purpose: To screen for the prevalence and type of cardiovascular disease (CVD) in people living with HIV (PLHIV) using cardiovascular MRI in a contemporary cohort with highly active antiretroviral therapy.
Methods and materials: All participants underwent a standardised MRI protocol for cardiac function, myocardial perfusion (regadenosone), and scar by late gadolinium enhancement (LGE). Myocardial fibrosis and oedema using native T1/T2-mapping were also assessed. Blood sampling was performed prior to MRI.
Results: 141 participants were identified (n=32 in category C/AIDS). 16 patients had previously documented (n=23) myocardial diseases: myocarditis, n=1 coronary artery disease (CAD), n=8 myocardial infarction, n=3 congestive heart failure, n=3, and arrhythmia, n=8. The mean value for hs-cTnT, CRP and NT-proBNP was 9±18ng/l, 0.3±0.6mg/l and 104±229ng/l. The mean current CD4-count was 695±346/µl, significantly (p<0.001) improved from initial HIV-diagnosis (336±265/µl). 14 subjects had impaired LV-EF (<50%) and 35 presented borderline LV-EF (50-55%). Myocardial LGE was present in 28 patients: non-ischemic pattern, n=16, ischemic pattern, n=11, and both patterns, n=1. 2 patients had relevant inducible ischaemia, whereas a pattern of microvascular disease (MVD) was found in 23 patients. 72 subjects had diffuse fibrosis and 25 had active inflammation. Elevated native T1/T2 was significantly associated with low (<350/µl), current, and initial CD4-count (χ^2=5.317,p=0.021; χ^2=3.841,p=0.050), just as with category C/AIDS (χ^2=4.949,p=0.026). Native T2 showed a significant correlation with initial CD4-count (r=-0.252,p=0.008) and current NT-proBNP (r=0.190,p=0.030), but not with other laboratory values.
Conclusion: PLHIV have prevalent and diverse cardiac involvement, which is predominantly non-ischaemic inflammatory in origin. Relevant ischaemia due to epicardial CAD is a minor presentation compared to MVD. Our MRI findings emphasise the role for in-depth phenotyping of CVD due to chronic inflammation, bearing a potential for personalised treatment.
Limitations: Visual assessment of LGE and MVD.
Ethics committee approval: Ethics committee approval and written informed consent.
Funding: Funding from DZHK was received.
Author Disclosures:
C. Arendt: Research/Grant Support at DZHK
D. Leithner: nothing to disclose
T. J. Vogl: nothing to disclose
T. Wolf: nothing to disclose
C. Stephan: nothing to disclose
E. Nagel: Research/Grant Support at DZHK
V. Puntmann: Research/Grant Support at DZHK
P. de Leuw: nothing to disclose
A. Haberl: nothing to disclose

RPS 603b-9 12:07

Selected clinical parameters and changes in cardiac magnetic resonance in patients with rheumatoid arthritis and ankylosing spondylitis without clinically apparent myocardial injury

W. Tanski, P. Gac, A. Chachaj, M. Sobieszczanska, R. Poreba, A. Szuba*; Wroclaw/PL (pawelgac@interia.pl)*

Purpose: The relationship between the occurrence of rheumatoid arthritis (RA) and ankylosing spondylitis (AS) and the cardiac magnetic resonance (CMR) changes in people without clinically overt heart disease.
Methods and materials: The study group consisted of 74 people (48.81±11.35 years): 29 patients with RA, 23 patients with AS, and 22 people from a control group. Blood samples were taken to assess laboratory parameters, disease activity was determined using activity scales, and CMR was performed.
Results: It was shown that the factors independently related to higher left ventricular mass index are AS occurrence, human B27 leukocyte antigen occurrence, higher neutrophil gelatinase-associated lipocalin concentration (NGAL), and higher body mass index (BMI). The lower right ventricular ejection fraction is a result of an independent effect of RA, AS, and higher NGAL. RA presence, methotrexate use, higher rheumatoid factor titer, higher NGAL, older age, and higher BMI should be considered independent risk factors for greater left ventricular myocardium hydration. RA occurrence, AS occurrence, type 2 diabetes occurrence, and a higher C-reactive protein concentration can be independently associated with a higher probability of non-ischaemic left ventricular myocardium injury. A larger volume of fluid in the pericardial sac is a result of an independent effect of higher NGAL, higher anti-cyclic citrullinated peptide antibodies titre, and higher DAS28 disease activity index. The use of steroids is a protective factor against larger volumes of pericardial fluid.
Conclusion: RA and AS in people without clinically apparent myocardial injury are associated with the occurrence of adverse changes in CMR. NGAL is the most useful clinical parameter for the purpose of predicting the risk of adverse changes in CMR in the studied group of patients with RA and AS.
Limitations: A small study group size. Only standard CMR sequences.
Ethics committee approval: Local Bioethics Committee.
Funding: No funding was received for this work.
Author Disclosures:
P. Gac: nothing to disclose
M. Sobieszczanska: nothing to disclose
R. Poreba: nothing to disclose
A. Szuba: nothing to disclose
W. Tanski: nothing to disclose
A. Chachaj: nothing to disclose

RPS 603b-10 12:13

The effects of cardiac geometry, microcirculation, and tissue characteristics on cardiac deformation in silent diabetic cardiomyopathy

J. Li, Z.-G. Yang, Y.-K. Guo, Y. Gao, X. Liu*; Chengdu/CN (jianglifs@163.com)*

Purpose: We evaluated the effects of LV geometry, myocardial microcirculation, and tissue characteristics on cardiac deformation in silent type 2 diabetes mellitus (T2DM) patients, utilising multiparametric cardiac magnetic resonance (CMR) imaging.
Methods and materials: A total of 55 clinically diagnosed T2DM patients and 29 healthy controls were evaluated. CMR-derived parameters including cardiac geometry, function, microvascular perfusion, T1 mapping, T2 mapping, and strain were analysed and compared between T2DM patients and controls.
Results: Compared with the controls, those with T2DM presented a higher remodelling index, decreased perfusion function, higher extracellular volume (ECV), higher T2 values, and decreased cardiac strain. Additional univariable and multivariable analysis revealed that a longer duration of diabetes was associated with a decreased longitudinal peak systolic strain rate (PSSR-L) (β = 0.195, p = 0.013), and remodelling index, and ECV tended to correlate with a longitudinal peak diastolic strain rate (PDSR-L) (remodelling index, β = −0.339, p = 0.000; ECV, β = −0.172, p = 0.026), while microvascular perfusion index and T2 value affected both PSSR-L (perfusion index, β = −0.328, p = 0.000; T2 value, β = 0.306, p = 0.000) and PDSR-L (perfusion index, β = 0.209, p = 0.004; T2 value, β = −0.275, p = 0.000) simultaneously.
Conclusion: T2DM patients demonstrated LV concentric remodelling, microvascular injury, myocardial fibrosis, myocardial oedema, and deformation dysfunction. In addition, the existing pathological changes have diverse effects on cardiac systolic and diastolic functions.
Limitations: A single-centre study. The studied variables are weakly correlated with LV deformation.
Ethics committee approval: The study was approved by the institutional ethics committee of our hospital (No. 2016-24).
Funding: 1·3·5 project for disciplines of excellence, West China Hospital, Sichuan University (ZYGD18013).
Author Disclosures:
J. Li: nothing to disclose
Z.-G. Yang: nothing to disclose
Y.-K. Guo: nothing to disclose
Y. Gao: nothing to disclose
X. Liu: nothing to disclose

RPS 603b-11 12:19

Combined dedicated lung and cardiac screening with third generation dual-source CT: potential for dose reduction

M. Vonder, M. Dorrius, R. Vliegenthart, G. de Bock*; Groningen/NL (marleenvonder@gmail.com)*

Purpose: Currently, two different CT acquisitions are used for dedicated lung cancer screening and dedicated cardiovascular screening of an individual. These acquisitions originate from older CT systems. The aim of this phantom study was to determine the accuracy of low-dose ECG-triggered chest CT for the quantification of coronary artery calcium compared to a dedicated full dose ECG-triggered cardiac CT.
Methods and materials: A phantom insert with 9 calcifications was placed in a thorax phantom simulating a small to medium patient size. The phantom was repeatedly scanned in high-pitch spiral mode with low-dose ECG-triggered chest protocol (chest equivalent quality reference of 20 mAs) and compared to default full dose ECG-triggered cardiac protocol (cardiac quality reference of 64 mAs) as reference. Mann-Whitney U testing was used to compare Agatston scores and noise levels, and a total radiation dose was logged. Potential dose reduction was calculated as the percentage of complete lung and cardiac examination.
Results: The combined acquisition protocol resulted in a similar median Agatston score (p=0.31) of 685 (IQR:669-699) and a similar noise level (p=0.095) of 22.0 HU (IQR:20.5-24.5) as the dedicated cardiac reference

protocol (median Agatston: 667 [IQR:654-692], noise: 20.0 HU [IQR:19.5-21.0]). The $CTDI_{vol}$ of only the cardiac region of the ECG-triggered chest protocol was 0.61 mGy (0.20 mSv) vs 0.86 mGy (0.28 mSv) for the reference protocol. If a dedicated cardiac acquisition can be eliminated, the potential dose reduction was 20% for small-medium patient size for complete lung and cardiac evaluation in one acquisition.
Conclusion: With the new protocol, the total radiation dose for combined lung and cardiac screening in one CT acquisition can potentially be reduced by 20% without compromising on CAC quantification and image quality.
Limitations: n/a
Ethics committee approval: n/a
Funding: No funding was received for this work.
Author Disclosures:
M. Vonder: nothing to disclose
M. Dorrius: nothing to disclose
G. de Bock: nothing to disclose
R. Vliegenthart: nothing to disclose

11:15 - 12:30 **Room M 2**

Interventional Radiology

RPS 609b

Experimental

Moderators:
N.N.
F. Pedersoli; Maastricht/NL

RPS 609b-1 11:15

Validation of a dose tracking software for skin dose map calculation using on-phantom measurements with radiochromic films

P. E. Colombo[1], F. Rottoli[1], M. M. J. Felisi[1], C. de Mattia[1], S. Riga[1], M. Sutto[1], C. Dillion[2], S. Massey[2], A. Torresin[1]; [1]*Milan/IT,* [2]*Scottsdale, AZ/US*
(paolae.colombo@ospedaleniguarda.it)

Purpose: To validate the algorithm within the radiation dose index monitoring software NEXO[DOSE]® (Bracco Injeneering SA, Lausanne). It provides the skin dose distribution in interventional radiology procedures.
Methods and materials: To determine the skin dose distribution in interventional radiology procedures, the software uses exposure parameters taken from the radiation dose structured report and additional information specific to each angiographic system. To test the algorithm accuracy, GafChromic® XR-RV3 films, wrapped on a cylindrical PMMA phantom, were irradiated with different setups and two different angiographic systems. The film measurements were compared in terms of absolute dose and geometric accuracy, with the ones that the software calculated on the same cylindrical model.
Results: The cumulative dose values estimated by the software are in correlation with the GafChromic® measurements (differences lower than 15%) within the regions of the higher dose, whereas we are more interested in assessing patient exposure. Concerning the geometric accuracy, the differences between the dose spatial distribution simulated and the measured ones are less than 3 mm (4%) in simple tests and 5 mm (5%) in setups closer to clinical practice. Moreover, similar results are obtained for the two different angiographic system vendors.
Conclusion: In the tests performed, NEXO[DOSE]® provides an accurate estimate of skin dose similar to or better than those obtained by other software packages. The validation on cylindrical geometry phantom proved that the calculation can be extended to anthropomorphic geometry and can be used to simulate the patient skin dose.
Limitations: The dose value discrepancies increase up to 33% in regions with lower doses because the software does not consider the out-of-field scatter contribution of the neighbouring fields.
Ethics committee approval: n/a
Funding: No funding was received for this work.
Author Disclosures:
P. E. Colombo: nothing to disclose
A. Torresin: nothing to disclose
M. M. J. Felisi: nothing to disclose
F. Rottoli: nothing to disclose
C. de Mattia: nothing to disclose
S. Riga: nothing to disclose
M. Sutto: nothing to disclose
S. Massey: Employee at PACSHealth, LLC, Scottsdale, AZ, USA
C. Dillion: Employee at PACSHealth, LLC, Scottsdale, AZ, USA

RPS 609b-2 11:21

Large biodegradable microspheres: evaluation using dynamic renal CT-perfusion in an experimental pig model

C. L. Schlett[1], T. Reichenbacher[2], D. F.-J. Vollherbst[2], T. Gockner[2], T. D. D. Do[2], S. Macher-Göppinger[3], P. L. L. Pereira[4], H.-U. Kauczor[2], C. Sommer[2]; [1]*Freiburg/DE,* [2]*Heidelberg/DE,* [3]*Mainz/DE,* [4]*Heilbronn/DE*
(christopher.schlett@post.harvard.edu)

Purpose: To compare relatively large new biodegradable and established non-biodegradable microspheres for the embolisation of the right kidney in a swine embolisation model using renal perfusion by dynamic CT imaging.
Methods and materials: Transarterial embolisation of the kidneys was performed from a central position within 9 swine using three different microspheres: L1 and L2 as a prototype (PharmaCept, Germany) of biodegradable starch microspheres (in-vitro biodegradation time/size-d_{50}/size-d_{100}: <52-72h/539µm/1240µm for L1 and <54h/569µm/1495µm for L2) and EmboSphere700-900 as commercially non-biodegradable microspheres. Dynamic contrast-enhanced CT was performed pre-interventional, after 1h, and 7d post-interventional; blood flow (BF) was derived from CT using Syngo volume-perfusion-CT-body. BF was measured across the entire kidney at the hilus (covering 10 mm z-axis) as well as stratified into 4 anatomic regions (dorsolateral, dorsomedial, ventrolateral, and ventromedial segments).
Results: CT derived a physiological renal BF of 181.03±31.4mL/100mL/min pre-interventional. Overall, post-interventional BF was reduced to 40.0% at 1h and recovered after 7d to 69.2% of the pre-interventional value. The observed relative BF decrease at 1h was lower for non-biodegradable than for biodegradable microspheres (-49.2±18.6% vs -64.0±18.0%, respectively) without reaching statistical significance (p=0.10). If analysed per anatomic section, there was a significantly larger BF decrease in the dorsal segments (β=0.28, p<0.0001) and in the lateral segments (β=0.14, p=0.008), independent of the used microspheres.
Conclusion: Renal perfusion after embolisation with relatively large microspheres varied significantly across anatomic locations, potentially due to flow and gravitational effects. Observed differences between biodegradable versus non-biodegradable microspheres did not reveal statistical significance.
Limitations: Limited power due to sample size.
Ethics committee approval: The study was approved by the Regional Council of Karlsruhe (35-9185.81/G-17/15) and followed the directive of the German Animal Protection Law.
Funding: The study was supported technically and financially by PharmaCept GmbH, Berlin, Germany without any publication restrictions.
Author Disclosures:
C. L. Schlett: nothing to disclose
T. Reichenbacher: nothing to disclose
D. F.-J. Vollherbst: nothing to disclose
T. Gockner: nothing to disclose
S. Macher-Göppinger: nothing to disclose
P. L. L. Pereira: nothing to disclose
H.-U. Kauczor: Speaker at Philips Healthcare
C. Sommer: Research/Grant Support at PharmaCept GmbH, Berlin, Germany
T. D. D. Do: nothing to disclose

RPS 609b-3 11:27

MR-guided high-power microwave ablation in hepatic tumours: initial experience in clinical routine

R. Hoffmann, M. T. Winkelmann, S. Clasen, J. Weiß, G. Gohla, K. Nikolaou; *Tübingen/DE (ruediger.hoffmann@med.uni-tuebingen.de)*

Purpose: Evaluation of the technical success and patient safety of high-power MR-guided microwave ablation using a wide-bore 1.5T MR system.
Methods and materials: 13 Patients (61.0 years ± 6.8 [standard deviation]) with 17 hepatic malignancies (6 hepatocellular carcinomas, 11 hepatic metastases) underwent MR-guided tumour ablation with a high-power, water-cooled microwave ablation system from 08/2018-09/2019. The mean tumour size was 13.7 mm ± 5.9 (range: 6-25 mm). Planning, applicator placement, therapy monitoring, and control imaging were carried out using a 1.5T MR system. Technical success and ablation zone diameters were assessed by contrast-enhanced post-ablative control MR imaging. The mean follow-up was 3.6 months ± 4.4 (range: 0-14 months).
Results: Technical success was achieved in all lesions. Lesions were treated using 1.5 ± 0.5 applicator positions with an ablation power of 100W. The mean energy applied was 70,6kJ ± 31,4kJ per tumour (range: 18-120 kJ). The mean total duration of energy application was 11.7 min ± 5.2 (range: 3-20 min) per tumour. Ablation zone short-axis and long-axis diameters were 29.0 mm ± 6.9 (range: 19-41 mm) and 39.6 mm ± 7.8 (range: 28-58 mm), respectively. 3 patients developed new tumour manifestations in the untreated liver during initial follow-up. No complications were observed.

Conclusion: MR-guided high-power microwave ablation provides safe and effective treatment of hepatic malignancies with short ablation durations.
Limitations: The small study population and short follow-up due to the relatively short availability of the MR-conditional microwave ablation system.
Ethics committee approval: Institutional review board approval and patient informed consent were obtained for this prospective study.
Funding: No funding was received for this work.
Author Disclosures:
R. Hoffmann: nothing to disclose
M. T. Winkelmann: nothing to disclose
S. Clasen: nothing to disclose
J. Weiß: nothing to disclose
G. Gohla: nothing to disclose
K. Nikolaou: nothing to disclose

RPS 609b-4 11:33
The joint application of T1 and T2 mapping magnetic resonance imaging (MRI) for the characterisation of the tumour microenvironment in an untreated rabbit hepatic cancer model
S. Keller, T. Borde, M. Shahryari, A. Kader, J. Brangsch, C. Reimann, M. R. Makowski*; Berlin/DE (sarah.keller@charite.de)*

Purpose: To characterise the tumour microenvironment of liver VX2 rabbit tumours using T2 and T1 mapping MRI.
Methods and materials: N=9 female New Zealand white rabbits with left-hepatic VX2 tumours received MRI scans at 14, 21, and 28 days following tumour implantation. MRI was performed on a 3T system (mMR Biograph, Siemens) using a head-neck coil. An axial T2map FLASH (TR/TE 207.4/1.32ms, slice thickness 3 mm), contrast-enhanced imaging (TR/TE 167/5.23ms, slice thickness 0.7 mm), and an axial pre-/post-contrast modified look-locker inversion recovery (MOLLI) (TR/TE 1155/2.45ms, slice thickness 3 mm) were performed. Gd-EOB-DTPA (Primovist, Bayer) at 0.025mmol/kg/KG was injected intravenously through an ear vein IV placement. Images were analysed using Horos (v4.0.0.0RC1). Tumours were segmented into a central, marginal, peripheral, and liver region. Histopathology was obtained in all tumours. For statistical analysis, a two-way ANOVA was applied using SPSS (v.25, IBM, Armonk, NY).
Results: The intrahepatic tumour was established successfully in all rabbits. Within 4 weeks, the tumour size increased from average (SD) 8.3 (1.2) to 14.3 (2.9) mm. Between 14 days and 21 days, T2 relaxation times were significantly decreased in the tumour centre (mean difference 18.6 ms; p=0.025). T2 relaxation times did not change between the tumour regions. Pre- and post-contrast T1 times significantly delineated the three tumour regions and liver parenchyma on days 21 and 28 ($p<0.05$). T1 times were not changed between the three groups.
Conclusion: T1 mapping delivers best results in discriminating tumour regions during longitudinal observations of untreated VX2 liver rabbit tumours, making it a promising technique for future experimental treatment studies.
Limitations: A small sample size using female New Zealand white rabbits.
Ethics committee approval: n/a
Funding: German Research Foundation (SFB1340 “Matrix inVision"), German Federal Ministry of Education and Research (LiSyM 031L0057).
Author Disclosures:
S. Keller: Research/Grant Support at DFG (SFB1340)
T. Borde: nothing to disclose
M. Shahryari: Research/Grant Support at BMBF (LiSyM 031L0057)
J. Brangsch: Research/Grant Support at DFG (SFB1340)
C. Reimann: Research/Grant Support at DFG (SFB1340)
M. R. Makowski: Research/Grant Support at DFG (SFB1340)
A. Kader: nothing to disclose

RPS 609b-5 11:39
Fabrication of adriamycin/Fe_3O_4 gelatin microspheres via a high-voltage electrospraying method for embolisation
J. Li, J. Ji, C. Lu, N. Zhang*; Lishui/CN (a15990007235@126.com)*

Purpose: Usually, adriamycin microspheres (ADM-MS) used in TACE are prepared by an emulsion-crosslinking method. However, the size of ADM-MS can’t be controlled conveniently. Here, we utilise electrospraying to fabricate uniform adriamycin/Fe_3O_4 magnetic gelatin microspheres for embolisation.
Methods and materials: ADM/Fe_3O_4-MS were obtained from a mixture of adriamycin and Fe_3O_4 nanoparticles in gelatin aqueous solution via high-voltage electrospraying method. In electrospraying, the liquid flowing out of a nozzle, which is maintained at high electric potential, is forced by the electric field to be dispersed into fine microspheres. The content of adriamycin and the release curve of the microsphere drug in vitro were measured. Furthermore, the microwave applied elevates to the microspheres temperature. The inhibition of VX2 cells under ADM/Fe_3O_4-MS with MTT assay was observed.
Results: ADM/Fe_3O_4-MS with a diameter range from 200-800μm can be obtained by adjusting the parameters of electrospraying, such as flow rate, voltage, and needle diameter. Meanwhile, ADM/Fe_3O_4-MS posses the sustained release of adriamycin capability. The percent of drug release from ADM/Fe_3O_4-MS after 26 days was about 76.2%. Both microwave heating and adriamycin can inhibit or kill the VX2 cells directly.
Conclusion: A targeted, microwave-sensitive and magnetic ADM/Fe_3O_4-MS is developed by a high-voltage electrospraying method. In electrospraying, the diameter ADM/Fe_3O_4-MS can be controlled to some extent via the parameter of electrospraying, such as voltage, flow rate, and needle diameter. The in vitro studies demonstrate that ADM/Fe_3O_4-MS have an extended sustained-release phase and anti-tumour effect. Furthermore, microwave activates the efficiency of chemotherapy based on increasing the thermal-agent effect of Fe_3O_4 nanoparticles in the tumour.
Limitations: ADM/Fe_3O_4-MS can be applied in the magnetic resonance imaging and achieve a visualised therapy which needs to be further described by data.
Ethics committee approval: n/a
Funding: No funding was received for this work.
Author Disclosures:
J. Li: nothing to disclose
J. Ji: nothing to disclose
C. Lu: nothing to disclose
N. Zhang: nothing to disclose

RPS 609b-6 11:45
Identification of the effects on PD-1 and Tim-3 expressions and the function of T lymphocytes in tumour-bearing mice by RFA
M. Xu, T. Y. Huang, X. Y. Xie*; Guangzhou, Guangdong/CN (xu2004m@sina.com)*

Purpose: To investigate the dynamic changes of immune function in patients with colorectal metastatic liver cancer after RFA.
Methods and materials: BALB/C mice bearing dual colorectal cancer were randomly divided into an ablation group and control group. The tumour on the right side was ablated and the growth of the contralateral tumour was observed by means of vernier caliper, ultrasonography, and pathological examination. T lymphocytes of blood, spleen, and TILs were harvested, and immune checkpoints (PD-1, Tim-3) at different times after ablation, as well as T cell function of secreting cytokines, were measured by flow cytometry, immunofluorescence, and immunohistochemistry.
Results: At the early stage after RFA treatment, a slight stagnation of the contralateral tumour was observed in the contralateral tumour, and the tumour volume was observed to be the smallest on the 3rd day before rapid growth resumed. The percentage of total TILs, CD8+, and CD4+ TILs in contralateral tumours was higher than that in the control group at 3, 9, and 12 days after ablation. PD-1 and Tim-3 were highly expressed on TILs and there was no significant difference in the expression level of PD-1 and Tim-3 in control groups at different times. The levels of PD-1+CD8+TILs, Tim-3+CD8+TILs, and PD-1+Tim-3+CD8+TILs in the ablated group decreased to a minimum of about 50% compared to the control group on the 3rd day, and then began to rise, being close to or exceeding the control group on the 12th day.
Conclusion: RFA can enhance the anti-tumour immunity of organism in the early 3 days, with inhibited tumour growth, increased percentage of TILs, and a remarkable decrease of PD-1 and Tim-3 expression on CD8+TILs.
Limitations: n/a
Ethics committee approval: IACUCC of Sun-Yat Sen University.
Funding: No funding was received for this work.
Author Disclosures:
M. Xu: nothing to disclose
X. Y. Xie: nothing to disclose
T. Y. Huang: nothing to disclose

RPS 609b-7 11:51
Low-dose CBCT based on optimised source-detector trajectories for C-arm
S. Hatamikia[1], A. Biguri[2], G. Kronreif[1], J. Kettenbach[1], T. Russ[3], W. Birkfellner[1]; *[1]Vienna/AT, [2]Southampton/UK, [3]Heidelberg/DE (sepidehhatamikia@yahoo.com)*

Purpose: We propose a target-based cone-beam computed tomography (CBCT) imaging framework in order to optimise the x-ray source-detector trajectory by incorporating prior information available in interventional images. The main aim was to design a CBCT with a minimum dose to the patient.
Methods and materials: A patient-specific model from a preoperative CT was used as a digital phantom for trajectory simulations. We introduced a trajectory optimisation scheme that tries to minimise the radiation dose by means of reducing projections while keeping a reasonable imaging quality at the region of interest of the reconstructed image. We used a structural similarity index (SSIM) as the objective function for the evaluation of the reconstructed image based on simulations. A Philips Allura FD20 Xper C-arm was used for the experiments.

We used an adaptive steepest descent projection onto convex sets (ASD-POCS) algorithm for the reconstruction. The performance of our framework was investigated with an Alderson-Rando head phantom. The dose was evaluated by the computed tomography dose index (CTDI).
Results: Our experiments based on the head phantom showed that our optimised trajectory could achieve a comparable image quality with respect to the reference C-arm CBCT while using one-quarter of projections. We used a feature similarity index (FSIM) in order to quantify the reconstruction results. The relative deviation of FSIM was achieved by 7.54% between the reconstructed image and the reference CBCT. Our results showed the CTDI per mAs delivered by the optimised trajectory was six times lower than by the standard trajectory.
Conclusion: We demonstrate that a minimal dedicated set of projections with optimised orientations is sufficient to localise targets and has a potential for low-dose CBCT interventions.
Limitations: n/a
Ethics committee approval: n/a
Funding: The Austrian Center for Medical Innovation and Technology (ACMIT).
Author Disclosures:
S. Hatamikia: nothing to disclose
A. Biguri: nothing to disclose
G. Kronreif: nothing to disclose
J. Kettenbach: nothing to disclose
T. Russ: nothing to disclose
W. Birkfellner: nothing to disclose

RPS 609b-8 11:57
Phase-contrast imaging based on the microbubble monitoring of radiofrequency ablation: an ex vivo study
P. Haopeng, H. Wei, L. Jian, T. Rongbiao, W. Zhiyuan, D. Xiaoyi, W. Qingbing, W. Zhongmin, C. Kemin*; Shanghai/CN*
(panghaopeng@126.com)

Purpose: To explore the potential of synchrotron radiation phase-contrast imaging for real-time microbubble formation monitoring during radiofrequency ablation.
Methods and materials: Radiofrequency ablation was performed on ex vivo porcine muscle tissue using unipolar and multi-tined expandable electrodes. Images of microbubble formation in the samples were captured by both synchrotron radiation phase-contrast imaging and absorption-contrast imaging. The synchronous ablation temperature was recorded. Ablation size was assessed by histologic examination.
Results: Microbubble formation during radiofrequency ablation could be visualised by synchrotron radiation phase-contrast imaging. The diameter of the microbubbles revealed on the image ranged from tens of microns to several millimetres, and these microbubbles first appeared at the edge of the RFA electrode when the target region temperature reached approximately 60℃ and rapidly extended outwards. The range of microbubbles corresponded to the ablation zone.
Conclusion: Phase-contrast imaging enabled real-time high-resolution visualisation of microbubble formation during radiofrequency ablation, indicating a potential for its use in ablation monitoring.
Limitations: An ex vivo study might not reflect actual microbubble transformation in vivo and the influence of microvessel perfusion and the heat sink phenomenon should be considered. The RFA zone of multi-tined expandable electrodes was larger than the field of the CCD and its range could not be measured by PCI. Although in our study, the range of microbubbles after RFA using unipolar electrodes was close to that measured on histological cross-sections, which contained complete and partial coagulation necrotic areas. The transition between complete coagulation necrosis and partial coagulation necrosis was gradual, and the boundary was indistinct.
Ethics committee approval: n/a
Funding: Shanghai municipal commission of health and family planning (No. 201640087).
Author Disclosures:
P. Haopeng: Investigator at Ruijin Hospital
W. Zhiyuan: Employee at Ruijin Hospital
H. Wei: Employee at Ruijin Hospital
L. Jian: Employee at Ruijin Hospital
T. Rongbiao: Employee at Ruijin Hospital
D. Xiaoyi: Employee at Ruijin Hospital
W. Qingbing: Employee at Ruijin Hospital
W. Zhongmin: Founder at Ruijin Hospital
C. Kemin: Research/Grant Support at Ruijin Hospital

RPS 609b-9 12:03
A preclinical endogenous rat HCC model system for the prospective evaluation of imaging-derived biomarkers in interventional tumour therapy
F. Lohöfer[1], G. Kaissis[1], E. Bliemsrieder[1], P. Bohrer[1], J. Werner[1], R. Buchholz[2], E. J. Rummeny[1], R. Braren[1], P. M. Paprottka[1]*; [1]Munich/DE, [2]Münster/DE*
(fabian.lohoefer@tum.de)

Purpose: To establish a preclinical model system for catheter-based interventions in hepatocellular carcinoma (HCC).
Methods and materials: HCC was induced in rats by oral administration of diethylnitrosamine (DEN) over 10 weeks. Tumour growth was monitored by weekly T2-weighted MRI. When tumours reached a size over 10 mm, MRI with DCE-imaging and T1-mapping were performed using a liver-specific contrast agent. Digital subtraction angiography (DSA) was then performed through a left common carotid artery approach. A 1.2 French catheter was navigated to the common hepatic artery. DSA was performed with a standardised flow rate. After DSA-imaging, Cis-Platin was injected selectively over the angiographic microcatheter. After 10 minutes, the animals were euthanised and the tumours were excised. Deposition of platinum and gadolinium was assessed by laser ablation inductively coupled plasma mass spectrometry (LA-ICP MS) on tissue slices.
Results: Contrast dynamic parameters (time to peak and influx/efflux slopes) correlated well between DSA and DCE imaging in HCCs. T1-mapping showed no significant uptake of liver-specific contrast agent in HCC. LA-ICP MS allowed for spatially resolved ex vivo quantification of gadolinium and platinum in the hepatic and tumour tissues. High arterial vascularisation in in vivo imaging correlated strongly with increased platinum concentrations.
Conclusion: The development of a transarterial chemoembolisation model in HCC-bearing DEN rats allows for sensitive quantification of tumour perfusion and chemotherapeutic agent uptake, validated with a spatially resolved, high-accuracy mass spectroscopy method.
Limitations: This is a preclinical proof of concept study with a limited number of animals.
Ethics committee approval: ROB-55.2Vet-2532.Vet_02-16-25.
Funding: No funding was received for this work.
Author Disclosures:
F. Lohöfer: nothing to disclose
E. J. Rummeny: nothing to disclose
G. Kaissis: nothing to disclose
E. Bliemsrieder: nothing to disclose
P. Bohrer: nothing to disclose
J. Werner: nothing to disclose
R. Buchholz: nothing to disclose
R. Braren: nothing to disclose
P. M. Paprottka: nothing to disclose

RPS 609b-10 12:09
Monodisperse microspheres based on PMMA (polymethyl methacrylate) hydrogels: a novel embolisation agent tested in a rabbit renal model
F. N. Fleckenstein, F. Streitparth, B. Gebauer, D. Geisel, D. C. Schmidt, R. W. W. Günther, W. M. Lüdemann*; Berlin/DE*
(willie-magnus.luedemann@charite.de)

Purpose: The effectivity of in vivo visibility and biocompatibility of novel, loadable, and potentially bioresorbable monodisperse microspheres for embolotherapy based on PMMA hydrogels was evaluated in a rabbit renal model.
Methods and materials: The microparticles were provided as anionic particles (300 µm) with a loading capacity for cationic substrates of up to 40% mass fraction and were tagged with 1% magnetite by the manufacturer. Particle embolisation of an interlobar artery via a 2.4F microcatheter was carried out in 24 rabbits. Contrast-enhanced (CE) magnet resonance imaging (MRI) was performed afterwards to demonstrate magnetite deposition and renal perfusion defects. The rabbits were sacrificed after follow-up angiography and MRIs taken in cohorts of 8 animals each after 7, 28, or 56 days. Changes to the parenchyma as well as signs of particle degradation and vessel recanalisation were evaluated histologically and angiographically.
Results: The embolisations were technically successful. Three animals had to be sacrificed prematurely due to complications not related to the renal embolisation. The wedge-shaped perfusion defects on angiography corresponded in shape and size with infarcts and magnetite depositions observed in CE T1w and native T2w MRI sequences, respectively. No relevant particle degradation or vessel recanalisation was observed. There was little heterophilic cellular infiltrate and vascular inflammation consistent with high biocompatibility.

Conclusion: The newly developed microparticles are easy to handle and effective embolisation agents with good biocompatibility. Recent advances in the reduction of chemical cross-linking to just a tenth encourages further in vivo testing of degradability.
Limitations: Renal arteries are end arteries; complete infarction is inevitable distal to the embolisation. This might negatively impact recanalisation and particle resorption.
Ethics committee approval: All experiments had institutional animal care and use committee approval.
Funding: German Federation of Industrial Research Associations (AIF).
Author Disclosures:
W. M. Lüdemann: nothing to disclose
F. N. Fleckenstein: nothing to disclose
B. Gebauer: nothing to disclose
R. W. W. Günther: nothing to disclose
D. Geisel: nothing to disclose
F. Streitparth: nothing to disclose
D. C. Schmidt: nothing to disclose

RPS 609b-11 12:15
Funnel-shaped catheter model decreases clot migration during mechanical thrombectomy
Y. Tanyildizi, E. Payne, T. Gerber, L. Seidmann, A. Heimann, O. Kempski, N. Keric, M. A. Brockmann, S. Kirschner*; Mainz/DE*

Purpose: One limitation of mechanical thrombectomy (MT) is clot migration during the procedure. This might be caused by abruption of the trapped thrombus at the distal access catheter (DAC) tip during stent-retriever retraction due to the cylindrical shaped tip of the DAC. Aiming to solve this problem, this study evaluates the proof-of-concept of a new designed funnel-shaped tip in an experimental in vitro setting.
Methods and materials: Two catheter models, one with a funnel-shaped tip and one with a cylindrical-shaped tip, were compared in an experimental setup. For MT, a self-made vessel model and thrombi generated from pig's blood were used. MT was performed 20 times for each device using two different stent-retrievers, 10 times respectively
Results: For the funnel-shaped model, MT was successful with both stent-retrievers (Trevo XP ProVue 3/20 mm; Trevo XP ProVue 4/20 mm) at the first pass in 9/10 times (90%), respectively. For the cylindrical-shaped model, MTs were successful at the first pass with the smaller stent-retriever 5/10 (50 %) and 6/10 (60%) for the larger stent-retriever.
Conclusion: The in vitro experiments show a better recanalisation rate for the funnel-shaped tip compared to the cylindrical-shaped tip. Further studies are needed to verify the safety and efficacy of the proposed funnel-shaped tip.
Limitations: A single in vitro experimental setting with missing in-vivo experiments due to a not yet feasible prototype of the novel DAC for in-vivo experiments.
Ethics committee approval: Animal experiments were carried out after receiving approval by the local government committee (Landesuntersuchungsamt Rheinland-Pfalz, Germany) under reference number 23 177-07/G 14-1-094 and in accordance with the German Animal Welfare Act (Tierschutzgesetz). All applicable international, national, and/or institutional guidelines for the care and use of animals were adhered to.
Funding: No funding was received for this work.
Author Disclosures:
Y. Tanyildizi: nothing to disclose
E. Payne: nothing to disclose
T. Gerber: nothing to disclose
L. Seidmann: nothing to disclose
A. Heimann: nothing to disclose
N. Keric: nothing to disclose
O. Kempski: nothing to disclose
M. A. Brockmann: nothing to disclose
S. Kirschner: nothing to disclose

RPS 609b-12 12:21
Photothermal-mediated local heating using a branched gold nanoparticle-coated stent to suppress stent-induced tissue hyperplasia in a rat's gastric outlet
M. Kim*; Jeju-si/KR (soir09@naver.com)*

Purpose: To investigate the effectiveness of photothermal (PT)-mediated local heating for suppressing stent-induced tissue hyperplasia and to evaluate in vivo temperature during local heating of a rat's gastric outlet.
Methods and materials: A branched gold nanoparticle (BGNP)-coated self-expandable metallic stent (SEMS) was produced for PT-mediated local heating under near-infrared laser irradiation. 45 rats were randomly divided into three groups (15 rats each). Group A received non-coated SEMS. Group B received BGNP-coated SEMS with local heating at 55°C. Group C received BGNP-coated SEMS without local heating. 5 rats in each group were sacrificed after heating. The remaining 10 rats were sacrificed 4 weeks after stent placement. The effectiveness of local heating was assessed by western blot and histopathological analysis results.
Results: BGNP-coated SEMSs were successfully fabricated. All procedures were successful in all rats. Stent-induced tissue hyperplasia-related variables were significantly lower in group B than in groups A and C (all $p<0.001$). The mean degree of CD31-positive deposition was significantly lower in group B than in groups A and C (all $p<0.001$). The mean degree of TUNEL-positive deposition was significantly higher in group B than in groups A and C (all $p<0.001$). Ki67-positive mesothelial monolayers were more prominent in groups A and C than in group B.
Conclusion: PT-mediated local heating suppressed tissue hyperplasia after stent placement in a rat's gastric outlet. The in vivo temperatures were significantly decreased compared to the in vitro temperatures during local heating.
Limitations: It is necessary to determine timing for local heating to suppress stent-induced tissue hyperplasia.
Ethics committee approval: Animal Board approval obtained.
Funding: Basic Science Research Program through the National Research Foundation of Korea (NRF) funded by the Ministry of Science, ICT and Future Planning (2019R1F1A1040357).
Author Disclosures:
M. Kim: nothing to disclose

11:15 - 12:30 **Room M 3**

Chest

RPS 604b

Deep learning in chest radiograph and chest CT interpretation

Moderators:
A. Farchione; Rome/IT
C. F. Muñoz-Nuñez; Valencia/ES

RPS 604b-K 11:15
Keynote Lecture
E. Neri*; Pisa/IT*

Author Disclosures:
E. Neri: nothing to disclose

RPS 604b-1 11:25
A clinical-radiomics nomogram based on radiographic features to assess pulmonary metastasis of osteosarcoma of the extremities
P. Yin, N. Hong*; Beijing/CN (yinping915@163.com)*

Purpose: Osteosarcoma (OS) is the most common primary malignant bone tumour in adolescents. Pulmonary metastasis (PM) occurs in more than half of patients at different stages of the disease course, which is one of the important factors affecting the long-term survival of OS. We aimed to develop and validate a clinical-radiomics nomogram based on radiographic and clinical features that could predict PM of OS of the extremities.
Methods and materials: 1,100 patients (PM=418, non-PM=682) with histologically proven OS of the extremities were retrospectively analysed and divided into a training set (n=770) and a validation set (n=330). Radiographic features and risk factors (sex, age, type, grade, treatment, etc.) associated with PM were evaluated. We compared the performance of models based on radiographic features, clinical data, and their combination. The area under the receiver operating characteristic curve (AUC) and accuracy (ACC) were used to evaluate different models.
Results: A combined model had a relatively higher performance than an individual one. A clinical-radiomics nomogram based on combined features achieved an AUC of 0.873 and ACC of 0.842, followed by a radiomics model (AUC=0.821, ACC=0.790) and clinical data (AUC=0.762, ACC=0.706) in the validation set.
Conclusion: The clinical-radiomics nomogram had a good performance in predicting PM of OS of the extremities, which would be helpful in clinical decision-making.
Limitations: All images were acquired over the course of several years and all of our imaging data come from a single-centre. A a multicenter study with a large sample size is needed in further study.
Ethics committee approval: This study was approved by the local ethics committee of our hospital.
Funding: No funding was received for this work.

Author Disclosures:
P. Yin: nothing to disclose
N. Hong: nothing to disclose

RPS 604b-3 11:31
Quantitative analysis of airway and parenchymal lesions in idiopathic pulmonary fibrosis using an artificial intelligence-based technology
T. Handa, K. Tanizawa, T. Oguma, N. Tanabe, T. Niwamoto, H. Shima, T. Kubo, K. Togashi, T. Hirai*; Kyoto/JP (hanta@kuhp.kyoto-u.ac.jp)*

Purpose: Previous studies showed that the severity of traction bronchiectasis (TBE) might be associated with prognosis in idiopathic pulmonary fibrosis (IPF). This study aimed to quantify airway volumes as an indicator of TBE together with parenchymal lesions on chest high-resolution computed tomography (HRCT) and investigate their clinical significance in patients with IPF.
Methods and materials: A total of 103 IPF patients who visited Kyoto University Hospital and underwent chest HRCT and pulmonary function tests were enrolled. An artificial intelligence-based image analysis software was developed in collaboration with FUJIFILM Corporation. The software automatically measured airway volumes peripheral to the main bronchi, as well as volumes of parenchymal lesions. The extents of these volumes were expressed as percentages to total lung volume and their associations with pulmonary function and survival were analysed.
Results: Airway volumes had a moderate negative correlation with %FVC and strong positive correlation with FEV1/FVC. In univariate analysis, airway volumes, as well as volumes of some parenchymal lesions including consolidation and interstitial lung disease (ILD) (the sum of ground-glass opacity, reticulation, and honeycombing), were significantly associated with survival. In multivariate analysis, consolidation (hazard ratio [HR], 1.54; 95% confidence interval [95%CI], 1.25–1.90) and ILD volumes (HR, 1.06; 95%CI, 1.02-1.10), but not airway volumes, were independently associated with survival.
Conclusion: Airway volumes are novel parameters associated with pulmonary function and survival in IPF. Consolidation volume might also be a novel prognostic imaging biomarker in IPF.
Limitations: This is a single-centre, retrospective study with a moderate number of patients. Serial changes of CT parameters were not assessed.
Ethics committee approval: The Institutional Review Board of Kyoto university approved this retrospective study (IRB approval number R1353).
Funding: This study was supported by a grant from FUJIFILM Corporation.
Author Disclosures:
T. Handa: Research/Grant Support at Teijin Pharma
K. Tanizawa: nothing to disclose
T. Oguma: nothing to disclose
N. Tanabe: nothing to disclose
T. Niwamoto: nothing to disclose
H. Shima: nothing to disclose
T. Kubo: nothing to disclose
K. Togashi: nothing to disclose
T. Hirai: Grant Recipient at FUJIFILM Corporation

RPS 604b-4 11:37
Radiomic-based nomogram: a novel technique to predict the EGFR mutation status for first-generation EGFR TKI therapy
Q. Weng[1], J. Hui[1], H. Wang[1], C. Lan[1], M. Chen[1], P. Pang[2], M. Xu[1], Z. Wang[1], J. Ji[1]*; [1]Lishui/CN, [2]Hangzhou/CN*

Purpose: To develop a radiomics-based nomogram for preoperative prediction the EGFR mutation in NSCLC patients.
Methods and materials: All patients underwent nonenhanced CT scan before surgery. A.K. software extracted 396 radiomic features. LASSO logistic regression was used for feature dimension reduction and radiomic features construction. We incorporated the independent clinical features into the radiomic features model. The performance was compared between the radiomic feature model and the joint prediction model.
Results: The radiomic signatures were significantly associated with EGFR activating mutation. Five clinical features were contributed as a clinical feature model. The radiomic-based nomogram suggested high accuracy and good calibration for prediction of EGFR status in the training cohorts. Though it showed a slight decrease of accuracy in validation cohorts, the significant difference wasn't found between the two models in prediction power (P=0.1547).
Conclusion: We developed a combined prediction model showing a favourable performance for non-invasively predicting EGFR activating mutation in NSCLC patients.
Limitations: This is a retrospective study and only lesions which went to surgery were chosen, there may be a selection bias. Our study performed in two institutions and the different reconstruction algorithms may affect the image quality. Thus, it is necessary to validate our findings in multiple centres. The CT images analysed in the present study were nonenhanced and whether the findings in this study are suitable for enhanced images needs further investigation
Ethics committee approval: Our study has been approved by institutional review board of two institutions.
Funding: This study was supported by Zhejiang Medical and Health Science Project (2019RC320 to QY. Weng).
Author Disclosures:
Q. Weng: nothing to disclose
J. Hui: nothing to disclose
H. Wang: nothing to disclose
C. Lan: nothing to disclose
P. Pang: nothing to disclose
M. Xu: nothing to disclose
Z. Wang: nothing to disclose
J. Ji: nothing to disclose
M. Chen: nothing to disclose

RPS 604b-5 11:43
3D computer-aided volumetry (CADv) system with AI system: a comparison of quantitative nodule component measurement accuracy and pulmonary nodule differentiation capability on repeated CT examination
Y. Ohno[1], K. Aoyagi[2], Y. Kishida[3], S. Seki[3], Y. Ueno[3], A. Yaguchi[4], T. Yoshikawa[3]*; [1]Toyoake/JP, [2]Otawara/JP, [3]Kobe/JP, [4]Kawasaki/JP (yohno@fujita-hu.ac.jp)*

Purpose: To compare the capability for nodule component measurement and nodule differentiation between computer-aided volumetry (CADv) with and without convolutional neural network (CNN) on repeated CT in routine clinical practice.
Methods and materials: 170 consecutive patients detected with 215 pulmonary nodules (103 malignant and 112 benign nodules) at initial CTs underwent follow-up CT, pathological and bacterial examinations, treatment, or more than 2 years follow-up. In this study, each CADv automatically assessed solid and GGO component as well as total nodule (TN) volumes. In each patient, TN volume change per day (TN/day) and doubling time (DT) were also automatically evaluated from two serial CTs at each CADv. To evaluate the accuracy of volume measurement, the gold standard of each volume was computationally determined by the STAPLE method. To determine the utility of CNN, the measurement error of each volume was compared between both CADvs by t-test. To compare the capability for nodule differentiation, ROC analysis was performed. Finally, diagnostic accuracies were compared among all indexes determined by both CADvs by McNemar's test.
Results: Measurement errors of GGO and TN with CNN were significantly smaller than those without CNN ($p<0.05$). The area under the curve (Az) of TN/day with CNN (Az=0.94) was significantly larger than that of others ($p<0.0001$). In addition, Az of DT with CNN (Az=0.67) was significantly larger than that without CNN (Az=0.58, p=0.03).
Conclusion: CADv with CNN is more useful than without CNN for quantitative nodule component assessment and nodule differentiation on routine CTs.
Limitations: A limited study population.
Ethics committee approval: This prospective study was approved by our institutional review board of Kobe University Graduate School of Medicine and written informed consent was obtained from each subject.
Funding: This study was financially and technically supported by Canon Medical Systems Corporation.
Author Disclosures:
Y. Ohno: Research/Grant Support at Canon Medical Systems Corporation
K. Aoyagi: Employee at Canon Medical Systems Corporation
Y. Kishida: nothing to disclose
S. Seki: nothing to disclose
Y. Ueno: nothing to disclose
A. Yaguchi: Employee at Toshiba Corporation
T. Yoshikawa: Research/Grant Support at Canon Medical Systems Corporation

RPS 604b-6 11:49
Objectively evaluating the labelling accuracy of the Stanford CheXpert dataset: a multi-reader study
H. Mahajan, R. S. Rajan, V. K. Agarwal, M. Murugavel, V. K. Venugopal, V. Mahajan*; New Delhi/IN (vasanthdrv@gmail.com)*

Purpose: To quantify the labelling accuracy of the CheXpert dataset released by Stanford University by comparing it with labels established by radiologists.
Methods and materials: 284 frontal chest x-rays were randomly extracted from the CheXpert dataset and read by 3 radiologists (R1, R2, R3) having 12, 14, and 32 years of experience, respectively. Each radiologist reported 'yes' or 'no' for all the labels provided in the CheXpert dataset. 'Support devices' were excluded due to the inherent unclear nature of the label. Percentage observed agreement was calculated for all three radiologists and the consensus of radiologists to the

CheXpert labels. In CheXpert, '-1' label was attributed to 'uncertain' presence of findings in the image. We evaluated 4 scenarios with '-1' treated as 'Yes', 'No', 'N/A', and a separate third label. Additionally, we intended to open-source our labels for these 284 images.
Results: The mean percentage observed agreement for R1 was 0.80, 0.83, 0.83, and 0.79, for R2 was 0.79, 0.82, 0.82, and 0.78, and for R3 was 0.79, 0.82, 0.82, and 0.78 for each of the four scenarios of '-1' labels. Percentage observed agreement between the consensus of 3 radiologists and CheXpert was highest for 'fractures' (0.94), 'pneumothorax' (0.93), and 'pneumonia' (0.87), and lowest for 'lung opacity' (0.63), 'atelectasis" (0.72), and 'pleural effusion' (0.76).
Conclusion: Our study demonstrates that labels extracted from Stanford's database using natural language processing are accurate and can be used for training and validating deep learning algorithms. More such open-source datasets can help in the development of many more algorithms.
Limitations: A small sample size of 284 x-rays is a major limitation of this study.
Ethics committee approval: n/a
Funding: No funding was received for this work.
Author Disclosures:
V. K. Venugopal: nothing to disclose
H. Mahajan: Other at Director, Mahajan Imaging Pvt. Ltd, Other at Research collaboration General Electric Company, Other at Research collaboration Philips NV, Other at Research collaboration Qure.ai, Other at Research collaboration Predible Health
V. K. Agarwal: nothing to disclose
R. S. Rajan: nothing to disclose
V. Mahajan: nothing to disclose
M. Murugavel: nothing to disclose

RPS 604b-7 11:55
Leveraging deep learning artificial intelligence in detecting mismatched anatomy in chest images acquired with abdomen protocol: prevalence analysis and performance metrics
K. Y. Younis, K. Nye, G. Rao*; Waukesha/US (kh.younis@gmail.com)*

Purpose: In 2018, the two highest volume categories of x-ray procedures performed in the main radiology departments were chest (44%) and abdomen/pelvis (18%). X-ray images may be acquired using a protocol for different anatomy, resulting in using incorrect x-ray exposure parameters and image processing algorithms. Using the incorrect DICOM tags may also prevent the consistent and reliable use of hanging protocols in PACS. We propose an AI algorithm to automatically detect the onset of protocol mismatch related to chest frontal x-ray images and issue a warning to the technologist, enabling the technologist to acquire the exposure again but with the right protocol.
Methods and materials: We curated 732 unique x-ray images acquired with an abdomen protocol from mobile and fixed x-ray systems at institutions in the USA and Ireland. All the images were evaluated by a radiologic technologist and divided into two groups, namely chest and abdomen. A deep learning chest frontal detection algorithm was trained on 29,778 unique x-ray images from USA and Canada. The performance of the algorithm was evaluated using a confusion matrix analysis on the 732 unique images.
Results: The anatomy mismatch prevalence changed among sites with an average of 11.2% of chest exams taken with the abdomen protocol and a maximum of 12% in a large hospital. The overall accuracy in detecting chest images and rejecting abdomen images obtained with abdomen protocol was 96.9%. The false-positive rate of flagging true abdomen images as chest was only 1.5%, but that is reasonable since they include a large portion of the lungs.
Conclusion: A deep learning algorithm can be used to warn a radiographer if a chest image is acquired using a protocol for a different anatomy.
Limitations: n/a
Ethics committee approval: n/a
Funding: No funding was received for this work.
Author Disclosures:
K. Y. Younis: Employee at GE Healthcare
K. Nye: Employee at GE Healthcare
G. Rao: Employee at GE Healthcare

RPS 604b-8 12:01
Quantitative image quality comparison of bone suppression images generated by dual-energy subtraction techniques and deep learning-based software
A. Son, K.-H. Do, G.-S. Hong, K.-W. Jo, K. P. Kim, J. H. Yun*; Seoul/KR (ayeon1230@gmail.com)*

Purpose: To investigate the quantitative image quality of bone suppression image (BSI) generated by deep learning-based (DL) software compared with dual-energy subtraction (DES) techniques.
Methods and materials: This prospective study included 40 adult patients who underwent two digital chest radiographs (CXR) using x-ray equipment with DES and x-ray equipment with DL software. In intercostal and bone regions, respectively, 720 region-of-interests (ROIs) were extracted from the original CXR and BSI. For the comparison of objective image quality, peak signal-to-noise ratio (PSNR) and structure similarity index (SSIM) were calculated from ROIs extracted from original CXR and BSI, and compared between DES techniques and DL software groups.
Results: In the intercostal regions, PNSR and SSIM of BSI generated by the DL software was significantly higher than those of DES technique (31.45±6.87 dB vs. 29.85±2.31 dB; and 97.51±8.76 % vs. 91.26±5.13 %; all P value < 0.001). In bone regions, PNSR of BSI generated by the DL software was significantly lower than that of DES technique (20.93±3.18 vs. 34.37±3.22 dB), but SSIM of BSI made by the DL software was significantly higher than that of DES technique (94.57±8.76 vs. 87.77±5.16 % in SSIM) (all P < 0.001).
Conclusion: DL software creates effective bone removal images while maintaining the image quality of the soft tissue.
Limitations: The image quality of the BSI generated by DES may be not an absolute criterion because the image quality of x-ray can be affected by x-ray exposure parameters.
Ethics committee approval: The present study protocol was reviewed and approved by the Institutional Review Board of Asan Medical Center (approval No. 2018-1348) and all patients gave written, informed consent.
Funding: This research was supported by a research grant from Samsung Electronics (2018).
Author Disclosures:
A. Son: Speaker at Department of Radiology, University of Ulsan College of Medicine & Asan Medical Center, Seoul, Republic of Korea
G.-S. Hong: Author at Department of Radiology, University of Ulsan College of Medicine & Asan Medical Center, Grant Recipient at Samsung Electronics (2018)
K.-H. Do: Author at Department of Radiology, University of Ulsan College of Medicine & Asan Medical Center
K. P. Kim: Author at Department of Nuclear Engineering, Kyung Hee University
J. H. Yun: Author at Department of Medicine, University of Ulsan College of Medicine & Asan Medical Center
K.-W. Jo: Author at Division of Pulmonary and Critical Care Medicine, University of Ulsan College of Medicine & Asan Medical Center

RPS 604b-9 12:07
Preoperative CT-based radiomics combined with intraoperative frozen section can diagnose invasive adenocarcinoma in pulmonary nodules: a multicentre study
G. Wu, H. C. Woodruff, S. Sanduleanu, T. Refaee, A. Jochems, R. Leijenaar, P. Lambin*; Maastricht/NL (g.wu@maastrichtuniversity.nl)*

Purpose: To develop a preoperative radiomics model and combine it with an FS and clinical data to distinguish invasive adenocarcinomas (IA) from preinvasive lesions/minimally invasive adenocarcinomas (PM).
Methods and materials: This multicentre study containing 623 lung adenocarcinoma patients was split by centre into training (n = 331), testing (n = 143), and external validation dataset (n = 149). Random-forest models were trained using radiomics features, results from FS, lesion volume, clinical and semantic features, and combinations thereof. The area under the curve (AUC) was used to evaluate model performances. The models were further assessed using diagnostic accuracy and calibration and decision curves.
Results: The radiomics-based model shows good classification performance and diagnostic accuracy for distinguishing IA from PM, with AUCs of 0.89, 0.89, and 0.88, in three datasets respectively, and with corresponding accuracies of 0.82, 0.79, and 0.85. Adding volume and FS significantly increases the performance of the model with AUCs of 0.96, 0.97, and 0.96, and with accuracies of 0.91, 0.94, and 0.93 in three datasets. There is no significant difference in AUC between the FS model with radiomics and volume against an FS with volume model alone, while the former has higher accuracy. The model combining all information shows minor non-significant improvements in AUC and accuracy compared to the FS model with radiomics and volume.
Conclusion: Radiomics are potential biomarkers for the risk of IA, especially in combination with FS, and could help guide surgical strategy for pulmonary nodules patients.
Limitations: A retrospective data collection and manual contour.
Ethics committee approval: The review boards approved this study and the informed consent was waived.
Funding: Supported by the Dutch Technology Foundation STW.

Author Disclosures:
G. Wu: nothing to disclose
S. Sanduleanu: nothing to disclose
T. Refaee: nothing to disclose
H. C. Woodruff: Shareholder at Oncoradimics SA
A. Jochems: nothing to disclose
R. Leijenaar: nothing to disclose
P. Lambin: Research/Grant Support at Varian medical, Research/Grant Support at Oncoradiomics, Research/Grant Support at ptTheragnostic, Research/Grant Support at Health Innovation Ventures, Research/Grant Support at DualTpharma, Other at Oncoradimics, Other at BHV, Other at Merck, Other at Convert pharmaceuticals, Shareholder at Oncoradiomics SA, Shareholder at Convert pharmaceuticals SA, Patent Holder at Oncoradimics, Patent Holder at ptTheragnostic/DNAmito

RPS 604b-10 12:13
Development and validation of a deep learning-based model for automatic detection of tuberculosis on radiographs
D. Wang[1], S. Wu[1], H. Wang[1], T. Zou[1], Y. Sun[2], S. Drago Gonzalez[2], Y. Shen[1]; *[1]Beijing/CN, [2]Wiesbaden/DE*

Purpose: To develop a deep learning (DL)-based model for the automatic and efficient detection of tuberculosis on radiographs and to validate its feasibility in clinical practice.
Methods and materials: In this proposed model, ResNeXt was utilised as the backbone while the RetinaNet was adopted to extract object features. The non-local module was embedded to capture the correlations between tuberculosis characteristics and the surrounding points. The model was trained, validated, and tested on a private dataset containing 1,678 x-rays manifested with tuberculosis at a ratio of 8:1:1. In addition, two public datasets were used to validate the robustness of the DL-based model. One consisted of 58 tuberculosis abnormal x-rays and 80 normal x-rays (Montgomery County X-ray Set) and the other contained 336 tuberculosis abnormal x-rays and 326 normal x-rays (Shenzhen Hospital X-ray Set). Area under the receiver operating characteristics (AUROC) score, detection recall, and precision were calculated to evaluate the model performance.
Results: DL-based model achieved an AUROC score of 0.9301, a recall of 0.8523, and a precision of 0.8240 in the local test dataset. In addition, the DL-based model demonstrated excellent performance in detecting tuberculosis for the two public datasets with the AUROC scores of 0.9588 (Shenzhen) and 0.9666 (Montgomery). In particular, the recall and precision were 0.8363 and 0.9623 for Shenzhen datasets while 0.8448 and 0.9609 for Montgomery datasets.
Conclusion: The proposed DL-based model was efficient and robust for automatic tuberculosis detection. It might be applied to assist radiologists in clinical practice.
Limitations: This study need to expand the sample size from other hospitals to increase the model robustness and the conclusion confidence.
Ethics committee approval: n/a
Funding: No funding was received for this work
Author Disclosures:
D. Wang: Employee at Infervision
Y. Sun: Employee at Infervision
S. Drago Gonzalez: Employee at Infervision
H. Wang: Employee at Infervision
S. Wu: Employee at Infervision
Y. Shen: Employee at Infervision
T. Zou: Employee at Infervision

RPS 604b-11 12:19
A comparison of ultra-low-dose chest CT with deep learning reconstruction and standard-dose chest CT with hybrid reconstruction
C. Steveson[1], J. Schuzer[2], S. Rollison[2], T. Machado[2], A. Jones[2], P. Julien-Williams[2], J. Moss[2], M. Chen[2]; *[1]Adelaide/AU, [2]Bethesda/US (chloe.steveson@medical.canon)*

Purpose: Deep convolutional neural network image reconstruction can reduce image noise and enable radiation dose reductions. The aim of this study is to investigate whether the use of a deep learning reconstruction algorithm allows for reduced radiation dose chest CT scanning.
Methods and materials: 105 consecutive patients with cystic lung diseases underwent a chest CT at standard and ultra-low radiation doses on a 320 detector row CT scanner. The standard dose scan was reconstructed using a soft tissue kernel with hybrid iterative reconstruction (AIDR3D) and the ultra-low-dose scan was reconstructed using a soft tissue kernel with deep learning reconstruction (AiCE) techniques. Cystic lung diseases were quantified as the percentage of lung volume occupied by cysts. Cyst scores were quantified by semi-automated software. The signal-to-noise ratio was calculated for each reconstruction. Data was analysed by linear correlation, paired t-test, and Bland-Altman.
Results: Patients averaged 49.1 years (range 27-76yrs), 91% were female. The mean radiation dose reduction was 97% (4.50 mSv ±2.24 mSv for standard dose vs. 0.14 mSv ±0.02 mSv for ultra-low-dose, p <0.001). The mean cyst score was 8.9±10.8 for standard dose AIDR 3D reconstruction and 8.5±11.3 for ultra-low-dose deep learning reconstruction, representing an insignificant difference of 0.38%. The linear correlation coefficient was excellent at 0.975 (p<0.001). Signal-to-noise for low-dose AiCE images was lower than to standard-dose AIDR3D images (4.20 vs. 7.38, respectively, p<0.001) but completely adequate for interpretation.
Conclusion: Deep learning reconstruction in conjunction with 97% radiation reduction has an excellent correlation with standard conventional chest CT.
Limitations: A single-centre study.
Ethics committee approval: Institutional ethics approval (National Institutes of Health, USA).
Funding: No funding was received for this work.
Author Disclosures:
C. Steveson: Employee at Canon Medical Systems
J. Schuzer: Employee at Canon Medical Research
S. Rollison: nothing to disclose
J. Moss: nothing to disclose
M. Chen: nothing to disclose
T. Machado: nothing to disclose
A. Jones: nothing to disclose
P. Julien-Williams: nothing to disclose

11:15 - 12:30 **Room M 4**

Neuro
RPS 611b
Multiple sclerosis

Moderators:
C. Gianni; Rome/IT
A. Rovira Cañellas; Barcelona/ES

RPS 611b-K 11:15
Keynote lecture
F. Barkhof; *Amsterdam/NL (f.barkhof@vumc.nl)*

Author Disclosures:
F. Barkhof: Advisory Board at Roche, Advisory Board at Biogen, Advisory Board at IXICO, Advisory Board at Merck, Grant Recipient at GE healthcare, Research/Grant Support at AMYPAD (IMI-EU)

RPS 611b-1 11:25
Brain atrophy in multiple sclerosis and clinically isolated syndromes: a 30-year follow-up
L. Haider[1], K. Chung[2], G. Birch[2], S. Mangesius[3], F. Prados[2], O. Ciccarelli[2], F. Barkhof[4], D. Chard[2]; *[1]Vienna/AT, [2]London/UK, [3]Innsbruck/AT, [4]Amsterdam/NL (l.haider@live.at)*

Purpose: Brain atrophy and the neurodegeneration underlying it starts early in multiple sclerosis (MS). However, the long-term clinical relevance of early atrophy is unknown.
Methods and materials: 132 people presenting with a clinically isolated syndrome were recruited between 1984-87 and followed-up clinically and with an MRI 1, 5, 10, 14, 20, and 30 years later. Third ventricular width, medullary width, and white matter lesions were measured at all available time points.
Results: At 30 years, 27 had a clinically isolated syndrome (CIS), 34 relapsing-remitting (RR) MS, 26 secondary progressive (SP) MS, and 16 had died due to MS-related (MSRD) causes. Of those who were alive, the mean expanded disability status scale (EDSS) in the CIS groups was 1 (0-2), in the RRMS group 1.5 (1-2), and in the SPMS group 6 (6-6,5).
Nested mixed effect models estimated significant faster atrophy rates in SPMS (p<0.0000) and MSRD patients (p<0.0000).
Using logistic regression, a reduction of 1 mm in the medullary width from baseline to 5 years, predicted a 6-fold increase in the probability of SPMS or MSRD over the next 25 years (p<0.013).
Atrophy rates within the first 5 years after CIS predicted a broad range of cognitive and motor function-based outcome measures at 30 years.

Conclusion: Our findings suggest that brain atrophy within 5 years of symptom onset predicts disability a decade or more later, indicating its relevannce prior to clinical progression.
Limitations: The analysis was restricted by the image quality of archival films analysed at baseline, one, and five-year follow-up.
Ethics committee approval: Approved by the National Research Ethics Service (15/LO/0650).
Funding: L.H. was supported by ECTRIMS/MAGNIMS and ESNR-Fellowships.
Author Disclosures:
L. Haider: nothing to disclose
K. Chung: Speaker at Teva, Biogen Idec, and Roche
G. Birch: nothing to disclose
S. Mangesius: nothing to disclose
F. Prados: nothing to disclose
O. Ciccarelli: Consultant at Novartis, Roche, Teva and Merck
F. Barkhof: Consultant at Bayer Schering Pharma, Sanofi-Genzyme, Biogen Idec, Teva, Merck Serono, Novartis, Roche, IXICO, GeNeuro, Apitope Ltd. and Jansen Research
D. Chard: Speaker at Excemed

RPS 611b-3 11:31
The bi-caudate ratio as an MRI marker of white matter atrophy in multiple sclerosis and ischaemic leukoencephalopathy
D. Serag, S. A. H. Hassanein; *Shebin El-Kom/EG*
(shaimaahamid@hotmail.com)

Purpose: To assess the value of the bi-caudate ratio as an MRI marker of white matter atrophy in multiple sclerosis and ischaemic leukoencephalopathy patients and to set a cut-off value to differentiate between patients with white matter atrophy and normal subjects.
Methods and materials: 115 patients (54 male and 61 female) (mean age {+SD}, 52.5 {+ 18.2} years) diagnosed with white matter leukoencephalopathy (MS in 51 patients and ischaemic leukoencephalopathy in 64 patients) and a control group of 60 subjects (27 male and 33 female) with normal white matter signal were scanned. The BCR was compared for both patients and controls. The BCR was compared for patients with MS and ischaemic leukoencephalopathy.
Results: BCR for the patients ranged from 0.13-0.27 mm (mean {± SD}=0.16±0.02), while for the control group it ranged from 0.05-0.13 mm (mean {± SD}=0.09±0.01). The difference between the two groups was statistically significant (P<0.001). A cut-off value of 0.13 was used to differentiate between the BCR in both patients and control groups with a sensitivity, specificity, and accuracy of 99.2%, 100%, and 99%, respectively. The difference in BCR for patients diagnosed with MS and ischaemic leukoencephalopathy was also statistically significant (P<0.001).
Conclusion: The bi-caudate ratio represents a linear measurement of subcortical atrophy that can be useful as a surrogate marker of global supra-tentorial white matter atrophy instead of the usually performed visual, and therefore subjective, assessment. It is an easily obtained measure that can be performed without complex time consuming volumetric studies. Our findings also revealed that the BCR is higher in patients with ischaemic leukoencephalopathy than in patients with MS.
Limitations: n/a
Ethics committee approval: n/a
Funding: No funding was received for this work.
Author Disclosures:
D. Serag: nothing to disclose
S. A. H. Hassanein: nothing to disclose

RPS 611b-4 11:37
A comparison study of three different methods for detection of T2/FLAIR signal changes in multiple sclerosis
R. Antulov[1], M. Kusk[1], V. Antonov[1], J. M. Christiansen[1], M. Dawari[1], E. M. H. Kruuse[2]; *[1]Esbjerg/DK, [2]Middelfart/DK*
(ronald.antulov@outlook.com)

Purpose: MRI is important in monitoring multiple sclerosis (MS) but conventional side-by-side reading (SBSR) of follow-up examinations for detecting new or changing T2/FLAIR lesions is time-consuming and prone to misdetection. Several recent articles presented methods for the detection of T2/FLAIR lesions based on commonly available software packages that accelerate the reading process. The aim was to compare two novel reading methods against SBSR in an everyday reading environment.
Methods and materials: 30 consecutive MS patients were included. MRI examinations were performed on the same 1.5T scanner and included a 3D-FLAIR sequence. 4 radiologists with different experience levels analysed two follow-up examinations, current and previous, respectively, on the same workstation. Automatic co-registration of the follow-up examinations along with colour coding of the current examination (CE) for the colour-coded reading (CCR) and contrast inversion of the CE for the inverted contrast reading (ICR) were performed. We analysed the specificity, sensitivity, positive predictive value (PPV), and negative predictive value (NPV) for the detection of new MS lesions (NMSL), MS lesion size changes (MSLSC), and reading time (RT). A senior neuroradiologist provided the reference standard.
Results: CCR showed the highest combined sensitivity [97.5%] and specificity [85%] for NMSL detection with a PPV of 93.1% and NPV of 95.4%. Regarding MSLSC detection, both CCR [60.9%] and ICR [80%] showed a higher combined sensitivity compared to SBSR [49%]. The combined mean RT showed a significant decrease when CCR [71s] and ICR [88s] were compared to SBSR.
Conclusion: CCR and ICR are valid alternatives to SBSR that reduce the RT while keeping or improving NMSL and MSLSC detection. Therefore such reading methods are recommended in everyday clinical routine.
Limitations: The number of included patients is limited.
Ethics committee approval: The IRB approved the study and waived the need for informed consent.
Funding: No funding was received for this work.
Author Disclosures:
R. Antulov: nothing to disclose
M. Kusk: nothing to disclose
V. Antonov: nothing to disclose
J. M. Christiansen: nothing to disclose
M. Dawari: nothing to disclose
E. M. H. Kruuse: nothing to disclose

RPS 611b-5 11:43
Cervical cord atrophy in MS: in search of a threshold area — a meta-analysis
A. Guarnera, C. C. C. Quattrocchi, V. Di Lazzaro, R. Papalia, B. B. Beomonte Zobel; *Rome/IT (guarneraalessia@gmail.com)*

Purpose: To investigate whether patients with MS present with significant cervical cord atrophy compared to healthy controls and to identify a cervical spinal cord area threshold that could discriminate patients with MS from healthy controls.
Methods and materials: Literature databases were searched (2001-2018) for cohort and case-control studies reporting measures of cervical cord areas on MRI scans in MS patients and controls to be included in the meta-analysis. Articles evaluating the size or changes in the size of MS plaques, non-homogeneous patient categories, and patients with MS undergoing experimental therapies were excluded.
Results: 17 studies were included, resulting in a total cohort of 1,545 patients and 505 controls. A significant statistical difference between progressive forms of MS (PMS, PPMS, and SPMS) patients and healthy controls cervical cord areas (p<00001) was ascertained. Based on a ROC curve, a cervical cord threshold area of 71 mm^2 (sensitivity 94%, specificity 100%) to determine progressive forms of MS patients from non-progressive forms of MS and healthy controls was identified (Younden index: 94%).
Conclusion: Cervical cord atrophy is statistically significant in PMS patients compared to healthy controls. The detection of a cervical cord trans-sectional area threshold of 71mm^2, measured by MRI in MS patients, could be used both in clinical practise to discriminate progressive forms of MS from healthy controls and non-progressive forms of MS and in clinical trials to validate the efficacy of established therapies and new therapies.
Limitations: The relative small number of studies analysed and the heterogeneity of sequences and methods used for cervical cord trans-sectional area measurements by the included studies.
Ethics committee approval: The study was approved by the institutional ethics board and adhered to the tenets of the declaration of Helsinki.
Funding: No funding was received for this work.
Author Disclosures:
A. Guarnera: nothing to disclose
C. C. C. Quattrocchi: nothing to disclose
V. Di Lazzaro: nothing to disclose
R. Papalia: nothing to disclose
B. B. Beomonte Zobel: nothing to disclose

RPS 611b-6 11:49
Brain connectivity changes in CMT1A patients: a resting-state functional MRI study
T. Perillo[1], G. Pontillo[2], S. Cocozza[3], R. Dubbioso[2], S. Tozza[2], F. Manganelli[2], M. Quarantelli[2], A. Brunetti[2]; *[1]Giugliano in Campania/IT, [2]Naples/IT*
(tperillo3@gmail.com)

Purpose: Evidence from different neuropathies demonstrated that peripheral nerve pathology can broadly influence brain connectivity, way beyond the involvement of the sensorimotor network. The aim of our study was to systematically investigate functional connectivity (FC) changes in the brain of Charcot-Marie-Tooth (CMT) 1A patients.

Methods and materials: In this observational cross-sectional study, we enrolled 18 right-handed patients with genetically confirmed CMT1A, along with 20 age- and sex-comparable healthy controls (HC). Resting-state (RS) fMRI data was analysed with a seed-based approach sampling 32 ROIs included in the SPM-based CONN toolbox and characterising an extended set of classical RS networks. Between-group differences for the distinct seeds were tested using the standard general linear model implemented in SPM12, covarying for age, sex, and mean motion, and correcting for multiple comparisons at the cluster level. The results of each analysis were considered significant for $p<0.05$ and were Bonferroni-corrected for multiple comparisons (0.05/32).
Results: In CMT1A patients compared to HC, several clusters emerged of increased FC relative to seeds within the default mode, dorsal attention, and language and salience networks, encompassing different supratentorial cortical areas ($p<0.001$).
Furthermore, a cluster of reduced FC relative to the occipital cortex was found in the left lentiform nucleus (p=3E-4).
Conclusion: CMT1A patients show extensive rearrangements of brain connectivity.
FC increase could reflect a reduction of the physiological anticorrelation between the default mode (DMN) and other networks (e.g. increased FC between hubs of the salience and dorsal attention networks and DMN nodes, namely posterior cingulate cortex and inferior parietal lobule), as well as a compensatory mechanism (e.g. increased FC within the language network).
Reduced FC between the occipital cortex and lentiform nucleus could represent a maladaptive disruption of the visual corticostriatal functional loop.
Limitations: n/a
Ethics committee approval: n/a
Funding: No funding was received for this work.
Author Disclosures:
T. Perillo: nothing to disclose
G. Pontillo: nothing to disclose
S. Cocozza: nothing to disclose
R. Dubbioso: nothing to disclose
S. Tozza: nothing to disclose
F. Manganelli: nothing to disclose
M. Quarantelli: nothing to disclose
A. Brunetti: nothing to disclose

RPS 611b-7 11:55

Investigation of brain structural plasticity in CMT1A patients: a combined VBM and TBSS study

E. A. Vola, G. Pontillo, S. Cocozza, R. Dubbioso, S. Tozza, F. Manganelli, M. Quarantelli, A. Brunetti; *Naples/IT*
(elena.a.vola@gmail.com)

Purpose: Although it is primarily a peripheral nervous system disease, several anecdotal reports of central nervous system (CNS) involvement have been described in different forms of Charcot-Marie-Tooth disease (CMT), including its most common subtype (CMT1A). The aim of this study was to investigate the presence of structural damage in the brain of CMT1A patients.
Methods and materials: 20 patients with genetically confirmed CMT1A were enrolled along with 20 age- and sex-comparable healthy controls (HC). Brain MRI exams included a 3D-GE-T1w for the voxel-based morphometry analysis (VBM) and diffusion tensor imaging (DTI) data for the tract-based spatial statistics (TBSS) analysis. CMT1A patients also underwent clinical and electrophysiological examinations including the determination of the CMT neuropathy score (CMTNS) as a global measure of disease severity and the compound motor action potential (CMAP) as an index of distal arm axonal damage.
Results: The VBM analysis revealed a cluster of significantly increased GM density in CMT1A patients compared to HC encompassing the right paravermian portions of the cerebellar lobules III, IV and V. No between-group differences emerged from the TBSS analysis when considering the DTI metrics. A significant negative correlation ($r=-0.738$, $p=0.003$) was found between the CMAP values and the age, sex, and TIV-adjusted z-scores of the first eigenvariate extracted from the cluster of significant between-group difference at the VBM analysis.
Conclusion: CMT1A patients show cerebellar grey matter modifications, which occur independently from central white matter microstructural alterations, possibly representing a structural plasticity mechanism which compensates for the primary peripheral nerve damage.
Limitations: n/a
Ethics committee approval: n/a
Funding: No funding was received for this work.
Author Disclosures:
E. A. Vola: nothing to disclose
G. Pontillo: nothing to disclose
S. Cocozza: nothing to disclose
R. Dubbioso: nothing to disclose
S. Tozza: nothing to disclose
F. Manganelli: nothing to disclose
M. Quarantelli: nothing to disclose
A. Brunetti: nothing to disclose

RPS 611b-8 12:01

The prediction of clinical disability in multiple sclerosis using a combined machine learning and texture analysis approach

S. Cocozza[1], R. Cuocolo[1], G. Pontillo[1], L. Ugga[2], M. Petracca[1], R. Lanzillo[1], V. Brescia Morra[1], A. Brunetti[1]; [1]*Naples/IT*, [2]*Scafati/IT*
(sirio.cocozza@unina.it)

Purpose: Despite the use of advanced MRI techniques, imaging biomarkers often fail to accurately predict the accumulation of physical disability in multiple sclerosis (MS) patients. The aim of our study was to investigate the possible role of radiomics for the prediction of disability in MS by applying a machine learning approach to texture analysis (TA) parameters.
Methods and materials: 79 patients with MS were recruited. All patients underwent a neurological examination with the determination of the expanded disability status scale (EDSS) as an index of clinical disability along with an MRI protocol on a 3T scanner including 3D-T1-weighted and 3D-FLAIR sequences.
On FLAIR images, hyperintense lesions were segmented, while T1-weighted volumes were used to segment white matter (WM) and both cortical and deep grey matter (GM). Features were extracted using open-source software (Pyradiomics v2.1.2) with a resulting dataset that was processed with a data mining software (Weka v3.8), while a regression support vector machine was used for EDSS score prediction.
Model validation was performed with a train-test approach, with the test group constituting 25% of the total population.
Results: MS patients (M/F=44/35; 41.5±11.0 years) showed a median EDSS score of 3.5.
The subset evaluator produced a dataset containing 47 features (22 from T1-weighted and 25 from FLAIR sequences, mainly derived from deep GM).
The support vector machine obtained a correlation coefficient of 0.87, with a mean absolute error of 0.5 and a root mean square error of 0.7.
Conclusion: Our results demonstrate that a machine learning-derived model including TA parameters mainly related to deep GM is able to predict physical disability in MS patients with significant accuracy.
Limitations: A single center, retrospective study.
Ethics committee approval: Study approved by the local ethics committee.
Funding: No funding was received for this work.
Author Disclosures:
S. Cocozza: Advisory Board at Amicus, Speaker at Sanofi, Speaker at Shire
R. Cuocolo: nothing to disclose
G. Pontillo: nothing to disclose
L. Ugga: nothing to disclose
M. Petracca: nothing to disclose
R. Lanzillo: nothing to disclose
V. Brescia Morra: nothing to disclose
A. Brunetti: nothing to disclose

RPS 611b-9 12:07

Impact of enhancement and lesion size on quantitative susceptibility mapping values of multiple sclerosis lesions

G. Manasseh[1], T. Hilbert[1], M. J. Fartaria[1], J. Deverdun[2], T. Kober[1], P.-P. P. Maeder[1], P. Hagmann[1], V. Dunet[1]; [1]*Lausanne/CH*, [2]*Montpellier/FR*
(gibran.manasseh@alumni.ethz.ch)

Purpose: Quantitative susceptibility mapping (QSM) is an emerging method used to characterise brain lesions in multiple sclerosis (MS). Our goals were to investigate the relation between QSM values and gadolinium (Gd)-enhancing MS lesions and to assess the relation between QSM values and lesion size.
Methods and materials: We performed a retrospective study on 73 MS patients who underwent a single-time-point brain MRI at 3T (MAGNETOM Skyra, Siemens Healthcare, Erlangen, Germany), including 3D FLAIR, T1-MPRAGE pre/post-Gd, and double-echo GRE (TE=20/40ms) sequences. The fully automated prototype method LeManPV was used for the automated lesion segmentation on 3D FLAIR and T1-MPRAGE pre-Gd images. A set of lesions was selected manually according to specific criteria. Active lesions were identified using T1-MPRAGE pre/post-Gd data. QSM maps were estimated from GRE images using a standard post-processing pipeline including RESHARP and TVSB algorithms. QSM lesions values were extracted using LeManPV lesion masks and compared between non-enhancing and enhancing lesions with the

Wilcoxon rank-sum test. The relation to size was evaluated with the Spearman coefficient.
Results: 3,894 lesions were found by the LeManPV method. We selected 985 lesions (25%), of which 35 (3.6%) were enhancing. We observed similar mean QSM values in enhancing and non-enhancing lesions (0.0026±0.0184 vs 0.0050±0.0176 ppm, p=0.32). For lesions with a volume greater than 70 µL, the difference was significant (-0.0044±0.0150 vs 0.0082±0.0177 ppm, p=0.028). In non-enhancing lesions, there was a very weak correlation between QSM values and lesions size for lesions ≥70 µL (rho=0.18, p=0.0015) but not for lesions <70 µL (rho=0.06, p=0.13).
Conclusion: On a single time-point, QSM values may be influenced by lesion size and enhancement status. This should be taken into account when QSM values are used to identify active MS lesions.
Limitations: n/a
Ethics committee approval: n/a
Funding: No funding was received for this work.
Author Disclosures:
G. Manasseh: Author at CHUV
T. Hilbert: Employee at Siemens Healthineers
M. J. Fartaria: Employee at Siemens Healthineers
J. Deverdun: nothing to disclose
T. Kober: Employee at Siemens Healthineers
P.-P. P. Maeder: nothing to disclose
P. Hagmann: nothing to disclose
V. Dunet: nothing to disclose

RPS 611b-10 12:13

Microscopic anisotropy imaging without the confounding effect of fibre orientation dispersion can significantly improve the characterisation of pathology in multiple sclerosis

K. Winther Andersen[1], S. Lasic[2], H. Lundell[1], M. Nilsson[2], D. Topgaard[2], F. Szczepankiewicz[2], H. Roman Siebner[1], M. Blinkenberg[1], T. B. Dyrby[1]; [1]Copenhagen/DK, [2]Lund/SE (samo@rwi.se)*

Purpose: Can tensor-valued diffusion encoding provide higher specificity in multiple sclerosis (MS)? In contrast to the traditional fractional anisotropy (DTI-FA), microscopic fractional anisotropy (µFA) obtained from tensor-valued diffusion encoding is not affected by fibre dispersion and might therefore be a better disease biomarker. We estimated DTI-FA and µFA in a group of relapsing-remitting (RRMS) and primary progressive (PPMS) MS patients and age-matched healthy controls (HC).
Methods and materials: 45 MS and 28 HC were scanned (14 PPMS, 26 RRMS, and 27 HC analysed) on a Philips Achieva 3T, 32-channel head-coil. DTI-FA from conventional DWI: 106 images 2x2x2 mm, 50 slices, scan time 21.5 min. µFA from tensor-valued DWI: 2.5x2.5x2.5 mm, 14 slices, scan time 16.2 min.
Results: Tissue pathology in normal-appearing white matter (NAWM) was reflected by µFA, but not DTI-FA. µFA was lowest in PPMS and highest in HC. DTI-FA tended to be higher in HC than in RRMS, but counterintuitively, higher DTI-FA was observed in PPMS than in RRMS, probably due to degenerated crossing fibres. µFA provides stronger correlations with clinical scores. Total lesion volume correlated with µFA but not DTI-FA. µFA negatively correlated with age but not DTI-FA.
Conclusion: Compared to traditional diffusion MRI, tensor-valued encoding can significantly improve the characterisation of pathology in MS.
Limitations: Lower image resolution may lead to partial volume effects reducing specificity.
Ethics committee approval: Approval by the ethics committee of the Capital Region of Denmark (protocol H-15006964) and written informed consent was obtained.
Funding: Danish Multiple Sclerosis Society (Grant Nr. A31910 and A27996).
VINNMER Marie Curie Industry Outgoing grant (Grant Nr. 013-04350).
Swedish Research Council (2014-3910)
Swedish Foundation for Strategic Research (Grant Nr. AM13-0090)
Lundbeck Foundation (Grant Nr. R186-2015-2138)
Author Disclosures:
S. Lasic: Employee at Random Walk Imaging
K. Winther Andersen: nothing to disclose
H. Lundell: nothing to disclose
M. Nilsson: Shareholder at Random Walk Imaging
D. Topgaard: Shareholder at Random Walk Imaging
H. Roman Siebner: nothing to disclose
M. Blinkenberg: nothing to disclose
T. B. Dyrby: nothing to disclose
F. Szczepankiewicz: nothing to disclose

RPS 611b-11 12:19

MR planimetric measurements for diagnosis and outcome prediction of multiple sclerosis

S. Mangesius[1], S. Pereverzyev[1], L. Lamplmayr[1], L. Lenhart[1], L. Haider[2], G. Bsteh[1], S. Wurth[1], F. Deisenhammer[1], E. R. R. Gizewski[1]; [1]Innsbruck/AT, [2]Vienna/AT (stephanie.mangesius@tirol-kliniken.at)*

Purpose: Brain volume change has been suggested as an MRI predictor of disability in multiple sclerosis (MS). However, volumetric measurements are not used routinely as no accepted methodology for clinical use exists to date. Easily applicable planimetric measurements are proposed for different neurologic disease entities. In this pilot study, we investigated whether planimetric measures predict the technically more complex volumetric measurements in MS patients.
Methods and materials: Neural networks (NNs) were used to predict the volumetric measures (grey matter [GM], white matter [WM], and cerebrospinal fluid [CSF]) with planimetric measures. The planimetric input variables were preselected using Spearman's correlation (SC) coefficient.
Results: Planimetric characteristics yielding a high correlation with volumetric characteristics were GM with frontooccipital diameter (FOD) (SC=0.98), midbrain diameter (M_d) (SC=0.92), pontine area (P_A) (SC=0.98), midbrain-to-pontine diameter ratio (SC=0.90), WM with transverse skull diameter (SC=0.89), FOD (SC=0.93), M_d (SC=0.85), P_A (SC=0.95), CSF with third ventricle width unaligned (SC=0.82), anterior segment of corpus callosum/genu (SC=-0.83), corpus callosum index (CCI) (SC=-0.83), and regional anterior CCI (SC=-0.92). The NNs constructed based on these measures predicted the volumes of GM, WM, and CSF with errors below 11% for GM, 5% for WM, and 15% for CSF.
Conclusion: Despite the small sample size, we observed high correlations between MR planimetric and volumetric measurements and were able to construct NNs with low prediction errors.
Limitations: Larger patient cohorts will allow separation in training and test sets to investigate MR planimetry as an easy to apply and robust imaging biomarker to evaluate cerebral and ventricular volume in patients with MS with similar accuracy as, and strong correlations with, volumetric measurements.
Ethics committee approval: The study has been approved by the ethical committee of the Medical University of Innsbruck.
Funding: No funding was received for this work.
Author Disclosures:
S. Mangesius: Grant Recipient at ESNR Pioneers and Past Presidents Award in the category of Diagnostic Neuroradiology, in Honor of Auguste Wackenheim 2018, Grant Recipient at ESR Invest in the Youth programme for the ECR 2019, Grant Recipient at travel grant from „Junge Radiologen“ for the ECR 2018, Research/Grant Support at ÖAW (Österreichische Akademie der Wissenschaften; GDNG_2018-041_MedCorpInn) 2018 outside the submitted work, Advisory Board at EAN Scientific Panel Neuroimaging
L. Lamplmayr: Research/Grant Support at Austrian Science Fund (FWF): project P 29514-N32
L. Lenhart: nothing to disclose
S. Pereverzyev: Research/Grant Support at Austrian Science Fund (FWF): project P 29514-N32
L. Haider: Research/Grant Support at ESNR Research Fellowship, Research/Grant Support at ECTRIMS-MAGNIMS Research Fellowship , Research/Grant Support at Austrian MS society
S. Wurth: Other at participated in meetings sponsored by, or received honoraria or travel funding from Biogen, Merck, Novartis, Sanofi Genzyme, Teva, Allergan, Ipsen Pharma and Roche
G. Bsteh: Other at participated in meetings sponsored by, received speaker honoraria or travel funding from Biogen, Cellgene, Merck, Novartis, Sanofi-Genzyme and Teva, and received honoraria for consulting Biogen, Roche and Teva
F. Deisenhammer: Speaker at Almirall, Biogen, Celgene, Genzyme-Sanofi, Merck, Novartis Pharma, and Roche, Research/Grant Support at Biogen, Research/Grant Support at Genzyme-Sanofi, Other at section editor of the MSARD Journal (Multiple Sclerosis and Related Disorders)
E. R. R. Gizewski: Speaker at lecture fees from Bracco and Bayer

11:15 - 12:30 **Room M 5**

Abdominal Viscera

RPS 601c

Diffuse liver disease

Moderators:
U. I. Attenberger; Mannheim/DE
C. Stoupis; Maennedorf/CH

RPS 601c-1 11:15

Non-invasive quantification of hepatic steatosis using conventional ultrasonography with liver biopsy as gold standard

G. Weijers; *Nijmegen/NL (Gert.Weijers@radboudumc.nl)*

Purpose: Quantitative analysis of conventional ultrasonography can be an attractive non-invasive alternative for liver biopsies to stage steatosis. We validated the computer aided ultrasound (CAUS) method for staging human steatosis against qualitative as well as a quantitative histopathology.
Methods and materials: In a cohort consisting of consecutive patients referred for liver biopsy (n=224), with a variety of clinical indications, biopsy and ultrasound examinations were performed. Histological examination revealed 87 patients with steatosis (NAFLD activity score (NAS): 1-3) and 128 patients with liver fibrosis score. A fully automated method applied to digitally scanned HE-slides was developed to estimate the steatosis proportional area (SPA) in order to obtain absolute steatosis values. Five ultrasound images per patient were analysed using the CAUS protocol, which determines depth-dependent histogram and parametric texture parameters after several pre-processing steps. Pearson correlations to NAS and SPA were obtained for all CAUS parameters. Data was divided (50-50%) into a training and test set in order to train (multiple linear regression analysis) and test (area under the receiver operation curve (AUROC)) independently.
Results: Best correlating parameters were the mean-echo-level (R=0.71, p<0.01) and the residual-attenuation-coefficient (R=0.77, p<0.01). High predictive performance with an AUC of 0.94 to NAS and 0.99 to SPA was found. Fibrosis was not found to be a confounding parameter for staging steatosis.
Conclusion: The excellent predictive performance values indicate the potential usage of the generic applicable CAUS method for steatosis screening and follow-up studies.
Limitations: CAUS accurately quantifies steatosis, but is so far not suitable for detection of fibrosis or cirrhosis. Therefore, CAUS should be seen as an additional offline tool performed by radiologists.
Ethics committee approval: Approved by the institutional review board (no.2016-2763).
Funding: No funding was received for this work.
Author Disclosures:
G. Weijers: nothing to disclose

RPS 601c-2 11:21

Non-invasive assessment of liver cirrhosis with multiphasic dual energy CT using iodine maps: correlation with model of end-stage liver disease score

D. Mastrodicasa[1], M. J. Willemink[2], C. Duran[3], V. Hinostroza[1], L. Molvin[1], M. Khalaf[1], R. B. Jeffrey[1], B. N. Patel[1];
[1]*Stanford, CA/US,* [2]*Menlo Park, CA/NL,* [3]*Boston, MA/US (domenico.mastrodicasa@gmail.com)*

Purpose: To determine whether multiphasic dual -energy (DE) CT iodine quantitation correlates with severity of chronic liver disease.
Methods and materials: 28 cirrhotic and 22 non-cirrhotic patients who underwent a multiphasic liver protocol DECT and had MELD scores available were included. All three phases (arterial, portal venous (PVP), and delayed) were performed in DE mode. ROIs were placed in the caudate, left and right hepatic lobe, in the aorta, common hepatic artery (CHA), and portal vein (PV) to measure iodine (I) values (mg I/ml). (λ) were calculated as follows: $I_{delayed-arterial}$/ time and $I_{delayed-PVP}$/ time. λ were correlated with MELD scores and the area under the curve of the receiver operating characteristic (AUROC) was calculated to distinguish cirrhotics and non-cirrhotics.
Results: Cirrhotic and non-cirrhotic patients had significantly different $\lambda_{delayed-PVP}$ for caudate (λ = 1.350 vs. 2.350, P<.0001), left (λ = 1.383 vs. 2.200, P<.004), and right (λ = 1.063 vs. 1.913 , P<.0001) lobe. $\lambda_{delayed-arterial}$ were significantly different for CHA (λ = 2.450 vs. 11.250, P<.023) and PV (λ = 2.750 vs. 3.750, P<.013). A significant correlation was found between MELD scores and $\lambda_{delayed-PVP}$ of caudate, left and right lobes (rho=0.340, P=.034; rho=0.393, P=.005; rho=0.368, P=.034, respectively). AUROC for caudate, left, and right lobe $\lambda_{delayed-PVP}$ in differentiating cirrhotics from non-cirrhotics were 0.794, 0.739, and 0.908, respectively.
Conclusion: Multiphasic DECT iodine quantitation over time is significantly different between cirrhotics and non-cirrhotics, correlates with MELD score, and it could serve as a non-invasive measure of cirrhosis and disease severity with high diagnostic accuracy.
Limitations: Retrospective study.
Ethics committee approval: IRB and HIPAA-compliant study.
Funding: Institutional grant by Siemens Healthineers.
Author Disclosures:
D. Mastrodicasa: Research/Grant Support at Siemens Healthineers
M. J. Willemink: Grant Recipient at American Heart Association, Speaker at Koninklijke Philips NV, Consultant at Arterys Inc, Shareholder at Segmed, Inc
V. Hinostroza: nothing to disclose
C. Duran: nothing to disclose
L. Molvin: Speaker at General Electric Company
M. Khalaf: nothing to disclose
R. B. Jeffrey: nothing to disclose
B. N. Patel: Speaker at General Electric Company

RPS 601c-3 11:27

Quantification of local 3D texture maps for detection of fibrosis in the liver

W. Hamilton[1], S. Carey[1], B. E. Hoppel[2], Z. Afraz[1], P. Rogalla[1]; [1]*Toronto/CA,* [2]*Vernon Hills, WI/US (william.hamilton@uhn.ca)*

Purpose: To develop a method for detection and staging of liver fibrosis from low-dose single-energy CT by quantifying spatial distributions of local 3D texture maps.
Methods and materials: 33 patients who underwent a four-phase liver CT were categorised as having healthy (F0 and F1) or fibrotic livers (F3 and F4). Spherical ROIs, radius 20mm, were extracted from each liver. The ROIs were selected from regions close to the liver surface, avoiding major vessels and lesions. To simplify patterns in tissue structure, a Gaussian filter was applied to each ROI before binning gray levels using k-means clustering with k=20. Local 3D texture maps were produced from each binned ROI using the PyRadiomics library. The maps were computed voxel-wise for spherical subsets of 5-voxel radius. As a proof of concept, features were extracted from local 3D variance maps only. To quantify the spatial distributions of the features as they varied across each map, entropy, variance, gray level run length, and size zone matrices were computed from each local variance map.
Results: The mean entropy, variance, run length non-uniformity, and zone size variance for healthy (SD)/fibrotic (SD) livers are 0.200(0.247)/0.392(0.440), 0.071(0.087)/0.121(0.160), 1700.68(1410.26)/548.071(186.141), 0.267(0.366)/0.027(0.029), respectively. Kruskal-Wallis tests demonstrate significant differences between distributions of healthy and fibrotic livers for run length non-uniformity (U=7.456, p=0.006), however distributions of variance (U=0.938, p=0.333), entropy (U=0.926, p=0.336), and zone size variance (U=2.370, p=0.123) did not demonstrate significant differences.
Conclusion: Our novel approach shows promise for quantification of fibrosis in the liver and circumvents the need for objective comparison of parameter-sensitive texture features, which suffer from poor interpatient standardisation. Run length non-uniformity may represent the leading feature for separating healthy from fibrotic livers.
Limitations: Number of livers analysed.
Ethics committee approval: Research ethic board approval.
Funding: MSH-UHN AMO Innovation Fund.
Author Disclosures:
W. Hamilton: nothing to disclose
P. Rogalla: nothing to disclose
S. Carey: nothing to disclose
B. E. Hoppel: Employee at Canon Medical Systems
Z. Afraz: nothing to disclose

RPS 601c-4 11:33

Liver vein to cava attenuation: a simple parameter to increase predictive value of caudate-right lobe ratio and liver segmental volume ratio to detect significant liver fibrosis on abdominal CT scans

J. Hrycyk, V. C. Obmann, C. Marx, W. Kajdi, D. Catucci, A. Berzigotti, L. Ebner, A. Christe, A. T. Huber; *Berne/CH (joris.hrycyk@insel.ch)*

Purpose: To investigate incremental value of liver vein to cava attenuation (LVCA) in combination with caudate-right lobe ratio (CRL-R) and liver segmental volume ratio (LSVR) to predict significant liver fibrosis on portal venous phase abdominal CT scans.
Methods and materials: 212 patients were retrospectively included: 107 consecutive patients with liver biopsy and portal venous phase abdominal CT within 6 months and 105 patients without liver fibrosis, based on liver MR elastography (<2.8 kPa). The patients were grouped into patients with clinically significant fibrosis (73 patients with fibrosis grade 2-4 in histology) and patients without clinically significant fibrosis (139 patients, 34 with fibrosis grade 0-1 and

105 patients without liver fibrosis based on MR elastography). CRL-R and LSVR were calculated alone and multiplied with LVCA (1: liver veins hyperdense, 2: isodense, 3: hypodense compared to vena cava, 4: liver veins not contrasted). Resulting scores were called liver imaging morphology and attenuation based fibrosis score (LIMA) and liver segmental volume and attenuation ratio (LSVAR). ROC-analysis was performed.
Results: LVCA-enhanced LIMA fibrosis score and LSVAR (AUC 0.76 and 0.80, p<0.001) performed better than CRL-R and LSVR (AUC 0.72 and 0.76, p<0.001). Simple LIMA fibrosis score showed similar performance as liver volumetry based LSVR, requiring time-consuming image post-processing.
Conclusion: LIMA fibrosis score, as a combination of LVCA and CRL-R, showed better performance than CRL-R alone and similar performance than time-consuming LSVR. LSVAR, as a combination of LVCA and LSVR was the overall best predictor for significant liver fibrosis.
Limitations: A limitation of the present study is its retrospective nature.
Ethics committee approval: An agreement of the local ethics commitee of Bern, Switzerland, was obtained.
Funding: No funding was received for this work.
Author Disclosures:
J. Hrycyk: nothing to disclose
V. C. Obmann: nothing to disclose
C. Marx: nothing to disclose
W. Kajdi: nothing to disclose
A. Berzigotti: nothing to disclose
L. Ebner: nothing to disclose
A. Christe: nothing to disclose
D. Catucci: nothing to disclose
A. T. Huber: nothing to disclose

RPS 601c-5 11:39
Quantitative measurement of hepatic fibrosis on gadoxetic acid–enhanced magnetic resonance imaging in patients with chronic liver disease: multicentre study
Y. R. Kim[1], Y. H. Lee[1], D. M. Kang[1], M. J. Kim[1], T.-H. Kim[1], K. W. Kim[2], Y. Y. Jeong[3], K.-H. Yoon[1]; *[1]Iksan/KR, [2]Seoul/KR, [3]Jeonnam/KR (sweetynn@naver.com)*

Purpose: The aims of this study were to compare coefficient of variation (CV) in MR hepatobiliary image and serum biomarkers such as aspartate aminotransferase to platelet ratio index (APRI) and fibrosis-4 index (FIB-4) values according to the histopathologic fibrosis score, to identify the diagnostic performance of CV map in diagnosing hepatic fibrosis.
Methods and materials: This study was a prospective multicenter study which included 71 patients who underwent liver MRI using gadolinium EOB-DTPA and liver biopsy or surgery. Patients were divided into 4 groups according to the liver fibrosis score; Group 1 (F0, 1), Group 2 (F2), Group 3 (F3), Group 4 (F4). To quantitatively measure the hepatic fibrosis, a hepatobiliary image was analysed to identify inhomogeneous signal intensities calculated from CV map in the liver parenchyma. We also evaluated the comparison study of among CV, APRI, and FIB-4. The diagnostic performance of the CV map for fibrosis and cirrhosis was evaluated using ROC curve.
Results: Mean CV values in each group were Group 1 (n=18): 3.50±0.36, Group 2 (n=8): 4.09±0.50, Group 3 (n=21): 4.45±0.70, and Group 4 (n=30): 5.49±1.12, respectively (p<0.001). Mean FIB-4 values were Group 1: 1.19±1.20, Group 2: 3.36±2.74, Group 3: 3.38±3.12, and Group 4: 4.86±3.39, respectively (p=0.001). Area under curves of CV values on ROC analysis were 0.930 for significant fibrosis, 0.874 for cirrhosis (p<0.001, respectively).
Conclusion: CV value based on hepatobiliary MR image provides accurate discrimination of hepatic fibrosis with reliable measurements and demonstrates high diagnostic performance.
Limitations: Small study populations. Various MR vendors/protocols.
Ethics committee approval: Approved by the institutional review board.
Funding: Supported by the grants of the National Research Foundation of Korea (NRF) (2016M3A9A7918501) and Bayer Korea. Ltd.
Author Disclosures:
Y. R. Kim: nothing to disclose
Y. H. Lee: nothing to disclose
T.-H. Kim: nothing to disclose
K. W. Kim: nothing to disclose
D. M. Kang: nothing to disclose
M. J. Kim: nothing to disclose
Y. Y. Jeong: nothing to disclose
K.-H. Yoon: Research/Grant Support at the National Research Foundation of Korea (NRF) , Research/Grant Support at Bayer Korea. Ltd.

RPS 601c-6 11:45
Functional liver imaging score derived from gadoxetic acid-enhanced MRI predicts outcomes in patients with chronic liver disease
L. Beer, N. Bastati-Huber, M. Mandorfer, S. Pötter-Lang, Y. Bican, G. Semmler, B. Simbrunner, T. Reiberger, A. Ba-Ssalamah*; Vienna/AT (lucian.beer@meduniwien.ac.at)*

Purpose: The aim of the study was to investigate the accuracy of the gadoxetic acid-enhanced MRI based functional liver imaging score (FLIS) in predicting hepatic decompensation and transplant-free survival (TFS) in patients with chronic liver disease (CLD).
Methods and materials: 265 with CLD met the inclusion criteria of this retrospective study. Those patients were retrospectively assigned a FLIS based on the sum of three hepatobiliary-phase features, each scored on an ordinal 0-2 scale: enhancement, excretion, and portal-vein-sign. FLIS scores of 0-3 and 4-6 indicate impaired and preserved liver function, respectively. Patients were further stratified into three groups: non-advanced CLD (non-ACLD); compensated advanced CLD (cACLD); and decompensated advanced CLD (dACLD). The predictive value of FLIS for first and/or further hepatic decompensation and for TFS was investigated using Kaplan-Meier analysis, log-rank tests, and Cox-regression.
Results: Intraobserver (correlation-coefficient κ=0.983; 95% confidence-interval [CI]:0.971-0.991) and interobserver (κ=0.931; 95%CI: 0.898-0.954) agreement for FLIS was excellent. In patients with cACLD, the FLIS was independently predictive of a first hepatic decompensation (adjusted-hazard-ratio, [aHR]: 3.72,95%CI: 1.1-12.64; P=.04), but not for further hepatic decompensations in patients with dACLD (aHR:1.43, 95%CI:0.92-1.94, P=.17). The FLIS was an independent risk factor for mortality in both patients with cACLD (aHR:7.44, 95%CI:2.74-20.17, P<.001) and those with dACLD (aHR: 3.84, 95%CI:1.16-9.48; P=.004).
Conclusion: A simple gadoxetic acid-enhanced MRI-derived FLIS can identify patients with advance chronic liver disease at increased risk for hepatic decompensation and mortality.
Limitations: Single-centre study.
Ethics committee approval: Approved by the Ethics Committee of the Medical University of Vienna.
Funding: No funding was received for this work.
Author Disclosures:
L. Beer: nothing to disclose
N. Bastati-Huber: nothing to disclose
M. Mandorfer: nothing to disclose
S. Pötter-Lang: nothing to disclose
A. Ba-Ssalamah: Speaker at Bayer
Y. Bican: nothing to disclose
G. Semmler: nothing to disclose
B. Simbrunner: nothing to disclose
T. Reiberger: nothing to disclose

RPS 601c-7 11:51
Multi-parameter magnetic resonance imaging for staging liver fibrosis and detecting macrophage polarisation
Y. M. Lu, D. Wang*; Shanghai/CN (lym1007@sjtu.edu.cn)*

Purpose: To evaluate MRI T1 and T1ρ mapping with calculation of extracellular volume (ECV) for diagnosis and grading of liver fibrosis, and to explore correlation between those parameters and macrophage polarisation in a rat model.
Methods and materials: Different degrees of fibrosis were induced in 60 male Sprague-Dawley rats by bile duct ligation (BDL) and carbon-tetrachloride (CCl4) injection. Liver fibrosis was graded by Sirius red and α-smooth muscle actin staining. The native T1 values, Tρ values, and ECV were assessed by using quantitative MRI mapping techniques at 11.7T. The METAVIR system was used for the staging of fibrosis. Expressions of M2-related factors were analysed with RT-PCR and immunohistochemistry.
Results: The T1 values in liver cirrhosis (F4) and significant fibrosis (≥ F2) after BDL were greater than in control animals (1246msec±52 vs 1124±34msec vs 1066±63, respectively, P<.001); T1ρ values in liver cirrhosis and significant fibrosis after BDL were also greater than in control animals (66.53±5,64 vs 37.76±6.48 vs 29.68±3.22, respectively, P<.001); ECV was greater in liver cirrhosis and significant fibrosis after BDL compared with control animals (33.6%±2.5 vs 26.03%±3.8 vs 16.65%±2.9, respectively; P< .001). Analogous T1, T1ρ, and ECV results were observed after CCl4 injection. Middle and high correlations were found between native T1, ECV and the expression of CD204, IL-10 and TGFβ1.

Conclusion: T1, T1ρ values, and ECV may be accurate methods for noninvasively assessing liver fibrosis. Elevation of T1 and ECV was associated with macrophage M2 polarisation.
Limitations: We didn't discuss the impact of other pathological factors to those paremeters.
Ethics committee approval: Approved by the Institutional Animal Care and Use Committee of Xinhua Hospital affiliated to Shanghai Jiao Tong University School of Medicine.
Funding: No funding was received for this work.
Author Disclosures:
Y. M. Lu: nothing to disclose
D. Wang: nothing to disclose

RPS 601c-8 11:57

Multiparametric MRI for activity grading and staging of hepatic fibrosis: role of T2-mapping, multi-gradient-echo MRI, and MR elastography

S. M. Skawran, H. Honcharova-Biletska, S. Blümel, D. Segna, C. Jüngst, A. Weber, C. Gubler, C. S. Reiner*; Zurich/CH*

Purpose: To evaluate whether T2-mapping, multi-gradient-echo-sequence, and MR-elastography (MRE) can diagnose activity grade and stage of hepatic fibrosis.
Methods and materials: 61 patients with suspicion of hepatic fibrosis undergoing MRI at 3.0T - including T2-mapping, multi-gradient-echo-sequence for proton-density-fat-fraction (PDFF), and MRE - and liver biopsy between 2015 and 2019 were prospectively analysed. ROIs were placed in the liver in the corresponding maps. Patients with probable iron overload were excluded (R2*>100s-1). Histologic inflammatory activity grading and fibrosis staging systems were applied according to underlying etiology and unified yielding activity grades G0-3 and fibrosis stages F0-4. The cohort was split into steatohepatitis (n=24) and all other etiologies (n=37). Descriptive statistics and ROC-analysis were performed.
Results: In the steatohepatitis group, PDFF was significantly higher in G2-3 vs G0-1 (p=0.02) with an AUC=0.779. T2-values were not significantly different between grades (p=0.06). Stiffness was significantly higher when any fibrosis was present (p=0.008) with an AUC=0.887. T2-values (p=0.84) and PDFF (p=0.84) were not significantly different across F0-F4. In the general fibrosis group, PDFF and T2-values were similar across G0-3 (p=0.81; p=0.10) and F0-F4 (p=0.17; p=0.06). Stiffness was significantly higher when any fibrosis was present (p=0.02) with an AUC=0.827 and for clinically relevant fibrosis (F2-4 vs. F0-1: p<0.001) with an AUC=0.846.
Conclusion: PDFF may serve as a marker for activity of steatohepatitis. MRE can identify fibrosis in steatohepatitis and in other etiologies of fibrosis. An independent role for T2-mapping could not be established.
Limitations: T2-mapping is susceptible to fat deposition, which might explain the limited value in our cohort. Whether it might have a role in a multiparametric model will be subject to further research.
Ethics committee approval: Prospective study approved by local ethics committee. Patients gave written informed consent.
Funding: No funding was received for this work.
Author Disclosures:
S. M. Skawran: nothing to disclose
H. Honcharova-Biletska: nothing to disclose
S. Blümel: nothing to disclose
D. Segna: nothing to disclose
C. Jüngst: nothing to disclose
A. Weber: nothing to disclose
C. Gubler: nothing to disclose
C. S. Reiner: nothing to disclose

RPS 601c-9 12:03

Evaluation of liver fibrosis and cirrhosis on the basis of T1 mapping considering acute inflammation, age, and liver volume as confounding factors

C. Breit, D. Boll, D. J. Winkel, M. Henkel, T. Heye*; Basel/CH*

Purpose: To evaluate confounding factors for the assessment of liver fibrosis by T1 mapping.
Methods and materials: 200 patients who underwent routine abdominal MRI at 1.5T and 3T scanners were retrospective included. 93 patients were defined as healthy based on the information of the hospital information system, 40 patients showed acute elevation of liver and bile parameters, and 67 subjects had a clinically or biopsy proven liver fibrosis or cirrhosis. A ROI based analysis of the T1 maps of the liver was performed. Additionally fat fraction, R2*, liver volume, laboratory parameters, sex, and age were regarded as potential confounding factors. Fibrosis was staged by using the Child-Pugh score and the METAVIR score.
Results: There was a significant difference at 1.5T between T1 values in patients without known fibrotic changes and normal laboratory parameters (574.8+/-56ms) and those with elevated liver enzymes and bile levels (657.4+/-73ms) or known fibrotic liver disease (643.8+/-83 ms). At 3T the T1 values for patients with liver fibrosis or cirrhosis (995+/-150.3ms) were significantly higher than for the healthy group (870+/-128ms) and not significantly higher than for patients with laboratory abnormalities (952.4+/-137ms). There was a significant, moderate positive correlation between T1 values and the Child-Pugh stage at 1.5T (ρ=0.38, p=0.0112) and a non-significant, moderate positive correlation at 3T (ρ=0.3, p=0.26). There was no correlation between age and T1 values at 1.5T and 3T.
Conclusion: T1 mapping is a reasonable method for the detection of liver fibrosis and cirrhosis. Age is no confounding factor hence age independent thresholds can be defined. Acute liver diseases are a confounding factor that need to be regarded.
Limitations: Retrospective study with potential selection bias.
Ethics committee approval: Informed consent waived.
Funding: No funding was received for this work.
Author Disclosures:
C. Breit: nothing to disclose
T. Heye: nothing to disclose
D. Boll: nothing to disclose
D. J. Winkel: nothing to disclose
M. Henkel: nothing to disclose

RPS 601c-10 12:09

T1 relaxation times of the liver and spleen to predict significant liver fibrosis: is there an additional value of normalisation to the blood pool?

V. C. Obmann, A. Christe, A. Berzigotti, J. T. Heverhagen, L. Ebner, C. Gräni, A. T. Huber*; Berne/CH (adrian.huber@me.com)*

Purpose: To analyse liver and spleen native T1 relaxometry values to predict significant fibrosis and their additional value when normalised to the blood pool.
Methods and materials: 156 patients without solid liver lesions on routine liver multidetector CT scans underwent liver MRI with gradient-echo based MR elastography (MRE) and shortened modified Look-Locker inversion recovery (shMOLLI) based T1 relaxometry. T1 relaxation times were measured in the right liver lobe and in the spleen, in the aorta and in the vena cava. MRE liver stiffness was compared with T1 relaxation times alone, as well as T1 relaxation times normalised to the blood pool in the vena cava and in the aorta. Pearson correlation, students t-test, and receiver operation characteristics (ROC) analysis were used to investigate the usefulness of different T1 relaxometry values to predict significant liver fibrosis, using a cutoff value of 3.5kPa in MRE.
Results: Correlation between T1 relaxometry values and MRE liver stiffness was r=0.49-0.59 (p<0.001) for T1 of the liver and for T1 of the liver normalised to blood pool, while T1 of the spleen was less useful (r=0.11-0.17). Both normalised and not normalised T1 values of the liver allowed to significantly separate patients with significant liver fibrosis from those without significant liver fibrosis (p<0.001). In ROC-analysis, T1 relaxometry values normalised to the blood pool did not perform better than T1 values alone.
Conclusion: Native T1 relaxation times of the liver allowed to predict clinically significant liver fibrosis, while T1 relaxation times of the spleen were less useful. There was no additional value of liver and spleen native T1 relaxometry values to predict significant fibrosis when normalised to the blood pool.
Limitations: Retrospective design. MRE as non-invasive gold-standard, no histology.
Ethics committee approval: Yes.
Funding: No funding was received for this work.
Author Disclosures:
A. T. Huber: nothing to disclose
V. C. Obmann: nothing to disclose
J. T. Heverhagen: nothing to disclose
L. Ebner: nothing to disclose
A. Christe: nothing to disclose
C. Gräni: nothing to disclose
A. Berzigotti: nothing to disclose

RPS 601c-11 12:15

Iron measurement by quantitative MRI-R2* at 3.0T and 1.5T

J. Yamamura[1], S. Keller[1], R. Grosse[1], B. P. Schönnagel[1], Z. J. Wang[2], P. Nielsen[1], R. Fischer[3]*; [1]Hamburg/DE, [2]Dallas, TX/US, [3]Oakland, CA/US (j.yamamura@uke.de)*

Purpose: To investigate the suitability of a 3.0T imager for iron measurements in comparison to 1.5T in the liver.
Methods and materials: Patients with transfusional siderosis, hereditary hemochromatosis, DBA, and controls (n=249) underwent a MRI-R2* at 1.5T and 3.0T. In patients with severe liver iron burden (LIC>2000 µg/g_{liver}), shorter echo times were used (TE=0.65). In-vivo LIC was determined from the specific hemosiderin/ferritin magnetic susceptibility as non-invasively measured by SQUID. R2* was determined from a mono-exponential fit with constant signal level offset.

Results: In patients, LIC ranged from 130 to 9700 µg/g_{liver} and in controls from 176 to 377µg/g_{liver}. At 1.5 and 3.0T, R2*ranged from 31-2236s^{-1} and from 41-2344s^{-1}, respectively. From a direct comparison between R2* at 3.0T and 1.5T, a non-linear relationship was found between R2*(3T) and R2*(1.5T) due to the higher relaxivity at 3T. Below R2*(1.5T) < 600 s^{-1}, a linear relationship with a ratio of R2*(3.0)/R2*(1.5T) = 1.85±0.04 could be obtained in contrast to expected ratio of 2:1. In order to overcome the saturation effect of the 3T relaxivity for severe liver iron overload, one has to put constraints on the signal amplitude.
Conclusion: For liver iron measurements in patients with LIC>3000µg/g_{liver} or >18mg/$g_{dry\ weight}$, 1.5T imagers are better suited than 3.0T unless ultrashort echo times can be used. For R2* rates below that level, 3.0T systems with 3D data acquisition are more advantageous.
Limitations: Realtively small sampling size. In the future, this result must be further studied in a multi-centre study.
Ethics committee approval: Informed consent was obtained from all participants before examination and the local IRB approved the study.
Funding: No funding was received for this work.
Author Disclosures:
J. Yamamura: nothing to disclose
S. Keller: nothing to disclose
R. Grosse: nothing to disclose
B. P. Schönnagel: nothing to disclose
Z. J. Wang: nothing to disclose
P. Nielsen: nothing to disclose
R. Fischer: nothing to disclose

RPS 601c-12 12:21
Quantitative MRI characterisation of NASH in a dietary rodent model
M. Dioguardi Burgio[1], P. Garteiser[2], F. Julea[2], A. Abyzov[2], V. Paradis[1], V. Vilgrain[1], B. van Beers[1]; [1]Clichy/FR, [2]Paris/FR (marco_dioguardi@hotmail.it)

Purpose: To assess the diagnostic performance of quantitative MRI parameters for the diagnosis of early non-alcoholic steatohepatitis (NASH) in a dietary rodent model.
Methods and materials: We included 74 mice (C57bl6) with 2 control groups fed with normal diet (for 5 and 17 weeks, N=7), 3 dietary groups (5, 11, and 16 weeks, N=10) fed with high fat diet deficient in choline and supplemented with methionine and 3 dietary groups (5, 11, and 16 weeks, N=10) fed with high fat diet. The liver was scanned with a 7T system. Proton density fat fraction (PDFF), R2*, mechanical properties at 400, 600, and 800Hz including storage modulus (G'), loss modulus (G''), damping ratio, shear modulus (G*), and G* frequency dispersion coefficient were obtained with dedicated imaging sequences. At histopathology, the grade of steatosis, ballooning, inflammation, and the fibrosis stage were assessed. NASH was diagnosed according to the FLIP algorithm. ROC analysis, Spearman correlations, and multivariate regression were used to test the variables.
Results: 19 mice had NASH including 15 with stage 1 fibrosis. 32 had simple steatosis. G'' at 400Hz had the largest AUROC for NASH (0.84; p<0.01) and for diagnosing NASH versus simple steatosis (0.80; p<0.01). Cutoff of G''>0.38 kPa had 89% sensitivity and 79% specificity for NASH diagnosis. PDFF correlated with steatosis (rho 0.81; p<0.01). At multivariate analysis, inflammation was the main determinant of the frequency dispersion coefficient.
Conclusion: At quantitative MRI, the loss modulus had the best diagnostic performance for diagnosing early NASH. Frequency dispersion coefficient might be a marker of liver inflammation.
Limitations: Use of two different high fat diets might be a source of bias.
Ethics committee approval: Animal board approval was obtained.
Funding: No funding was recieved for this work.
Author Disclosures:
M. Dioguardi Burgio: nothing to disclose
P. Garteiser: nothing to disclose
F. Julea: nothing to disclose
A. Abyzov: nothing to disclose
V. Paradis: nothing to disclose
V. Vilgrain: nothing to disclose
B. van Beers: nothing to disclose

11:15 - 12:30 **Tech Gate Auditorium**

Artificial Intelligence and Machine Learning

RPS 605c

Different views on artificial intelligence (AI) and machine learning (ML)

Moderators:
A. Agostini; Ancona/IT
P. Mc Laughlin; Cork/IE

RPS 605c-1 11:15
The use of AI-based applications in radiology and the liability of the medical practitioner: a law and economics analysis of the incentives towards automation in diagnosis
A. Bertolini[1], G. Vatteroni[2], F. Episcopo[1], A. Chiti[3], L. Balzarini[2]; [1]Pisa/IT, [2]Milan/IT, [3]Pieve Emanuele/IT (andrea.bertolini@santannapisa.it)

Purpose: To assess the impact on the radiologist's behaviour of the diffusion of different AI-based imaging technologies (AIT), taking into account civil liability rules.
AIT increase cooperation between man and machine in diagnosis, allowing greater precision in lesion detection or reducing the involvement of the practitioner in the analysis of clearly negative cases. Machines possess some degree of autonomy, often supervised by the human user, in the assessment of the case. From a legal perspective, this entails a possible new apportionment of civil liability between (i) the medical practitioner, (ii) the manufacturer/programmer, and (iii) the hospital/structure that decided to adopt the given AI-based solution.
We intend to show how liability would be apportioned and what incentives this provides to radiologists in using specific AITs.
Methods and materials: Being a law and technology study, we began by providing a description of the specific applications considered, focusing on (a) the level of automation the system displays, (b) the possibility for it to adopt decisions (e.g. rule out what appears to be a certainly negative case), (c) its declared overall precision, and (d) the role of the human user.
The liability apportionment analysis was performed according to the principles of micro-comparative law, taking into account the European legal system and theoretical law and economics (game theory).
Results: By taking into account the different AIT, we will describe how liability is apportioned between the mentioned parties involved (i, ii, iii above).
Conclusion: The awaited liability apportionment affects the behaviour of the radiologist, in particular, the tendencies towards (1) using the application, (2) relying on its output, and (3) diverging from its conclusion, eventually leading to some defensive-medicine approaches.
Limitations: n/a
Ethics committee approval: n/a
Funding: No funding was received for this work.
Author Disclosures:
A. Bertolini: nothing to disclose
L. Balzarini: nothing to disclose
A. Chiti: nothing to disclose
G. Vatteroni: nothing to disclose
F. Episcopo: nothing to disclose

RPS 605c-2 11:21
Attitudes and perceptions of UK medical students towards artificial intelligence and radiology: a multicentre survey
D. S. Poon, C. Sit, A. Azam, A. Amlani, K. Muthuswamy, R. Srinivasan, L. Monzon; London/UK (daniel.poon@kcl.ac.uk)

Purpose: To explore the attitudes of UK medical students regarding AI, their understanding, and career intention towards radiology. We also examined the state of education relating to AI amongst this cohort.
Methods and materials: Students from UK medical schools were invited to complete a survey consisting of Likert and dichotomous questions.
Results: 484 responses were received from 19 UK medical schools. 88% of students believed that AI will play an important role in healthcare and 49% reported they were less likely to consider a career in radiology due to AI. 89% of students believed that teaching in AI would be beneficial and 78% agreed that students should receive training in AI as part of their medical degree.

Only 45 students received any teaching on AI; none received such teaching as part of their compulsory curriculum. Students that received teaching in AI were more likely to consider radiology (p=0.01). Despite this, a large proportion of students in the taught group reported a lack of confidence and understanding required for the critical use of healthcare AI-tools.
Conclusion: UK medical students understand the importance of AI and are keen to engage. Medical school training of AI should be improved. Realistic use-cases and limitations of AI must be presented to students so they will not feel discouraged from pursuing radiology.
Limitations: Not all UK medical schools were represented in the current study and response rates differed between different institutions, potentially introducing bias. Associated limitations relating to survey-based observational studies would apply. For example, potential misunderstanding or misintrepretation of questions by the respondents.
Ethics committee approval: Minimal risk ethical approval was obtained from the King's College London research ethics office (KCL-MRA18/19-11127).
Funding: No funding was received for this work.
Author Disclosures:
D. S. Poon: nothing to disclose
C. Sit: nothing to disclose
A. Azam: nothing to disclose
A. Amlani: nothing to disclose
K. Muthuswamy: nothing to disclose
R. Srinivasan: nothing to disclose
L. Monzon: nothing to disclose

RPS 605c-3 11:27

The impact of artificial intelligence on the choice of radiology as a medical speciality by undergraduate medical students

G. Irene Brandes Garcia, A. Azzolini, U. Dos Santos Torres, E. A. S. Bretas, G. de Souza Portes Meirelles, G. D`ippolito*; Sao Paulo/BR (azzolini.anderson@gmail.com)*

Purpose: To evaluate the impact of artificial intelligence on the choice of radiology as a medical specialty by undergraduate medical students.
Methods and materials: In February 2019, an anonymous online survey was sent to Brazilian medical students from the city of São Paulo. The research contemplated questions such as how much students think they know about artificial intelligence (AI) technologies, how much AI discourages them from choosing radiology as a speciality, and if they believe that radiologist's job market is threatened.
Results: A total of 101 students answered the questionnaire, most enrolled in the internship years. More than half (52.5%) believed that the labour market for radiologists is threatened by AI and, even more surprisingly, among those students that had once considered radiology as a career, almost half (42.3%) discarded the speciality mainly due to the development of AI. At the same time, the majority of the overall participants (64.3%) claimed not to have good knowledge about these new technologies.
Conclusion: An expressive part of medical students believe that AI is a threat to the radiological practice and this perception may have an impact on their career choice. However, the majority claim to have insufficient knowledge about it.
Limitations: The main limitations of our study were the small number of participants, the fact that the students were from only one city, and that the majority of them were from the same university.
Ethics committee approval: This research was not registered on ethical boards since it was based on a voluntary online questionnaire and anonymity was reassured.
Funding: No funding was received for this work.
Author Disclosures:
A. Azzolini: nothing to disclose
G. Irene Brandes Garcia: nothing to disclose
U. Dos Santos Torres: nothing to disclose
E. A. S. Bretas: nothing to disclose
G. de Souza Portes Meirelles: nothing to disclose
G. D`ippolito: nothing to disclose

RPS 605c-4 11:33

How do expectations and attitudes towards artificial intelligence applications differ between radiologists and IT experts?

F. Jungmann, T. Jorg, R. Natalie, C. Düber, J. Stefanie, P. Mildenberger*; Mainz/DE*

Purpose: To investigate the opinion of radiologists and IT experts on artificial intelligence (AI) and its future impact on radiological work.
Methods and materials: During a national meeting for AI, eHealth, and IT-infrastructure in 2019, a survey was conducted to obtain the participants' opinion on AI in radiology. 131 participants (42 radiologists, 89 IT experts/non-radiologists) took part in the survey. A 7-point Likert scale (1: "I disagree at all" to 7: "I totally agree") was used to assess the views of radiologists, IT experts in hospitals, and healthcare companies.
Results: All participants agreed that medicine will become more efficient with the use of AI (5.98) and that plausibility checks will be important to be able to understand the decisions of the AI (6.30). All participants stated that the validation of AI algorithms in clinical studies is mandatory (6.32).
Radiologists rated the statement that AI will lead to a change in the working environment of all physicians significantly higher than non-radiologists (6.38 vs. 5.85, p=.04). The need to inform patients about the use of AI (4.12 vs. 5.2, p=.009) was rated significantly lower among radiologists.
Conclusion: Radiologists and IT experts share various attitudes regarding future use on AI, especially with regard to the improvement in medical care and the need to validate algorithms in clinical studies. The views of radiologists and IT experts differ on some specific issues, such as the impact of AI on physicians' work and whether patients need to be informed prior to the use of AI.
Limitations: Not all participants of the meeting participated in the study, so a selection bias is possible.
Ethics committee approval: n/a
Funding: No funding was received for this work.
Author Disclosures:
R. Natalie: nothing to disclose
F. Jungmann: nothing to disclose
T. Jorg: nothing to disclose
J. Stefanie: nothing to disclose
P. Mildenberger: nothing to disclose
C. Düber: nothing to disclose

RPS 605c-5 11:39

A European-wide needs assessment to prioritise technical procedures for simulation-based education in radiology

L. Nayahangan[1], E. Albrecht-Beste[1], L. Konge[1], B. Brkljacic[2], C. Catalano[3], B. B. Ertl-Wagner[4], K. Riklund[5], M. B. Bachmann Nielsen[1]*; [1]Copenhagen/DK, [2]Zagreb/HR, [3]Rome/IT, [4]Munich/DE, [5]Umeå/SE (leizl.joy.nayahangan@regionh.dk)*

Purpose: To identify and prioritise technical procedures that should be included in future simulation-based curricula for radiology trainees.
Methods and materials: A three-round Delphi process was initiated among key leaders chosen according to their leadership and educational role in the European Society of Radiology. Delphi round 1 identified all potential technical procedures that newly qualified radiologists should be able to perform. Round 2 explored and prioritised the procedures by investigating the frequency of procedures, the number of radiologists that should be able to perform the procedure, the feasibility for simulation training, and the risk and/or discomfort when performed by an inexperienced radiologist. Round 3 was an elimination and final ranking of the procedures. A consensus criterion of 2/3 was set a priori for inclusion in the final list.
Results: 71 key leaders across 27 countries agreed to participate and responded to round 1. Response rates for rounds 2 and 3 were 72% (51/71) and 82% (42/51), respectively. Round 1 identified 719 procedures; these were reduced to 34 procedures after removing duplicates and non-technical skills. In the final round, 8 procedures were eliminated, resulting in a final prioritised list of 26 technical procedures for simulation. The top 3 procedures include basic ultrasound (probe selection, image optimisation, and technical performance), ultrasound of the upper abdomen, and ultrasound of the kidneys, retroperinuem, abdominal wall, intestines, appendix, urinary bladder, pelvis, and scrotum.
Conclusion: This European-wide needs assessment promotes the development of simulation-based training programs targeted at current training needs. The prioritised list of technical procedures should guide the planning of future simulation-based education of radiology trainees.
Limitations: Although 27 countries participated, the selection process did not guarantee equal representation from every country.
Ethics committee approval: n/a
Funding: No funding was received for this work
Author Disclosures:
L. Nayahangan: nothing to disclose
E. Albrecht-Beste: nothing to disclose
L. Konge: nothing to disclose
B. Brkljacic: nothing to disclose
C. Catalano: nothing to disclose
B. B. Ertl-Wagner: nothing to disclose
K. Riklund: nothing to disclose
M. B. Bachmann Nielsen: nothing to disclose

RPS 605c-6 11:45

Medicine in the digital age: artificial intelligence in medical education

F. Jungmann, K. Deutsch, S. Kuhn*; Mainz/DE*

Purpose: To introduce a curricular course for medical students which addresses artificial intelligence (AI) in medical education for the first time.
Methods and materials: "Medicine in the digital age" represents an interdisciplinary course in medical school that is taught in 5 modules on digital topics such as medical apps, augmented reality, big data, individualised medicine, and AI.
The course was held in 3 consecutive terms. All 32 participants were questioned in focus groups using guideline interviews. The questions of the guideline were first formulated structurally and then in terms of content, from which the 3 interview focuses emerged: fields of applications of AI, Work 4.0, and critical reflection. The interviews were evaluated using qualitative content analysis according to Philipp Mayring.
Results: 47% of the students' statements could be assigned to Work 4.0, 31% to critical reflection, and 22% to fields of application of AI. Within the category Work 4.0, the topic human-machine interaction accounted for the largest share of statements with 56%. The fears and worries of the students concerning AI played only a minor role with 12% of the statements in this category. The category critical reflection describes a holistic view of medicine in the digital age on the level of social abstraction and self-reflection (e.g. practical implementation, ethics).
Conclusion: The course conveys the knowledge of digital tools, the acquisition of skills, and the development of an attitude towards AI. The students become aware of the process of change through the increasing digitalisation and recognise the necessity to acquire new competencies for their future.
Limitations: Currently, the course is offered within the scope of the compulsory elective week. An expansion for all students is the aim.
Ethics committee approval: n/a
Funding: No funding was received for this work.
Author Disclosures:
F. Jungmann: nothing to disclose
K. Deutsch: nothing to disclose
S. Kuhn: nothing to disclose

RPS 605c-7 11:51

How scientific mobility can help the future of radiology research: a radiology trainee's perspective

F. Pesapane*; Milan/IT (filippopesapane@gmail.com)*

Purpose: To provide a perspective of radiology fellows about the current trends and policy tools for promoting mobility among young radiologists, especially in the EU and USA.
Methods and materials: Evidence-based medicine requires multicentre collaboration to identify a best practice, standardise it, and share it. Mobility helps to uniform techniques and terminology in different countries, which are crucial to develop widely-shared guidelines.
Results: While the EU has many talented and skilled researchers, they account for a significantly lower share of the labour force than is the case in the USA.
Given advances in communication technology, a core group of networked researchers may go a long way towards helping a country with modest scientific resources achieve the analogue world-class excellence of the richest countries, in a broader win-win situation. However, these new avenues will require strong leadership and enhanced institutional autonomy. International organisations such as the ESR and RSNA can play a role to involve local centres into global science projects. With the help of these societies, a radiology trainee can easily take advantage of the international training opportunities that are currently offered by public or private grants, enhancing the scientific mobility and the cooperation among research centres of different countries.
Moreover, the cultural-knowledge and the networks developed during mobility can be used by the trainees to advance their career.
Conclusion: Today, it is not just being a certified radiologist that matters, the place where training is held plays a role when applying for a high-level position. Mobility of trainees is an indispensable prerequisite to facing new challenges, including the application of artificial intelligence to medical imaging, which will require a large multicentre collaboration.
Limitations: n/a
Ethics committee approval: n/a
Funding: No funding was received for this work.
Author Disclosures:
F. Pesapane: nothing to disclose

RPS 605c-8 11:57

Resident quality control (RQC): introducing a new method for monitoring residents' progress, strengths, and weaknesses, hence, tailoring and improving the residency program

H. Yashar, N. Leizarowitz, D. G. Shendler, D. G. Levy, D. Mercer, S. Adam, D. S. Barnes, A. Blachar*; Tel Aviv/IL (hilayashar1@gmail.com)*

Purpose: Residents' performance quality assurance and improvement is a priority for residency programs in all departments, let alone in radiology. There is a constant need for a general quality control system that covers all modalities in which residents are engaged.
Our radiology department implemented a residents' quality grading system (RQC). The goal of this system is to provide data that will demonstrate residents' progress and areas of strength and weaknesses, hence, tailoring the residency program individually.
Methods and materials: A computerised information system was developed and deployed. The system enables attending radiologists to grade residents' reports on a scale of 1-4, according to the following: 1) Complete agreement of the attending radiologist with the resident's report. 2) General agreement between reports, with minor changes. 3) Major changes without clinically significant impact. 4) Major changes with clinical significance that can gravely affect the patient.
The attending radiologist inserts the appropriate grade in the report and the resident is able to see it instantly.
Results: The RQC system has been implemented successfully in our department, with high compliance rates. Residents have been able to receive on-line feedback, understanding the clinical impact of their reports immediately. Moreover, the department is able to monitor a resident's progress and areas of weaknesses, thus directing his/her residency program accordingly.
Conclusion: RQC is a new system implemented by our radiology department with a high compliance rate, enabling constant feedback on residents' radiology reports. It continuously provides essential data that will impact residents' progress and quality of radiology reports, thus tailoring the residency program on an individual basis.
Limitations: Limitations include variability among evaluating radiologists, bias based on previous impression, shift workload, time of shift, and resident seniority.
Ethics committee approval: n/a
Funding: No funding was received for this work.
Author Disclosures:
A. Blachar: nothing to disclose
H. Yashar: nothing to disclose
D. Mercer: nothing to disclose
S. Adam: nothing to disclose
D. G. Levy: nothing to disclose
N. Leizarowitz: nothing to disclose
D. G. Shendler: nothing to disclose
D. S. Barnes: nothing to disclose

RPS 605c-9 12:03

Implementation of artificial intelligence: is the community ready? An international survey of 1,041 radiologists and residents

M. Huisman[1], E. R. Ranschaert[2], W. Parker[3], D. Mastrodicasa[4], M. Kočí[5], D. Pinto Dos Santos[6], T. Leiner[1], M. J. Willemink[7]*; [1]Utrecht/NL, [2]Turnhout/BE, [3]Vancouver/CA, [4]Stanford, CA/US, [5]Palo Alto, CA/US, [6]Cologne/DE, [7]Menlo Park, CA/NL (merel.huisman1@gmail.com)*

Purpose: Key opinion leaders predicting implementation issues will determine the course of AI (artificial intelligence) in radiology. The perception at large by radiologists and residents of AI remains unexplored. We investigated the existing knowledge and overall attitude towards AI by international radiologists and residents to help facilitate implementation.
Methods and materials: Between April-July 2019, a multi-language survey was accessible to radiologists and residents containing questions on awareness, knowledge, and attitude towards AI. Relationships of independent variables with an open and proactive attitude towards AI (readiness to use and learn about AI, to collaborate with data scientists, and agreement that radiologists should take the lead) were assessed using multivariable logistic regression.
Results: The survey was completed by 1,041 respondents from 54 countries (mean age 41 (range 24-74)). Most participants were male (n=670, 65%), radiologists (n=719, 69%), and working in non-academic centres (n=572, 55%) without formal research training (n=727, 70%). Over half had no knowledge of informatics/statistics (n=537, 52%). A minority had profound knowledge of AI (n=168, 16%). Almost half of the participants appeared to have an open and proactive attitude towards AI (n=501, 48%), which was significantly ($p<0.05$) associated with sex, age, working in an academic centre, having received formal research training, pre-existent knowledge on informatics/statistics, and professional social media use.

Conclusion: Almost half of the participants showed an open and proactive attitude towards AI, however, a substantial proportion had no knowledge of informatics/statistics. Pre-existent knowledge was independently associated with a positive attitude, indicating a need for additional training to facilitate implementation.
Limitations: Selection bias is presumably an issue in this survey, therefore the true percentage of the population having an open and proactive attitude is most likely lower.
Ethics committee approval: n/a
Funding: No funding was received for this work.
Author Disclosures:
M. Huisman: nothing to disclose
E. R. Ranschaert: nothing to disclose
W. Parker: nothing to disclose
D. Mastrodicasa: nothing to disclose
M. Kočí: nothing to disclose
D. Pinto Dos Santos: nothing to disclose
T. Leiner: nothing to disclose
M. J. Willemink: nothing to disclose

RPS 605c-10 12:09

Anticipated hurdles and incorporation into residency programs of artificial intelligence (AI): an international survey of 1,041 radiologists and residents

M. Huisman[1], E. R. Ranschaert[2], W. Parker[3], D. Mastrodicasa[4], M. Kočí[5], D. Pinto Dos Santos[6], T. Leiner[1], M. J. Willemink[7]; *[1]Utrecht/NL, [2]Turnhout/BE, [3]Vancouver/CA, [4]Stanford, CA/US, [5]Palo Alto, CA/US, [6]Cologne/DE, [7]Menlo Park, CA/NL (merel.huisman1@gmail.com)*

Purpose: Integration of AI education in residency programs is not yet common. As residency programs are already demanding, controversy exists as to what extent it should be incorporated, although it might accelerate the implementation of AI in radiology. We sought to explore the opinion of the radiology community and to identify commonly anticipated hurdles to implementation.
Methods and materials: Between April-July 2019, a multi-language survey was accessible to radiologists and residents including multiple-choice questions on the integration of AI in residency programs and the anticipated hurdles to implementation of AI in radiology.
Results: The survey was completed by 1,041 respondents from 54 countries, mean age 41 (range 24-74), mostly male (n=670, 65%), and radiologists (n=719, 69%). A majority (n=819, 79%) indicated AI should be incorporated in residency programs, the remainder indicated maybe (n=182, 18%) or disagreed (n=40, n=4%). A small majority indicated that AI should (n=241, 23%) or maybe should (n=359, 35%) become a radiology subspecialty, while almost half (n=437, 42%) disagreed. Indicated hurdles to implementation were mainly ethical/legal issues (n=630, 61%), limitations in digital infrastructure (n=356, 61%), lack of knowledge (n=584, 56%) of stakeholders (i.e. clinicians, radiology staff, or management), and generalisability of AI algorithms (n=400, 38%).
Conclusion: A large majority of responders favours incorporation of AI into radiology training. Anticipated hurdles to implementation were mainly ethical and legal issues, and a lack of knowledge and generalisability issues, which is in concordance with key opinion leaders. Based on these results, incorporation of AI training in residency programs seems highly advisable, including ethical and legal aspects as well as methodology to ensure safe and effective use of AI.
Limitations: Selection bias is present, therefore the opinion of the population will be more moderate.
Ethics committee approval: n/a
Funding: No funding was received for this work.
Author Disclosures:
M. Huisman: nothing to disclose
E. R. Ranschaert: nothing to disclose
W. Parker: nothing to disclose
D. Mastrodicasa: nothing to disclose
M. Kočí: nothing to disclose
D. Pinto Dos Santos: nothing to disclose
T. Leiner: nothing to disclose
M. J. Willemink: nothing to disclose

RPS 605c-11 12:15

The influence of AI-based computer-aided diagnosis systems on diagnosis confidence in medical experts with different levels of experience

J. F. M. Gawlitza[1], P. Fries[1], P. D. A. Heinzl[2], A. Bücker[1], E. Jussupow[2]; *[1]Homburg/DE, [2]Mannheim/DE (joshua.gawlitza@uks.eu)*

Purpose: With the current developments in artificial intelligence (AI), the future work of radiologists is likely to change as computer-aided diagnosis programs (CAiD) will be part of work-a-day life. We hypothesised that the diagnosis confidence of medical experts using CAiD systems will alter regarding their different experience levels.
Methods and materials: We developed a virtual diagnosing environment with a DICOM viewer, quantified computed tomography, and lung function parameters. 29 medical professionals (students to clinic directors) were exposed to 3 cases of either severe emphysema or lung fibrosis in a randomised order. The aim was a binary diagnosis: “COPD” or “not COPD”. After a first control case, a diagnosis was suggested to the reader from the CAiD (either “AI suggests: COPD” or “[…] not COPD”). The suggestion was experimentally manipulated, so it was once correct and once false. Besides accuracy, confidence in diagnosis was measured after every case.
Results: Medical students started with a-priori confidence in diagnosing COPD of 60%. Correct diagnosis suggestion of the AI system boosted confidence to 75%, while incorrect AI suggestion led to a significant drop in confidence to 50% ($p = 0.012$). No significant difference was found between the latter and a-priori confidence. A similar pattern was shown for medical students of higher semesters (ANOVA $p = 0.004$). No significant differences were found for medical doctors (ANOVA $p = 0.651$).
Conclusion: Our results suggest diagnosis confidence is more likely to be influenced in less experienced medical experts through AI-suggestions, either correct or false. Future education programs should address this problem and inform young residents about the pitfalls and benefits of AI-based CAiD systems.
Limitations: A small sample size due to a complex comprehensive setup. Binary diagnosis (low depth).
Ethics committee approval: n/a
Funding: No funding was received for this work.
Author Disclosures:
J. F. M. Gawlitza: nothing to disclose
P. Fries: nothing to disclose
A. Bücker: nothing to disclose
P. D. A. Heinzl: nothing to disclose
E. Jussupow: nothing to disclose

14:00 - 15:30 **Room X**

Student Session

S 7

My educational or social project at my university

Moderator:
C. Stroszczynski; Regensburg/DE

S 7-1 14:05

A simplified method to estimate the energy spectrum for megavoltage photon beams by monoenergetic depth dose library

P. Chakraborty, H. Saitoh; *Tokyo/JP*

Purpose: Although Monte Carlo simulation by using the specification of the linear accelerator (LINAC) is the most common method to determine the energy spectrum, it consumes a lot of computing time and the treatment head specification is not always easy to obtain. Therefore, a simplified method was discussed in this study to estimate the energy spectrum that can reproduce the depth dose agreed with the measured data. To estimate the energy spectrum, a monoenergetic depth dose library was provided. Characteristics of the energy spectrum as a function of distance from the central axis were also described in this study.
Methods and materials: The monoenergetic depth dose of 0.1MeV to 11MeV was simulated using the DOSRZnrc code with a history of 1000000000 to obtain better statistical accuracy. The energy spectrum was reconstructed using the monoenergetic depth dose library and a GRG (generalised reduced gradient) non-linear function was performed repeatedly until a good agreement between the calculated and measured depth dose was obtained.
Results: The total relative difference of the reconstructed and measured dose distribution was less than 1%, which provides good accuracy in the energy spectrum estimation.
Conclusion: A simplified method to estimate the energy spectrum incident on the surface of a water phantom was successfully implemented, which can be used as a fast energy spectrum estimation technique to obtain an accurate calculation of dose distribution.
Limitations: n/a
Ethics committee approval: n/a
Funding: No funding was received for this work.
Author Disclosures:
P. Chakraborty: nothing to disclose
H. Saitoh: nothing to disclose

S 7-2 14:15
Reduction of microwave ablation needle-related metallic artefacts from virtual monoenergetic images using dual-layer detector spectral CT in rabbit VX2 hepatocellular carcinoma models
G. Wang[1], Z. Wang[1], X. Lu[2], Z. Jin[1]; [1]Beijing/CN, [2]Shenyang/CN (wangguorong_1022@163.com)

Purpose: To investigate the ability and the optimal energy level of virtual monoenergetic images (VMIs) to reduce microwave ablation needle-related metal artefacts by dual-layer detector spectral CT (DLSCT).
Methods and materials: A total of 20 rabbit VX2 hepatocellular carcinoma models that underwent DLSCT-guided percutaneous microwave ablation were analysed. Conventional 120 kVp polychromatic images and energy levels 40-200 keV (with increments of 20 keV) of VMIs were reconstructed. Two independent radiologists evaluated image quality objectively and subjectively (5-point Likert scale: 1=worst, 5=excellent). The CT value and standard deviation (SD) of the region of interest (ROI) on the chosen image were recorded, including the most significantly hypointense artefact (ROI_1), hyperintense artefacts (ROI_2), and distant liver tissue less affected by artefacts of the same slice (ROI_3). The image noise was defined as SD of ROI_1 (SD_1) and ROI_2 (SD_2). The metallic artefact-induced deviation of the attenuation value was defined as the variance in the absolute value of CT value (|CT1-CT3|, |CT2-CT3|). Statistical analysis was performed to compare the difference between 120 kVp conventional images and each energy level of VMIs.
Results: Compared with conventional images, VMIs showed significant lower SD_1 specifically at an energy level of 40 and 200 keV, and lower SD_2 when energy levels were at 140~200 keV ($P<0.05$). At 140~200 keV, the values of |CT1-CT3|, |CT2-CT3| were lower than those of conventional images ($P<0.05$). VMIs at 160~200 keV yielded higher subjective image scores than those of conventional images ($P<0.05$).
Conclusion: VMIs from DLSCT can obviously reduce microwave ablation needle-related metal artefacts in rabbit VX2 hepatocellular carcinoma models. Importantly, 200 keV may be the optimal energy level for reducing artefacts objectively and subjectively.
Limitations: The small sample size.
Ethics committee approval: Approval obtained from the animal board.
Funding: No funding was received for this work.
Author Disclosures:
G. Wang: nothing to disclose
Z. Wang: nothing to disclose
Z. Jin: nothing to disclose
X. Lu: nothing to disclose

S 7-3 14:25
Missed lung cancers on radiographs and CT
Å. S. Lyslo, A. P. Parkar; Bergen/NO (aaselyslo@gmail.com)

Purpose: To retrospectively assess the rate of missed lung cancer on radiographs/CTs to identify the type of errors that occur and correlate the results to international guidelines for recommended miss rates for radiological lung cancer diagnosis.
Methods and materials: A manual search in PACS of CT thorax examinations from 01/10/2017-31/03/2019 was performed. CTs for cancer follow-up were excluded. Cases with lung cancers/indeterminate lesions were collected. Prior examinations (cut-off 2yrs) were searched for and each case classified:
1. Lesion not visible/no prior examinations/correct follow-up.
2. Lesion not reported.
3. Lesions reported but misinterpreted.
4. Lesions reported correctly but insufficiently conveyed to a clinician.
5. Lesions reported and conveyed correctly, but insufficient clinical follow-up.
6. Technical issues.
The time-lapse due to missed diagnosis was recorded.
Results: 2,266 CTs were initially reviewed and 50 were found to have lung cancer or indeterminate lesions.
The radiological diagnosis was correct in 41 (82%) cases.
35 (70%) were from group 1.
4 (8%) were from group 2.
5 (10%) were from group 3
6 (12%) were from group 5.
No cases were from group 4/6.
Of the 4 missed lesions, 2 were located in the left hilum and 1 each in the right and left upper lobe. Of the 5 misinterpreted lesions, 2 were considered an infection, 2 fibrosis, and 1 calcification.
Of the 6 without sufficient follow-up, 2 were elderly with advanced cancer and unable to undergo treatment, 2 postponed treatment themselves, and 2 were truly not followed up despite radiologists' recommendation.
The time-lapse ranged from 2-24 months.
Conclusion: The overall missed rate of lung cancer fulfilled international recommendations (>75%). Misinterpretation was a major issue as well as misses in the hilum. Education and training need to focus on that.
Limitations: As CT examinations for cancer follow-ups were excluded, new cancers occuring there could have been missed.
Ethics committee approval: Ethics committee review and data protection regulations were followed.
Funding: No funding was received for this work.
Author Disclosures:
Å. S. Lyslo: nothing to disclose
A. P. Parkar: nothing to disclose

S 7-4 14:35
Fully automated quantification of left ventricular volumes and function in cardiac MRI: an evaluation of a deep learning-based algorithm
B. Böttcher, E. Beller, A. Busse, F. Streckenbach, M.-A. Weber, F. Meinel; Rostock/DE

Purpose: To investigate the performance of a deep learning-based algorithm for fully automated quantification of left ventricular volumes and function in cardiac MRI.
Methods and materials: We retrospectively analysed CMR examinations of 50 patients (74% men, median age 57 years). The most common indications were known or suspected ischaemic heart disease, myocarditis, or cardiomyopathies. Fully automated volumetric analysis of left ventricular volumes and function was performed using a deep learning-based algorithm. The analysis was subsequently corrected by a cardiovascular imaging expert as necessary. Manual volumetric analysis was performed by two radiology trainees. The time required for analysis was recorded. Volumetric results were compared using Bland-Altman statistics.
Results: The fully automated volumetric analysis was successfully completed in all patients in a median of 8.4 seconds. With expert review and corrections, the analysis required a median of 110 seconds. The median time required for manual analysis was 3.5 minutes for a cardiovascular imaging fellow and 9 minutes for a radiology resident. Compared with the expert-corrected results, the fully automated algorithm showed a mean deviation of -2.1% for end-diastolic volume, +3% for end-systolic volume, -10% for stroke volume, and -7.5% for ejection fraction. No corrections were necessary for 10 patients (20%). In the remainder, corrections were made on a median of 2 slices. The most common correction was related to inclusion or exclusion of slices at the apex or base of the left ventricle.
Conclusion: The deep learning-based algorithm allows for a fully automated analysis of left ventricular volumes and function with good accuracy. Although manual corrections are required in most patients for precise results, this approach is very time-efficient compared to manual analysis.
Limitations: A limited number of 50 cases.
Ethics committee approval: n/a
Funding: No funding was received for this work.
Author Disclosures:
B. Böttcher: nothing to disclose
F. Meinel: Consultant at Agfa-Gevaert Healthcare GmbH
M.-A. Weber: nothing to disclose
E. Beller: nothing to disclose
A. Busse: nothing to disclose
F. Streckenbach: nothing to disclose

S 7-5 14:45
The diagnostic accuracy of regadenoson perfusion cardiac magnetic resonance imaging in individuals with known or suspected coronary artery disease
A. Azcona[1], M. Roncal Redin[2], I. Soriano[2], A. Paternain Nuin[2], A. Ezponda Casajus[2], G. Bastarrika Alemañ[2]; [1]Zizur Mayor/ES, [2]Pamplona/ES (andoniazcona@gmail.com)

Purpose: To determine the accuracy and diagnostic performance of regadenoson-induced stress perfusion cardiac magnetic resonance (CMR) imaging in routine clinical practice.
Methods and materials: 403 consecutive individuals with known or suspected coronary artery disease underwent conventional stress/rest perfusion CMR in a 1.5-Tesla MR system (MAGNETOM Aera, Siemens Healthineers) for clinical indication. An intravenous bolus of regadenoson (0.4mg) was employed as a stressor. Stress perfusion CMR studies were visually assessed for perfusion deficits. CMR results were compared with invasive coronary angiography, considering positive 50% stenosis in at least one coronary vessel.
Results: A total of 402 individuals (305 males, mean age 64±11.8 years) were retrospectively evaluated. One patient could not complete the examination due to severe chest pain requiring nitroglycerin. Most frequently, the test was performed in patients with chest pain and prior coronary revascularisation (34.7%). Stress-CMR resulted as positive in 123 patients (30.6%) and negative in 279 (69.4%). Invasive coronary angiography was performed in 102

individuals. Compared with coronary angiography, regadenoson stress perfusion CMR showed a sensitivity of 94.5% (95% CI, 86.6%-98.5%), specificity of 82.8% (64.2%-94.1%), positive predictive value of 93.2% (86.1%-96.8%), negative predictive value of 85.7% (69.5%-94%), and accuracy of 91.2% (83.9%-95.9%).
Conclusion: Regadenoson stress perfusion CMR has a high diagnostic accuracy for the detection of significant coronary artery disease in routine clinical practice.
Limitations: A retrospective study.
Ethics committee approval: n/a
Funding: No funding was received for this work.
Author Disclosures:
A. Azcona: nothing to disclose
M. Roncal Redin: nothing to disclose
A. Paternain Nuin: nothing to disclose
A. Ezponda Casajus: nothing to disclose
G. Bastarrika Alemañ: nothing to disclose
I. Soriano: nothing to disclose

S 7-6 14:55
The establishment of a student sonography course: from zero to over 1,000 in 2.5 years
L. Müller, J. Weimer*; Mainz/DE*

Purpose: Sonography is often the first imaging technique undergraduate medical students become familiar with. In German medical school, the curriculum is no defined space for practical skills training in imaging. Until 2017, there was only one available sonography device for training without any form of instruction for all medical students between year 3 and 6 at the Johannes-Gutenberg University Mainz. This was the motivation for establishing a new *peer-to-peer* student sonography course (*Sono-For-Klinik*, Mainz).
Methods and materials: In early 2017, we trained 22 student tutors with the help of the Departments of Radiology and Internal Medicine. Furthermore, we wrote a script with over 180 pages and created several teaching materials. Course rooms with electronic equipment and sonography devices were provided by the Rudolf-Frey-Lernklinik Mainz. Moreover, we linked in with external clinical partners who provided us with images and expertise. A standardised questionnaire was used for the evaluation of the course. The gained practical skills of the students were verified with objective structured clinical examinations.
Results: The first course was able to start in summer, 2017, with 60 students. The number of participants reached 151 in the next semester. Today, 1,040 students have participated in the course and 42 tutors have been trained. New sub courses (e.g. with a focus on echocardiography or FAST) have been created. We were certified as an official course by the *DEGUM* (German Society for Sonography) in 2018.
Conclusion: The need for practical imaging skills is huge among undergraduate students. Since the establishment of the course, all of our course capacities have been occupied. Due to self-motivation, it was possible to feed this need and to establish our educational project with over 1,000 participants in 2.5 years.
Limitations: The retrospective design.
Ethics committee approval: n/a
Funding: No funding was received for this work.
Author Disclosures:
L. Müller: nothing to disclose
J. Weimer: nothing to disclose

S 7-7 15:05
Is gadolinium-enhanced imaging necessary in the surveillance of non-operated cranial meningiomata?
P. J. Shah, K. E. Twentyman, S. Currie, I. Craven*; Leeds/UK (kathryn.twentyman@hotmail.co.uk)*

Purpose: Gadolinium use is not without risk and economic cost. With patient safety of paramount importance and in this time of increasing health economic scrutiny, consideration must be given to alternative safer and less-expensive diagnostic and surveillance imaging techniques without sacrificing outcomes. This study's purpose was to evaluate whether T2-weighted imaging (T2-MRI) can provide an accurate alternative to gold-standard T1-weighted post-gadolinium imaging (Gd-MRI) in the assessment of non-operated cranial meningiomata.
Methods and materials: 90 meningiomata (30 skull base, 30 infratentorial, and 30 supratentorial) were identified from a tertiary neuroscience centre database. Two neuroradiologists independently measured the single maximal diameter of meningioma on either axial T2-MRI or Gd-MRI without reference to the other sequence. Observers were blind to previous measurements and clinical reports. This was repeated after a washout period (2 weeks) to permit intra and interobserver correlation. Bland–Altman plots evaluated the level of agreement (set at +/-1 mm) between meningioma measurements obtained on T2W-MRI and Gd-MRI.
Results: Neuroradiologists showed excellent intra and interobserver concordance on both Gd-MRI and T2-MRI (intra and inter ICC>0.9, irrespective of meningioma location). On Bland-Altman plots, the mean difference in measurements of supratentorial, infratentorial, and skull base meningiomata using T2-MRI and Gd-MRI were 0.46 mm, 0.78 mm, and 1.64 mm, respectively.
Conclusion: T2-MRI should be considered as an alternative to Gd-MRI in the surveillance of non-operated meningiomata located in the supra and infratentorial compartments. Change to the surveillance regime may provide health and economic benefits. Gd-MRI is still indicated in the assessment of skull base meningiomata. Skull base tumours are often intimately related to other complex anatomical structures and the use of Gd-MRI may enhance local soft-tissue contrast in order to better define tumour extent.
Limitations: A single-centre, consultant-only study with a small sample and differing protocols.
Ethics committee approval: n/a
Funding: No funding was received for this work.
Author Disclosures:
K. E. Twentyman: nothing to disclose
P. J. Shah: nothing to disclose
S. Currie: nothing to disclose
I. Craven: nothing to disclose

S 7-8 15:15
3D printed models: the new revolutionary tool in medical education
A. S. Constantinescu[1], E. Liciu[2]*; [1]Voluntari/RO, [2]Bucharest/RO (andconstef@yahoo.com)*

Purpose: The purpose of this study was to evaluate the efficiency of using different 3D-printed models and the CTs of the patients from which the models were created for teaching sectional anatomy to medical students. Our hypothesis was that in order to understand sectional or radiological anatomy one must first create a three-dimensional reconstruction of that structure in their mind. By creating a physical 3D reconstruction using the patient's own CT, we can make sure that the model we created is more accurate and that the learning process would, therefore, be much easier.
Methods and materials: Two 3D-printing technologies (Fused deposition modelling and stereolithography) were used to create the following models: scoliosis, pelvic bone, coronary arteries, 2 aorta models, heart, and a tumour model. During 5 hands-on workshops with a total of 50 student participants, we presented this subject and we also provided a 5 question questionnaire at the end that we used to interpret the results.
Results: 80% of the students completely agreed that the 3D-printed models were useful in understanding sectional anatomy. 76% would use a similar model of another structure for the same purpose. 82% would recommend using a 3D-printed model to another student or colleague. 76% of the students agreed that a lot of credibility to this study method was attributed to the models being an accurate representation of the patients anatomical structure and over 96% of them would like to see 3D-printed models being implemented in university courses.
Conclusion: In conclusion, the questionnaire results showed that 3D-printed models can be a learning bridge from conventional to sectional anatomy.
Limitations: This learning method is completely dependent on the lecturer's public speaking and teaching skills.
Ethics committee approval: n/a
Funding: No funding was received for this work.
Author Disclosures:
A. S. Constantinescu: nothing to disclose
E. Liciu: nothing to disclose

14:00 - 15:30 **Coffee & Talk 1**

GI Tract

RPS 701

Upper GI tract: what is new?

Moderators:
A. Laghi; Rome/IT
S. J. Withey; London/UK

RPS 701-1 14:00
An application study of CT perfusion imaging in assessing metastatic involvement of perigastric lymph nodes in patients with gastric cancer
Z. Sun, S. Hu, L. Shao, L. Jin*; Wuxi/CN (qiong953780@163.com)*

Purpose: This study used CT perfusion imaging (CTPI) technology to evaluate the diagnostic efficacy in differentiating metastatic from inflammatory perigastric lymph nodes in patients with gastric cancer.
Methods and materials: A total of 115 perigastric lymph nodes of 60 patients with gastric cancer confirmed by gastroscopy underwent CTPI scan before an operation. The scan data was post-processed by using commercial software to calculate perfusion parameters including blood flow (BF) and permeability surface (PS), and to measure the size of lymph nodes. According to the postoperative pathology result, the lymph nodes were divided into two groups: metastatic nodes and inflammatory nodes. Perfusion parameters and the size of lymph nodes between two groups were respectively compared statistically, and a ROC analysis was used to determine the optimal cutoff value with sensitivity, specificity, and area under the curve (AUC).
Results: Examined perigastric lymph nodes were metastatic in 65 and inflammatory in 50. Mean values of perfusion parameters in metastatic and inflammatory lymph nodes, respectively, were BF of 90.05 versus 79.31 ml/100 mg /min ($p < 0.01$), and PS of 42.19 vs. 35.89 ml/100 mg /min ($p < 0.01$). Mean values of the size in metastatic and inflammatory lymph nodes were 1.34 cm versus 1.16 cm ($p > 0.05$). The sensitivity of 81.5%, the specificity of 66.0 %, and AUC of 0.784 for BF with a cutoff value of 80.76 ml/100 mg /min for differentiating metastatic from inflammatory nodes were higher than those of PS or the size of lymph nodes ($P < 0.05$).
Conclusion: BF might be a more effective marker than PS or the size of lymph nodes for differentiating metastatic from inflammatory nodes in gastric cancer patients.
Limitations: The unknown cardiac output of patients might influence CT perfusion values.
Ethics committee approval: n/a
Funding: No funding was received for this work.
Author Disclosures:
Z. Sun: nothing to disclose
S. Hu: nothing to disclose
L. Shao: nothing to disclose
L. Jin: nothing to disclose

RPS 701-2 14:06

Virtual gastroscopy performed with stomach CT protocol and its role in the staging of gastric cancer: our experience

G. Fontanella[1], C. A. T. Manganiello[1], S. de Lucia[1], M. Mancinelli[1], A. Festa[1], B. Brogna[1], S. Borrelli[2]; [1]*Benevento/IT,* [2]*Avellino/IT*
(giovanni.fontanella@hotmail.com)

Purpose: To establish the role of our gastric CT protocol, with additional virtual gastroscopy navigation, in the staging of gastric cancer.
Methods and materials: Between August 2018 and September 2019, we selected 34 patients (mean age 64.2, 58.82% male) and scanned them in our 160 detector row system, using a dedicated CT protocol with standard gastric fluid distention obtained with a 2 litre diluted sodium amidotrizoate and meglumine amidotrizoate solution. The studies were reviewed by two radiologists with gastrointestinal and abdominal imaging experience, either in standard 2D or 3D navigation mode. The results were then compared for accuracy, specificity, and sensitivity with the pathology data.
Results: The lesions we detected were divided in three T groups: T1/T2 (44.11%), T3 (26.47%), and T4 (29.42%). Sensitivity values were 77.9% for T1/T2, 87.1% for T3, and 100% for T4 lesions. Specificity values were 100% for T1/T2, 83.2% for T3, and 92.3% for T4 lesions. Global accuracy values were 85.9% for T1/T2, 82.2% for T3, and 91.0% for T4 lesions. Nodal status was evaluated as well, with 23 N-positive patients (73.52%); nodal staging sensitivity, specificity, and accuracy values were 91.0%. 64.2%, and 75.7%.
Conclusion: Our CT protocol with fluid distention of the stomach and 3D virtual navigation has shown to have high sensitivity, specificity, and overall global accuracy in the staging of gastric cancer, especially for the T status in the early stages (T1/T2) and nodal status, allowing a more accurate therapeutic planning, especially concerning patients eligible for surgery.
Limitations: Our study is monocentric and based on a relatively small number of patients (34).
Ethics committee approval: All patients were orally instructed and signed written informed consent obtained.
Funding: No funding was received for this work.
Author Disclosures:
G. Fontanella: nothing to disclose
C. A. T. Manganiello: nothing to disclose
S. de Lucia: nothing to disclose
M. Mancinelli: nothing to disclose
A. Festa: nothing to disclose
B. Brogna: nothing to disclose
S. Borrelli: nothing to disclose

RPS 701-3 14:12

Deep learning CT-based radiomics for prediction of treatment response to neoadjuvant chemoradiation in oesophageal squamous cell carcinoma

C. Xie[1], Y. Hu[2], L. Han[2], J. Fu[2], V. Vardhanabhuti[1], K. Chiu[1]; [1]*Hong Kong/HK,* [2]*Guangzhou/CN*

Purpose: Neoadjuvant chemoradiotherapy (NCRT) plus surgery improves long-term survival of patients with locally advanced esophageal squamous cell carcinoma (ESCC). Treatment response prediction remains a great challenge. We aimed to evaluate the value of deep learning radiomics models based on computed tomography (CT) for predicting pathologic complete response (pCR) in ESCC patients receiving NCRT.
Methods and materials: We identified 161 patients with ESCC (mean age: 58, male: 83.5%, pCR: 46.0%). A total of 2048 deep learning radiomics features were analysed by the convolutional neural network (Xception) from CT images. After feature selection, a radiomics signature was built with an extreme gradient boosting (XGBoost) algorithm. Two models were built. Model A, for post-NCRT evaluation, incorporates both pre-NCRT and post-NCRT CT images into the analysis, while Model B, for pretreatment assessment, was built based on pre-NCRT CT images only.
Results: Model A comprised 9 selected features and showed good discrimination performance in test set for treatment response to NCRT, with an accuracy of 0.78, area under the receiver operating characteristic curve (AUC) of 0.89, sensitivity of 0.70, and specificity of 0.96. Calibration curves demonstrated good agreement between the prediction probability and the observed pCR (Hosmer-Lemeshow test, P-value = 0.66). Decision curve analysis confirmed the clinical benefits. Model B was also found to have predictive potential, with an accuracy of 0.67, AUC of 0.73, sensitivity of 0.87, and specificity of 0.62.
Conclusion: Deep learning radiomics analysis based on CT demonstrated promising predictive value for NCRT treatment response in locally advanced ESCC. Both pretreatment and post-NCRT models could be potentially used for treatment strategy decision-making.
Limitations: Future studies in larger prospective cohorts are needed to further confirm clinical practicability.
Ethics committee approval: n/a
Funding: Supported by Grant No. 179 from the Health Ministry of China.
Author Disclosures:
C. Xie: nothing to disclose
V. Vardhanabhuti: nothing to disclose
Y. Hu: nothing to disclose
J. Fu: nothing to disclose
K. Chiu: nothing to disclose
L. Han: nothing to disclose

RPS 701-4 14:18

Contrast MRI features in differentiating early invasive squamous cell cancer from mucosal high-grade neoplasia of the oesophagus

J. Qu[1], H. Zhang[1], X. Yan[2], S. Wang[3]; [1]*Zhengzhou/CN,* [2]*Shanghai/CN,* [3]*Xi'an/CN (qjryq@126.com)*

Purpose: To evaluate the diagnostic accuracy of contrast-enhanced MRI in the differentiation of mucosal high-grade neoplasia (MHN) from early invasive squamous cell cancer (EISCC) of the oesophagus.
Methods and materials: 32 study participants with MHN (n=18) and EISCC (n=14) of the oesophagus were enrolled in this prospective study. Postoperative histopathologic analysis was the reference standard. All participants underwent MRI (MAGNETOM Skyra, Siemens Healthineers, Erlangen, Germany). Two radiologists, blinded to participants' data, independently evaluated enhancement degree and enhancement pattern. Diagnostic performance of the two features was compared using the Chi-square test; kappa values were assessed for reader performance.
Results: Surgery was performed within 3.8+2.5 days after MR imaging. Inter-reader agreement on image quality was excellent (Kappa value=0.801~0.902 for three sequences, $P<0.001$), and the agreement on MR features was also excellent (Kappa value=0.831, $P<0.001$). All 4 mass-like MHN were "heart-shaped" in appearance. The combined two features provided the best sensitivity, specificity, and AUC of 100%, 94.1%, and 0.987, respectively. There was no significant difference between the degree of enhancement and the combination of the two features.
Conclusion: Contrast MRI can differentiate MHN from EISCC in oesophagus, with the presence of "heart-shaped" appearance favouring the diagnosis of MHN.
Limitations: Limited sample size, because most MHN was removed by EMR/ESD. Dynamic enhanced images features were not analysed in this study because it remains difficult to acquire good image quality of dynamic enhanced images of the chest.
Ethics committee approval: This study was approved by the Hospital Ethics Committee and all participants signed the written informed consent form.
Funding: No funding was received for this work.

Author Disclosures:
J. Qu: Speaker at the Affiliated Cancer Hospital of Zhengzhou University
H. Zhang: Author at the Affiliated Cancer Hospital of Zhengzhou University
X. Yan: Consultant at MR Scientific Marketing, Siemens Healthineers
S. Wang: Consultant at MR Scientific Marketing, Siemens Healthineers

RPS 701-5 14:24
Prognostic value of pretreatment computed tomography-defined tumour characteristics in patients with oesophagal neuroendocrine carcinoma: a preliminary result
Y. Zhou; *Zhengzhou/CN*

Purpose: To determine the prognostic significance of pretreatment CT-defined tumour characteristics in patients with oesophagal neuroendocrine carcinoma (NEC).
Methods and materials: A total of 89 patients who had confirmed oesophageal NEC were included in our database from September 2012 to July 2019. A baseline CT scan was obtained less than 1 week before treatment was performed. Basic morphological image features and clinical data including patients' age, gender, tumour length, location, the depth of wall thickness, clinical symptoms, immunohistochemical expressions, tumour invasion depth, lymph node metastasis, distant metastasis, treatment strategy, tumour margin, necrosis, calcification, morphological subtype, enhanced homogeneity, enhanced pattern, and enhanced degree were recorded. Potential prognostic factors of survival were evaluated using a univariate Cox proportional hazard model based on forward stepwise selection from the variables.
Results: The median overall survival was 45 (range, 24.6-65.4) months. Overall survival was censored in 18 patients. The univariate Cox regression analysis indicated that only the enhanced degree as an independent factor influenced the overall survival [Hazard Ratio, 0.53; 95% confidence interval (CI), 0.333-0.842] (P=0.007).
Conclusion: The CT enhanced degree on venous phase demonstrated improved predictive ability for predicting the overall survival of NEC after treatment.
Limitations: We created a prognostic model for 5-year overall survival, which is not the only interesting outcome variable. Pretreatment CT texture analysis and pathological response after treatment might be other variables of interest for future studies.
Ethics committee approval: This study was approved by the Institutional Review Board (IRB). All patients enrolled in this study provided informed consent.
Funding: No funding was received for this work.
Author Disclosures:
Y. Zhou: nothing to disclose

RPS 701-7 14:30
Staging of duodenal adenocarcinoma with CECT
G. Litjens[1], S. Radema[1], L. Brosens[2], C. J. H. M. van Laarhoven[1], E. J. M. van Geenen[1], J. J. Hermans[1]; *[1]Nijmegen/NL, [2]Nijmegen/Utrecht/NL (g.litjens@radboudumc.nl)*

Purpose: To determine the accuracy of staging duodenal adenocarcinoma (DA) with contrast-enhanced CT. DA represents over 50% of small bowel adenocarcinomas. Patients usually present with aspecific symptoms, causing significant delays in diagnosis. Currently, it is unclear what would be the optimal diagnostic workup in DA.
Methods and materials: Retrospective evaluation of TNM-stage of DA on portal-venous CECT in 50 patients.
Results: The tumour was visible in 90% (45/50) of patients, isodens in 46% (23/50), hypodens in 30% (15/50), hyperdens in 2% (1/50), and of mixed density in 12% (6/50). Tumours were localised in all segments of the duodenum, but mostly in the pars descendens (22/50=44%). 35 patients underwent surgery with curative intent, 28 were resected, and 7 had unexpected metastases (N=4) or local invasion (N=3). The T-stage of the 28 resected patients was correct in 13 (13/28=46%), overestimated in 2 (2/28=7%), underestimated in 10 (10/28=36%), and in 3 patients the T-stage could not be determined. Of the 28 resected patients, 21 had suspicious lymph nodes (LNs), but only 13 of these had positive LNs at pathology. Of the 7 patients without suspicious LNs, 3 had positive LNs at pathology. In 12% (6/50), tumours in the duodenum were missed on endoscopy. In 27 patients with MRI, tumour visibility and extension could be better determined on the HASTE than on CECT.
Conclusion: CECT is probably not sufficient for staging DA. Compared to pathology, CECT underestimates the T-stage and cannot reliably detect LN metastases, which are highly prognostic. Future research concerning additional imaging modalities is needed to improve staging DA. We suggest that MRI could be a potential candidate.
Limitations: Retrospective and therefore non-uniform data.
Ethics committee approval: Informed consent waived and study approved by ethical committee.
Funding: No funding was received for this work.
Author Disclosures:
G. Litjens: nothing to disclose
J. J. Hermans: nothing to disclose
E. J. M. van Geenen: nothing to disclose
S. Radema: nothing to disclose
L. Brosens: nothing to disclose
C. J. H. M. van Laarhoven: nothing to disclose

RPS 701-8 14:36
The Oxford 1000 barium swallow study: our experience
M. Chen, H. F. D'costa; *Oxford/UK (d.mitch.chen@gmail.com)*

Purpose: A barium swallow is a fluoroscopic test of the upper gastrointestinal tract. It involves the use of ionising radiation and is operator dependent with respect to radiation exposure, which can be reduced with staff training.
In this observational study, 1004 barium swallow cases were evaluated for the relationship between radiation dose and staff level of training, and correlated with the final clinical/histologic diagnoses.
Methods and materials:
Data from 1004 barium swallows performed at our centre (M:F = 411:593) were retrospectively collected.
The radiation dose was first compared with the national diagnostic reference level (NDRL) and then with the operator training level, categorised as first-year residents, advanced radiographers, senior residents and consultants. At our centre, first-year radiology residents are trained by the advanced radiographers to perform barium swallows. Senior radiology residents perform the test independently in most cases.
40% of patients have subsequently had an oesophagogastroduodenoscopy (OGD). The patients were categorised by their final diagnoses.
Results:
The findings show 80% of the cases performed are within the NDRL and established statistically significant correlation ($p<0.05$) between radiation dose level and operator training level. There was no significant correlation between dose and final diagnosis. All histologically confirmed cases of malignancy were noted on the initial barium swallow tests apart from one, demonstrating the high sensitivity of the latter for malignancy.
Conclusion: This study demonstrates that radiation dose, though largely within the accepted range, is lowest for consultant GI radiologists with no difference in pathology identification. Re-visiting consultant supervised barium training will help further lower the radiation exposure to patients. Barium swallow study remains a valuable imaging modality for evaluating oesophageal pathologies in 21st century medicine.
Limitations:
Single-centre study.
Ethics committee approval: n/a
Funding:
No funding was received for this work.
Author Disclosures:
M. Chen: nothing to disclose
H. F. D'costa: nothing to disclose

RPS 701-9 14:42
Utility of dynamic oesophagogram in the grading of achalasic patients: comparison with static x-ray barium swallow and correlation with clinical subtypes
G. Fontanella[1], C. A. T. Manganiello[1], M. Mancinelli[1], A. Festa[1], S. de Lucia[1], B. Brogna[1], S. Borrelli[2]; *[1]Benevento/IT, [2]Naples/IT (giovanni.fontanella@hotmail.com)*

Purpose: To establish the role of the dynamic oesophagogram in the grading of achalasia, in comparison with our standard static barium swallow protocol, and evaluate its correlation with clinical/manometric subtypes classification.
Methods and materials: Between June 2017 and June 2019, we selected 109 patients (mean age 61.4, 56.68% male) and evaluated them, both with our static (SBS) and dynamic barium swallow (DBS) x-ray protocol. The studies were reviewed in blind by two radiologists with gastrointestinal and abdominal imaging experience. The results were then evaluated for accuracy, specificity, and sensitivity, and compared with the manometric/clinical grading, our gold standard.
Results: The patients were divided into 4 radiological grades for both SBS and DBS, according to morphological criteria (I-IV), corresponding to three clinical subtypes (1-3; subtype 3 accomodating radiological grades III-IV). Sensitivity values ranged between 78.1-100% for SBS and between 96.3-100% for DBS. Specificity values were substantially similar for both SBS and DBS, ranging

between 58-97%. Subtype grading accuracy was significantly higher for DBS in Subtype I (82.3 vs 70.7%).
Conclusion: Our dynamic oesophagogram protocol, compared with our static dynamic swallow, has shown to have similar specificity, better sensitivity, and global accuracy for the diagnosis of achalasia. This has been linked to the much higher sensitivity in dysmotility detection shown by DBS. Grading definition accuracy is particularly high for DBS when compared with the manometric/clinical staging. These results are promising and DBS could help guide therapeutic choices through a more precise patient stratification.
Limitations: Our study is monocentric and the number of patients is limited (109).
Ethics committee approval: Our study received ethical committee approval and each patient signed informed consent before examinations.
Funding: No funding was received for this work.
Author Disclosures:
G. Fontanella: nothing to disclose
C. A. T. Manganiello: nothing to disclose
M. Mancinelli: nothing to disclose
A. Festa: nothing to disclose
S. de Lucia: nothing to disclose
B. Brogna: nothing to disclose
S. Borrelli: nothing to disclose

RPS 701-10 14:48

A non-invasive model for predicting the malignant potential for gastrointestinal stromal tumours by using contrast-enhanced ultrasonography with gastric distention

T. Li, M. Lu*; Chengdu/CN (635598031@qq.com)*

Purpose: It is difficult to accurately identify the risk level of gastrointestinal stromal tumours (GISTs) without surgical pathological confirmation. The purpose of our study was to propose a non-invasive prediction model for diagnosing GISTs by using contrast-enhanced ultrasound (CEUS) with gastric distention.
Methods and materials: We retrospectively reviewed 36 GIST patients who underwent CEUS from May 2017 to August 2019. All lesions were certificated by pathology after surgery. The age of the patient, size of the lesion, necrosis, calcification in the lesion, perfusion parameters including arrival time (AT), peak intensity (PI), time to peak (TTP), and area under the curve (AUC) of the lesion and surrounding normal tissue were analysed. Logistic regression analyse were performed.
Results: Of the 36 GISTs, 19 were high-risk and 16 low-risk tumours, respectively. Compared with low-risk GISTs, high-risk GIST had faster AT (7.3s vs. 11.9s, $p < 0.001$), higher PI (15.2dB vs. 12.2dB, $p < 0.05$), and larger size (4.2cm vs. 2.2cm, $p < 0.001$). In multivariate logistic regression, AT (＜9.04s, odds ratio [OR] 34.26, 95% confidence interval [CI] 1.69–694.83), PI (＞15.21dB, OR 44.63, 95% CI 0.86–2323.87), and size (＞2.4cm,OR 47.11, 95% CI 2.64–840.55) were independent predictors of high-risk GIST and low-risk GIST.
Conclusion: The size, AT, and PI of the GISTs on CEUS can be used as parameters for a non-invasive risk level prediction model of GISTs. This model may be helpful in identifying different levels of GISTs before surgery.
Limitations: 36 GISTs were not sufficient enough, a larger sample size should be involved in the future study.
Ethics committee approval: This study was approved by the Institutional Review Board and Ethics Committee of Sichuan Cancer Hospital.
Funding: No funding was received for this work.
Author Disclosures:
T. Li: nothing to disclose
M. Lu: nothing to disclose

RPS 701-11 14:54

Differential diagnosis and mutation stratification of gastrointestinal stromal tumours on CT images using a radiomics approach

M. P. A. Starmans, M. J. M. Timbergen, M. Vos, M. Renckens, D. J. Grünhagen, G. J. van Leenders, S. Sleijfer, J. J. Visser, S. Klein*; Rotterdam/NL (m.starmans@erasmusmc.nl)*

Purpose: Gastrointestinal stromal tumours (GISTs) are rare mesenchymal tumours of the gastrointestinal (GI) tract and difficult to diagnose. Here, we evaluate radiomics for 1) distinguishing GIST from other GI tumours, and 2) predicting the GIST c-KIT mutational status and mitotic index.
Methods and materials: Patients treated at the Erasmus MC between 2004-2017 with GIST or non-GIST GI tumours with a venous phase CT scan were included. A clinician segmented the tumours from which 424 radiomics features were extracted. Sex, age, and tumour location were collected. Prediction models for GIST versus non-GIST, presence of c-KIT mutation and type (exon9 or exon11), and mitotic index (≤ 5/50 high power fields (HPF) vs. > 5/50 HPF) were created through an automated search amongst a variety of machine learning algorithms to find the combination that maximises performance. The evaluation was implemented through 100x random-split cross-validation, with 80% of the data used for training and model optimisation and 20% for testing. For comparison, a subset was scored by a radiologist.
Results: The dataset consisted of 122 non-GISTs (schwannomas, leiomyosarcomas, leiomyomas, gastric cancers, and lymphomas) and 125 GISTs. The GIST versus non-GIST radiomics model had a mean area under the curve (AUC) of 0.72; adding location improved the performance to 0.83; adding age and gender did not improve the performance. The radiologist had a similar performance (AUC of 0.72). The c-KIT mutation models (c-KIT, exon9, and exon11) only predicted the absence of mutations. The mitotic index model had an AUC of 0.60.
Conclusion: Our radiomics approach proved useful for distinguishing GISTs from other GI tumours, with a performance similar to a radiologist, but could not predict the GIST c-KIT mutational status or mitotic index.
Limitations: Potential location bias.
Ethics committee approval: Erasmus MC IRB (MEC-2017-1187).
Funding: NWO (#14929-14930).
Author Disclosures:
M. P. A. Starmans: nothing to disclose
M. J. M. Timbergen: nothing to disclose
M. Vos: nothing to disclose
M. Renckens: nothing to disclose
D. J. Grünhagen: nothing to disclose
G. J. van Leenders: nothing to disclose
S. Sleijfer: nothing to disclose
J. J. Visser: nothing to disclose
S. Klein: nothing to disclose

RPS 701-12 15:00

Gastrointestinal stromal tumours (GISTs): an imaging perspective

P. Gupta[1], V. Choudhary[2]; [1]*Jammu/IN*, [2]*New Delhi/IN (puneetgupta619@yahoo.com)*

Purpose: To list the clinical features and imaging findings of GISTs and describe how GISTs can be diagnosed on the basis of the imaging findings.
Methods and materials: We reported 22 cases of pathologically and surgically proven GISTs at our hospital. The aim of this retrospective study was to review the imaging features of 22 GIST cases. We also describe the clinical and pathological findings of this well-recognised entity.
Results: Gastrointestinal stromal tumours (GISTs) are the most common mesenchymal tumours of the gastrointestinal tract. CT is the imaging modality of choice for diagnosing GIST at initial presentation, staging, and monitoring of the disease during and after the treatment. The aim of imaging is to locate the lesion, define its morphological characteristics, evaluate local invasion, and detect distant metastasis. CT is the imaging of choice for these purposes. Multidetector CT can pick up most lesions > 2 cm. CT is also superior for the staging of GISTs and monitoring the disease during and after treatment. Radiologists can often predict the correct diagnosis at presentation by the appearance of a large exophytic gastrointestinal mass without significant lymphadenopathy.
Conclusion: Gastrointestinal stromal tumours (GISTs), which arise from the interstitial cells of Cajal, are the most common mesenchymal tumours of the gastrointestinal tract. The increasing recognition of GISTs and prolonged survival of the patients with GISTs have made imaging increasingly important not only for diagnosis but also for monitoring the effects of treatment. Computed tomography (CT) is the imaging modality of choice for these purposes.
Limitations: n/a
Ethics committee approval: n/a
Funding: No funding was received for this work.
Author Disclosures:
P. Gupta: nothing to disclose
V. Choudhary: nothing to disclose

RPS 701-13 15:06

Development and validation of a nomogram based on CT images and 3D texture analysis for preoperative prediction of the malignant potential in gastrointestinal stromal tumors

C. Ren*; Shanghai/CN (rencaiyue@163.com)*

Purpose: The purpose of this study is to develop and validate a nomogram for preoperative prediction of the malignant potential in GISTs.
Methods and materials: A total of 440 patients with pathologically confirmed GIST after surgery were retrospectively analysed. They were divided into the training (n=308) and validation set (n=132). CT signs and texture features of each patient were analysed and a predictive model was developed using the lasso regression. Then a nomogram based on selected parameters was developed. The predictive effectiveness of the nomogram was evaluated by the ROC and AUC. C-index and calibration plots were formulated to evaluate the reliability and accuracy of the nomogram by bootstrapping based on internal and

external validity. The clinical application value of the nomogram was determined through the DCA.
Results: 156 GIST patients with low-malignant and 284 with high-malignant potential were enrolled. The prediction nomogram consisting of size, cystoid variation, and meanValue had an excellent discrimination both in training and validation sets (AUCs (95% CI): 0.935 (0.908, 0.961), 0.933 (0.892, 0.974); C-indices (95% CI): 0.941 (0.912, 0.956) , 0.935 (0.901, 0.982); sensitivity: 81.4%, 90.6%; specificity: 75.0%, 75.7%; accuracy: 88.0%, 88.6%, respectively). The calibration curves indicated a good consistency between the actual observation and nomogram prediction for differentiating GIST malignancy. DCA demonstrated that the nomogram was clinically useful.
Conclusion: This study presents a prediction nomogram which can be conveniently used to facilitate the preoperative individualised prediction of malignancy in GIST patients.
Limitations: This study was a single-centre retrospective study. The sample selection was biased in this retrospective study.
Ethics committee approval: n/a
Funding: Grant 81871347 from the National Natural Science Foundation of China.
Author Disclosures:
C. Ren: nothing to disclose

RPS 701-14 15:12
Development and validation of a risk model based on deep learning method for preoperative prediction of occult peritoneal metastasis in gastric cancer
D. Liu[1], Z. Huang[1], B. Wu[1], P. Yu[2]; [1]*Chengdu/CN*, [2]*Beijing/CN (18720998339@163.com)*

Purpose: To develop a risk model using a contrast-enhancement computed tomography (CECT) based on deep learning method to predict occult peritoneal metastasis (OPM) in patients with gastric cancer (GC).
Methods and materials: A total of 567 GC patients (training (OPM-positive n=55, OPM-negative n=340) and internal validation (OPM-positive n=24, OPM-negative n=148) cohort) were subject to develop the risk model based on deep learning method (Xception). All patients' OPM status was diagnosed as negative by CECT and later confirmed by laparoscopy or surgery (OPM-positive n=79, OPM-negative n=488). The region of interest was manually drawn along the margin of the primary tumour and extracted information reflecting phenotypes of the primary tumour. In the training cohort, we used 5-fold cross-validation and fuse for the prediction results obtained separately on the internal validation cohort. Receiver operating characteristics (ROC) and the area under ROC (AUC) were used to measure the model's discrimination and the decision curve analysis was used to compare the benefit of the model and all-laparoscopy and none-laparoscopy schemes on the internal validation cohort.
Results: The AUC yield was 0.8273 (median AUC, range in [0.8115-0.9950]), 0.7606 (median AUC, range in [0.7515-0.7727]) and 0.8558 for the cross-validation training cohort, cross-validation validation cohort and internal validation cohort. Decision curve analysis showed that if the threshold probability in the clinical decision was less than 50%, the patient would benefit more from our model than either of the all-laparoscopy or none-laparoscopy schemes.
Conclusion: Our model has an excellent prediction ability of OPM using only CECT and may have significant clinical implications in the early detection of OPM for GC.
Limitations: The region of interest was delineated in one single slice.
Ethics committee approval: This retrospective study was approved by the institutional review board of our hospital and informed consent was waived.
Funding: No funding was received for this work.
Author Disclosures:
D. Liu: nothing to disclose
Z. Huang: nothing to disclose
B. Wu: nothing to disclose
P. Yu: nothing to disclose

RPS 701-15 15:18
Gastrointestinal stromal tumours (GISTs): the relationship between preoperative imaging features on contrast-enhanced computed tomography (CECT) and pathologic risk stratification
S. Guerri[1], G. Danti[2], G. Grazzini[2], A. Masserelli[2], S. Pradella[2], V. Miele[2]; [1]*Bologna/IT*, [2]*Florence/IT*

Purpose: To evaluate the association between imaging features of gastrointestinal stromal tumours (GISTs) on preoperative contrast-enhanced computed tomography (CECT) and risk of relapse according to Miettinen's risk classification.
Methods and materials: The preoperative CECT of all patients with a pathologically proven diagnosis of GIST who underwent surgery between January 2008 and June 2019 were retrospectively reviewed. Exclusion criteria were recurrent GISTs, "paediatric-type" GISTs, and treatment with Imatinib prior to surgery. The following imaging features were analysed: growth pattern (exophytic/endoluminal/mixed), calcifications (presence/absence), necrosis (presence/absence), signs of ulceration or fistulisation (presence/absence), internal foci of haemorrhage (presence/absence), margins (irregular/well-defined), enlarged feeding or draining vessels (presence/absence), type of CE (homogenous/heterogeneous), degree of CE (marked versus mild and moderate), ascites (presence/absence), lymphadenopathy (presence/absence), peritoneal implants, and liver and other organs metastasis (presence/absence). The Chi-Square statistic was used to examine the correlation between different imaging features and pathologic risk classes of surgical resection specimens.
Results: 54 patients (29 men, 25 women; median age 65±11 years; range: 30-84 years) were included in the study for a total of 56 primitive GISTs: 5 (8.9%) no risk, 13 (23.2%) very low risk, 17 (30.4%) low risk, 8 (14.3%) moderate risk, and 13 (23.2%) high risk. Necrosis (p<0.001), ulceration or fistulisation (p=0.004), haemorrhage (p=0.007), margins (p=0.005), enlarged vessels (p<0.001), type of CE (p<0.001), and metastasis (p<0.001) were found to be associated with the Miettinen's risk group.
Conclusion: The presence of necrosis, signs of ulceration or fistulisation, internal foci of haemorrhage, irregular margins, enlarged vessels, heterogeneous CE, and metastasis were significantly associated with high risk of relapse and CECT imaging may be useful for risk stratification.
Limitations: Retrospective and observational study design.
Ethics committee approval: n/a
Funding: No funding was received for this work.
Author Disclosures:
S. Guerri: nothing to disclose
G. Danti: nothing to disclose
G. Grazzini: nothing to disclose
S. Pradella: nothing to disclose
A. Masserelli: nothing to disclose
V. Miele: nothing to disclose

14:00 - 15:30 **Studio 2020**

Radiographers

RPS 714

Hot topics in computed tomography and radiotherapy practice

Moderators:
N.N.
J. Reponen; Oulu/FI

RPS 714-1 14:00
Radiation therapists and occupational burnout: a national survey in Italy
P. Cornacchione[1], F. Fellin[2], C. Galdieri[3], D. Pasini[1], D. Lambertini[4], S. Durante[5], D. Catania[3], M. Zanardo[3]; [1]*Rome/IT*, [2]*Trent/IT*, [3]*Milan/IT*, [4]*Reggio Emilia/IT*, [5]*Bologna/IT (patriziacornacchione@gmail.com)*

Purpose: To investigate occupational burnout levels among radiation therapists (RTT) in Italy and the possible associations with socio-demographic factors.
Methods and materials: The Italian Association of Radiation Therapists (AITRO) and the Italian Federation of Scientific Radiographers Societies (FASTeR) proposed a national online survey including the Maslach Burnout Inventory to RTTs. Italian RTTs count around 2,000 individuals. Mann-Whitney U and c^2 tests were used.
Results: We obtained 246 answers, 106 (43%) respondents were men, RTT age was <30yo for 44 respondents (18%), 31-40yo for 73 (30%), 41-50yo for 63 (25%), and >50yo for 66 (27%), and 235 (95%) RTTs worked full-time. RTTs had an overall high median emotional exhaustion (EE) score (37, IQR 31-46), and high depersonalisation (16, IQR 13-21) compared to occupational burnout references (≥27 and ≥13, respectively). The median score of personal achievement (PA) (31, IQR 28-34) was comparable to the reference (≤31). Using a subgroup analysis, females had significantly higher levels of EE (p=0.003). Having sons and working with paediatric patients did not show an impact on occupational burnout (p>0.086). A total of 67 (27%) RTTs stated that a specific stress management course was available at their workplace and it appeared related to a reduced EE score (p=0.005), while 60 (24%) respondents declared that they relied on psychological support relating to a reduced EE (p=0.035). High levels of EE, depersonalisation, and low levels of PA were present in 235 (96%), 193 (78%), and 130 (53%) participants, respectively.
Conclusion: Italian RTTs' levels of burnout exceed the reference value, especially for EE and depersonalisation. Future interventions aimed at preventing burnout stressors should be implemented in the radiation therapy work environment
Limitations: An Italian survey.

Ethics committee approval: n/a
Funding: No funding was received for this work.
Author Disclosures:
P. Cornacchione: nothing to disclose
F. Fellin: nothing to disclose
C. Galdieri: nothing to disclose
D. Pasini: nothing to disclose
D. Lambertini: nothing to disclose
S. Durante: nothing to disclose
D. Catania: nothing to disclose
M. Zanardo: nothing to disclose

RPS 714-2 14:06
Development of a training program for 3D CBCT image verification in prostate cancer
C. L. Coelho[1], S. Pinto[2], A. Dias[2], C. Castro[1]; [1]Porto/PT, [2]Aveiro/PT

Purpose: Cone-beam computed tomography (CBCT) is an important tool in patient position verification before radiotherapy treatment delivery. The purpose of this study was the development of a training program directed to therapeutic radiographers based on a 3D CBCT treatment verification in prostate cancer.
Methods and materials: An initial sample of 51 therapeutic radiographers answered a survey and performed the image verification of 10 clinical cases before integration into the training program. Participants performed the analysis of the same CBCT images and answered a survey of 4 closed questions and an open one related to their perception about the training program. To evaluate the shifts resulting from the image analysis, the t-test was used for paired samples, comparing the mean absolute deviation (MAD) in the 4 directions of the couch mechanical movements.
Results: A sample of 41 therapeutic radiographers completed all phases. No statistically significant differences were found in general and in subgroups of <2 years and >2 years' experience with CBCT (p>0.05). Professionals with more than 10 years of experience revealed an improvement in image analysis after the training program, with differences in the vertical shift before and after (p=0.001). No relation was observed between years of experience and the level of confidence.
Conclusion: This training program structure shows a level of effectiveness considered satisfactory for its implementation, as there is an educational need to update the programmatical contents related to the cross-sectional pelvic anatomy. Since decision-making is vital for treatment delivery, critical analysis of CBCT, and improving patient outcomes, it is important to include these contents in clinical practice.
Limitations: n/a
Ethics committee approval: n/a
Funding: No funding was received for this work.
Author Disclosures:
C. L. Coelho: Employee at Instituto Português de Oncologia Francisco Gentil do Porto
S. Pinto: Employee at Escola Superior de Saúde da Universidade de Aveiro, Investigator at IBIMED Universidade de Aveiro
A. Dias: Employee at Departamento de Economia, Gestão, Engenharia Industrial e Turismo da Universidade de Aveiro
C. Castro: Employee at Instituto Português de Oncologia Francisco Gentil do Porto

RPS 714-3 14:12
Offline adaptive radiation therapy for prostate cancer: using daily CBCT and deformable image fusion for correct replanning
L. Capone[1], F. Lusini[1], L. Nicolini[1], F. Cavallo[2], D. Di Minico[2], G. Triscari[1], V. Forte[2]; [1]Rome/IT, [2]Mirabella Eclano/IT (caponel@upmc.edu)

Purpose: Modern radiotherapy equipment allows different strategies to be implemented online or offline. The purpose of this work is to define an offline ART procedure capable of guaranteeing a correct replanning in prostatic treatments according to objective evaluation parameters.
Methods and materials: The treatment protocol of prostate patients involves emptying the rectum and filling the bladder. Daily checks are performed using CBCT images. For this study, 18 prostate patients were selected (medium and low risk). The analysis was carried out using Velocity v4.0 software (Varian medical system) on patients subjected to replanning (group B) and others (group A). In order to allow an effective quantitative comparison, the Dice coefficient and statistical indices of dispersion and distribution were taken into consideration.
Results: Dispersion of percentages linked to the volume of the rectum is greater in the cases related to group A (IQR=5.72%; Q1=-3.98%; Q2=-0.66%; Q3=1.74%) than in group B (IQR=5.05%; Q1=-2.66%; Q2=0.02%; Q3=2.39%). The distribution of bladder percentage changes in group A produced IQR=11.80%(Q1=-10.12%; Q2=-5.49%; Q3=1.67%) while in group B IQR=9.07% (Q1=-3.57%; Q2=0.95%; Q3=5.51%). The Dice coefficient in group A showed a daily overlap of the bladder on average equal to 0.92±0.13, while in group B, 0.93 ±0.07. The volume of the rectum, in both groups, had an average Dice coefficient equal to 0.85±0.14.
Conclusion: The Dice coefficient is a useful index to establish whether localisation of the volumes is superimposable to CT sim data it considers only their geometrical overlapping. Volumes averages are important, especially for the bladder, which is more subject to changes of this type, rather than to variations in spatial localisation.
Limitations: Only prostate patients treated with 80Gy were selected for this study.
Ethics committee approval: n/a
Funding: No funding was received for this work.
Author Disclosures:
L. Capone: Speaker at UPMC SAN PIETRO
F. Lusini: Author at UPMC SAN PIETRO
L. Nicolini: nothing to disclose
F. Cavallo: Investigator at UPMC SAN PIETRO
D. Di Minico: nothing to disclose
G. Triscari: nothing to disclose
V. Forte: nothing to disclose

RPS 714-4 14:18
Radiation exposure levels used for planning and verification during prostate radiotherapy treatment
R. G. Monteiro, M. Mariano, J. Santos; Coimbra/PT
(raquelmonteiro--@hotmail.com)

Purpose: The significant advances in science, particularly in the radiation therapy (RT) field, have an important role in promoting and improving patient care and cancer treatments. During this, the patient is exposed to radiation related to the RT treatment but also to other examinations that must be quantified. The aim of this study is to characterise RT planning and verification of radiation exposure, excluding the dose values directly related to the treatment.
Methods and materials: The dose files related to computed tomography (CT) (Siemens®) and cone-beam computed tomography (CBCT) integrated on the linear accelerator TrueBeam (Varian Medical Systems®) of 60 patients with prostate cancer were analysed.
Results: A total of 1,252 exams were analysed and the mean values of DLP were 351.95 mGy for CBCT, 791.22 mGy for CT without current modulation, and 491.43 mGy for CT with current modulation.
Conclusion: The effective dose during the planning and verification of radiation therapy treatment is relevant. Optimisation of this imaging modality must be taken into account in order to reduce the patient risk.
Limitations: The results of this study are directly related to the radiotherapy equipment technology.
Ethics committee approval: Institution ethical approval obtained.
Funding: No funding was received for this work.
Author Disclosures:
J. Santos: nothing to disclose
M. Mariano: nothing to disclose
R. G. Monteiro: nothing to disclose

RPS 714-5 14:24
Analysis of radiotherapy performance using quality indicators derived from automated treatment pathways
L. Capone, F. Lusini, L. Nicolini, F. Cavallo, D. Di Minico; Rome/IT
(caponel@upmc.edu)

Purpose: Quality indicators and evidence-based measures of health care that can be used with administrative data to track performance and clinical outcomes are standardised. This study analyses the quality indicators needed in a cancer centre accredited by international JCI standards that use only electronic procedures for managing their patient workflow.
Methods and materials: Tasks and activities related to patient flow management have been identified and recreated digitally in the EMR according to the workflow carried out based on the JCI standards. The analysis was based on data from January 2019-August 2019. The quality indicators selected were staff compliance in the use of automated activities, percentages of completion with automatic care pathway activities, and waiting times between the different activities of the treatment paths from the first radiotherapy consultation to the treatment.
Results: Staff compliance in the use of automated activities was on average higher (91%) in the first 4 months compared to the second (80%), with a clear decline in July.
Percentages of completion of the activities show the adherence already acquired to the closure of some tasks such as the time out of radiotherapy treatments (92%) and the closure of the folder (43%).
The waiting times of the activities are on average always higher than our reference standard, but there is an improvement trend in all the activities analysed.

Conclusion: The EMR system allows you to accurately analyse the performance delivered in radiotherapy departments, creating versatile quality indicators which can be customised through the creation of adhoc care pathways, making it possible to achieve high-quality levels in the accreditation phase by international commissions and guarantee the monitoring of areas that need improvement.
Limitations: n/a
Ethics committee approval: n/a
Funding: No funding was received for this work.
Author Disclosures:
L. Capone: Author at UPMC San Pietro
F. Lusini: Author at UPMC San Pietro
L. Nicolini: Author at UPMC San Pietro
F. Cavallo: Author at UPMC San Pietro
D. Di Minico: Author at UPMC San Pietro

RPS 714-6 14:30

Evaluation of the reproducibility abdominal compression with termoplastic mask in adrotherapeutic treatment with carbon ions and respiratory gating

L. Anemoni, A. Mancin, C. M. I. Diegoli, A. Vai, V. Vitolo, F. Valvo, S. Tampellini, A. Barcellini*; Pavia/IT*

Purpose: To evaluate the reproducibility over time of abdominal compression with a thermoplastic mask, identifying the position of the diaphragm on computed tomography (CT), and comparing the image dataset acquired in the simulation phase with those related to intra-treatment revaluations in the same respiratory phase.
Methods and materials: A group of 5 patients treated with carbon ions and respiratory gating was considered. The breathing signal was acquired through a pressure sensor placed between the patient and the thermoplastic mask. The 4D image datasets were reconstructed in at least 4 respiratory phases: (0% ex), 30% inspiration (30% in), 30% expiration (30% ex), and end-inspiration (100% in). The diaphragm was contoured on the dataset correspond to the maximum expirio phase. On a weekly basis, an intra-treatment CT revaluation was acquired for checking the consistency of the patient's anatomy and setup, acquired in the same way as the CT baseline. The difference between the positions of the mass centre of the diaphragm between CT planning and CT revaluation at the maximum expirio phase ($P_{diaframma}$ = √(x_diafr^2+y_diafr^2+z_diafr^2)) was used to evaluate the reproducibility of abdominal compression.
Results: A different position of the centre of mass was observed (1.3 ± 0.3 cm). During CT revaluation, there was a greater abdominal compression which cranially moves the diaphragm as happens during treatment.
Conclusion: Increase the time to be allowed to elapse (e.g. half/full day) between the mask packaging and CT acquisition.
Limitations: Patients who struggle to keep a constant breath for at least 20 minutes.
Ethics committee approval: n/a
Funding: No funding was received for this work.
Author Disclosures:
L. Anemoni: Author at Fondazione CNAO
A. Mancin: Author at Fondazione CNAO
V. Vitolo: Author at Fondazione CNAO
S. Tampellini: Author at Fondazione CNAO
F. Valvo: Author at Fondazione CNAO
A. Barcellini: Author at Fondazione CNAO
A. Vai: Author at Fondazione CNAO
C. M. I. Diegoli: Author at Fondazione CNAO

RPS 714-7 14:36

Planning and verification of radiation exposure in head and neck radiotherapy treatment

M. F. N. Coelho, M. Mariano, J. Santos*; Coimbra/PT*
(joanasantos@estescoimbra.pt)

Purpose: During head and neck radiotherapy treatment, the patient is exposed several times to radiation in addition to the treatment dose. This exposure is related to the different stages of the radiotherapy workflow, the computed tomography (CT) planning, and the cone-beam CT (CBCT) used for the different verifications throughout the treatment. This study aims to quantify patient radiation exposure in different radiotherapy treatment stages, from diagnosis to the end of the process, excluding the treatment dose.
Methods and materials: The dose values of planned CT and CBCTs performed on adult patients with primary head and neck tumours from October 2018-March 2019 were directly collected on the scanners. The examination doses were analysed and compared with the tumour location and treatment fractionation clinical decisions.
Results: The majority of the patients performed 24 CBCT during the treatment and 33 treatment fractionations. In head and neck radiotherapy treatment, the planning CT was the procedure that involved the higher examination dose value in comparison with the total CBCT exposures.
Conclusion: If the obtained examination dose values from planning and verification imaging were included in the dosimetry calculations, no differences were found in treatment fractionation.
Limitations: The number of patients with head and neck tumours during the data collection period.
Ethics committee approval: Ethical approval was obtained from the centre.
Funding: No funding was received for this work.
Author Disclosures:
J. Santos: nothing to disclose
M. F. N. Coelho: nothing to disclose
M. Mariano: nothing to disclose

RPS 714-8 14:42

Evaluation of radiation dose and image quality for comparison of state-of-the-art intraoperative cone-beam CT and preoperative MSCT for spine surgery navigation

M. Fujii[1], K. Doi[2], J. Miyagawa[1], N. Tamaru[1], M. Taniguchi[1], Y. Fujinaga[1]*;*
[1]Matsumoto/JP, [2]Willowbrook, IL/US (m_fujii@shinshu-u.ac.jp)

Purpose: To compare the patient dose and image quality of state-of-the-art intraoperative cone-beam CT (CBCT; Artis Pheno, SiemensHealthineers, Germany) and preoperative multi-slice CT (MSCT; Lightspeed VCT, GE, USA) for spine surgery navigation.
Methods and materials: Radiation dose measurements were performed using a torso anthropomorphic phantom (RAN-100; Phantom Laboratory, USA) with optically stimulated luminescence dosimeters (GD-352M; Chiyoda Technol, Japan). The dosimeters were attached to various landmarks on the phantom surface, in the centre-plane, in the breasts regions, and in other organs at risk. Dosimeter measurements were repeated 3 times each for CBCT and MSCT, and for each clinical protocol at our institution. Image quality was evaluated with modulation transfer function (MTF), noise power spectrum (NPS), and contrast-to-noise ratio (CNR) using a Catphan 700 phantom (Phantom Laboratory).
Results: The measured average dose for CBCT and MSCT was 42.4mGy and 46.4mGy, respectively. The spatial frequency at 10% MTF for CBCT and MSCT was 1.22cycle/mm and 1.09cycle/mm. NPS value at 0.5cycle/mm for CBCT and MSCT was 368 and 196, respectively. CNR for CBCT and MSCT was 16.9 and 29.0, respectively.
Conclusion: In our clinical protocols, CBCT was found to have a 9% lower radiation dose than MSCT, without significant degradation in image quality. Therefore, the CBCT protocol is recommended for use in spine surgery navigation when it is available.
Limitations: One paired equipment study of CBCT and MSCT. A one institutional, phantom study.
Ethics committee approval: n/a
Funding: No funding was received for this work.
Author Disclosures:
J. Miyagawa: nothing to disclose
M. Fujii: nothing to disclose
N. Tamaru: nothing to disclose
M. Taniguchi: nothing to disclose
Y. Fujinaga: nothing to disclose
K. Doi: nothing to disclose

RPS 714-9 14:48

Safe administration of contrast media: adding shine to the shades of grey

R. Hassan, P. P. Wali, A. Chethan Kumar, S. Kanumukullakshminarayana, B. Singh, S. Gopalan, A. Nagadi, H. C. Chadaga, A. Kumar*;*
Bangalore/IN
(Rosmi.h@columbiaindiahospitals.com)

Purpose: To understand the proper guidelines regarding administration of iodinated and gadolinium-based contrast agents, particularly in patients with renal compromise, in pregnancy, and lactation, and to clarify misconceptions regarding the diagnostic usage of contrast media.
There is a lack of proper understanding among clinicians and radiologists about the guidelines and approach to contrast administration in various clinical scenarios, which can lead to unnecessary delay or avoidance of useful diagnostic studies. Contrast-induced nephropathy is grossly overestimated by both radiologists and clinicians. The risk of undergoing a non-diagnostic non-contrast CT is probably higher than the potential risk of developing CIN even in patients with eGFR <30 ml/min.
Methods and materials: We conducted an audit among the radiology departmental staff and clinicians regarding the basic principles of contrast administration with a questionnaire with 10 questions (1st audit). The response was assessed on the same day and results regarding awareness were analysed. Lectures were conducted for radiologists, technicians, and clinicians regarding

recent guidelines related to contrast administration following which a 2nd audit was conducted after 6 months. The response was assessed and the improvement in awareness and implementation in routine practice was reviewed.
Results: Significant improvement in awareness was observed in second audit results among radiologists (80% vs 100%), residents (70% vs 100%), technicians (50% vs 90%), and clinicians (30% vs 80%).
Conclusion: It is of utmost importance that radiology residents and radiologists have a good understanding of the basic principles of contrast administration.
It is essential to adequately educate and train the radiographers for the judicious utilisation and optimisation of radiological studies and to ensure smooth workflow.
Limitations: The attrition among the responders.
Ethics committee approval: n/a
Funding: No funding was received for this work.
Author Disclosures:
A. Chethan Kumar: nothing to disclose
R. Hassan: nothing to disclose
P. P. Wali: nothing to disclose
B. Singh: nothing to disclose
S. Kanumukullakshminarayana: nothing to disclose
S. Gopalan: nothing to disclose
A. Nagadi: nothing to disclose
H. C. Chadaga: nothing to disclose
A. Kumar: nothing to disclose

RPS 714-10 14:54
Systematic review and meta-analysis on risk factors and interventions to prevent contrast media extravasations in patients undergoing computed tomography
S. Ding, C. Campeanu, N. Richli, G. Gullo*; Lausanne/CH*

Purpose: To identify risk factors for contrast medium extravasation at the injection site and interventions to prevent or reduce damages.
Methods and materials: To find studies that included patients undergoing computed tomography performed with intravenous contrast, 9 databases were searched, including PubMed, CINAHL, and Embase. This review evaluated risk factors (patient demographics, comorbidities, and medication history) and interventions (e.g. contrast agent, injection per se, the material used for injection, and the healthcare professionals involved). Articles were assessed by two independent groups of reviewers for methodological validity using the Joanna Briggs institute system for the unified management (JBI SUMARI). In one case, quantitative data from two cohort studies was pooled in a statistical meta-analysis.
Results: 15/2,151 articles were selected. 2 were randomised controlled trials and 13 were quasi-experimental and observational studies. The quality of these studies was considered moderate to low. Being of female sex and inpatient status appeared to be risk factors for extravasation. Furthermore, the volume extravasated could be affected by the injection rate, venous access site, and catheter dwelling time. Preliminary studies seemed to indicate the potential of extravasation detection accessories to identify extravasation and reduce the volume extravasated. The other interventions either did not result in a significant reduction in the frequency/volume of extravasation or the results were mixed across the studies.
Conclusion: Potential risks were identified and areas for possible interventions such as the use of new catheters for injection. Further studies, however, should be conducted with solid methodological designs to allow the development of high-quality strategies to reduce the risks associated with extravasation.
Limitations: Statistical pooling was not always possible due to the heterogeneity of the studies.
Ethics committee approval: n/a
Funding: HES-SO.
Author Disclosures:
C. Campeanu: nothing to disclose
S. Ding: nothing to disclose
N. Richli: nothing to disclose
G. Gullo: nothing to disclose

RPS 714-11 15:00
The individualisation of CT-protocols for suspected pulmonary embolism: a national survey
A. Rusandu, B. Dymbe, E. V. Mæland, J. R. Styve*; Trondheim/NO (albertina.rusandu@ntnu.no)*

Purpose: Given the extensive use of CT in radiation-sensitive patient groups, such as pregnant and paediatric patients, and the importance of the CT-protocol tailoring for both radiation dose and image quality, the purpose of this study was to determine the extent to which individualisation of CT-protocols is practised across the country.
Methods and materials: The cross-sectional study involved collecting CT-protocols along with a mini-questionnaire in order to obtain additional information about how the CT-examination is individualised. All public hospitals performing CTs for detecting pulmonary embolisms were invited and 41% participated.
Results: Tailoring a standard protocol to different patient groups was more common than using dedicated protocols. Most of the available radiation dose reduction approaches were used. However, the implementation of these strategies was not systematic. Children and pregnant patients were examined without using dedicated CT-protocols or protocol adjustments focusing on a radiation dose reduction in 30% and 39% of the hospitals, respectively.
Conclusion: There is a need for practice optimisation, especially for developing dedicated CT-protocols or guidelines for tailoring the existing protocol to paediatric and pregnant patients.
Limitations: The senior CT-radiographer of the department who answered the questions might not always have extensive knowledge of all the adhoc protocol adjustments made by other radiographers. The extent of adjusting CT-protocols when examining children or pregnant patients might be higher than reported.
Ethics committee approval: The need for approval from The Regional Committee for Medical and Health Research Ethics and the Norwegian Centre for Research Data was waived as the project did not involve any health related or personal information. Participants were informed about the study's aim and that an e-mail reply containing attached CT-protocols would be regarded as implied consent to participation.
Funding: No funding was received for this work.
Author Disclosures:
A. Rusandu: nothing to disclose
B. Dymbe: nothing to disclose
E. V. Mæland: nothing to disclose
J. R. Styve: nothing to disclose

RPS 714-12 15:06
Stroke imaging: a multiphase CT angiography standard protocol for the improvement for hub-and-spoke hospital organisation
E. Stefani[1], M. Centenaro[2], L. Baldo[2], E. Delazer[2], M. Gambarotto[2], G. Molena[2], T. Nistor[2]*; [1]Conegliano/IT, [2]Treviso/IT*

Purpose: To create a standardised study protocol that can be applied to all CT scanners in a hub-and-spoke hospital organisation design to diagnose ictus cerebri and to promote training events for radiographers who work in the radiology department.
Methods and materials: A multi-professional working group has been created involving radiographers and radiologists with great experience in a hub centre and in 4 spoke hospitals in the same geographic area.
Data are from a 4-month long study and have been compared to literature of the same hospital design.
The technology available (6 CT scanners from 16-256 slice) has been analysed to define standard scanning techniques, reconstruction algorithms, window settings, and necessary reformations in order to produce comparable diagnostic images of the brain in all hospitals of the radiology department.
The multi-professional group planned a specific training for 60 radiographers working in CT imaging in order to share technical features of the new operating model.
Results: The new multiphase CT angiography protocol was defined.
2 major training events were realised with a 90% commitment to the project.
After that the new protocol has been adopted in the hub and in 3 out of 4 spoke hospitals, according to the technology available (with 16 slice-CT scanners, not all angiographic phases can be taken appropriately).
Reliability and reproducibility of diagnostic images produced in spoke hospitals increased and the repetition of unnecessary CT examinations, when patients with acute ischaemic stroke arrived at the hub hospital for treatment, has been largely avoided.
Conclusion: Multiphase CT angiography represents the gold standard when studying ictus cerebri in hub and spoke organisations. The use of standard protocol allows for a time-saving and widely available technique.
Limitations: n/a
Ethics committee approval: n/a
Funding: No funding was received for this work.
Author Disclosures:
E. Stefani: Author at AULSS 2 Marca Trevigiana
G. Molena: Author at Università degli Studi di Padova
T. Nistor: Author at Università degli Studi di Padova
L. Baldo: Author at Università degli Studi di Padova
E. Delazer: Author at Università degli Studi di Padova
M. Gambarotto: Author at Università degli Studi di Padova
M. Centenaro: Author at AULSS 2 Marca Trevigiana

RPS 714-13 15:12
Good practices for radiographers: patient installation and centring for brain-CTs
V. Berclaz, C. Chevallier, C. Bruguier, J.-B. Ledoux; *Lausanne/CH (Virginie.Berclaz@chuv.ch)*

Purpose: The importance of patient centring when performing a CT is essential to provide good image quality and to ensure radioprotection. Because of time constraints, CT scans performed in the emergency department may have poor patient installation and centring, and thus lower quality.
Methods and materials: This retrospective study analysed brain-CT scans during a three-month period performed on various CT scanners in our institution. Centring was evaluated using DoseWatch. Straightness was assessed using SSDE view scout in the same software in order to identify the use of a head support (foam cushion or CT-head holder). The inclusion criteria was a brain-CT with at least native acquisition.
200 cases were randomly selected and subsequently divided into emergency-CT scans (100 cases) and routine/elective CT scans (50 cases each, performed during working hours). The same analysis was carried out after a workshop discussion with the CT radiographer's team concerning the preliminary results.
Results: After the workshop, we observed a change in practice. Radiographers adopted the use of the head support to improve centring. The preliminary results showed that centring was overall good, but still with outliers demonstrating a misuse of the chosen head support. Initially, 1% of cases were performed with a CT-head holder in the emergency-CT compared to 25% for the routine/elective CT. After the workshop, it increased to 5% and 35%, respectively. Straightness improved by 15% for the foam head cushion and a significant decrease in the number of outliers was observed after the workshop.
Conclusion: Radiographers performed CTs with better quality after the initial evaluation followed by a workshop, which is an effective and low-cost solution to improve CT image quality.
Limitations: n/a
Ethics committee approval: n/a
Funding: No funding was received for this work.
Author Disclosures:
C. Bruguier: nothing to disclose
V. Berclaz: nothing to disclose
C. Chevallier: nothing to disclose
J.-B. Ledoux: nothing to disclose

RPS 714-14 15:18
CT scan anthropometric study of the frontal sinus for sexual diagnosis: first results from a documented osteological collection (Portugal, 19th-20th centuries)
P. M. Martins[1], R. C. M. C. R. Gaspar[2], A. Silva[1], B. Magalhães[2]; *[1]Aveiro/PT, [2]Coimbra/PT (pmartins@ua.pt)*

Purpose: A recent body of evidence from the literature around the world has shown that the human sinuses are sexually dimorphic, which may be very useful both in forensic and archaeological contexts. The main goal of the present study is to ascertain if this sexual dimorphism is also present in Portuguese individuals.
Methods and materials: The present study included 30 crania ([15 females, 15 males]; age-at-death ranges from 19-87 years old; $\bar{x}$=44.57, SD=16.85 [males $\bar{x}$=41.47, SD=15.51 and females $\bar{x}$=47.67, SD=18.09]) from the International Exchange Skull collection stored at the University of Coimbra (Portugal). CT scans were performed using a Siemens Somatom Emotion 16-CT scanner with a study protocol for imaging the paranasal sinuses. 6 linear measurements were taken in both right and left frontal sinuses (RF and LF weight; RF and LF height; RF and LF anteroposterior length) using RadiAnt DICOM Viewer 4.0.1 (64-bit). 3 volumetric measurements, the nasofrontal angle (NFA), and 3Dmeshes were obtained with ITK-SNAP software.
Results: 5 measurements resulted in higher means in males (one is equal in both sexes), although, no significant differences were found in all the linear measures and volumes taken in the frontal sinuses. Nevertheless, females had a significantly higher mean (Student's t=-2,453; d.f.=27; p=0.021) for NFA. Age at death does not seem to play a role in the present results (Student's t=-1.008; d.f.=28; p=0.322).
Conclusion: The present results question if dimorphic differences between sinuses may be specific to certain populations and show that NFA may be useful for sexual discrimination. In the future, the maxillary sinuses, as well as their morphology/shape, should also be considered as parameters of analysis for sexual discrimination. Also, a large sample size should be considered.
Limitations: n/a
Ethics committee approval: n/a
Funding: FCTFellowship SFRH/BD/102980/2014.
Author Disclosures:
P. M. Martins: nothing to disclose
R. C. M. C. R. Gaspar: nothing to disclose
A. Silva: nothing to disclose
B. Magalhães: nothing to disclose

RPS 714-15 15:24
Values-based radiography: what patients, radiographers, and managers value in their examinations and treatments
A. Newton-Hughes[1], R. Strudwick[2]; *[1]Salford/UK, [2]Ipswich/UK (a.newton-hughes@salford.ac.uk)*

Purpose: While values-based practice is promoted in healthcare, little is known about stakeholder values in diagnostic and therapeutic radiography.
Methods and materials: This small project used audio-recorded focus groups and individual interviews in two geographically remote regions to identify the values of patients, radiographers, and managers.
Results: The results suggest that patients value the interpersonal elements of the examination e.g. smiles etc., and while they also value safety and efficiency, they assume that they will experience these. Patients particularly valued being able to see their images and have questions answered. Radiographers value giving the patient a good experience and enjoy learning from them. Radiographers assume that patients value their honesty and the care they show. Managers value a patient-centred approach and are also influenced by the need for service quality, while the radiographers believe that managers value and appreciate their staff.
Conclusion: While patients value seeing their images and having their questions answered, they advised that in diagnostic radiography they were seldom given access to their images. Conversely, in therapeutic radiography, the patients were able to review their images and valued this highly. Diagnostic patients reported being left with unanswered questions, which was not the case for radiotherapy. Both patient groups valued welcoming communication and diagnostic patients reported that this is not what they experienced.
Radiographers report that they value giving the patient a good experience and earning their trust, but in diagnostic radiography this is not always the patient experience.
While therapeutic and diagnostic patients shared the same values, their reported experiences were different.
Limitations: The small sample size.
Ethics committee approval: University and IRAS approval gained with participants providing signed consent.
Funding: This presentation details the findings of a research project funded by the College of Radiographers and Industry Partnerships Scheme.
Author Disclosures:
A. Newton-Hughes: nothing to disclose
R. Strudwick: nothing to disclose

14:00 - 15:30 **Coffee & Talk 2**

Breast

RPS 702

Artificial intelligence, radiomics and more: part 1

Moderators:
O. H. Arponen; Tampere/FI
K. Pinker-Domenig; New York; NY/US

RPS 702-K 14:00
Keynote lecture
R. Schulz-Wendtland; *Erlangen/DE (ruediger.schulz-wendtland@uk-erlangen.de)*

Author Disclosures:
R. Schulz-Wendtland: nothing to disclose

RPS 702-1 14:10
Breast cancer detection in mammography using artificial intelligence: a large-scale retrospective evaluation
K. H. Kim, H.-E. Kim, H. Nam, B.-K. Han, H. H. Kim, E.-K. Kim; *Seoul/KR (khkim@lunit.io)*

Purpose: To assess the feasibility of artificial intelligence (AI) as an effective diagnostic-support tool for breast cancer detection in mammography in terms of overall diagnostic performance and false-positive-findings per image (FPPI).
Methods and materials: A total of 170,230 exams of 4-view digital mammograms were retrospectively collected from multiple institutions, where 36,468 were cancer, 59,544 were benign, and 74,218 were normal. An AI-based diagnostic-support tool was developed and evaluated on validation data from 3 countries: South Korea (KR; 619 cancer, 620 benign, 619 normal), the United States (US; 250 cancer, 250 benign, 250 normal), and the United Kingdom (UK; 218 cancer, 218 benign, 218 normal). Overall diagnostic performance was measured with area under the ROC curve (AUROC), sensitivity, and specificity.

Breast radiologists annotated biopsy-confirmed cancer lesions by referring to radiology and pathology reports, and FPPI was measured for cancer (FPPI-C), benign (FPPI-B), and normal (FPPI-N) breasts respectively to evaluate AI in terms of false-positive, which was known to be the fatal weakness of traditional CAD software.
Results: Per-exam, AUROC, sensitivity, and specificity was 0.970, 90.3%, and 91.7% for KR, 0.953, 93.6%, and 80.2% for US, and 0.938, 91.7%, and 76.8% for UK. For FPPI analysis, cancer-side, benign-side, both-side of breasts of cancer, and benign, normal exams were used. FPPI-C, FPPI-B, and FPPI-N were 0.353, 0.054, and 0.025 for KR, 0.370, 0.162, and 0.025 for US, and 0.320, 0.236, and 0.056 for UK.
Conclusion: The AI-based diagnostic-support tool developed from large-scale mammograms can be used for breast cancer detection on mammography. It achieved 0.94-0.97 of AUROC and >90% of sensitivity with low false-positive-findings per image, especially in normal exams.
Limitations: Real clinical value needs to be investigated via reader studies.
Ethics committee approval: Approved by IRB. Informed consent was waived.
Funding: Lunit Inc.
Author Disclosures:
K. H. Kim: Employee at Lunit
H.-E. Kim: Employee at Lunit
H. H. Kim: nothing to disclose
B.-K. Han: nothing to disclose
E.-K. Kim: nothing to disclose
H. Nam: Employee at Lunit

RPS 702-2 14:16
Breast cancer detection in screening mammography using artificial intelligence: a multicentre retrospective reader study
H.-E. Kim[1], K. H. Kim[1], E. H. Lee[2], B.-K. Han[1], H. H. Kim[1], E.-K. Kim[1];
[1]Seoul/KR, [2]Bucheon/KR

Purpose: To assess the feasibility of artificial intelligence (AI)-based diagnostic-support software and whether it can be used to improve a radiologist's diagnostic performance in breast cancer screening under European double reading guidelines.
Methods and materials: A total of 320 exams of screening mammograms were retrospectively collected from two institutions; 80 cancer (proven by biopsy), 32 benign (proven by biopsy or follow-up imaging), and 48 normal exams respectively from each institution. A multi-reader multi-case study was conducted with 7 breast radiologists. Each radiologist read each case without and then with the assistance of Lunit INSIGHT MMG, an AI-based diagnostic-support software. Readers decided whether each case needed to be recalled in their first reading and then modified their decision by referring to the output of the software. Radiologist's performance was evaluated in terms of sensitivity and specificity as follows: 1) single reading (software-unaided), 2) double reading (majority voting of 3 readers, i.e. average of 35 possible combinations of 3 out of 7 readers), and 3) single reading (software-aided). Software standalone performance was also measured.
Results: Average sensitivity and specificity of radiologists based on their binary decision (i.e. recall or not) were 1) single reading (software-unaided): 80.0% and 72.3%, 2) majority voting of 3 radiologists (double reading simulation): 81.9% and 75.4%, 3) single reading (software-aided): 86.3% and 73.8%. Standalone performance of the diagnostic-support software was 88.8% (sensitivity) and 81.9% (specificity).
Conclusion: Radiologist's diagnostic performance was significantly improved; without vs with assistance of the software: 80.0% vs 86.3% (P<.001) in sensitivity and 72.3% vs 73.8% (P<.05) in specificity. Software-assisted performance in terms of sensitivity was better than the majority voting of multiple radiologists.
Limitations: Real clinical value needs to be investigated via prospective studies.
Ethics committee approval: Approved by IRB. Informed consent was waived.
Funding: Lunit Inc.
Author Disclosures:
H.-E. Kim: Employee at Lunit Inc.
K. H. Kim: Employee at Lunit Inc.
E. H. Lee: nothing to disclose
B.-K. Han: nothing to disclose
H. H. Kim: nothing to disclose
E.-K. Kim: nothing to disclose

RPS 702-3 14:22
Reducing the radiologist's workload by detecting normal mammograms with an AI system
A. D. Lauritzen[1], A. Rodriguez-Ruiz[2], M. C. von Euler-Chelpin[3], E. Lynge[3], I. Vejborg[3], M. Nielsen[3], N. Karssemeijer[2], M. Lillholm[4]; *[1]København/DK, [2]Nijmegen/NL, [3]Copenhagen/DK, [4]Roedovre/DK (al@di.ku.dk)*

Purpose: To investigate whether an AI system can detect normal mammographies in a breast cancer screening cohort.
Methods and materials: This retrospective study analysed 18,020 doubly read studies from the Danish Capital Region breast cancer screening program, comprised of 143 screen-detected cancers and 447 non-cancer recalls (false-positives). Using the deep learning-based image analysis tool, Transpara v1.5, all studies were sorted into 10 categories based on findings from four views. A high category (10) indicated a high probability of malignancy, while a low category (1) indicated a very low probability of malignancy. Normal studies were identified as being in category 5 or less. This study examined the number of studies, and non-cancer recalls, that can possibly be avoided by detecting normal studies before radiologist reading.
Results: Using category 5 or less as a threshold, 10,545 (58.52%) studies were classified as normal. Included were 5 screen-detected cancers (3.5%) and 106 non-cancer recalls (23.71%). Category 1 and 2 comprised of 4,738 (26.29%) studies, 26 non-cancer recalls (5.82%), and 2 screen-detected cancers (1.36%). Category 1 comprised of 2,627 (14.58%) studies, 12 non-cancer recalls (2.68%), and 0 screen-detected cancers.
Conclusion: The results show that the AI system can successfully identify normal mammographies with very few missed screen-detected cancers. Furthermore, a substantial amount of false-positive studies were identified as normal. The results suggest that AI systems could potentially effectively and safely reduce the number of studies that radiologists would have to examine by a considerable amount, and several false-positives could be avoided.
Limitations: Transpara identifies a few screen-detected cancers as normal. Having radiologists examine missed cases, future improvements could be made. The number of cancer cases was limited. Results should be confirmed on a larger study.
Ethics committee approval: n/a
Funding: Partially Eurostars project IBSCREEN ref. 9715.
Author Disclosures:
A. D. Lauritzen: nothing to disclose
A. Rodriguez-Ruiz: Employee at ScreenPoint Medical
M. C. von Euler-Chelpin: nothing to disclose
E. Lynge: nothing to disclose
I. Vejborg: nothing to disclose
M. Nielsen: nothing to disclose
N. Karssemeijer: CEO at ScreenPoint Medical
M. Lillholm: nothing to disclose

RPS 702-4 14:28
The value of 2D-AI-based CAD for second or third reading tested on 17,910 screening mammograms
S. H. Heywang-Köbrunner, A. Jänsch, C. Mieskes, M. Hertlein, A. Hacker;
Munich/DE (sylvia.heywang@referenzzentrum-muenchen.de)

Purpose: To test the capabilities of a new 2D-CAD program based on artificial intelligence and deep learning algorithms for systematic consecutive screen reading.
Methods and materials: For this purpose, 18,002 consecutive screening mammograms acquired in our screening unit between 1/2018-11/2018 were anonymised and processed by the CAD system (iCAD Inc.).
A call was considered positive if the case threshold exceeded 30 (which is a more specific threshold) and a hit was visible within the lesion on at least 1 view. Ground truth for benign lesions was a benign screening result (based on independent double reading), a benign consensus reading of cases considered suspicious by at least one reader, or a benign result after complete workup of cases considered suspicious at consensus reading. Malignancies were proven by percutaneous biopsy and surgery. We counted one diagnosis per patient. Patients with bilateral cancers obtained 1 diagnosis per breast.
Results: We excluded 45 drop-outs due to incomplete work-up (refused etc.), 40 cases with B3 lesions and 7 mammographically occult malignancies detected incidentally during assessment or preoperative staging. The evaluation was patient-based; only patients with bi-lateral cancers were evaluated breast-based. Using a case threshold of 30 CAD achieved a sensitivity of 91.5% (for 32 DCIS and 85 inv. cancers) and specificity of 80.2%; reader1: 84.6% and 91.6%; reader 2 89.7% and 91.5%.
Conclusion: Achieved results justify hopes to use novel CAD systems for a second (e.g. in countries with a shortage of readers) or third reading in the near future. Human consensus reading remains indispensable.
Limitations: n/a
Ethics committee approval: Not necessary since completely anonymised data was used.
Funding: No funding was received for this work.
Author Disclosures:
A. Jänsch: Employee at Reference Center Mammography Munich
S. H. Heywang-Köbrunner: Author at Reference Center Mammography Munich
C. Mieskes: Employee at Reference Center Mammography Munich
M. Hertlein: Other at Reference Center Mammography Munich
A. Hacker: Employee at Reference Center Mammography Munich

RPS 702-5 14:34

Mammographic case conspicuity: a comparison between a radiologist's assessment and a masking index

S. Hickman[1], J. Mainprize[2], R. Black[1], J. Kaggie[1], Y. Huang[1], M. Yaffe[2], F. J. Gilbert[1]; [1]Cambridge/UK, [2]Toronto/CA
(sarah.hickman3@nhs.net)

Purpose: Cancers can be difficult to detect or even missed due to dense breast tissue. This study investigated the relationship between density, characterised using a masking index, lesion conspicuity, and evaluated subjectively, and cases found by only one reader in a double reading mammography screening system.
Methods and materials: Using the TOMMY trial dataset, the contralateral breast mammogram of 566 invasive cancer cases were analysed with a masking algorithm based on density and tissue arrangement. Two radiologists independently classified each cancer as either subtle or obvious, assigned a conspicuity score (1-3), and provided their decision to recall the case or not. Lesion size, radiological feature, and density as measured by a visual analogue score (VAS) was recorded. A generalised linear mixed-effects model was used to account for the non-negative skewed nature of the data to associate the masking index and the radiologist assessments. Size, density, and feature were fixed effects. Random effects included intercepts for subjects, the site of test, and lesion side.
Results: There were 58 subtle and 508 obvious invasive cancers (median age 62 years). Median lesion size was 13 mm [IQR 9-19 mm] with median density VAS 31 [IQR 20-50]. The masking index reduced by 25.9% (p <0.0001) from subtle to obvious cases. The reduction was 16.2% (p=0.017) after the adjustment for size, radiological feature, and density VAS. With lower density (VAS <50), the masking index reduced by 28.4% (p=0.0003) from subtle to obvious cases following adjustment. However, this was not demonstrated in cases with higher density (VAS >=50).
Conclusion: The masking index corresponds with the radiologist's assessment and could provide a quantitative measure to target supplemental imaging.
Limitations: Small subtle case sample size.
Ethics committee approval: Dataset from ethically approved TOMMY trial.
Funding: CRUK programme grant.
Author Disclosures:
S. Hickman: Research/Grant Support at Cancer Research UK
F. J. Gilbert: Research/Grant Support at GE Healthcare, Research/Grant Support at Bayer, Consultant at Google DeepMind
M. Yaffe: nothing to disclose
R. Black: nothing to disclose
J. Mainprize: nothing to disclose
Y. Huang: nothing to disclose
J. Kaggie: nothing to disclose

RPS 702-6 14:40

Acceptability of 3D printed breast models and their impact on the decisional conflict of breast cancer patients

L. Santiago, E. Arribas, B. E. Adrada, D. Black, C. Checka, J. Lee, R. Volk; Houston, TX/US
(Lumarie.Santiago@mdanderson.org)

Purpose: To evaluate the acceptability and impact of 3D printed breast models (3DM) on treatment-related decisional conflict (DC) of breast cancer patients.
Methods and materials: Patients with breast cancer were accrued in a prospective single-institution trial. All patients underwent contrast-enhanced breast MRI (MRI). A personalised 3D printed breast model (3DM) was derived from MRI. DC was evaluated pre and post 3DM review. Acceptability was assessed post 3DM review.
Results: Pre and post 3DM DC evaluation and 3DM acceptability assessment were completed by 25 patients. Bilateral 3DM was generated in 2 patients with bilateral breast cancer. The mean patient age was 48.8 years (28-72). Tumour stage was Tis (7), 1 (8), 2 (8) and 3 (4). The nodal staging was 0 (19), 1 (7), and 3 (1). Tumours were unifocal (15), multifocal (8), or multicentric (4). Patients underwent mastectomy (13) and segmental mastectomy (14) with (20) or without (7) oncoplastic intervention. 7 patients underwent neoadjuvant therapy. The mean pre and post 3DM DC scores were 16.6 (SD 15.3) and 10.0 (SD 13.2). There was a significant reduction in overall DC post 3DM review indicating patients became more assured of their treatment choice (p=0.001). DCS reduction post 3DM was also observed in the uncertainty (p=0.18), informed (p=.005), values (p=0.41), and effective (p=0.001) DCS subscales. No significant reduction was observed in the support of DCS subscale (p=0.148). 3DM acceptability was rated as good/excellent in understanding their condition, disease size, surgical options, encouraging to ask questions, 3DM detail, 3DM size, and 3DM impartiality.
Conclusion: 3DM are an acceptable tool to decrease decisional conflict in breast cancer patients.
Limitations: Small sample size.
Ethics committee approval: Institutional review board approval. Informed consent obtained.
Funding: John S. Dunn Sr. Distinguished Chair Grant and Robert D. Moreton Distinguished Chair Grant.
Author Disclosures:
L. Santiago: nothing to disclose
B. E. Adrada: nothing to disclose
D. Black: nothing to disclose
C. Checka: nothing to disclose
J. Lee: nothing to disclose
E. Arribas: nothing to disclose
R. Volk: nothing to disclose

RPS 702-7 14:46

Improving radiologist performance in breast cancer detection with the concurrent use of an artificial intelligence tool

S. Pacilè[1], J. Lopez[2], P. Chone[3], T. Bertinotti[4], P. Fillard[4]; [1]Valbonne/FR, [2]Newport Beach/US, [3]Oakland/US, [4]Paris/FR (spacile@therapixel.com)

Purpose: To demonstrate and estimate the benefits that an artificial intelligence (AI) tool could bring to the breast cancer detection performance of radiologists.
Methods and materials: The study was designed as a multi-reader multi-case investigation with fully-crossed design so that each case was read by each reader both with and without the aid of AI. It involved 14 participants who read a set of digital mammography (DM) images, half of them without AI and the other half with the help of AI during one first session and complementary cases during a second session. The used dataset included 240 cases (80 true positives, 40 false negatives, 80 true negatives, and 40 false positives).
The AI tool (MammoScreen v1.0.0, Therapixel) that was used is a system designed to identify suspicious regions for breast cancer on DM and assess their likelihood of malignancy. Area under the ROC curve and sensitivity were assessed as endpoints.
Results: Among readers, 11 (79%) increased their AUC using the AI system. The average AUC across readers was 0.769 when reading unaided and 0.797 when using the AI system. The average difference in AUC was 0.028 (95% CI: 0.002, 0.055 and p = 0035). Likewise, average sensitivity was shown to be increased by 0.033 when using AI support (p = 0.021). Figure 1-2 provide case examples where 9 radiologists detected small invasive cancers only using AI, avoiding making a false negative.
Conclusion: The overall conclusion of this study is that the performance of radiologists in reading mammograms is improved with the concurrent use of this new AI-based tool.
Limitations: n/a
Ethics committee approval: The investigation protocol was approved by an IRB.
Funding: The study was sponsored by Therapixel.
Author Disclosures:
P. Fillard: Founder at Therapixel
S. Pacilè: Employee at Therapixel
J. Lopez: Investigator at Hoag
P. Chone: Employee at Therapixel
T. Bertinotti: Employee at Therapixel

RPS 702-8 14:52

Validation of a deep learning-based breast density estimation tool on a Danish screening cohort in the context of personalised risk-based screening

A. D. Lauritzen[1], M. C. von Euler-Chelpin[2], E. Lynge[2], I. Vejborg[2], M. Nielsen[2], M. Lillholm[3]; [1]København/DK, [2]Copenhagen/DK, [3]Roedovre/DK
(al@di.ku.dk)

Purpose: To validate a fully automatic density estimation tool on a screening cohort in terms of agreement with radiologists' BI-RADS and cancer risk segregation.
Methods and materials: This study was based on the Danish Capital Region breast cancer screening program from November 1st, 2012, to December 31st, 2013. 4-view FFDMs were available for 53,956 women. The cohort's median age (IQR) was 59 (54-65) and the cohort comprised of 568 cancers. Radiologist's BI-RADS 4th edition scores were available from two readers. Using a deep learning-based fully automatic tool developed by the University of Copenhagen, all FFDMs were scored for planimetric percent mammographic density (PMD). The correspondence between two-reader consensus BI-RADS and PMD was evaluated in terms of Spearman correlation and, after categorisation of PMD, with weighted kappa statistics (WKS). The latter was compared to the readers' interobserver WKS. In terms of cancer risk segregation, the area under the ROC-curve (AUC) was compared for PMD and consensus BI-RADS, both with age as a covariate in a logistic regression model.

Results: The correlation between PMD and consensus BI-RADS was 0.85. The WKS between PMD and consensus BI-RADS was 0.693, and the radiologist inter-observer WKS was 0.692. The AUC for cancer risk was 0.60 (0.57-0.62) for PMD+age and 0.59 (0.56-0.61) for consensus BI-RADS+age.
Conclusion: PMD matched radiologists' BI-RADS in terms of the agreement between categorised PMD and consensus BI-RADS and the radiologists' interobserver agreement; both were substantial. For cancer risk segregation, there was no significant difference between consensus BI-RADS and PMD. Regarding personalised screening using mammographic density as a risk factor, the results suggest that automated PMD would work as well as consensus BI-RADS of two radiologists.
Limitations: The two readers work at the same clinic.
Ethics committee approval: n/a
Funding: Partially Eurostars project IBSCREEN ref. 9715.
Author Disclosures:
A. D. Lauritzen: nothing to disclose
M. C. von Euler-Chelpin: nothing to disclose
E. Lynge: nothing to disclose
I. Vejborg: nothing to disclose
M. Nielsen: nothing to disclose
M. Lillholm: nothing to disclose

RPS 702-9 14:58

Reproducibility of a semiquantitative scoring system to assess breast arterial calcifications (SSS-BAC) on mammography

A. Cozzi, R. M. Trimboli, M. Codari, C. B. Monti, C. Nenna, D. Spinelli, D. Capra, M. Alì, F. Sardanelli*; Milan/IT (andrea.cozzi@gmail.com)*

Purpose: To propose a semiquantitative score system for BAC assessment (SSS-BAC) and estimate its intra- and inter-reader reproducibility.
Methods and materials: In this retrospective study, consecutive women who underwent screening mammography at our centre from 01/01/2018 to 31/01/2018 were retrieved and included according to BAC presence. Two readers (R1 and R2) independently applied the SSS-BAC to both mediolateral oblique views, obtaining a score as the sum of: 1) number of calcified vessels (from 0 to n), 2) calcium burden (0 or 1), and 3) length of calcified vessels (from 0 to 4). R1 repeated the assessment two weeks later. Reading time was recorded for both readers on a subgroup of 10 subjects. Cohen κ statistics and Bland–Altman analysis were used to assess intra- and inter-reader reproducibility.
Results: Of a total 408 asymptomatic women who underwent mammography during the study period, 57 (14%) had BAC, so that 114 medio-lateral oblique views were assessed. Median final score was 4 (interquartile range [IQR] 3–4) for R1 and 4 (IQR 2–4) for R2 (P=0.417) while median reading time was 156 seconds (IQR 99–314 seconds) for R1 and 191 (IQR 137–292 seconds) for R2 (P=0.743). Bland–Altman analysis showed a 77% intra-reader reproducibility (bias 0.193, coefficient of repeatability [CoR] 0.955) and a 64% inter-reader reproducibility (bias 0.211, CoR 1.516).
Conclusion: SSS-BAC showed high reproducibility and was applied in about 2–3 min. It could be utilised in future studies to stratify cardiovascular risk and in trials for cardiovascular events prevention in the female population.
Limitations: Single-centre study. Only two readers.
Ethics committee approval: Ethics committee approval was obtained.
Funding: No funding was received for this work.
Author Disclosures:
A. Cozzi: nothing to disclose
R. M. Trimboli: nothing to disclose
M. Codari: nothing to disclose
C. B. Monti: nothing to disclose
C. Nenna: nothing to disclose
D. Spinelli: nothing to disclose
D. Capra: nothing to disclose
M. Alì: nothing to disclose
F. Sardanelli: Advisory Board at Bracco, Grant Recipient at Bracco, Grant Recipient at Bayer, Grant Recipient at General Electric, Speaker at Bracco, Speaker at Bayer, Shareholder at General Electric

RPS 702-10 15:04

Deep learning-based calcification segmentation for imperfect mammography data

M. Jie[1], M. Xu[1], X. Lin[1], Y. Zhang[2], Z. Cao[2], S. Wu[1], L. Huang[1], M. Wu[1], Y. Wang[1]; *[1]Shenzhen/CN, [2]Palo Alto/US (majie688@hotmail.com)*

Purpose: Calcification detection from mammograms plays a vital role in early breast cancer diagnosis. We propose an automatic calcification segmentation solution based on deep learning framework and a series of novel pre-processing methods.
Methods and materials: We develop a series of novel pre-processing methods to normalise mammogram images and encourage the consistency of labels, and then a modified U-Net framework was applied to segment calcifications. Firstly, mammogram images were pre-processed, including window adjustment, breast region extraction, and artefact removal. Small patches with the size of 512*512 were extracted from original mammograms. Then, based on the size and shape, the calcification labels were classified as three types: dots, vessels, and clusters. To encourage the consistency of labels, the patches containing vessels were excluded from the training data. Then, a U-Net model with group normalisation was trained using the processed data. Finally, the obtained best two U-Net models were ensembled to segment calcifications. The training and evaluation were performed on an in-house dataset consisting of 1,776 mammograms with calcifications. Calcifications in this dataset were annotated by two experienced radiologists. The data was randomly split as training (60%), validation (20%), and test data (20%), respectively.
Results: In our evaluation, a predicted calcification is assumed as detected if more than 25% area is covered by the label. Recall at 1 false-positive per image for the three calcification types (dots, vessels, and clusters) are 0.691, 0.971, and 0.912. In comparison, recall at 5 false positives per image for these three calcification types reach 0.918, 1.00, and 0.988, respectively.
Conclusion: The developed pre-processing methods and the modified U-Net framework can effectively segment various types of calcifications.
Limitations: The size of the database is limited.
Ethics committee approval: n/a
Funding: No funding was received for this work.
Author Disclosures:
M. Jie: Employee at Shenzhen People's Hospital
M. Xu: Employee at Shenzhen People's Hospital
X. Lin: Employee at Shenzhen People's Hospital
Y. Zhang: Employee at PingAn Tech, US Research Lab
Z. Cao: Employee at PingAn Tech, US Research Lab
S. Wu: Employee at Ping An Technology
L. Huang: Employee at Ping An Technology
M. Wu: Employee at Shenzhen People's Hospital
Y. Wang: Employee at Shenzhen People's Hospital

RPS 702-11 15:10

Workflow reduction and performance using an FDA cleared platform for mammography triage

A. Watanabe[1], V. D. Lim[2], L. N. Tanenbaum[3]; *[1]Manhattan Beach, CA/US, [2]La Jolla/US, [3]New York, NY/US (alyssa90266@gmail.com)*

Purpose: To assess performance and potential for workflow reduction using a deep learning triage algorithm.
Methods and materials: An FDA-cleared deep learning (DL) algorithm (cmTriageTM, CureMetrix, Inc.) was used to analyse two data sets of 2D mammograms. The first set was comprised of 400 biopsy-confirmed malignant cases and 855 negative cases from 4 institutions (with at least one-year follow-up as validation of benignity). The second set of 597 sequential screening mammograms was obtained at a single academic institution between July 1 and July 31, 2013.
Results: The overall AUC of the triage software is 0.95 (CI = [0.94, 0.96]). In the first simulation, at the default setting, cmTriage performed with a specificity of 77% and sensitivity of 93% (95% CI = [0.90,0.96]). At very high sensitivity of 99% with 95% CI = [0.97,1.00]), the specificity was 40% and 40% of the cases could have been removed from the worklist.
In the second study, there was a worklist reduction of 30% (at high sensitivity) to 63% (at default) of the screening mammograms.
There was 60% recall reduction at default and 32% reduction at high sensitivity (all false). There was a 11% reduction of benign biopsies at default. The recall rate would be reduced by 44% and 30% respectively with no loss in sensitivity at either operating point. There were no missed cancers at the high sensitivity setting.
Conclusion: Pre-analysis of mammograms using this triage software has the potential to significantly improve radiologist performance and enhance workflow and productivity without impairing sensitivity.
Limitations: This was a retrospective study. The sample size of the two data sets is limited and expansion to larger data sets is needed.
Ethics committee approval: n/a
Funding: No funding was received for this work.
Author Disclosures:
A. Watanabe: Consultant at Curemetrix, Shareholder at Curemetrix
V. D. Lim: Consultant at Curemetrix

RPS 702-12 15:16

Mammographic breast density assessment using deep learning especially for Asian women: clinical implementation

J. Liu[1], F. Yang[1], J. Tao[1], L. Shi[2], J. Lv[2]; *[1]Wuhan/CN, [2]Hangzhou/CN (liu_jie0823@163.com)*

Purpose: As high density in Asian women increases, the existing evaluation model of European and American women's breast density is not applicable in

China. The aim of this work was to investigate a deep learning (DL)-based breast density classifier to consistently distinguish the “dense” category.
Methods and materials: In this prospective study, we collected 2,548 digital mammograms from 637 women. An independent assessment of breast density was performed by four experienced radiologists to form a gold standard. We then used the gold standard to verify the performance of the existing AI model, which was based on the ResNet-18 neural network trained on the original interpretation of 80,156 digital screening mammograms.
Results: The DL model showed excellent accuracy (81%) and good agreement with radiologists in the test set (k = 0.67; 95% confidence interval [CI]: 0.64,0.70). The recall and precision were 49.42% and 66.15% in group A, 82.87% and 67.05% in group B, 86.00% and 87.83% in group C, and 67.65% and 96.72% in group D, respectively.
Conclusion: The proportion of each classification affects the accuracy of the training set. We got better performance in the test set of group D compared to other studies because of the higher proportion. Therefore our DL model is more suitable for Asian women (19% in training set and 12% in the test set of group D), which will help to establish the risk assessment models of breast cancer for Asian women.
Limitations: There is a lack of data for more regions in Asia, such as Korea and Japan, and we are going to do a multicentre study.
Ethics committee approval: n/a
Funding: No funding was received for this work.
Author Disclosures:
J. Liu: Speaker at Union Hospital of Huazhong University of Science and Technology
F. Yang: Author at Union Hospital of Huazhong University of Science and Technology
J. Tao: Author at Union Hospital of Huazhong University of Science and Technology
L. Shi: Author at Yitu Healthcare
J. Lv: Author at Yitu Healthcare

RPS 702-13 15:22
Deep learning-based mass segmentation in mammograms
M. Jie[1], M. Xu[1], X. Lin[1], Z. Cao[2], Z. Yang[2], S. Wu[1], L. Huang[1], M. Wu[1], Y. Wang[1]; [1]*Shenzhen/CN,* [2]*Palo Alto/US (majie688@hotmail.com)*

Purpose: Interpreting mammograms is an expertise-required task. We propose an improved encoder-decoder structured CNN model deeplab v3+ for automatic mass segmentation in mammography.
Methods and materials: We collected ~2,250 mammograms with mass lesions from three public datasets (CBIS-DDSM, INbreast, and Breast Cancer Digital repository (BCD) and 910 retrospective mammograms with mass lesions from an in-house dataset (Jan 2017 to May 2019). An encoder-decoder structured CNN, deeplab, integrated with atrous spatial pyramid pooling and atrous depth-wise convolution, was leveraged to segment masses. With Xception as the backbone, a novel pixel-wise focal loss was developed to further improve the detected mass contours. The CBIS-DDSM data and our in-house dataset were randomly split as training (60%), validation (20%), and test data (20%), respectively. The other two datasets (INbreast and BCD), along with the training subset of CBIS-DDSM, constituted the training set, while the validation and test subsets of CBIS-DDSM were the sole validation and test sets. The best model obtained using the public datasets was further fine-tuned on the in-house training data and then applied to the in-house validation and test data, respectively.
Results: The FROC curve of the deeplab model with Xception as the backbone and with the images downsampled by 3 was the highest. The baseline deeplab model reports 0.78 (Average Precision(AP)) and 0.883 (recall). Our best model reports 0.805 (AP) and 0.977 (recall) on the public test data, and 0.901 (AP) and 0.94 (recall) on the in-house dataset.
Conclusion: This study demonstrates a CNN-based segmentation model deeplab v3+, embedded with atrous spatial pyramid pooling and atrous depth-wise convolution, with Xception backbone, for effectively mass segmentation in mammography.
Limitations: The bias caused by race difference is not well considered.
Ethics committee approval: n/a
Funding: No funding was received for this work.
Author Disclosures:
M. Jie: Employee at Shenzhen People's Hospital
M. Xu: Employee at Shenzhen People's Hospital
X. Lin: Employee at Shenzhen People's Hospital
Z. Cao: Employee at PingAn Tech, US Research Lab
Z. Yang: Employee at PingAn Tech, US Research Lab
S. Wu: Employee at Ping An Technology
L. Huang: Employee at Ping An Technology
M. Wu: Employee at Shenzhen People's Hospital
Y. Wang: Employee at Shenzhen People's Hospital

Cardiac

RPS 703

Cardiac function: advanced imaging techniques

Moderators:
N.N.

RPS 703-1 14:00
4D-flow-derived mitral valve vortex ring: the relationship with left ventricular function
C. Kräuter[1], U. Reiter[1], C. Reiter[1], V. Nizhnikava[1], M. Masana[2], A. Schmidt[1], M. Fuchsjäger[1], R. Stollberger[1], G. Reiter[1]; [1]*Graz/AT,* [2]*Barcelona/ES*

Purpose: The mitral valve (MV) vortex ring is a swirling blood flow structure formed during diastole that is thought to store the kinetic energy of blood entering the left ventricle (LV). Cardiac magnetic resonance four-dimensional phase-contrast (4D-flow) imaging allows for the analysis of the MV vortex ring. The aim of this study was to investigate the relation of absolute and relative vortex ring kinetic energy with systolic and diastolic LV function parameters.
Methods and materials: 21 healthy subjects (male/female 7/14; age 59±7 years) underwent realtime-cine and 4D-flow imaging at 3T. LV volumetric function parameters (ejection fraction, ventricular volumes, and peak filling rates) were determined from realtime-cine series with routine software. Pre-processing of velocity data as well as the measurement of peak early-(E) and late-(A)-diastolic transmitral velocities were performed by prototype software (4DFlow, Siemens Healthcare). MV vortex rings were automatically detected and evaluated by in-house software. Dependencies of early- and late-diastolic peak absolute and relative kinetic energy ($Ekin_{abs,E}$, $Ekin_{rel,E}$, $Ekin_{abs,A}$, and $Ekin_{rel,A}$) on LV function parameters were assessed by correlation analysis.
Results: Early- and late-diastolic MV vortex rings were detected in each subject. While LV volumetric function parameters did not correlate significantly with vortex ring kinetic energy, early- and late-diastolic peak transmitral velocities (E=74±12cm/s, A=67±13cm/s) showed strong correlations with the respective peak kinetic energies ($Ekin_{abs,E}$=1.48±0.66mJ, r=0.86; $Ekin_{rel,E}$=67.7±24.4J/m^3, r=0.90; $Ekin_{abs,A}$=1.09±0.55mJ, r=0.89; $Ekin_{rel,A}$=57.8±23.3J/m^3, r=0.93). Furthermore, the E/A ratio (E/A=1.14±0.23) correlated strongly with the ratio of peak kinetic energies ($Ekin_{abs,E}/Ekin_{abs,A}$=1.61±0.87, r=0.80; $Ekin_{rel,E}/Ekin_{rel,A}$=1.32±0.64, r=0.84).
Conclusion: MV vortex ring kinetic energy demonstrated a strong relation with peak transmitral inflow velocities, suggesting the MV vortex ring as a promising structure for studying LV diastolic function.
Limitations: A small number of subjects.
Ethics committee approval: Medical University Graz (24-126ex11/12).
Funding: OeNB-Anniversary-Fund No.17934.
Author Disclosures:
C. Reiter: nothing to disclose
C. Kräuter: nothing to disclose
U. Reiter: nothing to disclose
V. Nizhnikava: nothing to disclose
M. Masana: nothing to disclose
A. Schmidt: nothing to disclose
M. Fuchsjäger: nothing to disclose
R. Stollberger: nothing to disclose
G. Reiter: Employee at Siemens Healthcare Diagnostics GmbH

RPS 703-2 14:06
Quantitative assessment of left ventricular regional myocardial strain changes in patients with coronary chronic total occlusion using cardiac magnetic resonance: a pilot study
K. Liu, Z. Li, C. Xia, K. Diao; *Chengdu/CN*
(634270986@qq.com)

Purpose: To investigate the differences of regional strain parameters between myocardial segments dominated by the occlusive and non-occlusive vessels in patients with coronary chronic total occlusion (CTO) using cardiac magnetic resonance (CMR).
Methods and materials: 42 patients (30 men, 66.5±8.2 years) with CTO confirmed by coronary angiography (CAG) were enrolled and underwent bSSFP cine CMR on a Siemens 3.0T MRI scanner. 3D regional strain parameters of left ventricular (LV) myocardial segments were measured using tissue tracking procedure on CVI42 software, based on a standardised 17-segment model of AHA. These parameters included regional radial, circumferential and longitudinal peak strain (PS), peak systolic strain rate (PSSR), peak diastolic strain rate (PDSR), and peak displacement (PD). The occlusive vessel was

determined by CAG results and a two-independent t test was used to analyse the difference of strain parameters between myocardial segments dominated by the occlusive and non-occlusive vessels.
Results: Compared with myocardial segments dominated by non-occlusive vessels, the above strain parameters of myocardial segments dominated by occlusive vessel all decreased. There were significant differences on radial PS [(33.52±15.13) % vs. (20.64±10.51)%, P=0.007], circumferential PS [(-17.48±4.89) % vs. (-14.45±6.72) %, P=0.037], radial PSSR [(2.95±2.32) s-1 vs. (1.36±0.98) s-1, P=0.04], circumferential PSSR [(-1.05±0.39) s-1 vs. (-0.85±0.38) s-1, P=0.034], radial PD [(6.15±2.13) mm vs. (4.60±2.01) mm, P=0.003], and longitudinal PD [(6.15±3.87) mm vs. (4.43±2.59)mm, P=0.034].
Conclusion: Strain analysis by CMR can quantitatively evaluate LV myocardial deformation and detect early cardiac regional dysfunction, which has potential clinical value for identifying ischaemic myocardial segments in CTO patients.
Limitations: A lack of studies on the diagnostic performance of strain parameters.
Ethics committee approval: This study was approved by Institutional Medical Ethics Committee of our institute. Written informed consent was obtained from all patients.
Funding: "1.3.5" project for disciplines of excellence, West China Hospital, Sichuan University, China (ZYGD18019).
Author Disclosures:
K. Liu: nothing to disclose
Z. Li: nothing to disclose
C. Xia: nothing to disclose
K. Diao: nothing to disclose

RPS 703-3 14:12

Academic challenge meets reality: the transfer of a cardiac ventricle segmentation algorithm to clinical data

C. Anastasopoulos[1], P. Full[2], T. Akıncı D'antonoli[1], F. Isensee[2], P. Haaf[1], K. Maier-Hein[2], J. Bremerich[1], B. Stieltjes[1], G. Sommer[1]; [1]*Basel/CH,* [2]*Heidelberg/DE*

Purpose: To investigate the predictive power of an award-winning deep-learning ventricle segmentation (DLVS) trained on a publicly available data-set if applied to a clinical data-set without further training.
Methods and materials: 899 cardiac MRI data-sets with short-axis steady-state free precession cines that had been semi-automatically segmented for clinical reading were retrospectively included. Reported left/right ventricular (LV/RV) volumes and ejection fraction (EF) served as ground truth. Parameters were recalculated using a fully automatic DLVS, which won the MICCAI Automated cardiac diagnosis challenge. Cases were classified as normal or pathologic using established thresholds for indexed end-diastolic volume (EDVi), EF, and mass.
Results: DLVS showed good correlation to reported values for LV-EDVi (R^2 0.95), LV-EF (R^2 0.83), and mass (R^2 0.82). For RV-EDVi (R^2 0.62) and RV-EF (R^2 0.29), prediction deviated from reported values. According to the reports, 485/899 cases had reduced LV-EF (<57%), which was predicted by DLVS with a 79% accuracy, 7% false-positive, and 33% false-negative rate (FPR/FNR). Reduced RV-EF (≤50%; 231 cases) was predicted with a 75% accuracy, 18% FPR, and 48% FNR. LV dilatation (EDVi males >105, females >96mL/m^2; 233 cases) was predicted with a 94% accuracy, 7% FPR, and 3% FNR. RV dilatation (EDVi m>121, f>112mL/m^2; 42 cases) was predicted with a 91% accuracy, 7% FPR, and 31% FNR. LV hypertrophy (m>176, f>140g/m^2; 208 cases) was predicted with a 89% accuracy, 2% FPR, and 40% FNR.
Conclusion: Automatic segmentation of a large clinical sample delivered satisfactory results, especially for LV-EDVi. Nevertheless, deviations for other parameters were substantial and consequently led to a prominent number of clinical misclassifications. This indicates a need for more clinically representative data in challenges.
Limitations: Clinical reading volumetric results might not be suitable as ground truth.
Ethics committee approval: Ethics committee approval obtained.
Funding: No funding was received for this work.
Author Disclosures:
C. Anastasopoulos: nothing to disclose
P. Full: Grant Recipient at Kaltenbach-Stipendium
T. Akıncı D'antonoli: nothing to disclose
F. Isensee: nothing to disclose
P. Haaf: nothing to disclose
K. Maier-Hein: nothing to disclose
J. Bremerich: nothing to disclose
B. Stieltjes: nothing to disclose
G. Sommer: nothing to disclose

RPS 703-4 14:18

Retro-gated compressed sensing cardiac cine imaging: sharper borders and accurate ventricular quantification in 60 seconds

B. Longere[1], L. Grenier[1], J. Pagniez[1], V. Silvestri[1], A. Simeone[1], M. Schmidt[2], C. Forman[2], F. Pontana[1]; [1]*Lille/FR,* [2]*Erlangen/DE (fpontana@gmail.com)*

Purpose: To evaluate a newly developed segmented retro-gated compressed sensing (CS-RG) cine sequence in comparison with conventional segmented retro-gated multi-breath-hold balanced SSFP (SSFP-REF) and real-time single-breath-hold compressed sensing cine (CS-RT).
Methods and materials: 30 adult patients referred for CMR underwent a protocol on a 1.5T scanner (MAGNETOM Aera, Siemens Healthcare) including at least a short-axis stack and one vertical and one horizontal long axis slice using (a) the reference retro-gated multi-breath-hold cine SSFP-REF, (b) the single-breath-hold CS-RT cine sequence, and (c) the 3-breath-hold CS-RG prototype sequence. Two readers independently assessed LV and RV end-diastolic volume (EDV), end-systolic volume (ESV), ejection fraction (EF), and LV mass for each sequence. Image quality was objectively compared using edge-sharpness measurements and subjectively rated with a 4-point scale.
Results: The mean scan time of SSFP-REF was 485.4 ±83.3s with a mean of 15.0 ±1.2 breath-holds vs 23.9 ±5.2s with CS-RT and 58.3 ±15.1s with CS-RG (p<0.0001). Analysis of variance demonstrates no significant difference regarding mean LV and RV volumes (EDV, ESV), or EF and LVM (p >0.17). All images were rated as diagnostic with a similar subjective image quality between CS-RG and SSFP-REF mainly rated as excellent (p=0.31), higher than the score mainly rated as good, with CS-RT (p=0.0008). CS-RG demonstrated a significantly better edge sharpness than CS-RT (0.083 ± 0.013pixel^{-1}vs 0.070 ±0.011 pixel^{-1}; p=0.0004) and no significant difference with SSFP-REF (0.075 ± 0.016pixel^{-1}; p=0.0516).
Conclusion: CS-RG cine provides an accurate quantification of LV and RV functional parameters in 3 breath-holds and in around one minute without compromising the sharpness of myocardial borders and image quality.
Limitations: No major limitation except sample size.
Ethics committee approval: Each patient gave informed consent.
Funding: No funding was received for this work.
Author Disclosures:
F. Pontana: Speaker at Siemens Healthcare, Speaker at GE Healthcare, Speaker at Bracco, Speaker at Bayer
B. Longere: nothing to disclose
L. Grenier: nothing to disclose
J. Pagniez: nothing to disclose
V. Silvestri: nothing to disclose
M. Schmidt: Employee at Siemens Healthcare
C. Forman: Employee at Siemens Healthcare
A. Simeone: nothing to disclose

RPS 703-5 14:24

The role of strain analysis in patients with suspicious arrhythmogenic cardiomyopathy

G. Muscogiuri[1], F. Ricci[2], L. Fusini[1], M. Guglielmo[1], A. Baggiano[1], A. I. Guaricci[3], G. Cicala[4], M. Pepi[1], G. Pontone[1]; [1]*Milan/IT,* [2]*Rome/IT,* [3]*Bari/IT,* [4]*Parma/IT (g.muscogiuri@gmail.com)*

Purpose: To evaluate biventricular strain in the early diagnosis of AC.
Methods and materials: We retrospectively evaluated 38 patients who underwent cardiac magnetic resonance and myocardial biopsy suggestive for AC between 2016 and 2019.
MR images were transferred to an off-line dedicated workstation and global longitudinal (GLS), circumferential (GCS), and radial (GRS) strain were calculated using a dedicated tool. After the evaluation of volumes and function, the population was divided based on MR imaging criteria for the diagnosis of AC (Model 1). Model 2 divided the population into two parts, using EF of left ventricle (LV EF)≥55% as a cut-off value. Model 3 identified patients with a positive biopsy and the absence of imaging criteria for AC plus LV EF≥55%.
All the MR parameteres were compared with a healthy population who underwent cardiac MR for other purposes. A p value < 0.05 was considered statistically significant.
Results: In Model 1, a statistically significant difference (p<0.01) was observed for GLS, GCS, and GRS of LV between the normal population and the population with a positive biopsy. Similarly, significant results of Model 1 were observed for RV in terms of GCS and GRS.
In Model 2, a significant difference of left ventricle GLS and GRS was observed between patients with a positive biopsy and LV EF ≥ or < 55%.
In Model 3, the GRS (p: 0.02) and GCS (p: 0.003) resulted in statistically significant differences compared to the normal population.

Conclusion: An analysis of strain could be extremely helpful for the identification of patients that do not satisfy the criteria for diagnosis of AC.
Limitations: The population was composed exclusively by patients with a positive biopsy. It would be interesting to include patients with a negative biopsy.
Ethics committee approval: In process.
Funding: No funding was received for this work.
Author Disclosures:
G. Muscogiuri: nothing to disclose
F. Ricci: nothing to disclose
L. Fusini: nothing to disclose
M. Guglielmo: nothing to disclose
A. Baggiano: nothing to disclose
A. I. Guaricci: nothing to disclose
G. Cicala: nothing to disclose
M. Pepi: nothing to disclose
G. Pontone: nothing to disclose

RPS 703-6 14:30
Compressed sensing 4D flow assessment of parameters of left ventricular diastolic function
G. Reiter[1], C. Reiter[1], N. Jin[2], F. Testud[3], C. Kräuter[1], D. Giese[4], A. Triebl[1], M. Fuchsjäger[1], U. Reiter[1]; [1]*Graz/AT,* [2]*Chicago/US,* [3]*Malmoe/SE,* [4]*Erlangen/DE (gert.reiter@siemens-healthineers.com)*

Purpose: Cardiac magnetic resonance four-dimensional (4D) flow imaging is a potential technique for the characterisation of left ventricular (LV) diastolic function, which could substantially benefit from a reduction of scan times. The purpose of the present study was to investigate if the acceleration of whole-heart 4D flow imaging by compressed sensing (CS) could be employed to derive standard parameters of LV diastolic function.
Methods and materials: 11 adult cardiac patients with regular heart rhythm were prospectively recruited for 3T (Magnetom Skyra, Siemens Healthcare, Erlangen, Germany), ECG- and navigator-gated whole-heart 4D flow imaging with CS (acceleration-factor=7.6), and without CS (parallel acquisition acceleration-factor=3). Protocols of the prototype sequence were matched for spatial resolution and the number of reconstructed frames. For both data sets, early- (E) and late diastolic (A) transmitral peak velocities, systolic (S) and diastolic (D) pulmonary venous peak velocities, as well as early-diastolic peak mitral annular velocity (e'), were evaluated using a prototype software (4DFlow, Siemens Healthcare, Erlangen, Germany). The corresponding parameters of LV diastolic function E/A, S/D, and E/e' were calculated. The relationships of the velocity-ratios derived with and without CS were investigated by means of correlation and Bland-Altman analysis.
Results: CS acquisition reduced scan time significantly (369±92 s vs. 618±119 s, p<0.01). Velocity-ratios from CS measurements (E/A=1.35±0.31; S/D=1.11±0.33; E/e'=11.7±4.7) exhibited no significant bias compared to respective results without CS (E/A=1.44±0.31, p=0.15; S/D=1.16±0.29, p=0.13; E/e'=11.8±4.8, p=0.92), demonstrated small standard deviations of errors (0.17, 0.10 and 2.6 for E/A, S/D and E/e', respectively), and correlated strongly (r=0.85, 0.96 and 0.85 for E/A, S/D and E/e', respectively).
Conclusion: Compressed sensing allows substantial acceleration of whole-heart 4D flow imaging without a significant impact on the evaluation of standard parameters of LV diastolic function.
Limitations: A small subject number.
Ethics committee approval: Medical University Graz (25-044ex12/13).
Funding: OeNB Anniversary-Fund 17934.
Author Disclosures:
G. Reiter: Employee at Siemens Healthcare Diagnostics GmbH
C. Reiter: nothing to disclose
N. Jin: Employee at Siemens Medical Solutions USA
F. Testud: Employee at Siemens Healthcare AB
C. Kräuter: Grant Recipient at OeNB Anniversary Fund
D. Giese: Employee at Siemens Healthcare GmbH
A. Triebl: nothing to disclose
M. Fuchsjäger: nothing to disclose
U. Reiter: nothing to disclose

RPS 703-7 14:36
Extra-cellular volume (ECV) of the left and right ventricle as a marker to triage diastolic dysfunction
A. Kapoor, G. Mahajan, A. Kapoor; *Amritsar/IN (masatulak@aim.com)*

Purpose: To evaluate the role of extracellular volume estimation to triage left ventricle diastolic dysfunction.
Methods and materials: Informed consent was taken from 100 consecutive new patients with stage II diastolic dysfunction tissue doppler echocardiography with preserved ejection fraction > 50%. Pro BNP levels, demographic data, and treatment details were noted.
ECV of the left and right ventricle (LV and RV) was determined on cardiac MR (Siemens 1.5T Amira) using T1 MOLLI plain and contrast study. Patients were categorised into three groups: Group I) with normal ECV of RV and LV (<27%), Group II) with abnormal ECV of LV and normal ECV of RV, and Group III) with raised ECV of RV and LV.
Patient follow-up was for one year to determine the occurance of readmission or mortal event.
Results: There were 67 males and 43 females with a mean age of 67 years. 32 patients were in group I, 48 in group II, and 20 in group III. The mean pro BNP levels raised in group II in 72% patients and in 100 % in group III (p value 0.5). The mean ECV of LV and RV in groups I, II, III were 22%, 32%, and 37%, and 23%, 24%, and 35%, respectively (p<0.05). The one-year readmission was 6%, 15%, and 40% in group I, II, and III patients (p<0.01).
Conclusion: ECV estimation of LV and RV can triage patients of LV diastolic dysfunction, which has a significant effect on first-year hospital readmission. Pro BNP levels show a poor correlation with ECV.
Limitations: A small cohort of patients with left ventricle dysfunction, short follow-up of one-year, and the non-use of other serum fibrotic markers.
Ethics committee approval: n/a
Funding: No funding was received for this work.
Author Disclosures:
A. Kapoor: nothing to disclose
G. Mahajan: nothing to disclose
A. Kapoor: nothing to disclose

RPS 703-8 14:42
Age and sex-related influences on left atrial phasic function in type 2 diabetes mellitus patients from a Chinese population: a feature tracking cardiovascular magnetic resonance imaging
M.-T. Shen, Z.-G. Yang; *Chengdu/CN*

Purpose: Left atrial (LA) phasic function is tightly linked to T2DM and confers key prognostic information. The influences of age and sex on LA phasic function using FT-CMR in T2DM patients is unclear. Therefore, we used FT-CMR to assess LA phasic function in T2DM patients based on age and sex.
Methods and materials: 150 T2DM patients (64% men; mean age, 53.43±11.02 years) were eligible for FT-CMR analysis. LA longitudinal strain and strain rate at systolic were εs and SRs, early diastolic were εe and SRe, and late diastolic were εa and SRa, which reflected reservoir, conduit, and pump function, respectively. All parameters were analysed by CVI42 and compared in terms of age and sex.
Results: Women demonstrated higher conduit function (εe: 13.36±3.63% vs. 11.77±3.23%, p=0.014; SRe: -1.50±0.41 vs. -1.32±0.44, p=0.023) and lower pump function (εa: 9.75±2.83% vs. 10.90±2.81%, p=0.048; SRa: -1.16±0.41 vs. -1.41±0.42; P=0.002) than men, while the reservoir function was similar. Women showed age-dependent more pronounced reservoir functional decay and pump functional augment than men (P for interaction, <0.05). Increasing age was independently associated with deteriorated conduit function and augment pump function, even after accounting for baseline clinical covariates in multivariable models that incorporated LA volume, LAEF, LVEF, LV global strain, and LV mass/end-diastolic ratio (all P<0.001).
Conclusion: Our findings suggest that women with T2DM demonstrated higher conduit and lower pump function than men with T2DM, and aging deteriorated conduit and increased pump function in both sexes, being more prominent in women at advanced ages, and was independent of baseline characteristics.
Limitations: A limited sample size.
Ethics committee approval: n/a
Funding: National Natural Science Foundation of China (81471721, 81471722, 81771887, 81771897), and 1·3·5 project for disciplines of excellence, West China Hospital, Sichuan University (ZYGD18013).
Author Disclosures:
M.-T. Shen: nothing to disclose
Z.-G. Yang: nothing to disclose

RPS 703-9 14:48
Myocardial mass corrected strain yields high diagnostic performance to differentiate between health and disease
M. C. Halfmann, S. Benz, T. Leckebusch, T. Klimzak, M. Michael, M. Larisch, C. Düber, K.-F. Kreitner, T. Emrich; *Mainz/DE (Moritz.Halfmann@gmx.de)*

Purpose: Correction of feature tracking (FT) derived strain values to myocardial mass lead to an improvement in the diagnostic power in acute myocarditis and hypertensive heart disease. The purpose of this study was to evaluate this concept in a large cohort of various cardiomyopathies in comparison to healthy volunteers.
Methods and materials: This study incorporated 444 data sets of healthy volunteers (n=127) and various cardiac diseases with and without depressed ejection fraction (n=317). CINE images in typical short- and long axis orientation were used to calculate traditional parameters of cardiac function and volumes, as well as FT derived strain values. Subsequently, strain values were corrected

to myocardial mass (strain-ratio). For post-processing, a dedicated cardiovascular software tool was used (cvi42, Circle, Calgary, Canada). ROC-Analysis was used to compare the diagnostic power to differentiate between health and disease.
Results: Global longitudinal rStrain showed the highest diagnostic power to differentiate between health and disease with an AUC of 0.904, resulting in a sensitivity and specificitiy of 82.8% and 82.6%. For differentiation of health and disease, rStrain clearly outperformed EF (ΛAUC: 0.20), EDV (ΛAUC: 0.43), myocardial mass (ΛAUC: 0.04), and "naked" longitudinal strains (ΛAUC: 0.15).
Conclusion: Myocardial mass corrected strains are a powerful method to discriminate between health and various acute and chronic cardiomyopathies.
Limitations: A single-centre study and retrospective study design.
Ethics committee approval: All patients provided written informed consent. The study was approved by the local ethics committee (2018-13520/837.196.13/837.477.14).
Funding: No funding was received for this work.
Author Disclosures:
T. Emrich: nothing to disclose
M. C. Halfmann: nothing to disclose
S. Benz: nothing to disclose
T. Leckebusch: nothing to disclose
T. Klimzak: nothing to disclose
M. Michael: nothing to disclose
M. Larisch: nothing to disclose
C. Düber: nothing to disclose
K.-F. Kreitner: nothing to disclose

RPS 703-10 14:54

Global myocardial strains in pulmonary hypertension: association with severity of the disease

V. Nizhnikava, G. Reiter, U. Reiter, C. Reiter, C. Kräuter, G. Kovacs, H. Olschewski, M. Fuchsjäger*; Graz/AT (volha.nizhnikava@gmail.com)*

Purpose: Pulmonary hypertension (PH) is associated with left (LV) and right ventricular (RV) functional and myocardial alterations. Cardiac magnetic resonance (CMR) cine-imaging is used not only for the assessment of volumetric function but also for the determination of myocardial strain parameters.
The aim of the study was to compare associations of feature-tracking derived myocardial strain parameters with mean pulmonary arterial pressure (mPAP) and volumetric function in patients with PH.
Methods and materials: 34 patients with PH underwent right heart catheterisation for mPAP assessment (mPAP=44±11mmHg) and CMR cine realtime free-breathing imaging at 3T (Skyra, Siemens Healthcare) within 1±3 days. LV and RV volumetric parameters were evaluated from short-axis slices (Argus, Siemens Healthcare). Global radial (GRS), circumferential (GCS), and longitudinal (GLS) LV and RV strains and strain rates (GRS_{rate}, GCS_{rate}, and GLS_{rate}, respectively) were assessed from short-and four-chamber series (cvi42, Circle Cardiovascular Imaging) using a two-dimensional approach. Relations between parameters were analysed by regression and correlation analysis.
Results: Significant correlation with mPAP was found for the following strain parameters: RV-GRS (r=-0.43), systolic RV-GRS_{rate} (r=-0.41), RV-GCS (r=0.41), systolic LV-GRS_{rate} (r=0.42), and systolic LV-GCS_{rate} (r=-0.42).
All strain parameters correlated more strongly to respective ejection fraction (EF) than to mPAP: RV-GRS (r=0.62), systolic RV-GRS_{rate} (r= 0.45), and RV-GCS (r=-0.62) with RV-EF; systolic LV-GRS_{rate}(r=0.63) and systolic LV-GCS_{rate} (r=-0.54) with LV-EF. With the respective EF as the covariate, only partial correlations of LV strain parameters with mPAP remained significant (r=0.46 for systolic LV-GRS_{rate}, and r=-0.46 for systolic LV-GCS_{rate}).
Conclusion: In PH patients, global LV and RV strain parameters are more strongly associated with ventricular function than with the severity of PH. Consistent correlations of LV systolic strain rates with mPAP might be related to septal bowing.
Limitations: A single-centre study.
Ethics committee approval: NCT01725763.
Funding: OeNB-Anniversary-FundNr17934.
Author Disclosures:
G. Reiter: Employee at Siemens Healthcare Diagnostics GmbH
V. Nizhnikava: Grant Recipient at ESOR Fellowship
U. Reiter: nothing to disclose
C. Reiter: nothing to disclose
G. Kovacs: nothing to disclose
C. Kräuter: Grant Recipient at OeNB Anniversary Fund
H. Olschewski: nothing to disclose
M. Fuchsjäger: nothing to disclose

RPS 703-11 15:00

Feasibility and value of right atrial strain in patients with inoperable chronic thromboembolic pulmonary hypertension (CTEPH)

V. Bethke, A. Hasse, M. Richter, A. Brose, C. Liebetrau, C. B. Wiedenroth, K. Tello, G. Krombach, F. Roller*; Giessen/DE*

Purpose: Ventricular strain analysis showed promising results in patients with pulmonary hypertension. In contrast, right atrial (RA) strain is not yet well investigated. Therefore, the aim of this study was to assess the feasibility and value of RA strain in patients with inoperable chronic thromboembolic pulmonary hypertension.
Methods and materials: MRI at 1.5 Tesla and right heart catheterisation were performed before and 6 months after BPA in 30 consecutive CTEPH patients (mean age 63.4±10.6 years; 17 female). RA feature tracking strain analysis was performed (global longitudinal (GL) and global radial (GR)) and compared to 30 control patients (mean age 56.6±9.5 years; 19 female). Results were also correlated to right ventricular function (RVEF) and measures of pulmonary haemodynamic (mPAP and PVR).
Results: RVEF, mPAP, and PVR significantly decreased after BPA (all p<0.0001). Moreover, RA strain parameters decreased significantly after BPA (GL -15.1±6.9 to 18.5±4.8, p < 0.0005; GR 27.7±12.2 to 37.0±12.8, p=0.0001) and were significantly lower compared to the controls (GL -21.7 ± 5.2 and GR 49.3±19.5; p<0.0001). GR strain revealed a moderately significant correlation to RVEF (before BPA r=0.35; after BPA r=0.42, p=0.019), whereas only slight correlation trends to pulmonary haemodynamic (mPAP, PVR) were present.
Conclusion: RA strain was significantly lower in CTEPH patients compared to controls. Beside significant improvement of RV function and pulmonary haemodynamic, BPA also significantly improved RA strain. Moreover, RA strain showed a moderate correlation to RVEF. In addition to ventricular strain analysis, RA strain might enable new insights regarding atrioventricular coupling, therapy-effects, and monitoring and prognosis in CTEPH.
Limitations: A small study cohort.
Ethics committee approval: n/a
Funding: No funding was received for this work.
Author Disclosures:
V. Bethke: Author at UKGM
A. Hasse: Author at UKGM
M. Richter: Author at UKGM
A. Brose: Author at UKGM
C. Liebetrau: Author at UKGM
C. B. Wiedenroth: Author at UKGM
K. Tello: Author at UKGM
G. Krombach: Author at UKGM
F. Roller: Author at UKGM

RPS 703-12 15:06

U-Net convolutional neural network and B-spline deformable image registration for fully-automated strain calculation is feasible in the study of health in Pomerania

F. C. Laqua[1], P. L. Madsen[2], N. Hosten[1], R. Bülow[1]; *[1]Greifswald/DE, [2]Copenhagen/DK*

Purpose: To assess the feasibility of fully-automated myocardial strain estimation in a large epidemiological study since manual segmentation and strain estimation is time-consuming and prone to interoperator-variability.
Methods and materials: From the study of health in Pomerania (SHIP), 1,519 subjects from the general population (median age 52 years, 54.9% men) underwent steady-state-free-precession cine-CMR. A U-Net convolutional neural network (U-Net) was trained with 4-chamber, 2-chamber, and short-axis images of 991 probands from SHIP-TREND and used to predict left ventricular (LV) segmentation in end-diastole for the independent SHIP-CORE cohort. Time-series images were registered using deformable B-spline registration. In this manner, a set of indicator-points, derived from segmentation, was warped through the cardiac cycle. The movement of the indicator-points was visually assessed by two CMR experts. Global and segmental circumferential and longitudinal and radial myocardial strain curves were calculated following Green-Lagrangian formulation.
Results: Predicted segmentation was robust for LV myocard and cavity except for very apical and basal slices, with minor errors in the presence of banding-artefacts. In the vast majority of the assessed time-series, the indicator point-set followed wall motion and biologically plausible strain curves were calculated. Minor segmental tracking errors occurred with underlying motion and chemical-shift artefacts.
Conclusion: Fully-automated myocardial strain estimation combining deformable B-Spline registration with U-Net is feasible in a large population-based CMR study and presents a promising approach for even larger CMR studies like the German National Cohort and UK Biobank. Future research is needed for validation and comparison to manual software.

Limitations: No quantitative comparison with a reference-standard was undertaken. Comparison with commercially available software is ongoing.
Ethics committee approval: All individuals gave written informed consent. The study was approved by the Ethics Committee of the University of Greifswald.
Funding: This study is supported by the German Federal State of Mecklenburg-West-Pomerania.
Author Disclosures:
F. C. Laqua: nothing to disclose
R. Bülow: nothing to disclose
N. Hosten: nothing to disclose
P. L. Madsen: nothing to disclose

RPS 703-13 15:12

Pressure-volume relationship by stress cardiovascular magnetic resonance: feasibility and clinical implications

A. Meloni[1], A. de Luca[2], C. Nugara[3], C. Cappelletto[2], G. Aquaro[1], C. Grigoratos[1], G. Todiere[1], A. Barison[1], A. Pepe[1]; [1]*Pisa/IT,* [2]*Trieste/IT,* [3]*Palermo/IT (alessia.pepe@ftgm.it)*

Purpose: The variation between rest and peak stress end-systolic pressure-volume relation (ESPVR) is obtained during routine stress echocardiography and is an index of myocardial contractile performance.
This is the first study assessing the delta rest-stress ESPVR (DESPVR) by dipyridamole stress cardiovascular magnetic resonance (CMR).
Methods and materials: 100 consecutive patients (24 females, 63.76±10.17 years) who underwent dipyridamole stress-CMR were considered.
The ESPVR was evaluated at rest and peak-stress from raw measurement of systolic arterial pressure by sphygmomanometer and end-systolic volume by the biplane Simpson method. Wall motion and perfusion at rest and after dipyridamole were analysed. Macroscopic fibrosis was detected by the late gadolinium enhancement technique.
Results: The mean ESPVR at rest and peak stress was, respectively, 4.84±2.47 and 5.33±3.16 mmHg/mL/m2; mean ΔESPVR was 0.48±1.45 mmHg/mL/m2.
ΔESPVR was significantly lower in males.
ΔESPVR was not correlated to baseline left ventricular end-diastolic volume index or ejection fraction.
43 patients had myocardial fibrosis and showed significantly lower ΔESPVR values.
An abnormal stress CMR was found in 25 patients. The ΔESPVR was significantly lower in patients with abnormal stress CMR.
During a mean follow-up of 56.34±30.04 months, 24 cardiovascular events occurred. At receiver-operating characteristic curve analysis, a ΔESPVR<0.02 predicted the presence of future cardiac events with a sensitivity of 0.79 and a specificity of 0.68.
Conclusion: The noninvasive assessment of the ΔESPVR index during a dipyridamole stress-CMR exam was feasible. The ΔESPVR was independent from baseline LV dimensions and function, so it can be used for a comparative assessment of patients with different diseases. ΔESPVR by CMR can be a useful marker for additional prognostic stratification.
Limitations: n/a
Ethics committee approval: Ethics committee approval obtained.
Funding: No funding was received for this work.
Author Disclosures:
A. Pepe: nothing to disclose
A. Meloni: nothing to disclose
A. de Luca: nothing to disclose
C. Nugara: nothing to disclose
C. Cappelletto: nothing to disclose
G. Aquaro: nothing to disclose
C. Grigoratos: nothing to disclose
G. Todiere: nothing to disclose
A. Barison: nothing to disclose

RPS 703-14 15:18

Effectiveness of cardiovascular magnetic resonance combined strain value in the determination of ejection fraction

I. A. Abidoye[1], M. C. Halfmann[2], S. Benz[2], T. Leckebusch[2], T. Klimzak[2], M. Larisch[2], C. Düber[2], K.-F. Kreitner[2], T. Emrich[2]; [1]*Ado-Ekiti/NG,* [2]*Mainz/DE (ibukunabidoye@yahoo.com)*

Purpose: Strain parameters reflect cardiac deformation by analysing longitudinal and circumferential shortening as well as radial thickening of the myocardium. Theoretically, optimal myocardial contraction should be a result of all three deformation patterns. Therefore, we propose a new method (combined strain) to link strain values to cardiac function.
Methods and materials: In this retrospective cross-sectional study, we evaluated 444 subjects, both healthy (n=127) and diseased (n=317), with varying degrees of ejection fraction (EF) using CMR imaging at 3T (MAGNETOM Prisma, Siemens Healthineers, Erlangen, Germany). Left ventricular volumes and EF, as well as global strain values [radial (RS), circumferential (CS), and longitudinal (LS)], were acquired for the left ventricle using dedicated software (cvi42, Circle, Calgary, Canada). Combined strain (CoS) was calculated by the following equitation: CoS=RS+Absolute(CS+LS).
Results: Overall, absolute combined strain was found to have a higher correlation to EF than absolute longitudinal and radial strain, and a comparable correlation as absolute circumferential strain. The correlation was much stronger in patients with depressed EF than in those with normal EF. Sensitivity and specificity to predict reduced EF was higher in combined strain than in longitudinal or radial strain (AUC for CoS: 0.91 vs LS: 0.86 vs RS: 0.86).
Conclusion: In our large collective of healthy volunteers and magnitude of cardiomyopathies with and without depression of left ventricular function, the proposed concept of a combined strain outperformed radial and longitudinal strain in the evaluation of left ventricular function. The prognostic implications of these parameters have to be determined in prospective studies.
Limitations: A single-centre, retrospective study.
Ethics committee approval: All patients provided written informed consent. The study was approved by the local ethics committee (2018-13520/837.196.13/837.477.14).
Funding: No funding was received for this work.
Author Disclosures:
I. A. Abidoye: nothing to disclose
M. C. Halfmann: nothing to disclose
S. Benz: nothing to disclose
T. Leckebusch: nothing to disclose
T. Klimzak: nothing to disclose
M. Larisch: nothing to disclose
C. Düber: nothing to disclose
K.-F. Kreitner: nothing to disclose
T. Emrich: nothing to disclose

RPS 703-15 15:24

Left atrial strain imaging: a comparison between conventional and highly accelerated cine imaging

G. Bisso[1], C. Reichhardt[1], S. Altmann[1], I. A. Abidoye[2], C. Düber[1], K.-F. Kreitner[1], T. Emrich[1]; [1]*Mainz/DE,* [2]*Ado-Ekiti/NG (sebastian.a.altmann@web.de)*

Purpose: Feature-tracking (FT) derived strain imaging of the left atrium is a promising method for the detection of atrial function and (subclinical) dysfunction in cardiomyopathies (REF). FT relies on sufficient spatial and temporal resolution that allows corrects tracking of endo- and epicardial contours. Compressed sensing (CS) is a relatively new method to accelerate image acquisition by incoherent sub-sampling of k-space, transformation of sparsity, and iterative reconstructions. The aim of this study was to compare left atrial strain by FT between a conventional (Conv) and a CS-based CINE sequence.
Methods and materials: This prospective study included 32 healthy volunteers. Imaging was performed at 3T (MAGNETOM Prisma, Siemens Healthineers, Erlangen, Germany). CINE images (Conv and CS) in typical long axis orientations were used to calculate left atrial FT strain. Both sequences were comparable in regard to temporal and spatial resolution. Post-processing was performed with a dedicated cardiac imaging software (cvi42, Circle, Calgary, Canada).
Results: Left atrial reservoir, booster, and conduit strain differed significantly between CONV and CS (e.g. reservoir strain (Conv vs CS): 42.9 vs 27.6%, p<0.0001) (Table 2). Nevertheless, there was an almost linear correlation for reservoir and conduit strain, and a weaker correlation for booster strain.
Conclusion: FT strain parameters of the left atrium differ significantly between Conv and CS-based CINE images. These differences could be explained by different diastolic reference phases for FT and thin atrial walls for contour detection. Further research is needed to establish a potential correction factor and validate this in a larger cohort with normal and impaired atrial function.
Limitations: A single-centre study.
Ethics committee approval: All volunteers provided written informed consent to participate. The study was approved by the local ethics committee (2018-13520).
Funding: No funding was received for this work.
Author Disclosures:
G. Bisso: nothing to disclose
T. Emrich: nothing to disclose
C. Reichhardt: nothing to disclose
S. Altmann: nothing to disclose
I. A. Abidoye: nothing to disclose
C. Düber: nothing to disclose
K.-F. Kreitner: nothing to disclose

14:00 - 15:30 **Room Y**

CTiR 7
Clinical Trials in Radiology 2

Moderators:
F. J. Gilbert; Cambridge/UK
U. Mahmood; Oak Brook/US

CTiR 7-1 14:00
Diagnostic accuracy of dynamic contrast enhanced computed tomography in comparison with positron emission tomography in the characterisation of solitary pulmonary nodules: the SPUtNIk Trial
F. J. Gilbert[1], J. R. Weir-McCall[1], S. Harris[2], K. Miles[3], R. Rintoul[4], N. Qureshi[1], S. Dizdarevic[5], L. Little[2], L. Pike[3], D. Sinclair[3], A. Shah[6], R. Eaton[6], J. Jones[2], A. Clegg[2], V. Benedetto[7], J. Hill[7], A. Cook[7], D. Tzelis[8], L. Vale[8], L. Brindle[2], J. Madden[2], K. Cozens[2], K. Eichhorst[2], C. Peebles[2], A. Banerjee[2], S. Han[9], F.-W. Poon[9], A. Groves[3], L. Kurban[10], M. Callister[11], E. Crosbie[12], F. Gleeson[13], K. Karunasaagarar[14], O. Kankam[15], S. George[2]; *[1]Cambridge/UK, [2]Southampton/UK, [3]London/UK, [4]Papworth/UK, [5]Brighton/UK, [6]Stevenage/UK, [7]Preston/UK, [8]Newcastle/UK, [9]Glasgow/UK, [10]Aberdeen/UK, [11]Leeds/UK, [12]Manchester/UK, [13]Oxford/UK, [14]Sheffield/UK, [15]St. Leonards on Sea/UK (fjg28@cam.ac.uk)*

Purpose: To compare the diagnostic accuracy of dynamic contrast-enhanced computed tomography (DCE-CT) and ^{18}Fluorine-Fluorodeoxyglucose Positron Emission Tomography/Computed Tomography (PET/CT) for the diagnosis of solitary pulmonary nodules.
Methods and materials: In this prospective multicentre trial, 380 participants with an incidentally detected solitary pulmonary nodule (8-30mm), and no recent history of malignancy, underwent DCE-CT and PET/CT. All patients underwent either biopsy with histological diagnosis or completed 2 years of CT follow-up. PET/CT was considered positive if it met one of the following criteria: nodule tracer uptake equal to or greater than the mediastinum with irregular/spiculate morphology on CT or evidence of distant metastases. DCE-CT was considered positive if the degree of nodule enhancement was ≥20 Hounsfield units. The primary outcome measures were the comparative diagnostic accuracies of DCE-CT and PET/CT.
Results: Of 380 participants recruited, 312 (47% female, 68.1±9.0 years-old) completed the study. The median pulmonary nodule diameter was 14mm (IQR 11-19), with a 61% rate of malignancy. The sensitivity and specificity for DCE-CT was 95.2% (95%CI 91.2;97.5) and 29.3% (95%CI 22.0;37.8), and for PET/CT was 72.5% (95%CI 65.7;78.4) and 80.5% (95%CI 72.6;86.5). The area under the receiver operator characteristic curve (AUROC) was 0.63 (95%CI 0.58;0.67) for DCE-CT and 0.76 (95%CI 0.72;0.82) for PET/CT (p<0.001). Combining the tests resulted in a significant increase in the diagnostic accuracy over PET/CT alone (AUROC=0.89 (95%CI 0.86;0.93),p<0.001).
Conclusion: PET/CT has a superior diagnostic accuracy to DCE-CT for the diagnosis of solitary pulmonary nodules. However, combining the two techniques improves the diagnostic accuracy over either test alone.
Limitations: Results may not be generalisable to screening detected nodules.
Ethics committee approval: REC-12/SW/0206.
Funding: NIHR-HTA (09/22/117).
Author Disclosures:
J. R. Weir-McCall: nothing to disclose
K. Miles: nothing to disclose
F. J. Gilbert: Research/Grant Support at Google Deepmind, Research/Grant Support at GE Healthcare, Research/Grant Support at Bayer
S. Harris: nothing to disclose
R. Rintoul: nothing to disclose
N. Qureshi: nothing to disclose
L. Little: nothing to disclose
S. Dizdarevic: nothing to disclose
S. George: nothing to disclose
L. Pike: nothing to disclose
D. Sinclair: nothing to disclose
A. Shah: nothing to disclose
R. Eaton: nothing to disclose
J. Jones: nothing to disclose
A. Clegg: nothing to disclose
V. Benedetto: nothing to disclose
J. Hill: nothing to disclose
A. Cook: nothing to disclose
D. Tzelis: nothing to disclose
L. Vale: nothing to disclose
L. Brindle: nothing to disclose
J. Madden: nothing to disclose
K. Cozens: nothing to disclose
K. Eichhorst: nothing to disclose
C. Peebles: nothing to disclose
A. Banerjee: nothing to disclose
S. Han: nothing to disclose
F.-W. Poon: nothing to disclose
A. Groves: nothing to disclose
L. Kurban: nothing to disclose
M. Callister: nothing to disclose
E. Crosbie: nothing to disclose
F. Gleeson: nothing to disclose
K. Karunasaagarar: nothing to disclose
O. Kankam: nothing to disclose

CTiR 7-2 14:10
Discussant
M. Oudkerk*; Groningen/NL*

Author Disclosures:
M. Oudkerk: nothing to disclose

CTiR 7-3 14:15
Visibility of interval cancer on previous screening mammograms: comparison of digital mammography and digital breast tomosynthesis in population-based screening
P. Skaane, S. B. Brandal, S. Y. Yanakiev, E. E. Eben, T. Lie, R. Gullien*; Oslo/NO (PERSKA@ous-hf.no)*

Purpose: Review baseline screening examinations of interval cancer (IC) in a population-based program comparing DM and DM+Digital Breast Tomosynthesis (DBT).
Methods and materials: Oslo Tomosynthesis Screening Trial (OTST) (ClinicalTrials.gov NCT01248546) was a prospective study comparing DM and DM+DBT. The trial had a paired design with four arms for independent double reading 2D and 2D+DBT and a common consensus meeting before decision to recall. 24,301 women (50-69 years) were included. Four radiologists retrospectively reviewed baseline screening examinations of all interval cancers using the same breast-based 5-point rating scale applied in the screening program, and gave individual scores for each breast and for CC- and MLO-view, and separately for DM and DBT. A consensus meeting grouped the analysis as normal, nonspecific, and significant minimal signs, and false negative ("missed"). The two latter categories were defined as "actionable", i.e., potential detectable cancer.
Results: Screen-detected cancer was found in 230 women (four bilateral) and 51 IC (IC rate 2.1/1000) during a two-year follow-up period. Two IC developed among 938 women were recalled for reasons other than cancer. Of 14 IC among 2,856 women dismissed at consensus, 8 had a positive score for IC, and 5 at 2D, and 7 at DBT among dismissed were classified as actionable. 35 IC among 20,507 women had negative score in all four arms (none actionable at DM, 5 actionable at DBT). Totally 5 IC were considered actionable at 2D compared with 12 at DBT. Correct diagnosis of these 12 exams might have reduced the ICR for DBT-screening from 2.1/1000 to 1.6/1000.
Conclusion: More IC had the potential to be correctly detected at baseline DBT-screening compared with DM, probably due to both perception and characterisation errors.
Limitations: The material, including screening examinations, was enriched with cancers (and relatively few normal and benign cases) which might have increased the readers awareness for malignancies. Only one of the four reviewers was reader of the OTST.
Ethics committee approval: Oslo Tomosynthesis Screening Trial (OTST): Clinical Trials.gov nr.: NCT 01248546. Regional Ethics Committee reference number: 2010/144.
Funding: None.
Author Disclosures:
T. Lie: nothing to disclose
P. Skaane: Speaker at Hologic, GE Healthcare
S. B. Brandal: nothing to disclose
S. Y. Yanakiev: nothing to disclose
E. E. Eben: nothing to disclose
R. Gullien: nothing to disclose

CTiR 7-4 14:25
Discussant
N.N.
Author Disclosures: -

CTiR 7-5 14:30

Multicenter prospective comparison of the TROcar versus SELdinger technique for percutaneous Cholecystostomy: the TroSelC Trial

N. A. Arkoudis[1], L. Reppas[1], S. C. Spiliopoulos[1], M. Theofanis[2], P. M. Kitrou[2], K. Katsanos[2], K. Palialexis[1], D. Filippiadis[1], E. Brountzos[3]; [1]Athens/GR, [2]Patras/GR, [3]Haidari/GR (nick_arkoudis@hotmail.com)

Purpose: To compare the safety and efficacy of bed-side ultrasound-guided (US) Trocar versus US/fluoroscopy-guided Seldinger techniques for percutaneous cholecystostomy (PC).
Methods and materials: This is a prospective, two-center, non-inferiority study comparing bed-side US-guided Trocar PC (group T; 53 patients, mean age:74.31±16.19 years, male:28) versus US/fluoroscopy-guided Seldinger PC (group S; 52 patients, mean age: 79.92±13.38, male:26) in consecutive patients undergoing PC in two large tertiary university hospitals. Primary endpoints were technical success and procedure-related complications rates. Secondary endpoints included procedural duration, pain assessment, and clinical success in up to 3 months of follow-up.
Results: PC was successfully performed in all 105 patients (100%). Clinical success was similar between the two study groups (86.8% group T vs.76.9% group S; p=0.09). Mean procedural time was significantly lower in group T (1.77±1.62min vs. 4.88±2.68min group S; p<0.0001). Significantly more procedure-related complications were noted in group S compared to group T (11.5% vs. 1.9%; p=0.02). In group S, bile leak was 7.7%, abscess formation 1.9%, and gallbladder rupture 1.9%. No procedure-related death was noted. Minor bleeding occurred in one patient (1.9%) in group T, which auto-resolved. At 12 hours, pain score was significantly lower for patients in group T (0.78 ± 1 vs. 3.12 ± 1.36; p=0.0001).
Conclusion: Bed-side, US-guided Trocar PC was equally effective with less procedure-related complications, required less procedural time, and resulted in decreased post-procedural pain, compared to fluoroscopically-guided PC using the Seldinger technique.
Limitations: Relatively small number of patients included. Each center performed only one method for PC. Patients were not blinded to the study's method.
Ethics committee approval: Institutional board approval was obtained and an informed consent explaining the risks and benefits of the procedure was obtained in all cases.
Funding: No funding was received for this work.
Author Disclosures:
N. A. Arkoudis: nothing to disclose
L. Reppas: nothing to disclose
S. C. Spiliopoulos: nothing to disclose
M. Theofanis: nothing to disclose
P. M. Kitrou: nothing to disclose
K. Katsanos: nothing to disclose
K. Palialexis: nothing to disclose
D. Filippiadis: nothing to disclose
E. Brountzos: nothing to disclose

CTiR 7-6 14:40

Discussant

A. L. Bojanović; *Niš/RS*

Author Disclosures:
A. L. Bojanović: nothing to disclose

CTiR 7-7 14:45

Building an advanced medical image anonymisation system by integrating open-source tools in a large multi-center cross-modality AI imaging project

Y. Huang[1], W.-J. Lee[1], Y.-C. Chen[1], T.-D. Wang[1], C.-M. Chen[1], C.-Y. Lee[2], W.-C. Wang[1], C.-Y. Chou[1], Y.-C. Chang[1]; [1]Taipei/TW, [2]Miaoli/TW (squll1peter@gmail.com)

Purpose: Proper de-identification of medical images while maintaining research-relevant information and connection between cross-modality image studies is complex and cumbersome. We aimed to develop a medical image anonymisation system that integrates currently available open-source tools to overcome the de-identification difficulties in a large multi-center cross-modality AI imaging project.
Methods and materials: Cardiovascular images including cardiac CT, nuclear myocardial perfusion images, invasive coronary angiography, coronary fractional flow reserve, coronary optical coherence tomography, and intravascular ultrasound from eight institutes were retrospectively collected to build the database. The images were de-identified with an on-site standalone anonymiser then sent to the Core Lab for main de-identification process. The main de-identification processor is composed of an open-source DICOM server with a custom server-side script, a MIRC clinical trial processor with custom pipelines, and python scripts for special anonymisation and processing needs. Each component runs in a separate container but connect to the same virtual network. De-identification profile and server settings are versioned and tested in a separate container before publishing.
Results: A total of 12 million multi-center cross-modality cardiovascular images from 2000 patients were de-identified successfully while preserving research-relevant information and connection between cross-modality image studies. A special de-identification process for specific type of image annotation was developed and integrated into the main de-identification process.
Conclusion: We successfully built a medical image anonymisation system in a multi-center cross-modality cardiovascular imaging database by integrating available tools.
Limitations: (1) Lack of real time progress monitoring and feedback for end users. (2) Requires manual manipulation to redo de-identification with new profile.
Ethics committee approval: Research Committee of National Taiwan University Hospital.
Funding: Ministry of Science and Technology, Taiwan.
Author Disclosures:
W.-C. Wang: nothing to disclose
Y. Huang: nothing to disclose
W.-J. Lee: nothing to disclose
Y.-C. Chang: nothing to disclose
T.-D. Wang: nothing to disclose
C.-M. Chen: nothing to disclose
C.-Y. Chou: nothing to disclose
Y.-C. Chen: nothing to disclose
C.-Y. Lee: nothing to disclose

CTiR 7-8 14:55

Discussant

T. de Bondt; *Antwerp/BE (timo.debondt@gmail.com)*

Author Disclosures:
T. de Bondt: nothing to disclose

CTiR 7-9 15:00

Abbreviated MRI randomised study in breast cancer survivors: does it impact patient anxiety?

M. Mohallem Fonseca[1], T. Alhassan[2], D. Koszycki[1], B.-A. Schwarz[1], R. Segal[1], A. Arnaout[1], T. Ramsay[1], J. Lau[1], J. M. Seely[1]; [1]Ottawa, ON/CA, [2]Dubai/AE (jeseely@toh.on.ca)

Purpose: To determine if the addition of abbreviated breast MRI (A-MRI) to surveillance mammography (MG) impacted patient anxiety and if it improved cancer detection rate (CDR) in breast cancer survivors.
Methods and materials: A prospective parallel unblinded controlled trial was performed in a tertiary care academic center on women with a personal history of breast cancer who were randomised into two groups: surveillance with MG or MG plus A-MRI. The primary outcome was anxiety measured via four validated questionnaires at the time of enrollment, after notification of imaging results, and 6 months later, and compared between the two groups. Other parameters including recall, biopsy rates, and CDR were compared between MG and A-MRI.
Results: 199 patients were included, 105 women in A-MRI plus MG and 94 in MG groups. MRI recall rate was 26.6% (28/105), biopsy rate was 20% (21/105), with CDR 5.7% (6/105) - 6 cancers found by MRI alone. Compared to MRI alone, the rates of MG recall, biopsy and CDR were significantly lower: 4.5% (9/199, p<0.00001), 3.0% (6/199, p<0.00001), 0.5% (1/199, p<0.0039) respectively - 1 DCIS found in a patient who had MG only. Penn State Worry Questionnaire scores were similar for both groups and did not change over time, both moderately severe.
Conclusion: Compared to mammography alone, A-MRI had significantly higher cancer detection in breast cancer survivors. MRI was not associated with a "reassuring effect", but showed no increase in anxiety despite a higher rate of recalls and biopsies. Further work is needed to ensure an acceptable benefit-to-harm ratio.
Limitations: Potential for selection bias due to oncologist preference.
Ethics committee approval: Approved by the institutional review board and written informed consent was obtained.
Funding: Support was provided in part by the Ottawa Hospital Cancer Program.
Author Disclosures:
M. Mohallem Fonseca: nothing to disclose
T. Alhassan: nothing to disclose
D. Koszycki: nothing to disclose
B.-A. Schwarz: nothing to disclose
A. Arnaout: nothing to disclose
T. Ramsay: nothing to disclose
J. Lau: nothing to disclose
J. M. Seely: Consultant at Hoffman Roche
R. Segal: nothing to disclose

CTiR 7-10 15:10
Discussant
S. Perez Rodrigo*; Madrid/ES*

Author Disclosures:
S. Perez Rodrigo: nothing to disclose

CTiR 7-11 15:15
Diagnostic performance of ultrasound in patients with pancreatic ductal adenocarcinoma: a multi-centered population-based observational study
J. Kang, M. Abdolell, A. Costa*; Halifax, NS/CA (jessie-dain@Dal.Ca)*

Purpose: To evaluate the performance of ultrasound (US) in diagnosing patients with pancreatic ductal adenocarcinoma (PDAC) in our region.
Methods and materials: Patients diagnosed with PDAC between 2014-15 were identified by the Cancer Registry data. Their US requisitions, images, and reports were reviewed independently by a radiology resident and abdominal radiologist, and finalised via consensus. Examinations were excluded if a pancreatic lesion was known at the time of US.
The following data elements were extracted: clinical suspicion of PDAC, comment on image quality, detection of tumour, location, size, detection of secondary signs and liver metastases, suspicion of neoplasm raised, and follow-up recommendations. US were graded as true-positive, indeterminate, or false-negative. One-way ANOVA and chi-square tests were performed according to these subgroups.
Results: 113 US examinations on 107 patients (53 men, 54 women; mean 70 +/- 13 years) were included. Cancer was suspected clinically in 49 patients. 35/113 (31.0%) examinations commented on image quality, however only 49/113 (43.4%) visualised the tumour. There were 50 true-positives, 40 indeterminates, and 23 false-negatives. There was no difference in age, weight, tumour location, or size across subgroups. However, sex distribution, clinical suspicion of PDAC, comment on US quality, visualisation of tumour, detection of secondary signs, and liver metastases were significantly different ($p<0.005$). The number of examinations reporting suspicion of neoplasm or recommending follow-up also varied significantly ($p<0.0001$).
Conclusion: Assessment of PDAC with US is unreliable in our region, with a large proportion of indeterminate and false-negative studies. These results have important implications for radiologists reporting US and referring physicians relying on US for patient work-up.
Limitations: Retrospective study. Operator dependent nature of US.
Ethics committee approval: REB approval, PHIA adherence.
Funding: No funding was received for this work.
Author Disclosures:
J. Kang: nothing to disclose
A. Costa: nothing to disclose
M. Abdolell: CEO at Densitas Inc

CTiR 7-12 15:25
Discussant
T. Denecke*; Leipzig/DE (Timm.Denecke@medizin.uni-leipzig.de)*

Author Disclosures:
T. Denecke: Research/Grant Support at Guerbet, Siemens, be imaging, Investigator at Siemens, Bayer, be imaging, Speaker at Canon, Siemens, Bayer, be imaging

14:00 - 15:30 **Room M 1**

Hybrid, Molecular and Translational Imaging

RPS 706

Clinical utility of hybrid imaging with PET/CT/MRI

Moderators:
M. Gerwing; Münster/DE
M. Herranz; Shanghai/CN

RPS 706-K 14:00
Keynote lecture
J. Ferda*; Plzen/CZ (ferda@fnplzen.cz)*

Author Disclosures:
J. Ferda: nothing to disclose

RPS 706-1 14:10
Dynamic ^{18}F-FET PET as an independent prognostic factor in de-novo oligodendroglioma
M. Unterrainer, F. Vettermann, B. Suchorska, J. Herms, W. G. Kunz, M. Niyazi, P. Bartenstein, J.-C. Tonn, N. Albert*; Munich/DE (marcus.unterrainer@med.uni-muenchen.de)*

Purpose: Within the updated WHO classification, gliomas are stratified into molecular genetic subgroups. Among these, IDH-mutant, 1p/19q-codeleted gliomas (oligodendrogliomas) exert a favourable outcome compared to IDH-wildtype tumours such as glioblastoma. Therefore, the individual risk of treatment-associated morbidity has to be weight up. ^{18}F-FET PET increasingly gains clinical importance for glioma imaging, however, its prognostic value in de-novo oligodendroglioma is unclear and was evaluated.
Methods and materials: Patients with histologically verified de-novo oligodendroglioma (IDH-mutant and 1p/19q-codeleted) underwent MRI and dynamic ^{18}F-FET PET prior to therapy. ^{18}F-FET PET parameters (maximum/mean tumour-to-background ratio [TBR_{max}, TBR_{mean}], minimal time-to-peak [TTP_{min}], biological-tumour-volume [BTV]), contrast-enhancement, Karnofsky-Performance-Score (KPS) and subsequent treatment were assessed and correlated with the progression-free survival (PFS) as defined by Response-Assessment in Neuro-Oncology criteria (RANO) using Kaplan-Meier estimates and uni-/multivariate analyses.
Results: Seventy-six patients with de-novo oligodendroglioma (WHO grade II n=58, WHO grade III n=18) were included. During a median follow-up time of 67.5 months, 43/76 patients experienced tumour progression with a median PFS of 57.0 months. In univariate analyses, WHO grade (WHO grade II vs. III: median PFS 64.0 vs. 39.0 months, $p=0.035$) and TTP_{min} on dynamic PET (≤25 vs. >25 min: median PFS 50.0 vs. 104.0 months, $p=0.021$) were associated with PFS, whereas age, contrast enhancement, KPS, $TBR_{max/mean}$ and BTV were not ($p>0.05$). In multivariate analysis, both WHO grade (hazard ratio 2.4 (CI: 1.2–4.9), $p=0.019$) and TTP_{min} (hazard ratio 2.4 (CI: 1.1–5.2), $p=0.021$) were significant prognostic factors for PFS.
Conclusion: Within the molecular genetic subgroup of oligodendroglioma, TTP_{min} on dynamic ^{18}F-FET PET represents an independent prognostic imaging biomarker for PFS. Therefore, dynamic ^{18}F-FET PET in addition to histological and molecular genetic features might help to individualize the clinical management and decision making.
Limitations: Retrospective study.
Ethics committee approval: Approved by the ethics committee LMU.
Funding: No funding for this study was received.
Author Disclosures:
M. Unterrainer: nothing to disclose
F. Vettermann: nothing to disclose
B. Suchorska: nothing to disclose
J. Herms: nothing to disclose
W. G. Kunz: nothing to disclose
P. Bartenstein: nothing to disclose
J.-C. Tonn: nothing to disclose
N. Albert: nothing to disclose
M. Niyazi: nothing to disclose

RPS 706-2 14:16
Comprehensive functional evaluation of the spectrum of multi-system atrophy with 18F-FDG PET/CT and 99mTc TRODAT-1 SPECT: 5 years experience from a tertiary care centre
R. Verma, R. Ranjan, H. Mahajan, E. Belho, V. Gupta, N. Seniaray, N. Gupta, V. Mahajan*; New Delhi/IN (drharshmahajan@yahoo.com)*

Purpose: To elucidate the patterns of characteristic hypometabolism on 18F-FDG PET/CT in various subtypes of MSA and correlation with the patterns of uptake on Dopamine transporter imaging with 99mTc TRODAT-1 SPECT.
Methods and materials: A retrospective analysis of 65 patients of clinically suspected MSA was done. All the subjects underwent 99mTc TRODAT-1 SPECT study and 18F-FDG PET/CT scan on two separate days, between 2013 and 2018. The scans were analysed both qualitatively (visually) and semi-quantitatively. The FDG uptake patterns were recorded, and areas of hypometabolism that were two standard deviations from the mean were considered abnormal.
Results: All the subjects had an abnormal pattern of FDG uptake on PET scan, both on a visual inspection and semiquantitative analysis. In MSA-P subjects (n=22), diffuse predominant hypometabolism of the globus pallidus-putamen complex was noted with relative sparing of the caudate nuclei. In MSA-C subjects (n=23), characteristic hypometabolism was noted in the cerebellum and brainstem. In mixed subtypes (n=10), variable involvement of the basal ganglia, cerebellum, and brainstem was noted with frontoparietal hypometabolism. TRODAT scan was abnormal in all and showed pronounced asymmetry with prominent rostrocaudal gradient seen in the MSA-P subtype.

Conclusion: Dopamine transporter imaging agent 99mTc TRODAT-1 SPECT not only helps in the confirmation of Parkinsonian disorders but also demonstrates varying patterns of distribution in different subtypes of MSA. Characteristic patterns of hypometabolism may help in the differentiation of the subtypes of MSA in the presence of clinically overlapping symptoms.
Limitations: Retrospective design and semiquantitative assessment are the major limitations of this study.
Ethics committee approval: IRB approval was not required as it was a retrospective study.
Funding: No funding was received for this work.
Author Disclosures:
H. Mahajan: Other at Director, Mahajan Imaging Pvt Ltd Research collaboration, General Electric Company Research collaboration, Koninklijke Philips NV Research collaboration, Qure.ai Research collaboration, Predible Health
R. Verma: nothing to disclose
R. Ranjan: nothing to disclose
E. Belho: nothing to disclose
V. Gupta: nothing to disclose
N. Seniaray: nothing to disclose
V. Mahajan: nothing to disclose
N. Gupta: nothing to disclose

RPS 706-3 14:22

^{18}F-choline PET-CT in the localisation of parathyroid adenomas

A. Mazurek[1], M. Dziuk[1], A. Gizewska[1], S. Piszczek[1], N. Papachristodoulou[2]; *[1]Warsaw/PL, [2]Budapest/HU (andrzej_mazurek@wim.mil.pl)*

Purpose: The aim was to evaluate the usefulness of ^{18}F-choline (^{18}F-FCH) PET-CT for parathyroid adenoma detection in patients with hyperparathyroidism in comparison with neck ultrasound (US) and parathyroid 99mTc-MIBI scintigraphy.
Methods and materials: The 50 patients (45F/5M) underwent neck US, 99mTc-MIBI scintigraphy (subtractive and dual-phase planar and SPECT-CT imaging) and ^{18}F-FCH PET-CT within 6 months. The findings were classified as positive, inconclusive or negative in terms of images typical for parathyroid adenoma in each imaging modality. The localisation of possible parathyroid adenoma in subsequent surgical operation was performed based on the ^{18}F-FCH PET-CT images. The results were compared to the surgical and pathological findings and the follow-up evaluation. Additionally, laboratory tests were performed (plasma calcium and parathormone levels).
Results: Primary hyperparathyroidism was diagnosed in 46/50 and secondary in 4/50 patients. The mean radioactivity of ^{18}F-FCH was 215 MBq and the average time from radiotracer injection to scan was 67 minutes. 44 patients scanned with ^{18}F-FCH PET-CT were classified as positive, 3 as inconclusive and 3 as negative. In the neck US results, 6 patients were scored as positive, 8 as inconclusive and 36 as negative. The results of 99mTc- MIBI scintigraphy were as follows: 8 patients positive, 4 inconclusive, 38 negative. Thirty-five patients underwent surgery, in 30 out of them (85,7%) surgical treatment was effective. Among 35 patients, 11 had previously undergone unsuccessful surgery (none of those patients had previously performed ^{18}F-FCH PET-CT).
Conclusion: The ^{18}F-FCH PET-CT method demonstrates high accuracy in the detection of parathyroid adenomas compared to neck US and 99mTc-MIBI parathyroid scintigraphy, increasing the efficacy of surgical operation in patients with hyperparathyroidism.
Limitations: Not all patients underwent surgery.
Ethics committee approval: The ethics committee approved this study.
Funding: Funding agencies: Military Institute of Medicine, Affidea PET-CT Center Warsaw Poland.
Author Disclosures:
A. Mazurek: nothing to disclose
A. Gizewska: nothing to disclose
N. Papachristodoulou: Research/Grant Support at Affidea, Other at Affidea
S. Piszczek: Employee at Affidea; Military Institute of Medicine
M. Dziuk: Advisory Board at Affidea, Employee at Affidea; Military Institute of Medicine

RPS 706-4 14:28

RECIL vs Lugano for response assessment in FDG-avid Non-Hodgkin lymphomas: a head-to-head comparison in 54 patients

D. Leithner[1], A. Haug[2], D. P. B. Staber[2], M. Raderer[2], D. B. Kiesewetter[2], P. D. U. Jaeger[2], D. C. Kornauth[2], P. D. I. Simonitsch-Klupp[2], D. Berzaczy[2]; *[1]Frankfurt am Main/DE, [2]Vienna/AT (doris.leithner@gmail.com)*

Purpose: To compare the recently proposed RECIL classification to the established Lugano response classification for treatment response assessment in FDG-avid lymphomas, with a particular focus on the provisional response category of RECIL, termed "minor response" (MR).
Methods and materials: In 54 patients with FDG-avid Non-Hodgkin lymphomas (41 with diffuse large B-cell lymphoma and 13 with follicular lymphoma), [18F]FDG-PET/CT-based response according to RECIL (five response categories: complete remission (CR); partial remission (PR); minor response (MR); stable disease (SD); or progressive disease (PD)) and Lugano (four response categories: CR; PR; SD; or PD) was determined at the interim restaging after three immunochemotherapy cycles, and at the end-of-treatment (EOT) restaging after six immunochemotherapy cycles. Following the recording of MR, absolute and relative rates of agreement, as well as kappa (κ) coefficients were calculated.
Results: At the interim restaging, MR was observed in 8/54 patients (14.8%), all of which showed a responding disease according to Lugano. At EOT, MR was observed in only 3/54 patients (5.6%). When MR was recoded as PR, the overall agreement between RECIL and Lugano was 83.3% at the interim restaging (45/54 patients; κ=0.69, P<0.0001), and 90.7% at EOT (49/54 patients; κ=0.79, P<0.0001). When MR was recoded as SD, the overall agreement between RECIL and Lugano was 79.6% at the interim restaging (43/54 patients; κ=0.63, P<0.0001), and 90.7% at EOT (49/54 patients; κ=0.79, P<0.0001).
Conclusion: The RECIL and Lugano classifications yield comparable information about lymphoma treatment response in the majority of patients with FDG-avid lymphomas, especially at EOT. Minor response at the interim restaging according to RECIL is a common finding and generally indicates a favourable EOT outcome.
Limitations: Only two lymphoma subtypes were included.
Ethics committee approval: The study was approved by the local Ethics Committee; informed consent was waived.
Funding: No funding was received for this work.
Author Disclosures:
D. Leithner: nothing to disclose
A. Haug: nothing to disclose
M. Raderer: nothing to disclose
P. D. U. Jaeger: Speaker at Janssen, Speaker at AbbVie
D. C. Kornauth: nothing to disclose
D. Berzaczy: nothing to disclose
D. P. B. Staber: Speaker at Janssen, Speaker at AbbVie
P. D. I. Simonitsch-Klupp: nothing to disclose
D. B. Kiesewetter: nothing to disclose

RPS 706-5 14:34

Metabolic tumour volume as a prognostic biomarker in melanoma patients undergoing baseline ^{18}F-FDG-PET/CT: a comparison with serologic tumour markers and acute phase proteins

C. P. Reinert, S. Gatidis, D. H. Dittmann, C. Pfannenberg, K. Nikolaou, A. Forschner*; Tübingen/DE (christian.reinert@med.uni-tuebingen.de)*

Purpose: In this study, we investigated the correlation of serologic tumour markers and acute-phase proteins with whole-body metabolic tumour volume (MTV) in melanoma patients undergoing ^{18}F-FDG-PET/CT and the role of MTV as an imaging predictor for overall survival.
Methods and materials: A patient cohort with malignant melanoma undergoing ^{18}F-FDG-PET/CT between 04/2013 and 01/2015 was evaluated. Whole-body MTV was quantified using 50%-isocontour volumes of interests (VOIs) and then correlated with serum levels of LDH, S-100 protein, c-reactive protein (CRP) and alkaline phosphatase (AP), which were tested close to the timepoint of PET/CT. Overall survival (OS) between PET/CT and death was compared between patients with MTV above or below the cohort's median and pathological or non-pathological serologic parameters.
Results: 107 consecutive patients (65±13.1y) were included. ^{18}F-FDG-PET/CT revealed a median whole-body MTV of 2.74 [0–66.3] cm^3. We observed a strong correlation between LDH and MTV (r_P=0.73) and between S-100 and MTV (r_P=0.54), whereas CRP and AP showed a less significant or no correlation with MTV (r_P=0.66;r_P=0.30). For the differentiation between MTV above/below patient median, ROC analysis derived 212 U/l as cut-off value for LDH (AUC 0.82;sensitivity 0.77;specificity 0.70). MTV above the patient median was associated with reduced OS (43.1±2.7months) compared to MTV below the patient median (55.7±2.8months, p=.02). Correspondingly, elevated LDH was accompanied with reduced OS (39.3±5.1months) compared to normal LDH (50.1±2.3months, p=.03).
Conclusion: Whole-body MTV in ^{18}F-FDG-PET/CT appears to be an imaging biomarker for the disease progression in malignant melanoma which correlates well with established serologic parameters and proves to be a feasible imaging predictor for OS.
Limitations: Retrospective design.
Ethics committee approval: Approved by the institutional review board.
Funding: No funding was received for this work.

Author Disclosures:
C. P. Reinert: nothing to disclose
S. Gatidis: nothing to disclose
C. Pfannenberg: nothing to disclose
K. Nikolaou: Speaker at Siemens, Bayer, Bracco, Advisory Board at Siemens, Bayer, Bracco
D. H. Dittmann: nothing to disclose
A. Forschner: nothing to disclose

RPS 706-6 14:40
Impact of ^{18}F-FDG-PET/CT on clinical management in patients with cholangiocellular carcinoma
L. S. Kiefer, J. Sekler, B. Gückel, C. La Fougère, K. Nikolaou, S. Gatidis, C. Pfannenberg*; Tübingen/DE (lena.kiefer@med.uni-tuebingen.de)*

Purpose: To determine the impact of ^{18}F-FDG-PET/CT on clinical management in patients with cholangiocellular carcinoma (CCA).
Methods and materials: Patients with CCA undergoing clinically indicated PET/CT between 04/2013-08/2018 were prospectively included in the local PET/CT registry study. Questionnaire data from referring physicians regarding PET/CT indication (diagnosis/staging/suspected recurrence) and intended clinical management (non-treatment (watchful-waiting/additional tests)/palliative/curative treatment) were recorded before and after PET/CT. Post-PET/CT changes in clinical management were analysed. The outcome was determined using Kaplan-Meier-analysis.
Results: 27 patients (mean age: 60 years (IQR: 51.5-67.5 years), 56% males) with altogether 43 PET/CT-examinations were included. PET/CT indications were mainly "suspected recurrence" and "staging" (95.3%). Intended clinical management changed in 35 cases (81.4%) after PET/CT. Major changes (between non-treatment and treatment strategies) occurred in 27 cases (62.8%). Minor changes in non-treatment and among therapies were documented in 8 cases (18.6%). Additional tests (further imaging and/or biopsy) were intended in 21 (48.8%) and 9 (20.9%) cases before PET/CT. After PET/CT, imaging was performed in 1 (2.3%) and biopsy in 8 (18.6%) cases. In only one case biopsy was already planned before the PET/CT and performed afterwards, whereas in 8 cases, biopsy became unnecessary based on PET/CT results. Patients with intended curative treatment after PET/CT showed a mean survival of 2.21 years (95%-CI: 0.76-3.66 years), whereas patients with intended palliative or non-treatment showed a mean survival of 1.21 years (95%-CI: 0.72-1.69years) and 2.08 years (95%-CI: 1.27-2.89years).
Conclusion: ^{18}F-FDG-PET/CT influences clinical management in patients with CCA. It guides the decision for reasonable additional tests and helps to avoid unnecessary imaging and biopsy. Thus, a more appropriate and individualised treatment may be possible based on PET/CT results.
Limitations: Small cohort.
Ethics committee approval: The study was approved by the local institutional review board and ethics committee. Informed consent was obtained from all patients.
Funding: No funding was received.
Author Disclosures:
L. S. Kiefer: nothing to disclose
K. Nikolaou: nothing to disclose
C. La Fougère: nothing to disclose
S. Gatidis: nothing to disclose
C. Pfannenberg: nothing to disclose
B. Gückel: nothing to disclose
J. Sekler: nothing to disclose

RPS 706-7 14:46
Diagnostic efficiency of whole-body ^{18}F-FDG PET/MRI, MRI alone, and SUV and ADC values in the staging of primary uterine cervical cancer
A. Kiviniemi[1], S. Narva[1], I. Rinta-Kiikka[2], S. Hietanen[1], J. Hynninen[1], J. Virtanen[1]*; [1]Turku/FI, [2]Tampere/FI (aikast@utu.fi)*

Purpose: To assess the diagnostic performance of PET/MRI and MRI alone in the local and whole-body staging of cervical cancer, and to evaluate the benefit of standardised uptake value (SUV) and apparent diffusion coefficient (ADC) in staging.
Methods and materials: Consecutive patients with biopsy-proven cervical cancer and whole-body ^{18}F-FDG PET/MRI obtained before the definitive treatment were retrospectively identified. Local tumour spread, nodal involvement, and distant metastases were evaluated using PET/MRI or MRI dataset alone. Histopathology or clinical consensus with the follow-up imaging were used as reference standard. Tumour SUVmax and ADC were measured and the SUVmax/ADC ratio calculated. The area under the curve (AUC) was determined to predict diagnostic performance and Mann-Whitney U test was applied for group comparisons.
Results: In total, 33 patients who underwent surgery (n=23) or first-line chemoradiation (n=10) were included. PET/MRI resulted in higher AUC compared with MRI alone in detecting parametrial (0.89 vs 0.73), vaginal (0.85 vs 0.74), and deep cervical stromal invasion (0.96 vs 0.74), respectively. PET/MRI had higher diagnostic confidence than MRI in identifying patients with radical cone biopsy and no residual at hysterectomy (sensitivity 89% vs 44%). PET/MRI and MRI showed equal AUC for pelvic nodal staging (both 0.73), whereas AUC for distant metastases was higher using PET/MRI (0.80 vs 0.67). The tumour SUVmax/ADC ratio, but not SUVmax or ADC alone, was significantly higher in the presence of metastatic pelvic lymph nodes (P<0.05).
Conclusion: PET/MRI shows higher accuracy than MRI alone for determining not only distant metastasis but also local invasive tumour spread. Tumour SUVmax/ADC ratio may predict pelvic nodal involvement.
Limitations: No evaluation of interobserver variability.
Ethics committee approval: This study was approved by the institutional ethics committee and informed consent was waived.
Funding: Turku University Hospital Research Funds, Instrumentarium Science Foundation, Sigrid Jusélius Foundation, Orion Research Foundation.
Author Disclosures:
A. Kiviniemi: nothing to disclose
S. Narva: nothing to disclose
J. Virtanen: nothing to disclose
I. Rinta-Kiikka: nothing to disclose
S. Hietanen: nothing to disclose
J. Hynninen: nothing to disclose

RPS 706-8 14:52
The role of histopathological and biochemical parameters in predicting metastatic disease in Ga68 PSMA PET for prostate cancer
U. Aydos, Ü. Ö. Akdemir, S. Çetin, F. Ç. Budak, S. Gülbahar, M. Y. Koparal, T. S. Sozen, L. Ö. Atay*; Ankara/TR*

Purpose: The aim of this study was to evaluate the role of histopathological and biochemical parameters in the prediction of the presence and number of PSMA positive lesions consistent with the metastatic spread of prostate cancer on Ga68 PSMA PET images.
Methods and materials: Biochemical, histopathological, and imaging data of 302 prostate cancer patients who underwent Ga68 PSMA PET/CT or PET/MR imaging for primary staging were retrospectively analysed. Patients were divided into two groups as "PET-positive" and "PET-negative" according to the presence of pathologic extra-prostatic PSMA involvement. "PET-positive" cases were additionally divided into three groups: Group A (N1+, M0), Group B (1-3 distant metastases), Group C (>3 distant metastates).
Results: The mean age of patients was 66.8 ± 7.6 years. Imaging modality was PET/MR in 223 (73.8%) and PET/CT in 79 (26.2%) patients. Total PSA, PSA density (PSAD), and tumour tissue ratio were found to be higher in Group C compared to both groups. PSMA PET positivity was observed in 3.8% of the low-intermediate risk groups (ISUP 1-3 and total PSA≤20 and PSAD<0.15). This ratio was 46% (p<0.001) in the high-risk group (ISUP 4-5 or total PSA>20 or PSAD≥0.15) with a relative risk of 12. The logistic regression model to predict the presence of distant metastasis had an accuracy of 89.7%; with ALP, total PSA and ISUP Gleason grade as significant predictors (p<0.05).
Conclusion: In this study, Ga68 PSMA PET positivity was significantly higher in the high-risk patient group than in the low-intermediate risk groups. The regression model used for predicting the presence of distant metastasis on PET imaging was successful with high accuracy.
Limitations: This study was retrospective.
Ethics committee approval: n/a
Funding: No funding was received for this work.
Author Disclosures:
S. Gülbahar: nothing to disclose
U. Aydos: nothing to disclose
Ü. Ö. Akdemir: nothing to disclose
S. Çetin: nothing to disclose
F. Ç. Budak: nothing to disclose
M. Y. Koparal: nothing to disclose
T. S. Sozen: nothing to disclose
L. Ö. Atay: nothing to disclose

RPS 706-9 14:58
Prostate cancer heterogeneity in high b-value DWI correlates with ^{68}Ga-PSMA PET/CT: preliminary results
M. Mottola[1], F. Ferroni[2], D. Barone[2], M. A. Turci[1], M. Celli[2], F. Matteucci[2], G. Gavelli[2], G. Paganelli[2], A. Bevilacqua[1]*; [1]Bologna/IT, [2]Meldola/IT (margherita.mottola@unibo.it)*

Purpose: To investigate whether radiomic features computed on high b-value DWI sequences referring to tumour cellularity correlate with the ^{68}GA-PSMA PET/CT ligand, highly specific for the diagnosis of prostate cancer (PCa).
Methods and materials: This study retrospectively enrols 17 patients belonging to a multi-cohort investigation for the clinical impact of 3T-mpMRI and ^{68}GA-PSMA PET/CT in PCa diagnosis and staging. PCa lesions were contoured in consensus by two experienced radiologists in either DWI or T2w sequences, depending on where they were more visible. 40% of SUV_{max} was used as the threshold to contour lesions on PET images and, on these regions, the median of the last decile of SUV (SUV_{M90th}) was computed. Instead, 84 radiomic features were computed on b-2000 DWI lesions and their value was correlated to SUV_{M90th} through the absolute Spearman index (ρ).
Results: Several radiomic features showed excellent correlations with ^{68}GA-PSMA-SUV_{M90th}. In particular, the radiomic feature performing as the best is related to local tumour heterogeneity and showed ρ≥0.7 in 82% of patients, ρ≥0.5 in just two cases, and one-only patient yielded ρ=0.3.
Conclusion: The outcome reveals a rank correlation between the degrees of PCa cellularity heterogeneity and ^{68}GA- PSMA -SUV_{M90th}. In other words, a wider expression of membrane receptors for PSMA seems corresponding to an over-proliferation of cells, which theoretically is suggestive of tumour onset and malignancy progression.
Limitations: A wider cohort of patients is needed to better understand this correlation and to deepen the physiological and biomolecular causes of such behaviour.
Ethics committee approval: IRB approval, written informed consent was waived.
Funding: No funding was received for this work.
Author Disclosures:
M. Mottola: nothing to disclose
A. Bevilacqua: nothing to disclose
G. Gavelli: nothing to disclose
D. Barone: nothing to disclose
F. Ferroni: nothing to disclose
M. A. Turci: nothing to disclose
F. Matteucci: nothing to disclose
M. Celli: nothing to disclose
G. Paganelli: nothing to disclose

RPS 706-10 15:04

Assessment and evaluation of the significant role of 18F-FDG-PET/CT in determining the cause of fever of unknown origin (FUO) and inflammation of unknown origin (IUO)

S. M. Shaikh; *Hyderabad/IN (idrsikandar@gmail.com)*

Purpose: Fever of unknown origin (FUO) and inflammation of unknown origin (IUO) are becoming diagnostically challenging conditions with relevance to various medical advances and newer techniques. Diagnosis of these underlying disease conditions may be significantly improved by 18F-fluorodeoxyglucose positron emission tomography (18F-FDG-PET).
Methods and materials: Retrospective study to test the diagnostic utility of 18F-FDG-PET/CT in a large cohort of patients with FUO or IUO and to define parameters to increase the likelihood of diagnostic 18F-FDG-PET/CT. Patients under the FUO or IUO category underwent 18F-FDG-PET/CT scanning in addition to the standard diagnostic work-up. 18F-FDG-PET/CT results were classified as helpful or non-helpful in establishing the final diagnosis. Binary logistic regression was used to identify clinical parameters associated with a diagnostic 18F-FDG-PET/CT.
Results: 60 patients underwent FDG PET-CT, 18 with FUO, 35 with IUO and 7 had FUO or IUO previously (exFUO/IUO). The diagnosis was established in 24 patients (79.2%). The leading diagnoses were Tuberculosis (15.3%) in the FUO group, large vessel vasculitis (21.1%) and polymyalgia rheumatica (18.3%) in the IUO group and IgG4-related disease (15.4%) in the exFUO/IUO group. In 34 patients (56.7% of all patients and 71.6% of patients with a diagnosis), 18F-FDG-PET/CT was positive and helpful in finding the diagnosis. Predictive markers for a diagnostic 18F-FDG-PET/CT were an age over 50 years (p=0.019), C-reactive protein (CRP) level over 30 mg/L (p=0.002) and the absence of fever (p=0.001).
Conclusion: 18F-FDG-PET/CT scanning is helpful in evaluating the correct diagnosis in more than 50% of the cases presenting with FUO and IUO. Absence of intermittent fever, higher age and elevated CRP level increase the likelihood for a diagnostic 18F-FDG-PET/CT.
Limitations: Differentials of malignant foci cannot be ruled out.
Ethics committee approval: n/a
Funding: No funding was received for this work.
Author Disclosures:
S. M. Shaikh: nothing to disclose

RPS 706-11 15:10

Initial evaluation of 18F-FDG biodistribution in healthy and oncology subjects scanned using the uEXPLORER total-body PET/CT

Y. Abdelhafez, N. Omidvari, B. Spencer, R. D. B. Badawi, S. Cherry, L. Nardo; *Sacramento, CA/US (yabdelhafez@ucdavis.edu)*

Purpose: EXPLORER is a new generation PET/CT scanner with unprecedented sensitivity and total-body coverage. Its clinical implementation changes the way PET/CT is interpreted and the radiologist needs to gain familiarity with the new way that the functional anatomy is seen. This work aims to characterise aspects of the impact of this new technology on the visualisation of small structures through a semiquantitative evaluation.
Methods and materials: PET data from 19 subjects (healthy subjects, n=5, and oncology patients with limited disease, n=14) were acquired on the EXPLORER scanner for 20 min at 90-min post-injection of 18F-FDG. Data were reconstructed in 1-mm isotropic voxels using an OSEM iterative algorithm with 4 iterations and 20 subsets. At least 1-cm volumes of interest (VOIs) were placed on the liver (Lbkg), ascending aorta (AAbkg) and bone marrow at L3 vertebral body (L3), and smaller structures such as spinal cord (SC), adrenals (AG) and pituitary gland (PG). Semiquantitative values including the SUVmean, SUVmax and SUVpeak were recorded.
Results: SUVmean values for larger structures were: Lbkg=2.5±0.70; AAbkg=1.61±0.39; L3=2.39±1.33. For smaller structures, SUVmax & peak were: for SC, 4.13±0.1.42 & 2.70±0.59 (varied by region); for PG, 5.54±1.60 & 3.26±0.88; and for AGs, 4.64±2.14 & 2.73±0.92. When PG and AG values were normalised for Lbkg, their ratios were: 2.4 & 1.9 for SUVmax and 1.4 & 1.1 for SUVpeak, respectively. No significant differences were seen between healthy and cancer patients.
Conclusion: Initial EXPLORER scans in healthy and oncology subjects demonstrated that biodistribution values in small structures are higher than that usually seen from standard scanners. For example, the adrenals and pituitary gland uptake are higher than the liver background. This notion is critical to correctly interpret total-body PET/CT scans.
Limitations: Small sample size.
Ethics committee approval: IRB#1498688-1 &1341792-4
Funding: NIH R01 CA206187-01
Author Disclosures:
Y. Abdelhafez: nothing to disclose
N. Omidvari: nothing to disclose
B. Spencer: nothing to disclose
S. Cherry: Research/Grant Support at United Imaging, Other at UC Davis has a revenue sharing agreement with United Imaging Healthcare.
L. Nardo: nothing to disclose
R. D. B. Badawi: Research/Grant Support at United Imaging, Other at UC Davis has a revenue sharing agreement with United Imaging Healthcare.

RPS 706-12 15:16

Evaluation of the first integrated PET/dual-energy CT system in patients with lung cancer

S. S. Martin[1], M. van Assen[2], P. Burchett[3], J. G. Ravenel[3], A. Varga-Szemes[3], T. J. Vogl[1], U. J. Schoepf[3], C. N. de Cecco[4]; [1]*Frankfurt am Main/DE,* [2]*Groningen/NL,* [3]*Charleston, SC/US,* [4]*Atlanta, GA/US (simartin@outlook.com)*

Purpose: The aim of this study was to prospectively evaluate the first integrated positron emission tomography (PET)/dual-energy computed tomography (DECT) system in patients with lung cancer.
Methods and materials: In this single-center HIPAA compliant prospective trial, we included 25 patients (age range, 41-84 years; mean age, 62±12.8) with NSCLC (n=21) or SCLC (n=4) who were referred for a PET study between May 2017 and June 2018. All patients received contrast-enhanced imaging on a clinical PET/DECT system. Data analysis included PET-based standard uptake values (SUV_{max}) and DECT-based iodine densities of tumour masses and lymph nodes.
Results: SUV_{max} and iodine density parameters were measured in 33 malignant lung masses (18.0 and 2.3 mg/mL, respectively) and 56 enlarged mediastinal or hilar lymph nodes (8.4 and 2.2 mg/mL, respectively). A moderate correlation was found for SUV_{max} and iodine density values in tumour masses (r=0.53). SUV_{max} and iodine density values of lymph node metastases showed a weak correlation (r=0.36). Additionally, iodine quantification analysis provided no added value for the differentiation of malignant from benign lymph nodes with an area under the curve (AUC) of 0.52 using PET-based SUV_{max} analysis as the reference standard.
Conclusion: The integration of PET/DECT in lung cancer staging can provide additional insights in the assessment of primary lung cancer and on the correlation between tumour vascularisation and metabolic activity, offering an alternative for tumour characterisation improvements.
Limitations: This is a pilot study with a small study size of 25 participants. The histological subtypes at various stages were not investigated in our study.

Ethics committee approval: This prospective, single-center study was approved by the ethics committee of our university hospital. All study participants provided written informed consent.
Funding: This study was supported by a research grant from Siemens Healthineers.
Author Disclosures:
S. S. Martin: nothing to disclose
M. van Assen: nothing to disclose
P. Burchett: nothing to disclose
J. G. Ravenel: nothing to disclose
A. Varga-Szemes: Research/Grant Support at Elucid, Research/Grant Support at Siemens
T. J. Vogl: nothing to disclose
U. J. Schoepf: Research/Grant Support at Astellas, Research/Grant Support at Bayer, Research/Grant Support at Bracco, Research/Grant Support at Elucid, Research/Grant Support at Guerbet, Research/Grant Support at HeartFlow, Research/Grant Support at Siemens
C. N. de Cecco: Research/Grant Support at Guerbet, Speaker at Siemens, Research/Grant Support at Siemens

RPS 706-13 15:22
Prostate cancer lymph node metastasis assessment by artificial intelligence-based PET/CT detection
P. Borrelli[1], M. Larsson[1], J. Ulén[2], O. Enqvist[2], E. Trägårdh[2], H. Kjölhede[1], P. Hoilund-Carlsen[3], L. Edenbrandt[1]; [1]Gothenburg/SE, [2]Malmö/SE, [3]Odense/DK (pablo.borrelli@vgregion.se)

Purpose: First experience with automated artificial intelligence (AI)-based ^{18}F-choline-PET/CT detection of prostate cancer (PCa) lymph-node metastases.
Methods and materials: Cloud-based annotation (RECOMIA) was used by two nuclear-medicine specialists, who manually segmented lymph-node metastases in scans from 407 biopsy-proven PCa patients, 325 (80%) of which were used for training of a convolutional neural network (CNN), while 81 (20%) made up a validation group. Reader A annotated the total material blinded to training/validation designation. Reader B annotated the validation group blinded to Reader A and AI-based segmentation. CNN classified high tracer uptake suggesting lymph-node metastasis. A CNN-tool from prior studies was used to mask organs already segmented in the system.
Results: The AI-based tool failed in 1 validation patient weighing 123kg. In 18 of the remaining 80 validation patients both readers detected ≥1 lymph-node lesion and in 53 they agreed that no lesion was present. Inter-reader reliability, expressed by kappa, was 0.72 (95% CI 0.56-0.89). A total of 87 lymph-node lesions were detected by both readers; the AI-based tool detected 80 (92%) of these. Fifty-four were detected by one reader only; the AI-based tool detected 28 (52%) of these. The AI-based tool identified 219 suspicious lymph-nodes not detected by the readers or 2.7 per patient. Thus, the AI-based tool made 327 detections, of which 108 (33%) were considered lymph-node lesions by at least one reader.
Conclusion: Automated AI-based detection of lymph-node metastases is feasible and reproducible. The discrepancy between AI- and reader-based detection should be further investigated in prospective studies of PCa patients recognising the challenges of lymph-node detection and verification. The AI-based tools developed are available on request at (www.recomia.org) for research purpose.
Limitations: Further studies are needed.
Ethics committee approval: n/a
Funding: No funding was received for this work.
Author Disclosures:
P. Borrelli: nothing to disclose
J. Ulén: nothing to disclose
O. Enqvist: nothing to disclose
E. Trägårdh: nothing to disclose
H. Kjölhede: nothing to disclose
L. Edenbrandt: Employee at EXINI Diagnostics AB, Lund Sweden, Grant Recipient at EXINI Diagnostics AB, Lund Sweden
M. Larsson: nothing to disclose
P. Hoilund-Carlsen: nothing to disclose

16:00 - 17:30 **Room X**

Student Session

S 8

My scientific paper in the field of dose optimisation, abdominal imaging, musculoskeletal imaging

Moderator:
L. M. M. Sconfienza; Milan/IT

S 8-8 16:05
Coronary calcium scoring at 100 kV with tin filtration using a kV-independent reconstruction kernel
R. H. Savage[1], A. F. Abadia[1], S. S. Martin[2], A. Varga-Szemes[1], A. Fischer[3], U. J. Schoepf[1], C. Tesche[4], P. Sahbaee[1], V. Vingiani[5]; [1]Charleston, SC/US, [2]Frankfurt am Main/DE, [3]Charleston/US, [4]Munich/DE, [5]Rome/IT (SavageRo@musc.edu)

Purpose: To investigate the feasibility of a protocol for coronary artery calcium scoring (CACS) at 100kV with tin filtration (Sn100kV) to provide accurate Agatston scores and to asses its potential for radiation dose reduction using a software-based correction algorithm and a kV-independent kernel compared to the standard 120kV acquisition.
Methods and materials: We analysed image data of 114 patients who underwent a clinically-indicated CACS acquisition using the standard 120kV protocol and an additional Sn100kV CACS research scan. Datasets of the Sn100kV scans were reconstructed using a kV-independent kernel, which produced images with Hounsfield units equivalent to 120kV for bone and calcium. This enabled Agatston scoring without changing the original weighting threshold of 130HU, regardless of the original tube voltage chosen for image acquisition. The Agatston scores and radiation dose values were calculated and compared between the two protocols.
Results: Median Agatston scores derived from the standard 120kV and the Sn100kV protocol with the kV-independent kernel were 24.7 (IQR:0-171.1) and 21.4 (IQR:0-173.8), respectively (p=0.18). We found an excellent correlation for Agatston scores derived from the two different protocols with a Pearson's correlation of r=0.99. The dose-length-product was 11.4±4mGycm using the Sn100kV and 50.4±24.9mGycm using the standard 120kV protocol (p<0.01), resulting in significantly lowering the effective radiation dose by 77% (0.16±0.06mSv vs 0.7±0.35mSv, P<0.01) for scanning at Sn100kV. Additionally, 99% of patients were classified into the same risk category using the Sn100kV protocol.
Conclusion: CACS at Sn100kV using the kV-independent kernel is feasible and shows a high correlation compared to standard 120kV scanning. Furthermore, the radiation dose was significantly reduced using the low-kV protocol.
Limitations: A single-centre study with images read by only one radiologist.
Ethics committee approval: IRB-approved, informed consent waived.
Funding: No funding was received for this work.
Author Disclosures:
R. H. Savage: nothing to disclose
C. Tesche: nothing to disclose
V. Vingiani: nothing to disclose
A. F. Abadia: nothing to disclose
A. Varga-Szemes: Research/Grant Support at Siemens, Consultant at Elucid Bioimaging
P. Sahbaee: Employee at Siemens Healthineers
U. J. Schoepf: Research/Grant Support at Astellas, Bayer, Elucid Biomaging, GE, Guerbet, HeartFlow, Siemens, Consultant at Astellas, Bayer, Elucid Bioimaging, GE, Guerbet, HeartFlow, Siemens
S. S. Martin: nothing to disclose
A. Fischer: nothing to disclose

S 8-1 16:15
Evaluation of a tube voltage-tailored contrast media injection protocol for coronary CT angiography
R. H. Savage[1], V. Vingiani[2], U. J. Schoepf[1], A. F. Abadia[1], A. Fischer[1], M. van Assen[3], P. von Knebel Doeberitz[4], A. Varga-Szemes[1], S. S. Martin[5]; [1]Charleston, SC/US, [2]Rome/IT, [3]Groningen/NL, [4]Mannheim/DE, [5]Frankfurt am Main/DE (SavageRo@musc.edu)

Purpose: To evaluate a tube voltage-tailored contrast media (CM) application protocol utilising software support for patient-specific injection during coronary CT angiography (CCTA).

Methods and materials: In this HIPAA-compliant single-centre study, 120 patients referred to CCTA were prospectively assigned to a tube voltage-tailored CM injection protocol. Automated tube voltage selection (ATVS), which automatically adjusts kV to the patient's body habitus, ranged from 70-130kV by applying 10kV intervals. The iodine delivery rate (IDR) was adapted to the tube voltage level using dedicated software (Bayer/Medrad, Indianola, PA). The administrated CM volume ranged from 33mL at 70kV (IDR, 0.8gI/s) to 65mL at 130kV (IDR, 1.9gI/s). Attenuation measurements were performed in the aorta and coronary arteries to calculate quantitative signal-to-noise (SNR) and contrast-to-noise (CNR) ratios. Five-point scales were used to evaluate the overall image quality. Radiation metrics were assessed (Radimetrics™, Bayer) and compared between the protocols.
Results: The mean age of the study patients was 62.5±11.9 years. Image quality was rated as diagnostic in all patients. Contrast enhancement peaked at 7 kV ($p<0.001$), while SNR and CNR parameters showed no significant differences between the tube voltages ($p=0.085$). Additionally, no significant differences were found for subjective image quality parameters between the different protocols ($p=0.139$). The lowest radiation dose values were observed in the group of patients assigned to the 70kV protocol with a median effective radiation dose of 1.1mSv ($p<0.001$).
Conclusion: The proposed tube voltage-tailored injection protocol allows for an individualised scanning of patients undergoing CCTA with significant reductions of CM and radiation dose while simultaneously maintaining a high diagnostic image quality.
Limitations: The diagnostic accuracy of different tube voltage-tailored CM protocols was not investigated. The vendor-specific parameters for CM administration.
Ethics committee approval: IRB-approved, all subjects provided informed consent.
Funding: No funding was received for this work.
Author Disclosures:
R. H. Savage: nothing to disclose
V. Vingiani: nothing to disclose
U. J. Schoepf: Consultant at Astellas, Bayer, Elucid Bioimaging, GE, Guerbet, HeartFlow, Siemens, Research/Grant Support at Astellas, Bayer, Elucid Bioimaging, GE, Guerbet, HeartFlow, Siemens
A. F. Abadia: nothing to disclose
A. Fischer: nothing to disclose
M. van Assen: nothing to disclose
P. von Knebel Doeberitz: nothing to disclose
A. Varga-Szemes: Research/Grant Support at Siemens, Consultant at Elucid Bioimaging
S. S. Martin: nothing to disclose

S 8-2 16:25

Interventional cardiology: patient exposure to radiation and interoperator variability — a healthcare group investigation

J. Anderson[1], M. Zanardo[2], B. Smith[3], M. Maher[3], L. Fox[3], A. Anderson[3], L. A. Rainford[3]; [1]Balbriggan/IE, [2]Di Milano/IT, [3]Dublin/IE
(joseph.anderson@ucdconnect.ie)

Purpose: To evaluate both retrospective and prospective radiation exposure data in a cohort of patients undergoing IC examinations performed by different operators to analyse factors impacting radiation dose with a special focus on operator dependency and to seek operator perceptions on radiation protection training.
Methods and materials: Retrospective and prospective data collation and analysis of radiation parameters from 179 DCAs and 43 PCIs performed in a single centre (Sept 2018-June 2019) by 3 interventional cardiologists within a Siemens Artis imaging suite were conducted. The radiation parameters available for all patients were dose area product (DAP), total fluoroscopy time (FT), the number of cine runs, and the cumulative air kerma. Data collated for retrospective examinations included D.O.B, gender, previous cardiac history, operator, procedure type, access route, contrast agent, and contrast dose. In addition, patient BMI and the total examination duration and complexity was recorded for prospective data. Dose reference levels were calculated at the 3rd quartile. Operators compared against each other and with national/international standards. Cardiologists with consistently low DRLs were followed up with a semistructured interview.
Results: DRLs were determined by gender, patient BMI, previous cardiac history, type of IV approach, contrast dose, and the operator, and were within Irish and European DRLs. Significant interoperator variability ($p<0.001$) was noted. The cardiologist acknowledges his trainer and mentor who influenced him a lot with his technique, decision making, efficiency, and low radiation levels.
Conclusion: Radiation safety in interventional cardiology procedures is operator dependent. Further research is warranted in the standardisation of operator training with evolving technologies.
Limitations: The retrospective data collection, discontinuous sampling, procedure-specific rather than patient-specific statistical analysis, and the non-availability of occupational dosimetry.
Ethics committee approval: Ethics approval from UCD School of Medicine and Departmental with permission from Bon Secours Hospital, Dublin.
Funding: No funding was received for this work.
Author Disclosures:
J. Anderson: nothing to disclose
M. Zanardo: nothing to disclose
B. Smith: nothing to disclose
M. Maher: nothing to disclose
L. Fox: nothing to disclose
A. Anderson: nothing to disclose
L. A. Rainford: nothing to disclose

S 8-3 16:35

Scattered radiation in mobile chest AP in ICU

M. Antikainen, M. Sarjanoja, K. Tuomivaara, T. S. Schroderus-Salo, A. Henner; *Oulu/FI*

Purpose: To investigate scattered radiation in the mobile chest at different distances and heights around the patient's bed with varying kV values.
Methods and materials: The study utilised a MobileArt evolution high power type 32kW (manufactured 2010) mobile x-ray unit. Measurements were taken with a phantom laying supine and half-sitting on a bucky table for an AP chest x-ray. The mAs value was 1.2mAs, while the tube potential varied from 95kV-125kV. Scattered radiation was measured both from the phantoms side and caudally with RaySafe i2 dosimeters (868.3MHz). The distances were measured from the centre of the radiation field at 0.5 m, 1 m, 1.5 m, and 2 m. At each distance, doses were measured at 70 cm (bed level), 100 cm, 130 cm, and 160 cm from the floor.
Results: The amount of scattered radiation increased when kV was raised in both patient positions. With the patient supine with 95kV, the dose rate was 3,222mSv/h, while at 125kV, it was 5,154mSv/h. Scattered radiation decreased significantly when the distance increased. For example, with 125kV and measuring at 160 cm, with 0.5 m distance, the dose rate was 6,244mSv/h, but at 2 meters only it was 0,944mSv/h. The highest dose rates for both supine (5,154mSv/h) and half-sitting (6,244mSv/h) positions were measured at 0.5 m and 160 cm from the floor.
Conclusion: As expected, the higher the tube potential, the more and further radiation scatters in both positions. The highest dose rates were measured at 160 cm from the floor (radiographers neck-head level) and the lowest doses were at the patient's bed level. Noting the direction of scattering radiation is important to protect the surrounding patients and personnel.
Limitations: n/a
Ethics committee approval: No ethical approvement needed.
Funding: No funding was received for this work.
Author Disclosures:
M. Antikainen: nothing to disclose
M. Sarjanoja: nothing to disclose
K. Tuomivaara: nothing to disclose
T. S. Schroderus-Salo: nothing to disclose
A. Henner: nothing to disclose

S 8-4 16:45

Convolutional neural network-based volumetric segmentation of the liver compared with semi-automatic and manual methods

B. Budai, P. Borsos, P. Magyar, V. Bérczi, P. N. Kaposi; *Budapest/HU*
(bettinabudai.95@gmail.com)

Purpose: The manual segmentation of CT images for volumetric analysis of the liver can be time-consuming. Alternatively, partially, or fully computer-aided methods can reduce labour and processing time.
Methods and materials: 62 CT scans from patients examined for diffuse or focal liver diseases were retrospectively collected. The portal venous phase scans were reconstructed with a slice thickness of 5 mm and without an interslice gap. The area of the whole liver was manually segmented as the ground truth with 3D Slicer software. A grow-from-seeds method was used for semi-automatic three-dimensional segmentation of the livers. Either every third or pre-selected five axial slices were used in the grow-cut process, followed by an automatic hole filling, extrusion removing, and surface smoothing of the predicted volume. We developed in-house a volumetric, fully convolutional neural network (V-net) for automated liver segmentation. The network was trained on 51 scans after image preprocessing and data augmentation. The remaining 11 scans were used in the test set and prediction accuracy was estimated after 10-fold cross-validation.
Results: The predicted volume of 62 livers in semi-automatic segmentation where the area of the whole liver was manually delineated on every third slice showed a Dice coefficient of (DSC)=mean±SD=0.96±0.007, Hausdorff average distance of (Hd)=0.95±0.22 mm, and a Jaccard coefficient of (Jc)=0.93±0.012.

The accuracy of the semi-automatic segmentation using only five manually contoured slices was also excellent: DSC=0.94±0.013, Hd=1.83±0.67 mm, and Jc=0.88±0.023. Meanwhile, the V-net based segmentation has achieved DSC=0.87±0.024, Hd=4.25±0.76 mm, and Jc=0.77±0.043.
Conclusion: We conclude that a V-net model can be used for liver segmentation with similar accuracy to manual and semi-automatic methods, thus, expediting the clinical workflow.
Limitations: The size of the training and validation cohorts should be increased before a clinical application can be introduced.
Ethics committee approval: Approval obtained from the research ethics committee of our institution.
Funding: No funding was received for this work.
Author Disclosures:
B. Budai: nothing to disclose
P. Borsos: nothing to disclose
P. Magyar: nothing to disclose
V. Bérczi: nothing to disclose
P. N. Kaposi: nothing to disclose

S 8-5 16:55
Split-bolus and single-pass CT of the abdominal district
A. Missere, N. Raiano*; Naples/IT*

Purpose: To compare the various standard CT protocols and those performed with split-bolus and single-pass techniques, emphasising the advantages and differences in the abdominal district.
The several demonstrated protocols which have used split-bolus and single-pass techniques have the purpose of underlining a decrease of the radiation dose to the patient compared to the standard protocols. The optimisation of the protocol to reduce radiation dose becomes more remarkable considering the new 2013/59 EURATOM directive.
Methods and materials: The illustrated protocols referring to the abdominal district evaluate the diagnostic accuracy of patients with non-traumatic acute or inflammatory bowel disease, the detection and characterisation of focal liver lesions in oncologic patients, the detection of FNH, the pre-operative assessment of HCC, the evaluation of the resectability of pancreatic tumours, and the synchronous nephrographic and excretory phase in the uro-CT.
Results: The diagnostic efficacy of split-bolus and single-pass CT techniques is comparable to that of the multiphasic protocol CT.
Conclusion: The comparison between split-bolus and single-pass CT with multiphasic protocol CT is in terms of noise and CNR, with a reduction in radiation dose and in the number of images to film and store. This comparison demonstrates the diagnostic efficacy and the reduction of radiation dose with the split-bolus and single-pass CT protocols.
Limitations: The amount of contrast in some split-bolus CT protocols.
Ethics committee approval: Local ethics committee approval was obtained.
Funding: No funding was received for this work.
Author Disclosures:
A. Missere: Author at University of Naples "Federico II"
N. Raiano: Author at National Cancer Institute- IRCCS "Fondazione G. Pascale"

S 8-6 17:05
Vascular activity in rotator cuff tendinopathy: evaluation with conventional Doppler ultrasound and superb microvascular imaging (SMI)
C. C. Ooi, K. Q. Teng, S. K. Wong, G. M. Tan, V. C. Ma, S. N. Mohamed, P. C. Mohan, T. S. Howe, M. A. Png*; Singapore/SG*
(1602085@sit.singaporetech.edu.sg)

Purpose: Superb microvascular imaging (SMI) is an innovative Doppler technique for imaging minute vessels with slow velocity. The primary aim of this study was to elucidate the application of SMI in comparison with conventional colour Doppler (CD) and power Doppler (PD) in detecting neovascularity in the supraspinatus tendon. The secondary aim was to investigate the association between neovascularity and shoulder pain and functional disability.
Methods and materials: The supraspinatus tendon of consecutive patients presented with clinical suspicion of rotator cuff problems were evaluated with grey-scale (tendon enlargement, homogeneity, and hypoechogenicity), CD, PD, and SMI. Two radiologists independently graded the images. The relationship between neovascularity (on CD, PD, and SMI) and pain/disability as determined by a visual analog scale (VAS) and the Oxford shoulder score (OSS) was established.
Results: 59 patients (mean age 53, 39 females) were recruited. 34 (34/59: 58%) patients demonstrated no flow in all Doppler techniques while in 22 (22/59: 37%) patients, vascularity was detected in SMI but not with CD or PD ($p<0.01$). SMI positively correlated with hypoechogenicity on grey-scale ($p<0.01$), VAS ($p<0.001$), and OSS scores ($p<0.001$), while CDU and PDU did not show a significant relationship. The Kappa-coefficients of grey-scale, CD, PD, and SMI between the two reviewers were 0.87, 0.79, 0.74, and 0.85, respectively.
Conclusion: Neovascularity on SMI is associated with a hypoechogenic alteration of the supraspinatus tendon and is more related to shoulder pain and functional deficit compared to CD and PD. SMI is a feasible and reliable clinical tool. The supplementation of SMI to conventional ultrasound may increase the performance for diagnosing painful rotator cuff tendinopathy.
Limitations: A single-centre study with a small sample size.
Ethics committee approval: Approved by the Singapore Institute of Technology (SIT) Institutional Review Board.
Funding: No funding was received for this work.
Author Disclosures:
K. Q. Teng: nothing to disclose
V. C. Ma: nothing to disclose
C. C. Ooi: nothing to disclose
S. K. Wong: nothing to disclose
G. M. Tan: nothing to disclose
P. C. Mohan: nothing to disclose
T. S. Howe: nothing to disclose
M. A. Png: nothing to disclose
S. N. Mohamed: nothing to disclose

S 8-7 17:15
Body composition in elderly lung transplantation recipients assessed by pre-transplantation computed tomography scans predicts the outcome after lung transplantation
D. Kifjak, H. Prosch, S. Schwarz, A. Benazzo, P. Jaksch, M. Weber, W. Klepetko, K. Hoetzenecker, T. Schweiger*; Vienna/AT*
(daria.kifjak@meduniwien.ac.at)

Purpose: To predict the clinical outcome in elderly lung transplantation (LuTx) recipients after transplantation by semi-automated quantification of body composition in preoperative chest CT scans.
Methods and materials: This retrospective study included 114 patients ≥60 years who received LuTx at the Medical University of Vienna from December 1998-December 2018 and who underwent a chest CT within one year before transplantation. The mediastinal fat areas at the level of the carina and the dorsal muscle group (DMG) areas at the level of the 12th thoracic vertebral body were calculated semi-automatically using OsiriX (Pixmeo, Switzerland). The adjusted and normalised data was correlated with clinical parameters.
Results: The mean age at transplantation was 63±2.7 years. Fibrosis (40.4%) and COPD (50.9%) were the most common diagnoses. We identified three groups of patients according to body composition ("low risk": high muscle mass and low mediastinal fat (n=8), "high risk": low muscle mass and high mediastinal fat (n=12), and "intermediate": any other combination (n=94)). The "high risk" group patients compared to the "low risk" group patients had a significantly increased risk for wound infections (p=0.001), delirium (p=0.042), and tracheostomy (p=0.032). The time of ventilation (p=0.022; 480 vs 43 hours), the stay in the ICU (p=0.001; 38 vs 5 days), and the stay in hospital (p=0.001; 66 vs 19 days) were significantly longer in the "high risk" group compared to the "low risk" group.
Conclusion: The body composition in pre-transplantation chest CT scans of LuTx candidates is an objective and easily applicable tool for the identification of patients with a poor outcome after LuTx. In addition, it accentuates the pivotal importance of physical activity and rehabilitation in LuTx.
Limitations: The small sample size and single centre.
Ethics committee approval: Ethics committee approval obtained.
Funding: No funding was received for this work.
Author Disclosures:
D. Kifjak: nothing to disclose
H. Prosch: nothing to disclose
S. Schwarz: nothing to disclose
A. Benazzo: nothing to disclose
P. Jaksch: nothing to disclose
M. Weber: nothing to disclose
W. Klepetko: nothing to disclose
K. Hoetzenecker: nothing to disclose
T. Schweiger: nothing to disclose

16:00 - 17:30 **Room Y**

My Thesis in 3 Minutes

MyT3 8

Oncologic Imaging

Moderators:
C. Johnston; Dublin/IE
O. V. Kucheruk; Moscow/RU

MyT3 8-1 16:00

The value of diffusion-weighted MRI in differentiating benign from malignant rectal tumours and assessing the grading of the malignant tumours

A. H. Albu Mohammed, D. A. Al-Hilly*; Baghdad/IQ (ali_dawai@yahoo.co.uk)*

Purpose: To evaluate the value of the apparent coefficient of diffusion in the differentiation between benign and malignant rectal tumours and to assess the histological grading of the malignant tumours.
Methods and materials: A cross-sectional study was conducted in Medical City Complex. Forty patients with rectal tumours were included, and an MRI exam was done for all patient with diffusion weighted imaging as a part of the exam. All patients were followed up for a final histopathological result.
Results: A total of 40 patients, with 21 female and 19 male, their age range from 19-75 years with the mean age of 52.37 ± 14.14 years. All malignant rectal tumours showed restricted diffusion with lower ADC values in comparison to benign tumours (0.814 ± 0.14 vs 1.433 ± 0.27 * 10^{-3} mm^2 / sec). Also, there were statistically significant differences between grades of malignant tumours (well, moderate and poor differentiated) in which the poorly differentiated tumours have lower ADC value than moderate and well-differentiated tumours. In addition to that, the diffusion-weighted imaging revealed an increase in the number of detected lymph nodes when compared with conventional MRI exam without DWI (5.76 ± 3.26 vs 4.42 ± 1.95 lymph nodes).
Conclusion: Diffusion-weighted MR imaging is a valuable tool in the differentiation of benign from malignant rectal tumours with high sensitivity and specificity with the aid of ADC values calculated from the maps obtained by DWI and also in assessing the grading of malignancy.
Limitations: The susceptibility artefact of the diffusion-weighted imaging in addition to artifacts from the air and other contents of the bowel. Small tumours less than 1.5 cm.
Ethics committee approval: n/a
Funding: No funding was received for this work.
Author Disclosures:
A. H. Albu Mohammed: Author at Baghdad Medical City
D. A. Al-Hilly: Consultant at Baghdad Medical City

MyT3 8-2 16:04

Role of 18F-FDG PET-CT in detection and staging of hepatocellular carcinoma

H. Abdelhalim, M. Houseni, M. Elsakhawy, N. Abd Elbary, O. Elabd*; Shebeen El-Kom/EG (heba.abdelhalim@liver.menofia.edu.eg)*

Purpose: To evaluate the role of fluorine18-fluorodeoxyglucose positron emission tomography/computed tomography (18F-FDG-PET/CT) in detection of hepatocellular carcinoma (HCC), its regional and distant metastasis.
Methods and materials: A prospective study on 100 patients referred to our centre due to presence of hepatic focal lesions. As a part of investigation, 18-F-FDG PET/CT was done. Sensitivity of 18-F-FDG PET/CT to detect HCC, its nodal and distant metastasis was calculated.
Results: 18F-FDG-PET/CT has shown high sensitivity for the detection of primary HCC (93.4%), regional lymph nodal metastases (91.3%) and pulmonary deposits (88.2%). It demonstrated high specificity for detection of pulmonary deposits (95.2%). Metabolically active HCC lesions were detected in only 70% of cases with poorly differentiated HCC in 32 patients, moderately differentiated HCC in 23 patients and well-differentiated HCC in only 8 patients with P-value <0.001. We detected a significant difference in SUVmax value between the different grades of HCC (P-value < 0,001) with mean SUVmax 3.0±0.53 for well-differentiated HCC, 5.3±2.6 for moderately-differentiated HCC & 10.6±4.2 for poorly differentiated HCC.
Conclusion: 18F-FDG-PET/CT has high sensitivity in detection of high pathologic grades of HCC, lymph nodal as well as pulmonary deposits.
Limitations: Histopathology for HCC metastases was not available in all cases. The presence of enlarged reactive regional lymph nodes in cirrhotic patients caused increased false-positive nodal metastasis.
Ethics committee approval: The research programme and the informed consent have been approved by the ethics committee of the National Liver Institute, Menofia University, Egypt.
Funding: No funding was recieved for for this work.
Author Disclosures:
M. Elsakhawy: nothing to disclose
N. Abd Elbary: nothing to disclose
O. Elabd: nothing to disclose
M. Houseni: nothing to disclose
H. Abdelhalim: nothing to disclose

MyT3 8-3 16:08

Whole-body low-dose CT scan imaging quality and radiation dose in multiple myeloma: a comparison between 128-slice and 64-slice scanners

A. Ahmed, P. Kiely, J. Saunders*; Limerick/IE (a.ahmed2@nuigalway.ie)*

Purpose: Imaging is crucial for staging and monitoring multiple myeloma patients. Radiation exposure from these imaging is of particular concern in this patient group as they require repeated imaging of the whole body. The aim of this study is to assess the difference in radiation dose and objective image quality in multiple myeloma patients, comparing 64-slice and 128-slice CT scanner for whole-body imaging.
Methods and materials: This was a retrospective, single centre study involving patients who have histologically proven multiple myeloma and have had whole-body CT imaging on 128-slice and 64-slice CT scanner at University Hospital Limerick, evaluating image quality objectively and radiation exposure. Image quality analysis was performed by measured the signal to noise ratio and contrast to noise ratio. Radiation dose was automatically calculated for 32-cm body phantom by the CT scanner.
Results: Our study demonstrated that image quality is improved while using the 128-slice CT scanner, with significantly reduced radiation dose when compared to 64-slice scanner (9.57 mSv with 64-slice scanner vs 4.93 with 12-slice scanner). The improvement of image quality was statistically significant in two, out of the three anatomical sites measured.
Conclusion: Due to the improved image quality and reduced radiation dose, we recommend using the 128-slice CT scanner for staging and monitoring multiple myeloma patients.
Limitations: The main limiting factors of this study are the low sample size used and the fact this was a single centre study. Objective image quality was measured at three anatomical sites. More anatomical site comparisons would have led to a more comprehensive study.
Ethics committee approval: Study was approved by the local ethics committee.
Funding: No funding was recieved for this work.
Author Disclosures:
A. Ahmed: nothing to disclose
P. Kiely: nothing to disclose
J. Saunders: nothing to disclose

MyT3 8-4 16:12

Predicting response to therapy of locally advanced rectal cancer: radiomic analysis from MR imaging

M. Micilotta[1], G. Cappello[2], V. Giannini[2], A. Defeudis[2], S. Mazzetti[2], S. Cirillo[1], D. Regge[2]*; [1]Turin/IT, [2]Candiolo/IT (monicamicilotta@gmail.com)*

Purpose: To predict the response to neoadjuvant therapy in patients with locally advanced rectal cancer (LARC) using texture features of MRI staging examination, to customise therapeutic management.
Methods and materials: The dataset is composed of 52 patients acquired in two different institutions with different MR scanners and protocols. All colorectal cancers were manually segmented on the T2-w images. CRCs were classified as non-responders (R-) if their TRG score was >=3 and responder (R+) otherwise. 39 quantitative features were extracted from the largest segmented slice, including volume, mean, standard deviation, percentiles, skewness, kurtosis, and texture parameters from GLCM and GLRLM matrices from both T2w and ADC maps. Patients from institution A and B were randomly used as training and testing dataset. A stepwise logistic regression model was created using 70% of lesions (36) as a training set and 30% as testing set (16) randomly selected.
Results: The dataset included 21 R- and 31 R+ tumours. Accuracy on the training set was 98% (35/36), with sensitivity and specificity of 100% (21/21) and 95% (14/15), respectively. Accuracy on the testing set was 87% (14/16), with sensitivity, specificity, NPV and PPV of 86% (8/9), 89% (6/7), 89% and 86% respectively.
Conclusion: This study demonstrates the possibility to recognize, analyzing MRI staging examination, patients that will not respond to conventional neoadjuvant therapies, to customize treatment and avoid the use of ineffective therapies, preventing unnecessary toxicity and costs.
Limitations: This study is limited by a manual segmentation with consequent interobserver variability and an external validation dataset.

Ethics committee approval: Ethics committee approval obtained.
Funding: AIRC5x1000 - Ref. 9970, FPRC5x1000 Ministero Salute 2013, FPRC5x1000 Ministero Salute 2015.
Author Disclosures:
V. Giannini: nothing to disclose
M. Micilotta: nothing to disclose
A. Defeudis: nothing to disclose
S. Mazzetti: nothing to disclose
S. Cirillo: nothing to disclose
D. Regge: nothing to disclose
G. Cappello: nothing to disclose

MyT3 8-5 16:16
Pre-operative CT staging of borderline pancreatic cancer patients after neoadjuvant treatment: its accuracy in the prediction of vascular invasion and resectability
S. Ahmed*; Assiut/EG (shimaaabdalla@aun.edu.eg)*

Purpose: To assess the utility of MDCT-tumour vascular interface criteria for predicting vascular invasion and resectability in borderline pancreatic cancer (BRPC) patients after neoadjuvant therapy.
Methods and materials: Eighty-six patients with BRPC who finished neo-adjuvant therapy, showed no progression in preoperative CTs and underwent surgery were included. Two radiologists assessed preoperative CTs to predict vascular invasions and resectability status; the comparison was done with surgical and pathological findings.
Results: At preoperative MDCT, combined criteria of circumferential interface ≥ 180^0 and venous contour deformity (teardrop appearance, unilateral/ bilateral narrowing or occlusion) correctly predicted (89.4%) of venous invasions with an accuracy 93.2%. Combined criteria of circumferential interface ≥ 180^0 with contour deformity (narrowing, teardrop appearance, occlusion) or length of tumour contact > 2cm correctly predicted (71.4%) of arterial invasions with an accuracy 90.7%. Preoperative CT correctly predicted (94.4%) of R0 resections. In cases with no pathologic vascular invasion, criteria of preserved tumour vascular intervening fat/pancreas parenchyma, or lost intervening fat/parenchyma but with circumferential interface ≤ 90^o, preserved normal venous contour and patent lumen correctly predicted (96%) of R0 resections with an accuracy 94.1%. In cases with vascular invasion, combined criteria of circumferential interface < 180^o with preserved normal venous contour and patent lumen correctly predicted (93.3%) of R0 resections with an accuracy 85.1%.
Conclusion: Tumour vascular interface criteria are accurate in the prediction of vascular invasion after neo-adjuvant therapy. MDCT was helpful in the prediction of R0 resection in cases with no pathologic vascular invasion and cases with only venous involvement.
Limitations: We analysed only cases with no progression on pre-operative CT based on RECIST criteria, it may underestimate the number of R0 resections.
Ethics committee approval: IRB approval was obtained.
Funding: No funding was received for this work.
Author Disclosures:
S. Ahmed: nothing to disclose

MyT3 8-6 16:20
Measurement of the volume of a metabolically active tumour by PET/CT with 18F-FDG: a new criterion for the status of the disease in patients with multiple myeloma
A. Sergey, V. Troyan, S. V. Kozyrev, O. A. Rukavitsyn*; Moscow/RU (sergey-alexeev@rambler.ru)*

Purpose: Using PET/CT with 18F-FDG, determine the volume of the metabolically active tumour (MAT) and TLG, and the change in the dynamics of these parameters.
Methods and materials: The results of 99 PET/CT were analysed in 15 patients. After each study, the volume of the MAT, TLG, was measured. The results of PET/CT were differentiated according to the status of the disease at the time of the study, where “1” - stringent complete response and complete response “2” - very good partial response and partial response; "3" – stable disease; "4" - progressive disease.
Results: The results were divided into four groups: “1” (n = 36); “2” (n = 19); "3" (n = 8); “4” (n = 33). In group “1”, lower values of the MAT and TLG were observed compared with other groups — the median of the MAT = 1 [0; 2.95]; median TLG = 2 [0; 11]. In group “3”, high values of the MAT and TLG were observed compared to other groups — the median of the MAT = 190 [65.5; 326]; median TLG = 2,298 [107; 671]. In the subsequent pairwise comparison of medians, significant differences (p> 0.01) in the measurement of the MAT and TLG were detected by the MAT in the groups “1” and “2”; “1” and “3”; “1” and “4”; “2” and “4”; by TLG in the groups “1” and “3”; “1” and “4”; "2" and "4".
Conclusion: Metabolically active tissue volume and TLG statistically significantly change at different disease statuses. This suggests that this method can be used as an independent criterion for assessing the status of the disease in patients with MM
Limitations: n/a
Ethics committee approval: n/a
Funding: No funding was received for this work.
Author Disclosures:
A. Sergey: Author at Main Military Clinical Hospital named after academician N.N. Burdenko
O. A. Rukavitsyn: Author at Main Military Clinical Hospital named after academician N.N. Burdenko
V. Troyan: Author at Main Military Clinical Hospital named after academician N.N. Burdenko
S. V. Kozyrev: Author at Main Military Clinical Hospital named after academician N.N. Burdenko

MyT3 8-7 16:24
Multi-parameter model-based on dual-energy CT predicts mediastinal lymph node metastasis in lung cancer patients
X. Hu, Q. Gu, K. Zhang, P. Li, H. Shen*; Changsha/CN (649291883@qq.com)*

Purpose: To develop a multi-parameter model based on dual-energy CT imaging to predict the mediastinal lymph node metastasis in lung cancer patients.
Methods and materials: Forty-two patients prospectively underwent dual-energy computed tomography (DECT) and a gemstone spectral imaging (GSI) before surgery due to lung cancer. The mediastinal lymph node short diameter, enhancement degree and enhancement mode were evaluated. The lymph nodes CT value at different energy levels (40keV～190keV, interval 10 keV) and spectrum slope, iodine density were obtained. Logistic regression analysis was performed to find out the factors associated with lymph node metastasis, and CT subjective imaging model, DECT model and multi-parameter combined model were established, respectively. The performance of these classifiers was evaluated by the receiver operating characteristic curve (ROC) and compared with Delong test.
Results: A total of 74 lymph nodes were obtained in 42 patients, including 33 lymph nodes metastasis positive and 41 lymph nodes metastasis negative. Logistic regression analysis showed that the CT value at 100Kev and the slope of the energy spectrum curve were correlated with lymph node metastasis (P<0.05). The DECT model achieved the best performance [AUC=0.904; 95% confidence interval (CI) 0.832 to 0.976] in predicting the mediastinal lymph node metastasis with sensitivity and specificity of 0.805 and 0.939, which was better than that of CT subjective imaging model(AUC=0.776, P=0.004). The multi-parameter combined model did not improve the predictive performance (AUC= 0.920,P = 0.123), with sensitivity and specificity of 0.780 and 0.970.
Conclusion: DECT model can significantly improve the accuracy of preoperative diagnosis of mediastinal lymph node metastasis in lung cancer patients.
Limitations: The sample size is small. The model needs to be tested with external test data.
Ethics committee approval: n/a
Funding: No funding was received for this work.
Author Disclosures:
K. Zhang: Founder at First Hospital of Hunan University of Chinese Medicine
X. Hu: Author at First Hospital of Hunan University of Chinese Medicine, Speaker at First Hospital of Hunan University of Chinese Medicine, Owner at First Hospital of Hunan University of Chinese Medicine
Q. Gu: Research/Grant Support at People’s Hospital of Hunan Province
P. Li: Research/Grant Support at First Hospital of Hunan University of Chinese Medicine
H. Shen: Research/Grant Support at First Hospital of Hunan University of Chinese Medicine

MyT3 8-8 16:28
Qualitative assessment in radiotherapy of lung cancer using gemstone spectral imaging
L. Weihua, Y. Wang, F. Lin, Y. Lei*; Shenzhen/CN (18804511716@163.com)*

Purpose: To evaluate tumour responses in patients treated with radiotherapy for medically inoperable non-small cell lung cancer (NSCLC) by assessing intratumoral changes and damage of nearby tissues using gemstone spectral imaging (GSI).
Methods and materials: 26 cases of early-stage, biopsy-proved, medically inoperable lung cancer (NSCLC) underwent gemstone spectral imaging before and 1-6 weeks after radiotherapy. The CT images before and after radiotherapy were obtained and iodine concentration, water concentration and spectrum energy curve and CT values at 40-50 keV were measured. All the data were post-processed by using GSI viewer software. Tumour response was evaluated

by comparing tumour dimensions, volumes and damage of nearby tissues before and after radiotherapy with standard PET/CT evaluation criteria. Those measurements between pre- and post-treatment and two methods were compared by using SPSS 17.0.
Results: Mean CT values of a tumour and iodine content of the tumour region of interest (ROI) in post-therapy were significantly lower than that in pre-therapy (50.13±7.50 vs 78.82±11.81 (HU), 0.91±0.32 vs 2.65±0.35 (g/L), P<0.05 respectively), while water concentrations were found no significant difference between them. The results also exhibited that the radiotherapy can be targeted more precisely with the help of GSI with reduced damage of nearby healthy tissues. Using response evaluation criteria for solid tumours (RECIST), 14 patients demonstrated complete responses, 8 partial responses and 4 stable diseases, which is consistent with previous qualitative evaluation by PET/CT.
Conclusion: Gemstone spectral CT imaging is a noninvasive, precise and rapid screening method. By spectral imaging and material separation technology, it could provide more qualitative and quantitative assessment in radiotherapy of lung cancer.
Limitations: The authors have declared that no competing interests exist.
Ethics committee approval: The ethics committee of Shenzhen Second People's Hospital has given ethical approval.
Funding: No funding was received for this work.
Author Disclosures:
L. Weihua: nothing to disclose
Y. Wang: nothing to disclose
F. Lin: nothing to disclose
Y. Lei: nothing to disclose

MyT3 8-9 16:32

Exploring the implications of modified advanced lung cancer inflammation index on outcomes in patients with advanced non-small cell lung cancer

D. Goyal, A. Mahajan, K. Prabhash*; Mumbai/IN (devendragoyal4@gmail.com)*

Purpose: Sarcopenia and NLR are both predictive and prognostic marker in oncology. The objectives were to evaluate the prognostic value of modified ALI beyond original ALI and see the interaction between sarcopenia, SMD, NLR, ALI and mALI at baseline and post four cycles of chemotherapy and their effects on OS and PFS in patients with advanced NSCLC.
Methods and materials: This study consisted of a total of 285 advanced NSCLC patients. Morphometric parameters such as SMD, SMI and fat-free mass (FFM) were measured by CT at the L3 vertebra. ALI was defined as BMI x serum albumin/neutrophil-lymphocyte ratio (NLR) and mALI was defined as SMI x serum albumin/NLR.
Results: Based on the cut-off of <36.62 HU 185 (64.9 %) had poor muscle quality. Using the cut-offs described by Prado et al the prevalence of sarcopenia within the population was 162(56.8%). About 70% of patients were found to be suffering from sarcopenia across all the BMI categories and this was found to be significant. Patients having sarcopenia suffered from a higher incidence of chemotherapeutic drug toxicities 152 as compared to 121 amongst non-sarcopenics, but this was not found to be statistically significant. ROC curves were used to define poor ALI [<28.02] and mALI [<55.33]. Concordance was seen between ALI and mALI in the pre-treatment setting with 90% of patients with poor ALI having poor mALI and this was statistically significant.
Conclusion: Pre-and post-chemotherapy sarcopenia, SMD and mALI were statistically significant factors in predicting OS in both univariate and multivariate analysis. These biomarkers could potentially help triage patients for chemotherapy according to their tolerability and active nutritional intervention for better outcomes.
Limitations: Post-chemotherapy ALI could not be calculated.
Ethics committee approval: Approval was obtained.
Funding: No funding was received for this work.
Author Disclosures:
D. Goyal: nothing to disclose
A. Mahajan: nothing to disclose
K. Prabhash: nothing to disclose

MyT3 8-10 16:36

Application of the new anaesthetic protocol N.O.R.A. (non-operating room anaesthesia) for osteoid osteoma percutaneous treatment

A. Paladini[1], A. Borzelli[2], F. Pane[2], M. Spinetta[1], D. Negroni[1], A. Galbiati[1], I. Percivale[1], Z. Falaschi[1], G. Mazzucca[1]; [1]*Novara/IT,* [2]*Naples/IT (andreapaladini1988@gmail.com)*

Purpose: The purpose of this study is to verify the effectiveness and complications occurrence of radiofrequency ablation (RFA) in the treatment of osteoid osteoma (OO) in non-operating room anaesthesia (N.O.R.A.).
Methods and materials: From 2016 to 2019, 61 patients affected by OO (40 men and 21 women) with an age of 20.7 years on average (range, 4-51 years; 12 patients aged 20 years or younger) underwent computed tomography-guided percutaneous radiofrequency ablation (RFA) in N.O.R.A. (non-operating room anaesthesia). Lesion sites treated were: femur (27), tibia (22), pelvis (2), talar bone (3), distal radius (1), and humerus (6). Mean follow-up time was 36 months. In each case, anaesthesiologic support followed a new protocol (N.O.R.A. protocol), approved by our institute. Primary success rate, complications, symptom-free intervals, and follow-up results were evaluated.
Results: Pain relief (evaluated with visual analogue scale – VAS) was significant in 97% of patients; it disappeared within 24 hours of the procedure in 44 patients, within 3 days in 10 patients, and within 7 days in 7 patients. After 6 months of observation time, 60 of 61 patients were successfully treated and had no more complaints. In 2 patients, two major complications were found: infection of the site treated, healed with antibiotics, and a nerve lesion, healed with steroid therapy. No other complications were observed.
Conclusion: RFA is a highly effective, efficient, minimally invasive and a safe method for the treatment of OO following N.O.R.A. protocol.
Limitations: No randomisation of patients and poor follow-up were identified as limitations.
Ethics committee approval: n/a
Funding: No funding was received for this work.
Author Disclosures:
A. Paladini: nothing to disclose
A. Borzelli: nothing to disclose
F. Pane: nothing to disclose
M. Spinetta: nothing to disclose
D. Negroni: nothing to disclose
A. Galbiati: nothing to disclose
I. Percivale: nothing to disclose
Z. Falaschi: nothing to disclose
G. Mazzucca: nothing to disclose

MyT3 8-11 16:40

LDCT the saviour? Low-dose CT chest as a cost-effective tool for lung cancer screening in developing countries

A. V. Alexander, A. Babu*; Thiruvalla/IN (ashwinalexander@gmail.com)*

Purpose: Lung cancer is the leading cause of death worldwide. In developed countries, morbidity and mortality due to lung cancer are decreasing due to screening and early detection. In a low income country, high-resolution CT (HRCT) of the lung is almost 15 times the average daily wage. Hence, HRCT is scarcely used as a screening tool, and clinicians mainly rely on chest x-rays for diagnostic purposes which often reveals only the tip of the iceberg. This study aims to create awareness about the effectiveness of low-dose CT (LDCT) as a screening tool.
Methods and materials: This is a descriptive, retrospective study of all patients who underwent LDCT chest in our institution from 1st January 2018 to 31st March 2019. Patients with a history of carcinoma lung/previously detected nodules/mass lesions were excluded. From LDCT images and reports demographic details, diagnosis, lymphadenopathy, mass lesions, nodules and calcification were collected. They were categorised based on ACR guidelines. All images and reports were viewed by the authors personally to remove any interpersonal bias.
Results: Total number of patients included in the study was 649. Findings were detected in 62.5% of the sample, which included 11.4% had miliary lesions, 8.4% had nodules and 0.1% had a mass lesion. Of the total nodules detected 78% were non-calcified. In miliary lesions, 59% were non-calcified.
Conclusion: LDCT is an effective tool for screening pulmonary cancers in countries and regions with limited economic resources. In our study, the positive screen was 6.8% in the general population. If LDCT is deployed for screening targeted populations like smokers, the detection rate would be higher.
Limitations: n/a
Ethics committee approval: n/a
Funding: No funding was received for this work.
Author Disclosures:
A. V. Alexander: nothing to disclose
A. Babu: nothing to disclose

MyT3 8-12 16:44

Integrated PET/MRI for therapy response assessment of patients with Ewing sarcoma: preliminary results

J. Grueneisen[1], M. Chodyla[1], B. M. Schaarschmidt[2], O. Martin[2], M. Forsting[1], K. Herrmann[1], L. Umutlu[1]; [1]*Essen/DE,* [2]*Düsseldorf/DE (johannes.grueneisen@uk-essen.de)*

Purpose: To evaluate the clinical applicability of integrated PET/MRI for monitoring the effectiveness of primary systemic treatment of Ewing sarcoma patients.
Methods and materials: A total of 5 juvenile patients with the confirmation of an Ewing sarcoma and scheduled for the VIDE polychemotherapy regimen (6 cycles) underwent a PET/MR examination before the start (1st scan), after the second cycle (2nd scan) as well as after the end (3rd scan) of treatment. Two experienced physicians analysed the imaging datasets. They were instructed to

perform a whole-body tumour staging in each examination to identify all tumour lesions as well as to assess potential changes during treatment. Therapy response was defined according to the RECIST1.1 and PERCIST criteria. Histopathological analysis and follow-up imaging served as the reference standard.
Results: PET/MR examination of the primary tumours showed a slight decrease in size during treatment (mean size: 1st scan: 77.6mm; 2nd scan: 60.0mm (-22.9%); 3rd scan: 56.6mm (-27.2%), however revealed a significant reduction in metabolic activity (mean SUVmax: 1st scan: 5,9; 2nd scan: 2,3 (-61,0%); 3rd scan: 1,9 (-67.8%). Furthermore, in 4 cases distant metastases could be detected. One patient showed a metabolic complete response, while morphological analysis revealed stable disease. Three further patients revealed metabolic partial response, whereas, RECIST classified two patients as a partial responder and one patient as stable disease. One patient showed new FDG-avid metastases and was classified as a progressive disease.
Conclusion: Our preliminary results demonstrate a good diagnostic performance of integrated PET/MRI for staging and therapy monitoring juvenile patients with Ewing sarcomas, in combining morphological and metabolic information, accompanied with a reasonable radiation dose for the patient.
Limitations: This study was limited by patient cohort.
Ethics committee approval: The study was approved by the local ethics committee.
Funding: No funding was received for this work.
Author Disclosures:
O. Martin: nothing to disclose
J. Grueneisen: nothing to disclose
M. Chodyla: nothing to disclose
B. M. Schaarschmidt: nothing to disclose
M. Forsting: nothing to disclose
K. Herrmann: nothing to disclose
L. Umutlu: nothing to disclose

MyT3 8-13 16:48
Multi-parametric MRI approach for post-TACE HCC
M. Elmansy, M. Elrakhawy, M. A. El-Adalany*; Mansoura/EG (sasamansy90@gmail.com)*

Purpose: To evaluate the role of dynamic-combined subtraction and diffusion magnetic resonance imaging (MRI) in the differentiation between residual and necrotic lesions after treatment by trans-arterial chemoembolization (TACE).
Methods and materials: This prospective study included 50 cases of hepatocellular carcinoma (HCC) patients underwent TACE based on ethical respect and eligibility of patients to do MRI on a 1.5-tesla machine. Diffusion-weighted images (DWI) were done before the dynamic study at different levels. Apparent diffusion coefficient (ADC) maps and subtraction dynamic series were created using a workstation and ADC value was calculated. MR images were interpreted by two different levels experienced observers taking the follow-up findings as regard imaging and arterial hypervascularity blush on repeated TACE as our reference standard. The diagnostic accuracy of dynamic, DWI, subtraction and ADC values for both observers were determined and considered statistically significant at p-value <0.050.
Results: Dynamic and subtraction studies were superior to DWI as regard their diagnostic accuracy and had the same values. Dynamic and subtraction specificity was 90.5 and 95 % for observer 1 and 2 respectively whereas DWI was 76 and 81 % for the same observers respectively. There was a statistically significant difference in ADC value between residue (n=29) and non-residue (n=21) groups with cut-off value for complete ablation >0.94 and >1.05 for both observer (1) and (2) respectively. The absolute agreement and consistency between the two observers Cohen K =0.9 for both dynamic and subtraction and 0.78 for DWI.
Conclusion: Each MRI modality has its merit and accuracy in evaluation of HCCs post-TACE.
Limitations: No pathology due to biopsy sample error post-TACE. No available CT for all patients for comparison.
Ethics committee approval: n/a
Funding: No funding was received for this work.
Author Disclosures:
M. Elmansy: nothing to disclose
M. Elrakhawy: nothing to disclose
M. A. El-Adalany: nothing to disclose

MyT3 8-14 16:52
Multidisciplinary approach in the diagnosis of primary and secondary lung and pleura tumours in cases of synchronous and metachronous cancers
L. Petrychenko*; Dnipro/UA (petrychenkoliliana@gmail.com)*

Purpose: To increase preoperative diagnosis of lung and pleura tumours and to identify the belonging of metastases in the organs of the chest cavity in cases of multiple localisations of the oncological process with the help of CT-guided transthoracic trepan biopsy to obtain a histological material for verification and selection of a specific treatment.
Methods and materials: In the period from January to September 2019, we had made a transthoracic pulmonary biopsy of 27 patients with primary and secondary tumours and with lung and pleura nodes. 11 of them were patients with one localization of oncological process. There were 3 patients with primary non-verified tumours of the chest cavity. And 13 patients had multiple localisations of oncological process. The size of the nodes and tumours varied from 9mm to 11sm.
Results: Histological results were obtained from all investigated nodes and tumours of 27 patients. Biopsy gave a histological answer about the origin of the node or tumour, which made it possible to select the treatment for patients correctly and specifically. According to histological research, 3 patients had tumours and changes which were not related to the oncological disease. 6 patients were diagnosed lung cancer as the second localisation of oncological process. 18 patients had the continuation of the main process and we received the information about the genesis of metastases in cases of primary multiple localisation.
Conclusion: Obtainig a biopsy of tumour tissue makes it possible to get information about the genesis of metastases in cases of synchronous and metachronous cancers. CT guided transthoracic biopsy helps to get tumour tissue material, carry out molecular genetic studies and makes it possible to individualise approaches to the patient's treatment.
Limitations: n/a
Ethics committee approval: n/a
Funding: No funding was received for this work.
Author Disclosures:
L. Petrychenko: Author at Communal Enterprise , Speaker at Communal Enterprise

MyT3 8-15 16:56
Assessment of body composition using magnetic resonance imaging and association with clinical outcomes in patients with colorectal and lung cancer
N. Sakai, A. Bhagwanani, J. Khalasthry, M. Hall-Craggs, S. A. Taylor*; London/UK*

Purpose: To examine the relationship between body composition, as measured by MRI, and the clinical outcome of patients with colorectal and lung cancer.
Methods and materials: Patients with colorectal or lung cancer were prospectively recruited to two multicentre studies examining the use of whole-body MRI in cancer staging (February 2013-September 2016). MR images (Philips mDixon) of patients from 9 sites were post-processed by 2 radiologists using a semi-automated in-house segmentation tool to derive total body fat mass (FM), fat-free mass (FFM), skeletal muscle (SM) mass and SM fat fraction (FF), corrected for height. Body composition parameters were compared between lung and colorectal cancer patients using the t-test, and with a length of hospital stay (LHS), metastatic status and mortality using linear regression and t-tests.
Results: 74 patients with colorectal (42M, 32F; mean age 62.9±12.1) and 53 patients with lung cancer (28M, 25F; mean age 66.9±10.5) were included. Patients with lung cancer had significantly greater mean SM FF than those with colorectal cancer (p=0.0124), and lower FFM (p=0.0071) and SM (p=0.0084) indices. LHS in lung cancer patients was significantly associated with SM FF (p=0.035). We found no relationship between body composition and metastatic status or 12-month mortality.
Conclusion: Patients with lung cancer have lower FFM and SM indices consistent with a reduction in muscle mass compared to colorectal cancer patients. In lung cancer patients, increasing SM FF (i.e. fatty infiltration) was associated with a greater LHS. These findings may reflect differences in the underlying disease pathogenesis and have implications for management in terms of optimising nutritional support.
Limitations: Specific reasons for hospital stay were not recorded so further analysis of the relationship between LHS and body composition was not possible.
Ethics committee approval: Ethical approval and written informed consent received.
Funding: No funding was received for this work.
Author Disclosures:
N. Sakai: nothing to disclose
A. Bhagwanani: nothing to disclose
J. Khalasthry: nothing to disclose
M. Hall-Craggs: nothing to disclose
S. A. Taylor: nothing to disclose

MyT3 8-16 17:00

A preliminary study of spectral imaging characteristic differences among tumour tissue, transition tissue and normal tissue of pancreatic cancer

W. Wu, Y. Xu; *Guangzhou/CN (zai.sa@163.com)*

Purpose: To investigate the clinical value of gemstone spectral imaging (GSI) parameters changes among tumour tissue, transition tissue and normal tissue of pancreatic cancer on wide detector spectral CT.
Methods and materials: 19 adult-patients diagnosed as pancreatic cancer and 12 adult-patients as control group were performed 4 phases spectral-enhanced examination on revolution CT. For the patients with pancreatic cancer, ROIs were drawn separately from tumour tissue, transition tissue to normal tissue. Iodine(water) density and water(iodine) density were measured in late-arterial phase and fat(iodine) density was measured in plain phase. The data of tumour tissue, transition tissue and normal tissue of pancreatic cancer were compared with each other, and their differences with those of control group were analysed.
Results: For the patients with pancreatic cancer, from the tumour, the transition zone to the normal tissue, the iodine(water) values, water(iodine) values and fat(iodine) values were gradually increased. The values of iodine(water) and water(iodine) among groups were found significant differences with each other ($p<0.05$); there were no significant differences between the fat(iodine) values between tumour and transition zone, transition zone and normal tissue ($p>0.05$), while there was significant difference between tumour and normal tissue ($p<0.05$). Compared with the control group, there were significant differences among tumour, transition zone and normal tissue in iodine(water) values respectively ($p<0.05$); there were significant differences between the control group and tumour, transition zone in water(iodine) values and fat(iodine) values ($p<0.05$), but no significant difference with normal tissue ($p>0.05$).
Conclusion: Using spectral imaging parameters, the changes of "the tumour side to the transition zone to normal tissue" in pancreatic cancer can be evaluated and differentiated with the normal pancreas.
Limitations: No golden standard.
Ethics committee approval: This study was approved by the ethics committee.
Funding: No funding was received for this work.
Author Disclosures:
W. Wu: nothing to disclose
Y. Xu: nothing to disclose

MyT3 8-17 17:04

The role of diffusion-weighted magnetic resonance imaging in the assessment of response to treatment in cervical cancer patients after chemo-radiation therapy

G. Zanirato Rambaldi, M. Giannotta, A. Galuppi, E. Salizzoni; *Bologna/IT*

Purpose: To analyse the role of DW-MRI in early prediction of response to treatment in cervical cancer patients after chemo-radiation (RT).
Methods and materials: Between September 2017-August 2019, 68 women with histologically proven cervical cancer underwent DW-MRI in our centre before and after the completion of neoadjuvant RT. Two radiologists, with respectively 4-20 years of MR experience, measured tumour volume (TV) and ADC mean in consensus. Three regions of interest were drawn on a single DW image, avoiding areas of necrosis, and on the corresponding ADC map: the mean ADC was obtained. According to response evaluation criteria in solid tumours, treatment response was classified as complete (CR) partial (PR) response, stable disease (SD) or progression (PD). Comparisons were made with Mann-Whitney and Chi-square tests.
Results: 68 women aged between 31-85 years (average 55), affected by squamous cell carcinoma were analysed. The mean time from RT to the MRI was 23 days (range 2-55). CR was observed in 39 patients, PR in 17. No PD was observed. After RT, TV was higher in PR and SD than in CR ($p=0.001$). TV reduction was lower in PR than in CR ($p=0.01$). ADC was lower before RT than after, respectively 0.82 and 1.25 $*10^{-3}$ mm^2/s ($p<0.001$), and ΔADC was higher in CR than in SD ($p=0.035$); while no statistically significant differences were observed in ADC values in PR and SD, ADC in CR was higher than in PR, respectively 1.32 and 1.02 $*10^{-3}$ mm^2/s ($p<0.017$).
Conclusion: DW-MRI is useful for evaluating response to treatment after RT and for predicting CR.
Limitations: This study is a retrospective study and includes scarcer numerosity of population.
Ethics committee approval: n/a
Funding: No funding was received for this work.
Author Disclosures:
G. Zanirato Rambaldi: nothing to disclose
M. Giannotta: nothing to disclose
A. Galuppi: nothing to disclose
E. Salizzoni: nothing to disclose

MyT3 8-18 17:08

Correlation between diffusion-weighted MRI and the expression of PCNA and Ki-67 in cervical cancer cells

Z. Ma, X. Zhao; *Zhengzhou/CN (11430884@qq.com)*

Purpose: To investigate the changes of ADC and rADC values of DWI in patients with cervical cancer and their correlation with PCNA and Ki-67.
Methods and materials: Forty patients with cervical cancer were confirmed by pathology. All patients underwent magnetic resonance imaging and diffusion-weighted imaging before an operation. PCNA and Ki-67 immunohistochemical staining were performed during operation. The expression of PCNA and Ki-67 in cervical cancer patients with different differentiation degree was analysed by variance analysis. The correlation between PCNA, Ki-67, ADC and rADC was analysed by Pearson correlation analysis. SPSS 21.0 statistical software was used for statistical analysis of the data, $P < 0.05$ was statistically significant.
Results: The ADC value and rADC value of low differentiation group were lower than that of high differentiation group ($t = 2.118$, $P < 0.05$). There was no significant difference between the poorly differentiated group and the moderately differentiated group ($P > 0.05$). The expression of PCNA and Ki-67 increased with the decrease of differentiation. With the increase of PCNA and Ki-67 expression, the ADC value and r-ADC value decreased, and the difference was statistically significant ($P < 0.05$). After Pearson correlation test, ADC value was negatively correlated with Ki-67 and PCNA expression ($P < 0.05$).
Conclusion: The measurement of ADC and rADC values in DWI imaging of cervical cancer is helpful to evaluate and differentiate different pathological grades of cervical cancer and has potential as a non-invasive method for evaluating the degree of tumour proliferation.
Limitations: The pathological specimens obtained are not identical to the parts of the solid part of the tumours measured on ADC maps.
Ethics committee approval: n/a
Funding: No funding was received for this work.
Author Disclosures:
Z. Ma: Author at Third Affiliated Hospital of Zhengzhou University
X. Zhao: Founder at Third Affiliated Hospital of Zhengzhou University

MyT3 8-19 17:12

Does whole-body PET/MRI of abdominal cancers offer additional findings compared to contrast-enhanced CT?

S. G. Gür, B. Koyuncu Sökmen; *Istanbul/TR (bedriyekoyuncu@yahoo.com)*

Purpose: In this study, we aimed to compare the diagnostic value of contrast-enhanced CT and PET/MRI in patients with abdominal malignancy.
Methods and materials: Between January 2016 and May 2019, 77 patients with intraabdominal primary tumours with PET/MRI and contrast-enhanced CT examination were screened with retrospectively. PET/MRI and contrast-enhanced CT images of the patients were evaluated by two independent radiologists and the common consensus was obtained. Histopathological findings were taken as reference. Diagnostic value of two different modalities for the primary tumour, metastatic focus and lymphadenopathy were compared.
Results: PET/MRI and CT , respectively, regardless of the histology of the primary tumour, 100% of primary tumours (77 patients) and 98,7 % of primary tumours (76 patients); 100% of lymph node involvement(24 patients) and 91,6% of lymph node involvement (22 patients), 100% of distant metastases (36 patients) 97,2% of distant metastases (35 patients) has detected. There was no statistically significant difference between the PET/MRI and CT in terms of primary tumour ($p = 0.32$), lymph node metastasis ($p = 0.15$) and distant metastasis ($p = 0.32$). In addition, it provided additional information in 6,6% (1/15 patients) of patients in detecting multiple foci in hepatocellular carcinoma, regardless of our aim. In addition, PET/MRI detected undetectable brain and extremity metastases in 19.4% (7/36 patients) of patients compared with CT.
Conclusion: The biggest advantage of PET/MRI is the low ionising radiation. PET/MRI is superior to CT in lymph node and distant metastasis detection.
Limitations:
The main limitation of this study is low patient number.
Ethics committee approval:
The institutional review board approved the study; the requirement for informed consent was waived since the study was retrospective investigation.
Funding: No funding was received for this work.
Author Disclosures:
S. G. Gür: nothing to disclose
B. Koyuncu Sökmen: nothing to disclose

MyT3 8-20 17:16

Acoustic radiation force impulse elastography as a response evaluation tool for transarterial chemoembolisation in the treatment of hepatocellular carcinoma

J. Moideen, I. Subbanna, V. Bhargavi; *Bengaluru/IN (drjunise@gmail.com)*

Purpose: Trans-arterial chemoembolisation is chosen for patients with hepatocellular-carcinoma who falls into BCLC-stage B usually helps in the local control of the tumour burden. So it is necessary to monitor the results post TACE treatment for deciding further management. CECT/MRI abdomen is taken as the gold standard in considering the treatment response following treatment. In this study, we evaluated the role of ARFI-elastography to measure stiffness in deep tissues. As a response evaluation tool in HCC patients treated by TACE.
Methods and materials: A total of 95 lesions from 54 patients were evaluated with elastography before and after TACE procedure and findings were correlated with Triphasic CECT scans. The difference in enhancing areas in follow up CT scans were assessed and categorised and was compared with the difference in ARFI-Max values attained on ARFI-elastography on follow-up. It was also compared with the difference in stiffer areas within the lesion of follow-up. The lesions were categorised into lesions within a cirrhotic liver and lesions within a non-cirrhotic liver. Various parameters were compared using Kappa, weighted Kappa, Kruskal Wallis test and linear regression analysis.
Results: In our study, HCCs showed variable stiffness but predominantly the lesions were stiffer as compared to normal liver. Brighter areas on elastography represent the stiffer portions of the tumour which may represent the residual tumour post-treatment. There were 57 tumours in a cirrhotic background and 38 tumours in a non-cirrhotic background. We found that there is a statistically significant agreement on evaluation.
Conclusion: ARFI-elastography is a safe, non-invasive, rapid and novel technique which can be effectively used as a response evaluation tool after TACE in patients with hepatocellular-carcinoma especially when other imaging modalities are contraindicated.
Limitations: n/a
Ethics committee approval: n/a
Funding: n/a
Author Disclosures:
J. Moideen: nothing to disclose
I. Subbanna: nothing to disclose
V. Bhargavi: nothing to disclose

MyT3 8-21 17:20

Thermal effect of irreversible electroporation in pancreatic cancer

O. W. Kozak, S. Hac, T. Gorycki, B. Brzeska, K. Skrobisz, J. Pienkowska, M. Szymanski, M. Studniarek; *Gdansk/PL (oliwiak@gumed.edu.pl)*

Purpose: Irreversible electroporation (IRE) of the pancreas is an increasingly used method for unresectable pancreatic cancer that can be used in cytoreduction followed by surgical treatment and shows promising results in palliative care. It is claimed that IRE is not causing thermal effect comparing to radiofrequency and microwave ablation. Aim of the study is to assess the early post-IRE changes in signal intensities in the ablation zone with emphasis on thermal effect and vascularisation.
Methods and materials: We retrospectively analysed the MRI studies of 24 patients (10 F, 14M, aged 35-71) with unresectable pancreatic cancer during or shortly after chemotherapy. Standard IRE procedure was performed. MR images were performed on 1,5T and 3T scanners one day before IRE procedure and up to 7-days after. A standard protocol for pancreas was performed including T1W, TW2, DWI/ADC, DCE with subtraction series.
Results: Signal intensities in the ablated zone on T1-FatSat images after contrast media administration with subtraction was in the range 0-6,25. The ADC values after IRE were significantly higher compared to pre-IRE measurements. Signs of thermal effect were seen as gas bubbles close to the electrodes after CT-guided percutaneous procedures were performed. On MR images in 83,3% of patients, they were seen as small, hypointense zones in electrodes placement on T1-FatSat contrasted-enhanced images.
Conclusion: Low SI values in the ablated zones on T1-FatSat+CM images with subtraction proves that all vascular bed within the ablation zone was completely damaged. Growth of ADC values after IRE is the effect of cellular water displacement to intercellular space what is a sign of cytolysis. IRE can create thermal effect on exposed tissues.
Limitations: This study is limited by a small group of patients and that it is performed as a single centre study.
Ethics committee approval: All applied procedures were approved by a local ethical committee.
Funding: No funding was received for this work.
Author Disclosures:
O. W. Kozak: nothing to disclose
S. Hac: nothing to disclose
T. Gorycki: nothing to disclose
B. Brzeska: nothing to disclose
K. Skrobisz: nothing to disclose
J. Pienkowska: nothing to disclose
M. Szymanski: nothing to disclose
M. Studniarek: nothing to disclose

MyT3 8-22 17:24

The prognostic value of neutrophils lymphocyte ratio (NLR) in patients treated with trans-arterial chemoembolisation with epirubicin particles for hepatocarcinoma

A. G. Chimenti[1], G. Zanirato Rambaldi[1], M. Giannotta[1], A. Rebonato[2]; *[1]Bologna/IT, [2]Pesaro/IT (achimenti2801@gmail.com)*

Purpose: To analyse the prognostic value of the neutrophils lymphocyte ratio (NLR) in patients treated with trans-arterial chemoembolisation with epirubic particles (TACE) for hepatocarcinoma (HCC).
Methods and materials: From the review of the chart, the following data were collected: the white blood cells count, the percentage of neutrophils, the percentage of lymphocytes, the value of albumin and total bilirubin, INR, the value of alpha-fetus protein pre-TACE, creatinine, the value of GFR, the value of ferritin pre-TACE, the CHILD-PUGH class. The lymphocyte neutrophils ratio (NLR) was calculated.
Results: Between January 2012 and April 2015, 83 patients affected by HCC underwent TACE at our centre: 52 of them (39 males) were included. Survival after the first procedure was 1.60 years (range 0.25-4.27). The average NLR value was 3.15 (range 0.61-19.02; median 1.96). Patients were divided into two groups according to the median NLR value, showing a significant poor survival among patients with NLR>1.96 (p 0.0087).
Conclusion: The lymphocyte neutrophils ratio is an important prognostic value for patients affected by hepatocarcinoma undergoing drug eluting beads-TACE.
Limitations: This study is retrospective.
Ethics committee approval: n/a
Funding: No funding was received for this work.
Author Disclosures:
A. G. Chimenti: nothing to disclose
G. Zanirato Rambaldi: nothing to disclose
M. Giannotta: nothing to disclose
A. Rebonato: nothing to disclose

Friday, March 13

08:30 - 10:00 **Room C**

Interventional Radiology

RPS 909

Neuro-interventions

Moderators:
N.N.

RPS 909-1 08:30

Investigation of two FD stents' EMSA variation at a giant aneurysm neck by using virtual stent deployment

G. Guclu[1], T. Günaydın[1], C. Ünsal[1], A. B. Olcay[1], C. Bilgin[2], B. Hakyemez[2]; *[1]Istanbul/TR, [2]Türkiye/Bursa/TR (bahadir.olcay@yeditepe.edu.tr)*

Purpose: Flow diverter (FD) stents are typically used in the treatment of giant aneurysms. While these aneurysms may form and grow at the weak section of an artery wall, the use of FD restricts the blood flow going into aneurysm sac by diverting the blood flow through the parent artery when these stents are placed into the patients' aneurysm site.
Methods and materials: In the present study, a three-dimensional aneurysm site of a 41-year-old female patient was constructed using 220 digital subtraction angiography (DSA) images. The average hydraulic diameter of the left internal carotid artery (LICA) carrying aneurysm was calculated to be nearly 4.5 mm. Then, two FD stents, namely FRED 4518 and FRED 5014, were chosen for virtual stent deployment. It is noted that FRED 4518 has a 40% effective metal surface area (EMSA) and 18 mm working length while FRED 5014 has a 28% EMSA and 20 mm working length.
Results: Once the FD stents were placed into the artery separately using the virtual deployment method, the EMSA value of FRED 4518 decreased to 30.28% while FRED 5014's EMSA value became 21.67% at the patient's aneurysm neck due to the curly shape and non-uniform cross-sections of the parent artery.
Conclusion: This indicates that a decrease in FD's EMSA value can have an influence in haemodynamics inside an aneurysm sac by accelerating or decelerating the stagnation process.
Limitations: Radial forces in FD stents are not taken into account.
Ethics committee approval: Ethics committee approval obtained.
Funding: The Scientific and Technological Research Council of Turkey under the 1001 Program (Project no. 117M491).
Author Disclosures:
A. B. Olcay: Grant Recipient at Yeditepe University
C. Bilgin: nothing to disclose
G. Guclu: Speaker at Yeditepe University
T. Günaydın: nothing to disclose
C. Ünsal: nothing to disclose
B. Hakyemez: Shareholder at Uludag University

RPS 909-2 08:36

MRgFUS thalamotomy: the potential value of periprocedural parameters as a predictive tool for evaluating tremor treatment outcomes

M. Martino, A. Gagliardi, E. Tommasino, M. Allevi, F. Bruno, F. Arrigoni, A. Catalucci, P. Sucapane, C. Masciocchi*; L'Aquila/IT (aivlim@hotmail.it)*

Purpose: Therapeutic application for tremor treatment by transcranial high-intensity focused ultrasound (HIFU) demands a precise analysis of physical and control parameters to obtain optimal outcome. Our objective was to define the correlation between periprocedural parameters regarding HIFU procedures and treatment outcome.
Methods and materials: 57 patients with essential tremor (ET) and Parkinson disease (PD) tremor were treated using an MRgFUS brain system (ExAblate 4000, InSightec) in a 3T MR scanner (MR750, GE Healthcare). We retrospectively evaluated the intraprocedural MR-thermometry, measuring the accumulated thermal dose (ATD) size and temperature and the number of sonications and values of maximum energy delivered and temperatures reached. The periprocedural parameter profiles were correlated with the corresponding treatment outcome assessed using the Fahn-Tolosa-Marin scale after 1 day, 1 month, 3 months, and 6 months follow-up.
Results: Statistical analysis showed a mean ATD temperature significantly correlated with FTM scores after 1 day and 1 month follow up ($p<0.005$) We did not find any statistically significant correlation between ATD temperature and FTM in 3 and 6 months follow-up, or between clinical outcomes and other periprocedural parameters.
Conclusion: According to our preliminary results, intraprocedural ATD after the procedure may have a possible predictive value of treatment outcome after MRgFUS thalamotomy in patients with ET and PD tremor.
Limitations: The limited number of patients available could be a hindrance for statistical significativity.
Ethics committee approval: n/a
Funding: No funding was received for this work.
Author Disclosures:
M. Martino: nothing to disclose
A. Gagliardi: nothing to disclose
E. Tommasino: nothing to disclose
F. Bruno: nothing to disclose
F. Arrigoni: nothing to disclose
A. Catalucci: nothing to disclose
P. Sucapane: nothing to disclose
C. Masciocchi: nothing to disclose
M. Allevi: nothing to disclose

RPS 909-3 08:42

The impact of balloon guide catheter usage in a mechanical thrombectomy on tissue integrity of the penumbra

M. T. Berndt, T. Boeckh-Behrens, J. Kaesmacher, C. Zimmer, B. Friedrich, F. Mück, S. Wirth, C. Maegerlein*; Munich/DE (maria.berndt@tum.de)*

Purpose: During mechanical recanalisation of large vessel occlusions (LVO), the use of proximal flow arrest with balloon guide catheters (BGC) was shown to be associated with better angiographic and clinical outcome. It is unclear if there is a benefit for the structural integrity of the penumbral brain tissue. The aim of the study was to analyse possible microstructural alterations in the salvaged penumbra dependent on BGC-usage.
Methods and materials: All patients who underwent mechanical recanalisation of LVO of the anterior circulation were reviewed within a prospective stroke registry of a single comprehensive stroke centre. 65 patients received an admission CT-perfusion together with post-interventional diffusion tensor imaging. Technical details such as BGC-usage were correlated with microstructural integrity changes of the salvaged grey matter through a MD (mean diffusivity)-index. Moderation analysis was performed to test the interaction of BGC on the correlation between angiographic and clinical outcome.
Results: For all patients with complete reperfusion (TICI 3), microstructural integrity changes with a lowered MD-index were found within the salvaged penumbra for cases of non-BGC-usage (mean=0.02) compared to cases with BGC-usage (0.01, p=0.04). The benefit of complete reperfusion on good clinical outcome is moderated by the BGC-group (effect 2.78, p=0.01 vs for non-BGC:0.3, p=0.71).
Conclusion: The lowered MD-index early after mechanical recanalisation without the use of BGC can be interpreted as microstructural ischaemic damage of the salvaged penumbra, possibly caused by microembolisation without using proximal flow arrest. It was shown that achieving complete reperfusion in a setting of BGC-usage minimises penumbral damage and improves the long-term outcome.
Limitations: Results should be confirmed in a multi-centric setting.
Ethics committee approval: Approval by the local ethics committee. The need for patient consent was waived.
Funding: No funding was received for this work.
Author Disclosures:
M. T. Berndt: nothing to disclose
T. Boeckh-Behrens: nothing to disclose
C. Zimmer: nothing to disclose
B. Friedrich: nothing to disclose
F. Mück: nothing to disclose
S. Wirth: nothing to disclose
C. Maegerlein: nothing to disclose
J. Kaesmacher: nothing to disclose

RPS 909-4 08:48

Preliminary experience of endovascular embolisation of cerebral dural arteriovenous fistulas with SQUID 12

E. Lozupone, P. Trombatore, L. Milonia, F. D'argento, A. Alexandre, I. Valente, A. Pedicelli*; Rome/IT (PIETRO.TR@OUTLOOK.IT)*

Purpose: To show the effectiveness and safety of SQUID 12 in the embolisation of cerebral dural arteriovenous fistulas (cDAVF).
Methods and materials: From June 2017-January 2019, the authors retrospectively reviewed clinical, demographic, and embolisation data of 13 consecutive patients with cDAVF (3 IIb, 5 Cognard III, and 5 Cognard IV) who underwent embolisation using the SQUID 12. 4 patients were symptomatic for headache, 2 patients presented with vertigo and confusion, 2 patients with tinnitus, 1 patient with a bruit, and 1 patient with aphasia; 3 patients were asymptomatic. The number of arteries catheterised for embolisation, the total amount of embolic agent, the rate of occlusion, the time of the procedure, and

the rate of complication were recorded. Mid-term follow-up with MR and DSA was reviewed.
Results: In 11 patients, the cDAVF closure was accomplished at the end of the procedure; in one case, a double staged treatment was performed, while in another case, a small remnant was left. The average time of injection was 36 minutes and the average amount of SQUID 12 was 2.8 mL. One patient with a cDAVF of traverse sinus region (Cognard III) experienced a facial palsy which resolved after 2 weeks of corticosteroids; no other complications were recorded. Mid-term MR and angiographic follow-up confirmed complete occlusion of the cDAVFs in 12 patients; in 1 patient with an infratentorial fistula, a small relapse was detected.
Conclusion: The treatment of the DAVFs by using SQUID 12 seems to be effective and safe. The lower viscosity allow a distal migration of the agent, a lesser proximal reflux, and a deeper penetration in the cDAVF.
Limitations: A mall sample size and a retrospective study.
Ethics committee approval: n/a
Funding: No funding was received for this work.
Author Disclosures:
P. Trombatore: nothing to disclose
E. Lozupone: nothing to disclose
L. Milonia: nothing to disclose
F. D'argento: nothing to disclose
A. Alexandre: nothing to disclose
I. Valente: nothing to disclose
A. Pedicelli: Author at Emboflu

RPS 909-5 08:54

Radiation exposure of patients during interventional neuroradiology procedures

V. Opancina, R. Vojinovic*; Kragujevac/RS*

Purpose: To assess the doses received by patients during interventional neuroradiology procedures and to establish their dose range.
Methods and materials: Our study included all patients who underwent diagnostic and therapeutic interventional neuroradiology procedures from December 2017-June 2019 at our institution. The following variables were taken into account: dose area product, air kerma, and fluoroscopy exposure time. Peak skin dose was calculated from a published dose conversion formula for interventional procedures: PSD=249+5.2*DAP. We estimated an effective dose from DAP using a dose conversion factor, where DCC= ED/DAP, and calculated a brain dose using the ED and tissue weighing factor provided by ICRP-103.
Results: There were 224 cerebral angiographies, 55 aneurism embolisations, and 21 combined procedures. We calculated the total mean±SD and third quartiles for all dependent variables: DAP (93.95±50.48 Gy-cm^2; 116.23 Gy-cm^2), AK (595.23±382.07 Gy; 680.94 Gy), T (7.43±7.37 min; 9.26 min), ED (13.62±7.32 mSv; 16.85 mSv), and PSD (0.49±0.26 Gy; 0.60 Gy). Estimated brain doses for diagnostic, therapeutic, combined, and all procedures in total were 254.62 mGy, 227.84 mGy, 341.12 mGy, and 272.4 mGy. Post hoc analysis determined a Bonferroni correction of critical value which was significant for each test: DAP-procedure type (0.016), AK-procedure type (0.000), ED-procedure type (0.016), and PSD-procedure type (0.016).
Conclusion: Interventional neuroradiology procedures show significant variability in radiation dose due to patient constitution, radiologist expertise, and equipment factors. Knowing the doses can have a great benefit in terms of prevention of possible radiation effects.
Limitations: There is no standardised method for effective dose calculation.
Ethics committee approval: Approved by Institutional Ethics Committee.
Funding: No funding was received for this work.
Author Disclosures:
V. Opancina: nothing to disclose
R. Vojinovic: nothing to disclose

RPS 909-6 09:00

Quantitative collateral vessel density associated with the prognosis of mechanical thrombectomy on intracranial large vessel occlusion: an initial study based on CT perfusion imaging

Z. Shi, M. Yang, H. Wang, J. Lu*; Shanghai/CN (shizhangmd@smmu.edu.cn)*

Purpose: This study on acute ischaemic stroke caused by intracranial large vessel occlusion (LAO) aims to further evaluate the high-risk factors of the prognosis of mechanical thrombectomy (MT) by collateral vessel density (CVD) using F-STROKE software.
Methods and materials: This study was retrospectively analysed on 92 patients with acute ischaemic stroke caused by LAO from January 2018-October 2018. All patients underwent CT perfusion (CTP) examination before MT. The patients were divided into two groups according to 90d-mRS (0-2 points: good prognosis; 3-6 points: poor prognosis). F-stroke software was used for CTP image analysis to quantitatively obtain core infarct volumes, ischaemic penumbra volumes, mismatch ratios, and CVD. A multivariate logistic regression model was used to calculate the odds ratio (OR) and 95% confidence interval (95%CI). P<0.05 was considered statistically significant.
Results: A total of 87 patients with LAO (51.2±8.4 years; 57 males and 30 females) were included. The univariate analysis showed that the core infarction volume (P=0.017), mismatch ratio (P=0.040), CVD (P=0.003), and symptom improvement (P<0.001) were associated with the prognosis after MT. As multivariate logistic regression analysis showed, CVD (P=0.008; OR=13.296; 95%CI, 1.948-90.736) and symptom improvement (P=0.003; OR=13.824; 95%CI, 2.476-77.196) were two independent high-risk factors for the prognosis of MT. According to ROC, the AUC value of CVD and symptom improvement were 0.819 and 0.760, respectively.
Conclusion: For patients with LAO who underwent MT, CVD was an independent quantitative predictor to the prognosis after MT surgery.
Limitations: The retrospective analysis of the acquired data. We only used CT scans performed on acute stroke patients.
Ethics committee approval: n/a
Funding: No funding was received for this work.
Author Disclosures:
Z. Shi: nothing to disclose
M. Yang: nothing to disclose
H. Wang: nothing to disclose
J. Lu: nothing to disclose

RPS 909-7 09:06

Automated contrast-uptake measurements on single-phase CT angiography for stroke triage

P. Reidler, D. Puhr-Westerheide, L. Rotkopf, D. Apel, F. Dorn, S. Tiedt, M. P. D. L. Kellert, M. P. Fabritius, W. G. Kunz*; Munich/DE*

Purpose: To determine the clinical value of software-based automated cerebral attenuation measurements at CT angiography (CTA) to classify eligibility for late time window thrombectomy as established by DEFUSE 3 criteria using CT perfusion (CTP) imaging.
Methods and materials: We enrolled stroke patients with large vessel occlusion and complete imaging datasets including non-contrast CT, CTA, and CTP. X-ray attenuation in Hounsfield Units (HU) was measured at non-contrast CT and CTA data in all Alberta stroke program early CT score (ASPECTS) regions using automated software. Contrast uptake (CU) was defined per ASPECTS region as the absolute difference of attenuation on CTA minus non-contrast CT. All regional values were merged into a composite CTA-CU score using a linear regression model. Extent of the ischaemic core and target mismatch were determined at CTP. Receiver-operating-characteristics analysis was performed to calculate area-under-the-curve (AUC) for the classification of DEFUSE 3 criteria (core<70 mL, target mismatch>1.8).
Results: We included 79 patients with ischaemic core sizes of 17 mL (IQR: 9-46 mL). Automatic CU measurements were technically successful in all patients. CU values over all ASPECTS regions were significantly lower in the ischaemic compared to the non-ischaemic hemisphere, with a median of 4.2HU (IQR: 2.7–5.8HU, p<0.001). The composite CTA-CU score enabled significant classification of DEFUSE 3 thrombectomy criteria (AUC: 0.85, p<0.001, sensitivity: 91%, specificity: 67%) while outperforming visual ASPECTS.
Conclusion: As an observer-independent and quantifiable imaging biomarker, the composite CTA-CU score was able to classify CTP imaging criteria for late time window thrombectomy criteria.
Limitations: Limitations include the use of only one CT vendor, the global variability of CTA protocols, and the rather small study sample.
Ethics committee approval: The study was appoved by the local IRB.
Funding: No funding was received for this work.
Author Disclosures:
P. Reidler: nothing to disclose
W. G. Kunz: nothing to disclose
D. Puhr-Westerheide: nothing to disclose
L. Rotkopf: nothing to disclose
D. Apel: nothing to disclose
F. Dorn: nothing to disclose
S. Tiedt: nothing to disclose
M. P. D. L. Kellert: nothing to disclose
M. P. Fabritius: nothing to disclose

RPS 909-8 09:12

Prognostic value of semi-quantitative collateral assessment in the endovascular treatment of ischaemic stroke

M. V. M. Micelli, P. Palumbo, G. Bianchi, A. Izzo, F. Bruno, M. Varrassi, S. Carducci, A. V. Giordano, C. Masciocchi*; L'Aquila/IT (micelli.mvm@gmail.com)*

Purpose: To evaluate collateral circulation in patients with an acute ischaemic stroke (AIS) who underwent endovascular thrombectomy (ET) in order to investigate its value in the prediction of clinical outcome.
Methods and materials: We retrospectively investigated 120 patients with CTA-proven large vessel occlusion (LVO) treated with ET from January 2014-September 2019. Good collateral (GC), good recanalisation rate (RR), and clinical assessment (CA) were defined respectively by a collateral flow grading system (ASITN/SIR) score ≥2, a thrombolysis in cerebral infarction (TICI) score ≥2b, and the NIHSS scale before and 24 hours after ET.
Results: The patients were divided into two groups due to the presence of GC (63%) or not named worse collateral (WC) (37%). Each group was analysed in relation to onset time, TICI, and NIHSS using Spearman's rank correlation coefficient. Although analogue onset time of symptoms was considered, the 24h-NIHSS score was better in the GC-group than the WC-group ($p<0.001$). GC were also associated with a better RR ($p<0.05$).
Conclusion: In line with the recent randomised studies, the analysis of collateral and a better selection of patients have to be mandatory for a better clinical outcome.
Limitations: A small sample.
Ethics committee approval: n/a
Funding: No funding was received for this work.
Author Disclosures:
A. V. Giordano: nothing to disclose
M. V. M. Micelli: nothing to disclose
P. Palumbo: nothing to disclose
G. Bianchi: nothing to disclose
A. Izzo: nothing to disclose
M. Varrassi: nothing to disclose
S. Carducci: nothing to disclose
C. Masciocchi: nothing to disclose
F. Bruno: nothing to disclose

RPS 909-9 09:18

6 to 24 hours endovascular thrombectomy for large intracranial vessel occlusion without perfusion CT patient selection: a single-centre experience

F. Giubbolini[1], A. Pedicelli[1], A. Alexandre[1], A. Bartolo[1], I. Valente[1], E. Lozupone[1], F. D'argento[2], C. Colosimo[1]; [1]*Rome/IT*, [2]*Taviano/IT*
(Francesca.giubbolini@gmail.com)

Purpose: The effect of endovascular thrombectomy performed more than 6 hours after the onset of ischaemic stroke has been shown by the DAWN and DEFUSE-3 trials. In these trials, strict criteria were employed for patient selection, including perfusion CT. We performed a retrospective single-centre evaluation of patient treated 6 to 24 hours after stroke onset without perfusion CT selection.
Methods and materials: On a total of 212 patients who received endovascular thrombectomy for major intracranial vessel occlusion, we identified 55 patients who were treated 6 to 24 hours after stroke onset. Patients were selected on the basis of clinical and radiological criteria. Co-primary endpoints were the rate of functional independence (0, 1, or 2 on the mRS) at 90 days and post-treatment symptomatic intracranial haemorrhage (ECASS II criteria). Secondary endpoints were an early therapeutic response and successful recanalisation.
Results: Out of 55 patient, 22 (40%) were functionally independent at 90 days (mRS 0-2). Of these, 11 were mRS 0, 7 were mRS 1, and 4 were mRS 2, while the rate of symptomatic intracranial haemorrhage was 4 out 55 (7%). Early therapeutic response was achieved in 22 out of 55 patients (40%). Successful recanalisation was achieved in 44 out of 55 patients (80%).
Conclusion: Our data confirms that endovascular thrombectomy for large intracranial vessel occlusion in a later time window is safe and effective, even without CT-perfusion patient selection. A larger population of patients can potentially benefit from endovascular thrombectomy even without applying strict selection criteria, compared to DWAN and DEFUSE-3 trials.
Limitations: A retrospective, monocentric study with a small sample size.
Ethics committee approval: n/a
Funding: No funding was received for this work.
Author Disclosures:
F. Giubbolini: nothing to disclose
A. Pedicelli: nothing to disclose
A. Alexandre: nothing to disclose
A. Bartolo: nothing to disclose
I. Valente: nothing to disclose
E. Lozupone: nothing to disclose
F. D'argento: nothing to disclose
C. Colosimo: nothing to disclose

RPS 909-10 09:24

The clinical application of low-dose CT-guided craniocerebral puncture biopsy

Y. Lian, J. Dong, Z. Zhou, Z. Lu, Y. Pan; *Zhengzhou/CN*
(lybang0507@126.com)

Purpose: To investigate the clinical value and safety of CT-guided craniocerebral puncture biopsy.
Methods and materials: From March 2017-July 2019, 23 patients (14 males and 9 females, aged 17-80 years old with a mean age of 52.5 years old) with clinical neurological symptoms or signs underwent CT-guided craniocerebral puncture biopsy. Enhanced-MRI and MRS revealed that all patients had multi-intracranial space-occupying lesions. GE Lightspeed CT was used to perform the CT-guided craniocerebral puncture biopsy for pathological or bacteriological examinations. The number of scans, operation time, pathological type, and complications were counted and analysed.
Results: Of the 23 patients, a definite pathological diagnosis was made in 22 cases, with a high biopsy positive rate of 95.7% (22/23). Among them, an oncology-pathological diagnosis was obtained in 18 cases (18/22, 81.8%), including 8 cases of diffuse large B-cell lymphoma (8/18, 44.4%), 6 cases of astrocytoma (6/18, 33.3%), 3 cases of glioblastoma (3/18, 16.7%), and 1 case of metastatic composite small cell carcinoma (1/18, 5.6%). Inflammatory infectious disease was confirmed in 4 cases (4/22, 18.2%). One patient was diagnosed with cerebral gliosis hyperplasia but it was confirmed as a glioblastoma after surgery. The average operating time was 27 minutes and the mean DLP was 201.6 mGy*cm, with an average radiation dose of 0.42 mSv. 4 patients had a small amount of haemorrhage (about 0.5-1.5 ml) at the puncture site. No serious complications such as neurological damage, epilepsy, a large amount of intracranial haemorrhage, and intracranial infection occurred in all patients.
Conclusion: CT-guided craniocerebral puncture biopsy is minimally-invasive with fewer complications, low radiation dose, and a high pathological positive rate. It has great clinical value in the diagnosis of craniocerebral lesions.
Limitations: The radiation exposure.
Ethics committee approval: n/a
Funding: No funding was received for this work.
Author Disclosures:
Y. Lian: nothing to disclose
J. Dong: nothing to disclose
Z. Zhou: nothing to disclose
Z. Lu: nothing to disclose
Y. Pan: nothing to disclose

RPS 909-11 09:30

Contrast-enhanced ultrasound-guided transoral core-needle biopsy: a novel, safe, and well-tolerated procedure for obtaining high-quality tissue in patients with oral cancer

M. Lu, T. Wei; *Chengdu/CN*

Purpose: To determine the tolerability, safety, and effectiveness of contrast-enhanced ultrasound (CEUS)-guided transoral core-needle biopsy (CNB) for oral lesions.
Methods and materials: A consecutive series of 44 patients who underwent CEUS-guided transoral CNB of oral lesions at our hospital were evaluated retrospectively. CEUS-guided transoral CNB was performed by using an endocavitary transducer and needle guide device attached to the transducer shaft. Tolerability questionnaires were completed prior to and following the sampling procedures. The CEUS characteristics, successful biopsy rate, diagnostic performance, tolerability, and complications were assessed and recorded.
Results: CEUS improved the conspicuity of target lesions and the detection rate of internal liquefied necrosis compared with transoral US ($p<0.05$). The successful biopsy rate was 100%. Based on the final diagnosis, 29 malignant lesions (23 squamous cell carcinomas, 3 adenoid cystic carcinomas, 2 mucoepidermoid carcinomas, and one melanoma) and 15 benign lesions (8 inflammatory lesions, 5 pleomorphic adenomas, one schwannoma, and one haematoma), the sensitivity, specificity, positive predictive value (PPV), negative predictive value (NPV), and accuracy of this technique were 96.7%, 100%, 100%, 93.8%, and 97.7%, respectively. No significant difference in pain and swelling of the biopsied site from before and after the procedure was observed. No serious complications were observed.
Conclusion: CEUS-guided transoral CNB can be considered as a safe, well-tolerated, and effective technique for patients with suspected oral cancer.
Limitations: This study design was retrospective. This was a single-centre study with a small sample of cases. Studies with sufficient samples should be performed further.
Ethics committee approval: This study was approved by the Institutional Review Board and Ethics Committee of Sichuan Cancer Hospital. Informed consent was obtained before the ultrasonography examination and biopsy.

Funding: No funding was received for this work.
Author Disclosures:
M. Lu: Author at Ultrasound Medical Center, Sichuan Cancer Hospital Institute, Sichuan Cancer Center, School of Medicine, University of Electronic Science and Technology of China, Chengdu, China, 610041
T. Wei: Author at Ultrasound Medical Center, Sichuan Cancer Hospital Institute, Sichuan Cancer Center, School of Medicine, University of Electronic Science and Technology of China, Chengdu, China, 610041 ; North Sichuan Medical College, Nanchong, China, 637000

RPS 909-12 09:36

High blood pressure levels after endovascular treatment for ischaemic stroke are associated with worse outcome: results from the MR CLEAN registry

N. Samuels[1], R. van de Graaf[1], C. van Den Berg[1], J. Hofmeijer[2], Y. Roos[3], B. Roozenbeek[1], H. Lingsma[1], D. W. J. Dippel[1], A. van der Lugt[1]; *[1]Rotterdam/NL, [2]Arnhem/NL, [3]Amsterdam/NL (n.samuels@erasmusmc.nl)*

Purpose: Optimal blood pressure (BP) management in the acute period of ischaemic stroke remains uncertain, specifically in patients undergoing endovascular treatment (EVT). We evaluated the association between BP levels post-EVT and outcome, according to recanalisation status.
Methods and materials: We included patients from the MR CLEAN registry who underwent EVT from March 2014-June 2016 in 7 centres registering post-EVT BP values. The primary outcome was the functional outcome (modified Rankin scale) at 90 days. Secondary outcomes were sICH and early neurological deficit (NIHSS at 24h). BP parameters were mean, maximum, and minimum systolic (SBP), and mean arterial pressure (MAP) during the first 6 hours post-EVT. We used multilevel regression analysis to account for the repeated measures per patient to evaluate the association between BP and outcomes, adjusted for centre and prognostic factors, and we tested for interaction between BP and recanalisation status.
Results: In total, 867 patients were included for analyses. Mean SBP and MAP were 140 ± 22 mmHg and 99 ± 18 mmHg, respectively. Maximum SBP and MAP were associated with worse functional outcome (adjusted common odds ratio per 10mmHg (acOR) 0.93, 95% CI 0.88 to 0.98 and acOR 0.42, 95% CI 0.21 to 0.86) and higher NIHSS scores (β 0.55, 95% CI 0.33-0.77 and β 5.5, 95% CI 2.7 to 8.4). Maximum SBP was associated with higher sICH rates (adjusted OR 1.28, 95% CI 1.14 to 1.49). There was no effect of mean or minimum BP on outcome and no interaction between BP and recanalisation status.
Conclusion: Higher maximum SBP and MAP levels in the first 6 hours after EVT are associated with worse functional and neurological outcomes and higher sICH rates.
Limitations: n/a
Ethics committee approval: https://www.mrclean-trial.org
Funding: https://www.mrclean-trial.org
Author Disclosures:
N. Samuels: nothing to disclose
R. van de Graaf: nothing to disclose
C. van Den Berg: nothing to disclose
J. Hofmeijer: nothing to disclose
Y. Roos: Consultant at Stryker, Shareholder at Nico.lab
B. Roozenbeek: nothing to disclose
H. Lingsma: nothing to disclose
D. W. J. Dippel: Grant Recipient at Dutch Heart Foundation, Dutch Brain Foundation, the Netherlands Organisation for Health Research and Development, Health Holland Top Sector Life Sciences and Health, and unrestricted grants from AngioCare BV, Medtronic/ Covidien/EV3, MEDAC Gmbh/LAMEPRO, P
A. van der Lugt: Grant Recipient at Dutch Heart Foundation, AngioCare BV, Covidien/EV3, MEDAC Gmbh/LAMEPRO, Stryker, Penumbra, Inc, Medtronic

RPS 909-13 09:42

Repetitive transarterial chemoperfusion in recurrent malignant head and neck neoplasms: local response rate and survival

T. J. Vogl, A. Tröger, T. Stöver, T. Gruber-Rouh*; Frankfurt am Main/DE (t.vogl@em.uni-frankfurt.de)*

Purpose: To evaluate the response and survival of malignant recurrent neoplasms located in the head and neck area post repetitive transarterial chemoperfusion (TACP) as a palliative treatment method.
Methods and materials: 47 patients (33 males, 14 females) were treated in 4-week intervals using TACP with mitomycin C 8.5 mg/m², gemcitabine 1000 mg/m², and cisplatin 35mg/m². Before treatment, a multiparametric MRI was performed in order to evaluate the size, location, and volume of the tumour prior to TACP. After TACP, a CT scan was performed for the exclusion of possible side-effects. Tumour response was evaluated according to the RECIST criteria.
Results: TACP was well-tolerated without significant side-effects. According to the RECIST criteria, 29.79% (n=14) of the patients presented with partial remission (PR), 68.09% (n=32) showed stable disease (SD), and 2.13% (n=1) had progressive disease (PD). The median survival rate of the patients from the start of TACP therapy was 14.7 months. Patients with PR after the first treatment session presented with significantly better survival (p=0.03) with a mean of 21.4 months, while patients with SD only presented with a survival of 11.3 months.
Conclusion: TACP seems to be an effective palliative treatment option in patients with head and neck tumours.
Limitations: A limited number of patients were included.
Ethics committee approval: Approval by the Institutional Review Board.
Funding: No funding was received for this work.
Author Disclosures:
T. J. Vogl: nothing to disclose
A. Tröger: nothing to disclose
T. Stöver: nothing to disclose
T. Gruber-Rouh: nothing to disclose

RPS 909-14 09:48

Mechanical thrombectomy using TIGER

L. Will, V. Maus, S. Fischer*; Bochum/DE (Lena.Will@kk-bochum.de)*

Purpose: To evaluate the safety and efficacy of mechanical thrombectomy with a manually adjustable stent retriever (Tigertriever) in acute stroke.
Methods and materials: The Tigertriever is a manually expandable mesh intended for the treatment of acute ischaemic stroke. The unique design enables the operator to manually adjust the radial force to the vessel wall during mechanical thrombectomy.
A total of 39 thrombectomy procedures carried out at a single neurovascular centre with Tigertriever were analysed in retrospect.
Results: Of the 39, 22 were successful with the Tigertriever alone resulting in a TICI score of >2b in 100% with a medium of 1 attempt. In 17 cases, the strategy was combined with another thrombectomy device resulting in a final TICI score of >2b in 80% of these cases.
10 of the cases were arterial occlusions located distally to the circle of Willis treated with Tigertriever 13, a device compatible with a 0.0013-inch microcatheter. Mechanical thrombectomy in these distal occlusions was successful in 9 cases.
Conclusion: The Tigertriever represents an efficient and safe addition to the existing concepts for mTE. The Tiger 13 expands the opportunities to perform mTE in distal locations, especially due to the compatibility with a 0.013-inch microcatheter.
Limitations: n/a
Ethics committee approval: n/a
Funding: No funding was received for this work.
Author Disclosures:
L. Will: Author at Knappschaftskrankenhaus Bochum
V. Maus: Author at Knappschaftskrankenhaus Bochum
S. Fischer: Author at Knappschaftskrankenhaus Bochum

RPS 909-15 09:54

One-stop management with perfusion for transfer patients with stroke due to a large-vessel occlusion: feasibility and effects on in-hospital times

A. Brehm[1], I. Tsogkas[1], I. Maier[2], H. J. Eisenberger[2], Y. Pengfei[3], J. M. Liu[3], J. Liman[2], M.-N. Psychogios[1]; *[1]Basel/CH, [2]Göttingen/DE, [3]Changhai/CN (alex.brehm@usb.ch)*

Purpose:
In-hospital time delays lead to a relevant deterioration of neurologic outcomes in patients with stroke with large-vessel occlusions. At the moment, CT perfusion is relevant in the triage of late-window patients with stroke. We conducted this study to determine whether one-stop management with perfusion is feasible and leads to a reduction of in-hospital times.
Methods and materials: In this observational study, we reported the first 15 consecutive transfer patients with stroke with externally confirmed large-vessel occlusions who underwent flat panel detector CT (FDCT) perfusion and thrombectomy in the same room. Preinterventional imaging consisted of non-contrast FDCT and FDCT perfusion, acquired with a biplane angiography system. The FDCT perfusion was used to reconstruct an FDCT angiography to confirm the large-vessel occlusions. After confirmation of the large-vessel occlusion, the patient underwent mechanical thrombectomy. We recorded time metrics and safety parameters prospectively and compared them with those of transfer patients who we treated before the introduction of one-stop management with perfusion.
Results: 15 transfer patients underwent FDCT perfusion and were treated with mechanical thrombectomy from June 2017-January 2019. The median time from symptom onset to admission was 241 minutes. The median door-to-groin time was 24 minutes. Compared with 23 transfer patients imaged with multidetector CT, it was reduced significantly (24 minutes; 95% CI, 19-37 minutes, versus 53

minutes; 95% CI, 44–66 minutes; P< 0.001). Safety parameters were comparable between groups.
Conclusion: In this small series, one-stop management with perfusion led to a significant reduction of in-hospital times compared with our previous workflow.
Limitations: The observational design and the small number of patients.
Ethics committee approval: Patients were taken from a prospective acquired board certifed database. (Ethik vote number: 13/7/15An Göttingen). Additional consent was waived.
Funding: No funding was received for this work.
Author Disclosures:
A. Brehm: Research/Grant Support at Siemens
I. Tsogkas: nothing to disclose
I. Maier: nothing to disclose
H. J. Eisenberger: nothing to disclose
Y. Pengfei: nothing to disclose
J. M. Liu: nothing to disclose
J. Liman: nothing to disclose
M.-N. Psychogios: Research/Grant Support at Siemens

08:30 - 10:00 **Room N**

Artificial Intelligence and Machine Learning

RPS 905

Artificial intelligence and machine learning for ultrasound

Moderators:
V. Cantisani; Rome/IT
M. Huisman; Utrecht/NL

RPS 905-1 08:30

Fully automatic femur length measurement in ultrasound images by a novel hybrid approach based on a convolutional network
M. Ghelich Oghli[1], R. Gerami[2], S. Moradi[1], N. Sirjani[1], A. Shabanzadeh[2], P. Ghaderi[2], I. Shiri[3]; *[1]Karaj/IR, [2]Tehran/IR, [3]Geneva/CH*
(m.g31.mesu@gmail.com)

Purpose: 2D fetal ultrasound biometrics have been extensively used to establish (or confirm) the gestational age of the foetus, estimate its size and weight, and identify growth patterns and abnormalities. Among various parameters, femur length (FL) measurement suffers from inter and intraobserver variability. In this paper, we proposed a deep learning-based approach to calculate FL automatically.
Methods and materials: Our prepared dataset contained 315 2D ultrasound images of the foetal femur in the standard plane. The dataset was gathered from two distinct centres: (i) Alvand Medical Imaging Center, Tehran, Iran, and (ii) Laleh Hospital, Tehran, Iran.
To segment the femur in the ultrasound image, we had a pre-processing step. We used the superpixel algorithm to remove darker parts of the image, as the femur is typically the brightest part of the US image. Then we applied an image saliency algorithm to represent the salient features of the image. Finally, a novel convolutional network was trained on these pre-processed images to segment the femur. The proposed network, namely MFP-Unet, was a combination of Unet and feature pyramid network (FPN). After the segmentation process, a skeletonisation algorithm achieved the femur length.
Results: We used the mean absolute difference (MAD) and root mean square error (RMSE) for the measurements' errors. The values of errors were 0.18 mm and 0.12 mm for FL. The correlation between automatic and manual measurements was evaluated by the correlation graph and the R-value was 0.97.
Conclusion: According to the results, we have proposed a robust and useful algorithm for automatic femur length measurement that can be extended to nuchal translucency (NT) measurement based on providing dataset.
Limitations: The images should be taken in the second trimester.
Ethics committee approval: n/a
Funding: Med Fanavaran Plus.
Author Disclosures:
M. Ghelich Oghli: Speaker at Med Fanavaran Plus, Author at Med Fanavaran Plus
S. Moradi: Author at Med Fanavaran Plus
R. Gerami: Author at Aja University of Medical Sciences
A. Shabanzadeh: Author at Med Fanavaran Plus
I. Shiri: Author at Geneva University Hospital Geneva
N. Sirjani: Author at Med Fanavaran Plus
P. Ghaderi: Author at Med Fanavaran Plus

RPS 905-2 08:36

A ternary classification of chronic liver disease with a neural network using ultrasound B-Mode and shear-wave elastography examination parameters
P. Drazinos[1], I. Gatos[2], I. Theotokas[2], S. Yarmenitis[3], A. Soultatos[2], E. Panteleakou[2], P. Zoumpoulis[1]; *[1]Kifissia/GR, [2]Athens/GR, [3]Marousi/GR*
(p.drazinos@echomed.gr)

Purpose: Chronic liver disease (CLD) is one of the major causes of death and the major cause of hepatocellular carcinoma development. Accurate diagnosis regarding CLD progress is, therefore, very important. Our aim is to build and train a neural network (NN) classifier that will estimate the impact of parameters derived from an ultrasound (US) B-Mode and shear-wave elastography (SWE) examination in order to classify individuals into three main classes, F0-F1, F2-F3, and F4 fibrosis stages. Liver biopsy (LB) was considered as the 'gold standard'.
Methods and materials: Our dataset consisted of 315 individuals, 175 F0-F1, 52 F2-F3, and 88 F4 fibrosis stages. All individuals underwent a US examination performed by an experienced radiologist followed by an LB examination for individuals with fibrosis stage F1-F4. We randomly divided our dataset into 50% (training), 20% (testing), and validation (30%). For the training, 10-fold cross-validation (CV) was performed. The SWE measurements of the liver's right lobe (RL SWE), the existence of nodularity, and the known aetiology of each individual were used as inputs for the training and testing of a NN classifier.
Results: The NN classifier had a 10-fold CV accuracy of 88.78% and a 95% confidence interval (CI) of 88.52%-89.04%. The mean accuracy of the classifier on the test was 87.78% (95% CI 87.25%-88.31%). The mean area under the curve (AUC) for the test samples was 0.962 (95% CI 0.959-0.965). The validation accuracy was 84.63% (95% CI 84.27%-85.00%).
Conclusion: The NN classifier achieved good accuracy results in both training and testing and validation, and could be used to assist radiologists in CLD assessment in everyday clinical practice.
Limitations: n/a
Ethics committee approval: All subjects have signed informed consent.
Funding: No funding was received for this work.
Author Disclosures:
P. Drazinos: nothing to disclose
S. Yarmenitis: nothing to disclose
I. Gatos: nothing to disclose
I. Theotokas: nothing to disclose
P. Zoumpoulis: Equipment Support Recipient at Mindray
A. Soultatos: nothing to disclose
E. Panteleakou: nothing to disclose

RPS 905-3 08:42

A preliminary study of parametric imaging with a contrast-enhanced ultrasound to predict luminal A breast cancer
L. Tang, J. Jiang, M. Chen; *Shanghai/CN*

Purpose: To explore the use of parametric imaging as an imaging ensemble method to analyse breast contrast ultrasound images to diagnose or predict luminal A breast cancer in the early stage.
Methods and materials: 189 patients with breast cancer who underwent a contrast-enhanced ultrasound and obtained pathological findings before surgery were enrolled in this retrospective analysis. After extracting the TIC curve of each pixel in the ROI region of images, the relevant parameters PI, AUC, MTT, WiR, WoR, TTP, and RT in the curve were used as independent parameters for two-dimensional imaging. Each parameter was unified between 0 and 255 grey-levels to generate a parametric image grey-scale image. By transforming the index map and the palette axis, the three fluxes were superimposed to generate a parametric imaging colour map.
Results: There were 46 luminal A breast cancers and a total of 644 parameter imaging features. After the dimension reduction was selected and the features of repetition or the same meaning were eliminated, 3 effective features were finally selected. After the SVM output the probability value, RT_E2 had an AUC of 0.677, a sensitivity of 83.9%, a specificity of 71.7%, and an accuracy of 81.0%. The AUC, sensitivity, specificity, and accuracy of RT_Hm2 were 0.650, 77.4%, 70.3%, and 71.4%, respectively. Those of RT_Et2 reached 0.665, 63.6%, 69.6%, and 65.1%, respectively.
Conclusion: Parametric imaging features, combined with time and distribution characteristics, provide more comprehensive diagnostic information and offer the possibility of predicting luminal A breast cancer.
Limitations: The design of this study has limitations. The sample was biased for the different incidence rates.
Ethics committee approval: All patients signed written informed consent.
Funding: No funding was received for this work.

Author Disclosures:
L. Tang: Author at Department of Diagnostic Ultrasound, Tongren Hospital, School of Medicine, Shanghai Jiao Tong University
J. Jiang: Author at Department of Diagnostic Ultrasound, Tongren Hospital, School of Medicine, Shanghai Jiao Tong University
M. Chen: Author at Department of Diagnostic Ultrasound, Tongren Hospital, School of Medicine, Shanghai Jiao Tong University

RPS 905-4 08:48
Machine learning analysis in the prediction of placenta adhesion disorder in patients with placenta previa using ultrasound derived texture features
F. Verde, V. Romeo, R. Cuocolo, L. Sarno, S. Migliorini, A. Stanzione, M. D'armiento, A. Brunetti, M. P. S. Maurea*; Naples/IT (francescoverde87@gmail.com)*

Purpose: To predict the presence of placenta adhesion disorder (PAD) in patients with placenta previa using ultrasound (US) derived texture analysis (TA) features and a machine learning (ML) analysis.
Methods and materials: 53 patients (n=36 without PAS and n= 17 with PAS) with placenta previa who underwent endo-vaginal US examination for suspicion of PAD were retrospectively selected. 2D circle ROI was placed over homogeneous placental tissue. ROIs and corresponding images were then imported on a dedicated software (3D slicer, heterogeneity CAD) to extract first, second, and higher order TA features. ML analysis was subsequently run to identify the best performing method to correctly classify instances.
Results: A total of 688 TA features were extracted. 299 TA features showed an intraclass correlation coefficient values higher or equal to 0.75. No features showed low variance using a threshold of 0.0. Highly (r>0.8) correlated features were excluded, with 14 TA features further selected. Using these features with a bagged J48 algorithm, with each bag containing 70% of cases and 50 iterations, an accuracy of 82% was obtained.
Conclusion: ML analysis using TA featured extracted from US images may be useful to accurately identify PAS in patients with placenta previa.
Limitations: Limitations are related to a relatively small sample and a retrospective design.
Ethics committee approval: IRB approved, consent waived.
Funding: No funding was received for this work.
Author Disclosures:
A. Brunetti: nothing to disclose
F. Verde: nothing to disclose
V. Romeo: nothing to disclose
R. Cuocolo: nothing to disclose
L. Sarno: nothing to disclose
S. Migliorini: nothing to disclose
A. Stanzione: nothing to disclose
M. D'armiento: nothing to disclose
M. P. S. Maurea: nothing to disclose

RPS 905-5 08:54
Transfer learning radiomics based on multimodal ultrasound imaging for staging liver fibrosis: a pilot study
H. Ding, L.-Y. Xue, Y.-L. Zhu, W.-P. Wang, J.-H. Yu*; Shanghai/CN (13651886013@163.com)*

Purpose: To propose a transfer learning (TL) radiomics model that efficiently combines the information from grey-scale and elastogram ultrasound images for accurate liver fibrosis grading.
Methods and materials: Totally, 466 patients undergoing partial hepatectomy were enrolled, including 401 with chronic hepatitis B and 65 without fibrosis pathologically. All patients received elastography and got liver stiffness measurement (LSM) 2-3 days before surgery. We proposed a deep convolutional neural network by TL to analyse images of grey-scale modality (GM) and elastogram modality (EM). The TL process was used for liver fibrosis classification by Inception-V3 network which pretrained on ImageNet. The diagnostic performance of TL and non-TL was compared. The value of single modalities, including GM and EM alone, and multimodalities, including GM+LSM and GM+EM, was evaluated and compared with that of LSM and serological indexes. Receiver operating characteristic curve analysis was performed to calculate the optimal area under the curve (AUC) for classifying fibrosis of S4, ≥S3, and ≥S2.
Results: TL in GM and EM demonstrated higher diagnostic accuracy than non-TL, with significantly higher AUCs (all P < .01). Single-modal GM and EM both performed better than LSM and serum indexes (all P < .001). Multimodal GM+EM was the most accurate prediction model (AUCs are 0.950, 0.932, and 0.930 for classifying S4, ≥S3, and ≥S2, respectively) compared with GM+LSM, GM and EM alone, LSM, and biomarkers (all P < .05).
Conclusion: Liver fibrosis can be staged by a transfer learning modal based on the combination of grey-scale and elastogram ultrasound images, with excellent performance.
Limitations: A single-centre study.
Ethics committee approval: n/a
Funding: This study received funding from National Natural Science Foundation of China (grant number 81571675, 81873897, and 61471125).
Author Disclosures:
H. Ding: nothing to disclose
L.-Y. Xue: nothing to disclose
J.-H. Yu: nothing to disclose
Y.-L. Zhu: nothing to disclose
W.-P. Wang: nothing to disclose

RPS 905-6 09:00
Design and development of a convoluted neural network model for the detection and classification of ultrasound image-based thyroid nodules
B. Marconi Narvaez, F. Lubinus, Y. Arias, A. Ortiz*; Bucaramanga, Santander/CO (bmarconi1979@gmail.com)*

Purpose: To design a model based on convoluted neural networks capable of performing automatic detection of thyroid nodule (TN) on ultrasound (US) and classifying its risk of malignancy based on EU TIRADS 2017 criteria.
Also, to identify inter and intraobserver variability between a senior and junior radiologists for TN classification and compare levels of accuracy on classifying a TN between radiologists and a neural network model.
Methods and materials: The thyroid gland US image database (2,000 images) was acquired in grey-scale mode. Conversion from DICOM to JPG format was completed using PyDICOM library. Annotations and patient information from the image were deleted. Data augmentation methods were applied to increase the number of images (up to 6,000) for training the model. The convoluted neural network algorithm was designed by using TensorFlow 2.0 (Google). Two expert radiologists classified the US images based on EU TIRADS; only the matched images were selected for training the model. Training and validation of the model were completed by arranging different sets of neurons, convolution, and max-pooling layers. The CNN model and radiologist (1 senior and 1 junior) were tested by presenting 200 images choosen randomly from the database.
For the evaluation of interobserver variability, the Spearman correlation coefficient and Kruskall Gamma concordance were calculated. A secondary analysis was carried out using the criteria from the senior radiologist as a gold standard and the discriminatory capability (ROC curve) and the validity of the CNN model versus junior and senior radiologist were compared.
Results: Preliminary accuracy was 78% and a loss of 0.30%. Other statistical parameters are being calculated.
Conclusion: CNN models can be used as an assistance tool for the screening of thyroid nodes on US.
Limitations: Limited technical resources.
Ethics committee approval: Ethics committee approval was obtained.
Funding: No funding was received for this work.
Author Disclosures:
B. Marconi Narvaez: nothing to disclose
F. Lubinus: nothing to disclose
Y. Arias: nothing to disclose
A. Ortiz: nothing to disclose

RPS 905-7 09:06
No sonographer required: a feasibility study to investigate if midwives in resource-limited settings are able to acquire a prenatal ultrasound within two hours
T. L. A. van Den Heuvel, B. van Ginneken, C. L. de Korte*; Nijmegen/NL*

Purpose: Prenatal imaging is barely performed in resource-limited settings. This is mainly caused by a severe shortage of ultrasound devices and trained sonographers capable of acquiring and interpreting ultrasound images. We investigated if midwives in resource-limited settings are able to perform a predefined ultrasound acquisition protocol. This acquisition protocol consists of six predefined sweeps with the transducer over the abdomen of the pregnant woman. In previous research, we developed deep learning algorithms that can automatically interpret prenatal ultrasound images which were acquired using this protocol.
Methods and materials: A workshop was given to 5 midwives at St. Luke's Catholic Hospital in Wolisso, Ethiopia. The midwives had no prior knowledge of ultrasound. The workshop consisted of a presentation to introduce ultrasound imaging and the acquisition protocol. The midwives practised the acquisition protocol on each other to become familiar with the protocol. The midwives then went to the prenatal department to acquire the protocol from pregnant women.
Results: The midwives successfully acquired the protocol from all 72 pregnant women that visited the hospital. The protocol was acquired using the MicrUs EXT-1H (Telemed ultrasound medical systems, Vilnius, Lithuania). All midwives were able to perform the protocol within two hours of training.

Conclusion: The predefined ultrasound acquisition protocol can be taught within two hours to midwives without prior knowledge of ultrasound. Combining this protocol with algorithms that automatically interpret the ultrasound data has the potential to make implementation of prenatal screening in resource-limited settings much faster and easier, since it would avoid the need to train sonographers.
Limitations: This feasibility study only included five midwives from one city.
Ethics committee approval: This study was approved by the local ethics committee. Every woman in this study signed a written informed consent.
Funding: No funding was received for this work.
Author Disclosures:
T. L. A. van Den Heuvel: nothing to disclose
B. van Ginneken: nothing to disclose
C. L. de Korte: nothing to disclose

RPS 905-8 09:12
Automatic segmentation of the right ventricle from an ultrasound video using a novel deep learning approach
M. Ghelich Oghli[1], A. Alizadehasl[1], S. Moradi[2], N. Sirjani[2], A. Shabanzadeh[1], P. Ghaderi[1], I. Shiri[3]; [1]Tehran/IR, [2]Karaj/IR, [3]Geneva/SZ (m.g31.mesu@gmail.com)

Purpose: In contrast to more recent studies that disclosed the pivotal role of the right ventricle (RV) in pathological conditions, it has been considered a 'forgotten chamber' for decades. To quantify the RV function, fractional area change (FAC) is calculated through the apical 4-chamber view. As a prerequisite to estimate the RV area and FAC, the segmentation of the RV is necessary.
Methods and materials: We proposed an efficient approach for RV segmentation during the entire cardiac cycle. The presented architecture is based on an OSVOS network, which is a CNN architecture for semi-supervised video object segmentation. The network has three parts: the base, parent, and test networks. In the test phase, it gives the manual mask of one or more frames of the video. In summary, our contributions are:
1) The base network was trained on a CAMUS challenge dataset boosted by augmentation methods by a factor of 10.
2) The parent network was trained on our prepared dataset. It contained 142 apical 4-chamber videos with the annotation of RV endocardium.
3) The first frame of the cardiac cycle was segmented automatically using our previously presented method, MFP-Unet.
Results: The evaluation and comparison with the state-of-the-art approaches is performed using ROC curve, Dice coefficient (DC), Hausdorff distance (HD), and contour accuracy (CA). Our proposed network achieved 0.94 of AUC, 0.93 of DC, 0.57 cm of HD, 0.89 of CA, and these are the best results in comparison with PReMVOS, OSVOS-S, and ReConvNet.
Conclusion: The proposed architecture can capture the RV structure as well as manual expert tracing with an acceptable error range. The performance of the network could be improved by means of maintaining the training dataset and eliminating the augmentation procedure.
Limitations: There were no limitations.
Ethics committee approval: n/a
Funding: Med Fanavaran Plus.
Author Disclosures:
M. Ghelich Oghli: Author at Med Fanavaran Plus, Speaker at Med Fanavaran Plus
S. Moradi: Author at Med Fanavaran Plus
A. Shabanzadeh: Author at Med Fanavaran Plus
A. Alizadehasl: Author at Rajaie Cardiovascular, Medical & Research Center
N. Sirjani: Author at Med Fanavaran Plus
I. Shiri: Author at Geneva University Hospital
P. Ghaderi: Author at Med Fanavaran Plus

RPS 905-9 09:18
The accuracy of a CAD system to classify breast masses on ultrasound according to BI-RADS lexicon 5th edition
E. F. C. Fleury; *Sao Paulo/BR (edufleury@hotmail.com)*

Purpose: To determine the accuracy of a CAD system to classify breast masses on ultrasound according to BI-RADS lexicon 5th edition
Methods and materials: 83 breast masses consecutively referred for biopsy (31 malignant) were included. A 15 years experienced radiologist classified the masses according to criteria proposed by the BI-RADS. For classification, the B-Mode findings associated with the strain elastography findings were considered. The radiologist final classification was compared to that obtained by a semi-automated CAD system adopting similar classification criteria as proposed by the BI-RADS lexicon. To perform the CAD system classification, the same observer manually delimited the masses at the B-Mode images. The CAD classification system consists of 3 steps: 1) Use of machine learning to classify masses in B-mode. 2) Quantitative classification of masses by strain elastography. 3) Integration of 1 and 2. We evaluated the diagnostic accuracy and the area under the ROC curve for the two classifications. It was also assessed the agreement between the visual classification with the CAD system. As a gold-standard reference, histological results of biopsies were adopted.
Results: The AUC for the radiologist was 0.714 and the CAD system was 0.807. The interobserver agreement according to the Kappa test was 0.8 if positive or negative results were considered. For all BI-RADS final category, including categories 2, 3, 4, and 5, the agreement was 0.58. The system impacts more at BI-RADS category 3 where a downgrade to category 2 was observed. Half of the lesions classified as BI-RADS were downgraded to 2.
Conclusion: A CAD system can be used to classify breast masses by ultrasound with similar accuracy to a radiologist.
Limitations: Experimental software in a small sample size.
Ethics committee approval: Approved by Institutional Ethical Committee and Brazilian Research Platform.
Funding: No funding was received for this work.
Author Disclosures:
E. F. C. Fleury: Author at DL4MED

RPS 905-10 09:24
The classification of lymph node ultrasound images using texture analysis and machine learning
A. Bocoum[1], L. Chami[2], A. Giron[2], M. Lemahieu[3], O. Lucidarme[2], C. Nioche[1], I. Buvat[1], F. Frouin[1], C. Pellot-Barakat[1]; [1]Orsay/FR, [2]Paris/FR, [3]Gregy-sur-Yerre/FR (claire.barakat@inserm.fr)

Purpose: To differentiate malignant from benign ultrasound images of lymph nodes (LN) using texture analysis and machine learning models.
Methods and materials: The database consisted of 103 examinations of superficial LNs of patients (age: 54±18 years) who had undergone multi-parametric US imaging (B-mode, Doppler and shear-wave elastography) followed by a US-guided biopsy. Texture analysis was performed on all B-mode and elasticity images using the free LIFEx program (www.lifexsoft.org). Texture features relevant for LN discrimination were selected using univariate non-parametric comparisons of a means test ($p < 0.05$). Redundant correlated textural features (Pearson $R > 0.85$) were discarded. In addition, 20 conventional descriptive and quantitative clinical and imaging features (patient age, vascularisation degree, elasticity, etc.) were analysed. Using LN histology (benign/malignant) as classification outputs, various supervised machine learning algorithms implemented with SAS® Viya were trained (60% of the exams assigned to the training cohort) and subsequently tested on the remaining cohort.
Results: Of the 107 LNs, 35 (33%) were benign and 72 (67%) were malignant (20 carcinomas, 52 lymphomas). Of the 129 initial texture features, 38 were selected. Gradient boosting, logistic regression, and SVM achieved similar performances for the classification of LN in the test set (Youden-index: 0.80-0.81; misclassification rate: 9.5%-14.3%; AUC: 0.91-0.94). When using supervised classification without texture features, Youden was 0.56 only and the misclassification rate was 17%.
Conclusion: Textural analysis was found relevant to distinguish between malignant and benign LNs in our database, including a majority of lymphoma-related LN. Machine learning models involving textural features might facilitate LN diagnosis based on multi-parametric ultrasound imaging.
Limitations: The models must be evaluated on an external dataset.
Ethics committee approval: IRB approval (ID RCB: 2015-A01315-44).
Funding: FLI grant ANR-11-INBS-0006.
Author Disclosures:
C. Pellot-Barakat: nothing to disclose
O. Lucidarme: nothing to disclose
L. Chami: nothing to disclose
A. Giron: nothing to disclose
M. Lemahieu: nothing to disclose
C. Nioche: nothing to disclose
I. Buvat: nothing to disclose
F. Frouin: nothing to disclose
A. Bocoum: nothing to disclose

RPS 905-11 09:30
Ultrasound-based radiomics technology for assessing foetal lung maturity during pregnancy complications
Y. Du; *Shanghai/CN (duyanran44@126.com)*

Purpose: To evaluate and compare the development of foetal lungs with pregnancy complications and normal pregnancy during different gestational weeks using ultrasound-based radiomics technology.
Methods and materials: A total of 548 foetal lung ultrasound images of 491 single pregnant women were obtained during routine ultrasound examinations between 28 and 41 weeks of gestation before birth. Ultrasound-based radiomics technology was used to extract foetal lung image features. A standard machine-learning model was composed of feature transformation and a regression model

was used to evaluate the relationship between texture features, pregnancy complications, and gestational age.
Results: Foetal lung ultrasound images were divided into four groups: GDM group, GDM + pre-eclampsia group, pre-eclampsia group, and normal group. The accuracy of foetal lung texture analysis in estimating complications of different pregnancies at different gestational weeks was 80.1%-92.9%. The accuracy of the gestational age prediction model established by foetal lung image texture analysis of the normal and complication groups was 61.5–82.1%.
Conclusion: Ultrasound-based radiomics technology is a noninvasive way to assess foetal lung development during different pregnancy complications. The foetal lung maturity prediction model will be of great help in the assessment of foetal lung development during different pregnancy complications, for monitoring the medication of disease, and the choice of termination time.
Limitations: By expanding the sample size, the stability and accuracy of the model will be improved. The GDM groups were not subdivided according to the severity of diabetes mellitus, further emphasising the need to test and verify the differences between examiners and machines.
Ethics committee approval: n/a
Funding: This work was supported by the National Natural Science Foundation of China (Grant 61771143 and 61871135) and the Science and Technology Commission of Shanghai Municipality (Grant 18511102904 and 17411953400).
Author Disclosures:
Y. Du: nothing to disclose

RPS 905-12 09:36

Ultrasound-based radiomics approach: a potential method for the prediction of Ki-67 expression and differentiation grades in hepatocellular carcinoma

Y. Dong, Q. Zhang, Z. Yao, J. Yu, W. Wang*; Shanghai/CN (dr_mimi@163.com)*

Purpose: A radiomics approach can extract high-throughput image features, take full advantage of prognostic information from medical images, and provide prognosis information noninvasively. This study aimed to evaluate the correlation between liver ultrasound images based on a radiomics approach and Ki-67 expression differentiation grades of hepatocellular carcinoma (HCC).
Methods and materials: Clinical data and liver grey-scale ultrasound images of 93 operated-on and histopathologically proved HCC patients were retrospectively analysed. Two models were built to predict the Ki-67 expression and differentiation grades of HCC lesions based on grey-scale ultrasound images. Four radiomics approach steps were used: image segmentation, feature extraction, feature selection, and classification. Tumour regions from grey-scale ultrasound images were segmented to extract the wavelet, texture, and morphological features.
Results: By using a genetic algorithm with minimum-redundancy-maximum-relevance (mRMR), a Wisconsin Rank sum test, and sparse representation method, 452 grey-scale ultrasound image features were obtained and selected. The image features with the best discrimination performance were combined to establish our prediction models. With the same dataset, the area under the receiver operating characteristic curve (AUC) in the results reached 0.76 (Ki-67) and 0.87 (tumour differentiation grades).
Conclusion: A grey-scale ultrasound image based radiomics approach has potential application value in the clinical diagnosis and prognosis of Ki-67 expression and differentiation grades of HCC.
Limitations: The patient number is relatively limited. The stability evaluation of the radiomic analysis would be further improved by multicentre studies in the future.
Ethics committee approval: This study was approved by the institutional review board of our institution. Informed consent was waived before ultrasound examination. The procedure was in accordance with the declaration of Helsinki.
Funding: Supported by Shanghai Municipal Health and Family Planning Commission Research Project (Grant No. 201840215) and Shanghai Municipal Science and Technology Major Project (Grant No. 2017SHZDZX01).
Author Disclosures:
Y. Dong: nothing to disclose
W. Wang: nothing to disclose
Q. Zhang: nothing to disclose
Z. Yao: nothing to disclose
J. Yu: nothing to disclose

RPS 905-13 09:42

Preoperative prediction of microvascular invasion in hepatocellular carcinoma: the application of a radiomic algorithm based on grey-scale ultrasound images

W. Wang[1], Y. Dong[1], L. Zhou[2], W. Xia[2], Q. Zhang[1], X. Gao[2]; *[1]Shanghai/CN, [2]Suzhou/CN (puguang61@126.com)*

Purpose: To establish a radiomic algorithm based on grey-scale ultrasound images and to make preoperative predictions of microvascular invasion (MVI) in hepatocellular carcinoma (HCC) patients.
Methods and materials: In this retrospective study, 322 cases of histopathologically confirmed HCC lesions were included. The classifications based on preoperative grey-scale ultrasound images were performed in two stages: (1) classifier #1, MVI-negative and MVI-positive cases, and (2) classifier #2, MVI-positive cases were further classified as M1 or M2 cases. The gross-tumoural region (GTR) and peri-tumoural region (PTR) signatures were combined to generate gross- and peri-tumoural region (GPTR) radiomic signatures. The optimal radiomic signatures were further incorporated with vital clinical information. Multivariable logistic regression was used to build radiomic models.
Results: 1,595 radiomic features were extracted from each HCC lesion. At the classifier #1 stage, the radiomic signatures based on features of GTR, PTR, and GPTR showed area under the curve (AUC) values of 0.708 (95 % CI, 0.603 - 0.812), 0.710 (95 % CI, 0.609 - 0.811), and 0.726 (95% CI, 0.625 - 0.827), respectively. Upon incorporation of vital clinical information, the AUC of the GPTR radiomic algorithm was 0.744 (95 % CI, 0.646 - 0.841). At the classifier #2 stage, the AUC of the GTR radiomic signature was 0.806 (95 % CI, 0.667 - 0.944).
Conclusion: Radiomic algorithm based on grey-scale ultrasound images has potential value to facilitate preoperative prediction of MVI in HCC patients. The GTR radiomic signature may be helpful for further discriminating among MVI-positive patients.
Limitations: The possibility of a selection bias due to retrospective study.
Ethics committee approval: This study was approved by the institutional review board of Zhongshan Hospital. Informed consent was waived before ultrasound examination.
Funding: Shanghai Municipal Health and Family Planning Commission Research Project (Grant No. 201840215).
Author Disclosures:
W. Wang: nothing to disclose
Y. Dong: nothing to disclose
L. Zhou: nothing to disclose
W. Xia: nothing to disclose
Q. Zhang: nothing to disclose
X. Gao: nothing to disclose

RPS 905-14 09:48

A deep learning approach for multi-structure segmentation in echocardiography images

S. Moradi[1], A. Alizadehasl[1], M. Ghelich Oghli[1], N. Sirjani[2], A. Shabanzadeh[1], P. Ghaderi[1], I. Shiri[3]; *[1]Tehran/IR, [2]Karaj/IR, [3]Geneva/CH (shakiba.mrd71@gmail.com)*

Purpose: Most of the quantitative features in analysing echocardiography images are elicited from the cardiac chambers morphologies. Elevated atrial pressure or an increase in flow leads to atrial enlargement, and any changes on left ventricle morphology could be a sign of abnormality. Automatic segmentation makes the procedure more accurate and less operator-dependent, and these advantages leads to more precise prediction of the LV and left atrial (LA) volumes and ejection fraction. We proposed a deep learning (DL) approach for the segmentation of the LV endocardium, epicardium, and LA in apical 4-chamber view images.
Methods and materials: The dataset used is a publically available dataset of echocardiography images which is published in CAMUS challenge. The data contains 900 apical 4-chamber view images in end-systole (ES) and end-diastole (ED) frames. We used our DL architecture, which is recently introduced (MFP-Unet) for multi-structure segmentation. 720 ED and ES images (augmented by a power of 10) are used as the training dataset and 180 images are used for the testing procedure.
Results: The model achieved a Dice coefficient (DC) value of 95% for endocardium, 97% for epicardium, and 91% for LA segmentation at ED phase, and 92% DC, 95% DC, and 92% DC at ES phase. The Hausdorff distance was also used as a validation metric. It was 4.72 for epicardium, 4.83 for endocardium, and 5.11 for LA at ED phase, and 5.32, 5.5, and 5.18, respectively, at ES phase.
Conclusion: This study evaluated the power of our novel DL algorithm in echocardiographic image segmentation. It is shown that the proposed method is reliable and behaves similarly to clinical experts in calculating the clinical cardiac indices.
Limitations: n/a
Ethics committee approval: n/a
Funding: Med Fanavaran Plus.

Author Disclosures:
S. Moradi: Author at Med Fanavaran Plus, Speaker at Med Fanavaran Plus
A. Alizadehasl: Author at Rajaie Cardiovascular, Medical and Research Center
M. Ghelich Oghli: Author at Med Fanavaran Plus
N. Sirjani: Author at Med Fanavaran Plus
A. Shabanzadeh: Author at Med Fanavaran Plus
P. Ghaderi: Author at Med Fanavaran Plus
I. Shiri: Author at Geneva University Hospital Geneva

08:30 - 10:00 **Room Y**

My Thesis in 3 Minutes

MyT3 9

Artificial Intelligence and Machine Learning

Moderators:
F. Coppola; Bologna/IT
D. Pinto dos Santos; Cologne/DE

MyT3 9-1 08:30
To explore the value of CT radiomics in evaluating the biological behaviour of pancreatic cancer
Q. Gu*; Changsha/CN (729570216@qq.com)*

Purpose: To investigate whether CT radiomics can be used to assess the biological behaviour of pancreatic cancer before surgery.
Methods and materials: 94 histopathological confirmed pancreatic cancer patients who underwent CT scans were retrospectively included. The volume of interest (VOI) of the tumour on CT images was manually delineated and radiomics features were extracted by MaZda software. After feature reduction, radiomics models reflecting tumour biological behaviour (differentiation, lymph node metastasis) were established and the radiomics score(Rad-score)of each patient was calculated. The performance of each model was assessed by the receiver operating characteristic curve (ROC).
Results: There were no significant differences in both the differentiation degree group and lymph node metastasis group based on age and gender (P>0.05). The tumour location was statistically significant between the lymph node metastasis positive group and negative group (P=0.02). The radiomics model established by 7 CT radiomics features can predict the differentiation degree of pancreatic cancer. The area under the ROC curve（AUC） is 0.78 and 0.76 in the training group and validation group, respectively. The radiomics model established by 6 CT radiomics features can predict the lymph node metastasis of pancreatic cancer. The AUC is 0.77 and 0.74 in the training group and validation group, respectively.
Conclusion: CT radiomics have a great prospect in the non-invasive evaluation of the biological behaviour of pancreatic cancer. It has certain reference significance for preoperative evaluation of the malignant degree and is helpful to clinical treatment decision in pancreatic cancer.
Limitations: The sample size is small, and the results need to be confirmed with large sample studies. The model built in this study was validated with internal data but not tested with external test data.
Ethics committee approval: n/a
Funding: No funding was received for this work.
Author Disclosures:
Q. Gu: Author at The People's Hospital of Hunan Province, The First Hospital Affiliated of Hunan Normal University, Speaker at The People's Hospital of Hunan Province, The First Hospital Affiliated of Hunan Normal University

MyT3 9-2 08:34
Automated estimations of body weight prior to CT examinations using a 3D camera
M. S. May[1], F. Geißler[1], A. Wimmer[2], M. Saake[1], M. Kopp[1], R. Heiß[1], M. Uder[1], W. Wuest[1]; *[1]Erlangen/DE, [2]Forchheim/DE (matthias.may@uk-erlangen.de)*

Purpose: The aim of this study was to automatically assess the body weight prior to CT examinations.
Methods and materials: Body weight of 100 consecutive adult patients with an indication for CT was visually estimated by a technologist and a radiologist prior to the examination. The patients were additionally asked for their current anamnestic values before the true values were weighed. A roof-mounted 3D camera was used after patient positioning on the scanner's table to fit in an individual avatar using machine learning algorithm that was taught by the 200 preceding patients. Body weight was mathematically derived from this information.
Results: Mean body weight of our collective was 80 kg (± 19kg). The vast majority was examined wearing street-wear (94%), only few patients were wearing medical gowns (6%). Shoes were worn in 60% of the cases. Anamnestic values had a very low error from the ground truth (± 2%). Automated calculations (± 3%) were comparably precise, but estimations by radiologists (± 8%) and technologist (± 9%) were significantly worse. All assessment techniques tended to slightly underestimate the true values.
Conclusion: Automated weight assessment is feasible in a clinical routine setting with a high precision using a 3D camera and machine learning algorithms. This information could be used for automated contrast agent adaptations in future CT generations.
Limitations: Different interfering circumstances like large clothes, covers, positioning and other medical devices may bias the assessment of body weight by a 3D camera. The accuracy of the algorithm could be improved especially in these patients by increasing the number of cases in future projects.
Ethics committee approval: The study was approved by the local review board, written informed consent was obtained from each patient.
Funding: The study was funded by Siemens Healthcare GmbH.
Author Disclosures:
M. S. May: Speaker at Siemens Healthcare GmbH
F. Geißler: nothing to disclose
M. Saake: Speaker at Siemens Healthcare GmbH
M. Kopp: Speaker at Siemens Healthcare GmbH
R. Heiß: Speaker at Siemens Healthcare GmbH
M. Uder: Speaker at Siemens Healthcare GmbH
W. Wuest: Speaker at Siemens Healthcare GmbH
A. Wimmer: Employee at Siemens Healthcare GmbH

MyT3 9-3 08:38
A pilot study of radiomics signature-based on biparametric MRI for the preoperative prediction extrathyroidal extension in papillary thyroid carcinoma
S. Hu[1], X. Wang[2]; *[1]Wuxi/CN, [2]Zhenjiang/CN (hsd2001054@163.com)*

Purpose: To investigate the efficiency of radiomics signature to preoperatively predict aggressiveness histological feature extrathyroidal extension (ETE) in papillary thyroid carcinoma (PTC) with biparametric magnetic resonance imaging (bp-MRI) findings.
Methods and materials: For each patient, the images were manually segmented using ITK-SNAP software. 107 textural features were automatically calculated from the segmented region of interest (ROI). Random forest was used to do classification and the datasets were partitioned randomly 10 times to do training and testing with ratio 1:1. Furthermore, forward greedy feature selection based on feature importance was adopted to reduce overfitting. The classification accuracy was estimated on the test set using the area under the curve (AUC).
Results: After feature selection, the top 2 features of T2WI and the top 6 features of T2WI-FS achieve AUC 0.845 and 0.928, respectively. If the features in T2WI and T2WI-FS were combined, the performance of the model will decrease slightly (AUC 0.882 before and 0.913 after feature selection). Adding more radiomics feature filters on the T2WI-FS images to get more features does not improve the model performance (with AUC 0.891). Hyper parameters of the random forest model have negligible influence on the model performance with AUC mean 0.907 and std 0.006 for T2WI-FS images.
Conclusion: Radiomics features based on pre-contrast T2WI and T2WI-FS is helpful to predict aggressiveness histological feature ETE in PTC. And the T2WI-FS image features extracted without using any feature filters provide the best classification performance. The most important features are related to ROI size and the heterogeneity of the texture of ROI.
Limitations: The sample size of the study is small.
Ethics committee approval: The written informed consent was waived.
Funding: No funding was received for this work.
Author Disclosures:
S. Hu: nothing to disclose
X. Wang: nothing to disclose

MyT3 9-4 08:42
Ventriculoperitoneal shunt valve detection and identification using object detection with a faster RCNN
J. Haubold[1], A. Radbruch[2], M. Forsting[1], L. Umutlu[1], F. Nensa[1]; *[1]Essen/DE, [2]Heidelberg/DE (johannes.haubold@uk-essen.de)*

Purpose: Determining the pressure level of a ventriculoperitoneal (VP) shunt valve requires both the correct identification and finding the manufacturer's image for reading the pressure level. To reduce this effort, we have implemented a network for automated identification of the VP shunt valve and for an assignment of the manufacturer's image to read the pressure level.

Methods and materials: The collective (560 images of eight shunts) was split into 112 test images and 448 training images. For object detection, a Faster RCNN was trained. Subsequently, the detected label was used for a content-based image retrieval to assign the manufacturer's image for reading the pressure level. The mean average precision (mAP) at 0.5 intersections over union (IOU) was calculated to measure the precision.
Results: In the test set, a mAP of 0.77@0.5IOU was achieved for multiclass detection. In the next step, the fused images were demonstrated to a young resident in radiology. He was asked for each image whether the VP shunt was correctly identified. The assigned manufacturer's image for reading the pressure stage enabled the resident in radiology to correctly identify all misclassified VP shunt valves.
Conclusion: Using a Faster RCNN for an automated object detection it was possible to create a network with high performance for the identification of VP-shunts with a versatile mechanism to identify misclassifications.
Limitations: This study was performed in a single-centre because of the nature of machine learning more multi-centre data is needed for validation.
Ethics committee approval: This retrospective analysis was approved by the institutional review board of the University Hospital Essen. Informed consent was waived by the institutional review board, because of the retrospective character of the study.
Funding: No funding was received for this work.
Author Disclosures:
J. Haubold: nothing to disclose
F. Nensa: nothing to disclose
M. Forsting: nothing to disclose
A. Radbruch: nothing to disclose
L. Umutlu: nothing to disclose

MyT3 9-5 08:46
Deep convolutional neural networks-based coronary computed tomography angiography for CAD classification
Z. Huang, X. Wang, J. Xiao, Z. Li, Y. Xie, Y. Hu*; Wuhan/CN (304527885@qq.com)*

Purpose: We aimed to assess the utility of an automatic post-processing and reporting system based on CAD-RADS™ in suspected coronary artery disease patients.
Methods and materials: The model was designed for CAD-RADS assessment categories with automatic coronary tree segmentation and stenosis detection algorithm based on convolutional neural networks with the training of consecutive 2000 CCTA examinations. The diagnostic value of CAD-RADS classification, one-vessel CAD, two-vessel CAD, left main CAD and three-vessel CAD were performed by the model compared to radiologists with commercially-available automated segmentation and manual post-processing and also compared to invasive coronary angiography (ICA).
Results: Of the 322 patients in the study, 15, 9, 48, 96, 99, 35, 20 were classified as CAD-RADS 0, 1, 2, 3, 4A, 4B and 5 based on the model. The consistency test showed that the Kappa value of the model and radiologists was 0.639 (P<0.05). The Kappa value for diagnosing one-vessel CAD, two-vessel CAD, left main CAD and three-vessel CAD between the model and radiologists with CCTA is 0.758, 0.747, 0.869 and 0.596, respectively. The Kappa value for diagnosing one-vessel CAD, two-vessel CAD, left main CAD and three-vessel CAD between the model and ICA is 0.581, 0.494, 0.758 and 350, respectively. However, there is a poor agreement for detecting plaque characteristics between the model and radiologists with CCTA (Kappa value 0.349).
Conclusion: The CNN-based CAD-RADS in CCTA images is good consistency with the radiologists. However, the poor agreement for detecting plaque characteristics is remarkable in the study.
Limitations: This study is limited by the select bias and the fact that it is a retrospective study.
Ethics committee approval: The present study was approved by the institutional review board of the Central Hospital of Wuhan.
Funding: No funding was received for this work.
Author Disclosures:
Z. Huang: nothing to disclose
X. Wang: nothing to disclose
J. Xiao: nothing to disclose
Z. Li: nothing to disclose
Y. Xie: nothing to disclose
Y. Hu: nothing to disclose

MyT3 9-6 08:50
Impact of an artificial intelligence-based noise reduction algorithm on image quality in low-dose coronary CT angiography of obese patients
P. Liu, Y. Wang, M. Yu, Z. Liu, M. Wang, Z. Jin*; Beijing/CN*

Purpose: This study aims to assess the impact of artificial intelligence (AI)-based noise reduction algorithm on image quality (IQ) in low-dose (LD) coronary CT angiography (CCTA) for obese patients.
Methods and materials: Forty consecutive patients with BMIs ≥ 25 kg/m^2 underwent clinically indicated CCTA examinations on a NeuViz 128 CT scanner using a step-and-shoot mode with 100 kV and automatic current modulation. Images were reconstructed with an iterative algorithm (group A) and an AI-based noise reduction algorithm (group B), respectively. Image noise, signal-to-noise ratio (SNR) and contrast-to-noise ratio (CNR) were calculated on the aortic root (AO), left main artery (LM), left anterior descending artery (LAD), left circumflex artery (LCX), and right coronary artery (RCA) to evaluate IQ objectively. Subjective IQ scores were graded on a four-point scale (1: excellent, 4: poor).
Results: Compared to group A, group B yielded statistically significant reductions in image noise in the AO, LM, LAD, LCX and RCA of 63.97%, 38.63%, 21.29%, 24.38% and 29.99%, respectively. SNR and CNR both significantly increased in group B compared to group A (all P < 0.001). The subjective IQ scores in group B were superior to those in group A (1.57 ± 0.67 vs. 1.71 ± 0.67, P < 0.001). The effective dose was 2.3 ± 0.1mSv.
Conclusion: The AI-based noise reduction algorithm is an innovative and promising method that could effectively improve the IQ in LD CCTA for obese subjects.
Limitations: The diagnostic accuracy of coronary artery stenosis with AI-based noise reduction technology had not yet been evaluated using invasive coronary angiography as a standard examination.
Ethics committee approval: n/a
Funding: n/a
Author Disclosures:
P. Liu: nothing to disclose
Y. Wang: nothing to disclose
Z. Liu: nothing to disclose
M. Yu: nothing to disclose
M. Wang: nothing to disclose
Z. Jin: nothing to disclose

MyT3 9-7 08:54
Digitised patient history in computed tomography: data acquisition with mobile tablet computers
M. Kopp[1], F. Geißler[1], M. Wetzl[1], M. Wiesmüller[1], R. Heiss[1], T. Allmendinger[2], M. Uder[1], M. S. May[1]*; [1]Erlangen/DE, [2]Forchheim/DE*

Purpose: In contemporary healthcare systems, patient data is often unstructured and only available in hardcopy form. However, mobile tablet computers are a possibility to acquire digitized and structured patient data. Especially, for the indication of computed tomography (CT) consideration of critical patient history is mandatory. Also, high-quality reporting is supported by valid information about patient background. The aim of this study was to analyze the feasibility of structured, mobile tablet workflow for supporting informed consent discussion and reporting process. Secondly, the prevalence of critical patient history was evaluated.
Methods and materials: Mobile tablet computers were provided to consecutive patients, who answered independently a questionnaire (maximum 25 questions) concerning CT indication and general patient history. A specific software solution was used to provide structured access to all patient data for preparation of informed consent discussion and reporting process.
Results: In total 1159 patients answered the questionnaire with a mean age of 59.8 ± 15.3 years, 33% were female. Critical information on overall patient history was found for 54.9%. Evaluation of CT indication showed: 4.2% kidney disease, 3.4% diabetes medication, 3.1% claustrophobia, 1.6% allergic reactions to contrast agents and 1.4% thyroid hyperfunction. Furthermore, the patients indicated in 23.1% a pulmonary disease (most frequent: 4.5% asthma), in 12.1% a malignant disease and in 8.1% cardiovascular diseases.
Conclusion: Tablet-based acquisition of patient history is feasible and facilitates preparation of informed consent discussion and reporting process as critical patient history is frequent but easily accessible by using a specific software solution.
Limitations: Even higher patient numbers are necessary to obtain information about correlations between patient history, symptoms, CT related complications and the final radiology report.
Ethics committee approval: n/a
Funding: The study was funded by the Bavarian State Ministry of Economics, Transport and Technology.
Author Disclosures:
M. Kopp: Speaker at Siemens Healthineers
T. Allmendinger: Employee at Siemens Healthineers
M. Uder: nothing to disclose
F. Geißler: nothing to disclose
M. Wetzl: nothing to disclose
M. Wiesmüller: nothing to disclose
R. Heiss: nothing to disclose
M. S. May: Speaker at Siemens Healthineers

MyT3 9-8 08:58

Whole-tumour texture analysis of apparent diffusion coefficient maps for distinguishing lateral ventricle central neurocytoma from ependymoma

W. Wang, J. Cheng; *Zhengzhou/CN (weijianwang520@163.com)*

Purpose: We explored the role of whole-tumour texture analysis of apparent diffusion coefficient (ADC) maps for discriminating lateral ventricle central neurocytoma from ependymoma.
Methods and materials: We retrospectively evaluated findings in 35 patients with lateral ventricle central neurocytoma and 20 patients with ependymoma who underwent diffusion-weighted imaging (b = 0,800 s/mm(2)) at 3T with the acquisition of corresponding ADC maps. We derived texture analysis data from regions of interest drawn on all slices of the ADC maps in which tumour was visualised, including areas of necrosis and haemorrhage in the tumour. We used the t-test to evaluate the capacity of texture analysis parameters (variance, kurtosis,1th,10th percentiles) to discriminate central neurocytoma from ependymoma and analysed the receiver operating characteristic (ROC) curve to determine the optimum threshold value for each parameter and its corresponding sensitivity and specificity.
Results: Lateral ventricle central neurocytoma demonstrated significantly lower variance, kurtosis, 1th, 10th percentiles than ependymoma (P < 0.05). ROC curve analysis of the variance yielded the best area under the ROC curve (AUC; 0.93), the sensitivity of 90%, and specificity of 92%, with a cut-off value of 2008.
Conclusion: A whole-tumour texture analysis of ADC maps might be helpful for discriminating lateral ventricle central neurocytoma from ependymoma.
Limitations: It is small-scale retrospective research in which the number of patients per tumour is unbalanced. The correlation between ADC texture analysis parameters and histopathological characteristics needs further study.
Ethics committee approval: No ethics committee approval was obtained.
Funding: National Key R&D Program of China (2016YFC0106900): The investigation of equipment evaluation and clinical applications in magnetic resonance imaging.
Author Disclosures:
W. Wang: Author at First Affiliated Hospital of Zhengzhou University
J. Cheng: Author at First Affiliated Hospital of Zhengzhou University

MyT3 9-9 09:02

Convolutional neural networks for automated fracture detection and localisation on ankle radiographs

Q. Xie, B. Yin, Y. Lu, X. Li, D. Geng; *Shanghai/CN (474278641@qq.com)*

Purpose: To identify the feasibility and performance of using a deep convolutional neural network (DCNN) for fracture detection and localisation on ankle radiographs.
Methods and materials: A total of 8957 ankle radiographic studies were extracted from our institution picture archiving and communication system (PACS). Radiologists annotated all tibia and fibula fractures with bounding boxes. The dataset was split into training (90%) and validation (10%) sets and used to train fracture localisation models for images of anteroposterior, lateral, and oblique view. ResNeXt101 + FPN was implemented as a proposal network, whose output of proposal regions are fed into EfficientNet to be elaborately classified. The accuracy, sensitivity, false-negative rate, and area under the receiver operating characteristic curve (AUC) were evaluated on an unseen test set of 600 consecutive emergency department ankle radiographic studies acquired during 2019, orthopedist and radiologist with more than 10 years of orthopaedic professional experience in consensus as to the reference standard. The results were compared with those of medical professional groups. The authors also used a segmentation branch (CNN decoder) to confirm the validity of the model.
Results: In a classification metric, the algorithm achieved an AUC of 0.932 for identifying ankle fractures. An accuracy of 86.8% is realised with a sensitivity of 97.6%, a false-negative rate of 13.2%. In object detection metric, we accomplish an average precision (AP) of 0.95. The network presented a similar diagnostic performance to that of the orthopaedists in terms of these variables.
Conclusion: The ability of a two-stage RCNN not only to detect ankle fractures on ankle radiographs with a low false-negative rate but also have high accuracy for localising fracture lesions was demonstrated.
Limitations: Automated classification of an ankle fracture is not done.
Ethics committee approval: n/a
Funding: No funding was received for this work.
Author Disclosures:
Q. Xie: Author at Huashan Hospital
B. Yin: Author at Huashan Hospital
D. Geng: Author at Huashan Hospital
Y. Lu: Author at Huashan Hospital
X. Li: Author at Huashan Hospital

MyT3 9-10 09:06

Machine learning-based analysis of nasopharyngeal carcinoma: MRI radiomics for prediction of recurrence or metastasis

D. Bao, D. Luo, S. Dai, Y. Geng; *Beijing/CN (baodanhb@126.com)*

Purpose: To use machine learning-based magnetic resonance imaging radiomics to predict recurrence or metastasis in patients with nasopharyngeal carcinoma.
Methods and materials: This study retrospectively analysed 142 patients with nasopharyngeal carcinoma, and randomly assigned to the training and validation group at a ratio of 8:2. Feature selection was performed in the radiomic feature sets extracted from images of T2-weighted fat suppression (T2WI/FS) and contrast-enhanced T1-weighted (CE-T1WI) sequence respectively, and the combining feature set incorporating two sequences with variance threshold, select K best and the LASSO methods gradually. Two machine learning algorithms (Random Forest[RF]; Logistic Regression [LR]) were utilised for predictive model constructing. The diagnostic performance of the models was evaluated by receiver operating characteristic curves with indicators of accuracy, sensitivity, specificity and area under the curve, and compared by DeLong test.
Results: 10, 28, and 17 optimal features were selected from 1409 T2WI/FS, 1409 CE-T1WI, and 2818 combining features, respectively. Four-group models were constructed using the 10 T2WI/FS features ($Model_{T2/FS}$), 28 CE-T1WI features ($Model_{CE\text{-}T1WI}$), the combined 38 features ($Model_{combined}$) and 17 optimal features selected from the 2818 features ($Model_{optimal}$) . The $Model_{optimal}$ using RF algorithm showed the best prediction performance with accuracy, sensitivity, specificity, and area under the curve of train/test: 0.96/0.79, 0.96/0.86, 0.97/0.63, and 0.99/0.80, respectively.
Conclusion: Radiomics models based on baseline nasopharyngeal carcinoma magnetic resonance imaging has a high potential for recurrence or metastasis prediction, especially the $Model_{optimal}$ using RF algorithm. Moreover, except for $Model_{optimal}$, the RF was not superior to the LR algorithm for model construction.
Limitations: This was a retrospective single centre study.
Ethics committee approval: This retrospective study was approved by the ethics committee of our institution, and the requirement for informed consent was waived.
Funding: No funding was received for this work.
Author Disclosures:
D. Bao: nothing to disclose
D. Luo: nothing to disclose
S. Dai: nothing to disclose
Y. Geng: nothing to disclose

MyT3 9-11 09:10

Radiomics on ^{18}F-FDG PET and CT images can differentiate lymphomatous from metastatic lymphadenopathy

X. Ou[1], Z. Bo[1], J. Wang[2], F. Pang[1], J. Wu[1], Z. Zhao[1], P. Cao[1], X. Ma[1]; *[1]Chengdu/CN, [2]Nanjing/CN (drmaxuelei@gmail.com)*

Purpose: To assess the value of PET/CT radiomics combined with a large panel of machine-learning methods classifying lymphomatous and metastatic lymphadenopathy, and secondly to identify optimal machine-learning methods for radiomics-based malignant lymphadenopathy classification.
Methods and materials: PET and CT radiomic features from 492 lymph nodes were retrospectively analysed. Radiomic features were manually extracted using LIFEx software from PET and CT images within the same volume of interest (VOI). Five feature selection and nine classification methods were evaluated with independent training (n=394 lesions) and testing datasets (n=98 lesions). The performance of classification models was evaluated using the area under the curve (AUC), sensitivity and specificity.
Results: The ROC analysis revealed PET and CT radiomics with machine-learning methods possess a strong ability in differentiating malignant lymphadenopathy with the AUC up to 0.985. “Gradient Boosting Decision Tree (GBDT)” + “GBDT” achieved the highest classification AUC in the most differential assignments.
Conclusion: Radiomic features extracted from PET/CT images are efficient to differentiate between metastatic and lymphomatous lymphadenopathy using machine-learning methods. ”GBDT” + “GBDT” was found to be the optimal machine-learning method in our analysis.
Limitations: First, we didn’t compare the differences between malignant lymph nodes and inflammatory lymph nodes. Although the differential diagnosis of malignant and benign lymph nodes is not difficult and has been proven in the previous studies[13,22,25]. However, classifying of lymphadenopathy into metastatic, inflammatory and lymphomatous lymph nodes is frequently encountered in clinical practice. Second, although a large lymph nodes sample was included in this retrospective study, prospective studies are needed to verify our findings.
Ethics committee approval: This study was approved by the local ethics administration office. As this is a retrospective study, patients’ informed consent was waived.
Funding: No funding was received for this work.

Author Disclosures:
X. Ma: nothing to disclose
X. Ou: nothing to disclose
Z. Bo: nothing to disclose
J. Wang: nothing to disclose
F. Pang: nothing to disclose
J. Wu: nothing to disclose
Z. Zhao: nothing to disclose
P. Cao: nothing to disclose

MyT3 9-12 09:14
Segmentation of heart from chest x-ray images using U-net
L. A. Klarov, A. Timofeev, D. Zakharova, S. Permyakov, E. Nikiforov, D. Egorov*; Yakutsk/RU*

Purpose: The purpose of the study is the accurate selection of heart shadow from x-rays.
Methods and materials: We collected a dataset of 1300 chest x-rays and applied masks to them. For analysis, all x-rays were converted to jpg, and the mask was created in png. To isolate the heart, we used a 9-layer U-net convolutional neural network. With startup parameters learning rate = 1e-5, Adam optimiser, batch = 5 (3, 5), epochs = 800. The network was launched with samples of 400, 800 and 1300 images. In each run, a generator of additional images was used (5 to 1 image every epoch).
Results: The direct relationship is determined: an increase in the quality of segmentation with an increase in the number of x-rays in the dataset on the training sample. The quality of the test data is also affected by significant parameters when selecting lr, batch size. The parameter of epochs=800 shows good convergence on the graphs and was chosen as the most optimal. Samples with 400 and 600 images contain mask artefacts in the inner contour of the heart shadow. When sampling 1300 images, there are artefacts of determination beyond the outer contour.
Conclusion: The accuracy of the contours (the pulmonary artery and the left atrial abalone) and the presence of artefacts depend on the volume of the dataset. The selection of optimal hyperparameters also affects the results of segmentation in more global moments, such as determining the main fixation zones.
Limitations: The lower border of the heart remains fuzzy, even with a large number of images.
Ethics committee approval: n/a
Funding: No funding was received for this work.
Author Disclosures:
L. A. Klarov: nothing to disclose
A. Timofeev: nothing to disclose
D. Zakharova: nothing to disclose
S. Permyakov: nothing to disclose
E. Nikiforov: nothing to disclose
D. Egorov: nothing to disclose

MyT3 9-13 09:18
Whole-tumour texture analysis of apparent diffusion coefficient maps obtained using 3.0T MRI for distinguishing uterine endometrial carcinoma from endometrial polyps
W. Wang, J. Cheng, Y. Zhang*; Zhengzhou/CN*

Purpose: We explored the role of whole-tumour texture analysis of apparent diffusion coefficient (ADC) maps for discriminating uterine endometrial carcinoma and endometrial polyps.
Methods and materials: We retrospectively evaluated findings in 40 patients with uterine endometrial polyps and 50 patients with endometrial carcinoma who underwent diffusion-weighted imaging (b = 0,800 s/mm(2)) at 3T with the acquisition of corresponding ADC maps. We derived texture analysis data from regions of interest drawn on all slices of the ADC maps in which tumour was visualised, including areas of necrosis and haemorrhage in the tumour. We used the Mann-Whitney test to evaluate the capacity of texture analysis parameters (mean, skewness, kurtosis,50th,90th percentiles) to discriminate uterine endometrial carcinoma from endometrial polyps and analysed the receiver operating characteristic (ROC) curve to determine the optimum threshold value for each parameter and its corresponding sensitivity and specificity.
Results: Uterine endometrial carcinoma demonstrated significantly higher mean vales of ADC, skewness, kurtosis,50th,90th percentiles than endometrial polyps ($P < 0.05$). ROC curve analysis of the 90th percentile yielded the best area under the ROC curve (AUC; 0.92), sensitivity of 90%, and specificity of 95%, with a cut-off value of 198.
Conclusion: Whole-tumour texture analysis of ADC maps might be helpful for discriminating uterine endometrial carcinoma from endometrial polyps.
Limitations: It is small-scale retrospective research in which the number of patients per tumour is unbalanced. The correlation between ADC texture analysis parameters and histopathological characteristics needs further study.
Ethics committee approval: No approval was obtained.
Funding: National Key R&D Program of China (2016YFC0106900) The investigation of equipment evaluation and clinical applications in magnetic resonance imaging.
Author Disclosures:
W. Wang: Author at First Affiliated Hospital of Zhengzhou University
J. Cheng: Author at First Affiliated Hospital of Zhengzhou University
Y. Zhang: nothing to disclose

MyT3 9-14 09:22
Radiomics analysis of 18F-FDG PET/MR datasets for the prediction of therapy response of isolated limb perfusion in patients with soft-tissue sarcomas
J. Grueneisen[1], M. Chodyla[1], A. Demircioglu[1], M. Forsting[1], K. Herrmann[1], O. Martin[2], L. Umutlu[1]; [1]*Essen/DE,* [2]*Düsseldorf/DE (johannes.grueneisen@uk-essen.de)*

Purpose: To investigate the potential of radiomic analysis based on PET/MR-derived imaging parameters for the prediction of therapy response of isolated limb perfusion with melphalan and alpha-TNF (TM-ILP) in patients with soft-tissue sarcomas (STS).
Methods and materials: A total of 47 patients with the verification of a STS manifestation were prospectively enrolled for an integrated 18F-FDG PET/MR examination prior to neoadjuvant TM-ILP. The study protocol comprised the acquisition of several 18F-FDG PET- and MR-derived morphological After tumour segmentation, 17748 quantitative imaging features were extracted and tested for significance by a χ^2-test. Statistical modelling was performed using Random Forests and evaluated by repeated 5-fold cross-validation. Histopathological results after subsequent tumour resection served as reference standard and patients were categorized as responders/non-responders based on the grading scale by Salzer-Kuntschik.
Results: Histopathological analysis categorised 28 patients as therapy responders (Grade I-III) and 19 patients as non-responders (Grade IV-VI). For the differentiation between histopathological therapy response and non-response to TM-ILP, receiver operating characteristic analysis revealed an area under the curve (AUC) of 0.71. Furthermore, statistical analysis showed a positive predictive value of 76% to identify therapy responders in our patient cohort and a specificity of 74% to correctly define patients as non-responders.
Conclusion: Our preliminary results demonstrate the potential to predict therapy response of soft-tissue sarcomas under TM-ILP with a non-invasive imaging procedure, which has a high impact on further treatment and patients' prognosis. Accordingly, besides primary tumour staging, PET/MRI may have the potential to enhance the comprehensive pre-therapeutic evaluation of STS and improve patient therapy management.
Limitations: This study was limited by patient cohort.
Ethics committee approval: The study was approved by the local ethics committee. Written informed consent was obtained from all patients before each examination.
Funding: No funding was received for this work.
Author Disclosures:
J. Grueneisen: nothing to disclose
M. Chodyla: nothing to disclose
A. Demircioglu: nothing to disclose
M. Forsting: nothing to disclose
K. Herrmann: nothing to disclose
O. Martin: nothing to disclose
L. Umutlu: nothing to disclose

MyT3 9-15 09:26
Deep learning-based evaluation of normal bone marrow activity in ^{18}F-NaF PET/CT in patients with prostate cancer
S. Lindgren Belal[1], O. Enqvist[1], J. Ulén[1], L. Edenbrandt[2], E. Trägårdh[1]; [1]*Malmö/SE,* [2]*Gothenburg/SE (sarah.lindgren_belal@med.lu.se)*

Purpose: Bone marrow is the primary site of skeletal metastases in prostate cancer. ^{18}F-sodium fluoride (NaF) can detect activity due to malignancy, but also identifies irrelevant degenerative cortical uptake. Normal radiotracer activity in solely the marrow has yet to be described and could be the first step towards automated tumour burden calculation. We aimed to investigate the normal activity of ^{18}F-NaF in whole bone and bone marrow in patients with localised prostate cancer.
Methods and materials: ^{18}F-NaF PET/CT scans from 87 patients with high-risk prostate cancer from two centres were retrospectively analysed. All patients had a recent negative or inconclusive bone scan. In the first centre, a PET scan was acquired 1-1.5 hours after i.v. injection of 4 MBq/kg ^{18}F-NaF on an integrated PET/CT system (Gemini TF, Philips Medical Systems) (53/87). In the second centre, scanning was performed 1 hour after i.v. injection of 3 MBq/kg ^{18}F-NaF

on an integrated PET/CT system (Discovery ST, GE Healthcare) (34/87). CT scans were obtained in immediate connection to the PET scan. Automated segmentation of vertebrae, pelvis, femora, humeri and sternum were performed in the CT scans using a deep learning-based method. Bone <7 mm from skeletal surfaces was removed to isolate the marrow. SUV was measured within the remaining area in the PET scan.
Results: SUV_{max} and SUV_{mean} in the whole bone and bone marrow of the different regions were presented.
Conclusion: We present a deep-learning approach for evaluation of normal radiotracer activity. Knowledge about radiotracer uptake in normal bone prior to cancerous involvement is a necessary first step for subsequent tumour assessment and could be of value when implementing future tracers.
Limitations: n/a
Ethics committee approval: Lund, Sweden (552/2007).
Funding: This study was funded by Knut and Alice Wallenberg Foundation.
Author Disclosures:
S. Lindgren Belal: nothing to disclose
O. Enqvist: nothing to disclose
J. Ulén: nothing to disclose
L. Edenbrandt: Consultant at EXINI Diagnostics AB
E. Trägårdh: nothing to disclose

MyT3 9-16 09:30
Machine learning and radiomics analysis of breast MRI for prediction of grading, hormone receptor status and lymph node metastases in patients with breast cancer
M. Chodyla[1], J. Grueneisen[1], O. Martin[2], J. Haubold[1], M. Forsting[1], F. Nensa[1], L. Umutlu[1]; *[1]Essen/DE, [2]Düsseldorf/DE (Michal-Kamil.Chodyla@uk-essen.de)*

Purpose: To investigate the potential of MR-derived parameters for the prediction of grading, the hormone receptor status and lymph node metastases in patients with breast cancer.
Methods and materials: A total of 81 patients with BI-RADS 5 and 6 lesions were prospectively enrolled for a dedicated breast MRI examination prior to resection. The study protocol comprised diffusion-weighted imaging, T2-weighted imaging and dynamic contrast-enhanced T1-weighted imaging as well as consecutive subtraction imaging. After tumour segmentation, 13145 quantitative imaging features were extracted and tested for importance by the following feature selection methods: χ^2-test, t-test, Fisher-score, randomised logistic regression. Statistical modelling was performed using logistic regression, Random Forests or SVMs and evaluated by 5-fold cross-validation with 25 repeats. Histopathological results after subsequent tumour resection served as a reference standard.
Results: Prediction of the N-stage, as well as Elston-Ellis Grading, was moderately high with AUCs of 0.75 and 0.78, respectively. AUCs of prediction of the ER-status was moderate (0.68), while the prediction of Ki67 and HER2 status was weak (AUC = 0.61 and 0.56).
Conclusion: Our preliminary results demonstrate the potential for MR imaging-based tumour decoding and phenotyping of breast cancer with a prediction of N-stage and grading showing promising results. Prediction of the hormonal status was insufficient.
Limitations: The study was limited by small sample size and lack of control.
Ethics committee approval: This study was approved by the local ethics committee. Written informed consent was obtained from all patients before each examination.
Funding: No funding was received for this work.
Author Disclosures:
M. Chodyla: nothing to disclose
J. Grueneisen: nothing to disclose
O. Martin: nothing to disclose
J. Haubold: nothing to disclose
F. Nensa: nothing to disclose
L. Umutlu: nothing to disclose
M. Forsting: nothing to disclose

MyT3 9-17 09:34
Clinical value of MRI texture analysis for differentiating solitary fibrous tumours/hemangiopericytoma from angiomatous meningioma based on ADC and enhanced T1WI images
S. Zhang, J. Cheng*; Zhengzhou/CN*

Purpose: To explore the clinical value of preoperative texture analysis based on ADC and T1CE images in distinguishing solitary fibrous tumours/hemangiopericytoma and angiomatous meningioma.
Methods and materials: The clinical data and preoperative magnetic resonance imaging data of 24 patients with SFT/HPC and 20 patients with AM were retrospectively analysed. The histogram and GLCM parameters were analysed with Image J software to compare the difference between SFT/HPC and AM, and establish logistic regression model and plot the ROC curve for statistically significant parameters and joint parameters to confirm their efficacy in predicting SFT/HPC and AM.
Results: The Max, Min, Mean, Med of T1CE and ADC sequences of SFT/HPC are lower than AM (P<0.05, except MaxADC). The SD of T1CE sequences of SFT/HPC is larger than AM (P=0.031). The Kurt and Ske of T1CE and ADC sequences of SFT/HPC are larger than AM (P=0.003, p=0.001). ASM of ADC sequence of SFT/HPC is lower than AM (p=0.013); Con of T1CE sequence of SFT/HPC is lower than AM (p=0.027); Ent of ADC sequence of SFT/HPC was higher than AM (p=0.003); Among them, the AUC of Max, Min, Mean, Med, SD, Kurt of T1CE sequence and Min, Mean, Med, ASM, IDM, Ent of ADC sequence were greater than 0.7, and the AUC of MinT1CE, MedT1CE, and MeanT1CE were 0.970,0.964 and 0.960;multi-parameter joint analysis AUC and diagnostic efficacy (sensitivity, specificity, accuracy) were significantly improved.
Conclusion: This study shows that the analysis of tumour region texture of ADC and T1CE sequences has important clinical value for preoperative identification of SFT/HPC and AM.
Limitations: SFT/HPC and AM are rare, and the sample size is small.
Ethics committee approval: n/a
Funding: No funding was received for this work.
Author Disclosures:
S. Zhang: nothing to disclose
J. Cheng: nothing to disclose

MyT3 9-18 09:38
DoseGuard: a fully automated and fast Monte Carlo-based dose calculation system for interventional radiology
N. J. Staut, G. Paiva Fonseca, C. Jeukens, A. Vaniqui, M. Podesta, S. van Hoof, F. Verhaegen*; Maastricht/NL (nick.staut@smartscientific.nl)*

Purpose: Legislation regarding radiation dose registration creates the need for more accurate dose information. In interventional radiology, the patient dose and especially skin dose is of particular interest. Current calculation methods are based solely on the radiation dose structured report (RDSR) data or indirect dose metrics resulting in high inaccuracies. In this work, a more accurate and fully automated system is developed allowing for accurate calculations giving almost real-time feedback to the physician.
Methods and materials: An automated dose calculation system based on Monte Carlo simulations and computer vision were developed using three RGB-D cameras (Microsoft Kinect). The calibrated camera system determined the geometric relationship between the patient and x-ray source and combines this information with the RDSR data to create a fast Monte Carlo model and calculate the patient's skin dose. The patient is modelled using a family of mathematical (XCAT) phantoms. The system was tested on a clinical machine using an anthropomorphic RANDO-phantom and GafChromic film.
Results: Fully automated skin dose calculations can be performed under 10 seconds within a 10% uncertainty for all field sizes, and uncertainties below 5% for field sizes smaller than 15 cm x 15 cm. Initial tests show differences between film and simulations smaller than 5%. Organ doses can be calculated offline.
Conclusion: The built prototype shows that the combination of Monte Carlo simulation and computer vision has the potential to improve the accuracy of dose calculations in radiology. Even providing near the real-time skin dose feedback during interventional procedures allowing for the prevention of radiation-induced skin lesions. The system can also calculate organ doses to estimate the long term radiation effect.
Limitations: Only phantom measurements were performed.
Ethics committee approval: n/a
Funding: This work was partially funded by an EU Interreg Crossroads2 grant.
Author Disclosures:
M. Podesta: nothing to disclose
C. Jeukens: nothing to disclose
N. J. Staut: nothing to disclose
G. Paiva Fonseca: nothing to disclose
A. Vaniqui: nothing to disclose
S. van Hoof: nothing to disclose
F. Verhaegen: nothing to disclose

MyT3 9-19 09:42
A combination of eight cortical morphologic neuroimaging biomarkers could effectively differentiate tinnitus patients from healthy subjects: evidence from the application of machine learning
H. Lv, Z. Wang, P. Zhao, Y. Liu*; Beijing/CN (chrislvhan@126.com)*

Purpose: A large number of neuroanatomical alterations in patients with tinnitus were detected in many previous studies. However, the most probable cortical morphologic neuroimaging biomarkers that characterise tinnitus should only enrol a limited number of features.
Methods and materials: To test this hypothesis, we would apply the machine learning method to develop a feature selection method in order to differentiate tinnitus patients from healthy subjects. The brain regions with anatomical alterations in tinnitus patients were further validated. We firstly summarised 61

brain regions with significant morphologic alterations reported by previous studies and defined them as the features. From this feature pool, a hybrid feature selection algorithms combined with F-score and sequential forward floating selection (SFFS) was performed to select relevant features. The support vector machine (SVM) model was applied to analyse their performance and created a classifier. On a database of 46 tinnitus patients and 56 healthy controls, 5-fold cross-validation was used in this study to evaluate the accuracy of this classifier.
Results: A combination of eight brain regions was featured by the highest accuracy of classification in differentiating tinnitus patients from healthy controls effectively. Those brain regions including bilateral hypothalamus, left superior frontal gyrus (SFG), right rostal middle frontal gyrus, right insula, right inferior parietal lobule (IPL), and two neighbored nodes in left superior temporal gyrus (STG).
Conclusion: Our study elucidated the most characteristic anatomical changes in patients with tinnitus by applying SVM classifier, providing validated cortical morphologic neuroimaging biomarkers to differentiate tinnitus patients from normal controls.
Limitations: Results of cortical thickness and cortical surface area were not included. Larger datasets for training and testing will be more helpful.
Ethics committee approval: This study was approved by the medical research ethics committees and institutional review board of our institution.
Funding: NSFC61801311
Author Disclosures:
H. Lv: nothing to disclose
Z. Wang: nothing to disclose
P. Zhao: nothing to disclose
Y. Liu: nothing to disclose

MyT3 9-20 09:46
The correlation of artificial intelligence-based CAD-RADs by coronary computed tomography angiography with breast arterial calcification on mammography
X. Wang, Z. Huang, J. Xiao, Z. Li, Y. Hu*; Wuhan/CN*
(wangxiangwhch1971@163.com)

Purpose: This study sought to evaluate the association of breast arterial calcification (BAC) on breast screening mammography with coronary artery disease-reporting and data system (CAD-RADS™) based on artificial intelligence-coronary computed tomography angiography (CCTA).
Methods and materials: This prospective single-institution study included asymptomatic women over 40 who underwent CCTA and breast cancer screening mammography between 2018 were recorded. CAD-RADS™ was scored based on artificial intelligence. Mammograms were assessed visually for the presence and severity of BAC.
Results: 560 eligible women underwent a CCTA. Of these 214 patients also underwent mammography. In comparison to the low CAD-RADS (CAD-RADS< 3) group, the high CAD-RADS (CAD-RADS≥3) group, they more often had a history of hypertension (p=0.032), diabetes (p=0.011), hypercholesterolemia (p=0.024). They also had a statistically higher level of LDL-C (p=0.037), where HDL-C was lower than the low CAD-RADS group with (p=0.029). BAC was significantly higher in the high CAD-RADS group (p=0.008). A multivariate analysis, BAC (odd ratio [OR] 6.24, 95% confidence interval [CI]:3.39-15.45), diabetes (odd ratio [OR] 3.77, 95% confidence interval [CI]:2.16-7.98) and LDL-C (odd ratio [OR] 1.28, 95% confidence interval [CI]:1.04-4.71) were independent predictive factors for patients with high CAD-RADS patients.
Conclusion: There was a significant correlation between the severities of CAD detected by artificial intelligence and BAC. BAC, diabetes and LDL-C may be used as an additional diagnostic tool to predict the severity of CAD.
Limitations: This was a retrospective analysis. BAC was showed absence or present in the present study, more precise BAC quantification or semi-quantitative scale would be useful.
Ethics committee approval: The present study was approved by the institutional review board of the Central Hospital of Wuhan.
Funding: No funding was received for this work.
Author Disclosures:
X. Wang: nothing to disclose
Z. Huang: nothing to disclose
J. Xiao: nothing to disclose
Z. Li: nothing to disclose
Y. Hu: nothing to disclose

MyT3 9-21 09:50
Variations of standard quality control for clinical PET/MRI systems: a European perspective
A. Valladares[1], T. Beyer[1], R. Boellaard[2], Z. Chalampalakis[3], C. Comtat[3], L. Dal Toso[4], A. E. Hansen[5], J. Nuyts[6], I. Rausch[1]; *[1]Vienna/AT, [2]Amsterdam/NL, [3]Orsay/FR, [4]London/UK, [5]Copenhagen/DK, [6]Leuven/BE*
(alejandra.valladares@meduniwien.ac.at)

Purpose: Hybrid imaging systems play an important role in non-invasive disease characterisation. Therefore, stringent quality control (QC) procedures are required to ensure proper functionality of the systems and to gain accurate quantitative results. Here, we evaluate existing QC procedures for combined PET/MRI systems in clinical routine.
Methods and materials: Eight highly-experienced European imaging sites were surveyed about locally implemented PET/MRI QC procedures. The survey was based on existing recommendations on QC for stand-alone PET and MRI systems. In addition, relevant vendor-specific information on QC measures was collected.
Results: In total, five Siemens, two GE, and one Philips PET/MRI systems were reported. For all the systems, the centres reported performing the PET daily QC as implemented by the vendor. However, moderate to high variations were found across other tests and testing frequencies for the PET and MRI components of the systems. Based on the observed variability in QC procedures across sites and vendors, a consensus on QC procedures was reached. This consensus includes for the PET component: a daily QC as suggested by the local vendor, a quarterly cross-calibration measurement including the assessment of uniformity, and a yearly image quality test. For the MRI component, monthly coil checks and a quarterly MR IQ test including the assessment of signal-to-noise ratios and artefacts that could affect clinical scans and image quality.
Conclusion: Significant variations in daily QC procedures were observed across PET/MR imaging sites. A consensus on minimum QC procedures for clinical routine was proposed. This consensus can help assure high-quality examinations across sites.
Limitations: Specific applications will require additional tests.
Ethics committee approval: n/a
Funding: This work has received funding from the European Union's Horizon 2020 research and innovation programme under the MSCA No. 764458.
Author Disclosures:
A. Valladares: nothing to disclose
T. Beyer: nothing to disclose
R. Boellaard: Consultant at BMS
Z. Chalampalakis: nothing to disclose
C. Comtat: nothing to disclose
L. Dal Toso: nothing to disclose
A. E. Hansen: nothing to disclose
J. Nuyts: nothing to disclose
I. Rausch: nothing to disclose

08:30 - 10:00 **Room M 3**

Oncologic Imaging

RPS 916

Brain, head and neck tumours: advanced imaging and radiomics

Moderators:
G. Zanirato Rambaldi; Bologna/IT
C. Stippich; Heidelberg/DE

RPS 916-K 08:30
Keynote lecture
A. Radbruch*; Heidelberg/DE*

Author Disclosures:
A. Radbruch: nothing to disclose

RPS 916-1 08:40
GLINT GlucoCEST in neoplastic tumours at 3T: the first clinical results of GlucoCEST in brain tumours
T. Lindig[1], B. Bender[1], K. Herz[1], A. Deshmane[1], J. Schittenhelm[1], X. Golay[2], K. Scheffler[1], U. Ernemann[1], M. Zaiss[1]; *[1]Tübingen/DE, [2]London/UK*
(tobias.lindig@med.uni-tuebingen.de)

Purpose: Dynamic glucose enhanced (DGE) CEST imaging has almost only been shown at ultra-high field (UHF) due to the low effect size. The first results of 10 glioma patients of a DGE CEST method with fast 3D imaging developed for clinical field strength are shown herein.
Methods and materials: CEST saturated images at different frequency offsets were acquired at 160 time points before, during, and after glucose injection (0.3mg/kg) with 6.3s temporal resolution to detect accumulation in the brain. The total scan time was 16:45 min. 7 glioma patients with blood-brain barrier (BBB) leakage (6 WHO°4, IDH wild-type (WT) and 1 WHO°2, IDH positive), 3 glioma patients without BBB leakage (WHO°2, IDH positive; WHO°3, WT and WHO°4, WT), and 3 healthy controls were scanned with a clinical 3T system. After motion

and field inhomogeneity correction, the DGE images were analysed by subtracting each image from a pre-injection baseline image: $\Delta DGE(t)=DGE_{baseline}-DGE(t)$.
Results: In the high-grade gliomas with BBB leak, glucose uptake could be detected in the gadolinium-enhancing region and in tumour necrosis approximately 4 minutes after injection with a maximum increase of ΔDGE around 0.4% after approximately 9 minutes, whereas unaffected white matter ROIs did not show any significant DGE increase in accordance with previous UHF studies. Healthy controls and all 3 glioma patients without gadolinium enhancement showed no significant detectable DGE effect.
Conclusion: We demonstrated that stable DGE imaging can be accomplished at clinical field strength using optimised saturation and readout parameters. The first results are promising and indicate that glucoCEST corresponds more to the disruptions of the blood-brain barrier with gadolinium uptake than to the molecular tumour profile or tumour grading.
Limitations: n/a
Ethics committee approval: Approved, consent obtained.
Funding: EU Horizon2020, No667510.
Author Disclosures:
T. Lindig: nothing to disclose
B. Bender: nothing to disclose
K. Herz: nothing to disclose
A. Deshmane: nothing to disclose
J. Schittenhelm: nothing to disclose
X. Golay: nothing to disclose
K. Scheffler: nothing to disclose
U. Ernemann: nothing to disclose
M. Zaiss: nothing to disclose

RPS 916-2 08:46

T2-FLAIR mismatch in grade II and III gliomas: fifty shades of mismatch?
A. Desagneaux, S. Grand, M. D. C. Pasteris, M. D. J. Boutonnat, S. Charara, C. Berthet, A. Krainik, A. Kastler*; Grenoble/FR (desagneaux.andrea@gmail.com)*

Purpose: The identification of imaging criteria predictive of a specific molecular subtype has become a priority to enable accurate glioma subtypes diagnosis with imaging. We aimed to assess possible variants of the typical T2-FLAIR mismatch in grade II and III glioma tumours with correlation to both histologic and molecular findings.
Methods and materials: A single-centre retrospective study including WHO grade II and III gliomas with complete IDH and 1p19q status was conducted. Two types of mismatch were defined. Typical, as previously described, and atypical T2-FLAIR mismatch, defined as the presence of one or more of the following characteristics: very low signal in flair, thick T2-FLAIR rim hyperintensity, irregular shaped T2-FLAIR mismatch, incomplete rim, or peri T2-FLAIR mismatch tumoural spread.
Results: Among 39 included patients, 20 had IDH–mutant astrocytomas, 14 had IDH–mutant oligodendromas, and 5 had IDH-wild type. The T2-FLAIR mismatch was found in 16/20 astrocytoma IDH-mutant cases (80%), with an excellent inter-reader agreement (k of 0.89 (95% CI 0.76-1.01, p<0.001) and high PPV (100%), specificity 100%, NPV 82.6%, and sensibility 80%). The T2-FLAIR mismatch sign among IDH–mutant astrocytoma was present with a typical presentation in 6/20 (30%) cases and atypical presentation was present in 10/20 (50%) cases.
Conclusion: This study confirmed the usefulness of the T2-FLAIR mismatch to help to diagnose IDH-mutant astrocytoma. Atypical T2-FLAIR mismatch should also be considered, as this study has shown that broadening the definition of the already well-described T2-FLAIR mismatch may improve the MRI prediction accuracy of molecular subtypes in grade II and III gliomas.
Limitations: A retrospective study with a small sample.
Ethics committee approval: Study ethics approval (CECIC Rhône-Alpes-Auvergne, Clermont-Ferrand, IRB 5891).
Funding: No funding was received for this work.
Author Disclosures:
A. Desagneaux: nothing to disclose
S. Grand: nothing to disclose
S. Charara: nothing to disclose
C. Berthet: nothing to disclose
A. Kastler: nothing to disclose
A. Krainik: nothing to disclose
M. D. J. Boutonnat: nothing to disclose
M. D. C. Pasteris: nothing to disclose

RPS 916-3 08:52

MRI diffusion kurtosis imaging and a location-specific analysis for paediatric glioma grading
I. P. Voicu[1], A. Napolitano[1], M. Vinci[1], E. Miele[1], A. Carai[1], A. Carboni[1], A. Mastronuzzi[1], M. Caulo[2], G. S. Colafati[1]; *[1]Rome/IT, [2]Chieti/IT (paul.voicu@hotmail.it)*

Purpose: To investigate whether diffusion kurtosis imaging (DKI) can help differentiate low- and high-grade gliomas in paediatric patients.
Methods and materials: We retrospectively analysed preoperative MRIs including DKI in 69 children (8.3±4.3 years, 32 females) with gliomas, divided into a testing (n=58) and validation (n=11) cohort. Mean, axial, radial, and fractional anisotropy kurtosis values (MK, AK, RK, and kFA, respectively) were extracted from semiautomatically-segmented solid tumour volumes. For each metric we analysed: 1) conventional accuracy, 2) accuracy for location-specific subgroup analyses, hypothesising an opposite pattern in infratentorial midline gliomas compared to other locations, 3) location-specific overall accuracy and comparison with the conventional analysis model, and 4) model validation. Statistical analyses included t-test, ROC, and correlation analyses.
Results: 1) Conventional AUCs were 0.699, 0.658, 0.649, and 0.672 for MK, AK, RK, and kFA .
2) T-tests on 15 infratentorial midline gliomas (9 pHGG) and 43 other-location gliomas (10 pHGG) confirmed our hypotheses, yielding P<0.05 for all metrics except kFA. ROC analyses yielded AUCs of 0.925, 0.907, and 0.870 for MK, AK, and RK, respectively, in the infratentorial midline subgroup, and 0.906, 0.875, and 0.821 for MK, AK0 and RK0 respectively0 in other locations.
3) Whole-cohort location-specific estimates yielded AUCs of 0.900, 0.879, and 0.837 for MK, AK0 and RK0 respectively. Model comparisons yielded superiority for location-specific AUCs (P=0.01, P=0.01, and P=0.06 for MK, AK, and RK, respectively).
4) Validation on 11 patients yielded higher Matthews' correlation coefficient for location-specific metrics (0.82, 0.69, and 1 versus 0.31, 0.44, and 0.62 for MK, AK, and RK).
Conclusion: DKI accurately grades paediatric gliomas with a location-specific analysis.
Limitations: Further validation on more ample cohorts is needed.
Ethics committee approval: n/a
Funding: No funding was received for this work.
Author Disclosures:
I. P. Voicu: nothing to disclose
A. Napolitano: nothing to disclose
M. Vinci: nothing to disclose
E. Miele: nothing to disclose
A. Carai: nothing to disclose
A. Carboni: nothing to disclose
A. Mastronuzzi: nothing to disclose
M. Caulo: nothing to disclose
G. S. Colafati: nothing to disclose

RPS 916-4 08:58

Tumour microvascular normalisation enhancing CAR-T immunotherapy to glioblastoma via MRI
X. Chen, T. Xie*; Chongqing/CN (xiaochen229@foxmail.com)*

Purpose: To investigate whether tumour microvascular normalisation based on anti-angiogenesis could enhance CAR-T immunotherapy to solid tumours guided by MRI.
Methods and materials: Based on our previous studies on IL13R2α-CAR-T therapy in glioblastomas, we evaluated the effects of treatment with lower-dose bevacizumab on a NOD-SCID mice orthotopic glioblastoma model by 7.0T MRI to obtain the imaging biomarkers of tumour microvascular normalisation to determine the right time to transplant CAR-T cells. We used the USPIO-labelled cell tracking technique with MRI to evaluate the penetration and persistence of CAR-T cells in the tumour and functional MRI to assess the therapeutic effect.
Results: Tumour vascular normalisation appeared on day 3 and gradually faded away on day 7 after lower-dose bevacizumab treatment. The DCE-MRI and IVIM-MRI parameters show great potential in the non-invasive assessment of the normalisation window induced by bevacizumab. The K^{trans} value showed a significant decrease and the ADC value marked an increase in the combination therapy group 3 days after treatment compared to the monotherapy or the control groups, which were verified by immunohistochemical staining.
Conclusion: We established a combinational regimen that synchronises CAR-T therapy with tumour vascular normalisation. Moreover, we established an imaging platform and evaluation system for in vivo tracking of tumour vascular normalisation enhancing CAR-T immunotherapy to glioblastomas. These findings offer hope for developing new approaches that could enhance CAR-T therapy in solid tumours.
Limitations: n/a

Ethics committee approval: Human peripheral blood was obtained from healthy donors under an institutional review board-approved protocol. The use of laboratory animals was in compliance with the guideline of the National Institute of Health. All animal experiments were performed according to a protocol approved by the Animal Use Subcommittee.
Funding: National Natural Science Foundation of China (grant no. 81801672).
Author Disclosures:
X. Chen: nothing to disclose
T. Xie: nothing to disclose

RPS 916-5 09:04

Cerebral blood volume measurement at tumour-microvascularity derived from local image variance of susceptibility-weighted imaging in glioblastomas: correlation with IDH mutational status

H. Wu[1], X. Zhou[2], W. Zhang[1]; [1]*Chongqing/CN,* [2]*Shanghai/CN (cefradine1005@gmail.com)*

Purpose: To assess the clinical practice of rCBV value of tumour-microvascularity derived from local image variance (LIV) of susceptibility-weighted imaging (SWI) for IDH genotype prediction in glioblastomas (GBM).
Methods and materials: Preoperative MRI examinations of 78 GBM patients with a known IDH genotype were recruited. rCBVs derived from DSC-MRI was computed and normalised against the contralateral unaffected white matter value. rCBV and SWI images were coregistered to the MNI space. SWI-LIV were calculated according to the steiner translation theorem. The LIV regions were then extracted as ROI for rCBV measurement. The hot-spot ROI-based rCBV analysis was also conducted for confrontation. The discriminating potential for assessing IDH mutation status prediction was assessed by ROC curves.
Results: ROC analysis revealed that the rCBVs in SWI-LIV regions had a great ability to predict the IDH genotype with a sensitivity of 82.05% and a specificity of 97.06% (AUC=0.955). The SWI-LIV-based rCBV analysis has a superior diagnostic performance for IDH genotype prediction compared to the hot-spot ROI method (the difference between areas=0.077, z-score=1.697, and p=0.09).
Conclusion: Our study has proven that rCBVs in SWI-LIV regions has high prediction capabilities for the IDH mutation status in GBM patients. As SWI hypointensity is highly correlated with tumour microvascularity, the SWI-LIV-based ROI method is reliable to evaluate the haemodynamic change compared to the hot-spot based method.
Limitations: Lacking the microvascular-related biopsy data or pathologic sampling to comfirm the rCBV change in SWI-LIV regions.
Ethics committee approval: This study was approved by the institutional review board of the Army Medical University and was conducted in accordance with Health Insurance Portability and Accountability Act regulations.
Funding: The National Key R&D Program of China (2018YFC0115004) and grants from the Natural Science Foundation of China (81871421 and 81571660).
Author Disclosures:
H. Wu: nothing to disclose
X. Zhou: nothing to disclose
W. Zhang: nothing to disclose

RPS 916-6 09:10

Remodelling tumour microenvironments through inhibiting the glycolytic activator PFKFB3 to synergise with antiangiogenic therapy in glioblastoma: insights from multiparametric MRI and proteome profiling

J. Zhang, W. Zhang*; Chongqing/CN (ilovetqm@qq.com)*

Purpose: To investigate whether targeting tumour glycolysis by PFKFB3 blockade is a novel potential strategy to enhance antiangiogenic therapy in glioblastomas (GBM) and to evaluate treatment-related molecular characterisation and clinically translatable MR imaging biomarkers of tumour response.
Methods and materials: Patient-derived orthotopic GBM xenografts in mice were established and imaged before (baseline) and at different time points after treatment with bevacizumab (BEV), 3PO (PFKFB3 inhibitor), BEV and 3PO, and saline. The tumour volume, cellularity, neovascularisation, and metabolites were monitored by T_2WI, IVIM, DCE-MRI, and ^{1}H-MRS, respectively. Pathology and proteome microarray were analysed to correlate with imaging parameters and evaluate post-treatment molecular profiling.
Results: BEV treatment induced remarkable PFKFB3 expression compared with the control ($P<0.05$). 3PO enhanced BEV therapeutic efficacy by sustained vascular normalisation, improved oxygenate status, and reduced the expression of matrix metalloprotein-9. K^{trans} and f were positively correlated with microvascular density (r=0.8776; r=0.9177), hypoxia (r=0.5566; r=0.5681), and negatively vascular maturation (r=-0.4898; r=-0.5884). Only co-treatment improved vascular perfusion corresponding to increased D*. BEV activated glycolysis with a rising trend of Lac/Cr and lactate dehydrogenase-A level. Co-treatment inhibited multiple proangiogenic factors by downregulating VEGF-independent pathways.
Conclusion: Targeting PFKFB3 has much potential to abate BEV-induced glycolytic adaption resistance by remodelling tumour microenvironments and could be monitored through multiparametric MRI thoroughly. IVIM is a promising alternative to DCE-MRI to characterise tumour response.
Limitations: The patient-derived GBM xenografts were modelled from one patient specimen only. Taking the tumour inherent heterogeneity into account, large-scale studies based on xenografts obtained from different GBM patients are needed to recapitulate diversity tumour habits and draw a definite conclusion.
Ethics committee approval: This preclinical study was approved by the Animal Use Subcommittee of Daping Hospital, Army Medical University.
Funding: The National Natural Science Foundation of China (No.81511660 and 81871421).
Author Disclosures:
J. Zhang: nothing to disclose
W. Zhang: nothing to disclose

RPS 916-7 09:16

^{18}F-FET or ^{18}F-FCH PET/CT in the primary diagnosis of low-grade glioma: a pilot study

M. Hodolic[1], A. M. Krpan[2], A. T. Golubic[2], J. Nemir[2], G. Mrak[2], M. Zuvic[2], D. Huic[2]; [1]*Olomouc/CZ,* [2]*Zagreb/HR (marina.hodolic@gmail.com)*

Purpose: Gliomas are associated with varied survival, in part linked with their histological subtype. The diagnosis of low-grade glioma (LGG) is challenging, as conventional imaging modalities can often give inconclusive or equivocal results. Function imaging modalities can provide additional metabolic information. O- (2-[18F]-fluoroethyl) -L-tyrosine (^{18}F-FET) is radiopharmaceutical approved for the characterisation of glioma-suggestive brain lesions. ^{18}F-FET displays a high tumour-to-background ratio and no accumulation in inflammatory lesions. Because of low uptake in normal brain parenchyma, some centres use fluoromethyl-(18F)-dimethyl-2-hydroxyethyl-ammonium chloride (^{18}F-FCH) PET for the characterisation of glioma-suggestive brain lesions.
The aim of this study was to determine the diagnostic accuracy of ^{18}F-FET and ^{18}F-FCH PET/CT in patients with primary LGG.
Methods and materials: 11 patients aged 21-80 years with MRI-suspected LGG were involved. Patients underwent ^{18}F-FET and ^{18}F-FCH PET/CT within one week. Surgery and pathohistological diagnoses were performed in the next two weeks.
Results: 11/11 patients with suspected LGG underwent MRI, ^{18}F-FET and ^{18}F-FCH PET/CT. 9/11 patients underwent surgery and pathohistological diagnosis.
6 patients positive on ^{18}F-FET (SUVmax values ranging from 1.3-3.1) and negative on ^{18}F-FCH PET had a pathohistological diagnosis of LGG (2 ganglioma and 4 diffuse astrocytomas).
2 patients with ^{18}F-FET and ^{18}F-FCH PET avid lesion had a final diagnosis of glioblastoma multiforme.
1 patient negative on ^{18}F-FET and negative on ^{18}F-FCH PET had a diagnosis of focal cortical dysplasia.
2/11 patients are still waiting for surgery.
Conclusion: Appropriate radiopharmaceutical should be chosen before performing PET/CT in patients with newly diagnosed LGG. ^{18}F-FET seems to be more accurate than ^{18}F-FCH in the primary diagnosis of LGG.
Limitations: The small number of patients.
Ethics committee approval: The University Hospital Centre Zagreb, Croatia, approved this study.
Funding: 18F-FET was received for free.
Author Disclosures:
M. Hodolic: Consultant at Iason, Graz, Austria
D. Huic: nothing to disclose
A. M. Krpan: nothing to disclose
A. T. Golubic: nothing to disclose
J. Nemir: nothing to disclose
G. Mrak: nothing to disclose
M. Zuvic: nothing to disclose

RPS 916-8 09:22

The use of contrast clearance analysis for the post-therapeutic follow-up of brain tumours and metastases treated with radiotherapy

S. Mahmoudi, A. Toutaoui, T. Baroudi, R. Louelh*; Tizi Ouzou/DZ (abdelkader.toutaoui@gmail.com)*

Purpose: Contrast clearance analysis calculated from delayed-contrast-MRI is a novel methodology that enables the reliable differentiation between tumour and non-tumoural tissues in brain tumour patients. Analysis maps are calculated by subtracting 3D-T1-MRIs acquired 5 min post-contrast injection from those acquired 60-105 min later. We studied applications of this methodology for the post-therapeutic follow-up of patients in conventional/stereotactic radiotherapy.
Methods and materials: 10 patient treated in our department were included in this study. 5 patients with glioblastoma, 2 patients with germinoma, and 3 with brain metastases were scanned following the protocol. The first scan was

performed 4 months after the end of treatment. For 3 patients, 3 additional scans were performed every 3 months. 2 other patients had 2 more scans.
Results: 24 contrast clearance analysis maps were calculated for 10 patients. Detailed examples demonstrating the potential application of this method for the management of brain tumours are presented in this study. The potential application of the method for assessing the existence/absence of residual tumours after radiotherapy is demonstrated in the case of all patients with the first scan. The use of this technique for differentiating progression from treatment effects is demonstrated in the case of patients with 4 and 3 scan maps. In the case of 4 patients, a significant increase in the red volume in the maps was indicative of necrosis. For 1 patient, the map favoured pseudoprogression over progression. These evaluations are supported by clinical signs and tumour markers.
Conclusion: The contrast clearance analysis presents a novel model-independent approach providing efficient separation between tumour/non-tumour tissues. The presented results provide histological validation of analysis maps and demonstrate their potential contribution to the management of brain tumour patients.
Limitations: n/a
Ethics committee approval: n/a
Funding: No funding was received for this work.
Author Disclosures:
A. Toutaoui: nothing to disclose
S. Mahmoudi: nothing to disclose
T. Baroudi: nothing to disclose
R. Louelh: nothing to disclose

RPS 916-9 09:28

Early post-treatment assessment of multi-parametric MRI after stereotactic radiosurgery: can it predict the long-term response of brain metastases?

P. P. Arcuri, S. Roccia, A. Quattrone, G. Fodero, V. Aiello, C. Bertucci, E. Mazzei, D. Laganà*; Catanzaro/IT (arppaolo@alice.it)*

Purpose: Imaging criteria to evaluate the response of brain metastases to stereotactic radiosurgery (SRS) in the early post-treatment period remains an important need not yet resolved. The aim of this study is to correlate early (within 12 weeks) post-treatment multi-parametric MRI changes with long-term outcomes after treatment of brain metastases with SRS.
Methods and materials: We evaluated 24 patients with multi-parametric MRI techniques, including spectroscopy, diffusion, and perfusion imaging in the pre- and post-treatment early period for the differentiation of radiation-related changes and tumour recurrence after SRS in intracranial metastases. Patients were followed longitudinally until death, progression, or intervention. All patients presented with enlargement of the treated lesion, an increase in perilesional brain oedema, and aggravation of neurological signs and symptoms from 7-29 weeks after primary treatment. Kruskal–Wallis' non-parametric test was performed. Sensitivity, specificity, and accuracy were assessed. Fisher's exact test was used to evaluate statistical significance. Histology or radiological follow-up was the gold standard.
Results: A low apparent diffusion coefficient (ADC) $<1\times10^{-3}$ mm^2/s, a high relative cerebral blood volume (rCBV) ratio >2.3, and a high choline/creatine (Cho/Cr) ratio >1.9 suggested tumour recurrence. A high ADC $>1\times10^{-3}$ mm^2/s, a low rCBV ratio <2.3, and a Cho/Cr ratio <1.9 suggested SRS-induced radiation changes. Sensitivity, specificity, and diagnostic accuracy were, respectively: rCBV=82%, 79%, and 81%, ADC= 75%, 73%, and 79%, and Cho/Cr ratio=76%, 80%, and 82%.
Conclusion: Early post-treatment rCBV and, to a lesser extent, ADC values and Cho/Cr ratios may be used as imaging biomarkers to help predict the long-term response of brain metastases to SRS. This can help identify patients who will ultimately fail SRS and allow for timelier adjustments in the treatment approach.
Limitations: The different primitive neoplasms.
Ethics committee approval: n/a
Funding: No funding was received for this work.
Author Disclosures:
A. Quattrone: Author at CNR
P. P. Arcuri: Speaker at A.O. Pugliese Ciaccio, Author at A.O. Pugliese Ciaccio
S. Roccia: Author at A.O. Pugliese Ciaccio
G. Fodero: Author at A.O. Pugliese Ciaccio
V. Aiello: Author at Magna Graecia University
C. Bertucci: Author at A.O. Pugliese Ciaccio
E. Mazzei: Author at A.O. Pugliese Ciaccio
D. Laganà: Author at Magna Graecia University

RPS 916-10 09:34

The efficacy prediction of enzatiinib in brain metastases of crizotinib-resistant ALK-positive non-small-cell lung cancer (NSCLC) based on radiomics of brain MRI

D. H. Hou, S. J. Zhao, N. Wu*; Beijing/CN (1661874241@qq.com)*

Purpose: To investigate the feasibility of efficacy prediction of enzatiinib in brain metastases of crizotinib-resistant ALK-positive NSCLC based on radiomics of brain MRI.
Methods and materials: We enrolled ALK-positive NSCLC patients with brain metastases who progressed on crizotinib from 27 centres across China and acquired their clinical information and MRI images. The efficacy of patients was grouped according to progression-free survival (PFS=69 weeks). Radiomic features of T1-weighted contrast material-enhanced images on baseline were extracted using software A. K. and analysed in IPMs. Clinical characteristics analyses were performed using the statistical package R.
Results: By the latest evaluation date, this multicentre analysis included 69 brain metastases (mean size: 1.13 cm (0.46-3.25 cm); lesion location: 29 in frontal lobes, 6 in parietal lobes, 8 in occipital lobes, 10 in temporal lobes, 9 in cerebellums, and 7 in other parts) in 18 patients (10 women, 8 men; mean age: 51 years (36-66 years). Clinical characteristics (gender, age, lesion size, and location) were independent of the efficacy (P>0.05). Statistically significant differences were found in 2 radiomic features in multivariate analysis (p<0.05). Multivariate logistic regression models reconstructed with these radiomic features had predictive power for efficacy (AUC: 0.745, sensitivity: 0.714, and specificity: 0.714).
Conclusion: Radiomics provides prognostic value for PFS in patients receiving enzatiinib treatment.
Limitations: The study only included a small number of patients. We designed the study using a lesion-based approach reflecting the prognosis condition of patients, which may leaded to overfitting. We only analysed brain metastases but not meningeal metastasis.
Ethics committee approval: Approved by the local ethics review board. Patients provided written informed consent.
Funding: National Key R&D Program of China (2017YFC1308700), Chinese Academy of Medical Sciences Initiative for Innovative Medicine (2017-I2M-1-005).
Author Disclosures:
D. H. Hou: Author at cancer hospital chinese academy of medical sciences
S. J. Zhao: Investigator at cancer hospital chinese academy of medical sciences
N. Wu: Investigator at cancer hospital chinese academy of medical sciences, Consultant at cancer hospital chinese academy of medical sciences

RPS 916-11 09:40

MRI radiomics: tumour marker at the pretreatment prediction of response to neoadjuvant chemotherapy of nasopharyngeal carcinoma

J. Sun[1], S. Chen[2], J. Ding[2], F. Shan[1], C. Huang[2];
[1]Shaoguan/CN, [2]Stony Brook/CN
(sunjunqi1233668@sina.com)

Purpose: To develop and validate a non-invasive radiomic model to predict the response to cisplatin-based neoadjuvant chemotherapy in NPC patients using pretreatment contrast-enhanced T1WI MRI (CE-MRI) and T2WI.
Methods and materials: Currently, we have response data from 105 NPC patients who received the cisplatin-based neoadjuvant chemotherapy. 63 patients showed a response to neoadjuvant chemotherapy (by RECIST). Their pretreatment CE-MRI images were used for radiomic analysis. Regions-of-interest covering the whole tumour were manually delineated by a radiologist and a total of 850 radiomic features were extracted for each patient, including shape, texture, wavelet, and Laws features. The dataset was split into a training cohort (n=70) and a temporal validation cohort (n=35). Features with strong discriminative power were selected by pre-selection (Mann Whitney U-test p<0.05, Spearman correlation |r|<0.7) followed by a least absolute shrinkage and selection operator (LASSO) with 10-fold cross-validation in the training cohort. The prediction performance was evaluated in the temporal validation set. The receiver operating characteristic (ROC) analysis was performed with the optimal threshold determined by maximising the Youden index in the training set.
Results: In the training cohort, 4 radiomic features were selected for the prediction model, with an area under the ROC curve (AUC)=0.89, sensitivity=0.82, and specificity=0.90. The corresponding temporal validation results were 0.89, 0.67, and 0.86, respectively.
Conclusion: This study demonstrates the potential of using routine pretreatment CE-MRI to predict NPC patients' response to cisplatin-based neoadjuvant chemotherapy.
Limitations: The relatively small number of patients.
Ethics committee approval: n/a
Funding: Guangdong Medical Research Fund.
Author Disclosures:
J. Sun: nothing to disclose
S. Chen: nothing to disclose
J. Ding: nothing to disclose
F. Shan: nothing to disclose
C. Huang: nothing to disclose

RPS 916-12 09:46

Dual-energy 4D-CT of parathyroid adenomas not clearly localised by sestamibi scintigraphy and ultrasonography: a retrospective study

M. Woisetschlager[1], O. Gimm[1], K. Johansson[2], G. Wallin[3], I. Garcia[1], A. Spångeus[1]; [1]Linköping/SE, [2]Västervik/SE, [3]Örebro/SE

Purpose: To evaluate if four-dimensional dual-energy computed tomography (4D-DECT) and quantitative information can improve the localisation of PAs and better distinguish between PAs, lymph nodes (LNs), and the thyroid gland (Thy).
Methods and materials: 15 patients (mean age: 57±18.9 years; range: 22-82 years) with persistent or recurrent primary hyperparathyroidism underwent 4D-DECT in 3 different phases: no-contrast, arterial, and venous. Quantitative data was also determined, including Hounsfield unit (HU) values, dual-energy information (electron density [Rho], atomic number [Z], and dual-energy index [DEI]), and spectral information (keV).
Results: With regards to spectral information, lower energies showed greater HU differences between the 3 tissues than higher energies. In the venous phase, there were significant differences between all 3 tissues up to 100keV ($p<0.05$). For all energies, PA was significantly lower in HU than Thy in non-contrast images and higher than LN in the arterial phase ($p<0.05$). All 3 tissues differed significantly from each other in terms of HU in the venous phase at 90kV, 150kV, and mixed 0.8 images. Thy was significantly higher than PA and LN in non-contrast images for 90kV, 150kV, mixed 0.8, and Rho ($p<0.05$). LN was significantly lower than PA and Thy in the arterial phase for 90kV, 150kV, mixed 0.8, Rho, Z, and DEI ($p<0.05$).
Conclusion: There were significant differences between PA, LN, and Thy at different energies and contrast phases, as well as in their spectral information, which might enhance diagnostic accuracy and location. Dual-energy information from real non-contrast scans might be helpful in equivocal cases.
Limitations: The small number of participants and retrospective design.
Ethics committee approval: D/N: 2017/241-31.
Funding: No funding was received for this work.
Author Disclosures:
M. Woisetschlager: nothing to disclose
G. Wallin: nothing to disclose
O. Gimm: nothing to disclose
K. Johansson: nothing to disclose
I. Garcia: nothing to disclose
A. Spångeus: nothing to disclose

11:15 - 12:30 **Room B**

Musculoskeletal

RPS 1010a

Artificial intelligence (AI) and new techniques in MRI

Moderators:
L. M. Sconfienza; Milan/IT
R. Sutter; Zurich/CH

RPS 1010a-1 11:15

Computer-assisted diagnosis of hip dysplasia and femoroacetabular impingement FAI using automatic reconstruction of MRI-based 3D models of the hip joint: a deep learning-based study

T. Lerch, G. Zeng, F. Schmaranzer, N. Gerber, K. Siebenrock, M. Tannast; Berne/CH (till.lerch@insel.ch)

Purpose: Hip dysplasia and FAI are complex three-dimensional hip pathologies that can cause hip pain in young and active patients of child-bearing age. Imaging is static and based on 2D pelvic radiographs. Computer-assisted CT-based diagnosis of hip dysplasia and FAI was introduced for patient-specific planning of surgical treatment but MRI-based 3D models would offer a radiation-free alternative.
This study explores the difference between automatic and manual MRI-based 3D-models and if diagnostic parameters correlate between automatic and manual MR-based 3D-models.
Methods and materials: We performed an IRB-approved comparative, retrospective study of 31 hips of 26 symptomatic patients with FAI and hip dysplasia. We compared CT-and MR-based osseous 3D models of the hip joint of the same patients. A 3D-CT scan (isovoxel: 1 mm^3) of the entire pelvis and the distal femoral condyles were obtained. Preoperative MR arthrograms of the hip were obtained including axial-oblique T1 3D-VIBE sequence (0.8 mm^3 isovoxel) and two axial anisotropic (1.2 x1.2 x 1 mm) 3D-T1 VIBE DIXON sequences of the entire pelvis and the distal femoral condyles. Automatic reconstruction of MRI-based 3D models was performed using machine-learning (deep learning). Threshold-based manual reconstruction of CT- and MR-based 3D-models was performed using commercial software (AMIRA).
Results: The difference between MRI-based 3D-models was below 1 mm. The median difference was 0.2±0.1 mm for the proximal femur and 0.2±0.5 mm for the acetabulum. The Dice coefficient was 97% for the acetabulum and 98% for the femur. The correlation for 6 diagnostic parameters was excellent and significant ($r=0.99$, $p<0.001$) between automatic and manual MR-based 3D-models. The absolute difference was below 2°.
Conclusion: Automatic MRI-based 3D models can replace CT-based 3D-models for patients of childbearing age with hip dysplasia and FAI.
Limitations: A retrospective study.
Ethics committee approval: IRB approval was obtained.
Funding: No funding was received for this work.
Author Disclosures:
T. Lerch: nothing to disclose
M. Tannast: nothing to disclose
F. Schmaranzer: nothing to disclose
K. Siebenrock: nothing to disclose
G. Zeng: nothing to disclose
N. Gerber: nothing to disclose

RPS 1010a-2 11:21

To test the ability of artificial intelligence to differentiate between benign and malignant soft tissue masses in ultrasonography

L. Perronne[1], B. Wang[2], R. S. Adler[2]; [1]Paris/FR, [2]New York/US

Purpose: Ultrasound evaluation of superficial soft tissue masses is increasingly utilised in routine clinical practice. However, differentiating benign from malignant aetiologies may be challenging. Deep convolutional neural networks (CNNs) have shown the potential to classify images with good accuracy. We propose to test the ability of this methodology to differentiate between benign and malignant superficial soft tissue masses.
Methods and materials: A total of 760 ultrasound images from focused ultrasounds of superficial soft tissue masses were selected to train a CNN classifier. The dataset consisted of 523 images of benign soft tissue masses and 237 images of malignant masses, all confirmed by pathologic diagnosis. We selected the pre-trained VGG-16 architecture implemented on Keras. We performed a binary classification (benign and malignant). Then, we tried to differentiate between 3 subgroups of benign masses: lipomas, benign nerve sheath tumours, and vascular malformations.
Results: The test accuracy of the model to determine if the mass was benign or malignant mass was 0.75. The CNN outperformed two experienced musculoskeletal radiologists on a test sample dataset. The accuracy of the model to differentiate between the 3 benign subgroups test dataset was 0.66.
Conclusion: As an initial step, artificial intelligence (AI) shows promise in the differentiation of benign from malignant soft masses, outperforming two musculoskeletal radiologists. The addition of a larger variety and number of soft tissue masses will be necessary to establish the utility of AI as a useful tool going forward.
Limitations: The limited size of our dataset restricted the number of subgroups that could be investigated. We tested the accuracy of only two radiologists, which does not necessarily reflect the accuracy of radiologists with varying experience.
Ethics committee approval: This study has institutional board review approval.
Funding: No funding was received for this work.
Author Disclosures:
L. Perronne: nothing to disclose
B. Wang: nothing to disclose
R. S. Adler: nothing to disclose

RPS 1010a-3 11:27

Tumour margin infiltration in soft tissue sarcomas: prediction with 3T MR texture analysis

M. Kim[1], W.-H. Jee[1], Y. Lee[1], J. H. Hong[2], Y.-G. Chung[2], W.-J. Bahk[1]; [1]Gyeonggi/KR, [2]Seoul/KR

Purpose: To determine the value of MR texture analysis to assess tumour margin infiltration in soft tissue sarcomas at 3T MRI including IVIM DWI.
Methods and materials: 31 patients with pathologically confirmed soft tissue sarcomas after surgery who underwent 3T MRI including IVIM DWI were included in this study. Margin infiltration on pathology was used as a golden standard. Texture analysis was performed by drawing ROIs on axial T1- and T2-weighted images, contrast-enhanced (CE) T1-weighted images, high b value DWI, and ADC maps using software (TexRad). Mean, SD, entropy, MPP, skewness, and kurtosis were compared between sarcomas with an infiltrative margin and sarcomas with a circumscribed margin. A Mann-Whitney U test was performed. The ROC curve with AUC was obtained.
Results: Among 31 patients with sarcomas, 22 sarcomas had tumour margin infiltration at pathology. T1 kurtosis was significantly higher in sarcomas with an infiltrative margin than a circumscribed margin: 1.959 vs 0.12 ($p=0.017$). CE T1 kurtosis was significantly lower in sarcomas with an infiltrative margin than a

circumscribed margin: 0.563 vs 1.413 (p=0.020). The mean and MPP on DWI were higher in sarcomas with an infiltrative margin than a circumscribed margin: 404.4 vs 269.4 (p=0.082). AUCs of T1 kurtosis and skewness were 0.792 (95% CI, 0.628-955) and 0.601 (95% CI, 0.371-830), respectively. On DWI, AUC of mean and MPP was 0.702 (95% CI, 0.520-0.884). AUC of CE T1 mean and MPP was 0.630 (95% CI, 0.383-877). With a cutoff of 0.545 in T1 kurtosis, sensitivity and specificity for predicting tumour margin infiltration were 71% and 88%, respectively.
Conclusion: MR texture analysis may be reliable to predict the tumour margin infiltration in soft tissue sarcomas, particularly using T1 kurtosis at 3T.
Limitations: A retrospective study with potential selection bias and a small study population.
Ethics committee approval: Approved by IRB and informed consent was waived.
Funding: No funding was received for this work.
Author Disclosures:
W.-H. Jee: nothing to disclose
M. Kim: nothing to disclose
J. H. Hong: nothing to disclose
Y.-G. Chung: nothing to disclose
W.-J. Bahk: nothing to disclose
Y. Lee: nothing to disclose

RPS 1010a-4 11:33
Paediatric radiographic detection of the acute distal tibial fracture using trained AI-networks
Z. A. Starosolski, J. H. Kan, A. Annapragada*; Houston, TX/US (zastaros@texaschildrens.org)*

Purpose: Tibial fracture detection is a routine task in paediatric radiology. Its precision depends on knowledge of anatomy and experience-based training. Until recently, there were no computer-aided detection tools due to anatomical complexity, a variety of 2d projections, additional objects in the image, the presentation of pathology, the age of patients, and gender.
Methods and materials: We presented a CNN-based system that can automatise radiographic distal tibia fracture detection. The system used two connected CNNs. The first CNN was trained to localise the distal tibia using 500 normal and 500 pathological studies, including displaced and nondisplaced fractures. The images were manually annotated with a box containing the distal tibia. This CNN had a 98% accuracy with zero false-positives. The second CNN was chosen from previously developed CNNs trained on a different, broader set of manually segmented distal tibia images and had undergone the 10 fold cross-validation. The best CNN, which formerly achieved an accuracy of 95.9%, was selected for validation in this study.
Results: The whole system combined two models into the pipeline. An x-ray image was read and the distal tibia localised as an ROI. The ROI was transferred to the fracture detection algorithm. If the distal tibia was not localised, then it was not processed by the second model. The whole system achieved an area under the receiver-operating curve (AUC-ROC) of 0.89.
Conclusion: This method could become a computer-aided diagnosis (CAD) tool, accelerating the workflow in paediatric radiology departments.
Limitations: This study was limited to images acquired and read at a single institution.
Ethics committee approval: This work was conducted under a protocol approved by the Institutional Review Board.
Funding: No funding was received for this work.
Author Disclosures:
J. H. Kan: nothing to disclose
Z. A. Starosolski: nothing to disclose
A. Annapragada: nothing to disclose

RPS 1010a-5 11:39
Quantitative ultrashort echo time MRI (UTE-MRI) for the diagnosis of early cartilage degeneration: a comparison with T2 mapping
J. Yang[1], H. Shao[1], L. Wan[2], J. Du[2], G. Tang[1]*; [1]Shanghai/CN, [2]San Diego/US (yangjiaweitj@126.com)*

Purpose: To investigate the feasibility of using a quantitative ultrashort echo time MRI (UTE-MRI) technique to diagnose early cartilage degeneration and to compare the technique's diagnostic efficacy with T2 mapping.
Methods and materials: 20 patients with a total knee arthroplasty were obtained and underwent an MR scan on a clinical 3.0T scanner. 72 regions of interest were manually drawn on specimens for UTE-adiabaticT1ρ, UTE-T2*, and T2 measurement, and the corresponding cartilage-bone regions were further divided into normal (n=11, Mankin scores 0-1), mild (n=28, Mankin scores 2-5), moderate(n=21, Mankin scores 6-9), and severe (n=12, Mankin scores 10-14) degeneration groups based on histological measures of degeneration (Mankin scores) as a reference standard. Statistical analysis was performed to compare the differences among the groups.
Results: The UTE-adiabaticT1ρ in the normal group was significantly different from the mild group moderate group and severe group. The adiabaticT1ρ, UTE-T2*, and T2 values correlated significantly with Mankin scores, with UTE-adiabaticT1ρ and UTE-T2* markedly correlated with Mankin scores, and with T2 values weakly correlated with Mankin scores. The diagnostic efficacy of UTE-adiabatic T1ρ was better than UTE T2* mapping and T2 mapping for the diagnosis of early cartilage degeneration.
Conclusion: UTE-adiabaticT1ρ may provide a more promising imaging biomarker with potential application in more comprehensive diagnoses and the monitoring of cartilage degeneration compared to UTE-T2* and T2.
Limitations: The sample size was small. The study was performed ex vivo and the measurement condition was different from the real physiological environment. Additionally, this study could not utilise quantitative biochemical measurements for PG and the collagen of cartilage.
Ethics committee approval: The study was approved by Ethics Committee at our Hospital (Ethics Committee approval number: shsy-iec-ky-3964).
Funding: National Natural Science Foundation of China (81871325,81801656).
Author Disclosures:
L. Wan: nothing to disclose
J. Yang: nothing to disclose
H. Shao: nothing to disclose
G. Tang: nothing to disclose
J. Du: nothing to disclose

RPS 1010a-7 11:45
Dixon or DWI: quantitative discrimination between malignant and acute osteoporotic vertebral fractures
R. Donners, M. M. Obmann, D. Boll, D. Harder*; Basel/CH (ricardo.donners@usb.ch)*

Purpose: To compare Dixon MRI derived fat-fraction (FF) and ADC to discriminate between malignant and acute osteoporotic vertebral fractures.
Methods and materials: 1.5T MRI of 42 malignant and 27 acute osteoporotic vertebral fractures were retrospectively reviewed. Fractured vertebrae showed extensive hyperintensity on fluid-sensitive fat-suppressed sequences. FF was derived from axial T1 VIBE two-point Dixon images with dedicated in and opposed echo timing by dividing the fat-only sequence through the sum of the fat-plus water-only sequence. ADC maps were calculated from axial b50 and b900 images. ROI-based measurements of mean FF and ADC were performed for each fractured vertebra in the axial plane. A blinded MSK-radiologist classified fractures as malignant or osteoporotic based only on morphologic features, also noting diagnostic confidence. Diagnostic performance was compared by ROC curve analyses and discriminating cut-off values were derived. P<0.05 was deemed significant.
Results: FF and ADC were significantly smaller in malignant fractures (p<0.01). AUC was significantly larger for FF than for ADC (p=0.03). The FF AUC (0.92), sensitivity (86%), and specificity (85%) were not significantly inferior compared to the radiologist's interpretations (0.93, 98%, and 89%; each p>0.05). ADC AUC (0.78) and sensitivity (62%) were significantly smaller compared to the radiologist (each p<0.01). Low-reader confidence was reported in 11% of fractures. In this subgroup, the specificity of FF and ADC (83% each) exceeded the radiologist's specificity (50%).
Conclusion: Quantitative FF and ADC can distinguish malignant from acute osteoporotic fractures. FF showed superior diagnostic accuracy over ADC and was non-inferior to an MSK-radiologist's evaluation.
Limitations: The study size, retrospective design, lack of histopathology, and recall bias.
Ethics committee approval: This study follows the regulations of the local ethics committee. Patient consent was waived.
Funding: No funding was received for this work.
Author Disclosures:
R. Donners: nothing to disclose
M. M. Obmann: nothing to disclose
D. Boll: nothing to disclose
D. Harder: nothing to disclose

RPS 1010a-8 11:51
Shape-based machine learning for three-dimensional phenotyping of the lumbosacral spine and dural sac: a prediction of Fibrillin-1 gene mutations pathogenic for Marfan syndrome
F. Rengier, O. Naas, T. Norajitra, C. Lückerath, M. Karck, K. Maier-Hein, H.-U. Kauczor*; Heidelberg/DE (fabian.rengier@web.de)*

Purpose: To test our hypothesis that three-dimensional phenotyping of the lumbosacral spine and dural sac using shape-based machine learning enables the prediction of Fibrillin-1 gene mutations pathogenic for Marfan syndrome.
Methods and materials: 184 patients being evaluated for Marfan syndrome, 01/2012-12/2016, underwent 1.5T-MRI with 3D T2-weighted TSE-sequence of the lumbosacral spine with 1x1x1 mm³ spatial resolution. 110 patients (32.4±11.6 years, 50 female) agreed to genetic testing; 38 had a Fibrillin-1 gene

mutation pathogenic for Marfan syndrome (FBN1+) and 72 were tested negative (FBN1-). Shape-based machine learning allowed three-dimensional segmentation and quantification of volumes and volume ratios of vertebral bodies L3-L5 and dural sac segments L3-S1.
Results: Dural sac volumes were significantly enlarged in FBN1+ vs FBN1- patients (in mL): segment L3 12.5±3.0 vs 10.3±2.3, L4 11.8±3.5 vs 9.0±2.5, L5 11.7±4.4 vs 7.9±3.1, and S1 13.5±8.7 vs 5.3±3.1 (all p<0.001). Vertebral body volumes did not significantly differ between FBN1+ vs FBN1- patients. ROC analysis for the identification of FBN1+ patients showed AUCs of 0.797 for total lumbosacral dural sac volume, 0.660 for L3 volume ratio, 0.694 for L4 volume ratio, 0.766 for L5 volume ratio, 0.786 for S1 dural sac volume, and 0.753 for S1 to L4 dural sac volume ratio. Combined sensitivity, specificity, and positive and negative predictive values for identification of FBN1+ patients were 69%, 93%, 84%, and 85%.
Conclusion: Fibrillin-1 gene mutations were associated with a significantly altered three-dimensional phenotype of the lumbosacral spine and dural sac. Shape-based machine learning allowed identification of patients with Fibrillin-1 gene mutations with a high specificity and moderate sensitivity.
Limitations: Potential sources of bias are the retrospective study design and secondary exclusion of those patients without genetic testing.
Ethics committee approval: An ethics committee approved the study and waived written informed consent.
Funding: No funding was received for this work.
Author Disclosures:
F. Rengier: nothing to disclose
O. Naas: nothing to disclose
C. Lückerath: nothing to disclose
T. Norajitra: nothing to disclose
M. Karck: nothing to disclose
K. Maier-Hein: nothing to disclose
H.-U. Kauczor: nothing to disclose

RPS 1010a-9 11:57

Radiology improving the diagnosis and management of patients suffering with Ehlers-Danlos syndrome. An upright biomechanical MRI study
F. W. Smith; *London/UK (franciswsmith@hotmail.com)*

Purpose: The incidence of the hypermobile Ehlers-Danlos syndrome (hEDS) is larger than is generally understood, with many patients being misdiagnosed as suffering from ME or fibromyalgia. It is important to make the correct diagnosis to enable appropriate treatment.
Methods and materials: 112 consecutive patients with hEDS had MRI scans of the cervical spine and craniocervical junction performed in an upright MRI scanner, where the cervical spine angle was measured with the neck in neutral flexion and extension, and compared with an age-sex matched control group. MRI of the atlantoaxial joint was performed looking forwards, to the right, and to the left to assess for evidence of laxity of the craniocervical ligamentous complex. The cerebellar tonsillar station was also recorded.
Results: Patients with hEDS showed a decrease in their cervical spine angle in neutral 20% less than the control group (16º vs 20º), a 50% larger ability to flex the neck (-20º vs -11º), and a 45% greater angle in extension (55º vs 32º). 72% showed ligamentous laxity/instability of the cervical spine. 80% showed evidence of atlantoaxial instability.
43.5% demonstrated hindbrain herniation of greater than 5 mm, with no evidence of syringomyelia in a pattern distinctly different from the Chiari malformation.
Conclusion: It is important to be able to make accurate measurements of increased mobility and laxity of both the cervical spine and atlantoaxial joints in patients suffering from hEDS to allow for referral for the appropriate treatment, including surgery where indicated. It is also important for the reassurance of these patients, who have a physical disability, that they do have hEDS and are not psychologically disturbed or suffering from ME or fibromyalgia.
Limitations: n/a
Ethics committee approval: n/a
Funding: No funding was received for this work.
Author Disclosures:
F. W. Smith: nothing to disclose

RPS 1010a-10 12:03

Can sacrum height predict body height, age, and sex? A large population-based MRI study
F. Yahya[1], D. Cantré[2], K. Thierfelder[1], M.-A. Weber[1], S. Langner[1];
[1]Rostock/DE, [2]Roggentin/DE (Fathi.yahya@med.uni-rostock.de)

Purpose: Post-mortem identification of unknown deceased persons and age estimation in the living are central tasks of forensic scientists. Body height is traditionally derived from measurements of long bones. The sacrum is a centrally located bone that is relatively unsusceptible to environmental factors. The aim of the study was to investigate if sacrum height can be used to estimate body height, weight, age, and sex using datasets from a population-based magnetic resonance imaging (MRI) study.
Methods and materials: A total of 2,499 whole-body MRIs were evaluated. Sacrum height was measured in the median plane of sagittal T2-weighted images of the spine and associations with age, sex, and body height were analysed. Linear regression was used to derive formulas for body height estimation.
Results: Male participants had significantly (p<0.001) greater sacrum height (11.4 cm, standard deviation 1.1 cm, range: 7.9-14.6 cm) compared to female participants (10.9 cm, standard deviation 1.0 cm, range: 7.3-14.5 cm). The Pearson-correlation was r=0.44 for body height. The mean absolute difference (MAD) between calculated and measured body height was 4.9 cm for females and 4.8 cm for males. ROC cut-off to classify sex had a 60% sensitivity and 57.3% specificity.
Conclusion: Contrary to previous reports, sacrum height alone cannot be recommended to predict body height, age, or sex. It is not as reliable as predictions based on large bones.
Limitations: A population-based MR-study from a specific region of Germany. Not all participants in the study were included in the final analysis. There was no correlation with established techniques for age, sex, and height determination based on the analysis of long bones.
Ethics committee approval: Approved by the local ethics committee and all participants gave their written informed consent.
Funding: No funding was received for this work.
Author Disclosures:
F. Yahya: nothing to disclose
D. Cantré: nothing to disclose
K. Thierfelder: nothing to disclose
M.-A. Weber: nothing to disclose
S. Langner: nothing to disclose

RPS 1010a-11 12:09

The use of whole-body MRI in chronic recurrent multifocal osteomyelitis in children: our experience in 29 patients
M. Gónzalez[1], L. Rodríguez Díez[2], E. Ladera González[2], I. Barber Martinez[3], E. Iglesias[2], E. J. J. Inarejos Clemente[3]; *[1]Montevideo/UY, [2]Barcelona/ES, [3]Esplugues de Llobregat/ES*
(made.gonzalez@gmail.com)

Purpose: To describe the most common locations of involvement in chronic recurrent multifocal osteomyelitis (CRMO) in children using whole-body magnetic resonance imaging (WB-MRI).
Methods and materials: We retrospectively reviewed 29 patients (12 girls, 17 boys) with a diagnosis of CRMO from 2014-May 2019. All patients underwent WB-MRI using STIR sequences in axial and coronal planes, and sagittal planes to evaluate the spine. Imaging data was evaluated by a paediatric radiologist with more than 10 years of experience and a radiology fellow with 3 years of experience.
Results: The mean age at diagnosis was 11 years (3-16 years), but the mean age of clinical presentation was 10 years.
A total of 175 lesions were investigated. The lesions were multifocal in 28/29 cases (96.5%) and the number of lesions encountered per patient ranged from 1-28 lesions.
The most common sites of involvement were the pelvis and femur (21%), followed by tibia (19.3%), and the spine and humerus (7.4%). Other less frequent locations included clavicles (4.5%), tarsus (4%), foot (3.4%), radius and cuboid (2.8%), fibula (2.3%), and the sternum (1.7%). The involvement of the patella, ribs, carpus, and scapula was exceedingly rare, accounting for 0.6%.
The metaphysis of long bones was most frequently involved (56.4%), followed by epiphysis (13.6%). Bilateral lesions were 42.9%.
Conclusion: WB-MRI is the diagnostic modality of choice in patients with a clinical diagnosis of CRMO. Bilateral involvement of metaphysis and epiphysis of long bones, and the pelvis, are the most frequent areas of involvement.
Limitations: n/a
Ethics committee approval: n/a
Funding: No funding was received for this work.
Author Disclosures:
M. Gónzalez: nothing to disclose
I. Barber Martinez: nothing to disclose
E. J. J. Inarejos Clemente: nothing to disclose
E. Ladera González: nothing to disclose
L. Rodríguez Díez: nothing to disclose
E. Iglesias: nothing to disclose

RPS 1010a-12 12:15
Clinical validation of a deep learning-based bone age software: a feasibility study
W. W.-I. Lea, S.-J. Hong, H.-K. Nam, H. S. Yong, Z. Yang, J. Jeong, J. Kim; *Seoul/KR (lwooin17@gmail.com)*

Purpose: To evaluate the clinical performance of deep learning (DL)-based software for bone age assessment in a paediatric endocrinology clinic in South Korea.
Methods and materials: We compared the bone age estimated from commercial DL-based software (BoneAge, Vuno, Seoul, Korea) with the bone ages independently estimated by 3 physicians (1 musculoskeletal radiologist, 1 paediatric endocrinologist, and 1 radiology resident) using a Greulich-Pyle atlas. In total, 109 children (8 boys, 101 girls) aged between 4 and 17 years who visited the paediatric endocrinology clinic from December 2018 were enrolled. Fisher's exact test (two sides), Pearson's correlation coefficient, and root mean squared error (RMSE) were used to compare the bone ages of DL software and those of the 3 physicians. An intraclass correlation coefficient (ICC) evaluated inter-rater variation.
Results: Fisher's exact test showed significant differences between DL bone age and all 3 physicians' bone age ($p<0.025$). There were good correlations ($r=0.93$, 0.92, and 0.9, $p<0.05$), however, the RMSE values were 9.7, 13.1, and 9.9 months between the bone age of DL software and those of the musculoskeletal radiologist, paediatric endocrinologist, and radiology resident, respectively. RMSE values between the 3 physicians were 12.3, 18, and 14.8 months, with relatively good correlation with each other ($r=0.88$, 0.89, and 0.88, $p<0.05$). ICC values between the 3 physicians were 0.93, 0.84, and 0.87 each, with an overall ICC value of 0.92.
Conclusion: Bone age estimated by DL-based software showed good correlation with the bone ages estimated using a traditional Greulich-Pyle atlas by 3 physicians but showed statistically different values.
Limitations: A retrospective, single-centre study with a small number of patients
Ethics committee approval: n/a
Funding: No funding was received for this work.
Author Disclosures:
S.-J. Hong: nothing to disclose
W. W.-I. Lea: nothing to disclose
Z. Yang: nothing to disclose
H. S. Yong: nothing to disclose
H.-K. Nam: nothing to disclose
J. Jeong: nothing to disclose
J. Kim: nothing to disclose

11:15 - 12:30 **Room C**

Neuro

RPS 1011a

Brain tumours

Moderators:
A. I. Holodny; New York, NY/US
P. Naval Baudín; L'Hospitalet de Llobregat/ES

RPS 1011a-K 11:15
Keynote lecture
C. Majós; *Barcelona/ES (cmajos@bellvitgehospital.cat)*

Author Disclosures:
C. Majós: nothing to disclose

RPS 1011a-1 11:25
A longitudinal glioblastoma analysis of multi-parametric brain MRI using deep learning
M. Perkuhn[1], R. Shahzad[1], F. Thiele[2], P. Stavrinou[1], M. Schlamann[3], C. Kabbasch[1], J. Borggrefe[1]; *[1]Cologne/DE, [2]Aachen/DE, [3]Essen/DE (rahilshahzad@gmail.com)*

Purpose: Cytoreductive surgery, radiation, and chemotherapy are the cornerstones of glioblastoma (GB) therapy. Currently, response to therapy is assessed by MRI based on two-dimensional tumour measurements, which have inherent limitations around the tumour-cavity. Manual segmentation of the lesions is time-consuming and suffers from high inter-rater-variability. To overcome these limitations and allow for a user-independent volume assessment, this study aimed to train and evaluate a state-of-the-art deep learning model (DLM) for fully-automatic GB segmentation of contrast-enhancing tumours (CET), oedema (ED), and tumour cavities (TC) on clinical routine follow-up data.
Methods and materials: 94 subjects undergoing primary GB resection were included. T1, T2, FLAIR, and contrast-enhancing (CE) T1 sequences were obtained during the course of treatment follow-up. Ground truth segmentations for the tumour compartments were obtained by consensus reading. Data was split into a training set (80 subjects) and test set (14 subjects). A multi-parametric, multi-label DLM for GB segmentation was trained on postoperative scans of the training set. A transfer learning approach was also used by including a preoperative model trained on an additional 220 GB subjects.
Results: The DLM was tested on 85 longitudinal follow-up scans from the test set. Volume correlations (R) of DLM to manual segmentations were 0.89 (CET), 0.95 (ED), and 0.96 (TC). Automatic segmentation achieved Dice coefficients (±SD) of 0.35±0.33 (CET), 0.64±0.22 (ED), and 0.57±0.30 (TC). For CET>2 ml, the median Dice was 0.61.
Conclusion: The proposed fully-automatic approach is robust in detecting the different tumour compartments on routine follow-up data. A DLM which is sensitive to small CET's (<2 ml) is currently being developed. DLM's show a strong potential to provide automated deep-learning-based GB segmentation in longitudinal GB analysis that may facilitate RANO assessment and improve the radiologist's workflow.
Limitations: n/a
Ethics committee approval: The local ethics committee approved this retrospective study.
Funding: No funding was received for this work.
Author Disclosures:
R. Shahzad: Employee at Philips Research
M. Perkuhn: Employee at Philips Research
F. Thiele: Employee at Philips Research
P. Stavrinou: nothing to disclose
M. Schlamann: nothing to disclose
C. Kabbasch: nothing to disclose
J. Borggrefe: nothing to disclose

RPS 1011a-2 11:31
MRI characterisation of peri-operative brain haemodynamic alterations after awake surgery in diffuse low-grade gliomas
A. Coget, J. Deverdun, E. Le Bars, L. van Dokkum, F. Molino, N. Menjot de Champfleur; *Montpellier/FR (arthur.coget@gmail.com)*

Purpose: No data is currently available on postoperative haemodynamic variations after neurosurgery, while these presumed variations could have imaging, clinical, and physiopathological implications. Here, we aim to characterise perioperative brain perfusion modifications after awake surgery in a cohort of patients with diffuse low-grade gliomas using MRI.
Methods and materials: 53 patients with diffuse low-grade gliomas who underwent awake surgery were included in this study. MRI acquisitions on a 3.0T magnet including perfusion-weighted imaging GE-EPI with contrast agent were performed before, within 36 h, and three months after surgery. Mean perfusion parameter values, as well as their asymmetry index, have been estimated for each hemisphere and each ROI and then compared between the three time-points. ROIs were extracted from the AAL atlas.
Results: We observed haemodynamic alterations ipsilateral to the tumour resection, marked by a stronger asymmetry index between hemispheres and on all perfusion parameters. Regional differences in the evolution of the haemodynamic variations were found, including both transient postoperative modifications (e.g. in the putamen) and persistent postoperative alterations (e.g. in the precuneus). Finally, permanent haemodynamic impairments at 3 months post-surgery existed not only in specific regions but also translated to a general ipsilateral hemispheric impairment.
Conclusion: The observed post-operative regional differences and persisting modifications of the cerebral vascular autoregulatory processes ask for caution in the analysis and interpretation of perfusion and BOLD-based imaging immediately and long-term after brain surgery.
Limitations: A main limitation concerns the impact of post-operative brainshift that could induce misalignement between AAL maps and perfusion volumes between MRI sessions.
Ethics committee approval: The study was approved by the local ethical committee. Participants gave informed consent before inclusion.
Funding: No funding was received for this work.
Author Disclosures:
A. Coget: nothing to disclose
J. Deverdun: nothing to disclose
E. Le Bars: nothing to disclose
L. van Dokkum: nothing to disclose
F. Molino: nothing to disclose
N. Menjot de Champfleur: nothing to disclose

RPS 1011a-3 11:37

MRI evaluation of targeted adoptive immunotherapy for gliomas using biotinylated adoptive T lymphocytes

H. Zhang[1], S. Wu[2]; [1]Qingdao/CN, [2]Shanghai/CN (smwu19@fudan.edu.cn)

Purpose: To explore the biotinylation of adoptive T lymphocytes and its feasibility of targeted adoptive T cells immunotherapy (ACT) for gliomas based on biotin receptors.
Methods and materials: Adoptive CD8+ T lymphocytes were co-cultured with Sulfo-NHS-Biotin to form biotinylated adoptive T lymphocytes in vitro, and Alexa Four 647-labelled streptavidin was further co-cultured with biotinylated adoptive T lymphocytes. The proportion of glioma cells apoptosis and death were further analysed by FCM. Glioma cells recruiting biotinylated adoptive T cells were observed by CLSM and enhanced MRI to observe the size changes of in situ gliomas at different time points after targeted ACT. Using transferase-mediated deoxyuridine triphosphate-biotin nick end labelling (TUNEL), apoptosis was detected in tumour tissues and the proportion of glioma recruiting biotinylated adoptive T lymphocytes was analysed by FCM.
Results: FCM showed that the overall biotinylation efficiency of adoptive T lymphocytes reached 96.3%. The apoptosis proportion of glioma cells induced by biotinylated adoptive T lymphocytes (34.14%) was significantly increased. FCM showed that the proportion of biotinylated CD8+ T lymphocytes in the targeted glioma area was 4.77% and the total proportion of CD8+ T lymphocytes (8.89%) was more obvious than the control group (1.81%). Enhanced MRI found that only 20% of the individuals in the targeting group had a reduced tumour volume, but the mean value was not significantly different from the control group ($p>0.05$). In addition, the TUNEL apoptosis assay found that level of tumour cell apoptosis in the targeting group was only slightly better than the non-targeting group.
Conclusion: Biotinylation of adoptive T lymphocytes increases the proportion of gliomas recruited, enhancing the killing of glioma cells.
Limitations: n/a
Ethics committee approval: n/a
Funding: National Natural Science Foundation of China Research (Grant Nos. 81671732 and 51372260).
Author Disclosures:
H. Zhang: nothing to disclose
S. Wu: nothing to disclose

RPS 1011a-4 11:43

An unsupervised learning method for IDH mutation prediction in glioblastomas based on cumulative probability distribution curves in vascular habitats

H. Wu[1], W. Jiang[2], X. Zhou[3], W. Zhang[1]; [1]Chongqing/CN, [2]Hangzhou/CN, [3]Shanghai/CN (cefradine1005@gmail.com)

Purpose: To evaluate the clinical practice for an unsupervised learning method in IDH genotype prediction in malignant glioblastomas (GBM).
Methods and materials: Preoperative MRI examinations of 25 GBM patients with known IDH genotype were recruited into this study. Perfusion parameters were used to automatically draw the reproducible habitats related to vascular heterogeneity (i.e. high-angiogenic enhancing tumour habitats (HAT) and low-angiogenic enhancing tumour habitats (LAT)). We extracted the voxel matrix of each habitat to build cumulative probability distribution functions (CDF) and obtain the cohort-specific CDF via the function coefficient average. The Fréchet distance between the individual CDF and cohort-specific CDF and for the LOOCV was evaluated. In addition, the rCBV values at 25%, 50%, and 75% of peak height were used for the ROC analysis and KM survival analysis.
Results: Our model achieved 84% accuracy for IDH prediction in the training cohort and 80.0% in the validation cohort at the HAT habitat, in addition to 84% in the training cohort the validation cohort at the LAT habitat. Significant results were obtained for $rCBV_{C25}$ and $rCBV_{C50}$ in the HAT habitat (hazard ratios(HR), 3.29 [p=0.02] and 3.86 [p<0.00], respectively).
Conclusion: Our classifiers can provide natural boundaries for efficient discrimination of the IDH-wildtype and mutation cohort and is concise and robust in inter-institutional comparison for natural features and cohort-specific classifier.
Limitations: One primary limitation is the small sample size (n=25) in the analyses due to the single-institution, retrospectively collected data.
Ethics committee approval: This study was approved by the institutional review board of the Army Medical University and was conducted in accordance with Health Insurance Portability and Accountability Act regulations.
Funding: Natural Science Foundation of China (81571660 and 81871421).
Author Disclosures:
H. Wu: nothing to disclose
X. Zhou: nothing to disclose
W. Zhang: nothing to disclose
W. Jiang: nothing to disclose

RPS 1011a-5 11:49

A non-invasive in-vivo evaluation of IDH mutation status using 3T MR edited spectroscopy in brain glioma patients

D. Juskanic[1], J. Polakova Mistinova[2], M. Marjanska[3], S. Holly[1], L. Patrovic[1], M. Halaj[1], M. Sekeresova[1], K. Kolejak[1], M. Kavec[2]; [1]Nitra/SK, [2]Bratislava/SK, [3]Minneapolis/US

Purpose: The presence of isocitrate dehydrogenase (IDH) mutation is a major diagnostic and prognostic marker in gliomas. The proteomic footprint of IDH mutation is the intracellular presence of oncometabolite 2-hydroxy-glutarate (2HG), which is detectable by MR spectroscopy (MRS). The primary aim of the study was to evaluate the diagnostic performance of in-vivo MRS to determine IDH status. Spectral quality subanalysis was also performed.
Methods and materials: 39 spectra were acquired and reported prospectively in 36 consecutive patients with MR imaging appearance of CNS glioma from February 2018-June 2019 at a tertiary referral hospital with a neurosurgery department. Single voxel MRS data was acquired at a 3T system (Magnetom Skyra, Siemens) with a Mescher–Garwood point-resolved spectroscopy (MEGA-PRESS) sequence. Standard voxel size was 8 ml; adjustment to the tumour volume was an option. Postprocessing and an evaluation of the spectra were performed with LCModel. Positive finding was defined as detectability of 2HG peak with a CRLB value less than 60%. Immunohistochemistry or genetic test results were available to compare to the 18 spectra.
Results: Single voxel MEGA-PRESS MR spectroscopy provided 80% sensitivity (CI 95%, 0.44-0.96) and 75% specificity (CI 95%, 0.36-0.95) in the detection of 2HG. Spectral quality subanalysis revealed that the greatest limitation of the method is lower SNR, which resulted in an intermediate quality of 44% and a non-diagnostic test in 13% of all acquired spectra.
Conclusion: 2HG MR spectroscopy has a competing diagnostic accuracy considering its non-invasive, non-contrast, and radiation-free nature. It may be an integral part of advanced MR tumour protocol, aiding prognostic assessment and multidisciplinary treatment planning for glioma patients.
Limitations: SNR decreases after spectral subtraction, especially in smaller and subcortically located tumours.
Ethics committee approval: Ethics commitee approval. Written informed consent.
Funding: No funding received for this work.
Author Disclosures:
D. Juskanic: nothing to disclose
J. Polakova Mistinova: nothing to disclose
M. Marjanska: nothing to disclose
L. Patrovic: nothing to disclose
S. Holly: nothing to disclose
M. Sekeresova: nothing to disclose
K. Kolejak: nothing to disclose
M. Halaj: nothing to disclose
M. Kavec: Employee at Siemens

RPS 1011a-6 11:55

Topographical mapping of 436 newly diagnosed IDH wildtype glioblastomas with versus without MGMT promoter methylation

F. Incekara, S. R. van der Voort, S. Klein, M. J. van Den Bent, M. Smits; Rotterdam/NL

Purpose: O^6-methylguanine-methyltransferase (MGMT) promoter methylation status is an important prognostic factor for patients with glioblastomas (GBM). There are conflicting reports about the topographical distribution of GBM with versus without MGMT promotor methylation, possibly caused by molecular heterogeneity in GBM populations. We initiated this study to re-evaluate the topographical distribution of GBM with versus without MGMT promoter methylation.
Methods and materials: Preoperative T2-weighted/FLAIR and post-contrast T1-weighted MRI scans of patients aged 18 years or older with IDH wildtype GBM were collected. Tumours were semi-automatically segmented and the topographical distribution between GBM with versus without MGMT promoter methylation presented using frequency heatmaps. Voxel-wise differences were analysed using permutation testing with threshold-free cluster enhancement.
Results: 436 IDH wildtype GBM patients were included, 211 with and 225 without MGMT promoter methylation. Visual examination suggested that when compared with MGMT unmethylated GBM, MGMT methylated GBM were more frequently located near the bifrontal and left occipital periventricular area and less frequently near the right occipital periventricular area. Statistical analyses, however, showed no significant difference in topographical distribution between MGMT methylated versus MGMT unmethylated GBM.
Conclusion: This study re-evaluated the topographical distribution of MGMT promoter methylation in 436 newly diagnosed IDH wildtype GBM, which is the largest homogenous IDH wildtype GBM population to date, in light of the updated WHO 2016 classification. There was no statistically significant difference in anatomical localisation between MGMT methylated versus unmethylated IDH wildtype GBM.

Limitations: The retrospective design, potential selection and confounding biases.
Ethics committee approval: The study design was approved by the Medical Ethical Committee of Erasmus MC and HMC. (IRB: no informed consent needed due to retrospective nature of study).
Funding: The Dutch Cancer Society (KWF project number EMCR 2015-7859).
Author Disclosures:
F. Incekara: nothing to disclose
S. R. van der Voort: nothing to disclose
M. Smits: Speaker at speaker fees (paid to institution) by GE Healthcare, Other at independent reviewer for EORTC-1410 honorarium (paid to institution) for Parexel Ltd.
M. J. van Den Bent: nothing to disclose
S. Klein: nothing to disclose

RPS 1011a-7 12:01
Discriminative validity of DSC perfusion MRI and DWI for IDH mutation status
E. Cindil, N. Erdoğan, N. Dağ, M. N. Cerit, H. N. N. Şendur, A. Y. Öner, E. T. Tali*; Ankara/TR*

Purpose: Isocitrate dehydrogenase (IDH) mutation has a predictive prognostic value in high grade gliomas (HGG). The aim of this study was to investigate if dynamic susceptibility contrast perfusion (DSC) MRI is able to differentiate IDH mutationstatus in HGGs.
Methods and materials: 60 patients with HGG (21 glioblastomas, 17 anaplasticastrositomas; 14 IDH-mutant, 24 IDH-wild) who underwent 3T conventional MRI and DSC-MRI prior to a biopsy or surgery were included retrospectively. Perfusion (rCBV, PSR) and diffusion metrics (mean ADC, minimum ADC) in the tumour core and peritumoral non-enhancing area were measured. A Mann Whitney U test was used to detect statistically significant differences in metrics between IDH-mutant and IDH-wild type tumours. P>0.05 was considered significant.
Results: rCBV in the tumour core was the only parameter which showed statistically significant differences between IDH-mutant (meanrCBV=3.14) and IDH-wild tumour types (meanrCBV=5.29, p<0.001). The AUC value of rCBV was 0.86 with a sensitivity of 0.83 and a specificity of 0.79 at the best cut-off point of 3.26. There were no significant differences for other metrics for both the tumour core and peritumoural area between IDH-mutant and IDH-wild tumours.
Conclusion: rCBV's measurement of the tumour core may help to differentiate IDH mutation status in HGGs but it is not possible to differentiate by using other DSC perfusion metrics and DWI metrics of the tumour core and peritumoural non-enhancing area.
Limitations: The inadequate number of cases.
Ethics committee approval: The local institutional review board approved this retrospective study.
Funding: No funding was received for this work.
Author Disclosures:
N. Erdoğan: nothing to disclose
E. Cindil: nothing to disclose
N. Dağ: nothing to disclose
A. Y. Öner: nothing to disclose
E. T. Tali: nothing to disclose
M. N. Cerit: nothing to disclose
H. N. N. Şendur: nothing to disclose

RPS 1011a-8 12:07
Whole-brain apparent diffusion coefficient measurements correlate with survival in glioblastoma patients
A. Rulseh, J. Vymazal*; Prague/CZ (aarulseh@gmail.com)*

Purpose: Glioblastomas (GBM) are the most common malignant primary brain tumour and methods to improve early detection and evaluate the treatment response are highly desirable. We explored changes in whole-brain apparent diffusion coefficient (ADC) values with respect to survival (progression-free [PFS], overall [OS]) in a cohort of GBM patients followed at regular intervals until disease progression.
Methods and materials: A total of 43 subjects met the inclusion criteria and were analysed retrospectively. Histogram data was extracted from whole-brain ADC maps including skewness, kurtosis, entropy, median, mode, and 15th percentile (p15) and 85th percentile (p85) values, and linear regression slopes (versus time) were fitted. Regression slope directionality (positive/negative) was subjected to univariate Cox regression. The final model was determined by a LASSO on metrics above the threshold.
Results: Skewness, kurtosis, median, p15, and p85 were all below the threshold for both PFS and OS and were analysed further. The median regression slope directionality best modelled PFS (p=0.001; HR 3.3; 95% CI 1.6-6.7), while p85 was selected for OS (p=0.002; HR 0.29; 95% CI 0.13-0.64).
Conclusion: Our data showed tantalising potential in the use of whole-brain ADC measurements in following GBM patients, specifically serial median ADC values which correlated with PFS, and p85 values which correlated with OS. Whole-brain ADC measurements are fast and easy to perform and free of ROI-placement bias.
Limitations: Due to the retrospective design, detailed clinical information was not available and the assessment of potential prognostic benefit at individual time points was not possible.
Ethics committee approval: The study was approved by the institutional review boards or ethics committees of all participating centres, and all patients provided written informed consent.
Funding: Supported by MH CZ-DRO (NHH, 00023884). IG174301 and AZV MZ CR NV18-04-00457.
Author Disclosures:
A. Rulseh: nothing to disclose
J. Vymazal: Consultant at Novocure

RPS 1011a-9 12:13
Correlation of dynamic contrast-enhanced perfusion MRI with glioblastoma wild-type and brain metastases
P. M. M. Latorre Brajovic[1], L. Hernandez Martinez[2], C. Casado Pérez[2], J. Alonso Sánchez[2], A. Hilario Barrio[2], L. Koren Fernandez[2], P. Martin[2], A. C. Martinez de Aragon[2], A. Ramos Gonzalez[2]*; [1]Santiago/CL, [2]Madrid/ES, (pmlatorre@gmail.com)*

Purpose: Glioblastomas and metastatic brain tumours are the most common malignant brain tumours. It is often difficult to differentiate between these two neoplasms on conventional MR imaging. Our goal is to evaluate the role of the T1-weighted dynamic contrast-enhanced (DCE) MRI perfusion technique to differentiate between glioblastomas and metastatic lesions.
Methods and materials: DCE-MRI was retrospectively analysed in 19 patients with unique metastatic brain lesions and 22 patients with glioblastoma wild-type prior to any therapeutic intervention. DCE perfusion parameters calculated for the region of maximal tumoural enhancement were volume transfer constant (K^{trans}), efflux rate constant (K^{ep}), fractional volume of extravascular extracellular space (V_e), initial area under the gadolinium contrast agent concentration-time curve (IAUGC), contrast enhancement ratio (CER), and maximum slope of increase (Max Slope). Mann-Whitney U-tests were applied to these parameters.
Results: CER was significantly higher in metastasis (0.94) than in glioblastoma (0.67) (P=0.032). V_e was marginally higher in metastasis (0.37) than in glioblastoma (0.25) (P=0.055). The remaining perfusion parameters did not show statistically significant differences.
Conclusion: DCE-MRI showed that it has a limited potential to differentiate glioblastoma wild-type and metastases brain tumours. V_e and CER were the best parameters to discriminate between glioblastomas and metastases.
Limitations: It is a retrospective study with a small series of cases.
Ethics committee approval: n/a
Funding: No funding was received for this work.
Author Disclosures:
P. M. M. Latorre Brajovic: nothing to disclose
A. Hilario Barrio: nothing to disclose
J. Alonso Sánchez: nothing to disclose
L. Koren Fernandez: nothing to disclose
P. Martin: nothing to disclose
L. Hernandez Martinez: nothing to disclose
C. Casado Pérez: nothing to disclose
A. C. Martinez de Aragon: nothing to disclose
A. Ramos Gonzalez: nothing to disclose

RPS 1011a-10 12:19
The predictive power of MRI in identifying the pathological grading of meningiomas
F. Ballati[1], P. Lomoro[1], S. Sacco[1], C. Paganelli[2], G. Buizza[2], L. M. Farina[1], A. M. Bacila Turcanu[1], A. Iannalfi[1], L. Preda[1]*; [1]Pavia/IT, [2]Milan/IT (france.balla@hotmail.it)*

Purpose: To assess whether magnetic resonance imaging (MRI) can predict the histological WHO grading of meningiomas and if it is able to differentiate WHOI from WHOII and WHOIII.
Methods and materials: 76 patients with 77 histologically proven meningiomas were enrolled (43 WHOI, 27 WHOII, and 7 WHOIII). Data was derived from multiparametric MRI sequences: pre- and post-contrast T1, T2, FLAIR, and diffusion (DWI). T1 post-contrast was used to obtain lesion volume, which was rigidly registered on the ADC map obtained from DWI in order to derive multi-parametric imaging features based on conventional ADC and an intra-voxel-incoherent-motion (IVIM) model (i.e. ADC, D, D*, and f) within the whole tumour volume. Qualitative features from morphological images were also evaluated: tumour localisation, T1- and T2- signal intensity relative to grey matter, shape, tumour-brain interface, peritumoural oedema, capsular enhancement, and tumour enhancement (homogeneous vs inhomogeneous).

Results: Regarding DWI parameters, median values of ADC, D, and D* were higher for WHOI than WHOII and WHOIII meningiomas (p<0.05) in univariate analysis. Statistically significant differences (p<0.05) were also found in univariate analysis among qualitative features such as tumour localisation, T1- and T2- signal intensity relative to grey matter, tumour shape, peritumoural oedema, capsular enhancement, and tumour enhancement. Combining DWI and qualitative parameters, the median ADC and tumour enhancement resulted statistically different in multivariate analysis between the two groups (p<0.05), with an AUC of 0.98, a specificity of 0.93, and sensitivity of 0.97.
Conclusion: Both DWI and qualitative features could be potential predictors of meningiomas histological grade. Lower ADC and inhomogeneous tumour enhancement suggest a high-grade meningioma. In future, these features may be useful to characterise lesions with no histological diagnosis and for the application in tailored therapy treatments.
Limitations: n/a
Ethics committee approval: n/a
Funding: No funding was received for this work.
Author Disclosures:
F. Ballati: nothing to disclose
P. Lomoro: nothing to disclose
S. Sacco: nothing to disclose
C. Paganelli: nothing to disclose
G. Buizza: nothing to disclose
L. M. Farina: nothing to disclose
A. M. Bacila Turcanu: nothing to disclose
A. Iannalfi: nothing to disclose
L. Preda: nothing to disclose

RPS 1011a-11 12:25
T1-weighted dynamic contrast-enhanced MRI perfusion of chordoma: a biomarker and innovative follow-up imaging tool for assessing tumour response after proton therapy
A. Rajendran, N. Chidambaranathan, F. Abubacker Sulaiman*; Chennai/IN (adhithyan40@gmail.com)*

Purpose: We hypothesised that T1-weighted dynamic contrast-enhanced (DCE) MR imaging parameters and time-intensity curves can be used to characterise tumour response to proton therapy, detecting subsequent changes in chordoma vasculature, which may later predict parallel changes in tumour volume as detected by conventional MR imaging.
Methods and materials: We retrospectively analysed MRIs from patients with a pathology-proved chordoma of the sacrum, spine, or clivus. 15 patients with DCE-MR perfusion imaging (3T philips Ignenia Elition) before and after proton-therapy were enrolled. DCE-MR imaging was acquired on completion of routine MR imaging. Kinetic enhancement of tissues before and after contrast injection was obtained by using a 3D T1-weighted fast-spoiled gradient-echo sequence.
ROIs were drawn to encompass the entirety of the chordoma by 2 attending neuroradiologists. The area under the curve (AUC), wash-in and wash-out rates, and relative enhancement were the parameters analysed.
Dynamic concentration-time curves illustrate changes in MR imaging signal intensity as a function of time. Two curves for before and after RT were obtained for each patient.
Results: Chordoma lesions did not exhibit significant changes in tumour volume in response to therapy and limited the utility of conventional MR imaging in evaluating treatment efficacy and subsequent patient prognosis.
However, quantitative DCE parameters such as AUC and wash-in significantly decreased post-treatment. This change reflected the extent of vascular damage induced by proton therapy.
Characteristic dynamic MR signal intensity–time curves shifted to the left side post proton therapy and served as a biomarker in our study.
Conclusion: DCE-MR imaging presents a novel alternative to conventional MR imaging for tumour monitoring in patients with chordoma, providing insight into the physiologic and haemodynamic processes within a particular lesion.
Limitations: A retrospective study.
Ethics committee approval: n/a
Funding: No funding was received for this work.
Author Disclosures:
A. Rajendran: nothing to disclose
N. Chidambaranathan: nothing to disclose
F. Abubacker Sulaiman: nothing to disclose

11:15 - 12:30 **Room X**

Oncologic Imaging

RPS 1016

Breast and gynecologic advanced imaging and radiomics

Moderators:
R. Balaji; Chennai/IN
V. Romeo; Naples/IT

RPS 1016-K 11:15
Keynote lecture
V. Lehotska*; Bratislava/SK (viera.lehotska@ousa.sk)*

Author Disclosures:
V. Lehotska: nothing to disclose

RPS 1016-1 11:25
Automated MR phenotyping improves the prediction of survival in primary invasive breast cancer
M. Dietzel[1], R. Schulz-Wendtland[1], P. Clauser[2], M. Hammon[1], S. Ellmann[1], E. Wenkel[1], R. Zoubi[3], M. Uder[1], P. A. T. Baltzer[2]; *[1]Erlangen/DE, [2]Vienna/AT, [3]Ibbenbüren/DE*

Purpose: To investigate whether automated MRI-phenotyping improves the prediction of survival in PBC.
Methods and materials: Within this retrospective study, 314 consecutive patients with PBC received standard clinical-staging MRI examinations before the initiation of treatment.
Diagnostic work-up, treatment, and follow-up were done at 1 tertiary-care, academic breast-centre (disease-specific-survival/DSS=279; death from breast-cancer=35). The Nottingham prognostic index (NPI) was used as the reference method with which to predict the survival of breast cancer.
Automated MRI analysis was accomplished by commercially available, FDA-cleared software. Based on this analysis, MRI-phenotypes that provided a specificity >99% for DSS were identified by machine-learning algorithms (classification-and-regression trees). Results were 10-fold cross-validated.
The prediction of survival based on MRI-phenotypes, according to the NPI, and MRI-phenotypes plus the NPI in combination were investigated (Cox-regression and Kaplan-Meier statistics).
Results: Predictive accuracies for NPI and MRI-phenotypes alone were similar (P=0.5). MRI-phenotypes showed a high prevalence of 42.7% (134/314), practically ruling out the occurrence of death in these patients. 21.6% of these patients (29/134) would have been falsely predicted by NPI as at-risk for disease-specific death. Inclusion of MRI-phenotypes into the NPI significantly improved its prediction of survival by 31.5% (29/92), giving a hazard ratio (HR) of 8.5 compared to the standard NPI (HR_{NPI}=5.4; P=0.03). The potential improvement of survival prediction by MR-phenotypes was verified for molecular subtypes.
Conclusion: Automated MRI-phenotyping improved the prediction of survival in PBC. MRI-phenotyping based on standard breast MRI examinations might support the indication for more complex diagnostic procedures (genetic profiling, etc.). They could support the decision as to whether a more aggressive cytotoxic therapy is warranted or not.
Limitations: Multicentric validation of our initial results with a special focus on potential oncological implementation is pending.
Ethics committee approval: IRB approved.
Funding: No funding was received for this work.
Author Disclosures:
M. Dietzel: nothing to disclose
P. A. T. Baltzer: nothing to disclose
M. Uder: nothing to disclose
E. Wenkel: nothing to disclose
S. Ellmann: nothing to disclose
R. Schulz-Wendtland: nothing to disclose
R. Zoubi: nothing to disclose
M. Hammon: nothing to disclose
P. Clauser: nothing to disclose

RPS 1016-2 11:31

The assessment of uterine cervical cancer with intravoxel incoherent motion imaging (IVIM) and diffusion kurtosis imaging (DKI) at 3T

Y. Qi, Y. He, C. Lin, H. Zhou, X. Wang, H. Xue, Z. Jin*; Beijing/CN*

Purpose: To explore the application of intravoxel incoherent motion imaging (IVIM) and diffusion kurtosis imaging (DKI) in the diagnosis of cervical cancer and to analyse the correlations between IVIM-DKI with the pathology result.
Methods and materials: 64 patients with cervical cancer and 25 patients with normal uterine cervixes were enrolled. The pathological type and differentiation degree of cervical cancer were collected. The patients underwent female pelvis MR on a 3T MR scanner for diffusion imaging with b-values at 0, 10, 50, 100, 200, 800, 1,200, and 2,000 s/mm^2. IVIM results (D-IVIM, D*, and f) and DKI results (D-kurtosis and K) were derived from images with b=0~800 s/mm^2 and 0, 800~2,000s/mm^2 respectively. ROC analysis was used to identify cervical cancer. Spearman's non-parametric correlation was used to analyse the correlation between the pathological data and image results. ICC was calculated to assess the inter-class repeatability.
Results: D-IVIM were significantly lower in the cervical cancer group (0.92±0.20) than in the normal group (1.37±0.25) (p=0.000), with a sensitivity of 88.2% and specificity of 92.2% at 1.145. D-kurtosis were significantly lower in the cervical cancer group (1.19±0.24) than in the normal group (1.82±0.27) (p=0.000), with a sensitivity of 95.2% and 92.2% at 1.47. F values were lower in the cancer group (0.11±0.05) than in the normal group (0.20±0.09) (p=0.000). K-values were higher in the cancer group (1.05±0.24) than in the normal group (0.89±0.18)(p=0.003). The lower tumour differentiation degree, the lower D-kurtosis, and the higher K value (r=0.33, 0.47, all p<0.05). ICC ranged from 0.897-0.991.
Conclusion: IVIM and DKI have been applied for cervical cancer diagnosis, showing good diagnostic efficacy. IVIM-DKI results correlated with the tumour differentiation degree.
Limitations: Some patients did not undergo surgery and only biopsy pathology was available.
Ethics committee approval: This study was approved by ethics committee and written informed consent was obtained.
Funding: No funding was received for this work.
Author Disclosures:
Y. Qi: nothing to disclose
Y. He: nothing to disclose
C. Lin: nothing to disclose
H. Zhou: nothing to disclose
X. Wang: nothing to disclose
H. Xue: nothing to disclose
Z. Jin: nothing to disclose

RPS 1016-3 11:37

The effects of 8th edition TNM AJCC staging in breast cancers detected with a screening programme

A. Pittaro[1], G. Gennaro[1], V. Pasqualino[1], G. Romanucci[2], S. A. Montemezzi[3], F. Caumo[1]; *[1]Padua/IT, [2]Verona, loc. Marzana/IT, [3]Verona/IT*
(pittaroalice@gmail.com)

Purpose: In 2017, the American Joint Committee on Cancer (AJCC) updated the Cancer Staging Manual to the 8th edition, including a definition of a prognostic staging that incorporates TNM classification and tumour biomarkers. The purpose of this study is to compare the staging of screen-detected breast cancers using the 7th and 8th AJCC Cancer Staging Manual editions.
Methods and materials: The characteristics of 423 breast cancers detected in a screening programme from 2013-2016 were retrospectively reviewed. For each cancer, the anatomical stage based on the 7th TNM edition and the prognostic stage based on the 8th edition were calculated and differences analysed.
Results: The median age at diagnosis was 61 years (range 50-75 years). The anatomical stage was 0 in 13.9% of cases, IA in 63.1%, IB in 6.1%, IIA in 9.9%, IIB in 5.2%, IIIA in 0.7%, and IV in 0.9%, respectively. The application of TNM 8th edition changed the stage group in 18.2% of women with an upstage in 4.8% and a downstage in 13.2%. Among the upstaged group, 23.8% of cancers were luminal-A, 23.8% luminal-B, and 52.4% triple-negative. 4.8% were grade 1, 38.1% grade 2, and 57.1% grade 3. Among the downstaged group, 76.8% of women were luminal-A and 23.2% luminal-B. 23.2% were grade 1, 69.6% grade 2, and 7.1% grade 3. Major staging changes were observed in stage IA (3.3%), IIA (8.7%), and IIB (3.3%).
Conclusion: The adjunct of biomarkers to anatomical characteristics (TNM) can change the staging of breast cancers found in a screening programme, resulting most often in a downstage. The application of prognostic staging is important to better define the prognosis and the therapeutic approach, which should be oriented by cancer subtypes.
Limitations: The cancers that were screen-detected rarely include advanced stages.
Ethics committee approval: n/a
Funding: No funding was received for this work.
Author Disclosures:
A. Pittaro: nothing to disclose
G. Gennaro: nothing to disclose
V. Pasqualino: nothing to disclose
G. Romanucci: nothing to disclose
S. A. Montemezzi: nothing to disclose
F. Caumo: nothing to disclose

RPS 1016-4 11:43

The impact of ^{18}F-FDG PET/MR on therapeutic management in breast cancer patients: a prospective evaluation of staging algorithms

J. Kirchner[1], O. Martin[1], L. Umutlu[2], K. Herrmann[2], L. M. Sawicki[1], G. Antoch[1], C. Buchbender[1]; *[1]Düsseldorf/DE, [2]Essen/DE*
(Julian.Kirchner@med.uni-duesseldorf.de)

Purpose: To investigate whether the potential differences in staging between a traditional staging imaging algorithm and ^{18}F-FDG PET/MR leads to a change in patient management in breast carcinoma and to compare the diagnostic accuracy between the traditional staging algorithm and ^{18}F-FDG PET/MR for the TNM classification.
Methods and materials: In this prospective, multicentre cohort study, 56 women with newly diagnosed, therapy-naive breast cancer were included. All patients were examined by a traditional staging imaging algorithm and whole-body ^{18}F-FDG PET/MR including dedicated ^{18}F-FDG PET/MR breast examinations. Each patient was discussed twice in a separate tumour board session to determine a total of 3 therapy recommendations based on a traditional algorithm only, a traditional algorithm and ^{18}F-FDG PET/MR as well as histopathology, and ^{18}F-FDG PET/MR alone. The major changes in therapy recommendations and the differences between the traditional staging algorithm and ^{18}F-FDG PET/MR for the TNM classification were evaluated.
Results: Differences with major changes in therapy recommendations among the 3 tumour boards were seen in 23% patients, whereas in 14%, the recommendation based on the ^{18}F-FDG PET/MR was consistent with the recommendations from the tumour board with all available information. Therapy changes included therapy of the breast (3.5%), locoregional nodes (12.5%), and systemic therapy (9.0%).
Conclusion: Current guidelines should consider systemic staging with ^{18}F-FDG-PET/MRI as optional in breast cancer patients with an elevated pre-test probability for distant metastases at the time of initial diagnosis. Further scientific assessment of ^{18}F-FDG-PET/MR in this setting is necessary.
Limitations: Patient survival has not been assessed.
Ethics committee approval: The ethics committee of the Medical Faculties of the Universities of Duisburg-Essen and Düsseldorf approved the study.
Funding: Deutsche Forschungsgemeinschaft (DFG), the German Research Foundation (BU3075/2-1).
Author Disclosures:
J. Kirchner: nothing to disclose
L. Umutlu: nothing to disclose
O. Martin: nothing to disclose
K. Herrmann: nothing to disclose
G. Antoch: nothing to disclose
C. Buchbender: Grant Recipient at DFG
L. M. Sawicki: nothing to disclose

RPS 1016-5 11:49

Pretreatment identification of non-responders to neoadjuvant chemotherapy in breast cancer patients

L. Vanovcanova, I. Waczulikova, B. Vertakova-Krakovska, V. Lehotska*; Bratislava/SK (lucia.vanovcanova@ousa.sk)*

Purpose: To estimate the diagnostic performance of multiparametric breast MRI in the pretreatment identification of non-responders to neoadjuvant chemotherapy (NAC).
Methods and materials: 85 patients (median 44y) with locally advanced invasive breast carcinoma were enrolled in this retrospective study. All underwent a core-cut biopsy with histopathological analysis of ER, HER2, and Ki67. Baseline breast MRI was performed before NAC with an evaluation of T2, ADC coefficient, enhancement pattern, and necrosis. Based on these parameters, patients were designated as responders or non-responders. Levels of response to NAC were based on postoperative histology results: pathological complete response (pCR) as responding, pathological residual disease (pRD) as non-responding. An MRI-based predictive model supplemented by selected histopathological characteristics of breast carcinoma was constructed using logistic regression analysis. Agreement analysis and diagnostic performance measures (Cohen's kappa, sensitivity, specificity, positive predictive value (PPV), and negative predictive value (NPV)) were calculated. The AUC curve served as an overall measure of discriminative performance.

Results: Non-responders on initial MRI were non.significantly associated with 1.2 times higher odds for having pRD after NAC in comparison with responders. None of individual MRI features were significantly associated with pRD. Combining an MRI response prediction with histopathological characteristics significantly improved the model performance (for cut-off probability=0.5, sensitivity 89.1%, specificity 36.7%, correct classifications 70.6%, and AUC=72.4% (model deviance Chi-square test: p=0.044; ER+: OR=3.15, 95% CI 1.09-9.15, p=0.035), HER 2 (HER2+: OR=3.15, 95% CI 1.02–9.69, p=0.046), ki67 (ki67>30%: OR=2.26, p=0.125)).
Conclusion: Pretreatment identification of non-responders to NAC is crucial for the further complex management of patients with breast cancer. Multiparametric MRI supported by histopathological parameters of tumours is sufficiently predictive of non-responders to NAC.
Limitations: n/a
Ethics committee approval: n/a
Funding: No funding was received for this work.
Author Disclosures:
L. Vanovcanova: Author at 2nd Radiology Department, Faculty of Medicine, Comenius University in Bratislava, Bratislava, Slovakia and St. Elizabeth Cancer Institute, Bratislava, Slovakia
V. Lehotska: Consultant at 2nd Radiology Department, Faculty of Medicine, Comenius University in Bratislava, Bratislava, Slovakia and St. Elizabeth Cancer Institute, Bratislava, Slovakia
I. Waczulikova: Consultant at Department of Nuclear Physics and Biophysics, Faculty of Mathematics, Physics and Informatics, Comenius University in Bratislava, Bratislava, Slovakia
B. Vertakova-Krakovska: Consultant at 1st Department of Oncology, Faculty of Medicine, Comenius University in Bratislava, Slovakia and St. Elizabeth Cancer Institute, Bratislava, Slovakia

RPS 1016-6 11:55

Relaxation-compensated CEST (chemical exchange saturation transfer) MRI at 7T aids breast cancer diagnostics

D. Paech, L. Loi, F. Zimmermann, P. Bachert, M. Ladd, S. Bickelhaupt, S. Goerke, S. Schott, H.-P. Schlemmer*; Heidelberg/DE (d.paech@dkfz.de)*

Purpose: To investigate fat-corrected, relaxation-compensated amide proton transfer (APT) CEST MRI at 7 Tesla (7T) in patients with newly-diagnosed breast cancer.
Methods and materials: 10 patients with newly-diagnosed breast cancer and 7 healthy volunteers were included. APT CEST MRI was performed on a 7T whole-body scanner. APT signal intensities were quantified using a multi-Lorentzian fit analysis in the tumour area and in healthy fibroglandular breast tissue after correction of B_0/B_1-field inhomogeneities, fat signal contribution, and T_1- and T_2 -relaxation. Signal intensity differences between normal-appearing and tumour breast tissue were compared using the Mann–Whitney U test. Furthermore, Pearson's correlation analysis between tumour APT signal intensities and the Ki-67 proliferation index was performed.
Results: APT signals in breast cancer tissue (6.70±1.38%Hz) were significantly increased compared to normal-appearing fibroglandular breast tissue (p=0.001). Between patients with normal-appearing breast tissue (3.56±0.54%Hz) and the fibroglandular breast tissue of healthy volunteers (3.70±0.68%Hz), no differences were observed (p=0.88). A moderate positive correlation was found between the APT signal and the proliferation index Ki-67 (r=0.61, p<0.01).
Conclusion: Relaxation-compensated APT CEST MRI at 7T allowed a non-invasive differentiation of breast cancer lesions and normal-appearing breast tissue by quantifying increased protein-specific signal intensities in malignant tumours. Thus, APT CEST MRI represents a contrast agent-free method that may help to increase diagnostic accuracy in MR mammography.
Limitations: The relatively small sample size (n = 17) prevents generalisation of the results. However, statistically meaningful results were obtained. 7T MRI devices are not widely available, which limits an immediate clinical translation of the presented approach.
Ethics committee approval: This prospective, monocentric study was approved by the local ethics committee. Written informed consent was obtained.
Funding: No funding was received for this work.
Author Disclosures:
L. Loi: nothing to disclose
D. Paech: nothing to disclose
F. Zimmermann: nothing to disclose
P. Bachert: nothing to disclose
M. Ladd: nothing to disclose
H.-P. Schlemmer: nothing to disclose
S. Bickelhaupt: nothing to disclose
S. Goerke: nothing to disclose
S. Schott: nothing to disclose

RPS 1016-7 12:01

The predictive role of body composition parameters (BCP) assessed by computed tomography in operable breast cancer treated with neoadjuvant chemotherapy: a retrospective observational cohort study

S. Draisci, A. Pecchi, R. Bonacini, C. Omarini, P. Torricelli*; Modena/IT (stefanodraisci@gmail.com)*

Purpose: To establish the prognostic value of clinical and radiological body compositions parameters (BCP) on the tumour response to neoadjuvant chemotherapy (NC) in patients with operable breast cancer (BC).
Methods and materials: From 2005-2017, we retrospectively evaluated patients who underwent a CT examination before treatment and whose weight, height, age, and menopausal status information were available. BMI, liver-to-spleen ratio, subcutaneous fat area (SFA, cm^2), visceral fat area (VFA, cm^2) at L4 level, and skeletal muscle index (LSMI, cm^2/m^2) at L3 level were carried out combining clinical and radiologic findings. Tumour characteristics (stage, grade, and subtypes) were collected. This data was related to pathological complete response (pCR), overall survival (OS), and relapse free survival (RFS) by calculating odds and hazard ratios and their 95% confidence intervals through univariate logistic regression and univariate and multivariate Cox models, considering BMI subgroups, BCPs, and pCR.
Results: 407 patients were included, 55% with BMI <25 and 45% with BMI >25. 137 patients underwent CT examination. Hormonal receptor-positive BC was more frequent in overweight patients (p<0.05). Post-menopausal women had higher VFA, fatty liver disease, and obesity compared to premenopausal patients. High VFA and liver steatosis were negative predictive factors for pCR (pCR rate: 36% normal VFA vs 20% high VFA, p=0.048; no steatosis 32% vs steatosis 13%, p=0.056). No association between BMI classes and tumour response was detected. Neither BMI classes nor BCPs significantly influenced OS and RFS.
Conclusion: Visceral adiposity and hepatosteatosis were involved in chemosensitivity in BC patients treated with NC, and both can be reliably assessed by native CT scans.
Limitations: n/a
Ethics committee approval: n/a
Funding: No funding was received for this work.
Author Disclosures:
S. Draisci: nothing to disclose
A. Pecchi: nothing to disclose
C. Omarini: nothing to disclose
R. Bonacini: nothing to disclose
P. Torricelli: nothing to disclose

RPS 1016-8 12:07

Whole-body diffusion-weighted magnetic resonance imaging (WB-DWIBS/MRI) in peritoneal carcinomatosis from ovarian cancer: a diagnostic performance

F. J. Garcia Prado, E. Utrera, L. Reguera Berenguer, R. Saiz Martinez, E. Martin Illana, J. Blazquez Sanchez, T. Castellanos, R. Marquez, E. Grande Pulido*; Madrid/ES (javiergarciaprado@yahoo.es)*

Purpose: To assess the diagnostic performance (DP) and tumour burden correlation of whole-body DWI with background suppression MRI (WB-DWIBS/MRI) in peritoneal carcinomatosis (PC) of suspected OC using the peritoneal cancer index (PCI) referring to cytoreduction surgery.
Methods and materials: 39/217 patients with disseminated OC underwent cytoreduction and WB-DWIBS/MRI. The PCI scored tumour burden (0-3) in 13 anatomical regions (global range of 0-39). Two radiologists (Rad1/Rad2) assessed the PCI preoperatively and with surgical findings.
We evaluated regional and global DP, the interobserver agreement, statistical differences (McNemar test), and correlation (Pearson's test).
Results: Global evaluation: The overall positive scoring (PCI>0) for Rad1, Rad2, and surgery were 34.52%, 27.22%, and 31.76%, with a global average PCI 7.82, 8, and 8.44, respectively. The tumour burden correlation with surgery was 0.762 (p<0.001) for Rad1 and 0.642 (p<0.001) for Rad2. The sensibility, specificity, and accuracy were 0.84, 0.88, and 0.87. The global Kappa was 0.53. Regional evaluation: Kappa was moderate to substantial in 6/13 regions. The pelvis followed by the central region presented the highest number of positives and sensitivity. The bowel loops showed the lowest detection rate. Accuracy was over 0.86 in all regions for Rad1.
Conclusion: WB-DWIBS/MRI is a reliable imaging technique that is useful in preoperatively quantifying and depicting PC in OC to achieve complete cytoreductive surgery.
Limitations: A single institutional study. Occult selection bias as patients selected were also candidates for cytoreduction. Areas that may contraindicate resectability might be underevaluated. More than half were postoperative patients. DP may be affected. No direct comparison with other imaging techniques such as CT or PET/CT.

Ethics committee approval: Institutional review board approval and all patients signed written informed consent.
Funding: No funding was received for this work.
Author Disclosures:
F. J. Garcia Prado: Author at MD Anderson Cancer Center
L. Reguera Berenguer: Author at Instituto Tecnológico PET
E. Utrera: Author at MD Anderson Cancer Center
R. Saiz Martinez: Author at MD Anderson Cancer Center
E. Martin Illana: Author at MD Anderson Cancer Center
J. Blazquez Sanchez: Author at MD Anderson Cancer Center
R. Marquez: Author at MD Anderson Cancer Center
T. Castellanos: Author at Clínica Universidad de Navarra
E. Grande Pulido: Author at MD Anderson Cancer Center

RPS 1016-9 12:13
Using IVIM and DCE-MRI to monitor the focal perfusion status of uterine fibroids after high-intensity focused ultrasound
X. Lu, Y. Ban, H. Du, X. Wang, X. Ding*; Urumqi/CN (305844324@qq.com)*

Purpose: To assess the value of IVIM and DCE-MRI in monitoring microcirculation information after HIFU ablation of uterine fibroids.
Methods and materials: All 58 patients underwent IVIM and DCE-MRI scans before and 48h after therapy, and 27 patients underwent a third scan 3-6M after therapy. The apparent diffusion coefficient (ADC), diffusion coefficient (D), pseudo diffusion coefficient (D*), perfusion fraction (f), maximum slope of increase (MSI), and signal enhancement ratio (SER) of the uterine fibroid were compared.
Results: Compared to pretreatment, the f and MSI values of 48h after therapy were significantly higher, while the D* and SER values were lower. Compared to pretreatment, the f, D*, and MSI values of 3-6 months after therapy were significantly lower, while the SER values were higher. Compared to 48h after therapy, the f and MSI values of 3-6 months after therapy were significantly higher, while the D* and SER values were lower. When referred to the Pearson correlation result, SER was negatively correlated with f and positively correlated with D*.
Conclusion: Along with the MSI and SER values, the D* and f values of IVIM can also monitor microcirculation perfusion changes of uterine fibroids after HIFU. As IVIM-DWI is non-invasive and contrast agent-free, it may be an alternate choice in the evaluation of HIFU ablation.
Limitations: A larger patient population is needed for further validation. Its application in other types of tumours should be further evaluated.
Ethics committee approval: All procedures performed in studies involving human participants were in accordance with the ethical standards of the institution and with the 1965 Helsinki declaration and its later amendments or comparable ethical standards. Written informed consent was obtained.
Funding: National Natural Science Foundation of Xinjiang Uygur Autonomous Region, China (2018D01C298).
Author Disclosures:
Y. Ban: nothing to disclose
H. Du: nothing to disclose
X. Lu: nothing to disclose
X. Wang: nothing to disclose
X. Ding: nothing to disclose

RPS 1016-10 12:19
The application quantitative parameters of multiple models of multi-b value DWI-MRI in different pathological type, grade, and clinical stage of cervical cancer
J. Sun[1], F. Shan[1], C. Huang[2]; *[1]Shaoguan/CN, [2]Stony Brook/US (sunjunqi1233668@sina.com)*

Purpose: To investigate the application of quantitative parameters of a mono-exponential model, bi-exponential model, and stretching exponential model of multi-b value DWI-MRI in different pathological types, grades, and clinical stages of cervical cancer.
Methods and materials: 142 patients confirmed with cervical cancer cases were subjected to MRI routine sequence and multi-b value DWI-MRI sequence imaging. A mono-exponential model parameter (ADC), bi-exponential model parameters (D, D*, f), and stretching-exponential model parameters (DDC, α) were obtained by FUNCTOOL post-processing software. The multiple quantitative parameters of the 3 models were used to distinguish the pathological type, grade, and clinical stage of cervical cancer. ROC analysis was performed to identify meaningful parameters.
Results: 142 cases of cervical cancer were enrolled. ADC, f, and DDC values were statistically different in clinically high and low stages of cervical cancer ($P < 0.05$). ADC, f, DDC, and alpha values were statistically different in the cervical squamous cell carcinoma and adenocarcinoma group ($P < 0.05$). ADC and DDC values were statistically different in the poor differentiation and moderate-to-well differentiation of cervical cancer ($P < 0.05$). The alpha value has the highest AUC (0.723) and diagnostic power (a sensitivity of 78.9% and a specificity of 77.5%) in the cervical squamous cell carcinoma and adenocarcinoma group.
Conclusion: The multiple quantitative parameters of multiple models of multi-b value DWI-MRI can show diffusion, perfusion, and heterogeneity changes of cervical cancer. They can identify the pathological type, grade, and clinical stage of cervical cancer, which is conducive to the choice of cervical cancer treatment and prognosis evaluation.
Limitations: A relatively small number of patients. MR imaging was mostly performed after cervical cancer biopsy.
Ethics committee approval: n/a
Funding: No funding was received for this work.
Author Disclosures:
J. Sun: Author at yuebei people's hospital
F. Shan: nothing to disclose
C. Huang: nothing to disclose

RPS 1016-11 12:25
The role of quantitative MRI in assessing radiation response in uterine cervix cancer
V. Mahawar, A. Jajodia, A. K. Chaturvedi, A. S. Rao, S. Chauhan*; [1]New Delhi/IN (drmahawarvivek@gmail.com)*

Purpose: To compare quantitative MRI (ADC values) and clinical parameters in patients with cervical cancer.
Methods and materials: This MR study was retrospectively analysed in cervical cancer patients (n=133). Patients included in the study were non-surgical candidates with a locally advanced stage of 2B to 4A. Baseline MR imaging was done to assess the status of parametrial and ADC values. Post concurrent chemotherapy (CCT) and EBRT (external beam radiotherapy) assessment MRI was done and the ADC values were analysed in the region of interest. As per the institutional protocol, brachytherapy (ICRT/MUPIT) was done depending on the extent of parametrial invasion. The change of ADC values was charted separately, dividing the study groups into ICRT versus MUPIT. ICRT was given 100 patients and MUPIT 33. The 2 study groups were compared for the occurrence of recurrence and metastasis, stage, and nodal status, and statistical analysis was done to identify any significant correlation between baseline ADC, follow-up ADC, change in ADC, and recurrence-free survival among the groups.
Results: The occurrence of recurrence and metastasis, stage, and nodal status correlated among 2 groups as p=0.002, 0.549, 0.029, and 0.184, respectively. 24/33 (72%) patients in the MUPIT group were stage 3 and 4. 49/100 (49%) patients in the ICRT group were stage 2. Age, baseline ADC, follow-up ADC, change in ADC, and recurrence-free survival among the groups were p=0.711, 0.931, 0.112, <0.0001, and <0.0001, respectively). The median recurrence-free survival for the ICRT group was 25 months and 9 months for the MUPIT group.
Conclusion: A change in ADC is a potential surrogate marker for identifying between different choices of radiotherapy in uterine cervix cancer.
Limitations: The small cohort.
Ethics committee approval: Ethics committee approval obtained.
Funding: No funding was received for this work.
Author Disclosures:
V. Mahawar: nothing to disclose
A. Jajodia: nothing to disclose
A. K. Chaturvedi: nothing to disclose
A. S. Rao: nothing to disclose
S. Chauhan: nothing to disclose

11:15 - 12:30 **Coffee & Talk 1**

Interventional Radiology

RPS 1009a

Lymphatic and venous interventions

Moderators:
H. R. Portugaller; Graz/AT
K. K. Pyra; Lublin/PL

RPS 1009a-1 11:15
Endovascular stenting of the main veins in urology
O. B. Zhukov*; Moscow/RU (ob.zhukov@yandex.ru)*

Purpose: Stenting of the main veins in urology is a responsible step that requires a clear understanding of the subsequent haemodynamic changes.
Methods and materials: We performed more than 67 stentings of the major pelvic veins and retroperitoneal organs regarding aortomesenteric compression of the left renal vein, progression of the pelvic venous disease, recurrent ovarian-varicocele, varicocele, and chronic pelvic pain syndrome.

Results: Of 67 patients, 23 had a double block of upper and lower nutcracker syndrome. After confirming phlebohypertension, these patients received a nitinol-nickel stent (Zilver Cook, Protehge). In several cases, venous stents Wallsten-Uni endoprosthesis (Boston Scientific) were used.
Conclusion: The optimal diagnostic algorithm for the early detection of May Turner syndrome is a thorough examination using compression tests, asymmetry of venous blood flow in the iliac veins of more than 8 cm/s, and MRI phlebography of the inferior vena cava system, with the aim of spatial orientation of the level and floor of possible compression. Then, after phlebography and phlebotonometry with a gradient of more than 10 mm RT and in connection with the clinical picture of the disease, the installation of a venous stent
Limitations: n/a
Ethics committee approval: n/a
Funding: No funding was received for this work.
Author Disclosures:
O. B. Zhukov: nothing to disclose

RPS 1009a-2 11:21
INTACT-lymph: the current results of an interventional approach to lymphatic leakage
W. Flatz[1], T. Streitparth[1], M. Frölich[2], M. Seidensticker[1], J. Ricke[1], F. Streitparth[1]; [1]*Munich/DE,* [2]*Mannheim/DE (radiologie.muenchen@gmail.com)*

Purpose: To visualise the lymphatic vessels and detect lymphatic leakage, and to evaluate the therapeutic potential of intranodal and CT-guided lymphatic embolisation.
Methods and materials: In this prospective study, 16 patients suffering from lymphatic leakage due to different causes (e.g. nephrectomy, prostatectomy) resistant to conservative treatment were included. Intranodal lymphography using lipiodol, and in case of non-responding, a second intervention via CT-guided embolisation using lipiodol and/or histoacryl, was performed. Technical success was defined as a visualisation of the lymphatic system and visualisation of a leakage site. Clinical success was defined as a significant reduction of chylus collected via drainage (>90% reduction) with no significant increase of lymphatic leakage in control exams and an improvement in the quality of life (Karnofsky index).
Results: Lymphatic system visualisation and the detection of lymph fistula was successful in 94% of patients (15/16). The intervention was clinically successful in 81% of cases (13/16). One patient had to be treated for several other diseases and was lost to follow-up. One patient showed only a 25% reduction of chyle flow and was treated with a kidney transplant. A third patient had thoracic chyle leakage without visualisation of the site of leakage. Therapeutic embolisation using lipiodol alone was successful as a "one-stop-shop" in 63% of cases (10/16). In 8 patients, CT-guided embolisation was performed, 4 were clinically successful, 1 was partially successful, and 1 patient showed only partial improvement (Karnofsky-Index 50->70). Karnofsky-Index improved from 73 to 90 in all patients.
Conclusion: Direct intranodal lymphography is highly recommended for the visualisation and therapeutic occlusion of lymphatic leaks. Additional CT-guided embolisation using lipiodol and/or histoacryl improves the clinical outcome.
Limitations: A small patient number.
Ethics committee approval: Consent of local ethics committee was obtained (LMU Munich ethics commitee).
Funding: No funding was received for this work.
Author Disclosures:
W. Flatz: nothing to disclose
M. Frölich: Board Member at Smartradiology
T. Streitparth: nothing to disclose
M. Seidensticker: nothing to disclose
J. Ricke: nothing to disclose
F. Streitparth: nothing to disclose

RPS 1009a-3 11:27
25-years experience with transpedal lymphangiography in the management of postoperative therapy-refractory lymphatic leakage: final results with subgroup analyses
C. M. Sommer[1], F. Pan[1], T. D. D. Do[1], G. M. Richter[2], H. U. Kauczor[1], T. Hackert[1], M. Loos[1]; [1]*Heidelberg/DE,* [2]*Stuttgart/DE (cmsommer@gmx.com)*

Purpose: During the DCK (Deutscher Chirurgen Kongress) 2019, the preliminary results of our 25-year experience on transpedal lymphangiography in the management of postoperative therapy-refractory lymphatic leakage were presented. In this update, the final results with subgroup analyses are summarised.
Methods and materials: The final cohort consisted of 355 patients who underwent transpedal lymphangiography with the intention to cure postoperative therapy-refractory lymphatic leakage in different locations. Study goals included patient demographics and technical results, as well as complication and cure rates. Dedicated subgroups analyses were performed to outline predictors for a cure.
Results: Postoperative lymphatic leakage resulted from different highly complex surgical procedures in the neck, thorax, abdomen, pelvis, and/or lower extremity. The daily drainage volume was 1124±1336 ml. The technical success rate of the amount of injected iodised oil used and major and minor complication rates of transpedal lymphangiography were 87.2%, 10.3±4.3ml, and 0%, and 0.3%, respectively. The cure rate of transpedal lymphangiography was 42.6%. Positive predictors for cure were radiological extravasation/pooling of iodised oil under fluoroscopy, radiography, and, especially, CT (yes vs no; p=0.006), the type of lymphatic leakage (lymphatic fistula vs lymphocele; p=0.033), and the daily drainage volume (845±1067 vs 1316±1399; p=0.001).
Conclusion: Transpedal lymphangiography is feasible, safe, and effective in the management of postoperative therapy-refractory lymphatic leakage. Under consideration of positive predictors for a cure, different lymphatic second-line interventions should be scheduled prospectively as, according to our data, lymphatic second-line interventions can dramatically increase the cure rate (e.g. CT-guided ethanol 95% sclerotherapy shows a cure rate of 76.9% after clinically ineffective transpedal lymphangiography).
Limitations: A retrospective cohort study.
Ethics committee approval: All procedures were in accordance with the ethical standards of the institutional and/or national research committee and with the 1964 Helsinki declaration. Specific consent was obtained.
Funding: No funding was received for this work.
Author Disclosures:
C. M. Sommer: nothing to disclose
F. Pan: nothing to disclose
T. D. D. Do: nothing to disclose
G. M. Richter: nothing to disclose
H. U. Kauczor: nothing to disclose
T. Hackert: nothing to disclose
M. Loos: nothing to disclose

RPS 1009a-4 11:33
Early inferior vena cava filter retrieval strategy in trauma patients: the role of pre-retrieval contrast-enhanced CT
M. Kim, S. Y. Lee, H. Lee, J.-K. Lim*; Daegu/KR*

Purpose: To increase the retrieval rate of IVC filters with pre-retrieval contrast-enhanced CT evaluation.
Methods and materials: An active IVC filter retrieval strategy was established in March 2017. We reviewed pre-retrieval venous thromboembolism (VTE) CT findings, retrieval rate, indwelling time, anticoagulation therapy, and recurrence of VTE. Subgroup analyses were also performed before and after the active filter retrieval strategy establishment from 2010-2018.
Results: 177 IVC filter insertions were performed in trauma patients during the study period and all patients underwent CT prior to filter retrieval. CT findings were as follows: completely resolved VTE n=108 (61%), partially improved n=58 (33%), no change n=8 (5%), and aggravated n=3 (2%). The overall retrieval rate was 84% with a mean indwelling time of 32 days. In subgroup analyses, 95 (53%) were in the prior to strategy establishment (PSE) group and 82 (47%) were in the after strategy establishment (ASE) group. The retrieval rate was significantly higher in ASE than PSE 81/82 (99%) versus 68/95 (72%) (p<0.001). Anticoagulation therapy was applied in 63/95 (63%) of the PSE group and in 67/82 (82%) of the ASE group. The duration of anticoagulation was significantly reduced in the completely resolved VTE group (mean 78 days ± 126) than the residual VTE group (mean 133 ± 271) (p<0.001). There was no recurrent VTE during a mean follow-up of 24 month in the PSE group and 10 months in the ASE group.
Conclusion: This study showed an overall 84% IVC filter retrieval rate in trauma patients. After the active filter retrieval strategy setup, 99% of filters were safely retrieved in trauma patients. Pre-retrieval CT can help in the decision making of early filter retrieval and the planning of proper anticoagulation therapy.
Limitations: The inclusion of study subjects was restricted to trauma patients only. Our data was single institutional.
Ethics committee approval: n/a
Funding: No funding was received for this work.
Author Disclosures:
M. Kim: nothing to disclose
S. Y. Lee: nothing to disclose
H. Lee: nothing to disclose
J.-K. Lim: nothing to disclose

RPS 1009a-5 11:39

Endovascular percutaneous arteriovenous fistula creation: current evidence, technique, and single-centre experience

U. Salati, J. W. Ryan*; Dublin/IE (umersalati@gmail.com)*

Purpose: To assess endovascular arteriovenous fistula creation for haemodialysis in end-stage renal failure and compare its efficacy, primary and secondary patency, and cost-effectiveness to traditional surgically created arteriovenous fistulas (AVF).
We also present a systematic review of the current evidence for the effectiveness of endovascular fistula creation.
Methods and materials: The 4Fr WavelinQ (Becton, Dickinson and Company) device was used to create AVFs (radial artery-radial vein, ulnar artery-ulnar vein, and interosseous artery-interosseous vein) in all patients. Patients were followed for at least 3 months and primary and secondary patency was determined. Multiple patients were screened for suitability for the procedure and, ultimately, 7 cases were performed.
A cost comparison of percutaneous versus surgical AVF creation was also conducted.
Results: Procedural technical success was 100%. Primary patency at 6 weeks was 85%; coil embolisation of a venous pseudoaneurysm from a guidewire trauma, unfortunately, resulted in fistula thrombosis in one case. This patient went on to have a surgical fistula created.
2 needle cannulations were done in 2/7 patients at the time of this abstract (and expected to change).
A cost analysis of the procedure was performed and compared to surgically created AVFs; the percutaneous procedure cost an approximate €6,000 per patient, with 1 inpatient admission, and surgical fistulas cost an average of approximately €12,866 per patient with an average inpatient stay of 3 days.
Conclusion: Endovascular arteriovenous fistula creation is a safe and effective technique demonstrating at least non-inferiority to surgical AVFs and is significantly more cost-effective.
Limitations: A single-centre, single-arm study with limited numbers.
Ethics committee approval: Written informed consent obtained from all patients.
The device has CE Mark and FDA approval; ethics approval waived.
Funding: No funding was received for this work.
Author Disclosures:
U. Salati: nothing to disclose
J. W. Ryan: nothing to disclose

RPS 1009a-6 11:45

An alternative method for traditional surgical suturing in port catheter placement: glue

M. Aşık*; Istanbul/TR (muratasik219@yahoo.com)*

Purpose: A port catheter (PC) is a medical device that is used for long-term or short-term access to veins in patients having chemotherapy who require continuous medication. Our aim is to evaluate the efficacy and advantages of using glue for tissue adhesion in the closure of the skin incision for the reservoir when placing the PC.
Methods and materials: In all cases, except for 3 cases of the brand port catheter, a port reservoir was placed under the skin in the anterior wall of the chest. The subcutaneous fat tissue was covered with an absorbable suture to cover the reservoir. The skin tissue of the bioglue (Cryolife / Georgia-USA), which is ready in its injector, was closed by thinning.
Results: 39 patients (20 males, 19 females, mean age 57.1) who were scheduled to receive port catheter chemotherapy between January 2017 and December 2017 were included in the study. During the process, BioGlue was preferred for port closure of the skin tissue on the reservoir as tissue adhesion instead of surgical sutures. After the procedure, the patients were kept under observation for 1 hour to monitor for possible complications.
Conclusion: There are many complications, such as infection and especially bleeding, when placing a PC. The incidence of these complications increases with the traditional surgical suture closure of the skin. The vast majority of patients with PCs are immunosuppressed patients, where suture can cause opportunistic infections. Pain caused by skin closure with conventional surgical suture may also cause the procedure to be prolonged. Using glue instead of conventional suturing of the tissue is a cheaper and advantageous alternative.
Limitations: A retrospective, single-institutional, small-sample-sized study.
Ethics committee approval: Ethics committee approval obtained.
Funding: No funding was received for this work.
Author Disclosures:
M. Aşık: Investigator at Istanbul Medeniyet Universsity

RPS 1009a-7 11:51

Dynamic MR lymphangiography: a new technique for the assessment of the central lymphatic system in adults

S. Katsari, D. K. Gordon, P. P. Mortimer, P. S. Mansour, F. Howe, L. A. Ratnam*; London/UK (Katsari.sofia@gmail.com)*

Purpose: To describe the technique and utility of dynamic contrast-enhanced MR lymphangiography (DCMRL).
DCMRL enables imaging of the central lymphatic system and its relationship to anatomical structures, demonstrating flow rate, obstruction, and leakage from the lymphatic system. This provides important diagnostic information and could inform treatment such as thoracic duct embolisation or lymphovenous anastomosis.
Methods and materials: 8 adult patients with lymphatic abnormalities were examined in a tertiary lymphovascular referral centre using DCMRL. 1 patient had Noonan's syndrome, 1 patient had chylous ascites and effusions, and 6 patients had a primary lymphatic abnormality. Bilateral ultrasound-guided access into inguinal lymph nodes was carried and ultrasound contrast injected to confirm the position. DCMRL was performed in a 3T MRI scanner by injecting gadolinium into the inguinal lymph nodes. The central lymphatic system, including the pelvis, retroperitoneal lymphatics, and thoracic duct were assessed. Patients with lymphoedema in the lower extremities were re-scanned after walking for a short period.
Results: In 7 patients, DCMRL was successful in providing information about the central lymphatic system. In 2 of these patients, leakage of contrast was seen into the mediastinum and into pleural effusions. Abnormal lymphatic drainage was noted in all patients in either thoracic or abdominal lymphatics, or in both. In 1 patient, no drainage was seen into the central lymphatics, however, the contrast was seen to reflux into the scrotum and superficial tissues of the legs.
Conclusion: DCMRL has been successfully used to provide information about central lymphatic anatomy and to identify obstruction and leakage of lymphatic fluid. This novel technique offers possibilities for both diagnoses and treatment options for patients with lymphatic abnormalities.
Limitations: n/a
Ethics committee approval: n/a
Funding: No funding was received for this work.
Author Disclosures:
P. P. Mortimer: nothing to disclose
S. Katsari: nothing to disclose
F. Howe: nothing to disclose
L. A. Ratnam: nothing to disclose
D. K. Gordon: nothing to disclose
P. S. Mansour: nothing to disclose

RPS 1009a-8 11:57

Venous access devices and thrombotic complications incidence: implantation technique does matter

M. Cherkashin, A. Nikolaev, N. Berezina, D. Puchkov, N. Nikitina, D. I. Kuplevatskaya, K. Suprun, P. Yablonsky*; St. Petersburg/RU (mikhail.a.cherkashin@gmail.com)*

Purpose: To assess the role of totally implanted venous access devices (TIVAD) implantation errors in thrombotic complications.
Methods and materials: In this prospective study, we screened 428 patients with implanted venous access devices (395 port-systems (PS) and 33 peripherally inserted central catheters (PICC)). 64 patients (61 PS and 3 PICC) had venous thrombosis or device malfunctions during follow-up. These patients were included in the final analysis. The mean patients' age was 45 years (6-73). In all cases, venous ultrasound examination and angiography were performed.
Results: Thromboses were treated by low-molecular-weight heparins. In 7 cases, local thrombolysis was effective. In 2 patients, we performed device explantation due to the risk of thrombosis progression. The mean time for venous thrombosis development was 3 months after the intervention. In 1 case, non-massive pulmonary embolism was revealed.
We analysed a small group of patients with catheter malposition (n=15). In 46.6% (n=7), thrombosis was identified and we suggested device malposition as a serious VTE risk factor.
Different types of malpositions were identified: catheter placement errors, capsule placement errors, and complex malpositions.
Conclusion: TIVAD implantation errors are characterised by a high rate of thrombotic complications. The main reason is an underestimation of imaging support during implantation. In most cases of malposition, interventions were performed by ECG or ultrasound without a final x-ray.
Based on our analysis, we suggest maximizing direct x-ray or CT imaging during intervention. At least one shot must be performed in the final stage of implantation to assess the catheter tip position.
Limitations: A non-randomised single-center study.
Ethics committee approval: Approved by a local ethics board.
Funding: No funding was received for this work.

Author Disclosures:
M. Cherkashin: nothing to disclose
A. Nikolaev: nothing to disclose
N. Berezina: nothing to disclose
D. Puchkov: nothing to disclose
N. Nikitina: nothing to disclose
D. I. Kuplevatskaya: nothing to disclose
P. Yablonsky: nothing to disclose
K. Suprun: nothing to disclose

RPS 1009a-9 12:03

The efficacy of cutaneous anaesthesia in endovenous laser ablation of the great saphenous vein.

K. Singh, R. Malik, A. Kumar, R. S. Gupta*; Bhopal/IN (drkjsrandhawa@gmail.com)*

Purpose: To evaluate the safety and efficacy of cutaneous anaesthesia for pain control during injectable tumescent anaesthesia in endovenous laser ablation of the greater saphenous vein (GSV).
Methods and materials: An evaluation of 35 patients (25 male, 10 female), who had undergone endovenous laser ablation for greater saphenous vein insufficiency was done. All of these patients had undergone cutaneous application of cream-based skin anaesthetics consisting of lidocaine 2. 5%W/W and prilocaine 2. 5%W/W (TOPLAP cream) along the length of GSV to be ablated. The cream was applied at least an hour before cleaning and draping the patient for the procedure. To facilitate the application of the cream, GSV was marked under USG guidance. All patients received tumescent anaesthesia. All patients were asked to record the pain or discomfort using the visual analogue score (VAS) from the start of the procedure until the end of the GSV ablation. No intravenous analgesia or sedation was used.
Results: The mean recorded pain score was approximately 2.2 (range 1-4). Most of the patients had tolerable mild pain/discomfort with a pain score of 1-3. 4 patients complained of moderate pain with a VAS score of 4. However, the overall experience of patients was satisfactory, with patients having the ability to resume immediate ambulation and making endovenous laser ablation a walk-in walk-out procedure.
Conclusion: Cutaneous anaesthesia is a safe, adequate, and effective option to decrease and/or eliminate the intraoperative discomfort associated with tumescent anaesthesia injections and laser ablation during endovenous laser ablation of the greater saphenous vein.
Limitations: A limited sample size. Ethnicity and socio-economic background of the participants was not taken into consideration.
Ethics committee approval: n/a
Funding: No funding was received for this work.
Author Disclosures:
K. Singh: nothing to disclose
A. Kumar: nothing to disclose
R. Malik: nothing to disclose
R. S. Gupta: nothing to disclose

RPS 1009a-10 12:09

Assessment of the effectiveness of pelvic vein embolisation: a single-centre experience

C. Leonard, D. C. O Neill, M. P. Brassil, M. J. Lee*; Dublin/IE (carolaleonardo@gmail.com)*

Purpose: Pelvic congestion syndrome can arise from incompetent valves, typically in gonadal veins, resulting in pain. Pelvic vein embolisation is a minimally invasive treatment for pelvic congestion syndrome by embolising incompetent pelvic veins. The purpose of this retrospective study was to assess the efficacy of pelvic vein embolisation in the treatment of pelvic congestion syndrome.
Methods and materials: All patients treated with pelvic vein embolisation for pelvic congestion syndrome were analysed (2011-2019) in a university teaching hospital. A standardised questionnaire using a 0-10 numeric rating scale was used to assess pain scores and the impact on activities of daily living (ADLs), including work, socialising, exercise, and sleeping, before and after embolisation.
Results: 28 embolisation procedures were performed in 23 women. 5 patients underwent repeat embolisation for ongoing symptoms. The technical success of the procedure was 100% and there were only minor complications in 2 patients. 74% (17/23) response rate. The median pre-procedural pain score was 8 (IQR 7-8). This significantly reduced at 1-months to 5 (IQR 2.5-7.5) and at 12-months to 5 (IQR 0-8). 35% (n=6) of patients reported complete resolution of pain at 1 year. Improvement in the impact on ADLs was demonstrated across all domains and significantly in the impact on the exercise median before 8 (IQR 1-9) to 5 (IQR 6-9) after p=0.00694.
Conclusion: Pelvic vein embolisation results in reduced pain scores compared to their pre-operative values. Given that 4 had repeat venography without embolisation suggests a multifactorial component to the symptoms. Improvement in the impact on ADLs is demonstrated across all domains, particularly exercise. Information from this study will allow clinicians to convey the potential improvements in symptom parameters for patients undergoing embolisation for pelvic congestion.
Limitations: The sample size.
Ethics committee approval: Ethical approval received.
Funding: No funding was received for this work.
Author Disclosures:
M. J. Lee: nothing to disclose
C. Leonard: nothing to disclose
D. C. O Neill: nothing to disclose
M. P. Brassil: nothing to disclose

RPS 1009a-11 12:15

Hydrophilic guidewire usage in facilitating catheter advancement during the endovenous treatment of varicose veins

K. Hwang, S. W. Park, J. H. Hwang, Y. W. Kwon, J. Min*; Seoul/KR*

Purpose: To investigate the use of hydrophilic guidewires for facilitating catheter advancement during varicose vein treatment using radiofrequency ablation (RFA) or cyanoacrylate closure (CAC).
Methods and materials: From March 2016-April 2019, 463 limbs in 286 patients (126 male, mean age 53.7 years, range 21-88 years) with incompetent great saphenous vein were subjected to either RFA or CAC. Procedure records were reviewed for the use of a hydrophilic guidewire, the reason for guidewire usage, and the choice of guidewire diameter.
Results: In total, a hydrophilic guidewire was used to facilitate catheter advancement in the treatment of 92 of 463 limbs (19.8%). For RFA, a guidewire was used in the treatment of 53 of 321 limbs (16.5%). Among them, 15 limbs were due to vasospasm, while 38 were due to venous tortuosity. A 0.025-inch guidewire was used in 42 of 53 limbs (79.2%), and a 0.018-inch guidewire in 11 of 53 limbs (20.8%). For CAC, a 0.035-inch guidewire was used in 39 of 142 limbs (27.5%). Among them, 10 limbs were due to vasospasm, 23 due to venous tortuosity, and 6 due to repeated varicose vein engagement. All varicose vein treatment sessions were technically successful. No major complications occurred.
Conclusion: Hydrophilic guidewire usage could facilitate catheter advancement when it is hindered by vasospasm, tortuosity of the saphenous vein, or repeated engagement into varicosity. For RFA, the use of a 0.018-inch guidewire could provide better catheter advancement when a 0.025-inch guidewire passage through the radiofrequency catheter is difficult.
Limitations: This is a retrospective study from a single institute. There is no comparison with other methods.
Ethics committee approval: n/a
Funding: This study was supported by a KSIR grant.
Author Disclosures:
K. Hwang: Speaker at Konkuk University Medical Center, Author at Konkuk University Medical Center
S. W. Park: Author at Konkuk University Medical Center
J. H. Hwang: Author at Konkuk University Medical Center
J. Min: Author at Konkuk University Medical Center
Y. W. Kwon: Author at Konkuk University Medical Center

RPS 1009a-12 12:21

Assessment and treatment of low-flow venous malformations

R. M. Mousa, B. Hawthorn, T. Cavenagh, L. Mailli, J.-Y. Chun, L. A. Ratnam, R. A. Morgan*; London/UK (rolamousa87@gmail.com)*

Purpose: To outline the diagnostic features of LFVM and describe the efficacy of percutaneous sclerotherapy in their management.
Methods and materials: This study was done over two years, including 28 patients with LFVM, diagnosed with MRI and US. These patients underwent a total of 54 treatments. Management was divided into sessions, with each session consisting of multiple treatments (1 to 4) with an 8-week interval in between. Sclerotherapy procedures were done under local anaesthesia using ultrasound guidance. Compression was applied after the procedure where practicable. Subjective response to treatment was based on improvement in pain, swelling, discomfort, discolouration, and improvement of movement where applicable. The objective evaluation was based on a decrease in the size of the lesion on examination, change in the ultrasound appearances, and change in vascularity on colour Doppler evaluation.
Results: Approximately 93% of the patients reported a significant improvement of symptoms, which correlated with changes in US appearance and a decrease in the number of cystic spaces. 2 patients reported no significant resolution of the symptoms, which were correlated with no significant changes on US; both lesions were in the extremities (wrist and leg). Most patients complained of pain and swelling which resolved within a week of the procedure. No significant post-procedural complications were reported.

Conclusion: Treatment of LFVM with percutaneous sclerotherapy results in good outcomes for patients with a low complication rate. Accurate diagnosis of these lesions is critical to guide management.
Limitations: n/a
Ethics committee approval: Written consent was obtained from all patients.
Funding: No funding was received for this work.
Author Disclosures:
R. M. Mousa: Author at St Georges Hospital, Speaker at St Georges Hospital
B. Hawthorn: nothing to disclose
T. Cavenagh: nothing to disclose
L. Mailli: nothing to disclose
J.-Y. Chun: nothing to disclose
L. A. Ratnam: nothing to disclose
R. A. Morgan: nothing to disclose

11:15 - 12:30 **Room N**

Genitourinary

RPS 1007

Imaging in pregnancy and female tumours

Moderators:
G. Masselli; Rome/IT
T. Mokry; Heidelberg/DE

RPS 1007-1 11:15

ADNEX MR scoring system in the characterisation of ovarian lesions: retrospective external validation of malignancy prediction accuracy
A. Solopova, U. Nosova, V. Bychenko*; Moscow/RU (dr.solopova@mail.ru)*

Purpose: To evaluate the ADNEX MR scoring system accuracy in predicting ovarian tumour malignancy.
Methods and materials: A retrospective study was conducted on the basis of the analysis of pelvic MRI results of patients with ovarian lesions sent for clarifying diagnosis after ultrasound from 2018 to 2019, after excluding incomplete study protocols and observations without diagnosis verification. All ovarian lesions were analysed using the ADNEX MR scoring system algorithm.
Results: The study included 118 patients (average age 48.6 (26-81)) and 136 lesions: 33 (24.3%) were malignant and 7 (21.2%) were borderline epithelial sex cord stromal tumours with a low degree of malignancy. The distribution of malignant tumours among the studied groups showed that lesions with a score of 2 were found in 1.37% (1/73), with a score of 3 were found in 11.5% (3/26), with a score of 4 were found in 62.5% (10/16), and with a score of 5 were found in 90.5% (19/21). The ADNEX MR scoring system demonstrated high accuracy: a sensitivity of 91.3% (95% confidence interval [CI], 86.1% -94.8%) and specificity of 96.7% (95% CI, 92.3% -98.6%) in the malignancy prediction.
Conclusion: ADNEX MR scoring system is an informative method of ovarian tumour malignancy prediction, therefore implementation in the algorithm of preoperative diagnosis can be important for optimising the management tactics. The greatest difficulties in assessing arose when characterising borderline epithelial mucinous tumours and non-epithelial tumours with a low degree of malignancy.
Limitations: A retrospective, single-institution study.
Ethics committee approval: Ethics committee approval was obtained.
Funding: The study was funded by the Grant of the President of the Russian Federation.
Author Disclosures:
V. Bychenko: nothing to disclose
A. Solopova: nothing to disclose
U. Nosova: nothing to disclose

RPS 1007-2 11:21

Diagnostic value of individual MRI findings in abnormally invasive placenta
S. Sefidbakht[1], P. Iranpour[1], A. Teimouri[1], E. Khabbazi[1], Z. Gholami Bardeji[1], F. Zarei[1], P. Pishdad[1], H. Vafaei[1], B. Bijan[2]; *[1]Shiraz/IR, [2]Sacramento, CA/US (Arashteimourirad@gmail.com)*

Purpose: To evaluate the predictive value and accuracy of individual MRI findings in the diagnosis of abnormally invasive placenta (AIP).
Methods and materials: A retrospective PACS-based search was done for all the MRIs performed over 5 years in a tertiary referral centre for evaluation of possible AIP. The normal outcome was defined as an eventless vaginal delivery or cesarian section without the need for transfusion or hysterectomy. AIP was considered positive if pathologic prove was present. Patients with complicated deliveries but no hysterectomy or pathologic proof were excluded from the study. Individual findings evaluated included heterogeneity, dark placental bands, rounded edges, lumpy margins, and bulging uterine outline. Chi-square was used to compare findings. Sensitivity, specificity, PPV, and NPV for each individual finding were determined.
Results: Over a period of 2 years, 392 MRIs were done to further evaluate for possible AIP, of which 152 cases had a final diagnosis of AIP and 38 were lost to follow-up. Sensitivity, specificity, and overall accuracy of MRI for diagnosis of AIP were 93, 90%, and 89%. Dark bands were most accurate (sensitivity, specificity, and overall accuracy of 91, 78%, and 82%). Lumpy margins and loss of retroplacental hypo intense band were least accurate. A combination of retroplacental dark bands, anteroinferior low-lying/previa, and bulging uterine margins were the most accurate combination, slightly increasing the sensitivity, specificity, and overall accuracy to 93, 92, and 91% (based on a logistic regression method).
Conclusion: Not all the individual signs of AIP have the same diagnostic value in predicting the diagnosis. The single most useful determinant for the diagnosis was dark placental bands. The most useful combination of findings were a history of previous C/S, placenta previa, and dark placental bands. Adding other findings did not significantly raise the accuracy.
Limitations: n/a
Ethics committee approval: n/a
Funding: No funding was received for this work.
Author Disclosures:
H. Vafaei: nothing to disclose
A. Teimouri: nothing to disclose
S. Sefidbakht: nothing to disclose
P. Iranpour: nothing to disclose
E. Khabbazi: nothing to disclose
F. Zarei: nothing to disclose
P. Pishdad: nothing to disclose
B. Bijan: nothing to disclose
Z. Gholami Bardeji: nothing to disclose

RPS 1007-3 11:27

Comparative analysis of placental volume and vasculature in normal and foetal growth restricted (FGR) pregnancies
S. Jain, S. Hota, R. C. Shukla, M. Jain, T. Singh*; Varanasi/IN (shivijain1103@gmail.com)*

Purpose: To evaluate differences in placental volume and vasculature between normal and FGR pregnancies by three-dimensional ultrasound (3D-USG).
Methods and materials: 703 pregnant women with singleton foetus at gestation age (GA) of 6-9 weeks (GA confirmed through transvaginal ultrasound) were enrolled. At 28-36 weeks, 3D-USG assessment of placental volume (PV), vascularisation index (VI), flow index (FI), vascularisation flow index (VFI), and an estimated foetal weight (EFW) was done. Those with EFW < 10^{th} percentile for GA were placed in the FGR group and the rest in the normal group. Follow-up till delivery was done in 121 FGR and 153 normal pregnancies. The diagnosis was confirmed through birth-weight in 107 and 111 women, respectively. Receiver operator characteristic (ROC) curves were plotted; correlation coefficients of PV, VI, FI, VFI with EFW were calculated. A Student t-test and Mann-Whitney U test were used.
Results: A mean of PV, VI, and VFI were significantly lower ($p<0.001$) in FGR than normal (PV: 192.67 ± 24.07 vs 275.08 ± 94.82, VI: 3.26 ± 1.48 vs 10.53 ± 7.94, VFI: 2.44 ± 1.61 vs 5.46 ± 3.07) while FI had no significant difference between the two (FI: 46.41 ± 7.70 vs 49.19 ± 7.08, $p=0.07$). Area under ROC curve (AUC) were VI: 0.860, VFI: 0.799, PV: 0.791, and FI: 0.690. Sensitivity and specificity of cut-off values for PV (208 ml), VI (5.0), and VFI (3.2) were 74% and 69%, 91% and 75%, and 75% and 71%, respectively. PV showed a maximum correlation with EFW; 0.829 for FGR and 0.911 for normal pregnancies ($p<0.05$ each).
Conclusion: 3D-USG assessment of placental volume and vasculature serves as a complementary tool to EFW in discriminating FGR from normal pregnancies.
Limitations: A tertiary hospital-based study; results cannot be generalised at a community level.
Ethics committee approval: n/a
Funding: No funding was received for this work.
Author Disclosures:
S. Jain: nothing to disclose
S. Hota: nothing to disclose
R. C. Shukla: nothing to disclose
M. Jain: nothing to disclose
T. Singh: nothing to disclose

RPS 1007-4 11:33

The role of sonosalpingography (SSG) using normal saline in female subfertility: diagnostic or therapeutic?

R. Rastogi, N. Jain*; Moradabad/IN (rajulrst@yahoo.co.in)*

Purpose: Sonosalpingography (SSG) has been a less commonly used tool for assessing the patency of fallopian tubes in subfertile females. Its significance is undermined by laparoscopic evaluation (LE) that allows simultaneous therapeutic procedures to restore its patency if the obstruction exists. But LE is invasive and expensive.
Methods and materials: We performed this study with the aim of evaluating the role of SSG in the diagnosis of tubal obstruction, its cause, and relieving the obstruction.
50 subfertile females with a normal-appearing uterus and ovaries on transvaginal ultrasonography were included in our study. SSG was performed with an infusion of normal saline to evaluate tubal patency by recording free peritoneal spill. If peritoneal spill was absent bilaterally then the patient underwent laparoscopic evaluation. However, if unilateral or bilateral peritoneal spill was noted, then the patient was recruited for assisted reproductive techniques (ART) and the results were correlated with pregnancy.
Results: Out of 50 patients, SSG demonstrated free peritoneal spill unilaterally in 46 patients who conceived with ART during the following six months. In the remaining 4 patients with a lack of bilateral spill on SSG, 2 revealed unilateral partial block and 2 revealed bilateral tubal block on LE. In all patients, SSG correctly depicted the site of obstruction. In 9 patients, it revealed PID (tubercular) by demonstrating flimsy peritubal adhesions and in 14 patients, higher pressure exerted during SSG restored the patency with sharp abdominal pain.
Conclusion: Our study reveals that SSG is not only diagnostic but may also be a therapeutic tool. SSG should be used more often and can be used to at least segregate patients who prudently need laparoscopic evaluation.
Limitations: n/a
Ethics committee approval: n/a
Funding: No funding was received for this work.
Author Disclosures:
R. Rastogi: nothing to disclose
N. Jain: nothing to disclose

RPS 1007-5 11:39

The accuracy of the characterisation of adnexal masses with non-contrast pelvic MRI: an 11-year experience from a tertiary referral centre in the United Kingdom

H. Şahin[1], C. Panico[2], H. C. Addley[1], S. Ursprung[1], J. Smith[1], S. Freeman[1], V. Simeon[2], P. Chiodini[2], E. Sala[1]; [1]*Cambridge/UK,* [2]*Naples/IT (hilalcimen@gmail.com)*

Purpose: To assess the accuracy of non-contrast pelvic magnetic resonance imaging (MRI) for the characterisation of adnexal masses and evaluate the reproducibility of a new non-contrast adnex MRI scoring system used in a tertiary referral centre.
Methods and materials: Pelvic MRI examinations performed for adnexal mass characterisation or follow-up of endometriomas between the years 2008-2018 in our institution were retrospectively reviewed. In total, 484 patients with an adnexal mass who were either treated surgically or followed-up for at least one year were identified. After exclusion of patients without diffusion-weighted imaging (DWI), the final cohort included 297 patients with 356 adnexal masses. A randomised set of 100 patients was chosen from this cohort to assess the reproducibility of the proposed five-category scoring system. Various MRI features were assessed in both sets.
Results: There were 303 benign and 53 malignant tumours in the study cohort. ROC analysis of the used scoring system for predicting overall outcome showed an AUC of 0.93. A cut-off score of ≥4 was associated with malignancy with an accuracy of 93.82% and PLR of 18 for predicting malignancy, with a sensitivity of 84.91% and a specificity of 95.38%. In the analysis of MRI features of the reproducibility set, inter and intraobserver agreement was moderate-almost perfect for most of the features and the repeatability of the scoring system.
Conclusion: Non-contrast MRI scoring for adnexal mass characterisation seems to be promising with high accuracy and reasonable inter and intraobserver agreement. The validity of the scoring needs to be tested in multicentre prospective studies.
Limitations: A single-centre, retrospective study.
Ethics committee approval: Service evaluation approval is present.
Funding: No funding was received for this work.
Author Disclosures:
H. Şahin: nothing to disclose
C. Panico: nothing to disclose
H. C. Addley: nothing to disclose
S. Ursprung: nothing to disclose
J. Smith: nothing to disclose
S. Freeman: nothing to disclose
V. Simeon: nothing to disclose
E. Sala: nothing to disclose
P. Chiodini: nothing to disclose

RPS 1007-6 11:45

Integration of proteomics with CT-based qualitative and texture features in high-grade serous ovarian cancer patients: an exploratory analysis

L. Beer[1], H. Sahin[1], K. M. Darcy[2], J. B. Freymann[3], L. Maxwell[2], T. P. Conrad[2], E. Huang[3], E. Sala[1]; [1]*Cambridge/UK,* [2]*Bethesda/US,* [3]*Rockville/US (lucian.beer@meduniwien.ac.at)*

Purpose: To investigate the association between CT imaging traits and texture metrics with proteomic data in patients with high-grade serous ovarian cancer (HGSOC).
Methods and materials: This retrospective, hypothesis-generating study included 20 patients with HGSOC prior to primary surgery. Two readers independently assessed the contrast-enhanced computed tomography (CT) images and extracted 33 imaging traits. All sites of suspected HGSOC were manually segmented and grey-level correlation and matrix-based texture features were computed. 3 texture features that represented intra-and inter-site tumour heterogeneity were used for analysis. An integrated analysis of transcriptomic and proteomic data identified proteins with a conserved expression between primary tumour sites and metastasis. Correlations between protein-abundance and various CT features were assessed using the Kendall tau rank correlation coefficient and the Mann-Whitney U test, whereas the area under the receiver-operating characteristic-curve (AUC) was reported as a metric of the strength and the direction of the association.
Results: 8 proteins were identified as significantly associated with CT-based imaging traits, with the strongest correlation observed between the MRI1 protein and peritoneal disease in the liver/right upper quadrant (P<0.001, AUC=0.940). The abundance of 4 proteins was associated with texture features that represented intra and inter-site tumour heterogeneity, with the strongest correlation between the GSTM1 protein and cluster dissimilarity (p=0.024, =0.368).
Conclusion: This study provides the first insights into the potential associations between standard-of-care CT imaging traits and texture measures of intra-and intersite heterogeneity and the abundance of several proteins.
Limitations: A small sample, retrospective study.
Ethics committee approval: This was a multi-institutional, institutional review board-approved, and Health-Insurance Portability and Accountability Act (HIPAA)-compliant study.
Funding: The Mark Foundation for Cancer Research and the Cancer Research UK Cambridge Centre (C9685/A25177).
U.S. Department of Defense - Uniformed Services University of the Health Sciences (HU0001-16-2-0006).
National Cancer Institute (HHSN261200800001E).
Author Disclosures:
L. Beer: nothing to disclose
H. Sahin: nothing to disclose
K. M. Darcy: nothing to disclose
J. B. Freymann: nothing to disclose
L. Maxwell: nothing to disclose
T. P. Conrad: nothing to disclose
E. Huang: nothing to disclose
E. Sala: nothing to disclose

RPS 1007-7 11:51

Pre-treatment MRI radiomics-based response prediction model in locally advanced cervical cancer

L. Russo, B. Gui, S. Persiani, M. Miccò, L. Boldrini, D. Cusumano, R. Autorino, G. Ferrandina, R. Manfredi*; Rome/IT (lucarusso.md@gmail.com)*

Purpose: To investigate the potential of the radiomic approach to MRI to the predict pathological complete response to treatment (pCR) in patients with locally advanced cervical cancer (LACC). The second goal was to develop and validate this MRI signature, to apply the model out of the habitat where it was created.
Methods and materials: 183 patients with LACC (FIGO IB2-IVA) treated in two hospitals were enrolled, 156 patients for the training set and 27 for the validation set, respectively. All patients underwent neoadjuvant chemoradiation therapy followed by radical surgery.
For each patient, a staging 1.5T MR image was acquired. 230 radiomic features belonging to 4 families (fractal, statistical, textural, and morphological features) were extracted. Considering the application of all the filters used, 1,889 features were extracted. Features selection and model training were carried out following an iterative method, ad-hoc developed for this study. Model selection was

carried out using the area under the curve (AUC) of the receiving operator characteristic (ROC) curve as a target metric.
Results: 15 features were selected. The model showing the highest performance was a random forest with default parameters (RF_DEF). This model shows an AUC of 0.76 on the training and 0.82 on the external validation set.
Conclusion: Our radiomic model showed a good predictive value with a high AUCs both in the training and validation group, so it is able to predict the probability of pathological complete response in patients undergoing chemoradiation therapy using pre-treatment images.
The presented model is able to predict patients' response to treatment before commencement and use this information to support the clinical decision-making process.
Limitations: Further external validation cohort should be studied.
Ethics committee approval: Institutional ethics committee approved the study.
Funding: No funding was received for this work.
Author Disclosures:
L. Russo: nothing to disclose
B. Gui: nothing to disclose
M. Miccò: nothing to disclose
L. Boldrini: nothing to disclose
D. Cusumano: nothing to disclose
R. Autorino: nothing to disclose
G. Ferrandina: nothing to disclose
R. Manfredi: nothing to disclose
S. Persiani: nothing to disclose

RPS 1007-8 11:57

The variance of quantitative kurtosis imaging using ultra-high b-value DWI over the menstrual cycle: the influence of oral contraceptives

T. Mokry, A. Mlynarska-Bujny, J. Pantke, T. Kuder, J. Rom, H.-U. Kauczor, H.-P. Schlemmer, S. Bickelhaupt*; Heidelberg/DE*

Purpose: To evaluate the influence of contraceptives on the variability of quantitative kurtosis parameters of the ovaries over the menstrual cycle in diffusion-weighted magnetic resonance imaging (DWI).
Methods and materials: This IRB-approved prospective study included 30 volunteers with or without oral-contraceptives (n=15 for each group, mean 27.9y) from 07/2017-09/2019. MRI was performed using a 1.5T MRI (Aera) with a multi-b-value-epi-DWI 0,50, 100, 800, 1500, and 2000s/mm^2 at three timepoints during the menstrual cycle (T1=day 1-5, T2=day 7-12, and T3=day 19-24). Ovaries were 3D-segmented (b=800s/mm^2). Diffusion-kurtosis (K_{app}) was calculated. Quantitative parameters and coefficient-of-variation (CoeV) were analysed and compared between the groups using Students t-test after Shapiro-Wilk and Brown-Forsythe pretest.
Results: Amongst the women without oral contraceptives, the CoeV for kurtosis parameters was significantly elevated in comparison to the group with oral contraceptives at Timepoint1 (0.34 vs 0.30;p=0.04) and Timepoint2 (0.36 vs 0.32,p=0.018) of the menstrual cycle, however not at Timepoint3 (0.29 vs 0.30;p=0.28). Mean absolute K_{app} was not significantly different in between the women with and without oral contraceptives for Timepoint1=0.618±0.057 vs 0.637±0.039], p=0.14, and Timepoint2=0.606±0.062 vs 0.616±0.059, p=0.54, however, at Timepoint3, significant differences were observed (0.649±0.058 vs 0.596±0.062, p=0.0013).
Conclusion: Quantitative diffusion kurtosis imaging demonstrated a significantly higher coefficient of variation in women with a natural menstrual cycle compared to women using oral contraceptives in the follicular phase. The absolute mean values between the groups only differed significantly during the luteal phase. These findings should be considered when quantitatively applying kurtosis DWI in imaging of the ovaries.
Limitations: A limited number of volunteers, no intra-individual repeated measures, and the influence on suspicious lesions was not investigated.
Ethics committee approval: IRB approved.
Funding: No funding was received for this work.
Author Disclosures:
S. Bickelhaupt: Other at pending patents in the field of DWI
A. Mlynarska-Bujny: nothing to disclose
J. Pantke: nothing to disclose
T. Kuder: nothing to disclose
J. Rom: nothing to disclose
H.-P. Schlemmer: nothing to disclose
H.-U. Kauczor: nothing to disclose
T. Mokry: nothing to disclose

RPS 1007-9 12:03

Multiparametric MRI-based radiomics analysis for preoperative assessment of uterine cervical cancer aggressiveness

Y. Liu, Y. Zhang, Z. Ye*; Tianjin/CN (zywtj@hotmail.com)*

Purpose: To develop and validate models using multiparametric radiomic biomarkers to preoperatively evaluate cervical cancer aggressiveness regarding Ki-67 labelling index and lymphovascular invasion (LVI) status and to predict lymph node metastasis.
Methods and materials: 130 consecutive patients with biopsy-confirmed untreated uterine cervical cancer were enrolled in this prospective study. All underwent surgery within 2 weeks after MRI examination. Ki-67 index and LVI were assessed on whole-tumour slides with HE and IHC staining. Volumetric segmentation was performed by two radiologists who have proven consistency in a preliminary study. B1-field correction, cross-individual rescaling, and intensity normalisation were conducted to reduce the scanner-shifting variety and to promote reproducibility. 690 volumetric radiomic biomarkers were extracted from T1WI, T2WI, and DWI followed by a grouped-ElasticNet workflow to fuse multi-modality data. A structural equation model was used to infer model-wise relationships to validate the rationality of study hypotheses. Habitat descriptors were designed to visualise proposed integrated biomarkers.
Results: The radiomic model achieved AUC 0.79 (0.75, 0.83), a recall rate of 0.86 in LVI predicting, AUC 0.78 (0.74, 0.81), and a recall rate of 0.82 in Ki-67 predicting. 81% of metastatic lymph nodes were recognised with AUC 0.82 (0.74, 0.89), whereas only 33% had a minor-axis diameter greater than 1.0 cm. Among several priori hypotheses, LVI significantly mediated the predictive effect of Ki-67 on pelvic lymphonode metastasis status (p<0.01), which probably reflect pathophysiological facts.
Conclusion: It is feasible and effective to filtrate robust MR biomarkers to depict tumour aggressiveness and to predict lymph node metastasis risk, providing a non-invasive approach in clinical practice.
Limitations: Sample imbalance exists in metastatic lymph nodes that might limit efficiency.
Ethics committee approval: IRB approved with written informed consent from all patients.
Funding: Funded by NSFC Young Scientists Fund.
Author Disclosures:
Y. Liu: nothing to disclose
Y. Zhang: nothing to disclose
Z. Ye: nothing to disclose

RPS 1007-10 12:09

Diffusion-weighted imaging of cervical cancer: feasibility of ultra-high b value at 3T

Y. Qi, Y. He, C. Lin, X. Wang, H. Zhou, H. Xue, Z. Y. Jin*; Beijing/CN (qiyafei19910603@163.com)*

Purpose: To evaluate imaging quality and compare the signal intensity and ADC maps of ultra-high b-value (2,000 s/mm2; B2) images against those of 800 s/mm2 b-value (B1) images in DWI for cervical cancer.
Methods and materials: 60 patients diagnosed with cervical cancer by pathology were prospectively included. A female pelvis MRI using a 3T MR scanner was performed; B1 and B2 images were obtained for evaluation. Two radiologists blinded to scan parameters evaluated the images for background suppression, spatial distortion, image ghosting, lesion diagnostic confidence, and whole imaging quality using a 5-point scoring system. Scores were compared using a paired Wilcoxon test. Signal intensity (SI) of tumour tissue was measured in B1 and B2 images for tumour and normal reference tissues. Additionally, SI contrast ratios (CRs) were calculated and compared using the Mann-Whitney U test, ADC values of tumours, and normal tissues were measured, and tumour maximum diameters were calculated with T2W imaging.
Results: Background suppression, lesion diagnostic confidence, and whole imaging quality scores were higher in B2 than B1 images ($p < 0.001$). CRs of tumour-to-normal SI were also higher for B2 than B1 images ($p < 0.01$). Mean ADC values derived from B2 images showed better correlations with tumour differentiation grades than did those from B1 images. Tumour diameters measured by B2 imaging experienced a smaller bias.
Conclusion: B2 images in DWI demonstrated superiority in image quality and cervical cancer diagnosis to the commonly used B1 images in female pelvis.
Limitations: Though blinded, it is inevitable that observers could differentiate the B2 and B1 images. Pathologic diameters of the lesions were not available.
Ethics committee approval: This study was approved by ethics committee and written informed consent was obtained.
Funding: No funding was received for this work.
Author Disclosures:
Y. Qi: nothing to disclose
C. Lin: nothing to disclose
Y. He: nothing to disclose
X. Wang: nothing to disclose
H. Zhou: nothing to disclose
H. Xue: nothing to disclose
Z. Y. Jin: nothing to disclose

11:15 - 12:30 **Room O**

Breast

RPS 1002a

Contrast-enhanced x-ray imaging of the breast

Moderators:
G. G. Esen; Istanbul/TR
H. Preibsch; Tübingen/DE

RPS 1002a-1 11:15

Contrast-enhanced mammography (CEM): a systematic review and meta-analysis of diagnostic performance

A. Cozzi[1], C. B. Monti[1], C. G. Monaco[1], M. Zanardo[1], S. Schiaffino[2], R. M. Trimboli[1], G. Di Leo[2], L. A. Carbonaro[2], F. Sardanelli[2]; [1]Milan/IT, [2]San Donato Milanese/IT (andrea.cozzi@gmail.com)

Purpose: To appraise the diagnostic performance of contrast-enhanced mammography (CEM) through a systematic review and meta-analysis.
Methods and materials: After study protocol registration on PROSPERO, we performed in September 2019 a systematic search on MEDLINE/EMBASE for articles reporting the independent diagnostic performance of CEM. We then excluded studies with temporal subtraction CEM, not focused on lesion detection, evaluating response to neoadjuvant therapy, and not providing data for sensitivity and specificity calculation. For multi-reader studies, we analysed results from the most expert reader. We computed Chi-squared for sensitivity and specificity heterogeneity. We calculated pooled sensitivity, specificity, positive and negative likelihood ratios (LR), and diagnostic odds ratio (DOR). Moreover, we constructed a summary receiver operating characteristics (sROC) curve. Data was reported as point estimates and their 95% confidence intervals (CIs). Risk of publication bias was assessed by visually inspecting the ROC ellipse plot.
Results: From a total of 98 studies, published between 2003 and 2019, we included 50 studies as depicted in the flowchart. These studies involved 7516 patients (mean age ranging from 46–62 years) for a total of 6915 lesions. Chi-squared was significant for sensitivity and specificity (both p<0.001). Pooled sensitivity was 94.1% (95% CI 92.1−95.6%), pooled specificity 66.6% (95% CI 59.6−72.9%), positive LR 2.81 (95% CI 2.28−3.52), negative LR 0.09 (95% CI 0.07−0.11), and DOR 31.8 (95% CI 21.0−47.8). The sROC curve had an area under the curve of 0.921. Visual inspection of the ROC ellipse plot revealed no risk of publication bias.
Conclusion: CEM showed high sensitivity, while its suboptimal specificity could be explained by a lack of standardised descriptors and diagnostic categories, as well as by biased population selection.
Limitations: Possible data duplication in some of the included studies.
Ethics committee approval: No ethics committee approval needed.
Funding: No funding was received for this work.
Author Disclosures:
A. Cozzi: nothing to disclose
F. Sardanelli: Advisory Board at Bracco, Grant Recipient at Bayer, Grant Recipient at Bracco, Grant Recipient at General Electric, Speaker at Bayer, Speaker at Bracco, Speaker at General Electric
S. Schiaffino: Speaker at General Electric
M. Zanardo: nothing to disclose
C. B. Monti: nothing to disclose
C. G. Monaco: nothing to disclose
G. Di Leo: nothing to disclose
L. A. Carbonaro: nothing to disclose
R. M. Trimboli: nothing to disclose

RPS 1002a-2 11:21

Impact of contrast-enhanced mammography as a work-up technique for women recalled at breast cancer screening: preliminary results

C. G. Monaco[1], L. A. Carbonaro[2], S. Schiaffino[2], A. Cozzi[1], D. Spinelli[1], R. M. Trimboli[2], G. Di Leo[2], F. Sardanelli[1]; [1]Milan/IT, [2]San Donato Milanese/IT (cristianmonaco87@gmail.com)

Purpose: To evaluate contrast-enhanced mammography (CEM) ability to reduce biopsy rate (BR) in women recalled after first-level screening mammography.
Methods and materials: Recalled women 40-80 yrs were screened to undergo CEM alongside standard assessment (SA: tomosynthesis, additional views, ultrasound, and/or core- or vacuum-assisted biopsy). Exclusion criteria were breast cancer symptoms, allergies to contrast agents, renal failure, pregnancy, or breast implants. One of three radiologists (6-15 years of experience) independently evaluated SA or CEM recommending biopsies or 2-year follow-up. SA was performed independently of, and blinded to, CEM results. Taking SA results as reference standard, we calculated the potential BR after CEM (women candidate to biopsy for positive CEM/women who had CEM) to be compared with the real BR after SA (women who had biopsy following SA/women recalled for SA).
Results: Since January 2019, 181 women were recalled, 102 (56%) being eligible for this study. Ultimately 69/102 (68%) were enrolled and performed CEM. Compared to SA, there 8 were true positives, 52 true negatives, 7 false positives, and 2 false negatives (both ductal carcinoma in situ, DCIS), resulting in 80% sensibility (95% confidence interval [CI] 44–97%), 88% specificity (95% CI 77–95%), 53% positive predictive value (95% CI 27–79%), and 96% negative predictive value (95% CI 87–99%). CEM-BR was 13/69 (18.8%, 95% CI 10.4–30.1%) and SA-BR was 19/69 (27.5%, 95% CI 17.5–39.6%).
Conclusion: With an 80% sensitivity (false negatives represented only by DCIS) and an 88% specificity, CEM in recalled patients showed a potential BR reduction of about one third in comparison to SA.
Limitations: Preliminary results: only one third (n=69) of the planned sample size (n=197). Non-randomised, monocentric study.
Ethics committee approval: Ethics Committee approval was obtained.
Funding: This study was funded by GE Healthcare.
Author Disclosures:
C. G. Monaco: nothing to disclose
L. A. Carbonaro: nothing to disclose
S. Schiaffino: Speaker at general electric
A. Cozzi: nothing to disclose
D. Spinelli: nothing to disclose
R. M. Trimboli: nothing to disclose
G. Di Leo: nothing to disclose
F. Sardanelli: Speaker at Bracco, Speaker at Bayer, Grant Recipient at General Electric, Advisory Board at Bracco, Speaker at General Electric, Grant Recipient at Bracco, Grant Recipient at Bayer

RPS 1002a-3 11:27

Diagnostic value of the delayed image in contrast-enhanced spectral mammography for the assessment of malignancy in BI-RADS 4 mammographic findings

A. Ainakulova, Z. J. Zholdybay, D. Kaidarova, N. Inozemtseva; Almaty/KZ (ar89@list.ru)

Purpose: To assess the performance of the delayed image in CESM to diagnose breast cancer in BI-RADS 4 findings detected by mammography.
Methods and materials: Between May 2018 and May 2019, 150 women with BI-RADS 4 after standard mammography were performed CESM. CESM technique: image acquisition began at a 2-minute delay after the start of the contrast injection and was completed within 6 minutes after initiation of contrast administration. On 8-12 minutes, a set of additional bilateral (lesions of both breast) or monolateral (lesions of one breast) craniocaudal (CC) or mediolateral-oblique (MLO) views was acquired. All the lesions were histologically verified.
Results: 160 lesions were identified, 89 of which were malignant and 71 benign. Malignancy rates were 22.7% (10/44 BI-RADS 4a), 47.5% (29/61 BI-RADS 4b), and 90.9% (50/55 BI-RADS 4c). There were 86 true-positive, 63 true-negative, 8 false-positive, and 3 false-negative (one invasive cancer, two DCIS) CESM findings, effecting a sensitivity, specificity, PPV, and NPV of 96.9% (95%-CI 90.9–99.2%), 92.9% (95%-CI 86.5–97.9%), 92.2% (95%-CI 85.6–96.9%), and 97.2% (95%-CI 92.2–99.5%), respectively.
Conclusion: CESM is an accurate tool to further diagnose BI-RADS 4a and 4b lesions and may be helpful to avoid unnecessary biopsies. BI-RADS 4c lesions should be biopsied irrespective of CESM findings. Delayed image increases the specificity of the method by 10%.
Limitations: Small number of patients.
Ethics committee approval: n/a
Funding: No funding was received for this work.
Author Disclosures:
A. Ainakulova: nothing to disclose
Z. J. Zholdybay: nothing to disclose
D. Kaidarova: nothing to disclose
N. Inozemtseva: nothing to disclose

RPS 1002a-4 11:33

Diagnostic accuracy of contrast-enhanced digital mammography (CEDM) in breast cancer detection among women with dense breast in comparison to digital mammography and ultrasound

R. Sudhir, V. Koppula, K. Sannapareddy; Hyderabad/IN (rashmi4210@gmail.com)

Purpose: Comparative diagnostic accuracy of digital mammography, US, and contrast-enhanced digital mammography (CEDM) in breast cancer detection among women with dense breast with histopathological diagnosis as the gold standard.

Methods and materials: A prospective study on consecutive women >40 years with dense breast on conventional imaging who underwent CEDM and biopsy at our centre were included. Women with h/o pregnancy, renal insufficiency, or prior allergic reaction to iodinated contrast agent were excluded. On mammography and ultrasound, lesions were categorised based on ACR BI-RADS fifth edition. On CEDM, lesions were categorised based on the intensity and dynamic patterns of contrast enhancement. Moderate to intense enhancement with wash-out in delayed phase were considered malignant and lesions with no enhancement or progressive enhancement were considered benign lesions. Statistical analysis was done using SPSS software version 21.
Results: A total of 156 lesions, 87 malignant and 69 benign lesions, were included. For mammogram, US, mammogram and US combined, and CEDM, sensitivity was 92.7%, 71.3%, 94.2%, and 96.6%; specificity 52.2%, 75%, 82.6%, and 83%; and accuracy 73.5%, 76.3%, 85.7%, and 92%, respectively.
Conclusion: CEDM is an emerging tool with significantly better diagnostic efficiency and accuracy than the mammogram and US alone or combined, therefore it may play a promising role in early detection, diagnosis, staging, and follow-up of breast cancer in women with dense breast at lesser cost and much shorter examination time compared to MRI.
Limitations: Radiation exposure 1.5 times of conventional digital mammography. CEDM cannot be performed in women with renal insufficiency and a history of allergy to iodinated contrast. Depth of the lesion and chest wall invasion cannot be assessed as accurately as MRI.
Ethics committee approval: Approved from an ethics committee.
Funding: No funding was received for this work.
Author Disclosures:
R. Sudhir: Author at Basavatharakam Indo-American cancer hospital and reasearch centre,hyderabad, Consultant at Basavatharakam Indo-American cancer hospital and reasearch centre,hyderabad, Speaker at Basavatharakam Indo-American cancer hospital and reasearch centre,hyderabad
V. Koppula: Consultant at Basavatharakam Indo-American cancer hospital and reasearch centre,hyderabad, Speaker at Basavatharakam Indo-American cancer hospital and reasearch centre,hyderabad
K. Sannapareddy: Consultant at Basavatharakam Indo-American cancer hospital and reasearch centre,hyderabad

RPS 1002a-5 11:39

The comparative role of contrast-enhanced spectral mammography and contrast-enhanced MRI in preoperative diagnosis and management decision of sonomammography suspicious lesions

M. M. Gomaa, M. M. H. Hanafy, R. M. Kamal, S. A. Mansour, M. Hassan, G. Mohamed*; Cairo/EG (mohammedgomaa555@yahoo.com)*

Purpose: To compare the role of contrast-enhanced spectral mammography and dynamic contrast-enhanced MRI in the preoperative diagnosis of suspicious breast lesions detected on sonomammography and evaluation of disease extension of the proved breast cancer.
Methods and materials: This study included 171 lesions in 82 patients. All patients underwent digital mammography, breast ultrasound, CESM, and contrast-enhanced MRI breast. Results were correlated to histopathological details.
Results: Histological analysis: 51/171 (29.8 %) lesions were benign while 120/171 (70.2 %) were malignant.
The accuracy measures of CESM and DCE-MRI were higher than that of sonomammography. DCE-MRI sensitivity and NPV were significantly higher than CESM (p-value 0.014 and 0.013). The overall accuracy of MRI was better than CESM, however, no statistically significant difference was detected.
Axillary lymph nodes were assessed by SM, CESM, and MRI in cases with malignant lesions and their sensitivities were 93.8 %, 50 %, and 87.5 %, respectively, and their specificities were 90.3%, 93.5 %, and 93.5%, respectively.
Regarding multiplicity, both DCE-MRI and CESM were better than SM in their detection, with DCE-MRI superior to CESM.
Regarding size assessment, we found no correlation between SM and postoperative size, with weak agreement, high correlation, and agreement between CESM and postoperative size, slightly higher correlation and agreement between DCE- MRI and postoperative, with high correlation and agreement between CESM and DCE-MRI.
Conclusion: MRI is still the best study in preoperative diagnosis and management decision of breast cancer, however, contrast-enhanced spectral mammography is a feasible comparable technique with promising results.
Limitations: Different biological subtypes of included breast cancer patients.
Ethics committee approval: Approved by ethical committee of faculty of medicine at Cairo University. Written consent was obtained from all patients.
Funding: No funding was received for this work.
Author Disclosures:
M. M. Gomaa: nothing to disclose
M. M. H. Hanafy: nothing to disclose
R. M. Kamal: nothing to disclose
S. A. Mansour: nothing to disclose
M. Hassan: nothing to disclose
G. Mohamed: nothing to disclose

RPS 1002a-6 11:45

Contrast-enhanced digital mammography: what is the added value in the diagnostic work-up of microcalcifications?

A. Franconeri[1], D. de Benedetto[2], C. Bellini[2], M. C. Masciotra[3], R. Trapasso[2], G. Bicchierai[2], F. Di Naro[2], J. Nori[2], V. Miele[2]; *[1]Pavia/IT, [2]Florence/IT, [3]Campobasso/IT (afrancon88@gmail.com)*

Purpose: To assess the added value of contrast-enhanced digital mammography (CEDM) in the evaluation of microcalcifications.
Methods and materials: We retrospectively screened 1233 women who performed CEDM from September 2016 to August 2018. Inclusion criteria were the presence of microcalcifications on a mammogram, biopsy-proven histological diagnosis, and the absence of an associated mass. CEDM performed with no residual microcalcifications after biopsy were excluded. CEDM sensitivity, specificity, positive predictive value (PPV), negative predictive value (NPV), and accuracy were calculated. Microcalcifications morphology and associated enhancement were independently reviewed by 2 radiologists with 6 and 24 months of CEDM experience, respectively. Interobserver agreement was calculated with Cohen's kappa test.
Results: The final population included 138 women (52.99±9.92 years old). 87 microcalcifications presented enhancement: 45 out of 50 (90.0%) were carcinomas (B5), 26 out of 34 (76.5%) lesions with uncertain malignant potential (B3), and 16 out of 54 (29.6%) benign lesions (B2). All 5 B5 without enhancement were carcinomas in situ. Carcinoma in situ presented as mild to moderate progressive non-mass enhancement, invasive carcinoma as moderate to intense wash-out mass enhancement. Out of 8 B3 without enhancement, only 1 (12.5%) upgraded to carcinoma in situ. All morphologically different types of microcalcification presented high NPV and included rounded/punctiform calcification (VPN=94.4%). The overall diagnostic sensitivity of CEDM was 89.5%, with 57.0% specificity, 60.0% PPV, 88.2% NPV, and 70.6% accuracy. AUC was 0.81 according to ROC curve. Substantial agreement was observed between the two observers (K=0.71).
Conclusion: CEDM represents a novel technique with good ability in detecting and characterising microcalcifications. Morphology and distribution still play the most important role in the decision planning, however, CEDM can help when rounded/punctiform microcalcifications or B3 lesions are found.
Limitations: A retrospective study, small sample, and CEDM performed after biopsy.
Ethics committee approval: n/a
Funding: No funding was received for this work.
Author Disclosures:
A. Franconeri: nothing to disclose
D. de Benedetto: nothing to disclose
C. Bellini: nothing to disclose
M. C. Masciotra: nothing to disclose
F. Di Naro: nothing to disclose
R. Trapasso: nothing to disclose
J. Nori: nothing to disclose
V. Miele: nothing to disclose
G. Bicchierai: nothing to disclose

RPS 1002a-7 11:51

Evaluation of contrast-enhanced digital mammography (CEDM) in the preoperative staging of breast cancer: large-scale single-centre experience

G. Bicchierai, P. Tonelli, D. de Benedetto, F. Di Naro, D. Cirone, V. Miele, J. Nori*; Florence/IT (giulia.bicchierai@gmail.com)*

Purpose: One of the most important indications for contrast-enhanced breast imaging is the pre-surgical breast cancer (BC) staging. This is the large-scale single-centre experience evaluating the role of CEDM in pre-surgical staging. The aims of this retrospective study were to define the diagnostic performance of CEDM in the pre-surgical setting and to identify which type of patient may have a greater advantage of having CEDM.
Methods and materials: We selected 326 patients with BC who performed CEDM as preoperative staging and had breast cancer-related surgery at our institution. We analysed when CEDM led to additional imaging or biopsy and when it changed the type of surgery that was planned according to conventional breast imaging (CI) techniques (digital mammography, tomosynthesis, and ultrasound). CEDM diagnostic performance in the correct preoperative staging of BC of the whole population and into various subgroups were calculated.

Results: CEDM sensitivity for the index lesion was 98.8%, which led to additional breast imaging in 23.6% and additional biopsies in 17.5%. CEDM changed the type of surgery in 18.4%. In the preoperative BC staging, CEDM sensitivity, specificity, PPV, and NPV and accuracy resulted in 93%, 98%, 90%, 98%, and 98%, respectively. CEDM performance was better in patients with palpable lesions.
Conclusion: CEDM has an excellent diagnostic performance in the pre-surgical staging of BC. Symptomatic patients with palpable lesions benefitted most from CEDM, with a statistically significant difference.
Limitations: The most important limitations are the patient population we selected i.e. patients with histological-proven BC, not a screening population, which may have influenced the high rate of surgical change and the retrospective nature of the study.
Ethics committee approval: The local institutional review board (IRB) approved this retrospective analysis.
Funding: No funding was received for this work.
Author Disclosures:
V. Miele: nothing to disclose
G. Bicchierai: nothing to disclose
P. Tonelli: nothing to disclose
D. de Benedetto: nothing to disclose
F. Di Naro: nothing to disclose
D. Cirone: nothing to disclose
J. Nori: nothing to disclose

RPS 1002a-8 11:57

Preoperative evaluation of breast cancer: diagnostic performance of contrast-enhanced digital mammography compared to magnetic resonance imaging

C. Depretto[1], A. Liguori[1], A. Borelli[1], G. Boffelli[2], C. G. Monaco[1], F. Cartia[1], C. Ferranti[1], G. Scaperrotta[1]; [1]Milan/IT, [2]Pavia/IT
(cathie.dp@gmail.com)

Purpose: To compare the diagnostic performance of contrast-enhanced digital mammography (CEDM) and magnetic resonance imaging (MRI) in preoperative evaluations and to evaluate the effect of each modality on surgical management.
Methods and materials: From January 2018 to July 2019, 96 patients with newly diagnosed invasive breast cancer underwent CEDM and MRI. Imaging findings were correlated with pathological results and compared. The diagnostic performance in the detection of index and secondary cancers and occult contralateral cancers was compared. We also evaluated whether CEDM or MRI resulted in additional imaging and in changes in surgical management. Patients also completed a questionnaire indicating their preference between CEDM and MRI.
Results: 96 women with 113 target lesions were included in the analysis. CEDM demonstrated a similar sensitivity to MRI (96% vs 100%) in detecting target lesions. For the detection of secondary cancers in the ipsilateral breast and occult cancers in the contralateral breast, no significant differences were found between CEDM and MRI. CEDM resulted in minor false-positive results at additional imaging compared with MRI (7% vs 12%) and in minor changes in surgical management compared with MRI (19% vs 26%). 93 women replied to the questionnaire regarding the preference between CEDM versus RM and most preferred CEDM (71% vs 12%), mainly for the shorter examination time (90%).
Conclusion: CEDM demonstrated a diagnostic performance comparable with MRI in depicting index cancers, secondary cancers, and occult cancers in the contralateral breast. CEDM demonstrated minor false-positive results and minor changes in surgical management and it was preferred by women.
Limitations: We have only one set of preliminary results.
Ethics committee approval: This single-centre prospective study was approved by the Institutional Review Board and informed consent was obtained from all patients.
Funding: No funding was received for this work.
Author Disclosures:
C. Depretto: nothing to disclose
A. Liguori: nothing to disclose
A. Borelli: nothing to disclose
G. Boffelli: nothing to disclose
C. G. Monaco: nothing to disclose
F. Cartia: nothing to disclose
C. Ferranti: nothing to disclose
G. Scaperrotta: nothing to disclose

RPS 1002a-9 12:03

Contrast-enhanced digital mammography (CEDM) for monitoring the response of breast cancers to neoadjuvant chemotherapy: a comparison with MRI

D. Bernardi[1], A. Acquaviva[2], M. Valentini[3], V. Sabatino[3], M. Pellegrini[3], C. Fantò[3]; [1]Milan/IT, [2]Naples/IT, [3]Trent/IT
(Daniela.Bernardi@humanitas.it)

Purpose: To compare the performance of CEDM and MR in estimating the response to neoadjuvant chemotherapy (NAC) and assessing the size of the residual tumour.
Methods and materials: 63 women who underwent NAC for breast cancer had both CEDM and MR before starting (PRE), during (MID), and at the end of NAC (POST). One radiologist looked at CEDM while another looked at MR. Both reported, for each exam and NAC step, the largest diameter of the target lesion. Response to therapy was finally classified according to RECIST criteria, comparing MID- with PRE-NAC, then POST- with MID-NAC lesion-size. Pathological results used as a reference standard for comparison with the last CEDM and MR controls. Statystical analysis: Pearson correlation and Bland Altman plot to test the agreement for measurements and Chi-square test to evaluate the agreement for RECIST classification.
Results: There was consistent correlation between CEDM and MR measurements in PRE (0.94, IC 0.90-0.96), MID (0.92, IC 0.86- 0.95), and POST-NAC (0.92, IC 0.86-0.95).
The correlation was less consistent when comparing CEDM and MR POST NAC measurements with those of pathologists (respectively 0.64, 95% CI 0.44-0.77 and 0.63, IC 95% 0.44-0.77).
Classifying the response to therapy according to RECIST criteria, there was significative agreement between CEDM and MR both at MID-NAC (88.2%, p <0.0001) and POST-NAC (84.6%, p <0.0001). Comparing POST-NAC controls with pathologist response, the agreement was higher for MR (84.6%, p <0.0001) compared to CEDM (77%, p <0.0001).
MR showed significant higher sensitivity (79% vs 69%) and specificity (100% vs 91%) than CEDM in assessment complete response (CR)
Conclusion: CEDM performed similarly to MR in evaluating the response to NAC and may represent an alternative in case of contraindications or when MR is not available.
Limitations: A single-institution experience.
Ethics committee approval: IRB approval.
Funding: No funding was received for this work.
Author Disclosures:
D. Bernardi: nothing to disclose
C. Fantò: nothing to disclose
M. Valentini: nothing to disclose
A. Acquaviva: nothing to disclose
V. Sabatino: nothing to disclose
M. Pellegrini: nothing to disclose

RPS 1002a-10 12:09

Contrast-enhanced spectral mammography with a compact synchrotron source

L. Heck[1], M. Dierolf[1], T. Sellerer[1], K. Mechlem[1], B. Günther[1], S. Metz[2], D. Pfeiffer[2], K. Kröninger[3], J. Herzen[1]; [1]Garching/DE, [2]Munich/DE, [3]Dortmund/DE

Purpose: Contrast-enhanced spectral mammography (CESM) based on K-edge subtraction (KES) helps to identify uncertain findings in standard mammography. As CESM requires two acquisitions, dose reduction is a crucial issue. Here, two dual-energy dose-compatible CESM approaches were evaluated with a compact synchrotron source.
Methods and materials: In this study, two CESM techniques, the commonly used dual-energy KES imaging and a two-material decomposition, were evaluated at a quasi-monochromatic compact synchrotron x-ray source. For a better comparison to the laboratory results, clinical CESM images were performed. Low-energy attenuation-based images were acquired and images showing the contrast agent iodine were calculated with a modified mammographic accreditation phantom in both the clinical and the laboratory measurements.
Results: Confirmed by a higher contrast-to-noise ratio (CNR) and spatial resolution, improved image quality was achieved with both the aforementioned iodine image calculation methods. The spectral approach achieved even better results than KES. We demonstrate the reduction of the applied dose by up to 66% compared to the clinically applied dose at equal CNR. Additionally, the image quality of the laboratory results of the low-energy images also increased compared to the clinical examinations.
Conclusion: Our findings regarding the CNR and the spatial resolution suggest the great potential of the two-material decomposition approach as a means to improve the diagnostic quality and to reduce the dose in clinical examinations.
Limitations: This study suffers from the time-consuming energy change of the compact synchrotron x-ray source which takes about 30 minutes but can be reduced to a few seconds in the future. In addition, the energies could be optimised by oscillating directly around the absorption K-edge.
Ethics committee approval: n/a
Funding: Cluster of Excellence Munich-Centre for Advanced Photonics MAP, DFG EXC-158; Center for Advanced Laser Applications (CALA); DFG Research Training Group GRK 2274.

Author Disclosures:
K. Kröninger: nothing to disclose
L. Heck: Speaker at Technische Universität München, Author at Technische Universität München
M. Dierolf: nothing to disclose
T. Sellerer: nothing to disclose
K. Mechlem: nothing to disclose
B. Günther: nothing to disclose
S. Metz: nothing to disclose
D. Pfeiffer: nothing to disclose
J. Herzen: nothing to disclose

RPS 1002a-11 12:15
Dedicated spiral breast CT with a single-photon counting detector: initial results of the first 300 women
N. Berger, M. Marcon, T. Frauenfelder, A. Boss*; Zurich/CH*

Purpose: Initial clinical experiences using a dedicated spiral-breast CT (B-CT) with a single-photon counting detector.
Methods and materials: 300 consecutive women undergoing B-CT were evaluated on the reason of assignment for B-CT instead of mammography, a detection rate of breast cancer and, quality criteria of data acquisition. Furthermore, the number of additional ultrasound examinations due to unclear findings or dense breast tissue and reliability of the technical data acquisition were assessed.
Results: 591 B-CT acquisitions in 300 women were performed. The lack of breast compression (254 of 300, 84.7%) was the main reason to choose this method over mammography, which was desired due to personal reasons or mastodynia. 10 patients (0.3%) had implants hampering mammography. 102 possible lesions were detected in B-CT, including 4 cases of breast cancer (1.3% of all patients). Additional ultrasound was performed in 226 patients (102 due to detected lesions and 124 due to dense breast tissue). 3 malignant lesions were detected in an additional ultrasound (1% of all patients). As quality-criteria, the pectoralis muscle was included in 341 of 591 examinations, but a complete assessment of breast tissue was only possible in 149 examinations. No movement artifacts were noted. In 99% of all women, the examination could be realised.
Conclusion: The dedicated B-CT provides high-quality images and can be used as an alternative, in particular in those patients not otherwise willing to perform mammography because of the breast compression.
Limitations: Single-centre and retrospective study.
Ethics committee approval: The institutional review board approve this retrospective study.
Funding: No funding was received for this work.
Author Disclosures:
N. Berger: nothing to disclose
M. Marcon: nothing to disclose
T. Frauenfelder: nothing to disclose
A. Boss: nothing to disclose

RPS 1002a-12 12:21
Optimisation of photon-counting breast CT for spectral single-scan contrast-enhanced imaging: a phantom study
V. Ruth, D. Kolditz, C. Steiding, W. A. A. Kalender*; Erlangen/DE*

Purpose: Optimising the settings of a photon-counting breast CT (pcBCT) for spectral contrast-enhanced imaging from a single scan and evaluating the accuracy according to iodine quantification and the creation of virtual-unenhanced images (VNC).
Methods and materials: The settings of a pcBCT with 100µm detector element size and integrated charge-sharing correction were adapted to maximize the signal to noise ratio (SNR) between the contrast agent and soft tissue. Therefore, the energy threshold separating the x-ray spectrum was swept from 23.1keV to 50.6keV. Validation measurements were performed with contrast agent samples (2.5 to 25mg Iodine/ml) in phantoms with a 7.5 cm and 12 cm diameter. Iodine maps and VNC images were generated from a single scan using image-based material decomposition. Iodine concentrations and CT values were measured and compared to the known concentrations and reference CT values.
Results: Spectral single-scan contrast-enhanced pcBCT was feasible. Maximal SNRs were found at a threshold position of 32.5keV. Accurate iodine quantification (average RMSE of 0.56mg/ml) was possible down to 2.5 mg Iodine/ml. Minor changes of CT values compared to non-enhanced CT scans were observed in the VNC images -1.2±21.6HU and 4.9±67.4HU (7.5 and 12 cm phantom). The noise was increased by the decomposition by a factor of 2.62 and 4.87 (7.5 and 12 cm phantom) but did not compromise accurate iodine quantification.
Conclusion: Accurate iodine quantification and the creation of VNC images can be achieved using contrast-enhanced pcBCT from a single CT scan under the complete absence of temporal or spatial misalignment. Using iodine maps and VNC images, pcBCT has the potential to reduce dose, shorten examination and reading time, and to increase cancer detection rates.
Limitations: The CT scans presented were performed on a bench testing model of a commercially available pcBCT system.
Ethics committee approval: n/a
Funding: No funding was received for this work.
Author Disclosures:
V. Ruth: Employee at AB-CT - Advanced Breast-CT GmbH
D. Kolditz: Employee at AB-CT - Advanced Breast-CT GmbH
W. A. A. Kalender: Founder at AB-CT - Advanced Breast-CT GmbH
C. Steiding: Employee at AB-CT - Advanced Breast-CT GmbH

11:15 - 12:30 **Studio 2020**

Physics in Medical Imaging

RPS 1013

Advances in MRI

Moderators:
N.N.

RPS 1013-K 11:15
Keynote lecture
D. J. Lurie*; Aberdeen/UK (d.lurie@abdn.ac.uk)*

Author Disclosures:
D. J. Lurie: nothing to disclose

RPS 1013-1 11:25
Motion correction for super resolution 2D multislice MRI: application to prostate
S. Riederer, E. Borisch, R. Grimm, S. Kargar, A. Kawashima*; Rochester, MN/US (riederer@mayo.edu)*

Purpose: Describe how slice-to-slice displacement occurring in 2D multi-slice acquisition of overlapped slices can be corrected, allowing high quality reformats in other orientations.
Methods and materials: Super-resolution is a method which provides improved through-plane resolution in a 2D acquisition by using input data comprised of overlapped slices. T2-weighted spin-echo (T2SE) imaging is typically acquired in multiple passes to avoid slice-to-slice interference. The resultant e.g. axial images can be reformatted into other orientations, e.g. sagittal or coronal. For static objects, this can be effective. However, for subtle (≈1 mm) motion as in T2SE of the prostate, the reformats can have objectionable “scalloping” artefact. Here we describe a correction algorithm. Because consecutive axial slices are overlapped, they are highly correlated. Using cross-correlation we determine and correct for slice-to-slice displacement between adjacent slices. The knowledge that subsets of slices are acquired within the same pass allows additional constraints on the correction. The method was assessed in 16 patients undergoing prostate MRI. Each was imaged using 78 3-mm thick slices with 2 mm slice-to-slice overlap. Slice sets with and without motion correction were subjected to super-resolution processing, and sagittal reformats were evaluated for artefact inhibiting visualisation of the margin between the prostate and anterior rectal wall.
Results: In 13 of the 16 studies, the level of the artifact was reduced modestly or significantly. Plots displacements, used for correction, from a fiducial (X, Y) mean value in the transverse direction of all 78 slices acquired. Figure 2 compares sagittal reformats using uncorrected (left) and corrected (right) axial image sets.
Conclusion: Retrospective motion correction of T2SE axial images of the prostate allows high-resolution artefact-suppressed reformatting in other orientations.
Limitations: Limited number of studies.
Ethics committee approval: This study was approved by the IRB.
Funding: This work was funded (NIH RR018898).
Author Disclosures:
S. Riederer: nothing to disclose
E. Borisch: nothing to disclose
R. Grimm: nothing to disclose
S. Kargar: nothing to disclose
A. Kawashima: nothing to disclose

RPS 1013-2 11:31

Dynamic contrast-enhanced magnetic resonance imaging during free breathing for hepatic lesions: clinical applicably and limitations

M. C. Langenbach[1], L. Basten[2], D. Maintz[1], T. J. Vogl[2], T. Gruber-Rouh[2], J.-E. Scholtz[2], B. Kaltenbach[2]; [1]*Cologne/DE,* [2]*Frankfurt am Main/DE (marcel.langenbach@me.com)*

Purpose: To evaluate the clinical applicability and limitations of this new prototype volume-interpolated breath-hold examination (VIBE) with compressed sensing (VIBEcs) for rapid multiphase MRI with a free selectable variable temporal resolution for hypervascularised hepatic lesions.
Methods and materials: Twenty patients with hypervascularised hepatic lesions were included in this prospective study and underwent contrast-enhanced liver MRI at 3T. In all patients, VIBEcs was used for rapid arterial multiphase imaging. Results were analysed regarding image quality and clinical applicability of the dynamic lesion evaluation. Evaluation of image quality, visibility and conspicuity were performed by three independent radiologists, each with more than 5 years of experience, based on a 5-point Likert scale (5=excellent). Results were correlated with the lesion entity. Limitations for the use of VIBEcs in image acquisition were defined. Time curves of dynamic contrast enhancement were plotted for each patient and quantification of attenuation performed to isolate the optimal time-point for image acquisition.
Results: All patients were successfully evaluated. Individual setting of acquisition time point (best point 40.6 seconds) instead of fixed delay allowed high reading scores for image quality, visibility and conspicuity for all lesions (mean score >4). Lesion entity showed no significant impact on the reading performance (p=0.765). The limitation was defined as follows: small lesion size (<8mm), subdiaphragmatic localisation, large necrotic area (>80% of the lesions).
Conclusion: Free-breathing MRI with VIBEcs allows image acquisition with high temporal and spatial resolution using individual acquisition time points during contrast phase to gain optimal results with a robust acquisition protocol.
Limitations: The intention was to test the feasibility. Small patient cohort and a single centre.
Ethics committee approval: The study protocol was approved by the institutional review board. Written obtained consent was obtained by all patients prior to inclusion.
Funding: No funding was received for this work.
Author Disclosures:
L. Basten: nothing to disclose
M. C. Langenbach: nothing to disclose
D. Maintz: nothing to disclose
T. J. Vogl: nothing to disclose
T. Gruber-Rouh: nothing to disclose
J.-E. Scholtz: nothing to disclose
B. Kaltenbach: nothing to disclose

RPS 1013-3 11:37

Radiomics and 3T DCE-MRI in breast cancer: is it possible to predict the response to neo-adjuvant chemotherapy?

C. Cavedon, M. V. Bisighin, G. Benetti, C. Zerbato, L. Camera, S. A. Montemezzi; *Verona/IT (carlo.cavedon@aovr.veneto.it)*

Purpose: To obtain a predictive model based on MRI radiomic features for classification of new patients between responders and non-responders to neo-adjuvant chemotherapy (NAC).
Methods and materials: 60 patients who underwent pre-NAC 3T DCE-MRI and NAC due to breast cancer between January 2015 and October 2018 were included in the study. Two radiologists contoured the lesion in both the pre-contrast and third DCE-MRI scan with a semi-automatic tool. Images were resampled with square voxels (0.9 mm). 214 radiomic features were extracted for each patient, including textural metrics of GLCM, GLRLM, GLSZM, NGTDM and GLDM. Least absolute shrinkage and selection operator (LASSO) was used to select the most suitable grey-level quantization and for feature reduction. Logistic regression and support vector machine (SVM) were used to build a model based on the most significant features. The performance of the multivariable models was assessed by means of ROC analysis, using a leave-one-out cross-validation.
Results: Features including sphericity of the lesion, kurtosis and several higher order metrics turned out to be correlated with the radiological complete response to NAC ($p<0.05$). The multivariable logistic model, built with the 8 LASSO-selected features, showed sensitivity, specificity, and area under the ROC curve of 0.74, 0.79, and 0.76, respectively, whereas for the SVM model they were 0.67, 0.88, and 0.80.
Conclusion: The presented predictive model provides an indication on the potential of 3T DCE-MRI-based radiomics to predict NAC outcome. Even though the sensitivity of the model is not high enough to grant clinical use, it can provide a substantial support on decision making.
Limitations: This is a single-institution study.
Ethics committee approval: This study was approved by the institutional review board of the "Azienda Ospedaliera Universitaria Integrata - Verona".
Funding: No funding was received for this work.
Author Disclosures:
C. Cavedon: nothing to disclose
M. V. Bisighin: nothing to disclose
G. Benetti: nothing to disclose
C. Zerbato: nothing to disclose
L. Camera: nothing to disclose
S. A. Montemezzi: nothing to disclose

RPS 1013-4 11:43

A correction of MR field non-uniformity dedicated to breast imaging

F. Khalid[1], P. Akl[2], D. Sebbag Sfez[2], C. Malhaire[2], F. Frouin[1]; [1]*Orsay/FR,* [2]*Paris/FR (frederique.frouin@inserm.fr)*

Purpose: The aim of the study was to compensate for MR field non-uniformities of breast MRI on retrospective data sets, a prerequisite step to compute robust radiomic features.
Methods and materials: The N4ITK algorithm, widely used to correct for bias field in brain studies, was tested on breast images. As the preset values of the hyperparameters (adapted to cerebral MRI) were not relevant for breast, a grid search of hyperparameters was applied to define corrections relevant for different types of MR breast images. The method was applied to T1-weighted images acquired on a breast phantom and a retrospective dataset of 41 T1-weighted DCE MRI, acquired in our institution with a 1.5 T Magnetom MRI scanner, using two different coils. The impact of the correction was assessed by computing relative image intensities variation between left and right normal tissues in the pectoral muscles (PMr) and the healthy breast parenchyma (BPr), and in the inner and outer layers in the phantom.
Results: New default parameters of N4ITK (5 fitting levels, 50 iterations, mask on the breast region) were necessary for bias field correction. The comparison of PMr and BPr values before and after correction showed a significant reduction after N4ITK (p-value =0.05 for PMr, $< 10^{-5}$ for BPr). Similar trends were found on the phantom images.
Conclusion: Retrospective studies need a posteriori algorithms to correct for spatial non-uniformity. Optimised values of N4ITK correction were proposed for breast MRI. Even if perfectible, this fully automatic solution is already useful and should be easily embedded in further radiomic studies.
Limitations: Further investigations should characterise bias fields for each coil.
Ethics committee approval: Institutional Review Committees approved this retrospective study and waived informed consent.
Funding: No funding was received for this work.
Author Disclosures:
C. Malhaire: nothing to disclose
F. Frouin: nothing to disclose
F. Khalid: nothing to disclose
P. Akl: nothing to disclose
D. Sebbag Sfez: nothing to disclose

RPS 1013-5 11:49

Investigation of radiomic features repeatability and reproducibility in MRI with a dedicated pelvis phantom

L. Bianchini[1], J. Santinha[2], N. Loucao[2], F. Botta[1], D. A. Origgi[1], M. Cremonesi[1], N. Papanikolaou[2], A. Lascialfari[1]; [1]*Milan/IT,* [2]*Lisbon/PT (linda.bianchini@unimi.it)*

Purpose: The aim of this study was to evaluate the repeatability and the reproducibility of radiomic features on two 1.5 T MRI scanners of different vendor.
Methods and materials: T_2-weighted images of a dedicated pelvis phantom were acquired on scanner A, repeating the acquisitions 10 times without changing the sequence parameters. The phantom was repositioned and the acquisitions repeated. 16 regions of interest were drawn on the phantom inserts. PyRadiomics was used to normalise images and extract radiomic features on original and filtered images. The phantom was acquired on scanner B and the procedure repeated in the same way. To test repeatability - with and without phantom repositioning - the interclass correlation coefficient (ICC) for an absolute agreement was calculated pairwise for each radiomic feature comparing the acquisitions intra-scanner. In order to test reproducibility, the ICC (consistency and absolute agreement) was determined to compare the acquisitions inter-scanner.
Results: Repeatability: the features showing excellent repeatability (ICC > 0.9) were on average 97% for scanner A and 92% for scanner B (no repositioning). The features showing excellent repeatability when repositioning the phantom were 24% (scanner A) and 36% (scanner B). Reproducibility: the features with excellent consistency and agreement were 19% and 10% of the total

respectively. The most stable features were those extracted from wavelet filtered images and belonging to the first order and glrlm categories.
Conclusion: The radiomic features showed excellent repeatability when the experiment was performed without any variation. However, less than a quarter of the features proved excellent repeatability when the phantom was repositioned. A selection of the reproducible features should be carried out in case of multicentric studies, given the low reproducibility observed comparing two different scanners.
Limitations: n/a
Ethics committee approval: n/a
Funding: No funding was received for this work.
Author Disclosures:
L. Bianchini: nothing to disclose
J. Santinha: nothing to disclose
N. Loucao: Employee at Philips Healthcare
F. Botta: nothing to disclose
M. Cremonesi: nothing to disclose
D. A. Origgi: nothing to disclose
N. Papanikolaou: nothing to disclose
A. Lascialfari: nothing to disclose

RPS 1013-6 11:55

Transchelation of gadolinium ions from GBCA to glycosaminoglycans: linear vs macrocyclic GBCA

P. Schuenke, P. Werner, M. Taupitz, L. Schröder*; Berlin/DE (schuenke@fmp-berlin.de)*

Purpose: Several studies reported that gadolinium (Gd) can be retained in various tissues in patients treated with Gd-based contrast agents (GBCA). However, the exact mechanism of Gd deposition in tissue is not fully understood. In this study, we quantitatively investigate the transchelation of Gd ions from GBCA to glycosaminoglycans (GAGs) as a potential explanation for observed long-term enhancements in vivo.
Methods and materials: Linear and macrocyclic GBCAs were dissolved in water and GAG solutions with different concentrations of $ZnCl_2$. Using a saturation recovery MRI sequence, ROI-averaged, quantitative, time-resolved R_1 values were extracted from T_1-weighted image series. All MR measurements were performed on a 9.4T preclinical MRI system (Bruker, Germany).
Results: Using MR relaxometry, the release of Gd ions from GBCA was quantified and the higher stability of macrocyclic GBCAs was confirmed. The individual contributions to observed relaxation rates could be quantified. Further, the chelation of Gd ions in GAGs was proven using MR relaxometry and confirmed by means of isothermal titration calorimetry (ITC) measurements. The relaxivities of resulting Gd-GAG complexes were determined and found to be about eight times higher compared to GBCAs. At a physiological $ZnCl_2$ concentration (2 mM), about 20% of Gd ions were shown to be translated from Gd-DTPA to GAGs.
Conclusion: We could prove the transchelation of Gd ions from (linear) GBCA to glycosaminoglycans, which are ubiquitous in the human body. The fact that the resulting Gd-GAG complexes have very high relaxivities means that small amounts (~20% of linear GBCA dissociated) can have huge effects on T_1-weighted contrasts and thus could be an explanation for the observed long-term enhancements in vivo.
Limitations: The simple model system does not fully describe the in vivo situation.
Ethics committee approval: n/a
Funding: No funding was received for this work.
Author Disclosures:
P. Schuenke: nothing to disclose
M. Taupitz: nothing to disclose
P. Werner: nothing to disclose
L. Schröder: nothing to disclose

RPS 1013-7 12:01

Diffusion tensor distribution imaging: a novel framework for quantifying microscopic tissue heterogeneity in brain tumours

J. P. de Almeida Martins[1], S. Lasic[1], Y. Zheng[2], Q. Wei[3], S. Li[4], W. Sun[4], H. Xu[4], D. Topgaard[1]*; [1]Lund/SE, [2]Houston, TX/US, [3]Shanghai/CN, [4]Wuhan/CN (daniel.topgaard@fkem1.lu.se)*

Purpose: Conventional diffusion tensor imaging (DTI) metrics are challenging to interpret in terms of specific tissue properties. Here, we address this problem by designing novel acquisition and analysis protocols that quantify the sub-voxel composition of the living brain with nonparametric diffusion tensor distributions (DTDs).
Methods and materials: We used a UIH uMR 790 3T MRI system to scan three patients with biopsy-proven pathologies: meningioma, glioblastoma, and intracranial cyst. Data was acquired with a custom diffusion-weighted EPI sequence in less than five minutes and converted to voxel-wise DTDs using a model-free inversion algorithm. The spatially-resolved DTDs were converted to a novel set of 15 parameter maps informing about the diffusivity, anisotropy, and orientation of the microscopic tissue environments.
Results: Healthy tissues are all characterised by distinctive distributions that accurately capture their corresponding diffusion properties; white-matter: low diffusivity, high anisotropy; grey-matter: low diffusivity, low anisotropy; cerebrospinal fluid: high diffusivity, low anisotropy. The investigated pathologies showed different diffusion properties: meningioma presents low diffusivity and high anisotropy, glioblastoma exhibits low diffusivity and low anisotropy, and intracranial cyst displays an isotropic core enveloped by anisotropic tissue. Maps derived from the DTDs allowed a compact visualisation of sub-voxel composition and displayed good agreement with the expected tissue properties.
Conclusion: The proposed framework with spatially-resolved DTDs is capable of resolving and characterising sub-voxel tissue environments that are indistinguishable in conventional DTI. The novel statistical maps derived from the distributions displayed good contrast between different tissues types and provided valuable insight into the structural properties of the studied pathologies.
Limitations: This pilot study is limited by the low number of investigated patients.
Ethics committee approval: Study approved by the institutional review board of the Wuhan University Hospital.
Funding: Work funded by Random Walk Imaging AB and United Imaging Healthcare.
Author Disclosures:
D. Topgaard: Shareholder at Random Walk Imaging AB
S. Lasic: Employee at Random Walk Imaging AB
Y. Zheng: Employee at United Imaging Healthcare
Q. Wei: Employee at United Imaging Healthcare
S. Li: nothing to disclose
W. Sun: nothing to disclose
H. Xu: nothing to disclose
J. P. de Almeida Martins: Employee at Random Walk Imaging

RPS 1013-8 12:07

Diffusion-tensor imaging, fibre tracking: differences between probabilistic and deterministic approaches for neurosurgical planning

L. Berta, D. Lizio, L. Gennari, M. Rizzi, C. Regna Gladin, E. Marcati, M. Cenzato, G. Lo Russo, A. Torresin*; Milan/IT (alberto.torresin@unimi.it)*

Purpose: The reconstruction of fibre tracts (FT) of white matter in the brain from diffusion tensor imaging (DTI) data is daily performed at our centre for neurosurgery and stereo-electroencephalography planning in epilepsy patients. Aim of this study is to compare two different algorithms for FT.
Methods and materials: We selected 16 patients planned for neurosurgery and acquired with an echo-planar imaging sequence using a receive coil head SENSE 8-channel on a Philips Achieva 1.5T scanner (64 directions, b-value 1000mm^2/s). Cortico-spinal tracts were reconstructed with different algorithms using the same input data (i.e. DTI images and regions of interest for seed and waypoints). We used Intellispace Portal v8.0 (Philips Healthcare), a commercial platform for medical image management with a module for the deterministic reconstruction of FT, and the probabilistic algorithm PROBTRACKX by FSL v5.0.6, a free-distributed software for analysis of MRI brain images (https://fsl.fmrib.ox.ac.uk/fsl/fslwiki). For each patient, the tracts were compared in terms of the distance of their centre of gravity (DCoG) and Dice index (DI) calculated within each axial slice of the brain peduncle (BP), internal capsule (IC) and cerebral cortex (CC).
Results: The average DCoG in the BP, IC and CC were, respectively 5.2, 5.5, 9.3mm. The average DI values for the same anatomical sites were 30%, 43%, 12% with values within 0% and 70%, meaning a partial or absence of overlap of the FT reconstructed with the two methods.
Conclusion: The two algorithms for FT shows geometrical differences that cannot be ignored and should be discussed with the neurosurgery team.
Limitations: Clinical validation of FT reconstructed from DTI acquisition with neurophysiological data is mandatory.
Ethics committee approval: n/a
Funding: No funding was received for this work.
Author Disclosures:
L. Berta: nothing to disclose
A. Torresin: nothing to disclose
D. Lizio: nothing to disclose
L. Gennari: nothing to disclose
C. Regna Gladin: nothing to disclose
E. Marcati: nothing to disclose
M. Rizzi: nothing to disclose
M. Cenzato: nothing to disclose
G. Lo Russo: nothing to disclose

RPS 1013-9 12:13

Orientation-resolved means of diffusivities and transverse relaxation times in heterogeneous brain tissue

A. Reymbaut[1], J. de Almeida Martins[1], C. Tax[2], F. Szczepankiewicz[1], D. Jones[2], D. Topgaard[1]; [1]*Lund/SE,* [2]*Cardiff/UK*
(alexis.reymbaut@fkem1.lu.se)

Purpose: In white matter, the millimetre-scale resolution of diffusion MRI may encompass myelinated axons and unknown fractions of grey matter, cerebrospinal fluid, or pathological tissue. To tackle this heterogeneity, conventional approaches rely on assumptions regarding tissue properties. This work combines novel MRI acquisition and processing methods to extract voxel-scale nonparametric 5D distributions of diffusion tensors (microstructure) and T_2 (chemical composition) without the use of limiting assumptions. Orientation-resolved (fiber-specific) means of diffusivities and T_2 are then defined via orientation clustering within the 5D distributions.
Methods and materials: A healthy volunteer was scanned on a 3T Siemens MAGNETOM Prisma using an EPI sequence customised for tensor-valued diffusion encoding and variable echo times. A nonparametric 5D distribution of diffusion tensors and T_2 is estimated in each voxel via a Monte-Carlo inversion algorithm. This algorithm also provides uncertainty on the estimated distribution and orientation distribution functions (ODFs) of anisotropic components. Finally, orientation-resolved means of isotropic diffusivity ("size"), normalised anisotropy ("shape") and T_2 are computed using an in-house orientation-clustering algorithm.
Results: ODFs present orientations that are consistent with the known anatomy, and are estimated in all areas of the brain, including heterogeneous voxels that comprise white matter, cerebrospinal fluid and/or grey matter. In parallel, our clustering procedure yields the median and interquartile range (uncertainty) of the orientation-resolved means of sizes, shapes and T_2.
Conclusion: We tease apart intra-voxel fibres and separately characterise their respective microstructure and chemical composition. This work shows potential in the understanding and longitudinal tracking of brain development and neurodegenerative diseases.
Limitations: Pilot study limited by the low number of investigated subjects.
Ethics committee approval: Approved by the IRB of Cardiff University School of Medicine.
Funding: Work financially supported by the Swedish Foundation for Strategic Research (ITM17-0267) and the Swedish Research Council (2018-03697).
Author Disclosures:
A. Reymbaut: Employee at Random Walk Imaging AB
J. de Almeida Martins: Employee at Random Walk Imaging AB
C. Tax: nothing to disclose
F. Szczepankiewicz: nothing to disclose
D. Jones: nothing to disclose
D. Topgaard: Shareholder at Random Walk Imaging AB

RPS 1013-10 12:19

Natural abundance C13 magnetic resonance spectroscopy quantification of mono-and polyunsaturated fatty acids: influence of diet

R. Garcia-Alvarez[1], B. Bartnik-Olson[2], A. F. Rodríguez-Hernández[3], C. Modroño[3], J. L. González-Mora[3], N. Sailsuta[4]; [1]*Madrid/ES,* [2]*Loma Linda, CA/US,* [3]*Santa Cruz de Tenerife/ES,* [4]*Pasadena, CA/US (R.Garcia@ge.com)*

Purpose: Lipid composition of body fat can be a key indicator of nutritional status and other related human disorders. In vivo C13 magnetic resonance spectroscopy (MRS) enables the non-invasive study of fatty acids, notably two key unsaturated fatty acids: monounsaturated fatty acids (MUFA) and polyunsaturated fatty acids (PUFA). The purpose of this work is to utilise C13-MRS to quantify MUFA and PUFA in a cohort of healthy volunteers with well-established diets.
Methods and materials: A total of 13 carnivores (6 males, 7 females; mean age 49 ± 17 years) and 14 vegetarian (9 males, 5 females; mean age 43 ± 19 years) subjects were scanned on a clinical 3.0T GE Signa-HD scanner using a dual-tuned C13-H1 coil. The MRS acquisition consisted of a natural abundance non-decoupled C13 pulse sequence. MUFA and PUFA peaks were quantified in the frequency domain using a Marquardt fitting algorithm. Between-group differences in the PUFA/MUFA ratio were compared using a paired t-test.
Results: A non-decoupled, natural abundance C13-MRS spectrum from the calf muscle of a vegetarian subject in the region of mono and polyunsaturated lipid resonances was observed. Compared to carnivores, vegetarian subjects showed a lower PUFA/MUFA ratio (using 2-sided student t-test, p = 0.06).
Conclusion: This study demonstrated the feasibility to perform and quantify in-vivo non-decoupled natural abundance C13-MRS in the mono and polyunsaturated lipid region. PUFA/MUFA ratio differences between recruited carnivores and vegetarians were found to be non-statistically significant (p=0.06). Future work aims to increase statistical power by increasing the number of subjects. In general, this method can be used to monitor changes in lipid composition with diet.
Limitations: n/a
Ethics committee approval: All subject gave their informed consent.
Funding: No-funding was received for this work.
Author Disclosures:
R. Garcia-Alvarez: Employee at General Electric Healthcare
B. Bartnik-Olson: nothing to disclose
C. Modroño: nothing to disclose
J. L. González-Mora: nothing to disclose
A. F. Rodríguez-Hernández: nothing to disclose
N. Sailsuta: nothing to disclose

RPS 1013-11 12:25

Multimodal multi-parametric phantom of the fatty liver disease

O. Dynnyk, O. Omelchenko, O. Solodovnik, N. Marunchi; *Kiev/UA*
(Ol.Omelchenko@Gmail.Com)

Purpose: Fatty liver disease (FLD) inevitably leads to steatohepatitis, fibrosis, and cirrhosis. The main trend of FLD diagnosis by ultrasound is a multi-parametric approach (mp-US) with the simultaneous application of 4 techniques: B-mode, shear wave elastography (SWE) for fibrosis, SW dispersion for inflammatory activity (SWD), attenuation coefficient (AC) for steatosis. Proton density fat fraction (PDFF) MRI recognised as a reference method. The aim was to create multimodal training phantom for mp-US and correlation of the steatosis degree between AC and PDFF.
Methods and materials: We propose a phantom container of non-magnetic material with a filler. We used milk fat based phantoms with different fat concentration, as far as milk composed of spherical drops of triglycerides comparable to fat vacuoles in hepatocytes. 35 phantoms with different fat concentrations were studied: milk 2.5%, 3.2% and cream 5%, 10%, 12%, 15%, 20%. We simultaneously used SWE, SWD and AC by US equipment Aplio i-800 (Canon Medical) with a PVI-475BX convex probe. PDFF was performed using Titan 1.5T MRI (Canon Medical). Mass fraction of fat filler was also biochemically evaluated. Spearman's rank correlation coefficient was applied.
Results: Close correlation was obtained of the filler fat concentration between the AC (dB/cm/MHz), chemicaly mass fraction of fat (%) - 0.700 and PDFF (average value - 0.782, minimum - 0.747, maximum - 0.782), respectively.
Conclusion: A training phantom was created for the simultaneously used the mp-US technologies: SWE, SWD and AC. A high degree of correlation between the values of AC and MR-PPDF is determined our phantom as multimodal for steatomery.
Limitations: An additional variety of fat concentration might increase the accuracy of correlation.
Ethics committee approval: No patients or animals were tested in study.
Funding: No external fundings were used for the conduction of the study.
Author Disclosures:
O. Omelchenko: nothing to disclose
O. Dynnyk: nothing to disclose
O. Solodovnik: nothing to disclose
N. Marunchi: nothing to disclose

11:15 - 12:30 **Coffee & Talk 2**

Paediatric

RPS 1012a

Paediatric musculoskeletal imaging: what's new?

Moderators:
I. Barber Martinez; Esplugues De Llobregat/ES
A. Kanavaki; Athens/GR

RPS 1012a-1 11:15

Bone marrow signal on whole-body MRI in healthy asymptomatic children: a prospective observational study establishing novel reference standards

E. V. Brandis[1], P. K. K. Zadig[2], K. Rosendahl[3], D. Avenarius[2], B. Nguyen[1], L.-S. O. Müller[1]; [1]*Oslo/NO,* [2]*Tromsø/NO,* [3]*Bergen/NO (elisabeth@vonbrandis.net)*

Purpose: WBMRI enables the depiction and characterisation of diseases at an early stage and is embraced for use in children by many centres, although no studies addressing its precision, accuracy, and clinical validity are published. The signal in the bone marrow that may be interpreted as pathology is shown to be present in healthy children. We set out to examine healthy, asymptomatic children with WBMRI to establish normal reference standards for the skeleton in children.

Methods and materials: From 2018-2019, 160 volunteers 6-18 years were recruited for research-purposes only. Coronal T2dixon, T1tse, and DWI (b50 and b1000) from skull base to toes, on state of the art 1.5T scanners (Siemens and Philips), whole body-coil, no sedation, were performed. The scantime was 40-45 minutes. Scoring was performed by two radiologists in consensus, assessing the presence of signal changes suggestive of bone marrow oedema.
Results: All examinations were successful and high-quality images were obtained. Preliminary results of 80 children showed several expected and surprising signal changes that could be mistaken for pathology in a clinical setting.
Conclusion: Signal change is frequently seen on WBMRI in the skeleton of healthy children. This knowledge is crucial to avoid the overstaging of disease, particularly when assessing for lesions at a preclinical stage.
Limitations: Norway is a relatively homogeneous society regarding social status, physical activity, and body-habitus. The definition of "healthy" is challenging. The majority of children report minor intermittent musculoskeletal symptoms. We defined "asymptomatic" as no symptoms impairing everyday activity or necessitating consulting a doctor in the last 6 months. No histological correlation could be made.
Ethics committee approval: Approved by the Regional Committees for Medical Research Ethics, South East Norway, informed consent obtained from all participants/carers.
Funding: National grant (Helse Sør-Øst) for a three year PhD-program.
Author Disclosures:
E. V. Brandis: nothing to disclose
P. K. K. Zadig: nothing to disclose
K. Rosendahl: nothing to disclose
D. Avenarius: nothing to disclose
L.-S. O. Müller: nothing to disclose
B. Nguyen: nothing to disclose

RPS 1012a-2 11:21

Whole-body MRI of bone manifestations in patients with Gaucher disease type 1 after long-term treatment with enzyme replacement therapy

A. Lollert, K. Laudemann, E. Mengel, C. Hoffmann, M. Brixius-Huth, J. Hennermann, C. Düber, G. Staatz; *Mainz/DE*
(andre.lollert@unimedizin-mainz.de)

Purpose: To assess bone manifestations in patients with Gaucher disease type 1 (GD1) with whole-body magnetic resonance imaging (WB-MRI) and to evaluate the effects of different timing in initiating long-term enzyme replacement therapy.
Methods and materials: In 17 long-term treated (enzyme replacement therapy with alglucerase/imiglucerase for a median of 13 years) patients with GD1, we performed 2 WB-MRI examinations at a median interval of 13 months. MRI results were retrospectively stratified based on treatment initiation into two groups: "early" (age ≤ 12 years) and "late" (during adulthood). We assessed the occurrence of irreversible avascular necroses (AVN) and applied several semi-quantitative scores: the bone-marrow-burden (BMB) score, the Düsseldorf-Gaucher score (DGS), the vertebra-disc-ratio (VDR), and the Gaucher disease type 1 severity scoring system (GD-DS3).
Results: MRI assessments showed no AVN in the "early" treatment group. AVN were observed in 2 patients of the "late" group. The follow-up examinations showed slight improvements in the BMB-score (P=0.039), DGS (P=0.011), and VDR (P=0.047), with similar tendencies in both treatment groups. The GD-DS3 score only improved in the "late" treatment group (P=0.043).
Conclusion: The ongoing clinical value of enzyme replacement therapy with alglucerase/imiglucerase is supported by our data as WB-MRI-based scores stayed constant or slightly improved even after long-term treatment. Complications (i.e. AVN) were only observed in the "late" treatment group. The early initiation of enzyme replacement therapy may protect the bone.
Limitations: The relatively small study cohort and retrospective study design. The interval between MR examinations was rather short. However, we provided data from patients with very long treatment courses.
Ethics committee approval: Approval of the local independent ethics committee was not necessary due to the retrospective study design.
Funding: This study was financially supported by Genzyme GmbH.
Author Disclosures:
A. Lollert: nothing to disclose
K. Laudemann: nothing to disclose
E. Mengel: nothing to disclose
C. Hoffmann: nothing to disclose
M. Brixius-Huth: nothing to disclose
J. Hennermann: Research/Grant Support at Shire, Research/Grant Support at Genzyme GmbH
C. Düber: Research/Grant Support at Genzyme GmbH
G. Staatz: Research/Grant Support at Genzyme GmbH

RPS 1012a-3 11:27

Radiological investigation of suspected physical abuse in children

S. Drew[1], K. Stafford[2]; [1]*Cambridge/UK*, [2]*Camberley/UK*
(Stephdrew09@gmail.com)

Purpose: Radiological investigation should be performed where physical abuse of a child is suspected. Appropriate timely imaging is vital in view of the social and legal implications of the accompanying radiological reports. The aim of this work is to audit practice in a UK district general hospital and evaluate its adherence to national standards. These standards are set by the joint Royal College of Radiologists (RCR) and Royal College of Paediatrics and Child Health (RCPCH) publication: 'The radiological investigation of suspected physical abuse in children'.
Methods and materials: Patients who received an x-ray skeletal survey for suspected non-accidental injury from the 1st February 2017-26th March 2019 (n=27) were identified using the software Sunquest Integrated Clinical Environment (ICE). The mean age was 10 months, with a range of 11 days to 3 years and 5 months. The radiological reports and notes of these patients were analysed and used to evaluate adherence to standards.
Results: Good practice identified in this audit was that skeletal surveys were double reported 92.6% of the time. Areas requiring improvement included the speed of double reporting, attendance for the follow-up skeletal survey, and performance of CT head in the under 1-year-old group, with a follow-up MRI head and spine where indicated.
Conclusion: Improving adherence to standards requires co-operation between radiological and paediatric departments. Additional qualified radiologists can improve reporting speeds, as can appropriate outsourcing to local hospitals. Where CT or MR scans are decided against for clinical reasons, this should be clearly documented in the notes, and the integrity of 'the net' should be improved to avoid a loss to follow-up in children who are potentially at risk.
Limitations: n/a
Ethics committee approval: n/a
Funding: No funding was received for this work.
Author Disclosures:
S. Drew: nothing to disclose
K. Stafford: nothing to disclose

RPS 1012a-4 11:33

MRI patterns of muscle involvement in type 2 and 3 cohorts of patients with spinal muscular atrophy

L. Cristiano[1], T. Verdolotti[1], C. Brogna[1], T. Tartaglione[1], A. Pichiecchio[2], C. Cinnante[3], C. Colosimo[1], E. M. Mercuri[1]; [1]*Rome/IT*, [2]*Pavia/IT*, [3]*Milan/IT*
(laralu84@hotmail.it)

Purpose: To define a specific pattern of muscle involvement on MRI, assessing both fatty replacement and muscle atrophy, in a cohort of type 2 and type 3 SMA children and adults including both ambulant and non-ambulant patients.
Methods and materials: In this multicentric study, we prospectively enrolled consecutive SMA patients (March 2018-January 2019). Muscle MRI consisted of TSE/FSE T1-weighted sequences covering the entire lower limb. Each muscle was examined through its whole extension using Mercuri classification for fatty infiltration. Thigh muscles were also grouped in anterior, posterior, and medial compartments for atrophy classification.
Results: 55 patients were included and divided in 3 subgroups: 18 type 2 SMA, 11 type 3 who had lost ambulation, and 26 type 3 ambulant patients. The results showed large variability in type 2 and type 3, with various degree of proximal to distal gradient. At thigh level, the anterior compartment was more often involved while the adductor longus and other medial muscles were relatively spared. In the posterior compartment, the semitendinosus muscle was the most involved. At leg level, the soleus was predominantly involved. ANOVA was used to assess heterogeneity among different SMA types. A non-parametric Wilcoxon signed-rank test was used to compare difference according to an individual compartment.
Conclusion: Our results suggest that although there is an overall recognisable pattern of muscle involvement with abnormal signal within individual muscles associated with atrophy, there is a marked variability across patients with different age, functional level, and type of SMA. The variability observed may help to understand natural history and response to new treatments.
Limitations: A lack quantitative sequences (Dixon).
Ethics committee approval: Ethics committee approval obtained.
Funding: No funding was received for this work.
Author Disclosures:
L. Cristiano: nothing to disclose
C. Brogna: nothing to disclose
T. Verdolotti: nothing to disclose
T. Tartaglione: nothing to disclose
A. Pichiecchio: nothing to disclose
C. Cinnante: nothing to disclose
C. Colosimo: nothing to disclose
E. M. Mercuri: nothing to disclose

RPS 1012a-5 11:39

Diagnostic performance of morphometric vertebral fracture analysis (MXA) in children using a 33-point software program

F. F. Alqahtani[1], N. J. Crabtree[2], P. Bromiley[3], T. Cootes[3], P. Broadley[1], I. Lang[1], A. C. Offiah[1]; [1]Sheffield/UK, [2]Birmingham/UK, [3]Manchester/UK

Purpose: To evaluate the diagnostic accuracy of morphometric vertebral fracture analysis (MXA) using a 33-point software program designed for adults on dual-energy x-ray absorptiometry (DXA) images of children.
Methods and materials: Lateral spine DXA images of 420 children aged 5-18 years were retrospectively reviewed. VFA by an expert paediatric radiologist using Genant's SQ scoring system served as the gold standard. All 420 DXA scans were analysed by a trained radiographer, using semi-automated software (33-point morphometry). VFA of a random sample of 100 DXA was performed by an experienced paediatric clinical scientist. MXA of a random sample of 30 DXA images were analysed by 4 additional observers. Diagnostic accuracy and inter and intraobserver agreement (kappa statistics) were calculated.
Results: Overall sensitivity, specificity, false-positive (FP) and false-negative (FN) rates for the radiographer using the MXA software were 80%, 90%, 10%, and 20%, respectively, and for mild fractures alone were 46%, 92%, 8%, and 54%, respectively. Overall sensitivity, specificity, FP, and FN rates for the 4 additional observers using MXA were 89%, 79%, 21%, and 11%, respectively, and for mild fractures alone were 36%, 86%, 14%, and 64%, respectively. The agreement between the two expert observers was fair to good for VFA and MXA [kappa=0.29 to 0.76 (95% CI: 0.17-0.88) and 0.29 to 0.69 (95% CI: 0.17-0.83)], respectively.
Conclusion: MXA using a 33-point technique developed for adults is not a reliable method for the identification of mild vertebral fractures in children. A paediatric standard is required which not only incorporates specific vertebral body height ratios but also the age-related physiological changes in vertebral shape that occur throughout childhood.
Limitations: n/a
Ethics committee approval: n/a
Funding: This study funded as part of PhD project by Najran University.
Author Disclosures:
F. F. Alqahtani: nothing to disclose
N. J. Crabtree: nothing to disclose
P. Bromiley: nothing to disclose
T. Cootes: nothing to disclose
P. Broadley: nothing to disclose
I. Lang: nothing to disclose
A. C. Offiah: nothing to disclose

RPS 1012a-6 11:45

Magnetically-controlled growing rods in early-onset scoliosis: the clinical utility of ultrasound in monitoring distraction

F. Messina, F. Pucciarelli, L. Labianca, V. Giuliani, G. Moltoni, E. Rosati, D. Caruso, A. Laghi, G. Argento; *Rome/IT*
(fil.messina91@gmail.com)

Purpose: Magnetically-controlled growing rods (MCGR) are currently used as the gold standard for the treatment of progressive early-onset scoliosis (EOS) in skeletally immature patients. The goals of this study are to verify ultrasound's accuracy compared to the plain radiographs in distraction measurements and to evaluate the effectiveness of distraction procedures and determine the disparity between total length increase and programmed increase.
Methods and materials: Distraction procedure was performed at 2-monthly intervals with an increase of 3 mm in length at each occasion. At each follow-up, pre- and post-distraction assessment was performed with ultrasound and plain radiographs in order to confirm distraction length. Ultrasound evaluation was performed through two measurements with two different landmarks (called US-M1 and US-M2). Radiographic measurements were achieved on anteroposterior plain radiographs and were calibrated and corrected for magnification.
Results: 6 patients with EOS were included, 4 with a dual-rods system and 2 with a single rod. 16 distraction procedures were performed. The increase in total length compared to the planned distraction was 83.48%, measured on plain radiographs, 95.24% and 87.61%, respectively on US-M1 and US-M2 ultrasound measurements. Length increases in patients with dual rods were 75.76% on plain radiographs, 95% on US-M1, and 87.22% on US-M2, and in the case of patients with a single rod were, respectively, 98.9%, 96.67%, and 90%.
Conclusion: Ultrasound assessment in distraction measurement was as accurate as plain radiographs. The US-M1 landmark was found to be more reliable than US-M2. Increases in rod length were 16.52% and 4.76% lower than that programmed, measured respectively with plain radiographs and ultrasound (US-M1). With reference to the value of plain radiographs, a difference was found between dual rods versus single rod groups.
Limitations: The limited number of patients in rare conditions.
Ethics committee approval: n/a
Funding: No funding was received for this work.
Author Disclosures:
F. Messina: nothing to disclose
F. Pucciarelli: nothing to disclose
L. Labianca: nothing to disclose
V. Giuliani: nothing to disclose
G. Moltoni: nothing to disclose
E. Rosati: nothing to disclose
D. Caruso: nothing to disclose
A. Laghi: nothing to disclose
G. Argento: nothing to disclose

RPS 1012a-7 11:51

Radiological and clinical prognostic factors in children with atlantoaxial rotatory subluxation/fixation

L. Lotrecchiano[1], S. Guerri[1], M. Molinari[1], P. Zarantonello[1], A. Giugliano[2], L. Ceccarelli[1], G. Vara[1], G. Facchini[1], P. Spinnato[1]; [1]Bologna/IT, [2]San Gennaro Vesuviano/IT (ludovica.2611@gmail.com)

Purpose: Atlantoaxial rotary subluxation/fixation (AARS/F) is a rare cause of torticollis in children. Patients usually present with their head fixed in rotation with some degrees of flexion ('cock-robin' head position). CT permits the diagnosing and grading of the disease.
The purpose of our study was to evaluate the correlations between radiological and clinical factors and patients' prognosis.
Methods and materials: We retrospectively reviewed all CT studies and all clinical reports from our hospital archive of children diagnosed with AARS/F in the last 15 years.
Two expert musculoskeletal radiologists reviewed all CT studies, grading AARS/F according to the Fielding-Hawkins system. Moreover, C1-C2 rotation-degrees were calculated.
The outcome assessments were positive (complete clinical/radiological recovery at three months follow-up), and negative (disease persistence or relapse at three months follow-up).
All patients were treated conservatively after diagnosis (cervical traction/neck collar).
Results: We included 53 patients (mean age=8.7y – 26F, 27M) diagnosed with AARS/F in the study. In 7/53 subjects (13.2%), a negative clinical outcome was observed.
The presence of concomitant infection or inflammation at the head and neck region (Griesel's syndrome) was significantly associated with a negative outcome (p=0.001). Fielding-Hawkins grading was also well correlated with the patients' outcome (p=0.01). C1-C2 rotation-degrees was rather associated with the outcome, without reaching statistical significance (p=0.056). The presence/absence of a traumatic event that triggered AARS/F was not correlated with the patients' outcome (p=0.171).
Conclusion: The presence of concomitant infection/inflammation at head and neck regions in patients with AARS/F is the most important prognostic factor and is associated with poorer outcomes. The Fielding-Hawkins radiological grading system well correlates with the patients' outcome.
Limitations: A retrospective study.
Ethics committee approval: n/a
Funding: No funding was received for this work.
Author Disclosures:
L. Lotrecchiano: nothing to disclose
S. Guerri: nothing to disclose
M. Molinari: nothing to disclose
P. Zarantonello: nothing to disclose
A. Giugliano: nothing to disclose
L. Ceccarelli: nothing to disclose
G. Vara: nothing to disclose
P. Spinnato: nothing to disclose
G. Facchini: nothing to disclose

RPS 1012a-8 11:57

Morphometric assessment of the face with 3D "black bone" magnetic resonance imaging in patients with juvenile idiopathic arthritis

M. J. Kupka, J. Aguet, M. W. Wagner, C. J. J. Kellenberger; *Zurich/CH*
(michaeljkupka@gmail.com)

Purpose: To evaluate the feasibility of "black bone" magnetic resonance imaging for assessing craniofacial deformity in children with juvenile idiopathic arthritis.
Methods and materials: Black bone three-dimensional gradient-echo images (flip angle 5°, submillimetre isotropic resolution) from 10 children (median age 13 years, range 2-16 years), who underwent MRI of the temporomandibular joints, were evaluated with the multiplanar reconstruction tools of SECTRA PACS and Advantage Workstation. Intra- and inter-rater reliability was

investigated for measuring the height of the mandibular ramus and condyle, basal length of the mandible, gonion angle, and mandibular inclination angle by Bland Altman analysis and intraclass correlation coefficient.
Results: Black bone images required inversion of the signal intensity and removal of air before they could be processed with standard volume rendering tools. The reliability for linear measures was best on thin minimum intensity projection images (agreement bias <1 mm , range 4 mm, ICC 0.97–0.99). The variability of angle measures was higher (agreement bias <4°, range±8°, ICC 0.99).
Conclusion: Morphometric measures of the face can be obtained from black bone MRI with comparable reliability to that reported for cone-beam CT. Black bone MRI may be considered as a radiation-free alternative to CT in children with JIA.
Limitations: The small sample size.
Ethics committee approval: n/a
Funding: No funding was received for this work.
Author Disclosures:
M. J. Kupka: Author at Kinderspital Zürich
J. Aguet: nothing to disclose
M. W. Wagner: nothing to disclose
C. J. J. Kellenberger: nothing to disclose

RPS 1012a-9 12:03

The presence of globally-decreased perfusion on post-reduction MRI does not reliably predict proximal femoral growth disturbance at midterm follow-up in developmental dysplasia of the hip

F. Schmaranzer[1], M. Ferrer[2], P. Miller[2], S. Bixby[2], Y.-J. Kim[2], E. Novais[2]; *[1]Berne/CH, [2]Boston, MA/US*

Purpose: Post-reduction perfusion MRI has been previously introduced to assess femoral head perfusion but its prognostic value is unclear. We sought to determine whether globally-decreased femoral head perfusion predicts femoral growth disturbance at a minimum of 5 years after closed/open reduction for DDH.
Methods and materials: A retrospective analysis of patients undergoing closed/open reduction for DDH and post-reduction perfusion MRI within 24 hours was conducted. 94 hips (83 patients, mean 11±4 year follow-up) had a minimum 5-year radiographic follow-up. Of these, 45/49 hips had open/closed reduction. The Kalamchi/MacEwen classification of the proximal femoral deformity was used (grade 4; total damage to femoral epiphysis, -physis, -neck) at latest the radiographic follow-up. 1.5T MRI was performed including 2D coronal-, axial PD-w, and T1-w TSE images, before/after i.v. contrast injection (0.2 mmol/l Gd-DTPA^{2-}). Femoral head enhancement was graded as normal/asymmetric/focally/globally decreased. Multivariate regression analysis was performed and the diagnostic performance calculated.
Results: At follow-up, 11 hips (12%) had femoral growth disturbance. The prevalence of globally-decreased perfusion was higher (p=0.016) in hips with (36%, 4/11) compared to hips without growth disturbance (10%; 8/75) and was independently associated with femoral growth disturbance (OR: 6.2; 95%CI, 2 to 27; p=0.014). While the negative predictive value of globally-reduced perfusion was high (92%), its positive predictive value was low (36%) in predicting femoral growth disturbance.
Conclusion: Globally-decreased perfusion on post-reduction MRI does not reliably predict proximal femoral growth disturbance in DDH at mid-term. The aetiology of femoral growth disturbance after treatment of DDH is likely a multifactorial problem not solely attributed to decreased femoral head perfusion after closed/open reduction.
Limitations: A singe-centre study at a tertiary centre.
Ethics committee approval: IRB approaval was granted under a waiver for informed consent.
Funding: No funding was received for this work.
Author Disclosures:
F. Schmaranzer: Grant Recipient at SNF
M. Ferrer: nothing to disclose
P. Miller: nothing to disclose
S. Bixby: nothing to disclose
Y.-J. Kim: nothing to disclose
E. Novais: nothing to disclose

RPS 1012a-10 12:09

Which risk factors predict hip instability or developmental dysplasia of the hip in newborns?

C. Zichichi, G. Como, I. Mauro, L. Cattarossi, R. Girometti, C. Zuiani*; Udine/IT (clara.zichichi@gmail.com)*

Purpose: To investigate which risk factors are predictive of developmental dysplasia of the hip (DDH) or hip instability (HI) in newborns using hip ultrasound (HUS)-based diagnosis.

Methods and materials: We retrospectively analysed the clinical data of 1,017 newborns who underwent HUS from August 2016-December 2018. Included patients showed dependent risk factors (familiarity, macrosomia, twins, and podalic presentation), independent risk factors (doubt or positive Ortolani manoeuvre, hip click, skin folds asymmetry, and others), or coexistence of two or more risk factors (dependent or independent) for DDH. Each hip was analysed by one of two operators with 3- and 7-years' experience, respectively, using a high-frequency linear probe and the graft technique. Patients were divided into three groups according to HUS-related categorisation (1a-1b versus 2a-2b versus >2c).
We used the χ^2 test and built two different logistic regression models to asses which risk factors were predictive of HUS categorisation 2a-2b (HI) or >2c group (DDH).
Results: HUS categorised patients as 1a-1b in 872/1017 (85.7%), HI in 126/1017 (12.4%), and DDH in 19/1017 (1.9%), respectively. On multivariate analysis, HI was independently predicted by positive Ortolani manoeuvre (OR=10.16; p<0.0001) and the coexistence of two risk factors (OR= 2.64; p=0.014), which occurred in 15/126 (11.9%) and 10/126 (7.9%) cases, respectively. DDH was independently predicted by positive Ortolani manoeuvre (OR=74.64; p<0.0001), coexistence of > 3 risk factors (OR=186.6; p<0.0001), and skin folds asymmetry (OR=10.36; p=0.037), which occurred in 8/19 (42.1%), 2/19 (10.5%), and 1/19 (5.3%) cases, respectively.
Conclusion: HI and DDH are predicted by a limited number of risk factors, suggesting that indication of HUS should be restricted accordingly.
Limitations: A monocentric and retrospective design.
Ethics committee approval: Informed consent waived because of the retrospective design.
Funding: No funding was received for this work.
Author Disclosures:
C. Zichichi: nothing to disclose
G. Como: nothing to disclose
L. Cattarossi: nothing to disclose
I. Mauro: nothing to disclose
R. Girometti: nothing to disclose
C. Zuiani: nothing to disclose

RPS 1012a-11 12:15

Single fast high-resolution 3D T1 VIBE FS MR sequence versus CT in the evaluation of tarsal coalition in children and adolescents: a reliable radiation-free alternative?

V. Caturano, A. Bartoloni, A. Magistrelli, D. Barbuti, P. Toma, A. Bozzao, M. Cirillo*; Rome/IT (ale.bartoloni@gmail.com)*

Purpose: To evaluate the accuracy of a fast MR T1 VIBE fat-saturated (FS) 3D sequence in paediatric patients with tarsal coalition compared to CT.
Methods and materials: 15 patients (age range 9-18 years; 9 females, 6 males) with a diagnosis of the tarsal coalition on x-ray and CT were included in the study.
All patients underwent 3T MRI (Siemens Magnetom Vida).
Both feet were simultaneously examined with a single volumetric T1 VIBE FS sequence (acquisition in axial plane; TR: 9.42ms, TE: 4.92 ms, and voxel size <1 mm) using an 18-channel surface coil.
The time scan for the single sequence varied between 120-150 sec, depending on the size of the feet and patient age.
Images were independently evaluated by 3 paediatric musculoskeletal radiologists and the findings were compared with CT imaging.
Results: Of the 9 patients with calcaneonavicular coalition (unilateral: 5 cases, bilateral: 4 cases), 7 had a non-osseus type and 2 had an osteofibrous type. In 1 patient, an os calcaneus secondarius was detected.
Of the 5 patients with the talocalcaneal coalition (unilateral: 3 cases, bilateral: 2 cases), 4 had a non-osseus coalition and 1 had an osseous type.
1 patient had a bilateral non-osseus coalition involving the calcaneocuboid joint.
Providing a high contrast between bone and cartilage, the single volumetric MRI sequence of our protocol (T1 VIBE FS 3D) was comparable to CT both in the diagnosis of tarsal coalition and in the assessment of its location, extent, and type (osseus/non-osseous) in all patients.
Conclusion: Paediatric patients with tarsal coalition can be accurately studied with a single T1 VIBE FS 3D MR sequence instead of CT, without radiation exposure.
Limitations: Few cases were included in the study.
Ethics committee approval: n/a
Funding: No funding was received for this work.
Author Disclosures:
A. Bartoloni: nothing to disclose
V. Caturano: nothing to disclose
A. Magistrelli: nothing to disclose
D. Barbuti: nothing to disclose
P. Toma: nothing to disclose
A. Bozzao: nothing to disclose
M. Cirillo: nothing to disclose

RPS 1012a-12 12:21
The triangular fibrocartilage complex on high-resolution 3T magnetic resonance imaging in children: what is normal?
A.-S. van der Post, S. Jens, F. Smithuis, M. Obdeijn, M. Maas*; Amsterdam/NL (a.vanderpost@amsterdamumc.nl)*

Purpose: To define normal age-related triangular fibrocartilage complex (TFCC) morphology, homogeneity, and signal intensity on high-resolution 3.0 Tesla (3T) magnetic resonance imaging (MRI) in children.
Methods and materials: This cross-sectional study included 24 healthy children, aged 12-18 years, that did not participate in wrist-loading sports more than two times a week. They underwent a 3T MRI of one wrist, including proton-density (PD)-weighted images in three planes without fat saturation and PD-weighted coronal and T2-weighted axial images with fat saturation. Morphology, homogeneity, and signal intensity of TFCC components were assessed by 3 radiologists and 1 hand surgeon independently using a standardised score form that was developed by 1 physician experienced in TFCC-research and the 4 observers with several consensus meetings and test rounds.
Results: The cohort consisted of 12 girls and 12 boys with a mean age of 13.5 (SD, 1.1). Observers were consistent in defining anatomical variants and measurements. The observers reported anatomical variations in a substantial number of children. For instance, linear vertical increased the signal with disruption of the articular disc and diffuse increased the signal of the disc not extending to the joint surface. Also, general TFCC disc morphology, proximal and distal lamina, radio-ulnar ligaments, prestyloid recess, and meniscus homologue showed anatomical variants.
Conclusion: This study shows normal TFCC variation on high-resolution 3T MRI in healthy children, such as focal articular disc perforations. When interpreting MRI of the wrist in children, it is important to be aware of the TFCC anatomy and its normal variations.
Limitations: The sample size. Observers were aware that children were healthy and asymptomatic.
Ethics committee approval: Approved by the local medical ethical committee (reference number 2014_382#B2015303).
Funding: No funding was received for this work.
Author Disclosures:
A.-S. van der Post: nothing to disclose
S. Jens: nothing to disclose
M. Maas: nothing to disclose
M. Obdeijn: nothing to disclose
F. Smithuis: nothing to disclose

11:15 - 12:30 **Room E**

Emergency Imaging

RPS 1017

Pulmonary embolism and other

Moderators:
N.N.
Z. Serafin; Bydgoszcz/PL

RPS 1017-K 11:15
Keynote lecture
N.N.

RPS 1017-1 11:25
Shifting from double-rule-out towards whole body check-up: diagnostic yield of CT in patients with suspected aortic dissection
J. Vosshenrich, G. Sommer*; Basel/CH (jan.vosshenrich@usb.ch)*

Purpose: To assess the diagnostic yield of double-rule-out-CT in patients with suspected aortic dissection in an emergency setting.
Methods and materials: A total of 437 double-rule-out-CT studies performed from 09/2018 to 09/2019 at our institution and four remote hospitals (teleradiological coverage during on-call hours), were included. All studies were ordered by the respective emergency department to rule out aortic dissection. Images were acquired according to our routine double-rule-out protocol. Final radiological reports were manually reviewed to identify diagnoses that may explain patients' symptoms noted in the order sheet (severe chest pain or chest and abdominal pain). Total numbers of vascular and nonvascular findings were calculated.
Results: In 178 patients (40.7%) at least one finding that could explain patients' symptoms was identified. Vascular pathologies represented 16.0% (70) of findings and included 26 aortic dissections (5.9%), 20 pulmonary embolisms (4.6%), 16 aortic aneurysms (3.7%), 2 intramural aortic hematomas (0.5%), 2 aortic ruptures (0.5%) and 4 Leriche syndromes (0.9%). In contrast, 128 findings (29.3%) were of nonvascular origin, i.e. 21 pulmonary (4.8%), 42 cardiac (9.6%), 58 gastrointestinal or genitourinary (13.3%) and 7 musculoskeletal pathologies (1.6%). These included a variety of neoplastic, inflammatory and infectious diseases. 259 studies (59.3%) were negative without any relevant vascular or nonvascular finding.
Conclusion: Our results suggest that suboptimal patient preselection and inflationary use of double-rule-out-CT is an emerging issue in busy emergency departments.
Radiologists thus need to be aware to regularly encounter a vast amount of relevant nonvascular findings in these exams, some of which may be more difficult to detect than usual, as double-rule-out-CT is not considered the optimal imaging protocol for these pathologies.
Limitations: Retrospective, correlation with final radiologic reports only.
Ethics committee approval: n/a
Funding: No funding was received for this work
Author Disclosures:
J. Vosshenrich: nothing to disclose
G. Sommer: nothing to disclose

RPS 1017-2 11:31
Diagnostic performance of different low-dose levels for the detection of pulmonary embolism in computed tomography
M. T. Winkelmann, S. Afat, S. Walter, E. Stock, A. B. Brendlin, A. Othman*; Tübingen/DE (moritz.winkelmann@med.uni-tuebingen.de)*

Purpose: To evaluate the effects of dose reduction on diagnostic accuracy and image quality of pulmonary angiography CT(CTPA) in adults with suspected pulmonary embolism (PE) in clinical routine.
Methods and materials: 52 consecutive patients received CTPA for suspected PE. Realistic low-dose CT images were generated using an offline software (ReconCT, Siemens Healthineers), as either filter back projections(FBP) or as ADMIRE (strength 3 or 5) with 25%, 50% and 75% of the original dose. To assess image quality (overall image quality, noise, artefacts, and sharpness) and diagnostic confidence, a five-point scale was used. Patient-based and segment-based diagnostic accuracy was calculated for LDCT-reconstruction with original dose CTPA as a standard of reference.
Results: Among 52 patients, the prevalence of acute pulmonary embolism was moderate (15.5%). The median dose-length product and effective dose for all 52 scans was 275.3±140.5 mGy·cm and 3.9±1.9mSV. Overall subjective image quality was highest for ADMIRE 5 with 75% and lowest for FBP with 25% of the original dose (median [interquartile range]:5[5]vs.3[2-3], p<0.001. Patient-based diagnostic accuracy was high for all all LDCT datasets down to 25% for ADMIRE 3+5 (sensitivity:100%, negative predictive value [NPV]: 100%), and lower for FBP with 25% dose reduction (sensitivity: 93%; [NPV]: 97%). Segment-based diagnostic accuracy was high for ADMIRE 3+5 down to 25% dose reduction (sensitivity: 91.9%, specificity: 98.9%) and lowest for FBP with 25% dose reduction (sensitivity: 87.8%, specificity: 99%). Inter-rater agreement regarding the detection of PE was almost perfect at all doses and recons (kappa>0.95).
Conclusion: Our findings indicate that radiation dose reduction down to 25% of the original data via iterative reconstruction algorithms on a 3rd generation DE-CT scanner maintained the diagnostic accuracy and image quality for the assessment of PE in CTPA.
Limitations: Retrospective study design.
Ethics committee approval: Approved by the Ethics Committee (University of Tübingen).
Funding: No funding was received.
Author Disclosures:
M. T. Winkelmann: nothing to disclose
S. Afat: nothing to disclose
A. Othman: nothing to disclose
E. Stock: nothing to disclose
A. B. Brendlin: nothing to disclose
S. Walter: nothing to disclose

RPS 1017-3 11:37
What about incidental findings on emergency CT scanners?
P. Berge, A. Darsonval, C. Nedelcu, A. Paisant, C. Aubé*; Angers/FR (pierre.berge@chu-angers.fr)*

Purpose: The objective was to evaluate the prevalence and determinants of incidental findings (IFs) on MDCTs performed for an emergency department (ED). The secondary aims were to inventory additional investigations, their benefits, side effects, costs and the final diagnoses.
Methods and materials: One thousand consecutive patients (51.9-year-old +/- 22.7, 477 women) who underwent MDCT in the ED of our institution from January 2011 to November 2011 were retrospectively included. We collected: IFs (divided into low and high clinical significance), body areas covered, availability of prior imaging, radiologist's experience and subspecialty. In the subgroup of patients followed in our institution, we recorded the additional

investigations and their outcomes. Their costs were assessed according to the French health care system.
Results: Among the 1000 included patients, 232 had at least one IF and 122 at least one IF of high clinical significance (IFCS). A significant association with the presence of at least one IF was noted for the older patient, less-experienced radiologist, no subspecialty of the radiologist, abdominopelvic area, and the absence of prior imaging. In the subgroup of 16 patients followed in our institution, two diagnoses of malignancy were made (a gastro-intestinal stromal tumour and a Bosniak IV cystic renal lesion). One iatrogenic complication occurred (an acute urinary retention following the radiofrequency ablation of the Bosniak IV kidney cyst). Cost of the additional investigations was €41,247 (with an average of €2,578 per patient).
Conclusion: IFs on emergency MDCTs were frequent, rarely severe, rarely iatrogenic and costly.
Limitations: The subgroup of patients followed in our institution was small compared to the number of patients included.
Ethics committee approval: This study was approved by our local institutional ethics review board.
Funding: No funding was received for this work.
Author Disclosures:
P. Berge: nothing to disclose
C. Aubé: nothing to disclose
A. Darsonval: nothing to disclose
C. Nedelcu: nothing to disclose
A. Paisant: nothing to disclose

RPS 1017-4 11:43
CT-aortography as the diagnostic tool to determine the instability of the arterial wall in abdominal aortic aneurysms
D. Tutova, R. Muslimov, L. Kokov*; Moscow/RU (Danifo@mail.ru)*

Purpose: The purpose of this study is to explore and to reveal specific structural changes in the aorta and surrounding tissues with CT scans, which can be regarded as signs of aortic wall instability.
Methods and materials: CT studies were performed by a 160-slice CT scanner with native and arterial contrast phases. CT data of 104 patients with confirmed abdominal aortic aneurysm (AAA) were retrospectively studied. The assessment of such signs of instability of the aortic wall was based on the following findings: hyperattenuating crescent sign, fissuration of parietal thrombotic masses, draped aorta sing, aortic bleb, and periaortic stranding. In addition, the treatment tactics of patients were also studied.
Results: According to these findings, the patients were divided into 3 groups: 1. with ruptured AAA - in 28 (26.9%) cases. 2. with unruptured AAA, with one sign of instability - in 50 (48%) cases. 10 (20%) patients from this group underwent surgical treatment. 3. with unruptured AAA, with several signs of instability - in 26 (25.1%) cases. In this group, 6 patients underwent urgent surgical treatment, and 4 non-treated patients developed a rupture of AAA in the next few days, i.e. 38.4% of the cases.
Conclusion: CT can make a quick and comprehensive diagnosis of AAA. The high frequency of occurrence of signs of instability in the ruptured AAA indicates their high prognostic significance. The combination of 2 or more signs indicates a high risk of threatening rupture, which in combination with other factors can be considered as an indication for urgent surgical treatment. The most common CT signs of instability of the AAA include hyperattenuating crescent sign, a draped aorta sing and periaortic stranding.
Limitations: n/a
Ethics committee approval: n/a
Funding: No funding was received for this work.
Author Disclosures:
D. Tutova: Author at research institute named after N.V. Sklifosovsky, Speaker at research institute named after N.V. Sklifosovsky
R. Muslimov: Author at research institute named after N.V. Sklifosovsky
L. Kokov: Author at research institute named after N.V. Sklifosovsky

RPS 1017-5 11:49
Prognostic value of CT pulmonary angiography parameters in acute pulmonary embolism.
D. Cozzi, C. Moroni, E. Cavigli, A. Bindi, V. Miele, C. Caviglioli, P. Nazerian, S. Vanni, M. Bartolucci*; Florence/IT (dilettacozzi@gmail.com)*

Purpose: Patients with acute pulmonary embolism (APE) present with a different broad spectrum of prognoses. Computed tomographic pulmonary angiography (CTPA) is the first-line test in APE diagnostic algorithm, but its correlation with short-term outcome remains not clear at all. The aim of this study is to determine if CTPA findings can predict 30-day mortality of patients with APE in the emergency department.
Methods and materials: This is a retrospective, monocentric study involving 780 patients with APE, diagnosed at the emergency department of our institution between 2010 and 2018. These CTPA findings were evaluated: embolic-obstruction burden score (Qanadli score), common-pulmonary artery trunk diameter, right-to-left ventricular ratio, diameters of the azygos vein and coronary sinus. Comorbidities and fatal/non-fatal adverse outcomes within 30 days were recorded. Troponin I values were investigated and correlated with angiographic parameters with multiple logistic regression analysis.
Results: The all-cause and APE-related 30-day mortality rates were 5.9% and 3.6% respectively. Patients who died within 30 days were older and had higher prevalence rates of malignancy. Qanadli score and all CTPA parameters correlate with Troponin I level and the presence of RVD at echocardiography (p-values< 0.0001). Instead, RV/LV ratio and coronary sinus diameter correlate with 30-day mortality (p-values< 0.005). At the multivariate-logistic regression analysis, only coronary sinus and RVD remained significant with an HR = 2.5 (95% CI 1.1-5.6) and HR = 1.9 (95% CI 0.95-3.7), respectively.
Conclusion: These results suggest that CTPA quantification of right ventricular strain is an accurate predictor of 30-day mortality. In particular, it seems that a dilated coronary sinus (> 9 mm) has an additional prognostic value in association with echocardiographic signs of right-heart disfunction and high Troponin I levels.
Limitations: n/a
Ethics committee approval: Approval for this study is in progress.
Funding: n/a
Author Disclosures:
D. Cozzi: nothing to disclose
M. Bartolucci: nothing to disclose
C. Moroni: nothing to disclose
E. Cavigli: nothing to disclose
A. Bindi: nothing to disclose
V. Miele: nothing to disclose
C. Caviglioli: nothing to disclose
P. Nazerian: nothing to disclose
S. Vanni: nothing to disclose

RPS 1017-6 11:55
Present limitations of Artificial Intelligence in the emergency setting: performance study of a commercial, computer-aided detection algorithm for pulmonary embolism
K. Mueller-Peltzer[1], G. Negrao de Figueiredo[2], C. G. Trumm[2]*; [1]Freiburg/DE, [2]Munich/DE (katharina.mueller-peltzer@uniklinik-freiburg.de)*

Purpose: Since Artificial Intelligence is moving from an experimental stage to clinical implementation, the aim of our study was to evaluate the performance of a commercial, computer-aided detection (CAD) algorithm of pulmonary CT angiograms (CTPA) regarding the presence of pulmonary embolism (PE) in the emergency department.
Methods and materials: In this retrospective study, we included all CTPA studies performed in a large emergency department over a period of 36 months, which were analysed by two radiologists experienced in emergency radiology to set a standard reference. Original reports and CAD-results were compared regarding the detection of lobar, segmental and subsegmental PE. All CAD-findings were analysed concerning the underlying pathology. False-positive (FP) CAD findings were correlated to the contrast-to-noise-ratio (CNR).
Results: Expert reading revealed PE in 182 of 1,229 patients (49% men, 10-97 years) with a total of 504 emboli. The CAD algorithm reported 3,331 findings, of those 258 (8%) were true-positive (TP) while 3,073 (92%) were FP. CAD analysis showed a sensitivity of 47% (95% CI: 33-61%) on a lobar and 50% (95% CI 43-56%) on a subsegmental level. On average, there were 2.25 FP findings per study (median 2, range 0-25). There was no significant correlation between the number of FP and CNR (Spearman's Rank Correlation Coefficient = 0.09). Soft tissue (61.0%) and pulmonary veins (24.1%) were the most common underlying pathologies of FP findings.
Conclusion: Applied on a collective of a large emergency department, the tested commercial CAD algorithm faced relevant performance challenges that need to be addressed in future CAD development projects.
Limitations: A limiting factor of our study is its retrospective single centre study design.
Ethics committee approval:
The study was approved by the local institutional review board.
Funding: No funding was received for this work.
Author Disclosures:
K. Mueller-Peltzer: nothing to disclose
C. G. Trumm: nothing to disclose
G. Negrao de Figueiredo: nothing to disclose

RPS 1017-7 12:01
The role of a computer-assisted detection algorithm for the diagnosis of peripheral pulmonary embolism
A. Richter, F. Rengier, H.-U. Kauczor, T. F. Weber*; Heidelberg/DE*

Purpose: Aim of this study was to evaluate the performance of a computer-assisted detection algorithm (CAD) for the diagnosis of peripheral pulmonary embolism (PE) using a reduced contrast material dose CT acquisition protocol.
Methods and materials: Retrospective analysis of patients referred to CT for assessment of PE from July 2018 to December 2018. Patients with evidence of central PE at CT were excluded. CT pulmonary angiograms were obtained using a dual-layer detector CT and an injection technique comprising 55 ml contrast material (iodine concentration, 350 mg/ml) and 50 ml saline chaser with 4 ml/s flow rate. PE-CAD was performed using a dedicated image processing software designed for peripheral PE detection (Philips Intellispace Portal version 10, Haifa, Israel). Test performance statistics were calculated for PE-CAD detection of peripheral emboli with a radiologists' read serving as reference standard.
Results: 130 patients were included. 21 patients with 151 peripheral emboli were diagnosed with peripheral PE using the reference standard. 20 patients with peripheral PE were correctly identified by PE-CAD. PE-CAD was false positive in 46 patients without a final diagnosis of peripheral PE. On a per-patient basis, sensitivity, specificity, negative likelihood ratio, and positive likelihood ratio for PE-CAD were 95%, 58%, 0.08 and 2.26, respectively. On a per-embolus basis, sensitivity, specificity, negative likelihood ratio, and positive likelihood ratio for PE-CAD were 60%, 33%, 1.22, and 0.89, respectively.
Conclusion: Using a reduced contrast material dose CT acquisition protocol, PE-CAD is valuable for the exclusion of peripheral PE on a per-patient basis. Use of PE-CAD as a screening tool is limited by false positive findings.
Limitations: n/a
Ethics committee approval: n/a
Funding: n/a
Author Disclosures:
A. Richter: nothing to disclose
F. Rengier: nothing to disclose
H.-U. Kauczor: nothing to disclose
T. F. Weber: nothing to disclose

RPS 1017-8 12:07

Dual-energy CT for wrist fracture patients with negative radiographs: a prospective diagnostic test accuracy study

C. F. Müller[1], K. K. Gosvig[1], H. Børgesen[1], J. S. Gade[1], M. W. Brejnebol[1], A. Rodell[2], M. C. Nemery[1], M. Boesen[3]; [1]*Herlev/DK,* [2]*Ballerup/DK,* [3]*Frederiksberg/DK*

Purpose: To evaluate dual-energy CT (DECT) in diagnosing bone marrow edema (BME) and fractures in patients with clinical suspicion of a fracture but negative radiograph.
Methods and materials: 46 consecutive adult patients (50 wrists) with recent trauma and clinical suspicion of a fracture, but negative radiograph, were prospectively enrolled between January and November 2018. Wrists were evaluated with DECT (80kV and 150kV with tin filter) and MRI (1.5T) and images read independently by four blinded readers. Presence of BME and fracture was rated per bone. Reference standard for BME was the combined reading of MRI scans by all readers; for fracture a combined reading of MRI and DECT scans by all readers. A fifth radiologist arbitrated results in case of discrepancies. Diagnostic test accuracy (DTA) was calculated per reader and for readers combined.
Results: 750 bones in 50 wrists were assessed. 52 bones (18 radius, 15 scaphoid, 19 others) had BME and 41 bones had fractures (16 radius, 11 scaphoid, 14 others). For BME detection DECT had combined accuracy 95%, sensitivity 68% and specificity 98%. For fracture detection MRI had combined accuracy, sensitivity and specificity (97%, 76% and 99%) and DECT (97%, 85%, and 99%). Sensitivity for fracture detection was higher with DECT for all readers, but McNemar's tests were not significant.
Conclusion: DECT has a very high specificity and moderate sensitivity in detecting traumatic BME of the wrist. DECT and MRI have similar high sensitivity and specificity in detecting wrist fractures and are equivalent for the workup of patients with suspected wrist fractures with negative radiographs.
Limitations: NA
Ethics committee approval: The study was approved by the regional ethical review board. All patient gave written informed consent.
Funding: This work was supported by Innovation Fund Denmark.
Author Disclosures:
C. F. Müller: Employee at Siemens Healthineers, Research/Grant Support at Innovation Fund Denmark
K. K. Gosvig: nothing to disclose
H. Børgesen: nothing to disclose
J. S. Gade: Speaker at Siemens Healthineers
A. Rodell: Employee at Siemens Healthineers
M. Boesen: nothing to disclose
M. C. Nemery: nothing to disclose
M. W. Brejnebol: nothing to disclose

RPS 1017-9 12:13

Pulmonary embolism: epidemiology, use of clinical probability scores, and correlation between clinical, radiological and analytical variables. A retrospective, single-centre study

A. J. Láinez Ramos-Bossini, M. D. C. Pérez García, F. Garrido Sanz, S. Suárez Moreno, R. Gálvez López, M. Rivera Izquierdo*; Granada/ES (ajbossini@ugr.es)*

Purpose: To evaluate factors related to pulmonary embolism (PE), the explicit use of clinical probability scores (CPSs), and relevant CT findings in patients that underwent chest computed tomography angiography (CTA) for suspected PE in our hospital.
Methods and materials: Retrospective observational study of chest CTAs ordered for suspected PE in a Spanish tertiary hospital during 2018. Epidemiological, clinical, radiological and analytical variables, and the explicit use of CPSs were analysed. Four two-level CPSs were retrospectively calculated, and guideline adherence was analysed accordingly.
Results: In total, 534 patients (52.8% women, median age: 73 years) were included. PE prevalence was 23.0%. PE-exclusive and all-cause early mortality (<6 months) in patients with PE was 15.4% and 22.8%, respectively. CPSs were explicitly used in 15.2% of all cases. D-dimer tests were ordered in 88.2% of all cases. Although significant differences were observed among scale values, most CTA orders were justified according to retrospective CPSs and standard D-dimer values. Significant differences in clinical, analytical and CT findings were observed depending on PE subtype. RV/LV ratio >1 was significantly associated with cardiac damage markers and with other CT findings of right ventricular strain.
Conclusion: Despite the poor explicit use of CPSs, our results suggest that the yield of clinical gestalt assessment may be similar to that of CPS. PE subtype and CT markers of right ventricular strain should be always included in the radiological report given their prognostic implications. Prospective studies are further required to validate our results.
Limitations: The main limitations of the study concern its retrospective nature and the fact that it was performed at one institution.
Ethics committee approval: This study was approved by our Institutional Review Board.
Funding: No funding was received for this work.
Author Disclosures:
A. J. Láinez Ramos-Bossini: nothing to disclose
F. Garrido Sanz: nothing to disclose
M. D. C. Pérez García: nothing to disclose
S. Suárez Moreno: nothing to disclose
R. Gálvez López: nothing to disclose
M. Rivera Izquierdo: nothing to disclose

RPS 1017-10 12:19

Efficiency and impact of CT in ICU patients with unknown inflammatory focus

R. Martin[1], J. A. Luetkens[2], A. Faron[2], D. K. Thomas[2], D. Kuetting[2]; [1]*Dresden/DE,* [2]*Bonn/DE (ronmartin.uni@gmail.com)*

Purpose: To evaluate the efficiency and impact of computerized tomography (CT) on diagnosis and further diagnostic/therapeutic regimen in ICU patients with fever, systemic inflammatory response syndrome (SIRS) or sepsis with unknown focus of infection.
Methods and materials: Non-ECG-gated chest/abdominal CT examinations of ICU patients (internal medicine, surgery, heart surgery, neurology/neurosurgery) were prospectively analyzed for inflammatory foci. Both CT findings and changes in diagnostic/therapeutic regimen were analyzed. Prior CT, X-Ray, MRI, ultrasound examinations, bronchioalveolar lavage and urine analysis performed during the same ICU treatment but prior to the CT, were cross-checked to verify whether foci were actually new.
Results: In 99 out of 112 (88,4%) prospectively examined patients (34,8% female, mean age 64,8 years), a total of 147 possible foci (thoracic: n=92; abdominal: n=55) were detected. Of the 147 foci (58,5% defined as definite, 41,5% as questionable), prior examinations had suspected inflammatory focus in 80 cases. CT diagnosis led to 74 changes in therapy regimen in 58 of 99 Patients (59%): change/initiation of antibiotics: 52,7%, CT guided thoracic/abdominal puncture: 21,6%, operation: 8,1%, change in patient positioning: 8,1%; other: 9,5%. In 24 patients, CT findings led to 33 diagnostic follow-ups: endoscopy: 45,5%, microbiological testing: 24,2%, additional imaging: 18,2%, others: 12,1%.
Conclusion: CT examinations in ICU patients with unknown focus of infection leads to diagnosis in most cases as well as to adaption in therapy regimen and thus should be considered in patients with obscure clinical infection.
Limitations: Further research has to be done with a higher number of CTs and patients to outline the specific role and impact of CT in patients of unknown Focus of Infection.

Ethics committee approval: The Ethics Committee of the University Clinic of Bonn approved the study.
Funding: No funding was received for this work.
Author Disclosures:
R. Martin: nothing to disclose
J. A. Luetkens: nothing to disclose
A. Faron: nothing to disclose
D. Kuetting: nothing to disclose
D. K. Thomas: nothing to disclose

11:15 - 12:30 **Room F1**

Radiographers

RPS 1014a

Radiographer role and professional challenges

Moderators:
G. N. Paulo; Coimbra/PT
M. Szczerbo-Trojanowska; Lublin/PL

RPS 1014a-1 11:15

Occupational burnout among radiographers: findings from a national survey

L. P. V. Ribeiro[1], A. M. Baltazar[2], K. B. Azevedo[2], A. F. Abrantes[2], S. Rodrigues[2], O. Lesyuk[3], R. P. P. Almeida[2], J. Pinheiro[3];
[1]Parchal/PT, [2]Faro/PT, [3]São Brás de Alportel/PT
(luispedroribeiro@hotmail.com)

Purpose: Burnout is a complex phenomenon characterised by emotional exhaustion, social detachment, and feelings of low personal achievement. In this study, we aim to establish the prevalence of burnout among radiographers and to explore the factors influencing its development.
Methods and materials: A total of 205 radiographers from the country answered the Maslach Burnout Inventory (MBI), composed of 3 dimensions: emotional exhaustion, depersonalisation, and personal achievement associated with a sociodemographic and professional characterisation questionnaire. The questionnaire was made available online and confidentiality was assured to all participants.
Results: The global internal consistency of MBI accessed by the Cronbach's alpha was 0.776. Statistically significant differences were observed between rotational shift work and depersonalisation (t=2.482; p=0.014) and personal achievement (t=2.352; p=0.020). Using the one-way ANOVA, significant differences were observed between professional experience and professional satisfaction and the three MBI dimensions. The average burnout value was 22.9 (three levels, where the middle level ranges from 34-66). Regarding the burnout dimensions, emotional exhaustion was positioned in the middle level (out of three levels), while depersonalisation and personal achievement scored the highest level.
Conclusion: Radiographers in this research suffer from burnout syndrome. Rotational shiftwork is the major cause of depersonalisation and reduces the sense of personal achievement. Professional satisfaction is negatively affected by this syndrome. High emotional exhaustion and depersonalisation, and the low sense of personal achievement, are also common among professionals that work for more years. The health promotion for healthcare professionals should be addressed by healthcare facilities across the country.
Limitations: n/a
Ethics committee approval: The ethics committee approved the study and written informed consent was obtained.
Funding: No funding was received for this work.
Author Disclosures:
L. P. V. Ribeiro: nothing to disclose
A. M. Baltazar: nothing to disclose
K. B. Azevedo: nothing to disclose
A. F. Abrantes: nothing to disclose
S. Rodrigues: nothing to disclose
O. Lesyuk: nothing to disclose
R. P. P. Almeida: nothing to disclose
J. Pinheiro: nothing to disclose

RPS 1014a-2 11:21

The radiographer's role in Italy: a national survey on the development and growth of radiographers' skills

M. Giusti[1], S. Durante[2], P. Cornacchione[3], R. Ricci[1], M. Zanardo[4], N. Persiani[1];
[1]Florence/IT, [2]Bologna/IT, [3]Rome/IT, [4]Milan/IT

Purpose: A complete overview of the radiographers' professional profile plays a fundamental role in the assessment of possible development and growth of radiographers' skills. The aim of this study was to assess the Italian radiographers' profile.
Methods and materials: The Italian Federation of Scientific Radiographers Societies (FASTeR) proposed a national online survey, including 64 questions and sub-divided into different topics. Italian radiographers count around 28,000 individuals.
Results: We obtained 872 (3.1%) answers, 480 (55%) males, 392 (45%) radiographers had been working for less than 10 years, 610 (70%) had a bachelor degree, and 358 (41%) were highly specialised with a master degree (European qualification framework level 7). A total of 602 (69%) radiographers worked mostly as an employee in the public health sector, 637 (73%) in hospitals, and 732 (84%) full-time, earning in 40% of cases between 22,001-28,000€ gross per year. Radiographers have a good knowledge of the institutional/hospital organisation chart (663, 76%) and management (knowledge of the budget) of the employment institution. Radiographers duties included the optimisation and control (680, 78%) of the technological equipment. Selected future areas of professional growth were the technological sector with new technologies development (576, 66%), as well as healthcare professions management (567, 65%).
Conclusion: When analysing the actual role and skills of Italian radiographers, it is evident that the professional responsibility will increase through scientific research, management of new technologies, and department governance in the next years.
Limitations: An Italian survey.
Ethics committee approval: n/a
Funding: This study was supported and promoted by the Italian National Radiographers Federation and Technical, Rehabilitation and Prevention Health Professions (FNO TSRM PSTRP).
Author Disclosures:
M. Giusti: nothing to disclose
S. Durante: nothing to disclose
R. Ricci: nothing to disclose
M. Zanardo: nothing to disclose
P. Cornacchione: nothing to disclose
N. Persiani: nothing to disclose

RPS 1014a-3 11:27

Advanced and consultant AHP practice: a vision for the future

N. Barlow, R. Milner*; Rotherham/UK (nicholas.barlow@nhs.net)*

Purpose: Due to increasing clinical pressures, high vacancy rates, and significant referral growth, the Rotherham NHS foundation trust (TRFT) designed and implemented a new allied health professional (AHP)-led plain film (PF) reporting service. The aim was to increase performance, reduce clinical risk, improve quality, and increase value through lower cost per report.
Methods and materials: Following the appointment of the trust's first AHP consultant, the AHP PF workforce was restructured. This included increasing the scope of practice, increasing the number of reporting sessions, delivering in-service training, providing dedicated reporting sessions, and internally promoting and training new members of staff. Key stakeholders included radiologists/radiographers, referring clinicians, patients/the public, health education institutes, local commissioning bodies, and professional colleges.
Results: Since its implementation, there have been no serious incidents, complaints, or near misses. AHP's doubled the percentage of plain film reports from 40% to 80% of the total reports undertaken. The percentage of reports by medical colleagues reduced from 35% to 5%. Based on model hospital data, TRFT now has the highest proportion of reports provided by AHP's of any secondary care acute provider. The cost per report reduced by approximately 50%.
Conclusion: The results of this service re-design are highly encouraging through high levels of accuracy, reduced risk, a significant reduction in report TaT, patient satisfaction, and cost-effectiveness. Increased staff morale and major improvements in recruitment and retention have also been encountered.
Limitations: Support from local radiologists and clinicians was significant, as the pervading biases within some professional bodies worked against the overall plan. This service design was limited to a single hospital, however, we believe this service can easily be replicated in larger trusts within Europe.
Ethics committee approval: n/a
Funding: Trainee reporting radiographer posts were partly funded by Health Education England.
Author Disclosures:
N. Barlow: Consultant at Rotherham Hospital
R. Milner: Consultant at Rotherham Hospital

RPS 1014a-4 11:33

Patterns of movement of radiographers and professional qualifications recognition across the European Union

J. G. Couto[1], S. L. Mc Fadden[2], P. Bezzina[1], P. McClure[2], C. Hughes[2]; *[1]Msida/MT, [2]Newtownabbey/UK (jose.g.couto@um.edu.mt)*

Purpose: The 2005/36/EC directive established the process for the recognition of academic qualifications between EU member states, facilitating the movement of radiographers. The aim of this study was to investigate the patterns of movement of radiographers across the EU.
Methods and materials: A review of the Regulated Professions Database (RPD) was performed for 2015-2017. Data extracted included the number of radiographers applying for recognition of qualification that achieved recognition, required compensation measures (exam or adaptation period) before recognition, or were denied recognition. The direction of professional movement across countries was also investigated.
Results: 510 radiographers achieved recognition in another EU country each year. The UK, Ireland, and Germany are the countries receiving the most radiographers annually (203, 96, and 42, respectively). Most radiographers move away from Italy, Portugal, and the UK (108, 90, and 89, respectively).
France, Italy, and Finland required a higher proportion of applicants to undergo compensation measures (94%, 83%, and 80%, respectively). The countries of origin with a higher proportion of radiographers undergoing compensation measures were Estonia, Belgium, and Bulgaria (86%, 61%, and 50%, respectively).
The applicants with the highest proportion of rejected recognitions come from Romania (14%), Germany (13%), and the Czech Republic (11%).
Conclusion: Radiographers move between all EU member states. Two patterns of movement were identified: south to north, possibly due to higher wages, and between neighbouring countries, possibly as language was not a barrier. Negative replies and compensation measures seem to be caused by differences in training or lack of regulation of the profession.
Limitations: Data was not available for 21% of the EU countries. Some of the radiographers that achieved recognition may not move.
Ethics committee approval: n/a
Funding: PhD funded by the University of Malta.
Author Disclosures:
J. G. Couto: nothing to disclose
P. Bezzina: nothing to disclose
C. Hughes: nothing to disclose
P. McClure: nothing to disclose
S. L. Mc Fadden: nothing to disclose

RPS 1014a-5 11:39

Awareness of medical radiation exposure among patients

L. P. V. Ribeiro[1], D. V. Mestre[2], R. P. P. Almeida[2], A. F. Abrantes[2], O. Lesyuk[3], S. Rodrigues[2], K. B. Azevedo[2]; *[1]Parchal/PT, [2]Faro/PT, [3]São Brás de Alportel/PT (luispedroribeiro@hotmail.com)*

Purpose: Ionising radiation is widely used to diagnose many diseases and relevant hazards are known to be an important limitation to its application. It is believed that the awareness of radiation dose value is one of the main stages in patient radiation protection. Therefore, the main goal of this study was to survey patients' current knowledge level of medical exposure to ionising radiation.
Methods and materials: A self-applied questionnaire was used and assigned to the participants. The questionnaires consisted of two main sections to evaluate the sociodemographic data and the radiation knowledge/awareness and risks associated to medical imaging procedures. A total of 181 valid questionnaires were interpreted and statistically analysed through descriptive statistics and correlation tests.
Results: Most of the respondents were aware that general radiology uses ionising radiation (94.5%). Regarding magnetic resonance imaging, 49.3% of the participants thought that it used ionising radiation. Participants were quite divided when asked who should provide radiation information (54.14% chose the physician and 45.86% the radiographer). Furthermore, 27.62% and 45.3% think that they are not exposed to radiation at home and on a plane, respectively.
Conclusion: Patients had inadequate knowledge and mistaken beliefs about various aspects of ionising radiation and its effects. To communicate effectively, it is essential to devise methods and adequate resources for radiographers to convey correct and effective information. Furthermore, it would be appropriate to include lessons about radiation and side-effects in national education programs.
Limitations: The patients' literacy.
Ethics committee approval: The ethics committee approved the study and written informed consent was obtained.
Funding: No funding was received for this work.
Author Disclosures:
K. B. Azevedo: nothing to disclose
L. P. V. Ribeiro: nothing to disclose
D. V. Mestre: nothing to disclose
R. P. P. Almeida: nothing to disclose
A. F. Abrantes: nothing to disclose
O. Lesyuk: nothing to disclose
S. Rodrigues: nothing to disclose

RPS 1014a-6 11:45

An investigation of Irish radiographers' attitudes and opinions towards taking on the role of referrers

K. Davies; *Prosperous,Co. Kildare/IE (keisha.davies@ucdconnect.ie)*

Purpose: An amendment to S.I. 256 was introduced early in 2019 giving Irish radiographers the ability to refer patients for radiological examinations. The study gathered Irish radiographers' opinions and attitudes on this change in legislation and preparedness to taking on the role of referring.
Methods and materials: The questionnaire was distributed to 154 basic and senior grade radiographers in a total of 6 regional and local/rural hospitals in Ireland. The questionnaire consisted of 3 sections: awareness of the legislation, radiographers' opinions and attitudes towards the legislation, and preparedness to take on the role of referring.
Results: The study response rate was 31% (n=48). 56% of respondents were unaware of the incoming legislative change. 76% (n=38) were in agreement with the legislative change. 58% (n=28) stated 'better workflow' as the main benefit. 'Medico-legal risks' were cited by 40% (n=19) and 27% (n=13) cited 'lack of training' as their main concerns. 67% (n=32) said they felt prepared to take on the role of referring, with 83% (n=40) stating that they would require further training before taking on the role. Ongoing CPD was cited as the most suitable form of training by 44% (n=21).
Conclusion: Irish radiographers have a positive attitude towards taking on the role of referrers and believe it will benefit patient care. Concerns about medico-legal risks and lack of training were expressed. Attempts should be made to facilitate forms of training for Irish radiographers prior to the implementation of this legislation.
Limitations: The small sample size has an impact on the generalisability of results. A response rate of greater than 95% is considered excellent and reduces the likelihood of a non-response bias (Plantly and Carson, 2010).
Ethics committee approval: UCD ethics committee approval.
Funding: No funding was received for this work.
Author Disclosures:
K. Davies: nothing to disclose

RPS 1014a-7 11:51

A national course for radiographers/radiographer students for acting as an RPO

T. S. Schroderus-Salo[1], P. Leppäsaari[2], M. Petäjäjärvi[3], T. Saloheimo[4], S. Törnroos[5], L. Walta[6], K. Vironen[7], A. Henner[1]; *[1]Oulu/FI, [2]Kuopio/FI, [3]Tampere/FI, [4]Helsinki/FI, [5]Kirkkonummi/FI, [6]Turku/FI, [7]Vasa/FI (tanja.schroderus-salo@oamk.fi)*

Purpose: EU-directive was given on 13/12/2013 (2013/59/EURATOM) and it was meant to be implemented in national legislation by the latest on 06/02/2018. In Finland, the directive was implemented on 15/12/2018. This change in legislation offers radiographers the possibility to act as radiation protection officers (RPO) in plain radiography, veterinary, dental imaging, and mammography. The purpose of this study was to evaluate the pilot execution of the course made by 6 institutions.
Methods and materials: To the pilot course built on a Moodle platform involved 7 student radiographers, 5 radiographers, 2 teacher students (radiographers), and 1 teacher. All materials were performed in a group of teachers from 6 universities of applied sciences in Finland. All lectures were recorded. Students had tasks (measuring of scattered dose, HVL, and use of different QA phantoms) to do in groups in simulation environments or at radiological departments in hospitals.
Data was collected during the course from emails, discussion areas, and at the end of the written exam. The data was analysed by qualitative content analyse methods.
Results: According to the first results of the data, students felt the workload to be quite heavy and the time period too short. The exact number of workhours are available after the exam. Physics, optimising methods, and patient dose calculations are the most difficult parts, although they should be familiar to everyone. More results will be available when the course ends.
Conclusion: This course will be included in the radiography program in all Finnish UAS and it will run 3 times per academic year. The written exam will be held at the same time in all institutions. For students, this enables the possibility for individual participation in the course.

Limitations: The pilot is a small group.
Ethics committee approval: n/a
Funding: No funding was received for this work.
Author Disclosures:
A. Henner: nothing to disclose
T. S. Schroderus-Salo: nothing to disclose
S. Törnroos: nothing to disclose
M. Petäjäjärvi: nothing to disclose
P. Leppäsaari: nothing to disclose
L. Walta: nothing to disclose
T. Saloheimo: nothing to disclose
K. Vironen: nothing to disclose

RPS 1014a-8 11:57
Patient-centred care in diagnostic radiography: perceptions of service users, service deliverers, students, and educators
M. Hardy[1], E. Hyde[2]; *[1]Bradford/UK, [2]Derby/UK (M.L.Hardy1@bradford.ac.uk)*

Purpose: To elicit the meaning of patient-centred care (PCC) from the perspectives of service users (patients), service deliverers (radiographers and managers), radiography students, and educators, and determine whether these are aligned in terms of attached importance.
Methods and materials: A 2 stage approach was adopted.
Stage 1 was a web-based attitudinal survey to explore the understanding of PCC. Respondents were asked to indicate their level of agreement to paired (positive and negative phrasing) statements. The survey content was the same across participant groups but the phrasing was tailored to the respondent group. Pre-distribution piloting ensured the suitability of the survey language and questions. Data was analysed using descriptive statistics with the impact of statement phrasing analysed using a Wilcoxon signed-rank test.
Stage 2 was focus groups and telephone interviews with volunteer participants from stage 1. Situational vignettes were developed from stage 1 responses and participants were asked to discuss these to elicit a deeper understanding of PCC priorities from the differing perspectives. The interviews were audio-recorded and transcribed verbatim before being analysed thematically to draw out key themes. These were compared and contrasted across the participant groups.
Results: While the core components of PCC identified by all groups were technical competence, dignity and privacy, and human interaction, the interpretation and meaning placed on these and their relative importance within PCC varied. Importantly, only patients identified the environment as important to PCC. Similarly, only radiographers and radiography managers identified efficiency as important.
Conclusion: Patient-centred care does not hold the same meaning for the different participant groups. In order to truly deliver PCC, the differing values and interpretations need to be aligned.
Limitations: n/a
Ethics committee approval: Ethical approval was granted by the University of Derby.
Funding: This research was funded by the UK College of Radiographers Industry Partnership scheme.
Author Disclosures:
E. Hyde: Grant Recipient at Society & College of Radiographers, UK
M. Hardy: Grant Recipient at NIHR, Board Member at British Institute of Radiology

RPS 1014a-9 12:03
Compassionate patient care in diagnostic medical imaging
J. Bleiker, K. Knapp, S. Morgan-Trimmer, S. J. Hopkins*; Exeter/UK (j.bleiker@exeter.ac.uk)*

Purpose: Compassion is a poorly understood concept in medical imaging research, but an increase in its focus was recommended in the Francis report (2013). This study aimed to conceptualise compassion in diagnostic imaging.
Methods and materials: The project was conducted from within a constructivist paradigm. 34 semi-structured interviews were conducted with a purposive sample of DI ex-patients. 5 focus groups with approximately 6 student radiographers and 1 group of post-graduate radiographers were facilitated. Data was harvested from a Twitter journal club discussion between radiographers of the author's published literature review. Data was transcribed and analysed thematically.
Results: Compassion in DI is conceptualised according to three themes constructed from the data: 1) perceptible elements of the procedure, 2) underlying qualities, skills, and abilities of radiographers, and 3) moral and ethical foundations. Perceptions of an impersonal 'production line' technical procedure can be avoided and rapport developed by developing skills and abilities in asking targeted clinical questions and explanations, particularly during the introductory stage. Offering information about patients' x-ray images during the closing stages may compassionately reduce uncertainty and anxiety. Ethical practice need not necessarily include in every interaction expressions of compassion, feelings in a radiographer of caring about their patient, or feelings in patients of being valued. Contradictory organisational values were revealed in the data with an over-emphasis on an individuals responsibility for providing compassionate care.
Conclusion: The concept of compassion has depth, with surface appearances underpinned by moral values and behaviour-motivating drivers. The findings have implications for the scope of practice around training and competence in image interpretation and could inform future interventions to re-structure the communication and interpersonal components of patient examinations in DI.
Limitations: Maintaining focus in interviews.
Ethics committee approval: UoE approval granted.
Funding: No funding was received for this work.
Author Disclosures:
J. Bleiker: nothing to disclose
K. Knapp: nothing to disclose
S. Morgan-Trimmer: nothing to disclose
S. J. Hopkins: nothing to disclose

RPS 1014a-10 12:09
The EFRS Research Hub: promoting research in radiography
L. A. Rainford, R. J. Toomey*; Dublin/IE (louise.rainford@ucd.ie)*

Purpose: The importance of radiographer involvement in research, and research in radiographer practice, has long been recognised, although there continues to be calls for further development of a research culture in the profession. Imaging research often requires access to large numbers of radiographers or other professional participants, which can be very difficult, time-intensive and expensive to achieve.
The European Federation of Radiographer Societies (EFRS) in 2019 launched the inaugural EFRS Research Hub 2019 at the European Congress of Radiology, Vienna. The Hub aims to provide radiographers and allied researchers with opportunities to conduct and take part in high-quality research, thereby raising research awareness and involvement, and expanding the professional evidence base. The development of the Hub and a summary of research outcomes to date will be provided.
Methods and materials: A venue adjacent to the Radiographers' Lounge at ECR 2019 was secured and arranged at the congress venue. 7 research projects, catering to a spectrum of radiographer participants, were devised by researchers across 3 institutions. These included projects supported the work of 2 radiographer PhD researchers. Specialist software and equipment were supplied through in-kind vendor support.
Results: The Hub 2019 attracted 249 radiographer/radiography student participants hailing from over 30 countries. These participants participated 437 times over the 7 studies. The success of the Hub is a testament to the enthusiasm of radiographers. The EFRS approved the continuation and expansion of the Hub for ECR 2020.
Conclusion: The EFRS Research Hub offers a valuable opportunity for imaging researchers, promoting a research culture in radiography. The diversity of research undertaken at ECR2020 will expand and an activity review will be disseminated.
Limitations: n/a
Ethics committee approval: n/a
Funding: Partial funding: EFRS for the Research Hub.
Author Disclosures:
L. A. Rainford: nothing to disclose
R. J. Toomey: nothing to disclose

RPS 1014a-11 12:15
Ethical evidence in radiology research
A. M. M. Quadrado, J. Figueiredo, A. Santos*; Coimbra/PT (ana.m.quadrado@gmail.com)*

Purpose: As scientific research papers produce vital benefits for society, it is of utmost importance that researchers respect ethical parameters. Thus, the distribution of the response pattern of each project to the ethical precepts, previously defined as fundamental in a scientific investigation, should be evaluated.
Methods and materials: An original observational studies checklist was produced and validated to be fulfilled with the main ethical aspects of each research paper. The study sample comprised all research projects developed in the medical imaging and radiotherapy course, in 50 research projects in the areas of radiology, radiotherapy, and nuclear medicine, in Coimbra Health School. Descriptive analysis, using qualitative nominal variables and consisting of an exploration of absolute and relative frequencies, was implemented. Data collection was accomplished in a retrospective, observational, descriptive, and exploratory manner.
Results: The majority of papers didn't reveal ethical concerns. Only about 1/3 of scientific research revealed compliance with ethical aspects. As a positive standard of compliance, there was evidence of beneficence, non-maleficence, non-discrimination, respect for anonymity, and proportionality principle. As a negative pattern of compliance, there was no proof of respect for autonomy and

individual responsibility, free, informed, express and written consent, no stigmatisation, and neither respect for privacy nor respect for confidentiality.
Conclusion: Unfortunately, this research exposes the predomination of a lack of ethical indications produced by researchers investigations, revealing ethical culture failure.
It also shows the Institutional Research Ethics Committees and the National Data Protection Commission's flaw in allowing the publication of scientific papers without ethical evidence and orientation.
Without doubt, the Institutional Review Committees should undertake the review of such investigations to safeguard the rights and well-being of stakeholders.
Limitations: A large sample size.
Ethics committee approval: n/a
Funding: No funding was received for this work.
Author Disclosures:
A. Santos: nothing to disclose
A. M. M. Quadrado: nothing to disclose
J. Figueiredo: nothing to disclose

RPS 1014a-12 12:21
Postgraduate education in radiography: what is the bigger picture?
J. M. Grehan, M.-L. Ryan, J. Last, L. A. Rainford*; Dublin/IE*
(jennifer.grehan@ucd.ie)

Purpose: The roles of allied health professionals are changing constantly and radiographers today find themselves working in one of the fastest evolving professions in healthcare. In a technology-led environment, postgraduate education alongside continuing professional development (CPD) is fundamental to ensuring competency and high standards within diagnostic imaging. Following a European-wide EFRS radiography education survey, McNulty et al (2015) raised concerns as a lack of postgraduate radiography offerings were identified. This study was conducted to gain a snapshot of the landscape of radiography postgraduate education across Europe and internationally.
Methods and materials: A single page questionnaire totalling 13 closed questions was developed, comprising 4 topic areas: demographics, working practices, postgraduate education, and funding. This was administered over 4 days to radiographers as part of the EFRS Radiographers Research Hub at the European Congress for Radiology conference 2019. 100 responses were received.
Results: Participants from 27 countries completed questionnaires. The mean number of years qualified was 14 across a range of grades. 67% of participants had postgraduate qualifications with 45% stating they used their postgraduate education daily. 55% of countries stated having senior grade radiographers in charge of modalities, while only 20% required that these senior posts have postgraduate qualifications. 37% of countries reported no formal postgraduate offerings in the modalities of CT/MR/NM/US/IR. There was no standardisation of postgraduate funding with the majority of self-funding (36%).
Conclusion: This study identified a lack of standardisation across funding, representation in radiography departments, and availability. A positive perception towards postgraduate education was noted, however, barriers identified require strategic consideration.
Limitations: Participants were professionally active and attending ECR 2019. The data represents this subset of radiographers and further research is warranted outside of a conference setting.
Ethics committee approval: n/a
Funding: No funding was received for this work.
Author Disclosures:
J. M. Grehan: nothing to disclose
L. A. Rainford: nothing to disclose
J. Last: nothing to disclose
M.-L. Ryan: nothing to disclose

11:15 - 12:30 **Room F2**

Paediatric

RPS 1012b

Advanced imaging in paediatric cancers

Moderators:
M. C. Calcagno; Catania/IT
A. S. Littooij; Leiden/NL

RPS 1012b-K 11:15
Keynote lecture
P. D. Humphries*; London/UK*

Author Disclosures:
P. D. Humphries: disclosure/affirmation information not submitted

RPS 1012b-1 11:25
The effect of time-of-flight on reducing the injected [^{18}F] FDG activity for whole-body PET/CT imaging of paediatric oncology patients
H. Kertész[1], T. Beyer[1], T. Traub-Weidinger[1], J. Cal-Gonzalez[1], M. Hacker[1], T. Kitsos[2], K. London[2], P. Kench[2]; *[1]Vienna/AT, [2]Sydney/AU*
(hunor.kertesz@meduniwien.ac.at)

Purpose: To assess the effect of time-of-flight (TOF) on image quality at reduced count levels for whole-body [^{18}F] FDG-PET/CT studies of paediatric oncology patients.
Methods and materials: 29 paediatric oncology patients (12F/17M, (12±5)-y/o, 13≤BMI≤28) who underwent routine whole-body PET/CT examinations on a Siemens Biograph mCT system with TOF capability (500ps) were included. The mean activity concentration was (3.8±08) MBq/kg. Events were randomly removed from the LM data to simulate reduced levels of [^{18}F] FDG activity. All data was reconstructed using the vendor e7-tools with standard iterative image reconstruction OSEM, OSEM plus resolution recovery (PSF), and with and without TOF information. A 5 mm FWHM Gaussian post-filter was applied to all reconstructions. The reconstructed images were evaluated for noise, signal-to-noise-ratio (SNR) (liver), contrast-to-noise-ratio (CNR) (all lesions), and the SNR and CNR gains with TOF were calculated.
Results: When using OSEM, the mean noise level was 11% (6%-18%) and when adding the TOF information, the noise was reduced to 9% (6%-15%). For PSF reconstructions, the lowest noise level was obtained with PSF+TOF 8%. At 50% counts, the PSF+TOF mean noise level of 10% was close to 11% for the 100% counts OSEM images. A mean gain in the SNR and CNR of 1.2-1.3 was obtained when the TOF information was included. Assuming that image noise levels below 10% are acceptable for clinical work-up, VOI analysis of the liver indicated this level be achieved at 50% counts or more when using PSF+TOF.
Conclusion: A 50% dose reduction potential in paediatric PET/CT is possible when using a 10% acceptable threshold on noise levels and iterative reconstruction with PSF+TOF. This quantitative analysis will be complemented by the qualitative grading of image quality by clinical experts.
Limitations: n/a
Ethics committee approval: Ethics approval 2019/ETH00138.
Funding: Supported by the Austria-FWF Project I3451-N32.
Author Disclosures:
H. Kertész: nothing to disclose
T. Beyer: nothing to disclose
T. Traub-Weidinger: nothing to disclose
J. Cal-Gonzalez: nothing to disclose
M. Hacker: nothing to disclose
T. Kitsos: nothing to disclose
K. London: nothing to disclose
P. Kench: nothing to disclose

RPS 1012b-2 11:31
Oncologic imaging and H2020: the PRIMAGE project helping childhood cancer research with artificial intelligence
L. Marti-Bonmati[1], A. Alberich-Bayarri[1], R. Ladenstein[2], L. Cerda Alberich[1], B. Hero[3], B. Martínez de las Heras[1], G. Marti-Besa[1], M. Aznar[4], E. Neri[5]; *[1]Valencia/ES, [2]Vienna/AT, [3]Cologne/DE, [4]Madrid/ES, [5]Pisa/IT*
(Luis.Marti@uv.es)

Purpose: Digital clinical data (imaging, pathology, genomic analytics, and wearable sensors) and patient electronic records (clinical profiling, treatment, and endpoints) are key enabling factors in clinical practice. This change is promoting clinical innovation models via real-world data-driven inferences. PRIMAGE, a 4-year European Commission-financed project having 16 European partners, is one of the more ambitious medical imaging research projects dealing with artificial intelligence in the paediatric cancer environment: neuroblastoma and diffuse intrinsic pontine glioma (DIPG).
The aim was to construct as an observational in silico study involving high-quality repository with anonymised data (imaging, clinical, molecular, and genetics) for the training of machine learning and multiscale algorithms to finally have a clinical decision support (CDS) tool.
Methods and materials: The use of computational imaging allows the extraction of multiparametric data, multiscale models, visual analytics, and artificial intelligence, leading to a new era in radiomics, characterised by high-throughput extraction, storage, and analysis of a large amount of quantitative imaging features and parameters (imaging biomarkers).
Results: The new platform will able to provide quantitative relevant information (virtual biopsies) for early disease diagnosis, disease phenotyping, disease grading, targeting therapies, and the evaluation of disease response to treatment in children with neuroblastoma and DIPG.
Conclusion: PRIMAGE's CDS system, offered as an open cloud-based platform, will provide precise clinical assistance for phenotyping, treatment allocation, and patient endpoint estimations based on imaging biomarkers, tumour growth simulation, advanced visualisation, and machine-learning

approaches. Final results will be available for the scientific community at the end of the project, ready for translation to other malignant solid tumours.
Limitations: GDPR limitations on patients recruitment will be commented.
Ethics committee approval: The project has the ethics committee approval of the coordinator hospital and reserach institute.
Funding: H2020-SC1-DTH-2018-1 GA 826494.
Author Disclosures:
G. Marti-Besa: nothing to disclose
L. Marti-Bonmati: nothing to disclose
A. Alberich-Bayarri: CEO at Quibim SL
R. Ladenstein: nothing to disclose
L. Cerda Alberich: nothing to disclose
B. Hero: nothing to disclose
B. Martínez de las Heras: nothing to disclose
M. Aznar: CEO at Matical
E. Neri: nothing to disclose

RPS 1012b-3 11:37
Computer-aided detection (CAD) of pulmonary nodules in paediatric ultra-low-dose chest CT: a performance analysis
P. J. Kuhl, H. Huflage, T. A. Bley, S. Veldhoen; *Würzburg/DE (kuhl_p@ukw.de)*

Purpose: To evaluate the dose-dependency of a computer-aided detection (CAD) system for identifying pulmonary nodules in paediatric ultra-low-dose chest CTs (ULDCT).
Methods and materials: Two scan protocols for 100kV ULDCT using tin filtration differing in the reference mAs (ref.mAs) setup for automatic tube current modulation were compared.
146 consecutive scans of paediatric patients who underwent ULDCT were included and divided into 2 study groups: 48 patients (11.1±5.5 years) underwent ULDCT with 30 ref.mAs while 98 patients (13.5±5.5 years) were scanned using 96 ref.mAs.
Patients with inflammatory consolidations were excluded. Each scan was assessed for pulmonary nodules by two radiologists and each lesion was categorised by size (2-3 mm vs ≥3 mm). Each nodule marked by the CAD system was validated in consensus. The radiation dose was estimated in size-specific dose estimates (SSDE).
Results: Radiation dose in the 30 ref.mAs group was significantly lower (0.16±0.09 mGy) than in the 96 ref.mAs group (0.56±0.22 mGy, p<0.001).
There was no significant difference between the groups regarding total CAD errors (mean per scan 1.44±3.50 vs 1.37±2.24 for NS ≥2 mm and 0.85±2.24 vs 0.71±1.59 for NS ≥3 mm) resulting in resembling CAD sensitivities (0.43 vs 0.45 in nodule size (NS) ≥ 2mm; 0.65 vs 0.74 in NS ≥3 mm).
There was no significant correlation between SSDE and CAD errors for NS ≥2 mm (r=-0.054) and NS ≥ 3mm (r=-0.067).
Conclusion: Lowering the parameters for automatic tube current modulation in paediatric ULDCT results in significant dose reduction without compromising the evaluated CAD system.
Limitations: CAD sensitivity and specificity in this oncology-dominant study group was not satisfying in both scan protocols assessed.
Ethics committee approval: n/a
Funding: The project underlying this report was funded by the Deutsche Forschungsgemeinschaft (DFG), project number VE1008/1-1 and KO 2938/5-1.
Author Disclosures:
P. J. Kuhl: nothing to disclose
S. Veldhoen: nothing to disclose
H. Huflage: nothing to disclose
T. A. Bley: nothing to disclose

RPS 1012b-5 11:43
The value of diffusion-weighted MRI in the response assessment of nephroblastoma
A. M. Hötker[1], Y. Mazaheri[2], A. Lollert[3], J. Zheng[2], S. Müller[4], J.-P. Schenk[5], O. Akin[2], N. Graf[4], G. Staatz[3]; *[1]Zurich/CH, [2]New York, NY/US, [3]Mainz/DE, [4]Homburg (Saar)/DE, [5]Heidelberg/DE (andreas.hoetker@usz.ch)*

Purpose: To assess the value of diffusion-weighted MRI (DW-MRI) in the prediction of viable blastemal remnant after neoadjuvant chemotherapy in patients with nephroblastoma, which is considered a poor prognostic marker and may result in additional adjuvant treatment.
Methods and materials: This IRB- approved study included 37 paediatric patients who underwent DW-MRI prior and after completion of neoadjuvant chemotherapy for nephroblastoma and subsequent surgical resection. Two blinded radiologists volumetrically assessed each tumour and the parameters mean ADC, median ADC, 12.5th/25th/75th percentile, skewness, and kurtosis were calculated. The associations between the imaging features and blastemal remnant fraction were examined using over-dispersed Poisson regression.
Results: Inter-reader agreement was high for mean ADC, volume, skewness, and kurtosis (ICC: 0.74-0.96). In univariable analysis, pre-therapeutic ADC mean, median, 12.5th percentile, and skewness were significantly associated with the presence of blastemal remnant for reader 1 (p=0.009-0.044) and pre-therapeutic ADC mean, median, 12.5th/25th/75th percentile, and skewness for reader 2 (p=0.009-0.026). In a multivariable analysis, the ADC mean was significantly associated with blastemal remnant for both readers (reader 1: fraction ratio 1.33 (1.07, 1.65), p=0.014; reader 2: fraction ratio 1.1 (1.01, 1.2), p=0.034). Post-therapeutic MRI parameters were not significantly associated with blastemal remnant.
Conclusion: A higher pre-therapeutic ADC was significantly associated with a larger fraction of a blastemal remnant after neoadjuvant chemotherapy. This could allow for a more personalised chemotherapeutic regime in these patients and offer predictive information at the time of the initial diagnosis.
Limitations: The retrospective study design.
Ethics committee approval: IRB approved.
Funding: No funding was received for this work.
Author Disclosures:
A. M. Hötker: nothing to disclose
Y. Mazaheri: nothing to disclose
A. Lollert: nothing to disclose
S. Müller: nothing to disclose
J.-P. Schenk: nothing to disclose
J. Zheng: nothing to disclose
O. Akin: nothing to disclose
N. Graf: nothing to disclose
G. Staatz: nothing to disclose

RPS 1012b-6 11:49
Radiomic features as a marker of metastatic spread in Wilms' tumours
G. Fichera[1], L. Baffoni[2], T. Toffolutti[1], M. Zuliani[1], B. Giorgi[1], E. Quaia[1], C. Giraudo[1]; *[1]Padua/IT, [2]Montebelluna/IT (gfichera90@gmail.com)*

Purpose: To assess the role of radiomic analyses for characterising metastatic and localised paediatric renal Wilms' tumours.
Methods and materials: Paediatric patients affected by Wilms' tumours referred to our tertiary centre for staging (i.e. treatment naïve) from 2012-2018 and examined by contrast-enhanced computed tomography were included in this retrospective study. Patients matching the inclusion criteria were then subdivided according to the presence of metastases (i.e. mW and lW). One radiologist expert in paediatric imaging drew regions of interest along the margins of all primary tumours covering the entire volume using open-source software (3D Slicer). The same software was applied to extract 33 radiomic features from each patient belonging to three categories: first-order statistics, grey-level co-occurrence matrix (GLCM), and the grey-level run-length matrix (GLRLM). The Student's t-test was used to compare mW and lW patients for each radiomic feature (p<0.05). The accuracy of the variables showing a statistically significant difference was assessed by receiver operating characteristic curves.
Results: 32 patients (16 females, mean age±SD, 4±2.27 yrs) met the inclusion criteria and were analysed in this study. 10 patients were affected by metastatic disease (i.e. mW) and 22 by localised tumours (i.e. lW). Two features (one FOS, one GLRLM) showed a statistically significant difference between mW and lW: variance (p=0.043) and grey-level non-uniformity normalised (GLNUN; p=0.008). The area under the curve was good for GLNUN (AUC=0.805) and fair for the variance (AUC=0.655)
Conclusion: GLNUN can be considered as a robust radiomic marker of metastatic spread in Wilms tumours.
Limitations: Future studies addressing the clinical implications and considering the impact on the therapeutic treatment of our findings should be performed.
Ethics committee approval: Ethics committee approval obtained.
Funding: No funding was received for this work.
Author Disclosures:
G. Fichera: nothing to disclose
L. Baffoni: nothing to disclose
T. Toffolutti: nothing to disclose
M. Zuliani: nothing to disclose
B. Giorgi: nothing to disclose
E. Quaia: nothing to disclose
C. Giraudo: nothing to disclose

RPS 1012b-7 11:55
The feasibility and value of quantitative semi-automated diffusion-weighted imaging volumetry of neuroblastic tumours
S. Gassenmaier[1], I. Tsiflikas[1], J. Fuchs[1], R. Grimm[2], C. Urla[1], M. Ebinger[1], S. W. Warmann[1], J. F. Schäfer[1]; *[1]Tübingen/DE, [2]Erlangen/DE (sebastian.gassenmaier@med.uni-tuebingen.de)*

Purpose: To assess the feasibility and value of semi-automated diffusion-weighted imaging (DWI) volumetry of whole neuroblastic tumours with an apparent diffusion coefficient (ADC) map evaluation after neoadjuvant chemotherapy.
Methods and materials: Paediatric patients who underwent surgical resection of neuroblastic tumours at our institution from 2013-2019, and who received a preoperative MRI scan with DWI after chemotherapy, were included. Tumour volumetry was assessed with a semi-automated approach in DWI using a dedicated software prototype. Quantitative ADC values were calculated automatically of the total tumour volume after manual exclusion of necrosis. Manual segmentation in T1-weighted and T2-weighted sequences was used as a reference standard for tumour volume comparison.
Results: 27 patients with 28 lesions (neuroblastoma (NB): n=19, ganglioneuroblastoma (GNB): n=7, and ganglioneuroma (GN): n= 2) could be evaluated. The mean patient age was 4.5±3.2 years. The median volume of standard volumetry (T1w or T2w) was 50.2 ml (interquartile range (IQR): 91.9 ml) vs 45.1 ml (IQR: 98.4 ml) of DWI (p=0.145). Mean ADC values ($x10^{-6}$ mm^2/s) of the total tumour volume (without necrosis) were 1,187±301 in NB vs 1,552±114 in GNB/GN (p=0.037). The 5^{th} percentile of ADC values of NB (614±275) and GNB/GN (1,053±362) provided the most significant difference (p=0.007) with an area under the curve of 0.848 (p<0.001).
Conclusion: Quantitative semi-automated DWI volumetry is feasible in neuroblastic tumours with an integrated analysis of tissue characteristics by providing automatically calculated ADC values of the whole tumour as well as an ADC heatmap.
Limitations: Although the number of subjects is small, it represents one of the largest published cohorts with ADC analysis of neuroblastic tumours due to the low incidence of this disease.
Ethics committee approval: IRB approval obtained. Written informed consent waived.
Funding: No funding was received for this work.
Author Disclosures:
S. Gassenmaier: nothing to disclose
I. Tsiflikas: nothing to disclose
J. Fuchs: nothing to disclose
R. Grimm: Employee at Siemens Healthcare, Shareholder at Siemens Healthcare
C. Urla: nothing to disclose
S. W. Warmann: nothing to disclose
J. F. Schäfer: nothing to disclose
M. Ebinger: nothing to disclose

RPS 1012b-9 12:01

Dynamic contrast-enhanced perfusion MRI and diffusion-weighted imaging as an imaging biomarker for paediatric cancer

L. Cerda Alberich, G. Marti-Besa, A. Alberich-Bayarri, L. Marti-Bonmati*; Valencia/ES (leogibi230@gmail.com)*

Purpose: Neuroblastomas are the most frequent solid extracranial cancer in childhood. Its diagnosis, prognosis, and monitoring are based on the information provided by multiparametric magnetic resonance images. Our focus is to explore the utility of diffusion and perfusion changes in neuroblastomas as an early biomarker of diagnosis, using diffusion-weighted and dynamic contrast-enhanced MRIs.
Methods and materials: Multiple MR imaging real-word sequences were used from 30 patients. Volumes-of-interest were calculated and transferred to DCE perfusion and apparent diffusion coefficient (ADC) maps. Histogram analysis and clustering unsupervised ML algorithms were used to determine the values of the mean and standard deviation of the initial area under the curve at 60 seconds (IAUC60) and ADC for automatic differentiation of neuroblastic tumours. The resolution was estimated and the data was smeared accordingly to identify and remove the noise and low-quality voxels.
Results: Significant differences in the mean ADC were found for neuroblastic tumours: 1.0 for ganglioneuroma, 0.82 for ganglioneuroblastoma, and 0.52 for neuroblastoma, with an uncertainty of 0.11%, 42%, and 16%. This result improves tumour differentiation with respect to state-of-the-art voxel-by-voxel methodologies, which were found to be: 1.6 for ganglioneuroma, 1.7 for ganglioneuroblastoma, and 1.3 for neuroblastoma, with an uncertainty of 3.6%, 12%, and 17%. THe mean IAUC60 was found to have a value of 43 (and 14% uncertainty) for neuroblastoma, as opposed to a value of 17 (and 17% uncertainty) with state-of-the-art voxel-by-voxel methodologies.
Conclusion: The proposed novel technique to determine IAUC60 and ADC parameters holds promise for differentiating benign and malignant neuroblastic tumours.
Limitations: The dataset size and harmonisation among different machines and data collection techniques.
Ethics committee approval: La Fe Hospital received approval from the hospital's ethics committee.
Funding: Horizon2020. Topic:SC1-DTH-07-2018-RIA. GA:826494.
Author Disclosures:
L. Cerda Alberich: nothing to disclose
G. Marti-Besa: nothing to disclose
A. Alberich-Bayarri: nothing to disclose
L. Marti-Bonmati: nothing to disclose

RPS 1012b-10 12:07

The differentiation of low- and high-grade paediatric brain tumours by using intravoxel incoherent motion imaging and diffusion kurtosis imaging

D. She*; Fuzhou/CN (shedejun@126.com)*

Purpose: To demonstrate that a new set of parameters from IVIM and DKI can be used to improve the accuracy of MR imaging for differentiating among low- and high-grade paediatric brain tumours.
Methods and materials: 49 paediatric patients with histologically-proved brain tumours who underwent IVIM and DKI were recruited in this study. The mean, minimum, maximum IVIM [pure diffusion coefficient (D), pseudo-diffusion coefficient (D*), and perfusion fraction (f)], and DKI [diffusion kurtosis (K) and diffusion coefficient (Dk)] parameters were measured. The IVIM and DKI values were measured in solid tumour regions and in normal-appearing grey matter as a control. These values were compared between the low-and high-grade paediatric brain tumours by using the Mann-Whitney U test. Receiver-operating characteristic (ROC) analysis and logistic regression analysis were performed to evaluate the diagnostic performance of single-parametric and multiparametric models.
Results: None of the IVIM and DKI parameters exhibited significant differences in normal-appearing grey matter (P>0.05). The Dk and D values were lower, whereas the K and f_{min} values were higher in high-grade paediatric brain tumours than those in low-grade paediatric brain tumours (all p<0.05). The combination of DK_{min} and K_{max} provided the largest area under the ROC curve (0.955) in the ROC analysis compared with individual parameters (D_{min} 0.891, DK_{min} 0.933, K_{max} 0.923, and f_{min} 0.734), indicating an improved diagnostic performance for tumour grading.
Conclusion: The parameters derived from IVIM and DKI can be used to distinguish low-grade paediatric brain tumours from high-grade paediatric brain tumours. The combination of DKI parameters may serve as non-invasive and quantitative imaging parameters for grading paediatric brain tumours in vivo.
Limitations: A retrospective study covering a relatively small sample of subjects.
Ethics committee approval: n/a
Funding: No funding was received for this work.
Author Disclosures:
D. She: nothing to disclose

RPS 1012b-11 12:13

Post-transplant thymus restoration is a really good predictor of transplant outcomes?

M. Cuccaro, F. F. Zennaro, R. Simeone, F. M. Murru, N. Maximova*; Trieste/IT (michele.cuccaro1992@gmail.com)*

Purpose: To find a correlation between post-transplant thymic volume and thymopoiesis, to associate thymic renewal with early and long-term transplant outcomes, and to expand the role of the radiology team in transplant clinical decisions and the post-transplant management of paediatric patients.
Methods and materials: Thymic volume assessment and thymocytes analysis were performed before HSCT (baseline volume), at 3, 6, 12 months, and long-term after HSCT.
74 paediatric patients who underwent an allo-HSCT from 2002-2018 were included. The control group consisted of 311 paediatric patients undergoing chest MRI for orthopaedic reasons.
The analysis was performed with HOROS software. Manual thymus tracing was performed for each cut, with the generation of a 3D reconstruction and a volume calculation.
Statistical analyses were performed using WinStat and MedCalc.
Results: There is a statistically significant correlation between thymus volume and thymopoiesis with p<0.0001 and r=0.5720.
The average thymic volume at all evaluations is significantly greater in the subgroup without GVHD: 16.1 (±10.0) cm^3 vs 11.2 (±8.7) cm^3; p<0.05.
There is a significant difference in the average thymic volume between patients who survived after the HSCT (68.8 ± 48.46) and patients who did not (2.9 ± 2.11); p<0.0001.
Conclusion: The restoration of thymic volume is a good indicator of positive outcomes in allogeneic HSCT, while a restoration failure is related to transplant-related mortality.
Thymic MRI assessment is now part of the current clinical management of transplanted patients and improves their integrated care pathways.
The next aim will be to create specific sequences that allow us to analyse the microenvironment of thymic tissue (“virtual biopsy”).

Limitations: A monocentric and retrospective study with a limited sample of subjects.
Currently, our MRI protocol allows us to study only the thymic morphology but not the microenvironment of the thymic tissue.
Ethics committee approval: n/a
Funding: No funding was received for this work.
Author Disclosures:
M. Cuccaro: nothing to disclose
F. F. Zennaro: nothing to disclose
N. Maximova: nothing to disclose
R. Simeone: nothing to disclose
F. M. Murru: nothing to disclose

RPS 1012b-12 12:19
Ultrasound-guided core biopsy with smear cytology: the fastest route for diagnosis in paediatric oncology
A. Ilivitzki, B. Sokolovski, A. Ben Barak, S. Postovski, M. Ben Aarush*; Haifa/IL (ailivitzki@gmail.com)*

Purpose: In our hospital, ultrasound-guided fine-needle biopsy (US-guided FNB) is the first choice for tissue diagnosis in the paediatric population. In 2018, we added smear cytology in some of our biopsies, allowing for an immediate primary diagnosis. We retrospectively reviewed our experience with FNB assessing the accuracy rate, safety, and availability of the procedure, as well as the accuracy of the smear cytology and its added value for patient management.
Methods and materials: Paediatric ultrasound-guided biopsies done in our hospital from 01/2018-09/2019 were studied. Data collection included demographics, clinical and procedural data, and follow-up.
Results: 106 biopsies were performed on 91 patients, 15 of them on known oncologic patients. 96.2% of biopsies were performed within 36 hours. 79 tumours were correctly diagnosed and 1 malignancy was misdiagnosed as a benign lesion. 23 biopsies were correctly diagnosed as non-tumour. Smear cytology was performed in 30 cases; 25 tumours and 5 reactive lymph nodes. The cytologist correctly differentiated the tumour from inflammation in all cases and diagnosed the tumour in 24 of the cases. The sensitivity of ultrasound-guided FNB is 98.7%, specificity 100%, and accuracy 99%. The accuracy of smear cytology for differentiating tumours from non-tumours is 100% and for final diagnosis 97%.
Conclusion: We find ultrasound-guided FNB for suspected malignancy in the paediatric population highly available, safe, and accurate. In our small cohort, smear cytology was an excellent, real-time tool for differentiating tumour and non-tumour tissue, and in most cases allowed for early correct tumour diagnosis. This procedure may accelerate patient management and improve patient care.
Limitations: A retrospective study with a small cohort.
Ethics committee approval: All biopsies were done under informed consent. The local Helsinki committee approved the study.
Funding: No funding was received for this work.
Author Disclosures:
A. Ilivitzki: nothing to disclose
B. Sokolovski: nothing to disclose
A. Ben Barak: nothing to disclose
S. Postovski: nothing to disclose
M. Ben Aarush: nothing to disclose

11:15 - 12:30 **Room Y**

Radiographers

RPS 1014b

An array of applications: ultrasound and dual-energy x-ray absorptiometry

Moderators:
T. Herlihy; Dublin/IE
N.N.

RPS 1014b-1 11:15
Ultrasound practice in Europe: an EFRS survey
G. Harrison[1], M. R. V. Pedersen[2], B. Kraus[3], R. Martins Dos Santos[4], S. Noij-Rijkes[5]; *[1]London/UK, [2]Vejle/DK, [3]Vienna/AT, [4]Coimbra/PT, [5]Haarlem/NL (gillhaha@gmail.com)*

Purpose: The European Federation of Radiographer Societies (EFRS) are carrying out 3 on-line surveys to determine current views and practice of radiographers undertaking ultrasound examinations. The results of the first survey of EFRS national societies is presented here.
Methods and materials: An on-line survey was sent to 54 EFRS radiographer societies, asking for opinions and practice within their country to explore the actual and perceived role of radiographers within ultrasound.
Results: 27 countries responded (50% response rate) with 40 individual respondents providing valuable information. Radiologists perform ultrasound examinations in all but one county, 'specialist doctors' scan in 80% of countries followed by radiographers in 59%. Limitations to radiographer ultrasound practice included shortages of high-quality educational opportunities, legislation stating that only doctors can scan, and resistance from some clinical colleagues. Team working with radiology colleagues was seen as good practice to develop radiographers' skills and competence in ultrasound. Further advice was to gradually develop radiographer skills led by a few centres, ensure a rigorous audit is undertaken, and publish the outcomes to help build the case for wider implementation.
Conclusion: Radiographers' role extension into ultrasound is evident in some countries to a high level of independent practice. In other countries, radiographers either have some involvement in ultrasound scanning but not independent report writing or have no involvement at all. The results of the survey will be discussed within the presentation and suggestions provided for countries wanting to explore radiographer advancement in ultrasound.
Limitations: The survey was in English, which led to different interpretation of some questions.
Ethics committee approval: GDPR and consent were explained at the beginning of the voluntary, anonymous survey.
Funding: No funding was received for this work.
Author Disclosures:
G. Harrison: nothing to disclose
M. R. V. Pedersen: nothing to disclose
B. Kraus: nothing to disclose
R. Martins Dos Santos: nothing to disclose
S. Noij-Rijkes: nothing to disclose

RPS 1014b-2 11:21
Eye assessment by B-mode ultrasound and elastography
R. A. M. Santos, A. R. R. R. Garcês*; Coimbra/PT (rutemartinssantos@gmail.com)*

Purpose: To analyse and characterise ocular structures, namely the eyeball, optic nerve head, and periorbital fat by B-mode ultrasound and sonoelastography in healthy young subjects.
Methods and materials: 240 images were collected by B-mode ultrasound and by elastography in 30 healthy subjects. The exclusion criteria was an eye surgery whose procedure leaves this very sensitive. After collection, measurements were made for the thickness and echogenicity of the intraorbital fat, eyeball, and optic nerve, as well as the colour (RGB) fraction and strain-ratio elastography of the globe and ocular nerve.
Results: The values of elasticity vary from 36.24±11.71 a.u. for the red colour in the right eyeball to 102.42±15.72 a.u. for the green colour in the left eyeball, whereas for the optic nerves they range from 38.57±8.22 a.u. for the red colour of the left optic nerve up to 141.26±23.65 a.u. for the blue colour of the right optic nerve.
Conclusion: Sonoelastography is an imaging ultrasound exam capable of analysing ocular structures and measuring values that in the future may serve as a comparison for the analysis of ophthalmological pathologies.
Limitations: It is important to have a higher age range.
Ethics committee approval: Participants were fully informed of the purpose and procedures of the study and provided written informed consent. The study conformed to the guidelines of the declaration of Helsinki and was approved by the ethics committee of the Polytechnic Institute of Coimbra (No 42/2018).
Funding: No funding was received for this work.
Author Disclosures:
R. A. M. Santos: nothing to disclose
A. R. R. R. Garcês: nothing to disclose

RPS 1014b-3 11:27
Association between risk factors and testicular microlithiasis
M. R. V. Pedersen*; Vejle/DK (Malene.Roland.Vils.Pedersen@rsyd.dk)*

Purpose: Testicular microlithiasis (TML) and its clinical significance is not fully understood. TML and risk factors have been associated with testicular cancer. This study investigated the association between TML and socioeconomic and other pre-diagnostic factors.
Methods and materials: All men who had a scrotal ultrasound examinations at the department of radiology, Vejle Hospital, from 2001-2013 were included. They were categorised as patients with and without TML and compared with pre-diagnostic data from a nationwide registry.
Results: A total of 2,404 men (283 (11.8%) with TML and 2,121 (88.2%) without TML) were included. Overall, we found no statistically significant differences in demographics, socioeconomic characteristics, or testicular diseases in men with and without TML. Men with TML had more often been treated for infertility (OR

2.09, 95% CI 0.84-5.24) and testicular torsion (OR 1.58, 95% CI 0.34-7.36) compared to men without TML.
Conclusion: Treatment for infertility and torsion was non-significantly associated with TML and no other association was found. This data does not suggest early exposure to be related to TML.
Limitations: No information in the Danish National Patient Registry or PACS was available on testicular volume, because the testicular volume is not a standard record. Selection bias may be present. However, to compensate for this, a high number of patients were included in this study and the patients were included from a long interval (2001-2013).
Ethics committee approval: The study was approved by the Danish Data Protection Agency (2008-58-0035/2009-41-3471). According to Danish law, the study did not require patients consent or approval from the Committee on Health Research Ethics of Southern Denmark, since no biomedical intervention was performed.
Funding: The Region of Southern Denmark, the Danish Council of Radiographers, and the Lillebaelt Hospital Research Council.
Author Disclosures:
M. R. V. Pedersen: nothing to disclose

RPS 1014b-4 11:33
An ultrasound study to evaluate the effects of pulmonary rehabilitation in muscle mass in people with chronic obstructive pulmonary disease
P. M. Martins[1], A. A. André[2], S. de Francesco[1], P. Rebelo[1], C. Paixão[1], L. Noronha[3], A. Marques[1]; [1]Aveiro/PT, [2]Coimbra/PT, [3]Canoas/BR (pmartins@ua.pt)

Purpose: To evaluate the effects of pulmonary rehabilitation (PR) on the structure and function of the diaphragm, quadriceps, and biceps brachii muscles in people with chronic obstructive pulmonary disease (COPD).
Methods and materials: People with COPD were recruited from primary centres and hospitals. A group of age- and gender-matched healthy people were recruited. An US equipment (LogiqP6PRO, GE) with linear (11L) and convex (4C) probes was used. Rectus femoris and biceps brachii thickness (RF_T, BB_T) and their cross-sectional areas (RF_{CSA}, BB_{CSA}) were measured 3 times. Right diaphragmatic thickness at maximal inspiration (DT_{Insp}) and expiration (DT_{Exp}) were obtained. Diaphragmatic excursion (DE) was measured during normal breathing (DE_NB) and at maximal inspiration (DE_max_insp) using M-mode US. Quadriceps (QMS) and elbow (EMS) muscle strength were assessed with a handheld dynamometer, exercise tolerance with the 6-min walk test (6MWT) and 1-min sit-to-stand, before (T0) and after a 12-weeks PR programme. Non-parametric tests were used for data analysis (statistical significance was set to $p<0.05$).
Results: 25 people with COPD (9 female) aged 66.3±10.4 years, BMI=24.7±4.5 kg/m^2, and 10 healthy volunteers (4 female) aged 65.9±7.3 years, BMI=28.4±3.4 kg/m^2, were enrolled. Significant differences between COPD and healthy volunteers at baseline (T0) were found for thickness, RF_{CSA}, and BB_{CSA}. Significant increases were observed in people with COPD after PR for RF_T, RF_{CSA}, BB_T, BB_{CSA}, DT_{Insp}, 1 min sit-to-stand, 6MWT, and QMS ($0.001 \leq p \leq 0.019$). No other significant differences were found. Significant and moderate correlations were found between strength measures and muscle size ($0.404 \leq r_s \leq 0.580$).
Conclusion: There was an overall increase in muscle sizes after the PR programme. US measurements have shown to be a promising outcome measure for pulmonary rehabilitation.
Limitations: n/a
Ethics committee approval: Study received ethical approval from the Health Administration North and Centre, Portugal
Funding: 3R Project-Ref. FCT (SAICT-POL/23926/2016).
Author Disclosures:
P. M. Martins: nothing to disclose
A. A. André: nothing to disclose
C. Paixão: n/a
P. Rebelo: nothing to disclose
L. Noronha: nothing to disclose
A. Marques: nothing to disclose
S. de Francesco: nothing to disclose

RPS 1014b-5 11:39
Skin layer evaluation by ultrasound
R. A. M. Santos, V. Fonseca; *Coimbra/PT (rutemartinssantos@gmail.com)*

Purpose:
To evaluate the aging changes of the skin by ultrasound with B-mode.
Methods and materials: 28 participants were divided into 2 groups: 18-35 years and 35-70 years. Participants who had scars and/or tattoos were excluded. All participants answered personal and sociodemographic questions, such as age, ethnicity, sun exposure, and their use of sunscreen among others. Then, an ultrasound examination was performed on different areas of the skin.
Results: There was a higher subepidermic low echogenicity band index in the age group 18-29 years in the right hand, flexing of the right and left arms, and the neck. The epidermis was superior in the age group 37-64 years and, in relation to the neck, the hyperechogenic line was less visible also in this age group, which is suggestive of cutaneous aging.
Conclusion: This study showed that there are layers of skin, especially in the age group 18-29 years, that are aged. High-frequency ultrasound is an effective method for identifying and evaluating the different layers of the skin.
Limitations: The inability to have older individuals, upwards of 70 years, for comparing with the other age ranges.
Ethics committee approval: Participants were fully informed of the purpose and procedures of the study and provided written informed consent. The study conformed to the guidelines of the declaration of Helsinki and was approved by the ethics committee of the Polytechnic Institute of Coimbra (No 36/2019).
Funding: No funding was received for this work.
Author Disclosures:
R. A. M. Santos: nothing to disclose
V. Fonseca: nothing to disclose

RPS 1014b-6 11:45
Variability in liver transient elastography and acoustic radiation force impulse (ARFI) imaging-based elastography measures in a healthy paediatric cohort
A. McGee, M. Rowland, B. Bourke, L. A. Rainford; *Dublin/IE (allison.mcgee@ucd.ie)*

Purpose: In children, FibroScan transient elastography (TE) and acoustic radiation force impulse (ARFI) ultrasound elastography techniques are attractive, non-invasive tests for liver disease assessment. Since repeatability and reproducibility are hallmarks of any clinical test, this study aimed to determine the normal range of liver TE and ARFI measurements in healthy children and evaluate their repeatability and reproducibility.
Methods and materials: Healthy volunteer children had 2 independent measurements of liver stiffness, utilising FibroScan TE and ARFI imaging-based elastography, independently performed by two operators according to a protocol designed to reduce measurement confounders. For each elastography technique, the upper limit of normal (ULN) liver stiffness was determined. Measurement repeatability and reproducibility for both methods and multiple operators were examined with Bland and Altman plots and Lin's concordance correlation coefficient (CCC).
Results: 101 healthy children had two valid, independent liver stiffness measurements with TE and ARFI (Mean age: 12.4 years, SD: 2.57, M:F: 36%:65%). ULN values for liver stiffness were TE: 6.5 kPa and ARFI: 1.21 m/s. For repeat measurements, the 95% limits of agreement ranged from -0.72 kPa-+0.79 kPa for TE and from -0.13 m/s-+0.15 m/s for ARFI. Lin's CCC was p=0.85 (95%CI 0.81-0.89) for TE and p=0.61 (95%CI: 0.46-0.71) for ARFI-derived measures.
Conclusion: Despite operator expertise and efforts to reduce confounders, TE and ARFI measurements of liver stiffness in healthy volunteer children were not repeatable. Prescriptive elastography technique guidelines and the evaluation of the operator training protocol with a continued review of the operator performance to identify less expert operators is recommended to maintain and enhance diagnostic accuracy.
Limitations: n/a
Ethics committee approval: Full institutional ethical approval was obtained. Written informed consent from parents and informed assent from children were obtained.
Funding: The Health Research Board (Ireland) partly funded this research.
Author Disclosures:
A. McGee: nothing to disclose
L. A. Rainford: nothing to disclose
M. Rowland: nothing to disclose
B. Bourke: nothing to disclose

RPS 1014b-7 11:51
The impact of ageing on muscle morphology: an ultrasound study
R. A. M. Santos; *Coimbra/PT (rutemartinssantos@gmail.com)*

Purpose: To characterise the quadriceps muscle morphology in older institutionalised individuals and to evaluate the morphological muscle changes with physical activity.
Methods and materials: 36 older participants from a daycare centre were divided into two groups (18 subjects each). One of the groups performed an exercise program intervention for 8 weeks. All participants were submitted to ultrasound evaluation of the quadriceps femoris bilaterally, before and after the intervention program.
Results: 36 participants were recruited, with a mean age of 73.0±6.0 years. Vastus medialis (VM) and Vastus lateralis (VL) showed the largest, and the rectus femoris (RF) the smallest, muscle thickness (MT) for both right and left sides. For echo-intensity (EI) values, VL showed the highest values and VM the

lowest. When the two groups were compared, there were significant differences between the groups for MT and EI values ($p<0.05$).
Conclusion: There is a higher prevalence of sarcopenia in the elderly and institutionalised population. Ultrasound can be one of the strategies to prevent the sarcopenia showing positive effects on the practice of physical activity.
Limitations: The inability to use a data from the young group to compare and analyse the results.
Ethics committee approval: Participants provided written informed consent. The study conformed to the guidelines of the declaration of Helsinki and was approved by the ethics committee of the Polytechnic Institute of Coimbra.
Funding: On behalf of the AGA@4life Consortium. This work is co-financed by the European Regional Development Fund through the partnership agreement Portugal 2020-Regional Operation Program CENTRO2020 under the project CENTRO-01-0145-FEDER-023369 AGA@4life: AGA-comprehensive geriatric approach to promote an active and healthy ageing implementation of an integrated and multidisciplinary intervention program.
Author Disclosures:
R. A. M. Santos: nothing to disclose

RPS 1014b-8 11:57
Ultrasound evaluation of muscular mass and strength in handball players and sedentary age-matched controls
P. M. Martins[1], S. de Francesco[1], A. Baptista[1], I. Silva[1], L. Noronha[2], A. A. André[3]; [1]*Aveiro/PT,* [2]*Canoas/BR,* [3]*Coimbra/PT (silvia.francesco@ua.pt)*

Purpose: To evaluate quadriceps and biceps brachii muscle mass and quality in athletes and sedentary young controls in ultrasound (US) images. Furthermore, we aimed to establish a correlation between US and strength variables.
Methods and materials: 16 male handball players (20.25±1.77 years; BMI=26.16±3.02 kg/m^2) and 16 sedentary age-matched university students (20.94±2.96 years; BMI=23.35±3.10 kg/m^2) volunteered to participate in this study. An US equipment (LogiqP6PRO, GE) with linear (11L) probe was used. Three measures of quadriceps thickness (Q_T), rectus femoris thickness (RF_T), RF cross-sectional area (RF_{CSA}), vastus lateralis thickness (VL_T), and pennation angle of the RF (RF_{PA}) and VL (VL_{PA}) were obtained. Of the upper limb, biceps brachii thickness (BB_T) and BB_{CSA} were measured. The echo intensity of the RF and BB were evaluated (RF_{EI}, BB_{EI}). Isometric knee extension strength (IKES), isometric elbow flexor strength (IEFS), and handgrip strength (HGS) were determined with a hand-held dynamometer. Statistical significance was set to 0.05.
Results: Statistically significant differences between athletes and controls were found in BMI ($p=0.015$) and in the strength variables HS, IEFS, and IKES ($p<0.001$), and in the US variables RF_T, RF_{CSA}, RF_{PA}, BB_{CSA} ($p<0.001$), VL_T ($p=0.008$), and VL_{PA} ($p=0.004$). There was no significant difference between groups regarding muscle echo intensity variables BB_{EI} and RF_{EI}.
Positive and strong correlations were found for BB_{CSA} and IEFS ($r=0.75$; $p<0.001$) and RF_{CSA} and IKES ($r=0.76$; $p<0.001$). A moderate correlation was found between HGS and RF_{CSA} ($r=0.57$; $p=0.001$) and BB_{CSA}($r=0.58$; $p=0.001$).
Conclusion: The results shows that regular exercise has great impact in muscle size and strength. Furthermore, muscle architecture parameters evaluated with US can be used to non-invasively evaluate athlete performance.
Limitations: n/a
Ethics committee approval: Institutional board approval and written inform consent obtained.
Funding: No funding was received for this work.
Author Disclosures:
S. de Francesco: nothing to disclose
P. M. Martins: nothing to disclose
A. Baptista: nothing to disclose
I. Silva: nothing to disclose
L. Noronha: nothing to disclose
A. A. André: nothing to disclose

RPS 1014b-9 12:03
The role of physical activity on hamstring muscle morphology: a pilot ultrasound study
R. A. M. Santos, A. C. Tavares*; Coimbra/PT (rutemartinssantos@gmail.com)*

Purpose: To characterise and evaluate the morphological changes of the hamstring muscles through ultrasound parameters such as the pennation angle, fascicle length, cross-sectional area, echo-intensity, and muscle thickness.
Methods and materials: 22 young female divided into two groups (control group=11; athletes group=11) were submitted an ultrasound examination at 50% of the posterior region of the thigh for the semimembranosus and long portion of the femoral biceps muscles in the longitudinal and panoramic views.
Results: 22 athletes with a mean age of 23.27 years were evaluated. There were significant differences between the two groups in muscle morphology. The athletes' group showed higher values for muscle thickness, cross-sectional area, pennation angle, and fascicle length, and a lower values for muscle echo intensity.
Conclusion: Physical exercise causes changes in muscle morphology and ultrasound is a good method for the musculoskeletal assessment of athletes' performance since it is an imaging modality that allows the carrying out of comparative bilateral studies for athletes' performance follow-up and for preventive strategies to fight sedentarism.
Limitations: The low number of participants.
Ethics committee approval: Participants provided written informed consent. The study conformed to the guidelines of the declaration of Helsinki and was approved by the ethics committee of the Polytechnic Institute of Coimbra.
Funding: No funding was received for this work.
Author Disclosures:
R. A. M. Santos: nothing to disclose
A. C. Tavares: nothing to disclose

RPS 1014b-10 12:09
Dual-energy x-ray absorptiometry patient and staff radiation exposure: an experimental analysis
M. S. D. Nascimento, A. R. Clemente, Ó. M. D. C. Tavares, J. Santos*; Coimbra/PT (marianaimrnascimento@gmail.com)*

Purpose: Dual-energy x-ray absorptiometry (DXA) is broadly used to evaluate mineral bone density and consequently diagnose osteoporosis. DXA technology has evolved throughout time, implying differences in the acquisition mode and radiation exposure levels. This study aims to evaluate the examination and staff dose values in different DXA examinations performed in different technological equipment.
Methods and materials: 2 different DXA scanners, Lunar iDXA and Lunar DPX with narrow fan-beam and pencil-beam systems, respectively, were used in this study. Whole-body, lumbar spine, and left hip DXA acquisitions were performed on a PBU-60 anthropomorphic phantom and six Raysafe I3 dosimeters were placed in different positions in the room, in order to evaluate effective dose values in the possible room positions of the staff.
Results: The highest examination dose values were obtained on the Lunar iDXA scanner. The staff exposures values were higher on hip examinations and no exposure was detected during a whole-body examination.
Conclusion: The lower exposure values in DXA when compared to other medical imaging examinations are not negligible. The narrow fan-beam DXA scanner presented higher exposure values when compared with the pencil-beam technology.
Limitations: It was not possible to compare all DXA technology scanners.
Ethics committee approval: Ethical commmite approval was obtained.
Funding: No funding was received for this work.
Author Disclosures:
J. Santos: nothing to disclose
Ó. M. D. C. Tavares: nothing to disclose
M. S. D. Nascimento: nothing to disclose
A. R. Clemente: nothing to disclose

RPS 1014b-11 12:15
Total and regional bone density and body mass in male adolescents: comparison between soccer players and swimmers
J. Pinheiro[1], L. P. Ribeiro[2], M. Coelho-E-Silva[3]; [1]*Sao Bras/PT,* [2]*Faro/PT,* [3]*Coimbra/PT (pedro.alexandrex94@gmail.com)*

Purpose: To compare athletes from sports contrasting in mechanical impact: soccer versus swimming.
Methods and materials: Bone mineral content (BMC) and density (BMD), lean soft tissue, and fat tissue were assessed using dual-energy x-ray absorptiometry. Anthropometric measures such as stature, sitting height, body mass, and 6 skinfolds were also measured. A Shapiro-Wilk test was performed to assess normality distribution. Descriptive statistics consisted of the median, standard deviation, maximum, minimum, frequency, and mode. A comparison between soccer players and swimmers was performed using t-tests for independent samples.
Results: Soccer players (n=40) exhibit higher BMC for the whole body (1,528.4±108.3 vs 1,404.1±50.3) than swimmers (n=36) and for all specific regions of the body, except the upper limbs where swimmers exhibit higher BMC (195.7±35.2 vs 191.8±36.7). Soccer players have higher body mass (53.0±11.7 vs 44.2±9.6) and body mass index percentile for age (61.6±24.9 vs 42.5±27.2). Whole-body DXA shows a higher fat-free mass for soccer players (40.2±6.7 vs 35.5±5.4) and fat mass (20.9±3.5 vs 18.5±2.8).
Conclusion: Physical activity seems to promote and benefit bone mass gains during growth for specific regions of the skeleton. Soccer has a greater impact on specific regions of the pelvis and swimming on the upper limbs.
Limitations: The sample size.
Ethics committee approval: The ethics committee approved the study and written informed consent was obtained.

Funding: No funding was received for this work.
Author Disclosures:
J. Pinheiro: nothing to disclose
L. P. Ribeiro: nothing to disclose
M. Coelho-E-Silva: nothing to disclose

RPS 1014b-12 12:21
Total and regional bone density and body mass: comparison between normal and overweight male adolescents
J. Pinheiro[1], L. P. Ribeiro[2], M. Coelho-E-Silva[3]; [1]Sao Bras/PT, [2]Faro/PT, [3]Coimbra/PT (pedro.alexandrex94@gmail.com)

Purpose: To compare between normal and overweight/obese male adolescents.
Methods and materials: Bone mineral content (BMC) and density (BMD), lean soft tissue, and fat tissue were assessed using dual-energy x-ray absorptiometry. Anthropometric measures such as stature, sitting height, body mass, and 6 skinfolds were also measured. Descriptive statistics consisted of the median, interquartile range, maximum, and minimum. A comparison between overweight/obese and normal-weight male adolescents was performed using a Mann-Whitney U test.
Results: Overweight/obese (n=12, body mass index ≥85% percentile for age and gender) male adolescents exhibit higher BMD for the whole-body (1.110±0.137 vs 0.967±0.166; p=0.001) and specific regions of the skeleton than normal weight male adolescents (n=27, body mass index <85% percentile for age and gender) except for the upper limbs (0.741±0.160 vs 0.731±0.029; p=0.124) and the femoral shaft (1.122±0.200 vs 1.144±0.090; p=0.315). The mean body mass for overweight/obese subjects was 73.8±10.5 kg and for normal-weight subjects was 46.0± 3.8 kg. Body composition by DXA showed that overweight/obese subjects exhibit higher fat mass (FM) for the whole body (28.2±4.0 vs 17.7±5.3; p<0,001) but shows similar values for the upper limbs (1.9±0.01 vs 1.9±0.01; p=0.411). Overweight/obese subjects also exhibited higher lean soft tissue (LST) for the whole-body (54.2±7.7 vs 33.9±10.1; p<0.001) and specific regions.
Conclusion: Excess body mass may have an osteogenic effect on bone mass gains due to the extra load exerted on the skeleton.
Limitations: The sample size.
Ethics committee approval: The ethics committee approved the study and written informed consent was obtained.
Funding: No funding was received for this work.
Author Disclosures:
J. Pinheiro: nothing to disclose
L. P. Ribeiro: nothing to disclose
M. Coelho-E-Silva: nothing to disclose

11:15 - 12:30 **Coffee & Talk 3**

Head and Neck

RPS 1008

Temporal bone and auditory pathway

Moderators:
P. Golofit; Szczecin/PL
N.N.

RPS 1008-1 11:15
Reliability and clinical correlation of different grading scales in the MRI evaluation of endolymphatic hydrops
P. Malmierca Ordoqui[1], A. Paternain Nuin[1], A. Ezponda Casajus[1], M. Calvo Imirizaldu[1], A. C. Igual Rouilleault[1], V. Suárez Vega[2], R. Garcia de Eulate[1], N. Perez[1], P. Dominguez Echavarri[1]; [1]Pamplona/ES, [2]Madrid/ES (pmalmierca@unav.es)

Purpose: To analyse the degree of interobserver agreement in the detection and grading of endolymphatic hydrops (EH) with different scales and to correlate MRI findings with clinical information.
Methods and materials: 75 patients, diagnosed with unilateral definite Meniere's disease (MD), undergoing 3T-MRI of the inner ear were recruited. Cisternography, T2-FLAIR, and REAL IR imaging were performed 4 hours after intravenous contrast administration. Two independent radiologists blinded to clinical data analysed the images. Vestibular EH was evaluated using 4-stage (none/mild/moderate/severe), 3-stage (none/moderate/severe), and 2-stage (none/present) visual scales. Three-point (none/present/severe) and two-point (none/present) scales were employed for cochlear EH assessment. Discrepancies were solved by consensus. Interobserver agreement was evaluated with weighted-kappa (w-K) statistics. The association of pure tone audiometry (PTA) and caloric test with MR findings of EH was analysed with one-way ANOVA (p<0.05).
Results: Out of 75 patients, we identified EH in 90.6% of the clinically affected ear and in 17.3% on the silent side. Substantial or excellent interobserver agreement was found in all cases (mean w-K=0.83; range 0.7-0.91). The agreement was almost perfect with the 4-point vestibular EH scale (0.91±0.1). For cochlear EH, the highest consistency was obtained with the 2-point-scale (0.76±0.1). A statistically significant association was found between PTA and vestibular and cochlear EH, with all the scales. The strongest association was observed with the 2-stage cochlear (49.5±22 vs 25.4±21.5,F=45.1, p<0.001) and vestibular EH (54.8±20.1 vs 27.1±21.2,F=64.9, p<0.001) grading systems. The caloric test was also associated with 2-stage and 4-stage vestibular EH scales (F=4.5, p=0.034 and F=2.9, p=0.035, respectively).
Conclusion: A 4-stage vestibular EH grading system gave the best interobserver consistency. Vestibular and cochlear EH detected by MRI were associated with PTA and caloric tests, especially with the 2-scale grading system.
Limitations: A retrospective, single-institution study.
Ethics committee approval: Ethics committee approval obtained and informed consent waived.
Funding: No funding was received for this work.
Author Disclosures:
P. Malmierca Ordoqui: nothing to disclose
P. Dominguez Echavarri: nothing to disclose
A. Paternain Nuin: nothing to disclose
R. Garcia de Eulate: nothing to disclose
N. Perez: nothing to disclose
A. Ezponda Casajus: nothing to disclose
M. Calvo Imirizaldu: nothing to disclose
A. C. Igual Rouilleault: nothing to disclose
V. Suárez Vega: nothing to disclose

RPS 1008-2 11:21
Early radiologic manifestations of endolymphatic sac tumours in von Hippel-Lindau disease
J. F. Molto Garcia[1], H. J. Kim[2], P. Chittiboina[2], R. Lonser[2], J. Butman[2]; [1]Washington DC/US, [2]Bethesda/US (josemolto85@gmail.com)

Purpose: To characterise the imaging features of small (<1 cm) endolymphatic sac tumours (ELSTs) in von Hippel-Lindau disease (VHL).
Methods and materials: 19 VHL patients with 22 small ELST (3 with bilateral small ELSTs), 10 males and 9 females with ages between 11 and 74, were enrolled in a longitudinal natural history study of VHL.
High-resolution temporal-bone CT (<1.5 mm) and contrast enhanced MR (<3.0 mm, typically 1.5 thick/0.75 mm spacing T1-weighted) were available in all patients. Endolymphatic hydrops was evaluated in 9 cases using delayed FLAIR obtained 6-12 hours after contrast injection.
Results: Indirect MR findings: endolymphatic hydrops (4/9), intralabyrinthine haemorrhage (7/22), and enhancement within the ipsilateral vestibular aqueduct (13/22).
Direct MRI findings: intratemporal mass around the aqueduct (11/22) and distension/mass involving the extraosseous portion of the endolymphatic sac (10/22).
CT findings: erosion adjacent to the aqueduct (13/22) and asymmetric enlargement of the ipsilateral aqueduct (6/22).
Four cases were CT negative, no case was MRI negative, but 5 cases exhibited only “indirect” signs on MRI. One of these “indirect MRI only” cases were confirmed by erosion on CT.
Of the 4 cases with hydrops, 2 had neither intratemporal mass nor CT findings, and 1 had neither erosion nor intratemporal mass.
Conclusion: As VHL associated ELSTs cause irreversible audiovestibular morbidity independent of tumour size, early diagnosis and surgery have been advocated. ELSTs are locally invasive so that erosion on CT is diagnostic. Direct MRI tumour findings may be present when CT is negative. In some cases, radiologists must rely on indirect findings, e.g. intralabyrinthine haemorrhage or hydrops (requiring delayed FLAIR imaging) to establish the diagnosis of a small ELST.
Limitations: n/a
Ethics committee approval: n/a
Funding: No funding was received for this work.
Author Disclosures:
J. F. Molto Garcia: nothing to disclose
P. Chittiboina: nothing to disclose
R. Lonser: nothing to disclose
J. Butman: nothing to disclose
H. J. Kim: nothing to disclose

RPS 1008-3 11:27

Localisation evaluation of middle ear cholesteatoma with fusion of turbo spin-echo diffusion-weighted imaging and high-resolution computed tomography

X. Fan, Z. Liu*; Shenyang/CN (18940252031@163.com)*

Purpose: To assess the high-resolution computed tomography (HRCT) and turbo spin-echo diffusion-weighted imaging (TSE-DWI) fusion images in evaluating the anatomical location of cholesteatoma.
Methods and materials: A retrospective collection of 68 patients with clinically suspected middle ear cholesteatoma was performed. These patients underwent a TSE-DWI scan on a Philips Ingenia 3.0T superconductive MRI scanner and an ear HRCT scan on a Siemens Somatom Definition dual-source CT scanner. The fused image was produced using the intelligence space portal workstation to produce TSE-DWI-CT images. Subsequently, all patients underwent surgery within 14 days of the MRI scan. All data was analysed by receiver operating characteristic (ROC) to calculate the diagnostic performance of TSE-DWI-CT fusion images. According to the 2016 revised European Academy of Otolology and Neurootology/Japan Otological Society (EAONO/JOS) Joint Consensus Statements division of ear space (STAM system), Kappa statistical was used to calculate the consistency of TSE-DWI-CT fusion image division and localisation with intraoperative recording division and localisation.
Results: Based on the pathological results, patients were divided into a cholesteatoma group (n=50) and a non-cholesteatoma group (n=18). The use of TSE-DWI-CT fusion had greater diagnosis accuracy (92.65%) than HRCT (80.88%), P<0.05, the sensitivity and specificity of the diagnosis middle ear cholesteatoma were 94.00% and 88.89%. TSE-DWI-CT image fusion also showed increased localisation accuracy (88.82%), which was significantly improved compared with TSE-DWI (76.47%) and HRCT (61.76%).
Conclusion: The TSE-DWI-CT fusion image is a non-invasive, low-cost method for preoperative diagnosis of cholesteatoma and has a high diagnostic value for anatomical location of cholesteatoma, and can guide the choice of surgical planning.
Limitations: A small sample size and less negative patients.
Ethics committee approval: n/a
Funding: No funding was received for this work.
Author Disclosures:
X. Fan: nothing to disclose
Z. Liu: nothing to disclose

RPS 1008-4 11:33

Evaluation of necrotising external otitis on CT and MR: assessment of spreading patterns

L. van der Meer[1], C. Mitea[1], J. Waterval[1], D. Kunst[2], A. Postma[1]; *[1]Maastricht/NL, [2]Nijmegen/NL (liekevandermeer@gmail.com)*

Purpose: Necrotising external otitis (NEO) is a serious complication of the external otitis. NEO can be classified according to anterior, medial, intracranial, and crossed spreading patterns. Currently, there is no consensus on the optimal imaging modality for diagnosis. This study compares NEO spreading patterns and relevant subsites as assessed on MR and HRCT of the temporal bone in order to evaluate diagnostic comparability.
Methods and materials: We retrospectively examined 21 NEO patients who received an HRCT temporal bone and MR within a 3-month interval. Involvement of subsites and subsequent spreading patterns were assessed by a neuroradiologist blinded for the other imaging modality. The prevalence of spreading patterns by CT and MR were calculated and compared.
Results: In all patients, an anterior spreading pattern was noted on both MR and CT. Retrocondylar fat infiltration was the most consistent subsite of the anterior spreading pattern. The medial spreading pattern was seen in 7 patients at MR and in 5 of these 7 patients at CT, with parapharyngeal fat infiltration as the most consistent subsite. The intracranial spreading pattern matched in 1 out of 6 patients. The majority of patients showed a single (62%) and matching anterior spreading pattern at CT and MR.
Conclusion: The most common anterior spreading pattern of NEO can be assessed with CT as well as MR. However, the more complicated medial and intracranial spreading patterns as seen on MR could only be identified on CT in a small number of patients. Diagnosis of NEO at CT should therefore be complemented with additional imaging.
Limitations: The cohort consisted of a small number of included patients. A wide time interval between CT and MR was present, therefore a disease progression/regression between CT and MR is not excluded.
Ethics committee approval: n/a
Funding: No funding was received for this work.
Author Disclosures:
L. van der Meer: Other at Institutional grant - Siemens Healthcare
J. Waterval: nothing to disclose
D. Kunst: nothing to disclose
C. Mitea: Other at Institutional grant - Siemens Healthcare
A. Postma: Other at Institutional grant - Siemens Healthcare

RPS 1008-5 11:39

High-definition MRI for the evaluation of labyrinthic disorders

M. A. Esteves Da Cunha, T. Gillanders, M. Perez Akly, L. A. Miquelini, F. M. Olivera Plata, A. B. Granson, J. A. Funes, C. H. Besada*; Ciudad Autonoma De Buenos Aires/AR (maedacunha@gmail.com)*

Purpose: High definition magnetic resonance (HDMR) is the gold standard method in the study of the pathologies of the inner ear, however, there are no precise findings to determine a differential diagnosis between them. We investigated the usefulness of dedicated MR sequences in the characterisation of the intralabyrinthine pathology.
Methods and materials: We included patients evaluated between January 2010 and September 2019. Demographic and imaging data was collected. MRI images included high-resolution T2-weighted (HRT2), pre-enhanced T1-weighted (T1PE) and contrast-enhanced T1-weighted (T1CE). We placed ROIs on both labyrinths and in the fourth ventricle.
Results: MRI scans of 50 patients were analysed. The median age was 63.5 years (IQR 43-73). We found 18 (36%) patients with inflammatory labyrinthitis, 16 (32%) with intra-labyrinthine neurinoma, 9 (18%) with intra-labyrinthine haemorrhage, and 7 (14%) with ossifying labyrinthitis. All patients with intra-labyrinthine neurinoma had a low signal in HRT2, a mild-high signal in T1PE, and contrast enhancement. 14 patients with inflammatory labyrinthitis (77.8%) had low signal intensity in HRT2 and high signal in T1PE, and 13 patients (72.2%) had contrast enhancement. All patients with ossifying labyrinthitis had low signal intensity in HRT2 and 6 patients (87.5%) had high signal intensity in T1PE. All patients with haemorrhage had a high signal in pre-enhanced T1W. When we compared intra-labyrinthine neurinoma with inflammatory labyrinthitis, we found a significant difference in low signal intensity in HRT2 (p 0.001), T1PE (p 0.014), and in T1CE (p 0.003).
Conclusion: There are multiple entities that may alter the labyrinth signal in MR, some with similar radiologic patterns. We found differences in all the sequences studied between inflammatory labyrinthitis and intracochlear neurinoma.
Limitations: A diagnosis based on imaging findings without histopathology.
Ethics committee approval: Approved by an ethics committee.
Funding: No funding was received for this work.
Author Disclosures:
M. A. Esteves Da Cunha: nothing to disclose
M. Perez Akly: nothing to disclose
L. A. Miquelini: nothing to disclose
F. M. Olivera Plata: nothing to disclose
C. H. Besada: nothing to disclose
J. A. Funes: nothing to disclose
A. B. Granson: nothing to disclose
T. Gillanders: nothing to disclose

RPS 1008-6 11:45

Superior vestibular neuritis: improved detection using FLAIR sequence with delayed enhancement (1 hour)

A. Venkatasamy, T.-T. Huynh, A. Charpiot, N. Meyer, F. Veillon*; Strasbourg/FR (aina.vnkt@gmail.com)*

Purpose: Vestibular neuritis is a secondary cause of vertigo and new imaging protocols using delayed FLAIR with double-dose of gadolinium are proposed for its diagnosis. Our aim is to demonstrate that a single dose of gadolinium is sufficient.
Methods and materials: 33 patients with unilateral vestibular neuritis were compared to a control group. All patients underwent a FLAIR sequence one hour after intravenous injection of a single-dose of gadolinium at 1.5T. Two radiologists analysed the enhancement intensity of the superior (sup VN) and inferior vestibular nerve (inf VN), and ratios to the signal of the cerebellum were calculated (supVN/C). The statistics were performed using a Bayesian analysis.
Results: A strong enhancement of the sup VN was observed on the pathological side in 85% of patients with vestibular neuritis. The average signal intensity of the pathological sup VN (139 units ± 44) was more than two times the average intensity in the control group (58.5 units ± 5). The average ratios sup VN/C were significantly different between the pathological side in vestibular neuritis (2.43 units ± 0.63) and the control group (1.16 ± 0.14 (Pr(diff > 0) = 1). A delayed enhancement >71.5 units had a sensitivity of 96% and a specificity of 100% for the diagnosis of superior vestibular neuritis.
Conclusion: A delayed FLAIR sequence, acquired one hour after a single-dose of gadolinium injection, is a useful method for the diagnosis of vestibular neuritis. An enhancement of the sup VN >71.5 units was in favour of the diagnosis.
Limitations: A study on more patients should be performed to confirm the findings.
Ethics committee approval: The ethics committee of our institution approved the study (FC/ 2017-29) and it was registered on clinicaltrials.gov (NCT03452410).
Funding: No funding was received for this work.

Author Disclosures:
A. Venkatasamy: nothing to disclose
T.-T. Huynh: nothing to disclose
F. Veillon: nothing to disclose
A. Charpiot: nothing to disclose
N. Meyer: nothing to disclose

RPS 1008-7 11:51
The length of the organ of Corti in humankind: a meta-analysis study
B. Atalay, M. B. Eser, M. T. Kalcıoğlu, H. Ankaralı*; Istanbul/TR (bilgineser@hotmail.com)*

Purpose: The review question was: what is the length of the Corti organ (OC) in humankind?
Current studies offered that cochlear size might affect implant success in patients with hearing loss.
The hypothesis was: are the covariates (such as gender) affected the OC length?
Methods and materials: This meta-analysis was organised using the PRISMA statement.
The gender, age, country, continent, methods, and materials were determined as covariates, and this data was extracted from the studies.
OC was determined as an outcome. Data was pooled according to a random-effects model.
Meta-regression analysis was performed with Stata software (ver. 14.0) Metareg command. The overall effect was estimated with Metaan command.
Results: The review included 47 studies (n=3,976 material) and found that covariates weren't predictors of outcome.
Estimation of the between-study variance for the OC length (τ^2=0.7692) and the ratio of residual variance resulting from heterogeneity (I^2=0%) was statistically insignificant. Also, the coefficient determination of the model was R^2=19.18% (p=0.356). There wasn't a statistically significant relationship between the OC value and covariates.
The overall effect value for the OC length was 32.742 (CI %95:32.270-33.214) mm.
Conclusion: Evaluating each patient's OC size by imaging prior to cochlear implant surgery is important because of the wide variation.
The fact that there is a difference between spiral coefficient methods with the histological method (the gold standard for measuring the OC) necessitates the development of these methods.
Measurements that are made on images obtained by 3D reconstruction seem to be the future topics of radiology.
Limitations: The review includes only English language papers (except cites). There was no study from South America and Africa.
Ethics committee approval: n/a
Funding: No funding was received for this work.
Author Disclosures:
M. B. Eser: nothing to disclose
B. Atalay: nothing to disclose
M. T. Kalcıoğlu: nothing to disclose
H. Ankaralı: nothing to disclose

RPS 1008-8 11:57
Role of non-echo-planar diffusion-weighted images in the identification of recurrent cholesteatoma of the temporal bone
A. Guarnera, A. Romano, E. Covelli, G. Butera, M. Barbara, A. Bozzao*; Rome/IT (guarneraalessia@gmail.com)*

Purpose: To verify the specificity of non-EPI DWI-MRI in patients operated on for middle ear cholesteatoma who showed positivity at imaging performed 6 to 9 months after surgery and underwent second-look surgery.
Methods and materials: In a single-centre, a consecutive cohort of patients treated for cholesteatoma and undergoing 1.5T non-EPI DWI-MRI 6 to 9 months after surgery was evaluated. Patients showing a hyperintense signal in the middle ear underwent revision surgery and were included in the study, whilst the others were still under radiological follow-up and were excluded. Two radiologists independently placed an ROI inside the brightest part of the observed signal alteration on coronal HASTE-DWI images. The mean signal intensity (SI) and maximum (SImax) SI values were recorded for each patient. Signal intensity ratios (SIR) were calculated using the inferior temporal cortex (SIRT) and the background noise (SIRN) as references.
Results: 143 subjects (210 ears) were evaluated. 27 subjects (40 ears) showed a high signal lesion inside the middle ear and underwent revision surgery. 36 ears were confirmed to be affected by residual/recurrent cholesteatoma. In 4 ears, inflammatory tissue was found. According to the ROC analysis, SI, SIRT, and SIRTmax showed the best statistical values (AUC=1).
Conclusion: Residual/recurrent cholesteatoma can be accurately detected using quantitative evaluation of non-EPI DWI MRI, which may avoid a revision surgery if negative.
Limitations: The analysed cohort was relatively small. The design of this study excluded patients with normal DWI since false-negative DWI-MRI in post-surgical population is only 3% of cases.
Ethics committee approval: The study was approved by the Institutional Ethics Board and in line with the Declaration of Helsinki. Informed consent was obtained for MR examination.
Funding: No funding was received for this work.
Author Disclosures:
A. Guarnera: nothing to disclose
A. Romano: nothing to disclose
E. Covelli: nothing to disclose
G. Butera: nothing to disclose
M. Barbara: nothing to disclose
A. Bozzao: nothing to disclose

RPS 1008-9 12:03
Presence of vascular loop in patients with audio-vestibular symptoms: is it a significant finding? Evaluation with a 3-Tesla MRI 3D constructive interference steady state (CISS) sequence
M. A. Z. Teleb[1], N. Almansour[2]*; [1]Alexandria/EG, [2]Alahsa/SA (mamdouh_zidan@yahoo.com)*

Purpose: To evaluate the association of audio-vestibular symptoms with the presence of vascular loops and vascular contact in the cerebellopontine angle and the internal auditory canal using 3-Tesla magnetic resonance imaging.
Methods and materials: The study included 98 patients (196 ears); 51 females and 47 males, age range 11-73 years, mean 47.6±15 years. The healthy control group with no symptoms in either ear, n=60 (120 ears); 32 females and 28 males, age range 12-69 years, mean 45.3±15.8 years. The non-symptomatic ear in the patients were added to the healthy control group. Patients underwent a neuro-otologic evaluation to exclude an underlying pathologic process. The patients with neuritis or tumours at the CPA were not included in the study. No patients had previous CPA surgery or temporal bone trauma. All MR imaging examinations were performed by using a 3T (Magnetom Verio 3T; Siemens Medical Solutions, Erlangen, Germany). The imaging protocol consisted of axial T2-weighted images of the whole brain and coronal and axial T1-weighted images of the CPA before and after administration of intravenous contrast. 3D constructive interference steady state (CISS) imaging of the CPA was performed. The healthy control group was examined with the 3D CISS sequence in addition to the routine cranial MR imaging protocol.
Results: No statistically significant association was detected between the studied audiovestibular symptoms; tinnitus, deafness or vertigo and vascular loop (grades I-III) or vascular contact (type I-III) (p<0.05).
Conclusion: It was concluded that no possible role of the presence of vascular loop or vascular contact with the 8th cranial nerve in causing tinnitus, deafness or vertigo using 3D-CISS sequence assessment. Therefore, these findings are not certainly considered pathological but possibly to be normal anatomical variants.
Limitations: The sample size.
Ethics committee approval: n/a
Funding: No funding was received for this work.
Author Disclosures:
M. A. Z. Teleb: nothing to disclose
N. Almansour: nothing to disclose

RPS 1008-10 12:09
A critical appraisal of the quality of vertigo practice guidelines using the AGREE II tool: a EuroAIM initiative
F. M. Doniselli[1], M. Zanardo[1], A. Costa[1], V. Cuccarini[1], L. M. M. Sconfienza[1], M. Mazón Momparler[2], A. Rovira Cañellas[3], E. Arana Fernandez de Moya[2]*; [1]Milan/IT, [2]Valencia/ES, [3]Barcelona/ES (fabio.doniselli@gmail.com)*

Purpose: To assess the methodologic quality of guidelines for the management of vertigo and dizziness, and to compare their recommendations.
Methods and materials: In May 2019, a systematic search was performed using MEDLINE, EMBASE, the National Guideline Clearinghouse, and the National Institute for Health and Clinical Excellence to find practice guidelines for the management of vertigo and dizziness. The evaluation of guidelines quality was performed independently by four authors using the AGREE II tool. We excluded from the results those guidelines that were not primarily focused on vertigo and dizziness, such as national/international guidelines in which vertigo and dizziness were briefly mentioned.
Results: Our strategy of literature search identified 162 studies and 16 guidelines were selected for the appraisal. Only four guidelines reached the acceptance level in the overall result (at least 60%), with two of them reaching the highest scores (at least 80%). The highest scores were found in domain 6 “editorial independence” (median value=65%) and domain 4 “clarity of presentation” (median value=61%). The remaining domains showed a low level of quality: domain 2 "stakeholder involvement", domain 3 "rigour of development", and domain 5 “applicability” had median values of 23%, 25%, and

24%, respectively. Comparing with other EuroAIM evaluations, the quality of these guidelines was very low because of low involvement of the multidisciplinary team and no use of the AGREE II guidelines in the writing guidelines recommendations.
Conclusion: Considering all guidelines, only two had a "high" overall score, while 10/16 were rated as "low" quality. Future guidelines might take this into account to improve clinical applicability.
Limitations: Our team of evaluators was composed of three radiologists and an otolaryngologist.
Ethics committee approval: No ethics committee approval was required for this systematic review.
Funding: No funding was received for this work.
Author Disclosures:
F. M. Doniselli: nothing to disclose
M. Zanardo: nothing to disclose
A. Costa: nothing to disclose
V. Cuccarini: nothing to disclose
E. Arana Fernandez de Moya: nothing to disclose
L. M. M. Sconfienza: nothing to disclose
M. Mazón Momparler: nothing to disclose
A. Rovira Cañellas: nothing to disclose

RPS 1008-12 12:21
Characteristics of small-world connectivity and ninety cortical nodes in bilateral sensorineural hearing loss: a study using graph theoretical analysis
X.-M. Xu, T.-Y. Tang, G.-J. Teng*; Nanjing/CN (xmxu15@163.com)*

Purpose: To explore the topological characteristics of brain connectome following sensorineural hearing loss (SNHL) from the global level and nodal level.
Methods and materials: 36 subjects with long term bilateral SNHL and 37 matched HCs were recruited from the local hospital and community for this study. Every subject underwent pure tone audiometry tests, neuropsychological assessments, and MRI scanning. AAL atlas was employed to divide a brain into 90 cortical and subcortical regions of interest, then investigated the global and nodal properties of “small world” network in SNHL and control groups using a graph-theory analysis. The global characteristics included small worldness, cluster coefficient, characteristic path length, local efficiency, and global efficiency. Node properties included degree centrality, betweenness centrality, nodal efficiency, and a nodal clustering coefficient. Interregional connectivity analysis was also computed among 90 nodes to find alterations in the SNHL group.
Results: The SNHL group had significantly higher hearing thresholds and cognitive impairments as well as disrupted internal connections among 90 nodes. The SNHL group displayed lower AUC of cluster coefficient, path length lambda, but increased global efficiency. The opercular and triangular part of the inferior frontal gyrus, rectus gyrus, parahippocampal gyrus, precuneus, and amygdala showed abnormal local features. Some of these connectome alterations were correlated with duration and cognitive ability.
Conclusion: SNHL changed some topological properties, proving potential imaging biomarkers and treatment targets for future study.
Limitations: Small sample size and various duration of SNHL. Future work needs to recruit more subjects and control confounding factors.
Ethics committee approval: This study was approved by the ethics committee of our hospital and university (2016ZDSYLL031.0). Written informed consent was obtained from each enrollee at the beginning.
Funding: National Natural Science Foundation of China (81520108015).
Author Disclosures:
X.-M. Xu: nothing to disclose
G.-J. Teng: nothing to disclose
T.-Y. Tang: nothing to disclose

11:15 - 12:30 **da Vinci (Room D1)**

Abdominal Viscera

RPS 1001a

Advances in MRI techniques

Moderators:
N. Papanikolaou; Lisbon/PT
F. Regini; Firenze/IT

RPS 1001a-K 11:15
Keynote lecture
A. J. van der Molen*; Leiden/NL (a.j.van_der_molen@lumc.nl)*
Author Disclosures:
A. J. van der Molen: nothing to disclose

RPS 1001a-1 11:25
Influence of injection rate in determining the development of artifact during acquisition of dynamic arterial phase in Gd-EOB-DTPA MRI studies
C. Maino[1], D. Ippolito[2], A. Pecorelli[2], L. Riva[2], C. R. G. L. Talei Franzesi[1], S. Sironi[3]; *[1]Milan/IT, [2]Monza/IT, [3]Bergamo/IT*
(mainocesare@gmail.com)

Purpose: To assess whether modifications of injection rate of Gd-EOB-DTPA contrast media could influence the development of artifacts during arterial phase of liver MRI studies.
Methods and materials: All EOB-MRI studies performed at our institution between 2016 and 2018 were retrospectively evaluated. Each MRI study was acquired on 1.5 T scanner with our liver protocol: T1 in- and out-phase, T2 with and without fat-saturation, DWI, and 3D-T1 pre- and post i.v. injection of contrast media with different flow injection rate (1 mL/sec and 1.5 mL/sec). For each study, a single radiologist recorded the presence or the absence of artifacts during different acquisition phase: 1) all the examination; 2) only during the arterial phase; 3) only during portal venous phase; 4) both arterial and portal venous phase. The reviewer registered the injection flow rate of contrast medium for each examination.
Results: Of 748 MRI studies, 229 were excluded to the presence of artifacts in the entire examination. Of the remaining, 312 were obtained using a flow rate of 1 ml/s and 207 using a flow rate of 1.5 ml/s. Only 14 exams developed artifacts during the arterial phase using a flow rate of 1 ml/min, while a total of 84 when a flow rate of 1.5 ml/s was used (4% vs 40%). Comparing the different groups, the reduction of injection rate (1 ml/sec) statistically reduced the development of artifacts during arterial phase ($p<0.0001$).
Conclusion: Development of artifacts of Gd-EOB-DTPA liver-MR studies can be related to flow injection rate and the reduction of flow (1 mL or less) may help in the better assessment and acquisition of the arterial phase.
Limitations: Single-center study.
Ethics committee approval: Written informed consent.
Funding: No funding was received for this work.
Author Disclosures:
C. Maino: nothing to disclose
D. Ippolito: nothing to disclose
A. Pecorelli: nothing to disclose
C. R. G. L. Talei Franzesi: nothing to disclose
S. Sironi: nothing to disclose
L. Riva: nothing to disclose

RPS 1001a-2 11:31
Intrapatient and interobserver image quality analysis in liver MRI study with Gd-EOB-DTPA using two different multiarterial phase techniques
F. Castagnoli[1], V. Ruggeri[2], M. Bertuletti[1], M. Gatti[2], R. Inchingolo[3], R. Faletti[2], L. Grazioli[1]; *[1]Brescia/IT, [2]Turin/IT, [3]Matera/IT*
(francy-cast@hotmail.it)

Purpose: To evaluate intrapatient and interobserver variability in patients who underwent liver MRI with Gd-EOB-DTPA using two different multiarterial phase techniques.
Methods and materials: Two radiologists retrospectively analysed 154 prospectively enrolled patients who underwent liver MRI performed with 1.5T MAGNETOM Aera twice from February 2017 to March 2019, using two different multiarterial algorithms: CAIPIRINHA or TWIST-VIBE (Siemens Healthcare, Erlangen, Germany). For every patient, breath-holding time, BMI, sex, and age were recorded before the second MRI study. The phase without contrast media and every arterial phase (after administration of Gd-EOB-DTPA; dose: 0.025ml/kg; injection rate: 1ml/s) were evaluated using different scores to quantify Gibbs artefacts (present/absent), noise (present/absent), breath artefacts, and general quality of images (score 1-5, 1: “non-diagnostic”, 5: “absence of artefacts”/“optimal exam quality”).
Results: CAIPIRINHA always had better scores for every parameter considered, with the exception of noise score analysis. 37% of patients failed to obtain multiarterial phases: in particular 11% had only one arterial phase, 26% had two. Breath-holding time was the only parameter that influenced the performance of multiarterial techniques. TWIST-VIBE had a worse score for Gibbs and breath artefacts but a better noise score: 23% of patients in the basal phase had noise (vs46% in CAIPIRINHA), 18% in the first arterial phase (vs29%), 18% in the second arterial phase (vs30%), and 17% in the third arterial phase (vs31%).
Conclusion: CAIPIRINHA always allows the obtaining of diagnostic images without multiarterial phase only in 37% of cases. TWIST-VIBE always allows the obtaining of three arterial phases. Breath-holding time is the only parameter which can influence the preliminary choice between CAIPIRINHA and TWIST-

VIBE. TWIST-VIBE is preferable in very compliant patients, otherwise CAIPIRINHA is more appropriate.
Limitations: Limited cohort; non-homogeneous follow-up.
Ethics committee approval: Study approved by ethics committee.
Funding: No funding was received for this work.
Author Disclosures:
M. Bertuletti: nothing to disclose
F. Castagnoli: nothing to disclose
V. Ruggeri: nothing to disclose
M. Gatti: nothing to disclose
R. Inchingolo: nothing to disclose
R. Faletti: nothing to disclose
L. Grazioli: nothing to disclose

RPS 1001a-3 11:37

Gadoxetate disodium-enhanced MRI: assessment of arterial phase artifacts and hepatobiliary uptake in a large single centre series

N. Vietti Violi[1], P. Agriradi[2], A. Rosen[2], M. Cherny[2], A. Weiss[2], G. Hernandez Meza[2], J. S. Babb[2], S. Kihira[2], B. Taouli[2];
[1]Lausanne/CH, [2]New York, NY/US (nviettivioli@gmail.com)

Purpose: To assess the prevalence of arterial phase artifacts during MRI using gadoxetate disodium and its predictive factors as well as the quality of the hepatobiliary phase (HBP) in a large series.
Methods and materials: This retrospective single centre study included 851 patients (M/F: 537/314, mean age: 63y) with gadoxetate disodium MRI performed in 2017. The MRI protocol included unenhanced, dual arterial (AP1 and AP2), portal venous, transitional and HBP. Three independent radiologists graded dynamic images using a 5-scale score (1: no motion, 5: severe, nondiagnostic). Transient severe motion (TSM) was defined as a score ≥4 during at least one AP with a score ≤3 during other phases. HBP uptake was assessed using a 3-scale score (1: liver hyperintense to portal vein (PV), 2: liver isointense to PV, 3: liver hypointense to PV). The association between demographic, clinical, and acquisition parameters with TSM was tested in uni- and multivariate logistic regression.
Results: TSM related artifacts were observed in 103/851 patients (12.1%): 83 (9.8%) in one AP and 20 (2.3%) in both AP. 87/851 (10.2%) patients demonstrated limited contrast uptake at HBP. 6 patients (0.7%) presented TSM and limited HBP contrast uptake. Presence of TSM was significantly associated with age, presence of liver disease, and cancer on univariate logistical regression, but not in multivariate analysis (p>0.05). No association was found between imaging acquisition parameters and TSM.
Conclusion: TSM was present in 12.1% of gadoxetate disodium-enhanced MRIs and was poorly predicted based on clinical factors. TSM is rarely associated to limited HBP contrast uptake.
Limitations: Single center study.
Ethics committee approval: The institutional review board approved the study and waived informed consent.
Funding: Swiss National Science Foundation, fellowship:P2LAP3_178053.
Author Disclosures:
N. Vietti Violi: nothing to disclose
P. Agriradi: nothing to disclose
A. Rosen: nothing to disclose
M. Cherny: nothing to disclose
A. Weiss: nothing to disclose
G. Hernandez Meza: nothing to disclose
J. S. Babb: nothing to disclose
S. Kihira: nothing to disclose
B. Taouli: nothing to disclose

RPS 1001a-4 11:43

Relative enhancement of the liver during hepatobiliary phase after Gd-BOPTA administration: correlation with bilirubin levels and renal function

R. Valletta[1], M. Bonatti[2], F. Lombardo[1], G. Zamboni[1], G. Schifferle[2];
[1]Verona/IT, [2]Bozen/IT (riccardo.valletta@studenti.univr.it)

Purpose: To investigate if there is correlation between liver signal intensity during hepatobiliary phase (HBP) after Gd-BOPTA administration and liver/renal function.
Methods and materials: IRB-approved retrospective study, need for informed consent was waived. 75 consecutive patients (44 M, 31 F; mean age 63y) who underwent Gd-BOPTA-enhanced liver MRI (including HBP) on a 1.5T scanner between January 2018 and August 2019 were included. Liver signal intensity on unenhanced and HBP images was measured using round ROIs and normalised to paraspinal muscles. Subsequently, normalised relative enhancement (NRE) between unenhanced phase and HBP was correlated with patients' total bilirubin blood levels and eGFR.
Results: Mean total bilirubin was 1,73 mg/dl (0,27-23,23 mg/dl), while mean eGFR was 69,5 (48-135). There was a significant, weak negative correlation between NRE and total bilirubin (p=0.004; Spearman r=-0.329). No significant correlation was found between NRE and patients' eGFR.
Conclusion: Patients with higher bilirubin levels tend to show lower relative enhancement of the liver during HBP compared to patients with normal liver function. A supplementary dose of Gd-BOPTA could be considered in these patients in order to achieve an optimal quality of the examination, even if further investigations are needed.
Limitations: One limitating factor is the relatively small population.
Ethics committee approval: n/a
Funding: No funding was received for this work.
Author Disclosures:
R. Valletta: nothing to disclose
M. Bonatti: nothing to disclose
F. Lombardo: nothing to disclose
G. Zamboni: nothing to disclose
G. Schifferle: nothing to disclose

RPS 1001a-5 11:49

Visualising liver function by T1 relaxometry based quantification of hepatic concentration of a gadolinium-based liver specific contrast agent

C. Breit, T. Heye, D. J. Winkel, D. Boll*; Basel/CH*

Purpose: To evaluate whole-organ liver function non-invasively, to get spatial information on segmental liver metabolism, and determine a parameter which correlates with fibrotic changes.
Methods and materials: 72 healthy patients (mean 53 yrs, 19-87yrs) without histopathologically proven liver disease, 21 patients with temporary elevated liver enzymes (mean 66 yrs, 34-91 yrs), and 109 patients with biopsy proven liver fibrosis or cirrhosis (mean 61 yrs, 36-86yrs) underwent 1.5T (133) or 3T (69) routine MRI and were included. Fibrosis was classified by using the histopathologicy METAVIR and the clinical Child-Pugh Scores. Gd-concentration was quantitated based on T1 map-based calculations. Gd-concentration mapping was performed by using a look-locker approach prior to intravenous administration of hepatocyte specific contrast agent. Parenchymal fat fraction, R2*, liver volume, laboratory hepatic function parameters, gender, and age were aquired and used for classification based on machine learning algorithms.
Results: Mean Gd-concentration in the liver parenchyma was significant (p<0.0001) higher for healthy patients ([Gd]=0,51mcmol/l) than for those with liver fibrosis or cirrhosis (([Gd]=0.31mcmol/l) and with acute liver disease ([Gd]=0.28mcmol/l), even though there was no significant difference in Gd-concentration between patients with acute liver disease and those with known fibrosis or cirrhosis. There was a significant (p<0.0001) moderate negative correlation for the mean Gd-concentration and the METAVIR score (r=-0.44) as well as for the Child-Pugh stage (r=-0.35). There was a significant strong correlation between the bilirubin concentration and the Gd-concentration (r=-0.61, p<0.0001).
Conclusion: T1-based measuring of contrast agent concentration allows to non-invasively quantify liver function and is a potential predictor even for detection of early fibrotic changes. Furthermore, it is possible to get additional spatial information about liver metabolism by creating concentration maps.
Limitations: Retrospective study design.
Ethics committee approval: Informed consent waived.
Funding: No funding was received for this work.
Author Disclosures:
T. Heye: nothing to disclose
D. Boll: nothing to disclose
C. Breit: nothing to disclose
D. J. Winkel: nothing to disclose

RPS 1001a-6 11:55

Mapping of the liver function: impact of MR field strength on T1 reduction rate

D. Catucci, V. C. Obmann, A. Berzigotti, J. Hrycyk, W. Kajdi, C. Gräni, L. Ebner, A. Christe, A. T. Huber*; Berne/CH (verena.obmann@insel.ch)*

Purpose: To determine whether T1 reduction rate is dependent on field strength in patients with and without liver cirrhosis.
Methods and materials: 85 consecutive Gd-EOB-DTPA liver MRI scans with available T1 mapping pre- and post-contrast administration in equilibrium phase were analysed between September 2018 and January 2019. 44 exams were performed on a 1.5T system and 41 exams on a 3T system. Each of these two groups was then divided into patients with and without liver cirrhosis. T1-reduction rates were calculated as: (native T1 – post contrast T1) / native T1. Groups were compared using a Mann-Whitney-U test.
Results: At 1.5, 23 patients had cirrhosis, while 21 patients had no cirrhosis. At 3T, 17 patients had cirrhosis, while 24 patients had no cirrhosis. At both 3T and 1.5T, T1 reduction rate discriminated between patients with and without cirrhosis (p=0.001 and p>0.001). T1 reduction rates did not differ significantly between 3T

and 1.5T in patients with cirrhosis (median 60% vs. 59%; p=0.991) and without cirrhosis (median 75% vs. 75%; p=0.787).
Conclusion: This study shows that T1 reduction rate is comparable between 3T and 1.5T and may discriminate patients with and without liver cirrhosis as an imaging surrogate to map liver function.
Limitations: We acknowledge limitations to our study, mainly the retrospective study design and limited number of patients included.
Ethics committee approval: This study was approved by the cantonal ethics committee Bern. Written informed consent was given.
Funding: This project was funded by the Swiss National Science Foundation (SNF) grant # 320030_188591.
Author Disclosures:
V. C. Obmann: nothing to disclose
A. Berzigotti: nothing to disclose
D. Catucci: nothing to disclose
J. Hrycyk: nothing to disclose
W. Kajdi: nothing to disclose
C. Gräni: nothing to disclose
L. Ebner: nothing to disclose
A. T. Huber: nothing to disclose
A. Christe: nothing to disclose

RPS 1001a-7 12:01
Precision analysis for dual R2 MRI relaxometry in assessment of liver disease
H. Leao Filho[1], W. Chua-Anusorn[2], P. Clark[3]; [1]Sao Paulo/BR, [2]Camberra/AU, [3]Perth/AU (hiltonmlf@gmail.com)

Purpose: A quantitative MRI method (QMRI) was recently validated using multi-compartmental R2 relaxometry (MCR2R) to map liver fibrosis/inflammation in patients with non-alcoholic steatohepatitis. The study was designed to evaluate this method precision through examinations performed in volunteers on a 3T scanner at different times using the same parameters.
Methods and materials: 30 volunteers were recruited. They underwent exams on a 3T scanner after fasting for 4h. They were re-scanned on the same MRI and protocol less than 1 week apart. The protocols used a multi-spin echo sequence (MSE) to determine water extracellular fraction and R2 maps. We also acquired multi-gradient echo sequences (MGE) to calculate proton density fat fraction. All measures were performed by one radiologist with 13 years of experience using a ROI encompassing the whole liver area in a single slice. The repeatability of the measures was assessed through the within-subject coefficient of variation and repeatability coefficient.
Results: Extracellular water fraction (ECWF) mean values were 12.99% (±1.88) in the first exam and 13.06 (±1.9) in the second, ranging from 9.9 to 16.9%. The repeated scans were not statistically significantly different (T-test). The bias between scans was <0.1% ECWF. The repeatability coefficient between scans was 2.47% (absolute measure of ECWF), comparable to the 2xSD variation of ECWF obtained previously across each fibrosis grade, indicating that approximately 95% of patients would receive the correct fibrosis grade. The within-subject coefficient of variation was 6.86% (as a percentual).
Conclusion: The study showed good precision of the QMRI method for quantifying the extracellular water fraction (as a proxy for degree of fibrosis), with repeatability coefficient of 2.47%.
Limitations: Single institution. Small number of patients. One reader.
Ethics committee approval: Approved by ethics with informed consent.
Funding: No funding was received for this work.
Author Disclosures:
H. Leao Filho: nothing to disclose
P. Clark: CEO at MagnePath, Founder at MagnePath
W. Chua-Anusorn: CEO at MagnePath, Founder at MagnePath

RPS 1001a-8 12:07
A comparative study of diagnostic value of DWI MRI bewteen mono-exponential, bi-exponential, and non-Gaussian kurtosis models in pancreatic ductal adenocarcinoma
S. Peng; *Sichuan/CN (pengsk1986@126.com)*

Purpose: To investigate the diagnostic value of different DWI models (monoexponential, biexponential models multiple b values diffusion-weighted imaging, and non-Gaussian diffusion-weighted MRI) in poorly differentiated pancreatic ductal adenocarcinoma.
Methods and materials: 52 patients with poorly differentiated pancreatic ductal adenocarcinoma confirmed by surgery were collected. All patients underwent DWI (1.5T, Multi-b values : 0, 50, 100, 150, 200, 500, 800, 1000, 1500, 2000 s/mm2). Mean values of DWI-derived metrics $ADC_{standard}$, ADC_{slow}, ADC_{fast}, f, MK, and DK were calculated from regions of interest in all tumours and non-tumorous parenchyma and compared. ROC was used to evaluate the diagnostic efficiency.
Results: All lesions could be distinguished from non-lesions by three DWI sequences (ADC-DWI, DKI and IVIM). The $ADC_{standard}$, ADC_{fast} , f values, and MK showed significant differences between tumours and non-tumorous parenchyma (both $P < 0.05$). The area under the curve for ADC, D, D*, f, K, and DK were (0.705, 0.665, 0.648, 0.614), respectively. The ROC curve integrated with $ADC_{standard}$ and MD has better diagnostic efficiency (the area under ROC curve is about 0.754).
Conclusion: $ADC_{standard}$, ADC_{fast}, f, and MK could differentiate tumours from non-tumorous parenchyma. The combination of Gaussion distribution model and non-Gaussion distribution model has the potential to increase the diagnostic accuracy of DWI in patients with pancreatic ductal adenocarcinoma.
Limitations: Not enough cases and focused only on poorly differentiated pancreatic cancer.
Ethics committee approval: n/a
Funding: Sichuan science and technology program（2015SZ0030. Popularisation project of sichuan provincial commission of health and family planning（17PJ421.
Author Disclosures:
S. Peng: Author at Sichuan Provincial Hospital

RPS 1001a-9 12:13
MRI with diffusion-weighted imaging in the evaluation of abdominal Castleman's disease
W. Mingliang, Z. Mengsu; *Shanghai/CN (wang.mingliang@zs-hospital.sh.cn)*

Purpose: To analyse the MR imaging characteristics and ADC values of abdominal Castleman's disease (CD).
Methods and materials: The MR imaging data of 14 patients with CD were retrospectively reviewed. Image analysis included the location, size, shape, lesion margins, plain signal intensity, and enhancement pattern of the lesions and spleen. ADC values of the CD and spleen were measured on the images of ADC map.
Results: Of the 14 patients with CD, 9 cases were hyaline vessel type, the mean maximum diameter of the lesion was 5.1±2.4 cm, 5 cases were plasma cell type, and the mean maximum diameter of the lesion was 4.5±1.9 cm. All 14 lesions were round or elliptical. The lesions showed an equal or slightly lower signal intensity on T1WI and high or slightly higher signal intensity on T2WI, high signal intensity on DWI. All 14 cases were significantly enhanced in the arterial phase and persisted enhancement in the portal vein phase and in the delayed phase, which was consistent with the spleen. The mean ADC values of CD and spleen in 11 patients without cirrhosis were respectively $(1.12\pm0.18) \times 10^{-3} mm^2/s$ and $(1.13\pm0.15) \times 10^{-3} mm^2/s$, and there was no statistically difference (P=0.836).
Conclusion: The MR characteristics of Castleman's disease have certain characteristics. In particular, the signal characteristics of diffusion-weighted imaging and ADC values of lesions are consistent with the spleen, which is helpful for diagnosis and identification.
Limitations: The number of cases included in this study was small.
Ethics committee approval: The retrospective study was approved by the institutional review board of our hospital. Specific informed consent was not required according to Local Ethics Committee rules for retrospective study design.
Funding: No funding was received for this work.
Author Disclosures:
W. Mingliang: Author at Zhongshan Hospital, Fudan University
Z. Mengsu: Author at Zhongshan Hospital, Fudan University

RPS 1001a-10 12:19
T1-weighted fat-suppressed sequence: most specific way for time and cost-effective diagnosis of endometriosis with MRI
A. Dumbadze; *Tbilisi/GE (dumbadze.a@yahoo.com)*

Purpose: To determine the accuracy of the high specificity of hyperintensity foci presence on T1-weighted fat-suppressed images in the diagnosis of superficial and deep pelvic endometriosis in everyday practice.
Methods and materials: During 12 months, 40 patients (35.4 ± 7.2 years) referred to our institution with clinically suspected endometriosis underwent 3.0T MRI examination of pelvis without using i.v. contrast. Every examination included T1-weighted fat-sat sequences and was interpreted by two radiologists (with different experience). All patients with T1-W fat-sat hyperintensity foci proceded afterwards to minimally invasive diagnostic procedures as laparoscopy or cystoscopy for confirmation of endometriosis with histopathology.
Results: The two radiologists had an identical sensitivity of 80.3% (95% CI; 57.6-95.2). The specificity was 100% (95% CI; 82.4-100) for the young and 89.5% (95% CI; 66.9-98.7) for the experienced radiologist. The area under the ROC curve was 0.90 (95% CI; 0.81-0.99) for the young and 0.83 (95% CI; 0.70-0.96) for the experienced radiologist. The intraoperator variability was low with almost perfect reproducibility for the overall detection of lesions; k=0.90 (95%

CI; 0.77-1) for the young and k=0.85 (95% CI; 0.70-1) for the experienced radiologist.
Conclusion: Our results show that the characterisation of lesions by MRI, especially with using of T1-W fat sat sequence, is highly specific and moderately sensitive in the diagnosis of endometriosis, with high interoperator reproducibility. Pelvic protocols should always include the T1-W fat-sat sequence. In addition to its accuracy in distinguishing teratomas from endometriomas, it helps to better characterise adhesions and distinguishing from post-surgical scars. In future MRIs, it can be used to diagnose pelvic lesions and the accurate examination may replace the necessity of biopsy.
Limitations: n/a
Ethics committee approval: n/a
Funding: No funding was received for this work.
Author Disclosures:
A. Dumbadze: nothing to disclose

RPS 1001a-11 12:25
Impaired enhancement of portal vein on portal venous phase with Gd-EOB-DTPA compared to Gd-BOPTA in cirrhosis
F. Vernuccio, V. Greco, C. Gozzo, R. Cannella, M. Midiri, G. Brancatelli; *Palermo/IT (federicavernuccio@gmail.com)*

Purpose: This study compared enhancement of the portal vein with Gd-BOPTA and Gd-EOB-DTPA in cirrhotic patients.
Methods and materials: A total of 84 cirrhotic patients (30 women, 54 men) who underwent both Gd-EOB-DTPA– and Gd-BOPTA–enhanced liver MRI from 2008 to 2018 were retrospectively included. Interval time between Gd-BOPTA and Gd-EOB-DTPA MR studies was 10.7 months. Patients received a weight-dependent dose of Gd-EOB-DTPA (0.025 mmol/kg body) or Gd-BOPTA (0.1 mmol/kg body). Signal intensity of the portal vein, liver-to-portal vein contrast ratio, and image contrast of portal vein were calculated on portal venous phase for each exam and compared per patient through the Wilcoxon signed rank sum test. Statistical significance was set at $p<0.05$.
Results: Compared to Gd-BOPTA MRI, Gd-EOB MRI in the portal venous phase showed significantly lower portal vein signal intensity (1461.72 ± 360.56 vs. 1256.68 ± 327.71, respectively; $p<0.001$) and image contrast of the portal vein (0.27 ± 0.11 vs. 0.35 ± 0.11, respectively, $p<0.001$) and higher liver-to-portal vein contrast ratio (0.72 ± 0.11 vs. 0.64 ± 0.11, $p<0.001$).
Conclusion: At the recommended dose of hepatobiliary contrast agents, Gd-EOB-DTPA yields lower enhancement of the portal vein than Gd-BOPTA in cirrhotic patients. Gd-BOPTA might therefore enable better evaluation of the portal vein in cirrhotic patients.
Limitations: Retrospective design, small sample size and single-centre experience, lack of correlation with laboratory data or contrast dose.
Ethics committee approval: IRB approved, informed consent waived.
Funding: No funding was received for this work.
Author Disclosures:
F. Vernuccio: nothing to disclose
V. Greco: nothing to disclose
R. Cannella: nothing to disclose
M. Midiri: nothing to disclose
G. Brancatelli: nothing to disclose
C. Gozzo: nothing to disclose

11:15 - 12:30 **Darwin (Room D2)**

Breast

RPS 1002b

Interactions between breast radiology and pathology

Moderators:
E. Divjak; Zagreb/HR
M. Lesaru; Bucharest/RO

RPS 1002b-K 11:15
Keynote lecture
C. Kurtz; *Lucerne/CH (claudia.kurtz@luks.ch)*

Author Disclosures:
C. Kurtz: nothing to disclose

RPS 1002b-1 11:25
A retrospective review of recalled microcalcifications following breast cancer treatment
P. L. Gammack, M. Smith, M. Stewart; *Edinburgh/UK (pauline.gammack1@nhs.net)*

Purpose: This study focused on women with previously treated breast cancer who were recalled for further imaging due to microcalcifications. We aimed to determine our ability to characterise these; which factors increased risk of recurrence, timeframe of recurrence, and results of biopsies.
Methods and materials: Data was collected for patients recalled between June 2013 and February 2019, specifically time interval, original diagnosis, original mammographic appearance, and the outcome of recall.
Results: 194 women were recalled for microcalcifications for further views +/ biopsy. 126 were for ipsilateral to the original cancer, 66 contralateral, and 2 bilateral. 104 (54%) underwent biopsies, the remainder were considered benign. 66% confirmed recurrence/new cancer. 3 microcalcifications were recalled and not biopsied, then subsequently determined to be a recurrence. The time interval for recurrence ranged from 1 to 12 years, with an average of 4.4 years. 74% recurred within 5 years. Of the 40 ipsilateral recurrences, 29 had DCIS with their original cancer and 26 had microcalcifications in their initial cancer.
Conclusion: Our study proved that we perform well in the characterisation of mammographic calcifications in the treated breast. Biopsy rates were appropriate as a large percentage confirmed histological recurrence. Reassuringly, only 3 recurrences were missed (0.02% of all recalls). The presence of DCIS and calcifications in the original cancer increased the risk of recurrence. 25% of recurrences and new cancers were beyond 5 years of follow-up, suggesting that our health board's protocol of following up treated breast cancer for 10 years is appropriate.
Limitations: Data regarding previous mammogram/pathology results were not available for patients who were treated prior to electronic records. The record recalled patients is maintained manually by a mammographer and may not include all patients in the program.
Ethics committee approval: n/a
Funding: No funding was received for this work.
Author Disclosures:
P. L. Gammack: nothing to disclose
M. Smith: nothing to disclose
M. Stewart: nothing to disclose

RPS 1002b-2 11:31
Representative calcifications revisited: how many sequential breast calcifications are adequate for definitive diagnosis?
W. Teh, R. Uzvolk, M. Morgan, J. Rees, R. Felton; *London/UK (william.teh@nhs.net)*

Purpose: The Brevera breast biopsy device provides real-time visualisation of representative calcifications during biopsy potentially, allowing fewer samples, minimising trauma, and ensuring the accuracy of the biopsy. This study examines how many sequential specimens containing calcifications are required for accurate diagnosis.
Methods and materials: A prospective study using tomosynthesis-guided 9 gauge vacuum biopsy (VAB) of screen-detected microcalcifications with realtime imaging of specimen radiograph. A minimum of 12 samples or more until representative calcifications were obtained. Sequential imaging of breast specimens was correlated with the histological assessment for the presence of calcifications and pathology. Final correlation with any lesions undergoing vacuum excision for B3 (high-risk lesions) or surgery.
Results: 157 VABB were performed on 155 patients with calcifications ranging from 2-120 mm (mean 16.3 mm) with pathological calcifications confirmed in 152 (96.8%). 82 (52.2%) were benign, 20 (12.7%) B3 (high risk), 3 suspicious (1.9%), and 47 (29.9%) malignant. 43% of calcifications were obtained on the first specimen. For benign lesions, there was a 85% accuracy on the first positive specimen and 100% by the fourth. For DCIS, the diagnosis was obtained on the first positive specimen in 92% and 100% by the fourth. Three lesions (1 B3 and 1 B4) were upgraded to DCIS on vacuum excision. 10 DCIS were upgraded to the invasive disease at surgery in spite of representative calcifications in 3-7 specimens.
Conclusion: Realtime sequential visualisation of confirmed representative calcifications can reduce the number of samples required during biopsy. Lesions containing calcifications can be confidently diagnosed when 4 specimens containing calcifications are obtained. Careful correlation with direct histological analysis in the multidisciplinary meeting is required. Underestimation of invasive malignancy can still occur.
Limitations: Single institution. Ongoing to accrue numbers.
Ethics committee approval: n/a
Funding: Loan of equipment.

Author Disclosures:
W. Teh: Research/Grant Support at Hologic, Investigator at Royal Free London, Speaker at Royal Free London
R. Uzvolk: nothing to disclose
M. Morgan: nothing to disclose
J. Rees: nothing to disclose
R. Felton: nothing to disclose

RPS 1002b-3 11:37
Prevalence of papillary lesions in solitary dilated duct visualised by mammography
V. J. Ayres[1], L. Ramalho[2], L. D. M. Pompei[1], E. F. C. Fleury[3]; [1]*Santo André/BR,* [2]*Bg/BR,* [3]*Sao Paulo/BR (ayresve@gmail.com)*

Purpose: To determinate the prevalence, pathological significance, and risk factors associated with papillary lesions when solitary dilated duct is visualised at mammography.
Methods and materials: Prospectively evaluation of consecutive mammography was performed in a specialised breast cancer control centre, in accordance with local ethical approval. Patients that presented solitary dilated duct at mammography were later evaluated with ultrasonography (US). Cases that exhibited intraductal components were submitted to percutaneous biopsy, following anatomopathological correlation.
Results: In the period from March 17, 2016, to March 10, 2017, 9,035 mammographic exams were included, 8,125 (90%) representing screening and 910 (10%) diagnostic exams. The mammographic study identified 135 solitary dilated duct (SDD) cases (1.49%) and 94 (1.04%) of them followed US evaluation. Percutaneous and/or surgical biopsy were performed in all 24 cases with intraductal components and it revealed 8 papilloma lesions: 6 papillomas, one papillary lesion, and one sclerosing papilloma. Association with pathological papilloma findings with statistical significance ($p < 0.05$) using Chi Quadrado were menopause, parity, papillary discharge, breast density category (a) entirely fatty and (b) there are scattered areas of fibroglandular, microcalcifications on mammogram, and mass on ultrasound.
Conclusion: Solitary dilated duct findings without other suspicious signs at mammography benefits from US analysis for intraductal content's evaluation, which often represents benign findings. When associated with intraductal mass, biopsy should be considered and the expected result should be papilloma.
Limitations: The limitation was the 32 cases in which it was not possible to perform a complementary study of US.
Ethics committee approval: This paper had the local ethical committee approval and all participants provided written informed consent.
Funding: No funding was received for this work.
Author Disclosures:
L. Ramalho: nothing to disclose
V. J. Ayres: nothing to disclose
L. D. M. Pompei: nothing to disclose
E. F. C. Fleury: nothing to disclose

RPS 1002b-4 11:43
Role of contrast-enhanced imaging in the management of lesions of uncertain malignant potential (B3)
C. Bellini[1], A. Franconeri[2], G. Bicchierai[1], D. de Benedetto[1], F. Di Naro[1], J. Nori[1], V. Miele[1]; [1]*Florence/IT,* [2]*Pavia/IT (1chiarabellini@gmail.com)*

Purpose: To evaluate the role of contrast-enhanced digital mammography (CEDM) and dynamic contrast-enhanced magnetic resonance imaging (DCE-MRI) in the management of lesions of uncertain malignant potential (B3).
Methods and materials: We screened 374 women with histological diagnosis of B3 from July 2016 to December 2018, who underwent open excision (OE), vacuum-assisted excision (VAE), or with proof of stability on follow-up. We retrospectively included 252 patients who performed CEDM or DCE-MRI within 30 days before or after a biopsy. Positive predictive values (PPV) and negative predictive values (NPV) of B3 malignancy of the different contrast-enhanced imaging techniques were calculated. Fisher's exact test was used to compare CEDM and DCE-MRI groups. Contrast-enhanced imaging concordance was evaluated for B3 lesions, which underwent both techniques.
Results: 189 (75.0%) patients performed CEDM, 75 (29.8%) DCE-MRI, and 17 (6.7%) both. Out of 123 B3 enhancing on CEDM, 34 (27.6%) resulted in cancers (19 carcinomas in situ, 15 invasive), while out of 53 B3 enhancing onDCE-MRI, 24 (45.3%) resulted in cancers (17 carcinomas in situ, 7 invasive). Sensitivity and NPV of CEDM and DCE-MRI were 100%, specificity was 42.6% vs 43.1%, while accuracy was 52.9% vs 61.3%, respectively. In 11 lesions studied with both techniques, concordance was 100%.
Conclusion: Our results showed that contrast-enhanced imaging is a fundamental tool in B3 management with the high negative predictive value of malignancy since no upgraded B3 lesion showed enhancement. No differences between CEDM and DCE-MRI were found in the group which underwent both techniques.
Limitations: Restrospective study. Not every patient had undergone the two contrast-enhanced imaging techinques. Small sample of study.
Ethics committee approval: n/a
Funding: No funding was received for this work.
Author Disclosures:
C. Bellini: nothing to disclose
A. Franconeri: nothing to disclose
G. Bicchierai: nothing to disclose
D. de Benedetto: nothing to disclose
F. Di Naro: nothing to disclose
J. Nori: nothing to disclose
V. Miele: nothing to disclose

RPS 1002b-5 11:49
Cone-beam breast CT features associated with HER2/neu overexpression in patients with primary breast cancer
Y. Zhu, Y. Zhang, Y. Ma, Z. Ye*; Tianjin/CN (zhuyueqiang1985@126.com)*

Purpose: To identify the relationship between human epidermal growth factor receptor 2 (HER2) status and cone-beam breast CT (CBBCT) characteristics in surgically resected breast cancer.
Methods and materials: Preoperative CBBCT of patients with BI-RADS 4 or 5 lesions identified on mammography or ultrasound and dense or very dense breast tissue were retrospectively evaluated in 181 surgically resected breast cancers (triple-negative excluded) between October 2012 to August 2015. A set of CBBCT descriptors was semiquantitatively assessed by consensus double reading. Multivariate logistic regression analysis using backward elimination method (BEA) was performed to identify independent predictive factors of harbouring HER2/neu. Principle component analysis (PCA) was used to determine characteristics that might differentiate HER2 status. Receiver operating characteristic (ROC) curve analyses were conducted to determine the predictive capability.
Results: HER2 positive was found in 101 (55.8%) of 181 patients. Based on BEA, pathologic grade, maximum dimension, lobulation, ΔCT, and calcification morphology were confirmed as independent predictive factors of HER2/neu overexpression. PCA showed that calcification- and border-related characteristics were the most important for differentiation. ROC curve analyses showed that CBBCT features (AUC = 0.853) were superior to clinicopathologic features (AUC = 0.613, $P < 0.001$) and comparable to combination (AUC = 0.856, $P = 0.866$).
Conclusion: CBBCT features could be used to prognosticate HER2 status independently, which are potentially complementary to histopathologic result and helpful in guiding biopsy.
Limitations: We limited our analyses to non-triple-negative breast cancer, surgically resected, and non-preoperative treated specimens.
Ethics committee approval: The institutional review board approved this study and written informed consent was obtained from all patients.
Funding: National Key R&D Program of China (No. 2017YFC0112600 and 2017YFC0112601). National Natural Science Foundation of China (No. 81571671).
Author Disclosures:
Y. Zhu: nothing to disclose
Y. Zhang: nothing to disclose
Y. Ma: nothing to disclose
Z. Ye: nothing to disclose

RPS 1002b-6 11:55
Triple negative and HER2-positive breast cancers found by mammography screening associate with excellent prognosis
J. Alanko[1], R. Vanninen[2], M. Tanner[1], J. Isola[1]; [1]*Tampere/FI,* [2]*Kuopio/FI*

Purpose: To compare clinical and biological features and prognosis of screen detected and clinically detected breast cancers in women aged 50 to 68 years.
Methods and materials: We collected the mammograms and clinical data of 825 patients diagnosed with the invasive breast cancer for the first time in Tampere between 2006 and 2014. Of these, 572 cancers were found by screening mammography (69%), 171 cancers were diagnosed between the screening rounds (21%), and 82 cancers were found in women who had not participated in the screening program (10%).
Results: Of all cancers, 96 were HER2+ (12%) and 47 TN (6%). Majority of HER2+ (59%) and of TN breast cancers (57%) were found by screening.
Screen-detected tumours of HER2+ and TN subtype were smaller and less frequently node positive than those clinically detected. Of HER2+ cancers found by screening, T1 cancers were 79% and N0 81%, and TN cancers were T1 81% and N0 64%. From the screening, these percentages were clearly smaller. During the follow-up (average 7.3 years), distant metastases appeared in screen-detected HER2+ cancers for only 4% of patients and TN cancers for 7% of patients. When in interval and not participation groups, the amounts were evidently larger.

Conclusion: A significant number of HER2+ and TN cancers are found by mammography screening. Despite the fact that HER2+ and TN cancers are considered to be clinically aggressive, the screening showed that their prognosis in this data is very good and clearly better than the cancers found between the screening rounds.
Limitations: The evaluation is based on the results of a single screening unit and the number of cases is not very large.
Ethics committee approval: Approved by the ethics committee.
Funding: Supported by Eka Grant of The Finnish Medical Foundation.
Author Disclosures:
J. Alanko: nothing to disclose
R. Vanninen: nothing to disclose
M. Tanner: nothing to disclose
J. Isola: nothing to disclose

RPS 1002b-7 12:01

Ultrasonographic features of triple-negative invasive breast carcinomas are associated with mRNA-lncRNA signature and risk of recurrence

J. Li, J. Zhou, Y. Jiang, Y. Liu, Z. Shi, C. Chang, Z. Shao*; Shanghai/CN (jiaweili2006@163.com)*

Purpose: To evaluate the association between mRNA and lncRNA signatures, sonographic features, and risk of recurrence of triple-negative breast cancers (TNBC).
Methods and materials: Data of 114 TNBC patients whose pathological specimens accepted transcriptome analysis were retrospectively reviewed. The risk of recurrence was determined based on the association between transcriptome profiles and recurrence-free survival (RFS). Ultrasound images were assessed according to the breast imaging reporting and data system (BI-RADS). Multivariate logistic regression analysis was used to determine the sonographic features that were associated with the risk of recurrence.
Results: Selected from 183 mRNAs and 195 lncRNAs expressed in tumour tissues and adjacent normal tissues, there were three mRNAs (CHRDL1, FCGR1A, RSAD2) and two lncRNAs (HIF1A-AS2, AK124454) that were closely correlated with the RFS event of TNBCs. Of the three mRNAs, two were upregulated (FCGR1A and RSAD2) and one was downregulated (CHRDL1). Both HIF1A-AS2 and AK124454 were downregulated. We established an integrated mRNA-lncRNA signature for risk score of RFS: risk score= -1.225´CHRDL1+0.74´FCGR1A+0.219´RSAD2+0.482´HIF1A-AS2+0.571´AK124454. An optimum cut-off score of 0.793 was obtained to classify patients into high-risk and low-risk groups. The benign-like features such as regular shape, circumscribed margin, posterior acoustic enhancement, and no calcifications were significantly associated with the upregulated signature of HIF1A-AS2 and a high risk of recurrence ($p<0.05$). The malignant-like features like irregular shapes, uncircumscribed margin, no posterior acoustic enhancement, and calcifications were significantly associated with the downregulated signature of CHRDL1 and a low risk of recurrence ($p<0.05$).
Conclusion: Sonographic features of TNBCs are significantly associated with the risk of recurrence estimated from mRNA-lncRNA signatures.
Limitations: The retrospective review of the ultrasound images.
Ethics committee approval: n/a
Funding: National Natural Science Foundation of China project (No. 81627804, 81830058).
Author Disclosures:
J. Li: nothing to disclose
J. Zhou: nothing to disclose
Y. Jiang: nothing to disclose
Y. Liu: nothing to disclose
C. Chang: nothing to disclose
Z. Shao: nothing to disclose
Z. Shi: nothing to disclose

RPS 1002b-8 12:07

Role of T2-weighted-fs sequences in breast MRI in the evaluation of peritumoural oedema as a predictive marker for breast cancer aggressiveness: results of a retrospective monocentric study

M. Gerboni[1], M. Durando[1], E. Regini[2], G. Bartoli[1], S. A. S. Gentile[1], C. Costanza[1], G. Mariscotti[1], L. Bergamasco[1], P. Fonio[1]; *[1]Turin/IT, [2]Settimo Torinese/IT (mattia.gerboni@gmail.com)*

Purpose: To investigate the predictive role of peritumoural oedema assessed at MRI T2-STIR sequences in patients with invasive breast cancer considering disease free-survival and overall survival time.
Methods and materials: We conducted a retrospective study on 107 patients (mean age: 53 years) with biopsy-proven invasive breast cancers, who underwent preoperative breast MRI on 1.5 T scanner from January 2010 to July 2011. Images were reviewed by two radiologists in consensus, assessing peritumoural oedema on the basis of the degree of the signal intensity surrounding the tumour on T2-STIR images. The MRI protocol included pre-contrast T2-STIR images, DWI, and dynamic GRE T1 images before and after contrast injection, also with the subtraction technique. We categorised patients into two main groups according to the presence or absence of peritumoural oedema on T2-STIR sequences. We retrospectively collected other lesions characteristics, such as size, histology, molecular pattern, absence/presence of positive lymph nodes, and type of surgery. Statistical analysis was performed to assess the disease-free survival and overall survival using the Kaplan-Meier curves.
Results: The median follow-up of patients included in the study was 7.7 ± 1.3 years. Based on MRI findings, peritumoural oedema was found on 52 among 107 lesions (48.9%). In this group, recurrence occurred in 9 patients, while in the second group (absence of peritumoural oedema) in 4 patients. Disease-free survival according to Kaplan-Meier test did not statistically differ between the two groups ($p=0.11$). In the peritumoural oedema group, overall survival time was statistically ($p=0.045$) lower compared to the other group.
Conclusion: The presence of peritumoural oedema detected on MRI T2-STIR sequences could be considered as a valid ancillary feature of predictability of worse survival outcome.
Limitations: Small sample, monocentric study.
Ethics committee approval: n/a
Funding: No funding was received for this work.
Author Disclosures:
M. Gerboni: nothing to disclose
M. Durando: nothing to disclose
E. Regini: nothing to disclose
G. Bartoli: nothing to disclose
G. Mariscotti: nothing to disclose
L. Bergamasco: nothing to disclose
S. A. S. Gentile: nothing to disclose
C. Costanza: nothing to disclose
P. Fonio: nothing to disclose

RPS 1002b-9 12:13

Role of ^{18}F-FDG uptake on PET/CT in identifying androgen receptor expression in triple-negative breast cancer and the associated factors

H. Lee[1], H. S. Lim[2], S. Y. Ki[3], H. Park[1]; *[1]Gwang-ju/KR, [2]Jeollanamdo/KR, [3]Hwasun/KR (phm6284@naver.com)*

Purpose: To investigate the relationship between ^{18}F-FDG uptake and androgen receptor (AR) expression in triple-negative breast cancer (TNBC).
Methods and materials: Between July 2013 and April 2017, 163 patients with primary TNBC who underwent ^{18}F-FDG PET/CT were retrospectively categorised into AR-positive (n = 24) and AR-negative (n = 139) groups by immunohistochemical staining. SUV_{max} value and clinicopathologic features were compared between the two groups. The association between prognostic values and SUV_{max} was evaluated by the multiple regression model and the correlation analysis between SUV_{max} and clinicopathologic variables was performed.
Results: Median SUV_{max} was significantly higher in AR-negative group than in AR-positive group ($P = .034$). AR-positive group was significantly older ($P < .001$) and had more DCIS component ($P = .015$), and AR-negative group showed significantly high Ki67 proliferation ($P = .004$) and p53 overexpression ($P = .023$). In multiple regression analysis, tumour size, DCIS component, and histologic grade 1 were significantly associated with SUV_{max}. Tumour size, histologic grade 3, and Ki67 showed positive correlations with SUV_{max} ($P < .001$, Spearman's rho (ρ)= .485; $P = .027$, $\rho = .142$; $P < .001$, $\rho = .291$), while associated DCIS component, androgen receptor, and histologic grade 1 ($P < .001$, $\rho = -.333$; $P = .033$, $\rho = -.167$; $P < .001$, $\rho = -.252$, respectively) showed negative correlation with SUV_{max}.
Conclusion: There was significant difference of ^{18}F-FDG uptake with regard to AR expression in TNBC. SUV_{max} was significantly associated with tumour size, histologic grade, and associated DCIS component in TNBC.
Limitations: Small numbers of study cohorts in a single tertiary centre. Retrospective design - selection bias is inevitable.
Ethics committee approval: n/a
Funding: No funding was received for this work.
Author Disclosures:
H. Lee: nothing to disclose
H. S. Lim: nothing to disclose
S. Y. Ki: nothing to disclose
H. Park: nothing to disclose

RPS 1002b-10 12:19

Determination of morphological characteristics of primary breast cancer by focus diffusion-weighted MRI: comparison with conventional diffusion-weighted images and dynamic contrast-enhanced MRI

Y. Metin[1], N. Orhan Metin[2], F. Tasci[2], O. Ozdemir[1], S. Kul[3], A. Babatürk[1]; *[1]Ankara/TR, [2]Rize/TR, [3]Trebizond/TR (dr.andelib@gmail.com)*

Purpose: To compare the diagnostic accuracy and effectiveness of focus diffusion-weighted imaging (f-DWI), conventional diffusion-weighted imaging (c-

DWI), and dynamic-contrast enhanced magnetic resonance imaging (DCE-MRI) in determining the morphological characteristics of primary breast cancer.
Methods and materials: c-DWI, f-DWI, and DCE-MRI of newly diagnosed 155 breast cancer patient's images were evaluated retrospectively. Morphological features of the lesions and image quality were compared between all three imaging protocols by two radiologists. Apparent diffusion coefficient (ADC) values of the lesions were compared between f-DWI and c-DWI.
Results: Evaluation by the two readers of all primary breast cancers for the mean ADC values were 82.5 and 88 for f-DWI, and 92.5 and 94.5 for c-DWI, respectively, with the difference being statistically significant (p< 0.001). Both two readers identified that perceived signal to noise ratio (SNR) and sharpness obtained from f-DWI and DCE-MRI was significantly higher than c-DWI (p< 0.001). Distortion was also significantly less encountered at f-DWI than the conventional one. Qualitatively, there was no significant difference between f-DWI and DCE-MRI.
Conclusion: f-DWI allows higher quality images than the conventional one. This allows the morphological features to be identified at a similar accuracy to dynamic contrast-enhanced images with high resolution.
Limitations: In this study, only the morphological features of malignant lesions were compared and no difference was made between focal diffusion and conventional diffusion in the differentiation of benign and malignant lesions. In addition, focus diffusion-weighted imaging is obtained in a slightly longer period than conventional diffusion-weighted imaging.
Ethics committee approval: This retrospective study was approved by the institutional review board in our institution and written informed consent was obtained from all patients.
Funding: No funding was received for this work.
Author Disclosures:
Y. Metin: Author at Ankara University Faculty of Medicine
N. Orhan Metin: Author at Recep Tayyip Erdoğan University Faculty of Medicine
F. Tasci: Author at Recep Tayyip Erdoğan University Faculty of Medicine
O. Ozdemir: Author at Lokman Hekim University Faculty of Medicine
S. Kul: Author at Karadeniz Technical University Faculty of Medicine
A. Babatürk: nothing to disclose

RPS 1002b-11 12:25
Application of delayed contrast-enhanced MRI for improved accuracy in the evaluation of breast lesions
D. Daniels, N. Nissan, D. Last, S. Sharabi, Y. Mardor, M. Sklair-Levy; *Ramat Gan/IL (Dianne.Daniels@sheba.health.gov.il)*

Purpose: Contrast-enhanced MRI of the breast provides high sensitivity but variable specificity and may lead to excessive benign biopsies. Based on previous success with the application of delayed contrast MRI (DCM) in differentiating tumour/non-tumoural regions in brain tumours, we aim to study the feasibility of applying DCM to breast cancer patients in order to potentially reduce the number of benign unnecessary biopsies.
Methods and materials: 52 women undergoing breast MRI were scanned by standard DCE-MRI, as well as with DCM acquired 20 minutes post-contrast. Image analysis was provided via in-house developed software, affording colour-coded maps reflecting contrast accumulation/clearance (depicted red/blue in the maps) at the delayed time point. DCM maps were retrospectively compared with the results of the conventionally obtained diagnostic workup.
Results: A total of 69 lesions were evaluated. All 19 malignant and high-risk lesions correctly appeared blue in the DCM maps, while 42 of the benign lesions appeared red. Another eight lesions appeared mixed or blue. No false-negative cases were obtained. False-positive cases (blue for benign) were mainly due to haemangiomas, fat necrosis, and fibroadenomas with myxoid components. Standard DCE resulted in 100%/52%/44%/100% sensitivity/specificity/PPV/NPV to breast cancer, while DCM resulted in 100%/84%/70%/100%, respectively. Further comparison of DCM maps with histology specimens suggested that high vessel-density with vessel compression appeared blue in the maps while low vessel-density with dilated lumens appeared red.
Conclusion: DCM may provide improved specificity for the diagnosis of breast cancer. Further application aimed at the optimisation of biopsy planning is now underway.
Limitations: A pilot study with a limited number of participants. Future aims include protocol optimisation and the scanning of larger cohort.
Ethics committee approval: Approved by IRB committee. Written informed consent was waived.
Funding: Israel Science Foundation.
Author Disclosures:
S. Sharabi: nothing to disclose
Y. Mardor: nothing to disclose
N. Nissan: nothing to disclose
D. Daniels: nothing to disclose
D. Last: nothing to disclose
M. Sklair-Levy: nothing to disclose

11:15 - 12:30 **Descartes (Room D3)**

Interventional Radiology

RPS 1009b

Spine and bone

Moderators:
J. T. C. Baptista; Lisboa/PT
P. Popovic; Ljubljana/SI

RPS 1009b-1 11:15
Epidural pulsed radiofrequency (EPR) with access via sacral hiatus: therapeutic indications
F. Castelli[1], C. Di Lorenzo[2], A. M. Ragusa[3], B. Varsallona[2], A. Scavone[2], G. Scavone[2], M. V. V. Raciti[4], P. Aliffi[2], G. Galvano[2]; *[1]Verona/IT, [2]Catania/IT, [3]Biancavilla/IT, [4]Pavia/IT (fedicastelli@gmail.com)*

Purpose: To evaluate the effectiveness of EPR with access via sacral hiatus in patients affected by chronic lumbosciatalgia resistant to conservative treatment
Methods and materials: In this retrospective study, 120 patients were included (72 women and 48 men) who were affected by chronic lumbosciatalgia caused by discal protrusions or hernias for which no surgical or percutaneous treatment was provided; Pfirrmann's grade of discal degeneration 4 or 5 and discal calcifications. Pain symptoms were evaluated using the visual analogue scale (VAS) and the numeric pain rating scale (NPRS), including patients scoring above 7. After local anaesthesia, the sacral hiatus was located via AP and lateral fluoroscopically guided x-ray. By using a cannula, a catheter was introduced with a bipolar electrode at its distal extremity which was directed to the nerve roots requiring treatment. The catheter was introduced into the epidural space; once the target root was reached, a neurophysiological study was run to confirm the correct root via bioelectrical impedance and sensory and motor stimulation. Having ensured the correct positioning of the electrode, pulsed radiofrequency begun for 240 seconds. Then, a mix of steroids and local anaesthetic were injected via the same catheter.
Results: There was a significant reduction in pain in 75% of cases (90/120). VAS/NPRS scores were evaluated after treatment and after 2 weeks, 1, 3, 6, and 12 months, showing a significant improvement. VAS/NPRS pre-treatment average scores were 7.6 (+-0.3), after 1 month they had decreased to 2.3 (+-0.3), and after 12 months they were 2.8 (+-0.1). There were no peri and post-procedural complications.
Conclusion: In accordance with scientific literature evidence, this treatment proved effective in patients with chronic lumbosciatalgia with discopathy for which there are no surgical or percutaneous treatment indications.
Limitations: n/a
Ethics committee approval: n/a
Funding: No funding was received for this work.
Author Disclosures:
F. Castelli: Consultant at ARNAS Garibaldi Catania
C. Di Lorenzo: Consultant at ARNAS Garibaldi Catania
A. M. Ragusa: Consultant at ARNAS Garibaldi Catania
B. Varsallona: Consultant at ARNAS Garibaldi Catania
A. Scavone: Consultant at ARNAS Garibaldi Catania
G. Scavone: Consultant at ARNAS Garibaldi Catania
M. V. V. Raciti: Consultant at ARNAS Garibaldi Catania
P. Aliffi: nothing to disclose
G. Galvano: Consultant at ARNAS Garibaldi Catania

RPS 1009b-2 11:21
CT-guided screw fixation by interventional radiologists in traumatic injuries of the pelvic ring: screw accuracy placement and clinical outcome
F. Torre[1], C. Dekimpe[1], L. J. Pavan[1], O. Andreani[1], S. Guinebert[2], A. Prestat[1], N. Stacoffe[3], D. S. Palominos Pose[4], N. Amoretti[1]; *[1]Nice/FR, [2]Paris/FR, [3]Lyons/FR, [4]Santiago de Chile/CL*

Purpose: To report our clinical experience of CT-guidance fixation of pelvic ring traumatic fractures, evaluating screw placement accuracy, safety, complications, and clinical outcome.
Methods and materials: All consecutive patients who beneficiated from a CT-guided fixation of a sacroiliac or acetabular fracture in our radiology department after a high energy trauma from 11/2016-11/2018 were included. All procedures were realised under general anaesthesia with dual CT and fluoroscopic guidance by two experienced interventional radiologists. Treated fractures, unstable reduced posterior pelvic ring disruptions, with or without sacroiliac disjunction (TILE B or C), and minimally displaced acetabular fractures were minimally displaced. The primary outcome was screw placement accuracy. Secondary endpoints were patient radiation exposure, procedure time,

complications, clinical functional score (MAJEED score), and pain scale evaluation (VAS) during a follow-up period from 4-30 months.
Results: 32 patients were included (mean age 46 years) and 62 screws were placed. Screw placement was correct in 28/31 patients (87.5%, missing data of one patient). 2 patients presented with persistent pain after fixation due to a screw conflict. In both cases, screws were removed by an interventional radiologist after fracture consolidation, resolving the pain. The mean procedure time was 67 minutes and the mean patient radiation exposure was 965mGy cm. No major complications occurred. The mean follow up was 13 months. The mean postoperative MAJEED score was 84/100 and the mean pain score was 1.6/10.
Conclusion: This technique is an effective and safe procedure in undisplaced or minimally displaced pelvic fractures, allowing both accurate fixation and minimally invasiveness. The possibility of percutaneous removal allows resolution of any eventual unsatisfying screw positioning in a minimally invasive way.
Limitations: The retrospective design.
Ethics committee approval: Informed consent was obtained.
Funding: No funding was received for this work.
Author Disclosures:
F. Torre: nothing to disclose
L. J. Pavan: nothing to disclose
C. Dekimpe: nothing to disclose
O. Andreani: nothing to disclose
S. Guinebert: nothing to disclose
A. Prestat: nothing to disclose
N. Stacoffe: nothing to disclose
N. Amoretti: nothing to disclose
D. S. Palominos Pose: nothing to disclose

RPS 1009b-3 11:27

Percutaneous ozone nucleolysis for low back pain: any issues for spine biomechanics? 6 years of MRI imaging follow-up

E. Tommasino, P. Palumbo, F. Bruno, M. Varrassi, M. V. M. Micelli, F. Arrigoni, A. Splendiani, C. Masciocchi*; L'Aquila/IT (emanuele.tommasino@gmail.com)*

Purpose: To explore how O2-O3 chemiodiscolysis affects the biomechanics of the spine and the functional spinal unit and whether it accelerates lumbar spine degeneration.
Methods and materials: A total of 100 patients treated with an O2-O3 mixture, either periganglionic or intradiscal, 6 years before our study underwent MRI examination. An evaluation of the success rate was performed on both groups on the basis of the modifications of lumbar spine biomechanics, using well-defined markers of spine degeneration. Comparisons were made between the patients treated with the percutaneous O2-O3 intradiscal injection and the paraganglionic O2-O3 injection was used as a control group.
Results: Both treatments showed a significant reduction of disc height ($p<0.05$), although only the intradiscal injection obtained the decrease of disc area and protrusion ($p<0.05$). Similarly, in the periganglionic injection, the Pfirrman and Modic score markers of lumbar spine degeneration increased ($p<0.05$), whereas in the intradiscal injection they remained stable ($p>0.05$).
Conclusion: Biomechanical properties of the spine are not affected after the intradiscal injection of O2-O3. This study demonstrates that chemiodiscolysis, restoring the natural loads along the FSU, does not exacerbate lumbar spine degeneration.
Conversely, periganglionic injection, acting as a symptomatic treatment, does not delay lumbar spine degeneration.
Limitations: Although in the paraganglionic injection, we did not directly obtain any shrinkage of the disc, a protruded disc naturally reduces its own extrusion due to the dehydration of the NP.
Ethics committee approval: Approval of our medical ethical committee and informed consent was obtained.
Funding: No funding was received for this work.
Author Disclosures:
E. Tommasino: nothing to disclose
P. Palumbo: nothing to disclose
F. Bruno: nothing to disclose
M. Varrassi: nothing to disclose
M. V. M. Micelli: nothing to disclose
F. Arrigoni: nothing to disclose
A. Splendiani: nothing to disclose
C. Masciocchi: nothing to disclose

RPS 1009b-4 11:33

Systematic evaluation of low-dose MDCT for planning purposes of lumbosacral periradicular infiltrations

N. Sollmann, K. Mei, S. Schön, I. Riederer, F. K. Kopp, C. Zimmer, J. S. Kirschke, P. B. Noel, T. Baum*; Munich/DE (nico.sollmann@tum.de)*

Purpose: To evaluate image quality and confidence for planning of periradicular infiltrations using virtually lowered tube currents and in-house developed statistical iterative reconstruction (IR) for multi-detector computed tomography (MDCT).
Methods and materials: 20 patients (54.9±13.1 years) underwent MDCT for planning purposes of periradicular infiltrations at the lumbosacral spine (120 kVp/100 mAs). Planning scans were simulated as if they were performed at 50% (D50), 10% (D10), 5% (D5), and 1% (D1) of the tube current of original scanning. Image reconstruction was achieved with two levels of IR (A: similar in appearance to clinical reconstructions and B: ten times stronger noise reduction). Two readers (R1/R2) performed image evaluation including confidence for intervention planning (scoring: 1-high, 2-intermediate, and 3-low confidence).
Results: Level A of IR was favourable regarding overall image quality, artefacts, image contrast, and nerve root depiction, with preserved good scores down to D10 scans. The confidence for planning was not significantly different ($p>0.05$) between scans with tube currents virtually lowered down to 10% and original-dose scans when using level A of IR (R1: 1.2 ± 0.4, R2: 1.1 ± 0.3). Inter-reader agreement for planning confidence was good (Cohen's kappa: 0.62-1.00).
Conclusion: MDCT for lumbosacral periradicular infiltrations may be conducted with tube currents lowered down to 10% of the standard dose (equal to 10 mAs) without limitations in planning confidence.
Limitations: Evaluations were performed for procedure planning only and not for the sequential scans acquired during the intervention. The time needed for image reconstructions using IR can be long, hampering direct implementation into the clinical setting.
Ethics committee approval: This retrospective study was approved by the IRB.
Funding: University of Pennsylvania Research Foundation and Philips Healthcare.
Author Disclosures:
S. Schön: nothing to disclose
N. Sollmann: nothing to disclose
K. Mei: nothing to disclose
I. Riederer: nothing to disclose
F. K. Kopp: nothing to disclose
C. Zimmer: nothing to disclose
J. S. Kirschke: Research/Grant Support at Philips Healthcare
P. B. Noel: Research/Grant Support at Philips Healthcare
T. Baum: nothing to disclose

RPS 1009b-5 11:39

The predictive role of the lumbar disc FA (fractional anisotropy) map in diffusion tensor imaging (DTI) to select patients with low back pain who may benefit from intradiscal oxygen-ozone injections

E. Tommasino[1], M. Varrassi[1], M. Perri[2], A. Splendiani[1], F. Bruno[1], C. Masciocchi[1], A. Barile[1], E. Di Cesare[1]*; [1]L'Aquila/IT, [2]San Giovanni Rotondo/IT (emanuele.tommasino@gmail.com)*

Purpose: To assess annular fibers anisotropy through the intervertebral disc FA map to select patients suffering from low back pain of lumbar disc origin and who may benefit from intradiscal oxygen-ozone injection.
Methods and materials: A total of 75 patients suffering from low back pain were selected. Before treatment, they underwent MR examination on a 3T, with a standard protocol of conventional sequences (T2, T2 fat-sat, and T1 FSE) and one additional DTI sequence for assessing respectively lumbar disc pathology and the fractional anisotropy (FA) map of the involved intervertebral disc. Discography of the involved disc was also obtained under CT guidance in order to confirm MRI reports. Patients were randomly assigned into two groups. One control group (20 men, 16 women) underwent intraforaminal injection of steroids and anaesthetics. The remaining 39 patients in the study group (18 men, 21 women) underwent the same treatment with the addition of an intradiscal oxygen-ozone (O2-O3) injection. An ODI questionnaire was administered before and after the treatment. Results were compared with a $\chi 2$, t-test, and regression analysis.
Results: In cases of annular fissure without herniation or disc extrusion, O2-O3 intradiscal injection therapy was successful in 41% of the study group patients compared to 27.5% of the control group patients ($P<0.01$). The ODI questionnaire showed a significant improvement of symptoms in both groups ($P<0.01$). FA disc map values positively correlated with the annular fissuration and the positive outcome.
Conclusion: An FA disc map congruous with a rupture of annular fibres could be considered as a predictive sign of a response to oxygen-ozone lumbar intradiscal injection and should be included in the preoperative study.
Limitations: n/a
Ethics committee approval: Ethical approval was obtained by our medical committee.
Funding: No funding was received for this work.

Author Disclosures:
E. Tommasino: nothing to disclose
M. Varrassi: nothing to disclose
M. Perri: nothing to disclose
A. Splendiani: nothing to disclose
F. Bruno: nothing to disclose
C. Masciocchi: nothing to disclose
A. Barile: nothing to disclose
E. Di Cesare: nothing to disclose

RPS 1009b-6 11:45

The association between osteoarthritis features on MRI and the clinical outcome of transcatheter arterial embolisation therapy for knee osteoarthritis

T. A. van Zadelhoff[1], Y. Okuno[2], S. M. A. Bierma-Zeinstra[3], A. Moelker[4], E. Oei[3]; [1]Amsterdam/NL, [2]Tokyo/JP, [3]Rotterdam/NL, [4]Bergschenhoek/NL (tijmenvanzadelhoff@gmail.com)

Purpose: To explore the association between baseline MRI features related to knee osteoarthritis and the clinical outcome of patients undergoing transcatheter arterial embolisation (TAE) of neoangiogenesis around the knee for the treatment of pain caused by osteoarthritis.
Methods and materials: Baseline knee MR images of patients who underwent TAE were assessed semi-quantitatively using the MRI osteoarthritis knee score (MOAKS). Items scored included effusion and Hoffa synovitis, cartilage defects, bone marrow lesions (BMLs), and osteophytes. Absolute pain reduction was calculated from the Western Ontario and McMaster Universities osteoarthritis index (WOMAC) questionnaire pain subscore at baseline and at 6 months. Linear regression analysis adjusted for age, sex, and a baseline WOMAC pain score was used to measure the association between MRI signs at baseline and clinical outcome.
Results: 52 patients were analysed. The mean baseline pain score was 61.11 (SD=9.04) and the mean pain reduction was 35.46 (SD=20.97). Effusion-synovitis (MOAKS score 2-3) at baseline showed a negative association with WOMAC pain reduction (β: -.30; P<0.05). Hoffa synovitis showed a positive but not statistically significant association (β: .18; p>0.05). The amount and severity of cartilage full-thickness defects, BMLs, and osteophytes all had a negative association with pain reduction (β: -.42, β: -.38, and β: -.38, respectively; all p<0.05).
Conclusion: The presence of effusion-synovitis at baseline is associated with decreased pain reduction after TAE treatment. In general, the presence of more and a higher-grade of osteoarthritis-related MRI signs at baseline is associated with less reduction in the WOMAC pain score after TAE. This information could be useful when selecting patients for TAE treatment.
Limitations: Synovitis was assessed using non-contrast-enhanced MRI instead of contrast-enhanced MRI. This could potentially have caused underdiagnosis of synovitis.
Ethics committee approval: n/a
Funding: No funding was received for this work.
Author Disclosures:
T. A. van Zadelhoff: nothing to disclose
Y. Okuno: nothing to disclose
E. Oei: nothing to disclose
S. M. A. Bierma-Zeinstra: nothing to disclose
A. Moelker: nothing to disclose

RPS 1009b-7 11:51

Symptomatic low-grade lumbar isthmic lysis: trans-isthmic pars interarticularis screwing under CT and fluoroscopic guidance

L. J. Pavan[1], F. Torre[1], A. Kastler[2], P. Kugelstadt[1], N. Stacoffe[3], A. Prestat[4], A. Rudel[1], C. Dekimpe[1], N. Amoretti[1]; [1]Nice/FR, [2]Grenoble/FR, [3]Lyons/FR, [4]Nancy/FR

Purpose: To assess the accuracy of trans-isthmic percutaneous screwing under CT and fluoroscopic guidance in patients with symptomatic low-grade isthmic spondylolisthesis.
Methods and materials: 50 consecutive patients treated for trans-isthmic screwing at our centre were retrospectively included. Treatment indications were low-grade lumbar isthmic lysis and persisting low back pain (visual analog scale VAS>6) refractory to medical treatment and local infiltrations. Exclusion criteria were a neurological deficit, spinal posture impairment, lumbar surgery, refusal to undergo the procedure, high-grade spondylolisthesis, and coagulopathies. The procedure was carried out under local anaesthesia with CT and fluoroscopic guidance by an experienced interventional radiologist. The primary outcome was a technical success, assessed on postoperative CT using the same success criteria as surgical screw placement. The secondary outcome was pain decrease assessed with a VAS pain score preprocedural and at 1 year.
Results: 99 screws were positioned in 50 patients (28 females, 22 males, mean age 50±19 years [17-80y], bilateral screwing in 49 patients, unilateral in one patient). The average screw length was 27 mm [24-32 mm] and the mean procedure duration was 50 minutes [45-60 min]. Postoperative CT assessment showed satisfactory placement in 96/99 screws (technical success rate of 96.9%). No complications occurred intra or postoperatively.
The mean VAS pain score decreased from 7.8±1.6 [5-10] to 2.9±2.1 [0-7] at 1 year.
Conclusion: Percutaneous trans-isthmic screwing under CT and fluoroscopic guidance allows an accurate and safe pars-isthmic fixation in patients with symptomatic low-grade spondylolisthesis, with satisfying pain reduction following the procedure.
Limitations: A retrospective design.
Ethics committee approval: Local IRB approval was obtained (IRB 5891).
Funding: No funding was received for this work.
Author Disclosures:
N. Amoretti: nothing to disclose
L. J. Pavan: nothing to disclose
F. Torre: nothing to disclose
P. Kugelstadt: nothing to disclose
A. Kastler: nothing to disclose
N. Stacoffe: nothing to disclose
C. Dekimpe: nothing to disclose
A. Prestat: nothing to disclose
A. Rudel: nothing to disclose

RPS 1009b-8 11:57

Percutaneous treatment of vertebral body fractures in patients with vertebral metastases by using expandable SpineJack® intravertebral implants: the initial experience of 21 consecutive patients

C. Pusceddu, N. Ballicu, L. Melis; Cagliari/IT (clapusceddu@gmail.com)

Purpose: To evaluate the feasibility and effectiveness of the SpineJack® intravertebral implant in the treatment of pathological vertebral fractures in cancer patients. The primary aim of the treatment was pain palliation and recovery of the height of the vertebral body.
Methods and materials: 21 patients (10 men and 11 women, median age 62) with fractures of 24 vertebral metastases underwent CT fluoroscopy-guided percutaneous vertebral augmentation by bi-peduncular expandable SpineJack® insertion followed by vertebroplasty. 7 patients underwent MW ablation immediately before the osteosynthesis. We analysed the feasibility and complications of the procedure, the decrease in pain using a visual analogue scale (VAS), and the restoration of the anterior and middle height of the vertebral body, before and 1 week after the procedures. Patients were followed up for 14 months (range from 3-25 months).
Results: The procedure was technically successful in all treated vertebrae. Bone cement leakage occurred in 12 cases, but no symptoms were reported. No signs of root irritation or neurological deficit were observed. VAS score decreased from 7.1 (range, 4-8.7) to 1.2 (range, 0-3). The anterior and middle height of the vertebral body reduced in all patients with a deformity reduction and improvement of column stability.
Conclusion: This preliminary result suggests that the SpineJack ® procedure in vertebral pathological fractures is safe and effective, provides immediate benefits in terms of pain relief, functional recovery, and vertebral height restoration, with a rapid return to self-sufficiency.
Limitations: The small sample of patients and the short follow-up don't permit establishing the exact role of this approach in the treatment of patients with vertebral fractures of spinal metastases.
Ethics committee approval: n/a
Funding: No funding was received for this work.
Author Disclosures:
C. Pusceddu: nothing to disclose
N. Ballicu: nothing to disclose
L. Melis: nothing to disclose

RPS 1009b-9 12:03

A 7-year experience of magnetic resonance-guided focused ultrasound surgery (MRgFUS) ablation of bone lesions: results from an MSK interventional centre

F. Arrigoni, C. de Cataldo, P. Palumbo, M. Ruschioni, F. Formiconi, L. Zugaro, A. Barile, C. Masciocchi; L'Aquila/IT (arrigoni.francesco@gmail.com)

Purpose: To retrospectively evaluate clinical and radiological results of ablative procedures of focal benign bone lesions performed with a magnetic resonance-guided focused ultrasound surgery (MRgFUS) equipment.
Methods and materials: We retrospectively evaluated patients who underwent MRgFUS treatment on painful and symptomatic benign bone lesions from February 2012-October 2019. Patients were considered eligible for the procedure if the lesion was on the bone surface, i.e. accessible from the ultrasound beam, and if there were no contraindications to MRI. We evaluated

the success rate in terms of clinical and imaging results, complications, and relapse rates.
Results: Our population included 71 patients (40 males, 31 females, mean age at the time of treatment 29±16). In the last few years, since 2012, we successfully treated 66 lesions (success rate 93.5%): 51 osteoid osteomas and 15 epiphyseal lesions (6 intraarticular osteoblastomas, 4 fibroangiomas, 1 subperiosteal chondroma, 1 mixofibroma, 2 chondroblastomas, and 1 GCT recurrence). Pain control was obtained in all cases with a fast and definitive relief. No complication from the percutaneous approach was recorded (complication rate 0%). The advantage in HIFU treatment was also shown by the imaging follow-up (up to over 2 years), with significant bone densification and no pathologic fracture after thermal ablation. In 5 patients, we reported clinical and radiological relapse (relapse rate 6.5%): 1 tug lesion, 3 osteoid osteomas, and 1 osteoblastoma. All the disease relapse cases occurred before 2017, probably related to limited technical experience.
Conclusion: Our results confirm the validity of MRgFUS as the treatment of choice for benign superficial bone lesions because of its minimally invasive approach, high-profile of safety, and excellent effectiveness.
Limitations: A limited number of patients and an operator with progressively increasing experience.
Ethics committee approval: n/a
Funding: No funding was received for this work.
Author Disclosures:
C. de Cataldo: nothing to disclose
F. Arrigoni: nothing to disclose
P. Palumbo: nothing to disclose
M. Ruschioni: nothing to disclose
L. Zugaro: nothing to disclose
A. Barile: nothing to disclose
C. Masciocchi: nothing to disclose
F. Formiconi: nothing to disclose

RPS 1009b-10 12:09

Intravertebral cleft in percutaneous vertebroplasty: what else?

F. Torre[1], L. J. Pavan[1], A. Prestat[1], H. Vasseur[1], C. Ibba[1], N. Stacoffe[2], A. Kastler[3], P. Foti[1], N. Amoretti[1]; [1]*Nice/FR,* [2]*Lyons/FR,* [3]*Grenoble/FR*

Purpose: To compare the clinical outcome of CT and fluoroscopy-guided percutaneous vertebroplasty (PVP) in vertebral fractures with and without an intravertebral cleft.
Methods and materials: All patients treated at our centre with PVP from 11/2014-11/2015 under CT and fluoroscopic guidance were reviewed. Inclusion criteria were the presence of painful thoracolumbar osteoporotic vertebral fractures (VAS>5 under antalgic medication) with MRI confirmation, graded type II or III according to Genant's classification. Patients were divided into two groups according to the presence (group 2) of an intravertebral cleft (Kümmel disease) or not (group 1). Exclusion criteria were medullary compression, acute infection, active haemorrhage, and malignant vertebral fractures. Follow-up was done at day 1, months 1, 3, 6, and 1 year with a visual analogue scale (VAS) score for pain.
Results: 90 patients were included (mean age 79 years [70-92 years], 27 males and 63 females, 61 thoracic and 39 lumbar vertebral fractures). 50 patients (group 1) didn't have an intravertebral cleft before PVP, while 40 patients did (group 2). Vertebral fractures with a cleft were significantly more painful at preoperatory ($p<0.05$). Both groups demonstrated significant improvement in VAS results at follow-up after PVP ($p<0.05$). Group 2 (cleft) presented a larger decrease in pain compared to group 1 (no cleft). Cement leakage into an intervertebral disc was observed in 25/90 cases (27.7%), significantly more frequent in patients without a cleft (20/50, 40%) than in patients with a cleft (5/40, 12.5%)($p<0.0006$).
Conclusion: Fractures with an intravertebral cleft are more painful that those without a cleft and receive greater clinical benefit from PVP, with a larger VAS decrease and less intervertebral disc cement leakage in comparison to the group of osteoporotic fractures without a cleft.
Limitations: The retrospective design.
Ethics committee approval: IRB approval and informed consent was obtained.
Funding: No funding was received for this work.
Author Disclosures:
F. Torre: nothing to disclose
L. J. Pavan: nothing to disclose
A. Prestat: nothing to disclose
H. Vasseur: nothing to disclose
C. Ibba: nothing to disclose
N. Stacoffe: nothing to disclose
A. Kastler: nothing to disclose
P. Foti: nothing to disclose
N. Amoretti: nothing to disclose

RPS 1009b-11 12:15

Complications of image-guided thermal ablation of bone metastasis: a single-centre experience

G. Bianchi, F. Arrigoni, A. Izzo, C. de Cataldo, P. Palumbo, M. V. M. Micelli, L. Zugaro, A. Barile, C. Masciocchi; *L'Aquila/IT*

Purpose: To review complications following thermal ablation and cryoablation of painful bone metastasis and discuss the risks and clinical presentation of each complication, as well as how to treat and potentially avoid complications.
Methods and materials: We retrospectively evaluated 50 advanced cancer patients with painful bone metastasis (BM) treated by CT-guided percutaneous thermal ablation techniques (RFA, CA, or MWA) with palliative or curative intent in the last 4 years in our department. Curative treatment was performed to selected oligometastatic patients presenting with limited bone disease (<3 potentially treatable BM, each ≤3 cm in size). Patients with a painful bone metastasis (≥4/10 on a 0-10 VAS scale over the 24h) or higher risk of pathological fracture underwent palliative treatments.
Results: Axial bones were involved in 21 patients (42%). CA was performed in 31 cases (62%), RFA in 11 patients (22%), and MW ablation in 8 cases (16%). Complications were observed in 4 patients out of 50 (8%). An intramuscular haematoma was detected in 1 lesion located in the sacral wing. In 1 patient, an abscess developed after CA of an acetabular lesion. A lumbar artery pseudoaneurysm was observed following CA of an L2 secondary lesion. In 1 case, subcutaneous emphysema after CA of an ischiatic lesion was detected. In all the patients, the complications were successfully managed.
Conclusion: Percutaneous thermal ablation techniques are minimally invasive and a safe option in the management of BM. In our study, the low rate of complications observed is related to an appropriate patient selection made by a multidisciplinary team with 10-years experience in this field.
Limitations: A small sample size.
Ethics committee approval: n/a
Funding: No funding was received for this work.
Author Disclosures:
G. Bianchi: nothing to disclose
F. Arrigoni: nothing to disclose
A. Izzo: nothing to disclose
C. de Cataldo: nothing to disclose
P. Palumbo: nothing to disclose
M. V. M. Micelli: nothing to disclose
L. Zugaro: nothing to disclose
A. Barile: nothing to disclose
C. Masciocchi: nothing to disclose

RPS 1009b-12 12:21

Ablation, vertebroplasty, and radiotherapy in treating symptomatic spinal metastases: can a combined treatment ensure stability and disease control in a medium-long term follow-up?

C. de Cataldo, A. Izzo, G. Bianchi, M. Ruschioni, F. Formiconi, F. Arrigoni, L. Zugaro, A. Barile, C. Masciocchi; *L'Aquila/IT*
(camilladeca@hotmail.it)

Purpose: To assess the efficacy of the combined approach through ablation, vertebroplasty, and postoperative radiotherapy in the management of painful and lytic bone metastases in vertebral fractures or in vertebrae with increased fracture risk.
Methods and materials: We retrospectively evaluated clinical and radiological outcomes of 17 patients who consecutively underwent ablation, vertebroplasty, and radiotherapy. Treated patients had a life expectancy of at least 1 year and required analgesic therapies because of disabling back pain. 20 painful vertebral body metastases were treated, including vertebral fractures and impending vertebral fractures. Ablation and vertebral cementation were performed in a single session under TC guidance, with the purpose being the most radical removal of the metastasis and the injection of the least quantity of cement. The postoperative single session radiotherapy treatment was performed no longer than 10-days after the procedure. VAS and ECOG-PS were evaluated before and after treatment, as well as imaging lesion features.
Results: Patients showed an immediate, rapid, and persistent regression of the symptomatology. Clinical follow-up (mean 18±6 months) showed a decreased need for opioid pain medication and significantly decreased functional disabilities (mean improvement VAS score 2.5 points, mean improvement ECOG-PS 1.8 points). The radiological follow-up (mean 16±7 months) did not show local metastatic recurrence in terms of vertebral height and morphology variations or marginal osteolysis progression.
Conclusion: We strongly support the evidence of combining ablation, vertebroplasty, and radiotherapy as a promising option for the treatment of spinal metastatic lesions, both with a palliative and, in selected cases, curative purpose.
Limitations: A limited study population size.

Ethics committee approval: In accordance with the Helsinki declaration.
Funding: No funding was received for this work.
Author Disclosures:
C. de Cataldo: nothing to disclose
A. Izzo: nothing to disclose
G. Bianchi: nothing to disclose
M. Ruschioni: nothing to disclose
F. Formiconi: nothing to disclose
F. Arrigoni: nothing to disclose
L. Zugaro: nothing to disclose
A. Barile: nothing to disclose
C. Masciocchi: nothing to disclose

11:15 - 12:30 **Room G**

GI Tract

RPS 1001b

Colon cancer: techniques for detection and staging

Moderators:
L. Lambert; Prague/CZ
N.N.

RPS 1001b-K 11:15
Keynote Lecture
M. J. Gollub; *New York, NY/US (gollubm@mskcc.org)*

Author Disclosures:
M. J. Gollub: nothing to disclose

RPS 1001b-1 11:25
Investigating the use of CT colonographs in patients too frail for optical colonoscopy and their management outcome
S. C. Chin[1], G. Duncan[2]; *[1]Dundee/UK, [2]Perth/UK (sookcheng@doctors.org.uk)*

Purpose: CT colonographs (CTCs) are often used as an alternative investigation for colorectal malignancies (CRCs) for patients who are deemed too frail for colonoscopy. We hope to investigate if CTCs performed for this cohort of patients changes their management outcome.
Methods and materials: All CTCs performed from 01/06/14 to 30/06/18 with the keywords 'frail', 'unfit', or 'dementia', and patients coming from nursing homes, were identified. Patients where colonoscopy was attempted previously were excluded. As a control group (non-frail), 100 random CTCs were selected from 01/01/18 to 30/06/18. The CTC quality and findings were collected and categorised. For patients with suspected CRC or polyps, subsequent management and colonoscopy, surgical and pathology report (if applicable) were analysed. The correlation of CTC findings was recorded and any complications from subsequent intervention were also recorded. The Chi-square test was used to test for significance of differences between the groups.
Results: 57 patients met the inclusion criteria. The population group median age was 83 years old vs 67 years old. 46.6% of the study group's examinations were suboptimal quality ($p<0.005$). None of the suspected CRC and polyps <6mm in the study group had a subsequent intervention. Patients with polyps >6mm, 33.3% from the study group versus 83.3%, had an intervention. There was statistical significance in the number of CRC, polyps >6mm, and intervention rate of patients with suspected CRC.
Conclusion: For patients too frail to undergo colonoscopy, CTCs rarely changes their management outcome and a contrast-enhanced abdominopelvic CT examination may be sufficient to identify CRCs and facilitate potential future palliative intervention.
Limitations: Reliance on the accuracy of the provided clinical history to identify the study population and subjective assessment of the clinician to assess the patient's frailty.
Ethics committee approval: n/a
Funding: No funding was received for this work.
Author Disclosures:
S. C. Chin: nothing to disclose
G. Duncan: nothing to disclose

RPS 1001b-2 11:31
The evaluation of the redundant sigmoid colon on computed tomography images
N. Hürsoy[1], O. Aydemir[2], S. Ünal[3], E. Anamurluoğlu[4], H. E. Akkaya[5], M. Kul[4]; *[1]Rize/TR, [2]Konya/TR, [3]Trebizond/TR, [4]Ankara/TR, [5]Karaman/TR (nurhursoy@gmail.com)*

Purpose: To investigate the frequency of the redundant sigmoid colon on computed tomography images by using Kantor's criteria and to compare the results with the literature. We also aimed to emphasise the clinical importance of redundancy and to increase the awareness of radiologists for this condition.
Methods and materials: This retrospective study was performed with 500 patients who underwent CT scans in Turhal State Hospital from August to October 2017. Axial views were evaluated to detect the presence of the redundant sigmoid colon. The thickness of the rectus abdominis muscle, psoas muscle, subcutaneous fat, anteroposterior diameter of abdomen, and the transverse diameter between each anterior superior iliac spinae were measured. The presence of colonic diverticulae was also noted.
Results: The redundant sigmoid colon was detected in 93 patients with a frequency of 18.6%. Age and sex were not significantly different between both groups. The transverse diameter between each anterior superior iliac spinae was significantly shorter in patients with a redundant sigmoid colon.
Conclusion: Kantor's criteria is a useful method for evaluating the redundancy of the sigmoid colon on axial CT images. The frequency of the redundant sigmoid colon is nearly 20% and this condition is important since it is a major risk factor for volvulus, it causes incomplete optic colonoscopies, and is associated with irritable bowel syndrome.
Limitations: Limitations of design and number of patients.
Ethics committee approval: n/a
Funding: No funding was received for this work.
Author Disclosures:
N. Hürsoy: Speaker at RTE University
O. Aydemir: Author at Konya Health Department
S. Ünal: Author at Hackalı Baba State Hospital
E. Anamurluoğlu: Author at Guven Hospital
H. E. Akkaya: Author at Karaman State Hospital
M. Kul: Author at Ankara University

RPS 1001b-3 11:37
Dedicated MR imaging for staging of peritoneal metastases in colorectal cancer patients considered for CRS-HIPEC: the DISCO randomised multicentre trial
M. P. Engbersen[1], A. G. J. Aalbers[1], D. M. J. Lambregts[1], J. Nederend[2], I. de Hingh[2], R. G. H. Beets-Tan[1], N. F. M. Kok[1], M. J. Lahaye[1]; *[1]Amsterdam/NL, [2]Eindhoven/NL (m.engbersen@nki.nl)*

Purpose: To determine the value of dedicated MRI as a non-invasive staging method to evaluate whether complete CRS can be achieved via a randomised controlled trial.
Methods and materials: The study is set-up as a multicentre randomised controlled trial. Patients are eligible when they are considered for CRS-HIPEC after conventional CT staging. The participant will be randomly assigned to either the experimental arm A or the control arm B. Patients in arm A will undergo an MRI scan dedicated to PM, which includes diffusion-weighted, T2 weighted, and post contrast-enhanced T1 weighted imaging of the chest, abdomen, and pelvis. MRI assessment will determine whether the patient can directly proceed for CRS-HIPEC, or whether patients are not eligible for CRS-HIPEC. In borderline cases, a diagnostic laparoscopy (DLS) will be advised. Arm B patients will receive a standard of care, namely proceed to CRS-HIPEC and DLS if deemed necessary at MDT meeting. The primary outcome is the proportion of preventable surgical staging procedures. A preventable surgical procedure is defined as an exploratory laparotomy of a patient with clearly unresectable disease and a DLS or exploratory laparotomy of a patient with clearly resectable disease.
Results: The 270 patients are yet to be included.
Conclusion: If MRI staging can help surgeons in selecting patients who might benefit from CRS-HIPEC, it will spare curative patients unnecessary surgical staging and less open-close procedures in palliative patients. In addition, MRI will provide a clear overview of the abdominal disease for the surgeons to use for their preoperative planning.
Limitations: Need for pathological proof might need DLS.
Ethics committee approval: METC approval has been received.
Funding: Funding for this project is provided by ZonMw.

Author Disclosures:
M. P. Engbersen: nothing to disclose
M. J. Lahaye: Research/Grant Support at ZonMw
R. G. H. Beets-Tan: nothing to disclose
A. G. J. Aalbers: nothing to disclose
N. F. M. Kok: nothing to disclose
D. M. J. Lambregts: nothing to disclose
I. de Hingh: nothing to disclose
J. Nederend: nothing to disclose

RPS 1001b-4 11:43
Clinical impact of dedicated whole-body MR imaging in patients with advanced colorectal cancer
E. Nerad[1], M. P. Engbersen[1], D. M. J. Lambregts[1], E. M. Godfrey[2], N. F. M. Kok[1], A. G. J. Aalbers[1], R. G. H. Beets-Tan[1], M. J. Lahaye[1]; *[1]Amsterdam/NL, [2]Cambridge/UK*

Purpose: To evaluate the clinical impact of dedicated whole-body MRI (WB-MRI) in patients with stage IV colorectal cancer (CRC) on CT.
Methods and materials: This was a retrospective study of 42 patients with CRC referred to our specialist oncologic centre with suspicion of liver and/or peritoneal metastasis. All patients underwent an additional 3T WB-MRI at our institution, including pre/postcontrast T1, T2, and diffusion-weighted imaging (DWI). Multidisciplinary team (MDT) meeting notes were evaluated and if the result of WB-MRI changed the original treatment plan (based on the CT result), it was regarded as a significant clinical impact.
Results: All metastases detected on CT images were also detected with WB-MRI. WB-MRI changed the treatment strategy in 13 patients (31%). WB-MRI diagnosed additional liver and peritoneal metastases in 3 (7%) and 1 (2%) patients, respectively. WB-MRI confirmed or ruled out liver and peritoneal metastases in indeterminate CT studies in 1 (2%) and 6 (14%) patients, respectively. In one patient (2%), WB-MRI confirmed pulmonary metastasis in a lesion that was indeterminate with CT and in another patient (2%) WB-MRI detected an additional metastatic lesion in the anterior abdominal wall and potential renal malignancy.
Conclusion: Dedicated WB-MRI changed the treatment plan in almost one third (31%) of patients with stage IV CRC on CT. WB-MRI should be considered in this patient group to prevent undertreatment.
Limitations: Number of patients included.
Ethics committee approval: n/a
Funding: No funding was received for this work.
Author Disclosures:
E. Nerad: Author at Netherlands cancer institute, Speaker at Netherlands cancer institute
M. P. Engbersen: Author at Netherlands cancer institute
D. M. J. Lambregts: Author at Netherlands cancer institute
E. M. Godfrey: Author at Netherlands cancer institute
N. F. M. Kok: Author at Netherlands cancer institute
A. G. J. Aalbers: Author at Netherlands cancer institute
R. G. H. Beets-Tan: Author at Netherlands cancer institute
M. J. Lahaye: Author at Netherlands cancer institute

RPS 1001b-5 11:49
Low-volume reduced bowel preparation for CT colonography: a randomised controlled trial
N. Panvini[1], D. M. Bellini[1], M. Rengo[1], S. Vicini[2], I. Carbone[3], A. Laghi[3]; *[1]Latina/IT, [2]Sora/IT, [3]Rome/IT (npanvini88@gmail.com)*

Purpose: To investigate feasibility and patient tolerance of a reduced bowel preparation for CT colonography (CTC).
Methods and materials: Asymptomatic and symptomatic patients were enrolled in this multicentric randomised trial. All patients were randomly assigned (1:1 ratio, blocks of ten) to receive a reduced (52.5 g of Macrogol dissolved in 500 mL of water, RBP) or full (105 g of Macrogol in 1000 mL, FBP) bowel preparation and faecal tagging. Five readers performed a blinded subjective image analysis by means of 4-point Likert-scales from 0 (highest score) to 3 (worst score). Endpoints were the quality of large bowel cleansing and tolerance to the assigned bowel preparation regimen.
Results: 78 patients were randomly allocated to treatments (44 in FBP-group, 34 in RBP-group). Both groups resulted in optimal colon cleansing. Homogeneity of fluid tagging (median score 0 vs 0, p=0.075), volume of residual stools (median score 0 vs 0, p=0.082), and colonic distension (median score 0 vs 0, p=0.073) were similar for both groups. RBP resulted in better patient tolerance.
Conclusion: Reduced bowel preparation may provide better tolerance for patients undergoing CTC without affecting colon cleansing and image quality.
Limitations: The main limitation of our study is that the diagnostic accuracy has not been evaluated.
Ethics committee approval: The study protocol was approved by the Institutional Review Board of our Institution and written informed consent was obtained from all patients.
Funding: No funding was received for this work.
Author Disclosures:
N. Panvini: nothing to disclose
D. M. Bellini: nothing to disclose
M. Rengo: nothing to disclose
S. Vicini: nothing to disclose
I. Carbone: nothing to disclose
A. Laghi: nothing to disclose

RPS 1001b-6 11:55
Evaluation accuracy of US compared to CT for the diagnosis of colonic diverticulitis: prospective single-centre study
S. E. Gabrieli, M. Dahan, N. Granat, H. Neiman,, T. Gurvitz, E. Atar, G. Bachar; *Petah Tikva/IL (nadavgranat@gmail.com)*

Purpose: Diverticulitis is commonly diagnosed using CT. The major drawback of a CT scan is exposure to ionising radiation that increases the risk of malignancy. Our aim was to determine the diagnostic accuracy of US compared with CT for patients suspected for diverticulitis and to examine the possibility of using US as a primary tool in emergency department for the diagnosis of diverticulitis.
Methods and materials: A double-blind prospective analysis was conducted between 2015-2019 on 170 consecutive patients who were admitted to the emergency department suspected clinically for diverticulitis. Their medical history, clinical signs, and laboratory exams were reviewed. All patients underwent first US examination followed by an abdominal CT scan.
Results: 122 patients were identified with colonic diverticulitis as the final diagnosis by CT compared to 125 by US. Sensitivity and specificity of US examination were 93.6% (95% CI 87.37% - 97.0%) and 88.9% (95%CI 75.1%-95.8%), respectively.
The positive and negative predictive values for the diagnosis of simple diverticulitis by US were 95.9% and 83.3%, respectively. 19 patients were identified with complicated diverticulitis by CT compared to 17 patients by US (89.5%). In those two cases, a small tiny perforation was missed by US.
Conclusion: Our study shows that US has high sensitivity and specificity in the evaluation of patients with suspected diverticulitis and can replace CT examination as a primary tool in diagnosing simple colonic diverticulitis. CT examination can be reserved as a second tool in cases of suspected complicated diverticulitis.
Limitations: Single-centre study.
Ethics committee approval: The study was approved by our IRB committee.
Funding: No funding was received for this work.
Author Disclosures:
S. E. Gabrieli: nothing to disclose
N. Granat: nothing to disclose
E. Atar: nothing to disclose
M. Dahan,: nothing to disclose
H. Neiman,: nothing to disclose
T. Gurvitz: nothing to disclose
G. Bachar: nothing to disclose

RPS 1001b-7 12:01
The impact of mismatch repair status to the preoperative staging of local colon cancer
E. Erbs, S. R. Rafaelsen, J. Lindebjerg, L. H. Jensen, T. F. Hansen; *Vejle/DK (s.rafaelsen@dadlnet.dk)*

Purpose: Computed tomography (CT) scan is standard in preoperative local staging of colon cancer. Tumours with a deficient mismatch repair (dMMR) system are characterised by unique clinical and pathophysiologic aspects that may impact on the accuracy of the preoperative CT staging.
Methods and materials: Data from the Danish Colorectal Cancer Group national clinical database addressing a cohort of patients operated for stage I-III colon cancer in 2010-15 was analysed. The analyses of MMR status had been conducted consecutively through means of immunohistochemistry. All CT scans were blindly assessed by a certified radiologist.
Results: Data from 590 patients, operated at a specialised cancer centre were available for analyses. 135 (22.9%) of the patients had tumours demonstrating dMMR. The overall correlation of the clinical and pathological T-category was significant for both groups. There was inferior correlation between clinical (cN) and pathological (pN) N-category (p>0.05) in pMMR cancers with a higher degree of over-staging assessed by CT-scan compared to a significant correlation between cN and pN stage in pMMR cancers (p<0.01). Of the 91 dMMR tumours assessed node-positive by the preoperative CT scan, 59 (64.8%) showed no sign of metastatic involvement at the postoperative assessment.

Conclusion: The accuracy of preoperative lymph node staging in colon cancer by CT scan seems to differ depending on MMR status and may impact the clinical management including the neoadjuvant setting.
Limitations: This study is based on data from a national database and by that suffers from limitations related to this kind of research such as incomplete data registration.
Ethics committee approval: n/a
Funding: No funding was received for this work.
Author Disclosures:
S. R. Rafaelsen: nothing to disclose
E. Erbs: nothing to disclose
J. Lindebjerg: nothing to disclose
L. H. Jensen: nothing to disclose
T. F. Hansen: nothing to disclose

RPS 1001b-8 12:07

Effect of iterative model reconstruction algorithm on radiologists' performance in CT colonography

Y. Lian[1], J. Dong[1], W. Cao[2], J. Gao[1]; [1]*Zhengzhou/CN*, [2]*Guangzhou/CN (lybang0507@126.com)*

Purpose: To assess radiation dose and image quality of CT colonography (CTC) at 100 kVp with iterative model reconstruction algorithm (IMR) at 20 mAs compared with filtered back projection (FBP) at 50 mAs.
Methods and materials: 32 patients suspected with colon adenomatous polyp or adenocarcinoma were enrolled. All patients underwent CTC examination at 50mAs in a supine position and 20mAs in a prone position, with the same tube voltage at 100 kVp about two hours before fibro-colonoscope. Images were reconstructed using FBP and IMR. Two radiologists independently evaluated image quality. Qualitative image quality was assessed with a five-score scale. Image noise, signal-to-noise ratio, contrast-to-noise ratio, and effective radiation dose were recorded and calculated. Qualitative and quatitative values were analysed using the Wilcoxon signed rank test and the paired t test, respectively.
Results: 38 colon polyps or adenocarcinomas were detected in fibro-colonoscope examination. For 20 mAs with IMR (A group) and 50 mAs with FBP (B group), there is no statistically significant difference in lesion detection (reader 1: 35/38 vs 36/38, and reader 2: 31/38 vs. 33/38, p>0.05). However, qualitative image quality scores (3.9 vs 2.5), image noise ([12.77± 0.91] HU vs. [50.04±5.45] HU), SNRs (3.13±0.28 vs. 1.02±0.20), and CNRs (81.42±6.11 vs. 19.93±1.46) were significantly superior of 20 mAs with IMR, respectively (p<0.05). Compared with group B, the radiation dose of A group decreased significantly (0.42±0.03 mSv vs. 1.07±0.12mSv).
Conclusion: Image quality of CTC using 20 mAs with IMR reconstruction could be comparable to 50 mAs with FBP at the same tube voltage with no significant detection of polyp and radiation dose of the former was only 0.42 mSv, which was reduced by about 39.3%.
Limitations: Lacking data of patients with BMI>24.
Ethics committee approval: n/a
Funding: No funding was received for this work.
Author Disclosures:
Y. Lian: nothing to disclose
J. Dong: nothing to disclose
W. Cao: nothing to disclose
J. Gao: nothing to disclose

RPS 1001b-9 12:13

Extra-peritoneal findings on dedicated DW-MRI for colorectal cancer patients considered for CRS/HIPEC

I. van 't Sant, M. P. Engbersen, C. Gispen, D. M. J. Lambregts, N. F. M. Kok, A. G. J. Aalbers, R. G. H. Beets-Tan, M. J. Lahaye*; Amsterdam/NL*

Purpose: To examine the added value of preoperative DW-MRI in colorectal cancer patients considered for cytoreductive surgery and hyperthermic intraperitoneal chemotherapy (CRS-HIPEC) regarding extra-peritoneal findings over the standard diagnostic work-up.
Methods and materials: Between February 2016 and January 2019, all colorectal cancer patients with suspected peritoneal metastases (PM) who were considered for CRS-HIPEC and who underwent a preoperative DW-MRI in addition to standard diagnostic work-up (CT thorax/abdomen ± PET-scan) were included. The added value of DW-MRI was determined by scoring the number of extra-peritoneal findings that had not emerged in previous imaging, the number of previously uncertain findings that could be rejected or confirmed, and the number of findings that could be qualified as more or less likely. The reference standard was surgical results or follow-up imaging in patients that did not undergo surgery.
Results: Of the 153 included patients (M/F=83/70), 40 had a PET scan in addition to CT and DW-MRI scans. Mean delay between CT (±PET) and DW-MRI was 17 days (IQR:4-31). DW-MRI was scored as of added value in 39% (59/153) of cases. New extra-peritoneal findings were found in 14% (22/153), the majority being metastases in the abdominal wall (10), liver (5), and adnexa (4). 32 lesions previously characterised as possibly malignant could be refuted based on DW-MRI findings. In 85%, this concerned liver lesions. 8 malignant lesions were left unmentioned on imaging altogether, 5 of which were port-site metastases.
Conclusion: DW-MR imaging in colorectal cancer patients considered for CRS-HIPEC has an added value in detecting and clarifying extraperitoneal findings that are occult or indistinct on standard work-up imaging methods. These findings are important as they may form contraindications to otherwise futile CRS-HIPEC procedures.
Limitations: Retrospective nature.
Ethics committee approval: n/a
Funding: No funding was received for this work.
Author Disclosures:
M. P. Engbersen: nothing to disclose
I. van 't Sant: nothing to disclose
A. G. J. Aalbers: nothing to disclose
C. Gispen: nothing to disclose
N. F. M. Kok: nothing to disclose
R. G. H. Beets-Tan: nothing to disclose
D. M. J. Lambregts: nothing to disclose
M. J. Lahaye: nothing to disclose

RPS 1001b-10 12:19

Neural network-based diagnosis algorithm of appendicitis in patients with acute abdominal pain presenting to emergency department

J. J. Park, K. A. Kim, Y. Nam*; Seoul/KR*

Purpose: To investigate the feasibility of a neural network-based diagnosis algorithm of appendicitis by using CT for patients with acute abdominal pain visiting an emergency room (ER).
Methods and materials: For this retrospective study, a neural network-based diagnostic algorithm of appendicitis was developed using CT data of patients who visited ER with abdominal pain and underwent abdominopelvic CT between December 2018 and May 2019. For training, 3D isotropic cubes ($4\times4\times4cm^3$) including appendix were manually segmented and labelled as appendicitis or normal appendix. A 3D convolutional neural network was trained to perform binary classification for input 3D images. In the training process, cross-entropy loss was used and kernel size was 3. To reduce overfitting, data augmentation processes such as shifting, flipping, and adding random noises were adopted. 8-fold cross-validation was used. For each model, 64 subjects were used to train the network and the remaining 16 subjects were tested using the trained network algorithm. Diagnostic performance was assessed.
Results: 667 patients were involved, with 215 patients with acute appendicitis and 452 patients with normal appendix (331 men and 336 women; mean age, 45.6 years old). Accuracy of a neural network-based classification algorithm for diagnosis of appendicitis was 91.60 %. Sensitivity, specificity, positive predictive value, and negative predictive value were 90.65 %, 92.05 %, 84.35 %, and 95.42 %, respectively.
Conclusion: A neural network-based diagnosis algorithm was feasible with high diagnostic performance for acute appendicitis on CT of patients visiting ER with acute abdominal pain.
Limitations: We only included CT image in patients with normal and inflamed appendix. External validation was not performed. We manually extracted appendix. Automatic detection algorithm is under development.
Ethics committee approval: The institutional review board approved this study. Informed consent was waived due to the retrospective nature.
Funding: No funding was received for this work.
Author Disclosures:
J. J. Park: nothing to disclose
K. A. Kim: nothing to disclose
Y. Nam: nothing to disclose

RPS 1001b-11 12:25

Role of abdominal helical computed tomography in the diagnosis of adult intussception

D. Vo Tan, P. M. N. Do*; Ho Chi Minh/VN (duc.vt@ump.edu.vn)*

Purpose: To describe imaging characteristics of adult intussception (AI) on CT and to identify diagnostic values of them.
Methods and materials: Case series report including patients: defined AI on CT, over 18 years of age, having had surgery, with/without histo-pathology. Patients were divided into two groups: those with enteroenteric intussusception (EI) and those with intussusceptions involving colon (IC), including enterocolic and colocolic lesions.
Results: From 01/2014 to 01/2017 at University Medical Center, HCMC, there were 53 intussusceptions of 52 patients on CT (EI: 14_26%, IC: 39_74%). 33 of those had intussusception on surgery (EI: 10_3%, IC: 23_70%). Mean length of intussusceptions of both groups was 7,6±4,0cm (2,4-19,6). Mean diameter of intussusceptions was 4,7±1,1cm (2,2-7). Mean interposed fat thickness was 1±0,6cm (0,1-2,6). CT and surgery characteristics of patients in EI group were

of minor differences. The ratio of AI on CT with obstruction and with ischemia necrosis were both 3,8%. The outcome of diagnosing complications by CT and by surgery was comparable. Characteristics capable of predicting presence of intussusception on surgery were in EI group: lead point, length > 6cm, interposed fat thickness > 0,5 cm; in IC group: length > 5.65 cm, interposed fat thickness > 0,75 cm.
Conclusion: Characteristics capable of predicting the presence of intussusception on surgery are lead point, length, and interposed fat thickness.
Limitations: Retrospective and cross-sectional study.
Ethics committee approval: University of Medicine and Pharmacy at Ho Chi Minh City, Vietnam.
Funding: No funding was received for this work.
Author Disclosures:
D. Vo Tan: nothing to disclose
P. M. N. Do: nothing to disclose

11:15 - 12:30 **Room K**

Cardiac

RPS 1003a

Emerging applications: cardio-oncology and athletes' hearts

Moderators:
E. Pershina; Moscow/RU
A. Toth; Budapest/HU

RPS 1003a-K 11:15
Keynote lecture
T. Hazırolan*; Ankara/TR*

Author Disclosures:
T. Hazırolan: nothing to disclose

RPS 1003a-1 11:25
Cardiac deformation parameters measured by cardiac magnetic resonance in a cohort of highly-trained endurance athletes
B. Domenech Ximenos[1], M. Sanz-de la Garza[2], D. Lorenzatti[2], A. Sepulveda[3], F. Crispi[2], R. J. Perea[2], S. Prat Gonzalez[2], M. Sitges[2]; *[1]Girona/ES, [2]Barcelona/ES, [3]Santiago de Chile/CL (bl.domenech@gmail.com)*

Purpose: There is evolving evidence that the cumulative effects of intensive endurance exercise may induce a broad spectrum of cardiac adaptation/remodelling patterns. Even if the common features of the athlete's heart are well-known, whether changes in cardiac strain parameters occur in response to training is less well-studied. We aimed at understanding and characterising these changes in CMR derived-strain parameters in highly trained endurance athletes.
Methods and materials: 93 highly trained endurance athletes (>12 hours training/week at least during the last 5 years) and 72 age and gender-matched controls (52% male, mean age 35±5.1 years) underwent a resting-CMR. Biatrial and biventricular dimensions and function were assessed, as well as the presence of myocardial fibrosis by LGE. We evaluated radial, circumferential, and longitudinal strain of both ventricles and left atrium from feature tracking (FT) of cine images.
Results: High endurance training load was associated with larger bi-ventricular and bi-atrial sizes, mildly reduced the systolic function of both ventricles, as compared to controls (P < 0,05). LGE was significantly more prevalent in athletes (n=33, 35.4% vs 4,2%; P<0,001), with a constant pattern in the right ventricle (RV) insertion points. Left ventricle circumferential and radial strain, RV circumferential, radial and longitudinal strain, and left atrium strain were all lower in athletes than in controls; p<0.05.
Conclusion: The strain values from FT in our group of highly-trained endurance athletes were lower than in the control group. This was observed together with harmonic biventricular dilation and with the presence of LGE confined to the RV insertion point. The clinical impact of these strain values is currently uncertain and still warrants further investigation.
Limitations: No long-term follow-up available.
Ethics committee approval: Institutional review-board approval was obtained. Subjects provided written informed consent.
Funding: Partially funded by AGAUR(M. Sanz-de la Garza,MD,PhD). GrantDEP2013-44923-P.
Author Disclosures:
B. Domenech Ximenos: nothing to disclose
M. Sanz-de la Garza: nothing to disclose
D. Lorenzatti: nothing to disclose
A. Sepulveda: nothing to disclose
F. Crispi: nothing to disclose
R. J. Perea: nothing to disclose
S. Prat Gonzalez: nothing to disclose
M. Sitges: nothing to disclose

RPS 1003a-2 11:31
Non-invasive MRI evaluation of adjuvant chemotherapy effects on heart in breast cancer patients: 1-year follow-up in a single centre
C. de Cataldo[1], E. Cannizzaro[1], P. Palumbo[1], S. Torlone[1], M. C. de Donato[1], M. Latessa[2], S. Necozione[1], E. Di Cesare[1], C. Masciocchi[1]; *[1]L'Aquila/IT, [2]Sienna/IT (camilladeca@hotmail.it)*

Purpose: To evaluate the accuracy of a non-invasive MRI follow-up through strain analysis in the detection of anthracycline-induced left ventricular systolic dysfunction.
Methods and materials: We prospectively evaluated 36 breast cancer patients (mean age 53,4, range 39-67) undergoing anthracycline-based chemotherapy, between February 2018 and February 2019. All the patients underwent a non-enhanced cardiac magnetic resonance (CMR) before (Time 0), at 3-6 months (Time 1), and after 1 year (Time 2) from the beginning of chemotherapy. Global radial (GRS), circumferential (GCS), and longitudinal (GLS) strain values were assessed for each patient on each CMR examination through a dedicated software (Cvi42). Statistical analysis through Friedman's test and Post-hoc Test according to Conover was performed.
Results: We found statistically significant difference among strain values at Time 0, Time 1, and Time 2, respectively. [GLS median: 18,26±2,2 vs -15,09±1,6 vs -13,51±1,7(p<0,0001), GCS median: 18,51±2,9 vs -18,11± 1,7 vs -17,03±1,8(p<0,00001), and GRS: 29,56±3,9 vs 26,94±3,6 vs 24,86±3,4(p<0,00001)]. Median FE was 60±4% at Time 0, 56±5% at Time 1, and 53±2% at Time 2 (p<0,00001). 18 patients showed a GLS decrease with a compensatory GRS and GCS increase at Time 1, followed by a consensual decrease of all the values at Time 2. 11 patients showed a gradual decrease in all strain values from Time 0 to Time 2. 7 patients demonstrated no significant variation between strain values at Time 0 and 1, with a significant decrease at Time 2.
Conclusion: We support the validity of a non–enhanced CMR follow-up in breast cancer patients undergoing anthracyclines treatment in the detection of early myocardial impairment through strain analysis. It is a reliable post-processing tool deserving a definitive clinical validation.
Limitations: Small study specimen size.
Ethics committee approval: In accordance with the Helsinki Declaration.
Funding: No funding was received for this work.
Author Disclosures:
E. Di Cesare: nothing to disclose
E. Cannizzaro: nothing to disclose
S. Torlone: nothing to disclose
P. Palumbo: nothing to disclose
C. de Cataldo: nothing to disclose
M. C. de Donato: nothing to disclose
M. Latessa: nothing to disclose
S. Necozione: nothing to disclose
C. Masciocchi: nothing to disclose

RPS 1003a-3 11:37
Decreased myocardial deformation in athletes correlates with the degree of LV hypertrophy
J. Stáreková, C. Behzadi, G. K. Lund, G. H. Welsch, B. P. Schoennagel, K. Muellerleile, G. Adam, M. Regier, E. Tahir*; Hamburg/DE (j.starekova@uke.de)*

Purpose: To assess ventricular morphology and parameters of diastolic function between professional soccer players and competitive triathletes compared to sedentary controls using cine feature-tracking CMR.
Methods and materials: 23 soccer players (22±4 years), 19 triathletes (28±6 years), and 16 controls (26±3 years) underwent CMR. Chambers volume and left ventricular mass were determined and correlated with global myocardial strain. Peak systolic longitudinal (LS), circumferential (CS), and radial (RS) strains were analysed on cine CMR images using feature-tracking software.
Results: Athletes displayed higher myocardial mass (P<0.001) compared to the controls. The longitudinal ventricular strain was significantly reduced in athletes in comparison to the controls (P<0.01 for the right ventricle (RV) and P<0.05 for LV) as well as radial LV strain (P<0.05). Both athletic groups were characterised by eccentric hypertrophy. However, in comparison to triathletes, soccer players revealed higher LV mass (87±15 vs. 75±13 g/m2, P<0.05). Furthermore, soccer players experienced a greater decrease in the longitudinal strain of LV (-16±2 vs. -17±2%, P<0.05) and RV (-18±2 vs. -20±3%, P<0.05), as well as in radial LV strain (38±8 vs. 43±7%, P<0.05). An increase in LV mass correlated with a

decrease in the longitudinal strain (r=0.47, P<0.001) and radial strain (r=-0.28, P<0.05).
Conclusion: Reduction of global myocardial strain in athletes correlates with the level of LV hypertrophy. Detrimental effects on myocardial mechanics due to an increased level of sport-induced hypertrophy pronounced in soccer players cannot be excluded.
Limitations: The presence of myocardial fibrosis and its potential influence on LV strain cannot be excluded.
Ethics committee approval: Ethics comitee aproval (Ärztekammer Hamburg). Written informed consent was obtained.
Funding: No funding was received for this work.
Author Disclosures:
J. Stáreková: nothing to disclose
E. Tahir: nothing to disclose
G. Adam: nothing to disclose
G. K. Lund: nothing to disclose
B. P. Schoennagel: nothing to disclose
C. Behzadi: nothing to disclose
K. Muellerleile: nothing to disclose
M. Regier: nothing to disclose
G. H. Welsch: nothing to disclose

RPS 1003a-4 11:43

Coronary atherosclerosis in apparently healthy master athletes discovered during pre-participation screening: role of coronary CT-angiography (CCTA)

G. Rovere, R. Marano, B. Merlino, L. Natale, G. Savino, R. Manfredi*; Rome/IT*

Purpose: To assess the role of coronary CT-angiography (CCTA) and non-invasive detection of coronary atherosclerosis (cATS) in the assessment and clinical management of master athletes (MA) during the pre-participation screening (PPS).
Methods and materials: We retrospectively examined 167 MA who underwent CCTA in our hospital since 2006, analysing symptoms, stress-test ECG, cardiovascular risk profiles (SCORE), and CCTA findings.
Results: Among the whole enrolled population, 153 (91.6%) MA underwent CCTA for equivocal/positive stress-test ECG with/without symptoms, 13 (7.8%) just for clinical symptoms, and 1 (0.6%) due to family history. The CCTA showed the presence of cATS in 69 MA (41.3%), congenital coronary anomalies (anomalous origin or deep myocardial bridge) in 8 (4.8%), and both in 7 (4.2%). A negative CCTA was observed in 83 MA (49.7%). The risk-SCORE (age, hypertension, hypercholesterolemia, and smoking) was a good indicator for the presence of moderate/severe cATS on CCTA. However, mild/moderate cATS was present in 17.8% of MA clinically stratified at a low risk-SCORE.
Conclusion: CCTA may be helpful in the PPS of MA with an abnormal stress test ECG and/or clinical symptoms engaged in competitive sports with high cardiovascular involvement, while the invasive coronary angiography is more indicated in athletes with positive stress-test ECG and high clinical risk. Age, gender, presence of symptoms, and clinical risk-SCORE assessment may help sports-physicians/cardiologists to decide whether to request a CCTA or not.
Limitations: n/a
Ethics committee approval: n/a
Funding: No funding was received for this work.
Author Disclosures:
B. Merlino: nothing to disclose
G. Rovere: nothing to disclose
R. Marano: nothing to disclose
L. Natale: nothing to disclose
G. Savino: nothing to disclose
R. Manfredi: nothing to disclose

RPS 1003a-5 11:49

Instant impact of a competitive event on ventricular strain by feature tracking cardiac magnetic resonance imaging and changes in cardiac biomarkers in triathletes

M. L. Warncke, J. Stáreková, C. Jahnke, B. Scherz, K. Müllerleile, U. Radunski, G. Adam, G. Lund, E. Tahir*; Hamburg/DE*
(m.warncke@uke.de)

Purpose: To analyse the impact of an endurance competition on left (LV) and right ventricular (RV) function by feature-tracking strain analysis by cine cardiac magnetic resonance imaging (CMR) in competitive male and female triathletes.
Methods and materials: 50 asymptomatic triathletes (45 ±10 years, 20% female) with more than 10 weekly training hours were studied by CMR performed on a 1.5T system with a 5-channel cardiac coil before and after an endurance competition (1.3 ±0.5 km of swimming, 59.9 ±72.5 km of cycling, and 15.9 ±11.5 km of running). Functional and morphological LV parameters were determined using CVi42 (circle cardiovascular imaging). Global peak systolic longitudinal, radial, and circumferential myocardial strains were analysed using Segment (Medviso, Sweden). Blood tests were performed before the competition and at the time of the CMR.
Results: Troponin T (6 ±4 pg/ml vs. 51 ±77 pg/ml, P<0.0001), NT-proBNP (45 ±73 pg/ml vs. 116 ±99 pg/ml, P<0.0001), and creatine kinase isoenzyme MB (10 ±14 U/l vs. 32 ±19 U/l, P<0.0001) increased significantly after the competition. Radial and circumferential LV strain increased from baseline to post-competition with 39 ±11% vs. 44 ±11% (P<0.05) and -16 ±4% vs. -18 ±3% (P<0.05). LV longitudinal strain showed a trend for decrease (-17 ±2% vs. -17 ±2%, P=0.054). Circumferential RV strain increased significantly post-competition (-6 ±3% vs. -7 ±2%, P<0.01), whereas RV longitudinal strain remained constant (-9 ±3% vs. -9 ±4%, P=0.668). LV ejection fraction did not change (63 ±7% vs. 62 ±6%, P=0.607).
Conclusion: Cardiac biomarkers are markedly elevated following strenuous endurance exercise in healthy male and female triathletes with normal LV ejection fraction. LV radial, circumferential, and RV circumferential strain increases. LV longitudinal strain decreases post-competition.
Limitations: Different competition formats.
Ethics committee approval: n/a
Funding: No funding was received for this work.
Author Disclosures:
M. L. Warncke: nothing to disclose
J. Stáreková: nothing to disclose
C. Jahnke: nothing to disclose
B. Scherz: nothing to disclose
K. Müllerleile: nothing to disclose
U. Radunski: nothing to disclose
G. Adam: nothing to disclose
G. Lund: nothing to disclose
E. Tahir: nothing to disclose

RPS 1003a-6 11:55

Coronary CT-angiography in the clinical workflow of athletes with malignant anomalous origin of coronary arteries

F. Paciolla, R. Marano, G. Savino, L. Natale, B. Merlino, R. Manfredi*; Rome/IT*

Purpose: To assess the CCTA, added to clinical-profiles, in the diagnosis, management, and follow-up of athletes with anomalous-origin of left- (AOLCA) and right-coronary-artery (AORCA) from the wrong-sinus.
Methods and materials: Subjects with suspected AOLCA/AORCA at the trans-thoracic-echocardiography (TTE) or with inconclusive-TTE underwent CCTA to rule out/confirm and characterise the anatomical findings: partial- (pINT) or full-(INT) inter-arterial-course, high-take-off (HTO), acute-take-off-angle (ATO), slit-like-origin (SLIT), intramural-course (IM), intraarterial-course-length (LEN), and lumen-reduction/hypoplasia (HYPO).
Results: CCTA identified 28 athletes: 6-AOLCA (3-males, 20.3±11.0years), 22-AORCA (18 males, 29.1±16.5years); 26/28 (92.9%) suspected at TTE. Clinical symptoms were present only in 13 athletes (46.4%; 10-AORCA). Four subjects (3-AORCA) had abnormal rest ECG and 11 (40.7%) (9-AORCA) abnormal stress ECG. INT course was observed in 15 athletes (53.6%): 6/6-AOLCA and 9/22-AORCA (40.9%). HTO/ATO occurred in 1 and 3/6 AOLCA-patients, HTO in 12/22 (54.5%) and ATO in 21/22 (95.5%) in AORCA. Slit-like-origin was never recorded in AOLCA and present in 7/22 AORCA (31.8%). Suspected IM resulted in 3-AOLCA (50%), always with HYPO/ATO and in one case HTO, whereas IM was suspected in 6/22 AORCA (27.3%), in all cases with HYPO, observed in 12/22 AORCA (54.5%). No statistically significant differences resulted between asymptomatic/symptomatic subjects regarding the prevalence of pINT/INT-courses, HTO/ATO, and slitlike-ostium. A slight significant relationship between suspected proximal IM (r=0.47,p<0.05) and proximal HYPO of anomalous-vessel (r=0.65,p<0.01) resulted in AORCA and confirmed on AOLCA/AORCA pooled analysis (r=0.58,p<0.01 for HYPO). All AOLCA/AORCA athletes were disqualified from competitive sports and warned to avoid vigorous physical efforts. Surgery was recommended to all AOLCA athletes and to 13 AORCA (3-asymptomatic), but only 6 underwent surgery. No MACE/ischemic symptoms/signs occurred during a mean-follow-up of 49.6±39.5 months.
Conclusion: CCTA is an accurate/mandatory diagnostic technique for the detection of anomalous-coronary-anatomy and risk-stratification, providing essential information for safe/effective clinical management of athletes, with important prognostic and sport-activity implications.
Limitations: n/a
Ethics committee approval: n/a
Funding: No funding was received for this work.
Author Disclosures:
F. Paciolla: nothing to disclose
G. Savino: nothing to disclose
R. Marano: nothing to disclose
L. Natale: nothing to disclose
B. Merlino: nothing to disclose
R. Manfredi: nothing to disclose

RPS 1003a-7 12:01

Assessment of myocardial deformation in elite male weightlifters using cardiovascular magnetic resonance feature tracking technique

G. Ge, W. Xiaohua*; Beijing/CN (guogeegg@sina.com)*

Purpose: To assess the myocardial deformation in elite male weightlifters with cardiovascular magnetic resonance imaging (CMR) feature tracking technique.
Methods and materials: 14 elite Chinese male weightlifters and an age-, sex-matched cohort of 14 sedentary volunteers were enrolled. All participants underwent CMR scans at 3.0T and feature tracking technique was used to obtain global and regional left (LV) and right ventricular (RV) strain parameters.
Results: The LV global longitudinal (LV-GLS), circumferential (LV-GCS), radial strains (LV-GRS), and RV-GLS were significantly lower in weightlifters (-11.19±1.19%, -14.02±1.19%, 21.31±2.35% and -14.89±4.25%) than in volunteers (-14.50±1.84%, -16.62±1.24%, 27.01±3.18% and -18.75±3.54%, P<0.001). The LV peak systolic longitudinal, circumferential, radial-strain rate, and peak diastolic radial-strain rate were lower in weightlifters (-0.73±0.18, -0.88±0.13, 1.27±0.22 and -1.27±0.24) than in volunteers (-0.90±0.15, -0.98±0.12, 1.55±0.25 and -1.62±0.34, P<0.05). Differences in torsion, torsion rate, LV peak diastolic longitudinal and circumferential strain rate, RV-GRS, RV peak systolic and diastolic longitudinal or radial strain rates were non-significant (P>0.05). For segmental analysis, the basal anterior wall and mid-cavity to apical inferior walls of athletes had significantly lower LV GLS (P<0.05), while the inferior walls, inferolateral walls, and apical slice had significantly lower LV GCS and LV GRS compared with control volunteers (P<0.05).
Conclusion: Using CMR feature tracking technique, elite weightlifters demonstrated lower LV GLS, LV GCS, LV GRS, RV GLS, and segmental hypokinesis when compared to volunteers, which could be considered as a physiological adaptation to intensive training.
Limitations: There was a small number of participants. A direct comparison to athletes of other disciplines was not performed. All measurements were invariably acquired at rest.
Ethics committee approval: The Peking University Third Hospital Ethics Committee approved the study. Written informed consent was obtained from all subjects
Funding: No funding was received for this work.
Author Disclosures:
G. Ge: nothing to disclose
W. Xiaohua: nothing to disclose

RPS 1003a-8 12:07

Cardiac MRI texture analysis with semi-automatic segmentation: comparison between segmentation techniques and reproducibility

M. Orlando, N. Di Meo, G. M. Agazzi, M. Ravanelli, D. Farina*; Brescia/IT (matteo.orland@gmail.com)*

Purpose: To compare cardiac MR (CMR) texture analysis (TA) features extracted from the whole left ventricle (wLV-ROI) with those obtained on a representative single short-axis section with a circumferential ROI (c-ROI) or with a ROI on the interventricular septum (s-ROI).
Methods and materials: Retrospective single-centre study in 85 patients submitted to CMR from Jan 17 to Feb 18 with a negative report (i.e. no late gadolinium enhancement, no contractile dysfunction, normal LVEF, and volumes). MRI was performed with a 1.5-T system with cardiac coil; b-SSFP sequences in the short-axis at end-diastole were analysed using a freeware software (3DSlicer). wLV-ROI and c-ROI segmentation was performed semi-automatically with a brush tool on an intensity threshold-based mask; s-ROI was segmented manually. 107 TA features for segmentation were extracted with the pyRadiomics library. Interobserver and intraobserver agreement tests were performed in a subset of 20 patients after a 4-week pause. The intraclass correlation coefficient (ICC) was used to compare TA data from wLV-ROI, c-ROI, and s-ROI, and to measure inter and intraobserver agreement.
Results: The comparison between wLV-ROI and c-ROI, and between wLV-ROI and s-ROI, obtained ICC>0,8 for 5 first-order features: Median, RootMeanSquared, 90Percentile, 10Percentile, Mean. Additionally, 2 shape features had ICC>0,8 for c-ROI: Maximum2DDiameterSlice and MinorAxisLength. We observed good inter and intraobserver agreement for 76 features (ICC>0,8).
Conclusion: The agreement between TA features obtained with wLV-ROI and smaller samples is limited to first-order radiomic metrics suggesting the need for whole-ventricle analysis for diffuse myocardial disease. No superior order feature, except for 2 of shape, can be reliably obtained unless segmenting the whole LV. The reproducibility is good (ICC>0,8 for >70% of the features).
Limitations: Single-centre, retrospective, small sample.
Ethics committee approval: All patients gave written consent to CMR.
Funding: No funding was received for this work.
Author Disclosures:
M. Orlando: nothing to disclose
N. Di Meo: nothing to disclose
G. M. Agazzi: nothing to disclose
D. Farina: nothing to disclose
M. Ravanelli: nothing to disclose

RPS 1003a-9 12:13

Native T1 mapping early detects the cardiotoxicity caused by daunorubicin: verified by histological

R. Xu, H. Liu, Y. Guo, L. Chen*; Chengdu/CN (Xrongdoctor@163.com)*

Purpose: Daunorubicin (DNR) serves as the backbone of many anti-cancer treatment strategies, but DNR-induced cardiotoxicity was rarely reported compared with doxorubicin (DOX).
Methods and materials: 38 adult male New Zealand white rabbits weighing 2 to 4 kg were included in this study. There were divided into 3 groups including control subjects and the DNR subjects with 3 or 4 mg/kg respectively. The CMR imaging included the function, native T1 mapping, and LGE. The time points were 2 weeks and 4 weeks. Some subjects were sacrificed for histological evaluation at the end of CMR scan.
Results: In the group of controls rabbits and DNR rabbits, the EF was decreased from 2 weeks to 4 weeks (controls 62.32±7.95% vs. 2 weeks 56.29±5.64% vs. 4 weeks 52.41±11.35%). For the T1 mapping analysis, the global native T1 values in rabbits with 4mg/kg weekly at 2 and 4 weeks were significantly higher than the controls (P <0.05) and all modelling rabbit had higher T1 values than controls. Most of the DNR rabbits (94.68%) were without the presence of LGE and a few of the subjects (5.32%) showed the LGE positive in subendocardial or the free wall. The Masson stain showed diffuse extracellular collagen deposition in the LV myocardium.
Conclusion: Native T1 mapping could detect diffuse myocardial injury in 4 weeks caused by daunorubicin. The higher cumulative dose and longer time may result in a more severe myocardium injury.
Limitations: This is preliminary research and short of follow-up in the protection of the cardiotoxicity. And we will do further research for the comprehensive assessment of the myocardial injury.
Ethics committee approval: Our research was approved by the animal ethic institution.
Funding: This work is supported by the clinical research funding (K1519) in our institution.
Author Disclosures:
R. Xu: nothing to disclose
H. Liu: nothing to disclose
Y. Guo: nothing to disclose
L. Chen: nothing to disclose

RPS 1003a-10 12:19

Identifying early stages of doxorubicin-induced cardiotoxicity in rat model using 7.0 tesla cardiac magnetic resonance and creatine kinase isoenzymes

S. Wang, F. Gao*; Chengdu/CN*

Purpose: To identify early stages of doxorubicin (DOX)-induced cardiotoxicity in a rat model using 7.0-tesla cardiac magnetic resonance (CMR) combining creatine kinase isoenzymes (CKMB).
Methods and materials: 34 rats were included. 28 of these rats were injected with DOX (2.5mg/kg) through vena caudalis weekly and were divided into 4 subgroups. The first subgroup received DOX for four weeks and underwent CMR examination after 4 weeks. The other groups received DOX for six weeks and underwent CMR examination after 6, 8, and 10 weeks, respectively. 2 rats injected with physiological saline (2.5ml/kg) also performed CMR examination at the same time as each experimental subgroup. All these rats were sacrificed after CMR examination and venous blood was collected to detect CKMB. Ejection fraction (EF) for the left ventricle (LV) was quantified from all CMR images. Global radial (GRS), circumferential (GCS), and longitudinal strain (GLS) parameters of LV were also obtained by CMR tissue tracking (CMR-TT). All these parameters were compared between treatment groups and controls.
Results: The earliest DOX-induced cardiotoxicity CMR parameter was GLS（-17.84±2.50 vs -21.79±5.80, P=0.007）decreasing at week 6. EF, GCS, CLS, and GRS were declined at week 8 and week 10. For CKMB, it was significantly increased at week 4 (869.14±210.69u/L vs 417.50±9.20u/L, P=0.001) and all CMR parameters were not affected at this time. CKMB continued to rise at week 6 and week 8, however, it showed no significant difference between treatment groups and controls at week 10 (376.29±65.29u/L vs 443.50±16.26u/L, P=0.210).
Conclusion: CKMB and CMR-TT are an effective method to evaluate DOX-induced cardiotoxicity at an early stage.

Limitations: Small sample size.
Ethics committee approval: This study was approved by Institutional Animal Research Committee of our local institute.
Funding: National Natural Science Foundation of China (8193000682).
Author Disclosures:
S. Wang: nothing to disclose
F. Gao: nothing to disclose

RPS 1003a-11 12:25
Assessment of myocardial extracellular volume on routine body computed tomography in a cohort of breast cancer patients treated with anthracyclines
D. Capra, C. B. Monti, T. Bosetti, E. de Benedictis, A. Luporini, M. Alì, F. Sardanelli, F. Secchi*; Milan/IT (davide.capra@unimi.it)*

Purpose: To evaluate the feasibility of estimating myocardial extracellular volume (ECV) on routine thoracic contrast-enhanced CT in breast cancer patients, and, if feasible, to assess if a rise in ECV is associated with anthracyclines administration even in the absence of clinical symptoms or echocardiographic changes.
Methods and materials: Female patients with breast cancer who had undergone routine CT examinations at our institution before and shortly after the end of chemotherapy including anthracyclines were retrospectively evaluated. Patients without available haematocrit, with CT images with artefacts, or who had undergone radiation therapy of the left breast were excluded. Follow-up CT examinations were also analysed, when available. ECV was calculated on scans obtained at about 1, 3, and 7 min after contrast injection.
Results: 32 female patients (aged 57±13 years, mean±standard deviation) with pre-treatment haematocrit 38±4% and ejection fraction 64±6% were analysed. Pre-treatment ECV was 27.0±2.9% at 1 min, 27.4±3.8% at 3 min, and 26.4±3.8% at 7 min, similar to normal values reported for normal subjects in the literature. Post-treatment ECV (median interval: 89 days after treatment) was 31.1±4.9%, 32.5±5.0% and 30.0±5.1%, respectively. The values were significantly higher than pre-treatment values at all times ($p < 0.005$). ECV at follow-up (median interval: 135 days after post-treatment CT) was 31.0±4.5%, 30.0±3.4%, and 27.7±3.7%, respectively, without significant differences ($p > 0.548$) when compared to post-treatment values.
Conclusion: After anthracyclines treatment, ECV was significantly higher than pre-treatment values. In the follow-up, ECV remains higher than pre-treatment values.
Limitations: This study is limited by its small sample size and its retrospective, monocentric nature.
Ethics committee approval: Ethics Committee approval was obtained. Written informed consent was waived.
Funding: No funding was received for this work.
Author Disclosures:
D. Capra: nothing to disclose
C. B. Monti: nothing to disclose
T. Bosetti: nothing to disclose
E. de Benedictis: nothing to disclose
A. Luporini: nothing to disclose
M. Alì: nothing to disclose
F. Sardanelli: Grant Recipient at Bayer, Grant Recipient at General Electric, Grant Recipient at Bracco, Speaker at Bayer, Speaker at General Electric, Speaker at Bracco, Advisory Board at Bracco
F. Secchi: nothing to disclose

11:15 - 12:30 **Room M 1**

Neuro

RPS 1011b

Radiomics and deep learning in neuroimaging

Moderators:
A. Van Der Hoorn; Groningen/NL
N.N.

RPS 1011b-1 11:15
Automated deep learning-based meningioma segmentation in multiparametric MRI
K. R. Laukamp, L. Pennig, F. Thiele, R. P. Reimer, L. Goertz, D. Zopfs, M. Timmer, M. Perkuhn, J. Borggrefe*; Cologne/DE (kai.laukamp@uk-koeln.de)*

Purpose: Volumetric assessment of meningiomas represents a valuable tool for treatment planning and the evaluation of tumour growth as it allows for a more precise assessment of tumour size than conventional diameter methods. Segmentation data can be used for consecutive quantitative or radiomics analysis allowing for improved tumour characterisation. However, manual segmentations are time-consuming and therefore usually not performed. In this study, we established a dedicated meningioma deep learning model based on routine MRI-data and evaluated its performance for automated segmentation.
Methods and materials: MRI datasets (T1-/T2-weighted, T1-weighted contrast-enhanced [T1CE], and FLAIR) of 126 patients with intracranial meningiomas (grade I: 97, grade II: 29) were included. Preprocessing of imaging data included registration, skull-stripping, resampling, and normalisation. Target volumes for manual and automated segmentations included contrast-enhancing tumour volume in T1CE and the total lesion volume (union of lesion volume in T1CE and FLAIR [including solid tumour parts and surrounding oedema]). For automated segmentation, an established deep learning model architecture (3D-Deep-Convolutional-Neural-Network, DeepMedic, BioMedIA) operating on all four MR-sequences was trained using manual segmentations of two independent readers from 70 patients (training-group). The trained deep learning model was then validated on the 56 remaining patients (validation-group) by comparing automated to ground-truth manual segmentations, which were performed by two additional readers in consensus.
Results: In the validation-group, comparison of the deep learning model and manual segmentations revealed average Dice coefficients of 0.91±0.08 for the contrast-enhancing tumour volume and 0.82±0.12 for the total lesion volume. In the training-group, inter-reader variabilities of the two manual readers were 0.92±0.07 for the contrast-enhancing tumour volume and 0.88±0.05 for the total lesion volume.
Conclusion: Deep learning-based automated segmentation yielded high segmentation accuracy, comparable to manual inter-reader variabilities.
Limitations: Due to the retrospective study design, no evaluation of the actual clinical benefit could be applied.
Ethics committee approval: The study was approved by the institutional review board.
Funding: No funding was received for this work.
Author Disclosures:
K. R. Laukamp: nothing to disclose
L. Pennig: nothing to disclose
F. Thiele: Employee at Philips Healthcare
R. P. Reimer: nothing to disclose
L. Goertz: nothing to disclose
D. Zopfs: nothing to disclose
M. Timmer: nothing to disclose
M. Perkuhn: Employee at Philips Healthcare
J. Borggrefe: Other at Jan Borggrefe received an honorarium from Philips for scientific lectures.

RPS 1011b-2 11:21
Radiomics analysis in predicting the grade of meningiomas using monoexponential, biexponential, and stretched-exponential diffusion models
L. Lin, X. Chen, Y. Xue, Q. Duan*; Fuzhou/CN (84088100@qq.com)*

Purpose: Grading meningiomas before surgeries is particularly essential for therapeutic decisions and prognosis. The purpose of this study was to establish a radiomic model based on monoexponential, biexponential, and stretched-exponential diffusion models for non-invasively predicting the grade of meningiomas.
Methods and materials: Consecutive 107 patients who underwent MRI including multi-b values were histopathologically confirmed as having meningiomas. Apparent diffusion coefficient (ADC), true diffusion coefficient (D), pseudo diffusion coefficient (D*), perfusion fraction (f), distributed diffusion coefficient (DDC), and intravoxel water diffusion heterogeneity radiomics features were obtained based on solid components of the entire tumour. Optimal feature subsets were selected as using the support vector machine with a recursive feature elimination algorithm (SVM-RFE). Receiver operating characteristic curve (ROC) analysis was employed to assess the efficiency for grading the tumours.
Results: 7 radiomic features were selected in the training set, based on which radiomics model yielded area under the curve (AUC) values of 0.730 and 0.785 for the training and test sets. The accuracies/sensitivity/specificity of predicting the grade of meningiomas were 75.00%/70.37%/100.00%.
Conclusion: It is feasible to grade meningiomas by using a radiomics model built from monoexponential, biexponential, and stretched-exponential diffusion imaging.
Limitations: The number of high-grade meningiomas was relatively small. The acquisition times of the IVIM sequence were relatively long in this study.
Ethics committee approval: Written informed consent was obtained from all subjects in this study. Institutional review board approval was obtained.
Funding: Fujian Provincial Health and Family Planning Research Talent Training Program (grant No.2017-2-24; 2018-1-14), Startup Fund for scientific research: Fujian Medical University (grant number: 2017XQ1036), and Joint

Funds for the innovation of science and Technology: Fujian province (grant number: 2018Y9044).
Author Disclosures:
L. Lin: nothing to disclose
X. Chen: nothing to disclose
Y. Xue: nothing to disclose
Q. Duan: nothing to disclose

RPS 1011b-3 11:27
Radiomics analysis of enhancing residual tumours better predicts survival in post-surgery MRI patients with brain glioblastomas
A. Garcia-Ruiz[1], P. Naval Baudín[2], M. Ligero[1], A. Pons Escoda[1], N. Calvo[2], M. Cos Domingo[1], C. Majós Torró[1], R. Perez Lopez[1]; [1]*Barcelona/ES,* [2]*L'Hospitalet de Llobregat/ES*

Purpose: To extract radiomics first-order distribution and texture features from post-surgical enhancing tumours and explore their prognostic value in patients with brain glioblastomas.
Methods and materials: We retrospectively analysed 160 consecutive patients with glioblastoma multiforme treated with surgery and radiotherapy plus concomitant and adjuvant temozolomide from 2009-2017. Censored patients and those with images acquired later than 7 days from surgery were excluded. Subtraction of the T1-weighted and contrast-enhanced T1-weighted MRI was performed to obtain the enhancement map; the area of residual enhancement was semi-automatically segmented to obtain the enhancing mask. 96 radiomics features were extracted from the contrast-enhanced T1-weighted images (texture and first-order statistics). The population was split into training (80%) and test (20%) subpopulations. Feature selection was performed by minimum-redundancy-maximum-relevance and stepwise regression on the training set. Logistic regression and ROC curve analyses were performed to evaluate the prognosis into high/low survival (threshold at median survival of 16 months).
Results: 124 patients were included in the final analysis. A total of 10 radiomics features, including minimum intensity, contrast grey-level co-occurrence matrix, and inverse difference grey-level co-occurrence matrix features were selected. These features predicted short and long survival with an AUC=0.72 (95% CI 0.62-0.82, p<0.001) in the training and 0.71 (95% CI 0.49-0.92, p=0.044) in the test subpopulation.
Conclusion: The selected radiomics features quantifying tumour intensity and heterogeneity are able to predict longer or shorter patient survival in both the training and test subpopulations with similar/fair accuracy.
Limitations: In this retrospective study, the variability of image acquisition parameters was unavoidable. Manual segmentations might present interobserver variability. An external validation may confirm the applicability of the proposed method.
Ethics committee approval: Informed consent was waived by the Bellvitge University Hospital research ethics committee.
Funding: RPL is supported by La-Caixa-Foundation and Prostate-Cancer-Foundation.
Author Disclosures:
A. Garcia-Ruiz: nothing to disclose
P. Naval Baudín: nothing to disclose
A. Pons Escoda: nothing to disclose
N. Calvo: nothing to disclose
M. Cos Domingo: nothing to disclose
C. Majós Torró: nothing to disclose
R. Perez Lopez: Grant Recipient at La Caixa Foundation, Grant Recipient at Prostate Cancer Foundation
M. Ligero: nothing to disclose

RPS 1011b-4 11:33
MR textural features (radiomics) for assessing the response to treatment in patients with intracranial tuberculomas: a retrospective review
S. Khan, M. Awais, M. Wasay, M. Azeemuddin*; Karachi/PK (shahmeer.khan@aku.edu)*

Purpose: To study whether MR-based radiomic features can be used to assess the response to antituberculous treatment.
Methods and materials: We included 24 patients with intracranial tuberculomas diagnosed by either culture or histopathology who had a pre- and post-treatment brain MRI with contrast performed at our institute from July 2009-July 2019. Patients with coexisting demyelination, tumour, or history of surgery were excluded. 16 patients showed a treatment response while 8 showed no response. A textural analysis was performed using Lifex and 44 textural parameters were extracted. The region of interest (ROI) was manually drawn on post-contrast FLAIR images. An independent Sample's t-test was employed to study statistically different parameters in both groups. Logistic regression was performed to develop a model for predicting the response to treatment on the basis of MR radiomic features in differentiating patients with intracranial tuberculoma.
Results: MR radiomic parameters, histogram skewness and GLCM correlation, showed a statistically significant difference in patients who showed improvement versus those who did not ($\chi2=11.517$, p=0.003). The model explained 52.9% (Nagelkerke R2) of variance in predicting the response to treatment and correctly classified 83.3% of cases. ROC curve analysis for histogram skewness showed an area under the curve of 0.766 (p=0.037 and 95% CI =0.577-0.954).
Conclusion: MR textural parameters including histogram skewness and GLCM correlation can be used as imaging biomarkers to differentiate patients with intracranial tuberculomas who responded to treatment versus resistant cases.
Limitations: The small sample size and retrospective analyses.
Ethics committee approval: Ethics committee approval obtained.
Funding: No funding was received for this work.
Author Disclosures:
S. Khan: nothing to disclose
M. Awais: nothing to disclose
M. Azeemuddin: nothing to disclose
M. Wasay: nothing to disclose

RPS 1011b-5 11:39
Between and within rater agreement in white matter hyperintensity segmentation from manual rating and a supervised automated classifier (FSL-BIANCA)
L. Griffanti[1], I. Mattioli[2], V. Bordin[3], I. Bertani[3], S. Suri[1], E. Zsoldos[1], K. Ebmeier[1], C. Mackay[1], G. Zamboni[2]; [1]*Oxford/UK,* [2]*Modena/IT,* [3]*Milan/IT (ludovica.griffanti@ndcn.ox.ac.uk)*

Purpose: Volumetric quantification of white matter hyperintensities (WMH) is well established in research and is starting to be adopted clinically for structured reports.
Automated tools using machine learning should avoid time-consuming manual segmentation and give more objective results. However, supervised tools require segmentation examples to train the algorithm and the tools' performance is usually evaluated by comparing the output to manual masks, which suffer from between and within rater variability.
We aimed to evaluate whether our tool, FSL-BIANCA, can overcome the variability present in the manual training set and increase the consistency of automatic results.
Methods and materials: We used 24 MRI scans from the Whitehall II imaging sub-study.
Manual WMH segmentation was performed by two raters (R1, R2) and repeated by the second rater a year later (R2a, R2b).
The manual masks were used to train BIANCA and the automated WMH masks were generated using a leave-one-out approach.
Between and within rater agreement on manually and automatically segmented masks were calculated using a Dice index and results were compared with paired t-tests.
Results: The agreement between BIANCA outputs generated with masks from different raters is similar to the manual between rater agreement. BIANCA outputs trained with masks from R2 (a,b) are more consistent than the within rater agreement of manual masks.
Conclusion: Our results suggest that if the examples provided to BIANCA are sufficiently in agreement, the automated tool improves the consistency of the output. This also highlights the need to standardise the definition of WMH, especially if automated tools are planned to be used in multicentre studies.
Limitations: The limited amount of scans, raters (with different expertise), and re-tests.
Ethics committee approval: Ethics approval and consent from all participants were obtained.
Funding: MRC (G1001354), MRC-DPUK, and Parkinson's UK.
Author Disclosures:
L. Griffanti: nothing to disclose
I. Mattioli: nothing to disclose
V. Bordin: nothing to disclose
I. Bertani: nothing to disclose
S. Suri: nothing to disclose
E. Zsoldos: nothing to disclose
K. Ebmeier: nothing to disclose
C. Mackay: nothing to disclose
G. Zamboni: nothing to disclose

RPS 1011b-6 11:45
A comparison of different radiomics models in the prediction of haematoma expansion in patients with intracerebral haemorrhages
H. Xie, S. Ma, X. Zhang, X. Wang*; Beijing/CN (xiehuihui1030@163.com)*

Purpose: To compare the predictive performance of different models in predicting haematoma expansion (HE) in patients with intracerebral haemorrhages (ICH).

Methods and materials: 251 patients with ICH who underwent computed tomography (CT) shortly after symptom onset and follow-up CT within 24 hours were retrospectively recruited. Haematoma expansion was defined as a volume growth exceeding 6 mL or 33% from the baseline volume. Patients were randomly allocated into a training cohort (177: with HE, 74; without HE, 103) and a validation cohort (74: with HE, 34; without HE, 40). Baseline images were analysed. The radiological model was constructed based on conventional radiological features (shape, volume, etc.). Radiomics features were extracted and a radiomics signature was calculated for each patient. Combined models were constructed with both conventional radiological features and a radiomics signature using 5 different methods: a logistic regression model, decision tree, random forest, AdaBoost, and support vector machine model (SVM). The predictive performance of models was assessed with a receiver operating characteristic curve (ROC) analysis.
Results: The radiological model reached an AUC of 0.869 in the training cohort and 0.811 in the validation cohort. Combined models built with 5 different methods achieved high AUCs in both cohorts. Among them, the combined model using AdaBoost reached the highest AUC of 0.959 in the training cohort. The combined model using logistic regression reached the highest AUC of 0.924 in the validation cohort.
Conclusion: Combined models based on radiologic features and a radiomics signature yield high predictive performance in predicting HE in both cohorts.
Limitations: A retrospective study, limited sample size, and the study was performed in only one institution.
Ethics committee approval: This study was approved by local institutional review board and informed consent was waived.
Funding: No funding was received for this work.
Author Disclosures:
H. Xie: nothing to disclose
S. Ma: nothing to disclose
X. Wang: nothing to disclose
X. Zhang: nothing to disclose

RPS 1011b-7 11:51
Automated MRI brain volumetry: a software comparison
P. Kousis, P. Toulas, E. Lamprou*; Athens/GR (p_koussis@yahoo.gr)*

Purpose: The automated brain volumetry from MRI images is a modern tool to quantify brain anatomy in patients with conditions related to brain atrophy. There is much software available in the market. We choose Neuroquant (NQ) and Volbrain (VB) in order to investigate any differences between their volumetric measurements and how these differences affect their atrophy estimation.
Methods and materials: 26 patients with multiple sclerosis visited the MRI lab at Bioiatriki SA (Athens) with the query of brain volumetry. They scanned in GE Discovery 750 3.0T MR system and the exam protocol included a 3D T1 sequence without contrast enhancement. The parameters in 3DT1 were in accordance with NQ's directions. These same images were processed both with NQ and VB. Measurements from different brain structures were compared. The unpaired t-test was the statistical method used for data analysis. In patients with an atrophy result from NQ, the possible agreement with VB was checked.
Results: Whole-brain, hippocampus, cerebellum, and white matter measurements had or had not quite significant differences ($p>0.05$).
Intracranial cavity measurements had very significant differences.
Amygdale, putamen, and thalamus had extremely significant differences with a deviation from the bibliography average of 167.7% for NQ and 17.7% for VB, 35.9% for NQ and 3.3% for VB, and 0.7% for NQ and 29.3% for VB, respectively.
Conclusion: There are important differences in the measurements of some brain structures, with significant deviation from the bibliography average for both NQ and VB.
Although the initially unexpected differences, NQ and VB are both able to determine atrophy.
VB has smaller deviations from average values and, for the time, is free (10/d).
Limitations: The 3DT1 parameters should be constant during the study.
Ethics committee approval: n/a
Funding: No funding was received for this work.
Author Disclosures:
P. Kousis: nothing to disclose
P. Toulas: nothing to disclose
E. Lamprou: nothing to disclose

RPS 1011b-8 11:57
Deep learning AI technology matches lumbar spine MRI image quality at about 1/3 the scan time
L. N. Tanenbaum[1], W. Gibbs[2], S. Bash[3], L. Wang[4], H. Gandhi[4], P. Gulaka[4], A. Shankaranarayanan[5], T. Zhang[6]; *[1]Riverside, CT/US, [2]Pasadena/US, [3]Los Angeles/US, [4]Palo Alto/US, [5]Waukesha, WI/US, [6]Menlo Park, CA/US (nuromri@gmail.com)*

Purpose: To evaluate the performance of deep learning AI (DLAI) to match routine lumbar spine MRI image quality at highly reduced scan times.
Methods and materials: 27 consecutive patients (49+/-16 years old; 17 male) underwent standard of care (SOC) lumbar spine MRI exams on 1 of 3 different clinical 1.5T scanners. All subjects underwent an additional accelerated 2D sagittal T2 series processed by an FDA cleared convolutional neural network-based deep learning AI application trained on multivendor MR platforms (SubtleMR™). The sagittal T2 scan times averaged 2:12 (SOC) and 0:49 (DLAI=2.7x acceleration). 54 image series (27 SOC and DLAI) were randomised and independently rated by two board-certified neuroradiologists for perceived SNR, anatomy/pathology conspicuity, motion artefacts, and overall image quality on a 5-point Likert scale (1: non-diagnostic, 2: poor, 3: diagnostic, 4: good, and 5: excellent). A two-sided paired t-test was performed with $P<0.05$ considered as statistically significant.
Results: The average scores for perceived SNR, anatomy/pathology conspicuity, motion artefacts, and overall image quality (SOC/DLAI) were 5.0/4.9, 5.0/4.9, 4.9/4.8, and 5.0/4.9, respectively, for reader 1, and 4.4/4.3, 4.8/4.5, 4.7/4.7, and 4.4/4.2 for reader 2. No statistically significant difference between DL-accelerated scans and standard scans were present for all criteria and both readers.
Conclusion: Deep learning AI technology can match routine lumbar spine MR image quality at approximately 1/3 of the scan time.
Limitations: The limited number of subjects (27).
Ethics committee approval: IRB approved with written informed consent.
Funding: No funding was received for this work.
Author Disclosures:
L. N. Tanenbaum: Advisory Board at subtle, Advisory Board at icometrix, Advisory Board at curemetrix, Advisory Board at Enlitic, Speaker at GE, Speaker at Philips, Speaker at Siemens, Advisory Board at aidoc
W. Gibbs: nothing to disclose
S. Bash: Advisory Board at icometrix, Advisory Board at Coretechs
L. Wang: Employee at Subtle Medical
H. Gandhi: Employee at Subtle Medical
P. Gulaka: Employee at Subtle Medical
A. Shankaranarayanan: Employee at Subtle Medical
T. Zhang: Employee at Subtle Medical

RPS 1011b-9 12:03
Automated expert level localisation of perivascular spaces in the centrum semiovale and the basal ganglia
K. M. H. van Wijnen, F. Dubost, P. Yilmaz, M. P. D. M. A. Ikram, W. J. Niessen, H. H. H. Adams, M. W. Vernooij, M. de Bruijne*; Rotterdam/NL (k.vanwijnen@erasmusmc.nl)*

Purpose: Enlarged perivascular spaces (PVS) are a neuroimaging marker for cerebral small vessel disease. Manual annotation of PVS is challenging, time-consuming, and subject to observer bias. We developed and evaluated an automated method for the localisation of PVS in the two most clinically relevant regions: the centrum semiovale (CSO) and the basal ganglia (BG).
Methods and materials: We used T2-weighted 1.5T MRI scans from 2,202 subjects enrolled in the population-based Rotterdam scan study, 1,202 for method development, and 1,000 for evaluation. An expert rater annotated one predefined slice per brain region with a single dot per PVS. A separate set of 40 MRI scans was annotated twice to estimate intra-rater agreement, which was computed by considering both sets once as ground truth and computing the average sensitivity and false-positives per image (FPPI).
We trained a regression convolutional neural network to predict the intensity-based distance to the nearest PVS for each voxel. Subsequently, the predicted distance maps were thresholded to detect PVS.
Results: The intra-rater agreement showed an average sensitivity of 55.7% with 4.43 FPPI in the CSO and in the BG this was 73.2% and 2.09, respectively. Our method had similar performance with, for the same number of FPPI, an average sensitivity of 55.6% in the CSO and 75.3% in the BG.
Conclusion: Even for an expert rater, this is a challenging problem as shown by the intra-rater agreement. Our proposed method can annotate PVS fully automatically as well as an expert rater. This method could replace the time-consuming manual assessment of PVS in neurological studies.
Limitations: The single scanner, single protocol dataset; 1 slice per brain region annotated.
Ethics committee approval: Rotterdam scan study approved by the medical ethics committee of Erasmus MC.
Funding: NWO-P15-26, Quantib, ZonMw104003005.
Author Disclosures:
K. M. H. van Wijnen: Research/Grant Support at Quantib
F. Dubost: nothing to disclose
P. Yilmaz: nothing to disclose
M. P. D. M. A. Ikram: nothing to disclose
W. J. Niessen: Founder at Quantib
H. H. H. Adams: nothing to disclose
M. W. Vernooij: nothing to disclose
M. de Bruijne: nothing to disclose

RPS 1011b-10 12:09

The added diagnostic value of a model-based reconstruction algorithm in detecting acute trauma-related lesions in brain CT examinations in an emergency setting

C. Maino[1], D. Ippolito[1], S. Lombardi[1], L. Riva[1], C. R. G. L. Talei Franzesi[2], S. Sironi[3]; [1]Monza/IT, [2]Milan/IT, [3]Bergamo/IT (mainocesare@gmail.com)

Purpose: To evaluate the added value of a model-based reconstruction algorithm (IMR) in the assessment of traumatic and acute findings in emergency non-enhanced computed tomography (NECT) cranial scans in comparison to the standard hybrid iterative reconstruction approach (iDose).
Methods and materials: We evaluated 150 patients who underwent a 256-row NECT scan at the emergency department for head trauma. Images of the volumetric acquisition of the brain scan were reconstructed with iDose and IMR (2mm thickness), then were randomly evaluated by two radiologists who recorded the presence, nature, number, and location of the acute findings. Image quality evaluation was also performed using a 4-point scale (1: unacceptable, 4: more than average).
Results: IMR showed a higher detection rate of acute lesions in comparison to iDose (IMR identified 55 vs 15 subdural haemorrhages, 97 vs 44 subarachnoid haemorrhages, 11 vs 11 intraventricular haemorrhages, 42 vs 21 parenchymal haemorrhages, 48 vs 36 contusive lesions, and 62 vs 7 diffuse axonal injuries). We obtained significant intraobserver difference when comparing the two different reconstruction protocols ($p<0.05$), while no significant difference between the observers was found when evaluating each reconstruction protocol ($p<0.05$), obtaining high interobserver agreement ($k= 0.87$). IMR offered a higher image quality rating (3.32 vs 2.53), CNR (3.18 vs 2.1), and SNR (15.67 vs 8.53), and a lower noise index (2.13 vs 4.3) than iDose.
Conclusion: IMR, by offering high diagnostic image quality at a thinner slice, identifies a higher number of acute traumatic lesions than iDose with a significant reduction of noise and partial volume artefacts, thus representing a very useful diagnostic tool in assessing brain lesions of trauma patients.
Limitations: A single-centre study.
Ethics committee approval: Written informed consent was obtained from each patient.
Funding: No funding was received for this work.
Author Disclosures:
C. Maino: nothing to disclose
D. Ippolito: nothing to disclose
S. Lombardi: nothing to disclose
L. Riva: nothing to disclose
C. R. G. L. Talei Franzesi: nothing to disclose
S. Sironi: nothing to disclose

RPS 1011b-11 12:15

An advanced deep learning approach to automatically detect and segment intracranial aneurysms in patients with subarachnoid haemorrhages on CTA

R. Shahzad[1], L. Pennig[1], L. Goertz[2], F. Thiele[3], M. Perkuhn[1], J. Borggrefe[1]; [1]Cologne/DE, [2]Mannheim/DE, [3]Aachen/DE (rahilshahzad@gmail.com)

Purpose: To develop a deep learning model (DLM) for fully automated detection and segmentation of intracranial aneurysm in patients with subarachnoid haemorrhages (SAH) on CT-angiography (CTA).
Methods and materials: This retrospective single-centre study included 295 confirmed aneurysms from 253 patients with SAH (2010-2017). All patients from 2016-2017 (68 patients/79 aneurysms) provided the training-set, whereas subjects from 2010-2016 (185 patients/216 aneurysms) served as a test-set. Ground truth was established by independent manual segmentations of the aneurysms by a radiologist and neurosurgeon in a voxel-wise manner. CTA source images acquired using a standard clinical protocol for head/neck (n=222) and head (n=29) were pre-processed by extracting the brain mask and enhancing the blood vasculature. A 3D convolutional neural network (CNN) architecture based on DeepMedic was used for training 3 different DLMs using a different combination of vessel-enhanced input images as multiple-channels, as well as modifying the CNN parameters. An ensembling strategy was then used to generate the final DLM, optimised by using 5-fold-cross-validation.
Results: In the training-set, DLM achieved an aneurysm detection rate of 0.72, average false-positives (FP's)/scan of 0.21, a Dice coefficient of 0.74, and a volume correlation (r) of 0.97. Comparing the performance of the individual DLMs to the ensemble approach, we observed an increase of 37% (0.54 vs 0.74) with respect to Dice and a decrease of 90% with respect to FP's/scan (2.10 vs 0.21). On the independent test-set, sensitivity was 0.82 with an average of 0.81 FP's/scan, a Dice of 0.75, and r of 0.9.
Conclusion: The proposed DLM is robust in detecting and segmenting aneurysms in patients with SAH on routine CTA images. We also demonstrated a significant increase of performance by using an ensemble of different DLMs.
Limitations: n/a
Ethics committee approval: The local ethics committee approved this retrospective study.
Funding: No funding was received for this work.
Author Disclosures:
R. Shahzad: Employee at Philips Research
L. Pennig: nothing to disclose
L. Goertz: nothing to disclose
F. Thiele: Employee at Philips Research
J. Borggrefe: nothing to disclose
M. Perkuhn: Employee at Philips Research

RPS 1011b-12 12:21

Morphometry: a way to facilitate the diagnosis of dementia?

P. Malmierca Ordoqui, A. Paternain Nuin, M. Calvo Imirizaldu, A. C. Igual Rouilleault, B. Echeveste, M. Riverol, P. Dominguez Echavarri, M. A. Fernandez Seara, R. Garcia de Eulate; Pamplona/ES (pmalmierca@unav.es)

Purpose: To evaluate the reproducibility of morphometry MRI to assess atrophy in patients with a mild cognitive impairment (MCI).
Methods and materials: We retrospectively analysed MR images of 114 patients with MCI. One radiologist rated atrophy in 6 key brain regions bilaterally in T1-MPRAGE sequences using established visual rating scales.
Afterwards, atrophy was rated with a morphometry function (MorphoBox algorithm, Siemens prototype) which automatically estimates the volume of different brain regions and compares them with normative adjusted ranges. Maps with the different brain regions colour-coded indicated the degree of deviation (no deviations=green, mild=yellow, moderate=orange, and large=red). Using Fisher's tests, we evaluated the association between classifications (visual and morphometric) and between each classification and the actual clinical diagnosis, including all patients and including only those classified as normal or MCI/Alzheimer's disease (AD) by all methods.
Results: When all patients were included, there was no association between visual and morphometric classifications ($p=0.44$). However, if only normal or MCI/AD patients were considered, the association was close to significance ($p=0.073$). When all patients were included there was a significant association between the visual classification and clinical diagnosis ($p=0.006$), but no association between morphometry and clinical diagnosis ($p=0.29$). However, when only normal or MCI/AD patients were considered, the association between clinical diagnosis and visual classification was not significant ($p=0.43$), while the association between clinical diagnosis and morphometry was closer to significance ($p=0.0920$).
Conclusion: The morphometry function has a tendency to be significant when it comes to differentiating normal patients from MCI/AD. Nevertheless, it doesn't classify other dementias as well as visual classification.
Morphometry may represent a facilitating tool in the clinical assessment of MCI/AD, although further investigations are required.
Limitations: The small sample size.
Ethics committee approval: Ethics committee approval obtained.
Funding: No funding was received for this work.
Author Disclosures:
P. Malmierca Ordoqui: nothing to disclose
R. Garcia de Eulate: nothing to disclose
M. Calvo Imirizaldu: nothing to disclose
A. Paternain Nuin: nothing to disclose
P. Dominguez Echavarri: nothing to disclose
M. A. Fernandez Seara: nothing to disclose
B. Echeveste: nothing to disclose
M. Riverol: nothing to disclose
A. C. Igual Rouilleault: nothing to disclose

11:15 - 12:30 **Room M 2**

Imaging Informatics

RPS 1005a

Radiomics and texture analysis

Moderators:
A. Bink; Frankfurt am Main/DE
M. E. Mayerhöfer; Vienna/AT

RPS 1005a-1 11:15

Differentiating head and neck paraganglioma versus schwannoma using texture analysis: a preliminary analysis

A. Ghosh, S. R. Malla, A. S. Bhalla, S. Manchanda, D. Kandasamy; New Delhi/IN (soumyaranjan_aiims@yahoo.com)

Purpose: To investigate the value of T2-weighted based radiomics in the differentiation of head and neck paragangliomas and schwannomas.
Methods and materials: This retrospective study included patients presenting with neck masses who were imaged under our institutional protocol in 3T MRI scanner between January 2016 and March 2019. A total of 46 patients (36 paragangliomas and 16 schwannomas) were identified using a composite gold standard of histopathology, cytology, and DOTANOC PET CT. Fat-suppressed T2-DIXON axial images with TR-2500-3500msec, TE-90msec, 4 mm slice thickness and 190x190 mm-FOV were used for analysis.
First- and second-order texture-parameters were calculated from original and filtered images. Feature selection using F-statistics and collinearity analysis provided 10 texture parameters for further analysis. A Mann-Whitney-U test was used to compare the two groups and p-values were adjusted for multiple comparisons. AUC for the significant features was obtained.
Results: A total of 7 texture parameters were found to be significantly different between paragangliomas and schwannomas (adjusted $p < .05$). Laplacian of Gaussian intermediate, first-order kurtosis, wavelet HLL, grey-level co-occurrence matrix (glcm) correlation, and wavelet LHH glcm correlation each achieved a specificity of 93.5% in differentiating paraganglioma and schwannoma with AUC of 0.738, 0.819, and 0.689, respectively. A logistic regression model combined the 7 significant texture parameters to differentiate between paragangliomas and schwannomas, which obtained a sensitivity of 97.2% and specificity of 75%, with an AUC of 0.97 (0.87 to 0.99).
Conclusion: T2-weighted based radiomics could serve as a useful adjunct to conventional MRI in distinguishing head and neck paragangliomas from schwannomas, which may influence triage contrast administration or nuclear medicine based DOTANOC studies.
Limitations: These results are preliminary and thus require validation on a larger and independent data set to assess reproducibility for the potential for clinical translation.
Ethics committee approval: n/a
Funding: No funding was received for this study.
Author Disclosures:
S. R. Malla: Investigator at All India Institute of Medical Sciences, New Delhi
A. Ghosh: Investigator at ll India Institute of Medical Sciences, New Delhi
A. S. Bhalla: Investigator at All India Institute of Medical Sciences, New Delhi
S. Manchanda: Investigator at All India Institute of Medical Sciences, New Delhi
D. Kandasamy: Investigator at All India Institute of Medical Sciences, New Delhi

RPS 1005a-2 11:21

Radiomics-based approach for the diagnosis of osteoporosis using hip radiographs

K. Sang Wook, J. Lee, S.-J. Ye, H. D. Chae*; Seoul/KR*

Purpose: To evaluate the performance of a radiomics-model for the diagnosis of osteoporosis using hip radiographs.
Methods and materials: For the development dataset, 6,995 hip anteroposterior radiographs with dual-energy x-ray absorptiometry (DXA) were collected between 2010 and 2018. Both hip joints were automatically segmented using U-net, except for joints with fractures or metal prostheses. A total of 11,243 joints (normal 9,170, osteoporosis 2,073) were used for the development dataset and a temporally-separated validation dataset was comprised of 553 joints (normal 459, osteoporosis 74) from 300 hip anteroposterior radiographs between 2008 and 2009. T-scores on hip DXA were used as reference standards. Three clinical (age, sex, and weight) and 293 radiomics features were used to train the random forest and gradient boosting classifiers. Two radiologists assessed the possibility of osteoporosis using a 5-point scale and the performance of the radiologist was compared with the radiomics-model. Receiver-operating characteristic curve analysis was used to assess diagnostic performance.
Results: The diagnostic performance was AUC 0.809 (95% CI 0.774-0.842) for board-certified radiologists and AUC 0.760 (95% CI 0.721-0.796) for the radiology resident. The performance of the radiomics-model was AUC 0.830 (95% CI 0.796-0.861), sensitivity 74.3%, and specificity 79.5%, with an optimal cut-off probability of 0.318. The performance of the radiomics-model was significantly higher than the radiology resident ($P = 0.038$).
Conclusion: The radiomics-model for the diagnosis of osteoporosis using hip radiographs showed comparable diagnostic performance to those of the radiologists and may help in the automatic screening of osteoporosis in plain radiographs.
Limitations: Additional external validation is needed to assess the generalisability of the model.
Ethics committee approval: All datasets were collected under IRB approval in SNUH.
Funding: This work was supported by the National Research Foundation of Korea grant funded by the Korean government (No. NRF-2017M2A2A6A01071214).
Author Disclosures:
K. Sang Wook: nothing to disclose
J. Lee: nothing to disclose
S.-J. Ye: nothing to disclose
H. D. Chae: nothing to disclose

RPS 1005a-3 11:27

Quantitative ultrasound texture analysis of the foetal lung versus foetal pulmonary artery Doppler as a non-invasive predictor of neonatal respiratory distress syndrome (RDS)

N. Osman*; Minia/EG (nasrosman_7@yahoo.com)*

Purpose: To make a comparison between quantitative ultrasound texture analysis of the foetal lung (QuantusFLM) and pulmonary artery acceleration time/ejection time ratio (AT/ET) for the evaluation of foetal lung maturity.
Methods and materials: The prospective cohort study was conducted on 65 pregnant women selected from cases referred to the obstetrics and gynaecology department at Minia University Hospital from May 2018 to March 2019. All patients underwent ultrasound examination for foetal pulmonary artery acceleration time/ejection time ratio (AT/ET) as well as a grey-scale axial ultrasound image of the foetal lungs, which were analysed using the Quantus-FLM software online application. 25 patients were excluded from the study due to a foetal birth more than 48 hours after the ultrasound examination, corticosteroid administration in between the examination and delivery, congenitally malformed foetuses, neonatal sepsis, or respiratory distress due to causes other than neonatal RDS. After delivery, the neonates were grouped according to diagnosis of RDS as positive or negative.
Results: From the 40 eligible foetuses, 9 (22%) developed neonatal RDS. Both AT/ET and Quantus FLM results were significantly correlated with the development of neonatal RDS. AT/ET were significantly lower in feotuses developed RDS. A cutoff value of 0.305 for AT/ET predicted the development of RDS (sensitivity: 77.78%, specificity: 87.1%) while Quantus FLM predicted neonatal RDS with 88.9% sensitivity and 90.32% specificity.
Conclusion: Both AT/ET and Quantus-FLM may provide a noninvasive means of detecting the development of neonatal RDS with acceptable levels of sensitivity and specificity.
Limitations: Small numbers of patient study.
Ethics committee approval: This study is approved by our university ethics committee.
Funding: No funding was received for this work.
Author Disclosures:
N. Osman: Author at no company

RPS 1005a-4 11:33

Can MRI texture analysis of the pancreas predict postoperative pancreatic fistulas?

S. M. Skawran, P. Kambakamba, B. Baessler, M. Kupka, D. Eshmuminov, H. Petrowsky, C. S. Reiner*; Zurich/CH (stephan.skawran@usz.ch)*

Purpose: To evaluate whether a magnetic resonance imaging (MRI) texture analysis (TA)-based machine learning (ML) classifier can predict postoperative pancreatic fistulas (POPF) after pancreaticoduodenectomy (PD).
Methods and materials: 70 patients who underwent MRI before PD between 2010 and 2018 were retrospectively analysed. POPF was graded according to the international study group of pancreatic fistula and split into clinically relevant versus non-relevant or no POPF. On T1- and T2-weighted images, two regions of interest were placed in the pancreatic corpus and cauda. 1,350 radiomic features were extracted after standardised image processing using the open-source pyRadiomics library. The dataset was split into training and test sets. After feature reduction, a non-linear support vector machine (SVM) was trained on the 3 most important features. Logistic regression analyses were performed using these features and mean T1 and T2 signal intensity values (SImean). Diagnostic accuracy of the models was compared using areas under the receiver operating characteristics curve (AUCs).
Results: One T1 and two T2 higher-order texture features were identified as the most important variables for classification. All 3 variables showed significant differences between the two groups (all $p<0.02$). The trained SVM achieved an AUC of 0.68 when applied on the test dataset. In contrast, logistic regression models using only SImean from T1- and T2-weighted images resulted in an AUC of 0.51 [T1mean], 0.60 [T2mean], and 0.59 [combined] (all $p<0.001$).
Conclusion: MRI-texture analysis based on routine sequences provides a promising prediction of clinically relevant POPF.
Limitations: Studies were limited to one vendor. Cross-vendor-transferability remains to be elucidated. Image analysis was done by one reader. Reproducibility will be subject to further research.
Ethics committee approval: The local ethics committee approved this retrospective study and all patients gave written informed consent.
Funding: No funding was received for this work.

Author Disclosures:
S. M. Skawran: nothing to disclose
B. Baessler: nothing to disclose
C. S. Reiner: nothing to disclose
P. Kambakamba: nothing to disclose
H. Petrowsky: nothing to disclose
M. Kupka: nothing to disclose
D. Eshmuminov: nothing to disclose

RPS 1005a-5 11:39
The influence of different levels of adaptive statistical iterative reconstruction (ASIR) regarding computed tomography texture features
T. Polidori, D. Caruso, E. Muscogiuri, D. de Santis, A. Laghi*; Rome/IT (tiziano.polidori13@gmail.com)*

Purpose: To evaluate the influence of different levels of ASIR on computed tomography texture features.
Methods and materials: We analysed 10 patients who underwent unenhanced computed tomography (CT) scans of the abdomen with the same scanner (Revolution Evo, GE Healthcare, USA). Subsequently, we reconstructed raw data with 11 levels of ASIR (from 0 to 10), thus obtaining datasets with different percentages of blending between filtered back projection and iterative reconstruction. Two radiologists analysed the texture features of the liver, kidney, spleen, and muscle tissues using four different regions of interest (ROIs) that were cloned for all 11 different iteration levels datasets. Data was then elaborated with TexRad medical imaging software. 5 different radiomic features (mean, standard deviation, entropy, skewness, and kurtosis) were compared among the different reconstruction algorithms and spatial scaling factor (SSF) by using ANOVA test with Bonferroni correction.
Results: Different iteration levels significantly affect ($p<0.05$) standard deviation (SD) and entropy values for SSF 0, with a decrease of these parameters from 0 to 10 ASIR (e.g. statistically significant decrease of entropy between level 10 and 0-7). The influence of different ASIR levels on these parameters gradually faded with an increase in the SSF, thus no significant differences between all the radiomic values have been obtained from SSF 5 to 6. We did not find statistically significant differences between the values of mean, skewness, and kurtosis, regardless of the SSF value and the tissue.
Conclusion: We demonstrated that different ASIR levels moderately affect standard deviation and entropy with a declining trend from SSF 0 to SSF 5-6. Mean, skewness, and kurtosis are not significantly affected by different ASIR levels.
Limitations: A small study population.
Ethics committee approval: n/a
Funding: No funding was received for this work.
Author Disclosures:
T. Polidori: nothing to disclose
D. Caruso: nothing to disclose
E. Muscogiuri: nothing to disclose
D. de Santis: nothing to disclose
A. Laghi: nothing to disclose

RPS 1005a-6 11:45
Correlation between CT texture parameters and clinicopathological properties of regional lymph nodes in patients with colon cancer
D. Wen[1], J. Y. Sun[2]*; [1]Chengdu/CN, [2]Cheng Du/CN (snow88416@163.com)*

Purpose: To investigate the correlation between CT texture features and regional metastasis of regional lymph nodes in colon cancer patients.
Methods and materials: We collected 69 patients with colon cancer from January 2018 to March 2019. A CT-enhanced scan informed consent was signed one week before surgery and a full-abdominal enhanced CT scan was performed. A radiologist was responsible for marking the enlarged lymph nodes in the area. A gastrointestinal surgeon was responsible for the location of the lymph nodes of the ex vivo specimens. The image of the venous phase was exported to the CK texture analysis software platform, the largest cross-section of the matching lymph nodes was selected, and the contour was manually drawn, extracting a total of 41 texture parameters of labelled lymph nodes. The marker-matched lymph nodes were divided into LNM (-) group and LNM (+) group by labelling the lymph node metastasis (LNM) as a standard. The texture characteristic parameters of the two groups were analysed and the ROC and AUC were used for performance evaluation.
Results: A total of 69 patients with colon cancer were collected, the markers matched 101 lymph nodes, of which 15 were metastatic lymph nodes and 86 non-metastatic lymph nodes. After statistical analysis, the texture parameter inertia had a correlation with lymph node metastasis ($P<0.05$, AUC=0.671). The other 40 texture parameters had no obvious correlation with lymph node metastasis.
Conclusion: Some texture parameters of single lymph nodes in colon cancer patients have a correlation with their metastasis.
Limitations: The sample size was small and the research period not long enough.
Ethics committee approval: Approved by the Bioethics Committee of West China Hospital of Sichuan University.
Funding: No funding was received for this work.
Author Disclosures:
D. Wen: nothing to disclose
J. Y. Sun: nothing to disclose

RPS 1005a-7 11:51
Classification of non-enhancing glioma tumours by diffusion MRI with B-tensor encoding: an explorative study of tumour heterogeneity
J. Brabec, F. Durmo, F. Szczepankiewicz, B. Lampinen, L. Knutsson, P. Sundgren, M. Nilsson*; Lund/SE (jan.brabec@med.lu.se)*

Purpose: To classify gliomas based on the anisotropic and isotropic diffusional kurtosis obtained from dMRI with B-tensor encoding.
Methods and materials: 25 patients with glioma tumours were examined on a 3T scanner (MAGNETOM Prisma, Siemens Healthcare, Erlangen, Germany). A prototype spin-echo B-tensor encoding sequence was used with TR/TE=5300/80 ms/ms, resolution=2.3×2.3×2.3mm^3, two B-tensor shapes (linear and spherical), and four b-values between 0.1 and 2.0ms/μm^2. The mean diffusivity, anisotropic kurtosis, and isotropic kurtoses were obtained. The tumours were delineated on post-Gd T1w images. All five non-enhancing glioblastomas (WHO IV) and all four non-enhancing oligodendrogliomas (WHO II) were selected for analysis, where mean and standard-deviations were compared with a U-test.
Results: The anisotropic and isotropic kurtoses for a glioblastoma together with a post-Gd T1w image and a mean diffusivity map was mapped. In this example, the necrotic core was associated with lower anisotropic kurtosis. It also demonstrated higher isotropic kurtosis, with a contrast stronger than that of the mean diffusivity. Two non-enhancing tumours without a necrotic core (glioblastoma and oligodendroglioma) that appear similar on the T1w images were compared. Within the glioblastoma, the isotropic kurtosis showed a lower variability, whereas the oligodendroglioma showed higher variability, possibly due to higher tumour heterogeneity. This finding was corroborated, showing that the standard deviation of the isotropic kurtosis differs significantly between non-enhancing glioblastomas and oligodendrogliomas ($p=0.032$).
Conclusion: Non-enhancing glioblastomas and non-enhancing oligodendrogliomas had a significantly different standard deviation in isotropic kurtosis, which indicates that it can be used to distinguish them.
Limitations: Conclusions are based on a small sample size and will therefore be validated in a larger cohort.
Ethics committee approval: Informed written consent was obtained from all subjects. Approvals 2016/6 and 2017/866.
Funding: ALF (F2018/1490), Cancer Foundation (CAN2018/468), Swedish Research Council (VR2016-02199-3).
Author Disclosures:
J. Brabec: nothing to disclose
F. Szczepankiewicz: Patent Holder at Inventor of patents related to the study.
L. Knutsson: nothing to disclose
P. Sundgren: nothing to disclose
M. Nilsson: Grant Recipient at Research support from Random Walk Imaging (formerly Colloidal Resource)., Patent Holder at Patent applications in Sweden (1250453-6 and 1250452-8), USA (61/642 594 and 61/642 589), and PCT (SE2013/ 050492 and SE2013/050493)., Shareholder at Ownership interests in Random Walk Imaging.
F. Durmo: nothing to disclose
B. Lampinen: nothing to disclose

RPS 1005a-8 11:57
Whole-tumour histogram analysis of diffusion kurtosis imaging as a predictive biomarker of tumour response in locally advanced rectal cancer treated with neoadjuvant chemoradiation
Y. Sun, T. T. Tong, G. Yajia, C. Fu*; Shanghai/CN (12211230032@fudan.edu.cn)*

Purpose: To explore the predictive value of whole-tumour histogram analysis in diffusion kurtosis imaging to assess tumour response to neoadjuvant chemoradiation therapy in locally advanced rectal cancer.
Methods and materials: 43 enrolled patients were examined using MRI at two time points: 1-7 days before NCRT (pre-MRI) and within 1-7 days of NCRT completed (post-MRI). Pretreatment T stage, N stage, MRF, EMVI, tumour location and length, pretreatment CEA, and CA19-9 levels were recorded. According to tumour response, we classified the patients into pCR and non-pCR groups. Whole tumour volume of interest (VOI) was obtained by a semi-automatic segmentation method in both pre- and post-MRI. Then, ADC, K, and D histograms and corresponding parameters, difference histograms value between pre-MRI and post-MRI, were calculated. Histograms metrics of ADC,

K, and D, tumour characteristics, and their relationship with tumour response were evaluated by using logistics regression.
Results: Pre-K_{ske}, post-tumour volume, and ADC_{sd} (pre-post) were correlated with tumour response by using a Lasso regression model and then a radiological signature score was built. Pretreatment EMVI(+) (OR=9.231,p=0.048), MRF(+) (OR=5.317, p=0.030), higher rectal cancer (OR=4.110,p=0.021), CEA≥5ng/ml (OR=9.231, p=0.048), and a low radiological signature score (OR=14.428, p=0.011) could be associated with non-pCR in univariate analysis. Multivariate analysis identified that the pretreatment CEA≥5ng/ml (OR=42.311, p=0.044) and low radiological signature score (OR=1.312, p=0.007) would be independent factors to indicate a patient with non-pCR.
Conclusion: Whole-tumour histogram analysis of DKI is a valuable and easily available tool to predict tumour response. It will be helpful to stratify patients who are sensitive to NCRT in locally advanced rectal cancer.
Limitations: This study is not a large-scale randomised trial and comprises data from only one centre.
Ethics committee approval: n/a
Funding: No funding was received for this work.
Author Disclosures:
Y. Sun: nothing to disclose
T. T. Tong: nothing to disclose
G. Yajia: nothing to disclose
C. Fu: nothing to disclose

RPS 1005a-9 12:03
Quantitative comparison of a novel visualisation technique (gradient-intensity projection, GIP) with an average projection for ultra-low-dose CTs of the chest
S. Carey[1], B. E. Hoppel[2], W. Hamilton[1], S. Kandel[3], P. Rogalla[1]; [1]*Toronto, ON/CA,* [2]*Vernon Hills, WI/US,* [3]*Berlin/CA (sean.carey@uhn.ca)*

Purpose: To develop a thick-slab presentation technique (gradient-intensity projection) which can effectively mitigate the increased noise inherent in ultra-low-dose CT (ULDCT) while demonstrating superior image contrast as compared to average projection.
Methods and materials: The value of a voxel in the thick-slab output slice is computed as a weighted average of the voxels contained in each contributing slice of the input image at the same position in the slice. The weight of each contributing voxel is determined by computing the difference in HU value of that voxel with its neighbours in a 3x3 area in the input image. This creates a weighting matrix of the same size as the input image, where a higher weight reflects a higher intensity gradient at the position in the image (GIP). A moving average low-pass filter is applied to the weight matrix to provide local consistency and to reduce the contribution of speckle-noise while leaving the contribution of larger structures. Both projection techniques were applied to a thoracic ULDCT image (0.16 mSv) reconstructed using deep-learning reconstruction. The noise level was assessed by comparing the standard deviation of regions in the liver and in the air and contrasted by computing a GLCM on a circular ROI drawn over the lung vasculature. The entropy in the lung ROI was also assessed.
Results: The standard deviation of the ROIs in the liver for average/GIP was 8.89/9.89, in air 10.614/11.919, respectively (n.s.). The contrast of the lung vasculature (GLCM) was 2347.41/14353.05, the entropy 7.19/8.165, respectively, both p< 0.001.
Conclusion: Gradient-intensity projection offers significantly increased contrast of fine structures without a significant increase of image noise over average projection.
Limitations: Not yet clinically validated.
Ethics committee approval: n/a
Funding: No funding was received for this work.
Author Disclosures:
S. Carey: nothing to disclose
P. Rogalla: nothing to disclose
W. Hamilton: nothing to disclose
B. E. Hoppel: nothing to disclose
S. Kandel: nothing to disclose

RPS 1005a-10 12:09
Phantomless assessment of volumetric bone mineral density using virtual non-contrast images from spectral detector computed tomography
C. E. S. Zaeske[1], D. Zopfs[1], S. Lennartz[1], K. R. Laukamp[1], M. Merkt[2], R. P. Reimer[1], D. Maintz[3], J. Borggrefe[1], N. Grosse Hokamp[1]; [1]*Cologne/DE,* [2]*Coblenz/DE,* [3]*Münster/DE*

Purpose: To evaluate a phantomless assessment of volumetric bone mineral density (vBMD) based on virtual non-contrast images of arterial (VNC_a) and venous phase (VNC_v) derived from spectral detector CT (SDCT) as compared to true non-contrast images (TNC) and adjusted venous phase conventional images ($CI_{V(adjusted)}$).
Methods and materials: Retrospective inclusion of 104 patients with triphasic SDCT between January 2018 to April 2019 with subsequent reconstruction of TNC, VNC_a, VNC_v, and venous phase images (CI_V). Assessment of vBMD by two radiologists usnig an FDA/CE-cleared software, which determined average vBMD of the first 3 lumbar vertebrae in each reconstruction. CI_V was adjusted for contrast enhancement using earlier suggested formulae.
Results: No significant difference was found comparing vBMD values obtained from $CI_{V(adjusted)}$ and TNC images (91.79 ± 36.52 mg/cm^3 vs. 90.16 ± 41.71 mg/cm^3, p=1.00), whilst vBMD values obtained from VNC_a and VNC_v (42.20 ± 22.50 mg/cm^3 and 41.98 ± 23.3 mg/cm^3) were significantly lower as compared to TNC and $CI_{V(adjusted)}$ (all p≤0.01).
Conclusion: vBMD values obtained from adjusted venous phase images did not show significant differences to vBMD values derived from TNC images, and thus may be utilised for an opportunistic BMD screening in CT examinations. SDCT-derived virtual non-contrast images appear to systematically underestimate vBMD, hence appropriate adjustments are required prior to a possible clinical implementation.
Limitations: No correlation to the reference standard areal BMD measurements by DEXA was performed. No cross-vendor comparison was performed.
Ethics committee approval: n/a
Funding: No funding was received for this work.
Author Disclosures:
C. E. S. Zaeske: nothing to disclose
D. Zopfs: nothing to disclose
S. Lennartz: Research/Grant Support at Phillips
J. Borggrefe: Speaker at Phillips
D. Maintz: Speaker at Phillips
K. R. Laukamp: nothing to disclose
N. Grosse Hokamp: Speaker at Phillips, Research/Grant Support at Phillips
R. P. Reimer: nothing to disclose
M. Merkt: nothing to disclose

RPS 1005a-11 12:15
Supervised machine learning predictive modelling for primary versus secondary lung malignancy in CT-guided transthoracic biopsies
E. J. M. Barbosa Jr., D. Lindsay, N. Sachs, J. Gee; *Philadelphia, PA/US*

Purpose: CT-guided transthoracic biopsy (CTTB) is a minimally invasive method for the diagnostic evaluation of a variety of thoracic diseases. We leveraged a large cohort of CTTB patients to assess how well supervised machine learning models utilising clinical and imaging variables can predict pathology diagnosis in primary versus secondary lung malignancy.
Methods and materials: 588 patients were retrospectively identified, comprising of biopsies performed at our institution. Our model included variables such as age, race, sex, smoking history, smoking pack-years, history of prior cancer, immune status, nodule location, nodule size, nodule margin, and nodule shape. These variables were extracted from radiology reports and electronic medical records. Ground-truth was CTTB pathology diagnosis, classified as primary (60.5%) versus secondary (39.5%). We compared 3 supervised machine learning classifiers: random forest (RF), logistic regression (LR), and decision tree (DT), utilising a 75%/25% training/validation ratio for the CTTB cohort (10-fold cross-validation).
Results: The RF model produced AUC (area under the curve) of ROC (receiver operating characteristic) of 0.87 and accuracy of 0.81, the LR model produced AUC of ROC of 0.89 and accuracy of 0.81, whereas the DT model produced AUC of ROC of 0.79 and accuracy of 0.71.
Conclusion: CTTB, while accurate for pathologic diagnosis of thoracic lesions, can be costly and may entail significant risks. LR and RF models achieved up to 81% diagnostic accuracy, potentially allowing non-invasive prediction of primary versus secondary lung malignancy, a crucial distinction for patient management.
Limitations: A retrospective design.
Ethics committee approval: IRB approved, waiver of informed consent.
Funding: Funded by the NIH (USA).
Author Disclosures:
E. J. M. Barbosa Jr.: nothing to disclose
J. Gee: nothing to disclose
D. Lindsay: nothing to disclose
N. Sachs: nothing to disclose

RPS 1005a-12 12:21
Dominant language hemisphere detection by using a ML model informed by structural and functional connectivity
S. Pascual-Diaz, J. C. Pariente, E. Muñoz-Moreno, C. Garrido, E. Conde, N. Bargallo I Alabart; *Barcelona/ES (PARIENTE@CLINIC.CAT)*

Purpose: To develop a method to determine the language dominant hemisphere (LDH) by using structural, diffusion, and resting-state MRI.

Methods and materials: This study was performed on structural and functional neuroimaging data from 15 subjects. We define the LDH goal standard using MRI functional data with language and comprehension tasks.
For the structural analyses, whole-brain tractography reconstructions were performed using multi-shell, multi-tissue, constrained spherical deconvolution. We obtained the language-related tracts using a pre-trained convolutional neural network (Tractseg) and used them to obtain language connectivity matrices.
We obtained different indices from the volumetric acquisition (e.g. cortical thickness), diffusion-based parameters (e.g. FA), and graph theoretical indices derived from structural and functional language connectivity matrices. We performed a parametric statistical analysis for each of the metrics and used the significant indices to obtain single-subject laterality differences by training a ML-based classification algorithm.
Additionally, we compared the results obtained with our methodology using the standard laterality index approach.
Results: We found statistically significant differences for the cortical thickness in the superior temporal gyrus and in the MD for the uncinated tract. The ML model had an accuracy of 0.90 +/- 0.19 with a confusion matrix.
We did not find differences using the LI analysis.
Conclusion: Our results suggest that we can use this methodology to predict the LDH by using a ML classification model based on resting-state and diffusion from MRI data.
Limitations: The sample is not big enough for a ML-based study. This abstract is a proof of concept and we are now acquiring new subjects to validate the new methodology.
Ethics committee approval: n/a
Funding: This study is funded by a FIS project PI/012 and the European funding of regional development (FEDER).
Author Disclosures:
J. C. Pariente: nothing to disclose
S. Pascual-Diaz: nothing to disclose
E. Muñoz-Moreno: nothing to disclose
E. Conde: nothing to disclose
N. Bargallo I Alabart: nothing to disclose
C. Garrido: nothing to disclose

11:15 - 12:30 **Room M 3**

Abdominal Viscera

RPS 1001c

Liver imaging and beyond: giving answers to clinical questions

Moderators:
R. Dežman; Ljubljana/SI
A. Wetter; Essen/DE

RPS 1001c-1 11:15

Long-term evolution of hepatocellular adenomas at MR imaging follow-up
F. Vernuccio[1], R. Maxime[2], M. Dioguardi Burgio[2], F. Cauchy[3], S. Dokmak[2], D. Valla[2], J. Zucman-Rossi[3], V. Paradis[2], V. Vilgrain[2]; [1]Palermo/IT, [2]Clichy/FR, [3]Paris/FR (federicavernuccio@gmail.com)*

Purpose: Hepatocellular adenomas (HCAs) are rare benign liver tumours. Guidelines recommend continued surveillance for patients diagnosed with HCAs, but these recommendations are mainly based on small series or experts' opinion. The aims of this study were to analyse the long-term evolution of HCAs, including solitary and multiple lesions, and to identify predictive features of progression.
Methods and materials: In a retrospective cohort study, we included 118 patients (mean age 40±10 years old) with pathology-proven HCAs: 41 had solitary HCAs and 77 patients multiple HCAs. ß-catenin mutated HCAs and HCAs with foci of malignancy were defined at-risk of progression. MR exams were analysed and tumour evolution was evaluated using RECISTv1.1.
Results: In a median follow-up of 5.0 years, 37/41 (90%) patients with solitary HCAs and 55/77 (71%) patients with multiple HCAs showed stable or regressive disease. After resection of solitary HCAs, new lesions appeared only in 2/29 (7%) patients, both with HCAs at-risk of progression. Among patients with multiple HCAs, HNF-1α inactivated HCAs showed a higher rate of progression compared to inflammatory HCAs (11/26[42.3%] vs. 7/37[18.9%], p=0.043), and lower use and lesser duration of oral contraceptives intake (28/32 [87.5%] vs. 45/45 (100%), p=0.027, and mean 12.0±7.5 years vs. 19.2±9.2 years, p= 0.001, respectively).
Conclusion: 78% of HCAs showed long-term stability or regression. After resection of solitary HCAs, new lesions occurred only in HCAs at-risk of progression. Patients with multiple HCAs were more likely to show progressive disease, with HNF-1 α inactivated HCAs being the most common subtype showing progression.
Limitations: Retrospective design. A low number of unclassified, sonic hedgehog, or ß-catenin mutated in exon 7-8 HCAs. A lack of serial MRI exams. An adoption of RECIST 1.1 may have underestimated size changes.
Ethics committee approval: IRB approved; waiver of informed consent obtained.
Funding: No funding was received for this work.
Author Disclosures:
F. Vernuccio: nothing to disclose
R. Maxime: nothing to disclose
M. Dioguardi Burgio: nothing to disclose
F. Cauchy: nothing to disclose
S. Dokmak: nothing to disclose
D. Valla: nothing to disclose
J. Zucman-Rossi: nothing to disclose
V. Paradis: nothing to disclose
V. Vilgrain: nothing to disclose

RPS 1001c-2 11:21

Prediction of histopathological growth patterns by radiomics and CT-imaging in patients with operable colorectal liver metastases: a proof-of-concept study
M. P. A. Starmans[1], F. E. Buisman[1], F. Willemssen[1], S. R. van der Voort[1], D. J. Grünhagen[1], P. B. Vermeulen[2], C. Verhoef[1], S. Klein[1], J. J. Visser[1]; [1]Rotterdam/NL, [2]Antwerp/BE (m.starmans@erasmusmc.nl)*

Purpose: The histopathological growth pattern (HGP) is a prognostic factor in patients with colorectal liver metastases (CRLM). Currently, HGPs can only be obtained postoperatively through resection. We present a non-invasive, preoperative alternative using CT and radiomics.
Methods and materials: As a proof-of-concept, we aimed to distinguish two extrema: pure (i.e. 100%) desmoplastic HGP (dHGP) and pure replacement HGP (rHGP). The dataset consisted of CT scans from 76 patients with 93 CRLM (45 dHGP; 48 rHGP). Three clinicians manually delineated the lesions; one repeated process. Observer segmentation variability was determined using the dice similarity coefficient (DSC). From each segmentation, 410 radiomics features were extracted. Decision models were created for the segmentations of each observer separately and by training and testing on different observers. The models were created through an automated search amongst a variety of machine learning algorithms to find the combination that maximizes performance. The evaluation was implemented through a 100x random-split cross-validation, using 80% for training and model optimisation and 20% for testing.
Results: The mean inter-rater DSC was 0.69, indicating poor observer agreement. The single-observer radiomics models resulted in mean area under the curves (mAUCs) of 0.67, 0.61, and 0.70. The multiobserver radiomics models, trained on two observers and tested on the third, resulted in mAUCs of 0.72, 0.70, and 0.64. Thus, no substantial model differences were found among the segmentations of the observers.
Conclusion: Our radiomics model is able to associate quantitative CT imaging features with pure HGPs and generalises well to segmentations of an unseen observer. Pending further optimisation and validation, radiomics based on CT imaging may have potential as a non-invasive, preoperative surrogate for postoperative HGP assessment.
Limitations: Relatively small dataset.
Ethics committee approval: Erasmus MC IRB (MEC-2017-479).
Funding: NWO #14929-14930.
Author Disclosures:
M. P. A. Starmans: nothing to disclose
F. E. Buisman: nothing to disclose
F. Willemssen: nothing to disclose
J. J. Visser: nothing to disclose
S. R. van der Voort: nothing to disclose
D. J. Grünhagen: nothing to disclose
P. B. Vermeulen: nothing to disclose
C. Verhoef: nothing to disclose
S. Klein: nothing to disclose

RPS 1001c-3 11:27

MRI of atypical liver haemangioma: significant imaging features to differentiate accurately from cholangiocarcinoma
R. Boxhoorn, R. S. Dwarkasing, F. Willemssen, G. P. Krestin; Rotterdam/NL (rboxhoorn@gmail.com)*

Purpose: The purpose of this study was to evaluate liver lesions that were initially suspected of CCA on MRI and proved haemangioma on histopathology evaluation. Are there features of MRI that can reliably differentiate atypical haemangioma from CCA?

Methods and materials: Retrospectively we identified 16 consecutive patients with PA proven haemangiomas that were initially suspected of CCA on MRI. We compared these lesions with a group of 20 PA proven CCAs from the same search period. Two observers evaluated lesions qualitatively and quantitatively on morphologic features, signal intensity, DWI/ADC values, and contrast enhancement patterns.
Results: 16 patients with atypical haemangiomas were included: lesion size mean 6.3 cm; range 2.2 cm-11.2 cm. The control group consists of 20 CCA with size mean 6.9 cm; range 2.8 cm-13.5 cm. All lesions in both groups had heterogeneous signal intensities in T1W and T2W and, although progressive contrast enhancement was seen in both groups, haemangiomas demonstrated more intense enhancement in the early arterial phase. Perilesional arterial enhancement with iso-intensity in the portal-venous phase was observed in the majority (n=11) of haemangiomas, significantly more (p<0.001) than CCAs (n=1).
The average ADC mean of haemangiomas was 2.40±0.57 x 10^{-3} mm^2/s (range 1.55-3.55), significantly higher (p<0.0001) than for CCAs: 1.36±0.18 x 10^{-3} mm^2/s (range 0.95-1.62).
Conclusion: Atypical liver haemangiomas demonstrate significant higher ADC value and perilesional arterial enhancement than CCA and can be used to suggest the right diagnosis.
Limitations: Usual limitations and potential sources of bias associated with retrospective study design.
Ethics committee approval: n/a
Funding: No funding was received for this work.
Author Disclosures:
R. Boxhoorn: nothing to disclose
R. S. Dwarkasing: nothing to disclose
F. Willemssen: nothing to disclose
G. P. Krestin: nothing to disclose

RPS 1001c-4 11:33

New IVIM parameter PDR (perfusion/diffusion ratio) in discrimination of benign and malignant focal liver lesions

J. Podgorska, P. Kus, B. Gołębiewski, K. Pasicz, J. Jasieniak, A. Rogowska, W. Skrzyński, P. Kukołowicz, A. Cieszanowski*; Warsaw/PL*
(jpodgo@gmail.com)

Purpose: Intra-voxel incoherent motion (IVIM) imaging allows simultaneous assessment of the diffusion of water in the extracellular space and the microcirculation of blood in capillaries. The aim of the study was to assess the usefulness of IVIM parameters: true diffusion (D), pseudo-diffusion (D*), perfusion fraction (f,) and the author's own parameter, PDR (perfusion/diffusion ratio; the ratio of the speed of signal b loss as a result of IVIM, to the speed drop of signal b due to diffusion), in the differentiation of benign and malignant focal liver lesions (FLLs).
Methods and materials: We evaluated prospectively 50 patients (age: 25-80 years, mean 60) with 83 FLLs (24 benign and 59 malignant) examined on 3T MRI, including the IVIM (10 b values: 0-900 s/mm^2). Malignant lesions were confirmed histopathologically, benign lesions were verified by follow-up studies.
Results: Significant differences (p<0.05) between benign and malignant lesions were obtained for D parameter (median ± standard deviation: benign: 1.40±0.66x10^{-3} mm^2/s; malignant: 0.97±0.38x10^{-3} mm^2/s) and for the PDR (10.6±11.0; 4.0±20.6). No significant differences were found for f and D*. The analysis of ROC curves for D with a cut-off value of 1.05x10^{-3} mm^2/s showed 71% sensitivity, 72% specificity, 71% accuracy, and for the PDR with a cut-off of 5.18, 65%, 75%, 68%, respectively.
Conclusion: The study showed the usefulness of IVIM parameters: D and the PDR in differentiation of FLLs.
Limitations: There is a predominance of malignant over benign lesions in the study group.
Ethics committee approval: The research protocol was approved by the local ethics committee and written consent was obtained from all patients prior to the study.
Funding: No funding was received for this work.
Author Disclosures:
B. Gołębiewski: nothing to disclose
W. Skrzyński: nothing to disclose
A. Rogowska: nothing to disclose
P. Kus: nothing to disclose
K. Pasicz: nothing to disclose
J. Jasieniak: nothing to disclose
J. Podgorska: nothing to disclose
P. Kukołowicz: nothing to disclose
A. Cieszanowski: nothing to disclose

RPS 1001c-5 11:39

Hepatic uptake index in the hepatobiliary phase of Gd-EOB-DTPA-enhanced magnetic resonance imaging estimates functional liver reserve and predicts posthepatectomy liver failure

M. Donadon[1], E. Lanza[1], B. Branciforte[2], R. Muglia[2], C. Lisi[2], V. Pedicini[1], D. Poretti[1], L. Balzarini[1], G. Torzilli[1];
[1]Rozzano/IT, [2]Pieve Emanuele/IT
(riccardo.muglia@humanitas.it)

Purpose: Recent evidence suggests that gadolinium-ethoxybenzyl-diethylenetriamine penta-acetic acid-enhanced magnetic resonance imaging (Gd-EOB-DTPA MRI) may be used to evaluate liver function. We assessed whether the signal intensity of Gd-EOB-DTPA MRI might correlate with common use liver disease clinical score systems and posthepatectomy liver failure (PHLF) in patients undergoing hepatectomy for liver tumours.
Methods and materials: We retrospectively analysed 137 preoperative Gd-EOB-DTPA MRIs of patients undergoing hepatectomy from November 1st, 2015, and July 31st, 2018.
Mean signal intensity of liver (L_{20}) and spleen (S_{20}) were measured on T1-weighted single-breath-hold 3D fat-saturated gradient-echo sequences acquired 20 minutes after Gd-EOB-DTPA administration.
The hepatocellular uptake index (HUI) of liver volume (V_L) was calculated with the following formula $V_L[(L_{20}/S_{20})\text{-}1]$ and was tested with several clinical score systems for liver disease and to the occurrence of PHLF.
Results: Patients with unhealthy livers had significantly lower values of HUI in comparison with those with normal function. This was found for MELD score ≤9 vs. >9 (p=0.0488), BILCHE score ≤2 vs. >2 (p=0.0208), ALBI grades (p=0.0357), and Humanitas score ≤6 vs. >6 (p=0.0311). HUI was significantly lower in those patients with PHLF (p=0.001). Receiver operating characteristics curve analysis revealed valuable HUI ability in predicting PHLF (AUC=0.84; 95%CI=0.71-0.92; p<0.001), with a cutoff value of 574.33 (98% sensitivity; 83% specificity).
Conclusion: HUI measured on preoperative Gd-EOB-DTPA MRI identifies patients with unhealthy liver and predicts PHLF. This index could be used to discriminate those patients at higher risk of complications after hepatectomy.
Limitations: Patients with severely diseased liver were not included since they weren't considered candidates for hepatectomy. Other proposed methods of Gd-EOB-DTPA MRI signal intensity measurements weren't analysed for our cohort.
Ethics committee approval: Informed consent was obtained from each considered patient.
Funding: No funding was received for this work.
Author Disclosures:
R. Muglia: nothing to disclose
M. Donadon: nothing to disclose
E. Lanza: nothing to disclose
B. Branciforte: nothing to disclose
C. Lisi: nothing to disclose
V. Pedicini: nothing to disclose
D. Poretti: nothing to disclose
L. Balzarini: nothing to disclose
G. Torzilli: nothing to disclose

RPS 1001c-6 11:45

Improved display of hepatic arteries with multiple arterial phases using differential sub-sampling with cartesian ordering: comparison with single arterial phase and computed tomographic angiography

Z. Ye, Y. Wei, H. Tang, B. Song*; Chengdu/CN (948080771@qq.com)*

Purpose: To evaluate whether multiple arterial phases (MAP) using DISCO acquisition would improve the display of hepatic arteries when comparing to single arterial phase (SAP) and computed tomographic angiography (CTA).
Methods and materials: A total of 130 patients were enrolled. In part I of the study, 50 patients underwent MRI with MAP image and 50 patients with SAP images. In part II of the study, 30 patients underwent both MRI with MAP and CTA. Two readers independently assessed the hepatic arterial display on a four-point scale in terms of image quality and visualisation of hepatic arterial branches. The kappa test was used to evaluate the agreement between the two readers. Kruskal-Wallis test was used to compare the difference of arterial display and Bonferroni correction was used for further multiple comparisons of arteries.
Results: Moderate to excellent interobserver agreement was obtained for the arterial phase timing and degree of motion artifact (all kappa value > 0.65). For part I, the mean arterial display score obtained with MAP was higher than SAP imaging in the common hepatic artery (CHA, 3.68±0.47vs3.14±0.5), proper hepatic artery (PHA, 3.40±0.50vs2.88±0.44), left hepatic artery (LHA, 2.78±0.42vs2.40±0.57), right hepatic artery (RHA, 3.04±0.45vs2.72±0.54), left gastric artery (LGA, 3.10±0.42vs2.62±0.67), and gastroduodenal artery (GDA, 2.80±0.61vs2.42±0.76) (all p<0.01). For part II, MAP and CTA acquisition showed comparable image quality and arterial display score in CHA (3.50±0.51vs3.47±0.51, p=0.798), PHA (3.30±0.47vs3.30±0.53, p=0.935), LHA

(2.83±0.59vs3.03±0.41, p=0.122), RHA (3.10±0.48vs3.13±0.35, p=0.809), LGA (3.03±0.32vs3.00±0.37, p=0.710), and GDA(2.80±0.61vs2.80±0.48, p=0.659).
Conclusion: MAP using DISCO acquisition is superior than SAP and is comparable with CTA in the display of hepatic arteries.
Limitations: The diagnostic performance of these imaging methods in lesion detection and conspicuity was not evaluated.
Ethics committee approval: Local IRB approved this study and written informed consent were obtained.
Funding: No funding was received for this work.
Author Disclosures:
Z. Ye: nothing to disclose
H. Tang: nothing to disclose
Y. Wei: nothing to disclose
B. Song: nothing to disclose

RPS 1001c-7 11:51
CT texture analysis and liver regeneration: preliminary data on associating liver partition and portal vein ligation for staged hepatectomy (ALPPS) in liver malignancies
A. Borgheresi, A. Agostini, A. Mari, L. Ottaviani, D. Nicolini, M. Vivarelli, S. Maggi, A. Giovagnoni*; Ancona/IT (alessandra.borgheresi@gmail.com)*

Purpose: ALPPS is a two-stage liver resection: the splitting in-situ and portal vein ligation in the 1st step allow for rapid liver hypertrophy and completion of resection after 7-15 days (2nd step). Accurate patient selection is mandatory to avoid periprocedural liver failure.
The aim of this work is to evaluate the correlation of preoperative CT textural features with liver hypertrophy on virtual resection on CT after ALPPS 1st step.
Methods and materials: All ALPPS performed between January 2013 and January 2015 were retrospectively included. All patients were <70 yo with no-known cirrhosis or severe steatosis.
All CT were obtained with a 64-row CT (LighSpeed VCT, GE Healthcare) and performed at baseline and at 7th postoperative day after ALPPS 1st step with a tri-phasic CT protocol. The remnant liver volume (mL) was calculated with liver analysis on Syngo.via (Siemens Healthineers). The liver regeneration index (RI) was calculated as: $[(RLV_{7day}-RLV_{baseline})/RLV_{baseline}]\times100$. The texture analysis was performed on baseline CT with radiomics prototype (Syngo.via Frontier, Siemens Healthineers) on the segmented RLV at baseline. The correlation between RI>70% and texture features were calculated with univariate and multivariate analysis.
Results: 14 patients were included (10 F/4M) with a median age of 47 (25-75p: 41-62 yo) with a RI of 69% (25-75p: 52%-81%). Among texture parameters, gray level co-occurrence matrix (GLCM) contrast was an independent predictor of RI>70%.
Conclusion: The preliminary data on CT texture analysis in patients undergoing ALPPS show potential for prediction of liver hypertrophy after ALPPS 1st Step.
Limitations: This is a single-center study with a limited number of patients.
Ethics committee approval: n/a
Funding: No funding was received for this work.
Author Disclosures:
A. Borgheresi: nothing to disclose
A. Agostini: Speaker at Siemens Healthineers
A. Mari: nothing to disclose
L. Ottaviani: nothing to disclose
M. Vivarelli: nothing to disclose
S. Maggi: nothing to disclose
A. Giovagnoni: nothing to disclose
D. Nicolini: nothing to disclose

RPS 1001c-8 11:57
Liver size estimation revisited: why we should replace distance measurements in midclavicular line by automated volumetry
T. J. Weikert, D. J. Winkel, H.-C. Breit, L. Noordtzij, T. Heye, D. Boll*; Basel/CH (thomas.weikert@usb.ch)*

Purpose: To investigate the inter-rater reliability and validity of distance measurements in the mid-clavicular line (MCL) that are frequently reported as an estimate of liver size in cross-sectional imaging on a large dataset.
Methods and materials: We identified 275 consecutive abdominal CT examinations acquired at our institution in December 2018. The corresponding reports contain measurements of liver height in MCL. Firstly, to investigate inter-rater reliability, MCL distance measurements were performed independently by three radiology residents on a subset of 55 exams (coronal plane). ICC and the corresponding 95% confidence interval (CI) were calculated (absolute-agreement, two-way-random-effects model). Secondly, to assess validity, we calculated the Pearson correlation coefficient for actual liver volumes and the MCL distance measurements extracted from the corresponding clinically-approved reports. Liver volumes of all 275 datasets were determined by an AI-based organ volumetry software (NeuronX, Siemens Healthineers), whose validity had been previously proven. All measurements were performed on the portal-venous phase series (slice-thickness: 5 mm).
Results: Mean liver volume was 1775 ml (95% CI: 1693 ml–1856 ml). ICC for the MCL measurements of the three raters was 0.56 (95% CI: 0.39-0.70). The Pearson correlation coefficient for distance measurements in MCL and liver volumes was 0.58 (p<0.001).
Conclusion: The poor to moderate inter-rater reliability of MCL distance measurements of the liver as well as its only moderate correlation with actual liver volumes suggest that we should stop using them as an estimate for liver size. Instead, we should promote the integration of reliable automated liver volumetric measurements into our workflows.
Limitations: Only three readers. Measurement of liver volumes only in the coronal plane.
Ethics committee approval: Written informed consent was waived by the local ethics committee.
Funding: No funding was received for this work.
Author Disclosures:
T. J. Weikert: nothing to disclose
D. J. Winkel: nothing to disclose
H.-C. Breit: nothing to disclose
L. Noordtzij: nothing to disclose
T. Heye: nothing to disclose
D. Boll: nothing to disclose

RPS 1001c-9 12:03
Can CT textural analysis reliably differentiate peritoneal tuberculosis from peritoneal carcinomatosis?
N. Khan, M. Awais*; Karachi/PK (awais_aku@yahoo.com)*

Purpose: To determine whether quantitative CT texture parameters can reliably differentiate peritoneal tuberculosis (PT) from peritoneal carcinomatosis (PC).
Methods and materials: Patients with a biopsy confirmed diagnosis of PT or PC from 2010-2018 were enrolled. Textural analysis was performed using LIFEx software and 42 textural parameters were calculated. Student t-test was used to compare the individual textural parameters between the two groups. Logistic regression analysis was used to study the significant textural parameters for differentiating between study groups. Area under the receiver operating curve (ROC) for the significant textural parameters was calculated to determine the optimal cut-off values. A p-value of < 0.05 was considered statistically significant.
Results: 28 with PT and 36 with PC were included. Independent samples t-test showed statistically significant differences in multiple textural parameters in both groups. Logistic regression analysis using GLZLM HGZE parameter showed a maximum difference of -23.571 (p = .000) between the two groups. The logistic regression model was statistically significant 2 = 73.528 (p = 0.000). The model demonstrated 90.1% (Nagelkerke R2) of the variance and classified 97% of the cases correctly. (Sensitivity, specificity, positive predictive value, negative predictive values were 100%, 93.3%, 94.73%, and 100%, respectively). ROC curve was obtained from the data which showed an area under the curve of .965 (p = .000 and 95% CI= 0.913-1, respectively).
Conclusion: CTTA is reliable in differentiating between peritoneal tuberculosis and peritoneal carcinomatosis. The textural parameter GLZLM HGRE can be used as a model biomarker with 97% accuracy.
Limitations: The study was retrospective with a relatively small sample size.
Ethics committee approval: As a retrospective chart review, the study was approved by the institutional ethical review committee with a waiver of informed consent.
Funding: No funding was received for this work.
Author Disclosures:
N. Khan: nothing to disclose
M. Awais: nothing to disclose

RPS 1001c-10 12:09
Assessment of peritoneal carcinomatosis using iodine overlays from spectral detector computed tomography
S. Lennartz, D. Zopfs, N. Abdullayev, M. Le Blanc, K. Slebocki, A. Wagner, C. Wybranski, N. Grosse Hokamp, T. Persigehl*; Cologne/DE (simon.lennartz@uk-koeln.de)*

Purpose: Peritoneal carcinomatosis (PC) is a prognostically relevant metastatic condition which may be difficult to differentiate from postoperative alterations. The study aim was to determine whether PC could be distinguished more accurately from such benign peritoneal alterations (BPA) with a combination of spectral detector CT-derived conventional and color-coded iodine overlay images (CI/IO) as compared to CI only.
Methods and materials: 30 patients with PC and 30 with BPA with portal-venous phase abdominal SDCT were retrospectively included. Four radiologists determined presence/absence of PC for each patient and assessed lesion conspicuity, diagnostic certainty, and image quality using 5-point Likert scales. Subjective assessment was conducted in two sessions comprising solely CI and CI/IO between which a latency of 6 weeks was set. Iodine concentration and

attenuation of 30 PC/BPA lesions each were determined ROI-based to analyse quantitative lesion differentiation.
Results: Overall specificity at visual assessment was significantly higher when using CI/IO as compared to CI only (0.86 vs. 0.78;p<0.05), while sensitivity was comparable (0.79 vs. 0.81; p=1.0). In postsurgical patients, the overall increase in specificity was highest (0.91 vs. 0.80, p<0.05). Lesion conspicuity was rated higher in CI/IO (4(3-5),CI:3(3-4);p≤0.05), while diagnostic certainty was comparable (both 4(3-5);p=0.5). CI/IO received the highest rating for image quality and assessability of relevant anatomical structures (5(4-5). Quantitatively, iodine measurements facilitated differentiation between PC and BPA (AUC_{Iodine}=0.95, AUC_{HU}=0.90).
Conclusion: For visual differentiation between PC and BPA, a combination of IO/CI improves specificity at comparable sensitivity, particularly when assessing patients with a history of abdominal surgery. Iodine may facilitate quantitative lesion differentiation compared to HU, however, this should be validated further.
Limitations: The sample size was limited and the study design retrospective.
Ethics committee approval: Waived due to retrospective study design.
Funding: Else Kröner-Fresenius Stiftung(2016-Kolleg-19 to SL).
Author Disclosures:
S. Lennartz: Research/Grant Support at Philips Healthcare
D. Zopfs: nothing to disclose
N. Abdullayev: nothing to disclose
M. Le Blanc: nothing to disclose
K. Slebocki: nothing to disclose
A. Wagner: nothing to disclose
C. Wybranski: nothing to disclose
T. Persigehl: nothing to disclose
N. Grosse Hokamp: Speaker at Philips Healthcare, Research/Grant Support at Philips Healthcare

RPS 1001c-11 12:15
Analysis of non-enhanced CT characteristics in patients with ultra-long-term continuous ambulatory peritoneal dialysis
J. Guan, X. Hu, F. Zhang, Y. Peng*; Guangzhou/CN*

Purpose: To investigate the characteristics of patients with ultra-long-term continuous ambulatory peritoneal dialysis (CAPD) on non-enhanced CT.
Methods and materials: 23 patients with a history of more than 10 years of CAPD (Group A) and 109 patients who failed to receive 5 years of CAPD and turned to hemodialysis (Group B) were retrospectively enrolled. General information (gender, age, primary disease) and CT manifestations, including parietal peritoneum thickening, degree of parietal peritoneum calcification (mild: <5 foci of calcifications; severe: ≥15 foci of calcifications), calcification of mesostenium mesenteric margin/free margin, calcification of mesenteric region, and abdominal visceral arterial calcification) of both groups were compared. CT images in group A were collected at the 10th year of CAPD, and in group B were collected 3 months before stopping CAPD.
Results: There was no significant difference in general information between the two groups (P>0.05). The incidence of following CT findings had statistically significant difference between group A and B (P<0.01): (1) extensive thickening of parietal peritoneum (21.7% vs. 78.9%); (2) degree of parietal peritoneum calcification (mild: 30.4% vs. 9.2%; severe: 8.7% vs. 60.6%); (3) calcification of mesenteric region (4.3% vs. 32.1%); (4) calcification of mesostenium free margin (13.0% vs. 49.5%). However, there was no significant difference in calcification of mesostenium mesenteric margin (30.4% vs. 40.3%) or abdominal visceral arterial calcification (61.1% vs. 56.9%) (P>0.05).
Conclusion: Patients with ultra-long-term CAPD usually showed slight parietal peritoneum thickening to mild parietal peritoneum calcification on non-enhanced CT. Adverse factors for persistence of long-term CAPD can be monitored by non-enhanced CT.
Limitations: No autopsy was performed in this study and there was no evidence indicating the mechanism of stopping CAPD.
Ethics committee approval: n/a
Funding: No funding was received for this work.
Author Disclosures:
J. Guan: nothing to disclose
Y. Peng: nothing to disclose
F. Zhang: nothing to disclose
X. Hu: nothing to disclose

RPS 1001c-12 12:21
Distinguishing benign from malignant focal liver lesions (FLL) using the apparent diffusion coefficient (ADC): impact of post-processing on the diagnostic accuracy?
M. Dietzel[1], S. Ellmann[1], M. Saake[1], M. Hammon[1], M. Uder[1], R. Janka[1], P. A. T. Baltzer[2]; *[1]Erlangen/DE, [2]Vienna/AT*

Purpose: We investigated whether there is an impact of post-processing on ADC values of FLL.
Methods and materials: 51 consecutive cancer patients receiving standardised multiparametric liver-MRI for suspected FLL were prospectively recruited (1.5T: T2, dynamic T1 +/- Gd-EOB-DTPA; DWI: breath-hold EPI: TR/TE: 2100/62 ms, b0/b800).
Rescan-reliability of ADC values was addressed by double measurement of diffusion-weighted sequences giving ADC_1/ADC_2. Histological verification or imaging follow-up >24 months served as reference-standard (RS).
FLL were identified on dynamic T1 scans by two experienced blinded readers in consensus. Every FLL was assessed by one standardised region-of-interest (ROI) drawn into the most suspicious FLL-enhancement (automated ROI-transfer between sequences). Two ADC-metrics were investigated:
A) ADC_a (standard ADC-map by the proprietary scanner-software)
B) ADC_b (established open-source method)
Consequently four ADC-values were available to characterize each FLL (ADC_{1a}, …, ADC_{2b}). These four ADC-values were stratified by the RS (benign/malignant-FLL) and compared intraindividually (Friedman-test, Bland-Altmann-Plot, Area-under-the-ROC-curve/AUC-comparison; alpha=5%).
Results: 87 FLL in non-cirrhotic livers were diagnosed (42/45 malignant/benign, mean-age: 64years). For neither ADC_a (P=0.28) nor ADC_b (P=0.33) was a systematic or proportional bias observed comparing the initial and repeated scan. In malignant-FLL both for ADC_1 and for ADC_2 (median-difference: 0.60 and $0.57*10^{-3}$ mm^2/s) significant systematic (both P<0.001) and proportional bias (P<0.05) was observed if ADC_a was used instead of ADC_b (P<0.001). This bias was not observed for benign-FLL (P=0.88). Results translated to different intraindividual diagnostic performance between the four ADC-values. The biggest differences was observed between ADC_{1a} (AUC=0.79) and ADC_{1b} (AUC=0.71;P=0.004).
Conclusion: We identified a significant impact of post-processing methods on the ADC values of FLL. The results led to a different diagnostic accuracy depending on the post-processing method.
Limitations: Results should be validated in prospective trials with special focus on more ADC metrics and on longitudinal ADC comparison.
Ethics committee approval: n/a
Funding: No funding was received for this work.
Author Disclosures:
M. Dietzel: nothing to disclose
S. Ellmann: nothing to disclose
M. Uder: nothing to disclose
P. A. T. Baltzer: nothing to disclose
M. Saake: nothing to disclose
M. Hammon: nothing to disclose
R. Janka: nothing to disclose

11:15 - 12:30 **Room M 4**

Musculoskeletal

RPS 1010b

Hip, pelvis and lower extremity

Moderators:
P. D. Afonso; Lisbon/PT
T. J. Dietrich; St. Gallen/CH

RPS 1010b-1 11:15
3D structural parameters predict future total hip replacement better than current 2D radiographic standards: an AGES-Reykjavik study
T. Turmezei[1], G. M. Treece[1], A. H. Gee[1], S. Sigurjonsson[2], H. M. M. Jónsson[2], T. Aspelund[2], V. Gudnason[3], K. E. S. Poole[1]; *[1]Cambridge/UK, [2]Reykjavik/IS, [3]Kopavogur/IS (tom@turmezei.com)*

Purpose: To compare analysis of hip CT with 3D joint space mapping (JSM) against radiographic criteria in a predictive model for future total hip replacement (THR).
Methods and materials: We undertook a nested case-control study within the AGES-Reykjavik cohort of healthy older adults, all with a baseline 1 mm slice thickness hip CT. After 2:1 age and gender matching then exclusions, there were 80 cases with THR within 5 years versus 187 controls, mean age 74.4±4.9 years. The Kellgren and Lawrence grade (KLG) and minimum 2D (min2D) joint space width (JSW) were assessed at each hip. After JSM delivered 3D JSW maps for each hip, statistical shape modelling determined 3D joint shape modes (SM). Statistical parametric mapping (SPM) revealed significantly different regions of 3D JSW between groups. Receiver operating characteristics with area-under-the-curve (AUC) values were calculated for hip pain (HP), KLG, min2D, minimum 3D JSW from the SPM region of interest (ROI) divided by mean JSW (min3D), and SM.
Results: SPM revealed a region superiorly where JSW was significantly dependent on THR, narrower in cases by up to 1 mm (p<0.05); this was the ROI used in the predictive model. Hip pain was the poorest predictor (AUC=0.69).

KLG (0.72) and min2D (0.73) were outperformed by SM (0.74) and min3D (0.79). AUC increased with a combination of min3D and SM (0.81) and maximal when KLG was also included (0.86).
Conclusion: JSM results in better prediction of THR than 2D radiographic standards in healthy older individuals. These findings support the exploration of JSM application in clinical trials with the potential for stratification, prediction, and monitoring of osteoarthritis.
Limitations: n/a
Ethics committee approval:
See Harris et al. Am J Epidemiol. 2007;165(9):1076–1087.
Funding: The Cambridge NIHR Biomedical Research Centre, Wellcome Trust (100676/Z/12/Z), and National Institute on Aging (NO1-AG-1-210; Icelandic Government).
Author Disclosures:
T. Turmezei: nothing to disclose
G. M. Treece: Patent Holder at U.S. patent US8938109B2, “Image data processing systems for estimating the thickness of human/animal tissue structures”
A. H. Gee: nothing to disclose
S. Sigurjonsson: nothing to disclose
H. M. M. Jónsson: nothing to disclose
T. Aspelund: nothing to disclose
V. Gudnason: nothing to disclose
K. E. S. Poole: Patent Holder at U.S. patent US8938109B2, “Image data processing systems for estimating the thickness of human/animal tissue structures”

RPS 1010b-2 11:21
CT assessment of muscle mass and quality for hip surgery: a feasibility study
S. Zannoni, D. Albano, M. Jannone, L. Pedone, C. Messina, L. M. M. Sconfienza*; Milan/IT (stefaniazannoni@hotmail.com)*

Purpose: The segmentation of psoas muscles at L3 is used to estimate sarcopenia status. However, this parameter is not useful when CT is performed in other districts. Our aim was to correlate the estimation of muscle mass around the hip with that obtained using psoas segmentation at L3 on CT.
Methods and materials: A radiologist reviewed abdominal CTs performed on 50 consecutive patients (29 males; mean age: 69.6±11y). Regions of interest were drawn to assess cross-sectional areas (CSA) and attenuation of psoas muscles at the L3 level, which was considered as the standard. These values were correlated with CSA and attenuation of the iliopsoas, rectus femoris, sartorius, and tensor fascia latae at the hip, separately on each side. After applying the Bonferroni correction for multiple comparisons, statistical significance was set as $P<0.002$.
Results: We found a significant correlation between attenuation values of both psoae at L3 and those of all the other hip muscles ($P<0.001$, $r>0.491$). A significant correlation was observed between CSA of the right psoas and the other muscles ($P\leq0.001$, $r>0.459$), except for the tensor fascia latae at the lesser trochanter ($P=0.004$, $r=0.401$). We observed a significant correlation between CSA of the left psoas at L3 and that of the psoas and rectus femoris at the hip ($P=0.001$, $r=0.456$), with no significant correlation with tensor fascia latae and sartorius ($P\geq0.002$, $r\leq0.430$).
Conclusion: CT segmentation of hip muscles is highly correlated to that performed on the psoas at the L3 level, except for tensor fascia latae. These measurements could be used to evaluate sarcopenia in patients undergoing hip surgery.
Limitations: A small population.
Ethics committee approval: n/a
Funding: No funding was received for this work.
Author Disclosures:
D. Albano: nothing to disclose
S. Zannoni: nothing to disclose
C. Messina: nothing to disclose
L. M. M. Sconfienza: nothing to disclose
L. Pedone: nothing to disclose
M. Jannone: nothing to disclose

RPS 1010b-3 11:27
Does the use of magnetic resonance imaging in occult and suspected metastatic pathological neck of femur fractures affect the choice of surgical intervention?
B. Budair, M. J. H. Al-Tibi, T. Boutefnouchet*; Birmingham/UK (m.al-tibi@nhs.net)*

Purpose: Magnetic resonance imaging is often employed as the diagnostic modality of choice in occult and suspected pathological femoral neck fractures. The research question is: does the use of an MRI scan in occult and suspected metastatic pathological neck of femur fractures affect the choice of surgical intervention?
Methods and materials: A retrospective observational analysis was conducted of 104 consecutive patients who had an MRI scan of the hip from July 2009-August 2011 among a total population of 894 hip fractures managed in our institution. The findings of plain radiography, which preceded MRI, were recorded. The data was extracted from the medical records and an online image archiving system. Statistical analysis software SAS/STAT® SAS Institute Inc. USA© was used to conduct data collation and analyses.
Results: From a total of 894 femoral neck fractures treated in our institution, 100 patients had an MRI scan preoperatively for either an occult fracture or suspected fracture secondary to metastatic disease. MRIs confirmed the presence of 13 simple fractures. A total of 14 patients had pathological features suggestive of metastasis, of which 12 were clearly visible on plain radiographs. The surgical plan did not change after MRI for any of these pathological fractures.
Conclusion: Results of this study demonstrate that an MRI scan had an impact on treatment selection only when a simple but radiographically occult fracture is suspected, but not in the context of suspected metastatic pathological fractures.
Limitations: n/a
Ethics committee approval: Institutional agreement was obtained before the study. Ethics committee approval was not required to carry out this study.
Funding: No funding was received for this work.
Author Disclosures:
M. J. H. Al-Tibi: nothing to disclose
B. Budair: nothing to disclose
T. Boutefnouchet: nothing to disclose

RPS 1010b-4 11:33
Potential of susceptibility-weighted imaging for the reliable assessment of angle measurements reflecting hip morphology
S. M. Böker, L. Adams, U. L. Fahlenkamp, B. Hamm, M. R. Makowski*; Berlin/DE*

Purpose: To evaluate the potential of susceptibility-weighted magnetic resonance imaging (SWMR) for angle measurements reflecting hip morphology, using radiographs as a reference standard.
Methods and materials: 40 patients were examined (04/2014-01/2019) with standard MR-sequences, coronal SWMR, and radiographs in anteroposterior pelvic view. Coronal maximum intensity projection (MIP) images of both hips were reconstructed on SWMR and T1-weighted images. Sharp's angle, Tönnis angle, and the lateral centre-edge angle of Wiberg were measured on coronal SWMR, T1-weighted MIP-images, and radiographs. Measurements were compared by linear regression analysis and Blant-Altmann plots, using radiographs as a reference standard. Additionally, a ratio between the signal intensity of muscles and bone on SWMR and T1w MIP-images was calculated and compared between sequences.
Results: 40 patients were examined. 69 hip joints could be evaluated. Sharp's angle ($y=1.04x+1.77$, $R^2=0.80$), Tönnis angle ($y=0.86x+1.60$, $R^2=0.86$), and the lateral centre-edge angle of Wiberg ($y=0.94x+2.49$, $R^2=0.88$) showed a strong correlation between SWMR MIP-images and radiographs. The correlation between T1-weighted MIP-images and radiographs was moderate for Sharp's angle ($y=0.69x+14.54$, $R^2=0.37$) and the lateral centre-edge angle of Wiberg ($y=0.79x+3.18$, $R^2=0.40$). Tönnis angle could not be measured reliably on T1-weighted MIP-images. The ratio between the intensity of muscles and the femoral head was significantly higher on SWMR than on T1-weigted images ($p<0.001$).
Conclusion: Coronal SWMR MIP-images enable the reliable measurement of Sharp's angle, Tönnis angle, and the lateral centre-edge angle of Wiberg compared to radiographs with higher accuracy compared to T1w MIP-images.
Limitations: Metal implants cause strong susceptibility artefacts, especially on SWMR, with the consequence being that hips with implants could not be evaluated.
Ethics committee approval: The institutional review board approved this prospective study. Written informed consent was obtained from all subjects.
Funding: No funding was received for this work.
Author Disclosures:
S. M. Böker: nothing to disclose
M. R. Makowski: Grant Recipient at DFG
L. Adams: nothing to disclose
B. Hamm: Other at More than 50 records on the ICMJE disclosure form.
U. L. Fahlenkamp: nothing to disclose

RPS 1010b-5 11:39

Equivalence between MRI-based synthetic CT and conventional CT in the morphological assessment of the femoroacetabular joint

M. C. Florkow, K. Willemsen, F. Zijlstra, C. Wismans, B. van der Wal, H. Weinans, M. van Stralen, R. Sakkers, P. R. Seevinck; *Utrecht/NL (p.seevinck@umcutrecht.nl)*

Purpose: In paediatric orthopaedics, the use of potentially harmful CT could be avoided by generating synthetic CT (sCT) from radiation-free MR images. Although widely investigated for radiotherapy, sCTs have not been evaluated for orthopaedics. In this study, we compared clinically relevant measurements for hip dysplasia as performed on CTs and sCTs.
Methods and materials: 30 male prostate cancer patients without known orthopaedic conditions were included and scanned with MR and CT for radiotherapy treatment planning. Morphological assessment of the femoroacetabular joint was performed on CT and sCT reconstructions obtained from a BoneMRI prototype (BoneMRI v1.1-alpha, MRIguidance BV, Utrecht, the Netherlands). Clinical measurements for evaluation included centre-edge angle (CEA), sharp angle (SA), extrusion index (EI), acetabular index (AcetIncl), and femoral centre-to-midline distance (FCMD). Equivalence was tested for each measurement using a paired two-one sided test. The equivalency margins were defined using literature values of the intraobserver limit of agreement measured on x-ray. CT and sCT were considered equivalent for confidence intervals of the mean difference between the CT and the sCT within ±4.2° for CEA, ±5.6° for AcetIncl, ±2.9° for SA, ±6.1% for EI, and ±4.5 mm for FCMD.
Results: All measurements were proven equivalent between the CT and sCT. Bonferonni-corrected confidence intervals at 95% were -2.0° and 0.9° for the CEA, 0.3° and 1.4° for SA, -2.4% and 1.0% for EI, -1.5° and 0.9° for the AcetIncl, and 0 mm and 0.6 mm for FCMD. No patient presented a substantial difference for all measurements.
Conclusion: This study demonstrates that sCT is equivalent with CT for femoroacetabular morphological assessment in adults.
Limitations: Future studies are necessary to confirm these findings in paediatric patients.
Ethics committee approval: Medical-ethical approval was obtained.
Funding: Dutch Scientific Organisation NWO-TTW-15479.
Author Disclosures:
P. R. Seevinck: Founder at MRIGuidance BV, Shareholder at MRIGuidance BV, Research/Grant Support at Zimmer Biomet
M. van Stralen: Founder at MRIGuidance BV, Shareholder at MRIGuidance BV
M. C. Florkow: nothing to disclose
K. Willemsen: nothing to disclose
F. Zijlstra: nothing to disclose
H. Weinans: Research/Grant Support at Zimmer Biomet
R. Sakkers: nothing to disclose
B. van der Wal: Research/Grant Support at Zimmer Biomet
C. Wismans: Employee at MRIguidance BV

RPS 1010b-6 11:45

Improved performance of orthopaedic metal artefact reduction in virtual mono-energetic spectral images compared to conventional poly-energetic images: a total hip arthroplasty phantom study

V. Stuivenberg[1], R. H. H. Wellenberg[2], L. van de Riet[1], I. M. Nijholt[2], J. van Osch[2], R. W. van Hamersvelt[1], P. A. de Jong[1], T. Leiner[1], M. F. Boomsma[2]; *[1]Utrecht/NL, [2]Zwolle/NL (m.f.boomsma@gmail.com)*

Purpose: To investigate whether the use of metal artefact reduction for orthopaedic implants (O-MAR) resulted in more effective metal artefact reduction in virtual mono-energetic images (VMI) of a total hip arthroplasty (THA) phantom when compared to the reduction achieved with O-MAR in conventional poly-energetic images using poly-energetic images without O-MAR as reference.
Methods and materials: A THA phantom containing 18 hydroxyapatite calcium carbonate pellets, which represented the same modular bone density, was scanned on a dual-layer spectral detector CT scanner with or without unilateral prosthesis. To quantify the effect of metal artefact reduction, the following image quality parameters were assessed for each pellet: CT values (Hounsfield units), noise (measured as standard deviation), signal-to-noise ratio (SNR), and contrast-to-noise ratio (CNR). In a previous study, we found CT numbers are similar in 74keV VMI and 140kVp poly-energetic images, whereas 130keV showed optimal CNRs in the CT imaging of metal hip prostheses. Therefore, conventional poly-energetic 140kVp images reconstructed with iterative model-based reconstruction (IMR) and VMI extracted at 74keV and 130keV were all analysed with and without O-MAR.
Results: The use of O-MAR resulted in a reduction of metal artefacts in 140kVp poly-energetic images and 74 130keV mono-energetic images. When using 140kVp poly-energetic images without O-MAR as a reference, metal artefacts were most effectively reduced in 130keV mono-energetic images reconstructed with O-MAR.
Conclusion: Results of this quantitative THA phantom study showed that 130keV VMI combined with O-MAR resulted in a more effective metal artefact reduction compared to 74keV VMI and conventional poly-energetic images combined with O-MAR. The clinical value of our findings should be further investigated in patients with THA.
Limitations: The phantom quantification.
Ethics committee approval: n/a
Funding: No funding was received for this work.
Author Disclosures:
R. H. H. Wellenberg: nothing to disclose
M. F. Boomsma: nothing to disclose
T. Leiner: nothing to disclose
P. A. de Jong: nothing to disclose
I. M. Nijholt: nothing to disclose
R. W. van Hamersvelt: nothing to disclose
V. Stuivenberg: nothing to disclose
J. van Osch: nothing to disclose
L. van de Riet: nothing to disclose

RPS 1010b-7 11:51

Iliopsoas impingement after THR: our purpose of a diagnostic and therapeutic algorithm

A. Antón Jiménez[1], M. de Albert de Delas-Vigo[1], J. M. M. Escudero Fernández[1], D. Moreno Martínez[2], A. Gimeno[1], M. T. Veintemillas[1], L. Casas[1], C. Torrents[1], R. Dominguez[1]; *[1]Barcelona/ES, [2]Cornella de Llobregat/ES (alba.antonj@gmail.com)*

Purpose: To review iliopsoas impingement after a total hip replacement (THR) and the usefulness of US-guided infiltration as a diagnostic technique, to assess the effectiveness of the different treatment modalities for this condition, and to establish a relation between CT position parameters of the prosthesis and clinical response.
Methods and materials: This retrospective study from 2017-2019 included 35 patients (20 female; mean age 66.7 years; mean BWI 26.6) who underwent total hip replacement (60% right hip; 74.3% posterolateral surgical approach) at our institution. The mean time of pain appearance after THR was 11.1 months.
All patients had a positive test to anaesthesia and glucocorticoid US-guided infiltration of the iliopsoas tendon sheath. When pain recurrence appeared, endoscopic tenotomy was performed.
Inclination, corrected anteversion, medialisation, and axial and sagittal acetabular overhanging of the prothesis were measured on CT.
Therapeutic efficacy was evaluated by VAS and Harris score pre and post-treatment.
Results: 67% of the patients had a delayed pain recurrence after infiltration, which did not correlate with prothesis position CT parameters.
From the patients who underwent endoscopic tenotomy (n=13), the majority (n=8) had a total or partial positive clinical outcome.
High degrees of horizontal and vertical overhanging (>10 mm) correlated significantly with a negative response to treatment ($p<0.05$). So, CT parameters can help in clinical management decision (tenotomy vs acetabular change).
Conclusion: A US-guided anaesthesia and glucocorticoid infiltration test is a useful tool in iliopsoas impingement diagnosis and conservative treatment.
Endoscopic tenotomy will produce remission of pain in most of the patients. Nevertheless, an acetabular cup overhanging of >10 mm is a negative prognostic factor to surgical treatment response.
Limitations: n/a
Ethics committee approval: n/a
Funding: No funding was received for this work.
Author Disclosures:
A. Antón Jiménez: nothing to disclose
A. Gimeno: nothing to disclose
M. de Albert de Delas-Vigo: nothing to disclose
R. Dominguez: nothing to disclose
M. T. Veintemillas: nothing to disclose
L. Casas: nothing to disclose
C. Torrents: nothing to disclose
J. M. M. Escudero Fernández: nothing to disclose
D. Moreno Martínez: nothing to disclose

RPS 1010b-8 11:57

Integrity of the pectineal ligament in MRI correlates with radiographic superior pubic ramus fracture displacement

A. Klengel, H. Steinke, P. Pieroh, A. Höch, T. Denecke, C. Josten, G. Osterhoff; *Leipzig/DE (alexis.klengel@posteo.de)*

Purpose: Estimating the stability of pelvic lateral compression fractures solely by static radiographs can be difficult. The role of anterior pelvic soft tissues as potential secondary stabilisers of the pelvic ring has hardly been investigated. The purpose of this study was to assess the integrity of the pectineal ligament, a strong ligament along the pectineal line, and correlate it with the initial radiographic appearance of the pubic ramus fracture.

Methods and materials: The eligibility criteria included a pelvic lateral compression fracture with superior pubic ramus involvement, available post-traumatic radiographs (pelvis ap, inlet, and outlet), and MRI of the pelvis with fat-suppressed, fluid-sensitive coronal images within 6 weeks after the trauma. In a retrospective review, the degree of MR-morphologic alterations of the pectineal ligament was described (grade 0=intact, grade 3=rupture) and correlated to radiographic superior pubic ramus fracture displacement.
Results: 33 superior pubic ramus fractures in 31 patients were analysed. In the majority of fractures (72.7 %), associated MR-morphologic alterations of the pectineal ligament were present. Radiographic displacement and MRI grading showed a strong positive correlation (Spearman-Rho: 0.783, p<0.001). The sensitivity and specificity for a radiographic displacement of >3 mm on plain radiographs to detect a structural ligament lesion on MRI (grade 2 and higher) were 73% and 100% (Fisher's exact: p<0.001).
Conclusion: Radiographic displacement of superior pubic ramus fractures >3 mm is a strong indicator for a structural lesion of the pectineal ligament, which should be radiologically reported. Future studies should investigate the biomechanical importance of this ligament for pelvic ring stability.
Limitations: No surgical or histologic correlation. Heterogeneous MRI sequence protocols.
Ethics committee approval: Approval of the local institutional ethics committee was obtained.
Funding: No funding was received for this work.
Author Disclosures:
A. Klengel: nothing to disclose
H. Steinke: nothing to disclose
P. Pieroh: nothing to disclose
A. Höch: nothing to disclose
T. Denecke: nothing to disclose
C. Josten: nothing to disclose
G. Osterhoff: nothing to disclose

RPS 1010b-9 12:03

Quantification of metal artefact reduction of various MRI techniques in 10 common total hip arthroplasty implants: when less is more!

S. Shah[1], D. Dalili[1], J. Spence[1], S. Hill[1], H. Connolly[1], S. A. Jengojan[2], J. Fritz[3], G. Charles-Edwards[1], A. Isaac[1]; [1]London/UK, [2]Vienna/AT, [3]Baltimore, MD/US (Dr.amandaisaac@googlemail.com)

Purpose: To quantify the metal artefact reduction capabilities of various metal artefact reduction MRI pulse sequences in 10 commonly used total hip arthroplasty implants (THAI).
Methods and materials: 10 different THAI systems were imaged on a commercially available 1.5T MRI system in a water-based phantom. T1-weighted MRI was acquired without and with the following metal artefact reduction techniques (MARS): high receiver bandwidth, high transmit bandwidth, view-angle-titling (VAT) at 50% and 100%, and slice-encoded-metal-artefact-correction (SEMAC) with 6, 10, and 14 encoding steps. The size of signal voids and pile-ups were assessed by fitting Rician and Gaussian distributions around each implant. Line profiles implant stems were used to assess signal pile-up at bone-metal interfaces.
Results: MARS improved the signal void in 7/10 THAI, with SEMAC-14 outperforming all other methods and reducing the signal void from 6% to 22%. Signal pile-up was reduced in all implants with SEMAC-14 and VAT both performing the best, reducing pile-up from 28% to 75%. At the bone-metal interface of all 7 hip implants which had femoral stems, SEMAC reduced signal pile-up from 11% to 86%.
Conclusion: SEMAC reduces implant-induced signal void up to 22%, depending on the implant design and metallurgy. While all MARS methods reduce signal pile-up, SEMAC and VAT perform best. SEMAC, however, incurs a significant time-penalty, which may be problematic in certain scenarios. SEMAC significantly reduced signal pile-up at the bone-metal interface, improving the ability of MRI to diagnose periprosthetic complications and abnormalities including tumour recurrence, collections, fractures, muscle integrity, and AI-guided preoperative revision surgery planning.
Limitations: In vivo with only 10 implants.
Ethics committee approval: A quality assurance study.
Funding: No funding was received for this work.
Author Disclosures:
A. Isaac: nothing to disclose
S. Shah: nothing to disclose
G. Charles-Edwards: nothing to disclose
D. Dalili: nothing to disclose
J. Fritz: Advisory Board at Siemens
J. Spence: nothing to disclose
S. Hill: nothing to disclose
S. A. Jengojan: nothing to disclose
H. Connolly: nothing to disclose

RPS 1010b-10 12:09

Validation of a physical examination test for ischiofemoral impingement with correlation of MRI findings

Z. M. Ozdemir[1], T. Yıldırım[1], L. Karaca[1], A. Sağir Kahraman[1], Ü. Aydingöz[2]; [1]Malatya/TR, [2]Ankara/TR (zynpmaras@yahoo.com)

Purpose: To validate a physical examination test for ischiofemoral (IF) impingement and correlate MRI findings.
Methods and materials: The population of this prospective study comprised of a symptomatic group of 24 women with hip pain, who had positive MRI findings (IF space narrowing and oedema), and an age-matched group of 27 asymptomatic women. Each group underwent a physical examination test that entailed hip adduction, external rotation, extension, and knee flexion, both in the recumbent and upright standing positions, within 7 days of an MRI. VAS scores were noted before and after the test. A single radiologist quantitatively and qualitatively evaluated the IF and quadratus femoris (QF) spaces on 1.5T MR images.
Results: Mean ages were 56.0 (34-76) and 55.2 (34-79) years in symptomatic and asymptomatic groups, respectively (p>0.05). Likewise, BMIs were not statistically significantly different between the groups. IF and QF spaces were significantly narrower (p<0.001), ischial angles wider (p<0.001, right; p=0.002, left), and soft tissue oedema at the IF space was more common (p<0.001) in the symptomatic group, which also had higher VAS scores (p<0.001) that increased significantly during both the recumbent (p<0.001 for both sides) and upright (p=0.003, right; p<0.001, left) parts of the physical examination test.
Conclusion: A physical examination test that entails hip adduction, external rotation, extension, and knee flexion significantly increases symptoms of IF impingement that are correlated on MRI.
Limitations: A small number of patients. A single radiologist performing MRI evaluation.
Ethics committee approval: We obtained institutional review board approval and informed consent.
Funding: No funding was received for this work.
Author Disclosures:
Z. M. Ozdemir: nothing to disclose
T. Yıldırım: nothing to disclose
L. Karaca: nothing to disclose
A. Sağir Kahraman: nothing to disclose
Ü. Aydingöz: nothing to disclose

RPS 1010b-11 12:15

Glycosaminoglycan chemical exchange saturation transfer imaging of the talocrural joint in patients with osteochondral lesions and healthy volunteers

M. Boschheidgen[1], M. Frenken[1], A. Müller-Lutz[1], L. Kasprowski[1], G. Antoch[1], C. Schleich[1], S. Nebelung[2], D. B. Abrar[1]; [1]Düsseldorf/DE, [2]Aachen/DE (Matthias.Boschheidgen@med.uni-duesseldorf.de)

Purpose: To optimise a glycosaminoglycan chemical exchange saturation transfer (gagCEST) protocol for imaging of glycosaminoglycans (GAG) at 3T and to compare gagCEST values between patients with osteochondral lesions and healthy volunteers (HV).
Methods and materials: We used Bloch-McConnel simulations for optimising the gagCEST protocol. The following T1 and T2 relaxation times of cartilage at 3T were used: T1=1.2s and T2=0.039s. 11 HV (age 24±5 years) and 4 patients (age 32±9 years) with osteochondral lesions were examined with the optimised gagCEST protocol. In addition, T1 and T2 values were determined to evaluate if the relaxation times used in the simulation were accurate. Sequence parameters of the gagCEST sequence were: FOV=160x160 mm², slice thickness=5 mm, and TE/TR=3.5ms/7.2ms. 25 CEST images with a frequency offset between -3 ppm and 3 ppm, and one S0 image, were recorded.
Results: The optimisation with the Bloch-McConnel simulations showed an ideal B1 amplitude of 0.8 µT and a pulse and interpulse duration of 300 ms. We found a mean T1 time of 0.88±0.13s and a mean T2 time of 0.033±0.005s. These values significantly differed from the values used in the simulation. Nevertheless, further simulations revealed the same optimal pulse sequence parameters for the CEST sequence. HVs showed a significant higher gagCEST effect compared to patients (HV: MTRasym=(1.40±0.71)%; patients: MTRasym=(0.05±0.28)%, p<0.01).
Conclusion: The proposed gagCEST protocol showed good performance and could distinguish between HV and patients with osteochondral lesions.
Limitations: n/a
Ethics committee approval: n/a
Funding: No funding was received for this work.

Author Disclosures:
M. Boschheidgen: nothing to disclose
M. Frenken: nothing to disclose
A. Müller-Lutz: nothing to disclose
L. Kasprowski: nothing to disclose
G. Antoch: nothing to disclose
C. Schleich: nothing to disclose
S. Nebelung: nothing to disclose
D. B. Abrar: nothing to disclose

RPS 1010b-12 12:21
Patients with pincer FAI due to protrusio acetabuli or acetabular retroversion have intra- and extra-articular anterior subspine hip impingement on a 3D-CT-basedimpingement simulation
T. Lerch, F. Schmaranzer, I. Todorski, M. Hanke, C. Leibold, S. Steppacher, K. Siebenrock, M. Tannast*; Berne/CH (till.lerch@insel.ch)*

Purpose: Diagnosis and surgical treatment of hips with different types of pincer-FAI, such as protrusio acetabuli and acetabular retroversion, remains controversial as actual 3D acetabular coverage and location of impingement cannot be studied using standard 2D imaging. It remains unclear if pincer hips exhibit intra- or extra-articular FAI. Therefore, the purposes are to determine the impingement-free range of motion using osseous models based on 3D-CT scans and to determine the osseous intra-and extra-articular 3D impingement zones located using a 3D impingement simulation.
Methods and materials: This is a retrospective, comparative, controlled study involving 70 hips in 50 patients. 24 patients (44 hips) had symptomatic pincer-type FAI and 26 patients (26 hips) had normal hips. Surface models based on 3D-CT scans were reconstructed and compared for hips with acetabular retroversion (30 hips), protrusio acetabuli (14 hips), and normal asymptomatic hips (26 hips). Using CT-based 3D-models, impingement-free ROM and location of impingement were determined for all hips using validated 3D-collision detection software.
Results: The mean flexion was significantly ($p<0.001$) decreased in hips with protrusio acetabuli (104±9°) and acetabular retroversion (116±6°) compared to normal hips (125±13°). The mean internal rotation (IR) in 90° of flexion was significantly ($p<0.001$) decreased in hips with protrusio acetabuli (14±11°) compared to normal hips (32±9°).
The prevalence of extra-articular subspine impingement was significantly ($p<0.001$) higher (87%) in hips with acetabular retroversion compared to hips with protrusio acetabuli (14%) and normal hips (0%). The location of anterior acetabular impingement differed significantly ($p<0.001$) between hips with protrusio acetabuli and normal hips.
Conclusion: Extra-articular subspine impingement was detected in hips with acetabular retroversion. Osseous ROM and location of impingement differs between hips with protrusio acetabuli, acetabular retroversion, and normal hips. Patient-specific analysis of the location of impingement using 3D-CT could improve diagnosis and planning of treatment.
Limitations: A retrospective, single-centre study.
Ethics committee approval: IRB approval was obtained.
Funding: No funding was received for this work.
Author Disclosures:
T. Lerch: nothing to disclose
M. Tannast: nothing to disclose
K. Siebenrock: nothing to disclose
F. Schmaranzer: nothing to disclose
I. Todorski: nothing to disclose
M. Hanke: nothing to disclose
C. Leibold: nothing to disclose
S. Steppacher: nothing to disclose

11:15 - 12:30 **Room M 5**

Artificial Intelligence and Machine Learning

RPS 1005b

Artificial intelligence and machine learning in reporting and workflow

Moderators:
M. Fatehi; Tehran/IR
D. Pinto dos Santos; Cologne/DE

RPS 1005b-1 11:15
Radcount: an integrated system to represent essentials of the radiology examination and reporting processes
K. Nairz, J. Schuhmacher, P. Zingg, M. Sladek, M. Abu Baker, J. T. Heverhagen*; Berne/CH*

Purpose: Occupational processes can only run smoothly if all participants are getting relevant and essential information accurately, clearly, and without time lag. Current table-style process information from a single system (RIS) does not fulfil those criteria and presumably leads to inefficiencies.
Methods and materials: Patient-, process-, and time-information was obtained from the RIS relational database (GE, Oracle) and from the enterprise resource planning program (SAP) by ETL-programs. Time-stamps were directly extracted from DICOM images in a modality-independent manner. Process progression was calculated from those time points. A machine-learning tool (Prophet) was implemented to forecast daily patient numbers and increase the project ability. Data was visualised in a browser via an open-source client-server application or via a business intelligence software (Qliksense).
Results: RadCount prepares key numbers like throughput times, equipment occupancy, and patient lists in a visual and self-explaining manner. Predictive analytics technology was used to forecast the expected workload. Data was presented live and team-specifically, and thus facilitated the planning of radiological examination and diagnostic processes. Moreover, by combining data from different sources, typical interface problems were being alerted and hence could be prevented.
Conclusion: Radcount eliminated the problem of poor information transfer about VRE- and MRSA-infections at the interfaces. It also provided the data needed to devise an intelligent MR scheduling based on overbooking to manage no-shows. Its predictive functionality allows for resource management. Our solution is designed to be platform-independent and may be applicable to other platforms or high-throughput clinical processes. Thus, the tool proves oneself to enhance efficiency and safety.
Limitations: Radcount is expandable by further resolving the time sequence of the radiology processes.
Ethics committee approval: IRB exemption was obtained.
Funding: No funding was received for this work.
Author Disclosures:
K. Nairz: nothing to disclose
J. T. Heverhagen: nothing to disclose
J. Schuhmacher: nothing to disclose
M. Sladek: nothing to disclose
P. Zingg: nothing to disclose
M. Abu Baker: nothing to disclose

RPS 1005b-2 11:21
IILS: an intelligent imaging layout system to realise automatic imaging-report standardisation and to optimise intra-interdisciplinary clinical workflow
Y. Wang*; Nanjing/CN (wangzhang227@163.com)*

Purpose: To achieve imaging report standardisation and improve the quality and efficiency of the intra-interdisciplinary clinical workflow.
Methods and materials: We created a lung IILS based on deep learning for imaging report standardisation and workflow optimisation for the identification of nodules. Our IILS utilised a deep learning plus adaptive auto-layout tool, which trained and tested a neural network with imaging data from all the main CT manufacturers from 11,205 patients. Model performance was evaluated by the receiver operating characteristic curve (ROC) and calculating the corresponding area under the curve (AUC).
Results: Our IILS was clinically applicable due to the consistency with nodules detected by IILS, with its highest consistency of 0.94 and an AUC of 90.6% for malignant pulmonary nodules versus benign nodules with a sensitivity of 76.5% and specificity of 89.1%. Applying this IILS to a dataset of chest CT images, we demonstrated performance comparable to that of human experts in providing a better layout and aiding in diagnosis in 100% valid images and nodule display. The IILS was superior to the traditional manual system in performance, such as reducing the number of clicks from 14.45 ± 0.38 to 2, time consumed from 16.87 ± 0.38 sec to 6.92 ± 0.10 sec, number of invalid images from 7.06 ± 0.24 to 0, and missing lung nodules from 46.8% to 0%.
Conclusion: This IILS might achieve imaging report standardisation and improve the clinical workflow, therefore opening a new window for the clinical application of artificial intelligence.
Limitations: n/a
Ethics committee approval: This experiment was approved by the drum tower hospital ethics committee and written informed consent was obtained.
Funding: No funding was received for this work.
Author Disclosures:
Y. Wang: Speaker at NANJING DRUMTOWER HOSPITAL, NANJING, CHINA

RPS 1005b-3 11:27

Machine learning-based assistance to context-sensitively suggest ASPECT score during the reporting of neuroradiological emergencies

C. G. Cho[1], A. Junge[1], B. Kämpgen[2], V. Saase[1], A. Ulfert[1], E. L. Gonzalez[1], T. Ganslandt[1], H. Wenz[1], M. E. Maros[1]; [1]Mannheim/DE, [2]Rimpar/DE
(matt.maros@gmail.com)

Purpose: The Alberta stroke programme early CT score (APECTS) is a 10-point quantitative CT scan score that predicts the functional outcome of stroke patients and serves as a surrogate when selecting patients for neurointerventional procedures. Although ASPECTS is considered a biomarker, it is frequently missing from reports. Here, we investigated whether machine learning (ML)-based approaches can be utilised to assist radiologists in providing ASPECTS, hence improving report quality.
Methods and materials: We generated a stratified random sample (age, gender, and year) of CT cases (n=206) with a suspected ischaemic stroke or haemorrhage between 2015-2019. Conventional free-text reports were retrieved from local RIS. Two blinded readers (R1,exp.:3yrs; R2,exp.:7yrs) assessed the clinical question, referring department, the findings, and impressions of the reports, whether (pc-)ASPECTS had been or should have been provided (necessary:154[74.7%] vs. -not: 52[25.3%]). Further, the presence of ischaemia, haemorrhage, tumour, incidental findings, and procedures including CT-angiography/perfusion or previous imaging were recorded. These key features were also automatically detected using a RadLex-based proprietary information extraction software (www.empolis.com). Next, tree-based and elastic net ML-algorithms were fitted on training/validation/test sets to learn rules required for ASPECTS reporting.
Results: Cohen's kappa was 0.635 for "APECTS necessary" (p<0.0001) corresponding to 86.4% agreement between the readers. Among the investigated ML-models, the 10-fold cross-validated elastic net showed the best independet test set (n=20) performance of 95% accuracy (95%CI:75.1-99.87%,P[Acc>NIR]=0.024), 100% sensitivity, 93% specificity, 83.3% PPV, and 100% NPV on this imbalanced classification task.
Conclusion: ML-based assistance to context-sensitively suggest ASPECTS during the reporting of neuroradiological emergencies is feasible. It produces high-quality reports, which are better suited for cohort identification and downstream analyses.
Limitations: Retrospective single-centre data, which was counteracted by 10-fold CV.
Ethics committee approval: Nr.:2017-825R-MA.
Funding: CGC,BK,MEM gratefully acknowledge funding from BMWi-ZIM (grantno.:ZF4514602TS8).
Author Disclosures:
A. Ulfert: nothing to disclose
M. E. Maros: Consultant at SmartReporting GmbH
C. G. Cho: nothing to disclose
A. Junge: nothing to disclose
B. Kämpgen: Employee at EMPOLIS Information Management GmbH
V. Saase: nothing to disclose
E. L. Gonzalez: nothing to disclose
T. Ganslandt: nothing to disclose
H. Wenz: Consultant at SmartReporting GmbH

RPS 1005b-4 11:33

RANO check: a deep learning language model-based automatic response labelling using solely the findings sections of conventional free-text reports of brain tumours

M. E. Maros[1], A. Junge[1], V. Saase[1], C. G. Cho[1], B. Kämpgen[2], C. Groden[1], T. Ganslandt[1], H. Wenz[1]; [1]Mannheim/DE, [2]Rimpar/DE
(matt.maros@gmail.com)

Purpose: The response assessment in neuro-oncology (RANO) criteria for glioblastoma (GBM) and brain metastases are used for the standard response assessment of brain tumours in clinical trials. Human readers show large variations compared to deep learning (DL)-based segmentation tools. But the IT-infrastructure for such tools is scarcely available in most clinics. Therefore, we present DL-language model-based assistive tools that can generate RANO-GBM/BM labels solely using text from the findings section of a report.
Methods and materials: We performed a single-centre retrospective cohort study of 1,252 (GBM: 734[58.6%]; BM: 518[41.4%]) consecutive MRIs from 394 patients (GBM:243; BM:151) between 11/2011-07/2019. Conventional free-text reports were retrieved from the local RIS. The impressions were used to generate class labels. For training and inference, only the findings were used. RANO responses were distributed as follows: complete response (CR,n=94), partial response (PR,n=55), stable disease (SD,n=697), and progression (PD,n=406). We fitted universal language model fine-tuning (ULMFiT)[2] and fastText[3] models, which were task-specifically fine-tuned on binary (PD[32.4%] vs. CR+PR+SD[67.6%]) and multi-class RANO responses.
Results: Both FastText and ULMFiT showed an averaged accuracy ~79% on the binary RANO response task while showing significant differences (p<0.05) compared to the no information rate (NIR) of predicting the majority class (67.6%). ULMFiT showed a remarkable 79% specificity, 83% recall, and 47% precision. On the highly imbalanced multiclass RANO task, fastText and ULMFit showed ~68% and ~69% accuracies, respectively.
Conclusion: Computer-aided reporting using embedded DL-models is feasible, even for complex tasks such as RANO response assessment. Such models can support radiologists to improve report quality, thus strengthening radiological enpoints in clinical trials.
Limitations: Restricted general-domian German language model was used.
Ethics committee approval: Nr.:2017-825R-MA.
Funding: The authors gratefully acknowledge funding from BMWi-ZIM (MEM,CGC,BK grantnr.:ZF4514602TS8) and BMBF-MIRACUM (TG,MEM grantnr.:01ZZ1801E).
Author Disclosures:
V. Saase: nothing to disclose
M. E. Maros: Consultant at SmartReporting GmbH
A. Junge: nothing to disclose
C. G. Cho: nothing to disclose
B. Kämpgen: Employee at EMPOLIS Information Management GmbH
C. Groden: nothing to disclose
T. Ganslandt: nothing to disclose
H. Wenz: Consultant at SmartReporting GmbH

RPS 1005b-5 11:39

Automating quality control for standardised structured radiology reports using text analysis

C. Thouly[1], A. Dhrangadhariya[2], D. Fournier[1], H. Müller[2], H. Brat[1]; [1]Sion/CH, [2]Sierre/CH

Purpose: To assess a software prototype performance in measuring concordance between the indication and conclusion sections in standardised structured reports (SSRs) by comparing the results of automated and human evaluation.
Methods and materials: 200 randomly chosen French-language SSRs with "indication", "description" and "conclusion" sections were analysed. Indication and conclusion concordance regarding anatomy and disease was assessed by two expert radiologists and by a prototype software using falling rule-lists aided by MeSH (medical subject headings) terminology.
The software measured semantic similarity between any two MeSH codes with MeSHSim and an R-package with "-nodeSim" functionality. L'Extracteur de concepts multi-terminologique (ECMT) combining a rule-based and an NLP (natural language processing)-based approach was used to extract health-related concepts from French-language texts using French-language terminologies in HeTOP (health terminology/ontology portal), housing 70 health terminologies in 32 languages including MeSH and radiology lexicon (RadLex).
Results: Upon total concordance assessment between the indication and conclusion, the prototype reported 45% concordance for the anatomy information, while manual evaluation reported a 61% concordance. For disease information, the prototype reported 80% concordance versus 88% with the peer review. Based on ground truth, the algorithm accuracy for measuring anatomy concordance was 84% and for disease 92%. It took the experienced radiologists about 1.5 hours to conduct manual quality checks, but the prototype did it in a matter of seconds.
Conclusion: The automated prototype shows good performance compared to expert radiologists for the assessment of indication and conclusion concordance in SSRs. It also reduces the time and cost required for quality control.
Limitations: The prototype success is subject to the ability of ECMT to accurately extract the concepts from free texts and also upon availability of a particular concept in the MeSH vocabulary.
Ethics committee approval: n/a
Funding: No funding was received for this work.
Author Disclosures:
H. Brat: nothing to disclose
C. Thouly: nothing to disclose
A. Dhrangadhariya: nothing to disclose
D. Fournier: nothing to disclose
H. Müller: nothing to disclose

RPS 1005b-6 11:45

Automatic pre-population of normal chest x-ray reports using a high-sensitivity deep learning algorithm: a prospective study of clinical AI deployment

V. Mahajan, N. S. Batta, S. Gupta, V. K. Venugopal, H. Mahajan, M. Murugavel; *New Delhi/IN (vidur@mahajanimaging.com)*

Purpose: To evaluate a high-sensitivity deep learning algorithm for normal/abnormal chest x-ray (CXR) classification by deploying it in a real clinical setting.
Methods and materials: A commercially available deep learning algorithm (QXR, Qure.ai, India) was integrated into the clinical workflow for a period of 3 months at an outpatient imaging facility. The algorithm, deployed on-premise,

was integrated with PACS and RIS such that it automatically analysed all adult CXRs and reports for those which were determined to be “normal” were automatically populated in the RIS using HL7 messaging. Radiologists reviewed the CXRs as part of their regular workflow and ‘accepted’ or changed the pre-populated reports. Changes in reports were divided into ‘clinically insignificant’ and ‘clinically significant’ following which those CXRs with clinically significant changes were reviewed by a specialist chest radiologist with 8 years’ experience.
Results: A total of 1,970 adult CXRs were analysed by AI, out of which 388 (19.69%) were identified to be normal. 361/388 (93.04%) of these were accepted by radiologists and in 14/388 (3.60%) clinically less significant changes (e.g. increased broncho-vascular markings) were made in reports. Upon review of the balance 13/388 (3.35%) CXRs, it was found that 12 had truly clinically significant missed findings by AI, including 3 with opacities, 3 with lymphadenopathy, 3 with blunted CP angle, 2 with nodules, and 1 with consolidation.
Conclusion: This study shows that there is a great potential to automate the identification of normal CXRs to a great degree, with very high sensitivity.
Limitations: The evaluation is limited to the normal/abnormal classification of chest x-ray.
Ethics committee approval: Institutional ethics committee approval was obtained.
Funding: No funding was received for this work.
Author Disclosures:
V. Mahajan: nothing to disclose
V. K. Venugopal: Consultant at CARING, Other at Research collaboration, General Electric Company Research collaboration, Koninklijke Philips NV Research collaboration, Qure.ai Research collaboration, Predible Health
H. Mahajan: Other at Director, Mahajan Imaging Pvt Ltd Research collaboration, General Electric Company Research collaboration, Koninklijke Philips NV Research collaboration, Qure.ai Research collaboration, Predible Health
N. S. Batta: nothing to disclose
S. Gupta: nothing to disclose
M. Murugavel: nothing to disclose

RPS 1005b-7 11:51
AI-based understanding and visualisation of spinal MRI reports
K. Orbán, E. Szabó, A. Kicsi, P. Pusztai Phd, K. Szabó Ledenyi, P. Németh, L. Vidács Phd, Z. T. Kincses, T. Gyimóthy Dsc Phd*; Szeged/HU (orban.krisztina@outlook.hu)*

Purpose: We propose an artificial intelligence-based method for the comprehension of textual radiological reports. Thousands of reports are created annually which represent textual information that is often expressed in the native language of the radiologist. Comparison and later examination of their content are rather cumbersome. To our knowledge, we are the first to introduce an intelligent comprehension and detailed visualisation technique that supports Hungarian language reports.
Methods and materials: Our method relies on deep learning and various artificial intelligence procedures. The classification builds upon data from almost 500 anonymised reports manually annotated by two radiologists with 0.79 Cohen's kappa agreement. The classification process detects anatomic locations and pathologies with quantification, which are further specified with natural language processing techniques. Several linguistic characteristics are also addressed and negative statements and non-pathological disorders are separated.
Results: Our AI classification model achieves a three-class classification with an F-score of 90-96%. The recognised disorders are displayed in a tree structure and also highlighted in the text itself. Furthermore, they are also visualised on a schematic illustration indicating the anatomical position of the disorders. This detailed view is obtained automatically by AI and NLP methods and is not yet available in existing RIS applications.
Conclusion: We introduce an AI-based method for the automatic comprehension and visualisation of radiological reports, working currently with lumbar spine MRI reports written in Hungarian. The results can be used to filter the core of the report content and for quality assurance. Our process can be extended to other languages and to any field where large amounts of text are created routinely and would benefit from automatic processing.
Limitations: Our method currently supports reports written in Hungarian and concerning the spinal region.
Ethics committee approval: n/a
Funding: No funding was received for this work.
Author Disclosures:
L. Vidács Phd: Author at MTA-SZTE Research Group on Artificial Intelligence, University of Szeged
T. Gyimóthy Dsc Phd: Author at MTA-SZTE Research Group on Artificial Intelligence, University of Szeged
K. Orbán: Author at Department of Radiology, University of Szeged
E. Szabó: Author at Affidea Magyarország Kft.
A. Kicsi: Author at University of Szeged Department of Software Engineering
P. Pusztai Phd: Author at MTA-SZTE Research Group on Artificial Intelligence
K. Szabó Ledenyi: Author at University of Szeged Department of Software Engineering
P. Németh: Author at University of Szeged Department of Software Engineering
Z. T. Kincses: Author at Department of Radiology, University of Szeged

RPS 1005b-8 11:57
Radiology report generation using pointer networks: a step towards radiology report standardisation
A. Kharat[1], J. Tandale[2], A. Ahmad[2], R. Lokwani[2], A. Pant[2], A. Jaju[2], K. Saoji[2], A. Patil[2]*; [1]Maharashtra/IN, [2]Pune/IN (kharatamit75@gmail.com)*

Purpose: We study automated report generation using deep learning (DL) techniques to reduce radiologist's work load with the aim of creating report templates which can be used by radiologists.
Methods and materials: The dataset, available from 800+ bed hospital, contains 13,000 images along with their reports. The convolutional neural network (CNN) Chex-Net model for detecting pathologies was used, which is a 121-layer dense CNN called densenet. The original model was trained to detect 14 pathologies and we extended this model to 15 pathologies. We used the following steps to create a report template: 1) fed images into the ChexNet model to get 15 predicted probabilities for respective pathologies, 2) of the 15 predicted probabilities, the ones which exceeded the threshold value were said to be present in that image, and 3) we generate a template-based report combining the predicted pathologies with the heuristic rules provided by radiologists.
Results: A sequence to sequence (StS) model with pointer networks (PN) was used. Method: 1) The selected template is modified by a radiologist if needed and modifications by the radiologist are stored. 2) For the StS model, the created report is the input sequence while the modified report from the radiologist is the output sequence. 3) Mapping is learnt between these two sequences, one accounts for expert knowledge and the other utilises real-time expert output to further remove inconsistencies. For the randomly selected set of 100 studies, reports are generated using the proposed methodology. Generated reports are validated by 2 radiologists. Validation is done based on understanding and auto-generated reports to reduce the radiologist's time in writing reports.
Conclusion: More than 52% of reports were accepted for report generation by making minor changes and edits by our team of validating radiologists. This process can be a stepping stone towards radiology report standarisation.
Limitations: n/a
Ethics committee approval: n/a
Funding: No funding was received for this work.
Author Disclosures:
A. Kharat: Founder at deeptek.ai
J. Tandale: Employee at Deeptek
R. Lokwani: Employee at Deeptek
A. Pant: Founder at Deeptek
A. Ahmad: Employee at Deeptek
A. Jaju: Employee at deeptek
K. Saoji: Employee at deeptek
A. Patil: Founder at deeptek

RPS 1005b-9 12:03
Validation of a high precision semantic search tool using a curated dataset containing related and unrelated reports of clinically relevant search terms
V. K. Venugopal[1], N. Kumar[2], V. Jagannatha[2], V. Mahajan[1], H. Mahajan[1], S. Rajan[1], A. Shastry[2], R. Rao K.[2]*; [1]New Delhi/IN, [2]Bangalore/IN (vasanthdrv@gmail.com)*

Purpose: To validate a sematic search tool by testing the search results for complex terms.
Methods and materials: The tool consists of two pipelines: an offline indexing pipeline and a querying pipeline. The raw text from both reports and queries were first passed through a set of pre-processing steps; sentence tokenisation, spelling correction, negation detection, and word sense disambiguation. It was transformed into a concept plane followed by indexing or querying. During querying, additional concepts were added using a query expansion technique to include nearby related concepts. The validation was done on a set of 30 search queries, carefully curated by two radiologists. The reports that are related to the search queries were randomly selected with the help of keyword search and the text was re-read to determine its suitability to the queries. These reports formed the "related" group. Similarly, the reports that were not exactly satisfying the context of the search queries were categorised as the "not related" group. A set of 5 search queries and 250 reports were used for tuning the model initially. A total of 500 reports of the 10 search queries formed the corpus of the test set. The search results for each test query were evaluated and appropriate statistical analysis was performed.

Results: The average precision and recall rates on 10 unseen queries on a small corpus for respective queries containing related and unrelated reports were 0.54 and 0.42. On a larger corpus containing 60 K reports, the average precision for these 15 queries was 0.6.
Conclusion: We describe a method to clinically validate a sematic search tool with high precision.
Limitations: A small corpus of test reports.
Ethics committee approval: n/a
Funding: No funding was received for this work.
Author Disclosures:
V. K. Venugopal: Other at Research collaboration, General Electric Company Research collaboration, Koninklijke Philips NV Research collaboration, Qure.ai Research collaboration, Predible Health, Consultant at CARING
V. Mahajan: nothing to disclose
H. Mahajan: Other at Director, Mahajan Imaging Pvt Ltd Research collaboration, General Electric Company Research collaboration, Koninklijke Philips NV Research collaboration, Qure.ai Research collaboration, Predible Health
S. Rajan: nothing to disclose
V. Jagannatha: Employee at Philips Healthcare
N. Kumar: Employee at Philips Healthcare
A. Shastry: Employee at Philips Healthcare
R. Rao K.: Employee at Philips Healthcare

RPS 1005b-10 12:09

Decision support system for automated CT abdominal imaging protocol selection using natural language processing with machine learning

P. Rogalla[1], S. Carey[1], B. E. Hoppel[2], K. Noro[3], M. D. Y. Yamazaki[3], M. Y. Shimomura[3], M. Nakatsugawa[4]; *[1]Toronto, ON/CA, [2]Vernon Hills, WI/US, [3]Otawarai/JP, [4]Kawasaki/JP (kazumasa1.noro@medical.canon)*

Purpose: To evaluate the accuracy of a protocol recommendation engine with natural language processing with machine learning (NLP-ML) for automatic protocolling of abdominal CTs.
Methods and materials: 110,001 historical imaging requests for abdominal CT were extracted from a RIS database containing the executed imaging protocols and 16 associated patient information values (e.g. indication, primary diagnosis, and free-text comment). Keywords were extracted from the free-text comment by TF-IDF to create a bag-of-words feature. A multinomial naïve Bayes model was trained to classify the 9 most frequent protocols. A protocol recommendation engine with NLP-ML was developed, which interfaced to the RIS and provided radiologists with a recommended protocol and its probability based on the free-text imaging request. Three radiologists protocolled the imaging requests twice: first without and then with the aid of the protocolling engine. The radiologist categorised each recommendation as "good catch", agreement, minor error, and severe error. The accuracy of the protocolling engine was calculated by using the second selection as the ground truth.
Results: The protocolling engine's accuracy by a radiologist and an average was 84.7% (161/190), 88.0% (132/150), 90.8% (138/152), and 87.6% (431/492, p<0.001), respectively. Radiologists changed their protocolling based on the engine's recommendation ("good catch") in 2% (5/190), 1.3% (2/150), 2.6% (3/152), respectively, and on average in 2.0% (10/492) of the cases. On average, minor errors of the NLP-ML occurred in 11.2% and severe errors in 1.2% of all protocols.
Conclusion: A protocolling engine with NLP-ML shows promising accuracy and has the potential to eliminate the time consuming and tedious task of protocolling CT imaging requests.
Limitations: The number or selectable imaging protocols (9), number of readers (3), and body regions (abdomen).
Ethics committee approval: Institutional research ethics board approval.
Funding: Canon Medical Systems Corporation.
Author Disclosures:
K. Noro: Employee at Canon Medical Systems Corporation
P. Rogalla: Research/Grant Support at Princess Margaret Cancer Centre
S. Carey: Employee at Princess Margaret Cancer Centre
B. E. Hoppel: Employee at Canon Medical Research USA
M. Nakatsugawa: Employee at Canon Medical Systems Corporation
M. D. Y. Yamazaki: Employee at Canon Medical Systems Corporation
M. Y. Shimomura: Employee at Canon Medical Systems Corporation

RPS 1005b-11 12:15

Natural language processing enables a correlation of clinical information with positive findings in low-dose computed tomography in patients with suspected urolithiasis

T. Jorg[1], B. Kämpgen[2], P. Mildenberger[1], C. Düber[1], P. Mildenberger[1], F. Jungmann[1]; *[1]Mainz/DE, [2]Rimpar/DE (tobias.jorg@googlemail.com)*

Purpose: To automatically extract clinical and epidemiological information from past narrative radiological reports on low-dose computed tomography (CT) for suspected urolithiasis using natural language processing (NLP) and to correlate findings with clinical information.
Methods and materials: Narrative reports of low dose CT-examinations of the retroperitoneum from 04/2016 to 07/2018 (n=1714) were analysed using NLP. Reports were automatically structured based on RadLex® concepts. Manual feedback was used to test and train the NLP engine to reach adequate test accuracy (F1-Score ≥0.80). Chi-square test, phi-coefficient, and logistic regression were performed to determine the effects of clinical information on the positive hit rate of urolithiasis.
Results: Urolithiasis was affirmed in 72% of the reports. In 38% of the reports, at least one stone was described in the kidneys and in 45% in the ureter. In 22% of the reports, patients suffered from combined nephrolithiasis and ureterolithiasis.
Affirmed clinical information such as previous stone history and obstructive uropathy could be found significantly more frequently in reports with affirmed urolithiasis (p=.001). The combination of obstructive uropathy and loin pain showed the highest rate for positive urolithiasis with an odds ratio of 1.16.
Conclusion: Generating data from past radiological reports allows for the calculating of positive hit rates for pathologies, which can be used for epidemiological studies or to evaluate the appropriateness of CT-examinations. The evaluation of our data indicates that the occurrence of clinical information such as stone history and obstructive uropathy, or a combination of obstructive uropathy and loin pain, was higher in patients with affirmed urolithiasis. NLP can collect and monitor the data automatically in high quality.
Limitations: Clinical information may not be revealed correctly or entirely by the referring physicians which could lead to limitations.
Ethics committee approval: n/a
Funding: No funding was received for this work.
Author Disclosures:
T. Jorg: nothing to disclose
P. Mildenberger: nothing to disclose
F. Jungmann: nothing to disclose
P. Mildenberger: nothing to disclose
C. Düber: nothing to disclose
B. Kämpgen: nothing to disclose

RPS 1005b-12 12:21

Development of a software application for the automatic determination of CT protocols using natural language processing

A. Ciritsis, T. Frauenfelder, C. Rossi, A. Boss; *Zurich/CH (alexander.ciritsis@usz.ch)*

Purpose: To develop a software application for CT protocol determination using natural language processing (NLP) based on free-text classification and to evaluate the agreements by comparing protocols determined via NLP with those determined by radiologists.
Methods and materials: The database of report information system (RIS) was queried for a list of CT examinations with the referring department and its corresponding medical questioning, suspected diagnosis, and conducted CT protocol over a period of one year. For each of the departments referring patients to the radiological institution, three separate models for most common, less common, and rare protocols based on a support vector machine (SVM) and term frequency–inverse document frequency (TFIDF) were trained. Thereby, the medical questioning, as well as the suspected diagnosis by the referring department, served as features and the conducted CT protocol as a label.
Results: After data query in a total of 7,211 CT examinations with the referring department, corresponding medical questioning and suspected diagnosis were extracted. Medical questioning and suspected diagnosis formulated by the referring department were combined and preprocessed using predefined stop words and regular expressions before being translated into a feature space for the SVM via TFIDF. 15 different models for the most frequent referring departments were trained and model accuracy varied from 71% to 92%. For eventual implementation, a GUI implementing the previously trained models was developed.
Conclusion: NLP shows promising results in the automation and standardisation of CT protocol determination. The presented technology may be integrated into the clinical routine and result in a lean workflow for CT protocol determination in radiological institutions.
Limitations: Models were trained on clinical data from only one institution.
Ethics committee approval: Ethics committee approval obtained.
Funding: SPHN project NLPforTC.
Author Disclosures:
A. Ciritsis: nothing to disclose
T. Frauenfelder: nothing to disclose
A. Boss: nothing to disclose
C. Rossi: nothing to disclose

11:15 - 12:30 **Tech Gate Auditorium**

Cardiac

RPS 1003b

Transcatheter structural cardiac intervention: TAVI and beyond

Moderators:
F. Michallek; Berlin/DE
N.N.

RPS 1003b-K 11:15
Keynote lecture
C. Celeng; *Utrecht/NL (celengcsilla@gmail.com)*

Author Disclosures:
C. Celeng: nothing to disclose

RPS 1003b-1 11:25
Morphometric and subjective frailty assessment in transcatheter aortic valve implantation
M. Giannoudi[1], M. A. Waduud[2], M. Drozd[1], T. Slater[1], P. P. J. Sucharitkul[1], D. Blackman[1], J. Scott[1]; *[1]Leeds/UK, [2]Glasgow/UK (ll16ppjs@leeds.ac.uk)*

Purpose: To determine the prognostic impact of objective and subjective measures of frailty and their relationship to existing validated assessment methods after transcatheter aortic valve implantation (TAVI).
Methods and materials: Consecutive patients were identified from the Leeds Teaching Hospital Trust TAVI database. Frailty was quantified objectively by measuring total psoas muscle area (TPMA) on routine CT scans and subjectively using a clinician-based judgement of overall frailty, termed the Leeds-Subjective Assessment of Frailty in the Elderly (L-SAFE) score. Post-intervention morbidity and mortality were examined between these scoring systems and validated scoring systems.
Results: This study included 420 patients having undergone TAVI between January 2013 and December 2015. Median clinical follow-up was 4.0 years (IQR 2.9-5.0). Standardised measurements of TPMA were not associated with overall all-cause mortality (adjusted HR 1.11, 95% CI 0.94 to 1.31, p=0.206). The L-SAFE score was associated with the duration of hospital stay (adjusted regression co-efficient -0.93, 95% CI -1.71 to -0.15, p=0.019) and overall all-cause mortality (adjusted HR 0.66, 95% CI 0.53 to 0.82, p<0.001). Only the L-SAFE score significantly correlated with traditional methods of frailty assessment.
Conclusion: We demonstrate a purely subjective measure of frailty to be prognostic in determining post-TAVI morbidity and mortality when compared to the measurement of the TPMA.
Limitations: The retrospective nature of the study meant that there were elements of data that could not be collected. The biggest weakness is the lack of interobserver measurements for the L-SAFE score, however, this is the start of our team's work using this scoring system with the aim of further research including multiple assessor scores.
Ethics committee approval: n/a
Funding: No funding was received for this work.
Author Disclosures:
M. Giannoudi: nothing to disclose
M. A. Waduud: nothing to disclose
M. Drozd: nothing to disclose
T. Slater: nothing to disclose
D. Blackman: nothing to disclose
J. Scott: nothing to disclose
P. P. J. Sucharitkul: nothing to disclose

RPS 1003b-2 11:31
Possibility of estimating the aortic valve calcium score based on the angiographic phase of multidetector computed tomography performed before transcatheter aortic valve implantation
P. Gac, B. Kedzierski, P. Macek, G. Mazur, R. Poreba, K. Pawlas; *Wroclaw/PL (pawelgac@interia.pl)*

Purpose: To assess the possibility of estimating the aortic valve calcium score (AVCS) based on the angiographic phase of multidetector computed tomography (MDCT) performed before transcatheter aortic valve implantation (TAVI).
Methods and materials: The study group consisted of 31 patients who had undergone two-phase MDCT of the heart and large vessels before TAVI: the native phase for AVCS assessment and the angiographic phase for assessment of the aortic valve size and assessment of the access route. Mean age was 78.61±6.04 years. The semi-automatic evaluation of AVCS in slices thickness 3 mm and 2 mm ($AVCS_{native3.0}$ and $AVCS_{native2.0}$) was made on the basis of the native phase. Using the angiographic phase, AVCS was estimated for slices thickness 0.6 mm, with increased differentiation thresholds for contrasting aortic lumen with calcifications in the aortic valve from a typical 130 HU to 500 HU and 600 HU ($AVCS_{CTA0.6\ 500HU}$and $AVCS_{CTA0.6\ 600HU}$).
Results: AVCS measured by various methods were: $AVCS_{native3.0}$- 3640.58±2289.03, $AVCS_{native2.0}$- 3397.09±2138.25, $AVCS_{CTA0.6\ 500HU}$- 1871.94±1304.46, and $AVCS_{CTA0.6\ 600HU}$- 1586.06±1723.89. There were statistically significant positive linear correlation between AVCS values evaluated on the basis of the native phase and AVCS values estimated on the basis of the angiographic phase: r $AVCS_{native3.0}$ vs. $AVCS_{CTA0.6\ 500HU}$ - 0.90, r $AVCS_{native3.0}$ vs. $AVCS_{CTA0.6\ 600HU}$ - 0.40, r $AVCS_{native2.0}$ vs. $AVCS_{CTA0.6\ 500HU}$ - 0.89, and r $AVCS_{native2.0}$ vs. $AVCS_{CTA0.6\ 600HU}$ - 0.39. Using regression analysis, mathematical formulas for calculating native AVCS based on AVCS values estimated on the basis of angiographic phase were defined: $AVCS_{native3.0}$= 644.7+1.8 $AVCS_{CTA0.6\ 500HU}$, $AVCS_{native3.0}$= 2922.1+0.5 $AVCS_{CTA0.6\ 600HU}$, $AVCS_{native2.0}$= 689.2+1.6 $AVCS_{CTA0.6\ 500HU}$, and $AVCS_{native2.0}$= 2789.4+0.5 $AVCS_{CTA0.6\ 600HU}$.
Conclusion: AVCS can be reliably estimated using only the angiographic phase of MDCT of the heart and large vessels.
Limitations: Small size of study group
Ethics committee approval: Wroclaw Medical University Bioethical Committee.
Funding: No funding was received for this work.
Author Disclosures:
P. Gac: nothing to disclose
B. Kedzierski: nothing to disclose
P. Macek: nothing to disclose
G. Mazur: nothing to disclose
R. Poreba: nothing to disclose
K. Pawlas: nothing to disclose

RPS 1003b-3 11:37
CT-coronary angiography in high-pitch-TAVI-planning-CT: why it rarely works
P. Seitz, R. F. Gohmann, S. Gottschling, D. Holzhey, H. Thiele, M. Abdel-Wahab, C. Lücke, C. D. Krieghoff, M. Gutberlet; *Leipzig/DE*

Purpose: Depiction of the access-route and annular dimensions are essential prior to transcatheter-aortic-valve-implantation (TAVI). Seemingly coincidently, coronary-arteries are sometimes depicted diagnostically. In this analysis, we investigated factors influencing the diagnostic depiction of coronary-arteries in pre-TAVI-CT.
Methods and materials: 100 patients (46 women; mean age 79,0±5,9 years) were retrospectively included. All patients underwent dual-source-CT-scans (Siemens, Definition FLASH) in prospectively-ECG-triggered-high-pitch-mode after injecting 70 ml contrast-medium (Iomeprol 400 mg iodine/ml, Flow 3,5 ml/s) for evaluation of the access route and annular dimensions.
The number of diagnostic coronary-segments per patient (DSpP) was determined and set in relation to heartrate, BMI, coverage along the z-axis (CaZA), and heart-rhythm.
Results: Overall, 30.3% of coronary-segments were diagnostically depicted. Mean heartrate correlated inversely with DSsP (75±19 bpm; r=-0,35; p<0,001). CaZA (% of RR-interval) correlated inversely with DSpP (r=-0,33; p<0,001). CaZA correlated strongly with heartrate (r=0,71; p<0,0001). BMI correlated negatively with DSpP (r=-0,26; p<0,01).
DSpP was not significantly different between patients with atrial fibrillation and sinus rhythm (p=0,11). Mean heart rate variability was 15±23 bpm and showed no correlation to DSpP (p=0,11; r=0,256).
Conclusion: Fully diagnostic studies in high-pitch-TAVI-planning-CT are rare and only occur under very special circumstances (low heartrate and narrow CaZA). Nevertheless, relevant coronary-findings can frequently be observed with this technique.
The most significant factors influencing DSsP are CaZA, HR, and BMI. As all these parameters are either intrinsic to the patient or are difficult to influence in this patient collective, fully diagnostic exams are rare with this technique. However, limiting the FoV to optimise scan metrics could improve the frequency of fully diagnostic studies and should be investigated further.
Limitations: Retrospective study design.
Ethics committee approval: The study was approved by the local ethics committee.
Funding: No funding was received for this work.
Author Disclosures:
P. Seitz: nothing to disclose
D. Holzhey: nothing to disclose
R. F. Gohmann: nothing to disclose
M. Abdel-Wahab: nothing to disclose
S. Gottschling: nothing to disclose

H. Thiele: nothing to disclose
C. Lücke: nothing to disclose
C. D. Krieghoff: nothing to disclose
M. Gutberlet: nothing to disclose

RPS 1003b-4 11:43

Sinus of Valsalva thrombosis detected on computed tomography after transcatheter aortic valve replacement

S. J. Lim, H. J. J. Koo, J.-W. Kang, D. H. Yang; *Seoul/KR*
(vitamindasa@hanmail.net)

Purpose: Leaflet thrombosis after transcatheter aortic valve replacement (TAVR) has been reported recently, whereas thrombosis in the sinus of Valsalva has not been fully evaluated. We described the clinical and radiological findings of the patients with sinus of Valsalva thrombosis using cardiac computed tomography (CT).
Methods and materials: Between March 2011 and August 2019, 192 patients underwent cardiac CT after TAVR. In this study, after retrospective review of the CT images, we included 8 patients who had sinus of Valsalva thrombosis identified on cardiac CT. Patients demographics, the interval between TAVR and cardiac CT scan, location and CT attenuation of sinus of Valsalva thrombosis, and presence of concurrent leaflet thrombosis were collected.
Results: The median interval between TAVR and cardiac CT was 11 days. Sinus of Valsalva thrombosis was frequently detected in a non-coronary sinus (88%) and mainly located in the bottom of the sinus (100%), growing up to the sinotubular junction. 2 patients had concomitant leaflet thrombosis and 3 patients had subclinical ischemic stroke on the brain magnetic resonance imaging. All patients had taken aspirin and clopidogrel after TAVR for at least 6 months without anticoagulation.
Conclusion: Cardiac CT after TAVR can detect sinus of Valsalva thrombosis and attention should be paid to this potential source of systemic embolisation.
Limitations: Selection bias could not be avoided because it was a retrospective observational study. We could not know when the sinus of Valsalva thrombosis had developed because we obtained CT scans with various time intervals. We could not suggest the optimal antithrombotic therapy for the sinus of Valsalva thrombosis, leaflet thrombosis, or post-TAVR strokes.
Ethics committee approval: This study was approved by Institutional Review Board of our hospital (Approval number: 2019-0312). Informed consent; n/a
Funding: No funding was received for this work.
Author Disclosures:
S. J. Lim: nothing to disclose
H. J. J. Koo: nothing to disclose
J.-W. Kang: nothing to disclose
D. H. Yang: nothing to disclose

RPS 1003b-5 11:49

The impact of coronary artery disease and pre-procedural percutaneous coronary intervention on the short and long-term mortality after transcatheter aortic valve implantation

T. P. W. van Den Boogert, J. Vendrik, J. Gunster, M. van Mourik, B. Claessen, F. van Kesteren, N. R. Planken, J. Baan, J. Henriques; *Amsterdam/NL*
(t.p.vandenboogert@amsterdamumc.nl)

Purpose: Coronary artery disease (CAD) is a common concurrent condition in patients receiving transcatheter aortic valve replacement (TAVR), but consensus on the prognostic implications of CAD and its pre-procedural treatment with percutaneous coronary intervention (PCI) is missing. If we could select the coronary segments in which pre-procedural PCI treatment will have a positive effect on the outcome, we could evaluate these segments for CAD on pre-procedural CTA.
Methods and materials: An institutional TAVR database was complemented with data extracted from coronary angiography and PCI reports. The extent of CAD, lesion location, lesion severity, and the location of PCI were scored. Survival analysis was performed to investigate the impact on mortality within 3 years after TAVR.
Results: Among the 1,514 included patients, the mean age was 82 years, 55% were female, 31% had diabetes mellitus, and CAD prevalence was 55%. Survival analysis revealed no significant association of CAD extent on mortality, but significant LAD-lesions (≥70% DS) were significantly associated with increased 3-year and short-term mortality (HR:1.6, 95%CI:1.0-2.4 and HR:3.4, 95%CI:1.4-8.1, respectively). Pre-procedural PCI of unselected lesions was significantly associated with an increased 3-year and short-term mortality (HR:1.7, 95%CI:1.0-2.7 and HR:2.3, 95%CI:1.1-4.9, respectively), but selective PCI of proximal lesions resulted in comparable mortality rates.
Conclusion: Not the extent of CAD but only significant LAD lesions are independently associated with higher mortality after TAVR. Pre-procedural PCI of unselected lesions is also associated with higher mortality, but there was no significant difference in mortality between patients with and without selective pre-procedural PCI of proximal LAD and LM lesions.
Limitations: Single-centre, non-randomised cohort and we used CAG and PCI reports from local and referral hospitals.
Ethics committee approval: n/a
Funding: No funding was received for this work.
Author Disclosures:
T. P. W. van Den Boogert: nothing to disclose
N. R. Planken: nothing to disclose
J. Henriques: nothing to disclose
J. Vendrik: nothing to disclose
J. Gunster: nothing to disclose
M. van Mourik: nothing to disclose
B. Claessen: nothing to disclose
F. van Kesteren: nothing to disclose
J. Baan: nothing to disclose

RPS 1003b-6 11:55

Cardiac computed tomography versus transoesophageal echocardiography in preoperative sizing of ostium secundum atrial septal defect prior to transcatheter closure

S. T. Wong[1], T. Pressat-Laffouilhère[1], K. Warin Fresse[2], S. Bejar[1], F. Bauer[1], J.-N. Dacher[1]; [1]*Rouen/FR*, [2]*Nantes/FR*
(tatianawong27@gmail.com)

Purpose: To investigate the feasibility and accuracy of cardiac multidetector computed tomography (MDCT) prosthesis sizing of ostium secundum atrial septal defect (ASD).
Methods and materials: 70 consecutive patients were included in this retrospective bicentric study between May 2012 and June 2018. They underwent cardiac MDCT and transoesophageal echocardiography (TEE) before transcatheter closure of ASD; dimensions of the defect and peripheral rims were measured. Defect measurements obtained at TEE and MDCT were compared to prosthesis size. Our primary criterion was the comparison of ASD maximal diameter obtained at MDCT (CT-Dmax) to prosthesis size. Intraclass correlation coefficient (ICC), Bland Altman plots, and linear regression were calculated. Intraobserver and interobserver agreement were calculated for MDCT defect measurements.
Results: 43 patients were finally included for defect measurements: 17 did not undergo transcatheter closure and 10 had incomplete data. For CT-Dmax, ICC was 0.88 (CI95% = [0.78 – 0.93]; p=0.06), mean difference was – 0.82 +/- 5.73 mm, and regression linear equation was 0.9 x + 3.2 ($p < 0.001$). For maximal diameter at TEE versus prosthesis size, ICC was 0.46 (CI95% = [0.21 – 0.61]; $p = 0.003$), mean difference was – 6.06 +/- 8.26 mm, and regression linear equation was 0.91 x + 7.6 ($p < 0.001$). Intraobserver and interobserver agreement for CT-Dmax was 0.97 (CI95% = [0.95 – 0.98]) and 0.86 (CI95% = [0.73 – 0.93]), respectively.
Conclusion: MDCT is a reliable tool for sizing the defect of ostium secundum ASD, making it an accurate alternative to pre-procedural TEE.
Limitations: Retrospective and small cohort.
Ethics committee approval:
The institutional review board approved this retrospective study and informed consent was waived.
Funding: No funding was received for this work.
Author Disclosures:
S. T. Wong: nothing to disclose
T. Pressat-Laffouilhère: nothing to disclose
K. Warin Fresse: nothing to disclose
S. Bejar: nothing to disclose
F. Bauer: nothing to disclose
J.-N. Dacher: nothing to disclose

RPS 1003b-7 12:01

Role of CT in the preoperatory setting of transcatheter mitral valve interventions: which is the correct phase for mitral annulus sizing?

V. Nicoletti, A. Palmisano, D. Vignale, L. Pannone, C. Colantoni, A. Del Maschio, F. de Cobelli, A. Esposito; *Milan/IT (nicoletti.valeria@hsr.it)*

Purpose: Transcatheter mitral valve interventions (TMVI) are emerging as alternative treatments in patients with severe mitral regurgitation (MR) who are non-eligible for surgery. Cardiac CT plays a crucial role in TMVI planning, guiding the assessment of patient suitability, prosthesis sizing, and access planning. However, the entity of the modifications of mitral valve geometry throughout the cardiac cycle and the best phase for annulus sizing are still unclear.
Methods and materials: 44 patients with severe MR candidate to TMVI (3 type-I, 16 type-II, 10 type-IIIa, 15 type-IIIb according to Carpentier classification) and 21 patients without significative MR (control group) were retrospectively evaluated. Each patient underwent a multiphase (0-90%) retrospective ECG-gated cardiac CT. Mitral valve annulus was manually extracted every 10% steps

of the R-R interval, according to the recommended D-shape segmentation model.
Results: Patients with severe MR had enlarged left ventricle (LV-EDV=248,7±112,2 ml) and atrium (LA-ESV=201,6±71,1 ml) with reduced ejection fraction (EF=40,5±15,9%) compared to control patients (p<0,05). Moreover, MR patients showed larger maximum annular area (16,0±4,0 vs 9,5±1,8cm²; p<0,001), particularly in the case of type-II MR. Only the TT diameter showed no significant difference between the two groups (p=0,252). In MR patients, the largest annular area was found predominantly (48%;21/44) during systolic phases (20-40%), while in control patients (67%;14/21) during proto-diastolic phases (40-60%). In the remaining patients, the maximum area was randomly distributed among the remaining phases.
Conclusion: We can conclude that a multiphase acquisition with the inclusion of the systole and a personalised approach to the segmentation of the mitral annulus could be important for the correct planning of TMVI.
Limitations: Limited sample size. No comparative data in a population without MR.
Ethics committee approval: This study has been approved by the istitutional review board.
Funding: No funding was received for this work.
Author Disclosures:
V. Nicoletti: nothing to disclose
A. Palmisano: nothing to disclose
D. Vignale: nothing to disclose
L. Pannone: nothing to disclose
C. Colantoni: nothing to disclose
A. Del Maschio: nothing to disclose
F. de Cobelli: nothing to disclose
A. Esposito: nothing to disclose

RPS 1003b-8 12:07
Predictors of cerebral embolisation after percutaneous transfemoral aortic valve implantation: a RETORIC substudy
F. I. Suhai, A. Varga, B. Szilveszter, J. Karady, A. Panajotu, A. Bartykowszki, A. I. Nagy, B. Merkely, P. Maurovich-Horvat*; Budapest/HU*
(suhaiimi987@gmail.com)

Purpose: To evaluate the predictors, occurrence, and distribution of TAVI-related silent ischemic brain lesions using diffusion MRI.
Methods and materials: We investigated 109 consecutive patients from the prospective arm of the RETORIC study (NCT02826200) who underwent brain MRI one week after percutaneous transfemoral aortic valve implantation (TAVI). To determine the occurrence and distribution of periprocedural cerebral ischemic lesions, averaged diffusion-weighted images (trace), and mean diffusivity (MD) maps from the DTI dataset were used. To evaluate the aortic valve calcium score (AVCS), we assessed the preoperative prospectively ECG-triggered cardiac CT (256-slice MDCT). We also assessed the periprocedural factors such as periprocedural time and pre- and postdilatation. Linear regression analysis was performed to identify the independent predictors of TAVI-related ischemic lesions.
Results: After TAVI, a total of 918 new cerebral ischemic lesions were detected in 100/109 patients (92%). The median ischemic lesion volume was 237 µl (interquartile range 89.5-650) with a median lesion number of 6 (2-10) per patient. 759/918 lesions (83%) were supratentorial (389 left vs. 370 right). Most lesions (628/918, 68%) were subcortical; the left and right MCA territories were the most affected (left: 190/918, 21% vs. right: 177/918,19%). The vast majority of ischemic lesions were clinically silent (96%); 4% of patients had a stroke which was proven by MRI. The median AVCS was 2,769 (interquartile range 1,858-4,537). Ballon pre-dilatation during TAVI procedure showed significant correlation with increased total ischemic lesion volume (p<0.001, ß = 0.370) on univariate analysis, AVCS, periprocedural time, or post-dilatation were not associated with ischemic load on MRI (p>0.05).
Conclusion: Periprocedural ischemic lesions are frequent (92%), however, most of them are clinically silent. Only balloon pre-dilatation during TAVI was a predictor of increased ischemic load.
Limitations: n/a
Ethics committee approval: Written informed consent.
Funding: No funding was received for this work.
Author Disclosures:
F. I. Suhai: nothing to disclose
A. Varga: nothing to disclose
B. Szilveszter: nothing to disclose
J. Karady: nothing to disclose
A. Panajotu: nothing to disclose
A. Bartykowszki: nothing to disclose
A. I. Nagy: nothing to disclose
B. Merkely: nothing to disclose
P. Maurovich- Horvat: nothing to disclose

RPS 1003b-9 12:13
Combined coronary CT-angiography and TAVI-planning: a contrast-neutral and efficient routine approach to exclude significant coronary artery disease
R. F. Gohmann, P. Lauten, C. D. Krieghoff, P. Seitz, C. Lücke, M. Abdel-Wahab, D. Holzhey, H. Thiele, M. Gutberlet*; Leipzig/DE*
(robin.gohmann@gmx.de)

Purpose: To analyse the ability of coronary CT-angiography (cCTA) for ruling out significant coronary artery disease (CAD) during routine evaluation for transcatheter aortic valve implantation (TAVI) in patients with a high pre-test probability of CAD.
Methods and materials: 460 consecutive patients undergoing pre-TAVI-evaluation (238 women; mean-age 79,6±7,4 years) were retrospectively included. Patients with prior CABG were excluded. All patients were examined with a standard protocol consisting of a retrospectively gated CT-scan of the heart, immediately followed by a high-pitch scan of the vascular access route utilising a single bolus of 70 ml iodinated contrast-medium. No beta-blockers or nitrates were applied.
Heart rate and heart rate variability during the scan were 74,5±19,5 and 23,3±33,2 beats per minute; attenuation at the ascending was 465,4±145,4 HU. Images were evaluated for significant CAD (stenosis >50%); examinations where CAD could not be ruled out were read as positive. Patients routinely received invasive coronary angiography (ICA) 84,3% (388/460), which was omitted if the renal function was impaired and CAD could be ruled out on cCTA. All stenoses visually identified on ICA were graded qualitatively (QCA) using the same cut-off.
Results: cCTA could rule out for significant CAD in 40,2% (188/460). As detailed in the table, sensitivity, specificity, PPV, NPV, and accuracy per patient were 97,8%, 45,2%, 49,6%, 97,4%, and 63,9%, respectively. The stenoses additionally identified on ICA were located in the mid LAD, mid RCA, or obtuse marginal 1.
Conclusion: cCTA and pre-TAVI-evaluation can be performed jointly with no need for additional contrast medium or medication. cCTA is able to exclude significant CAD in a relatively high proportion of this high-risk collective. Thereby cCTA can reduce the number of ICA and the total amount of contrast-medium needed, with the potential of making pre-procedural-evaluation for TAVI-Planning safer and faster.
Limitations: Retrospective study design.
Ethics committee approval: This study was approved by the local ethics committee.
Funding: No funding was received for this work.
Author Disclosures:
R. F. Gohmann: nothing to disclose
P. Lauten: nothing to disclose
C. D. Krieghoff: nothing to disclose
P. Seitz: nothing to disclose
C. Lücke: nothing to disclose
M. Abdel-Wahab: nothing to disclose
D. Holzhey: nothing to disclose
H. Thiele: nothing to disclose
M. Gutberlet: nothing to disclose

RPS 1003b-10 12:19
Cardiac magnetic resonance imaging parameters of right ventricular function predict mortality in a cohort of patients undergoing transcatheter aortic valve implantation (TAVI)
J. Schmid, C. Kamml, D. Zweiker, D. Hatz, A. Schmidt, M. Fuchsjäger, A. Zirlik, J. Binder, P. Rainer*; Graz/AT (johannes.schmid@medunigraz.at)*

Purpose: Recent studies show that right ventricular (RV) function is closely associated with the outcome of different cardiac conditions. This study aims to evaluate the value of RV functional parameters obtained from cardiac magnetic resonance imaging (cMR) for predicting mortality in patients undergoing transcatheter aortic valve implantation (TAVI).
Methods and materials: Patients with severe aortic stenosis were prospectively recruited to undergo cMR before TAVI. After exclusion of 11 patients due to insufficient image quality, cMR images of 112 patients (mean age 82±6 years; 34% women) were analysed using dedicated tissue tracking software (Circle cvi42). Obtained parameters included RV ejection fraction (RV-EF), RV global longitudinal, circumferential strain (RV-GLS, RV-GCS), RV longitudinal systolic velocity (RV-vel), left ventricular ejection fraction (LV-EF), and left ventricular global circumferential strain (LV-GCS).
Results: Mean follow-up was 3.5±1.8 years. Mortality after one and three years was 14% (16/112) and 29% (32/112), respectively.
RV-EF, RV-GLS, and RV-vel significantly predicted 3-year-all-cause-mortality in univariate Cox-regression (p=0.012, p=0.033, p=0.007), while RV-GCS, LV-EF, and LV-GCS did not (p=0.25, p=0.32, p=0.33). Results remained significant for RV-EF and RV-vel when adjusted for sex and age (p=0.015, p=0.013).

In ROC-analysis, RV-EF, RV-GLS, and RV-vel (AUC=0.64; 0.62; 0.63) outperformed current clinical risk scores (EuroSCORE-II, AV-Score, STS-Score) in predicting 3-year-all-cause-mortality.
Conclusion: cMR-derived RV functional parameters, especially parameters of longitudinal contraction, predicted mortality in our cohort. They performed better than left ventricular functional parameters and currently used clinical risk scores, and may improve outcome-prediction after TAVI.
Limitations: Only patients without contraindications for cMR were included, which may potentially bias the study cohort.
Ethics committee approval: The study was approved by the local ethics committee. Patients provided written informed consent.
Funding: No funding was received for this work.
Author Disclosures:
J. Schmid: nothing to disclose
C. Kamml: nothing to disclose
D. Zweiker: nothing to disclose
D. Hatz: nothing to disclose
A. Schmidt: nothing to disclose
M. Fuchsjäger: nothing to disclose
J. Binder: nothing to disclose
P. Rainer: nothing to disclose
A. Zirlik: nothing to disclose

RPS 1003b-12 12:25
Imaging of the left atrial appendage prior to occluder device placement: introduction of a new single-contrast bolus dual-phase protocol adapted to spectral-detector CT
K. R. Laukamp[1], S. Dastmalchian[2], L. Ciancibello[2], L. Pennig[1], C. Nelles[1], T. Hickethier[1], R. Gilkeson[2], A. Gupta[2]; [1]Cologne/DE, [2]Cleveland, OH/US (kai.laukamp@uk-koeln.de)

Purpose: Preimplantation cardiac-CT is ideal for assessing left-atrial-appendage (LAA) regarding size for selection of proper device and detection of contraindications such as in situ thrombi. Due to poor contrast-medium distribution in arterial-phase, the distinction between artificial filling-defects versus true thrombi is difficult. A delayed-phase is required for confirmation, which needs a second bolus to maintain adequate contrast. In this study, we investigated if a second bolus can be omitted when virtual-monoenergetic-images (VMI) from dual-energy spectral-detector-CT (SDCT) are used to enhance contrast in the delayed-phase.
Methods and materials: 51 consecutive patients undergoing SDCT-imaging of the LAA were prospectively included. Imaging-protocol comprised dual-phase acquisitions with single-bolus contrast-injection. Conventional images (CI) from both phases and 40keV VMI from the delayed-phase were reconstructed. Mean and standard deviation of attenuation were calculated by placing regions-of-interest in the LAA, left-atrium (LA), and pericardial fat. Additionally, two radiologists evaluated conspicuity, homogeneity of contrast distribution, and diagnostic certainty for the presence of a thrombus.
Results: The difference of mean attenuation between LAA and LA was significantly lower in the delayed-phase (arterial-phase: 10.8±37.7HU, delayed-phase: 2.1±12.5HU, p<0.05), indicating more homogenous contrast distribution. The contrast of the LAA decreased significantly in the delayed-phase, but was significantly improved by VMI; attenuation and image quality parameters were comparable to CI of the arterial-phase (attenuation/SNR/CNR, CI arterial-phase: 263.9±116.9HU/13.9±7.3/6.4±3.9; CI delayed-phase: 106.2±35.2HU/5.8±3.1/1.0±0.9; VMI delayed-phase 256.6±108.5/17.7±10.7/4.7±3.4). The subjective reading confirmed the objective findings and showed significantly improved diagnostic certainty for the evaluation of the LAA when VMI of the delayed phase were used.
Conclusion: The investigated single-bolus dual-phase acquisition protocol improved visualisation of the LAA; homogeneity of contrast media was higher in the delayed-phase while VMI could maintain high contrast and image quality comparable to arterial-phase.
Limitations: No echocardiography for evaluaiton of presence of LAA-thrombus was available.
Ethics committee approval: IRB-approved.
Funding: No funding was received for this work.
Author Disclosures:
K. R. Laukamp: nothing to disclose
L. Ciancibello: nothing to disclose
S. Dastmalchian: nothing to disclose
L. Pennig: nothing to disclose
C. Nelles: nothing to disclose
T. Hickethier: nothing to disclose
R. Gilkeson: nothing to disclose
A. Gupta: nothing to disclose

14:00 - 15:30 **Room X**

Student Session

S 11

My scientific paper in the field of neuroimaging

Moderator:
D. Negru; Iasi/RO

S 11-1 14:05
Direct detection of metabolic changes in rat brain slices during perfusion arrest: implications for imaging of cerebral ischaemia with hyperpolarised MR
D. Shaul[1], B. Grieb[2], G. Sapir[1], S. Uppala[1], J. Sosna[1], J. M. Gomori[1], R. Katz-Brull[1]; [1]Jerusalem/IL, [2]Ravensburg/DE

Purpose: The DAWN trial has shown that patients with acute stroke who had a mismatch between clinical deficit and infarct volume could benefit from endovascular thrombectomy even 24h after the onset of stroke. As the assessment of the patients' neurological deficits is by definition a subjective assessment, it raises the need for an objective marker of salvageable brain tissue. Perfused brain slices prove an *ex-vivo* model of the brain in which the perfusion can be controlled. In this study, we were interested in monitoring instantaneous changes in lactate dehydrogenase (LDH) and pyruvate dehydrogenase (PDH) activities in perfused rat brain slices by hyperpolarised [1-^{13}C] pyruvate MRS. The slices were exposed to an ischaemic insult which was achieved by arrested-perfusion. In this model, [1-^{13}C] pyruvate delivery is not hindered by the blood-brain-barrier and therefore its metabolism by brain cells can be determined directly.
Methods and materials: Brain slices were produced from Sprague-Dawley rats (n=11) and placed in an NMR tube perfused with oxygenated aCSF. In the control group (n=6), well-oxygenated [1-^{13}C] pyruvate was administered continuously. In the arrested-perfusion group (n=5), the perfusion was stopped 30 seconds before the injection of [1-^{13}C] pyruvate. LDH and PDH activities were quantified by measuring the production of [1-^{13}C] lactate and [^{13}C] bicarbonate with product-selective-saturating-excitations that were designed to quantify enzymatic rates.
Results: During 94 seconds of ischaemic insult, LDH activity increased by 56±25% and PDH activity decreased by 51±16% (n=5). No significant changes in LDH nor PDH activities were observed in the control group (n=6).
Conclusion: Hyperpolarised [1-^{13}C] pyruvate MRS shows promise in identifying the dynamically changing ischaemic penumbra as it could detect rapidly and non-invasively temporal changes in cerebral metabolic activity following ischaemia.
Limitations: Further research is needed to test this approach *in-vivo*.
Ethics committee approval: The study was approved by the Hebrew-University Institutional-Animal-Care
Funding: Horizon-2020.
Author Disclosures:
D. Shaul: nothing to disclose
G. Sapir: nothing to disclose
J. M. Gomori: nothing to disclose
B. Grieb: nothing to disclose
R. Katz-Brull: nothing to disclose
S. Uppala: nothing to disclose
J. Sosna: nothing to disclose

S 11-2 14:15
Evaluation of the diagnostic role of shear-wave elastography in patients with carpal tunnel syndrome
S. A. Seyed Mokhtari[1], A. Mohammadi[2], A. Afshar[2]; [1]Tabriz/IR, [2]Urmia/IR (armanmxt@yahoo.com)

Purpose: To evaluate median nerve (MN) stiffness by quantitative shear-wave elastography (SWE) in patients with carpal tunnel syndrome (CTS).
Methods and materials: A total of 124 wrists of 62 patients (36 CTS patients and 26 healthy subjects), bilaterally, were enrolled in the study. All diagnoses in patients and controls were confirmed with nerve conduction studies (NCS). High-resolution ultrasonography (US) and SWE were performed on the MN and cross-sectional area (CSA) and nerve stiffness was measured. The t-test was performed to compare CSA and SWE of the nerve in the CTS, control, and subgroups based on NCS tests. ROC analysis was also performed. P<0.05 was considered as significant.
Results: Patients with CTS had higher elasticity values of MN (55.53±18.54 kPa) compared to control subjects (23.05±9.97 kPa) (P<0.0001). Patients with moderate-severe CTS had higher elasticity values (59.88±15.69 kPa) compared

to patients with mild CTS (46.79±20.47 kPa) (P=0.006). A 34.0-kPa cut-off value on SWE revealed a sensitivity, specificity, PPV, NPV, and accuracy of 92.85%, 90.74%, 92.85%, 90.74%, and 91.93%, respectively.
Conclusion: Median nerve stiffness at the carpal tunnel inlet is significantly higher in patients with carpal tunnel syndrome. These findings suggest that the SWE-based stiffness measurement of the median nerve was a useful diagnostic modality.
Limitations: We performed measurements from only the tunnel inlet and do not know how the nerve stiffness changes at the distal tunnel or the forearm level by SWE.
Ethics committee approval: Approved by the ethical committee of the Urmia University of Medical Sciences. Written informed consent was obtained from all patients.
Funding: No funding was received for this work.
Author Disclosures:
S. A. Seyed Mokhtari: nothing to disclose
A. Mohammadi: nothing to disclose
A. Afshar: nothing to disclose

S 11-3 14:25
Time-depended cardiovascular effects of intra-arterial milrinone and nimodipine application in cerebral vasospasm
J. Jentzsch, H. Merkel, S. Ziganshyna, K. Gaber, D. Lindner, S. Schob, U. Quäschling, K.-T. Hoffmann, C. Richter*; Leipzig/DE*

Purpose: Cerebral vasospasm is the major cause of morbidity and mortality in patients with ruptured cerebral aneurysms who survived an initial haemorrhagic event. A recent randomised clinical trial validated the significant benefit of intra-arterial treatment over conservative treatment. However, risk-benefit-profiles of the drugs used for pharmaceutical angioplasty have not yet been analysed. Our study compares the efficacy and side-effects of intra-arterial nimodipine versus milrinone in patients treated for symptomatic vasospasm.
Methods and materials: 35 patients were treated intra-arterially for severe cerebral vasospasm. 12 received nimodipine only, 6 received milrinone only, and 3 were treated with a combination of both. Totally, 144 procedures were reviewed, 82 finally included. Spasm-relief, dosage and duration of application, mean-arterial-pressure (MAP), the requirement for systemic vasopressor therapy, and functional outcomes after 3-6 months were reviewed.
Results: Both drugs strongly increased the calibre of MCA- and ACA-segments. Less markedly, they reduced the vasotonus of the intradural ICA-segments (192% vs 120%). The time required to achieve significant spasm-relief was much higher for nimodipine compared to milrinone (6mg:55min vs 20mg/20min). The effect on the vasotonus after milrinone application was dose-dependent (maximum increase in diameter: 187% vs 166%, 20mg vs10mg). Milrinone showed the maximum effect after 10 minutes, whereas nimodipine efficacy appeared in a more delayed manner. Comparing the compensatorily required vasopressor dosages to avoid critical drops in MAP and nimodipine demanded significantly more systemic vasopressor than milrinone (0.08+/-0.13µg/kg/min vs 0.07+/-0.07µg/kg/min). All except for one patient (nimodipine) developed DCI but unfavourable outcomes were lower in the nimodipine cohort (mRS mean 3 vs 4.2).
Conclusion: The immediate vaso-relaxing-effect of nimodipine is inferior to milrinone, but nimodipine may have additional neuroprotective effects. However, cardiovascular comorbidities, an initial Hunt and Hess scale and individual susceptibility to pharmaceutical agents, are most considerable confounders.
Limitations: A retrospective, unicentric study with a small sample size.
Ethics committee approval: Local IRB granted.
Funding: No funding was received for this work.
Author Disclosures:
J. Jentzsch: Author at University Hospital Leipzig
H. Merkel: Other at University Hospital Leipzig
S. Ziganshyna: Other at University Hospital Leipzig
K. Gaber: Other at University Hospital Leipzig
K.-T. Hoffmann: Other at University Hospital Leipzig
D. Lindner: Other at University Hospital Leipzig
C. Richter: Other at University Hospital Leipzig
U. Quäschling: Other at University Hospital Leipzig
S. Schob: Other at University Hospital Leipzig

S 11-4 14:35
The treatment of wide-necked bifurcation aneurysms with the use of a pCONus device and its complications: a meta-analysis
K. Krupa, I. Kucybała, P. Brzegowy, A. Urbanik*; Cracow/PL*
(kamilkrupa955@gmail.com)

Purpose: Endovascular treatment of wide-necked bifurcation aneurysms represents a technical challenge for interventional radiologists. In order to achieve better results of the embolisation, the pCONus device was developed. The aim of the study was to summarise the overall safety and efficacy of the pCONus device in the treatment of wide-necked bifurcation aneurysms.
Methods and materials: The major electronic medical databases were thoroughly searched to identify relevant studies. Data regarding the type of included studies, type of aneurysm, and its localisation, as well as results and complications of the treatment, were extracted from the eligible studies and included into a meta-analysis.
Results: A total of 9 studies (218 patients with 220 aneurysms) were included in the meta-analysis. The most common localisation of treated aneurysms was the middle cerebral artery with a pooled prevalence estimate (PPE) of 45.3%. Significantly less often aneurysms were located on the anterior communicating artery (PPE 29.7%) and the basilar artery (PPE 15.1%). Immediately after the procedure, in 41.6% of patients, RROC I (complete obliteration of the aneurysm) was observed. RROC II (residual neck) was present in 31.3% of patients, while RROC III (residual aneurysm) was present in 27.1% of patients. The results of short-term follow-up showed that most frequently RROC I was observed in 53.9% of cases. Less often, RROC II with a PPE of 24.9% was seen, followed by the RROC III with a PPE of 21.2%. The PPE of intraprocedural complications was 15.2%.
Conclusion: The use of a pCONus device with coiling in the treatment of wide-necked bifurcation aneurysms provides good occlusion rates and high safety.
Limitations: The low quality of evidence.
Ethics committee approval: n/a
Funding: No funding was received for this work.
Author Disclosures:
K. Krupa: Author at Jagiellonian University, Medical College
I. Kucybała: Author at Jagiellonian University, Medical College
P. Brzegowy: Author at Jagiellonian University, Medical College
A. Urbanik: Author at Jagiellonian University, Medical College

S 11-5 14:45
Stenting of intracranial stenosis in acute stroke: single-centre experience from the last decade
M.-S. Schüngel, S. Schob, K.-T. Hoffmann, U. Quäschling*; Leipzig/DE*
(Marie-Sophie.Schuengel@medizin.uni-leipzig.de)

Purpose: To summarise our experience from the last decade with stenting of symptomatic intracranial stenosis (SIS) causing acute, progressive stroke.
Methods and materials: Our retrospective study included 71 interventions (66 patients, mean age: 68.5 years) with average stenosis of 76% (modified NASCET-calculation). Balloon-expandable-stents (BES: Liberté, Pharos, Rebel, Coroflex) and self-expandable-stents (SES: Enterprise, Solitaire, Wingspan, Leo+Baby, p48MW_HPC, Silk Vista Baby) were applied. In total, 86 stents were used, but only 69 were implanted with adequate success. 77.3% of patients presented in the context of acute progressive stroke. Lysis (rtPA) was initiated in 12 patients.
Results: 77.3% were successfully treated. In 60.6%, BES, in 22.7%, SES+PTA ,and in 7.6%, other combinations (BES+SES+balloon, low-profile flow diverter) were used. In 9.1%, proper vessel-reconstruction failed.
77.3% regained at least partial functional independence (90days-mRS: ≤3), however, 22.7% died despite successful intervention. Except for one patient, all remaining presented with initial mRS-scores>3. 66.7% of deaths were related to poorly-collateralised basilar stenosis and 33.3% had high-grade stenosis at the C7/M1 segment.
Conclusion: SIS, especially in the posterior circulation, bears an extraordinarily high-risk for mortality and permanent disability despite early causative treatment. In this condition, collateralisation and comorbidities are most significant for the individual outcome. Off-label use of BES yields a good success-to-risk ratio, however, considerable stiffness and restricted manoeuvrability of BES empirically renders implantation impossible in demanding cases. Application of SES+balloon-PTA represents a promising bail-out-technique (especially with low-profile-flow-diverters) in these situations. Hence, considering the devastating natural course of SIS and accounting for the substantial evolution of neuro-interventional techniques which revolutionised stroke-treatment in the post-SAMMPRIS era, endovascular treatment of SIS has become obligatory especially, but not exclusively, during acute interventions as thrombectomy. Yet asymptomatic high-grade intracranial stenosis should be evaluated critically before deciding for conservative treatment only.
Limitations: Only single-centre experiences were presented.
Ethics committee approval: n/a
Funding: No funding was received for this work.
Author Disclosures:
M.-S. Schüngel: nothing to disclose
K.-T. Hoffmann: nothing to disclose
S. Schob: nothing to disclose
U. Quäschling: nothing to disclose

S 11-6 14:55
Patient feedback on the consenting process for radiologically-guided interventional procedures
H. Iqbal, A. Maqsood-Shah, G. Ayub*; Leeds/UK (ll15hi@leeds.ac.uk)*

Purpose: This audit assessed the local consenting practice in interventional radiology using a patient feedback form provided by the RCR. The questionnaire contained 14 questions looking at different aspects of consenting and recorded the patient's satisfaction in terms of yes, no, and not sure. The target was for 95% of patients answering 'yes' to all questions. In the first cycle, 30% of patients answered 'Yes' to all questions. Areas needing improvement included providing information leaflets and providing information about pain and procedure benefits. The action plan after the first cycle included providing feedback to the radiologists to improve awareness and providing leaflets in advance.
Methods and materials: In the second cycle, 33 patients filled out a questionnaire form within 48 hours of their procedure. The anonymised data was quantitatively analysed.
Results: 36% of patients answered 'Yes' to all questions, showing a 6% increase. 90% answered yes to 10 out of 14 questions when analysed separately, confirming good progress. 100% of patients understood their procedure and had enough information to give consent. 55% answered yes to having sufficient information regarding alternative treatment.
Conclusion: A separate analysis of questions showed improvements in most areas, although the overall improvement was small. The worst outcome was seen in the question regarding discussing alternative treatments. Arguably, the day of the procedure is unsuitable for these conversations due to time limitations and a lack of complete history. It is assumed these conversations have taken place by the referring clinical team. Actions to take forward include revision of the questionnaire; we feel the RCR set questionnaire is not well suited to our practice. We intend to analyse these results alongside the relevant consent form to look for discrepancies and a repeat audit is prudent.
Limitations: N/A
Ethics committee approval: N/A
Funding: No funding was received for this work.
Author Disclosures:
H. Iqbal: nothing to disclose
A. Maqsood-Shah: nothing to disclose
G. Ayub: nothing to disclose

S 11-7 15:05
Tibial nerve calliber in MR neurography is negatively correlated with conduction velocities and compound motor action potentials in patients with diabetic neuropathy
L. Schimpfle, D. J. Jende, F. Kurz, D. S. Kopf, D. J. Gröner, D. Z. Kender, P. D. P. Nawroth, M. Bendszus*; Heidelberg/DE*

Purpose: Diabetic polyneuropathy (DPN), being one of the most common and most burdening complications in patients with diabetes mellitus, is still poorly understood. Magnetic resonance neurography (MRN) allows for the detection of pathological changes in the tibial compartment of the sciatic nerve. The aim of this study is to combine MRN with clinical, serological, and electrophysiological patient assessments in order to achieve a better understanding of the pathophysiology and possible treatment options in DPN.
Methods and materials: MRN of the sciatic nerve at 3 Tesla (Siemens Magnetom TIM TRIO) was performed in 130 patients with diabetes mellitus using a T2-weighted, fat-suppressed sequence with the following parameters: Tr: 5970ms, TE: 55ms, FOV: 160x150 $mm^{2,}$ matrix size: 512x512, slice thickness: 4mm, interslice gap: 0.35 mm, voxel size: 0.5x0.3x4.0 mm^3)
Segmentation of the tibial compartment of the sciatic nerve was carried out manually using the software Image J (version 1.52o, 2019) while nerve lesions were quantified semi-automatically with MATLAB (version 7.14.0.0739 (R2012a)).
In addition, every patient underwent clinical, electrophysiological, and serological assessment. MRN and clinical data were subsequently correlated using GraphPad Prism (Version 8).
Results: At the time of abstract submission, preliminary results of 42 patients were available. The cross-sectional surface area (CSA) correlated negatively with tibial nerve conduction velocity (NCV) (r=-0.37, p<0.01) and negatively with tibial compound motor action potential (Amp) (r=-0.37,p<0.019).
Conclusion: The preliminary results described above indicate that the thickening of nerve fascicles seen in DPN patients results in poorer nerve conduction values (NCV, Amp) implying advanced nerve damage. With all 130 patients being analysed, we expect more correlations of nerve pathologies with clinical and serological data.
Limitations: A cross-sectional study.
Ethics committee approval: Ethics number: S-383/2016, clinicaltrials.gov identifier: NCT03022721.
Funding: No funding was received for this work.
Author Disclosures:
L. Schimpfle: nothing to disclose
F. Kurz: nothing to disclose
M. Bendszus: nothing to disclose
D. J. Jende: nothing to disclose
P. D. P. Nawroth: nothing to disclose
D. S. Kopf: nothing to disclose
D. J. Gröner: nothing to disclose
D. Z. Kender: nothing to disclose

S 11-8 15:15
Introducing medical students to functional MRI and neuroscience research: myopia may induce changes in visual cortex activation
N. Rodríguez Albacete[1], R. Acosta Hernández[1], B. García Martínez-Lozano[1], A. Inuggi[2], J. M. M. Garcia Santos[1]; *[1]Murcia/ES, [2]Milan/IT (nicorodriguezal96@gmail.com)*

Purpose: To assess differences in visual cortex BOLD signal between myopic and emmetropic subjects.
Methods and materials: fMRI EPI was performed using a block-design stimulation in 6 emmetropic (3 men) and 6 myopic (3 men) healthy young volunteers. Two medical students manually mined the following data in a commercial workstation: highest BOLD magnitude and cross-correlation coefficient (CCC) using a 9-voxel ROI, whole cluster BOLD magnitude/CCC, total activated pixels, and number of activated slices. Variables were compared between groups (Mann-Whitney U test) and correlated (Spearman's correlation) with age, myopia duration, and dioptres in myopic subjects. One of the students was further trained in imaging analysis within the Erasmus Program. He performed a two-sample t-test group comparison and multiple regression modelling dioptres and myopia duration as regressors within SPM software.
Results: Total activated pixels (P=0.046) were significantly higher in myopic subjects. Significant correlations were observed between the highest BOLD magnitude and number of activated slices (ρ -0.928; P=0.008), the highest CCC and total activated pixels (ρ 0.943; P=0.005), and the total activated pixels and number of activated slices (ρ 0.943; P=0.005) only in myopic subjects. In addition, the highest BOLD magnitude (ρ 0.986; P<0.001) and whole cluster CCC (ρ -0.899; P=0.015) were correlated with dioptres. Imaging analysis showed four significant voxels in the occipital lobe in myopic>emmetropic and none in myopic<emmetropic. Some voxels correlating positively to myopia duration and negatively to dioptres were also demonstrated.
Conclusion: Myopic may have more extensive activation than emmetropic subjects, which might be a first adaptive mechanism. Increasing peak activation might be a subsequent compensation.
Limitations: The sample size, short block length, and lack of refraction correction.
Ethics committee approval: Ethics committee approval waived.
Funding: No funding was received for this work.
Author Disclosures:
N. Rodríguez Albacete: nothing to disclose
R. Acosta Hernández: nothing to disclose
J. M. M. Garcia Santos: nothing to disclose
A. Inuggi: nothing to disclose
B. García Martínez-Lozano: nothing to disclose

14:00 - 15:30 **Coffee & Talk 1**

Physics in Medical Imaging

RPS 1113

Improving quality to build safety

Moderators:
N.N.
L. Sukupova; Prague/CZ

RPS 1113-K 14:00
Keynote lecture
H. Delis*; Patras/GR (hdelis@gmail.com)*

Author Disclosures:
H. Delis: nothing to disclose

RPS 1113-1 14:10
Achievable doses and diagnostic reference levels for computed tomography for EUCLID (European study on clinical DRLs) clinical indications: data from a multinational dose registry
D. Bos[1], S. Yu[2], J. Luong[2], P. Chu[2], Y. Wang[2], A. Wetter[1], R. Smith-Bindman[2]; *[1]Essen/DE, [2]San Francisco, CA/US*

Purpose: Radiation doses for computed tomography (CT) examinations are highly variable between patients, institutions, and countries. Achievable doses (target doses reflecting the 50% in distribution) and diagnostic reference levels (reference doses reflecting the 75% in distribution) are often created to help reduce unnecessary variation by providing guidance to radiologists and technologists. The European Society of Radiology has identified common indications for CT (EUCLID, European study on clinical DRLs) in order to create benchmarks.
Methods and materials: Standardised data on 2.3 million CT examinations in adults ages 18 years and older was collected between January 2016-December 2018 from 155 institutions across 7 countries as part of the UCSF international CT dose registry. This data was used to calculate the target and reference doses for each EUCLID indication for CT-dose index (CTDIvol) and dose-length product (DLP).
Results: The number of included patients for the EUCLID categories ranged from 3,176 (coronary angiography) to 721,263 (appendicitis). Doses were significantly different across the different categories. E.g., the target dose for DLP for suspected brain haemorrhage was 861 mGy-cm, whereas for chronic sinusitis was 250 mGy-cm. The observed target and reference doses for DLP in mGy-cm were: suspected brain haemorrhage target DLP=861 and reference DLP=1,067, chronic sinusitis 250 and 373, cervical spine trauma 450 and 962, pulmonary embolism 372 and 558, coronary calcium score 66 and 102, coronary angiography 497 and 915, lung cancer 329 and 555, hepatocellular carcinoma 1,304 and 2,016, abdominal pain 519 and 773, and appendicitis 661 and 1,059.
Conclusion: Reference and target dose levels for EUCLID clinical indications from diverse organisations can be used for dose optimisation and institutional evaluation, and to inform indication-specific dose-optimised protocols.
Limitations: n/a
Ethics committee approval: n/a
Funding: Funded by PCORI and NIH.
Author Disclosures:
D. Bos: nothing to disclose
J. Luong: nothing to disclose
S. Yu: nothing to disclose
P. Chu: nothing to disclose
Y. Wang: nothing to disclose
A. Wetter: nothing to disclose
R. Smith-Bindman: Research/Grant Support at US National Institutes of Health, Research/Grant Support at Patient- Centered Outcomes Research Institute, Research/Grant Support at Centers for Disease Control and Prevention, Research/Grant Support at the University of California Office of the President, Advisory Board at scientific advisory board, Speaker at Bayer Healthcare.

RPS 1113-2 14:16

Achievable doses and diagnostic reference levels for paediatric computed tomography for different age groups and clinical indications: data from a multinational dose registry

D. Bos[1], S. Yu[2], J. Luong[2], P. Chu[2], Y. Wang[2], R. Smith-Bindman[2]; [1]*Essen/DE,* [2]*San Francisco, CA/US*

Purpose: Radiation doses vary across patients, institutions, and countries. Achievable doses (target doses) and diagnostic reference levels (reference doses that should not be exceeded) for children by size and clinical indication would help physicians optimise their doses.
Methods and materials: Standardised computed tomography (CT) examinations were collected in children up to the age of 15 years between January 2016-December 2018 from 156 institutions across 7 countries as part of the UCSF international CT dose registry. Achievable doses (target doses, defined as the 50% in observed distribution) and diagnostic reference levels (reference doses, defined as the 75% in distribution) were calculated for the CT-dose index (CTDIvol) and dose-length product (DLP) stratified by age for the most common clinical indications for CT scanning.
Results: Data was analysed for 51,107 CT examinations including 6,373 (12%) in children under age 1, 10,928 (21%) in children aged 1-5, 13,759 (27%) in children aged 5-10, and 20,047 (39%) in children aged 10-15. For the anatomic area and clinical indication category, there was an increase in dose by age. The target doses for DLP for head CT increased from 211 mGy-cm among children <1 year old to 604 mGy-cm in children aged 10-15 and corresponding reference doses increased from 295 to 808 mGy-cm. Doses also varied significantly by indication. Among children aged 10-15, the target dose for a head CT was 808 mGy-cm, whereas it was 328 mGy-cm for CT sinus and 1,038 mGy-cm for trauma head CT.
Conclusion: Indication- and protocol-specific target and reference doses for paediatric CT examinations can help to reduce unnecessary variations in dose by providing guidance to radiologists and technologists, thereby reducing a potential harm of CT exposure.
Limitations: n/a
Ethics committee approval: n/a
Funding: Funded by PCORI and NIH.
Author Disclosures:
D. Bos: nothing to disclose
S. Yu: nothing to disclose
J. Luong: nothing to disclose
P. Chu: nothing to disclose
Y. Wang: nothing to disclose
R. Smith-Bindman: nothing to disclose

RPS 1113-3 14:22

A 3-years retrospective study of cumulative radiation exposure from recurrent imaging for oncological patients

I. Dyakov[1], V. Stoynova[2]; [1]*Sofia/BG,* [2]*Vienna/AT (iliya.dyakov@acibademcityclinic.bg)*

Purpose: To estimate the cumulative effective dose (CED) from diagnostic, radiotherapy treatment planning and follow-up imaging studies for oncological patients and review the potential for dose reduction through improved justification and optimisation.
Methods and materials: The study was performed in an oncological hospital in Sofia, Bulgaria. 6,318 patients who underwent CT studies during 2016-2019 were retrospectively reviewed by means of dose monitoring software Dose Watch (GE Healthcare). Patients with more than 3 CTs were identified and, for each of them, CED was estimated by adding radiography, fluoroscopy, and nuclear medicine studies retrieved from Dose Watch and PACS in 3 connected hospitals. Clinical appropriateness was evaluated by a comparison to existing guidelines.
Results: Out of 6,318 patients, 1,406 (22%) underwent 3 or more CT and other imaging studies. The CED of 718 (11.4%) of all patients exceeded 100 mSv and in 263 (4 %), it was above 200 mSv, with a maximum of 1,658 mSv. From all 5,806 procedures, 64% were CTs, followed by PET-CT (13%), radiography (7%), radiotherapy CT simulation (7%), SPECT-CT (6%), mammography (2%), and angiography (1%). The follow-up studies showed no dynamic of the disease in 11% of patients and no malignancy findings in 19%.
Conclusion: The recurrent imaging studies of oncological patients are well justified in most cases. No consensus was found between existing guidelines about the type and frequency of the follow-up imaging procedures. Optimisation of CT protocols for treatment planning and follow-up was identified as the priority. A unified exposure monitoring system at a regional or national level with access to individual exposure histories of patients would help improve the care and safety of oncological patients.
Limitations: n/a
Ethics committee approval: n/a
Funding: No funding was received for this work.
Author Disclosures:
I. Dyakov: nothing to disclose
V. Stoynova: nothing to disclose
J. Vassileva: nothing to disclose

RPS 1113-4 14:28

Dose optimisation for CT scans of the temporal bone using a spectral shaping tin filter

N. Saltybaeva, A. Stüssi, C. Blüthgen, S. Tanadini-Lang, M. Guckenberger, S. Winklhofer*; Zurich/CH (Sanata5@yandex.ru)*

Purpose: Despite the clinical benefits of computed tomography (CT), there are relevant concerns associated with radiation exposure to patients. Novel spectral shaping usually represented by a tin-filter (Sn) have already shown improved dose efficiency in chest and abdomen CTs. This study aims to investigate the feasibility of an Sn-filter in head CTs and to evaluate possible dose reduction.
Methods and materials: This retrospective study involved 20 patients (mean age 55.9±18.3 years). 12 patients underwent temporal bone CTs using conventional 120kVp-protocol (220 reference mAs) while 8 were scanned using 130kVp-Sn-protocol (420 reference mAs). Objective image quality for each patient was evaluated by the signal-to-noise ratio (SNR), calculated as the mean signal divided by the noise measured in the internal auditory canal (IAC), the external auditory canal (EAC), and squama temporalis (ST). Subjective image quality was evaluated by two experienced radiologists using a 5-point Likert scale (1=excellent, 2=good, 3=moderate, 4=fair, and 5=non–diagnostic). The radiation dose was assessed by the mean of CTDIvol values collected from patient dose reports. Finally, the differences in SNR and radiation dose between investigated protocols were checked for statistical significance using unpaired t-tests.
Results: The mean CTDIvol for the protocol with an Sn-filter was significantly lower than the one for the conventional protocol (26.8±2.5mGy vs 38.3±4.8mGy, p<0.001). SNR comparison has shown no significant difference between the two protocols (p=0.18, 0.11, and 0.35 for IAC, EAC, and ST, respectively). Subjective image quality assessment has shown substantial inter-reader agreement (79%) with moderate reliability (k=0.45). For both protocols, image quality for all the cases was rated as either “good” or “excellent”.

Conclusion: The study indicated that Sn-filtration in temporal bone CT allows for substantial dose reduction without compromising diagnostic image quality.
Limitations: The small cohort.
Ethics committee approval: Approved by the local ethics committee.
Funding: No funding was received for this work.
Author Disclosures:
N. Saltybaeva: nothing to disclose
A. Stüssi: nothing to disclose
C. Blüthgen: nothing to disclose
M. Guckenberger: nothing to disclose
S. Tanadini-Lang: nothing to disclose
S. Winklhofer: nothing to disclose

RPS 1113-5 14:34
Accelerated Monte Carlo simulation of patients' doses in interventional radiology procedures using the MC-GPU code
M. Ginjaume, M. A. Duch, D. Fernández Bosman, C. Delgado*; Barcelona/ES (david.fernandez.bosman@upc.edu)*

Purpose: The directive 2013/59/EURATOM establishes the need to establish quality assurance programmes and the assessment of patient dose, in particular, in practices such as interventional radiology (IR) and cardiology (IC). In the framework of the European project MEDIRAD, we have developed a method for organ dose and peak skin dose monitoring of patients undergoing IR/IC procedures based on the accelerated Monte Carlo code, MC-GPU.
Methods and materials: MC-GPU has been validated by comparing the simulations with experimental measurements using TLD using regular shaped phantoms made of tissue-equivalent materials under realistic conditions. In addition, several tools have been developed to accelerate the patient organ dose calculation for a complete IR/IC procedure. On the one hand, we have prepared an interface between radiation dose structured reports and the MC-GPU code. The tool automatically generates the input files needed for the simulation. The patient is represented by the voxelised anthropomorphic phantom "REX" (Schlattl H et. al. 2007). Moreover, a graphical interface has been implemented to have a 3D colour-map of the patient's dose in the different tissues.
Results: The results show good agreement between the simulations and the experimental measurements. Differences between measured and calculated doses for the different experimental configurations were, in general, lower than 10%. The computational time needed for the simulation of a single irradiation event is a few seconds using 2 GPU cards (GeForce GTX 1080Ti).
Conclusion: It has been verified that MC-GPU is a good tool for the assessment of the absorbed dose in the different organs and for the maximum skin dose determination in patients undergoing an IR procedure.
Limitations: n/a
Ethics committee approval: n/a
Funding: The Euratom research and training programme 2014-2018 under grant agreement No 755523.
Author Disclosures:
M. Ginjaume: Author at Institute of Energy Technologies
D. Fernández Bosman: Speaker at Institute of Energy Technologies
M. A. Duch: Author at Institute of Energy Technologies
C. Delgado: Author at Hospital Vall d'Hebron

RPS 1113-6 14:40
X-ray dark-field chest radiography: the first clinical implementation
K. Willer[1], T. Urban[1], W. Noichl[1], M. Frank[1], R. C. Schick[1], B. Renger[2], T. Koehler[3], J. Herzen[1], F. Pfeiffer[1]*; [1]Garching/DE, [2]Munich/DE, [3]Hamburg/DE (konstantin.willer@ph.tum.de)*

Purpose: To demonstrate the first successful implementation of x-ray dark-field chest radiography on patients and to provide a novel medical imaging tool that generates structure sensitive information for an improved diagnostic assessment of the lung's physical condition.
Methods and materials: A prototype scanner, capable of simultaneously acquiring dark-field and attenuation chest x-rays, has been developed and installed on-site for a first experimental study on COPD patients. The system is assembled from medical x-ray components and a 3-grating interferometer. Within the currently ongoing study, 78 patients have already been examined. The subject collective includes patients without lung disorders for reference and patients with mild to severe stages of COPD. Through a questionnaire, computed tomography, and spirometry, the individual severity of the disease is assessed.
Results: The dark-field and attenuation images are obtained simultaneously in one 7s scan at an average effective dose of 0.04 mSv. We found that healthy patients exhibit a distinct and homogeneous signal over the entire pulmonary region. Here, intact alveolar structure with a lot of air-tissue interfaces induces strong small-angle scattering. In contrast, a weak signal is obtained for COPD patients, where parenchyma degradation prevails.
Conclusion: These preliminary results indicate that x-ray dark-field radiography is capable of probing the lung's underlying microstructure, which remains inaccessible with currently deployed medical imaging methods, while it is highly affected by disorders such as emphysema, fibrosis, or lung cancer. Particularly with regard to the early detection of COPD, we consider the technique's transfer to a human application as a breakthrough.
Limitations: n/a
Ethics committee approval: The study was approved by the institutional ethics review board and the federal office for radiation protection. Participants gave written informed consent.
Funding: Partially funded by Philips, Hamburg, DE.
Author Disclosures:
K. Willer: nothing to disclose
T. Koehler: Employee at Philips GmbH
F. Pfeiffer: nothing to disclose
T. Urban: nothing to disclose
W. Noichl: nothing to disclose
M. Frank: nothing to disclose
R. C. Schick: nothing to disclose
B. Renger: nothing to disclose
J. Herzen: nothing to disclose

RPS 1113-7 14:46
X-ray dark-field chest radiography: scatter artefact reduction
T. Koehler[1], K. J. Engel[2], A. Yaroshenko[1], K. Willer[3], W. Noichl[3], T. Urban[3], A. A. Fingerle[4], D. Pfeiffer[4], F. Pfeiffer[3]*; [1]Hamburg/DE, [2]Eindhoven/NL, [3]Garching/DE, [4]Munich/DE (franz.pfeiffer@tum.de)*

Purpose: Dark-field x-ray imaging is a new technology to visualise the alveolar structure of lung tissue which relies on coherent small-angle x-ray scattering. Incoherent Compton scatter overlaying the dark-field signal impedes image formation and hampers diagnostic interpretation. The purpose was to develop and validate an algorithm to eliminate the contribution of Compton scatter to the dark-field signal.
Methods and materials: A slot-scanning dark-field x-ray system was used to acquire data of phantoms and subjects. Correction for Compton scattering was performed in a two-step approach. First, conventional x-ray transmission and dark-field images were generated by standard phase-retrieval. The conventional images were the input for a kernel-based scatter estimation method. Estimates for scattered intensity were calculated for each slot position and were accounted for as additional incoherent background radiation during a second-pass phase-retrieval.
Results: Dark-field images without scatter correction show artificial dark-field signal in areas with a large scatter fraction, i.e. in image areas of the spine, heart, and abdomen.
The developed scatter correction greatly reduces this artificial signal and allows for a better quantitative measurement of the true dark-field signal generated by lung tissue. Typically, the correction of the dark-field signal by application of the scatter correction algorithms is in the order of 30% in areas of the spine, 10% in the area of the heart, and 15% in the abdomen.
Conclusion: The developed method provides more quantitative dark-field signal.
Preclinical studies demonstrated the potential of dark-field radiography to detect early stages of various lung diseases. By using the proposed method, more accurate dark-field images are obtained.
Limitations: Evaluation was done on sample cases.
Ethics committee approval: The study was IRB approved. Patients signed informed consent.
Funding: Partially funded by Philips Medical Systems DMC GmbH.
Author Disclosures:
T. Koehler: Author at Philips GmbH Innovative Technologies, Employee at Philips GmbH Innovative Technologies
K. J. Engel: Author at Philips Research, Employee at Philips Research
A. Yaroshenko: Author at Philips Medical Systems DMC GmbH, Employee at Philips Medical Systems DMC GmbH
K. Willer: nothing to disclose
W. Noichl: nothing to disclose
T. Urban: nothing to disclose
A. A. Fingerle: nothing to disclose
D. Pfeiffer: nothing to disclose
F. Pfeiffer: nothing to disclose

RPS 1113-8 14:52
The probability and impact of a high radiation dose in patients undergoing CT examinations
C. Jeukens, H. Boere, B. A. J. M. Wagemans, P. J. Nelemans, E. C. Nijssen, J. E. Wildberger, A. M. H. Sailer*; Maastricht/NL (cecile.jeukens@mumc.nl)*

Purpose: To determine the probability of receiving a high radiation dose from single or multiple CT examinations and to assess the potential impact by

evaluating clinical indications for multiple CT examinations and associated prognosis of high-dose patients.
Methods and materials: All CT examinations performed at our institution between 01/07/2013-01/07/2018 for which radiation dose data was available were included. The effective dose received by single or multiple CT examinations was assessed for each patient using dose monitoring software. The probability of receiving a high dose (i.e. ≥50mSv (single) or ≥100mSv (multiple)) was evaluated using survival analysis for women, men, different age categories, and the total number of CT examinations received. Baseline characteristics and the probability of survival up to 4.5 years were assessed for high-dose patients, taking clinical indication into account.
Results: An effective radiation dose was available for 100,672 CT examinations performed amongst 49,978 patients, 649 of whom received a high radiation dose. The estimated high radiation dose probability was 0.43% for a single examination and 1.5% (men) to 1.9% (women) for repeated examinations over a period of 4.5 years. Factors increasing this probability are female sex, especially in the age category 51-64 (probability=3.02%), and >6 CT examinations (probability>16%). The impact on survival is limited because high-dose patients are often severely ill: 65% of high-dose CT examinations were oncology-related and 48% of high-dose patients died within 4.5 years from pre-existing medical conditions.
Conclusion: The probability of receiving a high radiation dose from CT examinations is small but not negligible. High-dose patients often had pre-existing conditions with a high risk of premature death. Consequently, the impact of a high radiation dose is expected to be small on a population level.
Limitations: The data originates from a single centre.
Ethics committee approval: The study was approved and written informed consent was waived.
Funding: No funding was received for this work.
Author Disclosures:
C. Jeukens: nothing to disclose
H. Boere: nothing to disclose
B. A. J. M. Wagemans: nothing to disclose
P. J. Nelemans: nothing to disclose
E. C. Nijssen: nothing to disclose
J. E. Wildberger: Grant Recipient at Agfa (Morstel, Belgium), Grant Recipient at Bayer Healthcare (Berlin, Germany), Grant Recipient at GE (Chicago, Illinois), Grant Recipient at Philips Healthcare (Best, the Netherlands), Grant Recipient at Optimed (Ettingen, Germany), Grant Recipient at Siemens Healthineers (Forchheim, Germany), Other at Bayer Healthcare (Berlin, Germany), Other at Siemens Healthineers (Forchheim, Germany)
A. M. H. Sailer: nothing to disclose

RPS 1113-9 14:58

First SSDE reference values for paediatric head CT examinations

A. S. L. Dedulle, K. Houbrechts, N. Fitousi, J. Jacobs, H. Bosmans*; Leuven/BE (an.dedulle@qaelum.com)*

Purpose: To investigate the water equivalent diameter (WED) and size-specific dose estimates (SSDE) for paediatric head computed tomography (CT) examinations on two CT devices.
Methods and materials: Paediatric brain CT examinations from one year were investigated for two Siemens devices, with one located at the emergency (ER) department (CT_1 and CT_{ER}). The WED of the middle slice of the CT series was determined and used to calculate the SSDE according to AAPM report 293. The paediatric patients were categorised into 5 age groups (A: 0-1y, B: 1-5y, C: 5-10y, D: 10-15y, and E: 15-18y). A Mann-Whitney test was used to compare the WED and SSDE of the age groups for both scanners.
Results: At CT_1 and CT_{ER}, respectively, 128 and 207 scans were carried out. The correlation between patient age and WED was significant (CT_1: r^2=0.73, CT_{ER}: r^2=0.71). The mean WED and SSDE of the age groups CT_1 were A: 14 cm, 16 mGy; B: 16 cm, 16 mGy; C: 17 cm, 19 mGy; D: 18 cm, 21 mGy; E: 18 cm, 29 mGy. For the same age groups, the WED was not significantly different (p>0.05) between the two devices. For the age groups up to 10 years (A-C), the SSDE was also not significantly different (p>0.05), however, SSDE differed significantly (p<0.05) for the age groups above 10 years (D-E), with a mean SSDE of 24 mGy and 31 mGy for CT_{ER}.
Conclusion: Several European documents suggest the use of patient weight rather than age for dose investigation purposes. As weight may not be available at the moment of dose monitoring, SSDE is a valid alternative. It can be calculated and scaled with $CTDI_{vol}$ (and therefore attenuation). We provide the first set of reference values.
Limitations: No access to the clinical indication of the head CT examinations.
Ethics committee approval: n/a
Funding: PhD grant from VLAIO [Grant No. HBC.2016.0233].
Author Disclosures:
A. S. L. Dedulle: Research/Grant Support at VLAIO [HBC.HBC.2016.0233], Employee at Qaelum NV
K. Houbrechts: nothing to disclose
N. Fitousi: Employee at Qaelum NV
J. Jacobs: CEO at Qaelum NV, Founder at Qaelum NV
H. Bosmans: Founder at Qaelum NV, Board Member at Qaelum NV

RPS 1113-10 15:04

The small-size detail detection performance of digital breast tomosynthesis, synthetic 2D, and conventional full-field digital mammography images for different mammography systems: a multicentre study

V. Ravaglia[1], L. Angelini[2], M. Bertolini[3], G. della Gala[4], S. Farnedi[1], P. Golinelli[5], L. Pagan[6], N. Scrittori[1], G. Venturi[7]*; [1]Ravenna/IT, [2]Rimini/IT, [3]Reggio Emilia/IT, [4]Sassuolo/IT, [5]Modena/IT, [6]Bologna/IT, [7]Forli'/IT (valentina.ravaglia@auslromagna.it)*

Purpose: To compare the small-size detail detection of combined modalities DBT+S (digital breast tomosynthesis and synthetic 2D) and DBT+FFDM (DBT and conventional full-field digital mammography) for mammography systems of different models and vendors.
Methods and materials: 15 different mammography systems of 9 different models were compared. We used a home-made phantom composed by CDMAM (Artinis), homogeneous PMMA slabs, and BR3D tissue-equivalent slabs (Cirs) containing an anatomic noise in order to obtain different phantom configurations equivalent to 32, 60, and 90 mm breast thicknesses.
The CDMAM phantom was composed of an aluminium slab with gold details of different diameter and thickness. For this study, we focused only on small details ranging from 0.5 to 0.1 mm that simulate microcalcifications.
We exposed at 2 different dose levels (one obtained with a clinical automatic exposure programme and the other with manual “fixed” parameters) and the processed images were successively divided into squared sub-images, each containing a detail of different size and contrast. The sub-images were rotated and displayed in random order on a 5MP calibrated monitor to 4 trained readers. The percentage correct rate for DBT+S and DBT+FFDM was evaluated.
Results: As an example, the percentage correct rate for 4 different systems for details 0.4 mm and 0.1 mm is shown.
Conclusion: For details greater than 0.4 mm, the combined modalities DBT+S and DBT+FFDM show a similar detectability in all the systems. For smaller details, the difference in the detection between the 2 combined modalities depends on the system.
Limitations: The use of a physical phantom, composed of aluminium and gold details, could affect the reconstruction algorithm for DBT and s-2D.
Ethics committee approval: n/a
Funding: No funding was received for this work.
Author Disclosures:
V. Ravaglia: Author at AUSL Romagna
G. Venturi: nothing to disclose
N. Scrittori: nothing to disclose
S. Farnedi: nothing to disclose
L. Angelini: nothing to disclose
M. Bertolini: nothing to disclose
G. della Gala: nothing to disclose
P. Golinelli: nothing to disclose
L. Pagan: nothing to disclose

RPS 1113-11 15:10

Image quality evaluation of a new high-resolution 3-D digital breast tomographic (DBT) imaging system

J. C. O' Driscoll[1], E. Ranahan[1], M. F. M. McEntee[2], J. McCullagh[1]*; [1]Cork/IE, [2]Sydney/AU (jessicadrscll1@gmail.com)*

Purpose: To compare the performance of the Hologic Selenia 3Dimensions, the newest generation high-resolution DBT imaging system with the Dimensions 8000 model, the standard resolution DBT imaging system. The high-resolution system saves pixels to their native detector resolution of 70 µm while the standard resolution system 2 x 2 rebins pixels to 140 µm for tomosynthesis acquisitions.
Methods and materials: Spatial resolution was assessed using a modulation transfer function (MTF). Contrast performance was analysed using a signal difference to noise ratio (SDNR) and the BR3D test object. Contrast detectability was evaluated using the CDMAM 3.4 test object. The noise was examined using the normalised noise power spectrum (NNPS). The mean glandular dose (MGD) was also assessed.
Results: The 70 µm high-resolution system demonstrated a mean improvement of the $MTF_{0.5}$ value by 40% and 27% in the x and y directions. An average reduction of 64% in SDNR was observed. The detection of features in the BR3D test object improved. The mean threshold gold thickness for the 0.1 mm detail size was 58% lower. Increased NNPS values of 8% at 0.5 mm^{-1} and 16% at 2

mm^{-1} were calculated. For breast thicknesses over 45 mm, MGD was reduced for 2-D imaging. Similar MGDs were calculated for both systems for volumetric imaging.
Conclusion: An overall improvement in image quality with no subsequent increase in patient dose for the 70 µm high-resolution system was demonstrated. Findings suggest that saving pixels to 70 µm provides an improvement in spatial resolution, improved visibility of pathological features, and enhanced detection of thinner discs at detail diameters similar to calcifications. Further work will examine whether these improvements impact clinical outcomes.
Limitations: n/a
Ethics committee approval: n/a
Funding: No funding was received for this work.
Author Disclosures:
J. C. O' Driscoll: nothing to disclose
E. Ranahan: nothing to disclose
J. McCullagh: nothing to disclose
M. F. M. McEntee: nothing to disclose

RPS 1113-12 15:16
The use of automatic software for quality controls to detect defective phantoms
G. Gennaro, F. Caumo*; Padua/IT (gisella.gennaro@iov.veneto.it)*

Purpose: To use a software package designed for the automation of routine quality control (QC) tests in digital mammography to detect phantoms with manufacturing defects.
Methods and materials: 24 Leeds TORMAS phantoms to be employed in routine tests of mammography units used within a regional screening programme were preliminarily tested to exclude the possible presence of defects. Two images of each test object were acquired using the same digital mammography equipment, one in a manual exposure mode to enhance possible differences while minimising variability due to the imaging system itself and one in an automatic exposure mode (AEC) with the phantom on the top of a 35 mm polymethyl-methacrylate (PMMA) stack to reproduce the same conditions as in the routine use. 15 image quality indices (IQIs) automatically calculated by the software tool used for routine tests were selected to evaluate phantom homogeneity and detect possible defects. Outliers were computed for each IQI and their impact on phantom homogeneity analysed.
Results: 8 outliers were found in 5 different IQIs from the images acquired in the manual mode associated to 7 phantoms. The impact of 4/7 outliers (57%) was mitigated in the images acquired with the PMMA in the AEC mode as used for routine tests; the 4 phantoms generating those outliers were thereby assumed to be acceptable. The 3 phantoms including outliers measurable from both datasets (without and with PMMA) were considered defective and were replaced with new phantoms.
Conclusion: Software tools employed for routine QC tests can be successfully used to test phantom quality and detect possible manufacturing defects.
Limitations: The limited number of images acquired per phantom due to time constraints.
Ethics committee approval: n/a
Funding: No funding was received for this work.
Author Disclosures:
G. Gennaro: nothing to disclose
F. Caumo: nothing to disclose

RPS 1113-13 15:22
The evaluation of the quality of education in courses on radiation protection in Germany
P. Strauß*; Münster/DE (patrick.strauss@ukmuenster.de)*

Purpose: In Germany, a specific qualification is required to get permission to justify medical exposure in accordance with German regulations to diagnose and applicate x-ray. For this, specific courses on radiation protection are legally mandatory. One focus is on the correct use of equipment for radiation protection and justifying medical exposure. For comparison, the legal bases of the course concepts in Switzerland and Austria were also examined.
Methods and materials: Investigators attended all mandatory courses on radiation protection for their entire length (basic, advanced, and up-to-date refresher courses). A total of 15 different courses from 6 different organisers were evaluated. Structured interviews with course organisers were conducted. The participants' prior and gained knowledge during the attended courses was determined separately by multiple-choice questions. Structured checklists were developed, assuring consistent evaluations of the courses. The investigator's methods and checklists were developed and affirmed by experts in workshops. Representatives of professional societies were interviewed.
Results: Following the evaluation, it was concluded that the quality of knowledge transfer was divergent. An increase of knowledge could always be confirmed statistically, but often the clinical relevance and up-to-date contents were missing. All investigated courses complied with the mandatory content guidelines. The compulsory up-to-date refresher courses were found to be refreshing basic knowledge mostly instead of presenting new developments and technologies in radiation protection.
Conclusion: To achieve a more appropriate learning situation in the courses, proposals are made, including a new target-group-specific course configuration with reduced attendance times. A specific course for radiation safety officers similar to Austria's concept is suggested. Subject catalogues for the redesigned courses were created and could be used for harmonisation throughout Europe.
Limitations: Only courses on radiation protection in Germany were evaluated.
Ethics committee approval: n/a
Funding: Funding by Bundesamt für Strahlenschutz.
Author Disclosures:
P. Strauß: nothing to disclose

14:00 - 15:30 **Coffee & Talk 2**

Vascular

RPS 1115

Pulmonary arteries, veins, aorta, carotid and lymphatics

Moderators:
N.N.
A. Van Der Lugt; Rotterdam/NL

RPS 1115-1 14:00
Response to balloon pulmonary angioplasty in treated versus untreated pulmonary arteries in CTEPH patients
Z. Zhai[1], H. Ota[2], M. Staring[1], J. Stolk[1], K. Sugimura[2], K. Takase[2], B. Stoel[1]*; [1]Leiden/NL, [2]Sendai/JP (z.zhai@lumc.nl)*

Purpose: Balloon pulmonary angioplasty (BPA) is a treatment of obstructed pulmonary arteries (PAs) for patients with inoperable chronic thromboembolic pulmonary hypertension (CTEPH). Since the effect of BPA in untreated (unobstructed) PAs is unknown, we investigated the treatment response in treated and untreated PAs by analysing CT pulmonary angiography (CTPA).
Methods and materials: We studied 22 consecutive CTEPH patients (20 female; age 67±14) who underwent CTPA and right-heart catheterisation (RHC) pre- and post-BPA. In consensus, 3 experts selected treated artery segments based on the BPA locations and approximately 5 untreated artery segments at a similar level. Post-BPA CTPA scans were registered to pre-BPA scans and local intravascular density changes were measured. The median density change in treated (MDC_T) and untreated segments (MDC_U) was calculated based on manual selections. The difference between MDC_U and MDC_T was tested by a paired t-test. The difference in density changes (ΔMDC) between treated and untreated PAs was calculated (MDC_T-MDC_U). Changes in RHC parameters included systolic, diastolic, and mean pulmonary artery pressure (ΔsPAP, ΔdPAP, and ΔmPAP) and in pulmonary vascular resistance (ΔPVR). The relation between haemodynamic changes and ΔMDC was studied with Spearman's correlation.
Results: MDC_T (51±85 HU) and MDC_U (-23±103 HU) were significantly different and in the opposite direction (p=0.001). ΔMDC was significantly correlated with ΔdPAP (R=-0.55, p=0.008) and ΔPVR (R=-0.47, p=0.026), and marginally correlated with ΔmPAP (R=-0.4, p=0.068).
Conclusion: Perfusion in treated PAs increased, whereas perfusion in untreated PAs decreased. Not only improved perfusion in treated arteries but also the normalisation in untreated arteries may play a significant role in improving haemodynamics by BPA.
Limitations: The normal vascular perfusion of healthy people is lacking.
Ethics committee approval: Approved by the local ethics committee and written informed consent from patients was obtained.
Funding: No funding was received for this work.
Author Disclosures:
Z. Zhai: nothing to disclose
H. Ota: nothing to disclose
M. Staring: nothing to disclose
J. Stolk: nothing to disclose
K. Sugimura: nothing to disclose
K. Takase: nothing to disclose
B. Stoel: nothing to disclose

RPS 1115-2 14:06

Pulmonary artery enlargement is independently associated with 1-year mortality in transcatheter aortic valve replacement patients: a retrospective longitudinal study

V. L. Turner[1], M. J. Willemink[1], A. Jubran[2], J. B. Kim[1], E. M. Maret[3], K. J. Moneghetti[1], F. Haddad[1], D. Fleischmann[1]; [1]*Stanford, CA/US,* [2]*Haifa/IL,* [3]*Stockholm/SE (vturner@stanford.edu)*

Purpose: Pulmonary hypertension has been shown to be an independent predictor of poor outcome in patients undergoing transcatheter aortic valve replacement (TAVR). In this retrospective longitudinal study we sought to evaluate whether pulmonary artery enlargement measured on pre-procedural computed tomography angiography (CTA) is associated with 1-year mortality in patients after TAVR.
Methods and materials: We retrospectively included 402 patients undergoing TAVR from July 2012-March 2016. Clinical parameters and pre-procedural CTA scans were retrospectively reviewed. Patients were followed for all-cause mortality. The main pulmonary artery (MPA) area and diameter were measured on pre-procedural CTAs near the bifurcation on double-oblique reformations. Kaplan-Meier and Cox proportional hazards regression analyses were performed.
Results: The median follow-up time of 402 patients was 433 (interquartile 339-797) days. A total of 56/402 (14%) died within 1 year after TAVR. MPA area ($p<0.001$) and the Society of Thoracic Surgery risk scores (STS-score) ($p=0.001$) were significantly larger in 1-year non-survivors (N=56) versus survivors (N=346). Multivariate Cox analysis adjusted for age, gender, STS score, cardiac risk, frailty, and NYHA classification showed that both MPA area (HR1.30 [95%-CI 1.16–1.46] per cm^2, $p<0.001$) and STS-scores (HR1.10 [1.02–1.20] per STS point, $p=0.0016$) were independently associated with 1-year mortality. The area under the curve for 1-year mortality was similar for MPA area (AUC=0.67 [95%-CI 0.59–0.75]) compared to STS-score (AUC=0.64 [95%-CI 0.57–0.72]). Kaplan-Meier analysis showed that the mortality of patients with a pre-procedural MPA area of ≥7.4 cm^2 was significantly higher compared to patients with a smaller MPA area of <7.4c m^2 (mortality 23% vs 9%; log-rank $p<0.001$).
Conclusion: The enlargement of MPA on pre-procedural CTAs is independently associated with post-procedural 1-year mortality in patients who undergo TAVR.
Limitations: A retrospective single-centre design. Further studies are needed to demonstrate the reproducibility of our results in other CT scanners and cohorts.
Ethics committee approval: n/a
Funding: No funding was received for this work.
Author Disclosures:
V. L. Turner: nothing to disclose
M. J. Willemink: Grant Recipient at American Heart Association, Grant Recipient at Koninklijke Philips NV, Consultant at Arterys, Inc, Founder at Segmed, Inc
A. Jubran: nothing to disclose
J. B. Kim: nothing to disclose
E. M. Maret: nothing to disclose
K. J. Moneghetti: nothing to disclose
D. Fleischmann: Research/Grant Support at Siemens AG
F. Haddad: nothing to disclose

RPS 1115-3 14:12

The cost-effectiveness of contrast-enhanced ultrasound (CEUS) for the detection of type I and III endoleaks after EVAR: the role of CEUS as the most cost-effective imaging modality

M. F. Froelich[1], W. G. Kunz[2], S. H. Kim[3], D.-A. A. Clevert[2], J. Rübenthaler[2]; [1]*Mannheim/DE,* [2]*Munich/DE,* [3]*Frankfurt am Main/DE*

Purpose: Follow-up after endovascular aortic repair (EVAR) is necessary to detect complications. Computed tomography or magnetic resonance angiography (CT-A/MR-A) are used as a standard of care. Contrast-enhanced ultrasound (CEUS) has been shown to be an imaging modality with equipollent diagnostic accuracy. The aim of this study was to determine the cost-effectiveness of this imaging method in comparison to others for the evaluation of type I and III endoleaks.
Methods and materials: A decision model based on Markov simulations estimated lifetime costs and quality-adjusted life-years (QALYs) associated with CT-A, MR-A, CEUS, and colour-Doppler. Model input parameters were obtained from recent literature. Probabilistic sensitivity analysis was performed to estimate the uncertainty of model results. Net monetary benefits, incremental costs, incremental effectiveness, and incremental cost-effectiveness ratios were derived from the probabilistic sensitivity analysis. The willingness-to-pay (WTP) was set to $100,000/QALY.
Results: In the base-case scenario for a WTP of $100,000 per QALY, CT-A and MR-A were dominated strategies resulting in lifetime costs of $20,374.77 for CT-A and $20,673.71 for MR-A, with expected effectiveness of 9.556 QALYs vs 9.564 QALYs. Colour-Doppler showed an expected cost of $19,868.57 with 9.532 QALYs whereas CEUS reached costs of $20,050.19 with 9.564 QALYs, resulting in an ICER of $5,720.91/QALY.
Conclusion: CEUS is a cost-effective imaging method for the evaluation of type I and III endoleaks in endovascular aortic repair surveillance.
Limitations: The average age of patients entering the model was set to 70 years, which is in line with existing literature for the likelihood of endoleaks, but neglects the fact that there must also be younger patients with endoleaks after EVAR.
Ethics committee approval: n/a
Funding: No funding was received for this work.
Author Disclosures:
M. F. Froelich: Employee at Smart Reporting GmbH
W. G. Kunz: nothing to disclose
S. H. Kim: nothing to disclose
D.-A. A. Clevert: nothing to disclose
J. Rübenthaler: nothing to disclose

RPS 1115-4 14:18

Value of dynamic perfusion computed tomography in the detection and classification of endoleaks after endovascular aortic repair (EVAR)

J. Stroeder[1], D. Kerner[1], A. Massmann[1], J. F. M. Gawlitza[1], A. Bücker[1], R. Kubale[2], P. Fries[1]; [1]*Homburg/DE,* [2]*Pirmasens/DE*

Purpose: To assess the value of dynamic perfusion computed tomography (CT) in the detection and classification of endoleaks in patients after EVAR.
Methods and materials: 10 patients (9 males/1 female; mean age 76.8 years +/- 5 years) after EVAR with known endoleaks diagnosed with contrast-enhanced ultrasound or standard CT were included. They underwent a contrast-enhanced dynamic perfusion CT using a third-generation dual-source scanner (Somatom Force, Siemens Healthineers, Erlangen, Germany) to identify the origin of the endoleaks. We retrospectively performed contrast attenuation measurements for all time points based on region of interest (ROI) measurements within the stent lumen and the perfused endoleak within the aneurysm sac and in the inferior mesenteric artery. Perfusion characteristics were graphed for the assessment using commercially available software (SyngoVia, Siemens Healthineers, Erlangen, Germany). Differences between areas under the curves (AUC) were analysed by ANOVA and Tukey's test.
Results: The contrast attenuation time curve pattern and the AUC for the perfused endoleak within the aneurysm sac is similar to the feeding vessel, allowing for differentiation between type 1 and type 2 endoleaks. The dynamic perfusion CT and the graphing of the findings was a helpful tool in the assessment of endoleak characteristics. Significance of AUC differences for Type 2 endoleaks was $p<0.0001$.
Conclusion: Dynamic perfusion CT helps to correctly identify and classify endoleaks after EVAR, which has a marked impact on patient management.
Limitations: A single-centre, retrospective study.
Ethics committee approval: Written informed consent was obtained.
Funding: No funding was received for this work.
Author Disclosures:
J. Stroeder: nothing to disclose
P. Fries: nothing to disclose
R. Kubale: nothing to disclose
A. Massmann: nothing to disclose
D. Kerner: nothing to disclose
A. Bücker: nothing to disclose
J. F. M. Gawlitza: nothing to disclose

RPS 1115-5 14:24

Dual-energy CT iodine mapping and virtual monochromatic series applications in the diagnosis of endoleak after endovascular aortic repair (EAVR) planning

P. Hou; *Zhengzhou/CN (houping1221@163.com)*

Purpose: To assess the diagnostic value of endoleak conspicuity amongst DECT monochromatic series, iodine mapping, and conventional images with follow-up CTA after EAVR planning.
Methods and materials: 19 patients that required follow-up CTA after EVAR with 23 endoleaks (17 medium endoleaks; 6 small endoleaks) underwent spectral CT to generate conventional 140-kVp polychromatic images (group A), monochromatic images with energy levels from 40 to 70keV (group B), and iodine mapping (group C). Clinical and operative outcomes were recorded as the reference standard. Two radiologists independently analysed lesion conspicuity to assess sensitivity and specificity.
Results: Sensitivity and specificity were both 100% for medium endoleaks on images among all groups. For small endoleaks in the comparison of the conventional images, sensitivity for detection increased from 63.6% (95% CI, 30.8-89.1%) to 98.1% (95% CI, 68.2-100%), 98.7% (95% CI, 75.5-100%), and 100% (95% CI, 71.5-100%) when iodine mapping, 50kev, and 60keV images were assessed, respectively. The number of false-positives were increased with

40keV images. The small endoleaks were poorly visualised in group A and 70kev images. Interobserver agreement were moderate (κ=0.45) and substantial (κ=0.63) among iodine mapping and monochromatic images, respectively.
Conclusion: Iodine mapping and virtual monochromatic images (50kev and 60kev levels) increase the conspicuity of endoleaks of the aorta, resulting in improved diagnostic accuracy compared with a review of conventional CT images alone.
Limitations: This investigation reflects our preliminary experience with a relatively small number of patients. Different detector configurations caused some variability in the imaging parameters.
Ethics committee approval: This prospective single-institution study was approved by the Human Research Committee of our institutional review board and all patients provided written informed consent.
Funding: No funding was received for this work.
Author Disclosures:
P. Hou: nothing to disclose

RPS 1115-6 14:30

The incidence of penetrating aortic ulcer (PAU) as a cause for non-aneurysmal rupture of the abdominal aorta: a single-centre experience

K. Andreychuk[1], N. Chernaya[2], V. E. Savello[1], N. N. Andreychuk[1], O. Krotova[1]; *[1]St. Petersburg/RU, [2]Moskow/RU (andreychuk@cvsurgery.ru)*

Purpose: Selected reports declare that spontaneous ruptures of non-aneurysmal, non-infected abdominal aortas are extremely rare. Many authors suppose the main cause is a penetrating aortic ulcer (PAU). Unfortunately, only single reports regarding single cases of PAU located in the abdominal aorta can be revealed. In this study, we analysed our experience in the diagnosis and management of complicated PAU in the abdominal aorta.
Methods and materials: 48 patients with non-aneurysmal rupture of the abdominal aorta due to PAU (median age 61 years; 32 women) were included in this report. In all cases, patients had clinical signs of internal bleeding, so aneurysmal rupture was suspected as the main cause on admission. The diagnosis was determined by ultrasound and CTA.
Results: The radiologic findings included typical signs of PAU (the same as the signs in the thoracic aorta) represented by non-dilated aorta with a strong calcified wall, single or multiple crateriform ulcers, and ulcer bottom defect with extravasation. In this area, retroperitoneal haematoma with contrast uptake was detected. In rare cases where the PAU and consequent rupture were located in the posterior wall of the aorta, a temporary restricted (two-stage) rupture without signs of continuing bleeding could be observed. The following histopathological examination confirmed PAU with wall destruction. The majority of patients underwent surgical repair (35 open and 9 endovascular). 7 patients died.
Conclusion: Our experience indicates that PAU in the abdominal aorta and following non-aneurysmal rupture is quite rare, but not a casuistic aortic emergency condition. This should be suspected in each case of non-traumatic retroperitoneal bleeding. The diagnostical and tactical approach should be the same as in cases of acute aortic syndrome based in the thoracic aorta.
Limitations: n/a
Ethics committee approval: n/a
Funding: No funding was received for this work.
Author Disclosures:
K. Andreychuk: nothing to disclose
N. Chernaya: nothing to disclose
V. E. Savello: nothing to disclose
N. N. Andreychuk: nothing to disclose
O. Krotova: nothing to disclose

RPS 1115-7 14:36

An evaluation of the changes of renal blood flow before and after an operation in patients with aortic dissection

D. Liu*; Beijing/CN (dongting0530@163.com)*

Purpose: To investigate the changes of renal CT perfusion in aortic dissection (AD) patients before and after an operation and to access the feasibility of the clinical diagnosis.
Methods and materials: 31 patients with AD who underwent 320-row CT renal perfusion before and after operation were included. Blood flow (BF), blood volume (BV), and the clearance of the bilateral kidneys were measured. A comparison of the difference of perfusion parameter values before and after the operation and various CT imaging signs of AD were observed.
Results: The BF values measured between the true lumen, false lumen, and overriding groups were different (p<0.05); the false lumen group was the lowest. The BV of the true lumen and the overriding group was statistically different (P<0.05) after the operation; the overriding group was the lowest while other groups had no significant difference (P>0.05). The value of BV and clearance decreased after the operation (P<0.05), BF had no significant difference (P>0.05), the BV of the false lumen group decreased (P<0.05), and BF and clearance had no significant difference (P>0.05). The perfusion parameters of the overriding group had no significant difference (P>0.05) before and after the operation.
Conclusion: Perfusion imaging using 320-slice dynamic volume CT can be used to evaluate haemodynamic features of the kidneys. Both surgical and interventional operations can affect renal perfusion. Perfusion imaging is helpful in evaluating the renal functional status preoperation and in discovering renal ischaemia postoperation.
Limitations: The number of participants included in this study was relatively small, which was based on a single-centre experience. Further studies based on the analysis of more cases are required.
Ethics committee approval: This prospective study was approved by our institutional review board.
Funding: No funding was received for this work.
Author Disclosures:
D. Liu: nothing to disclose

RPS 1115-8 14:42

A feasibility study of virtual non-contrast imaging derived from single-source fast kVp-switching dual-energy CTAs in patients with aortic dissection

B. Wen, J. Liu, L. Xu*; Beijing/CN (wwwyyner@163.com)*

Purpose: To study the feasibility of virtual non-contrast (VNC) imaging derived from single-source fast kVp-switching dual-energy arterial phase CTAs in evaluating the status of patients with aortic dissection and to calculate the potential radiation dose reductions.
Methods and materials: 50 consecutive patients with aortic dissection were examined with CT scans including TNC imaging using conventional single-energy mode at 120 kVp and arterial phase CTA utilising the rapid kVp-switching dual-energy CT technique (80 kV/Sn140 kV) of the aorta. VNC images were obtained from an arterial phase CTA dataset. Two radiologists independently evaluated the image quality of TNC and VNC images. The mean attenuation and image noise of various regions of the aorta and abdominal organs were measured on TNC and VNC images.
Results: Interobserver agreement was excellent. For almost all locations, the CT value and image noise were lower at VNC than at TNC. The CNR of different locations showed no significant difference. Subjective image score was lower for VNC (4.52±0.53 vs 4.31±0.51, P>0.05) but there were no cases rated non-diagnostic. The effective dose for dual-phase was 11.22±1.91mSv and for single-phase was 6.85±1.76 mSv. The dose saving by removing the TNC was 4.37±0.54 mSv (39.7%).
Conclusion: In patients with AD, the VNC images derived from single-source fast kVp-switching dual-energy CTs can provide comparable image quality to TNC images and reliable diagnostic information. Replacing TNC images will lower radiation dose by 39.7%.
Limitations: The study was only a single-centre study applicable to the GE revolution CT. Our results were vendor-specific and the results may vary with other patient populations.
Ethics committee approval: The study was approved by our hospital's ethics committee and all patients provided written informed consent.
Funding: No funding was received for this work.
Author Disclosures:
B. Wen: nothing to disclose
J. Liu: nothing to disclose
L. Xu: nothing to disclose

RPS 1115-9 14:48

High-frequency 3D lumen volume ultrasound is a sensitive method to detect early aneurysmal changes in elastase-induced murine abdominal aortic aneurysms

M. A. Waduud, P. Kandavelu, M. Reay, J. Scott, M. Bailey*; Leeds/UK (m.a.waduud@leeds.ac.uk)*

Purpose: To investigate the reproducibility of anterior-posterior diameter (APDmax) and three-dimensional lumen volume (3DLV) measurements of abdominal aortic aneurysms in a classical murine AAA model. We also investigated the sensitivity of each method to detect changes in AAA size.
Methods and materials: Peri-adventitial application of porcine pancreatic elastase (PPE AAA) or sham surgery was performed in two cohorts of mice. Cohort 1 was used to assess for observer variability with APDmax and 3DLV measurements. Cohort 2 highlighted the relationship between APDmax and 3DVL and the changes in AAA detected.
Results: There was no significant observer variability detected with APDmax measurement. Similarly, no significant intraobserver variability was evident with 3DLV, however, a small but significant interobserver difference was present. APDmax and 3DLV measurements of PPE AAA significantly correlated. Changes in the AAA morphology were detected earlier with 3DLV.

Conclusion: APDmax and 3DLV are both reliable methods of measuring an AAA. Both these methods correlate with each other. However, changes in AAA morphology are detected earlier with 3DLV, which is important in detecting subtle but important changes to aortic geometry in a laboratory setting.
Limitations: This was a proof-of-principle animal study.
Ethics committee approval: Animal work was carried out in accordance with the UK Animals (Scientific Procedures) Act 1986 under Home Office Project Licence PPL: P606320FB.
Funding: This work was funded by the British Heart Foundation (BHF). MAW is a BHF clinical training research fellow and MAB is a BHF intermediate clinical fellow.
Author Disclosures:
M. A. Waduud: nothing to disclose
P. Kandavelu: nothing to disclose
M. Reay: nothing to disclose
J. Scott: nothing to disclose
M. Bailey: nothing to disclose

RPS 1115-10 14:54

Sex differences in vulnerable plaque composition and morphology in patients with mild-to-moderate carotid artery stenosis

D. H. Dam-Nolen[1], N. C. van Egmond[1], M. E. Kooi[2], J. Hendrikse[3], P. J. Nederkoorn[4], P. J. Koudstaal[1], D. Bos[1], A. van der Lugt[1]; [1]*Rotterdam/NL,* [2]*Maastricht/NL,* [3]*Utrecht/NL,* [4]*Amsterdam/NL (h.nolen@erasmusmc.nl)*

Purpose: For not yet fully understood reasons, the stroke incidence rate is higher in men than in women. Carotid atherosclerosis is a major cause of ischaemic strokes. Several plaque components are important determinants for plaque progression and rupture. Sex differences in these so-called vulnerable plaque characteristics, including intraplaque haemorrhage (IPH), lipid-rich necrotic core (LRNC), thin or ruptured fibrous cap (TRFC), and ulcerations, may help further explain sex differences in strokes. This study aims to analyse sex differences in plaque composition and morphology in symptomatic patients.
Methods and materials: We selected 238 patients from the Plaque At RISK-study (PARISK), which included patients with recent ischaemic symptoms and <70% ipsilateral carotid artery stenosis. Plaque characteristics were assessed with MRI (n=224) and MDCTA (n=188). We used multivariable logistic regression analyses to assess the effects of sex on the presence and volume of plaque characteristics. Differences in volumes were analysed using multivariable linear regression models in those patients in whom the plaque component of interest was present.
Results: Men had significantly higher plaque burden (β=23.05, 95%CI:15.81-30.29). Men also had a higher prevalence of IPH (OR=3.29, 95%CI:1.54-7.50) and LRNC (OR=2.40, 95%CI:1.25-4.62) after an adjustment for age and plaque burden. These associations remained significant after additionally adjusting for cardiovascular risk factors and medication (OR=2.79, 95%CI:1.25-6.60; OR=2.48, 95%CI:1.23-5.07). In patients with IPH and/or LRNC in their symptomatic carotid plaque, the volume of IPH and LRNC was not significantly associated with sex after an adjustment for age and plaque burden. Sex was not associated with the presence of TRFC, ulcerations, and calcifications.
Conclusion: Vulnerable plaque components like IPH and LRNC are more common in men than women in symptomatic patients with mild-to-moderate carotid stenosis.
Limitations: n/a
Ethics committee approval: Institutional review board approval was obtained. All patients gave written informed consent.
Funding: No funding was received for this work.
Author Disclosures:
D. H. Dam-Nolen: nothing to disclose
N. C. van Egmond: nothing to disclose
M. E. Kooi: nothing to disclose
P. J. Nederkoorn: nothing to disclose
P. J. Koudstaal: nothing to disclose
J. Hendrikse: nothing to disclose
D. Bos: nothing to disclose
A. van der Lugt: nothing to disclose

RPS 1115-11 15:00

Carotid plaque neovascularisation detection and assessment accuracy with the contrast-enhanced ultrasound (CEUS) method

A. Lioznovs, M. Radzina, A. Lacis, A. Jukna, I. Briede, Y. Solskaya, L. Dronka, S. Pavlovics*; Riga/LV (lioznov1@gmail.com)*

Purpose: Contrast ultrasound (CEUS) is an effective method that can detect the presence of neovascularisation in unstable atherosclerotic plaques and significantly reduce cerebral stroke risk. The purpose of the study was to analyse the CEUS technique ability to confirm plaque instability in correlation with CTA and histological findings in order to determine the method's accuracy and limitations.
Methods and materials: During the prospective research, conducted from 2017-2019, 54 patients with 72 plaques detected with a duplex US were included. Every patient was analysed with CEUS, DUPLEX, and CTA to compare the accuracy of the imaging methods. 30 endarterectomies were performed and the histology of the atherosclerotic plaques was acquired. Based on CEUS results, two groups were identified: poor (grade 1) neovascularisation and well visible (grade 2) vasa vasorum. Each group was correlated with histological findings.
Results: The neovascularisation was diagnosed in 27/72 (37.5%) patients by CEUS. In 12 cases (16.7%), plaques showed grade 1 neovascularisation and in 15 cases (23.2%), grade 2. The presence of neovascularisation was proved by histology in all CEUS positive cases from 2-39 microvessels. Comparing the CEUS method and results of histology, a statistically significant correlation was found (r_s=0.099; p=0.704) and the method's sensitivity, specificity, positive predictive value, negative predictive value, and accuracy were 82.4%, 69.2%, 77.8%, 75%, and 76.7%, respectively. A statistically significant correlation between neovascularisation was found in terms of contrast time and CEUS for neovascularisation grades (0.633; p=0.06).
Conclusion: CEUS imaging provides additional information in the detection of plaque instability with high accuracy, sensitivity, and specificity, regardless of the stenosis grade and corresponding well to histological results.
Limitations: It was observed that calcified and partially calcified plaques had a smaller number of microinvasions, but no significant correlation was found, possibly due to the small number of patients (rs–0.9; p=0.31).
Ethics committee approval: n/a
Funding: No funding was received for this work.
Author Disclosures:
A. Lioznovs: nothing to disclose
M. Radzina: nothing to disclose
Y. Solskaya: nothing to disclose
A. Lacis: nothing to disclose
A. Jukna: nothing to disclose
L. Dronka: nothing to disclose
S. Pavlovics: nothing to disclose
I. Briede: nothing to disclose

RPS 1115-12 15:06

Vessel wall imaging using CT: an innovative dual-energy protocol for differentiating vascular pathologies

W. Zhou, A. C. C. Goh*; Sydney/AU (kimwx.zhou@gmail.com)*

Purpose: Vascular diseases have traditionally been evaluated with luminal imaging, however, pathologies such as fibromuscular dysplasia, intramural haematoma, vasculitis, and atheroma can be better differentiated if the vessel wall can be directly imaged (Alexander, 2017).
We describe a novel technique to image the blood vessel wall using dual-energy CT rather than the established techniques with MRI.
Methods and materials: Contrast-enhanced exams were performed on a clinical CT scanner with the capability for dual-energy and calcium suppression. Routine dual-energy scan protocol was selected, including gated and non-gated aortogram, pulmonary angiogram, renal/mesenteric angiogram, portal venous abdomen, and other angiographic studies of the head, neck, and limbs. Calcium suppressed image reconstruction was performed in addition to routine reconstructions using a selection of experimental parameters including calcium suppression strength, slice thickness, the field of view, and kernel sharpness.
Results: Using calcium suppression reconstruction, contrast-enhanced blood is effectively suppressed to negative modified-HU, allowing the direct visualisation of the vessel wall for the aorta, pulmonary vessels, portal vein, coeliac artery, superior mesenteric artery, and renal artery. Small visceral vessels of the chest and abdomen are also well reconstructed by this method to show the vascular wall.
Conclusion: Prior knowledge of vessel wall imaging has required the use of MRI. We propose a novel method for high-resolution CT imaging of vessel wall morphology, with advantages such as short exam time and better patient tolerance. This has the potential for improving the diagnosis and management of vasculopathies.
Limitations: The study is limited by the number of scans analysed and the lack of same-patient comparison with MRI as the existing gold standard of vessel wall imaging.
Ethics committee approval: n/a
Funding: No funding was received for this work.
Author Disclosures:
W. Zhou: nothing to disclose
A. C. C. Goh: nothing to disclose

RPS 1115-13 15:12
Inguinal lymphadenopathy as a predicting factor for primary amputation in patients after endovascular treatment
D. Raskin, S. Balan, O. Mozes, D. Silverberg, A. Aburamila, M. Halak, U. Rimon*; Ramat Gan/IL (oshry.mozes@sheba.health.gov.il)*

Purpose: To assess the correlation between inguinal lymph node characteristics and ipsilateral primary limb amputation rates in patients with ischaemic foot ulcers who underwent technically successful endovascular treatment.
Methods and materials: A retrospective review of patients who were endovascularly treated for ischaemic foot ulcers from January 2015-May 2017. Unilateral lymph node size, contrast enhancement, necrosis, and perinodular fat infiltration were assessed on pre-procedural computed tomography angiography. Primary endpoints were amputation and sepsis within six months following treatment. Independent samples t-tests and a Chi-square test of independence examined the relationship between lymph node characteristics and limb amputation and septic shock.
Results: Endovascular treatment of 202 limbs in 202 patients (135 males; median age 72.8 years [range, 42.2-93.7]) was technically successful. 42/202 (20.8%) patients underwent amputation and 6/202 (3%) patients had sepsis. There was a significant difference in lymph node sizes between the amputated and the non-amputated limbs (P=0.000). Lymph node characteristics were significantly related to amputation (P<0.001). Perinodular fat infiltration or increased node size were associated with the likelihood to undergo limb amputation than the others, respectively. Lymph node characteristics were also related to septic shock (P<0.05).
Conclusion: Limb amputation and ipsilateral lymph node size and characteristics are associated with the technically successful endovascular treatment of patients with ischaemic foot ulcers. Moreover, increased lymph node size and perinodular fat infiltration predicted limb amputation.
Limitations: A retrospective study restricted to the imaging characteristics of the inguinal lymph nodes of selected patients with ulcers lacking apparent infection.
Ethics committee approval: Institutional review board approval was obtained.
Funding: No funding was received for this work.
Author Disclosures:
D. Raskin: nothing to disclose
S. Balan: nothing to disclose
O. Mozes: nothing to disclose
D. Silverberg: nothing to disclose
A. Aburamila: nothing to disclose
M. Halak: nothing to disclose
U. Rimon: nothing to disclose

RPS 1115-14 15:18
The effect of different compression stockings on venous malformations: a systematic assessment of morphology and quality of life
R. Heiß, A. Dr. Mükke, M. S. May, W. Wuest, M. Uder, R. Janka, W. Lang*; Erlangen/DE (Rafael.Heiss@uk-erlangen.de)*

Purpose: To analyse the effect of different compression therapies on venous malformations (VM).
Methods and materials: Patients with VM in the upper and lower extremities (N=20) were eligible for the study. Patients were treated with compression stockings class I and II for 4 weeks in a randomised order. Patients and physicians were blinded to the compression class. The absolute volume of the VM was measured by segmentation in MRI images. The volume of the extremity was obtained by perimetry measurements (PER). Quality of life was assessed by the SF-12 score. MRI and PER were performed at baseline and after the wearing period of 4 weeks of each compression class.
Results: In comparison with baseline measurements, both compression classes showed a significant reduction of the volume of the VM in MRI scans (p<0.001), whereas the decrease of the lesions' volume was inforced by compression class II (p=0.039). In contrast, PER did not reveal significant differences in comparison to the baseline for both compression classes (p=0.26, p=0.055). No subgroup in the quality of life assessment showed a significant difference between compression classes.
Conclusion: MRI is an applicable tool for the systematic assessment of the total volume of VM. Both compression stockings class I and II reduce the total volume of VM, with superiority in class II. As there is no difference in the quality of life between both compression classes, class II compression stockings may be recommended for conservative treatment of patients with local swelling and pain caused by VM.
Limitations: The limited number of patients with intraindividual comparison of different interventions.
Ethics committee approval: IRB (Institutional Review Board) approval was obtained from Friedrich-Alexander-University Erlangen-Nuremberg, Germany (124_17 B).
Funding: Study was funded by medi GmbH & Co. KG, Bayreuth, Germany.
Author Disclosures:
R. Heiß: nothing to disclose
M. Uder: nothing to disclose
R. Janka: nothing to disclose
A. Dr. Mükke: nothing to disclose
W. Lang: nothing to disclose
M. S. May: nothing to disclose
W. Wuest: nothing to disclose

RPS 1115-15 15:24
The results of an ultrasound vein valve study change current saphenous therapy
J. C. Ragg, J. Grünwald*; Berlin/DE (jcr@gmx.eu)*

Purpose: Novel high-resolution ultrasound systems (16-32 MHz) allow for new insights in venous anatomy, physiology, and pathophysiology. Which novel information is depictable in particular in the detection of small structures like vein valves and low-flow phenomena?
Methods and materials: 1,300 consecutive patients, aged 6-92 years, were examined with the newest high-resolution ultrasound systems (16-23 MHz: Zonare One Pro, Mindray M9; Siemens Juniper 16 MHz, Vevo MD-peak 32 MHz), with a focus on the saphenous veins and their valves. Video loops of the intra- and epifascial systems were recorded for evaluation by 3 independent investigators.
Results: 3 groups of vein valve lesions could be detected, representing different origins. First, embryonic valve lesions showing commissural mismatch, incomplete, or missing cusps were found in 47% of candidates 6-8 years of age, comprising just one or two valves in 78% of the cases. A second mechanism was pressure-induced valve decompensation, marked by progredient dilatation and loss of functional reserve. It was seen after the age of 25 years and mainly concerned terminal GSV valves or medial perforators (76%). A third mechanism was stasis-related valve degeneration with a typical sonographic marker called "persistent aggregates" blocking the valve sinus increasing unto sclerotic degression or even loss of valve structures. Reflux of this mechanism was not seen before the age of 35 years, but was in 63.2% of the cases aged above 70 years.
Conclusion: Different kinds of valve lesions will need different therapies. Embryonic lesions need repair, pressure problems need internal compression, and just stasis-related early stages may benefit from stockings. Lesion-specific modalities for prevention and therapy now have to be evaluated.
Limitations: General limitations of ultrasound (e.g. obesity).
Ethics committee approval: n/a
Funding: No funding was received for this work.
Author Disclosures:
J. C. Ragg: nothing to disclose
J. Grünwald: nothing to disclose

14:00 - 15:30 **Room F2**

Chest

RPS 1104

New applications of advanced CT and MRI

Moderators:
N.N.

RPS 1104-1 14:00
µCT-monitoring of neutrophil elastase deficiency on a mouse model of cystic fibrosis-like lung disease
L. Zhu, Z. Zhou-Suckow, J. Salomon, D. Leitz, W. Stiller, W. Wagner, H.-U. Kauczor, M. O. Wielpütz*; Heidelberg/DE (monica_zhul@163.com)*

Purpose: Cystic fibrosis (CF) is characterised by chronic obstructive lung disease, driven by recurrent infections and inflammation. Our aim was to elucidate the value of micro-CT (µCT) for monitoring disease progression in a mouse model of CF-like lung disease and for quantifying effects of neutrophil elastase (NE) knock-out as a potential target for therapeutic intervention.
Methods and materials: 60 conserved lungs from mice with four different genotypes combining CF-like lung disease (Scnn1b-Tg) or wild-type (WT) with neutrophil elastase knock-out (Scnn1b-Tg/NE$^{-/-}$, WT/NE$^{-/-}$) were scanned by µCT (8.6µm resolution) three times (newborn, 5-6, and 14-16 days old). Alveolar size measured by mean linear intercepts (LM), lung volume, and air proportion were quantified on µCT.
Results: Average LM was similar in newborn mice among all four groups. At 5-6 days and 14-16 days, the alveolar size was larger in Scnn1b-Tg compared to WT (p<0.01), indicating the development of emphysema. Lung volume was significantly increased at 14-16d in Scnn1b-Tg (p<0.05) and air proportion was

increased from 5-6 days (p<0.01). Importantly, Scnn1b-Tg/NE$^{-/-}$ showed a significantly reduced air proportion at both 5-6 days and 14-16 days compared to Scnn1b-Tg alone, though the alveolar size and lung volume only showed a trend towards reduction be NE knock-out, indicating that NE knock-out reduces emphysema in CF-like lung disease.
Conclusion: µCT detects early development of emphysema in a mouse model of CF-like lung disease, which can potentially be mitigated by NE deficiency. Non-invasive imaging of µCT allows for longitudinal quantification of CF-like lung disease and it may be used as an endpoint for novel therapeutic trials in this mouse model.
Limitations: Data from adult mice has not yet been analysed and more parameters are being collected.
Ethics committee approval: Approved by the federal animal protection authority.
Funding: Supported by the German BMBF.
Author Disclosures:
L. Zhu: nothing to disclose
Z. Zhou-Suckow: nothing to disclose
J. Salomon: nothing to disclose
D. Leitz: nothing to disclose
W. Stiller: nothing to disclose
W. Wagner: nothing to disclose
H.-U. Kauczor: nothing to disclose
M. O. Wielpütz: nothing to disclose

RPS 1104-2 14:06

Application of ultra-high-resolution computed tomography target scan in lateral or oblique body position in predicting histological invasiveness of persistent pure ground-glass nodules

H. Ren, L. Xu, F. Sun, F. Liu, J. Cai, L. Yu, W. Guan, H. Xiao, H. Li*; Shanghai/CN (renhuadoc@163.com)*

Purpose: To retrospectively investigate whether ultra-high-resolution computed tomography (U-HRCT) target scan in lateral or oblique body position (scan protocol G) could predict histological invasiveness of pulmonary adenocarcinoma manifesting as persistent pure ground-glass nodules (pGGNs).
Methods and materials: 306 pathologically confirmed pGGNs in 260 patients who had undergone protocol G examinations were enrolled in this study. There were 213 preinvasive lesions (59 of atypical adenomatous hyperplasias and 154 of adenocarcinomas in situ) and 93 invasive pulmonary adenocarcinomas (IPAs) (53 minimally invasive adenocarcinomas and 40 invasive adenocarcinomas). The U-HRCT findings of the two groups were analysed on orthogonal multiplanar reformation images manually.
Results: Compared with preinvasive lesions, IPAs exhibited significantly larger diameter, higher mean and representative attenuation, lower relative attenuation and higher frequencies of heterogeneity, air bronchogram, bubble lucency, pleural retraction, and vascular convergence (P<0.01). Higher AUC and specificity could be achieved by using representative attenuation than mean attenuation or relative attenuation for predicting invasiveness. The multivariate logistic analysis revealed that larger diameter (OR=1.328, 95% confidence interval [CI]: 1.208-1.461) and higher representative attenuation (OR=1.005, 95% CI: 1.003-1.007) were significant predicting factors of IPAs from preinvasive lesions (P<0.05). The optimal cut-off of the maximum diameter for IPAs was larger than 10 mm.
Conclusion: The imaging features based on scan protocol G can effectively help predict histological invasiveness of persistent pGGNs.
Limitations: Some selected bias may be unavoidable. Intraobserver and interobserver variability were not analysed in this study. All scans and data used in our study were obtained on an available workstation provided by only one company. Therefore, further validation studies are required.
Ethics committee approval: This retrospective study was approved by the institutional review board.
Funding: This study was funded by 2018 Xinhua-uOttawa Joint Clinical Research Project.
Author Disclosures:
H. Ren: nothing to disclose
H. Li: nothing to disclose
F. Liu: nothing to disclose
J. Cai: nothing to disclose
F. Sun: nothing to disclose
L. Xu: nothing to disclose
L. Yu: nothing to disclose
W. Guan: nothing to disclose
H. Xiao: nothing to disclose

RPS 1104-3 14:12

Pulmonary MR imaging with ultra-short echo time (UTE): a comparison of vapabilities for nodule detection and lung-RADS classification with low- and standard-dose CTs

Y. Ohno[1], M. Yui[2], D. Takenaka[3], T. Yoshikawa[4]; *[1]Toyoake/JP, [2]Ohtawara/JP, [3]Akashi/JP, [4]Kobe/JP (yohno@fujita-hu.ac.jp)*

Purpose: To compare capabilities of pulmonary MR imaging with ultra-short echo time (UTE-MRI) for lung nodule detection and lung-RADS classification with thin-section low- and standard-dose CTs.
Methods and materials: 110 consecutive patients were examined with chest standard- and low-dose CTs (270 mA [SDCT] and 60 mA [LDCT]) and UTE-MRI. In each patient, the probability of presence at each pulmonary nodule was assessed on all three methods by means of a 5-point visual scoring system. In addition, all nodules were classified based on lung-RADS on each method by the same radiologists. To compare nodule detection capability, Jackknife alternative free-response receiver operating characteristic analysis was performed among all methods. To evaluate lung-RADS classification capability, inter-method agreements were also assessed by kappa statistics with χ^2 test performed.
Results: On comparison of nodule detection capability by consensus reading, figure-of-merits (FOMs) of all methods (UTE-MRI: FOM=0.89, LDCT: FOM=0.86, SDCT: FOM=0.89) had no significant difference (p>0.05). For lung-RADS classification, interobserver agreement of each method was determined as almost perfect (UTE-MRI: κ=0.92, p<0.0001; LDCT: κ=0.93, p<0.0001; SDCT: κ=0.96, p<0.0001). In addition, inter-method agreements were also assessed as almost perfect (UTE-MRI vs. LDCT: κ=0.86, p<0.0001; UTE-MRI vs. SDCT: κ=0.87, p<0.0001; LDCT vs. SDCT: κ=0.95, p<0.0001).
Conclusion: Pulmonary MR imaging with UTE is considered at least as valuable as low- and standard-dose CTs for lung nodule detection and lung-RADS classification.
Limitations: This study was performed as a comparison of nodule detection capability and lung-RADS classification among MRI and low- and standard-dose CTs. However, there was no direct comparison of screening capability among them.
Ethics committee approval: This prospective study was approved by the institutional review board of Kobe University Hospital and written informed consent was obtained from each subject.
Funding: This prospective study was supported by Canon Medical Systems Corporation.
Author Disclosures:
Y. Ohno: Research/Grant Support at Canon Medical Systems Corporation
M. Yui: Employee at Canon Medical Systems Corporation
D. Takenaka: nothing to disclose
T. Yoshikawa: Research/Grant Support at Canon Medical Systems Corporation

RPS 1104-4 14:18

Chronic lung allograft dysfunction (CLAD) after lung transplantation: comparing CT features between bronchiolitis obliterans syndrome, restrictive allograft syndrome, and non-CLAD patients

P. Agarwal[1], C. L. Schlett[1], A. Wielandner[2], P. Jaksch[2], C. Wassipaul[2], A. Benazzo[2], H. Prosch[2]; *[1]Freiburg/DE, [2]Vienna/AT (prerana.vkag@gmail.com)*

Purpose: To describe the CT features in patients with chronic lung allograft dysfunction (CLAD), including bronchiolitis obliterans syndrome (BOS) and restrictive allograft syndrome (RAS) post double-lung-transplantation(DLuTx), and compare these to non-CLAD patients to find the most valuable discriminating features between the two groups.
Methods and materials: This retrospective study analysed data of 451 patients who underwent DLuTx from 01/2008 to 12/2012 at Vienna-General-Hospital, Austria. After applying some exclusion criteria, patients were stratified based on clinical presentation and a pulmonary function test into BOS, RAS, and non-CLAD. The last available CT scan in each group was scored by two thorax radiologists in consensus, based on a semi-quantitative scoring system similar to one described previously. Data was analysed using logistic regression deriving area under the ROC curve (AUC).
Results: A total of 171 patients were included and median post-transplantation follow-up was 2,373 days. Of them, 41 were classified as BOS, 16 as RAS, and 114 as non-CLAD. There was a significant difference in almost all features between non-CLAD and CLAD (p<0.001). Four strongest CT features, airway-wall-thickening, peripheral ground-glass-opacities, sub-pleural thickening, and air-trapping, provided independent and incremental value with an AUC of 0.823 (95%CI:0.745-0.901) to differentiate between CLAD and non-CLAD. Within CLAD, two CT-parameters allowed nearly perfect separation of BOS from RAS: septal-and-non-septal-lines (AUC 0.936 [95%CI:0.870-1.000) and peripheral-consolidations (AUC 0.939 [95%CI:0.840-1.000).

Conclusion: Several CT features differ between CLAD and non-CLAD; within CLAD, septal-and-non-septal lines, as well as peripheral consolidations, allow a high accuracy to separate BOS from RAS. Imaging allows phenotyping of CLAD patients by identification of specific morphological features and can be used as an adjunct to lung function evaluation.
Limitations: A retrospective design, small sample size, and semi-quantitative scoring system.
Ethics committee approval: Approved by the IRB.
Funding: No funding was received for this work.
Author Disclosures:
P. Agarwal: nothing to disclose
C. L. Schlett: nothing to disclose
H. Prosch: nothing to disclose
A. Wielandner: nothing to disclose
P. Jaksch: nothing to disclose
A. Benazzo: nothing to disclose
C. Wassipaul: nothing to disclose

RPS 1104-5 14:24

Functional MRI diffusion and chemical shift imaging in the assessment of anterior mediastinal masses

Y. Sabri[1], M. A. Fouad[1], S. A. E. H. Abd El Rahman[2], Y. El Hinnawy[1];
[1]Cairo/EG, [2]Giza/EG (mona.fouad@kasralainy.edu.eg)

Purpose: To investigate the potential of non-contrast enhanced functional MRI modalities, including diffusion-weighted imaging (DWI) and chemical shift imaging (CSI), to characterise anterior mediastinal lesions and differentiate benign from malignant spectrum, as well as different subtypes in the same pathological category, in an attempt to improve non-invasive approaches for the diagnosis and follow-up of patients with mediastinal lesions.
Methods and materials: This study included 71 patients with anterior mediastinal lesions detected by multi-slice computed tomography (MSCT). All cases were evaluated by diffusion-weighted imaging, ADC mean and minimum values, assessed and chemical shift MRI imaging, chemical shift ratio (CSR), and signal intensity index (SII), and were calculated and compared.
Results: In diffusion-weighted imaging benign and malignant lesions cut off value was for the ADC mean (1.267 x10-3 mm2/sec) and for ADC min (1.215 x10-3 mm2/sec). For differentiation between sarcoidosis and malignant lymphadenopathy, the cut-off value for ADC mean was 1.298 x10-3 mm2/sec and ADC min was 1.215 x10-3 mm2/sec. In chemical shift imaging quantitative assessment, thymic hyperplasia showed lower CSR and higher SII values than the thymoma and thymic carcinoma, however, germ cell tumour showed borderline CSR and high SII.
Conclusion: Functional MRI findings, both qualitative and quantitative assessment using diffusion-weighted images and chemical shift MR-images of the anterior mediastinum, has a diagnostic potential to differentiate between benign and malignant tumours. Patient's demographics, the mediastinal compartment in question, and conventional MR findings were all taken into consideration.
Limitations: The limited number of cases in each group.
Ethics committee approval: This study was conducted after institutional and departmental ethical committee approval number I- 091016 and informed consent was obtained from patients or their authorised representatives.
Funding: No funding was received for this work.
Author Disclosures:
M. A. Fouad: Author at Cairo university medical school, Speaker at Cairo university medical school
Y. Sabri: Consultant at Cairo university medical school
S. A. E. H. Abd El Rahman: Author at Cairo university medical school
Y. El Hinnawy: nothing to disclose

RPS 1104-6 14:30

A comparison of capability for therapeutic effect prediction between CEST imaging and FDG-PET/CT in non-small cell lung cancer patients with chemoradiotherapy

Y. Ohno[1], M. Yui[2], T. Yoshikawa[3]; *[1]Toyoake/JP, [2]Ohtawara/JP, [3]Kobe/JP (yohno@fujita-hu.ac.jp)*

Purpose: To compare the capability of therapeutic effect prediction for chemoradiotherapy between chemical exchange saturation transfer (CEST) imaging at 3.5 ppm and FDG-PET/CT in non-small cell lung cancer (NSCLC) patients.
Methods and materials: 32 stage III NSCLC patients underwent CEST imaging, FDG-PET/CT, and chemoradiotherapy and follow-up examinations. All patients were then divided into recurrence (n=7) and non-recurrence (n=25) groups. From CEST data in each patient, magnetisation transfer ratio asymmetry (MTR_{asym}) map was computationally generated. In each lesion, MTR_{asym} and maximum value of standard uptake value (SUV_{max}) were assessed by ROI measurements. To compare each index between two groups, Student's t-test was performed. Then, multivariate logistic regression analyses were performed to investigate the discriminating factors of the two groups. Finally, disease-free between responders and non-responders assessed by each index were compared by the Kaplan-Meier method followed by a log-rank test.
Results: MTR_{asym} and SUV_{max} had significant differences between the two groups ($p<0.05$). Multivariate regression analyses identified MTR_{asym} (Odds ratio [OR]: 0.23, p=0.04) and SUV_{max} (OR: 0.09, p=0.008) as significant differentiators. Both indexes had significant differences in disease-free survival between the two groups (MTR_{asym}: p=0.01, SUV_{max}: p=0.0006).
Conclusion: CEST imaging has potential for predicting the therapeutic effect of chemoradiotherapy and is considered at least as valuable as FDG-PET/CT in NSCLC patients.
Limitations: No comparison of survival assessed by each index was considered as one of the limitations in this study.
Ethics committee approval: This prospective study was approved by the institutional review board of Kobe University Hospital and written informed consent was obtained from all patients.
Funding: It was financially and/or technically supported by Canon Medical Systems Corporation.
Author Disclosures:
Y. Ohno: Research/Grant Support at Canon Medical Systems Corporation
M. Yui: Employee at Canon Medical Systems Corporation
T. Yoshikawa: Research/Grant Support at Canon Medical Systems Corporation

RPS 1104-7 14:36

Non-contrast-enhanced assessment of lung perfusion in patients with cystic fibrosis during respiratory tract exacerbation using Fourier decomposition magnetic resonance imaging (FD-MRI)

A. Mazzaro[1], F. Serafini[2], P. Ciet[3], S. Bertolo[4], M. Ros[4], N. Landini[5], G. Morana[4]; *[1]Verona/IT, [2]Padua/IT, [3]Rotterdam/NL, [4]Treviso/IT, [5]Arezzo/IT (andrea.mazzaro1558@gmail.com)*

Purpose: To evaluate the potential of FD-MRI, a validated technique for lung perfusion assessment, in differentiating CF patients with respiratory tract exacerbation and its correlation with clinical parameters.
Methods and materials: We selected 32 consecutive CF patients at their visit, performing a clinical examination, spirometry, and pulmonary MRI. Patients with exacerbations, identified with a Pex score, underwent antibiotic treatment, while those who were stable were not treated. A second examination was performed after therapy in exacerbated and after 30 days in the stable patients. For FD-MRI, an untriggered two-dimensional SSFP coronal sequence was used. The data obtained was converted into perfusion maps by a specific FD software. Two readers independently analysed the maps for perfusion defects using a field-based scoring system (0-18). We assessed intra- and inter-rater agreement (Cohen's k), differentiation between stable and exacerbated (OR), and correlation with spirometry parameters (Kendall's Tau).
Results: There were 14 patients with exacerbation and 17 stable patients. The score showed an inter- and intra-rater agreement k of 0.85 and 0.93 ($p<0.05$). Exacerbated patients had a significantly higher score than stable patients in the first examination (OR:4.0, IC95%:1.4-12.3), while after therapy there wasn't any difference (OR:1.1, IC95%:0.4–2.5). The score showed an inverse correlation with FEV1, FEF, and FVC in exacerbated patients, both in the first (Tau: -0.59,-0.61,-0.66, p<0,05) and in second examinations (-0.41,-0.43,-0.58, $p<0.05$). No correlation was found for the stable patients.
Conclusion: The score applied to FD-MRI perfusion maps showed good reproducibility. It appeared to be effective in differentiating CF patients with pulmonary exacerbation and could play a role in monitoring as it seems correlated with spirometry parameters.
Limitations: A small patient population. There were very few studies about the clinical use of FD-MRI.
Ethics committee approval: Approved by local ethics committee. Informed consent obtained.
Funding: No funding was received for this work.
Author Disclosures:
A. Mazzaro: nothing to disclose
G. Morana: nothing to disclose
S. Bertolo: nothing to disclose
P. Ciet: nothing to disclose
M. Ros: nothing to disclose
F. Serafini: nothing to disclose
N. Landini: nothing to disclose

RPS 1104-8 14:42

Repeatability of the phase-resolved functional lung (PREFUL) MRI derived ventilation and perfusion dynamics in COPD and healthy controls

G. H. Poehler, A. Voskrebenzev, F. Klimes, L. Behrendt, T. F. Kaireit, M. Gutberlet, F. Wacker, J. Hohlfeld, J. Vogel-Claussen; *Hanover/DE (poehler.gesa@mh-hannover.de)*

Purpose: In COPD, patient-friendly imaging tools that integrate morphological and functional pulmonary assessment are currently translated into the clinic and clinical trials. Recently, based on conventional Fourier decomposition (FD), phase-resolved functional lung (PREFUL) MRI was established as a contrast-free, non-invasive 2D-imaging tool to detect and quantify regional pulmonary blood flow and ventilation dynamics in free-breathing (Voskrebenzev et.al MRM. 2017).
The purpose of this study was to assess the repeatability of PREFUL-MRI based ventilation and perfusion quantitative biomarkers in COPD and healthy volunteers.
Methods and materials: 28 COPD patients/12 healthy volunteers were examined twice on a 1.5T MR. Baseline and follow-up data of the lung PREFUL-MRI after 1 min (healthy volunteers)/after 14 days (COPD patients) was analysed using regional ventilation (RVent) flow-volume loops (FVL) by means of cross-correlation (ccVent) and quantified perfusion maps. Ventilation defect percentage based on correlation metrics (VDPcc), perfusion defect percentage (QDP), and ventilation/perfusion match based on cross-correlation (VQMcc) were calculated. Bland-Altman/power-calculation analyses were performed.
Results: Bland-Altman plots confirmed good reproducibility of V/Q PREFUL. A power calculation for n=30 using the data from this calculation revealed in COPD/healthy volunteers the smallest detectable difference of 0.031/0.017 RVent, 0.031/0.0017 ccVent, 2.4/2.3% QDP, 5.6/0.5% VDPccVent, and 4.5/6% VQMccVent. T-tests showed no significant differences between baseline and follow-up data (p>0.05).
Conclusion: Considering the high repeatability, contrast agent-free PREFUL-MRI derived ventilation and perfusion biomarkers in free-breathing are ready to be used as endpoints in clinical respiratory trials.
Limitations: n/a
Ethics committee approval: This study was approved by the local ethics commitee and all participants gave written informed consent.
Funding: No funding was received for this work.
Author Disclosures:
G. H. Poehler: nothing to disclose
A. Voskrebenzev: nothing to disclose
F. Klimes: nothing to disclose
L. Behrendt: nothing to disclose
T. F. Kaireit: nothing to disclose
M. Gutberlet: nothing to disclose
F. Wacker: nothing to disclose
J. Hohlfeld: nothing to disclose
J. Vogel-Claussen: nothing to disclose

RPS 1104-9 14:48

Acquiring CT scans in different respiratory phases in patients with pulmonary emphysema: a comparison of quantitative CT analysis and clinical data

L. Song[1], J. Leppig[2], R.-H. Huebner[2], D. B. C. Lassen-Schmidt[3], Z. Jin[1], F. Doellinger[2]; [1]*Beijing/CN,* [2]*Berlin/DE,* [3]*Bremen/DE*
(Jonas-Alexander.Leppig@charite.de)

Purpose: To investigate whether CT scans in maximum inspiration or expiration correlate more adequately with clinical data.
Methods and materials: 172 patients with COPD GOLD stage III or IV underwent non-enhanced thin-section MSCT at maximum inspiration and expiration, pulmonary function testing (PFT), exercise testing, and quality of life assessments within a narrow time frame. Quantitative CT (QCT) analysis was performed to determine total lung volume (TLV), total emphysema score (TES), and the 15th percentile of lung attenuation (P15) at both inspiration (IN) and expiration (EX) using MeVisPULMO 3D software. Spearman correlation analysis was used to correlate QCT analysis with PFT parameters and clinical measurements.
Results: QCT parameters showed a varying correlation with PFT, exercise testing, and quality of life assessments: e.g. TLVIN showed a very strong correlation with TLC (r=0.81, P<0.001), a moderate to strong correlation with RV, FVC, and FEV1/FVC (r=0.60, 0.56, -0.49, P<0.001). TLVEX showed a moderate to strong correlation with TLC, RV, and FEV1/FVC (r=0.75, 0.66, -0.43, P<0.001). P15Diff showed a moderate correlation with KCO% and TLCO% (r= 0.41, 0.40, P<0.001).
Conclusion: This study showed QCT parameters and PFT are complementary tools to evaluate pulmonary emphysema in patients of GOLD stages III and IV. TES and P15 at expiration might usefully reflect pulmonary function. Furthermore, P15 can be used as an effective parameter for evaluating lung diffusion capacity.
Limitations: As we investigated CT scans and clinical data of patients with pulmonary emphysema, our results might not be applicable to the full extent to different subgroups.
Ethics committee approval: n/a
Funding: No funding was received for this work.
Author Disclosures:
J. Leppig: nothing to disclose
F. Doellinger: nothing to disclose
L. Song: nothing to disclose
R.-H. Huebner: nothing to disclose
D. B. C. Lassen-Schmidt: nothing to disclose
Z. Jin: nothing to disclose

RPS 1104-10 14:54

Chest MRI in cystic fibrosis and chronic obstructive pulmonary disease: reproducibility and comparison with pulmonary function testing

M. O. Wielpütz[1], M. Eichinger[1], S. M. F. Triphan[1], S. Wege[1], H.-U. Kauczor[1], M. Puderbach[1], F. Risse[2], C. P. Heussel[1], G. Heussel[1]; [1]*Heidelberg/DE,* [2]*Biberach an der Riß/DE (wielpuetz@uni-heidelberg.de)*

Purpose: Recent studies support radiation-free morpho-functional magnetic resonance imaging (MRI) as a potential endpoint in cystic fibrosis (CF) lung disease and chronic obstructive pulmonary disease (COPD). Our aim was to determine the mid-term reproducibility of morphological and functional MRI abnormalities in clinically stable CF and COPD patients with repeat MRI studies one month apart, and to correlate morphological and perfusion abnormalities with spirometry.
Methods and materials: 15 CF (29.3±9.3y, FEV1%=66.59±15.83%) and 20 COPD (66.5±8.9y, FEV1%=42.04±13.26%) patients prospectively underwent clinical work-up, spirometry, and chest MRI twice one month apart (MRI1, MRI2). MRI scans were assessed using a validated MRI score, blinded for clinical and demographic data.
Results: The MRI morphology, perfusion, and global score did not differ between MRI1 versus MRI2 in patients with CF and COPD, with the exception of the MRI global score which increased slightly in COPD from 14.6±3.8 to 15.2±3.8 (p<0.05). Limits-of-agreement between MRI1 and MRI2 were approximately ±4 for the MRI global score. Importantly, FEV1% also did not change from MRI1 to MRI2. MRI scores showed a moderate inverse correlation with FEV1% in CF (r=-0.57 to -0.70, p≤0.001), but not in COPD, which was mostly due to a narrow range of disease severity.
Conclusion: Chest MRI abnormalities were highly reproducible within one month in clinically stable CF and COPD patients. Correlation with spirometry in CF further supports MRI's role as a sensitive and robust modality for the assessment of regional disease severity.
Limitations: Our study was performed in adult CF patients and the results may not be readily transferable to paediatric CF patients.
Ethics committee approval: This study was approved by the institutional ethics committee and written informed consent was obtained from all participants.
Funding: This study was funded by Boehringer Ingelheim Pharma GmbH & Co. KG, Germany.
Author Disclosures:
M. O. Wielpütz: Advisory Board at Vertex, Boehringer Ingelheim, Grant Recipient at Boehringer Ingelheim, Vertex
S. M. F. Triphan: nothing to disclose
M. Eichinger: nothing to disclose
S. Wege: nothing to disclose
H.-U. Kauczor: nothing to disclose
M. Puderbach: nothing to disclose
F. Risse: Employee at Boehringer Ingelheim
C. P. Heussel: Grant Recipient at Boehringer Ingelheim
G. Heussel: Grant Recipient at Boehringer Ingelheim

RPS 1104-11 15:00

Measuring ventilation inhomogeneity in cystic fibrosis using unenhanced functional 3D-UTE MRI

J. F. Heidenreich[1], A. Weng[1], C. Metz[1], T. Benkert[2], H. Hebestreit[1], T. A. Bley[1], H. Köstler[1], S. Veldhoen[1]; [1]*Würzburg/DE,* [2]*Erlangen/DE*
(Heidenreic_J@ukw.de)

Purpose: To assess the clinical feasibility of proton-based non-contrast-enhanced functional lung MR imaging with a 3D-UTE sequence for the monitoring of cystic fibrosis (CF).
Methods and materials: 20 CF patients and 10 healthy volunteers underwent functional lung MRI using a prototypical stack-of-spirals 3D-UTE sequence. Images from in- and expiration were acquired during single breath-holds. The fractional ventilation (FV) was calculated voxelwise from the signal intensity amplitude. The interquartile range of the ventilation rate (FV normalised to the mean of the entire lung) was calculated for each subject and compared between groups. For the CF patients, the IQR was correlated to the lung clearance index (LCI) from multiple breath washout and the results of pulmonary function tests (PFT). Mann-Whitney U tests and the Spearman correlation coefficient were used for statistical analyses.

Results: Ventilation maps revealed increased ventilation inhomogeneity in patients with CF. A significantly higher IQR was observed in patients with CF compared to healthy controls (mean ± standard deviation, 0.66 ± 0.16 vs. 0.50 ± 0.04, respectively; P= 0.007). In the patient group, the IQR correlated negatively with the obstruction markers FEV1/FVC ratio (Tiffeneau index), MEF25 (r = 0.70/0.78), and positively to the LCI (r = 0.90).
Conclusion: Increased IQR was found in patients with cystic fibrosis. IQR demonstrated a significant correlation to established markers for airway obstruction (Tiffeneau index, MEF25) and ventilation inhomogeneity (LCI). The interquartile range of the normalised FV could be used as a measure of ventilation inhomogeneity and thus for disease management in cystic fibrosis.
Limitations: n/a
Ethics committee approval: Approved by the institutional review board. Written informed consent was obtained from all participants.
Funding: Funded by the German Research Foundation (DFG), project number VE1008/1-1 and KO 2938/5-1.
Author Disclosures:
J. F. Heidenreich: nothing to disclose
A. Weng: nothing to disclose
C. Metz: nothing to disclose
T. Benkert: Employee at Siemens Healthcare GmbH
H. Hebestreit: nothing to disclose
T. A. Bley: nothing to disclose
H. Köstler: Research/Grant Support at DFG KO 2938/5-1
S. Veldhoen: Research/Grant Support at DFG VE1008/1-1

RPS 1104-12 15:06

Radiomic features: the biomarker used for distinguishing EGFR DEL19 and L858R sensitising mutation subtype

J. Ji[1], Q. Weng[1], H. Wang[1], J. Hui[1], C. Lan[1], M. Chen[1], P. Pang[2], M. Xu[1]; *[1]Lishui/CN, [2]Hangzhou/CN (lschrjjs@163.com)*

Purpose: The evidence that DEL 19 mutations are different from L858R mutation is accumulating since the different chemosensitivities. The aim of this study was to establish a CT derived approach to differentiate the EGFR DEL19 and EGFR L858R sensitising mutation in non-small cell lung cancer (NSCLC) patients.
Methods and materials: A total of 396 CT-based phenotypic characteristics were extracted from NSCLC preoperation images. On the basis of CT features extracted from 149 NSCLC patients, a CT-based phenotypic signature was proposed using a Cox regression model with LASSO penalty for the prediction of EGFR mutation. Furthermore, a joint prediction model incorporating the CT based image radiomic features and clinicopathologic characteristics was proposed for EGFR sensitising mutation subtype prediction.
Results: Of 396 radiomic features, 4 features were considered to be independent features represented as Rad-score. Cox regression was applied and 4 clinical features were selected. We found the radiomics signature showed good discrimination performance in both the primary and validation cohorts. In the training set, the radiomic signature successfully discriminated the EGFR DEL19 and EGFR L858R sensitising mutation (AUC=0.698, P<0.0001). Combining the imaging signature with a clinical feature model of EGFR status (AUC=0.778, P=0.0143) significantly improved prediction accuracy (AUC=0.874, P<0.0001). Furthermore, the joint prediction model showed a significant difference when compared to a radiomic signature model alone (P=0.0041, 95%CI: 0.0558-0.296) and with good calibration.
Conclusion: Radiomic features can be used as an approach to predict the EGFR sensitising mutation subtype between EGFR DEL19 and EGFR L858R. The clinical features enhanced the prediction accuracy of radiomic features model. Our study has implications for the use of imaging-based biomarkers in the clinic, as applies noninvasively, repeatedly, and at low cost.
Limitations: n/a
Ethics committee approval: This study has been approved by IRB.
Funding: No funding was received for this work.
Author Disclosures:
J. Ji: nothing to disclose
Q. Weng: nothing to disclose
H. Wang: nothing to disclose
J. Hui: nothing to disclose
C. Lan: nothing to disclose
M. Chen: nothing to disclose
P. Pang: nothing to disclose
M. Xu: nothing to disclose

RPS 1104-13 15:12

The prognostic utility of reporting the ordinal coronary artery calcification score in routine chest CTs to prevent cardiovascular events

H. Bernardo Fernandez[1], M. Perez-Peña Del Llano[2], A. Renilla[2]; *[1]Oviedo/ES, [2]Mieres/ES (hugo.bernardo@hotmail.com)*

Purpose: To establish a link between total coronary calcification (CAC), detected on routine chest CT exams following a visual ordinal scoring system (OSS), and the possibility of developing a cardiovascular event (CE) over time.
Methods and materials: A retrospective case-control study was conducted selecting patients referred to our hospital for CE during 2015-16 who had a previous chest CT done, then two same-gender control patients with chest CT performed the same day and in previous dates were added. A total of 84 patients were included. An OSS was used to evaluate length coronary calcification and correlated with the presence or absence of CE.
Probabilities and curves of disease-free survival were calculated with the Kaplan-Meier method. The differences between curves were evaluated with the log-rank test.
SPSS 20.0 statistical analysis software was used, including Pearson $\chi 2$ test, t-Student, or Mann-Whitney tests and ANOVA or Kruskal-Wallis for group comparison.
Statistical significance was considered at a 5% probability level ($p<0.05$).
Results: CAC was observed in 92.85% of cases and 64.81% of the controls, with the descent coronary artery being the most commonly calcified.
A significative relationship between the number of calcified arteries and the total score obtained in the visual scoring system with having suffered a CE (Pearson correlation 17 and 21 with $p< 0.001$, respectively) was found using the Chi-square test ($p< 0.001$) and survival Kaplan-Meier curve.
A score of >4.9 determined a strong posibility of CE in a 36 month follow-up period.
Conclusion: Performing a visual score of CAC in routine chest CT can provide prognostic information concerning cardiovascular risk and should be incorporated in all radiological reports.
Limitations: A retrospective study and small sample.
Ethics committee approval: n/a
Funding: No funding received for this work.
Author Disclosures:
H. Bernardo Fernandez: nothing to disclose
M. Perez-Peña Del Llano: nothing to disclose
A. Renilla: nothing to disclose

RPS 1104-14 15:18

A comparison of quantitative lung parenchyma and airway parameters in low and ultra-low dose computed tomography

O. Weinheimer[1], L. Yu[2], J. G. Fletcher[2], M. O. Wielpütz[1], C. P. Heussel[1], H.-U. Kauczor[1], C. J. Galban[3], T. E. Robinson[4], B. Bartholmai[2]; *[1]Heidelberg/DE, [2]Rochester, MN/US, [3]Ann Arbor, MI/US, [4]Palo Alto, CA/US (weinheimer@uni-heidelberg.de)*

Purpose: Various quantitative evaluation techniques of computed tomographic (CT) images have been proven to deliver useful and objective biomarkers describing lung parenchyma and airways. Because low dose (LD) CT is becoming the standard in lung CT imaging, the question arises how an ultra-low dose (ULD) CT at dose level like that in chest x-ray influences quantitative CT (QCT).
Methods and materials: In the present study, 198 individuals (age: 54.4±16.4yrs) with a clinical indication for low-dose CT, such as malignancy screening or follow-up of a known lung nodule, were scanned twice, once with LD (mean effective dose: ~2.18mSv) and once with ULD (~0.18mSv). Advanced modelled iterative reconstruction (ADMIRE) was used. LDCT was reconstructed with strength level 2 ($LDCT_2$), ULDCT with strength level 2, and 4/5 ($ULDCT_2$, $ULDCT_{4/5}$). Numerous fully automated QCT parameters were generated on global and lobar generation-based levels. LDCT served as ground truth.
Results: The mean lung volume (LV) for $ULDCT_2$ was 0.58% smaller compared to $LDCT_2$ ($ULDCT_{4/5}$: 0.60%) and the differences were not significant. The mean lung density (MLD) was significantly increased by 6.56HU ($ULDCT_{4/5}$: 3.73HU), linear regression parameters for $ULDCT_2$~$LDCT_2$: r^2=0.97, slope=0.99, intercept=0.52HU ($ULDCT_{4/5}$~$LDCT_2$: r^2=0.97, slope=1.01, intercept=13.6HU), largest deviations for the lingula with 6.85HU (2.15HU), r^2=0.94, slope=0.98, and intercept=-13.0HU (r^2=0.9, slope=0.86, intercept=-100.0HU). Airway wall percentages (WP) were significantly increased by 2.59% (1.04%), r^2=0.92, slope=0.89, and intercept=7.98% (r^2=0.93, slope=0.89, intercept=7.16%).
Conclusion: There are significant differences between QCT parameters in LDCT and ULDCT, however, they are strongly correlated. The accuracy of QCT parameters decreases for the lobes and for higher airway generations. Regarding these findings, ULDCT may be an alternative to LDCT. ADMIRE strength 4/5 generally delivered preferable results.
Limitations: Results are influenced by inspiration level.
Ethics committee approval: Study under Mayo Clinic IRB approval: #14-002156.
Funding: Dr. Fletcher received a research grant from Siemens Healthcare.
Author Disclosures:
O. Weinheimer: nothing to disclose
M. O. Wielpütz: nothing to disclose
H.-U. Kauczor: nothing to disclose
C. P. Heussel: nothing to disclose
C. J. Galban: nothing to disclose

T. E. Robinson: nothing to disclose
B. Bartholmai: nothing to disclose
L. Yu: nothing to disclose
J. G. Fletcher: Research/Grant Support at Siemens

RPS 1104-15 15:24
Reducing artefacts from contrast media in the thorax in dual-layer spectral detector CT: using virtual monoenergetic image reconstructions and orthopaedic metal-artefact-reduction algorithms
N. N. Pan[1], S. Wang[1], X. Lu[2]; [1]Tianjin/CN, [2]Shenyang/CN (pannannan1018@163.com)

Purpose: To assess the artefacts reduction caused by contrast media in the subclavian vein and axillary vein in patients with thoracic tumour in dual-layer spectral detector CT (DLCT) by virtual monoenergetic image (VMI) reconstructions and orthopaedic metal-artefact-reduction (MAR) algorithms.
Methods and materials: A total of 61 consecutive patients with a thoracic tumour who underwent enhanced chest CT examination were included. We reconstructed the same arterial CT dataset into conventional images (CI), VMI, CI with MAR algorithms (CI+MAR), and VMI with MAR algorithms (VMI+MAR). VMI and VMI+MAR were reconstructed at 100, 130, and 160 keV. Noise (SD), artefact index (AI), and attenuation in Hounsfield Units (HU) with a difference of the four reconstructed images were compared. Subjective image quality was compared in terms of diagnostic image quality and degree of artefact reduction using the Likert-scale.
Results: Attenuation difference and AI were decreased in VMI+MAR images at 100, 130, and 160 keV, compared with VMI images or CI+MAR images ($p < 0.05$), and they were all lower than CI images ($p < 0.05$). Furthermore, noise was reduced in VMI+MAR and VMI as compared to CI images ($p < 0.05$). In addition, soft tissue adjacent to contrast media showed better artefacts reduction and better assessment in VMI+MAR images than VMI images or CI+MAR images, and they were all better than CI images. ($p < 0.05$).
Conclusion: The combination of MAR and VMI showed significant reduction of artefacts caused by contrast media than each technique alone, and provided improved diagnostic confidence.
Limitations: We only analysed images obtained at three energy levels (100, 130, and 160keV). Individual patient characteristics such as circulation and anatomical differences could have also impacted the extent of artefact.
Ethics committee approval: n/a
Funding: No funding was received for this work.
Author Disclosures:
N. N. Pan: nothing to disclose
X. Lu: nothing to disclose
S. Wang: nothing to disclose

14:00 - 15:30 **Room Y**

CTiR 11
Clinical Trials in Radiology 3

Moderators:
M. Dewey; Berlin/DE
M. Mahoney; Cincinnati, OH/US

CTiR 11-1 14:00
MR CLEAN-MED - The effect of periprocedural medication in acute ischemic stroke treatment: acetylsalicylic acid, unfractionated heparin, both or neither? Interim results and protocol amendment
R. van de Graaf[1], B. Roozenbeek[1], V. Chalos[1], A. C. G. M. van Es[1], H. Lingsma[1], D. W. J. Dippel[1], A. van der Lugt[1], M. Clean Med Investigators[2]; [1]Rotterdam/NL, [2]Na/NL (r.a.vandegraaf@erasmusmc.nl)

Purpose: A considerable proportion of ischemic stroke patients do not recover despite fast and complete recanalisation after endovascular therapy (EVT). It is unknown whether periprocedural antithrombotic therapy can improve clinical outcome. This study assesses the effect of acetylsalicylic acid (ASA) and unfractionated heparin (UFH), alone, or in combination, in patients who undergo EVT.
Methods and materials: MR CLEAN-MED is a multicenter, prospective, randomised, open-label, blinded-endpoint trial using a 2x3 factorial design. We aim to enroll 1500 patients. Study interventions are intravenous treatment with ASA (300 mg) and/or UFH in a low-dose (5000 IU bolus, followed by 500 IU/hour x 6 hours) or moderate-dose (5000 IU bolus, followed by 1250 IU/hour x 6 hours). Primary outcome is the score on the modified Rankin Scale at 90 days. Safety endpoints include the occurrence of symptomatic intracerebral hemorrhage (sICH) and mortality.
Results: Sixteen Dutch and five French sites participated in the study. By October 2019, 270 patients were randomised. Following on receipt of the 4th safety report in April 2019, after inclusion of 132 patients, the data safety monitoring board recommended to stop enrollment in the moderate-dose UFH arm based on an increased sICH risk compared to the other treatment arms (22.7% vs. 5.7%; OR 4.88 95%CI 1.55-15.55[Table]). No patients were included in the moderate-dose UFH arm after receipt of this recommendation.
Conclusion: In MRCLEAN MED the effect of ASA and/or UFH during EVT on functional outcome will be evaluated further and the inclusion of patients in the ASA and low-dose UFH arms continues. Periprocedural treatment with moderate-dose UFH (5000 IU bolus, followed by 1250 IU/hour during 6 hours) is associated with increased sICH risks and should be avoided.
Limitations: N/A
Ethics committee approval: Medisch Ethische Toetsings Commissie Erasmus MC (Medical Ethical Committee Erasmus MC), 09/10/2017, ref: MEC-2017-366.
Funding: None.
Author Disclosures:
R. van de Graaf: nothing to disclose
B. Roozenbeek: nothing to disclose
V. Chalos: nothing to disclose
A. C. G. M. van Es: nothing to disclose
A. van der Lugt: Grant Recipient at Dutch Heart Foundation; Dutch Brain Foundation; European Union; The Netherlands Organization for Health Research and Development, Health Holland Top Sector Life Science; AngioCare BV; Covidien/EV3; MEDAC Gmbh/LAMEPRO; Top Medical/Concentric; Thrombolytic , Consultant at Erasmus MC received compensation from Stryker, Medtronic, Bracco Imaging Ltd
D. W. J. Dippel: Grant Recipient at Dutch Heart Foundation; Dutch Brain Foundation; European Union; The Netherlands Organization for Health Research and Development, Health Holland Top Sector Life Science; AngioCare BV; Covidien/EV3; MEDAC Gmbh/LAMEPRO; Top Medical/Concentric; Thrombolytic , Consultant at Erasmus MC received compensation from Stryker, Medtronic, Bracco Imaging Ltd
H. Lingsma: nothing to disclose
M. Clean Med Investigators: nothing to disclose

CTiR 11-2 14:10
Discussant
K. Dolić; Split/HR (kdolic79@gmail.com)

Author Disclosures:
K. Dolić: nothing to disclose

CTiR 11-3 14:15
The effect of density on recall, detection, and interval cancer rates in tomosynthesis plus digital mammography or digital mammography breast cancer screening: preliminary results from RETomo trial
V. Iotti[1], P. Giorgi Rossi[1], A. Nitrosi[1], V. Helin[2], E. Gauthier[2], C. Campari[1], V. Marchesi[1], R. Vacondio[1], P. Pattacini[1]; [1]Reggio Emilia/IT, [2]Villejuif/FR (valentina.iotti@ausl.re.it)

Purpose: The RETomo trial was a two-arm test-and-treat randomised controlled trial comparing tomosynthesis (DBT) plus digital mammography (DM) versus DM alone for breast cancer screening. We investigate interim analysis on recall, detection, interval cancer rate in the first round by breast density.
Methods and materials: Women (45-70yo) presenting for a screening mammography in ReggioEmilia, and previously screened with DM, were randomised to the experimental arm (DBT+DM) or to the control arm (DM), both with two projections and double reading (NCT02698202). Density was automatically assessed with DenSeeMammo software on the 4 DM projections. Recall, detection, and interval cancer rates were reported. All women were followed up to 24 months from recruitment or up to the second round.
Results: From March 2014-2016, 19566 women were recruited. Density assessment was available for 8651 women in the DM+DBT-arm and 8544 in the DM-arm. Recall rate was similar in both arms and increased with density from 1.9% in BI-RADS A to 4.2% in BI-RADS D. Detection rate, including ductal carcinoma in situ (DCIS), was 9.1/1000(79) and 4.7/1000(40) respectively. DBT+DM detected about two fold more cancers in all BI-RADS classes except A, but interaction could be due to chance (p=0.65). Interval cancers rate was similar in both arms (2.0/1000[17] and 1.9/1000[16] in DBT+DM and DM arm, respectively). Interval cancer rate increases with density in both arms (OR for the increase of one BI-RADS class 1.6, 95%CI 1.0-2.5).

Conclusion: DBT+DM detected more cancers independently from density, but without impact on interval cancer rate. Density increased recall rate and interval cancer rate in both arms.
Limitations: Interval cancers are only one of the outcomes to assess the efficacy of DBT in screening.
Ethics committee approval: ProvincialEthical Committee.
Funding: Partially funded by the Regione Emilia-Romagna and the Local Health Authority-IRCCS.
Author Disclosures:
V. Iotti: Speaker at GE Healthcare
C. Campari: nothing to disclose
P. Giorgi Rossi: nothing to disclose
V. Helin: Employee at Predilife
E. Gauthier: Employee at Predilife
A. Nitrosi: nothing to disclose
R. Vacondio: nothing to disclose
P. Pattacini: Speaker at GE Healthcare
V. Marchesi: nothing to disclose

CTiR 11-4 14:25
Discussant
P. Skaane; *Oslo/NO (PERSKA@ous-hf.no)*

Author Disclosures:
P. Skaane: Equipment Support Recipient at Hologic

CTiR 11-5 14:30
Whole-body MRI versus an FDG-PET/CT-based reference standard for staging of paediatric Hodgkin lymphoma: a prospective multicentre study
S. Spijkers[1], A. S. Littooij[1], A. Beishuizen[1], S. G. Elias[1], B. de Keizer[1], T. Kwee[2], N. Tolboom[1], R. A. J. Nievelstein[1]; *[1]Utrecht/NL, [2]Groningen/NL (suzannespijkers@outlook.com)*

Purpose: To assess the concordance of WB-MRI and FDG-PET/CT for staging in children with Hodgkin lymphoma (HL) in order to contribute to the development of evidence-based 'radiation reduced' imaging protocols in paediatric HL in the future.
Methods and materials: A total of 68 children with HL were included in this prospective, multicenter, international study. All participants underwent WB-MRI and FDG-PET/CT at staging. Two radiologist independently evaluated all WB-MR images in two separate readings: with and without DWI. The FDG-PET/CT examinations were evaluated by a nuclear medicine physician. An expert panel assessed all discrepancies between WB-MRI and FDG-PET/CT to derive the FDG-PET/CT-based reference standard. Concordance for correct classification of all disease sites between WB-MRI (both with and without DWI) and the reference standard was calculated, as well as PPV, NPV and Cohen's kappa statistics. Inter-observer agreement for the WB-MRI including DWI reading was calculated using kappa statistics.
Results: WB-MRI including DWI was concordant with the FDG-PET/CT-based reference standard for determining disease stage in 97% of the patients (66/68). Agreement between WB-MRI and the reference standard was very good for both nodal (κ=0.97, 95%CI 0.94-0.99) and extra-nodal (κ 1.00) staging. Kappa values for correct disease stage increased significantly with the addition of DWI (p=0.04). Inter-observer agreement between WB-MRI readers was good (κ=0.74, 95%CI 0.58-0.91).
Conclusion: WB-MRI with DWI showed excellent agreement with the FDG-PET/CT-based reference standard, but did not reach complete concordance for stage. The addition of DWI to the WB-MRI protocol in staging of paediatric HL was shown to improve staging agreement with the FDG-PET/CT-based reference standard.
Limitations: Main limitation: lack of a true gold standard.
Ethics committee approval: The local institutional review boards approved the study. Written informed consent was obtained.
Funding: Financially supported by Kinderen Kankervrij (projectnumber 87).
Author Disclosures:
S. Spijkers: nothing to disclose
R. A. J. Nievelstein: nothing to disclose
A. S. Littooij: nothing to disclose
N. Tolboom: nothing to disclose
B. de Keizer: nothing to disclose
T. Kwee: nothing to disclose
S. G. Elias: nothing to disclose
A. Beishuizen: nothing to disclose

CTiR 11-6 14:40
Discussant
E. L. Twomey; *Dublin/IE*

Author Disclosures:
E. L. Twomey: nothing to disclose

CTiR 11-7 14:45
Pivotal study of MRI-guided transurethral ultrasound ablation (TULSA) in men with localised prostate cancer
J. J. Futterer[1], D. Bonekamp[2], S. Arora[3], S. Raman[4], T. Tirkes[5], K. J. Macura[6], J. Chin[7], L. Klotz[8], S. Eggener[9]; *[1]Nijmegen/NL, [2]Hirschberg/DE, [3]Nashville/US, [4]Los Angeles/US, [5]Indianapolis, IN/US, [6]Baltimore, MD/US, [7]London, ON/CA, [8]Toronto, ON/CA, [9]Chicago/US (jurgenfutterer@gmail.com)*

Purpose: MRI-guided transurethral ultrasound ablation (TULSA) is an incision-free procedure for customised prostate ablation. We report one-year outcomes from the TULSA-PRO Ablation Clinical Trial (TACT).
Methods and materials: TACT enrolled 115 men with organ-confined prostate cancer (≤T2b, PSA ≤15 ng/ml, Gleason Grade Group 1-2) from 13 centers in five countries. TULSA was used for whole-gland ablation, sparing the urethra and urinary sphincter. Primary endpoints were adverse events and proportion of men with PSA reduction ≥75%. Secondary endpoints included one-year 10-core biopsy, mpMRI, prostate volume reduction, and quality-of-life.
Results: Median (IQR) age was 65 (59-69) years and PSA 6.3 (4.6-7.9) ng/ml. Pre-treatment, 72/115 (63%) men had Grade Group 2 (GG2) disease, and 98/115 (85%) had PI-RADSv2 score ≥3 MRI lesions. Ablation time was 51 (39-66) min for targeted prostate volumes of 40 (32-50) cc, with ablation coverage 98% (95-99%) on MRI thermometry.
Grade 3 adverse events occurred in 8% of men, all resolved, with no rectal injuries or Grade ≥4 events. At one year, 1% were incontinent (>1 pad/day), while 69/92 (75%) maintained erections sufficient for penetration. PSA reduction ≥75% was achieved in 110/115 (96%), decreasing 95% (91-98%) to nadir 0.34 (0.12-0.56) ng/ml. Prostate volume decreased from 37 to 2.8 cc. On one-year biopsy, GG2 disease was eradicated in 54/68 (79%) men; 72/111 (65%) had no evidence of any cancer.
Multivariate predictors of residual GG2 included intraprostatic calcifications at screening, thermal coverage of target volume, and one-year MRI lesions ($p<0.05$).
Conclusion: The TACT pivotal study of MRI-guided TULSA met its primary endpoint of ≥75% PSA reduction in 96% of patients, with low rates of severe toxicity and residual GG2 disease.
Limitations: Short-term outcomes, single-arm study.
Ethics committee approval: Ethics approved at all sites, all patients provided written informed consent.
Funding: Profound Medical.
Author Disclosures:
J. J. Futterer: Speaker at Profound Medical
D. Bonekamp: Speaker at Profound Medical
S. Arora: nothing to disclose
S. Raman: Consultant at Profound Medical
T. Tirkes: nothing to disclose
K. J. Macura: nothing to disclose
J. Chin: Consultant at Profound Medical
L. Klotz: Consultant at Profound Medical
S. Eggener: Consultant at Profound Medical

CTiR 11-8 14:55
Discussant
V. Panebianco; *Rome/IT (valeria.panebianco@uniroma1.it)*

Author Disclosures:
V. Panebianco: nothing to disclose

CTiR 11-9 15:00
Adherence to PI-RADS v2 minimum technical requirements in the PRECISION trial: a new quality control scoring system for multiparametric MRI of the prostate
F. Giganti, V. Kasivisvanathan, S. Punwani, M. Emberton, C. Allen, C. M. Moore, Precision Study Group Collaborators; *London/UK (giganti.fra@gmail.com)*

Purpose: The PRECISION trial was a multi-centre randomised study showing the superiority of MRI-targeted to standard TRUS-guided biopsy in 500 biopsy-naïve men across 23 centres from 11 countries. We report the results from the quality assurance work assessing scans from each trial site.

Methods and materials: Men were scanned using either a 3T or 1.5T scanner. Three centres used an endorectal coil and 4 did not administer antiperistaltic agents before multiparametric MRI.
64 out of 252 scans were chosen randomly and included scans from each site. Two expert radiologists reviewed the images in consensus using the PI-RADS v.2.1 guidelines. The quality of each scan was assessed using a 1-to-5 Likert scale, where 1 meant no MR sequences were of diagnostic quality and 5 meant each sequence was independently of diagnostic quality (Fig. 1).
Results: Four scans (6%) had a score of 2, 16 (25%) of 3, 27 (42%) of 4, and 17 (27%) of 5. MR quality was deemed of at least sufficient diagnostic quality (scoring ≥3) for 60 (94%) scans, with 44 (69%) being of good/excellent quality (scoring ≥4).
Adherence to minimum standards was highest for T2-WI, lower for DWI (slice thickness, number of b-values and lack of dedicated long b value sequences) and lowest for DCE (temporal resolution and absence of fat saturation/subtraction).
Conclusion: MRI and targeted biopsies outperform standard biopsy when sufficient attention is paid to high-quality scan acquisition and reporting. Whilst adherence to PI-RADS v2.1 minimum technical requirements in PRECISION was good overall, the greatest variability was in the DCE sequences.
Limitations: Further assessment of the utility of DCE imaging is warranted in the diagnostic setting.
Ethics committee approval: National Research Ethics Committee East Midlands, Leicester (15/EM/0188)
Funding: NIHR through a doctoral fellowship award (DRF-2014-07-146, to Dr. Kasivisvanathan) and a grant (2015001) from the EAU Research Foundation.
Author Disclosures:
F. Giganti: Grant Recipient at Dr. Francesco Giganti is funded by the UCL Graduate Research Scholarship, the Brahm PhD scholarship in memory of Chris Adams.
V. Kasivisvanathan: Speaker at EAU
S. Punwani: Grant Recipient at Prof. Shonit Punwani receives research support from the United Kingdom's National Institute of Health Research (NIHR) UCLH/UCL Biomedical Research Centre.
M. Emberton: Investigator at Prof. Mark Emberton receives research support from the United Kingdom's National Institute of Health Research (NIHR) UCLH/UCL Biomedical Research Centre. He is an NIHR Senior Investigator.
C. M. Moore: nothing to disclose
Precision Study Group Collaborators: nothing to disclose
C. Allen: nothing to disclose

CTiR 11-10 15:10
Discussant
D. Beyersdorff*; Berlin/DE*

Author Disclosures:
D. Beyersdorff: nothing to disclose

CTiR 11-11 15:15
MRI in addition to mammography screening in women with extremely dense breasts: outcome of the second (incident) round of the randomised DENSE trial
M. F. Bakker, S. V. de Lange, R. M. Pijnappel, W. B. Veldhuis, C. van Gils, O. B. O. T. Dense Study Group*; Utrecht/NL*

Purpose: To evaluate the incident vs. prevalent round of supplemental MRI screening for women with extremely dense breasts within a population-based screening program.
Methods and materials: Between 2011-2015, we randomised 40,373 screening participants (aged 50-75) with a negative mammography and extremely dense breasts (assessed with Volpara software) to supplemental 3.0-T MRI (n=8,061) or mammography screening only (n=32,312). In the prevalent (first) screening round, 4,783 women underwent MRI. Here we compare the results of the incident (second) MRI screening round with those of the prevalent round (presented earlier).
Results: After the prevalent screening round, 4,308 women (90%) had again undergone mammographic screening with a negative result and were eligible for the second round. Of them, 3,389 (79%) underwent supplemental MRI screening again. Reasons for discontinuation were time constraints, other health concerns, or MRI-related (e.g. claustrophobia).
Supplemental cancer detection rate with MRI was 5.9/1000 screens [95%CI:3.6-9.1], compared to 16.5/1000 [95%CI:13.3-20.5] in the prevalent round. For this, 3.2% [95%CI:2.6%-3.8%] of women were recalled for further diagnostic work-up, compared to 9.5% [95%CI:8.7%-10.4%] in the prevalent round.
Conclusion: As expected from an incident screening round, the cancer detection rate in this second round of supplemental MRI screening of women with extremely dense breasts is lower than in the prevalent round. Still, by adding MRI, the number of cancers detected almost doubled compared to normal mammography screening only. The false-positive rate decreased to one-third of the rate of the prevalent screening round.
Limitations: The incident screening round data on interval cancers are not yet available.
Ethics committee approval: Dutch Minister of Health, Welfare and Sport (2011/19); participants gave written informed consent.
Funding: UMC Utrecht, ZonMw, Dutch Cancer Society, Dutch Pink Ribbon/A Sister's Hope, Stichting Kankerpreventie Midden-West, Bayer AG Pharmaceuticals, and Volpara Health Technologies.
Author Disclosures:
M. F. Bakker: Research/Grant Support at Bayer AG Pharmaceuticals, Research/Grant Support at Volpara Health Technologies
C. van Gils: Research/Grant Support at Bayer AG Pharmaceuticals, Research/Grant Support at Volpara Health Technologies
W. B. Veldhuis: nothing to disclose
R. M. Pijnappel: nothing to disclose
S. V. de Lange: Research/Grant Support at Bayer AG Pharmaceuticals, Research/Grant Support at Volpara Health Technologies
O. B. O. T. Dense Study Group: nothing to disclose

CTiR 11-12 15:25
Discussant
A. O. Oktay Alfatli*; Izmir/TR*

Author Disclosures:
A. O. Oktay Alfatli: nothing to disclose

14:00 - 15:30 **Coffee & Talk 3**

Cardiac

RPS 1103

Anatomic and functional assessment of CAD with CCTA: what's new?

Moderators:
R. Faletti; Turin/IT
N.N.

RPS 1103-K 14:00
Keynote lecture
U. Hoffmann*; Boston/US*

Author Disclosures:
U. Hoffmann: nothing to disclose

RPS 1103-1 14:10
Functional prediction by corrected coronary opacification (CCO) from coronary computed tomography angiography (CCTA) in the assessment of not evaluable well-calcified plaque
P. Palumbo, E. Cannizzaro, S. Torlone, A. Corridore, M. C. de Donato, F. Cobianchi Bellisari, F. Sgalambro, E. Di Cesare, C. Masciocchi*; L'Aquila/IT (palumbopierpaolo89@gmail.com)*

Purpose: Coronary computed tomography angiography (CCTA) is a reliable tool in the diagnosis of obstructive coronary artery disease. However, heavily calcified plaques often require further functional examination to assess whether flow is limited. The purpose of our study was to determine whether changes in coronary opacification (CCO) can predict abnormal myocardial perfusion alteration.
Methods and materials: 75 patients with calcified plaques not properly evaluable with CCTA and subsequently assessed with adenosine-stress MRI were retrospectively included in our study. 19 patients underwent invasive coronary angiography (ICA) in coronary arteries. Per-vessel CCO analysis and per vessel fist-pass MRI perfusion qualitative and MPRI analysis were performed. Obtained values were compared with the severity of coronary stenosis and TIMI flow grade at the time of invasive coronary angiography.
Results: CCO identified abnormal TIMI with a sensibility, specificity, PPV, and NPV respectively of 100%, 83.3%, 77.8%, and 100%, with the best cutoff of 0.178. Very good correlation between CCO and TIMI was found (r = 0,83). Based on angiographic stenosis, CCO reported a sensibility, specificity, PPV, and NPV respectively of 88.9%, 90%, 88.9%, and 90%, with the best cutoff of 0.178. The optimal correlation was found with qualitative first-pass perfusion alteration and good correlation with MPRI (r = -0.72), and very good agreement between the two exams (kappa = 0.78, 95% CI 0.51 to 1)

Conclusion: CCO differences seem to have good capability in predicting qualitative first-pass perfusion or MPR alteration in a vessel-based analysis.
Limitations: Lack of functional ICA-derived FFR does not permit a comparison with current gold standard.
Ethics committee approval: The study was conducted in accordance with the declaration of Helsinki.
Funding: No funding was received for this work.
Author Disclosures:
P. Palumbo: nothing to disclose
E. Cannizzaro: nothing to disclose
S. Torlone: nothing to disclose
A. Corridore: nothing to disclose
M. C. de Donato: nothing to disclose
F. Cobianchi Bellisari: nothing to disclose
F. Sgalambro: nothing to disclose
E. Di Cesare: nothing to disclose
C. Masciocchi: nothing to disclose

RPS 1103-2 14:16

Coronary CT angiography-derived plaque quantification for the identification of lesion-specific ischemia

N. Zhao, Y. Gao, B. Lv*; Beijing/CN (15810686235@163.com)*

Purpose: To investigate the quantitative characteristics of coronary atherosclerotic plaques with haemodynamic significance and identify risk factors for lesion-specific ischemia as compared with invasive FFR.
Methods and materials: 162 patients (56.4 ± 8.8 years, 72% male) who underwent CCTA and ICA were prospectively enrolled. All patients were evaluated for conventional risk factors. The lumen area stenosis rate, minimum inner diameter, minimum lumen area, lesion length, plaque burden and volume ratios of fibrous, and lipid and calcification of plaques were measured from CCTA using a semi-automatic software prototype (Plaque analysis prototype, Siemens Healthineers). The differences between all CT parameters were compared in FFR ≤0.8 and >0.8 groups. The correlation between routine risk factors and CT parameters and haemodynamically significant plaques were analysed.
Results: 88/197 lesions were haemodynamically significant (FFR ≤0.8). In groups with invasive FFR ≤0.8, lesion length (30.20 vs. 23.07 mm), lumen area stenosis rate (78.05 vs. 65.50%), and diameter stenosis rate (52.79 vs. 40.98%) were significantly higher than FFR >0.8 group (all p<0.001). The minimum lumen area (1.57 vs. 2.25 mm^2) and minimum inner diameter (1.40 vs. 1.70 mm) of the FFR ≤0.8 group were lower with statistically significance (all p=0.001). In a multivariate analysis, the following parameters showed predictive value for lesion-specific ischemia: lesion length (OR=1.048, p<0.001) and diameter stenosis rate (OR=1.038, p = 0.015).
Conclusion: The lesion length and diameter stenosis rate portend predictive value to identify haemodynamically significant CAD (invasive FFR ≤0.8).
Limitations: Only plaque information and routine risk factors was explored for identifying flow-limiting lesions.
Ethics committee approval: This study was approved by the Institutional Review Board. Informed consent was obtained for all patients.
Funding: No funding was received for this work.
Author Disclosures:
N. Zhao: Investigator at FUWAI HOSPITAL, CAMS & PUMC, Author at FUWAI HOSPITAL, CAMS & PUMC
Y. Gao: Investigator at FUWAI HOSPITAL, CAMS & PUMC, Author at FUWAI HOSPITAL, CAMS & PUMC
B. Lv: Investigator at FUWAI HOSPITAL, CAMS & PUMC, Author at FUWAI HOSPITAL, CAMS & PUMC

RPS 1103-3 14:22

Coronary CT angiography derived plaque markers correlated with invasive instantaneous flow reserve for detecting haemodynamically significant coronary stenoses

D. Overhoff[1], G. Özdemir[1], U. J. Schoepf[2], I. Akin[1], D. Lossnitzer[1], M. Borggrefe[1], S. O. Schönberg[1], S. Baumann[1], S. Janssen[1]; *[1]Mannheim/DE, [2]Charleston, SC/US (daniel.overhoff@umm.de)*

Purpose: To compare morphological and anatomic plaque markers derived from coronary computed tomography angiography (cCTA) for the detection of lesion-specific ischemia with invasive instantaneous wave-free ratio (iFR®) as the reference standard.
Methods and materials: In our prospective study, we enrolled patients with suspected coronary artery disease (CAD) who had undergone cCTA using a low-dose third-generation dual-source CT and invasive coronary angiography (ICA) with iFR® measurement. Various plaque markers were assessed on cCTA. The discriminatory power of these markers for the detection of ischemia-inducing CAD was evaluated against invasive iFR®.
Results: Our study cohort included 39 patients. Among 54 vessel-specific lesions, 15 lesions (28%) were characterised as haemodynamically significant by iFR®≤0.89. The area under the curve (AUC) of lesion length/ minimal luminal diameter[4] (LL/MLD[4]) (0.84, p=0.0045) was greater than the AUC of minimal luminal area (MLA) (0.82, p=0.0085), MLD (0.81, p=0.0028), the degree of luminal diameter stenosis (0.81, p=0.0050), corrected coronary opacification (CCO) (0.79, p=0.0036), remodeling index (RI) (0.75, p=0.0073), and percentage aggregate plaque volume (%APV) (0.72, p=0.0172). LL, vessel volume (VV), total plaque volume (TPV), and calcified and non-calcified plaque volume (CPV/ NCPV) did not reach statistical significance, and were unable to discriminate between vessels with and without ischemia-inducing coronary stenosis.
Conclusion: LL/MLD[4], MLA, MLD, the degree of luminal diameter stenosis, CCO, RI, and %APV derived from cCTA can support the detection of haemodynamically significant coronary stenosis as compared with iFR®, with LL/MLD[4] showing the greatest discriminatory power.
Limitations: A small study cohort that may incur selection bias. Only a modest fraction of the assessed 54 lesions were haemodynamically relevant, which may have limited the validity in positive cases.
Ethics committee approval: Approved by IRB.
Funding: No funding was received for this work.
Author Disclosures:
D. Overhoff: nothing to disclose
D. Lossnitzer: nothing to disclose
S. Baumann: nothing to disclose
M. Borggrefe: nothing to disclose
S. O. Schönberg: nothing to disclose
U. J. Schoepf: Consultant at Siemens, Consultant at Gueberet, Consultant at Bayer
I. Akin: nothing to disclose
G. Özdemir: nothing to disclose
S. Janssen: nothing to disclose

RPS 1103-4 14:28

Performance of a deep learning algorithm for the evaluation of CAD-RADS classification with CCTA

G. Muscogiuri[1], M. Chiesa[1], L. Fusini[1], M. Guglielmo[1], A. Baggiano[1], A. I. Guaricci[2], G. Cicala[3], M. Pepi[1], G. Pontone[1]; *[1]Milan/IT, [2]Bari/IT, [3]Parma/IT (g.muscogiuri@gmail.com)*

Purpose: To develop a deep convolutional neural network (CNN) to classify coronary computed tomography angiography (CCTA) in the correct coronary artery disease reporting and data system (CAD-RADS) category.
Methods and materials: 288 patients who underwent clinically indicated CCTA were included in this single-centre retrospective study. The CCTAs were stratified by CAD-RADS scores by expert readers and considered as a reference standard. A deep CNN was designed and tested on the CCTA dataset and compared to on-site reading. The deep CNN analysed the diagnostic accuracy of the following three models based on CADRADS classification: Model A (CADRADS 0 vs CADRADS 1-2 vs CADRADS 3,4,5), Model 1 (CADRADS 0 vs CADRADS>0), and Model 2 (CADRADS 0-2 vs CADRADS 3-5). The time of analysis for both physicians and CNN were recorded.
Results: Model A showed a sensitivity, specificity, negative predictive value, positive predictive value, and accuracy of 47%, 74%, 77%, 46%, and 60%, respectively. Model 1 showed a sensitivity, specificity, negative predictive value, positive predictive value, and accuracy of 66%, 91%, 92%, 63%, 86%, and 89%, respectively. Conversely, Model 2 demonstrated the following sensitivity, specificity, negative predictive value, positive predictive value, and accuracy: 82%, 58%, 74%, 69%, 71%, and 78%, respectively. Time of analysis was significantly lower using CNN as compared to on-site reading (530.5±179.1vs104.3±1.4 seconds, p:0.01).
Conclusion: Deep CNN yielded accurate automated classification of patients with CAD-RADS.
Limitations: A small sample size was used for the study.
Ethics committee approval: In process.
Funding: No funding was received for this work.
Author Disclosures:
G. Pontone: nothing to disclose
G. Muscogiuri: nothing to disclose
M. Chiesa: nothing to disclose
L. Fusini: nothing to disclose
M. Guglielmo: nothing to disclose
A. Baggiano: nothing to disclose
A. I. Guaricci: nothing to disclose
G. Cicala: nothing to disclose
M. Pepi: nothing to disclose

RPS 1103-5 14:34

NETosis and cardiovascular disease in a cohort of patients with acute chest pain: correlations between coronary CT angiography and laboratory results

M. Fusaro[1], M. Rattazzi[1], G. Tessarin[2], C. Bortolanza[1], M. Tiepolo[1], C. Nardin[1], L. Tonon[1], G. Morana[1]; [1]*Treviso/IT,* [2]*Padua/IT (tessarin.giovanni@gmail.com)*

Purpose: Observational cohort study evaluating neutrophil extracellular traps (NET)-osis' activation in patients with acute coronary syndrome and in patients with and without coronary artery disease investigated with coronary CT angiography.
Methods and materials: We enrolled 27 patients with an acute coronary syndrome (ACS), 86 patients with non-complicated coronary artery disease (CAD) diagnosed with coronary computed tomography angiography, and 114 patients with no CT signs of coronary artery disease from March 2016 to October 2017. Each patient underwent blood sampling to assess circulating markers of NETosis, such as lactoferrin, proteinase PR3, PMN elastase, and neutrophil gelatinase-associated lipocalin (NGAL). The circulating levels of these markers were then compared between the three groups of patients.
Results: Increased levels of neutrophils and decreased levels of lymphocytes ($p<0.001$) were found in patients with acute coronary syndrome compared to the other two populations. Analysis of NETosis's markers showed a significant increase of NGAL and PMN-Elastase in ACS patients compared to the ones with NO-CAD (respectively, $p=0.005$ and $p=0.009$) and with CAD (respectively, $p=0.002$ and $p=0.010$). A significant increase of lactoferrin was also recorded in CAD versus NO-CAD populations ($p=0.014$). No significant differences for PR3 were found. Furthermore NGAL plasmatic levels resulted independently associated to ACS presence ($p=0.013$) also after traditional risk factors adjustment.
Conclusion: This study showed a significant increased level of some NETosis' markers in subjects with ACS compared to patients with and without CAD, suggesting a role of neutrophils activation in atherothrombotic complications of atherosclerosis.
Limitations: A limited number of patients analysed, especially patients with acute coronary syndrome.
Ethics committee approval: Approval of the ethics committee for the clinical trial of provinces of Treviso and Belluno (Italy). Written informed consent acquired.
Funding: No funding was received for this work.
Author Disclosures:
G. Tessarin: nothing to disclose
M. Fusaro: nothing to disclose
M. Rattazzi: nothing to disclose
C. Nardin: nothing to disclose
C. Bortolanza: nothing to disclose
M. Tiepolo: nothing to disclose
L. Tonon: nothing to disclose
G. Morana: Speaker at Bracco

RPS 1103-6 14:40

Comparison of pericoronary fat attenuation index in patients with and without plaque on cCTA by plaque type and stenosis severity

R. Ma, M. van Assen, D. Ties, G. J. Pelgrim, G. Sidorenkov, P. M. van Ooijen, P. van der Harst, R. van Dijk, R. Vliegenthart*; Groningen/NL (ericgeminim@gmail.com)*

Purpose: To investigate differences in fat attenuation index (FAI) between coronary arteries with and without plaque and relationships with plaque morphology.
Methods and materials: We retrospectively investigated 165 patients with clinically indicated cCTA between January 2015 and November 2017 (72 patients without and 93 patients with plaque). Scanning involved 3rd generation dual-source CT (SOMATOM Force, Siemens Healthineers) at 70kV. For healthy coronary arteries, FAI was measured at the proximal coronary segment. For diseased coronary arteries, FAI was measured across the plaque-causing most luminal narrowing. The first regression model compared FAI in healthy and diseased coronary arteries. A second model, including only diseased coronary arteries, evaluated the relationship of plaque-type and stenosis severity with FAI. Plaque type was divided into non-calcified, mixed, and calcified. Stenosis severity was categorised as minimal (1-24%), mild (25-49%), moderate (50-69%), and severe (70-100%).
Results: FAI in healthy and diseased coronary arteries were -98.0±10.1HU versus -100.5±10.1HU, -93.9±8.5HU versus -91.4±11.2HU, and -96.1±9.0HU versus -93.7±10.8HU for LAD, LCX, and RCA, respectively. There was a significant difference in FAI between healthy vessels and diseased vessels ($p=0.018$). FAI of non-calcified, mixed, and calcified plaque was -90.7±12.0HU, -95.0±10.5HU, and -97.9±10.8HU, with a significant difference between FAI of non-calcified and calcified plaque ($p=0.025$) and between non-calcified and mixed plaque ($p<0.001$). FAI of minimal, mild, moderate, and severe stenosis was -94.7±10.6HU, -95.5±11.2HU, -95.8±11.9HU, and -99.1±12.0HU. FAI was significantly different between minimal/mild and severe stenosis ($p=0.011/0.016$).
Conclusion: FAI showed differences by coronary plaque composition and degree of stenosis. These results may offer insight into the development of coronary artery disease and plaque vulnerability.
Limitations: The study lacked pathology results.
Ethics committee approval: The Medical Ethical Board waived the need for informed consent.
Funding: The first author was sponsored by the China Scholarship Council.
Author Disclosures:
R. Ma: nothing to disclose
M. van Assen: nothing to disclose
D. Ties: nothing to disclose
G. J. Pelgrim: nothing to disclose
G. Sidorenkov: nothing to disclose
P. M. van Ooijen: nothing to disclose
P. van der Harst: nothing to disclose
R. van Dijk: nothing to disclose
R. Vliegenthart: nothing to disclose

RPS 1103-7 14:46

FFR-CT in the evaluation of acute chest pain: concepts and first experiences

R. R. Bayer[1], A. M. Fischer[1], S. S. Martin[2], C. Tesche[3], A. Varga-Szemes[1], U. J. Schoepf[1]; [1]*Charleston, SC/US,* [2]*Frankfurt am Main/DE,* [3]*Munich/DE (bayer@musc.edu)*

Purpose: Fractional flow reserve derived from coronary CTA (FFR-CT) has demonstrated utility in the evaluation of coronary artery disease in stable outpatients. However, the utility of FFR-CT in the emergency department (ED) setting in patients with acute chest pain (ACP) is insufficiently studied. We evaluated 30-day clinical outcomes (major adverse cardiovascular events (MACE), revascularisation, and readmission) in patients presenting to the ED with ACP.
Methods and materials: Patients between the ages of 18-95 years who presented to our ED with ACP and underwent clinically indicated cCTA and FFR-CT were included. cCTA was acquired using 3rd generation dual-source CT and FFR-CT was performed HearFlow®. Patients were retrospectively evaluated for 30-day MACE, readmission, revascularisation, and additional testing.
Results: A total of 59 patients underwent CCTA and subsequent FFR_{CT}. 32 out of 59 patients (54%) had negative FFR_{CT} (≥0.80) out of whom 18 patients (55%) were discharged from the ED. Out of the 32 patients without functionally significant CAD by FFR_{CT}, 32 patients (100%) underwent no revascularisation and 32 patients (100%) had no MACE at the 30-day follow-up period. Conversely, there were 3 MACE in the group of 27 patients with an FFR_{CT} <0.8. The average turnaround time for FFR_{CT} results was 3.5 hrs.
Conclusion: This preliminary data demonstrates that cCTA and subsequent FFR_{CT} has the potential for accurate and safe evaluation of CAD in patients presenting to the ED with acute chest pain. In this small cohort of patients, FFR_{CT} yielded a negative predictive value of 100%.
Limitations: The limitations of the study included a small sample size at a single centre. The high disease prevalence and severe may have resulted in selection bias.
Ethics committee approval: IRB approval with waiver of consent.
Funding: Research support provided by HeartFlow.
Author Disclosures:
R. R. Bayer: Research/Grant Support at HeartFlow, Research/Grant Support at Bayer
A. M. Fischer: nothing to disclose
C. Tesche: nothing to disclose
A. Varga-Szemes: nothing to disclose
U. J. Schoepf: Research/Grant Support at Astellas, Research/Grant Support at Bayer, Research/Grant Support at Bracco, Research/Grant Support at Elucid Bioimaging, Research/Grant Support at Guerbet, Research/Grant Support at HeartFlow, Research/Grant Support at Siemens
S. S. Martin: nothing to disclose

RPS 1103-8 14:52

Comparative-effectiveness analysis of coronary CTA in patients with stable chest pain

X. Wu[1], A. Malhotra[2], H. Mojibian[1]; [1]*New Haven, CT/US,* [2]*Stamford, CT/US (ajay.malhotra@yale.edu)*

Purpose: To evaluate the comparative-effectiveness of CCTA as initial diagnostic and as follow-up imaging modality for patients with stable chest pain.
Methods and materials: A decision-analytic model was created over a 5-year span. Input parameters were based on randomised trials and long-term follow-up studies. Base case calculations, probabilistic sensitivity analysis, and two-

way sensitivity analyses were performed. Two sets of analyses (conservative and aggressive) were performed.
Results: The base case calculation shows coronary CCTA to be the optimal diagnostic modality in both conservative and aggressive management with an expected utility of 4.56 QALYs. Among functional imaging, using CCTA as a follow-up for equivocal results is shown to yield higher benefit than using any modality alone.
CCTA was the optimal initial diagnostic modality in 97.65% of the 10,000 Monte Carlo simulations.
CCTA remains the optimal strategy throughout the ranges when varying the pre-test probability of severe and moderate CAD from 0 to 40% and 0 to 70%. When varying the sensitivity of CCTA, the results show that CCTA is replaced by PET followed by CCTA when the sensitivity of CCTA is below 86.4%. When varying the sensitivity of SPECT, PET, and stress echocardiogram from 50% to 100%, CCTA remains the optimal strategy throughout the ranges. Two-way sensitivity analyses were performed varying the sensitivity of CCTA with the sensitivity of each functional imaging modality. CCTA remained the optimal strategy when the sensitivity was at least 5% higher than the other modality in absolute values.
Conclusion: CCTA is the optimal initial diagnostic modality for patients with stable chest pain, yielding the highest health benefit. CCTA also serves as a value follow-up modality in patients with equivocal functional imaging results.
Limitations: Limitations inherent to modeling study.
Ethics committee approval: n/a
Funding: No funding was received for this work.
Author Disclosures:
A. Malhotra: nothing to disclose
X. Wu: nothing to disclose
H. Mojibian: nothing to disclose

RPS 1103-9 14:58
Routine early postoperative CT imaging after CABG surgery: clinical value and unexpected findings
M. G. Karolyi, T. Gloor, M. O. Schmiady, H. Alkadhi*; Zurich/CH (mihaly.karolyi@usz.ch)*

Purpose: Cardiac CT angiography (CCTA) has evolved as the preferred imaging modality to follow-up patients who have undergone coronary artery bypass surgery (CABG). Yet, its clinical value in the early postoperative setting is not established. We evaluated the benefit of adding CCTA to our routine clinical workup after CABG.
Methods and materials: 215 patients (181 male, age 66±10 years) underwent CCTA within two weeks after CABG using third-generation dual-source CT with an effective radiation dose of 4.5±2.6 mSv. Graft patency and additional findings were registered and the change in clinical patient management after CCTA was evaluated.
Results: Graft occlusion or high-grade stenosis was revealed in 6.7% (32/215) of the patients, with 5.8% (19/329) of venous and 4.0% (13/323) of arterial grafts affected (p=0.22). Pleural effusion with lung atelectasis was recognised in 24% (51/215), residual pneumothorax in 12% (25/215), infiltration in 4% (9/215), and cardiac or vascular thrombus in 1.5% (3/215) of the patients, while additional incidental findings in 5.1% (11/215) of the patients, such as pathologic lymphadenopathy, lung nodule, unknown hepatic lesion, renal aneurysm, or hiatus hernia. No adverse events related to CCTA were documented. CCTA changed further clinical management in 31.3% (10/32) of the patients with occluded or stenosed grafts, and altogether in 11.6% (25/215) of the patients after CABG.
Conclusion: Early postoperative CCTA after CABG frequently reveals persistent postoperative and unexpected findings and may change management in about 1/3 of the patients with affected grafts. This effect on clinical outcomes should be evaluated in long term follow-up studies.
Limitations: Retrospective study design. No clinical follow-up.
Ethics committee approval: Approved by the institutional review board. Due to the retrospective study design, written informed consent of the patients was waived.
Funding: No funding was received for this work.
Author Disclosures:
M. G. Karolyi: nothing to disclose
M. O. Schmiady: nothing to disclose
H. Alkadhi: nothing to disclose
T. Gloor: nothing to disclose

RPS 1103-10 15:04
CAD-RADS in the era of FFR_{CT}: an observational study in an acute chest pain population
A. F. Abadia[1], D. Giovagnoli[1], U. J. Schoepf[1], R. R. Bayer[1], R. Steinbach[1], M. van Assen[2], A. Varga-Szemes[1], S. S. Martin[3]; [1]*Charleston, SC/US,* [2]*Groningen/NL,* [3]*Frankfurt am Main/DE (simartin@outlook.com)*

Purpose: Coronary artery disease reporting and data system (CAD-RADS) is a standardised classification system for coronary CT angiography (CCTA). We aimed to investigate the impact of fractional flow reserve (FFR_{CT}) derived from CCTA on CAD-RADS stratifications in patients presenting with acute chest pain (ACP).
Methods and materials: FFR_{CT} analysis was included in the diagnostic workup of 94 patients (mean age 65.7±9.6 years) who presented to the emergency department (ED) with ACP and were referred for CCTA. We evaluated the rate of CAD-RADS reclassifications from the initial interpretation of the CCTA study alone versus after FFR_{CT} results were obtained. Other reported data included downstream resource use and 90-day clinical outcomes.
Results: 3 patients were initially classified as CAD-RADS 1, 18 as CAD-RADS 2, 44 as CAD-RADS 3, and 29 as CAD-RADS 4 based on CCTA alone. No patient with an initial CAD-RADS 1, 2, or 4 classification was reclassified following the addition of FFR_{CT} results. However, in patients with CAD-RADS 3, where function testing is often recommended for further evaluation, 41% (18/44) were reclassified to CAD-RADS 2 after FFR_{CT} results were obtained. This assessment may decrease the rate of additional diagnostic testing by 64%. Additionally, no clinical events occurred in the group of patients with FFR_{CT} >0.80 at 90-day follow up.
Conclusion: Adding FFR_{CT} analysis in patients presenting with ACP substantially decreases equivocality in CCTA interpretation, drastically reduces CAD-RADS 3 classifications, and has the potential to obviate unnecessary downstream testing. One should consider an update to the CAD-RADS classification to account for the availability of FFR_{CT}.
Limitations: Single-centre, short follow-up time, small sample.
Ethics committee approval: IRB-approved. Informed consent waived.
Funding: No funding was received for this work.
Author Disclosures:
M. van Assen: nothing to disclose
A. F. Abadia: nothing to disclose
D. Giovagnoli: nothing to disclose
R. R. Bayer: Research/Grant Support at HeartFlow, Research/Grant Support at Bayer
U. J. Schoepf: Research/Grant Support at Astellas, Bayer, Elucid Bioimaging, GE, Guerbert, HeartFlow Inc., and Siemens, Consultant at Astellas, Bayer, Elucid Bioimaging, GE, Guerbert, HeartFlow Inc., and Siemens
A. Varga-Szemes: Research/Grant Support at Siemens, Consultant at Elucid Bioimaging
R. Steinbach: nothing to disclose
S. S. Martin: nothing to disclose

RPS 1103-11 15:10
Effect of calcification on diagnostic performance of computational fluid dynamic based FFR-CT identifying ischemia-specific lesions in patients with suspected CAD: a preliminary study from China
N. Zhao, Y. Gao, B. Lv*; Beijing/CN (15810686235@163.com)*

Purpose: To assess the effect of calcification on the diagnostic performance of FFR-CT for haemodynamically significant CAD with invasive FFR as a standard reference.
Methods and materials: 127 patients with suspected CAD (56.9 ± 8.9 years, 75.6% male) who underwent CCTA and ICA were prospectively enrolled. The performance of FFR-CT was compared in different conditions, including the presence and absence of calcification, different CAC scores, diffusivity index of calcification, and coronary segments with calcified plaques. The calcification-related parameters were compared among true positive, true negative, false positive, and negative groups of FFR-CT. The association between the parameters and ΔFFR (ΔFFR=FFR – FFR-CT) and performance of FFR-CT were analysed.
Results: 152 vessels of 127 patients had haemodynamically relevant stenosis. The vessel-based and patient-based sensitivity, specificity, and accuracy of FFR-CT were 74.63%, 77.65%, and 75.7%, and 79.37%, 76.56%, and 77.2%. The accuracy and specificity reduced with increased CAC scores (per-patient: 86.96% to 74.04%, 100% to 72.73%; per-target-vessel: 78.05% to 74.77%, 92% to 76.47%) and diffusivity index (per-target-vessel) (75% to 71.43%, 76.32% to 71.87%). The specificity was lower in the presence of calcification (per-patient: 100% vs. 72.55%; per-vessel: 92% vs. 76.27%) and more calcification related coronary segments and arteries groups. But all the differences between groups didn't reach statistical significance. The values of all parameters were non-significantly higher in the false negative group. In regression analysis, the number of coronary segments and arteries had a predictive value for diagnostic performance of FFR-CT (OR=1.426, p = 0.039; OR=0.355, p = 0.026).
Conclusion: The diagnostic performance of FFR-CT could be potentially negatively affected by calcification.
Limitations: The sample size of study is relatively small and subjectives of some subgroups are not enough.
Ethics committee approval: This study was approved by the Institutional Review Board. Informed consent was obtained from all patients.
Funding: No funding was received for this work.

Author Disclosures:
N. Zhao: Author at FUWAI HOSPITAL, CAMS & PUMC, Investigator at FUWAI HOSPITAL, CAMS & PUMC
Y. Gao: Author at FUWAI HOSPITAL, CAMS & PUMC, Investigator at FUWAI HOSPITAL, CAMS & PUMC
B. Lv: Author at FUWAI HOSPITAL, CAMS & PUMC, Investigator at FUWAI HOSPITAL, CAMS & PUMC

RPS 1103-12 15:16
Prognostic value of coronary CT angiography-derived plaque features and clinical parameter on adverse cardiac outcome using support vector machine learning
C. Tesche[1], B. Hedels[1], F. Straube[1], S. Hartl[1], B. Brück[1], M. J. Bauer[1], U. J. Schoepf[2], E. Hoffmann[1], U. H. Ebersberger[1]; [1]*Munich/DE,* [2]*Charleston, SC/US (tesche.christian@googlemail.com)*

Purpose: To evaluate the prognostic value of coronary CT angiography-derived plaque features and clinical parameter on adverse cardiac outcome using support vector machine (SVM).
Methods and materials: Data of 361 patients (61.9±10.3 years, 65% male) with suspected coronary artery disease (CAD) who underwent cCTA were retrospectively analysed. The occurrence of major adverse cardiac events (MACE) more than 90 days after cCTA was recorded. Several cCTA-derived plaque characteristics and conventional CT risk scores together with cardiovascular risk factors were provided to the supervised SVM learning algorithm to predict MACE. Performance of SVM was compared against conventional regression analysis.
Results: MACE was observed in 31 patients (8.6%) after a median follow-up of 4.5 years. Patients suffering MACE had significantly more obstructive CAD with a higher segment stenosis score, segment involvement score, and number of high-risk plaque features compared to controls (all p<0.05). Likewise, patients with MACE had a higher Framingham risk score, reflecting the clinical risk for cardiovascular events. The SVM algorithm showed a sensitivity and specificity of 0.94 and 0.87 for the prediction of MACE. The area under the curve (AUC) was 0.97 (95%CI 0.95-0.98) and showed significantly higher performance compared to regression analysis incorporating all available information (AUC 0.92, p<0.05).
Conclusion: A deep-learning SVM algorithm utilising cCTA-derived plaque information and clinical data improves the prediction of MACE when compared to regression analysis. A SVM based algorithm may improve the integration of patient's information to improve risk stratification.
Limitations: Retrospective single-centre study. Patient follow-up was performed using electronic medical records of the hospitals, therefore, we might have missed events occurring outside the hospital.
Ethics committee approval: Approved by the local ethical board with a waiver of informed consent.
Funding: No funding was received for this work.
Author Disclosures:
C. Tesche: nothing to disclose
B. Hedels: nothing to disclose
F. Straube: nothing to disclose
S. Hartl: nothing to disclose
B. Brück: nothing to disclose
M. J. Bauer: nothing to disclose
U. J. Schoepf: Consultant at Siemens, Research/Grant Support at Siemens
E. Hoffmann: nothing to disclose
U. H. Ebersberger: nothing to disclose

RPS 1103-13 15:22
Prognostic value of cCTA derived morphological and functional quantitative plaque markers using semi-automated plaque software
D. Overhoff[1], S. Baumann[1], F. Kaeder[1], U. J. Schoepf[2], S. O. Schönberg[1], M. Borggrefe[1], I. Akin[1], D. Lossnitzer[1], S. Janssen[1]; [1]*Mannheim/DE,* [2]*Charleston, SC/US (daniel.overhoff@umm.de)*

Purpose: In this study we analysed the prognostic value of coronary computed tomography angiography (cCTA) derived morphological and functional quantitative plaque markers and plaque scores for major adverse cardiovascular events (MACE).
Methods and materials: We analysed data of patients with suspected coronary artery disease (CAD). Various plaque markers were obtained using a semi-automated software prototype or derived from the results of the software analysis. Several risk scores were calculated and follow-up data concerning MACE was collected from all patients.
Results: A total of 131 patients (64±11 years, 73% male) were included in our study. MACE occurred in 11 patients within the follow-up period of 34±25 months. CAD-RADS score (OR=11.62), Syntax score (SS) (OR=1.11), Leiden-risk-score (OR=1.37), Duke jeopardy score (DJS) (OR=1.57), the index DJS/minimal luminal diameter (MLD) (OR=1.40), segment involvement score (SIS) (OR=1.76), total plaque volume (TPV) (OR=1.20), lipid-rich plaque volume (OR=1.23), and percentage aggregated plaque volume (%APV) (OR=1.32) were significant predictors for MACE (all p≤0.05). Also, the corrected coronary opacification (CCO) correlated significantly with the occurrence of MACE (p<0.0001). The CAD-RADS score, SS, and Leiden-risk score showed substantial sensitivity for predicting MACE (90.9%). The SS and Leiden-risk score displayed high specificities of 80.8% and 77.5%, respectively. These plaque markers and risk scores all provided high negative predictive value (NPV >90%).
Conclusion: The cCTA derived plaque markers of SIS, TPV, lipid-rich plaque volume, %APV, CCO, and the risk scores exhibited a predictive value for the occurrence of MACE and can likely aid in identifying patients at risk for future cardiac events.
Limitations: Since only patients with CAD were selected, the validity regarding individual CVRF may be affected. Also, the MACE/non-MACE groups were not matched for baseline characteristics.
Ethics committee approval: IRB approved study.
Funding: No funding was received for this work.
Author Disclosures:
F. Kaeder: nothing to disclose
D. Overhoff: nothing to disclose
S. Baumann: nothing to disclose
U. J. Schoepf: Consultant at Bayer, Consultant at Guerbet, Consultant at Siemens
S. O. Schönberg: nothing to disclose
M. Borggrefe: nothing to disclose
I. Akin: nothing to disclose
D. Lossnitzer: nothing to disclose
S. Janssen: nothing to disclose

14:00 - 15:30 **da Vinci (Room D1)**

Emergency Imaging

RPS 1117

Abdomen and brain

Moderators:
A. Blanco Barrio; Murcia/ES
N.N.

RPS 1117-K 14:00
Keynote lecture
I. Arkhipova; *Moscow/RU (iarkhipova1977@gmail.com)*

Author Disclosures:
I. Arkhipova: nothing to disclose

RPS 1117-6 14:10
Variability in non-contrast head CT image quality in Ireland: opportunities for tarameter optimisation and standardisation to improve stroke care
J. Hynes, D. Caldwell, P. Kenny, P. J. Macmahon; *Dublin/IE (johynes@tcd.ie)*

Purpose: Non-contrast computed tomography (NCCT) of the brain is a critical tool in the investigation of suspected acute ischaemic stroke. The recognition of subtle differences in attenuation values between normal brain parenchyma and regions of ischaemic tissue is crucial to accurate and timely diagnosis. Our study aims to identify which combination of CT acquisition parameters maximises the ability to detect these early changes. We also investigated the variation in imaging protocols for suspected acute stroke at different institutions in the regional hospital network.
Methods and materials: Uniformity images of the CATPHAN phantom were obtained under various combinations of kV, mAs, reconstruction kernel, slice thickness and strength of iterative reconstruction. Images were analysed by an in-house algorithm, based on the statistical method of Chao et. al., (2000) to objectively measure low contrast detectability. Data is presented as contrast-detail diagrams, i.e., the minimum separation in Hounsfield Units (HU) required to distinguish a low contrast object of a given equivalent diameter from the background. 12 CT scanners made by 3 different manufacturers across 6 hospitals were surveyed.
Results: Increasing mAs, slice thickness and utilising higher levels of iterative reconstruction objectively improve low contrast detectability in NCCT brain. Deviations in protocols across manufacturers and hospitals were found to result in variations in image quality.
Conclusion: Variations in acquisition protocol produce differences in image quality which may contribute to missed and/or delayed findings. Optimising low contrast detectability and ensuring standardisation between linked institutions offers the potential to make a meaningful improvement in modern stroke care.

Limitations: Standardisation will inevitably be limited by the variation in manufacturers, radiologists' preferences and scanner performance.
Ethics committee approval: n/a
Funding: No funding was received for this work.
Author Disclosures:
J. Hynes: nothing to disclose
D. Caldwell: nothing to disclose
P. Kenny: nothing to disclose
P. J. Macmahon: nothing to disclose

RPS 1117-1 14:16

Adrenal glands enhancement in computed tomography as a predictor of 24-hour mortality in critically ill patients

R. Winzer, J. Kühn, C.-J. Baldus, D. Seppelt, I. Platzek, R.-T. Hoffmann, D. Fedders*; Dresden/DE (robert.winzer@uniklinikum-dresden.de)*

Purpose: To assess the hyperattenuation of adrenal glands on contrast-enhanced computed tomography scans as a predictor of hospital mortality in critical care unit patients.
Methods and materials: Seventy-three patients (67.5 ±12.3 years of age) were included in this retrospective analysis. All patients underwent contrast-enhanced CT due to life-threatening indications. Attenuation of the adrenal glands in the portal venous phase was ROI-based assessed quantitatively by documenting Hounsfield units (HU) by two radiologists. From ROC analysis, Youden's J statistic was derived with death within 24 (48 and 72) hours as a classifier. Interrater agreement was assessed using intraclass correlation coefficient for measurements of the HU in adrenal glands and weighted kappa (k) after classifying patients with hyperdense adrenal enhancement (= enhancement above the threshold by ROC analysis).
Results: Fourteen patients (19%) died within 24 hours. In the portal venous phase HU means of both adrenal glands differed significantly between patients who died within 24 hours and those who survived (135.7 ± 46 HU vs 74.7 ± 24 HU; p=0.001). For portal venous phase, data ROI-based ROC analysis yielded for a Youden index of 0.79/0.85, a sensitivity of 100%/100% and a specificity of 79%/85% (p<.0001), a cut-off point of 93/95 HU for prediction of 24-hour mortality for rater 1 and 2, respectively. The AUC was 0.92/0.93. ICC of 0.99 and weighted kappa (k) of 0.84 indicated a high interrater agreement.
Conclusion: Venous hyperattenuation of adrenal glands on contrast-enhanced CT can predict 24-hour mortality quite well and can serve as a reproducible prognostic marker for the patient's outcome.
Limitations: Retrospective study.
Ethics committee approval: Ethics committee approval is given.
Funding: No funding was received for this work.
Author Disclosures:
R. Winzer: nothing to disclose
D. Fedders: nothing to disclose
J. Kühn: nothing to disclose
D. Seppelt: nothing to disclose
C.-J. Baldus: nothing to disclose
R.-T. Hoffmann: nothing to disclose
I. Platzek: nothing to disclose

RPS 1117-2 14:22

Do emergency physicians appropriately request a head CT in patients with new-onset seizure?

I. García Tuells, J. M. Plasencia Martinez, E. Antolinos, M. N. Plasencia, J. M. M. Garcia Santos, J. Trejo Falcón*; Murcia/ES (irenegt92@gmail.com)*

Purpose: To determine how Emergency Head Computed Tomography (EHCT) is requested in patients with new-onset seizure in our environment. EHCT would be appropriate if the new-onset seizure was focal, associated with neurological deficit or in certain contexts.
Methods and materials: Physicians from 3 hospitals (H1, H2, H3), regularly involved in emergency on-call duty, answered a five-question survey on EHCT appropriateness for new-onset seizures. Fisher's test was used to compare the answers (A) among hospitals, resident/staff physician, residence year and medical specialty.
Results: We obtained 39 surveys [H1 12 (20.77%), H2 18 (46.15%), H3 6 (23.08%)] from 31 residents (79.49%) [14 (45.16%) ≥3 years of training] and 8 staff physicians (20.51%). 31/39 (79.49%) were Family and Community Medicine Specialists (FCMS). 32/39 (82%) would request (A4+A5) EHCT whatever the kind of seizure (Q1). That was the most common response in FCMS (27/31 -87.1%- vs 5/8 -62%-, P=0.043) and in staff physicians (8/8 -100%- vs 24/31 -77.4%- P=0.042). 9/39 (23.07%) and 8/39 (20.51%) requested an EHCT (A4+A5) according to Radiology and Emergency Departments guidelines (Q4) or Emergency Department guidelines (Q5). Residents ≤2nd year (15/17 -88.23 - vs 6/14 -42.86%- P = 0.029) were not aware (A2+A3) of those guidelines (Q5). For 31/39 (79.45%) of the participants, the EHCT results did not modify (A2+A3) the clinical attitude (Q2) and 27/39 (69.20%) were not sure (A3) about EHCT detected relevant alterations in those patients (Q3). The answers were similar among hospitals.
Conclusion: On-call physicians routinely request CT scans for new-onset seizure ignoring current evidence. It is mandatory to go into quality improvement cycles promoted by radiology departments to improve current practices.
Limitations: Limitations were a potential Hawthorne effect and the small sample size.
Ethics committee approval: n/a
Funding: No funding was received for this work.
Author Disclosures:
E. Antolinos: nothing to disclose
I. García Tuells: nothing to disclose
M. N. Plasencia: nothing to disclose
J. M. Plasencia Martinez: nothing to disclose
J. M. M. Garcia Santos: nothing to disclose
J. Trejo Falcón: nothing to disclose

RPS 1117-3 14:28

The performance of artificial intelligence in the detection of intracranial haemorrhage on head computed tomography with clinical workflow integration

N. Watte, K. H. Nieboer, N. Buls, J. de Mey*; Brussels/BE (ninawatte@gmail.com)*

Purpose: To evaluate the performance of an artificial intelligence (AI) tool using a deep learning algorithm for detecting intracranial haemorrhage (ICH) on head computed tomographic (CT) exams with clinical workflow integration at the emergency department.
Methods and materials: We retrospectively collected a dataset at the emergency department, containing 500 consecutive head CT exams and their clinical reports, between Sept 1, 2019, and Oct 1, 2019. All CT exams were automatically pseudo-anonymised and transferred for ICH detection by an AI tool (Aidoc, Israel). We registered the number of studies that were successfully processed by AI, and we calculated the diagnostic performance by the positive (PPV) and negative (NPV) predictive values, sensitivity, and specificity. The original clinical radiology report and consensus by independent supervision were considered as the gold standard. Concordance was assessed by Cohen's k statistic.
Results: During a one-month implementation phase, the algorithm created a report for 388 studies (77,6%) during real-time radiology workflow; 22,4% failed, due to multiple possible technical issues, not further subject to this study. From the 388 processed studies, 31 (7,9%), were labelled by AI as having ICH. The expert readers detected 37 (9,5%) ICHs. The concordance between AI and expert reading was substantial (kappa=0,65). Algorithm performance for ICH revealed a 98% NPV and 61% PPV. The false-negative and false-positive rates were 6/337 (1,7%) and 20/37 (54%), respectively. The sensitivity and specificity were 84%.
Conclusion: In a clinical emergency setting, 77% of all head CT exams could be automatically evaluated by AI. With high specificity and negative predictive value, the AI tool shows the potential to rule out ICH. The positive predictive value remains moderate.
Limitations: We currently investigated 500 cases. Further research with 3000 CT exams is ongoing.
Ethics committee approval: n/a
Funding: n/a
Author Disclosures:
N. Watte: nothing to disclose
N. Buls: nothing to disclose
J. de Mey: nothing to disclose
K. H. Nieboer: nothing to disclose

RPS 1117-4 14:34

Diagnostic accuracy of multidetector CT in colonic ischaemia in the emergency department

G. Addeo[1], M. M. Lanzetta[1], G. Grazzini[1], D. Cirone[1], M. C. Bonini[2], S. Pradella[1], V. Miele[3]*; [1]Florence/IT, [2]Colle Val d'Elsa/IT, [3]Rome/IT (gloria.addeo@gmail.com)*

Purpose: To evaluate the diagnostic accuracy of MDCT (multidetector computed tomography), performed in an acute care setting in the diagnosis of primary CI (colonic ischaemia), with laparoscopic or laparotomic evaluation or surgery as the reference standard.
Methods and materials: The abdominal MDCT scans of 277 patients with clinical-laboratory suspicion of CI were retrospectively reviewed, 46 patients were excluded for secondary CI. The final study population consisted of 231 patients. CT was classified as positive for CI when the radiologist's interpretation showed a definitive diagnosis of CI; clear absence of CI was classified as a negative result. If the radiologist missed the relevant findings and failed to suspect CI, the CT report was defined as incorrect. The MDCT findings were

true positive, true negative, false positive, and false negative considering laparoscopic or laparotomic evaluation or endoscopy as the reference standard.
Results: In 41% of 231 patients included, CI was pathologically confirmed on the use of surgery. On the basis of the emergency radiology reports there were 30% true positive cases, 3,5% false positive, 11% false negative and 56% true negative. We calculated sensitivity, specificity, positive predictive value (PPV), negative predictive value (NPV) and diagnostic accuracy of MDCT obtaining: 73,4% sensitivity; 94% specificity; a PPV and a NPV of 90% and of 84%, respectively; 86% diagnostic accuracy.
Conclusion: Despite the successful CT imaging results in CI diagnosis, high colonic distention was the major cause leading to more false negative results even after intravenous administration of the contrast agent. Radiologists' experience and expertise have an important impact on their performance.
Limitations: Our investigation is in itself limited by its retrospective nature.
Ethics committee approval: The Hospital Institutional Review Board approved the study.
Funding: No funding was received for this work.
Author Disclosures:
G. Addeo: nothing to disclose
M. M. Lanzetta: nothing to disclose
D. Cirone: nothing to disclose
G. Grazzini: nothing to disclose
S. Pradella: nothing to disclose
V. Miele: nothing to disclose
M. C. Bonini: nothing to disclose

RPS 1117-5 14:40
Accuracy of Single-Pass Split-Bolus CT for detecting vascular injury in the spleen: a retrospective study in 111 patients with blunt splenic trauma
F. H. Berger[1], M. Edwards[2], T. Tromp[2], D. R. Kool[3], L. F. M. Beenen[3], B. Teunissen[3], M. Scheerder[3], M. Brink[2]; [1]*Toronto, ON/CA*, [2]*Nijmegen/NL*, [3]*Amsterdam/NL (Mobrink@hotmail.com)*

Purpose: To evaluate the diagnostic performance of Single-Pass Split-Bolus CT (SPSB-CT) for the detection of all splenic vascular injuries (SVI) and clinically relevant splenic vascular injuries in blunt trauma patients with proven splenic injury.
Methods and materials: Six-year single Level 1 trauma centre retrospective analysis of all blunt trauma patients with splenic injury on SPSB-CT. Patients were identified through electronic records. Data at the presentation and during 3 months follow-up were used. Two radiologists and one trauma surgeon, using all clinical and imaging data, defined the reference standard for the presence of SVI (AV fistula, pseudoaneurysms, active contrast extravasation) and clinically relevant SVI causing management changes or death. Four blinded radiologists evaluated initial SPSB-CT for SVI with binary (yes/no) and confidence (1-5) scores. Pooled sensitivity and specificity and observer agreement (Fleiss Kappa) statistics were calculated with 95% confidence intervals.
Results: 111 patients were included (male: 76%, mean age: 35, range 9-81) with 108 thoracoabdominal SPSB-CT (median DLP 455 mGycm), and 3 abdominopelvic SPSB-CT (mean DLP 243 mGycm). Mean aortic and hepatic enhancement was 310 HU and 109 HU. Incidence of SVI was 37/111 (33.3%), incidence of clinically relevant SVI was 27/111 (24.3%). For SVI, sensitivity was 85.8% (range 74.8% - 89.2%) and specificity was 89.9% (range 87.8% - 91.9%). For clinically relevant SVI, sensitivity was 88.9% (range 85.2% - 92.6%) and specificity was 81.9% (range 79.8% - 83.3%). Observer agreement was 88.1% with a Fleiss kappa of 0.76. At a 3 month follow-up, two patients had delayed splenic haemorrhage. No deaths related to missed SVI by SPSB-CT.
Conclusion: In blunt trauma splenic injury patients, SPSB-CT adequately detects splenic vascular injury with good inter-observer agreement.
Limitations: Retrospective, single-centre study.
Ethics committee approval: Ethics approval and informed consents was obtained.
Funding: No funding was received for this work.
Author Disclosures:
F. H. Berger: nothing to disclose
M. Edwards: nothing to disclose
T. Tromp: nothing to disclose
D. R. Kool: nothing to disclose
L. F. M. Beenen: nothing to disclose
B. Teunissen: nothing to disclose
M. Scheerder: nothing to disclose
M. Brink: nothing to disclose

RPS 1117-7 14:46
Detection of CVA and TIA at the emergency department triage: developing a prediction machine learning model
E. Druskin[1], E. Zimlichman[1], S. Soffer[2], S. Bader[1], Y. Barash[1], E. Konen[1], E. Klang[1]; [1]*Ramat Gan/IL*, [2]*Tel Aviv/IL*

Purpose: Suspected cerebrovascular accident (CVA) or transient ischemic accident (TIA) patients undergo head CT. Early identification of patients with CVA/TIA at the emergency department (ED) triage can expedite evaluation. Our aim was to develop a prediction model for CVA/TIA at triage time.
Methods and materials: We retrieved data for consecutive adult patients (1/2012 to 12/2018) who performed head CT in our ED. We obtained the following triage variables: chief complaint recorded by the triage nurse, demographics, vital signs, pain score, emergency severity index (ESI), comorbidities and home medications. Previous ED visits and hospitalisations were also computed. CVA/TIA diagnoses were verified using ICD9 coding. We used a gradient boosting model to predict CVA/TIA at the triage time. Included variables were used as input for the model. We trained the model on years 2012-2017 data and tested on the year 2018 data. We evaluated the AUCs of single variables and the full model to predict CVA/TIA. We used Youden's index to find the model's optimal sensitivity and specificity.
Results: The study cohort included 93,202 patients who underwent head CT in our ED. Among those, 7,280 patients (7.8%) were finally diagnosed with CVA/TIA. Variables with higher AUC included chief complaint (0.84), pain score (0.67), age (0.63) and systolic blood pressure (0.62). The full model showed an AUC of 0.87 (95% CI: 0.86 - 0.88) for detecting CVA/TIA at triage. The model showed a sensitivity of 84.1% and specificity of 75.0% for detecting CVA/TIA.
Conclusion: Nurse staff recorded chief complaint has a high accuracy for CVA/TIA. A machine-learning model may further expedite head CT scans for CVA/TIA at the triage.
Limitations: Retrospective single-centre study.
Ethics committee approval: Sheba Medical Center IRB approval. Informed consent was waived by the committee.
Funding: No funding was received for this work.
Author Disclosures:
E. Druskin: nothing to disclose
E. Zimlichman: nothing to disclose
S. Soffer: nothing to disclose
S. Bader: nothing to disclose
Y. Barash: nothing to disclose
E. Konen: nothing to disclose
E. Klang: nothing to disclose

RPS 1117-8 14:52
Identification of lodged projectiles on CT based on their shape, caliber measurements and dual-energy material differentiation
D. Gascho[1], N. Zoelch[1], E. Deininger-Czermak[1], C. M. S. Tappero[1], A. Buehlmann[1], P. Wyss[1], M. Thali[1], S. Schaerli[2]; [1]*Zurich/CH*, [2]*Basel/CH (dominic.gascho@irm.uzh.ch)*

Purpose: The purpose of this study was to assess the visual classification of bullets and the accuracy of calibre estimations on computed tomograpy, as well as the feasibility of dual-energy-based material differentiation.
Methods and materials: This postmortem study includes fatal gunshot wounds (n=10) with a projectile or bullet fragment lodged inside the body. The decedents underwent CT with 120 kVp. Two additional scans with tube voltages of 120 and 140 kVp (CT dose index: both 9 mGy) were performed over the anatomic region where the projectile was lodged. The shape of the projectile was assessed by an expert in ballistics using volume renderings. The calibres were estimated by measuring the diameter of the projectile on aligned multi-planar reconstructions. Two radiologists (experienced / little experienced in ballistics) performed the measurements. For each projectile, the dual-energy index (DEI) was calculated. The DEI was based on CT numbers obtained from ROI measurements at 120 and 140 kVp (Fig.1C&D).
Results: Non-fragmented bullets could be identified as semi-jacketed hollow-point (SJHP) bullets or full metal jacket (FMJ) bullets. The SJHP bullets demonstrated characteristic mushrooming on CT. The experienced radiologist was close to the actual calibre according to the measurements of the diameters of non-fragmented bullets. All lead bullets, whether fragmented or not, clearly differed from a bullet made of copper/zinc in their DEI.
Conclusion: CT can provide information regarding the type of ammunition used, which is crucial for the assessment of injuries. However, visual assessments and calibre estimations are only feasible for non-fragmented projectiles. The DEI-based material differentiation is not limited to non-fragmented projectiles and allowed a clear distinction between lead and copper/zinc bullets.
Limitations: This study is limited by the small number of cases.
Ethics committee approval: n/a
Funding: No funding was received for this work.
Author Disclosures:
D. Gascho: nothing to disclose
N. Zoelch: nothing to disclose
E. Deininger-Czermak: nothing to disclose
C. M. S. Tappero: nothing to disclose
A. Buehlmann: nothing to disclose
P. Wyss: nothing to disclose
M. Thali: nothing to disclose
S. Schaerli: nothing to disclose

RPS 1117-9 14:58

The accuracy of US and CT in diagnosing appendicitis with consideration of indeterminate examinations according to STARD guidelines

C. Crocker[1], M. A. Akl[2], M. Abdolell[1], M. Kamali[1], A. Costa[1]; [1]*Halifax/CA,* [2]*Makka/SA (andreufcosta@gmail.com)*

Purpose: To determine the accuracy of US and CT in diagnosing appendicitis at our institution, taking into account the number of indeterminate examinations in accordance with the Standards for Reporting Diagnostic Accuracy (STARD) guidelines.
Methods and materials: We evaluated 790 patients who underwent US, CT or both for evaluation of suspected appendicitis between May 2013-April 2015. Patient characteristics and US and CT results were recorded. The reference standard was histopathology or three months of medical record follow-up if surgery was not performed. 3x2 tables were generated, and sensitivity, specificity, overall test yield and accuracy were calculated according to STARD guidelines. For surgical cases, time to surgery (one-way ANOVA) and negative appendectomy rates (NAR, Fisher's exact test) were compared between patients who underwent US alone, CT alone, or both US and CT.
Results: There were 473/562 indeterminate US examinations (overall test yield, 15.8%); sensitivity and specificity were 98.5% and 54.2%, respectively. 13/522 CTs were indeterminate (overall test yield, 97.5%); sensitivity and specificity were 98.9% and 97.2%, respectively. Taking indeterminate studies into account, the accuracy was 13.7% for US and 95.6% for CT. Time to surgery was longer in patients who underwent US and CT (19.2±16 hours) vs. US alone (12.8±6.4, p=0.002), but not CT (15.8±8.6, p=0.07).
Conclusion: At our institution, a large proportion of US examinations are indeterminate for appendicitis. CT is the preferred first-line imaging test for evaluating appendicitis in non-pregnant adults.
Limitations: It is a single-centre and retrospective study. We did not include clinical or laboratory data, however, this also impacts patient diagnosis and management, and we did not re-interpret US and CT images.
Ethics committee approval: IRB approval was obtained and need for consent was waived.
Funding: No funding was received for this work.
Author Disclosures:
A. Costa: nothing to disclose
C. Crocker: nothing to disclose
M. A. Akl: nothing to disclose
M. Kamali: nothing to disclose
M. Abdolell: nothing to disclose

RPS 1117-10 15:04

Thin slices and maximum intensity projection reconstructions increase sensitivity to hyperdense artery sign in acute ischemic stroke

J. Rosskopf, B. L. Schmitz, T. Gräter*; Ulm/DE (johannes.rosskopf@uni-ulm.de)*

Purpose: To investigate the effect of different cranial nonenhanced CT (NECT) image reconstructions on correct detection of hyperdense artery sign (HAS) which is a frequently rising challenge particularly also for observers with lower practice level on NECT.
Methods and materials: Twenty-five of 100 patients' NECT image data presented with HAS. Sixteen observers with lower practice level on NECT evaluated independently and in a randomised order the three image reconstructions of each data set with thin slice 0.75 mm, thick slab 5 mm and 5 mm maximum intensity projection (MIP) and rated the likelihood of the presence of HAS in the middle cerebral artery.
Results: MIP and thin slice image reconstructions yielded significantly higher sensitivities for the correct detection of HAS than thick slab reconstructions (73%/73% vs 45%; $p < 0.05$). Sensitivity to HAS did not differ between using thin slice and MIP reconstructions (73% vs 73%). The interobserver reliability was moderate (κ, 0.4). Ranking of HAS detectability did not correlate with image reconstructions ($p > 0.05$ of ICC in a mixed model analysis).
Conclusion: MIP and thin slices reconstructions increased the sensitivity to HAS (73%) whereas thick slab reconstructions seemed to be rather less appropriate (45%). These findings might be important also in particular for observers with lower practice level on NECT.
Limitations: The observers in our study might have been biased in detecting clots by the appearance of early signs of infarction.
Ethics committee approval: n/a
Funding: No funding was received for this work.
Author Disclosures:
J. Rosskopf: nothing to disclose
B. L. Schmitz: nothing to disclose
T. Gräter: nothing to disclose

RPS 1117-11 15:10

Diffusion-weighted imaging can add value to emergency MRI for the diagnosis of acute appendicitis among pregnant women

Y.-C. Wong[1], L.-J. Wang[1], C.-H. Wu[2]; [1]*Taoyuan/TW,* [2]*New Taipei City/TW (ycwong@cgmh.org.tw)*

Purpose: We investigated whether or not diffusion-weighted imaging (DWI) can add value to emergency non-enhanced MRI for the correct diagnosis of acute appendicitis among pregnant women.
Methods and materials: From January 2018 to August 2019, 44 consecutive emergency MRI without contrast enhancement were performed to pregnant women for assessing acute right lower abdominal condition. Their median age was 33.0 years (IQR 27.0, 36.0) and median gestation age was 16 weeks (IQR 10.3, 24.9). All MRI examinations were retrospectively reviewed for acute appendicitis by two readers independently. The charts were reviewed for final diagnosis. The sensitivities, specificities, positive predictive value (PPV) and negative predictive value (NPV) of the variables for final diagnosis of acute appendicitis were computed.
Results: Among 44 patients, the final diagnosis of acute appendicitis was confirmed in 17 (38.6%). The final diagnosis of the other 27 patients was not acute appendicitis. They comprised 4 patients who underwent surgeries for other abdominal conditions and 23 patients who did not undergo surgery but were discharged without complications. Of 44 MRI examinations, 20 had DWI pulse sequence. Twenty four MRI did not have DWI. The final diagnosis was significantly associated with DWI ($p<0.001$), T2WI ($p<0.001$) and fat-saturated T2WI ($p<0.001$). The sensitivities, specificities, PPV and NPV of MRI overall diagnosis for acute appendicitis were 100.0% (95%CI 100.0, 100.0), 100.0% (95%CI 100.0, 100.0), 100.0%, 100.0% (with DWI) and 100.0% (95%CI 100.0, 100.0), 82.4% (95%CI 64.2, 100.5), 70.0%, 100.0% (without DWI).
Conclusion: DWI can add value to non-enhanced MRI for a correct diagnosis of acute appendicitis for pregnant women.
Limitations: Limitations were selection bias and a small number of subjects. The research was done at a single institution and discrepancies were resolved between 2 readers.
Ethics committee approval: n/a
Funding: No funding was received for this work.
Author Disclosures:
Y.-C. Wong: nothing to disclose
L.-J. Wang: nothing to disclose
C.-H. Wu: nothing to disclose

RPS 1117-12 15:16

Diagnostic accuracy of multidetector CT in primary acute mesenteric ischemia

M. Lanzetta, G. Addeo, M. C. Bonini, G. Grazzini, S. Pradella, V. Miele*; Florence/IT (monica.lanzetta@virgilio.it)*

Purpose: The purpose was to evaluate the diagnostic accuracy of multidetector CT in detecting primary acute mesenteric ischemia (AMI), considering laparoscopy, laparotomy, or other diagnoses confirmed by clinical-laboratoristic data as the reference standard.
Methods and materials: Initial MDCT scans in 231 patients with acute abdomen associated with metabolic acidosis and/or hyperlactatemia were retrospectively reviewed. CT was classified as positive or negative from the radiologist's report and considered true positive (TP) or false positive if laparoscopy/laparotomy or clinical status and serial MDCTs confirmed the diagnosis of AMI or not. A negative CT was considered true negative when laparoscopy/laparotomy excluded AMI or when CT findings oriented for another diagnosis were confirmed by clinical-instrumental data. Negative CT was considered false negative (FN) if laparoscopy/laparotomy confirmed the diagnosis of AMI. Moreover, all MDCTs were retrospectively evaluated by a skilled radiologist for the presence of vascular, bowel wall, mesenteric-peritoneal findings, and the involvement of other organs.
Results: Out of all 231 patients who underwent contrast-enhanced MDCT for acute abdomen and abnormal laboratory tests, 60 turned out to have AMI. MDCT shows a sensitivity of 82%, a specificity of 96%, a positive predictive value of 87%, a negative predictive value of 94% and a diagnostic accuracy of 92% in the diagnosis of AMI. Absent/decreased enhancement of the bowel wall was detectable in all patients with AMI; absent/decreased enhancement of the bowel wall, and colon involvement were more frequent in FN compared to TP; paper thin wall and peritoneal findings were more frequent in intestinal injury requiring resection.
Conclusion: MDCT plays a fundamental role in the diagnosis of AMI, making it possible to identify findings more correlated with ischemic damage requiring intestinal resection.
Limitations: Retrospective design from a single centre, lack of control group.
Ethics committee approval: Ethics committee approval was obtained.
Funding: No funding was received for this work.

Author Disclosures:
M. Lanzetta: nothing to disclose
G. Addeo: nothing to disclose
M. C. Bonini: nothing to disclose
G. Grazzini: nothing to disclose
S. Pradella: nothing to disclose
V. Miele: nothing to disclose

14:00 - 15:30 **Room K**

Genitourinary

RPS 1107

Prostate lesions scoring and treatment

Moderators:
M. De Rooij; Nijmegen/NL
M. Seçil; Izmir/TR

RPS 1107-1 14:00
DWI and PRECISE criteria in men on active surveillance for prostate cancer: a multicentre preliminary experience of different ADC calculations
F. Giganti[1], M. Pecoraro[2], D. Fierro[2], R. Campa[2], C. Allen[1], M. Emberton[1], C. Catalano[2], C. M. Moore[1], V. Panebianco[2]; [1]*London/UK,* [2]*Rome/IT (giganti.fra@gmail.com)*

Purpose: The PRECISE scoring system evaluates the likelihood of radiological progression in patients on active surveillance (AS) for prostate cancer (PCa) with serial multiparametric magnetic resonance imaging (mpMRI). A score of 1-2 denotes radiological regression, a score of 3 implies stability, and a score of 4-5 denotes progression. We assessed the inter-reader reproducibility of different apparent diffusion coefficient (ADC) calculations and their relationship to the PRECISE scores.
Methods and materials: Two radiologists retrospectively evaluated baseline and follow-up scans (performed on the same MR systems) in 30 patients from two different institutions. A PRECISE score was initially given in consensus. After at least 6 weeks to reduce the likelihood of being influenced by the consensus reading, each radiologist independently calculated the ADC for the lesion, non-cancerous tissue, and urine in the bladder. Normalised ADC ratios were calculated with respect to normal prostatic tissue (npADC) and urine. Spearman's correlation (ρ), intraclass correlation coefficients (ICC), differences in ADC, and ROC curves were computed.
Results: Interobserver reproducibility was very good (ρ>0.8; ICC>0.90). When considering patients with radiological regression/stability versus progression at follow-up mpMRI, lesion ADC was different between these groups (0.91 vs 0.73 × 10^{-3} mm^2/s; p=0.025). Differences between the two groups were seen in npADC ratio (0.68 vs 0.53; p=0.012). Cut-offs of 0.77 × 10^{-3} mm^2/s (lesion ADC) and 0.59 (npADC ratio) could differentiate the two groups (areas under the curve: 0.74 and 0.77, respectively).
Conclusion: The ADC correlates well with the PRECISE scores and it holds promise in the evaluation of radiological progression of PCa over time.
Limitations: A small cohort of patients and the absence of tissue verification by means of radical prostatectomy.
Ethics committee approval: n/a
Funding: European School of Radiology (2019 BRACCO fellowship) and ERASMUS+ programme.
Author Disclosures:
F. Giganti: Research/Grant Support at Dr. Giganti has received funding by the European School of Radiology (ESOR) under the umbrella of the 2019 BRACCO fellowship and the ERASMUS+ programme (University College London). He is also funded by the UCL Graduate Research Scholarship, the Brahm PhD
M. Pecoraro: nothing to disclose
D. Fierro: nothing to disclose
R. Campa: nothing to disclose
C. Allen: nothing to disclose
M. Emberton: Investigator at Prof. Emberton receives research support from the United Kingdom's National Institute of Health Research (NIHR) UCLH/UCL Biomedical Research Centre. He is an NIHR Senior Investigator.
C. Catalano: nothing to disclose
C. M. Moore: nothing to disclose
V. Panebianco: nothing to disclose

RPS 1107-2 14:06
Interobserver reproducibility of the PRECISE scoring system for prostate MRI on active surveillance: results from a two-centre pilot study
F. Giganti[1], M. Pecoraro[2], A. Stabile[3], V. Stavrinides[1], S. Cipollari[2], M. Emberton[1], C. Catalano[2], C. M. Moore[1], V. Panebianco[2]; [1]*London/UK,* [2]*Rome/IT,* [3]*Milan/IT (giganti.fra@gmail.com)*

Purpose: To assess the interobserver reproducibility of the PRECISE score for magnetic resonance imaging (MRI) in patients on active surveillance (AS) for prostate cancer (PCa).
Methods and materials: The PRECISE scoring system assesses the radiological progression of PCa over time. A score of 1 or 2 means regression of a previously visible lesion, a score of 3 denotes stability, and 4 or 5 suggests radiological progression. We retrospectively evaluated serial MRI scans in 80 men on AS from two different academic centres (40 from each centre) with biopsy-confirmed low- or intermediate-risk PCa (i.e. ≤ Gleason 3+4 and a prostate specific antigen ≤ 20 ng/ml) and ≥ 2 MR scans. Two radiologists reported all scans independently and gave a PRECISE score from the second scan onwards. Cohen's κ coefficients and percent agreement were computed.
Results: The agreement was substantial, both at a per-patient and a per-scan level (κ=0.71 and 0.61; percent agreement=79% and 81%, respectively) for each PRECISE score. The agreement was greater (κ=0.83 and 0.67; percent agreement=90% and 91%, respectively) when the PRECISE scores were grouped according to the absence/presence of radiological progression (PRECISE 1-3 vs 4-5). A higher inter-reader agreement was observed for the scans performed at one centre (κ=0.81 vs 0.55 on a per-patient level, and κ=0.70 vs 0.48 on a per-scan level, respectively). The discrepancies between institutions were less evident for percent agreement (80% vs 78% and 86% vs 75%, respectively).
Conclusion: We observed substantial reproducibility for PRECISE scoring of radiological change in men on AS, particularly when the clinical cut off a PRECISE score ≥ 4 for MRI-directed biopsy was used.
Limitations: Not all men underwent targeted rebiopsy during follow-up.
Ethics committee approval: n/a
Funding: 2019 Bracco Fellowship and Erasmus+ programme.
Author Disclosures:
F. Giganti: Grant Recipient at Dr. Giganti is funded by the UCL Graduate Research Scholarship and the Brahm PhD scholarship in memory of Chris Adams. He also received funding for this project by the ERASMUS+ programme (sponsored by the European Union and University College London) and
A. Stabile: nothing to disclose
M. Pecoraro: nothing to disclose
V. Stavrinides: nothing to disclose
S. Cipollari: nothing to disclose
M. Emberton: Investigator at Prof. Emberton Mark Emberton receives research support from the United Kingdom's National Institute of Health Research (NIHR) UCLH/UCL Biomedical Research Centre. He has been an NIHR Senior Investigator since 2014.
C. Catalano: nothing to disclose
C. M. Moore: nothing to disclose
V. Panebianco: nothing to disclose

RPS 1107-3 14:12
Clinical and economic impact of transperineal laser ablation (TPLA) in the treatment of benign prostatic hyperplasia (BPH)
G. Manenti, T. Perretta, S. Marsico, C. P. Ryan, D. D'amato, A. Turbanti, E. Finazzi Agrò, R. Floris; *Rome/IT*

Purpose: To assess the efficacy, safety, and economic impact of transperineal laser ablation (TPLA) in the treatment of benign prostatic hyperplasia (BPH).
Methods and materials: 30 patients (age 73.4 ± 8.4 years) with lower urinary tract symptoms underwent TPLA under local anaesthesia. Under ultrasound guidance by US/MRI fusion software, up to four 21G applicators were inserted into the prostatic tissue. The primary endpoint was the absence of relevant complications intra- and early (15 days) post-intervention. Secondary endpoints included the evaluation of total intervention time, ablation time, energy deployed, observation time, catheterisation time, IPSS, quality of life (QoL), peak urinary flow rates, post-void residual (PVR), and prostatic morphology and volume, evaluated with 3T mpMRI at 3, 6, and 12 months.
Results: No complications occurred intra- or early post-intervention. The mean ablation time was 33.3 minutes (range 25.3 min-max 42.4), the mean energy deployed was 12,137 J (range 7,204.4-max 14,3483 J), the mean hospital stay was 113 minutes, and the mean catheterisation time was 7.1 days (range 1.1-max 9.3 days). At 3 months, the mean IPSS improved from 22.3 to 7.4 (P < 0.001), the mean QoL from 3.4 to 1.7 (P < 0.001), the mean Q max from 5.1 to 12.5 mL/s, the mean PVR from 148.3 to 87.1, and the mean prostate volume from 54.9 to 42.3 mL.

Conclusion: TPLA is feasible, safe, and economical in the treatment of BPH. Our preliminary data demonstrates significant clinical results at 6 and 12 months.
Limitations: A small number of treated patients, short follow-up, and our first expierence with this technique.
Ethics committee approval: Protocol approved by the ethical committee of the Tor Vergata Hospital.
Funding: No funding was received for this work.
Author Disclosures:
S. Marsico: nothing to disclose
T. Perretta: nothing to disclose
G. Manenti: nothing to disclose
C. P. Ryan: nothing to disclose
D. D'amato: nothing to disclose
A. Turbanti: nothing to disclose
E. Finazzi Agrò: nothing to disclose
R. Floris: nothing to disclose

RPS 1107-4 14:18

Intra-reader comparison of PI-RADS 2 versus PI-RADS 2.1 in a large cohort: stable cancer detection performance with few changes in scoring

M. Rudolph[1], A. Baur[1], M. Haas[1], P. Asbach[1], S. Mahjoub[2], H. Cash[1], B. Hamm[1], T. Penzkofer[1]; [1]*Berlin/DE,* [2]*Cologne/DE*
(madhuri-monique.rudolph@charite.de)

Purpose: To evaluate the PI-RADS 2.1 scoring system in a lesion-based intra-reader comparison to the previous version 2, analysing cancer detection performance and intra-reader variability.
Methods and materials: 342 datasets (3.0T) of patients who received an MRI/TRUS biopsy (10-core systematic and targeted biopsies) were evaluated in a blinded/randomised setting. Lesions were marked and scored according to PI-RADS v2 and v2.1 by one of three experienced radiologists >6 months between the sessions. Histopathology was used as a reference and correlated with location and scoring of the readers' assessments.
Results: 366 lesions were found and 193 (53.76%) lesions harboured PCa. Significant cancer (csPCA, Gleason≥3+4) was detected in 135 (37.6%) lesions. 216 (60.17%) lesions were in the PZ with prevalence of csPCA at 87 (40.82%), 143 lesions (39.83%) in the TZ with prevalence of 48 (33.57%). Distribution of PI-RADS-scores and csPCa detection rates were: (PZ, PI-RADS 2/2.1) 1) 14.3%/15.4%, 2) 8.1%/13.0%, 3) 13.0%/10.0%, 4) 42.4%/42.9%, and 5) 72.1%/68.3%, and (TZ, PI-RADS 2/2.1) 1) 0.0%/6.3%, 2) 4.3%/7.4%, 3) 18.8%/8.3%, 4) 57.1%/40.0%, and 5) 59.3%/61.7% (all p>0.05). Cohen's kappa for PI-RADS 2 versus 2.1 was 0.59 and the weighted kappa was 0.77. PI-RADS v2/v2.1 AUC-ROC for significant cancer detection was 0.776/0.733 for PZ and 0.793/0.800 for TZ (p>0.05). The new segments (Left/Right Base PZm) were used in 31 of the lesions (9.06%).
Conclusion: The comparison of PI-RADS 2 versus 2.1 revealed slight changes with respect to cancer detection rate and scoring, with no detectable statistical significance in a large cohort. Intra-reader variability was moderate to good. ROC-performance was stable at a high level. The newly added segments are used in few instances.
Limitations: A retrospective design and MRI/TRUS gold standard (although less bias than prostatectomy cohort).
Ethics committee approval: IRB approved the study.
Funding: Berlin Institute of Health.
Author Disclosures:
M. Rudolph: nothing to disclose
T. Penzkofer: Research/Grant Support at Siemens Healthineers, outside of submitted work, Research/Grant Support at multiple companies outside of submitted work
A. Baur: Speaker at Bayer, outside of submitted work
M. Haas: nothing to disclose
P. Asbach: nothing to disclose
S. Mahjoub: nothing to disclose
H. Cash: nothing to disclose
B. Hamm: Other at multiple companies, outside of submitted work

RPS 1107-5 14:24

Do we practice what we preach? A systematic review of compliance to PI-RADSv2 acquisition protocol

A. Ponsiglione[1], R. Cuocolo[1], A. Stanzione[1], F. Verde[1], A. Ventimiglia[2], V. Romeo[1], M. Petretta[3], M. Imbriaco[1]; [1]*Naples/IT,* [2]*Castellamare di Stabia/IT,* [3]*Avellino/IT (andreaponsiglione@hotmail.it)*

Purpose: To assess the adherence in literature to technical parameters required by PI-RADSv2 guidelines.
Methods and materials: Multiple medical literature databases were systematically assessed by 3 investigators. Original studies regarding prostate magnetic resonance imaging (MRI) published after January 2016 were retrieved using an appropriate search string. Information about technical acquisition protocols and patient enrolment were collected from full text and/or supplemental materials for the analysis. Technical parameters were dichotomised in relation to their adherence to PI-RADSv2 guidelines.
Results: A total of 150 studies were included in the analysis. Of all papers, 15% reported protocol details regarding all technical specifications requested for T2-weighted (T2w) sequences, only 8% for diffusion-weighted imaging (DWI) and apparent diffusion coefficient (ADC) maps, whereas 10% did the same for dynamic contrast-enhanced (DCE) sequences. Overall, only 5% of all studies reported every technical parameter requested by PI-RADSv2, none of which completely met guidelines specifications.
Only 19% of studies were in line with PI-RADSv2 for all reported technical parameters. In particular, the adherence was lowest for T2w frequency in-plane resolution (12%), ADC maps low-b value (27%), and DCE imaging temporal resolution (43%). Furthermore, only 59% of studies reporting DWI high-b value followed recommendations.
Conclusion: Compliance to PI-RADSv2 in literature is greatly heterogeneous. Our results point out the need for a better diffusion of protocol standardisation and for less stringent indications of some technical parameters.
Limitations: Our analysis was limited to a relatively short period of time (34 months), even if it included exams from a wider range (2006–2018). The number of studies collected was high, while there was heterogeneous reporting of imaging protocol details.
Ethics committee approval: n/a
Funding: No funding was received for this work.
Author Disclosures:
M. Imbriaco: nothing to disclose
A. Ponsiglione: nothing to disclose
R. Cuocolo: nothing to disclose
A. Stanzione: nothing to disclose
F. Verde: nothing to disclose
V. Romeo: nothing to disclose
M. Petretta: nothing to disclose
A. Ventimiglia: nothing to disclose

RPS 1107-6 14:30

MRI-derived PRECISE scores for predicting radiological progression in prostate cancer patients on active surveillance

I. Caglič, N. Sushentsev, E. Sala, N. Shaida, B. Koo, A. Warren, C. Kastner, V. Gnanapragasam, T. Barrett*; Cambridge/UK*
(iztokcaglic@gmail.com)

Purpose: To validate the predictive value of the prostate cancer radiological estimation of change in sequential evaluation (PRECISE) MRI system in the follow-up of prostate cancer (PCa) patients on active surveillance (AS) and its correlation to disease progression on AS.
Methods and materials: 305 men enrolled in an AS programme between 2011 and 2018 were included. Disease progression on AS was defined as the end-point. Receiver operating characteristic curve analysis was performed, with the area under the curve (AUC) for PRECISE scores estimated for detection of progression. Kaplan–Meier curves compared progression-free survival (PFS) between PRECISE scores.
Results: Progression rate for the cohort was 16.7% (51/305) over a median follow-up of 52 months. The AUC, specificity, sensitivity, PPV, and NPV of the PRECISE system were 0.83, 0.77, 0.89, 0.57, and 0.95, respectively. PSA-Density and the Likert lesion-probability score were the only significant baseline parameters predictive of progression in multivariate analysis (OR=5575.0, p=0.008 and 1.7, p<0.001, respectively). Diagnostic performance of PRECISE was increased to AUC=0.92 (PPV=0.69 and NPV=0.94) when combined with the significant baseline predictors. Kaplan-Meier curves showed a significant difference in PFS between PRECISE scores 1-3 (94%) versus scores 4-5 (35.5%) at 5 years; p<0.001.
Conclusion: PRECISE MRI scoring has a good predictive value for men with PCa on AS. The high NPV of PRECISE can reduce the need for re-biopsy, whilst the moderate PPV for progression should trigger either closer monitoring or re-biopsy.
Limitations: A retrospective design. In 8 cases, PRECISE score 5 (i.e. T3a/T3b disease) triggered a direct switch to treatment, with pathological progression not definitively being confirmed.
Ethics committee approval: The Local Ethics Committee waived the need for informed consent.
Funding: No funding was received for this work.
Author Disclosures:
I. Caglič: nothing to disclose
N. Sushentsev: nothing to disclose
T. Barrett: nothing to disclose
C. Kastner: nothing to disclose
A. Warren: nothing to disclose
E. Sala: nothing to disclose
B. Koo: nothing to disclose
N. Shaida: nothing to disclose
V. Gnanapragasam: nothing to disclose

RPS 1107-7 14:36

Inter-reader agreement in multiparametric MRI reporting using prostate imaging reporting and data system version 2.1

G. Brembilla, P. Dell'oglio, A. Stabile, A. Damascelli, L. Brunetti, G. Cristel, A. Esposito, F. Montorsi, F. de Cobelli*; Milan/IT (brembilla.giorgio@hsr.it)*

Purpose: To evaluate the agreement among readers with different expertise in detecting suspicious lesions at prostate multiparametric MRI using prostate imaging reporting and data system version 2.1.
Methods and materials: We evaluated 200 consecutive biopsy naïve or previous negative biopsied men who underwent MRI for clinically suspicious prostate cancer (PCa) between May and September 2017. Of them, 132 patients underwent prostate biopsy. 7 radiologists (4 dedicated uro-radiologists and 3 non-dedicated abdominal radiologists) reviewed and scored all MRI examinations according to PI-RADS v2.1. Agreement on index lesion detection was evaluated with Conger's k coefficient, AC1 coefficient, percentage of agreement (PA), and indexes of specific positive and negative agreement. Clinical and radiological features that may influence variability were evaluated.
Results:
Agreement in index lesion detection among all readers was substantial (AC1: 0.738; 95%CI: 0.695-0.782). Dedicated radiologists showed higher agreement compared to non-dedicated readers. Clinical and radiological parameters that positively influenced agreement were PSA density ≥0.15 ng/ml/cc, pre-MRI high risk for PCa, positivity threshold of PI-RADS score >3, PZ lesions, the homogeneous signal intensity of the PZ, and subjectively easy interpretation of MRI. The positive specific agreement was significantly higher among dedicated readers, up to 93.4% (95%CI: 90.7-95.4) in patients harbouring csPCa. Agreement on absence of lesions was excellent for both dedicated and non-dedicated readers (respectively: 85.1% [95%CI 78.4-92.3]; and 82.0% [95%CI 77.2-90.1]).
Conclusion:
Agreement on index lesion detection among radiologists of various experience is substantial to excellent when using PI-RADS v2.1. Concordance on the absence of lesions is excellent across the readers' experience.
Limitations: A retrospective study, limited to a single-tertiary-care referral centre.
Ethics committee approval: This study was approved by our Institutional Review Board and written informed consent was obtained.
Funding: No funding was received for this work.
Author Disclosures:
G. Brembilla: nothing to disclose
P. Dell'oglio: nothing to disclose
A. Stabile: nothing to disclose
A. Damascelli: nothing to disclose
L. Brunetti: nothing to disclose
G. Cristel: nothing to disclose
A. Esposito: nothing to disclose
F. Montorsi: nothing to disclose
F. de Cobelli: nothing to disclose

RPS 1107-8 14:42

Diagnostic value of combining PI-RADS v2.1 with prostate-specific antigen density in prostate cancer

X. Wei, J. Zou, S. Zhong, G. Hu, J. Xu*; Shenzhen/CN (502498022@qq.com)*

Purpose: To investigate the diagnostic value of the prostate imaging reporting and data system version 2.1 (PI-RADS v2.1) and PSA-derived indicators, aiming at improving the diagnostic value of prostate cancer to guide clinical biopsy decision-making.
Methods and materials: 180 patients were analysed, with the biopsy results being benign prostatic hyperplasia (BPH) and prostate cancer (PCa) in 111 (61.67%) and 69 (38.33%) patients, respectively. The PI-RADS v2.1 was used to describe the MRI findings. The age, PSA, fPSA, and fPSA/tPSA of the patients were collected. PSAD was divided into three groups with cut-off points of 0.150 and 0.350. Univariate and multivariate analyses were performed to determine significant predictors of prostate cancer.
Results: The differences of the PI-RADS v2.1 score, age, PSA, fPSA/tPSA, PSAD, and PV between the PCa group and BPH group were statistically significant. The multivariate analysis revealed that the PI-RADS v2.1 score and PSAD were independent predictors for prostate cancer. Combining the PI-RADS v2.1 score and PSAD, when the PI-RADS v2.1 score ≤2 and PSAD ≤0.350 ng/mL/mL, or the PI-RADS v2.1 score was 3 and PSAD≤0.150 ng/mL/mL, the prostate cancer detection rate was low (9.10%), and prostate cancer cases in this range were all low-risk cancer (the Gleason score was 6). In contrast, a PI-RADS v2.1 score of 3 and PSAD>0.350 ng/mL/mL or a PI-RADS v2.1 score ≥4, was associated with the highest prostate cancer detection rate (76.00%), and most of the cases were high-risk cancer.
Conclusion: Patients with a PI-RADS v2.1 score ≤2 and PSAD ≤0.350 ng/mL/mL, or a PI-RADS v2.1 score of 3 and PSAD ≤0.150 ng/mL/mL might avoid unnecessary biopsies. The combination of PI-RADS v2.1 and PSAD did improve the diagnostic value of prostate cancer and assist in clinical guidance biopsy decision-making.
Limitations: A bias may exist.
Ethics committee approval: n/a
Funding: No funding was received for this work.
Author Disclosures:
X. Wei: nothing to disclose
J. Zou: nothing to disclose
S. Zhong: nothing to disclose
G. Hu: nothing to disclose
J. Xu: nothing to disclose

RPS 1107-9 14:48

Safe reduction of MRI-targeted biopsies in men with PI-RADSv2 category 3 lesions: cross-institutional validation of a multivariate risk model based on clinical parameters

D. Deniffel[1], K. Namdar[1], I. Gujrathi[2], E. Salinas-Miranda[1], A. Toi[1], N. Perlis[1], A. Finelli[1], F. Khalvati[1], M. A. Haider[1]; *[1]Toronto/CA, [2]Boston/US (ddeniffel@lunenfeld.ca)*

Purpose: To assess whether a risk model solely based on clinical parameters can reduce MRI-targeted biopsies of PI-RADSv2 category 3 index lesions without missing clinically significant (cs) prostate cancer (PCa) (ISUP≥grade 2).
Methods and materials: We retrospectively analysed 278 patients without a prior PCa diagnosis who underwent multiparametric MRI and MRI-targeted biopsy at 2 institutions. A multivariate model was fitted to the training cohort (institution 1; n=202), using the following clinical parameters: prostate volume, prior biopsy status, PSA density (PSAd), and age. Decision thresholds to rule out csPCa were determined within the PI-RADSv2 3 subgroup of the training cohort (n=115). The validation cohort (institution 2) consisted of 76 men with PI-RADSv2 3 index lesions. Using the area under the ROC curve (AUC), the performance of our model in the validation cohort was compared to PSAd, normalised ADC (nADC), lesion volume, and the MRI European randomised study of screening for PCa risk calculator (MRI-ERSPC-RC).
Results: Our model (AUC=0.80) outperformed PSAd (AUC=0.60; p=0.01), lesion volume (AUC=0.45; p=0.03), and the MRI-ERSPC-RC (AUC=0.39; p=0.0002), and was not inferior to nADC (AUC=0.68; p=0.13). Predefined thresholds for nADC and lesion volume resulted in a minor biopsy reduction by 5% (4/76) and 4% (3/76), respectively; the published threshold for the MRI-ERSPC-RC would have reduced biopsies by 93% (71/76), however, missing 83% (5/6) of csPCas. At a PSAd ≥0.083 ng/ml/ml and a risk threshold ≥0.082 for the multivariate model, the percentage of men who may have avoided biopsy was 21% (16/76) and 33% (25/76), respectively, without missing any csPCa (0/6).
Conclusion: Applying a risk model based on clinical parameters in men with PI-RADSv2 3 index lesions could result in 33% fewer biopsies being performed without missing any csPCa.
Limitations: A retrospective study.
Ethics committee approval: IRB-approved study.
Funding: OICR; DFG-fellowship [DE 3207/1-1].
Author Disclosures:
D. Deniffel: nothing to disclose
K. Namdar: nothing to disclose
I. Gujrathi: nothing to disclose
E. Salinas-Miranda: nothing to disclose
A. Toi: nothing to disclose
N. Perlis: nothing to disclose
A. Finelli: nothing to disclose
F. Khalvati: nothing to disclose
M. A. Haider: nothing to disclose

RPS 1107-10 14:54

MpMRI-targeted prostate biopsy only: does systematic biopsy belong in the past?

M. Klingebiel, T. Ullrich, C. Arsov, M. Quentin, D. Mally, P. Albers, G. Antoch, L. Schimmöller*; Düsseldorf/DE (Maximilian.Klingebiel@med.uni-duesseldorf.de)*

Purpose: To evaluate the prostate cancer (PCa) detection of targeted MRI/ultrasound fusion-guided biopsy (TB) and systematic transrectal ultrasound-guided biopsy (SB) in a large patient collective.
Methods and materials: Consecutive patients with 3T multi-parametric MRI of the prostate and subsequent TB plus SB from 01/2014 to 04/2019 were included in this study. Study endpoints were PCa detection of TB versus SB, and analyses of cases with only positive SB or Gleason upgrade by SB. Histopathological positive cores of TB and SB were retrospectively correlated with the MRI data.
Results: In total, 785 patients (65±9 years; median 8.1ng/ml) met the inclusion criteria. In 461 patients a PCa and in 342 patients a clinically significant PCa (csPCa; Gleason score ≥3+4=7) were verified. In 75 patients (16%), only SB detected a PCa, including 30 patients with csPCa (6.5%). In 50 of these cases

(26 csPCa), SB targeted the MRI index lesion missed by TB. 19 of 44 non-significant PCa (nsPCa) were not visible on MRI (43%). In 42 patients, SB resulted in a Gleason upgrade compared to TB. In 31 of these cases, TB missed the MRI centre of the PCa. In 12 patients, SB resulted in csPCa, whereas TB showed nsPCa (2.6%). In 175 patients, TB and SB showed equal results (38%). In 69 patients, TB resulted in a Gleason upgrade including 28 more csPCa (6%). In 101 patients, only TB detected the PCa, including 67 csPCa (15%).
Conclusion: Additional SB detected 9% more csPCa, which in the majority were correctly described on MRI, but missed by TB. Furthermore, SB over-detected 10% additional insignificant PCa. Thus, SB might be unnecessary and provide no benefit through the optimisation of TB.
Limitations: n/a
Ethics committee approval: Written informed consent was obtained.
Funding: No funding was received for this work.
Author Disclosures:
D. Mally: nothing to disclose
M. Klingebiel: nothing to disclose
T. Ullrich: nothing to disclose
C. Arsov: nothing to disclose
M. Quentin: nothing to disclose
P. Albers: nothing to disclose
G. Antoch: nothing to disclose
L. Schimmöller: nothing to disclose

RPS 1107-11 15:00

Preoperative MRI risk estimation and predictors of positive surgical margins in patients with prostate cancer undergoing radical prostatectomy

L. Schimmöller, M. Quentin, T. Ullrich, S. Dörfler, C. Arsov, P. Albers, G. Antoch*; Düsseldorf/DE (lars.schimmoeller@med.uni-duesseldorf.de)*

Purpose: To analyse multiparametric prostate MRI (mpMRI) examinations of patients with positive surgical margins (PSM) of the prostate cancer (PCa) after robotic assisted radical prostatectomy (RPE).
Methods and materials: Consecutive patients with PSM in one or more localisations after RPE and prior mpMRI for PCa detection from 01/2016 to 12/2018 were retrospectively included in this study. MpMRIs were analysed by two experienced readers in consensus regarding PCa visibility, capsule contact length (CCL), extracapsular extension (ECE), and location of PSM in relation to the histopathologic examination of the prostatectomy specimens.
Results: 44 patients with a postoperative tumour stage of 34% T2c, 25% T3a, and 41% T3b were included. PSM occurred at the posterior capsule in 14 patients, anterior in 13 patients, basal at the seminal vesicles (SV) in 7 patients, and in 16 patients apical at the membranous urethra. The PCa was visible on MRI in 97% of cases (n=41). An MRI correlate of ECE was seen in 56% (19/34), the contact to the urethra in 88% (13/16), and to the SV in 100% (7/7). Measurable ECE on MRI was found in 57% (mean 5.1±2.7mm) with a mean CCL was 21±13 mm.
Conclusion: PSM occurred mostly apical at the urethra, anterior, or posterior at the capsule margin or basal at the SV. MpMRI has a high ability to visualise PCa and determine cases with a risk of PSM. Measurable ECE, CCL, and distance to the membranous urethra should always be reported.
Limitations: n/a
Ethics committee approval: n/a
Funding: No funding was received for this work.
Author Disclosures:
P. Albers: nothing to disclose
L. Schimmöller: nothing to disclose
M. Quentin: nothing to disclose
T. Ullrich: nothing to disclose
C. Arsov: nothing to disclose
S. Dörfler: nothing to disclose
G. Antoch: nothing to disclose

RPS 1107-12 15:06

Feasibility of a 2nd generation MR-compatible remote-controlled manipulator for transrectal focal laser ablation in patients with prostate cancer

S. P. Hoogendoorn, J. G. R. Bomers, J. P. M. Sedelaar, J. J. Futterer*; Nijmegen/NL (Stefan.Hoogendoorn@radboudumc.nl)*

Purpose: To assess the feasibility of a 2nd generation MR-compatible remote-controlled manipulator (RCM) as an aid to perform transrectal MRI-guided focal laser ablation in men with histologically proven prostate cancer (PCa).
Methods and materials: Between March 2016 and May 2018, 17 consecutive patients with at least one focus of histologically proven PCa (Gleason ≥7) underwent transrectal MRI-guided focal laser ablation. An MR-compatible RCM (Soteria Medical) was used to steer the needle guide. Depending on the size of the lesion, several ablations were performed. For the evaluation of the workflow, the procedure times, the manipulation times, and the number of ablations were recorded. Complications were registered according to the clinical practice guidelines proposed by the Society of Interventional Radiology (SIR).
Results: All lesions were reachable with the MR-compatible RCM. The median procedure time was 125 minutes (range, 77-169 minutes) and the median manipulation time for laser-fibre movement was 34 minutes (range, 8-60 minutes). Per lesion, a median number of 5 ablations was performed (range, 2–7). One SIR grade B (urine-retention) and one grade C/D (urosepsis) complication were reported.
Conclusion: It is safe and feasible to perform transrectal MRI-guided focal laser ablation using a MR-compatible RCM.
Limitations: n/a
Ethics committee approval: n/a
Funding: No funding was received for this work.
Author Disclosures:
S. P. Hoogendoorn: nothing to disclose
J. G. R. Bomers: nothing to disclose
J. P. M. Sedelaar: nothing to disclose
J. J. Futterer: nothing to disclose

RPS 1107-13 15:12

Multiparametric MRI and targeted prostate biopsy: a comparison between In-Bore and TRUS-MRI fusion techniques performed by the same operator

S. Cipollari, R. Campa, M. Pecoraro, V. Salvo, M. Del Monte, C. Catalano, V. Panebianco*; Rome/IT (stefanocipollari@gmail.com)*

Purpose: To compare in-bore and of TRUS-MRI fusion MR targeted prostate biopsies performed by the same operator.
Methods and materials: A cohort of 820 patients with elevated PSA level and no previous positive biopsy who underwent prostate mpMRI were retrospectively reviewed. Patients underwent diagnostic high-field (3T and 1.5T) mpMRI (T2WI on axial and coronal planes, DWI with six b values up to 2000 s/mm2, DCE images). Two expert radiologists retrospectively evaluated the exams according to PI-RADS v2 and inter-reader agreement was calculated using K statistics. Targeted biopsy was performed in 223 patients; 106 underwent in-bore biopsy and the remaining 117 patients underwent TRUS-MRI fusion biopsy. MRI data was compared to histopathology data. Detection rates were calculated to evaluate the performance of the two different techniques.
Results: In-bore and fusion techniques did not significantly differ in overall prostate cancer detection (0.68 vs. 0.66, p=0.07). The in-bore biopsy was in the subgroup of lesions smaller than 0.3cc (mean diameter 8.3 mm) and in detection of clinically significant PCa (0.60 vs. 0.56, $p < 0.05$). A statistically significant difference in favour of the in-bore technique was found in terms of a higher per-core cancer detection (0.56, 95% CI 0.54–0.58 vs 0.4, 95% CI 0.38– 0.42) and a lower number of cores per-patient (3.22, 95% CI 3.02–3.42 vs 6.52, 95% CI 4.82–8.22)
Conclusion: In-bore and TRUS-MRI fusion techniques were comparable in terms of overall detection rate. The in-bore technique was superior in the detection of smaller lesions, in the PI-RADS 3 lesions, and in the per-core detection rate.
Limitations: Relatively small size and possible bias due to different scans.
Ethics committee approval: n/a
Funding: No funding was received for this work.
Author Disclosures:
M. Pecoraro: nothing to disclose
S. Cipollari: nothing to disclose
R. Campa: nothing to disclose
M. Del Monte: nothing to disclose
V. Salvo: nothing to disclose
C. Catalano: nothing to disclose
V. Panebianco: nothing to disclose

RPS 1107-14 15:18

MRI-directed high frequency (29MHz) TRUS-guided biopsies: an alternative to TRUS-MRI image fusion?

F. Cornud[1], A. Lefevre[1], P. Camparo[2], P. Soyer[1], M. Barral[1]; *[1]Paris/FR, [2]Amiens/FR (francois.cornud@imagerietourville.com)*

Purpose: Significant prostate cancer (sPCa) detection rate is increased by pre-biopsy MRI. However, MRI/ultrasound fusion biopsy entails targeting errors. In-bore MR-guided biopsy is precise, but not widely available. Very high frequency transrectal ultrasound (micro-ultrasound), as a second look examination after MRI, may localise tumour foci of sPCa.
Methods and materials: A total of 117 consecutive patients, mean age 64 ± 12yo, biopsy-naïve in 67% (79/117) of cases, non-suspicious rectal examination in 85% of cases (102/117), with a median PSA level of 8 ng/mL (range: 2-200ng/ml) and at least one focal lesion (MRI+) with a score>2 on biparametric-MRI (bp-MRI), were included. Transrectal biopsy of all lesions visible on micro-ultrasound (MUS+) was performed using a 29MHz transducer. MUS+/MRI+ and

MUS+/MRI- lesions were targeted without image fusion, which was only used for MUS-/MRI+ lesions. Tumours with a Gleason score ≥7 or a maximum cancer core length >3 mm were considered significant.
Results: A total of 144 focal lesions were analysed. Of them, 131 (131/144, 91%) were MUS+, including 114 (114/144, 79%) MUS+/MRI+ and 17 (17/144, 12%) MUS+/MRI- lesions. Significant cancer was detected in 70 lesions (70/114, 56%) in the MUS+/MRI+ group and in 4 lesions (4/17, 23.5%) in the MUS+/MRI- group. The 13 remaining lesions were MUS-/MRI+ without sPCa. The sensitivity and specificity of micro-ultrasound were 100 and 18%.
Conclusion: Micro-ultrasound, as a second look imaging modality, can localise tumour foci detected by bp-MRI and represents an attractive alternative to MRI-TRUS image-fusion.
Limitations: A single-centre study.
Ethics committee approval: n/a
Funding: No funding was received for this work.
Author Disclosures:
F. Cornud: nothing to disclose
M. Barral: nothing to disclose
P. Camparo: nothing to disclose
A. Lefevre: nothing to disclose
P. Soyer: nothing to disclose

RPS 1107-15 15:24
Soractelite™ transperineal laser ablation (TPLA) for the treatment of benign prostatic hyperplasia: results at 6 and 12 months
G. Patelli[1], G. Mauri[2], G. Iapicca[3], G. Manenti[4], T. Perretta[1], C. Ryan[4], R. Esposito[5], C. M. Pacella[6]; [1]*Seriate/IT,* [2]*Milan/IT,* [3]*Avellino/IT,* [4]*Rome/IT,* [5]*Cosenza/IT,* [6]*Albano Laziale Roma/IT (patellig@yahoo.it)*

Purpose: To investigate the safety and effectiveness of TPLA in patients with symptomatic benign prostatic hyperplasia (BPH).
Methods and materials: Under US guidance, up to 4 21G applicators were inserted in the prostatic tissue. A diode laser operating at 1064 nm was used. Change in IPSS, PVR, Qmax, QoL, and prostatic volume at 6 and 12 months, and any complications, were recorded.
Results: Data of 160 patients with at least 6 months follow-up and 83 patients with at least 12 months follow-up were analysed.
At 6 months, IPSS improved from 22.5 ± 5.1 to 7.7 ± 3.3 (P<0.001), PVR from 89.5 ± 84.6 to 27.2± 44.5 ml (P<0.001), Qmax from 8.0 ± 3.8 to 14.3 ± 3.9 ml/s (P<0.001), QoL from 4.5 ± 1.1 to 1.8 ± 1.0 (P< 0.001), and volume from 75.0 ± 32.4 to 60.3 ± 24.5 ml (P< 0.001).
At 12 months, IPSS improved from 22.5 ± 4.5 to 7.0 ± 2.9 (P<0.001), PVR from 71.7 ± 93.9 to 17.8 ± 51.0 ml (P<0.001), Qmax from 8.6 ± 5.2 to 15.0 ± 4.0 ml/s (P<0.001), QoL from 4.2 ± 0.6 to 1.6 ± 0.9 (P< 0.001), and volume from 87.9 ± 31.6 to 58.8 ± 22.9 ml (P< 0.001).
7/160 (4.3%) grade I and 1/160 (0.6%) grade III complication occurred.
Conclusion: SoracteLite™ TPLA allows significant improvement of IPSS, Qol, Qmax, PVR, and reduction of prostatic volume at 6 and 12 months
Limitations: A retrospective design.
Ethics committee approval: IRB approval was obtained.
Funding: No funding was received for this work.
Author Disclosures:
G. Patelli: nothing to disclose
G. Mauri: Consultant at Elesta SrL
G. Iapicca: nothing to disclose
G. Manenti: nothing to disclose
T. Perretta: nothing to disclose
C. Ryan: nothing to disclose
R. Esposito: nothing to disclose
C. M. Pacella: Consultant at Elesta SrL

14:00 - 15:30 **Room M 1**

Neuro

RPS 1111

Neurovascular diseases

Moderators:
N.N.

RPS 1111-1 14:00
Associations between cardiovascular function, brain volumes, and white matter hyperintensities
M. van Hout, I. Dekkers, J. J. M. Westenberg, A. Scholte, H. J. Lamb; *Leiden/NL (i.a.dekkers@lumc.nl)*

Purpose: To study whether vascular and left ventricular (LV) function is associated with total brain volume, grey and white matter volumes, and white matter hyperintensities (WMH) in the middle-aged general population.
Methods and materials: 4,366 participants of the UK-biobank underwent magnetic resonance imaging (MRI) to assess LV (ejection fraction (EF) and cardiac index (CI)) and brain parameters (total, grey, and white matter volumes and volume of WMH). The augmentation index (AIx) was used as a measure of arterial stiffness. An analysis of variance was used to test whether multivariate linear regression or polynomial splines should be performed using the cardiovascular function as determinants, brain volumes normalised for head size, and WMH as outcome variables, adjusting for known confounders. WMH were log-transformed to adjust for skewed distribution.
Results: EF was non-linearly associated with total brain volume and grey matter volume, with an optimal volume for an EF between 55 and 60% (P<0.001), but not associated with white matter volume. EF showed a negative linear association with WMH (β=1.005 mm^3 [-1.003; -1.008], P=0.03). In contrast, CI was not associated with total brain volume, grey matter volume, or WMH. CI did show a significant positive linear association with white matter volume (β=3.194 mm^3 [760; 5,627], P=0.01). AIx was not significantly associated with brain volumes or WMH.
Conclusion: A complex association exists between LV ejection fraction and brain structure, with an optimal grey matter volume for an EF between 55 and 60%. EF is negatively associated with WMH.
Limitations: Our observational cross-sectional design precludes causal inference and did not assess cognitive functioning.
Ethics committee approval: The study was approved by the National Research Ethics Service Committee (11/NW/0382).
Funding: No funding was received for this work.
Author Disclosures:
I. Dekkers: nothing to disclose
M. van Hout: nothing to disclose
J. J. M. Westenberg: nothing to disclose
A. Scholte: nothing to disclose
H. J. Lamb: nothing to disclose

RPS 1111-2 14:06
Vascular hyperintensities on a post-contrast 3D fast-spin-echo T1-weighted sequence: a sign of poor collateral pathways in sickle-cell disease cerebral vasculopathy?
C. Y. Provost[1], W. Ben Hassen[1], J. Benzakoun[1], L. Legrand[1], D. Calvet[1], P. Bartolucci[2], O. Naggara[1], C. Oppenheim[1], M. Edjlali-Goujon[1]; [1]*Paris/FR,* [2]*Créteil/FR (cyprovost@gmail.com)*

Purpose: Sickle cell disease (SCD) cerebral vasculopathy is characterised by progressive occlusion of cerebral arteries with the development of extensive collateral pathways to compensate. We aimed to evaluate the prevalence and meaning of post-contrast vascular hyperintensities (PCVH) on a 3D fast-spin-echo T1-weighted sequence in SCD.
Methods and materials: We included 19 SCD patients with cerebral artery occlusion and 50 SCD patients without occlusion, as detected on MR angiography at 3-Tesla. Two neuroradiologists blinded to clinical data and the other MRI sequences looked for PCVH on a post-contrast 3D fast-spin-echo T1-weighted sequence. We evaluated the concordance between the arterial distribution of occlusions and PCVH. Dynamic susceptibility contrast perfusion imaging was performed to measure Tmax values in the occluded arterial territory.
Results: Inter and intraobserver agreements for the detection of PCVH were excellent. PCVH was found in 14 of 19 patients (74%), with cerebral artery occlusion and only 1 of 50 patients (2%) without occlusion (p<0.001). This latter patient had bilateral severe stenosis of the cervical internal carotid arteries. The concordance between the arterial distribution of occlusions and that of PCVH was good to excellent (κ=0.73, 0.76, and 0.80 for the anterior, middle, and posterior cerebral arteries, respectively). Tmax values in the occluded arterial territory were higher in PCVH-positive patients compared to PCVH-negative patients (3 seconds versus 2 seconds, p<0.001).
Conclusion: PCVH in sickle cell disease is a sign of severe cerebral vasculopathy and is associated with marked hypoperfusion. It may represent poor collateral pathways.
Limitations:
The 3D fast-spin-echo T1-weighted sequence was only performed at 3-Tesla, thus limiting the generalisability of the findings.
Ethics committee approval: This study received ethics committee (Comité de Protection des Personnes Île-de-France Saint-Louis) approval.
Funding: No funding was received for this work.

Author Disclosures:
C. Y. Provost: nothing to disclose
M. Edjlali-Goujon: nothing to disclose
C. Oppenheim: nothing to disclose
D. Calvet: nothing to disclose
P. Bartolucci: nothing to disclose
W. Ben Hassen: nothing to disclose
J. Benzakoun: nothing to disclose
L. Legrand: nothing to disclose
O. Naggara: nothing to disclose

RPS 1111-3 14:12

White matter lesion volume in subjects with prediabetes, subjects with diabetes, and normoglycemic control subjects

S. Grosu[1], R. Lorbeer[1], F. Bamberg[2], C. L. Schlett[2], A. Peters[3], M. Heier[1], S. Rospleszcz[1], B. B. Ertl-Wagner[1], S. Stöcklein[1]; [1]*Munich/DE,* [2]*Freiburg/DE,* [3]*Neuherberg/DE*

Purpose: As white matter lesions (WML) of the brain are associated with an increased risk of stroke, cognitive decline, and depression, elucidating the associated risk factors is important. In addition to age and hypertension, prediabetes and diabetes may play important roles in the development of WML. Previous studies have, however, shown conflicting results. We aimed to evaluate the association between WML volume and prediabetes/diabetes.
Methods and materials: 400 subjects of the epidemiological KORA study cohort underwent 3T-MRI. WML were manually segmented on 3D-FLAIR images. An oral glucose tolerance test (OGTT) was administered to all participants without previously diagnosed type 2 diabetes. Linear and logistic regression analyses of WML volume and measures of diabetes and diabetes status were conducted while controlling for cardiovascular risk factors.
Results: The final study population consisted of 388 participants (57% male; age: 56.3±9.2 years). WML were found in 249 participants with a mean volume of 1755±5920 mm^3. 98 subjects had prediabetes and 51 established diabetes. Serum glucose concentration determined by OGTT, but not fasting glucose or HbA1c levels, showed a significant association with WML volume after adjustment (p=0.004). WML volume was significantly higher in subjects with prediabetes (p=0.023) and diabetes (p=0.003) compared to normoglycemic control subjects. However, these associations became insignificant after adjustment.
Conclusion: In this population without prior cardiovascular disease, we identified serum glucose concentration assessed by OGTT as a quantitative determinant of WML volume. Our data suggests that the effect of diabetes, and particularly prediabetes, on WML volume might be driven by impaired glucose tolerance.
Limitations: The limited sample size. Unmeasured confounding variables cannot be fully ruled out.
Ethics committee approval: Approved by the ethics committee of Ludwig-Maximilian-University Hospital, Munich.
Funding: German Research Center for Environmental Health and the German Research Foundation (DFG).
Author Disclosures:
S. Grosu: nothing to disclose
R. Lorbeer: nothing to disclose
F. Bamberg: nothing to disclose
C. L. Schlett: nothing to disclose
A. Peters: nothing to disclose
S. Rospleszcz: nothing to disclose
B. B. Ertl-Wagner: nothing to disclose
S. Stöcklein: nothing to disclose
M. Heier: nothing to disclose

RPS 1111-4 14:18

Acute symptomatic lacunar ischaemic stroke as the first presentation of small vessel disease: how common is it?

A. Guarnera[1], C. Barbato[2], L. Ulivi[2], S. Browning[3], D. Werring[3], R. Simister[3], R. Jager[3]; [1]*Rome/IT,* [2]*Florence/IT,* [3]*London/UK (guarneraalessia@gmail.com)*

Purpose: To investigate the prevalence of cerebral small vessel disease (SVD) in a consecutive cohort of patients presenting with acute symptomatic lacunar ischaemic strokes (ASLIS) and to ascertain how frequently an ASLIS represents the initial radiological manifestation of SVD.
Methods and materials: In a hospital trust, a database of 831 patients undergoing MRI for acute stroke from May 2018-February 2019 was retrospectively reviewed to identify patients with DWI+ASLIS. Patients with a history of trauma or cancer, haemorrhagic strokes, and large vessel disease were excluded. Patients were split into those with and without SVD by using established scoring systems. Subjects with evidence of SVD were assigned to three categories: arteriolosclerosis, probable/possible cerebral amyloid angiopathy (CAA), and mixed disease. Potential risk factors were evaluated by Fisher's and Student's tests, and calculating the odds ratio, between the groups of patients with and without evidence of SVD and among the subgroups of patients with SVD.
Results: Of 104 subjects included, 29 (28%) showed no evidence of SVD, while of the remaining 75 (72%), 59 (57%) had evidence of arteriolosclerosis, 4 (4%) of CAA, and 12 (11%) of mixed disease. Among the markers of SVD, white matter hyperintensity was the most common. Subjects with evidence of SVD were significantly more prone to be older, smokers, and affected by diabetes, hypercholesterolemia, and hypertension (OR:2.1).
Conclusion: In 2/3 of patients with ASLIS and a co-existing burden of SVD, arteriolosclerosis was predominant and subjects were likely to present cardiovascular risk factors. DWI+ASLIS was the first imaging manifestation of SVD in about 1\3 of subjects. These patients may have different pathophysiology, different risk of stroke recurrence, and need tailored therapy.
Limitations: The relative small cohort analysed.
Ethics committee approval: The study was approved by the institutional ethics committee.
Funding: No funding was received for this work.
Author Disclosures:
A. Guarnera: nothing to disclose
C. Barbato: nothing to disclose
L. Ulivi: nothing to disclose
S. Browning: nothing to disclose
D. Werring: nothing to disclose
R. Simister: nothing to disclose
R. Jager: nothing to disclose

RPS 1111-5 14:24

Dynamic computed tomography angiography (dCTA) for determining infarct size and collaterals in order to predict the clinical outcome after recanalisation of acute ischaemic stroke

E. Puglielli, P. Pierluigi, A. Bernardini, S. Roiati, N. Caputo*; Teramo/IT (edopug@hotmail.com)*

Purpose: To investigate the impact of dCTA weighting on the evaluation of collateral circulation using classic methods and their ability to predict infarct size and clinical outcome. The visualisation of pial collaterals may vary depending on whether the CTA is arterial (A), arterio-venous (AV), or venous (V) weighted.
Methods and materials: 190 consecutive patients (mean age=47 years, April 2009-September 2019) with classical onset underwent endovascular therapy in a single-centre using predominantly stent retrievers, neurotrombectomy devices, or thromboaspiration. Basal CT and dCTA were used for imaging. Two readers studied infarct volume on imaging of the collateral scores stratified by dCTA weighing with age, gender, occlusion aetiology, symptoms, national institutes of health stroke scale (NIHSS) median score at presentation, clot burden score (CBS), and modified Rankin scale (mRS) correlation.
Results: The median NIHSS score at presentation was 18 (range 3-36) and the onset to treatment time was 123 (76-187) minutes. dCTA scans were A-weighted in 135/190 (71.05%), AV in 25/190 (13.15%), and v-weighted in 30/190 (15.78%). Poor collateralisation (OR 12.50; 95% CI (3.9, 43); p<0.0001) and longer time to peak of maximum arterial enhancement (OR 3.1; 95% CI (1.93, 6.1); p <0.0001) were positively associated with a late venous phase cortical vein filling. All collateral scores were related to infarct volume irrespective of dCTA weighting (p<0.005). No association was shown between dCTA weighting, collateral grade, and clinical outcome.
Conclusion: dCTA weighting did not significantly impact collateral grade analysis with the three common collateral scores and there is a lack of evidence of their ability to predict final infarct size after recanalisation
Limitations: The possible error due to a small series.
Ethics committee approval: n/a
Funding: No funding was received for this work.
Author Disclosures:
E. Puglielli: nothing to disclose
P. Pierluigi: nothing to disclose
A. Bernardini: nothing to disclose
S. Roiati: nothing to disclose
N. Caputo: nothing to disclose

RPS 1111-6 14:30

The arterial remodelling ratio and normalised wall index of the middle cerebral artery are associated with leptomeningeal collateral status: a study of high-resolution vessel wall imaging

R. Tang[1], S. Liu[2], S. Xia[2], Z. Wang[1]; [1]*Beijing/CN,* [2]*Tianjin/CN (vickney1993@163.com)*

Purpose: Arterial stenosis is not sufficient for stratifying stroke risk. In this study, we evaluated atherosclerotic plaque features of the middle cerebral artery (MCA) using high-resolution vessel wall imaging (HR-VWI) and explored the correlation between plaque features and leptomeningeal collateral (LMC) status.
Methods and materials: 61 patients with intracranial atherosclerotic disease who underwent HR-VWI scans (September 2016-December 2018) were

retrospectively included. All patients presented with symptoms of ischaemic stroke or transient ischaemic attack with confirmed stenosis >30% in M1-2 segments. Plaque features were measured at the cross-section with most lumen narrowing (MLN) on HR-VWI. LMC was graded per patient on strategically acquired gradient echo (STAGE) derived magnetic resonance angiography (MRA) images using an established five-point collateral score (CS) system. Patients were divided into a poor (CS=0-2) or good (CS=3-4) LMC group. Independent two-sample t-tests, Mann-Whitney U-tests, or one-way analysis of variance was used as appropriate. Univariate and multivariate logistic regressions were conducted to identify the plaque features correlated with LMC status.
Results: Larger outer wall area (OWA), lumen area (LA_{MLN}), wall area, less stenosis percent (S%), M1 segment, and inferior wall distribution were found in the good LMC group compared with the poor LMC group (all p<0.05). Significant associations between the arterial remodelling ratio (ARR, odds ratio [OR] 3488.108, 95% confidence interval [CI] 1.198-2.637, p=0.004) and normalised wall index (NWI, OR 132.686, 95% CI 0.693-0.978, p=0.027) with LMC status were found.
Conclusion: Plaques in the poor or good LMC group exhibit different morphology and distribution features, among which ARR and NWI are associated with LMC status, which may help determine therapeutic decision-making in the clinical setting.
Limitations: n/a
Ethics committee approval: n/a
Funding: No funding was received for this work.
Author Disclosures:
R. Tang: nothing to disclose
S. Liu: nothing to disclose
Z. Wang: nothing to disclose
S. Xia: nothing to disclose

RPS 1111-7 14:36

The role of diffusion-weighted brain MR imaging in predicting outcomes after comatose cardiac arrest

K. Coursier[1], S. Vanden Berghe[2], S. A. Cappelle[3], K. Ameloot[4], F. de Keyzer[5], R. Peeters[4], S. van Cauter[4], S. Janssens[4], P. Demaerel[4]; *[1]Genk/BE, [2]Heule/BE, [3]Ypres/BE, [4]Leuven/BE, [5]Brussels/BE*
(kristof_coursier@hotmail.com)

Purpose: To assess a qualitative and quantitative approach to diffusion-weighted brain MR imaging (DWI) in order to investigate its role in predicting clinical outcomes after cardiac arrest.
Methods and materials: 75 patients underwent brain MR imaging within 5±2 days after a cardiac arrest. Two observers independently used a four-point Likert scale scoring template per assessed brain area on high b-value diffusion-weighted images (DWI). Intra and interobserver variability were tested using the intraclass correlation coefficient. ROC/AUC analysis was used for the outcome correlation with the clinical outcome defined by the cerebral performance category status at 180 days. Quantitative parameters on DWI were the percentage of voxels with apparent diffusion coefficient (ADC) <0.650 x 10^{-3} mm^2/s and the mean whole-brain ADC value.
Results: Intraobserver variability was excellent for the total cerebral cortex (TCC) score and for the total grey nuclei (TGN) score. Interobserver variability was excellent for the TCC and good to excellent for the TGN score. ROC analysis of the qualitative DWI showed a good correlation with the outcome for the TCC and for the TGN (AUC=0.83) score, whereas the quantitative DWI parameters correlated very poorly with the outcome (AUC 0.57-0.60).
Conclusion: Qualitative assessment of DWI acquired early after cardiac arrest provides valuable information to predict the outcome after cardiac arrest, while the correlation of the quantitative ADC assessment with the outcome was poor.
Limitations: n/a
Ethics committee approval: Study is based on a clinical trial that was approved by the ethics committee of UZ Leuven K.U.L., s58017.
Funding: Study is based on a clinical trial that was funded by a non-commercial TBM grant from the Flemish Government (IWT Flanders, Belgium).
Author Disclosures:
K. Coursier: nothing to disclose
S. Vanden Berghe: nothing to disclose
S. A. Cappelle: nothing to disclose
R. Peeters: nothing to disclose
S. van Cauter: nothing to disclose
P. Demaerel: nothing to disclose
F. de Keyzer: nothing to disclose
K. Ameloot: nothing to disclose
S. Janssens: nothing to disclose

RPS 1111-8 14:42

Homogeneity of the mean transit time allows for the discrimination of the functional outcome after aneurysmal subarachnoid haemorrhage

K. Jannusch, K. Beseoglu, M. Kaschner, N. A. Teichert, H. Nasri, A. K. Petridis, B. Turowski, J. Caspers, C. Rubbert; *Düsseldorf/DE*
(christian.rubbert@med.uni-duesseldorf.de)

Purpose: The pathogenesis leading to poor functional outcome after aneurysmal subarachnoid haemorrhage (aSAH) is multifactorial. CT perfusion imaging (CTP), especially the mean transit time (MTT), is increasingly used to monitor for delayed cerebral ischaemia. We hypothesise that the homogeneity (i.e. the standard deviation) of the MTT across the cortex on patient admission is predictive of the functional outcome.
Methods and materials: 147/630 consecutive subarachnoid haemorrhage patients (2008-2015) were retrospectively analysed (mean age 54.5, 66.7% female. Inclusion: aSAH, admission within 24h of ictus, CTP within 24h of admission, documented functional outcome after six months (modified Rankin scale grades; mRS). Exclusion: previous aSAH, CTP not evaluable).
MTT was recorded over 360° along the cortex in a 10 mm wide ribbon using a sliding window approach spanning 10° in 2° increments.
MTT standard deviation across the cortical ribbon (MTT_{SD}) was compared between mRS-dichotomised patient groups (≤2;>2) using a t-test. A logistic regression model (LRM) with stepwise regression using MTT_{mean}, MTT_{max}, MTT_{SD}, patient age, sex, world federation of neurosurgical societies and modified Fisher score, was assessed.
Results: F1 shows MTT_{SD}/mRS. MTT_{SD} was significantly different between patient groups (mRS ≤2;>2, p<0.001). After stepwise regression, the LRM retained MTT_{SD} (p=0.021), age (p=0.003), and Fisher score (p=0.0004). McFadden R^2=0.22 indicated a good to excellent model fit. The model's area under the receiver operating characteristics curve was 0.81.
Conclusion: Along with the Fisher score and patient age, the MTT_{SD} is predictive of functional outcome 6 month after aSAH ictus. MTT_{SD}, as a measurement of homogeneity, should be further evaluated for monitoring and prognostic assessments.
Limitations: Patients with detrimental pre-aSAH-mRS might have been included (unlikely at mean age of 54.5).
Ethics committee approval: The study was approved by the local ethics committee. The requirement for written informed consent was waived.
Funding: No funding was received for this work.
Author Disclosures:
C. Rubbert: nothing to disclose
K. Jannusch: nothing to disclose
K. Beseoglu: nothing to disclose
M. Kaschner: nothing to disclose
N. A. Teichert: nothing to disclose
H. Nasri: nothing to disclose
A. K. Petridis: nothing to disclose
B. Turowski: nothing to disclose
J. Caspers: nothing to disclose

RPS 1111-9 14:48

Feasibility study of 4D flow MRI to evaluate haemodynamics in patients with intracranial aneurysms

J.-G. Zhang, Z. Li; *Chengdu/CN (zjgscuhx@126.com)*

Purpose: To study the relationship between aneurysm morphology and haemodynamics in patients with intracranial aneurysms by using 4D flow technology. This study aims to explore its feasibility and value.
Methods and materials: In this study, clinical and imaging data of 25 patients with intracranial aneurysms were collected before surgery. After post-processing of 4D flow original phase images, the dynamic 3D images of blood flow velocity, wall shear stress (WSS), and velocity vector were created by the CVI42 software. The haemodynamic indexes including WSS, WSS ratio, shear concentration index (SCI), mean and maximum blood flow velocity, and mean and maximum instantaneous blood flow were measured and calculated. Meanwhile, the morphological parameters of aneurysms (including neck diameter, height, aneurysm width, parent diameter, neck diameter/parent diameter, aneurysm angle, etc.) were measured on digital subtraction angiography (DSA) images. Pearson's correlation was used to analyse the correlation between haemodynamic parameters (WSS, WSS ratio, and SCI) and other parameters.
Results: The WSS and WSS ratio was positively correlated with the ratio of neck diameter and parent diameter (r=0.578, 0.637, P<0.05), and SCI values were positively correlated with the aneurysm angle (r=0.395, P<0.05).
Conclusion: The haemodynamics of intracranial aneurysms is closely related to their morphology and the 4D flow MRI technique can dynamically and quantitatively evaluate the haemodynamic indicators of aneurysms, which has application value in exploring the mechanism of aneurysms and assessing the risk of aneurysm rupture.

Limitations: The small sample size.
Ethics committee approval: This study was approved by the ethics committee of West China Hospital and written informed consent was obtained.
Funding: 1.3.5 project for disciplines of excellence, West China Hospital, Sichuan University (Program Number: ZYGD18019). The recipient is Zhenlin Li.
Author Disclosures:
J.-G. Zhang: nothing to disclose
Z. Li: nothing to disclose

RPS 1111-10 14:54

Imaging of endovascularly treated intracranial aneurysms: comparing the novel technique of ASL-based silent-MR angiogram with 3D TOF-MR angiogram and digital subtraction angiogram

A. Rajendran[1], K. Chandrasekharan[2], D. K. Santhosh[2]; [1]*Chennai/IN,* [2]*Trivandrum/IN (adhithyan40@gmail.com)*

Purpose: To compare silent-MRA and 3D TOF-MRA in the evaluation of follow-up imaging of endovascularly treated intracranial aneurysms in comparison with DSA as the criterion standard for the assessment of the residual aneurysms and stent patency.
Methods and materials: A prospective analysis of consecutive patients with endovascularly treated aneurysms either by coiling or flow diverter who had follow-up imaging with TOF, silent-MRA, and DSA. The results were analysed by two neuro-radiologists independently. 3D TOF-MRA, silent-MRA, and DSA were evaluated for the size of the residual aneurysms and graded by the Raymond–Roy scale. The patency of the stent was also analysed. Images were analysed for the quality and graded on a 5-point scale. Kappa parameters were used to look for the agreement between the two methods. Scores were averaged and compared between techniques by using a Wilcoxon signed-rank test.
Results: 19 patients (4=stent-assisted coiling, 6=flow-diverters, and 9=simple or balloon-assisted coiling) were included.
The mean image quality score for residual aneurysm evaluation was 3.89+/-0.6 for TOF-MRA and 4.68+/-0.46 for silent-MRA. Scores of silent-MRA and 3D TOF-MRA differed significantly (P<0.05) according to the Wilcoxon signed-rank test.
The mean image quality score for the assessment of the stent or flow-diverter patency was 2.8+/-1.07 for TOF-MRA and 4.2+/-0.6 for silent-MRA. Scores of silent-MRA and 3D TOF-MRA differed significantly (P<0.05) for evaluating the stent or flow diverter patency.
Intermodality agreement values of 0.90 and 0.40 were obtained for DSA/silent-MRA and DSA/3D TOF-MRA, respectively.
Conclusion: Silent-MRA provides more accurate imaging information and better image quality than conventional TOF-MRA in the evaluation of residual aneurysms and stent patency by reducing the magnetic susceptibility artefacts.
Limitations: The limited number of cases.
Ethics committee approval: Ethics committee approval obtained.
Funding: No funding was received for this work.
Author Disclosures:
A. Rajendran: nothing to disclose
K. Chandrasekharan: nothing to disclose
D. K. Santhosh: nothing to disclose

RPS 1111-11 15:00

Follow-up of intracranial aneurysms treated with endovascular techniques: a comparison of the different methods with a review of the literature

E. Puglielli, G. Lanni, L. Conti, A. Gennarelli, N. Caputo; *Teramo/IT (edopug@hotmail.com)*

Purpose: To compare time-of-flight 3D-TOF magnetic resonance angiography (MRA), contrast-enhanced CE-MRA at 1.5-Tesla, computed tomography angiography (CTA), and digital subtraction angiography (DSA) for evaluating aneurysm occlusion and parent artery patency after coiling or stent-assisted coiling with a review of the recent literature.
Methods and materials: in this retrospective single-centre study, 427 patients were included if they had an intracranial aneurysm treated by coiling/stent-assisted coiling (April 2009-June 2019) followed by MRA (3D-TOF-MRA and CE-MRA), CTA or DSA, performed in an interval of 6, 12, or 24 months. Pooled sensitivity and specificity were calculated using the aneurysm occlusion status as defined by the Raymond-Roy occlusion grading scale.
Results: Vessels visualisation in the vicinity of the treated aneurysm was better in CTA, while regarding aneurysm occlusion, evaluation of the agreement with DSA was better for CE-MRA (K=0.51) than 3D-TOF-MRA (K=0.25). Diagnostic accuracies for the aneurysm remnant depiction were similar for 3D-TOF-MRA and CE-MRA (P=1). For TOF-MRA, the sensitivity and specificity of all aneurysms undergoing endovascular therapy were 87% and 93%, respectively, in accordance to the recent literature.
Conclusion: After coiling or stent-assisted coiling treatment, 3D-TOF-MRA and CE-MRA demonstrated good accuracy in detecting the aneurysm remnant, although it tends to overestimate. Vessels visualisation in the vicinity of treated aneurysm was better in CTA. Despite CE-MRA, agreement with DSA was better; there was no statistical difference between 3D-TOF-MRA and CE-MRA accuracies. Both MRAs were unable to provide a precise evaluation of the in-stent status but could detect the parent vessel occlusion. While digital subtraction angiography (DSA) remains the gold standard, magnetic resonance angiography (MRA) is attractive as a non-invasive follow-up technique.
Limitations: The small series.
Ethics committee approval: n/a
Funding: No funding was received for this work.
Author Disclosures:
E. Puglielli: nothing to disclose
G. Lanni: nothing to disclose
L. Conti: nothing to disclose
A. Gennarelli: nothing to disclose
N. Caputo: nothing to disclose

RPS 1111-12 15:06

Concordance between the simplified Edinburgh CT criteria and the modified Boston MRI criteria for cerebral amyloid angiopathy-associated (CAA) intracerebral haemorrhages (ICH)

F. Bruno, E. Tommasino, F. Cobianchi Bellisari, A. Barile, E. Di Cesare, C. Masciocchi, A. Splendiani; *L'Aquila/IT (federico.bruno.1988@gmail.com)*

Purpose: To evaluate the reproducibility of the Edinburgh CT criteria for cerebral amyloid angiopathy-associated (CAA) lobar intracerebral haemorrhage (ICH) in comparison to the modified Boston MRI criteria.
Methods and materials: We retrieved the images of 132 patients, with first-ever intracerebral hemorrhage diagnosed by non-contrast CT, in our Emergency department. The same patients underwent also MRI examination, to assess brain complications and were confirmed clinically with the diagnosis of cerebral amyloid angiopathy. Two blinded expert neuroradiologists independently evaluated CT images for the presence of the described CT signs for CAA ICH (finger-like projections, subarachnoid haemorrhage, lobar distribution).
Results: Using the simplified Edinburgh CT criteria, CAA-ICH was found in 89/100 patients (89%). The Boston criteria categorised 92 patients as having CAA-ICH. The concordance between the different diagnostic method was 92% (k= 0.82). Among CT signs, the presence of all CT signs resulted to have the highest specificity, while the highest diagnostic performance was recorded for SAH alone.
Conclusion: The concordance between the simplified Edinburgh criteria and the modified Boston criteria is high. Therefore, CT scores can be safely used in cases where MR is unsuitable, be it for contraindications or patient medical conditions.
Limitations: No histological confirmation.
Ethics committee approval: All procedures performed in studies involving human participants were in accordance with the ethical standards of the institutional and/or national research committee and with the 1964 Helsinki declaration.
Funding: No funding was received for this work.
Author Disclosures:
F. Bruno: nothing to disclose
E. Tommasino: nothing to disclose
A. Splendiani: nothing to disclose
A. Barile: nothing to disclose
E. Di Cesare: nothing to disclose
C. Masciocchi: nothing to disclose
F. Cobianchi Bellisari: nothing to disclose

RPS 1111-13 15:12

Clinical radiomics nomogram for the risk estimation of haematoma expansion after intracerebral haemorrhage

Y. Yang, Q. Chen, D. Zhu, J. Liu, M. Zhang, H. Xu, S. Huang; *Wenzhou/CN*

Purpose: Early haematoma expansion (HE) following intracerebral haemorrhage (ICH) is strongly associated with a poor outcome. The purpose of this study was to develop and validate a clinical radiomics nomogram for predicting HE in patients with acute spontaneous ICH.
Methods and materials: In total, 1,153 eligible patients were enrolled, of whom 864 (75%) were assigned to the derivation cohort and 289 (25%) to the validation cohort. Based on the LASSO algorithm or multivariate analysis, three models (the clinical model, the radiomics model, and the hybrid model incorporating both clinical and radiomics predictors) were constructed to predict HE. The Akaike information criterion (AIC) and likelihood ratio test (LRT) were used for comparing the goodness of fit of the three models, and the AUC was used to evaluate their discrimination ability for HE.
Results: The hybrid model (AIC=681.426; χ^2=128.779) was determined as the optimal model with the lowest AIC and highest Chi-square values compared with the radiomics model (AIC=767.979; χ^2=110.234) or clinical model (AIC=753.757; χ^2=56.448). The radiomics model had better discrimination ability for HE than

the clinical model in both derivation (p=0.009) and validation (p=0.022) cohorts. In both datasets, the clinical radiomics nomogram showed satisfactory discrimination and calibration in predicting HE (AUC=0.771, sensitivity=87.0%; AUC=0.820, sensitivity=88.1%; respectively).
Conclusion: Integrating CT-based radiomic signatures with clinical risk factors could optimise the predictive performance for HE. In the absence of CT angiography, the clinical-radiomics nomogram can offer an individualised tool for the risk stratification of HE with good sensitivity and may help select more ICH patients for anti-expansion clinical trials.
Limitations: The nomogram is derived from a single-centre analysis, thus lacking external validation.
Ethics committee approval: n/a
Funding: No funding was received for this work.
Author Disclosures:
Y. Yang: nothing to disclose
Q. Chen: nothing to disclose
J. Liu: nothing to disclose
D. Zhu: nothing to disclose
M. Zhang: nothing to disclose
H. Xu: nothing to disclose
S. Huang: nothing to disclose

RPS 1111-14 15:18
Quantification of carotid intraplaque haemorrhage: a comparison with manual segmentation and semi-automatic segmentation on magnetisation-prepared rapid acquisition with gradient-echo sequence
Y. J. Song[1], H.-S. Kwak[2]; [1]*Jeonju-si Jeollabuk-do/KR,* [2]*Jeonju/KR*
(twinklinglena@gmail.com)

Purpose: Carotid intraplaque haemorrhage (IPH) increases the risk of territorial cerebral ischaemic events but different sequences or criteria are used to diagnose and quantify carotid IPH. The purpose of this study was to compare manual segmentation and semi-automatic segmentation for the quantification of carotid IPH on magnetisation-prepared rapid acquisition with the gradient-echo (MPRAGE) sequence.
Methods and materials: 40 patients with 16-79% carotid stenosis and IPH on MPRAGE sequence were reviewed by 2 trained radiologists with more than 5 years of specialised experience in carotid plaque characterisation. Initially, the radiologists manually read the IPH based on the MPRAGE sequence. The IPH volume was then measured by 3 different semi-automatic methods: high signal intensity above 150%, 175%, and 200% than that of the adjacent muscle on MPRAGE sequence. The agreement on measurements between manual segmentation and semi-automatic segmentation was assessed using the intraclass correlation coefficient (ICC).
Results: There was good agreement between manual segmentation and the 3 criteria of semi-automatic segmentation for the quantification of IPH volume. ICC of each semi-automatic segmentation were as follows: 150% criteria: 0.87-0.96, 175% criteria: 0.85-0.96, and 200% criteria: 0.69-0.90. The agreement of total IPH length was good in all criteria of semi-automatic segmentation (ICC=150% criteria: 0.80-0.94, 175% criteria: 0.71-0.91, and 200% criteria: 0.60-0.87). ICC of 150% and 175% criteria were significantly better than that of 200% criteria (p<0.05).
Conclusion: ICC of 150% and 175% criteria for semi-automatic segmentation are more reliable for quantification of IPH volume. Semi-automatic classification tools may be beneficial in large-scale multicentre studies by reducing the image analysis time and avoiding bias between human reviewers.
Limitations: There was no histological confirmation. The relatively small number of patients.
Ethics committee approval: This study was conducted with institutional review board approval.
Funding: No funding was received for this work.
Author Disclosures:
Y. J. Song: nothing to disclose
H.-S. Kwak: nothing to disclose

RPS 1111-15 15:24
Accelerated time-of-flight magnetic resonance angiography using spiral imaging improves the conspicuity of intracranial arterial branches whilst reducing scan time
N. Sollmann, T. Greve, A. Hock, C. Zimmer, J. S. Kirschke*; Munich/DE*
(nico.sollmann@tum.de)

Purpose: To compare time-of-flight magnetic resonance angiography (TOF-MRA) acquired with compressed SENSE (TOF-CS) to spiral imaging (TOF-Spiral) for the imaging of brain-feeding arteries.
Methods and materials: 71 patients (60.2±19.5 years, 28.2% with pathology) who underwent TOF-MRA after the implementation of new scanner software enabling spiral imaging were analysed retrospectively. TOF-CS (standard sequence; duration: ~4 min) and the new TOF-Spiral (duration: ~3 min) were acquired. Image evaluation (vessel image quality and detectability, diagnostic confidence [1: diagnosis very uncertain-5: diagnosis very certain], quantitative measurement of aneurysm diameter, or degree of stenosis according to NASCET criteria) was performed by two readers. Quantitative assessments of pathology were compared to computed tomography angiography (CTA) or digital subtraction angiography (DSA).
Results: TOF-CS showed higher image quality for intraosseous and intradural segments of the internal carotid artery, while TOF-Spiral better depicted small intracranial vessels like the anterior choroidal artery. All vessel pathologies were correctly identified by both readers for TOF-CS and TOF-Spiral with high confidence (TOF-CS: 4.4±0.6 and 4.3±0.7; TOF-Spiral: 4.3±0.8 and 4.3±0.8) and good inter-reader agreement (Cohen's kappa: >0.8). Quantitative assessments of the aneurysm size or stenosis did not significantly differ between TOF-CS or TOF-Spiral and CTA or DSA (p>0.05), with excellent correlations between the measurements of both readers (ICC>0.95).
Conclusion: TOF-Spiral for the imaging of brain-feeding arteries enables reductions in scan time without drawbacks in diagnostic confidence. A combination of spiral imaging and CS may help to overcome the shortcomings of both sequences alone and could further reduce acquisition times.
Limitations: The retrospective design and comparatively low number of vessel pathologies observed among the enrolled patients.
Ethics committee approval: This retrospective study was approved by the IRB.
Funding: Philips Healthcare.
Author Disclosures:
N. Sollmann: nothing to disclose
T. Greve: nothing to disclose
A. Hock: Employee at Philips Healthcare
C. Zimmer: nothing to disclose
J. S. Kirschke: Research/Grant Support at Philips Healthcare

14:00 - 15:30 **Room M 3**

Abdominal Viscera

RPS 1101

Advances in CT techniques

Moderators:
N. Grosse Hokamp; Cologne/DE
T. Leiner; Utrecht/NL

RPS 1101-1 14:00
Comparison study between published contrast administration protocols for enhanced liver CT examination in adults
F. Zanca[1], B. Rizk[2], D. Racine[3], P. Pujadas[4], D. Fournier[5], H. Brat[5];
[1]*Leuven/BE,* [2]*Villars-sur-Glane/CH,* [3]*Lausanne/CH,* [4]*Paris/FR,* [5]*Sion/CH*
(federica.zanca@palindromo.consulting)

Purpose: To compare hepatic enhancement level and uniformity across adult patients, using different personalised contrast administration protocols proposed in literature.
Methods and materials: 623 patients undergoing a three-phase liver CT examination were prospectively included, using a standardised CT protocol (100 or 120 kV in the function of patient BMI, 5 ml/sec contrast media (CM) injection rate, 80 sec portal phase delay, Iopamidol 370mg Iodine/ml).
Patients were prospectively assigned to one of three specific CM administration protocol group: G1 (100ml fixed CM volume, n = 297); G2 (600mgI/kg of body weight, n = 98,); G3 (750mgI/kg of measured fat free mass (FFM), n=228). Impact of kV settings was accounted through measured liver parenchymal enhancement (CEI) scaling factors for each scanner.
The mean injected CM volume, iodine dose, and median CEI at 100kV were compared across groups (one-way ANOVA or Kruskall-Wallis, p<0.005). The variance of the distributions was assessed and CEI compared to a diagnostically appropriate level of 30-50HU.
Results: G3 mean contrast volume and iodine dose (93.1 ml, 34.4 mgI respectively) were significantly lower than G1 (100ml, 37.0 mgI) and G2 (109.5 ml, 40.5 mgI) (p<0.0001 for both). 87-94% of patients were over-enhanced with a significantly lower median CEI for G3 (65.6HU) than G2 (70.7HU) and G1 (77.5HU) (p<0.0001 for both). Only 8% (G1), 6% (G2), and 13% (G3) reached target enhancement. Variance decreased from 520 (G1) to 403 (G2) to 247 (G3).
Conclusion: The FFM-based protocol improved patient-to-patient liver enhancement uniformity, while significantly reducing the iodine load, although still overestimated for a large group of patients. Our kV scaling factors suggest that 600mgI/FFM@100kV would significantly reduce over-enhancement and target a homogeneous diagnostic value of 50 HU.
Limitations: n/a
Ethics committee approval: Approved.
Funding: No funding was received for this work.

Author Disclosures:
F. Zanca: nothing to disclose
H. Brat: nothing to disclose
P. Pujadas: Employee at GE Healthcare
D. Racine: nothing to disclose
B. Rizk: nothing to disclose
D. Fournier: nothing to disclose

RPS 1101-2 14:06
Standardisation of dual-energy CT iodine uptake of the abdomen: defining reference values in a big data cohort
I. Yel, C. Booz, S. S. Martin, L. Lenga, B. Kaltenbach, T. J. Vogl, M. H. Albrecht; *Frankfurt am Main/DE (Dr.IbrahimYel@gmail.com)*

Purpose: Despite a wealth of literature on dual-energy CT (DECT) iodine uptake in various pathologies, physiologic reference values for this technique for a confident clinical application have not been defined to date. Therefore, we investigated the iodine uptake of healthy abdominal and pelvic organs in a big data cohort.
Methods and materials: Consecutive portal-venous abdominal DECTs were reviewed and unremarkable exams were included (n=520; white/asian=489; mean age=59±15,5 years; 265w/255m). ROI-measurements were performed in the following anatomical regions (number of ROIs): liver (9), pancreas (3), spleen (3), adrenal glands (2), kidneys (6), prostate (4), uterus (2), urinary bladder wall (1), and lymph nodes (3). Iodine uptake was compared among different organs and subgroup analysis was performed (young vs old/male vs female).
Results: Overall mean iodine uptake values were as follows (mg/ml): liver=1.93±0.54, pancreas=2.06±0.57, spleen=2.55±0.65, adrenal glands=1.66±0.43, kidneys=6.28±1.36, prostate=1.11±0.52, uterus=1.07±0.74, bladder=0.69±0.29, and lymph nodes=0.75±0.21. Iodine uptake was comparable between liver/pancreas and liver/adrenal glands (p>=0.119). Women showed higher iodine uptake for liver (2.07±0.58vs1.79±0.45mg/ml), pancreas (2.29±0.57vs1.83±0.47mg/ml), spleen (2.81±0.65vs2.30±0.53mg/ml), adrenal glands (1.76±0.49vs1.56±0.33mg/ml), and kidneys (6.74±1.36vs5.83±1.20mg/ml) than men (p<0.001). In older patients, iodine uptake increased for liver (1.98±0.52vs1.87±0.54mg/ml), spleen (2.48±0.65vs2.63±0.64mg/ml), and kidneys (6.11±1.24vs6.45±1.45mg/ml) compared to younger subjects (p<=0.040). Only the uterus showed lower values in older women (0.77±0.45vs1.35±0.84mg/ml,p<0.001).
Conclusion: Physiologic iodine uptake values show age- and gender-related differences for the liver, spleen, and kidneys. Pancreas and adrenal glands show higher iodine perfusion in women. While prostate parenchyma seems unaffected throughout a lifetime, iodine supply of the uterus decreases in elderly women. Lymph nodes and bladder are unaffected by demographic influences.
Limitations: Monocentric study. Single device (Somatom Force).
Ethics committee approval: Approval by local IRB.
Funding: No funding was received for this work.
Author Disclosures:
I. Yel: nothing to disclose
C. Booz: Speaker at Siemens Healthineers
S. S. Martin: nothing to disclose
T. J. Vogl: nothing to disclose
L. Lenga: nothing to disclose
B. Kaltenbach: nothing to disclose
M. H. Albrecht: Research/Grant Support at Siemens Healthineers, Speaker at Siemens Healthineers

RPS 1101-3 14:12
Comparison of established dual-energy CT reconstructions with a novel virtual non-calcium based method to detect radiolucent gallstones
A. Almutairi, A. Alzahrani, A. Alosaimi, F. Azzumeea, M. F. A. Mohammed; *Riyadh/SA (mohammed.f.mohammed@gmail.com)*

Purpose: Cholelithiasis affects up to 15% of the population with recurrent ED visits. CT is often the first investigation for abdominal pain and offers higher sensitivity and specificity for the diagnosis of acute cholecystitis. However, up to 80% of gallstones are radiolucent. We hypothesise that a new dual-energy CT technique improves detection of stones compared to previously reported VMI techniques.
Methods and materials: Consecutive patients who received a dsDECT scan in the ED and an MRI or US study within 6 months of the dsDECT were included. An optimised VNCa algorithm was used to detect gallstones alongside 40 keV and 190 keV reconstructions by 2 abdominal radiologists. Sensitivity, specificity, PPV, NPV, and interobserver agreement were calculated and reported with 95% confidence intervals. US or MRI were considered the reference standard.
Results: 85 patients met the inclusion criteria. Modified VNCa correctly detected all 14 radiolucent stones with a sensitivity, specificity, PPV, NPV, and agreement of 100% [78% - 100%], 98.6% [92.4% - 99.9%], 93.3% [70.2% - 99.7], 100% [94.8% - 100%], and k = 0.88 respectively. Performance of 40 keV reconstructions was 35% [16.3% - 46.1%], 98.6% [92.4% - 99.9%], 83.3% [43.7% - 99.2%], and 88.6% [79.8% - 93.9%] and 50% [26.8% - 73.2%], 90.1% [81% - 95.1%], 50% [26.8% - 73.2%], and 90.1[81% - 95.1%] for 190 keV reconstructions.
Conclusion: A modified VNCa-based algorithm provides a highly sensitive and specific tool for detection of radiolucent gallstones, providing accurate and rapid diagnosis in the acute setting.
Limitations: A reterospective study. A small number of stones.
Ethics committee approval: IRB approved.
Funding: No funding was received for this work.
Author Disclosures:
M. F. A. Mohammed: nothing to disclose
A. Almutairi: nothing to disclose
A. Alzahrani: nothing to disclose
A. Alosaimi: nothing to disclose
F. Azzumeea: nothing to disclose

RPS 1101-4 14:18
Diagnose negative gallstones with dual-layer spectral detector CT
J. Liu[1], X. Lu[2]; [1]*Tianjin/CN,* [2]*Shanghai/CN (18522587288@163.com)*

Purpose: To investigate the clinical application of dual-layer spectral detector CT (DLCT) in the diagnosis of negative gallstones.
Methods and materials: Between March 2019 to September 2019, we retrospectively enrolled 17 patients (6 men; mean age, 46 years; age range, 28–65 years) with gallstones who were detected by the magnetic resonance cholangiopancreatography (MRCP) and were not detected by conventional CT imaging. All patients underwent unenhanced abdomenal CT scanning with DLCT. The 40 keV to 200 keV virtual monoenergetic images (VMI), effective atomic number (Z_{eff}), spectral HU curve of negative gallstoness, and bile were analysed.
Results: All negative gallstones were clearly diagnosed by DLCT. The attenuation of negative stones showed lower than bile on the VMIs. The difference of attenuation between gallstones and bile was the largest in $VMI_{40\ keV}$ (gallstones -55.26±12.54 HU, bile 19.56±11.91HU). The Z_{eff} also showed the significant difference (gallstones 6.01±0.19, bile 7.17±0.08). The slope of the spectral curve of the negative stones was positive, the spectral curve of bile was approximately straight, and the slope was almost zero.
Conclusion: DLCT can confirm the negative gallstones, which has high diagnostic value.
Limitations: There was a small sample size in our study. Some stones were too small, which may have led to measurement errors.
Ethics committee approval: n/a
Funding: No funding was received for this work.
Author Disclosures:
J. Liu: nothing to disclose
X. Lu: nothing to disclose

RPS 1101-5 14:24
Contrast media reduction in abdominal dual-energy CT: low keV virtual monoenergetic images restore diagnostic assessment and image quality
S. Lennartz[1], N. Grosse Hokamp[1], C. Zäske[1], D. Zopfs[1], G. Bratke[1], A. Glauner[1], D. Maintz[1], D.-H. Chang[2], T. Hickethier[1]; [1]*Cologne/DE,* [2]*Heidelberg/DE (simon.lennartz@uk-koeln.de)*

Purpose: Abdominal CT with reduced contrast media (CM) application would be beneficial for patients at risk for contrast-induced nephropathy yet may imply inferior assessability. The study evaluated if low-keV virtual monoenergetic images from abdominal spectral-detector CT (SDCT) with reduced contrast media ($RCM\text{-}VMI_{40keV}$) provide similar image quality as conventional scans with standard contrast media dose (SCM).
Methods and materials: 78 patients with abdominal SDCT were included: 41 patients at risk for adverse reactions who received 44 RCM scans with 50ml of CM and 37 patients who received 44 SCM scans with 100ml of CM. Both groups were matched for effective body diameter. $RCM\text{-}VMI_{40keV}$, conventional RCM, and SCM images were reconstructed. Attenuation and SNR of liver, pancreas, kidneys, lymph nodes, aorta, and portal vein were assessed ROI-based. CNR of lymph nodes vs aorta/portal vein were calculated. Two readers blinded against patients/reconstructions assessed organ/vessel contrast, lymph node delineation, image noise, and overall assessability using 4-point Likert scales.
Results: Lymph node attenuation was similar between $RCM\text{-}VMI_{40keV}$ and SCM images (p=0.83), while for all other ROIs, $RCM\text{-}VMI_{40keV}$ was superior (p<0.05). SNR was equal between $RCM\text{-}VMI_{40keV}$ and SCM images for all ROIs (p-range 0.23-0.99). CNR of lymph nodes vs aorta/portal vein was highest in $RCM\text{-}VMI_{40keV}$ (p<0.05). Qualitatively, $RCM\text{-}VMI_{40keV}$ received equivalent or higher scores than SCM in all criteria except for organ contrast, overall assessability, and subjective image noise for which SCM was superior. However, in these three categories, $RCM\text{-}VMI_{40keV}$ received proper or excellent scores in

88.6%/94.2%/95.4% of all cases. Conventional RCM were inferior in all quantitative/qualitative parameters.
Conclusion: VMI_{40keV} effectively antagonises contrast deterioration in CM-reduced abdominal SDCT, facilitating diagnostic assessment.
Limitations: The study did not investigate lesion detection.
Ethics committee approval: Waived due to retrospective study characteristics.
Funding: Else Kröner-Fresenius Stiftung (2016-Kolleg-19 to SL).
Author Disclosures:
D. Zopfs: nothing to disclose
S. Lennartz: Research/Grant Support at Philips Healthcare
N. Grosse Hokamp: Speaker at Philips Healthcare, Research/Grant Support at Philips Healthcare
C. Zäske: nothing to disclose
G. Bratke: nothing to disclose
A. Glauner: nothing to disclose
D.-H. Chang: nothing to disclose
T. Hickethier: Research/Grant Support at Philips Healthcare
D. Maintz: Speaker at Philips Healthcare

RPS 1101-6 14:30
Optimised virtual monoenergetic image for liver fibrosis staging using dual-layer spectral CT
R. Li, L. Wang, Y. Yang, F. Yan, Q. Han, X. Chen*; Shanghai/CN (lrk12113@rjh.com.cn)*

Purpose: To investigate the value of an optimised virtual monoenergetic image (VMI) for liver fibrosis staging using dual-layer spectral CT.
Methods and materials: 26 rabbit models of CCl_4-induced liver fibrosis were established and 4 untreated rabbits served as controls. Dynamic contrast-enhanced CT was performed including arterial phase [AP] and venous phase [VP] using dual-layer spectral CT. CT attenuation on VMI (40kev, 50kev, 60kev, 70kev) and conventional polyenergetic images (CPI) were measured by whole-liver volumetric ROI drawing on precontrast and enhancement images. $\Delta CT_{40\text{-}70kev}$ were calculated and correlated with the histopathological fibrosis stage to determine the optimised VMI.
Receiver operating characteristic (ROC) analysis was performed for assessing the diagnostic performance of the optimised VMI for fibrosis stage.
Results: On arterial phase, no significant correlation was identified between $\Delta CT_{40\text{-}70kev}$ and fibrosis stage or CPA ($P > 0.05$). On portal venous phase, ΔCT_{CPI}, $\Delta CT_{VMI\ 40}$, $\Delta CT_{VMI\ 50}$, $\Delta CT_{VMI\ 60}$, and $\Delta CT_{VMI\ 70}$ showed moderate correlation (r=0.453, P=0.012; r=0.595, P=0.001; r=0.543, P=0.002; r=0.498, P=0.005; and r=0.449, P=0.013; respectively) with fibrosis. $\Delta CT_{VMI\ 50}$ showed the highest correlation with fibrosis stage. $\Delta CT_{VMI\ 50}$ areas under ROC (AUROCs) were 0.861, 0.790, 0.831, and 0.740 for diagnosing fibrosis with ≥F1, ≥F2, ≥F3, and F4 stage, respectively.
Conclusion: $\Delta CT_{VMI\ 50}$ on portal venous phase may be a potential biomarker for liver fibrosis staging.
Limitations: This is an anmial study. The study should be further confirmed in patients.
Ethics committee approval: n/a
Funding: No funding was received for this work.
Author Disclosures:
R. Li: nothing to disclose
L. Wang: nothing to disclose
Y. Yang: nothing to disclose
F. Yan: nothing to disclose
Q. Han: nothing to disclose
X. Chen: nothing to disclose

RPS 1101-7 14:36
Virtual monoenergetic images for diagnosing small hepatocellular carcinoma using dual-layer spectral CT: optimal energy level and added value
Z. Fu[1], C. Xu[1], D. Li[1], Y. Tian[1], X. Chen[2], C. Du[1]; [1]Nanjing/CN, [2]Shanghai/CN (xingbiao.chen@hotmail.com)

Purpose: To determine the optimal keV setting for virtual monoenergetic images (VMI) derived from dual-layer spectral CT (DLCT) and added value for diagnosing small hepatocellular carcinoma (sHCC) in comparison with conventional 120 kVp polyenergetic images (PI).
Methods and materials: 64 patients with sHCC who underwent upper abdomen enhanced scan using DLCT were retrospectively enrolled and were diagnosed by pathology within one week before or after CT examination. PI and VMIs (40–100 keV with an interval of 10 keV) were reconstructed from the same acquisition. CT value of sHCC lesions and liver parenchyma at the same slice and image noise for PI and VMIs were recorded. The contrast-to-noise ratios (CNR) and signal-to-noise ratios (SNR) were calculated and compared with PI and VMIs. PI and VMIs were reviewed by 2 radiologists independently for the sHCC diagnosis using a 3-point scale and compared.
Results: Image noise from VMI_s had no significant difference with PI. With energy levels from 60keV to 40 keV, SNR of VMIs increased from 7.07±2.48 to 9.09±4.21 and all were significantly higher than PI (5.36, all P<0.05). CNR of VMI_{40keV} and VMI_{50keV} were 4.09±2.34 and 2.70±1.61, and both were significantly higher than PI (0.96±0.82, both P<0.05). The subject score for VMIs increased from 2.78±0.42 to 2.90±0.25 as the energy level increased from 60keV to 40keV. All subject scores for VMIs were significantly greater than for PI (2.53±0.51, all P<0.05).
Conclusion: The lowest energy level VMI_{40keV} provided the best SNR, CNR, subject score, and equivalent noise as PI on DLCT. Moreover, VMI_{40keV} improved the sHCC lesion conspicuity and increased the diagnostic confidence.
Limitations: Small population. VMI energy level interval was large.
Ethics committee approval: n/a
Funding: No funding was received for this work.
Author Disclosures:
X. Chen: Employee at Philips Healthcare
Z. Fu: nothing to disclose
C. Xu: nothing to disclose
C. Du: nothing to disclose
D. Li: nothing to disclose
Y. Tian: nothing to disclose

RPS 1101-9 14:42
Iodine accumulation in the liver in patients treated with amiodarone can be unmasked using material decomposition from multiphase spectral-detector CT
K. R. Laukamp[1], A. Hashmi[2], N. Grosse Hokamp[1], A. Gupta[2], S. Lennartz[1], P. F. Graner[2], T. Persigehl[1], R. Gilkeson[2], N. Ramaiya[2]; [1]Cologne/DE, [2]Cleveland, OH/US (kai.laukamp@uk-koeln.de)

Purpose: Amiodarone accumulates in the liver where it increases x-ray attenuation by its iodine-content. Liver damage indicated by steatohepatitis and a decrease of attenuation can thereby be masked. Therefore we evaluated liver-attenuation in patients treated and not treated with amiodarone using true-non-contrast (TNC) and virtual-non-contrast (VNC) images acquired with spectral-detector-CT (SDCT).
Methods and materials: 142 patients, of which 21 have been treated with amiodarone, receiving SDCT-examinations (unenhanced-chest [TNC], CT-angiography of chest and abdomen [CTA-Chest, CTA-Abdomen]) for transcatheter-aortic-valve-replacement (TAVR)-planning were included. TNC, CTA-Chest, CTA-Abdomen, and corresponding VNC-images (VNC-Chest, VNC-Abdomen) were reconstructed. Image-analysis was conducted using ROI-based measurements of mean-attenuation (HU). The liver-attenuation-index (LAI) was calculated as the difference between liver- and spleen-attenuation.
Results: Liver-attenuation and LAI derived from TNC-images of patients receiving amiodarone were higher (63.1±9.8HU versus 58.1±8.6HU, p=0.04; 16.8±7.9HU versus 9.7±8.1HU, p<0.001). Contrary to TNC, liver-attenuation and LAI were not higher in amiodarone patients in VNC-Chest (liver-attenuation, 56.3±8.3HU versus 55.3±5.8HU, p=0.35; LAI, 7.5±8.5HU versus 7.5±6.9HU, p=0.50) and in VNC-Abdomen (liver-attenuation, 59.2±6.4HU versus 58.7±5.8HU, p=0.62; LAI, 8.5±6.5HU versus 6.5±6.7HU, p=0.10). In patients untreated with amiodarone, VNC accurately subtracted iodine and depicted similar attenuation compared to TNC.
Conclusion: Patients treated with amiodarone showed higher liver-attenuation in TNC. In contrast, VNC revealed comparable liver-attenuation in patients treated and untreated with amiodarone, indicating that VNC accurately subtracted hepatic amiodarone-deposits in line to contrast-agent related iodine-uptake.
Limitations: Spectral imaging data for the unenhanced chest acquisition (TNC) was not routinely saved at our institution, therefore creation of VNC images was only possible for CTA-Chest and CTA-Abdomen. A ROI-based measurement of mean attenuation was conducted and not a volumetric assessment of the entire liver.
Ethics committee approval: This study was apporved by the institutional review board.
Funding: No funding was received for this work.
Author Disclosures:
K. R. Laukamp: nothing to disclose
A. Hashmi: nothing to disclose
N. Grosse Hokamp: Other at Nils Große Hokamp received speakers' honoraria from Philips Healthcare.
A. Gupta: nothing to disclose
S. Lennartz: Other at Nils Große Hokamp received speakers' honoraria from Philips Healthcare.
P. F. Graner: nothing to disclose
T. Persigehl: nothing to disclose
R. Gilkeson: nothing to disclose
N. Ramaiya: nothing to disclose

RPS 1101-10 14:48

Metal implants on abdominal CT: can split-filter dual-energy CT provide additional value over iterative metal artefact reduction?

H. M. Wichtmann[1], S. Yang[1], K. R. Laukamp[2], S. Manneck[1], K. Appelt[1], D. Boll[1], T. Heye[1], M. Benz[1], M. M. Obmann[1]; [1]*Basel/CH,* [2]*Cologne/DE*

Purpose: To assess metal artefact reduction in split-filter dual-energy CT (tbDECT) using virtual monoenergetic images (VMI) compared to 120kVp-equivalent mixed images (MIX) and iterative metal artefact reduction algorithm (iMAR).
Methods and materials: Abdominal tbDECT of 30 patients with total hip replacements (15 uni-, 15 bilateral) were included. Images were reconstructed as MIX and VMI (40 to 190 keV, 10 keV increments), with and without iMAR. Quantitative image quality was assessed using ROI-analysis of corrected attenuation-values [HU] and standard deviation (SD) for hypo- and hyperdense artefact on all reconstructions. Qualitative image quality was rated for overall image quality and vascular contrast on a 5-point Likert-scale (1: no artefact/contrast to 5: most artefact/contrast).
Results: Lowest artefact (both hypo- and hyperdense) was observed on MIX_{iMAR} (-10.6 and -0.6 HU), which was significantly lower compared to the standard MIX (p=0.006 and p<0.001). Comparison between MIX and VMI_{40keV} showed more artefact on VMI_{40keV} (p<0.001). Low keV $VMI_{iMAR-40keV}$ did not show more artefact than MIX_{iMAR} or MIX (p≥0.08). Image noise was highest for conventional low VMI_{40keV} (46.1 HU). Yet, $VMI_{iMAR-40keV}$ showed similar image noise compared to MIX (10.9 vs 12.4 HU, p=0.608). Qualitative image quality was rated best for VMI_{iMAR} at 140 keV (2.43), which was significantly better than MIX (4.07, p<0.001), but not MIX_{iMAR} (2.70, p=0.176). Low keV VMI_{iMAR} showed both improved image quality and vascular contrast compared to MIX (2.93 vs 4.07, p<0.001, 4.17 vs 2.70, p<0.001).
Conclusion: Abdominal tbDECT MIX_{iMAR} reconstructions provide the best image quality in patients with total hip replacements. High keV VMI_{iMAR} does not further decrease artefact. However, iMAR enables the use of low keV VMI_{iMAR} to boost iodine-based contrast with acceptable image quality.
Limitations: n/a
Ethics committee approval: IRB approved, need for informed consent waived.
Funding: No funding was received for this work.
Author Disclosures:
S. Yang: nothing to disclose
H. M. Wichtmann: nothing to disclose
K. R. Laukamp: nothing to disclose
S. Manneck: nothing to disclose
K. Appelt: nothing to disclose
D. Boll: nothing to disclose
T. Heye: nothing to disclose
M. Benz: nothing to disclose
M. M. Obmann: nothing to disclose

RPS 1101-11 14:54

Improved image quality in abdominal CT: promising results from a novel deep learning image reconstruction (DLIR) technique

T. Njølstad[1], A. Schulz[1], G. Pace[2], H. K. Andersen[1], A. C. T. Martinsen[1]; [1]*Oslo/NO,* [2]*Ancona/IT (tormund.njolstad@gmail.com)*

Purpose: To assess image quality in abdominal CT reconstructed with a novel deep learning image reconstruction (DLIR) technique in thin slices and compare with standardly applied hybrid iterative reconstruction (IR) technique in thick slices.
Methods and materials: 10 abdominal CT scans, performed on a GE Revolution CT scanner, were reconstructed with standardly applied IR technique (50% ASiR) for 2.5mm slices and a novel DLIR technique (TrueFidelity) for 0.625mm slices. Image contrast, noise, and contrast-to-noise ratio (CNR) were calculated for quantitative image quality analyses. Qualitative image quality was assessed independently by 3 radiologists, blinded to reconstruction method applied, along 9 visual grading image criteria on a five-point scale in a side-by-side comparative setting. Each patient was presented twice to evaluate intraobserver agreement and images were randomly selected to the right or left monitor to avoid situation bias. Odds ratios (OR) were evaluated using logistic regression.
Results: For quantitative analyses, CNR between the portal vein and liver parenchyma was significantly higher for images reconstructed with DLIR compared to IR (p=0.005). For visual grading, DLIR image quality was more frequently perceived as slightly better or clearly better across all visual grading criteria compared to IR. OR for DLIR perceived as better than IR was highly significant for visual reproduction of liver parenchyma, overall impression of image noise, texture, and contrast (p<0.001). OR for DLIR perceived as equal or better than IR was highly significant for all visual grading criteria (p<0.001).
Conclusion: Abdominal CT reconstructed in 0.625 mm slices using a novel DLIR technique shows markedly improved image quality when compared to 2.5 mm slices, with standardly applied IR across a variety of clinical image quality criteria.
Limitations: Pilot study.
Ethics committee approval: n/a
Funding: Supported by GE-Healthcare.
Author Disclosures:
T. Njølstad: nothing to disclose
A. Schulz: Other at Supported by GE Healthcare
H. K. Andersen: Other at Supported by GE Healthcare
G. Pace: nothing to disclose
A. C. T. Martinsen: Other at Supported by GE Healthcare

RPS 1101-12 15:00

Optimisation of abdominal CT using a new iterative reconstruction technique

G. Pace[1], M. Afadzi[2], A. Schulz[2], T. M. Aalokken[2], A. C. T. Martinsen[2], A. Giovagnoni[1]; [1]*Ancona/IT,* [2]*Oslo/NO (pacegenny@gmail.com)*

Purpose: To investigate the potential of a new statistical iterative reconstruction technique (ASIR-V) to balance the deterioration of image quality in abdominal computed tomography (CT) using thinner slice reconstructions (<2.5 mm).
Methods and materials: 10 patients underwent contrast-enhanced CT for oncological follow-up on a GE revolution CT (GE Healthcare, Milwaukee, WI), noise-index 29.0, automatic current modulation at 120kV. Reconstructions at 2.5, 1.25, and 0.625mm slice thickness with ASIR-V 0, 30, 50, 70, and 90%. Quantitative (contrast-to-noise ratio in the liver, portal vein, muscle, and abdominal aorta; image noise in spleen) and qualitative analyses (5-point scale, 10 criteria) of image quality were conducted. Comparison of median CNRs and image noise between the fourteen series and the 2.5 mm/ASiR-V 50% reconstructions was done using Dunnett's multiple comparison testing with 2.5 mm/ASiR-V 50% as the control group. The qualitative evaluation was analysed with visual grading regression (VGR).
Results: No reconstructed data set provided significantly better CNR than the control group. The 1.25 mm slices in combination with ASiR-V 70%-90%, and 0.625 mm with ASiR-V 90% showed statistically equal CNR in liver parenchyma, portal vein, muscle, and aorta (all p=1), and statistically lower image noise (all p<0.05) compared to the control group. The 1.25 mm data sets with ASIR-V 70% showed equal image quality in comparison to the control group in all criteria evaluated. Image was scored superior to the control group with 1.25 mm and ASIR-V 90% (p<0.02).
Conclusion: Abdominal CT images reconstructed at 1.25 mm slices with ASIR-V 70% provided an image quality equivalent to the standard protocol (2.5 mm slices, ASiR-V 50%) and might have the potential to demonstrate more subtle abnormalities and avoid partial volume effect.
Limitations: Few patients, few readers.
Ethics committee approval: Approved by an institutional review board. Written informed consent was waived.
Funding: No funding was received for this work.
Author Disclosures:
G. Pace: nothing to disclose
M. Afadzi: Other at Institutional research collaboration with GE Healthcare
A. Schulz: Other at institutional research collaboration with GE Healthcare
A. Giovagnoni: nothing to disclose
T. M. Aalokken: Other at insitutional research collaboration with GE Healthcare
A. C. T. Martinsen: Other at institutional research collaboration with GE Healthcare

RPS 1101-13 15:06

A randomised controlled trial proposing a straight forward 10-to-10 rule for individualised liver imaging based on tube voltage and body weight

B. Martens, J. E. Wildberger, B. M. F. Hendriks, S. M. van Kuijk, N. H. G. M. Peters, J. de Vos-Geelen, C. Mihl; *Maastricht/NL (bibi.martens@mumc.nl)*

Purpose: To optimise the CT liver protocol based on both body weight (BW) and tube voltage (TV). The rule of thumb was that 10kV TV reduction would lead to a 10% decrease in CM dose.
Methods and materials: 256 patients referred for a portal-venous-phase CT were randomly allocated to one of four groups. Group 1 (n=64): 120kV; 0.521gI/kg. In group 2 (n=63), TV was reduced (90kV), whereas the dosing factor remained unaltered: 0.521gI/kg. In group 3 (n=63), TV was reduced by 20kV with a subsequent 20% reduction in dosing factor (e.g. 100kV; 0.415gI/kg). Group 4 (n=66): 30 kV decrease with a 30% CM reduction: 90kV; 0.365gI/kg. Objective image quality (IQ) was evaluated by measuring the attenuation in Hounsfield units (HU), signal-to-noise ratio (SNR), and contrast-to-noise ratio (CNR). Subjective IQ was assessed by using a 5-point Likert scale regarding overall IQ. Statistical analysis was performed using SPSS (IBM, version 24.0).
Results: Mean attenuation values in group 1, 3, and 4 were comparable: 118.2±10.0; 117.6±13.9; 117.3±21.6 (p>0.90). Attenuation in group 2 was significantly higher, 141.0±18.2, in comparison to all other groups (p=<0.01). Patients were divided into two weight categories: 80kg and >80kg. No significant difference in attenuation was found between weight categories. CNR was

significantly higher in group 2 compared to the other three groups (p=<0.01). No significant differences in subjective IQ were found (p=0.383).
Conclusion: The proposed 10-to-10 rule is an easy to reproduce method leading to homogeneous enhancement of the liver, regardless of BW and TV.
Limitations: This is a single-centre study.
Ethics committee approval: Approved by the local ethics committee. Registered on ClinicalTrials.gov (NCT03735706). Written informed consent was obtained from all 256 patients.
Funding: No funding was received for this work.
Author Disclosures:
B. Martens: Research/Grant Support at Institutional research grants from Bayer and Siemens
J. E. Wildberger: Research/Grant Support at Institutional grants: Agfa, Bard, Bayer, GE, Optimed, Philips, Siemens. Speaker's bureau: Bayer, Siemens.
B. M. F. Hendriks: Research/Grant Support at Institutional research grants from Bayer and Siemens
S. M. van Kuijk: nothing to disclose
N. H. G. M. Peters: nothing to disclose
C. Mihl: Research/Grant Support at Institutional research grants from Bayer and Siemens and personal fees (speakers' bureau) from Bayer.
J. de Vos-Geelen: nothing to disclose

RPS 1101-14 15:12
3D-segmentation of visceral and subcutaneous adipose tissue on CT: influence of contrast-medium and -phase
R. F. Gohmann, P. Seitz, B. Temiz, S. Gottschling, C. D. Krieghoff, C. Lücke, M. Gutberlet*; Leipzig/DE (robin.gohmann@gmx.de)*

Purpose: To analyse the influence of contrast-medium and phase on the segmentation of adipose tissue.
Methods and materials: Exams of 31 patients undergoing routine multi-phasic CT containing a native scan at identical kV were retrospectively included. In addition to the native scan (n=31), patients had received an arterial (n=23), portal-venous (n=10), and/or venous scan (n=31) after intravenous injection of 90 ml iodinated contrast-medium. The volume of adipose tissue was quantified semi-automatically with a threshold between -190HU and -30HU. Absolute volumes of visceral and subcutaneous compartments were recorded separately and the relative difference between the native scan and contrast-phases ($[Vol_{contrast\text{-}phase}\text{-}Vol_{native\text{-}scan}]/Vol_{native\text{-}scan}$) was computed.
Results: Segmented volume of adipose tissue for subgroups on native, arterial, portal-venous, and venous scans was 4,79±2,21, 4,86±2,21, 4,29±2,09, and 4,49±2,35 dm^3 in the visceral and 5,90±3,44, 6,02±3,64, 6,71±3,35, and 5,72±3,22 dm^3 in the subcutaneous compartment, respectively.
Relative difference of volumes within patients between native and arterial, portal-venous, and venous phase was -4,7±3,0%, -8,6±5,8%, and -9,6±9,7% for the visceral and -0,4±4,6%, -1,0±6,5%, and -2,6±8,1% for the subcutaneous compartment, respectively.
Total and visceral volumes were significantly different between native scans and all contrast-phases (p<0,001); no significant isolated differences were observed for the subcutaneous compartment.
Conclusion: Segmented volumes of adipose tissue on CT decrease after injection of contrast-medium. This decrease in volume is less pronounced in early contrast-phases (e.g. arterial) and mainly takes place in the visceral compartment. This fact must be considered when utilising contrast-enhanced CTs for risk-stratification or evaluation of therapy-response as frequently practised in oncology.
Limitations: This study was retrospective in design, including patients with different indications for CT and underlying diseases, which might have influenced the observed changes of segmented adipose tissue after contrast injection.
Ethics committee approval: This study was approved by the local ethics committee.
Funding: No funding was received for this work.
Author Disclosures:
R. F. Gohmann: nothing to disclose
P. Seitz: nothing to disclose
B. Temiz: nothing to disclose
S. Gottschling: nothing to disclose
C. D. Krieghoff: nothing to disclose
C. Lücke: nothing to disclose
M. Gutberlet: nothing to disclose

RPS 1101-15 15:18
Dynamic segmental CT liver perfusion data analysis after portosystemic shunt procedure in patients with liver cirrhosis
N. Djuraeva[1], F. Nazirov[1], A. Babadjanov[1], A. Amirkhamzaev[1], U. R. Salimov[2], N. Vakhidova[1], A. Sultanov[1]; [1]*Tashkent/UZ,* [2]*Ghandy/AF (nika.kt@rambler.ru)*

Purpose: To study the dynamics of parameters of the CT liver perfusion in patients with liver cirrhosis after portosystemic shunting.
Methods and materials: Study included 50 patients (average age 43±1.5 years). The control group consisted of 10 healthy volunteers of comparable age. All patients underwent volumetric low-dose liver perfusion with a tube rotation speed of 0.275 sec, the amount of contrast medium 40 ml, Kv 100/80, MA 200/150, and effective dose (E) 17±1,2 mSv.
Results: In the group with liver cirrhosis (LC), there was an increase in global and regional changes in hepatic perfusion towards an increase in hepatic arterial blood flow (BF) and a decrease in portal BF with a decrease in the hepatic perfusion index (HPI). After portosystemic shunting, there was a positive shift in the portal BF by 87,44±6,1 (mL/100 mL/min) and HPI improvement by 31,4 % (p<0.05). There was also a decrease in the width of the portal and splenic veins by 17.1% and 16.5% (p<0.05), respectively.
Segmental analysis of HPI showed that the most pronounced improvement in hepatic blood flow was observed in I, IV, VII, VIII segments (17.4%).
Conclusion: Low-dose CT liver perfusion revealed significant positive shifts (p<0.05) after portosystemic shunting of the HPI index, more pronounced in central segments in patients with LC, restoring the balance between hepatic and portal blood flow, and reducing the pressure in the portal and splenic veins.
Limitations: n/a
Ethics committee approval: n/a
Funding: No funding was received for this work.
Author Disclosures:
N. Djuraeva: Author at RSSPMCS named after acad. V.Vakhidov
F. Nazirov: Author at RSSPMCS named after acad. V.Vakhidov
U. R. Salimov: Author at RSSPMCS named after acad. V.Vakhidov
A. Amirkhamzaev: Speaker at RSSPMCS named after acad. V.Vakhidov
A. Babadjanov: Author at RSSPMCS named after acad. V.Vakhidov
N. Vakhidova: Author at RSSPMCS named after acad. V.Vakhidov
A. Sultanov: Author at RSSPMCS named after acad. V.Vakhidov

14:00 - 15:30 **Room M 5**

Musculoskeletal

RPS 1110

Knee

Moderators:
Ž. Snoj; Ljubljana/SI
P. Van Dyck; Edegem/BE

RPS 1110-K 14:00
Keynote Lecture
S. Cappabianca*; Naples/IT (salvatore.cappabianca@unicampania.it)*

Author Disclosures:
S. Cappabianca: Speaker at Università della Campania L. Vanvitelli

RPS 1110-1 14:10
The importance of being minocycline chlorhydrate. Sclerosant acting antibiotic versus corticosteroids to treat symptomatic Baker cysts: a prospective study
I. Percivale[1], A. Paladini[1], M. Spinetta[1], A. Borzelli[2], F. Pane[2], D. Negroni[1], M. Cernigliaro[1], A. Carriero[1], G. Guzzardi[1]; [1]*Novara/IT,* [2]*Naples/IT (ilaperci@gmail.com)*

Purpose: A prospective study about the efficiency and safety on the use of a sclerosant antibiotic (minocycline chlorhydrate) versus steroids (triamcinolone acetonide) to treat patients with symptomatic Baker cysts.
Methods and materials: We prospectively enrolled 66 patients, randomised into two cohorts; cyst drainage followed by antibiotic injection and cyst drainage followed by steroids injection. 58 patients underwent 6 month clinical and radiologic follow-up. The primary end-point was a volume reduction of more than 40% with respect to the cyst native volume. Secondary end-points were duration, pain reduction (VAS), and cyst permanence (volume reduction less than 40%).
Results: The primary end-point has been reached in the 66.7 % of patients treated with antibiotics (mean volume reduction: 54%) and in the 35.7% of patients treated with steroids (mean volume reduction: 69%). Cyst permanence was seen in the 65% of cases treated with steroids and in the 34% of cases treated with antibiotics. We achieved a mean pain reduction (VAS) of 3.2 points. The procedural duration was higher in patients treated with antibiotics (15.5 min) compared to corticosteroids (8.6 min).
Conclusion: Both treatments are safe (no major or minor adverse events) but antibiotic injection is more efficient considering the primary end-point. Despite

an increased procedural time, patients with antibiotic treatment have a lower rate of cyst permanence.
Limitations: The limited number of patients and short follow-up.
Ethics committee approval: n/a
Funding: No funding was received for this work.
Author Disclosures:
I. Percivale: nothing to disclose
A. Paladini: nothing to disclose
M. Spinetta: nothing to disclose
A. Borzelli: nothing to disclose
F. Pane: nothing to disclose
D. Negroni: nothing to disclose
M. Cernigliaro: nothing to disclose
A. Carriero: nothing to disclose
G. Guzzardi: nothing to disclose

RPS 1110-2 14:16
The correlation between the anatomical variations of the knee joint and fat-pad pathologies and patellar tilt
A. H. Çilengir, Y. K. K. Çetinoğlu, M. F. Gelal, B. Dirim Mete, F. Elmalı, C. Kazimoglu, Ö. Tosun*; Izmir/TR (acilengir@gmail.com)*

Purpose: The correlation between patellar tilt, oedema in the superolateral portion of the infrapatellar fat pad, and chondromalacia was described in the literature. However, there is not enough information about other variations that may cause knee joint pathologies. A correlation with quadriceps patellar tendon angle (QPA) was not described. Our aim was to describe the correlation between knee joint variations and analyse accompanying fat-pad, cartilage, and tendon pathologies.
Methods and materials: A retrospective analysis of age, gender, side, femoral sulcus angle (SA), tibial tubercule-trochlear groove distance (TTTG), patellar tendon length (PTL), patellar height (PH), Insall-Salvati ratio (ISR), lateral trochlear inclination angle (LTI), trochlear facet asymmetry (TFA), trochlear depth (TD), trochlear dysplasia (TDis), suprapatellar-infrapatellar-prefemoral fat-pad oedema (SPE-IPE-PFE), suprapatellar effusion (SE), patellar and femoral chondromalacia (PC and FC), and quadriceps and patellar tendinopathy (QT and PT) on 406 knee MRIs with patellar tilt (PTi) was performed. The relationship between PTi, QPA, and other parameters were evaluated. 40 knee MRIs without PTi were selected as a control group.
Results: The presence of SPE-IPE-PFE, SE, PC, and FC was more frequent in the PTi group; SA, TT-TG, PTL, ISR, LTI, TFA, and TD values were significantly different between the two groups. The distribution of PTi was significantly related to TDis, PC, QT, SA, TT-TG, LTI, and TD in the PTi group. The distribution of QPA was significantly associated with TDis, IPE, PFE, QT, SA, and LTI in the PTi group. We calculated 10 degrees of PTi as a cut-off value for a superolateral portion of the infrapatellar fat-pad oedema.
Conclusion: Many anatomical variations of the knee joint, including QPA, are associated with fat-pad, cartilage, and tendon pathologies.
Limitations: The restrospective design.
Ethics committee approval: This study has approval from an institutional review board.
Funding: No funding was received for this work.
Author Disclosures:
A. H. Çilengir: nothing to disclose
Y. K. K. Çetinoğlu: nothing to disclose
M. F. Gelal: nothing to disclose
B. Dirim Mete: nothing to disclose
F. Elmalı: nothing to disclose
C. Kazimoglu: nothing to disclose
Ö. Tosun: nothing to disclose

RPS 1110-3 14:22
The assessment of medial meniscus extrusion on ultrasound using MRI as a reference standard
R. A. Zeitoun[1], H. Hossam El-Din[1], N. Eesa[1], S. F. Ismail[2]; *[1]Cairo/EG, [2]Giza/EG (raniazeitoun@gmail.com)*

Purpose: To assess medial meniscus extrusion using US on supine and standing (weight-bearing) positions as a sign of the presence of underlying meniscal tears. The study was done using MRI as a reference standard for the detection of tears.
Methods and materials: This observational analytic prospective study included 103 patients (48 females and 55 males), aged between 18-70 years. The US measured values of the medial meniscal extrusion on supine and standing positions were correlated to the MRI diagnosis of tears. The included patients were classified into two groups according to the presence or abscence of meniscal tears on MRI. Statistical analysis was performed for the obtained measurements for both groups and P<0.05 was considered significant. ROC curve was done to reach a cut-off value for extrusion as a sign of medial meniscus tear.
Results: 45 patients (43.68%) had medial meniscal tears (horizontal, vertical, branching, radial, root, and bucket-handle tears). The measured extrusion on supine and standing positions, as well as the difference between them in the two groups, all showed a significant P=0.001. The extrusion on standing position with a cutoff value of >3.3 mm showed a specificity (96.55%), positive predictive value (93.8%), and accuracy (83.5%) for the detection of a medial meniscus tear.
Conclusion: Measuring medial meniscus extrusion using ultrasonography, especially in a standing position, is a good sign to predict tears.
Limitations: The sample size and the number of patients with different subtypes of tears were not large enough for a powerful conclusion to correlate the value of extrusion and the subtype of tear.
Ethics committee approval: The study has been approved by the Ethical Committee of Faculty of Medicine, Cairo University, in compliance with the Helsinki declaration.
Funding: No funding was received for this work.
Author Disclosures:
R. A. Zeitoun: nothing to disclose
H. Hossam El-Din: nothing to disclose
S. F. Ismail: nothing to disclose
N. Eesa: nothing to disclose

RPS 1110-4 14:28
Evaluation of medial meniscal extrusion using weight-bearing ultrasound: correlation with MRI and meniscal tears
A. L. Falkowski[1], J. A. Jacobson[1], M. Cresswell[2], A. Bedi[1], V. Kalia[1]; *[1]Ann Arbor, MI/US, [2]Vancouver, BC/CA*

Purpose: To compare medial meniscal extrusion as seen on weight-bearing ultrasound compared with MRI and meniscal tears.
Methods and materials: Patients obtaining a routine knee MRI were prospectively evaluated with supine and weight-bearing ultrasound (US) of the medial meniscus. The position of the outer boundary of the medial meniscus on US images and MRI was measured relative to the tibia by a fellowship-trained musculoskeletal radiologist. A correlation was made to the presence or absence of a meniscal tear and statistical significance was calculated via a Student t-test.
Results: 50 knees from 49 subjects (23 male, 26 female; mean age 44±15 years) were included (18 right, 32 left; one bilateral). The mean medial meniscal extrusion on supine US was 1.3 mm (range -1.5-3.6 mm), with no significant difference compared with MRI (p=0.21), which increased to 2.1 mm on weight-bearing US. In the 38% (19/50) of subjects with meniscal tears on MRI, the mean medial meniscal extrusion on weight-bearing US was 2.13 mm (range 0-4.4 mm) with a change between supine and weight-bearing of 0.63 mm (range -1.8-2.7 mm). In the 62% (31/50) of subjects with no meniscal tear, the mean medial meniscal extrusion on weight-bearing US was 2.05 mm (range 0-3.8 mm) with a change between supine and weight-bearing of 0.87 mm (range -0.1-2.2 mm) and no significant difference between subjects with and without tear (p=0.805 and p=0.413).
Conclusion: Supine US was comparable with supine MRI for the assessment of medial meniscal extrusion. The presence of a meniscal tear did not result in increased medial meniscal extrusion on weight-bearing US compared with no meniscal tear.
Limitations: The reading of the images was performed by one reader.
Ethics committee approval: IRB-approved study with informed consent.
Funding: No funding was received for this work.
Author Disclosures:
A. L. Falkowski: nothing to disclose
J. A. Jacobson: nothing to disclose
M. Cresswell: nothing to disclose
A. Bedi: nothing to disclose
V. Kalia: nothing to disclose

RPS 1110-5 14:34
Agreement between cartilage morphology on MRI and weight-bearing CT and radiographs respectively for visualising patellofemoral OA features in the MOST study
N. Segal[1], B. Everist[1], K. Brown[1], J. He[1], J. Lynch[2], M. Nevitt[2]; *[1]Kansas City, KS/US, [2]San Francisco, CA/US (segal-research@kumc.edu)*

Purpose: The patellofemoral joint is frequently affected by osteoarthritis (PFOA) and is incompletely imaged on radiographs. Weight-bearing CT (WBCT) could offer advantages for visualisation. This study determined the agreement between the detection of cartilage damage on MRI and PFOA on WBCT and radiographs.
Methods and materials: The right knees of 60 people who did not have findings of PFOA at a prior clinic visit were randomly selected. WBCT and radiographs were read for an OARSI JSN score (0=none, 1=minimal, 2=moderate, and 3=total joint-space loss), and MRI was read for a MOAKS cartilage score (size and % of full-thickness) by 2 musculoskeletal radiologists, each with more than

10 years experience, who were blinded to the subject. Weighted kappa coefficients were calculated for agreement between modalities. Inter-reader reliability was assessed with weighted kappa statistics.
Results: The mean±SD age and BMI for the 60 participants (66.7% women) were 67.6±9.8 years and 30.0±5.3 kg/m2, respectively. There was a fair-to-moderate agreement between PFOA findings on WBCT and semi-quantitative scores of PF cartilage on MRI, while an agreement was none-to-slight between radiographic PFOA readings and MRI readings. Inter-rater reliability for the WBCT JSW {kappa=0.60 (0.48, 0.72)} and MRI MOAKS-CM {kappa=0.70 (0.61, 0.79)} readings were good.
Conclusion: PFOA scoring on WBCT agrees with MRI substantially better than does scoring on XR. At the same relative radiation level as radiographs (<0.10 mSv), WBCT imaging holds the potential to improve understanding of the weight-bearing patellofemoral joints beyond what is possible with radiographs.
Limitations: Radiologists were provided with written instructions, but no in-person training in the scoring systems used and no consensus readings were completed, potentially attenuating inter-rater agreement.
Ethics committee approval: Following an IRB-approved informed consent process, all participants provided written informed consent.
Funding: NIH R01AR071648, U01AG18832, and U01AG19069.
Author Disclosures:
N. Segal: Equipment Support Recipient at CurveBeam, LLC, Research/Grant Support at Flexion Therapeutics, Research/Grant Support at Pacira CryoHealth
B. Everist: nothing to disclose
K. Brown: nothing to disclose
J. He: nothing to disclose
J. Lynch: Consultant at Boston Imaging Core Labs (BICL)
M. Nevitt: nothing to disclose

RPS 1110-6 14:40
The efficacy of the anterior translation of the tibia in anterior cruciate ligament mucoid degeneration: an observational study
A. I. Saad, D. Waldron, A. Iqbal, S. Evans, S. L. James, R. Botchu*; Birmingham/UK (aisaad@hotmail.co.uk)*

Purpose: Mucoid degeneration (MD) of the ACL is a well-known pathological entity diagnosed on MRI. However, it can be confused with complete or partial tears of the ACL. Radiologists focus on the posterior femoral translation as a reliable secondary sign.
We encountered several patients with MD of the ACL who have a posterior translation exceeding 5 mm with an intact ACL. We investigated the likely cause of this with the means to abolish confusion and misdiagnosis of ACL tears.
Methods and materials: A retrospective search of our department's radiology system for knee MR imaging over 10 years. All patients had MD within the substance of the ACL and an intact ACL. We evaluated the measurement of the degree of posterior translation of the femur (PTF) in relation to the tibia. The data was categorised according to the length of the PTF (PTFM).
Results: We identified 464 consecutive cases with MD. The mean age was 52 years. There was a male predominance of 261 to 203 females. The average PTFM was 2.4 mm with a range of 0-20 mm. 85.6% of patients had a PTFM of <5 mm. 205 patients had no PTF. 192 cases had a PTFM range between 1-5 mm.
14.4% of patients had a PTFM >5 mm. Of them, 32.8% had a PTFM of 6 mm, 53.7% had a PTFM range between 7-9 mm, with the remaining 13.4% >9 mm.
Conclusion: It is essential to look for other secondary signs of ACL tears and not only focus on the PTFL and correlate this with clinical findings.
Limitations: This study was retrospective and no arthroscopic correlation has been assessed, as the diagnosis of MD was solely a radiological diagnosis.
Ethics committee approval: n/a
Funding: No funding was received for this work.
Author Disclosures:
A. I. Saad: nothing to disclose
D. Waldron: nothing to disclose
A. Iqbal: nothing to disclose
S. Evans: nothing to disclose
S. L. James: nothing to disclose
R. Botchu: nothing to disclose

RPS 1110-7 14:46
Attachment type of the posterior meniscofemoral ligament and clinical significance
H. J. Park, S. Ham*; Seoul/KR (sooyoun.ham@samsung.com)*

Purpose: To investigate the correlation between the attachment type of the posterior meniscofemoral ligament (pMFL) and the incidence of lateral meniscal tears.
Methods and materials: We retrospectively evaluated 191 patients who underwent knee MRIs. We assessed the attachment type of the pMFL (high vs low) and measured the thickness of the pMFL. Then we evaluated the presence of a meniscal tear or discoid meniscus. We assessed if there was a significant relationship between the mean thickness of the pMFL and the incidence of meniscal tears or a discoid meniscus according to the type of pMFL using independent t-tests. We also assessed the significance of the relationship between the mean thickness of the pMFL and the presence or absence of a meniscal tear or discoid meniscus using Pearson's Chi-square test.
Results: High type pMFLs were significantly thicker than low type pMFLs ($p<0.001$). There was no significant difference in the incidence of meniscal tears according to the type of pMFL. There was also no significant difference in pMFL thickness between patients with meniscal tears and those without meniscal tears.
Conclusion: High type pMFLs tend to be thicker than low type pMFLs, but the thickness is irrelevant to the incidence of meniscus injury.
Limitations: We could not completely exclude the possibility of selection bias and confounding factors because this was a retrospective study. We only included symptomatic patients who had knee MRI data, which could also contribute to a selection bias. We did not correlate pMFL results to the clinical outcomes.
Ethics committee approval: n/a
Funding: No funding was received for this work.
Author Disclosures:
H. J. Park: Author at Kangbuk Samsung hospital
S. Ham: nothing to disclose

RPS 1110-8 14:52
Chondrocalcinosis is associated with increased knee joint degeneration over 4 years: data from the osteoarthritis initiative
S. Foreman[1], A. S. Gersing[1], C. von Schacky[1], G. Joseph[2], J. Neumann[1], N. E. Lane[3], C. McCulloch[2], M. Nevitt[2], T. M. M. Link[2]; *[1]Munich/DE, [2]San Francisco, CA/US, [3]Sacramento, CA/US*

Purpose: To determine if the presence of calcium-containing crystals (CaC) is associated with increased knee joint degeneration over 4 years and to assess if the total number of CaCs deposited is a useful measure of disease burden.
Methods and materials: 70 subjects with CaCs in right knees at baseline were selected from the osteoarthritis initiative and matched to 70 subjects without evidence of CaCs. T1-weighted gradient-echo sequences were used to confirm the presence of CaCs and count the numbers of distinct circumscribed CaCs. Morphological abnormalities were assessed at baseline and 4-year follow-ups using the modified semi-quantitative whole-organ magnetic resonance imaging score (WORMS). Linear regression models were used to analyse the associations between the presence of CaCs at baseline and changes in WORMS and to analyse the associations between the numbers of circumscribed CaCs at baseline and changes in WORMS.
Results: Presence of CaCs was associated with increased cartilage degeneration in the patella (coefficient: 0.33; 95% confidence interval (CI): 0.04-0.63), the medial femur (coefficient: 0.51; 95% CI: 0.18-0.83), the lateral tibia (coefficient: 0.36; 95% CI: 0.01-0.71), and the medial and lateral meniscus (coefficient: 0.38; 95% CI: 0.00-0.75 and coefficient: 0.72; 95% CI: 0.12-1.32). Knees with higher numbers of CaCs had increased cartilage degeneration in the patella and medial femur (coefficient: 0.09; 95% CI: 0.05-0.14; $p<0.001$ and coefficient: 0.08; 95% CI: 0.02-0.14; $p=0.005$).
Conclusion: CaCs were associated with increased cartilage and meniscus degeneration over a period of 4 years. Assessing the number of CaC depositions may be useful to evaluate the risk of onset and worsening of degenerative disease.
Limitations: No synovial fluid was available for analysis.
Ethics committee approval: IRB approval (all centres).
Funding: NIAMS-R01AR064771.
Author Disclosures:
S. Foreman: nothing to disclose
A. S. Gersing: nothing to disclose
C. von Schacky: nothing to disclose
G. Joseph: nothing to disclose
J. Neumann: nothing to disclose
N. E. Lane: nothing to disclose
C. McCulloch: nothing to disclose
M. Nevitt: nothing to disclose
T. M. M. Link: nothing to disclose

RPS 1110-9 14:58

Quantitative analysis of knee joint cartilage by using T2* and T1rho relaxation times in professional female volleyball players and a healthy control group

K.-J. J. Maas[1], F. O. Henes[1], M. Regier[2], M. L. Warncke[3], M. Kaul[1], G. Schön[1], G. Adam[1], C. Behzadi[1]; *[1]Hamburg/DE, [2]Munich/DE, [3]Hamburg, HAMBURG/DE (k.maas@uke.de)*

Purpose: To analyse the effects of repetitive physical activity on T2* as well as T1rho relation time measurements of knee joint cartilage in professional female volleyball players and healthy controls.
Methods and materials: 24 professional female volleyball players (mean age: 25.5 years±3.6; BMI 21.1±1.3) and 24 female individuals (mean age: 27.5 years±2.9; BMI 21.3±1.9) underwent MRI including two separate quantitative techniques (T2* and T1rho) at 3T. 11 segments for medial and lateral knee compartments were defined and in each segment a horizontal segmentation into a deep and a superficial layer was performed. Arithmetic means from relaxation times were computed. Due to the cluster structure of the data, a random intercept model was estimated, if necessary.
Results: For female volleyball players, mean relaxation times were noted with 27.1 ms (CI: 26.7-27.5 ms) for T2* and 46.4 ms (CI: 45.8-47 ms) for T1rho. For the healthy control group, mean relaxation times were calculated with 23.5 ms (CI: 23.1-23.9 ms) for T2* and 41.5 ms (CI: 40.9-42.1 ms) for T1rho. T2* as well as T1rho relaxation times were generally prolonged in female volleyball players in comparison to healthy individuals. Significantly differences comparing T2* relaxation times were detected in 11 deep and 16 superficial cartilage layers, as well as 9 deep and 22 superficial layers for T1rho.
Conclusion: There is a tendency towards prolonged T2* and T1rho relaxation times in knee joint cartilage of professional female volleyball players compared to controls. For both imaging markers, more distinct results were detected for the superficial cartilage layer. These findings might be considered as initial stages of osteoarthritis in physically active female individuals.
Limitations: The population size.
Ethics committee approval: n/a
Funding: No funding was received for this work.
Author Disclosures:
K.-J. J. Maas: nothing to disclose
F. O. Henes: nothing to disclose
M. Regier: nothing to disclose
M. L. Warncke: nothing to disclose
M. Kaul: nothing to disclose
G. Schön: nothing to disclose
G. Adam: nothing to disclose
C. Behzadi: nothing to disclose

RPS 1110-10 15:04

Assessment of patellofemoral maltracking using 3.0T kinematic MRI

K.-J. J. Maas, J. Frings, M. L. Warncke, T. Dust, K.-H. Frosch, G. Adam, F. O. Henes; *Hamburg/DE (k.maas@uke.de)*

Purpose: Patellar maltracking is routinely described with subjective clinical tests, but until now remains challenging to be assessed objectively and standardised with a reproducible measurement technique. Kinematic MRI allows dynamic assessment of the patellofemoral joint with real-time muscle contraction. We aimed to implement kinematic MRI as a standardised and objective measurement technique to quantify patellar maltracking.
Methods and materials: 10 knees of patients with clinical patellar maltracking and 10 knees of healthy volunteers were evaluated. All participants underwent knee MRI at 3T in real-time by a radial 2-dimensional GRE sequence in sagittal and axial orientation at the patellar level through a range of flexion-extension (approximately 0-50°). Lateral maltracking as well as the patella tilt were measured. Maltracking was defined as the "delta" of the isometric centre of the patellar at the maximum point of flexion and extension compared to the perpendicular line from the posterior margins of the femoral condyles drawn through the centre of the trochlear sulcus.
Results: Lateral maltracking, as well as patella tilt, was significantly higher in symptomatic patients (maltracking mean: 1.03±0.55 mm, patella tilt mean: 21.8±10.58°) than in the volunteer group (maltracking mean: 0.13±0.11 mm, patella tilt mean: 3.8±2.78°) with p=0.0001. There was no lateral tracking within healthy volunteers greater than 27 mm. Lateralisation within symptomatic patients ranged from 0.54 to 2.64 mm. Lateral maltracking significantly correlated with increased patella tilt with r=0.9358 (p<0.0001).
Conclusion: Dynamic radial 2-dimensional GRE sequence allows exact dynamic assessment of patellar maltracking in symptomatic patients, providing kinematic MRI as a standardised and objective measurement technique.
Limitations: The size of the population included in this study.
Ethics committee approval: Ethics committee approval obtained.
Funding: No funding was received for this work.
Author Disclosures:
K.-J. J. Maas: nothing to disclose
M. L. Warncke: nothing to disclose
J. Frings: nothing to disclose
T. Dust: nothing to disclose
K.-H. Frosch: nothing to disclose
G. Adam: nothing to disclose
F. O. Henes: nothing to disclose

RPS 1110-11 15:10

Distal femoral cortical irregularity (DFCI): increased prevalence in competitive young alpine skiers

C. Stern, J. Galley, S. Fröhlich, L. Peterhans, J. Spörri, R. Sutter; *Zurich/CH (christoph.stern@gmx.de)*

Purpose: Tumour-like cortical irregularities at the posterior distal femur are common incidental findings in adolescents, but their origin is still debated. The purpose was to investigate the prevalence of irregularities at the tendinous attachment of the medial/lateral head of the gastrocnemius (MHG/LHG) and of the adductor magnus (AM) muscle in competitive young alpine skiers compared to young adults of the same age.
Methods and materials: Knee MRI examinations of 105 competitive young alpine skiers (age 13-16 years) and a control group (matched for gender, age, and extremity) of 105 adolescent patients were evaluated by two radiologists for the presence of cortical lesions at the femoral attachment site of the MHG, LHG, and AM tendon. Lesion diameters were measured on sagittal fat-suppressed MR images. Statistical analysis included Person's Chi-square, Student's t-test, and kappa statistics.
Results: Cortical lesions were found in 58.1% of competitive alpine skiers (61/105) compared to 26.7% in the control group (28/105)(p<0.001). In 2 skiers, more than one lesion per individual was found versus none for the control. Lesion distribution for competitive athletes and the control group were 60/63 (95%) and 26/28 (93%) lesions at the MHG, 3/63 (5%) and 1/28 (3.5%) at the LHG, and 0/63 (0%) and 1/28 (3.5%) at the AM attachment site, respectively. Inter-reader agreement was almost perfect (k=0.87). No substantial difference was observed for the average size of MHG lesions in athletes (3.7 mm) versus the control group (3.4 mm) (p=0.321).
Conclusion: A cortical irregularity of the distal femur at the tendon attachment sites is a frequent incidental finding on MRI, with a significantly increased prevalence in competitive young alpine skiers, supporting the theory of a stress-related origin. These irregularities should not be mistaken for malignancy.
Limitations: A retrospective control group.
Ethics committee approval: Ethics committee approval obtained.
Funding: No funding was received for this work.
Author Disclosures:
C. Stern: nothing to disclose
L. Peterhans: nothing to disclose
R. Sutter: nothing to disclose
J. Galley: nothing to disclose
S. Fröhlich: nothing to disclose
J. Spörri: nothing to disclose

RPS 1110-12 15:16

Volume and quantitative dynamic contrast-enhanced MR blood perfusion parameters of the infrapatellar fat-pad and their relationship with oedema and effusion in patients with patellofemoral pain

R. van der Heijden, B. A. de Vries, D. Poot, M. van Middelkoop, G. P. Krestin, E. Oei; *Rotterdam/NL (r.a.vanderheijden@erasmusmc.nl)*

Purpose: The infrapatellar fat-pad (IPFP) is implied as a source of pain in knee osteoarthritis (OA) and patellofemoral pain (PFP), a supposed precursor of OA. Inflammation or increased IPFP volume may have causative effects. The aim of this study was to quantitatively evaluate dynamic contrast-enhanced (DCE) MRI parameters as a surrogate measure of inflammation and volume of the IPFP, and explore their relationship with IPFP oedema and joint effusion in PFP patients.
Methods and materials: PFP patients and healthy control subjects underwent 3T MRI comprising non-fat saturated FSPGR and DCE-MRI. Motion was corrected by image registration. The IPFP was delineated on the FSPGR sequence using Horos software. Volume was calculated and quantitative perfusion parameters (Ktrans, Kep, Ve, and Vp) were extracted by fitting the extended Tofts' pharmacokinetic model. Differences in volume and DCE-MRI parameters between patients and controls were tested by linear regression analyses adjusted for confounders of sex, age, BMI, and sports participation. The same applied to IPFP oedema and effusion.
Results: 43 controls and 35 PFP patients were included. Volume and perfusion parameters were not statistically significantly different between groups. Knees with effusion showed a higher perfusion of the IPFP.
Conclusion: The IPFP has been implied as a possible source of knee pain, but its blood perfusion as a surrogate measure of inflammation and volume do not seem to play a role in patellofemoral pain. PFP patients with effusion showed higher perfusion, indicating inflammation, in contrast to controls.

Limitations: Due to the large intersubject variability, small differences in perfusion or volume could have been undetected. But given the small effect sizes, these would not be clinically relevant.
Ethics committee approval: Approved by the institutional review board and written informed consent obtained.
Funding: Partly funded by ESSR, RSNA, Erasmus University, and Dutch Artritis Foundation.
Author Disclosures:
B. A. de Vries: nothing to disclose
E. Oei: nothing to disclose
G. P. Krestin: nothing to disclose
D. Poot: nothing to disclose
R. van der Heijden: nothing to disclose
M. van Middelkoop: nothing to disclose

RPS 1110-13 15:22
Collective intelligence has increased diagnostic performance compared to expert radiologists in the evaluation of knee MRI
A. Campagner, C. Messina, D. Albano, S. Gitto, F. Cabitza, L. M. M. Sconfienza*; Milan/IT (carmelomessina.md@gmail.com)*

Purpose: As is widely known, the traditional diagnostic approach, which involves a single physician, can result in worrying error rates. Collective intelligence has recently been considered as a possible strategy to pool individual physicians' diagnoses and reduce misdiagnosis. Our aim is to present an investigation about the accuracy of these techniques on a real-world experiment of MR assessment.
Methods and materials: We asked 13 radiologists from a tertiary orthopaedic institution to identify abnormal exams among 417 knee MR images from the Standford MRNet dataset1 (which is a low-resolution imaging dataset used to train machine-learning predictive models). Radiologists were also asked to assess their confidence on their decisions and the perceived complexity of each case. We assessed each radiologist's accuracy in comparison with the accuracy rates obtained by leveraging collective intelligence techniques.
Results: The radiologists' panel obtained an average accuracy of 0.82-0.01 (95% confidence interval). Taking the majority annotation for each exam as the gold standard, we obtained an accuracy of 0.86. Weighing the annotations of the radiologists' by their confidence resulted in an accuracy of 0.87; considering only the most accurate raters, or selecting the most surprisingly popular annotation, we obtained an accuracy of 0.88, in either case. All collective intelligence techniques increased diagnostic accuracy in the cases for which the radiologists exhibited a greater misdiagnoses rate, on low-confidence and high-complexity cases.
Conclusion: Collective intelligence techniques were associated with increased diagnostic accuracy compared with the average of the individual radiologists and the most accurate ones. These promising results suggest that these techniques merit further consideration for applications in the ground-truthing of machine-learning models and, potentially, in clinical settings to reduce diagnostic error.
Limitations: n/a
Ethics committee approval: n/a
Funding: No funding was received for this work.
Author Disclosures:
C. Messina: Grant Recipient at Abiogen, Bracco, IBSA
D. Albano: nothing to disclose
L. M. M. Sconfienza: Grant Recipient at Abiogen, Bracco, Fidia
F. Cabitza: nothing to disclose
S. Gitto: nothing to disclose
A. Campagner: nothing to disclose

16:00 - 17:30 **Coffee & Talk 2**

Artificial Intelligence and Machine Learning

RPS 1205

Artificial intelligence and machine learning for x-ray imaging

Moderators:
L. Cornelissen; Groningen/NL
Y. Kovalenko; Kiev/UA

RPS 1205-1 16:00
Are pixel-level annotations necessary? Evaluation of their importance in detecting abnormalities in chest x-rays
T. R. Nimmada, P. Putha, M. Tadepalli, B. Reddy, A. M. Jagirdar, P. Rao, P. Warier*; Mumbai/IN (tarun.raj@qure.ai)*

Purpose: Pixel-level annotations are commonly used to segment and localise abnormalities in chest x-rays (CXRs), but they can also be used to improve the performance of classification models. In this study, we analyse the performance of models trained with and without pixel-level supervision to detect pulmonary consolidation in chest x-rays.
Methods and materials: A dataset of 2.5 million chest x-rays (D) along with their radiologist reports were used for this experiment. Labels were extracted using natural language processing techniques from reports. Pixel-level annotations were obtained for 5,000 consolidation positive cases with the help of 5 radiologists. Three training subsets were created: D1) 1 million CXRs (20,000 consolidation positives) sampled randomly from D without any pixel-level annotations, D2) 100,000 CXRs (5,000 consolidation positives) sampled randomly from D1 without pixel-level annotations, D3) D2 with pixel-level annotations. Classification models were trained using deep learning on D1 (M1) and D2 (M2) with labels extracted from reports. Models were trained on D3 (M3) using a hybrid of labels and annotations. An independent test set of 50,000 CXRs was used to assess the performance of M1, M2, and M3.
Results: The area under the receiver operating characteristic was used to compare the performance of models. AUC of M1, M2, and M3 were observed to be 0.90, 0.85, and 0.87 respectively. AUC of M3 is higher than that of M2 but lesser than M1.
Conclusion: While models trained with pixel-level supervision performed better than those without it, models trained on more labelled data showed the best performance. The influx of more labelled data into training improved the performance of more than pixel-level annotations.
Limitations: This method should be further evaluated on more abnormalities.
Ethics committee approval: n/a
Funding: No funding was received for this work.
Author Disclosures:
T. R. Nimmada: Employee at Qure.ai technologies pvt ltd
P. Putha: Employee at Qure.ai technologies pvt ltd
M. Tadepalli: Employee at Qure.ai technologies pvt ltd
B. Reddy: Employee at Qure.ai technologies pvt ltd
A. M. Jagirdar: Employee at Qure.ai technologies pvt ltd
P. Rao: Employee at Qure.ai technologies pvt ltd
P. Warier: CEO at Qure.ai technologies pvt ltd

RPS 1205-2 16:06
Sensitivity to user input in deep learning-based vertebral segmentation from lateral cervical spine x-rays
J. Spencer[1], J. Tabak[1], J. R. Meakin[1], G. Slabaugh[2], S. M. M. R. Al Arif[3], K. Knapp[1]; *[1]Exeter/UK, [2]London/UK, [3]Veldhoven/NL (K.M.Knapp@exeter.ac.uk)*

Purpose: Cervical spine injuries (CSIs) occur in approximately 4.3% of trauma patients in the UK. We investigate the sensitivity to user input on computer-aided detection software (CAD) designed to aid clinicians with CSI diagnosis.
Methods and materials: We collected 137 lateral cervical spine radiographs. Injury diagnosis is dependent on the results of a deep learning segmentation algorithm, which requires vertebrae centres as input. The data was expertly-annotated to define ground truth outlines of the C3–C7 vertebrae.
We used the Unet architecture with a modified loss function to account for vertebrae shape, training the network using 124 images. We defined a 'true centre' for each of the 13 test images and randomly varied the input centres from this point, measuring the resulting effect on segmentation performance.

Results: Segmentation accuracy relates to the ground truth outline. Consistency relates to the result using the 'true centre' as input (both using Jaccard index). With 100 pseudo-random variations of the input centres for 13 test images, with a mean accuracy of 0.85 and consistency of 0.92. With 'radius around true centre: percentage of tests, mean consistency, mean accuracy' we have '<=1 mm: 34%, 0.97, 0.88', '(1-2) mm: 26%, 0.94, 0.87', '(2-3) mm: 15%, 0.90, 0.85', '(3-4) mm: 8%, 0.85, 0.82'. We observed a crucial drop-off in performance outside a 2 mm radius of the true centres.
Conclusion: Sensitivity to user input is vital in assessing the role of CAD in the clinical pathway for CSIs. The results indicate that guidance for user selection should be to target within 2 mm of the vertebrae centre and clinician training should account for this.
Limitations: This is a develomental version of CSPINECAD.
Ethics committee approval: University of Exeter Ethics Committee approval.
Funding: Funded by the EPSRC and Wellcome Trust.
Author Disclosures:
K. Knapp: Grant Recipient at Wellcome, Speaker at ECR
J. Spencer: Grant Recipient at Wellcome
J. Tabak: Grant Recipient at Wellcome
J. R. Meakin: Grant Recipient at Wellcome
G. Slabaugh: Grant Recipient at EPSRC
S. M. M. R. Al Arif: nothing to disclose

RPS 1205-3 16:12
Is a deep learning algorithm equivalent to the radiologist in fracture detection on conventional x-rays?
G. H. Reichert[1], E. Zerbib-Attal[2], B. A. Naipeanu[1], A. Altar[1], M. Fontaine[1], R. Radjabaly[1], A. Bellamine[1], N. Javaud[1], N. Siauve[1]; *[1]Colombes/FR, [2]Paris/FR (guillaumereichert@hotmail.fr)*

Purpose: The increasing need for emergency imaging has led to a multiplication of conventional x-rays, especially in traumatic injury. At the same time, artificial intelligence (AI) programs are in development and deep learning algorithms could help the radiologist and the emergency room (ER) to screen for patients with fractures.
To determine the accuracy of a deep learning algorithm for the detection of fractures on conventional x-rays in ER patients.
Methods and materials: We use an algorithm (Rayvolve®) developed by Azmed® for fracture detection in the appendicular skeleton. The study was divided into 2 steps.
In step 1, 2,000 X-rays were selected from the ER of our hospital as the training population and were annotated for the status of fracture or not fractured, to train the algorithm.
In step 2, 126 patients were randomly selected by an emergency doctor as a test set. These x-rays were extracted and annotated by both a radiologist and the algorithm. The results of the algorithm were compared to those of the radiologist.
Results: In step 1, about 15% of the patients had a fracture.
In step 2, 26 x-rays with fractures were identified. Only 21/26 fractures were detected by the algorithm, which makes a sensitivity rate of 80.7%. Among the 100 patients with no fracture, 35/100 patients were annotated by the algorithm as fractured, which makes a sensibility rate of 35%. The positive predictive value was 37.5% and the negative predictive value was 92.9%.
Conclusion: This study shows that an algorithm like Rayvolve® could be a valuable computer-aided diagnostic tool for detecting fractures in ER. However, more fractures have to be annotated to improve the accuracy of the algorithm.
Limitations: n/a
Ethics committee approval: n/a
Funding: No funding was received for this work.
Author Disclosures:
G. H. Reichert: nothing to disclose
E. Zerbib-Attal: CEO at Azmed
B. A. Naipeanu: nothing to disclose
A. Altar: nothing to disclose
M. Fontaine: nothing to disclose
R. Radjabaly: nothing to disclose
A. Bellamine: nothing to disclose
N. Javaud: nothing to disclose
N. Siauve: nothing to disclose

RPS 1205-5 16:18
Adapting state-of-the-art deep learning detectors for diagnosing bone lesions in musculoskeletal x-rays
A. Attia, A. Joseph, E. Zerbib-Attal, L. Combaldieu, G. Fradet, N. Upendra*; Paris/FR*

Purpose: The explosion of usable data and compute power over the past decade saw deep learning (DL) transform traditional internet businesses. As of today, DL is enabling new products and services across a wavelength of sectors, of which healthcare (with a focus on assisted diagnosis on medical images) is poised to be one of the most impacted sectors. With an ever-increasing demand for medical image diagnosis and insufficient specialists to commensurate with this demand, DL seeks to turn the tables around and aide specialists with the diagnosing procedure by reducing time and ameliorating accuracy.
This paper documents how we at AZmed adapted a state-of-the-art DL detector for fracture detection, with the mission of augmenting a doctor's workflow. Our adaption involved experimenting with pre-processing techniques, pre-training datasets, backbones, and hyper-parameters tuning. The paper details the insights obtained from rigorous experimentation and astute training strategies realised as a result. Additionally, light is thrown on research conducted on feature map outputs of the network in an effort to better grasp the functioning and behaviour of our fracture detector.
Methods and materials: Train, validation, and test dataset.
Results: Yet to be published.
Conclusion: The performance of the detectors allows doctors to save time and to reduce medical errors.
Limitations: A retrospective study.
Ethics committee approval: n/a
Funding: No funding was received for this work.
Author Disclosures:
A. Joseph: Speaker at AZmed, Employee at AZmed
A. Attia: Founder at AZmed
E. Zerbib-Attal: Founder at AZmed
L. Combaldieu: Employee at AZmed
G. Fradet: Employee at AZmed
N. Upendra: Employee at AZmed

RPS 1205-6 16:24
The effect of hard attention on abnormality detection in chest x-rays
T. R. Nimmada, B. Reddy, P. Putha, M. Tadepalli, A. M. Jagirdar, P. Rao, P. Warier*; Mumbai/IN (tarun.raj@qure.ai)*

Purpose: Visual attention in image classification allows models to focus on the region of interest effectively. In this study, we describe the effect of hard attention, achieved by explicitly cropping the region of interest (ROI) in detecting 2 abnormalities (tracheal shift and scoliosis) in chest x-rays. We also compare the performance of models trained with and without attention.
Methods and materials: Deep learning models were trained on a dataset of 2.5 million chest x-rays to detect scoliosis and tracheal shift. To incorporate hard attention, we trained a deep neural network model to localise the mediastinum from chest x-rays. This model took an input image (of size HxW) and output a binary mask (M) of size HxW with a rectangular ROI (size hxw) encompassing the mediastinum. The ROI was dilated to the left and right to obtain a binary mask (M1) of ROI size hx2w. The ROI in mask M1 was eroded to get a new mask (M2) of ROI size (h/2)x2w. M1 and M2 were used as attention masks to crop the region of interest for scoliosis and tracheal shift, respectively. This served as input data on which classification models with attention were trained.
Results: We measured the area under the receiver operating characteristic (AUC) to compare the models trained with (m_a) and without attention (m_wa). For tracheal shift, AUC of m_a and m_wa were 0.95 and 0.92, respectively. For scoliosis, AUC of m_a and m_wa were found to be 0.95 and 0.88, repsectively.
Conclusion: We have shown that performance of classification models to detect tracheal shift and scoliosis can be improved with hard attention. Attention helps us incorporate domain knowledge while training.
Limitations: Metrics other than AUC should be measured for further evaluation.
Ethics committee approval: n/a
Funding: No funding was received for this work.
Author Disclosures:
T. R. Nimmada: Employee at Qure.ai technologies pvt ltd
B. Reddy: Employee at Qure.ai technologies pvt ltd
P. Putha: Employee at Qure.ai technologies pvt ltd
M. Tadepalli: Employee at Qure.ai technologies pvt ltd
A. M. Jagirdar: Employee at Qure.ai technologies pvt ltd
P. Rao: Employee at Qure.ai technologies pvt ltd
P. Warier: Employee at Qure.ai technologies pvt ltd

RPS 1205-7 16:30
Artificial intelligence in standard radiology: automatic x-ray diagnostic algorithm
M.-M. Benta, F. Birsasteanu, S. Dunarintu, S. Iarca, B. Bercean, C. Avramescu, A. Tenescu*; Timisoara/RO (marius.benta@yahoo.com)*

Purpose: To develop a performant chest x-ray pathology classification machine learning model for the "Pius Brînzeu" Emergency County Hospital, using publicly available datasets (CheXNet and CheXPert) as its backbone.
Methods and materials: The convolutional neural network algorithm trained on CheXNet and CheXPert was underperforming when tested on cases from the "Pius Brînzeu" Hospital. We extracted 48,000 anonymised radiographs of consenting patients from the hospital's PACS system. We labelled them by transforming their associated radiological reports into labels and retrain the

algorithm with the initial model used as pretraining. Three radiologists hand labelled 2,000 x-rays in the newly obtained dataset and drew class bounding boxes that indicated afflicted areas on the x-rays. We trained a third model with the adjusted dataset.
Results: AUC was used as the metric to compare model performance. We evaluated 3 models on a gold standard dataset containing 500 radiologist annotated images. The publicly trained model scored 0.809, the automatically labelled model scored 0.813, and the one that uses hand label radiographs scored 0.825.
Conclusion: Our results indicate that there is a clear benefit to adding hospital-specific images to the dataset. Hand labelling also increases performance over NLP labelling, which shows that NLP has limitations especially in languages that don't have a word stemmer, like Romanian.
We conclude that retraining a model that uses public data as its backbone with data specific to a hospital strongly increases the performance of the model in the hospital. The most important further improvements come from the quality of the new dataset.
Limitations: The of hand labelled dataset is small compared to the hospital dataset.
Ethics committee approval: The study was aproved by the local Ethical Commitee.
Funding: No funding was received for this work.
Author Disclosures:
M.-M. Benta: Advisory Board at Xvision
F. Birsasteanu: nothing to disclose
S. Dunarintu: nothing to disclose
S. Iarca: Founder at Xvision
B. Bercean: Founder at Xvision
C. Avramescu: Founder at Xvision
A. Tenescu: Founder at Xvision

RPS 1205-8 16:36
Cascading model architecture of convoluted neural networks to improve the performance of pathology detection in digital chest x-rays
A. Kharat[1], A. Ahmad[2], J. Tandale[2], R. Lokwani[2], S. Kasliwal[2], G. Naik[2], S. Kondal[2], A. Pant[2], K. Saoji[2]; [1]Maharashtra/IN, [2]Pune/IN (kharatamit75@gmail.com)

Purpose: The chest x-ray is the most commonly used diagnostic examination screening tool in radiology. Due to constrained resources and the image-driven nature of a diagnosis, we want to assess if machine learning (ML) can aid in pathology detection.
Methods and materials: The data source was a leading hospital (LH) of 800+ bed capacity. The dataset was anonymised and not publicly available. The dataset contained 26,000 x-rays and associated radiology reports but without pathology labels. Using findings in radiology reports, pathology labels were generated.
Results: We trained a Densenet-121 model. Our objective was to build a customised ML model for the detection of any of 15 different chest diseases that are trained more effectively for chest x-ray source-specific datasets. Our data was imbalanced. Training a deep learning (DL) model for these pathologies can be challenging. Solely relying on balancing techniques cannot be a reliable way to improve performance. We explored cascading models. Along with 15 pathology prediction model for improved performance, we trained the model for binary classification to check if a chest x-ray has a pathology or not using a team of two validating radiologists. We used a Densenet-121 model trained without transfer learning. This binary model is combined with 15-pathology model in a cascading way. We found that the cascading architecture was more performant than using only the 15-pathology model on the LH dataset. We found that. at a small compromise for accuracy. the sensitivity (recall) of pathologies was better using this model.
Conclusion: Using cascading architecture, we could improve Kappa, sensitivity/recall, and F1 score significantly for pathology detection in digital chest radiographs. Using the cascading model archiecture of CNN, radiologists can efficienctly manage and control the turn around time of the reporting process of digital radiographs by incorporating these techniques in workflow.
Limitations: n/a
Ethics committee approval: n/a
Funding: No funding was received for this work.
Author Disclosures:
A. Kharat: Founder at deeptek.ai
A. Ahmad: Employee at Deeptek
J. Tandale: Employee at Deeptek
R. Lokwani: Employee at Deeptek
S. Kasliwal: Employee at Deeptek
G. Naik: Employee at Deeptek
S. Kondal: Employee at Deeptek
A. Pant: Employee at Deeptek
K. Saoji: Employee at Deeptek

RPS 1205-9 16:42
Deep learning-based architecture for detection of tuberculosis in digital chest radiography: our experience in the Indian scenario
A. Kharat[1], A. Ahmad[2], R. Lokwani[2], G. Naik[2], J. Tandale[2], K. Saoji[2], A. Jaju[2], A. Patil[2], A. Pant[2]; [1]Maharashtra/IN, [2]Pune/IN (kharatamit75@gmail.com)

Purpose: Tuberculosis (TB) has infected 1% of the global population and is a major cause of death in developing countries.
Methods and materials: Deep learning (DL) was used to classify every digital chest x-ray (DX) into 3 types: abnormal (TB likely), abnormal (TB unlikely), and normal. A model trained on a combination of publicly available 'NIH DX dataset' and private anonymised hospital data was used. Dataset for modelling: 2,050 images with train-test ratio=78:22. Training set: 1,600 images with 530 abnormal TB, 530 abnormal non-TB, and 540 normal DX and test set consisting of 450 images equally balanced in the 3 classes with 150 images each. Basis: convolutional neural networks (CNN). DX divided into 3 predefined classes. Steps: 1] conversion of DX DICOM to PNG format, image resized to 224 x 224 and fed to the DenseNet-121 model for training, and 2] learning rate scheduler to reduce the learning rate to 1/10th of its initial value after every 10 epochs.
Results: Test set: 450 images.
Conclusion: CNN scores can potentially be used for TB screening in DX with a radiologist in the loop approach. TB screening programs to assist government hospitals using DL can be a game-changer in curbing TB. Instant alert triage can enable urgent sputum checks and initiation of antitubercular treatment before the patient leaves the hospital premise.
Limitations: n/a
Ethics committee approval: n/a
Funding: No funding was received for this work.
Author Disclosures:
A. Kharat: Founder at deeptek.ai
K. Saoji: Employee at Deeptek
A. Ahmad: Employee at Deeptek
R. Lokwani: Employee at Deeptek
G. Naik: Employee at Deeptek
J. Tandale: Employee at Deeptek
A. Pant: Founder at Deeptek
A. Patil: Founder at Deeptek
A. Jaju: Employee at Deeptek

RPS 1205-10 16:48
Breast cancer screening with denoised ultra-low-dose mammography
M. Sklair-Levy[1], M. Green[1], E. Konen[1], N. Kiryati[2], A. Mayer[1]; [1]Ramat Gan/IL, [2]Tel Aviv/IL (arnmayer@gmail.com)

Purpose: To assess a novel AI-based algorithm for the denoising of ultra-low-dose (ULD) digital mammography.
Methods and materials: A retrospective dataset of 16 digital mammography studies (each: bilateral CC and MLO) was obtained from a Senographe Pristina (GE Healthcare) imager in a standard breast cancer screening protocol. ULD mammograms were simulated by adding synthetic noise to the pixels, corresponding to 90% less radiation. A neural locally-consistent non-local block which preserves fine details (e.g. micro-calcifications) was proposed to denoise the images. The network was trained on a single case (4 views) and tested on the remaining 15. Comparision is given against 4 state-of-the-art denoising algorithms ([1], [2], [3], and [4]). Peak signal-to-noise ratio (PSNR) and structural similarity index (SSIM) quantified the similarity between denoised-ULD and normal dose image pairs.
Results: The proposed method outperformed all the compared algorithms: PSNR (proposed=38.92/second-best=38.27) and SSIM (proposed= 0.987/second-best=0.979).
Conclusion: A novel AI-based denoising algorithm was proposed and validated for the enhancement of synthetic ULD mammography. The proposed algorithm showed promising results, motivating future validation on real ULD mammography.
Limitations: Simuated data was used, real ULD data will be used in future research.
Ethics committee approval: IRB was obtained from our institution.
Funding: No funding was received for this work.
Author Disclosures:
A. Mayer: nothing to disclose
M. Sklair-Levy: nothing to disclose
M. Green: nothing to disclose
E. Konen: nothing to disclose
N. Kiryati: nothing to disclose

RPS 1205-11 16:54

Development and performance comparison of multi-task deep learning approaches for the severity assessment of radiographic hip osteoarthritis features

C. von Schacky[1], J. H. Sohn[2], F. Liu[3], S. C. Foreman[1], E. Ozhinsky[3], P. M. Jungmann[4], M. Nevitt[3], T. M. M. Link[3], V. Pedoia[3]; [1]Munich/DE, [2]Baltimore/US, [3]San Francisco, CA/US, [4]Freiburg/DE
(claudio.vschacky@hotmail.de)

Purpose: Radiographic features of hip osteoarthritis include joint space narrowing, osteophytes, subchondral sclerosis, and subchondral cysts. The aim was to develop, validate, and compare the performance of four multi-task deep learning approaches for grading radiographic hip osteoarthritis features.
Methods and materials: We used 15,364 hip joints (7,738 pelvic radiographs) from subjects of the Osteoarthritis Initiative. Each hip joint was graded for five osteoarthritis features and each feature for absence, mild, moderate, or severe presence. The data was split 80%/10%/10% for training/validation/ testing. The hip joint was detected with a trained RetinaNet for object detection. Then, four different approaches to solve this multi-task problem were evaluated and compared: single-model alone, single-model with classifier, multi-task learning, and fine-tuned multi-task learning. All models were based on a Densenet-161. Reliability was assessed with Cohen's Kappa.
Results: All multi-task approaches achieved higher reliability compared to single-model approaches. The highest reliability was achieved with a fine-tuned multi-task learning model with a Kappa of 0.58 for femoral osteophytes, 0.41 for acetabular osteophytes, 0.51 for joint space narrowing, 0.44 for subchondral sclerosis, and 0.53 for subchondral cysts.
Conclusion: This study shows that a variety of multi-task learning approaches can be used for grading radiographic hip osteoarthritis features and that multi-task learning might have advantages over single-model training.
Limitations: The training set only consisted of cases of one large scale dataset from a longitudinal OA study. It would increase the quality of the training set to add further samples with different demographic and imaging characteristics.
Ethics committee approval: Written informed consent was obtained from all participants. IRB approval was granted by this HIPAA-compliant study by the four participating US-based centres.
Funding: NIH-NIAMS: 5R01AR064771-05.
Author Disclosures:
C. von Schacky: nothing to disclose
F. Liu: nothing to disclose
S. C. Foreman: nothing to disclose
E. Ozhinsky: nothing to disclose
M. Nevitt: nothing to disclose
V. Pedoia: nothing to disclose
T. M. M. Link: nothing to disclose
J. H. Sohn: nothing to disclose
P. M. Jungmann: nothing to disclose

RPS 1205-12 17:00

Defending against adversarial attacks in the detection of pneumothoraces from chest radiographs: ensuring robustness in clinical AI applications

D. Kügler[1], A. M. Bucher[2], A. Distergoft[2], A. Rajkarnikar[3], M. Uecker[3], P. D. A. Kuijper[3], T. J. Vogl[2], D. A. Mukhopadhyay[4]; [1]Bonn/DE, [2]Frankfurt am Main/DE, [3]Darmstadt/DE

Purpose: Adversarial examples are small input changes with malicious intent that are imperceptible to the human eye yet can completely change the output of a deep neural network (DNN). In this investigation, we introduce controlled Gaussian noise administration, a practical defence against adversarial attacks on the detection of pneumothoraces from chest radiographs.
Methods and materials: We trained a DNN classifier (ResNet) on 9,265 manually annotated chest radiographs for the detection of pneumothoraces. Validation was tested on a dataset of 150 images containing comparable chest radiographs (I_C) against annotation of a trained radiologist reader. Each image was then attacked (I_A) with 4 gradient-based adversarial attack methods (BIM, DF, SMA, FGSM). In the defence dataset (I_D), we introduced controlled Gaussian randomness in increasing steps on a heuristic scale (steps 1-7).
Results: Classification by the human reader did not differ significantly between I_C and I_A (p=0.325). DNN classification accuracy dropped from 83.3% (I_C) to 16.6% (I_A; p<0.001). Best overall accuracy for I_D was found in step 5 (56%±12.6%; p<0.001). Optimal corrections steps varied highly between attack types (BIM, step1: 81.1%, p<0.001). Overall true-positive rates were 0.65 (I_C), 0.35 (I_A), and 0.56 (I_D; DF/SMA, step7: 0.9), overall false-positive rates were 0.1 (I_C), 0.9 (I_A), and 0.6 (I_D; BIM, step 3: 0.09). AUC overall was 0.775 (I_C), 0.225 (I_A), and 0.48 (I_D; BIM step2: 0.761). Steps 6 and 7 did not result in further improvement of overall accuracy (48.2%; p=0.152).
Conclusion: Even highly effective adversarial attacks can be effectively counteracted by the proposed method of controlled Gaussian noise administration. Comparable defence mechanisms should be integrated when transferring DNNs to clinical application.
Limitations: Effectiveness should be validated in a larger dataset.
Ethics committee approval: n/a
Funding: No funding was received for this work.
Author Disclosures:
A. M. Bucher: Other at Travel support: Bayer
D. Kügler: nothing to disclose
A. Distergoft: nothing to disclose
T. J. Vogl: Other at Travel support: Bayer
M. Uecker: nothing to disclose
A. Rajkarnikar: nothing to disclose
P. D. A. Kuijper: nothing to disclose
D. A. Mukhopadhyay: nothing to disclose

RPS 1205-13 17:06

On the robustness of a deep learning-based algorithm for detecting abnormalities in chest radiographs across different devices and view positions: a retrospective case-control study

S. Na, M. Kim, J. Park, C. M. Park, E. J. Hwang, S. Park; Seoul/KR
(sgpark@lunit.io)

Purpose: To validate the robustness of a deep learning-based algorithm that detects abnormal lesions in chest radiographs for a screening environment.
Methods and materials: To verify the robustness of a deep learning-based algorithm, we collected datasets from Seoul National University Hospital. 2,673 chest radiographs taken from 27 x-ray devices were collected to verify the robustness across different x-ray devices. These radiographs were then divided into two groups of which 661 cases (479 abnormal and 182 normal) were computed radiography (CR) and 2,012 cases (1,449 abnormal and 563 normal) were digital radiography (DR). 2,625 (2,028 abnormal and 597 normal) posterior-anterior (PA) images and 1,729 (1,580 abnormal and 149 normal) anterior-posterior (AP) images were collected to verify the robustness across different view positions. These two datasets were reviewed by board-certified radiologists. For the deep learning-based algorithm, we used LUNIT INSIGHT CXR 3 to predict 10 major radiologic findings in chest radiographs. This algorithm was trained with 147,823 images using various augmentation schemes such as photometric and geometric jittering for making itself more robust to radiographs taken with various settings.
Results: The algorithm achieved AUC of 96.54 and 97.09 for CR and DR, respectively. The p-value of DeLong's test for the difference between two AUCs was 0.4802. Moreover, for PA and AP images, it achieved AUC of 97.29 and 96.67 for PA and AP, respectively. The p-value was calculated to be 0.3182.
Conclusion: Chest radiographs have tremendous heterogeneity due to various devices and methods in taking chest radiographs. Our experimental results showed that a well-generalised algorithm can be robust in detecting abnormalities on chest radiographs in a screening environment.
Limitations: More validation of the robustness from various sites could be useful.
Ethics committee approval: n/a
Funding: No funding was received for this work.
Author Disclosures:
S. Park: Employee at Lunit, Founder at Lunit
S. Na: Employee at Lunit
J. Park: Employee at Lunit
M. Kim: Employee at Lunit
C. M. Park: Research/Grant Support at Lunit
E. J. Hwang: nothing to disclose

RPS 1205-14 17:12

Clinical validation of a deep learning-based bone age software in healthy Korean children

W. W.-I. Lea, S.-J. Hong, H.-K. Nam, H. S. Yong, Z. Yang, J. Jeong, E. Noh;
Seoul/KR (lwooin17@gmail.com)

Purpose: To evaluate the clinical performance of a deep learning (DL)-based bone age software in healthy Korean children.
Methods and materials: This retrospective study included 371 healthy children (217 boys, 154 girls) aged between 4 and 17 years who visited the department of paediatrics for growth check-ups between January 2017 to December 2018. A total of 553 left-hand radiographs of 371 healthy Korean children were assessed using a commercial DL-based bone age software (BoneAge, Vuno, Seoul, Korea). Two sample t-test, Fisher's exact test (two side), Pearson's correlation coefficient, root mean squared error (RMSE), concordance rate, and Bland-Altman analysis were used to evaluate the clinical performance of DL software by comparing with their chronologic age.
Results: Two sample t-test (p<0.001) and Fisher's exact test (p=0.011) showed there is a significant difference between the normal chronological age and the bone age estimated by DL software. Between the two variables, there was a good correlation (r=0.96, p<0.001), however, the RMSE value was 15.2 months.

With a 12-months cut-off, the concordance rate was 58.8%. The Bland-Altman plot showed that the DL software had a tendency to estimate the bone age younger than the chronologic age, especially in children under the age of 10 years.
Conclusion: DL-based bone age software showed a low concordance rate and a tendency to estimate the bone age younger than the chronologic age in healthy Korean children.
Limitations: A retrospective study, single-centre trial, with a small number of patients.
Ethics committee approval: n/a
Funding: No funding was received for this work.
Author Disclosures:
W. W.-I. Lea: nothing to disclose
S.-J. Hong: nothing to disclose
H.-K. Nam: nothing to disclose
H. S. Yong: nothing to disclose
Z. Yang: nothing to disclose
J. Jeong: nothing to disclose
E. Noh: nothing to disclose

RPS 1205-15 17:18
A cloud-based intelligent system for bone age determination in athletes: making AI available for sport imaging
M. Fatehi[1], R. Nateghi[1], P. Fatehi[1], F. Pourakpour[1], A. Sami[2]; *[1]Tehran/IR, [2]Shiraz/IR (mansoor.fatehi@gmail.com)*

Purpose: In order to implement fair play principles, FIFA has developed a bone age grading system consisting of I-VI levels which can be used in teenage athletes using MRI as a modality without ionising radiation. This grading system requires a particular imaging protocol and reporting guideline. The purpose of this paper is to describe an online cloud-based AI-enabled reporting system to provide the automated grading of wrist MR studies uploaded by football clubs or authorities.
Methods and materials: The football players of the national team were studied by Siemens Avanto 1.5 using a knee coil, following dedicated FIFA protocol, resulting in 9 coronal sections in T1W sequence. An AI model was developed in MATLAB. 72 cases with 648 slices were augmented to 11,034 images to train the model and then tested by 30 cases resulting in 420 images after augmentation. The system was adapted to a web-based application to get an MRI data set as an input and provide a grading report.
Results: The system was able to provide a grading report within 30 seconds after the upload of the study with an accuracy of 98-100% compared to trained experienced MSK radiologist familiar with the FIFA system.
Conclusion: The system provides fast reliable grading capacity to be available to any football federation or authority, as well as football clubs, to get the report from anywhere. The system is independent of the interpreting physician with immediate results available for decision making.
Limitations: The intelligence of the grading system needs to be adapted to different races and geographical background to be applicable for a wide international scale.
Ethics committee approval: n/a
Funding: No funding was received for this work.
Author Disclosures:
M. Fatehi: nothing to disclose
R. Nateghi: nothing to disclose
F. Pourakpour: nothing to disclose
A. Sami: nothing to disclose
P. Fatehi: nothing to disclose

16:00 - 17:30 **Room Y**

My Thesis in 3 Minutes

MyT3 12
Radiographers

Moderators:
M. Gardarsdottir; Reykjavik/IS
F. Zarb; Msida/MT

MyT3 12-1 16:00
Survey of radiologists', radiology residents', and radiographers' knowledge regarding contrast materials and management of associated adverse reactions
F. Khan, M. Samad, G. Wahid; *Peshawar/PK (islamianfellow@hotmail.com)*

Purpose: To assess the knowledge of radiology personnel regarding the contrast media and management of associated adverse reactions.
Methods and materials: The survey conducted from 21st February to 31st March 2019 in five major hospitals of Peshawar, Pakistan. A 30-item questionnaire was adopted from the existing literature containing both open and closed-ended questions and a pilot study was conducted among 25 radiology personnel to assess the face validity of the tool. Universal sampling technique was adopted. Hospital ethical review committee approval was granted.
Results: 15.2%,46.7% and 28.6% correctly classified contrast media used in radiology, iodinated contrast media on the basis of ionicity and osmolality respectively. 63% chose severe contrast material induced allergic reaction as type I hypersensitivity reaction while 56.2% correctly identified the features of iodinated contrast media associated with lesser side effects. Only 6.7% of people had read the ACR 2018 manual on contrast media. Regarding the risk factors for acute adverse reactions and signs/symptoms of anaphylaxis 13.3% and 7.6% responded correctly. Twenty-eight percent of participants correctly identified epinephrine as the initial medication in an anaphylactic reaction. Regarding epinephrine, 43.8%,6.7%, and 8.6% of participants knew the preferred route of administration, concentration, and dose. More than sixty-five percent of participants could name a single intravenous corticosteroid and antihistamine.
Conclusion: Radiology personnel's knowledge regarding contrast material and management of severe contrast material-induced allergic reactions is unsatisfactory.
Limitations: The response rate was low and hence sample size.
Ethics committee approval: Ethical review committee approval was granted.
Funding: No funding was received for this work.
Author Disclosures:
F. Khan: Other at Hayatabad Medical Compex, Author at Hayatabad Medical Complex, Investigator at Hayatabad Medical Complex
M. Samad: Consultant at Hayatabad Medical Complex, Author at Hayatabad Medical Complex, Employee at Hayatabad Medical Complex
G. Wahid: Consultant at Hayatabad Medical Complex, Author at Hayatabad Medical Complex, Employee at Hayatabad Medical Complex

MyT3 12-2 16:04
An experimental approach to the development of a 3D printed model of the hand and wrist for use in undergraduate radiography teaching
L. Kennedy; *Waterford/IE (laura.kennedy.3@ucdconnect.ie)*

Purpose: The impact of 3D printing in all industries is steadily increasing. The cost of 3D printing, which was once a deterrent, has declined, allowing for easier access to the technology and the benefits it has to offer the healthcare industry. As research highlights the shift away from conventional teaching at third-level, methods of achieving a hands-on learning approach are being explored. Radiography students have benefited greatly from the use of radiographic anthropomorphic while training. However, such phantoms are very costly for educational facilities. The importance of projection radiography in diagnosing wrist pathology cannot be disputed. Evidence shows problems that can arise from improper positioning of the wrist can cause morbidity in the patient. Thus the aim of the research project is to 3D print an anthropomorphic radiographic model of the hand and wrist for use in undergraduate radiography teaching.
Methods and materials: Materials were tested for their suitability to print various components of the model, the model was designed using CAD software and printed with specific parameters. Following the PDSA cycle the model was created. A beta test of success was carried out on undergraduate students.
Results: A 3D printed model of the hand and wrist was successfully developed with experimental materials. The model was well received in beta testing.
Conclusion: 3D printed models can provide an accurate and cost-effective alternative to radiographic anthropomorphic phantoms for undergraduate teaching, with opportunities for customisation knowing little boundaries.
Limitations: Funding was the primary limitation of the study which was carried out at the undergraduate level.
Ethics committee approval: The ethical exemption was granted by the School of Medicine Undergraduate Research Ethics Committee (UREC SM) on the 04th of February 2019, UREC number UREC-SM-2018-86.
Funding: No funding was received for this work.
Author Disclosures:
L. Kennedy: Author at University College Dublin

MyT3 12-3 16:08
Estimation of pituitary gland volume and its correlation with age and gender: a magnetic resonance study
T. D. C. Cabrita[1], A. F. Abrantes[1], L. P. V. Ribeiro[2], S. Rodrigues[1], R. C. M. C. R. Gaspar[3], R. P. P. Almeida[1], K. B. Azevedo[1]; [1]Faro/PT, [2]Parchal/PT, [3]Coimbra/PT (tiagocabrita123@hotmail.com)

Purpose: To determine the dimensions of normal pituitary gland and correlate with age and gender, in order to obtain standard reference values.
Methods and materials: Head MRI scans of 410 patients with clinically normal pituitary function (173 males and 237 females) were retrospectively analysed and in the age range 10-90 years. T1-weighted images were reviewed in order to obtain volumetric measurements of the pituitary gland using RadiAnt DICOM Viewer software® (V.4.2.1). The height, width and depth of the pituitary were obtained from mid-sagittal and coronal planes, while the volume was calculated from these measured parameters. The data obtained were stratified based on age and gender for analysis.
Results: Females had greater pituitary height (5.59±1.29 mm), width (13.08±2.21 mm), and volume (398.98±123.80 mm^3) compared to males (5.53±1.23 mm, 12.59±2.09 mm and 378.58±106.46 mm^3, respectively). However, males had greater depth values (10.56±1.34 mm) compared to females (10.54±1.49 mm), having a positive correlation between depth and gender (r = 0.113, P= 0.022). Significant differences between pituitary height, width and volume with age were found and they correlated negatively with increasing age (r = −0.157, P= 0.001; r = −0.129, P = 0.009; and r = −0.140, P = 0.004, respectively). Also, it was possible to identify that these parameters have a peak at age range 41-50 for females, that may result due the intense hormonal activity at this age. Regarding the gender, no significant differences between pituitary height, width and volume were found.
Conclusion: We have provided reference values for the normal pituitary gland dimensions in the Portuguese population, in order to facilitate assessment and diagnosis in patients with abnormalities of the hypothalamic-pituitary axis.
Limitations: N/A
Ethics committee approval: Ethics committee approved the study.
Funding: No funding was received for this work.
Author Disclosures:
T. D. C. Cabrita: nothing to disclose
A. F. Abrantes: nothing to disclose
L. P. V. Ribeiro: nothing to disclose
S. Rodrigues: nothing to disclose
R. C. M. C. R. Gaspar: nothing to disclose
R. P. P. Almeida: nothing to disclose
K. B. Azevedo: nothing to disclose

MyT3 12-4 16:12
Radiographer's communication skills in private imaging facilities
A. C. M. Gonçalves[1], S. Rodrigues[2], L. P. V. Ribeiro[3], A. F. Abrantes[2], R. P. P. Almeida[2], O. Lesyuk[4], B. Vicente[5]; [1]Tavira/PT, [2]Faro/PT, [3]Parchal/PT, [4]São Brás de Alportel/PT, [5]Olhão/PT (catarina.3@live.com)

Purpose: Effective communication is at the heart of quality health care. In radiography a considerable part of the working day is spent relating to others. Radiographers should base themselves on interpersonal competences throughout their daily work routine, to promote quality in diagnosis, patient safety and technical excellence. The aim of this study was the exploration of patient's perceptions regarding the performance of the Radiographer in terms of interpersonal communication skills in private imaging facilities.
Methods and materials: The instrument used was the questionnaire "Communication Assessment Tool" adapted to the professional reality of the radiographer. A final sample of 150 valid questionnaires including 15 questions with a five-point Likert scale ("poor" to "excelent") was used. The paper-based instrument was delivered and filled by the patients after the performance of imaging procedures from two private hospitals. The results were reported as a percentage of "excellent" ratings and mean scores.
Results: The average "excellent" response rate was 45% (= 4). The issues rated "excellent" relate to respect (55.3%, = 4.43) and to the use of accessible language (57.3%, = 4.41). The worst-rated "excellent" issues are related to the encouragement to ask questions (29.3%, = 3.75) and the understanding of the radiographer in face of patients' health problems (32%, = 3.99). Significant differences were found between age, gender, context and shift.
Conclusion: Radiographers' communication skills were evaluated with good levels of patient confidence with the radiological examinations. Despite the overall positive results, radiographers should have a marked impact on their communication with patients because they are often one of the first health professionals that patients see.
Limitations: n/a
Ethics committee approval: Ethics committee approved the study and written informed consent.
Funding: No funding was received for this work.
Author Disclosures:
A. C. M. Gonçalves: nothing to disclose
S. Rodrigues: nothing to disclose
L. P. V. Ribeiro: nothing to disclose
A. F. Abrantes: nothing to disclose
R. P. P. Almeida: nothing to disclose
O. Lesyuk: nothing to disclose
B. Vicente: nothing to disclose

MyT3 12-5 16:16
Ultrasound evaluation of abdominal muscles in asymptomatic and patients with chronic low back pain: the role of a radiographer
B. Vicente[1], A. F. Abrantes[2], L. P. V. Ribeiro[3], S. Rodrigues[2], J. Pinheiro[4], M. V. C. Reis[2], R. P. P. Almeida[2]; [1]Olhão/PT, [2]Faro/PT, [3]Parchal/PT, [4]São Brás De Alportel/PT (biancaicvicente@gmail.com)

Purpose: Abdominal muscles are one of the important elements to support the lumbar spine. Evaluation of muscle thickness using ultrasonography is considered to be a source of information from muscles characteristics. The aim of this study was to investigate whether there were differences between chronic low back pain (CLBP) and healthy subjects in abdominal muscles thickness using ultrasound.
Methods and materials: A sample of 23 CLBP patients and 20 controls was recruited. Four abdominal muscles (Rectus Abdominis (RA), External Oblique (EO), Internal Oblique (IO) and Transversus Abdominis (TA)), were bilaterally measured by a trained radiographer at rest and while contracted.
Results: The pattern of relative muscle thickness was IO > RA > EO > TA, bilaterally, both at rest and while contracted. The mean for RA, EO, IO and TA muscles thickness in asymptomatic subjects were (11.05, 3.735, 14.335, 4.015) at rest and (11.03, 3.295, 12.685, 3.63) while contracted, respectively. The mean for RA, EO, IO and TA muscles thickness in patients with CLBP were (11.11, 2.945, 15.565, 3.955) at rest and (10.99, 2.525, 13.645, 3.44) while contracted, respectively. Significant differences in the thicknesses of the abdominal muscles were measured during rest and while contracted, as well as between both genders. However, no significant differences were found between CLBP patients and control group.
Conclusion: Despite the results, ultrasound measurements of abdominal muscles are reliable, and radiographer can play a key role in this field. However, the validity of using thickness change as a measure of muscle function, their correlation with other clinical features and the effect of specific retraining all require further investigation.
Limitations: Sample size
Ethics committee approval: Ethics committee approved the study and written informed consent was delivered to the participants.
Funding: No funding was received for this work.
Author Disclosures:
B. Vicente: nothing to disclose
A. F. Abrantes: nothing to disclose
L. P. V. Ribeiro: nothing to disclose
S. Rodrigues: nothing to disclose
J. Pinheiro: nothing to disclose
M. V. C. Reis: nothing to disclose
R. P. P. Almeida: nothing to disclose

MyT3 12-6 16:20
Sentinel lymphatic nodes scintigraphy in patients with vulvar cancer
E. Zykov, A. Ilyin, A. Meldo, G. Bozhukhin, G. Lungu, V. M. Moiseenko, S. Maksimov, K. Shelekhova; St. Petersburg/RU (zykov4@yandex.ru)

Purpose: Sentinel lymphatic nodes scintigraphy (SLN) allows for intraoperative choosing the optimal volume of surgery in patients with vulvar cancer without any clinical data on the presence of the metastasis in the inguinal lymph nodes. Purpose of the study was to evaluate the significance of SLN scintigraphy in patients with vulvar cancer in the stage of intraoperative planning.
Methods and materials: The study included 46 patients with vulvar cancer cT1N0M0 (average age 72 years old). To confirm the degree of cN0, MRI of the pelvis with contrast enhancement were performed. All patients underwent preoperational scintigraphy of SLN. The radioactive pharmacological preparation (RPP) Tc99m-Technephite 90-150 MBq in the volume of 0,7-1,0 to the patient was administered 3-16 hours before surgery. The scanning was conducted 30-60 minutes after the injection of RPP in the static mode in a prone position in two projections.
Results: The RPP accumulation in regional lymph nodes during SLN scintigraphy was detected in 100% of the patients. In the case of intraoperative histological examination, metastatic lesions of SLN were revealed in 9 patients (20%). With the expansion of surgery volume and subsequent histological evaluation, metastases in other excised lymph nodes were detected in three cases. In six cases, metastases were found in one lymph node only. In 37

patients (80%) there were no metastatic lesion of SLN. This allowed avoiding of lymphadenectomy.

Conclusion: SLN scintigraphy with biopsy as a clarifying diagnostic method allows individualising the volume of operative intervention.
Limitations: This study has no limitations.
Ethics committee approval: n/a
Funding: No funding was recieved for this work.
Author Disclosures:
E. Zykov: nothing to disclose
A. Meldo: nothing to disclose
A. Ilyin: nothing to disclose
G. Bozhukhin: nothing to disclose
G. Lungu: nothing to disclose
V. M. Moiseenko: nothing to disclose
S. Maksimov: nothing to disclose
K. Shelekhova: nothing to disclose

MyT3 12-7 16:24

An investigation of post-registration PET/CT radiography training in Ireland

R. E. Whelan, K. Curran, L. A. Rainford*; Dublin/IE (rachel.whelan@ucdconnect.ie)*

Purpose: A well-trained workforce is essential in a PET/CT department. There is a lack of published literature regarding the training and education of PET/CT radiographers in Ireland. This study investigated the PET/CT training offered in Ireland and investigated in which areas further training might be beneficial for PET/CT radiographers in Ireland.
Methods and materials: An online questionnaire was distributed to PET/CT radiographers across Irish centres. Open and closed questions were asked about PET/CT training and further training areas. The questionnaire sought information regarding participants' individual training, important areas for training, and participant demographics.
Results: Questionnaire responses (n=26) were received from 7 of 9 sites nationally (estimated staff response rate of 74% within these sites). 'In-house' induction PET/CT training programmes varied in duration from 1-2 weeks long to more than 9 weeks long. Observation and shadowing were among the most commonly used approaches to training. The use of a competency checklist during training and the level of agreement that the training fully prepared the participant to work independently in PET/CT were significantly associated ($p<0.024$, $r=0.672$). Radiation protection, pathology, radiopharmaceutical administration, artefactual variants and critical situations associated with contrast media/radiopharmaceuticals were identified as important training topics.
Conclusion: Key training areas were identified. Changes in practice - for example the introduction of a new Gallium service - were identified as matters that may affect future training needs. Further research is warranted to identify how the training needs identified should be addressed.
Limitations: The participant responses are representative of Irish PET/CT radiographers therefore further research is recommended to collect data from other European countries for comparison.
Ethics committee approval: This study was performed following ethical permission from the School of Medicine, University College Dublin.
Funding: No funding was received for this work.
Author Disclosures:
R. E. Whelan: nothing to disclose
L. A. Rainford: nothing to disclose
K. Curran: nothing to disclose

MyT3 12-8 16:28

Has the radiographer practice changed in the use of anti-scatter grid with the introduction of digital detectors: a scoping review

C. Campeanu*; Lausanne/CH (cosmin.campeanu@hesav.ch)*

Purpose: To scrutinise the changes in radiographer's practice regarding the use of the anti-scatter grid in flat-panel digital imaging.
Methods and materials: The scoping review method was applied to identify gaps in the existing literature and to formulate recommendations for practice and/or policy changings. The three major databases for healthcare literature have been consulted: Medline, CINAHL and EMBASE using a combination of key-words (anti-scatter grid, digital radiography, radiographers practice).
Results: 149 studies were identified. After title and abstract reading, 25 articles were selected and 12 were retained for analysis/discussion based on inclusion criteria. The studies were divided into four groups: paediatric imaging, musculoskeletal and chest imaging in adults and "virtual-grid-like" radiographies. Based on phantom-studies of paediatric abdomen, specific recommendations were provided for grid-use decision-making: the patient should be over 14cm thickness with small FOV (21x18cm) at 80kVp. For adults, the removal of the anti-scatter grid can promote a dose reduction (up to a maximum of 418%) on specific anatomical areas such as shoulder and "virtual-grid-like" bedside chest radiographies, while keeping diagnostic image quality. This study was already clinically assessed, being possible a direct introduction on practice. The non-grid lateral cervical spine and horizontal beam hip radiographies need a further clinical assessment before changing the practice.
Conclusion: The introduction of digital detectors has potential to change radiographers practice regarding the use of anti-scatter grid. However, this change can be clinically implemented in just 2 specific radiographic examinations: AP shoulder and bedside chest acquisitions. Further clinical research should be designed considering the irradiated volume (measured thickness multiplied by the displayed FOV), through multiple parameters variations and different anatomical areas.
Limitations: This was an extensive scoping review but no experimental research was conducted to complement the findings.
Ethics committee approval: Not applicable.
Funding: Not applicable.
Author Disclosures:
C. Campeanu: nothing to disclose

MyT3 12-9 16:32

An investigation into the necessary considerations when giving patients online access to their health records

N. Seymour[1], M. D. Davis[2]*; [1]Cork/IE, [2]Dublin/IE (niall.seymour@ucdconnect.ie)*

Purpose: The use of electronic health records is becoming widespread and with this comes the desire of many patients to have easy access to their stored imaging and healthcare records. This study aimed to investigate, on a global and national level, the necessary considerations for any stakeholder intending on giving patients online access to their health records.
Methods and materials: A rapid structured literature review was conducted to gain an international perspective on the primary concerns that arise when giving patients online access to their records. This review was supported by conducting interviews with people working in the Republic of Ireland who have experience relevant to this area. All data gathered was analysed quantitatively using NVivo, a qualitative data analysis programme.
Results: A total of 49 articles and seven interviews were subjected to thematic analysis, from which six key considerations have been identified. These are as follows: (1) accessibility and engagement barriers, (2) security, (3) results, (4) proxy access (5) patient-generated health data and (6) resources.
Conclusion: Giving patients online access to their health records has the potential to bring significant benefits to patients and healthcare providers. Addressing important considerations could help ensure that giving patients online access to their health records can be secure, beneficial and not cause unnecessary worry or concern for patients or unnecessary strain on healthcare providers.
Limitations: Given the time constraints for this research project, an in-depth analysis of each consideration identified was not possible. However, this study has provided an overview of the key considerations, which is a valuable starting point from which stakeholders could begin planning patient portal implementation.
Ethics committee approval: Exemption from a full ethical review was granted by the Undergraduate Research Ethics Committee in University College Dublin on November 5, 2018.
Funding: No funding received.
Author Disclosures:
N. Seymour: nothing to disclose
M. D. Davis: nothing to disclose

MyT3 12-10 16:36

Nutritional support in cancer patients: radiographers' perceptions

A. Y. Dimitrova, P. Jones, G. van Dijk*; Msida/MT (angelina.y.dimitrova@gmail.com)*

Purpose: This study aimed to explore the perceptions of radiographers employed in an oncology centre regarding their ability to identify patients needing nutritional advice and to provide patients with the appropriate dietary support.
Methods and materials: A non-experimental, quantitative approach was employed. An existing questionnaire was modified, using published guidelines to suit the aim of this study, and distributed to all radiographers working in the radiotherapy department of the selected oncology centre. Data were analysed using descriptive statistics.
Results: With a response rate of 85% (n=22), 86% (n=19) of participants indicated that patients asked for nutritional advice. 36% (n=8) of the respondents did not have previous training on nutritional interventions. All participants expressed interest in receiving additional information or training regarding nutritional management of side effects and identification of cases needing a referral to a dietitian. 82% (n=18) of participants stated that a protocol for referrals to dietitians was available at their clinical site, however, only two respondents indicated that they referred patients to a dietitian. All radiographers

are self-rated as knowledgeable in identifying patients in need of dietary interventions and delivering the appropriate nutritional support. This was supported by the high level of agreement between literature recommendations and radiographers' responses.
Conclusion: Findings suggest that radiographers perceive themselves as knowledgeable and provide patients with the appropriate nutritional support. However, only two radiographers referred patients to dietitians and all radiographers indicated that they would like additional support. The researcher, therefore, proposed additional training, implementation of scripted nutritional advice and further studies into the lack of referrals to the dietetic team.
Limitations: Participants may have responded in their favour or sought assistance, leading to biased results. Use of close-ended questionnaires may have restricted data, limiting explanation of complex issues.
Ethics committee approval: N/A
Funding: No funding was received for this work.
Author Disclosures:
A. Y. Dimitrova: nothing to disclose
G. van Dijk: nothing to disclose
P. Jones: nothing to disclose

MyT3 12-11 16:40
SAFMEDS to improve medical students and trainees accuracy in interpreting chest radiographs: a pilot study
K. Dunne, D. Byrne, S. Lydon, P. McCarthy, C. Madden*; Galway/IE (kevindunne04@gmail.com)*

Purpose: To develop an efficient and effective educational tool that students can use in a self-directed manner to improve their chest x-ray (CXR) interpretation skills.
Methods and materials: Third-year medical students and medical interns took part in this study. Participants completed a pre-intervention assessment which required them to indicate a diagnosis for 25 CXR images. No clinical information accompanied the images. Participants then: 1) received a tutorial on CXR interpretation, and; 2) independently used a behavioural instructional methodology called SAFMEDS ("say-all-fast-minute-each-day-shuffled"), which involved 60-second practice trials with a set of flashcards depicting CXR images, for six weeks. Subsequently, participants completed a post-intervention. Dependent t-tests were used to compare the performance of each group at the pre-intervention and post-intervention assessments.
Results: A total of 13 third-year medical students, and 14 medical interns completed the pre-intervention assessment with a mean overall accuracy of 34.2% and 63.1% respectively. Post-intervention accuracy increased to 67.6% (n=11, p= <0.001) for the medical students and 77.3% (n=9, p= 0.02) for the medical interns.
Conclusion: SAFMEDS produced statistically significant improvements in accuracy for both groups in just six weeks when interpreting CXRs. This is in line with other research which has shown the efficacy of SAFMEDS in varied educational domains. As SAFMEDS constitutes a self-directed learning resource it is potentially a very valuable tool given the ever-increasing class sizes in medicine, and increasingly busy medical curricula, which impacts upon the time available to students in the class to master essential clinical skills.
Limitations: This study was limited by small sample size, single institution and only ten diagnoses included.
Ethics committee approval: Approval for the study was granted by the Research Ethics Committee at the National University of Ireland, Galway.
Funding: Received from National Doctors Training and Planning.
Author Disclosures:
K. Dunne: nothing to disclose
D. Byrne: nothing to disclose
S. Lydon: nothing to disclose
P. McCarthy: nothing to disclose
C. Madden: nothing to disclose

MyT3 12-13 16:44
Evaluation of haemodynamic changes in the middle cerebral artery in smokers: an ultrasonography study
M. D. P. Brazuna[1], L. P. V. Ribeiro[2], S. Rodrigues[1], A. F. Abrantes[1], R. P. P. Almeida[1], M. V. C. Reis[1], K. B. Azevedo[1]; *[1]Faro/PT, [2]Parchal/PT (marciobrazuna@hotmail.com)*

Purpose: The effect of cigarette smoking on the brain is not clearly understood but is probably multidirectional and complex, predominantly affecting the circulatory system, both general and cerebral. Transcranial Doppler (TCD) ultrasonography is a noninvasive bedside monitoring technique that can evaluate cerebral blood flow haemodynamics in the intracranial arterial vasculature. This study aims to evaluate haemodynamic changes induced by smoking habits in the middle cerebral artery.
Methods and materials: Mean flow velocity (MFV), peak systolic velocity (PSV), end-diastolic velocity (EDV), resistive index (RI) and pulsatility index (PI) were determined in the middle cerebral artery by a trained radiographer. A sample of 34 volunteer participants (17 smokers and 17 non-smokers) were examined using a dedicated ultrasound equipment for the TCD and a comparative study of the haemodynamic parameters measured in both groups was performed.
Results: The mean values of the blood flow velocities measured in the smoking volunteer participants (MFV=53.74cm/s; PSV=89.02cm/s; EDV=38.10cm/s) were lower compared to non-smokers (MFV=59.85cm/s; PSV=99.94cm/s; EDV=39.82cm/s), worsening with the intensity of their smoking habits. Smoking subjects also had a higher blood pressure on average. All these phenomena presented a greater magnitude in male subjects.
Conclusion: The findings provide additional novel evidence of the adverse effects of cigarette smoking on the human brain since smoking has negative effects on middle cerebral artery and haemodynamics. Therefore, smoking is a risk factor for alterations in middle cerebral artery haemodynamics and male smokers are more likely to develop vascular changes. Radiographers can play a key role in the detection of pathophysiological changes from a preventive perspective.
Limitations: This study is limited by the sample size.
Ethics committee approval: Ethics committee approved the study and written informed consent was delivered to the participants.
Funding: No funding was received for this work.
Author Disclosures:
M. D. P. Brazuna: nothing to disclose
L. P. V. Ribeiro: nothing to disclose
S. Rodrigues: nothing to disclose
A. F. Abrantes: nothing to disclose
R. P. P. Almeida: nothing to disclose
M. V. C. Reis: nothing to disclose
K. B. Azevedo: nothing to disclose

MyT3 12-14 16:48
Ultrasound measures of abdominal aortic caliber and quadriceps femoris muscle thickness: influence of physical activity and body mass index
H. S. Ponte[1], L. P. V. Ribeiro[2], S. Rodrigues[1], A. F. Abrantes[1], A. D. M. Ribeiro[3], R. P. P. Almeida[1], M. V. C. Reis[1], T. C. P. L. Guerreiro[4]; *[1]Faro/PT, [2]Parchal/PT, [3]Portimão/PT, [4]Santiago Do Cacém/PT (henrique_s_ponte@hotmail.com)*

Purpose: To evaluate the influence of physical activity level, body mass index (BMI) and gender on the ultrasound measurement of abdominal aortic caliber and quadriceps femoris muscle thickness.
Methods and materials: The International Physical Activity Questionnaire (IPAQ) was applied to 52 healthy volunteers to evaluate the health-related physical activity (PA) and BMI values were determined through a body composition analysis scale. Measurements of quadriceps femoris muscle thickness and abdominal aortic caliber were performed from B-mode ultrasound images, acquired twice by two independent radiographers. The thickness of the rectus femoris and vastus intermedius (RFVIMT), vastus medialis (VMMT) and vastus lateralis (VLMT) were measured. Standardised images of the aorta were recorded at three different levels: below the level of the origin of the splenic artery (AAC-SA), below the level of the origin of the renal arteries (AAC-RA) and 1-3 cm above the bifurcation (AAC-B).
Results: IPAQ showed that 21.2% of participants had a low PA level, 25.0% had a moderate PA level and 53.8% had a high PA level. Regarding BMI, 7.7% of the volunteers were classified as underweight, 63.5% as normal, 21.2% as overweight and 7.7% as obese. Significant positive correlations were observed between BMI and ACC-RA (r = 0.298, P= 0.032), BMI and RFVMIT (r = 0.638, P= 0.000), BMI and VLMT (r = 0.442, P= 0.001). Significant negative relationships were observed between gender and AAC-B (r = - 0.424, P= 0.002) and between gender and VMMT (r = - 0.536, P= 0.000).
Conclusion: A healthy lifestyle with proper physical activity levels is essential for the prevention of major cardiovascular diseases, obesity, muscular weakness, among others. However, further studies in this field are required.
Limitations: This study was limited by the sample size.
Ethics committee approval: Ethics committee approved the study.
Funding: No funding was received for this work.
Author Disclosures:
H. S. Ponte: nothing to disclose
L. P. V. Ribeiro: nothing to disclose
S. Rodrigues: nothing to disclose
A. F. Abrantes: nothing to disclose
A. D. M. Ribeiro: nothing to disclose
R. P. P. Almeida: nothing to disclose
M. V. C. Reis: nothing to disclose
T. C. P. L. Guerreiro: nothing to disclose

MyT3 12-15 16:52

Radiographers in cath-lab: new operating procedures to improve quality assurance and patient safety

F. Aragona[1], E. Stefani[2], M. Coccato[2], M. Centenaro[1], S. Cuman[3]; [1]*Treviso/IT,* [2]*Conegliano/IT,* [3]*Varese/IT*

Purpose: To analyse logistics arrangements in a modern cath-lab and to develop operating procedures for radiographers to improve teamwork and dose reduction during coronary angiography and angioplasty. To underline how multi-professional approach and competence enhancement affect quality during cardiac interventional procedures.
Methods and materials: Data produced are from international guidelines and from the literature review. Human and technological resources have been analysed. Cath-lab of the study has been compared to three major labs of regional heart disease-hub hospitals. Phantom based quality assurance measurements have been taken before the implementation of new operating producedures. A squared radiation field has been used to test dose amount with a normal and a low dose protocol.
Results: Operating procedures have been developed in order to define professional roles and responsibilities. Teamwork improved quality of services by sharing the procedures created. Dose reduction is expected to be significant with correct application of protocols and resultant time decrease. According to physical measurements, the use of low-dose protocol does not affect image quality.
Conclusion: Consciousness and cooperation between professionals are essential in a cath-lab. It allows a better interventional activities organisation, timing optimisation and risk management. The use of the low-dose protocol is recommended during angiography and angioplasty.
Limitations: n/a
Ethics committee approval: n/a
Funding: No funding was received for this work.
Author Disclosures:
F. Aragona: Author at Università degli Studi di Padova
E. Stefani: Author at AULSS 2 Marca Trevigiana
M. Centenaro: Author at AULSS 2 Marca Trevigiana
S. Cuman: Author at AULSS 2 Marca Trevigiana
M. Coccato: Author at AULSS 2 Marca Trevigiana

MyT3 12-16 16:56

The environment preventing female radiological technologists from improving their career prospects: filling the duration of their pregnancy and child-rearing

T. Nakamura[1], S. Suzuki[2], K. Kato[3], S. Kamiya[4], S. Asegawa[1]; [1]*Shizuoka/JP,* [2]*Toyoake/JP,* [3]*Kanagawa/JP,* [4]*Nagoya/JP*

Purpose: There is a wide variety of diagnostic equipment for breast cancer and is becoming more technologically advance as years go by. A lot of female radiological technologists are worried about returning to work after taking maternity leave or childcare leave, some might be worried about being rusty with their skills and knowledge when returning to work, so we wanted to conduct this study to be able to help them with their reinstatement at work. The study aims to determine the necessary environment in order to balance work and child-rearing of female radiological technologists.
Methods and materials: Questionnaire surveys and interviews were conducted for technologists who can't participate in study sessions due to various problems including parenting, and examine the responses and what's the necessary environment in order to balance work and child-bearing.
Results: The results showed that regular study meetings should be done, where they can learn with children in the community, can freely participate, and can allow them to deepen the connection and share their concerns between technologists participating in the study group, and this kind of study will help support female radiological technologists who would like to continue working while reducing anxiety on return after childcare leave.
Conclusion: This type of study that can participate with children can hope to raise the level of child bearing generations of technicians and furthermore continue education during the childcare period that had previously hindered female career progress.
Limitations: This study conducted a survey of specific people and organisations.
Ethics committee approval: Obtained approval from our ethics committee (ECD2018-002).
Funding: No funding was received for this work.
Author Disclosures:
T. Nakamura: nothing to disclose
S. Suzuki: nothing to disclose
K. Kato: nothing to disclose
S. Kamiya: nothing to disclose
S. Asegawa: nothing to disclose

MyT3 12-17 17:00

Development of radiographer scheduling system considering skills and training: a case study

K. Hidaka, T. Miyamoto*; Suita/JP (hidaka@hp-rad.med.osaka-u.ac.jp)*

Purpose: Radiographers are limited human resources. From the long-term perspective of hospital administration, staff training is also an important issue. Allocating appropriate shifts is difficult for radiographers who manage the scheduling. Our objective is to construct an integer programming model of radiographer scheduling that considers the skills and training of radiographers to compare the results of computational experiments using real data.
Methods and materials: A mathematical optimisation model was constructed with the scheduling of radiographers as an integer programming problem. More than one staff member is allocated each day by modality, room, and time zone as a shift. Radiographer skills were set at three skills: self, trainer, and responsible skill. We included 32 restrictions, such as off-duty and the upper limit of the number of night shifts. Shifts were scheduled by minimising each radiographer's workload. We compared the workload of radiographers between shifts using actual data collected over two months in 2018 and the radiographer scheduling model to derive shifts. Analysis conditions were as follows: the number of staff 59, shifts 2379, trainee staff 2, modalities 15, rooms 57, days 38, the workload of daytime shift 1, swing shifts 3, and graveyard shifts 5.
Results: All staff were allocated shifts and off-duty without constraint violation. By optimising scheduling, the staff workload was equalised. The workload of each staff member could be reduced as compared to scheduling performed by the shift creator (average workload of optimisation model 36.8, real data 37.0), and the load of the shift creator could be reduced (calculation time was short, i.e. <30s).
Conclusion: It was useful for radiographer scheduling management to allocate shifts by optimising the workload.
Limitations: n/a
Ethics committee approval: n/a
Funding: This work was supported by JSPS KAKENHI (Grant-in-Aid for Scientific Research (C), Grant Number JP17KO9235).
Author Disclosures:
K. Hidaka: Speaker at Division of Radiology, Department of Medical Technology, Osaka University Hospital, Research/Grant Support at JSPS KAKENHI Grant-in-Aid for Scientific Research (C)
T. Miyamoto: Research/Grant Support at JSPS KAKENHI Grant-in-Aid for Scientific Research (C), Author at Graduate School of Engineering, Osaka University

MyT3 12-18 17:04

A radiographers' preceptorship: educational needs in the United Arab Emirates

M. M. Abuzaid[1], W. Elshami[1], S. Hamid[2], M. A. Musallam[1]; [1]*Sharjah/AE,* [2]*Waterford/IE (mabdelfatah@sharjah.ac.ae)*

Purpose: Acting as preceptors, radiographers play an integral role in the preparation of the next generations. Therefore, hearing and responding to their stories is essential to the quality of the radiology education programme. The study investigates the educational needs of radiographer's preceptors and factors affecting their preceptorship role.
Methods and materials: A cross-sectional study among hospitals in the UAE who received students for radiography training. A survey covered demographics, education, practice, training, needs assessment scale, course content, and a teaching methods assessment scale.
Results: One-hundred twelve out of one hundred thirty invited radiographers from hospitals across the UAE responded. The preceptorship is un-paid services. 32.4% were nationals, 67.6% ex-pats, 48.6% males, 51.4% females, 63% baccalaureate (43%) diploma and (6%) master degree. 21% indicated that they did not receive dedicated preceptor training. The maximum training duration provided by local universities ranged from one to two days per academic years. The training concentrated on practice roles, regulation, and communications skills and students evaluation. 85% believed that a proper preceptor-training programme would improve preceptorship skills and students outcome. 62% were able to identify the barriers to preceptor training.
Conclusion: Standard and dedicated training programmes are required to enhance the quality of preceptorship and students practical experience. Precept knowledge and teaching skills can support education strategies for new radiographers generation.
Limitations: Surveying of department managers on their perceptions towards the preceptor-training programme.
Ethics committee approval: Approved by the University of Sharjah, Research and Ethics Committee.
Funding: No funding was received for this work.
Author Disclosures:
M. M. Abuzaid: Author at University of Sharjah
W. Elshami: Advisory Board at University of Sharjah
S. Hamid: Author at Depended Researcher
M. A. Musallam: Author at Ministry of Health And Prevention

MyT3 12-19 17:08

The impact of talking to "experts by experience" on students' empathy scores

G. Harrison, A. Harris*; London/UK (gillhaha@gmail.com)*

Purpose: This study aims to assess medical ultrasound students' empathy scores in response to interaction with 'experts by experience'.
Methods and materials: Students completed the Toronto Empathy Questionnaire[5] before and after an interactive teaching and learning session with four 'patients'. Students completed a short questionnaire and were asked to reflect on what they had learnt and how it might impact their future practice. 23 students (48%) participated in the study at a single institution across two cohorts. A further cohort will be recruited.
Results: Twenty empathy scores were valid. Females had higher mean empathy scores initially and after the session, however males had a higher overall increase in mean empathy score after the interactions. Empathy scores increased or stayed the same for 75% of students. The event met or exceeded students' expectations.
Conclusion: Mean empathy levels were higher than published norms and increased or remained the same for three quarters of students after the session. Empathy can lead to improved trust between health care provider and patient, compliance with instructions and treatment, patient satisfaction and outcomes, so it is important to ensure ways to increase empathy and compassion are incorporated into the curriculum. Students highlighted various ways to change practice in light of this session, which would impact on patient care and communication.
Limitations: Students were self-selecting, which may impact on the results.
Ethics committee approval: Ethics approval was granted from the School of Health Sciences, City, University of London.
Funding: No funding was received for this work.
Author Disclosures:
G. Harrison: Investigator at City, University of London
A. Harris: Investigator at City, University of London

MyT3 12-20 17:12

Using a standardised patient to authentically replicate the clinical experience during a trauma simulation for third-year radiological technology students in a Canadian undergraduate programme

S. Lea, R. Macleod*; Halifax, NS/CA (stephanie.lea@dal.ca)*

Purpose: Third-year radiological technology students at Dalhousie University must demonstrate the required knowledge, skills, and competence to safely, accurately, and efficiently perform complex radiographic examinations on a trauma patient. Student competency is assessed by a simulation; this simulation was not previously designed following established standards of best practice and lacked authenticity. Adding a standardised patient to simulation has been reported to improve authenticity in nursing and medical literature, but this has not been investigated in a radiography programme.
Methods and materials: Fourteen third-year radiological technology students completed a timed (30 minute) trauma simulation; this was the first time a standardised patient has been used as part of a simulation. Using open-ended interview questions students were individually interviewed and they described their experience participating in a trauma simulation that used a standardised patient. The transcripts were compiled and coded; phenomenological thematic analysis was used and resultant themes were verified with participants.
Results: Students enjoyed having a standardised patient as part of the simulation and stated that it made the experience realistic and authentic. Students found that they needed to employ their patient care and communication skills much more than in previous simulation experiences.
Conclusion: Standardised patients add authenticity to the radiological technology trauma simulation and students' patient care and communication skills can be more accurately assessed. This model of simulation will continue to be part of the Dalhousie radiological technology programme.
Limitations: The authors acknowledge they are both the designers of the simulation and educators of the students participating in the simulation; participation in the study was completely voluntary. As this is a qualitative study the results cannot be generalisable.
Ethics committee approval: The study went through REB and a written consent form was completed.
Funding: No funding was received for this work.
Author Disclosures:
S. Lea: nothing to disclose
R. Macleod: nothing to disclose

Saturday, March 14

08:30 - 10:00 **Room B**

Breast

RPS 1302

Imaging-guided breast biopsy innovations

Moderators:
T. Sella; Jerusalem/IL
N.N.

RPS 1302-1 08:30

Shear-wave elastography-guided core-needle biopsy for the determination of breast cancer molecular subtypes

A. Peker, P. Balci, I. Başara Akin, H. A. Özgül, S. O. Aksoy, D. Gurel*; Izmir/TR (doktorpeker@gmail.com)*

Purpose: To investigate the role of shear-wave elastography-guided (SWE) core-needle biopsy for the accurate determination of breast cancer immunohistochemical subtypes.
Methods and materials: This study was conducted between May 2018 and April 2019 and included adult patients who had a lesion larger than 1 cm and were referred for a core-needle biopsy. Patients were divided into two groups by block randomisation. B-Mode ultrasonography-guided biopsy (control group, group 1) and SWE-guided biopsy (group 2) were performed in a total of 60 lesions. The biopsy in the control group was recorded as biopsy A, the SWE-guided biopsy from the relatively rigid area of the lesion was recorded as biopsy B, and the biopsy from the relatively less rigid area of the lesion was recorded as biopsy C. Diagnosis and immunohistochemical results were recorded and compared with the surgical results.
Results: The mean lesion sizes were 33.2 ± 22.6 mm in group 1 and 27.8 ± 11.9 mm in group 2. Sensitivity was 96.7% in biopsy A and 100% in biopsy B and C. Benign-malignant accuracy was 94.7%, 100%, and 90%, and diagnostic accuracy was 89.5%, 100%, and 90% in biopsy A, B, and C, respectively. When immunohistochemical markers were evaluated in one patient (14.3%) at biopsy A, Her2 receptor status was wrong. When the 10% difference in ER, PR, and Ki67 rates were considered significant, the accuracy of ER was highest in biopsy B as 77.8% (p = 0.04). Accuracy in immunohistochemical subtyping was 100% in biopsy B, and 71.4% in biopsy A and C (p = 0.08).
Conclusion: SWE-guided core-needle biopsy of breast lesions increased sensitivity, diagnostic accuracy, and accuracy in immunohistochemical subtyping to 100%.
Limitations: See attached file.
Ethics committee approval: Approved by the institutional ethics committee.
Funding: Funded by the University Department of Scientific Research Projects.
Author Disclosures:
A. Peker: nothing to disclose
P. Balci: nothing to disclose
I. Başara Akin: nothing to disclose
H. A. Özgül: nothing to disclose
S. O. Aksoy: nothing to disclose
D. Gurel: nothing to disclose

RPS 1302-2 08:36

Ultrasound-guided tattooing of axillary lymph nodes in patients prior to neoadjuvant therapy and the identification of tattooed nodes at the time of surgery

N. Rotbart[1], T. Allweis[2], T. Menes[3], Y. Rapson[4], H. Cernik[2], I. Bokov[2], O. Golan[3], O. Givon Madhala[1], A. Grubstein[1]*; [1]Petah Tikva/IL, [2]Rehovot/IL, [3]Tel Aviv/IL (noarotbart@yahoo.com)*

Purpose: Breast cancer patients with lymph node metastases at diagnosis often undergo neoadjuvant therapy. Identification of a LN which regressed after NAC remains a challenge. A new concept of targeted axillary lymph node dissection has recently been proposed which involves the removal of a node with documented metastases in addition to the removal of the nodes most likely to harbour disease.
The aim of the study was to evaluate the possibility of tattooing biopsied nodes prior to NAT and identifying them at the time of surgery.
Methods and materials: Carbon suspension was injected into axillary LNs before starting NAC. During surgery, an attempt was made to identify the tattooed LN, which was removed and sent for pathological evaluation. All patients underwent a sentinel lymph node biopsy and/or axillary lymph node dissection as mandated by their clinical status.
Results: 63 patients underwent tattooing of involved axillary lymph nodes. At surgery, a tattooed node was identified in 60 patients (95.2%). Of 50 patients in whom both radioactivity and tattoo were identified in axillary LNs, 40 (80%) lymph nodes were radioactive and tattooed, however in 10 patients (20%) the tattooed LN was not radioactive.
Conclusion: Ultrasound-guided tattooing of involved axillary lymph nodes prior to neoadjuvant therapy is a safe, effective, and easily performed method of marking these nodes for future identification at the time of surgery. We found the tattooing was helpful in identifying the marked LN in the majority of cases. In our study, the identification rates of tatooed nodes was about 95.2%.
Limitations: The main limitation was the small number of patients.
Ethics committee approval: The study protocol was approved by our institutional review board and patients signed informed consent prior to injection.
Funding: No funding was received for this work.
Author Disclosures:
N. Rotbart: nothing to disclose
T. Allweis: nothing to disclose
T. Menes: nothing to disclose
Y. Rapson: nothing to disclose
H. Cernik: nothing to disclose
I. Bokov: nothing to disclose
O. Golan: nothing to disclose
O. Givon Madhala: nothing to disclose
A. Grubstein: nothing to disclose

RPS 1302-3 08:42

Stereotactic 9-gauge vacuum-assisted breast biopsy: how many specimens do we need?

B. M. Den Dekker, P. J. van Diest, S. de Waard, H. Verkooijen, R. M. Pijnappel*; Utrecht/NL (bm.den.dekker@hotmail.com)*

Purpose: To determine the minimum number of stereotactic 9-gauge vacuum-assisted breast biopsy (VABB) specimens required to establish a final histopathological biopsy diagnosis of mammographically suspicious lesions.
Methods and materials: A total of 120 women referred for VABB of 129 mammographically suspicious lesions were included (December 2017-October 2018). Stereotactic 9-gauge VABB was performed, acquiring twelve specimens per lesion. Calcification retrieval was assessed with individual specimen radiography. Each specimen was histologically analysed in chronological order and findings were compared with the final histopathological result after assessment of all 12 specimens and with results of surgical excision. Cumulative diagnostic yield per specimen was calculated.
Results: In total, 131 VABB procedures were performed in 120 women (mean age 59y). In 95% (95%CI 90%-98%) of the procedures, a final histopathological biopsy diagnosis was reached after 6 specimens. After 9 specimens, the final diagnosis was established in all 131 cases. In the 41 patients with a DCIS or invasive diagnosis at biopsy, there were 8 procedures (20%) where calcifications were retrieved before the diagnostic specimen was obtained. Underestimation of subsequent resection diagnosis occurred in 6 out of 30 excised lesions classified as DCIS(20%) and in 1 out of 4 excised high-risk lesions.
Conclusion: With 6 stereotactic 9-gauge VABB specimens, a final histopathological biopsy diagnosis could be established in 95% (95%CI 90%-98%) of the procedures. Taking 9 specimens seems to be optimal. Ending the stereotactic VABB procedure as soon as calcifications are retrieved may cause false-negative results.
Limitations: Study-pathologist was not blinded to study design and clinical histopathological result. Fixed biopsy protocol was used, irrespective of lesion size and location relative to the needle.
Ethics committee approval: Approval from the IRB of the UMCU and written informed consent from study participants was obtained.
Funding: Funding was received from Hologic.
Author Disclosures:
B. M. Den Dekker: Research/Grant Support at Hologic
P. J. van Diest: nothing to disclose
S. de Waard: nothing to disclose
H. Verkooijen: nothing to disclose
R. M. Pijnappel: nothing to disclose

RPS 1302-4 08:48

Failure of stereotactic core-needle biopsy in women recalled for suspicious microcalcifications at screening mammography: frequency, causes, and final outcome in an observational follow-up study

J. L. R. Lameijer[1], L. Duijm[2]*; [1]Eindhoven/NL, [2]Nijmegen/NL (joostlameijer@gmail.com)*

Purpose: To determine the failure rate of stereotactic core-needle biopsy (SCNB) and its causes and final outcome in women recalled for microcalcifications at screening mammography.
Methods and materials: We included a series of 466,647 screens obtained in a Dutch screening region between January 2009 and January 2017. Radiology

reports and pathology results were obtained of all recalls during two-year follow-up.
Results: A total of 2,815 women (19.9% of 14,142 recalls) were recalled for suspicious microcalcifications. SCNB was indicated in 2,220 women, of which 10 refused a biopsy. Breast cancer (DCIS or invasive cancer) was diagnosed in 671 of 2,210 women (30.4%). SCNB was technically not feasible in 36 women (1.6%, 36/2,210), of which ten underwent surgical biopsy (5/10 positive). Pathology showed no calcifications and no malignancy in the SCNB specimen in 30 women after SCNB (1.5%, 30/1,974), of which 5 proved to have breast cancer at subsequent surgery. The remaining 25 women, without a diagnosis of breast cancer two years after the recall, underwent follow-up imaging (n=14), surgical excision with the benign outcome (n=4), or were asked to re-attend the screening programme without follow-up (n=7). Breast cancer was diagnosed in 15% of women (10/66) who experienced either SCNB cancellation due to technical limitations, or whose SCNB yielded no malignancy in the absence of calcifications in the specimen.
Conclusion: Although the failure rate of SCNB is very low, a close surveillance with a low threshold for surgical biopsy is warranted as we found that breast cancer was present in 15% of these women.
Limitations: Due to differences in programmes, our data may not be extrapolated to other screening programmes.
Ethics committee approval: Ethical approval was waived.
Funding: No funding was received for this work.
Author Disclosures:
J. L. R. Lameijer: nothing to disclose
L. Duijm: nothing to disclose

RPS 1302-5 08:54
Conventional imaging occult DCIS diagnosed on MRI-guided biopsy: can we predict upgrade on surgical pathology?
Y. Amitai[1], T. Menes[2], A. M. Scaranelo[1], S. Kulkarni[1], S. Ghai[1], R. Fleming[1], V. Freitas[1]; [1]*Toronto, ON/CA,* [2]*Tel Aviv/IL (yoavslava@yahoo.com)*

Purpose: To identify clinical and imaging features of upgrade for invasive disease in patients with conventional imaging occult ductal carcinoma in situ (DCIS) diagnosed on MRI-guided biopsy.
Methods and materials: Results of consecutive patients with MRI-detected pure DCIS, occult on conventional imaging (CI) including mammography and ultrasound performed in a tertiary academic hospital in 2009-2018, were reviewed. Women were divided into 2 groups based on the gold standard final pathology: Pure DCIS or DCIS with an invasive component. Final surgical pathology was used to validate MRI results.
Results: 50 patients fulfilled the inclusion criteria and formed the study cohort. 46 patients (92%) had non-mass enhancement (NME) yielding pure DCIS diagnosis compared to 4 enhancing masses. The most common NME distribution was focal (22, 48%). The most common kinetic pattern was persistent (24, 48%). Overall, 12 patients (24%) were upgraded to invasive malignancy on final pathology. The only parameter showing statistically significant association with upgrade was kinetic characteristics; 10 (40%) of the women with plateau or washout kinetics, versus 2 (8%) of the women with progressive kinetics were upgraded to invasive cancer on surgery (P=0.034). On multivariate analysis, progressive kinetics remained inversely associated with upgrade when compared to washout kinetics (OR=0.012; P<0.021; 95% CI 0.02;0.73).
Conclusion: The washout kinetic pattern of enhancement proves to be the best predictor of invasion in conventional imaging occult DCIS diagnosed on MRI-guided biopsy. It may have implications for treatment planning as sentinel lymph node biopsy may be considered in the primary surgical procedure for this subset of patients. Larger studies should be encouraged to consolidate our findings.
Limitations: Retrospective design. High level of interobserver variability in DCIS. No diffusion calculations.
Ethics committee approval: n/a
Funding: No funding was received for this work.
Author Disclosures:
Y. Amitai: nothing to disclose
T. Menes: nothing to disclose
A. M. Scaranelo: nothing to disclose
S. Kulkarni: nothing to disclose
S. Ghai: nothing to disclose
R. Fleming: nothing to disclose
V. Freitas: nothing to disclose

RPS 1302-6 09:00
Tomosynthesis-guided vacuum-assisted biopsy for mammographic low-contrast, non-calcific lesions: technical and pathologic results
C. Faggioli[1], K. Jerman[2], A. Linda[2], R. Girometti[2], C. Zuiani[2]; [1]*Gorizia/IT,* [2]*Udine/IT*

Purpose: To evaluate technical and pathologic outcomes of tomosynthesis-guided vacuum-assisted biopsy (DBT-VAB) performed on low-contrast, non-calcific lesions (LC-NCL) found at mammography.
Methods and materials: Of women referred to DBT-VAB in our institution between January 2017 and March 2018, we retrospectively included 152 patients with 154 sonographically occult LC-NCL. Two radiologists with 15 and 2 years of experience in breast imaging worked in consensus to review mammographic examinations, radiology reports, and pathology reports to record patients' and lesions' features, the rate and reasons for technical failure, as well as pathologic and follow-up results (up to 12 months).
Results: DBT-VAB was unfeasible in 14/154 LC-NCL (9%) presenting as architectural distortions (11/14), asymmetry (2/14), and opacity (1/14). Reasons were lack of target visualisation and deep location in 13/14 and 1/14 cases, respectively. None of the patients developed malignancy at imaging follow-up. DBT-VAB was performed in the remaining 140/154 (91%) LC-NCL, including 66/140 (47%) architectural distortions, 46/140 (33%) opacities, 19/140 (14%) asymmetries, and 9/140 (6%) mixed lesions. Complications occurred in 11/138 (8%) patients, including 9 haematomas, 1 vasovagal reaction, and 1 subcutaneous emphysema. Biopsy found 25/140 (18%) malignant lesions (B5), 36/140 (26%) high-risk lesions (B3), 76/140 (54%) benign lesions (B2), and (2%) normal tissue in 3/140 cases (B1). After surgical excision, 7/36 high-risk lesions were upgraded to malignancy (2 invasive and 5 DCIS), corresponding to an underestimation rate of 19%. Additionally, surgical excision and/or follow-up demonstrated malignancy in 2/9 cases of imaging-pathology discordant B2 lesions. No malignancy was found at surgical excision of B1 lesions. Overall, the malignancy rate was 24%.
Conclusion: DBT-VAB was feasible in the majority of LC-NCL, with a few complications. About one-fourth of LC-NCL was malignant, supporting the need for biopsying those mammography findings.
Limitations: Monocentric and retrospective design.
Ethics committee approval: Informed consent waived because of the retrospective design.
Funding: No funding was received for this work.
Author Disclosures:
A. Linda: nothing to disclose
C. Faggioli: nothing to disclose
K. Jerman: nothing to disclose
R. Girometti: nothing to disclose
C. Zuiani: nothing to disclose

RPS 1302-7 09:06
Value of targeted fusion US with virtual mammographic navigation in B3 lesions
V. E. Gazhonova, M. Efremova, E. Bachurina, T. Kuleshova, H. Khlustina; *Moscow/RU (vx969@yandex.ru)*

Purpose: To evaluate the role of second-look targeted fusion MMG/US navigation in BI-RADS 3 lesions in comparance to standard HHUS.
Methods and materials: 45 women with 50 B3 lesions on mammography followed by ultrasound were studied by two experts for breast US (GV18y.exp; PI25 y.exp) blinded to each other results. The first radiologist performed standard HHUS and the second fusion ultrasound with virtual mammographic navigation. Fusion US and conventional HHUS were performed on My LAB Twice (ESAOTE) with a linear transducer BL433 (3-18MHz). 25 B3 lesions were biopsied under US and 10 with stereotactic MMG, 15 follow up for 2 years. The ROC-curves were compared for both methods.
Results: B3 lesions were upgraded to B5 by HHUS in 14 pts, and in 20 by fusion US, with cancer proven in 18 pts. B3 lesions were downgraded to B2 in 20 by HHUS, and in 25 by fusion US, none of them appearing to have cancer. ROC-curve analysis showed that fusion was superior to HHUS with AUC 0,889 (95%CI 0,768 to 0,960), and 0,794 (95%CI 0,656 to 0,895), respectively. Fusion US were superior to HHUS in the cases of grouped microcalcifications and subtle less than 4 mm B3 lesions. Agreement in BIRADS category between the examiners was 0,82.
Conclusion: Fusion US with virtual mammographic navigation may help in identify microcalcification and subtle less than 4 mm B3 lesions, thus increasing the diagnostic performance of targeted US.
Limitations: Limitations of the study were consecuted patients with B3 lesions and a small group of cancer patients.
Ethics committee approval: Written consent was received from all patients. The examination was approved by the Institutional Ethical Committee.
Funding: No funding was received for this work.
Author Disclosures:
V. E. Gazhonova: nothing to disclose
M. Efremova: nothing to disclose
E. Bachurina: nothing to disclose
T. Kuleshova: nothing to disclose
H. Khlustina: nothing to disclose

RPS 1302-8 09:12

Calcified lesions with a low risk of malignancy on mammography and uncertain malignant potential (B3) detected at stereotactic vacuum-assisted breast biopsy

Z. C. Milosevich, V. Urban, K. Obradovic, N. Adzic, M. Nadrljanski; *Belgrade/RS*

Purpose: To analyse the management and outcome of calcified lesions with a low risk of malignancy on mammography (BI-RADS category 4a) and uncertain malignant potential (B3) detected at stereotactic vacuum-assisted breast biopsy (SVAB).
Methods and materials: Retrospective analysis of 91 consecutive SVAB procedures was performed. Inclusion criteria were BI-RADS category 4a calcified lesions on screening mammography and histologic diagnosis of B3 lesions. The three groups of patients were defined, based on the post-biopsy multidisciplinary team decisions, as 1) with a definite histology after surgical excision, 2) with breast dynamic contrast-enhanced magnetic resonance imaging (DCE-MRI) after SVAB, prior to surgical excision, and 3) the group that is followed by annual physical assessment and mammography. Malignancy rates were evaluated for each group.
Results: The first group consisted of 13 patients (14.3%), the second of 20 (22.0%), and the third of 58 (63.7%). Atypical ductal hyperplasia lesions (isolated or associated with other B3 lesions) were found in 45.0% patients, papillary lesions in 31.9%, lobular intraepithelial neoplasia in 15.4%, flat epithelial atypia in 6.6%, and radial scar in 1.1%, with no significant difference of B3 lesions histologic types between the three groups (p=0.09). An upgrade to malignancy in the first group was 38.5% (5 patients) and in the second, 20.0% (4 patients). Taking into account the absence or presence of angiogenesis on DCE-MRI, a negative predictive value of DCE-MRI was 92%. In the third group, 1-year to 6-year follow-up was negative for breast malignancy.
Conclusion: The rates of upgrade to malignancy in our study were high, up to 38.5%. The post-biopsy DCE-MRI may be an useful tool for further management of B3 lesions.
Limitations: Retrospective analysis study.
Ethics committee approval: n/a
Funding: No funding was received for this work.
Author Disclosures:
Z. C. Milosevich: nothing to disclose
V. Urban: nothing to disclose
K. Obradovic: nothing to disclose
N. Adzic: nothing to disclose
M. Nadrljanski: nothing to disclose

RPS 1302-9 09:18

Comparison of calcification retrieval performance between upright tomosynthesis-guided and prone stereotactic vacuum-assisted breast biopsy

T. Uematsu; *Shizuoka/JP (t.uematsu@scchr.jp)*

Purpose: To compare the calcification retrieval performance of upright tomosynthesis-guided vacuum-assisted breast biopsy (Tomo VAB) with that of prone stereotactic vacuum-assisted breast biopsy (ST VAB).
Methods and materials: A retrospective review of records revealed 176 calcification lesions not detected by ultrasound in 176 women who underwent Tomo VAB or ST VAB. A mean of 6 specimens per lesion were obtained using 9-gauge or 11-gauge needle. Calcification retrieval success was defined as identification of calcifications on specimen radiographs. Procedure time, estimated exposure dose, and complications were also evaluated.
Results: During the study period, 88 ST VAB in 88 patients and 88 Tomo VAB in 88 patients were performed. Each calcification retrieval success rate was the same (99% vs 99%). No complications were observed in either group. Mean procedure time was shorter with Tomo VAB vs ST VAB (16 vs 26 min, respectively; p<.001), and fewer estimated exposure doses were acquired with Tomo VAB vs ST VAB (4.35mGy vs 9.6mGy, respectively; p<.001) as during Tomo VAB, only 3 reference tomosynthesis images were generally obtained, while 8 reference 2D images were generally obtained during ST VAB.
Conclusion: Tomo VAB has the same degree of clinical performance for diagnosing calcifications as ST VAB and can be performed in less than two thirds of the ST VAB procedure time and with about half of the exposures in ST VAB.
Limitations: This study had some limitations, mainly resulting from its retrospective single-institution nature and small patient numbers. Another limitation is that our comparison groups were not randomised but were rather divided by time.
Ethics committee approval: This retrospective study was approved by our institutional review board and the requirement to obtain informed consent was waived.
Funding: No funding was received for this work.
Author Disclosures:
T. Uematsu: nothing to disclose

RPS 1302-10 09:24

The value of contrast-enhanced ultrasound in breast cancer biopsy

Y. Zhu, Y. Chen, J. Jiang; *Shanghai/CN (tttmax2004@126.com)*

Purpose: To investigate the value of contrast-enhanced ultrasound (CEUS) in breast cancer biopsy.
Methods and materials: A total of 49 consecutive patients with biopsy-confirmed breast cancer were enrolled in this retrospective cohort study. All patients underwent CEUS to evaluate the homogeneity of perfusion of breast lesions. For lesions showed homogeneous enhancement on CEUS, the centre part and peripheral part were biopsied respectively. For heterogeneously enhanced lesions, the biopsies were thus performed targeting both the enhanced regions and non-enhanced regions. The sample adequacy rate and core cancer involvement of the biopsy cores taken from the enhanced regions were compared with those from the non-enhanced regions.
Results: A total of 53 breast cancer lesions were biopsy-confirmed in 49 patients. CEUS revealed homogeneous enhancement in 8 of 53 breast cancers (15.1%) and heterogeneous enhancement in 45 of 53 breast cancers (84.9%). The sampling adequacy rate was 98.5% for biopsy cores taken from the enhanced regions, significantly higher than those from the non-enhanced regions (72.9%, P<0.01). The core cancer involvement was higher in enhanced regions than non-enhanced regions (median: 55% vs 30%, P<0.01).
Conclusion: CEUS can differentiate the active area and necrotic fibrosis area of breast tumours by displaying the microvessels and might be the possible solution to the problem of biopsy site selection.
Limitations: This study might be limited by its retrospective study design and that all the patients were enrolled with biopsy-proven breast cancer.
Ethics committee approval: This retrospectively designed, single-institution study was approved by the local institutional review board (XHEC-D-2019-015).
Funding: No funding was received for this work.
Author Disclosures:
Y. Zhu: nothing to disclose
Y. Chen: nothing to disclose
J. Jiang: nothing to disclose

RPS 1302-11 09:30

Vacuum-assisted excision (VAE) as an alternative to open surgical excision for B3 lesions in a screening clinical unit

I. Allajbeu, K. Taylor, P. L. Moyle, C. Breast Unit, F. J. Gilbert; *Cambridge/UK (ia359@cam.ac.uk)*

Purpose: To investigate the usage of VAE techniques as an alternative approach to open excision diagnostic procedure for B3 lesions in clinical practice.
Methods and materials: Retrospective data collection was via K62, National Health Service Breast Screening Programme (NHSBSP) database, to identify all patients diagnosed with B3 lesions on biopsy between April 2015-March 2019. Audit standard was NHSBSP No.49 guidelines on B3 lesions. Mammographic findings, biopsy type, management, and final pathology results were recorded for each patient. Upgrade/downgrade rates were calculated for each subtype and compared with the previous years.
Results: 105 patients had B3 histopathology on core biopsy (CB), 14 G or vacuum-assisted biopsy (VAB) 9G. From these, 72 patients had VAE, either stereotactic or under ultrasound, and 20 surgical excision as second line, decided by MDT. 70 of the B3 lesions stayed the same/were downgraded to B2 in their final histopathology. 2 of the B3 lesions were upgraded to B5a (high grade DCIS) by VAE as second line. There was a progressive increase in second-line VAE from 58% in 2015 and to 80% in 2019. The unit was 94% concordant with the standard in terms of performed investigation for each lesion subtype.
Conclusion: The data shows our VAE policy saves patients having unnecessary operations for benign disease.Therefore, VAE should always be considered as an alternative pathway to the open surgical excision for the majority of B3 lesions in concordance with the official guidelines. This would potentially reduce the benign open biopsy rate whilst maintaining accuracy of cancer diagnosis. Management of all B3 lesions should be discussed in the MDT meetings.
Limitations: Single-centre study with a limited number of patients and data.
Ethics committee approval: n/a
Funding: No funding was received for this work.
Author Disclosures:
I. Allajbeu: nothing to disclose
K. Taylor: nothing to disclose
F. J. Gilbert: nothing to disclose
C. Breast Unit: nothing to disclose
P. L. Moyle: nothing to disclose

RPS 1302-12 09:36
Ultrasound-guided core-needle biopsy of the axillary lymph nodes in different subtypes of newly diagnosed breast carcinoma
M. Jafari, M. Gity, A. Olfatbakhsh, K. Rezaei Kalantari; *Tehran/IR (maryjafarimd@gmail.com)*

Purpose: To assess the diagnostic accuracy of US-guided core needle biopsy (CNB) in the detection of axillary LN metastasis in different subtypes of breast cancer.
Methods and materials: From May 2018 through May 2019, in a prospective study of 1153, 153 cases with biopsy-proven breast cancer showed suspicious axillary LNs in ultrasound. They underwent axillary sampling and then pathologic correlation. 65 patients met the inclusion criteria.
Results: Axillary US-guided CNB correctly identified 55 (84.5%) of the 65 involved LNs. The sensitivity, specificity, positive/negative predictive values, and positive/negative likely hood ratio (LR) of CNB were 75.5 %, 93.7%, 92.5%, 78.9%, 12.2, and 0.25 respectively (p value< 0.001). Interestingly, we found that in hormone-positive tumours, the sensitivity and PPV of axillary CNB were higher, 80.9% and 94.4% respectively (p<0.001). In Her-2 negative cancers, the sensitivity of CNB was more, with no statistically significant difference.
Conclusion: CNB is a fast, simple and minimally invasive technique with a high LR (+) in ruling in and good LR (-) in ruling out the axillary metastasis. Because of the reliability of CNB in preoperative diagnosis of LN metastasis, we could suggest avoiding sentinel LN surgery in post-CNB negative cases similar to post-CNB positive cases. Biological markers seem to affect the CNB pathologic results; this emphasis should be investigated in the studies with larger sample size.
Limitations: The limitations of CNB are including mistargeting of the LN, the discordance of postoperative pathology and biopsy in micrometastasis, the failure of biopsy of deeply located/small-sized LN, trauma to the adjuscent tissue, and pain.
Ethics committee approval: This study achieved ethical approval from the Institutional Board of Motamed cancer institute (ACECR) with approval number of 9610101.
Funding: No funding was received for this research.
Author Disclosures:
M. Jafari: nothing to disclose
M. Gity: nothing to disclose
A. Olfatbakhsh: nothing to disclose
K. Rezaei Kalantari: nothing to disclose

RPS 1302-13 09:42
Breast biopsy performed the same day as diagnostic imaging: does it impact patient care?
K. Coffey, E. Cheang, V. Mango, E. A. Morris, D. D'alessio; *New York, NY/US (coffeyk@mskcc.org)*

Purpose: To determine the time to surgery for patients undergoing diagnostic breast imaging and breast biopsy on the same day compared to patients with imaging and biopsy on separate days.
Methods and materials: Retrospective case-control study reviewing 300 patients from 1/1/2009 to 1/1/2017 was performed. Review included 150 patients with diagnostic breast imaging and breast biopsy performed the same day compared to 150 patients with biopsy performed on days following imaging. Time interval from diagnostic imaging to biopsy, pathological diagnosis, surgical consultation, and surgery was determined.
Results: Same-day biopsies were more often performed in younger patients (55 vs 65 years) with a history of breast cancer (58.9% vs 30.0%), BRCA mutation (4.5% vs 0.8%), clinical symptoms (17.9% vs 10.0%), or a BI-RADS 5 lesion (2.7% vs 1.7%). No significant difference was observed in the time from biopsy to pathologic diagnosis (2.0 vs 1.7 days, p=.056) or from diagnosis to surgical consultation (11.5 vs 13.4 days, p=.43). The time between diagnostic imaging and surgical consultation was significantly shorter in the same-day group (13.3 vs 26.4 days, p<.001). The time from diagnostic imaging to surgery was shorter in the same-day group, however not statistically significant (37.8 vs 45.8 days, p=.16).
Conclusion: Same-day breast biopsies decreased the time from diagnostic imaging to surgical consultation (p<.001) in symptomatic and high-risk patients and may be valuable to patient care even without a statistically significant effect on time to surgery.
Limitations: Limitations include a small sample size.
Ethics committee approval: The United States Institutional Review Board approved this retrospective study with a waiver of informed consent.
Funding: No funding was received for this work.
Author Disclosures:
K. Coffey: nothing to disclose
D. D'alessio: nothing to disclose
E. A. Morris: nothing to disclose
V. Mango: nothing to disclose
E. Cheang: nothing to disclose

RPS 1302-14 09:48
Association of retrospective peer review and positive predictive value of magnetic resonance imaging-guided vacuum-assisted needle biopsies of breast
C. Yalniz[1], J. Rosenblat[2], D. Spak[1], W. Wei[1], M. Scoggins[1], H. C. Le-Petross[1], M. Dryden[1], B. E. Adrada[1], B. E. Dogan[3]; *[1]Houston, TX/US, [2]Los Angeles, CA/US, [3]Dallas, TX/US (mjdinok@yahoo.com)*

Purpose: To evaluate the association between retrospective peer review of breast magnetic resonance imaging-guided vacuum-assisted needle biopsies and positive predictive value of subsequent magnetic resonance imaging-guided biopsies.
Methods and materials: In January 2015, a weekly conference was initiated in our institution to evaluate all breast magnetic resonance imaging-guided vacuum-assisted needle biopsies performed over January 1, 2014-December 31, 2015. During these weekly conferences, 6 anonymised cases were discussed and the faculty voted on whether they agree with the biopsy indication, accurate sampling, and radiology-pathology correlation. We retrospectively compared the magnetic resonance imaging indication, benign or malignant pathology rates, lesion types, and the positive predictive value of magnetic resonance imaging-guided vacuum-assisted needle biopsy in the years before and after initiating this group peer review.
Results: The number of dynamic contrast-enhanced magnetic resonance imaging and magnetic resonance imaging-guided vacuum-assisted needle biopsies before and after initiating the review was 1447 vs 1596 (p=0.0002), and 253 (17.5%) vs 203 (12.7%) (p=0.04), respectively. The positive predictive value of magnetic resonance imaging-guided biopsy significantly increased after group review was implemented (positive predictive value in 2014=%39.1 and positive predictive value in 2015=%48.8) (p=0.03).
Conclusion: Our study showed an association between retrospective peer review of past biopsies and increased positive predictive value of magnetic resonance imaging-guided vacuum-assisted needle biopsies in our institution.
Limitations: A retrospective study performed in a single institution. The small number of patients included decreased the power of the statistical results. MRI-directed ultrasound and ultrasound guided biopsy rates are not included in this study.
Ethics committee approval: This was an institutional review board approved, HIPAA compliant, retrospective case review in which the requirement for patient informed consent was waived.
Funding: No funding was received for this work.
Author Disclosures:
C. Yalniz: nothing to disclose
J. Rosenblat: nothing to disclose
D. Spak: nothing to disclose
W. Wei: nothing to disclose
M. Scoggins: nothing to disclose
H. C. Le-Petross: nothing to disclose
M. Dryden: nothing to disclose
B. E. Adrada: nothing to disclose
B. E. Dogan: Consultant at Endomag, Inc. Cambridge, U.K

08:30 - 10:00 **Room F2**

Genitourinary

RPS 1307

Prostate MRI for differential diagnosis

Moderators:
J. Belfield; Liverpool/UK
M. T. El-Diasty; Jeddah/SA

RPS 1307-1 08:30
Blood oxygenation level-dependent MR imaging for the differentiation of prostate cancer with benign tissue: a preliminary experience
Y. Kim, C. Kim; *Seoul/KR (ytyson@naver.com)*

Purpose: To evaluate the feasibility of blood oxygenation level-dependent (BOLD) magnetic resonance imaging (MRI) in differentiating prostate cancer with benign tissue.
Methods and materials: 145 patients (mean age, 66.8 years) with biopsy-proven prostate cancer who underwent 3-T BOLD MRI at 3T were enrolled. BOLD MRI was performed using a multiple fast-field echo sequence to acquire 12 T2*-weighted images. The R2* value (rate of spin dephasing, 1/sec) was measured in the index tumour (n=145) and the benign peripheral (PZ, n=138) and transition zones (TZ, n=141), and the results were compared. The reproducibility of R2* measurements was evaluated.

Results: Tumour R2* values (26.1 ± 5.9) were significantly different from benign PZ (28.1 ± 9.8) and TZ (22.1 ± 4.0) (P < 0.001). For predicting the tumour, the area under the receiver operating characteristics curve of R2* was 0.606, with the optimal cutoff value of 22.8 (1/sec), resulting in a 73.8% sensitivity and 52% specificity. At the Altman-Bland test, the mean differences in R2* values were 4.9% for tumours, 9.5% for benign PZ, and 2.8% for benign TZ, respectively. There were no associations between tumour R2* and the Gleason score, age, prostate volume, PSA, or tumour size.
Conclusion: BOLD MRI at 3T appears to be a feasible technique for differentiating prostate cancer with benign tissue. However, a further study is required for direct clinical application.
Limitations: A retrospective study at a single institution. Potential errors of R2* measurements.
Ethics committee approval: Our institutional review board approved this retrospective study and the requirement for informed consent was waived.
Funding: No funding was received for this work.
Author Disclosures:
Y. Kim: nothing to disclose
C. Kim: nothing to disclose

RPS 1307-2 08:36

Age-related and zonal anatomical changes in the microstructure of normal human prostatic tissues: a preliminary study with VERDICT MRI
X. Wang, F. Lin, Y. Lei, Y. Wang*; Shenzhen/CN (1263165281@qq.com)*

Purpose: To identify differences in the histological features of the prostate by age- and region-related changes in normal prostatic tissues by using VERDICT (vascular, extracellular, and restricted diffusion for cytometry in tumours) MRI.
Methods and materials: In total, 31 male volunteers were included in the study. The derived VERDICT parameters (the fIC, fEES, and vascular fraction fVASC) were analysed with a histogram. Based on the whole prostate volume and the PZ, CG, and AS ROIs, histogram parameters were computed. Two-way ANOVA and Pearson correlation coefficients were performed.
Results: There were significant differences between the histogram parameters and regions of the prostate (P < 0.05). In the PZ, there was a correlation between age and the mean, median, skewness, and entropy of the fIC (all P < 0.05). Age was significantly correlated with the statistics of the fEES (all P < 0.001). In the CG, age was found to have a significant positive correlation with the entropy of the fIC (P < 0.001). There was a significant positive correlation between age and the mean, median, and entropy of the fEES (all P < 0.001). Similar to the PZ (P < 0.001), age also showed a significant positive correlation with the entropy of the fVASC (P < 0.001), but no correlation with other parameters of the fVASC.
Conclusion: VERDICT MRI successfully reveals microstructural changes across anatomical zones and age groups in normal prostate glands.
Limitations: A relatively small sample size.
Ethics committee approval: This study was approved by the institutional human ethics board and all participants provided signed consent prior to entry into the study.
Funding: No funding was received for this work.
Author Disclosures:
X. Wang: Speaker at The First Affiliated Hospital of Shenzhen University
F. Lin: Author at The First Affiliated Hospital of Shenzhen University
Y. Lei: nothing to disclose
Y. Wang: nothing to disclose

RPS 1307-3 08:42

Utility of a quantitative ADC/DCE model in dynamic contrast enhancement (DCE)-positive, upgraded PI-RADS-3-to-4 lesions
A. A. Tavakoli[1], P. Badura[1], T. Tubtawee[1], V. Schütz[1], D. Tichy[1], A. Stenzinger[1], M. Hohenfellner[1], H.-P. Schlemmer[1], D. Bonekamp[2]; *[1]Heidelberg/DE, [2]Hirschberg/DE (S.tavakoli@gmx.de)*

Purpose: To study the value of a quantitative ADC/DCE regression model in predicting clinically significant prostate cancer (csPCa) in an analysis of DCE-positive upgraded PI-RADS-3-to-4 lesions.
Methods and materials: Clinical lesions reported in 3T MR exams with suspicion for csPCa were segmented on ADC maps and a visually identified early DCE time point. DCE was normalised to minimally enhancing parenchyma (DCEnorm). Logistic regression models included mean ADC and mean ADC/DCEnorm. The binary outcome was a Gleason grade group (GGG) >=2 and the maximum targeted GGG was used for patient-based analysis. In a subset of PI-RADS-3-to-4 upgrades, the model performance of the mean ADC was compared to the model performance of combined ADC/DCEnorm.
Results: Of 308 successful exams, 274 patients had 454 MR lesions that served as biopsy targets. 211 patients had a total of 275 MR lesions in the PZ. 34 patients received a PI-RADS-3-to-4 upgrade due to the radiologist's DCE assessment. Of these 34 patients, 9 had GGG ≥2 after biopsy, 2 had GGG=1, and 23 had no malignancy. Sensitivity/specificity of the mean ADC model was 56%/80%, whereas sensitivity/specificity of the model mean ADC model/DCEnorm was 100%/76%. 25 lesions were overcalled by the clinical assessment, whereas n=6 were false-positive for the combined ADC/DCEnorm model and n=5 for the ADC only model.
Conclusion: A quantitative regression model of a mean ADC/normalised DCE yielded reduced false-positive calls in comparison to clinical PI-RADS-3-to-4 calls without a loss of sensitivity. The ADC only model also reduced false-positive calls but missed 4 out of 9 csPCa.
Limitations: Our results quantify DCE utility for PI-RADS-3-to-4 upgraded lesions, however, do not provide guidance on increasing the detection rate of PI-RADS-3 calls.
Ethics committee approval: Ethics committee approval with written informed consent waived (S-156/2018).
Funding: No funding was received for this work.
Author Disclosures:
A. A. Tavakoli: nothing to disclose
P. Badura: nothing to disclose
T. Tubtawee: nothing to disclose
V. Schütz: nothing to disclose
D. Tichy: nothing to disclose
A. Stenzinger: Consultant at Astra Zeneca, BMS, Novartis, Roche, Illumina, Thermo Fisher, Board Member at Astra Zeneca, BMS, Novartis, Thermo Fisher
M. Hohenfellner: nothing to disclose
H.-P. Schlemmer: Other at Consulting fee: Siemens, Curagita, Profound, Bayer, Consultant at Curagita, Bayer, Research/Grant Support at BMBF, Deutsche Krebshilfe, Dietmar-Hopp-Stiftung, Roland-Ernst-Stiftung, Speaker at Siemens, Curagita, Profound, Bayer
D. Bonekamp: Speaker at ProfoundMedical Inc. Patrick

RPS 1307-4 08:48

Quantifying age-related differences in diffusion tensor imaging biomarkers for the male urethral sphincter complex of prospective prostate cancer patients
A. S. C. Verde, J. Santinha, A. Gaivao, N. Loucao, J. Fonseca, C. Matos, N. Papanikolaou*; Lisbon/PT (nickolas.papanikolaou@research.fchampalimaud.org)*

Purpose: Urinary incontinence is a major post-surgical complication that diminishes prostate cancer patients' quality of life. This study's purpose was to explore the feasibility of diffusion tensor imaging to access age and disease-related differences in the male urethral complex.
Methods and materials: 95 consecutive patients with a clinical suspicion of prostate cancer underwent a multi-parametric MRI examination including a diffusion tensor imaging (DTI) sequence with 16 directions and a b-value=600 s/mm^2. The proximal and distal sphincters and the membranous urethra were reconstructed using a deterministic tractography algorithm. DTI metrics, including tract length and density, fractional anisotropy (FA), axial diffusivity (AD), mean diffusivity (MD), radial diffusivity (RD), and 14 additional histogram metrics, were analysed. Pearson or Spearman correlations and linear regressions were performed between age and each DTI metric. Differences in DTI metrics between age and disease groups (healthy controls, benign prostatic hyperplasia, and prostate cancer patients) were accessed by analysis of variance (ANOVA) or the non-parametric Kruskal-Wallis test. Post-hoc t-tests were used to identify statistically significant differences between groups.
Results: Statistically significant changes with age were found in MD and RD distributions. Particularly, older subjects evidenced lower RD kurtosis in the proximal sphincter, lower MD maximum in the distal sphincter, and higher MD median absolute deviation in the membranous urethra. No statistically significant differences were found in DTI metrics between disease groups.
Conclusion: Age should be included as a covariate in the model that uses sphincters' DTI biomarkers to predict the post-surgical urinary continence recovery time.
Limitations: The minimum patients' age under study and the patients' heterogeneity within each disease group.
Ethics committee approval: The Champalimaud Foundation EC approved the DTI acquisitions, additional to the mpMRI.
Funding: No funding was received for this work.
Author Disclosures:
N. Papanikolaou: Advisory Board at Advantis Medical Systems, Founder at MRIcons
A. S. C. Verde: nothing to disclose
A. Gaivao: nothing to disclose
C. Matos: nothing to disclose
J. Fonseca: nothing to disclose
N. Loucao: Employee at Philips Healthcare
J. Santinha: nothing to disclose

RPS 1307-5 08:54

Risk stratification of patients with prostate cancer: promising results with high b-value DWI radiomic features

M. Mottola[1], F. Ferroni[2], D. Barone[2], G. Gavelli[2], A. Bevilacqua[1]; [1]*Bologna/IT,* [2]*Meldola/IT (margherita.mottola@unibo.it)*

Purpose: To investigate the potential role of radiomic features computed on high b-value diffusion-weighted imaging (DWI) to perform risk stratification of patients with a clinical suspicion of prostate cancer (PCa).
Methods and materials: 42 patients of our institution, representing 7 risk levels, were retrospectively enrolled in the study and grouped into 4 classes of risk: (a) clinically significant (CS) PCa split over 4 levels (ISUP=2÷5), (b) non-clinically significant (NCS) PCa (ISUP=1) patients with a negative biopsy, and (c) positive mpMRI (NP) or (d) negative mpMRI (NN). After computing radiomic features on DWI b=2000s/mm^2, the correlation between radiomic features and risk level was investigated through two steps, (i) Spearman index (ρ) and (ii) Kruskal-Wallis and Wilcoxon tests ($p<0.05$), for multi- and pairwise- comparison of the 4 classes, respectively.
Results: The mean of the local coefficient of variation (CV_L-m), a measure of local dispersion of DWI values, resulted in the most discriminant radiomic features among the four classes ($p\sim10^{-6}$), able to rank the four increasing risk classes with ρ=0.81, with a high pairwise separability ($p\leq0.026$). ρ=0.81 was also achieved when correlating the CV_L-m with all 7 increasing risk level groups.
Conclusion: This study allows performing an early stratification of all 7 PCa risk levels. Increasing values of CV_L-m in DWI images describe a higher degree of local heterogeneity in accordance with tissue over-proliferation and, consequently, an increasing level of tumour aggressiveness.
Limitations: The number of patients could be low for a proper stratification of the cohort in 7 classes. However, the excellent results achieved when using CV_L-m values to correctly rank all risk levels give CV_L-m the most promising role in depicting PCa risk progression.
Ethics committee approval: IRB approval and written informed consent was waived.
Funding: No funding was received for this work.
Author Disclosures:
M. Mottola: nothing to disclose
A. Bevilacqua: nothing to disclose
G. Gavelli: nothing to disclose
D. Barone: nothing to disclose
F. Ferroni: nothing to disclose

RPS 1307-6 09:00

Why a b-value of 1,400 s/mm2 or higher is optimal for evaluating prostatic index lesions on synthetic diffusion-weighted imaging

S. Y. Cha, S. Y. Park*; Seoul/KR*

Purpose: PI-RADS recommends the use of high-b-values of 1,400 s/mm2 or greater for diffusion-weighted imaging (DWI) interpretation. However, lesion signal intensity on DWI decreases as b-values increase. Thus, the fundamental reasons regarding optimal b-value range are still unclear. We qualitatively and quantitatively analysed the optimal b-value range for calculated DWI (cDWI) in the prostate.
Methods and materials: 92 patients who underwent DWI and targeted biopsy for index lesions were retrospectively included. We generated cDWI for a range of b-values, 1,000-3,000 s/mm2, using dedicated software and true DWI data of b-values of 0, 100, and 1,000 s/mm2. We assumed lesion conspicuity would be best when background (benign prostatic areas [bP] and periprostatic areas [pP]) signal intensities (SI) become homogeneous. We firstly analysed the b-value showing the best visual conspicuity (qualitative analysis) and then assessed the b-value showing same SI between bP and pP (quantitative analysis). The 95% confidence interval of a qualitative or quantitative b-value was considered as the optimal b-value range.
Results: Optimal b-value ranges for qualitative and quantitative analyses were 1,761-1,805 s/mm2 and 1,640-1,771 s/mm2 (med, 1,790 vs 1,705 s/mm2; p= 0.003) for reader 1, and 1,835-1,895 s/mm2 and 1,705-1,841 s/mm2 (med, 1,872 vs 1,763 s/mm2; p= 0.022) for reader 2, respectively. Bland-Altman plots consistently demonstrated the mean difference of less than 100 s/mm2 between qualitatively and quantitatively determined b-values for the two readers.
Conclusion: Calculated b-values showing homogeneous SI between bP and pP seem to be optimal for evaluating prostatic index lesions on cDWI. Our qualitative and quantitative findings consistently suggest the use of a b-value of 1,600-1,900 s/mm2.
Limitations: The data analyses were performed retrospectively. We evaluated patients of a single institution. Further prospective and external validation studies are required.
Ethics committee approval: n/a
Funding: No funding was received for this work.
Author Disclosures:
S. Y. Cha: nothing to disclose
S. Y. Park: nothing to disclose

RPS 1307-7 09:06

Accelerated, high-resolution quantitative T2 mapping at 3T for the detection of prostate cancer

A. M. Bucher[1], A. Polk[1], R. Strecker[2], B. Kaltenbach[1], D. T. Hilbert[2], E. Weiland[2], T. J. Vogl[1], B. Bodelle[1]; [1]*Frankfurt am Main/DE,* [2]*Erlangen/DE*

Purpose: To test the reliability of the latest-generation, fast, high-resolution T2-mapping prototype sequence supporting parallel imaging and model-based reconstruction ($T2_M$) in the detection of malignant prostate lesions of the peripheral zone.
Methods and materials: We included 350 image series (T2-weighted-imaging, diffusion-weighted-imaging, T1-weighted pre-contrast-imaging, dynamic contrast-enhancement, and $T2_M$) from 50 multiparametric MRI datasets at 3 Tesla (MAGNETOM Prisma^{fit}, Siemens Healthcare, Erlangen, Germany), clinically indicated for suspected prostate cancer (pCA). The standard multiparametric prostate protocol was rated for the occurrence of prostate lesions. In 22 cases, there was biopsy-confirmed pCA in the peripheral zone. Regions of interest (ROI) were drawn on axial $T2_M$ (0.7x0.7x3.0mm^3, 16 echoes with delta TE 10.8ms, TR 5000msec) for each examination: on 3 slices (apex, mid-base, and base) to measure healthy prostate tissue of the peripheral and transitional zone and for confirmed malignant lesions on the most representative slice. The average and minimum values of transverse relaxation time (T2) in each ROI were recorded.
Results: The average acquisition time for $T2_M$ was 4:36 min. Healthy prostate tissue had a mean T2 of 151.3±42.6ms in the peripheral zone and 95.1±22.5ms in the transitional zone. The mean T2 in the peripheral zone was significantly reduced for confirmed pCA (71.6±13.3ms, p=0.001). T2 measurements could differentiate infiltration of the transitional zone from peripheral pCA (p=0.001). When comparing minimal values of $T2_M$, we found a good distinction between healthy tissue and pCA (healthy: 99.4±19.9ms, malignant: 52.0±10.6ms; p=0.001).
Conclusion: The detection of malignant prostate tissue is feasible using quantitative measurements from high-resolution T2-mapping sequences with a good distinction of pCA. $T2_M$ could be added with an acceptable acquisition time.
Limitations: Results should be confirmed in a larger cohort.
Ethics committee approval: Ethics committee review granted approval and informed consent was waived.
Funding: No funding was received for this work.
Author Disclosures:
A. M. Bucher: Other at Travel support: Bayer
T. J. Vogl: Other at Travel Support: Bayer
R. Strecker: Employee at Siemens Heathineers
B. Bodelle: nothing to disclose
E. Weiland: Employee at Siemens Heathineers
B. Kaltenbach: nothing to disclose
A. Polk: nothing to disclose
D. T. Hilbert: Employee at Siemens Heathineers

RPS 1307-8 09:12

Advanced postprocessing in diffusion-weighted imaging of the prostate: impact on image quality and lesion detectability

D. Zinsser[1], J. Weiß[1], M. Esser[1], M. Nickel[2], A. E. E. Othman[1]; [1]*Tübingen/DE,* [2]*Erlangen/DE (dominik.zinsser@med.uni-tuebingen.de)*

Purpose: To investigate the effect of advanced postprocessing consisting of adaptive combination and motion correction of multiple acquisitions in diffusion-weighted magnetic resonance prostate imaging and its potential to improve image quality and prostate cancer detection.
Methods and materials: We retrospectively evaluated clinically indicated multiparametric 3T-MRI-examinations of 53 patients (mean age 68.8±10 years) including diffusion-weighted imaging of the prostate with and without prototypical advanced postprocessing for the extraction of trace-weighted images from the original diffusion-weighted acquisitions. Two readers rated image quality, artefacts, distortion, and detectability of lesions in high b-value images (b=1000/calculated 2000 s/mm²) of both datasets using a 4-point Likert scale (1=poor, 4=excellent). Measurements of signal intensity of the peripheral zone and lesions were carried out. This enabled us to calculate the ratio of signal intensity of lesions to the peripheral zone and therefore produce a quantitative comparison of lesion detectability. Lesions were assessed according to PI-RADS V2.
Results: With advanced postprocessing, image quality was rated significantly better for b1000 (4 vs 3, p=0.0001) and b2000 (3 vs 2, p=0.0006) while artefacts were rated significantly better for b2000 (3(IQR 3-3) vs 3(IQR 2-3), p=0.0005). No significant differences for distortion were found. Due to improved lesion/tissue contrast with advanced postprocessing, detectability of lesions was qualitatively and quantitatively better for b1000 (4 vs 3, p=0.0084; 1.36 vs 1.31, p<0.0001) and b2000 (4(IQR 4-4) vs 4(IQR 3-4), p=0.0003; 3.24 vs 2.92, p<0.0001). With advanced postprocessing, two additional lesions (overall 38 instead of 36) were found.

Conclusion: Advanced postprocessing significantly improves image quality and reduces artefacts in diffusion-weighted prostate imaging. Furthermore, it significantly enhances the detection of potentially malignant lesions and enables the recognition of more suspect lesions compared to standard diffusion-weighted imaging.
Limitations: n/a
Ethics committee approval: Written informed consent was waived.
Funding: No funding was received for this work.
Author Disclosures:
D. Zinsser: nothing to disclose
J. Weiß: nothing to disclose
M. Esser: nothing to disclose
M. Nickel: Employee at Siemens Healthcare GmbH
A. E. E. Othman: Grant Recipient at Bayer Vital GmbH

RPS 1307-9 09:18
Updated PI-RADS 2.1: does it affect the diagnostic outcome of multiparametric prostate MRI?
J. Knapp, M. Sinn, C. Berliner, L. Well, G. Adam, D. Beyersdorff, M. Sauer; *Hamburg/DE (m.sauer@uke.de)*

Purpose: To evaluate whether the recent update on PI-RADS (2.1) has significant impact on the assessment of multiparametric prostate MRI (mpMRI) in comparison to PI-RADS 2.0.
Methods and materials: 125 consecutive patients (median age 65 years) underwent standardised, in-house mpMRI at 3T in the first quarter of 2019. All examinations were re-assessed retrospectively according to PI-RADS 2.1, acknowledging the updates on DWI scoring in the transitional zone (TZ), volumetry (e.g. used for PSA density calculation), and lesion localisation. Relevant clinical parameters, as well as subsequent diagnostics and therapies, were co-registered. P-values were determined by paired Student's t-tests.
Results: In 125 MRIs, 23 lesions were upgraded (PI-RADS "2" to "3") due to PI-RADS 2.1 DWI criteria, but only 2 of these 23 lesions replaced the previous index lesion. Therefore, the overall PI-RADS score was only two times increased (PI-RADS "2" to "3", ~ "equivocal biopsy target"), one time decreased (PI-RADS "2" to "1"), and remained unchanged in 122 cases. Analysis of the overall PI-RADS scores of all patients demonstrated no significant differences (p=0.57). 8 index lesions were topographically relocated within the new sector map to the additionally defined sectors. The updated recommendations on prostate volumetry demonstrated a mean deviation of 6.4 ml compared to previous PI-RADS 2.0 without significant differences (p=0.38). Correlation in linear regression was good (r^2=0.83; CI:0.85-1.0).
Conclusion: PI-RADS 2.1 updates had no significant impact on the overall MRI scores, especially with respect to biopsy guidance. Revised volumetry does not cause significant changes compared to PI-RADS 2.0.
Limitations: A retrospective, single-reader, and single-centre analysis.
Ethics committee approval: Informed consent was waived by the ethics committee.
Funding: No funding was received for this work.
Author Disclosures:
M. Sauer: nothing to disclose
C. Berliner: nothing to disclose
G. Adam: nothing to disclose
J. Knapp: nothing to disclose
M. Sinn: nothing to disclose
L. Well: nothing to disclose
D. Beyersdorff: nothing to disclose

RPS 1307-10 09:24
Comparison of abbreviated MRI protocols for the detection of prostate cancer in a cohort of radical prostatectomy patients: a multi-reader study
F. Bonato, G. Giannarini, L. Di Mico, L. Cereser, G. Como, C. Zuiani, R. Girometti; *Udine/IT*
Purpose: To compare multiparametric magnetic resonance imaging (mpMRI)-derived abbreviated protocols in detecting prostate cancer (PCa).
Methods and materials: We retrospectively included 108 patients (mean age 64.8 years) who performed mpMRI to stage biopsy-proven clinically-localised PCa before radical prostatectomy between January 2016-May 2019. Examinations were performed on a 3.0T magnet with a prostate imaging reporting and data system version 2 (PI-RADSv2)-compliant protocol. Two readers (R1 and R2, with an experience of <600 and <250 examinations) blinded to definitive pathology, independently analysed mpMRI examinations, attributing a PI-RADSv2 score to each observation on a per-sequence basis. A study coordinator assessed the final PI-RADSv2 category of each observation by combining readers' categorisations according to the following combinations: fast-MRI (diffusion-weighted imaging+T2-weighted imaging), fast-MRI+dynamic contrast-enhanced imaging (DCE), biparametric MRI (bpMRI), and mpMRI. Based on pathology results, we calculated the cancer detection rate (CDR) and false-discovery rate (FDR) (false-positives/true-positives + false-positives) of each protocol. The analysis was performed on the index lesion, using category ≥3 as the cut-off.
Results: 108 index lesions predominated in the peripheral zone, showing a median Gleason score 3+4 and pT stage ≤2c in 74% of cases. Fast-MRI, fast-MRI+DCE, and bpMRI equalled mpMRI, showing 78.7% (95%CI 69.6-85.8) and 77.8% (95%CI 68-6-85.0) CDR, and 10.5% (95%CI 5.0-19.3) and 9.6% (95%CI 4.4-18.3) FDR for R1 and R2, respectively. Fast-MRI+DCE upgraded 53.8% and 90% of category 3 assignments achieved with fast-MRI by R1 and R2, respectively. Upgraded cases were true-positives in 95% of cases.
Conclusion: In a medium-to-low experience setting, fast-MRI+DCE was the abbreviated protocol better balancing CDR and minimising PI-RADS 3 assignments.
Limitations: A monocentric and retrospective study.
Ethics committee approval: Informed consent acquisition was waived due to the retrospective design.
Funding: No funding was received for this work.
Author Disclosures:
F. Bonato: nothing to disclose
G. Giannarini: nothing to disclose
L. Di Mico: nothing to disclose
L. Cereser: nothing to disclose
G. Como: nothing to disclose
C. Zuiani: nothing to disclose
R. Girometti: nothing to disclose

RPS 1307-11 09:30
Accuracy of a double-reading strategy using abbreviated prostate MRI in patients with prostate cancer candidate to active surveillance
S. Maresca, C. Zuiani, L. Cereser, G. Como, M. Lorenzon, R. Girometti; *Udine/IT (silviomaresca@gmail.com)*

Purpose: To investigate the diagnostic performance for index prostate cancer (iPCa) of a double-reading strategy with an abbreviated magnetic resonance imaging (aMRI) protocol in patients candidate to active surveillance.
Methods and materials: Between February 2015 and November 2018, we retrospectively included 54 men with biopsy-proven low-risk prostate cancer candidate to active surveillance who underwent 3.0T multiparametric magnetic resonance imaging (mpMRI) before a confirmatory biopsy. Three radiologists (R1, R2, and R3) with average-to-low experience in mpMRI, blinded to clinical history and biopsy results, reviewed examinations under the form of aMRI (transverse T2-weighted imaging and diffusion-weighted imaging). Prostate imaging reporting and data system version 2.1 (PI-RADSv2.1) was used for categorising aMRI observations. Using category ≥4 as the cut-off and a confirmatory biopsy as a reference standard, we assessed the sensitivity and specificity for iPCa of single readings (R1, R2, and R3), as well as the readings resulting from the combination of R1+R2, R2+R3, and R1+R3. In double-reading, a case was assessed positive if suspicious for at least one reader.
Results: Saturation targeted confirmatory biopsy was performed with the transperineal approach. At biopsy, iPCas included 42/54 (78%) low-risk lesions. The remaining 12/54 (22%) patients were reclassified to the intermediate-to-high-risk category. Sensitivity/specificity for R1, R2, and R3 were 67% (95%CI 35-90)/57% (95%CI 41-72), 83% (95%CI 52-98)/60% (95%CI 43-74), and 42% (95%CI 15-72)/79% (95%CI 63-90), respectively. Double-reading provided a sensitivity/specificity of 83% (95%CI 52-98)/50% (95%CI 34-66) for R1+R2, 83% (95%CI 52-98)/57% (95%CI 41-72) for R2+R3, and 75% (95%CI 43-95)/55% (95%CI 39-70) for R1+R3, respectively.
Conclusion: A double-reading approach using an abbreviated magnetic resonance imaging (aMRI) protocol improved the sensitivity for iPCa in patients candidate to active surveillance.
Limitations: A retrospective design.
Ethics committee approval: IRB-approved.
Funding: No funding was received for this work.
Author Disclosures:
S. Maresca: nothing to disclose
C. Zuiani: nothing to disclose
L. Cereser: nothing to disclose
G. Como: nothing to disclose
M. Lorenzon: nothing to disclose
R. Girometti: nothing to disclose

RPS 1307-12 09:36
In-vivo tissue characterisation of prostate cancer: an extreme gradient boosting algorithm to predict Gleason scores in multiparametric MRIs of the prostate
S. Ellmann, M. Schlicht, M. Dietzel, M. Hammon, R. Janka, M. Saake, B. Wullich, M. Uder, T. Bäuerle; *Erlangen/DE (stephan.ellmann@uk-erlangen.de)*

Purpose: Radiomic features extracted from routine MRI sequences are increasingly used for in-vivo tissue characterisation. The aim of this study was

to develop a computer-aided diagnosis (CADx) algorithm to predict the Gleason score (GS) of prostate cancers (PCa) in multiparametric MRIs of the prostate (mpMRI).
Methods and materials: 83 PCa reported in mpMRI were included in this retrospective study. Histopathology of TRUS-guided biopsy cores with reported GS served as a standard of reference (SOR). mpMRIs were performed following international guidelines and current practice. Imaging parameters included lesion size, T2w-signal intensity, diffusion restriction, prostate volume, and dynamic parameters (wash-in, wash-out, peak enhancement intensity, the initial area under the curve, and time-to-peak) along with zonal anatomy (peripheral zone vs central gland), patient age, and serum PSA level. Predicting the GS was defined as a regression problem. Using the above-mentioned parameters, an extreme gradient boosting algorithm was trained to predict the lesions' GS. A leave-one-out cross-validation was applied to ensure generalisability. Performance optimisation was focused on minimising the root-mean-square-error (RMSE). Inter-reader agreement of the imaging parameters was assessed using intraclass correlation coefficients (ICC).
Results: Histopathological assessment revealed n=17 Gleason-6 PCa, n=45 Gleason-7 PCa, n=8 Gleason-8 PCa, and n=13 Gleason-9 PCa. The CADx reached an RMSE of 0.653. Predicted and observed GS correlated significantly (P<0.0001, r=0.503). All imaging parameters featured excellent inter-reader agreement (all ICC≥0.87).
Conclusion: This study describes a CADx for GS prediction of PCa in mpMRI with high accuracy and excellent inter-reader agreement.
Limitations: Limitations include the retrospective and monocentric study design.
Ethics committee approval: The ethics committee approved this study, with a waiver of informed consent.
Funding: This work was supported by the German Research Foundation (DFG, CRC 1181-Z02).
Author Disclosures:
S. Ellmann: nothing to disclose
M. Schlicht: nothing to disclose
M. Dietzel: nothing to disclose
M. Hammon: Advisory Board at Siemens Healthineers
R. Janka: Advisory Board at Siemens Healthineers
B. Wullich: nothing to disclose
M. Uder: Advisory Board at Siemens Healthineers
T. Bäuerle: nothing to disclose
M. Saake: Advisory Board at Siemens Healthineers

RPS 1307-13 09:42

Follow-up of patients within PI-RADS category 3: analysis of an advisable control interval

S. Dörfler, L. Schimmöller, M. Quentin, T. Ullrich, C. Arsov, P. Albers, G. Antoch*; Düsseldorf/DE*
(Stephan.Doerfler@med.uni-duesseldorf.de)

Purpose: To analyse follow-up (FU) mpMRI in patients within a PIRADS category of 3.
Methods and materials: This retrospective single-centre study includes consecutive patients with a PIRADS category 3, ≥1 follow up mp-MRI (T2WI, DWI, DCE), and target plus systematic TRUS-guided biopsy or transurethral resection (TUR-P) as histological reference standard between 2012-2018. Study endpoints were analyses of PIRADS, PSAD, PSA, and prostate volume during FU MRIs with subgroup analyses of patients with a positive histology.
Results: Of 89 included patients (median PSA 6.6ng/ml; PSAD 0.13ng/ml/ml) with a FU period of 31±18 month, PCa was detected in 19 cases (median PSA 6.0ng/ml; PSAD 0.13ng/ml/ml) and csPCA in 5 cases (median PSA 5.5ng/ml; PSAD 0.13ng/ml/ml). Only the PI-RADS score, but not PSA, PSAD, or prostate volume, showed a significant difference in FU MRIs. Prostate volume rose in biopsy-negative cases (median initial 53 ml to 68 ml in FU; p=0.07). There was a significant PIRADS downgrade in cases with a negative biopsy during FU after 36 to 48 month (p=0.001) and a significant PI-RADS upgrade after 13 to 24 month in cases with verified PCa (p=0.02).
Conclusion: There was a very low rate of csPCA in PIRADS 3 patients. Patients with PCA and an initial PI-RADS 3 showed an upgrade to PIRADS 4 in FU MRI within 13-24 months. In cases with a negative biopsy, there seems no benefit to follow-up MRIs earlier than 36-48 months in cases of stable PSAD.
Limitations: n/a
Ethics committee approval: Review board approval and written informed consent obtained.
Funding: No funding was received for this work.
Author Disclosures:
S. Dörfler: nothing to disclose
L. Schimmöller: nothing to disclose
M. Quentin: nothing to disclose
T. Ullrich: nothing to disclose
C. Arsov: nothing to disclose
P. Albers: nothing to disclose
G. Antoch: nothing to disclose

RPS 1307-14 09:48

Fractal analysis of perfusion MRI for predicting prostate cancer grading: validation of previously established cutoffs

F. Michallek[1], H. Huisman[2], B. Hamm[1], M. Dewey[1]; *[1]Berlin/DE, [2]Nijmegen/NL (florian.michallek@charite.de)*

Purpose: MRI is used for detecting prostate cancer (CaP), however, non-invasive grade prediction remains challenging. The perfusion pattern might allow non-invasive prediction of CaP-grading by quantifying chaos of perfusion. This study validates the fractal analysis of perfusion-MRI for CaP grade prediction.
Methods and materials: The openly available PROSTATEx2-dataset (testing cohort) was analysed with the Gleason grade group (GGG) from MRI-guided biopsies as a reference. Fractal analysis was applied to dynamic contrast-enhanced MRI-sequences (3Tesla, 3D-turbo-flash gradient-echo, resolution around 1.5x1.5x4 mm, each 3.5 seconds). Fractal dimension (FD) cutoffs were established in a previous study to predict low, intermediate, and high GGG1-4 CaP, and were validated in this study. GGG agreement with FD was assessed by quadratic-weighted kappa-statistics. Performance of fractal analysis was compared to an apparent diffusion coefficient (ADC) analysis.
Results: A cohort of 72 CaP in 64 patients was studied. Significant FD differences were found in pairwise GGG predictions (p<0.005), except for the highest groups (GGG4, n=8, vs GGG5, n=6). Using previously established FD thresholds, very good agreement of fractal analysis with GGG was achieved with quadratic-weighted kappa κ_{FD}=0.88 [CI: 0.79-0.98] for multi-class prediction. In comparison, ADC differences were significant for predicting GGG1 vs GGG2-5 CaP (p≤0.02) with moderate performance (κ_{ADC}=0.36 [CI: 0.12-0.59]). The differentiation of GGG4 from GGG5 CaP was neither reliable by fractal analysis nor ADC analysis.
Conclusion: Using previously determined FD thresholds for predicting CaP grading, fractal analysis achieved a high agreement with GGG and outperformed ADC analysis in an independent cohort.
Limitations: The differentiation of GGG4 from GGG5 CaP was neither reliable by fractal analysis nor ADC analysis.
Ethics committee approval: n/a
Funding: No funding was received for this work.
Author Disclosures:
F. Michallek: Grant Recipient at F.M. has received grant support from the German Research Foundation (DFG, project number: 392304398) and the Digital Health Accelerator of the Berlin Institute of Health., Patent Holder at F.M. has filed a patent application on fractal analysis of perfusion imaging (together with Marc Dewey, PCT/EP2016/071551).
H. Huisman: nothing to disclose
B. Hamm: nothing to disclose
M. Dewey: Grant Recipient at M.D. has received grant support from the Heisenberg Program of the German Research Foundation (DFG) for a professorship (DE 1361/14-1), the Digital Health Accelerator of the Berlin Institute of Health, and the DFG graduate program on quantitative biomedic, Other at M.D. was elected European Society of Radiology (ESR) Research Chair (2019–2022) and the opinions expressed in this article are the author's own and do not represent the view of ESR. M.D. is also the editor of Coronary CT Angiography and Cardiac CT, both p, Patent Holder at M.D. has filed a patent application on fractal analysis of perfusion imaging (together with Florian Michallek, PCT/EP2016/071551)., Speaker at M.D. has received lecture fees from Toshiba Medical Systems, Guerbet, Cardiac MR Academy Berlin, and Bayer (Schering-Berlex).

RPS 1307-15 09:54

mpMRI detection of suspected prostate cancer with a negative biopsy: can radiomic features help radiologists?

A. Bevilacqua[1], M. Mottola[1], F. Ferroni[2], G. Gavelli[2], D. Barone[2]; *[1]Bologna/IT, [2]Meldola/IT (margherita.mottola@unibo.it)*

Purpose: To investigate whether DWI-based radiomics features could differentiate patients with a clinical suspicion of PCa and negative TRUS-biopsy that have a positive mpMRI from patients where mpMRIs do not show any evidence.
Methods and materials: The records of 17 patients undergoing 3T-mpMRI for suspected PCa subsequently not confirmed at TRUS-biopsy were extracted from our institutional database. The ground truth was available for only a few. 7 patients did not report evidence at mpMRI, while 10 patients showed suspected PCa lesions, contoured in consensus by two radiologists. 84 image-based radiomic features were computed on high b-value DW-MRI sequences of all patients of the two groups. The ROC curve was computed for each feature and the one yielding the highest AUC was selected. Its discrimination power was also assessed via a Wilcoxon rank-sum test (p<0.001).
Results: The mean of local skewness (S_L-m), related to local inhomogeneities of DWI values, confirms radiologist reports in 94% of cases, with AUC=0.93 (95% CI, 0.56-1.00), specificity=100%, and sensitivity=86% (one false-positive only). Median S_L-m values in patients with suspected PCa were greater than 30% ($p \sim 10^{-4}$) with respect to patients showing no evidence at mpMRI.

Conclusion: DWI-based radiomic features strongly support mpMRI evidence in cases of suspected, and for some patients clear, PCa although TRUS-biopsy is negative. These outcomes suggest further investigation on the role that these extremely promising features could have in PCa patient's stratification.
Limitations: Although it confirmed the mpMRI evidence to be PCa for the few patients where the ground-truth was available, for most of them it was not at our disposal because patients did not belong to a dedicated study.
Ethics committee approval: IRB approval, written informed consent was waived.
Funding: No funding was received for this work.
Author Disclosures:
M. Mottola: nothing to disclose
A. Bevilacqua: nothing to disclose
G. Gavelli: nothing to disclose
D. Barone: nothing to disclose
F. Ferroni: nothing to disclose

08:30 - 10:00 **Room Y**

My Thesis in 3 Minutes

MyT3 13

Abdominal and Gastrointestinal

Moderators:
A. Torregrosa Andres; Valencia/ES
M. G. Pezzullo; Brussels/BE

MyT3 13-1 08:30

Comparison of CT findings in successful and unsuccessful non-operative management of acute appendicitis

C. Civan Kuş, D. Tüney, C. Yegen, T. Demirbas, C. Ilgın*; Istanbul/TR (drceydacivan@hotmail.com)*

Purpose: Although acute appendicitis standard treatment has been performed surgically, it has been seen that treatment is possible with antibiotic and non-operative observation in recent years. In this study, we aimed to determine whether CT findings in patients diagnosed with acute appendicitis should be used for directing treatment.
Methods and materials: A total of 60 patients, who underwent abdominal CT and antibiotic treatment for acute appendicitis were retrospectively evaluated. Patients who were treated with antibiotics were followed up for at least six months to determine the recurrent disease rate and CT findings of successful and unsuccessful medical treatment cases were compared. Appendiceal wall thickness, diameter, wall contrast enhancement, intraabdominal free fluid, periappendiceal fat stranding severity, perirectal lymph node, appendicolith and adjacent organ findings in CT of groups were compared with chi-square and Mann-Whitney-U tests.
Results: A total of 60 patients were evaluated. Because of 6 of the 60 patients who received medical treatment didn't complete the 6-month follow-up period, and 17 of them couldn't be followed-up, 23 patients have not been included in the research. As a result, at the end of the 6-month follow-up, 23 of the 37 medical treatment patients were successful and 14 of them were unsuccessful. Comparing the CT findings of the successful and unsuccessful medical treatment groups, just the severity of appendix wall enhancement was found statistically significant (p=0.005). After at least 6 months follow-up, the recurrent disease rate of patients who received medical treatment was 38%.
Conclusion: The likelihood of unsuccessful treatment increases when the severity of appendix wall contrast enhancement is evident in patients treated with medical therapy. The recurrent disease rate of medical treatment after at least 6 months follow-up was 38%.
Limitations: Retrospective study.
Ethics committee approval: Ethics committee approval obtained.
Funding: No funding was received.
Author Disclosures:
C. Civan Kuş: nothing to disclose
D. Tüney: nothing to disclose
C. Yegen: nothing to disclose
T. Demirbas: nothing to disclose
C. Ilgın: nothing to disclose

MyT3 13-2 08:34

Dynamic contrast-enhanced MR imaging of rectal cancer using a golden-angle radial stack-of stars VIBE sequence: pharmacokinetic analysis and associations with different histopathological findings

Y. Li, Z. Li, C. Xia*; Chengdu/CN (18108087220@163.com)*

Purpose: To explore the role of pharmacokinetic analysis of perfusion parameters derived from golden-angle radial stack-of stars VIBE sequence in discriminating tumour characteristics and the associations with histopathological findings.
Methods and materials: 56 pathologically confirmed rectal cancer patients who received radial VIBE DCE-MRI examination were enrolled in our study. Pharmacokinetic parameters were correlated with tumour histopathological findings including staging, perineural lymphatic invasion and Ki67. The comparison of K^{trans}, Kep, V_e and iAUC between tumour and normal tissue was performed. Correlation between different pharmacokinetic parameters and pathological findings were calculated. Logistic regression analyses were used to determine the association between PNI, lymphatic metastasis and pharmacokinetic parameters.
Results: The values of K^{trans}, V_e and iAUC were significantly higher in tumour than in normal tissue; all $P<0.05$, the same as K_{ep}, $p<0.05$. Those parameters did not demonstrate statistical signifcance in correlating with N staging and Ki67 except for T staging and K^{trans}; the correlation coefficient r_s was 0.374, p=0.038. Combined K^{trans}, K_{ep}, V_e and iAUC can predict PNI as high as 78.1%. Combined K_{ep}, V_e and iAUC reached 79.4% in predicting lymphatic metastasis.
Conclusion: Pharmacokinetic parameters derived from golden-angle radial stack-of stars VIBE sequence can distinguish tumour from normal tissue. The combination of K^{trans}, K_{ep}, V_e and iAUC can act as a potential predictor of PNI and in combination with K_{ep}, V_e and iAUC as a promising predictor of lymphatic metastasis in rectal cancer patients.
Limitations: Limitations are the small sample size, participants belonging to different staging and the classification and differentiation groups, which may affect the objective evaluation.
Ethics committee approval: The study was approved by our institutional review board and written informed consent was obtained from all participants.
Funding: 1.3.5 project for disciplines of excellence, West China Hospital, Sichuan University
Author Disclosures:
Y. Li: nothing to disclose
Z. Li: nothing to disclose
C. Xia: nothing to disclose

MyT3 13-3 08:38

Computed tomography volumetric analysis of rate and factors affecting liver regeneration in liver transplant recipients

A. Jayant[1], T. B. S. Buxi[2], K. S. Rawat[1], P. Singh[1]*; [1]New Delhi/IN, [2]Gurgaon/IN, (abhishekjayant@gmail.com)*

Purpose: The purpose of this study was to assess liver regeneration with CT volumetry in patients who have undergone liver transplantation and to evaluate factors impacting liver regeneration in these patients.
Methods and materials: The study was done in the Department of Radiodiagnosis at Sir Ganga Ram Hospital. 34 patients were included in this study. Inclusion criteria: all adult patients who underwent living donor liver transplantation at our centre and gave consent for participation in our study. Exclusion criteria: paediatric liver transplant patients and acute liver failure patients. After taking valid consent, demographic, clinical and laboratory parameters, as well as pre-operative graft weight of these patients, were noted. CT was done on the 7th and 30th post-transplant day and The volume was calculated using CT volumetry software. Percentage and absolute growth of graft on these days were calculated. Correlation of various pre-transplant variables (age, sex, height, weight, BMI, BSA, MELD score, graft lobe, pre-transplant graft volume, graft to recipient weight ratio and indication for liver transplant) with graft regeneration was assessed.
Results: Rapid regeneration of graft was noted with a mean absolute and percentage regeneration on the 30th day being 685.4 ± 200.3cc and 119.2 ± 44%. Significant (p value <0.05) and positive correlation was found between weight, BMI, BSA, graft volume, graft to recipient weight ratio (GRWR) and 30th-day graft volume.
Conclusion: We concluded that graft regeneration in liver transplant recipients is a rapid and continuous process in the first thirty days. There is a positive and significant correlation between graft regeneration and pre-transplant variables as well as recipient's weight, BMI, BSA, graft volume and GRWR.
Limitations: The study is limited by the relatively small sample size of 34 patients and the fact that is was a time bound study.
Ethics committee approval: The study was approved by the institute's ethics committee.
Funding: No funding was received for this work.
Author Disclosures:
A. Jayant: nothing to disclose
T. B. S. Buxi: nothing to disclose
K. S. Rawat: nothing to disclose
P. Singh: nothing to disclose

MyT3 13-4 08:42

Can CT findings predict the surgical outcome in patients of adhesive small bowel obstruction: a retrospective cum prospective study

P. Singh[1], S. S. Ghuman[2], T. B. S. Buxi[3], A. Jayant[1]; [1]New Delhi/IN, [2]Noida/IN, [3]Gurgaon/IN (priyanka.dolly21@gmail.com)

Purpose: The purpose of this study is to assess the accuracy of MDCT findings as predictors for impending surgical intervention in patients with adhesive small bowel obstruction.
Methods and materials: The study was done in the Department of Radiodiagnosis (CT) at Sir Ganga Ram Hospital. The study was done in two phases. In the first phase, 75 retrospective cases meeting the inclusion criteria were included in this study. 8 MDCT features: small bowel dilatation, bowel wall thickening, degree of obstruction, small bowel air-fluid level, small bowel faeces sign, mesenteric fatty stranding, the presence of transition point and the presence of intraperitoneal free fluid were assessed in these patients. Sensitivity, specificity, positive predictive value, negative predictive value and the accuracy of these features for the prediction of surgical outcome were evaluated. Correlations of these features individually and in combination were assessed with surgical management. In the second phase of our study, the validity of the results obtained in the retrospective group was tested by applying them to 25 prospective cases.
Results: In the retrospective group, small bowel dilatation (>4cm) and high-grade obstruction were found to be statistically significant and a positive predictor of surgical outcome in patients of adhesive small bowel obstruction both individually and in combination. The model generated on the basis of the retrospective data showed an outstanding discrimination between surgical and conservative management when applied on prospective cases, thus validating our results.
Conclusion: MDCT features of small bowel dilatation >4cm and high-grade obstruction can both independently and in combination predict surgical outcome in patients with adhesive small bowel obstruction.
Limitations: There is no widely accepted definition for the grade of obstruction. The clinical status of the patient was not taken into consideration.
Ethics committee approval: Approved by the ethical committee of our institutuion.
Funding: No funding was received for this work.
Author Disclosures:
P. Singh: nothing to disclose
S. S. Ghuman: nothing to disclose
T. B. S. Buxi: nothing to disclose
A. Jayant: nothing to disclose

MyT3 13-5 08:46

Contrast-enhanced CT-based textural parameters as potential prognostic factors of survival for colorectal cancer patients receiving targeted therapy

H. Xu, H. Liang; Chengdu/CN (xhydoris@gmail.com)

Purpose: This study was designed to estimate the clinical significance of the contrast-enhanced computed tomography textural features for the prediction of survival in colorectal cancer patients receiving targeted therapy (bevacizumab and cetuximab).
Methods and materials: The LifeX software was used to extract the textural parameters of the tumour lesions in the contrast-enhanced computed tomography. Progression-free survival and overall survival were estimated using the Kaplan–Meier method. Univariate and multivariate analyses using the Cox proportional hazards model were performed to assess the prognostic value of textural parameters.
Results: Eighty colorectal cancer patients receiving targeted therapy (bevacizumab 42; cetuximab 38) were included. In the multivariate analysis, 8 textural parameters were revealed to be independent predictors of progression-free survival and overall survival, including skewness, kurtosis, homogeneity, energy and entropy of gray-level co-occurrence matrix, LRE, LRHGE, and contrast. Further, sphericity, compacity, LRLGE, LZGE and SZLGE were shown to be significantly associated with progression-free survival, while entropy and energy form a histogram-based matrix. Dissimilarty, SRE, SRLGE, RP, LZE, LZLGE and LZHGE were significantly associated with the overall survival.
Conclusion: In conclusion, our study provides preliminary evidences that several radiomic parameters derived from CT images were prognostic factors and predictive markers for CRC patients who are candidates for targeted therapy (bevacizumab and cetuximab).
Limitations: First of all, patients in this study were from a single centre. Secondly, the population was relatively small although we reviewed a relatively large database. Finally, there is subjectivity in the process of manually drawing VOIs. Thus, further studies are needed to validate the results of our study.
Ethics committee approval: This study was approved by the Ethics Administration Office of our hospital.
Funding: No funding was received for this work.
Author Disclosures:
H. Liang: Speaker at Chengdu University of TCM
H. Xu: Author at West China School of Medical, Sichuan University

MyT3 13-6 08:50

Diagnostic accuracy of ultrasound in the detection of amoebic liver abscess

S. Khan, W. A. Mirza; Karachi/PK (shahmeer.khan@aku.edu)

Purpose: The purpose of this study was to determine the diagnostic accuracy of ultrasound in the detection of amoebic liver abscess in patients undergoing liver abscess aspiration at the Department of Radiology (Aga Khan University Hospital).
Methods and materials: Setting: Department of Radiology, Aga Khan University Hospital, Karachi. Duration of the study with dates: The study was carried out over a period of six months from 22-01-2019 to 21-07-2019. Subjects and Methods: A total of 105 cases undergoing liver abscess aspiration were included in the study. Ultrasound was performed by a sonologist / radiologist with a minimum of 5 years experience of abdominal sonography. The same interpreted the images. Patient demographics and sonographic features were recorded on a proforma.
Results: The mean age of the patients was 49.3±17.5; 74 (70.5%) male and 31 (29.5%) female patients. A single lesion was found in 98 patients (93.3%) and multiples lesions in 7 patients (6.7%). Out of 105 patients, the location of the lesion was right in 93 (88.6%) and left in 12 patients (11.4%). Ultrasound showed a sensitivity of 97.5%, specificity 82.6%, PPV 95.2%, NPV 90.4% and diagnostic accuracy 94.2%, in the detection of amoebic liver abscess. Stratification for age, gender, number of lesions and location of lesions was also carried out.
Conclusion: In conclusion, ultrasonography is highly sensitive in diagnosing amoebic liver abscess. Ultrasound is an ideal, safe, sensitive, non-invasive and easily available imaging modality for the diagnosis. Ultrasound is an excellent imaging modality for the identification and location of the ALA, for the estimation of size and volume, and for the evaluation of complications.
Limitations: The study does not enumerate how these features would help to differentiate from a pyogenic abscess.
Ethics committee approval: Ethical review committee exemption was obtained.
Funding: No funding was received for this study.
Author Disclosures:
S. Khan: nothing to disclose
W. A. Mirza: nothing to disclose

MyT3 13-7 08:54

Contrast-enhanced ultrasonography (CEUS) vs dynamic contrast-enhanced MRI (DCE-MRI) for the characterisation of focal liver lesions: where do we stand?

K. Sood, Y. Agarwal, S. Gupta, R. Prasad; New Delhi/IN (komalsood16@gmail.com)

Purpose: To compare and determine the role of CEUS and DCE-MRI in the diagnostic evaluation of focal liver lesion and to qualitatively classify lesions using contrast washout patterns on CEUS (LI-RADS).
Methods and materials: An observational cross-sectional study was performed on 102 patients. All patients with focal liver lesions on grayscale ultrasound were included in the study except for those with simple cysts, patients with COPD, CKD (GFR<30 ml/min/1.73 m²), IHD and patients with contraindications to MRI. First CEUS was done on our subject and a provisional classification of the lesion using LI-RADS was done using the washout pattern of the contrast followed by DCE-MRI on which the lesion was classified again using LI-RADS. The final diagnosis was confirmed by histopathology. Results of these non-invasive modalities were then compared to histopathology (gold standard).
Results: For the contrast-enhanced ultrasound studies, sensitivity is 90% (95% CI 88-90), specificity is 82% (95% CI 80–84), and 41 for diagnostic odds ratio (DOR); for the CEMRI studies, sensitivity is 88% (95% CI 86-90), specificity is 83% (95% CI 81–85), and 35.80 for DOR.
Conclusion: CEUS can be a promising and cost-effective modality for focal liver lesions as compared to DCE-MRI for an initial evaluation. It not only shows comparable results in identifying the final diagnosis but also makes use of a contrast agent which gets excreted through lungs (SF6) and hence can easily be used in patients with liver/renal disease.
Limitations: The only limitation to our study is that CEUS is operator-dependent, so specificity of CEUS can further be increased when performed by the same and experienced sonologist.
Ethics committee approval: Approval taken.
Funding: No funding for this study was received.

Author Disclosures:
K. Sood: Author at V.M.M.C. & Safdarjung Hospital, Investigator at safdarjung hospital, Speaker at safdarjung hospital
Y. Agarwal: Consultant at V.M.M.C. & Safdarjung Hospital
S. Gupta: Consultant at V.M.M.C. & Safdarjung Hospital
R. Prasad: Consultant at V.M.M.C. & Safdarjung Hospital

MyT3 13-8 08:58

Reproducibility of intravoxel incoherent motion of liver on a 3.0T scanner: free-breathing and respiratory-triggered sequences acquired with different numbers of excitations

A. Cieszanowski, K. Pasicz, M. Naduk-Ostrowska, J. Podgorska, E. Fabiszewska, W. Skrzyński, J. Jasieniak, I. Grabska, P. Kukołowicz; *Warsaw/PL (naduk.martyna@gmail.com)*

Purpose: To optimise the IVIM imaging of the liver on a 3T scanner by assessing parameter reproducibility on free-breathing (FB) and respiratory-triggered (RT) sequences acquired with different numbers of signal averages (NSA).
Methods and materials: 20 subjects underwent IVIM MRI on a 3T scanner using four different echo-planar sequences, each with 10 b values: 0-900 s/mm2. Images were acquired with FB and RT with NSA = 1-4 (FBNSA1-4, RTNSA1-4) and with NSA = 3-6 (FBNSA3-6, RTNSA3-6). For the assessment of the reproducibility of IVIM-derived parameters (f, D, D*), each subject was scanned again with an identical protocol during the same session. IVIM parameters were calculated. The distribution of IVIM-parameters for each DWI sequence was given as the median value with first and third quartile. Inter-scan reproducibility for each IVIM parameter was evaluated using the coefficient of variance and Bland-Altman difference. Differences between FB sequence and RT sequence were tested using the non-parametric Wilcoxon signed-rank test.
Results: The mean coefficient of variance (%) for f, D, and D* ranged from 60 to 64, from 58 to 84, and 99 for FBNSA1-4 sequence; from 50 to 69, from 41 to 97, and from 82 to 88 for RTNSA1-4 sequence; from 22 to 27, 15, and from 70 to 80 for FBNSA3-6 sequence; and from 21 to 32, from 12 to 17, and from 50 to 80 for RTNSA3-6 sequence, respectively.
Conclusion: Increasing the NSA for IVIM acquisitions allows us to improve the reproducibility of IVIM-derived parameters. The sequence FBNSA= 3-6 was optimal in terms of reproducibility and acquisition time.
Limitations: The number of studied subjects was limited to 20.
Ethics committee approval: The study was approved by the Institutional Review Board, and all volunteers signed an informed consent form.
Funding: No funding was received for this work.
Author Disclosures:
M. Naduk-Ostrowska: nothing to disclose
A. Cieszanowski: nothing to disclose
J. Podgorska: nothing to disclose
J. Jasieniak: nothing to disclose
K. Pasicz: nothing to disclose
E. Fabiszewska: nothing to disclose
W. Skrzyński: nothing to disclose
P. Kukołowicz: nothing to disclose
I. Grabska: nothing to disclose

MyT3 13-9 09:02

A model based on liver stiffness measured by shear-wave elastography and future liver remnant ratio to predict post-hepatectomy liver failure in patients with hepatocellular carcinoma

H. Long; *Guangzhou/CN (longhaiy@hotmail.com)*

Purpose: This study aimed to develop a clinical model based on liver stiffness for predicting post-hepatectomy liver failure (PHLF) among patients with hepatocellular carcinoma (HCC).
Methods and materials: Patients undergoing upper abdominal CT or MRI and liver stiffness (LS) measured by shear wave elastography (SWE) prior to hepatectomy for HCC between August 2018 and September 2019 were enrolled prospectively. 80 consecutive patients in our center were enrolled as a derivation set and another 40 patients served as an independent internal validation set. Future liver remnant ratio was estimated based on a three-dimensional reconstruction of the liver and virtual surgery simulation. PHLF was defined per the International Study Group of Liver Surgery (ISGLS) criteria. Multivariate logistic analysis was used to establish the predictive model. The discriminative ability of the model was determined by area under curve (AUC) and compared with commonly predictive systems. A nomogram based on the model was established to display the risk of PHLF.
Results: PHLF occurred in 29 patients (36.3%) in the derivation set. A model based on the basis of future liver remnant ratio, liver stiffness and clinical signs of portal hypertension (CSPH), had a good discrimination ability with AUC of 0.903 (95% confidence interval[CI]: 0.826-0.981, p<0.001) and calibration ability (P=0.116). The model showed satisfactory discrimination ability in the validation set with AUC of 0.815. The AUC of our model was significantly bigger than those of conventional predictive systems in the derivation patients (corresponding AUC, 0.649–0.703).
Conclusion: This model provides good preoperative prediction of PHLF in patients with HCC.
Limitations: Limitations were the small sample size and the fact that the external validation cohort was not available at the time.
Ethics committee approval: This research was approved by the Ethics Committee for the First Affiliated Hospital of Sun Yat-sen University.
Funding: No funding was received for this work.
Author Disclosures:
H. Long: nothing to disclose

MyT3 13-10 09:06

A game-changer for non-transfusion-dependent thalassemia patients: T2* MRI in liver and myocardium iron quantification

G. Nagenthran, P. R. Radhakrishnan, R. J. D. Santosham, B. Jeevanandham; *Chennai/IN (g3nagikrish@gmail.com)*

Purpose: To study the correlation of liver (LIC) and myocardial (MIC) iron concentration using T2* MRI with serum ferritin in non-transfusion-dependent thalassemia patients.
Methods and materials: In this prospective study done between September 2016 and 2018, thirty patients of non-transfusion-dependent thalassemia (17 males and 13 females) were studied. Serum ferritin was determined using the chemiluminescent method. T2* MRI was done using 1.5T Seimens Magentom Avanto. Post-processing: T2* analysis spreadsheet. Inclusion criteria: patients who were diagnosed with non-transfusion-dependent thalassemia (NTDT) - age: 5-50 years. Exclusion criteria: patients on chelation therapy, patients with fever or active infections and patients with contraindications to MR imaging.
Results: Out of 30 patients, 24 had a liver iron overload and only 1 patient had a myocardial iron overload. There was a non-linear correlation between LIC and serum ferritin (P-value <0.01). The rate of change of serum ferritin was not proportional to LIC. No correlation was found between MIC and serum ferritin. A negative correlation was found between LIC and haemoglobin. Liver iron concentration increases as age increases, indicating the accumulation of iron over time. A significant positive correlation was found between LIC and liver size and spleen size (P-value <0.01).
Conclusion: Since the serum ferritin level does not reflect the level of liver iron overload in non-transfusion-dependent thalassemia patients, the assessment of liver iron concentration using the T2* relaxometry method helps in the early detection of iron overload, the early initiation of chelation therapy and the prevention of complications.
Limitations: Respiratory artifact can cause false interpretation.
Ethics committee approval: The Ethics committee approval was obtained.
Funding: NIL
Author Disclosures:
G. Nagenthran: nothing to disclose
P. R. Radhakrishnan: nothing to disclose
B. Jeevanandham: nothing to disclose
R. J. D. Santosham: nothing to disclose

MyT3 13-11 09:10

Calculating the cut-off value of the damping index using the ROC curve to identify Child-Pugh C patients

N. K. Agrawal[1], A. N. Kamble[2]; [1]*Mohali/IN,* [2]*New Delhi/IN*

Purpose: The Child-Pugh score is based on clinical indices and lab results and gives the idea about patient's severity about liver disease. The Child-Pugh C score carries the grave prognosis. In emergency settings, all the values might not be known. Thus it becomes important to have a proxy for laboratory indices which can be promptly and non-invasively done. Thus, we looked at Doppler ultrasound as an alternative. Previous studies have shown that Colour Doppler is useful in prognosticating patients with liver disease. However, very few studies have used objective parameters like the damping index to assess the severity of liver failure objectively, to be used as a prognostication marker.
Methods and materials: 30 patients with portal hypertension underwent Doppler ultrasound. The damping index was calculated by a reader who was blinded to the patient's Child-Pugh score. SPSS was used to calculate the ROC curve. Middle hepatic artery waveform was taken, then the damping index was calculated, dividing the minimum velocity by maximum velocity.
Results: The damping index of 0.56 has good sensitivity (94%) and specificity (84%) to identify the Child-Pugh C patients (p-value <0.001).
Conclusion: The damping index can be used as an alternative to identify Child-Pugh score C patients who have severe liver disease and carry a bad prognosis. Kim et al have shown a 0.6 cut off of DI for a severe portal hypertension (hepatic venous pressure gradient >12 mm Hg) sensitivity of 75.9% and a specificity of 81.8%. Thus the findings of our study support the hypothesis that the damping index can be a useful parameter in evaluating patients with liver disease, especially for their prognostication.

Limitations: The study sample size is small and it was done in one centre.
Ethics committee approval: Institutional ethic committee approval was obtained.
Funding: No funding was received for this study.
Author Disclosures:
N. K. Agrawal: nothing to disclose
A. N. Kamble: nothing to disclose

MyT3 13-12 09:14

Is visual estimation of liver lobe proportion sufficient to decide on the adequate distribution of the chemotherapeutic agent in uveal melanoma patients undergoing hepatic artery infusion?

T. Goeser, J. Grueneisen, J. M. Ludwig, Y. Li, L. Umutlu, M. Forsting, J. Theysohn, B. M. Schaarschmidt*; Essen/DE*

Purpose: In uveal melanoma patients, hepatic metastases can be treated by intraarterial hepatic chemo infusion (IHC). If both liver lobes have to be treated separately due to anatomical variants, the volume proportion of both lobes are visually estimated on angiographic images in order to adapt the correct distribution of the chemotherapeutic agent. The aim of this study was to compare the visually estimated volume proportions on angiographic images with measured volume proportions between both lobes on CT to determine a potential aberrance.
Methods and materials: In this retrospective study, patients with uveal melanoma that underwent separate IHC of the right and the left liver lobe and received pre- and post-treatment CT were included. Volume measurements were performed for both liver lobes pre-and post-treatment and the volume proportions prior to the intervention were compared with the volume proportions described in the angiographic report by the interventional radiologist.
Results: A total of 31 patients (mean age: 64.9, 16 female, 15 male) were eligible for the analysis. The mean aberrance between volume proportions measured in CT and the estimated values described in the angiographic report was 6,8%. In 9 cases, an aberrance of more than 10%, in one patient an aberrance of more than 20% was observed.
Conclusion: In uveal melanoma patients with liver metastases, the visual pre-estimated volume proportion between the right and the left liver lobe is normally matching the measured values. In singular cases with atypical liver anatomy, it might be necessary to perform a volume measurement in order to decide on an appropriate distribution of the chemotherapeutic agent.
Limitations: Small cohort, retrospective study design.
Ethics committee approval: Informed consent was waived by the institutional review board.
Funding: No funding was received for this work.
Author Disclosures:
T. Goeser: nothing to disclose
B. M. Schaarschmidt: nothing to disclose
L. Umutlu: nothing to disclose
M. Forsting: nothing to disclose
J. Theysohn: nothing to disclose
J. Grueneisen: nothing to disclose
J. M. Ludwig: nothing to disclose
Y. Li: nothing to disclose

MyT3 13-13 09:18

The effect of glycemic-control on renal triglyceride content assessed by proton MR spectroscopy in patients with type 2 diabetes mellitus

I. Dekkers[1], M. B. Bizino[1], E. H. M. Paiman[1], J. W. A. Smit[2], I. M. Jazet[1], A. de Vries[1], H. J. Lamb[1]*; [1]Leiden/NL, [2]Nijmegen/NL (i.a.dekkers@lumc.nl)*

Purpose: Since renal steatosis is a potential driver of diabetic kidney disease, and tight glycemic control can reduce the risk of diabetic nephropathy, we assessed whether glycemic control influences renal triglyceride content (RTGC). Furthermore, we compared GLP-1 receptor agonist liraglutide vs standard glucose-lowering therapy.
Methods and materials: In this single-centre parallel-group trial, T2DM patients were randomised to liraglutide or placebo added to standard care (metformin/sulfonylurea-derivative/insulin). Participants were included if RTGC measurement using proton-spectroscopy (^{1}H-MRS) met the quality criteria. The change in RTGC after 26 weeks of glycemic control and the difference of RTGC change between treatment groups was analysed using ANCOVA while adjusting for baseline differences. Between-group differences in RTGC were tested using non-parametric tests.
Results: Fifty out of 85 T2DM patients (59%) of the MAGNA VICTORIA studies who underwent ^{1}H-MRS had renal spectra that met the quality criteria and were included in the present study. The baseline study population consisted of 50 T2DM patients with a mean age of 56.5±9.1 years (range 33–73 years; 46% males). The baseline median RTGC was 0.23% [25th, 75th percentile; 0.12, 0.36], compared to 0.14% [0.09, 0.23] at the follow-up (p=0.06). The mean HbA1c was 61.6±8.4 mmol/mol at the baseline, which changed to 56.3±9.5 mmol/mol at the follow-up (p=0.046). An analysis of covariance did not show a significant association between liraglutide and difference in RTGC after adjustment for baseline RTGC (p=0.33).
Conclusion: Twenty-six weeks of glycemic control resulted in lower RTGC with a trend towards significance. These findings warrant the need for larger clinical studies on glycemic control and renal steatosis.
Limitations: Although renal outcomes were pre-specified, the MAGNA VICTORIA studies were powered for other primary endpoints than RTGC.
Ethics committee approval: The study was approved by the institutional review board.
Funding: The study was funded by the Dutch Kidney Foundation and Novo Nordisk.
Author Disclosures:
I. Dekkers: nothing to disclose
M. B. Bizino: nothing to disclose
E. H. M. Paiman: nothing to disclose
J. W. A. Smit: nothing to disclose
I. M. Jazet: nothing to disclose
A. de Vries: nothing to disclose
H. J. Lamb: nothing to disclose

MyT3 13-14 09:22

Improvement of ultrasonographical differential diagnosis of gastric lesions: the value of contrast-enhanced sonography with gastric distention

T. Li, M. Lu*; Chengdu/CN*

Purpose: The purpose of this retrospective study is to evaluate the diagnostic value of contrast-enhanced sonography plus gastric distention sonography and the Double Contrast-enhanced Ultrasound (DCUS) in gastric lesions.
Methods and materials: 107 cases with pathology confirmed gastric lesions were retrospectively reviewed, DCUS and oral contrast agent ultrasound (US) were performed in all cases prior to the operation. Perfusion parameters including arrival time (AT), peak intensity (PI), time to peak (TTP), area under the curve (AUC) of the lesion and surrounding normal tissue were analysed. A reader blinded to pathology results was asked to rate and compare each case with surgical or resection biopsy pathology results.
Results: From the 107 gastric lesions, 75 were malignant gastric lesions (33 gastric cancers, 42 gastrointestinal stromal tumours (GISTs)) and 32 were benign gastric lesions (11 inflammatory masses and 21 polypoid adenomas). Compared with US, DCUS achieved a higher value in sensitivity (90.6% vs 70.6%), specificity (75% vs 62.5%), and overall accuracy (85.9% vs 68.2%). When US was tested against DCUS, the increase in the correct diagnoses value was significant (P = .01). Gastric cancer had faster AT, higher PI and AUC than normal tissue (P<0.05); gastric cancer and GIST had faster AT than polypoid adenoma (P<0.05).
Conclusion: The combination of different CEUS enhancement characteristics with quantitative perfusion parameters may provide a promising tool helping to differentiate gastric cancer and GIST from benign lesions.
Limitations: Due to an insufficient number of partial cases, we did not evaluate the diagnostic accuracy by each pathological type.
Ethics committee approval: This study was approved by the Institutional Review Board and Ethics Committee of the Sichuan Cancer Hospital.
Funding: No funding was received for this work.
Author Disclosures:
T. Li: nothing to disclose
M. Lu: nothing to disclose

MyT3 13-15 09:26

Shear-wave elastography method in the diagnosis of acute appendicitis

C. Yıldırım[1], Ö. Tunçyürek[2]*; [1]Aydin/TR, [2]Nicosia/CY (cihatyil50@gmail.com)*

Purpose: Acute appendicitis (AA) is the most seen disease with acute abdominal pain. Our purpose is to assess shear-wave elastography (SWE) in the diagnosis of acute appendicitis and to compare SWE findings and postoperatively histopathologic results of appendicitis.
Methods and materials: Patients with right lower quadrant pain underwent ultrasonography (US) between 01.01.2018 and 01.05.2019. If appendices visualized with US, the tissue elasticity of the appendices was measured by SWE. Besides, the presence of free fluid in the peritoneal cavity, lymph node and peri-appendicular inflammation were recorded for AA diagnosis in US. The demographics of the patients were also recorded. US-SWE results were compared with histopathologic scores of inflammation statistically with the Mann-Whitney U test.
Results: 84 patients were evaluated with US. 36 patients had findings for AA diagnosis. All patients diagnosed with AA were operated. There was a significant difference between the inflammation score and SWE results (p<0.001). According to the ROC curve analysis, the sensitivity and specificity of shear-wave elastography US in the diagnosis of acute appendicitis were calculated as 77% and 65%, respectively.

Conclusion: The SWE method is currently under development. Several types of SWE methods are used for the diagnosis of several diseases as a helper, routinely. In AA, the perforation risk is related to the inflammation score. The SWE method may be useful in the diagnosis of early AA when US findings are insufficient and to predict the risk of perforation due to its correlation with inflammation intensity.
Limitations: Limitations in this study are that the shear-wave elastography measurements can be affected by tissue depth and respiratory movements and that the size of the sampling window can not be changed.
Ethics committee approval: Ethical committee approval and written consent forms were obtained.
Funding: No funding was received for this work.
Author Disclosures:
C. Yıldırım: nothing to disclose
Ö. Tunçyürek: nothing to disclose

MyT3 13-16 09:30
Comparison of spin-echo echo-planar imaging (SE-EPI), MR elastography with gradient-recalled echo (GRE), MR elastography and correlation with transient elastography (TE)
J. Yoon, E. S. Lee, H. J. Park, B. I. Choi, S. B. Park*; Seoul/KR (yoonjw1203@caumc.or.kr)*

Purpose: To compare the liver stiffness (LS) values obtained by newly developed spin-echo echo-planar imaging (SE-EPI) MR elastography (MRE) with conventional gradient-recalled echo (GRE) MRE in the same condition. In addition, to assess the statistical correlation of the obtained LS values with those of transient elastography (TE).
Methods and materials: From April 2018 to September 2019, we retrospectively included a study population who underwent liver MRE with both SE-EPI and GRE sequences in the same session. Among them, we excluded patients without TE within one year and finally enrolled 43 patients. LS measurements for MRE were performed using free-drawing region-of-interest and reliable TE measurements were defined as the median value of 10 measurements with interquartile range/median (IQR/M) ≤30%. We compared technical success rates, median LS values and areas of confidence for MRE measurements between SE-EPI and GRE sequences using paired t-test. We also evaluated the correlation co-efficient between LS values obtained by each MRE sequence and TE, respectively.
Results: The technical success rate of MRE in SE-EPI was significantly higher than that of GRE (100% vs. 86.0%, p=0.03). LS values from SE-EPI and GRE MRE were not significantly different (SE-EPI; 3.78kPa vs. GRE; 3.54kPa, p=0.08). The areas of confidence for MRE measurements were significantly larger in SE-EPI than those of GRE MRE (8215.1981 vs. 2691.4759 mm2, p<0.001). The LS values from two MRE sequences were significantly correlated with those from TE (SE-EPI; r=0.64, p<0.001 vs. GRE; r=0.61, p<0.001).
Conclusion: SE-EPI MRE is technically stable, and LS values obtained by this sequence would be reliable. LS values obtained by GRE and SE-EPI MREs are significantly correlated with those by TE.
Limitations: The MRE examinations were performed using a single MR unit.
Ethics committee approval: n/a
Funding: No funding was received for this work.
Author Disclosures:
J. Yoon: Speaker at Chung-Ang university hospital, Author at Chung-Ang university hospital
E. S. Lee: Author at Chung-Ang university hospital
H. J. Park: Author at Chung-Ang university hospital
B. I. Choi: Author at Chung-Ang university hospital
S. B. Park: Author at Chung-Ang university hospital

MyT3 13-17 09:34
CT signs evaluation in predicting the site of gastrointestinal tract perforation: a review of 100 operated patients
S. Ferraro, M. Giannotta, G. Zanirato Rambaldi, F. Dardi, P. E. Orlandi, M. Imbriani*; Bologna/IT (sissina9@libero.it)*

Purpose: The aim of this study was to retrospectively evaluate the accuracy of CT for preoperative determination of the site of surgically proven gastrointestinal (GI) perforation and to determinate the most predictive findings in this diagnosis.
Methods and materials: We retrospectively reviewed the abdominal CT of 100 patients who had a surgically proven GI perforation (64 males; aged between 32-92 years) performed in our centre, from March 2017 to March 2019. IV contrast agent was used in 83 patients. Two observers, respectively with 25 and 4 years of radiological experience, blinded to the surgical diagnosis, reached a consensus prediction of the site of perforation using the presence of the following CT findings: extra-luminal air (grade and distribution), defect in the wall, wall thickening, abnormal wall enhancement, peritoneal fluid, fat-stranding and inflammatory masses. We also evaluated these signs in predicting perforation due to peptic ulcer disease vs diverticulitis, respectively the most common cause of upper and lower GI perforation. A Chi-Square test was used to analyse the results.
Results: 37 patients presented an upper GI perforation and 63 a lower GI perforation. Severe free air (p=0.04), free air in the supra-mesocolic compartment (p=0.00) and peritoneal fluid (p=0.00) resulted in strong predictors of upper GI perforation, while mild and moderate free air (p=0.04) and fat-stranding (p=0.00) indicated a lower GI perforation. 35 patients had a peptic ulcer disease and 28 patients had diverticulitis. Free air in the supra-mesocolic compartment (p=0.00) and peritoneal fluid (p=0.00) suggested a perforation due to peptic ulcers, while free air in pelvis and retroperitoneum (p=0.03), fat-stranding (p=0.00), abnormal wall enhancement (p=0.05) and inflammatory masses (p=0.05) indicated a perforation due to diverticulitis.
Conclusion: CT is highly accurate for distinguishing upper from lower GI perforation.
Limitations: 17 patients performed unenhanced CT.
Ethics committee approval: n/a
Funding: n/a
Author Disclosures:
S. Ferraro: nothing to disclose
M. Giannotta: nothing to disclose
G. Zanirato Rambaldi: nothing to disclose
F. Dardi: nothing to disclose
P. E. Orlandi: nothing to disclose
M. Imbriani: nothing to disclose

MyT3 13-18 09:38
Value of CT enterography for predicting the incidence and short-term surgery in patients with Crohn's fistulising disease in the era of biologics
G. Minyi*; Guangzhou/CN (wfbbq@163.com)*

Purpose: To analyse the value of CT enterography (CTE) in predicting the incidence in patients of perianal fistulising disease and the risk of surgical treatment within one year, to provide the evidence for guiding clinical evaluation and rational selection of treatment options.
Methods and materials: 279 cases of newly diagnosed Crohn's disease patients were analysed retrospectively. All patients were followed-up for one year. CTE imaging parameters were recorded and pelvic MR images were evaluated with regard to the presence of anal fistulas.
Results: 204 patients were eligible for the analysis. The presence of colonic involvement was seen in 47/88 (53.41%) cases in the anal fistula group (Group 1) and in 38/116 (32.76%) cases in the non-anal fistula group (Group 2) (P=0.006). The bowel wall enhancement in Group 1 mainly manifested as type 1 and type 2 as 69/88 (78.41%) compared with type 3 and type 4 in Group 2 as 78/116 (67.25%)(P＜0.001). Rectal involvement was present in 12/18 (69.62%) cases of the surgical group (Group 3) vs 22/53 (41.51%) of the non-surgical group (Group 4), luminal stenosis in 15/18 cases (83.33%) of Group 3 vs 4/18 cases (22.22) in Group 4, intra-abdominal fistula in 33/53 (62.27%) of Group 3 vs 2/53 (3.77%) of Group 4. In the multivariate analysis, rectal involvement (OR 1.911 (1.102 to 4.185), P＜0.001), luminal stenosis (OR 2.627 (1.760 to 6.024), P=0.028) and intra-abdominal (OR 1.337 (1.093 to 3.585), P=0.006) increased the risk of surgery.
Conclusion: Colonic involvement and bowel wall enhancement can predict the onset of perianal fistulising disease. Rectal involvement, luminal stenosis, and intra-abdominal fistula increase the risk of short-term surgery for perianal fistulising disease.
Limitations: Limitations were: 1. Single-centre, selection bias; 2. Very few patients did not use enema; 3. Few patients' drug treatment was not standardised.
Ethics committee approval: n/a
Funding: No funding was received for this study.
Author Disclosures:
G. Minyi: Author at The sixth affiliated hospital of Sun Yat-sen University

MyT3 13-19 09:42
The role of CT gastric volumetry in sleeve gastrectomy
M. S. T. M. Elfeshawy, A. E. Mohamed, E. Sokker*; Cairo/EG (mst1200@yahoo.com)*

Purpose: The study is aimed at the correlation between the operative gastric volume reduction and body weight reduction after surgery.
Methods and materials: Our study included 30 cases; all were overweight/obese individuals. There were 20 females and 10 males. All patients underwent MSCT abdomen with oral contrast. Post-processing in form of multi-planner reformatting and 3D reconstruction was performed in all cases before and 3 months after sleeve gastrectomy.
Results: The collection and correlation of preoperative and postoperative data revealed that the percentage of operative gastric volume reduction ranged between 76% and 98% with a mean value of about 84%, while the percentage of body weight reduction ranged between 7% and 24% with a mean value of

about 15%. The correlation between body weight and gastric volume measured preoperatively in the studied patients was found to be insignificant, which means that the stomach volume does not have a direct impact on body weight.
Conclusion: MSCT volumetric study of the stomach is the gold standard imaging technique for the evaluation of the gastric size in the preoperative and postoperative stages in the context of bariatric sleeve gastric surgery. Gastric volume does not have a direct impact on body weight in obese individuals. Further evaluation of gastric volume and bodyweight of the studied patients one year after surgery is recommended for a continuous observation as well as monitoring the rate of weight loss and incidence of gastric pouch dilatation.
Limitations: Patients who are candidates for gastric reduction surgery other than sleeve gastrectomy. Patients with recurrent weight gain after a previous gastric reduction procedure.
Ethics committee approval: An approval of the study was obtained from Al-Azhar University Academic and Ethical Committee. Every patient signed an informed written consent for the acceptance of the operation.
Funding: No funding was received for this study.
Author Disclosures:
M. S. T. M. Elfeshawy: nothing to disclose
A. E. Mohamed: nothing to disclose
E. Sokker: nothing to disclose

MyT3 13-20 09:46
CT gastroscopy: a convenient tool to evaluate gastric mass lesions
S. Siddharth, P. Narang, D. S. Srivastava, P. Gupta*; New Delhi/IN (siddharthsharma100@gmail.com)*

Purpose: The purpose of this study was to assess the role of computed tomography gastroscopy (CTG) in the evaluation and treatment planning of gastric mass lesions (GML) and to compare the diagnostic accuracy of the same with conventional endoscopy (CE).
Methods and materials: 26 patients with GML detected by CE and confirmed by histopathology prospectively underwent a 256 slice CT scan at a tertiary care centre between August 2017 and September 2018. CTG was done after distending the stomach by oral effervescent agents and insufflation of air through foley's catheter inserted via nasopharyngeal route. CTG images were developed by a dedicated software. GML morphology on CTG was compared to CE using appropriate statistical tools and Kappa value was calculated to find the agreement.
Results: All lesions (100%) diagnosed by CE were successfully detected on CTG. Sensitivity and specificity for evaluating lesion size were 92.9% and 50% respectively, while PPV and NPV were 68.4% and 85.7% respectively. The sensitivity for evaluating the length of the stricture was 100% with 73.1% accuracy. Sensitivity and PPV for the detection of the surface of lesions were 65.4% and 100% respectively, with 65.4% accuracy. Kappa value of 0.79 suggested a good intermodality agreement.
Conclusion: CTG helps in identifying lesions and has bright prospects in cases with obstructive pathology where CE provides limited information. A combined interpretation of axial and 3D images is necessary to make an accurate diagnosis. Being a non-invasive technique with fewer complications it can be carried out in a safe, compliant and effective manner for complete evaluation of GML.
Limitations: Limitations were the small sample size and the single-centre experience. Patient preparation is stringent and cumbersome. Radiation dose is an issue in the paediatric population.
Ethics committee approval: n/a
Funding: No funding was received for this study
Author Disclosures:
S. Siddharth: nothing to disclose
P. Narang: nothing to disclose
D. S. Srivastava: nothing to disclose
P. Gupta: nothing to disclose

MyT3 13-21 09:50
Radiologic findings of ampullary cancer on contrast-enhanced MRI (CEMRI) with a liver-specific contrast agent: pay attention to the 30-min delayed scan
I. Son, S. Hong, N. Lee, S. Kim*; Busan/KR*

Purpose: To determine the radiologic findings of ampullary cancer on contrast-enhanced MRI (CE-MRI) with a liver-specific contrast agent.
Methods and materials: This retrospective study included 120 patients (65 male and 55 female; mean age: 70.62 years) who were suspected to have ampullary cancer and who performed CE-MRI with a liver-specific contrast agent from January 2015 to January 2019. We collected data including the presence of the bulging ampulla, size, T1/T2-signal intensity, enhancement patterns, diffusion restriction of the ampulla, the extent of common bile duct (CBD) and pancreatic duct dilatation, the change of shape in distal CBD, CBD wall thickening and asymmetry, the contrast secretion to duodenum on a 20-min and a 30-min delayed scan. We also reviewed the pathologic and clinical diagnostic information. In addition, we performed a subgroup analysis according to the presence of the bulging ampulla. Univariate and multivariate analysis was performed to determine the malignancy-associated factor.
Results: 54 patients had ampullary cancer and 66 patients had a benign condition. On the multivariate analysis, diffusion restriction (p=0.028) and heterogeneous enhancement (p=0.045) of the ampulla, no change of shape in distal CBD (p=0.010), and no contrast secretion to duodenum 30-min delayed scan (p=0.001) were significantly associated with ampullary cancer. On the subgroup analysis, the presence of diffusion restriction and the extent of CBD dilatation, no contrast secretion to duodenum 30-min delayed scan was significantly associated with ampullary cancer in the group with the bulging ampulla. In the group without the bulging ampulla, no contrast secretion to duodenum 30-min delayed scan is the only significant factor for ampullary cancer.
Conclusion: Diffusion restriction and heterogeneous enhancement of the ampulla, no change of shape in distal CBD, and no contrast secretion to duodenum 30-min delayed scan were significantly associated with ampullary cancer. Among them, no contrast secretion to duodenum 30-min delayed scan is the only significant factor regardless of the presence of the bulging ampulla.
Limitations: Single centre, retrospective study with a small number of subjects.
Ethics committee approval: n/a
Funding: No funding was received for this work.
Author Disclosures:
I. Son: nothing to disclose
S. Hong: nothing to disclose
N. Lee: nothing to disclose
S. Kim: nothing to disclose

MyT3 13-22 09:54
MRI-guided microwave ablation of hepatic malignancies: feasibility, efficacy, safety and follow-up
N. Yang*; Shanghai/CN (eoslulu@foxmail.com)*

Purpose: To investigate the feasibility, technical success, safety and follow-up of hepatic malignancies microwave ablation under MRI-guidance.
Methods and materials: From August 2015 to February 2019, 26 patients (38 lesions) were enrolled. T1WI, T2WI, DWI and enhanced MRI were performed as pre-treatment and follow-up (range on 3-36 months). The feasibility evaluation included the successful detection of target tumour and the tumour delineation under MRI during targeting. The technical success was defined as a successful performance of the ablation procedure as initially intended and the achievement of a coagulation zone covering the target tumour with ＞5mm margin. The technique efficacy was evaluated on a contrast-enhanced MR follow-up imaging 4 weeks later. The safety evaluation was based on procedure-related complications according to the clinical practice guidelines of the society of interventional radiology.
Results: 100% primary efficacy rate was achieved and no major complication were observed. The 3D visualisation image has given more and precise information for evaluation and follow-up. 60W/5 MIN ablation power was given in lesions under 1 cm in which the ratio of the ablation zone volume to applied energy and sphericity was calculated. 6 lesions with incomplete circle on reconstructed DWI immediately postprocedural, and persistent hyperintense signal (rang on 3 days to 1 week) was developed into new lesions in the next 6-12 months.
Conclusion: MRI-guidance is feasible and effective in the planning and evaluation of microwave ablation in hepatic malignancies. The available clinical data strongly supports the advantages of 3D-reconstructed image tumour assessment over the one based on routine axial image.
Limitations: Our study has many pitfalls: 1. The relatively small sample size of patients, 2. A lack of imaging-pathologic data, 3. Further studies are required to reveal the inner linking between microstructural changes with a signal on multi-b-value DWI and on the early stage after ablation.
Ethics committee approval: n/a
Funding: No funding was received for this work.
Author Disclosures:
N. Yang: nothing to disclose

08:30 - 10:00 **Room M 1**

Imaging Informatics

RPS 1305

Imaging informatics in Europe and beyond

Moderators:
J. Fernandez-Bayo; Sabadell/ES
S. Gatidis; Tübingen/DE

RPS 1305-1 08:30

The current state of knowledge of imaging informatics amongst Spanish radiologists

D. D. Eiroa Gutiérrez[1], M. Fdez. Del Castillo Ascanio[2], N. Roson Gradaille[1], R. Mast Vilaseca[1], K. Ramirez Tucas[1], V. Pantoja Ortiz[2]; [1]*Barcelona/ES,* [2]*Santa Cruz de Tenerife/ES (contrasteyodado@gmail.com)*

Purpose: To evaluate general knowledge and concerns about trends on imaging informatics among radiologists currently working in Spain (both residents and attending physicians).
Methods and materials: Type of study: a cross-sectional survey. Inclusion criteria: a radiologist currently working in Spain (public and private). Survey preparation: a survey comprising a total of 20 questions was confectioned, inquiring about technical issues and ethical and professional perspectives. Outcome measures: observational statistical analysis, mainly of frequencies, was carried out.
Results: Most of the 223 surveyed radiologists [52 (23.32%) residents and 171 (76.68%) attending radiologists (AR)] work in National Health Services, at least partly. The most heard-of technologies were machine learning (72.55%) and artificial intelligence (67.26%), with the latter (22.59%) and algorithms (18.39%) being the most used technologies among the surveyees.100% of respondents considered they should pursue academic training in IT and new technologies and around 98% of them reckon it should be included in the speciality's academic program. However, 76.23% of the interviewees think there is not enough time in four years of academic training to include said skills and competencies. Moreover, the main issue expressed by the respondents was patient safety.
Conclusion: Although most of the main commercial technologies are recognised by Spanish radiologists, there is a lack of knowledge of the underlying methods used. There is a will to learn about these topics, although there is no time during residency years. The main concern is patient safety, which highlights the ethical implications of the implementation of such technologies.
Limitations: The main limitation is the selection bias due to convenience sample. A larger sample would allow to draw better conclusions. A higher participation, particularly among residents, was desired.
Ethics committee approval: n/a
Funding: No funding was received for this work.
Author Disclosures:
D. D. Eiroa Gutiérrez: nothing to disclose
M. Fdez. Del Castillo Ascanio: nothing to disclose
R. Mast Vilaseca: nothing to disclose
N. Roson Gradaille: nothing to disclose
V. Pantoja Ortiz: nothing to disclose
K. Ramirez Tucas: nothing to disclose

RPS 1305-2 08:36

Should we perform all the radiological tests that are requested?

P. Fraga Rivas[1], C. Benito Vicente[1], L. Garcia Del Salto Lorente[1], M. I. Diez Perez de las Vacas[1], J. de Miguel Criado[2], F. Aguilera Del Hoyo[1], A. Marco Sanz[2]; [1]*Madrid/ES,* [2]*Coslada/ES (fragarivas@gmail.com)*

Purpose: To present a computer system to assess the justification in radiology that allows us to evaluate the requested examinations, the justification of exposures being applied and determining whether patients fit the recommended criteria for the procedure, and to evaluate its use in a radiology service in the last 6 months
Methods and materials: We have a tool in the electronic history that allows the evaluation of radiological requests before they are cited. When the radiologist considers the test is indicated, they proceed to its validation, and then it can be cited. Otherwise, they deny the indication and the test is cancelled or changed to another imaging test more appropriate to clinical suspicion. Any change in the request is communicated to the petitioning physician.
Results: Of the 84,342 requests made in the last semester of 2018, we included in this validation system all the CT, MR, Doppler, biopsy, and puncture tests, which represent 10,342 requests (12.2%). 10,044 requests were considered indicated but were not indicated 249 (0.29%). We analyse the results by radiological modality, service, petitioning physician, and diagnostic suspicion. We evaluated those tests that, not being indicated, have been modified to other tests more adjusted to the clinical suspicion.
Conclusion: Justification of radiographic examinations is the practice of evaluating requested radiological examinations to assess for clinical merit and appropriateness based on clinical notes and patient information. We believe that our validation process has been useful in the radiological management of the patient, in reducing the radiation received, and in avoiding unexpected findings that divert the main diagnosis in unjustified tests. Radiologist who actively participate in the decision-making process of justification of an examination will ultimately contribute towards improved patient care and management.
Limitations: n/a
Ethics committee approval: n/a
Funding: No funding was received for this work.
Author Disclosures:
P. Fraga Rivas: nothing to disclose
F. Aguilera Del Hoyo: nothing to disclose
C. Benito Vicente: nothing to disclose
L. Garcia Del Salto Lorente: nothing to disclose
J. de Miguel Criado: nothing to disclose
M. I. Diez Perez de las Vacas: nothing to disclose
A. Marco Sanz: nothing to disclose

RPS 1305-3 08:42

National diagnostic imaging trends in Spain: 2010-2017

A. Perez Girbes, M. P. Barreda Solana, V. Navarro Aguilar, A. Torregrosa Andres; *Valencia/ES (aperezgirbes@gmail.com)*

Purpose: To describe the national trends in diagnostic imaging used in Spain from 2010 to 2017 in public and private healthcare.
Methods and materials: Data was obtained from National Hospitals Statistics, an annual report published on the Spanish Health Ministry webpage (https://www.mscbs.gob.es/estadEstudios/estadisticas/estHospiInternado/inforAnual/homeESCRI.htm). Included variables were annual examinations rate per 1,000 inhabitants, annual scanners/rooms per million inhabitants, and a ratio between the number of examinations per scanner/room. Included modalities were CT, MR, PET-CT, SPECT, digital angiography, mammography, conventional radiography, and scintigraphy.
Results: For cross-sectional imaging, annual national examinations rates per 1,000 inhabitants increased 114.8% for PET-CT (1.62 to 3.48), 51.4% for MR (47.58 to 72.04), 42.5% for SPECT (2.40 to 3.42), and 33.4% for CT (83.13 to 110.92). In 2017, public healthcare accounted for 81% of PET/CT examinations, 61% of MR studies, 87% of SPECT examinations, and 83% of CT.
Conventional radiography and mammography also increased their examination rates by 9.9% and 38.1%, respectively. Conversely, digital angiography and scintigraphy decreased by 1.8% and 12.5%. All modalities except conventional radiography and scintigraphy increased the number of scanners/rooms per million inhabitants.
Conclusion: All diagnostic imaging modalities significantly increased the number of examinations per 1,000 inhabitants in Spain between 2010 and 2017, except digital angiography and scintigraphy.
Limitations: This is an observational study for a period of 8 years. Data should be used carefully due to amount of aggregation.
Ethics committee approval: n/a
Funding: No funding was received for this work.
Author Disclosures:
A. Perez Girbes: nothing to disclose
M. P. Barreda Solana: nothing to disclose
A. Torregrosa Andres: nothing to disclose
V. Navarro Aguilar: nothing to disclose

RPS 1305-4 08:48

The effect of changing the method of teaching radiology to interactive clinically-based learning on the achievements of medical students in imaging

U. Wachsman, I. Shelef, Y. Lior, G. Ben- Arie; *Beer-Sheva/IL (gal_b_a@yahoo.com)*

Purpose: To evaluate the efficacy of changing teaching methods in the 4th year medical school radiology course from lecture-based teaching to interactive clinical case-based teaching.
Methods and materials: We compared the assessments in the radiology course taken from 4th year medical students during 2018-2019. In the first year, teaching was primarily done via conventional lectures. In the following year, case-based teaching with interactive web application named “NEARPOD” was employed to motivate student participation. The student knowledge assessments were comprised of identical post-test questions, encompassing 5 images of common diagnoses such as pneumothorax, pneumonia, normal chest x-ray (CXR), subdural haematoma, and ischaemic stroke. We also compared

pre- and post-tests taken in the later year, similarly, composed of 5 different images of common radiographic diagnoses.
Results: 72 students answered the post-test in the first year and 50 students answered in the following year. 55 students answered the pre-test in that year. Post-test student achievements following the methodological changes were significantly higher when compared with the control group (p <0.001). Students provided positive feedback to the methodological teaching changes.
Conclusion: Our study shows that teaching radiology in a clinical case-based manner, combined with web-based interactive applications, results in significant improvements, specifically in identifying key imaging pathologies, as compared to conventional lecture-based teaching.
Limitations: n/a
Ethics committee approval: n/a
Funding: No funding was received for this work.
Author Disclosures:
U. Wachsman: nothing to disclose
I. Shelef: nothing to disclose
G. Ben- Arie: nothing to disclose
Y. Lior: nothing to disclose

RPS 1305-5 08:54
Professional social media use is associated with having received advanced scientific training: results from an international survey in 1,041 radiologists and residents
M. Huisman[1], E. R. Ranschaert[2], W. Parker[3], D. Mastrodicasa[4], M. Kočí[5], D. Pinto Dos Santos[6], T. Leiner[1], M. J. Willemink[7]; [1]*Utrecht/NL,* [2]*Turnhout/BE,* [3]*Vancouver/CA,* [4]*Stanford, CA/US,* [5]*Palo Alto, CA/US,* [6]*Cologne/DE,* [7]*Menlo Park, CA/NL (merel.huisman1@gmail.com)*

Purpose: Social media use has increased substantially over the last decade, particularly in medical professional fields. We intended to characterise current social media use for professional purposes in the international radiology community.
Methods and materials: A web-based survey was accessible from April to July 2019 and included questions on demographics, professional background, and social media use. Multivariable logistic regression was used to assess independent predictors for professional social media use.
Results: Participants (n=1,041) were working in 54 different countries, mostly Europe (n=867, 83%). Slightly more than half (n=553, 53%) indicated the use of social media for professional purposes. Among participants who used social media, LinkedIn was most frequently mentioned (n=360, 65%), followed by Facebook (n=199, 36%), Twitter (n=115, 21%), and Instagram (n=99, 18%). Professional social media use was inversely associated with age (OR 0.98 (0.97-0.99), p<0.001), and positively associated with advanced scientific training (PhD/research fellowship; OR 1.65 (1.24-2.18), p<0.001) after adjusting for gender and region. There were no significant differences in professional social media usage between residents, fellows, and radiologists; academic and non-academic participants or gender. Male gender was a predictor for Twitter use (p<0.05), female gender for Instagram use (p<0.05). Working in Europe was a predictor for Twitter and Instagram usage (p<0.001). Advanced scientific training was a predictor for LinkedIn and Twitter (p<0.001). There were no predictors for Facebook.
Conclusion: Our international survey indicates radiologists and residents with advanced scientific training more frequently use social media for professional purposes, especially LinkedIn and Twitter. European radiology professionals more frequently use Instagram or Twitter for professional purposes.
Limitations: "Social media use for professional purposes" is subjective as indicated by the participants.
Ethics committee approval: n/a
Funding: No funding was received for this work.
Author Disclosures:
M. Kočí: nothing to disclose
M. Huisman: nothing to disclose
E. R. Ranschaert: nothing to disclose
W. Parker: nothing to disclose
D. Mastrodicasa: nothing to disclose
D. Pinto Dos Santos: nothing to disclose
T. Leiner: nothing to disclose
M. J. Willemink: nothing to disclose

RPS 1305-6 09:00
First peer review experience among a French teleradiology community
M. Schertz[1], E. Morau[2], G. Sozeau[2], M. Cavet[1]; [1]*Paris/FR,* [2]*Montpellier/FR (schertzmathieu@hotmail.fr)*

Purpose: Peer review is seldom reported in France and double reading has been recommended in teleradiology. We therefore report our peer review experience among a community of teleradiologists.
Methods and materials: Peer review was performed anonymously and on a voluntary basis. Over one year, randomised CT and MRI cases were reviewed within our RIS-embedded system. The rate of review, discrepancies, doctor's participation, and satisfaction were reported. The discrepancy scoring system derived from the RADPEER program.
Results: Over a period of one year, 1,691 (1.1%) of 155,879 cases were reviewed: 89.7% (1,517) were qualified as concordant, 6.0% (102) as a minor discrepancy, 4.3% (72) as a major discrepancy, and 3.4% (54) as major discrepancies likely to be clinically significant.
52 of 65 radiologists (80%) participated in the review. 85% of them were overall satisfied with the peer review system, 88% felt that being reviewed was beneficial for them, 48% felt that reviewing others was beneficial for them.
All discrepancies likely to be clinically significant were consensually revised and the updated conclusions shared with the referring clinicians.
Conclusion: We highlight the feasibility of peer review on a voluntary basis within our network of teleradiologists. The recorded rate of discrepancies likely to be clinically significant was below the rates previously published (4). Participation and satisfaction among radiologists were high.
We therefore recommend the continuation of peer review in our community and encourage other teams to do so.
Limitations: n/a
Ethics committee approval: RIS-embedded system approuved by the CNIL (Comité national d'Informatique et des Libertées).
Funding: No funding was received for this work.
Author Disclosures:
M. Schertz: nothing to disclose
M. Cavet: nothing to disclose
E. Morau: nothing to disclose
G. Sozeau: nothing to disclose

RPS 1305-7 09:06
Innovation in radiology using a needs-based approach: clinical radiologists' experience
R. A. Rippel, A. El-Zein; *Oxford/UK (radoslaw.rippel@gmail.com)*

Purpose: To present our experience and promote the learning and utilisation of a needs-based innovation approach in clinical radiology.
Methods and materials: Need-based innovation is a methodology enabling a structured approach to screening for problems worth pursuing followed by a thorough system for idea generation and product development.
Oxford Biodesign offers two programmes which focus on a systematic approach to clinical-needs finding. Fellowship is a 9 month full immersion course taking participants from observations, through clinical needs finding, needs assessment, generation of solutions, stakeholders assessment, and market research, all the way to prototyping and start-up with seed funding. The short programme follows a similar curriculum, however, it is run as a series of two-hour interactive sessions once a week during the academic year.
Results: Needs-based innovation is a systematic approach to problem-finding and solution generation which is well-tailored to the complex and high-barrier entry field of medical device and digital health industries. Clinician participation in the programme not only enables the team to benefit from the clinical insight but also enables the clinician to experience a broader view of healthcare and different cognitive approach to the clinical environment. In this presentation, we will demonstrate our project outcomes and their potential impact on clinical practice. In addition, we showcase our experience of participation in both of the programmes as well as the road to innovation in radiology.
Conclusion: Radiology is a rapidly developing, technology-based clinical speciality. Use of the systematic need led innovation is an effective way to guide radiologists and develop collaborations focused on medical innovation, including digital health and medical device development.
Limitations: n/a
Ethics committee approval: n/a
Funding: The Oxford Biodesign Programme is supported by institutions such as the European Institute of Innovation and Technology (EIT).
Author Disclosures:
R. A. Rippel: nothing to disclose
A. El-Zein: nothing to disclose

RPS 1305-8 09:12
Challenges, opportunities, and strategies of global health radiology in low-middle income countries (LMIC): an excerpt review
S. L. Shem[1], H. Umdagas[2], F. B. Nkubli[3], D. Z. Joseph[4], M. Z. Ibrahim[2]; [1]*Gombe/NG,* [2]*Zaria/NG,* [3]*Maiduguri/NG,* [4]*Kano/NG (samuelshemm@gmail.com)*

Purpose: More than half of the world's population lacks adequate medical imaging services according to the World Health Organisation (WHO). However, radiology plays an important role in public health initiative programs such as tuberculosis, trauma, breast cancer screening, and maternal-infant health. The purpose of this study was to identify challenges, opportunities, and strategies of

radiology in global health initiatives in low-middle income country where resources may be scarce.
Methods and materials: White paper reports of RAD-AID conferences on international radiology for developing countries since inception in 2009 were reviewed. Additionally, resources from national and international organisations that published data such as the World Bank and the World Health Organisation (WHO) were reviewed, as well as the medical literature databases from the Cochrane Library and PubMed. Search terms such as global health radiology, challenges, and strategies were used.
Results: Establishment and sustainability of medical imaging services was a major long-standing challenge of radiology global health initiative programs in many low-income countries. To overcome this barrier, certain components of sustainability were identified as strategies to the implementation and optimisation of radiology services including economic development, technological innovation, clinical imaging models' implementation, educational approaches, and the integration of public health to radiology.
Conclusion: Components of radiology global health initiative programs should consider economic sustainability, information technology innovation, tested clinical models, education, and public health policies as keys to optimising radiological services in low middle-income countries.
Limitations: No known bias.
Ethics committee approval: n/a
Funding: No funding was received for this work.
Author Disclosures:
S. L. Shem: nothing to disclose
H. Umdagas: nothing to disclose
F. B. Nkubli: nothing to disclose
M. Z. Ibrahim: nothing to disclose
D. Z. Joseph: nothing to disclose

RPS 1305-9 09:18
First national teleradiology pilot project in the Saudi Ministry of Health
S. Alshaikh[1], A. Aldosari[1], H. Alasmari[1], M. Almuaiqel[1], M. Mutabi[1], Q. Alalwan[2], A. F. T. Gashgari[3]; *[1]Riyadh/SA, [2]Al-Hassa/SA, [3]Dammam/SA (salshaikh@moh.gov.sa)*

Purpose: The need for high-quality radiology reports is necessary for accurate and better diagnosis. However, due to the lack of subspecialised consultant radiologists in the Ministry of Health remote hospitals, this is a real challenge. The need for qualified medical physicists is another major concern for image quality assessment. Moreover, the impact of technologists and imaging protocols was investigated. The goal of this project is to establish a National TeleRadiology Platform (NTRP) to provide high-quality radiology reports for remote hospitals.
Methods and materials: The NTRP has been established to provide a centralised national radiology reporting system for remote hospitals. All remote hospitals send their radiology CT and MRI cases to one pool at the NTRP. The radiologists from all referral hospitals can access the pool remotely via NTRP for reporting. The final report is sent back to the remote hospitals within a pre-defined turn-around time (TAT). The reimbursement for radiologists' workloads has been estimated using the relative value unit (RVU). The NTRP serve routine cases and urgent cases were covered as a second opinion.
Results: The number of reported cases per month increased from 130 reports in July 2018 to 1,360 reports in September 2019. The percentage of reported cases performed with CT and MRI modalities were 65% and 35%, respectively.
Conclusion: The quality of reports was improved for remote hospitals. The clinicians started to request advanced exams with advanced protocols for subspecialised cases. The referrals from these hospitals to do subspecialided exam is no longer needed, in addition to the direct cost saving on hiring subspecialised radiologists. Based on the promising outcomes, the service was expanded from 10 to 20 remote hospitals.
Limitations: n/a
Ethics committee approval: n/a
Funding: No funding was received for this work.
Author Disclosures:
A. F. T. Gashgari: nothing to disclose
M. Mutabi: nothing to disclose
S. Alshaikh: nothing to disclose
A. Aldosari: nothing to disclose
H. Alasmari: nothing to disclose
M. Almuaiqel: nothing to disclose
Q. Alalwan: nothing to disclose

RPS 1305-10 09:24
Relative value unit system: a new approach for quantifying radiologists' workloads
S. Gelmez; *Istanbul/TR (sgelmez@yahoo.com)*

Purpose: Proper understanding and accurate quantification of the workload of radiologists is needed to effectively plan the workflow. Relative value unit (RVU) systems are used to assign values to radiologists' activities. Different methods, mainly based on reporting times, are used in various countries to create RVU tables. In this study, a more comprehensive method, taking in more input variables in accordance with the complexity level of local case-mix data, was used to assign RVUs.
Methods and materials: A total of 20 radiologists from 3 linked hospitals analysed the radiologic examinations from the reporting perspective and stated the subjective mean exam RVU and exam subgroup RVUs of 34 different types of CT, MRI, and ultrasonography examinations. Time and experience needed, extra time and effort that should be spent completing a report, and potential medicolegal issues associated with the reporting were considered in the assessment. In order to address the inherent variability of the workload, radiologic examinations were subgrouped according to the complexity level of the examination. Final exam RVU's were determined using the median as the central tendency because the data was skewed. RVU tables were generated according to the results.
Results: The workload of radiologists is difficult to measure. Reporting time based measurements have got many procedural bias. Variability and the complexity levels of the radiologic studies should be addressed to correctly assess the RVUs.
Conclusion: Working further on different local units is advised and the local units should be classified in order to create more accurate global RVU tables.
Limitations: The main concern in this study is the local case-mix data, so the final RVUs may not be representative of global or other local units.
Ethics committee approval: Ethics committee approval obtained.
Funding: No funding was received for this work.
Author Disclosures:
S. Gelmez: nothing to disclose

RPS 1305-11 09:30
Data mining of metrics from a report comparison tool can reveal daytime and shift dependent trends in the quality of residents' reports
J. Vosshenrich, I. Nesic, J. Cyriac, D. Boll, E. M. Merkle, T. Heye; *Basel/CH (jan.vosshenrich@usb.ch)*

Purpose: To investigate the feasibility of detecting daytime and shift dependent trends in residents' reporting with the help of a report comparison tool.
Methods and materials: In 2017, we developed a report comparison tool tracking changes between residents' preliminary and final reports signed by staff radiologists on a word level. Additional quantitative metrics (e.g. similarity index (0 to 1) and the ratio of added words) are automatically calculated for each report and stored in a local database.
Data for all CT reports from 2018 was retrieved along with metadata of the reported exams (e.g. date and time). Following data aggregation per weekday and shift (day-, late-, and night-shift), analysis was performed using trending line graphs.
Results: While trending line graphs of the mean report similarity, the mean number of added, and the mean number of deleted words from preliminary reports remained relatively stable over the week during day-shifts, a gradual decrease in the mean report similarity from 0.87 to 0.35 could be observed for reports created by residents over the course of their week of night-shifts (residents in our department perform 7 night-shifts in a row). The accompanying continuous rise in the mean number of added words suggests an increase in overlooked/misinterpreted findings.
When looking at the acquisition time of reported exams, a slight decrease in report similarity was observed during day-shifts in the afternoon on several weekdays. The similarity was also frequently lower in late-shifts compared to day-shifts.
Conclusion: Our results show that data mining from report comparison tools can reveal shift dependent trends in the completeness of preliminary reports and may be used as a quality measure or even indicator of a necessary rescheduling of radiologists' shifts to maintain high report quality.
Limitations: n/a
Ethics committee approval: n/a
Funding: No funding was received for this work.
Author Disclosures:
J. Vosshenrich: nothing to disclose
I. Nesic: nothing to disclose
J. Cyriac: nothing to disclose
D. Boll: nothing to disclose
E. M. Merkle: nothing to disclose
T. Heye: nothing to disclose

RPS 1305-12 09:36
MR site assessment using a Power BI-based reporting platform
P. Szatmari, R. Illing, L. Refi*; Budapest/HU*

Purpose: To monitor and report the performance of MR installations using a Power BI-based reporting platform.
Methods and materials: A vendor-neutral analytics tool (the 'agent') has been developed for use on selected magnetic resonance imaging (MRI) systems to monitor protocols used, image quality, and operational metrics. Data from these systems are collated centrally and displayed on a PowerBI interface (Microsoft, Redmond, USA). Reports generated from the interface are generated and distributed to a network of 210 personnel every month; the system also allows data access for the users on a web-based and a mobile-based platform for those requiring real-time access. The processed data is used by the operational and clinical management to evaluate and optimise the performance on both the country and centre level. Operational teams have used one of these metrics ('time between scans') to target centres in which efficiency gains could be made.
Results: The agent has been installed on a network of 112 MR systems in 11 countries. By using this data, the team in Lithuania, operating 9 MR systems, have been able to make proactive operational improvements, increasing the number of patients from 27.64 per day to 28.32 per day, and the machine utilisation rate from 75.75% to 79.91%, on average. On a price per scan basis of Eur119, this works out to be a gain of Eur19 420 overall for the country network per year.
Conclusion: By combining Power BI-based reporting and operational improvement methods, efficiency gains can be made, increasing utilisation by 4.16% or Eur19 420 per year.
Limitations: n/a
Ethics committee approval: n/a
Funding: No funding was received for this work.
Author Disclosures:
P. Szatmari: nothing to disclose
L. Refi: nothing to disclose
R. Illing: nothing to disclose

RPS 1305-13 09:42
Value-based workflow in radiology: what to expect from the PACS orchestrator
C. C. C. Quattrocchi, P. D'alessio, G. Carosi, I. Galdino, A. Ricciardi, C. A. Mallio*; Rome/IT (c.quattrocchi@unicampus.it)*

Purpose: To assess the impact of the PACS orchestrator management platform on the workflow of an imaging centre in terms of efficiency, workload, and turn-around times.
Methods and materials: This study was not subject to review by the institutional ethical committee as data was collected from those archived by the RIS-PACS of the hospital within a quality improvement initiative. Data was extracted by means of a tailored statistics output from RIS-PACS of our imaging centre after the implementation of the PACS orchestrator (Philips Healthcare, IT), a management platform embedded in the PACS. The following key performance indicators (KPI) of workflow were used: number of patients per full-time equivalent radiologist (FTE), number of procedures per FTE, relative value units (RVU)/FTE/year), difficulty index, and turn-around-time. The data was compared with earlier data (Jan 2017-Aug 2019) extracted from RIS at our institution.
Results: We showed the changes measured on the key performance indicators after the implementation of the PACS orchestrator, with statistical analysis of data compared with a period of two years of data collected in our institution as part of the institutional quality improvement program.
Conclusion: Management platforms show promise in increasing process capability in terms of individual workloads and turn-around times in radiology, and to expand the frame of performance of radiologists to non-clinical domains.
Limitations: A single-institution study where interventions are routinely made to correct for undesired trends of quality, safety and workflow efficiency. The quality of reports was not measured, as we only relied on the number of complaints from patients to the hospital. The average time-based RVUs have their limitations as the study ascribable time may be biased by specific clinical assets.
Ethics committee approval: n/a
Funding: No funding was received for this work.
Author Disclosures:
C. C. C. Quattrocchi: nothing to disclose
P. D'alessio: nothing to disclose
G. Carosi: nothing to disclose
I. Galdino: nothing to disclose
A. Ricciardi: nothing to disclose
C. A. Mallio: nothing to disclose

RPS 1305-14 09:48
Assessment of the user acceptance of a radiology information system (RIS) and picture archiving and communication system (PACS) at a hospital in Qatar
P. S. Mahajan, A. Sanousi, N. Al Maslamani*; Doha/QA (medmantra.com@gmail.com)*

Purpose: To evaluate user acceptance related to the RIS-PACS implementation in a clinical imaging department. To evaluate the degree to which the 3 constructs (deduced value, appreciated operational simplicity, and change) influence user acceptance and to assess whether socio-demographic variables explain user acceptance.
Methods and materials: User acceptance levels among employees of the clinical imaging department at Al-Khor Hospital were assessed using a modified "model for adoption of technology (MAT)". 54 RIS-PACS questionnaire surveys were put in place to obtain user characteristics data, 6 items for deduced value (DV), 4 items for appreciated operational simplicity (AOS), 4 items for change construct, and 9 items for behaviour (acceptance) construct. Each item on the list used a five-point Likert scale for grading.
Results: DV scored highly (4.31 out of 5), AOS 4.14 points, change scored 4.27, and acceptance level scored 3.88 points. Three constructs explained 42% of RIS-PACS variation in user acceptance, the most significant predictor being change construct explained by 32% of user variation. Users stated that the new RIS-PACS had a great impact on their work as it significantly improved overall service quality. Gender, age, profession, and frequency of RIS-PACS use did not alter the acceptance level. The influence of culture on the level of acceptance of RIS-PACS did not appear to have any influence.
Conclusion: Prior to RIS-PACS implementation, user acceptance should be assessed, as better user acceptance boosts chances of a successful adoption. Training programs are advised prior to its implementation. Healthcare organisations should measure all given factors influencing RIS-PACS acceptance. This will optimise system productivity and help in the realisation of its vast benefits.
Limitations: Reasons for low acceptance levels among particular professional groups and other promising predictors of user acceptance need to be explored.
Ethics committee approval: Ethics committee approval obtained.
Funding: No funding was received for this work.
Author Disclosures:
P. S. Mahajan: nothing to disclose
A. Sanousi: nothing to disclose
N. Al Maslamani: nothing to disclose

RPS 1305-15 09:54
Problem-specific detailed structured reporting: moving towards intelligent reporting based on musculoskeletal referral guidelines
M. Fatehi[1], A. Sami[2]*; [1]Tehran/IR, [2]Shiraz/IR (mansoor.fatehi@gmail.com)*

Purpose: The current practice of radiology is mostly based on template-driven reporting methods, so structured reporting can produce lengthy reports due to the necessity of completeness of the subparts. But the referring physicians prefer short reports pointing to the most relevant information in a concise manner. The purpose of this paper is to describe the experience of using an automated system to modify the subparts of the reporting template.
Methods and materials: We analysed all MSK guidelines in the ACR appropriateness criteria to achieve a wide range of real clinical problems expected to be solved by the radiologist. We used all MSK reporting templates in the RSNA-ESR library and disintegrated them into sub-templates, each focusing on a particular subset of information. We then mapped each sub-segment of the templates to the list of the clinical conditions and their variants. A system was developed to put the sub-segments together according to the selected clinical condition.
Results: We found 259 clinical condition variants sorted into 29 musculoskeletal referral guidelines. On the other hand, we subdivided 30 RSNA-ESR templates for MSK imaging into distinct modules, summing up to 87 segments. The system could compose flexible templates according to the selected clinical situation, helping the user to adapt the length and content of the template to the needed extent.
Conclusion: The system provides a flexible template builder, intelligently tailored to the clinical condition of the patient, drawn from the request form or entered by the interpreting radiologist, thereby enabling the radiologist to be more efficient in terms of timing and relevance of the report content.
Limitations: For those templates with less extensive details and itemised components, we prepared similar templates following the same concepts.
Ethics committee approval: n/a
Funding: No funding was received for this work.
Author Disclosures:
M. Fatehi: nothing to disclose
A. Sami: nothing to disclose

11:15 - 12:30 **Room B**

Artificial Intelligence and Machine Learning

RPS 1405a

Artificial intelligence and machine learning in the brain

Moderators:
M. De Bruijne; Rotterdam/NL
A. Mazumder; London/UK

RPS 1405a-K 11:15
Keynote lecture
N.N.

RPS 1405a-1 11:25
The added value of molecular genetic group as a prognostic indicator of overall survival and progression-free survival in glioma patients: machine learning based analysis
S. Zhang; *Guangzhou/CN (shui7515@126.com)*

Purpose: Glioma could be categorised as five molecular groups based on three biomarkers: IDH mutation, 1p/19q codeletion, and TERT promoter mutation. We aimed to explore the added value of the molecular group in predicting survival outcome of glioma.
Methods and materials: A total of 573 patients with confirmed glioma between January 1, 2011, and December 31, 2016, were included. The clinical and imaging findings and molecular biomarkers were retrospectively collected for analysis. An improved causal assumption inferring algorithm from the additive noise model was employed to discover the risk factors combination for progression-free survival (PFS) and overall survival (OS). Cox regression and seven machine learning models with 10-fold cross-validation were developed to predict PFS and OS based on the discovered risk factors. AUC was used to compare the prognostic performance of models.
Results: WHO grade, tumour location, and the molecular group were the three risk factors for PFS and OS. The support vector machine model achieved the highest AUC of 0.835 (95% confidence interval [CI]: 0.802-0.864) in predicting PFS and 0.871 (95% CI: 0.840-0.897) in predicting OS. The addition of the molecular group to the models could improve the predictive performance and the naive Bayes model obtained the highest AUCs of 0.854 (95% CI: 0.822-0.882) and 0.894 (95% CI: 0.866-0.918) in predicting PFS and OS, respectively.
Conclusion: The results showed good performance of machine learning-based clinical models for survival outcome prediction in glioma. The accuracy of clinical models could be increased by combining molecular group.
Limitations: We did not perform external validation with independent datasets for generalisation.
Ethics committee approval: This retrospective study was approved by the local Institutional Review Board before data collection and analysis.
Funding: No funding was received for this work.
Author Disclosures:
S. Zhang: nothing to disclose

RPS 1405a-2 11:31
Machine learning-based MRI texture analysis for predicting 1p/19q codeletion status of lower-grade gliomas
B. Kocak, E. Ş. Durmaz, E. Ateş, I. Sel, S. T. Turgut Güneş, O. Korkmaz Kaya, A. Zeynalova, O. Kılıckesmez; *Istanbul/TR (drburakkocak@gmail.com)*

Purpose: To evaluate the value of the machine learning (ML)-based MRI texture analysis for predicting 1p/19q codeletion status in lower-grade gliomas (LGG), using various ML algorithms.
Methods and materials: For this retrospective study, 107 patients with LGG were included from a public database. 10 different training and unseen test data splits were created using stratified random sampling. Radiomic features were extracted from conventional T2-weighted and contrast-enhanced T1-weighted MRI images. Dimension reduction was done using collinearity analysis and feature selection. Classifications were done using adaptive boosting, k-nearest neighbours, naive Bayes, neural network, random forest, stochastic gradient descent, and support vector machine. Friedman test and pairwise posthoc analyses were used for comparison of classification performances based on the area under the curve (AUC) metric.
Results: Overall, the performance of the ML algorithms was statistically significantly different, $\chi2(6) = 40.46$, $p<0.001$. In the pairwise analysis, 5 algorithms outperformed others, adjusted $p<0.05$. Mean AUC and accuracy values for the top 5 algorithms ranged from 0.813 to 0.871 and from 79.4% to 81.9%, respectively, with no statistically significant difference, adjusted $p>0.05$. The ML algorithm with the highest mean rank and stability was naive Bayes with a mean AUC and accuracy of 0.869 and 80.6%, respectively.
Conclusion: The ML-based MRI texture analysis might be a promising non-invasive technique for predicting the 1p/19q codeletion status in LGGs. Using this technique along with various ML algorithms, more than four-fifths of the LGGs can be correctly classified.
Limitations: Potential and most important limitations of the study are retrospective study design, dependency on the limited data on the public database, and a lack of other MRI sequences.
Ethics committee approval: No ethics committee approval was obtained because this work is based on a publicly available database.
Funding: No funding was received for this work.
Author Disclosures:
B. Kocak: nothing to disclose
E. Ş. Durmaz: nothing to disclose
E. Ateş: nothing to disclose
I. Sel: nothing to disclose
S. T. Turgut Güneş: nothing to disclose
O. Korkmaz Kaya: nothing to disclose
A. Zeynalova: nothing to disclose
O. Kılıckesmez: nothing to disclose

RPS 1405a-3 11:37
Prediction for the grading of stereotactic biopsy glioma targets based on preoperative MRI textural analysis
W. Rui, H. Pang, Q. Xie, Y. Ren, S. Duan, Y. Zhang, Z. Yao; *Shanghai/CN*

Purpose: To explore the value of textural analysis based on T1-weighted brain volume with gadolinium contrast enhancement (T1 BRAVO+C) images for the grading of glioma targets by stereotactic biopsy.
Methods and materials: A total of 36 diffuse glioma cases and 64 puncture targets were included in the study. All patients underwent a preoperative MR scan and intraoperative MR-guided stereotactic puncture biopsy. All cases had a histopathological diagnosis of WHO grade II or III diffuse gliomas. ROIs consistent with puncture targets were delineated on T1 BRAVO+C images and texture features were automatically calculated using Omni Kinetics software. Mann-Whitney rank-sum test was used to analyse texture differences between grade II and III ROIs. ROC curves evaluated the diagnostic value of textural analysis for grading glioma targets. The cutoff value was set according to the Youden index.
Results: Texture features, including max intensity ($P=0.001$), 95th quantile (0.002), range (< 0.001), variance (< 0.001), standard deviation (< 0.001), sum variance (0.022), and cluster prominence (< 0.001) were higher in grade III gliomas than grade II. Whereas, grade II gliomas showed increased uniformity ($P=0.001$) and short-run low grey-level emphasis values (0.018). Diagnostic efficiency of high-order grey-level run-length matrix features was slightly lower than first- and second-order features. AUC was 0.887 (95% confidence interval: 0.805-0.969, $P<0.001$) with combined texture features.
Conclusion: Textural analysis of T1 BRAVO+C images is valuable for grading glioma (WHO II and III) and may help in guiding artificial intelligence selection of preoperative puncture targets.
Limitations: Biopsy samples couldn't achieve 100% “point to point”.
Ethics committee approval: Institutional Review Board approval was obtained. All included patients signed written informed consent.
Funding: No funding was received for this work.
Author Disclosures:
Z. Yao: nothing to disclose
Y. Zhang: nothing to disclose
W. Rui: nothing to disclose
H. Pang: nothing to disclose
Q. Xie: nothing to disclose
Y. Ren: nothing to disclose
S. Duan: nothing to disclose

RPS 1405a-4 11:43
Glioma segmentation in sparse label applications: a federated learning solution
S. Niehaus[1], L. Lampe[1], A. Merola[2], G. Mihai[2], J. Reinelt[2], N. Scherf[3]; [1]*Berlin/DE,* [2]*Leipzig/DE,* [3]*Dresden/DE (sebastian.niehaus@aicura-medical.com)*

Purpose: Accurate tissue segmentations are essential for clinical applicability. We propose an improved approach to segmentation using federated learning for the decentralised training of a convolutional neural network (CNN) on heterogeneous MRI datasets of glioma patients.
Methods and materials: We split the BRATS-dataset (braintumorsegmentation.org) into three virtual hospitals (VHs) and added a fourth VH with data from a subsample of 121 patients of a publicly available

dataset (figshare.com/articles/brain_tumor_dataset/1512427). Two VHs (54 and 69 patients respectively) have contrast-enhanced T1-weighted MRIs with five classes [necrosis (N), oedema (E), enhancing tumour tissue (ETT), non-enhancing tumour tissue (N-ETT), and background]. One VH has only a binary segmentation map (61 images). The last VH has only unlabelled data (120 images). We trained the CNN with a federated learning setup without central data aggregation. In each VH where segmentations were available, a segmentation model was trained. An autoencoder was trained in each VH to learn volume reconstruction. Noise and rotation were used for data augmentation. In the federated learning merging process of the different models, only the decoder path of the CNN was combined into a global model.
Results: For the evaluation, we used the Dice similarity score and evaluated the performance classwise. The CNN trained with federated learning [evaluation score: 0.43 (N), 0.56 (E), 0.34 (ETT), and 0.74 (N-ETT)] outperformed results obtained with a baseline model [0.28 (N), 0.38 (E), 0.29 (ETT), and 0.54 (N-ETT)] trained in a single VH.
Conclusion: The proposed federated learning setup is superior for training CNNs on radiological data with sparse labelling, improving performance, and allowing for the use of larger datasets without compromising patient confidentiality.
Limitations: The experiments are limited to a single modality.
Ethics committee approval: n/a
Funding: No funding was received for this work.
Author Disclosures:
L. Lampe: Employee at AICURA medical GmbH
S. Niehaus: Employee at AICURA medical GmbH
A. Merola: Employee at AICURA medical GmbH
J. Reinelt: Employee at AICURA medical GmbH
G. Mihai: Employee at AICURA medical GmbH
N. Scherf: nothing to disclose

RPS 1405a-5 11:49
Deep learning radiomics algorithm for glioma (DRAG) for predicting survival in gliomas
A. Mahajan, S. Rane, U. Baid, M. Akolkar, S. Talbar, A. Moiyadi, S. Gupta*; Mumbai/IN (drabhishek.mahajan@yahoo.in)*

Purpose: Segmentation of brain tumours from multi-modal MR imaging remains a challenge and deep learning has a potential role in diagnosis, prognosis, and survival prediction. The project aimed at tumour segmentation and finding potential radiomic features for predicting overall survival.
Methods and materials: The proposed method was trained and validated on BRATS 2018 dataset. We developed a patch-based 3D-Unet model for tumour segmentation and evaluated the efficiency of radiomic features for overall survival prediction. Radiomic features were extracted from all four MR modalities for OS prediction. The training dataset included 210 high-grade-gliomas (HGG) and 75 low-grade-gliomas (LGG), while the validation set consisted of 66 cases. The trained model was validated on 191 sets of patient data from our hospital.
Results: All 285 training datasets were used in the model training process. The results were based on all 46 validations dataset. The final mean Dice indexes of the enhanced tumour (ET), whole tumour (WT), and tumour core (TC) were 0.75, 0.89, and 0.81, which shows our approach outperforms other submissions of the BRATS18 challenge. The method achieved good performance with Dice scores of 0.88, 0.83, and 0.75 for whole tumour, tumour core, and enhancing tumour, respectively. For the prediction of survival categories (<300 & >=300 days), the neural network demonstrated an accuracy of 70.2% in the training subset and 62.5 and 63.6% in the validation and testing subsets, respectively. The accuracy was 73% for the entire training dataset. The AUC was 0.799.
Conclusion: Our study demonstrates that transfer learning-based deep features are able to generate prognostic imaging signatures for OS prediction and patient stratification for GBM, indicating the potential of deep imaging feature-based biomarkers in the preoperative care of GBM patients.
Limitations: n/a
Ethics committee approval: Ethics committee approval obtained.
Funding: No funding was received for this work.
Author Disclosures:
A. Mahajan: nothing to disclose
S. Rane: nothing to disclose
U. Baid: nothing to disclose
M. Akolkar: nothing to disclose
S. Talbar: nothing to disclose
A. Moiyadi: nothing to disclose
S. Gupta: nothing to disclose

RPS 1405a-6 11:55
Smart protocol: real-time brain MRI pathology detection by deep learning for online protocol control
A. Pai[1], B. Low[1], L. Sørensen[1], M. Lillholm[1], M. D. E. B. Dam[1], R. Lauritzen[1], R. Kashyape[2], M. Nielsen[1]; [1]*Copenhagen/DK,* [2]*Nashik/IN (rskashyape@gmail.com)*

Purpose: Brain MRI protocols are determined prior to the patient entering the scanner and information collected during scanning rarely influences the scanning protocol. Real-time detection of pathologies may guide the choice of MRI sequences most informative for diagnosis while the patient is still in the scanner. Hereby, the scanner may be used optimally, patient discomfort minimised, and downstream reading and reporting prioritised.
Methods and materials: 2 million radiology reports were automatically scanned using natural language processing for pathologies, selecting 5,000 brain MRI studies obtained in collaboration with Medall Diagnostics, India, reflecting the most predominant pathologies; infarcts (hyperacute and acute) and tumours. Infarcts and tumour pathologies were annotated pixel-wise by trained annotators under a radiologist's supervision and quality control. Two sets of MRI brain protocols for clinically normal patients, patients with tumours, and patients with infarcts (and both) were established: A) standard clinical protocol and B) smart protocol (consisting of 4 base sequences and up to 2 additional specialised pathology specific sequences).
Results: On an independent dataset of 88 scans, the turn around time from scanning a sequence to reporting results back to the hospital system was less than 60 seconds. The specificity and sensitivity for detection was for tumour 95% (88-99%) and 78% (52-94%), and for infarcts 75% (63-85%) and 100% (83-100%). In a study with simulated protocols, on an average, 1.25 fewer sequences were acquired per patient and an overall 0.23 specialised sequences were missed for patients with pathology.
Conclusion: Turn around time is sufficiently low to influence protocol selection in clinical practice. Accuracy and fewer sequences acquired allow for the informing of the MRI operator, potentially saving scanner time, contrast administration, and patient recall. This has led to a trial installation in several hospitals.
Limitations: n/a
Ethics committee approval: n/a
Funding: No funding was received for this work.
Author Disclosures:
A. Pai: Shareholder at Cerebriu A/S
M. Nielsen: Board Member at Cerebriu A/S, Shareholder at Cerebriu A/S
L. Sørensen: Employee at Cerebriu A/S
M. Lillholm: Shareholder at Cerebriu A/S
M. D. E. B. Dam: Shareholder at Cerebriu A/S
R. Lauritzen: CEO at Cerebriu A/S, Board Member at Cerebriu A/S, Shareholder at Cerebriu A/S
B. Low: Employee at Cerebriu A/S
R. Kashyape: nothing to disclose

RPS 1405a-7 12:01
Classifying brain metastatic disease by an unknown cancer primary organ site using whole-brain clinical MRI data: a 3D convolutional neural network approach
S. Namjoshi, E. McTyre, M. Chan, C. Cramer, G. Lesser, R. Strowd, S. Tatter[1], W. Zhang, C. T. Whitlow*; Winston-Salem, NC/US (cwhitlow@wakehealth.edu)*

Purpose: Treatment decisions for brain metastatic disease are driven by knowledge of primary organ site cancer histology, which can require invasive biopsy. We propose an automated deep learning algorithm and image-preprocessing pipeline for rapid non-invasive imaging-based identification of brain metastatic tumour histology based on conventional whole-brain T1-weighted MRI data. Using whole-brain data obviates the need for brain tumour segmentation, which can be time intensive. We hypothesise that whole-brain imaging features will be sufficiently discriminative, allowing for accurate diagnosis of the primary organ site of malignancy.
Methods and materials: This single-site retrospective diagnostic study was comprised of patients (n=1,302) referred for gamma knife radiosurgery from July 2000 to May 2019. Contrast-enhanced T1-weighted brain MRI exams (n=2,104 MRIs) acquired from these patients were minimally preprocessed (voxel resampling and signal intensity rescaling/normalisation), requiring only seconds per MRI dataset, and used to train a 3D convolutional neural network (CNN) for determining the primary organ site associated with brain metastatic disease in one of three classes (breast, lung, and melanoma).
Results: After nested 10-fold cross-validation, our algorithm achieved best AUCs of 0.987 [95%CI: 0.983,0.991] (breast vs lung) and 0.988 [95%CI: 0.984,0.991] (lung vs melanoma). Although breast versus melanoma demonstrated low AUC with images alone (0.550), the algorithm performed better after the incorporation of demographic data (AUC = 0.704).

Conclusion: Our results demonstrate a robust CNN algorithm for effectively classifying metastatic tumour histology types for breast and lung based on conventional whole-brain MRI, without need for tumour segmentation. Further refinement may offer an invaluable tool to expedite primary organ site cancer identification for brain metastatic disease and perhaps improve patient outcomes and survival.
Limitations: Limitations include relatively small sample size and our retrospective approach from a single institution.
Ethics committee approval: IRB-approved.
Funding: NIH:P30CA01219, P01CA207206, R01CA074145.
Author Disclosures:
C. T. Whitlow: nothing to disclose
S. Namjoshi: nothing to disclose
E. McTyre: nothing to disclose
M. Chan: nothing to disclose
C. Cramer: nothing to disclose
G. Lesser: nothing to disclose
R. Strowd: nothing to disclose
S. Tatter: nothing to disclose
W. Zhang: nothing to disclose

RPS 1405a-8 12:07

Can we predict a brain metastases primary site by using deep learning algorithms, even in small datasets?

Y. Çuşkun[1], B. Alparslan[1], K. Kaplan[1], F. Çalışkan[1], O. Tavas[1], E. Dervişoğlu[1], H. M. Ertunç[1], A. K. Sivrioglu[2]; [1]*Kocaeli/TR,* [2]*Istanbul/TR (burcu.alparslan@gmail.com)*

Purpose: To investigate the feasibility of deep learning algorithms in the classification of brain metastases according to their origin.
Methods and materials: 177 patients with brain metastases from lung cancer (n=99), breast cancer (n=44), and other cancer types (n=37) were evaluated in our single-centre retrospective study. The dataset was derived by radiologists from pretreatment brain MR images of patients including 4 sequences: pre- and postcontrast T1-weighted spin-echo (T1W SE), fluid-attenuated inversion recovery (FLAIR), and apparent diffusion coefficient (ADC) maps. Since the sequence plans were different from each other, a 4-path convolutional neural network (CNN) had been developed in which the sequences images were given separately to the algorithm. We used 124 patients' data for training and 53 patients' data for testing in our 3-class (lung, breast, and others) and 2-class (lung and breast) CNN models.
Results: The accuracy of classification in the 3-class model was 74.07%, the area under the ROC curve (AUC) for lung cancer class was 0.87, for breast cancer 0.89, and for the others group 0.75. The two-class model had a higher accuracy of 81.48% and AUC of 0.76.
Conclusion: Deep learning algorithms using multisequence MRI can give satisfactory results in classifying brain metastases even in small datasets. What about with 'big data?'
Limitations: A small dataset.
Ethics committee approval: The study was approved by Kocaeli University institutional review board.
Funding: No funding was received for this work.
Author Disclosures:
B. Alparslan: nothing to disclose
Y. Çuşkun: nothing to disclose
K. Kaplan: nothing to disclose
F. Çalışkan: nothing to disclose
O. Tavas: nothing to disclose
E. Dervişoğlu: nothing to disclose
H. M. Ertunç: nothing to disclose
A. K. Sivrioglu: nothing to disclose

RPS 1405a-9 12:13

Deep convolutional neural network for automated segmentation of brain metastasis trained on clinical data acquired during six years of stereotactic radiosurgery

K. Bousabarah, P. D. M. Kocher, P. D. M. Ruge, J.-S. Brand, P. D. V. Visser-Vandewalle, D. H. Treuer; *Cologne/DE*

Purpose: Deep convolutional neural networks (DCNN) have demonstrated enormous performance in many segmentation tasks in medical imaging. Brain metastasis, with their large variability in imaging appearance, remain a challenge. To properly evaluate the clinical performance of a state-of-the algorithm in this task, we collected a clinically representative set of imaging data acquired for stereotactic radiosurgeries between 2013 and 2019.
Methods and materials: Registered MR images (contrast-enhanced T1, T2, and FLAIR) and the contour data containing the delineated lesions were restored from our treatment planning system. The data (509 patients with 1,223 metastasis) was split into a training (469 patients) and a test (40 patients) set. Ground truth segmentations on the test data were individually checked by a senior oncologist with 25 years of experience (MK). In addition to a conventional U-Net, a U-Net with multiple outputs (moU-Net) and a U-Net (sU-Net) only trained on small lesions (< 0.4ml) were employed.
Results: The U-Net, moU-Net, and the sU-Net detected brain metastasis with a sensitivity of 69%, 69%, and 51%, respectively. The sU-Net performed better at detecting small lesions (64% sensitivity) compared to the conventional U-Net (48%) and the moU-Net (48%). An ensemble of those networks had a sensitivity of 79%/74%, with a mean false-positive rate of 0.8/0.175 and a mean Dice score of 0.7/0.71, depending on if the segmentations were merged through summation or averaging.
Conclusion: We demonstrated that DCNNs trained on data collected during clinical practice produce state-of-the-art results and that in-house development of such algorithms is a feasible option. It was furthermore shown that a single network fails to generalise and that an ensemble of differently trained networks is superior.
Limitations: A single-centre study.
Ethics committee approval: n/a
Funding: No funding was received for this work.
Author Disclosures:
K. Bousabarah: nothing to disclose
P. D. M. Kocher: nothing to disclose
D. H. Treuer: nothing to disclose
P. D. M. Ruge: nothing to disclose
J.-S. Brand: nothing to disclose
P. D. V. Visser-Vandewalle: nothing to disclose

RPS 1405a-10 12:19

CNN based deep learning enhances 3D FLAIR brain perceived quality, SNR, and resolution at ~30% less scan time

L. N. Tanenbaum[1], S. Bash[2], W. Gibbs[3], L. Wang[4], H. Gandhi[4], P. Gulaka[5], A. Shankaranarayanan[6], T. Zhang[7]; [1]*Riverside, CT/US,* [2]*Los Angeles/US,* [3]*Pasadena/US,* [4]*Palo Alto/US,* [5]*Menlo Park/US,* [6]*Waukesha, WI/US,* [7]*Menlo Park, CA/US (nuromri@gmail.com)*

Purpose: To evaluate the capability of deep learning (DL)-based image processing of brain MRI to improve quality while reducing acquisition times.
Methods and materials: With IRB approval and patient consent, 11 patients (age: 48+/-15 years; 7 female) undergoing clinical brain 1.5T MRI exams underwent an accelerated sagittal 3DFLAIR scan (average scan time reduction 27.1%+/-3.5%) in addition to the institution's routine protocol, which included a submillimeter isotropic 3DFLAIR. A third image set was created by processing the faster series with an FDA-cleared CNN-based DL algorithm (SubtleMR™). The 3 sets (standard series (SS), accelerated series (AS), and DL processed accelerated series (DL)) were randomised and presented side-by-side for pair-wise comparisons (33) and evaluated for relative (1) image sharpness, (2) perceived SNR, and (3) lesion/anatomy conspicuity. Each series was also independently scored on overall quality. A two-sided paired t-test was performed for overall image quality, with $P<0.05$ considered statistically significant. Average image preference and 95% confidence interval were calculated for each paired series and reader.
Results: Overall quality scores (SS/AS/DL) were 4.0/3.1/5.0, 4.0/3.2/5.0, and 4.8/4.5/5.0 for reader 1-3. Paired t-test results suggested that DL is significantly better than SS ($P<0.05$) for reader 1 and 2, but not for reader 3 ($P=0.10$). When presented side-by-side, DL is superior (significantly superior for reader 1 and 2, mildly superior for reader 3) for image sharpness, perceived SNR, and lesion/pathology conspicuity when compared with SS or AS.
Conclusion: CNN-based DL image processing of 3DFLAIR brain MRI produces a boost in perceived image quality, SNR, and resolution despite a ~30% reduction in scan time.
Limitations: A limited number of subjects and imaging methods tested.
Ethics committee approval: Approved by IRB.
Funding: No funding was received for this work.
Author Disclosures:
L. N. Tanenbaum: Speaker at GE, Siemens, Philips, Bracco, Guerbet, Shareholder at Enlitic, aidoc, icometrix, nous, curemetrix
S. Bash: Advisory Board at icometrix, Advisory Board at coretechs
W. Gibbs: nothing to disclose
L. Wang: Employee at Subtle Medical
H. Gandhi: Employee at Subtle Medical
P. Gulaka: Employee at Subtle Medical
A. Shankaranarayanan: Employee at Subtle Medical
T. Zhang: Employee at Subtle Medical

RPS 1405a-11 12:25

Brain metastases in malignant melanoma: fully automated detection and segmentation on MRI using a deep learning model

L. Pennig[1], S. Lennartz[1], L. Goertz[1], F. Thiele[2], M. Perkuhn[1], J. Borggrefe[1], L. Caldeira[1], K. R. Laukamp[1]; [1]Cologne/DE, [2]Aachen/DE
(lenhard.pennig@uk-koeln.de)

Purpose: Given the growing demand for magnetic resonance imaging (MRI) of the head in patients with malignant melanoma and consecutively associated workload, physician fatigue with the inherent risk of missed diagnosis poses a relevant concern. The automatisation of detection and segmentation of brain metastases could serve as a tool for lesion preselection and assessment of therapeutic success in an oncological follow-up. The purpose of this study was the development and evaluation of a deep learning model (DLM) for fully automated detection and segmentation of brain metastases in melanoma patients on multiparametric MRI, including heterogenous data from different institutions and scanners.
Methods and materials: In this retrospective study, we included MRI scans (05/2013-10/2018; T1-/T2-weighted, T1-weighted contrast-enhanced (T1CE), T2-weighted fluid-attenuated inversion recovery) from 54 melanoma patients (mean age 63.54±13.83 years, 24 females) with 102 metastases at initial diagnosis. Independent manual segmentations of the metastases (based on T1CE) in a voxel-wise manner by two radiologists provided the ground truth of metastases count and segmentation. A 3D convolutional neural network (DeepMedic, BioMedIA) initially trained on glioblastomas was used receiving additional dedicated training applying five-fold cross-validation (5-FCV). For comparison of segmentation accuracies, Dice coefficients were calculated.
Results: The mean size of metastases was 2.35±7.81 cm^3 [range: 0.003–66.6 cm^3]. The glioblastoma DLM achieved a detection rate of 0.47 and a reasonable segmentation accuracy (median Dice: 0.64). After 5-FCV training, detection rate 0.87 ($p<0.001$) and segmentation accuracy (median Dice: 0.74, $p<0.05$) increased.
Conclusion: After dedicated training, our DLM detects brain metastases of malignant melanoma on multiparametric MRI with high accuracy. Despite small lesion size and heterogenous scanner data, automated segmentation achieved good volumetric accuracy compared to manual segmentations.
Limitations: A retrospective study.
Ethics committee approval: Ethics committee approval obtained and consent waived.
Funding: No funding was received for this work.
Author Disclosures:
L. Pennig: nothing to disclose
S. Lennartz: nothing to disclose
L. Caldeira: nothing to disclose
F. Thiele: Employee at Philips Healthcare
L. Goertz: nothing to disclose
M. Perkuhn: Employee at Philips Healthcare
J. Borggrefe: Speaker at Philips Healthcare
K. R. Laukamp: nothing to disclose

11:15 - 12:30 **Room C**

Breast

RPS 1402a

Artificial intelligence, radiomics and more: part 2

Moderators:
S. Jeganathan; Perth/AU
H. Sartor; Lund/SE

RPS 1402a-1 11:15

The application of model-adaptive artificial intelligence algorithms in breast ultrasound imaging

A. Abate[1], R. Giovanazzi[2], C. Di Bella[2], S. de Beni[3], S. D'onofrio[3], M. Cereseto[3], G. Querques[2], V. Besostri[4], R. Corso[2]; [1]Lesmo/IT, [2]Monza/IT, [3]Esaote/IT, [4]Pavia/IT (abate.anna75@gmail.com)

Purpose: Application of model-adaptive artificial intelligence (AI) algorithms in breast ultrasound (US) to improve diagnostic confidence and optimise daily clinical workflow.
Methods and materials: In 6 months, 50 female patients (mean age:45 ys) underwent breast US, using MyLab9 system (Esaote, Italy) with electromagnetic-tracking options (BreastNav), linear transducer (L4-15) with dedicated tracking sensor. On 11 patients, with a benign nodule detected for the first time, US follow-up examination was performed after 3 months with BreastNav that reproduces on a virtual-model the actual morphology of the patient's breast. Furthermore, BreastNav allows re-evaluation on follow-up US or US-guided biopsy procedures, the area previously highlighted by a target.
Results: Before US examination, a registration phase between the virtual-model and US was performed and 6 anatomical markers were selected. The model automatically adapts the shape of the breast to provide 1:1 correlation in "real-time" with US. BreastNav records 3D-US datasets and reproduces their positions on a virtual-model, reshaping it according to the pressure applied by the probe and providing immediate visual feedback on where US has been performed. Moreover, it is possible to put a target on the lesion and save it with the patient's study. During follow-up US, BreastNav technology shows the previously saved target, US reference image, and probe position in order to quickly identify the interested lesion. Furthermore, traffic-light feedback helps to identify the exact transducer spatial position to reach the archived target. In all patients, BreastNav correctly traced through AI-modelling technique the lesion indicated by the target, even with different breast morphologies and patient's position.
Conclusion: The AI algorithm of BreastNav technology supports follow-up examination of breast lesions, providing a visual feedback (target, probe position, and inclination) and simplifying clinical workflow.
Limitations: n/a
Ethics committee approval: n/a
Funding: No funding was received for this work.
Author Disclosures:
A. Abate: Speaker at ASST Monza, Author at ASST Monza
R. Giovanazzi: Author at ASST Monza
C. Di Bella: Author at ASST Monza
S. de Beni: Author at ESAOTE/ITALY
S. D'onofrio: Author at ESAOTE/ITALY
M. Cereseto: Author at ESAOTE/ITALY
G. Querques: Author at ASST Monza
V. Besostri: Author at ASST Monza
R. Corso: Author at ASST Monza

RPS 1402a-2 11:21

Classification of benign and malignant breast lesions using ultrasound shear wave elastography features: a non-black-box machine learning approach

A. Angelakis[1], H. Sportouche[2]; [1]Athens/GR, [2]Aix-en-Provence/FR
(ath.angelakis@gmail.com)

Purpose: To tune a non-black-box robust machine learning model on a relatively big, heterogeneous and multicentric data-set including shear wave elastography (SWE) features in order to classify benign and malignant breast lesions achieving high specificity and sensitivity.
Methods and materials: The data-set consisted of 1,989 breast lesions (995-994, benign-malignant determined by cytopathology or follow-up) coming from 16 European/American and 22 Asian centres with BI-RADS 2-5 scores. Features of the initial data-set were age, palpability, mobility, SWE lesion shape, and homogeneity of the mass. From measures on 3 SWE images we also included the SWE lesion dimension, the maximal and mean SWE values in Q-Box areas on lesion and fatty tissue, and the ratio of mean SWE values on lesion versus fatty tissue. We used feature engineering and tuned a CatBoost classifier of 97 iterators of depth 11.
Results: The performance of a 10-fold Cross-Validation was: sensitivity: 0.8732, specificity: 0.8983, and ROC-AUC: 0.8858 with 95% CI [0.849 - 0.930]. On an unseen validation dataset, the model's performance was: sensitivity: 0.8918, specificity: 0.8963, and ROC-AUC: 0.8941. The BI-RADS performance was: sensitivity: 0.9758, specificity: 0.5175, and ROC-AUC: 0.7466, and on the validation data-set was: sensitivity: 0.9837, specificity: 0.5233, and ROC-AUC: 0.7535. The SWE Emax performance was: sensitivity: 0.8490, specificity: 0.8182, and ROC-AUC: 0.8336, and on the validation data-set: sensitivity: 0.8864, specificity: 0.8031, and ROC-AUC: 0.8447.
Conclusion: In this study, we used a heterogeneous data-set of breast lesions and we tuned a gradient boosted tree classifier trained on SWE features. It achieved high classification scores outperforming conventional approaches (BI-RADS and SWE cut-off value). The model's result may be considered from radiologists during an examination's medical report.
Limitations: n/a
Ethics committee approval: n/a
Funding: No funding was received for this work.
Author Disclosures:
A. Angelakis: nothing to disclose
H. Sportouche: Employee at SuperSonic Imagine

RPS 1402a-3 11:27

Quantitative analysis of contrast-enhanced ultrasound imaging omics in evaluating the efficacy of adriamycin combined with cetuximab in the treatment of triple-negative breast cancer in nude mice

L. Tang, Q. Liu, M. Chen*; Shanghai/CN (13661657380@163.com)*

Purpose: To evaluate the effect of two-dimensional contrast-enhanced ultrasound (CEUS) on the chemotherapy of triple-negative breast cancer in nude mice and to find out the changes of haemodynamics in the tumours during the treatment.
Methods and materials: A female BALB/c nude mouse model of triple-negative breast cancer was established by human breast cancer MDA-MB-231 cells. Esaote Mylab90 ultrasound instrument and SonoVue contrast agent were used. Contrast-enhanced ultrasound (CEUS) was performed before administration of adriamycin combined with cetuximab on the 1st, 3rd, and 5th day, and before execution on the 7th day. The images were quantitatively analysed by contrast-enhanced imaging omics. On the basis of delineating the tumour boundary, different ROI regions were extracted respectively (more details are shown in the attached picture).
Results: 16 nude mice in the experimental group completed the 7-day experiment, while 5 in the control group failed to reach the 7-day survival period. All parameters basically reflected the characteristics of increasing with the number of days of treatment, which indicated the normalisation of blood vessels in lesions (more details are shown in the attached picture).
Conclusion: MTT, TTP, and BI values in the quantitative analysis of two-dimensional contrast-enhanced ultrasound imaging omics showed an upward trend during the treatment of adriamycin combined with cetuximab, which is expected to be helpful in predicting the efficacy of combined therapy for triple-negative breast cancer and will be more suggestive in the prediction of curative effect.
Limitations: The number of mice used in our experiment is not large enough and there may be selection bias from ultrasound instrument and quantitative analysis software.
Ethics committee approval: Our animal experimental research has been approved by the Animal Ethics Committee of Shanghai Jiaotong University School of Medicine.
Funding: National Natural Science Foundation of China.
Author Disclosures:
L. Tang: nothing to disclose
Q. Liu: nothing to disclose
M. Chen: nothing to disclose

RPS 1402a-4 11:33

Automated assessment of image quality in digital breast tomosynthesis in a screening setting: more positioning errors for women with large breasts

G. G. Waade, A. S. Danielsen, S. Hofvind*; Oslo/NO (gugi@oslomet.no)*

Purpose: To analyse mammographic image quality criteria related to positioning among women in a screening setting.
Methods and materials: An automated software assessed the left mediolateral oblique mammogram from 5,668 women participating in the tomosynthesis trial in Bergen, January 2018-May 2019, to obtain information about image quality. Image quality criteria were defined as nipple in profile, pectoral muscle shape, and inframammary fold (IMF) appearance (its visibility and/or presence of skin folds). We investigated proportions of image quality errors and used a log-binomial regression model to produce adjusted risk ratios (RR) with 95% confidence intervals (95%CI) of image quality errors for women with small (<700cm^3), relative to medium (700-1200cm^3), and large (>1200cm^3) breasts, adjusted for mammographic density (dense versus non-dense) and age.
Results: A total of 3,913 (69%) of the 5,668 mammograms included one or more image quality errors: nipple not in profile (20.1%, 1138/5668), pectoral muscle not straight (32.8%, 1857/5668), and issues with IMF appearance (42.9%, 2434/5668). Women with medium-sized or large breasts had a higher RR of image quality errors compared to women with small breasts (RR: 1.06, 95%CI: 1.01-1.11 and RR: 1.22, 95%CI: 1.17-1.29, respectively).
Conclusion: A large proportion of images contained positioning errors. Women with large breast are more likely to have mammograms of suboptimal image quality compared to women with small breasts.
Limitations: Further research is needed to investigate the clinical implications of these findings.
Ethics committee approval: The Regional Committee for Medical and Health Research Ethics approved the trial (2015/424).
Funding: The trial received funding by the Norwegian Cancer Society (190184-2017).
Author Disclosures:
G. G. Waade: nothing to disclose
S. Hofvind: nothing to disclose
A. S. Danielsen: nothing to disclose

RPS 1402a-5 11:39

Reading breast tomosynthesis examinations with an AI decision support system: improving cancer detection accuracy

R. M. Mann, A. Rodriguez Ruiz, A. Gubern Merida, N. Karssemeijer, I. Sechopoulos*; Nijmegen/NL (alejandro.rodriguezruiz@screenpointmed.com)*

Purpose: To compare the breast cancer detection accuracy of radiologists reading breast tomosynthesis (DBT) examinations unaided versus supported by an artificial intelligence (AI) system.
Methods and materials: A cancer-enriched, retrospective, fully-crossed, multi-reader, multicase, HIPAA-compliant study was performed. Four-view DBT examinations from 240 women were included. All examinations (in total 71 breasts with cancer lesions, 70 breasts with benign findings, and 339 normal breasts) were interpreted by 9 qualified radiologists (median experience 8 years, range 4-23), once with and once without AI support (Transpara, ScreenPoint Medical). The readers provided a level of suspicion for each breast. When using AI support, radiologists were shown an examination-based cancer likelihood score as well as marked lesions and lesion-based cancer likelihood scores. The area under the receiver operating characteristic curve (AUC) was compared between both reading conditions at a per breast-level, using mixed-models analysis of variance for multiple repeated clustered measurements. Reading time differences for normal examinations were also measured.
Results: On average, the AUC was higher with AI support than with unaided reading (0.861 vs 0.820, respectively; P = .001). The AUC of the stand-alone AI system was similar to the average AUC of the radiologists unaided (0.840 vs 0.820, 95% CI: -0.038, +0.078). Reading time per normal case showed an average reduction of -21% when using AI, with 8 of 9 readers having shorter reading time.
Conclusion: Radiologists improved their cancer detection in breast tomosynthesis examinations when using an AI system for support, while simultaneously reducing reading time.
Limitations: Retrospective laboratory study. Single vendor of AI and DBT images.
Ethics committee approval: HIPAA-compliant.
Funding: Study sponsored by ScreenPoint Medical.
Author Disclosures:
A. Rodriguez Ruiz: Employee at ScreenPoint Medical
R. M. Mann: nothing to disclose
A. Gubern Merida: Employee at ScreenPoint Medical
N. Karssemeijer: CEO at ScreenPoint Medical
I. Sechopoulos: nothing to disclose

RPS 1402a-6 11:45

Predicting malignant mass in digital breast tomosynthesis using a multi-objective feature selection radiomics model

Z. Fengxia, W. Xu, C. Wen, W. Chen, G. Qin*; Guangzhou/CN (3425262945@qq.com)*

Purpose: To apply a multi-objective feature selection radiomics model that considers sensitivity and specificity simultaneously for predicting the malignancy of the mass-like lesions in digital breast tomosynthesis (DBT).
Methods and materials: A total of 963 cases with diagnosed mass-like lesions were retrospectively used for model training and testing. Patients with infiltrating ductal carcinoma (IDC), ductal carcinoma in situ (DCIS), invasive lobular carcinoma (ILC), adenofibroma, cystic hyperplasia, cyst, and hyperplasia were included. The follow-up time was about 24 months and malignant cases were confirmed by biopsy or surgical pathology. DBT images were contoured and reviewed by 3 radiologists each with more than 5 years' experience in breast diagnosis. For MO-FS, we developed a modified entropy-based termination criterion (METC) that stops the algorithm automatically and used the evidential reasoning approach (SMOLER) to automatically select the optimal solution from the Pareto-optimal set.87. Image features including intensity features, textural features, and geometric features were extracted and selected based on the multi-objective model. Support vector machine (SVM) with radial basis function kernel was used for building the predictive model.
Results: In the prediction model, accuracy, area under the receiver operating characteristic curve (AUC), sensitivity, and specificity were used as the evaluation criteria. The multi-objective radiomics model shows a diagnostic accuracy of 75.6%, AUC of 81.9%, a sensitivity of 76.4%, and a specificity of 81.5%.
Conclusion: This study demonstrated the feasibility of using a multi-objective radiomics model on DBT images to predict the malignancy of the mass-like lesions. The model can handle many mass-like lesions in breast cancer screening and allow for improving the accuracy of diagnosis and increasing the radiologists' work efficiency.
Limitations: This is not a multi-centere study.
Ethics committee approval: n/a
Funding: Supported by Natural Science Foundation of Guangdong Province, China, 2018A0303130215.

Author Disclosures:
Z. Fengxia: nothing to disclose
W. Xu: nothing to disclose
C. Wen: nothing to disclose
W. Chen: nothing to disclose
G. Qin: nothing to disclose

RPS 1402a-7 11:51

Radiomic standardisation of breast MRI to predict pathological complete response to neoadjuvant chemotherapy

P. Akl[1], F. Khalid[2], D. Sebbag-Sfez[1], F. Frouin[2], C. Malhaire[1]; [1]*Paris/FR,* [2]*Orsay/FR (piaakl@gmail.com)*

Purpose: To optimise and standardise breast MRI texture measurements performed as part of a neoadjuvant chemotherapy (NAC) protocol by defining a data preprocessing method before radiomic index extraction, then testing the ability of textural analysis to predict a pathologic complete response (pCR).
Methods and materials: A clinical dataset of 76 patients, acquired using two scanners and three coils with locally advanced breast tumour diagnosis treated at Institut Curie, were analysed retrospectively. A bias field correction was systematically applied and evaluated through a mean relative difference parameter between left and right ROIs in normal tissues: breast parenchyma (BP) and pectoral muscles (PM). Images were then standardised using the sternum as reference tissue. Tumours were segmented and 48 radiomic features (RF) were extracted from 3D corrected and standardised images using the LIFEx software.
Results: Relative differences in normal breast and pectoral muscles were significantly reduced (p-value < 0.001 for both BP and PM) using bias field correction. Pathological analysis indicated that 35 (46%) patients were complete responders. The most robust RF for pCR prediction was “GLCM correlation”, showing an AUC under the ROC curve equal to 0.68. In addition, multivariate analysis taking into account different coils and scanners type and molecular subtypes showed no significant difference for this RF.
Conclusion: This study showed that retrospective bias field correction in breast MRI could improve regional quantitative analyses. This correction was combined with image standardisation on T2 weighted MR images and showed that "GLCM_correlation" is a promising and robust predictor of pCR in breast cancer.
Limitations: This study should be confirmed on a larger number of patients.
Ethics committee approval: The Institutional Review Committees approved this retrospective study and waived informed consent.
Funding: No funding was received for this work.
Author Disclosures:
P. Akl: nothing to disclose
F. Khalid: nothing to disclose
D. Sebbag-Sfez: nothing to disclose
F. Frouin: nothing to disclose
C. Malhaire: nothing to disclose

RPS 1402a-8 11:57

Radiomics-based MR features in HER2 overexpressing breast cancer receiving neoadjuvant chemotherapy: correlation with pathologic response

A. Bitencourt[1], P. Gibbs[2], C. Rossi[1], I. Daimiel Naranjo[3], R. Lo Gullo[2], K. Pinker-Domenig[2], E. A. Morris[2], M. Morrow[2], M. S. Jochelson[2]; [1]*Sao Paulo/BR,* [2]*New York, NY/US,* [3]*Madrid/ES (almirgvb@yahoo.com.br)*

Purpose: To use magnetic resonance (MR)-based radiomic features to assess tumour heterogeneity in HER2 overexpressing breast cancer patients receiving neoadjuvant chemotherapy (NAC) and correlate these findings with a pathologic response.
Methods and materials: This retrospective single-centre study included 311 patients with HER2 overexpressing invasive breast carcinoma who received NAC following pretreatment MRI. Pathologic complete response (pCR) was defined as no residual invasive carcinoma in the breast (ypT0/is) after surgical resection. A breast radiologist performed 3D segmentations of the tumour in the first minute post-contrast sequence using ITK-SNAP software. Enhancement maps were calculated as the percentage increase in signal from the pre-contrast image to the first post-contrast image. Radiomics and statistical analysis were performed using publicly available CERR software and MATLAB.
Results: Mean tumour size by MRI was 4.7 cm (range: 0.9-14.8 cm). The index tumour presented as mass in 47.3%, non-mass enhancement (NME) in 10.9%, and both mass and NME in 41.8%. Most tumours were multifocal on MRI (65.9%). Overall pCR rate was 62.7% (195/311). 12 radiomics parameters demonstrated significant differences between pCR and non-pCR groups. After ROC and correlation analysis 3 radiomic parameters were retained and advanced to modelling alongside clinical parameters, including lesion type (mass/NME/both), multifocality, size, and nodal status. A robust model was developed utilising coarse decision trees and 5-fold cross-validation. The final model utilised 5 parameters (2 clinical and 3 radiomic) for a diagnostic accuracy of 86.2% (268/311).
Conclusion: A model including both clinical and radiomics-based MR features can be used to assess tumour heterogeneity and predict pCR after NAC in HER2 overexpressing breast cancer patients.
Limitations: Retrospective design.
Ethics committee approval: IRB approved.
Funding: NIH/NCI Cancer Center Support Grant (P30-CA008748) and Breast Cancer Research Foundation.
Author Disclosures:
M. S. Jochelson: nothing to disclose
C. Rossi: nothing to disclose
A. Bitencourt: nothing to disclose
P. Gibbs: nothing to disclose
I. Daimiel Naranjo: nothing to disclose
R. Lo Gullo: nothing to disclose
K. Pinker-Domenig: nothing to disclose
E. A. Morris: nothing to disclose
M. Morrow: nothing to disclose

RPS 1402a-9 12:03

Combined contrast-enhanced magnetic resonance and diffusion-weighted imaging radiomic signatures for the assessment of breast cancer molecular subtypes

D. Leithner[1], M. S. Jochelson[1], J. V. M. Horvat[2], M. A. Marino[3], D. B. Avendano[4], D. Martinez[5], S. Thakur[6], E. A. Morris[1], K. Pinker-Domenig[1]; [1]*New York, NY/US,* [2]*002, SP/BR,* [3]*Messina, AT/IT,* [4]*Monterrey, NUEVO LEON/MX,* [5]*New york/US,* [6]*New York/US (doris.leithner@gmail.com)*

Purpose: To investigate the clinical value of radiomic features derived from contrast-enhanced magnetic resonance imaging (CE-MRI) and diffusion-weighted imaging (DWI) for the assessment of breast cancer receptor status and molecular subtypes.
Methods and materials: 91 patients with biopsy-proven breast cancer (luminal A, n=49; luminal B, n=8; HER2-enriched, n=11; triple-negative (TN), n=23) who underwent 3T CE-MRI and DWI were included in this IRB-approved study. Radiomic features (co-occurrence and run-length matrix, absolute gradient, autoregressive model, Haar wavelet transform, and geometry) were extracted from manually drawn ROIs (total number of features per lesion, n=704) on initial CE-MR images and ADC maps. The 5 best features for the differentiation of subtypes were selected separately for CE-MRI and ADC using the probability of error and average correlation coefficients. Following principal component analysis, a multi-layer perceptron feed-forward artificial neural network (MLP-ANN) was used for radiomics-based classification, with 10 iterations, and histopathology as a reference standard. 70% of the cases were used for training, and 30% for validation.
Results: MLP-ANN yielded an overall median area under the receiver-operating-characteristic curve (AUC) of 0.80 (0.77-0.85) for separation of TN from other cancers, with accuracies of up to 81.3% in the training and 84.0% in the validation datasets. The separation of luminal A and TN cancers yielded an overall median AUC of 0.76 (0.71-0.90), with up to 83.3% for training, and 79.2% for validation. All other AUCs were below 0.75.
Conclusion: Combination of radiomic features extracted from CE-MRI and DWI may aid in the non-invasive differentiation of TN and luminal A cancers from other breast cancer subtypes.
Limitations: Manual delineation of cancers.
Ethics committee approval: Approved by the Institutional Review Board; informed consent was waived.
Funding: NIH/NCI Cancer Center Support Grant, Susan G. Komen Foundation, Breast Cancer Research Foundation, Austrian Nationalbank "Jubiläumsfond".
Author Disclosures:
D. Leithner: nothing to disclose
M. S. Jochelson: Speaker at General Electric
J. V. M. Horvat: nothing to disclose
M. A. Marino: nothing to disclose
D. B. Avendano: nothing to disclose
S. Thakur: nothing to disclose
E. A. Morris: nothing to disclose
K. Pinker-Domenig: Speaker at EUSOBI, Speaker at IDKD 2019
D. Martinez: nothing to disclose

RPS 1402a-10 12:09

Radiomic features of axillary lymph nodes based on pharmacokinetic modelling DCE-MRI allow preoperative diagnosis of their metastatic status

H. B. Luo, Y. Y. Liu, J. Ren, P. Zhou; *Chengdu/CN (rohbin@163.com)*

Purpose: To study the feasibility of radiomic features extracted from axillary lymph nodes in diagnosing their metastatic status of breast cancer.
Methods and materials: 176 axillary lymph nodes in breast cancer, consisting of 87 metastatic axillary lymph nodes（ALNM) and 89 negative axillary lymph nodes proven by surgery, were retrospectively reviewed. Each selected axillary lymph node's 106 radiomic features based on pharmacokinetic modelling DCE-MRI and 5 conventional image features were obtained. The LASSO regression was used to select useful radiomic features. Logistic regression was used to develop diagnostic models for ALNM. Delong test was used to compare the diagnostic performance among different models.
Results: The 106 radiomic features were reduced to 4 ALNM diagnosis-related features by LASSO. 4 diagnostic models including the conventional model, pharmacokinetic model, radiomic model, and combined model were developed and validated. The Delong test showed that the combined model had the best diagnostic performance, with an AUC of 0.972 in the training cohort and 0.979 in the validation group. The diagnostic performance of the combined model and radiomic model were better than that of the pharmacokinetic model and the conventional model.
Conclusion: The radiomic features of axillary lymph nodes demonstrated promising application in diagnosing ALNM of breast cancer.
Limitations: There might be some selection bias in the study as it is difficult to accurately match the selected axillary lymph nodes visible on DCE-MRI with the metastatic nodes proved by the resection and biopsy. The semi-automatic features extraction approach may cause some interobserver heterogeneity. This was only a single-centre study.
Ethics committee approval: Our institutional review board approved this study and waived the need for informed consent.
Funding: The Key R&D Projects of the Science and Technology Department in Sichuan Province (grant number 2018SZ0183).
Author Disclosures:
H. B. Luo: nothing to disclose
Y. Y. Liu: nothing to disclose
J. Ren: nothing to disclose
P. Zhou: nothing to disclose

RPS 1402a-11 12:15

Parenchymal radiomics in cone-beam breast CT: comparison with mammography and implication for cancer risk estimation

Y. Zhu, Y. Zhang, Y. Ma, Z. Ye; *Tianjin/CN (zhuyueqiang1985@126.com)*

Purpose: To investigate the potential advantage of parenchymal radiomics in cone-beam breast CT (CBBCT) compared to mammography (MG) for breast cancer risk estimation.
Methods and materials: Bilateral CBBCT and MG from 233 women (147 malignant and 86 benign patients who had unilateral disease) were retrospectively collected from a CBBCT clinical trial (NCT01792999) between May 2012 to November 2014. Parenchymal radiomic features were computed from retroareolar region in contralateral normal breast parenchyma. Principal component analysis (PCA) was applied to obtain orthogonal radiomic components. Breast percent density (PD) was evaluated with software. Correlation analysis and linear regression were performed to determine the association between radiomic features and breast PD with increasing levels of risk. Age was also considered as an additional predictor in multivariate models.
Results: Overall, CBBCT radiomic features demonstrated stronger correlations with breast PD than MG. When dividing population into groups of increasing levels of risk according to breast PD, CBBCT radiomic features appeared to be more discriminative, having regression lines with overall steeper slopes, higher R^2 estimates, and lower P values. Linear regression of PCA radiomic features as predictors of PD also demonstrated significantly stronger associations with CBBCT (R^2 = 0.375) than with MG (R^2 = 0.069). The association was strongest when age was combined (R^2 = 0.439).
Conclusion: Parenchymal radiomic features were more strongly correlated to breast PD in CBBCT than in MG. CBBCT parenchymal radiomics could provide a more accurate characterisation of breast parenchymal patterns, which could ultimately improve breast cancer risk estimation.
Limitations: Our study cohort was a diagnostic population.
Ethics committee approval: The institutional review board approved this study and written informed consent was obtained from all patients.
Funding: National Key R&D Program of China (No. 2017YFC0112600), National Natural Science Foundation of China (No. 81571671).

Author Disclosures:
Y. Zhu: nothing to disclose
Y. Zhang: nothing to disclose
Y. Ma: nothing to disclose
Z. Ye: nothing to disclose

RPS 1402a-12 12:21

Artificial intelligence breast cancer risk estimation from CT thorax scans

S. de Buck[1], J. Bertels[1], C. van Bilsen[2], T. Dewaele[2], C. van Ongeval[1], H. Bosmans[1], J. Vandevenne[2], P. Suetens[3]; *[1]Leuven/BE, [2]Genk/BE, [3]Leuven - Heverlee/BE*

Purpose: Breast glandularity is associated with breast cancer risk. Systematic scoring of glandularity on CT thorax examinations performed for another clinical reason could find patients at risk, but it is currently cumbersome and not standard practice. Automated scoring would give access to this information. We propose a novel method to automatically segment the breast volume on CT thorax examinations and estimate glandularity.
Methods and materials: We used an artificial neural network with a U-Net-like architecture to automatically segment the breast region. A retrospective study was conducted on a dataset of 23 postmenopausal women that had a CT thorax examination for another clinical reason. The images were manually segmented to serve as a gold standard. The image/segmentation pairs were randomly separated in a training (15 patients) and a testing (8 patients) set. We computed 2 risk scores in the segmented breast: the glandular fraction (HU>40) and volumetric breast density (VBD), based on the average HU in comparison to pure fat and gland. Segmentation accuracy was validated by Dice overlap between predicted and manually segmented regions. Risk score correlation was assessed by the Pearson coefficient.
Results: We obtained a Dice overlap score of 0.84±0.03. The Pearson coefficient between predicted and ground-truth values of the glandular fraction and VBD amounted to 0.99 and 0.98 respectively.
Conclusion: We present a first, novel artificial intelligence-based approach to automatically compute the volume of the breast by a convolutional neural network and determine cancer risk scores based on CT thorax examinations performed for another reason. Results show excellent correspondence between the automated method and expert observers.
Limitations: Despite a limited population, good results are shown.
Ethics committee approval: A retrospective study on anonymised images, waived by the ethical committee (ZOL).
Funding: No funding was received for this work.
Author Disclosures:
S. de Buck: nothing to disclose
J. Bertels: nothing to disclose
C. van Bilsen: nothing to disclose
T. Dewaele: nothing to disclose
C. van Ongeval: nothing to disclose
H. Bosmans: nothing to disclose
J. Vandevenne: nothing to disclose
P. Suetens: nothing to disclose

11:15 - 12:30 **Room X**

Vascular

RPS 1415

Advances in vascular imaging

Moderators:
R. Schernthaner; Vienna/AT
U. Hoffmann; Boston, MA/US

RPS 1415-1 11:15

Flow-controlled angiography for the assessment of vascular patency, permeability, and leakage in bioengineered kidneys

S. Cohen[1], S. Hirschberg[2], S. Partouche[1], M. Gurevich[1], V. Tennak[1], V. Mezhybovsky[1], E. Nesher[1], E. Mor[3], E. Atar[1]; *[1]Petah Tikva/IL, [2]Salit/IL, [3]Ramat Gan/IL (sarit.soffer@gmail.com)*

Purpose: Perfusion decellularisation is a promising method for the generation of non-immunogenic organs from allogeneic and xenogeneic donors. A number of imaging modalities are used to assess vascular integrity in bioengineered organs, including fluoroscopic angiography, with no consistency in the method used. None of these techniques addressed changes in permeability, while the demonstration of patency was limited to visualisation of arterial tree. The goal of this study was to evaluate the use of fluoroscopic angiography performed under

controlled flow conditions for the assessment of vascular integrity in bioengineered kidneys.
Methods and materials: Porcine kidneys underwent ex vivo fluoroscopy before and after perfusion decellularisation, under controlled flow conditions. Arterial and venous patency were defined as the visualisation of contrast medium (CM) in distal capillaries and the renal vein, respectively. For permeability assessment, grey-scale intensity within the parenchyma was measured and the washout index (W_{index}) was calculated at several time points during a washout phase. Extravasation of CM was documented following iatrogenic injury.
Results: No differences in patency were detected in decellularised kidneys compared with native kidneys. However, a significantly lower W_{index} was calculated for decellularised kidneys, indicating a delayed CM clearance and increased vascular permeability. Focal opacities representing extravasation of CM into the parenchyma were only detected in decellularised kidneys. Iatrogenic leakage was equally detectable in both groups, with DSA scans revealing even minimal CM leakage.
Conclusion: Quantitively assessment of permeability should be coupled with patency when studying the effect of perfusion decellularisation on kidney vasculature. Flow-controlled fluoroscopic angiography based on the proposed methodology is an accessible, accurate, and sensitive method that should be adopted as the method-of-choice for vascular assessment in bioengineered organs.
Limitations: Larger sample sizes are needed to confirm our findings.
Ethics committee approval: Performed in accordance with IRB guidelines.
Funding: No funding was received for this work.
Author Disclosures:
S. Hirschberg: nothing to disclose
S. Cohen: nothing to disclose
S. Partouche: nothing to disclose
M. Gurevich: nothing to disclose
V. Tennak: nothing to disclose
E. Mor: nothing to disclose
E. Nesher: nothing to disclose
E. Atar: nothing to disclose
V. Mezhybovsky: nothing to disclose

RPS 1415-2 11:21

The evaluation of early haemodynamic changes in rabbit aorta atherosclerosis by high frame rate V-flow imaging

Y. Dong, Y. Qiu, Q. Zhang, D. Yang, W. Wang*; Shanghai/CN (dr_mimi@163.com)*

Purpose: To evaluate the change of V Flow and wall shear stress (WSS) parameters in the evaluation of early-stage aorta atherosclerosis (AS) in rabbit models.
Methods and materials: Rabbit AS models were established by feeding high-fat forage in healthy New Zealand rabbits (n=7). Ultrasound evaluations were performed once per week since the 14th week. A Mindray Resona 7s ultrasound system equipped with a L9-3U linear array transducer (3-9 MHz) and updated V Flow imaging function was used. The maximum WSS (WSSmax) value and mean WSS (WSSmean) value were compared with the blood flow volume (BFV) and peak systolic velocity (PSV) value measured by colour Doppler flow imaging (CDFI). Histopathological results after 34 weeks were used as the gold standard to make a correlation analysis with the WSS value.
Results: On the 34th week, pathological results showed typical fatty streak changes on the wall of the aorta. Since the 37th week, AS plaques could be detected. The WSS values of the aorta changed with the progression of AS, which began to decrease at the 14th week, increased between the 20th-27th week, and gradually decreased after the 27th week. A significant difference was found between the WSS values and the baseline values ($P<0.05$). Statistical results showed earlier statistical changes of WSSmax and WSSmean values while comparing with PSV and BFV values.
Conclusion: The WSS value measured by V Flow technology changed dynamically during the progress of aorta AS in rabbit models. WSS values might have potential clinical value in the evaluation of early haemodynamics changes in AS.
Limitations: The number of animals were limited.
Ethics committee approval: This animal study was approved by the ethics committee of Zhongshan Hospital, Fudan University.
Funding: Shanghai Municipal Science and Technology Innovation Action Plan Clinical Medicine Project (Grant No. 17411954200).
Author Disclosures:
Y. Dong: nothing to disclose
Y. Qiu: nothing to disclose
Q. Zhang: nothing to disclose
D. Yang: nothing to disclose
W. Wang: nothing to disclose

RPS 1415-3 11:27

The detection of shear stress in haemodialysis arteriovenous fistulae by ultrasound vector flow imaging

J. Ding[1], R. Zhao[1], Q. Yang[1], Y. Du[2], L. Zhu[2], H. Gan[1], M. Wang[1]*; [1]Beijing/CN, [2]Shenzhen/CN (yigang1982@gmail.com)*

Purpose: Altered blood flow and wall shear stress (WSS) in arteriovenous fistulae (AVF) might make the access stenosis, causing the dialysis procedure to become ineffective. The stenosis of AVF commonly occurs in three specific sites: the anastomosis floor (Type-I), on the inner wall of the swing segment (Type-II), and after the curved region when the vein straightens out (Type-III). WSS in these sites could be measured by V Flow, which is a high-frame-rate ultrasound vector flow imaging (VFI) implemented based on multi-directional Doppler techniques.
Methods and materials: This study established the first quick measurement of vascular WSS by V Flow in AVF (available on a clinical system, Resona 7 manufactured by Mindray, Shenzhen, China). 15 haemodialysis patients were included; 9 males and 6 females. The dialysis age was 38.0±25.1 months. The mean age of the fistula was 21.4±18.6 months. Each fistula was functioning for dialysis access at the time of our examination.
Results: The level of mean WSS in Type-I, -II, and -III sites were 0.9±0.6Pa, 1.2±0.5Pa, and 0.8±0.4Pa. The level of max WSS was 2.7±1.3Pa, 4.2±2.5Pa, and 1.7±0.7Pa in these sites. It was found that the WSS level of Type-III was significantly lower than the others ($P<0.05$), except the mean WSS in Type-I and -III ($P=0.6$). The level of fistulae flow rates was about 559±126.5 ml/min measured by V Flow.
Conclusion: The ultrasound VFI technique is convenient to study the changes of WSS and flow in AVF. The lowest WSS in Type-III might explain that this site is the most susceptible site for stenosis. WSS is expected to be a sensitive and non-invasive method for the early prediction stenosis of AVF.
Limitations: A pilot study.
Ethics committee approval: Approved by the Hospital Review Board.
Funding: Supported by Hospital funding YN2017QN04.
Author Disclosures:
J. Ding: Author at PEKING UNIVERSITY INTERNATIONAL HOSPITAL
R. Zhao: Author at PEKING UNIVERSITY INTERNATIONAL HOSPITAL
M. Wang: Author at PEKING UNIVERSITY INTERNATIONAL HOSPITAL
L. Zhu: Author at SHENZHEN MINDRAY BIO-MEDICAL ELECTRONICS CO., LTD.
Y. Du: Author at SHENZHEN MINDRAY BIO-MEDICAL ELECTRONICS CO., LTD.
H. Gan: Author at PEKING UNIVERSITY INTERNATIONAL HOSPITAL
Q. Yang: Author at PEKING UNIVERSITY INTERNATIONAL HOSPITAL

RPS 1415-4 11:33

Ferumoxytol MR angiography: a novel imaging technique for vascular mapping before haemodialysis arteriovenous fistula creation

A. Tan, S. Stoumpos, P. Hall Barrientos, A. Radjenovic, D. Kingsmore, R. S. Kasthuri, G. Roditi, P. Mark*; Glasgow/UK (alfred.research@gmail.com)*

Purpose: Doppler ultrasound (DUS) is routinely performed for vascular mapping prior to haemodialysis arteriovenous fistula (AVF) creation but has the disadvantage of not visualising the central vasculature. Ferumoxytol, an iron oxide nanoparticle, provides an alternative to gadolinium contrast for magnetic resonance angiography (MRA). We assessed the clinical utility of ferumoxytol-enhanced MRA (FeMRA) before autogenous upper limb AVF creation compared with DUS.
Methods and materials: In a prospective comparative study, paired FeMRA and DUS were obtained the same day. Vessels were evaluated for diameter, stenosis or occlusion, arterial disease, and central stenosis by independent readers. Interclass correlation coefficients (ICC) and Bland-Altman plots examined inter- and intra-reader variability. Based on accepted standards for AVF creation, an algorithm was designed to predict the AVF outcome relying on mapping findings. Logistic regression models were created with AVF success as the dependent variable and age, sex, and DUS or FeMRA mapping as the independent variables.
Results: 59 patients (mean age 59 years) had FeMRA and DUS, and 51 AVF were created. FeMRA showed excellent inter- and intra-reader repeatability (ICC 0.84-0.99). In addition to identifying 15 central vasculature stenoses, FeMRA explicitly characterised anatomical abnormalities and variants in arm vessels. On multivariable regression analyses, FeMRA mapping independently predicted AVF success in models including [OR: 6.49 (95% CI 1.70-24.79); p=0.006] and excluding central stenoses [OR: 4.58 (95% CI 1.25-16.83); p=0.02].
Conclusion: FeMRA better predicted the AVF successful outcome compared to DUS and has the added advantage of identifying central vessels pathology.

Limitations: The translation of study protocol to clinical practice. Ferumoxytol is not yet licensed as a contrast agent for MRI and used off-label.
Ethics committee approval: The study was approved by the institutional review board [Research Ethics Committee (REC) reference: 16/NS/0099, NCT02997046].
Funding: No funding was received for this work.
Author Disclosures:
A. Tan: nothing to disclose
S. Stoumpos: nothing to disclose
G. Roditi: nothing to disclose
P. Mark: nothing to disclose
D. Kingsmore: nothing to disclose
A. Radjenovic: nothing to disclose
P. Hall Barrientos: nothing to disclose
R. S. Kasthuri: nothing to disclose

RPS 1415-5 11:39
A magnetic micro-robot for aneurysm coiling with magnetic particle imaging
A. C. Bakenecker, F. Wegner, H. Schwenke, K. Lüdtke-Buzug, T. Friedrich, J. Barkhausen, T. M. Buzug*; Lübeck/DE (bakenecker@imt.uni-luebeck.de)*

Purpose: To introduce a new approach for aneurysm coiling by using a magnetic micro-robot, which is steered by the magnetic fields of a magnetic particle imaging (MPI) scanner in an in vitro study.
Methods and materials: For in vitro phantom experiments, a high precision model of a middle cerebral artery was used, which was 3D-printed and filled with water. For the micro-robot, we used a 3D-printed helically shaped swimmer, which can be navigated by magnetic fields. The required homogeneous magnetic fields of low amplitude (about 10 mT) and rotating field vector are generated by a commercial MPI scanner (Bruker BioSpin, Ettlingen, Germany). Low rotation frequencies (around 10 Hz) are applied and the swimmer follows the rotation. Due to the swimmers' shape, a forward movement is induced. The magnetic fields are pre-calculated according to the pathway the swimmer has to cope. The swimmer has a length of 3.0 mm and a width of 1.2 mm, fitting the blood vessels of the phantom. It is coated with magnetic nano and microparticles to introduce magnetic properties. The magnetic nanoparticles could serve as tracer material for visualisation with MPI.
Results: The swimmer can be navigated by external magnetic fields through a blood vessel towards an aneurysm within a vessel phantom. The magnetic fields were applied with an MPI scanner, which allowed the visualisation of the swimmer.
Conclusion: The first in vitro experiments demonstrate the feasibility of steering a micro-robot by pre-calculated magnetic fields of an MPI scanner through a vessel phantom towards an aneurysm, which paves the way for an untethered coiling procedure.
Limitations: In vitro experiments were performed without flow.
Ethics committee approval: n/a
Funding: The Federal Ministry of Education and Research, Germany (BMBF), Grant No. 13GW0230B (FMT).
Author Disclosures:
A. C. Bakenecker: nothing to disclose
F. Wegner: nothing to disclose
H. Schwenke: nothing to disclose
K. Lüdtke-Buzug: nothing to disclose
T. Friedrich: nothing to disclose
J. Barkhausen: nothing to disclose
T. M. Buzug: nothing to disclose

RPS 1415-6 11:45
The safety of a new stent design during magnetic particle imaging and magnetic resonance imaging
U. Grzyska[1], T. Friedrich[1], J. Haegele[2], T. M. Buzug[1], J. Barkhausen[1], F. Wegner[1]; *[1]Lübeck/DE, [2]Neuss/DE (ulrike.grzyska@gmx.de)*

Purpose: To evaluate the heating of a recently developed re-dilatable stent for the treatment of aortic coarctation in neonates and small children during magnetic particle imaging (MPI) and magnetic resonance imaging (MRI).
Methods and materials: All measurements were performed using a recently developed cobalt-chromium stent (BabyStent, Osypka) with a new stent design which allows for re-dilatation and adjustment of the diameter from 6 to 16 mm. At a diameter of more than 12 mm, the stent loses radial integrity while fracturing at dedicated breaking points. Temperature measurements were performed with fibre-optic thermometers during 7-minute MPI and MRI scans. 6 different stent diameters (6, 8, 10, 12, 14, and 16 mm) were evaluated in this study.
Results: In MPI, all stents with continuous struts showed a temperature increase (max. 2.3 K). The measured temperature differences increased with growing diameters up to 12 mm, whereas the stents with discontinuous struts at 14 and 16 mm showed nearly no heating. In contrast to MPI, the investigated stents showed no heating during the MRI measurements.
Conclusion: The stents showed no heating during MRI and only clinically insignificant heating during MPI and can safely be examined with both modalities. However, in MPI, the stent diameter and the strut design influence the temperature difference.
Limitations: The absence of flow could be a potential limitation of our study. To prevent potential cooling effects, we consciously created a worst case scenario study with static conditions and stents surrounded by air.
Ethics committee approval: n/a
Funding: The German Federal Ministry of Education and Research BMBF, grant number 13GW0071D.
Author Disclosures:
U. Grzyska: nothing to disclose
T. Friedrich: nothing to disclose
J. Haegele: nothing to disclose
T. M. Buzug: nothing to disclose
J. Barkhausen: nothing to disclose
F. Wegner: nothing to disclose

RPS 1415-7 11:51
The identification of intra-individual flow variation of intracranial aneurysms on phase-contrast MR and the influence on computational haemodynamics
Y. Wang[1], X. Liu[2], E. Kao[3], H. Haraldsson[3], M. Ballweber[3], M. Alastair[3], D. Saloner[3]; *[1]Chengdu/CN, [2]Beijing/CN, [3]San Francisco/US (wangyuting_330@163.com)*

Purpose: Patient-specific inlet artery flow has been applied in intracranial aneurysm simulations. This study aims to identify the intra-individual flow variation in phase-contrast MR (PCMR) and how it influences the following computational haemodynamics.
Methods and materials: 2D PCMRs were performed in a longitudinal patient cohort of intracranial aneurysms to determine the inlet flow boundary condition. The intraclass correlation coefficient (ICC) and the coefficient of variance (CV) across 3 time points were used to identify reproducibility and variation. Computational fluid dynamics were performed using the original flow and flow with the corresponding variation, respectively. The wall shear stress (WSS), low shear area (LSA), time-averaged wall shear stress (TAWSS), and oscillatory shear index (OSI) were compared.
Results: 51 patients (14 males; mean age: 62 years; mean follow-up interval: 7.2 months) were included. The reproducibility of the flow and velocity was good, with ICCs of 0.71-0.90. A 10% CV of mean flow was identified. The variation of flow data was smaller than the velocity data ($p<0.05$). The variation of flow and velocity at the end-diastolic phase was larger than that of the mean and systolic phase ($p<0.01$). A 10% of flow variance would lead to haemodynamic changes including 20% of WSS at the systolic phase, 19.6% of WSS at diastolic phase, 5.0% of LSA at systolic phase, 5.2% of LSA at diastolic phase, 20.1% of TAWSS, and 4.6% of OSI.
Conclusion: The flow should be preferred rather than the velocity in choosing inlet boundary conditions due to a smaller variance. A 10% of flow variation could lead to a series of haemodynamic changes. LSA is a more stable parameter than WSS.
Limitations: n/a
Ethics committee approval: Under IRB approval of UCSF. All subjects gave informed written consent.
Funding: No funding was received for this work.
Author Disclosures:
Y. Wang: nothing to disclose
X. Liu: nothing to disclose
E. Kao: nothing to disclose
H. Haraldsson: nothing to disclose
M. Ballweber: nothing to disclose
M. Alastair: nothing to disclose
D. Saloner: nothing to disclose

RPS 1415-8 11:57
The potential of ferumoxytol as a contrast media in computed tomography: a phantom study
A. Parakh, A. O'shea, M. Harisinghani, A. Kambadakone, R. Gupta, B. Ghoshhajra, S. Hedgire*; Boston, MA/US (aoshea1@mgh.harvard.edu)*

Purpose: To investigate the potential of ferumoxytol as a vascular contrast agent using dual-source dual-energy CT (DECT).
Methods and materials: 10 10-ml syringes were filled with increasing dilutions of ferumoxytol with saline in increments of 3 mg/ml ranging from 0-27 mg/ml. The syringes were placed within an attenuation phantom that was scanned using single-energy CT (SECT) at 120 kVp and DECT (100/Sn150) protocols. Attenuation (HU) for all syringes was measured on SECT and virtual monoenergetic images (VME) at 40-190 keV on DECT. Generally, an

intravascular attenuation of 250 HU is deemed acceptable for evaluating vasculature on CT. Therefore, the attenuation of different concentrations of ferumoxytol at varying energy levels was compared with 250HU.
Results: The maximum attenuation observed for the syringe containing 27 mg/ml ferumoxytol was 146HU at SECT and 435HU at 40keV-DECT. Attenuation values higher than 250 HU were observed for concentrations of 18 mg/ml at 40-42keV, 21 mg/ml at 40-44keV, 24 mg/ml at 40-50keV, and 27 mg/ml at 40-55keV. For concentrations between 18-27 mg/ml, HU at SECT were 96, 104, 122, and 146 HU, respectively. Compared to SECT, 40keV, and 50keV images increased the attenuation of ferumoxytol two-to-three-folds.
Conclusion: Use of low keV (40-50keV) monoenergetic images using 100/Sn150 kVp spectra on a dual-source dual-energy CT platform increases the attenuation of ferumoxytol compared to 120-kVp SECT substantially. CT imaging with this agent may be feasible for assessing vasculature in selected patient populations who can not receive iodinated or gadolinium contrast media for vascular CTA/MRA studies.
Limitations: This setup was a phantom without circulation dynamics. Further studies using clinically appropriate concentrations of ferumoxytol and simulated haemodynamics are required to assess the feasibility of using this contrast agent.
Ethics committee approval: n/a
Funding: No funding was received for this work.
Author Disclosures:
A. Parakh: nothing to disclose
A. O'shea: nothing to disclose
M. Harisinghani: nothing to disclose
A. Kambadakone: Research/Grant Support at GE Healthcare, Research/Grant Support at Philips Healthcare
R. Gupta: nothing to disclose
S. Hedgire: nothing to disclose
B. Ghoshhajra: Board Member at Society of Cardiovascular Computed Tomography, Grant Recipient at NIH, Research/Grant Support at Institutional - Siemens Healthcare Cardiac CT Research (fellow support), Shareholder at Apple

RPS 1415-9 12:03

Virtual monochromatic images in low tube current dual-energy spectral imaging combined with adaptive statistical iterative reconstruction V in head CT angiography: a phantom and clinical study

T. Song, Z. Li*; Chengdu/CN*

Purpose: To analyse the value of combining virtual monochromatic spectral (VMS) image and adaptive statistical iterative reconstruction V (ASiR-V) in low tube current dual-energy spectral imaging in head computed tomography angiography (CTA), and to explore the optimal VMS and ASiR-V levels.
Methods and materials: An anthropomorphic PBU-60 angiographic head phantom and 40 patients (randomly divided into two groups with 20 patients in each group) were examined on a revolution CT with spectral imaging mode at two different tube currents. Images of different energy levels in the low tube current group (with 280mA) were reconstructed with the combination of filtered back projection (FBP), 20%, 40%, 60%, and 80% ASiR-V. VMS images at 70keV in the routine tube current group (with 445mA) were reconstructed with FBP only.
Results: The SNR and CNR of the simulated cerebral vessels and subjective scores of the 55 keV VMS images with ASiR-V 60% and ASiR-V 80% in the low tube current patient group were higher than that of the 70 keV FBP images in the routine tube current group. The radiation dose of group A was lower than group B.
Conclusion: VMS images in low tube current spectral imaging combined with ASiR-V can significantly reduce the radiation dose and ensure image quality in head CTA. The 55 keV VMS images with ASiR-V 60% and 80% provide higher image quality.
Limitations: A single-centre study.
Ethics committee approval: This study was approved by the biomedical ethics committee of our hospital.
Funding: 1.3.5 project for disciplines of excellence, West China Hospital, Sichuan University (ZYGD18019).
Author Disclosures:
T. Song: nothing to disclose
Z. Li: nothing to disclose

RPS 1415-10 12:09

The effectiveness of dual-layer spectral detector CT for reducing the amounts of contrast agents and injection flow rate

T. E. Kim[1], Y. H. Chung[2], T. H. Nam[1], S. A. Kwon[1]; *[1]Seongnam/KR, [2]Seoul/KR, (20309@snubh.org)*

Purpose: To investigate the utility of a method for dual-energy computed tomography (DECT) using a low flow-rate and volume of contrast when the aorta CT angiography is progressed.
Methods and materials: 64 patients who underwent aorta CT angiography with 256MDCT and 128DECT were enrolled in this study. In cases of 256MDCT, we administered 130 mL of contrast at a rate of 3.0 mL/sec. In cases of 128DECT, we administered 50 mL of contrast at a rate of 1.5 mL/sec. Additional MonoE (60keV) images were reconstructed from a DECT examination. For quantitatively evaluation, two radiographers measured the CT number, standard deviation, and CNR. The measurement regions were two points as descending aorta and SMA. For qualitative evaluation, two radiologists evaluated the level of aortic enhancement based on three-point scaling at the region of the brachiocephalic artery, SMA, and IMA.
Results: Results in quantitative evaluation from the average CNR results, the MDCT cases were shown as 93±11 and 76±7 from the descending aorta and SMA. The DECT cases were shown as 108±14 and 86±13 from the descending aorta and SMA, respectively. The results of qualitative evaluation, the good results (over 3.5 points with P>0.05) at the evaluation have been reported. This means there are few statistical differences between the two methods.
Conclusion: Image reconstruction based on the spectral method using DECT for the scanning of aorta angiography reduced the dosage of the contrast agent by 62.5% and the injection flow rate by 50% without a decrease of the image quality. Therefore, the DECT aorta protocol is a useful technique in patients with kidney failure and poor IV.
Limitations: The lack of experiments with varying amounts of contrast agents.
Ethics committee approval: n/a
Funding: No funding was received for this work.
Author Disclosures:
T. E. Kim: Author at Seoul National University Bundang Hospital
Y. H. Chung: nothing to disclose
T. H. Nam: nothing to disclose
S. A. Kwon: nothing to disclose

RPS 1415-11 12:15

The validation of iodine contrast flow velocity quantification from time-resolved CT-angiography in a flow phantom

P. T. Boonen[1], N. Buls[1], J. Vandemeulebroucke[2], G. van Gompel[1], Y. J. F. de Brucker[1], D. Aerden[1], T. Leiner[3], J. de Mey[1]; *[1]Jette/BE, [2]Brussels/BE, [3]Utrecht/NL (pieter.thomas.boonen@vub.be)*

Purpose: To demonstrate the feasibility and reliability of flow velocity measurements using time-resolved CT-angiography in a dynamic flow phantom.
Methods and materials: All experiments were performed with a single lumen flow phantom with a 6 mm inner diameter. Saline was infused at varying injection rates with a contrast injector (Dual Shot GX 7-Nemoto) and the contrast bolus (2 mL iomeprol 350 at 0.33 mL/s) was subsequently injected using a syringe injector (Alaris GH Syringe Pump). The two injectors were connected to a silicone tube which was contained within a solid 2% agar-agar solution to mimic soft tissue.
Saline was injected at 6 flow rates to achieve the following reference velocities: 21.2 mm/s, 38.9 mm/s, 60.1 mm/s, 81.4 mm/s, 99.0 mm/s, and 120.3 mm/s. For each velocity, 6 consecutive time-resolved CTA acquisitions were performed (Revolution CT, GE Healthcare), each consisting of 20 repeated axial acquisitions with an interscan delay of 1.2s at 160 mm (256x0.625 mm) collimation. The mean centerline flow velocities were automatically assessed and differences and correlations with reference settings were evaluated with the Wilcoxon signed-rank test and the Pearson correlation.
Results: From the CT image data, the average obtained velocities were 21.6±5.6 mm/s, 34.5±6.8 mm/s, 61.5±3.1 mm/s, 76.3±14.5 mm/s, 104.9±27.0 mm/s, and 143.6±42.1 mm/s. No significant difference was observed with the reference velocities ($p=0.912$) and a significant linear correlation was found ($r=0.903$, $p<0.01$). Up to 99.0 mm/s, the measurement error was confined within 12%.
Conclusion: The results of this study suggest that mean flow velocities within the range of typical blood flow velocities (40 mm/s-70 mm/s) can be accurately measured with high precision in a 6 mm flow phantom using time-resolved CTA.
Limitations: Of minor importance.
Ethics committee approval: n/a
Funding: Fonds Wetenschappelijke Onderzoek Vlaanderen (FWO).
Author Disclosures:
P. T. Boonen: nothing to disclose
N. Buls: nothing to disclose
J. Vandemeulebroucke: nothing to disclose
G. van Gompel: nothing to disclose
Y. J. F. de Brucker: nothing to disclose
D. Aerden: nothing to disclose
J. de Mey: nothing to disclose
T. Leiner: nothing to disclose

RPS 1415-12 12:21
DKI evaluation of crossed cerebellar diaschisis after MCAO cerebral infarction in rats
Z. Ma, X. Zhao; *Zhengzhou/CN (11430884@qq.com)*

Purpose: To observe the expression of NMDA, apoptosis, and the effect on nerve function recovery in a rat model of middle cerebral artery occlusion (MCAO). Diffusion kurtosis imaging (DKI) was used to evaluate crossed cerebellar diaschisis (CCD) to provide an experimental and theoretical basis for clinical treatment.
Methods and materials: MCAO models were established in rats. Every 12 rats were randomly divided into a control group, 6-hour group, 12-hour group, 24-hour group, 48-hour group, 7-day group, and 14-day group. The rats were scanned by MRI at the above time points. Rats were sacrificed for H&E staining, immunohistochemical staining, and TUNEL staining to detect the expression of NMDA in the core infarct area and cerebellum, and to analyse the relationship between the parameters of MRI and molecular biology.
Results: The values of MD, ADC, and FA in MCAO rats were all lower than those of the control group and the parameters of contralateral cerebellum were lower than those of ipsilateral cerebellum ($P<0.05$), reaching the lowest value at 12 hours, while the values of MK were opposite. The expression of NMDA showed an upward trend, higher than that of the control group, which reached the maximum in 24 hours ($P<0.05$, and that in the contralateral cerebellum was higher than that in the ipsilateral cerebellum.
Conclusion: NMDA can be a novel treatment target for CCD and the parameters of MRI can predict the occurrence and development of CCD.
Limitations: Continuous dynamic scanning has not yet been used in the experiment.
Ethics committee approval: n/a
Funding: No funding was received for this work.
Author Disclosures:
Z. Ma: Author at Third Affiliated Hospital of Zhengzhou University
X. Zhao: Research/Grant Support at Third Affiliated Hospital of Zhengzhou University

11:15 - 12:30 **Coffee & Talk 1**

Interventional Radiology

RPS 1409a

Interventional practice, dose management and education

Moderators:
V. Bérczi; Budapest/HU
N.N.

RPS 1409a-K 11:15
Keynote lecture
G. Carrafiello; *Milan/IT*

Author Disclosures:
G. Carrafiello: nothing to disclose

RPS 1409a-1 11:25
Cost awareness of interventional radiology devices among radiology trainees
M. Courtney[1], D. Mulholland[1], D. O'Neill[1], C. Redmond[2], M. J. Lee[1], T. Farrell[1]; *[1]Dublin/IE, [2]Tullamore/IE (michael.courtney@tcd.ie)*

Purpose: Numerous disposable devices are consumed daily in interventional radiology (IR) suites globally. Trainees receive no formal training or assessment on the cost and identification of these devices. Educating specialists on disiposable devices has shown to reduce costs in other disciplines. This study aims to assess radiology trainees' ability to identify and estimate the costs of common disposable interventional radiological devices and identify deficiencies in postgraduate radiology teaching in terms of healthcare economics.
Methods and materials: The postgraduate radiology training body of a European country was consulted to obtain numbers of all current radiology trainees. Trainees were invited to partake in a questionnaire via email. An anonymous online survey consisting of 26 multiple-choice questions (MCQs) was administered. Respondents were asked to provide their year of training and subspecialty of interest. Respondents were asked to identify 13 devices, using in vivo and ex vivo images. The devices were a PICC line, Angioseal closure device, tunnelled dialysis catheter, Port-A-Cath, pigtail drainage catheter, guidewire, biopsy needle, micropuncture kit, angioplasty balloon, IVC filter, covered metal vascular stent, gastrostomy tube, and an EVAR graft. They were asked to estimate the cost of each device. Trainees were deemed correct if they responded within 25% of true cost.
Results: The questionnaire was delivered to 82 radiology trainees; the response rate was 60% (49/82). No trainee accurately estimated the cost for all 13 devices assessed. The cost of devices was underestimated by trainees 48.9% of the time and overestimated 32.3% of the time.
Conclusion: Radiology trainees are deficient in cost awareness of a number of common IR devices used. A health economics module in postgraduate radiology training may improve the efficiency of healthcare expenditure within radiology departments.
Limitations: n/a
Ethics committee approval: n/a
Funding: No funding was received for this work.
Author Disclosures:
M. Courtney: nothing to disclose
D. Mulholland: nothing to disclose
D. O'neill: nothing to disclose
C. Redmond: nothing to disclose
M. J. Lee: nothing to disclose
T. Farrell: nothing to disclose

RPS 1409a-2 11:31
A pilot study to compare the perception of image quality using smart glasses and a conventional monitor
S. Dorey[1], S. Al-Islam[2], J. D. Thompson[1], A. England[1]; *[1]Manchester/UK, [2]Blackburn/UK (shaun.dorey@tgh.nhs.uk)*

Purpose: Due to the hands-free nature of smart glasses, they have the potential to be useful in interventional environments where sterility has to be ensured and where the clinician has both hands occupied with surgical tasks. A visual grading analysis (VGA) study was performed to compare the perceived image quality of fluoroscopy images using smart glasses and a conventional monitor.
Methods and materials: 10 observers (3rd-year student radiographers) evaluated 4 anonymised fluoroscopic images for 4 criteria (representation of soft tissue structures, bone, contrast filled structures, and clear definition of a guidewire). Each criterion was rated on a scale of 1-5, with a higher number representing a more positive response.
The evaluation was completed with a pair of prototype Epson BT-35E smart glasses (Epson, Japan) in a controlled environment (dimmed ambient lighting with no adjustments made to the brightness, contrast, or magnification settings). The same images were also displayed on an Iiyama ProLite B2206WS monitor (Iiyama, Japan) within the same controlled environment. The area under the visual grading characteristic (AUC_{VGC}) was used as the figure of merit (FOM). The image evaluation would be considered statistically different if the 95% confidence interval (CI) of the AUC_{VGC} did not include 0.5.
Results: The AUC_{VGC} and 95% CI was 0.519 (0.425, 0.618), p=0.610, for the comparison of the image evaluation with smart glasses and a conventional monitor. This means that no significant difference was detected for the evaluation of image quality in this pilot data.
Conclusion: There were promising early results for the image quality provided by smart glasses in comparison to a conventional monitor. A larger-scale study, also considering dynamic imaging, is now required.
Limitations: n/a
Ethics committee approval: Application HST1819-279 approved University of Salford.
Funding: CoRIPS Student Research Award.
Author Disclosures:
S. Dorey: Author at Tameside and Glossop Integrated Care NHS Foundation Trust, Grant Recipient at Society and College of Radiographers
S. Al-Islam: Author at Royal Blackburn Hospital
J. D. Thompson: Author at University of Salford
A. England: Author at University of Salford

RPS 1409a-3 11:37
Endovascular simulation training: a tool to increase enthusiasm for interventional radiology among medical students
F. Stoehr[1], S. Schotten[1], M. B. B. Pitton[1], C. Düber[1], F. Schmidt[1], N. L. Hansen[2], B. Baessler[2], R. Kloeckner[1], D. Pinto Dos Santos[2]; *[1]Mainz/DE, [2]Cologne/DE (fabianstoehr@hotmail.de)*

Purpose: Interventional radiology (IR) is a growing field but is underrepresented in most medical school curricula. We tested whether endovascular simulator training improves attitudes towards IR among medical students.
Methods and materials: We conducted this prospective study at two university medical centres, where 4th-year medical students completed a 90-minute IR course. The class consisted of a theoretical part and a practical part, involving endovascular simulators. Using smartphones/tablets, students completed questionnaires before the course, after the theoretical part, and after the practical part. On a 7-point Likert scale, they rated their interest in IR, knowledge

about IR, the attractiveness of IR, and the likelihood to consider IR as a subspecialty. We used a crossover design to prevent position-effect bias.
Results: The seminar/simulator parts led to higher scores for all items compared to baseline: interest in IR (pre-course 5.2 vs post-seminar/post-simulator 5.5/5.7), knowledge of IR (pre-course 2.7 vs post-seminar/post-simulator 5.1/5.4), attractiveness in IR (pre-course 4.6 vs post-seminar/post-simulator 4.8/5.0), and the likelihood of choosing IR as a subspecialty (pre-course 3.3 vs post-seminar/post-simulator 3.8/4.1). Although the seminar and simulator both led to a significant improvement, the effect was significantly stronger for the simulator training compared to the seminar for all items (all $p<0.05$).
Conclusion: Endovascular simulator training in medical school significantly increases students' interest in IR, knowledge about IR, positive attitude toward IR, and the likelihood of potentially choosing IR as a subspecialty. Implementing dedicated IR courses that include practical simulator training might ease recruitment problems in the field.
Limitations: We minimised response bias by using an anonymous, untraceable survey design and ad-hoc completion of each questionnaire during the course.
Ethics committee approval: n/a
Funding: No funding was received for this work.
Author Disclosures:
F. Stoehr: nothing to disclose
S. Schotten: nothing to disclose
M. B. B. Pitton: nothing to disclose
C. Düber: nothing to disclose
F. Schmidt: nothing to disclose
N. L. Hansen: nothing to disclose
B. Baessler: nothing to disclose
R. Kloeckner: nothing to disclose
D. Pinto Dos Santos: nothing to disclose

RPS 1409a-4 11:43
Augmented reality in training: can CT-guided intervention be simulated accurately?
D. Amiras[1], P. Pratt[1], T. Hurkxkens[1], C. Watura[1], B. Pitrola[1], S. Rostampour[2], M. Hammady[1]; [1]*London/UK,* [2]*Luton/UK (bhavnapitrola@gmail.com)*

Purpose: Computed tomography (CT)-guided interventions are taught across the world mostly using a traditional mentored approach on real patients. However, it is well established that simulation is a valuable training tool in medicine. This project assessed the feasibility and acceptance of replicating a CT-guided intervention using a bespoke software application within an augmented reality head-mounted display (ARHMD): the Microsoft HoloLens.
Methods and materials: A bespoke application was written to simulate the process of performing a CT-guided procedure using augmented reality. Virtual patients were generated using CT datasets obtained from the cancer imaging archive. A mesh of a virtual patient was projected into the field of view of the operator and a virtual CT slice simulating the needle position generated on voice command. In order to provide tactile feedback, a mock biopsy phantom was made using agar jelly. ChArUco markers were used to track both the needle and phantom using RGB cameras built into the ARHMD.
The application was trialled by senior international radiologists and radiology registrars-in-training with a structured feedback questionnaire evaluating face validity and technical aspects.
Results: Good feedback was received from participants regarding realism, usability, and the accuracy of the application.
Conclusion: The study showed it is possible to replicate a CT-guided procedure with augmented reality and that this could be used as a training tool.
Limitations: There is no comparison made to traditional CT training techniques, although a further study will address this. A limited CT dataset was used to simulate patient subjects and this could be increased with further study.
Ethics committee approval: The CT datasets from the cancer imaging archive have ethical approval for re-use. No other ethical approval was required.
Funding: No funding was received for this work.
Author Disclosures:
D. Amiras: Speaker at Microsoft
P. Pratt: nothing to disclose
M. Hammady: nothing to disclose
C. Watura: nothing to disclose
T. Hurkxkens: nothing to disclose
S. Rostampour: nothing to disclose
B. Pitrola: nothing to disclose

RPS 1409a-5 11:49
RDIM software for patient peak skin dose assessment: comparison with radiochromic film measurements
M. M. J. Felisi[1], P. E. Colombo[1], S. Riga[1], F. Rottoli[1], F. Barbosa[1], A. Rampoldi[1], C. Dillion[2], S. Massey[2], A. Torresin[1]; [1]*Milan/IT,* [2]*Scottsdale, Arizona/US (marco.felisi@unimi.it)*

Purpose: To evaluate the accuracy of the algorithm for calculating the skin dose distribution in interventional radiology procedures, provided by the radiation dose index monitoring software NEXO[DOSE]® (Bracco Injeneering SA, Lausanne).
Methods and materials: To obtain the skin dose distribution, the software uses exposure parameters taken from the radiation dose structured report (primary/secondary angles, source-to-isocenter distance, kV, Kerma-Area Product (KAP), air-Kerma at interventional reference point, and additional filters), angiographic system information (table attenuation and KAP correction factor), and other factors, such as the backscatter factor and ratio of mass-energy absorption coefficients. The software had been previously validated on a geometrical phantom. GafChromic® XR-RV3 films were positioned under the patient's back to evaluate the software accuracy in clinical conditions. The interventional procedures (18 cases including prostatic artery embolisation, uterine fibroid embolisation, transjugular intrahepatic portosystemic shunt, and transarterial chemoembolisation) were performed with two Philips Integris Allura FD20 and a Siemens Artis Zeego.
Results: The peak skin dose (PSD) values were in a range from 0.2 Gy to 10 Gy. The differences between estimated and measured PSD were lower than 25%, except in one case where a discrepancy of 65% was probably due to an uncorrected geometric evaluation or to the film positioning. The mean deviation is 0.7%±20.6%.
Conclusion: We observed a good correlation ($r=0.980$, $p<0.0001$) between film measurements and software estimates. This study suggests that NEXO[DOSE]® software can be considered as a valuable dose calculation tool to optimise existing practices and monitor the follow-up required for patients who have received high doses, without using radiochromic films which are expensive and time-consuming.
Limitations: The analysis of a limited number of cases due to incorrect film positioning.
Ethics committee approval: n/a
Funding: No funding was received for this work.
Author Disclosures:
M. M. J. Felisi: nothing to disclose
S. Riga: nothing to disclose
P. E. Colombo: nothing to disclose
F. Rottoli: nothing to disclose
F. Barbosa: nothing to disclose
C. Dillion: Employee at bPACSHealth, LLC, Scottsdale, AZ, USA
A. Rampoldi: nothing to disclose
S. Massey: Employee at bPACSHealth, LLC, Scottsdale, AZ, USA
A. Torresin: nothing to disclose

RPS 1409a-6 11:55
Monte Carlo study of 3D stray radiation during interventional procedures
K. S. Alzimami*; Riyadh/SA (kalzimami@ksu.edu.sa)*

Purpose: In interventional medical procedures, other than the highly important issue of optimising image quality and patient exposure in use of the primary beam, there remains a continuing need for the study of staff exposures from the scattered radiation. Herein, an investigation is made of the 3D stray radiation distribution, the simulation being made of a realistic interventional scenario through the use of the Monte Carlo code Geant4 (version 10.3).
Methods and materials: The simulation was conducted based on the HDRK-Man computational phantom and a GE Infinia 3/8" C-arm machine, focusing on the effect of variation of kVp and field of view (FoV) on the scattered particles spatial distribution. Scatter fraction distributions were simulated for x-ray tube outputs (and half-value layers, HVL) of 60 kVp (2.3 mm Al), 80kVp (3.2 mm Al), and 120 kVp (4.3 mm Al), and FoV of 15, 20, 25, and 30 cm. The distributions are obtained for different height levels, corresponding to the lens of the eye, lung and prostate, and all radiosensitive organs.
Results: At fixed FoV, results reveal an inverse relationship between ESAK and kVp. A change in kVp from 60 to 80 has a greater effect than from 80 to 120. For a change in FoV at fixed kVp, the scatter fraction remains constant. For a given value of FoV, ESAK is seen to increases with a decrease in kVp, supporting existing literature.
Conclusion: The typically adopted locations of the various members of staff during interventions, in accordance with their role, is found to be an optimal choice. From such findings, we urge for the implementation of appropriate in-house protocols in seeking to mitigate the potential deleterious effects of radiation to members of staff.
Limitations: n/a
Ethics committee approval: n/a
Funding: No funding was received for this work.
Author Disclosures:
K. S. Alzimami: nothing to disclose

RPS 1409a-7 12:01

The eye lens dose of the interventionalist: measurement in practice

E. J. Meijer[1], D. van Zandvoort[1], J. W. H. Kruimer[2], C. V. Pul[3]; [1]*Eindhoven/NL,* [2]*Woerden/NL,* [3]*Veldhoven/NL (e.meijer@mmc.nl)*

Purpose: Early in 2018, the new eye lens dose limit of 20 mSv per year for occupational exposure to ionising radiation was implemented in the European Union. Dutch guidelines state that monitoring is compulsory above an expected eye lens dose of 15 mSv/year. In this study, we assess whether the eye lens dose of interventionalists in the Máxima Medical Centre, the Netherlands, would exceed 15 mSv/year and whether the measured eye lens dose measurements can be individually related to regular personal dosimeter measurements.
Methods and materials: The eye lens dose, Hp(3), of interventional radiologists (n=2), cardiologists (n=2), and vascular surgeons (n=3) was measured during six months, using thermoluminescence dosimeters (Mirion dosimetry services) on the forehead. Simultaneously, the surface dose, Hp (0.07), and whole-body dose, Hp (10), were measured using regular dosimeters outside the lead skirt at chest level. The dosimeters were simultaneously refreshed every four weeks. The observed dose data was extrapolated to one year to check compliance with the year limit.
Results: A clear relation was observed between the two dosimeters: Hp(3)≈0,25 Hp(0,07). The extrapolated year dose for the eye lens did not exceed 15 mSv for any of the interventionalists (average 3 to 10 studies/month).
Conclusion: The eye lens dose can be monitored indirectly through regular dosimeter at chest level. Additionally, all interventionalists remain below the dose limit and compulsory monitoring limit for the eye lens dose. We cannot generalise our findings to other hospitals because of too many variables involved, such as procedure type, the orientation of the tube, and the position of the interventionalist. Nevertheless, a limited monitoring period can give substantial information on the yearly eye lens dose.
Limitations: Findings are not generalisable to other hospitals due to many variables.
Ethics committee approval: n/a
Funding: No funding was received for this work.
Author Disclosures:
E. J. Meijer: nothing to disclose
D. van Zandvoort: nothing to disclose
J. W. H. Kruimer: nothing to disclose
C. V. Pul: nothing to disclose

RPS 1409a-8 12:07

Endovascular technologies for radiation oncology: how to protect patients from potential bleeding during radiotherapy and proton therapy in cases of vessel tumour invasion

M. Cherkashin, I. Sonkin, N. Vorobyov, N. Martynova, N. Berezina, A. Oleynik, A. Mikhaylov*; St. Petersburg/RU (mikhail.a.cherkashin@gmail.com)*

Purpose: To evaluate individual approaches of different endovascular techniques for bleeding prevention during conventional external beam or proton radiotherapy in patients with a pelvic tumour mass and vessel invasion.
Methods and materials: This is an ongoing case study. In 2018-2019, 3 patients (colorectal cancer, chondrosarcoma, and locoregional ovarian cancer) with vessel tumour invasion were included. 1 patient has an invasion into the internal iliac vein (IIV) and 2 have an invasion into external and common iliac veins (ECIV). Vein involvement was confirmed by CT and MR-angiography and conventional contrast angiography. Venous tumour invasion was characterised by a high bleeding risk during irradiation. Every case was discussed by the tumour board with intervention radiologists. The IIV patient underwent selective vein embolisation by coils and the ECIV patients underwent endovascular stenting by stent graft. Radiation therapy (2 external beam VMAT, 1-proton therapy) was performed.
Results: All patients were irradiated without bleeding complications. 2 patients with stent-grafts during the first follow-up (months 3) had no signs of venous insufficiency i.e. endovascular devices also prevent vein occlusion in postradiation period. For outcome tracking the individual, a program was developed; visits and control MRI at 3, 6, and 12 months and angiography on demand (by the decision of an interventional radiologist). From an oncology perpective, these patients are still under surveillance.
Conclusion: Internal bleeding during radiotherapy is a rare but potentially life-threatening complication. Multidisciplinary discussion with an interventional radiologist allows identification and risk minimisation endovascular technologies. Coil embolisation may be useful for internal iliac vein tumour invasion and angioplasty and stenting by stent-graft for external and common iliac vein involvement.
Limitations: A small number of subjects. Heterogeneous data sampling. The uncommon incidence of these types of clinical cases.
Ethics committee approval: The study was approved by a local ethical board.
Funding: No funding was received for this work.
Author Disclosures:
M. Cherkashin: nothing to disclose
I. Sonkin: nothing to disclose
N. Vorobyov: nothing to disclose
N. Martynova: nothing to disclose
N. Berezina: nothing to disclose
A. Oleynik: nothing to disclose
A. Mikhaylov: nothing to disclose

RPS 1409a-9 12:13

Monte Carlo study of scattered radiation during CBCT studies

Y. Toufique, J. Goracy, I. Delakis, C. E. Kelly, N. Apps, V. Bahun, W. Mubarak, O. Bouhali*; Doha/QA (yassine.toufique@qatar.tamu.edu)*

Purpose: Staff exposure to radiation during an interventional procedure with cone-beam CT (CBCT) can be higher than standard interventional fluoroscopic studies. This dose is due to scattered radiation during the operation. In this work, we study the origin and the impact of scatter using a GATE (GEANT4 application for tomographic emission) simulation toolkit. First, we validate a numerical model of a C-arm x-ray system from Siemens named ARTIS ZEEGO by the estimation of the computed tomography dose index (CTDI) using two polymethylmethacrylate (PMMA) phantoms. In addition, we present the validation of the GATE-modelled x-ray tube named MEGALIX Cat Plus by comparing the simulated energy spectrum with the calculated one by the SpekCalc software.
Methods and materials: Radiation doses (CTDI) were measured using PMMA head and body phantoms with diameters of 16 and 32 cm, respectively, and a height of 15 cm. Both phantoms contain five different positions (at centre and 3h, 6h, 9h, and 12h positions in the phantoms). Radiation measurements were performed at the 5 holes using a 100 mm long pencil chamber.
Results: For various voltage (kVp) levels of the x-ray tube, the results of simulated x-ray spectrums show a good agreement with calculated ones (SpekCalc). A difference in the K-characteristic x-ray intensity was observed. The relative difference between simulated and measured CTDI value for Siemens ARTIS ZEEGO at different kVp were less than 5%. Simulations demonstrated the distribution of scatter in the equipment and highlighted areas of potential high occupational doses.
Conclusion: In this study, we demonstrated the feasibility of modelling a complete CBCT study from the x-ray tube to the absorbed dose and the scattered one.
Limitations: A limitation in Monte Carlo tools and a lack of details about some CBCT components.
Ethics committee approval: n/a
Funding: No funding was received for this work.
Author Disclosures:
Y. Toufique: nothing to disclose
C. E. Kelly: nothing to disclose
N. Apps: nothing to disclose
J. Goracy: nothing to disclose
I. Delakis: nothing to disclose
V. Bahun: nothing to disclose
W. Mubarak: nothing to disclose
O. Bouhali: nothing to disclose

RPS 1409a-10 12:19

Leveraging technology to build an interventional oncology practice

S. H. Shah*; New York, NY/US (shahs1@mskcc.org)*

Purpose: Telemedicine has been utilised in primary care to increase access for patients. As the patient acceptance of this practice has grown, specialists have also begun to utilise telehealth visits. We tested the feasibility of starting an IR TeleHealth practice and studied the impact with a focus on days from IR referral to consult and from IR referral to biopsy.
Methods and materials: Telehealth visits were performed either by a physician or advanced practice provider at a single academic medical centre. The total patient encounters were analysed from 2017-2019. Visit types were categorised by standard documentation criteria. Time saved by the patient and physician not having to travel between locations was studied. Days from IR referral to consult and days from IR referral to biopsy were studied.
Results: In our experience, there were 325 telehealth encounters. Patients saved a total of $10,524 in travel costs and 279 hours of travel time. A total of 521 hours of travel time was saved by physicians and a total of $76,000 was saved by the practice. Days from IR referral to a clinic consult decreased from 2.7 days to 0.33 days and days from IR referral to biopsy decreased from 17.2 days to 12.2 days.
Conclusion: Leveraging telehealth can increase access to care for patients and allow for more efficient use of physician resources. In addition, telehealth could decrease the time from the referral to the initial office consult and could decrease

both the time to the clinic consultation and the IR procedure since many of these patients could potentially be seen on the same day as the referral.
Limitations: The equipment cost and regulations/compliance issues.
Ethics committee approval: n/a
Funding: No funding was received for this work.
Author Disclosures:
S. H. Shah: nothing to disclose

RPS 1409a-11 12:25
Does interventional radiology undergraduate exposure hold the key to workforce shortage? A multicentre/cross-sectional study in the United Kingdom
M. E. E. R. Elsakka[1], Y. Al-Obudi[1], H. M. A. Elgendy[2], M. Zamir[1]; [1]*London/UK,* [2]*Leicester/UK (Mohamed.elsakka@doctors.org.uk)*

Purpose: Interventional radiology (IR) is an evolving sub-speciality, although its representation in the undergraduate curriculum is not. This has prompted the cardiovascular and interventional radiology society of Europe (CIRSE) to introduce an undergraduate curriculum. With a shortage of 500 IR consultants, we aim to assess IR representation in the undergraduate curriculum across the United Kingdom.
Methods and materials: An 18-question questionnaire, influenced by the CIRSE undergraduate curriculum, was circulated across 18 hospitals in the United Kingdom. Recently graduated doctors were targeted to assess their understanding of IR given that they would have theoretically been exposed to the entire undergraduate curriculum and only have limited postgraduate experience.
Results: 280 replies were received. One-third of the cohort demonstrated poor exposure to general radiology, although this figure soared to 76% for IR. Only 13% of the respondents experienced a dedicated IR section in their undergraduate curriculum. Only two students were aware of international/national IR undergraduate curricula. More than 80% of respondents did not consider a career in radiology for various reasons, with 30% citing a lack of exposure. 40% of junior doctors were not aware of radiation exposure in IR. Similarly, less than half of the cohort correctly identified both the training route for IR and the imaging modalities used. Nonetheless, 80% of the respondents thought coronary stenting was being performed by IRs. Finally, the majority of the cohort welcomed radiology attachments and IR lectures as preferred teaching methods, the inclusion of IR undergraduate curriculum, and a two-week postgraduate exposure.
Conclusion: Despite current efforts, radiology, especially IR, is still falling behind in undergraduate curriculum representation. This study confirms that improved IR undergraduate exposure is a key factor in tackling national shortages of IRs.
Limitations: National, not international, study.
Ethics committee approval: n/a
Funding: No funding was received for this work.
Author Disclosures:
M. E. E. R. Elsakka: nothing to disclose
H. M. A. Elgendy: nothing to disclose
Y. Al-Obudi: nothing to disclose
M. Zamir: nothing to disclose

11:15 - 12:30 **Room N**

Artificial Intelligence and Machine Learning

RPS 1405b

Artificial intelligence and CT radiomics

Moderators:
M. Kolossvary; Budapest/HU
T. Penzkofer; Berlin/DE

RPS 1405b-1 11:15
An externally validated prognostic model based on CT radiomics to improve risk-stratification in head and neck cancer patients
S. A. Keek[1], F. Wesseling[2], L. Licitra[3], K. Scheckenbach[4], T. Hoffmann[5], M. Ravanelli[6], R. Leemans[7], T. Poli[8], P. Lambin[2]; [1]*Maastricht, LIMBURG/NL,* [2]*Maastricht/NL,* [3]*Milan/IT,* [4]*Düsseldorf/DE,* [5]*Ulm/DE,* [6]*Brescia/IT,* [7]*Amsterdam/NL,* [8]*Parma/IT (s.keek@maastrichtuniversity.nl)*

Purpose: Patients with locoregionally advanced head and neck squamous cell carcinoma (HNSCC) have high relapse and mortality rates. Imaging-based decision support could help improve prognosis by preventing unnecessary treatment or escalating treatment for suitably stratified patients. We investigate whether a CT radiomics-based prognostic model for TNM-7 stage-III and –IV HNSCC improves risk-stratification compared to the new gold standard of TNM-8.
Methods and materials: 699 retrospective (training) and 138 prospective (validation) stage III-IV (M0) HNSCC patients from 6 European hospitals were collected from the BD2Decide database (ClinicalTrials: NCT02832102). Patients were treated with surgery and/or (chemo-) radiotherapy. TNM-8 guidelines occasionally restaged III-IV into stage I-IV, depending on HPV status. A multivariable Cox regression model was trained to predict overall survival (OS) based on radiomics features derived from the gross tumour volume (GTV) of the primary tumour. ComBat harmonisation was used to improve the interchangeability of features between the different centres. Patient stratification was assessed through Kaplan-Meier (KM) survival curves and a log-rank test for significance (p-value<0.05). The accuracy of the prediction was reported through the concordance-index (CI).
Results: A 4-feature radiomics signature (four-filtered texture) can significantly group the validation cohort into two distinct risk groups ($p < 0.05$), with a CI of 0.69. TNM-8 staging can determine two risk groups ($p < 0.05$), albeit with a higher CI of 0.70. A model built on volume can also stratify the validation cohort ($p<0.05$, CI of 0.719).
Conclusion: A model based on radiomics significantly predicts OS in TNM-7 Stage-III and -IV HNSCC patients, but is not able to outperform TNM-8 staging.
Limitations: The radiomics model does not take HPV status into account and further analysis within subgroups may yield better results.
Ethics committee approval: n/a
Funding: European Union Horizon 2020 research/innovation program (689715).
Author Disclosures:
S. A. Keek: nothing to disclose
L. Licitra: Consultant at AstraZeneca, Consultant at Bayer, Consultant at Bristol-Myers Squibb, Consultant at Boehringer Ingelheim, Consultant at Debiopharm, Consultant at Eisai, Consultant at Merck Serono, Consultant at MSD, Consultant at Novartis, Consultant at Roche, Consultant at Sobi, Research/Grant Support at AstraZeneca, Research/Grant Support at Boehringer Ingelheim, Research/Grant Support at Eisai, Research/Grant Support at Merck Serono, Research/Grant Support at MSD, Research/Grant Support at Novartis, Research/Grant Support at Roche, Other at Bayer, Other at Bristol-Myers Squibb, Other at Debiopharm, Other at Merck Serono, Other at MSD, Other at Sobi
K. Scheckenbach: nothing to disclose
T. Poli: nothing to disclose
P. Lambin: Research/Grant Support at Varian Medical, Research/Grant Support at Oncoradiomics, Research/Grant Support at ptTheragnostic, Research/Grant Support at Health Innovation Ventures, Research/Grant Support at DualTpharma, Other at Oncoradiomics, Other at BHV, Other at Merck, Other at Convert pharmaceuticals, Shareholder at Oncoradiomics SA, Shareholder at Convert pharmaceuticals SA, Patent Holder at Oncoradiomics, Patent Holder at ptTheragnositc/DNAmito
T. Hoffmann: Consultant at MSD, Other at Bristol-Myers Squibb, Other at Merck Serono
R. Leemans: Other at MSD
M. Ravanelli: nothing to disclose
F. Wesseling: nothing to disclose

RPS 1405b-2 11:21
Test-retest reproducibility of radiomics features in the computed tomography of interstitial lung disease: a pilot study
F. Prayer, J. Hofmanninger, S. Röhrich, J. Pan, A. Willenpart, M. Weber, G. Langs, H. Prosch*; Vienna/AT*

Purpose: To investigate the reproducibility of publically available radiomics features in prospective test-retest chest CT data of patients with fibrosing interstitial lung disease (fILD). To provide libraries of robust features with regard to reconstruction protocol.
Methods and materials: 30 fILD patients received repeated CT scans on a single scanner. Image data was reconstructed using sharp/i70f, intermediate/i50f, and soft/i30f kernels, and 1/3 mm slice thickness. Radiomics features (n=86) were extracted from fibrotic and healthy lung tissue, ROIs and ROCs obtained. Test-retest feature intra-class correlation (ICC) using unchanged reconstruction parameters and a fILD radiomics feature performance score (RFPS) (ROC*ICC) were calculated. The impact of altered reconstruction parameters was investigated using ICCs of features between test CT reconstructed using a sharp kernel and thin slices, and test and retest CT reconstructed using different parameters.
Results: Median ICCs (constant parameters) for i70f/1mm, i50f/1mm, i30f/1mm, i70f/3mm, i50f/3mm, and i30f/3mm were 0.927, 0.929, 0.938, 0.929, 0.923, and 0.929, respectively. Median RFPS for i70f/1mm, i50f/1mm, i30f/1mm, i70f3mm, i50f3mm, and i30f/3mm were 0.893, 0.895, 0.912, 0.892, 0.903, and 0.903, respectively. Median ICCs (altered parameters: i70f/1mm vs. rest) for i50f/1mm, i30f/1mm, i70f/3mm, i50f/3mm, and i30f/3mm were 0.829, 0.537, 0.621, 0.425,

and 0.242, and 0.752, 0.483, 0.576, 0.412, and 0.263, for test and retest, respectively.
Conclusion: Altered reconstruction parameters, particularly slice thickness, for retest CT may reduce radiomics feature reproducibility. RFPS and ICCs provided may facilitate robust, reconstruction protocol-specific feature selection in future studies.
Limitations: This pilot study included a limited sample size.
Ethics committee approval: This prospective study was approved by the institutional review board.
Funding: This work was kindly supported by a research grant from Boehringer Ingelheim.
Author Disclosures:
F. Prayer: Research/Grant Support at Boehringer Ingelheim
J. Hofmanninger: Research/Grant Support at Boehringer Ingelheim
S. Röhrich: Research/Grant Support at Boehringer Ingelheim
J. Pan: Research/Grant Support at Boehringer Ingelheim
A. Willenpart: Research/Grant Support at Boehringer Ingelheim
M. Weber: Research/Grant Support at Boehringer Ingelheim
G. Langs: Research/Grant Support at Boehringer Ingelheim
H. Prosch: Research/Grant Support at Boehringer Ingelheim

RPS 1405b-3 11:27
CT high-resolution images-based radiomics analysis for differentiating lung cancer from tuberculosis
C. Tian[1], X. Chunchao[1], X. Li[2], X. Wang[2]; [1]Chengdu/CN, [2]Shanghai/CN
(tianchuan101995@163.com)

Purpose: To establish and validate a CT high-resolution images-based radiomics model for differentiating lung cancer from tuberculosis.
Methods and materials: 243 patients with lung cancer and 243 patients with tuberculosis who underwent CT examinations one month before pneumocentesis biopsy were respectively included in this study. The pneumocentesis biopsy was regarded as the golden standard. ITK-SNAP was used to segment draw the region of interest and generate the 3D volume of the lesion. All data was divided into a training cohort (ncancer=ntuberculosis=170) and validation cohort (ncancer=ntuberculosis=73) by using stratified sampling and 10-fold cross-validation with proportion 7:3. The texture features extracted by artificial intelligent kit (A.K.) were selected by using Spearman and Support vector machine recursive feature elimination feature selection method. The remaining features were included in the model developed by logistic regression analysis and presented with a radiomics nomogram. The receiver operator characteristics (ROC) analysis was performed to validate the radiomics model curves.
Results: There were a total of 696 features extracted. After data redundancy and dimension reduction, 17 features were used to develop the prediction model. A nomogram for distinguishing these two diseases, with an AUC of 0.894 (accuracy, 0.826; precision, 0.81; SE, 85.3%; and SP, 80%) for training set and 0.856 (accuracy, 0.767; precision, 0.767; SE, 76.7%; and SP, 76.7%) for the validation data was successfully plotted.
Conclusion: A CT high-resolution image-based radiomics has the potential for distinctions between lung cancer and tuberculosis, indicating that radiomics could play an important role in before-pneumocentesis biopsy.
Limitations: This is a retrospective, single-centre cohort study.
Ethics committee approval: n/a
Funding: No funding was received for this work.
Author Disclosures:
C. Tian: Speaker at West China Hospital of Sichuan University, Author at West China Hospital of Sichuan University
X. Chunchao: Author at West China Hospital of Sichuan University
X. Li: Author at Translational Medicine Team, GE Healthcare
X. Wang: Author at Translational Medicine Team, GE Healthcare

RPS 1405b-4 11:33
Biological validation with gene expression profiling of a CT-radiomics signature for predicting response to immunotherapy
M. Ligero, A. Garcia-Ruiz, C. Rubio-Perez, P. Nuciforo, J. Seoane, M. Escobar Amores, R. Dienstmann, E. Garralda, R. Perez Lopez; Barcelona/ES (mligero@vhio.net)

Purpose: To biologically validate the CT-radiomics signature predictive of response to immune-checkpoint-inhibitors by correlating the CT-radiomics score with gene expression profiling data from tumour samples and to compare the performance of radiomics only and combined with clinical data to predict response to immune-checkpoint-inhibitors in patients with advanced solid tumours.
Methods and materials: In this retrospective study, a predictive signature was derived from 239 metastases of 85 consecutive patients treated with immune checkpoint inhibitors (monoclonal anti-PD-1/anti-PD-L1 antibodies) monotherapy in phase I clinical trials from August 2012 to May 2018. Validation was performed in 112 lesions from 46 consecutive patients with urinary bladder cancer treated with anti-PD-1/PD-L1 monotherapy (Cohort 2). Radiomics variables were extracted from all lesions per patient in the pre-treatment CT scan and an elastic-net model was implemented. Biological validation was pursued studying the association (Mann-Whitney analyses) of the CT-radiomics score with RNA signatures of cytotoxic cells in an independent cohort of 20 patients. A regression model was applied to combine radiomics and clinical variables.
Results: In Cohort 1 (training), the radiomics signature associates with a response (area under the curve [AUC] 0.74;$P=2.96x10^{-10}$). In Cohort 2 (validation), the radiomics signature predicts a response with AUC=0.70 ($P=1x10^{-3}$). A high radiomics score associates with cytotoxic-enriched immunophenotype (P=0.035). The model combining radiomics and clinical variables slightly improve the capacity for predicting response AUC=0.76 ($P=1.02x10^{-5}$) in the training set and AUC=0.78 ($P=5x10^{-4}$) in the validation set.
Conclusion: CT-radiomics signature at baseline predicts the response to immune checkpoint inhibitors and, likely, reflects tumour immunophenotype. Integrating radiomics and clinical data improve the prediction performance.
Limitations: The biological validation was performed in a relatively small cohort.
Ethics committee approval: Approved by the institutional review board. Informed consent was waived.
Funding: Funded by BBVA, La Caixa-Foundation,Prostate Cancer Foundation.
Author Disclosures:
M. Ligero: nothing to disclose
A. Garcia-Ruiz: nothing to disclose
R. Dienstmann: nothing to disclose
P. Nuciforo: nothing to disclose
C. Rubio-Perez: nothing to disclose
J. Seoane: Research/Grant Support at Northem Biologics, Research/Grant Support at Roche-Glucart, Research/Grant Support at Mosaic Biomedicals, Founder at Mosaic Biomedicals
M. Escobar Amores: nothing to disclose
R. Perez Lopez: nothing to disclose
E. Garralda: nothing to disclose

RPS 1405b-5 11:39
Radiomics of small renal masses on multiphasic CT: accuracy of machine learning-based classification models for the differentiation of RCC and AML without visible fat
R. Yang, J. Wu, L. Sun, S. Lai, Y. Xu, X. Liu, Y. Ma, X. Zhen; Guangzhou/CN
(yangrm0708@gmail.com)

Purpose: To investigate the discriminative capabilities of different machine-learning based classification models on the differentiation of small (< 4 cm) renal angiomyolipoma without visible fat (AMLwvf) and renal cell carcinoma (RCC).
Methods and materials: This study retrospectively collected 163 patients with pathologically proven small renal mass, including 118 RCC and 45 AMLwvf patients. Target region of interest (ROI) delineation, followed by texture feature extraction, were performed on a representative slice with the largest lesion area on each phase of the four-phase CT images. 15 concatenations of the four-phasic features were fed into 224 classification models (built with 8 classifiers and 28 feature selection methods), classification performances of the 3,360 resultant discriminative models were compared, and the top-ranked features were analysed.
Results: Image features extracted from the unenhanced phase (UP) CT image demonstrated dominant classification performances over features from the other three phases. The two discriminative models 'SVM + t_score' and 'SVM + relief' achieved the highest classification AUC of 0.90. The top-10 ranked features from UP included 1 shape feature, 5 first-order statistics features, and 4 texture features, where the shape and first-order statistics features showed superior discriminative capabilities in differentiating RCC versus AMLwvf through the t-SNE visualisation.
Conclusion: Image features extracted from UP is sufficient to generate accurate differentiation between AMLwvf and RCC using a machine-learning-based classification model.
Limitations: The present study included only three RCC subtypes. Texture features were extracted from two-dimensional (2D) ROI on each representative axial section rather than from three-dimensional (3D) ROI. Kinetic pattern was not analysed in the current study.
Ethics committee approval: This case-control retrospective study was institutional review board approved and HIPAA compliant, with a waiver of informed patient consent.
Funding: No funding was received for this work.
Author Disclosures:
R. Yang: nothing to disclose
J. Wu: nothing to disclose
L. Sun: nothing to disclose
S. Lai: nothing to disclose
Y. Xu: nothing to disclose
X. Liu: nothing to disclose
Y. Ma: nothing to disclose
X. Zhen: nothing to disclose

RPS 1405b-6 11:45

Repeatability and reproducibility of radiomics features in spectral CT using an anthropomorphic abdomen phantom

L. Caldeira, J. Holz, S. Lennartz, D. Maintz, N. Grosse Hokamp; *Cologne/DE (liliana.caldeira@uk-koeln.de)*

Purpose: To evaluate repeatability and reproducibility of radiomics features in spectral CT using an anthropomorphic abdomen phantom.
Methods and materials: The phantom was scanned repetitively using different radiation doses ($CTDI_{vol}$ of 10, 15, and 20 mGy) using a spectral detector computed tomography scanner (SDCT). Scanning was repeated three times each. Different spectral results were reconstructed: conventional, virtual non-contrast (VNC), iodine density, iodine no-water, MonoE 50KeV, electron density, and Z-Effective. 34 three-dimensional regions-of-interest (ROIs) were defined analytically and fully-automated. 93 radiomics features were extracted employing the pyradiomics-package. In total, 93x7x3x3 extracted features were analysed. Repeatability and reproducibility were assessed using the concordance correlation coefficient (CCC).
Results: Features with excellent and moderate reproducibility, as indicated by a CCC>0.8 and CCC>0.6, respectively, for the different image reconstructions were identified. Percentage of features with CCC>0.8 varied between 16% (Z-Effective with 10 mGy) and 89% (iodine no-water with 15 mGy). Furthermore, the total number of features with CCC>0.8 and CCC>0.6 increases with dose. In total there were 205 features with excellent repeatability and reproducibility, but only 13 features for all image reconstructions were identified. Among all reconstructions, first-order features show the best reproducibility and repeatability (~50%). CCCs between different radiation doses were further assessed showing good reproducibility (>80% of features).
Conclusion: This study comprises the first systematic evaluation of repeatability and reproducibility using spectral reconstruction images from SDCT. While first-order features show a good repeatability and reproducibility, care has to be taken when using features with medium and poor reproducibility for classification tasks.
Limitations: Only phantom images were assessed; a translation onto patients is desirable. Images did not undergo pre-processing which holds potential to improve repeatability and reproducibility.
Ethics committee approval: n/a
Funding: No funding was received for this work.
Author Disclosures:
L. Caldeira: nothing to disclose
J. Holz: nothing to disclose
N. Grosse Hokamp: Speaker at Philips
S. Lennartz: nothing to disclose
D. Maintz: Speaker at Philips

RPS 1405b-7 11:51

Multicentre validation of a radiomics-based model for the diagnosis of idiopathic pulmonary fibrosis

T. Refaee[1], B. Bondue[2], G. van Simaeys[2], A. Ibrahim[1], G. Wu[1], H. C. Woodruff[1], P. A. Gevenois[2], S. Goldman[2], P. Lambin[1]; [1]*Maastricht/NL,* [2]*Brussels/BE (t.refaee@maastrichtuniversity.nl)*

Purpose: The most common idiopathic interstitial lung disease (ILD) is idiopathic pulmonary fibrosis (IPF), which is determined by the presence of usual interstitial pneumonia (UIP) in high resolution computed tomography (HRCT). If a patient diagnosed with ILD of an unknown cause is suspected of having IPF with a UIP pattern, an invasive biopsy is recommended. We investigated the ability of machine learning models based on radiomic features to identify IPF patients using thin-section CT, aiding in diagnostic and treatment selection towards precision medicine.
Methods and materials: A total of 259 patients from two separate collections were available for this study. 158 patients from the Lung Tissue Research Consortium consisted of two groups: group A (n=80) included patients with IPF/UIP and group B (n=78) included patients with non-IPF ILDs, both confirmed by biopsy. 101 patients collected retrospectively from Erasmus University Hospital consisted of two groups with identical clinical findings as group A and B respectively (n=52 and n=49). Each lung was automatically contoured and divided into four sectors. A random forest classifier model was created and the performance was assessed using the area under the receiver operator characteristics curve (AUC).
Results: Feature selection yielded one clinical (age) and seven radiomic features as inputs for the model. The AUC of the classification model, when applied to the basal sector of the lung, was 0.75 in training and 0.80 in testing. The positive predictive value was 73% and the negative predictive value was 75%.
Conclusion: Quantitative image analysis could potentially decrease the need for biopsies, providing a low-cost, non-invasive, observer-independent, and reproducible classification of fibrotic lung diseases. Future work includes adding further datasets for model validation and feature harmonisation methods.
Limitations: The sample size is low. There is a big variation in image acquisition and CT parameters.
Ethics committee approval: Was not needed (retrospective study).
Funding: grant P14-19 Radiomics STRaTegy.
Author Disclosures:
T. Refaee: nothing to disclose
B. Bondue: nothing to disclose
G. van Simaeys: nothing to disclose
A. Ibrahim: nothing to disclose
H. C. Woodruff: Research/Grant Support at Varian medical , Research/Grant Support at OncoRadiomics, Research/Grant Support at ptTheragnostic, Research/Grant Support at Health Innovation Ventures, Research/Grant Support at DualTpharma, Consultant at OncoRadiomics, Consultant at BHV, Consultant at Merck, Consultant at Convert pharmaceuticals, Shareholder at OncoRadiomics, Shareholder at Convert pharmaceuticals, Patent Holder at OncoRadiomics, Patent Holder at ptTheragnostic/DNAmito, Other at ptTheragnostic/DNAmito, Other at OncoRadiomics, Other at Health Innovation Ventures
P. A. Gevenois: nothing to disclose
P. Lambin: Shareholder at OncoRadiomics
G. Wu: nothing to disclose
S. Goldman: nothing to disclose

RPS 1405b-8 11:57

Prediction of tumour progression and recurrence in patients with hepatocellular carcinoma undergoing transarterial chemoembolisation as a bridge to transplant using CT radiomics features

E. Salinas-Miranda, K. Namdar, F. Khalvati, D. Deniffel, P. Abreu, T. Ivanics, G. Sapisochin, M. A. Haider, P. Veit-Haibach; *Toronto/CA (emmanuels7@gmail.com)*

Purpose: To evaluate the performance of an arterial phase CT radiomics model in predicting tumour progression prior to transplant or post-transplant recurrence in patients with hepatocellular carcinoma (HCC) who underwent pre-transplant transarterial chemoembolisation (TACE)
Methods and materials: In this retrospective study, we analysed the baseline contrast-enhanced CTs of 91 patients with HCC listed for liver transplantation prior to bridging therapy with TACE. Using the PyRadiomics library (v2.2), 1,441 radiomic features were extracted from the largest HCC volume in the arterial phase. After removing features with variance below 0.05, 762 features remained. Principal component analysis (PCA) was applied for feature reduction and the first 22 components were kept in the model. The binary classification task was done using a support vector machine (SVM) classifier. The performance of the model was evaluated by area under the receiver operating characteristic curve (AUC) using 5-fold cross-validation. The primary endpoint of the radiomics classifier was the combined event of tumour progression prior to transplant or post-transplant recurrence.
Results: The combined event occurred in 37% of patients (34/91) with 21.9% of patients (20/91) having tumour progression and1 5% of patients (14/91) having tumour recurrence. The mean time from listing to transplant, listing to progression, and listing to recurrence was 182, 335, and 670 days, respectively. The mean follow-up time was 1,308 days. The mean AUC for the prediction of pre-transplant tumour progression or post-transplant tumour recurrence was 0.81 (95% confidence interval: 0.76-0.85). The best radiomic model at a threshold of 0.387 achieved a sensitivity and specificity (at maximum Youden index) of 85% and 83%, respectively.
Conclusion: An arterial phase-based radiomics model can predict tumour progression and recurrence in HCC-patients listed for transplant who undergo TACE
A machine-learning driven radiomics algorithm may provide a useful tool for risk stratification of HCC patients listed for transplant. Further prospective validation is required.
Limitations: A retrospective study and single institution cohort. Radiomic features were obtained from single arterial-phase.
Ethics committee approval: An IRB approved study.
Funding: No funding was received for this work.
Author Disclosures:
E. Salinas-Miranda: nothing to disclose
K. Namdar: nothing to disclose
F. Khalvati: nothing to disclose
D. Deniffel: nothing to disclose
P. Abreu: nothing to disclose
T. Ivanics: nothing to disclose
G. Sapisochin: nothing to disclose
M. A. Haider: nothing to disclose
P. Veit-Haibach: nothing to disclose

RPS 1405b-9 12:03
CT-radiomics quantification towards a more accurate immunotherapy response assessment
A. Antón Jiménez[1], M. Ligero[1], S. Roche[1], R. Mast Vilaseca[2], N. Roson[1], M. Escobar[1], R. Perez Lopez[1]; [1]Barcelona/ES, [2]Hospitalet de Llobregat/ES (alba.antonj@gmail.com)

Purpose: To develop an immunotherapy response model based on the change of radiomic features from baseline to follow-up for a more accurate response assessment.
Methods and materials: This retrospective study included 67 consecutive patients with metastatic solid tumours treated in phase I clinical trials with immune checkpoint inhibitors (anti-PD1/PD-L1). Baseline contrast-enhanced CT and follow-up CT after 8 weeks of treatment were evaluated. One target lesion per patient was delineated and radiomics features were extracted using pyradiomics. An analysis of variance (ANOVA) was implemented as a feature selector. Featured differences between baseline and follow-up that showed significant differences for clinical benefit were selected and a logistic regression model was generated. Log-rank analysis of Kaplan-Meier data was conducted to determine associations between the radiomics score and overall survival.
Results: From 105 radiomic features from first-order, shape, and texture matrices, four features differed between baseline and follow-up (total energy, small area low grey-level emphasis, coarseness, and surface) associated with a response in the validation set ($p<0.05$). Prediction capacity of the radiomics model showed an AUC of 0.79 (95% CI 0.69-0.90; $p<0.05$). Patients with a higher radiomics score showed longer survival ($p<0.05$).
Conclusion: The change in radiomics features from baseline to follow-up after treatment classifies responder and non-responder patients and associates with overall survival.
Limitations: A retrospective study with a limited number of patients.
Ethics committee approval: Approved by the ethics committee.
Funding: No funding was received for this work.
Author Disclosures:
A. Antón Jiménez: nothing to disclose
M. Ligero: nothing to disclose
S. Roche: nothing to disclose
R. Mast Vilaseca: nothing to disclose
N. Roson: nothing to disclose
M. Escobar: nothing to disclose
R. Perez Lopez: nothing to disclose

RPS 1405b-10 12:09
A preliminary study of radiomic classifiers for identifying small cell lung cancer from non-small cell lung cancer
C. Y. Zhang, S. H. Liu, H. L. Yu, S. L. Liu, Z. X. Zhang; Qingdao/CN (shihe528@126.com)

Purpose: To establish a radiomics model and a nomogram for identifying small cell lung cancer from non-small cell lung cancer based on enhanced CT images.
Methods and materials: From January 2014 to June 2018, 202 cases of small cell lung cancer and 266 cases of non-small cell lung cancer were enrolled into our primary cohorts. All patients underwent enhanced CT scan and all lesions were pathologically confirmed. Our primary cohorts were randomly divided into a training group (n=327) and a verification group (n=141) according to 7:3. 396 radiomics features were automatically extracted by AK software. Data reduction and feature selection were performed using the LASSO regression model. Logistic regression analysis was used to establish a multivariate predictive model for identifying small cell lung cancer and non-small cell lung cancer. In addition, a nomogram model combining the radiomics features and clinical information was established in order to raise the diagnostic efficiency.
Results: The established radiomics label contained 14 omics features. The diagnostic efficiency of the radiomics label performed well in differentiating small cell lung cancer and non-small cell lung cancer. The area under the ROC curve (AUC) was 0.86 (training group, 95%CI:0.834～0.889) and 0.82 (verification group, 95%CI:0.802～0.851), respectively. Compared with the clinical parameter prediction model (AUC=0.86, 95%CI:0.836～0.890) and the image histology label (AUC=0.82, 95%CI:0.802～0.851) in the validation group, the AUC of the nomogram was 0.94 (95%CI:0.895～0.991) in the validation group and the accuracy was 86.2%.
Conclusion: The radiomics label and the nomogram have good diagnostic efficiency for identifying small cell lung cancer from non-small cell lung cancer.
Limitations: This study is a single-centre, retrospective study.
Ethics committee approval: n/a
Funding: No funding was received for this work.
Author Disclosures:
C. Y. Zhang: Author at The affiliated hospital of Qingdao University
S. H. Liu: Author at The affiliated hospital of Qingdao University
H. L. Yu: Author at The affiliated hospital of Qingdao University
S. L. Liu: Author at The affiliated hospital of Qingdao University
Z. X. Zhang: Author at The affiliated hospital of Qingdao University

RPS 1405b-12 12:15
A comparison between routine and targeted CT-based radiomics classification models for predicting malignant pulmonary nodules
G. Tao[1], Y. Chen[1], J. Ye[1], H. Yu[1], X. Ye[1], X. Li[2], Z. Zhou[2]; [1]Shanghai/CN, [2]Beijing/CN (121058820@qq.com)

Purpose: To compare the results of conventional and targeted CT-based radiomic classification models distinguishing benign and malignant pulmonary nodules.
Methods and materials: The two datasets were comprised of routine and targeted lung CT images of 349 patients with pathological results respectively. We built classification models to predict the malignancy of pulmonary nodules based on a radiomics method. To achieve the best result on both datasets, we used diverse feature selection methods and machine learning algorithms.
Results: The AUC, accuracy, sensitivity, and specificity of the radiomic model based on routine lung CT images were 0.77, 60.16%, 58.15%, and 78.79%, respectively. By contrast, the AUC, accuracy, sensitivity, and specificity of the radiomic model based on targeted lung CT images were 0.84, 75.72%, 76.36%, and 69.70%, respectively. The result showed that targeted CT images have an edge over routine CT images on predicting malignancy of pulmonary nodules.
Conclusion: Because of the use of target scanning, we obtain more sufficient and more accurate image data, and the large matrix, small FOV, and thin layer thickness reduce the voxel, making the quantitative analysis results more accurate. We have demonstrated that a radiomic classification model based on targeted CT images has better performance compared to a model based on routine CT images. Therefore, target CT combined with radiomic classification models can provide a more accurate diagnosis of pulmonary nodules, thus helping select proper treatment or follow-up strategies.
Limitations: This work has not been verified by a multicentre trial, which is considered to be our future work.
Ethics committee approval: This retrospective study was approved by the institutional review board of Shanghai Chest Hospital (KS1956).
Funding: Interdisciplinary Program of Shanghai Jiaotong University (YG2017QN661), Shanghai Municipal Health Commission Project (20184Y0219)(2019SY063), Science and Technology Commission Shanghai Municipal Project (18511102902)(19411965200), Shanghai Key Laboratory Open Project (STCSM18DZ2270700).
Author Disclosures:
G. Tao: nothing to disclose
J. Ye: nothing to disclose
Y. Chen: nothing to disclose
X. Li: nothing to disclose
X. Ye: nothing to disclose
H. Yu: nothing to disclose
Z. Zhou: nothing to disclose

11:15 - 12:30 **Room O**

Breast

RPS 1402b

Hand-held, contrast-enhanced, and automated whole-breast ultrasound

Moderators:
G. Adelsmayr; Graz/AT
A. Vourtsis; Athens/GR

RPS 1402b-1 11:15
The clinical efficacy of second-look ultrasound (SLUS) following breast MRI in breast cancer imaging: does SLUS change management?
A. J. Jameel, A. S. Mehdi, K. Edmonds, D. Khafaf, T. Seaton, D. Cunningham; London/UK (aia.s.mehdi@gmail.com)

Purpose: To evaluate our institutional experience of second-look ultrasound (SLUS) for targeted breast lesions identified on breast MRI. To determine our SLUS lesion detection rate (LDR), positive predictive value (PPV), and the effect on patient management (PM).
Methods and materials: A retrospective review of SLUS at our institution between January 2016-2017 identified 316 patients who underwent breast ultrasound following breast MR. All non-SLUS cases were excluded and 66 patients with 73 target lesions were included. The index lesion (inital ultrasound identified/ MR indication), the target lesion (MR identified/ SLUS indication), and the SLUS were analysed with regard to imaging characteristics (location, size, morphology, enhancement), histopathology, and MDT outcomes to assess the efficacy of SLUS and its LDR, PPV, and PM.

Results: 57 of 73 target lesions were identified on SLUS: LDR 78.1%.
The MR imaging characteristics of the 73 target lesions were: 74.0% <10mm, 26.0% > 10mm, 84.2% mass-like enhancement, 14.0% non-mass enhancement, 1.8% no enhancement.
Of the 57 target lesions detected on SLUS: 42.1% were biopsy-proven malignant (n=24) - PPV of 63.4%. 29.8% were biopsy-proven benign (n=17) - NPV 93.6%. 28.1% were not biopsied due to stable benign radiological features or patient refusal (n=16).
SLUS confirmed suspected findings in 71.9% (n=41) and changed management in 36.8% (n=21), causing upstaging to WLE or mastectomy.
Conclusion: Our study demonstrates the utility of SLUS breast imaging with 78.1% LDR, PPV 63.4%, and NPV 93.6%. SLUS changed patient management in 71.9% upstaging to WLE or mastectomy. SLUS is a pivotal imaging tool in the radiological assessment of breast lesions.
Limitations: 1 year data, limited sample size.
Ethics committee approval: n/a
Funding: No funding was received for this work.
Author Disclosures:
A. J. Jameel: nothing to disclose
A. S. Mehdi: nothing to disclose
D. Khafaf: nothing to disclose
T. Seaton: nothing to disclose
D. Cunningham: nothing to disclose
K. Edmonds: nothing to disclose

RPS 1402b-2 11:21
Evaluation of additional MR-detected breast mass using quantitative analysis of contrast-enhanced ultrasound and its comparability to MR findings
S. Y. Lee, O. Woo, H. S. Shin, S. E. Song, K. R. Cho, B. K. Seo, S. Y. Hwang; *Seoul/KR (adimsum@gmail.com)*

Purpose: To evaluate the diagnostic performance of contrast-enhanced ultrasound (CEUS) in evaluating breast mass and to determine whether kinetic pattern results comparable to dynamic contrast-enhanced MRI (DCE-MRI) can be obtained using quantitative analysis of CEUS.
Methods and materials: In this single-centre prospective study conducted from January 2016 to December 2018, a total of 71 breast cancer participants who had additional MR-detected mass with 2nd look US correlation were included. For these masses, a single radiologist performed the CEUS exam. Two radiologists then reviewed all the images for quantitative and qualitative analysis and were subsequently categorised according to BIRADS by consensus. The diagnostic performance of CEUS was analysed by comparing the BIRADS category to the final pathology results. The degree of agreement between kinetic patterns shown by CEUS and DCE-MRI was evaluated using weighted kappa analysis.
Results: Of the 71 US-correlated additional MRI-detected masses, 53 (75%) were malignant and 18 (25%) were benign. The diagnostic performance of CEUS for these masses was excellent with 84.9% sensitivity, 94.4% specificity, and 97.8% positive predictive value. Among the 53 malignant masses, there were 37 (71%) IDC, 8 (15%) DCIS, and 7 (13%) ILC. A total of 57/71 (80%) masses had correlating kinetic patterns and showed good agreement (weighted kappa = 0.66) between CEUS and DCE-MRI evaluations. Benign masses showed excellent agreement (0.84) while agreement in malignant masses was fair (0.38). Among different malignant types, IDC showed good agreement (0.62) while DCIS and ILC showed no agreement (0.14 and 0.10).
Conclusion: Diagnostic performance of CEUS for additional MR-detected breast mass was excellent. Accurate kinetic pattern evaluation that is fairly comparable to DCE-MRI can be obtained for benign and IDC masses by using CEUS.
Limitations: n/a
Ethics committee approval: n/a
Funding: No funding was received for this work.
Author Disclosures:
S. Y. Lee: nothing to disclose
O. Woo: nothing to disclose
H. S. Shin: nothing to disclose
S. E. Song: nothing to disclose
K. R. Cho: nothing to disclose
B. K. Seo: nothing to disclose
S. Y. Hwang: nothing to disclose

RPS 1402b-3 11:27
Clinical utility of second-look ultrasound with prone MRI virtual navigation in breast lesions detected on MRI alone: a preliminary study
R. Qi, L. Bao; *Hangzhou/CN (qirx1816@126.com)*

Purpose: To evaluate the clinical utility of second-look ultrasound (US) with MRI virtual navigation in the prone position for MRI-detected incidental breast lesions.
Methods and materials: Between June 2016 and February 2019, 24 consecutive patients with 26 additional BI-RADS category 4 or 5 lesions that were detected on MRI but occult on second-look US were enrolled in the study. All suspicious lesions were located with US/MRI fusion virtual navigation in the prone position and then underwent US-guided biopsy or surgical excision. The detection rate was calculated compared with pre/postoperation MRI and pathological results. The MRI features and pathological types of these lesions were analysed.
Results: A total of 24 lesions were successfully located with virtual navigation and performed with US-guided biopsy or localisation, and the detection rate of virtual navigation was 92.3% (24/26). 21 (87.5%, 21/24) proved to be benign lesions and 3 (12.5%, 3/24) malignant lesions at pathology. The remaining 2 lesions exhibited no abnormal findings on second-look US with virtual navigation and could be judged to be benign as there was no change during MRI follow-up after 6 months. Of the 26 MRI-detected lesions, 24 (92.3%, 24/26) were non-mass enhancements and 2 (7.6%, 2/26) were masses.
Conclusion: The lesions detected on MRI but not visible on US tend to be benign. Second-look US with virtual navigation in the prone position can be an effective method for the evaluation of such lesions and can significantly increase the rate of US-guided interventional procedures which are preferable for MRI-guided ones.
Limitations: Accurate alignment is difficult between different imaging modalities.
Ethics committee approval: The study was approved by our hospital's institutional review board.
Funding: Medical Health Science and Technology Project of Zhejiang Provincial Health Commission (2019PY061).
Author Disclosures:
R. Qi: nothing to disclose
L. Bao: nothing to disclose

RPS 1402b-4 11:33
Ultrasound evaluation of breast ductal carcinoma in situ
S. Paolicelli[1], N. Troiano[2], M. Carbone[1], M. Telegrafo[1], M. Moschetta[1]; *[1]Bari/IT, [2]Modugno/IT (simonapaolicelli@gmail.com)*

Purpose: To evaluate the role of ultrasound (US) for detecting and characterising breast ductal carcinoma in situ (DCIS) of the breast.
Methods and materials: US features of 178 preoperative lesions in 170 patients affected by DCIS were retrospectively evaluated by using the BIRADS ultrasound lexicon considering the lesion pattern (mass type, non-mass type, or occult), the presence of microcalcifications, architectural, and ductal distortions. For "mass-like" lesions, shape, margins, and echogenicity were considered. The ultrasound recognition rate of lesions and the distribution of ultrasound patterns was calculated, evaluating any statistically significant differences among the different lesion patterns.
Results: 63/178 lesions (35%) were detected by ultrasound; 52 (83%) were "mass-like" type and 11 (17%) "non-mass-like" type (6 architectural distortions, 5 ductal distortions) ($p < 0.05$). In 10 patients (6%), breast lesions were identified only by US. The most common US appearance of DCIS finding in mass-type lesions was an irregular shape (79%), indistinct margins (87%), and hypoechogenicity (94%) ($p < 0.05$). Microcalcifications associated with mass-type lesions were found in 23 cases (37%).
Conclusion: US can allow a diagnosis of DCIS of the breast in case of mass-type lesions. The most common US finding is represented by mass-type, hypoechogenic lesion, and indistinct margins. Microcalcifications and architectural distortions are the most frequent US findings in non-mass lesions.
Limitations: A limited number of patients.
Ethics committee approval: Yes.
Funding: No funding was received for this work.
Author Disclosures:
S. Paolicelli: nothing to disclose
N. Troiano: nothing to disclose
M. Carbone: nothing to disclose
M. Telegrafo: nothing to disclose
M. Moschetta: nothing to disclose

RPS 1402b-5 11:39

Assessment of NACT response in locally advanced breast cancer patients: a prospective comparison of grey scale ultrasound and contrast-enhanced ultrasound

A. Sharma, S. B. Grover, A. Katyan, .. Chintamani, D. C. Ahluwalia*; New Delhi/IN (anante266@gmail.com)*

Purpose: To compare the role of grey scale ultrasound and contrast-enhanced ultrasound (CEUS) in evaluating the response to neoadjuvant chemotherapy (NACT) in patients with locally advanced breast cancer (LABC).
Methods and materials: This prospective IRB approved study comprised of 40 patients of LABC receiving NACT. Both studies were performed in 4 stages: before each of the 3 cycles of LABC and immediately prior to surgery. Grey scale ultrasound was done to evaluate tumour size. This was followed by contrast-enhanced ultrasound using a 4.8 ml bolus intravenous injection of second-generation ultrasound contrast agent. The CEUS quantitative parameters recorded were time to peak (TTP), mean transit time (MTT), and area under curve (AUC). Pathological tumour response (pTR) was evaluated after modified radical mastectomy, using the Miller Payne grading system. Statistical analysis was done for sensitivity, specificity, PPV, and NPV of each technique.
Results: In the series of patients evaluated, 28 patients showed good pTR and 12 patients showed poor pTR. Grey scale ultrasound changes for size of tumour demonstrated sensitivity of 71.5%, specificity of 79.3%, PPV of 78.5%, and NPV of 73.8%, whereas quantitative CEUS parameters showed a sensitivity of 87.6%, specificity of 88.3%, PPV of 91.1%, and NPV of 82.4% in patients with good pTR. An increase in time to peak (TTP) after each cycle of NACT was the most accurate quantitative parameter.
Conclusion: CEUS study using quantitative parameters was more sensitive and specific as compared to grey scale ultrasound changes of size measurements. CEUS quantitative parameters can be very useful for modifying individualised patient based NACT regimens.
Limitations: Single-centre study.
Ethics committee approval: Informed consent was taken from all patients. Animal Board approval n/a.
Funding: No funding was received for this work.
Author Disclosures:
A. Sharma: Author at VMMC and Safdarjung Hospital, New Delhi
S. B. Grover: Author at VMMC and Safdarjung Hospital, New Delhi
.. Chintamani: nothing to disclose
D. C. Ahluwalia: nothing to disclose
A. Katyan: n/a

RPS 1402b-6 11:45

False-negative axillary ultrasound in patients with newly diagnosed invasive breast cancer: is there a correlation with preoperative findings?

C. Manzone, M. Durando, L. Bergamasco, E. Regini, G. Bartoli, G. Mariscotti, P. Fonio*; Turin/IT (chiaramanzone@hotmail.it)*

Purpose: To investigate false-negative results of preoperative axillary ultrasound (AUS) in patients with breast cancer and to identify features related to false-negatives.
Methods and materials: 124 consecutive patients with newly diagnosed invasive breast cancer who underwent preoperative AUS between January-June 2018 were retrospectively included. All patients underwent sentinel lymph node biopsy or axillary lymph node dissection and pathology outcomes were considered as a gold standard. True and false-negative AUS groups were statistically compared in terms of age, BMI, tumour size, subtype, grade, estrogen receptor (ER), progesterone receptor (PR), HER2 status, proliferation index, lymphovascular invasion (LVI), and growth pattern (unifocal or multifocal).
Results: Out of the 106 patients with normal AUS, 27 (25%) were found to be node-positive on pathologic assessment. On univariate analysis, LVI was found to be significantly different between true and false-negative groups [24%(19/79) versus 89%(24/27), p<0.0001]. Breast tumour size was smaller in the true-negative group with an average size of 14.0±9.0mm (versus 19.6±8.6mm, p=0.01). The presence of a higher grade and a multifocal growth pattern were more likely in the false-negative group [40%(32/79) versus 15%(4/27), p=0.03 and 90%(71/79) versus 67%(18/27), p=0.015]. There was no significant difference in age, BMI, subtype, ER, PR, and HER2 status and proliferation index. On multivariate analysis, only the presence of LVI achieved statistical significance [p<0.0001, OR 21.81(CI 95% 5.61–84.83)].
Conclusion: Our results suggest that patients with false-negative AUS are more likely to have larger (>20mm) multifocal and higher grade (G2-G3) invasive cancers. In this setting, preoperative AUS results should be interpreted cautiously.
Limitations: Small sample size. Retrospective, single-centre study. Low number of lobular subtype (18%).
Ethics committee approval: n/a
Funding: No funding was received for this work.
Author Disclosures:
C. Manzone: nothing to disclose
M. Durando: nothing to disclose
L. Bergamasco: nothing to disclose
E. Regini: nothing to disclose
G. Bartoli: nothing to disclose
G. Mariscotti: nothing to disclose
P. Fonio: nothing to disclose

RPS 1402b-7 11:51

Comparison between execution and reading time of 3D automatic breast ultrasound (ABUS) versus hand-held ultrasound (HHUS): results from the TOMUS study

N. Brunetti, S. de Giorgis, J. P. Zawaideh, F. Rossi, S. Tosto, A. Tagliafico, M. Calabrese*; Genoa/IT (nicole.brunetti.1992@gmail.com)*

Purpose: Breast density is an independent risk factor for breast cancer. Mammography is supplemented with hand-held ultrasound (HHUS) to increase sensitivity. Automatic breast ultrasound (ABUS) is an alternative to HHUS. Our study wanted to assess the difference in execution and reading time between ABUS and HHUS.
Methods and materials: N=221 women were evaluated consecutively between January 2019 and June 2019 (average age 53 years; range 24-89) within a multicentric comparative prospective trial between tomosynthesis and HHUS. The execution and reading time of ABUS and HHUS was calculated with an available stop watch. Time started for both procedures when the patient was ready on the examination table to be examined to the end of image acquisition and interpretation.
Results: No patients interrupted the exam due to pain or discomfort. N=221 women underwent ABUS and HHUS, n=11 patients refused to undergo both procedures due to time constraints and refused ABUS, therefore 210 patients were enrolled with both ABUS and HHUS available. The average time to perform and read the exam was 5 minutes for HHUS (DS ±1.5) with a maximum time of 11 minutes and a minimum of 2 minutes. The average time with ABUS was 17 minutes (DS ±3.8, with a maximum time of 31 minutes and a minimum time of 9 minutes). The ABUS technique took longer to be performed in all patients, with an average difference of 11 minutes (range 3-23 minutes) per patient, p<0,001.
Conclusion: A significant difference was observed in the execution and reading time of the two exams, where the US method was more rapid and tolerated.
Limitations: A potential sources of bias.
Ethics committee approval: The study received IRB approval and informed consent was obtained from all participating patients.
Funding: No funding was received for this work.
Author Disclosures:
N. Brunetti: nothing to disclose
S. de Giorgis: nothing to disclose
J. P. Zawaideh: nothing to disclose
S. Tosto: nothing to disclose
F. Rossi: nothing to disclose
A. Tagliafico: nothing to disclose
M. Calabrese: nothing to disclose

RPS 1402b-8 11:57

Could conventional US and contrast-enhanced US be helpful for breast cancer prediction based on MR imaging BI-RADS category 4 lesions?

J.-M. Xu*; Shanghai/CN (junmei_510@126.com)*

Purpose: To prospectively estimate the predicting value of US and CEUS for breast cancer in MR imaging BI-RADS 4 lesions and to determine whether the integration of US and CEUS into MR imaging BI-RADS 4 lesions improves the diagnostic performance.
Methods and materials: A total of 163 breast MR imaging BI-RADS 4 lesions in 163 women who underwent US and CEUS simultaneously before ultrasound-guided core biopsy or surgery were included. A multivariate logistic regression analysis was performed to assess 26 independent variables for prediction of malignancy. ROC curve analysis was used to evaluate the diagnostic performance.
Results: Of the 163 MR imaging BI-RADS 4 lesions, 49 (30.1%) were benign and 114 (69.9%) were malignant. Enhancement area enlargement (OR: 64.28) was the strongest independent predictor for breast malignancy, followed by hyperechoic halo sign (OR: 33.75), fast-in and/or fast-out patterns (OR: 27.76), and spiculation (OR: 20.38)(all P<0.05). The areas (Az) under the ROC curve for enhancement area enlargement and fast-in and/or fast-out patterns were greater than those for the significant independent variables of hyperechoic halo sign and spiculation. The Az, sensitivity, and specificity were 0.70-0.85, 53.5%-76.4%, and 85.7%-95.7% on US, respectively, and 0.86-0.89, 90.4%-95.6%, and 75.5%-87.8% on CEUS, respectively.
Conclusion: Conventional US and CEUS are both promising for breast cancer prediction in MR imaging BI-RADS 4 lesions, with higher sensitivity on CEUS and higher specificity on US. They can be used as a meaningful supplement to MR imaging in the diagnosis of BI-RADS 4 breast lesions and thus has the potential to avoid unnecessary biopsy.

Limitations: Our study only enrolled patients with MR imaging BI-RADS 4 lesions, so selection bias may be present.
Ethics committee approval:
This study was institutional review board-approved and informed consent was obtained from all patients.
Funding: No funding was received for this work.
Author Disclosures:
J.-M. Xu: nothing to disclose

RPS 1402b-9 12:03

The role of automated breast ultrasound (ABUS) in correlation to contrast-enhanced spectral mammogram (CESM) in the staging of breast cancer

M. H. Helal, S. A. Mansour, R. Hussien*; Cairo/EG (r_hkhaled@hotmail.com)*

Purpose: To evaluate the role of ABUS in correlation to CESM in the loco-regional staging of breast cancer.
Methods and materials: The study is a prospective analysis that included 75 female patients with proved breast cancers. Evaluation was in regard to the size, multiplicity, and the stromal invasion around the tumour. Cases were subjected to automated breast ultrasound and contrast-based mammography, which was performed using low and high exposures following i.v. injection of a contrast agent.
Results: Eligible cases were 62 in number. CESM and ABUS showed high accuracy of assessment of the tumour multiplicity (82.2%). ABUS showed a higher accuracy of the stromal involvement (93.5%) than CESM (66.1%). There was no significant difference in the size between the pathology and the CESM. The latter showed a percentage of agreement of 38.7%. Yet, there was a statistical significance ($p < 0.001$) between the ABUS and the pathology in the detection of the size of the tumour.
Conclusion: ABUS is a non-invasive modality that can be used for the staging of breast cancer. It provided accurate assessment of the stromal involvement and multiplicity of the cancer. CESM outperformed ABUS in the measurement of the size of the index cancer.
Limitations: Not all cases performed mastectomy, which may affect the study outcome.
Ethics committee approval: The study had an Ethics committe approval and patients gave informed written consent.
Funding: No funding was received for this work.
Author Disclosures:
S. A. Mansour: nothing to disclose
M. H. Helal: nothing to disclose
R. Hussien: nothing to disclose

RPS 1402b-10 12:09

Influence of breast density on patient's compliance during conventional hand-held breast ultrasound (US) or automated breast ultrasound (ABUS)

S. de Giorgis, N. Brunetti, J. P. Zawaideh, F. Rossi, A. Garlaschi, M. Calabrese, A. Tagliafico*; Genoa/IT (degiorgis.sara@libero.it)*

Purpose: To study the influence of breast density on patient's compliance during conventional hand-held breast ultrasound (US) or automated breast ultrasound (ABUS).
Methods and materials: Between January 2019 and June 2019, n=221 female patients (mean age: 53; age range: 24-89) included in a multicentric prospective comparative trial comparing digital breast tomosynthesis and US underwent both US and ABUS. All participants had independently interpreted US and ABUS regarding patient's compliance. The diagnostic experience with US or ABUS was described with a modified testing morbidities index (TMI), a validated instrument for assessing the short-term quality of life related to diagnostic testing. The scale ranged from 0 (the worst possible experience) to 5 (an acceptable experience). Pain or discomfort before and during testing, fear or anxiety before and during testing, and embarrassment during testing were recorded. Standard statistics were used to compare data of US and data of ABUS.
Results: None of the patients interrupted the ABUS exam. The mean TMI score was 4.6 (SD ± 0.5) for US and 4.3 (SD ± 0.8) for ABUS. The overall difference between the patient's experience on US and ABUS was statistically significant with $p<0.0001$. The difference between the patient's experience in women with BI-RADS 4 for breast density was statistically significant with $p<0.02$ in favour of US (4.7 ± 0.4) vs 4.5 (SD ± 0.6) for ABUS. Patients' experience with breast density 1 was better for US (4.7 ± 0.4) vs 4.3 (SD ± 0.6) for ABUS, $p<0.01$. Pain or discomfort during testing was higher in patients >40 years.
Conclusion: Compliance of ABUS was lower than US, especially in women <40 years. Breast density did not influence the ABUS experience.
Limitations: A potential sources of bias.
Ethics committee approval: The study received IRB approval.
Funding: No funding was received for this work.
Author Disclosures:
S. de Giorgis: nothing to disclose
N. Brunetti: nothing to disclose
J. P. Zawaideh: nothing to disclose
F. Rossi: nothing to disclose
A. Garlaschi: nothing to disclose
M. Calabrese: nothing to disclose
A. Tagliafico: nothing to disclose

RPS 1402b-11 12:15

A non-invasive differential diagnosis of breast cancer by the new concept of full breast ultrasonography: improvements of the initial assessment of the disease's extension

A. C. Georgescu, S. Bondari, E. Andrei, A. Manda*; Craiova/RO (acgeorges.radiology@gmail.com)*

Purpose: The non-invasive radiological-imaging differential diagnosis of breast cancer (BC) is still unsatisfactory due to the less specific descriptors and the non-anatomical scanning and interpreting. We aimed to improve sonomorphology for a better differential diagnosis and a better assessment of the initial extension of breast diseases through the new integrative concept of full breast ultrasonography (FBU), represented by the radial ductal scanning, colour Doppler, and strain sonoelastography.
Methods and materials: We conducted a retrospective study of 1,223 consecutive FBU in 944 patients, referred for screening, diagnostic, or follow-up in two imaging centres with different equipments, and we compared the initial US BI-RADS assessment with the pathological reports or the follow-up exams for the benign findings. Statistical analysis included the evaluation of the sensibility and specificity of the technique and other correlations of the findings.
Results: The US BI-RADS assessment was in accordance with the pathological reports in 99.2% cases. We found no significant correlation between BC-Density-Age, but significant association of BC + Benign pathology. The benign findings were multiple, combined, and with unpredictable evolution (regression or progression to the atypia or DCIS). The suspect infra-centimetric findings had short-interval follow-up (2-3 months). BC represented unifocal lesion in 60% of cases, multifocal and lobar type in 38% of cases, and multicentric lesions in 2% of cases. The most important descriptor for BC was the incident angle of the plunging artery and, when associated with a score 4 or 5 Ueno, the accuracy was close to 100%.
Conclusion: FBU offered a new hierarchy of the US descriptors, useful differential diagnosis of breast tumours, and anatomical redefinition of the multifocality and multicentricity of BC, with better initial evaluation of the disease's extension.
Limitations: Initial study.
Ethics committee approval: n/a
Funding: No funding was received for this work.
Author Disclosures:
A. C. Georgescu: Speaker at Prima Medical MedLife Romania, Author at Pan Med Laboratories
S. Bondari: Author at Prima Medical MedLife Romania
E. Andrei: Author at Prima Medical MedLife Romania
A. Manda: Author at Prima Medical MedLife Romania

RPS 1402b-12 12:21

Is US-texture analysis a useful instrument to discriminate fibroadenomas from complex fibroadenomas and benign phyllodes tumours?

I. Başara Akin, H. A. Özgül, M. K. Şimşek, C. Altay, M. Seçil, P. Balci*; Izmir/TR (haozgul@hotmail.com)*

Purpose: Although BIRADS 4A refers lesions with low malignancy suspicion, benign pathologic diagnoses such as fibroadenomas, complex fibroadenomas (CF), and benign phyllodes tumours (BPT) are commonly expected in this category lesions. Fibroadenomas are the most frequent benign tumours of the breast. CFs are subgroups of fibroadenomas with additional histopathologic features. The risk of developing breast carcinoma was found to be higher in patients with CF than in those with fibroadenomas. BPTs have a potential of malignant transformation. There is substantial overlap in sonographic features between phyllodes tumours and fibroadenomas. In this study, we aimed to use US texture analysis (USTA) to discriminate fibroadenomas from CFs and BPTs.
Methods and materials: We analysed the texture of 95 patients with histologically proven 32 fibroadenomas, 32 BPTs, and 31 CFs. Texture analysis was performed using LIFEx software on the largest slice of each lesion in B-mode US. First order texture histogram parameters (skewness, kurtosis, entropy) were evaluated. A comparison was made with an unpaired t-test.
Results: There were statistical significances in all lesions in terms of skewness ($p=0.00$) and kurtosis ($p=0.003$). In the evaluation of sub-groups with each other, there was statistical significance between fibroadenomas and both CFs and BPTs in terms of both skewness ($p=0.001$) and kurtosis ($p=0.009$). However, there was no statistical significance between CFs and BPTs according to all parameters.

Conclusion: In benign BIRADS 4A lesions, USTA is a potential biomarker to discriminate fibroadenomas from CFs and BPTs, which have a higher possibility of malignant transformations than fibroadenoma. USTA could have a contribution to US examination in the distinction of fibroadenoma.
Limitations: The number of patients was limited. Additionally, texture analyses were performed by one observer.
Ethics committee approval: n/a
Funding: No funding was received for this work.
Author Disclosures:
I. Başara Akin: Author at Dokuz Eylül University, School of Medicine, Department of Radiology
H. A. Özgül: Author at Dokuz Eylül University, School of Medicine, Department of Radiology
M. K. Şimşek: Author at Dokuz Eylül University, School of Medicine, Department of Radiology
C. Altay: Author at Dokuz Eylül University, School of Medicine, Department of Radiology
M. Seçil: Author at Dokuz Eylül University, School of Medicine, Department of Radiology
P. Balci: Author at Dokuz Eylül University, School of Medicine, Department of Radiology

11:15 - 12:30 **Studio 2020**

Neuro

RPS 1411a

Arterial spin labeling brain perfusion

Moderators:
A. Majos; Lodz/PL
M. Mannil; Zürich/CH

RPS 1411a-1 11:15

Application of post labeling delay time in 3D-pseudo continuous arterial spin labeled perfusion imaging in normal children

S. Tang*; Chongqing/CN (sltang66@163.com)*

Purpose: To explore the application value of PLD in 3D-pcASL perfusion imaging in normal children and to find the optimal PLD values for children at each age group.
Methods and materials: 5 groups of children, with 50 patients in each group, who underwent routine MRIs with normal results were included. The patients were stratified according to the following ages: <1 month, 1 to 6 months, 6 to 12 months, 1 to 3 years, 3 to 6 years, and 6 to 18 years. All patients received 3D-pcASL scanning. The PLD values were set to 1,025 ms, 1,525 ms, or 2,025 ms. In subjective evaluations, the SNR and CBF of 3D-pcASL perfusion images under different PLD values were compared and analysed.
Results: For patients in the < 1 month group and 1 to 6 months group, when the PLD value was 1,025 ms, the brain CBF values and SNR values were higher than those of the images with PLD values of 1,525 ms and 2,025 ms. For patients in the 6 to 12 months group, 1 to 3 years group, 3 to 6 years group, and 6 to 18 years group, when the PLD value was 1,525 ms, the brain CBF values and SNR values were higher than those of the images with PLD values of 1,025 ms and 2,025 ms.
Conclusion: The optimal PLD value for infants who are aged ≤6 months is 1,025 ms. The optimal PLD value for children >6 months to 18 years old is 1,525 ms.
Limitations: The deficiency of this study is that some children used sedatives during the examination.
Ethics committee approval: Ethics committee approval obtained.
Funding: No funding was received for this work.
Author Disclosures:
S. Tang: Author at Children's Hospital of Chongqing Medical University

RPS 1411a-2 11:21

Is multi-delay arterial spin labelling a better biomarker of cerebral perfusion in sickle cell cerebral vasculopathy?

C. Y. Provost[1], S. Lion[1], R. M. Lebel[2], J. Benzakoun[1], L. Legrand[1], D. Calvet[1], P. Bartolucci[3], M. Edjlali-Goujon[1], C. Oppenheim[4]; *[1]Paris/FR, [2]Calgary/CA, [3]Créteil/FR, [4]Paris Cedex 14/FR (cyprovost@gmail.com)*

Purpose: Arterial spin labelling (ASL) is a promising non-invasive MRI perfusion technique but remains challenging to use in sickle cell disease (SCD) cerebral vasculopathy, which results in long arterial transit times (ATT) through collateral pathways. We aimed to validate multi-delay ASL for cerebral blood flow (CBF) measurements in SCD patients with cerebral vasculopathy.
Methods and materials: We performed single-delay ASL (labelling duration=1,500 milliseconds, post-labelling delay=2,025 milliseconds) and multi-delay ASL (labelling duration=4,000 milliseconds, 7 post-labelling delays: 2,000-5,000 milliseconds) on a 3-Tesla MRI scanner in 21 patients with SCD cerebral vasculopathy. Dynamic susceptibility contrast MRI was used to assess the disease severity and to identify cortical regions with normal (<2 seconds), moderate (2-4 seconds), and severe (>4 seconds) Tmax. Normalised relative CBF (rCBF), ATT, and Tmax values were automatically extracted from 20 cortical regions.
Results: Single-delay ASL measured lower rCBF that were 93%, 89% ($p<0.001$), and 84% ($p=0.011$) of the multi-delay ASL values in cortical regions of normal, moderate, and severe Tmax, respectively. Compared to multi-delay ASL, single-delay ASL underestimated rCBF by 16% in regions with severe Tmax ($p=0.014$), especially in anterior and middle cerebral artery perfusion territories. ATT was correlated with Tmax in cortical regions with severe Tmax ($\rho=0.56$, $p<0.001$). ATT maps were visually comparable to that of Tmax.
Conclusion: Non-invasive multi-delay ASL improves CBF assessment in SCD cerebral vasculopathy, particularly in cortical regions with long ATT. It could reduce the need for contrast injection in patients difficult to infuse.
Limitations: No reference standard such as [^{15}O]-water positron emission tomography was available to validate the accuracy of rCBF measurement from ASL.
Ethics committee approval: The study was approved by the Comité de Protection des Personnes Île-de-France Saint-Louis Ethics Committee.
Funding: The Agence Régionale de Santé Ile-de-France.
Author Disclosures:
C. Y. Provost: nothing to disclose
M. Edjlali-Goujon: nothing to disclose
C. Oppenheim: nothing to disclose
P. Bartolucci: nothing to disclose
R. M. Lebel: nothing to disclose
S. Lion: nothing to disclose
D. Calvet: nothing to disclose
J. Benzakoun: nothing to disclose
L. Legrand: nothing to disclose

RPS 1411a-3 11:27

Multi-delay ASL with reduced-resolution pre-scan transit time maps for the assessment of cerebral perfusion in Moyamoya disease: a comparison with conventional 3D-ASL

Y. Zeng, S. Zhou, X. Zhang, Y. Chen, J. Fu, S. Duan, J. Qu, D. Geng, J. Zhang*; Shanghai/CN (18211220088@fudan.edu.cn)*

Purpose: The cerebral haemodynamics of Moyamoya disease (MMD) is complex and conventional arterial spin labelling (ASL) with a fixed post-labelling delay (PLD) time can easily misestimate the cerebral perfusion. We aimed to explore the value of a multi-delay ASL with reduced-resolution pre-scan transit time (TT) maps in obtaining cerebral perfusion information in MMD compared to the conventional 3D-ASL.
Methods and materials: 46 patients with MMD underwent both multi-delay ASL and 3D ASL-MRI. All brain regions based on the automated anatomical labelling (AAL-90) atlas were divided into 5 groups according to the TT values measured in TT maps from multi-delay ASL-MRI. The cerebral blood flow (CBF) values in 4,140 brain regions in all patients were also measured.
Results: The CBF values in multi-delay ASL and 3D-ASL were significantly different ($p<0.001$). At TT≤1,000 ms, 1,000 ms$<$TT≤1,500 ms, and 1,500 ms $<$TT≤2,000 ms, the respective CBF values in multi-delay ASL were lower than the corresponding CBF values in 3D-ASL value ($p<0.001$ for all comparisons). However, at 2,000 ms$<$TT≤2,500 ms, the multi-delay ASL value was higher than the 3D-ASL value ($p<0.001$). Although the fifth group (TT$>$2,500 ms) included only 5 brain regions of 3 patients, the CBF values from multi-delay ASL were all higher than those from 3D-ASL.
Conclusion: The CBF can be corrected by using a series of low-resolution TT maps from the multi-delay ASL-MRI. This approach possibly provides more accurate cerebral perfusion information for the assessment of MMD.
Limitations: The application of the multi-delay ASL was not explored in more depth.
Ethics committee approval: The study was approved by ethics committee of our hospital and written informed consent was obtained.
Funding: The National Key Research and Development Program of China (Grant No.2016YFA0203700).

Author Disclosures:
Y. Zeng: Author at Huashan Hospital, Fudan University, Speaker at Huashan Hospital, Fudan University
S. Zhou: Author at Huashan Hospital, Fudan University
X. Zhang: Author at Huashan Hospital, Fudan University
Y. Chen: Author at Huashan Hospital, Fudan University
J. Fu: Author at Huashan Hospital, Fudan University
S. Duan: Author at GE Healthcare China
J. Qu: Author at GE Healthcare China
D. Geng: Author at Huashan Hospital, Fudan University
J. Zhang: Author at Huashan Hospital, Fudan University, Research/Grant Support at Huashan Hospital, Fudan University

RPS 1411a-4 11:33

Cerebrovascular reserve derived from ASL may differentiate between affected and unaffected vascular territories in patients with Moyamoya disease

M. Fahlström, P. Enblad, A. Lewén, J. Wikström*; Uppsala/SE (markus.fahlstrom@radiol.uu.se)*

Purpose: To compare cerebrovascular reserve (CVR) in affected and unaffected vascular territories in patients with Moyamoya disease (MMD) using ASL.
Methods and materials: 9 patients with MMD were included before or after revascularisation surgery of unilaterally or bilaterally affected vascular territories. All patients were examined on a 3T MR scanner. CBF maps, based on 3D-pCASL acquisition, were acquired before and 5, 15, and 25 minutes after an i.v. acetazolamide (ACZ) injection and registered to each patient's 3D-T1-weighted image. A vascular territory template was spatially normalised to the patient-specific space. CBF values were extracted from regions supplied by the middle and anterior cerebral arteries and categorised as affected or unaffected based on DSA. CVR was calculated as CBF augmentation post-ACZ injection relative to baseline. A post label delay of 2,500 ms and large regions-of-interests were used to account for possible arterial transit time artefacts.
Results: A total of 19 examinations were analysed, generating 76 vascular territories (12 unaffected and 64 affected). Average CVRs (CI95%) in unaffected vascular territories were 60% (46-73%), 54% (44-64%), and 46% (38-54%) at 5, 15, and 25 minutes after ACZ injection, respectively. Corresponding values in affected vascular territories were 42% (38-47%), 40% (36-45%), and 38% (34-42%). Differences between unaffected and affected vascular territories were significant at 5 minutes (p=0.006) and 15 minutes (p=0.017), but not at 25 minutes (p=0.095).
Conclusion: CVR derived from ASL can differentiate between unaffected and affected vascular territories. ASL has potential as a non-invasive diagnostic method in patients with MMD.
Limitations: The small number of unaffected vascular territories is a potential source of bias.
Ethics committee approval: Approved by the regional ethics committee (DNR 2019/01316). Written informed consent was given.
Funding: No funding was received for this work.
Author Disclosures:
M. Fahlström: nothing to disclose
J. Wikström: nothing to disclose
P. Enblad: nothing to disclose
A. Lewén: nothing to disclose

RPS 1411a-5 11:39

Establishing a potential imaging biomarker in spinocerebellar ataxia type 3: the application of voxel-based morphometry and ASL

M. Hu, J. Zhao, H. Qiu, J. Chu, C. Wu*; Guangzhou/CN (humanshi_may@163.com)*

Purpose: To uncover the changes of whole-brain grey-matter (GM) based on voxel-based morphometry (VBM) and to obtain cerebral blood flow (CBF) maps of the significantly altered regions in VBM. Further, to establish a potential imaging biomarker for the diagnosis of spinocerebellar ataxia type 3 (SCA3).
Methods and materials: 20 symptomatic SCA3 patients (mean age: 39.7y), 5 pre-symptomatic SCA3 patients (mean age: 27.3y), and 20 age- and gender-matched healthy controls (HCs) (mean age: 37.6y) were included in this study and underwent whole-brain T1-MPRAGE and pASL. Their clinical information was also collected.
Results: Compared with HCs, SCA3 symptomatic patients had a significantly reduced GM volume in the right anterior cerebellum lobe (RACL) (P<0.001, FWE correction). However, no significant GM volume differences were found between pre-symptomatic and symptomatic SCA3 patients or was found between the HCs and pre-symptomatic SCA3 group. Further, when the extracted RACL CBF values in symptomatic SCA3 and HCs were compared, CBF values were significantly higher in symptomatic SCA3 patients ($CBF_{symptomatic\ group}$: 56.0±31.7 (mL/(100g×min) vs CBF_{HCs}: 29.6±22.0 (mL/(100g×min); P <0.05). ROC analysis showed that the CBF values of RACL had high diagnostic value (AUC=0.75) and the specificity, sensitivity, and cut-off value for the diagnosis of symptomatic SCA3 were 75%, 84.2%, and 29.8 mL/(100 g×min).
Conclusion: Compared with HCs, the GM volume had significantly reduced in the RACL of SCA3 symptomatic patients, whereas the CBF values of the same patients in RACL had complementary increased. The CBF value in RACL might serve as a non-invasive and promising diagnostic biomarker for SCA3 patients with a high sensitivity.
Limitations: The sample size is relatively small.
Ethics committee approval: This study has been approved by the ethics committee of The First Affiliated Hospital of Sun Yat-Sen University.
Funding: No funding was received for this work,
Author Disclosures:
M. Hu: Speaker at The First affiliated Hospital of Sun Yat-Sen University, Author at The First affiliated Hospital of Sun Yat-Sen University
J. Zhao: Author at The First affiliated Hospital of Sun Yat-Sen University
H. Qiu: Author at The First affiliated Hospital of Sun Yat-Sen University
J. Chu: Author at The First affiliated Hospital of Sun Yat-Sen University
C. Wu: Author at The First affiliated Hospital of Sun Yat-Sen University

RPS 1411a-6 11:45

ASL MRI brain imaging studies in patients with diabetic retinopathy

Q. He*; Kunming/CN (ynheqian@163.com)*

Purpose: To evaluate cerebral perfusion in diabetic retinopathy patients by magnetic resonance ASL imaging.
Methods and materials: 10 diabetic retinopathy patients without hypertension selected from June 2017-March 2019 were included in study group A, 24 non-retinopathy patients were included in study group B, and 22 healthy volunteers were included in control group C. Magnetic resonance head scanning, MRA, and ASL scanning were performed on the three groups of subjects at rest. SPM software based on MATLAB was used to convert and preprocess the obtained images and the activation points of each brain region were calculated. The ROI was manually marked in the activated brain region. According to the ROI activation diagrams of different brain regions obtained by preprocessing, an area of approximately 20 mm^2 and the average CBF value of the corresponding ROI and its mirror ROI were measured.
Results: The average CBF values of the left cerebellar hemisphere, left cerebellar tonsil, bilateral inferior temporal gyrus, left straight gyrus, left cingulate gyrus, and bilateral medial frontal gyrus in group A were lower than those in group B and group C (P<0.05), and the average CBF values of the pons and left anterior central gyrus in group A were higher than those in group B and group C (P<0.05).
Conclusion: MRI brain ASL imaging showed abnormal perfusion in the cerebral motor centre, visual projection area, limbic system, and other areas in patients with diabetic retinopathy, indicating that changes in cerebral microcirculation may occur simultaneously in diabetic retinopathy.
Limitations: Few cases were enrolled.
Ethics committee approval: Ethics committee approval obtained.
Funding: Supported, in part, by Core Grant 2018FE001(-267) from a special joint fund from Yunnan Provincial Department of Science and Technology and Kunming Medical University, Kunming, Yunnan, China.
Author Disclosures:
Q. He: Author at Yunnan second people's hospital, Investigator at Yunnan second people's hospital, Speaker at Yunnan second people's hospital

RPS 1411a-7 11:51

Perfusion abnormalities detected by MR pseudo-continuous arterial spin labelling (pCASL) in patients with porphyria

G. Castorani[1], D. Vergara[2], D. Grasso[3], C. Borreggine[4], G. Valle[5], C. C. Guida[5], A. Simeone[5], T. Popolizio[5], G. Guglielmi[6];
[1]Foggia/IT, [2]Naples/IT, [3]Manfredonia/IT, [4]Casamassima/IT, [5]San Giovanni Rotondo/IT, [6]Andria/IT (giulia.castorani90@gmail.com)

Purpose: Acute intermittent porphyria (AIP) is a rare inherited disorder presenting with abdominal, neurologic, and psychiatric symptoms.
Several studies documented brain perfusion defects by single-photon emission tomography (SPET) in subjects affected by AIP. PCASL is a non-invasive MRI technique for measuring tissue perfusion with a lot of potential clinical applications. Our purpose is to evaluate the role of pCASL and to compare it with SPET findings in this cohort of patients.
Methods and materials: 50 patients (26 group; 24 control) with AIP were included in the study. All subjects underwent MR examination using a 3T MR scanner with conventional sequences and pCASL, and had been studied by single-photon emission computed tomography. Two blinded neuroradiologists evaluated MR images and two experienced observers (20 years and 25 years) reviewed by consensus all SPECT images.
Results: Conventional MRI showed no significant findings in all patients. All presented a variable pattern of SPECT including multiple mild to moderate perfusion cortical defects, bilateral or asymmetric. The most involved regions

were temporal, frontal, and parietal lobes. We found a similar pattern of hypoperfusion with pCASL in 20 patients. 2 patients were excluded because of movement artefacts. 3 subjects didn't manifest any significative perfusion alteration.
Conclusion: pCASL represents an important and reliable alternative to others more expensive or invasive techniques, like PET or SPECT, for measuring cerebral perfusion in AIP patients. It could become a useful tool in research and clinical practice.
Limitations: The retrospective nature of the study; difficult in the control group.
Ethics committee approval: Patient consent was obtained.
Funding: No funding was received for this work.
Author Disclosures:
G. Castorani: nothing to disclose
D. Vergara: nothing to disclose
D. Grasso: nothing to disclose
C. Borreggine: nothing to disclose
G. Valle: nothing to disclose
C. C. Guida: nothing to disclose
A. Simeone: nothing to disclose
G. Guglielmi: nothing to disclose
T. Popolizio: nothing to disclose

RPS 1411a-9 11:57

The use of arterial spin labelling in acute ischaemic stroke and transient ischaemic attack

C. B. Brito[1], P. Vilela[1], X. Golay[2]; [1]*Lisbon/PT,* [2]*London/UK*
(catarinaborgesbrito@gmail.com)

Purpose: Arterial spin labelling (ASL) is a non-invasive and quantitative imaging method to evaluate brain perfusion and angiography (4D-MRA ASL) using magnetically labelled arterial blood water as an endogenous tracer. The aim of this review is to discuss the applications of ASL in the setting of acute ischaemic stroke (AIS) and transient ischaemic attack (TIA).
Methods and materials: A literature review was conducted searching the electronic databases PubMed and SCOPUS from inception to May 2019 to identify relevant peer-reviewed English publications. Qualitative and quantitative ASL imaging data were extracted.
Results: After screening 404 titles and abstracts, and 41 full-text articles, 34 studies were included. ASL is an accurate and fairly versatile technique that provides useful imaging information required by the current AIS treatment guidelines. ASL has a high sensitivity (>85%) and accuracy for the detection of the arterial occlusion site. This technique is successful in depicting the ischaemic penumbra, with a tendency to show larger volumes than dynamic-susceptibility contrast MRI perfusion. ASL can reliably rule-out stroke by recognising its mimics and may even help to sustain the diagnosis of minor stroke/TIA, monitor clinical evolution, and stratify the risk of future stroke. The new 4D-MRA ASL defines the arterial occlusion site and collateral circulation status, which helps to predict the clinical outcome.
Conclusion: ASL has proven to be an accurate alternative for stroke evaluation, allowing quantitative brain perfusion analysis, the definition of occlusion site, and collateral delineation with 4D-MRA. This technique is especially important when contrast agents are contraindicated, repeated image is needed, or the paediatric population is implicated. It is very effective for TIA/minor stroke evaluation.
Limitations: Available studies have small sample sizes and use different approaches to evaluate perfusion, limiting the comparability of results.
Ethics committee approval: n/a
Funding: No funding was received for this work.
Author Disclosures:
C. B. Brito: nothing to disclose
P. Vilela: nothing to disclose
X. Golay: nothing to disclose

RPS 1411a-10 12:03

MRI spectroscopy and arterial spin labelling in migraine patients

G. Singla[1], D. S. Thakur[2], D. S. Sharma[2]; [1]*Karnal/IN,* [2]*Shimla/IN*
(drgazalsingla2212@gmail.com)

Purpose: A migraine is a common disabling primary headache disorder of high prevalence. We tried to evaluate the neuro-imaging findings in patients with migraines with conventional and advanced MRI sequences.
Methods and materials: 44 patients with migraines and 14 well-matched controls received conventional MRI brain scanning, 3D multi-voxel spectroscopy, and arterial spin labelling. Ratios of N-acetyl aspartate (NAA)/choline (Ch), NAA/creatine(Cr), Cho/Cr, lactate(Lac)/NAA, and myoinositol(mI)/NAA were taken in each thalamus.
ASL images were analysed for any blood flow related abnormalities. Values were taken in both cerebral hemispheres in the frontal cortex, in both thalami, and in both cerebellar hemispheres.
Results: Few migraine patients showed T2/FLAIR white matter hyperintensities ($p>0.05$). There was reduced NAA/Cho and NAA/Cr ratios in the thalamus of the contralateral side of migraine headache ($p<0.05$).
NAA/Cho and NAA/Cr ratios were decreased in migraine patients when compared to controls ($p< 0.05$). Increased duration of illness was associated with decreased NAA/Cho and NAA/Cr ratios ($p<0.05$).
A significant decrease in perfusion in the ipsilateral brain in patients with ipsilateral migraine headache was noted.
Conclusion: MRS and ASL can help detect changes that are not readily detected on conventional MRI. MR spectroscopy can detect changes in the mean metabolite concentration in the thalami of migraine patients, which can predict the severity of the disease. MR perfusion using ASL can evaluate the perfusion changes. From such data, biomarkers can be developed in the future for early diagnosis. Also, medications can be developed targeting the thalamus for managing this disease more precisely.
Limitations: n/a
Ethics committee approval: n/a
Funding: No funding was received for this work.
Author Disclosures:
G. Singla: nothing to disclose
D. S. Thakur: nothing to disclose
D. S. Sharma: nothing to disclose

RPS 1411a-11 12:09

Arterial spin labelling-based MR perfusion in epilepsy: an imaging tool in the presurgical evaluation in epilepsy (a 50 case study)

A. Joshi, S. Jagtap, N. Kurwale, S. Patil*; Pune/IN*
(draniruddha.joshi@gmail.com)

Purpose: Accurate identification of the epileptogenic zone is an important prerequisite in the presurgical evaluation of refractory epilepsy.
The arterial spin labelling (ASL) non-contrast perfusion technique not only provides structural abnormalities but also a functional characterisation of abnormalities, and may play a vital role in structural MRI negative epilepsy.
Methods and materials: We examined 50 patients with intractable epilepsy. On the basis of their clinical and electrophysiological findings, 32 patients had temporal lobe epilepsy, 3 had post-ischaemic scar lesions, 9 had focal seizures, and 6 had dysplastic lesions.
MRI was performed using a 3.0-T Skyra (Siemens). ASL was performed with a pulsed sequence using a QUIPSII perfusion mode. Relative cerebral blood flow maps for ASL were calculated for contrast-enhanced perfusion-weighted imaging using Syngo perfusion (MR) software.
An epilepsy protocol was used: axial T2W, sagittal T1W and sagittal 3D FLAIR, SWI, and diffusion-weighted imaging with 62-direction scanning. Interictal FDG PET/CT was used for comparison with ASL.
Results: All cases with temporal lobe epilepsy showed hypoperfusion in the affected temporal lobe on both the interictal PET and ASL maps. In those cases where a cortical lesion was visible on imaging and corresponded with an alteration seen on PET, the same result seen on ASL perfusion.
Conclusion: The perfusion maps obtained with ASL corresponded well with the PET perfusion and EEG results in patients with intractable epilepsy.
ASL not only allows the localisation of the epileptogenic focus but also provides the functional characterisation of abnormalities identified by MRI. ASL is a non-contrast, non-radiation useful supplementary investigation. It has the potential to make MRI a one-stop-shop in epilepsy evaluation.
Limitations: Despite a slightly reduced resolution with ASL, we found a correlation between ASL, PET, and electrophysiological data.
Ethics committee approval: n/a
Funding: No funding was received for this work.
Author Disclosures:
S. Jagtap: nothing to disclose
A. Joshi: Author at DMH PUNE
N. Kurwale: nothing to disclose
S. Patil: nothing to disclose

RPS 1411a-12 12:15

CT-perfusion and MR-ASL in the differential diagnosis of glioblastomas and primary CNS lymphomas

A. Batalov, R. Afandiev, N. Zakharova, E. Pogosbekian, S. Goriainov,
A. Bykanov, I. Pronin, A. Potapov*; Moscow/RU (batalov89@gmail.com)*

Purpose: To study the possibilities of MR-ASL and CT-perfusion (CTP) in the differential diagnosis of glioblastomas (GB) and primary CNS lymphomas (PCNSL).
Methods and materials: On the basis of ASL, we measured the tumour blood flow (TBF) in 119 patients with GB and 16 patients with PCNSL. All patients were examined on a 3T MR-scanner. The pseudo-continuous ASL (pcASL) technique was used to calculate TBF. Post-processing of ASL data was conducted on the workstation using the ReadyView program. Using CT perfusion, we estimated haemodynamic parameters (CBF, CBV, MTT, and PS) in 23 patients with GB

and 15 patients with PCNSL. Post-processing was done using a CT-perfusion 4D program (AW Server 3.2 GE). All parameters (ASL and CTP) were normalised to intact white matter.
Results: ASl-TBF in GB was significantly higher than in PCNSL (p<0.001). The cut-off=109 ml/100g/min, AUC=0.885, sensitivity=93.8%, and specificity=73,1%. CTP-CBF and CBV in GB was significantly higher than in PCNSL (p<0.0001). The cut-off for CBF was 56.5 ml/100g/min (AUC=0.942, sensitivity=73.3%, and specificity=100%) and the cut-off for CBV was 4.4 ml/100g (AUC=0.965, sensitivity=100%, and specificity=82,6%). MTT and PS in GB was significantly lower than in PCNSL (p=0.008 for MTT, p<0.0001 for PS). The cut-off for MTT was 4.6s (AUC=0.759, sensitivity=80%, and specificity=69,6%) and the cut-off for PS was 7.6 ml/100g/min (AUC=0.968, sensitivity=86.7%, and specificity=100%).
Conclusion: ASL and CTP are reliable quantitative techniques for the differential diagnosis between GB and PCNSL. The study was supported by RFBR №18-29-01018.
Limitations: A small number of patients in the study group.
Ethics committee approval: n/a
Funding: The study was supported by Russian Foundation for Basic Research №18-29-01018.
Author Disclosures:
S. Goriainov: nothing to disclose
A. Batalov: nothing to disclose
R. Afandiev: nothing to disclose
N. Zakharova: nothing to disclose
E. Pogosbekian: nothing to disclose
A. Bykanov: nothing to disclose
I. Pronin: nothing to disclose
A. Potapov: nothing to disclose

11:15 - 12:30 **Coffee & Talk 2**

Genitourinary

RPS 1407a

Is there any news in CT protocols for renal masses and stones evaluation?

Moderators:
M. Basta Nikolic; Novi Sad/RS
J. Richenberg; Brighton/UK

RPS 1407a-1 11:15

Substantial radiation dose reduction with consistent image quality using a novel low-dose stone composition protocol
P. Apfaltrer[1], A. Dutschke[1], P. A. T. Baltzer[1], C. Schestak[1], M. Özsoy[1], C. Seitz[1], T. H. Helbich[1], H. Ringl[1], G. Apfaltrer[2]; *[1]Vienna/AT, [2]Graz/AT*

Purpose: To assess a novel low-dose CT-protocol, combining a 150kV spectral filtration unenhanced protocol (Sn150kVp) and a stone targeted dual-energy CT (DECT) in patients with urolithiasis.
Methods and materials: 232 (151 male, 49±16.4 years) patients with urolithiasis who had received a low-dose non-contrast enhanced CT (NCCT) for suspected urinary stones either on a third-generation dual-source CT system (DSCT) using Sn150kVp (n=116, group 1) or on a second-generation DSCT (n=116, group 2) using single-energy (SE) 120kVp. For group 1, a subsequent dual-energy CT (DECT) with a short stone-targeted scan range was performed. Objective and subjective image quality was assessed. Radiation metrics were compared.
Results: 534 stones (group 1: n=242 stones; group 2: n=292 stones) were found. In group 1, all 215 stones within the stone-targeted DECT-scan range were identified. 11 calculi (5.12%) were labelled as uric acid (UA) while 204 (94.88%) were labelled as non-UA calculi. DE analysis was able to distinguish between UA and non-UA calculi in all collected stones. There was no significant difference in the overall signal-to-noise ratio between group 1 and group 2 (p=0.819). On subjective analysis, both protocols achieved a median Likert rating of 2 (p=0.171). The mean effective dose was significantly lower for combined Sn150kVp and stone-targeted DECT (3.34±1.84mSv) compared to singe-energy 120kVp NCCT (4.45±2.89mSv) (p<0.001), equaling a 24.9% dose reduction.
Conclusion: The evaluated novel low-dose stone composition protocol allows substantial radiation dose reduction with consistent high diagnostic image quality.
Limitations: A retrospective design.
Ethics committee approval: Institutional review board approved.
Funding: No funding was received for this work.
Author Disclosures:
P. Apfaltrer: Speaker at Siemens Healthcare
A. Dutschke: nothing to disclose
P. A. T. Baltzer: nothing to disclose
C. Schestak: nothing to disclose
M. Özsoy: nothing to disclose
C. Seitz: nothing to disclose
T. H. Helbich: nothing to disclose
H. Ringl: nothing to disclose
G. Apfaltrer: nothing to disclose

RPS 1407a-2 11:21

Comparison of ultra-low-dose CT with standard-dose CT for urolithiasis
Y. S. Shim, S. H. Park, J. Lee; *Incheon/KR (peaceilv@naver.com)*

Purpose: To evaluate the radiation dose exposure, diagnostic performance, and image quality of ultra-low-dose non-contrast CT using an advanced modelled iterative reconstruction (ADMIRE) algorithm with spectral filtration for the detection of urolithiasis.
Methods and materials: 145 consecutive patients underwent non-contrast CT using third-generation dual-source scanner to obtain two datasets: 16.7% (ultra-low-dose CT) and 100% (standard-dose CT) tube loads with spectral filtration. The performance of ultra-low-dose CT for detection of stones was analysed by two readers and compared with that of standard-dose CT. Image quality was measured subjectively and objectively.
Results: 171 stones were detected in 79 patients. The mean effective radiation doses of ultra-low-dose CT was 0.3 mSV. The sensitivity and specificity values for the diagnosis of stones measuring ≥3 mm was 95.1% and 100% for ultra-low-dose CT. The sensitivity and specificity for all stone detection was 74.9% and 97.8% for ultra-low-dose CT. The image quality was lower for ultra-low-dose CT than for standard-dose CT (P<0.01).
Conclusion: Ultra-low-dose CT can be achieved with radiation doses close to KUB radiography. Ultra-low-dose CT with spectral filtration can be used to detect stones measuring ≥3 mm and be used as a follow-up imaging modality as an alternative to KUB radiography.
Limitations: The small number of obese patients and the relatively small number of ureteric stones. Due to the difference in image quality between ultra-low-dose and standard-dose CT scans, there was a limit to the extent that the readers could be blinded. The 3 mm slice thickness might impact the ability to detect small stones.
Ethics committee approval: Approval for the study was obtained from the institutional review board of Gil Medical Center.
Funding: No funding was received for this work.
Author Disclosures:
J. Lee: nothing to disclose
Y. S. Shim: nothing to disclose
S. H. Park: nothing to disclose

RPS 1407a-3 11:27

Variations in CT protocols and radiation doses for haematuria and renal colic: comparing practices in 20 European countries
F. Homayounieh[1], V. Gershan[2], R. Singh[1], M. Kalra[1], J. Vassileva[3]; *[1]Boston, MA/US, [2]Skopje/MK, [3]Vienna/AT (vgersan@gmail.com)*

Purpose: CT is commonly used for evaluating patients with haematuria and renal colic. We assessed variations in radiation doses and CT protocols for the evaluation of haematuria and renal colic in 20 European countries.
Methods and materials: IAEA surveyed practices in 51 hospitals from 20 European countries and obtained information for three CT protocols (haematuria, renal colic, and routine abdomen-pelvis CT) for 1,276 patients: patient information (weight and clinical indication), scanner information (vendor, scanner name, and number of detector rows), parameters (number of phases, scan start and end locations, mA, and kV), and radiation dose descriptors (CTDIvol and DLP). Two radiologists assessed the appropriateness of clinical indications and scan phases using the ESR referral guidelines and ACR appropriateness criteria. Descriptive statistics and Student's t tests were performed.
Results: Most institutions used 3-6 phase CT haematuria protocols (80%, median DLP 1,793-3,618 mGy.cm) which were associated with 2.4-4.9-fold higher dose compared to 2-phase protocol (20%, 740 mGy.cm) (p<0.0001). Likewise, 52% patients were scanned with 3-5 phase routine CT protocol (1,574-2,945 mGy.cm) as opposed to 37% single-phase routine CT (676 mGy.cm). The median DLPs for renal colic CT (516 mGy.cm; 77% had single-phase CT and 23% acquired 2-5-phases for renal colic protocol) were significantly lower than median DLPs with the other two CT protocols (p<0.0001). Most institutions did not change scan parameters (such as kV, mA, scan length) for multiphase protocols.

Conclusion: Although most institutions use low-dose CT for renal colic, large variations in haematuria and routine abdomen-pelvis CT protocols result in huge radiation doses (up to 2,945-3,618 mGy.cm). Scan parameters are not adjusted when acquiring CT with multiple phases.
Limitations: Most of the data came from developing nations with a heterogeneous number of patient studies.
Ethics committee approval: n/a
Funding: No funding was received for this work.
Author Disclosures:
V. Gershan: nothing to disclose
F. Homayounieh: nothing to disclose
R. Singh: nothing to disclose
M. Kalra: Research/Grant Support at Siemens Healthineers and Riverain Tech
J. Vassileva: nothing to disclose

RPS 1407a-4 11:33
The efficacy of CT urography using low-osmolar reduced-dose contrast agent and reduced radiation dose in patients with chronic kidney disease
H. S. Park, S. H. Kim, S. H. Cho, M. Kim*; Daegu/KR (mirank1210@naver.com)*

Purpose: To prospectively compare the image quality of CT urography with IOHEXOL 240 at 80-kVp to that with IOBITRIDOL 350 at 120-kVp in patients with or without chronic kidney disease.
Methods and materials: Among 400 patients > 60 years who underwent CT urography, 200 patients with eGFR < 45 mL/min scanned using IOHEXOL 240 at 80-kVp, and in eGFR < 45 mL/min with IOBITRIDOL 350 at 120-kVp were selected. Two radiologists measured quantitative (SNR, CNR, and CT value ratio of the bladder) and qualitative image quality (urinary tract opacification, visual image noise, artefact, and overall image quality) between the two groups with the same inclusion criteria.
Results: There were significantly higher SNR in IOHEXOL 240 at 80-kVp (renal cortex, liver parenchyma, and psoas muscle) except for the abdominal aorta ($P < 0.05$ for all). There were no significant differences in CNR and CT value ratio of the bladder between two groups ($P > 0.05$ for all). There were significant differences in the opacification score, visual image noise, artefacts, and overall image quality between the two groups ($P > 0.05$ for all).
Conclusion: CT urography with the use of IOHEXOL 240 at 80-kVp showed a dose reduction and no significant differences regarding the image.
Limitations: There are some technical parameters that have a significant impact on contrast agent enhancement, such as the rate of infusion, amount of iodine injected, and body composition and cardiac output
We did not use the techniques of abdominal compression or intravenous hydration because these techniques may be a burden for the patient.
The study suffers from selection bias, as patients were selected to perform CT urography by various referring clinicians that had a high clinical suspicion for urinary tract pathology.
Ethics committee approval: n/a
Funding: No funding was received for this work.
Author Disclosures:
H. S. Park: nothing to disclose
S. H. Kim: nothing to disclose
S. H. Cho: nothing to disclose
M. Kim: nothing to disclose

RPS 1407a-5 11:39
Effective radiation dose reduction in CT with iterative reconstruction in patients with urinary stones
S. H. Kim, H. S. Park, S. H. Cho*; Daegu/KR (warpaludin@gmail.com)*

Purpose: To prospectively compare the image quality and visibility of urinary stones on CT images to obtain multiple radiation exposures within the same patient reconstructed with SAFIRE.
Methods and materials: This prospective observational study included 760 patients (45.5 years ± 12.8, 452 men and 248 women) known to have urinary stones between January 2016 and December 2018. Patients underwent CT with simultaneous acquisition of 6 exposures per patient from the same patient (100% FBP, 75%, 50%, 37.5%, 25%, and 12.5% SAFIRE). Two radiologists independently assessed qualitative measurement, including overall image quality, noise, and visibility of the stones using a five-point scale. Quantitative measurement, including CT number, image noise, SNR, CNR, and corresponding FOM, were compared by using the Student t-test for comparison of 100% and 5 other radiation doses.
Results: Qualitative overall image quality, noise, and visibility of the stones by location at 37.5% dose were rated as non-inferior to those at 100% exposure, except for the visualisation of smaller stones < 3 mm. The CT images with 50% exposure had increased SNR and CNR compared with those of 100% exposure. The CT images with 37.5% exposure reconstructed with SAFIRE had significantly more noise and lesser CNR than CT images reconstructed with FBP compared with FOMnoise and FOMCNR. The size-specific dose estimation was 4.1m Gy±0.8 at 37.5% exposure.
Conclusion: CTs performed at 37.5% exposure reconstructed with SAFIRE prove diagnostically acceptable for the detection of clinically relevant stones.
Limitations: We did not use the techniques of abdominal compression because the technique may be a burden for patients, especially those with chronic heart failure or diabetes.
Ethics committee approval: n/a
Funding: No funding was received for this work.
Author Disclosures:
H. S. Park: nothing to disclose
S. H. Kim: nothing to disclose
S. H. Cho: nothing to disclose

RPS 1407a-6 11:45
Iodine parameters in triple-bolus dual-energy CT correlate with perfusion CT biomarkers of angiogenesis in renal cell carcinoma
D. Manoharan, A. Netaji, C. J. Das, S. Sharma*; New Delhi/IN (dineshkimi@gmail.com)*

Purpose: To determine the degree of relationship between PCT parameters and iodine concentration metrics derived from triple-bolus DECT and to compare the radiation dose delivered.
Methods and materials: This single-centre, IRB approved, prospective study was conducted from October 2015 to September 2017. 23 consenting adults (15 men, 8 women; mean age: 56 ± 13 [range, 25–78] years) with RCCs underwent consecutive PCT and triple-bolus DECT. Triple-bolus DECT consisted of synchronous corticomedullary, nephrographic, and delayed-phase scans acquired using a dual-source DECT scanner. Two readers independently analysed blood flow (BF), blood volume (BV), and permeability (PMB) from the PCT, and iodine density (ID) and the iodine ratio (IR) from the triple-bolus DECT. Size-specific dose estimates (SSDE) of both groups were calculated.
Results: Inter-reader agreement was good for PMB (intraclass correlation coefficient [ICC]=0.812) and BF (ICC=0.849) and excellent for BV (ICC=0.956), ID (ICC=0.961), and IR (ICC=0.956). Very strong positive correlations were found between BV and ID ($P < 0.001$) and BV and IR ($P < 0.001$). Strong positive correlations were found between BF and ID ($P < 0.001$) and BF and IR ($P < 0.001$). The correlations between PMB and ID (P=0.01) and PMB and IR (P=0.02) was moderate. The mean SSDE of triple-bolus DECT was significantly lower than that of PCT ($P < 0.001$).
Conclusion: Quantitative iodine metrics derived from triple-bolus dual-energy CTs showed a significant correlation with CT parameters in renal cell carcinoma, with a significantly lower radiation dose.
Limitations: Low dose perfusion protocols were not used. Volume ROI was not taken.
Ethics committee approval: IRB approval and patient consent was obtained.
Funding: No funding was received for this work.
Author Disclosures:
D. Manoharan: nothing to disclose
S. Sharma: nothing to disclose
A. Netaji: nothing to disclose
C. J. Das: nothing to disclose

RPS 1407a-7 11:51
A normalised dual-energy iodine ratio best differentiates renal cell carcinoma subtypes among quantitative imaging biomarkers from perfusion CT and dual-energy CT
D. Manoharan, A. Netaji, K. Diwan, C. J. Das, S. Sharma*; New Delhi/IN (dineshkimi@gmail.com)*

Purpose: To compare diagnostic performances of PCT and DECT in differentiating RCC subtypes.
Methods and materials: After IRB approval, this retrospective study included 51 patients (mean age, 49.7 ± 13.2 years; range, 19–71 years; 11 women and 40 men) with different RCC subtypes (36, 9, and 7 with clear-cell, papillary, and chromophobe subtypes, respectively) who underwent both PCT and DECT before surgery/biopsy between January 2014 and December 2018. Three independent readers measured blood flow, blood volume (BV), and permeability using PCT, and iodine concentration and iodine ratio (IR) using DECT. Multivariable logistic regression analysis was performed to assess PCT and DECT models. Inter-reader agreement was calculated using the intraclass correlation (ICC) coefficient. Size-specific dose estimates of the two methods were compared.
Results: BV (ICC, 0.929) and IR (ICC, 0.850) were the most reproducible parameters. PCT and DECT were significant models ($p<.05$, all) for differentiating clear-cell RCC from papillary and chromophobe RCC, whereas neither model was significant in differentiating papillary RCC from chromophobe RCC ($p>.05$). There was no significant difference in diagnostic accuracy between PCT and DECT ($p>.05$). IR was the only independent predictor of non-clear-cell RCC in models from all readers ($p<.05$). It had an AUC of 0.95, and

sensitivity, specificity, and accuracy with IR cut-off of 63.72% were 0.88, 0.87, and 0.87, respectively. The mean size-specific dose estimate was lower with DECT than with PCT (p<.001).
Conclusion: Perfusion CT and dual-energy CT had comparable and high diagnostic accuracy in differentiating renal cell carcinoma subtypes, with the iodine ratio being the best independent predictor. Further, dual-energy CT involved significantly lower radiation dose.
Limitations: n/a
Ethics committee approval: IRB approval was obtained and informed consent was waived.
Funding: No funding was received for this work.
Author Disclosures:
D. Manoharan: nothing to disclose
A. Netaji: nothing to disclose
K. Diwan: nothing to disclose
C. J. Das: nothing to disclose
S. Sharma: nothing to disclose

RPS 1407a-8 11:57

A retrospective evaluation of pathologic CT findings in a fast-track haematuria program

O. Graumann[1], J. Madsen[1], M. C. Kobel[2], C. B. Ipsen[3], J. B. Jensen[4], A. Makki[4]; [1]Odense/DK, [2]Vejle/DK, [3]Herning/DK, [4]Aarhus/DK (olegraumann@dadlnet.dk)

Purpose: Asymptomatic microscopic haematuria is one of the most common clinical findings requiring urological evaluation in adults. Often, no pathologic CT findings are seen among younger patients. Thus, CTs expose them to potential unnecessary radiation. The purpose of this study was to systematically evaluate pathologic CT findings for patients under primary investigation in the fast-track program for cancer in the urinary tract (UT) and other patients with haematuria, focusing mainly on findings of cancer in the UT.
Methods and materials: Using the radiology information system (RIS) as well as electronic patient records, data was obtained for all patients undergoing CT urography after referral in the fast-track program for cancer in the UT due to haematuria from 11 March, 2013, to 30 June, 2015, at a large university hospital.
Results: The study material was 2,365 CT urographies performed in 2,314 patients. In the group of patients with unexplained macroscopic haematuria, 101 cancers (8.77 %) were found in 1,152 CT urographies. In the group of patients older than 40 years with recurrent microscopic haematuria and relevant symptoms, 8 cancers (2.40 %) were found in 326 CT urographies. For the same patient group but with no relevant symptoms, 10 cancers (1.81 %) were found in 551 CT urographies.
Conclusion: The majority of pathologic CT findings for patients under primary investigation for haematuria were found in the group of macroscopic haematuria. Our study, therefore, supports a narrowing of the indication criteria for haematuria fast-track programs for cancer in the UT and in patients with asymptomatic haematuria.
Limitations: The study was retrospective and carried out in a single centre.
Ethics committee approval: n/a
Funding: No funding was received for this work.
Author Disclosures:
O. Graumann: nothing to disclose
J. Madsen: nothing to disclose
M. C. Kobel: nothing to disclose
C. B. Ipsen: nothing to disclose
J. B. Jensen: nothing to disclose
A. Makki: nothing to disclose

RPS 1407a-9 12:03

Size of kidney stones in computed tomography: the influence of acquisition and image reconstruction parameters

R. P. Reimer[1], J. Salem[1], M. Merkt[2], S. Lennartz[1], D. Zopfs[1], K. Sonnabend[1], A. Heidenreich[1], D. Maintz[1], S. Haneder[1], N. Grosse Hokamp[1]; [1]Cologne/DE, [2]Coblenz/DE (robert.reimer@uk-koeln.de)

Purpose: Computed tomography (CT) is the imaging modality of choice in suspected urolithiasis. Information obtained from CT includes the presence, location, and size of the stones, with the latter frequently determining treatment decision. While there is a consensus regarding how to perform measurements, the influence of other factors possibly impairing accurate measurement, including radiation dose and reconstruction techniques, is unknown.
Methods and materials: 47 kidney stones of different composition were scanned using a 256 row MDCT using a 3D-printed, semi-anthropomorphic phantom. The size was measured manually with a digital caliper (Man-M). Stones were imaged with 2 and 10 mGy. Images were reconstructed using filtered-back-projection, hybrid-iterative, and model-based iterative reconstruction algorithms (FBP, HIR, and MBIR) with different kernels and denoising levels. All stones underwent semi-automatic, threshold-based segmentation for computation of maximum diameter. Statistics were conducted using ANOVA ± correction for multiple comparisons.
Results: Overall stone size as compared to manual measurements was overestimated in CT (8.8±2.9 vs 10.0±3.1 mm, p<0.05) showing a good correlation (R^2=0.66). Radiation dose and denoising levels did not significantly influence measurements (p>0.05). MBIR and sharp kernels showed the closest agreement with Man-M (9.3±3.1 vs 8.8±2.9 mm, p<0.05). Differences within single stones were as high as 40% (e.g. Man-M: 5.9 mm, CT: 7.3-12 mm).
Conclusion: CT-based measurements tend to overestimate stone size as compared to manual measurements. CT-based measurements appear independent of radiation dose and denoising, however, reconstruction algorithms and kernels demonstrate a relevant impact on size measurements. The smallest differences were found when using model-based iterative reconstruction algorithms with a sharp kernel.
Limitations: This is a retrospective single-centre study only investigating reconstruction techniques of one vendor. Comparisons between reconstruction techniques of different vendors were beyond the scope of this study.
Ethics committee approval: IRB-approval given.
Funding: No funding was received for this work.
Author Disclosures:
R. P. Reimer: nothing to disclose
J. Salem: nothing to disclose
M. Merkt: nothing to disclose
S. Lennartz: Research/Grant Support at Philips Healthcare (Travel/Research Support)
D. Zopfs: nothing to disclose
A. Heidenreich: nothing to disclose
D. Maintz: Speaker at Philips Healthcare
S. Haneder: nothing to disclose
N. Grosse Hokamp: Speaker at Philips Healthcare
K. Sonnabend: nothing to disclose

RPS 1407a-10 12:09

Imaging protocols for CT urography: results from a consensus conference of the French Society of Genitourinary Imaging

R. Renard Penna; Paris/FR (raphaele.renardpenna@gmail.com)

Purpose: To develop technical guidelines for computed tomography urography.
Methods and materials: The French Society of Genitourinary Imaging organised a Delphi consensus conference with a two-round Delphi survey followed by a face-to-face meeting. Consensus was strictly defined using a priori criteria.
Results: 42 expert uro-radiologists completed both survey rounds with no attrition between the rounds.
96 (70%) of the initial 138 statements of the questionnaire achieved a final consensus. An intravenous injection of 20 mg of furosemide before iodinated contrast medium injection was judged mandatory. Improving the quality of excretory-phase imaging through oral or intravenous hydration of the patient, or through the use of an abdominal compression device, was not deemed necessary. The patient should be imaged in the supine position and placed in the prone position only at the radiologist's request. The choice between single-bolus and split-bolus protocols depends on the context, but split-bolus protocols should be favoured whenever possible to decrease patient irradiation. Repeated single-slice test acquisitions should not be performed to decide the timing of excretory phase imaging; instead, excretory phase imaging should be performed 7 minutes after the injection of the contrast medium. The optimal combination of unenhanced, corticomedullary phase and nephrographic phase imaging depends on the context. Suggestions of protocols are provided for 8 different clinical situations.
Conclusion: This expert-based consensus conference provides recommendations to standardise the imaging protocol for computed tomography urography.
Limitations: This consensus meeting did not address all clinical situations and did not take into consideration dual-energy CT
Ethics committee approval: n/a
Funding: Société d'Imagerie Génito-Urinaire.
Author Disclosures:
R. Renard Penna: nothing to disclose

RPS 1407a-11 12:15

Urinary calculi detection with CT-urography: our experience using the nephro-pyelographic phase alone

R. Ciabattoni[1], I. Campo[2], L. Basso[3], C. Sachs[1], M. A. A. Cova[1]; [1]Trieste/IT, [2]Conegliano/IT, [3]Genoa/IT (ciabattoni.riccardo@gmail.com)

Purpose: To evaluate whether the nephro-pyelographic phase of CT-urography alone, without the unenhanced phase, is sufficient to identify and localise urinary calculi.

Methods and materials: In this single-centre retrospective study, images were acquired using a 64-slice Toshiba multidetector CT scanner. Patients who underwent a CT-urography with split bolus or triphasic technique between 2016 and 2019 were included. Images were evaluated randomly and independently by two radiologists with 7 and 25 years of urogenital imaging experience. Patients with no urinary calculi identified or missing one of the CT-urography phases were excluded. The number of calculi identified on each phase was recorded.
Using Cohen's method, the intra-reader agreement was calculated comparing the unenhanced and the nephro-pyelographic phases analysed by each radiologist. The inter-reader agreement was calculated comparing the unenhanced phases and the nephro-pyelographic phases analysed by the two radiologists
Results: Of the 479 enrolled patients, 65 were included in the study (47 M, 18 F). The first radiologist identified 64 calculi in the unenhanced phases and 66 in the nephro-pyelographic phases. The second radiologist identified 76 calculi in the unenhanced phases and 74 in the nephro-pyelographic ones.
The intra-reader agreements were 0.912 and 0.963, respectively. The inter-reader agreements were 0.772 and 0.713, with comparable and reproducible statistical results
Conclusion: The use of a nephro-pyelographic phase alone has greater sensitivity and specificity than the unenhanced phase in localising urinary calculi and in differentiating them from other calcifications while delivering a lower radiation dose to the patient.
Limitations: The main limitation of the nephro-pyelographic phase, which occurred in one patient in our series, is in detecting calculi with the same density of iodinated urine, visible only in the unenhanced phase.
Ethics committee approval: n/a
Funding: No funding was received for this work.
Author Disclosures:
R. Ciabattoni: nothing to disclose
I. Campo: nothing to disclose
L. Basso: nothing to disclose
C. Sachs: nothing to disclose
M. A. A. Cova: nothing to disclose

RPS 1407a-12 12:21
Automated detection of kidney stones on CT images using a pre-trained ResNet
C. E. S. Zaeske, K. Bousabarah, J. Salem, D. Maintz, A. Heidenreich, S. Haneder, N. Grosse Hokamp*; Cologne/DE*

Purpose: A deep learning-based algorithm was developed to assist radiologists in detecting kidney stones. We demonstrates how the availability of pre-trained neural networks and the optimisation of the training process allow for the rapid development of powerful algorithms with low sample sizes.
Methods and materials: CT images from 52 patients with 114 kidney stones were labelled by a radiologist in training and used to train a ResNet50 pre-trained on ImageNet. To compensate for the small sample size and class imbalance, image augmentations and weighted sampling were used. Images were clipped using Hounsfield Units [-100, +1000] and normalised based on ImageNet statistics. The algorithm was trained using the one-cycle policy and the results were validated using 5-fold cross-validation.
Results: Classifications were evaluated per slice (2d) for the whole image series (3d). The mean accuracy, sensitivity, and precision of the classifier per slice were 0.94, 0.67, and 0.43, respectively. In 3d, we considered a kidney stone as detected if any slice containing the stone was correctly classified. Using this method, the mean sensitivity was measured to be 0.87.
Conclusion: Since most kidney stones were identified by the algorithm, it may allow for faster detection of kidney stones and thus a reduction of workload once implemented in clinical routine. Using pre-trained models and optimised training methods such as the used one-cycle policy allow for the rapid training of clinically useful decision support systems.
Limitations: The specificity of the algorithm regarding distractors such as phleboliths is yet to be determined. A specific comparison between radiologists using and not using the algorithm in the diagnostic setting to determine the time saving effect was out of the scope of this study.
Ethics committee approval: n/a
Funding: Koeln Fortune Program/University of Cologne.
Author Disclosures:
N. Grosse Hokamp: Speaker at Phillips, Research/Grant Support at Phillips
C. E. S. Zaeske: nothing to disclose
K. Bousabarah: nothing to disclose
J. Salem: nothing to disclose
A. Heidenreich: nothing to disclose
D. Maintz: Speaker at Phillips
S. Haneder: nothing to disclose

11:15 - 12:30 **Room E**

Chest

RPS 1404a

Implementing lung cancer screening

Moderators:
C. De Margerie-Mellon; Paris/FR
N.N.

RPS 1404a-1 11:15
Volume doubling times of lung adenocarcinomas: correlation with predominant histologic subtypes and prognosis
S. Park, S. M. Lee*; Seoul/KR*

Purpose: To investigate differences in VDT between the predominant histologic subtypes of lung adenocarcinomas and to assess the correlation between VDT and prognosis.
Methods and materials: This retrospective study included patients who underwent at least two serial CT scans before surgery between July 2010 and December 2018. Three-dimensional tumour segmentation was performed on two CT scans and VDTs were calculated. VDTs were compared between predominant histologic subtypes and lesion types using Kruskal–Wallis tests. Disease-free survival (DFS) was obtained from patients undergoing surgery before July 2017. A Cox proportional hazards model was used to determine predictors of DFS.
Results: Out of 268 patients (mean age, 64 years; 143 men), there were 30 lepidic, 87 acinar, 109 papillary, and 42 solid/micropapillary predominant subtypes. The median VDT was 528.8 days (range, 30.9–2,911.4 days) for all lung adenocarcinomas. VDTs differed significantly across subtypes (P<0.001), being shortest in solid/micropapillary subtypes (229.2 days). In terms of lesion type, solid lesions had significantly shorter VDTs than subsolid lesions (P<0.001).
In the 148 patients included in the survival analysis, 35 had disease recurrence or died. The multivariate analysis identified VDT (≥400 or <400 days) as an independent risk factor for DFS (hazard ratio, 2.310; P=0.024), as well as TNM stage and lesion type. Adding VDT to TNM stage and lesion type led to significant improvement in model performance (C-index, 0.767 vs. 0.795; P=0.037).
Conclusion: VDTs varied significantly according to the predominant histologic subtypes of lung adenocarcinoma, and VDT had additional prognostic value for DFS.
Limitations: Retrospective in nature. A selection bias.
Ethics committee approval: Informed patient consent was waived by the institutional review board.
Funding: Funding from the Basic Science Research Program through the National Research Foundation of Korea funded by the Ministry of Science, ICT & Future Planning.
Author Disclosures:
S. Park: nothing to disclose
S. M. Lee: nothing to disclose

RPS 1404a-2 11:21
Identifying participant subgroups in a lung cancer CT screening setting based on competing risks at the baseline scan
A. Schreuder[1], C. Jacobs[1], N. Lessmann[1], M. Broeders[1], M. Silva[2], I. Isgum[3], P. A. de Jong[3], N. Sverzellati[2], M. M. Prokop[1], U. Pastorino[4], C. M. M. Schaefer-Prokop[5], B. van Ginneken[1]*; [1]Nijmegen/NL, [2]Parma/IT, [3]Utrecht/NL, [4]Milan/IT, [5]Amersfoort/NL (antoniusschreuder@gmail.com)*

Purpose: Cardiovascular disease (CVD) and COPD are the main competing causes of death which diminish the benefits of lung cancer (LC) CT screening. Being able to identify participants at risk may encourage a multidisciplinary preventative approach towards reducing overall mortality.
Methods and materials: The model derivation (n=23,096) and validation cohorts (n=2,287) were formed using data from the NLST and MILD trials, respectively. CT measures of CVD and COPD were extracted using computer algorithms, and nodule features were provided by the trials. Risk models were developed to predict four outcomes: LC incidence, LC mortality, CVD mortality, and COPD mortality. For each outcome, a Cox regression model was derived from combining patient characteristics and CT features from the baseline scans.
Results: In the NLST, 756 were diagnosed with LC (3.4%) and 259 (1.2%), 435 (2.0%), and 0.5% died of LC, CVD, and COPD, respectively, after five years' follow-up. 34.2% (259/756) of the LC patients died. Among those who also had a CVD and COPD mortality risk above the 0.9 quantile, this proportion increased to 48.4% (45/93) (Figure 1). In participants with a low LC risk and high CVD and COPD mortality risks, respectively, 0.8% were diagnosed with LC (3/362) and 7.5% died (27/362) ("high" and "low" risk defined in Figure 2). Among those with

a high LC risk and low CVD and COPD mortality risks, 16.0% were diagnosed with LC (150/940) and 2.1% died (20/940).
Conclusion: LC screening participants can be stratified into groups based on LC, CVD, and COPD risk and may benefit from personalised follow-up protocols. Participants with a high LC risk and low risk of CVD or COPD deaths may benefit most from screening.
Limitations: A retrospective design. Recalibration required.
Ethics committee approval: n/a
Funding: No funding was received for this work.
Author Disclosures:
A. Schreuder: nothing to disclose
C. Jacobs: Grant Recipient at MeVis Medical Solutions AG
N. Lessmann: nothing to disclose
M. Silva: Other at Roche
I. Isgum: nothing to disclose
N. Sverzellati: Other at Roche
U. Pastorino: Grant Recipient at Italian Ministry of Health, Grant Recipient at Italian Association for Cancer Research, Grant Recipient at Fondazione Caripolo
C. M. M. Schaefer-Prokop: nothing to disclose
B. van Ginneken: Shareholder at Thirona BV, Founder at Thirona BV, Other at MeVis Medical Solutions AG
M. Broeders: nothing to disclose
P. A. de Jong: nothing to disclose
M. M. Prokop: Speaker at Bracco, Speaker at Bayer, Speaker at Toshiba, Speaker at Siemens, Grant Recipient at Toshiba

RPS 1404a-3 11:27
Variation in LungRADS™ scoring for screen detected lung nodules
H. C. Schmidt[1], M. McInnis[1], C. Dennie[2], D. Langer[1], M. Ang[1], A. Khan[1], P. Jain[1], M. Tammemagi[3], G. Darling[1]; [1]*Toronto, ON/CA,* [2]*Ottawa/CA,* [3]*Thorold/CA (heidi.schmidt@uhn.ca)*

Purpose: To determine the Canadian feasibility of a provincial scale roll-out of an organised lung cancer screening program, Cancer Care Ontario (CCO) implemented the multicentre High Risk Lung Cancer Screening Pilot (HRLCSP) in 2017. One of the integral components of the HRLCSP is radiology quality assurance (QA) to support consistency in performing and interpreting screening scans. Participating radiologists were required to attend a workshop, including a pre-workshop quiz.
Methods and materials: Before the HRLCSP workshop, 43 participating radiologists (chest radiologist without specific experience in lung cancer screening) received the LungRADS™ classification chart and a PowerPoint presentation with 20 questions regarding the scoring and follow-up of 16 different examples of CT images with screen-detected nodules. They were asked to score the nodule examples according to the LungRADS™ classification system. Responses were compared to the consensus of expert radiologists, which served as the reference standard.
Results: The LungRADS™ scores assigned by the participating radiologists varied significantly and were different from the reference standard. For the 20 questions, the correct answers ranged from 42% to 93%, with a mean of 74%. Nodule scores were both overestimated as well as underestimated.
Conclusion: Scoring screen-detected nodules using LungRADS™ does vary significantly and radiologist training before reading for a screening program is important for quality and consistency. The application of a pre-workshop quiz allows for the tailoring of the workshop content to address specific knowledge gaps.
Limitations: n/a
Ethics committee approval: n/a
Funding: No funding was received for this work.
Author Disclosures:
H. C. Schmidt: nothing to disclose
D. Langer: nothing to disclose
M. Ang: nothing to disclose
A. Khan: nothing to disclose
M. Tammemagi: nothing to disclose
M. McInnis: nothing to disclose
G. Darling: nothing to disclose
C. Dennie: nothing to disclose
P. Jain: nothing to disclose

RPS 1404a-4 11:33
Comparative cost-effectiveness of dynamic contrast-enhanced computed tomography versus positron emission tomography in the characterisation of solitary pulmonary nodules: the SPUtNIk trial
D. Tzelis[1], F. J. Gilbert[2], L. Vale[1], V. Benedetto[3], A. Clegg[3], S. Harris[4], J. R. Weir-McCall[2], K. Miles[5], S. George[4]; [1]*Newcastle/UK,* [2]*Cambridge/UK,* [3]*Preston/UK,* [4]*Southampton/UK,* [5]*Brighton/UK (jweirmccall@doctors.net.uk)*

Purpose: To compare the cost-effectiveness of dynamic contrast-enhanced computed tomography (DCE-CT) and ^{18}Fluorine-Fluorodeoxyglucose positron emission tomography/computed tomography (PET-CT) based approaches for the diagnosis of solitary pulmonary nodules (SPN).
Methods and materials: In this prospective multicentre trial, 380 participants with indeterminate SPN (8-30 mm) underwent DCE-CT and PET-CT. All patients completed 2 years follow-up with a collection of subsequent investigations, management strategy, and outcome. The cancer prevalence, diagnostic accuracy, and test outcome results of the SPUtNIk trial were used in an economic evaluation decision model. Further data on complications of the tests and survival came from a systematic review and meta-analysis. NHS tariff costs and the literature were used for cost estimates. The economic evaluation was reported as a cost-consequence analysis and the incremental cost per correctly managed case over a two-year time horizon was also calculated.
Results: Sequential DCE-CT and PET-CT were most accurate (84.4±1.4%) for the management of SPN compared with DCE-CT (77.8±2%) or PET-CT alone (82±1.6%). However, the combined modality approach was most costly in the cost-consequence analysis (£4058±210). A DCE-CT strategy was the least costly (cost=£3305±199) followed by PET/CT (£4014±206). For all correctly managed cases, the ICER for DCE-CT/PET-CT over DCE-CT was £11,323. For DCE-CT/PET-CT versus DCE-CT, the incremental cost per correctly managed case was £11,323. PET/CT would not be cost-effective compared to either DCE-CT or DCE-CT/PET-CT.
Conclusion: If society is not willing to pay more than £11,323 per accurately managed case, DCE-CT is a cost-effective strategy. Above this value, DCE-CT/PET-CT is the most cost-effective strategy. With the greater availability and access to CT, and lower cost, consideration should be given to using DCE-CT as the first-line test for indeterminate pulmonary nodules.
Limitations: Limited availability of utility data and long-term costs.
Ethics committee approval: REC-12/SW/0206.
Funding: NIHR-HTA (grant no:09/22/117).
Author Disclosures:
J. R. Weir-McCall: nothing to disclose
F. J. Gilbert: Research/Grant Support at Google Deepmind, Research/Grant Support at GE Healthcare, Research/Grant Support at Bayer
L. Vale: nothing to disclose
D. Tzelis: nothing to disclose
S. Harris: nothing to disclose
K. Miles: nothing to disclose
S. George: nothing to disclose
A. Clegg: nothing to disclose
V. Benedetto: nothing to disclose

RPS 1404a-5 11:39
Quality assurance in lung cancer screening by computed tomography: optimised ultra-low radiation dose by beam filtering in a randomised study
M. Silva[1], G. Milanese[1], S. Sestini[2], M. Ruggirello[2], A. Marchianò[2], N. Sverzellati[1], U. Pastorino[2]; [1]*Parma/IT,* [2]*Milan/IT (mariosilvamed@gmail.com)*

Purpose: To test different protocols of ultra-low radiation dose computed tomography (ULDCT) by x-ray spectrum shaping for lung cancer screening (LCS).
Methods and materials: Based on a former anthropomorphic phantom study, 375 subjects were prospectively randomised to one of the following ULDCT protocols: fully automated exposure control (both voltage and current - "ULDCT1"), fixed tube voltage (Sn100kVp) and current according to patient size (140mAs or 210mAs – "ULDCT2"), and a hybrid approach with fixed tube voltage and automatic exposure control for current ("ULDCT3" Sn100-100refmAs and "ULDCT4" Sn150-20refmAs). Each subject underwent double CT acquisition with one of the above protocols and the low-dose CT (LDCT: 120kVp, 25mAs). Intrasubject CT dose index (CTDIvol) and dose-length product (DLP) were compared (mean and standard deviation reported). An analysis of variance to compare ULDCT protocols was undertaken.
Results: CTDIvol was 1.62 (0) mGy in LDCT compared to ULDCT: 0.59 (0.21), 0.72 (0.15), 0.51 (0.16), and 0.66 (0.17).
DLP was 65 (6) mGycm in LDCT compared to ULDCT: 24 (8), 29 (7), 21 (7), 27 (8).
ULDCT3 showed lower CTDIvol than any ULDCT protocol ($p<0.001$) and lower DLP than ULDCT2 and 4 ($p<0.001$). Conversely, ULDCT2 appeared the less convenient approach for dose saving, with CTDIvol and DLP higher than ULDCT1 and 3 ($p<0.001$).
Conclusion: Optimised ULDCT protocols with x-ray spectrum shaping by tin-filter can be used with fixed tube voltage at Sn100 kVp and automatic control of tube current (ULDCT3) to aim at the sharpest optimisation of radiation dose. Fixed techniques are less effective in reducing doses.

Limitations: Image quality will be tested for consistency of each optimised protocol within LCS workflow by dedicated post-processing platform (detection and semi-automatic volume of nodule).
Ethics committee approval: Prot INT 21/11 and further amendments.
Funding: Italian Ministry of Health, AIRC, Fondazione Cariplo, Lombardy Region.
Author Disclosures:
M. Silva: nothing to disclose
G. Milanese: nothing to disclose
S. Sestini: nothing to disclose
M. Ruggirello: nothing to disclose
A. Marchianò: nothing to disclose
N. Sverzellati: nothing to disclose
U. Pastorino: nothing to disclose

RPS 1404a-6 11:45
Improving diagnostic accuracy for pulmonary nodules with the combination of morphological characteristics and spectral CT-specific multiparameters
Z. Ren, T. He*; Xianyang/CN*
(rzl19900220@163.com)

Purpose: To demonstrate the value of improving pulmonary nodules (PN) diagnostic accuracy by combining the morphological characteristics and spectral CT-specific parameters.
Methods and materials: 173 patients with pulmonary nodules (61 benign pulmonary nodules (BPN) and 112 malignant pulmonary nodules (MPN)) underwent dual-phase contrast-enhanced spectral CT. Monochromatic and material decomposition images were reconstructed. The morphological characteristics of PN were observed on 70keV images. The CT values from 40keV to 140keV, Effective-Z, blood concentration (BC), iodine concentration (IC), water concentration (WC) of PN, and the aorta at the same level were measured to calculate the slope of spectral HU curve (λ), normalised blood concentration (NBC), normalised iodine concentration (NIC), and normalised water concentration (NWC). The receiver operating characteristic (ROC) curve was drawn to evaluate the diagnostic performance of differentiating BPN from MPN.
Results: The two patient groups were similar demographically (P>0.05). The incidence of bronchial truncation, irregular shape, lobulation, pleural effusion, and vascular invasion in MPN was significantly higher than those in BPN (P<0.05). The CT values from 40keV to 90keV, $\lambda_{40keV\text{-}90keV}$, $\lambda_{100keV\text{-}140keV}$, $\lambda_{40keV\text{-}140keV}$, BC, IC, NBC, NIC, and Effective-Z values of BPN were significantly higher than those of MPN (P<0.05), while both lesions had similar CT values from 100keV to 140 keV and WC and NWC values (P>0.05). The diagnostic accuracy in differentiating BPN and MPN (AUC 0.891) with combined morphological characteristics and spectral CT-specific parameters was significantly higher than that of only using morphological characteristics (AUC 0.726) or spectral multiparameters (AUC 0.843).
Conclusion: Morphological characteristics with a combination of spectral CT multiparameter spectral CT can help to improve the diagnostic accuracy in differentiating pulmonary nodules.
Limitations: Tha sample size was small.
Ethics committee approval: n/a
Funding: No funding was received for this work.
Author Disclosures:
Z. Ren: nothing to disclose
T. He: nothing to disclose

RPS 1404a-7 11:51
Using spirometry to identify high-risk individuals not eligible for lung cancer screening
R. Aggarwal, A. Lam, G. Liu, J. Kavanagh*; Toronto/CA (jokavana@tcd.ie)*

Purpose: To determine if FEV1 can identify a high-risk subgroup of individuals traditionally excluded by current lung cancer screening eligibility criteria.
Methods and materials: Spirometry (2009-2013) was administered in a lung screening program and patient outcomes were tracked until 2017. The addition of forced-expiratory-volumes-at-one second, FEV1, to four different screening-eligibility criteria, (DLST, NLST, NELSON, and OLSP) was retrospectively assessed to identify high-risk individuals. Sensitivity, specificity, and the number needed to screen at various FEV1 cutoffs were compared to determine the optimal clinical cutoff.
Results: In 1,161 participants, optimal clinical cutoffs for FEV1 were 90%, 90%, 90%, and 85% for the DLST, NLST, NELSON, and OLSP, respectively. Respectively, the sensitivity was increased significantly by 33%, 28%, 28%, 16%, specificity was reduced by 19%, 25%, 24%, 22%, and NNS was reduced by 122, 7, 10, -3 when compared to original criteria alone.
Conclusion: Spirometry can identify a high-risk subpopulation missed by original lung screening criteria, particularly when self-reported COPD is not included. Inclusion of spirometry-identified airway obstruction screening-eligibility criteria into screening programs that lack another method for COPD assessment increases sensitivity.
Limitations: A retrospective single-institution study. The FEV1 cutoffs were chosen by the authors pragmatically to maximise sensitivity as well as keeping specificity acceptable.
Ethics committee approval: Approval was obtained through the University Health Network (UHN) Research Ethics Board (REB 06-0639). Recruitment began in June 2003 and concluded in December 2009 as part of the Lusi Wong Princess Margaret Early Lung Cancer Detection Program (PM-ELCAD).
Funding: This study was supported by the Lusi Wong Fund, the Princess Margaret Cancer Foundation, the Alan Brown Chair in Molecular Genomics (to GL), and the University of Toronto Comprehensive Research Experience for Medical Students programme.
Author Disclosures:
J. Kavanagh: nothing to disclose
A. Lam: nothing to disclose
R. Aggarwal: nothing to disclose
G. Liu: Advisory Board at Takeda,Astrazeneca,BMS,Bayer,Roche,Novartis,Abbyvie,Merck, Research/Grant Support at Takeda,Merck,Astrazeneca, Speaker at Astrazeneca, EMD serono

RPS 1404a-8 11:57
Pulmonary nodule growth: can follow-up be shortened with a high-end or an ultra-high-resolution CT scanner?
D. Grob, S. Schalekamp, L. J. Oostveen, W. J. van der Woude, C. Jacobs, M. M. Prokop, I. Sechopoulos, M. Brink*; Nijmegen/NL*
(Dagmar.Grob@radboudumc.nl)

Purpose: To determine the interscan variability of pulmonary nodule volume measurements in CT scans acquired with state-of-the-art wide-area and ultra-high-resolution CT systems.
Methods and materials: In this prospective study, patients with at least two non-calcified solid pulmonary nodules suspicious for metastases on previous CT scans were imaged twice with either a high-end 320-detector CT (MDCT, Aquilion ONE Genesis, Canon, slice thickness 0.5 mm, 512x512 matrix) or an ultra-high-resolution CT (UHRCT, Precision, Canon, 0.25 mm, 1024x1024). In between scans, an off-and-on table strategy was used to simulate follow-up scans with no nodule growth. Semi-automated volumetric nodule segmentation and volume estimation (max. 4 per patient, effective diameter 4-15 mm) were performed on a lung screening workstation (Veolity). 95%-limits of agreement (LOA) and the time to estimate actual nodule growth rate at a nodule volume doubling time (VDT) of 400 days were calculated.
Results: 17 patients (60 nodules, average volume: 218 mm^3) were imaged on the MDCT and 27 patients (90 nodules, 177 mm^3) on the UHRCT at a similar dose (mean dose-length-product: 126.6 mGycm vs. 127.2 mGycm, respectively (p=0.98)). The 95%-LOA was ±7.0% for the MDCT and ±5.9% for the UHRCT (p=0.07). Therefore, the minimum required interscan period to detect a VDT of 400 days is only 33-39 days.
Conclusion: Both scanners result in low interscan variability, especially compared to current clinical standards, which requires a volume change of 25% (the current 95%-LOA) as significant nodule growth. Therefore, the follow-up period to detect pulmonary nodule growth could be dramatically shortened from three to about one month, reducing patient anxiety and the potential for stage shift in lung nodule management.
Limitations: Pulmonary metastases instead of incidental nodules were measured.
Ethics committee approval: Review board approval and written informed consent were obtained.
Funding: Canon provided financial funding.
Author Disclosures:
I. Sechopoulos: Research/Grant Support at Canon Medical Systems, Speaker at Siemens Healthineers, Research/Grant Support at Siemens Healthineers, Speaker at Hologic
S. Schalekamp: nothing to disclose
D. Grob: Research/Grant Support at Canon Medical Systems
L. J. Oostveen: Research/Grant Support at Canon Medical Systems
M. M. Prokop: Grant Recipient at Canon Medical Systems, Speaker at Canon Medical Systems, Speaker at Bracco, Speaker at Bayer, Grant Recipient at Siemens Healthineers , Speaker at Siemens Healthineers , Other at Departmental spinoff - Thirona , Other at Departmental licence agreement - Mevis Medical Solutions
M. Brink: Research/Grant Support at Canon Medical Systems
W. J. van der Woude: nothing to disclose
C. Jacobs: Grant Recipient at MeVis Medical Solutions AG, Other at Royalties from MeVis Medical Solutions AG

RPS 1404a-9 12:03

The classification of pulmonary nodules by Lung-RADS 1.1: a randomised prospective analysis of four ultra-low dose CT protocols in a lung cancer screening trial

G. Milanese[1], M. Silva[1], M. Ruggirello[2], S. Sestini[2], F. Sabia[2], A. Marchianò[2], N. Sverzellati[1], U. Pastorino[2]; [1]Parma/IT, [2]Milan/IT

Purpose: To analyse the intrasubject agreement between low-dose (LDCT) and ultra-low-dose CT (ULDCT) for LungRADS1.1 in a lung cancer screening (LCS) setting.
Methods and materials: 375 subjects underwent single-breath-hold double CT acquisition protocol, including both standard LDCT scan (120kVp, 25mAs) and one of the following ULDCT protocols: fully automated exposure control ("$ULDCT_1$"), fixed tube-voltage and current according to patient size ("$ULDCT_2$": Sn100kVp, 140mAs/210mAs), or hybrid approach with fixed tube-voltage and automated exposure control for current ("$ULDCT_3$": Sn100kVp-100mAs_{ref}; "$ULDCT_4$": Sn150kVp-20mAs_{ref}).
Prospective LDCT reading was performed by semi-automatic software for the detection and segmentation of pulmonary nodules (PN). After a wash-out time of at least 2 weeks, two independent readers repeated the same process on ULDCT, without manual corrections. Dominant PNs (dPNs) were selected from both LDCT and ULDCT according to volumetric LungRADS1.1.
Agreement was assessed by means of Cohen's weighted-kappa test.
Results: Intrasubject inter-scanning protocol variation for LungRADS1.1 was: κ_{ULDCT1}=0.8461, κ_{ULDCT2}=0.9030, κ_{ULDCT3}=0.8813, and κ_{ULDCT4}=0.9033 for $Reader_1$, and κ_{ULDCT1}=0.8469, κ_{ULDCT2}=0.9029, κ_{ULDCT3}=0.7896, and κ_{ULDCT4}=0.7844 for $Reader_2$.
Inter-reader agreement by ULDCT was: κ_{ULDCT1}=0.8726, κ_{ULDCT2}=0.8899, κ_{ULDCT3}=0.8466, and κ_{ULDCT4}=0.8590.
$Reader_1$ missed dPNs in 11/98 (11.2%) $ULDCT_1$, 12/94 (12.8%) $ULDCT_2$, 16/88 (18.1%) $ULDCT_3$, and 14/95 (14.7%) $ULDCT_4$. Missing of LDCT dPNs did not affect management by $ULDCT_3$.
$Reader_2$ missed dPNs in 13/98 (12.2%) $ULDCT_1$, 9/94 (9.6%) $ULDCT_2$, 11/88 (12.5%) $ULDCT_3$, and 8/95 (8.4%) $ULDCT_4$. Missing of LDCT dPNs would have affected management by $ULDCT_3$ for 1 subject (shift from $LungRADS_3$ to $LungRADS_2$).
Conclusion: Intrasubject and inter-reader agreement for LungRADS between LDCT and ULDCT ranged from good to very good. $ULDCT_3$ scanning protocol can be proposed for the purposes of LCS.
Limitations: Single CT and CAD used.
Ethics committee approval: Prot-INT21/11 and further amendments.
Funding: Italian Ministry of Health, AIRC, Fondazione Cariplo, Lombardy Region.
Author Disclosures:
G. Milanese: nothing to disclose
M. Silva: nothing to disclose
M. Ruggirello: nothing to disclose
F. Sabia: nothing to disclose
A. Marchianò: nothing to disclose
N. Sverzellati: nothing to disclose
U. Pastorino: nothing to disclose
S. Sestini: nothing to disclose

RPS 1404a-10 12:09

Deep learning in discriminating atypical lung nodules: a diagnostic test

Y. Zhang[1], Y. Liu[1], H. Han[2], F. Qu[1], N. Huang[2], Z. Ye[1]; [1]Tianjin/CN, [2]Beijing/CN

Purpose: To test the feasibility and efficiency of a deep learning model to discriminate challenging atypical lung nodules.
Methods and materials: 5,912 surgically confirmed benign nodules since 2014 were initially included. Then preliminary screening was performed by three radiologists to filtrate atypical nodules following longest-diameter ≤3cm, part-solid or solid, no calcification, or adipose inside nodule on pre-contrast CT slices. So far, a total of 380 nodules including 190 malignant nodules and 190 atypical benign nodules diagnosed in 2019 comprised our research dataset. 24 semantic features and a diagnostic opinion were also recorded. A centre-cropped 3D convolutional neural network (CNN) which has previously proved efficiency in differentiating nodules on low-dose CT scans was trained with the LIDC-IDRI dataset and a private screening dataset. Receiver operating characteristic analysis was performed to evaluate the purposed study. An instance figure was uploaded to demonstrate the radiographic appearance of 4 included nodules.
Results: Only 79 (20.8%) atypical nodules were directly given correct diagnosis by radiologists without any follow-up suggestion. For initial CNN, the average precision on our dataset was 57.3% and the average AUC was 0.64, with 53.1% sensitivity and 60% specificity. After feeding CNN with additional new atypical samples, the average precision increased to 73% and the average AUC was 0.78, with 78.3% sensitivity and 70.0% specificity.
Conclusion: Deep learning has shown potential in recognising atypical nodules at base-line examinations. However, the critical role of the dataset in our study implies most datasets based on follow-up labels may not be enough. Deepening and broadening of the training dataset probably benefits further application of deep learning in radiology.
Limitations: Sample augmentation is still on-going to overcome distribution overlapping and to further improve performance.
Ethics committee approval: n/a
Funding: No funding was received for this work.
Author Disclosures:
Y. Zhang: nothing to disclose
Y. Liu: nothing to disclose
F. Qu: nothing to disclose
N. Huang: nothing to disclose
Z. Ye: nothing to disclose
H. Han: nothing to disclose

RPS 1404a-11 12:15

Multi-detector computed tomography diagnosis of the different pathological types of cystic lung cancer

L. Zheng[1], Y. Li[2]; [1]Shanghai/CN, [2]Zhangjiagang/CN
(zhenglinfeng04@aliyun.com)

Purpose: To analyse MDCT findings of different pathological types of cystic lung cancer (CLC).
Methods and materials: 28 cases with pathologically proved CLC were retrospectively collected and general clinical data and MDCT findings were analysed. Then imaging features of these CLC were further interpreted including lesion size, location, morphological classification, ground-glass opacity sign, shape, margin, tumour-lung interface, the relationship of tumour and bronchus, residual separation in the airspace, pleural indentation, and associated bullae.
Results: Of 28 CLC cases, 18 cases of adenocarcinomas, 3 cases of microinvasive adenocarcinomas, 6 cases of squamous carcinomas, and one adenosquamous carcinoma. The average age of patients in the adenocarcinoma cases and the squamous cell carcinoma cases were 60.56±8.03 and 66.00±7.93 years old, respectively, which was higher than the microinvasive adenocarcinoma cases (49.33±16.17 years old) (p=0.048). For the lesion size, the cases of adenocarcinoma (1.99±0.69 cm) and squamous cell carcinoma (2.45±0.87 cm) were larger than that of the cases of microinvasive adenocarcinoma (0.73±0.23 cm) (p=0.008). Ground-glass sign was mainly found in adenocarcinoma (14 cases, 77.8%) and microinvasive adenocarcinoma (3 cases, 100.0%), however, only one case (16.7%) of squamous cell carcinoma showed this sign (p=0.012). 5 cases of squamous cell carcinoma showed bronchial cut-off sign, which was more common than in the adenocarcinoma (2 cases) (p=0.003). There were no significant differences for other imaging features in different pathological types of CLC (p>0.05).
Conclusion: For the different pathological type of CLC, there are relatively typical CT imaging findings, e.g. the ground-glass opacity was frequently observed in adenocarcinoma while the bronchial truncation sign was common in squamous cell carcinoma. It is important to do dynamic follow-up CT for atypical lesions of CLC.
Limitations: Small size cases. A lack of follow-up data.
Ethics committee approval: n/a
Funding: No funding was received for this work.
Author Disclosures:
L. Zheng: nothing to disclose
Y. Li: nothing to disclose

RPS 1404a-12 12:21

Lung-RADS category and smoking status can predict adherence to recommendations in a real-world low-dose CT lung cancer screening program

E. J. M. Barbosa Jr.[1], M. Hershman[2]; [1]Philadelphia, PA/US, [2]Tucson/US

Purpose: Low-dose CT lung cancer screening (LCS) can decrease lung cancer related mortality in persons with a significant smoking history, however, it is hindered to low adherence to follow up recommendations.
Methods and materials: We retrospectively enrolled all persons who underwent multiple (2 or more) LCS exams from 2014 to 2019 at our institution and recorded patient demographics, lung-RADS category, outcomes, and adherence to screening recommendations. We assessed predictors of adherence via univariate and multivariate logistic regression (MLR).
Results: 260 persons returned for follow-up scans (57.7% had 2, 34.2% had 3, 7.7% had 4, and 0.4% had 5). 43/260 (16.5%) had positive scans, of which 28/260 (10.8%) were lung-RADS category 3, 8/260 (3.1%) were 4A, 6/260 (2.3%) were 4B, and 2/260 (0.8%) were 4X. 143 persons were current smokers at the time of the baseline LDCT and 117 persons were former smokers who quit within the last 15 years before the baseline LDCT. Overall adherence was 43.0% but increased progressively with higher lung-RADS (33.2%-100%) and with former smoker status (50.0%, vs 36.2% for current smokers). Smoking status and a positive lung-RADS category were the only statistically significant predictors of adherence in MLR modelling.

Conclusion: Adherence to LCS recommendations, which is crucial to maximize the benefits of LCS and allow early diagnosis of lung cancer, is less than 50% and is lower in persons who are current smokers and with negative LCS exams, offering a roadmap for targeted performance improvement, which healthcare systems can leverage to improve LCS cost-effectiveness and maximize its societal benefits.
Limitations: A retrospective design.
Ethics committee approval: IRB approved.
Funding: No funding was received for this work.
Author Disclosures:
E. J. M. Barbosa Jr.: nothing to disclose
M. Hershman: nothing to disclose

11:15 - 12:30 **Room F1**

Abdominal Viscera

RPS 1401

Dos and don'ts for liver imaging reporting and data system (LI-RADS)

Moderators:
N. Borojevic; Warrington/UK
C. S. Reiner; Zürich/CH

RPS 1401-1 11:15

LI-RADS category 5 hepatocellular carcinoma: preoperative gadoxetic acid–enhanced MRI to predict early recurrence after curative resection
H. Wei, H. Jiang, B. Song*; Chengdu/CN (weih_cat@163.com)*

Purpose: To identify preoperative gadoxetic acid enhanced-magnetic resonance (MR) imaging biomarkers for prediction of early recurrence (2 years) after curative resection for liver imaging reporting and data system category 5 (LR-5) hepatocellular carcinoma (HCC).
Methods and materials: Between July 2015 and July 2018, this retrospective study evaluated consecutive treatment-naïve, high-risk patients who underwent gadoxetic acid–enhanced MR examination within 1 month before surgical resection for HCC. All MR images were reviewed by two independent radiologists. Predictive clinical and imaging features for early recurrence were identified by univariate and multivariate analysis.
Results: A total of 126 patients with 167 LR-5 HCCs were included; 62 (49.2%) patients had postoperative tumour recurrence within 2 years. Four MR imaging features and serum AFP were independently associated with early recurrence: peritumoural hypointensity on hepatobiliary phase (HBP) (odds ratio [OR] = 6.68; 95% CI: 1.437, 31.081), corona enhancement (OR = 3.997; 95% CI: 1.238, 12.905), tumour size >5 cm (OR = 3.629; 95% CI: 1.137, 11.586), multifocality (OR = 3.141; 95% CI: 1.011, 9.763), and AFP level > 400 ng/mL (OR = 3.262; 95% CI: 1.242, 8.569). The AUCs of the combined models comprising only predictive MR imaging features and MR features along with serum AFP were 0.783 (95% CI: 0.704, 0.862) and 0.797 (95% CI: 0.719, 0.875), respectively.
Conclusion: In high-risk patients with LR-5 HCC, preoperative HBP peritumoral hypointensity, corona enhancement, tumour size, multifocality, and serum AFP can be used to predict early recurrence after curative hepatectomy.
Limitations: The retrospective design may cause a selection bias.
Ethics committee approval: n/a
Funding: This work was supported by the National Natural Science Foundation of China (No. 81771797).
Author Disclosures:
H. Wei: nothing to disclose
H. Jiang: nothing to disclose
B. Song: nothing to disclose

RPS 1401-2 11:21

What proportion of clinically reported LI-RADS 5 observations do not meet LI-RADS 5 criteria?
J. Birnbaum[1], C. B. Sirlin[2], V. Chernyak[3]; *[1]Bronx/US, [2]San Diego, CA/US, [3]Bronx, NY/US (vichka17@hotmail.com)*

Purpose: Liver imaging reporting and data system (LI-RADS) category 5 (LR-5) denotes 100% certainty of hepatocellular carcinoma. The assignment of LR-5 is based on combinations of major features (size, arterial phase hyperenhancement [APHE], "washout" [WO], enhancing "capsule", threshold growth). The goal of this study is to assess the proportion of LR-5 observations reported clinically that did not meet LR-5 criteria based on reported major features using LI-RADS v2017 and v2018.
Methods and materials: All MR and CT reports using a standardised LI-RADS macro between 4/17–8/19 were reviewed. For each reported LR-5 observation, all major features and LI-RADS version (v2017 or v2018) were extracted from the clinical report. Based on the reported major features, we determined whether LR-5 criteria were met for each observation.
Results: 237 observations in 181 patients (68% male, mean age 65.6 years) were reported as LR-5, including 137 (58%) reported with v2017 (median size 23 mm) and 100 (42%) with v2018 (median size 18 mm). 9/137 (7%) v2017 LR-5 observations and 4/100 (4%) v2018 LR-5 observations did not meet LR-5 criteria based on reported major features. Of the 9 incorrectly categorised v2017 observations, 3 (33%) lacked APHE, 1 (11%) was < 10 mm, 1 (11%) was 16 mm new observation with APHE only, and 4 (44%) were 10-19 mm with APHE and WO as the only other major feature. Of the 4 incorrectly categorised v2018 observations, 3 (75%) lacked APHE and 1 (25%) was < 10 mm.
Conclusion: Based on reported major features, 4-7% of clinically reported LR-5 observations do not meet LR-5 criteria. Methods such as education and decision support tools may help to reduce the frequency of these reporting errors.
Limitations: Retrospective single institution study.
Ethics committee approval: IRB-approved. Informed consent was waived.
Funding: No funding was received for this work.
Author Disclosures:
V. Chernyak: Consultant at Bayer
C. B. Sirlin: Advisory Board at AMRA, Advisory Board at Guerbet, Advisory Board at VirtualScopics, Advisory Board at Bristol Myers Squibb, Consultant at Exact Sciences, Consultant at IBM/Watson Health , Consultant at Fulcrum Therapeutics, Consultant at AMRA, Consultant at Bayer, Consultant at GE Healthcare, Research/Grant Support at Celgene, Research/Grant Support at Philips, Research/Grant Support at ACR Innovation, Research/Grant Support at GE US, Research/Grant Support at GE Digital, Research/Grant Support at Bayer, Research/Grant Support at GE MRI, Research/Grant Support at Siemens, Research/Grant Support at GE Healthcare, Research/Grant Support at Gilead, Speaker at GE Healthcare, Speaker at Bayer
J. Birnbaum: nothing to disclose

RPS 1401-3 11:27

Diagnostic criteria for recurrent hepatocellular carcinoma in gadoxetic acid enhanced MRI: are LR4 observations enough for the diagnosis of recurrence?
H. Kim, J.-I. Choi, S. Y. Youn, D. W. Kim, S. E. Rha*; Seoul/KR (heesoo2423@gmail.com)*

Purpose: Current diagnostic criteria for HCC are focusing on HCC naïve patients and there are no established diagnostic criteria for recurrent HCC. We evaluated the diagnostic performance of LI-RADS version 2018 using gadoxetic acid-enhanced MRI in patients with a prior history of HCC.
Methods and materials: We enrolled 51 consecutive patients who: 1) underwent liver transplantation or resection for HCC between 2013 to 2018 in our institute, 2) had gadoxetic acid-enhanced MRI within one month before transplantation or resection, 3) prior history of treatment of HCC, and 4) did not have more than five HCCs or infiltrative tumours. Two radiologists reviewed gadoxetic acid-enhanced MRIs and determined the presence of LR3, LR4, and LR5 observations except previously treated tumours based on LI-RADS version 2018 in consensus.
Results: Sensitivity for recurrent HCC of LR5 and LR5+LR4 observations were 32.4% and 89.2%, respectively. PPV for LR5, LR4, and LR3 observations were 100%, 70.0%, and 44.4%, respectively. 100% of LR4 observations determined by major features only (LR4m) were HCC. But PPV of LR4 observations upgraded from LR3 using ancillary features (LR4u) was 62.5%. For LR4u observations, PPV of observations with arterial enhancement (LR4ua) and without arterial enhancement (LR4un) were 81.3% and 25.0%, respectively. Sensitivity and PPV for LR5+LR4n+LR4ua observations were 83.7% and 91.2%, respectively.
Conclusion: The sensitivity of LR5 observations for the detection of recurrent HCC was very low. Regarding LR4 observations as HCC reduces the PPV. Presuming LR4 observations with arterial enhancement as HCC may compromise both sensitivity and PPV.
Limitations: Selection bias for retrospective design.
Ethics committee approval: IRB approved this study and waived informed consent.
Funding: National R&D Program for Cancer Control, Ministry of Health & Welfare, and Republic of Korea (HA15C0004).
Author Disclosures:
H. Kim: nothing to disclose
J.-I. Choi: Grant Recipient at Guerbet Korea, Advisory Board at Bayer Korea, Grant Recipient at Bracco Korea, Grant Recipient at Central Medical Service
S. Y. Youn: nothing to disclose
D. W. Kim: nothing to disclose
S. E. Rha: nothing to disclose

RPS 1401-4 11:33

Indeterminate lesions (LI-RADS 3 and 4) lacking arterial phase hyperenhancement on CT and MRI in the cirrhotic liver: outcome and role of ancillary features

A. Inzerillo[1], G. Porrello[2], F. Vernuccio[2], R. Cannella[2], M. Midiri[2], G. Brancatelli[2]; [1]Lascari/IT, [2]Palermo/IT (inzerilloagostino@gmail.com)

Purpose: To retrospectively evaluate LI-RADS ancillary imaging features and outcomes of indeterminate lesions lacking APHE in cirrhotic patients.
Methods and materials: In this retrospective study, we included indeterminate lesions (LR-3 and LR-4) up to 3 cm lacking APHE in consecutive cirrhotic patients imaged with CT or MRI. All MRI exams were performed with Gd-EOB-DTPA. All lesions were individually evaluated to determine LI-RADS major and ancillary imaging features at diagnosis and outcome. Reference standard was based on pathology and imaging follow-up.
Results: 27 lesions lacking APHE, 20 LR-3 and 7 LR-4, in 12 cirrhotic patients (10M, 2F) were included. HCC was proved for 4 [15%] of 27 lesions, including 1 of 10 (10%) lesions imaged with CT, and 3 of (17%) 17 lesions imaged with MRI. Not-HCC malignancy was diagnosed in 1 lesion imaged with MR. Imaging analysis of these 5 malignant lesions showed none of the ancillary features suggesting malignancy on the lesion imaged with CT. Conversely, at least one ancillary feature suggesting malignancy was detected in the remaining 4 lesions imaged with MR (i.e., hepatobiliary phase hypointensity in 4, restricted diffusion in 3, fat in the mass in 3, and T2-hyperintensity in 2).
Conclusion: HCC is identified in 10% and 17% of indeterminate LR-3 or LR-4 lesions lacking APHE imaged with CT or Gd-EOB-DTPA MRI, respectively. MRI may allow the detection of LI-RADS ancillary features suggesting malignancy and therefore those lesions requiring more aggressive management.
Limitations: Small sample size, retrospective design, no inter-reader assessment.
Ethics committee approval: IRB approved, waiver of informed consent obtained.
Funding: No funding was received for this work.
Author Disclosures:
A. Inzerillo: nothing to disclose
M. Midiri: nothing to disclose
G. Porrello: nothing to disclose
F. Vernuccio: nothing to disclose
R. Cannella: nothing to disclose
G. Brancatelli: nothing to disclose

RPS 1401-5 11:39

Modified LI-RADS for diagnosis of hepatocellular carcinoma on gadoxetic-acid-enhanced MR imaging: a prospective comparative study

Y. Qin, H. Jiang, B. Song; Chengdu/CN (qinyun@wchscu.cn)

Purpose: To develop modified liver imaging reporting and data systems (mLI-RADS) with gadoxetic acid-enhanced magnetic resonance imaging (EOB-MRI) and compare its diagnostic accuracy with the original version 2018 (v2018) LI-RADS for hepatocellular carcinoma (HCC) in high-risk patients.
Methods and materials: Totally 278 patients with 885 nodules (440 HCCs, size range: 0.3-14.6 cm) were enrolled from July 2015 to October 2018 and underwent EOB-MRI. Major and ancillary imaging features and LI-RADS categories of all liver observations were evaluated based on v2018 LI-RADS by two independent radiologists. We constructed four mLI-RADS with: i) restricted diffusion and hepatobiliary phase hypointensity upgraded as additional major features (M1), ii) "capsule" instead of enhancing "capsule" regarded as an additional major feature (M2), iii) size categories of "＜10 mm" and "10-19 mm" combined as "＜20 mm" (M3), and iv) M1+M2+M3 (M4). Per-lesion sensitivity and specificity of these criteria were compared using McNemar's test.
Results: Per-lesion sensitivity, specificity, and accuracy by consensus were 59%, 98%, and 78% for LR-5 or LR-TIV contiguous with LR-5 mass with v2018 LI-RADS. These measures were 68%, 97%, and 81% for M1, 60%, 98%, and 78% for M2, 73%, 98%, and 85% for M3, and 75%, 97%, and 86% for M4. M1 ($p=0.003$), M3 ($p<0.001$), and M4 ($p<0.001$) all demonstrated significantly higher sensitivity than v2018 LI-RADS without substantial affect of specificity (p=0.290-1.000).
Conclusion: Compared with v2018 LI-RADS, mLI-RADS on EOB-MRI exhibits diagnostic advantages for HCC in high-risk patients.
Limitations: All lesions of every patients were enrolled, but bootstrap analysis was not used to handle clustering effect.
Ethics committee approval: Ethical approval by the institutional review board and informed consent were obtained.
Funding: No funding was received for this work.
Author Disclosures:
Y. Qin: nothing to disclose
H. Jiang: nothing to disclose
B. Song: nothing to disclose

RPS 1401-6 11:45

Analysis imaging features of LI-RADs M on MRI using hepatocyte-specific agent and correlation with pathologic diagnosis

K. Lim, H. Kwon, J. Cho; Pusan/KR (nonomori85@naver.com)

Purpose: To analyse the image features for the diagnosis LI-RADs M on MRI using hepatocyte-specific agent and its correlation with pathologic diagnosis.
Methods and materials: Between March 2016 and February 2019, 65 LI-RADS M underwent MRI at 3T using a hepatocyte-specific agent and pathologic confirmation. Two independent radiologists evaluated the presence or absence of rim enhancement, peripheral washout, delayed central enhancement, targeted on TP or HBP, targeted restriction, infiltrative pattern, marked diffusion restriction, necrosis, severe ischemia and biliary dilatation, and surface retraction of each observation. The agreement of image features was assessed with an intraclass coefficient (ICC). The frequency of consensus image features was analysed and compared with pathologic diagnosis using the paired t-test.
Results: The agreement of image features was moderate to excellent. On pathologic diagnosis, there were HCC (35.4%), IHCC (27.7%), HCC-CC (7.7%), metastasis (15.4%), inflammation (10.8%), and rarely sarcoma, lymphoma (<5%). The biliary dilatation and surface retraction was significantly correlated to IHCC ($p<0.05$). The infiltrative pattern was correlated to chronic inflammation. Other image features were not correlated to specific pathologic diagnosis.
Conclusion: The presence of LR-M features and biliary dilatation or capsular retraction may be helpful in the diagnosis of IHCC without a biopsy. If only LR-M image features without biliary dilatation or capsular retraction are present, then a biopsy is essential for the accurate diagnosis. However, the infiltrative pattern may be an inflammatory disease which is not malignant, so it should be carefully considerate when making a diagnosis.
Limitations: A small number studied. Single institution. Retrospective study.
Ethics committee approval: IRB approval was provided.
Funding: No funding was received for this work.
Author Disclosures:
H. Kwon: nothing to disclose
J. Cho: nothing to disclose
K. Lim: nothing to disclose

RPS 1401-7 11:51

The diagnostic performance of LI-RADS v2018 and the value of major features and ancillary features in the diagnosis of 10-19 mm hepatocellular carcinoma (HCC) on gadoxetatic acid MRI

S. Xie, J. Chen, Y. Zhang, D. Rong, L. Sun, J. Wang; Guangzhou/CN (xiesidong2001@163.com)

Purpose: Recent updates in LI-RADS v2018 have changed diagnostic criteria for 10-19 mm HCC, but few studies investigated the diagnostic performance of LI-RADS v2018 for small HCC using gadoxetatic acid MRI. We retrospectively assessed the diagnostic performance of LI-RADS v2018 for 10-19 mm HCC in Chinese patients with chronic liver disease and explored several modifications of LI-RADS aiming to improve the sensitivity for diagnosing HCC without decreasing specificity on gadoxetatic acid MRI.
Methods and materials: Between June 2015 and April 2017, 111 patients at high risk for HCC who had up to 10-19 mm observations detected on gadoxetatic acid MRI and had no history of previous treatment for hepatic lesions were retrospectively studied. LI-RADS MRI features were reviewed by two independent radiologists in consensus. Observations were categorised according to LI-RADS v2018 and several modified versions of LI-RADS, which allow major features and ancillary features favoring HCC (AFs-HCC) to upgrade LR-4 to LR-5. Sensitivities, specificities, and accuracies of LR-5 for HCC were determined and compared.
Results: A total of 129 observations in 111 patients were included, which were 86 (66.7%) HCCs, 40 (31.0%) benign lesions, and 3 (2.3%) non-HCC malignancies (Table 3). The diagnostic performance of LR-5 defined by LI-RADS v2018 for 10-19 mm HCC was modest with a sensitivity, specificity, and accuracy of 58.6%, 97.6%, and 71.3%, respectively. Comparing to LI-RADS v2018, mLI-RADS IV (APHE+HBP hypointensity[no "washout"]=LR-5) and mLI-RADS III (APHE+TP hypointensity[no "washout"] =LR-5) showed highest sensitivities (77.0%, 73.6%) ($P<0.001$, $P<0.001$) and accuracies (82.2%, 81.4%) ($P<0.001$, $P=0.001$) while maintaining high specificities (92.9%, 97.6%) ($P=1.000$, $P=0.500$) (Table 6) (Figure 1).
Conclusion: In our study we found that comparing to LI-RADS v2018, mLI-RADS IV, and mLI-RADS III improved sensitivity without decreasing specificity of LR-5 for small HCC.
Limitations: Our study has several limitations. First, we conducted our study retrospectively at a since centre, thus confirmation is warranted in a prospective multicentre setting. Second, the number of patients in our study was relatively small. Further studies with a large patient population are needed to validate the presented result in our study. Finally, the reference standard for the final diagnosis was composite and not based on a histologic diagnosis alone. This may have caused selection bias.

Ethics committee approval: IBR approval was obtained.
Funding: This work was funded.
Author Disclosures:
S. Xie: Author at The 3rd Affiliated Hospital of Sun Yat-sen University
J. Chen: Author at The 3rd Affiliated Hospital of Sun Yat-sen University
Y. Zhang: Author at The 3rd Affiliated Hospital of Sun Yat-sen University
D. Rong: Author at The 3rd Affiliated Hospital of Sun Yat-sen University
J. Wang: Author at The 3rd Affiliated Hospital of Sun Yat-sen University
L. Sun: Author at The 3rd Affiliated Hospital of Sun Yat-sen University

RPS 1401-9 11:57

Diagnostic accuracy of single-phase CT texture analysis for prediction of LI-RADS v2018 category

S. Puttagunta, C. van der Pol, A. M. Kulkarni, I. Carrión Martinez, J. Wat, M. Ferri*; Hamilton/CA (drputtaguntamyhead@gmail.com)*

Purpose: To determine if texture analysis (TA) can classify liver observations likely to be hepatocellular carcinoma (HCC) based on the liver imaging reporting and data system (LI-RADS) using single portal-venous phase (PVP) CT.
Methods and materials: This retrospective cohort study included 64 consecutive LI-RADS observations, 38 LI-RADS 5, 12 LI-RADS 4, and 14 LI-RAD 3, on CT over a 19-month period. Each observation was segmented on PVP images and TA features including mean Hounsfield Unit (HU), median, minimum, maximum, standard deviation, skewness, kurtosis, and entropy were extracted. The final LI-RADS category was established by two fellowship-trained abdominal radiologists on multiphase CT. PVP TA features for LI-RADS observations were compared using Kruskal-Wallis and two sample t tests. Logistic regression was used for prediction of LI-RADS group. Diagnostic accuracy was assessed using receiver operating characteristic curves and Youden's method. P<0.05 defined statistical significance.
Results: Multiple PVP TA features were associated with the LI-RADS group including the mean HU (P=0.003), median (P=0.002), minimum (P=0.010), maximum (P=0.013), standard deviation (P=0.009), skewness (P=0.007), and entropy (P<0.001). On logistic regression, skewness remained significant (P=0.016) and could predict LI-RADS group with an area-under-the-curve (AUC)/sensitivity (SN)/specificity (SP) of 0.78/70%/79%. When the logistic regression model incorporated all significant features on univariate analysis, the AUC/SN/SP improved to 0.98/96%/100%.
Conclusion: TA features on PVP CT can differentiate liver observations likely and unlikely to be HCC based on LI-RADS with high diagnostic accuracy. This may preclude the need to immediately recall some patients for additional multiphase imaging.
Limitations: Retrospective design. Sample size. 2D TA was performed and 3D TA may have provided more data.
Ethics committee approval: Research Ethics Board approved.
Funding: No funding was received for this work.
Author Disclosures:
S. Puttagunta: nothing to disclose
C. van der Pol: nothing to disclose
A. M. Kulkarni: nothing to disclose
I. Carrión Martinez: nothing to disclose
J. Wat: nothing to disclose
M. Ferri: nothing to disclose

RPS 1401-11 12:03

Comparison of current guidelines for the noninvasive diagnosis of hepatocellular carcinoma using gadoxetic acid-enhanced MRI: diagnostic performances in liver transplantation candidates

S. Jeon, J. M. Lee, I. Joo, J. Y. Park, J. Yoo*; Seoul/KR*

Purpose: To compare the diagnostic performances of current guidelines for diagnosis of HCC in liver transplantation (LT) candidates using gadoxetic acid-enhanced liver MRI (Gd-EOB-MRI).
Methods and materials: In this retrospective study, 81 patients (119 HCCs and 35 non-HCCs) with liver cirrhosis who underwent preoperative Gd-EOB-MRI and subsequent LT were included. Per-lesion imaging diagnoses of HCCs were made using four different guidelines (American Association for the Study of Liver Disease (AASLD), European Association for the Study of the Liver (EASL), Asian Pacific Association for the Study of the Liver (APASL), and Korean Liver Cancer Association-National Cancer Center (KLCA-NCC) guidelines), and patient allocation was determined according to the Milan criteria (MC). Comparisons of per-lesion sensitivity, specificity, and accuracy of patient allocation between guidelines were performed using logistic regression with generalised estimating equations.
Results: For diagnosis of HCC, AASLD guidelines showed the highest specificity (97.4%) followed by EASL and KLCA-NCC guidelines (92.1% and 92.1%, P>0.99 and =0.15, respectively, in comparison to AASLD), while the specificity of APASL guidelines was demonstrated to be significantly lower than that of AASLD guidelines (78.9% vs. 97.4%, P=0.006). APASL and KLCA-NCC guidelines (75.9% and 65.6%) showed significantly higher sensitivities than AASLD/EASL (34.5% and 38.8%, respectively; all Ps<0.001). For organ allocation, KLCA-NCC showed higher accuracy in selecting unsuitable candidates (with non-HCC malignancies or beyond MC HCCs) than EASL (68.4% vs. 31.8%; P=0.001).
Conclusion: For diagnosis of HCCs using Gd-EOB-MRI in LT candidates, AASLD guidelines provided the highest specificity, followed by EASL, KLCA-NCC, and APASL guidelines, with a statistically significant difference found only with APASL guidelines. KLCA-NCC guidelines provided the most accurate selection of unsuitable LT candidates.
Limitations: Retrospective design.
Ethics committee approval: Approved by IRB with a waiver of informed consent.
Funding: No funding was received for this work.
Author Disclosures:
S. Jeon: nothing to disclose
J. M. Lee: nothing to disclose
I. Joo: nothing to disclose
J. Y. Park: nothing to disclose
J. Yoo: nothing to disclose

RPS 1401-12 12:09

Long-term evolution of LR-2, LR-3, and LR-4 observations in cirrhotic patients with hepatitis C treated with direct-acting antivirals

R. Cannella, S. Greco, F. Vernuccio, G. Cabibbo, C. Cammà, V. Di Marco, M. Midiri, G. Brancatelli*; Palermo/IT (rob.cannella89@gmail.com)*

Purpose: To assess the long-term evolution of observations with low (LR-2), intermediate (LR-3), and high (LR-4) probability for hepatocellular carcinoma (HCC) in cirrhotic patients with hepatitis C treated with direct-acting antivirals (DAA).
Methods and materials: This retrospective study assessed 2017 consecutive HCV patients treated with DAA between 2015 and 2019. Inclusion criteria were: i) cirrhosis or prior history of HCC, ii) available contrast-enhanced liver imaging studies (CT or MRI), iii) multiple follow-ups before and after DAA, and iv) at least one indeterminate lesion before DAA. Two radiologists reviewed imaging studies, recorded major imaging features, and categorised each lesion according to the LI-RADSv2018. Differences in evolution before and after DAA were evaluated using the Pearson $\chi 2$ or Fisher exact test. The cumulative risk of LR-5 was calculated by using the Kaplan-Meier method.
Results: Final population included 67 patients (mean age 69.5±10.8 years) with 109 observations (mean size 11.8±6.7 mm), including 31 (28.4%) LR-2, 67 (61.5%) LR-3, and 11 (10.1%) LR-4, with a mean follow-up of 44±23 months. Evolution of indeterminate observations to LR-5 was more common before DAA than after DAA (before DAA: 0 (0%) LR-2, 11 (16.4%) LR-3, and 8 (72.7%) LR-4 evolved to LR-5 vs. after DAA: 1 (3.2%) LR-2, 10 (14.9%) LR-3, and 1 (9.1%) LR-4 evolved to LR-5; p<0.001). Cumulative risk for LR-5 evolution was 15.5% at 6 months, 23.8% at one year, and 37.6% at two years. LI-RADS category was significantly associated with risk of progression into LR-5 (p<0.001).
Conclusion: The use of DAA therapy does not increase progression of indeterminate lesions into definitively HCC.
Limitations: Retrospective, small sample, lack of cohort of HCV cirrhotic patients not treated with DAA.
Ethics committee approval: IRB-approved study, informed consent was waived.
Funding: No funding was received for this work.
Author Disclosures:
R. Cannella: nothing to disclose
S. Greco: nothing to disclose
F. Vernuccio: nothing to disclose
G. Cabibbo: nothing to disclose
C. Cammà: nothing to disclose
V. Di Marco: nothing to disclose
M. Midiri: nothing to disclose
G. Brancatelli: Speaker at Bayer

11:15 - 12:30 **Room F2**

Musculoskeletal

RPS 1410a

Spine and inflammatory disorders

Moderators:
M. S. Posadzy; Poznan/PL
W. J. Rennie; Leicester/UK

RPS 1410a-1 11:15

Evaluation of the diagnostic accuracy of the RA magnetic resonance imaging (MRI) scoring system (RAMRIS) in wrist and metacarpophalangeal (MCP) joints in patients with rheumatoid arthritis (RA)

H. Wu, G. Zhang*; Guangzhou/CN*

Purpose: To validate the relationship of the RA MRI scoring system (RAMRIS) and the Sharp/Van der Heijde score on radiography with 28-joint count disease activity score (DAS28) in therapy-naive patients with RA.
Methods and materials: We analysed radiograph and MRI data of unilateral wrist and metacarpophalangeal (MCP) joints in 408 patients with newly diagnosed rheumatoid arthritis. Two readers scored synovitis, bone marrow oedema, bone erosion, joint space narrowing, and tenosynovitis according to RAMRIS. Radiographs were scored according to the SvH method. Correlations between RAMRIS, SvH scores, and DAS28 were determined. Low to moderate (≤5.1) and high (>5.1) disease activity were divided. The differences of RAMRIS and SvH scores in the 2 groups were compared.
Results: Synovitis, tenosynovitis, and MCP (2-5) scores were positively associated with DAS28 (all p<0.05). The tenosynovitis and MCP (2-5) scores of the low to moderate disease activity groups (7.93 ± 3.97, 11.21 ± 5.3, respectively) were significantly lower than those of the high disease activity group (10.11± 4.47, 13.97 ± 5.25, respectively) (P=0.021 and P=0.025, respectively). The total scores of RAMRIS in the high disease activity group (39.19 ± 18.24) were significantly different from those of the low to moderate disease activity groups (32.48 ± 20.52, P=0.025)
Conclusion: Synovitis, tenosynovitis, and MCP scores can be used to assess the activity of RA. The tenosynovitis, MCP, and total scores of RAMRIS may be helpful for differentiating high, moderate, and low disease activity.
Limitations: The study only included inpatients and may not be entirely generalisable to other populations. This study was also limited in the evaluation of DAS-28.
Ethics committee approval: Our study was approved by the ethics committee of our hospital and informed consent was obtained.
Funding: No funding was received for this work.
Author Disclosures:
H. Wu: nothing to disclose
G. Zhang: nothing to disclose

RPS 1410a-2 11:21

High-resolution MRI assessment of flexor tendon pulleys in psoriatic arthritis for disease detection and differentiation from rheumatoid arthritis using a 16-channel hand coil

D. B. Abrar[1], M. Frenken[1], M. Boschheidgen[1], S. Nebelung[2], P. Sewerin[1], G. Antoch[1], D. McGonagle[3], C. Schleich[1]; *[1]Düsseldorf/DE, [2]Aachen/DE, [3]Leeds/UK*

Purpose: To evaluate the value of 3-Tesla magnetic resonance imaging (MRI) changes of flexor tendon pulleys for the differentiation of psoriatic (PsA) and rheumatoid arthritis (RA) using a novel 16-channel high-resolution hand coil.
Methods and materials: 17 patients with active PsA, 20 patients with active RA, and 16 healthy controls (HC) were evaluated by high-resolution 3T MRI using the dedicated 16-channel hand coil. Images were analysed by 3 independent readers for the degree of inflammatory changes, the thickness of flexor tendon pulleys, and the comparison to the outcome measures for RA clinical trials PsA MRI score (PsAMRIS) and to its sub-scores: synovitis, flexor tenosynovitis, bone oedema, bone erosion, periarticular inflammation, and bone proliferation.
Results: Flexor tendon pulleys were thicker in PsA than in RA patients (mean difference 0.16 mm, p<0.001) and HC (mean difference 0.2 mm, p<0.001) and showed a higher degree of associated inflammatory changes (mean difference from RA: 4.7, p=0.048; mean difference HC: 14.65, p<0.001). Additionally, there was a strong correlation of accessory pulley inflammation and total PsAMRIS and its acute-inflammatory sub-scores (for second digit: synovitis r=0.72, flexor tenosynovitis r=0.7, overall PsAMRIS r=0.72, p<0.05). Similar correlations between MRI determined pulley inflammation and synovitis, flexor tenosynovitis, and periarticular inflammation were evident in digits 3-5. Weaker correlations between pulley inflammation and PsAMRIS and its inflammatory subscores were evident in RA.
Conclusion: The assessment of MRI changes of flexor tendon pulleys is potentially beneficial for disease detection in PsA, as well as for its distinction from RA and HC.
Limitations: A small study population and a different disease duration of the study groups.
Ethics committee approval: Study was approved by the local ethics comittee.
Funding: No funding was received for this work.
Author Disclosures:
D. B. Abrar: nothing to disclose
M. Frenken: nothing to disclose
M. Boschheidgen: nothing to disclose
S. Nebelung: nothing to disclose
P. Sewerin: nothing to disclose
D. McGonagle: nothing to disclose
G. Antoch: nothing to disclose
C. Schleich: nothing to disclose

RPS 1410a-3 11:27

The semi-automated algorithm for the detection of bone marrow oedema lesions in patients with axial spondyloarthritis

I. Kucybała, J. Polak, Z. Tabor, A. Urbanik, W. Wojciechowski*; Cracow/PL (iwona.kucybala@gmail.com)*

Purpose: To create an efficient tool for the semi-automated detection of bone marrow oedema lesions in patients with axial spondyloarthritis (axSpA).
Methods and materials: MRI examinations of 22 sacroiliac joints of patients with confirmed axSpA-related sacroiliitis (mean SPARCC score: 24.3±26.1) were included in the study. The design of our algorithm is based on Maksymowych et al. evaluation method and consists of the following steps: manual segmentation of bones (T1W sequence), automated detection of reference signal region, sacroiliac joint central lines and ROIs, a division of ROIs into quadrants, and automated detection of inflammatory changes (STIR sequence). As a gold standard, two sets of manual lesion delineations were created. Two approaches to the performance assessment of lesion detection were considered: pixel-wise (detections compared pixel by pixel) and quadrant-wise (quadrant to quadrant). Statistical analysis was performed using Spearman's correlation coefficient.
Results: The correlation coefficient obtained for pixel-wise comparison of semi-automated and manual detections was 0.87 (p=0.001, 95% CI 0.83-0.92), while for quadrant-wise analysis was 0.83 (p=0.001, 95% CI 0.75-0.89). The correlation between two sets of manual detections was 0.91 for pixel-wise comparison (p=0.001, 95% CI 0.86-0.94) and 0.88 (p=0.001, 95% CI 0.82-0.92) for the quadrant-wise approach. Spearman's correlation between two manual assessments was not statistically different from the correlation between semi-automated and manual evaluations, both for pixel- (p=0.14) and quadrant-wise (p=0.17) analysis. The average single-slice processing time was 0.64±0.30 seconds.
Conclusion: Our method allows for highly objective detection of bone marrow oedema lesions in patients with axSpA. The quantification of both affected pixels and quadrants using our semi-automated algorithm have comparable reliability to manual assessment.
Limitations: Time-consuming manual segmentation of bones.
Ethics committee approval: Jagiellonian University Bioethics Comittee approval No.1072.6120.16.2019.
Funding: No funding was received for this work.
Author Disclosures:
I. Kucybała: nothing to disclose
J. Polak: nothing to disclose
Z. Tabor: nothing to disclose
A. Urbanik: nothing to disclose
W. Wojciechowski: nothing to disclose

RPS 1410a-4 11:33

How tin filtration affects the value of an effective radiation dose in CT of the sacroiliac joints: can CT replace x-ray in patients with suspected sacroiliitis?

E. Korcakova, J. Štěpánková, D. Suchy, P. Hosek, K. Bajcurova, J. Pernicky, H. Mirka*; Plzen/CZ (korcakovae@fnplzen.cz)*

Purpose: To calculate values of an effective radiation dose given by tin-filtrated ultra-low dose computed tomography (TFULDCT) in a cohort of patients referred with suspected sacroiliitis. For comparison, the effective radiation doses given by x-ray in the same group were calculated. We evaluated the accuracy of TFULDCT and x-ray for detecting bone changes in sacroiliac joints (SI).
Methods and materials: Effective radiation dose was calculated by an experienced radiation physicist using ImpactDose 2.3, patient model-real patient data (CT Imaging GmbH, Germany), and PCXMC 2.0 (x-ray, STUK Finland). Datasets of 30 consecutive patients examined by TFULDCT and x-ray were

evaluated independently by 3 radiologists. Every investigator blindly evaluated the CT and x-ray studies and decided whether the finding was positive, negative, or uncertain for sacroiliitis. The results were statistically evaluated.
Results: The median value of an effective radiation dose received by TFULDCT of SI joints in our cohort was 0.11 mSv (0.06-0.34 mSv). The median of an effective radiation dose for x-ray in the same patient cohort was 0.22 mSv (0.09-0.58 mSv). CT provides a statistically significantly more reliable distinction between positive and negative cases than x-ray. X-ray had a greater number of unclear findings.
Conclusion: Our results show that TFULDCT significantly reduces the effective radiation dose and in the examination of SI joints achieves lower values than an x-ray. TFULDCT can be used for monitoring patients with axial spondylartitis because it has a high accurancy in assessing the bone changes and does not burden patients with a high radiation dose.
Limitations: n/a
Ethics committee approval: n/a
Funding: No funding was received for this work.
Author Disclosures:
E. Korcakova: nothing to disclose
J. Štěpánková: nothing to disclose
D. Suchy: nothing to disclose
P. Hosek: nothing to disclose
K. Bajcurova: nothing to disclose
J. Pernicky: nothing to disclose
H. Mirka: nothing to disclose

RPS 1410a-5 11:39
Glycosaminoglycan remodelling of lumbar intervertebral discs in elite rowers throughout their annual training cycle
M. Frenken, L. Kasprowski, M. Boschheidgen, B. Bittersohl, G. Antoch, C. Schleich, S. Nebelung, D. B. Abrar*; Düsseldorf/DE (miriam.frenken@med.uni-duesseldorf.de)*

Purpose: To assess the glycosaminoglycan (GAG) content of lumbar intervertebral discs (IVD) in elite rowers (ER) at different stages of their annual training cycle compared to healthy volunteers (HV) using GAG chemical exchange saturation transfer (gagCEST).
Methods and materials: 205 lumbar IVD of 21 ER (23 ±3 years, 9 female, 11 male) and 25 HV (27 ±2 years, 13 female, 12 male) were prospectively examined with 3T magnetic resonance imaging (MRI). Standard T2-weighted (T2w) sequences were used for morphological grading according to the Pfirrmann classification. GAG content of the nucleus pulposus (NP) and annulus fibrosus was determined with gagCEST in non-degenerated discs according to Pfirrmann. ER were examined during the peak of their competition preparation (T0) and 6 months later during the peak of their post-competition recovery period (T1).
Results: At T0 we found significantly higher gagCEST values in ER compared to HV (NP: 4.26 ±2.37% vs 3.38 ±1.72%, p<0.05; confidence interval (CI) 0.32%/1.44%; AF: 2.75 ±1.7% vs 1.961 ±1.23%, p<0.01; CI 0.4%/1.2%). At T1, gagCEST values decreased and illustrated no significant difference compared to HV (NP: 3.55 ± 2.31%, p=0.531, CI 0.038%/0.73%; AF: 2.31 ±1.57%, p=0.073, CI 0.03%/0.74%).
Conclusion: Compared to HV, lumbar IVD of ER show significantly higher gagCEST values during the peak of their competition preparation and similar values during the recovery period, indicating a GAG remodelling effect by training. The results suggest that physical activity (rowing) potentially prevents molecular GAG depletion in the lumbar IVD.
Limitations: Observations over a one-year training cycle, no long-term results beyond that.
Ethics committee approval: n/a
Funding: No funding was received for this work.
Author Disclosures:
M. Frenken: nothing to disclose
L. Kasprowski: nothing to disclose
M. Boschheidgen: nothing to disclose
B. Bittersohl: nothing to disclose
G. Antoch: nothing to disclose
C. Schleich: nothing to disclose
S. Nebelung: nothing to disclose
D. B. Abrar: nothing to disclose

RPS 1410a-6 11:45
Degeneration at atypical spinal segments in patients with abdominal aortic aneurysms
N. A. Farshad-Amacker, M. Farshad, J. Galley, R. Sutter, T. Götschi, U. J. Mühlematter*; Zurich/CH (nadja.farshad@balgrist.ch)*

Purpose: Abdominal aortic aneurysms (AAA) affect vascular perfusion of the lumbar spine by compromising its direct vascular supply. AAA treatment with endovascular aortic aneurysm repair (EVAR) completely occludes the direct vascular supply to the lumbar spine. We hypothesised that patients with AAA and patients with EVAR show a different pattern of spinal degeneration compared to controls without AAA.
Methods and materials: Patients who underwent EVAR with computed tomography images (CT) >6 months prior (n=52), at the time of EVAR (n=100), and >1 year after EVAR (n=100) were included and compared to an age- and gender-matched control group without AAA (n=94). Degeneration scores, levels with the most severe degeneration, and levels with the progression of degeneration were analysed in CT and compared at different time points. Statistics included Fisher's exact test, Wilcoxon's signed-rank test and a Mann-Whitney U test.
Results: Levels of most severe degeneration were located more commonly in the mid-lumbar area in AAA patients compared to control subjects (p=0.016) with significantly more endplate erosions (p=0.001). However, EVAR did not result in an additional accelerated degeneration.
Conclusion: AAA is associated with atypical location of lumbar spinal degeneration at the mid-lumbar segments, but EVAR does not seem to additionally accelerate the degenerative process. This observation underlines the importance of disc and endplate vascularisation in the process of spinal degeneration.
Limitations: The retrospective design.
Ethics committee approval: The ethical committee approved this retrospective study.
Funding: No funding was received for this work.
Author Disclosures:
N. A. Farshad-Amacker: nothing to disclose
J. Galley: nothing to disclose
R. Sutter: nothing to disclose
T. Götschi: nothing to disclose
U. J. Mühlematter: nothing to disclose
M. Farshad: nothing to disclose

RPS 1410a-7 11:51
Ultrasound evaluation of nail and extensor digitorum tendon involvement in psoriatic patients
L. Wang, L. Qiu*; Chengdu/CN (liyunwang1992@qq.com)*

Purpose: To evaluate ultrasound manifestations of the nail involvement in psoriatic patients, compare them with healthy individuals, and search for correlations between ultrasonography and clinical features.
Methods and materials: 37 psoriatic patients and 42 healthy volunteers were included. PASI index, mNAPSI index, and psoriatic area were recorded of all patients. 6 ultrasonography parameters in B mode and power Doppler concerning the nail plate, the bed, the matrix, the proximal nail fold, and extensor digitorum tendon of each finger in all subjects were evaluated and compared.
Results: The incidence of US abnormal morphology in the nail plate was significantly higher in psoriatic patients than healthy controls (55.98% vs 4.05%). The nail plate, the bed, the matrix, the proximal nail fold, and the extensor digitorum tendon were significantly thicker in psoriatic patients (0.82±0.25 vs 0.66± 0.09mm, 1.78±0.63 vs 1.48±0.33 mm, 2.81±0.51 vs 2.55±0.46 mm, 0.96±0.23 vs 0.89±0.13 mm, and 1.07±0.38 vs 1.00±0.29 mm, $p < 0.05$, respectively). The largest area under the curve (AUC) was obtained from the nail plate (AUC=0.749). No statistical difference was found in power Doppler ultrasound grading between both groups. The thicknesses of the nail plate, the bed, and the matrix were positively correlated with PASI index, mNAPSI index, and psoriasis area.
Conclusion: The changes of the nail unit and extensor digitorum tendon can frequently be found by ultrasound in psoriatic patients. Special attention might be paid to the ultrasonographic morphology and thickness of the nail plate.
Limitations: We did not evaluate nails with other imaging methods.
Ethics committee approval: The Clinical Trials and Biomedicine Ethics Committee of West China Hospital of Sichuan University approved this study and informed consent was obtained.
Funding: The National Natural Science Foundation of China (81671696).
Author Disclosures:
L. Wang: nothing to disclose
L. Qiu: nothing to disclose

RPS 1410a-8 11:57
The role of ultrasonography in monitoring long-standing rheumatoid arthritis
M. L. Dura, P. Zuchowski, P. Gorgolewski, S. Jeka*; Bydgoszcz/PL (p.zuchowski81@gmail.com)*

Purpose: In the course of rheumatoid arthritis (RA) there may occur irreversible inflammatory-destructive changes within joints. In later stages of RA, joint pain often results from destructive changes instead of an active inflammatory process in the synovial membrane. The aim of this study was to assess the cause of joint

pain in patients with long-standing RA (LSRA) in whom low disease activity was diagnosed through a disease activity score (DAS28).
Methods and materials: 53 patients with RA were enrolled in the study, each with low disease activity (DAS28 (CRP) <3.2) and disease history of 8 years or more. Participants had their metacarpophalangeal (MCP) II-V and proximal interphalangeal (PIP) I-V joints evaluated through physical examination. Joints exhibiting pain were further subjected to power Doppler ultrasound (PDUS) and grey-scale ultrasound (GSUS) examination.
Results: 954 joints in total were evaluated through physical examination, with pain found in 218 (22%) joints in 41 (77%) patients. In 218 joints examined through PDUS, an active inflammatory process was found in 171 (78%) joints. In the remaining 47 (22%) joints, the pain was related to irreversible destructive changes, including the presence of bone erosion in radiographs and membrane hypertrophy determined via GSUS. In the group of 41 patients with joint pain determined through physical examination, in 6 (15%) it was related to the presence of irreversible destructive changes and not an active inflammatory process.
Conclusion: US examination allows the designating of patients with LSRA in whom joint pain is connected with irreversible destructive changes in joints. In such a patient group, it may be advisable to terminate or alter the standard therapy for patients with active RA.
Limitations: A small study group.
Ethics committee approval: n/a
Funding: No funding was received for this work.
Author Disclosures:
P. Zuchowski: nothing to disclose
M. L. Dura: nothing to disclose
P. Gorgolewski: nothing to disclose
S. Jeka: nothing to disclose

RPS 1410a-9 12:03

The importance of lumbrical muscle enhancement on bilateral dynamic contrast-enhanced hand MRIs of patients with arthralgia: a possible diagnostic MRI-clue for rheumatoid arthritis

Z. Akkaya, A. Gürsoy Çoruh, A. H. Elhan, G. Sahin*; Ankara/TR (zehraakkaya@gmail.com)*

Purpose: To investigate the significance of lumbrical muscle enhancement (LME) in patients with hand arthralgia.
Methods and materials: Blinded to the diagnoses, dynamic contrast-enhanced bilateral hand MRIs of 100 patients (F:M=88:12) with hand arthralgia taken from 2014-2019, using 3.0T and 1.5T scanners, were retrospectively evaluated by 2 radiologists for the presence of LME. When identified, the degree of enhancement was graded as weak or strong.
Patients were stratified in 3 groups according to their final diagnoses as rheumatoid arthritis (RA)(n=41), control (fibromyalgia, osteoarthritis(OA), and rheumatological disease-ruled out cases)(n=31), and other arthritides groups (n=28)(spondyloarthropathy, Behçet's, Sjögren's, erosive OA, systemic lupus erythematosus, dermatomyositis, and polymyalgia rheumatica).
Categorical variables were compared by using Chi-Square/Fisher's exact tests. The difference among groups for continuous variables was evaluated by one-way ANOVA/Kruskal Wallis ANOVA. A multiple comparison test was used to know which groups differed from others where applicable. The agreement between raters was assessed by Cohen's Kappa(κ) statistic. P values <0.05 were considered significant.
Results: The mean patient age was 47.2±11.2. Age and gender were not significantly different among groups (p=0.17, p= 0.84, respectively). The RA group showed significantly more (p<0.001) and a stronger degree of enhancement (p=0.001) with substantial inter-rater-correlations for right and left hands (κ=0.739, κ=0.671, respectively, p<0.001). Right hands of RA and control patients showed significantly more LME (p=0.001, p=0.033, respectively).
Conclusion: In comparison to controls and other arthritides cases, RA patients demonstrated a significantly higher rate and degree of LME on MRIs with substantial inter-rater-correlations. This could indicate a subtle but important radiological clue for the diagnosis and differential diagnosis of RA.
Limitations: Due to the difficulty in recruiting patients with definitely established diagnoses, patient numbers were low in the arthritides group for individual disease analyses.
Ethics committee approval: Hospital Ethics Review Board approval was obtained.
Funding: No funding was received for this work.
Author Disclosures:
Z. Akkaya: nothing to disclose
G. Sahin: nothing to disclose
A. Gürsoy Çoruh: nothing to disclose
A. H. Elhan: nothing to disclose

RPS 1410a-10 12:09

T2 mapping of the sacroiliac joints in patients with axial spondyloarthritis: a pilot study

D. Albano[1], R. Bignone[2], V. Chianca[1], R. Cuocolo[3], C. Messina[1], L. M. M. Sconfienza[1], F. Ciccia[2], M. Midiri[2], M. Galia[2]; [1]*Milan/IT,* [2]*Palermo/IT,* [3]*Naples/IT (albanodomenico@me.com)*

Purpose: To determine whether T2-mapping of the sacroiliac joints (SIJs) might help to identify patients with spondyloarthritis.
Methods and materials: This pilot study included 21 biologic-naive patients with axial spondyloarthritis (10 males; mean age=43±12years; range=19-57) and 21 controls (14 males; mean age=34±10; range=28-71) who prospectively underwent SIJs MRI at 1.5T, including a multislice multi-echo spin-echo sequence. Standard MRIs were reviewed to assess the SIJs according to the assessment of spondyloarthritis international society (ASAS) criteria and spondyloarthritis research consortium of Canada (SPARCC) MRI index. T2 maps were used to draw regions of interests in the cartilaginous part of the SIJs. Disease activity was assessed using a BASDAI questionnaire. The Bland-Altman method, ROC curve analysis, Chi-square, Mann-Whitney U, Pearson's and Spearman's correlation coefficient were used for data analysis.
Results: MRI was positive for sacroiliitis in 6/21 patients (29%). Interobserver reproducibility of T2 values was 88% (coefficient of repeatability=5.9, bias=0.96, p<0.001). Mean T2 values of patients (59.2±2.9ms, range: 54.3-66.3ms) were significantly higher (p<0.001) than those of controls (39.6±3.4ms, range: 33.6-46.6ms). A T2 value of 50.5ms yielded 100% sensitivity and 100% specificity to differentiate patients from controls. Mean T2 values on the iliac side of the SIJs of patients (62.8±9.8 ms) were significantly higher than on the sacral side (56.4±11.3 ms; p<0.001). No significant association/correlation was found between T2 values and BASDAI, disease duration, SPARCC, ASAS criteria, HLA-B27-positivity, age, and gender (p≥0.197).
Conclusion: T2 values of the SIJs were significantly higher in patients than in healthy controls, making this tool potentially helpful for early identification of patients with spondyloarthritis.
Limitations: A small sample size and a lack of follow-up.
Ethics committee approval: IRB approval was obtained. All patients provided their written informed consent.
Funding: No funding was received for this work.
Author Disclosures:
D. Albano: nothing to disclose
R. Bignone: nothing to disclose
V. Chianca: nothing to disclose
R. Cuocolo: nothing to disclose
C. Messina: nothing to disclose
L. M. M. Sconfienza: nothing to disclose
F. Ciccia: nothing to disclose
M. Midiri: nothing to disclose
M. Galia: nothing to disclose

RPS 1410a-11 12:15

Loss of glycosaminoglycans in lumbar intervertebral discs in patients with ankylosing spondylitis

D. B. Abrar[1], M. Frenken[1], M. Boschheidgen[1], S. Nebelung[2], G. Antoch[1], P. Sewerin[1], X. Baraliakos[3], C. Schleich[1]; [1]*Düsseldorf/DE,* [2]*Aachen/DE,* [3]*Herne/DE*

Purpose: To evaluate the glycosaminoglycan (GAG) content of lumbar intervertebral discs (IVD) in patients with ankylosing spondylitis (AS) using GAG chemical exchange saturation transfer (gagCEST).
Methods and materials: 325 lumbar IVD of 40 patients with AS (mean age 50 ±10 years) and 25 healthy control patients (HC) were prospectively examined with 3T magnetic resonance imaging (MRI). MRI protocol contained morphological T2-weighted (T2w) images to grade IVD according to the Pfirrmann classification and biochemical imaging with gagCEST to calculate a region of interest (ROI) of the nucleus pulposus (NP) and annulus fibrosus (AF). Prior to the statistical testing of gagCEST effects in patients and HC, IVD were classified according to Pfirrmann.
Results: Significantly lower gagCEST values of NP and AF were found in non-degenerative IVD (Pfirrmann 1 and 2) of AS patients compared to HC (NP: 1.88 % ±1.21% vs 3.38 % ±1.71%; p<0.01; confidence interval (CI): 0.89%/2.11%. AF: 1.11 % ± 1.07 % vs 1.96 %± 1.23 %; p<0.01; CI 0.39%/1.3%).
Conclusion: GagCEST analysis of morphologically non-degenerative IVDs in T2w images showed significantly lower GAG values in patients with AS in the NP and AF compared to HC.
Limitations: A small study population and differences in disease duration and treatment.
Ethics committee approval: Written and inforfmed consent. Approval by the local ethics committee.
Funding: No funding was received for this work.

Author Disclosures:
D. B. Abrar: nothing to disclose
G. Antoch: nothing to disclose
M. Frenken: nothing to disclose
S. Nebelung: nothing to disclose
C. Schleich: nothing to disclose
P. Sewerin: nothing to disclose
X. Baraliakos: nothing to disclose
M. Boschheidgen: nothing to disclose

RPS 1410a-12 12:21
Reduction of metal artefacts caused by titanium peduncular screws at the spine using monoenergetic images and the MARS (metal artefact reduction software) system in dual-energy computed tomography
L. Ceccarelli, F. Ponti, P. Spinnato, R. Clinca, L. Lotrecchiano, A. M. Chiesa, G. Facchini*; Bologna/IT*

Purpose: To evaluate the reduction of metal artefacts in patients with titanium peduncular screws at spine level using standard acquisitions, monoenergetic images (mono-E), and monoenergetic image + MARS (mono-E+MARS) acquired with dual-energy computed tomography (CT).
Methods and materials: 25 patients (15 women, 10 men) who had undergone vertebral stabilisation with titanium peduncular screws were studied using dual-energy CT (GE, Discovery 750 HD) with standard acquisitions (QC), 100 to 140 keV monoenergetic reconstructions and 140keV+MARS reconstruction.
A quantitative evaluation was performed using ROI to measure attenuation (Hounsfield Unit (HU)) at the most hyperdense and most hypodense artefacts caused by titanium peduncular screws.
A qualitative analysis was also performed based on subjective evaluation by two radiologists in terms of image quality and the reduction of artefacts.
Results: A comparison of the mean attenuation values showed a significant ($p<0.0001$) reduction of artefacts in 140keV+MARS images compared to monoenergetic and conventional images at the level of the most hyperdense and hypodense artefacts.
Monoenergetic reconstructions showed a significant ($p<0.0001$) reduction of artefact compared to conventional images.
Monoenergetic images were qualitatively richer in diagnostic information.
Conclusion: Mono-E+MARS showed a quantitatively greater reduction of artefacts from titanium peduncular screws at spine level, although monoenergetic images were better from a diagnostic point of view.
Limitations: The retrospective nature of the study.
Ethics committee approval: We obtained ethics committee approval.
Funding: No funding was received for this work.
Author Disclosures:
L. Ceccarelli: nothing to disclose
R. Clinca: nothing to disclose
F. Ponti: nothing to disclose
P. Spinnato: nothing to disclose
A. M. Chiesa: nothing to disclose
G. Facchini: nothing to disclose
L. Lotrecchiano: nothing to disclose

11:15 - 12:30 **Room Y**

Cardiac

RPS 1403a

Epicardial fat, coronary calcifications and cardiovascular risk stratification: what's new in cardiac imaging?

Moderators:
G. Krombach; Giessen/DE
G. Muscogiuri; Milan/IT

RPS 1403a-1 11:15
Exposure to environmental tobacco smoke estimated using the SHSES scale and epicardial adipose tissue thickness in patients with hypertension
P. Gac, M. Poreba, P. Macek, G. Mazur, R. Poreba*; Wroclaw/PL (pawelgac@interia.pl)*

Purpose: To assess the relationship between the exposure to environmental tobacco smoke (ETS) estimated using the SHSES scale and epicardial adipose tissue thickness (EATT) in patients with hypertension.
Methods and materials: The study included 96 people with hypertension (69.32±9.54 years). All patients were assessed for exposure to ETS based on the SHSES scale and 128-slice coronary computed tomography (coroCT) was performed. Based on the SHSES scoring criterion, subgroups of subjects were identified: A) without ETS exposure (0 SHSES points, n=50), B) low ETS exposure (1-3 SHSES points, n=11), C) moderate ETS exposure (4-7 SHSES points, n=20), and D) high ETS exposure (8-11 SHSES points, n=17). Based on the images obtained in coroCT, EATT was measured. The maximum measurement taken along the anterior free wall of the right ventricle was taken as EATT.
Results: In the studied group, EATT was 5.75±1.85 mm. EATT was statistically significantly higher in subgroup D than in subgroups A and B (A: 5.28±1.64 mm, B: 5.04±2.64 mm, D: 7.04±2.64 mm, p_{A-D} and $p_{B-D}<0.05$). There was a positive linear correlation between exposure to ETS expressed by the number of points on the SHSES scale and EATT ($r=0.44$, $p<0.05$). In the regression analysis, it has been documented that higher SHSES scores, higher BMI, and higher systolic and diastolic blood pressure values are independent risk factors for higher EATT, while the use of ACE inhibitors and β-blockers are independent protection factors against higher EATT.
Conclusion: In patients with hypertension, there is a positive relationship between exposure to environmental tobacco smoke estimated using the SHSES scale and epicardial adipose tissue thickness.
Limitations: A single-centre study.
Ethics committee approval: Local Bioethical Committee.
Funding: No funding was received for this work.
Author Disclosures:
P. Gac: nothing to disclose
M. Poreba: nothing to disclose
P. Macek: nothing to disclose
G. Mazur: nothing to disclose
R. Poreba: nothing to disclose

RPS 1403a-2 11:21
Principal shape components derived from shape analysis of left coronary artery bifurcation correlated weakly with calcium score in a cohort with intermediate cardiovascular risk
Y. Huang, W.-J. Lee, S.-J. Chen, Y.-C. Chen, C.-L. Ko, T.-D. Wang, C.-M. Chen, Y.-C. Chang*; Taipei/TW (squll1peter@gmail.com)*

Purpose: A wide left coronary artery bifurcation angle has been reported to be associated with the severity of coronary artery disease, but it may not reflect complex three-dimensional vessel morphology. This study aimed to utilise statistical shape analysis to categorise and quantify the shape patterns of left coronary artery bifurcation, and correlate the shape changes to coronary calcium scores.
Methods and materials: Coronary CT angiography obtained from 406 subjects with intermediate cardiovascular risks were retrieved from a cross-modality multicentre cardiovascular imaging database. The centrelines of the left coronary artery adjacent to bifurcation was extracted and manually corrected. Statistical shape analysis of these centerlines was performed and the most significant principal components were determined by a scree test. The correlations between shape quantification results and coronary calcium scores were examined with the Pearson correlation coefficient. Patients were stratified into a high-calcium score group (Agatston score>100) and a low calcium score group.
Results: The scree test yielded 5 most significant shape patterns, explaining 76% of changes. The derived principal components were used on 178 subjects with available clinical information. There was a weak correlation: the calcium scores of LAD and LCX increased with wider bifurcating angle and shorter LM length (PC#1) (Pearson correlation coefficient: 0.18 for LM and 0.17 for LCx). The calcium score was independent of a simple acute turn at proximal LCX (PC#3). The differences in shape patterns were not significant between the high-calcium score group and the low-calcium score group.
Conclusion: Statistical shape analysis provided comprehensive shape change pattern observation. The calcium score of the left coronary artery was weakly correlated with LM length and bifurcating angle, and was independent of simple acute proximal turn of LCX.
Limitations: Shape analysis is subjected to intepretation.
Ethics committee approval: Aproved by NTUH research ethic committee.
Funding: No funding was received for this work.
Author Disclosures:
C.-L. Ko: nothing to disclose
Y. Huang: nothing to disclose
W.-J. Lee: nothing to disclose
S.-J. Chen: nothing to disclose
Y.-C. Chen: nothing to disclose
T.-D. Wang: nothing to disclose
Y.-C. Chang: nothing to disclose
C.-M. Chen: nothing to disclose

RPS 1403a-3 11:27

Coronary artery calcification with high-pitch chest CT using 256-detector row wide-volume CT scanner: comparison with dedicated calcium scoring CT

J. M. Shin, T. H. Kim, S. Y. Lee, S. J. Ki, C. H. Park*; Seoul/KR (sjaemin@yuhs.ac)*

Purpose: To assess the reliability of non-gated non-contrast chest CT (NCCT) with a wide coverage and fast gantry rotation time reconstructed at different slice thicknesses in quantification of coronary artery calcification (CAC) compared to ECG-gated calcium scoring cardiac CT (CaCT).
Methods and materials: Patients aged ≥50 who clinically required NCCT were prospectively enrolled. All CT scans were performed with 256-detector rows (z-axis coverage: 16 cm) and a gantry rotation time of 280 ms. NCCT was performed and immediately followed by CaCT. NCCT images were reconstructed at 0.625, 1.25, and 2.5 mm slice intervals. The CAC score was calculated using the Agatston method and also divided into four standard categories (0, 1-100, 101-400, and >400). Interobserver and intertechnique agreements were evaluated.
Results: 26 patients (14 males, mean age=66.04±6.97 years) were enrolled. The correlation of CAC scores between CaCT and NCCT with each slice thickness was almost perfect. The mean differences between CaCT and NCCT with a slice thickness of 0.625, 1.25, and 2.5 mm were 37.54, 6.67, and -41.04, respectively, in Bland-Altman plots. Intertechnique concordance of the four Agatston scoring categories was high with linear weighted kappa values of 0.599, 0.609, and 0.597 for NCCT and with a slice thicknesses of 0.625, 1.25, and 2.5 mm, respectively.
Conclusion: CAC quantification with NCCT using wide-detector, high-pitch, and high–temporal resolution scanning modes is almost perfectly consistent with CaCT and the strongest correlation was shown at a slice thickness of 1.25 mm.
Limitations: The patient number was small for the results to be generally accepted and iterative reconstruction used in this study might influence the absolute value of the CAC scores.
Ethics committee approval: Institutional review board of Gangnam Severance Hospital approved this study and all patients gave written informed consent.
Funding: No funding was received for this work.
Author Disclosures:
J. M. Shin: nothing to disclose
T. H. Kim: nothing to disclose
S. Y. Lee: nothing to disclose
S. J. Ki: nothing to disclose
C. H. Park: nothing to disclose

RPS 1403a-4 11:33

Altered cardiac structure and function below recent risk-thresholds: a population-based cardiac magnetic resonance study

F. C. Laqua[1], R. Bülow[1], S. Gross[1], T. Ittermann[1], H. Völzke[1], S. Felix[1], M. Dörr[1], N. Hosten[1], P. L. Madsen[2]; *[1]Greifswald/DE, [2]Copenhagen/DK*

Purpose: To determine alcohol-associated cardiac remodeling and sex-specific differences by cardiac magnetic resonance imaging (CMR) in a low-risk population-based sample.
Methods and materials: In the Study of Health in Pomerania, 1,134 voluntaries (median age 51 years, 55.7% men) underwent gadolinium-enhanced CMR between 2008 and 2012. In a cross-sectional approach, left ventricular (LV) and left atrial (LA) structure and function were related to self-reported alcohol intake over the past month in multivariable linear regression models adjusted for a priori specified clinical and socio-demographic confounders.
Results: 75% of the investigated population consumed less than recently recommended limits of 100 g/week. Only in men was alcohol intake associated with a linearly greater LV mass ($\beta_{fullmodel}$=0.140(0.049;0.23) d (95%-CI); p=0.003), cardiac output ($\beta_{fullmodel}$=0.0093(0.002;0.02) l $min^{-1}g^{-1}$ d; p=0.008), and a lower systemic vascular resistance ($\beta_{fullmodel}$=-0.020(-0.04;-0.002) mmhg l^{-1}min g^{-1}d; p=0.030). In contrast, alcohol intake was associated with greater LV wall-stress ($\beta_{fullmodel}$=1.21(0.3;2.1) mmHg g^{-1}d; p=0.008) in women only. For neither men nor women was alcohol intake related to LV end-diastolic volume, LA maximal volume, LV ejection fraction, or late gadolinium enhancement.
Conclusion: Even in a low-risk drinking population, alcohol intake for men is dose-dependently associated with peripheral vasodilation and a greater LV mass, independent from hypertension. In contrast, despite unchanged geometry, women's hearts are exposed to greater LV wall-stress. Cardiac structure and function is altered below currently recommended risk-thresholds for alcohol intake.
Limitations: The character of an observational study limits the ability to confirm causal relationships. Regression-dilution bias may arise from using alcohol consumption during the past month as a proxy for usual/cumulative consumption.
Ethics committee approval: All individuals gave written informed consent and the study was approved by Ethics Committee of the University of Greifswald.
Funding: This study is supported by the German Federal State of Mecklenburg-West-Pomerania.
Author Disclosures:
F. C. Laqua: Other at Bayer Healthcare GmbH refunded expenses in connection with a congress participation
R. Bülow: nothing to disclose
S. Felix: nothing to disclose
N. Hosten: nothing to disclose
P. L. Madsen: nothing to disclose
M. Dörr: nothing to disclose
T. Ittermann: nothing to disclose
S. Gross: nothing to disclose
H. Völzke: nothing to disclose

RPS 1403a-6 11:39

Metabolic syndrome and ectopic fat deposition in subclinical type 2 diabetes mellitus as determined by 1H-Magnetic resonance spectroscopy

Y. Gao[1], Z.-G. Yang[1], R. Shi[1], L. Jiang[2]; *[1]Chengdu/CN, [2]Guangzhou/CN (304789161@qq.com)*

Purpose: The purpose of this study was to assess the effects of MetS and ectopic fat deposition on LV structure changes in subclinical type 2 diabetes mellitus (T2DM).
Methods and materials: 53 T2DM patients and 20 healthy controls were prospectively enrolled. All of them performed CMR (3.0-T, Siemens Medical Solutions, Germany). We excluded patients with known cardiovascular disease and cardiovascular-related symptoms. We divided patients into MetS group and non-MetS group. Single-voxel ^{1}H-MRSS was performed to detect the myocardial triglyceride content using the post-processing software (jMRUI, version 6.0).
Results: Myocardial TG content was significantly higher in T2DM patients compared with controls (1.54±0.63 vs. 0.61±0.22 %, p < 0.001). GLS was lower in the MetS group than the non-MetS group and normal controls (all p<0.001). The MetS group had a significantly reduced upslope value (2.10±1.19 vs. 2.93±0.78, p<0.001) and an increased TTM value (36.09±14.57 vs. 24.77±11.01, p<0.001) than the controls. A correlation existed between the myocardium TG content and GLS (r = 0.339, p <0.05) and TTM (r = 0.415, p <0.05). ROC analysis showed that 1.56 was the optimal cutoff values of myocardium TG content that predicted the risk of LV deformation (AUC=0.71).
Conclusion: T2DM patients with MetS will cause more serious damage to the myocardium and myocardial TG content is negatively correlated with LVGLS and perfusion.
Limitations: The sample size was too small. A single-centre study, therefore an inclusion bias.
Ethics committee approval: n/a
Funding: This work was supported by the 1·3·5 project for disciplines of excellence, West China Hospital, Sichuan University (ZYGD18013) and the National Natural Science Foundation of China (81471721, 8147172281641169, 81771887 and 81771897).
Author Disclosures:
Y. Gao: nothing to disclose
Z.-G. Yang: nothing to disclose
R. Shi: nothing to disclose
L. Jiang: nothing to disclose

RPS 1403a-7 11:45

Association of coffee consumption with MRI markers of cerebral small vessel disease, cardiac function, and fat depots in a population-based study cohort

E. Beller[1], R. Lorbeer[2], D. Keeser[2], F. Meinel[1], S. Grosu[2], F. Bamberg[3], C. L. Schlett[3], B. B. Ertl-Wagner[4], S. Stöcklein[2]; *[1]Rostock/DE, [2]Munich/DE, [3]Freiburg/DE, [4]Toronto, ON/CA (ebba.beller@gmail.com)*

Purpose: Coffee is one of the most popular beverages in the world and even small health effects may have a large impact on public health. Therefore, we sought to determine the relationship between coffee consumption and cerebral small vessel disease (SVD), cardiac function, or fat depots, using a whole-body magnetic resonance imaging (MRI) protocol.
Methods and materials: MRI markers of SVD, cardiac function, and fat depots were obtained in a population-based study cohort without cardiovascular disease. A blended approach was used to estimate habitual coffee consumption. Associations of coffee intake with total brain volume, white matter lesions, cerebral microbleeds, total (TAT) and visceral adipose tissue (VAT), hepatic proton density fat fraction ($PDFF_{hepatic}$), and cardiac function were assessed by linear regression.

Results: In a sample of 132 women (mean age 56.3±8.8years) and 168 men (mean age 56.2±9.3years), habitual coffee consumption was positively associated with MR-based cardiac function parameters including late diastolic filling rate, stroke volume ($p<0.01$ each), and ejection fraction ($p<0.05$) when adjusting for age, sex, smoking, hypertension, diabetes, LDL, triglycerides, cholesterol, and alcohol consumption. Coffee consumption was negatively associated with VAT when adjusting for age, sex, smoking, hypertension, diabetes, LDL, triglycerides, and cholesterol ($p<0.05$), but not after additional adjustment for alcohol consumption. There was no significant association between coffee consumption and early diastolic filling rate, end-diastolic and end-systolic volume, TAT, $PDFF_{hepatic}$, or SVD parameters.
Conclusion: We found a significant positive and independent association between coffee intake and MRI-based systolic and diastolic cardiac function. Coffee consumption also seems to be inversely associated with VAT, but not independent of alcohol consumption. A significant association between coffee consumption and SVD was not observed.
Limitations: No difference between coffee preparation method or type of coffee was made.
Ethics committee approval: Ethic committee approved.
Funding: No funding was received for this work.
Author Disclosures:
E. Beller: nothing to disclose
R. Lorbeer: nothing to disclose
D. Keeser: nothing to disclose
F. Meinel: nothing to disclose
S. Grosu: nothing to disclose
F. Bamberg: nothing to disclose
C. L. Schlett: nothing to disclose
B. B. Ertl-Wagner: nothing to disclose
S. Stöcklein: nothing to disclose

RPS 1403a-8 11:51
Coronary artery calcium scoring: towards an update of the international standard
G. D. van Praagh[1], J. Wang[1], N. R. van der Werf[2], M. Greuter[3], D. Mastrodicasa[1], K. Nieman[4], D. Fleischmann[1], M. J. Willemink[1]; [1]Stanford, CA/US, [2]Utrecht/NL, [3]Groningen/NL (gijsvanpraagh@live.nl)

Purpose: Improvements of CT technology over the last decade allow for improved acquisition and reconstruction methods of coronary artery calcium (CAC) quantification. Currently, CAC-CT requires a relatively high radiation dose and inter- and intra-scan reproducibility is suboptimal. This study aimed to optimise the standard for CAC-quantification using low-kVp protocols with improved reproducibility on state-of-the-art CT systems from two major vendors.
Methods and materials: An anthropomorphic thoracic phantom with cardiac calcification insert containing 9 cylindrical calcifications and 2 additional extension rings was used. Images were acquired with new-generation CT systems from two vendors using routine protocols and a variety of tube voltages (120-80 kVp), tube currents (≤75% dose reduction), slice thicknesses (3/2.5 and 1/1.25 mm), and reconstruction techniques (filtered back projection and iterative reconstruction (IR)). Every protocol was scanned 5 times after repositioning of the phantom to asses reproducibility. Calcifications were quantified as Agatston and volume scores. Routine scores were compared to other scores using Friedman's tests and post-hoc Wilcoxon signed-rank tests with Bonferroni correction.
Results: Reducing tube potential to 100 kVp, radiation dose with 25%, and slice thickness to 1/1.25 mm, respectively, combined with high IR-levels, resulted in similar total Agatston scores ($P>0.05$). Total volume slightly reduced to values closer to the physical volume ($P>0.05$). Moreover, intrascanner CAC-score variability decreased with 1-9%. Analysis per calcification showed that variability and CAC-scores decreased in higher density calcifications. In lower density calcifications, CAC-scores increased due to increasing HU-values. On average, 6/9 lesions were detected with traditional slice thickness, while 7/9 were detected with thin-slice images.
Conclusion: This multivendor study showed protocol-optimisation resulted in reduced radiation doses without affecting total Agatston scores, volume scores closer to the physical volume, and improved reproducibility.
Limitations: n/a
Ethics committee approval: n/a
Funding: No funding was received for this work.
Author Disclosures:
G. D. van Praagh: nothing to disclose
J. Wang: nothing to disclose
N. R. van der Werf: nothing to disclose
M. Greuter: nothing to disclose
D. Mastrodicasa: nothing to disclose
K. Nieman: nothing to disclose
D. Fleischmann: Grant Recipient at Siemens Healthineers
M. J. Willemink: Grant Recipient at American Heart Association, Grant Recipient at Philips Healthcare, Consultant at Arterys, Inc., Founder at Segmed, Inc.

RPS 1403a-9 11:57
Increased epicardial adipose tissue accumulation as a predictor for essential hypertension in non-obese adults
A. Dobrovolskij[1], D. Austys[2], V. Jablonskienė[2], V. Dobrovolskij[2], N. Valeviciene[2], R. Stukas[2]; [1]Coblenz/DE, [2]Vilnius/LT (adobrovolskij@gmail.com)

Purpose: Essential hypertension (EH) is identified as one of the most important risk factors for cardiovascular morbidity in industrialised countries. Epicardial adipose tissue (EAT) is considered to be an important factor in the development of cardiovascular diseases. The pathophysiological mechanisms of EAT remain unclear to this day. Diverging results are presented regarding the association between EAT and EH. Moreover, there has been insufficient research on EAT association with different stages of EH. Our aim was to evaluate the association between size of EAT depots and the risk of EH, taking into account its stage.
Methods and materials: There were 258 non-obese adult patients investigated with different cardiovascular diseases, 157 of whom had EH and 101 who did not. Patients with EH were classified to 3 groups according to the stage of hypertension. Volume and thickness of EAT depots on ventricular free walls (6 locations) and grooves (5 locations) were measured using cardiac magnetic resonance tomography images, and then compared between groups. For the prediction of EH, a regression model was constructed.
Results: Overall, EAT thickness (in all locations) and volume were higher among hypertensive patients ($p<0.001$). Mean EAT thickness and volume were larger in the stage 1 hypertension group than among normotensive patients ($p<0.05$). Furthermore, the volume of EAT was lower in the stage 1 than in the stage 2 hypertension group ($p<0.05$). However, the EAT depots did not differ between severe and the estage 2 hypertension group. EAT volume, patients' age, body mass index, and dyslipidaemia status were independent with EH associated factors in a predictive model.
Conclusion: Significant differences in EAT accumulation between hypertensive and normotensive patients show that EAT measurements may serve as a risk indicator for EH as well as a predictor of hypertension severity.
Limitations: n/a
Ethics committee approval: Ethics committee approval provided.
Funding: No funding was received for this work.
Author Disclosures:
A. Dobrovolskij: nothing to disclose
D. Austys: nothing to disclose
N. Valeviciene: nothing to disclose
V. Jablonskienė: nothing to disclose
R. Stukas: nothing to disclose
V. Dobrovolskij: nothing to disclose

RPS 1403a-10 12:03
Impact of blending weight in hybrid iterative reconstruction on coronary artery calcium score based on cardiac CT
Z. Liu; Beijing/CN (liuzhuormyy@sina.cn)

Purpose: To investigate the impact of blending weight in hybrid iterative reconstruction (ASIR-V) on coronary artery calcium scores and risk classification based on cardiac CT.
Methods and materials: The non-contrast ECG-gated cardiac CT images of 100 patients were reconstructed using different blending weights of ASIR-V, including FBP (0% ASIR-V), 20% ASIR-V, 40% ASIR-V, 60% ASIR-V, 80% ASIR-V, and 100% ASIR-V. The average CT value and standard deviation (SD) in the ascending aorta and the maximum value of calcified plaque were compared among the different reconstructions. Agatston score, mass score, volume score, and risk classification based on Agatston score were also compared.
Results: An increased percentage of ASIR-V was associated with a reduction in SD of ascending aorta and the 3-types of calcium scores ($P<0.05$). Agatston scores were 170.2±387.3, 168.6±385.3, 166.4±381.9, 164.6±379.4, 162.9±376.7, and 161.1±374.1 for reconstructions, with 0%, 20%, 40%, 60%, 80%, and 100% ASIR-V, respectively. Mass scores were 23.62±52.56, 23.49±52.23, 23.32±52.30, 23.20±53.10, 23.15±52.83, and 22.99±52.41 mg, respectively. Volume scores were 68.7±140.7, 67.8±139.8, 67.0±139.6, 65.7±137.2, 64.8±135.9, and 64.0±135.0 mm^3, respectively (all $P\leq0.001$). There was no statistically significant difference in the average value in the ascending aorta and plaque maximum value ($P>0.05$) ASIR-V led to the risk reclassification to a lower category in 10 patients, including 8 from low to very low, and 2 from moderate to low based on Agatston scores.

Conclusion: ASIR-V results in image noise and calcium score reduction and may result in risk reclassification to a lower category.
Limitations: The results of this single-centre study were limited to only one scanner and one iterative reconstruction algorithm. The sample size of patients was small, which may affect the statistical results for the calcium score and risk reclassification.
Ethics committee approval: n/a
Funding: No funding was received for this work.
Author Disclosures:
Z. Liu: nothing to disclose

RPS 1403a-11 12:09
The fight between CAD-RADS and the calcium score: who is the winner?
R. Malagò[1], G. Tabacco[1], S. Peretto[1], M. Poletti[2], M. Mochen[3], G. Salandini[1], M. Pernigotto[1], G. Mansueto[1]; [1]*Verona/IT,* [2]*Cles/IT,* [3]*Dimaro/IT*

Purpose: To compare the prognostic value of CAD-RADS classification with the calcium score relative risk.
Methods and materials: With a series population from a single-centre study of 1,918 pts (1,167 M, 751 F, mean age 63yrs) who underwent CA-MDCT from April 2008 to September 2019, we reconstructed and scored each exam, classifying the detected lesions and plaques according to the CAD-RADS system. 1,850/1,918 pts underwent additional pre-contrast coronary artery calcium protocol (Ca score). We determined the calcium burden of atherosclerotic plaques in these exams, according to Agatston method, and the relative risk of coronary events adjusted for patients age and gender. A correlation between the Agatston score and CAD-RADS was obtained using a Spearman test.
Results: Patients with significant stenosis (CAD-RADS 3) showed an extensive degree of coronary artery calcification (average value of Ca score: 1,052), with a discrete to moderate relative risk (76%). Patients with an occluded vessel (CAD-RADS 5) had a higher degree of coronary artery calcification (average value of Ca score: 1,929) and a moderate to high relative risk (87%).
Good correlation was recorded between calcium score and CAD-RADS, in case of Ca score 0 and CAD-RADS 0-1 and CAD-RADS 4 and 5 and Ca score severe (Rho 0.9 and 0.86 respectively P< 0.001), significant but a lower correlation in case of a moderate Ca score and CAD-RADS 3 (rho 0-67 p<0.001).
Conclusion: CAD-RADS better describes the overall plaque extension and degree of significance than a Ca score.
Limitations: Study population is not homogeneous for risk factors.
Ethics committee approval: n/a
Funding: No funding was received for this work.
Author Disclosures:
G. Tabacco: nothing to disclose
R. Malagò: nothing to disclose
S. Peretto: nothing to disclose
M. Poletti: nothing to disclose
G. Salandini: nothing to disclose
G. Mansueto: nothing to disclose
M. Mochen: nothing to disclose
M. Pernigotto: nothing to disclose

RPS 1403a-12 12:15
Fully automated calcium scoring algorithms for phantom experiments
G. D. van Praagh[1], N. R. van der Werf[2], M. Voet[3], J. Wang[1], D. Fleischmann[1], M. Greuter[3], T. Leiner[2], M. J. Willemink[1]; [1]*Stanford, CA/US,* [2]*Utrecht/NL,* [3]*Groningen/NL (gijsvanpraagh@live.nl)*

Purpose: Anthropomorphic phantoms containing calcifications are often used in coronary calcium scoring (CCS) studies. Manually quantifying CCS is highly time consuming. Accordingly, we aimed to develop and validate a fully automatic method for CCS in a commercially available phantom using two commonly used computer-programming languages.
Methods and materials: An anthropomorphic thorax phantom with cardiac calcification insert containing 9 cylindrical calcifications was used. An extension ring was used to simulate larger patients. Scans were acquired on an electron-beam tomography system and 5 state-of-the-art CT systems from 4 major vendors using routine protocols with 130 and 120 kVp, respectively, 3 mm slice thickness and filtered back-projection. To simulate interscan variability, each acquisition was repeated 5 times after repositioning the phantom. The robustness of CCS quantification-algorithms was assessed by evaluating a variety of settings on one CT-system. CCS was determined with vendor-specific software and quantified as an Agatston score. We developed 2 fully automated algorithms in 2 programming languages: MATLAB and Python. Besides CCS, image quality analysis functions were implemented into the algorithm (standard-deviations of a water-equivalent region-of-interest and noise power spectrum). To assess CCS accuracy of the algorithms, CCS was compared with their values obtained with the vendor-specific software using Bland-Altman and intraclass correlation analyses.
Results: Both algorithms achieved high agreements with vendor-specific software for Agatston scores (mean ± 95% confidence-interval for MATLAB and Python, respectively: -0.3% ± 4.0% and -0.1% ± 3.8%; ICCs were excellent for MATLAB and Python: 1.00 (1.00-1.00) for both). Output of the algorithms from one scan was given in <5 seconds.
Conclusion: We developed two algorithms to fully automatically quantify calcifications and evaluate image quality in a commercially available phantom with excellent agreement compared to vendor-specific software.
Limitations: n/a
Ethics committee approval: n/a
Funding: No funding was received for this work.
Author Disclosures:
G. D. van Praagh: nothing to disclose
N. R. van der Werf: nothing to disclose
M. Voet: nothing to disclose
J. Wang: nothing to disclose
D. Fleischmann: Grant Recipient at Siemens Healthineers
M. Greuter: nothing to disclose
T. Leiner: Grant Recipient at Philips Healthcare
M. J. Willemink: Grant Recipient at American Heart Association, Grant Recipient at Philips Healthcare, Consultant at Arterys, Inc., Founder at Segmed, Inc.

11:15 - 12:30 **Coffee & Talk 3**

Head and Neck
RPS 1408
Maxillofacial and sinonasal imaging

Moderators:
M. Horta; Lisbon/PT
H. B. Eggesbo; Oslo/NO

RPS 1408-K 11:15
Keynote lecture
S. Bayraktaroğlu*; Izmir/TR (selenb2000@gmail.com)*

Author Disclosures:
S. Bayraktaroğlu: nothing to disclose

RPS 1408-1 11:25
The role of computed tomography staging imaging in the prediction of the pathological depth of invasion (DOI) in oral cancer
M. Pietragalla[1], L. G. Locatello[2], C. Nardi[2], F. Mungai[1], L. Bonasera[2], C. Taverna[2], L. Novelli[2], S. Colagrande[2], V. Miele[2]; [1]*Pistoia/IT,* [2]*Florence/IT (michelepietragalla@hotmail.it)*

Purpose: Depth of invasion (DOI) has been introduced into the latest TNM classification of oral squamous cell carcinoma(OSCC) as a required parameter to correctly define T staging and prognosis. Despite its primarily pathologic definition (pDOI), there is increasing evidence that radiological DOI (rDOI) can preoperatively predict its final value even though a standard and practical definition is lacking. We wanted to assess the clinical impact and utility of computed tomography-derived (CT) rDOI in a cohort of OSCC patients and to better define its measurement.
Methods and materials: We retrieved 58 cases of OSCC operated on at our institution from 2016-2019. After accounting for plane-specific shrinkage factors and different oral subsites, we compared pDOI and rDOI for each spatial plane by a paired difference test and correlation coefficient. Radiological accuracy and survival analysis were also determined to identify the rDOI's clinical value.
Results: For the lateral tongue, pDOI was more strongly related with axial rDOI (ρ=0.923, P<0.01). For the hard palate, the best plane was the sagittal one (P<0.01). In floor-of-mouth (FOM) lesions and cheek buccal mucosa, the strongest correlation was with coronal rDOI (P<0.01). Sagittal scans seem to be the best to evaluate the dorsum of the tongue and retromolar trigone. Gengiva (P<0.01) was more correctly evaluated in the coronal plane. The overall accuracy of rDOI restaging was 75.41%. Disease-free survival seems to be worse as rDOI increases, although differences are not statistically significant (log-rank, P=0.204).
Conclusion: CT-derived rDOI can be of great value in the preoperative assessment of OSCC. We have identified specific spatial planes where its measurement is more strongly related to final pathological report and we hope that a standardisation of imaging and pathological analysis is needed.

Limitations: n/a
Ethics committee approval: Informed consent obtained.
Funding: No funding was received for this work.
Author Disclosures:
L. G. Locatello: nothing to disclose
M. Pietragalla: nothing to disclose
C. Nardi: nothing to disclose
C. Taverna: nothing to disclose
F. Mungai: nothing to disclose
V. Miele: nothing to disclose
L. Novelli: nothing to disclose
S. Colagrande: nothing to disclose
L. Bonasera: nothing to disclose

RPS 1408-2 11:31

Correlation of MRI derived parameters and SUV uptake obtained from FDG- PET-CT with human papillomavirus status in oropharyngeal squamous cell carcinomas

A. Jajodia, V. Mahawar, A. S. Rao, A. K. Chaturvedi*; New Delhi/IN (drmahawarvivek@gmail.com)*

Purpose: A favourable response to (chemo) radiotherapy (CCRT) is seen in human papillomavirus (HPV)-positive OPSCC patients. The apparent diffusion coefficient (ADC) derived from MRI has been shown to predict treatment response. We evaluated the correlation between the clinico-demographic profile of oropharyngeal squamous cell carcinomas patients (OPSCC patients), HPV status, and ADC values with SUV uptake obtained from FDG- PET-CT.
Methods and materials: The study population was obtained from a historical cohort diagnosed with HPV-related OPSCC. A total of 105 OPSCC patients who had undergone molecular testing for HPV status by p16 with immuno-histochemistry (IHC) were identified. 96 patients had pretreatment imaging (either PET-CT or MRI) and post CCRT imaging was included. Imaging was evaluated by head and neck radiologists to calculate the mean ADC and SUV max. Pearson's Chi-square and ANOVA analyses were performed to evaluate the correlation.
Results: 26 OPSCC were HPV-positive. HPV-positive HNSCC showed significant association with smoking (p=0.016), grade (p=0.013), the stage of the tumour (p<0.0001), T status (p=0.011), response to CCRT (p00.026), lymph nodes (p=0.042), and ADC values on follow-up imaging (p=0.007). The change in ADC was significantly correlated with P16 status (p=0.010) and percentage change in p16 status was marginally correlated (P=0.058).
Conclusion: In OPSCC patient's positive HPV status correlates with the follow-up mean apparent diffusion coefficient. The complementary prognostic value of the post-treatment apparent diffusion coefficient might be partially ascribed to patients with a positive HPV status. Further studies are reasonable to determine whether PET-CT is a useful imaging biomarker in comparison to ADC to risk-stratify patients with HPV-related OPSCC.
Limitations: A small cohort.
Ethics committee approval: Ethics committee approval obtained.
Funding: No funding was received for this work.
Author Disclosures:
V. Mahawar: nothing to disclose
A. Jajodia: nothing to disclose
A. S. Rao: nothing to disclose
A. K. Chaturvedi: nothing to disclose

RPS 1408-3 11:37

Redirection of parasagittal cuts of magnetic resonance imaging for the temporomandibular joint

M. K. Zayet*; Cairo/EG (mohamed.zayet@dentistry.cu.edu.eg)*

Purpose: Magnetic resonance imaging (MRI) is the main imaging modality in the diagnosis of temporomandibular disorders. Furthermore, sagittal cuts are the chief plane in diagnosing these disorders. This study aimed to investigate the capability of parasagittal cuts taken parallel to the lateral pterygoid muscle in depicting the structures of the temporomandibular joint.
Methods and materials: 20 symptomatic temporomandibular joint (TMJ) patients performed MRI bilaterally using traditionally used parasagittal cuts and another plane parallel to the lateral pterygoid muscle. Four-point scale was used to assess the clarity of articular disc position, disc morphology, cortical bone, and overall quality of the images of both investigated techniques in closed and open positions. Moreover, the final diagnosis of the cases was obtained in each technique.
Results: The mean and standard deviation of muscular aligned cuts in the clarity of revealing disc position, disc position, cortical bone, and overall image quality in closed position were 2.83± 0.39, 2.63± 0.49, 2.53± 0.51, and 2.83± 0.39, respectively, while those for traditional plane were 2.55± 0.50, 2.43± 0.50, 2.80± 0.41, and 2.53± 0.51, with the same order. In the open position, the same investigated points got 2.80± 0.41, 2.73± 0.45, 2.73± 0.45, and 2.80± 0.41 in muscular aligned images, and 2.78± 0.42, 2.65± 0.48, 2.82± 0.39, and 2.78± 0.42 in the traditional plane. Both techniques provided the same diagnosis in 97.5% of cases.
Conclusion: Parasagittal magnetic resonance images taken parallel to the lateral pterygoid muscle have higher image quality than a traditional plane in revealing temporomandibular structures.
Limitations: Small number of cases (40 temporomandibular joints).
Ethics committee approval: The study was approved by the research ethics committee of Faculty of Dentistry, Cairo University (19-4-18).
Funding: No funding was received for this work.
Author Disclosures:
M. K. Zayet: nothing to disclose

RPS 1408-4 11:43

Visualisation of mandible fractures with the affection of the inferior alveolar nerve with high-resolution MRI sequences

E. Burian, L. Ritschl, M. Probst*; Munich/DE (e.burian@gmx.net)*

Purpose: Computed tomography (CT) or cone-beam computed tomography (CBCT) are the gold standards in clinical traumatology imaging when structures of the head and neck region are involved. However, CT and CBCT harbour inherent limitations in regards to soft tissue visualization. In mandible fractures, the inferior alveolar nerve (IAN) is at particular risk for damage. The aim of this study was to assess the IAN pre- and postoperatively and correlate elevated signal-to-noise-ratios (SNR) with potential sensitivity impairment.
Methods and materials: 18 patients suffering from a mandible fracture were examined on a 3T scanner. The conducted sequence protocol consisted of a 3D STIR, 3D WATS, and a 3D T1 FFE "black bone"-sequence (15 min scan time). Nerve function was assessed as normal, hypesthesia, anesthesia, or allodynia.
Results: The 3D T1 TFE sequences allowed for fracture detection in all patients. The 3D STIR sequence showed the highest SNR with regard to potential nerve damage (p<0.05). Besides some diagnostic accuracy in fracture detection like with CT, the direct visualisation of nerve structures was possible. Positive clinical nerve testing correlated with physiological SNR and hypoesthesia correlated with increased SNR (p<0.05).
Conclusion: The study highlights the feasibility of MRI for fracture detection and affection of the IAN. The applied sequence protocol showed comparable diagnostic power in detecting mandible fractures as with CT. Additionally, a reliable assessment of potential IAN damage with a good correlation to clinical sensory testing could be achieved.
Applying the described sequence protocol allowed for precise fracture detection as well as reliable nerve damage assessment.
Limitations: Motion artefacts due to a scan time of approximately 10 min.
Ethics committee approval: Ethics committee approval obtained.
Funding: No funding was received for this work.
Author Disclosures:
E. Burian: nothing to disclose
M. Probst: nothing to disclose
L. Ritschl: nothing to disclose

RPS 1408-5 11:49

In vitro validation of a digital subtraction radiography (DSR) system in detecting root canal (RC) density changes

G. Trifylli[1], I. C. Mackie[2]*; [1]Nikaia/GR, [2]Manchester/UK (gtrifili@yahoo.com)*

Purpose: To calculate the accuracy and reliability of a DSR system when in vitro changes were made on anterior maxillary incisor teeth, which simulate post-traumatic complications (e.g. continued root development and pulp canal obliteration).
Methods and materials: Subtle RC density changes were made through filing 15 teeth which were then placed in customised acrylic sockets in a skull. Baseline and subsequent digital radiographs were taken after the use of 40, 60, and 90 K file size, and after no filing. During the image acquisition stage, standardised conditions, in terms of image geometry and density, were achieved by using a cephalostat method of head stabilisation (cephalostat headset and a customized film holder) and software for image processing. DSR was applied and the subtraction images represented small, medium, large, or no RC density change (gain or loss). Radiographic assessment slides were done by 3 observers. Observer A assessed the slides at two different times.
Results: DSR sensitivity (0.93-0.96 at a possible cut-off point, 0.78-0.82 at a probable cut-off point, and 0.44-0.62 at a definite cut-off point), specificity (perfect: 1.00), Youden's J index (range between 0.44 and 0.96 at all the cut-off points), intraexaminer agreement (wk: 0.96, 95% CI: 0.93-0.99) and interexaminer agreement (wk range: 0.90-0.95, 95% CI: 0.83-0.98) were calculated. The results were analysed in relation to the site, size, and kind (gain or loss) of the density change.
Conclusion: DSR led to a more accurate and reproducible diagnosis. Highly accurate dignoses of small lesions at a low degree of confidence (sensitivity: 0.80-0.87) proved DSR to be a diagnostically useful tool, particularly when early detection of tooth density change is needed.

Limitations: n/a
Ethics committee approval: n/a
Funding: No funding was received for this work.
Author Disclosures:
G. Trifylli: Speaker at Dental Department, General State Hospital of Nikaia-Piraeus "Ag. Panteleimon", Greece.
I. C. Mackie: Consultant at Department of Oral Health and Development, University of Manchester, England

RPS 1408-6 11:55

Densitometric analysis of the condyle and axis in determining osteoporotic risk: a CBCT study

A. Uri, B. Evlice*; Adana/TR (alevuri@gmail.com)*

Purpose: To evaluate the usefulness of radiological density measurements of mandibular condyle (MC) and axis vertebra (AV) in patients with a risk of osteoporosis according to mental index (MI) values.
Methods and materials: Cone-beam computed tomography (CBCT) images of 96 patients were retrospectively analysed. Radiological density values of AV and MC (left and right), and measurements of MI (left and right), were performed from the areas formed by reference lines in the coronal section. Demographic data of patients such as age and gender were recorded. Patients were divided into two groups according to the mean age and into two categories as high and low risk according to the risk of osteoporosis by taking MI values (cut-off value: 3.0 mm) into the consideration. ROC curve analysis was used to determine the power of MC and AV's radiological densities to explain the risk of osteoporosis.
Results: There was a statistically significant difference between gender and MI values, and age groups and MC, AV, and MI values. In addition, MC and AV mean values were significantly lower in patients with a high risk of osteoporosis than in low-risk patients. There was a positive correlation between MC, AV, and MI variables in different strengths. Finally, the results of the ROC curve analysis showed that MC was more powerful with a lower difference than AV in determining the risk of osteoporosis.
Conclusion: MC and AV measurements are considered to be important predictors in determining the osteoporotic risk.
Limitations: The cut-off value of MI was considered as 3.0 mm, however, this value might be related to race or ethnicity.
Ethics committee approval: Ethics committee approval obtained.
Funding: No funding was received for this work.
Author Disclosures:
A. Uri: nothing to disclose
B. Evlice: nothing to disclose

RPS 1408-7 12:01

Radiomorphometeric evaluation of the clivus in an Indian paediatric population visiting a tertiary dental hospital: a cone-beam computed tomography study

A. Chaurasia*; Lucknow/IN (chaurasiaakhilanand49@gmail.com)*

Purpose: To determine the age and sex-related changes in clivus length and clivus width. Clivus width and clivus length were also evaluated for the age prediction of individuals.
Methods and materials: The CBCT images of 150 study subjects obtained from Carestream 9000cc (USA) CBCT machine at 90 Kvp, 4 mA for 11.3 seconds at FOV (17"×13.5"), voxel size of 300 in the age group of 6 to 17 years (76 male, 74 female) were chosen prospectively. The clivus length and clivus width were measured using trophy Dicom ink software on axial and sagittal images (DICOM images). An unpaired t-test and ANOVA test were used for comparison between groups. Pearson correlation coefficients were used to evaluate the correlations. The data analysis was done using SPSS version 21.0.
Results: Irrespective of age and sex, the mean clivus width was 28.8±3.98 and mean clivus length was 42.7±3.98. Statistically, no significant difference was observed between males and females ($p>0.05$) with clivus width. However, the clivus length was statistically significant ($p<0.001$) in both male and female populations. The clivus width and clivus length was directly associated with age. The mathematical equations derived from linear regression analysis can be used in the prediction of the age of an individual if the clivus width/clivus length is known.
Conclusion: The clivus measurements on CBCT can be used to predict the age of an individual in medicolegal disputes. As the Pearson correlation coefficient showed through strong associations between the clivus measurements, age, and gender, clivus measurements can be used to differentiate between the sex of humans and helps in age determination. Clivus dimensions can be used as an additional parameter in age and sex determination in inconclusive medicolegal cases.
Limitations: n/a
Ethics committee approval: Ethics committee approval obtained.
Funding: No funding was received for this work.
Author Disclosures:
A. Chaurasia: Author at King George Medical University, Consultant at King George Medical University

RPS 1408-8 12:07

Comparison of the diagnostic value of CT signs of lacrimal sac dilatation in patients with dacryocystitis with verbal reporting and virtual endoscopy

A. Ageev[1], A. Dergilev[2], V. A. Obodov[1], A. Obodov[1]; *[1]Yekaterinburg/RU, [2]Novosibirsk/RU (ageev.artem@gmail.com)*

Purpose: To specify normal and pathologic values and intervals of main numeric CT signs of lacrimal sac dilatation to compare the diagnostic value of those CT signs and to compare the diagnostic value of virtual endoscopy (VE) and conventional text reports for LS position description for intraoperative navigation purpose.
Methods and materials: 102 adult patients with dacryocystitis were included in this study. 204 CT volumes including lacrimal sacs (LS) and nasolacrimal ducts (NLD) images were obtained.
The main group included CT images of 123 LS and NLD on the affected side.
The control group included CT images of 81 LS and NLD of the same patients on the intact side, excluding patients with bilateral dacryocystitis.
Pearson's Chi-square test and receiver operating characteristic curve (ROC) analysis were applied to the collected data.
Results: CT signs of normal LS volume were specified: volume ≤0,29±0.1 cm^3 (sensitivity 73.17%, specificity 90.12%), height ≤13.9±1.3 mm (sensitivity 68.29%, specificity 74.07%), width ≤5.9±0.2 mm (sensitivity 65.85%, specificity 91.36%), and depth ≤6.55±0.4 mm (sensitivity 89.43%, specificity 74.07%).
The diagnostic value of CT signs of LS dilatation was found regressing in the following sequence: volume (area under the curve, AUC=0.886), depth (AUC=0.865), width (AUC=0.841), height (AUC=0.734), upper dislocation (AUC=0.586), and forward dislocation (AUC=0.564).
Significant differences in the diagnostic accuracy of text reports and VE were found: χ^2=52.61 ($P<0.0001$) and AUC difference 0.418±0.03 (VE AUC=0.992±0.01, text reports AUC=0,574±0,1).
Conclusion: LS volume is the most accurate CT sign of LS dilatation in patients with dacryocystitis. VE is better for LS position description than text reports and thus VE is recommended for routine clinical use.
Limitations: The numeric criteria of LS dilatation in children and other races will probably be different.
Ethics committee approval: n/a
Funding: No funding was received for this work.
Author Disclosures:
A. Ageev: nothing to disclose
A. Dergilev: nothing to disclose
V. A. Obodov: nothing to disclose
A. Obodov: nothing to disclose

RPS 1408-9 12:13

Evaluation through dacryo-CT of the relapse of epiphora after dacryocystorhinostomy

G. Salandini, M. Maturi, E. Genco, F. de Cecco, S. Mehrabi, G. Mansueto*; Verona/IT (giulia.salandini06@gmail.com)*

Purpose: To evaluate computed tomography dacryocystography (dacryo-CT) as an imaging method to identify the relapse of stenosis in patients with a recurrence of epiphora after dacryocystorhinostomy, as well as providing useful information to plan a new surgical operation.
Methods and materials: A retrospective study was performed including patients who underwent a dacryo-CT from January 2014-September 2019 in the AOUI of Verona. Patients who underwent dacryocystorhinostomy and presented with a recurrence of epiphora were identified.
The following qualitative variables were considered: relapse of stenosis, failure of the surgical shunt, patency of the nasolacrimal duct downstream, and the presence of anatomical variants.
Results: Patients who underwent dacryo-CT after dacryocystorhinostomy were 10 in total, 8 who underwent a monolateral dacryocystorhinostomy and 2 who underwent a bilateral dacryocystorhinostomy.
5 males and 5 females patients, aged between 32 and 88, were examined.
7 of the 10 patients had a relapse of stenosis of the lacrimal drainage apparatus.
Among the patients with a failure of the surgical shunt, 4 had a nasal septal deviation, 2 had sinusitis, and 1 presented with a total opacification of the maxillary sinus due to possible relapse of his previous underlying disease (inverted papilloma).
Among the 3 patients who had regular patency of the surgical shunt after the dacryocystorhinostomy, 1 developed contralateral stenosis of the nasolacrimal duct and 1 developed a mucocele of the lacrimal sac in the same side of the dacryocystorhinostomy, which was regularly patent.

Conclusion: Dacryo-CT is an optimal imaging method to identify the causes of failure of surgery and to plan a possible second operation.
Limitations: The low sample size and the retrospective nature of the study.
Ethics committee approval: n/a
Funding: No funding was received for this work.
Author Disclosures:
G. Salandini: nothing to disclose
M. Maturi: nothing to disclose
E. Genco: nothing to disclose
F. de Cecco: nothing to disclose
S. Mehrabi: nothing to disclose
G. Mansueto: nothing to disclose

RPS 1408-10 12:19
Assessment of the internal nasal valve angle by computed tomography: a new method proposal and a revision of current techniques
N. Janovic, A. Janovic, B. Pavlovic, M. Dimitrijevic, M. Djuric*; Belgrade/RS (aleksa.janovic@stomf.bg.ac.rs)*

Purpose: To test a new CT method for the internal nasal valve (INV) angle measurement and compare it with current techniques and endoscopy.
Methods and materials: 40 INV angles in 20 adult patients (mean age 38.25±10.9) were measured on CT images using a "nasal base view (NBV)" method and a new method and compared by Student's t-test. All patients were candidates for functional endoscopic sinus surgery (FESS) and preoperative CT examination. The exclusion criteria were a history of external nose trauma, septoplasty, esthetic nasal reconstructions, and diseases that may distort the INV angle. Angles were also measured on endoscopic images and correlated statistically with CT techniques. Measurements were made by two radiologists independently, and the interclass correlation coefficient (ICC) was calculated.
Results: INV angles were not significantly different between NBV and the new method (t=-1.256, p=0.216), although the new method provided slightly higher angles (NBV 11.19 ± 3.62 vs. the new method 11.86 ± 3.90). Both methods correlated significantly with angles measured on endoscopy images, but a much stronger correlation was detected with the new CT method (R=0.387, p=0.014 vs. R=0.808, p<0.001). The new CT method showed a stronger level of agreement (ICC=0.930) between radiologists in contrast to the NBV method (ICC=0.658).
Conclusion: A stronger correlation with nasal endoscopy and a better reproducibility gives priority to the new CT method for the INV angle measurement in daily radiological practice.
Limitations: A relatively small number of patients might limit the study. The INV narrowing was not diagnosed in all patients who participated in the study.
Ethics committee approval: The study was approved by the Ethics Committee of the Faculty of Medicine, No. 29/V-1.
Funding: No funding was received for this work.
Author Disclosures:
A. Janovic: nothing to disclose
N. Janovic: nothing to disclose
B. Pavlovic: nothing to disclose
M. Dimitrijevic: nothing to disclose
M. Djuric: nothing to disclose

RPS 1408-11 12:25
MRI detects chronic rhinosinusitis in infants and preschool children with cystic fibrosis
M. O. Wielpütz, O. Sommerburg, F. Wuennemann, E. Optazaite, M. Stahl, H.-U. Kauczor, I. Baumann, M. A. Mall, M. Eichinger*; Heidelberg/DE (wielpuetz@uni-heidelberg.de)*

Purpose: Chronic rhinosinusitis (CRS) contributes to the disease burden of patients with cystic fibrosis (CF). However, its onset and progression in infants and preschool children with CF remain poorly understood. Our aim was to determine the prevalence and extent of CRS in early CF using magnetic resonance imaging (MRI).
Methods and materials: MRI was performed in 67 infants and pre-school children with CF (mean age 2.3±2.1y, range 0-6y), and 30 non-CF controls (3.5±2.0y). Paranasal sinus dimensions and structural abnormalities including mucosal swelling, mucopyoceles, and nasal polyps of the maxillary, frontal, sphenoid, and ethmoid sinuses, and in addition medial maxillary sinus wall deformation, were assessed using a novel CRS MRI scoring system.
Results: Pneumatisation and dimensions of paranasal sinuses did not differ between the two groups. MRI detected an increased prevalence of mucosal swelling (83% vs 17%, P<0.001), mucopyoceles (75% vs 2%, P<0.001), polyps (26% vs 7%, P<0.001), and maxillary sinus wall deformation (68% vs 2%, P<0.001) in CF compared to controls. Furthermore, the extent of these abnormalities was also increased with an MRI sum score of 22.9±10.9 in CF compared to 4.5±7.6 in non-CF controls (P<0.001).
Conclusion: MRI detected normal dimensions of paranasal sinuses and a high prevalence and severity of paranasal sinus abnormalities due to CRS in infants and preschool children with CF without radiation exposure. Our results support the development of MRI for sensitive non-invasive diagnosis and the monitoring of CRS in young children with CF, and as an outcome measure for clinical trials.
Limitations: We did not assess the relationship between structural abnormalities and disease burden obtained by a questionnaire.
Ethics committee approval: Approved by the institutional ethics committee and informed written consent was obtained from parents or legal guardians.
Funding: Supported by the German BMBF, the Mukoviszidose e.V., and the Einstein Foundation.
Author Disclosures:
M. O. Wielpütz: Grant Recipient at Vertex, Boehringer Ingelheim, Advisory Board at Vertex, Boehringer Ingelheim
O. Sommerburg: nothing to disclose
F. Wuennemann: nothing to disclose
E. Optazaite: nothing to disclose
M. Stahl: Grant Recipient at Vertex
H.-U. Kauczor: Advisory Board at Boehringer Ingelheim, Research/Grant Support at Siemens, Philips, Speaker at Siemens, Philips, Boehringer Ingelheim, Astra Zeneca, MSD Sharp & Dome
I. Baumann: nothing to disclose
M. A. Mall: Advisory Board at Bayer, Vertex, Boehringer Ingelheim, Polyphor, Arrowhead, ProQR, Spyryx, Santera, Enterprise Therapeutics, Research/Grant Support at German Ministry for Education, Einstein Foundation, Mukoviszidose e.V., Speaker at Bayer, Vertex, Boehringer Ingelheim, Polyphor, Arrowhead, ProQR, Spyryx, Santera, Galapagos, Sterna, Enterprise Therapeutics, Celtaxys
M. Eichinger: nothing to disclose

11:15 - 12:30 **da Vinci (Room D1)**

Cardiac

RPS 1403b

Paediatric cardiology and congenital heart disease

Moderators:
O. Duvernoy; Uppsala/SE
N.N.

RPS 1403b-K 11:15
Keynote lecture
J.-N. Dacher*; Rouen/FR*

Author Disclosures:
J.-N. Dacher: nothing to disclose

RPS 1403b-1 11:25
Imaging of the pulmonary vasculature in congenital heart disease without gadolinium contrast: intraindividual comparison of a novel compressed SENSE accelerated 3D REACT with 4D CE-MRA
L. Pennig[1], A. Wagner[1], K. Weiss[1], S. Lennartz[1], D. Maintz[2], T. Hickethier[1], C. P. Naehle[3], A. Bunck[1], J. Doerner[3]*; [1]Cologne/DE, [2]Münster/DE, [3]Bonn/DE (lenhard.pennig@uk-koeln.de)*

Purpose: To compare a novel compressed SENSE accelerated (factor 9) ECG- and respiratory-triggered 3D relaxation-enhanced angiography without contrast and triggering (REACT-non-CE-MRA) with standard non-ECG-triggered time-resolved 4D contrast-enhanced MRA (4D CE-MRA) for imaging of the pulmonary vasculature in patients with congenital heart disease (CHD) at 1.5T.
Methods and materials: This retrospective analysis of 25 patients (06/2018-04/2019) with known or suspected CHD was independently conducted by two radiologists executing measurements on REACT-non-CE-MRA and 4D CE-MRA on 7 dedicated points (inner-edge): main pulmonary artery (MPA), right and left pulmonary artery, right superior and inferior pulmonary vein, left superior (LSPV), and inferior pulmonary vein. The image quality for arteries and veins was evaluated on a four-point scale in consensus.
Results: 23 of 25 patients presented with CHD. There was a high interobserver agreement for both methods of imaging at the pulmonary arteries (ICC ≥ 0.96); at pulmonary veins, REACT-non-CE-MRA showed a slightly higher agreement, pronounced at LSPV (ICC 0.946 vs 0.895). Measurements in 4D CE-MRA reached higher diameter values compared to REACT-non-CE-MRA at the pulmonary arteries with significant difference (e. g. MPA: mean 0.408 cm, p=0.002). REACT-non-CE-MRA (average acquisition time 07:01 ± 02:44 min)

showed significantly better image quality than 4D CE-MRA at the pulmonary arteries (3.84 vs 3.32, p=0.0002) and veins (3.32 vs 2.72, p=0.0152).
Conclusion: Compressed SENSE accelerated 3D REACT-non-CE-MRA allows for reliable and fast imaging of the pulmonary vasculature with higher image quality and slightly higher interobserver agreement than 4D CE-MRA without contrast agent and associated disadvantages. Therefore, it represents a clinically suitable technique for patients requiring repetitive imaging of the pulmonary vessels, e.g. patients with CHD.
Limitations: A retrospective study. No comparison to DSA.
Ethics committee approval: Ethics committee approval was given and consent was waived.
Funding: No funding was received for this work.
Author Disclosures:
L. Pennig: nothing to disclose
A. Wagner: nothing to disclose
K. Weiss: Employee at Philips Healthcare
S. Lennartz: nothing to disclose
D. Maintz: Speaker at Philips Healthcare
T. Hickethier: nothing to disclose
C. P. Naehle: nothing to disclose
A. Bunck: nothing to disclose
J. Doerner: nothing to disclose

RPS 1403b-2 11:31
Long-term follow-up of extracardiac Fontan procedure by CCT and CMR
M. Caicoya[1], M. Bret Zurita[1], I. Miguelsanz Martínez[2], E. Cuesta López[1], F. Gutiérrez-Larraya Aguado[1], E. Sanchez Pascual[1]; [1]Madrid/ES, [2]Tres Cantos/ES (martin.boto@gmail.com)

Purpose: In over 20 years of experience in congenital cardiopathy imaging in our tertiary hospital, we have witnessed the evolution of univentricular heart (UVH) surgery up to the arrival of Fontan procedure. We want to describe the late complications of patients with extracardiac Fontan correction and to familiarise radiologists with technical considerations for optimal image acquisition to avoid diagnostic pitfalls.
Methods and materials: Cardiac computed tomography (CCT) was performed in a 320-MDCT (Aquillion one, Canon Medical Systems S.A.®), with acquisition of an EKG-gated arterial phase and a 70 s-delayed phase (whole thorax). Cardiac-MRI (CMR) was obtained in a 3T system (Magnetom Skyra, SIEMENS®). EKG-gated dark and bright-blood, cine turbo-FLASH, PC in ascending aorta and AV valve, 3D Angio-MRI (wide FOV including upper abdomen) in arterial and venous phases, and late gadolinium enhanced sequences were obtained. Gadolinium contrast (3 mmol/Kg b.w.) was administered.
Results: We recruited 20 patients (18-26 years old). The mean follow-up period was 14 years. 9 (45%) patients had right and 11 (55%) patients had left morphological UVH. The average EF was 53.8%. 2 cases had ventricular EF<45%. Fontan stenosis was found in 4 patients (20%). 9 cases (45%) showed AV regurgitation and 2 patients (10%) presented with aortic regurgitation. Vascular complications (n=13) included 9 (45%) veno-venous and 2 (10%) arteriovenous fistulae. 10 cases (50%) had hepatic lesions.
Conclusion: CMR and MDCT are essential for follow-up and detection of late complications of extracardiac Fontan correction. The appearance of these complications may indicate the start of the Fontan failure.
Special imaging acquisition protocols are required for optimal evaluation of Fontan connections and complications.
Limitations: n/a
Ethics committee approval: n/a
Funding: No funding was received for this work.
Author Disclosures:
M. Caicoya: nothing to disclose
I. Miguelsanz Martínez: nothing to disclose
M. Bret Zurita: nothing to disclose
E. Cuesta López: nothing to disclose
F. Gutiérrez-Larraya Aguado: nothing to disclose
E. Sanchez Pascual: nothing to disclose

RPS 1403b-3 11:37
Is IVIM enough to assess hepatic injury in post-repair tetralogy of Fallot?
S. Baş Özkök, M. Sorkun; *İstanbul/TR (minealacagoz@gmail.com)*

Purpose: Although congestive hepatopathy is well explained in Fontan circulation and intravoxel incoherent motion (IVIM) was performed for liver injury, no reports have been published about liver injury in post-repair TOF patients by IVIM parameters. We aimed to research in post-repair TOF patients whether cardiac MRI (CMR) and laboratory findings correlate with liver injury by IVIM parameters.

Methods and materials: 30 patients with post-repair TOF (15.46±7.64 years old, F/M: 15/15) and 25 healthy controls (18.53±5.73 years old, F/M: 15/10) were included. IVIM sequences were revealed after CMR examination by a 1.5T scanner and 32-channel phased-array surface coil.
IVIM values (D, D*, and perfusion fraction) were measured by locating ROI in 8 segments of the liver. Pulmonary artery regurgitation fraction (RF), right and left end-diastolic volume index (LVEDVI, RVEDVI), and ejection fraction (LV-EF, RV-EF) were correlated with IVIM parameters in post-repair TOF patients.
Results: Mean LVEDVI, LV-EF, RVEDVI, RV-EF, and pulmonary artery RF were 92.3±21.43ml/m^2, 48.63±5.96%, 172.57±41.32ml/m^2, 39.53±6.37%, and 46.03±10.83, respectively. There was a significant difference between DWI, DTrue, and perfusion fraction of post-repair TOF (DWI: 177.50±126.78 mm^2/second versus 205.70±82.15 mm^2/second (p = 0.00318), DTrue 0.00165±0.0005 mm^2/second versus 0.00144±0.0008 mm^2/second, D* 0.068±0.075 versus 0.079±0.074 mm2/second (p = 0.12602), perfusion fraction 34.68±16.95% versus 29.57±12.56% (p =0.00001), and D*fraction 0.365±0.089 % versus 0.380±0.077%, respectively). There was no statistically significant correlation between IVIM parameters and CMRI measurements.
Conclusion: Liver injury can be seen independently from cardiac parameters. Evaluation of the liver should be added to annual cardiac check-ups. DWI, DTrue, and perfusion fraction parameters can be used for evaluating liver injury in post-repair TOF patients and assessing capillary perfusion and connective tissue/cell density by IVIM sequences.
Limitations: A relatively small sample size. A lack of histopathologic correlation with imaging.
Ethics committee approval: Institutional Review Board approval. Written informed consent was obtained.
Funding: No funding was received for this work.
Author Disclosures:
M. Sorkun: nothing to disclose
S. Baş Özkök: nothing to disclose

RPS 1403b-4 11:43
Multiparametric myocardial mapping of paediatric cardiac tumours: preliminary results in comparison with conventional cardiac MR evaluation
V. Bordonaro, D. Curione, T. P. Santangelo, P. Ciancarella, C. Napolitano, P. Ciliberti, A. Secinaro; *Rome/IT (bordonaroveronica@gmail.com)*

Purpose: To evaluate the diagnostic role of native T1, ECV, and T2 values of paediatric cardiac tumours.
Methods and materials: We retrospectively included 8 paediatric patients (mean age 8.25 ± 3.62 years, range 2-16; 6 femmine) with suspected cardiac masses (2 fibromas, 2 angiomas, 1 rhabdomyoma, 1 teratoma, 1 myxoma, and 1 lipoma) who underwent cardiac MRI on a 1.5T scanner using T2 and pre- and post-contrast T1 mapping sequences. Native T1, ECV, and T2 values were obtained as an average among 3 non-overlapping ROIs placed into the lesion and an additional ROI covering the whole mass. The analysis was performed by two experienced readers, blinded to the suspected diagnosis.
Results: The 2 fibromas showed native T1 values of 972 ± 96 ms, ECV values of 100% ± 2, and T2 of 47 ± 2 ms. The 2 angiomas had native T1 of 1,310 ± 48 ms and ECV of 57% ± 5 and T2 of 78 ± 2 ms. The rhabdomyoma had native T1 of 1,420 ms, ECV of 29%, and T2 of 73 ms. The teratoma showed native T1 values of 1,378 ms, ECV of 29%, and T2 of 58 ms. The myxoma had native T1 values of 1,644 ms, ECV of 74%, and T2 of 126 ms. The lipoma showed native T1 values of 215 ms, undetectable ECV, and T2 of 89 ms.
Conclusion: Preliminary data obtained from this small series of paediatric tumours suggests that ECV values trend towards a higher reproducibility and better correlates with the suspected diagnosis derived from a conventional MRI approach compared to native T1 and T2 values (e.g. ECV=100% in fibromas, normal ECV in rhabdomyoma, and ECV equal to plasmatic component in angiomas).
Limitations: n/a
Ethics committee approval: n/a
Funding: No funding was received for this work.
Author Disclosures:
V. Bordonaro: nothing to disclose
D. Curione: nothing to disclose
T. P. Santangelo: nothing to disclose
P. Ciancarella: nothing to disclose
C. Napolitano: nothing to disclose
P. Ciliberti: nothing to disclose
A. Secinaro: nothing to disclose

RPS 1403b-5 11:49

Possibilities of CT-angiocardiography in single ventricle defect diagnostics

T. Tazhigaliyeva; *Nur-Sultan/KZ (torgyn.tazhigaliyeva@gmail.com)*

Purpose: To explore the possibilities of CT-angiocardiography in the single ventricle of the heart (SVH) diagnostics.
Methods and materials: Studies were conducted in the radiology department of JSC "National Research Cardiac Surgery Center" from October 2011 to December 2018, inclusive. 1,844 patients with suspected CHD were examined, 125 (6,8%) of whom had a SVH: females - 59 (47,2%), males - 66 (52,8%).
Results: The studies results of 125 SVH patients were analysed; 70 (56%) via right ventricular hypoplasia (type A), 32 (25.6%) via left ventricular hypoplasia (type B), and 23 (18.4%) via a single ventricle (type C).
A single ventricle was diagnosed at the age of 1 up to 6 months in 74 (59.2%) patients, from 6 months to 1 year in 14 (11.2%) patients, from 1 to 5 years in 18 (14.4%) patient, from 5 to 10 years in 4 (3.2%) patients, and over 10 years in 15 (12%) patients.
SVH with other CHDs combination: atrial septal defect in 86 (68.8%) patients, patent ductus arteriosus in 70 (56%) patients, transposition of the great arteries in 51 (40.8%) patients, ventricular septal defect in 57 (45.6%) patients, pulmonary atresia in 28 (22.4%) patients, anomalous pulmonary veins drainage in 26 (20.8%) patients, patent foramen ovale in 19 (15.2%) patients, double superior vena cava in 15 (12%) patients, and coarctation of the aorta in 9 (7.2%) patients.
89 (71.2%) patients were operated on and 36 (28.8%) were not operated on, of which 56 had positive outcomes (62.9%) and 34 resulted in death (38.2%).
Conclusion: CT-angiocardiography is a highly informative and minimally invasive method for SVH diagnostics, replacing invasive methods such as cardiac catheterisation and angiocardiography. Sensitivity was 96.7%, specificity was 97.4%, and accuracy was 96.7%.
Limitations: n/a
Ethics committee approval: n/a
Funding: No funding was received for this work.
Author Disclosures:
T. Tazhigaliyeva: nothing to disclose

RPS 1403b-6 11:55

Correlation between changes in cardiac iron and hepatic iron in paediatric patients with thalassemia major

A. Pepe[1], A. Meloni[1], A. Filosa[2], L. Pistoia[1], E. Grassedonio[3], R. Righi[4], P. Preziosi[5], V. Positano[1], M. Casale[2]; [1]*Pisa/IT,* [2]*Naples/IT,* [3]*Palermo/IT,* [4]*Ferrara/IT,* [5]*Rome/IT (alessia.pepe@ftgm.it)*

Purpose: We evaluated if changes in myocardial iron overload (MIO) were related to baseline hepatic iron or changes in hepatic iron overload in children with thalassemia major (TM).
Methods and materials: We considered 68 TM patients enrolled in the MIOT project with <18 years at the first MRI and who performed a follow-up study at 18±3 months.
Myocardial and hepatic iron burdens were quantified by the T2* technique. Liver T2* values were converted into liver iron concentration (LIC) values.
Results: Baseline global heart T2* values were 29.72±11.21 ms and 16 patients showed baseline MIO (T2*<20 ms).
Mean percentage changes in global heart T2* values per month were 0.66±1.70 and they were significantly higher in patients with baseline MIO (1.99±2.53% vs 0.25±1.09% ms; P=0.002).
Percentage changes in global heart T2* values/month were not associated to initial MRI LIC values (R=0.048; P=0.695) or to final MRI LIC values (R=-0.134; P=0.277).
No correlation was detected between % changes in heart T2* and MRI LIC values (R=-0.244; P=0.067).
Conclusion: In paediatric TM patients, changes in MIO are not correlated to baseline MRI LIC values and changes in hepatic iron. Our data seems to not support the hypothesis that it is necessary to clean the liver before removing MIO.
Limitations: The limited sample size, however, TM is a rare disease.
Ethics committee approval: The study complied with the Declaration of Helsinki. The institutional review board approved this study. For all patients, parents gave their informed consent to the protocol.
Funding: The MIOT project receives "no-profit support" from industrial sponsorships (Chiesi Farmaceutici S.p.A. and ApoPharma Inc.).
Author Disclosures:
A. Pepe: nothing to disclose
A. Meloni: nothing to disclose
L. Pistoia: nothing to disclose
A. Filosa: nothing to disclose
E. Grassedonio: nothing to disclose
R. Righi: nothing to disclose
P. Preziosi: nothing to disclose
V. Positano: nothing to disclose
M. Casale: nothing to disclose

RPS 1403b-7 12:01

Biventricular cardiac strain in patients with a tetralogy of Fallot: a cardiac magnetic resonance study

C. B. Monti[1], G. Guarnieri[1], U. Barbaro[2], D. Capra[1], M. Alì[1], F. Sardanelli[1], F. Secchi[1]; [1]*Milan/IT,* [2]*Messina/IT (caterinab.monti@gmail.com)*

Purpose: To evaluate left (LV) and right ventricular (RV) strain and their modifications over time in patients with a tetralogy of Fallot (ToF).
Methods and materials: We retrospectively evaluated patients with ToF with two cardiac magnetic resonances (CMR) performed between 2014 and 2019. We segmented epicardium and endocardium in both ventricles in long-axis end-systolic and end-diastolic cine images, and calculated LV and RV volumes, ejection fraction (EF), global longitudinal (GLS), and radial and circumferential strain for the LV and RV. We conducted analyses overall and divided patients into two groups according to whether they underwent pulmonary valve replacement between the two CMRs (Group-1) or not (Group-0).
Results: Our study population included 46 patients, of which 30 belonged to Group-0 and 16 to Group-1. EF remained unvaried from the first to the second CMR overall (from 55%,60-63% to 55%,50-60%, p=0.563,) and in subgroups (Group-0 from 57%,48%-65% to 55%,49-62%, p=0.534, Group-1 from 54%, 51-58% to 53%, 50-60%, p=0.763). Overall, RV GLS increased (p=0.017) from the first (-22.8%,-26.3--21.1) to the second CMR (-20.1%,-23.1--16.9%). In Group-0, RV-GLS increased (p=0.034) from the first (-23%,-26.9—21.9%) to the second CMR (-20.5%,-25.3– -16.7%), while in Group-1, RV-GLS remained unvaried (p=0.238) from the first (-22.6%,-24.8—19.6%) to the second CMR (-19.6%,-22.6—17%).
Conclusion: RV-GLS may represent an early biomarker of RV functional deterioration in patients with ToF. Furthermore, pulmonary valve replacement may stall the worsening of RV GLS.
Limitations: A retrospective, monocentric study. A small study sample.
Ethics committee approval: Ethics committee approval was obtained, informed consent was waived due to the retrospective nature of the study.
Funding: No funding was received for this work.
Author Disclosures:
F. Sardanelli: Grant Recipient at Bayer, Grant Recipient at General Electric, Grant Recipient at Bracco, Speaker at Bayer, Speaker at General Electric, Speaker at Bracco, Advisory Board at Bracco
C. B. Monti: nothing to disclose
G. Guarnieri: nothing to disclose
U. Barbaro: nothing to disclose
D. Capra: nothing to disclose
M. Alì: nothing to disclose
F. Secchi: nothing to disclose

RPS 1403b-8 12:07

Right versus left ventricular blood pool ratio in T2 mapping: a simple method for detecting left-to-right shunts by CMR

T. Emrich[1], T. Schöler[1], I. A. Abidoye[2], T. Deisler[1], A. L. Emrich[1], P. Wenzel[1], C. Düber[1], A. Varga-Szemes[3], K.-F. Kreitner[1]; [1]*Mainz/DE,* [2]*Ado-Ekiti/NG,* [3]*Charleston, SC/US (tilman.emrich@gmail.com)*

Purpose: Left-to-right shunts (L-R-Shunt) lead to volume overload of the right ventricular system, pulmonary hypertension, and alterations of the RV myocardium, resulting in adverse cardiac events. CMR is able to detect L-R-Shunts by comparison of phase-contrast measurements of pulmonary and aortic flow (Qp/Qs-ratio), which is not routinely done in clinical CMR. T2-mapping is generally used for the analysation of myocardial oedema. Additionally, it is sensitive to the oxygenation of blood. This work evaluates an easy screening tool for the evaluation of L-R-Shunts using T2-mapping.
Methods and materials: We retrospectively analysed the ratio of T2-relaxation times of the LV/RV blood pool and Qp/Qs-ratio by phase-contrast-imaging from 5 patients with established relevant L-R-shunts. 7 healthy volunteers were used as a control group. Qp/Qs-ratio was calculated by dedicated measurements of pulmonary and aortic flow. In routinely acquired T2-maps of the mid-ventricular slice, the ratio between left and right ventricular blood pool T2-relaxation time was calculated.
Results: Compared to the control group, the L-R-Shunt-group showed relevant elevation of Qp/Qs and RV volume overload. T2 RV/LV-Ratio was significantly raised in patients with L-R-Shunts (0.93vs0.70, p=0.005). A ratio of >0.82 showed a 100% sensitivity and 85.7% specificity for detection of L-R-Shunts, resulting in a positive and negative predictive value of 83.3%, resp 100%. Alterations could also be depicted easily by visual assessment.

Conclusion: RV-LV blood pool T2-relaxation time ratio seems to be an easy and reliable method for the screening of L-R-Shunts. Elevated ratios of >0.82 should lead to a dedicated evaluation of Qp/Qs-ratio to determine the relevance of an L-R-Shunt. Despite its promising application, our preliminary results need to be validated in a larger study cohort.
Limitations: A single-centre study.
Ethics committee approval: The study was approved by the local ethics committee (2018-13520/837.196.13/837.477.14).
Funding: No funding was received for this work.
Author Disclosures:
T. Emrich: nothing to disclose
T. Schöler: nothing to disclose
I. A. Abidoye: nothing to disclose
T. Deisler: nothing to disclose
A. L. Emrich: nothing to disclose
P. Wenzel: nothing to disclose
C. Düber: nothing to disclose
K.-F. Kreitner: nothing to disclose
A. Varga-Szemes: Research/Grant Support at MUSC, Research/Grant Support at Siemens Healthineers, Consultant at Elucid Bioimaging

RPS 1403b-9 12:13
Anomalous ductus arteriosus connection and its relationship with the right aortic arch
M. Xie, H. Cao, L. Hong*; Wuhan/CN (Xiemx@hust.edu.cn)*

Purpose: To analyse the sonographic features of anomalous ductus arteriosus (DA) connection in the fetus and to investigate the relationship between anomalous ductal connection and the right aortic arch (RAA).
Methods and materials: Detailed fetal echocardiography was performed on 5,080 pregnancies referred to our hospital from 2014 to 2018. The three-vessel-trachea (3VT) view and DA transverse and long-axis view were chosen to observe the connection, course, dimension, and flow direction of DA. The presence of left/right/double-sided DA or aortic arch, vascular ring, and associated cardiovascular anomalies were evaluated.
Results: 41 fetuses (25.4±3.5 weeks) had anomalous DA connection and RAA was detected in all 41 cases. 21 fetuses (29/41) demonstrated a right-sided DA which abnormally connected between the pulmonary trunk (PT) or right pulmonary artery (RPA) and descending aorta (DAo). The other 12 cases (12/41) revealed a left-sided DA abnormally connected between the left pulmonary artery (LPA) and left subclavian artery (LSA). No vascular ring around the trachea was detected in all 41 cases. 5 cases (5/41) were isolated anomalous DA connection with RAA, while the remaining 36 cases (36/41) all demonstrated associated cardiac anomalies, including a tetralogy of Fallot (14/41), pulmonary atresia (9/41), double outlet right ventricle (6/41), transposition of the great arteries (3/41), and other cardiac anomalies. Reversed flow across DA was observed in 13 cases.
Conclusion: In our study, anomalous DA connection was always associated with RAA without forming vascular ring. The right-sided DA with anomalous connection between PT/RPA and DAo was more frequently seen than the left-sided DA abnormally connecting between LPA and LSA. DA abnormal connection is always accompanied with other cardiovascular anomalies.
Limitations: The embryonic developmental mechanisms of anomalous DA connection and its relationship with RAA still need further investigation.
Ethics committee approval: n/a
Funding: No funding was received for this work.
Author Disclosures:
M. Xie: nothing to disclose
H. Cao: nothing to disclose
L. Hong: nothing to disclose

RPS 1403b-10 12:19
Application of prospective ECG-gated multiphase scanning for coronary CT in children with different heart rates
S. Tang*; Chongqing/CN (sltang66@163.com)*

Purpose: To explore the application of prospective ECG-gated multiphase scanning in coronary CT imaging in children with different heart rates.
Methods and materials: In the control group, 200 children aged 2-4 years who underwent coronary CT examination in our hospital from January 2017 to December 2017 were retrospectively selected. They were divided into 5 groups according to the heart rate frequency: ＜75 beats/min, 75-85 beats/min, 86-95 beats/min, 96-105 beats/min, or 106-120 beats/min, with 40 in each group. Each child was treated with retrospective ECG-gated scanning technology. 6 groups of phase images were reconstructed: 40%, 45%, 50%, 70%, 75%, and 80%. The optimal phase was selected for coronary artery reconstruction.
Results: For the 2 groups with the same heart rate, the radiation dose in the study group was 72% lower than that in the control group. There was no significant difference in coronary artery image quality between the 2 groups at the optimal phase.
Conclusion: Applying prospective ECG-gated multiphase scanning technology to children's coronary CT imaging can significantly reduce the scanning radiation dose of children without affecting the quality of coronary artery image.
Limitations: The study was limited to children aged 3-4 years. Children with a heart rate higher than 120 beats/min were not included in the study, which needs to be further improved in future studies.
Ethics committee approval: The study protocol was approved by the Human Ethics Committee of the Children's Hospital of Chongqing Medical University. Written informed consent was obtained from the parents or guardians of all patients before the examinations.
Funding: No funding was received for this work.
Author Disclosures:
S. Tang: Author at Children's Hospital of Chongqing Medical University, Chongqing,China

11:15 - 12:30 **Darwin (Room D2)**

Radiographers

RPS 1414

Improving magnetic resonance imaging practice

Moderators:
N.N.

RPS 1414-K 11:15
Keynote lecture
C. Malamateniou*; London/UK (christina.malamateniou@city.ac.uk)*

Author Disclosures:
C. Malamateniou: nothing to disclose

RPS 1414-1 11:25
Radiographer's assessment of referrals for CT and MR imaging using a web-based data collection tool
C. Chilanga[1], K. B. Lysdahl[1], H. M. Olerud[1], R. Toomey[2], A. Cradock[2], L. A. Rainford[2]; *[1]Kongsberg/NO, [2]Dublin/IE (chiluten72@gmail.com)*

Purpose: To investigate radiographers' compliance with guidelines in assessing CT and MRI referrals and determine factors that influenced their performance.
Methods and materials: 5 referral scenarios for each of CT and MRI were distributed to radiographers who volunteered at the EFRS Research Hub at ECR 2019. A web-based data collection tool designed by Ziltron Ltd was used. The radiographers were required to determine the appropriateness of each referral, highlight any concerns, and recommend suitable alternative investigations if applicable. An overall performance score from 0-5 was calculated and a linear regression analysis was used to determine factors that influenced the radiographers' performance.
Results: 91 (n= 5l CT, n=40 MRI) radiographers participated. 58% and 57% of responses were consistent with recommended guidelines for CT and MRI, respectively. Possession of an MSc qualification in CT was a significant predicting factor of consistency with the guidelines (p=0.02). Being a radiographer in a lead professional role and/or an educator was a significant predicting factor for a greater consistency with the guidelines (p=0.01) in MRI, and approached significance for CT (p=0.06). The routine use of referral guidelines was reported by 80% of participants.
Conclusion: Over 50% of the radiographers' responses complied with guidelines.
Limitations: There may be a selection bias as participants were ECR 2019 attendees and predominantly working in Europe. Caution in translating the outcomes beyond this cohort is warranted. Additionally, the referral cases were designed with minimal text to enable easy comprehension for non-native English participants, however, the impact of language must be considered.
Ethics committee approval: Ethical approvals were obtained from the UCD Institutional UREC in Ireland and NSD (reference number 776616) in Norway.
Funding: No funding was received for this work.
Author Disclosures:
C. Chilanga: nothing to disclose
K. B. Lysdahl: nothing to disclose
H. M. Olerud: nothing to disclose
R. Toomey: nothing to disclose
A. Cradock: nothing to disclose
L. A. Rainford: nothing to disclose

RPS 1414-2 11:31

Image quality assessment of cervical and lumbar spine MRIs

T. E. C. D. Sousa[1], L. P. V. Ribeiro[2], A. F. Abrantes[3], A. D. M. Ribeiro[1], S. Rodrigues[3], K. B. Azevedo[3], N. F. Pinto[3], R. P. P. Almeida[3]; [1]Portimão/PT, [2]Parchal/PT, [3]Faro/PT (tiagosousa10@gmail.com)

Purpose: To assess if the image quality from cervical and lumbar spine MRI examinations meets the quality criteria previously established in a radiology department.
Methods and materials: A retrospective study was conducted in a public radiology department using a random sample of 450 cervical and lumbar spine MRI examinations grouped in 15 smaller samples, each one with 30 exams. Using a quality criteria checklist organised into 4 main groups, the conformities and non-conformities found were recorded and used to establish 3 types of quality control chars: the proportion of conformities and non-conformities (p chart), the total number of non-conformity exams (np chart), and the total number of non-conformities in each sample (c chart), in order to suggest corrective actions for improvement.
Results: Considering all exams, 289 were classified as conforming (64.22%) and 171 were classified as non-conforming (38%). Considering the non-conform exams group for the cervical spine, the quality criteria "motion artefacts" presented the highest number of non-conformities (55.56%), followed by "aliasing artefact" (31.11%). For the lumbar spine non-conform exams group, the quality criteria "cross-talk artefact" presented the highest number of non-conformities (45.59%), followed by "aliasing artefact" (21.32%) and "motion artefacts" (20.59%).
Conclusion: The existence of suitable quality control of the image is essential to achieve high-quality standards. Strategies for improving radiographers performance and scientific knowledge must be implemented to ensure that spine MRI examinations are performed in compliance with all the quality criteria established. Therefore, it is essential to implement a checklist for a systematic evaluation based on a quality control program.
Limitations: n/a
Ethics committee approval: The ethics committee approved the study.
Funding: No funding was received for this work.
Author Disclosures:
T. E. C. D. Sousa: nothing to disclose
L. P. V. Ribeiro: nothing to disclose
A. F. Abrantes: nothing to disclose
A. D. M. Ribeiro: nothing to disclose
S. Rodrigues: nothing to disclose
K. B. Azevedo: nothing to disclose
N. F. Pinto: nothing to disclose
R. P. P. Almeida: nothing to disclose

RPS 1414-3 11:37

A comparison of female pelvic MR image quality: Saudi and Irish perspectives

S. Al Dahery; *Jeddah/SA (shrooq_talal@hotmail.com)*

Purpose: Optimisation of MRI sequences is crucial to ensure high image quality for an accurate diagnosis. The aim is to compare the female pelvic MR image quality acquired from Saudi and Irish MR departments and evaluate the factors impact on it.
Methods and materials: Axial and sagittal T2W MR images were retrospectively collected from (9 Irish; 90 cases) and (10 Saudi; 94 cases) hospitals. Signal intensities of the fundus, gluteus maximus muscle, and the background noise standard deviation were obtained to calculate SNR/CNR. The images were evaluated by 8 expert observers and qualitative evaluation scores were recorded. An intervention was performed to improve image quality in a Saudi centre which had recorded low image quality for several criteria during phase one/two. Resultant images were collected and reviewed.
Results: Variation in the matrix and voxel sizes caused a statistically significant difference in SNR for axial T2W MR images. There was a significant difference in CNR due to the differences in the TR/TE. Statistically significant differences in CNR were recorded for the sagittal images, as the matrix and voxel sizes differed. There was no difference in SNR for sagittal images. Using thinner slices in the uterine T2W sequences resulted in better visualisation of the zonal layers.
Conclusion: A range of currently applied female pelvic MR protocols were identified across Irish and Saudi hospitals which resulted in image quality variations. MR image quality can be optimised by using a robust multi-phase optimisation process as evidenced following the optimisation intervention.
Limitations: The inability to fully explore the impact of patient BMI on image quality.
Ethics committee approval: Exemption from full ethical approval was granted by the Irish Institutional Human Research Ethics Committee and by the relevant IRB in MOH for Saudi hospitals.
Funding: King Abdullah Scholarship.
Author Disclosures:
S. Al Dahery: Speaker at UCD

RPS 1414-4 11:43

Simulated magnetic resonance imaging (MRI) by radiographers to reduce the sedation of paediatric patients

M. Champendal, G. Gullo, L. Marmy; *Lausanne/CH*

Purpose: To develop updated recommendations that are evidence-based to perform simulations as a strategy to prepare paediatric patients for MRI examinations when reducing the use of sedation.
Methods and materials: A systematic review using the Joanna Briggs Institute system for unified management (JBI SUMARI) was performed to identify studies published after 2010. Sedation, anxiety, paediatric*/child, mock MRI/play therapy were included in the search using a 6S model. The databases consulted were National Guidelines Clearinghouse, Nice, HealthEvidence, JBI, Cochrane, Uptodate, Tripdatabase, PubMed, Cinhal, and Google Scholar. 3 independent reviewers assessed articles and Gradepro software was used to rate each recommendation.
Results: 5/266 articles were selected. One was a systematic review, 2 were randomised controlled trials, and 2 were quasi-experimental and observational studies. 2 recommendations graded as B came up: paediatric patients' preparation with an MRI simulation is efficient between 4 and 11 years old. The relative risk of sedation was reduced to almost 50% for patients prepared with a simulated MRI compared to those without preparation. A modified Yale preoperative anxiety scale (mYPAS) test was suggested as a tool to select patients that can be exposed to a simulation when the score is less than 33.
Conclusion: The simulation of an MRI to prepare paediatric patients for this examination is a strategy that can work, but only in specific circumstances and mainly for an age superior to 4 years old. Simulation can reduce anxiety, ensuring a successful examination without sedation. Further studies, however, should be conducted to very if this strategy can be applied to other imaging modalities even using the same simulation setting.
Limitations: Only a few studies were available.
Ethics committee approval: n/a
Funding: No funding was received for this work.
Author Disclosures:
M. Champendal: nothing to disclose
G. Gullo: nothing to disclose
L. Marmy: nothing to disclose

RPS 1414-5 11:49

Technique and protocols for cardiothoracic time-resolved contrast-enhanced MRA sequences: a systematic review

M. Zanardo[1], F. Sardanelli[1], L. A. Rainford[2], C. B. Monti[1], J. G. Murray[2], F. Secchi[1], A. Cradock[2]; [1]Milan/IT, [2]Dublin/IE

Purpose: To review current cardiothoracic applications of time-resolved magnetic resonance angiography (TR-MRA) sequences, focusing on contrast agent (CA) protocols, adopted technical parameters, and acquisition schemes.
Methods and materials: A systematic search of the literature (Medline/EMBASE) was performed in May 2019 to identify articles utilising TR-MRA sequences. The study design, year of publication, population, magnetic field strength, type, dose and injection parameters of CA and injection, and technical parameters of TR-MRA sequences were extracted.
Results: Of 117 retrieved articles, 16 matched the inclusion criteria. The study design was prospective in 9/16 (56%) articles and the study population ranged from 5-185 patients for a total of 506 patients who underwent cardiothoracic TR-MRA. Magnetic field strength was 1.5T in 13/16 (81%) and 3T in 3/16 (19%) articles. The administered CA was gadobutrol (Gadovist) in 6/16 (37%) articles, gadopentetate dimeglumine (Magnevist) in 5/16 (31%), gadobenate dimeglumine (Multihance) in 2/16 (13%), gadodiamide (Omniscan) in 2/16 (13%), and gadofosveset trisodium (AblavarTM) in 1/16 (6%). CA showed highly variable doses among studies: a fixed amount or based on patient body weight (0.02-0.2 mmol/kg) was injected with a flow rate ranging from 1-5 mL/s. Sequences were "TWIST" in 13/16 (81%), "TRICKS" in 2/16 (13%), and "CENTRA" 1/16 articles (6%).
Conclusion: Results identified that a variety of technical approaches were adopted throughout different studies, highlighting a lack of standardisation and consensus. TR-MRA sequences are currently adopted in different clinical settings with different technical approaches, mostly due to different CA dose and type. Further studies are warranted in order to establish appropriate parameters for TR-MRA, especially in relation to CA protocols.
Limitations: No quality assessment was performed in the included studies.
Ethics committee approval: n/a
Funding: No funding was received for this work.

Author Disclosures:
F. Secchi: nothing to disclose
A. Cradock: nothing to disclose
M. Zanardo: nothing to disclose
F. Sardanelli: Grant Recipient at Bayer, Grant Recipient at General Electric, Grant Recipient at Bracco, Speaker at Bayer, Speaker at General Electric, Speaker at Bracco, Advisory Board at Bracco
L. A. Rainford: nothing to disclose
C. B. Monti: nothing to disclose
J. G. Murray: nothing to disclose

RPS 1414-6 11:55

The efficacy of the GRASE sequence compared to the compressed sensing technique for breath-hold three-dimensional MR cholangiopancreatography in patients with hyperintense bile on T1-weighted images

D. Morimoto, T. Hyodo, M. Itou, H. Fukushima, K. Kamata, M. Takenaka, K. Miyagoshi, M. Kudo, K. Ishii*; Osaka-Sayama/JP (morimoto-d@med.kindai.ac.jp)*

Purpose: To compare the image quality of single breath-hold (BH) three-dimensional (3D) MRCP using GRASE with that of the compressed sensing (CS) technique.
Methods and materials: We retrospectively identified 44 patients with hyperintense bile on T1-weighted fat-suppressed images who underwent BH 3D MRCP using both GRASE and CS with a 1.5T scanner. Maximum intensity projection MRCP images were reviewed for visibility of the right, left, and common hepatic duct, common bile duct, gallbladder (GB), cystic duct, and pancreatic duct (PD), motion artefact, background suppression, and overall image quality using a 5-point scale (1=poor; 5=excellent). The scores and availability rates, the latter defined as a visibility score of ≥3, were compared between GRASE and CS using a Wilcoxon signed-rank test and McNemar's test, respectively.
Results: The median visibility scores of each biliary segment were significantly higher in GRASE than CS ($p \leq 0.001$ for all). No significant difference was found for the PD ($p=0.396$). The motion artefact score was not significantly different ($p=0.313$). GRASE had significantly lower background suppression scores ($p<0.001$) and higher overall image quality scores ($p<0.001$) than CS. GRASE had significantly higher rates of availability on the basis of visibility of the GB (44/44 vs 29/44, $p<0.001$) and cystic duct (39/44 vs 19/44, $p=0.001$) than CS. Similar but non-significant trends were observed for the other biliary segments.
Conclusion: BH 3D MRCP with GRASE provides better image quality and higher availability for depiction of the biliary ducts than CS in patients with hyperintense bile on T1-weighted images.
Limitations: Non-consecutive patients might lead to a selection bias.
Ethics committee approval: IRB approval was obtained and informed consent was waived.
Funding: No funding was received for this work.
Author Disclosures:
D. Morimoto: nothing to disclose
T. Hyodo: nothing to disclose
M. Itou: nothing to disclose
H. Fukushima: nothing to disclose
K. Kamata: nothing to disclose
M. Takenaka: nothing to disclose
K. Miyagoshi: nothing to disclose
M. Kudo: nothing to disclose
K. Ishii: nothing to disclose

RPS 1414-7 12:01

The impact of phase-encoding direction on calculated ADC values in DW-MRI of normal bone marrow in the distal femur and proximal tibial

A. Alqattan, A. McGee, E. Delahunt, A. Cradock, S. Eustace, J. McNulty*; Dublin/IE (abrar.alqattan@ucdconnect.ie)*

Purpose: Multiple artefacts can cause variation in the calculated apparent diffusion coefficients (ADCs) for defined anatomical regions, resulting in unreliable quantification in DW MRI. The appropriate selection of parameters and phase-encoding (PE) direction are essential to minimise artefacts. The aim of this preliminary study was to evaluate the impact of PE-orientation on mean ADC for normal bone marrow at sites associated with ACL injury-related bone bruising.
Methods and materials: A standard knee protocol and optimised axial-DWI sequences acquired with the same parameters except for the PE-direction (anterior-posterior (AP) and right-left (RL)) were performed on 15 healthy individuals (18-35 years). For each subject, 30 50mm^2 regions-of-interest (ROIs) were placed on locations associated with ACL-related bone bruising: anterior, medial, and posterior ROIs in the medial and lateral tibial condyles (TC) and medial and lateral femoral condyles (FC). Mean ADC values were calculated and the effect of PE-direction (AP vs RL at b50_600s/mm^{2}and b50_ 800s/mm^2) was evaluated.
Results: The calculated mean ADC for all ROIs with an AP PE-direction was higher than RL PE-direction (diff=0.0066; SE=0.005) for b50_600s/mm^2 and marginally lower (diff=0.0007; SE=0.007) for b50_800s/mm^2. In the FCs, the effect of AP PE-direction was higher than the RL PE-direction by 0.019 (b50_600s/mm^2) and by 0.0398 (b50_800s/mm^2). The mean ADC was marginally lower in (TCs) by -0.005 and -0.025 for both b-value image sets. These results indicate marginal and non-statistically significant differences in mean ADCs for DWIs acquired in two PE-directions (p=0.11).
Conclusion: For healthy volunteers, the use of an AP or RL PE-direction has a minimal impact on ADCs, however, mean ADCs may be affected by changing the PE-direction in subjects with ACL-related bone bruising or ACL reconstructions, which will be evaluated in further research.
Limitations: n/a
Ethics committee approval: Institutional ethical approval obtained.
Funding: Part-funded by the Kuwait Cultural Office.
Author Disclosures:
A. Alqattan: nothing to disclose
A. McGee: nothing to disclose
E. Delahunt: nothing to disclose
A. Cradock: nothing to disclose
S. Eustace: nothing to disclose
J. McNulty: nothing to disclose

RPS 1414-8 12:07

Patient satisfaction of the Aspetar MRI service

T. Smith, M. N. A. Mohamed, H. Lloyd, S. Allenjawi, M. Farooq*; Doha/QA (mrinawas@gmail.com)*

Purpose: Patient satisfaction is important as the quality of care directly impacts on the income of health care facilities (Lang et al 2013). Numerous studies on patient satisfaction surveys have been conducted internationally, however, few have focused on MRI services, with virtually no cultural information related to Middle-Eastern populations. From the data collected, we hope to identify areas of weakness in dissatisfaction from our clients. We hope to enhance the image of the radiology department through improved revenue and public positivity.
Methods and materials: After IRB approval, all patients above the age of 18 years who had had an MRI examination were provided with a patient satisfaction survey questionnaire in either Arabic, French, or English. The survey was voluntary and anonymous with 500 surveys taken in a period of 6 months. The questionnaires asked for the patient's demographics, excluding identifiable data, and covered the key factors of competence, communication, sense of confidence, physical environment, and staff demeanour.
Results: There was no significant difference between nationality and satisfaction. The appointment of a scan within 3 days showed a significance in competence, communication, and sense of confidence. Waiting time showed significance in the department's competence, where the best satisfaction was within 15 minutes. For patients who had to wait more than 30 minutes, women were more dissatisfied than men of all participants.
Conclusion: The overall experience with the service of MRI was excellent and 98% would recommend that Aspetar MRI provides the best services and better patient care. Waiting times can impact on patient satisfaction for those who stay more than 15 minutes in waiting areas before proceeding to their scan and this needs to be addressed in the future.
Limitations: n/a
Ethics committee approval: Consent obtained.
Funding: No funding was received for this work.
Author Disclosures:
M. N. A. Mohamed: Investigator at Aspetar, Author at Aspetar, Employee at Aspetar
T. Smith: Investigator at Aspetar, Speaker at Aspetar, Author at Aspetar, Employee at Aspetar
H. Lloyd: Author at Aspetar, Investigator at Aspetar, Employee at Aspetar
S. Allenjawi: Author at Aspetar, Advisory Board at Aspetar
M. Farooq: Research/Grant Support at Aspetar, Board Member at Aspetar

RPS 1414-9 12:13

Patient perceptions of radiographer communication skills in MRI examinations

R. P. Sousa[1], O. Lesyuk[2], L. P. V. Ribeiro[3], S. Rodrigues[4], R. P. P. Almeida[4], A. F. Abrantes[4], A. D. M. Ribeiro[5]; *[1]Sagres/PT, [2]São Brás de Alportel//PT, [3]Parchal/PT, [4]Faro/PT, [5]Portimão/PT (rpsousa16@gmail.com)*

Purpose: The improvement of results in healthcare through the transmission of information to the patient using empathy and trust is already a verified hypothesis. Healthcare professionals should base themselves on interpersonal competencies throughout their daily work routine to promote quality in medical imaging, patient safety, and technical excellence. The aim of this study was the exploration of the patient's perceptions regarding the performance of

radiographers in terms of interpersonal communication skills during MRI procedures.
Methods and materials: The instrument used was the questionnaire "communication assessment tool" (Makoul et al. 2007) adapted to the professional reality of radiographers. 110 valid questionnaires (including 15 questions with a 5-point Likert scale) from patients aged from 18-85 years old were conducted. The paper-based instrument was delivered and filled by the patients after the performance of MRI procedures in 2 public hospitals.
Results: The internal consistency of the questionnaire was excellent (Cronbach's alpha=0.964). The highest ratings were for radiographer behaviour items, such as "used an accessible language" (4.62), "respect for the patients" (4.58), and "he paid attention to me" (4.53). The lowest ratings were "encouraged to make questions" (3.88), "involved patients in decision-making process" (4.06), and "talk with patients about the next following steps" (3.81).
Conclusion: Radiographers communication skills were evaluated with good levels of patient confidence with the MR examinations. Despite the overall positive results, this area of health service delivery must be accorded the attention it deserves to continually improve patient satisfaction through improved communication.
Limitations: The sample size.
Ethics committee approval: The ethics committee approved the study and written informed consent was obtained.
Funding: No funding was received for this work.
Author Disclosures:
R. P. Sousa: nothing to disclose
O. Lesyuk: nothing to disclose
L. P. V. Ribeiro: nothing to disclose
S. Rodrigues: nothing to disclose
R. P. P. Almeida: nothing to disclose
A. F. Abrantes: nothing to disclose
A. D. M. Ribeiro: nothing to disclose

RPS 1414-10 12:19
A survey to explore magnetic resonance imaging safety in Greece
N. Stogiannos[1], C. Westbrook[2]; [1]*Corfu/GR,* [2]*Cambridge/UK (nstogiannos@yahoo.com)*

Purpose: To explore specific MRI safety policies in Greece and compare them with the recommendations of the American College of Radiology (ACR). The null hypothesis was that there are no significant differences between the safety policies employed in Greece and the ACR's safety guidelines.
Methods and materials: All the MRI units currently operating in Greece were included in this study. Census sampling method was used. This resulted in a sample size of 307 MR scanners, operating both in a public/private or inpatient/outpatient environment. A specific questionnaire was distributed to the participants, with pre-coded closed questions. Statistical analysis was performed on IBM Spss statistical software, version 24.0. Descriptive statistics were performed to analyse the results. Pearson's Chi-square test was used to measure possible relationships between variables.
Results: Out of 307 MR scanners, 104 valid responses were received. The response rate was 33.87%, while the level of statistical significance was $p<0.05$. The margin of error was 7.9 percentage points at the 95% confidence interval. Cronbach's alpha coefficient was 0.686.
Conclusion: Greek MRI units reported a relatively good level of compliance with the recommendations of the ACR. However, a high lack of MR safe equipment was noticed, as well as some inconsistencies regarding the optimal zoning system. Specific safety measures are recommended to enhance MRI safety in Greece. Further research is needed.
Limitations: The item non-response bias. The generalisation of the results cannot be achieved due to the relatively low response rate.
Ethics committee approval: Written informed consent was obtained. Approval was given from the scientific committees of all public hospitals in line with the Greek legislation.
Funding: No funding was received for this work.
Author Disclosures:
C. Westbrook: nothing to disclose
N. Stogiannos: nothing to disclose

RPS 1414-11 12:25
Assessment of MRI safety knowledge and concepts in radiographers and other medical staff
V. M. F. Silva[1], D. Santos[2], A. Santos[2], J. Santos[2]; [1]*Porto/PT,* [2]*Coimbra/PT (vitorsoft@gmail.com)*

Purpose: There are risks and hazards related to MRI examinations. Therefore, it is extremely important to ensure both professionals and patients' protection from MRI risks and hazards. MRI risks and hazards professionals' knowledge is crucial for better practices.
The main purpose was to evaluate the knowledge about MRI safety of radiographers and medical physicians (radiology and neuroradiology), considering their experience, education, and background.
Methods and materials: This study was directed to radiographers and medical physicians working in public, private, and public-private institutions through an online questionnaire with 20 questions. The analysis of the influence of the experience in MRI was made with a Student t-test for independent samples and a Mann-Whitney test. Statistical analysis of the influence of extracurricular formation on MRI was performed using the ANOVA test.
Results: 128 complete replies were obtained, 102 from radiographers, 15 from radiologists, and 3 from neuroradiologists.
It was found that MRI experience and education were statistically significant ($p\leq0.05$) in concerns about MRI safety knowledge when compared to professionals without MRI experience and education.
Conclusion: This study focuses on the impact of continuing education, highlighting the importance of training dedicated to the area of professional performance related to MRI safety.
Limitations: The sample could be bigger.
Ethics committee approval: n/a
Funding: No funding was received for this work.
Author Disclosures:
V. M. F. Silva: nothing to disclose
D. Santos: nothing to disclose
A. Santos: nothing to disclose
J. Santos: nothing to disclose

11:15 - 12:30 **Descartes (Room D3)**

Oncologic Imaging

RPS 1416a

Chest malignancies: advanced imaging and radiomics

Moderators:
I. Vasyliv; Kiev/UA
T. C. McLoud; Boston, MA/US

RPS 1416a-1 11:15
A comparison of postoperative recurrence evaluation among FDG-PET/MRI, whole-body MRI, FDG-PET/CT, and conventional methods in non-small cell carcinoma patients
Y. Ohno[1], M. Yui[2], K. Aoyagi[2], T. Yoshikawa[3]; [1]*Toyoake/JP,* [2]*Otawara/JP,* [3]*Kobe/JP (yohno@fujita-hu.ac.jp)*

Purpose: To compare the capability for postoperative recurrence evaluation among FDG-PET/MRI, whole-body MRI, FDG-PET/CT, and conventional methods based on guidelines in non-small lung cancer (NSCLC) patients.
Methods and materials: 484 consecutive postoperative NSCLC patients (289 men, 195 women; mean age 69 years) prospectively underwent whole-body MRI, integrated PET/CTs, and conventional radiological methods, as well as a follow-up or pathological examinations. All patients were divided into recurrence (n=42) and non-recurrence (n=442) groups based on pathological and follow-up examinations. All co-registered PET/MRIs were generated by means of our proprietary software. The probability of postoperative recurrence in each patient was visually assessed on all methods by means of a 5-point visual scoring system. To compare diagnostic performance among all methods, receiver operating characteristic analyses were performed. The diagnostic accuracy of postoperative recurrence was statistically compared by using McNemar's test.
Results: The area under the curves (AUCs) of PET/MRI (AUC=0.99) was significantly larger than others (MRI and PET/CT: AUC=0.97, $p<0.05$; conventional methods: AUC=0.94, $p<0.05$). When feasible threshold values were applied, the accuracy of PET/MRI (97.7%) was significantly higher than others (MRI: 96.3%, $p<0.05$; PET/CT: 94.8%, $p<0.05$; conventional methods: 90.0%, $p<0.05$). The accuracy of MRI was significantly higher than PET/CT and conventional methods ($p<0.05$). In addition, the accuracy of PET/CT was significantly higher than conventional methods ($p<0.05$).
Conclusion: FDG-PET/MRI has better the potential for postoperative recurrence evaluation than others in postoperative NSCLC patients.
Limitations: Qualitative visual assessment for postoperative recurrence.
Ethics committee approval: This prospective study was approved by the institutional review board of Kobe University Hospital, and written informed consent was obtained.
Funding: Canon Medical Systems, Bayer Pharma and Daiichi Sanky Co., Ltd.

Author Disclosures:
Y. Ohno: Research/Grant Support at Canon Medical Systems Corporation
M. Yui: Employee at Canon Medical Systems Corporation
K. Aoyagi: Employee at Canon Medical Systems Corporation
T. Yoshikawa: Research/Grant Support at Canon Medical Systems Corporation

RPS 1416a-3 11:21

Dynamic perfusion area-detector CT (ADCT) versus FDG-PET/CT: the capability for therapeutic outcome prediction in small cell lung cancer patients with limited disease

Y. Ohno[1], Y. Fujisawa[2], K. Fujii[3], N. Sugihara[2], S. Seki[4], T. Yoshikawa[4]; [1]Toyoake/JP, [2]Otawara/JP, [3]Tokyo/JP, [4]Kobe/JP
(yohno@fujita-hu.ac.jp)

Purpose: To directly compare the capability for therapeutic outcome prediction among dynamics contrast-enhanced (CE-) perfusion area-detector CT (ADCT) and FDG-PET/CT in small cell lung cancer (SCLC) patients evaluated as limited disease (LD).
Methods and materials: 43 consecutive and pathologically diagnosed SCLC patients assessed as LD underwent PET/CT, dynamic CE-perfusion ADCT, chemoradiotherapy, and follow-up examination. In each patient, therapeutic outcomes were assessed based on RECIST guideline. All patients were divided into 2 groups as follows: responder (CR+PR: n=33) and non-responder (SD+PD: n=10) groups. The total tumour perfusion (TTP) and tumour perfusions from pulmonary (TPP) and systemic (TPS) circulations calculated by the dual-input maximum slope method from dynamic ADCT data and SUV_{max} were assessed at each targeted lesion. The average value of each index from all targeted lesions was compared between responders and non-responders by Student's t-test. To compare the differentiation capability in the 2 groups, all indexes as having significant difference were assessed by ROC analysis. Differentiation capability was compared among all indexes as having a significant difference between the 2 groups by McNemar's test.
Results: There were significant differences in all indexes except TPP ($p<0.05$). The area under the curve (AUC) of TPS (AUC=0.92) was significantly larger than that of SUV_{max} (AUC=0.73, p=004). When applied, each feasible threshold value and the accuracy of TTP (83.7%) and TPS (93.0%) were significantly higher than that of SUV_{max} (76.7%, $p<0.05$).
Conclusion: Dynamic CE-perfusion ADCT has a better potential for predicting the therapeutic outcome than PET/CT in SCLC patients with limited disease.
Limitations: No comparison of survival.
Ethics committee approval: This prospective study was approved by the institutional review board of Kobe University Hospital and written informed consent was obtained.
Funding: Canon Medical Systems Corporation.
Author Disclosures:
Y. Ohno: Research/Grant Support at Canon Medical Systems Corporation
Y. Fujisawa: Employee at Canon Medical Systems Corporation
K. Fujii: Employee at Canon Medical Systems Corporation
N. Sugihara: Employee at Canon Medical Systems Corporation
S. Seki: nothing to disclose
T. Yoshikawa: Research/Grant Support at Canon Medical Systems Corporation

RPS 1416a-4 11:27

Radiological classification of sub-solid lung nodules to differentiate three subtypes of early pulmonary adenocarcinoma

X. Cui[1], M. A. Heuvelmans[1], S. Zheng[1], H. J. M. Groen[1], M. Dorrius[1], M. Oudkerk[1], G. de Bock[1], R. Vliegenthart[1], Z. Ye[2]; [1]Groningen/NL, [2]Tianjin/CN
(cuixiaonan1988@163.com)

Purpose: To design a CT reporting system for the classification of sub-solid lung nodules to differentiate early pulmonary adenocarcinoma subtypes (SSNs) in clinical patients.
Methods and materials: We retrospectively identified 437 SSNs from 2011-2017 with pathological confirmation. SSNs were divided into a training group (N=291) and a testing group (N=146). In multinomial univariable and multivariable logistic regression, CT characteristics were analysed to identify factors discriminating between 3 adenocarcinoma subtypes [pre-invasive lesions (PLs), minimally invasive adenocarcinoma (MIA), and invasive adenocarcinoma (IA)]. The resulting differentiating factors were included in a classification and regression tree (CART) model. Subsequently, a CT reporting system was constructed for SSNs based on the optimised classification model. The classification performance was validated in the testing group.
Results: The most important differentiating factors based on CT-derived characteristics of sub-solid nodules were visual density (non-solid or part-solid), core (present or absent), diameter of solid component (≤6 mm or >6 mm), and semantic features (vacuole sign, pleural indentation, and vascular invasion). Overall sensitivity, specificity, and diagnostic accuracy of CT reporting system were 89.0% (95%CI: 84.8%-92.4%), 74.6% (95%CI: 70.8%-78.1%), and 79.4% (95%CI: 76.5%-82.0%) for the training group, and 84.9% (95%CI: 78.1%-90.3%), 68.5% (95%CI: 62.8%-73.8%), and 74.0% (95%CI: 69.6%-78.0%) in the testing group, respectively.
Conclusion: A CT reporting system for sub-solid pulmonary nodules helps to differentiate 3 adenocarcinoma subtypes. The classification tool can be used to assist clinicians in making follow-up recommendations or decisions with regards to surgery in patients with SSNs.
Limitations: This study is a single-centre retrospective study. The results may be limited to the local population.
Ethics committee approval: n/a
Funding: Royal Netherlands Academy of Arts and Sciences (PSA_SA_BD_01).
Author Disclosures:
M. A. Heuvelmans: nothing to disclose
X. Cui: nothing to disclose
S. Zheng: nothing to disclose
M. Oudkerk: nothing to disclose
H. J. M. Groen: nothing to disclose
M. Dorrius: nothing to disclose
G. de Bock: nothing to disclose
R. Vliegenthart: nothing to disclose
Z. Ye: nothing to disclose

RPS 1416a-5 11:33

Preoperative staging of tumours with mediastinal invasion: cine-MRI versus CT in the detection of cardiac and vascular involvement

N. Gennaro, U. Cariboni, F. Fazzari, V. M. Giudici, A. Rossi, O. G. Santonocito, P. Novellis, M. Infante, L. Balzarini, L. Monti; Rozzano/IT
(nicolo.gennaro@st.hunimed.eu)

Purpose: The accurate staging of tumours invading the mediastinum provides surgeons with critical information for patient selection and surgical planning. Contrast-enhanced CT is currently used for presurgical staging.
The aim of the study is to assess whether cine-MRI improves accuracy in the detection of neoplastic infiltration of critical mediastinal vascular and cardiac structures compared to contrast-enhanced CT, thus possibly expanding the spectrum of patient candidates to radical surgery.
Methods and materials: From 2008-2018, 32 patients (17M, 25F, mean age 56±14 years) diagnosed with neoplasms invading the mediastinum (lung cancer, n=16; sarcoma, n=7; thymic tumours, n=6; carcinoid, n=1; teratoma, n=1; germ cell tumours, n=1) underwent both contrast-enhanced CT and ECG-gated cine-MRI for preoperative staging. Imaging studies were reviewed by 2 expert cardio-radiologists.
The presence/site of infiltration of critical (aorta, myocardium, and pulmonary arteries) and non-critical vascular structures were noted and analysed separately. CT and MRI diagnostic performances were assessed using the postoperative anatomopathological report as a reference standard.
Results: Cine-MRI showed better diagnostic accuracy (90.2% vs 70.5%, p=0.03) in the detection of cardiac, aortic, and pulmonary artery involvement compared to CT. MRI excluded invasion of the myocardium and critical vascular structures in 8/32 (23.5%) patients that were initially considered non-surgical candidates according to CT findings.
Conclusion: Cine-MRI is more accurate than contrast-enhanced CT for the pre-operative assessment of mediastinal tumours with extensive contact with the heart or the great vessels. In our series, cine-MRI refined resectability in 23.5% of patients considered as non-surgical candidates according to contrast-enhanced CT findings.
Limitations: The limited number of patients and the unavailability of synchronised-CT studies for comparison with ECG-gated cine-MRI.
Ethics committee approval: ERB approved.
Funding: No funding was received for this work.
Author Disclosures:
N. Gennaro: nothing to disclose
U. Cariboni: nothing to disclose
L. Monti: nothing to disclose
O. G. Santonocito: nothing to disclose
F. Fazzari: nothing to disclose
V. M. Giudici: nothing to disclose
P. Novellis: nothing to disclose
M. Infante: nothing to disclose
L. Balzarini: nothing to disclose
A. Rossi: nothing to disclose

RPS 1416a-7 11:39

Prognostic 18F-FDG PET markers for immune-checkpoint inhibitor therapy in patients with non-small cell lung cancer

D. Kifjak, L. Beer, A. Haug, M. E. Mayerhöfer, M. Hochmair, H. Prosch; *Vienna/AT (daria.kifjak@meduniwien.ac.at)*

Purpose: To identify 18F-FDG-PET-CT quantitative imaging markers for survival in patients with advanced non-small cell lung cancer (NSCLC) treated with PD-1/PD-L1 inhibitors.
Methods and materials: This prospective, single-centre study included 40 patients with NSCLC who underwent 18F-FDG-PET-CT before and 8-12 weeks after the start of treatment with a PD-1/PD-L1 inhibitor. We semi-automatically extracted the following parameters: SUV_{Peak}, TLG (total lesion glycolysis), MTV (metabolic tumour volume), SLR (the spleen-to-Liver ratio), and the bone marrow-to-liver ratio at baseline and the follow-up scan. Each parameter at baseline was dichotomised using the median and percent changes of the parameter were dichotomised using ≤50% reduction as the threshold, respectively. We assessed progression-free survival (PFS) and overall survival using the Kaplan-Meier test and Cox regression analysis.
Results: In the univariate analysis, high baseline TLG (hazard ratio (HR): HR=3.05), MTV (HR=3.05), SLR (HR=2.70) as well as changes in TLG (HR=5.84), SUV_{peak} (HR=7.40) and MTV (HR=3.70) were associated with increased mortality ($p<0.05$). In the multivariate analysis, only the high baseline SLR (adjusted aHR=3.51, p=0.008) and changes in TLG (aHR= 6.90, $p<0.001$) were independently associated with increased mortality. Similarly, these parameters were associated with reduced PFS, while in the multivariate analysis, only changes in TLG were independently associated with reduced PFS (aHR=3.54, p=0.003).
Conclusion: Changes in the metabolically active tumour burden correlate with PFS and overall survival. Increased metabolic activity of the spleen at the start of the therapy is an independent risk factor for mortality.
Limitations: The small sample size and single-centre study. Different PD-1 and PD-1L inhibitors.
Ethics committee approval: Ethics committee approval obtained.
Funding: Oesterreichische Nationalbank (grant 16886), "Fond für interdisziplinäre Krebsforschung der Stadt Wien," and the Theodor Koerner Fund.
Author Disclosures:
D. Kifjak: nothing to disclose
L. Beer: nothing to disclose
A. Haug: nothing to disclose
M. E. Mayerhöfer: nothing to disclose
M. Hochmair: nothing to disclose
H. Prosch: nothing to disclose

RPS 1416a-8 11:45

The optimisation of the CT window setting to differentiate pre-invasive from invasive sub-solid lung nodules

X. Cui[1], S. Fan[1], M. A. Heuvelmans[2], H. J. M. Groen[2], M. Dorrius[2], M. Oudkerk[2], G. de Bock[2], R. Vliegenthart[2], Z. Ye[1]; *[1]Tianjin/CN, [2]Groningen/NL (cuixiaonan1988@163.com)*

Purpose: To determine the best CT window width setting to differentiate pre-invasive from invasive sub-solid pulmonary nodules.
Methods and materials: We retrospectively identified 437 pathologically confirmed SSNs. A solid lesion component on CT images was regarded as a marker of invasiveness (suggestive of MIA or IA). We used a fixed window level (WL) of 35 Hounsfield units and adjusted the window width (WW) until a solid component became visible. This WW was recorded. The best WW cut-off to distinguish invasive and pre-invasive lesions was based on the receiver operating characteristic curve. This WW was defined as the "core" window width. Sub-solid nodules were subsequently categorised as part-solid or non-solid based on the identification of a solid component on the two WW settings, mediastinal window setting (WW/WL, 350/35 HU) and core window setting. The test characteristics were compared.
Results: 88/437 lung lesions were pre-invasive (17 atypical adenomatous hyperplasias and 71 adenocarcinomas in situ) and 349 were invasive (233 minimally invasive adenocarcinomas and 116 invasive adenocarcinomas). The best WW to detect a solid component in SSNs was 1175 HU with AUC of 0.80. Sensitivity, specificity, positive predictive value, negative predictive value, and diagnostic accuracy for invasiveness of the SSN were 51.3%, 84.1%, 92.7%, 30.3%, and 57.9% for normal mediastinal window setting and 87.7%, 60.2%, 89.7%, 55.2%, and 82.2%, respectively, for the new core window setting. Of the 233 MIA lesions, 191 (82.0%) were categorised as part-solid based on the core window setting compared to 72 (32.2%) based on the mediastinal window setting.
Conclusion: A new window setting (WW/WL, 1175/35 HU) outperformed the regular mediastinal window setting (WW/WL, 350/35 HU) for detecting a solid component in SSNs.
Limitations: n/a
Ethics committee approval: n/a
Funding: Royal Netherlands Academy of Arts and Sciences-PSA_SA_BD_01.
Author Disclosures:
X. Cui: nothing to disclose
S. Fan: nothing to disclose
M. A. Heuvelmans: nothing to disclose
H. J. M. Groen: nothing to disclose
M. Dorrius: nothing to disclose
M. Oudkerk: nothing to disclose
G. de Bock: nothing to disclose
R. Vliegenthart: nothing to disclose
Z. Ye: nothing to disclose

RPS 1416a-9 11:51

CT evaluation of NSCLC treated with PD-1/PD-L1 inhibitors: experience of long term follow-up

M. Porta[1], D. Ippolito[1], C. Talei Franzesi[1], M. S. Capici[1], C. Maino[1], L. Riva[1], S. Sironi[2]; *[1]Monza/IT, [2]Bergamo/IT (m.porta9@campus.unimib.it)*

Purpose: Immunotherapy may lead to atypical patterns of tumour response such as pseudoprogression where an initial appearance of an enlarged lesion is followed by tumour regression due to infiltration and recruitment of various immune cells, such as T or B lymphocytes.
The aim of our study is to evaluate the type of response in patients with advanced stage NSCLC treated with PD-1/PD-L1 inhibitors.
Methods and materials: We retrospectively examined 35 patients with advanced-stage NSCLC (24 adenocarcinomas, 9 squamous cell carcinomas, and 1 undifferentiated carcinoma) treated with PD-1/PD-L1 inhibitors.
All patients underwent CT examination (256-row scanner) every 8 weeks, with a minimum of 3 and maximum of 6 CTs for each one. The images were evaluated using iRECIST criteria and all target lesions were analysed with "Intellispace Portal 10.1" software using the "tumour tracking" application for semi-automatic analysis.
Results: Atypical responses were observed in 12 patients (34%); one of them showed pseudoprogression (3%) while 11 showed dissociated responses (31%). No hyperprogression was identified. Patients with dissociated responses had significantly lower median survival than patients with pseudoprogression or typical response ($p<0.05$). Overall, 11 patients showed progression disease (31%) while 24 patients demonstrated partial response or stable disease (69%).
Conclusion: Our results demonstrated a low incidence of pseudoprogression according to the literature (ranging from 0.6% to 5% for patients with NSCLC treated with PD-1/PD-L1 inhibitors). Therefore, increased the tumour burden will reflect true progression than pseudoprogression in most patients.
Whereas, the still-controversial "dissociated response" showed a high occurrence in our study with a poor prognosis.
Limitations: A retrospective study with low availability of patients with at least 3 comparable CTs.
Ethics committee approval: n/a
Funding: No funding was received for this work.
Author Disclosures:
M. Porta: nothing to disclose
D. Ippolito: nothing to disclose
C. Talei Franzesi: nothing to disclose
C. Maino: nothing to disclose
L. Riva: nothing to disclose
S. Sironi: nothing to disclose
M. S. Capici: nothing to disclose

RPS 1416a-10 11:57

The relationship of FDG and iodine-related parameters in non-small cell lung cancer: the potential benefit of PET/CT with dual-energy CT scan in therapy response monitoring

J. Baxa[1], M. Pesek[1], M. Svaton[1], B. Schmidt[2], M. Sedlmair[2], J. Ferda[1]; *[1]Pilsen/CZ, [2]Forchheim/DE (baxaj@fnplzen.cz)*

Purpose: To assess the relationship of FDG uptake and iodine-related parameters in non-small cell lung cancer (NSCLC) with a focus on the therapy response monitoring and prediction.
Methods and materials: Patients (n=45) with confirmed NSCLC stage IIIB and IV who were not qualified for concomitant chemoradiotherapy were included in the study. FDG-PET/CT using single-source dual-energy CT (DE-CT) was performed for staging and early follow-up (after the 2nd cycle of chemotherapy). The correlation of FDG uptake and iodine-related values was assessed and compared with the therapy response.
Results: A strong correlation was found between volumetric FDG parameters (MTV=metabolic tumour volume and TLG=total lesion glycolysis) and the total iodine uptake (mg) using the Spearman correlation coefficient in staging (r=0.0.874, 0.894) and follow-up (r=0.935, 0.934). We also found a significant correlation of change in these values after 2 cycles of therapy. In the prediction

analysis, we proved a significant correlation of iodine uptake, MTV, and TLG with the outcome, and iodine uptake was found as a possible strong predictor (r=0.711; p<0.0001). The change in iodine uptake after chemotherapy correlated with an early therapy effect (r=0.659; p<0.0001).
Conclusion: Our results suggest possible interchangeability in functional assessment. Iodine uptake and volume metabolic parameters were found as predictors of early therapy effect and could be used for a personal approach in therapy conducting.
Limitations: The number of patients and short follow-up period.
Ethics committee approval: The study was approved by institutional ethics committee and patents signed informed consent.
Funding: The Ministry of Health of the Czech Republic, grant nr. 17-30748A.
Author Disclosures:
J. Baxa: nothing to disclose
M. Pesek: nothing to disclose
M. Svaton: nothing to disclose
B. Schmidt: Employee at Siemens Healthineers
M. Sedlmair: Employee at Siemens Healthineers
J. Ferda: nothing to disclose

RPS 1416a-11 12:03
Pseudo or real progression in advanced lung cancer immunotherapy: just a matter of size?
M. C. Sciandrello, A. Ferraris, D. Tore, A. Carisio, G. Bartoli, A. Depaoli, C. Guarnaccia, M. C. Martina, P. Fonio*; Turin/IT (mariaclotilde.sciandrello@gmail.com)*

Purpose: To evaluate early radiological findings that help to discriminate between pseudoprogression and true disease progression in patients with advanced lung cancer treated with immunotherapy.
Methods and materials: We retrospectively evaluated CT scans of 62 patients with non-small cell lung cancer (NSCLC) treated with PD-1 inhibitor using the iRECIST criteria and considering the invasion of adjacent healthy tissues as a possible predictor of true progression. Patients considered in unconfirmed progressive disease (iUPD) underwent a second CT scan 4-8 weeks after suspected progression.
Results: During follow-up, 39 iUPDs were documented; 23 cases after the first cycle of immunotherapy and 16 later, during treatment. The patients presented different CT scan findings: 4 with new lesions, 28 with an increase in the volume of preexisting lesions, and 7 cases of mixed response were documented. Local aggressive tumour behaviour with an invasion of nearby healthy structures was documented in 5 patients. A restaging CT scan performed 4-8 weeks later confirmed true progression (immune confirmed progressive disease, iCPD) in 36 cases, thus leading to a suspension of immunotherapy. All cases of local aggressive behaviour were confirmed as true progression. Only 3 cases of true pseudoprogression were reported (4.8%).
Conclusion: In our experience, the rate of pseudoprogression did not exceed 5%, which is in line with the literature. In clinical practice, considering local cancer aggressiveness could be a useful criterion to allow a more confident differential diagnosis between pseudo and real progression in addition to dimensional iRECIST criteria. This observation, that should be validated in a larger population, could help in identifying a subgroup of patients at a higher risk of real progression, which might be a useful element for clinical decision making.
Limitations: The poor sample, limited to advanced lung cancer.
Ethics committee approval: n/a
Funding: No funding was received for this work.
Author Disclosures:
A. Ferraris: nothing to disclose
M. C. Sciandrello: nothing to disclose
D. Tore: nothing to disclose
A. Carisio: nothing to disclose
G. Bartoli: nothing to disclose
A. Depaoli: nothing to disclose
C. Guarnaccia: nothing to disclose
M. C. Martina: nothing to disclose
P. Fonio: nothing to disclose

RPS 1416a-12 12:09
A nomogram based on CT images and 3D texture analysis for preoperatively differentiating thymic epithelial tumours
C. Ren*; Shanghai/CN (rencaiyue@163.com)*

Purpose: To develop and validate a nomogram in preoperatively predicting pathological classification for thymic epithelial tumour (TET) patients.
Methods and materials: 172 patients with pathologically confirmed TET were retrospectively analysed. They were randomly divided into a training set (n=120) and a validation set (n=52). Preoperative clinical demographics, CT signs, and texture features of each patient were analysed and predictive models were developed using the lasso regression. The predictive effectiveness of models was evaluated and compared by the AUC and DeLong test. A nomogram based on selected parameters was developed. C-index and calibration plots were formulated to evaluate the reliability and accuracy of the nomogram.
Results: 120 patients with low-risk TET (LTET) (A1, AB, and B1 thymoma) and 72 patients with high-risk TET (HTET) (B2, 3 thymoma, and thymic adenocarcinoma) were enrolled in this study. A clinical model, CT model, texture model, and the combination model were established and the AUCs of the 4 models in differentiating LTET from HTET were 0.64, 0.82, 0.86, and 0.94, respectively. The DeLong test showed the combination model held the highest predictive efficiency (p<0.05). A predictive nomogram was developed by the combination model's 4 independently risk factors. The internal and external validated C-index values for the nomogram were 0.89 and 0.96, respectively. The calibration curves indicated a good consistency for differentiating TET classification.
Conclusion: The nomogram we developed on this basis was verified to have clinical utility and has the potential to assist clinicians in making treatment recommendations for TET patients.
Limitations: The results need to be confirmed by further prospective and multicentric studies.
Ethics committee approval: n/a
Funding: The National Natural Science Foundation of China (Grant Nos.: 81871347).
Author Disclosures:
C. Ren: nothing to disclose

11:15 - 12:30 **Room G**

Interventional Radiology

RPS 1409b

Peripheral arterial interventions

Moderators:
Z. Bansaghi; Budapest/HU
N.N.

RPS 1409b-K 11:15
Keynote lecture
K. S. Koulia*; Athens/GR (kkoulia@gmail.com)*

Author Disclosures:
K. S. Koulia: nothing to disclose

RPS 1409b-1 11:25
Dose management capability of digital variance angiography (DVA): a 70% reduction of radiation dose in lower limb angiography
M. Gyánó[1], K. Szigeti[1], S. Osváth[2], J. Kiss[1], C. Csobay-Novák[1], B. Nemes[1]; *[1]Budapest/HU, [2]Budakeszi/HU (mgyanostb@gmail.com)*

Purpose: In previous clinical studies, digital variance angiography (DVA) provided higher SNR and better image quality than digital subtraction angiography (DSA). The observed quality reserve might provide an opportunity for the reduction of radiation exposure in x-ray angiography. Our aim was to evaluate the potential of DVA to reduce x-ray dose in lower limb angiography.
Methods and materials: In this prospective clinical study (OGYÉI2830/2017), we enrolled 30 patients with normal renal function undergoing elective lower limb angiography. We compared the signal-to-noise ratio (SNR) of DSA and DVA image-pairs in three regions (abdominal, femoral, and crural) obtained by the Siemens Extremities Care preset (E, 1.2 Gy/frame) or by a low-dose protocol (R, 0.36 microGy/frame). Visual evaluation of all images was performed by specialists using a 5-grade rating scale. The quality of DSA-E and DVA-R images was also compared.
Results: The SNR of DVA images were consistently higher (2.7-3.1-fold) than the corresponding DSA images. Even DVA-R had better SNR than DSA-E (2.1-fold). Altogether, 256 image-pairs were evaluated. DVA images had a significantly higher Likert-score than the corresponding DSA images (E: 3.90±0.07 vs 3.56±0.08, p<0.05; R: 3.60±0.08 vs 3.29±0.09, p<0.05) but there was no difference between DSA-E and DVA-R (3.56±0.08 vs 3.60±0.08). In 77% of all comparisons, DVA-R had at least as good quality as DSA-E with the following regional differences: abdominal 62%, femoral 74%, and crural 84%.
Conclusion: Our data shows that DVA allows for a very substantial (70%) x-ray dose reduction in lower limb angiography without affecting the quality and diagnostic value of angiograms.
Limitations: A single-centre trial.
Ethics committee approval: National Institute of Pharrmacy and Nutrition, license number: OGYÉI2830/2017.
Funding: No funding was received for this work.

Author Disclosures:
M. Gyánó: Employee at Kinepict Health Ltd.
K. Szigeti: Patent Holder at Kinepict Health Ltd.
S. Osváth: Patent Holder at Kinepict Health Ltd.
J. Kiss: Employee at Kinepict Health Ltd.
C. Csobay-Novák: nothing to disclose
B. Nemes: nothing to disclose

RPS 1409b-2 11:31
Endovascular thromboaspiration in acute superior mesenteric artery thromboembolic occlusion

S. Perissi[1], M. Femia[2], U. G. Rossi[2], P. Rigamonti[2], A. M. Ierardi[3], G. Carrafiello[2], M. Cariati[2]; *[1]Genoa/IT, [2]Milan/IT, [3]Varese/IT*

Purpose: Acute thromboembolic occlusion of the superior mesenteric artery (AMS) is a condition with an unfavourable prognosis. Early diagnosis and timely treatment, either surgical or endovascular, is fundamental to restoring blood flow to the ischaemic intestine and to reduce the possible necrotic bowel tracts. The aim of our work is to describe the management of acute AMS thromboembolic occlusion through endovascular thrombus aspiration.
Methods and materials: We reviewed the charts of 41 patients from 2017-2019 with MD-CT diagnosis of acute AMS thromboembolic occlusion and initial signs of bowel ischemia. 35/41 patients underwent endovascular thrombus aspiration through femoral access, with co-axial technique for the treatment of the AMS trunk and its collateral. In the remaining 6 patients, the same technique was performed with subsequent transcatheter selective thrombolytic therapy (12 hours) for the treatment of small distal branches residual thrombi. A follow-up with MD-CT was performed 15 days after the endovascular procedure.
Results: Technical success was achieved in 39/41 patients (95%) and clinical success in 37/41 (90%). 35/41 patients (85%) had postprocedural patency of the main trunk of the SMA and its distal branches with no bowel resection. 4/41 patients (10%) underwent partial resection of the necrotic intestine. 2/41 patients (5%) died after massive bowel ischemia.
Conclusion: Acute thromboembolic occlusion of SMA is a potentially fatal vascular emergency which requires early diagnosis and rapid restoration of mesenteric blood flow. Percutaneous endovascular revascularisation techniques are a valuable alternative to surgical thrombectomy as a first-line therapy.
Limitations: The potential sources of bias.
Ethics committee approval: n/a
Funding: No funding was received for this work.
Author Disclosures:
P. Rigamonti: nothing to disclose
S. Perissi: nothing to disclose
M. Femia: nothing to disclose
U. G. Rossi: nothing to disclose
A. M. Ierardi: nothing to disclose
G. Carrafiello: nothing to disclose
M. Cariati: nothing to disclose

RPS 1409b-3 11:37
A retrograde anterior tibial approach for SFA recanalisation: an alternative to the conventional antegrade technique

G. Falcone[1], F. Fanelli[1], A. Cannavale[2], F. Mondaini[1], E. Casamassima[1], G. Gabbani[1], V. Miele[1]; *[1]Florence/IT, [2]Rome/IT*

Purpose: To report our initial experience on retrograde recanalisation of femoropopliteal occlusions (CTO) through the anterior tibial artery (ATA).
Methods and materials: 33 patients (23 male, mean age 68y) with symptomatic CTO (claudication <50mt, Rutherford class ≥iii) of the femoropopliteal segment (mean length 97.4 ± 3.76 mm) underwent a retrograde approach via ATA. In all cases, antegrade recanalisation was unsuccessful. ATA access was performed under ultrasound guidance using a micropuncture set. Recanalisation of the obstructed segment was performed using a support catheter in combination with a 0.035"/0.018" guidewire. After recanalisation, angioplasty and/or stenting was performed through the femoral approach in a standard way.
Results: Technical success with recanalisation of the CTO segment was achieved in all patients. Endoluminal recanalisation was possible in 31 cases (93.9%), while in 2 patients, subintimal revascularisation (6.1%) was performed. The mean recanalisation time was 11' ± 3' (range 5'-15'). The final treatment was performed with a drug-coated-balloon in 24 patients and a drug-eluting stent in the remaining 9. Haemostasis of the ATA was obtained with balloon inflation (inflation time 3-4 minutes) in 26 cases (78.7%), and manual compression in 7 (21.2%). No complications occurred during or after the procedure. Patency of ATA was assessed by USCD in all patients before discharge and after 30 days.
Conclusion: Retrograde ATA access is a feasible and safe approach for complex femoropopliteal recanalisation. Several advantages are reported in comparison to other retrograde accesses (popliteal, pedal, etc.).
Limitations: The population size.
Ethics committee approval: n/a
Funding: No funding was received for this work.
Author Disclosures:
G. Falcone: nothing to disclose
F. Fanelli: nothing to disclose
A. Cannavale: nothing to disclose
F. Mondaini: nothing to disclose
E. Casamassima: nothing to disclose
G. Gabbani: nothing to disclose
V. Miele: nothing to disclose

RPS 1409b-4 11:43
Percutaneous angioplasty with a drug-coated balloon (DCB-PTA) in femoropopliteal arterial disease

G. Mazzarella, D. Laganà*; Catanzaro/IT (gmazzarella@tim.it)*

Purpose: To evaluate the efficacy and safety of percutaneous angioplasty with DCB-PTA as a therapeutic treatment in femoropopliteal steno-occlusions. We evaluated and compared the primary patency at 12 months of both TASC type A and B lesions and TASC type C and D lesions.
Methods and materials: From May 2016-August 2019, 87 patients (34 TASC A, 38 TASC B, 14 TASC C, and 6 TASC D) were treated. After having crossed the steno-occlusions and pre-dilatation with an uncoated balloon, an angioplasty with a paclitaxel-coated balloon was performed. A computed tomographic angiography (CTA) of the lower limbs was made to plan the treatment, while the results were evaluated with ultrasonography (CDUS) after 1, 3, and 6 months from the procedure, and with a CTA after 1 year.
Results: DCB-PTA was made in our study population without early and late clinically adverse events related to the PTA. During the procedure, no distal embolisms or complications to the access site occurred and in 69 patients an immediate resolution of the lesion was obtained. The primary patency at 12 months for TASC type A and B lesions was 81% with target lesion revascularisation (TLR) in 12 patients, while the primary patency at 12 months for TASC type C and D lesions was of 70% with target lesion revascularisation (TLR) in 6 patients.
Conclusion: DCB-PTA is a convenient therapeutic treatment and shows early and late efficacy in TASC A and B lesions. In contrast, it shows less efficacy in terms of restenosis in TASC type C and D lesions but still represent a good alternative.
Limitations: The experience of a single centre.
Ethics committee approval: n/a
Funding: No funding was received for this work.
Author Disclosures:
G. Mazzarella: nothing to disclose
D. Laganà: nothing to disclose

RPS 1409b-5 11:49
The efficacy of different embolisation techniques in relation to the different patterns of arterial bleeding: a retrospective analysis of 83 consecutive cases treated in emergency conditions

G. Bianchi, A. Iacopino, G. Campidoglio, P. Palumbo, A. Pace, M. Varrassi, S. Carducci, A. V. Giordano, C. Masciocchi*; L'Aquila/IT*

Purpose: To assess the efficacy of different embolic endovascular materials used to control acute arterial bleeding caused by traumatic or iatrogenic conditions.
Methods and materials: We retrospectively evaluated 83 patients (age range 14-81 years) who underwent embolisation procedures in emergency conditions to control acute abdominal bleedings. Technical success, recurrency rate, and complications were assessed in relation to the pattern of arterial bleeding and to the different embolisation techniques and materials (coils, glue, gel foam, covered stents, and plugs).
Results: The majority of cases were traumatic and iatrogenic bleeding, respectively, 30 and 42 patients ($p<0.001$). The most frequent bleeding patterns were blush in 75% of cases (single or multiple), pseudoaneurysms (15%), pseudoaneurysms with fistulisation (5%), and oozing bleeding (5%). Technical success was 99% for all the procedures. Treatment failures occurred in complex arterial bleeding patterns (pseudoaneurysms and pseudoaneurysms with fistulisation). In 1% of cases, a subsequent embolisation was necessary. In general, the complication rate was less than 1%.
Conclusion: Arterial bleeding is potentially life-threatening and can be treated with interventional angiographic techniques. Technical success, low recurrency rate, and a low percentage of complications are related to appropriate procedural planning. Our study demonstrates the efficacy of many embolic endovascular materials in controlling different patterns of bleeding. A multidisciplinary approach is essential, as well as the integration and review of laboratory data and other imaging studies.

Limitations: A small sample size.
Ethics committee approval: n/a
Funding: No funding was received for this work.
Author Disclosures:
G. Bianchi: nothing to disclose
A. Iacopino: nothing to disclose
G. Campidoglio: nothing to disclose
A. Pace: nothing to disclose
P. Palumbo: nothing to disclose
M. Varrassi: nothing to disclose
S. Carducci: nothing to disclose
A. V. Giordano: nothing to disclose
C. Masciocchi: nothing to disclose

RPS 1409b-6 11:55

Texture analysis of an arterial graft thrombus on CT angiography: does it correlate with the age of the thrombus and can it predict the success of catheter-directed thrombolysis?

A. K. Verma[1], R. Thornhill[2], S. Ryan[2], A. Hadziomerovic[2], K. R. Smyth[2], G. French[2], A. Gupta[2]; [1]*Lucknow/IN,* [2]*Ottawa/CA*
(drverma.gilbert25@gmail.com)

Purpose: To characterise a graft thrombus using quantitative texture analysis on CT angiography in relation to the thrombus age and clinical profile of a patient and its implication on catheter-directed thrombolysis
Methods and materials: This retrospective study included 67 patients with thrombotic grafts occlusion of the lower extremities referred for catheter-directed thrombolysis. Selected images from pre-procedure CT angiograms were retrieved in a defined study interval, de-identified and assigning each a unique identifier. The clinical data was collected and thrombolysis angiograms from PACS were reviewed for dose of tPA, complications, and the final result.
Thrombi on pre-procedure CTAs were manually segmented and saved as regions-of-interest for subsequent texture analysis. Various textural features were extracted for each ROI. The relationship between each textural feature and (a) the clinical age of the thrombus, (b) the dose of tPA administered, and (c) thrombolysis response (as TIMI grade flow) was explored using Spearman's rho correlation coefficients.
Results: The clinical age of the thrombus was positively correlated with grey-level skewness [p=0.0085], angular second moment [p=0.0031], and negatively correlated with sum entropy, entropy, and both run-level and grey-level non-uniformity.
tPA doses adjusted for the length of the graft segment thrombosed have a positive correlation with the mean grey-level, entropy, difference entropy, as well as both run-level and grey-level non-uniformity. It has a negative correlation with the angular second moment, suggesting decreased grey-level homogeneity associated with larger doses of tPA required.
Textural features were not significantly related to post thrombolysis flow across the re-canalised segment calculated as TIMI grade flow.
Conclusion: CT texture analysis features can be used to predict the age of the graft thrombi as well as the tPA dose required per cm length of the thrombosed graft.
Limitations: A single-centre study.
Ethics committee approval: Ethics committee approval obtained.
Funding: No funding was received for this work.
Author Disclosures:
A. K. Verma: nothing to disclose
A. Gupta: nothing to disclose
A. Hadziomerovic: nothing to disclose
S. Ryan: nothing to disclose
R. Thornhill: nothing to disclose
G. French: nothing to disclose
K. R. Smyth: nothing to disclose

RPS 1409b-7 12:01

Non-contrast-enhanced magnetic resonance imaging for the visualisation and quantification of an endovascular aortic prosthesis, their endoleaks, and aneurysm sacs at 1.5T

M. Salehi Ravesh[1], P. Langguth[1], J. A. Pfarr[1], I. Koktzoglou[2], R. Edelmann[3], J. Graessner[4], O. Jansen[1], J.-B. Hövener[1], J. P. Schaefer[1]; [1]*Kiel/DE,* [2]*Evanston/US,* [3]*Illinois/US,* [4]*Hamburg/DE (Mona.SalehiRavesh@uksh.de)*

Purpose: After an endovascular aortic aneurysm repair (EVAR), a follow-up at 1, 6, and 12 months is recommended for the remainder of the patient's life. The diagnostic standard methods for diagnosing endoleaks and the visualisation of aneurysms in EVAR-patients are invasive digital subtraction angiography (DSA), contrast-enhanced (CE) computed tomographic angiography (CE-CTA), and magnetic resonance angiography (CE-MRA). These techniques, however, require the use of iodine- or gadolinium-based contrast agents with rare, but possibly life-threatening side-effects such as renal impairment, thyrotoxicosis and allergic reactions, nephrogenic systemic fibrosis, and cerebral gadolinium deposition. The aim of this prospective study was to compare a non-contrast-enhanced MRI protocol (consisting of four MRI methods) with DSA and CE-CTA for the visualisation and quantification of an endovascular aortic prosthesis, their endoleaks, and aneurysms.
Methods and materials: 8 patients (mean age 76.8 ± 4.9 years, 63% male), whose thoracic, abdominal, or iliac aneurysms were treated with a different endovascular prosthesis and suffered from type I-V endoleaks were examined on a 1.5 Tesla MR system. Quiescent-interval slice selective MR angiography (QISS-MRA), 4-dimensional (4D)-flow MRI, T1- and T2-mapping, and DSA and CE-CTA were used for the visualisation and quantification of the endoprosthesis, endoleaks, and aneurysms in these patients.
Results: QISS-MRA provided good visualisation of endoleaks and comparable quantification of the aneurysm size with respect to CE-CTA and DSA. The 4D-flow MRI provided additional information about the wall shear stress, which could not be determined using DSA. In contrast to CE-CTA, T1- and T2-mapping provided detailed information about heterogeneous areas within an aneurysm sac.
Conclusion: Compared to DSA and CE-CTA, the proposed MRI methods provide improved anatomical and functional information for various types of endoprostheses and endoleaks.
Limitations: The small number of patients.
Ethics committee approval: No. D 517/18.
Funding: No funding was received for this work.
Author Disclosures:
M. Salehi Ravesh: nothing to disclose
P. Langguth: nothing to disclose
J. A. Pfarr: nothing to disclose
J.-B. Hövener: nothing to disclose
O. Jansen: nothing to disclose
I. Koktzoglou: nothing to disclose
R. Edelmann: nothing to disclose
J. Graessner: nothing to disclose
J. P. Schaefer: nothing to disclose

RPS 1409b-8 12:07

Risk factors for macroembolisation in femoropopliteal interventions using the SpiderFX filter embolic protection device

K. M. Treitl, M. Czihal, M. Treitl; *Munich/DE*
(karlamaria.treitl@med.uni-muenchen.de)

Purpose: To assess the safety and efficacy of a filter embolic protection device (FEPD) in the treatment of femoropopliteal peripheral arterial occlusive disease (PAOD).
Methods and materials: The monocentric retrospective study included 244 cases (mean age 71.4 ± 10.9 years; mean lesion length 13.2 ± 12.9 cm; 60.4%/39.6% Fontaine stage II/III-VI) in which a FEPD was used during recanalisation. The clinical outcome and FEPD-related complications (retrieval/placement/vasospasm/peripheral embolisation) were assessed. The degree of filter filling was semi-quantitatively classified (5-point-scale) and risk factors for filter macroembolisation (FME; grade 4 and 5) were calculated by multivariate analysis.
Results: Balloon angioplasty ± stenting (BAP), directional atherectomy ± BAP ± stenting (DA), and rotational thrombectomy ± BAP ± stenting (RT) were performed in 141, 61, and 42 cases, respectively. Revascularisation was successful in 96.7%. FEPD placement and retrieval failed in one case each (0.4%). Vasospasm requiring medical spasmolysis, peripheral embolisation, and FME occurred in 11, 10, and 91 cases, resulting in FEPD-related complication rates of 4.5%, 4.1%, and 37.3%, respectively. Peripheral embolisation and FME were more frequent in the BAP- and RT-groups (BAP: 4.9%/36.2%; RT: 4.8%/47.7%; DA: 1.6%/32.8%). Total occlusion, lesion length>19 cm, visible thrombus, atherectomy, and diabetes mellitus were identified as risk factors for FME after BAP and DA.
Conclusion: The FEPD is safe and efficient in capturing embolic debris during recanalisation in femoropopliteal PAOD, but a residual risk of embolisation remains, especially in RT.
Limitations: n/a
Ethics committee approval: The study protocol followed the principles of the Declaration of Helsinki and was approved by the institutional ethical review board. The indication for endovascular treatment was determined in an interdisciplinary consensus conference according to the current national guidelines. Written informed consent was obtained.
Funding: No funding was received for this work.
Author Disclosures:
K. M. Treitl: nothing to disclose
M. Czihal: nothing to disclose
M. Treitl: nothing to disclose

RPS 1409b-9 12:13
Endovascular limb revascularisation in no-option critical limb ischaemia: distal deep foot vein arterialisation
G. Cangiano[1], M. Silvestre[2], F. Pane[2], A. Borzelli[2], M. Coppola[2], A. Paladini[3], F. Corvino[2], F. Amodio[2], R. Niola[2]; [1]*San Sebastiano al Vesuvio/IT,* [2]*Naples/IT,* [3]*Novara/IT (kekkopane@hotmail.it)*

Purpose: To describe our experience in treating no-option critical limb ischaemia patients employing endovascular techniques for distal deep venous arterialisation.
Methods and materials: We retrospectively reviewed 16 patients between 2016-2018 (11 M, 5F; mean age 65 years) not eligible for surgical or endovascular approaches for revascularisation and major amputation candidates. After several failed attempts of standard or alternative intraluminal arterial recanalisation, we tried a subintimal approach using a 0.014 inch and 300 cm-long guidewire supported by a 2×40 mm low-profile balloon catheter. Taking advantage of the presence of heavy calcification in the distal portion of the foot artery, we intentionally pursued entry into a distal vein from a subintimal channel through the artery. In case of failure, we attempted the creation of an iatrogenic fistula with a pioneer plus catheter after we placed covered stents to ensure its patency.
Results: In 10 patients, we were able to revascularise the foot with the first technique, in 6 patients we performed the second one. In one case, it was necessary to embolise a collateral vein which was stealing arterial blood from the angiosomic target. Major amputation was observed in one patient. In two cases, we had minor amputations. In 11 cases, we achieved successful wound healing during 6 month follow-up after the procedures. In 81% of patients (13/16), we observed 3-month-fistula patency. One patient died due to other cardiovascular reasons.
Conclusion: Distal deep venous arterialisation proved to be an effective, safe, and promising technique to improve recanalisation rates and limb salvage in no-options critical limb ischaemia patients. However, we need further trials and investigations to improve the rate of success and employ it safely in daily clinical practice.
Limitations: A small sample.
Ethics committee approval: n/a
Funding: No funding was received for this work.
Author Disclosures:
F. Pane: nothing to disclose
G. Cangiano: nothing to disclose
M. Silvestre: nothing to disclose
A. Borzelli: nothing to disclose
M. Coppola: nothing to disclose
A. Paladini: nothing to disclose
F. Corvino: nothing to disclose
F. Amodio: nothing to disclose
R. Niola: nothing to disclose

RPS 1409b-10 12:19
Postpancreatectomy haemorrhage (PPH) after pancreaticoduodenectomy (PD): what is the role of interventional radiology (IR)?
D. Palumbo[1], G. Guazzarotti[1], S. Gusmini[1], P. Marra[2], M. Salvioni[1], M. Venturini[1], F. de Cobelli[1]; [1]*Milan/IT,* [2]*Bergamo/IT*

Purpose: To evaluate the role of IR in the diagnosis and management of PPH.
Methods and materials: From 01/2015-05/2019, 656 patients underwent PD. PPH has been classified on the basis of bleeding onset (early if within 24 hours after surgery; delayed when occurring later) and severity (mild or severe according to the amount of blood loss and transfusion requirements) into three grades according to 2007 ISGPS classification.
The source of bleeding, bleeding pattern, type of material used for embolisation, and technical success have been systematically recorded for each PPH.
Results: 58 (8.8%) patients had at least one PPH episode, for a total of 70 PPH (6 early grade b, 14 late grade b, and 50 grade c). Early PPH patients underwent upfront surgery, whereas late PPH episodes were first evaluated with CT scan. Late grade b were then treated conservatively and late grade c all underwent IR procedures.
In this subset, diagnostic angiography revealed the bleeding source in 47/50 (94%) cases (gastroduodenal [15/50, 30%], hepatic [14/50, 28%], superior mesenteric [14/50, 28%], inferior epigastric [2/50, 4%], and dorsal pancreatic artery [2/50, 4%]).
We observed active bleeding in 28 cases (56%), pseudoaneurysms in 21 (42%), and irregular vessels in 16 (32%).
IR permitted an efficient treatment of PPH in 46/47 cases with positive diagnostic angiography (technical success: 97.8%) using, sometimes in combination, covered stent (22/46, 47.8%), coil (21/46, 45.6%), and embolising particles or cyanoacrylic glue (13/46, 28.3%).
Conclusion: IR has a fundamental role in the diagnosis and treatment of PPH, in particular of grade c PPH.
Limitations: The need for prospective validation.
Ethics committee approval: Patients' consent was collected according to the ethics committee requirements in all those who had previously signed a procedure-specific informed consent covering retrospective studies.
Funding: No funding was received for this work.
Author Disclosures:
D. Palumbo: nothing to disclose
G. Guazzarotti: nothing to disclose
S. Gusmini: nothing to disclose
P. Marra: nothing to disclose
M. Salvioni: nothing to disclose
M. Venturini: nothing to disclose
F. de Cobelli: nothing to disclose

RPS 1409b-11 12:25
Type II endoleak: go straight!
G. Falcone[1], F. Fanelli[1], A. Cannavale[2], E. Chisci[1], M. Citone[1], S. Michelagnoli[1], V. Miele[1]; [1]*Florence/IT,* [2]*Rome/IT*

Purpose: Type II endoleaks represent the most common complication after endovascular aortic aneurysm repair (EVAR).
Methods and materials: 50 patients, 31 male, with post-EVAR type-II endoleak underwent percutaneous direct sac puncture. The procedures were performed under local anaesthesia.
Sac puncture was done using a 20G needle under rotational-angiography guidance. A coaxial system (4Fr catheter+2.7 microcatheter) was used to navigate within the sac. During the follow-up period, all patients underwent contrast-enhanced ultrasound (CEUS) at 6 and 12 months.
Results: Technical success with complete embolisation of the aneurysmatic sac was achieved in all cases. No complications, correlated to the direct percutaneous sac puncture, or to Onyx injection, occurred. The time of the procedure varied between 36 and 68 minutes (mean 51.36 minutes). The mean fluoroscopy time was 16.7 minutes. Posterior left access was used in 41 cases, posterior right access in 6 cases, and an anterior approach in 3 cases. In 19 cases (38%), one or more feeding vessels were visualised and embolised. Sac embolisation was achieved using Onyx+microcoils in 31 cases (62 %) and Onyx alone in 19 cases (38%). The mean amount of Onyx was 4.5 cc. After a 1-year follow-up, 34 cases (68%) of sac shrinkage were reported and in 16 patients (32%), the sac diameter remained stable.
Conclusion: Direct sac embolisation using Onyx, in combination with or without microcoils represents a safe and valid technique to solve type II endoleaks.
Limitations: The population size.
Ethics committee approval: n/a
Funding: No funding was received for this work.
Author Disclosures:
G. Falcone: nothing to disclose
F. Fanelli: nothing to disclose
A. Cannavale: nothing to disclose
E. Chisci: nothing to disclose
M. Citone: nothing to disclose
S. Michelagnoli: nothing to disclose
V. Miele: nothing to disclose

11:15 - 12:30 **Room K**

Genitourinary

RPS 1407b

Multimodality approach in imaging of the uterus and endometriosis

Moderators:
M. Garbajs; Ljubljana/SI
D. Negru; Iasi/RO

RPS 1407b-K 11:15
Keynote lecture
N. Rubtsova; *Moscow/RU*

Author Disclosures:
N. Rubtsova: nothing to disclose

RPS 1407b-1 11:25
A new MR scoring system for pelvic endometriosis: a feasibility study
S. Kitai[1], A. Tamura[1], Y. O. Tanaka[1], Y. Ota[2], H. Kobori[3], R. Konno[4], R. Shiokawa[1], N. Okada[1], A. Nishimoto-Kakiuchi[1]; [1]*Tokyo/JP,* [2]*Kurashiki/JP,* [3]*Soka/JP,* [4]*Saitama/JP (kitai@jikei.ac.jp)*

Purpose: The revised classification of endometriosis by the American Society for Reproductive Medicine was widely used in evaluating pelvic endometriosis. However, it was not well correlated to the severity of symptoms and obstetrical outcomes as it heavily depended on the size of the ovarian endometriotic cyst. Some trials had been made to make classifications reflecting clinical importance. However, there is no widely accepted system to date. The purpose of this study is to establish a new evaluation scale for the severity of pelvic endometriosis, including adhesion and deeply infiltrating endometriosis (DIE), which are more clinically meaningful.
Methods and materials: 60 cases with pelvic endometriosis were retrospectively evaluated using the same scoring system with MR and laparoscopy, independently. Three radiologists evaluated MR images including sagittal and axial T1-, T2-, and fat-saturated T1-weighted images obtained with 1.5T superconducting MR systems. Two gynaecologists also evaluated recorded video during laparoscopic surgery. Both decisions were made by consensus reading. The score included adhesions between uterus and bladder, uterus and ovaries, uterus and rectum, ovaries and rectum, and bilateral ovaries and fibrotic plaque on the posterior uterine aspect, respectively. The Pearson's coefficient of correlation of the total score between MR and laparoscopy was calculated. We also studied the concordance rate of each score.
Results: The Spearman's rank correlation coefficient between the MR and laparoscopy was 0.81. The concordance rate of each score was 0.52-0.97.
Conclusion: Our new MR scoring system emphasised adhesion and DIE was feasible to evaluate the severity of endometriosis.
Limitations:
A limited number of cases.
Ethics committee approval: Approved by the ethics committees of Kurashiki Medical Center, Medical Topia Soka Hospital and Chugai Pharmaceutical Co., LTD.
Funding:
No funding was received for this work.
Author Disclosures:
S. Kitai: Advisory Board at Chugai Pharmaceutical Co., LTD
A. Tamura: Advisory Board at Chugai Pharmaceutical Co., LTD
Y. O. Tanaka: Advisory Board at Chugai Pharmaceutical Co., LTD
Y. Ota: Research/Grant Support at Chugai Pharmaceutical Co., LTD, Investigator at Chugai Pharmaceutical Co., LTD
H. Kobori: Research/Grant Support at Chugai Pharmaceutical Co., LTD, Advisory Board at Chugai Pharmaceutical Co., LTD
R. Konno: Research/Grant Support at Chugai Pharmaceutical Co., LTD, Advisory Board at Chugai Pharmaceutical Co., LTD
R. Shiokawa: Employee at Chugai Pharmaceutical Co., LTD
N. Okada: Employee at Chugai Pharmaceutical Co., LTD
A. Nishimoto-Kakiuchi: Employee at Chugai Pharmaceutical Co., LTD

RPS 1407b-2 11:31

Non-inferiority analysis of endometriomas using DIXON sequence in comparison with conventional pre-contrast volumetric T1 (VT1) sequence

M. M. Filisbino[1], F. H. C. Souza[1], L. E. Paiva[1], M. D. P. Estrela[2], D. M. D. Araújo[1], A. Skaf[1], H. M. L. Filho[1]; [1]São Paulo/BR, [2]Barretos/BR *(marianamarins2810@hotmail.com)*

Purpose: To assess the non-inferiority of a DIXON sequence (DiS) in relation to VT1 in endometrioma evaluation, between readers, using subjective and quantitative analysis.
Methods and materials: 100 consecutive MRIs performed between April 2016-April 2018 were evaluated, half with the word endometriomas in the report and half with normal exams.
The exams were randomly distributed to two readers, a fellow with one year experience and a junior radiologist with 3 years of experience in pelvic imaging. The readers did two sessions: first, they were instructed to look only at DiS, and second, after a month interval to reduce memory bias, only at the VT1 sequence. The following criteria were evaluated: the presence of an endometrioma, size, signal ratio (SR), and laterality.
The SR was assessed with a region of interest (ROI) placed in the lesion and in the ipsilateral vertebral musculature.
Results: Of the 50 endometriomas cases, 3 were excluded due to incomplete data.
The agreement was perfect between readers in the 50 cases without endometriomas.
The intraobserver agreement was 96.9% for the first reader and 92.8% for the second, with kappa (k) values of 0.94 and 0.85, respectively. Interobserver agreement was 94.9% using VT1 and 92.8% for the DiS, with k values of 0.89 and 0.85, respectively.
The signal ratio was 1.78 using DiS and 2.05 for VT1, with p value=0.005.
Conclusion: The DIXON sequence is effective as the conventional T1 sequence for the evaluation of endometriomas, showing good agreement between observers, even without a higher signal ratio, as we postulated previously.
Limitations: A small sample and single institution.
Ethics committee approval: n/a
Funding: No funding was received for this work.
Author Disclosures:
M. M. Filisbino: nothing to disclose
F. H. C. Souza: nothing to disclose
L. E. Paiva: nothing to disclose
M. D. P. Estrela: nothing to disclose
D. M. D. Araújo: nothing to disclose
A. Skaf: nothing to disclose
H. M. L. Filho: nothing to disclose

RPS 1407b-3 11:37

MR classification of deep pelvic endometriosis: description and impact on surgical management

S. Lamrabet, A. Crestani, A. Bekhouche, C. Owen, C. Touboul, E. Darai, I. Thomassin; *Paris/FR (samia.lamrabet@gmail.com)*

Purpose: To retrospectively test the performance and reproducibility of MR Enzian classification and to develop a new MR classification, including lateral endometriosis, and to evaluate their ability to predict postoperative complications.
Methods and materials: Between 2017/01/01 and 2018/12/31, 150 women (mean age 34,5 years, 20-52 years) with deep endometriosis (DE) at MR imaging with a subsequent surgery were recruited. Two radiologists (junior and senior) independently reviewed MR images and rated DE according to MR Enzian classification and a new radiological classification named deep pelvic endometriosis index (dPEI), grading the severity of DE in low (≤2 compartments), moderate (3 or 4 compartments), and high extensive (≥5 compartments).
Results: MR and surgical Enzian classification were concordant for A lesions in 78.7% (118/150), for B lesions in 34.7% (52/150), and for C lesions in 82.7% (124/150). Operative time and hospital stay were longer in A2 compared to A0, B2 to B0, C3 to C2, and C2 to C0 ($p<0.001$) in high extensive compared to moderate extensive DE, and in moderate to low extensive DE ($p<0.01$). Patients with a vagina or rectosigmoid involvement had, respectively, 6 and 3 times more frequent complications according to Clavien Dindo ($p<0.001$). Postoperative dysuria was correlated to the presence of A lesions (OR=6.82, p=0.001), parametrial lesions (OR=6.6, p=0.0002), a moderate or high extensive DE according to dPEI (OR=4.15, p=0.001), unilateral lateral pelvic involvement (OR=3.6, p=0.03), and C lesions (OR= 2.6, p=0.04).
Conclusion: MR imaging is accurate to predict postoperative complications, helping clinicians to preoperatively inform patients of the specific risk of surgery for DE.
Limitations: A highly experienced centre. No long term follow up.
Ethics committee approval: Our institutional ethics committees approved the study and granted a waiver of informed consent.
Funding: No funding was received for this work.
Author Disclosures:
S. Lamrabet: Author at Tenon Hospital
I. Thomassin: Author at Tenon Hospital, Investigator at Tenon Hospital
A. Bekhouche: Consultant at Tenon Hospital
A. Crestani: Author at Tenon Hospital
C. Owen: Consultant at Tenon Hospital
C. Touboul: Author at Tenon Hospital, Investigator at Tenon Hospital
E. Darai: Author at Tenon Hospital, Consultant at Tenon Hospital

RPS 1407b-4 11:43

Minimal endometriosis: is it a valid MRI diagnosis? A retrospective correlation study between readers with distinct expertise levels

H. Leao Filho, E. Soares Souza, M. Figueiredo Alves, M. Sousa Castro, A. Skaff; *São Paulo/BR (hiltonmlf@gmail.com)*

Purpose: With increasing MRI usage for female pelvic pain evaluation, we are seeing an increase of minimal deep endometriosis diagnosis showing very subtle/subjective findings.
The study's purpose was to evaluate subtle/minimal endometriosis findings on MRI, assessing inter and intraobserver concordance between radiologists with different expertise levels.
Methods and materials: We conducted a retrospective study selecting 100 female pelvic MRI exams from 2015-2018. We searched for 50 normal MRI reports and 50 other examinations were chosen using keywords describing incipient/subtle endometriosis in the radiology reports.
The MRIs were independently analysed by three radiologists with different experience levels (two assistants with 15 and 3 years of expertise and one fellow with 1 year of expertise). They were blinded to clinical data and original reports. The readers filled a questionnaire determining the presence (or absence) and location of pelvic endometriosis. After a 2 months interval (memory bias), all the

readers re-evaluate the exams. The imaging criteria was revised with all the readers with practical cases before the study started.
Results: The intraobserver analysis was poor or weak in most compartments, with kappa (k) values varying between 0.24-0.48 for torus uterinus (TU-mean: 0.37) and 0.21-0.41 for utero-sacral ligaments (USL-mean: 0.36). The other areas reached lower k values, with the exception of ovaries (mean: 0.62).
The interobserver analysis was also low, with intraclass correlation values of 0.039 for TU and 0.032 for USL. Even if the studies were analysed by the presence of at least one area positive, the ICC was also poor, reaching 0.018.
Conclusion: Inter and intraobserver agreement were poor for assessing subtle/minimal endometriosis with pelvic MRI. These findings were independent of the reader's experience level.
Limitations: A single-centre study with a small number of patients and no pathological confirmation.
Ethics committee approval: Ethics approval, informed consent waived.
Funding: No funding was received for this work.
Author Disclosures:
H. Leao Filho: nothing to disclose
M. Figueiredo Alves: nothing to disclose
A. Skaff: nothing to disclose
M. Sousa Castro: nothing to disclose
E. Soares Souza: nothing to disclose

RPS 1407b-5 11:49
Role of preoperative transvaginal ultrasound mapping in the surgical management of deep infiltrating endometriosis: a prospective study
S. M. M. M. M. El-Maadawy, C. Nagy*; Dubai/AE (samarmaadawy@gmail.com)*

Purpose: To assess the accuracy of a new transvaginal ultrasound (TVS) mapping system in defining the size and location of deep infiltrating endometriosis (DIE) with laparoscopic and histologic confirmation.
Methods and materials: Our study included 51 patients showing features of DIE by TVS with subsequent laparoscopic and histologic evaluation. Data was collected from October 2017 to September 2019. All patients were examined by the same radiologist with GE E8 (GE Healthcare) ultrasound machine using a transvaginal 5-9 MHz transducer. Conventional 2D and 3D volume acquisition using volume contrast imaging (VCI) and tomographic ultrasound imaging (TUI) was used. Accurate mapping of the extent of DIE was recorded using a dedicated mapping sheet during TVS by the radiologist and at laparoscopy by the same surgeon who was blinded to TVS mapping. Results were correlated with histopathology findings.
Results: Laparoscopy detected DIE in all 51 patients. Depending on the locations of DIE, the accuracy of TVS ranged from 73%-98%. The lowest sensitivity (47%) and accuracy (73%) was seen in a TVS diagnosis of vaginal DIE with a positive likelihood ratio (LR+) of 2.8, while the highest accuracy (98%) was seen in detecting bladder lesions with LR+ of 47. 5 cases showed additional scar endometriosis with 100% accuracy.
Conclusion: We believe that the new TVS mapping is accurate in detecting the extent of DIE, which may help in preoperative evaluation and intraoperative management to tailor the surgical approach, thus improving patient outcomes.
Limitations: The high incidence of DIE in the sample due to patient selection and setting of the study as a referral centre for endometriosis.
Ethics committee approval: Informed consent was obtained from all patients.
Funding: No funding was received for this work.
Author Disclosures:
S. M. M. M. M. El-Maadawy: nothing to disclose
C. Nagy: nothing to disclose

RPS 1407b-6 11:55
Benign or malignant endometrium: can functional MRI techniques like diffusion-weighted magnetic resonance imaging (DW-MRI) and dynamic contrast-enhanced (DCE-MR) help us in differentiation?
M. Gulati, A. Garg, R. Dixit, G. Gandhi, N. Khurana*; New Delhi/IN (gulati_malvika92@yahoo.com)*

Purpose: To compare findings of conventional MRI, DWI, and DCE-MRI in benign and malignant endometrial lesions.
Methods and materials: 44 adult female patients with sonographically suspected endometrial lesions underwent MR imaging of the abdomen and pelvis (T1, T2WI, DWI, and DCE MRI). Conventional MR images were analysed for morphological features. The presence or absence of restricted diffusion was assessed on DWI and ADC values were calculated. Using DCE images, enhancement characteristics were studied and time-signal intensity (TIC) curves were generated. Appropriate tests for statistical analysis were applied. The ROC curve was applied to determine the ADC threshold value to differentiate between the malignant and benign lesions. The imaging diagnosis was finally compared with histopathological examination or follow-up imaging.
Results: Of 44 patients, 16 had benign lesions and 28 harboured malignant lesions. Conventional MR findings found to have a significantly higher frequency in benign lesions were a brightly hyperintense signal on T2WI, smooth tumour/endo-myometrial interface, and the presence of well-defined cystic areas within the mass ($p<0.01$). Diffusion restriction was seen only in 2/16 benign cases, however, was demonstrated in all the malignant cases ($p<0.01$). Using a ROC curve, cut off ADC value of $<0.859 \times 10^{-3}$ mm^2/sec was seen to have a sensitivity, specificity, PPV, and NPV of 100%, 89.3%, 100%, and 93.2%, respectively, for predicting malignant endometrial lesions. On dynamic imaging and TIC analysis, the increasing trend of enhancement was found to have a sensitivity of 86.2% and specificity of 81.2% for benign lesions.
Conclusion: Newer functional MR techniques of DWI and DCE-MR can significantly add to conventional MR imaging in differentiating benign from malignant endometrial lesions.
Limitations: A small sample size.
Ethics committee approval: Approval from an institutional ethical committee obtained.
Funding: No funding was received for this work.
Author Disclosures:
M. Gulati: nothing to disclose
A. Garg: nothing to disclose
R. Dixit: nothing to disclose
G. Gandhi: nothing to disclose
N. Khurana: nothing to disclose

RPS 1407b-7 12:01
Multiple-b values of diffusion-weighted imaging (DWI) for grading endometrial cancer
O. Zhang, X. Zhao, H. Ouyang*; Beijing/CN (18810683722@163.com)*

Purpose: To investigate multiple-b value DWI derived parameters in assessing the pathological grade of endometrial cancer (EC) preoperatively.
Methods and materials: 43 consecutive patients with EC confirmed by pathology underwent multiple-b value DWI with 13 b values on a 3.0T MR scanner preoperatively. Multiple-b value DWI derived parameters, including apparent diffusion coefficient (ADC), true diffusivity (D), perfusion-related diffusivity (D*), and perfusion fraction (f), were measured by two radiologists independently and were compared between three groups identified by three histological grades by using the ANOVA. After combining G1 and 2 groups, a binary logistic regression model was used to calculate the the predictive probability of combined parameters indicating statistical significance in identifying high-grade EC. ROC curve was employed to determine the diagnostic efficiency of these parameters.
Results: Significant differences of ADC and D values were found between G1 and G3 (P=0.001 and 0.010), between G2 and G3 of EC (P=0.009 and 0.025), while f values were significantly lower in G3 than those in G1 (P=0.010). There was no significant difference of D* between those three groups. The largest AUC was observed by using ADC to distinguish G3 from G1-2 (AUC=0.825). Moreover, the combined parameter showed better diagnostic performance and the combination of D and f values had the highest AUC in the prediction of high-grade EC (AUC: 0.828). With the cut-off larger than 0.289, the sensitivity and specificity were 85.7% and 72.4%, respectively.
Conclusion: Multiple-b value DWI derived parameters could provide additional information for grading EC, which could be helpful in treatment planning and prognosis evaluation.
Limitations: We performed 13 b values for a multiple-b value DWI protocol which prolonged the scan time.
Ethics committee approval: Review board approval and written informed consent obtained.
Funding: No funding was received for this work.
Author Disclosures:
O. Zhang: nothing to disclose
H. Ouyang: nothing to disclose
X. Zhao: nothing to disclose

RPS 1407b-8 12:07
Three-dimensional turbo-spin-echo amide proton transfer MR imaging for type I endometrial carcinoma: correlation with Ki-67 proliferation status
Y. He, C. Lin, Y. Qi, X. Wang, H. Zhou, H. Xue, Z. Jin*; Beijing/CN (ylhe_526@163.com)*

Purpose: To evaluate the utility of 3-dimensional amide proton transfer-weighted (APTw) imaging for type I endometrial carcinoma (EC) and the correlation with the Ki-67 labelling index.
Methods and materials: 54 consecutive patients suspected of endometrial lesions underwent APTw and IVIM imaging on a 3T MR scanner. APT values, calculated based on the asymmetry of the acquired Z-spectrum with respect to water frequency, using 3D TSE volume acquisition with B0 correction, were independently measured by two radiologists on 22 postoperative pathological confirmed type I EC lesions as well as IVIM-derived parameters (Dt, D*, f). A Student's t-test and Mann-Whitney U test were used to compare the differences of APT values and IVIM-derived parameters between different histological grades and Ki-67 proliferation groups. ROC analysis was performed. Pearson's

correlation analysis was performed between the APT values, IVIM-derived parameters, and Ki-67 labelling index.
Results: APT values of Ki-67 low-proliferation group (<30%, n=8) were 2.466 ± 0.191, significantly lower than the high-proliferation group (>30%, n=14) with APT values of 3.093 ± 0.142 (p=0.016). AUC was 0.768. The APT values of type I EC were moderately positively correlated with Ki- 67 labelling index (r=0.583, p=0.004). There were no significant difference of D_t (p=0.843), D*(p=0.262), and f(p=0.553) between the low-proliferation group and high-proliferation group. No correlation was found between IVIM-derived parameters and Ki-67 labelling index (D_t, p=0.717; D* p=0.151; f, p=0.153).
Conclusion: 3D TSE APTw imaging is feasible in type I endometrial carcinomas. APT values positively moderately correlate with Ki-67 proliferation status.
Limitations: The sample size was small. We selected the single largest area, not the whole volume, of EEA for APT values measurement.
Ethics committee approval: Approved by our institutional review board. Written informed consent was obtained.
Funding: Beijing Natural Science Foundation (grant No. 7184234).
Author Disclosures:
C. Lin: nothing to disclose
Y. He: nothing to disclose
Y. Qi: nothing to disclose
X. Wang: nothing to disclose
H. Zhou: nothing to disclose
H. Xue: nothing to disclose
Z. Jin: nothing to disclose

RPS 1407b-9 12:13
Myometrial invasion by endometrial carcinoma: which sequence is more useful with 3.0 Tesla imaging
L. Karaca[1], A. Sağir Kahraman[1], Z. Ozdemir[1], E. Yılmaz[1], A. Akatlı[1], G. Mert Dogan (balaban)[2], H. Kural[1]; [1]*Malatya/TR*, [2]*Izmir/TR*
(karacaleyla4@gmail.com)

Purpose: To investigate the different sequences of 3 Tesla magnetic resonance imaging and histopathological analysis in assessing myometrial invasion in endometrial carcinoma.
Methods and materials: In this prospective study, 61 women with diagnosed endometrial cancer were examined using 3 Tesla MR and hysterectomy; histopathologic was examined. MRI protocol included DWI, T2-weighted images, dynamic contrast T1-weighted images, and zoom it DWI. Apparent diffusion coefficient (ADC) maps were also obtained. ADC was calculated using both DWI and zoom it DWI.
All series images were examined by endometrium distance to explain myometrial invasion. Histopathological confirmation was conducted following a hysterectomy.
Results: All sequences and histopathological results were compared with the paired sample t-test. There was no significant difference between diffusion and zoom it diffusion to evaluate invasion deep.
In assessing the depth of myometrial invasion, there was a high correlation between histopathological results and both sequences (0.940). Zoom it DWI sequences provided more precise assessment than other T1-weighted image and T2-weighted image sequences.
When all sequences were evaluated, dynamic T1-weighted contrast images were the most inconsistent with pathological results.
Conclusion: In the evaluation of the depth of myometrial invasion by endometrial carcinoma 3 Tesla MR imaging and zoom it, DWI has more value than other conventional sequences.
Limitations: Our study is limited by the relatively small number of patients. In addition, the reader knew the diagnosis of endometrial carcinoma.
Ethics committee approval: Inönü University Scientific Research and Publication Ethics Committee approval.
Funding: No funding was received for this work.
Author Disclosures:
L. Karaca: nothing to disclose
A. Sağir Kahraman: nothing to disclose
Z. Ozdemir: nothing to disclose
E. Yılmaz: nothing to disclose
G. Mert Dogan (balaban): nothing to disclose
H. Kural: nothing to disclose
A. Akatlı: nothing to disclose

RPS 1407b-10 12:19
A machine learning-based approach for predicting the malignant potential of T2-hyperintense mesenchymal and mixed tumours of the uterus by fusing T2WI features and clinical information
T. Wang, W. Peng, J. Gong; *Shanghai/CN*
(wangtt_shca@126.com)

Purpose: To develop a machine-learning method to predict the malignant potential of T2-hyperintense uterine mesenchymal and mixed tumours by fusing T2WI features and clinical information.
Methods and materials: This retrospective study enrolled 141 patients with T2-hyperintense uterine mesenchymal and mixed tumours (111 patients in the training cohort and 30 in the validation cohort). A total of 960 radiomics features were initially computed and extracted from each 3D segmented tumour depicting on T2-weighted MR images. A univariate feature selection method was used to select high-performance features. We used an SVM machine-learning classifier to build two models by using selected clinical and radiomics features, respectively. Receiver operating characteristics curve (ROC) analysis was used to assess the performance of each model and compared with two radiologists.
Results: 3 clinical and 5 radiomics features were selected for prediction models. The clinical-radiomics fusion model can significantly improve the performance (AUC: 0.87±0.03, p<0.001) compared with a T2 MR image-based model (0.78±0.04) and clinical information based model (0.74±0.05), respectively. Two radiologists achieved no significant difference in AUC values (0.85 vs 0.82, p=0.37). In comparison, the fusion model yields significantly higher performance compared with two radiologists (p<0.001).
Conclusion: The clinical-radiomics fusion model can improve the performance in characterising T2-hyperintense uterine mesenchymal and mixed tumours, and can outperform experienced radiologists.
Limitations: The sample size was relatively small. We only included patients with T2-hyperintense uterine mesenchymal and mixed tumours, introducing a selection bias. Only T2WI were used for radiomics feature analysis in our study , to minimise variability in acquisition parameters. Other useful sequences such as DWI or dynamic contrast-enhanced images were not used.
Ethics committee approval: n/a
Funding: No funding was received for this work.
Author Disclosures:
T. Wang: Speaker at Fudan University Shanghai Cancer Center, Author at Fudan University Shanghai Cancer Center
W. Peng: Author at Fudan University Shanghai Cancer Center, Research/Grant Support at Fudan University Shanghai Cancer Center
J. Gong: Author at Fudan University Shanghai Cancer Center

RPS 1407b-11 12:25
Diffusion kurtosis imaging of endometrial carcinoma
S. Satta, M. Dolciami, F. Di Stadio, S. Capuani, L. Manganaro, C. Catalano; *Rome/IT (seresatta@gmail.com)*

Purpose: To assess the usefulness of diffusion kurtosis imaging (DKI) as a noninvasive method for detecting and evaluating endometrial cancer (EMC).
Methods and materials: 18 consecutive patients with a histological diagnosis of EMC by biopsy and 19 healthy volunteers were enrolled. They underwent an MR exam with diffusion-weighted imaging (DWI), acquired using multiple b values (from b 0 to b 2500 s/mm2) for each subject. DKI parameters were calculated for each voxel, to obtain K (kurtosis) and D (diffusivity). We also evaluated conventional ADC. All DWI images were processed using an in-house program developed with MatLab software (R2016a; MathWorks, Natick, MA). For K and D maps, regions of interest (ROIs) were manually drawn approximately equivalent in size to tumoural tissue and myometrium for EMC and to endometrium and myometrium for healthy patients, using DWI and T2W as references. Mean ± SD of K, D, and ADC values for uterine wall layers and EMCs were calculated and differences analysed using an Anova test.
Results: ADC (*10-3 mm2/s): EMC 0.87±0.22; healthy 0.96±0.23; p - D (*10-3 mm2/s): EMC 1.05±0.30; healthy 1.14±0.25; p - K (u.a.): EMC 1.12±0.30; healthy 0.63±0.18; p 0.015. K significantly discriminated between a tumour and healthy tissue (p=0.015), whereas D and ADC didn't discriminate.
Conclusion: Kurtosis imaging seems to be more sensitive compared to conventional diffusion imaging in detecting EMC. These results are promising and the difference between EMC and healthy layers may be used to precisely predict myometrial infiltration during MR examination.
Limitations: A limited number of patients.
Ethics committee approval: The study was approved by an ethics committee. Every patient gave written informed consent.
Funding: No funding was received for this work.
Author Disclosures:
S. Satta: nothing to disclose
M. Dolciami: nothing to disclose
S. Capuani: nothing to disclose
F. Di Stadio: nothing to disclose
L. Manganaro: nothing to disclose
C. Catalano: nothing to disclose

11:15 - 12:30 **Room M 1**

Hybrid, Molecular and Translational Imaging

RPS 1406

From hyperpolarised MRI to multimodal imaging probes

Moderators:
S. Aime; Turin/IT
I. Pashkunova-Martic; Vienna/AT

RPS 1406-K 11:15
Keynote lecture
X. Golay*; London/UK*

Author Disclosures:
X. Golay: nothing to disclose

RPS 1406-1 11:25
Virtual metabolic biopsies using hyperpolarised carbon-13 MRI to unravel metabolic heterogeneity in renal tumours
S. Ursprung, R. A. Woitek, M. A. McLean, A. S. Costa, A. Warren, C. Frezza, E. Sala, G. Stewart, F. A. Gallagher*; Cambridge/UK (su263@cam.ac.uk)*

Purpose: Renal cell cancer is the most common renal neoplasm and has recently been recognised for its genetic and metabolic intratumoural heterogeneity, contributing to tumour evolution, aggressiveness and treatment failure. Hyperpolarised [1-^{13}C]pyruvate (hp^{13}C-pyruvate) magnetic resonance imaging (hpMRI) allows the non-invasive assessment of pyruvate metabolism, but it is not known how this correlates with tissue-based molecular assays.
Methods and materials: Tumour metabolism was imaged in three patients with renal tumours using hpMRI. Following injection of hp^{13}C-pyruvate, metabolic images were acquired from 3 cm thick axial slices using an 8-channel-array coil on a 3T MRI with a temporal and spatial resolution of 4 s and 1.7 x 1.7 cm in-plane. Lactate concentrations measured using liquid chromatography-mass spectrometry (LC-MS) on perfused and ischaemic tissue samples were correlated with hpMRI-based metabolite signals.
Results: The tumours demonstrated a higher exchange rate for the hp^{13}C-label between pyruvate and lactate (k_{PL}: 0.010 ± 0.004s^{-1}, mean ± S.D.) than the normal kidney (0.003 ± 0.001s^{-1}). The parametric maps demonstrated intratumoural metabolic heterogeneity with at least two metabolically distinct tumour regions in each patient and higher metabolic heterogeneity in higher-grade tumours. Metabolic differences observed on imaging were replicated in tissue samples obtained before and after vascular exclusion, despite showing signs of ischaemia. A strong positive correlation (rho = 0.73, p = 0.003) was observed between lactate SNR on imaging and tissue concentrations measured with LC-MS (Figure 2).
Conclusion: Hyperpolarised ^{13}C-pyruvate demonstrates metabolic intratumoural heterogeneity in renal cancer and imaging-based lactate levels correlate with steady-state tissue lactate concentrations. Hyperpolarised imaging may guide biopsies to regions of metabolically aggressive regions of the tumour.
Limitations: Limited patient number with ongoing recruitment.
Ethics committee approval: UK-REC-Numbers: 15/EE/0378, 03/018
Funding: Funding by Wellcome Trust, Cancer Research UK.
Author Disclosures:
S. Ursprung: nothing to disclose
M. A. McLean: nothing to disclose
R. A. Woitek: nothing to disclose
A. Warren: nothing to disclose
C. Frezza: nothing to disclose
E. Sala: Speaker at Siemens
F. A. Gallagher: nothing to disclose
G. Stewart: Grant Recipient at Pfizer, Grant Recipient at AstraZeneca, Grant Recipient at Intuitive Surgical, Consultant at Merck, Consultant at Pfizer, Consultant at EUSA Pharma, Consultant at Cambridge Medical Robotics, Speaker at Pfizer
A. S. Costa: nothing to disclose

RPS 1406-2 11:31
Assessing tumour cell death in vivo using deuterium magnetic resonance spectroscopic imaging
F. Hesse, V. Somai, F. Kreis, F. Bulat, K. Brindle*; Cambridge/UK (friederike.hesse@cruk.cam.ac.uk)*

Purpose: To demonstrate that fast deuterium MRI can be used for detecting cell death and to assess early tumour treatment response.
Methods and materials: Methods for detecting early evidence of cell death were investigated in three different tumour models (blood, breast and colorectal cancer) by applying a fast 3D deuterium MRI pulse sequence with a time resolution of 5 minutes, following a bolus injection of [2,3-$^{2}H_2$] fumarate, before and 48 h or 24 h after treatment with a chemotherapeutic or a novel targeted agent, respectively. In vitro experiments were conducted on a 14.1 T high-resolution NMR spectrometer, whereas in vivo results, were gained on a 7.0 T horizontal bore magnet.
Results: Deuterium metabolic imaging (DMI) experiments in vivo were conducted in the same tumour models on three mice each to generate metabolic maps with high spatiotemporal resolution. A fast chemical shift imaging sequence allowed to assess tumour conversion of [2,3-$^{2}H_2$]fumarate to [2,3-$^{2}H_2$]malate following a bolus injection of labelled fumarate. Within 48 h of drug treatment, the malate/fumarate ratio increased significantly from 0.034 ±0.06 to 0.33 ±0.11 (p=0.04).
Conclusion: Deuterium MR spectroscopic images can provide quantitative and spatially resolved measurements of cell death imaging. This study demonstrates the potential of DMI for assessing early tumour responses to treatment in the clinic.
Limitations: Deuterium tracer possesses a relatively low sensitivity, which may constrain imaging spatiotemporal resolution. Injecting higher concentrated substrates remedied this limitation.
Ethics committee approval: Animal experiments were carried out in compliance with a project and personal license issued by the Home Office, approved by the Cancer Research UK, Cambridge Institute Animal Welfare and Ethical Review Body.
Funding: No funding was received for this work.
Author Disclosures:
F. Hesse: nothing to disclose
V. Somai: nothing to disclose
F. Kreis: nothing to disclose
F. Bulat: nothing to disclose
K. Brindle: nothing to disclose

RPS 1406-3 11:37
Improving longitudinal transversal relaxation of gadolinium chelate using silica coating magnetite nanoparticles
K. Xu, W. Zhang*; Chongqing/CN (292494513@qq.com)*

Purpose: Precisely and sensitively diagnosing diseases - especially early and accurate tumour diagnosis in clinical magnetic resonance scanner - is a highly demanding but challenging task. Gadolinium (Gd) chelate is the most common T_1 MRI contrast agent at present. However, traditional Gd-chelates are suffering from low relaxivity, which hampers its application on clinical diagnosis. Currently, the development of nano-sized Gd based T_1 contrast agent, such as incorporating gadolinium chelate into nanocarriers, is an attractive and feasible strategy to enhance the T_1 contrast capacity of Gd chelate. The objective of this study was to improve the T_1 contrast ability of Gd-chelate by synthesizing nanoparticles (NPs) for accurate and early diagnosis in clinical diseases.
Methods and materials: A reverse microemulsion method was used to coat iron oxide (IO) with a tunable silica shell and to form cores of NPs IO@SiO2 at step one. Then, Gd-chelate was loaded on the surface of the silica-coated iron oxide NPs. Finally, the Gd-based silica coating magnetite NPs IO@SiO2-DTPA-Gd was developed, and we tested the ability to detect tumour cells on a cellular level.
Results: The r_1 value of IO@SiO_2-DTPA-Gd with the silica shell thickness of ~ 11 nm is about 33.6 mM^{-1}s^{-1}, which is approximately six times higher than Gd-DTPA. Based on its high T_1 contrast ability, IO@SiO_2-DTPA-Gd can effectively detect tumour cells on a cellular level.
Conclusion: Our findings revealed an improvement of T_1 relaxation that was not only caused by the increase of molecular tumbling time caused by the IO@SiO_2 nanocarrier but also by the generated magnetic field caused by the iron oxide NPs. This nanostructure with high T_1 contrast ability may open a new approach to constructing a high-performance T_1 contrast agent.
Limitations: The study is limited by a lack of MRI detecting in vivo.
Ethics committee approval: n/a
Funding: Funding by the National Natural Science Foundation of China (No.81871421).
Author Disclosures:
K. Xu: Author at Daping Hospital
W. Zhang: Founder at Daping Hospital

RPS 1406-4 11:43

Extradomain-B fibronectin-targeting nanoprobe for FL/PA/CT trimodal accurate imaging and risk-stratification of breast cancer

D. Yao, Y. Wang, D. Wang; *Shanghai/CN (yaodefan@126.com)*

Purpose: Extradomain-B fibronectin (EDB-FN) is a marker for epithelial-to-mesenchymal transition (EMT), a biological process associated with tumour invasion, metastasis and drug resistance. EDB-FN is highly expressed in the extracellular matrix of aggressive human breast cancers. For non-invasive accurate detection and risk-stratification of breast cancer, a peptide-targeted gold nanorod, Pep-Sq@AuNRs, is synthesised for sensitive fluorescent, photoacoustic and computed tomography (FL/PA/CT) imaging of extradomain-B fibronectin in aggressive breast tumours.
Methods and materials: An EDB-FN-targeted peptide modified gold nanorod, Pep-Sq@AuNRs, was synthesized using a three-step process, and this probe is composed of three moieties. The first moiety is an EDB-FN-targeted peptide (Pep), preferably targeting EDB-FN. The second moiety is a NIR fluorescent dye (Sq), of which its essential properties of NIR FL/PA imaging and phototherapy. The third moiety is gold nanorods (AuNRs), acting as CT/PA contrast agent.
Results: This complex probe can effectively target aggressive MDA-MB-231 triple-negative breast cancer in mice, but not in low-risk slow-growing MCF-7 tumours. The NIR FL/PA signals were activated by EDB-FN for imaging, and the AuNRs were used for CT imaging and photothermal/photodynamic therapy (PTT/PDT). These results demonstrate that trimodal imaging with Pep-Sq@AuNRs may provide accurate detection and risk-stratification of breast cancer.
Conclusion: In summary, we developed a novel platform, Pep-Sq@AuNRs, as a model to distinguish aggressive MDA-MB-231 triple-negative breast cancer and low-risk slow-growing MCF-7 tumours in mice. The results demonstrate that Pep-Sq@AuNRs could effectively target the aggressive MDA-MB-231 triple-negative breast cancer and kill cancer cells by PTT/PDT.
Limitations: There are no limitations to this study.
Ethics committee approval: The animal handling was approved by the Ethics Committee of Xinhua Hospital, affiliated to Shanghai Jiao Tong University School of Medicine.
Funding: The National Natural Science Foundation of China (81901870) and Shanghai Sailing Program (18YF1415600).
Author Disclosures:
D. Yao: nothing to disclose
Y. Wang: nothing to disclose
D. Wang: nothing to disclose

RPS 1406-5 11:49

Novel complementary molecular imaging tools to monitor immunometabolic crosstalk in a rabbit model of liver cancer

L. J. Savic[1], L. Doemel[2], I. Schobert[1], M. Lin[2], R. J. Bucala[2], N. Goldberg[3], F. Hyder[2], D. Coman[2], J. Chapiro[2]; *[1]Berlin/DE, [2]New Haven, CT/US, [3]Jerusalem/IL (lynn-jeanette.savic@charite.de)*

Purpose: To establish novel complementary molecular imaging tools for non-invasive monitoring of metabolic (extracellular pH, pHe) and immune activities of the liver tumour microenvironment.
Methods and materials: Fifteen VX2 liver tumour-bearing rabbits were used: A) Nine rabbits underwent pHe-mapping after conventional transarterial chemoembolisation (cTACE, n=3), cTACE with pHe-buffering bicarbonate (n=3), or as untreated controls (n=3). B) Three rabbits received ^{160}Gadolinium-labeled anti-HLA-DR antibodies intra-arterially to detect antigen-presenting cells. C) Three animals received rhodamine-conjugated small iron oxide nanoparticles (SPION) intravenously to detect macrophage distribution. MRI was performed on clinical 3T-scanners before and 24hrs after treatment, including pHe, T1- and T2-weighted imaging. Immunohistochemistry (IHC) staining of HLA-DR and CD11b, Prussian blue staining, fluorescence microscopy of rhodamine, and imaging mass cytometry (IMC) of gadolinium were compared to MRI signal distribution.
Results: pHe-mapping of untreated tumours revealed tumour acidosis (pHe=6.75±0.02) compared to liver parenchyma (7.19±0.02, p<0.001). Bicarbonate-cTACE significantly increased tumour-pHe (6.98±0.03) compared to controls (p=0.024) and cTACE alone (pHe=6.86±0.05, p=0.008). Moreover, acid neutralisation was accompanied by restored immune cell infiltration in the peritumoral rim, which was not detectable after cTACE alone. T1-weighted MRI with^{160}Gadolinium-labelled antibodies revealed localised peritumoural ring enhancement, which corresponded to gadolinium distribution patterns detected by IMC. T2-weighted MRI with SPION showed curvilinear signal hypointensity due to selective peritumoral SPION deposition in macrophages.
Conclusion: ^{160}Gadolinium- and SPION-based molecular imaging allows for specific labelling of peritumoural immune cells that are eliminated by cTACE and restored with acid neutralisation as detected by pHe-sensitive MRS. Thus, these monitoring tools may improve the assessment of susceptibility and response to immuno-oncological and loco-regional therapies.
Limitations: Limited spatial resolution and limited number of subjects (pilot project).
Ethics committee approval: Animal protocols were approved by the Animal Care and Use Committee.
Funding: Funding by the National Institutes of Health (R01 CA206180, EB-023366) and the Society of Interventional Oncology.
Author Disclosures:
L. J. Savic: Research/Grant Support at SIO Research Grant, Research/Grant Support at Leopoldina Research Fellow
I. Schobert: Research/Grant Support at BMEP
L. Doemel: nothing to disclose
R. J. Bucala: Research/Grant Support at NIH
D. Coman: Research/Grant Support at NIH
F. Hyder: Research/Grant Support at NIH
J. Chapiro: Research/Grant Support at SIO Research Grant, Research/Grant Support at NIH
M. Lin: Research/Grant Support at NIH, Advisory Board at Visage
N. Goldberg: Research/Grant Support at NIH

RPS 1406-6 11:55

Target-specific in vivo imaging of tumour-immune interaction: evaluation of the regulatory protein S100A9

A. Helfen, J. Rieß, A. Schnepel, O. Fehler, M. Gerwing, M. Masthoff, W. Heindel, M. Wildgruber, M. Eisenblaetter; *Muenster/DE, (anne.helfen@ukmuenster.de)*

Purpose: Tumour progression and metastasis depend on tumour-infiltrating immune cells, which form a characteristic inflammatory tumour microenvironment (TME). As a promoter of tumour invasion and TME formation, the protein heterodimer S100A8/A9 released by activated infiltrating monocytes is associated with poor prognosis. Our aim was to develop an in vivo imaging tool as a biomarker for TME influence on tumour behaviour.
Methods and materials: From syngeneic murine breast cancer tumours 4T1 (highly malignant) and 67NR (low malignancy), wildtype (wt) and S100A9 knock out cells (CRISPR/cas9-method, ko) were created and implanted into either female BALB/c wildtype or S100A9$^{-/-}$-mice (n=10 each). At 4mm tumour diameter, anti-S100A9-Cy5.5-driven fluorescence reflectance imaging has been performed 0 and 24h after injection (contrast-to-noise ratios of fluorescence intensities in arbitrary units, AU). In vivo imaging was correlated with immunohistology, Western Blot and FACS analyses.
Results: In S100A9$^{-/-}$-mice fluorescence signals were significantly reduced for wildtype (4T1: 62,9 vs. 43,02AU;p=0,048, 67NR:52,73 vs. 27,26;p=0,033) and S100A9$^{-/-}$-tumours (4T1ko:65,33 vs. 42,51AU;p=0,005; 67NRko:54,61 vs. 34,19AU; p=0,006). However, no significant differences were detected for 4T1ko and 67NRko cells as compared with wildtype cells (4T1:p=0.543, 67NR:p=0.85). In all subgroups, the fluorescence signal was significantly higher in 4T1 as compared to 67NR tumours, reflecting their higher malignant potential. Imaging results were confirmed by ex-vivo analyses. Furthermore, FACS indicated an immune cell shift to immature monocytes within the S100A9-positive TME.
Conclusion: Our results in the 4T1/67NR breast cancer model confirm a secretion of S100A8/A9 by components of the TME, while tumour cells do apparently not release S100A8/A9. S100A9-specific in vivo imaging reflects tumour malignancy and may serve as a biomarker for TME formation and activity.
Limitations: n/a
Ethics committee approval: Animal board approval No.:84-02.04.2017.A011.
Funding: This work has been funded by DFG/Cluster of Excellence grant (PP-2017-01).
Author Disclosures:
A. Helfen: nothing to disclose
J. Rieß: nothing to disclose
A. Schnepel: nothing to disclose
O. Fehler: nothing to disclose
M. Gerwing: nothing to disclose
M. Masthoff: nothing to disclose
W. Heindel: nothing to disclose
M. Wildgruber: nothing to disclose
M. Eisenblaetter: nothing to disclose

RPS 1406-7 12:01

Cathepsin B-activated nanoparticles for multimodal imaging-guided photodynamic therapy to breast cancer

Y. Wang, D. Yao, D. Wang; *Shanghai/CN (wangyanshu_1992@sina.com)*

Purpose: Breast cancer is one of the most devastating malignancies in women. Photodynamic therapy (PDT) is widely investigated as alternative treatment for breast cancer due to its unique advantages. In light of upregulated cathepsin-B (CTSB) in breast cancer, we synthesized a targeted near-infrared activatable

probe (Pep-SQ@USPIO) for MRI/fluorescent/photoacoustic (MRI/NIR FL/PA) imaging-guided PDT.
Methods and materials: Pep-SQ@USPIO based on USPIO core modified with Pep-SQ. The sequence of Pep-SQ consisted of two moieties: the first moiety is fibronectin targeted peptide which labelled with a green fluorescent group, naphthalimide; the second moiety is a NIR fluorescent dye (SQ), of which it's essential properties of NIR FL/PA imaging and PDT. The two moieties linked via a cathepsin B-sensitive peptide (GFLG) linker. Transmission electron microscopy images, hydrodynamic size profiles, absorption spectra, cck-8 assay and oxidative stress elevation were acquired. The influence of "turn on" the fluorescence signal was studied in vitro and in vivo. The in vivo mice with tumour model was applied to evaluate imaging and photodynamic therapy efficacy.
Results: Pep-SQ@USPIO is almost nonfluorescent with inactivated phototoxicity and successfully applied to MR/PA imaging. After cancer cellular uptake, the cleavage of the GFLG substrate by CTSB led to recovering the quenched NIR FL signal, resulting in a high tumour/normal signal ratio. Upon treatment with 660 nm laser irradiation, generated reactive oxygen species (ROS) would produce PDT and enable remarkable tumour inhibition.
Conclusion: This tumour-specific theranostic probes can precisely diagnose and exerts further selective treatment, which may address challenges faced by traditional medicine in breast cancer.
Limitations: n/a
Ethics committee approval: All the experimental protocols were approved by the Ethics Committee of Xinhua Hospital affiliated to Shanghai Jiao Tong University School of Medicine.
Funding: Funding by the National Natural Science Foundation of China (NSFC 81371621).
Author Disclosures:
Y. Wang: nothing to disclose
D. Wang: nothing to disclose
D. Yao: nothing to disclose

RPS 1406-8 12:07

Functionalised nanoparticles for bone micro-fractures with spectral photon-counting CT

C. Lowe[1], F. Ostadhossein[2], M. Moghiseh[1], M. Anjomrouz[2], R. K. Panta[1], A. Y. Raja[1], A. P. H. Butler[1], D. Pan[3], M. Collaboration[1]; [1]*Christchurch/NZ,* [2]*Urbana/US,* [3]*St. Louis, MO/US (Mahdieh.moghiseh@otago.ac.nz)*

Purpose: We visualise bone microdamage with functionalised nanoparticles in excised human phalanx and whole rat specimens. Spectral photon-counting CT using a MARS scanner allowed characterisation of bone microdamage, microarchitecture, mineralisation, and composition. Such characterisation is essential to assess bone quality and the toughening mechanism of bone.
Methods and materials: Biological specimens involved imaging of the excised human phalanx followed by incubation in ligand targeted hafnia nanoparticles (HfO_2 NPs) and two rat specimens which were anaesthetised and received scalpel-induced bone microdamage in one hind limb. One rat received functionalised, and the other received non-functionalised, HfO_2 NPs via intramuscular injection. Five hours post-injection, the animals were euthanised and scanned with MARS scanner. MARS is a small-bore photon-counting scanner employing energy resolving detectors and an x-ray tube operated at clinical x-ray energies, 118kVp. Four energy bins (30-45, 45-65, 65-80, 80-118 keV) and energy resolution of 3.5 keV, were used for imaging, with a cubic reconstruction voxel size of 90 µm.
Results: The MARS scanner produced quantitative images of HfO_2 nanoparticles, bone, and soft tissue using energy-dependent differences in x-ray attenuation. For the excised phalanx, HfO_2 nanoparticles highlighted expected regions of bone microdamage at high specificity (> 70% identification success for ≥ 10 mg/mL). In the injured rat limb, measured delivery of ligand targeted HfO_2 nanoparticles was 6.4 mg.
Conclusion: We have shown that spectral photon-counting imaging enables specific identification and quantification of HfO_2 functionalised nanoparticles that were targeted at bone microfractures, an important capability for the assessment of bone quality.
Limitations: n/a
Ethics committee approval: The ethics committee approval was obtained from Illinois Institutional Animal Care and Use Committee at the University of Illinois Urbana Champaign (protocol #17125).
Funding: MBIE number: UOCX1404,MARS bioimaging Ltd. D.P. recipient of academic grants from NIH, NSF and DoD.
Author Disclosures:
M. Moghiseh: Shareholder at MARS Bioimaging Ltd, Employee at MARS Bioimaging Ltd
C. Lowe: nothing to disclose
F. Ostadhossein: nothing to disclose
M. Anjomrouz: Employee at MARS Bioimaging Ltd
R. K. Panta: Employee at MARS Bioimaging Ltd, Shareholder at MARS Bioimaging Ltd
A. Y. Raja: Employee at MARS Bioimaging Ltd
A. P. H. Butler: Employee at MARS Bioimaging Ltd, Founder at MARS Bioimaging Ltd, Board Member at MARS Bioimaging Ltd, Shareholder at MARS Bioimaging Ltd, Investigator at Ministry of Business, Innovation and Employment (MBIE)
D. Pan: Founder at Of three University based start ups. None of these entities, however, supported this work, Grant Recipient at NIH, NSF and DoD.
M. Collaboration: Employee at MARS Bioimaging Ltd, Shareholder at MARS Bioimaging Ltd, Grant Recipient at Ministry of Business, Innovation and Employment (MBIE)

RPS 1406-9 12:13

Quantification of various calcium crystals for gout, pseudo-gout and other arthropathies using spectral photon-counting CT

Y. Sayous[1], I. Bernabei[2], A. Viry[2], N. Busso[2], A. P. H. Butler[1], L. Stamp[1], F. Becce[2], A. Y. Raja[1], M. Collaboration[1]; [1]*Christchurch/NZ,* [2]*Lausanne/CH (yann.sayous@gmail.com)*

Purpose: To confirm a method for distinguishing various calcium crystals in a range of arthropathies, in preparation for planned imaging studies of excised specimens and patients. Distinguishing crystal-associated arthropathies non-invasively and early in the disease course remains a challenge with traditional imaging techniques. Our method provides 3D maps of 90 μm^3 voxels of crystal type that should allow earlier treatment options.
Methods and materials: A MARS spectral photon-counting scanner was used to scan calibration rods of three concentrations of each of monosodium urate (MSU), calcium pyrophosphate (CPP) and calcium hydroxyapatite (HA). The images were acquired using four energy channels (20-30, 30-40, 40-50 and 50-80 keV) with a 3.5 keV resolution. The crystal types were distinguished by comparing energy-dependent attenuation coefficients. First, to assess the performance of the system, receiver operating characteristic curves were used. Then the system was tested on the different rods to evaluate identification efficiency.
Results: System performance demonstrates, using pairwise areas under the curves (AUC), that all concentrations of MSU were readily differentiated from the two higher concentrations of CPP and HA with an AUC > 0.90. The highest concentrations of CPP and HA (200 mg/cm^3) were well differentiated from each other, while 100 mg/cm^3 of CPP and HA showed a fair differentiation. The tests from the rods demonstrate that spectral photon-counting CT can identify high concentrations of CPP and HA (correct identification up to 80%) and significant ability to identify MSU (correct identification up to 90%).
Conclusion: We are able to identify and quantify important calcium crystals across a range of clinically relevant concentrations. This enables us to study arthropathies in excised samples and patients using existing MARS research and human scanners.
Limitations: n/a
Ethics committee approval: n/a
Funding: MBIE UOCX1404, MARS Bioimaging Ltd, Medtechcore.
Author Disclosures:
A. Y. Raja: Employee at MARS Bioimaging Ltd
Y. Sayous: Research/Grant Support at MARS Bioimaging Ltd
I. Bernabei: nothing to disclose
A. Viry: nothing to disclose
N. Busso: nothing to disclose
A. P. H. Butler: Board Member at MARS Bioimaging Ltd, Employee at MARS Bioimaging Ltd, Founder at MARS Bioimaging Ltd, Shareholder at MARS Bioimaging Ltd, Grant Recipient at MBIE
F. Becce: nothing to disclose
M. Collaboration: Employee at MARS Bioimaging Ltd, Shareholder at MARS Bioimaging Ltd, Grant Recipient at MBIE
L. Stamp: nothing to disclose

RPS 1406-10 12:19

Histology of atherosclerotic plaque compared with tissue components measured using a spectral photon-counting CT

S. Dahal[1], E. Searle[2], S. Gieseg[2], A. Y. Raja[2], A. P. H. Butler[2], M. Collaboration[2]; [1]*Kathmandu/NP,* [2]*Christchurch/NZ*

Purpose: To confirm a method for non-invasively measuring four tissue components in atherosclerotic plaques. We compare the histology of plaques to 3D quantitative images of fat, water, calcium, and iron generated by a spectral photon counting CT.
Methods and materials: Arterial plaques obtained from carotid endarterectomy and scanned with a MARS spectral photon-counting CT. Following MARS imaging, the plaques were decalcified and fixed, then stained for protein, lipid, and iron. Histological photos were then taken of the stained tissue slices. The MARS scanner was operated at 120kVp with four energy channels with 3.5 keV resolution. This provided 3D maps of 90 µmcubic voxels of the four tissue components. Reference materials for calibration were ferric nitrate,

hydroxyapatite, oil, and water. The four maps of tissue components were compared to corresponding regions within the histological images.
Results: We will present tissue component maps alongside histological images. The images show: 1) regions of lipid deposits; 2) micro and macro calcification; 3) iron deposition; 4) thickness of the fibrous cap; 5) and ulcerations.
Conclusion: We have confirmed that the four maps of tissue components agree with histological analysis. Our technique non-invasively measures key features of some unstable plaque. The measurements are quantitative and in 3D. This enables us to study plaque in excised samples and patients using existing MARS research and human scanners.
Limitations: n/a
Ethics committee approval: CTY/01/04/036
Funding: MBIE, MARS Bioimaging Ltd, MedTechCORE.
Author Disclosures:
E. Searle: nothing to disclose
S. Dahal: Shareholder at MARS Bioimaging Ltd
S. Gieseg: Shareholder at MARS Bioimaging Ltd
A. P. H. Butler: Board Member at MARS Bioimaging Ltd, Employee at MARS Bioimaging Ltd, Shareholder at MARS Bioimaging Ltd, Founder at MARS Bioimaging Ltd, Grant Recipient at Ministry of Business Innovation and Employment
A. Y. Raja: Employee at MARS Bioimaging Ltd
M. Collaboration: Employee at MARS Bioimaging Ltd, Shareholder at MARS Bioimaging Ltd, Grant Recipient at Ministry of Business Innovation and Employment

RPS 1406-11 12:25
CT radiogenomic characterisation of non-small cell lung carcinoma with EGFR and ALK mutation
G. Sharma, R. Sudhir, V. Koppula*; Hyderabad/IN*
(ggaurav.sharma@yahoo.co.in)

Purpose: Radiogenomics, focussing on defining relationships between "image phenotypes" and "molecular phenotypes", is currently considered a promising new paradigm for extending clinical imaging into the era of molecular imaging. The purpose of this study is to assess the association between CT imaging features of non-small cell lung carcinoma with EGFR and ALK mutation and HPE and demographic correlation in NSCLC with EGFR & ALK mutation.
Methods and materials: A prospective observational study, conducted at our institute, for a period of 18 months. Patients with pre-treatment CT chest of the primary tumour at our institution with the histological diagnosis of non-small cell lung carcinoma and data on EGFR and/or ALK rearrangement status were included in this study.
Results: A total of 156 patients, 87/156 (55.8%) males and 69/156 (44.2%) females were included in the study. This study demonstrated that the female gender (p=0.0065), spiculated margin (p=0.0195), GGO (p=<0.0001), pleural retraction (p=0.0023), absence of emphysema (p=0.0003), nodule in primary tumour lobe (p=0.0321), pleural effusion on same side of the tumour (p=0.0003) and metastatic lymphangitis carcinomatosis (MLC) (p=0.0004) were significantly associated with EGFR positivity, while bigger a size of a lesion (p=0.0259), central distribution (p=0.0215) of the primary lesion, pleural retraction (p=0.022), nodules in non-tumour lobe (p=0.003) and MLC (p=0.0159) were significantly associated with ALK mutation status.
Conclusion: This study affirms previous studies for a few CT characteristics and also found new correlations between CT imaging characteristics and the molecular status of NSCLC, providing supporting evidence for molecular targets that can be treated using molecular drugs.
Limitations: Limitations were the relatively smaller sample size for ALK mutation and that the pattern of contrast enhancement was not studied.
Ethics committee approval: n/a
Funding: No funding was received for this work.
Author Disclosures:
G. Sharma: nothing to disclose
R. Sudhir: nothing to disclose
V. Koppula: nothing to disclose

11:15 - 12:30 **Room M 2**

Neuro

RPS 1411b

Stroke

Moderators:
N.N.

RPS 1411b-K 11:15
Keynote lecture
C. Tramontini*; Bogotá/CO (ctramontinij@gmail.com)*

Author Disclosures:
C. Tramontini: Speaker at Roche, Speaker at Novartis, Speaker at Merck

RPS 1411b-1 11:25
Mothership and drip-and-ship: does the initial treatment strategy in acute ischaemic stroke impact the outcome?
D. A. Weiss, C. Rubbert, M. Kaschner, P. D. M. S. Jander, M. Gliem, J.-I. Lee, C.-A. Haensch, B. Turowski, J. Caspers*; Düsseldorf/DE*
(DanielArvid.Weiss@med.uni-duesseldorf.de)

Purpose: Two strategies of initial patient care exist in endovascular thrombectomy (ET) depending on the site of initial admission: the mothership (MS) and drip-and-ship (DnS) principles. This study compares both strategies to clarify if one of them is superior in terms of patient outcome.
Methods and materials: 202 patients undergoing ET for anterior circulation ischaemic stroke were enrolled. Group comparisons in three-months modified Rankin scales (mRS) between both admission strategies were performed with the Mann-Whitney-U test and Spearman-correlation between admission strategy and mRS were analysed. A binary logistic regression (BLR) model was performed including mRS as the dependent variable and admission strategy, NIHSS, age, and onset-to-recanalisation-time as independent variables. Corresponding statistical tests were additionally performed in subgroups of patients with ET only or ET and intravenous thrombolysis (IVT).
Results: There were no significant group differences in three-month mRS between MS and DnS. However, a significant correlation between three-month mRS and admission strategy with lower mRS in MS principle was found in the subgroup of patients undergoing ET only. In patients treated with IVT and ET, this correlation was not significant. BLR showed a high explanation of variance in all models but no significant results for admission strategy.
Conclusion: The MS principle is superior to DnS in patients treated with ET only, probably due to time delay in the latter. However, in patients undergoing both IVT and ET, both strategies do not differ significantly. This indicates that bridging IVT is useful to reduce the unfavourable effect of transportation delay when local infrastructure necessitates DnS.
Limitations: The number of patients. No randomisation by intention.
Ethics committee approval:
Approval by the local institutional review-board (ID: 5468R). Written informed consent was obtained.
Funding: No funding was received for this work.
Author Disclosures:
D. A. Weiss: nothing to disclose
C. Rubbert: nothing to disclose
M. Kaschner: nothing to disclose
P. D. M. S. Jander: nothing to disclose
M. Gliem: nothing to disclose
J.-I. Lee: nothing to disclose
C.-A. Haensch: nothing to disclose
B. Turowski: nothing to disclose
J. Caspers: nothing to disclose

RPS 1411b-2 11:31
CT-perfusion before and immediately after mechanical thrombectomy improves outcome prediction beyond clinical, angiographic, and standard imaging characteristics in patients with acute ischaemic stroke
G. Brugnara, M. Foltyn, U. Neuberger, S. Nagel, P. Ringleb, M. Bendszus, M. Möhlenbruch, J. Pfaff, P. Kickingereder*; Heidelberg/DE*
(gianluca.brugnara@med.uni-heidelberg.de)

Purpose: To investigate the value of CT-perfusion obtained before and immediately after mechanical thrombectomy (MT) for the outcome prediction in patients with acute ischaemic stroke.
Methods and materials: CT-perfusion was performed both before and immediately after MT in 42 patients. Perfusion maps (CBV, CBF, MTT, TMax, and TTP) were calculated and areas of hypoperfusion were segmented in the

baseline exam. Quantitative data was extracted from the segmented area at baseline and the corresponding area after MT. Full clinical and interventional data was available. Patient outcome was defined with the modified Rankin scale (mRS) at 90 days into mRS≤2 (good outcome) and mRS>2 (bad outcome). Multivariable logistic regression was performed to assess the value of baseline clinical data, ASPECTS, TICI score, and pre- and post-treatment CT-perfusion parameters for predicting the treatment outcome.
Results: Inclusion of both pre- and post-treatment CT-perfusion (in addition to clinical parameters, ASPECTS, and TICI score) yielded the best performance with an AUC of 0.903 (95% CI, 0.802-1.000). Specifically, pre- and post-treatment TTP (OR=0.401/1.51, p=0.012/0.029) as well as age (OR=1.113, p=0.041) were independent predictors of treatment failure. The performance of this model was significantly higher (p=0.013) compared to a model that included only pre-treatment characteristics (baseline CT-perfusion, clinical parameters, and ASPECTS) with an AUC of 0.830 (95% CI, 0.699-0.961). Models without CT-perfusion parameters performed significantly worse with an AUC of 0.780 (95% CI, 0.642-0.918) when based on clinical/angiographic parameters and ASPECTS only (p=0.023).
Conclusion: CT-perfusion parameters obtained immediately after MT improve the treatment outcome prediction in patients with acute ischaemic stroke beyond baseline clinical/angiographic parameters, ASPECTS, and pre-treatment CT-perfusion parameters.
Limitations: The small patient sample and lack of multicentric data.
Ethics committee approval: Approval obtained prior to analysis.
Funding: No funding was received for this work.
Author Disclosures:
G. Brugnara: nothing to disclose
S. Nagel: nothing to disclose
M. Foltyn: nothing to disclose
P. Ringleb: nothing to disclose
U. Neuberger: nothing to disclose
M. Bendszus: nothing to disclose
M. Möhlenbruch: nothing to disclose
J. Pfaff: nothing to disclose
P. Kickingereder: nothing to disclose

RPS 1411b-3 11:37

Correlation of histopathologic thrombi composition with CT/CT angiography, stroke aetiology, and thrombolysis administration in patients with endovascular treatment of acute ischaemic stroke

A. Klepanec[1], J. Haring[1], J. Harsany[1], M. Mako[1], M. Hoferica[1], M. Durovka[1], I. Mrvová[1], P. Janega[2], G. Krastev[1]; [1]Trnava/SK, [2]Bratislava/SK
(andrej.klepanec@gmail.com)

Purpose: To evaluate the correlation between histopathologic thrombus composition, stroke aetiology, radiological findings on non-enhanced CT (NECT), and CT angiography (CTA) and thrombolysis administration in patients undergoing endovascular treatment of acute ischaemic stroke.
Methods and materials: From August 2017-July 2018, we prospectively collected thrombi extracted from 138 consecutive patients during endovascular treatment of acute ischaemic stroke. Histopathologic composition of red blood cells, thrombocytes with fibrin, and leukocytes in thrombi were evaluated with morphometric analysis. Correlation between histopathologic thrombus composition, stroke aetiology, radiological findings on NECT, and CTA and thrombolysis administration was performed. Statistical analysis was performed with GraphPad Prism version 8.2 software (GraphPad Software, La Jolla, California).
Results: There was a significant increase in thrombus density on NECT with the increase of erythrocytes composition (p=0.007) and a decrease of thrombocytes with fibrin composition in thrombus (p=0.008). There was a significant correlation between dense artery sign on NECT and stroke aetiology (p=0.002) with a significant increase of dense artery sign on NECT in patients with atrial fibrillation (p<0.0001). No correlation between thrombus composition and stroke aetiology was found. Thrombus density on NECT and CTAG was significantly associated with stroke aetiology (p=0.0002 and p=0.046). Bridging intravenous thrombolysis did not influence the composition of erythrocytes and thrombocytes with fibrin in extracted thrombi (p>005).
Conclusion: Increased thrombus density on NECT correlates with increased erythrocytes and decreased thrombocytes with fibrin composition. Patients with atrial fibrillation have a significant increase in dense artery sign on NECT. Systemic thrombolysis does not influence the histopathologic thrombus composition.
Limitations: A single-centre study.
Ethics committee approval: The study was approved by the local ethics committee.
Funding: No funding was received for this work.
Author Disclosures:
A. Klepanec: nothing to disclose
M. Durovka: nothing to disclose
I. Mrvová: nothing to disclose
P. Janega: nothing to disclose
G. Krastev: nothing to disclose
M. Hoferica: nothing to disclose
M. Mako: nothing to disclose
J. Haring: nothing to disclose
J. Harsany: nothing to disclose

RPS 1411b-4 11:43

Cost-effectiveness of thrombectomy for ischaemic stroke patients presenting beyond 6 hours of the last known-to-be-well based on the AURORA meta-analysis

W. G. Kunz, D. Puhr-Westerheide, M. Unterrainer, M. P. Fabritius, P. Reidler; *Munich/DE (wolfgang.kunz@med.lmu.de)*

Purpose: The AURORA meta-analysis (analysis of pooled data from randomised studies of thrombectomy more than 6 hours after last known-well) included patients that were randomised to endovascular thrombectomy (EVT) or to medical management (MM) presenting with large vessel occlusion stroke beyond 6 hours of symptom onset or last known-to-be-well. Based on 5 pooled trials, EVT showed clear clinical benefits. We aimed to determine the cost-effectiveness of EVT in this context.
Methods and materials: A decision model estimated lifetime costs and quality-adjusted life-years (QALY) associated with EVT or MM. The analysis was performed in a US setting from a societal perspective. Input parameters were based on the most recent and best available evidence, including pooled outcome data from 5 randomised trials. Probabilistic sensitivity analyses (PSA) were performed using 10,000 Monte Carlo simulations to estimate uncertainty. Incremental costs (IC), effectiveness (IE), and cost-effectiveness ratios (ICER) were derived.
Results: Based on outcome data of 458 patients randomised within the AURORA meta-analysis, the base-case analysis identified EVT as the strategy that resulted in incremental QALYs and cost-savings over the projected lifetime compared to MM (IC: -$17,902; IE: +1.71 QALYs; ICER: EVT dominant). Adjusting for all input parameter uncertainty in PSA, EVT was the preferred strategy with acceptability rates of >99.9% at all willingness-to-pay thresholds ranging from $10,000 to $150,000 per QALY. Simulations led to 94.46% dominant/cost-saving iterations.
Conclusion: EVT is projected to provide considerable long-term clinical benefit whilst also leading to considerable long-term cost-savings in the management of patients with large vessel occlusion stroke presenting beyond 6 hours of symptom onset or last known-to-be-well.
Limitations: The cost calculations were conducted in the United States and the absolute amount cannot be converted to other countries. Yet, the overall findings of considerable cost-savings associated with EVT in extended time windows can be assumed for other care settings.
Ethics committee approval: n/a
Funding: No funding was received for this work.
Author Disclosures:
W. G. Kunz: nothing to disclose
M. Unterrainer: nothing to disclose
P. Reidler: nothing to disclose
D. Puhr-Westerheide: nothing to disclose
M. P. Fabritius: nothing to disclose

RPS 1411b-5 11:49

Reasons for failed recanalisation in mechanical thrombectomy of the posterior circulation

C. Weyland, U. Neuberger, M. A. Möhlenbruch; *Heidelberg/DE (charlotte.weyland@med.uni-heidelberg.de)*

Purpose: Why does mechanical thrombectomy (MT) of the posterior circulation sometimes fail? Failed MT in the posterior circulation has not been investigated and leads to a fatal outcome in most cases, while reasons for failed MT in the anterior circulation have been recently well defined.
Methods and materials: In this retrospective analysis of an institutional review board-approved prospective stroke database in a comprehensive stroke centre, we compared patients with successful and failed MT of the posterior circulation from March 2009-April 2019 (group A: mTICI 0-1 vs group B: mTICI 2-3). Cases of failed recanalisation were further investigated for reasons of MT failure. Statistical analysis included univariate and multivariate analysis for investigating clinical or interventional predictors of MT failure.
Results: 225 patients were analysed (group A: 30 and group B: 195). Group A showed a significantly lower follow-up pASPECTS after MT, a higher NIHSS at discharge, and a higher mRS 90 days after the stroke onset. The main reasons for a failed recanalisation were futile vascular access, a failed passage of the occluded vessel, and complications after passing the occlusion. Stent-assisted PTA was an independent predictor for MT failure and played a decisive role in most of the failed MTs atherosclerosis.
Conclusion: For the first time, this study depicts futile vascular access, failed passage of the vessel occlusion, and interventional complications to be main reasons for recanalisation failure in MT of the posterior circulation.

Atherosclerosis and the struggle with stent-assisted PTA in the posterior circulation are, opposed to failed MT in the anterior circulation, the main sources of revascularisation failure.
Limitations: The mono-centre retrospective approach.
Ethics committee approval: n/a
Funding: No funding was received for this work.
Author Disclosures:
C. Weyland: nothing to disclose
U. Neuberger: nothing to disclose
M. A. Möhlenbruch: Board Member at Codman, Advisory Board at Medtronic, Advisory Board at Microvention, Advisory Board at Stryker

RPS 1411b-6 11:55
Quantitative analysis of iodine in multiphase CT angiography: a potential tool for diagnosing stroke
V. Fransson[1], H. Mellander[2], J. Wasselius[2], K. Ydström[3]; [1]Lund/SE, [2]Malmö/SE, [3]Höör/SE (veronica.fransson@skane.se)

Purpose: Can quantitative measurements in vascular territories of the brain in multiphase CT angiography (MP-CTA) provide the same information as CT-perfusion (CTP) and be used to identify ischaemic regions after cerebral stroke?
Methods and materials: Patients were included on the basis of having undergone MP-CTA and CTP on a local dual-energy CT on suspicion of cerebral stroke. Another criteria was for the spectral-based images to be available for retrospective analysis. 9 patients were found, 5 without detected perfusion deficits on CTP and 4 with. Iodine density and HU, corresponding to a conventional 120 kV image and to a virtual mono-energetic image using 40 keV-photons, were measured in vascular territories of the brain for all phases of the MP-CTA exam and in the non-contrast CT. Iodine density and HU were plotted as functions of the imaged phase. The plots were evaluated by comparing the left and right hemispheres. Delayed arrival of the contrast material was deemed indicative of ischaemia. These results were then compared to the results of the CTP in order to see if a correlation could be found.
Results: Patients without detected perfusion deficits displayed little or no difference between hemispheres. Patients with perfusion deficits showed signs of ischaemia in some or all regions as the CTP. Iodine density generated a larger separation between healthy and ischaemic tissue than HU.
Conclusion: Quantitative analysis of MP-CTA shows the potential for being able to provide the same information as the CTP. Measurements performed on iodine density, instead of HU, generated a larger separation between sick and healthy tissue making it a more sensitive method.
Limitations: The limited patient material and data acquisition based on vendor-specific software.
Ethics committee approval: This study was approved by the ethics committee.
Funding: No funding was received for this work.
Author Disclosures:
V. Fransson: Author at Skåne University Hospital, Speaker at Skåne University Hospital
H. Mellander: nothing to disclose
J. Wasselius: nothing to disclose
K. Ydström: nothing to disclose

RPS 1411b-7 12:01
Automated cerebral attenuation measurements on single-phase CT angiography in stroke: a replacement for CT-perfusion?
P. Reidler, D. Puhr-Westerheide, M. P. Fabritius, L. Rotkopf, S. Maurus, D. Apel, T. Liebig, W. G. Kunz; *Munich/DE*

Purpose: To address the performance of automated attenuation measurements on CT angiography source images (CTASI) to detect ischaemic areas, the infarction core, and predict the final infarction in acute ischaemic stroke.
Methods and materials: In a retrospective analysis, we used software-based automated segmentation and Hounsfield unit (HU) measurements for all regions of the Alberta stroke program early CT score (ASPECTS) on CTASI in patients with large-vessel-occlusion (LVO) stroke. To normalise the values, we calculated relative HU (rHU) as a ratio of the affected/unaffected hemisphere. For the classification of ischaemic areas, the regional ischaemic core, and final infarction by rHU-values, we used simultaneously acquired CTP-data and follow-up imaging as a ground truth. Receiver-operating-characteristics analysis was performed to calculate the area-under-the-curve (AUC).
Results: 79 patients were included. rHU-values presented a significant classification of ischaemic involvement in all 10 regions of the ASPECTS with AUC from 0.72-0.99 ($p<0.001$, except M4-cortex $p=0.002$). Classification of the ischaemic core resulted in lower AUC values (0.55-0.87), however, it still provided a significant classification for all regions except M3- and M5-cortex. The final infarction was predicted with AUC values from 0.65-0.85, significant in all regions except M3- and M5-cortex.
Conclusion: Automated attenuation measurements on CTASI present an excellent performance in detecting ischaemic regions in LVO stroke patients. Significant classification of the regional ischaemic core and the prediction of the final infarction was able for most ASPECTS regions. This technique has the potential for stroke imaging triage and to reduce the use of CTP.
Limitations: The small study sample, the use of only one CT vendor (Siemens), and the global variability of CTA protocols.
Ethics committee approval: The study was approved by the IRB according to the declaration of Helsinki.
Funding: No funding was received for this work.
Author Disclosures:
P. Reidler: nothing to disclose
D. Puhr-Westerheide: nothing to disclose
M. P. Fabritius: nothing to disclose
W. G. Kunz: nothing to disclose
D. Apel: nothing to disclose
L. Rotkopf: nothing to disclose
S. Maurus: nothing to disclose
T. Liebig: nothing to disclose

RPS 1411b-8 12:07
Artificial intelligence in stroke: evaluating the automated scoring of collaterals in acute stroke on computed tomography scans
M. Politi[1], A. Podlasek[2], R. Namias[2], S. Gerry[2], O. Joly[2], G. Harston[2], P. Papanagiotou[3], I. Q. Q. Grunwald[4]; [1]Athens/GR, [2]Oxford/UK, [3]Bremen/DE, [4]Chelmsford/UK (mariapoliti@hotmail.com)

Purpose: Computed tomography angiography (CTA) collateral scoring can identify patients most likely to benefit from mechanical thrombectomy and more likely to have good outcomes.
Our purpose was to generate an e-CTA collateral score (CTA-CS) for patients eligible for thrombectomy.
Methods and materials: A machine learning approach categorised collateral flow in 98 patients who received mechanical thrombectomy and generated an e-CTA collateral score (CTA-CS) for each patient. 3 experienced neuroradiologists (NRs) estimated the CTA-CS, first without and then with knowledge of the e-CTA output, before finally agreeing on a consensus score.
Results: e-CTA improved the intraclass correlation coefficient (ICC) between neuroradiologists from 0.58 (0.46-0.67) to 0.77 (0.66-0.85, $p=0.003$). e-CTA, without NR input, agreed with the consensus score in 90% of scans with the remaining 10% within 1 point of the consensus (ICC 0.93, 0.90-0.95). Sensitivity and specificity for identifying favourable collateral flow (collateral score 2-3) were 0.99 (0.93-1.00) and 0.94 (0.70-1.00), respectively.
Conclusion: e-CTA provides a real-time and fully automated approach to collateral scoring with the potential to independently quantify collateral scores even without expert rater input.
Limitations: The CTA-CS was generated under experimental conditions by specialist NRs without the time pressures of real-world clinical scenarios. In many healthcare settings, ready access to specialist neuroradiology input is not available. As such, the benefit of an automated e-CTA score may be greater than demonstrated here. Although NRs in this study were blinded to clinical data, all patients had a confirmed stroke and large vessel occlusion, knowledge of which was available to the expert scorers.
Ethics committee approval: The Freiburg ethics commission granted approval for the study (0171140).
Funding: e-STROKE SUITE, Brainomix Ltd., Oxford, UK.
Author Disclosures:
M. Politi: nothing to disclose
R. Namias: nothing to disclose
I. Q. Q. Grunwald: Consultant at Brainomix
S. Gerry: nothing to disclose
G. Harston: Employee at Brainomix
O. Joly: Consultant at Brainomix
P. Papanagiotou: nothing to disclose
A. Podlasek: nothing to disclose

RPS 1411b-9 12:13
Clinical decision support for visual ASPECTS cut-off values in patient selection for guideline-compliant thrombectomy using automated quantification of attenuation changes
D. Puhr-Westerheide, P. Reidler, S. Tiedt, L. Rotkopf, M. P. Fabritius, P. D. L. Kellert, F. Dorn, F. A. Wollenweber, W. G. Kunz; *Munich/DE (daniel.puhr-westerheide@med.uni-muenchen.de)*

Purpose: Large vessel occlusion (LVO) stroke leads to variable attenuations in ASPECTS regions on non-contrast CT (NCCT). Current guidelines recommend thrombectomy for patients with visually-assessed ASPECTS≥6 in the early time window. Our aim was to test the diagnostic performance of an automated assessment of regional hypoattenuation to identify evidence-based ASPECTS cut-off values for thrombectomy.
Methods and materials: We included 200 patients with an LVO stroke of the anterior circulation undergoing NCCT on admission. To ensure unbiased attenuation measurements, patients with prior contrast administration, prior

infarction, or pre-existing cerebral lesions were excluded. The ASPECTS was visually determined by two expert readers in consensus. An automated software tool was used to calculate the relative Hounsfield unit (rHU) values for ASPECTS regions compared to the non-ischaemic hemisphere. A composite rHU-ASPECTS, a score incorporating rHU from all regions, was used for comparison with the visually-assessed ASPECTS in regression analysis and receiver-operating-characteristics analysis.
Results: The median age was 74 years, median ASPECTS was 8 (IQR: 7-10), and 176 patients (88%) had an ASPECTS ≥6. We found a strong association of composite rHU-ASPECTS with visual ASPECTS in univariate regression (b=-0.560, p<0.001). Visually-rated early ischaemic signs in ASPECT regions were correctly identified by rHU values for all regions except the M1, M3, and M4. The highest discriminative value was found in the lentiform nucleus (AUC=0.892, p<0.001), the internal capsule (AUC=0.813, p<0.001), the caudate nucleus (AUC=0.779, p<0.001), and the insular cortex (AUC=0.776, p<0.001). The composite rHU-ASPECTS showed a high discriminative value for the identification of patients with ASPECTS<6 (AUC=0.779, p<0.001).
Conclusion: Automated assessment of regional hypoattenuations identified expert-classified visual ASPECTS cut-off values and may serve as a method to standardise stroke patient selection for thrombectomy.
Limitations: The retrospective, single-centre design.
Ethics committee approval: n/a
Funding: No funding was received for this work.
Author Disclosures:
D. Puhr-Westerheide: nothing to disclose
P. Reidler: nothing to disclose
S. Tiedt: nothing to disclose
L. Rotkopf: nothing to disclose
M. P. Fabritius: nothing to disclose
P. D. L. Kellert: nothing to disclose
F. A. Wollenweber: nothing to disclose
F. Dorn: nothing to disclose
W. G. Kunz: nothing to disclose

RPS 1411b-10 12:19
The effect of different thresholds for CT-perfusion volumetric analysis on estimated ischaemic core and penumbral volumes
S. O. Karhi[1], O. I. Tähtinen[2], J. Aherto[1], H. P. Matikka[1], H. Manninen[1], O. Nerg[1], M. Taina[1], P. Jäkälä[1], R. Vanninen[1]; [1]Kuopio/FI, [2]Tampere/FI *(simkar@student.uef.fi)*

Purpose: This retrospective single-centre study compared three threshold settings for automated analysis of the ischemic core (IC) and penumbral volumes using computed tomographic perfusion (CTP) and their accuracy for predicting final infarct volume (FIV) in patients with anterior circulation acute ischaemic stroke (AIS).
Methods and materials: 52 consecutive AIS patients undergoing mechanical thrombectomy (November 2015–March 2018) were included. Perfusion images were retrospectively analysed using a single CT neuro perfusion application (syngo.via 4.1, Siemens Healthcare GmbH). 3 threshold values (S1–S3) were derived from another commercial package (RAPID; iSchema View) (S1), up-to-date syngo.via default values (S2), and adapted values for syngo.via from a reference study (S3). The results were compared with FIV determined by follow-up non-contrast CT.
Results: The median IC volume (mL) was 24.6 (interquartile range: 13.7-58.1), with S1 and 30.1 (20.1-53.1) with S2/S3. After removing the contralateral hemisphere from the analysis, the median IC volume decreased by 1.33 (0-3.14), with S1 versus 9.13 (6.24-14.82) with S2/S3. The median penumbral volume (mL) was 74.52 (49.64-131.91), 77.86 (46.56-99.23), and 173.23 (125.86-200.64) for S1, S2, and S3, respectively. Limiting the analysis to the affected hemisphere, the penumbral volume decreased by 1.6 (0.13-9.02), 19.29 (12.59-26.52), and 58.33 mL (45.53-74.84) for S1, S2, and S3, respectively. The correlation between IC and FIV was highest in patients with successful recanalisation in <113 min (r=0.881 for S1; r=0.877 for S2/S3).
Conclusion: Optimising threshold settings significantly improves the accuracy of the estimated IC and penumbral volumes. International consensus guidelines based on larger multicentre studies should be established to support the standardisation of volumetric analysis in clinical decision-making.
Limitations: The small patient population and CTP brain coverage limited to 10 cm leading to potential underestimation of IC or penumbral volume.
Ethics committee approval: Approved by the Hospital Research Ethics Board.
Funding: Governmental funding from the Hospital Research Commission.
Author Disclosures:
S. O. Karhi: nothing to disclose
O. I. Tähtinen: nothing to disclose
H. P. Matikka: nothing to disclose
H. Manninen: nothing to disclose
O. Nerg: nothing to disclose
M. Taina: nothing to disclose
P. Jäkälä: nothing to disclose
R. Vanninen: nothing to disclose
J. Aherto: nothing to disclose

RPS 1411b-11 12:25
Virtual monoenergetic dual-energy CT reconstructions at 80 keV are optimal for early stroke detection
D. Dodig[1], S. Kovacic[1], Z. Matana Kaštelan[1], N. Bartolovic[1], S. Jurkovic[1], D. Miletic[1], Z. Rumboldt[2]; [1]Rijeka/HR, [2]Charleston, SC/US *(doris_5na5@yahoo.com)*

Purpose: Virtual monoenergetic (VM) dual-energy CT (DECT) imaging enables grey-to-white matter contrast-to-noise ratio optimisation, potentially increasing the visibility of ischaemic brain oedema. The aim of our study was to compare the diagnostic accuracy of early stroke detection on VM to weighted average (WA) reconstructions.
Methods and materials: Consecutive patients with brain DECT scanned within 12 hours of stroke symptom onset were prospectively included in the study. Patients having had other significant brain pathology were excluded. Two neuroradiologists evaluated in consensus WA and VM reconstructions (from 40 to 190 keV at 10 keV increments) for early stroke signs on a 4-point Likert scale: 1=stroke definitely present, 2=stroke probably present, 3=probably no stroke, and 4=definitely no stroke. A follow-up CT and/or MRI served as the standard of reference. Statistical evaluation was performed by ROC analysis.
Results: 44 patients (73%) developed stroke and 16 (27%) had no signs of a stroke on follow-up imaging. Ischaemic brain oedema detection was significantly more accurate on VM reconstructions at 80 keV compared to WA images with AUC 0.784 (95% CI 0.710, 0.858) and 0.685 (95% CI 0.588, 0.781), respectively (p=0.0339).
Conclusion: VM reconstructions at 80 keV are superior to polychromatic images for early stroke detection and are recommended for standard clinical protocol.
Limitations: Follow-up imaging served as the standard of reference, however, elapsed time and received treatment could have significantly influenced changes in brain pathology, thus making the comparison with initial brain DECT uncertain. Concurrent DWI MRI imaging would have been the preferred gold standard.
Ethics committee approval: Institutional review board approved this study. Informed consent was waived.
Funding: No funding was received for this work.
Author Disclosures:
D. Dodig: nothing to disclose
Z. Matana Kaštelan: nothing to disclose
S. Kovacic: nothing to disclose
S. Jurkovic: nothing to disclose
D. Miletic: nothing to disclose
Z. Rumboldt: nothing to disclose
N. Bartolovic: nothing to disclose

11:15 - 12:30 **Room M 3**

Oncologic Imaging

RPS 1416b

Multiple myeloma and lymphoma: advanced imaging and radiomics

Moderators:
O. A. Westerland; London/UK
N.N.

RPS 1416b-2 11:21
An MRI-DWI visual scale for tumour response evaluation in lymphomas
S. Kharuzhyk, E. Zhavrid, A. Dziuban; *Minsk/BY (skharuzhyk@nld.by)*

Purpose: To develop an MRI-DWI visual scale for tumour response evaluation in lymphomas and to compare its effectiveness with the PET/CT Deauville scale.
Methods and materials: The study included 97 patients with lymphoma. Post-treatment whole-body MRI-DWI was interpreted using a 5-level scale: 1=all lymph nodes (LNs) ≤1 cm in short-axis size with no extra lymphatic lesions, 2=LNs >1 cm and extra lymphatic organ lesions with signal intensity (SI)>muscles on ADC maps with no bone marrow (BM) lesions, 3=LNs >1 cm and organ lesions with SI equal to muscles on ADC maps with no BM lesions, 4=LNs >1 cm and/or organ lesions with SI<muscles on ADC maps and/or BM lesions, and 5=increase of lesions size and/or appearance of new lesions. Post-treatment PET/CTs were interpreted using a 5-level Deauville scale. Treatment response was classified as complete (CR, scores 1-3) or non-complete (NCR,

scores 4-5). Progression-free survival (PFS) and overall survival (OS) were compared in patients with CR and NCR.
Results: The number of chemotherapy courses was 3-8. According to MRI-DWI, 85 patients achieved CR and 12 NCR, PET/CT 75 and 22, respectively. The tumour response category coincided in 83 (86%) patients. 2-year PFS in patients with MRI-DWI CR and NCR was 87% and 22% (p=0.0), 3-year OS 93% and 64% (p=0.003), respectively. 2-year PFS in patients with PET/CT CR and NCR was 89% and 46% (p=0,0), 3-year OS 92% and 75% (p=0.013), respectively.
Conclusion: A simple MRI-DWI visual scale for tumour response evaluation in lymphomas was proposed. A high concordance with the PET/CT Deauville scale was demonstrated. The proposed MRI-DWI scale may be used as a non-irradiative alternative to the Deauville scale.
Limitations: n/a
Ethics committee approval: n/a
Funding: No funding was received for this work.
Author Disclosures:
S. Kharuzhyk: nothing to disclose
E. Zhavrid: nothing to disclose
A. Dziuban: nothing to disclose

RPS 1416b-3 11:27
The correlation between shear-wave velocity in newly diagnosed lymphomas and the degree of intra-tumoural fibrosis: a proof of principle
K. Ekert, H. Bösmüller, M. Horger*; Tübingen/DE*

Purpose: To evaluate the role of shear-wave elastography for the potential characterisation of lymphoma subtypes through a comparison to the amount of intra-tumoural collagen.
Methods and materials: This was a prospective study including 24 patients (age 56.26 years, range, 17.95-83.39; 7 females) with histologically proven lymphomas who underwent shear-wave elastography and Masson-Trichrome staining of tumour tissue. Ultrasound-guided biopsies and ARFIs were performed in the same involved node in one session. A mean of 7.3 (range, 5-8) measurements quantifying the mean shear-wave velocity (SWV) (m/s) elasticity of lymphoma tissue were measured. The patients belonged to 3 larger groups of Hodgkin's lymphoma (HL), follicular lymphoma (FL), and diffuse large B-cell lymphomas (DLBCL). The amount of collagen contained in the tumours was quantified by Masson-Trichrome staining.
Results: The mean and max SWV in our patient series were 3.35 (±0.23) m/s and 5.98 m/s. In the subgroup of HL, the mean and max SWV were 3.17 (±0.31) m/s and 4.53 m/s, in the subgroup of FL they were 2.84 m/s (±0.88) and 3.98 m/s, and in DLBCLs, 4.72 (±0.85) m/s and 5.98 m/s were measured, respectively. The corresponding mean percentage of collagen was 20.0% (±20.0) for HL, 22.0% (±10.2) for FL, and 14.6% (±12.7) for DLBCL. SWV-values correlated significantly with the amount of collagen in the tissue both in the entire patient series (p<0.001) as well as in differentiating DLBCL from HL (p=0.01) and FL (p=0.006).
Conclusion: Shear-wave velocity in lymphomas correlates with the amount of collagen, in particular, in DLBCL and could be used for tumour characterisation and differentiation.
Limitations: The small cohort size. However, it is continuously growing.
Ethics committee approval: The ethics committee approved this study.
Funding: No funding was received for this work.
Author Disclosures:
K. Ekert: nothing to disclose
M. Horger: nothing to disclose
H. Bösmüller: nothing to disclose

RPS 1416b-4 11:33
The influence of the MRI protocol on staging smoldering multiple myeloma patients according to the new SLIM–CRAB criteria
M. Wennmann[1], L. Kintzelé[1], T. Hielscher[1], G. Langs[2], M. Piraud[3], H.-U. Kauczor[1], J. Hillengass[4], B. Menze[3], M.-A. Weber[5]; *[1]Heidelberg/DE, [2]Vienna/AT, [3]Munich/DE, [4]Buffalo/US, [5]Rostock/DE*

Purpose: To investigate the spatial distribution of focal lesions (FLs) in whole-body MRI (wb-MRI) in smoldering multiple myeloma (SMM) patients and consequently the influence of the field of view of MRI (spinal vs wb) for upstaging SMM patients to multiple myeloma requiring systemic therapy according to the new SLIM-CRAB criterion ">1FL in MRI".
Methods and materials: The cohort consisted of 63 patients with overall 220 wb-MRI during follow-up and at least semiannual clinical follow-up until progression or for at least 3 years. All included wb-MRIs were performed on one of two identical 1.5 Tesla MRI systems at our site. Details on the wb-MRI protocol have been published before.
Results: In 23/220 wb-MRI cases, >1FL was apparent in spinal imaging, resulting in an indication for therapy regardless of further findings when wb-imaging was completed. When no FL was apparent in spinal imaging, only 16/171 cases revealed >1FL in wb-imaging. In 26 cases where 1 FL was revealed in spinal MRI, 12 showed >1FL when imaging was extended to wb-MRI.
Conclusion: When wb-MRI is not diagnostic standard in staging SMM patients due to time, cost, or technical restrictions, and spinal MRI is performed instead, the protocol for the subgroup of patients with 1 FL in the spine should be extended to wb-MRI, as half of these patients reveal >1FL in wb-MRI with the consequence of indication for systemic therapy according to the new SLIM-CRAB-criteria.
Limitations: The retrospective study design and the limited case number.
Ethics committee approval: This study was approved by the institutional ethics committee with a waiver of informed consent.
Funding: The Deutsche Forschungsgemeinschaft (DFG; WE 2709/3-1 and ME 3511/3-1) and the Austrian Science Fund (FWF; I2714-B31).
Author Disclosures:
M. Wennmann: nothing to disclose
L. Kintzelé: nothing to disclose
T. Hielscher: nothing to disclose
G. Langs: nothing to disclose
M. Piraud: nothing to disclose
H.-U. Kauczor: nothing to disclose
J. Hillengass: Advisory Board at Amgen, BMS, Celgene, Janssen, Novartis, Takeda, Consultant at Amgen, Celgene, Research/Grant Support at Celgene, Sanofi, Other at Travel Support: Amgen, BMS, Celgene, Janssen, Novartis, Takeda; Honoraria: Amgen, BMS, Celgene, Janssen, Novartis, Takeda
B. Menze: nothing to disclose
M.-A. Weber: nothing to disclose

RPS 1416b-5 11:39
Radiogenomics in multiple myeloma
N. de Vos, J. C. Dutoit, M. Behaeghe, T. van Den Berghe, P. Vlummens, K. L. A. Verstraete*; Ghent/BE (devos.nicolas90@gmail.com)*

Purpose: To study the association between magnetic resonance imaging (MRI) features and genetic abnormalities in patients newly diagnosed with smouldering multiple myeloma (SMM) or multiple myeloma (MM).
Methods and materials: This retrospective study included 26 patients with a new diagnosis of SMM or MM. Patients underwent whole-body MRI (conventional MRI, diffusion-weighted imaging (DWI), and/or dynamic contrast-enhanced MRI (DCE)) from January 2016-October 2019. Extensive genomic testing (array comparative genomic hybridisation (array CGH), copy number variation sequencing (CNV sequencing), and/or fluorescence in situ hybridisation (FISH)) was performed within 2 months of the whole-body MRI. Fisher's exact test was used to test for non-random associations between MR imaging features and genomic abnormalities.
Results: 26 patients were included (women/men 14/12, mean age±standard deviation 63±10 years, range 41-77). 15 patients were diagnosed with SMM (58%), while 11 patients were diagnosed with MM (42%). 13 patients (50%) had focal lesions. In patients with focal lesions, favourable genetics (hyperdiploidy) were more common than in patients without focal lesions (p<0.05). In patients without focal lesions, unfavourable genetics (hypodiploidy) were more common than in patients with focal lesions (p<0.05). No statistically significant differences in genetic abnormalities were found in patients with increased diffusion restriction or steep first-pass enhancement (p>0.05).
Conclusion: In patients with a new diagnosis of SMM or MM, unfavourable genetics (hypodiploidy) are more common in patients without focal lesions, while favourable genetics (hyperdiploidy) are more common in patients with focal lesions.
Limitations: A retrospective monocentric study with a limited number of patients.
Ethics committee approval: The study was approved by the institutional review board of the Ghent University Hospital.
Funding: No funding was received for this work.
Author Disclosures:
T. van Den Berghe: nothing to disclose
N. de Vos: nothing to disclose
K. L. A. Verstraete: nothing to disclose
J. C. Dutoit: nothing to disclose
M. Behaeghe: nothing to disclose
P. Vlummens: nothing to disclose

RPS 1416b-6 11:45
Magnetic resonance imaging in multiple myeloma: a focus on hip and proximal femur bone lesions and the MY-RADS score
F. Rossi, A. Dominietto, L. Torri, P. Francaviglia, G. Succio, A. Conte, S. Gualco, A. Tagliafico*; Genoa/IT (federossi0590@gmail.com)*

Purpose: Multiple myeloma (MM) is a haematological malignancy characterised by the clonal proliferation of plasma cells that determines bone lesions with different patterns of involvement. Due to prolonged corticosteroid therapy, MM patients have an increased risk of pathological fractures and osteonecrosis of

the proximal femur. According to the Durie & Salmon PLUS criteria and new MY-RADS score, MRI is of prognostic relevance to evaluate the disease extent (medullary and extra-medullary lesions).
Methods and materials: We reviewed MRI data from January 2018-August 2019 of n=52 patients (29 men and 23 women; mean age 65±13years) with MM at the level of the hip (including the proximal femur). Hip lesions have been classified according to the MY-RADS score and lesion characteristics in a diffuse pattern, focal pattern, mixed pattern, osteonecrosis, and pathological fractures. Descriptive statistical analysis was performed to summarise the dataset.
Results: Among the 52 selected MM patients, a total of n=40 (40/52; 77%) reported at least one hip lesion, n=10 patients at least two hip lesions (10/52; 20%), and n=2 (2/52; 3%) subjects had no lesions. According to hip lesions classification, n=6 osteonecrosis of the femoral head, n=26 diffuse pattern, n=10 focal pattern, n=15 mixed pattern, and n=5 pathological fractures were observed. Intra and interobserver agreement of MY-RADS score were 0.78 and 0.65, respectively.
Conclusion: MRI detects bone lesions in the hip and proximal femur in 97% of patients. In n=11/52, 21% of patients, a surgical consult was necessary. MRI allows the differentiation of bone pattern involvement in MM, which is useful for risk stratification using the MY-RADS score.
Limitations: The retrospective nature of the study and relatively small number of patients.
Ethics committee approval: The retrospective study protocol was approved by our institutional review board.
Funding: No funding was received for this work.
Author Disclosures:
F. Rossi: nothing to disclose
A. Dominietto: nothing to disclose
L. Torri: nothing to disclose
P. Francaviglia: nothing to disclose
G. Succio: nothing to disclose
A. Conte: nothing to disclose
S. Gualco: nothing to disclose
A. Tagliafico: nothing to disclose

RPS 1416b-7 11:51

An increased bone mineral density as an adverse prognostic factor in patients with systemic mastocytosis

J. Krammer, M. Jawhar, W.-K. Hofmann, S. O. Schönberg, A. Reiter, P. Riffel; *Mannheim/DE (philipp.riffel@umm.de)*

Purpose: Systemic mastocytosis (SM) is characterised by the expansion of clonal mast cells that infiltrate various organ systems. The extent of organ infiltration and subsequent organ damage distinguishes between indolent SM (ISM, nearly normal life expectancy) and advanced SM (AdvSM, poor prognosis). In ISM patients, the measurement of the bone mineral density (BMD) frequently reveals osteoporosis. In contrast, the association between increased BMD and osteosclerosis, respectively, and the various SM subtypes is unclear.
Methods and materials: BMD values in 61 patients (ISM, n=29, 48%; AdvSM, n=32, 52%) were correlated with clinical parameters and prognosis. Osteoporosis was defined as a BMD T-score of ≤-2.5 SD. Increased BMD and osteosclerosis were defined as a Z-score of >1 SD and >2 SD, respectively.
Results: Osteoporosis was detected in 11/29 (38%) patients with ISM and 2/32 (6%) patients with AdvSM (p=0.004). Osteosclerosis was only detected in AdvSM patients (16/32, 50%). AdvSM patients with an increased BMD had higher levels of bone marrow mast cell infiltration, serum tryptase, and alkaline phosphatase (p<0.05). Consequently, the prognosis of AdvSM patients with increased BMD was significantly inferior compared to those without increased BMD.
Conclusion: Osteoporosis is a common feature in ISM. Increased BMD is frequent in AdvSM but not in ISM patients, while osteosclerosis is restricted to AdvSM patients. Elevated BMD is associated with a more aggressive phenotype and inferior survival.
Limitations: Disease duration could not be determined reliably because some patients were not able to recall the start of their symptoms and the exact timing of their disease diagnosis.
Ethics committee approval: The requirement of informed patient consent was waived by the institutional review board as this is a retrospective study. The study was performed in compliance with HIPAA guidelines.
Funding: No funding was received for this work.
Author Disclosures:
P. Riffel: nothing to disclose
J. Krammer: nothing to disclose
S. O. Schönberg: nothing to disclose
M. Jawhar: nothing to disclose
A. Reiter: nothing to disclose
W.-K. Hofmann: nothing to disclose

RPS 1416b-8 11:57

Prognostic value of whole-body low-dose CT (WBLDCT) in the staging and restaging of patients with multiple myeloma (MM): a long period follow-up

T. P. Giandola[1], D. Ippolito[1], M. Ragusi[1], M. Porta[2], C. Maino[1], C. R. G. L. Talei Franzesi[3], S. Sironi[4]; *[1]Monza/IT, [2]Senago/IT, [3]Milan/IT, [4]Bergamo/IT (t.giandola@hotmail.it)*

Purpose: To evaluate, with WBLDCT, the prognostic features of bone marrow involvement and behaviour in patients with MM during a long follow-up period considering the dimensional parameter of bone lesions and according to the different infiltration pattern of disease.
Methods and materials: 100 patients with a clinical diagnosis of MM that underwent unenhanced WBLDCT scans followed during a long period (3-7 years) were enrolled in this study. WBLDCT was performed on 256-slice scanner with a tube voltage of 120kV and a tube current-time product of 40mAs. The whole skeleton was divided into 5 anatomic districts (the skull, spine sternum and ribs, pelvis, and upper/lower limbs) and evaluated in terms of infiltration pattern (focal, diffused, and combined) and the distribution of the disease. Moreover, the osteolytic bone lesions were categorised according to the maximum axial diameter (MAD), having 10 mm as the cut-off value.
Results: 63% of patients presented with the focal pattern, 22% had the diffuse pattern, and 15% had the combined pattern.
During follow-up, when considering the cut-off value >10 mm in MAD, 86 (82%)/105 analysed lytic lesions remained dimensionally unchanged, 11% showed a dimensional increase, and 7% showed a dimensional decrease.
59 patients with a lytic/combined pattern presented with multifocal lytic lesions with a MAD <10 mm and among them, 88% of the patients presented a dimensional stability of the lytic lesions, 2% showed a dimensional decrease of their lesions, and only 10% had a minimal dimensional increase (average of 5 mm) of the lytic lesions.
In patients with the diffuse pattern (38%), neither a modifications of the pattern nor a development of focal lytic lesions occurred during the follow-up.
Conclusion: WBLDCT represents a reliable imaging-based tool for the proper management of MM patients, which is useful to define the behaviour of different bone involvement, showing that the diffuse form of small lytic lesions (<10 mm) deserve less frequent follow-up.
Limitations: n/a
Ethics committee approval: n/a
Funding: No funding was received for this work.
Author Disclosures:
T. P. Giandola: nothing to disclose
D. Ippolito: nothing to disclose
M. Ragusi: nothing to disclose
C. R. G. L. Talei Franzesi: nothing to disclose
M. Porta: nothing to disclose
C. Maino: nothing to disclose
S. Sironi: nothing to disclose

RPS 1416b-9 12:03

The role of computed tomography texture analysis using dual-energy-based bone marrow imaging for multiple myeloma characterisation: a comparison with histology and established serologic parameters

C. P. Reinert, E. Krieg, M. Esser, K. Nikolaou, M. Horger; *Tübingen/DE (christian.reinert@med.uni-tuebingen.de)*

Purpose: To identify textural features on dual-energy CT (DECT) bone marrow images in multiple myeloma which correlate with the degree of medullary involvement assessed by histology and myeloma-related serologic parameters.
Methods and materials: 56 patients (63.9±11.8y) who underwent unenhanced DECT were evaluated. All patients had a bone marrow biopsy and current serum levels of immunoglobulins and serum-free light chains (SFLC). Using DECT post-processing, bone marrow images were reconstructed. The vertebral bodies T10-L5 were segmented for quantification of 1st, 2nd, and higher-order textural features based on a pyradiomics library, which were compared between myeloma stages, serologic parameters, and the presence/absence of osteolyses. Absolute values of textural features were correlated with the degree of bone marrow infiltration.
Results: 1st order features were higher in patients with stage 2/3 compared to stage 1 (p<0.02), whereas the 2nd order feature "GLCM cluster prominence" was lower (p<0.04). The 1st order "entropy", 2nd order GLCM features, and the higher-order "GLRLM high grey-level run emphasis" were lower in patients with elevated SFLC or pathological kappa/lambda ratios (p<0.03). In contrast, "GLRLM run variance" was higher (p<0.03), which was also observed in patients with osteolyses (p<0.007). The degree of bone marrow infiltration was positively correlated with 1st order features (e.g. "uniformity"; r_P=0.49; p<0.0001), whereas "entropy" and GLCM features were negatively correlated (e.g. "difference entropy"; r_P=-0.54; p<0.0001).
Conclusion: CT-textural features applied on non-calcium bone marrow images correlate well with myeloma-related serologic parameters and histology, showing a more uniform tissue structure with increasing medullary infiltration and

could be used as an additional imaging biomarker for the non-invasive assessment of medullary involvement.
Limitations: A retrospective study.
Ethics committee approval: Approved by the review board.
Funding: No funding was received for this work.
Author Disclosures:
C. P. Reinert: nothing to disclose
E. Krieg: nothing to disclose
K. Nikolaou: Speaker at Siemens, Bayer, Bracco, Advisory Board at Siemens, Bayer, Bracco
M. Horger: Speaker at Siemens Healthineers, Advisory Board at Siemens Healthineers
M. Esser: nothing to disclose

RPS 1416b-10 12:09

Advantages of whole-body diffusion-weighted MRI (WBMRI) versus whole-body low-dose CT in young patients affected by multiple myeloma (MM): a retrospective analysis

F. Castagnoli[1], A. Villanacci[1], V. Angelini[2], A. Belotti[1], B. Frittoli[1], L. Grazioli[1];
[1]Brescia/IT, [2]Naples/IT (francy-cast@hotmail.it)

Purpose: To compare CT and WBMRI in staging and follow-up during and post-therapy in young MM patients.
Methods and materials: From September 1, 2018-July 31, 2019, 219 WBMRI were performed with a Magnetom Aera 1.5T (Siemens Healthcare, Erlangen, Germany) using established protocols.
We reviewed 121 exams (89 patients, median age: 58.3). All had a histological report by bone marrow biopsy and a low-dose CT was performed.
Results: In 28/89 patients, we found a diffuse infiltration pattern at WB-DWI defined as hyperintensity in STIR sequences, hypointensity T1, and signal restriction in DWI of the spongy vertebral body. In 26 cases, the diagnosis was confirmed by a histological bone marrow report, with 2 false-positives and high concordance between the two methods. The plasma cell infiltration rate did not correlate with the grade of signal restriction on DWI. Instead, the DWI/ADC values correlated with the response to therapy.
In 43/89 patients (48.3%), the WBMRI protocol showed extraskeletal findings (benign and malignant) that previous CT-staging did not report; some of them (3 breast cancer, 4 prostatic cancer, 1 renal cell carcinoma, 1 HCC, 1 colon cancer, and 1 jugular thrombosis) changed the clinical treatment.
Conclusion: WBMRI is a functional imaging technique comprising anatomical and functional sequences with an emerging role in the management of MM patients. It allows highly sensitive detection of diffuse bone marrow infiltration patterns and focal lesions according to the International Myeloma Working Group Consensus Reccomandation (June 2019).
In our study, we found that, when available, WBMRI should be the first choice in young patients with MM to avoid radiation exposure.
Limitations: A retrospective study.
Ethics committee approval: n/a
Funding: No funding was received for this work.
Author Disclosures:
F. Castagnoli: nothing to disclose
A. Villanacci: nothing to disclose
V. Angelini: nothing to disclose
B. Frittoli: nothing to disclose
L. Grazioli: nothing to disclose
A. Belotti: nothing to disclose

RPS 1416b-11 12:15

The diagnostic efficacy of whole-body low-dose CT in the staging of patients with multiple myeloma compared to whole-body magnetic resonance imaging

T. P. Giandola[1], D. Ippolito[1], M. Ragusi[1], M. Porta[2], C. Maino[1],
C. R. G. L. Talei Franzesi[3], S. Sironi[4]; [1]Monza/IT, [2]Senago/IT, [3]Milan/IT,
[4]Bergamo/IT (t.giandola@hotmail.it)

Purpose: To compare the diagnostic efficacy of whole-body low-dose CT (WBLDCT) with whole-body magnetic resonance imaging (WBMRI) in the evaluation of bone marrow involvement and behaviour in different infiltration patterns in patients with multiple myeloma (MM).
Methods and materials: 44 patients with histologically-confirmed MM underwent WBLDCT and WBMRI. Unenhanced WBLDCT was performed on a 256-slice scanner with a tube voltage of 120 kV and tube current-time product of 40mAs. WBMRI was performed on a 1.5T with the acquisition of T1 TSE and T2 STIR sequences (coronal and sagittal plane), and axial DWIBS sequences, with different b-values (0.500 and 1,000 mm2/s). The whole skeleton was divided into 5 anatomic districts (the skull, spine, sternum and ribs, and upper and lower limbs) and evaluated in terms of infiltration patterns. WBLDCT findings were then compared with WBMRI findings.
Results: On WBMRI, 24%of patients presented with osteolysis (focal/combined pattern) with a total of 204 lytic lesions detected (3% in the skull, 10% in the upper limbs, 25% in the pelvis and lower limbs, 45% in the spine, and 17% in sternum and ribs). 10% of patients had a diffused pattern, 4% had the salt and pepper pattern, and 6% had a normal pattern.
On WBLDCT, 30% of patients presented with osteolysis (focal/combined pattern) with a total of 206 lytic lesions detected (33% in the skull, 10% in the upper limbs, 12% in pelvis and lower limbs, 45% in the spine, and 16% in sternum and ribs). 8% of patients had a diffuse pattern and 6% with no bone involvement. WBLDCT also detected 10 hyperattenuating lesions not recognisable to WBMRI. Moreover, 9% of patients presented an extraosseous involvement, which only WBRMI was able to detect.
Conclusion: WBLDCT is a reliable imaging technique able to detect small lytic lesions which are difficult to detect in MRI, such as skull lesions and hyperattenuating lesions. Conversely, WBMRI is more specific in discriminating diffuse bone involvement and detecting extraosseous disease.
Limitations: n/a
Ethics committee approval: n/a
Funding: No funding was received for this work.
Author Disclosures:
M. Ragusi: nothing to disclose
T. P. Giandola: nothing to disclose
D. Ippolito: nothing to disclose
M. Porta: nothing to disclose
C. Maino: nothing to disclose
C. R. G. L. Talei Franzesi: nothing to disclose
S. Sironi: nothing to disclose

RPS 1416b-12 12:21

Iodine concentration of healthy lymph nodes of the neck, axilla, and groin in dual-energy CT

A. Sauter[1], S. Ostmeier[1], J. Nadjiri[1], D. Deniffel[2], E. J. Rummeny[1], D. Pfeiffer[1];
[1]Munich/DE, [2]Toronto, ON/CA (ostmeiersophie@gmail.com)

Purpose: Lymph nodes (LN) are examined in every CT scan. Until now, an evaluation is only possible with morphological criteria. With dual-energy CT (DE-CT) systems, iodine concentration (IC) can be measured which could conduct an improved evaluation. The purpose of the study was to define standard values for IC of cervical, axillary, and inguinal LN in DE-CT, as these do not yet exist despite their clinical relevance.
Methods and materials: Imaging data of 297 patients who received a DE-CT in a portal-venous phase and showed healthy LN was retrospectively collected from the institutional PACS system. No present history of malignancy, inflammation, or trauma in the examined region was present. For each patient, the IC of the 3 largest LN of the examined area was measured. Normalisation to different structures was performed.
Results: The normalisation of the IC of LN to artery, vein, muscle, or a combination of those, did not lead to a decreased value-range. The smallest range and confidence interval of IC was found when using absolute values of IC for each region. Hereby, the mean values (95% confidence interval) for IC of LN were found: 2.09 mg/ml (2.00-2.18 mg/ml) for the neck, 1.24 mg/ml (1.16-1.33 mg/ml) for the axilla, and 1.11 mg/ml (1.04-1.17 mg/ml) for the groin.
Conclusion: The current study suggests standard values for IC of LN in DE-CT which could be used to differentiate between healthy and pathological lymph nodes.
Limitations: IC could be affected by the used CT-protocol.
Ethics committee approval: The retrospective study was approved and conducted in accordance with the guidelines of the institutional review board. Informed consent was waived by the institutional review board due to the retrospective design of the study.
Funding: No funding was received for this work.
Author Disclosures:
A. Sauter: nothing to disclose
S. Ostmeier: nothing to disclose
J. Nadjiri: nothing to disclose
D. Deniffel: nothing to disclose
E. J. Rummeny: nothing to disclose
D. Pfeiffer: nothing to disclose

11:15 - 12:30 **Room M 4**

Musculoskeletal

RPS 1410b

Tumours and bone density

Moderators:
S. Mariani; L'Aquila/IT
M. Reijnierse; Leiden/NL

RPS 1410b-1 11:15

Feasibility of MRI/DWI for the evaluation of treatment response in multiple myeloma: can ADC values predict treatment response?

A. Paternain Nuin, P. Malmierca Ordoqui, A. Ezponda Casajus, J. J. Rosales Castillo, M. Calvo Imirizaldu, M. Elorz, M. J. Garcia-Velloso, J. D. D. Aquerreta Beola*; Pamplona/ES (alberpanu@gmail.com)*

Purpose: To analyse the feasibility of diffusion-weighted MRI (DWI) for predicting treatment response in multiple myeloma (MM) lesions compared to FDG PET-CT.
Methods and materials: 20 patients with MM undergoing same-day whole-body MRI and FDG-PET/CT for the evaluation of treatment response were retrospectively recruited. Overall, 63 whole-body MRIs were evaluated. 3 significant bone lesions were analysed for each patient. Quantitative analysis of ADC maps and SUVmax of each lesion were evaluated in the subsequent studies. Variation of ADC values was compared with the variation of SUVmax for each lesion, which was considered the reference standard for this study. Differences between the mean ADC value in lesions from patients with clinical progression and patients with treatment response were also analysed, considering the criteria of the international myeloma work group (IMWG). Data analysis was performed using SPSS 21.0 software (Spearman's rank correlation coefficient and Student's t-test). Two-tailed p values were used for all statistical assessment and $p<0.05$ was considered statistically significant.
Results: An inverse, high, and significant correlation between the variations of the ADC value and SUVmax ($r=-0.686$; $p<0.01$) was found. There were also significant differences in mean ADC values between lesions from patients with clinical progression and patients with treatment response (757.69 vs 1377.95, $p<0.01$).
Conclusion: Variations of ADC values in DWI can be used to assess treatment response in patients with MM.
Limitations: A retrospective study limited to a single centre and MRI protocol. The sample consisted of 20 patients in advanced stages.
Ethics committee approval: n/a
Funding: No funding was received for this work.
Author Disclosures:
A. Paternain Nuin: nothing to disclose
P. Malmierca Ordoqui: nothing to disclose
J. D. D. Aquerreta Beola: nothing to disclose
M. Elorz: nothing to disclose
A. Ezponda Casajus: nothing to disclose
M. Calvo Imirizaldu: nothing to disclose
M. J. Garcia-Velloso: nothing to disclose
J. J. Rosales Castillo: nothing to disclose

RPS 1410b-2 11:21

Dual-energy CT virtual non-calcium technique in the diagnosis of osteoporosis: a correlation study with quantitative CT

Z. Liu, Y. Zhang, Y. Jiang*; Xi'an/CN (00505014@163.com)*

Purpose: To evaluate the diagnostic value for osteoporosis of dual-energy CT (DECT) based on the virtual non-calcium (VNCa) technique.
Methods and materials: Prospective dual-energy CT scanning was performed on the lumbar region of 55 patients with chronic low back pain, with a standard QCT phantom placed at the waist during scanning. Using the QCTPro analysis system, the BMD of each vertebral body was measured. Based on the VNCa technique, the quantitative parameters were measured, including the CT value of calcium (contrast media, CM), CT value of mixed energy images (regular CT value, rCT), calcium density(CaD), and fat fraction (FF), by using Siemens dual-energy analysis software with a specially modified configuration file. Pearson's test was used to analyse the correlation between BMD and these parameters, and to establish a regression equation. The diagnostic efficiency for osteoporosis of the equation was evaluated by ROC curve.
Results: The CM, rCT, CaD, and FF were significantly correlated with BMD (r-values were 0.885, 0.947, 0.877, and 0.492, respectively, and all $P<0.01$), the regressive BMD (rBMD) could be expressed with an equation as $rBMD=54.82-0.19*CM+20.03*CaD-1.24*FF$. Taking $rBMD<81.94 mg/cm^3$ as the threshold, the sensitivity and specificity were 90.0% and 92.0%, respectively, and the AUC was 0.966 ± 0.009 ($P<0.01$).
Conclusion: The calcium and fat quantitative related parameters of DECT have a good correlation with the BMD measured by QCT, and it may serve as an alternative method for the quantitative evaluation of osteoporosis in terms of mineral content and bone marrow fat composition.
Limitations: We try our best to ensure ROI "point-to-point" correspondence to reduce the generation of system errors.
Ethics committee approval: This research was approved by the Ethics Committee of Xi'an Jiaotong University Affiliated Honghui Hospital.
Funding: The Natural Science Foundation of Shaanxi Province (2017JM8152).
Author Disclosures:
Z. Liu: nothing to disclose
Y. Zhang: nothing to disclose
Y. Jiang: nothing to disclose

RPS 1410b-3 11:27

3D calcium maps of bone mineral density using spectral photon-counting CT

A. Matanaghi[1], C. Leary[2], P. Walker[1], M. Rajeswari Amma[1], J. Clark[1], N. Gilchrist[1], A. Y. Raja[1], A. P. H. Butler[1], M. Collaboration[1]; *[1]Christchurch/NL, [2]Portland, OR/US (aysouda.matanaghi@postgrad.otago.ac.nz)*

Purpose: We assessed 3-dimensional changes to bone-mineral density during decalcification and fracture healing processes. Characterising these changes has direct relevance to a wide range of clinical situations including fracture risk, bone healing, and other diseases affecting bone.
Methods and materials: 3D calcium maps at 90 µm voxel size were obtained using a MARS spectral photon-counting CT. Measured calcium densities ranged from 0-1200 mg/ml.
In a decalcification study, 4 excised ovine femur bones were demineralised in 2.5% nitric acid at different time intervals (0, 3, 6, and 16 days). Atomic absorption spectrometry was performed on 251 times diluted nitric acid solution (collected at each interval) and compared with MARS 3D calcium maps of the biological sample.
In a fracture healing study, 4 sheep were administered strontium daily until sacrifice at week 2, 4, 6, and 8 after an induced fracture. Excised tibias were scanned and mineral content values from MARS were compared with DXA.
Results: For decalcification, measured cortical BMD and total BMD (on 100 slices) decreased across the time 880 ± 170 to 440 ± 200 mg/cm^3 and 410 ± 230 to 213 ± 180 mg/cm^3, respectively. The trend was consistent with the atomic absorption spectrometry measurements of calcium loss into the nitric acid solution.
In assessing bone healing, MARS calcium maps show an increasing trend in cortical bone-mineral content as the fracture heals in all 4 sheep (1.04, 1.17, 1.31, and 1.72g). Total bone mineral content measurements with MARS and DXA correlated within 5 and 8% of each other.
Conclusion: Spectral photon-counting CT with a MARS scanner can quantify and visualise in 3D the changes in bone mineralisation. This will impact research, diagnosis, and management of a wide range of bone conditions.
Limitations: n/a
Ethics committee approval: Animal ethics committee: AEC2018-31A.
Funding: No funding was received for this work.
Author Disclosures:
A. Matanaghi: nothing to disclose
C. Leary: nothing to disclose
P. Walker: Shareholder at MARS Bioimaging Limited
M. Rajeswari Amma: nothing to disclose
J. Clark: nothing to disclose
N. Gilchrist: nothing to disclose
A. P. H. Butler: Board Member at MARS Bioimaging Limited, Shareholder at MARS Bioimaging Limited, Employee at MARS Bioimaging Limited, Founder at MARS Bioimaging Limited, Grant Recipient at The Ministry of Business, Innovation and Employment
M. Collaboration: Employee at MARS Bioimaging Limited, Shareholder at MARS Bioimaging Limited
A. Y. Raja: Research/Grant Support at The Ministry of Business, Innovation and Employment, Employee at MARS Bioimaging Limited, Shareholder at MARS Bioimaging Limited

RPS 1410b-4 11:33

Accuracy, precision, and reliability of bone mineral density (BMD) measurements by dual-energy CT (DECT): an initial ex-vivo study

L. Qin, F. Yan, L. Du*; Shanghai/CN (tevez10@126.com)*

Purpose: To investigate the accuracy, precision, and reliability of volumetric bone mineral density (vBMD) derived by dual-energy CT (DECT).

Methods and materials: 23 patients who underwent total hip arthroplasty were enrolled. Femoral heads were excised to rectangles for scanning. A dual-source DECT scanner (Definition flash, Siemens) was used to create dual-energy images under 80/Sn140 and 100/Sn140 kVp scanning conditions. They were subsequently scanned by single-energy CT and dual-energy x-ray absorptiometry (DEXA) to produce QCT-vBMD and BMM (bone mineral mass), respectively. DECT images were loaded to post-processing workstation (Examine, Siemens) for the calculation of DE-vBMD and BMM.
Results: At both scanning protocols conditions, DE-vBMD was excellently correlated with QCT-vBMD. Similarly, DE-BMM was strongly correlated with QCT-BMM and DEXA-BMM. Substantial agreement was found between QCT-BMM and DEXA-BMM. Agreement of interobserver and intraobserver of DE-vBMD was also good. Higher DECT-derived vBMD was found under 100/Sn140 kVp. Under 80/Sn140 kVp, DECT-derived vBMD and BMM were significantly higher than those from QCT and DEXA, with a mean difference that ranged from 7.8% to 57.6% for DE-vBMD, and 5.6% to 36.3% for DE-BMM, respectively. Linear regression analysis was carried out to calibrate 80/Sn140 kVp DE-vBMD (=0.6×DE-vBMD+48.493).
Conclusion: DECT allows for vBMD and BMM, which were strongly correlated with measurements derived from QCT and DEXA with high reliability and precision. Furthermore, after linear regression calibration, DECT could potentially provide accurate vBMD and BMM, and opportunistic screen patients undergoing DECT for other clinical indications.
Limitations: No DECT examinations were performed before surgeries. The assessment of osteoporosis was generally performed in the lumbar vertebrae. Whether contrast-enhancement DECT had impact on the measurements was unknown.
Ethics committee approval: Approved by the institutional review board of our institution. Written informed consent was obtained.
Funding: No funding was received for this work.
Author Disclosures:
L. Qin: nothing to disclose
F. Yan: nothing to disclose
L. Du: nothing to disclose

RPS 1410b-5 11:39

MRI patterns indicate treatment success and tumour relapse following radiofrequency ablation of osteoblastoma

L. Kintzelé[1], S. C. Brandelik[1], F. Wuennemann[1], M.-A. Weber[2], B. Lehner[1], H.-U. Kauczor[1], C. Rehnitz[1]; [1]*Heidelberg/DE,* [2]*Rostock/DE (kintz_l@hotmail.com)*

Purpose: To explore the typical magnetic resonance imaging (MRI) pattern of osteoblastoma (OB) after radiofrequency ablation treatment (RFA) and to derive signs that indicate treatment success or relapse.
Methods and materials: A total of 43 follow-up MRI examinations on 15 OB patients that underwent a total of 19 RFAs were analysed retrospectively. An early follow-up group (1-4 months after RFA) and late follow-up group (8-131 months after RFA) were created. Groups were differentiated depending on clinical treatment success. Images were analysed for the presence of central nidus enhancement (CNE), peripheral nidus enhancement (PNE), perifocal bone marrow oedema (PBME), and fatty nidus conversion (FNC).
Results: Every patient (n=14/14) in the treatment success group showed a target-like appearance with negative CNE and positive PNE or PBME at early follow-up. PNE was present in 93% (n=13/14) and PBME in 71% (n=10/14) of early follow-up images. At late follow-up, the target-like appearance was observed in 25% (n=5/20) of exams and 20% (n=4/20) for both PNE and PBME. FNC was not observed at early follow-up but occurred in 55% (n=11/20) of late follow-up exams. All three included MRI exams at clinical recurrence showed strong CNE, PNE, and extensive PBME in contrast to exams of the treatment success group.
Conclusion: The target-like appearance of OB indicates treatment success in early follow-up MRI exams. PNE and PBME typically reduce over time and can lead to FNC in successfully treated patients. CNE recurrence with PNE and extensive PBME are signs of relapse. PNE and PBME do not indicate treatment failure at early follow-up.
Limitations: The retrospective study design and limited patient number due to the rareness of osteoblastoma.
Ethics committee approval: The study was performed with a waiver of informed consent by the local review board.
Funding: No funding was received for this work.
Author Disclosures:
L. Kintzelé: nothing to disclose
S. C. Brandelik: nothing to disclose
F. Wuennemann: nothing to disclose
M.-A. Weber: nothing to disclose
B. Lehner: nothing to disclose
H.-U. Kauczor: nothing to disclose
C. Rehnitz: nothing to disclose

RPS 1410b-6 11:45

Benign versus malignant soft tissue tumours: differentiation with 3T MR texture analysis including intravoxel incoherent motion diffusion-weighted imaging

Y. Lee[1], W.-H. Jee[1], Y. Hwang[1], Y.-G. Chung[2], W.-J. Bahk[1]; [1]*Gyeonggi/KR,* [2]*Seoul/KR*

Purpose: To investigate the value of MR texture analysis (TA) to differentiate malignant from benign soft tissue tumours at 3T MRI including IVIM DWI.
Methods and materials: 69 patients with pathologically confirmed soft tissue tumours (29 benign and 40 malignant) who underwent 3T MRI including IVIM DWI were retrospectively enrolled. TA was performed on axial T1WI, T2WI, CET1, high-b value DWI, and ADC map using software (TexRAD). Mean, SD, entropy, MPP, skewness, and kurtosis were calculated according to different Laplacian of Gaussian spatial filters: SSF 0, 2, 4, and 6. The ROC curve was obtained. Student's t-test and multivariate logistic regression analysis were performed. The ROC curve with AUC was obtained.
Results: SSF 4 showed overall higher AUCs than other SSFs, although there were no significant differences in different SSFs. AUCs of the mean of DWI, ADC, T2WI, and CET1 were 0.709 (95% CI, 0.586-0.831), 0.851 (0.751-0.951), and 0.772 (0.656-0.887), which were significantly different between benign and malignant soft tissue tumours ($p<0.05$). AUCs of kurtosis of DWI, T1WI, and CET1 were 0.748 (0.632-0.864), 0.732 (0.610-0.855), and 0.806 (0.700 -0.913), which were significantly higher in malignant tumors ($p<0.05$). AUCs of entropy of DWI, ADC, and T2WI were 0.763 (0.653-0.874), 0.763 (0.653-0.874), and 0.769 (0.657-0.880), which were significantly higher in malignant tumours ($p<0.05$). AUCs of MPP of ADC and CET1 were 0.734 (0.605-0.864) and 0.744 (0.624-0.864), which was significantly lower in malignant tumours ($p<0.05$). AUC of combined ADCmean and CEkurtosis was 0.883 (0.783-0.943) with a sensitivity and specificity of 83% and 86%.
Conclusion: MR TA may be reliable and accurate in differentiating malignant from benign soft tissue tumours at 3T including IVIM-DWI.
Limitations: A retrospective study with selection bias and relatively small study population.
Ethics committee approval: Approved by IRB and informed consent was waived.
Funding: No funding was received for this work.
Author Disclosures:
W.-H. Jee: nothing to disclose
Y. Hwang: nothing to disclose
Y.-G. Chung: nothing to disclose
W.-J. Bahk: nothing to disclose
Y. Lee: nothing to disclose

RPS 1410b-7 11:51

MR imaging-guided high intensity focused ultrasound for painful bone metastases: standard versus dedicated conformal bone system

C. Gasperini[1], M. P. P. Aparisi Gomez[2], P. Ghanouni[3], T. Frisoni[1], D. Donati[1], A. Napoli[4], A. Bazzocchi[1]; [1]*Bologna/IT,* [2]*Valencia/ES,* [3]*Stanford/US,* [4]*Rome/IT (chr.gasperini@gmail.com)*

Purpose: MR-imaging-guided high intensity focused ultrasound (MRgHIFU) is a treatment option for painful bone metastases. A bone-dedicated system has been developed (conformal bone system (CBS)) aiming at extended treatment approaches and increased patient comfort. The purpose of this work was to compare CBS with the conventional system (CS) in terms of safety and efficacy.
Methods and materials: A matched-pair analysis study was conducted to compare the therapeutic effects of the two systems. CBS and CS-treated groups were matched 1:1 by age, sex, pre-treatment pain score on the NRS, and treated site. The primary endpoint was the rate of response to treatment (complete and partial) at 3 months after treatment according to the international consensus on palliative radiotherapy endpoints for future clinical trials in bone metastases criteria. Secondary endpoint included the rate of major and minor complications according to the common terminology criteria for adverse events, version 5.0.
Results: According to the criteria for patient eligibility and matching, a total of 28 patients (14 CBS,14 CS) with bone metastasis were enrolled for analyses (mean age: 61 in CBS group, 57 in CS group); 57% were male and 43% were female. Results showed that both CBS and CS were effective. The mean NRS at baseline was 6.7±2.6 and 6.5±2.8 for CBS and CS group, respectively. The primary endpoint occurred in 12 patients in the CBS group and in 10 in the CS group (cumulative event rate 86% vs 71%, p=0,6483). No adverse events over grade 2 were documented in both groups.
Conclusion: CBS provides a similar overall treatment response rate compared to CS and is equally safe. With this study we enhanced its feasibility for painful bone metastasis in selected patients.
Limitations: The small sample size and limited follow-up period to report clinical responses.
Ethics committee approval: n/a
Funding: No funding was received for this work.

Author Disclosures:
C. Gasperini: nothing to disclose
M. P. P. Aparisi Gomez: nothing to disclose
P. Ghanouni: nothing to disclose
T. Frisoni: nothing to disclose
D. Donati: nothing to disclose
A. Napoli: nothing to disclose
A. Bazzocchi: nothing to disclose

RPS 1410b-8 11:57

Treatment effects on osteoporotic vertebral compression fractures: a clinical long-term study of pain evaluation after vertebroplasty and kyphoplasty

T. J. Vogl, C. Hackbarth, N. N. N. Naguib; *Frankfurt am Main/DE*
(t.vogl@em.uni-frankfurt.de)

Purpose: To evaluate treatment effects on osteoporotic vertebral compression fractures (VCFs) by using percutaneous vertebroplasty (PFP) and percutaneous kyphoplasty (PKP) and to document whether these effects are still detectable several years after the end of therapy.
Methods and materials: From January 2002-February 2015, 49 patients who received PVP or PKP were evaluated. The surgical protocols and radiologically assisted CTs were retrospectively evaluated related to the occurrence of cement leakage. A special questionnaire regarding pain development before and after the procedure was analysed prospectively. The measurement of pain quality was based on the visual analogue scale (VAS).
Results: VAS score was on average 7.0 before and 3.7 after therapy with a significant difference (p≤0.001) in the change of VAS scores in all patients. Considering the reduction of VAS over time of observation, there was no significant difference in the occurrence of symptoms (p=0.694) and no difference in the decrease in VAS over time. In 10 patients (22.73%), at least one cement leakage was recorded by CT scan. There was no significant difference in the occurrence of cement leakage and the change in VAS (p=0.146). After therapy, 79.6% of all patients reported an increase in mobility and 83.7% reported a rise in quality of life.
Conclusion: Both PVP and PKP significantly reduce the pain in VCFs. These results are still being observed more than 10 years after the end of treatment.
Limitations: Other interventions overlapped with the therapeutic approach documented here. Evaluation of pain before and after therapy was based on the subjective feelings of the individual patients. Comparison with non-surgical fracture treatment or a placebo group is missing.
Ethics committee approval: This study was approved by our local ethical committee. Written informed consent was obtained.
Funding: No funding was received for this work.
Author Disclosures:
T. J. Vogl: nothing to disclose
C. Hackbarth: nothing to disclose
N. N. N. Naguib: nothing to disclose

RPS 1410b-9 12:03

Diffusion-weighted magnetic resonance and T1 heterogeneity predicts the response to treatment in sarcomas

D. Moreno Martínez[1], A. Gimeno[2], I. Ramos Oliver[2], M. de Albert de Delas-Vigo[2], C. Torrents[2], L. Casas[2], J. M. M. Escudero Fernández[2], R. Dominguez[2], M. T. Veintemillas[2]; [1]*Cornella de Llobregat/ES,* [2]*Barcelona/ES*
(daniel.mm@icloud.com)

Purpose: To identify MRI findings, pathological findings, and tumour-related factors that predict the response to treatment and its association with survival of soft tissue sarcomas.
Methods and materials: 41 patients with 23 complete cases were retrospectively analysed. All patients had a multiparametric MRI 1.5T, including conventional (T1-weighted, T2-weighted, and contrast-enhanced T1-weighted imaging) and functional (DCE-MR imaging and DW imaging with ADC mapping) sequences at the diagnoses, from 2011-2018. The analysis was done from the diagnosis MRI until the last MRI, chest-CT, or death. ADC values were reported using global regions of interests (gROIs) including all the tumuor in one slide and specific ROIs (sROIs) in the areas of lower ADC values. Other data was also reported (T1-T2 heterogeneity, presence of blood or fat, and contrast enhancement type). Pathological data after the percutaneous biopsy and the resected specimen was reported.
Results: Higher values of gROIs were related with less mortality (p=0.03) and less fibrosis post-treatment (p<0.05). Higher sROIs values were related with more fibrosis post-treatment (p=0.02) and less mortality (p=0.01). Higher T1-heterogeneity was related to less fibrosis post-treatment (p<0.05). We also found that higher values of fibrosis post-treatment were related to less mortality.
Conclusion: Higher values of diffusion are related to less mortality and the absence of areas with low ADC values are related to a good response to therapy. Higher values of T1-heterogeneity are related to a bad response to treatment (less fibrosis post-treatment). There is a positive association with fibrosis post-treatment and survival.
Limitations: The subjective reporting of the non-quantitative data and that not all patients had all data.
Ethics committee approval: n/a
Funding: No funding was received for this work.
Author Disclosures:
D. Moreno Martínez: nothing to disclose
A. Gimeno: nothing to disclose
M. de Albert de Delas-Vigo: nothing to disclose
C. Torrents: nothing to disclose
L. Casas: nothing to disclose
J. M. M. Escudero Fernández: nothing to disclose
R. Dominguez: nothing to disclose
M. T. Veintemillas: nothing to disclose
I. Ramos Oliver: nothing to disclose

RPS 1410b-10 12:09

Bone marrow oedema detection using dual-energy CT: application in sacroiliitis

M. Chen[1], J. L. Jaremko[2], F. van Den Bosch[1], N. Herregods[1], P. Carron[1], D. Elewaut[1], L. B. O. Jans[1]; [1]*Ghent/BE,* [2]*Edmonton, AB/CA*
(Min.Chen@ugent.be)

Purpose: To evaluate the diagnostic performance of dual-energy computed tomography (DECT) for sacroiliac bone marrow oedema (BME) detection in patients suspected for spondyloarthritis.
Methods and materials: Patients aged 18-55 years with suspicion for spondyloarthritis underwent DECT and 3.0 Tesla MRI of the sacroiliac joints on the same day. Virtual non-calcium (VNCa) images were calculated from DECT images for BME detection, using a three-material decomposition algorithm for bone mineral, red bone marrow, and yellow bone marrow. Each sacroiliac joint was divided into four quadrants for analysis. VNCa images were scored by two readers independently: 0=normal bone marrow and 1=BME. A quadrant was recorded as BME present if either of the readers scored '1' for the quadrant. Diagnostic performance was assessed with reference to MRI. CT numbers were measured on VNCa images. ROC analyses were performed to determine the cut-off values for BME detection.
Results: 40 patients (16 men, 24 women) were included. The sensitivity and specificity of BME detection by DECT were 65.4% and 94.2%. AUCs for CT numbers in the ilium and sacrum were 0.90 and 0.87, respectively. Cut-off values of -44.4 HU (iliac quadrants) and -40.8 HU (sacral quadrants) yielded sensitivities of 76.9% and 76.7% and specificities of 91.5% and 87.5%, respectively.
Conclusion: VNCa images are useful for BME detection in patient suspected for sacroiliitis.
Limitations: The sample size of the present study is small and the prevalence of BME is relatively low. The final clinical diagnosis was not taken into consideration for analysis.
Ethics committee approval: Institutional review board approved this study. Written informed consent was obtained.
Funding: The study is partially funded by the Young Researchers Grant awarded by the European Society of Musculoskeletal Radiology.
Author Disclosures:
J. L. Jaremko: nothing to disclose
M. Chen: nothing to disclose
N. Herregods: nothing to disclose
P. Carron: nothing to disclose
F. van Den Bosch: nothing to disclose
D. Elewaut: nothing to disclose
L. B. O. Jans: nothing to disclose

RPS 1410b-11 12:15

A novel computed tomography-based scoring system of intra-articular mineralisation of the knee: BUCKS (Boston University calcium knee score)

M. Jarraya[1], T. Neogi[1], J. Lynch[2], D. T. Felson[1], M. Nevitt[2], A. Guermazi[1]; [1]*Boston, MA/US,* [2]*San Francisco, CA/US*
(mohamedjarraya@gmail.com)

Purpose: To describe and assess the reliability of a novel computed tomography (CT) scoring system, the Boston University calcium knee score (BUCKS), for evaluating intra-articular mineralisation.
Methods and materials: We included subjects from the multicenter osteoarthritis study (MOST), a NIH-funded longitudinal cohort of older adults with or at risk of knee OA. Subjects underwent CT of bilateral knees. Each knee was scored at 28 locations (14 cartilage, 6 meniscus, 6 ligaments, 1 joint capsule, and 1 vessel). A musculoskeletal radiologist scored cartilage, meniscus, and vascular features using a score from 0-3. The joint capsule, posterior meniscal roots, ACL/PCL, and collateral ligaments were scored 0 or 1. 31 subject CTs

were reread 12 weeks later by the same reader and by a second reader, and agreement was evaluated using weighted kappa.
Results: The intra-reader reliability ranged from 0.93 for ligaments to 1.0 for joint capsules. The inter-reader reliability ranged from 0.92 for cartilage to 1.0 for joint capsules.
Conclusion: BUCKS demonstrated excellent reliability and is a potentially useful CT-based tool for studying the role of calcium crystals in knee OA.
Limitations: The concern for radiation exposure and inability to distinguish between the different types of calcium crystals.
Ethics committee approval: This study was approved by the institutional review boards at the University of Iowa, University of Alabama, Birmingham, University of California, San Francisco, and Boston University Medical Center.
Funding: The MOST Study is supported by NIH grants from the National Institute on Aging to Drs. Lewis (U01-AG-18947), Torner (U01-AG-18832), Nevitt (U01-AG-19069), and Felson (U01-AG-18820). This study was also supported by Dr. Neogi (K24 AR070892) and P60 AR047785.
Author Disclosures:
M. Jarraya: nothing to disclose
A. Guermazi: Founder at Boston Imaging Core Lab (BICL), Consultant at Merck Serono, Consultant at Ortho-Trophix, Consultant at Genzyme, Consultant at TissueGene
J. Lynch: nothing to disclose
D. T. Felson: nothing to disclose
M. Nevitt: nothing to disclose
T. Neogi: nothing to disclose

RPS 1410b-12 12:21
Angulation neutralising gyrating evaluation line-up (ANGEL) rib reconstructions in low-dose thoracic CT examinations of myeloma patients
J. Neubauer, L. Waibel, I. Dietrich, C. Neubauer*; Freiburg/DE*

Purpose: To compare reporting time and diagnostic accuracy for osteolysis between angulation neutralising gyrating evaluation line-up (ANGEL) rib reconstructions and standard axial reconstructions in low-dose thoracic CT examinations of myeloma patients.
Methods and materials: This retrospective study included myeloma patients who underwent low-dose thoracic CT examinations in our institution over a 1 year period. ANGEL rib and standard axial reconstructions were calculated. DICOM files were anonymised. 2 radiologists (3 years experience) independently evaluated osteolysis for each rib and measured the reporting time. Two radiologists (>6 years experience) established the reference standard using all reconstructions available. For differently evaluated cases, consensus reading was performed. P<0.05 was considered to denote statistical significance.
Results: 49 consecutive patients were included. Reporting time for ANGEL rib reconstructions and standard axial reconstructions were 97s and 80s for reader 1 (P=0.04) and 310s and 219s for reader 2 (P<0.001). Sensitivity, specificity, PPV, and NPV of ANGEL rib reconstructions and standard axial reconstructions for osteolyses were 0.52, 0.95, 0.61, 0.93 and 0.54, 0.94, 0.57, 0.94 for reader 1 (P>0.63) and 0.43, 0.96, 0.60, 0.92 and 0.53, 0.99, 0.97, 0.94 for reader 2 (P<0.04).
Conclusion: Reading time was longer in ANGEL rib reconstructions. Diagnostic accuracy of ANGEL rib reconstructions was worse in one reader and the same in the other. ANGEL rib reconstructions, therefore, cannot substitute standard axial reconstructions.
Limitations: This is a retrospective study. The reference standard was established by two experienced radiologists, partly using consensus reading.
Ethics committee approval: Our ethics committee approved this study.
Funding: No funding was received for this work.
Author Disclosures:
J. Neubauer: nothing to disclose
L. Waibel: nothing to disclose
I. Dietrich: nothing to disclose
C. Neubauer: nothing to disclose

11:15 - 12:30 **Room M 5**

Chest

RPS 1404b

Latest techniques in imaging of pulmonary vascular disease

Moderators:
L. Ebner; Berne/CH
N.N.

RPS 1404b-1 11:15
CTPA with a conventional CT at 100 kVp versus a spectral-detector CT at 120 kVp: a comparison of radiation exposure, diagnostic performance, and image quality
A. Sauter[1], N. Shapira[2], F. K. Kopp[1], J. K. Aichele[3], J. H. W. Bodden[1], A. Knipfer[1], J. Nadjiri[1], E. J. Rummeny[1], P. B. Noel[4]; *[1]Munich/DE, [2]Haifa/IL, [3]Pfaffenhofen/DE, [4]Philadelphia, PA/US (andreas.sauter@tum.de)*

Purpose: Dual-energy CT systems are nowadays widely used in clinical routine. However, concerns regarding radiation dose exist and quality of virtual-monoenergetic imaging with low kVp-levels compared to real low-kVp imaging is of interest. The purpose of this study was to compare CT pulmonary angiographies (CTPAs) as well as phantom scans obtained at 100 kVp to virtual monochromatic images (VMI) obtained with a spectral detector CT (SD-CT) at equivalent dose levels.
Methods and materials: 60 patients with suspected pulmonary embolism (PE) were included using a conventional CT (C-CT) and a SD-CT with the same mean CT dose index (4.85 mGy), respectively. C-CT was performed with 100 kVp and SD-CT was performed with 120 kVp. For SD-CT, VMIs with 40, 60, and 70 keV were calculated. All datasets were evaluated by three blinded radiologists regarding image quality, diagnostic confidence, and diagnostic performance. The contrast-to-noise ratio (CNR) for different iodine concentrations was evaluated in a phantom study.
Results: CNR was significantly higher with VMI at 40 keV compared to all other datasets. Subjective image quality, as well as a sensitivity and specificity, showed the highest values with VMI at 60 keV and 70 keV. A significant difference to 100 kVp (C-CT) was found for image quality. The highest sensitivity was found using VMI at 60 keV.
Conclusion: Higher levels of diagnostic performance and image quality were achieved with SD-CT compared to C-CT. In the clinical setting, SD-CT may be the modality of choice as additional spectral information can be obtained.
Limitations: As two different CT-systems were compared, examinations of different patients had to be compared and results could be biased.
Ethics committee approval: Institutional review board (IRB) approval was obtained for this retrospective study.
Funding: No funding was received for this work.
Author Disclosures:
A. Sauter: nothing to disclose
N. Shapira: Employee at Philips
F. K. Kopp: nothing to disclose
J. K. Aichele: nothing to disclose
J. H. W. Bodden: nothing to disclose
A. Knipfer: nothing to disclose
J. Nadjiri: nothing to disclose
E. J. Rummeny: nothing to disclose
P. B. Noel: nothing to disclose

RPS 1404b-2 11:21
Dual-energy CT in patients with suspect acute pulmonary embolism: a diagnostic accuracy systematic review and meta-analysis
A. Cozzi[1], C. B. Monti[1], M. Zanardo[1], S. Schiaffino[2], F. Sardanelli[1], F. Secchi[1]; *[1]Milan/IT, [2]San Donato Milanese/IT (andrea.cozzi@gmail.com)*

Purpose: To review the diagnostic performance of dual-energy CT (DECT) in diagnosing acute pulmonary embolism (PE).
Methods and materials: The study protocol was registered on PROSPERO and reported according to PRISMA. In February 2019, a systematic search was performed on MEDLINE/EMBASE for articles reporting the diagnostic performance of DECT for acute PE. Pooled sensitivity, specificity, positive and negative likelihood ratios (LR), and diagnostic odds ratio (DOR) were calculated according to the approach by Reitsma. A summary receiver operating characteristics (sROC) curve was constructed. Data was reported as an estimate and 95% confidence interval (CI). The pooled effective radiation dose for the chest (ChERD) was calculated using the random effect model. The impact of the year of publication on ChERD was evaluated through meta-regression analysis and risk of publication bias was assessed using the Egger test.
Results: Of 159 initially retrieved articles, 14 were included (23 independent study parts), totalling 993 patients with a median age range of 40-68 years and males from 32 to 79%. 12 studies used dual-tube/dual-detector DECT and 2 rapid-kV-switching DECT. Lower voltages ranged from 80-100 kVp and high voltages from 135-140 kVp. Pooled sensitivity was 84.1% (95% CI 78.3−88.6%), specificity 88.6% (95% CI 83.9−92.1%), positive LR 7.52 (95% CI 5.21−10.60%), negative LR 0.18 (95% CI 0.13−0.25%), and DOR 42.8 (95% CI 24.2−70.3%). The area under the curve of sROC was 0.93. ChERD showed high heterogeneity (I^2=97%) with 4.52 mSv (95% CI 3.68−5.36 mSv) pooled estimate. At meta-

regression, the year of publication did not impact on the radiation dose (r=0.152, p=0.703). The risk of publication bias was significant (Egger test p=0.006).
Conclusion: DECT diagnostic performance in acute PE is comparable to that of single-energy CT with comparable ChERD.
Limitations: Non-uniform use of DECT and reader experience.
Ethics committee approval: No Ethics Committee approval needed.
Funding: No funding received for this work.
Author Disclosures:
A. Cozzi: nothing to disclose
C. B. Monti: nothing to disclose
M. Zanardo: nothing to disclose
S. Schiaffino: Speaker at General Electric
F. Sardanelli: Speaker at General Electric, Speaker at Bracco, Speaker at Bayer, Grant Recipient at General Electric, Advisory Board at Bracco, Grant Recipient at Bayer, Grant Recipient at Bracco
F. Secchi: nothing to disclose

RPS 1404b-3 11:27

The feasibility and diagnostic performance of a contrast-enhanced ultra-low-dose CT protocol with a reduced scan range at 0.56 mSv on a 3rd generation dual source scanner to detect pulmonary embolism

A. B. Brendlin, S. Afat, K. Nikolaou, A. Othman*; Tübingen/DE (andreas.brendlin@gmail.com)*

Purpose: To evaluate the feasibility of a contrast-enhanced ultra-low-dose (ULD) protocol with reduced scan range (RSR) in patients with clinically suspected pulmonary embolism (PE) compared to ULD at original scan range (OSR).
Methods and materials: We included 82 consecutive patients (64 ± 16 years; 45 women) on a 3rd generation dual-source-scanner. Realistic simulations were used to generate datasets with 25% radiation dose OSR using ADMIRE 3 and 5, and 25% RSR ADMIRE 3 and 5, resulting in 328 datasets (4 sets each). Image noise was defined as mean standard deviation of HU-values measured bilaterally in the paraspinal muscles. The effective radiation dose was compared. All datasets were reviewed by three radiologists independently for image quality, diagnostic confidence, and presence/absence of PE. The diagnostic accuracy of ULD-RSR datasets was calculated using original dose datasets as a reference standard.
Results: Image noise between 100% OSR (20.54 ± 3.37), 25% Admire 3 (16.31 ± 2.58), and 25% Admire 5 (12.19 ± 2.71) differed significantly ($p \leq 0.001$). At 0.56 mSv, the effective radiation dose of ULD-RSR was significantly lower than standard protocol (3.55 mSv), as well as for either ULD or RSR alone ($p \leq 0.001$). Image quality was outstanding in each category (5; IQR 4-5) with excellent reliability (ICC ≥ 0.814, 95%CI 0.731-0.875). There was no impairment by reduction of scan range or radiation dose ($p \geq 0.54$). The sensitivity of ULD-RSR-CT was 0.947 and specificity 0.981.
Conclusion: On a 3rd generation dual-source-scanner, the radiation dose can be reduced to 16% of the original dose (0.56 mSv) in the detection of PE by combining mAs-reduction with a reduction of scan range and iterative reconstruction, while maintaining excellent image quality and accuracy.
Limitations: A retrospective design.
Ethics committee approval: Local ethics committee approved.
Funding: No funding was received for this work.
Author Disclosures:
A. B. Brendlin: nothing to disclose
S. Afat: nothing to disclose
A. Othman: nothing to disclose
K. Nikolaou: nothing to disclose

RPS 1404b-4 11:33

Prevalence and patterns of lung disease in patients with vascular Ehlers Danlos Syndrome (vEDS): CT features and histological correlations

S. Boussouar[1], A. Benattia[1], L. Gibault[1], F. Capron[1], P.-Y. Brillet[2], P. A. Grenier[1], M. Frank[1], E. Mousseaux[1], O. Sanchez[1]; *[1]Paris/FR, [2]Bobigny/FR (samia.boussouar@aphp.fr)*

Purpose: To describe and characterise clinical and CT imaging of lung involvement in patients with vEDS.
Methods and materials: All consecutive vEDS patients referred to a tertiary referral centre for vEDS between 2000 and 2016 were included. Chest computed tomography (CT) scans performed at initial vascular workup were retrospectively reviewed by two chest radiologists for lung involvement and analysed in respect of medical history and type of variant. 5 histologic samples from surgery were analysed.
Results: 136 patients (83 females and 53 males, 37 years) with molecularly confirmed vEDS were included. Identified pathogenic variants were glycine substitutions in 83 (61%) patients, splice-site and in-frame insertions-deletions in 42 (31%), and variants leading to haploinsufficiency in 11 (8%). 49 (36%) patients were current or former smokers. 24 (17.6%) patients had a history of respiratory complications including pneumothorax (n=17), haemothorax (n=4), and haemoptysis (n=3) leading to thoracic surgery in 11 patients.
Lung abnormalities were detected in CT scans in 78 (57.3%) patients. Emphysema (mostly centrilobular and paraseptal) was identified in 44 (32.3%) patients, without significant differences between smokers and nonsmokers. Clusters of calcified small pulmonary nodules were present in 9 (6.6%) patients and cavitated nodules in 4 (2.9%). Histological samples from surgery showed emphysema lesions with disruptions of alveoli in 3 cases, accompanied by diffuse haemorrhage increased haemosiderinic resorption.
Conclusion: In patients with vEDS, the most frequent CT feature observed, even in asymptomatic patients, is emphysema areas, suggesting a rupture of the alveolar walls. The identification by radiologists of this pattern may facilitate the diagnostic screening of undiagnosed probands.
Limitations: A retrospective study. No respiratory functional examinations.
Ethics committee approval: Written informed consent.
Funding: No funding was received for this work.
Author Disclosures:
S. Boussouar: nothing to disclose
A. Benattia: nothing to disclose
L. Gibault: nothing to disclose
F. Capron: nothing to disclose
P.-Y. Brillet: nothing to disclose
P. A. Grenier: nothing to disclose
M. Frank: nothing to disclose
O. Sanchez: nothing to disclose
E. Mousseaux: nothing to disclose

RPS 1404b-5 11:39

Machine learning-based cardiac chamber segmentation in CTPA for the noninvasive detection of pulmonary hypertension

M. A. Fink, C. Melzig, B. Egenlauf, E. Grünig, H.-U. Kauczor, C. P. Heussel, F. Rengier*; Heidelberg/DE*

Purpose: To assess machine learning-based cardiac chamber segmentation in computed tomography pulmonary angiographies (CTPA) for the noninvasive detection of pulmonary hypertension (PH).
Methods and materials: 56 consecutive patients undergoing right heart catheterisation (RHC) with a measurement of mean pulmonary arterial pressure (mPAP) and CTPA for suspected PH within 3 weeks between 08/2013 and 09/2014 were retrospectively reviewed. Cardiac chamber segmentation was performed automatically by a machine learning-based commercially available software and manually corrected if deemed necessary. Cardiac chamber volumes (right and left ventricles (RV/LV) and right and left atria (RA/LA)) were indexed to body surface area.
Results: 37 patients were diagnosed with PH (mean mPAP 38±11 mmHg) and 19 patients had a normal mPAP (mean 17±4 mmHg). Manual correction of the segmentation was performed in 15 cases (27%). In patients with PH, RA, and RV were significantly enlarged (87±45 vs. 44±19 ml/m^2 and 102±39 vs. 63±23 ml/m^2) and right to left atrial and ventricular ratios significantly increased (1.8±0.9 vs. 1.1±0.4 and 2.7±1.4 vs. 1.4±0.4) (all $p<0.001$). AUCs for the detection of PH were 0.83, 0.85, 0.76, and 0.83 for RA, RV, and atrial and ventricular ratio, respectively. A cutoff value for RV of 63 ml/m^2 allowed the diagnosis of PH with sensitivity, specificity, and positive and negative predictive values of 87%, 74%, 86%, and 74%, respectively.
Conclusion: Machine learning-based automated cardiac chamber segmentation in CTPA allowed noninvasive detection of PH as confirmed by RHC with good diagnostic accuracy.
Limitations: A retrospective and single-centre study with a limited number of patients.
Ethics committee approval: Ethics committee approved study and waived written informed consent.
Funding: License for the segmentation software provided by Philips.
Author Disclosures:
C. Melzig: nothing to disclose
B. Egenlauf: nothing to disclose
M. A. Fink: nothing to disclose
E. Grünig: nothing to disclose
H.-U. Kauczor: nothing to disclose
C. P. Heussel: nothing to disclose
F. Rengier: nothing to disclose

RPS 1404b-6 11:45

Machine learning model for predicting 30-day all-cause mortality in patients who were diagnosed with pulmonary embolism in the emergency department

N. Cahan[1], H. Greenspan[1], Y. Barash[2], S. Soffer[2], E. M. Marom[1], S. Apter[3], E. Konen[2], E. Klang[2]; *[1]Tel Aviv/IL, [2]Ramat Gan/IL, [3]Tel Hashomer/IL (noa.cahan@gmail.com)*

Purpose: Pulmonary embolism (PE) is a life-threatening condition. Rapid and accurate risk stratification can decrease PE mortality rates. We aimed to develop a machine learning 30-day mortality predictive model using clinical data.
Methods and materials: This retrospective study was approved by our institutional review board. We retrieved data for consecutive patients who underwent CT-angiography between 1/2012 to 12/2018 in our emergency department (ED) and were diagnosed with PE. Clinical variables included demographics, vital signs, chief complaint, medical history, home medications, blood tests, previous ED visits, and hospitalisations. The solution applies a machine learning-based classification algorithm, specifically, gradient boosting decision tree model (CatBoost). The model was trained on 2012-2017 data and tested on 2018 data. We evaluated the AUCs of single variables and of the entire model. We used Youden's index to find the model's optimal sensitivity and specificity.
Results: Our dataset included 367 patients, 38 of whom (10.3%) died within 30 days of diagnosis. Single variables with higher AUC included pulse (0.72), Di-Dimer (0.71), and arrival by ambulance (0.71). The entire model achieved an AUC of 0.84 (95% CI: 0.757-0.926) for predicting PE severity. 78.4% of the test cases were correctly risk stratified, based on the 30-day mortality label. Using Youden's index, the model showed a sensitivity of 90.9% and specificity of 77.7% for predicting death within 30 days.
Conclusion: Our model allows effective risk stratification of individuals with PE, which could improve the ability to direct preventative and health surveillance resources. To the best of our knowledge, the system is the first such fully automated solution.
Limitations: A retrospective single-centre study with a relatively small number of patients.
Ethics committee approval: Approved by our institutional review board.
Funding: No funding was received for this work.
Author Disclosures:
N. Cahan: nothing to disclose
H. Greenspan: nothing to disclose
Y. Barash: nothing to disclose
E. M. Marom: Other at Voxellence, Speaker at Bristol-Myers Squibb, Speaker at Boehringer Ingelheim, Speaker at Merck Sharp & Dohme
E. Konen: nothing to disclose
E. Klang: nothing to disclose
S. Apter: nothing to disclose
S. Soffer: nothing to disclose

RPS 1404b-7 11:51

Contrast medium administration for chest CT: a European protocol survey

M. K. Henning, T. M. Aaloekken, A. C. T. Martinsen, S. Johansen*; Oslo/NO (meid@ous-hf.no)*

Purpose: To investigate different contrast medium (CM) administration regimes for chest CT used by members of the European Society of Thoracic Imaging (ESTI).
Methods and materials: An online questionnaire was e-mailed to 650 ESTI members. The survey focused on CM protocols. In particular, questions referred to CM concentration, the use of fixed CM volume or weight/body composition tailored CM administration, injection rate, kV, and fixed delay or use of bolus tracking for chest CT.
Results: The overall response rate was 15.2%. Approximately 44% of the respondents used 350 mgI/ml and 54.5% used fixed CM volume regime. The injection rate varied between 1.5 to 5 ml/sec. Around 42% of respondents used fixed kV varying between 80 to 140 kVp and the majority used kV-modulation. Nearly 52% of the respondents used bolus tracking with a duration of 20-90 seconds.
Conclusion: Our survey showed a large variation in CM protocols used across Europe. There is a clear preference of using fixed CM administration regime for thoracic CT. More attention to the optimisation and establishment of a standard CM administration protocol in chest CT is needed.
Limitations: The name of the country and hospital were not recorded by the online survey. This may result in the involvement of several or no hospitals from each country responding to the survey. However, this cannot have such a major impact on the results achieved in this study as the aim of the study was to collect as many protocols as possible.
Ethics committee approval: The study was approved by the Norwegian Ethical Committee/Data Protection Officer at Oslo University Hospital.
Funding: No funding was received for this work.
Author Disclosures:
M. K. Henning: nothing to disclose
T. M. Aaloekken: nothing to disclose
A. C. T. Martinsen: nothing to disclose
S. Johansen: nothing to disclose

RPS 1404b-8 11:57

An evaluation of breast shielding combined with low-dose CTPA protocol for use in pregnancy

C. D. Gillespie, A. Yates, M. Hughes, M. C. Murphy, M. Rowan, F. Ni Ainle, F. Bolster, S. J. Foley, P. J. Macmahon*; Dublin/IE (ayates989@gmail.com)*

Purpose: To determine if breast dose benefit can be obtained using in-plane bismuth breast-shields when combined with a low-dose CTPA protocol and to assess the impact on image quality.
Methods and materials: A low dose CTPA protocol was evaluated by phantom and patient study, using a 128 slice iterative-reconstruction and auto-modulation enabled CT-scanner with a limited scan range. A RANDO phantom scanned using three protocols (80, 100, and 20kv) and 20 patients undergoing low-dose CTPA in pregnancy were evaluated with and without bismuth breast-shields.
TLDs measured surface breast dose in patients and breast and uterine doses in the phantom at various gestations. Image quality was assessed by ROI-analysis of noise at shield level. Signal and contrast-to-noise-ratios and a subjective 5-point image-quality score were applied to patient CTPAs. Dose and image quality for low-dose CTPA alone was compared to low-dose CTPA protocol with shields.
Results: Phantom breast doses ranged from 0.84-2.26mGy without shield and 0.32-1.3mGy with shield, conferring 57% reduction in dose (range 39%-76%). Patients' average surface breast dose was 1.3mGy without shield (0.76-2.12mGy) and 0.68mGy (0.44-1.0mGy) with shields, conferring 48% reduction.
The phantom data demonstrates increased noise for shielding groups, the greatest for the lowest kV parameters. However, in the patient study both subjective quality scores, SNR (no-shield: 11.2±3.7, shield: 10.8±2.6, p=0.74), and CNR (no-shield: 10.0±3.3, shield: 9.3±2.4, p=0.6) were comparable between groups.
Foetal doses in the phantom study were highest at term (0.28, 0.86 and 1.4mGy at 80, 100 and 120kV) and ranged from 0.005-0.42mGy for trimester 1–3.
Conclusion: Combining low-dose CTPA protocols with breast-shielding confers additional breast dose savings of approximately 50% without significantly impacting image quality. This yields doses ranging from 0.4-1mGy, approaching doses quoted for low-dose-perfusion-only scintigraphy.
Limitations: A limited sample size.
Ethics committee approval: Ethics approval obtained.
Funding: No funding was received for this work.
Author Disclosures:
M. Rowan: nothing to disclose
C. D. Gillespie: nothing to disclose
A. Yates: nothing to disclose
S. J. Foley: nothing to disclose
P. J. Macmahon: nothing to disclose
M. C. Murphy: nothing to disclose
M. Hughes: nothing to disclose
F. Ni Ainle: nothing to disclose
F. Bolster: nothing to disclose

RPS 1404b-9 12:03

Pseudo-embolic perfusion defects in pulmonary arterial hypertension (PAH) and pulmonary veno-occlusive disease (PVOD): evaluation with dual-energy CT lung perfusion in 63 patients

B. Lefebvre, M. Kyheng, N. Lamblin, P. Degroote, M. Fertin, J.-B. Faivre, J. Remy, M. Remy-Jardin*; Lille/FR (martine.remy@chru-lille.fr)*

Purpose: To investigate the frequency and characteristics of PE-type perfusion defects in PAH and PVOD.
Methods and materials: 63 patients with PAH (n=51) and PVOD (n=12) underwent dual-energy CT in the diagnostic workup of pre-capillary PH. Chest CT angiography was obtained with a dual-source CT system (1st (n=2), 2nd (n=4), and 3rd (n=43) generation) and reconstruction of standard morphologic and lung perfusion images using the lung PVB software. Lung perfusion analysis included a quantitative (mg I/mL) and qualitative (segmental assessment of perfusion defect) evaluation completed by comparative analysis with morphologic images.
Results: In the overall study population: (a) lung perfusion was homogeneous in 22 patients (35%) and heterogeneous in 41 patients (65%), (b) when rated as heterogeneous, lung perfusion showed bilateral defects (41/41; 100%) with a mean percentage of 89.9% of segments with perfusion defects, and (c) there was a single type of perfusion abnormality (patchy defects: 16/41; 39%; nonsystematised hypoperfusion: 9/41; 22% or PE-type defects : 1/41; 2.4%) or a mixed pattern (15/41; 36.6%). Comparison between PAH and PVOD showed (a) no significant difference in the frequency of perfusion abnormalities (p=0.31), mean percentage of segments with abnormal perfusion (p=0.91), patchy defects per patient (p=0.23), or nonsystematised hypoperfusion (p=0.41), but (b) a higher proportion of segments with PE-type defects in PVOD (16.7% vs 2.3%; p=0.041). PE-type perfusion defects were seen in 8 patients (8/61; 12.7%) (PAH: n=5; PVOD: n=3), rated as mild (4/8) or marked (4/8), and seen with the concurrent presence of centrilobular micronodules/GGO (3/8), mosaic attenuation (4/8), or normal lung.

Conclusion: PE-type defects were identified in 12.7% of PAH/PVOD patients with morphologic abnormalities avoiding a misdiagnosis of CTEPH.
Limitations: n/a
Ethics committee approval: Waiver of patient informed consent.
Funding: No funding was received for this work.
Author Disclosures:
M. Remy-Jardin: Research/Grant Support at Siemens Healthineers
B. Lefebvre: nothing to disclose
M. Kyheng: nothing to disclose
N. Lamblin: nothing to disclose
P. Degroote: nothing to disclose
M. Fertin: nothing to disclose
J. Remy: Consultant at Siemens Healthineers
J.-B. Faivre: nothing to disclose

RPS 1404b-10 12:09

Salvage of suboptimal enhancement of pulmonary artery in pulmonary CT angiography studies: rapid kVp switch dual-energy CT experience

A. Çinkooğlu, S. Bayraktaroğlu, R. Savas*; Izmir/TR (acinko@gmail.com)*

Purpose: To explore the potential improvement in pulmonary artery opacification and to assess the change in image quality parameters in VMI using fast switch kVp dual-energy CT.
Methods and materials: Computed tomography angiography (CTA) images of 877 patients with a diagnosis of PE were reviewed. 60 patients with suboptimal enhancement (<200 HU) were involved. Standard images (140 kVp) and VMI from 40 to120 keV were generated. Attenuation, noise, SNR, and CNR were measured in the pulmonary artery (PA). Using the VMIs, the best image was determined as the image with main PA opacification greater than 200 HU and image quality ≥3. 56 studies that met these criteria were considered as salvaged. At this best energy level, quantitative parameters were compared with standard images.
Results: The attenuations of VMIs at 40, 45, 50, 55, 60, 65, and 70 keV were significantly higher than standard images ($p< 0.001$). Similar findings were observed with SNR and CNR. In the salvaged patients, the average increase in mean PA attenuation was 62% (from 172.61±23.4 to 280.55±40.7), the average increase in SNR was 38% (from12.1±5.3 to 16.7±7.1), and the average increase in CNR was 48% (9.2±4.3 to 13.7±6) ($p< 0.001$).
Conclusion: Low keV VMI reconstructions significantly increase PA attenuation, CNR, and SNR compared to standard image reconstructions. Suboptimal CT studies can be salvaged using low keV VMIs.
Limitations: The study design is retrospective and includes a single-centre experience. To determine the adequacy of PA opacification level in CTA, we accepted a limit of 200 HU. There is no single predetermined standard value that can be used in this regard for pulmonary CTA.
Ethics committee approval: Approved by the Institutional Review Board(Approval Number:19-3.1T/70).
Funding: No funding was received for this work.
Author Disclosures:
A. Çinkooğlu: nothing to disclose
S. Bayraktaroğlu: nothing to disclose
R. Savas: nothing to disclose

RPS 1404b-11 12:15

Application of the dual-layer spectral detector CT on CTPA with a low dose of iodine contrast agent and low injection rate

X. Sui[1], W. Song[1], Z. Y. Jin[1], H. Du[1], X. Lu[2], S. Yu[1]*; [1]Beijing/CN, [2]Shenyang/CN (lena_sui@vip.163.com)*

Purpose: To evaluate the feasibility of the dual-layer spectral detector CT on CTPA with a low dose of iodine contrast agent and low injection rate.
Methods and materials: 53 patients with suspected pulmonary embolism had a CTPA with 20ml 370 mg I/ml at 2ml/s. All chest CT examinations were performed using a dual-layer detector spectral CT unit. Two series of images were obtained, including conventional images at 120kVp and virtual monoenergetic spectral images at 40keV. The ROIs were placed at the main pulmonary arteries (PA) and right and left PA. The CNR, SNR, and image quality scores were compared at 120kVp and 40keV. The sensitivity, specificity, PPV, and NPV for the detection of pulmonary embolism were compared between conventional images and virtual monoenergetic spectral images at 40keV.
Results: CNR of main PA, right, and left PA at 40keV images were 24.3±43.3, 22.2±29.8, 22.6±30.3, and SNR were 26.4±44.5, 24.4±31.3, 24.7±31.8, respectively. CNR on conventional images were 5.9±6.1, 5.6±4.7, 5.7±4.9, and SNR were 7.6±7.0, 4.7±1.9, 7.2±5.7, respectively. CNR and SNR at 40keV were significantly higher than conventional images ($P<0.05$). Subjective image quality score of virtual monoenergetic images at 40keV was higher than conventional images but there was no significant difference (Z=-1.2, P=0.25). 26 patients showed PE. Compared with conventional images, the sensitivity, specificity, PPV, and NPV at 40keV were higher in the detection of pulmonary embolism.
Conclusion: Virtual monoenergetic images at 40keV on dual-layer spectral CT with a low dose of iodine and low flow rate increased the detection of PE, while preserving image quality. At the same time, it reduced the risks of contrast media-induced nephropathy and contrast agent extravasation.
Limitations: This is a small number study.
Ethics committee approval: Written informed consent was obtained.
Funding: No funding was received for this work.
Author Disclosures:
H. Du: nothing to disclose
X. Sui: nothing to disclose
W. Song: nothing to disclose
Z. Y. Jin: nothing to disclose
X. Lu: nothing to disclose
S. Yu: nothing to disclose

RPS 1404b-12 12:21

Dual-energy contrast-enhanced CT compared to lung perfusion scintigraphy to assess pulmonary perfusion in patients with severe emphysema

H. A. Gietema[1], K. Walraven[1], R. Posthuma[1], C. Mitea[1], D. J. Slebos[2], L. Vanfleteren[3]*; [1]Maastricht/NL, [2]Groningen/NL, [3]Gothenburg/SE (hester.gietema@mumc.nl)*

Purpose: Endoscopic lung volume reduction (ELVR) with endobronchial valves is a highly effective treatment for patients with severe emphysema, but treatment success depends on thorough patient selection. Next to high-resolution computed tomography (HRCT) of the lung parenchyma and the assessment of distribution in pulmonary perfusion is crucial in defining patient eligibility and target lobe selection. The latter is commonly performed with lung perfusion scintigraphy. We hypothesised that the iodine overlay calculated from contrast-enhanced dual-energy CT images added to the standard HRCT could provide appropriate perfusion estimates.
Methods and materials: 40 patients, screened for ELVR, were included in this analysis. Pulmonary perfusion was assessed with lung perfusion scintigraphy and dual-energy contrast-enhanced CT scans. Perfusion distribution was calculated for each lung and for the upper, middle, and lower thirds of both lungs with the planar technique. The same regions of interest (ROI) were chosen at the iodine overlay.
For each ROI mean, the difference in estimated perfusion was calculated and limits of agreement were assessed. For each patient, the mean absolute difference was for ROIs was calculated.
Results: Perfusion distribution over both lungs showed good correlation (r=0.8) but was significantly different between both techniques. ($p<0.001$). The mean difference for each selected ROI between lung perfusion scintigraphy and iodine overlay was -2,8% ±3.1% (right middle part) to 2,3% ± 3,8% (left lower part). Limits of agreement were -9% - 10%.
Limits of agreement of mean absolute differences per region of interest were 0.75-5.6%.
Conclusion: Quantification of perfusion distribution using planar 99mTc perfusion scintigraphy and iodine overlays calculated from dual-energy contrast-enhanced CTs correlates well with acceptable variability.
Limitations: Outliers and significant differences in pulmonary perfusion distribution were seen, for which further research is required.
Ethics committee approval: A waiver was received.
Funding: No funding was received for this work.
Author Disclosures:
H. A. Gietema: nothing to disclose
K. Walraven: nothing to disclose
R. Posthuma: nothing to disclose
C. Mitea: nothing to disclose
D. J. Slebos: nothing to disclose
L. Vanfleteren: nothing to disclose

11:15 - 12:30 **Tech Gate Auditorium**

Neuro

RPS 1411c

New and advanced neuroimaging

Moderators:
N.N.

RPS 1411c-1 11:15

Intraoperative imaging findings in transcranial MR imaging-guided focused ultrasound treatment at 1.5T MRI

R. Cannella[1], C. Quarrella[1], M. D'amelio[1], A. Napoli[2], T. V. Bartolotta[1], C. Catalano[2], M. Midiri[1], R. Lagalla[1], C. Gagliardo[1]; [1]Palermo/IT, [2]Rome/IT
(rob.cannella89@gmail.com)

Purpose: To assess the intraoperative neuroimaging findings in patients treated with transcranial MR-guided focused ultrasound (tcMRgFUS) thalamotomy using 1.5T equipment in comparison with the 48-hours follow-up.
Methods and materials: 50 prospectively-enrolled patients undergoing unilateral tcMRgFUS thalamotomy for either medication-refractory essential tremor (n=39) or Parkinson tremor (n=11) were included. Two radiologists evaluated the presence and size of concentric lesional zones (i.e. zone I, zone II, and zone III) and the presence of oedema extending to the internal capsule on 2D T2-weighted sequences acquired intraoperatively after the last high-energy sonication and at 48-hours follow-up. Sonication parameters including the number of sonications, delivered energy, and treatment temperatures were also recorded. Differences in the lesion pattern and size were assessed using the McNemar test and paired t-test, respectively.
Results: All three concentric zones were visualised intraoperatively in 26 (52%) patients after the last high-energy sonication. Zone I was visible in 29 (58%) cases at intraoperative imaging but was significantly more commonly visualised at 48-hours (96%, p<0.001). The diameter of zone I and II and the thickness of zone III significantly increased at 48-hours (p<0.001). Diameters of zone I and zone II measured intraoperatively demonstrated a significant correlation with thermal maps temperatures (p≤0.006). The maximum average temperature significantly correlated with zone II diameter at 48-hours (p=0.038). A threshold of 56.5° had a sensitivity of 71.4% and a specificity of 60.5% for zone II >10 mm at 48-hours.
Conclusion: Intraoperative imaging may accurately detect typical lesional findings before completing the treatment. These imaging characteristics significantly correlate with sonications parameters and 48-hours follow-up.
Limitations: The different tremor aetiologies, lack of long-term imaging appearance or clinical outcome evaluation, and tcMRgFUS software updates over time.
Ethics committee approval: An IRB-approved study. Informed consent was waived.
Funding: No funding was received for this work.
Author Disclosures:
R. Cannella: nothing to disclose
C. Quarrella: nothing to disclose
M. D'amelio: nothing to disclose
A. Napoli: nothing to disclose
T. V. Bartolotta: nothing to disclose
C. Catalano: nothing to disclose
M. Midiri: nothing to disclose
R. Lagalla: nothing to disclose
C. Gagliardo: nothing to disclose

RPS 1411c-2 11:21

The correlation between 3T-MRI findings and the clinical outcome in patients submitted to MRgFUS thalamotomy: beyond what we can see

A. Corridore, M. C. de Donato, P. Cerrone, F. Bruno, M. Varrassi, F. Arrigoni, A. Catalucci, P. Sucapane, C. Masciocchi; *L'Aquila/IT*
(antonella.corridore@gmail.com)

Purpose: To evaluate MRI findings on a 3-Tesla-MRI in patients submitted to Vim thalamotomy through MRgFUS in the medium-long-term follow-up.
Methods and materials: We recruited 57 patients affected by essential tremor (25) or tremor due to Parkinson's disease (32) submitted to thalamotomy by MRgFUS in our centre. These patients performed MRI-controls after 1 day, 1 month, 6 months, and 1 year. A complete neurological evaluation was performed at the same time intervals and a correlation between the imaging findings and clinical outcome was performed.
Results: We depicted a progressive reduction of the lesion size (about 8% after 1 month, 30% after 6 months, and 50% after 1 year). SWI sequences were the most reliable in lesion depiction in long-term follow-up: in 68% of cases, no visible lesion was identified in other sequences but was always depicted in SWI sequences. Correlation analysis of lesion size evaluated on follow-up MRI did not show any statistically significant correlation with the clinical outcome (FTM scale) at any interval. Correlation analysis of postprocedural imaging findings with side-effects and complications showed a significant correlation between oedema extension below the AC-PC line and the presence/persistence of ataxia at all follow-up intervals. Lateral lesion extension toward the internal capsule was related to motor complications.
Conclusion: The size of the lesion doesn't show a relationship with the clinical outcome or represent an index of treatment success. The correlation with perilesional oedema can be useful in the clinical evaluation of the medium-long-term side-effects.
Limitations: Further studies with more numerous samples and long-term follow-up are necessary to confirm the stability of the clinical result after a thalamotomy in patients with smaller but potentially more effective lesions.
Ethics committee approval: In accordance with Helsinki declaration.
Funding: No funding was received for this work.
Author Disclosures:
A. Corridore: nothing to disclose
M. C. de Donato: nothing to disclose
P. Cerrone: nothing to disclose
F. Bruno: nothing to disclose
M. Varrassi: nothing to disclose
F. Arrigoni: nothing to disclose
A. Catalucci: nothing to disclose
P. Sucapane: nothing to disclose
C. Masciocchi: nothing to disclose

RPS 1411c-3 11:27

Mapping the cortical connections of the ventral intermediate nucleus with tractography in patients undergoing MRI-guided HIFU thalamotomy

P. Malmierca Ordoqui, A. Paternain Nuin, A. Ezponda Casajus, M. Calvo Imirizaldu, M. C. Rodríguez Oroz, R. Garcia de Eulate, J. Guridi, O. Parras, P. Dominguez Echavarri; *Pamplona/ES (pmalmierca@unav.es)*

Purpose: To evaluate the optimal pre-treatment tractography seed point in the cortex for VIM localisation based on the final HIFU lesion position on post-treatment MRI.
MRI-guided high-intensity focused ultrasound (HIFU) is an effective therapeutic approach for the ablation of the ventral intermediate nucleus (VIM) of the thalamus in drug-refractory tremor. Cortical connections of VIM might differ from person to person. For treatment planning, the best seed points at the cortex are not defined.
Methods and materials: 47 patients with medication-refractory essential tremor or Parkinson disease undergoing VIM ablation contralateral to the patient's hand dominance were recruited. VIM ablations were performed using a HIFU equipment fully compatible with a 3-Tesla MR scanner (Magnetom Skyra, Siemens Healthineers, Erlangen, Germany).
Pre-treatment DTI was co-registered with post-treatment 3D T2WI sequences. The VIM lesion was used as a seed for the DTI-based tractography. Cortical connections were registered and the distance to the mid-sagittal plane was quantified at the juxtacortical white matter on axial T2WI.
Results: HIFU was effective for immediate tremor control. According to cortical connections, patients were allocated into 4 groups: the medial aspect of the primary motor cortex (mM, n=19), intermediate region of the primary motor cortex (between m-M and hand-knob, iM, n=17), hand-knob region of the primary motor cortex (hM, n=2), and supplementary motor area (SMA, n=9). The mean distance from the mid-sagittal plane at these sites was 10.6±1.9 (mM), 17.7±3.2 (iM), 21.9±4.5 (hM), and 9.3±2.2 (SMA) mm.
Conclusion: Seeding of the HIFU-induced VIM lesions on co-registered pre-treatment DTI showed connections predominantly to the primary motor cortex medial to the hand-knob region. This area should be the recommended cortical seeding point for pre-treatment DTI as it will correctly delineate the final treatment location in most patients.
Limitations: The small sample size.
Ethics committee approval: Ethics committee approval obtained.
Funding: No funding was received for this work.
Author Disclosures:
P. Malmierca Ordoqui: nothing to disclose
P. Dominguez Echavarri: nothing to disclose
A. Ezponda Casajus: nothing to disclose
R. Garcia de Eulate: nothing to disclose
M. C. Rodríguez Oroz: nothing to disclose
A. Paternain Nuin: nothing to disclose
O. Parras: nothing to disclose
J. Guridi: nothing to disclose
M. Calvo Imirizaldu: nothing to disclose

RPS 1411c-4 11:33

How anxiety influences brain activity: a connectometry study

M. Porcu[1], P. Garofalo[1], F. Destro[1], A. Operamolla[1], A. Caneglias[2], E. Scapin[1], L. Saba[1]; [1]*Monserrato/IT,* [2]*Cagliari/IT (micheleporcu87@gmail.com)*

Purpose: It is known from the literature that anxiety correlates with reduced interhemispheric connectivity on resting-state functional connectivity. The aim of this study is to verify this hypothesis with the connectometry technique.
Methods and materials: We recruited 20 healthy subjects (13 males, 7 female; age 25-80). Each patient on the same day performed the Italian version of the trait scale of the state-trait anxiety inventory (STAI-I) for the assessment of a situation independent general condition of anxiety and then underwent an MR examination on a 3T scanner (Vantage Titan 3T - Canon) with a 32 channel head coil. The MR protocol included a 12 direction DW sequence for the connectometry analysis. The connectometry analysis was performed using a linear regression model to consider the effects of the STAI-I score, choosing three different T-score thresholds (T-threshold) values (1, 2, and 3). Results were considered statistically valid for p-value adjusted for a false discovery rate (p-FDR)<0.05. The network topology analysis measured the influence of the STAI-I score on brain networks.
Results: The connectometry analysis identified several white matter bundles negatively correlated to STAI-I score for T-threshold=3, in particular at the level of corpus callosum (48% of the total amount of tracts identified). Several properties of the network influenced the network topology analysis.
Conclusion: Anxiety is characterised by reduced interhemispheric connectivity measured with the connectometry technique.
Limitations: The small number of patients recruited and the low number of directions used in the DW sequences.
Ethics committee approval: The study was approved by the local ethical committee. Informed consent was obtained.
Funding: No funding was received for this work.
Author Disclosures:
P. Garofalo: nothing to disclose
M. Porcu: nothing to disclose
L. Saba: nothing to disclose
A. Operamolla: nothing to disclose
F. Destro: nothing to disclose
E. Scapin: nothing to disclose
A. Caneglias: nothing to disclose

RPS 1411c-5 11:39

Three-dimensional magnetic resonance fingerprinting at 3.0T: a preliminary clinical evaluation

G. Di Salle, G. Buonincontri, M. Cencini, M. Tosetti, P. Cecchi, G. Migaleddu, M. Cosottini, G. Donatelli*; Pisa/IT*

Purpose: Magnetic resonance imaging has great relevance in CNS pathology, mainly thanks to the multiple, excellent contrasts between tissues. Among its limitations stand long scan times and sensitivity to patients' motion. The present work compared conventional MR sequences with three-dimensional SSFP MR-fingerprinting (MRF) with spiral projection k-space trajectories. Through such technique, acquisition of quantitative data of T1, T2, and proton density allows for the post-hoc synthesis of conventional qualitative contrasts with reduced motion sensitivity. The aim of this study was to compare MRF with conventional MRI in examining normal and pathological brain structures.
Methods and materials: The signal-to-noise ratio (SNR) and contrast-to-noise ratio (CNR) were calculated on one phantom and two healthy volunteers. Assessment of absolute and relative contrast between grey and white matter, and qualitative evaluation of both normal encephalic structures and pathological findings representation, was conducted in 10 patients with different diseases, part of a protocol including 250 patients.
Results: SNR and CNR were comparable between MRF and conventional imaging (p>0.05 for all comparisons, except higher SNR of conventional FLAIR sequences in white matter, p=0.016). In MRF, absolute contrast was higher in T1-weighted (p=0.01) but lower in T2-weighted and FLAIR images. Relative contrast was higher in T1-weighted (p=0.0003) and comparable in T2-weighted and FLAIR images. Although not superior to conventional imaging in anatomical detail, MRF alone provided sequences with high diagnostic confidence in 7/10 patients, while the others needed further MR scans to reach conclusive diagnoses.
Conclusion: MRF is a promising tool for MRI in that it may preserve a good diagnostic accuracy while reducing the detriment of a long scan time.
Limitations: The small sample size.
Ethics committee approval: Approved by the local ethics committee.
Funding: Italian Ministry of Health, Health Service of Tuscany (research project GR-2016-02361693).
Author Disclosures:
G. Di Salle: nothing to disclose
M. Cencini: nothing to disclose
G. Buonincontri: nothing to disclose
M. Tosetti: nothing to disclose
P. Cecchi: nothing to disclose
G. Migaleddu: nothing to disclose
M. Cosottini: nothing to disclose
G. Donatelli: nothing to disclose

RPS 1411c-6 11:45

Magnetic resonance image compilation (MAGiC): utility in epilepsy imaging

R. Vadapalli, A. S. Vadapalli*; Hyderabad/IN (rammohanvsv@gmail.com)*

Purpose: To evaluate the utility of synthetic imaging in refractory epilepsy imaging.
Methods and materials: 40 patients with refractory seizures aged 12-54 years (Mean age 33+6, M:F ratio 3:2) underwent MR exams on a 3T Pioneer scanner (GE Healthcare, Milwaukee) using an epilepsy protocol+MAGIC sequence.
The conventional epilepsy protocol was supplemented with the synthetic MAGIC sequence, which is one scan yielding 6 contrasts: T1, PD T2FLAIR, STIR DIR, PSIR with quantitative T1 and T2 maps (4 minutes).
The images were randomised and independently assessed for diagnostic quality, morphologic legibility, and diagnostic radiologic findings by two independent neuroradiologists compared to the conventional protocol.
The interobserver variability was recorded using Kappa statistics.
Results: The overall diagnostic quality of synthetic MR images was superior to conventional MR imaging for epilepsy on a 5-level Likert scale (P<0.001; mean synthetic-conventional, -0.344±0.312; Δ=0.5; lower limit of the 95% CI, -0.398).
The legibility of synthetic and conventional morphology agreed in >95%, except in the basifrontal cortex and insulo opercular region in T1 and T1 FLAIR (all, >80%). Synthetic T2 FLAIR had more obvious artefacts, including +19.4% of cases with flow artefacts and +12.5% cases with white noise artefacts.
Interobserver variability was in acceptable limits (Cohen's kappa 0.9).
Conclusion: Synthetic MR imaging (MAGIC) with multiple contrasts is an useful adjunct tool in the comprehensive epilepsy protocol for reducing time penalties.
Limitations: iSyntheic image datasets are still 2D datasets. 3D synthetic imaging data is emerging and high-resolution 3D FLAIR T1 and T2 are still needed for a comprehensive evaluation.
Ethics committee approval: Waiver of informed consent by ERB.
Funding: No funding was received for this work.
Author Disclosures:
R. Vadapalli: Consultant at GE Health care
A. S. Vadapalli: nothing to disclose

RPS 1411c-7 11:51

Synthetic diffusion-weighted imaging (MAGIC DWI) in stroke imaging: a study of 52 cases

R. Vadapalli[1], A. S. Vadapalli[2]; [1]*Hyderabad/IN,* [2]*London/UK (rammohanvsv@gmail.com)*

Purpose: To evaluate the role of multi b-value synthetic diffusion-weighted imaging in the evaluation of stroke.
Methods and materials: 52 patients who presented with symptoms suggestive of stroke with ages of 39-81 years (mean age 49.5+/-10 years; M: F ratio 2:3) were evaluated by a dedicated stroke protocol and supplemented by an additional 2-minute synthetic magic DWI multi b-value protocol after a waiver from IRB.
The parameters of synthetic DWI sequence are as follows: multi b-value DWI acquisition with b-values of 0-1,000 and synthesis of b-values of 1,500 and 2,000, with the maximum b-value not exceeding 2,500.
The sensitivity of the detection of infarcts on conventional DWI was compared to MAGIC DWI.
Results: Of 52 patients, 31 had multiple acute lacunar infarcts in the MCA territory and MCA and PCA watershed zones, 21 in the infratentorial region including the brain stem and cerebellum, and 6 with a sensitivity of 92% and specificity of 97% with conventional DWI.
Using the MAGIC DWI with the synthesis of multiple b-values between 1,000 to 2,500, the sensitivity and specificity significantly improved to 97% and 99%, with an NPV of 99%.
Conclusion: Multi B-value ultra-fast synthetic MAGIC DWI, which is a synthetic diffusion technique, is a powerful adjunct tool to the conventional stroke protocol offering the user a retrospective synthetic slider to generate multi b-value data from 100-2,500, increasing the sensitivity of stroke detection with no time or SNR penalties.
Limitations: B-values above 2,500 are not feasible. The ADC value can be calculated until 1,000.
Ethics committee approval: Ethics committee approval and informed consent obtained.
Funding: No funding was received for this work.
Author Disclosures:
R. Vadapalli: Consultant at GE health care
A. S. Vadapalli: nothing to disclose

RPS 1411c-8 11:57

3D high-resolution myelin imaging using synthetic MRI

M. J. B. Warntjes, P. Johansson, P. Lundberg, A. Tisell*; Linköping/SE (marcel.warntjes@cmiv.liu.se)*

Purpose: Quantitative assessment of myelination is an important clinical biomarker in treatment and follow-up. Myelin can be measured using synthetic MRI; the measurement of the R1 and R2 relaxation and proton density PD, in conjunction with a myelin model, can provide myelin partial volume maps for the entire brain. Recently, a 3D acquisition method was developed for high-resolution, isotropic synthetic MRI. The purpose of this work was to compare myelin detection using 2D and 3D.
Methods and materials: The 3D QALAS sequence is a segmented spoiled gradient-echo sequence with 5 parallel acquisitions, interleaved with a T2 preparation and inversion pulse. The 2D MDME sequence (MAGiC) is a saturation recovery multi-slice TSE sequence with multi-echo read-out. A group of 12 volunteers was acquired two times with 3D QALAS and two times with MDME, both at 1.5T and 3T.
Results: The mean myelin volume for the entire group was 183 mL and the mean brain volume was 1,300 mL (14.1%). A high correlation was found between volumes determined by QALAS and MDME. The Pearson correlation coefficient was 0.94 and the mean difference was 0±13 mL. The difference between measurement 1 and 2 was -2±10 mL at 1.5T and 1±13 mL at 3T for QALAS, whereas it was 0±4 mL at 1.5T and -3±4 mL at 3T for MDME.
Conclusion: Myelin measurements using 3D QALAS provides very similar values of myelin and brain volumes in comparison to 2D MDME. The advantage of 3D QALAS is the ability to view the data in all orientations.
Limitations: A small number of subjects, all of which were healthy.
Ethics committee approval: The study was approved by the local ethical board. All participants provided written informed consent.
Funding: No funding was received for this work.
Author Disclosures:
P. Lundberg: nothing to disclose
P. Johansson: nothing to disclose
M. J. B. Warntjes: Board Member at SyntheticMR, Consultant at SyntheticMR
A. Tisell: nothing to disclose

RPS 1411c-9 12:03

In vivo description of the cerebral microvascular structures of a preterm newborn: the feasibility of superb microvascular imaging (SMI)

A. Barletta[1], P. A. Bonaffini[1], M. Balbi[1], A. Surace[1], A. Caroli[2], S. Gerevini[1], S. Sironi[1]*; [1]Bergamo/IT, [2]Ranica/IT (ninnibarletta@gmail.com)*

Purpose: To explore the potential of superb microvascular imaging (SMI) technology in visualising brain microvessels in preterm neonates of different gestational ages (GA).
Methods and materials: A retrospective, observational, single-centre study including 15 newborns (8 females) was conducted. Preterm patients were equally divided into GA groups according to the WHO sub-categories: extremely (GA< 28 weeks, EP), very (28-31 weeks and 6 days, VP), and moderate to late preterm (32-37 weeks, MLP). All patients underwent transcranial ultrasound (US) using a Toshiba Aplio500 scanner (Canon Medical Systems Corporation) and a linear 14 MHz transducer. Exams were performed during the first day of life via the anterior fontanel including superficial and deep scans (each on coronal and parasagittal planes). Based on their SMI morphology and location, microvessels were classified as extrastriatal (subdivided into cortical and medullary), striatal, or thalamic. Two examiners independently classified the vessels as visible (echogenic linear structures) or invisible. To assess the association between vessel visibility and GA, a binomial logistic regression analysis (separate for each microvessel group) was performed, taking visibility as a dependent variable and both examiners and GA as predictor variables.
Results: A statistically significant difference among GA groups was found in sex ($p=0.030$), GA by definition ($p=0.002$), weight at birth ($p=0.007$), and the Apgar score within 1 minute ($p=0.024$). GA significantly contributed to the visibility of superficial vessels ($p<0.05$ for both cortical and medullary ones) but not striatal and thalamic vessels.
Conclusion: SMI-US is a feasible tool for visualising and assessing intraparenchymal brain microvasculature in pre-term neonates. The morphology and distribution of the brain microvessels seen in the current study are consistent with those described in previous anatomical and radiological research.
Limitations: The retrospective analysis of images.
Ethics committee approval: Written informed consent was obtained.
Funding: No funding was received for this work.
Author Disclosures:
A. Barletta: nothing to disclose
P. A. Bonaffini: nothing to disclose
A. Caroli: nothing to disclose
M. Balbi: nothing to disclose
A. Surace: nothing to disclose
S. Gerevini: nothing to disclose
S. Sironi: nothing to disclose

RPS 1411c-10 12:09

The validity of SyMRI in the assessment of the neonatal brain

V. Schmidbauer, M. C. Diogo, S. A. Jengojan, K. Goeral, A. Berger, D. Prayer, G. Kasprian*; Vienna/AT (schmidbauervictor@gmail.com)*

Purpose: To assess the diagnostic accuracy of T1- and T2-weighted contrasts generated by the MR data post-processing software SyMRI for neonatal brain imaging.
Methods and materials: A total of 32 neonates were included in this retrospective study. 4 independent rating neuroradiologists assessed the neonatal brain on the basis of conventional and SyMRI generated T1- and T2-weighted contrasts. The sensitivity and specificity of both methods were calculated and compared with each other.
Results: Compared to conventionally acquired T1- and T2-weighted images, SyMRI-generated contrasts showed a lower sensitivity but a higher specificity [SyMRI: sensitivity: 0.88, confidence interval (CI): 0.72-0.95; specificity: 1, CI: 0.89-1/conventional MRI: sensitivity: 0.94, CI: 0.80-0.98; specificity: 0.94, CI: 0.80-0.98].
Conclusion: T1- and T2-weighted images, generated by SyMRI showed a comparable diagnostic accuracy to conventionally acquired contrasts. In addition to semi-quantitative imaging data, SyMRI provides diagnostic images and leads to more efficient use of available imaging time in neonatal brain MRI.
Limitations: The small sample size.
Ethics committee approval: The protocol of this study was approved by the local ethics commission and performed in accordance with the declaration of Helsinki.
Funding: No funding was received for this work.
Author Disclosures:
V. Schmidbauer: nothing to disclose
M. C. Diogo: nothing to disclose
S. A. Jengojan: nothing to disclose
K. Goeral: nothing to disclose
A. Berger: nothing to disclose
D. Prayer: nothing to disclose
G. Kasprian: nothing to disclose

RPS 1411c-11 12:15

Sodium MRI in mild traumatic brain injury

H. Grover, Y. Qian, F. Boada, K. Lakshman, S. Flanagan, Y. Lui*; New York/US (hemalgrover@gmail.com)*

Purpose: Metabolic derangements are known to occur after traumatic brain injury (TBI). Animal models point to initial Na^+ influx causing membrane depolarisation. White matter, particularly the corpus callosum (CC), is susceptible to damage. The purpose of this study is to compare the distribution of the total sodium concentration (TSC) in the CC between patients of mild TBI (mTBI) and controls using sodium MRI.
Methods and materials: 11 patients (6 M, 5 F; 20-52 years) with a history of mTBI and 10 healthy controls were studied. Sodium MRI scans were performed on a Siemens Prisma3T scanner using a custom 8-channel dual-tuned (1H-23Na) Tx/Rx head coil. Twisted projection imaging was used (FOV=220 mm, matrix size=64, TE/TR=0.3/100 ms, FA=90, and TA=10.3 min).
Sodium MR images were visually inspected in conjunction with proton MPRAGE. TSC was measured in genu, body, and splenium with 5 mm regions of interest (ROI). To assess for reproducibility, 5 measurements were independently taken within each area. A comparison was made between cohorts with a significance level of 0.05. To assess the distribution of TSC along the CC in the anterior-posterior dimension, the TSC genu/splenium ratio was calculated.
Results: TSC was higher in the genu (51.59 vs 45.6 mmol, $p=0.049$) and lower in the splenium (50.80 vs 41.88 mmol, $p=0.01$) in mTBI patients compared to controls. The genu/splenium ratio was also higher in patients (1.2 vs 0.9, $p=0.001$). On visual inspection, mTBI subjects demonstrated a reversal of the normal TSC anterior-posterior gradient in the CC compared with controls.
Conclusion: TSC distribution in the CC is altered after mTBI. Since changes in extracellular Na^+ concentration are transient after brain injury, detected alterations in TSC are believed to be attributable to changes in the intracellular Na^+ concentration. Our work supports the notion of ongoing Na^+ channelopathy after injury affecting callosal white matter such as perturbed expression of sodium channels.
Limitations: The small sample size.
Ethics committee approval: Institutional IRB approved study.
Funding: NIH-R01.
Author Disclosures:
H. Grover: nothing to disclose
Y. Lui: Research/Grant Support at NIH R01 grant
Y. Qian: nothing to disclose
S. Flanagan: nothing to disclose
F. Boada: nothing to disclose
K. Lakshman: nothing to disclose

RPS 1411c-12 12:21

What have we learnt from delving deeper? Is MR-guided focused ultrasound targeting the zona incerta with the ventral intermedius nucleus an effective treatment for essential tremor long-term?

A. J. Jameel[1], W. M. W. Gedroyc[1], D. Nandi[1], B. Jones[1], O. Kirmi[2], S. Malloy[1], Y. F. Tai[1], P. Bain[1], G. Charlesworth[1]; [1]*London/UK,* [2]*Oxford/UK*
(ayesha.jameel@nhs.net)

Purpose: Magnetic resonance-guided focused ultrasound (MRgFUS) is a non-invasive treatment for essential tremor (ET) that allows targeted thermal ablation of brain tissue. Previous studies demonstrate targeting the thalamic ventral intermedius nucleus (Vim) as an effective treatment in ET. This paper describes the world's first trial using MRgFUS to target both the Vim and the inferior zona incerta (ZI).
Methods and materials: This prospective study enrolled 13 patients with medication refractory ET for a unilateral MRgFUS procedure. Tremor severity and functional impairment were assessed at baseline and regular intervals post-treatment for 24 months, using the clinical rating scale for tremor (CRST).
BFS spirals were also collated intraoperatively, immediately pre-procedure and after targeting the Vim and ZI. All spirals were scored by 3 blinded neurologists. The percentage improvement in the spiral scores after Vim and ZI ablation were compared and analysed.
Results: In all patients, there was successful thermal ablation of the target tissue at both Vim and ZI with improvement in all parameters stable over 24 months. The CRST tremor score improved by 73.5% (treated arm) and 24% (non-treated arm).
The intraoperative BFS scores demonstrated the additional benefit of targeting the ZI was 21.8%; improvement after Vim lesioning was 27.9%, but after both Vim and ZI lesioning was 49.7%.
One patient (7.69%) experienced a significant adverse event; post-treatment unilateral hemi-chorea persistent at 2 years.
Conclusion: Our study provides further evidence that MRgFUS is an effective curative treatment for ET and demonstrates the additional benefit of targeting the thalamic Vim with the inferior ZI. Improvement in the tremor scores of the non-treated arm shows the positive bilateral effects of targeting the ZI.
Limitations: The limited sample size.
Ethics committee approval: REC approved.
Funding: Commercial Grant - Insightec. Equipment - Imperial Health Charity
Author Disclosures:
A. J. Jameel: Other at InsightTec PL- partial funding for research fellow salary
P. Bain: nothing to disclose
W. M. W. Gedroyc: Grant Recipient at InsighTec Plc, Equipment Support Recipient at Imperial Healthcare Charit
D. Nandi: nothing to disclose
B. Jones: nothing to disclose
O. Kirmi: nothing to disclose
S. Malloy: nothing to disclose
Y. F. Tai: nothing to disclose
G. Charlesworth: nothing to disclose

14:00 - 15:30 **Studio 2020**

Oncologic Imaging

RPS 1516

Gastrointestinal and pancreatic advanced imaging and radiomics in oncology

Moderators:
G. Kaissis; München/DE
S. Kharuzhyk; Minsk/BY

RPS 1516-1 14:00

CT texture analysis of gastrointestinal stromal tumours (GIST)

E. Tabone[1], G. Cappello[2], V. Giannini[2], A. Defeudis[2], R. Cannella[3], T. V. Bartolotta[3], D. Regge[2]; [1]*Turin/IT,* [2]*Candiolo/IT,* [3]*Palermo/IT*

Purpose: To evaluate the association between radiomic biomarkers extracted from baseline CT imaging and the mitotic count, tumour mutational profile, and prognostic Miettinen classification.
Methods and materials: This retrospective multicentre observational study included 63 histologically proven GISTs. Each lesion was manually segmented and 37 texture features were extracted both on a single slice and on the entire tumour volume. The reference standards were pathological findings and the Miettinen classification. Patients were dichotomised with the mitotic count (≤5/50HPF vs >5/50HPF), mutational status (c-KIT mutation vs PDGFRα and Wild-Type), and patient prognosis (good prognosis class: none, very low, and low risk vs poor prognosis class: intermediate and high risk). Univariate analyses using the Mann-Whitney test and multivariate analysis were performed and a stepwise logistic regression model to predict the patients' prognosis was developed using 70% of patients as the training set and the remaining 30% as the test set.
Results: 8 3D-features discriminated lesions with a low or high mitotic-count (best AUC 0.81, best sensitivity 86%, and best specificity 93%). 6 3D-parameters detected GISTs based on the mutational group (best AUC 0.77, best sensitivity 75%, and best specificity 79%) and 3 parameters correlated with the risk class (best AUC 0.76, best sensitivity 72%, and best specificity 85%). In the differentiation between GIST at a lower or higher risk of recurrence, the regression model used 6 different features and obtained AUC 0.78, sensitivity 65%, specificity 79%, VPN 71%, and VPP 73% on the training set, and AUC 0.83, sensitivity 88%, and specificity 75% on the test set.
Conclusion: Our results show a good correlation between radiomics features, disease aggressiveness, mutational profile, and the risk of recurrence. Results are promising but validation on external datasets will be necessary to confirm the role as an imaging biomarker.
Limitations: n/a
Ethics committee approval: n/a
Funding: No funding was received for this work.
Author Disclosures:
D. Regge: nothing to disclose
E. Tabone: nothing to disclose
T. V. Bartolotta: nothing to disclose
G. Cappello: nothing to disclose
V. Giannini: nothing to disclose
A. Defeudis: nothing to disclose
R. Cannella: nothing to disclose

RPS 1516-2 14:06

The prognostic role of diffusion kurtosis imaging for advanced gastric cancer after neoadjuvant chemotherapy

J. Fu, L. Tang, Q. Shi, Z. Li, Y.-S. Sun, J. Ji; *Beijing/CN*
(18410259295@163.com)

Purpose: To investigate whether DKI parameters are associated with overall survival (OS) in patienta with advanced gastric cancer after neoadjuvant chemotherapy.
Methods and materials: From 2014-2016, 46 consecutive patients with a biopsy-proven gastric cancer who underwent pre-neoadjuvant chemotherapy MRI with DKI (b=0, 200, 500, 800, 1,000, 1,500, and 2,000s/mm^2) were enrolled in this retrospective study. The region of interest was manually drawn on the specific slice showing the largest area of the tumour. Three parameters of DKI were calculated automatically: apparent diffusion coefficient (ADC, b=800s/mm^2), kurtosis (K), and diffusivity (D) value. Cox proportional hazards analyses were performed to determine the relationship between DKI parameters, neoadjuvant pathologic T-stages, tumour location, histologic subtype, and OS.
Results: The median follow-up was 37.7 months and 11 patients had died at a median time of 16.6 months. There was no significant difference in pre-treatment DKI parameters between the histologic subtypes. The ADC and K values were associated with a negative prognosis ($p=0.048$, $p<0.001$). Cox analysis showed that the K value ([HR], 1.011; 95% [CI]: 1.005, 1.018; $p<0.001$) was the representative predictor of OS. The optimum threshold point was 0.618.
Conclusion: DKI parameters can potentially provide prognostic information complementary to ADC for gastric cancer patients after neoadjuvant chemotherapy.
Limitations: The relatively small population in our study might result in bias in the results. We only explored the correlation between pre-neoadjuvant chemotherapy (pre-NACT) DKI parameters and overall survival, not all prognostic factors such as DKI parameters of post-NACT or PFS.
Ethics committee approval: This study was approved by our local institute review board.
Funding: No funding was received for this work.
Author Disclosures:
J. Fu: nothing to disclose
L. Tang: nothing to disclose
Z. Li: nothing to disclose
Q. Shi: nothing to disclose
J. Ji: nothing to disclose
Y.-S. Sun: nothing to disclose

RPS 1516-3 14:12

A radiomics approach to characterise the deficient DNA mismatch repair system and predict survival in colorectal cancer patients

Y. Y. Huang, Y. Li, Z. Liu; *Guangzhou/CN (yikiann@126.com)*

Purpose: To develop and validate a radiomic signature to characterise the deficient mismatch repair (MMR) system and investigate its prognostic value for survival prediction in colorectal cancer patients (CRC).
Methods and materials: The training cohort included 170 CRC from January 2008-December 2010. The independent validation cohort contained 91 patients from January 2011-December 2013. 92 features were extracted from tumours on venous-phase CT. We developed a radiomic signature to characterise MMR status (deficient MMR [dMMR] vs proficient MMR [pMMR]) with a Lasso regression model with discrimination and calibration performance assessed and validated, followed by a prediction performance of the radiomic signature for the overall survival (OS) assessed and validated.
Results: The radiomic signature, consisting of 3 features, was associated with MMR status (P<0.001 for both cohorts). The radiomic signature showed good discrimination (C-index: 0.815 [95% CI :0.693, 0.931] in the training cohort; 0.815 [0.712, 0.914] in the validation cohort) and good calibration. This MMR-related radiomic signature was found significantly associated with OS (training cohort: p=0.008, validation cohort: p=0.028) and was a significant predictor for OS when validated (C-index=0.66; 95% CI: 0.55–0.76; p<0.001). OS was significantly improved in the high-radiomic-score group (HR: 2.506, 95% CI: 1.071–5.863; p:0.034).
Conclusion: Our study presents a radiomic signature to characterise a deficient MMR system, which was shown to be predictive of OS in CRC. This study, through applying radiomics to correlate molecular subtypes with OS, suggests that radiomics might offer a non-invasive way to predict survival by identifying imaging features that could reflect underlying molecular drivers. This study might shed light on patient stratification for 'omics'-guided therapies and envision the future of precision medicine.
Limitations: The retrospective nature of data collection and the lack of external validation.
Ethics committee approval: Ethical approval by the institutional review board was obtained for this retrospective analysis with informed consent waived.
Funding: The National Natural Scientific Foundation of China (No.81771912 and 81701782).
Author Disclosures:
Y. Y. Huang: nothing to disclose
Y. Li: nothing to disclose
Z. Liu: nothing to disclose

RPS 1516-4 14:18
The utility of radiomics at baseline rectal MRI to predict the clinical complete response of rectal cancer after chemoradiation therapy
E. J. Ortiz[1], F. Tixier[1], J. S. Golia Pernicka[2], V. Paroder[1], D. Bates[1], N. Horvat[1], M. J. Gollub[1], H. Veeraraghavan[1], I. Petkovska[1]; [1]*New York, NY/US,* [2]*Bridgeport, CT/US (ejoh85@gmail.com)*

Purpose: To investigate the significance of T2-weighted-based radiomic data extracted from baseline rectal MRI combined with qualitatively assessed imaging features in predicting the clinical complete response after neoadjuvant CRT for rectal cancer.
Methods and materials: A retrospective study of patients with locally advanced rectal cancer who underwent rectal MRI before neoadjuvant CRT from October 2011–January 2015 followed by surgery was conducted. The reference standard for the pathologic complete response was the surgical histopathologic specimen after CRT. Qualitatively assessed imaging features were extracted from our institutional standardised radiology report. In radiomics analysis, one radiologist manually segmented the primary tumour on T2-weighted images for 102 patients to be used as the training set; two different radiologists independently segmented 66/102 patients to be used as the validation set. Using CERR software, 108 radiomics features were extracted. The Wilcoxon test was used to identify scanner-independent features. Subsequently, a least absolute shrinkage operator analysis was used to extract a radiomics score. A support vector machine model combining the radiomics score and qualitatively assessed clinical descriptors was compared against both clinical and radiomics-only models using the deLong test.
Results: 102 patients were included. The radiomics score produced an AUC of 0.75. Comparable results using the validation set were AUC=0.69 and 0.71 for each radiologist, respectively. The SVM model using the qualitative features had an accuracy of 67% (sensitivity 42%, specificity 72%); when adding the radiomics score, the accuracy increased to 74% (sensitivity 58%, specificity 77%).
Conclusion: The prediction of the clinical response to stratify patients before neoadjuvant therapy may be obtained by combining a radiomics-based score and qualitatively assessed features from pre-treatment rectal MRI.
Limitations: The manual segmentation, radiomics analyses based on T2-weighed images only, and imbalanced dataset.
Ethics committee approval: Institutional IRB approval.
Funding: Funding in part through the NIH/NCI Cancer Center Support Grant P30CA008748 and the Colorectal Cancer Research Center CC50367 at MSKCC.
Author Disclosures:
E. J. Ortiz: nothing to disclose
J. S. Golia Pernicka: nothing to disclose
V. Paroder: nothing to disclose
D. Bates: nothing to disclose
N. Horvat: nothing to disclose
M. J. Gollub: nothing to disclose
H. Veeraraghavan: nothing to disclose
I. Petkovska: nothing to disclose
F. Tixier: nothing to disclose

RPS 1516-5 14:24
Data mining for the evaluation of response to neoadjuvant chemoradiotherapy in locally advanced rectal cancer using a decision tree algorithm
F. Landolfi[1], M. Rengo[1], S. Badia[2], S. Picchia[2], E. Iannicelli[1], A. Laghi[1]; [1]*Rome/IT,* [2]*Latina/IT (federica.landolfi@uniroma1.it)*

Purpose: To develop and validate a decision tree model based on high-resolution T2-weighted (T2w) magnetic resonance (MR) images features, to discriminate between complete responder (CR) and partial/non-responder (P/NR) patients with locally advanced rectal cancer (LARC) after neoadjuvant chemoradiotherapy (CRT).
Methods and materials: A population of 65 patients (training cohort; 23 CR and 42 P/NR) was selectedto train a J48 classifier algorithm in identifying CR and P/NR patients, analysing images acquired on a 3 Tesla scanner. The developed model was validated on a population of 30 patients (validation cohort; 9 CR and 21 P/NR) who underwent MR on a 1.5 Tesla scanner.4 features, manually measured by 2 expert radiologists on pre and post CRT T2wimages were used to build the model: the tumour volume before and after therapy, MR tumour regression grade (MR-TRG) assessed according to Mandard score, volume reduction ratio (VRR), and T2 signal reduction ratio (DSI). All patients underwent surgical resection and histopathology was employed as the standard reference.
Results: The model correctly classified 26 (86.67%) patients with a mean absolute error of0.16%. Only 4 patients (13.33%) were misclassified: 3 CR classified as P/NR and1 P/NR classified as CR. The sensitivity for the identification of CR was 0.67, thespecificity 0.95.
Conclusion: The model, based only on manually-extracted features from T2w images, provided a high accuracy (86.67%) in the evaluation of CRT response, correctly classifying 95% of P/NR and 67% of CR. In the emerging scenario of a "wait and see" policy, these results could prove to be a very useful tool in the identification of P/NR patients, thus avoiding a delay of surgery in patients with a residual tumour and a surgical overtreatment in patients with complete response to CRT.
Limitations: A retrospective study with a small population sample.
Ethics committee approval: n/a
Funding: No funding was received for this work.
Author Disclosures:
F. Landolfi: nothing to disclose
M. Rengo: nothing to disclose
S. Badia: nothing to disclose
S. Picchia: nothing to disclose
E. Iannicelli: nothing to disclose
A. Laghi: nothing to disclose

RPS 1516-7 14:36
The impact of a structured report on the quality of preoperative CT staging of pancreatic ductal adenocarcinoma
M. Di Marco, F. Vernuccio, R. Cannella, S. Pellegrino, F. Allegra, D. G. Castiglione, G. Salvaggio, M. Midiri, G. Brancatelli; *Palermo/IT (davidegiuseppecastiglione@gmail.com)*

Purpose: To test whether a standardised structured radiology report improves the quality of preoperative CT staging of pancreatic ductal adenocarcinoma (PDA) compared to conventional free-text reports.
Methods and materials: In this retrospective, single-centre study, we included 27 patients (mean age, 64±11.1 years) with pathologically proven PDA operated on between 2015-2018 and imaged with pancreatic CT. 4 readers independently reported CT scans with both free-text and a structured report. The differences in reported morphologic and vascular features were assessed through a McNemar Test. The intra-reader and inter-reader agreements were calculated.
Results: 216 (108 conventional and 108 structured) reports were analysed. Encasement of the left gastric artery, gastroduodenal artery, and splenic artery was described in up to 14.8% using free-text reports and up to 29.6% using a structured report, resulting in low intra-reader agreement (k=0.033-0.216). Inter-reader agreement improved with a structured report compared to free-text reports for the left gastric artery (ICC=0.844 vs ICC=0.493, respectively), gastroduodenal artery (ICC=0.730 vs ICC=0.449, respectively), portal vein (ICC=0.847 vs ICC=0.638, respectively), portal confluence (ICC=0.848 vs

ICC=0.422, respectively), superior mesenteric vein (ICC=0.765 vs ICC=0.695, respectively), and the splenic vein (ICC=0.921 vs ICC=0.841, respectively).
Conclusion: The use of structured reports improves the quality of preoperative CT staging of pancreatic adenocarcinoma by significantly reducing the number of missed morphological and vascular features of PDA. Moreover, structured reporting results in a significant improvement of inter-reader agreement compared to free-text reports.
Limitations: The limited number of patients, retrospective nature, potential to miss unexpected findings not included in the template, potential testing or learning effect, and lack of time constraints for reporting.
Ethics committee approval: IRB approved. Waiver of informed consent obtained.
Funding: No funding was received for this work.
Author Disclosures:
M. Di Marco: nothing to disclose
F. Vernuccio: nothing to disclose
R. Cannella: nothing to disclose
S. Pellegrino: nothing to disclose
F. Allegra: nothing to disclose
D. G. Castiglione: nothing to disclose
G. Salvaggio: nothing to disclose
M. Midiri: nothing to disclose
G. Brancatelli: Other at lecture fees from Bayer

RPS 1516-8 14:42
Low-energy virtual monoenergetic images from DECT can improve the accuracy of CT perfusion calculations
S. Skornitzke, H.-U. Kauczor, W. Stiller*; Heidelberg/DE*
(Stephan.Skornitzke@med.uni-heidelberg.de)

Purpose: Virtual monoenergetic images (VMI) from dual-energy computed tomography (DECT) can improve image quality in contrast-enhanced abdominal CT imaging. A translation to CT perfusion could increase measurement accuracy by improving the delineation of changes in contrast agent concentrations.
Methods and materials: Dual-source DECT scans were acquired in 17 patients with pancreatic carcinomas with a DECT perfusion protocol consisting of 34 acquisitions at 80kV$_p$/Sn140kV$_p$ over 51 seconds. VMIs were calculated for energy levels between 40keV and 150keV in 5keV steps (Monoenergetic+, Siemens Healthineers). Perfusion maps of blood flow were calculated using the maximum-slope model for VMIs and polyenergetic 80kV$_p$ images. Perfusion maps were quantitatively evaluated in terms of blood flow in healthy tissue and the carcinoma, the contrast between tissue types, noise, and contrast-to-noise ratio (CNR), comparing VMIs to 80kV$_p$ images.
Results: The measured blood flow increased with energy level from 114±37ml/100ml/min (healthy tissue) and 46±25ml/100ml/min (carcinoma) for 40keV to 129±59ml/100ml/min (healthy tissue) and 76±50ml/100ml/min (carcinoma) for 150keV, compared to 114±37ml/100ml/min (healthy tissue) and 47±27ml/100ml/min (carcinoma) for 80kV$_p$ images. The differences between tissue types were statistically significant for all VMIs and 80kV$_p$ images ($p<0.05$). The measured blood flow was not significantly different between VMIs and 80kV$_p$ images for energies below 110keV. Noise in perfusion maps was reduced for low-energy VMIs (40keV:19ml/100ml/min; 80kV$_p$:23ml/100ml/min) and CNR was higher (40keV:3.7±1.9; 80kV$_p$:3.2±1.6) compared to 80kV$_p$ images. The differences in noise and CNR were statistically significant for all energy levels except those between 60keV and 75keV.
Conclusion: CT perfusion maps calculated from low-energy VMIs show improved quantitative image quality compared to conventional polyenergetic 80kV$_p$ images.
Limitations: Further evaluation of diagnostic image quality and patient radiation exposure seems necessary.
Ethics committee approval: Institutional review board approval and written informed consent were obtained.
Funding: No funding was received for this work.
Author Disclosures:
S. Skornitzke: Shareholder at Investment funds containing shares of healthcare companies
H.-U. Kauczor: nothing to disclose
W. Stiller: nothing to disclose

RPS 1516-9 14:48
The apparent diffusion coefficient (ADC) allows early prediction of response after prophylactic DC vaccination for pancreatic ductal adenocarcinoma (PDAC) prevention
A. J. Shangguan[1], M. Figini[2], L. Pan[3], J. Yang[1], A. Eresen[1], Y. Velichko[1], V. Yaghmai[1], Z. Zhang[1]; *[1]Chicago, IL/US, [2]London/UK, [3]Suzhou/CN*
(junjie.shangguan@northwestern.edu)

Purpose: We evaluated ADC as an imaging biomarker for the prediction of response to prophylactic DC vaccination in a Panc02 mouse model of pancreatic cancer,
Methods and materials: 20 mice were randomly assigned to treatment or control groups. The animals underwent 3 intraperitoneal injections of DC vaccines, mature DCs, Panc02 lysates, or no treatment, followed by tumour induction via Panc02 cell injection into the pancreas and weekly MRI scans. ADC was calculated from DW-MRI using MatLab. ΔADC is the ADC difference between 1 and 3w after tumour induction. Tumour tissue was collected for histology. Statistical analysis was performed on GraphPad Prism. The receiver operating curve (ROC) was generated.
Results: The ΔADC of the vaccines group was higher than the control groups and correlated with a diminished tumour volume, survival, and % interstitial collagen on histology. Prophylactic DC-vaccination also induced an anti-tumour immune response in vivo, a decreased tumour volume, and prolonged survival. Survival >49d was considered positive events for ROC. Distance analysis and Youden indexing both showed that optimal cut-off values were $-8.52\text{x}10^{-5}$ and $-9.24\text{x}10^{-5}$, with specificities of 0.9 and 0.7, and an odds ratio of 2.33.
Conclusion: ΔADC can predict the response to prophylactic DC vaccination in a Panc02 mouse model of pancreatic cancer.
Limitations: Our study only tracked up tumour growth for 3 weeks and did not track serum pro-inflammatory cytokines in mice. However, 3-time points are a sufficient number of time points for tracking tumour growth in MRI studies. We also demonstrated in vivo anti-tumor cell-mediated cytotoxicity using LDH assay.
Ethics committee approval: All animal protocols were approved by the institutional animal care and use committee.
Funding: The National Institutes of Health of USA, Radiology Society of North America, Fischel Fellowship, and Eisenberg Award.
Author Disclosures:
A. J. Shangguan: nothing to disclose
M. Figini: nothing to disclose
L. Pan: nothing to disclose
J. Yang: nothing to disclose
A. Eresen: nothing to disclose
Y. Velichko: nothing to disclose
V. Yaghmai: nothing to disclose
Z. Zhang: nothing to disclose

RPS 1516-10 14:54
The value in preoperative detection of pancreatic neuroendocrine tumours with spectral images derived from dual-layer spectral detector CT
Y. Yang, R. Li, J. Xu, Q. Han, X. Chen, F. Yan*; Shanghai/CN*
(yyz01a15@rjh.com.cn)

Purpose: To investigate the added value of spectral images derived from dual-layer spectral detector CTs (DLCT) for pancreatic neuroendocrine tumour (pNET) preoperative detection in comparison to 120-kVp conventional polyenergetic images (PI).
Methods and materials: 23 patients were pathologically confirmed of pNET after operations were enrolled. PI, iodine density map, and virtual monoenergetic images (VMI) were reconstructed. One resident and one senior radiologist independently interpreted the images to lesion localisation using PI and subsequently combined PI and spectral images. The CT value and iodine density of the lesion and pancreatic parenchyma were collected. CNR were calculated and compared between VMIs and PI. Lesion detection accuracy was recorded and compared with and without spectral images.
Results: There were 26 confirmed lesions among 23 patients. The detected tumours increased from 20 to 24 with additional spectral information compared to only with PI for the resident radiologist, and from 23 to 25 for the senior radiologist. The sensitivity of the preoperative diagnosis of pNET increased from 76.9% to 92.3%, and from 88.5% to 96.2%, respectively. The CT value of the lesion with VMI$_{40keV}$ was significantly higher than with PI; 179.3±35.3 HU vs 504.1±129.3 HU in the artery phase and 148.3±25.9 HU vs 401.8±87.4 HU in the portal phase. The CNR of the lesion with VMI$_{40keV}$ was higher than with PI; 3.4±1.8 HU vs 12.8±6.6 in the artery phase and 2.7±1.6 HU vs 10.2±5.8 in the portal phase (all $p<0.001$).
Conclusion: Preoperative diagnostic performance for pNET can be significantly improved with spectral images derived from DLCT. VMI$_{40keV}$ provided the best conspicuity and highest CNR of the lesion.
Limitations: The number of patients was relatively small.
Ethics committee approval: Written informed consent obtained.
Funding: No funding was received for this work.
Author Disclosures:
R. Li: nothing to disclose
Y. Yang: nothing to disclose
J. Xu: nothing to disclose
Q. Han: Employee at Philips Clinical Medical Research Division,Shanghai
X. Chen: Employee at Philips Clinical Medical Research Division,Shanghai
F. Yan: nothing to disclose

RPS 1516-11 15:00

Iodine concentration and tissue density in dual-energy contrast-enhanced CT as a potential quantitative parameter in early detection of local pancreatic cancer recurrence

R. M. Mathy, F. Fritz, W. Stiller, H.-U. Kauczor, S. Skornitzke*; Heidelberg/DE*

Purpose: Early diagnosis of local pancreatic cancer recurrence remains challenging. We quantitatively evaluated the diagnostic potential of dual-energy (DE) contrast-enhanced CT for distinguishing recurrent carcinoma from the unspecific postoperative soft-tissue formation (PSF).
Methods and materials: After potentially curative pancreatic carcinoma resection, 36 consecutive patients with PSF were examined with DECT, acquiring 34 images ($80kV_p/140kV_p$) every 1.5s starting 13s after the bolus injection (80ml contrast agent, 370mg/ml, flow rate 5ml/s). Corresponding time points of arterial, pancreatic, and early venous phase (delay 10s, 19s, and 30s) were calculated from bolus trigger times in prior conventional CTs. Iodine and $120kV_p$-equivalent (M0.5) images were calculated. Regions of interest were placed in each soft-tissue formation. The diagnosis of local recurrence was confirmed by regular follow-up or by histological study.
Results: The final diagnosis was a local recurrence in 23 patients and unspecific PSF in 13 patients. The early venous average iodine concentration in recurrent carcinomas was significantly higher than in unspecific PSF (1.4mg/ml vs 0.9mg/ml, p=0.02). Arterial and pancreatic phase iodine concentrations in recurrent carcinomas were higher than in unspecific PSF, but not significant (1.2mg/ml vs 1.0mg/ml, p=0.24; 1.3mg/ml vs. 1.2mg/ml, p=0.48, respectively). Early venous density of recurrent carcinoma in $120kV_p$-equivalent images was significantly higher (70HU vs 48HU, p=0.008). The ROC-curve analysis for early venous iodine concentrations (AUC=0.76) suggests cut-off values >=1.5mg/ml for local recurrence (specificity 0.92, sensitivity 0.57) and <=0.5mg/ml for unspecific PSF (specificity 0.96, sensitivity 0.45).
Conclusion: In difficult cases, measuring iodine concentrations or density in PSF in (early) venous phase DECT can be a valuable additional parameter for differentiating local recurrence from unspecific PSF.
Limitations: The initial purpose of this study was evaluating CT-perfusion, so the protocols were not optimised for evaluating DECT-data.
Ethics committee approval: Institutional review board approval and written informed consent were obtained.
Funding: Supported by BMBF-grant 031L0163.
Author Disclosures:
F. Fritz: nothing to disclose
R. M. Mathy: nothing to disclose
W. Stiller: Advisory Board at Philips Medical Systems
H.-U. Kauczor: nothing to disclose
S. Skornitzke: Shareholder at Investment funds containing shares of healthcare companies

RPS 1516-12 15:06

Portal radiomics in pancreatic head cancer: the relationship to the superior mesenteric vein resection margin

Y. Bian, X. Fang, L. Wang, J. Lu, G. Jin, H. Zhang*; Shanghai/CN (bianyun2012@foxmail.com)*

Purpose: To accurately identify the relationship between the portal radiomics score (rad-score) and the pathologic superior mesenteric vein (SMV) resection margin in patients with cancer in the head of the pancreas.
Methods and materials: 181 patients with pathologically confirmed cancer in the head of the pancreas who underwent multislice computed tomography within one month of resection from January 2016-December 2018 were retrospectively investigated. For each patient, 1,029 radiomics features of the portal phase were extracted, which were reduced using the least absolute shrinkage and selection operator (LASSO) logistic regression algorithm. Multivariate logistic regression models were used to analyse the association between the portal rad-score and SMV resection margin.
Results: Patients with negative (R0) and positive (R1) margins accounted for 70.17% (127) and 29.83% (54) of the cohort, respectively. The rad-score, which is based on 11 selected portal phase features, was significantly associated with the SMV resection margin status (P<0.05). Multivariate analyses confirmed a significant and independent association between the portal rad-score and SMV resection margin (P<0.0001); a higher portal rad-score was associated with R1 resection (P for trend <0.0001).
Conclusion: The portal rad-score is independently and positively associated with the risk of the SMV R1 resection in pancreatic head cancer.
Limitations: Retrospective in nature, the results were established based on data obtained from a single centre, and the available samples were limited.
Ethics committee approval: This retrospective single-centre cross-sectional study was reviewed and approved by the Biomedical Research Ethics Committee of Changhai Hospital.
Funding: National Science Foundation for Scientists of China (81871352, 81701689), Top Project of the Military Medical Science and Technology Youth Training Program (17QNP017).
Author Disclosures:
Y. Bian: nothing to disclose
X. Fang: nothing to disclose
L. Wang: nothing to disclose
J. Lu: nothing to disclose
G. Jin: nothing to disclose
H. Zhang: nothing to disclose

RPS 1516-13 15:12

A radiomics approach to pancreatic adenocarcinoma characterisation compared to the routine evaluation of CE-MDCT tissue attenuation features

V. Tikhonova, I. Gruzdev, E. V. Kondratyev, G. Karmazanovsky*; Moscow/RU (vdovenkobc28@mail.ru)*

Purpose: Attenuation characteristics of the pancreatic ductal adenocarcinoma (PDAC) and contrast material uptake vary depending on the histological grade and pancreatic parenchyma condition. The purpose of this study was to compare dynamic contrast enhancement (DCE) and radiomics features in predicting pancreatic adenocarcinoma grades. The data obtained from an analysis of the radiomics of pancreatic cancer can subsequently be used to predict the prognosis of patients with PDAC and for the inclusion of big data analysis in the diagnosis process.
Methods and materials: 62 consecutive patients with histologically-confirmed PDAC who underwent CE-MDCT were enrolled in the study. We compared the mean lesion attenuation and relative tumour enhancement ratio (RTE) of different types of PA and radiomics features using arterial, venous, and delayed-phase MDCT scans.
Results: Tumour attenuation parameters showed significant association with the PDAC grade, especially when calculated using both venous and delayed-phase images. RTE_{del} showed a significant difference between low and high-grade PDAC (-0.17±0.3 vs -0.06±0.09, p<0.005). RTEart showed a significant difference between intermediate and high-grade PDAC (-0.52±0.23 vs -0.67±0.19, p<0.05). We identified different radiomics features that best correlated with the PDAC grade (MPP, kurtosis, SSF etc). The diagnostic performance of joint CE-MDCT features with radiomics signature increased compared with CE_MDCT features alone (sensitivity 97.3 vs 91.3%, specificity 84.1 vs 80%).
Conclusion: The analysis of radiomics features and DCE features is useful for PDAC grade prediction.
Limitations: The study was single-centred with standardised CE-MDCT protocols. We plan to test the robustness of texture analysis in future studies.
Ethics committee approval: n/a
Funding: No funding was received for this work.
Author Disclosures:
V. Tikhonova: nothing to disclose
I. Gruzdev: nothing to disclose
E. V. Kondratyev: nothing to disclose
G. Karmazanovsky: nothing to disclose

RPS 1516-14 15:18

Pancreatic solid pseudopapillary neoplasm: CT imaging appearance correlation with invasive behaviours

W. Mingliang, Z. Mengsu*; Shanghai/CN (wang.mingliang@zs-hospital.sh.cn)*

Purpose: To investigate the CT imaging appearance of pancreatic solid pseudopapillary neoplasm (pSPN) in predicting pathological invasive behaviours.
Methods and materials: The clinical data and CT data of 103 patients with solid pseudopapillary neoplasm confirmed by surgical resection and pathology were retrospectively analysed. According to the pathological results, all cases were divided into two groups (the invasive group and non-invasive group). Image analysis included tumour number, location, size, shape, calcification, haemorrhage, fibrous pseudo capsule, and the proportion of cystic or solid component. The density of the solid components in all lesions was measured in plain scan, the arterial phase, and venous phase of CT images. The differences between the two groups were statistically analysed.
Results: All 103 cases of pSPN had a single lesion. 38 cases were in the invasive group and 65 cases were in the non-invasive group. There were statistically significant differences in the fibrous pseudo capsule and the proportion of cystic or solid component between the two groups (P<0.05). There were no significant differences in neoplasm maximum diameter, location, morphology, calcification, haemorrhage, pancreaticobiliary dilatation, and pancreatic atrophy between the two groups (P>0.05). The density in the venous phase (76.65±16.71) in the invasive group was higher than that in the non-invasive group (70.09±12.02) and the difference was statistically significant (P<0.05).

Conclusion: The pSPN has no capsule or incomplete capsule, more solid components, and obvious enhancement of the solid components in the tumour in the venous phase, which may suggest that the tumour has more invasive behaviour.
Limitations: There was no delay scan for CT scans.
Ethics committee approval: The retrospective study was approved by the institutional review board of our hospital.
Funding: No funding was received for this work.
Author Disclosures:
W. Mingliang: nothing to disclose
Z. Mengsu: nothing to disclose

RPS 1516-15 15:24
The rate of muscle loss measured with CT is a prognostic marker in patients with unresectable pancreatic cancer receiving FOLFIRINOX
E. Salinas-Miranda, F. Khalvati, D. G. O'kane, X. Dong, D. J. Knox, O. Bathe, V. Baracos, D. S. Gallinger, M. A. Haider*; Toronto, ON/CA (emmanuels7@gmail.com)*

Purpose: To assess the prognostic value of body composition biomarkers assessed by CT in pancreatic cancer patients (PC) undergoing FOLFIRINOX chemotherapy.
Methods and materials: We analysed the pre-treatment and first follow-up CT of 64 PC patients enrolled in a trial receiving FOLFIRINOX. Skeletal muscle, intraabdominal fat, subcutaneous fat, and intramuscular fat were measured as normalised cross-sectional areas (cm^2/m^2) at the L3-level. SliceOmatic software v5.0 was used. We calculated the rate of muscle loss (RML) over a follow-up time of 90 days. The associations between CT body composition measurements and clinical variables with time to progression (TTP) and overall survival (OS) were determined using a Cox proportional hazard analysis. Statistically significant variables in univariate analysis were included for multivariate analysis.
Results: In the multivariate analysis, the rate of muscular loss was significantly associated with OS and TTP, with a hazard ratio (HR) of 2.61 (CI: 1.37-4.95, p=0.003) and 1.92 (CI: 1.17-3.15, p=0.009), respectively. The optimal cut-point of RML was 8.18 cm^2/m^2 per 90 days for OS (HR:2.21, CI: 1.23-3.98, p<0.007) and 6.02 cm^2/m^2 per 90 days for TTP (HR:2.95, CI: 1.5-5.46, p<0.001). None of the remaining body composition measurements was associated with OS or TTP in multivariate analysis. RML remained significant in the prognostication for OS while the RECIST status at the first follow-up did not.
Conclusion: In patients with locally advanced and metastatic PC, the high RML between the first and second CT is associated with worse survival and earlier tumour progression.
The RML from baseline to the first follow-up CT in patients receiving FOLFIRINOX may add value to response prediction in PC and help with therapy modulation or nutritional intervention. Further prospective validation is required.
Limitations: A retrospective study with a low sample size.
Ethics committee approval: IRB approved the study.
Funding: Ontario Institute for Cancer Research and the Translational Research Initiative in Pancreatic Cancer and Clinician Investigator Program was granted to Masoom Haider.
Author Disclosures:
F. Khalvati: nothing to disclose
D. G. O'kane: nothing to disclose
E. Salinas-Miranda: nothing to disclose
X. Dong: nothing to disclose
D. J. Knox: nothing to disclose
O. Bathe: nothing to disclose
V. Baracos: nothing to disclose
D. S. Gallinger: nothing to disclose
M. A. Haider: nothing to disclose

14:00 - 15:30 **Room Y**

My Thesis in 3 Minutes

MyT3 15
Genitourinary

Moderators:
D. Junker; Hall in Tirol/AT
E. Rud; Oslo/NO

MyT3 15-1 14:00
Diagnostic value of attenuation measurement of the kidney on unenhanced helical CT in obstructive urolithiasis
H. H. Shanbhag*; Mumbai/IN (harshitha.shanbhag91@gmail.com)*

Purpose: The aim of this study was to evaluate the diagnostic value of attenuation measurement of kidney on NCCT (non-contrast CT) in comparison with other secondary signs of obstructive urolithiasis.
Methods and materials: 150 patients with acute unilateral flank pain, above the age of 18 years underwent NCCT, 50 control subjects admitted for other acute abdominal emergencies without urinary complains were included. Attenuation values were measured with ROI (40 mm^2) in upper, middle, lower portion of renal parenchyma (cortex). Mean attenuation value (Hounsfield units) was calculated for each kidney. A difference in mean attenuation values was calculated . Presence or absence of hydroureter, perinephric fat stranding, soft tissue rim surrounding the ureteral stone was noted.
Results: Among 150 patients with documented renal stones, mean attenuation of obstructed kidneys was 28.81+/-2.18HU (range 26.63-30.99). Mean attenuation in controls was 36.40 +/- 2.93 (range 33.47-39.33). A renal parenchymal density difference of 5.4 HU or greater had 86.26% sensitivity, 98.26% specificity, 99.17% positive predictive value, 69.36% negative predictive value, and 86% accuracy in predicting the presence of acute obstructing ureteral stone. It was more sensitive, specific and accurate compared to secondary signs such as hydroureter, perinephric stranding and soft tissue rim sign.
Conclusion: Renal parenchymal density difference of greater than or equal to 5.4HU is valuable sign of acute ureteral obstruction which showed better diagnostic accuracy than other secondary signs with advantage of being the only measurement-based parameter.
Limitations: Due to retrospective design, relationship between attenuation difference and duration of pain could not be evaluated.
Ethics committee approval: Institutional ethics committee approval was obtained. Written informed consent was taken from patients prior to the scan.
Funding: No funding was received for this work.
Author Disclosures:
H. H. Shanbhag: nothing to disclose

MyT3 15-2 14:04
Predictors of infectious complications following transrectal ultrasound-guided prostate biopsies in an Irish prostate cancer centre
R. R. Durganaudu, M. M. Morrin, R. Dunne*; Dublin/IE (durganar@tcd.ie)*

Purpose: The incidence of infectious complications following transrectal ultrasound (TRUS)-guided prostate biopsies is on the rise. In this study, we compared post-biopsy infection rates in patients who underwent mp-MRI targeted vs non-targeted TRUS-guided biopsies, and also aimed to identify other predictors of infectious complications.
Methods and materials: Retrospective review was performed on 525 patients who underwent TRUS biopsies in Beaumont Hospital between 1/01/2017 and 31/07/2018. Infection rates in both targeted and non-targeted biopsy groups were compared using Pearson's chi-square test. Other characteristics of patients with and without infections were compared using Mann-Whitney U test, Pearson's chi-square test and Fisher's exact test as appropriate. Binomial logistic regression analyses were then performed to identify possible predictors of infectious complications.
Results: Infectious complications occurred in 20 (3.8%) out of 525 patients. A total of 209 (39.8%) biopsies were targeted. Of the 20 patients who developed infectious complications, seven (35%) underwent targeted biopsies. The difference in infection rates in targeted and non-targeted biopsy groups was not statistically significant. Analysis of other associated patient characteristics revealed significantly higher median prostate-specific antigen (PSA) values in patients who developed infectious complications (p<0.05). On binomial logistic regression, none of the variables investigated were found to be significant predictors of infectious complications in our institution.
Conclusion: Rising infection rates post TRUS-guided biopsies is a concerning trend with significant implications. While our study did not identify any statistically significant predictors of infectious complications in our institution, it had helped uncover areas of research that could be explored further to help shape future policies.
Limitations: This study was limited by (1) small sample size, (2) retrospective nature of the study which affected accessibility of some data, and (3) that it is a single centre study.
Ethics committee approval: Approved audit.
Funding: No funding was received for this work.
Author Disclosures:
R. R. Durganaudu: Author at Tallaght University Hospital, Dublin
M. M. Morrin: Consultant at Consultant Radiologist, Beaumont Hospital
R. Dunne: Consultant at Consultant Radiologist, Beaumont Hospital

MyT3 15-3 14:08
Retrospective study of endovascular therapy for renal bleedings of arterial origin
A. Fialkovska[1], B. Glodny[2], J. Petersen[3]; *[1]Mannheim/DE, [2]Innsbruck/AT, [3]Birgitz/AT*

Purpose: It was intended to compare interventional super-selective embolisation regarding renal parameters, clinical course and outcome to other therapeutical options and by that improving the approach to the treatment of acute renal bleedings of arterial origin.
Methods and materials: Patients with renal injuries due to bleeding of arterial origin, pseudoaneurysms or arteriovenous fistulas underwent transcatheter arterial embolisation. The analysis included data of the technical and clinical success of embolotherapy, differences performing endovascular treatment during the clinical course and whether the post-interventional modified parenchymal renal volume amplifies the risk of developing renovascular hypertonia and chronic kidney disease.
Results: A total of 167 patients was included. The technical success rate was 100 % and a clinical success rate of 92.5 % was achieved. Recurrent bleeding occurred in 14 patients (8.4 %). 6 (42.9 %) were re-embolised and 5 (35.7 %) underwent total nephrectomy. Recurrent bleedings tended to occur in correlation with subcapsular haematomas ($p < 0.001$). Renal function was measured by glomerular filtration rate and creatinine several times. It revealed no significant changes ($p > 0.05$). Patients with discontinuity of renal fascia were at a higher risk of parenchymal loss ($p = 0.0237$). The post-interventional renal volume loss was insignificantly low and over a period of 15 years, neither contributed to the progression of renovascular hypertonia nor to deterioration of renal parameters.
Conclusion: This study verified that there was neither a positive correlation between a reduced post-interventional parenchymal renal volume and a progression of renovascular hypertonia nor deteriorating renal laboratory parameters. Furthermore, the choice of embolisation material and the appropriate catheter-technique are decisive for reducing fluoroscopy time.
Limitations: Not all the patients' data was available.
Ethics committee approval: n/a
Funding: No funding was received for this work.
Author Disclosures:
A. Fialkovska: nothing to disclose
B. Glodny: nothing to disclose
J. Petersen: nothing to disclose

MyT3 15-4 14:12
Multivessel Doppler in the evaluation of IUGR
H. Pobbati*; Hyderabad/IN (hvardhan2004@gmail.com)*

Purpose: To evaluate the role of colour Doppler sonography in the evaluation of pregnancy with intrauterine growth restriction. The uteroplacental circulation, which are the two maternal uterine arteries. The foeto-placental circulation, which is the umbilical artery. The foetal circulation, which includes the foetal middle cerebral artery.
Methods and materials: The study included 30 antenatal women who were diagnosed as having a foetus with intrauterine growth restriction based on greyscale ultrasound findings and referred for obstetric Doppler ultrasound if the following inclusion criteria and exclusion criteria were met. The inclusion criteria were: singleton pregnancy with a gestational age of more than 28 weeks. Women with reliable dating of pregnancy confirmed by an early first-trimester ultrasound examination using CRL or BPD or with known LMP will be selected. Multiple pregnancies and foetuses with congenital anomalies. Doppler US evaluation was performed following a detailed clinical history and US biometry. The scanners and transducers used: the greyscale real-time ultrasonographic examinations were performed using ALOKA PROSOUND SSD – 3500SX and PHILIPS HD 11XE. The transducers used for the study were 3.5MHz convex array transducer.
Results: The sensitivity of uterine artery Doppler study to detect adverse perinatal outcome was 83% when two Doppler parameters were considered.
Conclusion: Assessment of both the uteroplacental circulation and the fetoplacental circulations together is more sensitive to predict a perinatal outcome, than the assessment of each alone. In suspected IUGR, cerebro-umbilical ratio (MCA/UA PI) is a better predictor of adverse perinatal outcome than an abnormal MCA PI or umbilical artery PI. Best results are obtained when we use MCA/UA PI ratio, rather than PIs of a middle cerebral artery and umbilical artery separately.
Limitations: This study is limited by the lack of patient follow-up.
Ethics committee approval: Not applicable.
Funding: No funding was received for this work.
Author Disclosures:
H. Pobbati: nothing to disclose

MyT3 15-5 14:16
Magnetic resonance imaging and three-dimensional transperineal ultrasound evaluation of pelvic floor dysfunction in symptomatic women: a prospective comparative study
E. F. A. M. Tantawy, M. A. A. Basha, R. Almolla, H. Almassry*; Zagazig/EG (Dr_Engy_tantawy@yahoo.com)*

Purpose: To investigate magnetic resonance imaging (MRI) and 3-dimensional transperineal ultrasound (3D-TPUS) features of pelvic floor dysfunction (PFD) in symptomatic women in correlation with digital palpation and to define cut-offs for Hiatal dimensions that can predict muscle dysfunction.
Methods and materials: This is a prospective study included 73 women with symptoms suggesting PFD. 3D-TPUS, MRI, and digital palpation of levator ani muscle were performed for all patients. Levator hiatal antro-posterior (LHap) diameter and area (LH area) were measured at rest and at maximum muscle contraction.
Results: The reduction in LHap diameter and LH area during contraction was significantly less in women with underactive pelvic floor muscle contraction (UpfmC) than those who have a normal pelvic floor muscle contraction (NpfmC) by digital palpation ($p <0.001$). Statistically significant positive correlations ($p <0.001$) were found between Modified Oxford Score (MOS) and 3D-TPUS and MRI regarding the reduction in the LHap diameter ($r= 0.8, 0.82$, respectively) and LH area ($r= 0.6, 0.7$, respectively). A reduction in LHap <6.5% on 3D-TPUS and <7.6% on MRI, predicted UpfmC with sensitivities of 46% and 83%, respectively. A reduction in LH area <3.4% on 3D-TPUS and <3.8% on MRI predicted UpfmC with sensitivities of 75% and 88.5%, respectively. MRI was more sensitive in detecting levator avulsion (63%) than 3D-TPUS (27%).
Conclusion: MRI and 3D-TPUS have a strong positive correlation with palpation, and at certain cut-offs for Hiatal dimensions, they can be used as complementary and objective tools to improve the diagnosis and management planning of PFD.
Limitations: This study is limited by small sample size.
Ethics committee approval: Written consent from patients are obtained and our study was proved by our ethics committee according to the ethical principles of the Declaration of Helsinki.
Funding: No funding was received for this work.
Author Disclosures:
E. F. A. M. Tantawy: Speaker at zagazig university, Speaker at zagazig university
M. A. A. Basha: nothing to disclose
R. Almolla: nothing to disclose
H. Almassry: nothing to disclose

MyT3 15-6 14:20
Comparison of multiparametric prostate MRI and PSMA gallium PET-CT efficiency: the intraductal component and cribriform pattern in intraprostatic tumour focus
A. Arslan, M. B. Tuna, L. Güner, Y. Sağlıcan, A. R. Kural, E. Karaarslan*; Istanbul/TR (arslanaydan@gmail.com)*

Purpose: The aim of our study was to compare the efficacy of PET and MRI in detecting the intraductal component and cribriform pattern in patients with clinically significant prostate cancer who underwent radical prostatectomy.
Methods and materials: Thirty patients who underwent radical prostatectomy between June 2015 and April 2018 were included in the study. The intraductal component and cribriform pattern of each tumour focus were also identified with whole-mount histopathologic analysis correlation.
Results: The presence of intraductal component did not create a statistically significant difference in visibility of the index tumour on MRI and PET. However, in terms of total tumoral lesions, the visibility on MRI is statistically significant. The presence of cribriform pattern did not show a statistically significant difference in detection of the tumour on MRI and PET.
Conclusion: Cribriform pattern was found to be less visible than intraductal carcinoma by MRI.
Limitations: Our study was retrospective. It has a limited number of patients. Thirty patients were evaluated according to 67 clinically significant tumour foci.
Ethics committee approval: This study is approved by the institutional review board.
Funding: No funding was received for this work.
Author Disclosures:
A. Arslan: Author at Acıbadem Mehmet Ali Aydınlar University
M. B. Tuna: Author at Acıbadem Mehmet Ali Aydınlar University
L. Güner: Author at Acıbadem Mehmet Ali Aydınlar University
Y. Sağlıcan: Author at Acıbadem Mehmet Ali Aydınlar University
A. R. Kural: Author at Acıbadem Mehmet Ali Aydınlar University
E. Karaarslan: Author at Acıbadem Mehmet Ali Aydınlar University

MyT3 15-7 14:24
Comparison of ADC-ratio vs mean ADC value of multiparametric MRI to predict the aggressiveness of prostate cancer
X. Wang[1], V. Schütz[1], M. Görtz[1], D. Tichy[1], P. D. A. Stenzinger[1], M. Hohenfellner[1], H.-P. Schlemmer[1], D. Bonekamp[2]*; [1]Heidelberg/DE, [2]Hirschberg/DE (xianfeng.wang@dkfz-heidelberg.de)*

Purpose: To evaluate the usefulness of various apparent diffusion coefficient (ADC) ratios vs ADC in determining the aggressiveness of prostate cancer (PCa).

Methods and materials: 261 consecutive patients who underwent 3T MRI on a single scanner followed by MRI-transrectal US fusion biopsy within one month were included. A board-certified radiologist retrospectively reviewed all MRIs blinded to clinical information and placed 3D regions of interest (ROI) on focal lesions. Mean ADC (mADC) of each lesion and reference regions: normal-appearing peripheral zone (PZNL) and transition zone (TZNL), right and left internal obturator muscle (RIOM, LIOM), and the urinary bladder were calculated. Different ADC ratios were calculated as mADC/reference. Clinically significant PCa (sPC) was defined as Gleason Grade Group≥2. Independent t-test was used to differentiate the ADC metrics between sPC and non-sPC. Receiver operating characteristics (ROC), and the DeLong test was used to assess the differences of the area under the curve (AUC, 95%-CI).
Results: 392 lesions (302 in the peripheral zone) found in 253 men were included in the final study cohort. ADC metrics except ADC ratio (RIOM,LIOM) (p=0.43 and 0.53) showed a statistically significant difference between sPC and non-sPC (P<0.01). mADC showed the highest ROC-AUC of 0.67([0.61;0.72]),followed by ADC ratio PZNL with ROC-AUC of 0.66([0.60;0.71]) while, e.g. ADC ratio TZNL had ROC-AUC of 0.60 ([0.54;0.66]) which was significantly lower compared to mADC (p=0.002).
Conclusion: A highly standardised single-scanner ADC measurement could not be improved upon using any of the ADC ratio parameters.
Limitations: ADC ratios may still be advantageous when comparing data from multiple scanners and institutions.
Ethics committee approval: The institutional ethics committee approved the study and waived written informed consent (S-156/2018).
Funding: No funding was received for this work.
Author Disclosures:
X. Wang: nothing to disclose
V. Schütz: nothing to disclose
M. Görtz: nothing to disclose
D. Tichy: nothing to disclose
P. D. A. Stenzinger: Consultant at Astra Zeneca,BMS,Novartis,Roche, Illumina, Thermo Fisher, Board Member at Astra Zeneca,BMS,Novartis,Thermo Fisher
M. Hohenfellner: nothing to disclose
H.-P. Schlemmer: Consultant at Siemens,Curagita,Profound,Bayer, Board Member at Curagita, Grant Recipient at BMBF,Deutsche Krebshilfe,Dietmar-Hopp-Stiftung, Roland-Ernst-Stiftung
D. Bonekamp: Speaker at Profound Medical Inc.

MyT3 15-8 14:28
Radio-frequency ablation of renal cancer T1a with externally cooled multitined expandable electrodes
F. Pagnini, U. V. Maestroni, S. Ferretti, S. Buti, M. de Filippo*; Parma/IT (f.pagnini90@gmail.com)*

Purpose: To retrospectively evaluate the mid-term outcomes of percutaneous radio-frequency ablation (RFA) with multitined expandable electrodes externally cooled with saline solution in patients with T1 renal cell carcinoma (RCC).
Methods and materials: In this retrospective study, we evaluated 53 RCC in 47 patients treated with CT-guided RFA in 56 procedures (2015-2019). All patients were staged T1, N0, M0 prior to RFA. Mean tumour size was 23.79 mm. A 4-tined expandable RFA electrode cooled with pump-circulating saline was used. Efficacy was evaluated verifying complete tumour necrosis (no contrast enhancement on imaging) at the end of the procedure and on subsequent controls. Follow-up observation period was 5 years. Minor/major complications, hospitalization days, serum creatinine before-after RFA (compared using paired t-test) and pain (evaluated with NRS) were considered as safety indicators. Overall survival was also calculated (Kaplan-Meier method).
Results: Of 47 patients, 40/47 had 1 treatment (primary effectiveness rate 87,5%), 5/47 had 2 treatments and 1/47 had 3 treatments for residual disease, 1/47 had 3 treatments for multiple RCC. There were no relapses, no mid-long term complications; 5 minor (8,9%) and 1 major (1,7%) complications during the perioperative period were reported. Mean before and after RFA serum creatinine rates were respectively 1.08 mg/dl and 1.11 mg/dl (p-value: 0.4117). NRS median value: 0.8. Hospitalisation days median value: [2.8 ± 1.9] days. 91,4 % of all patients survived, with a median overall survival time of 65 months.
Conclusion: Mid-term results show that CT-guided RFA with multitined expandable electrodes externally cooled with saline solution is an effective and safe treatment in patients with RCC staged T1N0M0. Data reported in our study are in line with data reported in the literature from patients treated with other devices.
Limitations: This is a monocentric study, observing few cases.
Ethics committee approval: n/a
Funding: No funding was received for this work.
Author Disclosures:
F. Pagnini: nothing to disclose
U. V. Maestroni: nothing to disclose
S. Ferretti: nothing to disclose
S. Buti: nothing to disclose
M. de Filippo: nothing to disclose

MyT3 15-9 14:32
Role of MRI to evaluate kidney volume in AKPD patients
G. Di Nino, E. Grassedonio, M. Guarneri, L. La Grutta, G. Salvaggio, F. Midiri, M. Galia, T. V. Bartolotta, M. Midiri*; Palermo/IT*

Purpose: Patients with ADPKD (autosomal dominant polycystic kidney disease) show a progression disease hard to predict with common prognosis factors. We know the gradual expansion of the cysts increases the renal volume. A prognostic classification based on the renal volume measured with magnetic resonance imaging (MRI) corrected for height and age (HtTKV, height-adjusted total kidney volume) was developed. The proposed classification defines 5 classes (from A to E) of patients with a different risk of GFR decline based on renal growth rate and annual GFR reduction.
Methods and materials: 25 patients (age 24-57) with ADPKD (14F / 11M) were followed clinically and radiologically with abdominal MRI (GE 1.5T, T1, T2, DWI). The MRI was used to calculate HtTKV. The renal volume was calculated by the Mayo clinic's web-based programme and MRI images by an algorithm based on the ellipsoid equation (π / 6xLxWxD), 4 major measurements (L,W,D,coronal, sagittal ,axial sequences), then correlating these values to the patient's age and height, GFR, we obtained the patient class.
Results: The GFR range was (12-128) and the HtTKV (230 and 2078 mL/m). The patients were divided in 5 classes (4 class A, 7 B, 6 C, 5 D, 3 E). Patients in class A had normal value, 1/7 class B (GFR <60 ml / min / 1.73m2), class C: 4/6 (GFR <60 ml / min / 1.73m2).
Conclusion: Our study shows the utility of renal MRI-based volume in patients with ADPKD to analyse prediction factors.
Limitations: This study was limited by the number of patients due to a rare genetic disease.
Ethics committee approval: n/a
Funding: No funding was received for this work.
Author Disclosures:
E. Grassedonio: Author at A.O.U.P Paolo Giaccone
G. Di Nino: Author at A.O.U.P Paolo Giaccone, Speaker at A.O.U.P Paolo Giaccone
M. Guarneri: Author at A.O.U.P Paolo Giaccone
L. La Grutta: Author at A.O.U.P Paolo Giaccone
G. Salvaggio: Author at A.O.U.P Paolo Giaccone
F. Midiri: Author at A.O.U.P Paolo Giaccone
M. Galia: Author at A.O.U.P Paolo Giaccone
T. V. Bartolotta: Author at A.O.U.P Paolo Giaccone
M. Midiri: Author at A.O.U.P Paolo Giaccone

MyT3 15-10 14:36
Texture analysis of MRI for differential diagnosis of renal masses
M. Erşen[1], H. T. Sanal[1], M. Taşar[1], A. Keskin[2], M. Ş. Güneş[2]; [1]*Ankara/TR,* [2]*Istanbul/TR (mehmetersen@gmail.com)*

Purpose: The purpose is to investigate texture analysis findings', the structure analysis application in radiological imaging, efficacy in the differential diagnosis of kidney masses renal cell carcinoma (RCC) and oncocytoma, contribution to the classification of RCC subtypes and relationship with the nuclear stage of RCC.
Methods and materials: Retrospectively 32 patients who underwent renal MRI between November 2016-2018, having pathological diagnosis were included. The cases were divided into groups according to their pathological diagnoses (21 clear-cell-RCC, five papillary-RCC, three chromophobe-RCC, three oncocytoma; out of 21 clear-cell RCC cases 10 were low-stage, 10 were high-stage). Texture feature selection/extraction processes were applied on 2D axial images with MaZda software. Fisher's coefficient and POE+ACC methods were used for feature selection. Features were analysed with canonical discriminant analysis.
Results: The success rate in distinguishing the RCC subtypes from each other and from oncocytoma were found to be different when images of different sequences were used. With the evaluation of texture parameters on T2W and 70 sec contrast-enhanced T1W, 100%; SPAIR-T2W 89.3%, ADC 75.9%, out-of-phase 93.3% and 30 sec contrast-enhanced T1W 95% of the cases were classified correctly. All of the cases were classified correctly according to the data on ADC and 70-sec contrast-enhanced T1W images, the sequences which were used in distinguishing between low stage and high stage of clear cell RCC cases.
Conclusion: Texture-based analysis parameters can be used on MRI in differentiating RCC from oncocytoma, in classifying the RCC subtypes, and in discriminating clear-cell-RCC nuclear stage.
Limitations: Small size of case groups, the absence of lipid-poor angiolipoma and three different MR devices for image acquisiation were the main limitations of this study.
Ethics committee approval: Non-invasive ethical approval was obtained.
Funding: No funding was received for this work.

Author Disclosures:
M. Erşen: nothing to disclose
H. T. Sanal: nothing to disclose
M. Taşar: nothing to disclose
A. Keskin: nothing to disclose
M. Ş. Güneş: nothing to disclose

MyT3 15-11 14:40
68Ga-PSMA PET/CT in biochemically recurrent prostate cancer: when do we miss it and why?
I. Zelsky; *Yekaterinburg/RU (zelskii78@gmail.com)*

Purpose: 68Ga-PSMA PET/CT is being increasingly used for prostate cancer recurrence identification, however, the detection rate among patients varies from 66% to 85%. The aim of our study was to analyse the influence of several variables on the detection rate, some of them with possible influence on PSMA expression.
Methods and materials: This was a retrospective study of 312 men with biochemical failure after radical prostatectomy or radiation therapy, with or without ongoing androgen deprivation therapy (ADT), who received a 68Ga-PSMA PET/CT between 05/2018 and 08/2019. The goal was to determine the relationship among pre-scan PSA level, PSA doubling time, PSA velocity, Gleason score, ADT and the probability of identifying PSMA-avid disease. For statistical analysis, a p-value of <0.05 was considered statistically significant. Univariate and multivariate logistic regression analysis was applied.
Results: In 77% of patients, at least a single lesion with characteristics suggestive of recurrent PCa was detected. A positive 68Ga-PSMA PET/CT scan was associated with PSA doubling time and ADT.
Conclusion: We think that blockade of androgen receptor (AR) signalling oncogenic pathway activates phosphoinositide 3-kinase (PI3K) pathway, which leads to rapid PSA increasing and PSMA overexpression. So, in a patient with ADT we can detect a very small amount of tumour cells. But AR and PI3K signalling pathways have the reciprocal negative feedback loop, so activated AR inhibits PSMA expression. Therefore, patients without ongoing ADT have less PSMA on tumour cells, and detection thereof using a PSMA-ligand requires more tumour volume. Probably due to this fact we miss small tumour lesions in patients with low PSA values and without ongoing ADT using 68Ga-PSMA PET/CT.
Limitations: Not all variables were available for all patient.
Ethics committee approval: Written informed consent was obtained.
Funding: No funding was received for this work.
Author Disclosures:
I. Zelsky: nothing to disclose

MyT3 15-13 14:44
Multiple mathematical models of diffusion-weighted imaging for evaluation of prognostic features in endometrial cancer
O. Zhang, X. Zhao, H. Ouyang; *Beijing/CN (18810683722@163.com)*

Purpose: To investigate monoexponential, biexponential, and stretched-exponential models of diffusion-weighted imaging (DWI) for the assessment of prognostic features in endometrial cancer (EC).
Methods and materials: 61 consecutive EC patients confirmed by pathology underwent multiple-b value DWI (0-1200s/mm^2) preoperatively at 3.0T MR scanner. The apparent diffusion-weighted (ADC), biexponential model-derived parameters (D, D* and f) and stretched-exponential model-derived parameters (DDC and α) were measured by two radiologists independently. All parameters were compared between the deep and superficial of myometrial invasion, with and without cervical stromal infiltration (CSI), presence and absence of lymphovascular invasion(LVSI). ROC curve and intraclass correlation coefficient analysis were used for statistical evaluation in predicting prognostic factors of EC.
Results: Except for D* values, all of the parameters were significantly lower in tumours with deep myometrial invasion(DMI) than those invading superficial myometrial wall and the AUC was largest for ADC values(AUC:0.794). There was a significant difference between groups with and without CSI for ADC and f values and the f values exhibited best diagnostic performance in the prediction of CSI(AUC:0.825). The presence of LVSI had significant lower ADC, f and DDC values than those absences of LVSI and the DDC values showed the best diagnostic performance in the diagnosis of LVSI (AUC:0.759).
Conclusion: The current study demonstrated that the prediction of prognostic factors for EC is feasible by multiple mathematical DWI models, which could be conducive to the pre-treatment risk classification to facilitate the selection of the optimal therapeutic approach and meet the demand for greater personalisation of cancer care.
Limitations: It was a single-centre study with relatively small sample size and 13 b-values for the multiple b-value of DWI protocol prolonged the scan time.
Ethics committee approval: Information about review board approval and written informed consent.
Funding: No funding was received for this work.
Author Disclosures:
O. Zhang: nothing to disclose
X. Zhao: nothing to disclose
H. Ouyang: nothing to disclose

MyT3 15-14 14:48
High b-values in DWI for prostate cancer detection: what to acquire and what to compute?
M. Schoeniger[1], H. Seuss[1], F. Laun[1], J. Martin[1], T. Kuder[2], R. Janka[1], A. Cavallaro[1], M. Uder[1], M. Hammon[1]; *[1]Erlangen/DE, [2]Heidelberg/DE (Hannes.Seuss@googlemail.com)*

Purpose: The aim of this study was to compare the diagnostic quality of acquired and computed high b-value images in diffusion-weighted magnetic resonance imaging (DWI) of the prostate in a setting, where the signal-to-noise ratio (SNR) is increased at high b-values by means of larger voxel sizes.
Methods and materials: 34 patients with a PI-RADS 4/5 lesion in the peripheral zone were included. DWI was acquired (aDWI) with four b-values (0, 800, 1500, and 3000 s/mm²) at 3T. The nominal resolution was adapted to roughly keep the SNR constant. Computed-DWI (cDWI) were generated with the respective unweighted image and the acquired b-values, e.g. b3000 from b0 and b800 (cDWI3000-800). This resulted in two acquired and two computed images for each b-value (including b0) summarising to ten images. The three b0 images were pooled. Four readers performed a forced-choice pairwise comparison for representative lesions of all ten images and assessed lesion conspicuity and the ability to locate the lesion.
Results: Concerning lesion conspicuity, cDWI3000-1500 scored highest (6.71) followed by cDWI1500–800 (5.71), and cDWI1500–3000 (5.14). For the ability to localise the lesion, cDWI800-1500 scored highest (5.82), followed by aDWI800 (5.41), and cDWI1500-3000 (5.40).
Conclusion: In this study diagnostic performance of DWI in prostate magnetic resonance imaging was achieved for the combination of acquired b1500 and computed b3000. Therefore, we recommend to acquire images as high as b1500 and to compute the remaining images.
Limitations: Potentially the most important limitation is that whole-mount prostate histology data were not available because prostatectomy is rarely performed at our hospital.
Ethics committee approval: Institutional review board approval was obtained.
Funding: This study has received funding by the Deutsche Forschungsgemeinschaft (grant LA 2804/6-1).
Author Disclosures:
H. Seuss: nothing to disclose
M. Schoeniger: nothing to disclose
F. Laun: nothing to disclose
J. Martin: nothing to disclose
T. Kuder: nothing to disclose
R. Janka: nothing to disclose
A. Cavallaro: nothing to disclose
M. Uder: nothing to disclose
M. Hammon: nothing to disclose

MyT3 15-15 14:52
Multiparametric magnetic resonance imaging (mp-MRI) in the evaluation of prostate cancer based on PIRADS V2 on 1.5 T without endorectal coil
S. M. Ingole, R. U. Mehta, Z. Kazi; *Mumbai/IN (ingole.sarang@gmail.com)*

Purpose: To evaluate the role of multiparametric magnetic resonance imaging (mp-MRI) for the assessment of prostate cancer based on PIRADS V2 on 1.5T without endorectal coil.
Methods and materials: 45 patients with clinical suspicion of prostate cancer were retrospectively evaluated by 18 channel 1.5T MRI with body matrix coil, over a period of 24 months. All cases were evaluated using mp-MRI protocol i.e. T2W with DWI, DCE; interpreted using PIRADSv2 and correlated with histopathology.
Results: Mean age was 67 years and mean PSA was 38.2 ng/ml. 86% of all malignancies were in the peripheral zone. 80% of the cohort had prostate cancer, 11% had BPH and 9% had chronic prostatitis. PIRADS score for T2W showed good sensitivity (81%) but low specificity (67%) while PIRADS score for DWI with a sensitivity of 92% and specificity of 78% had overall accuracy better than T2W alone. Mean ADC value (x 10-6 mm2/s) was 732±160 in prostate cancer, 1009±161 in chronic prostatitis, 1142 ± 82 in BPH and 663 in case of microabscesses. Low ADC values (<936) has shown good correlation (AUC-0.87) with the presence of cancer foci. An inverse correlation was observed between Gleason score and ADC values in proven cases of cancer. DCE has shown 100% sensitivity / NPV, but moderate specificity (67%) in predicting malignancy. The final PIRADS score had almost 100% sensitivity and NPV with good overall PPV (95%).

Conclusion: T2W and DWI remain mainstay in diagnosis of prostate cancer on mp-MRI. DCE can be problem solving tool. Because assessment on mp-MRI can be subjective, use of PIRADSV2 guidelines are helpful in accurate interpretation.
Limitations: The endorectal coil was not used and sample size was small.
Ethics committee approval: n/a
Funding: No funding was received for this work.
Author Disclosures:
S. M. Ingole: Investigator at Saifee Hospital
R. U. Mehta: Consultant at Saifee Hospital
Z. Kazi: Consultant at Saifee Hospital

MyT3 15-16 14:56
Detection of peritoneal metastases from ovarian cancer: a comparison between 3T MRI and surgical findings
M. A. Szadkowska, J. P. Pałucki, J. Kuśnierz, M. E. Gumowska, K. Sloboda, J. M. Poziemska, M. Bidziński, A. Cieszanowski*; Warsaw/PL (maszadkowska@hotmail.com)*

Purpose: The aim of this study was to assess the effectiveness of 3T MRI in the detection of peritoneal carcinomatosis from ovarian cancer using intraoperative findings as a reference.
Methods and materials: 25 patients diagnosed with ovarian cancer, aged between 35 and 69 (mean age - 54), underwent MRI examinations at our institution between March 2017 and November 2018. The inclusion criteria were: pathologically confirmed diagnosis of ovarian cancer, preoperative 3T MRI examination performed at our institution, potentially resectable peritoneal metastases, eligibility to cytoreductive surgery (CRS, potentially followed by HIPEC procedure). The examinations were performed using a 3T MRI scanner. The MRI protocol included T1W-sequences (coronal and axial) before and after administration of gadolinium-based contrast agent, T2W-sequences (coronal and axial) and axial DWI/ADC scans. The patients underwent surgical exploration of the peritoneal cavity and the findings were reported according to PCI-scale (Peritoneal Carcinomatosis Index). The studies were retrospectively analysed by an experienced radiologist with a special interest in urogenital radiology and PCI scores were assigned and compared region to region to the results of the surgical evaluation.
Results: The overall sensitivity and the overall specificity of MRI were 60,00% and 73.94, respectively. MRI proved to be the most sensitive in region 6 (pelvis, 91,67%), 1 (right upper region, 83,33%) and 4 (left flank, 72,73%), whereas the lowest sensitivity was noted in small bowel and small bowel mesentery (regions 9- 25%, 10- 37.50%, 11- 25% and 12 - 42.86%).
Conclusion: The preoperative 3T MRI proved to be moderately effective, yet still useful, in the detection of peritoneal carcinomatosis from ovarian cancer.
Limitations: The limitations of this study were: retrospective design, relatively small sample.
Ethics committee approval: n/a
Funding: No funding was received for this work.
Author Disclosures:
M. A. Szadkowska: nothing to disclose
J. P. Pałucki: nothing to disclose
J. Kuśnierz: nothing to disclose
M. E. Gumowska: nothing to disclose
K. Sloboda: nothing to disclose
J. M. Poziemska: nothing to disclose
M. Bidziński: nothing to disclose
A. Cieszanowski: nothing to disclose

MyT3 15-17 15:00
Documenting the radiation diagnosis of stress urinary incontinence in females
H. Nechyparenka*; Grodno/BY (salejanna@mail.ru)*

Purpose: Improving the efficiency of diagnostics of cystocele and stress urinary incontinence (SUI) using methods of diagnostic radiology.
Methods and materials: A comprehensive examination of the data of 73 patients with genital prolapse (GP) with the help of a modified Pad-test and MRI.
Results: We modified the well-known Pad-test by intravenous injecting of solution of indigocarmine and an iodine-containing contrast preparation. After the test, a visual assessment of the sanitary pad and it's radiography was done. The main advantage of the modification is the ability to visually confirm the fact of involuntary loss of minimal volumes of urine by detecting the spot of indigocarmine on the sanitary pad and the contrast stain on the x-ray film of the pad after Pad-test. A colored spot on the pad and a contrasting shadow on the roentgenogram of the gasket is a documentary confirmation of the involuntary loss of the contents of the bladder – a sign of SUI. The procedure was used in 21 patients who suspected a minimal SUI. A positive Pad-test is a documentary confirmation of minimum volume SUI and an indication for MRI investigation. If, according to the results of static MRI, damage of the ligaments of the urethra and/or value of the urethral inclination angle (UIA) is more than 30º, a dynamic MRI needs to be done. At values of UIA according to the results of dynamic MRI over 35º, cystocele is diagnosed and classified.
Conclusion: The modified Pad-test confirms and documents the minimum SUI. An MRI of the pelvis detects and documents all cases of the presence of SUI in women with GP, allows for an objective diagnosis of the cystocele.
Limitations: No limitations identified.
Ethics committee approval: The positive decision of the ethics committee obtained.
Funding: No funding was received for this work.
Author Disclosures:
H. Nechyparenka: nothing to disclose

MyT3 15-18 15:04
Dual-energy computed tomography in the diagnostics of urolithiasis
L. Kapanadze, N. S. Serova, V. Rudenko, K. Alexandrova*; Moscow/RU (Lidakap@rambler.ru)*

Purpose: To assess the diagnostic possibilities of dual-energy computed tomography (DECT) in the evaluation of urinary stones composition "in vivo".
Methods and materials: A total of 91 patients: men (n=68; 75%) and women (n=23; 25%) aged from 20 to 70 years old with urolithiasis were examined at Sechenov University. Before the surgery, all patients underwent DECT (Canon, Japan) in order to predict the chemical composition of urinary stones in vivo. Shockwave lithotripsy (SWL) was performed in 53 patients (58,2%), percutaneous nephrolithotripsy (PCNL) – in 18 (19,7%) patients, ureterolithotripsy (URS) – in 20 (22,1%) patients. In the postoperative period, all the stones or their fragments (n=91; 100%) were examined using a comprehensive physicochemical analysis (x-ray phase analysis, electron microscopy, infrared spectroscopy).
Results: In order to increase the diagnostic efficiency of DECT, we performed a comprehensive analysis of five specific DECT indicators (stone density at 135 kV, Z eff of the stone, DER, DEI, DED) using discriminant analysis instead of the one indicator - the dual-energy ratio (DER) - which is more commonly used. Using discriminant analysis with five specific DECT indicators resulted in higher values of sensitivity, specificity and overall accuracy: for vevellite – 95,2%, 89,8%, 92,3%, for Ca-containing stones without vevellite – 85,3%, 96,4%, 92,3% and for uric acid and struvite stones – 100%, 100%, 100%.
Conclusion: Dual-energy computed tomography in the preoperative period is a highly informative method for reliable assessment of the chemical composition due to its high diagnostic value. DECT in patients with urolithiasis allows optimising the tactics of surgical treatment and the individualisation of metaphylaxis taking into account the type of stone formation.
Limitations: No limitations identified.
Ethics committee approval: n/a
Funding: No funding was received for this work.
Author Disclosures:
L. Kapanadze: nothing to disclose
N. S. Serova: nothing to disclose
V. Rudenko: nothing to disclose
K. Alexandrova: nothing to disclose

MyT3 15-19 15:08
Dynamic perfusion computed tomography in assessing of urogenital allografts
I. O. Shchekoturov, R. F. Bakhtiozin, A. L. Istranov*; Moscow/RU (samaramail@bk.ru)*

Purpose: To demonstrate the technique and possibilities of perfusion computed tomography in assessing of the urogenital allografts state.
Methods and materials: We examined 36 patients (n = 100%) using dynamic perfusion computed tomography. 27 of them (n = 75%) diagnosed with transsexualism, underwent a female-to-male sex change operation using phalloplasty and consistent urethroplasty after 6 months. 9 (n = 25%) patients had different urogenital diseases such as: posttraumatic urethral stricture, microphallia etc. A free revascularised microsurgical allograft - skin-muscular thoracodorsal was used for the reconstruction of the penis, and for the reconstruction of the urethra was used skin-fascial radial allograft.
Results: Processing of the data showed that in the early postoperative period there was a decrease in the level of arterial blood flow in the allograft tissue compared with preoperative indicators due to congestion and oedema. Then, an gradually increase in the level of arterial blood flow is observed due to the formation of anastomoses between the flap and the recipient's tissues and the further improvement of their function, as well as a decrease in the severity of oedema and congestion in the flap. The blood flow recovery in the flap to normal preoperative values was registered by the end of the first month after surgery.
Conclusion: Dynamic perfusion CT is a more modern and advanced diagnostic method for grafts assessing than three-phase computed tomography. This method provides additional information about allograft state and allows to

measure perfusion indicators at the capillary level with high spatial and temporal resolution in numerical values.
Limitations: There is no limitations.
Ethics committee approval: The study was approved by the Institutional Review Board of Sechenov University, and informed consent was obtained from all study participants.
Funding: No funding was received for this work.
Author Disclosures:
I. O. Shchekoturov: Speaker at Federal State Autonomous Educational Institution of Higher Education I.M. Sechenov First Moscow State Medical University of the Ministry of Health of the Russian Federation (Sechenov University), Author at Federal State Autonomous Educational Institution of Higher Education I.M. Sechenov First Moscow State Medical University of the Ministry of Health of the Russian Federation (Sechenov University)
R. F. Bakhtiozin: Author at Federal State Autonomous Educational Institution of Higher Education I.M. Sechenov First Moscow State Medical University of the Ministry of Health of the Russian Federation (Sechenov University)
A. L. Istranov: Author at Federal State Autonomous Educational Institution of Higher Education I.M. Sechenov First Moscow State Medical University of the Ministry of Health of the Russian Federation (Sechenov University)

MyT3 15-20 15:12

Bladder pathology: is it that easy?

C. A. B. Oliveira, V. Mendes, A. C. G. Costa*; Braga/PT*
(carlosaboliveira2014@gmail.com)

Purpose: To review bladder pathology with a multimodality approach and to define criteria when bladder pathology was found.
Methods and materials: Review 300 cases with bladder pathology.
Results: The bladder can be approached by many modalities. Ultrasound provides anatomic detail, vascularity and nodules identification. CT is the next step and the gold standard with uro-CT the most commonly used protocol. The six points were defined: (1) imaging findings, (2) ureterovesical junction (UVJ) permeability, (3) bladder wall thickness, (4) presence of nodules/masses, (5) neurogenic bladder, (6) pelvic masses and other findings. The imaging findings included: ultrasound a wall focal (nodule) or diffuse parietal thickening, vascularity; CT - diffuse or nodular parietal thickening with enhancement. 53% of patients had pathology of the UVJ including lithiasis, masses and compression. Bladder wall thickness was defined as pathologic superior to 3mm when distended and superior to 5. Nodules/ masses from the bladder where found in 13 %, from the ureter in 4 % and form the prostate in 3 % of cases, adnexal masses and uterine masses in 12 %. Signs of the neurogenic bladder were present in 64 % of cases and graded from mild to moderate and advanced. Other findings included lithiasis, other urothelial cancers, and intestinal pathology.
Conclusion: Bladder pathology is a common problem for radiologists and careful attention and awareness are a demand.
Limitations: This study is limited by one-radiologist read and its limited sample.
Ethics committee approval: N/A
Funding: No funding was received for this work.
Author Disclosures:
C. A. B. Oliveira: nothing to disclose
V. Mendes: nothing to disclose
A. C. G. Costa: nothing to disclose

MyT3 15-21 15:16

Renal duplex in evaluation acute glomerulonephritis in children with laboratory and histopathological correlation

R. M. Ellessy[1], R. H. Hashem[2], S. M. Kamel[1], D. Salah[1]; [1]*Giza/EG,* [2]*Cairo/EG*
(rehamellessy@gmail.com)

Purpose: Acute glomerulonephritis is an entity of renal disease in which immunologic mechanism cause damage to the basement membrane. The current study evaluates the renal vascular resistance in patients with acute glomerular diseases by measuring main renal and intrarenal arterial resistance (upper, mid and lower polar) (RI) of both kidneys and to correlate with laboratory data (creatinine, proteinuria) and histopathology.
Methods and materials: The study was conducted on twenty (20) patients with the age ranging from 3-13 years old. Cases with a non-glomerular cause of acute kidney injury, obstructive uropathy and known reno-vascular lesion were excluded from the current study.
Results: The mean RI of either main renal or parenchymal arteries is elevated in tubulointerstitial affection (mean value in main renal = 0.65, mean value in parenchymal arteries = 0.62) when compared to mean RI in cases without tubulointerstitial affection (mean value in main renal arteries = 0.59, mean value in parenchymal arteries = 0.57). The presence of crescent is not correlated with RI values in main renal and parenchymal arteries, creatinine level is positively correlated (p-value 0.1) with RI of the main renal arteries, no significant statistical correlation between RI indices and proteinuria (albumin /creatinine ratio).
Conclusion: RI index of the main renal artery may assist to predict creatinine level and severity of renal dysfunction although RI is elevated in tubulointerstitial cases still can not help in differentiation between different pathological affection.
Limitations: Limitation in the current study is a small sample size. Further recommendations are to include larger sample size, renal Doppler indices correlation with further lab assessment such as B_2 microglobulin and application of artificial intelligence and soft wares to assess renal echogenicity.
Ethics committee approval: n/a
Funding: No funding was received for this work.
Author Disclosures:
R. M. Ellessy: Author at KASR AL AINY HOSPITAL
R. H. Hashem: Consultant at KASR AL AINY HOSPITAL
S. M. Kamel: Consultant at KASR AL AINY HOSPITAL
D. Salah: Consultant at KASR AL AINY HOSPITAL

MyT3 15-22 15:20

Vesicoureteral reflux imaging in paediatric patients: can cystosonography replace micturating cystourethrogram?

P. Lomoro[1], A. Citterio[1], I. Simonetti[2], A. L. Nanni[1], V. Fichera[3], L. Preda[1], M. S. Prevedoni Gorone[1]; [1]*Pavia/IT,* [2]*Naples/IT,* [3]*Florence/IT*
(lmr.pcl89@gmail.com)

Purpose: Vesicoureteral reflux (RVU) is an abnormal condition, in which urine flows backwards from the bladder to the ureters and renal pelvis. If untreated, it may lead to recurrent urinary tract infections (UTIs), reflux nephropathy chronic renal failure. Currently, micturating-cystourethrogram (MCUG) and radionuclide-cystogram (RNC) are the most commonly performed techniques for the diagnosis of RVU; both involve exposure to ionising radiations. However, in the last years, cysto-sonography (CSG) has also been introduced in clinical practice. The aim of this study is to prove the non-inferiority of CSG compared to MCUG, through a comparative analysis, in order to start introducing it as first-line technique, to reduce radiation dose.
Methods and materials: 97 paediatric patients (49 boys and 48 girls) with UTIs were enrolled in the study. As first, after positioning of a urinary catheter, each patient underwent a CSG by the intravesical introduction of contrast agent (1ml-SonoVue), immediately followed by MCUG with intravesical iodinated-contrast-medium. Passive and active RVU was sought after spontaneous urination or abdominal press operation.
Results: The comparison of the results demonstrated a consistent concordance of the findings, further confirming the sensitivity of CSG in the diagnosis of RVU in the paediatric patient. During the ultrasound examination, it was also possible to assess the renal parenchyma and the possible dilation of the calicopyelic system as further findings useful for the purposes of the diagnostic classification of the patient.
Conclusion: Cystosonography is a sensitive diagnostic technique that allows to identify RVU and to evaluate possible morphological alterations of the renal parenchyma avoiding the use of ionising radiation.
Limitations: The limitation of this study are that it is a single centre study and that it refers to a short period of time.
Ethics committee approval: Patients were enrolled in the study, after informed parental consent.
Funding: No funding was received for this work.
Author Disclosures:
P. Lomoro: Speaker at Department of Diagnostic Medicine Institute of Radiology, IRCCS San Matteo University Hospital Foundation, Pavia, Italy., Author at Department of Diagnostic Medicine Institute of Radiology, IRCCS San Matteo University Hospital Foundation, Pavia, Italy.
A. Citterio: Author at Department of Diagnostic Medicine Institute of Radiology, IRCCS San Matteo University Hospital Foundation, Pavia, Italy.
I. Simonetti: Author at Department of Advanced Biomedical Sciences, University of Naples Federico II, Naples, Italy.
A. L. Nanni: Author at Department of Diagnostic Medicine Institute of Radiology, IRCCS San Matteo University Hospital Foundation, Pavia, Italy.
M. S. Prevedoni Gorone: Author at Department of Diagnostic and Interventional Radiology and Neuroradiology of IRCCS San Matteo University Hospital Foundation, Pavia, Italy.
V. Fichera: Author at Department of Pediatrics, Anna Meyer Children's University Hospital, Florence, Italy.
L. Preda: Research/Grant Support at Department of Clinical, Surgical, Diagnostic and Pediatric Sciences, University of Pavia, Pavia, Italy

MyT3 15-23 15:24

Computed tomography of pelvic varicocele in adolescents with urological pathology

U. Polyakova, I. Melnikov, M. Ublinskiy*; Moscow/RU (poliiinka.u@gmail.com)*

Purpose: The pathogenesis of pelvic venous insufficiency is multifactorial. Predisposing factors for the development of pelvic varicocele include a family history of varicose veins, previous pelvic surgery, aorto-mesenteric forceps, hormonal influences and multiple pregnancies in women. The purpose of this

study is to reveal the causes of pelvic varicocele in adolescents with urological pathology diagnosed by computed tomography.
Methods and materials: Three adolescents (2 girls, 14 and 17 years old, and 1 boy, 17 years old) with previously diagnosed urological pathology - pyeloectasia, had CT scan with intravenous contrast (Ultravist 370) on a 16-slice CT system and The Extended Brilliance Workspace (Philips) were used. Scanning area: abdomen and pelvis, scanning parameters: layer thickness 2,0 mm, voltage 120 kV.
Results: When analysing the images obtained, severe aorto-mesenteric forceps were detected in all patients.
Conclusion: We suppose that the main cause of varicocele in adolescents of both sexes is aortro-mesenteric forceps.
Limitations: n/a
Ethics committee approval: n/a
Funding: No funding was received for this work.
Author Disclosures:
U. Polyakova: nothing to disclose
M. Ublinskiy: nothing to disclose
I. Melnikov: nothing to disclose

MyT3 15-24 15:28
Preoperative radiographic predictors of major vascular reconstructions in patients with testicular cancer undergoing postchemotherapy residual tumour resection (PC-RPLND)
M. Boschheidgen, A. Nini, T. Ullrich, A. Hiester, C. Winter, P. Albers, G. Antoch, L. Schimmöller*; Düsseldorf/DE (Matthias.Boschheidgen@med.uni-duesseldorf.de)*

Purpose: To provide a complete resection of residual tumour in testicular cancer patients, major vascular surgery (MVS) is necessary and requires multidisciplinary planning and adequate resources to optimise outcome. To evaluate the probability to correctly predict MVS in patients undergoing postchemotherapy retroperitoneal lymph node dissection (PC-RPLND) for testicular cancer.
Methods and materials: From 504 RPLNDs performed in 434 patients (2008-2018), 78 patients submitted to PC-RPLND after 1st line chemotherapy with MVS, like caval and/or aortic replacement or reconstruction and available preoperative CT-scans were included in this study. Preoperative imaging was reviewed blinded to operative details. Statistical analyses were performed to evaluate predictors of MVS.
Results: Of 78 patients, 16 (21%) underwent MVS. Kruskall-Wallis tests showed statistically significant differences between transverse and sagittal tumour diameter, tumour volume, cava- and aorta-tumour contact angle and contact length (in cm) ($p<0.005$). Outstanding discrimination (>0.9) was found for cava-tumour contact angle. The optimal cut-off of 5 cm for transverse tumour diameter was confirmed (SENS 0.75 and 1-SPEC 0.18, CI95% 0.8-1). Cava-tumour contact angle had SENS 0.93 and 1-SPEC 0.17 with a cut-off of 98° (CI95% 0.9-1). At MVA aorta- (cut-off 64°) and cava-tumour contact angle (cut-off 98°) and poor IGCCCG score represented the three most important predictors of MVS ($p<0.05$). The model constructed has a PPV 100%, NPV 87% and an accuracy of 88%.
Conclusion: Presence of aorta-tumour contact angle >64°, cava-tumour contact angle >98° on CT scans and poor IGCCCG score identify correctly 9 out of 10 patients requiring MVS at the time of PC-RPLND. These patients may be referred to specialised centres capable to adequately perform this multidisciplinary surgery.
Limitations: n/a
Ethics committee approval: n/a
Funding: No funding was received for this work.
Author Disclosures:
M. Boschheidgen: nothing to disclose
A. Hiester: nothing to disclose
A. Nini: nothing to disclose
T. Ullrich: nothing to disclose
C. Winter: nothing to disclose
P. Albers: nothing to disclose
G. Antoch: nothing to disclose
L. Schimmöller: nothing to disclose

16:00 - 17:30 **Room C**

Musculoskeletal

RPS 1610

Knee and lower extremities

Moderators:
A. Barile; L'Aquila/IT
N.N.

RPS 1610-1 16:00
Intra- and inter-rater reliability of a new osteoarthritis radiographic scale for anterior cruciate ligament deficient knees
R. E. A. Walker[1], F. Mulji[1], P. Bertiche[2], D. J. Hunter[1], D. Chan[1], N. G. Mohtadi[1]; *[1]Calgary/CA, [2]Cordoba/AR (rewalker@ucalgary.ca)*

Purpose: To compare intra- and inter-rater reliability of a new scale to the international knee documentation committee (IKDC) scale for assessing radiographic osteoarthritis (OA) in anterior cruciate ligament (ACL) deficient subjects.
Methods and materials: Preoperative/postoperative weight-bearing, bilateral posteroanterior semi-flexed radiographs from 44 subjects with ACL deficiency were presented as standard unblinded, showing surgical tunnels/hardware with the affected knee identified, and blinded, surgical tunnels/hardware digitally removed with the affected knee not identified. Radiographs were randomised and independently assessed by 3 raters for OA using a new scale and the IKDC scale on two occasions.
The new scale separately evaluates joint space narrowing (JSN), joint space uniformity (JSU), and osteophytes for both medial and lateral tibiofemoral compartments with a comparison to the unaffected side. JSN was graded as normal, detectable, obvious <50%, obvious >50%, and bone-on-bone, JSU as uniform/non-uniform, and osteophytes as present/absent.
Cohen's and Fleiss kappa statistics were used to measure the intra- and inter-rater reliability of the new and IKDC scales.
Results: Intra-rater reliability was moderate to substantial for the new scale and IKDC, except fair reliability for one rater (unblinded radiographs) for lateral tibiofemoral joint uniformity. Kappa values were statistically significant ($p<0.01$). Inter-rater reliability ranged from slight to substantial for all categories of the new scale with statistically significant Kappa values ($p<0.05$), except for agreement on lateral osteophytes (standard unblinded). For both scales, intra- and inter-rater reliability was higher for blinded radiographs.
Conclusion: Intra-rater reliability of the new OA scale for ACL-deficient knees is moderate to substantial and the same or better than IKDC. Inter-rater reliability for JSN is comparable to IKDC. Blinding surgical tunnels/hardware and the affected side may remove rater biases when assessing radiographic OA.
Limitations: The comparison to unaffected knees assumes the knee is normal.
Ethics committee approval: The study received local ethics board approval. Informed written consent was obtained.
Funding: Grant funding from Workers' Compensation Board, Alberta.
Author Disclosures:
P. Bertiche: nothing to disclose
R. E. A. Walker: nothing to disclose
F. Mulji: nothing to disclose
D. J. Hunter: nothing to disclose
D. Chan: nothing to disclose
N. G. Mohtadi: Research/Grant Support at Workers' Compensation Board - Alberta

RPS 1610-2 16:06
Feasibility and reproducibility of 3D joint space mapping at the knee with standing CT data from the Multicentre Osteoarthritis Study (MOST)
T. Turmezei[1], S. B. L. Low[1], N. Segal[2], G. M. Treece[3], A. H. Gee[3], J. Lynch[4], K. E. S. Poole[3]; *[1]Norwich/UK, [2]Kansas City, KS/US, [3]Cambridge/UK, [4]San Francisco, CA/US (tom@turmezei.com)*

Purpose: Joint space mapping (JSM) can deliver 3D joint space width distribution (JSW) from CT imaging. The purpose of this study is to demonstrate its feasibility and reproducibility at the knee.
Methods and materials: 23 individuals were selected as a convenience sample from the Multicentre Osteoarthritis Study (MOST) with a full Kellgren and Lawrence grade (KLG) range. A prototype commercial cone-beam CT scanner (LineUp, CurveBeam, Warrington, PA) took fixed-flexion weight-bearing images of both knees with a 0.37 mm isotropic voxel reconstruction. JSM measured tibiofemoral JSW in 3D, with results mapped onto average joint surfaces for analysis. For feasibility, the side with worse KLG was taken, randomly if equal, for statistical parametric mapping (SPM) to ascertain the dependence of JSW

on KLG. For reproducibility, 3 knee sets were used for training of a novice, followed by a comparison of the remaining 20 against an expert.
Results: For each increment in KLG, there was a significant reduction in JSW up to 0.75 mm medially ($p<0.05$) and a non-significant increase in JSW up to 0.5 mm laterally. Global interoperator bias was -0.02 mm, the limits of agreement ±0.33 mm, and the root mean square coefficient of variation (RMSCV) 3.45%. Spatially localised results were even better with limits of agreement down to 0.1 mm and RMSCV down to 1% in central joint regions.
Conclusion: JSM at the knee is feasible, reproducible, and readily learned, meaning it could have an important role in the structural assessment of knee osteoarthritis in future research studies. The next step is to apply JSM in larger numbers to explore the relationship of 3D JSW distribution with clinical outcome measures such as pain, disability, and joint replacement.
Limitations: n/a
Ethics committee approval: http://most.ucsf.edu/IRBapproval.asp.
Funding: No funding was received for this work.
Author Disclosures:
T. Turmezei: nothing to disclose
S. B. L. Low: nothing to disclose
N. Segal: nothing to disclose
G. M. Treece: Patent Holder at U.S. patent US8938109B2, “Image data processing systems for estimating the thickness of human/animal tissue structures”.
A. H. Gee: Patent Holder at U.S. patent US8938109B2, “Image data processing systems for estimating the thickness of human/animal tissue structures”.
J. Lynch: nothing to disclose
K. E. S. Poole: nothing to disclose

RPS 1610-3 16:12

The natural history of new horizontal meniscal tears in individuals at risk for and with mild to moderate osteoarthritis: data from the osteoarthritis initiative

M. S. Posadzy[1], G. B. Joseph[1], C. McCulloch[1], M. Nevitt[1], J. Lynch[1], N. E. Lane[2], T. M. Link;
[1]San Francisco, CA/US, [2]Sacramento, CA/US

Purpose: To study the natural history of new horizontal meniscal tears and to determine if they are associated with the progression of cartilage degeneration in individuals at risk for or with mild to moderate knee osteoarthritis over a period of 4 years.
Methods and materials: Individuals who developed a new meniscal tear in the right knee were selected from the osteoarthritis initiative cohort 3T MRIs. Knee structural changes were monitored after 4 years using a modified whole-organ magnetic resonance imaging score (WORMS). Horizontal type tears were differentiated from non-horizontal tears. The control group included individuals without a meniscal tear at any timepoint matched according to BMI, gender, race, and age. Linear regression analysis was used to compare cross-sectional and longitudinal changes in cartilage WORMS scores between the groups.
Results: 41/75 subjects (54.6%) developed horizontal tears, 24 at the medial meniscus (with 17/24 (70.8%) at the posterior horn), 16 tears at the lateral meniscus (11/16 (68.75%) at the body), and one patient developed a tear in both menisci. Over 4 years, there were 30/41 (73.2%) horizontal tears but only 22/34 (64.7%) non-horizontal tears remained stable. Individuals with a new tear had higher WORMS scores at baseline ($p<0.05$). The overall progression of cartilage degeneration over 4 years was not significantly different between horizontal tear and control groups (WORMS total knee summary score: $p>0.597$, 95%CI=-0.57-1.00).
Conclusion: New horizontal meniscal tears tended to be stable over 4 years and no statistically significant differences in overall cartilage progression were found when compared to a matched control group.
Limitations: Only subjects developing meniscal tear over a two-year period of observation were included.
Ethics committee approval: Informed consent was reviewed and approved by institutional review boards of all participating centres.
Funding: The osteoarthritis initiative is funded by the NIH.
Author Disclosures:
M. S. Posadzy: nothing to disclose
G. B. Joseph: nothing to disclose
C. McCulloch: nothing to disclose
M. Nevitt: nothing to disclose
J. Lynch: nothing to disclose
N. E. Lane: nothing to disclose
T. M. Link: nothing to disclose

RPS 1610-4 16:18

Deep convolutional neural-network-based detection of ACL tears: a multicentre comparison of diagnostic accuracy with a surgical reference standard

C. Germann, G. Marbach, F. Civardi, S. Fucentese, R. Sutter, C. W. A. Pfirrmann, B. Fritz; *Zurich/CH*

Purpose: To clinically validate a novel, deep convolutional neural network (DCNN) for the detection of surgically proven ACL tears in a large patient cohort and to analyse the effect of MR examinations from different institutions, varying protocols, and field strengths.
Methods and materials: 512 consecutive patients were retrospectively included who underwent knee MRIs either in our (n=278) or at an outside institution (n=234), followed by knee arthroscopy in our institution. All MRIs were evaluated for a full-thickness ACL tear by three radiologists and the DCNN independently. The surgical reports served as a reference standard. Statistics included sensitivity, specificity, ROC curve analysis, and kappa-statistics. A $p<0.05$ was considered to represent statistical significance.
Results: An ACL tear was present in 45.7% (234/512) and absent in 54.3% (278/512) of patients. In comparison to any of the three readers, the DCNN showed a similar sensitivity of 96.1% (all $p\geq0.118$), but a significantly lower specificity of 93.1% (all $p<0.001$) and area under the curve (AUC) of 0.935 (all $p<0.001$). Subgroup analysis showed a significantly lower sensitivity, specificity, and AUC of the DCNN for patients examined at an outside institution (92.5%, 87.1%, and 0.898) in comparison to patients examined in our institution (99.0%, 94.4%, and 0.967), with $p=0.026$, $p=0.043$, and $p<0.05$, respectively. No significant differences of the DCNN assessments existed regarding field strength (1.5T or 3T MRI; all $p\geq0.753$). The agreement between the radiologists was almost perfect with kappa=0.984.
Conclusion: In our multi-institutional cohort (different institutions, varying protocols) our DCNN detects complete ACL tears with similar sensitivity and slightly lower specificity than specialised radiologists and with a similar accuracy than published meta-analyses.
Limitations: Possible selection bias because only patients with subsequent arthroscopic surgery were included. Only binary classification; no tear versus full-thickness tear.
Ethics committee approval: Approved by the local ethics committee.
Funding: No funding was received for this work.
Author Disclosures:
C. Germann: nothing to disclose
B. Fritz: nothing to disclose
R. Sutter: nothing to disclose
C. W. A. Pfirrmann: nothing to disclose
S. Fucentese: nothing to disclose
G. Marbach: Employee at Balzano AG
F. Civardi: Employee at Balzano AG

RPS 1610-5 16:24

Abbreviated 4 sequence protocol versus standard 6 sequence protocol for ankle MRIs: A retrospective check-list-based quantification of the value of additional sequences to the standard sequence

S. Rajan, G. Nanda, V. K. Venugopal, M. Murugavel, V. Mahajan, H. Mahajan, S. Gupta; *New Delhi/IN*

Purpose: To quantify the value provided by adding two sequences to an abbreviated 4-sequence scan protocol.
Methods and materials: This was a retrospective study of 79 MRIs of the ankle performed on a 3.0T scanner for various indications. Two sets of images were anonymised and randomised, one with three-plane FSPD and three-plane T1W images, the second with three-plane FSPD and axial T1 images. The four-sequence study was first read by two MSK radiologists with 16 years’ and 13 years’ experience using a standard 14-point checklist-based reporting template. This was followed by a washout period of 15 days and then the six-sequence study was read using the same template. The imaging findings were compared using Krippendorf’s alpha coefficient, which corrects for chance agreement.
Results: Only two features, ankle joint pathologies and subtalar articular pathologies, returned Krippendorf’s alpha scores greater than 0.67 for any radiologist suggesting no significant additional value. The other 12 features related to midtarsal joints, bones around the ankle joint, anterior talofibular ligaments, calcaneofibular ligaments, deltoid ligaments, spring ligaments, syndesmotic ligaments, lateral tendons, posteromedial tendons, Achilles tendons, anterior tendons, and plantar fascias scored below 0.67 for both radiologists implying a significant difference in the findings.
Conclusion: We conclude that the current standard of care 6 sequence multiplanar protocol offers significant additional value in 12 of the 14-checklist items as compared to the abbreviated four sequence protocol. Hence it is necessary for optimal imaging of the ankle joint.
Limitations: The relatively small number of cases.
Ethics committee approval: n/a

Funding: No funding was received for this work.
Author Disclosures:
V. K. Venugopal: nothing to disclose
S. Rajan: nothing to disclose
G. Nanda: nothing to disclose
M. Murugavel: nothing to disclose
V. Mahajan: nothing to disclose
H. Mahajan: nothing to disclose
S. Gupta: nothing to disclose

RPS 1610-6 16:30

Graft healing following anterior cruciate ligament reconstruction: a longitudinal DTI study

P. van Dyck[1], M. Froeling[2], E. de Smet[1], P. Verdonk[3], C. H. Heusdens[1], A. Ribbens[4], T. Billiet[4]; [1]*Edegem/BE,* [2]*Utrecht/NL,* [3]*Deurne/BE,* [4]*Leuven/BE (pieter.van.dyck@uza.be)*

Purpose: To investigate the ability of diffusion tensor imaging (DTI) to monitor graft healing following anterior cruciate ligament (ACL) reconstruction.
Methods and materials: 28 patients who underwent ACL reconstruction were enrolled prospectively and invited to undergo clinical and DTI follow-up at 3, 8, and 14 months postoperatively. DTI was acquired at 3T using single-shot SE-EPI (b-values: 0/400/800s/mm^2, 10 directions; TR/TE: 1300/45ms; voxel size: 1.5×1.5×6.0mm^3; FOV 768×768×60mm). Fibre tractography (FT) was performed to delineate the ACL graft. The posterior cruciate ligament (PCL) served as a control. Fractional anisotropy (FA), mean diffusivity (MD), axial diffusivity (AD), and radial diffusivity (RD) were calculated within the FT volumes. Data was compared using a linear mixed-effects model for all repeated measures and paired t-tests between different time points ($p<0.05$).
Results: All knees were stable during clinical follow-up. 72 DTI datasets were analysed. ACL grafts showed a significant decrease of FA over time ($F=9.05$, $p=0.003$), with the strongest decrease between 8 and 14 months postoperatively ($T=-2.55$, $p=0.002$). FA values of the PCL did not change over time ($F=0.01$, $p=0.94$). Diffusivities did not significantly change over time in ACL grafts or PCL according to the mixed-effects model ($p>0.05$). However, ACL grafts showed initial increase of diffusivities between 3 and 8 months postoperatively and decreasing values thereafter (reaching significance for AD: $T=-2.26$, $p=0.039$), while PCL showed continuing decreasing values.
Conclusion: Our study has shown the potential of longitudinally monitoring DTI values of ACL grafts following reconstruction. Our results indicate incomplete healing at 14 months postoperatively.
Limitations: A small sample size and no histological correlation.
Ethics committee approval: Approval by the institutional review board and written informed consent was obtained (B300201627688).
Funding: PVD is supported by research foundation FWO-Vlaanderen, Belgium (1831217N).
Author Disclosures:
P. Verdonk: nothing to disclose
P. van Dyck: Research/Grant Support at FWO-Vlaanderen
M. Froeling: nothing to disclose
E. de Smet: nothing to disclose
T. Billiet: Employee at Icometrix
A. Ribbens: Employee at Icometrix
C. H. Heusdens: nothing to disclose

RPS 1610-7 16:36

3D TSE MRI diagnostic accuracy compared to 2D TSE MRI for the detection of meniscal injuries with arthroscopic correlation

R. I. E. Yasin, W. A. Gouda; *Menofia/EG (rabab_yasin@outlook.com)*

Purpose: To compare 3D PD fat-suppressed space turbo spin-echo (TSE) and conventional 2D PD sequences at 3T MRI in the detection of meniscal tears.
Methods and materials: Dedicated MR knee imaging of 100 sequential patients with suspected meniscal injuries was retrospectively analysed by two independent radiologists in a novel study design using both a 2D PD standard multiplanar TSE MR technique and 3D PD TSE technique. The result was compared to arthroscopic results (arthroscopy was performed after MRI study) which were considered as a gold standard test. We determined the sensitivity, specificity, and interobserver agreement for each sequence.
Results: The 3D TSE shows statistically higher sensitivity and specificity (100% and 100%) for the detection of meniscal radial tear compared to the 2D sequence (67% and 96%). No significant difference was found between the sensitivity and specificity of both techniques regarding the detection of horizontal, longitudinal, root, flap, and bucket handle tears. There was higher interobserver agreements on 3D TSE SPACE than 2D sequences for radial, root, and bucket handle tears.
Conclusion: At 3T MRI, the 3D PD fat-suppressed space turbo spin-echo (TSE) has higher diagnostic performance compared to the routine 2D TSE protocol for the detection of meniscal radial tears and similar results as regarding the other types of tears with the advantage of faster acquisition.
Limitations: n/a
Ethics committee approval: Written and informed consent was obtained.
Funding: No funding was received for this work.
Author Disclosures:
R. I. E. Yasin: nothing to disclose
W. A. Gouda: nothing to disclose

RPS 1610-8 16:42

The utility of axial strain elastography in youth basketball players with a clinical diagnosis of patellar tendinopathy

R. E. A. Walker[1], O. B. A. Owoeye[2], Y. Chadha[3], J. P. Wiley[1], L. McLeod[1], T. Hubkarao[1], L. Palacios-Derflingher[1], C. A. Emery[1]; [1]*Calgary/CA,* [2]*St. Louis/US,* [3]*Toronto/CA (rewalker@ucalgary.ca)*

Purpose: To evaluate the diagnostic accuracy of axial strain elastography (ASE) for clinically diagnosed patellar tendinopathy (PTP) in youth basketball players.
Methods and materials: 52 participants (23 with PTP) were recruited from local youth basketball programs in 2016/17 and underwent sonographic assessment of bilateral patellar tendons, including ASE. Sonographers/sonologists were blinded to the case-control status of participants (PTP unilateral/PTP bilateral/no PTP). Images were partitioned, randomised, and archived for interpretation by two fellowship-trained musculoskeletal radiologists.
Using a graduated colour strain map (red-yellow-green-blue), two raters evaluated axial strain elastograms of the proximal patellar tendon and recorded tendons as 'soft'(>2/3 red), 'hard'(>2/3 blue), or 'intermediate' (neither 'hard' nor 'soft'). 'Soft' tendons were considered pathologic and cross-tabulated with clinically diagnosed PTP and controls to calculate accuracy, sensitivity, and specificity. The agreement was assessed between raters.
Results: 104 patellar tendons were scanned with ASE. 9 nondiagnostic exams were excluded, leaving 95 tendons for assessment. The inter-rater reliability was moderate (Kappa=0.491). The percent agreement was 76.8%. Of disagreements, 18/22 (81.8%) related to differences between classifying a tendon as 'soft' versus 'intermediate'. For reader 1, the accuracy of ASE compared to the clinical evaluation was 53% (42%-63%), sensitivity was 18% (7%-35%), and specificity was 71 (58%-82%). For reader 2, accuracy was 59% (48%-69%), sensitivity was 24% (11%-42%), and specificity was 77% (65%-87%).
Conclusion: ASE classification of tendons as 'soft', 'hard', or 'intermediate' stiffness had moderate inter-rater reliability. Further standardisation of definitions regarding ASE classification of tendons as 'normal' or 'pathologic' could improve inter-rater reliability.
As an isolated instrument, the accuracy of ASE for clinically diagnosed patellar tendopathy was poor.
Limitations: B-mode images visible on ASE elastograms could bias the reader.
Ethics committee approval: Local institutional ethics approval. Each participant provided written consent.
Funding: NBA/GE Orthopedics and Sports Medicine Collaboration Grant on Tendinopathy. Sport Injury Prevention Research Centre is supported by the International Olympic Committee.
Author Disclosures:
R. E. A. Walker: Research/Grant Support at NBA/GE Orthopedics and Sports Medicine Collaboration Grant on Tendinopathy
L. McLeod: nothing to disclose
Y. Chadha: nothing to disclose
L. Palacios-Derflingher: Research/Grant Support at NBA/GE Orthopedics and Sports Medicine Collaboration Grant on Tendinopathy
C. A. Emery: Research/Grant Support at NBA/GE Orthopedics and Sports Medicine Collaboration Grant on Tendinopathy
J. P. Wiley: Research/Grant Support at NBA/GE Orthopedics and Sports Medicine Collaboration Grant on Tendinopathy
O. B. A. Owoeye: Research/Grant Support at NBA/GE Orthopedics and Sports Medicine Collaboration Grant on Tendinopathy
T. Hubkarao: nothing to disclose

RPS 1610-9 16:48

Femur lengthening via a retrograde approach with the motorised intramedullary lengthening nail: 10-year follow-up MRI results

R. Donners, A. H. Krieg, D. Harder; *Basel/CH (ricardo.donners@usb.ch)*

Purpose: To establish MRI findings of the knee after leg lengthening via a retrograde femoral approach by using a motorised intramedullary lengthening nail in comparison to the healthy contralateral knee.
Methods and materials: In this prospective self-controlled single-centre study, 13 patients were included. All received unilateral retrograde femoral lengthening with a motorised intramedullary nail (FITBONE®, Wittenstein intens GmbH, Igersheim, Germany) and the follow-up time was 10-12 years. MRI of the contralateral knee of each patient served as a control. Exclusion criteria were MRI-contraindications, previous contralateral knee surgery, or severe trauma.

Standard MSK 3T-MRI images were assessed for joint effusion, synovial proliferation, cartilage defects, fibrotic changes of Hoffa's fat pad, and quadriceps femoris muscle atrophy compared to the healthy contralateral knee. Cartilage defects were graded according to the ICRS-classification system. Patient demographics, range of motion, and pain were noted.
Results: 13/13 postoperative knees showed fibrosis of Hoffa's fat pad, 0/13 in the control group. Moderate to severe cartilage defects (grade II-IV) of the trochlear groove were found in 13/13 postoperative knees in the insertion area. 1 healthy knee showed mild trochlear cartilage defects (grade I). 6/13 postoperative knees showed retropatellar cartilage defects. 10/13 patients showed postoperative atrophy of the medial and lateral vastus muscle compared to the control side. No case showed signs of chronic synovitis or relevant amounts of joint effusion. All patients were pain-free and showed a full range of motion.
Conclusion: Retrograde femoral lengthening with a motorised intramedullary nail may be associated with femoropatellar cartilage defects, arthrofibrosis, and muscle atrophy. Without corresponding clinical impairment, these findings may be normal in long-term follow-up.
Limitations: A small cohort and no different surgical method for comparison.
Ethics committee approval: Ethics board approval and written patient consent obtained.
Funding: No funding was received for this work.
Author Disclosures:
A. H. Krieg: nothing to disclose
R. Donners: nothing to disclose
D. Harder: nothing to disclose

RPS 1610-10 16:54

The role of shear-wave elastography in the diagnostic evaluation of plantar fasciitis

H. Y. Y. R, R. Chandra, D. K. Singh, N. Kumar, B. K. Nayak*; New Delhi/IN (harshith25yr@gmail.com)*

Purpose: To evaluate the added advantage of shear-wave elastography (SWE) over grey-scale sonography in the diagnosis of plantar fasciitis and to obtain a reproducible and reliable sonoelastographic shear stress cut-off value.
Methods and materials: In this prospective case-control study, 30 consenting patients having unilateral heel pain for >6 months and clinically diagnosed as unilateral heel pain were included. Patients were examined by the lead author and a faculty radiologist by B-mode sonography (for plantar fascia thickness), followed by SWE, obtaining a colour map for shear characteristics and quantitative data (shear velocity in cm/s and shear stress in kPa) using a 1x1 cm ROI placed at the position of the highest shear on the colour map. Sensitivity and false-positive rates with extrapolated specificity, PPV, and NPV were calculated, and shear stress cut-off values were obtained using the Chi-square test and ROC curve analysis. The unaffected foot from respective cases was taken as control (normal) for the study.
Results: Of 30 examined cases, mean thickness of plantar fascia was significantly higher (5.4 mm) in the affected foot compared to the unaffected (2.9 mm), with a standard ROC cut-off of 3.7 mm (sensitivity 93%, false-positive rate 10%). The mean shear stress in the plantar fascia on the affected side (60.1kPa) differed significantly from the unaffected side (150.7kPa). Taking 97.5kPa as the shear stress cut-off, considering affected patients having values below this cut-off, sensitivity was 81.8% and the false-positive rate was 10.6%. Extrapolated specificity, PPV, and NPV were 89.4%, 88.5%, and 83.1%. AUC was 0.91.
Conclusion: SWE shows superior diagnostic accuracy compared to grey-scale sonography in patients with plantar fasciitis and promises the potential for routine use in addition to B-mode US for the assessment of plantar fasciitis cases.
Limitations: A limited number of patients.
Ethics committee approval: Ethic committee approval obtained.
Funding: No funding was received for this work.
Author Disclosures:
B. K. Nayak: nothing to disclose
H. Y. Y. R: nothing to disclose
R. Chandra: nothing to disclose
N. Kumar: nothing to disclose
D. K. Singh: nothing to disclose

RPS 1610-11 17:00

The prevalence of midtarsal (Chopart) sprains in the setting of acute ankle injury in professional soccer players

M. T. Leiderer, G. H. Welsch, I. Molwitz, M. L. Warncke, K.-J. J. Maas, P. Bannas, G. Adam, F. O. Henes*; Hamburg/DE (m.leiderer@uke.de)*

Purpose: To evaluate the prevalence of midtarsal joint injury and its association with ankle sprain in professional soccer players after acute ankle trauma.
Methods and materials: 48 ankle MRIs of 43 professional soccer players with acute trauma (all male; mean age 21 y; range 15-31 y), acquired from January 2012-September 2019, were enrolled in the study. 3 scans were performed on a 1.5 Tesla, the remaining 46 on a 3 Tesla scanner with a routine ankle MRI protocol. A retrospective review of all MR images was undertaken in consensus by two experienced musculoskeletal radiologists. Acute tear (complete and partial) of the ligaments of the midtarsal and the ankle joint was assessed. In particular, MR images were scrutinised for injury to the dorsal calcaneocuboid, bifurcate, short and long plantar, spring, and dorsal talonavicular ligaments.
Results: Overall there were 36 cases with an ankle sprain, 19 with deltoid, 27 with lateral collateral ligament injuries, and 7 with a syndesmosis injury. Acute midtarsal joint injury was present in 13 cases (27.1%). In 9 of these, the midtarsal injury was concomitant with an ankle sprain or syndesmosis injury. In total, there were 22 midtarsal ligamentous injuries including the calcaneocuboid (4 complete, 5 partial) and calcaneonavicular (3 complete, 1 partial) parts of the bifurcate ligament, the dorsal calcaneocuboid ligament (1 complete, 2 partial), and the dorsal talonavicular ligament (2 complete, 4 partial). The plantar ligaments and the spring ligament were intact in all cases.
Conclusion: A midtarsal sprain is commonly associated with an acute ankle injury in professional soccer players. Radiologists must ensure that midtarsal injuries do not remain unrecognised, as accurate diagnosis of midtarsal sprain in MRI is important for effective clinical management.
Limitations: n/a
Ethics committee approval: n/a
Funding: No funding was received for this work.
Author Disclosures:
M. T. Leiderer: nothing to disclose
K.-J. J. Maas: nothing to disclose
I. Molwitz: nothing to disclose
F. O. Henes: nothing to disclose
G. Adam: nothing to disclose
P. Bannas: nothing to disclose
G. H. Welsch: nothing to disclose
M. L. Warncke: nothing to disclose

RPS 1610-12 17:06

Tenosynovitis at the metatarsophalangeal joints: a feature of rheumatoid arthritis? Results from a large cross-sectional MRI and anatomical study of tendon sheaths of the forefoot

Y. J. Dakkak, F. Jansen, M. de Ruiter, M. Reijnierse, A. van der Helm-van Mil*; Leiden/NL (y.j.dakkak@lumc.nl)*

Purpose: Recent MRI-studies revealed that tenosynovitis in the hands is associated with rheumatoid arthritis (RA). Although the forefoot is a preferential location for RA-inflammation, it is unknown whether MRI-detected tenosynovitis at the metatarsophalangeal (MTP)-joints is associated with RA. Additionally, anatomic literature leaves it undetermined if tendons at MTP-joints are surrounded by a synovial sheath. These questions were investigated.
Methods and materials: 634 persons were included: 157 newly presenting RA-patients, 284 patients with other early arthritides, and 193 symptom-free persons. All underwent MRI of unilateral MTP (1-5)-joints. Images were scored by two independent readers for tenosynovitis, synovitis, and bone marrow oedema. Its association with RA was analysed using logistic regression. Macroscopically, 14 forefeet of donated bodies were examined at the flexor-tendons and extensor-tendons for the presence and course of tendon sheaths. Tissue surrounding tendons was injected with blue-dyed resin or silicon. The presence of a sheath was also studied by light-microscopy.
Results: MRI-detected tenosynovitis was associated with RA (OR 2.4 (95%CI 1.5-3.8, P<0.001) for flexor and OR 3.1 (95%CI 1.9-5.2, P<0.001) for extensor tendons). The sensitivity of tenosynovitis in RA was 42%. The specificity compared to other arthritides was 78% and compared to symptom-free persons 98%. Macroscopically, all extensor and flexor tendons crossing MTP-joints demonstrated clearly demarcated sheaths surrounding tendons. Microscopy revealed a synovial sheath at flexor and extensor tendons.
Conclusion: Flexor and extensor tendons at metatarsophalangeal-joints are surrounded by a tenosynovium. MRI-detected tenosynovitis at metatarsophalangeal-joints was associated with, and specific for, rheumatoid arthritis, both when compared to patients with other arthritides and healthy controls.
Limitations: Our study is cross-sectional; additional longitudinal studies on the diagnostic value are needed.
Ethics committee approval: Ethics committee approval obtained.
Funding: European Research Council and the Dutch Arthritis Foundation.
Author Disclosures:
Y. J. Dakkak: nothing to disclose
F. Jansen: nothing to disclose
M. Reijnierse: nothing to disclose
M. de Ruiter: nothing to disclose
A. van der Helm-van Mil: nothing to disclose

RPS 1610-13 17:12
Effectiveness of ultrasound-guided treatment of plantar fasciitis: corticosteroid injection versus dry needling
A. Iozzelli, A. Cipriani*; Macerata/IT (aiozzelli@sirm.org)*

Purpose: To evaluate the efficacy and safety of ultrasound-guided treatment of plantar fasciitis using corticosteroid injection (CS) compared to the dry needling technique (DN).
Methods and materials: We enrolled 20 patients (12 females, 8 males, age 43.8±8.4 y) suffering from chronic plantar fasciitis, randomly allocated to the DN or the CS group. DN consisted of ultrasound-guided needling (18-gauge Chiba needle) of the plantar fascia calcaneal insertion with lidocaine 2%. The CS technique consisted of ultrasound-guided injection over the plantar fascia calcaneal insertion of 40mg/1ml triamcinolone acetonide with 1 ml lidocaine 2%. Evaluation of pain using the visual analogue scale (VAS, range 0-10) was obtained at baseline, 1 week, and 1, 6, and 12 months after the procedures. Morphology of plantar fascia and complications were recorded.
Results: The baseline VAS score was 8.19±1.2. CS resulted in superior pain reduction than DN at 1 week (1.50±1.35 vs 4.64±1.63, p=0.03) and 1 month (1.60±1.58 vs 3.73±1.35, p=0.04). Both techniques showed similar results at 6 months (2.50±1.18 vs 2.18±1.33, p>0.05) and DN resulted in better outcome at 12 months (DN=1.36±1.50 vs CS=4.00±2.45, p=0.03). The thickness of plantar fascia did not differ between the groups. No relevant complications were reported.
Conclusion: Our study demonstrates that DN could be an effective and safe option for the treatment of chronic plantar fasciitis, with better results in pain reduction than CS at 6 and 12 months follow-up. Conversely, CS gave immediate and short-term relief.
Limitations: The limited number of patients could affect the result of our study.
Ethics committee approval: Written informed consent was obtained from all patients.
Funding: No funding was received for this work.
Author Disclosures:
A. Iozzelli: nothing to disclose
A. Cipriani: nothing to disclose

RPS 1610-14 17:18
Quantitative 2D versus 3D geometric analysis on bones and joints in weight-bearing and non-weight-bearing cone-beam CT images
S. Berardo[1], M. Broos[2], J. G. G. Dobbe[2], M. Maas[2], G. J. Streekstra[2], R. H. H. Wellenberg[2]; *[1]Novara/IT, [2]Amsterdam/NL (berardo.sara@gmail.com)*

Purpose: The increasing use of cone-beam CT to diagnose ankle and foot problems urges the development of quantitative 3D analysis tools that deliver geometrical parameters corresponding to well-known 2D counterparts. We compared estimates of geometrical parameters from both cone-beam CT and radiographs as differences can be expected between 2D and 3D analyses.
Methods and materials: WB and non-WB cone-beam CT-images of the left and right hindfoot and forefoot were acquired on a Planmed verity cone-beam CT-scanner. Geometric analyses were performed on images of the foot in 2D using simulated radiography images and 3D using custom analysis software. Measurements included the calcaneal pitch, Meary's angle, the angle between 1st and 2nd metatarsal (MTT), the talocalcaneal angle, and cuboid height.
Results: 5 patients were included with a mean age of 39.6 years. All measurement results were statistically different in 2D and 3D (p<0.001). The average calcaneal pitch decreased in 2D and in both 3D WB compared to non-WB results. Meary's angle decreased in 2D measurements, however, increased using 3D measurements. The average angle between MTT1-2 increased in both approaches. During WB, the talocalcaneal angle decreased in both lateral-lateral and anterior-posterior 2D views and increased in 3D. Cuboid height decreased between non-WB and WB images by 1.3 and 6.5 mm in 2D and 3D images respectively (p<0.001).
Conclusion: The geometric parameters evaluated in 2D were different compared to 3D, which is likely caused by over-projection and the specific point of view. We expect that 3D measurement tools are more univocal and therefore more suitable for future use. Also, switching to 3D enables advanced analysis such as obtaining joint space maps.
Limitations: Sample-size, 2D and 3D comparisons, and multiple observers.
Ethics committee approval: n/a
Funding: No funding was received for this work.
Author Disclosures:
R. H. H. Wellenberg: nothing to disclose
M. Broos: nothing to disclose
M. Maas: nothing to disclose
G. J. Streekstra: nothing to disclose
J. G. G. Dobbe: nothing to disclose
S. Berardo: nothing to disclose

RPS 1610-15 17:24
Establishing quantitative measures for detecting subtle calcaneonavicular coalition: a case-control study
S. Rajan, V. K. Venugopal, H. Mahajan, V. Mahajan, S. Gaur*; New Delhi/IN (drsriramrajan@gmail.com)*

Purpose: We propose to determine if calcaneonavicular distance measurement could differentiate between normal patients and subtle forme fruste of calcaneonavicular coalition.
Methods and materials: 77 consecutive subjects presenting with foot pain and referred for MRI were evaluated. We assessed the calcaneonavicular distance on axial T1 images, and the anterior process calcaneum (APC) and posterior extension of navicular on sagittal images. The presence or absence of calcaneonavicular coalition was assessed. 15 normal volunteers without foot pain were also assessed.
Results: In patients with an obvious coalition, the mean calcaneonavicular distance was 1.5 mm (+0.52), the mean length of APC was 9.99 mm (+ 1.7), and the extra-articular length of the navicular bone was 11.18 mm (+2.29). The corresponding measurements in patients with foot pain but no obvious coalition were 3.91 mm (+2.19), 9.9 mm (+1.11), and 11.97 mm (+2.77), and in the normal volunteers were 3.99 mm (+1.49), 10.93 mm (+1.63), and 12.55 mm (+1.2). A support vector machine classifier was trained to classify coalition using 77 patients and 15 normal volunteers with 5-fold cross-validation. Accuracies of about 88 % were achieved when these three measurements were employed. A principal component analysis estimated the variance explained at 43 %, 35%, and 22% for the 3 components, respectively, implying all 3 components have significant predictive value in classifying coalition.
Conclusion: The 3 measures described in this study can be reliably used to detect subtle calcaneonavicular coalition on MRI of the ankle joints.
Limitations: The small sample size for normal controls.
Ethics committee approval: IRB approval was obtained.
Funding: No funding was received for this work.
Author Disclosures:
S. Rajan: nothing to disclose
V. K. Venugopal: nothing to disclose
H. Mahajan: nothing to disclose
V. Mahajan: nothing to disclose
S. Gaur: nothing to disclose

16:00 - 17:30 **Room X**

Student Session

S 16

My scientific paper in the field of oncologic imaging

Moderator:
P. K. Prassopoulos; Thessaloniki/GR

S 16-1 16:05
Comparison of hydrochloric acid infusion radiofrequency ablation with microwave ablation in an ex vivo liver model
H. Deng, T.-Q. Zhang, X. Jiang, J. Huang*; Guangzhou/CN (denghanx@sysucc.org.cn)*

Purpose: Normal saline infusion radiofrequency ablation (NSRFA) is a widely accepted treatment for tumours up to 3 cm in diameter. Microwave ablation (MWA) and hydrochloric acid infusion radiofrequency ablation (HRFA) may be better alternatives for larger tumours, but few studies comparing these 2 modalities have been published. Thus, this study is aiming to compare ablation zone sizes and shapes resulting from HRFA and MWA, using NSRFA as a control in an ex vivo bovine liver model.
Methods and materials: A total of 90 ablation procedures were performed prospectively, each using 3 modalities: NSRFA, HRFA, and MWA. For each modality, 5 ablation procedures were performed for each combination of power (80W, 100W, or 120W) and duration (5, 10, 20, 30, 45, or 60 minutes). Ablation zone outcome parameter includes transverse diameter (TD), longitudinal diameter (LD), volume (V), front distance (FD), and spherical ratio (SR).
Results: For ablation duration up to 30 minutes, the mean TD after HRFA and MWA did not differ significantly (β=0.13, *P*=.20). For ablation durations greater than 30 minutes, the mean TD was significantly larger after HRFA than after MWA (β=1.657, P<.001). The largest TD (9.46 cm) and the most spherical ablation zone (i.e. highest SR, 0.95) resulted from HRFA performed with 100W power for 60 minutes.
Conclusion: Both MWA and HRFA with power settings of 80W to 120W and a duration of 30 minutes are capable of treating tumours of 5 cm or less. For

tumours of 7 cm or larger, HRFA with power settings 100W and duration of 30 minutes or longer is a better option than MWA.
Limitations: THe ex vivo model is partly different from the clinical patient.
Ethics committee approval: n/a
Funding: National Natural Science Foundation of China, No. 81771955.
Author Disclosures:
H. Deng: nothing to disclose
T.-Q. Zhang: nothing to disclose
J. Huang: nothing to disclose
X. Jiang: nothing to disclose

S 16-2 16:15

Review of the clinical effectiveness of PET-CT scans in the management of sub-solid pulmonary lesions at the Oxford Lung Cancer MDT in the last 5 years

M. Rinaldi[1], F. B. F. Botta[1], A. Di Gioia[1], A. Sykes[2], F. Gleeson[2], L. Srinivasan[2], D. Stavroulias[2], F. Di Chiara[2], N. Rahman[2]; [1]*L'Aquila/IT,* [2]*Oxford/UK (martabrinaldi@gmail.com)*

Purpose: The pre-operative assessment for lung cancer surgery includes a total body FDG PET/CT as a mandatory investigation for solid and sub-solid lesions. We sought to evaluate the clinical effectiveness of a PET-CT scan in the management of sub-solid nodules. We additionally assessed the relationship between SUVmax and nodule type.
Methods and materials: We retrospectively analysed 407 patients who underwent lung resections and received complete imaging work-up. A consultant radiologist confirmed the sub-solid nature of 94 lesions: 27 GGOs and 67 PSN. We then compared the histopathology results with CT and PET-CT.
Results: Comparing PET/CT staging to pathological staging, PET overstaged (p=0.013) a high proportion of patients with GGOs (42.9%) and PSN (19.4%), whereas the number understaged by PET were not significantly different (p=0.11).
Then, assessing PET/CT and CT concordance, we demonstrated that these investigations were never discordant with GGO and rarely (4.5%) in PSN (p=0.050).
Regression analysis assessed the correlation between SUVmax and nodule type, even when size was taken into account, and both size and nodule type were independent predictors of increasing SUVmax (p<0.001).
Conclusion: This study suggests that PET/CT rarely adds information for PSN and never for GGO compared with CT, whereas the relationship between SUVmax and nodule type revealed that GGO and PSN had significantly lower SUVmax than solid, suggesting a different behaviour of these lesions.
Thus, there is a strong argument for stopping PET for GGOs and careful consideration in PSN given the low likelihood of change from the CT findings. Further studies should test cost and clinical effectiveness of a PET/CT scan (£89,300 for this cohort of patients) in the management of sub-solid lesions.
Limitations: The retrospective assessment of data.
Ethics committee approval: n/a
Funding: No funding was received for this work.
Author Disclosures:
L. Srinivasan: nothing to disclose
M. Rinaldi: nothing to disclose
F. Di Chiara: nothing to disclose
F. B. F. Botta: nothing to disclose
A. Di Gioia: nothing to disclose
A. Sykes: nothing to disclose
F. Gleeson: nothing to disclose
D. Stavroulias: nothing to disclose
N. Rahman: nothing to disclose

S 16-3 16:25

CT texture analysis in PET-negative lung cancer

J. Daffinà, D. Caruso, M. A. Tipaldi, M. Zerunian, T. Polidori, F. Pucciarelli, E. Ronconi, M. Rossi, A. Laghi*; Rome/IT (daffinajulia@gmail.com)*

Purpose: To differentiate benign from malignant lung nodules in PET-negative cases based on CT texture analysis (CTTA).
Methods and materials: We retrospectively analyzed 53 patients with lung nodules with a negative PET scan (standardised uptake value [SUV] <2.5) who underwent a CT-guided lung biopsy (CTLB). Based on the pathological report, the population was divided into two groups: malignant and benign lesions. A dedicated software (TexRAD) was used to segment target nodules, drawing a region of interest (ROI) for each CT slice which displayed the lesion. CT texture parameters, including kurtosis, standard deviation, mean, and skewness were extrapolated for each spatial scale image filtration (SSF) of texture parameters. P<0.05 was statistically significant. The receiver operating characteristic curve (ROC) was calculated considering as dependent variables each of the texture parameters and a dichotomous variable indicating the histological diagnosis (0=malignant, 1=benign) as independent.
Results: Kurtosis showed significant difference for each SSF (all P≤0.0013; SSF0 1.50±5,70 vs 0.99±4.22; SSF2 1.83±6.18 vs 0.30±3.06; SSF3 1.80±6.81 vs -0.09±1.91; SSF4 1.90± 5.38 vs 0.07±2.65; SSF5 1.3±3.77 vs 0.17±3.33; SSF6 0.88±2.5 vs 0.35±3.67) and was considered the best parameter to differentiate malignant from benign pulmonary nodules. The ROC analysis showed significant area under the curves (AUC) for kurtosis at SSF3 (P<0.001; AUC 0.654), skewness at SSF4 (P<0.001; AUC 0.642), and for standard deviation at SSF0 (P<0.001; AUC 0.821).
Conclusion: CTTA was useful in identifying significant features that can distinguish malignant from benign pulmonary lesions in cases without an altered glucose metabolism at the PET scan.
Limitations: The retrospective design.
Ethics committee approval: IRB approved.
Funding: No funding was received for this work.
Author Disclosures:
D. Caruso: nothing to disclose
M. Rossi: nothing to disclose
M. A. Tipaldi: nothing to disclose
T. Polidori: nothing to disclose
M. Zerunian: nothing to disclose
A. Laghi: nothing to disclose
E. Ronconi: nothing to disclose
F. Pucciarelli: nothing to disclose
J. Daffinà: nothing to disclose

S 16-4 16:35

MRI bias correction with an implicitly trained convolutional neural network

A. T. Simkó, T. Löfstedt, J. Jonsson, A. Garpebring, T. Nyholm*; Umeå/SE (attila.simko@umu.se)*

Purpose: Bias field correction deals with the intra-volume intensity inhomogeneities in magnetic resonance imaging (MRI) data. It has little significance for visual diagnosis yet it is a crucial step for the automation of radiotherapy solutions. Extensive research and evaluation show that the often used and well-established correction methods typically require parameter tuning for the given dataset or are expensive to compute.
Methods and materials: A novel method has been introduced, allowing for the training of a convolutional neural network (CNN) on non-medical images, making the model general and evaluating it for bias field correction on medical MRI data.
Results: The proposed method has been compared to an optimised N4ITK in three experiments. It produces nearly identical results to N4ITK for a benchmark test and similar results in a coefficient of variation, mean absolute error, mean error, and structural similarity for a BrainWeb-based experiment, with an average speedup factor of 137. Different methods performed best for the different investigated tissue types. It was also tested for real cases, often producing more radio realistic bias fields in the cases where N4ITK struggles. Also, no datasets were encountered where the method would not improve image quality.
Conclusion: Training a convolutional neural network implicitly, through the relation of the outputs of two similar training samples, is possible, omitting the need for true target data. The achieved model is not only generalised but also achieves comparable accuracy to N4ITK with a significant speedup.
Limitations: No numerical evaluation for real cases.
Ethics committee approval: n/a
Funding: Support obtained from the Cancer Research Foundation in Northern Sweden and from Karin and Krister Olsson.
Author Disclosures:
A. T. Simkó: nothing to disclose
T. Nyholm: nothing to disclose
J. Jonsson: nothing to disclose
A. Garpebring: nothing to disclose
T. Löfstedt: nothing to disclose

S 16-5 16:45

Pancreatic ductal adenocarcinoma: rim enhancement at CT imaging predicts histologic grade

M. Shantarevich, A. Egorkina, G. Karmazanovsky, E. V. Kondratyev, A. Kriger, A. Kurochkina, D. Kalinin*; Moscow/RU (shantarevichm@list.ru)*

Purpose: Survival rates and the prognosis of patients with pancreatic adenocarcinoma (PA) directly depends on the histologic grade of the tumour. The purpose of this study was to identify features and quantitative parameters at preoperative CT imaging for predicting the histologic grade of the tumour.
Methods and materials: 81 patients with histologically-verified pancreatic ductal adenocarcinoma (11 PA grade 1, 47 PA grade 2, and 23 PA grade 3) and preoperative CT imaging performed in the native, arterial, and portal phases (10 and 40 seconds since reaching the threshold density value on aorta), with the tube voltage 120 kV, were enrolled in this study. We compared mean absolute tumour and pancreatic parenchyma attenuation between groups for each contrast enhancement phase. For each patient, the presence of rim

enhancement was assessed and defined as irregular peripheral hyperdensity with a relatively hypodense central area on dynamic-enhanced images.
Results: The mean tumour density in the arterial phase was 51.1±17.6 HU, median 49 HU. The mean tumour density in the venous phase was 63.0±18.9 HU, median 63 HU. Among PA grade 1, in 81.8% the rim enhancement was not observed. PA grade 2 was found in 85.71% cases where it was impossible to unequivocally speak out in favour of the absence or presence of the rim enhancement. In the presence of the rim enhancement in 96.42%, PA was grade 2 or grade 3. The density of PA grade 1 in 90.91% was <63 HU and the density of PA grade 3 in 69.57% was ≥63 HU.
Conclusion: Rim enhancement of PA was associated with more aggressive histologic tumour grades.
Limitations: n/a
Ethics committee approval: n/a
Funding: No funding was received for this work.
Author Disclosures:
A. Kriger: nothing to disclose
M. Shantarevich: nothing to disclose
A. Kurochkina: nothing to disclose
A. Egorkina: nothing to disclose
G. Karmazanovsky: nothing to disclose
E. V. Kondratyev: nothing to disclose
D. Kalinin: nothing to disclose

S 16-6 16:55

Determinants of ADC in the bone marrow of healthy individuals: effects of sex, age, and fat fraction

L. Bombelli[1], A. Colombo[1], G. Signorelli[1], A. Rossi[2], P. Summers[1], R. Grimm[3], M. Bellomi[1], G. Petralia[1]; [1]Milan/IT, [2]Meldola/IT, [3]Erlangen/DE
(bombelli.luca@virgilio.it)

Purpose: In literature, there is little documentation of ADC values in normal bone marrow and of the effects of physiological factors. The aim of this study is to evaluate how sex, age, and fat (evaluated from %FF) affect the ADC values measured in the bone marrow of healthy individuals.
Methods and materials: We processed the diffusion-weighted images of WB-MRI examinations in 100 asymptomatic individuals, 50 men and 50 women aged 30-79 years. The mean value of ADC in bone marrow (ADCbm) was estimated by fitting the histogram extracted from the images with a semi-automatic segmentation technique. The %FF value was measured as the average of ROIs drawn in specific positions (iliac bone, D10, L4). Gender differences were assessed with the Mann-Whitney U test, while ADCbm correlations with age and %FF were assessed with the Spearman correlation coefficient (ρ).
Results: The values of ADCbm were significantly higher in women than in men (respectively 458.1±63.3 $\mu m^2/s$ and 383.0±58.4 $\mu m^2/s$, $p<0.01$). A significant negative correlation of ADCbm with age ($\rho=-0.46$, $p< 0,001$) was observed in women but was absent in men ($\rho=-0.04$, $p=0.79$). Moreover, there was a negative correlation between ADCbm and %FF in both women and men (respectively: $\rho=-0.52$, $p<0.001$ and $\rho=-0.28$, $p<0.05$).
Conclusion: There was a significant difference between ADCbm values of men and women. The negative correlation between ADCbm and age in women is likely related to menopause, while that between ADCbm and %FF, present in both sexes, appears to be a separate process.
Limitations: Calculate ADCbm and %FF with two different approaches.
Ethics committee approval: Approved by an internal review board.
Funding: No funding was received for this work.
Author Disclosures:
L. Bombelli: nothing to disclose
A. Colombo: nothing to disclose
G. Signorelli: nothing to disclose
A. Rossi: nothing to disclose
P. Summers: nothing to disclose
M. Bellomi: nothing to disclose
G. Petralia: Speaker at Siemens
R. Grimm: Employee at Siemens

S 16-7 17:05

Radiomics signature of the human papillomavirus (HPV) status in oropharyngeal squamous cell carcinoma (OPSCC)

S. P. Haider[1], A. Mahajan[1], T. Zeevi[1], P. Baumeister[2], C. Reichel[2], K. Sharaf[2], B. Judson[1], B. Burtness[1], S. Payabvash[1]; [1]New Haven/US, [2]Munich/DE
(stefan.haider.mdf@gmail.com)

Purpose: HPV-positive and HPV-negative forms of OPSCC are biologically distinct entities, with different prognosis, treatment strategies, and divergent AJCC/UICC staging schemes. Using feature selection and machine-learning classification algorithms, we identified the radiomics signature of HPV on pre-treatment FDG-PET and non-contrast CT scans.
Methods and materials: All data was retrieved from the Cancer Imaging Archive. Patients with OPSCC, known HPV-status, and pre-treatment PET/CT were included. The primary tumour and metastatic cervical nodes were separately segmented on PET scans; segmentations were then copied and adapted to the coregistered CT. A set of 1,040 radiomics features was extracted from each segmentation and per imaging modality.
To predict HPV-status, minimum-redundancy-maximum-relevance (MRMR) feature selection and random forest (RF) machine learning classifiers were applied in 5-fold cross-validation, repeated x10. The area-under-the-curve of receiver-operating-characteristic-curves (AUC-of-ROC) averaged across validation folds is reported.
Results: Of 114 included OPSCC cases, 87 had HPV-positive and 27 had HPV-negative forms. In addition to primary tumour lesions, 119 HPV-positive and 51 HPV-negative metastatic cervical nodes were analysed.
The primary tumour RF models achieved an averaged AUC-of-ROC of 0.69 (PET), 0.75 (CT), and 0.73 (PET/CT), based on 20 features selected by MRMR from the respective feature sets. In comparison, the averaged AUC of lymph node RF models was 0.66 (PET) and 0.64 (CT), based on 20 MRMR-features. PET-based lymph node models were non-predictive.
Conclusion: Radiomics feature extraction from FDG-PET and non-contrast CT scans, combined with machine learning classifiers, can generate imaging biomarkers for HPV-status in OPSCC primary tumours and metastatic lymph nodes, which may aid pathologists in HPV-classification if standard immunohistochemical staining is equivocal or supplement the immunohistochemical tests in subjects requiring second-line testing.
Limitations: n/a
Ethics committee approval: n/a
Funding: No funding was received for this work.
Author Disclosures:
S. P. Haider: nothing to disclose
S. Payabvash: nothing to disclose
P. Baumeister: nothing to disclose
C. Reichel: nothing to disclose
K. Sharaf: nothing to disclose
B. Judson: nothing to disclose
B. Burtness: nothing to disclose
A. Mahajan: nothing to disclose
T. Zeevi: nothing to disclose

S 16-8 17:15

Repeatability of quantitative WB-MRI analysis in patients with bone metastases

G. Saia[1], A. Colombo[1], A. Rossi[2], A. Azzena[1], F. Zugni[1], P. Summers[1], R. Grimm[3], M. Bellomi[1], G. Petralia[1]; [1]Milan/IT, [2]Meldola/IT, [3]Erlangen/DE
(giulia.saia.gs@gmail.com)

Purpose: WB-MRI is increasingly recommended for the evaluation of patients with metastatic bone diseases. A semi-automatic technique for the segmentation of diffusion-weighted images in WB-MRI examination has been developed to allow quantitative evaluation of tumour burden in bone metastases. The aim of this study was to evaluate the intra and interobserver repeatability of quantitative analysis of ADC in healthy and metastatic bone marrow in patients with bone metastases from breast cancer (BCa) and prostate cancer (PCa).
Methods and materials: 4 independent observers processed WB-MRI examinations from 20 patients with bone metastases (10 women with BCa and 10 men with PCa). Segmentation of bone marrow was performed applying a threshold on high b-value diffusion-weighted images and manually removing misclassified non-bone regions. The total volume of bone marrow (V_{bm}) and first-order ADC statistics were then obtained. We measured repeatability using intraclass correlation coefficients (ICC) and Bland-Altman method.
Results: We observed good to excellent ICC values in 4 parameters: ADC_Mean with intra and interobserver ICCs respectively of 0.92 (0.85-0.96, CI 95%) and 0.85 (0.75-0.92), ADC_Median 0.92 (0.85-0.96) and 0.88 (0.79-0.93), ADC_5% 0.9 (0.81-0.94) and 0.8 (0.69-0.88), and ADC_Skewness 0.9 (0.80-0.94) and 0.86 (0.76-0.92). Bland-Altman bias and limits of agreement calculated for ADC_Mean were, respectively, -1.1% and -13.7%–12.1%, and 5.0% and -18.8%–15.3% in intra and interobserver analysis. Repeatability was higher in BCa patients than in PCa patients.
Conclusion: While bias was almost 5 times greater for interobserver relative to intra, the limits of agreement were increased by only about 25%.
Limitations: Difficulties in segmenting PCa patients data likely led to lower repeatability in these patients relative to BCa patients.
Ethics committee approval: Approved by internal review board.
Funding: No funding was received for this work.

Author Disclosures:
G. Saia: nothing to disclose
A. Colombo: nothing to disclose
A. Rossi: nothing to disclose
A. Azzena: nothing to disclose
F. Zugni: nothing to disclose
P. Summers: nothing to disclose
M. Bellomi: nothing to disclose
G. Petralia: Speaker at Siemens
R. Grimm: Employee at Siemens

16:00 - 17:30 **Coffee & Talk 1**

Interventional Radiology

RPS 1609

Genitourinary interventions

Moderators:
B. Peynircioğlu; Ankara/TR
R. Nolz; Vienna/AT

RPS 1609-1 16:00

Thermal ablation of central renal tumours performed with a retrograde cold pyeloperfusion technique

G. Mauri[1], D. Rossi[2], G. Bonomo[1], P. della Vigna[1], D. Maiettini[3], G. M. Varano[4], L. Mascagni[4], F. Orsi[1]; *[1]Milan/IT, [2]San Donato Milanese/IT, [3]Perugia/IT, [4]Rome/IT (duccio.rossi@unimi.it)*

Purpose: To assess treatment safety and efficacy following thermal ablation of centrally located renal tumours performed with retrograde pyeloperfusion.
Methods and materials: From November 2011-December 2018, 54 patients (17 females, 37 males, mean age 69, range 41-89) underwent 64 renal ablations for centrally located renal tumours, 58/64 (90.6%) renal cell carcinomas (RCC), 5/64 (8%) oncocytomas, and one metastasis. Inclusion criteria consisted of biopsy-proven renal masses <4 cm (T1a); the average lesion size was 32.5 mm (range 16-67 mm). 7 mono-renal patients underwent 13/64 (13%) procedures. Microwave (MWA), radiofrequency (RFA), or their combination were the ablation techniques of choice, 33/64 RFA (52%), 29/64 (45%) MWA, and 2/64 (3%) MWA+RFA. All treatments were performed with ultrasound- and CT-guidance under general anaesthesia and a simultaneous retrograde cold pyeloperfusion technique in a dedicated angiography room setting.
Results: The primary technical success overall was reached in 57/64 cases (89%). Primary technical efficacy at 1 month overall was reached in 48/64 (75%) lesions. 12 lesions underwent a second treatment, with a secondary efficacy of 54/64 (84%). 2/54 (4%) underwent nephrectomy. At a median follow-up of 26.5 months, 3/54 patients died of unrelated events. The mean procedure duration overall was 32 minutes (range 2-160 minutes). Adverse events (AEs) were reported in 15/64 lesions (23%), 5/64 (8%) major AEs and 10/64 (16%) minor AEs.
Conclusion: Percutaneous thermal ablation of central renal tumours associated with protective pyeloperfusion is a safe and effective treatment option allowing for kidney function preservation and radical results in a large majority of cases. This technique can be useful for avoiding nephrectomy in mono-renal patients.
Limitations: The retrospective nature of the study.
Ethics committee approval: The protocol was approved by the ethics committee.
Funding: No funding was received for this work.
Author Disclosures:
D. Rossi: nothing to disclose
G. Mauri: Consultant at Elesta SrL
G. Bonomo: nothing to disclose
P. della Vigna: nothing to disclose
D. Maiettini: nothing to disclose
G. M. Varano: nothing to disclose
L. Mascagni: nothing to disclose
F. Orsi: nothing to disclose

RPS 1609-2 16:06

A minimally-invasive approach to symptomatic uterine fibroids: fibroids location as a predictor of treatment efficacy

P. Palumbo, A. Iacopino, A. V. Giordano, M. Di Luzio, S. Carducci, M. Varrassi, S. Mascaretti[3], G. Mascaretti, C. Masciocchi; *L'Aquila/IT (palumbopierpaolo89@gmail.com)*

Purpose: To retrospectively evaluate the comparing efficacy of MRgFUS and UAE in the treatment of different location-type uterine fibroids.
Methods and materials: 71 women consecutively treated for symptomatic uterine fibroids were enrolled in our study. Primary (clinical) and secondary (imaging efficacy evaluation) outcomes were evaluated. Pre-procedural and 1-year post-treatment MRI examinations were analysed.
Results: 27 patients were treated by UAE. The overall success rate was 94.63%. The response rate was 100% in submucosal groups and 87.5% and 72.73% in intramural and transmural groups, respectively. A significant difference was observed between transmural and both submucosal and intramural post-treatment severity scores (p=0.006 and 0.017, respectively), while no differences were observed between submucosal and intramural groups (p=0.33). No difference was found between the three groups in the Kaplan-Meier analysis (Log-rank: p= .74). 44 patients were treated with MRgFUS. The overall success rate was 83.01%. Notably, RR was 66.67% in the submucosal group, and 64.71% and 55.56% in intramural and transmural groups, respectively. A significant difference was observed between transmural and both submucosal and intramural post-treatment scores (p=0.016 and 0.017, respectively), while no differences were observed between submucosal and intramural groups (p=0.637). A significant difference was found between the three groups according to the Kaplan-Meier analysis (Log-rank: p=0.001).
Conclusion: MRgFUS and UAE are highly effective techniques in the treatment of symptomatic uterine fibroids. Fibroid type analysis should be considered for adequate treatment planning, especially for FUS treatment, which finds the primary indication for submucosal fibroids.
Limitations: The single-centre analysis and the retrospective analysis.
Ethics committee approval: Our study was conducted in accordance with the declaration of Helsinki.
Funding: No funding was received for this work.
Author Disclosures:
P. Palumbo: nothing to disclose
A. Iacopino: nothing to disclose
A. V. Giordano: nothing to disclose
M. Di Luzio: nothing to disclose
S. Carducci: nothing to disclose
M. Varrassi: nothing to disclose
S. Mascaretti: nothing to disclose
G. Mascaretti: nothing to disclose
C. Masciocchi: nothing to disclose

RPS 1609-3 16:12

CT-guided biopsy of the adrenal gland in patients suspected of lung cancer

C. Lückerath, B. Högerle, P. Flechsig, E. Herpel, M. Eichhorn, H. Winter, H.-U. Kauczor, C. P. Heußel, G. Heußel; *Heidelberg/DE (christian.lueckerath@med.uni-heidelberg.de)*

Purpose: To confirm adrenal metastasis of suspected lung cancer and for molecular tumour characterisation, a biopsy is required. CT-guided biopsy offers 3D visualisation of adjacent anatomical structures in real-time and a detection of complications.
Methods and materials: A retrospective analysis of all CT-guided biopsies of the adrenal glands performed from 2016-2018 at Thoraxklinik Heidelberg to evaluate outcome and complications and to identify potential risk factors.
Results: 53 CT-guided biopsies were performed in 50 patients (24 left/29 right). No transrenal, transsplenic, transpancreatic, or transpulmonal path was chosen. Anticoagulation was paused according to the guidelines in 16/22 cases. No major complications like death, abscess, pneumothorax, or Hb-relevant bleeding occurred. In 22 patients, a small local haematoma with a median size of 6 ml without further treatment was observed. 20 patients reported pain within the first hours after the intervention, which was easily treated with metamizole. 1 of those 15 patients with a transhepatic pathway showed an incidental arterioportal fistula in a follow-up CT, which did not require further action. The intervention duration from local anaesthesia to the control scan was a median 16 minutes, with a range of 7-35 minutes, and was well tolerated by the patients. Malignancy was confirmed in 92%. In 2 cases, an adenoma was detected; one lesion showed high FDG-uptake and the other high density on CT. In 2 cases, a definite determination was not possible.
Conclusion: CT-guided biopsy of the adrenal gland is a safe, fast, and reliable method to verify and characterise metastases in patients suspected of lung cancer. Pathways, patient positioning, investigator experience, and procedural manoeuvres are essential and will be communicated.
Limitations: A relatively small number of procedures.
Ethics committee approval: Ethics committee approval obtained.
Funding: No funding was received for this work.

Author Disclosures:
C. Lückerath: nothing to disclose
H. Winter: nothing to disclose
C. P. Heußel: nothing to disclose
B. Högerle: nothing to disclose
P. Flechsig: nothing to disclose
E. Herpel: nothing to disclose
M. Eichhorn: nothing to disclose
H.-U. Kauczor: nothing to disclose
G. Heußel: nothing to disclose

RPS 1609-4 16:18
Application of a novel image-processing method: digital variance angiography (DVA) in prostatic artery embolisation (PAE)
L. S. Alizadeh[1], T. J. Vogl[1], J. Kiss[2]; [1]*Frankfurt am Main/DE,* [2]*Budapest/HU (leona.alizadeh@outlook.de)*

Purpose: To compare the performance of digital variance angiography (DVA) versus conventional digital subtraction angiography (DSA) for its utility in image-guidance during prostatic artery embolisation (PAE) of benign prostatic hyperplasia. DVA is a novel x-ray image processing algorithm for the visualisation of contrast motion.
Methods and materials: We evaluated angiographic acquisitions of 15 patients (mean age 67.47, SD 9.76, range 42-82) undergoing PAE at our institution. For quantitative image-quality comparison, signal-to-noise ratio (SNR) of DSA and DVA image pairs were compared using multiple regions of interest (ROI) for each image. Qualitative image-quality evaluation was done in a randomised blinded trial by three experienced interventional radiologists using clinically relevant criteria (e.g. visibility of feeding- and collateral-branches, size of examinable arteries, and detectability of the prostatic artery). Fleiss' kappa-test was used to determine interrater agreement.
Results: DVA images provided 1.79 times higher SNR than DSA (median value, Q1-Q3 interval was 1.46-2-32). The visual evaluation indicated that DVA provided higher quality images than DSA since 90.6% of comparison evaluators preferred DVA over DSA images. The inter-rater agreement was 93.8% and Fleiss's kappa was 0.38 ($p<0.01$).
Conclusion: In PAE, DVA-imaging enhances the visualisation of anatomical structures compared to DSA-imaging via significant SNR reduction. The new technology might improve the safety and efficacy of the intervention. As an additional advantage, the observed quality reserve of DVA might also reduce the radiation dose and the amount of contrast agent.
Limitations: A retrospective trial. Aspects of workflow, radiation-dose, and intervention time have to be investigated in an upcoming prospective trial comparing DVA versus DSA directly in the intervention room.
Ethics committee approval: This study was approved by our institutional ethics board.
Funding: No funding was received for this work.
Author Disclosures:
L. S. Alizadeh: nothing to disclose
T. J. Vogl: nothing to disclose
J. Kiss: Employee at Kinepict Health

RPS 1609-5 16:24
Uterine fibroid embolisation efficacy and safety: 15 years experience in an elevated turnout rate centre
A. Paladini[1], I. Percivale[1], M. Spinetta[1], S. Bor[2], D. Negroni[1], M. Cernigliaro[1], A. Borzelli[3], F. Pane[3], G. F. Buoni[4]; [1]*Novara/IT,* [2]*Santhià/IT,* [3]*Naples/IT,* [4]*Turin/IT (20027467@studenti.uniupo.it)*

Purpose: To evaluate the effectiveness and safety of UFE as an alternative to surgery in the treatment of uterine fibromatosis.
Methods and materials: 255 patients (aged 26-55) with symptomatic UF, indicated for surgery, followed in our centre (2000-2014), with single or multiple fibroids, and pain and/or functional/compressive disorders underwent embolisation; an injection of PVA particles (150-900 µm) from the distal portion of uterine arteries (ascending section). The primary end-point was a flow-stop distally to the injection site, disappearance of the lesion design, and the preservation of flow in the main trunk of UA. The secondary end-point was the control of pain and functional/compressive disorders during follow-up (2-7 years).
Results: The procedure was performed bilaterally in 250 patients (98%). The mean duration was 47 min (average fluoroscopy: 10-50 min).
Post-embolisation pelvic pain (according to a VAS score) was on average 2.2 at discharge (24h). Follow-up at 2 years showed a resolution of menstrual disorders in 78% of patients and improvement in 14%, pain disappeared in 66%, significant improvement of menstrual flow and HCT/HB levels, and adecrease in total uterine (57.7%)/dominant fibroid (76.1%) volume. There was recurrence in 18 patients.
Conclusion: UFE represents an excellent alternative to surgical treatment. It is safe, tolerable, and effective both in the short and long term, with evident advantages in economic and social terms.
Limitations: A retrospective study without randomisation.
Ethics committee approval: n/a
Funding: No funding was received for this work.
Author Disclosures:
A. Paladini: nothing to disclose
F. Pane: nothing to disclose
M. Spinetta: nothing to disclose
S. Bor: nothing to disclose
D. Negroni: nothing to disclose
M. Cernigliaro: nothing to disclose
I. Percivale: nothing to disclose
A. Borzelli: nothing to disclose
G. F. Buoni: nothing to disclose

RPS 1609-6 16:30
The great migration: predicting intramural uterine fibroid migration after uterine artery embolisation
E. Y. Auyoung[1], L. A. Ratnam[2], R. Das[2], S. M. M. M. Ameli Renani[2], L. Mailli[2]; [1]*Basingstoke/UK,* [2]*London/UK (e.auyoung@doctors.org.uk)*

Purpose: To analyse pre-UAE MR images with a view to predicting migration of intramural fibroids post-UAE to better advise patients of the procedural risks.
Methods and materials: We retrospectively reviewed all patients referred for UAE for symptomatic fibroids at our institution over one year. Patients without a pre-procedural MRI and a six-month post-procedural MRI were excluded from the study. Both pre- and post-UAE images were independently reviewed by two radiologists with subsequent consensus review. In each, dominant intramural fibroids were identified and the following measurements taken: a) 3-dimensional maximal measurements, b) the shortest distance between the fibroid and the endometrial wall, and c) the shortest distance between the fibroid and the serosal wall. Paired sample t-tests and two-sample t-tests were used to compare between pre- and post-UAE variations and between migrated and non-migrated intramural fibroids, respectively.
Results: 35 dominant intramural fibroids were identified, of which, 8 migrated to become submucosal fibroids, while 5 were either partially or completely expelled. All migrating fibroids had a pre-UAE minimum distance from the endometrium of 1-2.4 mm and a maximum fibroid diameter greater than 5.1 cm, and none of the non-migrating fibroids had both these characteristics together.
Conclusion: Not only is it distressing to patients to have post-procedural pain and bleeding, but fibroid migration could also increase infection risks and affect fertility. Our study found that intramural fibroids with a minimum endometrial distance less than 2.4 mm and a maximum fibroid diameter greater than 5.1 cm have a high likelihood of migrating after UAE.
Limitations: Small sample size and low statistical power.
Ethics committee approval: n/a
Funding: No funding was received for this work.
Author Disclosures:
E. Y. Auyoung: nothing to disclose
L. Mailli: nothing to disclose
L. A. Ratnam: nothing to disclose
R. Das: nothing to disclose
S. M. M. M. Ameli Renani: nothing to disclose

RPS 1609-7 16:36
Investigating the clinical value of colour-coded pelvic parametric x-ray angiography for image guidance in prostatic artery embolisation for benign prostatic hyperplasia
L. S. Alizadeh, T. J. Vogl, A. Zinn; *Frankfurt am Main/DE (leona.alizadeh@outlook.de)*

Purpose: A major challenge in prostatic artery embolisation (PAE) is an adequate and distinct visualisation of the feeding prostatic vessels and other branches of the internal iliac arteries. Novel colour-coded parametric images calculated from raw angiographic image data provide additional information compared to common digital subtraction angiography (DSA). Our objective was to investigate the clinical value of parametric images in a PAE setting.
Methods and materials: We retrospectively examined the selective internal iliac artery image series of 26 patients (mean age: 67.47; SD: 9.76; range: 42-82) undergoing PAE. We generated 230, parametric, colour-coded-delay-angiograms (CDAs) from raw image data obtained from a latest-generation angiography system. Three experienced interventional radiologists evaluated the image quality using a 5-point-Likert scale based on clinically relevant criteria (e.g. the identification of dominant feeding arteries, stenoses, and non-target collaterals).

Results: Subjective image quality was evaluated with mean scores of 4.16 (range 3-5; std.deviat.+-0.73), significantly higher for DA compared to the mean scores of 3.43 (range 2-5; std.deviat.+-1.80) for standard DSA. Evaluators agreed CDAs provided more information than the simple BW angiograms (87%), the image would be useful to select the dominant feeding artery (93%), and the functional stenoses of the branches could also be determined (84%). The inter-rater agreement, Fleiss' kappa, and significance were 81%, 0.19, $p<0.05$, 85%, 0.32, $p<0.01$, and 79%, 0.11, $p<0.05$, respectively.
Conclusion: Parametric delay images calculated from x-ray angiography series provide more information than standard angiograms and hold additional information about the branches of the internal iliac artery. Decision-making based solely on CDAs will require an appropriate prospective safety assessment.
Limitations: Colour-coded-parametric-angiography has to be tested in upcoming prospective trials to prove our results for real-time image guidance.
Ethics committee approval: University hospital ethics committee approval obtained.
Funding: No funding was received for this work.
Author Disclosures:
L. S. Alizadeh: nothing to disclose
T. J. Vogl: nothing to disclose
A. Zinn: nothing to disclose

RPS 1609-8 16:42

Which women affected by uterine fibroids can be selected for MRgFUS treatment? Our experience

I. Capretti, L. P. Vazzana, S. Iafrate, E. Cannizzaro, F. Arrigoni, M. Di Luzio, S. Mascaretti, G. Mascaretti, C. Masciocchi*; L'Aquila/IT (luciavazzana@gmail.com)*

Purpose: To demonstrate that a careful selection of patients is important to predict the execution of treatment and a good result.
Methods and materials: 228 women with uterine fibroids were submitted to c.e. MRI to evaluate the possibility of MRgFUS treatment. The ablation results were evaluated by the non-perfused volume (NPV) on contrast-enhanced MR images acquired after the treatment.
Results: 115 women out of 228 (50.4%) were considered suitable for treatment (good MRI features of the dominant fibroids and adequate acoustic window); 15 of them obtained an incomplete result and other treatments (a second MRgFUS, uterine artery embolisation (UAE), or surgery). The mean value of the NPV ratio was 67.4%, assessed immediately after the treatment. 113 patients out of 228 were not eligible for the treatment: 8/113 women had an abdominal scar, 39/113 patients showed interposition bowel, reverse uterine position, or inadequate acoustic window, and 66/113 had inappropriate features of the fibroids such as number, side (i.e. pedunculate position), big size, or high vascularisation.
Conclusion: MRgFUS is a mini-invasive treatment and it is well tolerated by patients. A correct selection is necessary to achieve a risk-free treatment and good clinical results.
Limitations: The radiological evaluation according to criteria in the literature for the MRgFUS treatment.
Ethics committee approval: n/a
Funding: No funding was received for this work.
Author Disclosures:
F. Arrigoni: nothing to disclose
I. Capretti: nothing to disclose
L. P. Vazzana: nothing to disclose
S. Iafrate: nothing to disclose
E. Cannizzaro: nothing to disclose
M. Di Luzio: nothing to disclose
S. Mascaretti: nothing to disclose
G. Mascaretti: nothing to disclose
C. Masciocchi: nothing to disclose

RPS 1609-9 16:48

Results after endovascular uterine artery embolisation in the treatment of symptomatic leiomyoma

D. Tazhibaev, B. Abishev*; Nur-Sultan/KZ (tazhibaev74@mail.ru)*

Purpose: To evaluate fibroid size using ultrasonography (US) and magnetic resonance imaging (MRI) after uterine artery embolisation (UAE) of leiomyoma.
Methods and materials: 1,023 women with symptomatic leiomyoma were treated by bilateral transcatheter UAE. Angiography and embolisation were performed using 5F Cobra and Roberts uterine catheters by 355-1,000µm of PVA particles. The size of particles depended on the uterine artery diameter and anastomosis between the uterine and ovary arteries. The mean age was 29.5 years (range: 19-47).
Results: The moderate reduction of leiomyoma size was observed one month after UAE. The reduction of fibroid size after 1 month was 18.4% by US and 17.3% by MRI, after 3 months was 40.7% by US and 42.9% by MRI, after 6 months was 60.4% by US and 61.8% by MRI, after 12 months was 72.5% by US and 74.7% by MRI, and after 24 months was 70.8% by US and 72.2% by MRI. Doppler US-control showed a blood flow decrease during the first month after UAE; in 3 months, blood flow data was restored in uterine arteries. We also noticed a significant reduction or disappearance of clinical symptoms such as pain, menorrhagia, and pressure symptoms. The partial vascularisation of leiomyoma was only detected in one case 24 months after UAE.
Conclusion: UAE is an effective, minimal-invasive form of leiomyoma treatment. MRI and US are the modalities that can accurately estimate fibroid changes and blood flow in uterine arteries. The tendency of fibroid shrinkage after UAE is well-defined in the period from 1-24 months. After UAE, the blood supply of myometrium is restored according to US Doppler data in the period from 1-3 months.
Limitations: n/a
Ethics committee approval: n/a
Funding: No funding was received for this work.
Author Disclosures:
D. Tazhibaev: nothing to disclose
B. Abishev: nothing to disclose

RPS 1609-10 16:54

Melting time analysis of radiographic ice-balls during thawing in renal cryoablation: a proposal for the optimal time of cryoprobe removal

M. J. Kim, S. Y. Park*; Seoul/KR (minje1107.kim@samsung.com)*

Purpose: Cryoprobe removal before sufficient thawing may lead to tissue injury and bleeding. We analysed the melting time of radiographic ice-balls during thawing in renal cryoablation by using ultrasound (US) examination.
Methods and materials: A consecutive 27 patients who underwent percutaneous cryoablation with cryoprobes of 2-4 for a renal tumour (median size, 1.9 cm; range, 1.1-4.1 cm) were evaluated. Reconstructed CT images obtained during freezing were used to measure the radiographic ice-ball volume. After completing a last freezing, the melting time of the radiographic ice-ball was analysed with US. The melting time was defined as the time of complete disappearance of intrarenal posterior acoustic shadowing generated by a radiographic ice-ball, which was analysed by two independent radiologists. After removing the cryoprobes, the degree of perirenal haematoma was assessed (i.e. <1 cm versus ≥1 cm in thickness). Serum haemoglobin (Hb) was also investigated before and after cryoablation.
Results: The median radiographic ice-ball volume was 30.3 cm^3 (range, 21.0-62.8 cm^3). The median melting time of radiographic ice-balls on US was 13 and 14 minutes for radiologist 1 and 2 (range, 9-15 minutes for both radiologists) ($p>0.05$). A positive correlation was found between melting time and radiographic ice-ball volume (Spearman's rho, 0.647 and 0.484 for radiologist 1 and 2). Perirenal haematomas of ≥1cm in thickness were seen in two patients (7.4%). No patient required treatment for the bleeding. The median decrease of serum Hb was 0.3 g/dl.
Conclusion: Ice-balls of renal cryoablation may require 15 minutes for complete melting, which may be considered as the optimal time for cryoprobe removal.
Limitations: A small, single-institution study.
Ethics committee approval: n/a
Funding: No funding was received for this work.
Author Disclosures:
M. J. Kim: nothing to disclose
S. Y. Park: nothing to disclose

RPS 1609-11 17:00

Pregnancy results: favourable outcomes and fertility perspectives in women treated by MRgFUS for uterine fibroids

L. P. Vazzana, I. Capretti, S. Iafrate, F. Arrigoni, M. Di Luzio, S. Mascaretti, G. Mascaretti, C. Masciocchi*; L'Aquila/IT (luciavazzana@gmail.com)*

Purpose: To discuss fertility perspectives in women treated by MRgFUS and to report pregnancy after this procedure.
Methods and materials: 15 patients aged between 26 and 47 (mean age 36.4) affected by uterine fibroids who wanted to get pregnant were treated in our department with MRgFUS. This study evaluated the findings of 15 patients presenting with a difficulty to conceive and uterine fibroids smaller than 5.5 cm. We preliminarily excluded the other causes of infertility with a gynaecological evaluation. All patients had only one treatment. We made a c.e. MRI in order to control the non-perfused-volume immediately after treatment and then after 3, 6, and 12 months from the procedure.
Results: After 12 months from the treatment, 11 patients had complete reabsorption of the necrotic areas and 4 had partial reabsorption. 7 months later, the patients started the course to become spontaneously pregnant. 3 succeeded and 1 has already given birth at term to a healthy infant without any perinatal complications. Another patient with partial reabsorption of the necrotic area gave birth to a baby and another is now in her seventh month of pregnancy.

Conclusion: MRgFUS permits a significant reduction of the clinical symptomatology and is a valid alternative method to surgery in fertile women, without any complications in case of uterine implanting.
Limitations: A small group of patients.
Ethics committee approval: n/a
Funding: No funding was received for this work.
Author Disclosures:
L. P. Vazzana: nothing to disclose
I. Capretti: nothing to disclose
S. Iafrate: nothing to disclose
F. Arrigoni: nothing to disclose
M. Di Luzio: nothing to disclose
S. Mascaretti: nothing to disclose
G. Mascaretti: nothing to disclose
C. Masciocchi: nothing to disclose

RPS 1609-12 17:06

Percutaneous thermal ablation of small renal tumours: a singe-centre experience

G. Dar, N. Goldberg, A. Lorber, L. Appelbaum*; Jerusalem/IL*
(gili.dar@mail.huji.ac.il)

Purpose: Percutaneous ablation has been proven as a safe and effective treatment for small renal tumours. The treatment has been available in Israel for over 15 years. We will present the results of a single-centre experience, the largest ablation service in Israel.
Methods and materials: A retrospective study of 199 percutaneous renal tumour ablations was conducted. All patients (mean age 68 (±12); 53/146 female/male) were treated using ablation (microwave ablation 42%, radiofrequency ablation 50%, and cryoablation 8%) during 2013-2019. The average tumour diameter was 25 mm (10-58 mm); 104 tumors were exophytic, 69 were endophytic, and 26 were mixed. In 85 of the cases (42%), a biopsy was performed prior to the ablation. The pathological report revealed that 38 (44%) were clear-cell RCC, 10 (12%) were papillary type RCC, 2 (2%) chromophobe type RCC, 12 (14%) oncocytic tumour, 14 (16%) non-diagnostic, and 9 (12%) other. The monitoring protocol after treatment included imaging after 1, 3, 6, and 12 months subsequent to treatment and later annually; the median follow-up time was 26 months (1-122).
Results: Evidence of tumour recurrence was observed in 25 patients (12.6%); 13 were treated successfully by another ablation session. Cases in which recurrence was observed were characterized by a tumour larger than 30 mm (10-56). 10 of the lesions were central (endophytic).
Conclusion: Percutaneous ablation is a safe and effective treatment for small renal tumours. 89% of long-term complete ablation may be reached. In cases of remnant tumour tissue or recurrence, ablation can be repeated with good results.
Limitations: A single-centre study.
Ethics committee approval: In process.
Funding: No funding was received for this work.
Author Disclosures:
G. Dar: nothing to disclose
N. Goldberg: Consultant at Angiodynamics, Consultant at Cosman Company, Consultant at Xact Robotics
A. Lorber: nothing to disclose
L. Appelbaum: nothing to disclose

RPS 1609-13 17:12

Clinical and economic impact of transperineal laser ablation (TPLA) for treating focal unilateral prostate cancer

G. Manenti[1], T. Perretta[1], S. Marsico[1], C. P. Ryan[1], D. D'amato[1], M. Martins-Favre[2], S. Regusci[2]*; [1]Rome/IT, [2]Geneva/CH*

Purpose: To evaluate the therapeutic success, complications, and economic impact of transperineal US-guided focal laser ablation by US/MRI fusion software as a primary treatment for focal unilateral prostate cancer.
Methods and materials: 24 patients with newly diagnosed, histopathologically-proven, focal unilateral prostate cancer were treated with US-guided transperineal focal laser ablation as a primary treatment. The inclusion criteria were no previous prostate treatment, a PSA level ≤20, a Gleason score ≤7, and stage ≤ T2b N0M0 with 3T multi-parametric MRI-visible index lesion (PIRADS ≥ 4). After the ablation, a 3T mpMRI of the prostate was obtained. Follow-up consisted of mpMRI at 1, 3, 6, and 12 months and a US/MRI fusion-guided biopsy at 6 and 12 months.
Results: 24 patients were successfully treated with transperineal US-guided focal laser ablation. No complications occurred. The IPSS and SHIM did not significantly change after treatment. The mean operation time was 38.2 minutes (range 32.6-42.5), the mean ablation time was 21.7 minutes (range 18.3-26.8), the mean energy deployed was 3606J (range 3212-3804), the mean hospital stay was 113 minutes (range 55-178), and the mean catheterisation time was 261 minutes (range 95-412). At the 6- and 12-month follow-up, prostate mpMRI and US/MRI fusion-guided biopsy showed neither evidence of local residual disease nor recurrence.
Conclusion: Transperineal US-guided focal laser ablation as a primary treatment for prostate cancer has shown encouraging results. Ten-year follow-up with an international registry is intended to confirm oncological long-term prostate cancer with index lesion control.
Limitations: A small number of treated patients, short follow-up, and our first experience with this technique.
Ethics committee approval: Protocol approved by the ethical committee of Policlinico Tor Vergata (Rome).
Funding: No funding was received for this work.
Author Disclosures:
S. Marsico: nothing to disclose
G. Manenti: nothing to disclose
T. Perretta: nothing to disclose
C. P. Ryan: nothing to disclose
D. D'amato: nothing to disclose
M. Martins-Favre: nothing to disclose
S. Regusci: nothing to disclose

RPS 1609-14 17:18

Decision-making between radiofrequency and cryoablation based on tumour size, central location, and nearness to the collecting system for the management of cT1 RCC: a comparative study of 408 patients

T. Ramtohul[1], A. Méjean[1], M.-O. Timsit[1], C. Delavaud[2], J.-B. Quere[1], O. Helenon[1], J.-M. Correas[1]*; [1]Paris/FR, [2]Houilles/FR*
(toulsie@me.com)

Purpose: To evaluate our decision-making between RFA and CA based on tumour size, central position, and nearness to the collecting system on technical efficacy and oncologic outcomes for cT1 RCC.
Methods and materials: All cT1 RCC from 2005-2019 were included. Patients treated before 2013 were included in the RFA group and patients treated after 2013 were included in the CA or RFA group, where CA was performed for large (≧35 mm) central tumours or RCC with a nearness to the collecting system, while RFA was performed for smaller (<35 mm) and non-central RCC. The IPTW based on clinical and tumour features was applied. The primary success was compared using logistic regression, while local recurrence-free survival was compared using Cox proportional hazards regression. Clavien complications and the change in renal function (MDRD) were also evaluated.
Results: Data from 408 patients were analysed. The primary success rate was higher in the CA or RFA group compared to the RFA group (97.1% vs 87.1%, p<0.001). Local recurrence-free survival was better in the CA or RFA group compared to the RFA group (HR=0.49; 95%CI: 0.28-0.84; p=0.01). Survival without metastases was not different (p=0.65). The incidence of Clavien grade ≥2 adverse events (p=0.30) and the change of renal function (p=0.35) was similar.
Conclusion: Our decision-making between CA and RFA achieved a better primary success rate and local recurrence-free survival compared to RFA alone, with excellent oncologic outcomes for RFA in selected patients and also for large and central RCC mainly treated with CA.
Limitations: The retrospective design.
Ethics committee approval: Institutional review board approval was obtained to review the medical records of patients who underwent ablation of RCC at Necker University Hospital.
Funding: No funding was received for this work.
Author Disclosures:
T. Ramtohul: nothing to disclose
J.-M. Correas: Consultant at Supersonic Imagine, Consultant at Toshiba MS, Consultant at Philips US, Consultant at Bracco SA
C. Delavaud: nothing to disclose
J.-B. Quere: nothing to disclose
O. Helenon: nothing to disclose
A. Méjean: Consultant at Novartis, Consultant at Janssen, Consultant at Ipsen, Consultant at Ferring, Consultant at BMS, Consultant at Roche
M.-O. Timsit: nothing to disclose

RPS 1609-15 17:24

Adrenal glands haemorrhages: embolisation in an acute setting

F. Giurazza, F. Corvino, F. Pane, M. Silvestre, M. Coppola, R. Niola*; Naples/IT*
(francescogiurazza@hotmail.it)

Purpose: Acute adrenal haemorrhages are a rare event compared to other abdominal visceral injuries because of the anatomic localisation of the adrenal glands. The main causes are trauma and ruptured neoplasms.
This manuscript reports on a single-centre experience of transarterial embolisations of adrenal haemorrhages in an emergency setting.

Methods and materials: In this retrospective analysis from 2010 to date, 17 patients (12 men and 5 women, mean age: 59.8 years) presenting with adrenal bleedings were treated by endovascular embolisation.
The aetiology was traumatic in 7 cases, ruptured neoplasm in 8 cases, and spontaneous in 2 patients assuming oral anticoagulant therapy.
After thin slice contrast-enhanced CT, a super-selective embolisation was conducted with different embolising agents according to the type of vessel lesion and operator preference.
Results: Technical success rate, considered as an interruption of adrenal bleeding detectable at angiography, was 94.1%.
Clinical success rate, considered as haemodynamic stability restoration within 24 hours from the procedure, was 82.3%.
The vessels involved were the superior adrenal artery in 5 patients, the middle adrenal artery in 8 patients, the inferior adrenal artery in one patient, and more than one adrenal artery in 3 patients.
No procedure-related major complications occurred and no patients had infarctions, necrosis, abscess formation, or required long-term steroid supplementation.
Conclusion: Acute adrenal haemorrhages can be safely and effectively managed by catheter-directed embolisations. The source of bleeding has to be carefully investigated at CT and angiography as adrenal glands present with a wide and complex vascular arterial network.
Limitations: This is a retrospective analysis and therefore bias selections should be considered. The number of patients is small, however, this is due to the low frequency of the scenario.
Ethics committee approval: n/a
Funding: No funding was received for this work.
Author Disclosures:
F. Giurazza: nothing to disclose
F. Corvino: nothing to disclose
F. Pane: nothing to disclose
M. Silvestre: nothing to disclose
R. Niola: nothing to disclose
M. Coppola: nothing to disclose

16:00 - 17:30 **Coffee & Talk 2**

Neuro

RPS 1611

Functional MRI and diffusion tensor imaging

Moderators:
D. Auer; Nottingham/UK
N.N.

RPS 1611-1 16:00

Resting-state functional magnetic resonance imaging in predicting the long-term functional outcome after acute ischaemic stroke

E. Camacho-Ramos[1], A. Jimenez-Pastor[1], C. Biarnés[2], A. Alberich-Bayarri[1], S. Pedraza[2], J. Serena[2], M. Terceño[2], Y. Silva[2], J. Puig[2]; [1]Valencia/ES, [2]Girona/ES (educamacho@quibim.com)

Purpose: Stroke is one of the main causes of disability in adults. Resting-state functional magnetic resonance imaging (rs-fMRI) is able to map functional-anatomic networks by analysing spontaneously correlated low-frequency activity fluctuations across the brain. However, the role of rs-fMRI to predict the functional outcome after acute stroke remains unclear. We aimed to evaluate the impact of rs-fMRI at 72h after stroke symptoms onset to predict the functional outcome at 1-year follow-up.
Methods and materials: 35 reperfused stroke patients (12 female, age: 68±14 years, 3-day national institutes of health stroke scale (NIHSS) score: 6±5) were consecutively scanned 72 hours after symptom onset. A modified Rankin scale (mRS) was used to evaluate functional outcome at 90 days (patients with good functional outcome, mRS ≤2; poor outcome, mRS>2). Image pre-processing included motion and slice-timing correction, outliers' detection, brain tissue segmentation, MNI space normalisation, smoothing, and band-pass filtering to remove undesired components. Region-of-interest analyses were performed to calculate the correlation coefficients for every pairwise region and a weighted general linear model was used to discover significative differences ($p<0.05$ FWE) between groups.
Results: Patients with good outcome presented higher intra-network connectivity, while patients with poor outcome showed lower inter-network connectivity. To predict the 1-year functional outcome after a stroke, the 3-day NIHSS score was the most relevant predictor. An accuracy of 74.3% was obtained through a discriminant model using only clinical scores. Adding anatomical networks increased accuracy to 88.6%, 97.1% (including functional networks), and 100% (with clinical and imaging variables).
Conclusion: These results show the relevance of rs-fMRI in the acute phase to predict the long-term functional outcome in stroke patients.
Limitations: The sample size.
Ethics committee approval: n/a
Funding: No funding was received for this work.
Author Disclosures:
E. Camacho-Ramos: nothing to disclose
A. Jimenez-Pastor: nothing to disclose
C. Biarnés: nothing to disclose
A. Alberich-Bayarri: nothing to disclose
S. Pedraza: nothing to disclose
J. Serena: nothing to disclose
J. Puig: nothing to disclose
Y. Silva: nothing to disclose
M. Terceño: nothing to disclose

RPS 1611-2 16:06

The application of resting and task state fMRI in common exotropia

Y. Song[1], J. Chu[2], H. Han[1]; [1]Xiamen/CN, [2]Guangzhou/CN (xiaohongmao1992@163.com)

Purpose: This study applied brain resting and task state fMRI to detect the changes of brain activity and explore the mechanism of neurological damage in adult patients with common exotropia.
Methods and materials: 20 patients (M:10, F:10) and 20 age- and sex-matched controls with normal corrected visual acuity from 18 to 26 years of age were enrolled in this study. Two independent samples t-tests were employed to measure the differences of regional homogeneity (ReHo) and amplitude of low-frequency fluctuation (ALFF) in the resting-state fMRI and the brain-activity difference in the visual stimuli task fMRI of two groups.
Results: Compared with healthy controls, patients had significantly higher ReHo in the right middle occipital gyrus and the left supramarginal gyrus, and lower values in the right cingulate gyrus, the right precentral gyrus, the right superior temporal gyrus, and the left frontal sub-gyral lobe ($P<0.05$). Patients showed a reduced ALFF in the left superior parietal lobe, the right middle cingulate gyrus, the left anterior cingulate gyrus, and the right inferior temporal gyrus ($P<0.05$). Moreover, under the condition of binocular 2D visual task stimulus, the brain activity increased in the left superior frontal gyrus, the right superior orbital frontal gyrus, the bilateral inferior orbital frontal gyrus, and the left rectus gyrus in the patient group. Meanwhile, the brain activity of the left postcentral gyrus and the left precuneus gyrus increased under binocular stereo-stimulation.
Conclusion: Common exotropia may lead to disorders in the processing of visual-spatial information and the control of emotion and attention.
Limitations: The small case sample.
Ethics committee approval: n/a
Funding: No funding was received for this work.
Author Disclosures:
Y. Song: nothing to disclose
J. Chu: nothing to disclose
H. Han: nothing to disclose

RPS 1611-3 16:12

BOLD fMRI mapping of the language network: comparative assessment of task-based and resting-state fMRI

V. Lolli[1], S. Wastling[2], L. Mancini[2]; [1]Brussels/BE, [2]London/UK (valentina.lolli@erasme.ulb.ac.be)

Purpose: Task-based fMRI is the method of choice for determining the hemispheric dominance of language function. One important limitation is that the technique depends on the patient's ability to perform the task.
The aim of our study was to test the feasibility of using resting-state fMRI instead of task-based approaches.
Methods and materials: 15 healthy native English speakers underwent resting-state fMRI and two language fMRI paradigms: a verbal fluency (VF) and one verb generation (VG).
Task-based fMRI was analysed using both a general linear model (GLM) in the SPM software and independent component analysis (ICA).
Resting-state fMRI data was analysed by using both ICA and principal component analysis (PCA) using the SPM CONN toolbox, assuming a fixed number of 20 components. Resting-state networks were extracted by using both an automated template procedure and visually by two experts (VL and LM).
Results: The VG paradigm was more accurate than the VF paradigm or combination of the two and was therefore selected for further analyses.
Some of the networks labelled as language networks by the software were considered inappropriate and discarded by the experimenters.
There was a poor overlap between resting-state and task-related areas of activation as assessed by calculating the Dice similarity coefficients (mean:

0.1815) using the masks from the VG task GLM analysis, and the selected resting-state components.
The laterality index (LI) values of resting-state networks were significantly lower (mean: -0.0165) than the LI of the VG task map (0.4846).
Conclusion: Our results do not support the use of resting-state fMRI instead of task-based fMRI for hemispheric dominance assessment.
Limitations: Our sample is relatively small and heterogenous.
Ethics committee approval: Written informed consent was obtained from all subjects.
Funding: This work was part of the UCLH Project ID number: 09/H0716/18.
Author Disclosures:
V. Lolli: nothing to disclose
S. Wastling: nothing to disclose
L. Mancini: nothing to disclose

RPS 1611-4 16:18

Machine learning analysis in the diagnosis of medication overuse headache: a resting-state functional magnetic resonance imaging study
C. Yang, L. Yao, S. Lui*; Chengdu/CN*

Purpose: Medication-overuse headache (MOH) is a psychiatric comorbidity associated with chronic migraine. As machine learning is capable of identifying subtle disease patterns on a single subject level, we sought to determine the differences between MOH patients from healthy controls by using a machine learning classifier on resting-state functional MRIs (rs-fMRI).
Methods and materials: 34 patients with MOH and 41 age and sex-matched healthy controls were recruited. Smooth mean regional homogeneity (smReHo) was obtained via DPARSFA. Support vector machine (SVMs) algorithms based on PRoNTo toolbox were used to explore the utility for smReHo in the differentiation of patients and controls individually. Finally, Pearson's correlation between the MOH patients and clinical measurement was investigated.
Results: The balanced accuracy of the correct classification of MOH and controls was 72.03% for smReHo ($p<0.001$ during 1,000 permutation testing). Areas contributing to classification accuracy mainly included in right Heschl's gyrus (3.23%), left temporal pole, and right inferior temporal gyrus. The direct comparison showed that MOH patients had significantly decreased smReHo activation in the right Heschl's gyrus ($p<0.05$, FDR corrected), which was corresponding to the highest weight area by machine learning classifier. A negative correlation was observed between the duration of medication intake and smReHo activation in the right Heschl's gyrus ($r=-0.433$, $p<0.05$).
Conclusion: With machine learning computational analyses, our study was able to diagnose MOH patients on a single subject level by demonstrating decreased regional function in MOH patients, notably involving the right Heschl's gyrus, suggesting the right Heschl's gyrus might play an important role in the pathogenesis of MOH.
Limitations: Studies with larger samples may be required for further verification.
Ethics committee approval: n/a
Funding: No funding was received for this work.
Author Disclosures:
C. Yang: nothing to disclose
L. Yao: nothing to disclose
S. Lui: nothing to disclose

RPS 1611-5 16:24

The reorganisation of language networks after temporal lobe epilepsy surgery: a clinical fMRI study
O. Foesleitner[1], K.-H. Nenning[2], V. Schmidbauer[2], B. Sigl[2], J. Hainfellner[2], G. Langs[2], D. Prayer[2], G. Kasprian[2]*; [1]Heidelberg/DE, [2]Vienna/AT (benjamin.sigl@meduniwien.ac.at)*

Purpose: The reorganisation of language is common in epilepsy patients and a relevant factor in surgical therapy. The non-invasive gold standard in presurgical evaluation is language fMRI. fMRI network analysis could reveal subtle changes in language network architecture so far invisible with standard analyses and thus provide relevant additional information. We aimed to investigate the reorganisation processes of language networks in surgical patients with temporal lobe epilepsy (TLE) using standard fMRI activation and recent network analysis.
Methods and materials: Task-based language fMRIs were performed on 28 TLE patients (16 right/12 left) before and after surgery, and on 22 healthy controls. FMRI activation analysis, a derived laterality index, and functional connectivity of global and language networks were used to investigate language architecture. Naming, semantic, and phonematic verbal fluency were correlated with imaging parameters.
Results: Both left and right TLE were associated with widespread language network alterations, particularly ipsilesional, before, and more pronounced after surgery. Preoperatively, mesiotemporal connectivity was decreased in left TLE, while postoperatively bihemispheric changes with a shift to more atypical language laterality (especially frontal) occurred. In right TLE, right intrahemispheric frontotemporal functional connectivity was attenuated before and further decreased after surgery, while those patients with stronger connectivity scored worse in semantic verbal fluency. Better postoperative naming ability was generally accompanied by stronger interhemispheric frontal connectivity. In all cases, network analysis revealed more widespread alterations than activation analysis.
Conclusion: The reorganisation of language function is a visualisable phenomenon in left and right TLE, both before and after surgery. Functional connectivity analysis reveals more widespread network changes than fMRI activation analysis and may offer a more comprehensive view on language architecture. Some connectivity measures may serve as biomarkers for language performance.
Limitations: n/a
Ethics committee approval: n/a
Funding: No funding was received for this work.
Author Disclosures:
B. Sigl: nothing to disclose
O. Foesleitner: nothing to disclose
K.-H. Nenning: nothing to disclose
V. Schmidbauer: nothing to disclose
J. Hainfellner: nothing to disclose
G. Langs: nothing to disclose
D. Prayer: nothing to disclose
G. Kasprian: nothing to disclose

RPS 1611-6 16:30

Dynamic functional connectivity alterations of trigeminal neuralgia in resting-state fMRIs
X. Wan[1], P. Zhang[2], W. Wang[1], X. Su[1], S. Zhang[1], Q. Gong[1], Q. Yue[1]*; [1]Chengdu/CN, [2]Lanzhou/CN (awan1204@163.com)*

Purpose: Functional connectivity abnormalities, such as default mode network (DMN), have been reported previously in trigeminal neuralgia (TN) of which chronic pain is a common symptom. However, little is known about the dynamic functional connectivity (dFC) in patients with TN.
Methods and materials: 29 patients with TN were enrolled in this study and underwent rest-functional MRI scanning along with 24 age-, sex-, and education-matched healthy control (HC) subjects. A sliding-window approach was used to study the dFC based on the GIFT (group ICA of fMRI toolbox).
Results: The functional networks were arranged into DMN, auditory network (AUD), visual network (VIS), and ventral attention network (VAN). Dynamic analysis suggested 4 distinct connectivity 'states' across the entire group (state I for 24%, state II for 16%, state III for 35%, and state IV for 25%) and a larger proportion of state III and a smaller proportion of state IV were observed compared with HC group ($p=0.0000$ and $p=0.0058$, respectively). Furthermore, the TN group showed decreased connections between networks (DMN-VIS, AUD-VIS, and VIS-VAN). Our analyses showed that increased dwell time in the state IV was associated with the presence of pain in TN.
Conclusion: Our study indicates that chronic pain in TN is characterised by altered temporal properties in dynamic connectivity. Further studies on dynamic functional connectivity could help to better understand the progressive dysfunction of networks in TN.
Limitations: Correlation analysis is in progress.
Ethics committee approval: n/a
Funding: No funding was received for this work.
Author Disclosures:
X. Wan: nothing to disclose
W. Wang: nothing to disclose
P. Zhang: nothing to disclose
Q. Yue: nothing to disclose
Q. Gong: nothing to disclose
X. Su: nothing to disclose
S. Zhang: nothing to disclose

RPS 1611-7 16:36

Resting-state network plasticity in low-grade glioma patients before and after resection: maintaining language skills
L. van Dokkum, S. Moritz Gasser, J. Deverdun, G. Herbet, N. Menjot de Champfleur, H. Duffau, F. Molino, E. Le Bars*; Montpellier/FR (l-vandokkum@chu-montpellier.fr)*

Purpose: Diffuse low-grade gliomas (DLGG) have a slow infiltrating character, allowing for simultaneous plasticity and maintaining the patients' functional capacity. Here we addressed whether and how anatomical disconnection following left-hemispheric DLGG growth and resection interferes with resting-state connectivity, specifically in relation to language.
Methods and materials: 39 native French persons with a left DLGG were included and underwent awake surgical resection of the tumour. The anatomical disconnectivity risk following the DLGG volume and the resection, and the functional connectivity of resting-state fMRI images in relation to language, were evaluated prior to and three months after surgery. Resting-state connectivity

patterns were compared with 19 healthy controls. Language was assessed with a picture-naming task.
Results: Adaptive plasticity was observed in regions around the tumour/cavitas area, with increased connectivity of the left and right inferior parietal lobule with the left inferior temporal gyrus. Picture naming was surprisingly not dependent on the connectivity of the language network, but of the connectivity of regions know to be involved in semantics, in which their specific role could be explained in the light of the broader resting-state network they took part in. Also, the recruitment of the frontoparietal attention network was observed.
Conclusion: A whole-brain approach with specific clinical data input is required for meaningful resting-state analysis in case of lesions. Pre-surgical local plasticity and functional compensation by increased task-directed attention allow a relative high level of performance maintenance after DLGG resection.
Limitations: All participants underwent intensive speech-language rehabilitation post-surgery, which might have trained and strengthened attentional resources. The compensational strategy might thus have been learned.
Ethics committee approval: The study received local ethical committee's approval. Participants gave informed consent.
Funding: LabEx NUMEV (n° AN-10-LABX-20) and CHU Montpellier (AOI n° 2010-A01313-36).
Author Disclosures:
E. Le Bars: nothing to disclose
L. van Dokkum: nothing to disclose
S. Moritz Gasser: nothing to disclose
J. Deverdun: nothing to disclose
G. Herbet: nothing to disclose
N. Menjot de Champfleur: nothing to disclose
H. Duffau: nothing to disclose
F. Molino: nothing to disclose

RPS 1611-8 16:42
Thalamic structural connectivity abnormalities in minimal hepatic encephalopathy: a probabilistic tractography study
T.-X. Zou, N.-X. Huang, H.-J. Chen*; Fuzhou/CN (ztx6861@163.com)*

Purpose: There have been accumulating studies demonstrating thalamic related structural, functional, and metabolic abnormalities in minimal hepatic encephalopathy (MHE). We conducted the first study to investigate thalamic-related structural connectivity alterations in MHE.
Methods and materials: Diffusion based probabilistic tractography was used to determine the structural connection between the thalamus and the cortical/subcortical regions in 22 cirrhotic patients with MHE, 30 cirrhotic patients without MHE (NHE), and 30 healthy controls. DTI (diffusion tensor imaging) measurements of these thalamic connections, including connectivity strength (CS), fractional anisotropy (FA), mean diffusivity (MD), axial diffusivity (AD), and radial diffusivity (RD), were calculated and compared across three groups. Neuropsychological assessment was performed as well. The correlation analysis was conducted to investigate the relationship between neuropsychological performance and the measurements about thalamic connections. Machine-learning classification analysis was performed to estimate whether diffusion measurements can distinguish MHE from NHE.
Results: The probabilistic tractography revealed thalamic structural connection, which was disturbed in cirrhotic patients (reflected by decreased CS/FA and increased MD/AD/RD). Abnormal thalamic connection primarily involved the prefrontal cortex, sensorimotor cortex, parietal cortex, medial temporal cortex, hippocampus, and striatum. Thalamic connectivity abnormalities deteriorated from NHE to MHE and correlated with patients' impaired neuropsychological performance. The relatively high classification accuracy was obtained using CS as a discriminating index.
Conclusion: Our results demonstrated the altered thalamic structural connectivity with both cortical and subcortical regions in MHE. The disturbed thalamic connectivity may underlie the mechanism about cognitive deficits in MHE and can serve as biomarker for the diagnosis of MHE and monitoring disease progression.
Limitations: The cross-sectional design.
Ethics committee approval: The Research Ethics Committee of Fujian Medical University Union Hospital, China.
Each subject provided a written informed consent.
Funding: The National Natural Science Foundation of China (No.81501450).
Author Disclosures:
T.-X. Zou: nothing to disclose
N.-X. Huang: nothing to disclose
H.-J. Chen: nothing to disclose

RPS 1611-9 16:48
Assessment of translingual neurostimulation in the treatment of children with cerebral palsy in the late residual stage by means of a functional MRI
A. Sokolov, A. Efimtsev, D. Chegina, T. Ignatova, V. Fokin*; St. Petersburg/RU (falcon.and@mail.ru)*

Purpose: Constant stimulation of the nervous system is one of the most popular ways to activate neural networks in order to activate the brain and initiate neuroplasticity processes. The purpose of the study was to evaluate the impact of translingual neurostimulation of the brain to balance, coordination of movement, and the ability to form new motor skills in children with cerebral palsy in the late residual stage.
Methods and materials: This study involved 6 children with cerebral palsy, a form of spastic diplegia. Patients had intact intellect and no seizures in anamnesis. All children received standard treatment, including massage, medical-gymnastics with simulators, 10 daily sessions of physical therapy and neurostimulation of the brain (using a device for electrotactile stimulation called PoNS (portable neurostimulator)).
Patients underwent functional MRI of the brain before the start of, and at the end of, the course of treatment. The research was carried out using movement functional paradigms for each extremity (both feet and hands) and an active "count" paradigm for patients who could perform the task for the count and depending on clinical status, and passive movement or sensory paradigms were performed for those who could not. Postprocessing was carried out using the software package SPM 12.
Results: All patients noted decreased muscle tone and improved balance and coordination functions after neurostimulation. According to obtained fMRI data, patients who underwent translingual neurostimulation showed increased activation in the right-hand motor area and activation in the foot motor area in response to the stimuli.
Conclusion: Translingual neurostimulation is innovative in the field of neurostimulation, non-invasive, and safe and easy to use. fMRI active paradigms, with proper and high-quality implementation, is an auxiliary method for the objective control of treatment efficiency.
Limitations: n/a
Ethics committee approval: n/a
Funding: No funding was received for this work.
Author Disclosures:
A. Sokolov: nothing to disclose
A. Efimtsev: nothing to disclose
V. Fokin: nothing to disclose
D. Chegina: nothing to disclose
T. Ignatova: nothing to disclose

RPS 1611-10 16:54
Altered structural and functional connectome in unilateral sudden sensorineural hearing loss
W. Fan*; Wuhan/CN (fwl@hust.edu.cn)*

Purpose: To investigate the alterations of brain structural and functional connectome in unilateral sudden sensorineural hearing loss (USSHL) patients.
Methods and materials: We constructed functional-structural connectomes for USSHL patients (41 for the left side and 44 for the right side) and 85 controls. Graph theoretical analysis was employed to evaluate the network properties of functional-structural brain connectome. Moreover, we quantified coupling between functional-structural connectome by the correlation between functional-structural connectome edges within non-zero structural connectivity areas. The coupling of functional-structural brain connectome was compared by using permutation tests. To investigate the clinical relevance of altered brain network topologies in USSHL, Pearson's correlation analysis was performed between the clinical variables and the topological properties.
Results: Compared with the control groups, both groups of USSHL patients exhibited a significantly increased clustering coefficient, global efficiency, and local efficiency, but a significantly decreased characteristic path length in functional brain connectome, while a significant decrease clustering coefficient and local efficiency in structural brain connectome. In addition, the primary increased nodal strength was observed in limbic and paralimbic systems primarily as well as in the auditory network brain areas. More importantly, the coupling strength of structural-functional connectome was decreased and exhibited a negative correlation with some USSHL clinical variables in patients.
Conclusion: Detectable alteration of network organisation already occurred in USSHL patients within the acute period at the global and regional level. The functional connectome is characterised by a shift toward small-worldization while the structural connectome is toward randomisation, which may indicate a plastic reorganisation procedure of the brain to compensate for the loss of hearing in USSHL. Moreover, the degree of coupling between structural-functional connectome was decreased, which may reflect the pathophysiological mechanisms of USSHL.

Limitations: n/a
Ethics committee approval: n/a
Funding: NSFC (81701673).
Author Disclosures:
W. Fan: nothing to disclose

RPS 1611-11 17:00
On the relevance of functional-structural correlations in the multimodal MRI workup of neurosurgical cases
L. R. Kozák, G. Gyebnár*; Budapest/HU (lrkozak@gmail.com)*

Purpose: To investigate whether multimodal network graph analyses are relevant in the discussion of the combined fMRI-DTI pre-surgical evaluation of language networks.
Methods and materials: A retrospective cross-sectional evaluation of our 39 consecutive patients who underwent pre-surgical BOLD fMRI with 4 language tasks (TR=3s, 3x3x3 mm voxels) was conducted. DTI (32 encoding directions, b=800 s/mm^2, 2 mm isotropic resolution) was done with a standard SPM12 (https://www.fil.ion.ucl.ac.uk/spm) pipeline for fMRI, with the resulting activation maps further analysed using ICN_Atlas (Kozák et al., NeuroImage, 2017) with AAL atlas ROIs (Tzourio-Mazoyer et al., Neuroimage, 2002). DTI data was analysed using ExploreDTI with whole-brain tractography (Leemans et al., ISMRM, 2009) resulting in AAL-based connectivity matrices. Structural connectiome characteristics calculated with the brain connectivity toolbox (Rubinov and Sporns, NeuroImage, 2010) were compared against fMRI-based language network parameters using conventional parametric statistics in Matlab, focusing on Broca's and Wernicke's areas bilaterally.
Results: fMRI lateralisation correlated significantly with structural connectome graph parameters in a task-dependent fashion. The temporal lateralisation of speech comprehension and auditory decision and the frontal lateralisation of picture naming and synonym decision showed significant positive correlations with network metrics-based lateralisation parameters of the temporoparietal areas. The lateralisation of frontal language areas was also reflected in the lateralisation of arcuate fasciculus (AF).
Conclusion: The temporal lobe language networks seem to have a defining role in whole-brain language organisation, shown by the observed functional-structural correlations that are in line with previous literature (Wylie and Regner, Neurosci, 2014; Propper er al., Brain Cogn, 2010). A proper multimodal presurgical workup is important for preserving language function.
Limitations: The heterogeneity of age and pathologies, and DTI data instead of HARDI.
Ethics committee approval: Semmelweis University IRB #153/2019 (retrospective cross-sectional).
Funding: NRDIO Hungary OTKA-K128040 [LRK, GG]; EFOP-3.6.3-VEKOP-16-2017-00009, ÚNKP-19-3-III [GG].
Author Disclosures:
L. R. Kozák: nothing to disclose
G. Gyebnár: nothing to disclose

RPS 1611-12 17:06
Diffusion tensor tractography (DTT): an objective method of determining clinically relevant, compressive, spinal cord myelopathy
R. Rastogi, N. Jain*; Moradabad/IN (rajulrst@yahoo.co.in)*

Purpose: Magnetic resonance imaging (MRI) is the gold-standard imaging tool for compressive spinal cord myelopathy (CSCM). Diffusion tensor imaging (DTI), especially fibre-tracking or tractography (DTT), has been considered superior to routine MRI in predicting prognosis and urgency of decompression. This study aims to evaluate DTT as an advanced dimension of MRI in patients with CSCM in predicting the necessity of decompression management.
Methods and materials: 12 patients with clinical signs of CSCM underwent conventional MRI and DTI examination with a high-resolution matrix on a 1.5T magnet system. 3D-colour-coded maps were obtained in the sagittal and coronal planes. The presence or absence of parenchymal signal alteration and change in colour-code of the neural fibre tracts in the spinal cord, in addition to the integrity and homogeneous thickness of the fibre tracts on DTT, was evaluated. A near-homogeneous blue colour in the spinal cord and cauda equina was considered normal in our study, with the blue colour representing diffusion in the craniocaudal direction. Alteration in colour, thickness, and integrity, especially at the level of compression on T2W images, was considered significant.
Results: Out of 12 patients, 9 had signs of CSCM secondary to infective spondylodiskitis, 1 secondary to a disk protrusion, 1 secondary to a disk extrusion, and 1 secondary to the metastatic collapse of the vertebra.
In 8/12 patients with no spinal cord parenchymal signal alteration on T2W images, DTT revealed significant alteration in the colour-code both at and above the level of compression, signifying altered diffusion.
Conclusion: DTT is a more sensitive indicator of spinal cord compression than conventional MRI by revealing colour alterations, thinning and loss of integrity of spinal nerve fibre tracts, and providing an easy and fast tool to predict the need for surgical decompression.
Limitations: n/a
Ethics committee approval: n/a
Funding: No funding was received for this work.
Author Disclosures:
R. Rastogi: nothing to disclose
N. Jain: nothing to disclose

RPS 1611-13 17:12
The role of the waist-to-hip ratio in brain networks: a connectometry study
M. Porcu, E. Scapin, P. Garofalo, A. Caneglias, F. Destro, A. Operamolla, L. Saba*; Cagliari/IT (micheleporcu87@gmail.com)*

Purpose: It is known from the literature that BMI influences cerebral networks. The purpose of this study is to evaluate the influence of the waist-to-hip ratio (W-H ratio) on brain networks by using the connectometry technique.
Methods and materials: We recruited 30 healthy subjects (12 males, 18 female; age 25-80). The waist and hip circumferences of every patient were measured in order to calculate the W-H ratio and on the same day an MR examination was performed on a 3T scanner (Vantage Titan 3T, Canon) with a 32 channels head coil. The MR protocol included a 40 directions DW sequence for the connectometry analysis. The connectometry analysis was performed using a linear regression model to consider the effects of the W-H ratio, choosing three different T-score thresholds (T-threshold) values (1, 2, and 3). Results were considered statistically valid for a p-value adjusted for the false discovery rate (p-FDR) <0.05. The network topology analysis measured the influence of the W-H ratio on brain networks.
Results: The connectometry analysis identified several white matter bundles negatively correlated to the W-H score for T-threshold=2 and 3. Several properties of the network were influenced in the network topology analysis.
Conclusion: The W-H ratio influences brain networks. More studies are needed in order to fully understand these results.
Limitations: The small number of patients recruited and the DW parameters adopted, in particular, the low b-values.
Ethics committee approval: The study was approved by the local ethical committee. Informed consent was obtained.
Funding: No funding was received for this work.
Author Disclosures:
M. Porcu: nothing to disclose
P. Garofalo: nothing to disclose
E. Scapin: nothing to disclose
F. Destro: nothing to disclose
A. Operamolla: nothing to disclose
A. Caneglias: nothing to disclose
L. Saba: nothing to disclose

RPS 1611-14 17:18
Neural correlates of insight and analytical anagram solving: fMRI study
E. Kremneva, D. Sinitsyn, I. Bakulin, A. Poidasheva, A. Medyntsev, D. Lagoda, L. Legostaeva, N. Suponeva, M. Piradov*; Moscow/RU (kremneva@neurology.ru)*

Purpose: Insight is the sudden and unpredictable appearance of a problem's solution. The role of various brain structures in the generation of the insight phenomenon remains poorly understood. We aimed to study the neural correlates of the insight process during fMRI.
Methods and materials: We performed fMRIs in 32 healthy subjects with a paradigm that involved solving anagrams. After giving an answer, the participants labelled their strategy as 'insight' or 'analytical'. The data was analysed using a GLM with predictors corresponding to different stimulus types and button presses. A random-effects analysis for the population was performed using a t-test over the individual contrast images.
Results: Areas activated during 'insight' problem-solving compared to rest included bilateral middle/superior frontal gyri, bilateral anterior insula, left frontal operculum, left precentral gyrus, left supplementary motor cortex, left superior parietal lobule, left putamen, left pallidum, right cerebellum, and bilateral inferior occipital gyri. Areas activated during 'analytical' problem-solving compared to rest included right superior frontal gyrus, bilateral anterior insula, left frontal operculum, left precentral gyrus, left supplementary motor cortex, bilateral superior parietal lobules, right cerebellum, left putamen, and bilateral inferior occipital gyri. Activation of the left precentral gyrus, left supplementary motor cortex, and right cerebellum during both insight and analytical solving can be attributed to right-hand movement for keystroke at the "solving" moment. The contrast between the 'insight' and 'analytical' problem-solving did not contain significant clusters at FWE<0.05.

Conclusion: Both analytical and insight solving are associated with the activation of multiple brain regions without significant difference in activation areas between strategies. Future studies using different paradigms and combined methods (fMRI, EEG, NIBS, etc.) are needed to elucidate neural correlates of insight.
Limitations: n/a
Ethics committee approval: Ethics committee approval obtained.
Funding: RFBR according to research project № 18-00-01100 (K) (18-00-01078).
Author Disclosures:
E. Kremneva: nothing to disclose
D. Sinitsyn: nothing to disclose
I. Bakulin: nothing to disclose
A. Poidasheva: nothing to disclose
A. Medyntsev: nothing to disclose
D. Lagoda: nothing to disclose
L. Legostaeva: nothing to disclose
N. Suponeva: nothing to disclose
M. Piradov: nothing to disclose

RPS 1611-15 17:24
Language lateralisation in tumour patients and healthy controls using functional MRI and diffusion tractography
A. Q. Y. Al Busaidi[1], E. Gangemi[2], S. Wastling[1], A. S. van Den Berg[3], L. D'anna[1], L. Mancini[1], T. A. Yousry[1]; [1]*London/UK,* [2]*Rome/IT,* [3]*Dordrecht/NL (ayisha.albusaidi@nhs.net)*

Purpose: Our retrospective study investigates whether a correlation exists between functional language lateralisation using fMRI and structural lateralisation using diffusion data of language tracts in controls and tumour patients.
Methods and materials: 15 controls and 61 patients were included and underwent structural, functional, and diffusion imaging on 3T MRI. Subjects performed verbal fluency and verb generation language fMRI tasks, and a laterality index (LI) was calculated using data from the cerebral hemisphere and the contralateral cerebellar hemisphere. The diffusion tracts included the long fibres of the arcuate fasciculus, anterior and posterior short fibres of the arcuate fasciculus, uncinate fasciculus, inferior longitudinal fasciculus, inferior fronto-occipital fasciculus, and frontal aslant tract. An asymmetry index (AI) for each fibre pair was calculated using the tract volume derived from single tensor (ST) and spherical deconvolution (SD) diffusion data, as well as using the hindrance modulated orientational anisotropy (HMOA) derived from the SD method. A linear regression analysis between fMRI LI and DTI AI was performed.
Results: In all subjects, there was no significant correlation between fMRI LI and DTI AI for any of the tracts.
Conclusion: Our results do not justify replacing fMRI with tractography in the assessment of language lateralisation. The discordant results between ST- and SD-based asymmetry indices indicate that the structural lateralisation is less robust than the functional one.
Limitations: The predominately left-sided tumour distribution is due to the retrospective design, as included patients had all been selected clinically for presurgical assessment. The number of right-handed, left-handed, and ambidextrous subjects was not balanced. Disrupted or infiltrated fibres were excluded.
Ethics committee approval: The National Hospital for Neurology and Neurosurgery and Institute of Neurology Joint Research Ethics Committee approval was obtained.
Funding: No funding was received for this work.
Author Disclosures:
A. Q. Y. Al Busaidi: nothing to disclose
E. Gangemi: nothing to disclose
S. Wastling: nothing to disclose
A. S. van Den Berg: nothing to disclose
L. D'anna: nothing to disclose
L. Mancini: nothing to disclose
T. A. Yousry: nothing to disclose

16:00 - 17:30 **Room Y**

My Thesis in 3 Minutes

MyT3 16

Cardiac

Moderators:
C. A. Minoiu; Bucharest/RO
R. Salgado; Antwerp/BE

MyT3 16-1 16:00
Diagnostic and clinical value of dual-source computed tomography in pulmonary atresia with ventricular septal defect
X.-Z. Zhou, K. Shi, Z.-G. Yang*; Chengdu/CN (xinzhuzhou@126.com)*

Purpose: To explore the diagnostic and clinical value of dual-source CT (DSCT) in pulmonary atresia with ventricular septal defect (PA-VSD).
Methods and materials: The clinical and imaging data of 35 patients with PA-VSD confirmed by surgery or digital subtraction angiography (DSA) were retrospectively analysed. The results of preoperative transthoracic echocardiography (TTE) and DSCT were compared with those of surgery or DSA.
Results: DSCT and TTE all have high sensitivity and specificity in the diagnosis of intracardiac anomalies and anomalies of great vessels, the difference is not statistically significant ($p > 0.05$), while the sensitivity of DSCT in diagnosing PA-VSD patients with major aortopulmonary collateral arteries (MAPCAs) was higher than that of TTE (100% vs 68.75%). The incidence of MAPCAs in the group of the large ventricular septal defect (57.7%) is higher than non-large ventricular septal defect group (11.1%) diagnosed by DSCT, the difference is statistically significant（$p=0.018$, < 0.05. Based on DSCT images, McGoon ratio, Nakata index and TNPAI index of patients were measured. There were significant differences in McGoon ratio and TNPAI index between different treatment groups ($p < 0.05$).
Conclusion: DSCT can accurately diagnose PA-VSD and associated cardiovascular malformations, evaluate the development of pulmonary artery and anatomical characteristics of MAPCAs. It has great reference value for diagnosis and the choice of treatment methods of PA-VSD.
Limitations:
Firstly, the sample size of this study is relatively small, which limits the application of the research results. Secondly, because this study is a retrospective study, the surgical methods are affected by the personal habits of the operator partly, which makes the results of the study have certain limitations and need further verification of randomised clinical trials.
Ethics committee approval: Institutional Review Board at West China Hospital of Sichuan University approved this study.
Funding: No funding was received for this work.
Author Disclosures:
X.-Z. Zhou: nothing to disclose
K. Shi: nothing to disclose
Z.-G. Yang: nothing to disclose

MyT3 16-2 16:04
The feasibility and radiation dose of single-beat coronary CT angiography in patients with atrial fibrillation
C. Zhao, Z. Yang*; Beijing/CN (chenglin.zhao@163.com)*

Purpose: To evaluate the feasibility and radiation dose of single-beat coronary CTA in patients with atrial fibrillation (AF) compared sinus rhythm (SR).
Methods and materials: From 2016 to 2017, 20 patients with AF (group A) and 20 patients with SR (group B) were referred for CCTA with120 kVp tube voltage and auto mAs. The objective IQ including image noise, signal-to-noise ratio (SNR) and contrast-to-noise ratio (CNR) were compared respectively. The subjective IQ was evaluated by two radiologists in consensus (1 excellent, 2 good, 3 adequate, 4 poor). The effective radiation dose was calculated for each patient.
Results: Group A (8 male, 12 female, mean age 59.1±15.1years, BMI 28.4±5.1kg/cm^2), group B (8 male, 12 female, mean age 54.8±18.6 years, BMI 29.0±6.5 kg/cm^2) ($p>0.05$) were recruited. The image noise, CNR and SNR of the 2 groups were 28.7±5.8(A) vs 29.1±5.6(B) ($p>0.05$), 18.4±5.1(A) vs 18.5±6.7(B) ($p>0.05$) and 15.3±4.4(A) vs 15.4±5.9(B) ($p>0.05$). The subjective IQ of the 2 groups based on patients were all rated as diagnosable and the scores were 1.4±0.7(A) vs 1.6±0.7(B) ($p>0.05$); based on the artery segments, 261 segments (A) and 258 segments (B) of the 2 groups were evaluated, 100% (261/261) and 99.6% (257/258) were rated as diagnosable and the scores were 1.16±0.4(A) vs 1.24±0.5(B) ($p=0.02$). The mean effective radiation dose (ED) were 3.5mSv±1.1mSv vs 2.9 mSv±1.2mSv, ($p>0.05$).

Conclusion: Single-beat CCTA using wide-detector CT could achieve high rate of success and good IQ for AF patients and with acceptable ED compared with SR patients.
Limitations: A systematic comparison of diagnostic accuracy between CCTA and the gold standard of invasive coronary angiography has not been performed.
Ethics committee approval: We performed this study with the approval of the local institutional review board.
Funding: No funding was received for this work.
Author Disclosures:
C. Zhao: nothing to disclose
Z. Yang: nothing to disclose

MyT3 16-3 16:08

Screening potential of low-dose chest CT in assessing the degree of coronary arteries calcification

O. V. Styazhkina, K. Zhuravlev, V. E. Sinitsyn*; Moscow/RU (olya-mma@mail.ru)*

Purpose: Coronary artery calcinosis is a specific biomarker of coronary atherosclerosis. It is often detected on chest CT scans. Today the popularity of lung cancer screening with low-dose CT is growing. The aim of the study is to compare the diagnostic value of low-dose chest CT for the assessment of calcium score in comparison with the standard gated calcium scoring.
Methods and materials: Non-gated low-dose chest CT and gated calcium scoring were performed in 251 asymptomatic patients. The Agatston calcium score values obtained from low-dose CT and gated scans were analysed independently by two radiologists. Inter-observer and inter-technique agreement were evaluated (data with "zero" calcium scores was excluded). Inter-technique differences in a stratification of patients into five risk categories (scores 0, 1-100, 101-400, 401-1000 and> 1000) using the kappa coefficient (k) were analysed.
Results: The sensitivity of non-gated calcium scoring compared to the standard technique was 95%, specificity - 99%. The proportion of "zero" calcium score values in our study was 31% (79 patients). The inter-technique concordance was quite high, both with the inclusion of "zero" values ($r=0.981$, $p<0.05$) and without them ($r=0.978$, $p<0.05$). The inter-observer agreement was 0.998. The inter-technique agreement in the stratification of patients into the five risk groups according to the calcium score values was also high: $k = 0.846$. Effective radiation dose in low-dose chest CT was significantly lower than in the case of gated calcium scoring (0.96 ± 0.26 vs 1.51 ± 0.22 mSv, $p<0.01$).
Conclusion: The study showed that non-gated low-dose chest CT can be effectively used both for lung cancer screening and coronary calcium scoring with lower radiation exposure to patients than in gated calcium score.
Limitations: No limitations were identified.
Ethics committee approval: n/a
Funding: No funding was received for this work.
Author Disclosures:
K. Zhuravlev: nothing to disclose
V. E. Sinitsyn: nothing to disclose
O. V. Styazhkina: nothing to disclose

MyT3 16-4 16:12

Diagnostic performance of myocardial CT perfusion imaging for the detection of obstructive coronary artery disease: intraindividual comparison of half scan and multisegment reconstruction

D. Preuß, G. Garcia, M. Laule, M. Dewey, M. Rief*; Berlin/DE (daniel.preuss@mailbox.org)*

Purpose: To compare the diagnostic performance of half scan reconstruction (HSR) and multisegment reconstruction (MSR) of myocardial CT perfusion (CTP) imaging for the detection of obstructive coronary artery disease (CAD).
Methods and materials: A total of 134 consecutive patients (median age, 65.7 years; interquartile range, 55.9-70.2) prospectively underwent CTP. 93 patients had multisegment acquisition and were retrospectively interpreted for perfusion defects. In these patients, we performed both HSR and MSR and compared their diagnostic performance using ≥50% diameter stenosis in the supplying artery on quantitative coronary angiography as the reference standard. AUC and diagnostic performance were compared using DeLong et al.´s and McNemar´s approaches.
Results: Per-patient analysis revealed an overall AUC of HSR and MSR of 0.79 [95% confidence interval: 0.69, 0.88] and 0.65 [0.53, 0.78] (P= .01), respectively. Diagnostic accuracy of HSR was superior to MSR in patients with known CAD (74% (50 of 68) vs 63% (43 of 68); P< .001) and low heart rate variability (70% (39 of 56) vs 59% (33 of 56); P= .001). Diagnostic performance of HSR and MSR was the same in patients with suspected CAD (72% (18 of 25) vs 76% (19 of 25); P= .99) and heart rates ≥75 beats per minute (67% (20 of 30) vs 70% (21 of 30); P= .24).
Conclusion: HSR of myocardial CTP has a higher diagnostic performance than MSR in patients with known CAD and low heart rate variability. The two reconstruction methods have the same diagnostic performance in patients with suspected CAD and high heart rates.
Limitations: The subgroups have only a small number of patients.
Ethics committee approval: IRB approval and written informed consent were obtained.
Funding: No funding was received for this work.
Author Disclosures:
D. Preuß: nothing to disclose
G. Garcia: nothing to disclose
M. Dewey: Research/Grant Support at Heisenberg Program of the DFG for a professorship (DE 1361/14-1) and FP7 Program of the European Commission for the randomized multicenter DISCHARGE trial (603266-2, HEALTH-2012.2.4.-2), Research/Grant Support at Institutional master research agreements exist with Siemens Medical Solutions, Philips Medical Systems, and Toshiba Medical Systems. The terms of these arrangements are managed by the legal department of Charité - Universitätsmedizin Berlin., Speaker at Lecture fees from Toshiba Medical Systems, Guerbet, Cardiac MR Academy Berlin, and Bayer (Schering-Berlex), Board Member at Editor of the Cardiac Section of European Radiology
M. Rief: nothing to disclose
M. Laule: nothing to disclose

MyT3 16-5 16:16

CT-angiographic graft patency after minimally invasive multivessel coronary bypass surgery

O. Drozdova, M. Snegirev*; St. Petersburg/RU (olyadrozdova@yandex.ru)*

Purpose: Minimally invasive multivessel coronary artery bypass grafting (MICS CABG) has shown its safety, effectiveness and high rates of reproducibility, but graft patency data is lacking. In this study we retrospectively analyse CT-angiographic graft patency and mid- to early long-term outcomes in patients, subjected to MICS CABG in our institution.
Methods and materials: 245 patients were subjected to MICS CABG by small left side thoracotomy approach between July 2014 and December 2018. LITA harvesting, proximal and distal anastomoses were performed under direct vision. SVG/radial artery conduits were harvested endoscopically. Patients were examined with 128-slice CT coronary angiography. Angiographic results achieved for 127 (51.8%) patients (mean follow-up 31.1±7.8 months, range 15 – 45 months).
Results: All patients achieved complete revascularisation. The mean number of grafts was 2.6±0.5. Perioperative mortality was 0.4% (1 patient). There were 2 conversions to sternotomy (0.8%), 4 reopenings for bleeding (1.6%), 3 perioperative MI (1.2%) and 1 CVA (0.4%). 22 (9.0%) patients received transfusions. 83.2% of patients were followed-up clinically (range 12 – 56 months). Long-term mortality was 4.4% (9 patients). Stroke at follow-up occurred in 3 patients (1.5%). Repeat revascularisation was performed in 5 cases (2.4%). Overall graft patency rate in the examined patients was 89.8%. LITA graft patency rate was 98.4%. SVG grafts were patent in 84.0% of cases.
Conclusion: MICS CABG allows complete surgical revascularisation with the standard alignment of coronary grafts. Excellent perioperative and longer-term clinical results with promising angiographic graft patency rates have been achieved.
Limitations: This study is limited by the fact that it is a retrospective study.
Ethics committee approval: n/a
Funding: No funding was received for this work.
Author Disclosures:
O. Drozdova: Speaker at St.-Petersburg Municipal hospital №40
M. Snegirev: Author at St.-Petersburg Municipal hospital №40

MyT3 16-6 16:20

Evaluation of segmental viable myocardium using low-dose dobutamine stress cardiac MRI with tissue tracking

B. He, F. Gao*; Chengdu/CN (bohetmu@163.com)*

Purpose: To detect survived myocardium by low-dose dobutamine stress with tissue tracking using cardiac magnetic resonance (CMR) imaging and evaluate the prognosis of survived myocardium.
Methods and materials: In 24 adult SD rats, the left anterior descending coronary artery was occluded for half hours and released. Low-dose dobutamine stress cardiac cine-MR and late gadolinium enhancement were both performed to analyse wall motion of left ventricle. A three-dimensional and two-dimensional strain of anterior wall and anterior septum, include global peak longitudinal strain (GPLS), radial strain (GPRS), circumferential strain (GPCS), peak radial strain (PRS) and circumferential strain (PCS), were measured at baseline, after reperfusion and dobutamine stress. Triphenyl tetrazolium chloride (TTC) and Evans blue staining were applied to assess viable or nonviable myocardium.
Results: During baseline, statistical significance of GPLS, GPRS, GPCS, PRS and PCS dose are not present between viable and nonviable myocardium group ($P>0.05$), same as that observed after reperfusion except strain decrease without significance ($P>0.05$). While low-dose dobutamine stressing, PRS and

PCS of viable myocardium group increased significantly compared with that detected after reperfusion (P<0.05). Significant variances were presented between viable and nonviable myocardial group during stress. In addition, there was a significant difference between two-dimensional strain measured from cine-MR at rest and with stress. Strain variance of nonviable myocardium group during dobutamine stress dose not observe compared that detected after reperfusion (P>0.05).
Conclusion: The application of low-dose dobutamine stress cardiac MR with tissue tracking may provide an objective and accurate method to evaluate survived myocardium.
Limitations: The data still has to be interpreted with caution given the small sample size.
Ethics committee approval: This study was approved by Institutional Animal Research Committee of our local institute.
Funding: The study was funded by the National Natural Science Foundation of China (8193000682).
Author Disclosures:
B. He: nothing to disclose
F. Gao: nothing to disclose

MyT3 16-7 16:24

Myocardial CT perfusion imaging for the detection of obstructive coronary artery disease: should interpretation of perfusion defects be different depending on disease status?

D. Preuß, G. Garcia, M. Laule, M. Rief, M. Dewey*; Berlin/DE (daniel.preuss@mailbox.org)*

Purpose: To investigate whether perfusion defect (PD) interpretation of myocardial CT perfusion (CTP) should be different in patients with suspected or known coronary artery disease (CAD) for the detection of obstructive CAD.
Methods and materials: A total of 134 consecutive patients with known or suspected CAD prospectively underwent CTP. Rest and stress PDs were retrospectively interpreted in four reading categories (RC): RC 1 (stress volume positive), RC 2 (rest or stress volume positive), RC 3 (stress-induced PDs positive), RC 4 (stress-induced and partially reversible PDs positive). Detection of ≥50% diameter stenosis in the supplying artery on quantitative coronary angiography (reference 1) and intervention (reference 2) served as the reference standards.
Results: When using reference 1, per-patient analysis revealed AUCs of RC 1-4 of 0.74, 0.65, 0.62, and 0.72, respectively, in patients with known CAD. In these patients, AUC of RC 1 was higher than RC 3 (P= .03) and, respectively, AUC of RC 4 was higher than RC 3 (P= .006). In patients with suspected CAD, AUCs of RC 1-4 were the same (0.83, 0.86, 0.85, 0.88; all P> .05). When using reference 2, AUCs of RC 1-4 in patients with known CAD (0.61, 0.60, 0.67, 0.69) and, respectively, in patients with suspected CAD (0.75, 0.80, 0.76, 0.80) were the same at per-patient level analysis (all P> .05).
Conclusion: In patients with known or suspected CAD, every stress PD should be judged positive to detect obstructive CAD in myocardial CTP regardless of its presentation in rest.
Limitations: Study design is retrospective.
Ethics committee approval: IRB approval and written informed consent were obtained.
Funding: No funding was received for this work.
Author Disclosures:
D. Preuß: nothing to disclose
G. Garcia: nothing to disclose
M. Laule: nothing to disclose
M. Rief: nothing to disclose
M. Dewey: Research/Grant Support at Heisenberg Program of the DFG for a professorship (DE 1361/14-1) and FP7 Program of the European Commission for the randomized multicenter DISCHARGE trial (603266-2, HEALTH-2012.2.4.-2), Research/Grant Support at Institutional master research agreements exist with Siemens Medical Solutions, Philips Medical Systems, and Toshiba Medical Systems. The terms of these arrangements are managed by the legal department of Charité - Universitätsmedizin Berlin., Speaker at Lecture fees from Toshiba Medical Systems, Guerbet, Cardiac MR Academy Berlin, and Bayer (Schering-Berlex), Board Member at Editor of the Cardiac Section of European Radiology

MyT3 16-8 16:28

CT texture analysis of the myocardium in patients affected by aortic stenosis: a potential new tool?

F. Vaccher, G. M. Agazzi, M. Filippini, C. Fiorina, L. Lupi, M. Ravanelli, D. Farina*; Brescia/IT (filippo.vaccher0@gmail.com)*

Purpose: To assess the potential of texture analysis (TA) of native images of the interventricular septum to detect structural myocardial changes in patients with aortic valve stenosis (AVS), candidates to transcatheter aortic valve replacement (TAVI).
Methods and materials: Retrospective single-centre study on 210 CT-angiography exams performed for TAVI planning. Scans were obtained with dual-source CT scanner (Somatom Definition Flash, Siemens, Erlangen) with retrospective ECG-gated acquisition and bolus-tracking technique. Two-dimensional TA was performed using commercial software (TexRAD Ltd, Cambridge, UK), with a filtration histogram method, on polygonal regions-of-interest (ROI) manually drawn by a single operator on native axial sections reconstructed in diastole and systole; ROIs encompassed the interventricular septum below aortic valve level. Septal thickness (ST), ejection fraction (EF), and aortic valve area (AVA) were recorded in each patient, in order to correlate such parameters with TA features. Statistical analysis was carried out using the least absolute shrinkage and selection operator (LASSO) linear regression model. Significance was fixed at P=0,05.
Results: After LASSO analysis 10 TA features were significantly correlated with ST; a radiomic score was calculated (mean value 14,57) with linear regression coefficient 1,3389 ($p=2,22x10^{-11}$; $R^2=0,2299$). 12 TA features were significantly correlated with EF; a radiomic score was calculated (mean value 52,33) with linear regression coefficient 1,2790 ($p=5,39x10^{-16}$; $R^2=0,2804$). 8 TA features were significantly correlated with AVA; a radiomic score was calculated (mean value 0,6670) with linear regression coefficient 1,9824 ($p=2,55x10^{-5}$; $R^2=0,08807$).
Conclusion: TA features extracted for myocardial septum correlate with morphologic and functional parameters in patients affect by SA. The correlation with ST suggests a possible correspondence between TA features and myocardial fibrosis or disarray.
Limitations: The single-centre study, study design retrospective, small sample.
Ethics committee approval: All patients gave written consent to CT.
Funding: No funding was received for this work.
Author Disclosures:
F. Vaccher: nothing to disclose
G. M. Agazzi: nothing to disclose
M. Filippini: nothing to disclose
L. Lupi: nothing to disclose
M. Ravanelli: nothing to disclose
D. Farina: Speaker at BAYER 2018 honorary for a single lecture
C. Fiorina: nothing to disclose

MyT3 16-9 16:32

Early evaluation on left ventricular remodelling in patients with type 2 diabetes mellitus using MR tissue tracking

Y. Li, Z. Li, C. Xia*; Chengdu/CN (18108087220@163.com)*

Purpose: To estimate the clinical value of MR tissue tracking in the assessment of left ventricular remodeling in patients with type 2 diabetes mellitus.
Methods and materials: 29 patients with T2DM as well as 21 healthy controls were enrolled. Cardiac magnetic resonance（CMR）was used to obtain left ventricular function parameters while MR tissue tracking to get peak strains (PS. Radial PS, circumferential PS and longitudinal PS were calculated with global and 16 regional segments in DM and healthy controls. Together with LVEF, LVEDV and LV Mass, peak strains were compared between DM and controls.
Results: LVEF and global longitudinal PS, basal longitudinal PS were statistical significantly smaller for DM (-16.51±2.76 vs -18.00±2.15, $P<0.05$; and -11.26±3.69 vs -13.35±3.16 $P<0.05$; respectively). Global and segmental PS had a statistical significant correlation with LVEF (r=0.63, 0.407, 0.571, 0.517, -0.765, -0.667, 0.627, 0.243, 0.615, 0.655 , $P<0.05$ separately). Global and basal radial PS, mid longitudinal PS had a significant-good correlation with HaB1C (r=-0.375, -0.367, 0.381, $P<0.05$); separate PS had a poor diagnostic value while the union of apical radial PS, basal circumferential PS, global/basal/apical longitudinal PS had a relatively good sensitivity and specify to distinguish DM from healthy controls.
Conclusion: There is a statistically significant difference between DM and healthy controls on peak strain, which serves an early measurement of left ventricular remodelling which could potentially be included as a supplementary diagnostic procedure in the evaluation of DM.
Limitations: We didn't discuss the left ventricular systolic function of DM.
Ethics committee approval: The study was approved by our institutional review board and written informed consent was obtained from all participants.
Funding: 1.3.5 project for disciplines of excellence, West China Hospital, Sichuan University.
Author Disclosures:
Z. Li: nothing to disclose
Y. Li: nothing to disclose
C. Xia: nothing to disclose

MyT3 16-10 16:36
Clinical implications of measuring epicardial adipose tissue quantity
A. Jermendy; *Budapest/HU (adam.jermendy@gmail.com)*

Purpose: Various adipose tissue compartments play an important role in the development of cardiometabolic diseases. The quantity of different fat compartments is influenced by genetic and environmental factors. In a classical twin study we sought to assess the heritability of epicardial adipose tissue (EAT) quantity in comparison to that of abdominal subcutaneous (SAT) and visceral adipose tissue (VAT) compartments. Furthermore, we aimed to evaluate the role of EAT in the pathomechanism of coronary artery disease (CAD).
Methods and materials: We investigated 202 healthy adult twin subjects in whom CT based EAT, SAT and VAT quantity measurement, as well as coronary CT angiography, was performed. For the heritability assessment, intra-pair correlations were calculated and robust structural equation modelling was used. We performed logistic regression analysis to evaluate the association between CAD and clinical risk factors.
Results: We demonstrated in our study that genetics have substantial, while environmental factors have only a modest influence on EAT, SAT and VAT volumes. Our findings show that common and specific genetic effects both play an important role in developing these phenotypes. None of the phenotypic appearances of EAT, SAT and VAT proved to be completely independent of the other two. According to our results, EAT quantity shows a significant association with the presence of CAD supporting the concept that EAT may have a role in the pathomechanism of developing CAD.
Conclusion: As the presence of strong genetic predisposition does not automatically translate to the development of clinical disease phenotype, early and continuous preventive efforts should be implemented in order to prevent obesity. Our results also suggest that it seems reasonable to involve EAT quantity into cardiovascular risk assessment tools.
Limitations: The limitations of this study lay in the fact that it is a single-centre, cross-sectional study.
Ethics committee approval: n/a
Funding: No funding was received for this work.
Author Disclosures:
A. Jermendy: nothing to disclose

MyT3 16-11 16:40
The use of CTPA in the evaluation of heart failure in the acute setting
L. O'halloran[1], J. O'brien[2]; [1]*Limerick/IE,* [2]*Dublin/IE (liamoh@gmail.com)*

Purpose: Heart failure is a clinical diagnosis characterised by non-specific symptoms such as dyspnoea, fatigue and oedema. The European Society of Cardiology recommends obtaining objective measures for heart failure in order to confirm a diagnosis. However, it can be challenging to obtain objective measures such as echocardiography in the acute setting. CTPA is conventionally used to outrule pulmonary embolus, however, CTPA provides great detail of the heart and lungs as a whole. The aim of this study was to investigate what role CTPA could play in diagnosing heart failure.
Methods and materials: We reviewed 230 CTPA results, of these we confirmed which of these patients had heart failure by confirming a heart failure diagnosis with BNP and echocardiogram criteria. We divided the groups into those who had heart failure and those that did not. We then analysed which features found on CTPA were most specific for a diagnosis of heart failure.
Results: In our study the most specific signs were shown to be left ventricular enlargement, left atrial enlargement and right ventricular enlargement. This was demonstrated using chi-square analysis; right ventricular enlargement (value = 5.426 P=0.02), left atrial enlargement (value = 4.9 P=0.027) and left ventricular enlargement (value = 5.692 P=0.017).
Conclusion: Several findings on CTPA were demonstrated to be quite specific for a diagnosis of heart failure which includes left ventricular enlargement, left atrial enlargement and right ventricular enlargement. Acute physicians should utilise, if available, recent CTPA results while awaiting echocardiography in determining the presence of heart failure in patients.
Limitations: Study based at a single centre. A prospective study would have highlighted CTPA's clinical utility.
Ethics committee approval: Obtained from University Hospital Limerick's ethics committee.
Funding: No funding was received for this work.
Author Disclosures:
L. O'halloran: nothing to disclose
J. O'brien: nothing to disclose

MyT3 16-12 16:44
Compared with the left atrium, left atrial appendage function and myocardial remodeling, play a greater role in relapse of AF after radiofrequency ablation
X. Tian, C. Li, Y. Yuan; *Shijiazhuang/CN (tianx25@139.com)*

Purpose: To evaluate the role of the left atrium and left atrial appendage in the recurrence of atrial fibrillation (AF) after radiofrequency ablation.
Methods and materials: 63 patients with AF who underwent radiofrequency ablation for the first time were enrolled. According to the recurrence of AF after radiofrequency ablation, the patients were divided into the recurrence group (n = 20 cases) and non-recurrence group (n = 43 cases). All patients underwent a 256-slice spiral CT examination before the operation. The maximum volume of LAA (LAAVmax), minimum volume of LAA (LAAVmin), LAA emptying fraction (LAAEF), and LAA ejection volume (LAAEV), LAA volume strain (LAA-VS), maximum volume of LA (LAVmax), minimum volume of LA (LAVmin), LA emptying fraction (LAEF), LA ejection volume (LAEV), and LA volume strain (LAVS) were measured.
Results: The LAAVmax, LAAVmin, LAVmax, and LAVmin in the recurrence group were higher than those in the non-recurrence group ($P < 0.05$), while LAAEF, LAEF and LAA-VS in the recurrence group were lower than those in the non-recurrence group ($P < 0.05$). There was no difference in LA-VS between the two groups. LAAEF was an independent predictor of recurrence after radiofrequency ablation of AF. LAAEF < 44.68% had the highest predictive value for recurrence after radiofrequency ablation.
Conclusion: LAAEF is a predictor of recurrence after radiofrequency ablation of AF. Compared with LA volume strain, LAA volume strain which represented fibrosis of LAA myocardia is more useful in evaluating myocardial remodelling associated with recurrence of AF.
Limitations: Our team paid attention to patients' ECG and ambulatory ECG results through a clinic or telephone follow-up, but asymptomatic atrial fibrillation attacks may be omitted, leading to underestimation of recurrence rate.
Ethics committee approval: n/a
Funding: No funding was received for this work.
Author Disclosures:
X. Tian: nothing to disclose
C. Li: nothing to disclose
Y. Yuan: nothing to disclose

MyT3 16-13 16:48
A comparative study between cardiac computed tomography and magnetic resonance imaging in the assessment of cavopulmonary anastomosis
M. A. I. Gamal Elden[1], F. R. M. Elkafrawy[2], A. Soliman[3], M. Salah[4], A. Elmogy[1], A. Mourshed[1], A. Samir[1], S. Romeih[3], W. Elmozy[1]; [1]*Cairo/EG,* [2]*Alexandria/EG,* [3]*Aswan/EG,* [4]*Zagazig/EG (marwagamal2014@gmail.com)*

Purpose: Could MRI replace CT in the detection of veno-venous collaterals in cases of cavopulmonary anastomosis?
Methods and materials: The study involves 11 patients (three adult and eight children) who have complex heart anomalies and underwent bidirectional Glenn. They should have a normal renal function with no general contraindication for MRI, like claustrophobia or non-compatible pacemaker or cochlear implant. They were assessed by using MDCT and short protocol MRI (TWIST, contrast-enhanced (CE) 3D whole-heart and flow studies). The study is descriptive.
Results: The study includes four female and seven male patients. We arranged the results into minor and major collaterals detected by CT and CE 3D navigator as well as capability of the twist technique to show the contrast through both pulmonary arteries and if there are collaterals or not. CT and CE 3D navigator show minor and major venous collaterals with similar accuracy. Twist technique shows the contrast passing through both pulmonary arteries and collaterals yet it could not visualise the collaterals in four cases. MRI, the only method, to calculate flow in the venous collaterals.
Conclusion: CE 3D navigator beside TWIST technique can replace cardiac CT in the assessment of Glenn and collaterals. Additionally, MRI can measure the flow.
Limitations: The small number of cases.
Ethics committee approval: Written consent was taken from patients and/or their guardian to do CT and short protocol MRI.
Funding: No funding was received for this work.
Author Disclosures:
S. Romeih: nothing to disclose
W. Elmozy: nothing to disclose
A. Samir: nothing to disclose
A. Elmogy: nothing to disclose
F. R. M. Elkafrawy: nothing to disclose
M. A. I. Gamal Elden: nothing to disclose
M. Salah: nothing to disclose
A. Soliman: nothing to disclose
A. Mourshed: nothing to disclose

MyT3 16-14 16:52
Optimised short breath-holding time protocol for subtraction coronary CT angiography
N. Xu, J. Xing, X. Meng*; Shanghai/CN*

Purpose: Subtraction CT angiography(CCTA) using a 320-slice CT scanner has recently been introduced for patients with severe calcifications. Subtraction CCTA can remove calcification from CCTA images, and reduce the misevaluation of luminal stenosis degree caused by calcification artefacts. But many patients are unable to finish the scanning protocol due to the long breath-holding time, which limits its clinical application. We explored an optimised subtraction CCTA method with a short breath-holding time. The purpose of this study was to evaluate whether the short breath-Holding time protocol for subtraction CCTA could provide better image quality compared with the conventional CCTA.
Methods and materials: A total of 12 patients with coronary calcifications were enrolled in this study. The optimised subtraction CCTA was performed using the bolus-tracking method. The mask scan was acquired before the postcontrast scan during a single breath-hold. The patients' breath-holding times were recorded. The subtraction image was obtained by subtracting the mask image data from the postcontrast image data. Subjective image quality was evaluated using a 4-point scale.
Results: The mean breath-holding time was 10.12 ± 0.75 seconds (range, 8.9–11 seconds). Average image quality was significantly increased from 2.42 ± 0.67 with conventional CCTA to 3.0 ± 0.43 with subtraction CCTA ($P < 0.05$).
Conclusion: The optimised subtraction CCTA method allows the breath-holding time to be shortened to <12 seconds and provided better image quality compared with the conventional CCTA. The technique may be applied to patients who are unable to perform a long breath-hold and improve the success rate of subtraction CCTA.
Limitations: It is a small sample research up to now. The research is going on.
Ethics committee approval: n/a
Funding: No funding was received for this work.
Author Disclosures:
N. Xu: nothing to disclose
J. Xing: nothing to disclose
X. Meng: nothing to disclose

MyT3 16-15 16:56
Very low volume of contrast material in pre-TAVI CT: how low can we get?
P. Olga, A. Wolak, R. Wolff, Y. Almagor, N. R. Bogot*; Jerusalem/IL (olgapich@mail.ru)*

Purpose: To evaluate and compare the image quality of pre-TAVI (transaortic valve implantation) CT protocol of high pitch using weight adapted reduced contrast media (CM) injection vs standard pre-TAVI protocol.
Methods and materials: Retrospective analysis of 117 (73 females) consecutive patients undergoing pre-TAVI CT on Siemens FORCE scanner. 95 patients (mean age 81±7; weight 70kg±13) using FLASH high pitch single combined heart-aorta acquisition. CM volume (Omnipaque350) and injection rate administrated per weight. 23 patients (age 79±9;80kg±24) in the standard protocol control group underwent spiral cardiac scan followed by high pitch aortic acquisition. In both groups, scan was triggered by bolus-tracking. Attenuation values (HU) and contrast-to-noise ratio (CNR) were measured at the aortic root, abdominal aorta and femorals. Image quality considered sufficient at attenuation >200HU.
Results: CM volume and injection rate were significantly lower in FLASH group compared to control group (39±9ml/ 3±0.5ml/sec vs 75±8ml/ 4.2±0.8 ml/sec; $p<0.05$). DLP in FLASH was 303±104 vs 1175±772 in control. Image quality was sufficient in FLASH and control groups respectively: root-89 (93%) vs 19 (82%) of patients, abdominal aorta-94 (99%) vs 20 (87%) and femorals-85 (89%) vs 20 (87%) (P=NS). Non-significant difference in attenuation and CNR found between two groups for root (350±100HU/16 vs 348±256HU/15.6) and abdominal aorta (372±98/HU30 vs 416±257HU/30.5). Significant decrease in femorals attenuation and CNR in FLASH group (301±109HU/23 vs 449±221HU/33; $p<0.05$). Patient weight and DLP were lower in FLASH group ($p<0.05$).
Conclusion: Using single high pitch cardiac-aortic pre-TAVI CT scan with weight-adjusted injection allows significant CM volume and radiation dose reduction with preserved images quality.
Limitations: Single institution study. The standard group was smaller than FLASH group.
Ethics committee approval: Approved by the IRB, informed consent waved.
Funding: N/A
Author Disclosures:
P. Olga: nothing to disclose
N. R. Bogot: nothing to disclose
A. Wolak: nothing to disclose
R. Wolff: nothing to disclose
Y. Almagor: nothing to disclose

MyT3 16-16 17:00
Heart rate-dependent degree of motion artefacts in coronary CT angiography acquired by a dedicated cardiac CT scanner
M. Vecsey-Nagy, B. Szilveszter, A. Jermendy, M. Kolossvary, J. Simon, Z. Drobni, B. Merkely, P. Maurovich--Horvat*; Budapest/HU (nagy.milan33@gmail.com)*

Purpose: Currently used wide detector CT scanners enable precise assessment of coronary artery disease (CAD). However, no data is available regarding the degree of motion artefacts in images acquired by the recently introduced 560-slice CardioGraphe (CG) scanner. We aimed to assess the heart rate (HR) dependent presence and degree of motion artefacts in coronary CT angiography (CCTA) scans acquired by CG compared to a conventional 256-slice CT scanner.
Methods and materials: In this retrospective study, we have compared the images of 75 patients who underwent CCTA with CG (240 ms rotation time) to 75 scans acquired by a 256-slice CT scanner (270 ms rotation time). The mean age of the groups was 57.3 years, 49.3% males. Motion artefacts were assessed using a Likert-type scale, ranging from 1 to 4 (1: non-diagnostic, 2: severe motion artefacts, 3: mild motion artefacts, 4: no motion artefacts). The patients were divided into 3 equal groups (50-50-50 patients) according to HR ranges during image acquisition (51-60/min, 61-70/min, above 71/min). The image quality of each of the three groups in both scanners was compared using Wilcoxon rank-sum test.
Results: The CG scanner had a better image quality, with reduced motion artefacts as compared to the 256-slice scanner (mean Likert-score 2.7 ± 0.9 vs 2.3 ± 0.7, respectively, $p<0.003$). The CG images had higher Likert-scores in all 3 heart rate ranges (51-60/min, 61-70/min, 71+/min), which was statistically significant in the lower 2 ranges ($p=0.025$, $p=0.043$, $p=.156$, respectively).
Conclusion: The new 560-slice CG scanner allows for CCTA image acquisition with reduced motion artefacts as compared to a 256-slice scanner. The beneficial effect of fast gantry rotation was especially present at HR below 70/min.
Limitations: Not applicable.
Ethics committee approval: Not applicable.
Funding: Not applicable.
Author Disclosures:
M. Vecsey-Nagy: nothing to disclose
B. Szilveszter: nothing to disclose
A. Jermendy: nothing to disclose
M. Kolossvary: nothing to disclose
J. Simon: nothing to disclose
Z. Drobni: nothing to disclose
B. Merkely: nothing to disclose
P. Maurovich--Horvat: nothing to disclose

MyT3 16-17 17:04
Radiological visualisation in the diagnosis of potentially life-threatening conditions of an athlete's pathological heart
B. Sergey[1], V. Sukhov[2], D. Pospelov[2], E. Achkasov[1]; *[1]Moscow/RU, [2]St. Petersburg/RU (sabondarev@yandex.ru)*

Purpose: Frequency of fatal cardiac abnormalities development in athletes resulted in an increase in mortality, which reaches 75%. With the evidence of such dangerous changes development, it becomes extremely important to make an early diagnosis of these.
Methods and materials: We examined 11 male athletes 18-23 yo without significant family history regarding the pathology of cardiovascular system, involved for 14±2 yrs in playing sports with anamnestic presence of chronic physical fatigue and heart pains that underwent clinical examination, biochemical blood tests, ECG, stress-echocardiography, 12-leads Holter-monitoring, myocardial scintigraphy with 123I-MIBG, 99mTc-tetrofosmin rest/stress SPECT and, gadolinium-enhanced MRI.
Results: Biochemical markers of cardiomyocytes' acute damage were concordant to the clinical significance of these disorders matching to complaints severity of cardiac arrhythmias. Along with these data no violations of morphology, size and function of myocardium were revealed. Results of myocardial SPECT, stress ECG-test, stress echocardiography, daily Holter monitoring had no signs of myocardial ischemia. We didn't have laboratory and other data for inflammatory myocardial damage. Early phase 123I-MIBG scintigraphy (15' p.i.) showed impaired tracer accumulation in apex, anterolateral and inferior walls down to 61-67%. In the delayed phase (240' p.i.) less significant decrease of radiopharmaceutical uptake was noted. Diffuse-focal decrease of tracer uptake by myocardial perfusion SPECT with 99mTc-tetrofosmin not exceeding 8% of LV was noted in the anteroseptal region with improvement after the physical exercise test.
Conclusion: The combined use of diagnostic methods, such as SPECT, CE-MRI, stress echocardiography, make it possible to carry out differential diagnosis, to exclude acute coronary insufficiency, acute inflammatory damage of heart, regarding changes as a variant of takotsubo syndrome.

Limitations: This study is limited by its sample.
Ethics committee approval: All patients provided informed consent for examination, treatment, data processing and use of data in scientific work.
Funding: No funding was received for this work.
Author Disclosures:
B. Sergey: Author at Sechenov Univercity
V. Sukhov: nothing to disclose
D. Pospelov: nothing to disclose
E. Achkasov: nothing to disclose

MyT3 16-18 17:08

Relationships between coronary atherosclerotic morphology of computed tomography coronary angiography and myocardial perfusion abnormalities

A. Maltseva, K. W. Zavadovsky, A. Mochula, K. Kopeva, E. Grakova*; Tomsk/RU (maltseva.alina.93@gmail.com)*

Purpose: The purpose was to assess the relationships between morphological CT-characteristics of coronary atherosclerosis and myocardial perfusion downstream in patients with an intermediate pretest probability of stable coronary artery disease (SCAD).
Methods and materials: The study group comprised 68 patients (42 men, age 63 (56;68) years) who underwent coronary computed tomography angiography (CCTA) as well as stress-rest MPI (with CT attenuation correction) on the hybrid system GE Discovery NM/CT 570C. The patients were divided into two groups: 1) moderate and large stress perfusion defect extent (SSS≥9); 2) small perfusion defect extent (SSS<9).
Results: According to the univariate logistic regression, maximum stenosis (OR 1,04; CI 1,02-1,06; p=0,0001), the sum of stenoses (OR 1,01; CI 1,00-1,01; p=0,02), Segment Stenosis Score (OR 1,14; CI 1,04-1,25; p=0,04) and CT_SS (OR 1,32; CI 1,12-1,56; p=0,01), the presence of stenosis >50% (OR 5,4; CI 1,69-17,16; p=0,004), noncalcified (OR 1,79; CI 1,11-2,87; p=0,017) and circular features (OR 2,99; CI 1,48-6,04; p=0,002) of the atherosclerotic plaques were the independent determinants of moderate and large perfusion defect. By the results to multivariable logistic analysis the combination of several CT-characteristics of coronary atherosclerosis did not improve the prognostic model.
Conclusion: Segment Stenosis Score, CT_SS as well as the noncalcified structure and circular geometry of the atherosclerotic plaques are the most significant independent predictors of moderate and large stress perfusion defects. These CT morphological characteristics could be used for risk stratification in patients with an intermediate pretest probability of SCAD.
Limitations: This is the relatively small size of the study population.
Ethics committee approval: The local research ethics committee approved this study.
Funding: No funding was received for this work.
Author Disclosures:
A. Maltseva: Author at Cardiology Research Institute, Tomsk National Research Medical Center, Russian Academy of Sciences, Tomsk, Russia
K. W. Zavadovsky: Author at Cardiology Research Institute, Tomsk National Research Medical Center, Russian Academy of Sciences, Tomsk, Russia
K. Kopeva: Author at Cardiology Research Institute, Tomsk National Research Medical Center, Russian Academy of Sciences, Tomsk, Russia
E. Grakova: Author at Cardiology Research Institute, Tomsk National Research Medical Center, Russian Academy of Sciences, Tomsk, Russia
A. Mochula: Author at Cardiology Research Institute, Tomsk National Research Medical Center, Russian Academy of Sciences, Tomsk, Russia

MyT3 16-19 17:12

Aortic valve calcification scoring with computed tomography: the impact of advanced modelled iterative image reconstruction

R. M. M. Hinzpeter, F. Maisano, A. M. Kasel, F. Tanner, H. Alkadhi, M. Eberhard*; Zurich/CH (Ricarda.Hinzpeter@usz.ch)*

Purpose: To investigate whether advanced modelled iterative reconstruction (ADMIRE) of CT scans affects aortic valve calcification (AVC) scoring and likelihood categorisation of severe aortic stenosis.
Methods and materials: In this IRB-approved retrospective study, we included 100 consecutive patients with symptomatic aortic stenosis (median age: 77 years; 39 females) undergoing CT prior to transcatheter aortic valve replacement between 03/2019 and 10/2019. CT scans dedicated to calcium scoring were performed according to current guidelines and reconstructed with filtered back projection (FBP) and ADMIRE at strength levels 1-5. AVC Agatston scores were evaluated using a commercially available software platform. Gender-specific AVC Agatston score cut-off values were applied according to the current European Society of Cardiology recommendations to assign patients to different likelihood categories of aortic stenosis (unlikely to very likely). AVC scores are shown as median and interquartile-range (IQR). Friedman test was applied to analyse interval- and ordinal-scaled data.
Results: Each reconstruction algorithm produced statistically significant numerical AVC Agatston scores (p<0.001). Median AVC Agatston score for image reconstruction with FBP was 2527 (IQR: 1602-3673) and decreased with increasing ADMIRE strength levels. Image reconstruction with ADMIRE at strength level 5 showed the lowest median AVC Agatston score (2281, IQR: 1357-3362). Likelihood categorisation of severe aortic stenosis was significantly different between image reconstruction algorithms (p<0.001). For image reconstruction with FBP, 55 cases were assigned to the “very likely” category, compared to 44 cases performing image reconstruction with ADMIRE at strength level 5.
Conclusion: Image reconstruction of CT scans dedicated to AVC scoring with ADMIRE causes a significant decrease of AVC scores with increasing ADMIRE strength levels and therefore affects likelihood categorisation of severe aortic stenosis.
Limitations: This study is performed in a single-site, one vendor.
Ethics committee approval: The IRB approved, written informed consent obtained.
Funding: No funding was received for this work.
Author Disclosures:
M. Eberhard: nothing to disclose
R. M. M. Hinzpeter: nothing to disclose
F. Maisano: nothing to disclose
A. M. Kasel: nothing to disclose
F. Tanner: nothing to disclose
H. Alkadhi: nothing to disclose

MyT3 16-20 17:16

Histological validation of cardiac magnetic resonance T1 mapping for evaluation the variation in myocardial infarction on day 1, day 7 and 3 months in a swine model

L. Zhang, Y. Guo, H. Xu, M. Yang, R. Xu, Z. Yang, C. Fu*; Chengdu/CN (zhanglu_scu2018@163.com)*

Purpose: Our aims were to explore 1) how native T1 and extracellular volume (ECV) measured on CMR changed with time in infarcted myocardium; 2) the correlation between ECV and native T1 against histology-evaluated ECV.
Methods and materials: A total of 22 pigs were subjected to occlude anterior descending artery and underwent serial CMR examinations at acute (within 24h, n = 22), subacute (7 days, n = 13) and chronic (3 months. n = 6) after myocardial infarction (MI). The CMR protocol included cine, Modified Look-Lock Inversion (MOLLI) recovery and late gadolinium enhancement (LGE). Hematoxylin-eosin and Masson trichrome staining were conducted following scanning. The CMR exams and histopathological staining were performed in the same day.
Results: Infarcted native T1 changed with peaking at 7 days while a progressively increasing was observed in ECV during 3 months. The histology-evaluated ECV demonstrated a well correlation in the comparison with native T1 (acute, $r = 0.89$, $p < 0.001$; subacute, $r = 0.94$, $p < 0.001$; chronic, $r = 0.83$, $p < 0.001$); Also, a high correlation was found when compared with CMR-measured ECV (acute, $r = 0.89$, $p < 0.001$; subacute, $r=0.96$, $p < 0.001$; chronic, $r = 0.82$, $p < 0.001$).
Conclusion: Both native T1 and ECV in infarcted myocardium demonstrated dynamical changed with time. This may be explained by the severe interstitial oedema and the progressive collagenous deposition. These results have implication for the timing of CMR imaging early after MI.
Limitations: The experimental setup did not allow for baseline examination and early imaging after MI.
Ethics committee approval: This study was approved by the institutional ethics review board.
Funding: No funding was received for this work.
Author Disclosures:
L. Zhang: Author at West china second university hospital, Speaker at West china second university hospital
Y. Guo: Author at West china second university hospital
H. Xu: Author at West china second university hospital
M. Yang: Author at West china second university hospital
R. Xu: Author at West china second university hospital
Z. Yang: Author at In infarcted myocardium, (A) native T1 time was peaking at 7 days, while (B) ECV presented a progressively increasing at 3-month after MI. Error bars represent the standard deviation (SD). * p<0.05
C. Fu: Author at In infarcted myocardium, (A) native T1 time was peaking at 7 days, while (B) ECV presented a progressively increasing at 3-month after MI. Error bars represent the standard deviation (SD). * p<0.05

MyT3 16-21 17:20

Evaluation of image quality and radiation dose with prospective ECG-gated 80-slice CT angiography, in 182 consecutive children examinations with congenital heart disease

P. de Cambourg, P. Guérin, H. Necib, K. Warin Fresse; *Nantes/FR*

Purpose: Computed tomography angiography (CTA) is a reliable imaging tool to evaluate children congenital heart disease (CHD) but requires radiation exposure. This study aims to investigate image quality and radiation dose with a prospective electrocardiogram (ECG)-gated 80-slice CTA, in 182 consecutive children examinations with CHD.
Methods and materials: 182 consecutive examinations performed with a prospective ECG-gated 80-slice CTA from March 2016 to December 2017 in Nantes university hospital were retrospectively analysed. Radiation dose was assessed by dose length product (DLP) and effective dose (E). The objective quality image was assessed by contrast to noise ratio (CNR) and subjective quality image by two radiologists with a 10-point scale evaluating visualisation of coronary arteries. Correlation between quality image, radiation dose, age, weight, heart rate was analysed.
Results: DLP and E were 29.3±15.5mGy.cm and 0.6±0.2mSv respectively. Agreement between radiologists for subjective image quality was 0.79. Subjective image quality score was significantly better ($p<0.01$) with higher age, weight, DLP and lower heart rate in univariate analysis. CNR was significantly lower with increasing weight and DLP ($p<0.05$) but there was no correlation between CNR and age and heart rate.
Conclusion: Prospective ECG-gated 80-slice CTA is performing for the evaluation of children CHD with good image quality and low radiation dose. Visualisation of small structures is better when age and weight increase, heart rate decreases and when the radiation dose is more important. CNR evolves in the opposite side to subjective image quality score. It seems less appropriate to assess image quality from the clinical view of the radiologist.
Limitations: The study is retrospective.
Ethics committee approval: n/a
Funding: No funding was received for this work.
Author Disclosures:
P. de Cambourg: nothing to disclose
K. Warin Fresse: nothing to disclose
P. Guérin: nothing to disclose
H. Necib: nothing to disclose

MyT3 16-22 17:24

Myocardial extracellular volume assessment in a cohort of oesophagal cancer patients using routine contrast-enhanced CT

D. Capra, C. B. Monti, C. Gumina, A. Luporini, F. Lombardi, E. Asti, L. Bonavina, F. Sardanelli, F. Secchi; *Milan/IT (davide.capra@unimi.it)*

Purpose: To reproduce the feasibility of estimating myocardial extracellular volume fraction (ECV) through routine contrast-enhanced computed tomography (CT) in a cohort of oesophagal cancer patients and to investigate the correlation between an increase in ECV and exposure to radiation therapy.
Methods and materials: After ethics committee approval, patients with oesophagal cancer who had undergone routine CT examinations before and after radiation therapy were retrospectively analysed. For each patient, we considered pre-treatment CT and the post-treatment CT with the longest follow-up interval available. Patients with pre-existing cardiovascular conditions, who previously had undergone cardiotoxic chemotherapy, or with heavily artefacted CT images were excluded. ECV was measured using round regions of interest (ROI) in the septum at mid-level, accounting for movement by excluding borders, and in the left ventricular blood pool at the same level. Septal ECV was calculated using the formula proposed by Bandula et al. T-test for paired data was used to compare distributions.
Results: Twenty-one subjects were analysed, with a mean age of 64±18 years, four of which were women. Pre-treatment mean ECV was 27.89±3.54% and post-treatment mean ECV at follow-up was 32.08±4.51% with a median interval of 197 days. Post-treatment ECV was significantly higher than pre-treatment ECV ($p<0.001$).
Conclusion: ECV in oesophageal cancer patients showed to be significantly higher after treatment. Its rise after radiation therapy could play a role in the screening of myocardial condition in oesophageal cancer patients undergoing such treatment.
Limitations: This study is limited by its small sample size and its retrospective, monocentric nature.
Ethics committee approval: Ethics committee approval was obtained. Written informed consent was waived.
Funding: No funding was received for this work.
Author Disclosures:
C. Gumina: nothing to disclose
D. Capra: nothing to disclose
C. B. Monti: nothing to disclose
A. Luporini: nothing to disclose
F. Lombardi: nothing to disclose
E. Asti: nothing to disclose
L. Bonavina: nothing to disclose
F. Sardanelli: Grant Recipient at Bayer, Grant Recipient at General Electric, Grant Recipient at Bracco, Speaker at Bayer, Speaker at General Electric, Speaker at Bracco, Advisory Board at Bracco
F. Secchi: nothing to disclose

Sunday, March 15

08:30 - 10:00 **Coffee & Talk 1**

Radiographers

RPS 1714

Medical imaging challenges: nuclear medicine and radiography

Moderators:
D. O'Leary; Newcastle/UK
N.N.

RPS 1714-1 08:30

Preclinical multimodal imaging for a new theranostic approach in oncology

M. Gulizia, J. N. Hyacinthe, O. Lorton, L. A. Crowe, R. Salomir*; Geneva/CH*

Purpose: In the framework of developing theranostic nanotechnology in oncology, we develop and optimise methods to improve local deposition of PFOB nanodroplets in tumours using high-intensity-focused ultrasound (HIFU). We optimised a multimodal imaging pre-clinical protocol to evaluate the efficacy of HIFU modulated accumulation of nanodroplets in tumours.
Methods and materials: We compared treatment and control groups. We grafted tumour 4T1 cells subcutaneously. We injected retro-orbital 300 µl of PFOB. HIFU treatment was performed after injection and guided with MRI. We used MR-thermometry for the temperature control induced by HIFU. The PFOB was analysed with 19F-MRI and fluorescence imaging. We compared concentrations 1 and 24 hours post-treatment to evaluate the efficacity of the HIFU.
Results: The treatment group presented with higher concentrations of PFOB in the tumour. We used a Mann-Whitney U test. P=0.0339 (alpha 0.05). HIFU treatment probably increased the PFOB deposited in the tumour. The MR thermometry sequence was sufficient for this control. The 19F MRI sequence qualitatively showed colocalisation of fluorine in the tumour but was not quantitative enough. Fluorescence imaging allowed quantification of PFOB.
Conclusion: We demonstrated the feasibility of a mechanical HIFU procedure to significantly increase the local deposition of PFOB nano-emulsion in tumours. This work opens promising perspectives for developing a theranostic approach in oncology. The means of control are sufficient for this study.
Limitations: The limited sample size.
Ethics committee approval: In vivo experiments have been conducted under the Swiss law for animal experimentation [Art.18 (LPA), Art.141 (OPAn), Art.30 Ordonance sur l'expérimentation animale]. Experimental protocol has been evaluated and approved by the cantonal veterinary office of [GE/140/1].
Funding: ERANet EuroNanoMed2 program (grant "Sonotherag") and the Swiss National Foundation of Science (grant 31NM30_152045).
Author Disclosures:
M. Gulizia: Author at HEDS
R. Salomir: Author at HUG, Research/Grant Support at HUG
J. N. Hyacinthe: Author at HEDS
O. Lorton: Author at HUG
L. A. Crowe: Author at HUG

RPS 1714-2 08:36

Multimodal and theranostic iodinated-porphyrins contrast agents: synthesis, x-ray attenuation, and cytotoxicity evaluation

R. M. S. C. Pereira[1], C. Luis[2], M. D. G. P. M. S. Neves[1], R. Fernandes[2], M. D. A. F. Faustino[1]; *[1]Aveiro/PT, [2]Porto/PT (ruimpereira@ua.pt)*

Purpose: Porphyrins, due to their chemical, photophysical, and biological properties, could conjugate in a single molecule; drug properties with multimodal and/or theranostics applications. Such properties can be an excellent answer to the challenging demand of novel contrast media acting as multimodal and theranostic agents (MTCA). Those type of compounds were already studied in magnetic resonance (MRI) and near-infrared fluorescence imaging, but very few studies were developed in iodinated contrast media. Our aim was to develop new iodinated-porphyrin contrast agents with suitable x-ray beam attenuation and low toxicity, which can potentially be used as MTCA.
Methods and materials: Iodinated-porphyrin derivatives were prepared through 3 synthetic approaches. X-ray beam attenuation was assessed measuring Hounsfield units (HU) after compound exposure to a standardised computed tomography scan. Cytotoxicity was assessed in 3 cell lines exposed to the new iodinated-porphyrins derivatives using the MTT cellular viability assay. Results were internally compared with iomeprol, a contrast agent already on the market.
Results: 12 stable iodinated-porphyrin derivatives were successfully obtained with moderate to good yields. All compounds showed an x--ray beam attenuation ability similar to iomeprol (iomeprol: 488.2±1.2 HU; compounds: min-Por7 with 461.2±2.5 HU; max-Por4 with 483.5±2.6 HU). 7 of the iodinated-porphyrin derivatives showed similar viability to iomeprol, although only Por1 and Por2 presented better IC_{50} than iomeprol.
Conclusion: All synthesised compounds showed a proper x-ray beam attenuation ability to been used as contrast media. Por1 and Por2 (the last one with multimodal properties) showed decreased cytotoxicity when compared with iomeprol. Also, Por5, Por11, and Por12 showed promisor cytotoxicity evaluation results.
Limitations: Only toxicity in the dark was evaluated.
Ethics committee approval: n/a
Funding: Financial support for the QOPNA research Unit (FCT UID/QUI/00062/2019) by University of Aveiro and FCT/MCT.
Author Disclosures:
R. M. S. C. Pereira: nothing to disclose
M. D. A. F. Faustino: nothing to disclose
C. Luis: nothing to disclose
M. D. G. P. M. S. Neves: nothing to disclose
R. Fernandes: nothing to disclose

RPS 1714-3 08:42

Iodinated contrast media and their effect on thyroid function: routines and practices among diagnostic imaging departments in Norway

A. Rusandu, B. Sjøvold, E. Hofstad, R. J. Reidunsdatter*; Trondheim/NO (albertina.rusandu@ntnu.no)*

Purpose: In order to minimise adverse effects or injuries related to the effect of iodinated contrast media (ICM) on the thyroid, international guidelines recommend developing routines for the identification and management of patients at risk of developing thyroid dysfunction. This study aimed to investigate thyroid-related ICM administration routines among diagnostic imaging departments in Norway.
Methods and materials: A cross-sectional survey including 24 hospitals and 75 respondents (37 radiographers and 15 radiologists) with a 69% response rate was conducted. The survey covered routines for assessment and the management of risk-patients and rationale for the routines.
Results: The findings show a variation in routines among hospitals. The use of checklists as recommended by international guidelines was quite modest (15%), the respondents preferred other methods to identify risk and contraindications. Only 20% reported checking for scheduled thyroid scintigraphy or radioactive iodine therapy. 42% did not have thyroid-related ICM routines and the main reported reason was a lack of knowledge on the topic. Radiographers and radiologists expressed uncertainty about each other's roles and routines.
Conclusion: This study revealed the need for optimisation of routines regarding ICM administration to thyroid-related risk-patients. Training courses and activities that improve the interprofessional network might facilitate effective implementing of the guidelines.
Limitations: The low number of participant radiologists, which might reduce the precision of estimate and mask potential significant differences between the occupational groups.
Ethics committee approval: The Regional Committee for Medical and Health Research Ethics waived the need for approval as the project was considered a quality assurance project which did not involve any health-related or personal information. Participants were informed about the purpose of the study and that submitting the survey was regarded as implied consent.
Funding: No funding was received for this work.
Author Disclosures:
A. Rusandu: nothing to disclose
B. Sjøvold: nothing to disclose
E. Hofstad: nothing to disclose
R. J. Reidunsdatter: nothing to disclose

RPS 1714-4 08:48

A statistical comparison of a triage tool with exercise myocardial perfusion scan (MPS) data in a cohort of Maltese patients

K. Borg Grima[1], P. Bezzina[2], L. A. Rainford[3]; *[1]Naxxar/MT, [2]Malta/MT, [3]Dublin/IE (karen.borg-grima@um.edu.mt)*

Purpose: To investigate whether the results of a pre-determined triage tool recorded a statistically significant relationship with MPS results. The triage tool had been designed to assist in identifying patients who might not achieve the necessary exercise level.
Methods and materials: The triage tool was composed of 11 clinical questions and was used to collect data from 300 patients referred for MPS exercise stress testing in the state general hospital in Malta. Data was collected from March-June 2018. Scan data included the duration of exercise stress tests, results of the Duke treadmill score, summed stress score (SSS), and the total perfusion deficit (TPD).
Results: The tool demonstrated statistical significance in identifying patients who had a reduced functional ability, therefore being incapable of successfully completing their MPS treadmill exercise stress test. Gender (p<0.001), chest

pain when walking uphill (p<0.001), and the presence of previous revascularisation procedures (p=0.015) were all found to be statistically related to the treadmill exercise test duration. Moreover, a statistical significance was found between the triage tool results and the results of the DTS (p<0.001), SSS (p=0.048), and the TPD (p<0.001) scores.
Conclusion: The findings of the study identified that out of 82 participants who had a positive triage tool result, 93.9% had an inconclusive exercise stress test, confirming the value of this tool as a means of triaging patients prior to undergoing MPS exercise stress tests.
Limitations: The sample of participants was taken over a specific period of time, therefore further research is recommended to collect data prospectively over a longer timeframe.
Ethics committee approval: This study was performed following ethical permission from the University of Malta Research Ethics Committee.
Funding: No funding was received for this work.
Author Disclosures:
K. Borg Grima: nothing to disclose
P. Bezzina: nothing to disclose
L. A. Rainford: nothing to disclose

RPS 1714-5 08:54
The optimisation of computed tomography dose levels in ^{18}F-FDG PET-CT oncology examinations
R. A. F. Nunes, J. M. T. E. Rio, J. Santos*; Coimbra/PT (nunesritafa@gmail.com)*

Purpose: To evaluate CT dose values used on PET-CT with ^{18}F-FDG for oncology examinations and to optimise the institution practices in order to reduce patient exposure.
Methods and materials: The study was carried out in two phases. A retrospective phase, phase 1, analysed the clinical practice based on CT dose descriptors, acquisition parameters, and the influence of arm position on whole-body PET-CT protocols with ^{18}F-FDG on Philips Gemini GXL 16 and Siemens Biograph 6 equipment. Diagnostic reference levels (DRL's) were established per CT scanner. During phase 2, several protocols were tested on a PBU-60 anthropomorphic phantom in order to analyse the dose reduction in comparison to the current protocol. Objective image quality analysis was performed based on regions of interest.
Results: The obtained DRLs were in accordance with the literature. Significant differences were founded in examination dose values performed with different patient arm positioning. Significant differences were also founded in CT dose values per equipment PET-CT scanner using the same protocol.
Conclusion: This study contributed to the harmonisation of the procedures of ^{18}F-FDG PET-CT in oncological patients. Experimental tests revealed the potential for optimisation with a lower impact on image noise.
Limitations: The experimental tests were similar, however, the PET-CT equipment technology differences didn't allow the testing of the exact the same protocols.
Ethics committee approval: Ethical approval was obtained from the institution.
Funding: No funding was received for this work.
Author Disclosures:
J. Santos: nothing to disclose
J. M. T. E. Rio: nothing to disclose
R. A. F. Nunes: nothing to disclose

RPS 1714-6 09:00
An assessment of mobile radiography services in nursing homes using the model for assessment of telemedicine applications
E. Kjelle, K. B. Lysdahl, A. M. Myklebust, H. M. Olerud*; Kongsberg/NO (elin.kjelle@usn.no)*

Purpose: To assess mobile radiography services in nursing homes using the model for assessment of telemedicine applications (MAST).
Methods and materials: As MAST is a multidisciplinary assessment, multiple methods were used. Six out of 7 domains in MAST was assessed. A systematic literature review and statistical analysis were used to assess the following domains: (1) health problem and description of the application, (2) safety, (3) clinical effectiveness, and (4) patient perspectives. Cost-analysis using a decision-model was used for assessment of (5) economic aspects. Individual semi-structured interviews were used to assess (6) organisational aspects.
Results: Mobile radiography services were found to be safe with adequate image quality and the examinations affecting treatment and care (domains 1-3). The number of examinations was significantly higher in areas with mobile radiography; 0.5 per nursing home beds compared to 0.36 without this service; p=<0.001 (domain 1). The treatment given became more personalised when an examination was made in the nursing home. Patients and their relatives prefered mobile radiography (domain 4). In domain 5, mobile radiography was found to reduce costs by 30% compared to hospital-based services, a significant difference; p=<0.001. Managers experienced a need for organisational change when implementing mobile radiography (domain 6).
Conclusion: A mobile radiography service is a safe, high-quality telemedicine service, which contributes to increasing the quality of care and reducing costs. However, to facilitate a full-scale implementation of these services, there seems to be a need for changing the way health services are funded and managed.
Limitations: This PhD-project on mobile radiography services was mainly assessed in a Norwegian context, limiting its transferability.
Ethics committee approval: Approved by REC - project no. 2468. Approved by NSD - ref. 45739
Funding: No funding was received for this work.
Author Disclosures:
E. Kjelle: nothing to disclose
K. B. Lysdahl: nothing to disclose
A. M. Myklebust: nothing to disclose
H. M. Olerud: nothing to disclose

RPS 1714-7 09:06
Consideration of anatomical side markers by radiographers and student radiographers
L. A. Rainford, J. M. Grehan, M. O'connor, J. G. Stowe, M. D. Davis, E. McDermott, R. Toomey*; Dublin/IE (louise.rainford@ucd.ie)*

Purpose: The advent of digital radiography facilitated the easy addition of digital anatomical side markers to medical images, however, this is not considered best practice. Reported here is a subset of a larger study investigating how qualified medical doctors, radiographers, and students review image quality in general, with a particular focus on the importance of anatomical side markers.
Methods and materials: The research participants were 57 qualified radiographers and 65 student radiographers who volunteered at the EFRS Research Hub 2019 . They completed an image-viewing task whereby they reviewed 26 projection radiographs and decided if the images were ready to be sent to the PACS system for reporting. They could respond: a) optimal=send to PACS, b) acceptable=but could be improved, and c) unacceptable=action required before sending. They were not prompted to consider side markers or any other factors in particular. 8 images had no side marker, 7 had a digital marker, and 11 a lead marker.
Results: Participants rated 21.71% (qualified)/23.27% (students) of images with no marker as optimal, with a further 38.6%/39.42% rated "acceptable", implying that 60.31%/62.69% of images would be sent to PACS without a marker. 32.75% of images with a digital marker were rated "optimal=send to PACS".
Conclusion: Radiographers may underestimate the importance of anatomical side markers and further research is warranted.
Limitations: Selection bias; participants were present at ECR and therefore may be more research/professionally active. Participants from some countries/institutions may be overrepresented. Language may have inhibited understanding of the task in participants without English as a first language.
Ethics committee approval: The home institution Human Research Ethics Committee declared the work exempt from full review.
Funding: No funding was received for this work.
Author Disclosures:
L. A. Rainford: nothing to disclose
R. Toomey: nothing to disclose
J. M. Grehan: nothing to disclose
M. O'connor: nothing to disclose
J. G. Stowe: nothing to disclose
M. D. Davis: nothing to disclose
E. McDermott: nothing to disclose

RPS 1714-8 09:12
Radiographer optimisation of AEC use: keeping it "automatic" but taking back "control"
K. Matthews, J. Creedon, A. Dalton, E. Higgins, R. Motyer*; Dublin/IE (kate.matthews@ucd.ie)*

Purpose: This presentation reports 4 separate but associated studies which shared the common aim of establishing whether the use of automatic exposure control in direct digital radiography could be better optimised in some Irish hospitals.
Methods and materials: Various phantoms (PIXY without and with added layers of fat; ATOM paediatric phantoms age 1,5, 10, and 15) were x-rayed in 3 hospitals to simulate chest, pelvis, and lumbar spine radiography. AEC settings such as patient size and system speed were varied in order to change the dose constant controlling the AEC. The dose area product (DAP) and exposure index (EI) were recorded. Selected images were evaluated; noise levels were measured through the calculation of the signal-difference-to-noise ratio (SDNR) and the visual image quality was assessed through a visual grading analysis

(VGA). At each site, all measurements were compared with those obtained at prevailing clinical exposures.
Results: Radiographers can manipulate the AEC dose constant using the patient size and system speed selections. Such manipulations produced considerable (up to 54%) reduction in DAP. While DAP and SDNR values decreased with reduced AEC dose constant, the visual image quality as appraised by VGA was preserved to a point, demonstrating the maintenance of diagnostic image quality. The dose and image quality data from these phantom experiments showed consistent findings across examinations representing adults, obese adults, and children.
Conclusion: For the examinations tested, the dose constant programmed into the AEC in all sites results in an unnecessarily large dose.
Radiographers can and should manipulate the AEC settings to control automatic exposure and thus better optimise examinations.
Limitations: A phantom study is appropriate to this experimental research. The findings justify further investigation of AEC manipulation during patient examinations with an evaluation of clinical images.
Ethics committee approval: n/a
Funding: No funding was received for this work.
Author Disclosures:
K. Matthews: nothing to disclose
E. Higgins: nothing to disclose
R. Motyer: nothing to disclose
J. Creedon: nothing to disclose
A. Dalton: nothing to disclose

RPS 1714-9 09:18
The effect of non-optimal tube voltage on radiation dose in lumbar spine radiography
E. Alukić, N. Mekis*; Ljubljana/SI*

Purpose: To investigate how exposure parameters or, more precisely, the tube voltage affects radiation dose to the patient in lumbar spine imaging.
Methods and materials: The data for patient weight, height, image field size, and DAP were collated for 100 patients that were referred for lumbar spine radiography on 2 different x-ray units. The first unit used the tube voltage in line with the European guidelines (79kV) while the other unit's tube voltage was not in line with the EU guidelines (63 kV). The data was collected only for the AP projection. After the data collection, the calculations of BMI, effective dose, and dose to selected organs were calculated using a PCXMC2.0 Monte Carlo simulation program.
Results: No statistically significant difference was found between the BMIs of the compared groups (p=0.671). When the optimal exposure parameters were used, the DAP value was lower by 79% (p<0.001), the effective dose by 62% (p<0.001), and the average dose to the organs by 73% (p<0.001). The image field was significantly larger when the optimal parameters were used. Therefore, the dose difference should be even higher when the optimal exposure parameters were used if the field size would be the same.
Conclusion: Based on the results, we can conclude that the DAP, effective dose, and dose to organs are significantly higher when the exposure parameters used are not in line with the European guidelines.
Limitations: The data was obtained for AP projection only and the image quality was not assessed in the study.
Ethics committee approval: The national medical ethics committee and patient consent form were obtained prior to the study.
Funding: No funding was received for this work.
Author Disclosures:
N. Mekis: Speaker at University of Ljubljana, Faculty of Health Sciences
E. Alukić: nothing to disclose

RPS 1714-10 09:24
The optimisation of the lateral lumbar spine projection using an air-gap technique
A. Bellizzi, F. Zarb*; Msida/MT (andrea.bellizzi.15@um.edu.mt)*

Purpose: To investigate the feasibility of replacing an anti-scatter grid with an air-gap technique to achieve a dose reduction for lateral lumbar spine radiography while maintaining image quality on a direct digital radiography (DDR) system.
Methods and materials: The study comprised of 2 phases. Phase 1 was an experimental study using an anthropomorphic phantom to identify the optimal air-gap technique. Phase 2 was performing lateral projections of the lumbar spine on patients (n=50). Patients were randomly assigned into a control group (n=25, imaged using the anti-scatter grid) and an experimental group (n=25, imaged using the air-gap technique). The dose area product (DAP) of all examinations was recorded, keeping all other variables constant. Image quality evaluation was performed by 5 radiologists performing absolute visual grading analysis (VGA) using an image quality score tool, with the resultant scores analysed using visual grading characteristics (VGC).
Results: A 10 cm air-gap in conjunction with a source-to-image distance (SID) of 121 cm was found as the optimal air-gap technique. The clinical application of this technique resulted in a statistically significant (p<0.05) reduction in the radiation dose of 72% in terms of DAP. Image quality scores were higher for the anti-scatter grid but the variation between the image quality of the two techniques was not significant (p>0.05).
Conclusion: The results imply that replacing the anti-scatter grid with an optimal air-gap technique in lateral lumbar spine digital radiography provides a significant dose reduction whilst still maintaining diagnostic image quality.
Limitations: Differences in lateral thickness was a variable, limited by matching mean thickness for both groups. More air-gap/SID combinations were available, but particular distances were due to the physical room limitations.
Ethics committee approval: Approval obtained from the University of Malta Research and Ethics Committee.
Funding: No funding was received for this work.
Author Disclosures:
A. Bellizzi: nothing to disclose
F. Zarb: nothing to disclose

RPS 1714-11 09:30
The influence of optimal collimation on radiation dose and image quality in thoracic spine radiography
A. Pažanin[1], D. Škrk[2], N. Mekis[2]; [1]*Dubrovnik/HR,* [2]*Ljubljana/SI (apazanin@gmail.com)*

Purpose: To determine the change of radiation dose to the patient and impact on image quality when the collimation referred to in the professional literature is used for thoracic spine radiography.
Methods and materials: The study was performed on 84 patients who were referred for thoracic spine radiography in a Croatian hospital using a CR imaging system. Patients were randomly divided into 2 equal groups. The first group was imaged with the current collimation protocol and the second group with the collimation protocol mentioned in the professional literature. For each patient, weight and height, image-field size, exposure conditions, and DAP were measured while the effective dose and absorbed organ doses were calculated using the PCXMC Monte-Carlo simulation method. Image quality was assessed by 2 radiologists and 1 radiographer using the image software ViewDEX.
Results: There was no statistically significant difference in BMIs between the groups. With the optimal usage of collimator, it was found that the size of the primary field in the AP projection was reduced by 45% (p<0.001) and in the LAT projection by 41% (p<0.001). The study also showed reduced values of DAP for AP projection by 34% (p=0.007) and for LAT projection by 23% (p=0.040). The effective dose was reduced by 54% (p<0.001) for AP projection and 29% (p<0.001) for LAT projection. The mean absorbed dose to selected organs decreased by 26% in the AP projection and 28% in the LAT projection. Image quality evaluation showed improvement in AP projection by 13% (p=0.001) and in LAT projection by 15% (p<0.001).
Conclusion: Optimal collimation in thoracic spine imaging has a strong influence on the reduction of patient exposure to radiation and the improvement of image quality.
Limitations: n/a
Ethics committee approval: Ethics committee approval obtained.
Funding: No funding was received for this work.
Author Disclosures:
A. Pažanin: nothing to disclose
D. Škrk: nothing to disclose
N. Mekis: nothing to disclose

RPS 1714-12 09:36
Automating a generic performance assessment of plain radiography imaging systems
R. Us, N. Mekis*; Ljubljana/SI (rok3us@gmail.com)*

Purpose: To produce a transparent algorithm with the capacity to quickly and cheaply measure the relative performance of plain radiography imaging systems (IS).
Methods and materials: We used an ETR-1 test plate in combination with several plain radiography IS based on both CR and DR detector technology. We collected 20 radiographs for each focal spot (FS) setting using every IS. The test plate was placed at 20 mm intervals along the z-axis in order to reveal the potential impact of the anode heel effect and focal effect on image quality. We used exposures of 0.5 mAs at 81 kVp in order to avoid noise elimination and saturation. We upgraded our pilot FIJI macro to include affine image transformation functionality and DICOM header interaction. The macro was used to carry out the consistent characterisation of ETR-1's line-pair segments. This data was exported to a series of spreadsheets which were subjected to

percentile-based formatting as well as an absolute threshold. We also compared equivalent data points belonging to different FS sizes using subtraction.
Results: Our results take the form of 1 spreadsheet for each combination of IS and FS setting, containing contrast maintenance values for 20 different spatial frequencies belonging to each exposure. Percentile-based formatting revealed a deterioration of image quality at the margin of every FOV. This effect was more pronounced on the anode side. Threshold implementation revealed minimum levels of contrast at spatial frequencies consistent with each datasets' respective IS limiting spatial resolution. Subtraction revealed that larger FS produce lower quality radiographs.
Conclusion: Our upgraded FIJI macro appears to possess the capacity to produce useful and accurate assessments of image quality in plain radiography.
Limitations: Only one set of exposure conditions was used.
Ethics committee approval: n/a
Funding: No funding was received for this work.
Author Disclosures:
R. Us: nothing to disclose
N. Mekis: nothing to disclose

RPS 1714-13 09:42
Exposure factors selection: a new model for patients with obesity in projection radiography
S. J. M. Alqahtani, K. Knapp, J. R. Meakin, R. M. Palfrey*; Exeter/UK (sa512@exeter.ac.uk)*

Purpose: High radiation doses and dose variations when imaging obese patients are reported in the literature. This is of concern, especially with the high prevalence of obesity. This study reports new exposure factor prediction models that can be implemented in digital radiography.
Methods and materials: Dose optimisation experiments were conducted using a factorial design method. 5 bespoke phantoms with different sizes were used along with a Multi Fusion Max Siemens unit. Image quality was assessed physically and visually, and the DAP used as the dose measure. A mAs prediction model was produced based on the exposure factors (kVp, SID, and filtration) of images with the highest FOM. The data was analysed using Minitab software.
Results: Fixed kVp (75) with 125 cm of SID and 0.3 mm filtration of Cu were observed to produce the best image quality with the lowest dose across all phantoms. The mAs best prediction model was created based on fixed kVp, SID, and filtration with r^2=98.
Conclusion: The results of the current study prove a promising future for image quality improvement in obese patients. A mAs prediction model can be used as a preliminary guide to optimising image quality and minimising radiation dose in obese patients. More studies need to be conducted using other CR and DR systems.
Limitations: Only one digital system was used and the study focused on lumbar spine radiograph.
Ethics committee approval: No ethical approval was needed.
Funding: The PhD fund through Najran University.
Author Disclosures:
S. J. M. Alqahtani: nothing to disclose
K. Knapp: nothing to disclose
J. R. Meakin: nothing to disclose
R. M. Palfrey: nothing to disclose

RPS 1714-14 09:48
The optimisation of DR chest x-ray images using artificial intelligence: a pilot study
G. de Vries[1], A. England[2], H. Bijwaard[1], A. van der Heij-Meijer[3], P. H. Hogg[2]; *[1]Haarlem/NL, [2]Salford/UK, [3]Groningen/NL (geert.devries@inholland.nl)*

Purpose: Contemporary approaches to optimisation often involve physical phantoms which represent human anatomy. Images are analysed using mathematical techniques. Inferences are then made to predict whether abnormalities would be visible in human images. Such approaches have limitations, such as that some abnormalities are not included and phantoms are simple representations of anatomy. We report our initial work to determine whether artificial intelligence (AI) can be used in dose optimisation with anthropomorphic phantoms containing abnormalities.
Methods and materials: A deep convolutional neural network (DCNN) was trained on human chest x-ray images. PBU-60 anthropomorphic chest phantom images with synthetic nodules at 5 different locations and a 'no nodule condition' were acquired using 65kVp-125kVp in 10kVp steps; mAs was set to automatic exposure control (AEC) level, quarter, half, double, and four times AEC. SID was 200 cm. For each nodule condition, 4 phantom thicknesses were used: 0 cm, 2.5 cm, 5 cm, and 7.5 cm of PMMA. ROC area under the curve (AUC), sensitivity, and specificity were calculated from the output probabilities of DCNN for each kVp-mAs combination. Adequate image quality was considered at AUC >0.9, sensitivity>0.9, and specificity>0.6.
Results: For all exposures, >AEC the AUC was ≥0.9. Image quality was adequate for tube load half AEC at 85kVp suggesting possible dose reduction, for AEC at 85-95kVp suggesting mid-range tube potential settings as optimal, and for double AEC at 75-95kVp and four times AEC at 65-105kVp supporting the dose creep phenomenon.
Conclusion: These preliminary results suggest AI has the potential to be used in dose optimisation with anthropomorphic chest phantoms.
Limitations: n/a
Ethics committee approval: n/a
Funding: No funding was received for this work.
Author Disclosures:
G. de Vries: nothing to disclose
P. H. Hogg: nothing to disclose
A. England: nothing to disclose
A. van der Heij-Meijer: nothing to disclose
H. Bijwaard: nothing to disclose

RPS 1714-15 09:54
Radiographers' practice and the main reasons for the use of fluoroscopy to position patients during conventional radiography procedures
L. Hirschi[1], S. Rey[2], R. Le Coutre[2], M. Champendal[2]; *[1]La Chaux-de-Fonds/CH, [2]Lausanne/CH*

Purpose: To identify if fluoroscopy is used to guide the patients' positioning during conventional radiography procedures in clinical practice and the main reasons to do it.
Methods and materials: A questionnaire was developed, tested, and distributed to radiographers working in radiological departments that collaborated with an educational institution in French-speaking Switzerland. The questionnaire was composed of 32 questions exploring socio-demographic aspects, professional experience, context, and radiographic practice. Descriptive statistics and thematic analysis were performed according to the nature of the questions.
Results: The participation rate was 33% (87/264). From those participants, 39% were using fluoroscopy to guide the positioning of patients that needed radiographs of the spine, knee, and shoulder. They were working mainly in private practice (67%). The main reasons presented to use fluoroscopy were radioprotection, patient size, patient collaboration, previous surgeries, and to achieve a higher level of image quality. The radiographers that were not using fluoroscopy presented reasons as reducing radiation exposure time and dose and that the competence, professional experience, and practice were solid enough to achieve the adequate results to respond to the clinical demands.
Conclusion: In general, radiographers are not using fluoroscopy to guide patient positioning except in contexts that are more challenging, such as non-collaborative patients or after surgeries. It seems that experience and expertise are important aspects to reduce the use of fluoroscopy during radiography examinations. Further work is necessary to identify the limitations and benefits of using fluoroscopy. Radiographers' training to harmonise practice is also important to increase competences and confidence.
Limitations: Only French-speaking Switzerland was included and no evidence was provided to verify which practice (use or non-use of fluoroscopy) is the most appropriated.
Ethics committee approval: n/a
Funding: No funding was received for this work.
Author Disclosures:
M. Champendal: nothing to disclose
L. Hirschi: nothing to disclose
R. Le Coutre: nothing to disclose
S. Rey: nothing to disclose

08:30 - 10:00 **Room O**

Interventional Radiology

RPS 1709

TIPS and liver venous intervention

Moderators:
G. Elizondo-Riojas; Monterrey/MX
P. Lucatelli; Rome/IT

RPS 1709-K 08:30
Keynote lecture
N.N.

RPS 1709-1 08:40

Transjugular intrahepatic portosystemic shunt for the treatment of veno-occlusive disease after liver transplantation: a single-centre experience

R. Miraglia[1], I. Petridis[1], L. Maruzzelli[1], C. Cannataci[2], G. Sparacia[1], G. Mamone[1], A. Luca[1]; [1]*Palermo/IT,* [2]*Msida/MT*
(christinecannataci@gmail.com)

Purpose: Veno-occlusive disease (VOD) is a rare and life-threatening vascular disease, usually seen after haematopoietic stem cell transplantation, but reported also in liver transplant (LT) recipients. Treatment is based on the use of supportive measurements (diuretics, paracentesis) or the employment of anticoagulants and profibrinolytic-antithrombotic agents. Recently, the role of a transjugular intrahepatic portosystemic shunt (TIPS) has been proposed in patients not responsive to medical treatment. However, little data is available on the efficacy and long term follow-up. We present our experience in using the TIPS as a treatment for VOD in LT recipients not responsive to medical treatment.
Methods and materials: Retrospectively, charts of all adults LT recipients who underwent TIPS creation in a single-centre, using ePTFE covered stent, from 2004-2019 were reviewed. In 3 cases, TIPS was performed as a rescue treatment for VOD not responsive to medical treatment.
Results: All patients had a histological diagnosis of VOD performed 2, 5, and 6 months after LT, respectively. 2 patients had refractory ascites and 1 had refractory hydrothorax. Technical success of TIPS was obtained in all cases with a significant reduction of the portosystemic pressure gradient (PPG) (baseline PPG 17, 15, and 10 mmHg, respectively, final PPG 7, 5, and 5 mmHg, respectively). No immediate or delayed complications were reported. Clinical success was achieved in all 3 patients. No patients had post-TIPS hepatic encephalopathy. Until today, all patients are still alive and in good clinical conditions with a follow-up of 130, 49, and 27 months, respectively.
Conclusion: In our experience, TIPS creation was associated with good clinical outcome in the long term in LT recipients with VOD not responsive to medical treatment.
Limitations: A small number of patients.
Ethics committee approval: n/a
Funding: No founding was received for this work.
Author Disclosures:
R. Miraglia: nothing to disclose
L. Maruzzelli: nothing to disclose
I. Petridis: nothing to disclose
C. Cannataci: nothing to disclose
G. Sparacia: nothing to disclose
G. Mamone: nothing to disclose
A. Luca: nothing to disclose

RPS 1709-2 08:46

Transitional care for patients with cirrhosis: a multidisciplinary care model for the prevention of complications post-TIPS

C. Li, Y. Xu*; Shanghai/CN (181659616@qq.com)*

Purpose: To evaluate the efficacy of transitional care interventions of multidisciplinary teams for patients with cirrhosis post-TIPS.
Methods and materials: 68 patients who had undergone TIPS were randomly allocated to a control or intervention group. Patients in the control group received conventional care and patients in the intervention group received conventional care combined with transitional care. The compliance behaviour, the incidence of HE and shunt dysfunction, Child-Pugh scores, and ammonia of the two groups were compared at 1, 3, 6, and 12 months post-TIPS.
Results: Repeated measures analysis of variance showed significant group effects from 1, 3, 6, and 12 months post-TIPS for the compliance behaviour scores of the two groups. The intervention group had significantly higher compliance behaviour scores than the control group 1, 3, and 6 months post-TIPS, respectively. The incidences of HE in the intervention group were significantly lower than the control group 12 months after TIPS. The incidences of shunt dysfunction in the intervention group were significantly lower than the control group 12 months after TIPS. The group effects, time effects, and group*time interaction showed no significant difference in Child-Pugh scores and blood ammonia between the two groups.
Conclusion: Post-TIPS transitional care interventions increase the accessibility of patients to scientifically informed nursing, significantly improve patients' compliance behaviour and health, and decrease the incidence of HE and shunt dysfunction.
Limitations: n/a
Ethics committee approval: Review board approved.
Funding: The Foundation of the Shanghai Public Health Bureau, 201740143. The Project of Medical Key Specialty of Shanghai Municipality, ZK2015A22.
Author Disclosures:
C. Li: nothing to disclose
Y. Xu: nothing to disclose

RPS 1709-3 08:52

Portal vein embolisation is effective in moderately severe liver fibrosis/cirrhosis

J.-P. Kühn[1], F. Schaab[1], S. Bund[1], C. Baldus[1], M.-L. Kromrey[2], R.-T. Hoffmann[1]; [1]*Dresden/DE,* [2]*Greifswald/DE*
(jens-peter.kuehn@uniklinikum-dresden.de)

Purpose: Preoperative portal vein embolisation (PVE) increases future remnant liver (FRL) volume before hemihepatectomy. It is critically discussed when PVE fails in patients with early-stage fibrotic/cirrhotic liver diseases. The purpose of this study was to analyse the hypertrophy rate following PVE in different stages of liver fibrosis/cirrhosis.
Methods and materials: In a retrospective review, patients with malignant liver diseases and PVE of the right lobe were selected from our clinical database. All PVEs were realised by ipsilateral access and using the embolic agent n-butyl-2-cyanoacrylate. Computed tomographic volumetry was performed before and 3-6 weeks after PVE to assess the hypertrophy rate of the left lobe. Patients were characterised by the presence of liver diseases using Child-Pugh scores: A) no cirrhosis and B) moderately severe liver disease. The hypertrophy rate was compared to the severity of liver fibrosis/cirrhosis using a Mann-Whitney-Test.
Results: 56 patients with malignant liver diseases, 17 women/39 men, mean age of 64.5±10.3 years, underwent PVE of the right lobe. Patients had the following Child-Pugh scores: A) 41 patients and B) 15 patients. The overall hypertrophy rate was 25.9±25.4%. Hypertrophy rates did not differ significantly between stages of liver diseases: Child-Pugh A) 26.0±27.2% and Child-Pugh B) 21.3±17.4%; p=0.374.
Conclusion: PVE is an excellent approach to induce FLR hypertrophy before hemihepatectomy, not only in patients with no cirrhosis (Child-Pugh A), but also in patients with a moderate fibrosis/cirrhosis (Child-Pugh B).
Limitations: A limited number of patients with parenchymal liver diseases.
Ethics committee approval: The study was IRB approved.
Funding: No funding was received for this work.
Author Disclosures:
J.-P. Kühn: nothing to disclose
F. Schaab: nothing to disclose
S. Bund: nothing to disclose
C. Baldus: nothing to disclose
M.-L. Kromrey: nothing to disclose
R.-T. Hoffmann: nothing to disclose

RPS 1709-4 08:58

Endovascular treatment of congenital portosystemic shunts: a single-centre prospective study

M. D. Ponce Dorrego*; Madrid/ES (mdponcedorrego@gmail.com)*

Purpose: To assess clinical outcomes of endovascular (EV) treatment of congenital portosystemic shunts (CPSS) and establish a classification system for CPSS to guide closure device selection.
Methods and materials: In 15 patients with CPSS (aged 2 days to 21 years, 10 male) referred for EV treatment from 2014-2017, data was collected prior to treatment (age, sex, medical history, clinical and analytical data, urine trimethylaminuria, abdominal ultrasound, and body-CT), at the time of intervention (shunt anatomical and haemodynamic characteristics, device selected, and closure success) and at the postprocedural time points: during hospital stay and at one year (clinical, analytical, and imaging data).
Results: 1 patient was not treated because the shunt was too wide. Treatment was successful in 12 participants. Migration of the device was observed in 2 and acute splanchnic thrombosis in 1. The changes produced were expansion of portal veins (p=0.005), thrombopenia resolution (p=0.131), ammonia normalisation (p=0.003), increased prothrombin activity (p=0.043), decreased GOT, GPT, GGT, and bilirubin (p=0.007, p=0.056, p=0.036, and p=0.013, respectively), and disappearance of trimethylaminuria and regression of liver nodules (p=0.001). Amenorrhea was resolved in 1 patient and acute liver failure in another.
Conclusion: EV closure of CPSS is effective in inducing expansion of the portal branches. No restrictions exist except shunt width. Congenital absence of the portal vein and side-to-side shunts can be treated.
Limitations: Patients are aged between 2 days and 21 years. This can be considered both a limitation (reduced homogeneity of patient characteristics) and strength (results can be extrapolated to patients with no age restrictions).
Ethics committee approval: Procedural informed consent and written consent for inclusion in the study were obtained and the study protocol was approved by the ethics committee.
Funding: No funding was received for this work.
Author Disclosures:
M. D. Ponce Dorrego: Investigator at Hospital La Paz, Speaker at Hospital La Paz

RPS 1709-5 09:04

A simple CT-based score model/nomogram for predicting technical success and midterm outcomes in TIPS treatment for symptomatic portal cavernoma

X. Niu[1], Y. Chen[2]; [1]Chengdu/CN, [2]Guangzhou/CN (niu19850519@163.com)

Purpose: To investigate the clinical significance of a CT-based score model/nomogram for predicting technical success and midterm outcomes in transjugular intrahepatic portosystemic shunt (TIPS) treatment for the symptomatic cavernous transformation of the portal vein (CTPV).
Methods and materials: Patients with symptomatic CTPV who had undergone TIPS from January 2011-December 2016 were retrospectively analysed. The CTPV was graded with a 1-5 score based on contrast-CT imaging findings of the diseased vessel. Outcome measures were technical success rate, stent patency rate, and midterm survival. The nomogram was constructed and verified by calibration and decision curve analysis.
Results: A total of 84 patients (50 men, 34 women; mean age, 52.9±14.6 years) were enrolled. Inter-reader agreement of CTPV score was κ=0.83. TIPS were successfully placed in 82% of patients (69/84). The independent predictor of technical success was a CTPV score (odds ratio [OR] 1.91, 95% confidence interval [CI] 0.86, 3.62, P=0.024, AUC=0.90). The independent predictors for primary TIPS patency were a CTPV score and splenectomy (OR 4.12, 95% CI 0.86, 7.67, P=0.034, and OR 3.91, 95% CI 0.62, 6.76, P=0.041, respectively). The survival rates differed significantly between the TIPS success and failure groups. The clinical nomogram was constructed by patient age, model for end-stage liver disease (MELD), and a CTPV score. The calibration curves and decision curve analysis verified the usefulness of the CTPV score-based nomogram for clinical practice.
Conclusion: TIPS should be considered a safe and feasible therapy for patients with symptomatic CTPV. Furthermore, the CT-based score model/nomogram might aid interventional radiologists with therapeutic decision-making.
Limitations: A small, retrospective study.
Ethics committee approval: n/a
Funding: Health and Family Planning Commission of Chengdu (Sichuan, China) (grant 2015080) and Sichuan Province (grant 17PJ430).
Author Disclosures:
X. Niu: nothing to disclose
Y. Chen: nothing to disclose

RPS 1709-6 09:10

Variation of perfusion of the liver in cirrhotic patients undergoing TIPS placement for refractory ascites: a DCE-MRI study

L. Nocetti[1], R. Scaglioni[1], L. Turco[1], C. Caporali[1], M. Bianchini[1], G. Guidi[1], P. Torricelli[1], S. Colopi[2], F. Schepis[1]; [1]Modena/IT, [2]Rubiera/IT (luca.nocetti@gmail.com)

Purpose: Patients with cirrhosis often develop severe complications of portal hypertension such as refractory ascites that can be treated by a transjugular intrahepatic portosystemic shunt (TIPS). By shunting the portal blood supply to the systemic circulation, TIPS makes liver perfusion dependent on the efficiency of the hepatic arterial buffer response. Dual input mono compartment (DIMC) DCE-MRI is an MR perfusion technique useful in quantifying the contribution of the hepatic artery and portal vein to liver perfusion in the basal condition. In this work, we tested DCE-MRI to monitor liver perfusion before and after TIPS placement.
Methods and materials: TIPS procedure and baseline DCE-MRI were performed the same day; post-TIPS DCE-MRI when the patients' conditions were permissive. All the MRI studies were performed on a 1.5T Achieva Philips, 5ch body coil, with 3DSPGR sequence, TR/TE/FA:5ms/1.66ms/15°, matr:256x256, 11 slices 8 mm thk, para-coronal acquisition, 90dyns, 2s/dyn. A bolus of 0.1 mmol/kg Gd-DTPA was injected after 8dyns. ROIs on input vessels and liver contours were drawn by an expert radiologist. After the images conversion to traces concentration, the DIMC model was applied with in-house "FANTASTIC" software. Portal flow rate (PFR), arterial flow rate (AFR), hepatic flow rate (HFR), the arterial fraction (AF), and the mean transit time (MTT) were calculated.
Results: 21 patients (16 males), 63±11 years with cirrhosis and refractory ascites were included. After TIPS placement, a significant reduction of HFR, PFR, and MTT was observed (p<0.0005, p<0.0001, p< 0.0008, respectively), as well as an increase of the AF (p<0.0001). AFR was found increased although not significative (p=0.094).
Conclusion: MR perfusion can be a valid tool to monitor residual liver perfusion in cirrhotic patients undergoing TIPS implant.
Limitations: The need to analyse the relationship with clinical events such as hepatic encephalopathy.
Ethics committee approval: The study was approved by the local ethics committee.
Funding: No funding was received for this work.
Author Disclosures:
S. Colopi: nothing to disclose
L. Nocetti: nothing to disclose
F. Schepis: Grant Recipient at Gore and Cook
R. Scaglioni: nothing to disclose
C. Caporali: nothing to disclose
P. Torricelli: nothing to disclose
G. Guidi: nothing to disclose
L. Turco: nothing to disclose
M. Bianchini: nothing to disclose

RPS 1709-7 09:16

Successful right portal vein embolisation with ONYX in oncologic patients with massive hepatic right lobe involvement

A. Borzelli[1], F. Pane[1], A. Paladini[2], F. Amodio[1], E. Cavaglia[1], R. Niola[1]; [1]Naples/IT, [2]Novara/IT (antonio.borzelli@libero.it)

Purpose: To evaluate the feasibility and efficacy of ONYX as embolisation agent in preoperative right portal vein embolisation to induce adequate left liver lobe hypertrophy before extended right hepatectomy.
Methods and materials: 23 patients (mean age 58.3 years; 12 males, 11 females) with a radiological diagnosis (TC/RM) of extensive involvement of the only right liver lobe by cholangiocarcinoma (7), metastases (9), and HCC (16), with an undamaged left hepatic lobe and future remnant liver <30%, in patients with normal liver, and <40% in cirrhotic patients were included. All patients underwent sonographically-guided percutaneous puncture of the portal vein, performed with a 21G Chiba-needle and selective catheterisation of the main right branch and its ramifications with 5 Fr catheter and 2.7 Fr microcatheter. In all cases, we used ONYX-18. All patients underwent a CT scan before the right portal vein embolisation and another CT scan 1 month after it was performed to calculate the total liver volume, tumour volume, future remnant liver, and degree of induced compensatory left lobe hypertrophy.
Results: Technical success was achieved in all patients (23) with complete embolisation of the right portal vein branch. In no cases did we observe reflux of ONYX in the left portal vein branch and no major complications.
Conclusion: ONYX proved to be a safe and effective embolic agent for preoperative right portal vein embolisation, as it allows complete embolisation of right portal branches, even the smaller distal branches, with a very low risk of reflux and higher probability to determine a satisfactory left lobe hypertrophy. It is still very expensive, but we hope that its cost will lower in the future to allow its wider employment.
Limitations: A retrospective and single-institution study.
Ethics committee approval: n/a
Funding: No funding was received for this work.
Author Disclosures:
A. Borzelli: nothing to disclose
F. Pane: nothing to disclose
A. Paladini: nothing to disclose
F. Amodio: nothing to disclose
E. Cavaglia: nothing to disclose
R. Niola: nothing to disclose

RPS 1709-8 09:22

Percutaneous closure of portosystemic shunts other than lienorenal shunts in patients with portal hypertension for recurrent hepatic encephalopathy and bleeding

V. H. Ananthashayana[1], A. Mukund[1], Y. Patidar[2], S. K. Sarin[1], C. Ashok[1]; [1]New Delhi/IN, [2]Delhi/IN (drvenk.rdaiims@gmail.com)

Purpose: To determine the feasibility of a percutaneous approach in embolising non-lienorenal variceal shunts secondary to portal hypertension for recurrent encephalopathy and recurrent bleeding.
Methods and materials: We retrospectively evaluated patients from January 2014-August 2019 who underwent percutaneous closure of variceal shunts other than lienorenal shunts secondary to portal hypertension. A total of 15 patients were found to have undergone shunt closure by percutaneous approach as management for recurrent hepatic encephalopathy (14 patients) and recurrent bleeding (1 patient). We assessed the safety, feasibility, procedural complications, and clinical outcomes of each patient.
Results: Shunt closure and variceal embolisation were performed successfully in all patients. Percutaneous access was achieved through a transhepatic, transplenic, and direct paraumbilical approach by ultrasound and fluoroscopic guidance. Periplenic varix embolisation was performed in 5 patients, perigastric varix embolisation was performed in 4 patients, and umbilical varix embolisation was performed in 5 patients. Both mesocaval and perisplenic varix was embolised in one patient. Embolic materials used were N-butyl cyanoacrylate, coil, and vascular plug devices. There were no procedure-related complications.

Conclusion: Percutaneous access for shunt closure and varix embolisation is a simple alternative image-guided procedure in patients with portal hypertension for recurrent hepatic encephalopathy and bleeding.
Limitations: n/a
Ethics committee approval: n/a
Funding: No funding was received for this work.
Author Disclosures:
V. H. Ananthashayana: Author at Institute of Liver and biliary Sciences, New Delhi
A. Mukund: Author at Institute of Liver and biliary Sciences, New Delhi
Y. Patidar: Author at Institute of Liver and biliary Sciences, New Delhi
S. K. Sarin: Author at Institute of Liver and biliary Sciences, New Delhi
C. Ashok: Author at Institute of Liver and biliary Sciences, New Delhi

RPS 1709-9 09:28

The safety and efficacy of portal vein embolisation in patients with prior left lateral liver resection

V. van Den Bosch[1], M. F. Schulze-Hagen[1], F. Pedersoli[2], P. Isfort[1], U. Neumann[1], C. K. Kuhl[1], P. Bruners[1], M. Zimmermann[1]; [1]*Aachen/DE,* [2]*Maastricht/NL (vvandenbosch@ukaachen.de)*

Purpose: To investigate the safety and efficacy of right portal vein embolisation (PVE) following a left lateral liver resection.
Methods and materials: In this retrospective study, we included 13 patients without liver cirrhosis, aged 58.7±27.6 years, who were scheduled to undergo staged hepatectomy consisting of resection of liver segments II and III, followed by right-sided PVE and eventually right-sided hepatectomy (segments V-VIII), thus leaving segments IV (±I) as the future liver remnant (FLR). Using standardised multi-phase CT, we determined the total functional liver volume (TFLV) and volume of the FLR before and at 3-4 weeks after PVE. Patient data was retrospectively analysed for peri- and postinterventional complications, especially with regard to liver function, which was assessed by serum levels of albumin, total bilirubin, ALT, and AST pre-PVE, 1-day post-PVE, and 3-4 weeks post-PVE .
Results: The mean TFLV was 1,550cc before PVE and 1,668 cc after PVE. The mean pre-PVE FLR volume was 328cc and the mean post-PVE FLR volume was 505cc, indicating a mean volume increase of the FLR of 69.4±35.0%. The mean FLR/TFLV ratio post-PVE was 30.0% (range: 22.9-43.0%). PVE was successfully performed in all patients without any peri- or post-interventional complications. Although 11/13 patients developed mild transient elevation of AST and ALT after the PVE, values returned to baseline within 4 weeks. Based on FLR hypertrophy and liver function tests, all 13 would have been candidates for the completion of right-sided hepatectomy after PVE, however, since 3 patients were found to have new metastases within the FLR, a total of 10/13 eventually proceeded to surgery.
Conclusion: PVE of the right portal vein is safe and efficacious in patients who previously underwent left lateral liver resection.
Limitations: n/a
Ethics committee approval: n/a
Funding: No funding was received for this work.
Author Disclosures:
V. van Den Bosch: nothing to disclose
M. Zimmermann: nothing to disclose
P. Bruners: nothing to disclose
F. Pedersoli: nothing to disclose
C. K. Kuhl: nothing to disclose
P. Isfort: nothing to disclose
U. Neumann: nothing to disclose
M. F. Schulze-Hagen: nothing to disclose

RPS 1709-10 09:34

Non-invasive assessment of portal hypertension with spectral CT iodine density: a correlation study with HVPG

J. Dong, R. Wang, F. Liu*; Beijing/CN (dongjianradiology@163.com)*

Purpose: To investigate the feasibility of spectral CT iodine density in the evaluation of portal hypertension by correlation with the hepatic venous pressure gradient (HVPG) in patients with liver cirrhosis.
Methods and materials: 31 patients with liver cirrhosis were recruited in this study and all performed 3 phases of contrast-enhanced spectral CT before TIPS, with the HVPG recorded. Multiple regions of interest (ROIs) in liver parenchyma, aorta, and portal vein were selected, and the mean liver parenchymal iodine density (ID) from the arterial phase, venous phase, and delayed phase were recorded. ID of the liver (IDLAP) and spleen (IDSAP) parenchyma for the arterial phase, venous phase (IDLVP), and ID of the portal vein in venous phase (IDPVP) were measured and correlated with HVPG.
Results: No correlation was found between the liver and spleen volume, IDLAP, IDSAP, IDSVP, and IDLVP with HVPG. IDPVP was found to be independently correlated with the HVPG (P<0.01). With the threshold set as 54.3, IDPVP demonstrated 69.5% sensitivity, 62.1% specificity, 72.6% positive predictive value, and 64.7% negative predictive value in the diagnosis of clinically significant portal hypertension (HVPG ≥12mmHg), respectively.
Conclusion: Spectral CT iodine density demonstrates feasibility in the evaluation of clinically significant portal hypertension in liver cirrhosis as a non-invasive imaging modality.
Limitations: The small number of patients in a single clinical centre.
Ethics committee approval: This prospective study had hospital institutional review board and ethics committee approval.
Funding: No funding was received for this work.
Author Disclosures:
J. Dong: nothing to disclose
R. Wang: nothing to disclose
F. Liu: nothing to disclose

RPS 1709-11 09:40

3D/2D-fusion of preprocedural multi-detector-computed-tomography and intraprocedural fluoroscopy for the guidance of portal vein puncture during transjugular intrahepatic portosystemic shunt placement

T. Meine[1], T. Werncke[1], M. Kirstein[1], S. K. Maschke[1], C. Dewald[1], L. S. Becker[1], F. Wacker[1], B. C. Meyer[2], J. B. Hinrichs[1]; [1]*Hanover/DE,* [2]*Berlin/DE (becker.lena@mh-hannover.de)*

Purpose: Current guidance techniques for portal vein puncture rely on the acquisition of an intraprocedural C-arm computed tomography (CACT). This could increase the radiation exposure to the patient. The purpose of this study was to assess the technical success, puncture complications, and procedural characteristics of TIPS placement using image fusion of preprocedural multidetector-computed-tomography (MDCT) and intraprocedural fluoroscopy for portal vein puncture guidance.
Methods and materials: From 11/2018-06/2019, 27 consecutive patients (18 men, 59 years) with elective TIPS placement were included. A 3D vascular map (3D-VM) was generated by drawing polylines in the hepatic and portal veins on MDCT, which was acquired for the evaluation of the TIPS procedure. Afterwards, the 3D-VM was semi-automatically registered to fluoroscopic images in two perpendicular views and served as a real-time overlay during the intervention to guide the portal vein puncture. Technical success, puncture complications, and procedural characteristics such as overall procedural time (OPT), puncture time (PT), and the dose area product (DAP) were recorded and compared to the literature.
Results: TIPS placement by use of 3D/2D-fusion was technical successful with a significant reduction of the PSG (PSGpre-TIPS15±3mmHg, PSGpost-TIPS4±3mmHg; p<0.00001). No major complications occurred. The OPT was 64±29 min and the PT was 14±6 min, which is comparable to the literature. The DAP of 10748±9384uGy*m2 was lower than the reported DAP for CACT-assisted TIPS procedures.
Conclusion: TIPS placement using 3D/2D-fusion is effective, fast, and safe. It has the potential to reduce radiation exposure to the patient by at least 30% compared to published CACT-assisted TIPS procedures.
Limitations: A small, retrospective study without a control cohort. Large cohort studies are required to confirm the benefits for the patients.
Ethics committee approval: The Human Subjects Research Review Board of the Hanover Medical School approved our retrospective study and written informed consent was obtained.
Funding: No funding was received for this work.
Author Disclosures:
T. Meine: nothing to disclose
F. Wacker: Consultant at Siemens
J. B. Hinrichs: nothing to disclose
C. Dewald: nothing to disclose
L. S. Becker: nothing to disclose
T. Werncke: Consultant at Siemens
M. Kirstein: nothing to disclose
S. K. Maschke: nothing to disclose
B. C. Meyer: Consultant at Siemens

RPS 1709-12 09:46

Application of a liver biopsy as a treatment strategy determinant in Budd-Chiari syndrome

F. Rafiee, A. Rasekhi, B. Geramizadeh, H. Laalinia, P. Keshavarz*; Shiraz/IR (faranakrafiee1367@gmail.com)*

Purpose: Budd-Chiari syndrome (BCS) is hepatic venous outflow obstruction. The primary goal of treatment is the resolution of hepatic congestion in order to improve liver perfusion and preserve hepatocytes function. Medical management, recanalisation of stenotic or occluded hepatic veins, portosystemic shunting, and eventually liver transplantation are the treatment options. The aim of this study is to determine if angioplasty intervention can

substitute the portosystemic shunting by means of a new histopathological grading system for zone 3 congestion in BCS.
Methods and materials: In a retrograde study, we reviewed 34 cases of BCS, diagnosed on radiology/pathology basis, who underwent a biopsy of the explanted liver prior to transplantation. Alongside the extent and amount of irreversible fibrosis, we emphasised other pathologic changes including sinusoidal and central venular dilatation. The pathologic slides were rechecked and, according to a new congestion scoring system, patients were categorised considering the extent of central venular and sinusoidal dilatation. Total scores of 3-8 were applied for each patient.
Results: According to radiologic findings, 11 patients were in the proximal type subgroup, all representing a histopathologic score of 4 or less (score 3 in 6 patients, score 4 in the others). The remaining 23 patients were in the distal type category, including 7 patients with score 5 and the rest demonstrating score 6 or more. After pathological/radiological correlation, the study revealed that the more proximal the location of the venous obstruction was, the less sinusoidal and central venular dilatation.
Conclusion: The use of histopathology is beyond determining the presence of fibrosis. Liver biopsy results are useful in predicting the site of venous obstruction in BCS, thus considered as valuable pretreatment findings.
Limitations: The small sample volume.
Ethics committee approval: n/a
Funding: No funding was received for this work.
Author Disclosures:
F. Rafiee: nothing to disclose
A. Rasekhi: nothing to disclose
B. Geramizadeh: nothing to disclose
H. Laalinia: nothing to disclose
P. Keshavarz: nothing to disclose

RPS 1709-13 09:52
Transjugular intrahepatic portosystemic shunt using the new GORE VIATORR controlled expansion endoprosthesis: a single-centre experience
R. Miraglia[1], L. Maruzzelli[1], G. Sparacia[1], G. Mamone[1], A. Di Piazza[1], M. Milazzo[1], C. Cannataci[2], C. Gozzo[1], A. Luca[1]; [1]*Palermo/IT,* [2]*Msida/MT*
(christinecannataci@gmail.com)

Purpose: To evaluate the mid-term clinical efficacy and complications of transjugular intrahepatic portosystemic shunt (TIPS) creation using the new controlled expansion ePTFE covered stent (VCX) for portal hypertension complications.
Methods and materials: From 7/2016-6/2019, 139 consecutive patients received TIPS using VCX in a single centre.
Results: TIPS indications were refractory ascites (n=89), variceal bleeding (n=41), and other (n=9). The mean MELD score was 12.0 ± 4.6 (6-33). The mean age was 59.1 ± 10.4 (10-78) and the mean follow-up was 12.2 months (± 8.0, range 1-33). In 9 patients (cavernoma n=4, massive thrombosis n=4, and Budd-Chiari n=1), TIPS was directly dilated to 10 mm in diameter. In 122 patients, TIPS was dilated to 8 mm with a final PSG<12 mmHg or a PSG reduction≥40%, compared to the baseline PSG. In 8 patients, not reaching the haemodynamic target, the stent was further dilated to 10 mm in diameter during the same session, reaching the haemodynamic target. Overall clinical success was achieved in 118/139 (85%) patients (80% in refractory ascites, 95% variceal bleeding, and 80% other). Overt hepatic encephalopathy was observed in 21 patients (15%). TIPS revision was performed in 18 patients (13%). 3 patients (2%) underwent stent reduction. 28 patients (20%) died during follow-up of causes not related to TIPS. 17 patients (12%) underwent a liver transplant.
Conclusion: VCX can help to optimise the haemodynamic target during TIPS creation with a good clinical outcome and a reasonably low complication rate.
Limitations: A longer follow-up is necessary to confirm this data.
Ethics committee approval: n/a
Funding: No funding was received for this work.
Author Disclosures:
R. Miraglia: nothing to disclose
L. Maruzzelli: nothing to disclose
G. Mamone: nothing to disclose
G. Sparacia: nothing to disclose
A. Luca: nothing to disclose
A. Di Piazza: nothing to disclose
M. Milazzo: nothing to disclose
C. Cannataci: nothing to disclose
C. Gozzo: nothing to disclose

08:30 - 10:00 **Coffee & Talk 2**

Artificial Intelligence and Machine Learning

RPS 1705

Artificial intelligence: technical aspects

Moderators:
J. I. Peltonen; Helsinki/FI
N.N.

RPS 1705-1 08:30
The worrisome impact of an inter-rater bias on neural network training
O. Shwartzman, H. Gazit, I. Shelef, T. Riklin-Raviv*; Beersheba/IL*
(orshw@post.bgu.ac.il)

Purpose: We quantitatively evaluated the impact of inter-rater bias in manual segmentations of medical images on the output of artificial neural networks (ANNs).
Consistent differences in manual image annotations influence supervised ANNs' training processes. Thus, automatic segmentations of ANNs trained on different sources will be consistently different as well.
Methods and materials: MRIs of MS patients annotated by two radiologists with different levels of expertise were collected. CT scans of intracranial haemorrhage (ICH) patients were annotated twice: manually and semi-manually. We trained an ANN (U-Net) on annotations from one source and tested its output segmentations on annotations from another source, using Dice scores as matching criteria.
We used classifier ANNs to test (using hit-rate) if two sets of automatic segmentations produced by two identical U-Nets that were trained on different source segmentations could be distinguished. We calculated MS-lesion loads and ICH volumes based on the raters' and the U-Nets' segmentations and compared the differences.
Results: Lower Dice scores were obtained between the outputs of ANNs trained on annotations of one rater and tested on another (cross-evaluation experiment). Classification hit-rates were higher for U-Nets that were trained on different sources than for the sources' annotations themselves: ICH 0.92 (manual) versus 0.95 (automatic); MS 0.9 (manual) versus 0.93 (automatic). Differences in volumes calculated based on automatic segmentations of ANNs, trained on different sources, increased and became more consistent.
Conclusion: Segmentation bias between different raters is amplified in ANNs' training as the ANNs generalise the manual segmentation examples to the test data. Therefore, ANNs' segmentation and volume calculation, for the same input images, can be significantly different depending on the training sources.
Limitations: Testing specific segmentation ANN architecture.
Ethics committee approval: n/a
Funding: No funding was received for this work.
Author Disclosures:
O. Shwartzman: Author at Ben Gurion University of the Negev, Speaker at Ben Gurion University of the Negev
H. Gazit: Author at Ben Gurion University of the Negev
T. Riklin-Raviv: Author at Ben Gurion University of the Negev
I. Shelef: Author at Ben Gurion University of the Negev

RPS 1705-2 08:36
Aging AI: how machine learning models go out of sync
O. Pianykh[1], C. Crowley[2]; [1]*Newton Highlands, MA/US,* [2]*Boston/US*
(opiany@gmail.com)

Purpose: To investigate whether the accuracy of machine learning models used in radiology degrades with time.
Methods and materials: Machine learning (ML) gains an increasing role in radiology. Currently, most ML models use the same static "train once, deploy everywhere" approach. However, the environments and data used by these models evolve all the time. As a result, static models run into the risk of becoming outdated.
To verify this hypothesis, we used a full year of operational patient records from Massachusetts General Hospital. We trained several ML models to predict operational events, such as patient wait times or imaging delay times. We varied the age of the training data between 0 (current) and 12 months, and we varied the volume of the training set from 1 to 12 months. The performance of the trained models was then assessed based on the prediction accuracy for one month of test data. The goal was to see whether the size or the age of the training dataset affects the accuracy of the model results.
Results: A random forest model provided the most accurate prediction with R^2=0.65. AI models needed at least 1 month of training data volume to become accurate. However, the age of the training data had a visible effect on the model

accuracy: models trained on data older than 8 months produced significantly less accurate results.
Conclusion: As AI becomes increasingly present in radiology, more attention should be paid to maintaining high AI model accuracy. To stay accurate, AI models must be retrained/reevaluated on a regular basis.
Limitations: ML model quality may depend on the data available at each facility.
Ethics committee approval: n/a
Funding: No funding was received for this work.
Author Disclosures:
O. Pianykh: nothing to disclose
C. Crowley: nothing to disclose

RPS 1705-3 08:42

Cloud computing in combination with multi-scale deep reinforcement learning for 3D-landmark detection applied on whole-body organ volumetric analyses for the building of organ-specific databases

D. J. Winkel[1], H.-C. Breit[1], A. Ezzi[2], B. Stieltjes[1]; [1]*Basel/CH,* [2]*Princeton/US*

Purpose: To showcase a fully automated workflow combining deep reinforcement learning (DRL) for whole-body volumetric analyses and cloud-based post-processing and storing of data on 10,508 whole-body organ volumes.
Methods and materials: 431 retrospectively acquired multiphasic CT datasets with 10,508 volumes were included in the analysis (10,344 abdominal organ volumes, 164 lung volumes). AI-based whole-body organ volumes were determined using a multi-scale DRL for 3D body markers detection and 3D structure segmentation. The algorithm was trained for whole-body organ volumetry on 5,000 datasets. The data was uploaded to a cloud-based application with integrated DRL software, allowing to group data by diseases. Total processing time for all volumes and mean calculation time per case was recorded. Repeated measures analysis of variance (ANOVA) were conducted to test for robustness, considering the contrast phase and slice thickness. Final whole-body organ metrics were automatically outputted in comma-separated values format.
Results: The algorithm calculated organ volumes for the liver, spleen, and right and left kidney (mean volumes in mL: 1868.6, 350.19, 186.30, and 181.91, respectively), and for the right and left lung (2363.1 and 1950.9). We found no significant effects of the variable contrast phase or the variable slice thickness on the organ volumes. The mean computational time per case was 10 seconds. The total computational time for all volumes was 1 hour and 11 minutes.
Conclusion: We were able to show that DRL in combination with cloud computing enables a fast processing of substantial amounts of data, allowing to build up organ-specific databases.
Limitations: n/a
Ethics committee approval: n/a
Funding: D.J.W receives research support from the Swiss Society of Radiology and the Research Fund Junior Researchers of the University Hospital Basel (grant no. 3MS1034).
Author Disclosures:
D. J. Winkel: Employee at Siemens Healthineers
B. Stieltjes: nothing to disclose
H.-C. Breit: nothing to disclose
A. Ezzi: Employee at Siemens Healthineers

RPS 1705-4 08:48

Adversarial attacks in the detection of pneumothoraces from chest radiographs: addressing a vulnerability of deep neural network classifications in the clinical setting

A. M. Bucher[1], A. Distergoft[2], D. Kügler[3], A. Rajkarnikar[2], M. Uecker[2], T. J. Vogl[1], D. A. Mukhopadhyay[2]; [1]*Frankfurt am Main,* [2]*Darmstadt/DE,* [3]*Bonn/DE*

Purpose: Adversarial attacks are malicious changes to the input images that are below the detection level of a human reader, yet can completely falsify the classification of a deep neural network (DNN). We tested the vulnerability of a state-of-the-art DNN classifier in the detection of pneumothoraces by several adversarial attack variations.
Methods and materials: A state-of-the-art DNN architecture (ResNet) was trained on 9,265 chest radiographs and the locations of pneumothoraces were manually annotated. We tested a total of 600 modified images (I_A) based on 150 comparable chest x-ray images (I_C). Attack categories were basic iterative method (BIM), fast sign gradient method (FGSM), deep fool attack (DF), and saliency map attack (SAM). Annotation by a trained radiologist reader was performed for each test image.
Results: The accuracy of classification by the human reader was comparable between groups (I_C: 98.6%, I_A: 99.3%, p=0.325). DNN classification for I_C was an accuracy of 83.3%, FPR: 0.1, FNR: 0.35. Classification was significantly falsified for I_A with an accuracy of 16.7%, FPR: 0.9, FNR: 0.65; p<0.001. True-positive rates were 0.65 (I_C) and 0.35 (I_A), and true-negative rates were 0.9 (I_C) and 0.1 (I_A; p<0.001). AUC was 0.78 (I_C) and 0.23 (I_A, p<0.001). Attack strength measured by accuracy, FNR, FPR, and AUC were comparable across attack categories (p>0.1 each).
Conclusion: A wide range of adversarial attacks were highly effective to falsify DNN-based detection of pneumothorax from chest x-rays. This vulnerability needs to be carefully addressed when transferring DNN classifiers into the clinical setting.
Limitations: Effectiveness should be validated in a larger dataset.
Ethics committee approval: n/a
Funding: No funding was received for this work.
Author Disclosures:
A. M. Bucher: Other at Travel support: Bayer
T. J. Vogl: Other at Travel support: Bayer
D. Kügler: nothing to disclose
A. Distergoft: nothing to disclose
A. Rajkarnikar: nothing to disclose
M. Uecker: nothing to disclose
D. A. Mukhopadhyay: nothing to disclose

RPS 1705-5 08:54

An intelligent way to choose a training dataset for annotation to improve the segmentation accuracy of a deep segmentation network model

H. Haque[1], M. Hashimoto[2], N. Uetake[1], N. Toda[3], M. Jinzaki[2]; [1]*Hino/JP,* [2]*Tokyo/JP,* [3]*Shinjuku/JP (hasnine.haque@ge.com)*

Purpose: The annotating process is tedious and time-consuming. Effectively selecting a minimum number of representative unannotated training datasets out of a large-scale heterogeneous dataset is challenging. Our purpose was to identify training datasets iteratively and retrain current model to segment thigh muscle and produce state-of the-art segmentation performance.
Methods and materials: IRB-approved 3,000 clinical CT images were used for this study. A 3D-UNet base model, which was previously trained to segment thigh volume into 11 muscle classes by a small cohort of reference datasets, was used. An iterative active learning framework was developed which identified the datasets out of all datasets where base model segmentation prediction had a higher uncertainty in prediction and could produce a positive effect on segmentation accuracy if used for re-training. Identified datasets were further clustered by their similarity features and 10 representative datasets were selected for annotation in each iteration. All re-trained models performance was evaluated by randomly selected 18 test thigh volume datasets. We compared the average surface distance (ASD) as a segmentation performance metric when the base model was re-trained by the same number of randomly chosen datasets.
Results: After the second iteration, the evaluation indicates a 53% improvement in median ASD over all muscle class as compared to a 22% increase when re-trained with randomly chosen datasets. Paired t-test with a statistical significance score ($p < 0.005$) shows clear improvement of the segmentation performance.
Conclusion: Retraining a base model with the identified datasets by the active learning framework achieved higher segmentation accuracy in comparison to when trained with a randomly selected dataset. To keep the segmentation performance at the expected range for growing datasets, the framework finds the effective training datasets for annotation and reduces unnecessary annotation workload.
Limitations: The current model does not support images with a metal artefact.
Ethics committee approval: IRB Keio University School of Medicine.
Funding: AMED JP19lk1010025.
Author Disclosures:
H. Haque: Research/Grant Support at Keio University School of Medicine, Employee at GE Healtcare
M. Hashimoto: Employee at Keio University School of Medicine
N. Uetake: Employee at GE Healthcare
M. Jinzaki: Employee at Keio University School of Medicine, Grant Recipient at AMED
N. Toda: Employee at Keio University School of Medicine

RPS 1705-6 09:00

Can AI pick up significant abnormalities missed on the original read, hence contributing to QA?: a deeper dive into the abnormalities detected by AI versus the original radiologist

A. K. Sahu, B. Aggarwal; *New Delhi/IN (drsahuamit@gmail.com)*

Purpose: To evaluate the accuracy of deep learning in detecting clinically relevant abnormalities in chest x-rays in outpatient tertiary care centres and comparing it with the radiologist's read.
Methods and materials: 5,000 random chest x-rays from outpatient departments of 5 tertiary care centres were sent to deep learning as anonymised data for analysis. Abnormalities specified were nodule, calcification, cavity, consolidation, and blunting CP angle. After analysing, a deep learning algorithm provided 400 x-rays, mentioning specified abnormalities. Selected x-rays were

blindly read by 3 radiologists who gave their interpretation on specific abnormalities. A comparison was made between the primary read, AI read, and the interpretation of the 3 radiologists to pick up clinically relevant findings which were missed in primary read.
Results: Comparing the original reports of 403 cases, 3 radiologist majority opinion agreed with the AI for 75 ruled as normal and 188 as a missed finding in the original report. Individual radiologist concordance with AI with Cohen's Kappa values were 0.648, 0.789, and 0.457. Out of the discordant set, AI reads on cardiomegaly, opacity, and blunting of CP angle were positive for 79.75 and 41 cases. The highest concordance between the AI read and reporting radiologist was for cardiomegaly: 47 cases where all three radiologists agreed. The most common discordance was cardiomegaly, with reviewing radiologist agreement of 27%. The most significant missed finding by the AI read was cardiomegaly, with a total of 72 and blunting of CP angle of 6 cases; parenchymal opacities in 19 cases.
Conclusion: A deep learning algorithm can detect clinically relevant abnormalities in chest x-rays, which can be missed by radiologists, as small nodules, lung parenchymal/pleural calcification, and blunted CP angles, thus increasing diagnostic accuracy.
Limitations: n/a
Ethics committee approval: n/a
Funding: No funding was received for this work.
Author Disclosures:
A. K. Sahu: nothing to disclose
B. Aggarwal: nothing to disclose

RPS 1705-7 09:06

RECOMIA: a cloud-based platform for artificial intelligence research in radiology

P. Borrelli[1], O. Enqvist[1], J. Ulén[1], R. Kaboteh[1], E. Trägårdh[2], L. Edenbrandt[1]; *[1]Gothenburg/SE, [2]Malmö/SE (pablo.borrelli@vgregion.se)*

Purpose: The Research Consortium for Medical Image Analysis (RECOMIA) is a not-for-profit organisation with the objective of promoting research in the fields of artificial intelligence (AI) and medical imaging. RECOMIA aims at minimising the time and effort researchers need to spend on technical aspects such as display and transfer of DICOM images, legal aspects such as de-identification, GDPR, and HIPAA compliance, and quality aspects such as display tools so that medical experts can review and correct AI-segmentations in a cloud-based DICOM-viewer.
Methods and materials: Radiologists and nuclear medicine specialists have used the RECOMIA platform to manually annotate up to 100 organs in more than 300 CT studies. Not all organs were annotated in all images; in total, more than 10,000 were annotated. The manual annotations were used to train convolutional neural networks (CNN) to perform automated organ segmentation in CT images. The CT scans were split into training (80%) and validation (20%) groups.
Results: The CNN-based segmentations were compared to the manual segmentations of the validation group. There was agreement on 93.7% of the manually-labelled pixels. Conversely, there was agreement on 94.7% of the automatically-labelled pixels. The pixels considered background both manually and by the CNN are not included in these numbers. The run-time of the CNNs was about 2 minutes on a desktop computer.
Conclusion: AI-based tools can provide highly accurate and reproducible organ segmentation, similar to those obtained manually by radiologists, but much faster. We continue to train new CNNs to continuously improve performance. The tools developed in this project are available by request at www.recomia.org for research purposes.
Limitations: The tools are not for clinical use and not available for commercial purposes.
Ethics committee approval: n/a
Funding: No funding was received for this work.
Author Disclosures:
P. Borrelli: nothing to disclose
O. Enqvist: nothing to disclose
J. Ulén: nothing to disclose
R. Kaboteh: nothing to disclose
E. Trägårdh: nothing to disclose
L. Edenbrandt: Employee at EXINI Diagnostics AB, Lund Sweden, Grant Recipient at EXINI Diagnostics AB, Lund Sweden

RPS 1705-8 09:12

Integrating machine learning pipelines into clinical workflows with DICOM message queues

V. Saase, A. Junge, H. Wenz, C. Groden, M. E. Maros*; Mannheim/DE (vsaase@gmail.com)*

Purpose: We present a prototype that implements a modular, distributed, and parallel analysis pipeline in MRI reporting workflows of neuroradiology. The modular software architecture allows us to quickly exchange parts of the pipeline for experiments and testing while ensuring the stability and performance of the remaining system. We integrate image viewing, structured reporting, and monitoring by using custom user interfaces and well-established open-source software.
Methods and materials: Our implementation comprises multiple submodules: a web-based structured reporting editor, a machine learning-based MRI perfusion pipeline, a traditional rule-based processing pipeline, a viewer application, a PACS connection, and a high-performance database. We use DICOM metadata as messages for the standardised communication between modules. Modules are implemented in various programming languages, thus enabling us to choose the best tools for the specific requirements and lowering the entry barrier for less experienced developers. Modules can be distributed across the network, making use of dedicated hardware, thereby reducing the need for moving bulk data across slow connections.
Results: A pilot trial with 10 stroke reports and 10 tumour reports (Nreader=3) showed that reporting was significantly faster ($p<0.05$), more structured ($p<0.05$), and contained more repeatable quantitative measurements ($p<0.05$) when compared to our legacy system.
Conclusion: Flexible, standardised, and open source software is the way forward in the quest to integrate machine learning workflows into clinical practice, improving quality and performance.
Limitations: This study is a proof of concept of a tool bridging clinical work and research. The development of specific modules will be needed when transferring it to other sites. We are prohibited from distributing our software for clinical use by European law.
Ethics committee approval: The project was approved by the local ethics committee (2017-825R-MA, 2017-828R-MA).
Funding: No funding was received for this work.
Author Disclosures:
V. Saase: nothing to disclose
M. E. Maros: nothing to disclose
H. Wenz: nothing to disclose
C. Groden: nothing to disclose
A. Junge: nothing to disclose

RPS 1705-9 09:18

The methodology of the formation of databases for machine learning

A. Meldo, T. Trophimova, O. Tsyganskaya, K. Malinovskaya, I. Prokhorov*; St. Petersburg/RU (anna.meldo@yandex.ru)*

Purpose: To create a general methodology of the generation of databases for machine learning algorithms
Methods and materials: 450 anonymised chest CTs were included in the dataset. The RadiAnt DICOM Viewer has been chosen for modifying and dealing with the dataset. The prepared dataset was archived on the server of the oncological centre before the morphological diagnostics. Then the data was anonymised with the DicomCleaner™, renaming them with a special code. We used nodule's shape, internal, and external structure as a feature and represented them into histograms for radiomix. After the morphologic confirmation, we assigned some class label to each case.
Results: We created the database LIRA (Lung Image Resource Annotated) for the development and testing of CAD. All cases were confirmed morphologically. In our study, 65% of LCs had a typical CT, 26% of CT images corresponded to different diseases which require an additional differential diagnostic criteria, and 9% of LC cases were extremely difficult to recognise by means of CT due to an atypical visualisation image. Class labels for subsets were "typical LC", "atypical", and "not cancer".
Conclusion: One of the conditions for successfully using the medical CAD systems is a correctly created database which corresponds with clinical and radiological interpretation. We would like to point out that the main proposed idea of the methodology of creating the medical databases can be formulated as follows: structurisation of the data, their homogenisation and verification of diseases, and the inclusion of the "atypical" cases and cases which look similar to studying disease. The dataset LIRA contains class labels for each nodule to develop the differential diagnostic intellectual algorithm.
Limitations: n/a
Ethics committee approval: n/a
Funding: The reported study was funded by Russian Science Foundation, project number 18-11-00078.
Author Disclosures:
I. Prokhorov: nothing to disclose
A. Meldo: Author at St.Petersburg Clinical Research center of specialized types of medical care (oncological)
T. Trophimova: nothing to disclose
O. Tsyganskaya: nothing to disclose
K. Malinovskaya: nothing to disclose

RPS 1705-10 09:24
Super AI and supermodalities: the future of radiology?
D. Gicovate; *Jerusalem/IL (dgicovate@yahoo.com)*

Purpose: To research possible future directions for AI technology in radiology. We analyse the suitability of a hypothetical "super AI" technology capable of integrating multiple studies simultaneously. Additionally, we compare super AI with the possibility of developing a multi-modality-scanner ("supermodality").
Methods and materials: Super AI: combining AI packages will be possible to get better disease diagnosis.
We analysed some factors to develop such technology:
A) The time factor between different studies.
B) The patient position.
C) Modality technology.
D) The radiologist as an integrator of knowledge.
E) The contrast agent.
Supermodality: multimodality machines developed are the PET-MRI. PET-CT, CT-ultrasound-registration, etc, are common hospital practices.
What about a single machine that can scan using different technologies? Will it reduce the time to diagnose?
Results: Those new machines will suppose a completely new paradigm and new radiologist knowledge, and new contrast agents, may be needed.
Conclusion: Different AI packages can discover different findings in different kinds of studies. Combining modalities or combining AI packages will substantially improve diagnosis.
Two different strategies can be adapted to produce a more complete diagnosis in a multi-exam scenario:
1) To develop a super AI system, as a software solution, capable of analysing and integrating the data of different AI packages
2) To develop a new generation of machines: a super modality that scans the patient using several technologies at the same time (CT + MRI + ultrasound + etc.) and reducing patient positioning, time differences, contrast agents factors, and others.
Limitations: Both kinds of technologies do not exist today. Even if the software solution (super AI) is the easy one, and probably the most possible to develop in the next few years, a mix of the two strategies will be the only way to reach the next level of radiology.
Ethics committee approval: n/a
Funding: No funding was received for this work.
Author Disclosures:
D. Gicovate: Consultant at DGicovate, Employee at Hadassah University Hospitals

RPS 1705-11 09:30
The impact of radiomic feature selection on clinical modelling
J. van Lunenburg, W. H. K. Chiu; *Hong Kong/HK (jurgen@hku.hk)*

Purpose: Software choice often dictates what radiomic features can be extracted from images. This study analyses how different feature sets affect clinical models in two cancer cohorts: PET oesophagus (in-house dataset) and CT lung (open dataset).
Methods and materials: 95 patients (65 training and 30 validation cohorts) who had undergone pre-treatment 18F-FDG-PET studies were included and classified as those who achieved complete pathological response (pCR) and those who did not. The primary tumours were segmented using a fixed threshold approach, radiomic features were extracted, features were annotated according to the international biomarker standardisation initiative. Feature reduction with the minimum redundancy maximum relevance method was performed. Logistical regression and random forest models for clinical outcomes were constructed and compared using ROC curves, decision curves, and McNemar's test.
Results: Of the 5 feature sets tested, AUC values for the two models ranged between 0.6 and 0.87. Reduced feature sets did not have much overlap (10-25%) and showed substantial differences in their ability to predict outcomes with our models and datasets. A combined superset showed the best performance (AUC 0.87) but did not show much reduction in feature correlation.
Conclusion: High-dimensional data requires extensive feature reduction and increased scrutiny for overfitting, but if a proper methodology is applied, the results of combining multiple feature sets may be beneficial for modelling with radiomics in cancer.
Limitations: The PET dataset is not very large (low incidence and expensive modality) and the event frequency is slightly below 40%. The fixed threshold segmentation may be less accurate for lesion size, but it was chosen to maximise radiomics stability.
Ethics committee approval: The study was approved by the local ethics committee in accordance with the Helsinki Declaration and all patient information was anonymised prior to analysis.
Funding: No funding was received for this work.
Author Disclosures:
J. van Lunenburg: nothing to disclose
W. H. K. Chiu: nothing to disclose

RPS 1705-12 09:36
Practical implementation of artificial intelligence solutions in a multi-country healthcare organisation
R. Illing[1], A. Juhos[1], T. Sparkes[2], I. Fulop[1], R. Fenyi[1], O. Dumitroiu[3], K. Katsari[2]; *[1]Budapest/HU, [2]Amsterdam/NL, [3]Bucharest/RO (katia.katsari@affidea.com)*

Purpose: The value proposition of artificial intelligence (AI) solutions in healthcare have been well described and it is apparent that 'narrow AI' will have a role in every stage of the clinical workflow. The deployment of AI solutions in the clinical workflow of a multi-country healthcare organisation has many challenges, but establishing a systematic and unified framework can lead to successful outcomes. By defining measurable performance indicators, it is possible to track in real-time whether actions give benefits to all stakeholders; patients, referrers, and business partners.
Methods and materials: In order to establish the framework of AI deployment in the clinical workflow, working groups were formed at a group and country level between clinical, legal, data protection, digital, operational, commercial, and marketing to identify all areas of relevance in a project management approach.
Results: A unified framework of AI deployment was identified in eight steps:
- The selection criteria for AI solutions, pilot centres, and countries.
- A legal review including medical device class, intended use, and data protection impact assessment.
- A technical architecture review including digital infrastructure requirements and the integration of an AI solution.
- The definition of workflows for the assessment of AI solution benefits.
- The training of healthcare professionals.
- The definition of key performance indicators.
- The commercialisation process.
- The preparation of stakeholders' information and communication strategy and material.

Conclusion: The framework designed is robust enough to encompass the introduction of different AI solutions across the network. However, minor methodological adjustments are required for each specific AI solution to meet the requirements of use and implementation.
Limitations: n/a
Ethics committee approval: n/a
Funding: No funding was received for this work.
Author Disclosures:
K. Katsari: nothing to disclose
R. Illing: nothing to disclose
T. Sparkes: nothing to disclose
A. Juhos: nothing to disclose
I. Fulop: nothing to disclose
O. Dumitroiu: nothing to disclose
R. Fenyi: nothing to disclose

RPS 1705-13 09:42
The role of a deep learning-based artificial intelligence diagnostic system in assisting the establishment of the gold standard in clinical validation studies
P. Borrego[1], E. Ladera González[1], P. Sousa[1], M. T. D. Maristany Daunert[1], D. Wang[2], Y. Shen[2], S. Drago[1], Y. Sun[3], J. Munuera[1]; *[1]Barcelona/ES, [2]Beijing/CN, [3]Wiesbaden/DE (pepmunuera@hotmail.com)*

Purpose: The gold standard is critical for clinical validation studies but usually time-consuming for researchers. This project aimed to explore whether a deep learning (DL)-based artificial intelligence (AI) diagnostic system would benefit the researchers in establishing the gold standard by reducing the discrepancies between them.
Methods and materials: In this study, we utilised 196 CXR scans which were diagnosed as either pneumonia or effusion and employed the DL AI system (InferRead DR Chest Research, Infervision) to study its effects in eliminating the discrepancies when generating the gold standard. Two senior radiologists participated in the reader study. They reviewed the CXR images with and without the aid of an AI diagnostic system at an interval of 4 weeks. Discrepancies of their reviewing results were analysed and evaluated by Cohen's Kappa index.
Results: There were 18 cases that were diagnosed differently by the two senior radiologists when they reviewed the CXR images alone. With the assistance of the AI diagnostic system, the number of differentially diagnosed cases dropped to 7 cases, leading to a 61.1% reduction in discrepancies. Of note, the Kappa scores increased from 0.806 to 0.928 after utilising the AI diagnostic system. In particular, according to the ground truth of these CXR images, utilisation of the AI diagnostic system eliminated 17 discrepancy cases in which 8 false-positive cases and 7 false-negative cases were corrected. Meanwhile, among the 6 new introduced discrepancy cases, one was a false-positive case that was corrected by one radiologist with the help of the AI system.

Conclusion: A DL-based AI diagnostic system greatly reduced the diagnostic discrepancies among radiologists and could be utilised to assist the establishment of a gold standard in clinical validation studies.
Limitations: n/a
Ethics committee approval: n/a
Funding: No funding was received for this work.
Author Disclosures:
J. Munuera: nothing to disclose
P. Borrego: nothing to disclose
E. Ladera González: nothing to disclose
P. Sousa: nothing to disclose
M. T. D. Maristany Daunert: nothing to disclose
D. Wang: nothing to disclose
Y. Shen: Employee at Infervision
S. Drago: Employee at Infervision
Y. Sun: Employee at Infervision

RPS 1705-14 09:48
The utility of artificial intelligence/machine learning for the detailed evaluation of contrast media comparison studies
J. W. Patriarche[1], D. Patriarche[2], A. Kuhn[3], M. J. Kuhn[4]; *[1]Bellevue/US, [2]Ottowa/CA, [3]Milwaukee/US, [4]Peoria, IL/US (mkuhn6@gmail.com)*

Purpose: Contrast media comparison studies with artificial intelligence/machine learning (ML) software provides opportunities to look at enhancement characteristics quantitatively, providing greater clarity, reliability, and reproducibility.
Methods and materials: Using the change detector software produced by A.I. Analysis, Inc. (Seattle, WA), 24 patients with biopsy-proven glioblastoma multiforme were evaluated. Each patient had received equal doses of gadoteridol and gadobutrol within a 2-10 day time period. The software performs a novel ML enhancement calculation that automatically rates the degree of enhancement from 0.0 to 1.0 per voxel and the change in enhancement from -1.0 to +1.0. ROIs were manually defined for regions that were non-enhancing and unchanging, as well as enhancing and changing. Mean calculated enhancement values of actually non-enhancing regions were compared between subtraction and the ML technique. Mean calculated contrast to background ratio (CBR) values of actually enhancing/changing regions were compared between the subtraction and ML technique.
Results: For the actually unchanging/non-enhancing regions, the median ratio of mean calculated enhancement for subtraction technique versus AI technique was 13.34. The p-value using the ratio paired t-test was $<10^{-12}$. For the actually changing/enhancing regions, the average ratio of CBR between the ML technique and the subtraction technique was 7.6. The p-value using the ratio paired t-test was $<10^{-12}$.
Conclusion: The ML technique permits an automatic and reproducible calculation of enhancement, as well as a change in enhancement between MR studies. The ML technique provides enhancement and change in enhancement maps that are dramatically darker in the non-enhancing regions, and provide a much greater contrast for the actually enhancing/actually changing regions.
Limitations: n/a
Ethics committee approval: Insititutional review board approval was received.
Funding: No funding was received for this work.
Author Disclosures:
M. J. Kuhn: nothing to disclose
J. W. Patriarche: Founder at A.I. Analysis, Inc.
D. Patriarche: Founder at A.I. Analysis, Inc.
A. Kuhn: nothing to disclose

RPS 1705-15 09:54
Deep learning for natural language processing (NLP) in radiology
V. Sorin, Y. Barash, E. Konen, E. Klang*; Ramat Gan/IL (verasrn@gmail.com)*

Purpose: Natural language processing (NLP) enables the conversion of free text into structured data. Recent innovations in deep learning technology provide improved NLP performance. We aimed to survey deep learning NLP fundamentals and review radiology related research.
Methods and materials: This systematic review followed the PRISMA guidelines. We searched for deep learning NLP radiology studies published up-to September 2019. MEDLINE, Scopus, and Google Scholar were used as search databases.
Results: 10 relevant studies published between 2017 and 2019 were identified. Deep learning models applied for NLP in radiology are convolutional neural networks (CNN), recurrent neural networks (RNN), long short-term memory (LSTM), and attention networks. Deep learning NLP applications in radiology includes flagging of diagnoses such as PE and fractures, labelling follow-up recommendations, and automatic selection of imaging protocols. Deep learning NLP models perform equally or better than traditional NLP models.
Conclusion: Research and the use of deep learning NLP in radiology is increasing. An acquaintance with this technology can help prepare radiologists for the coming changes in their field.
Limitations: This systematic review has several limitations. First, heterogeneity of studies and variability in measures between studies prevented a meta-analysis. Second, we limited our search to radiology applications. Deep learning NLP is implemented for the analysis of many kinds of medical texts, not just limited to our field. Finally, deep learning for NLP is a rapidly expanding topic. Thus, there may be concepts and applications published after our review was performed.
Ethics committee approval: n/a
Funding: No funding was received for this work.
Author Disclosures:
V. Sorin: nothing to disclose
Y. Barash: nothing to disclose
E. Klang: nothing to disclose
E. Konen: nothing to disclose

08:30 - 10:00 **Room E**

Genitourinary

RPS 1707

Kidney and bladder problem solving: a different approach

Moderators:
I. Sjekavica; Zagreb/HR
N.N.

RPS 1707-1 08:30
3T blood-oxygen-level dependent (BOLD) MRI in renal transplants for the differentiation between acute rejection (AR) and acute tubular necrosis (ATN)
A. Ramadan, M. Shaaban, M. H. K. Khalifa, M. Zeid, N. Baddour, O. Ezz*; Alexandria/EG (doctoradelramadan@gmail.com)*

Purpose: To assess the diagnostic accuracy of 3T BOLD-MRI for the differentiation of AR and ATN in the transplanted kidney.
Methods and materials: This study included 75 renal graft recipients from living donors in 22 months. They were divided into group A, including 32 recipients with stable graft function, group B, and group C, including 25 and 18 recipients with pathologically proven AR and ATN, respectively. Each recipient was subjected to 3T BOLD-MRI using a breath-hold multiple fast-field echo sequence to obtain R2* maps in coronal planes. Qualitative analysis at colour-coded R2* maps and quantitative analysis by placing ROIs on R2* maps, measuring mean ±SD of C-R2* and M-R2*, and calculating MCR were performed. The ANOVA test was applied for comparison between different groups. ROC curve analysis determined the recommended cutoff values with corresponding sensitivity, specificity, PPV, NPV, and accuracy.
Results: The study included 75 adult recipients; 32 as control and 43 with graft dysfunction. Pathology was 25 AR (group B) and 18 ATN (group C). Qualitative analysis showed a visual difference between different groups. Quantitative analysis revealed significantly higher C-and M-R2* values in the ATN group (21.20±2.54/s and 31.01±3.99/s) than in group A (14.96±1.61/s and 26.38±3.12/s) and the AR group (14.83±2.86/s and 22.28±5.29/s), respectively. For the prediction of ATN versus AR, the recommended cutoff value was >18.93/s and >26.35/s for C-R2* and M-R2*, respectively, with high sensitivity and specificity, and 90.7% accuracy. MCR was lower in the AR and ATN groups than in the control group, but no difference was found between the AR and ATN groups.
Conclusion: 3T BOLD-MRI is promising for the evaluation of renal grafts with the potential ability to differentiate between AR and ATN cases.
Limitations: n/a
Ethics committee approval: n/a
Funding: No funding was received for this work.
Author Disclosures:
A. Ramadan: nothing to disclose
M. H. K. Khalifa: nothing to disclose
O. Ezz: nothing to disclose
M. Shaaban: nothing to disclose
M. Zeid: nothing to disclose
N. Baddour: nothing to disclose

RPS 1707-2 08:36

Renal allograft dysfunction evaluation using BOLD-MRI

M. E. Abou El-Ghar, H. M. Farg, B. Ali-El-Dein, A. Refaie, T. El-Diasty; *Mansoura/EG (maboelghar@yahoo.com)*

Purpose: To evaluate the role of BOLD-MRI using 3T magnet in the discrimination of renal allograft acute rejection from ATN in the early post-transplant period.
Methods and materials: This prospective study included 78 live-donor renal allograft recipients; 28 with normal function (group 1), 15 with AR (group 2), and 35 with ATN (group 3). Cortical R2* (CR2*), medullary R2* (MR2*), and medullary over cortical R2* ratio (MCR) were measured.
Results: The mean medullary R2* value (24.3 ± 2.5/sec) was significantly greater than the cortical R2* value (18.2 ± 2.2/sec) in normally functioning allografts ($p < 0.001$). The mean MR2* level was significantly lower in the acute rejection (AR) group (20.5 ± 2.5/sec) compared to the normal group (24.3 ± 2.5/sec, $P<0.001$) and ATN group (27.1 ± 1.9/sec, $P < 0.001$). There was also a significant difference in MR2* levels between the ATN group and the normal group ($p < 0.001$). The MCR was higher in the ATN group (1.44 ± 0.22) compared to the AR group (1.17 ± 0.14) and normal functioning group (1.35 ± 0.22), with a significant difference between the 3 groups ($p= 0.001$). The mean CR2* was higher in the ATN group (19.2 ± 2.5/sec) compared to the normal group (18.2 ± 2.2/sec) and AR group (17.5 ± 1.8/sec).
Conclusion: BOLD-MRI is a valuable non-invasive diagnostic technique that can differentiate between AR and ATN in kidney transplants by measuring the changes in intra-renal tissue oxygenation.
Limitations: We included only cases in the early transplant period.
Ethics committee approval: The study protocol was approved by our local institutional transplant committee. Informed consent was obtained from patients.
Funding: No funding was received for this work.
Author Disclosures:
M. E. Abou El-Ghar: nothing to disclose
H. M. Farg: nothing to disclose
B. Ali-El-Dein: nothing to disclose
A. Refaie: nothing to disclose
T. El-Diasty: nothing to disclose

RPS 1707-3 08:42

Medullary oxygenation: an important index for evaluating renal function in chronic kidney disease

P. Xin Long, T. Xin Kui; *Beijing/CN (mrpxl@126.com)*

Purpose: BOLD-MRI can provide regional measurements of oxygen content using deoxyhaemoglobin paramagnetic characteristics. Chronic kidney disease (CKD) can affect oxygenation levels in renal parenchyma, which influences the clinical course of the disease. Furosemide may make Na+ -K+ -ATP pump work reduction and oxygen consumption decrease. The goal of this study was to assess renal oxygenation levels in CKD using BOLD-MRI when injecting furosemide.
Methods and materials: 18 healthy subjects and 39 patients with CKD underwent a renal scan using a multi-gradient-recalled-echo (mGRE) sequence with 16 echoes, and 28 of 39 patients underwent the same sequence 7 minutes after injecting furosemide. R2* values of three regions of interest (ROI) of the renal cortex and medulla were measured and their average values were calculated. The difference of R2* was compared between the healthy subjects and all patients. According to eGFR, 28 patients with injected furosemide were divided into a normal eGFR group (group 1,≥90 mL/min/1.73 m^2) and an abnormal eGFR group (group 2,<90 mL/min/1.73 m^2), and the changes of R2* in the two groups after injection were compared. 28 of the 39 patients were confirmed by ultrasound-guided puncture and the other 11 patients had a similar diagnosis based on clinical symptoms and investigations.
Results: Medullary R2*(MR2*) were significantly lower in patients (78 kidneys, MR2*=28.81±4.65 s^{-1}) than in controls (36 kidneys, MR2*=31.18±1.87s^{-1}), $P<0.05$. Medullary to cortical R2* ratios of patients (1.78±0.26) was significantly decreased compared to controls (1.94±1.14), $P<0.01$. After injecting furosemide, R2* variance of the medulla (ΔMR2*＝MR2*pre－MR2*post) in group 1 (6.63±0.66) was higher than that of group 2 (4.03±0.64), $p＜0.01$.
Conclusion: Medullary R2* values in BOLD-MRI when injecting furosemide were an effective index for evaluating renal oxygenation in CKD.
Limitations: No differentiating specific pathogenesis of CKD.
Ethics committee approval: Informed consent was obtained from all participants.
Funding: No funding was received for this work.
Author Disclosures:
P. Xin Long: nothing to disclose
T. Xin Kui: nothing to disclose

RPS 1707-4 08:48

Veno-arterial index (VAI): a promising tool for renal transplant rejection

F. Lubinus[1], E. Zuñiga[1], S. Vera[1], E. Villarreal[1], M. Ochoa[1], J. C. Mantilla[2]; *[1]Bucaramanga/CO, [2]Floridablanca/CO (flubinus@hotmail.com)*

Purpose: In transplant rejection, there is an increase in venous flow velocities and a decrease in arterial flow velocities, probably due to graft hardening.
Methods and materials: A diagnostic study was carried out between January 2014 and May 2018. Renal transplanted patients who underwent percutaneous renal biopsy were studied. The veno-arterial index (VAI) was obtained by measuring the flow velocity in the segmental vein at the level of the renal medulla (VFV) and dividing this value by the velocity of the systolic peak of the segmental artery (PSV) in this same location.
Results: 78 records of patients who underwent renal biopsy were analysed. 32 patients (41.5%) suffered from transplant rejection, with 29 presenting with acute rejection. Prior to the study, a normal baseline value of the VAI was obtained by measuring the VAI in 70 individuals without known urological pathology, obtaining a VAI with a median value of 0.30 (range 0.18-0.44). In transplant rejection, the median VAI was 0.67. In kidneys with a negative biopsy for rejection, the median VAI was 0.41 ($p=0.007$), higher than that obtained for the general population which was 0.30 ($p=0.0001$). In subacute and acute rejection, the index was higher (VAI: 0.725). For the severity of rejection, the difference was also statistically significant ($p = 0.0001$).
Conclusion: The results of this study show that the veno-arterial index (VAI) is a useful parameter which could predict transplant rejection when elevated.
Limitations: Studies with a larger number of patients are required to confirm this hypothesis and to obtain a more accurate value of the VAI.
Ethics committee approval: Approved by the ethics committee.
Funding: No funding was received for this work.
Author Disclosures:
F. Lubinus: nothing to disclose
E. Zuñiga: nothing to disclose
S. Vera: nothing to disclose
E. Villarreal: nothing to disclose
M. Ochoa: nothing to disclose
J. C. Mantilla: nothing to disclose

RPS 1707-5 08:54

Quantitative analysis of wash-out parameters on an MRI DCE T1 weighted-sequence in adrenal lesions with a heterogeneous signal drop on chemical shift imaging

R. Galatola, A. Stanzione, F. Verde, V. Romeo, R. Liuzzi, P. P. Mainenti, E. Guadagno, A. Brunetti, S. Maurea; *Naples/IT (galatolaroberta@gmail.com)*

Purpose: To assess the significance of a qualitative heterogeneous pattern of signal drop on chemical shift (CS) magnetic resonance imaging (MRI) of adrenal lesions (AL) employing quantitative parameters obtained from CS and dynamic contrast-enhanced (DCE) sequences.
Methods and materials: This retrospective study included 3T MRI examinations with AL, for which histopathology, functional imaging, or follow-up data were available as a reference standard. Two radiologists qualitatively grouped AL on CS sequences, showing homogeneous (group A), heterogeneous (group B), and no (group C) signal drop. They manually drew 2D ROIs on CS and DCE images to obtain three quantitative parameters: adrenal signal intensity index (ASII), absolute (AWO), and relative washout (RWO). ANOVA analysis and a post-hoc Dunn's test were used to compare these values among the three groups.
Results: 66 AL were included, divided into groups A (n=19), B (n=23), and C (n=24). ASII values resulted as significantly different among the three groups ($p<0.001$) with the following median values: 71%, 53%, and 0.03%, respectively. AWO and RWO values were not significantly different between groups A and B, showing percentages (AWO: 54% and 46% and RWO: 33% and 29%, respectively) suggestive of a benign nature. Indeed, 98% of lesions were benign, mostly (86%) represented by adenomas. Conversely, AWO and RWO values of group C resulted as significantly different ($p<0.001$) and lower (20% and 9%, respectively) than other groups. Indeed, 58% of these lesions were non-adenomas and the remaining percentage were lipid-poor adenomas.
Conclusion: According to our results, AL showing a qualitative heterogeneous pattern of signal drop on CS images are mainly benign and represented by adenomas, showing dynamic quantitative parameters similar to those with a homogeneous signal drop on CS sequence.
Limitations: A retrospective design and small population.
Ethics committee approval: IRB approved, consent waived.
Funding: No funding was received for this work.

Author Disclosures:
R. Galatola: nothing to disclose
A. Stanzione: nothing to disclose
F. Verde: nothing to disclose
V. Romeo: nothing to disclose
R. Liuzzi: nothing to disclose
P. P. Mainenti: nothing to disclose
E. Guadagno: nothing to disclose
A. Brunetti: nothing to disclose
S. Maurea: nothing to disclose

RPS 1707-6 09:00
Role of diffusion-weighted imaging in the characterisation of renal masses
A. Sever, M. Yalçın, A. A. Demir, Y. Savas*; Istanbul/TR*
(mdalpersever@gmail.com)

Purpose: To investigate the role of diffusion-weighted imaging in the characterisation of renal masses.
Methods and materials: Between January 2014 and December 2018, patients who had a histopathologically-proven renal tumour were reviewed retrospectively. Patients who had preoperative MRIs were included for the study. Diffusion-weighted images were taken and ADC maps were calculated automatically by the MRI unit. The average ADC values of masses were measured. SPSS was used to evaluate the statistical data.
Results: Of the 142 patients, 108 had malignant masses and 34 had benign masses. Of the malignant patients, 59 had clear-cell RCC, 19 had papillary RCC, 14 had chromophobe RCC, 9 had TCC, and 7 had other rare subtypes. Of the benign patients, 6 had oncocytoma, 3 had angiomyolipoma, and 14 had papillary adenomas, metanephric adenomas, and infectious pseudotumours. 11 had benign cystic lesions of the kidneys.
The difference between ADC values of malignant and benign masses wasn't statistically significant (0.92 vs 0.88 × 10^{-3} mm^2/s; p>0.05). Clear-cell RCCs had higher ADC values than non-clear-cell RCCs (1.09 vs 0.73 × 10^{-3} mm^2/s; p<0.05). RCCs had higher ADC values than non-RCCs (0.96 vs 0.69 × 10^{-3} mm^2/s; p<0.05). Oncocytomas had higher ADC values than chromofobe RCCs (1.27 vs 0.73 × 10^{-3} mm^2/s; p<0.05). The difference between low-grade RCCs (Fuhrman grade 1-2) and high-grade RCCs (Fuhrman grade 3-4) was statistically significant. Low-grade RCCs had higher ADC values (1.06 vs 0.9 × 10^{-3} mm^2/s; p<0.05).
Conclusion: ADC measurements may help in the differentiation of certain renal masses. It should be encouraged to be used in appropriate situations.
Limitations: The retrospective nature of the study.
Ethics committee approval: Ethics committee approval obtained.
Funding: No funding was received for this work.
Author Disclosures:
A. Sever: nothing to disclose
M. Yalçın: nothing to disclose
A. A. Demir: nothing to disclose
Y. Savas: nothing to disclose

RPS 1707-7 09:06
The change of total kidney volume after renal transplant in patients with autosomal polycystic renal disease: does it play a role in the indications and optimal timing decision for native kidney resection?
L. Marcolin, L. M. Cacioppa, M. Ruggeri, G. Scalas, N. Sciascia, I. Capelli, R. Golfieri, G. La Manna*; [1]Bologna/IT*
(laura.cacioppa@gmail.com)

Purpose: Autosomal dominant polycystic kidney disease (ADPKD) is characterised by a progressive enlargement of kidney cysts, often leading to end-stage disease with the need for renal transplantation (RT) and native kidney nephrectomy (NN). Few studies have investigated the appropriate timing for NN and the role of the change in total kidney volume (TKV) after RT in NN indications.
Methods and materials: From January 2008 to December 2018, all polycystic patients who underwent RT in our centre were recorded and retrospectively reviewed. TKVs were evaluated with volumetric analyses on computed tomography (CT) scans performed before and one year after RT in patients who underwent RT alone, and in those scheduled for RT who also required NN. Mean TKV values were height/age, adjusted according to imaging classification of ADPKD (hTKV) and compared.
Results: A total of 182 RTs were collected; 50 patients (27.5%) underwent NN (29 bilateral and 21 unilateral). NN procedures were pre-RT, post-RT, and simultaneous to RT in 54 (76%), 11 (15.5%), and 6 (8.5%), respectively; 34 (47.9%) due to symptoms occurrence and 37 (52.1%) to allow graft positioning. The median age was 54,6 ± 8,7. The mean hTKVs showed a non significant post-RT reduction in the group submitted to RT alone (1866.1±1005.2 vs 1863.2±1075.4 ml/m;p=ns). Compared to those submitted to RT alone, patients who underwent NN showed a higher mean pre-RT hTKV (2301.7±1100.7 vs 1651±994.3 ml/m;p=0.1).
Conclusion: Despite the natural course of native polycystic kidneys, after RT is not well known and indications and timing of NN in patients scheduled for RT are controversial. Our study showed how TKV could be a measurable tool to determine critical kidney volumes at risk of complication and requiring future NN. Decisions for or against NN should take into account TKV reduction after RT and the presence of symptoms, complications, or unavailable graft space in order to avoid additive risks.
Limitations: n/a
Ethics committee approval: n/a
Funding: No funding was received for this work.
Author Disclosures:
L. M. Cacioppa: nothing to disclose
L. Marcolin: nothing to disclose
M. Ruggeri: nothing to disclose
N. Sciascia: nothing to disclose
I. Capelli: nothing to disclose
G. Scalas: nothing to disclose
R. Golfieri: nothing to disclose
G. La Manna: nothing to disclose

RPS 1707-9 09:12
VI-RADS: do we really need all multiparametric data?
J. Gmeiner, N. Garstka, S. Sevcenco, P. A. T. Baltzer*; Vienna/AT*
(jasmingmeiner@yahoo.de)

Purpose: To investigate the diagnostic performance of the overall VI-RADS score and its individual parameters in assessing muscle invasivness and grade of bladder cancer (BCa).
Methods and materials: In this IRB-approved, prospective single-centre cross-sectional observational study, patients with BCa underwent preoperative multiparametric MRI at 3T including T2w, DWI, and DCE images. Evaluation according to the VI-RADS scoring system was performed by two radiologists independently, blinded to histological findings. The performance of mpMRI and VI-RADS for determining muscle invasiveness and grade of BCa was compared by using ROC analysis.
Results: The median age of 45 included patients was 67.6, range 28-90 years. Among 45 BCa, 13 (29%) were identified as muscle-invasive and 32 (71%) as non-invasive BCa. The AUC for VI-RADS to predict muscle invasion was 0.975 (95% CI: 0.877 to 0.999) and 0.866 for VI-RADS to distinguish high-grade from low-grade BCa (95% CI 0.728 to 0.951). There was no significant difference between the AUC of single parameters (DCE, T2w and DWI) compared to the total VI-RADS score (p=1.000, p=0.408, p=0.264 for muscle invasion; p=1.000, p=0.2644, p=0.828 for grading).
Conclusion: Our results indicate that VI-RADS is an effective clinical decision rule to diagnose BCa grading and invasiveness. The inclusion of multiple parameters does not seem to be necessary. Therefore, contrast-enhanced sequences may be omitted as BCa patients regularly suffer from renal insufficiency.
Limitations: Besides a small sample size, the main limitation of this study is the observational character that did not investigate the effect of VI-RADS on clinical decision making.
Ethics committee approval: The study protocol was approved by the Ethics Committee of the Medical University of Vienna.
Funding: No funding was received for this work.
Author Disclosures:
J. Gmeiner: Author at Medical University of Vienna
N. Garstka: nothing to disclose
S. Sevcenco: nothing to disclose
P. A. T. Baltzer: nothing to disclose

RPS 1707-10 09:18
Diffusion tensor imaging (DTI) images + T2-weighted 3D CUBE sequences: a potential additional tool to mpMRI in differentiating non-muscle from muscle-invasive bladder cancer on a 3T scanner
D. Fierro, M. Pecoraro, S. Cipollari, R. Campa, V. Salvo, C. Catalano, V. Panebianco*; Rome/IT (fierrodavide852@hotmail.com)*

Purpose: To determine whether the association of diffusion tensor imaging (DTI) sequences + T2-weighted 3D CUBE to the standard mpMRI protocol could aid in differentiating muscle-invasive bladder cancer (MIBC) from non-muscle-invasive bladder cancer (NMIBC).
Methods and materials: 61 patients were enrolled and underwent mpMRI before tumour resection. Exams were performed on a 3T scanner (GE Discovery 750) with a 32 channel BodyCoil, DTI sequences (matrix 100x100, TR:3485, TE:55, Auto InvTime:248, thickness (thk): 3.0 mm, gap: 0.5 mm, field of view (FOV) 26, b value: 0 (2 NEX), 1,000 (4 NEX), 16 directions) and T2-weighted (CUBE) 3D isotropic (matrix: 260x260, TR: Auto, TE:120, thl: 1.4 mm, FOV 26, echo-train-length (ETL):100) were acquired and reconstructed with WorkStation

(FiberTrack program, GE, ADW 4.7). Two radiologists reported the exams, blinded to pathology results. Accuracy was determined using histopathology as a reference standard.
Results: A total of 61 exams were analysed. All NMIBC (n=41) lesions were correctly defined by the DTI + T2-weighted 3D CUBE image set. Overall accuracy of the setting protocol completed by FiberTrack and MultiPlanar reconstructions was 90% to differentiate NMIBC from MIBC.
Conclusion: Association of DTI + T2-weighted 3D CUBE sequences on MpMRI appears to be a reliable staging tool for bladder cancer. With further validation, mpMRI + DTI sequences + T2-weighted 3D CUBE could precede cystoscopic resection, allowing for prompt detection of muscle invasiveness fastening therapeutic pathways.
Limitations: A small sample size in a single institution.
Ethics committee approval: n/a
Funding: No funding was received for this work.
Author Disclosures:
D. Fierro: nothing to disclose
M. Pecoraro: nothing to disclose
S. Cipollari: nothing to disclose
R. Campa: nothing to disclose
V. Salvo: nothing to disclose
V. Panebianco: nothing to disclose
C. Catalano: nothing to disclose

RPS 1707-11 09:24

Evaluation of diffusion kurtosis imaging versus standard diffusion-weighted imaging in the assessment of the pathological grade of clear-cell renal cell carcinoma

J. Cao, B. He, X. Luo, X. Sun*; Zibo/CN (cjf19810629@163.com)*

Purpose: To evaluate the role of diffusion kurtosis imaging in the characterisation of clear-cell renal cell carcinoma compared with standard diffusion-weighted imaging.
Methods and materials: 80 patients with histologically proven ccRCC were evaluated by DKI and DWI on a 3-T scanner. All ccRCCs were classified as grade 1 (n=15), grade 2 (n=22), grade 3 (n=24), and grade 4 (n=19) according to the Fuhrman classification system. Regions of interest were drawn on the maps of the apparent diffusion coefficient, fractional anisotropy, mean diffusion coefficient, mean diffusion kurtosis, axial kurtosis, and radial kurtosis. The differences in DWI and DKI parameters were evaluated and a receiver operating characteristic analysis was performed.
Results: ADC value could be used to discriminate G1 vs G3, G1 vs G4, G2 vs G3, G2 vs G4, and G3 vs G4 ($P < 0.05$), except for G1 vs G2. All the DKI parameters except for FA could be used to discriminate G1 vs G2, G1 vs G3, G1 vs G4, G2 vs G4, and G3 vs G4 ($P < 0.05$), whereas MD, MK, and Kr could discriminate G2 vs G3 ($P < 0.05$). Moreover, ROC analysis showed that the MK values exhibited the best performance.
Conclusion: DKI could provide better performance than conventional DWI in grading ccRCC.
Limitations: The number of ccRCC patients was relatively small. When the lesion is small or there is an unresolved necrotic area in the lesion, the ROI fails to completely avoid the necrotic tissue in the lesion and the results may be biased.
Ethics committee approval: This study was approved by the local institutional review board and informed consent was obtained from all patients.
Funding: No funding was received for this work.
Author Disclosures:
J. Cao: nothing to disclose
B. He: nothing to disclose
X. Luo: nothing to disclose
X. Sun: nothing to disclose

RPS 1707-12 09:30

Imaging protocols for renal multiparametric MRI and MR urography: results of a consensus conference from the French Society of Genitourinary Imaging

O. Rouviere*; Lyon/FR (olivier.rouviere@netcourrier.com)*

Purpose: To develop technical guidelines for magnetic resonance imaging aimed at characterising renal masses (multiparametric magnetic resonance imaging and mpMRI) and the bladder and the upper urinary tract (magnetic resonance urography and MRU).
Methods and materials: The French Society of Genitourinary organised a Delphi consensus conference with a two-round Delphi survey followed by a face-to-face meeting. Two separate questionnaires were issued for renal mpMRI and for MRU. Consensus was strictly defined using a priori criteria.
Results: 42 expert uro-radiologists completed both survey rounds with no attrition between the rounds. 56/84 (66.7%) statements of the mpMRI questionnaire and 44/71 (62%) statements of the MRU questionnaire reached a final consensus. For mpMRI, there was consensus that no injection of furosemide was needed and that the imaging protocol should include T2-weighted imaging, dual-chemical shift imaging, diffusion-weighted imaging (use of multiple b-values; maximal b-value: 1000 s/mm²) and fat-saturated single-bolus multiphase (unenhanced, corticomedullary, nephrographic) contrast-enhanced imaging; late imaging (more than 10 minutes after injection) was judged as optional. For MRU, the patients should void their bladder before the examination. The protocol must include T2-weighted imaging, anatomical fast T1/T2-weighted imaging, diffusion-weighted imaging (use of multiple b-values; maximal b-value: 1000 s/mm²), and fat-saturated single-bolus multiphase (unenhanced, corticomedullary, nephrographic, excretory) contrast-enhanced imaging. An intravenous injection of furosemide is mandatory before the injection of contrast medium. Heavily T2-weighted cholangiopancreatography-like imaging was judged optional.
Conclusion: This expert-based consensus conference provides recommendations to standardise magnetic resonance imaging of kidneys, ureter, and bladder.
Limitations: Consensus statements represent a low level of evidence.
The consensus conference did not address MR examinations aimed at evaluating bladder cancer local staging, nor protocol variations in children or pregnant women.
Ethics committee approval: n/a
Funding: This work was funded by the French Society of Genitourinary Imaging (Société Française d'Imagerie Génito-urinaire)
Author Disclosures:
O. Rouviere: nothing to disclose

RPS 1707-13 09:36

Validation of vesical imaging reporting and data systems in bladder tumours: assessment of muscle invasion

S. H. Kim, H. S. Park, S. H. Cho*; Daegu/KR (warpaludin@gmail.com)*

Purpose: To retrospectively determine the diagnostic values of a VI-RAD score for the detection of muscle invasion in patients with bladder tumours.
Methods and materials: This study included 347 consecutive patients with 339 tumour lesions who were previously diagnosed by CT imaging and subsequently underwent bladder multiparametric MR imaging between January 2015 and March 2019. Lesions level analyses were performed by using an overall score of VI-RADS. Histologic examination of TURBT was used as the reference standard. Two radiologists assessed the diagnostic scores of tumours with muscle invasion by using cutoff values of ≥ 4 and ≥ 3. Cutoff values for VI-RADS scores were estimated from operating points of AUC analyses. Sensitivity, specificity, PPV, NPV, and accuracy were calculated to assess the utility of VI-RADS
Results: The interobserver agreement was excellent for three different MR imaging at the lesion level. T2W and DW imaging had a similar diagnostic accuracy of 79.3% for tumour lesions with muscle invasion compared to the overall score of 80.2%, with a cutoff value of 4. The overall VI-RAD score showed an accuracy of 80.2%, with a cutoff value of ≥ 4, granting a sensitivity of 91.3%, specificity of 76.0%, PPV of 83.3%, and NPV of 78.9%. When we applied an arbitrary overall score of ≥ 3, accuracy was 63.7%, sensitivity was 94.6%, specificity was 43.9%, PPV was 51.6%, and NPV was 63.7%.
Conclusion: VI-RADS has an overall good performance for the diagnosis of tumours with muscle invasion.
Limitations: The current study was a single-centre retrospective study with a small number of participants. As a consequence, a statistical significance was not observed in comparing each result. For these results to be more definitive, prospective studies with larger numbers of patients are required.
Ethics committee approval: n/a
Funding: No funding was received for this work.
Author Disclosures:
H. S. Park: nothing to disclose
S. H. Kim: nothing to disclose
S. H. Cho: nothing to disclose

RPS 1707-14 09:42

Validation of a prospective assessment of the vesical imaging-reporting and data system (VI-RADS) in high-risk non-muscle invasive bladder cancers (NMIBC) candidate for repeated transurethral resection

M. Pecoraro, S. Cipollari, R. Campa, F. Del Giudice, G. Simone, E. de Berardinis, C. Catalano, V. Panebianco*; Rome/IT (pecoraro.martina1@gmail.com)*

Purpose: To prospective validate VI-RADS in NMI-and-MIBC discrimination at TURBT. To identify HR-NMIBCs who could avoid Re-TURBT and to detect those at a higher risk for under-staging after TURBT.
Methods and materials: Patients with a BCa suspicion were offered multiparametric magnetic resonance imaging (mpMRI) before TURBT. According to VI-RADS, a cutoff ≥3 to define MIBC was assumed. TURBT reports were compared with preoperative VI-RADS scores to assess the accuracy of mpMRI in discriminating NMI-and-MIBC. HR-NMIBCs Re-TURBT reports were

compared with preoperatively recorded VI-RADS scores to assess mpMRI accuracy in predicting Re-TURBT outcomes. Sensitivity, specificity, and positive and negative predictive (PPV, NPV) values were calculated for mpMRI performance in patients undergoing TURBT and for HR-NMIBCs candidate for Re-TURBT. ROC curve and K statistics were calculated
Results: 231 patients were enrolled. MpMRI showed a sensitivity, specificity, PPV, and NPV in discriminating NMI-from-MIBC at initial TURBT of 91.9% (95%CI:82.2–97.3), 91.1% (95%CI: 85.8–94.9), 77.5% (95%CI:65.8–86.7), and 97.1% (95%CI:93.3–99.1), respectively. Area under curve (AUC) was 0.94 (95%CI:0.91–0.97). Within HR-NMIBCs (n=114), mpMRI before TURBT showed a sensitivity, specificity, PPV, and NPV of 85% (95%CI:62.1–96.8), 93.6% (95%CI: 86.6–97.6), 74.5% (95%CI: 52.4–90.1) and 96.6% (95%CI: 90.5–99.3), respectively, to identify patients with MIBC at Re-TURBT. AUC was 0.93 (95%CI: 0.87–0.97).
Conclusion: VI-RADS is accurate for discriminating NMI-and-MIBC. Within HR-NMIBCs, VI-RADS could improve the selection of patients' candidate for Re-TURBT in the future.
Limitations: MpMRI cannot yet be adopted for CIS and the sample is small in a single-centre.
Ethics committee approval: Approved by an ethical committee with a waiver of informed consent.
Funding: No funding was received for this work.
Author Disclosures:
M. Pecoraro: nothing to disclose
S. Cipollari: nothing to disclose
R. Campa: nothing to disclose
F. Del Giudice: nothing to disclose
G. Simone: nothing to disclose
E. de Berardinis: nothing to disclose
C. Catalano: nothing to disclose
V. Panebianco: nothing to disclose

RPS 1707-15 09:48
The potential of apparent diffusion coefficient values as an independent marker for tumour aggressiveness in non-muscle-invasive bladder cancer
A. Rahota[1], P. Medan[2], B. Petresc[3], A. Tamas-Szora[2], R. Rahota[1], N. Crisan[2], A. Lebovici[2]; [1]Oradea/RO, [2]Cluj/RO, [3]Tg. Mures/RO

Purpose: To determine whether the apparent diffusion coefficient (ADC) measured from diffusion-weighted imaging reflects quantitative information of the histological grading and clinical aggressiveness of non-muscle-invasive bladder cancer.
Methods and materials: We prospectively enrolled 25 bladder tumours that have undergone 1.5T MRI DW images using b-values of 0, 50, and 800 s/mm2 in axial and sagittal planes. ADC values and their relationship with histological factors were measured for each lesion. The pathology report was considered a gold standard diagnosis.
Results: 14 lesions were low grade (LG) and 11 high grade (HG). 11 lesions were staged as pTa and 14 as pT1. The mean ADCs of LG and HG tumours were 1.25 × 10−3 mm2/s, respectively, 0.80 × 10−3 mm2/s, with a difference that was statistically significant (p<0.001). The cut-off value in the receiver operating characteristic (ROC) curve for differentiating LG and HG according to ADC values was 0.87 × 10−3 mm2/s (Se=72.7%, Sp=100%), with an area under curve (AUC) of 0.90. The mean values of ADC of pTa and pT1 tumours were 1.24 × 10−3 mm2/s and 0.80 × 10−3 mm2/s, respectively (p<0.001). No significant difference was found among the values of ADCs of axial versus sagittal acquisitions for tumours located on the lateral walls (1.12 × 10−3 mm2 /s vs. 1.21 × 10−3 mm2/s, p=0.56), or for tumours located on the inferior and superior walls (1.15 × 10−3 mm2/s vs 1.08 × 10−3 mm2/s, p=0.56).
Conclusion: DW imaging with ADC measurement could become a novel non-invasive method for predicting tumour aggressiveness in bladder cancer.
Limitations: A preliminary study and small sample size.
Ethics committee approval: All patients gave written informed consent.
Funding: No funding was received for this work.
Author Disclosures:
A. Lebovici: nothing to disclose
A. Rahota: nothing to disclose
A. Tamas-Szora: nothing to disclose
N. Crisan: nothing to disclose
R. Rahota: nothing to disclose
B. Petresc: nothing to disclose
P. Medan: nothing to disclose

08:30 - 10:00 **Room Y**

My Thesis in 3 Minutes

MyT3 17
Head and Neck

Moderators:
Y. J. F. De Brucker; Brussels/BE
A. Germano; Barcarena/PT

MyT3 17-1 08:30
Performance of HRCT temporal bone in the evaluation of non-otologic anatomical variations in temporal bone and their implications in procedure planning of cochlear implant surgery: a prospective study
S. Agarwal, A. Prakash, N. Mannan, M. Grover; *Jaipur/IN (srishtiagarwal243@gmail.com)*

Purpose: Cochlear implantation is the recommended treatment for patients presenting with severe to profound pre- or post-lingual sensorineural hearing loss. Imaging plays a pivotal role in the selection of candidates. A pre-operative knowledge of variant anatomy helps in the planning of the surgical approach and aids in identifying potential complications.
Methods and materials: Patients suffering from profound to severe sensorineural hearing loss with the candidacy for cochlear implantation were evaluated by high-resolution CT of the temporal bone (HRCT). A total of 100 cases were referred from July 2018 to February 2019 and were included in the study after taking patient consent. Many anatomical variants were observed including mastoid pneumatisation, level of middle cranial fossa dura, Korner's septum, mastoid emissary vein, sigmoid sinus and jugular bulb position, bony facial canal, position of mastoid segment of facial nerve canal with respect to round window for visualisation of round window during surgery and alignment of cochlear basal turn with respect to axis of internal carotid artery canal for round window accessibility.
Results: The pre-cochlear implant imaging had a sensitivity of 97.22% and diagnostic accuracy of 90% in identifying accessibility of round window when correlating with intra-operative findings. Surgeon acceptability was a highlight of this study.
Conclusion: Pre-cochlear implantation imaging in addition to performing the accepted role of imaging of the middle and internal ear anatomy is also crucial in the identification of various non-otologic landmarks which affect procedure planning and possible complications. Attention to these small but significant details can greatly improve surgical outcome.
Limitations: There is possibility that changes could have happened in the period between imaging and surgery which was appreciated in surgery and was absent during imaging.
Ethics committee approval: n/a
Funding: No funding was received for this work.
Author Disclosures:
S. Agarwal: nothing to disclose
A. Prakash: nothing to disclose
M. Grover: nothing to disclose
N. Mannan: nothing to disclose

MyT3 17-2 08:34
Noise-optimised virtual monoenergetic imaging of dual-energy CT: effect on contrast agent artifacts reduction on carotid CTA examination
J. Fu, Y. Zeng, J. Zhang; *Shanghai/CN (kdidjs_fu@163.com)*

Purpose: Artefacts of contrast agent in the subclavian vein often affect the display of cervical arteries at the corresponding level. We aimed to evaluate the effects of noise-optimised virtual monoenergetic imaging (VMI+) reconstructions on reducing these artefacts, compared to traditional virtual monoenergetic imaging (VMI) and linearly blended (F_0.6) reconstructions in patients underwent carotid CTA and recommend a better energy level to show calcified plaque.
Methods and materials: Ten patients who underwent carotid CTA were evaluated retrospectively. Images were reconstructed with F_0.6, VMI and VMI+ at 20-keV intervals from 40 keV to 140 keV. Attenuation and noise were measured in the cervical arteries at the worst level obstructed by the contrast agent artefacts of each patient. The artefact index (AI) and iodine SNR were calculated.
Results: The AI values for the cervical arteries were lowest in the 140keV VMI+ series, which were lower compared to all the VMI and F_0.6 images (all p<0.029), but showed no significant differences compared to the 120keV VMI+ series (p=0.684). The SNR was highest in the 40keV VMI+ series, and there were no significant differences compared to the highest SNR in the VMI images and F_0.6 (P≥0.529), even compared to the 60-120keV VMI+ (p≥0.052).

Conclusion: DECT with 120keV VMI+ efficiently reduced artefacts of contrast agent without affecting image quality of carotid CTA, and 120keV can be used as an additional energy level in the VMI+ reconstruction to better show calcified plaques in the cervical arteries affected by the artefacts.
Limitations: A small number of patients with severe artefacts of contrast agent on carotid CTA were obtained.
Ethics committee approval: This was approved by the institutional review board of Huashan Hospital of Fudan University.
Funding: This study was funded by the Shanghai Rising-Star Program (Grant No. 16QA1400900).
Author Disclosures:
J. Fu: Author at Huashan Hospital of Fudan University
Y. Zeng: Author at Huashan Hospital of Fudan University
J. Zhang: Author at Huashan Hospital of Fudan University

MyT3 17-3 08:38
Ultra-high frequency ultrasound (UHFUS) of the minor salivary gland in patients with Sicca syndrome
A. Marcucci, S. Vitali*; Pisa/IT*

Purpose: The aim of this study was to assess the usefulness of ultra-high frequency ultrasound (UHFUS), with frequencies up to 70 MHz and resolution up to 30 µm, for the examination of the minor salivary glands in primary Sjögren's syndrome (pSjS). In particular we assessed the diagnostic accuracy of UHFUS, and the improvement of bioptic sampling under UHFUS guidance.
Methods and materials: Seventy-eight patients with Sicca syndrome suspected secondary to pSjS (72 females and 6 males) with a mean age of 56 years (standard deviation=±15 years) were enrolled. The following UHFUS parameters were evaluated: glands distribution, parenchymal inhomogeneity (score 0-3, from absent inhomogeneity to evident), fibrosis, and vascular pattern and degree of vascular intensity (by means of echo color-Doppler analysis). The minor salivary gland of the lower lip with more significant UHFUS abnormalities was marked with a dermographic pen and underwent biopsy for calculation of the focus score (FS).
Results: In 38/78 cases (48.7%) pSjS was diagnosed on the basis of ACR/EULAR criteria. Glands with UHFUS score≥1 were considered suggestive of pSjS (sensitivity=100%, specificity=26.7%, NPV=100% and PPV=50%). We found a good correlation between the FS and the following UHFUS parameters: lateral inhomogeneity (r=0.532), central inhomogeneity (r=0.496), central fibrosis (r=0.398). Under UHFUS guidance, the percentage of adequate bioptic samples increased from 62.5% in 2017 to 83.6% in the period 2018/2019.
Conclusion: UHFUS findings accurately predict the FS. Moreover, this modality provides reliable guidance for biopsy. The 100% negative predictive value makes UHFUS suitable as a screening tool for pSjS, with the potential to avoid unnecessary biopsies.
Limitations: The small number of patients enrolled.
Ethics committee approval: Ethics committee approval was obtained.
Funding: No funding was received for this work.
Author Disclosures:
A. Marcucci: Author at University of Pisa
S. Vitali: Author at University of Pisa

MyT3 17-4 08:42
Response evaluation of choroidal melanoma after brachytherapy using diffusion-weighted magnetic resonance imaging (DW-MRI): preliminary findings
F. Bitencourt[1], A. Bitencourt[1], J. D. O. Souza[1], N. Neves[2], M. Chojniak[1], R. Chojniak[1]; [1]São Paulo/BR, [2]Salvador/BR (almirgvb@yahoo.com.br)

Purpose: To evaluate the role of diffusion-weighted magnetic resonance imaging (DW-MRI) in the evaluation of patients with choroidal melanoma at the time of diagnosis and in the evaluation of therapeutic response after brachytherapy.
Methods and materials: We performed a prospective, unicentric study approved by the research ethics committee, which included patients with choroidal melanoma and indication for brachytherapy. Three DW-MRI examinations were proposed for each patient, one before and two after treatment. The apparent diffusion coefficient (ADC) value was calculated on DW-MRI and compared with local tumour control assessed by ophthalmologic follow-up.
Results: From 07/2018 to 06/2019, 19 patients were included, of which 13 underwent follow-up examinations. Patients' ages ranged from 24 to 78 years and 52.9% were male. At the ocular ultrasound, the mean tumour thickness and diameter were 6.3 mm and 11.5 mm, respectively. At initial MRI, most tumours presented high or intermediate signal at T1 (82.3%) and a low signal at T2 (70.6%). Two patients (15.4%) showed signs of tumour progression during follow-up. There was no statistically significant difference in tumour size between MR before and after treatment, however, there was a significant reduction in mean ADC in patients with progression (p = 0.02).
Conclusion: DW-MRI has shown to be useful in assessing patients with choroidal melanoma and mean ADC values can be used for response assessment, allowing early identification of patients at risk for progression after brachytherapy.
Limitations: This study was limited by the small number of cases.
Ethics committee approval: The IRB approval was obtained.
Funding: This study was funded by the São Paulo Research Foundation - FAPESP (grant n. 2016/05967-5).
Author Disclosures:
A. Bitencourt: nothing to disclose
F. Bitencourt: nothing to disclose
R. Chojniak: nothing to disclose
M. Chojniak: nothing to disclose
J. D. O. Souza: nothing to disclose
N. Neves: nothing to disclose

MyT3 17-5 08:46
The evaluation of the maculopathy using dynamic contrast-enhanced MRI in patients with proliferative diabetic retinopathy
Z. Chen, M. Liu, L. Ma*; Beijing/CN (yyqf@hotmail.com)*

Purpose: To evaluate the macular change in the patients with diabetic retinopathy using dynamic contrast-enhanced magnetic resonance imaging (DCE-MRI) technique.
Methods and materials: Twenty patients with diabetic retinopathy (DR) and 20 normal controls (NC) were included. The fast spoiled gradient recalled sequence was used to perform dynamic contrast T1WI enhancement on 3.0T MR system. The macular region, optic papilla and nasal retina were performed with quantitative DCE-MRI evaluation using Omni-Kinetics software.
Results: The maximal concentration, the area under the concentration-time curve (AUCconcentration-time) and maximal slope of macular region were significantly higher in DR [0.270 (0.03,1.20) mmol/100ml, 2.71 (0.04,9.91) mmol*min and 0.38 (0.06,3.18) mmol/min, respectively] than that [0.169(0.03,0.72) mmol/、1.25 (0.13,10.41) mmol*min and 0.245 (0.06,1.34) mmol/min] in NC (U value = 515.00 and P value = 0.080, U value = 433.00 and P value = 0.000, and U value = 563.00 and P value = 0.023, respectively). The receiver operating characteristic curve (ROC) analysis demonstrated that the area under AUCconcentration-time was 0.729±0.058 with the cut-off value 1.479 mmol*min (sensitivity 80.00% and specificity 62.50%) for macular region.
Conclusion: The quantitative DCE-MRI technique could be used to evaluate the maculopathy associated with the diabetic retinopathy.
Limitations: The limits of this study are that the region of interest (ROI) in the retinochoroidal complex, the enhanced concentration of choroid was also included in the regions, would not truly reflect retinopathy entirely based on the current MRI technique.
Ethics committee approval: This study was approved by the Chinese PLA General Hospital institutional review board, and written informed consent were obtained from all subjects.
Funding: No funding was received for this work.
Author Disclosures:
Z. Chen: nothing to disclose
L. Ma: nothing to disclose
M. Liu: nothing to disclose

MyT3 17-6 08:50
The relationship of severity of migraine and the optic nerve sheath diameter measured by ultrasonography in patients admitted to an emergency department
I. Kanbur[1], H. Topacoglu[2]; [1]Vienna/AT, [2]Istanbul/TR (drinciferkanbur@gmail.com)

Purpose: ONSD (optic nerve sheath diameter) measured by ultrasonography would be different in patients with migraine with aura than in patients with migraine without aura.
Methods and materials: 49 patients were enrolled. Patients were excluded from the study if they were haemodynamically unstable, needed emergency intervention, had an anatomical eye abnormality, had an eye disease that increased the ONSD or had a headache secondary to organic disease. Patients were assessed for headache type according to the criteria determined by the International Headache Society (IHS). The Siemens Acuson P500 portable ultrasound device in ocular imaging mode with a 10-MHz surface tissue probe was used bedside for the evaluation of the ONSD and eye segment diameter. The ONSD was scanned in the sagittal and transverse planes. Additionally, the eye segment diameter measurements were performed on both eyes. All measurements were repeated three times and then the mean value was recorded.
Results: There was no significant difference in the eye segment mean diameters between patients with and without pulsating pain (p > 0.05). There

was also no significant difference in the eye segment mean diameters between patients with and without aura using the Mann–Whitney U-test ($p > 0.05$).
Conclusion: In this study, we found that there was a statistically insignificant increase in the ONSD in patients with migraine with aura compared to the patients without aura and also in patients with pulsating pain compared with patients without pulsating pain. We could not find any differences in the transverse diameter, anteroposterior diameter, anterior camera depth, and eye globe volume in patients with and without aura.
Limitations: This study is limited by the following: the small number of participants, no control group, no follow-up measurements, and the inclusion of just migraine patients.
Ethics committee approval: n/a
Funding: No funding was received for this work.
Author Disclosures:
I. Kanbur: nothing to disclose
H. Topacoglu: nothing to disclose

MyT3 17-7 08:54
Volumetric analysis of the maxillary, sphenoid and frontal sinuses in computerised tomography: a comparative study using volume rendering in patients of the Hospital Universitario in Monterrey, Mexico
I. A. Garza Rico, R. A. Cuéllar Lozano, R. Pinales Razo, N. G. Jasso Ramirez*; Monterrey/MX (dra.ingridgarza@gmail.com)*

Purpose: To measure the volume and measurements of the maxillary, sphenoid and frontal sinuses and in healthy Mexican patients, using computed tomography (CT) scans.
Methods and materials: A retrospective, case series study in a single academic centre, CT scans of 210 subjects, 10 of every age, between 0 and 20 years of age, performed between January 2016 and November 2017 in the Hospital Universitario of Monterrey, Mexico. A comparative analysis of the volume and dimensions of the paranasal sinuses was performed using multiplanar reformating and volume rendering with segmentation. Patients with prior history of trauma, surgery, and pathology of the paranasal sinuses were excluded. The study population was subdivided by gender and age.
Results: A total of 210 CT scans were analysed, 104 (49.5%) males and 106 (50.5%) females. The groups were subdivided by age (<5, 6-10, 11-15 and >16 years). The largest volumes were reached by 16 to 20 years of age. In the 6-10 age group, the females had larger volumes than the males. The males had a tendency to present larger volumes in general. There is a high correlation in between the volume of sinus and its contralateral r (0.01) and there is also a significant relation of the sinus volume and age Z (<0.004).
Conclusion: There is a clear volumetric correlation according to age and gender, there is a direct relation between a sinus and its contralateral homologous. The expected volume development can influence clinical decision making in this age group.
Limitations: The normal variants of the paranasal sinuss were not part of the study design.
Ethics committee approval: This study was approved by the Ethics Comitee of the Hospital Universitario.
Funding: No founding was received for this work.
Author Disclosures:
I. A. Garza Rico: nothing to disclose
R. A. Cuéllar Lozano: nothing to disclose
R. Pinales Razo: nothing to disclose
N. G. Jasso Ramirez: nothing to disclose

MyT3 17-8 08:58
Role of magnetic resonance imaging in patients with temporomandibular joint pain
P. M. A. D. Mohamed Abouelhoda, R. A. M. A. Helal, A. A. Megahed*; Cairo/EG (bosi_123@hotmail.com)*

Purpose: To assess the role of MRI in the assessment of patients suffering from temporomandibular joint pain presented to the El-Demerdash Hospital.
Methods and materials: A cross-sectional study is done on 50 patients presented to El-Demerdash hospital presented by temporomandibular joint (TMJ) pain. MRI was done on our 1.5 T machine with the following conventional sequences: axial T1 images sagittal oblique images, oriented along the long axis of the mandible, acquired at closed and open mouth positions, obtained with a fast-spin echo, a PD, and a T2* gradient echo technique. Coronal thin sections of ≤3 mm T2 sequences. Image interpretation was done commenting upon the articular surfaces, articular disc position and morphology, joint space, lateral pterygoid muscle as well as bony abnormalities.
Results: 64% of the cases had TMJ pain due to disc displacement. 18% of the cases had TMJ pain due to arthritis. 6% of the cases had TMJ pain due to fracture. 6% of the cases had TMJ pain due to infection. 4% of the cases had TMJ pain due to tumour. 2% of the cases had TMJ pain due to lateral pterygoid muscle abnormality
Conclusion: MRI is the technique of choice for assessing patients presented with TMJ pain identifying its different pathologies. Having a systemic pattern in image interpretation is important for the radiologist to detect early signs of TMJ dysfunction, thereby avoiding its progression to an irreversible phase.
Limitations: The study was done on a small number of patients. The positioning of the patient during the imaging was limited due to severe pain and limited open-mouth view.
Ethics committee approval: The research ethics committee in the El-Demerdash Hospital approved the research with informed consent form for patients or their parents who are invited to participate in the research.
Funding: No funding was received for this work. Agreement to reduce the MR price was provided.
Author Disclosures:
P. M. A. D. Mohamed Abouelhoda: nothing to disclose
R. A. M. A. Helal: nothing to disclose
A. A. Megahed: nothing to disclose

MyT3 17-9 09:02
Normal thyroid stiffness in healthy adults using real-time shear wave and strain elastography and factors that influence the measurement of stiffness
M. Z. Mohammad Zakir[1], P. Chatterjee[2], R. Ravikumar[3]; [1]Nagpur/IN, [2]Guwahati/IN, [3]Chennai/IN (drmohammadzuber@gmail.com)

Purpose: Elastography is a non-invasive technique to determine tissue stiffness. Elastography estimation is of two types qualitative (compression) and quantitative (shear wave or ARFI) method. The aim of this study is to define a normal range of thyroid stiffness in healthy individuals using the above methods. Also, our objective is to determine various factors affecting in determining the elastography values.
Methods and materials: In our study 812 healthy subjects underwent the examination of the stiffness of the thyroid gland and various factors like age, gender, position during the test, BMI, size of ROI, depth of ROI etc which affect the stiffness measurement were studied. In the strain elastography (compression) the red colour coding was taken as stiffer areas and blue as normal tissue; green was intermediate tissue type.
Results: The mean value of ARFI (shear wave or quantitative) in the 812 subjects were 1.32 +/- 0.55 m/s. In the strain elastography (compression) all subjects' thyroid gland demonstrated blue colour coding representing normal parenchyma. The stiffness was found more in the elderly and with higher BMI subjects. The values were more consistent when measured in the mid-segment of the lobe of the thyroid gland. The values were slightly higher in female subjects. The size and depth of ROI do not affect the measurement.
Conclusion: The sonoelastography of the thyroid gland is an important non-invasive tool to assess the stiffness of thyroid gland in pathological conditions. The factors which affect the elastography measurement should be avoided or considered while measuring the elastography values. Elastography is a non-invasive technique to assess the tissue stiffness and to differentiate normal and abnormal areas in the tissue.
Limitations: The single-centre study design limited this study.
Ethics committee approval: n/a
Funding: No funding was received for this work.
Author Disclosures:
M. Z. Mohammad Zakir: nothing to disclose
P. Chatterjee: nothing to disclose
R. Ravikumar: nothing to disclose

MyT3 17-10 09:06
MDCT evaluation of neck masses in adults
A. Kotwal, A. N. Kamble*; New Delhi/IN*

Purpose: To study the role of multi-detector computed tomography (MDCT) in the evaluation of neck masses in adults in the Lady Hardinge Medical College, New Delhi. To correlate MDCT findings with clinical/perioperative/pathological follow-up findings whenever possible.
Methods and materials: The hospital-based descriptive observational study conducted from November 2015 to March 2017 in the department of radio-diagnosis. The study population was adults (>18 years) with neck masses. The sample size was 33 patients. The inclusion criteria was the following: age ≥ 18 years with clinically detected neck masses and neck masses detected on ultrasonography who were referred for MDCT and incidentally diagnosed neck masses by MDCT. The exclusion criteria were the following: a history of trauma of neck area and pregnancy. The study instruments were clinical proforma and PHILIPS BRILLIANCE 40 slices multi-detector CT. The methodology used included clinical evaluation and CT. Plain and contrast-enhanced scans using non-ionic contrast media were performed sequentially from the base of the skull to the 4th thoracic vertebra. Multi-planar reconstruction was created.
Results: Nodal masses were the most common masses (39.4%). These included metastatic (27.27%), lymphomatous (6.06%), tubercular adenopathy (6.06%). Non-nodal masses constituted 60.6%, included salivary gland lesions

(30%), thyroid masses (30%), masses of developmental origin (15%), neurogenic (10%), vascular (5%), mesenchymal origin (5%) and inflammatory masses (5%). 84.6% of the nodal masses were malignant, 15.3% were benign. 25% of the non-nodal masses were malignant, 75% were benign. In total, 48.48% had malignant lesions and 51.5% of the cases had benign lesions.
Conclusion: MDCT ensure anatomical localisation, characterisation and lesion extent of the neck masses.
Limitations: This study was performed as a single centre study and is limited by small sample size.
Ethics committee approval: The study was approved by the institutional ethical committee and written informed consent was taken by each patient.
Funding: This study was funded by our institute.
Author Disclosures:
A. Kotwal: nothing to disclose
A. N. Kamble: nothing to disclose

MyT3 17-11 09:10
Neurologic dysphagia: does the percutaneous endoscopic gastrostomy (PEG) treatment really decrease the incidence of aspiration pneumonia?
L. Perrucci, M. Stantieru, M. Giganti, R. Galeotti*; Ferrara/IT (dott.perrucciluca@gmail.com)*

Purpose: Our goal has been to determine if PEG treatment determined a reduction of pneumonia cases in a population with neurologic functional dysphagia.
Methods and materials: 20 patients with neurogenic dysphagia have been retrospectively examined. In 13 PEG-treated patients were evaluate the thorax x-rays and CT to find signs of pneumonia. The observation period is between 500 days before and after the endoscopic surgical procedure. Other seven patients were treated only with rehabilitation; the same evaluation was referred to the radiographic dynamic study of the swallowing (DSS - also called a videofluoroscopic study of the swallowing, VFSS). All 20 patients performed a DSS to confirm or exclude the presence of aspiration, this latter only determining the aspiration nature of pneumonia. The exact Fisher test was applied to each group and subgroup.
Results: In the first group analysed of the 13 PEG-treated patients, 7 presented pneumonia before the procedure and the prevalence increased of 8/13 after it, six of whom did not present before. Regarding those ones without aspiration at DSS(low-risk for pneumonia) presented an increase of the cases from 3/8 to 5/8. In the remaining five patients with aspiration (high-risk pneumonia with the burden of aspiration pneumonia defined at DSS) the ratio decreased from 4/5 to 3/5. No significant p-value has merged at the Fisher tests. In the second group of seven patients, who were not treated with PEG the Fisher test on pneumonia cases was not significant as well, but the prevalence of pneumonia was higher than in the other subgroups (6/7).
Conclusion: The DSS helped to distinguish patients with aspiration, and therefore with aspiration pneumonia, where the PEG treatment determined a reduction of pneumonia cases. In the other subgroups the prevalence of pneumonia increased.
Limitations: Nothing to declare.
Ethics committee approval: Nothing to declare.
Funding: nothing-to-declare
Author Disclosures:
M. Stantieru: nothing to disclose
L. Perrucci: nothing to disclose
M. Giganti: nothing to disclose
R. Galeotti: nothing to disclose

MyT3 17-12 09:14
Comparative efficacy of neck ultrasonography, ^{99m}Tc Sestamibi scan and ^{18}F- Choline PET/CT in the preoperative localisation of suspected cases of parathyroid adenoma in primary hyperparathyroidism
T. Neeliyath Thazha Kuni[1], A. Sood[2], R. Kr[1], S. K. Bhadada[2], B. R. Mittal[2], A. Behra[2], U. N. Saikia[2], D. S. Rao[3]*; [1]Calicut/IN, [2]Chandigarh/IN, [3]Detroit, MI/US (DRTHANSEER@GMAIL.COM)*

Purpose: This study was conducted to compare the effectiveness of ultrasonography of the neck, ^{99m}Tc-sestamibi and ^{18}F-fluorocholine PET/CT imaging in the preoperative localisation of parathyroid lesions in patients with primary hyperparathyroidism.
Methods and materials: Fifty-four patients of PHPT were included in this prospective study who underwent preoperative localisation of the parathyroid lesion(s) using three diagnostic modalities followed by surgery. The sensitivity, positive predictive value (PPV) and accuracy of the three imaging procedures to accurately detect abnormal parathyroid glands were determined using histopathology as the gold standard.
Results: FCH PET/CT detected 52 out of 54 patients and 52 out of 56 lesions with histopathologically proven parathyroid adenomas on patient-based and lesion-based analysis respectively. Preoperative USG, MIBI and FCH PET/CT localised abnormal parathyroid gland(s) in 39 (72.2%), 43 (79.6%) and 54 (100%) patients respectively. The sensitivity and PPV were 69.3% and 87.1% for USG, 80.7% and 97.6% for MIBI, and 100% and 96.3% for FCH PET/CT. The accuracy was 62.9%, 79.6% and 96.3% for USG, MIBI and FCH PET/CT respectively in the patient-wise analysis. In six patients with ectopic lesions, FCH PET/CT demonstrated higher sensitivity and accuracy than MIBI and USG (100% vs 66.6% and 16.7% respectively).
Conclusion: Among the three imaging techniques tested simultaneously, FCH PET/CT was superior for accurate preoperative localisation of parathyroid adenomas, especially for ectopic or small parathyroid lesions.
Limitations: Various statistical measures like specificity, negative predictive value and serum PTH cut off values for FCH PET/CT could not be calculated in our study, as none of the patients was negative on FCH PET/CT imaging.
Ethics committee approval: The ethics committee approval was obtained.
Funding: No funding was received for this work.
Author Disclosures:
T. Neeliyath Thazha Kuni: nothing to disclose
A. Sood: nothing to disclose
R. Kr: nothing to disclose
S. K. Bhadada: nothing to disclose
B. R. Mittal: nothing to disclose
A. Behra: nothing to disclose
U. N. Saikia: nothing to disclose
D. S. Rao: nothing to disclose

MyT3 17-13 09:18
Role of neck imaging reporting and data system (NI-RADS) in the prediction of local and regional recurrence of head and neck squamous cell carcinoma
T. Taha, M. M. M. Ashour, H. A. K. Abdel Hameed, Z. M. Abdel Hafeez, A. S. Abdelrahman*; Cairo/EG (manar.ashour@gmail.com)*

Purpose: To assess the diagnostic performance of the ACR NI-RADS.
Methods and materials: 116 follow-up scans for 55 patients treated from primary HNSCC were included in combined retrospective and prospective study that was conducted in Ain-Shams University Hospitals. Scans timings followed our institution protocol; the first follow-up performed eight weeks after finishing treatment. A choice between CE-CT/MRI or PET-CT determined by the clinical scenario. Scans were reported using the ACR NI-RADS template, scores were assigned to each scan; one for the primary tumour site and one for neck nodes. The assigned NI-RADS scores were correlated to patients' outcomes according to our gold standard: tissue pathological examination and/ or follow-up scans, with follow-up duration that extended for twelve months, except for two patients. We calculated the rate of disease recurrence for each score. We compared the diagnostic performance of the different NI-RADS templates for CE-CT; PET-CT and CE-MRI. We also assessed the diagnostic performance of the templates' imaging findings describing the primary tumor site morphological changes, enhancement, and FDG activity, and describing the neck nodes correlated to outcome. Data analysis was done by IBM SPSS (V.25.0, IBM Crop., USA, 2017-2018).
Results: We had 232 targets for primary tumour sites and for lymph nodes. Tumour recurrence occurred in 53 targets. Recurrence rates for each NI-RADS category. A significant correlation between template morphological and enhancement findings and patients' outcomes at the primary site and LNs. PET/CT template had the highest accuracy, sensitivity, and specificity.
Conclusion: The performance of the ACR NI-RADS reporting system is excellent with a good correlation with the outcome.
Limitations: This study is limited by the sample volume and time period.
Ethics committee approval: The ethics committee approval and written informed consent were obtained.
Funding: No funding was received for this work.
Author Disclosures:
M. M. M. Ashour: nothing to disclose
T. Taha: nothing to disclose
A. S. Abdelrahman: nothing to disclose
Z. M. Abdel Hafeez: nothing to disclose
H. A. K. Abdel Hameed: nothing to disclose

MyT3 17-14 09:22
A comparative study for diagnostic performance of shear wave elastography and diffusion-weighted MRI in cervical lymph nodes
V. S. Öztürk, E. Ertekin*; Aydin/TR (md.suhaozturk@gmail.com)*

Purpose: The aim of this study was to investigate the potential diagnostic value of point shear wave elastography (pSWE) and the contribution of concurrent diffusion-weighted MRI to diagnostic performance prospectively in patients with cervical lymphadenopathy.
Methods and materials: 188 cervical lymph nodes of 144 patients were included in the study. All patients with or without an underlying malignancy were included in the study and all lymph nodes were evaluated before the treatment or histopathological sampling. US characteristics were recorded, stiffness and

ADC values of lymph nodes were measured. Lymph nodes were divided into benign and malign groups with histopathological findings, clinical and sonographic follow-up.
Results: Short axis, hilus morphology, vascularisation patterns, pSWE, and ADC values were significant parameters in logistic regression tests between the two groups. The median stiffness of malign nodes were higher and the average ADC values were lower than others also the lowest ADC values were measured in lymphoproliferative disorders (p<0.001). Area under the curve values for pSWE and diffusion MRI were 0.846 (95% CI, 0.789-0.903), 0.796 (95% CI, 0.725-0.868), respectively. Tissue stiffness had the highest diagnostic accuracy with 80.3%. Accuracy rate increased to 87.2% from 83.5% when the pSWE was combined with the conventional US. No differences were detected when the DWI findings were added to these.
Conclusion: The use of pSWE combined with B-mode US may be sufficient for the differentiation of lymph nodes and will reduce the number of biopsies. The main role of DWI in cases which underwent ultrasonography, may be specific to lymphoproliferative disorders rather than lymph node characterisation.
Limitations: Study group was heterogeneous and not all cases had pathological evaluation.
Ethics committee approval: The ethics committee approval and written informed consent were obtained.
Funding: No funding was received for this work.
Author Disclosures:
V. S. Öztürk: nothing to disclose
E. Ertekin: nothing to disclose

MyT3 17-15 09:26
Role of magnetic resonance apparent diffusion coefficient in assessment of solitary thyroid nodule
E. H. A. Emara[1], H. Mansour[2], A. Bessar[2], I. Lebda[2]; [1]*Kafr El-Shaikh/EG,* [2]*Zagazig/EG (emademara85@yahoo.com)*

Purpose: To evaluate the role of apparent diffusion coefficient values in differentiating between malignant and benign solitary thyroid nodules and its correlation with histopathological results as the reference standard.
Methods and materials: 30 patients with solitary thyroid nodules were included and evaluated by ultrasound, colour Doppler ultrasound, conventional magnetic resonance imaging (MRI), MRI with diffusion-weighted imaging (DWI-MR) using b-values (500, 1000 mm^2/s) with ADC value measurement. Fine needle aspiration was done after DW-MRI to avoid affecting diffusion characters of the nodules. Histopathological examinations were done for all cases after surgery and correlated with the imaging finding.
Results: 24 nodules were benign (12 adenomatous hyperplasias, nine follicular hyperplasias, and three solitary nodular goiters) and six nodules were malignant (three papillary carcinoma and three follicular carcinoma). The mean ADC value of benign thyroid nodules (2.1± 0.2× 10–3 mm^2/s – 1.87± 0.3× 10–3 mm^2/s) was statistical significance higher than malignant ones (1.06± 0.2× 10–3 mm^2/s - 0.970.3× 10–3 mm^2/s) using b-values 500, 1000 mm^2/s (P=0.001 and 0.001) respectively. The mean ADC value of benign and malignant nodules done using b-values 1000 mm^2/s was statistical significance higher than using b-values 500 mm^2/s (P=0001). A cut-off ADC value of (1.5) has been suggested as a reference point to differentiate benign from malignant nodules with (83.3 % sensitivity, 96.0% specificity, 83.3 % PPV and 96.02% NPV, P=.001) using b-values 500 mm^2/s and (100 % sensitivity, 100% specificity, 100% PPV and 100% NPV, P=.001) using b-values 1000 mm^2/s.
Conclusion: ADC value calculation is a good quantitative measurement that can differentiate benign from malignant solitary thyroid nodules with recommendable b-value 1000 mm2/s.
Limitations: This study is limited by the motion artefact, a small number of patients and difficult to detect nodules < 5mm.
Ethics committee approval: n/a
Funding: No funding was received for this work.
Author Disclosures:
E. H. A. Emara: nothing to disclose
H. Mansour: nothing to disclose
A. Bessar: nothing to disclose
I. Lebda: nothing to disclose

MyT3 17-16 09:30
Preoperative assessment of extrathyroidal extension of papillary thyroid carcinomas by ultrasound and magnetic resonance imaging: a comparative study
S. Hu[1], X. Wang[2]; [1]*Wuxi/CN,* [2]*Zhenjiang/CN (hsd2001054@163.com)*

Purpose: The purpose of this study was to assess the diagnostic performance of preoperative ultrasonography (US) and magnetic resonance imaging (MRI) for the prediction of extrathyroidal extension (ETE) in patients with papillary thyroid carcinoma (PTC) and to compare the diagnostic performances of US and MRI for predicting ETE.
Methods and materials: This retrospective study was approved by our institutional review board. Preoperative US and MRI were performed for 225 patients who underwent surgery for PTCs between May 2014 and December 2018. For each case, the US and MRI features of ETE were retrospectively and independently investigated by two radiologists. The diagnostic performance of US and MRI, including their sensitivity, specificity, positive predictive value (PPV), and negative predictive value (NPV) for ETE, as well as their accuracy in predicting ETE was analysed.
Results: US showed higher sensitivity and NPV than MRI in the prediction of minimal ETE (87.5 vs 71.3, p=0.006 and 76.2 vs 61.7 p=0.046, respectively). MRI showed higher sensitivity than US for assessing extensive ETE (85.4 vs 66.7, p=0.005). The specificity and PPV of MRI were significantly higher than those of US (p=0.025 and p=0.025, respectively) for assessing overall ETE.
Conclusion: Preoperative US should be used as the first line of predicting minimal ETE and MRI should be added to assess assessing extensive ETE. Compared with US, MRI has higher specificity and PPV in detecting overall ETE of PTC.
Limitations: Selection bias may have existed.
Ethics committee approval: This retrospective study was approved by the institutional review board and written informed consent was waived.
Funding: No funding was received for this work.
Author Disclosures:
S. Hu: nothing to disclose
X. Wang: nothing to disclose

MyT3 17-17 09:34
Advanced protocol of MSCT data post-processing in orbital trauma
O. Pavlova, N. S. Serova, D. Davydov*; Moscow/RU*
(dr.olgapavlova@gmail.com)

Purpose: To establish the advanced diagnostic protocol of MSCT data postprocessing in patients with orbital trauma in order to select the correct treatment tactics and provide optimal preoperative planning.
Methods and materials: A total of 107 patients with orbital trauma (100%) were admitted to the hospital on the 1-2 day after the injury. MSCT was performed using Canon Aquilion One 640, data postprocessing was performed using workstation Vitrea Core. The analysis of MSCT data included standard visualisation of bone and soft tissue injury of orbital structures as well as developed techniques including orbital volume measurements, evaluation of inferior orbital wall defects, analysis of globe position and assessment of periorbital soft tissue density.
Results: Postprocessing of MSCT data according to the developed techniques compared to the standard visualisation of bone and soft tissue injury allowed to reveal additional increased traumatic orbital volume in 21 patients (19%); additional enophthalmos in 9 patients (8%); determination of 4 types of inferior orbital wall defects: small inferior orbital defects (n=18; 17%), moderate defects (n=31; 29%), severe defects (n=37; 35%) and total defects (n=20; 19%) as well as detailed assessment of periorbital soft tissue density: oedema (n=60; 56%), haematoma (n=10; 9%), atrophy (n=28; 27%), no changes (n=9; 8%), p<.001.
Conclusion: The advanced techniques of orbital volume measurements, inferior orbital wall defects evaluation, analysis of globe position and assessment of periorbital soft tissue density statistically significantly increased the efficiency of MSCT data analysis in patients with orbital trauma in order to define the correct treatment tactics.
Limitations: No limitations were identified.
Ethics committee approval: n/a
Funding: No funding was received for this work.
Author Disclosures:
O. Pavlova: nothing to disclose
N. S. Serova: nothing to disclose
D. Davydov: nothing to disclose

MyT3 17-18 09:38
Clinical value of mobile CT head examination in patients with intensive care unit
P. Jin, C. Xia, Z. Li*; Chengdu/CN*

Purpose: To investigate the timeliness, economy, radiation dose and clinical value of mobile CT head scan in intensive care patients.
Methods and materials: The clinical data of 80 patients with progressive intracranial haemorrhage were analysed retrospectively, mobile CT and conventional CT examination were performed in each of 40 cases. On two groups of a bleeding area of image quality was evaluated by two senior radiologists and records of two patients completed the inspection time, radiation dose and statistical analysis of the results.
Results: All patients were successfully completed by a CT head scan. The time required for a mobile CT group examination was (9.21±2.13 min), significantly lower than that of the normal group (47.43±7.10 min), the difference was statistically significant. The effective radiation dose was (1.52±0.00 mSv), lower than the normal group (1.90±0.40 mSv), the difference was statistically

significant. Two groups of bleeding area image quality by which difference was not statistically significant. The examining flow of mobile CT group was reduced three links and three medical staff than the normal group.
Conclusion: Mobile CT examination has higher timeliness and reduces the risk of mobile CT scanning in intensive care patients, saved labor cost and reduced radiation dose, could be better served for the ICU patients who had head CT examining needs.
Limitations: In this study, the body mass index, age and patients were not quantitatively analysed before or after surgery, and further studies will be conducted in the follow-up work.
Ethics committee approval: n/a
Funding: This study was funded by the 1.3.5 project for disciplines of excellence, West China Hospital, Sichuan University.
Author Disclosures:
Z. Li: Research/Grant Support at at west china hospital of Sichuan university
P. Jin: Author at west china hospital of Sichuan university
C. Xia: Research/Grant Support at west china hospital of Sichuan university

MyT3 17-19 09:42
Role of diffusion tensor imaging in the evaluation of patients with cervical spondylotic myelopathy: a cross-sectional study
V. S. Arunachalam, S. Saxena, R. Dev, P. Sharma, U. Chauhan, S. Sharma, N. Chatterjee*; Rishikesh/IN (drvenkat07@gmail.com)*

Purpose: To ascertain any correlation of diffusion tensor imaging (DTI) parameters - fractional anisotropy (FA) and apparent diffusion coefficient (ADC) with standard MR findings and clinical severity.
Methods and materials: Patients presenting with cervical myelopathy to neurosurgery/orthopedic outpatient department and without recent traumatic history, neuroparenchymal pathology or contraindication to MRI and agreeing to undergo MRI were examined with MRI of the cervical spine. In addition to standard MRI sequences for imaging the cervical spinal cord, diffusion tensor imaging based on single-shot EPI with 20 diffusion directions, each encoded with b-values of 0mm2/s and 1000mm2/s was performed in both sagittal and axial planes. Postprocessing of the raw DTI data was done using ready view developed by GE (Advantage4.7). Stenotic and non-stenotic levels were compared with Kang's grading and DTI parameters. Baseline clinical severity was assessed based on modified Japanese Orthopaedic Association (mJOA) score. Using SPSS(ver23), Anova's test was done to assess different Grade individuals. Pearson's correlation of FA with ADC, Kang's grade and mJOA score were calculated.
Results: 43 patients were included in the study. Mean FA values recorded at stenotic (0.346) was less than non-stenotic (0.600) levels. A negative correlation of -0.661 and -0.362 was recorded between FA and ADC and stenotic grading (Kang's), respectively. Level of significance was recorded at 0.013.
Conclusion: Diffusion tensor imaging can serve as a potential tool for understanding pathophysiology thereby complementing anatomical information from standard sequences and aid in prognostication of patients with cervical spondylotic myelopathy prior to surgical and non-surgical management.
Limitations: Changes in DTI parameters were not recorded following treatment. Technical limitations of DTI may be overcome by using HARDI and Q space imaging.
Ethics committee approval: Institutional ethics committee approved the study. Written informed consent was obtained from all patients.
Funding: No funding was received for this work.
Author Disclosures:
V. S. Arunachalam: nothing to disclose
S. Saxena: nothing to disclose
R. Dev: nothing to disclose
S. Sharma: nothing to disclose
N. Chatterjee: nothing to disclose
U. Chauhan: nothing to disclose
P. Sharma: nothing to disclose

MyT3 17-20 09:46
Non-contrast-enhanced carotid MRA: clinical evaluation of a novel ungated radial quiescent-interval slice-selective MRA at 1.5T
S. Peters[1], M. Huhndorf[1], J.-K. Ulf[1], I. Koktzoglou[2], R. Edelman[2], J. Graessner[3], M. Both[1], O. Jansen[1], M. Salehi Ravesh[1]; [1]*Kiel/DE,* [2]*Evanston, IL/US,* [3]*Hamburg/DE (Mona.SalehiRavesh@uksh.de)*

Purpose: Non-contrast-enhanced MRA techniques have experienced a renaissance due to the known correlation between the use of gadolinium-based contrast agents and the development of nephrogenic systemic fibrosis and the deposition of gadolinium in some brain regions. The purpose of this study was to assess the diagnostic performance of ungated non-contrast-enhanced radial quiescent-interval slice-selective MRA of the extracranial supra-aortic arteries in comparison with conventional contrast-enhanced MRA in patients with clinical suspicion of carotid stenosis.
Methods and materials: In this prospective study, both MRA pulse sequences were performed in 31 consecutive patients (median age, 68.8 years; 19 men). For the evaluation, the cervical arterial system was divided into 35 segments (right and left side). Three blinded reviewers separately evaluated these segments. An ordinal scoring system was used to assess the image quality of arterial segments and the stenosis grading of carotid arteries.
Results: Overall venous contamination in quiescent-interval slice-selective MRA was rated as “none” by all readers in 84.9% of the cases and in 8.1% of cases in contrast-enhanced MRA (p=0.0001). The visualisation quality of arterial segments was considered good to excellent in 40.2% for the quiescent-interval slice-selective MRA and in 52.2% for the contrast-enhanced MRA (p=0.0001). The diagnostic accuracy of ungated quiescent-interval slice-selective MRA concerning the stenosis grading showed a total sensitivity and specificity of 85.7% and 90.0%, respectively.
Conclusion: Ungated quiescent-interval slice-selective MRA can be used clinically as an alternative to contrast-enhanced MRA without a significantly different image quality or diagnostic accuracy for the detection of carotid stenosis at 1.5T.
Limitations: The number of patients in our single-centre study was relatively small.
Ethics committee approval: The ethics committee approval was obtained (No. D 508/18).
Funding: This study was funded by the National Institutes of Health under award number R01EB027475.
Author Disclosures:
M. Salehi Ravesh: nothing to disclose
S. Peters: nothing to disclose
M. Huhndorf: nothing to disclose
J.-K. Ulf: nothing to disclose
I. Koktzoglou: Research/Grant Support at e National Institutes of Health under award number R01EB027475
R. Edelman: Research/Grant Support at e National Institutes of Health under award number R01EB027475
J. Graessner: Employee at Siemens Healthcare GmbH
M. Both: nothing to disclose
O. Jansen: nothing to disclose

08:30 - 10:00 **Coffee & Talk 3**

Chest

RPS 1704

The dark side of chest imaging

Moderators:
N.N.

RPS 1704-1 08:30
Agreement between consultant radiologists and reporting radiographers in chest radiograph reporting: a consecutive clinical series
N. H. Woznitza[1], A. Devaraj[1], N. Hayes[1], D. Togher[1], N. Arumalla[1], E. Skyllberg[1], B. Ghimire[1], Z. Shah[1], D. R. Baldwin[2]; [1]*London/UK,* [2]*Nottingham/UK (nicholas.woznitza@nhs.net)*

Purpose: To investigate chest radiograph (CXR) reporting by radiographers.
Methods and materials: A prospective, single-site trial. 12-month consecutive CXRs referred from primary care were independently reported by consultant radiologists (CR;n=13) and reporting radiographers (RR;n=3). Respiratory physicians, blinded to the reporter, compared reports for agreement. Discordant cases were reviewed by thoracic radiologists, blinded to the reporter, who reached the index diagnosis and graded report elements (observation, interpretation, recommendations, and usefulness). The number of CR and RR generated CT scans and lung cancers diagnosed were recorded.
Results: 8,685 of 9,136 (95.1%) CXRs were included. Agreement and insignificant disagreement between CR/RR reports occurred in 5,981 (68.9%) and 1,347 (15.5%) of cases, respectively. 1,357 (15.6%) of CR/RR reports had clinically significant disagreement. Thoracic radiology review has been performed for 908 of 1,357 (66.9%) discordant reports. Both reports were correct in 292 (32.2%), CR report correct in 255 (28.1%), RR report correct in 271 (29.8%), and neither report correct in 90 (9.9%). Thoracic radiologists were no more likely to agree with a CR or RR report (p=0.49;CI=-0.03,0.07). RR reports were non-inferior to CR reports for observation (764 vs 768;p=0.787,CI=-0.037-0.029), interpretation (758 vs 763;p=0.742,CI=-0.039-0.028), and recommendations (692 vs 656;p=0.06,CI=-0.003-0.082), and not clinically different for usefulness (870 vs 832;p<0.001,CI=0.02-0.063). 350 CT scans were generated by CRs or RRs; 103 both CR/RR, 149 CR only, and 98 RR only. 31 of 49 lung cancers were diagnosed on a radiology generated CT; n=22 both CR/RR, n=5 CR only, and n=4 RR only (CR PPV=10.7%;RR PPV=12.9%).

Conclusion: CXR reporting by RR appears to be comparable to CR, with similar accuracy and use of further tests.
Limitations: A single-site study with a small number of observers, mitigated by prospective data collection and a large consecutive clinical series.
Ethics committee approval: NHS-HRA:17/LO/0870.
Funding: Cancer Research UK EDAG 2016.
Author Disclosures:
N. H. Woznitza: Consultant at InHealth
A. Devaraj: nothing to disclose
N. Hayes: nothing to disclose
D. Togher: nothing to disclose
N. Arumalla: nothing to disclose
E. Skyllberg: nothing to disclose
B. Ghimire: nothing to disclose
Z. Shah: nothing to disclose
D. R. Baldwin: nothing to disclose

RPS 1704-2 08:36
Measuring the cost of convenience: a multi-reader comparison of chest x-rays reported on a smartphone screen versus a medical grade monitor
V. Mahajan, H. Mahajan, A. Sharma, P. Garg, V. K. Venugopal, S. Gupta, M. Barnwal*; New Delhi/IN*

Purpose: Commonly in the developing world, photographs of medical images are sent through WhatsApp to radiologists for reporting in emergency situations with limited availability of PACS and trained radiologists. We studied the risks associated with such practice by replicating this process in a multi-reader chest x-ray (CXR) study.
Methods and materials: 200 CXRs from 4 outpatient imaging centres were pulled from PACS and anonymised and read by 3 radiologists; R1, R2, and R3 having 32-, 15-, and 6-years' experience, respectively. CXRs were read in two phases. In Phase-1 (P-1), photographs of CXRs, viewed on a non-medical screen, were taken using a smartphone (RedMi-Y1, 13MP camera) and sent to radiologists through WhatsApp who also read the images on smartphones (OnePlus-5T, iPhone 6, and RedMi-4). In Phase-2 (P-2), after a 2-week washout period, the radiologists reported the same CXRs on medical-grade monitors (27 inches, NEC). The findings in the CXRs were recorded under the labels: atelectasis, consolidation, infiltration, pneumothorax, oedema, emphysema, fibrosis, pleural thickening, effusion, cardiomegaly, nodule/mass, and normal study. Sensitivity and specificity were calculated for each label from P-1 for individual radiologists using their own findings and from P-2 as ground truth.
Results: Average sensitivity and specificity across all findings were 80% and 97%. The highest average sensitivity was for pleural effusion (84%) and lowest for pleural thickening (15%). The highest average specificity was for pneumothorax and oedema (99% for both), and the lowest for infiltration (94%). Pneumothorax, pleural effusion, consolidation, and mass/nodules were missed in 8, 6, 1, and 2 cases by R1; 3, 14, 3, and 8 cases by R2; and 2, 2, 3 and 12 cases by R3.
Conclusion: Reading CXRs on mobile phones can lead to significant errors.
Limitations: A small sample size.
Ethics committee approval: n/a
Funding: No funding was received for this work.
Author Disclosures:
V. Mahajan: nothing to disclose
M. Barnwal: nothing to disclose
V. K. Venugopal: Other at Research collaboration, General Electric Company Research collaboration, Koninklijke Philips NV Research collaboration, Qure.ai Research collaboration, Predible Health, Consultant at CARING, MAHAJAN IMAGING
H. Mahajan: Other at Director, Mahajan Imaging Pvt Ltd Research collaboration, General Electric Company Research collaboration, Koninklijke Philips NV Research collaboration, Qure.ai Research collaboration, Predible Health
A. Sharma: nothing to disclose
P. Garg: nothing to disclose
S. Gupta: nothing to disclose

RPS 1704-3 08:42
Extra validation and reproducibility results of a commercial deep learning-based automatic detection algorithm for pulmonary nodules on chest radiographs at tertiary hospital
K. E. Shin, J. S. Park, J. W. Lee, Y. Koo, S. Byun*; Bucheon/KR (sweetperi@naver.com)*

Purpose: To extra-validate and evaluate the reproducibility of a commercial deep learning-based automatic detection (DLAD) algorithm for pulmonary nodules on chest radiographs and to compare its performance with radiologists.
Methods and materials: This retrospective study enrolled 434 chest radiographs (normal to abnormal ratio, 242:192) from 378 patients that visited a tertiary hospital. DLAD performance was compared with two radiology residents and two thoracic radiologists. Abnormality assessment (using the area under the receiver operating characteristics, AUROC) and nodule detection (using jackknife alternative free-response ROC, JAFROC) were compared among three groups (DLAD only, radiologist without DLAD, and radiologist with DLAD). A subset of 56 paired cases, having two chest radiographs taken within a 7-day period, were assessed for intraobserver reproducibility using the intraclass correlation coefficient. Independent characteristics of pulmonary nodules detected by DLAD were assessed by multiple logistic regression analysis.
Results: The AUROC for abnormality detection for the three groups were 0.872, 0.929, 0.963, respectively ($p<0.05$), whereas the JAFROC analysis of nodule detection was 0.912, 0.834, and 0.948 ($p<0.05$). Reproducibility was 0.80, 0.67, and 0.80, which shows an increase in radiologists using DLAD ($p<0.05$). Nodules detected by DLAD were more solid, round-shaped, and well-marginated without masking ($p<0.05$).
Conclusion: Extra validation results of DLAD showed high ROC results and there was a significant improvement in the performance when radiologists used DLAD. Reproducibility by DLAD alone showed good agreement and there was an improvement from moderate to good agreement for radiologists using DLAD.
Limitations: This is a retrospective study, increasing the possibility of selection bias and limiting the ability to demonstrate a cause-and-effect relationship.
Ethics committee approval: The Institutional Review Board approved this retrospective study with a waiver of informed consent.
Funding: No funding was received for this work.
Author Disclosures:
K. E. Shin: nothing to disclose
J. S. Park: nothing to disclose
J. W. Lee: nothing to disclose
Y. Koo: nothing to disclose
S. Byun: nothing to disclose

RPS 1704-4 08:48
Quantification of regional and temporal lung ventilation in xenon-enhanced dual-energy CT imaging
N. Buls[1], S. Bayat[2], G. van Gompel[1], S. Verbanck[3], E. Invers[3], T. van Cauteren[1], J. de Mey[1]; *[1]Brussels/BE, [2]Grenoble/FR, [3]Jette/BE (Gert.vangompel@uzbrussel.be)*

Purpose: To assess the dynamics of lung ventilation using xenon-enhanced dual-energy CT (Xe-DECT) of an animal in a normal and bronchoconstricted state.
Methods and materials: Six anesthetised New Zealand white rabbits who received Xe-DECT scans using xenon gas as a contrast agent with a concentration of 70% Xe-30% oxygen, administered by mechanical ventilation via tracheostomy. Dynamic DECT scans (Revolution CT, GE Healthcare) were obtained over multiple breathing cycles during a Xe gas wash-in (WI) and wash-out (WO) sequence by performing 15 repetitive acquisitions with a 1,01s interscan delay. In addition, bronchoconstriction was induced by inhaled methacholine (40 mg/ml) and all scan sequences were repeated. Material decomposition was applied to isolate Xe from the image data and parametric ventilation maps were created to quantify Xe concentration in the segmented lungs. We compared the evolution of the regional Xe concentration (mg Xe/mL) in a normal and bronchoconstricted state.
Results: In a normal state, the maximum Xe concentration in the lungs was 1.60±0.45 mg/mL, which was reached after 15.6±6.9 s. During WO, a 50% decrease in Xe concentration was observed after 12.1±1.3s. The parametric maps clearly showed the increase and decrease of Xe concentration during the WI and WO sequences. After induction of bronchoconstriction, local ventilation defects could be visually detected. Animals showed a reduced Xe concentration in affected areas (1.27±0.68 mg/mL) compared to a normal state (1.91±0.65 mg/mL), and also higher concentration in non-affected areas (2.26±0.71 mg/mL) compared to a normal state.
Conclusion: This animal study suggests that Xe-DECT can be used to acquire spatial and dynamic data of lung ventilation as well as to detect hypoventilated regions due to bronchoconstriction.
Limitations: Only six animals were used in this study.
Ethics committee approval: Animal board approval was obtained.
Funding: Work supported by UZ Brussel department of Radiology.
Author Disclosures:
N. Buls: nothing to disclose
S. Bayat: nothing to disclose
G. van Gompel: nothing to disclose
S. Verbanck: nothing to disclose
E. Invers: nothing to disclose
T. van Cauteren: nothing to disclose
J. de Mey: nothing to disclose

RPS 1704-5 08:54

Non-contrast-enhanced 3D-UTE MRI for pulmonary imaging of immunocompromised patients during haematopoietic stem cell transplantation

C. Metz[1], D. Böckle[1], J. F. Heidenreich[1], A. Weng[1], T. Benkert[2], G. U. Grigoleit[1], T. A. Bley[1], H. Köstler[1], S. Veldhoen[1]; [1]*Würzburg/DE,* [2]*Erlangen/DE (metz_c1@ukw.de)*

Purpose: To evaluate the feasibility of non-contrast-enhanced 3D-UTE MRI for pulmonary imaging in immunocompromised patients during haematopoietic stem cell transplantation (HSCT).
Methods and materials: 28 patients with an indication for allogeneic HSCT were included in this prospective single-centre study and underwent thoracic MRI before HSCT initiation, in case of suspected pneumonia, and before discharge following completion of HSCT. MRI was acquired using a prototypical stack-of-spirals 3D-UTE sequence within a single breath-hold. Clinically indicated MDCT and a clinically used T2 weighted sequence were used as diagnostic reference. 3D-UTE MR and T2 weighted MR image sets were separately reviewed by two radiologists regarding presence of pleural effusions (PE), ground-glass opacities (GGO), and consolidations. Each MDCT used as reference for MRI results was assessed regarding the same items in consensus reading.
Results: A total of 62 MRI scans were acquired without periprocedural complications. 3D-UTE MRI allowed for sufficient imaging of pulmonary consolidations (sensitivity 78%, specificity 82%, PPV 84%, and NPV 76%). Regarding PE (sensitivity 54%, specificity 99%, PPV 92%, and NPV 89%) and GGO (sensitivity 49%, specificity 87%, PPV 45%, and NPV 88%), the diagnostic performance was lower. Overall consistency rate was high (79-90%). Inter-rater agreement was moderate to substantial (PE=0.62, GGO=0.57, consolidations=0.70). 3D-UTE was equivalent (54%) or superior (43%) when compared to T2 weighted MRI in detecting ground-glass opacity areas and consolidations.
Conclusion: With an acquisition time similar to MDCT, radiation-free and contrast-free 3D-UTE MRI can be expected to play a major role in future pulmonary imaging, for example, in diagnostics and follow-up of immunocompromised patients with pneumonia.
Limitations: n/a
Ethics committee approval: n/a
Funding: The project was funded by Deutsche Forschungsgemeinschaft. The Department receives a research grant from Siemens Healthcare GmbH, which is not specifically directed towards authors.
Author Disclosures:
C. Metz: Author at Universitätsklinikum Würzburg
D. Böckle: Employee at Universitätsklinikum Würzburg
J. F. Heidenreich: Employee at Universitätsklinikum Würzburg
A. Weng: Employee at Universitätsklinikum Würzburg
T. Benkert: Other at Siemens Erlangen
T. A. Bley: CEO at Universitätsklinikum Würzburg
H. Köstler: Other at Universitätsklinikum Würzburg
S. Veldhoen: Consultant at Universitätsklinikum Würzburg
G. U. Grigoleit: Consultant at Universitätsklinikum Würzburg

RPS 1704-6 09:00

Automated lung segmentation in chest radiographs using convolutional neural networks trained by means of a database augmented with a generative adversarial neural network

R. López-González[1], M. Roca-Sogorb[2], F. Garcia-Castro[2], A. Alberich-Bayarri[2]; [1]*Alzira/ES,* [2]*Valencia/ES (lopgon.rafael@gmail.com)*

Purpose: Automated lung segmentation in chest x-rays can bring many benefits for the optimisation of image analysis pipelines, such as lung textures quantification and pathologies classification. Our goal was to improve lung segmentation by using convolutional neural networks (CNN) and a database augmented by means of a generative adversarial neural network (GAN).
Methods and materials: Three public datasets of chest radiographs with manual segmentation masks of the lungs were gathered for the purpose of training CNNs. To increase the variability of the dataset, the radiographs from healthy subjects were augmented by means of a GAN. Additionally, 100 manually segmented cases from the ChestXray14 database were used for testing purposes.
To evaluate different deep learning approaches, a deeply-supervised UNET and a Mask R-CNN were trained with the augmented samples. The performance of both models was measured by means of the Dice score coefficient between the predictions and the manual segmentations of the ChestXray14 database.
Results: The model based on the deeply-supervised UNET architecture obtained an average Dice score of 0.94 for the right lung and 0.95 for the left lung. The model based on the Mask R-CNN architecture obtained an average Dice score of 0.96 for the right lung and 0.96 for the left lung.
Conclusion: Optimising the segmentation of the lungs in chest radiographs is feasible by means of convolutional neural networks trained with augmented data. The use of these techniques allows the learning of robust segmentation models and refining them with the generation of realistic augmented data.
Limitations: The main limitation of the study was that the models were evaluated in a test set of 100 images. A larger test database should be collected.
Ethics committee approval: n/a
Funding: No funding was received for this work.
Author Disclosures:
R. López-González: Employee at QUIBIM
M. Roca-Sogorb: Employee at QUIBIM
F. Garcia-Castro: Employee at QUIBIM
A. Alberich-Bayarri: CEO at QUIBIM, Shareholder at QUIBIM

RPS 1704-7 09:06

Visualisation of combined dark-field and attenuation chest x-rays from patients

R. C. Schick[1], W. Noichl[1], T. Urban[1], M. Frank[1], K. Willer[1], J. Mohr[2], T. Köhler[3], J. Herzen[1], F. Pfeiffer[1]; [1]*Garching/DE,* [2]*Karlsruhe/DE,* [3]*Hamburg/DE (rafael.schick@tum.de)*

Purpose: Using a clinical prototype for x-ray dark-field chest radiography, attenuation, differential-phase, and dark-field radiographs of the human chest are obtained to investigate the diagnostic value for chronic obstructive pulmonary disease and emphysema. Therefore, different visualisation concepts of combined dark-field and attenuation images are evaluated.
Methods and materials: In the hue-saturation-visibility colour space, the two images are fused together by entering different channels of the colour space: the dark-field signal determines the hue and saturation channel while the transmission value determines the value channel. In the red-green-blue-alpha colour space, the combination is achieved by a superposition of the two images using the transparent alpha-channel. For this purpose, the dark-field signal strength is encoded by a colour map while also defining a transparency map. The colour map is subsequently superimposed on the attenuation image using the transparency map.
Results: For each patient, an individually adjustable overlay is available to the radiologists as an additional tool to identify and evaluate possible diagnostic findings as well as to assess the strength of the signal of different lung regions.
Conclusion: The combined visualisation of both the attenuation and dark-field chest radiographs allows the correlation of the strength of the dark-field signal, i.e. the amount of intact alveolar structures with the accurate spatial position in the thorax accessible in the attenuation image, and thus provides a valuable tool to further investigate the clinical benefit of dark-field imaging.
Limitations: Perfectly registered images as obtained by the prototype for x-ray dark-field chest radiography are required.
Ethics committee approval: The study was approved by the ethics committee and by the national radiation protection agency. Participants gave written informed consent.
Funding: Partially funded by Philips Medical Systems DMC GmbH, Hamburg, Germany.
Author Disclosures:
R. C. Schick: nothing to disclose
T. Urban: nothing to disclose
W. Noichl: nothing to disclose
M. Frank: nothing to disclose
K. Willer: nothing to disclose
J. Mohr: nothing to disclose
T. Köhler: Employee at Philips Medical Systems DMC GmbH, Hamburg, Germany
J. Herzen: nothing to disclose
F. Pfeiffer: nothing to disclose

RPS 1704-8 09:12

X-ray dark-field chest radiography: optimal noise filtering for best image quality

Y. N. Leonhardt[1], J. H. W. Bodden[1], K. Willer[2], M. Frank[2], A. A. Fingerle[1], T. Koehler[3], D. Pfeiffer[1], E. J. Rummeny[1], F. Pfeiffer[1]; [1]*Munich/DE,* [2]*Garching/DE,* [3]*Hamburg/DE*

Purpose: To demonstrate an optimal noise reduction technique and optimal level of noise reduction in x-ray dark-field radiography of the human chest.
Methods and materials: X-ray dark-field radiographs of the chest were taken of lung-healthy human subjects and patients at different stages of chronic obstructive pulmonary disease (COPD) (58 patients; 64.6 ± 12.2 years; 31% female) with a grating-based prototype dark-field scanner with a field of view similar to conventional chest radiographs (37 x 37 cm²), and the acceleration voltage set to 70 kVp. The level of noise allowed in the reconstruction was defined as σ. During the reconstruction algorithm, different levels of noise reduction were applied ($\sigma_{min} = 10^{-5}$; $\sigma_{max} = 7.0$) and the raw image, as well as the reconstructed images, were assessed by two experienced radiologists in terms of image definition and noise independently.

Results: A noise level of σ = 1 was unanimously perceived to lead to the optimal image quality in in-vivo dark-field chest x-ray radiographs.
Conclusion: Moderate noise reduction in in-vivo dark-field chest x-ray radiographs may lead to an improvement in image quality in contrast to the raw image, while a high amount of noise reduction may lead to a loss of anatomical information. Thereby, noise reduction may increase usability in a clinical setting as well as in future investigations with regard to the evaluation of diseases, e. g. improved diagnosis and staging of COPD.
Limitations: n/a
Ethics committee approval: This ongoing prospective study was institutional review board (IRB) approved and the dark-field contrast x-ray imaging device has been approved for use in humans by the Federal Office for Radiation Protection.
Funding: Partially funded by Philips Medical Systems DMC GmbH, Hamburg, Germany.
Author Disclosures:
Y. N. Leonhardt: nothing to disclose
J. H. W. Bodden: nothing to disclose
K. Willer: nothing to disclose
M. Frank: nothing to disclose
A. A. Fingerle: nothing to disclose
T. Koehler: nothing to disclose
D. Pfeiffer: nothing to disclose
E. J. Rummeny: nothing to disclose
F. Pfeiffer: nothing to disclose

RPS 1704-9 09:18

X-ray dark-field chest radiography: reconstruction of image signals from a scanning moiré system used in a first patient study

W. Noichl[1], F. de Marco[1], K. Willer[1], T. Urban[1], M. Frank[1], R. C. Schick[1], T. Koehler[2], J. Herzen[1], F. Pfeiffer[1]; [1]*Garching/DE,* [2]*Hamburg/DE*

Purpose: To develop a robust approach for the image reconstruction within the scopeof a first clinical patient experiment on x-ray dark-field chest radiography investigating its potential benefits for the diagnosis of pulmonary disorders.
Methods and materials: Images were acquired using an x-ray grating interferometer tailored to clinical dark-field imaging of the human chest, operating at 70kVp. Three gratings were placed in the x-ray beam path, the first and second generating an intensity pattern, which was then analysed, utilising the third one. Conventionally, this is done by acquiring images at different relative positions of the gratings. Since constraints given by the fabrication process and alignment difficulties prevent the use of full-field gratings, the interferometer was moved continuously to obtain the necessary field of view of 37×37cm^2. Consequently, moving the gratings with respect to each other needed to be avoided to keep acquisition times sufficiently short (7s). Instead, by a slight misalignment of the gratings, a so-called moiré fringe pattern was formed. The contrast of these fringes was reduced by small-angle scattering within the tissue, which constitutes the dark-field signal and could be extracted by combining several of these displaced fringe patterns.
Results: An attenuation image, comparable to a conventional radiograph, and a dark-field image were computed from the overlapping raw detector images obtained from the scanning system.
Conclusion: Dark-field images can be obtained from a scanning setup meeting clinical requirements concerning coverage and acquisition speed.
Limitations: Due to the scanning acquisition scheme, there are some well-localised residual fringe artifacts caused by cardiac motion.
Ethics committee approval: The study was approved by the national radiation protection agency and the institutional review board.
Funding: Partially funded by Philips Medical Systems DMC GmbH, Hamburg, Germany.
Author Disclosures:
T. Urban: nothing to disclose
W. Noichl: nothing to disclose
F. de Marco: nothing to disclose
K. Willer: nothing to disclose
M. Frank: nothing to disclose
R. C. Schick: nothing to disclose
T. Koehler: Employee at Philips Research, 22335 Hamburg, Germany
J. Herzen: nothing to disclose
F. Pfeiffer: nothing to disclose

RPS 1704-10 09:24

X-ray Darkfield Chest Radiography: Evaluation of Diagnostic Image Quality in Inspiration and Expiration

C. Müller-Leisse[1], T. Urban[2], R. C. Schick[2], G. Zimmermann[1], T. Koehler[3], D. Pfeiffer[1], A. A. Fingerle[1], E. J. Rummeny[1], F. Pfeiffer[1]; [1]*Munich/DE,* [2]*Garching/DE,* [3]*Hamburg/DE (tina.ml@web.de)*

Purpose: To evaluate the first dark-field chest x-ray images on living humans and to assess image quality and visual impression, comparing inspiration and expiration.
Methods and materials: We have recently designed, constructed, and commissioned a worldwide first experimental prototype for grating-based dark-field chest radiography. 54 patients with either an overall inconspicuous chest CT or signs of pulmonary emphysema were selected and underwent conventional chest x-ray in inspiration as well as dark-field imaging in expiration and inspiration, posterior-anterior respectively.
All images were evaluated by two blinded radiologists analysing the images in terms of quality and signal strength, comparing those in expiration and inspiration. Clinical information (history of lung emphysema yes/no) was later taken into account.
Results: We found that both images in inspiration and expiration using x-ray dark-field radiography show good quality and appear to be feasible for clinical use.
Looking at one of the dark-field images only was enough to identify pulmonary diseases such as pulmonary emphysema, although having both dark-field radiographs in inspiration and expiration helped to confirm the diagnosis and gave additional information to understand dynamic changes during breathing.
Conclusion: The first dark-field x-ray images on living humans show promising results with high potential clinical value in inspiration as well as expiration. To detect pulmonary diseases such as pulmonary emphysema, it is enough to have either one inspiratory or expiratory image, however, having both gave additional information about dynamic pulmonalry changes during breathing.
Limitations: In this rather early state, we only have a limited number of examinations to analyse. We expect more concrete and significant results during the course of our study.
Ethics committee approval: An approval by the institutional review board (IRB) was obtained.
Funding: Partially funded by Philips Medical Systems DMC GmbH, Hamburg, Germany.
Author Disclosures:
C. Müller-Leisse: nothing to disclose
T. Koehler: Employee at Philips Germany
T. Urban: nothing to disclose
R. C. Schick: nothing to disclose
A. A. Fingerle: nothing to disclose
D. Pfeiffer: nothing to disclose
E. J. Rummeny: nothing to disclose
F. Pfeiffer: nothing to disclose
G. Zimmermann: nothing to disclose

RPS 1704-11 09:30

X-ray dark-field chest radiography: discussion of image signal dependencies of patients biometric data

F. Meurer[1], M. Frank[2], W. Noichl[2], G. Zimmermann[1], T. Koehler[3], A. A. Fingerle[1], D. Pfeiffer[1], E. J. Rummeny[1], F. Pfeiffer[2]; [1]*Munich/DE,* [2]*Garching/DE,* [3]*Hamburg/DE*

Purpose: To discuss the dependence or independence of x-ray dark-field radiography signal intensity and biometric data of healthy lungs.
Methods and materials: A grating-based dark-field chest x-ray prototype has been constructed and approved by the federal office for radiation protection to enable chest x-ray radiography of the human lung. Lung scans of 54 patients were included in this evaluation. Three from each other independent radiologists, trained in assessment of dark-field images, rated the overall dark-field signal intensity with a five-point ordinal scale. Furthermore, a quantitative evaluation of the signal intensity was performed. Statistical tests were made to find differences between different ages, various body mass indices, and the sex of the study participants.
Results: Present preliminary results indicate that there is no strong difference in objective and especially subjective evaluation of the dark-field signal intensity for different genders or various body mass indices. Only the participant's age shows a slight but significant negative correlation with signal intensity in objective evaluation. In a subjective rating, there was no difference.
Conclusion: The present preliminary results indicate that the dark-field signal intensity of the healthy lung is not correlated with gender and body weight. Just age and signal intensity correlate slightly negatively with each other in objective analysis. This is important because it indicates that any changes in the signal levels are more likely to be caused by lung diseases rather than biometric differences in patients.
Limitations: n/a
Ethics committee approval: This patient study has been approved by the institutional review board (IRB).
Funding: Partially funded by Philips Medical Systems DMC GmbH, Hamburg, Germany.

Author Disclosures:
F. Meurer: nothing to disclose
W. Noichl: nothing to disclose
M. Frank: nothing to disclose
F. Pfeiffer: nothing to disclose
D. Pfeiffer: nothing to disclose
A. A. Fingerle: nothing to disclose
E. J. Rummeny: nothing to disclose
G. Zimmermann: nothing to disclose
T. Koehler: Employee at Philips Medical Systems

RPS 1704-12 09:36
X-ray dark-field chest radiography: comparison of 70 kVp grating-based attenuation chest x-ray image quality with conventional chest x-rays
M. Renz[1], M. Kattau[2], T. Urban[2], G. Zimmermann[1], T. Köhler[3], D. Pfeiffer[1], A. A. Fingerle[1], E. J. Rummeny[1], F. Pfeiffer[1]; [1]Munich/DE, [2]Garching/DE, [3]Hamburg/DE (martin.renz@tum.de)

Purpose: To compare attenuation chest x-rays acquired with a grating-based prototype dark-field chest x-ray system to conventionally acquired chest x-rays regarding image quality and diagnostic confidence.
Methods and materials: A grating-based prototype system capable of acquiring dark-field and attenuation chest x-rays at 70 kVp was constructed. Due to limited grating size, it employs a slot-scanning image acquisition procedure with an acquisition time of 7 seconds. In our clinical study, 79 patients have been included so far. With every examination using our grating-based dark-field system, the attenuation signal is obtained simultaneously with the dark-field signal. As a reference, conventional chest x-rays are included for every patient using a standard clinical x-ray system operating at 125 kVp. On both systems examinations in p.-a. and lateral view are conducted. Visual comparison of grating-based and conventional chest x-ray was quantified by three independent readers.
Results: The utilisation of slot-scanning in our grating-based setup, as well as lower kVp, leads to reduced scatter and therefore higher contrast compared to conventional imaging. Long local exposure of 700 ms due to scanning procedure causes minimal blurring of the aortic and mediastinal silhouette. Visually quantified image quality and diagnostic confidence ratings of attenuation chest x-rays acquired with our prototype dark-field chest x-ray system were on par with ratings of conventional clinical chest x-rays. In both imaging variants, pulmonary parenchyma, as well as vascular, bronchial and osseous structures, are well differentiated.
Conclusion: Simultaneously acquired attenuation chest x-rays obtained by our prototype dark-field chest x-ray system are similar to conventional chest x-ray imaging regarding the diagnostic value.
Limitations: n/a
Ethics committee approval: This study is approved by the IRB.
Funding: Partially funded by Philips Medical Systems DMC GmbH, Hamburg, Germany.
Author Disclosures:
M. Renz: nothing to disclose
T. Urban: nothing to disclose
T. Köhler: Employee at Philips Research, 22335 Hamburg, Germany
D. Pfeiffer: nothing to disclose
E. J. Rummeny: nothing to disclose
F. Pfeiffer: nothing to disclose
A. A. Fingerle: nothing to disclose
M. Kattau: nothing to disclose
G. Zimmermann: nothing to disclose

RPS 1704-13 09:42
X-ray dark-field chest radiography: correlation of results from the first COPD-patient study to CT-based COPD analysis
A. Sauter[1], M. Kattau[2], K. Willer[2], G. Zimmermann[1], A. A. Fingerle[1], T. Koehler[3], D. Pfeiffer[1], E. J. Rummeny[1], F. Pfeiffer[2]; [1]Munich/DE, [2]Garching/DE, [3]Hamburg/DE (andreas.sauter@tum.de)

Purpose: To compare living human emphysema quantification using the first x-ray dark-field chest radiograph examinations versus CT.
Methods and materials: In total, 500 patients will be included in this study. So far, 79 patients were recruited after receiving a clinical CT-scan with contrast showing no pulmonary pathologies besides emphysema. For each patient, four dark-field images of the thorax (posterior-anterior and lateral, in inspiration, and in expiration) were performed using a clinical prototype. All images were evaluated by three radiologists who were blinded to the GOLD-stadium regarding signal strength. Based on the rating for signal strength, grading of emphysema was performed. The CT-examination of each patient was evaluated with dedicated software (IntelliSpace Portal, Philips GmbH) regarding the percentage of emphysematous lung tissue. Consequently, the correlation between visual dark-field signal and resulting grading of emphysema and CT based emphysema quantification was evaluated.
Results: The results from this first clinical dark-field chest radiography demonstrate a high correlation of CT and dark-field images regarding the grading of pulmonary emphysema. Dark-field images obtained in inspiration showed a better correlation with CT compared to dark-field images obtained in expiration. Posterior-anterior images showed a better correlation than lateral images, but the latter are useful for anatomical assignment.
Conclusion: Detection and grading of COPD is possible with dark-field x-ray radiography with a high correlation to CT, resulting in decreased radiation exposure (0.04 mSv) as well as fewer time expanses.
Limitations: Only a relatively small number of patients was included. For further evaluation, more patients have to be examined.
Ethics committee approval: The study was institutional review board (IRB) approved. All patients signed informed consent.
Funding: Partially funded by Philips Medical Systems DMC GmbH, Hamburg, Germany.
Author Disclosures:
A. Sauter: nothing to disclose
K. Willer: nothing to disclose
A. A. Fingerle: nothing to disclose
T. Koehler: Employee at Philips
D. Pfeiffer: nothing to disclose
E. J. Rummeny: nothing to disclose
G. Zimmermann: nothing to disclose
F. Pfeiffer: nothing to disclose
M. Kattau: nothing to disclose

RPS 1704-14 09:48
X-ray dark-field chest radiography: a correlation of first results from COPD-patients with lung function tests
A. A. Fingerle, K. Willer, W. Noichl, A. Sauter, G. Zimmermann, T. Köhler, D. Pfeiffer, E. J. Rummeny, F. Pfeiffer; Munich/DE (alexander.fingerle@tum.de)

Purpose: To investigate dark-field chest x-ray for the detection and staging of chronic obstructive pulmonary disease (COPD) by correlation of dark-field signal strength to lung function tests in a first patient study.
Methods and materials: In this ongoing prospective clinical study, 79 of 500 adult study participants (250 patients with different stages of COPD and 250 patients without lung diseases) were enrolled. Dark-field chest x-rays were acquired using a grating-based prototype imaging setup operating at 70 kVp in scanning mode. As a reference, conventional chest x-ray, whole-body plethysmography, and COPD assessment test were performed. Clinically indicated computed tomography scans were also included in the study. Visual assessment of dark-field signal strength using a 5-point ordinal scale was performed by three independent readers. In addition, dark-field signal strength was quantitatively evaluated. Results were correlated with findings of lung function tests.
Results: Dark-field signal strength correlated with the Tiffeneau-Pinelli index, which is given as the ratio of forced expiratory volume in 1 second (FEV1) to forced vital capacity (FVC), and FEV1 as a percent of predicted measured in whole-body plethysmography.
Conclusion: Dark-field signal strength may serve as a diagnostic marker of pulmonary function in COPD by visualising structural changes of the lung parenchyma. As a novel imaging modality, dark-field chest x-ray may have the potential to facilitate early diagnosis of COPD and improve the monitoring of the clinical course of disease while requiring less cooperation than spirometry.
Limitations: n/a
Ethics committee approval: This study was approved by the institutional review board and the federal office for radiation protection. Written consent was obtained from all patients.
Funding: Partially funded by Philips Medical Systems DMC GmbH, Hamburg, Germany.
Author Disclosures:
A. A. Fingerle: nothing to disclose
K. Willer: nothing to disclose
W. Noichl: nothing to disclose
A. Sauter: nothing to disclose
G. Zimmermann: nothing to disclose
T. Köhler: Employee at Koninklijke Philips NV
D. Pfeiffer: nothing to disclose
E. J. Rummeny: nothing to disclose
F. Pfeiffer: nothing to disclose

RPS 1704-15 09:54
Dark-field chest radiography: influence of the breathing state on image appearance
T. Urban[1], K. Willer[1], W. Noichl[1], M. Frank[1], R. C. Schick[1], J. Mohr[2], T. Koehler[3], J. Herzen[1], F. Pfeiffer[1]; [1]Garching/DE, [2]Karlsruhe/DE, [3]Hamburg/DE (theresa.urban@tum.de)

Purpose: To evaluate the first clinical dark-field chest x-ray images with respect to the breathing state of the patient.
Methods and materials: We constructed a clinical prototype for dark-field chest radiography suitable for human chest imaging, with an overall acquisition time of 7 seconds and a tube voltage of 70kVp. So far, more than 80 patients have been examined in posterior-anterior orientation in inspiration and expiration, with an average effective dose of 0.04mSv per radiograph.
Results: The dark-field signal in the lung can vary in strength due to both a difference in lung thickness as well as microstructural variations. In inspiration, the dark-field signal is quite homogeneous over the lung, which can be attributed to a homogeneous distribution of alveolar size and density. In expiration, the dark-field signal is higher, particularly in the lower parts of the lung. This is likely caused by an increase of air-tissue interfaces in the beam path due to the compression of lung parenchyma. The difference in dark-field signal between the two breathing states allows spatially identification of the regions of the lung that change micro-morphologically and thus participate in the ventilation of the lung.
Conclusion: This technique provides spatial information about microstructural changes in the lung and thus the physiological activity of different lung regions during breathing. The change in signal strength illustrates its sensitivity to the microstructure of the lung, promising a distinct diagnostic value of dark-field images for the assessment of lung diseases.
Limitations: At this rather early state of the ongoing study, there is a limited number of examinations.
Ethics committee approval: The study was approved by the ethics committee and by the national radiation protection agency. Participants gave written informed consent.
Funding: Partially funded by Philips Medical Systems DMC GmbH, Hamburg, Germany.
Author Disclosures:
T. Urban: nothing to disclose
K. Willer: nothing to disclose
W. Noichl: nothing to disclose
R. C. Schick: nothing to disclose
M. Frank: nothing to disclose
J. Mohr: nothing to disclose
T. Koehler: Employee at Philips Medical Systems DMC GmbH, Hamburg, Germany
J. Herzen: nothing to disclose
F. Pfeiffer: nothing to disclose

08:30 - 10:00 **Room M 1**

Musculoskeletal

RPS 1710

Upper extremities and facial bones

Moderators:
H. M. Brogger; Oslo/NO
B. J. Schwaiger; Munich/DE

RPS 1710-K 08:30
Keynote Lecture
M. Zanetti; Zurich/CH (marco.zanetti@hirslanden.ch)

Author Disclosures:
M. Zanetti: nothing to disclose

RPS 1710-1 08:40
A ten-year survey of different treatment approaches to tendinopathy of the supraspinatus tendon: PRP (platelet-rich plasma) or physical therapy?
G. Campidoglio[1], F. Bruno[2], S. Mariani[2], F. Arrigoni[2], L. Zugaro[2], A. Barile[2], C. Masciocchi[2]; [1]Rome/IT, [2]L'Aquila/IT (giuseppe.campidoglio@gmail.com)

Purpose: To evaluate clinical and morphological results of PRP treatment in patients with chronic tendinopathy of the supraspinatus tendon with a 10-year follow-up.
Methods and materials: We retrospectively evaluated, through clinical and MR examination, all patients selected for intratendinous PRP injections for the treatment of the supraspinatus degeneration between 2008 and 2018. The instrumental follow-up included MRI scans performed before and at the time of the follow-up. The patients were also evaluated with both clinical and functional examinations, namely the VAS and constant score.
Results: A total of 86 patients were treated and 57 were included in the analysis with pre and post-treatment examinations. 60 patients matched for age, sex, and disease duration were enrolled as a control group. Among all patients treated, 8 underwent surgical repair and 7 conservative therapy, 3 showed a low VAS score and bad clinical outcome, and 4 only a low VAS. Overall, 26 patients presented with VAS <4, whereas 20 with VAS=0. Among the control group, 8 patients underwent surgical repair and 18 alternative therapies. 4 patients showed a low VAS score and bad clinical outcome and 4 only a low VAS.
Conclusion: Our experience suggests that intratendinous injection of PRP did not modify the long-term natural history of tendinopathy. Nevertheless, it showed a significant impact on the VAS score and constant score.
Limitations: The small sample size of analysis.
Ethics committee approval: n/a
Funding: No funding was received for this work.
Author Disclosures:
G. Campidoglio: nothing to disclose
F. Bruno: nothing to disclose
S. Mariani: nothing to disclose
F. Arrigoni: nothing to disclose
L. Zugaro: nothing to disclose
A. Barile: nothing to disclose
C. Masciocchi: nothing to disclose

RPS 1710-2 08:46
3D isotropic MR-arthrography in the abduction-external rotation position to evaluate on-track/off-track lesions in anterior shoulder instability
F. Formiconi, M. Ruschioni, C. Gianneramo, F. Bruno, F. Arrigoni, S. Mariani, L. Zugaro, A. Barile, C. Masciocchi; L'Aquila/IT (formiconifrancesco@gmail.com)

Purpose: To evaluate the ability of shoulder three-dimensional (3D) magnetic resonance arthrography (MRA) and additional ABER (abduction-external rotation) scans to assess bipolar bone loss and detect on-track/off-track lesions in traumatic shoulder instability, by using MPR CT images as reference.
Methods and materials: 25 consecutive patients (14 male, 11 female, range 20-44) with clinical evidence of anterior shoulder instability. All patients underwent 3D-CT of the shoulder and direct shoulder MRA using three-dimensional (3D) isotropic PD sequences in standard and ABER position. Two blinded independent observers randomly evaluated the images twice to assess the glenoid track, the Hill-Sachs interval, and to predict engagement by using the "on-track/off-track" method. The intra and interobserver agreement was calculated.
Results: Out of 25 defect combinations, 13 were codified as non-engaging and 12 as engaging by using the "on-track/off-track" method. The intraobserver reliability was 0.921 for 3D-CT and 0.786 for MRA. The interobserver agreement ranged from "substantial" to "almost perfect" for both glenoid track and Hill-Sachs interval measurements ($p<0.005$). ABER MRA predicted engagement accurately in 23 cases (91.3%).
Conclusion: MRA using 3D isotropic PD sequences is a reliable method in assessing defects of bone in patients affected by anterior shoulder instability and bipolar bone loss by using the "on-track/off-track" method. The same sequence in the ABER position could predict the presence of engaging lesions.
Limitations: The small sample size.
Ethics committee approval: n/a
Funding: No funding was received for this work.
Author Disclosures:
F. Formiconi: nothing to disclose
M. Ruschioni: nothing to disclose
C. Gianneramo: nothing to disclose
F. Bruno: nothing to disclose
F. Arrigoni: nothing to disclose
S. Mariani: nothing to disclose
L. Zugaro: nothing to disclose
A. Barile: nothing to disclose
C. Masciocchi: nothing to disclose

RPS 1710-3 08:52
CT evaluation of different outcomes after variations of Bristow-Latarjet operations in a 1-year follow-up
Y. Zhao, H. Yuan; Beijing/CN (stormare_7@sina.com)

Purpose: The Bristow-Latarjet operation (coracoid translocation), which has developed different variations, is an effective treatment of shoulder recurrent dislocation. Our research is to investigate the merit and demerit of these variations by analysing CT images in a 1-year follow-up.

Methods and materials: 200 patients with shoulder recurrent dislocation who had a Bristow-Latarjet operation in our hospital were involved. They were divided into 6 groups. 25 cases were bone block fixed with anchor (G1), 52 cases inlay with single screw (G2), 15 cases no-inlay with single screw (G3), 67 cases inlay with single pair of buttons (G4), 14 cases with double screws (G5), and 27 cases with double pairs of buttons (G6). The size of bone block and un-union were evaluated in CT on the postoperative day, and at 3, 6, and 12 months.
Results: The increase of step below articular surface compared to postoperative day: G2>G4 in 3 months ($p<0.05$); G6>G1, G2, and G4 while G2>G4 in 6 months ($p<0.05$); G6>G1, G2, G3, and G4 in 12 months ($p<0.05$). The decrease of bone length along the tunnel: G1, G4, and G6>G2 while G6>G3, G4, and G5 in 6 months ($p<0.05$); G1, G4, and G6>G2 while G6>G3 in 12 months ($p<0.05$). The un-union rates in 3 months were 70% (significantly high), 2.73% (significantly low), 50%, 17.2%, 45.5%, and 30.4%, but were not significantly different in other stages.
Conclusion: Bone block absorption perpendicular to the articular was more after fixed with a single screw rather than buttons inlay and with double pairs of buttons rather than single fixation and anchor. Bone block absorption along the tunnel was more after fixed with buttons than a screw and with a single pair of buttons than double. Bone block un-union happened more in the early stage after fixed with anchor and less after fixed with a single screw inlay.
Limitations: A limited number of cases in some groups.
Ethics committee approval: n/a
Funding: No funding was received for this work.
Author Disclosures:
Y. Zhao: nothing to disclose
H. Yuan: nothing to disclose

RPS 1710-4 08:58

Visualisation of the coracoglenoid ligament in shoulder MR on 3DPD images and the evaluation of its association with shoulder pathologies

S. Rajan, R. S. Rajan, N. S. Batta, H. Mahajan, V. Mahajan, M. Murugavel, V. K. Venugopal*; New Delhi/IN (drsriramrajan@gmail.com)*

Purpose: To assess the visualisation of the coracoglenoid ligament (CGL) on PD CUBE images in 100 consecutive MR shoulder and to assess the association of absent visualisation of this ligament with pathologies of the shoulder.
Methods and materials: 100 consecutive MR shoulders were anonymised and retrospectively reviewed by three subspecialty musculoskeletal radiologists with 16 years, 15 years, and 12 years' experience on PD 3D CUBE images by triangulation on sagittal and axial images. The ligament was scored as 1-3 scale (not seen, indeterminate, and well seen). Posterosuperior labral tears, long head biceps tendon pathology, tear of the supraspinatus and subscapularis tendons, biceps pulley lesions, rotator interval ligaments, and synovial thickening in the rotator interval were also scored on a 1-3 scale (not seen, indeterminate, and well seen). Appropriate statistical tests were performed.
Results: The CGL was well seen on 82% cases by R1, in 78% by R2, and 70% by R3. The CGL was defined as absent in 13% cases by R1, 18% by R2, and 8% by R3 (with additional cases marked as wispy/thin CGL). Cases where CGL was not seen due to rotator interval synovial thickening was marked 5% by R1, 4% by R2, and 22% by R3. Amongst the cases with absent CGL, 69% had associated SLAP tear and 38% had associated long head of biceps tendon pathology. The rest of the pathologies did not have a significant association with CGL absence.
Conclusion: We demonstrate a consistent visualisation of the coraco-glenoid ligament on plain 3D PD images and an association of the absence of this ligament with SLAP tear and lesser degree of association with long head of biceps tendon pathology.
Limitations: The absence of surgical correlation.
Ethics committee approval: n/a
Funding: No funding was received for this work.
Author Disclosures:
R. S. Rajan: nothing to disclose
M. Murugavel: nothing to disclose
S. Rajan: nothing to disclose
N. S. Batta: nothing to disclose
H. Mahajan: Other at Director, Mahajan Imaging Pvt Ltd Research collaboration, General Electric Company Research collaboration, Koninklijke Philips NV Research collaboration, Qure.ai Research collaboration, Predible Health
V. Mahajan: nothing to disclose
V. K. Venugopal: Consultant at CARING, Other at Research collaboration, General Electric Company Research collaboration, Koninklijke Philips NV Research collaboration, Qure.ai Research collaboration, Predible Health

RPS 1710-5 09:04

T2 mapping at 3T MRI detects glenoid labral matrix changes in patients with and without superior labral anterior to posterior (SLAP) lesions of the shoulder using arthroscopy as a reference

C. Rehnitz, F. Wuennemann*; Heidelberg/DE (felix.wuennemann@med.uni-heidelberg.de)*

Purpose: Using arthroscopy as a gold standard, we prospectively evaluated T2 mapping of the shoulder regarding matrix changes of the labrum in patients with and without superior-labral-anterior-to-posterior (SLAP) lesions.
Methods and materials: T2 mapping was performed at 3T in 18 consecutive patients (12 men) with shoulder pain followed by shoulder arthroscopy. Two independent raters performed a region-of-interest-analysis in the superior labrum using the colour-coded T2 map. Inter-rater correlation coefficients (ICCs) were calculated. Cut-off values and their sensitivities/specificities including 95% confidence intervals (CI) for detection of SLAP lesions were assessed using arthroscopy as reference. $P<0.05$ was considered significant.
Results: The mean age did not differ significantly between n=12 patients with SLAP lesions and n=6 patients without SLAP lesions (55.5 vs 46.2 years, p=0.22). The mean T2 value in labra with proven SLAP lesions was significantly higher compared to those with no SLAP lesions (mean, 37.7±10.6 ms vs 20.8±2.4 ms, p=0.0001). A complete data separation was present, as the maximum T2 value (21.2) in labra with no SLAP lesion was lower than the minimum value in labra with lesions (27.8). Therefore cut-off values between 21.2 and 27.8 ms resulted in a sensitivity of 100% (95%CI:[73.5%-100.0%]) and specificity of 100% (95%CI:[54.1%-100.0%]). ICC was 0.97 and 95%CI:[0.9-0.99].
Conclusion: Higher T2 values in labra containing SLAP lesions indicate a higher degree of damage to the collagen network within the matrix. T2 mapping may be used as an additional tool to evaluate the biochemical labral matrix changes at the shoulder.
Limitations: The small sample size.
Ethics committee approval: Written informed consent. Approved by ethics committee of the University of Heidelberg.
Funding: No funding was received for this work.
Author Disclosures:
C. Rehnitz: nothing to disclose
F. Wuennemann: nothing to disclose

RPS 1710-6 09:10

Ultrasound evaluation of subdeltoid fluid collection and supraspinatus tendon thickness after surgical repair of the supraspinatus tendon and correlation with clinical results

H. J. Park, D. Y. Ahn*; Seoul/KR (cat3305@nate.com)*

Purpose: To investigate whether the repaired tendon thickness and sub-deltoid fluid collection after rotator cuff repair, which was seen on follow-up ultrasound (US), are correlated with clinical outcome and to assess whether these factors lead to different clinical outcomes depending on the surgical method.
Methods and materials: This retrospective study included 54 patients who underwent supraspinatus tendon repair with a suture-bridge or single-row technique and follow up US. Two radiologists independently measured the thickness of the repaired supraspinatus tendons and fluid collection in sub-deltoid space. We assessed the relationship between the sonographic parameters, including repaired supraspinatus tendon thickness and sub-deltoid fluid collection, with the clinical outcome represented by the Korean shoulder scoring system (KSS) score using correlation coefficients (R).
Results: There was a significant relationship between sub-deltoid fluid collection and the pain of the patients ($p\leq0.05$), although every category showed an inverse relationship with the fluid thickness. The ICC values for sonographic imaging parameters between interpreters ranged from 0.910 to 0.946, showing excellent reproducibility.
Conclusion: Sub-deltoid fluid collection of repaired supraspinatus tendons measured on postoperative US can be a useful method in predicting the patient's subjective clinical outcome, especially pain, regardless of age or surgical technique.
Limitations: This was a retrospective study. The measurement of sonographic parameters was based on captured images that had been taken prior to assessment and therefore it was not a real-time measurement.
Ethics committee approval: n/a
Funding: No funding was received for this work.
Author Disclosures:
H. J. Park: Author at Kangbuk Samsung hospital
D. Y. Ahn: nothing to disclose

RPS 1710-7 09:16

Semi-dynamic MRI of the extensor digitorum tendons in Jaccoud arthropathy

T. P.-E. Kirchgesner, M. Stoenoiu, N. Michoux, X. Libouton, F. Houssiau, B. Vande Berg; *Brussels/BE (thomas.kirchgesner@uclouvain.be)*

Purpose: To test the hypothesis that Jaccoud arthropathy (JA) in systemic lupus erythematosus (SLE) patients is associated with abnormal extensor digitorum (ED) tendons displacement during flexion of the metacarpophalangeal (MCP) joints.
Methods and materials: 16 SLE patients with JA (JA+), 12 SLE patients without JA (JA-), and 24 control subjects were included in the study. Transverse spin-echo T1-weighted MR sequences of the MCP joints in flexion and in extension were obtained in each hand of SLE patients and in one randomly-selected hand of control subjects. Two radiologists separately measured the amplitude and the direction of the displacement of the ED tendons with respect to the midline at the level of the MCP joints. Statistical analysis included two-way ANOVA with random effects to assess differences in amplitude ($p<0.0083$), Fisher-Freeman-Halton's exact test to assess differences in direction ($p<0.0063$), and Gwet's AC1 score to determine interobserver agreement.
Results: The amplitude of the displacement of the ED tendons was statistically significantly higher in JA+ patients than JA- patients and controls in flexion for both readers ($p<0.0001$) and in extension for one reader ($p<0.0048$). Ulnar deviation of the ED tendons was statistically significantly more frequent in JA+ patients than in JA- patients and controls in flexion and in extension for both readers ($p<0.0001$).
Conclusion: JA is associated with the abnormal displacement of the ED tendons in flexion and extension. Abnormal displacement of the ED tendons is absent in patients without JA.
Limitations: In the absence of anatomical correlation, we are unable to precisely determine the anatomic lesions associated with the instability of the ED tendons.
Ethics committee approval: This study was approved by our institutional ethics committee. All study participants provided written informed consent.
Funding: No funding was received for this work.
Author Disclosures:
T. P.-E. Kirchgesner: nothing to disclose
M. Stoenoiu: nothing to disclose
N. Michoux: nothing to disclose
X. Libouton: nothing to disclose
F. Houssiau: nothing to disclose
B. Vande Berg: nothing to disclose

RPS 1710-8 09:22

Assessment of cartilage disorders after distal radius fracture using biochemical and morphological non-enhanced magnetic resonance imaging

V. Mori, C. Schleich, D. B. Abrar, M. Frenken, G. Antoch, L. Oezel, S. Gehrmann, L. Wollschläger; *Düsseldorf/DE (valentina.mori@med.uni-duesseldorf.de)*

Purpose: To assess radiocarpal cartilage after distal radius fracture with intra-articular and extra-articular extension using multiparametric, non-enhanced magnetic resonance imaging (MRI).
Methods and materials: In this prospective study, multiparametric MRIs of the radiocarpal cartilage were performed in 26 participants (16 male, 10 female; mean age 39.5±14.7 years, range 20-70 years) using a 3-Tesla MRI. The cohort consisted of 14 patients with distal radial fractures and 12 healthy volunteers. The radiocarpal cartilage was assessed using morphological (DESS, TrueFISP) and biochemical (T2*) MRI sequences without the application of an intravenous contrast agent. The modified Outerbridge classification system for morphological analyses and region-of-interest biochemical analysis were applied to assess the degree of cartilage damage in each patient.
Results: Morphological cartilage assessment showed no significant difference between the DESS sequence and the reference standard, TrueFISP ($p= 0.75$). In the morphological (DESS, TrueFISP) and biochemical (T2*) assessments, patients with intra-articular fractures did not show greater cartilage damage than those with extra-articular fractures (DESS, $p=0.62$, TrueFISP, $p=0.32$, and T2*, $p=0.97$). Significantly greater cartilage degradation was observed after distal radius fracture compared to controls (DESS, $p=0.0001$, TrueFISP, $p=0.0001$, and T2*, $p=0.009$).
Conclusion: Magnetic resonance imaging using advanced, multiparametric sequences facilitates accurate, non-invasive assessment of cartilage changes after distal radius fracture without the need for a contrast agent. Post-traumatic radiocarpal cartilage damage did not differ between fractures with intra- and extra-articular extension, but patients with fractures showed significantly higher cartilage degradation compared to healthy controls.
Limitations: A small sample size. No arthroscopic or histological confirmation. Missing inter- and intra-reader reliability for biochemical imaging.
Ethics committee approval: 5087R. Approved by the local review board.
Funding: No funding was received for this work.
Author Disclosures:
V. Mori: nothing to disclose
C. Schleich: nothing to disclose
D. B. Abrar: nothing to disclose
M. Frenken: nothing to disclose
G. Antoch: nothing to disclose
L. Oezel: nothing to disclose
S. Gehrmann: nothing to disclose
L. Wollschläger: nothing to disclose

RPS 1710-9 09:28

Defining the normal reference range for the cross-sectional area of the median nerve at the wrist and forearm using high-resolution ultrasonography in asymptomatic Asian adults

M. Rauf, F. Raza, R. Nazir, B. Yawar Faiz, R. Aqeel; *Islamabad/PK (mari23392@gmail.com)*

Purpose: Ultrasonography (USG) is a reliable, inexpensive, readily available, and painless modality for the diagnosis of carpal tunnel syndrome. However, the main sonographic criteria of the cross-sectional area (CSA) of the median nerve shows a wide normal variation depending on regional and ethnical differences, which warrants the establishment of the normal range of variability in the dimensions of the median nerve in the local population. In our experience, the normal average cross-sectional area of the median nerve in the asymptomatic adult Asian population is relatively small compared to other populations worldwide.
Methods and materials: 500 asymptomatic patients/1,000 median nerves were evaluated by high-resolution USG using Toshiba Aplio 500 at the distal wrist crease and mid-forearm 12 cm above the distal wrist crease by 3 expert radiologists independently over a period of 2 years (July 2017-July 2019).
Results: The median nerve CSA in our population at the right wrist was 6.8±1.9 mm^2 while at the left wrist was 6.6±1.9 mm^2. The CSA at the right forearm was 5.3 ± 1.4 mm^2 while at the left forearm was 5.2±1.5 mm^2 ($P<0.001$). Also, the CSA was relatively larger in males than females.
Conclusion: The CSA of the median nerve at the wrist and forearm in the Asian population is relatively smaller compared to other populations worldwide. This further enforces the idea to define normal reference range for CSA of the median nerve by obtaining normative data for our population.
Limitations: Only Pakistani asymptomatic adults included. Results should be correlated with other available Asian population data as well as data available worldwide for better reference range determination.
Ethics committee approval: Approved by our institutional review board.
Funding: No funding was received for this work.
Author Disclosures:
M. Rauf: nothing to disclose
F. Raza: nothing to disclose
R. Nazir: Consultant at shifa international hospital islamabad pakistan
B. Yawar Faiz: Consultant at shifa international hospital islamabad pakistan
R. Aqeel: Consultant at shifa international hospital islamabad pakistan

RPS 1710-10 09:34

Direct visualisation of finger flexor pulley injuries at 3T and 7T MRI: an ex vivo feasibility study

R. Heiß[1], C. Lutter[2], R. Janka[1], M. Uder[1], V. Schöffl[3], F. W. Roemer[1], T. Bayer[3]; *[1]Erlangen/DE, [2]Rostock/DE, [3]Bamberg/DE (Rafael.Heiss@uk-erlangen.de)*

Purpose: To evaluate the feasibility and to compare image quality and diagnostic performance of 3T and 7T magnetic resonance imaging (MRI) protocols for the direct depiction of finger pulley ruptures using anatomic preparation as the reference.
Methods and materials: 30 fingers from 10 human cadavers were examined at 3T and 7T before and after being subjected to single and multiple iatrogenic pulley ruptures. MRI protocols were comparable in duration. Two experienced radiologists evaluated the MRIs and defined the location and morphology of finger pulley lesions. Image quality was graded according to a 4-point Likert scale. The diagnostic performance was assessed with anatomic preparation as a gold standard. Interobserver agreement was calculated using Cohen's Kappa coefficients (κ).
Results: In a comparison of 7T versus 3T sensitivity and specificity for the detection of A2, A3 and A4 pulley lesions were comparable with 100% versus 95%, respectively, 98% versus 100%. In the assessment of A3 pulley lesions sensitivity of 7T was superior to 3T MRI (100% vs 83%), whereas specificity was lower (95% vs 100%). Image quality assessed before and after iatrogenic rupture was comparable with 2.74 for 7T and 2.61 for 3T, reflecting adequate image quality in average, whereas the visualisation of the A3 finger flexor pulley

before rupture creation was significantly better for 7T ($p<0.001$). Interobserver variability was substantial at 7T ($\kappa=0.90$) and 3T ($\kappa=0.80$).
Conclusion: MRI at 3T and 7T allows direct visualisation and characterisation of traumatic A2, A3, and A4 pulley lesions with higher agreement rates for 7T. High-field MRI is a modern approach for the pre-surgical evaluation compared to indirect techniques such as ultrasound depending of bowstringing.
Limitations: An ex-vivo cadaver study.
Ethics committee approval: Ethics commettee approval was obtained from Friedrich-Alexander-University Erlangen-Nuremberg, Germany (260_15 Bc).
Funding: No funding was received for this work.
Author Disclosures:
R. Heiß: nothing to disclose
C. Lutter: nothing to disclose
R. Janka: nothing to disclose
M. Uder: nothing to disclose
V. Schöffl: nothing to disclose
F. W. Roemer: Shareholder at Frank Roemer is shareholder of BICL, LLC
T. Bayer: nothing to disclose

RPS 1710-11 09:40

Low-dose CT scanning of the clavicula for age estimation: loss of confidence?

S. Gassenmaier, J. F. Schäfer, K. Nikolaou, I. Tsiflikas*; Tübingen/DE (sebastian.gassenmaier@med.uni-tuebingen.de)*

Purpose: Computed tomography (CT) features are the reference standard in evaluating the ossification process of the medial clavicular epiphysis for forensic age diagnostics in adolescents and young adults. Consequently, the highest efforts on radiation reduction are warranted. Therefore, the aim of this study was to investigate the feasibility of low-dose CT of the clavicula for age estimation.
Methods and materials: 207 non-contrast chest CT of 144 patients born between 1988–2012, performed in 2018 due to various clinical indications, were included in this retrospective study. The mean patient age was 16.9±6.6 years. Patients were divided into a low-dose (LD; n=146) and high-dose (HD; n=61) group. Image quality and ossification stages (using the 5-stage classification including the subgroups 2a-3c) were assessed by two radiologists independently. Confidence levels were evaluated for subgroups 2a-3c. Radiation dose was determined via dosimetry software.
Results: A dose simulation with a z-axis reduction to depict the clavicula only resulted in a median exposure of 0.1 mSv (IQR: 0.0) in LD compared to 0.9 mSv (IQR: 0.6) in HD ($p<0.001$). The median image quality was rated significantly worse in LD compared to HD with a median of 3 (IQR: 1) versus 4 (IQR: 0) by both readers on a Likert-scale ranging from 1-4 ($p<0.001$ for both readers). There was an almost perfect agreement for the ossification stages between both readers with a Cohen's kappa of 0.83 ($p<0.001$). Median confidence levels of both readers were not significantly different between LD and HD (reader 1: $p=0.186$; reader 2: $p=0.074$).
Conclusion: Low-dose CT of the clavicula for age estimation is possible without a loss of confidence.
Limitations: No randomisation regarding scanning protocol was performed due to the retrospective character.
Ethics committee approval: IRB approval obtained. Informed consent waived.
Funding: No funding was received for this work.
Author Disclosures:
S. Gassenmaier: nothing to disclose
I. Tsiflikas: nothing to disclose
J. F. Schäfer: nothing to disclose
K. Nikolaou: nothing to disclose

RPS 1710-12 09:46

Significant differences in dynamic contrast-enhanced perfusion MRI of healthy regions and histologically confirmed medication-related osteonecrosis of the jaw

F. A. Huber, S. Morgenroth, P. Schumann, N. J. Rupp, R. Guggenberger*; Zurich/CH (florian.huber@usz.ch)*

Purpose: To investigate differences in perfusion-MRI parameters between healthy and pathologic regions in patients with a histologically confirmed medication-related osteonecrosis of the jaw (MRONJ).
Methods and materials: in a retrospective analysis, standard parameters of dynamic contrast-enhanced (DCE) perfusion MRI of 22 patients, who received the examinations as part of a dedicated clinical MRI protocol for MRONJ assessment, were evaluated. Same sized regions of interest were placed into a representative bone of defined regions. All regions were assessed qualitatively by a blinded expert radiologist as ground truth (4-point Likert-scale; normal, mild-severe changes). Furthermore, histologic confirmation was present for the resected regions.
Results: The mean patient age was 75.2 years (+/- 9.9; 12 female patients). Wash-in (0.15 vs 0.05) and positive enhancement integral (PEI; 0.17 vs 0.11) values were significantly higher in MRONJ-affected regions than in healthy jaw areas ($p<0.05$ for both). Furthermore, DCE-parameters partially correlated with qualitative expert ratings (wash-in, PEI, initial area under the curve, all $p<0.05$).
Conclusion: DCE-MRI reveals significantly different bone perfusion in MRONJ-affected regions of the mandible and maxilla compared to the healthy jaw. Disease extent according to MRI data was larger than visible necrotic areas during clinical examination and may help to evaluate the severity of this adverse drug effect.
Limitations: This is a retrospective single-centre and single-scanner investigation. All perfusion data was retrieved from MRONJ-diagnosed patients. While clinical and radiological assessment did not indicate pathologic alterations in regions defined as healthy, possible subvisual alterations of the healthy jaw may represent a limitation. However, a control-cohort of healthy volunteers was not used for ethical reasons.
Ethics committee approval: Written consent by all patients and IRB approval was given.
Funding: No funding was received for this work.
Author Disclosures:
F. A. Huber: nothing to disclose
S. Morgenroth: nothing to disclose
P. Schumann: nothing to disclose
N. J. Rupp: nothing to disclose
R. Guggenberger: nothing to disclose

RPS 1710-13 09:52

The value of the frontonasal suture as a specific personal identification: evaluation on three-dimensional cinematic rendering computed tomography images

N. Pattamapaspong, S. Chumsaengsri, S. Ruengdit, C. Madla, K. Mekjaidee, S. Prasitwattanaseree, P. Mahakkanukrauh*; Chiang Mai/TH (nuttaya@gmail.com)*

Purpose: Specific personal identification (fingerprint or DNA matching) is strong evidence in forensic examinations but is mostly lost with decomposition. Sutures on skulls are commonly preserved. The morphology of frontonasal sutures varies among individuals and can be clearly demonstrated by three-dimensional CT (3DCT) images using a new rendering technique. Cinematic volume rendering is a new technique which improves the clarity of 3DCT images and can display skull sutures. We asked whether 3DCT images of the frontonasal suture created by the cinematic volume rendering technique can be used as specific personal identification.
Methods and materials: CT images of 50 dry skulls were reformatted to 3DCT images by using a cinematic volume rendering technique on a commercially available workstation (syngo.via, version VB20). Photographs of the dry skulls were adjusted by a blurring effect on Photoshop. Four readers (an anatomist, forensic anthropologist, forensic doctor, and radiologist) responded to three questionnaires, firstly matching a 3DCT image with the photographs of dry skulls, secondly determining minimum levels of clarity of the suture on dry skull photographs that they can use for matching, and thirdly determining the level of clarity which 3DCT displayed using photographs of dry skulls as a reference.
Results: Correct matching rates were high for all readers (98-100%). The mean values of visual grading analysis scores for clarity of the sutures on 3DCT (63-77%) are higher than that of the minimum level that each reader required for matching (37-50%) ($p<0.001$, $p=0.0039$).
Conclusion: 3DCT images of the frontonasal suture created by cinematic volume rending can be used for personal identification. If a clinical CT of the skull of a missing person is available, 3DCT images can be later reformatted and used as pre-mortem data.
Limitations: n/a
Ethics committee approval: n/a
Funding: No funding was received for this work.
Author Disclosures:
N. Pattamapaspong: nothing to disclose
S. Chumsaengsri: nothing to disclose
S. Ruengdit: nothing to disclose
C. Madla: nothing to disclose
K. Mekjaidee: nothing to disclose
S. Prasitwattanaseree: nothing to disclose
P. Mahakkanukrauh: nothing to disclose

10:30 - 12:00 **Room X**

Breast

RPS 1802

Breast cancer treatment monitoring

Moderators:
M. A. Orsi; Milan/IT
N.N.

RPS 1802-1 10:30

Selective axillary dissection after neoadjuvant chemotherapy in patients with lymph node positive breast cancer (CLYP study): interim report of a prospective study

C. M. L. Trombadori, R. Rella, M. Conti, E. Bufi, M. Romani, L. Zagaria, G. Franceschini, P. Belli, R. Manfredi*; Rome/IT*
(charlotte.trombadori@gmail.com)

Purpose: To evaluate the accuracy of image-guided localisation and removal of lymph nodes containing known metastases in breast cancer patients treated with neoadjuvant chemotherapy (NACT).
Methods and materials: 64 patients with breast cancer and nodal metastases who underwent NACT between 2017 and 2019 were prospectively enrolled. A clip was placed in the sampled node. After NACT, patients underwent sentinel lymph node (SLN) dissection, removal of the clipped node (CN), and subsequent axillary lymphadenectomy (ALND). Pathological results of SLN and CN were compared to ALND to assess the false-negative rate (FNR).
Results: Axillary pathological complete response at ALND was 43,8%. FNR of SLN was 25%, with 9 false-negative (FN) events in 36 patients with residual disease. In 6/9 patients with FN SLNs, the CN contained metastases, resulting in an FNR of 8.3%. Basing on the number of abnormal nodes on initial staging, in patients with 1-3 abnormal nodes (21 patients) residual disease was identified in 10 patients at ALND (47,6%). The SLN didn't reveal metastases in 4/10 patients (FNR=40%) while the CN didn't reveal metastases in 1 patient (FNR=10%). In >4 abnormal nodes (43 patients), the FNRs of SLN and CN were 19,2% and 7,7%, respectively. According to radiological response to NACT, in patients with complete radiological response (cRR) (38 patients), the FNR of SLND was 35.3% (6 FN events in 17 patients with residual disease). In 4/6 patients with FN SLNs, the CN contained metastases, with an FNR of 11,7%. In patients without cRR (26 patients), the FNRs of SLN and CN were 15.8% and 5.3%, respectively.
Conclusion: CN could improve accuracy of axillary staging in node-positive patients who received NACT, especially in N1-stage and in patients with cRR.
Limitations: Nodal-stage on initial staging.
Ethics committee approval: The study was approved by an ethics committee.
Funding: No funding was received for this work.
Author Disclosures:
C. M. L. Trombadori: nothing to disclose
R. Rella: nothing to disclose
M. Conti: nothing to disclose
E. Bufi: nothing to disclose
M. Romani: nothing to disclose
G. Franceschini: nothing to disclose
P. Belli: nothing to disclose
R. Manfredi: nothing to disclose
L. Zagaria: nothing to disclose

RPS 1802-2 10:36

Evaluation of longer duration use of wire-free SCOUT 31-516 days prior to surgery of breast and axillary lesions in neoadjuvant chemotherapy patients: a pilot study

M. K. Hayes, H. Wright, E. Bloomquist*; Hollywood, FL/US*
(hayesmac@comcast.net)

Purpose: To assess the long-term performance of wire-free SCOUT localisation in the breast and axilla in neoadjuvant chemotherapy patients prior to surgery.
Methods and materials: Adult female breast cancer patients had wire-free SCOUT localisation (WFL) prior to neoadjuvant treatment and surgery between February 13, 2017, and July 3, 2019. Electronic medical record and surgical pathology determined the study endpoints.
Primary: Rate of successful surgery using WFL prior to NACT.
Secondary: Number of days to surgery, success rate of WFL placement, stability, and device-related complications.
Results: 38 WFL (16 breast and 22 axilla) were successfully placed prior to NACT in 34 patients, age 29-74 (mean 52) years. All (100%) underwent definitive breast cancer surgery after 32 to 516 (average 198) days. Standard imaging (MG, US, MRI, CT) was used to monitor response to NACT, specimen radiograph and surgical pathology reports documented no significant SCOUT migration (>5mm), no adverse events, and no obscuration of target tissue in 16/16 MRI exams.
Conclusion: Since longer-duration SCOUT WFL lead to successful surgery without adverse events or limitations on MRI, this study suggests the possibility of a clinically relevant paradigm shift regarding the timing of preoperative localisation. WFL prior to NACT response maintains flexible options for the surgical team, including de-escalation of breast or axillary lymph node surgery.
Limitations: This single-institution pilot was limited by a small study size. A multi-centre study including other WFL devices (TAG, MAGSEED, SmartClip) may provide further generalised knowledge for breast treatment teams.
Ethics committee approval: This prospective pilot study was approved by the institutional review board and written informed consent was obtained.
Funding: No funding was received for this work.
Author Disclosures:
M. K. Hayes: Consultant at Hologic, Inc, Merit, Inc, QT Ultrasound, Inc.
H. Wright: nothing to disclose
E. Bloomquist: nothing to disclose

RPS 1802-3 10:42

MRI prediction of response to neoadjuvant chemotherapy in breast cancer: a comparison between patients with and without tumoral calcifications on mammography

T. Sella, B. Simor, B. Maly, E. Carmon*; Jerusalem/IL*
(tamarse@hadassah.org.il)

Purpose: MRI is documented as the most accurate imaging modality to evaluate response to neoadjuvant chemotherapy (NAC). consequently, surgical planning is mandated by post-NAC MRI findings. However, if the tumour demonstrates extensive calcification on mammography (MG) at diagnosis, complete excision of calcifications is the common practice, regardless of MR findings. The purpose of this study was to examine the ability of MRI to predict complete response in tumours with versus without calcifications on MG.
Methods and materials: We retrospectively analysed pre and post NAC MG and MRI in 114 consecutive patients at a single institution, 64 (56%) with non-calcified tumours and 50 (44%) with calcifications on MG which correlated in extent with the suspicious enhancement on MRI. Response to NAC was assessed on MRI and compared with post-surgical pathology. Statistical analysis was performed using Chi-square or Fisher exact test, $p< 0.05$ considered significant.
Results: Demographics and tumour characteristics were similar in both groups. MRI predicted response to NAC equally in both groups showing 40% vs 41% complete, 52% vs 53% partial, and 8% vs 6% no response in patients with calcifications compared to no calcifications respectively (p=0.958). Concordance between MRI prediction and response on pathology was equal between the 2 groups, 70% with calcifications and 69% without, p=0.886. Among discordant cases, there was a small non-significant tendency for overestimation of response by MRI in patients without calcifications (19% vs 12%, p=0.24). Mastectomy was more commonly performed in patients with calcifications (66%) than those without (52%).
Conclusion: MRI predicts response to NAC equally in patients with calcified versus non-calcified tumours. Post NAC surgical planning based on MR findings should be considered in patients with tumour calcifications similar to those without.
Limitations: A retrospective study.
Ethics committee approval: Informed consent was waived.
Funding: No funding was received for this work.
Author Disclosures:
T. Sella: nothing to disclose
E. Carmon: nothing to disclose
B. Simor: nothing to disclose
B. Maly: nothing to disclose

RPS 1802-4 10:48

DWI-based response evaluation after neoadjuvant systemic treatment of breast cancer: comparison with RECIST-based criteria

R. Ota[1], M. Kataoka[1], M. Iima[1], M. Honda[2], S. Kanao[1], T. Kataoka[1], M. Toi[1], K. Togashi[1]*; [1]Kyoto/JP, [2]Osaka/JP (ota_rie0624@kuhp.kyoto-u.ac.jp)*

Purpose: To evaluate treatment response based on diffusion-weighted imaging (DWI) after neoadjuvant systemic treatment (NST). DWI score based on signal patterns on DWI were compared to RECIST-based evaluation.
Methods and materials: Breast cancer patients who underwent dynamic contrast-enhanced (DCE) MRI and received NST followed by surgery between 2014 and 2019 (n=116) were analysed.
MRI protocols were as follows: T1WI, T2WI, DWI (TR/TE=7000/62 ms; b=0, 1000 sec/mm2), and DCE-MRI performed on 3.0 Tesla scanner (Siemens AG, Erlangen, Germany) with 18 or 16 channel dedicated breast coils. The MRIs were retrospectively evaluated by two radiologists with 20 and 3 years experience of breast MRI, and the target lesions were given a 3-point score .

The RECIST-based evaluation was further classified into 3 groups (PD, SD, PR/near CR/CR).
Pathological evaluation: pCR was defined as no residual invasive or non-invasive cancer in breast tissue on histopathology from surgical resection (in situ lesion was allowed). Statistical analysis was performed with MedCalc. The diagnostic performance of DWI parameters in discriminating pCR was assessed using a receiver operating characteristic (ROC) analysis. For RECIST-based criteria, they were grouped as pCR or non-pCR.
Results: Among 116 cases, 40.5% (47/116) achieved pCR while 59.5% (69/116) were categorised as non-pCR on pathology. The DWI score was strongly associated with residual disease. ROC analysis showed area under the ROC (AUC) of 0.96 (95% confidence interval: 0.91-0.99). ROC analysis of RECIST-based evaluation showed AUC of 0.70 (95% Confidence interval: 0.60-0.78).
Conclusion: DWI-based evaluation of residual disease is a useful approach of breast cancer following NST.
Limitations: Visual assessment.
Ethics committee approval: This study protocol was approved by our institutional review board.
Funding: No funding was received for this work.
Author Disclosures:
R. Ota: nothing to disclose
M. Kataoka: nothing to disclose
M. Iima: nothing to disclose
K. Togashi: nothing to disclose
S. Kanao: nothing to disclose
M. Toi: nothing to disclose
T. Kataoka: nothing to disclose
M. Honda: nothing to disclose

RPS 1802-5 10:54
Muscle mass loss after neoadjuvant chemotherapy in breast cancer: estimation on breast magnetic resonance imaging using pectoralis muscle area
F. Rossi, L. Torri, S. de Giorgis, M. Calabrese, A. Tagliafico*; Genoa/IT*

Purpose: Sarcopenia is widely considered a predictor of poor survival and toxicity in breast cancer patients. The aim of this study was to evaluate if there is pectoralis muscle area (PMA) variation, reflecting a loss of skeletal muscle mass, on consecutive MRI examinations during neoadjuvant chemotherapy.
Methods and materials: A total of n=110 consecutive patients (mean age 56±11years) who were treated with NAC for histologically proven primary breast cancer between January 2017 and January 2019, and in whom tumour response was checked with standard breast MRI, were included. Two radiologists calculated the pectoralis muscle cross-sectional area before and after NAC.
Results: The time between the two MRI examinations, before starting NAC, and after completion of three cycles of NAC was 154,8±34 days. PMA calculated pre-NAC (8,14 cm^2) was larger than PMA calculated post-NAC (7,03 cm^2), ($p<0.001$). According to RECIST criteria, there were no significant differences between responders (complete or partial response) and no responders ($p=0.362$). The multivariate regression analysis did not show any significant relationships between ΔPMA and age, the time between MRI exams, estrogen and progesterone receptor status, human epidermal growth factor receptor status (HER-2), Ki-67 expression, lymph nodes status, RECIST criteria, or histological type and grade. Inter-reader ($k=0.72$) and intra-reader agreement (0.69 and 0.71) in PMA assessment were good.
Conclusion: Pectoralis muscle mass variation, reflecting loss of skeletal muscle mass, in breast cancer patients undergoing NAC can be estimated directly on standard breast MRI.
Limitations: Known limitations are the retrospective nature of the study and the lack of a control-group.
Ethics committee approval: The study was approved by our institutional review board. Written informed consent was obtained.
Funding: No funding was received for this work.
Author Disclosures:
F. Rossi: nothing to disclose
M. Calabrese: nothing to disclose
L. Torri: nothing to disclose
S. de Giorgis: nothing to disclose
A. Tagliafico: nothing to disclose

RPS 1802-6 11:00
The value of different tumour regression of MRI in evaluating the efficacy of neoadjuvant chemotherapy for breast cancer
X. Mei, J. Ma, X. Lin, C. Yi*; [2]Shenzhen/CN*
(2635063963@qq.com)

Purpose: To analyse the different shrinkage pattern of breast tumors in magnetic resonance imaging (MRI) after neoadjuvant chemotherapy (NAC) and to evaluate the efficacy of different shrinkage pattern in chemotherapy.
Methods and materials: Data from 50 patients who were diagnosed with unilateral breast cancer underwent NAC before surgery after the eighth cycle of NAC was analysed retrospectively. All patients underwent MRI scan with contrast enhancement. The shrinkage pattern was classified into 3 categories: concentric shrinkage, fragment-like shrinkage, and mixed shrinkage. All the patients were divided into pathological complete response (pCR) group and N-pCR group according to the histopathologic tumour response. The χ^2 test were used to compare the baseline characteristics of pCR and N-pCR groups, as well as the tumour enhancement pattern and shrinkage pattern of the molecular types. Associations were evaluated using binary logistic regression models.
Results: 16 patients achieved pCR and 34 patients had a residual disease (N-pCR). Age, menopausal status, tumour size, lymph node, T stage, molecular typing, ER, PR, ki-67 status, and tumour enhancement mode on MRI showed no significance between pCR and N-pCR groups (all $p>0.05$), while only HER2 status and shrinkage pattern a significant difference ($p<0.05$ in both). Interobserver agreement regarding shrinkage pattern was moderate after NAC (Kappa value 0.719). There were no statistically significant differences in tumour shrinkage pattern and MRI tumour enhancement among the molecular types (all $p>0.05$). There were statistically significant differences in MRI tumour enhancement in the tumour shrinkage pattern ($p<0.05$). Logistic model showed that tumour shrinkage pattern after NAC and HER2 status were independent factors for predicting pCR.
Conclusion: Shrinkage pattern and HER2 status can be independent factors for predicting pCR.
Limitations: A retrospective study.
Ethics committee approval: LL-KT-201801162.
Funding: Shenzhen science and technology research and development fund (JCYJ20180305164740612).
Author Disclosures:
X. Mei: Author at Shenzhen People's Hospital,Second Clinical Medical College of Jinan University, Speaker at Shenzhen People's Hospital,Second Clinical Medical College of Jinan University
J. Ma: Author at Shenzhen People's Hospital,Second Clinical Medical College of Jinan University
X. Lin: Author at Shenzhen People's Hospital,Second Clinical Medical College of Jinan University
C. Yi: Author at Shenzhen People's Hospital,Second Clinical Medical College of Jinan University

RPS 1802-7 11:06
The combined use of ADC with DCE-MRI in early assessing of response to neoadjuvant chemotherapy in patients with breast invasive ductal carcinomas
L. Liu, W. Peng, B. Yin, Y. J. Gu*; Shanghai/CN*
(llbbsy@163.com)

Purpose: To combine the dynamic contrast-enhanced magnetic resonance imaging (DCE-MRI) and ADC value to serve as early response markers in breast cancer after NAC.
Methods and materials: Between July 2014 and July 2016, 50 patients who received NAC were considered to be eligible. All patients underwent a pretreatment breast routine ultrasonography, MRI, DCE-MRI, and DWI. 50 patients underwent these examinations four times prior to treatment. 1st, 2nd, and following the final cycle of NAC. Responses were measured by routine MRI and ultrasonography using the response evaluation criteria in solid tumours (RECIST).
Results: The areas under the ROC curve were 0.627 for the ultrasonography in early assessment of the response to NAC. The areas under the ROC curve were 0.735 for routine MRI in early assessment of the response to NAC. There was a significant difference between responders and nonresponders in K^{trans}, Kep, and TTP after the first cycle of therapy （$P=0.022<0.05$). Among various perfusion parameters, the largest areas under the ROC curve were 0.84 for Kep, then that of K^{trans}(0.75). In a combined examination, the largest areas under the ROC curve was 0.88 and that of combined ADC and K^{trans} was the second (0.84).
Conclusion: Kep and K^{trans} are superior to routine MRI and ADC value in the early assessment of the response to NAC. Combined ADC with Kep and ADC with K^{trans} are the most recommended parameters that may help determine individual treatments.
Limitations: The number of cases was small. All cas-es were invasive ductal carcinoma. This might affect the evalua-tion results.
Ethics committee approval: Information about review or animal board approval and written informed consent.
Funding: No funding was received for this work.

Author Disclosures:
L. Liu: nothing to disclose
W. Peng: nothing to disclose
B. Yin: nothing to disclose
Y. J. Gu: nothing to disclose

RPS 1802-8 11:12
Impact of pathologic complete response definition on MRI diagnostic performance after neoadjuvant systemic therapy
D. A. Hashem, M. T. El-Diasty, A. Khazindar, A. Abusanad, S. Bakhsh, A. Bin Mahfuoz*; Jeddah/SA (Dalia-hashim@hotmail.com)*

Purpose: Determining disease extent after neoadjuvant chemotherapy (NAC) is essential for accurate surgical planning. Achieving pathologic complete response (pCR) has shown to have favourable prognosis in certain tumour subtypes, however, the definition of pCR varies between authors and can affect the interpretation of results at systematic reviews. We aimed to investigate the diagnostic accuracy of post-NAC MRI with reference to different pCR definitions.
Methods and materials: Records of patients with locally advanced breast cancer who underwent NAC followed by mastectomy between January 2016 and January 2019 were retrospectively reviewed. Post-treatment MRI was correlated with residual disease on final histopathology. Two definitions for pCR were used; the first was an absence of both invasive and in situ components, and the second was an absence of invasive component only. Diagnostic accuracy of post treatment MRI was tested against both definitions separately.
Results: 52 women (mean age, 47.4 years; range 28-74) with 56 breast masses were eligible for the study. Complete MRI response was noted in 22 (39%) masses. pCR was achieved in 14 (25%) and 25 (44.6%) masses using the first and second pCR definitions respectively. Negative predictive value (NPV) and overall accuracy of MRI for detecting residual disease was 50% and 75%, respectively, using the first pCR definition. With the second pCR definition, NPV and accuracy were 77.3% and 76.8%, respectively.
Conclusion: MRI NPV for residual disease was higher with the second pCR definition, however, overall accuracy was not different. MRI accuracy in detecting residual disease after NAC is not adequate to replace pathological assessment.
Limitations: Retrospective design, small sample size, and at single institution.
Ethics committee approval: This retrospective study was approved by the institutional review board with waiving of the informed consent.
Funding: No funding was recieved for this work.
Author Disclosures:
D. A. Hashem: nothing to disclose
M. T. El-Diasty: nothing to disclose
A. Bin Mahfuoz: nothing to disclose
A. Khazindar: nothing to disclose
A. Abusanad: nothing to disclose
S. Bakhsh: nothing to disclose

RPS 1802-9 11:18
Early prediction of axillary lymph node metastasis and their response to neoadjuvant systemic therapy with ^{18}F-FDG PET/CT in breast cancer patients
C. M. de Mooij, C. Mitea, F. Mottaghy, M. B. I. Lobbes, M. Smidt, T. van Nijnatten*; Maastricht/NL (c.demooij@maastrichtuniversity.nl)*

Purpose: To assess the value of ^{18}F-FDG PET/CT in predicting the presence of axillary lymph node metastasis (ALNM) and their response to neoadjuvant systemic therapy (NST) in breast cancer patients.
Methods and materials: We analysed 37 patients with breast cancer that underwent ^{18}F-FDG PET/CT prior to NST. Maximum standardised uptake values of the primary tumour (SUV-T) and the most FDG-avid lymph node (SUV-LN) and their ratio (NT ratio) were calculated. Patients with and without suspicious ALNM based on prior imaging were compared regarding their SUV values. ALNM response following NST was classified according to the Pinder classification. Patients were defined as responders (Pinder 1-3) and non-responders (Pinder 4). The association of SUV_{max} with ALNM response was assessed using ROC analyses.
Results: Of 37 patients, 25 (68%) had suspicion for ALNM. Patients with suspected ALNM showed significantly higher SUV-LN (1.5 vs. 6.1) and NT ratio (0.3 vs. 1.0), but no significant difference in SUV-T (6.0 vs. 8.3) was found. Non-significant differences between responders and non-responders of SUV-T (7.5 vs. 8.2), SUV-LN (5.6 vs. 5.1), and NT ratio (0.9 vs. 0.7) were found. The AUCs for SUV-T, SUV-LN, and NT ratio were 0.544, 0.630, and 6.11, respectively. An SUV-LN cutoff value of 3.5 had a sensitivity of 75% and a specificity of 49% in identifying patients who responded to NST.
Conclusion: ^{18}F-FDG PET/CT showed promising results in predicting ALNM and their response to NST in breast cancer patients.
Limitations: These results are preliminary, hence the low sample size.
Ethics committee approval: The need for informed consent was waived by a local ethics committee.
Funding: No funding was received for this work.
Author Disclosures:
C. M. de Mooij: nothing to disclose
T. van Nijnatten: Grant Recipient at Siemens
C. Mitea: nothing to disclose
M. Smidt: Grant Recipient at Xavier
M. B. I. Lobbes: nothing to disclose
F. Mottaghy: nothing to disclose

RPS 1802-10 11:24
MRI response evaluation after neoadjuvant chemotherapy: what are the factors of radiologic-pathologic discordance?
S. Mevlütoğlu[1], Ö. Aslan[1], I. G. Bilgen[1], A. O. Oktay Alfatli[1], L. Yeniay[1], O. Zekioğlu[2]*; [1]İzmir/TR, [2]Bornova-İzmir/TR (sevdamevlutoglu@hotmail.com)*

Purpose: To assess which clinicopathologic and radiologic factors influence magnetic resonance imaging (MRI) performance in the demonstration of radiologic response (false positive/negative results) in breast cancer after neoadjuvant chemotherapy (NAC).
Methods and materials: A total of 80 patients with breast cancer who underwent breast MRI before and after NAC was included in this study. All patients were diagnosed with core-needle biopsy before treatment for histological tumour type and immunohistochemical markers. Pathological examination was referenced as a gold standard after complete surgical excision. Complete radiological response (rCR) to NAC was accepted when the main lesion site showed no early enhancement on dynamic MRI.
Complete pathologic response (pCR) was described as the complete absence of invasive cancer in the surgical material.
The clinicopathologic and radiologic factors which influence the radiologic-pathologic correlation were analysed.
Results: The mean age of cohort was 43.5 years (range:24-64).
MRI analysis after NAC showed rCR in 44 cases (55%), while pathological analysis of surgical specimens after NAC detected pCR in 43 cases (53.8%).
Based on MRI findings, the radiologic-pathologic discordance was in 23 of 80 cases. Multivariate analysis of radiologic findings to identify predictors: dense breast parenchyme (BIRADS type C-D), multifocal multicentric lesions, high parenchyme enhancement, and non-mass enhancement in post-treatment MR imaging. Also, there were significantly more frequent cases of tumour nuclear histologic grade luminal B subtype.
Conclusion: Patients with dense breast parenchyme (BIRADS type C-D), high parenchyme enhancement, multifocal multicentric lesions, luminal B, invasive ductal type cancer, and non-mass enhancement in post-treatment MR imaging are significantly associated with radiologic-pathologic discordance on MR imaging after NAC. These patient populations should be evaluated in depth.
Limitations: A retrospective study, limitation in the number of patients.
Ethics committee approval: n/a
Funding: No funding was received for this work.
Author Disclosures:
S. Mevlütoğlu: nothing to disclose
Ö. Aslan: nothing to disclose
I. G. Bilgen: nothing to disclose
A. O. Oktay Alfatli: nothing to disclose
L. Yeniay: nothing to disclose
O. Zekioğlu: nothing to disclose

RPS 1802-11 11:30
Assessment of the usefulness of monitoring tumour volume and stiffness in evaluating neoadjuvant chemotherapy treatment responses in breast cancer
K. S. Dobruch-Sobczak, H. Piotrzkowska-Wróblewska, Z. Klimoda, J. Litniewski*; Warsaw/PL*

Purpose: To determine whether a classifier based on two US parameters (volume and stiffness) is predictive of treatment responses from the first courses of neoadjuvant chemotherapy (NAC).
Methods and materials: Prospective US analysis was performed in patients with breast cancer qualified for NAC, before and 7 days after the first four courses of NAC. US examinations with strain sonoelastography were performed using linear transducer L14-5. Tumour volume and tumour stiffness (using Tsukuba scale) were evaluated. The resistant malignant cells [RMC] (ranging from 0–100%) were assessed by a pathologist postoperatively. Histopathological examination classifies tumours as responding (RT) and non-responding (N-RT). RT included those with a reduction in cellularity ≥30% while

N-RT was <30%. Correlation analysis, univariate, and multivariate logistic regression analysis were used for statistical assessment.
Results: A total of 42 breast cancer in 30 patients (mean age 56.4y) were examined. A statistically significant correlation was found between stiffness, volume, and RMC ($p<0.05$) after 2, 3, and 4 courses of NAC. In logistic regression, the best results were after the 3rd course of NAC. Using only stiffness as a prognostic parameter, we obtained a sensitivity of 37%, specificity of 87%, PPV 70%, NPV 63%, and for volumes respectively: 47%, 77%, 74%, and 67%. The classifier using both parameters showed a sensitivity of 73%, specificity 75%, PPV 68%, and NPV 78%.
Conclusion: The use of two US parameters, volume and stiffness, are highly predictive of tumour response after the 3rd NAC cycle and performed better than single parameters.
Limitations: A small group.
Ethics committee approval: The study was approved by the institutional bioethical review board of each participating institution.
Funding:
The study was supported by the grant, 2016/ 23/B/ST8/03391 to JL from the National Science Centre, Poland (funder's website: https://ncn.gov. pl/).
Author Disclosures:
K. S. Dobruch-Sobczak: nothing to disclose
H. Piotrzkowska-Wróblewska: nothing to disclose
Z. Klimoda: nothing to disclose
J. Litniewski: nothing to disclose

RPS 1802-12 11:36

Breast MRI affects overall survival but not disease-free survival in breast cancer patients: a retrospective population-based study

T. van Nijnatten[1], L. van Tiel[2], A. C. Voogd[1], K. Groothuis-Oudshoorn[2], S. Siesling[3], M. B. I. Lobbes[4]; [1]*Maastricht/NL,* [2]*Twente/NL,* [3]*Utrecht/NL,* [4]*Sittard-Geleen/NL (Thiemo.nijnatten@mumc.nl)*

Purpose: To evaluate the effect of breast MRI on overall survival (OS) and disease-free survival (DFS) of patients with invasive breast cancer in the Netherlands.
Methods and materials: We selected all women from the nationwide cancer registry diagnosed with invasive breast cancer (a) between 2011-2013 for the OS-cohort and (b) in the first quarter of 2012 for the DFS-cohort. The study population was divided into a MRI and non-MRI group. In addition, subgroups were created according to breast cancer subtype: invasive carcinoma of no special type (NST) versus invasive lobular carcinoma (ILC). OS and DFS were compared between the MRI and non-MRI group using the Kaplan-Meier method and the log-rank test. Cox proportional hazard regression analysis was performed to estimate hazard ratio (HR) with a 95% confidence interval (CI). To account for missing data, multiple imputation was performed.
Results: Of the 31,756 patients included in the OS-cohort (70% non-MRI and 30% MRI), 27,752 (87%) were diagnosed with invasive carcinoma NST and 4,004 (13%) with ILC. Multivariable Cox regression showed that breast MRI had a tendency towards better OS (HR 0.91, 95%-CI 0.74-1.11) and was statistically significant for patients aged >50 years (overall). Of the 2,464 patients included in the DFS-cohort (72% non-MRI and 28% MRI), 2,161 (88%) were diagnosed with invasive carcinoma NST and 303 (12%) with ILC. Multivariable Cox regression analysis showed that breast MRI was not significantly associated with DFS (HR 1.16, 95%-CI 0.81-1.67).
Conclusion: Breast MRI was not significantly associated with an improved DFS and revealed a tendency towards an improved OS, which was only significant for patients aged >50.
Limitations: Retrospective and observational design.
Ethics committee approval: n/a
Funding: No funding was received for this work.
Author Disclosures:
T. van Nijnatten: Research/Grant Support at Siemens
M. B. I. Lobbes: Research/Grant Support at GE Healthcare
L. van Tiel: nothing to disclose
A. C. Voogd: nothing to disclose
K. Groothuis-Oudshoorn: nothing to disclose
S. Siesling: nothing to disclose

RPS 1802-13 11:42

The accuracy of a MRI scan for the prediction of pathological response (pCR) in neoadjuvant chemotherapy (NACT)

E. Giannotti, P. M. Moseley, T. Abdel-Fatah, J. Walker, K. D. Jethwa, S. Chan; *Nottingham/UK (ytteb84@hotmail.com)*

Purpose: To investigate the accuracy of MRI in evaluating response to neoadjuvant chemotherapy (NAC) in primary breast cancer and to determine if the presence of DCIS/LCIS can influence the accuracy.
MRI has a high specificity for the correct detection of residual tumour after NAC, but low sensitivity (correct identification of complete pathological response (pCR) PPV 48% has been reported).
Methods and materials: A cohort of 461 consecutive patients who received NAC in a single cancer centre (2007–2019) with post-NAC pre-surgery MRI and surgery pathology data were analysed. 'Gold Standard' for the response was pCR in the surgical specimen. Radiological complete response (rCR) was defined as 0 mm and non-rCR defined as ≥1 mm, using maximum tumour diameter on MRI.
Results: In the whole cohort, MRI sensitivity (probability of identifying a pCR from rCR)=71.0% (88/124), and specificity (probability of correctly identifying non-pCR from non-rCR)=81.0% (273/337).
The presence of DCIS/LCIS in the surgical sample reduces the accuracy of MRI assessment, sensitivity by 24.8% (with=53.1% vs without=77.9%), and specificity by 2.4% (with=78.6% vs without=81.0%), increasing overestimation of disease size. False-negative rate (probability of rCR incorrectly identifying pCR) is 46.9% with DCIS/LCIS versus 22.1% without DCIS/LCIS.
Conclusion: This analysis showed that there is a need to improve the accuracy of MRI assessment of pCR.
There is an urgent need to identify variables which can improve this invaluable tool to optimise treatment planning.
Introducing a volumetric and texture AI-driven analysis may increase the accuracy and confidence of MRI with positive clinical benefit leading to better patient treatment and less invasive approach to surgery.
Limitations: A retrospective study. Further researches needed.
Ethics committee approval: n/a
Funding: No funding was received for this work.
Author Disclosures:
J. Walker: nothing to disclose
E. Giannotti: nothing to disclose
P. M. Moseley: nothing to disclose
T. Abdel-Fatah: nothing to disclose
K. D. Jethwa: nothing to disclose
S. Chan: nothing to disclose

RPS 1802-14 11:48

Bone marrow signal intensity on breast MRI in women with breast cancer

I. Bokov[1], P. M. Sklair Levy[2], D. M. Ben-David[2], D. O. Haisraely[2]; [1]*Rehovot/IL,* [2]*Ramat Gan/IL (inna5566@gmail.com)*

Purpose: Women with breast cancer receiving neoadjuvant chemotherapy undergo breast MRI as part of treatment response assessment. Incidental sternal bone marrow enhancement may be demonstrated and be confused with pathologic findings. Our goal was to evaluate bone marrow enhancement on MRI prior to and upon completion of neoadjuvant treatment.
Methods and materials: A retrospective study between the years 2012-2017 included 109 consecutive women with breast cancer and treated with neoadjuvant chemotherapy. MRI was performed before and after treatment to evaluate response. The neoadjuvant regimen included AC-T in adjunct with G-CSF (bone marrow stimulating agent) and steroids. Bone marrow signal intensity was measured at the sternum, before and after contrast injection. Chest wall muscle signal intensity was used as a reference. The index was calculated as bone marrow signal intensity divided by muscle signal intensity prior, upon completion, and 1 year after completion of neoadjuvant treatment. MRI was performed on average 80 days from the end of treatment. Statistical correlation between bone marrow index, age, disease stage, and time from the end of treatment.
Results: The mean patient age was 50 and 98% were diagnosed with invasive ductal carcinoma. Bone marrow index prior to neoadjuvant treatment was 1.9, upon completion of treatment 3.5, and 1.4 at 1 year follow up. Age was found to be inversely correlated to bone marrow index, the bone marrow index was found to be significantly higher in women younger than 48y. No statistical correlation was found between the time of MRI from the end of treatment and disease stage.
Conclusion: MRI bone marrow signal intensity may be high in women with breast cancer upon completion of NAT. It may be secondary to treatment with GCSF. This should not be confused with pathological enhancement suspicious of metastatic disease.
Limitations: n\a
Ethics committee approval: n\a
Funding: No funding was received for this work.
Author Disclosures:
I. Bokov: nothing to disclose
P. M. Sklair Levy: nothing to disclose
D. M. Ben-David: nothing to disclose
D. O. Haisraely: nothing to disclose

RPS 1802-15 11:54

Which MRI morphologic criteria can better predict the response after neoadjuvant chemotherapy (NAC) in axillary lymph nodes (ALN)?

V. Ruggeri, M. Durando, G. Mariscotti, E. Regini, G. Bartoli, I. Castellano, P. Fonio*; Turin/IT (vruggerim@gmail.com)*

Purpose: To investigate which MRI morphologic criteria can predict residual disease in ALNs in patients who have undergone NAC.
Methods and materials: From 2017 to 2019, 60 consecutive patients with advanced breast cancer who underwent 1,5 T MRI before and after NAC were retrospectively collected. Pre- and post-NAC MRI were retrospectively analysed by two dedicated radiologists in consensus, blinded to histological results, evaluating both quantitative (number and diameter) and qualitative criteria (irregular margins, absence of fatty hilum, cortical thickness>3mm, perifocal oedema, rim enhancement, and asymmetry comparing with contralateral side) related to ALNs. ALNs status was evaluated by sentinel ALN biopsy or axillary dissection and nodal pathological response classified according to Pinder's criteria [complete response (pCR) versus no-complete response (no-pCR)]. Statistical analysis (Chi-square or Fisher's exact tests for categorical variables, non-parametric Mann-Whitney test for continuous variables) was performed to compare pCR versus no-pCR cases.
Results: At baseline MRI, no-pCR cases ALNs were characterised by loss of fatty hilum (93.3% versus 44.4% in pCR, p=0.02), presence of rim enhancement (86.7% versus 11.1% in pCR, p=0.001), asymmetry (93.3% versus 44,4% in pCR, p=0.02), average cortical thickness significantly larger (9.5 versus 3.7 mm, p=0.004) than pCR cases. At post-NAC MRI, average cortical thickness was significantly (p=0.01) larger in no-pCR patients compared to pCR (4.5 versus 1.8 mm). Considering as suspicious ALN with at least one of the above characteristics, MRI sensitivity, specificity, positive and negative predictive values, and accuracy for assessing ALNs response were 88.2%, 77.8%%, 88.2%, 77.8%, and 84.6%, respectively.
Conclusion: Based on our results, supporting the use of MRI in assessing nodal response after NAC, abnormal ALNs cortical thickness seems to be the most reliable parameter associated to no-pCR.
Limitations: Small sample, monocentric study.
Ethics committee approval: n/a
Funding: No funding was received for this work.
Author Disclosures:
V. Ruggeri: nothing to disclose
M. Durando: nothing to disclose
G. Mariscotti: nothing to disclose
E. Regini: nothing to disclose
G. Bartoli: nothing to disclose
I. Castellano: nothing to disclose
P. Fonio: nothing to disclose

10:30 - 12:00 **Coffee & Talk 1**

Cardiac

RPS 1803

Myocarditis and MINOCA syndromes

Moderators:
R. F. Gohmann; Leipzig/DE
L. Natale; Rome/IT

RPS 1803-1 10:30

Right ventricular myocarditis: the great imitator of cardiac magnetic resonance. A retrospective hystologically-based comparison with ARVC

F. Cilia, N. Galea, L. Marchitelli, G. Cundari, G. Mancuso, G. Pambianchi, I. Carbone, C. Catalano, M. Francone*; Rome/IT (fcilia91@hotmail.it)*

Purpose: Isolated right ventricular involvement in myocarditis (RV-myo) is an uncommon event, sharing overlapped clinical and morphological manifestations with arrhythmogenic right ventricular cardiomyopathy (ARVC), consisting of regional wall motion abnormalities, RV enlargement, impaired ejection fraction (EF), and late gadolinium enhancement (LGE). The two conditions have shown to be misdiagnosed with CMR in approximately 50% of cases.
Methods and materials: From a database of 12 consecutive patients undergoing endomyocardial biopsy (EMB) with an initial CMR suspicion of ARVC, we retrospectively identified 8 cases with a histological diagnosis of ARVC and 4 with RV-myo. Biventricular volumes, CMR tissue abnormalities, and clinical data were systematically compared and matched with current CMR diagnostic criteria of ARVC.
Results: 2 ARVC patients presented with a long-standing history of syncope, whereas 1 RV-myo patient presented with acute chest pain. In the remaining 9 cases, clinical presentations were highly overlapped, consisting of ECG abnormalities, variably associated with palpitations, and no troponin raise. CMR data showed comparably enlarged RV-EDV between ARVC and RV-myo (EDV/BSA respectively 117,3±32,4mL/m^2 vs.124,9±46mL/m^2,p>0.05) and reduced ejection fraction (EF:40,3±14,6% vs. 33,8±15,3%,p>0.05). RV-LGE was noted in 7/12 cases (n=3 ARVC; n=4 RV-myo), predominately involving RV free wall. Homogeneous intraventricular thickening was also observed in 2/4 RV-myo patients associated with coexisting tissue oedema. According to current CMR diagnostic criteria, the diagnosis of ARVC was established in 6/8 patients with ARVC and 2/4 with RV-myo.
Conclusion: Our results confirmed highly overlapped morpho-functional and tissue abnormalities in both pathological entities, introducing a relevant interpretation bias recalling the need for invasive characterisation in selected cases.
Limitations: A very limited study population.
Ethics committee approval: IRB and written informed consent was obtained.
Funding: No funding was received for this work.
Author Disclosures:
N. Galea: nothing to disclose
F. Cilia: nothing to disclose
M. Francone: nothing to disclose
C. Catalano: nothing to disclose
G. Pambianchi: nothing to disclose
G. Mancuso: nothing to disclose
I. Carbone: nothing to disclose
G. Cundari: nothing to disclose
L. Marchitelli: nothing to disclose

RPS 1803-2 10:36

Non-contrast enhanced diagnosis of acute myocarditis based on the 17-segment heart model using 2D-feature tracking magnetic resonance imaging

M. Salehi Ravesh[1], M. Eden[1], P. Langguth[1], T.-C. Piesch[1], J. K. Lehmann[1], A. Lebenatus[1], D. Hautemann[2], O. Jansen[1], M. Both[1]*; [1]Kiel/DE, [2]Leiden/NL (Mona.SalehiRavesh@uksh.de)*

Purpose: To investigate the diagnostic value of myocardial deformation analysis based on the 17-segment heart model using non-contrast enhanced (CE) 2D tissue feature tracking (2D-FT) technique.
Methods and materials: 70 patients with suspected myocarditis underwent a cardiovascular magnetic resonance (CMR) examination at 1.5 Tesla. A contrast-agent-free part of this CMR protocol was additionally performed in 40 healthy volunteers (HV). Besides standard CMR data sets, 2D-FT derived segmental and global longitudinal, radial, and circumferential deformation parameters were analysed. The 2D-FT results were compared to the combined findings from CMR imaging and endomyocardial biopsy (EMB).
Results: Patients were assigned to 3 groups depending on their ejection fraction (EF) (<40%, 40-55%, and ≥55%). Compared to HV, impaired EF (<55%) was significantly correlated to reduced segmental and global strain and strain rate values. The circumferential deformation analysis was more sensitive to myocardial changes than longitudinal and radial analysis. The segmental strain/strain rate had an accuracy of 84.3%/70.0% for the diagnosis of acute myocarditis, stated by EMB and CMR in 42 of 70 patients. In patients with preserved EF, acute myocarditis could be ruled out using only segmental strain analysis with a negative predictive value of 87.5%.
Conclusion: In patients with suspected myocarditis, the deformation analysis based on the 17-segment heart model provides valuable information about functional myocardial inhomogeneity. This quantitative approach could be used in addition to the clinical standard CMR protocol and represents a promising tool in the framework of a prospective automatised multiparametric CMR imaging analysis.
Limitations: The cut-off values in this work were determined according to the results in our HV.
Ethics committee approval: No. D 407/18.
Funding: No funding was received for this work.
Author Disclosures:
M. Salehi Ravesh: nothing to disclose
M. Eden: nothing to disclose
P. Langguth: nothing to disclose
T.-C. Piesch: nothing to disclose
J. K. Lehmann: nothing to disclose
A. Lebenatus: nothing to disclose
D. Hautemann: Employee at Medis bv
O. Jansen: nothing to disclose
M. Both: nothing to disclose

RPS 1803-3 10:42

Tissue characterisation by parametric mapping and strain cardiac magnetic resonance for the detection and monitoring of myocardial injury in fulminant myocarditis

H. Li, H. Zhu, L. Xia*; Wuhan/CN (haojie8393@163.com)*

Purpose: To investigate whether multiparametric cardiac magnetic resonance (CMR) could detect and monitor inflammation myocardial alterations in fulminant myocarditis.
Methods and materials: 19 patients (35 ± 14 years, 37% male) with a clinical diagnosis of fulminant myocarditis underwent CMR examinations at 3.0T in the acute phase and at 3-months follow-up. The control group consisted of 19 healthy volunteers. The CMR protocol included cine, black blood T2-weighted imaging, T1 mapping, T2 mapping, and late gadolinium enhancement (LGE). Cardiac strain was evaluated by feature tracking.
Results: The left ventricular mass index (64 [57, 76] versus 52 [47, 63], P<0.05) and interventricular septum thickness (10.5 [9, 11.3] versus 8.3 [6.6, 9.8], P<0.001) in the acute stage was significantly higher compared with controls and normalised at the chronic stage. All quantitative inflammation metrics, including oedema ratio, LGE mass, native T1, T2, and extracellular volume were significantly (all P<0.001) decreased in the follow-up scan, but still higher than controls. Compared with the controls, strain indices were all significantly (all P<0.001) impaired in the acute stage. Native T1 and T2 values led to excellent diagnostic accuracy for discriminating fulminant myocarditis from healed myocarditis, with AUC of 0.947 and 0.931.
Conclusion: Multiparametric CMR could detect and monitor inflammation myocardial injuries in patients with fulminant myocarditis. Native T1 and T2 values achieved excellent diagnostic performance in distinguishing acute from healed myocarditis.
Limitations: Though the diagnosis of FM was made by strict clinical criteria and typical CMR findings, the lack of EMB makes the myocardial histopathological verification unavailable.
Ethics committee approval: The study was approved by our Institutional Review Board and written informed consent was obtained prior to CMR.
Funding: National Natural Science Foundation of China (No. 81873889).
Author Disclosures:
H. Li: nothing to disclose
H. Zhu: nothing to disclose
L. Xia: nothing to disclose

RPS 1803-4 10:48

Mapping cardiac magnetic resonance (CMR) for early prediction of unfavourable left ventricle remodelling in acute myocarditis: a MIAMI study

A. Palmisano[1], G. Benedetti[2], M. Gatti[3], R. Faletti[3], N. Galea[4], M. Francone[4], A. Del Maschio[1], F. de Cobelli[1], A. Esposito[1]*; [1]Milan/IT, [2]London/UK, [3]Turin/IT, [4]Rome/IT (palmisano.anna@hsr.it)*

Purpose: A pixel-wise mapping technique resulted in more sensitive than conventional CMR images in the diagnosis of acute myocarditis. The role in the detection of subtle inflammation is still under investigation and imaging predictors of outcomes are still largely unknown.
Methods and materials: 68 patients with clinical suspicions of myocarditis underwent cardiac MR (CMR) at a 1.5T scanner for the evaluation of morpho-functionality, hyperaemia with ce-SSFP images, oedema with STIR and T2 mapping, scarred myocardium with LGE, native-T1, and ECV. When clinically indicated endomyocardial biopsy (EMB) was performed, a second CMR was performed 2 months after baseline. 45 healthy volunteers underwent CMR as the control group.
Results: Acute myocarditis was confirmed in 45 patients by both CMR and EMB. An Infarct-like presentation was the most frequent (25 patients, 56%). At baseline CMR, LV-EDV was 135 ml with EF.53%, LL criteria were positive (T2-ratio: 2.8, Hyperemia: 13%, LGE: 6%), and T1, T2 mapping, and ECV were significantly higher than normal values without difference among clinical presentation (p>0.05). Mapping parameters showed excellent diagnostic accuracy in the acute (AUC: 95%, 98%, and 90% for T1 map, T2 map, and ECV) and convalescent phases (90%, 85%, and 89% for T1 map, T2 map, and ECV). At short-term follow-up, a slight recovery of EF was experimented on with a reduction of all LL and mapping parameters. The modification of native-T1 values correlated to the recovery of EDV (R=0.8242, p=0.0005) and ejection fraction (R= -0.4559, p=0.0378).
Conclusion: Lower recovery of T1 value in the convalescent phase is associated with higher EDV and lower EF.
Limitations: A imited sample size and relatively short follow-up.
Ethics committee approval: The study was approved by Institutional Review Board. Aall study participants signed informed consent.
Funding: The study was granted by the Italian Ministry of Health.
Author Disclosures:
A. Palmisano: nothing to disclose
G. Benedetti: nothing to disclose
R. Faletti: nothing to disclose
M. Gatti: nothing to disclose
N. Galea: nothing to disclose
M. Francone: nothing to disclose
A. Del Maschio: nothing to disclose
F. de Cobelli: nothing to disclose
A. Esposito: nothing to disclose

RPS 1803-5 10:54

Agreement between old and new Lake Louise criteria for the diagnosis of acute myocarditis with a different clinical onset

G. Cundari, G. de Rubeis, A. Ascione, S. Coco, F. Catapano, F. Cilia, N. Galea, C. Catalano, M. Francone*; Rome/IT (cundarigiulia@gmail.com)*

Purpose: To compare the diagnostic performance of old and new Lake Louise criteria (oLLC and nLLC) in suspected acute myocarditis patients among various clinical presentations: infarct-like [IL], cardiomyopathic [CM], and arrhythmic [A].
Methods and materials: 110 patients with a clinical suspicion of acute myocarditis underwent 1.5T cardiac magnetic resonance. The protocol included cine–SSFP, T2wSTIR, early and late gadolinium-enhancement, T2-mapping, and native and post-Gd T1-mapping. 3 patients were excluded for unknown clinical hystory. Cohen's k test was used to assess the level of agreement and a McNemar test to compare the diagnostic proportion between oLLC and nLLC among different clinical presentations.
Results: The frequency of clinical presentations were 56/107 (52%) IL, 29/107 (27%) CM, and 22/107 (20.5%) A. A diagnosis was performed in 45/110 (40.9%) patients with oLLC and in 69/110 (62.7%) with nLLC [k=0,48[0,33-0,62], p<0.01. A statistically significant difference in the agreement of oLLC and nLLC was found for CM and A presentations [15/29(51,7%) vs 7/29(24,1%), k= 0,46[0,19-0,73] p<0.01 and 11/22(50%) vs 4/22(18,2%), k=0,36[0,063-0,66], p<0.05, respectively]. No statistical difference was found for IL onset [nLLC 41/56(73,2%) vs oLLC 33/56(58,9%), k=0,45[0,22-0,69], p>0.05]. Mapping sequences allowed for the diagnosis of acute myocarditis when oLCC were negative in 5/56 (9%) for IL, 3/29 (10%) for CM, and 4/22 (18%) for A. In particular, with T1-mapping and ECV, T1 criterion was met in 9/56 (16%) IL, 7/29 (24%) CM, and 8/22 (36%) A onset (p>0.05), and, with T2-mapping, T2 criterion in 13/56 (23%) IL, 9/29 (31%) CM, and 8/22 (36%) A onset (p>0.05).
Conclusion: The degree of agreement between oLLC and nLLC was moderate for overall, IL, and CM presentations, and fair for A. nLLC allowed for a diagnosis of more acute myocardites than oLLC in CM and A onsets.
Limitations: Bioptic diagnosis of acute myocarditis was made only in few patients.
Ethics committee approval: Informed consent was obtained.
Funding: No funding was received for this work.
Author Disclosures:
G. Cundari: nothing to disclose
G. de Rubeis: nothing to disclose
A. Ascione: nothing to disclose
S. Coco: nothing to disclose
F. Catapano: nothing to disclose
F. Cilia: nothing to disclose
N. Galea: nothing to disclose
C. Catalano: nothing to disclose
M. Francone: nothing to disclose

RPS 1803-6 11:00

Early T1 shortening (eT1sh): a new CMR parameter to detect myocardial hyperemia in acute myocarditis

A. Palmisano[1], G. Benedetti[2], R. Faletti[3], M. Gatti[3], N. Galea[4], M. Francone[4], F. de Cobelli[1], A. Del Maschio[1], A. Esposito[1]*; [1]Milan/IT, [2]London/UK, [3]Turin/IT, [4]Rome/IT (palmisano.anna@hsr.it)*

Purpose: To evaluate T1-mapping based approaches for the quantification of hyperemia in patients with acute myocarditis.
Methods and materials: 55 subjects (40 patients with acute myocarditis [AM]; 15 age- and sex-matched healthy control subjects [HC]) underwent 1.5T CMR. T1 mapping was acquired before (native T1) and 2 minutes after gadoliunium administration (early-enhanced T1). 3 different T1 mapping-based parameters were calculated: early enhanced T1-rt (eT1), early T1-rt shortening (eT1sh), and early relative T1-rt shortening (erT1sh). Optimal cut-off values and their diagnostic performances in the identification of AM were calculated.
Results: In AM patients, median eT1 was 275.6 ms [252-297], eT1sh was 75% [73%-78%], and erT1sh was 2.15 [1.83-2.59], all being significantly higher with respect to HC (p=0.0014, p<0.0001, and p<0.0001, respectively). eT1sh showed the best diagnostic performance with excellent AUC (97%, 95% confidence interval, CI: [93%-100%]). A reduction of eT1sh ≥69.5% identified AM with very

high sensitivity (93%), specificity (100%), NPV (83%), PPV (100%), and accuracy (95%). eT1 had a good AUC (92.5%, 95% CI: [86%-99%]), slightly worse than eT1sh. eT1≤331 ms identified AM with 93% sensitivity, 87% specificity, 81% NPV, 95% PPV, and 91% accuracy. erT1sh showed the worst diagnostic performance with 78% AUC (95% CI: [66%-91%]). erT1sh>1.9 identified AM with 68% sensitivity, 87% specificity, 50% NPV, 93% PPV, and 73% accuracy.
Conclusion: eT1sh showed the best diagnostic performance in the identification of AM. It can be a promising alternative method for the detection of hyperemia in AM.
Limitations: A relatively small sample size.
Ethics committee approval: The study was approved by the Institutional Review Board. Written informed consent was obtained.
Funding: The study was partially granted by the Italian Ministry of Health
Author Disclosures:
A. Palmisano: Grant Recipient at Italian Ministry of Health
G. Benedetti: nothing to disclose
R. Faletti: Grant Recipient at Italian Ministry of Health
M. Gatti: nothing to disclose
N. Galea: Grant Recipient at Italian Ministry of Health
M. Francone: nothing to disclose
F. de Cobelli: nothing to disclose
A. Del Maschio: nothing to disclose
A. Esposito: Grant Recipient at Italian Ministry of Health

RPS 1803-7 11:06

Derived-CMR strain efficacy in myocardial inflammation: a retrospective comparison with standard practice

P. Palumbo, C. de Cataldo, S. Torlone, G. Campidoglio, F. Cobianchi Bellisari, F. Sgalambro, S. Necozione, E. Di Cesare, C. Masciocchi*; L'Aquila/IT (palumbopierpaolo89@gmail.com)*

Purpose: A major role in the diagnosis of myocarditis is played by new CMR-based biomarkers. The aim of the study was to investigate the diagnostic capabilities of tissue-tracking (TT) strain analysis in patients with a CMR-based diagnosis of myocarditis.
Methods and materials: 43 patients with a CMR-based diagnosis of myocarditis according to the standard Lake Louise criteria were retrospectively analysed. 27 healthy participants were selected as a control group. Cine-RM data was used for the analysis. Dedicated TT-software was used to perform radial, circumferential, and longitudinal strain for global, per-plane (basal, middle, and apical), and segmental (AHA 16-segments standard) evaluation in short and long-axis left ventricle images.
Results: Patients with myocarditis showed significantly reduced LV radial and circumferential strain values, both in global and per-plane evaluation (GRS: 23.39 ±7.16% vs. 31 ±7.15%)(GCS: -14.90 ±3.69% vs. -18.21 ±2.52%)(RSbas: 21.92 ±6.47% vs. 29.25 ±6.28%)(CSbas: -14.21 ±3.38 vs. -17.50 ±2.46%), compared with healthy participants. Good accuracy was found according to the ROC analysis (AUC up to 0.824). No significant correlations were found with oedema, while a significant correlation was found between segmental radial and LE (p-value:0.019), and an interesting trend between segmental circumferential and LE (p-value:0.087).
Conclusion: Tissue-tracking strain analysis has proved accurate in the evaluation of patients diagnosed with myocarditis based on standard Lake Louise criteria. Tissue-tracking strain analysis could improve diagnostic accuracy in clinical practice, adding useful information over the standard findings.
Limitations: A lack of mapping sequence, especially in elderly examination, does not permit an adequate comparison with revisited Lake Louis criteria.
Ethics committee approval: The study was conducted in accordance with the declaration of Helsinki.
Funding: No funding was received for this work.
Author Disclosures:
P. Palumbo: nothing to disclose
C. de Cataldo: nothing to disclose
S. Torlone: nothing to disclose
C. Masciocchi: nothing to disclose
G. Campidoglio: nothing to disclose
E. Di Cesare: nothing to disclose
F. Cobianchi Bellisari: nothing to disclose
F. Sgalambro: nothing to disclose
S. Necozione: nothing to disclose

RPS 1803-8 11:12

Coronary inflammation by CT pericoronary fat attenuation in MINOCA and Tako-Tsubo syndrome

N. Gaibazzi, C. Martini, A. Botti, A. Pinazzi, B. Bottazzi, A. Palumbo*; Parma/IT (alepalumbo@gmail.com)*

Purpose: The pericoronary fat attenuation index (pFAI) emerged as a marker of coronary artery inflammation (CAI), measurable by standard coronary CT angiography (CCTA). It compares well with the gold standard for the CAI assessment and can predict future cardiovascular events. pFAI could prove invaluable in differentiating CAI from a noninflammatory status, helping to unravel the mechanisms subtending an event classified as myocardial infarction with nonobstructive CA (MINOCA) or Tako-Tsubo syndrome (TTS).
Methods and materials: Patients admitted with MINOCA and TTS between 2011-2018, who had both CCTA and cardiac MR during/shortly after the acute phase, were selected and pFAI measured in their CCTA. pFAI was also measured in control subjects who had CCTA for atypical chest pain workup, no obstructive CAD found in their CCTA, and no cardiac events at a 2-year follow-up.
Results: In the n=106 MINOCA/TTS, mean pFAI was 68.378.29 vs. 78.036.20 in the n=106 controls (P<0.0001), and the difference confirmed also when comparing mean pFAI in each CA between MINOCA/TTS and controls (P<0.0001). Nonobstructive coronary plaques at CCTA, high-risk plaques in particular, were more frequently found (P<0.01) in the MINOCA/TTS group versus controls.
Conclusion: In MINOCA and TTS pts, CCTA is not only able to detect angiographically invisible atherosclerotic plaques, but its diagnostic yield can be expanded using the simple measurement of pFAI to characterise pericoronary fat tissue. In MINOCA/TTS, mean pFAI demonstrates higher values compared with controls, a finding that has been associated with CAI.
Limitations: The drug therapy was not recorded. We cannot exclude an effect of drugs used in acute coronary syndromes on pFAI in our MINOCA/TTS group.
Ethics committee approval: The study was approved by Institutional Review Board and Research Ethics Committee and all subjects gave written informed consent.
Funding: No funding was received for this work.
Author Disclosures:
C. Martini: nothing to disclose
N. Gaibazzi: nothing to disclose
A. Palumbo: nothing to disclose
B. Bottazzi: nothing to disclose
A. Botti: nothing to disclose
A. Pinazzi: nothing to disclose

RPS 1803-9 11:18

Differentiating chronic myocarditis from non-ischemic dilated cardiomyopathy using segmental T1 mapping

M. T. A. Wetscherek[1], C. Lücke[2], P. Lurz[2], M. Gutberlet[2]*; [1]Cambridge/UK, [2]Leipzig/DE*

Purpose: To determine the T1-relaxation time differences between chronic myocarditis (CM) and non-ischemic dilated cardiomyopathy (DCM) using an overall and segmental approach on native T1 mapping.
Methods and materials: We performed a retrospective analysis of 62 cases, including 52 consecutive patients who had a presentation at >14 days from initial symptoms and underwent CMR as part of a complete diagnostic work-up for clinically suspected myocarditis in accordance to current guidelines. 26 patients were included in each of the CM and DCM groups and 10 individuals served as normal controls. The CMR protocol at 1.5T included non-contrast T1-mapping using a 5(3)3 MOLLI acquisition. We analysed a mid-myocardial slice for overall and segmental myocardial T1-relaxation. A Wilcoxon rank sum test was used to assess the differences between the groups.
Results: The overall median and interquartile range was 1060 [1002-1155] ms for CM and 1058 [1034-1093] ms for DCM, showing no significant difference between the two groups. The overall T1-relaxation time was significantly higher in both groups compared to controls, T1-relaxation 1007 [966-1036] ms, (p<0.05). In CM, we found no statistical difference in T1-relaxation between the lateral and septal segments, while the septal values were significantly higher compared to the values in the lateral wall segments in DCM (p<0.001). We found significantly higher T1-relaxation in the inferoseptal segment in DCM, 1120 [1088-1154] ms, compared to CM, 1075 [1042-1136] ms, (p=0.04).
Conclusion: A per-segment approach can help to differentiate chronic myocarditis and non-ischemic DCM, while an overall approach can only differentiate both groups from healthy subjects.
Limitations: The small sample size.
Ethics committee approval: This study approved by the institutional ethics committee. Written informed consent was obtained.
Funding: MW was funded by ESOR/ESCR cardiovascular fellowship program.
Author Disclosures:
M. T. A. Wetscherek: nothing to disclose
P. Lurz: nothing to disclose
M. Gutberlet: nothing to disclose
C. Lücke: nothing to disclose

RPS 1803-10 11:24

A multiparametric native CMR approach to acute and chronic cardiac diseases with increased myocardial mass using mapping and feature-tracking strain

M. C. Halfmann, S. Benz, C. Düber, R. Kloeckner, T. Muenzel, P. Wenzel, K.-F. Kreitner, T. Emrich; *Mainz/DE (Moritz.Halfmann@gmx.de)*

Purpose: The diagnoses of acute myocarditis (AM) and hypertensive heart disease (HHD) remain difficult and are commonly based on a combination of clinical expertise and a multi-parameter diagnostic workup including contrast-enhanced cardiac magnetic resonance imaging (CMR). It was our purpose to evaluate a multiparametric set of native imaging parameters for their diagnostic accuracy.
Methods and materials: A total of 33 AM and 21 HHD patients who had been referred to our department between 09/2014 and 09/2017, as well as 50 carefully selected healthy volunteers, (HV) underwent CMR at 3T. Subsequent feature-tracking strain analysis and native T1/T2 mapping were performed and results were processed in the form of binary logistic regressions. Cut-off values, areas under the curve (AUC), and corresponding sensitivities and specificities were derived from receiver operator characteristic curves.
Results: For HV vs AM, the combination of global circumferential strain, myocardial mass per body surface area (MYM), and T1 values performed best (AUC .92, 94% sensitivity, 76% specificity). In HV vs HHD, the triad of global longitudinal strain, MYM, and T1 values discriminated best between groups (AUC of .99, 100% sensitivity, 84% specificity), and in AM vs HHD, the combination of GLS, MYM, and T2 values outperformed all others (AUC .92, 90% sensitivity, 76% specificity).
Conclusion: Different distinct pathophysiologies behind the diseases lead to different sets of best-performing parameters. The proposed multiparametric approaches were able to precisely discriminate between healthy individuals and patients, as well as different patient populations, without the need for contrast agents.
Limitations: The retrospective design prevented endomyocardial biopsies as the current gold standard for diagnosing AM. However, because of the invasiveness and possible sampling errors, only few patients routinely have biopsies in clinical routine.
Ethics committee approval: n/a
Funding: No funding was received for this work.
Author Disclosures:
P. Wenzel: nothing to disclose
M. C. Halfmann: nothing to disclose
S. Benz: nothing to disclose
T. Muenzel: nothing to disclose
R. Kloeckner: nothing to disclose
C. Düber: nothing to disclose
K.-F. Kreitner: nothing to disclose
T. Emrich: nothing to disclose

RPS 1803-11 11:30

Gender-neutral FT-CMR strain ratios improve the discriminatory accuracy in acute and chronic heart conditions

M. C. Halfmann, S. Benz, C. Düber, R. Kloeckner, T. Muenzel, P. Wenzel, K.-F. Kreitner, T. Emrich; *Mainz/DE (Moritz.Halfmann@gmx.de)*

Purpose: Hypertensive heart disease (HHD) and acute myocarditis (AM) can both present with increased myocardial mass despite different pathophysiology. The differentiation between them remains difficult. The accompanying distinct patterns of altered myocardial deformation, however, can be investigated using a feature tracking (FT)-CMR strain. Hence, the aim was to evaluate whether new strain ratios including the myocardial mass per body surface area (MyoMass/BSA) yield additional value in the differentiation between both diseases and healthy volunteers.
Methods and materials: Patients with AM (n=43) and HHD (n=28) underwent CMR at 3T between 09/2014 and 09/2017. A group of 61 healthy volunteers (HV) served as normal controls. FT-strain analysis was performed and natural strain values were evaluated for gender and age-specific differences. Subsequently, gender-neutral strain parameters were calculated and indexed to the MyoMass/BSA, leading to ratio strains. These were then evaluated for their discriminatory accuracy by means of areas under the curve (AUC), sensitivity, and specificity.
Results: There were statistically significant differences in strains between genders ($p<0.05$) but not between age groups. For the differentiation between HV and AM, the global circumferential strain ratio performed best (AUC 0.86, 79% sensitivity, and 82% specificity). In discriminating between HV and HHD, as well as AM and HHD, the global longitudinal strain ratio outperformed all other parameters (AUCs 0.96/0.79, 92%/89% sensitivity, and 86%/66% specificity, respectively).
Conclusion: The calculated ratios provide additional value in the differentiation of diseases with increased myocardial mass. As there is no need for additional sequences, time, or even contrast agents, strain ratios have the potential to be a powerful addition into currently developing multiparametric native diagnostic approaches.
Limitations: The etrospective design did not allow for endomyocardial biopsies.
Ethics committee approval: n/a
Funding: No funding was received for this work.
Author Disclosures:
M. C. Halfmann: nothing to disclose
S. Benz: nothing to disclose
C. Düber: nothing to disclose
R. Kloeckner: nothing to disclose
T. Muenzel: nothing to disclose
P. Wenzel: nothing to disclose
K.-F. Kreitner: nothing to disclose
T. Emrich: nothing to disclose

RPS 1803-12 11:36

The prevalence and spectrum of cardiovascular MR features of myocardial infarction with non-obstructed coronary arteries: first results from the First Moscow City Hospital registry

E. Pershina, V. E. Sinitsyn, A. Shilova, D. Shchekochikhin, M. Gilyarov, A. Nesterov, A. Svet; *Moscow/RU (pershina86@mail.ru)*

Purpose: To analyse cardiovascular MR (CMR) features in myocardial infarction with non-obstructed coronaries (MINOCA) patients in an emergency hospital.
Methods and materials: The registry included the consecutive patients presenting to the emergency department between 2018 and 2019 with cardiac chest pain, elevated troponin (>0.04 ng/ml), and non-obstructed coronaries (according to results of cardiac catheterisation). They were referred to CMR performed with 1.5T scanner including cine-MR, T2-weighted images, and sequences with late gadolinium enhancement (LGE). Patients were divided into 4 categories based on their CMR findings: myocardial infarction (MI), myocarditis, hypertrophic cardiomyopathy (HCM), and normal CMR. Cases with apical ballooning without LGE were diagnosed as takotsubo syndrome (TS).
Results: 28 MINOCA patients (average age 61.6±13.4, 44% male) were included in the registry. CMR was performed 8 days (median) after patients' admission. 32.1% of patients presented with ST-elevation MI (STE). The average troponin T level was 0.64±0.18 ng/ml. CMR was able to identify the cause for the troponin rise in 75% of the patients. 25% of them had myocarditis, 25% acute MI, 13.2% HCM, and 7.1% TS. The results of CMR were normal in 25%. There was no difference between patients with and without ST-segment elevation according to the patterns of MR findings (p=0.6). Troponin levels, age, and sex did not significantly differ between the groups (p=0.15, p=0.29, and p=0.11, respectively).
Conclusion: The registry preliminary revealed that patients with MINOCA represent a heterogeneous cohort with different underlying causes with similar clinical and demographical data. CMR was able to establish the correct diagnosis in 75% of cases. There is a probability that the prevalence of TS was underestimated due to substantial time gap between admission and CMR.
Limitations: A single-centre registry.
Ethics committee approval: n/a
Funding: No funding was received for this work.
Author Disclosures:
E. Pershina: nothing to disclose
A. Nesterov: nothing to disclose
V. E. Sinitsyn: nothing to disclose
A. Shilova: nothing to disclose
D. Shchekochikhin: nothing to disclose
M. Gilyarov: nothing to disclose
A. Svet: nothing to disclose

RPS 1803-13 11:42

Correlation between native T1 and T2 mapping and MRI strain parameters in patients with myocarditis: a pilot study

M. Muca[1], L. Pagnan[2], M. G. Belgrano[1], M. A. A. Cova[1]; *[1]Trieste/IT, [2]Sgonico/IT*

Purpose: To research the correlation between T1 and T2 mapping and feature tracking parameters in cases of myocarditis and comparison of T1 and T2 mapping values between patients with myocarditis and those considered at low-risk of cardiomyopathy.
Methods and materials: 28 patients (19 with myocarditis; 9 at low-risk of cardiomyopathy) were enrolled retrospectively from November 2017 to October 2018. All patients underwent standard cardiac magnetic resonance (CMR) and T1 and T2 mapping sequences. Mapping and strain parameter evaluation were performed with two dedicated softwares.
Results: Native T1 mapping values for a basal slice and T2 mapping values for basal and apical slice were significantly increased in patients with myocarditis compared to low-risk patients (p-value, respectively, 0.03, 0.04, and 0.05).
A positive and significant correlation (p=0.02) between increased values of T1 mapping for a medium slice and decreased peak longitudinal strain in patients

with myocarditis was observed. Also, a positive correlation between increased native T1 mapping values and decreased values of peak circumferential strain (p=0.01), peak short-axis radial strain (p = 0.009), and peak long axis radial strain (p=0.02) was observed for the medium slice in these patients.
Conclusion: Our study suggests the utility of systematic use of T1 and T2 mapping sequences and feature tracking analysis in CMR as an integral part of the diagnosis and management of myocarditis identifies potentially high-risk patients with latent ventricular dysfunction.
Limitations: In our institution, reference values of T1 and T2 mapping aren't yet available. A higher prevalence of susceptibility artefacts in the inferolateral region was observed. Endomyocardial biopsy was performed only in one case of myocarditis. The small sample of patients enrolled may have influenced the results we obtained.
Ethics committee approval: n/a
Funding: No funding was received for this work.
Author Disclosures:
M. Muca: nothing to disclose
L. Pagnan: nothing to disclose
M. G. Belgrano: nothing to disclose
M. A. A. Cova: nothing to disclose

RPS 1803-14 11:48
Cardiac CT with triple-rule-out (TRO) and late iodine enhancement (LIE) acquisition in the evaluation of patients presenting with acute troponin elevation
D. Vignale[1], A. Palmisano[1], E. Boccia[1], M. Gatti[2], R. Faletti[2], F. Moroni[1], D. de Stefano[3], F. de Cobelli[1], A. Esposito[1]; *[1]Milan/IT, [2]Turin/IT, [3]Rome/IT (vignale.davide@hsr.it)*

Purpose: To evaluate the diagnostic yield of the late iodine enhancement (LIE) acquisition added to the triple-rule-out CT (TRO-CT) performed in patients presenting with acute symptoms and troponin elevation without clinical/electrocardiography criteria for acute myocardial infarction (AMI).
Methods and materials: 60 consecutive patients with acute symptoms, troponin elevation, and no diagnostic criteria for AMI underwent TRO-CT to diagnose acute aortic syndromes, obstructive coronary artery disease (CAD-RADS≥4), and pulmonary embolism (PE). Patients with a negative TRO-CT underwent LIE acquisition to evaluate the presence and pattern of LIE and to quantify the myocardial extracellular volume fraction (ECV). Obstructive CAD was confirmed by invasive coronary angiography and myocardial disease by cardiac magnetic resonance.
Results: The male to female ratio was 35:25. The median age was 71 years [IQR=47-78]. Peak median troponinT (n=46) was 49.0 ng/L[IQR=20.4-195.7] and peak median troponinI (n=14) was 4.1 ng/L[IQR=1.2-11.8]. Reported symptoms were chest pain (n=31[51%]), dyspnoea (n=16[26%]), palpitations (n=6[11%]), loss of consciousness (n=5[8%]), and other (n=14[23%]). TRO-CT identified 19 (32%) obstructive CAD, 1 (1%) acute aortic syndrome, 5 (8%) PE, 1 (1%) CAD+PE, and 1 (1%) CAD+acute aortic syndrome. LIE acquisition was performed in the remaining 33 (55%) TRO-negative patients. 2 (3%) had LIE with ischemic pattern, 16 (27%) LIE with non-ischemic pattern [13 (22%) myocarditis, 3 (5%) idiopathic dilated cardiomyopathy], 3 (5%) increased ECV suggestive for amyloidosis, 2 (3%) cardiac metastasis, 2 (3%) tako-tsubo cardiomyopathy, 1 (1%) pericarditis, and 1 (1%) basal hyperdensity of myocardium suggestive for haemosiderosis. 6 (10%) patients were negative to TRO and LIE and did not report major cardiovascular adverse events after a mean follow-up of 419 days.
Conclusion: LIE acquisition increases the diagnostic value of TRO-CT, finding a diagnosis in 82% of TRO-negative patients and allowing a safe discharge of TRO- and LIE-negative patients.
Limitations: A single-centre study, small sample size, and short follow-up.
Ethics committee approval: The study was approved by the institutional review board.
Funding: No funding was received for this work.
Author Disclosures:
D. Vignale: nothing to disclose
A. Palmisano: nothing to disclose
E. Boccia: nothing to disclose
M. Gatti: nothing to disclose
R. Faletti: nothing to disclose
F. Moroni: nothing to disclose
D. de Stefano: nothing to disclose
F. de Cobelli: nothing to disclose
A. Esposito: nothing to disclose

RPS 1803-15 11:54
Pericardial effusion is a marker of increased cardiac mortality in thalassemia major patients
A. Meloni[1], L. Pistoia[1], G. Restaino[2], N. Schicchi[3], R. Righi[4], A. Vallone[5], N. Dello Iacono[6], V. Positano[1], A. Pepe[1]; *[1]Pisa/IT, [2]Campobasso/IT, [3]Ancona/IT, [4]Ferrara/IT, [5]Catania/IT, [6]San Giovanni Rotondo/IT (alessia.pepe@ftgm.it)*

Purpose: This is the first prospective study evaluating if the presence of pericardial effusion (PE) is associated with increased cardiac mortality in thalassemia major (TM).
Methods and materials: 1,259 patients (648 females, 31.02±8.64 years) enrolled in the MIOT were prospectively followed from their first CMR scan. CMR was used to quantify myocardial iron overload (MIO) by a multislice T2* approach and to assess biventricular function parameters and PE by cine sequences.
Results: PE was present in 25 (2.0%) patients. Patients with and without PE were comparable for age, sex, percentage of patients with MIO (global heart T2*<20 ms), and biventricular parameters. The mean follow-up time was 44.55±20.35 months and there were 15 deaths, 9 due to cardiac causes. Cardiac mortality was greater for patients with PE versus those without PE (8.0% vs 0.6%, P=0.013). PE was a significant predictive factor for cardiac death (hazard ratio-HR=19.25, 95%CI=3.96-93.66, P<0.0001. PE remained a significant prognosticator for death also in a multivariate model including MIO.
Conclusion: PE is quite rare in TM patients and is not related to MIO, but an important role in its development could be played by the 'iron-induced' pericardial siderosis. PE is a strong predictor for cardiac death, independent from the presence of MIO. The non-invasive diagnosis of PE is important for a more complete definition of the cardiac involvement of TM patients and the estimation of the prognosis.
Limitations: A low number of events.
Ethics committee approval: The study complied with the Declaration of Helsinki. All patients gave their informed consent. The project was approved by the institutional ethics committee.
Funding: The MIOT project receives "no-profit support" from industrial sponsorships (Chiesi Farmaceutici S.p.A. and ApoPharma Inc.).
Author Disclosures:
A. Pepe: nothing to disclose
L. Pistoia: nothing to disclose
G. Restaino: nothing to disclose
A. Vallone: nothing to disclose
N. Schicchi: nothing to disclose
R. Righi: nothing to disclose
N. Dello Iacono: nothing to disclose
V. Positano: nothing to disclose
A. Meloni: nothing to disclose

10:30 - 12:00 **Coffee & Talk 2**

Head and Neck

RPS 1808

Imaging of the neck: more than thyroid

Moderators:
N.N.

RPS 1808-1 10:30
Multiparametric intraoral ultrasound of oral lesions: the correlation of B-mode, contrast-enhanced ultrasound, and shear-wave elastography with histopathology
M. Lu, T. Wei*; Chengdu/CN*

Purpose: To evaluate the diagnostic value of multiparametric ultrasound consisting of B-mode intraoral ultrasound, contrast-enhanced ultrasound (CEUS), and shear-wave elastography (SWE) in identifying benign and malignant oral lesions.
Methods and materials: A consecutive series of 29 patients (age range, 31-81 years; mean 61±12 years; 18 male and 11 female) were evaluated in this study retrospectively. B-mode, CEUS, and SWE examinations were performed in each case using an endocavitary transducer prior to operation. The quantitative parameters were recorded for each modality. The diagnostic performances of each modality and their combined use were evaluated with the receiver operating characteristic (ROC) curve and descriptive statistics.
Results: Of the 32 lesions, there were 21 malignant lesions and 11 benign lesions. Compared with separate B-mode, CEUS, and SWE examination, multiparametric ultrasound showed the highest value in sensitivity, specificity, PPV, NPV, and overall accuracy of 90.5%, 81.8%, 90.5% 81.8%, and 87.5%, respectively. Multiparametric ultrasound achieved larger area under the curve

(AUC) in ROC curve analysis and reduced the number of false-positive findings significantly (P<0.05).
Conclusion: Multiparametric intraoral ultrasound consisting of B-mode, contrast-enhanced ultrasound, and shear-wave elastography yields additional valuable quantitative data to single ultrasound modalities for the diagnosis of oral lesions.
Limitations: This study design was retrospective and the sample size was relatively small.
Ethics committee approval: Institutional Review Board and Ethics Committee of Sichuan Cancer Hospital was approved for this retrospective study and informed consent was obtained for every patient.
Funding: No funding was received for this work.
Author Disclosures:
M. Lu: Author at Ultrasound Medical Center, Sichuan Cancer Hospital Institute, Sichuan Cancer Center, School of Medicine, University of Electronic Science and Technology of China, Chengdu, China, 610041
T. Wei: Author at Ultrasound Medical Center, Sichuan Cancer Hospital Institute, Sichuan Cancer Center, School of Medicine, University of Electronic Science and Technology of China, Chengdu, China, 610041;North Sichuan Medical College, Nanchong, China, 637000

RPS 1808-2 10:36
High-resolution ultrasonography (HRUS) in periapical dental lesions
R. Rastogi, N. Jain*; Moradabad/IN (rajulrst@yahoo.co.in)*

Purpose: To evaluate the efficacy of high-resolution ultrasonography (HRUS) in the diagnosis of periapical lesions. Conventionally, the diagnosis of periapical lesions of the teeth has been based on clinical, radiological, and histopathological examinations. However, conventional radiological procedures do not allow for the differentiation between cystic and non-cystic periapical lesions. Recently, USG has been used to provide more detailed information. Limited studies have been done to evaluate periapical lesions using USG with colour Doppler and power Doppler.
Methods and materials: 60 patients having inflammatory periapical lesions of maxillary or mandibular anterior teeth and requiring endodontic surgery were included in this study. We used conventional periapical radiographs as well as USG with colour Doppler and power Doppler for the diagnosis of these lesions. Their diagnostic performances were compared against histopathologic examination.
Results: HRUS examination with colour Doppler and power Doppler identified 58 (38 cysts and 20 granulomas) of 60 periapical lesions accurately, with a sensitivity of 100% for cysts and 90.91% for granulomas, and a specificity of 90.91% for cysts and 100% for granulomas. In comparison, conventional intraoral radiography identified only 42 lesions (sensitivity of 78.9% for cysts and 45.4% for granulomas, and specificity of 45.4% for cysts and 78.9% for granulomas).
Conclusion: HRUS imaging with colour Doppler and power Doppler is superior to conventional intraoral radiographic methods for diagnosing the nature of periapical lesions in the anterior jaws. This study reveals the potential of USG examination in the study of other jaw lesions.
Limitations: n/a
Ethics committee approval: n/a
Funding: No funding was received for this work.
Author Disclosures:
R. Rastogi: nothing to disclose
N. Jain: nothing to disclose

RPS 1808-3 10:42
B-mode, colour Doppler, and shear-wave elastography ultrasound features to predict cervical traumatic neuromas after lateral neck dissection in thyroid cancer patients: a cross-sectional study
V. Marcos, F. L. Pereira, M. Schelini, M. H. Tsunemi, R. B. Domingues, M. Kulcsar, A. O. Hoff, M. C. Chammas, R. M. C. D. Freitas*; São Paulo/BR (ricardomcfreitas@gmail.com)*

Purpose: Cervical traumatic neuromas (CTN) following lateral neck dissection for thyroid cancer may be misdiagnosed as metastatic lymph nodes. The purpose of this study was to present the B-mode, colour Doppler, and shear-wave elastography (SWE) ultrasound (US) features of the CTNs and the differences from lymphadenopathies.
Methods and materials: 79 patients with US CTNs features were selected from 206 patients who underwent cervical US after neck dissection if the following was present: 1) nodule continuity with cervical plexus, 2) posterolateral location, 3) fusiform morphology, 4) hypoechogenic internal lines, and 5) Doppler-flow absence. 31 patients (group 1, n=38 nodules) underwent fine-needle aspiration biopsy (FNAb). Two radiologists blinded to the cytological results evaluated 26 patients (n=31 nodules, group 1) with B-mode, colour Doppler, and SWE. US features (except SWE) were then compared to 42 patients (n=48 nodules, group 2) who had biopsy-proven metastatic (n=32) or reactive lymphadenopathies (n=16).
Results: All group 1 nodules had a CTN diagnosis according to cytologic confirmation (n=15) and pain exacerbation during nodule puncture and undetectable thyroglobulin/calcitonin in FNAb washout fluid (n=38). B-mode, colour Doppler, and SWE US features were similar (p>0.05) between the biopsy-proven (n=11) and indeterminate-cytology CTNs (n=20). CTNs had a mean elastic score of 2, a shear-wave velocity of 3.2±0.5 cm/s, and an elasticity index of 33.3±11.3 kPa. The above-mentioned US CTNs features such as 1) and 4) showed a sensitivity, specificity, and accuracy of 0.95, 0.93, and 0.98, and 0.92, 1.00, and 0.97, respectively, to differentiate the CTNs from cervical metastatic or reactive lymphadenopathies.
Conclusion: Continuity with the cervical plexus and the hypoechogenic internal lines with a moderate soft elastic score were the key US features for CTNs.
Limitations: The small population was a study limitation.
Ethics committee approval: IRB approval and written informed consent was obtained.
Funding: No funding was received for this work.
Author Disclosures:
R. M. C. D. Freitas: nothing to disclose
M. Schelini: nothing to disclose
V. Marcos: nothing to disclose
M. Kulcsar: nothing to disclose
F. L. Pereira: nothing to disclose
M. C. Chammas: nothing to disclose
R. B. Domingues: nothing to disclose
A. O. Hoff: nothing to disclose
M. H. Tsunemi: nothing to disclose

RPS 1808-4 10:48
Role of B-scan USG as a primary tool in closed globe ocular blunt trauma and correlation with ophthalmoscopy and intraoperative observations: a study from a resource-poor hospital in rural India
S. Ghosh[1], J. Bardhan[2], A. Mondal[3], T. Dhibar[2]*; [1]Birbhum/IN, [2]Kolkata/IN, [3]Bankura/IN (samikghosh1988@gmail.com)*

Purpose: Blunt ocular trauma is a leading cause of acquired blindness globally, encompassing all age groups. This study intends to illustrate the role of high-frequency ultrasonography in accurately describing different ocular pathologies, especially those involving posterior segment, and comparing these findings with those observed during ophthalmoscopy and/or surgical exploration whenever feasible.
Methods and materials: In this 1-year-long descriptive study, conducted in a rural Indian hospital, high-frequency (HF, 5-12 MHz) USG was performed in 111 patients, irrespective of age, with a history of blunt ocular trauma within the last 2 years. Ocular findings were observed. Patients with active surface infection, impending/frank globe rupture and pre-existing ocular disorders were excluded. Routine ophthalmoscopic examination and operative interventions were done whenever necessary. Statistical analysis was conducted at the end.
Results: HF-USG proved to be comparable to ophthalmoscopy in terms of sensitivity and specificity. Vitreous haemorrhage (VH) was the most commonly detected pathology (49.5%), followed by retinal detachment (19.8%) and traumatic cataract (18.9%). Among VH, 27.2% were in combination with retinal detachment (RD) and cataract, while 16.4% in combination with posterior vitreous detachment (PVD). For VH, USG sensitivity and specificity was 100% and 93%. For other pathologies, specificity was 100% for all except PVD (97%). Sensitivity was 100%, 91%, 86%, 80%, and 70% for choroidal detachment, retinal detachment, PVD, ectopia lentis, and cataract, respectively. VH had a significant correlation with posterior vitreous detachment, choroidal detachment, traumatic cataract, post-traumatic ectopia lentis, and small globe size (p<0.05). Traumatic cataract had significant correction with traumatic ectopia lentis and day of presentation after injury (p<0.05)
Conclusion: HF-USG is an accurate and sensitive modality, especially in resource-poor hospitals, for the short/long-term assessment of posterior segment ocular pathologies due to ocular blunt trauma.
Limitations: A loss to follow-up.
Ethics committee approval: Ethics committee approval obtained.
Funding: No funding was received for this work.
Author Disclosures:
S. Ghosh: nothing to disclose
J. Bardhan: nothing to disclose
A. Mondal: nothing to disclose
T. Dhibar: nothing to disclose

RPS 1808-5 10:54
A 2-year retrospective analysis of the diagnostic performance of core-needle biopsy (CNB) versus fine-needle aspiration cytology (FNAC) in the evaluation of parotid gland lesions
Z. Saloojee, F. Hosseini-Ardehali*; London/UK (zzsaloojee@gmail.com)*

Purpose: To compare the relative diagnostic performance of FNAC and CNB in parotid gland (PG) lesions.
Methods and materials: Data from FNAC and CNB performed over a 2-year period was reviewed. Samples were included if the clinico-radiological suspicion was a PG neoplasm. Biopsies of lesions arising outside the PG, metastases, and microbiological aspirations were excluded as were recurrent pleomorphic adenomas. For excised lesions, final histopathology was assessed for concordance with the biopsy samples.
Results: 183 biopsies were obtained: 154 FNAC and 77 CNB. Of 154 FNAC, 27 were inadequate (82% adequacy rate), 85 yielded a cytological diagnosis (67% diagnostic rate), and 48 subsequently underwent CNB. From 76 CNB, 74 samples were adequate for diagnosis (97%) and 61 yielded a histopathological diagnosis (80%). Of 12 inadequate FNAC who had a CNB, 10 (83%) were diagnostic. In 68 of 183 patients, final excision histopathology was obtained: 82% FNA concordance and 92% CNB concordance. FNA sensitivity for malignancy was 60.0% (95% CI: 14.66%-94.73%) and FNA specificity was 90.2% (95% CI: 76.87-97.28%). CNB sensitivity was 100.00% (95% CI: 73.54%-100.00%) and specificity was 93.75% (95% CI: 69.77%-99.84%).
Conclusion: CNB demonstrates superior performance with regard to sensitivity, specificity, and histopathological concordance compared to FNA, with no complications in our study. This study is in line with published studies in this field suggesting the preferential use of CNB over FNA may be warranted in the evaluation of primary PG lesions.
Limitations: This was a retrospective, observational study. In cases where the cytology/histology was equivocal, interpretation was made by the authors on the final interpretation by consensus.
A relatively low number of lesions with final histopathological data (n=68) compared to total biopsy sample size (n=183).
Ethics committee approval: n/a
Funding: No funding was received for this work.
Author Disclosures:
Z. Saloojee: nothing to disclose
F. Hosseini-Ardehali: nothing to disclose

RPS 1808-6 11:00
The added value of preoperative multiparametric ultrasound in primary hyperparathyroidism: correlation with scintigraphy and histology
S. Pavlovics, M. Radzina, A. Ozolins, Z. Narbuts, P. Prieditis, M. Tirane*; Riga/LV (pavlovics.sergejs@gmail.com)*

Purpose: To evaluate the sensitivity and specificity of ultrasound and scintigraphy findings of histologically confirmed hyperplastic and neoplastic parathyroid glands in patients with primary hyperparathyroidism.
Methods and materials: This was a prospective study (02.2019–until this moment). 37 patients (aged 49-77 years, of whom 31 were women) with primary hyperparathyroidism scheduled for parathyroidectomy in Pauls Stradins Clinical University Hospital (PSKUS) were enrolled in the study. B-mode ultrasound, colour Doppler, superb microvascular imaging, elastography (strain-ratio and shear-wave, compared to the thyroid gland), contrast-enhanced ultrasound (SonoVue 2ml+Sol. NaCl 0.9% 10ml bolus) images were obtained and postprocessing performed. Results were compared with scintigraphy and postoperative histology.
Results: 48 suspicious nodules were surgically removed, of which 26 were solitary adenomas and 4 atypically localised adenomas. 4 patients had more than one parathyroid lesion. Most characteristic ultrasound features of parathyroid adenomas were hypoechoic, well-defined lesions with increased echogenicity in the central part (79%) and peripheral-central vascularisation (67%) with feeding vessel (100%), with the average size of an adenoma being 1.4x0.8 cm. Adenomas presented as soft lesions on elastography (average SR 0.98kPa and average 2D-SWE 21kPa). CEUS showed peripheral hypervascularity in the early arterial phase (median=9s), quickly reaching peak contrast concentration (median=16s), following early wash-out (median=30s). The most common histological type of adenoma was a chief-cell adenoma. Multiparametric ultrasound had a sensitivity and specificity of 91% and 58%, respectively, PPV 86% and NPV 70% compared to scintigraphy 69% and 43%, PPV 80%, NPV 30%, and a combination of both methods achieved a sensitivity of 95%, specificity 45%, PPV 75%, and NPV 83%.
Conclusion: Multiparameter ultrasound showed better sensitivity and specificity compared to scintigraphy, but combining both modalities improved sensitivity.
Limitations: An insufficient amount of patients.
Ethics committee approval: University of Latvia and PSKUS ethics committee approval and written informed consent was obtained.
Funding: No funding was received for this work.
Author Disclosures:
S. Pavlovics: nothing to disclose
M. Radzina: nothing to disclose
A. Ozolins: nothing to disclose
Z. Narbuts: nothing to disclose
P. Prieditis: nothing to disclose
M. Tirane: nothing to disclose

RPS 1808-7 11:06
Predictive value of head and neck CT arteriography in the intraoperative bleeding volume of carotid body tumours
Y. Chen, T. Su, H. Liu, Z. Jin, Z. Zhang, Y. Qi, J. Wang*; Beijing/CN (bjchenyu@126.com)*

Purpose: To investigate the predictive value of head and neck CT angiography (CTA) in intraoperative haemorrhage of carotid body tumours.
Methods and materials: Head and neck CT images of 36 patients with carotid body tumours confirmed by pathology were retrospectively analyzed. The intraoperative bleeding volume ＜500 ml group and intraoperative bleeding volume ≥500 ml group were compared and analysed. The patient's age, sex, Shamblin classification, size of the lesion, number of blood supply arteries, course of the disease, plain scan, and enhanced CT value were analysed. The ROC curve was established to determine the number of blood supply arteries, the maximum diameter of upper and lower, the longest diameter of the axis, and the sensitivity and specificity of the Shamblin type in judging the blood volume during the operation.
Results: The amount of bleeding during the operation of carotid body tumours is related to the age of the patients, the maximum diameter of tumours, the longest diameter of axes, Shamblin classification, and the number of blood supply arteries. The AUC of the number of blood supply artery is larger than the other parameters, which can better predict intraoperative blood loss in patients with CBT.
Conclusion: The number of blood supply artery detected in CTA is the best parameter to predict intraoperative blood loss.
Limitations: The selected cases are few and lack of validation of research. Dual-energy data wasn't analysed.
Ethics committee approval: This retrospective study was performed with institutional review board approval. Informed consent was obtained.
Funding: Prof. Zhengyu Jin received research grants from National Public Welfare Basic Scientific Research Project of Chinese Academy of Medical Sciences (2018PT32003).
Dr. Yu Chen received research grants from Fundamental Research Funds for the Central Universities (3332018006).
Author Disclosures:
Y. Chen: nothing to disclose
T. Su: nothing to disclose
H. Liu: nothing to disclose
Z. Zhang: nothing to disclose
Z. Jin: nothing to disclose
Y. Qi: nothing to disclose
J. Wang: nothing to disclose

RPS 1808-8 11:12
Characterisation of head and neck paragangliomas by multiparametric MR imaging: a comparison with other deep soft-tissue tumours of the neck
E. Arsovic, S. Akkari, U. Scemama, M. Montava, J. P. Lavieille, N. Fakhry, D. Taieb, A. Varoquaux*; Marseilles/FR*

Purpose: To identify quantitative MR biomarkers that allow distinction between paragangliomas and other deep soft-tissue tumours of the neck.
Methods and materials: A retrospective review of head and neck paragangliomas (HNPGL) patients evaluated by both ^{18}F-DOPA PET/CT, and time-resolved MRA sequences, between 2009-2019 was performed. A control group of 36 vascular space lesions (33 patients), investigated during the same period, was also analysed, including nerve sheath tumours, metastatic lymph nodes from squamous cell carcinomas or from UCNT, arterio-venous malformations, and temporal bone meningiomas. Semi-quantitative parameters of enhancement were extracted from time-intensity curves on time-resolved MRA sequences and ADC was assessed for each lesion. The image quality of curves was scaled (1-3). A gold standard was obtained for all cases.
Results: 50 patients with 60 HNPGL were included, including 20 patients with germline mutations in one of the SDH genes (SDHx). All semi-quantitative parameters extracted from time intensity-curves were significantly different between HNPGL and other vascular space tumours, including wash-in obtained par linear regression, time-to-peak, and wash-out. Nerve sheath tumours exhibited higher ADC values than lymph nodes. Classification and a regression tree (CART) clearly distinguished HNPGL from other tumours with a very high accuracy. The features were also shown and formed distinct groups on principal

component analysis. No significant difference was observed between sporadic and SDHx mutated HNPGL.
Conclusion: Our study clearly identifies a multiparametric MRI signature of paragangliomas that provides a strong impetus for switching from qualitative to quantitative analysis of deep soft-tissue tumours of the neck.
Limitations: A retrospective study, a limited number of patients, and various MRA sequences, althought this allows for comparison between them.
Ethics committee approval: The study was approved by an institutional review board.
Funding: No funding was received for this work.
Author Disclosures:
E. Arsovic: nothing to disclose
S. Akkari: nothing to disclose
U. Scemama: nothing to disclose
M. Montava: nothing to disclose
J. P. Lavieille: nothing to disclose
N. Fakhry: nothing to disclose
D. Taieb: nothing to disclose
A. Varoquaux: nothing to disclose

RPS 1808-9 11:18

Abbreviated MRI protocol in head and neck imaging: an alternative approach in the imaging of tumours in the head and neck

C. Loberg, B. Turowski, C. Rubbert, P. D. K. Scheckenbach, M. Kaschner, J. Caspers, D. Jansen, H. Nasri*; Düsseldorf/DE (christina.loberg@med.uni-duesseldorf.de)*

Purpose: Patients suffering from cancer of the head and neck are often impaired when undergoing head and neck MRI. Quality of MRI imaging is often impaired and appropriate assessment is not possible. We investigated whether an abbreviated protocol (AP) was suitable for patient assessment.
Methods and materials: We conducted a retrospective observational reader study in 480 studies of 377 patients suspected of having a tumour of the head and neck, recurrence or metastasis. Expert radiologists reviewed the T2w and pre- and postcontrast images first to search for significant enhancement in correlation to anatomic region. Thereafter, the regular full diagnostic protocol (FDP) consisting of additional DWI, STIR coronal, and T1w fatsat pre- and post-contrast in transversal and coronal orientation was analysed.
Results: MRI acquisition time for FDP was 17:53 min versus 9:82 min for the AP. Average time to read the complete AP was 5:30 min versus 11 min for the FDP. The comparison of diagnostic accuracy did not differ significantly between reading the AP and the complete FDP protocol (100%). NPV was high with 98.9% for complete AP and FDP readings. The specificity and positive predictive value of AP readings did not differ significantly from those of FDP reading (95.3% vs 94.8%).
Conclusion: Abbreviated MRI of the head and neck could be a viable alternative to a full-diagnostic protocol to minimise artefacts and improve patients compliance. In the case of unclear findings, additional MRI sequences can be added.
Limitations: A single-centre study in patients with different kind of malignancies of the head and neck with different treatments. The examination was performed at 1.5 to 3T field strength.
Ethics committee approval: Ethic committee approval and informed written consent obtained.
Funding: No funding was received for this work.
Author Disclosures:
C. Loberg: nothing to disclose
B. Turowski: nothing to disclose
M. Kaschner: nothing to disclose
P. D. K. Scheckenbach: nothing to disclose
C. Rubbert: nothing to disclose
H. Nasri: nothing to disclose
D. Jansen: nothing to disclose
J. Caspers: nothing to disclose

RPS 1808-10 11:24

Detection of laryngeal and hyoid fractures in forensic post-mortem CT: a comparison of standard post-mortem CT with dedicated high-resolution cervical CT acquisitions

A. M. Bucher[1], S. Heinbuch[2], A. Koppold[1], D. M. Kettner[1], P. D. M. Verhoff[1], M. Beeres[3], B. Bodelle[1], T. J. Vogl[1]; *[1]Frankfurt am Main/DE, [2]Homburg/DE, [3]Rüsselsheim/DE*

Purpose: To evaluate the detection rate of laryngeal and hyoid fractures in suspected homicide victims with suspicion of strangulation in forensic CT imaging and high-resolution reconstructions from dedicated laryngeal CT against autopsy findings.
Methods and materials: We included 20 consecutive post-mortem head and neck CT examinations (third-generation dual-source CT). For each case, a standard-of-care head and neck spiral (CT_N) and an additional high-resolution scan of the hyoid and larynx (CT_L) was acquired. Tube voltage was 120kV with a reference tube current of 300mAs (CT_N) and 350 mAs (CT_L). CT_N was reconstructed with standard reformations of the neck in axial, coronal, and sagittal orientations (3 mm slice thickness, 2 mm increment). CT_L was reconstructed in anatomically oriented sections (1 mm slice thickness, 1 mm increment). Image reporting was performed independently for standard reconstructions (CT_N) and additionally for isolated reimaging of laryngeal structures (CT_L). Macroscopic correlation by autopsy report was available for all cases. Fracture location was recorded in a binary fashion for all anatomic laryngeal regions.
Results: A total of 140 anatomical regions were compared per group. Sensitivity of fracture detection from CT_N was 45%, which was significantly increased on CT_L scans to 82% ($p<0.001$). Specificity was comparable between methods (CT_N: .97, CT_L: 0.96; $p=0.920$). Youden-index was improved from 0.43 to 0.78 in CT_L ($p<0.001$).
Conclusion: Post-mortem CT imaging provides an adequate detection rate with dedicated high-resolution acquisition and reconstruction protocol but is not adequate for fracture detection with standard parameters of clinical cervical protocol. A dedicated high-resolution CT of the larynx and hyoid should be used to guide autopsy.
Limitations: Results should be confirmed in a larger cohort.
Ethics committee approval: Ethics approval was granted, informed consent was waived.
Funding: No funding was received for this work.
Author Disclosures:
A. M. Bucher: Other at Travel support: Bayer
T. J. Vogl: Other at Travel support: Bayer
S. Heinbuch: nothing to disclose
P. D. M. Verhoff: nothing to disclose
D. M. Kettner: nothing to disclose
B. Bodelle: nothing to disclose
A. Koppold: nothing to disclose
M. Beeres: nothing to disclose

RPS 1808-11 11:30

Clinical assessment of metal artefact reduction methods in dual-energy CT in head and neck CT examinations

L. Xing*; ZhengZhou/CN (chenwan@hnair.com)*

Purpose: To determine the effect of iterative metal artefact reduction (iMAR) technique in reducing dental metallic artefacts in head and neck CT examinations.
Methods and materials: 30 patients with dental prosthesis implants were prospectively collected and the original data was reconstructed respectively in an iMAR group (Group A) and a conventional iterative reconstruction group (Group B). The CT and SD values of the two groups of images were measured respectively. The difference between the two groups was compared by a paired t-test.
Results: There was no significant difference in CT values on the opposite side of the same layer without artefacts ($P>0.05$). The CT values in Group A were significantly reduced in the high-density artefact area ($p<0.05$), while significantly increased in the low-density artefact area ($p<0.05$), and were closer to the CT values in the corresponding anatomical areas at the opposite side of the same layer. In terms of image noise, SD values in each measurement area of group A's images were lower than those of group B and significantly lower in high-density and low-density areas ($p<0.05$). In terms of subjective score, the results of the two groups of image evaluation are excellently consistent (Kappa=0.945, $p<0.05$). The subjective score of group A was significantly higher than that of the control group (group A:4.23±0.32, group B:2.11±0.51; $P<0.05$).
Conclusion: IMAR technique can significantly reduce metal artefacts around dental implants, correct CT values of surrounding tissues, help to accurately observe tissue structures around implants, and improve image quality, which has great clinical application value.
Limitations: The sample size is small and the results may be biased when the sample size is large.
Ethics committee approval: n/a
Funding: No funding was received for this work.
Author Disclosures:
L. Xing: nothing to disclose

RPS 1808-12 11:36

Dual-layer CT-derived 3-dimensional iodine quantification for inherent iodine of thyroid parenchyma: clinico-pathologic correlation and phantom validation

Y. H. Lee*; Ansan-Si/KR*

Purpose: The thyroid gland, as an inherently iodine-rich organ, shows uniquely higher attenuation in contrast to other neck structures on pre-contrast CT images. However, its attenuation varies among different thyroid disorders. We correlated iodine concentration (IC, mgI/ml) of thyroid parenchyma derived from

dual-energy CT (DECT) datasets with hormonal status and pathologic results with phantom validation.
Methods and materials: We retrospectively enrolled 227 patients (M:F=70:157, age= 47.9±10.6Yr) who consecutively underwent both US and neck CT examination before thyroid surgery during the past two years. On the additional iodine map from pre-contrast images obtained by dual-layer detector DECT scanner (120kVp), 3-dimensional IC measurement was done at the thyroid parenchyma sonographically devoid of nodules. After that, we statistically determined the mean IC of thyroid parenchyma depending on the thyroid hormonal status and pathologic results. A gammex phantom containing 7 iodine chambers with different IC ranging from 2 to 20mgI/ml was used to validate the accuracy of our scan parameters to calculate IC.
Results: Among the 165 euthyroid patients, the mean parenchymal IC was significantly lower in patients with pathologically proven Hashimoto's thyroiditis than those devoid of thyroiditis (0.95±0.49 vs 1.44±0.50, p<0.01). In the other 56 hyper-/hypothyroidism patients, the mean parenchymal IC was 0.35±0.59. From the phantom study for IC quantification, measurement error ranged from -0.2% to 2.0% with our DECT protocols.
Conclusion: DECT iodine quantification for inherent iodine could be helpful to understand thyroid parenchymal disorders.
Limitations: Limited to the specific technical parameters, for example, type of DECT or scanning condition.
Ethics committee approval: IRB-approved study.
Funding: Basic Science Research Program through the National Research Foundation of Korea(NRF) funded by the Ministry of Education (2018R1D1A1B07045730).
Author Disclosures:
Y. H. Lee: Research/Grant Support at Basic Science Research Program through the National Research Foundation of Korea(NRF)

RPS 1808-13 11:42
Evaluation of the role of dual-energy computed tomography (DECT) in thyroid nodules
S. Sagar, A. Kumar, N. Khandelwal, N. Panda, P. Dey, U. Nahar*; Chandigarh/IN*

Purpose: To assess the role of DECT in differentiating benign from malignant thyroid disease (BTD vs MTD).
Methods and materials: A prospective study was done between October 2017-October 2018 in our tertiary centre. DECT was performed using a 128-slice dual-source scanner (Siemens Somatom Definition Flash) for indications including staging, loco-regional extent, nodal status, and metastatic workup. Non-contrast (NC) and post-contrast (PC) sequences were evaluated for nodule size, attenuation value (A_v), and iodine concentration (I_c). FNA/histopathology was used as a gold standard.
Results: A total of 30 patients (21 females) having a mean age of 47.4 years were included. 15 patients had BTD and 15 patients had MTD including papillary carcinoma (n=9, 60%) and non-papillary malignancies (n=6, 40%). Benign nodules were larger than malignant nodules (mean size 42.9 vs 24.7mm respectively, p=0.013). MTD had higher PC A_v (mean HU 116.4) than BTD (82.6), while they had lower NC A_v (48.7 vs 62.1, p=0.006). MTD had higher PC I_c than BTD (2.83 mg/ml vs 1.32 mg/ml, p=0.001). The difference between PC I_c and NC I_c was defined as ΔI_c and that between PC A_v and NC A_v was defined as ΔAv. MTD had higher ΔI_c and ΔA_v than BTD (2.45mg/ml vs 0.93mg/ml, p=0.001 and 67.7 vs 20.5, p=0.002). PC A_v cut-off of 99.5 HU had 80.0% sensitivity and 86.7% specificity for identifying MTD (AUC 0.80). ΔI_c and ΔA_v cut-off of 1.12mg/ml and 36.7 had a sensitivity of 86.7% and 80.0% and a specificity of 86.7% and 86.7% (AUC 0.86 and 0.84, respectively).
Conclusion: DECT helps differentiate benign and malignant thyroid disease with a high sensitivity and specificity.
Limitations: n/a
Ethics committee approval: n/a
Funding: No funding was received for this work.
Author Disclosures:
S. Sagar: nothing to disclose
A. Kumar: nothing to disclose
N. Khandelwal: nothing to disclose
N. Panda: nothing to disclose
P. Dey: nothing to disclose
U. Nahar: nothing to disclose

RPS 1808-14 11:48
Can morphological analysis be useful for the detection and characterisation of adenomas in parathyroid MRI?
C. Z. Karaman, V. S. Öztürk, O. Abdullayev*; Aydin/TR (md.suhaozturk@gmail.com)*

Purpose: To review the preoperative MRI of patients with primary hyperparathyroidism who underwent surgery for parathyroid adenoma (PtA) and to investigate the morphological features that help differential diagnosis.
Methods and materials: Parathyroid MRIs of 184 patients from 2015-2018 were reviewed. Only 69 patients were operated on. 5 patients were excluded and 5 patients had bilateral lesions. In summary, 69 lesions from a total of 64 patients were analysed. Axial, sagittal, and coronal fat-saturated T2W TSE and axial pre/post-contrast T1W TSE sequences were obtained in a 1.5T MR system. T2W hyperintensity, oblonged morphology, "reverse-D" appearance, strong enhancement, and the extension to paraesophageal region were investigated. Sensitivity, specificity, and positive and negative predictive value were calculated for each finding (p<0.05).
Results: 56 were classified as parathyroid adenoma and 8 as non-PtA, pathologically. MR was negative in 5 lesions. The mean lesion size was 15 mm (4-44.8 mm). Of the 56 adenomas, 51 were T2A hyperintense while 38 showed strong enhancement. Oblonged morphology was present in 40 adenomas, "reverse D" appearance in 36, and paraesophageal extension in 16 adenomas. None of non-PtA lesions showed extension. There was a statistical significance for the strong enhancement (p=0.019) and sensitivity, specificity, and accuracy values were 70%, 75%, and 71%, respectively. The “reverse D” appearance described for the first time in the literature has been shown to be a common finding in adenomas and sensitivity, specificity, and accuracy values were 64%, 63%, and 64%, respectively.
Conclusion: Images on the sagittal plane may contribute to a morphological analysis for PtA in parathyroid MRI and oblonged morphology with reverse D appearance may facilitate the diagnosis.
Limitations: The number of non-adenoma lesions was little.
Ethics committee approval: Ethics committee approved.
Funding: No funding was received for this work.
Author Disclosures:
V. S. Öztürk: nothing to disclose
C. Z. Karaman: nothing to disclose
O. Abdullayev: nothing to disclose

RPS 1808-15 11:54
Advanced visualisation of peroneal artery perforators prior to autologous transplantation in head and neck surgery by dual-energy CTA and semiautomatic vessel unfolding
M. Wiesmüller, W. Wuest, R. Heiss, C. Treutlein, M. Uder, M. S. May*; Erlangen/DE (marco.wiesmueller@uk-erlangen.de)*

Purpose: Visualisation of peroneal vessels prior to autologous transplantation of osteomyocutaneous fibular flap for mandibular reconstruction is essential for surgical success. Our aim was to improve and simplify the pre-surgical diagnostics of peroneal perforators using a dedicated dual-energy CTA protocol and semiautomatic vessel unfolding algorithm.
Methods and materials: CTA of the lower limbs was performed in 20 patients using dual-energy acquisitions from a third-generation dual-source CT and a high iodine flux (7mL/s, 350 mg/mL). Monoenergetic reconstructions (40 keV) were automatically reconstructed from the scanner and used for the semiautomatic centreline labelling of the peroneal arteries and their lateral perforators on a post-processing console using a dedicated vascular workflow. Curved MIP reconstruction was regarded as a gold standard. Vessel unfolding reconstruction was performed using a prototype software application. Number and length of perforator arteries were compared between curved MIP reconstruction, thin slice MIP in coronal orientation, posterior VRT, and coronal vessel unfolding of each lower limb.
Results: The vessel unfolding algorithm was applicable in all patients and significantly more perforator arteries could be detected compared to thin slice MIP and VRT reconstructions. The mean perforator length was only 7% shorter than in the gold standard, whereas values from thin slice MIP and VRT were significantly shorter. Bone superposition was less frequent in vessel unfolding compared to thin slice MIP.
Conclusion: The combination of low monoenergetic reconstructions and vessel unfolding allows for a comprehensive and precise presentation of small peroneal perforator vessels prior to autologous transplantation.
Limitations: A limited number of patients in this preliminary study.
Ethics committee approval: n/a
Funding: No funding was received for this work.
Author Disclosures:
M. Wiesmüller: nothing to disclose
R. Heiss: nothing to disclose
M. S. May: nothing to disclose
M. Uder: nothing to disclose
W. Wuest: nothing to disclose
C. Treutlein: nothing to disclose

10:30 - 12:00 **Room F2**

Oncologic Imaging

RPS 1816

Liver tumours: advanced imaging, radiomics and treatment effects

Moderators:
J. Amorim; Porto/PT
N.N.

RPS 1816-1 10:30

Abbreviated MRI for HCC screening: a comparison of non-contrast, dynamic contrast-enhanced, and hepatobiliary phase sets

N. Vietti Violi[1], S. Lewis[2], J. Liao[2], M. Hulkower[2], G. Hernandez Meza[2], J. S. Babb[2], S. Kihira[2], K. Sigel[2], B. Taouli[2]; [1]Lausanne/CH, [2]New York, NY/US (nviettivioli@gmail.com)

Purpose: To compare the diagnostic performance and cost-effectiveness of AMRI sets extracted from a complete gadoxetic acid-enhanced MRI for HCC screening in a high-risk population.
Methods and materials: This retrospective study included 237 consecutive patients (M/F: 146/91, mean age: 58y) with chronic liver disease who underwent gadoxetic acid-enhanced MRI for HCC screening in 2017. Two radiologists independently reviewed 3 AMRI sets extracted from the complete exam: non-contrast [NC-AMRI: T2-weighted imaging (wi)+diffusion-weighted imaging (DWI)], dynamic-AMRI (Dyn-AMRI: T2wi+DWI+dynamic T1wi), and HBP-AMRI [T2wi+DWI+T1wi obtained during the hepatobiliary phase (HBP)]. Each patient was classified as HCC-positive or HCC-negative. The reference standard combined all available patient data. Estimated set characteristics, including historical US data, were incorporated into a cost-effectiveness analysis.
Results: The reference standard identified 13/237 patients with HCC (prevalence 5.5%, size 33.7±30 mm). The pooled sensitivities were 61.5% for NC-AMRI (95% confidence intervals: 34.4-83%), 84.6% for Dyn-AMRI (60.8-95.1%), and 80.8% for HBP-AMRI (53.6-93.9%), without significant difference between sets (p-range: 0.06-0.16). The pooled specificities were 95.5% (92.4-97.4%), 99.8% (98.4-100%), and 94.9% (91.6-96.9%), respectively, with a significant difference between Dyn-AMRI and the other sets (p<0.01). All AMRI methods were effective compared to US, with a life-year gain of 3-12 months compared to US against incremental costs of $11,494-$11,823.
Conclusion: NC-AMRI has limited the sensitivity for HCC detection, while HBP-AMRI and Dyn-AMRI showed excellent sensitivity and specificity, the latter being slightly higher for Dyn-AMRI. Initial cost-effectiveness estimates showed that all AMRI models are effective compared to US.
Limitations: Dyn-AMRI assessed using gadoxetic acid.
Ethics committee approval: The institutional review board approved the study and waived informed consent.
Funding: Swiss National Science Foundation, fellowship P2LAP3_178053.
Author Disclosures:
N. Vietti Violi: nothing to disclose
S. Lewis: nothing to disclose
J. Liao: nothing to disclose
M. Hulkower: nothing to disclose
G. Hernandez Meza: nothing to disclose
J. S. Babb: nothing to disclose
S. Kihira: nothing to disclose
K. Sigel: nothing to disclose
B. Taouli: nothing to disclose

RPS 1816-2 10:36

The predictive value of the liver imaging reporting and data system with contrast-enhanced ultrasound (v2017) in the risk of hepatocellular carcinoma in a high-risk population

J. Ding, L. Long, H. Zhou, Y. Zhou, Y. Wang, X. Jing; *Tianjin/CN*

Purpose: To explore the clinical value of the liver imaging reporting and data system (LI-RADS) version 2017 with contrast-enhanced ultrasound (CEUS) for the risk prediction of hepatocellular carcinoma (HCC).
Methods and materials: 571 patients with HCC risk factors received CEUS examination in our centre. 270 patients with 395 nodules were enrolled in this study according to the inclusion criteria. The final diagnostic reference standard was decided by surgical pathology or ultrasound-guided biopsy pathology. Each nodule was classified according to CEUS LI-RADS v2017. The diagnostic accuracy of the projections of CEUS LI-RADS v2017 for HCC was analysed retrospectively.
Results: 270 patients with 295 nodules included 245 HCCs, 13 intrahepatic cholangiocarcinomas (ICC), 8 combined hepatocellular cholangiocarcinomas (CHC), 2 metastatic neoplasms of other cellular origins, and 27 benign nodules. The numbers of LR-3, LR-4, LR-5, and LR-M categories were 16 (5.4%), 28 (9.5%), 183 (62.0%), and 68 (23.1%), and the positive predictive value (PPV) of LR-3, LR-4, and LR-5 was 43.8%, 60.7%, 98.4% for HCC, respectively. The sensitivity, specificity, and positive predictive value of the LR-5 category for HCC were 73.5%, 94.0%, and 98.4%.
Conclusion: CEUS LI-RADS v2017 classification standard has reliable risk prediction value for patients with high-risk factors of HCC, which the LR-5 category has a higher positive predictive value for patients at risk of HCC. However, the differential diagnosis between HCC and other non-HCC malignancies still remains to be further studied for LR-M observations.
Limitations: Due to the nature of the retrospective study, LR-1 and LR-2 categories nodules were not pathologically diagnosed and were not included in this study.
Due to pathological reasons, the proportion of LR-3 category nodules in this study is relatively small, which may lead to selection bias.
Ethics committee approval: n/a
Funding: No funding was received for this work.
Author Disclosures:
J. Ding: Author at Tianjin Third Central Hospital
L. Long: Author at Tianjin Third Central Hospital
H. Zhou: Author at Tianjin Third Central Hospital
Y. Zhou: Author at Tianjin Third Central Hospital
Y. Wang: Author at Tianjin Third Central Hospital
X. Jing: Author at Tianjin Third Central Hospital

RPS 1816-3 10:42

Direct-acting antiviral agents in HCV patients and risk of occurrence and recurrence of HCC: is it still a clinical dilemma?

F. Vernuccio, R. Cannella, S. Greco, G. Cabibbo, V. Di Marco, C. Cammà, M. Midiri, G. Brancatelli; *Palermo/IT (federicavernuccio@gmail.com)*

Purpose: To evaluate the intra-individual rate of occurrence and recurrence of hepatocellular carcinoma (HCC) in patients with hepatitis C virus (HCV) after sustained virologic response to direct-acting antivirals (DAA).
Methods and materials: We retrospectively included consecutive HCV patients with sustained virologic response to DAA from 2015-2019 imaged with CT or MRI. We excluded patients lacking pre-DAA and post-DAA imaging follow-up. A combined reference standard (imaging and pathology) was used for HCC diagnosis. Two radiologists reviewed imaging studies, categorised each lesion, and assessed treatment response according to LI-RADS v2018. Intra-individual differences in HCC occurrence and recurrence were evaluated with the McNemar test. The incidence rate of HCC after DAA therapy was calculated.
Results: The final cohort included 65 patients (mean age: 70±10 years old). Overall, pre-DAA and post-DAA mean follow-ups were 47±26 months, 25±25 months, and 24±15 months, respectively (pre-DAA vs post-DAA: p=0.472). HCC occurrence was demonstrated in a significantly larger number of patients before DAA than after DAA (n=48 (73.8%) vs n=25 (38.5%), respectively; p=0.002). After DAA, HCC occurred with a mean interval of 18±16 months and 60% (n=15) of HCC occurred after one year. Conversely, HCC recurrence was similar before and after DAA (n=5 (7.7%) vs n=12 (18.5%), respectively; p=0.092).
Conclusion: HCC occurrence is significantly reduced in patients with a sustained virologic response to DAA. Conversely, HCC recurrence is not significantly affected by DAA.
Limitations: The retrospective study design, small sample, and lack of cohort of HCV patients not treated with DAA.
Ethics committee approval: IRB-approved. Informed consent was waived.
Funding: No funding was received for this study.
Author Disclosures:
F. Vernuccio: nothing to disclose
R. Cannella: nothing to disclose
S. Greco: nothing to disclose
G. Cabibbo: nothing to disclose
V. Di Marco: nothing to disclose
C. Cammà: nothing to disclose
M. Midiri: nothing to disclose
G. Brancatelli: nothing to disclose

RPS 1816-4 10:48

Subcentimeter hepatocellular carcinoma in treatment-naïve patients: non-invasive diagnostic criteria and tumour staging on gadoxetic acid-enhanced MRI

M.-S. Park[1], S. H. Hwang[1], S. Park[2], S. Y. Kim[1]; [1]Seoul/KR, [2]Goyang-si, Gyeonggi-do/KR (radpms@yuhs.ac)

Purpose: To define the optimal non-invasive diagnostic criteria of subcentimeter hepatocellular carcinomas (HCC) and to evaluate the effect on tumour staging in treatment-naïve patients.
Methods and materials: This study included 110 treatment-naïve patients at risk of HCC eligible for curative treatment who had subcentimeter lesions

(n=136) on gadoxetic acid-enhanced magnetic resonance imaging (MRI). New diagnostic criteria for subcentimeter HCC was developed using logistic regression analysis. Subgroup analysis was performed for patients with co-existing HCC ≥1 cm (Co-HCC). The accuracy of MR staging with and without using the new criteria was compared by a generalised estimating equation test using pathologic staging as reference standards.
Results: 19.1% (26/136) of subcentimeter lesions were HCCs. 50% of subcentimeter lesions found in patients with co-HCCs were HCC, whereas 5.9% of them without co-HCCs were HCC (p=0.001). The presence of co-HCC, arterial phase hyperenhancement (APHE), and hypointensity on transitional phase (TP) were independent factors for diagnosing subcentimeter HCC. Compared with APHE and the hypointensity on portal venous phase (PVP), the new criteria (co-HCC, APHE, and hypointensity on TP) tended to show a higher sensitivity (46.2% vs 61.5%, p=0.185) and specificity (97.3% vs. 98.2%, p = 0.563). In patients with co-HCC, the new criteria outperformed APHE and hypointensity on PVP in terms of sensitivity (40.9% vs 72.7%, p=0.001) with comparable specificity (96.3% vs 92.6%, p=0.308). Including subcentimeter HCCs improved the accuracy of MR staging from 84.5% to 94.5% (p=0.001).
Conclusion: In patients with co-HCC, subcentimeter HCC can be accurately diagnosed when a lesion shows APHE and hypointensity on TP on gadoxetic acid-enhanced MRI. Our new criteria can improve the accuracy of tumour staging in treatment-naïve patients at risk of HCC.
Limitations: n/a
Ethics committee approval: n/a
Funding: No funding was received for this work.
Author Disclosures:
M.-S. Park: nothing to disclose
S. H. Hwang: nothing to disclose
S. Park: nothing to disclose
S. Y. Kim: nothing to disclose

RPS 1816-5 10:54

Does LI-RADS v2018 add significant diagnostic value over LI-RADS v2017 in the categorisation of hepatic observation?

M. A. A. Basha[1], S. Abdelaziz Aly[2]; [1]Zagazig, AL/EG, [2]Benha/EG (Mohammad_basha76@yahoo.com)

Purpose: To investigate the added value of LI-RADS v2018 over LI-RADS v2017 in the categorisation of hepatic observation.
Methods and materials: In this prospective study, 211 patients with 268 liver observations detected during US surveillance underwent hepatic CT and MRI examinations, histopathology, and clinical and radiological follow-up. Two radiologists evaluated the observations and independently assigned an LI-RADS category to each observation based on LI-RADS v2017 and LI-RADS v2018. We evaluated the inter-reader agreement (IRA) with Kappa statistics and compared the diagnostic performance of LI-RADS v2018 and LI-RADS v2017 by Fisher's exact test using histopathology as the reference standard.
Results: LI-RADS v2018 yielded a better accuracy, sensitivity, and specificity for the categorisation of hepatic observation than LI-RADS v2017 (94.3 vs 91.8, 93.4 vs 90.8, 93.5 vs 91.2, respectively). There was no significant difference between using LI-RADS v2018 and LI-RADS v2017 in the categorisation of hepatic observation (p=0.23). The IRA of the LI-RADS scores among LI-RADS v2018 and LI-RADS v2017 was excellent (κ=0.9524).
Conclusion: Although LI-RADS v2018 improved the diagnostic performance of LI-RADS in the categorisation of hepatic observation, there was no significant difference between using LI-RADS v2018 and LI-RADS v2017.
Limitations: All MRI examinations were performed with an extracellular gadolinium contrast agent. We did not include contrast-enhanced US. We only considered untreated observations.
Ethics committee approval: Institutional review board approval was obtained. Written informed consent was obtained from all patients.
Funding: No funding was received for this work.
Author Disclosures:
M. A. A. Basha: Author at Zagazig University, Speaker at Zagazig University
S. Abdelaziz Aly: Author at Benha University

RPS 1816-6 11:00

The prognostic value of LI-RADS classification in patient candidates for orthotopic liver transplantation

I. Vicentin[1], A. Coppola[2], G. Platania[3], D. Volterra[1], D. Ricci[1], M. Pecorilla[1], C. Sgrazzutti[1], A. Vanzulli[4]; [1]Milan/IT, [2]Cava De' Tirreni/IT, [3]Gravina Di Catania/IT, [4]Segrate/IT (vicentin.ilaria@gmail.com)

Purpose: To evaluate the prognostic value of LI-RADS classification of liver nodules in cirrhotic patients assessed before orthotopic liver transplantation (OLT) in predicting HCC-specific survival.
Methods and materials: We considered 245 patients who underwent OLT from 2005-2015 at our institute with CT or MRI available both at the time of insertion in the transplant list and within 4 months before OLT. CT and MRI exams were read by 2 radiologists in consensus. Liver nodules were classified into 7 categories according to the LI-RADS classification: LR-3, LR-4, LR-5, LR-M, LR-TIV, LR-TR viable, and LR-TR not viable; we excluded patients in whom it was not possible to assign a category (LR-NC) and nodules with LR-TR equivocal. To predict HCC-specific survival, we used Metroticket2calculator, which considers the number of nodules, size of the largest nodule, and α-fetoprotein value. We considered LR-5+LR-TR viable+LR-TIV nodules, then we included LR-4 nodules, and finally, we added LR-3 nodules. We used the c-index to assess prognostic accuracy in survival prediction. We compared c-indexes from the 3 models based on LI-RADS with a c-index obtained by calculating the number and maximum size of nodules obtained from a multidisciplinary tumour board meeting (MDTB).
Results: 555 nodules were categorised: 111 LR-3, 54 LR-4, 175 LR-5, 1 LR-TIV, 1 LR-M, 63 LR-TR viable, and 150 LR-TR not viable. The c-index calculated by applying MetroTicket parameters was 0.6 when considering LR-5+LR-TIV+LR-TR nodules, 0.6 when also including LR-4 nodules, and 0.65 when including LR-3 nodules.The c-index calculated by applying Metroticket parameters obtained from from MDTB was 0.72.
Conclusion: The best prognostic value based on the Metroticket 2.0 algorithm is obtained by considering the number and size of liver nodules obtained from MDTB. The LI-RADS classification showed similar prognostic value (P>0.05) only when including a low (LR-3), intermediate (LR-4), and high probability (LR-5) of malignancy nodules.
Limitations: A retrospective study.
Ethics committee approval: n/a
Funding: No funding was received for this work.
Author Disclosures:
I. Vicentin: Author at Ospedale Maggiore Niguarda
A. Coppola: Author at Ospedale Maggiore Niguarda
G. Platania: Author at Ospedale Maggiore Niguarda
D. Volterra: nothing to disclose
D. Ricci: nothing to disclose
M. Pecorilla: nothing to disclose
C. Sgrazzutti: nothing to disclose
A. Vanzulli: nothing to disclose

RPS 1816-7 11:06

Contrast-enhanced ultrasound adds value to the differentiation of hepatic neuroendocrine neoplasms from hepatocellular carcinomas

J. Huang, X. Xie; Guangzhou/CN (hjingzhi@mail2.sysu.edu.cn)

Purpose: The liver is the most common metastatic site for neuroendocrine neoplasms. Ultrasonography is widely used to detect focal liver lesions, but it is difficult to characterise hepatic neuroendocrine neoplasms (hNEN) from hepatocellular carcinomas (HCC). We investigated the value of contrast-enhanced ultrasound (CEUS) to distinguish hNEN from HCC in non-cirrhotic liver parenchyma.
Methods and materials: From January 2014-June 2019, 92 patients who underwent liver CEUS examinations followed by a pathological diagnosis of neuroendocrine neoplasms in our institution were retrospectively evaluated in the study. At the same time, 92 patients with histologically-proven HCC without liver cirrhosis were randomly selected from the database as a control group. For each lesion, conventional ultrasound features and CEUS parameters, including enhancement pattern and washout time, were evaluated. In addition, the diagnostic accuracy of ultrasonic parameters for the differentiation of hNENs and HCCs was assessed using a receiver operating characteristics (ROC) curve analysis.
Results: hNEN and HCC showed significant differences in the number of nodules (P<0.001), enhancement level in portal phase (P<0.001), and the start of contrast washout time (P<0.001). Compared with HCCs, hNENs more often showed multiple lesions, less likely demonstrated iso-enhancement in the portal phase, and a quicker start of the contrast washout. When using the number of nodules and washout time on CEUS as the differential diagnosis of hNEN and HCC, the area under the ROC curve was 0.934 (p<0.001, 95% CI=0.897-0.972) with 75.0% sensitivity, 75.6% specificity, and 84.8% accuracy.
Conclusion: Contrast-enhanced ultrasound improves the differentiation of hNEN and HCC in non-cirrhotic livers, with a combination of the number of nodules and washout time on CEUS showing the strongest diagnostic performance.
Limitations: A single-centre and retrospective-designed study.
Ethics committee approval: n/a
Funding: No funding was received for this work.
Author Disclosures:
J. Huang: Author at The First Affiliated Hospital, Sun Yat-Sen University, Speaker at The First Affiliated Hospital, Sun Yat-Sen University
X. Xie: Investigator at The First Affiliated Hospital, Sun Yat-Sen University, Consultant at The First Affiliated Hospital, Sun Yat-Sen University

RPS 1816-8 11:12

The development and validation of a radiomics nomogram for predicting transcatheter arterial chemoembolisation refractoriness of hepatocellular carcinoma

J. S. Kim, H. Sheen, J. K. Lee, S. Y. Baek*; Seoul/KR (truth0508@nate.com)*

Purpose: To develop and validate a radiomics nomogram for the pretreatment prediction of transcatheter arterial chemoembolisation (TACE) refractoriness with pre-therapeutic dynamic CT in patients with hepatocellular carcinoma without metastasis.
Methods and materials: This study included 80 patients with HCC treated with TACE, except for any vascular involvement, from July 2016-November 2018, after exclusion. The datasets were split into a training set (80%) and a test set (20%) for feature selection and we did 10-fold cross-validation. 40 radiomic features were extracted from arterial-phase CT using LIFEx. A lasso regression model was used for radiomics signature selection and the selected signatures were validated using a Mann-Whitney U test. The radiomics nomogram was based on the multivariate logistic regression model incorporated the rad score (radiomics score), CT image factors (enhancement, homogeneous arterial, heterogeneous portal, capsule, Bilobar, and multiple), and clinical factors (age, sex, and logAFP). For optimising the radiomics nomogram, multiple backward stepwise elimination methods were investigated. We also evaluated the radiomics nomogram using ROC and a confusion matrix. All statistical analyses were performed using RStudio software.
Results: The rad score, which consisted of GLZLM (grey-level zone length matrix), LZLGE (long-zone low grey-level emphasis), and GLZLM-GLNU (grey-level nonuniformity), was significantly associated with TACE refractioness ($p<0.05$) and a higher odds ratio (≥1.0). Predictors contained in the individualised prediction nomogram included rad score and Biolbar. The radiomics nomogram showed a good predicting performance: 0.91 AUC, 0.75 sensitivity, 0.91 specificity, 0.75 precision, and 0.87 accuracy.
Conclusion: This study presents a radiomics nomogram that incorporates the rad score and CT image factor (Biolbar), which can be conveniently used to facilitate the pretreatment prediction of TACE refractoriness.
Limitations: A retrospective study.
Ethics committee approval: Informed consent was waived due to the retrospective nature of the analyses.
Funding: No funding was recieved for this work.
Author Disclosures:
J. S. Kim: nothing to disclose
H. Sheen: nothing to disclose
J. K. Lee: nothing to disclose
S. Y. Baek: nothing to disclose

RPS 1816-9 11:18

Gadoxetic acid MRI for the assessment of HCC response to Yttrium 90 radioembolisation: correlation with histopathology

N. Vietti Violi[1], S. Hectors[2], J. Gnerre[2], A. Law[2], M. I. Fiel[2], B. Taouli[2];
[1]Lausanne/CH, [2]New York, NY/US (nviettivioli@gmail.com)

Purpose: To assess the diagnostic performance of gadoxetic acid MRI for evaluating the response of hepatocellular carcinoma (HCC) to Yttrium 90 transarterial radioembolisation (RE) using pathology as the reference standard.
Methods and materials: This retrospective study included 48 consecutive patients (M/F 36/12, mean age 62 y) with HCC treated by RE, followed by surgery (liver resection/transplantation:14/34), with MRI using gadoxetic acid within 90 days before surgery. Two independent radiologists evaluated the following criteria: the percentage of necrosis on subtraction images based on late arterial, portal venous and hepatobiliary (HBP) phases, modified (m)RECIST, LI-RADS, and apparent diffusion coefficient (ADC). Data was correlated to the percentage of necrosis on pathology. Inter-reader agreement for the radiologic percentage of necrosis was assessed using an interclass correlation coefficient (ICC). Receiver operating characteristic analyses were used to determine the prediction of complete pathologic necrosis (CPN). Correlation between radiologic and pathologic percentage of necrosis was assessed using Pearson's correlation.
Results: Histopathology demonstrated 71 HCCs (mean size: 2.8±1.7 cm), including 42 with CPN. There was an excellent inter-reader agreement for assessing the radiologic percentage of necrosis (ICC 0.82-0.89). The percentage of tumour necrosis, mRECIST, and LI-RADS were all significant ($p<0.0001$) predictors of CPN (AUC 0.80-0.82 for the radiologic percentage of necrosis and AUC 0.73-0.75 for mRECIST and LI-RADS), while ADC was not a significant predictor of CPN (AUC 0.63). The radiologic percentage of necrosis was significantly correlated to the histopathologic degree of tumour necrosis ($r=0.66-0.8$, $p<0.0001$).
Conclusion: Image subtraction has an excellent diagnostic performance for predicting CPN in HCC treated with RE; better than mRECIST, LI-RADS, and ADC.
Limitations: Few patients included: 42 patients/72 lesions.
Ethics committee approval: The institutional review board approved the study and waived informed consent.
Funding: Swiss National Science Foundation, fellowship P2LAP3_178053.
Author Disclosures:
N. Vietti Violi: nothing to disclose
S. Hectors: nothing to disclose
J. Gnerre: nothing to disclose
A. Law: nothing to disclose
M. I. Fiel: nothing to disclose
B. Taouli: nothing to disclose

RPS 1816-10 11:24

Advanced hepatocellular carcinoma treated with sorafenib: a prediction of overall survival using an integrated model based on pretreatment CT texture features and sarcopenia

T. Polidori, M. A. Tipaldi, D. Caruso, E. Ronconi, M. Zerunian, M. Rossi, A. Laghi*; Rome/IT (tiziano.polidori13@gmail.com)*

Purpose: To determine whether texture features on pretreatment contrast material–enhanced computed tomographic (CT) images combined with an analysis of sarcopenia can predict the overall survival (OS) in patients with advanced hepatocellular carcinoma (HCC) treated with sorafenib.
Methods and materials: We retrospectively evaluated 54 patients with advanced hepatocellular (HCC) treated with sorafenib from September 2008-August 2013. The inclusion criteria for this study were available pre-treatment computed tomography (CT) at the same hospital and available OS. 14 patients met these criteria and were enrolled in the study. CT texture and sarcopenia analysis were performed on pretreatment portal venous images. We analysed CT texture first level features (mean, standard deviation, entropy, mean of positive pixels, kurtosis, and skewness) at different anatomic scales ranging from fine to coarse texture. Sarcopenia was defined by a reduced skeletal muscle index calculated from an L3 section CT image. Statistical analysis was performed with SPSS 24.
Results: The normality distribution of continuous variables was assessed using a Shapiro-Wilk test and a univariate analysis was performed via the appropriate test (Chi-squared, Mann-Whitney U, and a 2-tail paired t-test) in order to identify variables which affected overall survival. Sarcopenia and 4 texture features were significant ($p<0.05$): mean, entropy, mpp, and skewness. These factors were combined to create a hybrid texture-clinical score, using coefficients derived from a multivariate Cox proportional-hazards regression model. The performance of the model was calculated using the Kaplan-Meier survival analysis (log rank=24.763, $p<0.001$).
Conclusion: Texture analysis combined to sarcopenia analysis can help predict overall survival in patients with advanced hepatocellular carcinoma (HCC) treated with sorafenib.
Limitations: The small population study.
Ethics committee approval: n/a
Funding: No funding was received for this work.
Author Disclosures:
M. Zerunian: nothing to disclose
T. Polidori: nothing to disclose
M. A. Tipaldi: nothing to disclose
D. Caruso: nothing to disclose
M. Rossi: nothing to disclose
A. Laghi: nothing to disclose
E. Ronconi: nothing to disclose

RPS 1816-11 11:30

Molecular imaging of tumour extracellular pH in a 3D organotypic in vitro model for liver cancer

I. Schobert[1], C. Hamm[1], L. Adam[1], J. Chapiro[2], J. Duncan[2], F. Hyder[2], D. Coman[2], L. J. Savic[1]; *[1]Berlin/DE, [2]New Haven, CT/US (isabel.schobert@charite.de)*

Purpose: To establish non-invasive magnetic resonance spectroscopy (MRS)-based imaging of extracellular pH (pH_e) for the monitoring of metabolic activity in a 3D organotypic in vitro model of liver cancer.
Methods and materials: Liver tumour cell lines with varying metastatic potential (VX2, HepG2, HuH7, and SNU475) and non-tumoural hepatocytes (THLE2) were cultured in monolayer and 3D collagen-I-based cell cultures to mimic an organotypic fibrotic liver tumour microenvironment. Non-invasive MRS-based pHe-mapping was employed on a 9.4T MR scanner using biosensor imaging of redundant deviation in shifts (BIRDS) in 3D cell cultures to compare metabolic activity among cell lines a) without treatment, b) supplemented with 25mmol/L

D-glucose, and c) treated with anti-glycolytic 3-bromopyruvate. Imaging findings were correlated with immunohistochemistry stainings indicative of tumour metabolism (GLUT-1) and acidity (LAMP-2).
Results: MRS-based pH_e-mapping revealed lower pH_e of VX2 (pH_e=6.7±0.03) and HuH7 (pH_e=6.79±0.05) compared to HepG2 (pH_e=6.91±0.12) and SNU475 (pH_e=6.93±0.03), while THLE2 hepatocytes showed physiologic liver pH_e (pH_e=7.1±0.02). Upregulation of GLUT-1 confirmed the hyperglycolytic phenotype of liver tumour cells. Incubation with 25mmol/L glucose significantly increased acidity in 3D cell cultures with VX2 (Δ0.28, p<0.001), HepG2 (Δ0.06, p<0.001), and HUH7 (Δ0.11, p<0.001), respectively. In turn, treatment with 3-bromopyruvate resulted in a gradual increase of pH_e in all cancer cell lines, where commonly used viability assays were insensitive to detect any therapy-induced effects.
Conclusion: As most liver tumours are hyperglycolytic, creating microenvironmental acidosis via excess lactate secretion, MRS-based pH_e-mapping revealed lower pH_e in cell lines with high metastatic potential. Therefore, this study introduces a translational model to image tumour-pH_e as a functional molecular biomarker for the metabolic phenotype, tumour aggressiveness, and potential use for testing of drug effects in vitro.
Limitations: The limited spatial resolution; no direct pH-measurement validation (31P-MRS was performed as validation).
Ethics committee approval: n/a
Funding: NIH-R01CA206180, NIH-R01EB023366.
Author Disclosures:
I. Schobert: nothing to disclose
C. Hamm: nothing to disclose
L. Adam: nothing to disclose
J. Chapiro: Research/Grant Support at NIH R01 CA206180, Research/Grant Support at SIO
J. Duncan: Research/Grant Support at NIH R01 CA206180
F. Hyder: Research/Grant Support at NIH R01 CA206180, Research/Grant Support at NIH R01 EB023366
D. Coman: Research/Grant Support at NIH R01 CA206180, Research/Grant Support at NIH R01 EB023366
L. J. Savic: Research/Grant Support at NIH R01 CA206180, Research/Grant Support at SIO

RPS 1816-12 11:36

A prospective study of 18F-FDG-PET/CT with integrated diagnostic multi-phasic contrast CT in the initial staging of hepatocellular carcinoma: the impact on staging systems

H. Abdelhalim[1], M. Houseni[2], M. Elsakhawy[2], N. Abd Elbary[2], O. Elabd[2];
[1]Shibin El Kom/EG, [2]Shebein ElKom/EG
(heba.abdelhalim@liver.menofia.edu.eg)

Purpose: To evaluate the role of fluorine 18-fluorodeoxyglucose positron emission tomography/computed tomography (18F-FDG-PET/CT) with integrated multiphasic contrast CT in the staging of hepatocellular carcinoma (HCC) and its effect on the initial management plan.
Methods and materials: A prospective analysis included 100 patients (91 males and 9 females) suspected to have HCC and referred to our centre for staging and treatment. All patients underwent imaging by 18F-FDG-PET/CT with integrated multiphasic contrast CT. Imaging findings were interpreted separately and with after image fusion. BCLC stage and compliancy with Milan criteria were assessed. Results were compared to reference data detected by histopathology and/or follow-up 18-F-FDG PET/CT.
Results: 18F-FDG-PET/CT with integrated multiphasic contrast CT demonstrated higher sensitivity and specificity than separate CECT for the detection of primary HCC (93.4% and 58.3%), regional lymph nodal metastases (91.3% and 40.3%), and pulmonary deposits (88.2% and 95.2%). Regarding the BCLC staging system, 18F-FDG-PET/CT with integrated multiphasic contrast CT showed accurate HCC staging in 53 patients (53%) compared to only 44 patients (44%) for separate CECT. Regarding the Milan criteria, 18F-FDG-PET/CT with integrated multiphasic contrast CT was accurate in 65 cases (65%) compared to only 60 cases (60%) for separate CECT.
Conclusion: 18F-FDG-PET/CT with integrated multiphasic contrast CT improves the initial staging of HCC and can significantly change the initial management plan.
Limitations: Histopathologic confirmation of metastases was not possible in all cases.
The criteria we used to determine metastasis may have some underestimation, even though the study was prospective.
Ethics committee approval: Institutional Review Board approval of National Liver Institute, Menofia University, Egypt.
Funding: No funding was received for this work.
Author Disclosures:
O. Elabd: nothing to disclose
H. Abdelhalim: nothing to disclose
M. Elsakhawy: nothing to disclose
M. Houseni: nothing to disclose
N. Abd Elbary: nothing to disclose

RPS 1816-13 11:42

The role of portal vein thrombosis in the assessment of perfusion analysis during dynamic computed tomography in patients with advanced hepatocellular carcinomas

A. Pecorelli[1], D. Ippolito[1], C. Maino[1], G. Querques[1], C. Talei Franzesi[1], S. Sironi[2]; *[1]Monza/IT, [2]Bergamo/IT (pecorelli.anna@gmail.com)*

Purpose: To investigate whether portal vein thrombosis (PVT) influences perfusion computed tomography (pCT) analysis in patients with advanced hepatocellular carcinomas (HCC) treated with sorafenib.
Methods and materials: 106 pCT consecutively performed in 38 patients with advanced HCC were analysed. Patients were divided according to the presence or absence of PVT. pCT was based on the acquisition of 16 dynamic slices/scan per 40 scans, performed on a 256-slice MDCT scanner after i.v. bolus injection of 50 ml iodinated contrast agent (350 mgI/ml) at a flow rate of 5 ml/s. The following pCT parameters were calculated for both normal liver parenchyma and HCC: hepatic perfusion (HP, ml/s/100g), arterial perfusion (AP, ml/s), portal perfusion (PP, ml/s), and hepatic perfusion index (HPI, %). Continuous variables were expressed as mean and standard deviation.
Results: No statistically significant differences were found in HP, AP, PP, and HPI values of HCC lesions between patients with and without PVT. pCT analysis of normal liver parenchyma showed that HP was significantly higher in patients with PVT in comparison to those without (14.6±5.4 vs 18.1±11.3, p=0.002) while HPI was significantly lower (24.1± 28.1 vs 13.2± 13.2, p=0.002). No differences were found in AP and PP values.
Conclusion: The presence of PVT causes parenchyma perfusion changes related to the reduction of portal venous flood and the increase of arterial blood flow, however, these haemodynamic changes do not modify the perfusion analysis of HCC lesions due to the development of typical unpaired arteries that are not associated with portal vein branches. This behaviour also allows the performance of pCT analysis in patients with advanced HCC and PVT.
Limitations: A retrospective study.
Ethics committee approval: IRB approval was granted.
Funding: No funding was received for this work.
Author Disclosures:
A. Pecorelli: nothing to disclose
D. Ippolito: nothing to disclose
C. Maino: nothing to disclose
G. Querques: nothing to disclose
C. Talei Franzesi: nothing to disclose
S. Sironi: nothing to disclose

RPS 1816-14 11:48

Virtual monoenergetic images from spectral detector CT (SDCT) facilitates washout assessment in arterially hyper-enhancing liver lesions

R. P. Reimer, N. Grosse Hokamp, A. Fehrmann Efferoth, A. Krauskopf, J. R. Kröger, T. Persigehl, D. Maintz, A. Bunck; *Cologne/DE*
(robert.reimer@uk-koeln.de)

Purpose: Recent studies have demonstrated that virtual monoenergetic images (VMIs) improve soft tissue contrast and conspicuity for hypodense liver lesions. This study investigates whether this translates into a benefit for washout assessment of arterially hyper-enhancing liver lesions in delayed-phase CT images.
Methods and materials: Our retrospective study was approved by the institutional review board. 60 arterially hyper-enhancing lesions in 30 patients (age: 65±9yrs, M/W: 20/10) were included. All patients underwent multi-phase contrast-enhanced SDCT (unenhanced, arterial, portal-venous, and delayed) for HCC work-up. MRI, CEUS, or biopsy within 3 months served as a standard of reference to determine the lesions as hepatocellular carcinomas (HCC) or non-HCCs. VMIs (40-200keV, 10keV-increment) and conventional images (CI) were reconstructed. Regions-of-interest were placed in lesions, liver parenchyma, and muscle on delayed phase; washout (HU_{liver}-HU_{lesion}) and the lesion-to-liver ratio (LLR) were calculated. Visual analysis was performed on 40, 60, 80keV, and CI by 3 radiologists. On a 5-point Likert scale, conspicuity and confidence of washout-evaluation were assessed. Statistical assessment was performed using ANOVA adjusted for multiple comparisons and a Wilcoxon test.
Results: The lesion size was 3.0±2.4 cm. Irrespective of reconstruction technique and keV-levels, washout and LLR were significantly higher on delayed phase images in HCC (n=50) compared to non-HCC lesions (n=10) (p<0.05). In HCC lesions, washout and LLR were significantly higher in VMIs with 40keV compared to CI and higher VMI keV-levels (p<0.05; e.g. washout in 40keV vs CI: 26.2±22.8 vs 11.8±8.5). Subjective analysis confirmed the best washout-evaluation (p<0.05) and confidence of evaluation in 40keV (p>0.05).
Conclusion: By increasing the lesion contrast, VMIs with low keV-values from SDCT, especially using 40keV, significantly improve the qualitative and quantitative assessment of washout in hyper-enhancing liver lesions.
Limitations: A retrospective, single-centre study.
Ethics committee approval: IRB-approval given.
Funding: No funding was received for this work.

Author Disclosures:
R. P. Reimer: nothing to disclose
N. Grosse Hokamp: Speaker at Philips Healthcare
A. Fehrmann Efferoth: nothing to disclose
A. Krauskopf: nothing to disclose
J. R. Kröger: nothing to disclose
T. Persigehl: nothing to disclose
D. Maintz: Speaker at Philips Healthcare
A. Bunck: nothing to disclose

RPS 1816-15 11:54
Intravoxel incoherent motion diffusion-weighted imaging in the differentiation of solid hepatic lesions using a volumetric approach: new frontiers!
M. Puglia[1], M. A. Bali[2], S. Picchia[3], M. Orton[4], S. Doran[5], T. Feiweier[6], D.-M. Koh[4], G. Morana[7]; [1]Pozzuoli/IT, [2]Brussels/BE, [3]Latina/IT, [4]London/UK, [5]Sutton/UK, [6]Erlangen/DE, [7]Treviso/IT (martapuglia@alice.it)

Purpose: To analyse the valence of an IVIM model and ADC value for the characterisation of solid focal liver lesions (FLLs) using a volumetric approach in 4 groups: benign vs malignant, FNH vs adenoma, hypervascular benign vs hypervascular malignant, and hypervascular malignant vs hypervascular malignant.
Methods and materials: 100 patients with 104 FLLs (77 malignant-27 benign) underwent liver 1.5T MRI for routine examination sequences using IVIM diffusion-weighted imaging with 11 b-values (0-800 s/mm2). The apparent diffusion coefficient (ADC) and IVIM-derived parameters, such as pure diffusion coefficient (D), pseudo diffusion coefficient (Ds), perfusion fraction (f), and their product (fDs) were computed with a volumetric approach and compared with the groups. A ROC curve analysis was performed to assess their diagnostic value.
Results: ADC and D were significantly lower in the malignant group than in the benign group (ADC mean: 1.38±0.36 vs 1.60±0.58; D mean 0.88±0.29 vs 1.05±0.30) × 10-3 mm2/s, and in the hypervascular malignant than hypervascular benign (ADC mean 1.38±0.33 vs 1.60±0.72; D mean: 0.90±0.21 vs 1.05±0.29) × 10-3 mm2/s. Ds did not show statistical differences. FDs were significantly lower in the hypovascular malignant than in the hypervascular malignant group (mean 9.96±1.03 vs 12.7±8.5) × 10-3 mm2/s. F was also lower in the hypovascular malignant than in the hypervascular malignant group
Conclusion: Compared with ADC, the IVIM model values using a volumetric approach improves the characterisation of FLLs.
Limitations: A retrospective study and a selection bias could be possible. A larger patient cohort may be useful to validate our results.
Ethics committee approval: n/a
Funding: No funding was received for this work.
Author Disclosures:
M. Puglia: nothing to disclose
S. Picchia: nothing to disclose
M. A. Bali: nothing to disclose
M. Orton: nothing to disclose
S. Doran: nothing to disclose
T. Feiweier: nothing to disclose
D.-M. Koh: nothing to disclose
G. Morana: nothing to disclose

10:30 - 12:00 **Room Y**

My Thesis in 3 Minutes

MyT3 18

Neuro

Moderators:
N.N.
I. Trofimenko; Moscow/RU

MyT3 18-2 10:34
Role of diffusion tensor imaging as a biomarker for cases with a history of optic neuritis in multiple sclerosis patients
M. A. S. M. Soliman; Cairo/EG (moataz_As20@hotmail.com)

Purpose: Using DTI for assessment of optic nerve integrity in MS patients with optic neuritis, and the possible affection of the contralateral optic nerve.
Methods and materials: Case-control cross-sectional observational study on 54 RRMS patients (17 males and 37 females; mean age: 31.35 ± 7.82 SD) according to Revised McDonald Criteria. Age and sex-matched healthy volunteers were recruited as control with a mean age of 29.54 ± 8.35 SD. Using 3 ROI for ON and one for chiasm. Comparing DTI results with previous OCT and optic nerve sheath diameter in patients records.
Results: 54 (40.3%) nerves affected and 54 non-affected optic nerves (40.3%) in the patient group and 26 (19.4%) normal control optic nerves. FA values in the proximal segment with a mean 0.52 + 0.04 SD among the control group. And 0.27 + 0.05 SD, 0.27 + 0.04 SD in affected and nonaffected eyes of patients respectively. There was a significant statistical difference between the patient and control groups for all four FA values ($p < 0.001$). No statistically significant difference between the FA values obtained from the affected and un-affected optic nerves within the patient group with a P-value of 0.1.
Conclusion: Quantitative DTI FA values were able to detect axonal loss in MS-related optic neuritis, with a similar degree of axonal loss in the contra lateral healthy optic nerve so it can be used for assessment of optic nerve integrity and response to therapy.
Limitations: Six months drop period between OCT and MRI data aquisition. Poor assessment of optic nerve at the orbit apex.
Ethics committee approval: n/a
Funding: No funding was received for this work.
Author Disclosures:
M. A. S. M. Soliman: nothing to disclose

MyT3 18-4 10:38
A prospective study to evaluate the role of MRI with MR spectroscopy of ring-enhancing lesions in the brain
S. S. Tonpe; Secunderabad/IN (sudhanshutonpe@gmail.com)

Purpose: To differentiate neoplastic from non-neoplastic brain lesions using conventional and advanced MR imaging techniques.
Methods and materials: Contrast MRI and MRS were done on 50 patients with GE Optima 1.5 Tesla MRI-machine referred with clinically suspected space-occupying lesions (SOL) and patients with incidental/diagnosed ring-enhancing lesion by CT scan were enrolled in the study from June-18 to June-19. The data will be entered in MS EXCEL spreadsheet and analysis will be done using Statistical Package for Social Sciences (SPSS) VERSION 22.0.
Results: Out of 50 cases, 22 are tuberculomas, 16 are NCC, 5 are abscess, 5 metastasis, 1 case of pilocytic astrocytoma and 1 tumefactive demyelination. Males were predominantly affected (31 cases - 62% of the cases) than females (19 cases - 38 %). 21-30 years is the most common age group involved (28% of the cases) and seizures are the most common presenting complaint (84%). The single lesion was noted in 34 % of patients whereas the rest 66% presented with multiple cases. Follow-up CT/MRI in 26 patients show resolution of the lesion and its associated perilesional oedema.
Conclusion: MRI is non-invasive and non-radiating is an ideal imaging modality. MRS helps in the characterisation of various ring-enhancing lesions.
Limitations: MRS could not be performed in four cases due to the presence of lesion close to the bone. MRS helps in the characterisation of various ring-enhancing lesions. However, no lesion can be diagnosed based on the findings of MRS as the sole criteria.
Ethics committee approval: After obtaining a written informed consent the patient was evaluated with Contrast MRI and MRS. The gold standard for diagnosis of brain mass is biopsy with histopathologic evaluation; however, most of the patients were followed up to correlate the findings with clinical imaging follow-up.
Funding: No funding was received for this work.
Author Disclosures:
S. S. Tonpe: nothing to disclose

MyT3 18-5 10:42
Genetic and environmental effects on the morphology and haemodynamics of the Circle of Willis: cross-sectional magnetic resonance angiography and transcranial ultrasound twin studies
B. Forgo[1], D. L. Tarnoki[1], T. Horváth[1], E. Medda[2], C. Baracchini[3], A. Sas[4], C. Oláh[4], L. Kostyal[5], A. Tarnoki[1]; [1]Budapest/HU, [2]Rome/IT, [3]Padua/IT, [4]Miskolc/HU, [5]Malyi/HU (fbia021@gmail.com)

Purpose: Increasing evidence supports that Circle of Willis (CoW) variants predispose to cerebrovascular ischaemia. However, results on the factors determining CoW variants are sparse and conflicting. We aimed to determine whether CoW morphology and haemodynamics are associated with genetic or environmental factors in twins.
Methods and materials: We investigated two separate twin populations: 1) 120 volunteer members of the Hungarian Twin Registry underwent time-of-flight magnetic resonance angiography (TOF-MRA) to record hypoplasia/aplasia in each CoW artery. 2) 64 volunteer members of the Italian Twin Registry were examined by transcranial colour-coded duplex sonography to investigate CoW haemodynamics. Concordance rates of CoW variants and raw heritability of haemodynamic traits were calculated. Cardiovascular risk factors were

compared within twin pairs discordant for CoW morphology using paired t-test and Fisher's exact test.
Results: The average age was 52±21 and 43±23 years in the first and second twin group, respectively. Concordance rates were higher in dizygotic than in monozygotic twins regarding anterior (0.47 and 0.22, respectively) and posterior (0.85 and 0.69, respectively) CoW variants. Cardiovascular risk factors did not differ significantly within monozygotic twin pairs discordant for CoW morphology ($p>0.05$ for body-mass index, hypertension, hypercholesterolemia and smoking, respectively). Raw heritability of CoW haemodynamics was low to moderate (0.00-0.56).
Conclusion: Our results support the dominance of environmental factors on both morphology and haemodynamics of the CoW. However, no cardiovascular risk factor was identified as a predictor of CoW variants. Consequently, our results stimulate further research aiming at specifying the environmental factors affecting CoW morphology.
Limitations: Major limitations include small sample size, and low spatial resolution and flow-dependence of TOF-MRA.
Ethics committee approval: The regional ethical committees approved the study (approval number: 1046-260/2014; 189/2014, 2014/10/21). All participants signed informed consent.
Funding: No funding was received for this work.
Author Disclosures:
B. Forgo: nothing to disclose
D. L. Tarnoki: nothing to disclose
T. Horváth: nothing to disclose
E. Medda: nothing to disclose
C. Baracchini: nothing to disclose
A. Sas: nothing to disclose
C. Oláh: nothing to disclose
L. Kostyal: nothing to disclose
A. Tarnoki: nothing to disclose

MyT3 18-6 10:46
Discrimination of intracranial ring-enhancing lesions using diffusion-weighted imaging, MR spectroscopy and diffusion tensor imaging
M. S. A. Faragalla*; Mansoura/EG (msaadfarag@gmail.com)*

Purpose: To differentiate intracranial ring-enhancing lesions using DWI, DTI and MRS.
Methods and materials: Forty-six patients examined by (1) DWI: mean ADC value, (2) MRS: calculated Cho/Cr ratio, (3) DTI: mean fraction anisotropy.
Results: Mean ADC values in the cystic part showed no significant difference between the primary tumours and secondary tumours (P-value = 0.07), while mean ADC value measured in the centre of abscess shows a significant difference from tumours (P= 0.002). No statistically significant difference between the ADC values measured in the enhancing wall of the primary tumours, secondary tumour and abscess; (P= 0.09).While mean ADC values measured in peritumuoral oedema could differentiate tumour infiltration from vasogenic oedema show a slightly significant difference with (P-value = 0.04). In MR Spectroscopy, the mean Cho/Cr ratio of tumours (4.2 ± 1.23) was significantly higher than abscess (1.65 ± 0.45) (P=0.006). And it's also noted that the mean value of the intralesional Cho/Cr ratio of tumour recurrence groups were significantly higher than radiation necrosis group (P-value =0.02). ROC curve analysis demonstrated a cut off value of 1.9. As regard DTI, the mean FA measured in peritumoural oedema surrounding the primary tumours demonstrates higher value than the FA measured in the peritumoural oedema of metastases, 0.235 and 0.147 respectively. ROC curve demonstrated cut-off value of 0.165.
Conclusion: DWI, MRS and DTI provided a greater confidence in differentiation of (primary from metastatic tumours), (tumours from abscesses) and (radiation necrosis from tumour recurrence).
Limitations: The studies measured ADC value from a single slice of ADC maps, which may cause observer bias. The study was performed on two MRI machines which may show slight differences and variability in results.
Ethics committee approval: Approved by Institutional Research Board, Mansoura University.
Funding: No funding was received for this work.
Author Disclosures:
M. S. A. Faragalla: Author at Mansoura University Hospitals

MyT3 18-7 10:50
The influence of antiretroviral therapy on brain imaging in HIV infection
E. Bakulina, T. Trofimova*; St. Petersburg/RU (Bakulina26region@gmail.com)*

Purpose: To study the neuroimaging in HIV-infected patients with different levels of CD4 cells, plasma HIV RNA, ART status.
Methods and materials: The eligibility criteria: HIV+, performed brain MRI, an adult. Examination data of 410 patients included a history of HIV infection, opportunistic diseases, current CD4 count, plasma HIV RNA, pathogen identification in CSF. Statistic analysis included chi-square (with Yates correction), Fisher's, the Mann-Whitney, Wald criteria.
Results: Regular ART was associated with a lower incidence of: large asymmetric lesions, caudate nuclei involvement, perilesional oedema, ring contrast enhancement. Duration of ART for more than five years reduces the incidence of brain involvement in HIV, contrast enhancement, white matter lesions, the involvement of the frontal lobes and basal nuclei. Lower current CD4 cells were associated with large asymmetric lesions, the involvement of the basal ganglia and posterior fossa, perilesional oedema and mass effect, blooming artefact on T2*, ring and nodular contrast enhancement. Plasma HIV RNA above 50 copies/ml was associated with diffuse white matter lesions, large asymmetric lesions, the involvement of the cerebellum, perilesional oedema. In major cases of CNS-IRIS we observed acute inflammatory demyelination, which was characterised by the appearance of new focal lesions, as well as the increase of old ones, atypical patterns of contrast enhancement: perivascular, peripheral, nodular, leptomeningeal.
Conclusion: ART and dependent on its current CD4 cells, plasma HIV RNA had an influence on the severity of brain structural damage. With the disease progression, the most vulnerable regions were basal ganglia and cerebellum despite ART. The atypical PML were significantly more often visualised in CNS-IRIS.
Limitations: This study was limited by its retrospective design, qualitative neuroradiological criteria, and several data were incomplete.
Ethics committee approval: The study approved by the ethics committee in accordance with the criteria ICH GCP. All patients have signed informed consent.
Funding: No funding was received for this work.
Author Disclosures:
E. Bakulina: nothing to disclose
T. Trofimova: nothing to disclose

MyT3 18-8 10:54
Comparison of 3D DIR, 3D FLAIR and 2D FLAIR pulse sequences for imaging in demyelinating disorder (in multiple sclerosis) at 3 Tesla
K. Nekar, P. P. Wali, R. Ananthasivan, U. Acharya*; Bangalore/IN (drkrishna3thi23@gmail.com)*

Purpose: Comparing 3D DIR sequence with that of 3D FLAIR and 2D FLAIR sequence in order to find out the h sensitivity in the detection of multiple sclerosis (MS) lesions and in addition we would like to further evaluate which among the 3D sequences would have higher sensitivity and specificity in picking up demyelinating lesions in the brain.
Methods and materials: Study population (minimum of 30 cases) will include patients who are being evaluated for demyelination disorders with MRI. Imaging was performed on a 3T Philips MR system using 3D DIR, 3D FLAIR sequences with the same parameters, including FOV, matrix, slice thickness, voxel size, and a number of signals averaging (NSA) in addition to routine T1, T2, diffusion-weighted and 2D FLAIR.
Results: Descriptive and inferential statistical analysis has been carried out in the present study. Results on continuous measurements are presented on mean ± SD (min-max) and results on categorical measurements are presented in number (%). Significance is assessed at 5 % level of significance. The following assumptions on data are made. Wilcoxon Signed rank test has been used to find the significance of the median score in two groups.
Conclusion: DIR brain imaging had the highest sensitivity in the detection of supratentorial lesions compared to3D FLAIR and 2D flair. In addition, the lesions obtained with 3D DIR images were more easily visualised.
Limitations: Patients with cardiac pacemakers and metallic implants will not be subjected to MRI. Motion disorder and claustrophobia, if severe, may make the examination difficult.
Ethics committee approval: The study is approved by a diplomate of the national board.
Funding: No funding was received for this work.
Author Disclosures:
K. Nekar: Author at MANIPAL HOSPITALS
P. P. Wali: Author at COLUMBIA ASIA HOSPITAL
R. Ananthasivan: Author at MANIPAL HOSPITAL
U. Acharya: Author at MANIPAL HOSPITAL

MyT3 18-9 10:58
Therapy results of pericallosal aneurysms: a retrospective unicentre study
C. Deuschl[1], M. Darkwah Oppong[1], K. Wrede[1], A. Radbruch[2], M. Forsting[1], I. Wanke[1], C. Mönninghoff[1]; [1]Essen/DE, [2]Heidelberg/DE *(cornelius.deuschl@uk-essen.de)*

Purpose: This retrospective unicentre study aims to compare treatment results of ruptured and unruptured pericallosal artery aneurysms (PAAs) regarding

postprocedural complications, patient outcome and aneurysm recurrence after endovascular (EVT) and neurosurgical treatment (NT).
Methods and materials: A total of 67 patients with PAA were admitted to our hospital, 44 patients with subarachnoidal haemorrhage (SAH) due to a ruptured PAA and 23 patients with unruptured PAA. The radiographic features of PAA were collected from pretreatment DSA. In addition, demographic, clinical and radiographic parameters of all patients were recorded. The outcome was measured based on the modified Rankin Scale (mRS) at six months after admission (favourable mRS score, 0-2 vs unfavourable mRS score, 3-6).
Results: Overall 46 patients underwent EVT and 21 patients NT. Six months after discharge of the SAH patients 24 had a favourable outcome (mRS 0-2) and 16 patients with unfavourable outcome (mRS 3-6). The mortality rate of patients with SAH was 10.1% (n=4) and was alike compared to former studies (11%) on patients with ruptured PAA. Overall aneurysm recurrence was found in six patients (9.4%). All patients with unruptured PAA had a favourable outcome.
Conclusion: EVT and NT of PAAs showed comparable good results, although aneurysm recurrence occurres more often after EVT.
Limitations: The crucial issue of this retrospective analysis is the lower quality/completeness of data compared with prospective data storage.
Ethics committee approval: The ethical approval for this study was provided by the local ethics committee (13-5580-BO).
Funding: No funding was received for this work.
Author Disclosures:
C. Deuschl: nothing to disclose
M. Forsting: nothing to disclose
K. Wrede: nothing to disclose
A. Radbruch: nothing to disclose
C. Mönninghoff: nothing to disclose
M. Darkwah Oppong: nothing to disclose
I. Wanke: nothing to disclose

MyT3 18-10 11:02
High-resolution MR imaging of cortical layers and their structural alterations in stroke and epilepsy patients
E. Lotan, D. Tanne, Y. Assaf*; Tel-Aviv/IL*

Purpose: We aimed to utilise a non-invasive in-vivo MR-based imaging modality and analysis framework to detect and characterise the laminar components of the human cerebral cortex in stroke and epilepsy patients compared with healthy controls (HC).
Methods and materials: Using 3T-MRI we calculated T1-component probability maps and showed that the T1-signal of the cortex can be divided into 5-6 distinct Gaussian distributions centred at different values, which represent different cortical laminar classes. For the stroke patients, we explored in-vivo if in patients (n=20) with chronic lacunar infarct, involving the corticospinal-tracts (CST), the cortical layers of the connected primary motor cortex (M1) are differently affected. We performed tractography using the infarcts as the seed areas to reconstruct the CST and identified the connected M1. For epilepsy patients (focal cortical dysplasia (FCD) and periventricular nodular heterotopia (PNH); n=9 each) we determined the laminar composition of 78 cortical regions of interest of the automated anatomical labelling (AAL) atlas, which was divided into 1000 sub-areas with equal volume.
Results: For stroke patients we showed focal cortical thinning in the connected M1 and specifically only in its deepest laminar portion as compared to the non-affected contralateral cortex (P<0.001), supporting the concept of secondary neurodegeneration. For epilepsy patients we found widespread cortical dyslamination compared to the HC, supporting evidences of epilepsy as a network disease with disrupted brain connectivity.
Conclusion: Our findings provide a method to calculate and characterise the laminar architecture of the cortex, which was implemented to stroke and epilepsy patient groups. Our method may be used as a sensitive imaging biomarker, and could potentially elucidate pathophysiologic mechanisms and facilitate patient management towards developing individually tailored treatment.
Limitations: Not applicable.
Ethics committee approval: Approved by institutional IRB.
Funding: Not applicable.
Author Disclosures:
E. Lotan: nothing to disclose
D. Tanne: nothing to disclose
Y. Assaf: nothing to disclose

MyT3 18-11 11:06
Application of low radiation dose combined spectrum and ASIR-V iterative reconstruction in CT scanning of ischaemic stroke: a feasibility study
Y. You*; Chengdu/CN (1390178629@qq.com)*

Purpose: To explore the application of low-dose combined spectrum in CT scan of ischaemic stroke.
Methods and materials: Group A (n=30) used the low-dose scan parameters: 80 kV, 50 mA, and the images were reconstructed by 50% ASIR-V. Head and neck (CTA) Scanning with Spectrum CT, 80-140 kV, 200 mA, the contrast agent volume was 20ml and the flow rate was 4ml/s. The images were reconstructed with 40 keV and 80% ASIR-V. Group B (n=30) used routine scan parameter: CTP:80 kV, 150 mA, CTA :100 kV, 350 mA, the contrast agent volume was 50ml and the flow rate was 5ml/s. The images were reconstructed by FBP. The contrast agent volume was 40ml and the flow rate was 5ml/s in CTP. The quantitative evaluation included: CTP parameters of the hypothalamic, frontal and temporal lobes without perfusion defects at the basal ganglia level, the CT and SD values of the head-neck CTA segments, and the CNR values of M1. The CTP and CTA image quality were also subjectively evaluated by two senior radiologists using a four-point grading scale.
Results: All CTP and CTA images were diagnostic. There were no significant differences in the subjective image, CTP parameters, CTA internal carotid artery and middle cerebral artery and CT value of common carotid artery. There were significant differences in SD and CNR in the common carotid artery. The effective dose and the contrast agent in group A were 58.5% and 23% lower than group B.
Conclusion: The use of low radiation dose combined spectrum and ASIR-V iterative reconstruction in CT scanning of ischaemic stroke.
Limitations: The simple size is relatively small.
Ethics committee approval: Approved by the ethics committee of our hospital.
Funding: No funding was received for this work.
Author Disclosures:
Y. You: Employee at west china hospital of Sichuan University

MyT3 18-12 11:10
A novel ANG-BSA/Car/ICG MNPs integrated for targeting therapy of glioblastoma
F. Lin*; Shenzhen/CN (foxetfoxet@gmail.com)*

Purpose: The existence of the blood-brain barrier has led to almost all chemotherapeutic drugs and gene drugs failing to effectively achieve and play a role in glioblastoma. So far, the survival rate of glioblastoma patients has hardly improved. In this study, we are aimed to construct an integrated nanoprobe based on albumin nanoparticles for targeted diagnosis and treatment of glioblastoma.
Methods and materials: We constructed bovine serum albumin nanoparticles (ANG-BSA/Car/ICG MNPs) containing SPIO, carmustine and ICG coupled ANG. The in vitro and in vivo MRI/FL dual-mode imaging of glioblastomas in vitro and in vivo were systematically evaluated in order to evaluate the penetration ability of blood-brain barrier and tumour-specific targeting effect. At the same time, through experiments with the control group, we evaluated the ability of ANG-BSA/Car/ICG MNPs to inhibit tumour.
Results: In vitro experiments, we verified that the targeting ability of nanoprobes to glioblastoma cells was significantly better than the control group. In addition, in vivo experiments, nanoprobes significantly increased the accumulation of brain tumours compared with the control group. This targeting imaging and drug delivery system provides an efficient strategy for targeted therapy and intraoperative localisation of glioblastoma.
Conclusion: ANG-BSA/Car/ICG MNPs present a promising potential in multifunctional therapeutic of glioblastoma, and we anticipate that this nanoplatform will be a perfect candidate in glioblastoma theranostic.
Limitations: This study was limited by the lack of comparison with other nanoplatforms.
Ethics committee approval: All animal experiments were approved and conducted according to the principles of the Institutional Animal Care Committee from the Shenzhen Second People's Hospital.
Funding: This study is supported by a grant from Basic Plan Program of Shenzhen, China (No. JCYJ20180228163333734).
Author Disclosures:
F. Lin: nothing to disclose

MyT3 18-13 11:14
Imaging as the new yardstick for diagnosing peripheral mononeuropathies: a comparison between high-resolution ultrasound and MR neurography with an approach to diagnosis
A. Agarwal Chandra, U. Jaipal, M. Bagarhatta, M. Agarwal, A. Chandra*; Jaipur/IN (a.agarwal.1992@gmail.com)*

Purpose: Peripheral neuropathies are a group of disorders which affect the peripheral nervous system and have been conventionally diagnosed using electrodiagnostic studies. This study was carried out to assess the role of imaging in diagnosing peripheral neuropathy as exact anatomical localisation of

the pathology is possible using high-resolution ultrasound (HRUS) and MR neurography, the modalities assessed in this study.
Methods and materials: A prospective study was carried out in a resource-limited setting on 180 peripheral nerves in 131 patients with symptoms of peripheral neuropathy after taking IRB approval. Each patient underwent HRUS and MR neurography, findings of which were then compared and statistically analysed assuming electrodiagnostic findings as to the gold standard.
Results: Overall, the diagnostic accuracy was highest for the proton density fat saturated (PDFS) MR sequence (93.89%) followed closely by HRUS (80%). The sensitivity was highest for PDFS sequence while the T1 MR sequence had the highest specificity. Combined diagnostic accuracy of both modalities was calculated to be 93.33% with a negative predictive value of 80%. HRUS and MRI equally detected the cases with nerve discontinuity, while neuromas were better identified on MRI.
Conclusion: With the advent of higher frequency probes and improved MR field strength, imaging of peripheral nerves is possible with better accuracy. Imaging assessment of nerves allows anatomical delineation with the identification of the exact site of involvement. This comparative study demonstrates the role of imaging in diagnosing peripheral neuropathies with the accuracy of MRI as high as 93.89% which may serve as an imaging gold standard. HRUS, being quicker, cost-effective and a comparable accuracy of 80% can serve as a reliable screening tool.
Limitations: Resource-limited setting and lack of newer sequences like DTI and DWI.
Ethics committee approval: The IRB approved.
Funding: No funding was received for this work.
Author Disclosures:
A. Agarwal Chandra: nothing to disclose
U. Jaipal: nothing to disclose
M. Bagarhatta: nothing to disclose
M. Agarwal: nothing to disclose
A. Chandra: nothing to disclose

MyT3 18-14 11:18

Evaluation of parameter changes in lateral lumbosacral radiography of patients with and qithout lumbar spinal stenosis in magnetic resonance imaging (MRI)

N. Merd, D. Gündüz*; Isparta/TR*

Purpose: To investigate the effect of lumbar spinal stenosis (LSS) on objective parameters reflected on radiographs and to adapt existing radiographic indexes to the diagnosis of LSS.
Methods and materials: LSS was determined by measuring the midline anteroposterior (AP) spinal canal diameter on axial T2-weighted images in lumbosacral MRI. Fifty patients with LSS and 50 patients without LSS were classified as. Lateral lumbosacral radiographs of the patients were evaluated retrospectively and on radiographs, pelvic incidence (PI), pelvic tilt (PT), sacral slope (SS), lumbar lordosis (LL), L5 incidence (L5I), L5 slope (L5S), sacral table angle (STA), sagittal vertebral corpus height (SBH), sagittal vertebral corpus width(SBW), peduncular width(PW), foraminal width (FW), posterior pedicle margin (PPM) were measured, SBW/PW and SBW/PPM ratios were calculated.
Results: In the LSS group, PI was significantly higher ($p = 0.029$). FW ($p < 0.001$) and PW ($p < 0.005$) values were significantly lower in the LSS group for each level. In the LSS group, SBH levels were lower ($p=0.041$) at L4 level, SBW levels were higher at L2-5 levels ($p < 0.005$) and PPM values were lower at S1 level only ($p < 0.005$). In the LSS group, the SBW / PW ratio for each level, the SBW / PPM ratio at L4 and L5 levels were significantly higher ($p < 0.005$). In the ROC analysis of parameters with significant differences between LSS and control groups, the cut-off values of significant parameters and levels were calculated.
Conclusion: The results of our study are useful for classifying patients with and without spinal narrow canals, but further studies are required.
Limitations: Inclusion of patients with a single level of a narrow canal in the patient group, not classifying spinal stenosis as developmental or congenital.
Ethics committee approval: n/a
Funding: No funding was recieved for this work.
Author Disclosures:
N. Merd: nothing to disclose
D. Gündüz: nothing to disclose

MyT3 18-15 11:22

Automated quantification pipeline (AQuaPi) for the non-invasive measurement of the cerebral metabolic rates of glucose using a fully-integrated PET/MRI

L. K. Shiyam Sundar[1], O. Muzik[2], I. Rausch[1], M. Hienert[1], E. Pataraia[1], E.-M. Klebermass[1], T. Traub-Weidinger[1], T. Beyer[1], M. Bauer[1]; *[1]Vienna/AT, [2]Detroit, MI/US (lalith.shiyamsundar@meduniwien.ac.at)*

Purpose: To introduce AQuaPi, a fully-automated pipeline for PET/MRI to non-invasively determine the cerebral metabolic rate of glucose (CMRGlc) images.
Methods and materials: The pipeline needs the following inputs: (1) PET list-mode data, (2) attenuation correction (AC) map, (3) MR angiography (MRA) images, (4) T1-w MRI and (5) MR navigators. The processing pipeline includes two main components: (i) an image-derived input function (IDIF) component and (ii) a quantification component (QC). The IC component calculates an IDIF by first determining a volume-of-interest through automated segmentation of the MRA, followed by MR navigator-based motion correction (MC) and an MR-based partial volume correction (PVC). The QC then uses the IDIF to generate CMRGlc images. To validate the pipeline, 10 healthy volunteers underwent [18F]FDG test-retest PET/MRI examinations in an integrated PET/MR. Arterial blood samples (AIF) were collected as a reference standard. Pseudo-CT images derived from T1-w MR were used for AC. Absolute percentage difference (APD) in regional MRGlc values (IDIF vs AIF) were determined in the following 6 brain regions: corpus callosum (CC), brainstem (BS), cerebellum (CB), thalamus (TH), anterior cingulate cortex (ACC) and the superior frontal cortex (SFC).
Results: The APD between CMRGlc values obtained from AIF and IDIF were: (5.9 ±3.2%) for CC, (5.9 ±3.3%) for BS, (5.8 ±3.4%) for CB, (5.5 ±3.1%) for ACC, (5.8 ±3.14%) for TH and (5.9 ±3.3%) for the SFC.
Conclusion: We have developed a fully-automated open-source processing pipeline which allows non-invasive determination of absolute CMRGlc values in a clinical setting.
Limitations: Inter- and intra-variability of CMRGlc is high.
Ethics committee approval:
Written informed consent was obtained from all the subjects along with ethics board approval.
Funding:
This work was supported by the Austrian Science Fund KLI482-B31.
Author Disclosures:
L. K. Shiyam Sundar: Author at Medical University Of Vienna
O. Muzik: nothing to disclose
I. Rausch: nothing to disclose
M. Hienert: nothing to disclose
E. Pataraia: nothing to disclose
M. Bauer: nothing to disclose
E.-M. Klebermass: nothing to disclose
T. Traub-Weidinger: nothing to disclose
T. Beyer: nothing to disclose

MyT3 18-16 11:26

Value of routine T_2WI histogram in differential diagnosis of glioblastoma

Z. Ma, X. Zhao*; Zhengzhou/CN (11430884@qq.com)*

Purpose: To study the diagnostic value of T_2 global greyscale histogram in the differential diagnosis of glioblastoma, central nervous system lymphoma and solitary metastasis of three tumour types.
Methods and materials: A retrospective analysis in our hospital had brain MRI examination and 95 cases of pathologically confirmed patients, including 29 cases of glioblastoma (male 13 cases, female 17 cases, mean age 51.2 + 14.5, 10 ~ 69 years old), central nervous system lymphoma 38 cases (male 19 cases, female 21 cases. The average age of 57.1 + 12.5, range 33 to 81 years), 28 cases of solitary metastases (male 15 cases, female 13 cases, average age 59.8, range 36 to 76 years). In three groups of MR T2 axial images with Mazda software will each layer level tumour regions of interest and analyse the global grey histogram, and of the three group parameter features were analysed. The statistical significance between the various parameters.
Results: Through histogram analysis of nine parameters, these nine parameters were statistically significant (all $P < 0.05$), including mean, variance, kurtosis, skewness, Perc.01%, Perc.10%, Perc.50% , Perc.90% and Perc.99%.
Conclusion: T_2 global gray histogram analysis has certain value in differential diagnosis of glioblastoma, central nervous system lymphoma and solitary metastasis, and it can provide new ideas and methods for differential diagnosis.
Limitations: As a retrospective study, it may have a selective bias in clinical cases.
Ethics committee approval: n/a
Funding: No funding was received for this work.
Author Disclosures:
Z. Ma: Speaker at Third Affiliated Hospital of Zhengzhou University, Author at Third Affiliated Hospital of Zhengzhou University, Investigator at Third Affiliated Hospital of Zhengzhou University
X. Zhao: Research/Grant Support at Third Affiliated Hospital of Zhengzhou University

MyT3 18-17 11:30

Compare the characteristics of different types of spontaneous intracranial artery dissection on high-resolution MRI vessel wall imaging

B. Tian, X. Tian, Z. Shi, J. Lu*; Shanghai/CN (bing.tian@hotmail.com)*

Purpose: To compare the characteristics of different types of spontaneous intracranial artery dissection on high-resolution MRI (HR-MRI) vessel wall imaging.
Methods and materials: Fifty-six patients with approved spontaneous intracranial artery dissection were scanned on a 3T Siemens Skyra scanner with pre- and post-contrast 3D T1-weighted SPACE. Patients were divided into four groups based on the morphological characteristics of pre-contrast 3D T1-weighted SPACE imaging. Type 1 corresponded to classic dissecting aneurysms, type 2 aneurysms were segmental ectasias, type 3 aneurysms were dolichoectatic dissecting aneurysms and type 4 aneurysms were saccular aneurysms unrelated to the branching zones. Consistency of clinical staging (acute, subacute, chronic stage) and imaging types was evaluated. The characteristics of spontaneous intracranial artery dissection were evaluated including intraluminal contrast enhancement, and artery wall enhancement (grade 0, similar to that of normal vessel walls; grade 1, less than or similar to that of muscle; and grade 2, greater than that of muscle). The characteristics of spontaneous intracranial artery dissection were compared among different types.
Results: Of the 56 aneurysms, 48 were located in the vertebrobasilar system, and the other eight aneurysms were located in the anterior circulation. There were 22 patients for type 1, 10 for type 2, 14 for type 3, and 10 for type 4. Patients were classified into acute (n=18), subacute (n=18), and chronic (n=20) stages according to the time intervals from symptom onset. The clinical staging was in good consistency with imaging types (p=0.000, r=0.732). There was significantly different of intraluminal contrast enhancement and vessel wall enhancement among the four types groups (p=0.030).
Conclusion: The 3T HR-MRI reveals the vessel wall characteristics and provides distinguishing findings between different types of spontaneous intracranial artery dissection.
Limitations: This study was limited by a small number of study groups.
Ethics committee approval: n/a
Funding: No funding was received for this work.
Author Disclosures:
B. Tian: nothing to disclose
X. Tian: nothing to disclose
Z. Shi: nothing to disclose
J. Lu: nothing to disclose

MyT3 18-18 11:34

Brain MRI follow-up in children with tuberous sclerosis complex: is gadolinium enhancement always necessary?

A.-L. Gaillard[1], J.-F. Chateil[2], M. Havez-Enjolras[3], A. Crombe[2], P. Bessou[2]; *[1]Saint-Maur-Des-Fossés/FR, [2]Bordeaux/FR, [3]Merignac/FR (a.lisegaillard@gmail.com)*

Purpose: Subependymal giant cell astrocytoma (SEGA) is a brain tumour developed in 10-26% of individuals with tuberous sclerosis complex (TSC). Since they are located near the foramen of Monro, SEGAs can cause obstructive hydrocephalus, leading to increase morbidity and mortality. It is recommended to follow TSC patients with contrast-enhanced (CE) MRIs, but the repetitive use of gadolinium-based contrast agents (GBCAs) may cause gadolinium deposits. Our aim was to compare the performance of CE and non-CE MRI to diagnose SEGA.
Methods and materials: Thirty-five TSC patients were enrolled in this retrospective single-centre study from September 2007 to January 2019 (15/35 (43%) males and 20/35 (57%) females). The inclusion criteria were: diagnosis of TSC on clinical and genetic arguments (according to international TSC consensus conference held in 2012) and at least three-brain MRIs performed for follow-up with a contrast agent injection. In total, 70 MRIs were selected (25 MRIs in the SEGA group and 65 MRIs in the non-SEGA group), two consecutive MRIs per patient were anonymised. Three radiologists performed a double-blinded review of the non-CE and CE MRI sequences. The diagnostic performances were calculated (sensitivity, specificity, positive/negative predictive values and inter and intra-observer agreements).
Results: The performances for the detection of SEGA were good and similar between the CE and non-CE MRIs. Inter-observer agreement was excellent for the two groups (range of Kappa coefficient: 0.81-0.93, p<0.001). The size of nodules near the Monro foramen, intense and heterogeneous contrast enhancement and modifications between two consecutive MRI were significantly associated with the presence of SEGA.
Conclusion: The performances of CE and non-CE MRIs are similar and excellent for detecting SEGA, raising the question of reducing unnecessary gadolinium-chelates injection for TSC patients.
Limitations: n/a
Ethics committee approval: n/a
Funding: No funding was received for this work.
Author Disclosures:
A.-L. Gaillard: nothing to disclose
J.-F. Chateil: nothing to disclose
A. Crombe: nothing to disclose
P. Bessou: nothing to disclose
M. Havez-Enjolras: nothing to disclose

MyT3 18-19 11:38

Role of transcranial ultrasound with Doppler and strain elastography in neonatal hypoxic-ischaemic encephalopathy with magnetic resonance imaging as the gold standard

A. Singh, U. Jaipal, D. A. Bhandari*; Jaipur/IN (DrAsthaSingh@outlook.com)*

Purpose: To compare and correlate the diagnostic role of neurosonography with spectral Doppler and strain elastography in neonatal hypoxic-ischaemic encephalopathy with MRI as the gold standard. To assess the role of diffusion-weighted Imaging in early identification and extent of ischemic injury.
Methods and materials: A prospective study was conducted on 50 patients under one month age with a clinical picture of neonatal encephalopathy, a history of perinatal asphyxia and low Apgar score. All patients were graded by Sarnat and Sarnat grading. Neurosonography with spectral Doppler of the anterior cerebral artery and strain elastography was done with 3-7 MHz probe on anterior fontanelle. Elastographic scores were assigned on a five-point colour scale.3 Tesla MRI was done with DWI (diffusion-weighted images). Ultrasound findings were correlated with MRI in various areas of the brain parenchyma and the role of DWI was evaluated by SPSS v.20.0.
Results: The diagnostic accuracy, sensitivity and specificity of neurosonography compared to MRI were 82%, 82.6% and 75% respectively. DWI detected mild ischaemic changes when other MR sequences were negative. Neurosonography detected all cases of germinal matrix haemorrhage and showed better sensitivity for thalamic, basal ganglia and periventricular white matter lesions. Altered RI values of ACA were seen in 59% of moderate and severe cases. Diagnostic accuracy of Elastographic score was 76.67% with a specificity of 86.67% (95%CI;59.54%-98.34%) and sensitivity of 66.67% (95%CI;33.38%-88.18%).
Conclusion: Neurosonography is an effective screening tool for detecting ischaemic encephalopathy. Raised elasticity of periventricular white matter in neonatal encephalopathy points towards its promising role in early diagnosis. DWI detects ischaemic changes earlier than conventional MRI which is important in initiating early management.
Limitations: This study was limited by its small sample size.
Ethics committee approval: Approval was taken from the ethical committee of SMS Medical College.
Funding: No funding was received for this work.
Author Disclosures:
A. Singh: nothing to disclose
U. Jaipal: nothing to disclose
D. A. Bhandari: nothing to disclose

MyT3 18-20 11:42

Correlation of childhood head injury with clinical and imaging characteristics of Dyke-Davidoff-Masson syndrome

F. Y. Chew, C. Y. Song, W.-C. Shen, Y.-F. Chen*; Taichung/TW (c_fyang@hotmail.com)*

Purpose: To investigate the correlation between childhood head injury and clinical-radiological features of Dyke-Davidoff-Masson Syndrome (DDMS).
Methods and materials: A total of 33 patients with a diagnosis of cerebral hemiatrophy at our institution between January 2012 to July 2019 were retrospectively review. Patients of this study must fulfil the following criteria: (i) clinical presentation of seizure; (ii) radiological manifestations with ipsilateral sulcal enlargement, ipsilateral lateral ventricular dilatation, and ipsilateral calvarial thickening. The patients were distributed into two groups based on the present or absent of childhood head injury. Clinical and imaging characteristics were compared and analysed. Raw data are presented as frequencies and percentages for categories and mean for the age at presentation. Fisher's exact test was used to assess the association between two categorical variables.
Results: There are 14 patients (eight males, six females) aged 1 to 46 years (mean age±SD=20.7±13.8) were included. There are eight patients with childhood head injury and six patients without history of childhood head injury. Clinical features recognised in these two groups are hemiplegia (87.5% vs 66.7% respectively, p=0.539), mental retardation (87.5% vs 66.7%,p=0.539) and psychiatric disorders (37.5% vs 16.7%, p=0.580). Of these patients, radiological appearances of wallerian degeneration and hyperpneumatisation of paranasal sinus (75% vs 50%, p=0.580); elevation of orbital roof (75% vs 33.3%,p= 0.277); hperpneumatisation of the mastoid and elevation of petrous ridge (62.5% vs 16.7%, p=0.138) were found in these two groups. The formation of porencephaly

and midline structural shift were identified among the patients (87.5% vs 16.7%, p=0.026).
Conclusion: The clinical-radiological manifestations of DDMS vary widely. The patients with childhood head injury were more likely to have the formation of porencephaly and midline structural shifts.
Limitations: This study was limited by a small number of patients and by the lack of detailed history and clinical information due to the retrospective nature of this study.
Ethics committee approval: n/a
Funding: No funding was received for this work.
Author Disclosures:
F. Y. Chew: nothing to disclose
W.-C. Shen: nothing to disclose
Y.-F. Chen: nothing to disclose
C. Y. Song: nothing to disclose

10:30 - 12:00 **Room G**

Vascular

RPS 1815

MR in vascular imaging

Moderators:
S. Haneder; Cologne/DE
N.N.

RPS 1815-K 10:30
Keynote lecture
N.N.

RPS 1815-1 10:40
A comparison of time-of-flight MR angiography with sparse under-sampling with TOF-MRA in the evaluation of intracranial aneurysms: digital subtraction angiography as a reference standard
X. Xu, W. Peng, C. Xia, Z. Li*; Chengdu/CN*
(1278240499@qq.com)

Purpose: To compare the performance of time-of-flight with sparse undersampling MRA and TOF-MRA in the image quality and evaluation of size parameters of intracranial aneurysms with DSA as the reference standard.
Methods and materials: 54 aneurysms from 46 patients who underwent TOF-MRA, TOFu-MRA, and DSA were included. For objective image quality, the contrast-to-noise ratio (CNR) and signal-to-noise (SNR) of two MRA images were compared. The subjective image quality was assessed using a 5-point score scale by two experienced observers and the interobserver agreement was determined. With DSA as the reference, the neck, height, and width of aneurysms in two MRAs were measured and compared on maximum intensity projection (MIP) image datasets, respectively.
Results: The SNRs and CNRs in TOFu-MRA (SNR=24.21±8.06; CNR=17.08±7.44) were significantly higher than those in TOF-MRA (SNR=18.94±6.44; CNR=13.27±6.00) (P<0.001). With an excellent interobserver agreement (κ values=0.94), the subjective image quality was significantly improved when the sparse TOF was used ($P < 0.05$). For measurement of size parameter, there were significant differences between TOF-MRA and TOFu-MRA among the three groups (neck, 3.63±2.22 vs 3.52±2.16; width, 4.62±4.59 vs 4.64±4.71; height, 4.62±4.59 vs 4.64±4.71, all P<0.05). Moreover, in the Bland-Altman plot analysis, TOFu-MRA showed no significant differences between DSA.
Conclusion: Compared with conventional TOF, sparse TOF could assess intracranial aneurysms more accurately with a better image quality and the same acquisition time.
Limitations: Further optimisation of the image quality with regard to NO settled protocol parameters would be needed.
Ethics committee approval: The study has been approved by the West China Hospital ethics committee.
Funding: 1.3.5 project for disciplines of excellence, West China Hospital, Sichuan University (ZYGD18019).
Author Disclosures:
X. Xu: nothing to disclose
W. Peng: nothing to disclose
C. Xia: nothing to disclose
Z. Li: nothing to disclose

RPS 1815-2 10:46
Quantification of the gradient of lumen narrowing of the internal carotid artery on an atherosclerotic plaque from magnetic resonance angiography for the stratification of the risk of cerebral stroke
W. Y. Ussov[1], A. Maksimova[1], V. E. Sinitsyn[2], S. P. Yaroshevsky[1], E. E. Bobrikova[1], O. Belichenko[2]; *[1]Tomsk/RU, [2]Moscow/RU*
(wolfussov@yandex.ru)

Purpose: We proposed a new index of haemodynamic severity of atherosclerotic stenosis of carotid arteries: gradient of narrowing of arterial lumen GNL={(S_{norm}–$S_{stenosis}$)/$D_{norm-stenosis}$}, mm^2/mm, i.e. as ratio of difference between the areas of cross-sections of the artery at the levels of most prominent stenosis and of normal non.stenosed artery closest to it, to the distance between them.
Methods and materials: 25 patients were studied, all with a stenosis of the internal carotid artery (ICA) >50%, (ECST), mono (n=22), or bilateral (n=3). 11 people without ICA stenosis served as the control group. In all participants, MR-angiography was carried out, with the calculation of the GNL on the ICA stenoses. Brain MRI was also carried out on all participants in T1-, T2-, PD-, and flair-weighted protocols.
Results: Patients were assigned to group 1 (n=12, without brain damages), and group 2 (n=13, evidence of earlier ischaemic damages). Group 1 and group 2 did not differ in stenosis % by ECST (74.9±4.25% vs 77.8±3.8%, p<0.05).
Group 1 and group 2 did differ in GNL (2.47±0.41 mm^2/mm and 4.60±0.51 mm^2/mm, p>0.02). GNL in 12 of 13 patients of group 2 was >3.35 mm^2/mm and 9 of 12 in group 1 demonstrated GNL <3.35 mm^2/mm. 2 died due to stroke (GNL 5.5 and 8.6 mm^2/mm)
In controls, the GNL was <0.75 mm^2/mm.
Conclusion: The GNL index, as mm^2/mm, is of diagnostic and prognostic value in carotid atherosclerosis.
Limitations: n/a
Ethics committee approval: All studies were approved by the local ethics committee.
Funding: No funding was received for this work.
Author Disclosures:
W. Y. Ussov: nothing to disclose
A. Maksimova: nothing to disclose
V. E. Sinitsyn: nothing to disclose
S. P. Yaroshevsky: nothing to disclose
E. E. Bobrikova: nothing to disclose
O. Belichenko: nothing to disclose

RPS 1815-3 10:52
A combination method of non-enhanced 3D-TOF MRA, 3D pCASL, and 3D t-ASL: a new quantitative assessment of territorial perfusion shifts and territorial CBF changes in MMD pre-and post-surgery
X. Gao, J. Sun, D. Ma*; Hangzhou/CN*
(10301010213@fudan.edu.cn)

Purpose: To explore intracerebral perfusion and territory shifts conducted by each main artery in Moyamoya disease pre-and post-surgery.
Methods and materials: 27 MMD patients underwent non-enhanced 3D t-ASL, 3D-TOF MRA, and 3D pCASL within one week before and after surgery. T-ASL maps and perfusion shifts of unilateral ICA and bilateral VA were obtained. Perfusion shifts were further subdivided and compared according to MRA. T-ASL images were coregistered to each ASL-CBF maps and created into binary masks. The CBF value was extracted by ASL-CBF maps and all these masks, respectively. A paired t-test was used to compare the surgical side, non-surgical side ICA-CBF, and bilateral VA-CBF, respectively, pre-and post-surgery. Independent two samples t-test was used to compare territorial CBF and its changes before surgery between the haemorrhagic group and the ischaemic group.
Results: 27 (7 haemorrhagic, 13 ischaemic) were enrolled. 4 distinct categories of perfusion territory shifts were observed on t-ASL. Perfusion territory shifts were divided into 2 categories. 7 perfusion territory shifts vanished and 6 appeared after surgery, including both 2 categories. There were significant CBF improvement in the surgical side ICA territory (p=0.004, 95% CI: 3.409-15.150, mean=9.27), non-surgical side ICA territory (p=0.043, 95% CI: 0.130-7.033, mean=3.58), and bilateral VA territory (p=0.003, 95% CI: 2.394-10.332, mean=6.36) after surgery. One patient had decreased CBF in all territories and postoperative ischaemic stroke.
Conclusion: The combination method of non-enhanced 3D-TOF MRA, 3D pCASL, and 3D t-ASL can quantitatively assess territorial perfusion shifts and CBF changes in MMD pre-and post-surgery in a non-invasive, non-radioactive manner. CBF increases in surgical side ICA, non-surgical side ICA, and bilateral VA after surgery.
Limitations: The sample size.
Ethics committee approval: Ethics committee approval obtained.
Funding: The National Natural Science Funds of China (NO.81702371).

Author Disclosures:
X. Gao: nothing to disclose
D. Ma: nothing to disclose
J. Sun: nothing to disclose

RPS 1815-4 10:58

The benefits of time-resolved imaging (TRI) in May Thurner syndrome (MTS): a correlation with the degree of iliac vein compression

D. M. D. Araújo[1], M. D. P. Estrela[2], M. M. Filisbino[1], A. Skaf[1], S. D. T. O. Cantoni[1], F. H. C. Souza[1], L. E. C. Paiva[1], H. Leao Filho[1]; [1]São Paulo/BR, [2]Barretos/BR (dyandramoreira@hotmail.com)

Purpose: To assess the benefits of TRI in patients with clinical suspicion of MTS. The main objective is to correlate the presence of a collateral venous pattern in the left inferior limb with the compression degree in the left common iliac vein (LCIV). We also aim to asses the inter and intraobserver variability in the degree of LCIV compression using different techniques.
Methods and materials: This retrospective study included 112 patients submitted to MRI-angiography with TRI sequences using intravenous contrast infusion on the left foot, between October 2014-May 2019. We selected 97 patients who did not undergo any interventional procedures and with an appropriated exam. One senior radiologist reviewed the images looking for collateral venous drainage and measured the maximal degree of LCIV compression. One fellow with 1 year of vascular training measured the maximal degree of venous compression in different sequences, without knowledge of the results from the senior radiologist. The readings took place at different times with each sequence to mitigate memory bias.
Results: We found a statistically significant difference between the presence of collateral venous drainage and the degree of compression with a median LCIV of 0.4 (0.3-0.7) cm in patients without collaterals (67) and a median LCIV of 0.3 (0.2-0.3) cm in patients with collaterals (30), with a p<0.001.
The intraclass correlation (ICC) between techniques by the fellow was 0.81 (IC95%: 0.73-0.87), with a mean variation of 0.11 cm. The ICC between the fellow and senior radiologist was worse, reaching 0.57-0.77 between techniques.
Conclusion: Time-resolved imaging allows a dynamic assessment of collaterals in MTS patients that correlates with the degree of LCIV compression in patients with MTS, but there is relevant variation between readers and techniques.
Limitations: A small sample and single institution.
Ethics committee approval: n/a
Funding: No funding was received for this work.
Author Disclosures:
D. M. D. Araújo: nothing to disclose
M. D. P. Estrela: nothing to disclose
M. M. Filisbino: nothing to disclose
A. Skaf: nothing to disclose
S. D. T. O. Cantoni: nothing to disclose
F. H. C. Souza: nothing to disclose
L. E. C. Paiva: nothing to disclose
H. Leao Filho: nothing to disclose

RPS 1815-6 11:04

A comparison of non-contrast 2D-bSSFP MRI sequence in Marfan patients at 1.5T and 3T: the influence of image quality, discrimination of the aortic wall, and aortic surgery on aortic diameter measurements

M. Avanesov, J. M. Weinrich, M. Sinn, A. Lenz, F. von Düring, M. L. Warncke[2], E. Tahir, G. Adam, P. Bannas; Hamburg/DE (maxim.avanesov@gmx.de)

Purpose: In Marfan patients, accurate aortic diameter measurements are crucial for life-long monitoring. We compared the influence of overall image quality, amount of image artefacts, contrast-to-noise-ratio (CNR), and aortic root surgery on the reliability of aortic measurements of non-contrast MRA in Marfan patients at 1.5T and 3T.
Methods and materials: 40 Marfan patients were prospectively evaluated by non-contrast 2D-bSSFP MRA of the aorta at 1.5T and after 12 months at 3T before (n=24) and after aortic surgery (n=16). Two readers independently rated the image quality and the presence/amount of artefacts on Likert scales at 9 (8) aortic levels before (after) aortic surgery. The CNR of the delineated aortic wall was separately calculated for each aortic level.
Results: Aortic imaging at 3T provided significantly superior CNR and more reproducible aortic diameters compared to 1.5T. Interobserver variances of aortic measurements were significantly smaller at the sinuses of the valsalva, sinotubular junction, mid-ascending aorta, and proximal descending aorta in pre-surgical patients (p<0.05). After aortic surgery, the majority of the advantages of 3T were mitigated by a significantly impaired image appearance due to the higher number of susceptibility/flow artefacts at 3T compared with 1.5T. This resulted in significantly higher aortic diameter variances at the mid-graft and distal anastomosis.
Conclusion: Non-contrast aortic imaging at 3T results in a higher CNR and more reproducible aortic measurement in pre-surgical Marfan patients compared to 1.5T. Most of these advantages are mitigated in post-surgical Marfan patients due to increased susceptibility/flow artefacts at 3T.
Limitations: The time delay between measurements at 1.5T/3T, differences of exact technical parameters at 1.5T/3T, and the measurements only in para-sagittal planes.
Ethics committee approval: Written informed consent was assessed. IRB approved this work.
Funding: No funding was received for this work.
Author Disclosures:
M. Avanesov: nothing to disclose
J. M. Weinrich: nothing to disclose
M. Sinn: nothing to disclose
A. Lenz: nothing to disclose
F. von Düring: nothing to disclose
M. L. Warncke: nothing to disclose
E. Tahir: nothing to disclose
G. Adam: nothing to disclose
P. Bannas: nothing to disclose

RPS 1815-7 11:10

Loss of kinetic energy over the aortic arch after surgical repair of acute aortic dissection: a prospective 4D flow study

T. Emrich, N. Ring, C. Bussalb, C. Noll, M. Thalheimer, M. C. Halfmann, C. Düber, K.-F. Kreitner, D. S. Dohle; Mainz/DE (natalie.ring90@gmail.com)

Purpose: 4D flow is an emerging imaging technique. Beside traditional flow parameters, 4D flow enables the calculation of advanced parameters like wall shear stress or the loss of kinetic energy. The aim of this prospective study was to evaluate differences in the loss of kinetic energy over the aortic arch between healthy volunteers and aortic dissection patients after surgical repair with implantation of an antegrade stent-graft ("frozen elephant trunk"; FET).
Methods and materials: In 17 healthy volunteers (HV) and 11 patients, 4D flow imaging was performed using a 4D flow prototype on a 3-Tesla MRI scanner. All patients had undergone aortic surgery for treatment of acute aortic dissection (type A) with supracoronary aortic replacement and "frozen elephant trunk" antegrade stent-graft implantation. 4D flow measurements and a calculation of the loss of kinetic energy (LoE) were performed with a dedicated 4D flow software tool (cvi42, Circle, Calgary, Canada) from the aortic annulus to the descending aorta.
Results: The mean maximum and average LoE was 2-3 times higher over the aortic arch in FET patients compared to healthy volunteers (mean maximum LoE FETvsHV: 9.0± 6.1 vs 3.7±1.3 mW; p=0.016 and mean average LoE FETvsHV: 2.4±1.3 vs 0.9±0.3 mW; p=0.003).
Conclusion: FET repair of acute aortic dissection leads to a significant increase in the loss of kinetic energy measured by 4D flow MR imaging. The prognostic implications of these changes on end-organ perfusion and cardiac remodelling have to be determined in prospective studies.
Limitations: A single-centre study without invasive correlation.
Ethics committee approval: All patients provided written informed consent. The study was approved by the local ethics committee (2018-13520).
Funding: No funding was received for this work.
Author Disclosures:
T. Emrich: nothing to disclose
N. Ring: nothing to disclose
C. Bussalb: nothing to disclose
C. Noll: nothing to disclose
M. Thalheimer: nothing to disclose
M. C. Halfmann: nothing to disclose
C. Düber: nothing to disclose
K.-F. Kreitner: nothing to disclose
D. S. Dohle: nothing to disclose

RPS 1815-8 11:16

Non-contrast self-navigated 3D whole-heart MR angiography: performance in aortic root evaluation prior to transcatheter aortic valve intervention

M. J. Pamminger[1], C. Kranewitter[1], C. Kremser[1], B. Henninger[1], G. Reiter[2], D. Piccini[3], G. Klug[1], A. Mayr[1]; [1]Innsbruck/AT, [2]Graz/AT, [3]Lausanne/CH

Purpose: To evaluate the image quality, interobserver reliability, and diagnostic accuracy of self-navigated non-contrast 3D whole-heart magnetic resonance angiography (MRA) for transcatheter aortic valve intervention (TAVI) evaluation in comparison to standardised contrast-enhanced CT angiography (CTA).
Methods and materials: A whole-heart 1.5T MRA was performed in 34 patients (84 years [IQR 79-86], 50% male) for aortic root sizing and coronary ostia height measurement. A subgroup of 19 (56%) patients underwent additional CTA as a gold standard. Image quality was assessed by a 4-point Likert scale, continuous

MRA and CTA measurements were compared with regression and Bland-Altman analysis, with valve sizing by kappa statistics.
Results: The median image quality of MRA was 1.5 [IQR 1.5-2.5]. In 4 patients (12%), 1 coronary ostium each (right coronary artery 3, left main artery 1) was not clearly definable on MRA. The interobserver correlation was substantial to excellent (r=0.61-0.92) with a bias of 19 mm^2 for the annulus area (lower limit of agreement -59 mm^2, upper limit of agreement 98 mm^2; p=0.009). Aortic root and ostia height measurements by MRA and CTA showed substantial to excellent correlation (r=0.65-0.90) with no significant bias (all p≥0.333). The mean annulus area for MRA was 414±71 mm^2 and for CTA 422±80 mm^2 (r=0.9) with bias of -8 mm^2 (lower limit of agreement -79 mm^2, upper limit of agreement -62 mm^2; p=0.333). Regarding prosthetic valve sizing, there was complete consistency between MRA and CTA-based decisions (κ=1).
Conclusion: Self-navigated non-contrast 3D whole-heart MRA enables reliable aortic root measurements without a significant difference to standardised CTA. Prosthesis sizing by MRA measurements would completely match a CTA-based choice. However, in some cases, coronary ostia may not be definable.
Limitations: The comparison of MRA and CTA was only performed in 19 patients.
Ethics committee approval: Local ethics comittee approval was obtained.
Funding: No funding was received for this work.
Author Disclosures:
M. J. Pamminger: nothing to disclose
C. Kranewitter: nothing to disclose
C. Kremser: nothing to disclose
B. Henninger: nothing to disclose
G. Reiter: Consultant at Siemens Healthcare Diagnostics GmbH
D. Piccini: Employee at Siemens Healthcare Switzerland
G. Klug: nothing to disclose
A. Mayr: nothing to disclose

RPS 1815-9 11:22

The role of time-resolved magnetic-resonance-angiography (TRMRA) in the characterisation of soft-tissue vascular anomalies (VA)

A. Sangwan, A. Goyal, A. Kumar, R. Sharma, D. Kandasamy, A. S. Bhalla, D. S. Arava, D. M. Singhal, D. R. Dawar*; New Delhi, Delhi/IN, (ankitsangwanaiims@gmail.com)*

Purpose: To assess the usefulness of time-resolved magnetic-resonance-angiography (TRMRA) in the characterisation of suspected soft-tissue vascular anomalies.
Methods and materials: A retrospective analysis of TRMRA done in patients with suspected VA from December 2017-May 2019 was conducted. TWIST (Siemens) and 4D-TRAK (Philips) sequences were acquired for a 3 minute post-contrast injection. The time-of-onset (TO), time-to-peak (TTP), the pattern of contrast enhancement, presence of feeding arteries, and draining veins were noted. 99 patients were included (60 males, 39 females, age-range 1-65 years) and the diagnosis was confirmed on a composite gold standard.
Results: 29 venous malformations showed gradual progressive filling-in of cystic spaces starting at 8.8+/-3.3s with peak enhancement at 110.3+/-41.08s. 22/29 showed intense-moderate CE with the draining vein in 17/29. 12 arteriovenous malformations (AVMs) started filling at 0.25+/-0.86s with a peak enhancement at 11.58+/-2.9s with hypertrophied feeding arteries, early draining veins, and tubular morphology in all cases. 16/22 cases of fibro adipose VA showed dysplastic veins, non-hypertrophied feeders, and phlebectasia. The mean TO was 8.85+/-4.89s and TTP was 73.66+/-49.38s. 18 vascular tumours enhanced early, homogeneously and intensely (TO 3.27+/-2.94s, TTP 19+/-9.69s), showing the parenchymal type of CE. 12/18 tumours showed hypertrophied feeding arteries and early draining veins. 7 neurofibromas also showed a parenchymal pattern but with delayed onset (5.71+/-5.49s) and peak (84.14+/-51.72s). There was a significant difference between TO and TTP in vascular tumours and neurofibromas (p=0.05, 0.0001, respectively). A significant difference was also seen between TTP of VMs and FAVA (p=0.0005). There was a good correlation with DSA findings (9/12 AVMs, 12/18 tumours).
Conclusion: TRMRA provides dynamic perfusion information for characterisation of VA. It provides vascular roadmaps and helps to assess the feasibility of embolisation/sclerotherapy.
Limitations: A subjective evaluation.
Ethics committee approval: Ethics committee approval obtained.
Funding: No funding was received for this work.
Author Disclosures:
A. Sangwan: nothing to disclose
A. Goyal: nothing to disclose
A. Kumar: nothing to disclose
R. Sharma: nothing to disclose
D. Kandasamy: nothing to disclose
A. S. Bhalla: nothing to disclose
D. S. Arava: nothing to disclose
D. M. Singhal: nothing to disclose
D. R. Dawar: nothing to disclose

RPS 1815-10 11:28

Time-resolved contrast-enhanced magnetic resonance angiography in patients with congenital heart disease: image quality using two different doses of a contrast agent

C. B. Monti, G. Dellaferrera, M. Zanardo, D. Capra, A. Cozzi, F. Sardanelli, F. Secchi*; Milan/IT (caterinab.monti@gmail.com)*

Purpose: To compare the image quality between two datasets of time-resolved, contrast-enhanced magnetic resonance angiography (TR-MRA) with different doses of gadobutrol in congenital heart disease (CHD) patients.
Methods and materials: CHD patients who underwent TR-MRA at our institution were retrospectively evaluated and divided into 2 groups according to the dose of gadobutrol they received: 0.10 mmol/kg (group A) or 0.15 mmol/kg (group B). Signal intensity of 6 different vascular structures, superior vena cava (SVC), ascending aorta (AAo), descending aorta (DAo), pulmonary artery (PA), left pulmonary artery (LPA), and right pulmonary artery (RPA), were reported along with the standard deviation of signal intensity of the background at each timepoint of TR-MRA. The signal-to-noise ratio (SNR) was subsequently calculated for each structure and timepoint. Peak SNRs for each structure were compared between the groups.
Results: A total of 40 patients were included in this study, 20 in group A and 20 in group B. Peak SNRs in group A were SVC: 97.05 (76.10-137.34), AAo: 123.27 (88.69-192.49), DAo: 109.94 (89.10-174.68), PA: 136.03 (93.66-205.37), LPA: 137.84 (82.43-190.33), and RPA: 146.55 (84.50-197.92). Peak SNRs in group B were SVC: 96.71 (49.34-121.72), AAo: 119.11 (79.65-177.98), DAo: 116.56 (87.64-184.21), PA: 126.97 (80.94-170.79), LPA: 124.80 (81.51-176.62), and RPA: 119.56 (80.16-174.25). There were no significant differences in peak SNRs of any structure (p≥0.301).
Conclusion: In CHD patients, TR-MRA may be performed using a dose of 0.10 mmol/kg of gadobutrol instead of 0.15 with no loss of image quality.
Limitations: A retrospective, monocentric study.
Ethics committee approval: Ethics committee approval was obtained. Informed consent was waived due to the retrospective nature.
Funding: No funding was received for this work.
Author Disclosures:
C. B. Monti: nothing to disclose
G. Dellaferrera: nothing to disclose
M. Zanardo: nothing to disclose
D. Capra: nothing to disclose
F. Sardanelli: Advisory Board at Bracco, Grant Recipient at Bracco, Grant Recipient at Bayer, Grant Recipient at General Electric, Speaker at Bracco, Speaker at Bayer, Speaker at General Electric
F. Secchi: nothing to disclose
A. Cozzi: nothing to disclose

RPS 1815-11 11:34

The influence of the pulses and flip angle on the quality of the non-enhanced renal arterial MR images

Y. Wang, F. Hu, S. Yan, D. Ren*; Chengdu/CN (369141717@qq.com)*

Purpose: To investigate the influence of the frequency of pulses and the flip angle on the quality of the non-enhanced renal arterial MRA.
Methods and materials: We prospectively recruited 14 volunteers [19 men, 6 women; age=23.8±2.61].Each volunteer was scanned 6 times with different flip angles (45°, 90°, and 135°) and frequency of pulses (1 or 3 times) with 1.5T MR NATIVE True-FISP sequences. The quality of the images and renal arterials presentation were graded ranging from 0-3 and 1-3, respectively. The average value of the bilateral renal arterials score was used for analysis. ICC was used to test the agreement between the two observers. Factorial analysis was used to compare image quality scores and renal artery scores between different scanning groups.
Results: The interobserver agreement of image quality and renal artery scores were good (ICC =0.77-0.88, 0.80-0.98). There was no difference in image quality and renal artery scores between different pulse groups (p=0.191, 0.177). There was a significant overall difference of image quality and renal artery scores between different flip angle groups (p=0.01, 0.00). There were no statistical significant differences for the interaction of pulse and flip angel in image quality and renal artery scores (p=0.87, 0.52). The image quality and renal artery scores were highest in 135° group.
Conclusion: Different pulse times have no significant effect on the image quality and renal artery display of NATIVE True-FISP sequences. For the flip angel, 135° is the better choice.
Limitations: A lack of objective quantitative parameters. The effect of blood flow velocity on image quality was not considered.
Ethics committee approval: Approved by the hospital ethics review committee.
Funding: No funding was received for this work.

Author Disclosures:
Y. Wang: nothing to disclose
F. Hu: nothing to disclose
S. Yan: nothing to disclose
D. Ren: nothing to disclose

RPS 1815-12 11:40
Free-breathing fast low-angle shot quiescent-interval slice-selective MR angiography for the improved detection of vascular stenoses in the pelvis and abdomen
A. Varga-Szemes[1], E. A. Aherne[2], U. J. Schoepf[1], T. Todoran[1], I. Koktzoglou[3], R. Edelman[4]; [1]*Charleston, SC/US,* [2]*Dublin/IE,* [3]*Evanston/US,* [4]*Illinois/US (vargaasz@musc.edu)*

Purpose: To evaluate the image quality and diagnostic accuracy in the pelvis and abdomen of free-breathing fast low-angle shot (FLASH)-based quiescent interval slice-selective (QISS) techniques in comparison to standard QISS in patients with peripheral artery disease (PAD), using CTA as the reference.
Methods and materials: 27 patients (69±10y) with PAD underwent non-contrast MRA using standard bSSFP-based QISS and prototype free-breathing radial-FLASH and Cartesian-FLASH-based QISS at 3T. A subset of patients (n=22) also underwent CTA as the reference standard. 9 arterial segments per patient were evaluated spanning the abdomen, pelvis, and upper thigh regions. Objective (signal intensity ratio (SIR) and relative standard deviation (SD)) and subjective image quality (4-point scale) and stenosis (>50%) were evaluated by two readers and compared using a one-way analysis of variance, Wilcoxon, and McNemar tests, respectively.
Results: A total of 179 vascular segments were available for analysis by all QISS techniques. No significant difference was observed among bSSFP, radial-FLASH, and Cartesian-FLASH-based techniques in SIR (p=0.428) and relative SD (p=0.220). Radial-FLASH-based QISS demonstrated the best image quality (p<0.0001) and the highest inter-reader agreement (κ=0.721). The sensitivity values of bSSFP, radial-FLASH, and Cartesian-FLASH-based QISS for the detection of >50% stenosis were 76.0%, 84.0%, and 80.0%, respectively, while specificity values were 97.6%, 94.0%, and 92.8%, respectively. Moreover, FLASH-based QISS consistently reduced off-resonance artefacts compared to the bSSFP-based approach.
Conclusion: Free-breathing FLASH-based QISS MRA techniques provide improved image quality and sensitivity, high specificity, and reduced off-resonance artefacts for vascular stenosis detection in the abdomen and pelvis.
Limitations: The limited sample size and lack of a control group.
Ethics committee approval: IRB-approved with written informed consent obtained.
Funding: NIH-NHLBI.
Author Disclosures:
A. Varga-Szemes: Investigator at Siemens, Consultant at Elucid Bioimaging
E. A. Aherne: nothing to disclose
U. J. Schoepf: Grant Recipient at Astellas, Bayer, Elucid Bioimaging, GE, Guerbet, HeartFlow, Siemens, Consultant at Elucid Bioimaging, Guerbet, HeartFlow, Siemens
T. Todoran: nothing to disclose
I. Koktzoglou: Grant Recipient at Siemens
R. Edelman: Grant Recipient at Siemens

RPS 1815-13 11:46
Stent lumen visualisation and quantification with magnetic particle imaging: a systematic in vitro study with 21 endovascular stents
F. Wegner[1], A. von Gladiss[1], J. Haegele[2], U. Grzyska[1], M. M. Sieren[1], K. Lüdtke-Buzug[1], T. M. Buzug[1], J. Barkhausen[1], T. Friedrich[1]; [1]*Lübeck/DE,* [2]*Neuss/DE (franz.wegner@uksh.de)*

Purpose: To investigate whether magnetic particle imaging (MPI) can visualise and quantify the lumen of endovascular stents.
Methods and materials: We investigated 21 commercially available stents (diameter: 3-10 mm, material: stainless steel, nitinol, platinum-chromium, cobalt-chromium) which were implanted in silicone vessel phantoms. All phantoms (stented phantoms and reference phantoms without stents) were filled with tracer dilution (1:100, Resovist, l'rom Pharmaceuticals, Tokio, Japan) and visualised with a preclinical commercially available MPI scanner (Bruker Biospin, Ettlingen, Germany). The quantification of the lumina was performed on the xz-planes of the images based on a calibrated signal intensity threshold.
Results: The visualisation of the stent lumen is feasible without any material induced artefacts. Between the stented phantoms and the reference phantoms there was no visual or quantitative difference observed (stented phantoms/reference phantoms vs nominal diameter r=0.98). The root mean square inaccuracy of stent lumen quantification was below half the spatial resolution.
Conclusion: In principle, MPI is able to depict and quantify the lumina of endovascular stents accurately without material induced effects.
Limitations: The in vitro study design and that we only used a single tracer concentration.
Ethics committee approval: n/a
Funding: This study was partially funded by the Federal Ministry of Education and Research BMBF grant numbers 13GW0071D, 13GW0069A, 13GW0230B, and 01DL17010A.
Author Disclosures:
A. von Gladiss: nothing to disclose
F. Wegner: nothing to disclose
J. Haegele: nothing to disclose
U. Grzyska: nothing to disclose
M. M. Sieren: nothing to disclose
K. Lüdtke-Buzug: nothing to disclose
T. M. Buzug: nothing to disclose
J. Barkhausen: nothing to disclose
T. Friedrich: nothing to disclose

10:30 - 12:00 **Tech Gate Auditorium**

Artificial Intelligence and Machine Learning

RPS 1805

Deep learning based scanning, image reconstruction, and quality assurance

Moderators:
R. Mirón Mombiela; Herlev/DK
A. Trianni; Udine/IT

RPS 1805-K 10:30
Keynote lecture
V. Gershan*; Skopje/MK (vgersan@gmail.com)*

Author Disclosures:
V. Gershan: nothing to disclose

RPS 1805-1 10:40
Automatic scan range delimitation in CT topogram images of the chest using deep learning
K. S. Moon, A. Demircioglu, L. Umutlu, K. Nassenstein*; Essen/DE (moon.kim.mail@gmail.com)*

Purpose: To automate the scan range delimitation in topograms of chest CT exams using deep learning techniques. Automation of this process would free the radiographer from this routine task and could potentially reduce the radiation exposure for the patient due to a stronger restriction of the scan range.
Methods and materials: A total of 1,150 chest topograms of patients (mean age=64.6 years) with pleural effusion (N=360), with atelectasis (N=82), with both diseases (N=21), or without both diseases (N=411) were extracted retrospectively from our PACS, and the scan range was delimitated in each topogram by two radiologists in consensus. A conditional generative adversarial neural network (CGAN) for image-to-image translation was trained on 1,000 topograms to generate virtual scan range delimitations. Quantitative evaluation was performed on 150 randomly selected topograms by computing the absolute difference of the predicted scan delimitations and those of the two expert radiologists.
Results: Automated scan range delimitation showed an excellent agreement with the scan range delimitation of the radiologists. The mean absolute difference between expert radiologists and the prediction of the neural network was 3.77 +/- 0.74 mm and 5.87 +/- 1.29 mm at the upper and lower limit, respectively.
Conclusion: An automated scan range delimitation of chest CT scans using deep learning techniques was trained and evaluated by comparing the scan range with the annotations of two senior radiologists. The results indicate that the conditional generative adversarial network can generate scan range delimitations that are comparable to those of expert radiologists.
Limitations: More training data could potentially increase overall performance. Evaluation from external sites is required to establish the method.
Ethics committee approval: Ethics committee approval was obtained.
Funding: No funding was received for this work.

Author Disclosures:
K. S. Moon: nothing to disclose
A. Demircioglu: nothing to disclose
L. Umutlu: nothing to disclose
K. Nassenstein: nothing to disclose

RPS 1805-2 10:46

Elevating clinical brain and spine MR image quality with deep learning reconstruction

L. N. Tanenbaum[1], S. Bash[2], M. Thomas[3], M. Fung[3], R. M. Lebel[4], S. Banerjee[5]; [1]Riverside, CT/US, [2]Los Angeles/US, [3]New York, NY/US, [4]Calgary/CA, [5]Menlo Park/US (nuromri@gmail.com)

Purpose: In the quest for increasing image quality, MR throughput can suffer and manoeuvre, which creates faster scans trade-off quality. There is a need to enhance images without prolonging scan time. Recently, deep learning-based reconstruction methods have shown promise to enhance image value. We evaluated the impact of a new deep learning image reconstruction (DLR) method for both noise reduction and improved image sharpness in clinical MR exams of the brain and spine.

Methods and materials: The investigational DLR leverages a deep convolutional residual encoder network trained on a >10K image database to create images with enhanced SNR and spatial resolution. 28 patients were scanned using clinical 2D brain (3T-7 and 1.5T-4) or spine (3T-12 and 1.5T-5) protocols. K-space data was reconstructed with both conventional and DLR (tuned to 75% noise reduction). Two neuroradiologists independently rated 93 pairs of conventional and DLR images side-by-side. Ratings were based on overall IQ, lesion conspicuity, perceived SNR and resolution, CNR, image texture, and artefact using a 5-point Likert scale (5=excellent, 1=non-diagnostic). A Wilcoxon signed-rank test was used to compare the ratings and inter-rater reliability between readers was assessed using the Bennett S score.

Results: DLR showed statistically significant improvement over conventional images in overall image quality (4.74±0.49 vs 3.27±0.70, p<0.05), lesion conspicuity (4.65±0.49 vs 3.24±0.52, p<0.05), contrast (4.59±0.61 vs 3.50±0.59, p<0.05), perceived resolution (4.66±0.61 vs 3.36±0.59, p<0.05), perceived SNR (4.72±0.60 vs 3.33±0.53, p<0.05), and image texture (4.66±0.60 vs 3.13±0.38, p<0.05). There was a substantial inter-rater agreement with an average S score of 0.66.

Conclusion: Overall IQ improved with DLR with higher perceived SNR, CNR, and spatial resolution compared to the conventional method. Future work will assess whether this technique can accelerate acquisitions while preserving quality.

Limitations: A limited series.

Ethics committee approval: Approved with subject consent.

Funding: No funding was received for this work.

Author Disclosures:

L. N. Tanenbaum: Advisory Board at GE, Siemens, Philips, Bracco, Geurbet, Shareholder at Icometrix, Curemetrix, Nous, AIDOC, Enlitic
S. Bash: Advisory Board at icometrix, Coretechs
M. Thomas: Employee at GE
M. Fung: Employee at GE
R. M. Lebel: Employee at GE
S. Banerjee: Employee at GE

RPS 1805-3 10:52

The effect of deep learning reconstruction on image quality in chest CT

J. Schuzer[1], J. Pack[2], C. Wen[3], C. Steveson[4], S. Rollison[5], J. Yu[2], M. Chen[5]; [1]Vernon Hills/US, [2]Long Beach/US, [3]Orange, CA/US, [4]Adelaide/AU, [5]Bethesda/US (jschuzer@mru.medical.canon)

Purpose: To investigate the effect of a deep learning image reconstruction algorithm on image quality in chest CT scans.

Methods and materials: With institutional ethics approval, 100 consecutive patients underwent chest CT at standard radiation doses on a 320-detector row CT scanner with the following scan parameters: Helical scan, 0.5 mm x 80 detector rows, 120 or 100kV, and automatic exposure control, 0.275s rotation speed and standard pitch. Each scan was reconstructed at 0.5 mm volume and 3 mm axial, coronal, and sagittal slices with both lung and soft tissue kernels using the clinical standard hybrid IR (AIDR3D) and deep learning reconstruction (AiCE) techniques. Images were evaluated for overall image quality, noise, presence of artefacts, contrast, visibility of small structures, and diagnostic confidence using a 4-point Likert scale. SNR and CNR were calculated for each reconstruction. Data was analysed by a paired t-test.

Results: Patients averaged 51.5 years (range 26-78), 77% were female with mean body mass index 27.5±7.1 kg/m2. In image quality, noise, contrast, and visibility of small structures, AiCE performed better than AIDR (3.71 vs 3.06, p <0001; 3.84 vs 2.95, p <0001, 3.66 vs 3.12, p <0001; 3.75 vs 3.16, p < 0001, respectively). The presence of artefacts and diagnostic confidence was not statistically significant for both reconstruction techniques (3.01 vs 2.98, p = 0.49; 4 vs 3.96, p = 0.32, respectively). Signal-to-noise for AiCE images was higher than AIDR3D images (21.0 vs. 16.3 respectively, p <0001). Contrast-to-noise for AiCE images was higher than AIDR3D images (29 vs 23.4 respectively, p <0001).

Conclusion: Deep learning reconstruction improves image quality in chest CT.

Limitations: A single-centre study.

Ethics committee approval: IRB approval National Institutes of Health, USA.

Funding: No funding was received for this work.

Author Disclosures:

J. Schuzer: Employee at Canon Medical Systems
J. Pack: nothing to disclose
C. Wen: nothing to disclose
C. Steveson: Employee at Canon Medical Systems
S. Rollison: nothing to disclose
J. Yu: nothing to disclose
M. Chen: nothing to disclose

RPS 1805-4 10:58

The effect of deep learning reconstruction on image quality in abdominal CT

J. Schuzer[1], J. Pack[2], C. Wen[3], C. Steveson[4], S. Rollison[5], J. Yu[2], M. Chen[5]; [1]Vernon Hills/US, [2]Long Beach/US, [3]Orange, CA/US, [4]Adelaide/AU, [5]Bethesda/US (jschuzer@mru.medical.canon)

Purpose: To investigate the effect of a deep learning image reconstruction algorithm on image quality in abdomen CT scans.

Methods and materials: With institutional ethics approval, 100 consecutive patients underwent abdominal CT at standard radiation doses on a 320-detector row CT scanner with the following scan parameters: Helical scan, 0.5 mm x 80 detector rows, 120 or 100kV, and automatic exposure control, 0.5s rotation speed and standard pitch. Each scan was reconstructed at 0.5 mm volume and 3 mm axial, coronal, and sagittal slices with a soft tissue kernel using the clinical standard hybrid IR (AIDR3D) and deep learning reconstruction (AiCE) techniques. Images were evaluated for overall image quality, noise, presence of artefacts, contrast, visibility of small structures, and diagnostic confidence using a 4-point Likert scale. SNR and CNR was calculated for each reconstruction. Data was analysed by a paired t-test.

Results: Patients averaged 51.1 years (range 19-78), 77% were female with mean BMI 27.5±7.1. In image quality, noise, contrast, and visibility of small structures, AiCE performed better than AIDR (3.69 vs. 3.08, p <0.001; 3.87 vs. 2.84, p <0.001, 3.72 vs. 3.17, p <0.001; 3.87 vs. 3.25, p < 0.001, respectively). The presence of artefacts and diagnostic confidence was not statistically significant for both reconstruction techniques (2.98 vs 2.95, p = 0.26; 3.98 vs. 3.95, p = 0.26, respectively). Signal-to-noise for AiCE images was higher than AIDR3D images (4.58 vs. 3.24 respectively, p <0.001). Contrast-to-noise for AiCE images was higher than AIDR3D images (18.48 vs. 13.31 respectively, p <0.001).

Conclusion: Deep learning reconstruction improves image quality in abdominal CT.

Limitations: A single-centre study.

Ethics committee approval: IRB approval National Institutes of Health/USA.

Funding: No funding was received for this work.

Author Disclosures:

J. Schuzer: Employee at Canon Medical Systems
C. Wen: nothing to disclose
J. Pack: nothing to disclose
C. Steveson: Employee at Canon Medical Systems
S. Rollison: nothing to disclose
J. Yu: nothing to disclose
M. Chen: nothing to disclose

RPS 1805-5 11:04

High resolution T2-weighted MRI of the abdomen using deep learning reconstruction

S. Funayama[1], T. Wakayama[2], R. Lebel[3], D. Tamada[1], H. Onishi[1], U. Motosugi[1]; [1]Yamanashi/JP, [2]Hino/JP, [3]Waukesha/US (akchan.acts@gmail.com)

Purpose: To evaluate the feasibility of a deep learning-based reconstruction technique (DLRecon) in clinical abdominal MRI with both standard and high-resolution short scan protocols.

Methods and materials: This study included 23 patients who underwent abdominal MRI. Each patient underwent 3 types of respiratory-triggered T2 weighted fast spin-echo (Discovery MR750 3.0T; GE Healthcare) with the following parameters: standard T2WI (std-T2WI, matrix, 320x192; thickness, 5 mm; NEX, 2), high-resolution T2WI (HR-T2WI, NEX, 1; matrix, 452x192), and super high-resolution T2WI (sHR-T2WI, NEX, 1; matrix, 452x192; thickness, 2.5 mm). The acquired data was reconstructed with and without DLRecon. DLRecon is a new deep learning-based MR reconstruction which comprises of a deep convolutional residual encoder network trained using a database of over 10,000 images to achieve images with high SNR and high spatial resolution. The depiction of anatomical details of the pancreas and the liver, motion artefact,

blurring, and overall quality were assessed to test the differences between those with and without DLRecon. The signal-to-noise ratio (SNR) of liver parenchyma and the spleen-to-liver signal intensity ratios were also calculated.
Results: The depiction of the anatomical details in the pancreas, blurring, and overall quality were improved with DLRecon. The SNR with DLRecon (std-T2WI, 9.99±3.94) was significantly higher than without DLRecon (9.08±2.9, p=0.01). Contrast between the liver and spleen was unaltered, with statistically equivalency at a threshold of 0.2 (std-T2WI, p<0.0001). All the above result trends were the same for HR-T2WI and sHR-T2WI.
Conclusion: The DLRecon provided improved SNR and less burring in abdominal T2WI compared to standard reconstruction for standard and high-resolution protocols.
Limitations: A retrospective study and a small number of patients.
Ethics committee approval: This study was approved by the institutional review board.
Funding: No funding was received for this work.
Author Disclosures:
S. Funayama: nothing to disclose
R. Lebel: Employee at GE Healthcare
D. Tamada: nothing to disclose
H. Onishi: nothing to disclose
T. Wakayama: Employee at GE Healthcare
U. Motosugi: nothing to disclose

RPS 1805-6 11:10
Influence of a novel deep learning noise reduction technology on filtered back-projected CT images in comparison to iterative reconstruction
A. Steuwe, O. T. Bethge, L. M. Sawicki, J. Böven, J. Morawitz, G. Antoch, J. Aissa; *Düsseldorf/DE (joel.aissa@med.uni-duesseldorf.de)*

Purpose: The software PixelShine (AlgoMedica, Germany) advertises with high-quality images even for low-dose CT acquisitions by reducing noise with deep learning algorithms while maintaining image information. This study aimed at an objective and subjective analysis of the image quality of processed datasets.
Methods and materials: This IRB-approved retrospective study included 27 patients (19 male) who received low-dose abdominal CT (Somatom Definition Flash, Siemens Healthineers) between November 2014 and February 2016. Images were reconstructed with filtered back-projection (FBP, B30f) and iterative reconstruction (IR, I30f, level 3, SAFIRE). Subsequently, FBP-images were post-processed using PixelShine (B30f-PS, PixelShine version 1.2.104, sharpening level 2, noise level 14, processing strength A8, soft kernel settings). CT numbers (mean and standard deviation (noise)) in 6 ROIs (background, paravertebral muscle, fat, spleen, liver, and bladder) and subjective image quality were compared for the different datasets.
Results: Image noise reduced significantly for B30f-PS-datasets compared to B30f- and I30f-datasets (-38 to -50% and -12 to -30% for soft tissues, respectively). CT numbers in liver, spleen, bladder, and fat were constant for all datasets, whereas significant differences were notable for background (B30f-PS vs B30f, and B30f vs I30f) and muscle (B30f-PS vs B30f, and B30f-PS vs I30f). In general, PixelShine improved image quality of B30f datasets considerably. Compared to I30f datasets, liver tissue looked more homogeneous, confirming a lower noise level. Beam-hardening artefacts were neither reduced nor enhanced.
Conclusion: PixelShine reduces noise while maintaining image information with its deep learning algorithm. Especially for older CT scanners, where IR is not available, PixelShine allows to increase image quality. For new scanners, PixelShine allows to reduce patient dose while maintaining image quality.
Limitations: n/a
Ethics committee approval: IRB-approved retrospective study.
Funding: No funding was received for this work.
Author Disclosures:
A. Steuwe: nothing to disclose
O. T. Bethge: nothing to disclose
L. M. Sawicki: nothing to disclose
J. Böven: nothing to disclose
J. Morawitz: nothing to disclose
J. Aissa: nothing to disclose
G. Antoch: nothing to disclose

RPS 1805-7 11:16
Deep learning reconstruction in ultra-low-dose abdominal CT: comparison with hybrid-iterative reconstruction
P. Rogalla[1], S. Kandel[2], B. E. Hoppel[3]; *[1]Toronto, ON/CA, [2]Berlin/CA, [3]Vernon Hills, WI/US (Patrik.Rogalla@uhn.ca)*

Purpose: To evaluate whether deep learning reconstruction (DLR) based on convolutional neural network provides superior image quality in ultra-low-dose abdominal CT compared to the hybrid-iterative reconstruction method.
Methods and materials: 62 patients underwent a CT of the abdomen (135kV, 20-40mA weight-based, 0.5s rotation time, 0.5*80 detector rows, 1.0 mSv reference dose). Four series were reconstructed with 0.5 mm slice thickness: (A) hybrid-iterative IR (AIDR), (B) DLR (combined), (C) DLR (sharp), and (D) DLR (smooth). All images were presented as 3 mm thick slices, 4 on 1 on a 4k monitor in random order and without image annotation. Using forced ranking, 2 readers evaluated the series in the categories of conspicuity, noise texture, low/high contrast detectability, artefacts, and overall appeal. The readers also graded image quality on a Likert scale (1=excellent, 10=low quality). Inter-reader agreement was calculated for all categories. Image noise (SD) was measured in external and intra-abdominal air and liver.
Results: DLR series (B) was generally preferred (rank 1) over all other reconstructions by both readers in all patients and in all categories (p<0.001). The overall mean rank of series (A)/(B)/(C)/(D) were 4.0/2.47/1.10/2.46 and the Likert scores were 6.9/3.4/1.97/3.6, respectively. Inter-reader agreement for forced ranking was k=0.80 and for the Likert score was k=0.78. SDs were 17.23/8.31/7.04/6.32 for external air, 21.5/10.8/10.3/8.3 for intra-abdominal air, and 23.1/9.9/9.3/7.25 for liver tissue, respectively, all p<0.0001 except in group B and C for intra-abdominal air and liver.
Conclusion: Deep learning reconstruction provides superior subjective image quality in ultra-low-dose abdominal CT compared to the current standard-of-care iterative method.
Limitations: The number of readers (2) and patients (62).
Ethics committee approval: Ethics approval was obtained.
Funding: No funding was received for this work.
Author Disclosures:
P. Rogalla: Research/Grant Support at Canon Medical Systems
S. Kandel: nothing to disclose
B. E. Hoppel: Employee at Canon Medical Systems

RPS 1805-8 11:22
Objective and qualitative IQ analyses of deep learning image reconstruction in multiphasic CT imaging of the liver: a patient and phantom study
F. Legou[1], P. Roux[1], V. Barrau[1], H. Pasquier[2], C. Legoff[2], M. Milliner[3], J.-L. Sablayrolles[1]; *[1]Saint Denis/FR, [2]Buc/FR, [3]Creteil/FR (legou.francois@gmail.com)*

Purpose: To evaluate the clinical benefits on image quality (IQ) of TrueFidelity, a deep learning image reconstruction (DLIR), in multiphasic liver CT compared to adaptive statistical iterative reconstruction V (ASIRV) in patients and on a phantom.
Methods and materials: 66 patients underwent a multiphasic liver CT during a 1-month-period. The protocol was tailored according to patient morphology: 80 kV for a body mass index (BMI) <25; 100 kV for 25<BMI<30, and 120 kV for BMI>30. IQ of patient images reconstructed with DLIR and ASIRV50 was assessed on portal phase by measuring liver parenchyma contrast and signal-to-noise ratios (CNR, SNR), and qualitatively by two radiologists using a 5-point Likert-scale. Phantom images acquired with similar protocols were evaluated by computing the noise power spectrum and the task-based modulation transfer function (MTF_{task}).
Results: Compared to ASIRV50, CNR and SNR were significantly improved with DLIR by 71% and 56% at 80, 83% and 77% at 100, and 61% and 60% at 120 kV, respectively (p<0.01 or less). Qualitative IQ was also improved with DLIR for each patient morphology (p<0.0001). On the phantom, compared to ASIRV50, DLIR reduced the noise magnitude by 31% at 80, 100, and 120kV while maintaining a coarser texture (noise mean frequency was 0.22 vs 0.21, 0.23 vs 0.21, and 0.25 vs 0.22 mm^{-1}, respectively). DLIR improved the MTF_{task} at 80, 100, and 120kV (spatial frequency at which the MTF_{task} reduces to 50% was 0.43 vs 0.36, 0.43 vs 0.39, and 0.41 vs 0.37 mm-1, respectively).
Conclusion: Compared to ASIRV50, DLIR improves the IQ of liver CT by reducing image noise without smoothing texture and by improving spatial resolution.
Limitations: IQ of the arterial phases haven't been assessed by the time of the submission. Results under completion.
Ethics committee approval: SFR approval.
Funding: No funding was received for this work.
Author Disclosures:
F. Legou: nothing to disclose
P. Roux: nothing to disclose
V. Barrau: nothing to disclose
J.-L. Sablayrolles: nothing to disclose
H. Pasquier: Employee at GE Healthcare
C. Legoff: Consultant at GE Healthcare
M. Milliner: nothing to disclose

RPS 1805-9 11:28
Evaluation of automated quality control of multicentre clinical trial CT data using spine localisation based on a machine learning method
S. Lee[1], C. Page[2], P. Galette[3], P. Murphy[2], B. Glocker[1]; *[1]London/UK, [2]Stevenage/UK, [3]Upper Providence/US (sarahlee@amallisconsulting.com)*

Purpose: Consistent image quality across multiple centres in clinical trials is crucial. The quality control is typically done by centralising data followed by manual checks prior to radiological review. For evaluating the feasibility of automating the QC process, we developed a software tool, Automatic Visual Quality Control (AutoVQC), that automatically locates the spine, calculates the anatomical field of view (FOV), and detects imaging artefacts using machine learning. AutoVQC was applied to in-house CT data from a multicentre clinical trial.
Methods and materials: The quality of CT scans (in total, 459 series from 62 subjects acquired at 7 sites) was evaluated using AutoVQC, which recognises the anatomical FOV of the images using random forests and detects artefacts such as missing slices. AutoVQC returns two values between 0 (foot) and 1 (top of the head) indicating the FOV in the canonical body axis and the outcome: pass or artefacts. The QC outcome was reviewed and classified as true-positive, true-negative, false-positive, and false-negative, where positive and negative indicate QC pass and artefacts, respectively.
Results: AutoVQC returned the spine localisation result within one minute per series. The result was reviewed for sufficient data quality for subsequent analyses and accurate corresponding canonical body axis range. From all 459 series evaluated, accuracy 0.93, precision 0.89, recall 0.98, and specificity 0.87 were achieved. The causes of artefacts included missing slices, non-axial image orientation, poor image quality, and the presence of multiple series in one single folder.
Conclusion: The initial evaluation of AutoVQC on multicentre study data demonstrated the potential of incorporating it into clinical trial image data management/analysis workflow for quality control of images based on automated spine localisation.
Limitations: A medium sample size.
Ethics committee approval: n/a
Funding: This work was supported by GSK.
Author Disclosures:
S. Lee: Consultant at GlaxoSmithKline, Consultant at GE Healthcare, Founder at Amallis Consulting LTD, Other at Director, Amallis Consulting LTD
B. Glocker: Consultant at GlaxoSmithKline
C. Page: Employee at was an employee of GlaxoSmithKline at the time of project, Shareholder at GlaxoSmithKline
P. Murphy: Employee at GlaxoSmithKline, Shareholder at GlaxoSmithKline
P. Galette: Employee at GlaxoSmithKline, Shareholder at GlaxoSmithKline

RPS 1805-10 11:34

Artificial intelligence for image-quality control of chest radiographs

K. I. Nousiainen, T. Mäkelä, A. Piilonen, J. I. Peltonen*; Helsinki/FI (katri.nousiainen@hus.fi)*

Purpose: To develop artificial intelligence for evaluating chest radiograph image-quality.
Methods and materials: We considered 3 different features of the image quality: inclusion, rotation, and inspiration. The inclusion was further divided into 4 edges: sin, dex, top, and bottom. The data comprised of 2,019 posteroanterior chest radiographs in an upright position. We annotated the images based on the European Commission's guidelines on quality criteria for diagnostic radiographic images. The inclusion criteria were divided into three classes: too tight, correct, and too wide. The rotation and inspiratory were divided into two classes: ok and not ok. We increased the amount of the image data for the inclusion by cropping the correct images to meet the too-tight criteria and for the inclusion and the rotation by flipping the images horizontally. The image histograms were equalized and the images were resized to a resolution of 512x512 pixels. Approximately 100 and 200 images were extracted for validation and test data, respectively. We trained ResNet50 and DenseNet121 networks with the remaining images.
Results: Resnet50 and Densenet121 both performed accurately for the inclusion detection in sin- and dex-edges. Densenet121 performed better for the inclusion detection in top- and bottom-edges as well as in the patient rotation and inspiration detection. The AUC was > 0.92 for the inclusion detection in all four edges in three classes. The AUC was > 0.71 and > 0.89 for the rotation and the inspiration, respectively.
Conclusion: Artificial intelligence can be used in a clinical setting as instant feedback of the chest radiograph image-quality. Additionally, the trained networks provide a tool for long-term quality control of a radiography unit.
Limitations: Data from only one centre was used.
Ethics committee approval: n/a
Funding: No funding was received for this work.
Author Disclosures:
K. I. Nousiainen: nothing to disclose
T. Mäkelä: nothing to disclose
A. Piilonen: nothing to disclose
J. I. Peltonen: nothing to disclose

RPS 1805-11 11:40

Adaptive versus fixed artificial intelligence (AI)-based preprocessing for noise reduction applied to routine non-contrast computed tomography scans

C. T. Whitlow[1], A. Hasegawa[2], J. Tan[1], R. Neelmegh[3], J. Vij[3]; *[1]Winston-Salem, NC/US, [2]Chapel Hill/US, [3]Sunnyvale/US (cwhitlow@wakehealth.edu)*

Purpose: Preprocessing CT material density images is a common step for noise reduction, which improves diagnostic image quality. Our study aimed to determine the utility of adaptive artificial intelligence (AI)-based preprocessing for adjusting parameters across each CT slice compared to a similar "fixed" AI-based version that applies the same parameters across all slices. We hypothesised that the adaptive AI-based approach would decrease noise levels across different imaging exams more than the fixed approach.
Methods and materials: This retrospective single-site observational study used head (n=569) and lung-nodule screening (n=276) CT exams acquired over the month prior to analysis on 64-MDCT scanners at standard-dose parameters. Original data was reconstructed as thin-section CT: 1) without preprocessing, 2) with fixed AI-based preprocessing, and 3) with adaptive AI-based preprocessing. The noise was computed as the dependent variable in each case using a manually coded software script and between-group analyses was conducted.
Results: There was a significant ($p<0.05$) between-group reduction in noise level variation, with decreases in noise for the AI-processed compared to the non-processed CT data and greater for the adaptive versus fixed AI-based algorithm. In particular, the standard deviation (SD) for the mean noise was markedly lower for the adaptive versus fixed AI-based algorithm, indicating decreases in image variability across scans.
Conclusion: The adaptive AI-based preprocessing algorithm outperformed the fixed method. In particular, SD differences between methods were more substantial, suggesting less variability in noise levels across cases for the adaptive method. Future investigation is necessary to determine if this algorithm produces image quality that improves sensitivity/specificity for the detection and diagnosis of clinically-relevant pathology.
Limitations: Limitations include relitively small sample-size and retrospective single-site design.
Ethics committee approval: IRB-approved.
Funding: No funding was received for this work.
Author Disclosures:
C. T. Whitlow: nothing to disclose
J. Tan: nothing to disclose
A. Hasegawa: Employee at AlgoMedica
R. Neelmegh: Founder at AlgoMedica
J. Vij: Founder at Algomedica

RPS 1805-12 11:46

Towards AI models that retain accuracy in the real world: a slice-level head CT artefact detector improves the performance of deep learning models

M. Maniparambil[1], S. Chilamkurthy[1], S. Tanamala[1], M. Biviji[2], P. Rao[1]; *[1]Mumbai/IN, [2]Nagpur/IN (mayug.maniparambil@qure.ai)*

Purpose: CT images often have artefacts due to subject motion. These cause mimics leading to false-positives (FPs) for AI models. In this study, we train an artefact-detector model and use this to make a subdural haemorrhage (SDH) detection model robust to artefacts.
Methods and materials: In FP's of the SDH model deployed at an urban outpatient centre, we found that 54% had artefacts. Visually inspecting these scans, we found that the models recognised motion-artefacts as SDH because both were hyperdense areas close to the cranium. We used a manually annotated dataset of 452 scans to train a convolutional neural network (CNN) to detect if a CT slice has artefacts or not. The original SDH model was also a CNN that predicted if a slice contained SDH. This model predicted scan as SDH positive if any slice was predicted positive. We modified this model by discounting the slices predicted as containing artefacts.
A validation dataset collected from the above centre from 06/18 to 01/19 contained 712 scans, of which 42 had SDH and 1,447 (total 22,131) slices had artefacts. Sensitivity and precision were used as metrics for SDH models, while slice-wise AUC for an artefact model.
Results: The original SDH model (sensitivity=1[90%CI 0.93-1] and precision=0.54[90%CI 0.44-0.64]) had 35 false-positives and 0 false-negatives. Quantitative analysis of FPs confirmed that 19 (54%) were due to CT artefacts. Our trained artefact model had slice-wise AUC of 96% [90%CI 0.952-0.967]. The proposed modification to the SDH model (sensitivity=1[90%CI 0.93-1] and precision=0.7[90%CI 0.62-0.81]) had reduced the FPs to 18 (decrease of 48.5%) without introducing any false-negatives.

Conclusion: AI can be trained to effectively detect artefact-ridden slices. This can be used to request reacquisition of an artefact containing scans or make other AI models robust to artefacts.
Limitations: n/a
Ethics committee approval: n/a
Funding: No funding was received for this work.
Author Disclosures:
M. Maniparambil: Employee at Qure.ai
S. Chilamkurthy: Employee at Qure.ai
S. Tanamala: Employee at Qure.ai
M. Biviji: nothing to disclose
P. Rao: Employee at Qure.ai

RPS 1805-13 11:52
Deep learning-based reduction of moving CT metal artefacts
T. Lossau, H. Nickisch, T. Wissel, S. Hakmi, A. Saalbach, C. Spink, M. Morlock, M. Grass*; Hamburg/DE (axel.saalbach@philips.com)*

Purpose: Non-static metal implants like pacemakers frequently lead to heavy streak-shaped artefacts in reconstructed CT image volumes. The reliable evaluation of neighbouring anatomy, for instance with regard to inflammation or calcification, might thereby be limited. Furthermore, motion precludes application of standard second pass metal artefact reduction (MAR) methods, which implicitly assume a static object during CT acquisition. We propose a MAR pipeline which is robust regarding motion and applicable on a wide range of scanner types, acquisition modes, and contrast protocols.
Methods and materials: The MAR pipeline uses raw projection data and is therefore independent of 3D motion blur. It is comprised of three convolutional neural network ensembles which are trained from scratch. First, SegmentationNets identify metal-affected line integrals in the input raw projection data. Second, values within the predicted metal shadow are treated as missing data and refilled based on surrounding line integrals by means of the InpaintingNets. The CT volume without metal is obtained by filtered backprojection of the inpainted sinogram. Finally, the ReinsertionNets determine metal positions in the image domain based on the segmented metal shadow.
Results: The data for supervised learning is generated by introducing synthetic metal implants into the projection data of 14 metal-free clinical cases with desired acquisition settings. A pacemaker lead model ensures sensible insertion positions, pathways, and motion trajectories by taking the cardiac anatomy and concomitant ECG-data into account.
Conclusion: The fully automatic pipeline is tested on 9 clinical cases with real pacemakers, whereby ECG-gated, as well as ungated contrast-enhanced CT, scan types are included. Significant metal artefact reduction is achieved.
Limitations: While empirical evaluation was restricted to pacemaker leads, applicability to other metal implants is very likely.
Ethics committee approval: n/a
Funding: No funding was received for this work.
Author Disclosures:
T. Wissel: Employee at Philips Research
T. Lossau: Employee at Philips Research
H. Nickisch: Employee at Philips Research
S. Hakmi: nothing to disclose
C. Spink: nothing to disclose
M. Morlock: nothing to disclose
M. Grass: Employee at Philips Research
A. Saalbach: Employee at Philips Research

C

Scientific and Educational Exhibits (C)

Full EPOS™ presentations are published at **epos.myESR.org** and can be cited by a Digital Object Identifier (DOI), if selected so during poster submission.